Key Words:
ELLWF
PA

Retention:
Permanent

E-Area Low-Level Waste Facility
DOE 435.1 Performance Assessment

JULY 2008

Washington Savannah River Company LLC
Savannah River Site
Aiken, SC 29808

Prepared for the U.S. Department of Energy under
Contract No. DE-AC09-96SR18500

Printed in the United States of America

Prepared for
U.S. Department of Energy

TABLE OF CONTENTS

APPENDICES

This page intentionally left blank.

LIST OF ACRONYMS AND ABBREVIATIONS

ACRONYMS

ALARA	As Low As Reasonably Achievable
ATTA	Advanced Tactical Training Area
CA	Composite Analysis
CAP-88	Clean Air Act Assessment Package – 1988
CB/TS	core barrels/thermal shields
CDP	cellulose degradation products
CFR	Code of Federal Regulations
CIG	Component-in-Grout
CLSM	controlled low strength material
CPT	cone penetrometer
CQF	Cognizant Quality Function
CSRA	Central Savannah River Area
CTF	Cognizant Technical Function
DAE	differential-algebraic equation
DAS	Disposal Authorization Statement
D&D	Decontamination and Decommissioning
DOD	Department of Defense
DOE	Department of Energy
DRF	dose release factor
DSA	Documented Safety Analysis
EDE	effective dose equivalent
EDST	Eastern Daylight Savings Time
EIS	Environmental Impact Statement
ELLWF	E-Area Low-Level Waste Facility
EMOP	E-Area Monitoring Program
EPA	Environmental Protection Agency
ET	Engineered Trench
ETP	Effluent Treatment Plant
GCL	geosynthetic clay liner
GSA	General Separations Area
HD	holddown
HDPE	high density polyethylene
HELP	Hydrologic Evaluation of Landfill Performance
IL	intermediate-level
ILNT	Intermediate-Level Non-Tritium
ILT	Intermediate-Level Tritium
ILV	Intermediate-Level Vault
KAPL	Knolls Atomic Power Laboratory
LAWV	Low-Activity Waste Vault
LAZ	lower aquifer zone

ACRONYMS AND ABBREVIATIONS

ACRONYMS – continued

LLW	low level waste
LLWF	Low Level Waste Facility
LVZ	Lower Vadose Zone
MCL	maximum contaminant level
MEI	maximally-exposed individual
MMI	Modified Mercalli Intensity
MWMF	Mixed Waste Management Facility
NCRP	National Council on Radiation Protection and Measurements
NESHAP	National Emissions Standards for Hazardous Air Pollutants
NOAA	National Oceanic and Atmospheric Administration
NPDES	National Pollutant Discharge Elimination System
NR	Naval Reactor
NRCDA	Naval Reactor Component Disposal Area
ORWBG	Old Radioactive Waste Burial Ground
OSC	Operational Soil Cover
PA	Performance Assessment
QA	quality assurance
QAP	Quality Assurance Procedure
RHS	right-hand side
SA	Special Analysis
SCDHEC	South Carolina Department of Health and Environmental Control
SDCF	scenario dose conversion factors
SLIT #	Specific set of 5 individual slit trenches that form a slit trench unit (e.g., SLIT8, set of 5 STs within the 656-ft-long x 157-ft-wide footprint immediately due east of the NRCDA)
SLITc	Central grouping of slit trench units composed of SLIT1 through SLIT7
SLITe	Eastern grouping of slit trench units composed of 8 future eastern slit trench unit footprints
SLITw	Western grouping of slit trench units composed of SLIT8 plus 5 future western slit trench unit footprints
SOF	sum of fractions
SQA	software quality assurance
SREL	Savannah River Ecology Laboratory
SRNL	Savannah River National Laboratory
SRS	Savannah River Site
ST	Slit Trench
SWMF	Solid Waste Management Facility
TPBAR	tritium-producing burnable absorber rods
UAZ	upper aquifer zone
UDQE	Unreviewed Disposal Question Evaluation
USEPA	United States Environmental Protection Agency
USGS	United States Geological Survey

ACRONYMS AND ABBREVIATIONS

ACRONYMS – continued

UTC	Universal Time Coordinated
UTR	Upper Three Runs
UVZ	Upper Vadose Zone
VZMS	vadose zone monitoring system
WAC	Waste Acceptance Criteria
WITS	Waste Information Tracking System
WMA	Wildlife Management Area
WMAP	Waste Management Area Project
WSRC	Washington Savannah River Company

ACRONYMS AND ABBREVIATIONS

ABBREVIATIONS

ρ_b	bulk density
Bq	Becquerel
cfs	cubic feet per second
Ci	curie
cm	centimeter
d	day
D_{eff}	effective diffusion coefficient
ft	foot
g	gram
hr	hour
in	inch
K_d	sorption coefficient
kg	kilogram
km	kilometer
ksi	kilopounds per square inch
L	liter
m	meter
mCi	millicurie
MeV	megaelectron volt
µg	microgram
mg	milligram
min	minute
mL	milliliter
mrem	millirem
msl	mean sea level
pCi	picocurie
pmol	picomole
psi	pounds per square inch
s	second
Sv	Sievert
yr	year

PART A

1.0 EXECUTIVE SUMMARY

2.0 SYNOPSIS

This page intentionally left blank.

1.0 EXECUTIVE SUMMARY

This Performance Assessment for the Savannah River Site (SRS) E-Area Low-Level Waste Facility (ELLWF) has been prepared to meet requirements of Chapter IV of the Department of Energy Order 435.1-1. The Order specifies that a Performance Assessment should provide reasonable assurance that a low-level waste disposal facility will comply with the performance objectives of the Order. The Order also requires assessments of impacts to water resources and to hypothetical inadvertent intruders for purposes of establishing limits on radionuclides that may be disposed near-surface. According to the Order, calculations of potential doses and releases from the facility should address a 1,000-year period after facility closure.

The point of compliance for the performance measures relevant to the all-pathways and air-pathway performance objective, as well as to the impact on the water resources assessment requirement, must correspond to the point of highest projected dose or concentration beyond a 100-m buffer zone surrounding the disposed waste following the assumed end of active institutional controls 100 years after facility closure. During the operational and institutional control periods, the point of compliance for the all-pathways and air-pathway performance measures is the SRS boundary. However, for the water resources impact assessment, the point of compliance remains the point of highest projected dose or concentration beyond a 100-m buffer zone surrounding the disposed waste during the operational and institutional control periods. For performance measures relevant to radon and inadvertent intruders, the points of compliance are the disposal facility surface for all time periods and the disposal facility after the assumed loss of active institutional controls 100 years after facility closure, respectively.

The E-Area Low-Level Waste Facility is located in the central region of the SRS known as the General Separations Area. It is an elbow-shaped, cleared area, which curves to the northwest, situated immediately north of the Mixed Waste Management Facility. The E-Area Low-Level Waste Facility is comprised of 200 acres for waste disposal and a surrounding buffer zone that extends out to the 100-m point of compliance. Disposal units within the footprint of the low-level waste facilities include the Slit Trenches, Engineered Trenches, Component-in-Grout Trenches, the Low-Activity Waste Vault, the Intermediate-Level Vault, and the Naval Reactor Component Disposal Area. Radiological waste disposal operations at the E-Area Low-Level Waste Facility began in 1994.

E-Area Low-Level Waste Facility closure will be conducted in three phases: operational closure, interim closure, and final closure. Operational closure will be conducted during the 25-year operation period (30-year period for Slit and Engineered Trenches) as disposal units are filled; interim closure measures will be taken for some units. Interim closure will take place following the end of operations and will consist of an area-wide runoff cover along with additional grading over the trench units.

Final closure of all disposal units in the E-Area Low-Level Waste Facility will take place at the end of the 100-year institutional control period and will consist of the installation of an integrated closure system designed to minimize moisture contact with the waste and to serve as a deterrent to intruders.

Radiological dose to human receptors is analyzed in this PA in the all-pathways analysis, the inadvertent intruder analysis and the air-pathway analysis, and the results are compared to the relevant performance measures. For the all-pathways analysis, the performance measure of relevance is a 25-mrem/yr effective dose equivalent (EDE) to representative members of the public, excluding dose from radon and its progeny in air. For the inadvertent intruder, the applicable performance measures are 100-mrem/yr EDE and 500 mrem/yr EDE for chronic and exposure scenarios, respectively.

The relevant performance measure for the air pathway is 10-mrem/yr EDE via the air pathway, excluding dose from radon and its progeny in air. Protection of groundwater resources is addressed by comparing calculated compliance point concentrations in groundwater with the relevant performance measure, which was determined to be the Safe Drinking Water Act maximum contaminant levels (MCLs) for beta-gamma and alpha-emitting radionuclides, and for radium and uranium. Radon fluxes for each disposal unit are calculated and compared to the average flux of 20 $pCi/m^2/s$ upper limit specified in the relevant performance objective.

Thirty-five parent radionuclides are addressed in the groundwater transport calculations, 15 radionuclides in the air-pathway calculations, and 78 parent radionuclides in the intruder analysis for all disposal units. Radon-222 fluxes are also evaluated for all disposal units. Two pathways have been identified as of possible consequence: 1) leaching of the wasteforms resulting in contamination of local groundwater, and 2) gaseous diffusion into the atmosphere above the disposal units. For the inadvertent intruder analyses, only the chronic resident and chronic post-drilling scenarios are considered plausible.

By comparing the calculated groundwater concentrations, all-pathway and air-pathway doses, intruder doses, and radon fluxes to respective performance measures, preliminary inventory limits are developed for each disposal unit. The potential effects of overlap of groundwater plumes from the various disposal units are then considered, as well as sensitivity and uncertainty in the groundwater concentration calculations, and the preliminary limits are adjusted as necessary. The final radionuclide disposal limits are compared with projected radionuclide inventories for each disposal unit, and sums of fractions of limits are calculated.

These limits are summarized in Table 1-1, by reporting only the maximum sum of fractions (SOF) calculated for each unit. None of the maximum SOFs is greater than one; therefore, there is a reasonable expectation that all of the performance measures set forth in DOE Order 435.1 will continue to be met throughout the life of the E-Area Low-Level Waste Facility.

Table 1-1. Summary of Impacts from E-Area Low-Level Waste Facility

Disposal Unit	Maximum SOF	Performance Measure	Major Nuclides
ST			
East	9.3E-01	4 mrem/year beta-gamma 12-100 years	I-129, H-3, C-14
Central	9.3E-01	4 mrem/year beta-gamma 12-100 years	Tc-99, I-129, H-3
West	9.5E-01	4 mrem/year beta-gamma 0-12 years	I-129, H-3
ET	9.6E-01	4 mrem/year beta-gamma 12-100 years	Tc-99, C-14, I-129, H-3
CIG	9.6E-01	4 mrem/year beta-gamma 125-1125 years	C-14, H-3, I-129
LAWV	9.2E-01	4 mrem/year beta-gamma	I-129, C-14
ILV	8.2E-01	4 mrem/year beta-gamma 200-1100 years	I-129
NRDCA			
643-7E	2.6E-01	10 mrem/year Air	C-14
642-26E	1.3E-01	10 mrem/year Air	C-14

Based on considerations of the point of assessment and the required points of compliance for the Composite Analysis, it is further concluded that the impact of the E-Area Low-Level Waste Facility Performance Assessment results on the Composite Analysis are negligible. A qualitative analysis evaluating the application of the As-Low-As-Reasonably-Achievable principle in the Performance Assessment process indicates that the goal of the process is attained based on technical and public policy considerations. These considerations place the points of compliance with performance measures at locations near the E-Area Low-Level Waste Facility that are not likely to be accessed by individuals and that are likely to exhibit higher concentrations than those to which individuals would realistically be exposed.

This page intentionally left blank.

2.0 SYNOPSIS

2.1 PURPOSE AND ORGANIZATION OF PA REPORT

This site-specific PA of the E-Area Low-Level Waste Facility (ELLWF) fulfills the DOE Order 435.1 requirement that such an assessment be prepared and maintained for DOE low-level waste (LLW) disposed of after September 26, 1988 (DOE M 435.1-1. IV.P. (2), DOE 1999a). The PA must provide reasonable assurance that the facility design and method of disposal will comply with the performance objectives of the Order, which are concerned with protection of public health and safety in limiting doses to members of the public and limiting releases of radon. The PA must also, for purposes of establishing limits on radionuclides that may be buried near-surface, assess impacts to hypothetical inadvertent intruders and impacts to water resources.

The organization of the PA report is depicted in Figure 2-1, and can be described as follows. Part C of the report provides the informational basis from which subsequent analyses have been performed. The Background Chapter in Part C provides facility- and site-specific information common to all of the disposal units in the E-Area LLWF, as well as general information relevant to identification of radionuclides and pathways of importance and the framework of the analytical techniques employed to evaluate environmental concentrations and dose. A general discussion of how the PA results will be used; and the approach to evaluating model sensitivity and uncertainty is also included in the Part C Background Chapter.

The Appendices in Part C provide tabulated information in support of the Part B analyses of performance specific to the disposal units in the E-Area LLWF. Most of this information is generated in the PA process (e.g., Appendix A containing the water table flux and peak groundwater concentrations), and represents intermediate results that are used in the final performance evaluation in Chapter 7 of Part B. Other appendices provide more in-depth discussions of background information (e.g., Appendix G, Data Supporting the Hydrogeologic Conceptual Model) or of specific analyses (e.g., Appendix F, Sensitivity and Uncertainty Study of the E-Area Trenches).

Part B of the report contains most of the analytical details pertinent to the assessment of performance of the individual disposal units and the performance of the facility as a whole. This part relies on the information provided in Part C and on several critical data packages developed in support of the E-Area LLWF PA and cited frequently throughout the Part B chapters. Chapters 1 through 5 provide analytical details specific to developing environmental concentrations and dose attributed to the individual disposal units. Chapter 6 addresses potential interactions of groundwater plumes from the various disposal units. Chapter 7 considers the results of the first five chapters and the plume interaction and sensitivity and uncertainty analyses results in terms of the measures of performance arising from the performance objectives and assessment requirements.

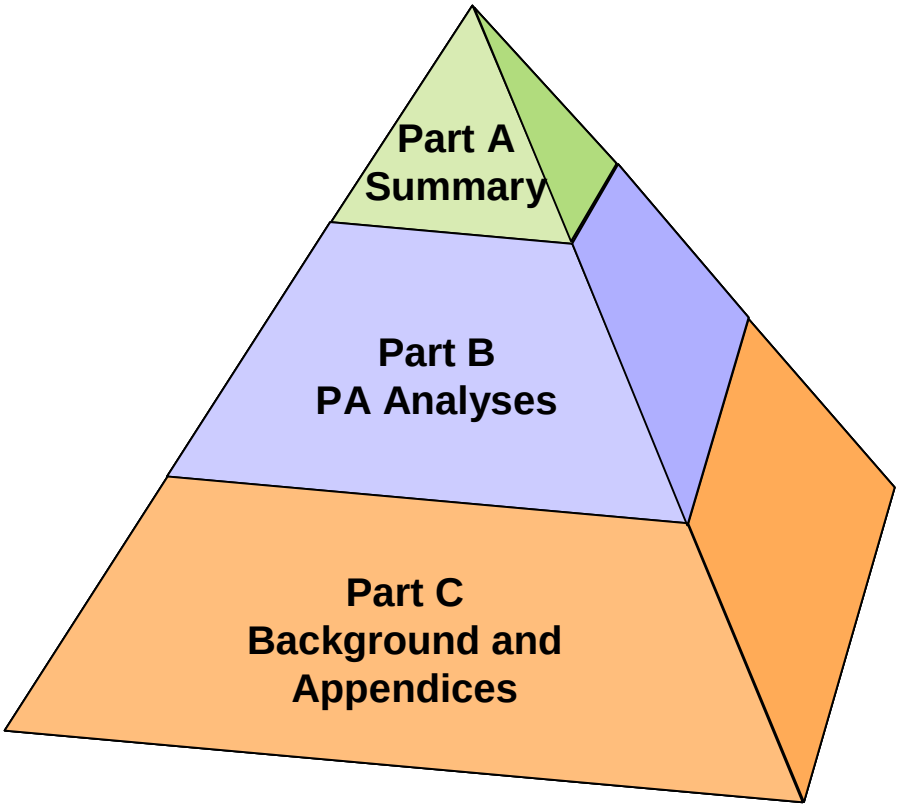

Figure 2-1. E-Area LLWF PA Report Organization

Finally, Part A of the E-Area LLWF PA provides a summary of the facility, performance objectives and assessment requirements, and PA results. All information provided in Part A is considered in greater detail in Part B.

2.2 DISPOSAL SITE, OPERATIONS, AND LIFECYCLE

The E-Area LLWF is located in the central region of the SRS known as the General Separations Area (GSA). Radiological waste disposal operations at the ELLWF began in 1994. The ELLWF is comprised of 200 acres for waste disposal and a surrounding buffer zone that extends out to the 100-m point of compliance for all disposal units. The current ELLWF area developed for disposal consists of approximately 100 acres. It is an elbow-shaped, cleared area, which curves to the northwest, situated immediately north of the Mixed Waste Management Facility (MWMF). Disposal units within the footprint of the LLWF include the Slit Trenches, Engineered Trenches, Components-In-Grout (CIG) Trenches, the Low Activity Waste Vault (LAWV), the Intermediate Level Vault (ILV), and the Naval Reactor Component Disposal Areas (NRCDAs).

The Slit Trenches, Engineered Trenches, and CIG Trenches are below-grade earthen disposal units. During the operational period, the Slit Trenches and Engineered Trenches are designed to accept low-level waste consisting of soil, debris, rubble, wood, concrete, equipment, and job control waste, which may be contained within B-25 boxes, B-12 boxes, 55-gallon drums, SeaLand containers, and other metal containers. The CIG Trenches are designed to accept large radioactively contaminated equipment and other smaller waste forms such as B-25 boxes to fill in the space around and above the large equipment. In addition, grout is poured around, between, and over the component(s) in order to encapsulate the component(s).

The LAWV is an above-grade, reinforced concrete vault, which is designed to contain predominately B-25 boxes and B-12 boxes, drums and/or concrete containers. The ILV is a below-grade, reinforced concrete vault built to accommodate intermediate-activity waste including tritium crucibles, job control waste, scrap hardware, and contaminated soil and rubble. The NRCDAs are above-grade gravel pads for the disposal of Naval Reactor Waste Shipping/Disposal Casks containing NR components. During the operational period, retired naval reactor components contained within casks are placed on the NRCDA as disposed in place.

ELLWF closure will be conducted in three phases: operational closure, interim closure, and final closure (Phifer et al. 2006). Operational closure will be conducted during the 25-year operation period (30-year period for Slit and Engineered Trenches) as disposal units are filled, and interim closure will be conducted after disposal operations have ceased for the Slit and Engineered Trenches and the CIG Trenches. Where needed, reinforced concrete mats are being installed over each CIG Trench segment after each is filled to provide structural support out to a period of 300 years for the integrated cap installed at final closure. Static surcharging and/or dynamic compaction will be conducted at the end of the 100-year institutional control period at the Slit Trenches and Engineered Trenches when the efficiency of the subsidence treatment will be greater due to container corrosion and subsequent strength loss. Dynamic compaction will not be carried out over any Slit or Engineered Trench (such as those containing M-Area glass and ETP Carbon Columns) that has been designated not to undergo such compaction (Phifer et al. 2006).

Prior to final closure of the NRCDAs, the space around, between, and over the casks will be filled with a structurally suitable material capable of supporting the final closure cap without resulting in differential subsidence.

Final closure of all disposal units in the ELLWF will take place at the end of the 100-year institutional control period (WSRC 2004). Final closure will consist of the installation of an integrated closure system designed to minimize moisture contact with the waste and to provide an intruder deterrent. The integrated closure system will consist of one or more closure caps installed over all the disposal units and a drainage system.

2.3 PERFORMANCE MEASURES

The performance objectives for DOE LLW disposal facilities are stated in DOE M 435.1-1.IV.P. (1) (DOE 1999a):

"Low-level waste disposal facilities shall be sited, designed, operated, maintained, and closed so that a reasonable expectation exists that the following performance objectives will be met for waste disposed of after September 26, 1988:

(a) Dose to representative members of the public shall not exceed 25 mrem (0.25 mSv) in a year total effective dose equivalent from all exposure pathways, excluding the dose from radon and its progeny in air

(b) Dose to representative members of the public via the air pathway shall not exceed 10 mrem (0.10 mSv) in a year total effective dose equivalent, excluding the dose from radon and its progeny.

(c) Release of radon shall be less than an average flux of 20 pCi/m^2/s (0.74 Bq/m^2/s) at the surface of the disposal facility. Alternatively, a limit of 0.5 pCi/l (0.0185 Bq/l) of air may be applied at the boundary of the facility."

The DOE 435.1 requirement for assessment of the protection of water resources is found in DOE M 435.1-1.IV.P. (2). (g), which states (DOE 1999a):

(g) "For purposes of establishing limits on radionuclides that may be disposed of near-surface, the performance assessment shall include an assessment of impacts to water resources."

The guide for DOE 435.1 (DOE 1999b) states "DOE M 435.1-1 does not specify the level of protection for water resources that should be used in a performance assessment for a specific low-level waste disposal facility. Rather, a site-specific approach, in accordance with a hierarchical set of criteria should be followed."

At SRS, the appropriate measure for protection of water resources has been determined to be the Safe Drinking Water Act MCLs. The MCLs (EPA 2000; EPA 2001) are shown in Table 2-1.

Table 2-1. Maximum Contaminant Levels

Component	Maximum Contaminant Level
Beta-Gamma Dose	4 mrem/year
Gross Alpha	15 pCi/L
Radium	5 pCi/L
Uranium	30 µg/L

The DOE 435.1 requirement for assessment of inadvertent intruder analysis is found in DOE M 435.1-1.IV.P. (2). (h), which states (DOE 1999a):

> (h) "For purposes of establishing limits on the concentration of radionuclides that may be disposed of near-surface, the performance assessment shall include an assessment of impacts calculated for a hypothetical person assumed to inadvertently intrude for a temporary period into the low-level waste disposal facility. For intruder analyses, institutional controls shall be assumed to be effective in deterring intrusion for at least 100 years following closure. The intruder analyses shall use performance measures for chronic and acute exposure scenarios, respectively, of 100 mrem (1 mSv) in a year and 500 mrem (5 mSv) total effective dose equivalent excluding radon in air."

The Order specifies that the PA shall include calculations for a 1,000-year period after closure of potential doses to representative future members of the public and potential releases from the facility to provide a reasonable expectation that the performance objectives identified are not exceeded (DOE 1999a). The point of compliance must correspond to the point of highest projected dose or concentration beyond a 100-m buffer zone surrounding the disposed waste.

2.4 SUMMARY OF KEY ASSUMPTIONS

Numerous assumptions were made in assessing the performance of the E-Area LLWF, which are noted and discussed in Chapters 1 through 6 of Part B. A summary of the key assumptions common to most of the analyses done in support of the PA are listed below. A list including key assumptions specific to each disposal unit is given in Appendix B.

2.4.1 Construction, Operation, and Closure Assumptions

- Disposal unit dimensions are appropriately defined in Phifer et al. (2006)
- All interim and final closure details are as described in Phifer et al. (2006)
- The operational period lasts for 30 years for the Slit and Engineered Trenches, and for 25 years for all other units; the institutional control period for 100 years
- Final closure of the entire E-Area LLWF will be carried out at the end of the institutional control period using the closure details documented in Phifer et al. (2006), based on the conceptual E-Area Closure Plan (WSRC 2004)

2.4.2 Groundwater Pathway

- "Best" estimate for physical and hydraulic properties of all subsurface materials from Phifer et al. (2006) are valid
- Material transport properties, including effective, total, and diffusive porosities, molecular diffusivity, and particle density are consistent with the values reported in Phifer et al. (2006)
- Longitudinal and transverse dispersivity coefficients are zero, except for the slit and engineered trench transport calculations, where they are set to 10% and 1%, respectively
- "Best estimate" K_ds and solubilities recommended by Kaplan (2006)
- Non-cementitious K_ds assigned values for Sandy Sediment or Clayey Sediments from Kaplan (2006)
- Radiological half-lives from Cook (2007)
- Model gridding sufficiently conforms with disposal unit dimensions to adequately simulate flow and transport
- Lateral extent of vadose zone model sufficient to support boundary condition specifications
- Infiltration rates adequately bound all plausible scenarios

2.4.3 Intruder Pathway

- Erosion barrier in closure cap will prevent excavation into the disposed waste for all units, and will limit resident-intruder exposures by maintaining at least 10 ft of soil material between the ground surface and the top of the disposed waste

2.4.4 Air Pathway

- Radionuclide migration from waste zone to ground surface assumed to occur by diffusion in vapor-filled pores only

2.4.5 Radon Pathway

- Radon migration from waste zone to ground surface assumed to occur by diffusion in vapor-filled pores only

2.4.6 All-pathways

- Based on pathway screening, only two pathways are considered for transport of radionuclides from the disposed waste into the environment; leaching of the wasteform resulting in contamination of groundwater local to E-Area and gaseous diffusion into the atmosphere local to E-Area.
- Because maximum exposures via the air pathway will occur at different times and locations than maximum exposures due to groundwater, contributions from the air transport pathway are considered separately.

2.5 OVERVIEW OF PA ANALYSES

In this PA, radiological dose to human receptors is analyzed in the all-pathways analysis, the inadvertent intruder analysis and the air-pathway analysis, and the results are compared to the relevant performance measures. Protection of groundwater resources is addressed by comparing calculated compliance point concentrations in groundwater with Safe Drinking Water Act MCLs for beta-gamma and alpha-emitting radionuclides, and for radium and uranium. Radon fluxes for each disposal unit are calculated and compared to the average flux of 20 $pCi/m^2/s$ upper limit specified in the relevant performance objective.

In preparation for making the required analyses, screening to identify radionuclides and environmental pathways of concern was conducted. The results of the screening calculations identified 35 parent radionuclides to be addressed in the groundwater transport calculations, 15 radionuclides to be addressed in the air-pathway calculations, and 78 parent radionuclides to be addressed in the intruder analysis. For the groundwater and air-pathway analyses, these results were also limited by the list of radionuclides in the projected inventories for the disposal units.

For radionuclides that were not screened out but were not in the projected inventory, trigger values were developed, based on very conservative assumptions, which can be used as surrogate disposal unit limits. Radon-220 was considered insignificant with respect to radon flux due to its short half-life, and only Rn-222 fluxes were evaluated. Radioactive progeny were considered in the screening analyses.

Of 47 pathways identified by which radionuclides released from the ELLWF have the potential for reaching humans, only two were identified as of possible consequence:
1) leaching of the wasteform resulting in contamination of local groundwater, and
2) gaseous diffusion into the atmosphere above the disposal units. For the inadvertent intruder analyses, two exposure scenarios were identified as plausible, based on consideration of potential acute and chronic scenarios – the chronic resident and chronic post-drilling scenarios.

Water infiltration rates through the various cover systems used for the E-Area LLWF disposal units are estimated in this PA with the EPA-sanctioned HELP model (Schroeder et al. 1994). Environmental transport from each disposal unit to and within the media of concern (groundwater and air) was simulated for each disposal unit. The PORFLOW numerical code (ACRI 2004) was used to simulate transport of radionuclides to the water table and, for volatile radionuclides, to the ground surface. This code was also used to simulate transport in groundwater to the points of assessment. Air transport of volatile radionuclides reaching the ground surface was simulated using CAP-88 (EPA 2006). Radionuclide-specific groundwater and air concentrations, as well as radon fluxes, were calculated in these simulations. Ingrowth of radioactive progeny was included in these analyses.

By comparing the calculated groundwater concentrations, all-pathway and air-pathway doses, intruder doses, and radon fluxes to respective performance measures, preliminary inventory limits were developed for each disposal unit (Chapters 1 through 5 of Part B). Groundwater plume interaction factors were developed (Chapter 6 of Part B) to adjust the groundwater-based inventory limits as necessary to account for potential plume overlap. Adjustments to the calculated limits are made, based on the plume interaction factors and results of sensitivity and uncertainty analyses (Chapter 7 of Part B).

2.6 DISPOSAL LIMITS

The final radionuclide disposal limits (tabulated in Chapter 7 of Part B) are compared with projected radionuclide inventories (Appendix C) and the SOF of limits for each disposal unit are provided. These limits are summarized in Table 2-2, by reporting only the largest SOF calculated for each unit.

Table 2-2. Summary of Impacts from E-Area LLWF

Disposal Unit	Maximum SOF	Performance Measure	Major Nuclides
ST			
East	9.3E-01	4 mrem/year beta-gamma 12-100 years	I-129, H-3, C-14
Central	9.3E-01	4 mrem/year beta-gamma 12-100 years	Tc-99, I-129, H-3
West	9.5E-01	4 mrem/year beta-gamma 0-12 years	I-129, H-3
ET	9.6E-01	4 mrem/year beta-gamma 12-100 years	Tc-99, C-14, I-129, H-3
CIG	9.6E-01	4 mrem/year beta-gamma 125-1125 years	C-14, H-3, I-129
LAWV	9.2E-01	4 mrem/year beta-gamma	I-129, C-14
ILV	8.2E-01	4 mrem/year beta-gamma 200-1100 years	I-129
NRDCA			
643-7E	2.6E-01	10 mrem/year Air	C-14
642-26E	1.3E-01	10 mrem/year Air	C-14

2.7 INTERPRETATION OF RESULTS

Achieving reasonable assurance that disposal units will meet DOE 435.1 performance objectives requires a thoughtful consideration of uncertainty in PA model design, model inputs, and facility operations. For this PA, uncertainties were addressed in the groundwater pathway by employing a combination of conservative modeling assumptions, deterministic sensitivity analyses, and preliminary probabilistic uncertainty analyses. Details of these analyses and results are presented in the respective PA modules.

For the E-Area disposal units, a tiered approach for addressing uncertainty in PORFLOW-based groundwater concentration calculations was carried out, which involved adopting conservative assumptions for some portions of the groundwater pathway analysis, and conducting qualitative sensitivity analysis. For the Slit and Engineered Trenches, a sensitivity analysis was conducted in which additional percentages of non-crushable waste was assumed to be present and a sum-of-fractions (SOF) analysis was conducted for four highly-mobile radionuclides that contribute the most to the SOF (i.e., H-3, C-14, Tc-99, and I-129 and their special waste forms).

For the CIG, K_d values, timing of cementitious material aging and grout effective diffusivity were selected for sensitivity analysis. For the ILV, sorption coefficients and effective diffusion coefficients were judged to be the dominant contributors to radionuclide concentration uncertainty, and sensitivity runs were conducted by varying these two parameters. For the LAWV, K_d, D_{eff}, vault cracking, and infiltration were identified for sensitivity runs. Sensitivity runs were conducted by varying all except infiltration rates, since uncertainty in infiltration has not yet been defined. The results of the sensitivity analyses can be evaluated by considering the impact of independently varied parametric values on the summed fraction of each radionuclide's disposal limit for the disposal unit of interest.

For the Slit and Engineered Trenches, CIG Trenches, and NRCDAs, a probabilistic uncertainty analysis was conducted using a commercial program, GOLDSIM. Inputs to the GOLDSIM model for the Slit and Engineered Trenches, CIG Trenches, and NRCDAs were treated as stochastic (random) variables and assigned statistical distributions based on data and/or professional judgment. The parameters selected for variable input were those having the most significant effect on the calculated groundwater concentrations and dose, as determined by previous sensitivity analyses, or professional judgment. The Monte Carlo analysis performed by the GOLDSIM program generates a statistical distribution of groundwater concentration and dose.

The results of the sensitivity and uncertainty analyses do not suggest that the PORFLOW-derived radionuclide disposal limits should be reduced to account for uncertainty.

2.8 IMPACT ON COMPOSITE ANALYSIS

The results of the CA for the SRS (WSRC 1997) concluded that the predominant sources of radionuclides contributing to the calculated dose at the identified points of assessment were facilities other than the E-Area waste disposal facility. The points of assessment for the CA are as follows. For the hypothetical future public individual, the points of assessment are the mouths of UTR and FMB (where creek water is undiluted by the Savannah River, but still accessible by the public), and the Savannah River at the Highway 301 bridge. For the hypothetical future public population, the points of assessment are the Savannah River at the Highway 301 bridge and the water treatment plants at Beaufort-Jasper, SC and Port Wentworth, GA. These were selected based on considerations of the points of maximum concentration accessible by the public, consistent with site plans for future use and control.

The primary dose limit of 100 mrem/yr and dose constraint of 30 mrem/yr are applicable to the CA. The current E-Area PA considers performance measures for groundwater and air (media by which members of the public may be exposed to radionuclides at the points of assessment) that are considerably less than these limits and constraints and the points of assessment for the CA are far enough removed from the vicinity of E-Area that considerable dispersion and decay in transit would occur. Therefore, it is concluded that the impact of the ELLWF PA results on the CA are negligible.

2.9 ALARA ANALYSIS

DOE's approach to radiation protection for LLW disposal is based on the performance objectives listed in the Order (DOE 1999a), which specify maximum doses for various pathways, and on the ALARA principle, which requires doses to be maintained as low as reasonably achievable. The requirement is stated in DOE (1999a):

> "Performance assessments shall include a determination that projected releases of radionuclide to the environment shall be maintained as low as reasonably achievable (ALARA)."

In addition to providing a reasonable expectation that the performance objectives described in DOE M 435.1-1.IV.P, the PA also needs to show that LLW disposal is being conducted in a manner that maintains releases of radionuclides to the environment ALARA. The goal of the ALARA process is attainment of the lowest practical dose level after taking into account social, technical, economic, and public policy considerations.

For the ELLWF PA, the point of compliance was selected to be the point of highest calculated dose or concentration beyond a 100-m buffer zone surrounding the waste after the institutional control period. The results of groundwater and air dispersion modeling indicate this location of highest dose or concentration is very close to the 100-m distance from the waste. However, the SRS Future Use Plan (DOE 1998) indicates that that the current SRS boundaries will remain unchanged; thus, no member of the public would have unrestricted access to the E-Area LLWF. Because the E-Area LLWF is a much greater distance from the site boundary than 100 meters, and groundwater potentially affected by releases from the E-Area LLWF is completely intercepted by UTR creek, the PA results protect the public to a much greater degree than would be required under the Future Use Plan. Considerable more dispersion of any radionuclides released to groundwater or air would occur if the closest access point to the disposal facility is the SRS site boundary. Therefore, the principle of ALARA is satisfied based on these technical and public policy considerations.

2.10 USE OF PA RESULTS

The primary use of the PA results is to develop radionuclide disposal limits for each of the disposal units. Limits are developed by ratio of the maximum impact (e.g., all-pathways dose) calculated for a specific time period for a unit inventory of each radionuclide to the respective performance measure (e.g., 25 mrem/year). The PA-derived limits are expressed in terms of curies per disposal unit.

The PA results also allow a comparison of projected radionuclide inventories at closure with the PA-derived radionuclide disposal limits. Compliance with performance measures is assessed by dividing the projected inventory at closure for each radionuclide in a particular disposal unit with the disposal limits determined for that unit. Summing the limit fractions for each performance measure and time period allows the sum-of-fractions to be calculated. A SOF less than one indicates compliance with the performance measure. The SOF method of assessing compliance assures future compliance despite changing projected inventories.

The PA sensitivity and uncertainty results are useful in determining which parameters of the disposal facility future PA maintenance activities should focus on. These activities may include development of more rigorous analytical techniques, or enhanced efforts to more accurately quantify environmental, or other physical, parameters.

2.11 REFERENCES

ACRI (Analytic & Computational Research, Inc.). 2004. *PORFLOW User's Manual*, Version 5.0, Rev: 5. Available at http://www.acricfd.com/download/papers/PORFLOW.pdf

Cook, J. R. 2007. *Radionuclide Data Package for Performance Assessment Calculations Related to the E-Area Low-Level Waste Facility at the Savannah River Site*, WSRC-STI-2006-00162, Rev. 0, Savannah River National Laboratory, Aiken, SC

DOE (Department of Energy). 1998. *Savannah River Site Future Use Plan*, March 1998.

DOE (Department of Energy). 1999a. *Radioactive Waste Management Manual of 7-09-99*, DOE M 435.1-1, U.S. Department of Energy, Washington, DC.

DOE (Department of Energy). 1999b. *Format and Content Guide for U.S. Department of Energy Low-Level Waste Disposal Facility Performance Assessments and Composite Analyses*, U.S. Department of Energy, Washington, DC.

EPA (Environmental Protection Agency). 2006. *CAP88-PC Version 3.0 User Guide*. Office of Radiation and Indoor Air, Washington, DC.

EPA (Environmental Protection Agency). 2000. *National Primary Drinking Water Regulations; Radionuclides; Final Rule*, 40 CFR Parts 141 and 142, U. S. Environmental Protection Agency, Washington, DC.

EPA (Environmental Protection Agency). 2001. Implementation Guidance for Radionuclides, appendix I, Comparison of Derived Values of Beta and Photon Emitters, EPA 816-D-00-002, U. S. Environmental Protection Agency, Washington, DC.

Kaplan, D. I. 2006. *Geochemical Data Package for Performance Assessment Calculations Related to the Savannah River Site (U)*, WSRC-TR-2006-00004, Rev. 0, Washington Savannah River Company, Savannah River Site, Aiken, SC.

Phifer, M. A., Millings, M. R., and Flach, G. P. 2006. Hydraulic Property Data Package for the E-Area and Z-Area Vadose Zone Soils, Cementitious Materials, and Waste Zones, WSRC-STI-2006-00198, Rev. 0, Washington Savannah River Company, Aiken, SC.

Schroeder, P. R., Dozier, T. S., Zappi, P. A., McEnroe, B. M., Sjostrom, J. W., and Peyton, R. L. 1994. *The Hydrologic Evaluation of Landfill Performance (HELP) Engineering Documentation for Version 3*. EPA/600/R-94/168b. Office of Research and Development, United States Environmental Protection Agency (EPA), Cincinnati, Ohio. September 1994.

WSRC (Westinghouse Savannah River Company). 1997. *Composite Analysis, E-Area Vaults and Saltstone Disposal Facilities*, WSRC-RP-97-311, Rev. 0, Westinghouse Savannah River Company, Aiken, SC.

WSRC (Westinghouse Savannah River Company). 2004. *Closure Plan for the E-Area Low-Level Waste Facility*, Rev. 5, WSRC-RP-2000-00425, Rev. 4, May 2004, Westinghouse Savannah River Company, Aiken, SC.

This page intentionally left blank.

CHAPTER 1

SLIT AND ENGINEERED TRENCHES

This page intentionally left blank.

1.0 SLIT AND ENGINEERED TRENCHES

LIST OF FIGURES

LIST OF TABLES

This page intentionally left blank.

1.0 SLIT AND ENGINEERED TRENCHES

1.1 EXECUTIVE SUMMARY

The Slit and Engineered Trench disposal units are shallow land burial facilities for the disposal of a high volume of very low activity waste. These units are constructed as needed.

Slit And Engineered Trench disposal limits through the 1,000-year compliance period have been developed for the following pathways: groundwater protection, all pathways, inadvertent intruder (resident scenario and post-drilling scenario), air, and radon. All instances of groundwater protection and all-pathways "limits" in this chapter refer to "preliminary limits" only, because they do not account for plume interaction or uncertainties. Table 1-1 through Table 1-11 provide these disposal limits for the Slit Trench and Engineered Trench disposal units, respectively. Limits for the Slit Trenches are presented for three groupings of Slit Trenches - the East Slit Trenches, Central Slit Trenches, and West Slit Trenches. In Chapter 7 these limits will be adjusted in consideration of the result of the uncertainty analyses reported in this chapter and the plume interaction analysis reported in Chapter 6.

Trigger values for radionuclides that are not screened out of the groundwater and air analyses and have not been specifically analyzed are given in Tables 4-4 and 4-5, respectively, in the Part C Background Chapter. The trigger values have been developed using conservative screening methodologies and can be used as surrogate disposal unit limits should any of the listed radionuclides be proposed for disposal.

Table 1-1. Preliminary Groundwater Protection Limits for East Slit Trenches

	Beta-Gamma			Gross Alpha			Radium Limit			Uranium Limit
	(Ci/Disposal Unit)			(Ci/Disposal Unit)			(Ci/Disposal Unit)			(Ci/Disposal Unit)
Parent Nuclide	**0-12 yrs**	**12-100 yrs**	**100-1130 yrs**	**0-1000 yrs**	**1000-1120 yrs**	**1120-1130 yrs**	**0-1000 yrs**	**1000-1120 yrs**	**1120-1130 yrs**	
Am-241	2.4E+10	2.1E+06	7.8E+03	3.9E+02	4.6E+02	4.6E+02	---	---	---	1.2E+12
Am-243	---	4.8E+16	2.9E+03	5.5E+02	1.6E+02	1.5E+02	---	---	---	1.1E+13
C-14	3.1E-01	2.6E-01	6.0E+00	---	---	---	---	---	---	---
C-14_NR.Pump	---	---	1.8E+00	---	---	---	---	---	---	---
Cf-249	7.6E+17	3.9E+12	1.4E+05	2.4E+03	8.4E+02	7.8E+02	---	---	---	6.5E+13
Cf-251	---	---	1.0E+09	1.1E+03	3.4E+02	3.2E+02	---	---	---	6.8E+18
Cl-36	1.1E-01	9.2E-02	2.1E+00	---	---	---	---	---	---	---
Cm-244	---	---	7.8E+18	2.9E+12	3.2E+11	2.7E+11	1.4E+19	1.1E+19	1.1E+19	3.7E+19
Cm-245	1.0E+14	1.3E+09	4.3E+03	1.9E+02	7.5E+01	6.9E+01	---	---	---	1.2E+12
Cm-246	---	---	6.8E+15	5.8E+02	1.7E+02	1.6E+02	1.3E+16	4.7E+15	4.3E+15	1.7E+14
Cm-247	---	---	2.2E+04	4.6E+02	1.3E+02	1.2E+02	---	---	---	1.2E+14
Cm-248	---	---	2.3E+10	5.5E+02	1.6E+02	1.4E+02	---	---	---	2.9E+18
H-3	6.1E+00	5.7E+00	1.6E+04	---	---	---	---	---	---	---
H-3_ETF.Carbon	---	---	6.7E+04	---	---	---	---	---	---	---
I-129	2.1E-04	1.4E-04	4.2E-03	---	---	---	---	---	---	---
I-129_ETF.Carbon	---	---	1.2E-01	---	---	---	---	---	---	---
I-129_ETF.GT.73	1.6E+00	4.2E-01	1.6E-01	---	---	---	---	---	---	---
I-129_F.Carbon	2.1E+01	5.6E+00	2.1E+00	---	---	---	---	---	---	---
I-129_F.CG.8	8.1E-03	2.1E-03	2.9E-03	---	---	---	---	---	---	---
I-129_F.Dowex.21K	1.1E+00	2.9E-01	1.1E-01	---	---	---	---	---	---	---
I-129_F.Filtercake	9.2E-03	2.4E-03	3.1E-03	---	---	---	---	---	---	---
I-129_H.Carbon	9.3E+00	2.5E+00	9.3E-01	---	---	---	---	---	---	---
I-129_H.CG.8	6.1E-02	1.6E-02	1.0E-02	---	---	---	---	---	---	---
I-129_H.Dowex.21K	2.5E+00	6.6E-01	2.5E-01	---	---	---	---	---	---	---
I-129_H.Filtercake	1.0E-01	2.8E-02	1.5E-02	---	---	---	---	---	---	---
K-40	1.6E-01	1.1E-01	1.1E+00	---	---	---	---	---	---	---
Mo-93	2.4E-01	1.9E-01	2.4E+00	---	---	---	---	---	---	---
Nb-94	1.2E-01	1.0E-01	2.3E+00	---	---	---	---	---	---	---
Ni-59	---	1.1E+10	7.1E+00	---	---	---	---	---	---	---

Table 1-1. Preliminary Groundwater Protection Limits for East Slit Trenches - continued

	Beta-Gamma			Gross Alpha			Radium Limit			Uranium Limit
	(Ci/Disposal Unit)			(Ci/Disposal Unit)			(Ci/Disposal Unit)			(Ci/Disposal Unit)
Parent Nuclide	**0-12 yrs**	**12-100 yrs**	**100-1130 yrs**	**0-1000 yrs**	**1000-1120 yrs**	**1120-1130 yrs**	**0-1000 yrs**	**1000-1120 yrs**	**1120-1130 yrs**	
Np-237	1.4E+04	4.5E+00	1.2E+00	6.1E-02	1.0E-01	2.2E-01	---	---	---	1.8E+08
Pd-107	---	1.3E+12	8.6E+02	---	---	---	---	---	---	---
Pu-238	---	---	1.3E+07	4.6E+05	1.5E+05	1.4E+05	4.6E+05	1.5E+05	1.4E+05	8.3E+18
Pu-239	5.9E+18	6.2E+12	7.3E+06	6.6E+06	5.7E+06	5.7E+06	---	---	---	1.3E+17
Pu-240	---	---	2.0E+16	1.1E+10	1.2E+09	1.0E+09	3.6E+16	2.8E+16	2.7E+16	1.4E+17
Pu-241	9.1E+12	3.0E+08	2.4E+05	1.2E+04	1.4E+04	1.4E+04	---	---	---	3.5E+13
Pu-242	---	---	1.3E+14	1.0E+10	1.1E+09	8.8E+08	4.3E+12	1.5E+12	1.4E+12	1.2E+17
Pu-244	---	---	7.5E+10	9.4E+09	9.4E+08	7.9E+08	1.5E+18	1.1E+18	1.0E+18	1.2E+18
Ra-226	6.4E+18	6.5E+07	3.1E+00	9.3E-02	3.8E-02	3.7E-02	9.3E-02	3.8E-02	3.7E-02	---
Se-79	---	---	---	---	---	---	---	---	---	---
Sn-126	---	---	---	---	---	---	---	---	---	---
Sr-90	2.8E+16	9.1E+06	1.8E+02	---	---	---	---	---	---	---
Tc-99	3.1E-01	1.4E-01	3.1E+00	---	---	---	---	---	---	---
Th-230	---	5.2E+10	1.1E+01	4.6E-01	1.3E-01	1.2E-01	4.6E-01	1.3E-01	1.2E-01	---
Th-232	1.8E+18	3.9E+10	2.2E+04	2.3E+04	5.2E+04	6.7E+04	3.0E+04	6.9E+04	8.9E+04	---
U-233	---	---	2.1E+13	5.7E+13	5.3E+12	4.5E+12	---	---	---	6.9E+14
U-234	---	2.0E+15	3.2E+03	1.2E+02	3.8E+01	3.5E+01	1.2E+02	3.8E+01	3.5E+01	2.1E+15
U-235	1.1E+10	2.8E+04	4.4E+00	3.4E+00	3.5E+00	4.0E+00	---	---	---	1.1E+12
U-236	---	---	2.0E+11	2.6E+11	2.1E+11	2.1E+11	3.5E+11	2.8E+11	2.8E+11	2.2E+13
U-238	---	---	4.2E+06	1.5E+05	5.0E+04	4.6E+04	1.5E+05	5.0E+04	4.6E+04	1.1E+11
Zr-93	2.3E+00	5.4E-01	6.2E-01	---	---	---	---	---	---	---

Note: Limits reported as "---" indicate that there is no limit or that the limit $\geq$ 1E+20.

Note: Groundwater limits in this table are to be considered preliminary. Adjustments are made in the groundwater limits as appropriate based on consideration of plume overlap effects from adjacent units in Chapter 6 and interpretation of sensitivity and uncertainty analyses in Chapter 7. Final limits are to be found in results tables in Chapter 7.

Table 1-2. Preliminary Groundwater Protection Limits for Center Slit Trenches

	Beta-Gamma			Gross Alpha			Radium Limit			Uranium Limit
	(Ci/Disposal Unit)			(Ci/Disposal Unit)			(Ci/Disposal Unit)			(Ci/Disposal Unit)
Parent Nuclide	**0-12 yrs**	**12-100 yrs**	**100-1130 yrs**	**0-1000 yrs**	**1000-1120 yrs**	**1120-1130 yrs**	**0-1000 yrs**	**1000-1120 yrs**	**1120-1130 yrs**	
Am-241	4.6E+09	2.1E+06	1.3E+04	2.6E+02	1.5E+02	1.4E+02	---	---	---	1.9E+12
Am-243	---	6.2E+16	5.6E+02	7.8E+01	3.0E+01	2.8E+01	---	---	---	1.4E+12
C-14	2.9E-01	2.9E-01	1.0E+01	---	---	---	---	---	---	---
C-14_NR.Pump	---	---	2.9E+00	---	---	---	---	---	---	---
Cf-249	1.4E+17	3.7E+12	3.8E+04	3.7E+02	1.6E+02	1.5E+02	---	---	---	1.1E+14
Cf-251	---	---	2.0E+08	1.5E+02	6.5E+01	6.1E+01	---	---	---	9.5E+17
Cl-36	1.0E-01	1.0E-01	3.5E+00	---	---	---	---	---	---	---
Cm-244	---	---	1.0E+18	8.2E+10	1.1E+10	9.3E+09	1.9E+18	1.5E+18	1.4E+18	1.2E+18
Cm-245	2.0E+13	1.2E+09	1.4E+03	4.2E+01	1.6E+01	1.5E+01	---	---	---	2.1E+12
Cm-246	---	---	9.1E+14	8.2E+01	3.2E+01	3.0E+01	1.3E+16	4.3E+15	3.9E+15	2.3E+13
Cm-247	---	---	4.2E+03	6.5E+01	2.5E+01	2.3E+01	---	---	---	1.6E+13
Cm-248	---	---	3.7E+09	7.7E+01	3.0E+01	2.8E+01	---	---	---	3.4E+17
H-3	5.5E+00	5.6E+00	2.7E+04	---	---	---	---	---	---	---
H-3_Concrete	1.3E+01	1.3E+01	6.3E+04	---	---	---	---	---	---	---
H-3_ ETF.Carbon	---	---	6.6E+04	---	---	---	---	---	---	---
I-129	1.7E-04	1.6E-04	7.4E-03	---	---	---	---	---	---	---
I-129_ETF.Carbon	---	---	2.0E-01	---	---	---	---	---	---	---
I-129_ETF.GT.73	1.4E+00	6.8E-01	2.7E-01	---	---	---	---	---	---	---
I-129_F.Carbon	1.8E+01	9.1E+00	3.5E+00	---	---	---	---	---	---	---
I-129_F.CG.8	6.9E-03	3.5E-03	4.2E-03	---	---	---	---	---	---	---
I-129_F.Dowex.21K	9.3E-01	4.7E-01	1.9E-01	---	---	---	---	---	---	---
I-129_F.Filtercake	7.8E-03	3.9E-03	4.4E-03	---	---	---	---	---	---	---
I-129_H.Carbon	7.9E+00	4.0E+00	1.6E+00	---	---	---	---	---	---	---
I-129_H.CG.8	5.2E-02	2.6E-02	1.7E-02	---	---	---	---	---	---	---
I-129_H.Dowex.21K	2.1E+00	1.1E+00	4.2E-01	---	---	---	---	---	---	---
I-129_H.Filtercake	8.9E-02	4.5E-02	2.6E-02	---	---	---	---	---	---	---
I-129_Mk50A	4.2E+00	1.7E+00	4.6E-01	---	---	---	---	---	---	---
K-40	2.2E-01	1.6E-01	1.9E+00	---	---	---	---	---	---	---
Mo-93	2.2E-01	2.2E-01	4.1E+00	---	---	---	---	---	---	---
Nb-94	1.1E-01	1.1E-01	3.9E+00	---	---	---	---	---	---	---
Ni-59	6.8E+19	4.0E+09	4.8E+00	---	---	---	---	---	---	---

Table 1-2. Preliminary Groundwater Protection Limits for Center Slit Trenches – continued

	Beta-Gamma (Ci/Disposal Unit)			Gross Alpha (Ci/Disposal Unit)			Radium Limit (Ci/Disposal Unit)			Uranium Limit (Ci/Disposal Unit)
Parent Nuclide	**0-12 yrs**	**12-100 yrs**	**100-1130 yrs**	**0-1000 yrs**	**1000-1120 yrs**	**1120-1130 yrs**	**0-1000 yrs**	**1000-1120 yrs**	**1120-1130 yrs**	
Np-237	2.8E+03	4. 6E+00	2.0E+00	1.0E-01	1.9E-01	4.5E-01	---	---	---	2.5E+08
Pd-107	---	4.9E+11	5. 8E+02	---	---	---	---	---	---	---
Pu-238	---	---	1.2E+07	4.4E+05	1.4E+05	1.3E+05	4.4E+05	1.4E+05	1.3E+05	1.8E+17
Pu-239	1.1E+18	7.9E+12	1.3E+07	1.1E+07	7.9E+06	7.7E+06	---	---	---	3.9E+15
Pu-240	---	---	2.7E+15	3.1E+08	3.8E+07	3.3E+07	4.9E+15	3.8E+15	3.6E+15	4.2E+15
Pu-241	1.7E+12	2.9E+08	3.9E+05	7.7E+03	4.4E+03	4.2E+03	---	---	---	5.9E+13
Pu-242	---	---	1.2E+14	2.8E+08	3.4E+07	2.9E+07	4.4E+12	1.4E+12	1.3E+12	3.8E+15
Pu-244	---	---	2.5E+09	2.6E+08	3.1E+07	2.6E+07	2.0E+17	1.5E+17	1.4E+17	3.6E+16
Ra-226	2.7E+17	3.0E+07	3.5E+00	7.5E-02	4.6E-02	4.6E-02	7.5E-02	4.6E-02	4.6E-02	---
Ra-226_Cooling.Tower	---	1.4E+12	1.6E+01	2.6E-01	1.2E+00	9.8E-01	2.7E-01	1.2E+00	9.8E-01	---
Se-79	---	---	3.8E+19	---	---	---	---	---	---	---
Sn-126	---	---	---	---	---	---	---	---	---	---
Sr-90	1.2E+15	4.0E+06	8.4E+01	---	---	---	---	---	---	---
Sr-90_Mk50A	1.6E+18	3.8E+09	4.7E+04	---	---	---	---	---	---	---
Tc-99	1.9E-01	1.6E-01	5.3E+00	---	---	---	---	---	---	---
Tc-99_Mk50A	6.2E+03	1.5E+03	4.0E+02	---	---	---	---	---	---	---
Th-230	---	2.4E+10	1.0E+01	3.7E-01	1.3E-01	1.2E-01	3.7E-01	1.3E-01	1.2E-01	---
Th-230_Cooling.Tower	---	1.2E+15	1.2E+02	2.3E+00	2.1E+00	2.0E+00	2.3E+00	2.1E+00	2.0E+00	---
Th-232	7.1E+16	4.5E+09	3.1E+03	3.2E+03	7.4E+03	9.4E+03	4.2E+03	9.9E+03	1.2E+04	---
U-233	---	---	5.5E+11	1.4E+12	1.4E+11	1.2E+11	---	---	---	1.9E+13
U-234	---	8.9E+14	3.0E+03	1.1E+02	3.6E+01	3.4E+01	1.1E+02	3.6E+01	3.4E+01	4.5E+13
U-234_MGlass	---	1.3E+18	1.2E+06	4.3E+04	1.5E+04	1.4E+04	4.3E+04	1.5E+04	1.4E+04	2.6E+16
U-235	2.0E+09	3.5E+04	7.3E+00	5.7E+00	5.9E+00	7.0E+00	---	---	---	1.5E+10
U-235_MGlass	2.7E+12	2.0E+07	2.9E+03	2.4E+03	2.2E+03	2.3E+03	---	---	---	9.0E+12
U-235_Paducah.Cask	6.6E+13	4.8E+08	3.1E+04	2.7E+04	2.4E+04	2.4E+04	---	---	---	9.9E+13
U-236	---	2.7E+19	2.7E+10	3.6E+10	2.9E+10	2.8E+10	4.8E+10	3.9E+10	3.7E+10	4.6E+11
U-236_MGlass	---	---	1.9E+13	2.5E+13	2.0E+13	1.9E+13	3.3E+13	2.7E+13	2.6E+13	2.7E+14
U-238	---	---	3.9E+06	1.5E+05	4.6E+04	4.3E+04	1.5E+05	4.6E+04	4.3E+04	2.4E+09
U-238_MGlass	---	---	1.5E+09	5.6E+07	1.8E+07	1.7E+07	5.6E+07	1.8E+07	1.7E+07	1.4E+12
Zr-93	1.7E+00	7.5E-01	8.8E-01	---	---	---	---	---	---	---

Note: Limits reported as "---" indicate that there is no limit or that the limit $\geq$ 1E+20.

Note: Groundwater limits in this table are to be considered preliminary. Adjustments are made in the groundwater limits as appropriate based on consideration of plume overlap effects from adjacent units in Chapter 6 and interpretation of sensitivity and uncertainty analyses in Chapter 7. Final limits are to be found in results tables in Chapter 7.

Table 1-3. Preliminary Groundwater Protection Limits for West Slit Trenches

	Beta-Gamma			Gross Alpha			Radium Limit			Uranium Limit
	(Ci/Disposal Unit)			(Ci/Disposal Unit)			(Ci/Disposal Unit)			(Ci/Disposal Unit)
Parent Nuclide	**0-12 yrs**	**12-100 yrs**	**100-1130 yrs**	**0-1000 yrs**	**1000-1120 yrs**	**1120-1130 yrs**	**0-1000 yrs**	**1000-1120 yrs**	**1120-1130 yrs**	
Am-241	1.5E+09	2.4E+06	1.7E+04	1.0E+02	6.8E+01	6.7E+01	---	---	---	2.6E+12
Am-243	---	7.9E+16	2.5E+02	2.5E+01	1.3E+01	1.2E+01	---	---	---	4.1E+11
C-14	3.7E-01	3.8E-01	1.6E+01	---	---	---	---	---	---	---
C-14_NR.Pump	---	---	4.2E+00	---	---	---	---	---	---	---
Cf-249	4.1E+16	4.2E+12	1.7E+04	1.2E+02	7.0E+01	6.8E+01	---	---	---	1.5E+14
Cf-251	---	---	8.7E+07	4.9E+01	2.8E+01	2.7E+01	---	---	---	2.9E+17
Cl-36	1.3E-01	1.3E-01	5.4E+00	---	---	---	---	---	---	---
Cm-244	---	---	2.7E+17	6.1E+09	9.2E+08	8.0E+08	5.0E+17	3.8E+17	3.7E+17	9.3E+16
Cm-245	5.9E+12	1.4E+09	6.4E+02	1.4E+01	7.0E+00	6.7E+00	---	---	---	2.8E+12
Cm-246	---	---	2.6E+14	2.6E+01	1.4E+01	1.3E+01	1.7E+16	5.1E+15	4.7E+15	6.6E+12
Cm-247	---	---	1.9E+03	2.1E+01	1.1E+01	1.0E+01	---	---	---	4.8E+12
Cm-248	---	---	1.3E+09	2.5E+01	1.3E+01	1.2E+01	---	---	---	8.6E+16
H-3	6.7E+00	7.4E+00	4.2E+04	---	---	---	---	---	---	---
H-3_ETF.Carbon	---	---	5.6E+01	---	---	---	---	---	---	---
I-129	2.1E-04	2.1E-04	9.4E-03	---	---	---	---	---	---	---
I-129_ETF.Carbon	---	---	3.0E-01	---	---	---	---	---	---	---
I-129_ETF.GT.73	1.7E+00	1.0E+00	4.0E-01	---	---	---	---	---	---	---
I-129_F.Carbon	2.3E+01	1.3E+01	5.2E+00	---	---	---	---	---	---	---
I-129_F.CG.8	8.7E-03	5.1E-03	5.9E-03	---	---	---	---	---	---	---
I-129_F.Dowex.21K	1.2E+00	6.9E-01	2.8E-01	---	---	---	---	---	---	---
I-129_F.Filtercake	9.8E-03	5.8E-03	6.3E-03	---	---	---	---	---	---	---
I-129_H.Carbon	9.9E+00	5.9E+00	2.3E+00	---	---	---	---	---	---	---
I-129_H.CG.8	6.5E-02	3.8E-02	2.5E-02	---	---	---	---	---	---	---
I-129_H.Dowex.21K	2.7E+00	1.6E+00	6.2E-01	---	---	---	---	---	---	---
I-129_H.Filtercake	1.1E-01	6.6E-02	3.8E-02	---	---	---	---	---	---	---
K-40	3.2E-01	2.4E-01	2.6E+00	---	---	---	---	---	---	---
Mo-93	2.9E-01	2.9E-01	6.4E+00	---	---	---	---	---	---	---
Nb-94	1.4E-01	1.5E-01	5.9E+00	---	---	---	---	---	---	---
Ni-59	9.5E+17	3.8E+09	5.3E+00	---	---	---	---	---	---	---
Np-237	1.0E+03	5.3E+00	2.73E+00	1.4E-01	2.6E-01	6.1E-01	---	---	---	4.1E+08

Table 1-3. Preliminary Groundwater Protection Limits for West Slit Trenches – continued

	Beta-Gamma			Gross Alpha			Radium Limit			Uranium Limit
	(Ci/Disposal Unit)			(Ci/Disposal Unit)			(Ci/Disposal Unit)			(Ci/Disposal Unit)
Parent Nuclide	**0-12 yrs**	**12-100 yrs**	**100-1130 yrs**	**0-1000 yrs**	**1000-1120 yrs**	**1120-1130 yrs**	**0-1000 yrs**	**1000-1120 yrs**	**1120-1130 yrs**	
Pd-107	---	4.6E+11	6.5E+02	---	---	---	---	---	---	---
Pu-238	---	---	1.4E+07	5.2E+05	1.7E+05	1.6E+05	5.2E+05	1.7E+05	1.6E+05	1.0E+16
Pu-239	3.4E+17	1.0E+13	1.7E+07	8.9E+06	2.4E+06	2.1E+06	---	---	---	3.1E+14
Pu-240	---	---	6.9E+14	2.2E+07	3.2E+06	2.8E+06	1.3E+15	9.7E+14	9.4E+14	3.3E+14
Pu-241	5.3E+11	3.3E+08	5.3E+05	3.1E+03	2.0E+03	2.0E+03	---	---	---	7.8E+13
Pu-242	---	---	1.4E+14	2.0E+07	2.8E+06	2.4E+06	5.4E+12	1.7E+12	1.5E+12	2.9E+14
Pu-244	---	---	2.1E+08	1.8E+07	2.5E+06	2.2E+06	5.2E+16	3.8E+16	3.6E+16	2.8E+15
Ra-226	6.8E+15	3.0E+07	4.6E+00	8.9E-02	6.1E-02	6.2E-02	8.9E-02	6.1E-02	6.2E-02	---
Se-79	---	---	6.8E+17	---	---	---	---	---	---	---
Sn-126	---	---	---	---	---	---	---	---	---	---
Sr-90	2.9E+13	2.2E+06	5.9E+01	---	---	---	---	---	---	---
Tc-99	2.2E-01	2.0E-01	7.4E+00	---	---	---	---	---	---	---
Th-230	1.1E+19	2.4E+10	1.3E+01	4.2E-01	1.6E-01	1.5E-01	4.2E-01	1.6E-01	1.5E-01	---
Th-232	1.5E+15	9.4E+08	8.3E+02	8.4E+02	2.0E+03	2.5E+03	1.1E+03	2.7E+03	3.3E+03	---
U-233	---	---	3.0E+10	6.5E+10	7.6E+09	6.4E+09	---	---	---	1.1E+12
U-234	---	8.8E+14	3.7E+03	1.3E+02	4.4E+01	4.2E+01	1.3E+02	4.4E+01	4.2E+01	2.6E+12
U-235	6.2E+08	4.4E+04	9.8E+00	7.6E+00	7.9E+00	9.4E+00	---	---	---	9.1E+08
U-236	---	5.6E+18	7.1E+09	9.5E+09	7.5E+09	7.2E+09	1.3E+10	1.0E+10	9.6E+09	2.7E+10
U-238	---	---	4.7E+06	1.8E+05	5.6E+04	5.2E+04	1.8E+05	5.6E+04	5.2E+04	1.4E+08
Zr-93	2.1E+00	1.1E+00	1.2E+00	---	---	---	---	---	---	---

Note: Limits reported as "---" indicate that there is no limit or that the limit $\geq$ 1E+20.
Note: Groundwater limits in this table are to be considered preliminary. Adjustments are made in the groundwater limits as appropriate based on consideration of plume overlap effects from adjacent units in Chapter 6 and interpretation of sensitivity and uncertainty analyses in Chapter 7. Final limits are to be found in results tables in Chapter 7.

Table 1-4. Preliminary Groundwater Protection Limits for Engineered Trenches

	Beta-Gamma			Gross Alpha			Radium Limit			Uranium Limit
	(Ci/Disposal Unit)			(Ci/Disposal Unit)			(Ci/Disposal Unit)			(Ci/Disposal Unit)
Parent Nuclide	**0-12 yrs**	**12-100 yrs**	**100-1130 yrs**	**0-1000 yrs**	**1000-1120 yrs**	**1120-1130 yrs**	**0-1000 yrs**	**1000-1120 yrs**	**1120-1130 yrs**	
Am-241	2.5E+11	1.4E+07	2.8E+04	1.4E+03	1.4E+03	1.4E+03	---	---	---	3.4E+12
Am-243	---	5.1E+17	2.3E+04	5.2E+03	1.3E+03	1.1E+03	---	---	---	1.0E+14
C-14	1.1E+00	6.5E-01	1.5E+01	---	---	---	---	---	---	---
Cf-249	9.0E+18	2.9E+13	7.6E+05	2.0E+04	6.3E+03	5.8E+03	---	---	---	2.2E+14
Cf-251	---	---	7.8E+09	1.0E+04	2.7E+03	2.4E+03	---	---	---	6.3E+19
Cl-36	3.9E-01	2.3E-01	5.2E+00	---	---	---	---	---	---	---
Cm-244	---	---	5.8E+19	8.6E+13	8.3E+12	7.0E+12	9.9E+19	8.1E+19	7.8E+19	---
Cm-245	1.2E+15	9.3E+09	2.0E+04	1.2E+03	4.8E+02	4.4E+02	---	---	---	4.1E+12
Cm-246	---	---	6.4E+16	5.5E+03	1.3E+03	1.2E+03	3.8E+16	1.6E+16	1.5E+16	1.6E+15
Cm-247	---	---	1.7E+05	4.3E+03	1.0E+03	9.2E+02	---	---	---	1.1E+15
Cm-248	---	---	2.0E+11	5.1E+03	1.2E+03	1.1E+03	---	---	---	3.0E+19
H-3	2.2E+01	1.6E+01	4.1E+04	---	---	---	---	---	---	---
H-3_ETF.Carbon	---	---	1.8E+05	---	---	---	---	---	---	---
I-129	1.0E-03	3.9E-04	1.1E-02	---	---	---	---	---	---	---
I-129_ETF.Carbon	---	---	5.9E-01	---	---	---	---	---	---	---
I-129_ETF.GT.73	6.8E+00	2.1E+00	8.0E-01	---	---	---	---	---	---	---
I-129_F.Carbon	9.1E+01	2.7E+01	1.0E+01	---	---	---	---	---	---	---
I-129_F.CG.8	3.5E-02	1.1E-02	1.1E-02	---	---	---	---	---	---	---
I-129_F.Dowex.21K	4.7E+00	1.4E+00	5.4E-01	---	---	---	---	---	---	---
I-129_F.Filtercake	3.9E-02	1.2E-02	1.2E-02	---	---	---	---	---	---	---
I-129_H.Carbon	4.0E+01	1.2E+01	4.6E+00	---	---	---	---	---	---	---
I-129_H.CG.8	2.6E-01	7.9E-02	4.4E-02	---	---	---	---	---	---	---
I-129_H.Dowex.21K	1.1E+01	3.2E+00	1.2E+00	---	---	---	---	---	---	---
I-129_H.Filtercake	4.5E-01	1.3E-01	7.3E-02	---	---	---	---	---	---	---
K-40	5.3E-01	3.2E-01	3.0E+00	---	---	---	---	---	---	---
Mo-93	8.5E-01	4.4E-01	6.2E+00	---	---	---	---	---	---	---
Nb-94	4.3E-01	2.5E-01	5.8E+00	---	---	---	---	---	---	---
Ni-59	---	3.8E+11	2.2E+01	---	---	---	---	---	---	---
Np-237	1.5E+05	2.7E+01	4.6E+00	2.3E-01	2.8E-01	3.3E-01	---	---	---	4.8E+08
Pd-107	---	4.7E+13	2.7E+03	---	---	---	---	---	---	---

Table 1-4. Preliminary Groundwater Protection Limits for Engineered Trenches – continued

	Beta-Gamma (Ci/Disposal Unit)			Gross Alpha (Ci/Disposal Unit)			Radium Limit (Ci/Disposal Unit)			Uranium Limit (Ci/Disposal Unit)
Parent Nuclide	**0-12 yrs**	**12-100 yrs**	**100-1130 yrs**	**0-1000 yrs**	**1000-1120 yrs**	**1120-1130 yrs**	**0-1000 yrs**	**1000-1120 yrs**	**1120-1130 yrs**	
Pu-238	---	---	4.8E+07	1.6E+06	5.6E+05	5.1E+05	1.6E+06	5.6E+05	5.1E+05	---
Pu-239	6.9E+19	6.2E+13	2.6E+07	2.0E+07	1.8E+07	1.8E+07	---	---	---	3.5E+18
Pu-240	---	---	1.5E+17	3.4E+11	3.1E+10	2.6E+10	2.5E+17	2.1E+17	2.0E+17	3.8E+18
Pu-241	9.8E+13	2.0E+09	8.4E+05	4.2E+04	4.3E+04	4.3E+04	---	---	---	1.1E+14
Pu-242	---	---	4.5E+14	3.1E+11	2.7E+10	2.3E+10	1.3E+13	5.3E+12	4.9E+12	3.3E+18
Pu-244	---	---	1.9E+12	2.8E+11	2.5E+10	2.0E+10	1.1E+19	8.2E+18	7.9E+18	3.1E+19
Ra-226	---	1.9E+09	1.1E+01	3.1E-01	1.3E-01	1.2E-01	3.1E-01	1.3E-01	1.2E-01	---
Se-79	---	---	---	---	---	---	---	---	---	---
Sn-126	---	---	---	---	---	---	---	---	---	---
Sr-90	2.6E+18	2.7E+08	5.7E+02	---	---	---	---	---	---	---
Tc-99	1.6E+00	3.6E-01	7.7E+00	---	---	---	---	---	---	---
Th-230	---	1.6E+12	4.4E+01	2.0E+00	5.0E-01	4.6E-01	2.0E+00	5.0E-01	4.6E-01	---
Th-232	---	1.2E+12	1.5E+05	1.5E+05	3.9E+05	5.2E+05	2.0E+05	5.2E+05	6.9E+05	---
U-233	---	---	7.8E+14	2.4E+15	2.0E+14	1.7E+14	---	---	---	2.4E+16
U-234	---	6.1E+16	1.2E+04	4.4E+02	1.4E+02	1.3E+02	4.4E+02	1.4E+02	1.3E+02	8.2E+16
U-235	1.1E+11	2.6E+05	1.4E+01	1.0E+01	1.1E+01	1.1E+01	---	---	---	2.8E+13
U-236	---	---	1.5E+12	1.8E+12	1.6E+12	1.5E+12	2.4E+12	2.1E+12	2.0E+12	8.5E+14
U-238	---	---	1.6E+07	4.7E+05	1.8E+05	1.7E+05	4.7E+05	1.8E+05	1.7E+05	4.4E+12
Zr-93	8.2E+00	1.5E+00	1.7E+00	---	---	---	---	---	---	---

Note: Limits reported as "---" indicate that there is no limit or that the limit ≥ 1E+20.

Note: Groundwater limits in this table are to be considered preliminary. Adjustments are made in the groundwater limits as appropriate based on consideration of plume overlap effects from adjacent units in Chapter 6 and interpretation of sensitivity and uncertainty analyses in Chapter 7. Final limits are to be found in results tables in Chapter 7.

Table 1-5. Preliminary All-Pathways Radionuclide Disposal Limits for East Slit Trenches

	(Ci/Disposal Unit)		
Parent Nuclide	**130 - 200 yrs**	**200-1000 yrs**	**1000-1130 yrs**
Am-241	6.0E+02	1.2E+02	1.5E+02
Am-243	2.3E+10	2.1E+02	5.6E+01
C-14	7.7E+00	7.7E+00	7.7E+00
C-14_NR.Pump	3.2E+00	1.9E+00	5.5E+02
Cf-249	1.4E+06	7.4E+02	2.5E+02
Cf-251	3.2E+18	3.1E+02	9.0E+01
Cl-36	1.3E+00	1.3E+00	1.3E+00
Cm-244	---	1.1E+12	1.1E+11
Cm-245	5.9E+03	6.6E+01	2.5E+01
Cm-246	---	2.2E+02	5.8E+01
Cm-247	5.2E+12	1.8E+02	4.8E+01
Cm-248	---	5.1E+01	1.3E+01
H-3	2.7E+06	2.7E+06	2.7E+06
H-3_ETF.Carbon	1.8E+06	8.5E+08	---
I-129	3.2E-01	3.2E-01	3.2E-01
I-129_ETF.Carbon	1.4E+01	7.4E+00	7.0E+00
I-129_ETF.GT.73	2.0E+01	1.0E+01	9.7E+00
I-129_F.Carbon	2.6E+02	1.4E+02	1.3E+02
I-129_F.CG.8	1.8E-01	2.5E-01	8.8E-01
I-129_F.Dowex.21K	1.3E+01	7.1E+00	6.7E+00
I-129_F.Filtercake	1.9E-01	2.6E-01	8.4E-01
I-129_H.Carbon	1.1E+02	5.9E+01	5.6E+01
I-129_H.CG.8	7.7E-01	6.4E-01	6.1E-01
I-129_H.Dowex.21K	3.1E+01	1.6E+01	1.5E+01
I-129_H.Filtercake	1.3E+00	1.0E+00	9.3E-01
K-40	3.0E+00	3.9E+00	5.8E+01
Mo-93	1.4E+01	1.4E+01	1.4E+01
Nb-94	1.6E+00	1.6E+00	1.6E+00
Ni-59	1.4E+07	2.6E+03	1.8E+03
Np-237	2.7E-02	1.9E-02	3.1E-02
Pd-107	2.1E+07	4.1E+03	2.7E+03
Pu-238	2.3E+10	1.4E+06	4.0E+05
Pu-239	3.9E+07	7.9E+05	7.2E+05
Pu-240	1.8E+19	4.5E+09	3.9E+08
Pu-241	2.1E+04	3.7E+03	4.5E+03
Pu-242	3.2E+18	4.2E+09	3.6E+08
Pu-244	---	3.9E+09	3.3E+08
Ra-226	4.0E+01	2.7E-01	1.1E-01

Table 1-5. Preliminary All-Pathways Radionuclide Disposal Limits for East Slit Trenches – continued

	(Ci/Disposal Unit)		
Parent Nuclide	**130 - 200 yrs**	**200-1000 yrs**	**1000-1130 yrs**
Se-79	---	---	---
Sn-126	---	---	---
Sr-90	4.8E+04	3.4E+03	3.6E+10
Tc-99	5.3E+00	5.3E+00	5.3E+00
Th-230	1.3E+03	1.3E+00	3.6E-01
Th-232	2.3E+05	6.1E+04	1.4E+05
U-233	---	1.8E+12	1.6E+11
U-234	2.3E+06	3.6E+02	1.0E+02
U-235	3.1E+00	4.2E-01	4.3E-01
U-236	3.5E+13	6.6E+11	3.3E+11
U-238	1.7E+10	4.3E+05	1.3E+05
Zr-93	1.0E+01	4.0E+00	3.7E+00

Note: Limits reported as "---" indicate that there is no limit or that the limit $\geq$ 1E+20.
Note: All-pathways limits in this table are to be considered preliminary. Adjustments are made in the all-pathways limits as appropriate based on consideration of plume overlap effects from adjacent units in Chapter 6 and interpretation of sensitivity and uncertainty analyses in Chapter 7. Final limits are to be found in results tables in Chapter 7.

Table 1-6. Preliminary All-Pathways Radionuclide Disposal Limits for Center Slit Trenches

	(Ci/Disposal Unit)		
Parent Nuclide	**130 - 200 yrs**	**200-1000 yrs**	**1000-1130 yrs**
Am-241	7.4E+02	9.3E+01	5.3E+01
Am-243	3.4E+10	2.9E+01	1.1E+01
C-14	1.3E+01	1.3E+01	1.3E+01
C-14_NR.Pump	3.5E+00	3.1E+00	1.2E+02
Cf-249	2.2E+06	1.1E+02	4.9E+01
Cf-251	4.2E+18	4.4E+01	1.7E+01
Cl-36	2.3E+00	2.3E+00	2.3E+00
Cm-244	---	3.2E+10	3.6E+09
Cm-245	7.7E+03	1.5E+01	5.6E+00
Cm-246	---	3.0E+01	1.1E+01
Cm-247	7.4E+12	2.6E+01	9.2E+00
Cm-248	2.8E+19	7.2E+00	2.6E+00
H-3	4.8E+06	4.8E+06	4.8E+06
H-3_Concrete	1.1E+07	1.1E+07	1.1E+07
H-3_ETF.Carbon	1.7E+06	1.3E+09	---
I-129	5.3E-01	5.3E-01	5.3E-01
I-129_ETF.Carbon	2.5E+01	1.3E+01	1.2E+01
I-129_ETF.GT.73	3.3E+01	1.7E+01	1.6E+01
I-129_F.Carbon	4.4E+02	2.3E+02	2.1E+02
I-129_F.CG.8	2.5E-01	4.1E-01	1.3E+00
I-129_F.Dowex.21K	2.2E+01	1.2E+01	1.1E+01
I-129_F.Filtercake	2.7E-01	4.4E-01	1.3E+00
I-129_H.Carbon	1.9E+02	1.0E+02	9.4E+01
I-129_H.CG.8	1.3E+00	1.1E+00	1.0E+00
I-129_H.Dowex.21K	5.1E+01	2.7E+01	2.5E+01
I-129_H.Filtercake	2.2E+00	1.7E+00	1.6E+00
I-129_Mk50	7.6E+01	2.8E+01	8.9E+01
K-40	4.9E+00	6.1E+00	3.0E+01
Mo-93	2.5E+01	2.5E+01	2.5E+01
Nb-94	2.7E+00	2.7E+00	2.7E+00
Ni-59	1.1E+06	2.5E+03	1.2E+03
Np-237	3.3E-02	3.1E-02	5.9E-02
Pd-107	1.8E+06	3.9E+03	1.8E+03
Pu-238	2.7E+09	1.3E+06	3.8E+05
Pu-239	5.1E+07	1.4E+06	1.2E+06
Pu-240	1.5E+18	1.2E+08	1.3E+07
Pu-241	2.6E+04	2.8E+03	1.6E+03
Pu-242	3.9E+17	1.2E+08	1.2E+07
Pu-244	---	1.1E+08	1.1E+07

Table 1-6. Preliminary All-Pathways Radionuclide Disposal Limits for Center Slit Trenches - continued

	(Ci/Disposal Unit)		
Parent Nuclide	**130 - 200 yrs**	**200-1000 yrs**	**1000-1130 yrs**
Ra-226	6.2E+00	2.2E-01	1.3E-01
Ra-226_Cooling.Tower	1.2E+04	7.7E-01	2.9E+00
Se-79	---	---	4.0E+19
Sn-126	---	---	---
Sr-90	7.1E+03	1.6E+03	2.8E+10
Sr-90_Mk50	3.6E+06	9.1E+05	3.9E+12
Tc-99	9.0E+00	9.0E+00	9.0E+00
Tc-99_Mk50	1.9E+03	6.0E+02	2.0E+03
Th-230	1.7E+02	1.1E+00	3.6E-01
Th-230_Cooling.Tower	5.8E+05	6.6E+00	5.7E+00
Th-232	2.0E+04	8.4E+03	2.0E+04
U-233	---	4.5E+10	4.5E+09
U-234	2.8E+05	3.3E+02	9.9E+01
U-234_MGlass	4.6E+08	1.3E+05	4.1E+04
U-235	3.8E+00	6.9E-01	7.4E-01
U-235_MGlass	8.8E+03	3.1E+02	2.8E+02
U-235_Paducah.Cask	1.2E+05	3.3E+03	3.0E+03
U-236	2.9E+12	6.9E+10	1.4E+10
U-236_MGlass	3.9E+15	4.3E+13	8.7E+12
U-238	2.1E+09	4.3E+05	1.2E+05
U-238_MGlass	3.5E+12	1.6E+08	4.8E+07
Zr-93	1.1E+01	5.7E+00	5.2E+00

Note: Limits reported as "---" indicate that there is no limit or that the limit $\geq$ 1E+20.
Note: All-pathways limits in this table are to be considered preliminary. Adjustments are made in the all-pathways limits as appropriate based on consideration of plume overlap effects from adjacent units in Chapter 6 and interpretation of sensitivity and uncertainty analyses in Chapter 7. Final limits are to be found in results tables in Chapter 7.

Table 1-7. Preliminary All-Pathways Radionuclide Disposal Limits for West Slit Trenches

	(Ci/Disposal Unit)		
Parent Nuclide	**130 - 200 yrs**	**200-1000 yrs**	**1000-1130 yrs**
Am-241	9.5E+02	3.9E+01	2.5E+01
Am-243	4.6E+10	9.4E+00	4.7E+00
C-14	1.8E+01	1.8E+01	1.8E+01
C-14_NR.Pump	4.6E+00	4.4E+00	2.1E+02
Cf-249	2.9E+06	3.7E+01	2.1E+01
Cf-251	9.2E+17	1.4E+01	7.7E+00
Cl-36	3.2E+00	3.2E+00	3.2E+00
Cm-244	---	2.4E+09	3.1E+08
Cm-245	1.0E+04	5.1E+00	2.5E+00
Cm-246	1.2E+18	9.8E+00	4.9E+00
Cm-247	9.8E+12	8.3E+00	4.1E+00
Cm-248	3.1E+17	2.3E+00	1.1E+00
H-3	6.5E+06	6.5E+06	6.5E+06
H-3_ETF.Carbon	1.5E+03	1.2E+06	---
I-129	6.6E-01	6.6E-01	6.6E-01
I-129_ETF.Carbon	3.6E+01	1.9E+01	1.8E+01
I-129_ETF.GT.73	4.9E+01	2.5E+01	2.4E+01
I-129_F.Carbon	6.5E+02	3.4E+02	3.2E+02
I-129_F.CG.8	3.6E-01	6.1E-01	1.6E+00
I-129_F.Dowex.21K	3.3E+01	1.8E+01	1.7E+01
I-129_F.Filtercake	3.8E-01	6.4E-01	1.6E+00
I-129_H.Carbon	2.8E+02	1.5E+02	1.4E+02
I-129_H.CG.8	1.9E+00	1.6E+00	1.5E+00
I-129_H.Dowex.21K	7.6E+01	4.0E+01	3.7E+01
I-129_H.Filtercake	3.2E+00	2.6E+00	2.3E+00
K-40	6.6E+00	8.7E+00	4.5E+01
Mo-93	3.4E+01	3.4E+01	3.4E+01
Nb-94	3.7E+00	3.7E+00	3.7E+00
Ni-59	2.0E+05	2.8E+03	1.3E+03
Np-237	4.2E-02	4.2E-02	8.0E-02
Pd-107	3.0E+05	4.3E+03	2.0E+03
Pu-238	7.2E+08	1.5E+06	4.6E+05
Pu-239	6.7E+07	1.6E+06	6.3E+05
Pu-240	2.6E+17	8.8E+06	1.1E+06
Pu-241	3.3E+04	1.1E+03	7.4E+02
Pu-242	1.0E+17	8.3E+06	1.0E+06
Pu-244	5.3E+19	7.6E+06	9.1E+05
Ra-226	2.0E+00	2.6E-01	1.8E-01

Table 1-7. Preliminary All-Pathways Radionuclide Disposal Limits for West Slit Trenches - continued

	(Ci/Disposal Unit)		
Parent Nuclide	**130 - 200 yrs**	**200-1000 yrs**	**1000-1130 yrs**
Se-79	---	9.7E+18	7.2E+17
Sn-126	---	---	---
Sr-90	2.2E+03	1.1E+03	3.3E+10
Tc-99	1.4E+01	1.4E+01	1.4E+01
Th-230	4.6E+01	1.2E+00	4.5E-01
Th-232	3.6E+03	2.2E+03	5.3E+03
U-233	---	2.2E+09	2.6E+08
U-234	7.3E+04	3.8E+02	1.2E+02
U-235	4.9E+00	9.2E-01	1.0E+00
U-236	5.3E+11	8.4E+09	1.0E+09
U-238	5.5E+08	5.2E+05	1.5E+05
Zr-93	1.3E+01	8.0E+00	7.4E+00

Note: Limits reported as "---" indicate that there is no limit or that the limit $\geq$ 1E+20.
Note: All-pathways limits in this table are to be considered preliminary. Adjustments are made in the all-pathways limits as appropriate based on consideration of plume overlap effects from adjacent units in Chapter 6 and interpretation of sensitivity and uncertainty analyses in Chapter 7. Final limits are to be found in results tables in Chapter 7.

Table 1-8. Preliminary All-Pathways Radionuclide Disposal Limits for Engineered Trenches

	(Ci/Disposal Unit)		
Parent Nuclide	**130 - 200 yrs**	**200-1000 yrs**	**1000-1130 yrs**
Am-241	1.8E+03	4.3E+02	4.7E+02
Am-243	6.7E+10	2.0E+03	4.3E+02
C-14	2.1E+01	2.1E+01	2.1E+01
Cf-249	4.2E+06	6.2E+03	1.8E+03
Cf-251	1.0E+19	2.9E+03	7.0E+02
Cl-36	3.6E+00	3.6E+00	3.6E+00
Cm-244	---	3.4E+13	2.7E+12
Cm-245	1.7E+04	3.9E+02	1.6E+02
Cm-246	---	2.0E+03	4.5E+02
Cm-247	1.6E+13	1.7E+03	3.7E+02
Cm-248	---	4.8E+02	1.0E+02
H-3	7.4E+06	7.4E+06	7.4E+06
H-3_ETF.Carbon	4.7E+06	2.1E+09	---
I-129	7.7E-01	7.7E-01	7.7E-01
I-129_ETF.Carbon	7.5E+01	3.8E+01	3.6E+01
I-129_ETF.GT.73	1.0E+02	5.2E+01	4.8E+01
I-129_F.Carbon	1.3E+03	6.8E+02	6.3E+02
I-129_F.CG.8	6.5E-01	9.0E-01	1.5E+00
I-129_F.Dowex.21K	6.9E+01	3.5E+01	3.3E+01
I-129_F.Filtercake	7.2E-01	9.2E-01	1.4E+00
I-129_H.Carbon	5.9E+02	3.0E+02	2.8E+02
I-129_H.CG.8	3.9E+00	3.0E+00	2.6E+00
I-129_H.Dowex.21K	1.6E+02	8.0E+01	7.5E+01
I-129_H.Filtercake	6.7E+00	5.1E+00	4.4E+00
K-40	7.9E+00	9.9E+00	1.7E+02
Mo-93	3.8E+01	3.8E+01	3.8E+01
Nb-94	4.2E+00	4.2E+00	4.2E+00
Ni-59	1.6E+08	5.6E+03	1.0E+04
Np-237	8.3E-02	7.1E-02	8.7E-02
Pd-107	2.4E+08	8.5E+03	1.6E+04
Pu-238	1.9E+11	4.7E+06	1.5E+06
Pu-239	1.1E+08	2.4E+06	2.1E+06
Pu-240	---	1.3E+11	1.0E+10
Pu-241	6.3E+04	1.3E+04	1.4E+04
Pu-242	2.7E+19	1.3E+11	9.3E+09
Pu-244	---	1.2E+11	8.4E+09
Ra-226	3.3E+02	9.1E-01	3.5E-01
Se-79	---	---	---
Sn-126	---	---	---
Sr-90	4.0E+05	1.1E+04	1.9E+11

Table 1-8. Preliminary All-Pathways Radionuclide Disposal Limits for Engineered Trenches - continued

	(Ci/Disposal Unit)		
Parent Nuclide	**130 - 200 yrs**	**200-1000 yrs**	**1000-1130 yrs**
Tc-99	1.3E+01	1.3E+01	1.3E+01
Th-230	1.1E+04	5.9E+00	1.3E+00
Th-232	2.4E+06	4.1E+05	1.0E+06
U-233	---	7.4E+13	5.8E+12
U-234	1.9E+07	1.3E+03	3.8E+02
U-235	9.3E+00	1.2E+00	1.3E+00
U-236	3.6E+14	4.9E+12	3.6E+12
U-238	1.4E+11	1.4E+06	4.9E+05
Zr-93	2.7E+01	1.1E+01	1.0E+01

Note: Limits reported as "---" indicate that there is no limit or that the limit $\geq$ 1E+20.
Note: All-pathways limits in this table are to be considered preliminary. Adjustments are made in the all-pathways limits as appropriate based on consideration of plume overlap effects from adjacent units in Chapter 6 and interpretation of sensitivity and uncertainty analyses in Chapter 7. Final limits are to be found in results tables in Chapter 7.

Table 1-9. Intruder-Based Radionuclide Disposal Limits for Slit and Engineered Trenches – Resident and Post-drilling Scenarios for 1000 Years

Radionuclide	Slit Trenches		Engineered Trenches	
	Resident Limit (Ci/Unit)	Post-drilling Limit (Ci/Unit)	Resident Limit (Ci/Unit)	Post-drilling Limit (Ci/Unit)
Ac-227	3.1E+07	4.2E+03	2.0E+07	4.3E+03
Ag-108m	3.6E+01	2.3E+03	2.4E+01	2.4E+03
Al-26	3.9E+00	1.6E+03	2.6E+00	1.7E+03
Am-241	6.2E+05	1.4E+03	4.1E+05	1.4E+03
Am-242m	1.6E+05	1.4E+03	1.1E+05	1.4E+03
Am-243	3.9E+02	1.1E+03	2.6E+02	1.2E+03
Ar-39	---	3.6E+07	---	3.7E+07
Ba-133	4.3E+09	8.2E+06	2.8E+09	8.5E+06
Bi-207	9.9E+04	2.3E+04	6.6E+04	2.4E+04
Bk-249	1.4E+05	4.9E+05	9.4E+04	5.1E+05
C-14	---	2.0E+03	---	2.1E+03
Ca-41	---	1.2E+04	---	1.2E+04
Cd-113m	---	3.0E+04	---	3.1E+04
Cf-249	3.7E+02	1.3E+03	2.4E+02	1.3E+03
Cf-250	3.8E+13	2.6E+05	2.5E+13	2.7E+05
Cf-251	1.4E+03	1.2E+03	9.0E+02	1.2E+03
Cf-252	7.5E+11	5.3E+07	5.0E+11	5.5E+07
Cl-36	---	2.5E+01	---	2.6E+01
Cm-242	2.6E+09	7.0E+05	1.8E+09	7.3E+05
Cm-243	4.1E+07	2.2E+04	2.7E+07	2.2E+04
Cm-244	4.4E+11	1.0E+05	2.9E+11	1.0E+05
Cm-245	2.4E+03	7.7E+02	1.6E+03	7.9E+02
Cm-246	1.0E+11	1.5E+03	6.8E+10	1.5E+03
Cm-247	7.9E+01	1.3E+03	5.2E+01	1.3E+03
Cm-248	5.5E+06	3.9E+02	3.6E+06	4.1E+02
Co-60	2.0E+09	8.3E+08	1.3E+09	8.6E+08
Cs-134	1.5E+19	4.8E+17	9.9E+18	5.0E+17
Cs-135	---	2.4E+04	---	2.5E+04
Cs-137	2.1E+06	2.4E+04	1.4E+06	2.5E+04
Eu-152	2.3E+06	6.5E+05	1.5E+06	6.7E+05
Eu-154	4.1E+07	1.1E+07	2.7E+07	1.2E+07
Eu-155	4.0E+18	2.4E+11	2.7E+18	2.4E+11
H-3	---	2.1E+06	---	2.1E+06
I-129	7.3E+09	3.8E+02	4.8E+09	3.9E+02

Table 1-9. Intruder-Based Radionuclide Disposal Limits for Slit and Engineered Trenches – Resident and Post-drilling Scenarios for 1000 Years - continued

Radionuclide	Slit Trenches		Engineered Trenches	
	Resident Limit (Ci/Unit)	Post-drilling Limit (Ci/Unit)	Resident Limit (Ci/Unit)	Post-drilling Limit (Ci/Unit)
K-40	6.7E+01	5.1E+02	4.4E+01	5.3E+02
Kr-85	9.9E+10	1.2E+09	6.5E+10	1.2E+09
Mo-93	---	4.7E+05	---	4.9E+05
Na-22	2.7E+15	5.9E+14	1.8E+15	6.2E+14
Nb-93m	---	1.2E+08	---	1.3E+08
Nb-94	9.6E+00	2.7E+03	6.4E+00	2.8E+03
Ni-59	---	4.2E+05	---	4.3E+05
Ni-63	---	3.0E+05	---	3.1E+05
Np-237	1.7E+02	1.1E+02	1.1E+02	1.1E+02
Pa-231	8.1E+01	1.2E+02	5.4E+01	1.3E+02
Pb-210	1.4E+11	2.2E+03	9.3E+10	2.2E+03
Pd-107	---	8.7E+05	---	9.1E+05
Pu-238	1.3E+07	3.6E+03	8.9E+06	3.7E+03
Pu-239	3.8E+06	1.5E+03	2.5E+06	1.5E+03
Pu-240	1.2E+09	1.5E+03	8.0E+08	1.5E+03
Pu-241	1.9E+07	4.1E+04	1.2E+07	4.2E+04
Pu-242	6.9E+08	1.5E+03	4.6E+08	1.6E+03
Pu-244	4.4E+01	1.3E+03	2.9E+01	1.3E+03
Ra-226	9.1E+00	7.1E+01	6.0E+00	7.4E+01
Ra-228	1.3E+08	2.5E+07	8.7E+07	2.6E+07
Rb-87	---	1.5E+04	---	1.6E+04
S-35	---	---	---	---
Sb-125	5.0E+16	7.4E+14	3.3E+16	7.7E+14
Sc-46	---	---	---	---
Se-79	---	2.4E+04	---	2.5E+04
Sm-151	---	5.9E+06	---	6.2E+06
Sn-121m	---	1.6E+06	---	1.7E+06
Sn-126	8.7E+00	2.1E+03	5.7E+00	2.1E+03
Sr-90	---	1.6E+03	---	1.7E+03
Tc-99	1.0E+09	2.4E+03	6.9E+08	2.5E+03
Th-228	6.6E+18	3.4E+18	4.4E+18	3.6E+18
Th-229	9.0E+01	5.0E+02	6.0E+01	5.2E+02
Th-230	1.9E+01	1.9E+02	1.2E+01	2.0E+02
Th-232	4.4E+00	1.5E+02	2.9E+00	1.5E+02

Table 1-9. Intruder-Based Radionuclide Disposal Limits for Slit and Engineered Trenches – Resident and Post-drilling Scenarios for 1000 Years - continued

Radionuclide	Slit Trenches		Engineered Trenches	
	Resident Limit (Ci/Unit)	Post-drilling Limit (Ci/Unit)	Resident Limit (Ci/Unit)	Post-drilling Limit (Ci/Unit)
U-232	3.2E+03	9.4E+02	2.1E+03	9.7E+02
U-233	9.3E+02	2.2E+03	6.2E+02	2.3E+03
U-234	3.8E+03	3.4E+03	2.5E+03	3.5E+03
U-235	5.0E+02	2.2E+03	3.3E+02	2.3E+03
U-236	2.8E+07	3.9E+03	1.8E+07	4.1E+03
U-238	9.7E+02	4.0E+03	6.4E+02	4.2E+03
W-181	---	---	---	---
W-185	---	---	---	---
W-188	---	---	---	---
Zr-93	---	9.5E+05	---	9.8E+05

Note: Limits reported as "---" indicate that there is no limit or that the limit $\geq$ 1E+20.
Note: Limits for special wasteforms (e.g., Mk50A, Cooling Tower) are the same as the limit for generic radionuclide.

Table 1-10. Overall Slit and Engineered Trench Air-Pathway Disposal Limit

Radionuclide	0 - 125 Year Trench Disposal Limits (Ci)	125 –1125 Year Trench Disposal Limits (Ci)	Overall Trench Air-Pathway Disposal Limit (Ci)
C-14	2.9E+05	3.5E+12	2.9E+05
Cl-36	1.5E+05	3.4E+10	1.5E+05
H-3	1.1E+07		1.1E+07
I-129	9.5E+02	1.6E+04	9.5E+02
S-35	4.5E+06	---	4.5E+06
Sb-124	1.5E+05	---	1.5E+05
Sb-125	6.6E+03	---	6.6E+03
Se-75	9.0E+04	---	9.0E+04
Se-79	5.5E+04	8.2E+09	5.5E+04
Sn-113	4.8E+05	---	4.8E+05
Sn-119m	5.6E+05	---	5.6E+05
Sn-121	---	---	---
Sn-121m	5.8E+04	2.7E+09	5.8E+04
Sn-123	7.8E+06	---	7.8E+06
Sn-126	1.3E+02	7.1E+05	1.3E+02

Note: Limits reported as "---" indicate that there is no limit or that the limit $\geq$ 1E+20.
Note: Limits for special wasteforms (e.g., Mk50A, Cooling Tower) are the same as the limit for generic radionuclide

Table 1-11. Slit and Engineered Trenches Disposal Limits for Radon Parent Radionuclides

Parent Source (1Ci)	Maximum Instantaneous Rn-222 flux at Land Surface ($pCi/m^2/sec$)	Time to Max (years)	Disposal Limit Per Unit Area [1] (Ci/m^2)	Slit Trench Disposal Limit [2] (Ci/SLT)	Engineered Trench Disposal Limit [3] (Ci/ET)
Pu-238	1.59E-08	125	1.26E+09	7.7E+12	1.1E+13
Ra-226	5.52E+00	1	3.62E+00	2.2E+04	3.3E+04
Th-230	2.91E-01	125	6.88E+01	4.2E+05	6.2E+05
U-234	1.69E-04	125	1.18E+05	7.2E+08	1.1E+09
U-238	2.00E-08	125	1.00E+09	6.1E+12	9.1E+12

[1] Disposal Limit per unit area (Ci/m^2) = 20 $pCi/m^2/s$ / Maximum Instantaneous Rn-222 flux at Land Surface
[2] Slit Trench Disposal Limit = Disposal Limit per unit area (Ci/m^2) × 6098 m^2
[3] Engineered Trench Disposal Limit = Disposal Limit per unit area (Ci/m^2) × 9063 m^2
Note: Limits for special wasteforms (e.g., Ra-226 and Th-230 Cooling Tower) are the same as the generic radionuclide.

1.2 INTRODUCTION AND GENERAL APPROACH

Slit Trench and Engineered Trench disposal limits through the 1,000 year compliance period have been developed for the following pathways: groundwater protection, air, all-pathways, inadvertent intruder (resident scenario and post-drilling scenario), and radon. All instances of groundwater protection and all-pathways "limits" in this chapter refer to "preliminary limits" only, because they do not account for plume interaction or uncertainties. A groundwater transport analysis has been conducted to determine maximum well concentrations (as a function of time) within a 100-m compliance region surrounding each of the three Slit and Engineered Trench groupings. The main analysis tool employed was the PORFLOW code, which handles both flow and transport of radionuclide chains (i.e., parents and daughters) in porous media. Two-dimensional flow and transport analyses were conducted to describe in detail the migration of species from the trenches through the vadose zone to the underlying water table.

The results from these 2-D vadose zone simulations (treated as source terms) were then input into a 3-D aquifer transport model to compute maximum groundwater concentrations of radionuclides within the 100-m compliance region. Preliminary groundwater protection disposal limits over the 1,000-year compliance period for the Slit and Engineered Trenches were developed from the computed maximum groundwater concentrations using the Future Limits feature of the all-pathways application (Koffman 2006a). Additionally preliminary all-pathways disposal limits over the 1,000-year compliance period for the Slit and Engineered Trenches were also developed from the computed maximum groundwater concentrations using the all-pathways application (Koffman 2006a).

An air-pathway analysis has been conducted to determine air-pathway disposal limits for 15 potentially volatile radionuclides over the 1,000 year compliance period for the Slit and Engineered Trenches. The PORFLOW code was utilized for diffusional transport of radionuclides out of the trench waste zones to the ground surface and the CAP88 code was utilized for subsequent atmospheric transport and dose calculations. A one-dimensional PORFLOW diffusional transport analysis was conducted to determine the flux of species to the ground surface from the trench waste zones. The atmospheric transport and dose calculation results obtained using CAP88 were combined with the flux of species at the ground surface to develop air-pathway disposal limits.

An inadvertent intruder analysis has been conducted to determine inadvertent intruder disposal limits over the 1,000-year compliance period for the Slit and Engineered Trenches. The analysis was conducted using an automated inadvertent intruder computer application developed at SRNL (Koffman 2006b) for the resident and post-drilling inadvertent intruder scenarios.

A radon pathway analysis has been conducted to determine radon pathway disposal limits for 5 radon-producing parent radionuclides over the 1,000 year compliance period for the Slit and Engineered Trenches. A one-dimensional PORFLOW diffusional transport analysis was conducted to determine the flux of radon to the ground surface from the Slit and Engineered Trench waste zones.

Within Chapter 7, Integration and Interpretation, the individual Slit and Engineered Trench disposal limits developed herein will be adjusted in consideration of the results of the Slit and Engineered Trench uncertainty analyses reported in this chapter and the plume interaction analysis reported in Chapter 6 Integrated Facility Analysis.

1.3 SLIT AND ENGINEERED TRENCHES GENERAL DESCRIPTION AND LIFECYCLE

1.3.1 Slit Trench General Description and Lifecycle

Slit Trenches are below grade earthen disposal units with essentially vertical side slopes. The excavated soil is stockpiled for later placement over disposed waste. Slit Trenches are generally 20 feet deep, 20 feet wide, and 656 feet long. Ten feet to 14 feet of undisturbed soil separates each trench. A set of five, 20-foot wide Slit Trenches, are grouped together within a 157-foot wide by 656-foot long footprint.[1] Eight such footprints, designated Slit 1 through 8, have been currently sited, and waste has been placed within all seven units. Figure 1-1 provides the layout of the Slit 1 through 8 footprints relative to future Slit footprints (shown in grey cross-hatch) and to other E-Area LLWF disposal unit types.

During the 30-year operational period, low-level waste consisting of soil, debris, rubble, wood, concrete, equipment, and job control waste is disposed within the Slit Trenches. Job control waste consists of potentially contaminated protective clothing (plastic suits, shoe covers, lab coats, etc.), plastic sheeting, etc. The waste may be disposed as bulk waste or contained within B-25 boxes, B-12 boxes, 55-gallon drums, Sealand containers, and other metal containers. Trench excavation begins at one end of the trench and only proceeds as needed toward the other end of the trench in order to minimize the area of open trench and the time the trench section is open. Waste placement in turn begins at one end of the trench and proceeds toward the other end. Bulk waste is pushed into the trench from one end. Containerized waste and large equipment are typically placed in one end of the trench with a crane. Figure 1-2 provides operational photographs of Slit Trenches. Eventually containerized waste areas of the trench are filled in with either bulk waste or clean soil to fill the voids between adjacent containers and the trench wall. Slit Trenches are typically filled to within four feet below the top of the trench with waste and daily cover, if required.

[1] The assumption that five individual Slit Trenches make up one Trench Unit was incorporated in this analysis. The area of five nominal individual trenches makes up 64% (or 0.64) of the area of the nominal trench Unit footprint. Thus, WMAP can adjust individual trench dimensions as long as their total area within a Unit does not make up LESS than 64% of the Unit area and that the individual trenches are spread out, i.e., not inordinately clustered together within the Unit footprint.

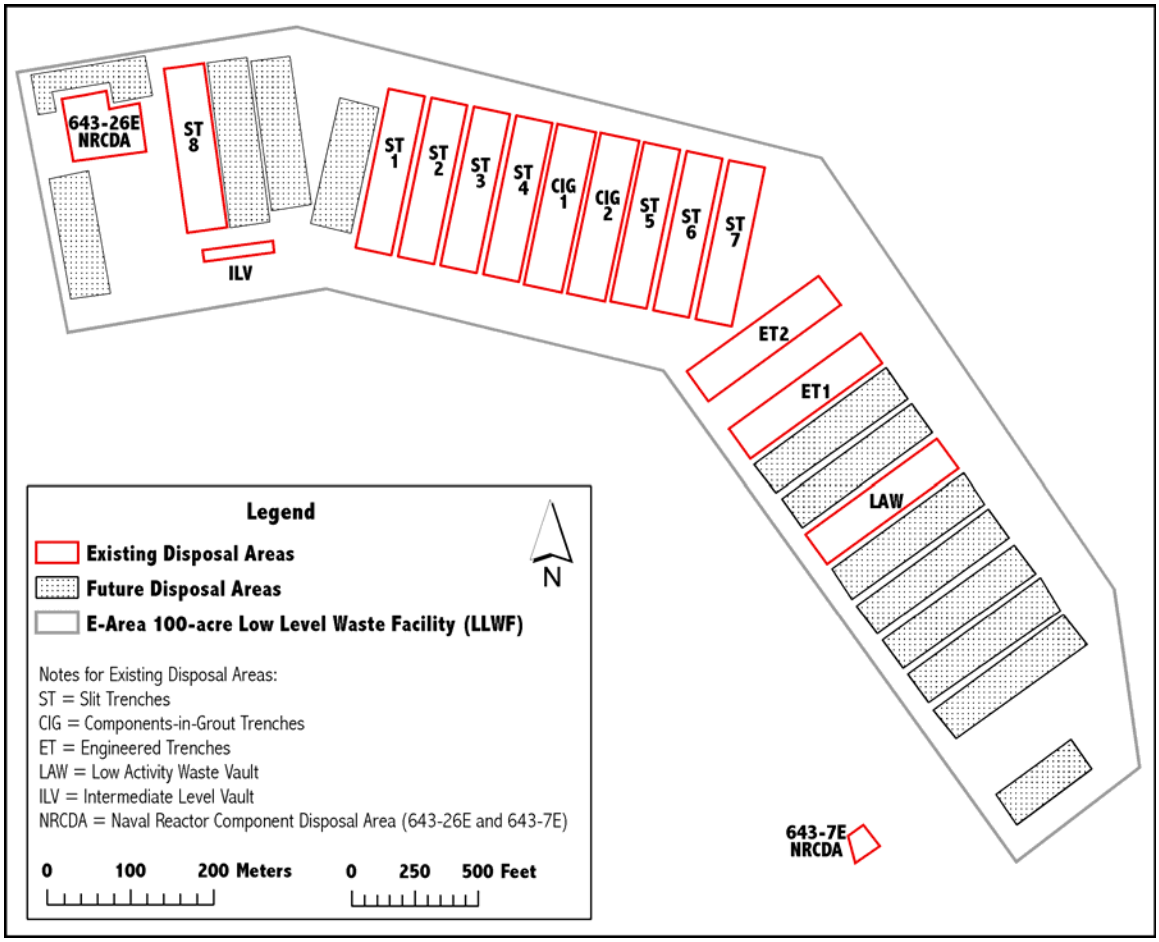

Figure 1-1. Location of Slit and Engineered Trench Footprints within the E-Area LLWF

Figure 1-2. Operational Slit Trench Photographs

Operational closure of the Slit Trenches will be conducted in stages. Once a section of the Slit Trench is filled, the stockpiled clean soil is bulldozed in a single lift over that section of trench to produce a minimum 4-foot thick clean soil layer over the waste (i.e., operational soil cover). The operational soil cover is graded to provide positive drainage off and away from the disposal operation. Subsequent trench sections are filled with waste, covered with an operational soil cover, and graded to promote positive drainage until the entire trench is filled and covered. The only mechanical compaction that the soil and waste in the trench receive is from the bulldozer and other heavy equipment moving over the top of a completely backfilled trench. Once a set of five Slit Trenches (i.e., the 157-foot wide by 656-foot long footprint) is filled, completely covered with the 4-foot soil cover, and a vegetative cover of shallow rooted grass is established, it is considered operationally closed. After operational closure the subsidence potential of Slit Trenches is highly variable due to waste variability. The subsidence potential could range from zero for bulk waste to 13.5 feet for B-25 boxes containing low-density waste stacked four high (Phifer and Wilhite 2001; Phifer 2004). Additionally, in order to minimize future subsidence of the final closure cap, limits on the disposal of containers with significant void space that are considered non-crushable (i.e., containers that will not be stabilized by dynamic compaction) have been imposed (Hang et al. 2005; Swingle and Phifer 2006).

At the end of the operational period, an interim runoff cover will be installed and maintained during the 100-year institutional control period (i.e., interim closure). The interim runoff cover will involve the placement of up to an additional 2-foot of soil over the Slit Trenches, which is graded to promote even greater drainage off the trenches. The interim runoff cover will consist of the surface application of a high density polyethylene (HDPE) geomembrane or geotextile fabric with spray on asphalt emulsion or some other water-shedding material. It will extend a minimum of 10 feet beyond the edge of all sides of the trenches.

Final closure of the Slit Trenches will take place at final closure of the entire E-Area LLWF, at the end of the 100-year institutional control period. Static surcharging and/or dynamic compaction of the Slit Trenches will be conducted at the end of the 100-year institutional control period, when the efficiency of the subsidence treatment will be greater due to container corrosion and subsequent strength loss. Final closure will consist of the installation of an integrated closure system designed to minimize moisture contact with the waste and to provide an intruder deterrent. The integrated closure system will consist of one or more closure caps installed over all the disposal units and a drainage system. Figure 1-3 provides the anticipated Slit Trench closure cap configuration. The closure cap will be installed with the crestline running lengthwise down the center of the unit (McDowell-Boyer et al. 2000; Cook et al. 2004; Phifer 2004; Phifer et al. 2006).

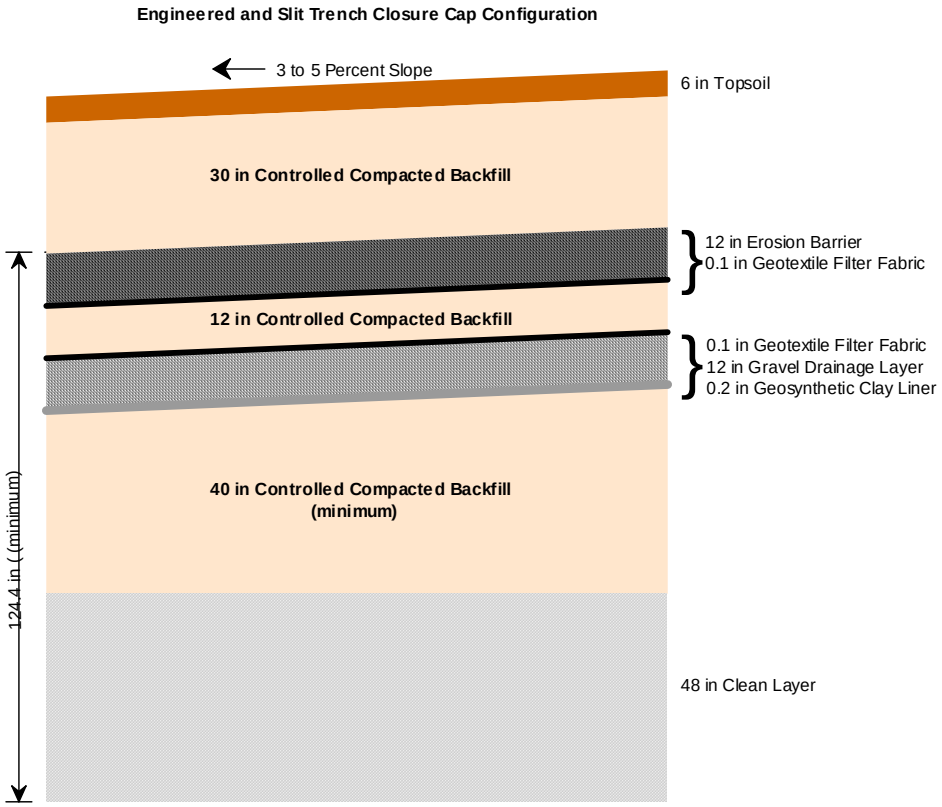

Figure 1-3. Slit and Engineered Trench Closure Cap Configuration

1.3.2 Engineered Trench General Description and Lifecycle

The ETs are below-grade earthen, drive-in, disposal units. The excavated soil is stockpiled for later placement over disposed waste. Currently two ETs are located in the E-Area LLWF. ET #1 is approximately 650 feet long by 150 feet wide (bottom dimensions) and varies in depth from 16 to 25 feet. It is designed to contain approximately 19,000 B-25 boxes of waste (Swingle and Phifer 2006). ET #1 consists of the following:

- A berm around the top on the sides where the local terrain slopes toward the trench
- Side slopes ranging from 1.25:1 (horizontal:vertical) to 1.5:1 that are covered with an erosion control matting and seeded
- A vehicle access ramp to the bottom
- A bottom consisting of compacted soil, a geotextile filter fabric, and approximately 6 inches of granite crusher run (from bottom to top) sloped to a sump
- A sump with 1-to-1 side slopes and a geotextile fabric and a polyethylene geoweb slope cover, infilled with 4,000-psi concrete covering the sump side slopes and sump bottom

Engineered Trench #2 is approximately 656 feet long by 160 feet wide (bottom dimensions) and varies in depth from 14 to 23 feet. It is also designed to contain approximately 19,000 B-25 boxes of waste. ET #2 is essentially identical to ET #1 except it does not contain a sump. The bottom of ET #2 is sloped to a low point where a 24 inch steel pipe takes water from ET#2 to the ET #1 sump (Swingle and Phifer 2006).

During the operational period low-level waste contained within B-25 boxes, B-12 boxes, 55-gallon drums, Sealand containers, components, and/or other metal containers are stacked by forklift or placed by crane within the Engineered Trench. The B-25 boxes are stacked in rows four high (approximately 17 feet high) with a forklift, beginning at the end of the trench opposite the access ramp. The stacks of B-25 boxes are generally placed immediately adjacent to one another with as little void space as possible between the stacks. Figure 1-4 provides operational photographs of ET #1 and ET #2.

Operational closure of the Engineered Trenches will be conducted in stages. As a sufficient number of B-25 rows are placed, the stockpiled clean soil is bulldozed in a single lift over some of the completed rows to produce a minimum 4-foot-thick clean soil layer over them (i.e., operational soil cover). The depth of both ETs at their west ends is less than the height of a stack of 4 B-25 boxes; therefore, soil is mounded above the original grade to provide adequate operational soil cover. This operational soil cover is only applied to that portion of the completed rows that still allows maintenance of a safe distance from the working face (i.e., where new boxes are placed in the stack) within the trench.

Engineered Trench #1 Aerial View

Engineered Trench #1 Interior View

Engineered Trench #2 View from Berm

Figure 1-4. Operational Engineered Trench Photographs

The operational soil cover is graded to provide positive drainage off the trench and away from the working face. Placement of the B-25 boxes continues until the trench is filled with boxes. At that point, the minimum 4 feet of operational soil cover is placed over the remaining portion of the trench; the entire area is graded to provide positive drainage off the trench, a vegetative cover of shallow rooted grass is established, and it is considered operationally closed. After operational closure, the subsidence potential of Engineered Trenches has been estimated at 13.5 feet due to stacked B-25 boxes containing low-density waste (Phifer and Wilhite 2001). Additionally in order to minimize future subsidence of the final closure cap, limits on the disposal of containers with significant void space that are considered non-crushable (i.e., containers that will not be stabilized by dynamic compaction) have been imposed (Swingle and Phifer 2006).

At the end of the operational period, an interim runoff cover will be installed and maintained during the 100-year institutional control period (i.e., interim closure). The interim runoff cover will involve the placement of up to an additional 2-foot of soil over the Engineered Trenches, which is graded to promote even greater drainage off the trenches. The interim runoff cover will consist of the surface application of a high density polyethylene (HDPE) geomembrane or geotextile fabric with spray on asphalt emulsion or some other water-shedding material. It will extend a minimum of 10 feet beyond the edge of all sides of the trenches.

Final closure of the Engineered Trenches will take place at final closure of the entire E-Area LLWF, which is at the end of the 100-year institutional control period. Static surcharging and/or dynamic compaction of the Engineered Trenches will be conducted at the end of the 100-year institutional control period, when the efficiency of the subsidence treatment will be greater due to container corrosion and subsequent strength loss. It is assumed that this subsidence treatment essentially eliminates future subsidence potential except in those areas containing non-crushable containers with significant void space (Swingle and Phifer 2006). Final closure will consist of the installation of an integrated closure system designed to minimize moisture contact with the waste and to provide an intruder deterrent. The integrated closure system will consist of one or more closure caps installed over all the disposal units and a drainage system. Figure 1-3 provides the anticipated Engineered Trench closure cap configuration (McDowell-Boyer et al. 2000; Cook et al. 2004; Phifer 2004; Phifer et al. 2006).

1.4 PRINCIPAL DISPOSAL UNIT DESIGN FEATURES

1.4.1 Slit Trench Principle Design Features

1.4.1.1 Slit Trench Structural Stability and Cover Integrity

After operational closure, the subsidence potential of Slit Trenches is highly variable due to waste variability. The subsidence potential could range from zero for bulk waste to 13.5 feet for B-25 boxes containing low-density waste stacked four high. Subsidence over bulk waste is expected to occur within the 100-year institutional control period due to waste consolidation and soil infilling (Phifer and Wilhite 2001; Phifer 2004). Subsidence over B-25 boxes containing low-density waste stacked four high is expected to occur between 50 and 500 years after burial due to container corrosion and subsequent collapse (derived from Jones and Phifer [2002] based upon a 50% volumetric corrosion loss of the B-25 lid and/or sides).

Prior to performance of subsidence treatment near the end of the 100-year institutional control period, both the operational cover and the interim runoff cover will be maintained and any subsidence-induced damage to the covers will be appropriately repaired. Significant subsidence-induced damage to those areas of the covers overlying trench portions containing containerized waste is not anticipated due to the inherent structural integrity of the containers until significant corrosion has occurred. However some subsidence-induced damage is anticipated to those areas of the covers overlying trench portions containing bulk waste.

Due to the Slit Trench subsidence potential, static surcharging and/or dynamic compaction of the Slit Trenches will be conducted prior to installation of the final E-Area LLWF closure cap near the end of the 100-year institutional control period. At that time, the efficiency of the subsidence treatment will be greater due to container corrosion and subsequent strength loss. Dynamic compaction will not be carried out over any Slit Trench area (such as those containing M-Area glass and ETP Carbon Columns) that has been designated not to undergo dynamic compaction. It is assumed that this subsidence treatment essentially eliminates future subsidence potential except in those areas designated not to undergo dynamic compaction or containing non-crushable containers with significant void space.

The final closure cap will be installed after subsidence treatment near the end of the 100-year institutional control period (Phifer 2004). However, since some areas are designated not to undergo dynamic compaction or contain non-crushable containers with significant void space, limited subsidence damage to the final closure cap is anticipated in these areas.

Additionally, after installation it is assumed that no closure cap maintenance will be performed other than that required for establishment of the vegetative cover. Therefore, it is assumed that the hydraulic properties of the closure cap will immediately begin to degrade after construction due to the following (Phifer and Nelson 2003; Phifer 2004):

- Formation of holes in the upper GCL by pine forest succession
- Reduction in the saturated hydraulic conductivity of the drainage layers due to colloidal clay migration into the layers
- Erosion of layers that provide water storage for the promotion of evapotranspiration

1.4.1.2 Slit Trench Water Infiltration

During the operational period, water infiltration through the waste is minimized by minimizing the area of open trench and the operational soil cover, which is graded to provide positive drainage off the trench and away from the working face. The interim runoff cover (see Cook et al. 2000, Rev. 4) minimizes water infiltration through the waste during the 100-year institutional control period. The interim runoff cover, which is maintained during institutional control, minimizes infiltration into the soil column overlying the waste. The final closure cap minimizes infiltration through the waste during the post-institutional control period. However, after installation it is assumed that no cap maintenance will be performed other than that required for establishment of the vegetative cover. Therefore, the hydraulic properties of the cap are assumed to degrade over time, resulting in increased infiltration through the cap over time.

1.4.1.3 Slit Trench Inadvertent Intruder Barrier

Inadvertent intrusion into Slit Trench waste is not considered feasible during the operational and institutional control periods, due to facility security during these periods. However, it is assumed that inadvertent intrusion could occur during the post-institutional control period. The closure cap (see Figure 1-3) includes an erosion barrier designed to maintain a minimum of 10 ft of clean material above the waste. This provides a barrier to excavation into the waste, since it is assumed that excavations for residential construction do not exceed 10 ft (McDowell-Boyer et al. 2000). However, it is not assumed to provide a barrier to drilling into the waste.

1.4.2 Engineered Trench Principle Design Features

1.4.2.1 Engineered Trench Structural Stability and Cover Integrity

During the operational period, B-25 boxes are stacked one on top of another and the stacks are generally placed immediately adjacent to one another with very little void space between the stacks. During placement of the operational soil cover, the lid of the top B-25 box in a stack is assumed to collapse into the box and the lower three boxes in the stack are assumed to remain undamaged (Phifer and Wilhite 2001). At that point, the matrix of B-25 boxes provides significant structural stability to support the operational soil cover.

It has been estimated that an Engineered Trench, containing B-25 boxes of waste stacked four high, has a subsidence potential of approximately 13.5 feet (Phifer and Wilhite 2001; Phifer 2004). It has also been estimated that subsidence over B-25 boxes containing low-density waste stacked four high will occur between 50 and 500 years after burial due to container corrosion and subsequent collapse (derived from Jones and Phifer 2002 based upon a 50% volumetric corrosion loss of the B-25 lid and/or sides). It has been further estimated that dynamic compaction of an Engineered Trench containing B-25 boxes at the end of the operational period would at best reduce the subsidence potential by 50 percent (Phifer and Wilhite 2001). However, the efficiency of subsidence treatment increases with time due to B-25 box corrosion and subsequent loss of strength. Therefore, rather than performing subsidence treatment (i.e., static surcharging and/or dynamic compaction) of the Engineered Trenches at the end of the operational period, it will be performed at the end of the 100-year institutional control period, when its efficiency will be greater. With performance of the subsidence treatment at the end of the 100-year institutional control period, it is assumed that essentially all future subsidence potential is eliminated, except in those areas containing non-crushable containers with significant void space.

Prior to performance of the subsidence treatment at the end of the 100-year institutional control period, both the operational cover and the interim runoff cover will be maintained, and any subsidence-induced damage to the covers will be appropriately repaired. However, significant subsidence-induced damage to the covers is not anticipated due to the inherent structural integrity of the stacked B-25 boxes until significant corrosion has occurred (Phifer 2004).

Additional work is currently in progress to better estimate the anticipated time period of B-25 box structural collapse following burial. Additionally, the timing of the use of static surcharging and/or dynamic compaction on the Engineered Trenches to achieve more efficient results is currently in progress. While B-25 containers stacked four high is the typical configuration currently placed in the Engineered Trenches, other containers are also placed there. These containers include 55-gallon drums, B-12 containers (of similar construction, but with about half the capacity of B-25s), Sealand containers (20 ft- and 40 ft-long shipping containers), and a few other types of steel containers. To date, only the long-term structural stability of B-25s has been evaluated; however, the estimate of how much collapse will be realized at the time of compaction is thought to be bounded by the B-25 box analysis.

The final E-Area LLWF closure cap will be installed at the end of the 100-year institutional control period (Phifer 2004). As outlined above, subsidence treatment of the Engineered Trenches will be performed immediately prior to installation of the final closure cap. At that time, the subsidence treatment will be more effective, and it is assumed that such treatment will minimize subsidence potential. However, since some areas contain non-crushable containers with significant void space, limited subsidence damage to the final closure cap is anticipated in these areas. Additionally, after installation it is assumed that no closure cap maintenance will be performed other than that required for establishment of the vegetative cover.

Therefore, it is assumed that the hydraulic properties of the closure cap will immediately begin to degrade after construction due to the following (Phifer and Nelson 2003; Phifer 2004):

- Formation of holes in the upper GCL by pine forest succession
- Reduction in the saturated hydraulic conductivity of the drainage layers due to colloidal clay migration into the layers
- Erosion of layers that provide water storage for the promotion of evapotranspiration

1.4.2.2 Engineered Trench Water Infiltration

During the operational period, water infiltration through the waste is minimized by the following:

- Berms surrounding the Engineered Trench, which prevent run-on
- Metal containers, which divert water
- The trench bottom, which is sloped to a sump from which water can be pumped
- The operational soil cover, which is graded to provide positive drainage off the trench and away from the active face, where new waste is being emplaced.

The interim runoff cover and the metal containers minimize water infiltration through the waste during the 100-year institutional control period. The interim runoff cover, which is maintained during institutional control, minimizes infiltration into the soil column overlying the waste, and the metal containers divert water around the waste while they remain intact (see Cook et al. 2000, Rev. 4). The final closure cap minimizes infiltration through the waste during the post-institutional control period. However, after installation it is assumed that no cap maintenance will be performed other than that required for establishment of the vegetative cover. Therefore, the hydraulic properties of the cap are assumed to degrade resulting in increased infiltration through the cap over time.

1.4.2.3 Engineered Trench Inadvertent Intruder Barrier

Inadvertent intrusion into the Engineered Trench waste is not considered feasible during the operational and institutional control periods, due to facility security during these periods. However, it is assumed that inadvertent intrusion could occur during the post-institutional control period. The closure cap includes an erosion barrier designed to maintain a minimum of 10 ft of clean material above the waste. This provides a barrier to excavation into the waste, since is assumed that excavations for residential construction do not exceed 10 ft (McDowell-Boyer et al. 2000). It is not assumed, however, to provide a barrier to drilling into the waste.

1.5 SLIT AND ENGINEERED TRENCHES WASTE CHARACTERISTICS

1.5.1 Slit Trench Waste Characteristics

1.5.1.1 Waste Form

Waste destined for Slit Trench disposal can generally be described as contaminated soil, rubble, wood debris, large components, miscellaneous tanks, and job control waste. Job control waste consists of potentially contaminated protective clothing (plastic suits, shoe covers, lab coats, etc.), plastic sheeting, etc. The waste may be disposed as bulk waste or contained within B-25 boxes, B-12 boxes, 55-gallon drums, Sealand containers, and other metal containers. Some limited amounts of elemental carbon have been disposed in the Slit Trenches in Effluent Treatment Plant (ETP) Carbon Columns. Slit Trench waste radioactivity levels are generally lower than for waste destined for vault disposal. The trenches have been accepting high volumes of waste from the Decontamination and Decommissioning (D&D) program. The curie levels are, however, relatively low.

1.5.1.2 Radionuclide Inventory

The forecasted radionuclide inventory at closure for the Slit and Engineered Trench units is provided in Appendix C. Inventories are presented for 4 groupings of trench units, as described:

SLITc - The central grouping of Slit Trench units composed of SLIT1 through SLIT7 (see Figure 1-1).

SLITe - The eastern grouping of Slit Trench units composed of 8 future Slit Trench unit footprints.

SLITw - The western grouping of Slit Trench units composed of SLIT8 plus 5 future western Slit Trench unit footprints.

Engineered Trenches - The grouping of the ET1 and ET2 units.

1.5.1.3 Waste Volume

The 21 Slit Trench "footprints" shown in Figure 1-1, are equivalent to approximately 19 standard footprints that are 157-foot wide by 656-foot long. Each standard footprint generally contains 5 trenches each with waste dimensions of 16 ft high by 20 ft wide by 650 ft long. This produces a trench footprint waste volume capacity of approximately 1,040,000 ft^3. Therefore, the capacity of the 19 equivalent standard footprints is 19,760,000 ft^3.

1.5.1.4 Packaging Criteria

Packaging criteria are described in the SRS 1S Manual, Waste Acceptance Criteria (WSRC 2006).

1.5.1.5 Pre-Disposal Treatment Methods

Generators follow SRS Waste Acceptance Criteria (WAC) requirements for packaging and shipping waste to applicable waste disposal facilities in E Area.

1.5.1.6 1.5.1.6 Waste Acceptance Restrictions

Waste acceptance for disposal in trenches must conform to criteria in the SRS WAC (WSRC 2006).

1.5.1.7 Security Classification of Wastes

A very small (insignificant) fraction of disposed LLW contains classified material. The security issues related to the disposal of this material are addressed in the SRS/SWMF security program.

1.5.2 Engineered Trench Waste Characteristics

1.5.2.1 Waste Form

Engineered Trench disposed low-level waste is contained within B-25 boxes, B-12 boxes, 55-gallon drums, Sealand containers, and/or other metal containers, which are stacked by forklift or placed by crane. B-25 boxes are the predominant disposal containers utilized. The B-25 boxes are stacked in rows four high (approximately 17 ft high) with a forklift. Container contents are mostly steel, paper, and plastic.

There are two Engineered Trenches. In Engineered Trench #2, container stacking begins at the end of the trench opposite the access ramp. In Engineered Trench #1 containers are stacked on both sides of the access ramp. The stacks of B-25 boxes are generally placed immediately adjacent to one another with as little void space as possible between the stacks.

1.5.2.2 Radionuclide Inventory

The 20-year projected inventory for the two Engineered Trenches is given in Part C.

1.5.2.3 Waste Volume

There are two Engineered Trenches. Engineered Trench #1 is approximately 650 feet long by 150 feet wide (bottom dimensions) and varies in depth from 16 to 25 feet. It is designed to contain approximately 19,000 B-25 boxes of waste (Swingle and Phifer 2006). Engineered Trench #2 is approximately 656 feet long by 160 feet wide (bottom dimensions) and varies in depth from 14 to 24 feet. It is also designed to contain approximately 19,000 B-25 boxes of waste. ET #2 is essentially identical to ET #1 except it does not contain a sump. The bottom of ET #2 is sloped to a low point where a 24 inch steel pipe takes water from ET#2 to the ET #1 sump (Swingle and Phifer 2006). Each B-25 box is designed to contain 90 cubic feet of waste; therefore each Engineered Trench can contain approximately 1,700,000 ft^3 of waste.

1.5.2.4 Packaging Criteria

Packaging criteria are described in the SRS 1S Manual, Waste Acceptance Criteria (WSRC 2006). The PA Process sets many of the criteria that are the basis for the WAC.

1.5.2.5 Pre-Disposal Treatment Methods

Generators follow SRS WAC (WSRC 2006) requirements for applicable pre-disposal treatment for the E-Area low-level waste disposal facilities. The PA Process sets many of the criteria that are the basis for the WAC.

1.5.2.6 Waste Acceptance Restrictions

Waste acceptance for disposal in Engineered Trenches must conform to criteria put forth in the SRS WAC (WSRC 2006). The PA Process sets many of the criteria that are the basis for the WAC.

1.6 SLIT AND ENGINEERED TRENCHES GROUNDWATER TRANSPORT ANALYSIS

This section documents the development of preliminary groundwater protection limits for the Slit and Engineered Trenches. The limits developed within this section are considered preliminary, since they do not take into consideration the effects of plume overlap from adjacent units or the results of sensitivity and uncertainty analyses. The effects of plume overlap are considered in Chapter 6, and the interpretation of sensitivity and uncertainty analyses is conducted in Chapter 7. Final limits are provided in Chapter 7.

1.6.1 Relation of Current Analysis to Previous Analyses

In this Performance Assessment, a re-evaluation of the groundwater transport was required for all radionuclides that could not be screened out due to numerous changes to the conceptual model of the Slit and Engineered Trenches, which were embodied within the deterministic model. The list includes 38 generic radionuclides and 20 special wasteform radionuclides. Thirty-five of the 38 generic radionuclides are identified as those radionuclides remaining after the screening analysis and listed in Table 4-1 of Part C (Background Chapter), while the special wasteforms are listed in Section 1.6.3.3. The remaining three generic radionuclides are included because their current inventories exceed the relevant trigger values (see discussion in Section 4.1.1 of the Background Chapter in Part C).

The key aspects of the new groundwater transport analysis include the following:

- Entirely new conceptual and deterministic models of the vadose zone for the Slit and Engineered Trenches were an extensive revision of the aquifer model, though still based on the calibrated GSA flow model (Flach 2004).
- Development of revised flow and transport properties for different materials (Phifer et al. 2006; Kaplan 2006).
- Updated estimates of water infiltration with respect to time (Phifer 2004) were utilized, in part, to establish steady-state flow periods for flow and transport simulations.
- Recognition that some of the waste disposed in trenches might not compact at the time of dynamic compaction (at the end of institutional control), thus posing a threat to compact and cause subsidence at a later date as corrosion degrades individual waste packages.
- Recognition that the presence of cellulose rich waste materials disposed in the trenches may produce cellulose degradation products (CDPs) that impact the mobility of different radionuclides.

1.6.2 Overview of Groundwater Transport Analysis

Groundwater transport analysis involved the establishment of two separate deterministic, numerical models, one for the vadose (unsaturated) zone and another for the aquifer zone (saturated). The vadose zone models were developed as 2-D, cross-sectional models, one to represent a typical Slit Trench and the other for a typical Engineered Trench. The aquifer model is fully 3-D, based upon the General Separations Area groundwater model, as described in Flach (2004). In each case the approach was to first establish a steady-state flow field through which contaminant migration was simulated with respect to time. For the vadose zone model, multiple steady-state periods were defined, corresponding to different infiltration rates for different time periods, for use with transient contaminant transport simulation.

The results of the transport models were combined in various ways to evaluate the effect of multiple individual trenches that make up each specific Slit Trench unit as well as the individual Engineered Trenches.

The vadose zone flow models were configured to be consistent with the latest E-Area Closure Plan (Phifer 2004a) and incorporate the different materials (e.g., backfill materials and natural sediments) described in this plan. Several features were incorporated to improve the previous analyses, including updated estimates of physical, hydraulic and transport properties for each of the materials within the modeled domains as well as the consideration of the presence of "non-crushable" waste materials within the trenches. Another consideration was that CDPs may be present within Slit and Engineered Trench waste, which would have the effect of enhancing the mobility of different radionuclides.

Contaminant transport simulations were performed for the radionuclides that could not be screened out with respect to possibly causing adverse exposure to human beings, as described in Taylor (2006) and for 20 additional special wasteform radionuclides. The approach for transport simulations was to introduce a unit source term of 1 mole of each parent radionuclide into the waste zone and determine the fractional mass flux exiting the vadose zone with respect to time. The mass flux exiting the vadose zone was then introduced to the aquifer model and, ultimately, the groundwater concentration with respect to time was determined at the 100-m compliance location.

In this analysis, four scenarios were evaluated which are thought to bracket the range of plausible results, considering operational constraints. The scenarios were conceived to account for the presence or absence of non-crushable (steel) waste packages and the presence or absence of CDPs within the trench waste zones. Non-crushable waste containers are those that do not fully compact during the subsidence treatment (e.g., dynamic compaction, static surcharge) just prior to final cover installation after the institutional control period. These containers could ultimately result in accelerated damage to the overlying closure cap from eventual container corrosion and collapse, which would cause slumping in the overlying soil and cap materials. This in turn would induce much higher infiltration into the depressions. The assumption in this analysis is that only 10% of the waste disposed in any disposal unit will be of the robust, non-crushable, variety. This percentage is to be administratively controlled during the operational period. CDPs may be present within the trenches in varying degrees and would impact the mobility of the radionuclides to varying degrees. Thus, a scenario was evaluated using radionuclide K_ds that reflect the presence of CDPs.

To summarize, the four scenarios are:

1. 0% non-crushable waste with no CDPs present
2. 0% non-crushable waste with CDPs present
3. 10% non-crushable waste with no CDPs present
4. 10% non-crushable waste with CDPs present

1.6.3 Groundwater Transport Conceptual Model

In this section, a discussion of the scenarios and conceptual models developed for evaluating subsurface transport of radionuclides released from the Trenches over time is provided. Key inputs and assumptions associated with implementation of these models are provided in Appendix B.

1.6.3.1 Operations, Closure and Degradation Scenarios

During the Operations period of the Trenches, there is no closure cap in place, only the fill material placed above the waste material (within the upper 4 feet of each trench) as it is filled with waste material. During the period of institutional control (100 years), an interim runoff cover (see Sections 1.4.1.1 and 1.4.2.2) is to be placed over the trenches and maintained, thus limiting infiltration. Following that, compaction of the trenches is to be conducted followed by emplacement of the final closure cap.

At the end of institutional control, the trenches will be compacted and a final closure cap placed over the E-Area disposal facilities. Studies indicate that the 16-foot thickness of waste could potentially compact to a 2.5-foot thickness, over which additional soil will be added and compacted to bring the trench up to the land surface (Phifer et al. 2001). Following that the permanent closure cap is to be emplaced. A detailed description of the Slit and Engineered Trenches, their operations and closure, is provided in Section 1.3.

For the E-Area Trenches, the operations period commenced at an earlier time (~5 years) than for other E-Area facilities. Thus, to more accurately represent actual field conditions, this extended operations period is incorporated into the Slit and Engineered Trench analysis as a 30-year operations period compared to the 25-year operations period that is assumed for all other E-Area disposal facilities. This difference is expressed as a longer simulation time in the vadose zone models for the Slit and Engineered Trenches.

In this analysis it is recognized that some non-crushable waste may be present in the trenches at the end of institutional control, when dynamic compaction is implemented. Therefore, two closure scenarios have been evaluated, one in which it is assumed that no non-compacted waste material is present and another in which 10% of the overall trench length is assumed to be non-crushable. If non-crushable waste containers are present at the time of compaction, they pose a threat to the integrity of the closure cap at a later time after corrosion degrades the containers to the extent that they collapse and cause slumping of the overlying soil and cap materials. In the first scenario the closure cap degradation is gradual over the PA period of assessment, the result of progressively deeper penetration of pine roots. Under the second scenario, the closure cap degradation is assumed to occur by the development of potholes into which surface runoff of precipitation in the immediate area preferentially flows. This analysis assumes that 10% of the trench closure area subsides in a random pattern due to this type of collapse immediately after the final cover is installed, based on the analysis documented in Hang et al. (2005).

1.6.3.2 Infiltration Boundary Conditions

Infiltration rates for the Slit and Engineered Trenches were calculated using the HELP model (see Phifer 2004) and modified to evaluate infiltration under a scenario whereby not all of the waste containers are crushed at the time of emplacement of the final closure cap. Baseline estimates of the infiltration rate through the closure cap are for the scenario in which all waste is assumed to be crushable at the time of final cover installation and therefore the closure cap is only degraded slowly by pine root encroachment.

Conditions under the scenario whereby the closure cap also fails due to the presence of non-crushable waste at the time of dynamic compaction impact the rate of water infiltration through time. Non-crushable containers retain their void space after the static surcharge is applied to individual trenches at the end of the institutional control period. However, these containers are still subject to corrosion and, in time, will collapse and likely cause the final closure cap to subside. The subsiding cover is thought to result in an increased rate of infiltration, and this effect is assumed to occur immediately after the final closure cap is constructed.

In the groundwater analysis part of this investigation, vadose zone flow simulations were performed by defining a series of time-periods during which steady, average conditions were assumed to prevail. The specific periods were established based on conditions that relate to closure (e.g., operations period, institutional control period) as well as the different calculated water infiltration rates through the closure cap. The time periods listed in Table 1-12 represent periods within the vadose zone model when hydraulic conditions remain constant, thus a steady infiltration rate is applied for the duration of that period. Throughout the remainder of this chapter, time zero (0) is regarded to be the beginning of facility operations (a 30-year period). The infiltration rates presented in Table 1-12 represent a steady rate that applies to each of these time periods.

Also, in Table 1-12, the column labeled “Case 01” presents the infiltration rates calculated for the scenario where the closure cap degrades only by gradual pine root encroachment. The infiltration rates presented in the column labeled “Case 11” correspond to the scenario where the presence of non-crushable waste causes enhanced damage to the closure cap, which results in much higher infiltration rates. Infiltration rates for Case 11 represents the average infiltration rates for subsided E-Area trenches throughout the PA compliance period of 1000 years. The subsided trenches are assumed to occur randomly throughout the disposal unit. The values listed in Table 1-12 were derived from the HELP model infiltration analysis (see Phifer et. al. [2006]). The infiltration rates for Case 01 and Case 11 are illustrated graphically in Figure 1-5 for the full 1000-year PA compliance period.

Table 1-12. Infiltration rates associated with Case 01 and Case 11 for the Slit and Engineered Trenches

Model Period	Time Range (years)	Case 01 Infiltration (cm/yr)	Case 11 Infiltration (cm/yr)	Period Description
TI01	0 to 30	40	40	Operations
TI02	30 to 130	0.91	0.91	Institutional Control
TI03	130 to 180	0.25	81.51	Post Institutional Control
TI04	180 to 230	0.27	81.50	"
TI05	230 to 280	0.64	81.03	"
TI06	280 to 330	1.38	80.12	"
TI07	330 to 380	2.11	79.21	"
TI08	380 to 430	2.85	78.30	"
TI09	430 to 480	3.69	77.27	"
TI10	480 to 530	4.63	76.10	"
TI11	530 to 580	5.57	74.94	"
TI12	580 to 630	6.51	73.77	"
TI13	630 to 680	7.45	72.61	"
TI14	680 to 730	8.51	71.32	"
TI15	730 to 830	10.27	69.17	"
TI16	830 to 930	12.62	66.32	"
TI17	930 to 1030	14.97	63.46	"
TI18	1030 t o 1130	17.32	60.61	Post Institutional Control

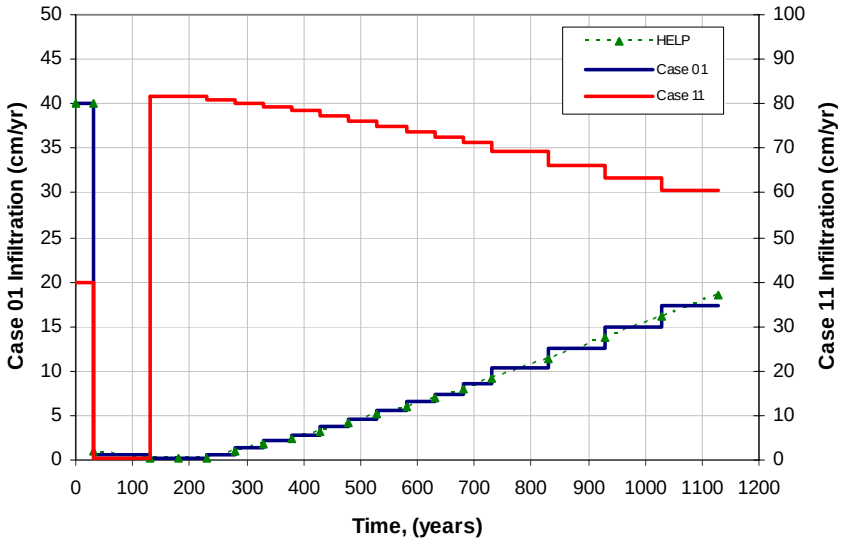

Figure 1-5. Slit and Engineered Trenches infiltration rates for Case 01 and Case 11

1.6.3.3 Slit and Engineered Special Wasteforms

The Slit and Engineered Trenches have been in active operation since the mid 1990s. The current estimated inventory of radionuclides is presented in Part C, as has been mentioned. In addition to the base 35 generic radionuclides that must be analyzed for each disposal facility in the E-Area Performance Assessment, there are three more generic radionuclides (Cf-249, Cf-251, Cm-246) analyzed for the trenches, since their current inventories exceed the relevant trigger values. The trigger values for these radionuclides are given in Tables 4-4 and 4-5 in the Part C Background chapter. In addition to these, an additional 20 "special" radionuclides associated with specific waste streams were also analyzed.

This investigation recognizes that CDPs may or may not be present within the waste zones of the Slit and Engineered Trenches. Hence, K_d values associated with each special wasteform are presented in Table 1-13 for the scenarios where CDPs are either present or not present. These values were derived from calculations made as a part of this investigation to quantify the rate of dissolution and/or diffusion of the radionuclide from each specific wasteform.

With respect to the Special wasteforms, certain disposal restrictions identified in earlier Special Analyses still apply in this PA. These restrictions are identified in the Key Assumptions that are listed in Appendix B. Specifically, these include: restrictions that apply to the disposal of high-concentration I-129 wasteforms and which are identified in Collard (2001); restrictions that apply to the disposal of the Paducah Cask special wasteform and which are identified in Collard (2001); restrictions that apply to the ETP special wasteforms and which are identified in Collard and Hiergesell (2004); and restrictions that limit the disposal of certain types of waste in the vicinity of the M-Area Glass special wasteforms and which are identified in Cook and Yu (2002).

Table 1-13. Special Wasteform radionuclides and associated K_d values

Special Wasteform	WITS Designation	Waste Zone K_d (no CDP present) ml/g	Waste Zone K_d (CDP present) ml/g
C-14_NR.Pump	C-14 N	0	0
H-3_ETF.Carbon	H-3 C	0	0
I-129_ETF.Carbon	I-129 C	7,400	3,700
I-129_ETF.GT.73	I-129 I	10,000	5,000
I-129_F.Carbon	I-129 B	132,500	66,250
I-129_F.CG.8	I-129 G	50	25
I-129_F.Dowex.21K	I-129 D	6,800	3,400
I-129_F.Filtercake	I-129 J	56.7	28.35
I-129_H.Carbon	I-129 A	58,100	29,050
I-129_H.CG.8	I-129 H	380	190
I-129_H.Dowex.21K	I-129 E	15,600	7,800
I-129_H.Filtercake	I-129 F	650	325
I-129_Mk50A	I-129 R	0	0
Ra-226 Cooling Tower	Ra-226T	*	*
Sr-90_Mk50A	Sr-90 R	0	0
Tc-99_Mk50A	Tc-99 R	0	0
Th-230 Cooling Tower	Th-230T	*	*
U-234_MGlass	U-234 G	0	0
U-235_MGlass	U-235 G	0	0
U-235_Paducah.Cask	U-235 P	0	0
U-236_MGlass	U-236 G	0	0
U-238_MGlass	U-238 G	0	0

* Cooling Tower wastes (Ra-226 and Th-230) are represented by the generic radionuclide in the presence of CDP.

1.6.3.4 Vadose Zone Flow and Transport Conceptual Model

Conceptual models were formulated for the vadose zone and groundwater zone as part of the Slit and Engineered Trenches groundwater transport analysis. The vadose zone conceptual models are for a 2-dimensional view of a typical (individual) Slit Trench and a typical (individual) Engineered Trench and are illustrated in Figure 1-6 and Figure 1-7, respectively. In these models the dimensions of the trench area are made to correspond exactly to the dimensions of Slit and Engineered Trenches. In Figure 1-6 the representations of different materials of the Slit Trench conceptual model are indicated by the different shaded areas where the outline of a typical 20-ft wide by 20-ft deep trench is imbedded within native soil materials.

The orange material is the Upper Vadose Zone and the yellow material is the Lower Vadose Zone. Within the trench there are 3 sub-zones identified, these being the Lower waste zone, the Upper waste zone and the Soil fill zone. The Upper and Lower waste zones occupy the lower 16 feet of the trench and comprise the zone that is initially filled with waste material and soil as each trench is filled. The Soil fill zone, indicated by the gray shading, occupies the upper 4 feet of the trench and is the zone into which clean backfill soil is placed to cover waste material as trench filling progresses.

At the end of the Institutional Control period, 100 years after the end of the Operations period, the waste material and soil fill in the slit trenches will be compacted prior to placement of the final closure cap. It is estimated that all of the uncompacted waste material from the Upper waste zone and the soil fill will be displaced into the Lower waste zone, which will occupy the lower 2.5 ft of the trench. Soil will be filled in and compacted to the land surface above the Lower waste zone prior to construction of the final closure cap.

In Figure 1-7, the representations of different materials of the Engineered Trench conceptual model are indicated by the different shaded areas where the outline of a typical Engineered Trench, in the form of a trapezoid, is imbedded within native soil materials. The width of the base is 160 ft, while the width just below the gray soil cover is 208 ft.

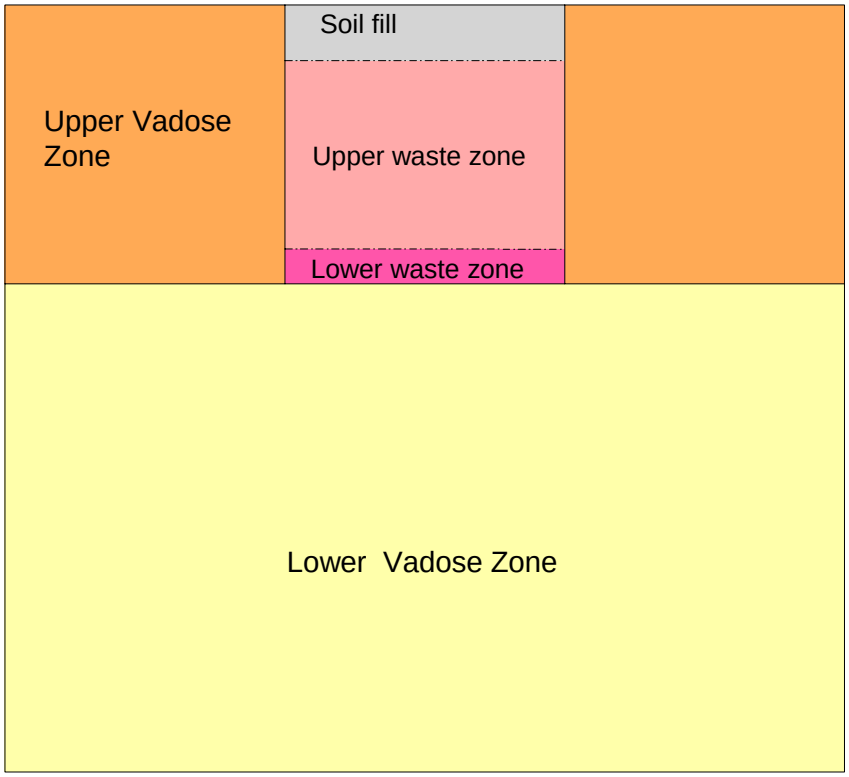

Figure 1-6. Vadose Zone Conceptual Model for a Typical Slit Trench

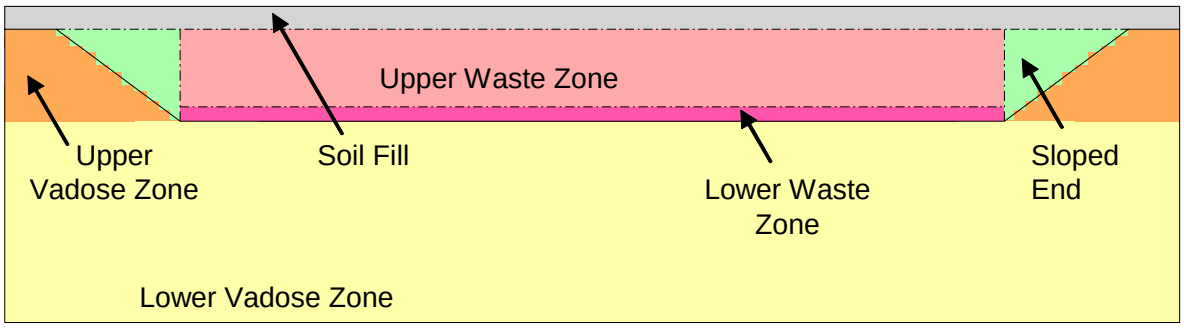

Figure 1-7. Vadose Zone Conceptual Model for a Typical Engineered Trench

Similar to the Slit Trench (Figure 1-6), the orange material in Figure 1-7 is the Upper Vadose Zone and the yellow material is the Lower Vadose Zone. Within the trench, three sub-zones are identified, the Lower waste zone (dark pink), the Upper waste zone (light pink), and the sloped-sides waste zone (green). These waste zones occupy the lower 16 feet of the trench and are the zones that are initially filled with waste material and soil as each trench is filled. Waste is not placed within the sloped trench ends; however, they are backfilled with soil as the waste zone is filled. The Soil fill zone, indicated by the gray shading, occupies the upper 4 feet of the model and is the zone into which clean backfill soil is placed to cover waste material as trench filling progresses.

At the end of the Institutional Control period, 100 years after the end of the Operations period, the waste material and soil fill in the Engineered Trenches will be compacted prior to placement of the final closure cap. It is estimated that all of the uncompacted waste material from the Upper waste zone and the soil fill will be displaced into the Lower waste zone, which will occupy the lower 2.5 ft of the trench. It is likely that uncompacted waste in the sloped sides will be displaced into a narrow band along the sloped surface. Soil will be filled in and compacted to the land surface above the Lower waste zone and the compacted layer in the sloped sides prior to construction of the final closure cap.

Throughout much of E-Area, the interface between the two natural soil zones occurs at an elevation of 264 ft. above mean sea level. Bottom of the model is the nominal long-term average elevation of the water table beneath E-Area. The land surface elevation and elevation of the long-term average water table vary across the E-Area, as does the depth from land surface to the water table. Based on well data from E-Area (see Hiergesell et al. 2003), the average depth from the land surface to the water table is approximately 55 to 65 ft, which is the basis of selecting 35 ft as a representative vertical distance between the base of a Slit or Engineered Trench and the water table in this conceptual model. The base of the Slit and Engineered Trenches are both 20 ft below grade, hence the distance from the land surface to the water table (55 ft) is consistent with the low end of the range of depths based on well data.

The physical and water flow properties, including porosity, bulk density, particle density, saturated hydraulic conductivity, characteristic curves (saturation/suction head/relative permeability), and effective diffusion coefficients of the different zones in Figure 1-6 and Figure 1-7 are discussed in detail in a separate report, Phifer et al. (2006). Likewise, the transport properties, distribution coefficients, K_ds, and solubility limits are discussed in detail in a separate report, Kaplan (2006). These properties of individual materials are briefly discussed below.

The Upper and Lower waste zones, the sloped sides of the ET, as well as the Soil fill zone, are initially represented as Operational Soil Cover, pre-compaction. After the Institutional Control period, compaction of the waste material and backfilling with compacted soil takes place and all of these zones are then represented as Operational Soil Cover (i.e., post-compaction material for the scenario where all of the waste in a trench is assumed to be crushable).

In the scenario whereby non-crushable waste is assumed to be present in the waste zone, the operational soil cover (OSC) material above the lower waste zone retains the pre-compaction properties after 100 years, under the assumption that subsidence after dynamic compaction disturbs the trench fill. The properties of these two materials as well as the Upper and Lower Soil zones are presented in Table 1-14.

Table 1-14. Physical and Flow Properties of Vadose Zone Materials

Material Type	Sat. K_v (cm/yr)	K_h/K_v	Effective porosity	Particle density (g/cm^3)
Operational Soil Cover (OSC) pre-compaction	3.8E+03	1.0	0.46	2.65
Operational Soil Cover (OSC) post-compaction	4.4E+02	1.0	0.27	2.65
Upper Vadose Zone	2.7E+02	7.1	0.39	2.70
Lower Vadose Zone	2.9E+03	3.6	0.39	2.66

Note: Values obtained from Phifer et al. (2006).

Transport properties

For trench simulations, two geochemical states are thought to be plausible and are hence evaluated separately. These are the no cellulose case, in which baseline K_d values are assigned for each radionuclide simulated and the CDP case in which different K_d values were assigned (see Kaplan 2006).

The K_ds were established for each of the 58 radionuclides evaluated for the Slit and Engineered Trenches. The basis for selecting values for these properties is related to the environmental settings (e.g., clayey sediment, sandy sediment or cementitious material) as they migrate with the contaminant plume through the subsurface. The rationale for selecting values used in the modeling involves the establishment of a "best" estimate and a "reasonably conservative" estimate for K_d. The "best estimates" are based on the determination of a central value of the literature, SRS site-specific environmental data or on expert judgment (Kaplan 2006). The "reasonably conservative" values were based on the lower limit of multiple K_d value measurements or the upper limit of solubility measurements (Kaplan 2006). For this investigation the "best estimate" values were utilized. This rationale, which is applied to both cases evaluated, with or without CDPs, where the non-CDP K_d values and the factor for modifying the K_d when CDPs are assumed to be present, have been obtained from Table 15 in Kaplan (2006).

For the purposes of assigning K_d values, certain backfill and natural soil materials have been simplified to be considered either "clayey" or "sandy". In this way Kd values associated with individual radionuclides are determined in a consistent fashion. Among the materials in the vadose zone, this classification is as presented in Table 1-15 along with the associated effective diffusion coefficient (D_{eff}) associated with each.

Table 1-15. Assignment of K_d by Material Type

	"Sand" K_ds	"Clay" K_ds	D_{eff} (cm2/yr)
Operational Soil Cover (OSC), pre		X	167.25
Operational Soil Cover (OSC), post		X	126.23
Upper Vadose Zone		X	167.25
Lower Vadose Zone	X		167.25

1.6.3.5 Saturated Zone Flow and Transport Conceptual Model

The aquifers of primary interest for the Slit and Engineered Trenches are the Upper Three Runs (UTR) and Gordon aquifers. Potential contamination from the trenches is not expected to enter the deeper Crouch Branch aquifer because an upward gradient exists between the Crouch Branch and Gordon aquifers near Upper Three Runs stream. Figure 1-8 is a cross-sectional schematic representation of groundwater flow patterns in the Upper Three Runs and Gordon aquifers along a north-south cross-section running through the center of the study area, shown with significant vertical exaggeration. Although not indicated on this diagram, the Slit and Engineered Trenches are situated at the land surface on the Upper Three Runs side of the groundwater divide.

Groundwater flow in the Upper Three Runs aquifer is driven by recharge, with nearby streams intercepting flow from higher elevations. The underlying Gordon aquifer is strongly influenced by discharge to Upper Three Runs stream, and recharged from both the overlying Upper Three Runs and underlying Crouch Branch Aquifer. Therefore the predominant flow pattern within the Gordon Aquifer is in the horizontal direction toward the discharge zone adjacent to, and beneath, Upper Three Runs stream. Flow across the Myers Branch confining Unit is a small fraction of total recharge to the Gordon aquifer, and can be neglected in comparison to recharge from the Upper Three Runs aquifer.

Groundwater flow in the Upper Three Runs Aquifer is predominantly horizontal with a smaller, vertically-downward component. Near groundwater divides located between surface water drainages, the vertical component of groundwater flow is stronger and downward due to the decreasing hydraulic head with increasing depth. In areas along Fourmile Branch, shallow groundwater moves generally in a horizontal direction and deeper groundwater has vertically upward potential to the shallow aquifers. In these areas, hydraulic heads increase with depth. Due to the position of the Slit and Engineered Trenches on the Upper Three Runs side of the groundwater divide, horizontal groundwater movement within the Upper Three Runs Aquifer beneath the Slit and Engineered Trenches is entirely toward Upper Three Runs stream. A more complete description of these units is presented in Part C (Background Chapter) of this report.

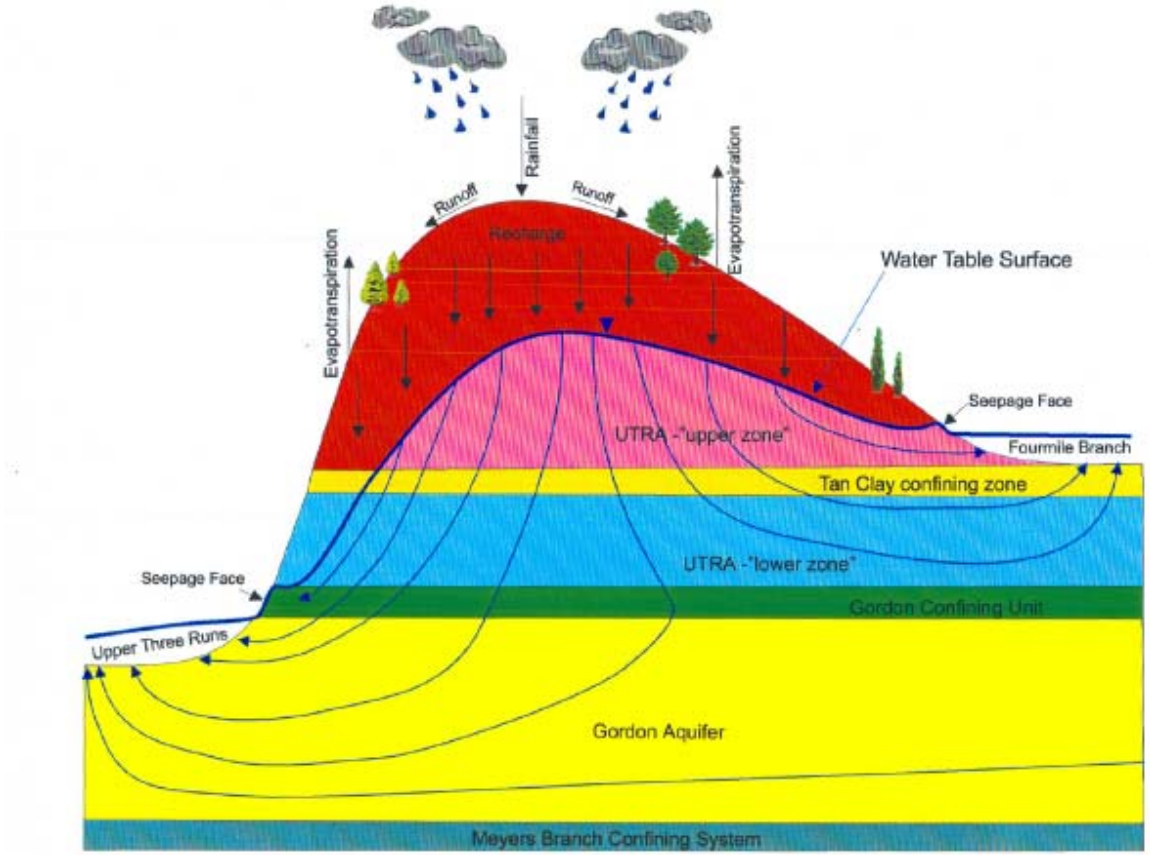

Figure 1-8. Generalized hydrogeologic cross-section near E-Area

The saturated hydraulic conductivity field is heterogeneous within hydrogeologic units and reflects variations present in the characterization data. The average horizontal conductivities in the saturated "upper" UTR aquifer zone, "lower" UTR aquifer zone, and Gordon aquifer unit are approximately 10, 13, and 38 ft/d, respectively. The average vertical conductivities for the "tan clay" confining zone and the Gordon confining unit are $6x10^{-3}$ and $1x10^{-5}$ ft/d, respectively. Particle density and porosity values were assigned based on classifying the aquifer materials as either "sandy" or "clayey". Sandy materials associated with aquifers are estimated to have a particle density of 2.66 and porosity of 0.38, while clayey materials are estimated to have a particle density of 2.67 g/cm^3 and porosity of 0.43 (see Flach 2004).

Transport properties in the saturated zone were also assigned based on the distinction between "sandy" and "clayey" materials. Effective dispersivity values of 0.18 and 0.14 were assigned for nodes representing sandy and clayey sediments, respectively. Likewise, K_d values for transport calculations were assigned based upon the "sandy" versus "clayey" distinction (aquifers vs. confining units) with specific values being selected as recommended in Kaplan (2006).

1.6.4 Groundwater Transport Deterministic Model Description

Numerical models were developed for both the vadose zone and saturated (groundwater) zone of the subsurface to facilitate simulations of radionuclide migration away from the Slit and Engineered Trenches through time. These models utilized the flow and transport code PORFLOW and were constructed to implement the conditions described in flow and transport conceptual models of both the vadose and saturated zones, as described in Sections 1.6.3.4 and 1.6.3.5 respectively, and to evaluate the 4 scenarios identified in Section 1.6.2.

The general approach to developing the numerical models was to construct 2D cross-sectional models of the vadose zone for typical, individual Slit and Engineered Trenches. The saturated zone model was extracted from the fully 3D groundwater (flow only) model, previously developed for the region surrounding the E-Area and described in Flach (2004), for the appropriate sub-domain surrounding the Slit and Engineered Trenches.

While a steady-state flow field previously existed for the saturated zone, steady-state flow fields for the 2-D vadose zone models were developed for the Slit and Engineered Trenches. The time period for each steady-state flow field was selected based on field operations and temporal changes in infiltration rates, as described in Section 1.6.3.2.

In general, three criteria were applied in the calibration process for these flow fields to determine if an acceptable degree of convergence had been achieved; these are summarized here as: 1) a global mass balance error 2) local mass balance error in the regions with insignificant contaminant mass, and 3) local mass balance error in regions with significant contaminant mass. Tolerances for these criteria were established as $< 1E\text{-}3$, $< 1E\text{-}1$ and $< 1E\text{-}2$, respectively. While mass balance errors were significantly less than these tolerances, they define the maximum mass balance error permitted for any simulation. The strength of this approach is that the convergence measures are defined directly in terms of readily available flow simulation outputs. A weakness is ambiguity in the mass balance tolerances. A high degree of convergence was achieved for vadose zone flow simulations.

Transport of radionuclides through the vadose and saturated zones was simulated in transient mode through the series of vadose zone steady-state flow fields and the steady-state groundwater flow field. The fractional mass fluxes exiting the vadose zone domain were utilized as the source term for the saturated zone transport simulations. The approach was to sequentially simulate each generic radionuclide and special wasteform radionuclide and account for in-growth and decay for all progeny. The simulation strategy was to introduce 1 mole of parent radionuclide into the waste zone at the start of the simulation to evaluate the peak groundwater concentrations for each parent radionuclide (or its progeny) at a distance greater than 100 m from the individual trenches. Overall simulation lengths were established to evaluate exposures for the full PA compliance period of 1,000 years. However, simulation periods were adjusted for certain shorter-lived radionuclides to eliminate unnecessary computation.

Four simulation scenarios were evaluated for both the Slit and Engineered Trenches, as described in the Vadose zone conceptual model, Section 1.6.2. These included the following cases:

1. 0% non-crushable waste with no CDPs present
2. 0% non-crushable waste with CDPs present
3. 10% non-crushable waste with no CDPs present
4. 10% non-crushable waste with CDPs present

The first two cases are the scenarios in which all waste is considered to be crushable (or 0% non-crushable) and the infiltration rates are incorporated to reflect an intact closure cap in the post-institutional control period. The latter two cases are the scenarios in which a portion of the waste is considered to be non-crushable and the infiltration rates are incorporated to reflect the damaged closure cap in the post-institutional control period. To evaluate the scenarios 3 and 4, vadose simulations with 100% non-crushable waste were conducted. The resulting contaminant fluxes exiting the vadose zone were combined with the resulting contaminant fluxes from the 0% non-crushable waste simulations in the proportion of 0.1 to 0.9 such that effective mass fluxes for the 10% cases were obtained. These fluxes were then utilized as input to the aquifer model. The presence or absence of CDPs was implemented by utilizing the appropriate K_d values for each radionuclide for each scenario. The results from the simulation of these 4 scenarios were utilized to calculate doses contributed to hypothetical individuals. The establishment of facility limits considered the results of all 4 scenarios, selecting the most restrictive scenario (highest groundwater concentration over the PA period of interest) to set the limits.

1.6.4.1 Waste and Vadose Zone Flow and Transport Models

General vadose model development

The following general considerations apply to the development of the 2D vadose zone models for both the Slit Trenches and Engineered Trenches. Grid spacing for the development of the 2D vadose zone models was implemented to accommodate more refinement near interfaces of materials having contrasting hydraulic properties. Conversely, larger spacing was incorporated in parts of the domain that were less important (i.e., removed from locations of significant contaminant mass) to reduce computational requirements. The general rule for transitioning from wide to narrow node spacing at material interfaces was applied in construction of the grid to insure that no element was more than twice the x or y dimension of its neighboring elements. Similarly, the general rule with regard to the aspect ratio of the x and y dimensions of model elements (ratio < 8:1) was applied throughout the domain.

Slit Trench Vadose Zone Models

The Slit Trench Vadose Zone model grid was constructed to implement the conceptual model of the vadose zone, as described in Section 1.6.3.4. The model domain extends vertically from the base of the closure cap to the water table. The trench itself is 20 ft deep by 20 ft wide. It represents a cross-sectional view of a typical, individual Slit Trench and extends
20 feet beyond the edge of the trenches on both sides, a distance judged sufficient to ensure that flow along the lateral model boundaries is vertical. The vertical distance from the base of the trench was established at 35 feet to represent the actual depth to the long-term average regional water table, as described in Section 1.6.3.4. Spacing of nodes was implemented to allow the interfaces of model elements to correspond exactly to the physical dimensions of an individual Slit Trench as well as the interfaces of different material type zones within the domain. Figure 1-9 illustrates the configuration of this grid and the different material zones, which are color coded, and which are identified and described in Section 1.6.3.4.

The domain consists of a 46 by 48 array of nodes. Grid spacing was implemented to accommodate more refinement near interfaces of materials having contrasting hydraulic properties. Conversely, larger spacing was incorporated in parts of the domain that were less important (i.e., removed from locations of significant contaminant mass) to reduce computational requirements.

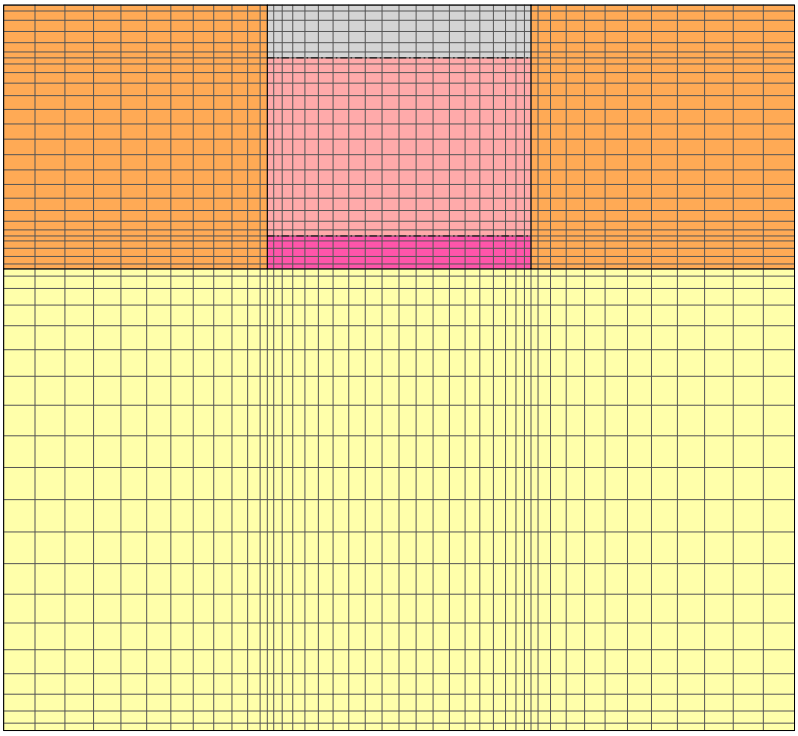

Figure 1-9. Slit Trench Vadose Zone Model Grid

Temporally, the flow model was implemented by simulating steady-state flow fields for each of the steady-state time periods identified in Section 1.6.3.2. The velocity fields associated with each of these periods were then used to simulate transient transport for the generic radionuclides and special wasteforms analyzed in this investigation.

The upper boundary of each steady-state flow model was established as a specified flux boundary with the flux defined as the infiltration rate associated with that period. Within the transport models, this boundary was established as no-flux (C=0) with respect to the contaminant transport. The side boundaries were established as no-flux boundaries with respect to both advection and contaminant flux (F=0, C=0). The lower boundary was assigned a prescribed pressure, P = 0, with respect to advection and was permitted to calculate contaminant flux by advection and diffusion.

This model domain was populated with material properties and infiltration rates as well as transport properties that reflected each of the 4 simulation scenarios described in Section 1.6.4. Specific flow and transport properties are presented in Sections 1.6.3.2 and 1.6.3.4.

In the transport simulations, each parent radionuclide and its progeny were simulated individually. One mole of parent was introduced uniformly throughout the Upper and Lower Waste Zones. After the Operations Control period (when trench compaction occurs), all of the contaminant mass in the Upper Waste Zone was transferred to the Lower Waste Zone. Flow and transport properties were changed for the Soil Fill, Upper Waste and Lower Waste zones at this point to reflect those of compacted backfill material.

Each of the 4 bounding scenarios described in Section 1.6.4 were evaluated. Output flux files were created for each radionuclide for each of the four scenarios. The resulting mass flux files include mass flux for both parent and progeny. For each radionuclide and its progeny, the total output mass for 5 individual Slit Trenches was combined to produce the composite output for an individual Slit Trench Disposal Unit. The mass flux output files for multiple Slit Trench Units were then combined to produce the source term input files for the different aquifer models.

Engineered Trench Vadose Zone Models

The Engineered Trench model grid was constructed to implement the conceptual model of the vadose zone, as described in Section 1.6.3.4. The model domain extends vertically from the base of the closure cap to the water table.

The cross-sectional outline of an Engineered Trench is a trapezoid, which is imbedded within native soil materials. The width of the base is 160 ft while the width at the upper surface is 208 ft. The domain extends 10 ft laterally, on both sides, beyond the upper boundary of the Engineered Trench. This boundary extends 34 ft beyond the Engineered Trench base. This distance is judged to be sufficient to assure that flow along the lateral model boundaries is vertical.

The vertical distance from the base of the trench was established at 35 ft to represent the actual depth to the long-term average regional water table, as described in Section 1.6.3.4. Spacing of nodes was implemented to allow the interfaces of model elements to correspond exactly to the physical dimensions of an individual Engineered Trench as well as the interfaces of different material type zones within the domain. Figure 1-10 illustrates the configuration of this grid and the different material zones, which are color coded, and which are identified and described in Section 1.6.3.4.

The domain consists of a 70 by 46 array of nodes. Compared to the Slit Trench vadose zone model grid, more nodes were required in the x-dimension to accommodate the wider profile of the Engineered Trenches and the sloping sides. Grid spacing was implemented to accommodate more refinement near interfaces of materials having contrasting hydraulic properties. Conversely, larger spacing was incorporated in parts of the domain that were less important (i.e., removed from locations of significant contaminant mass) to reduce computational requirements.

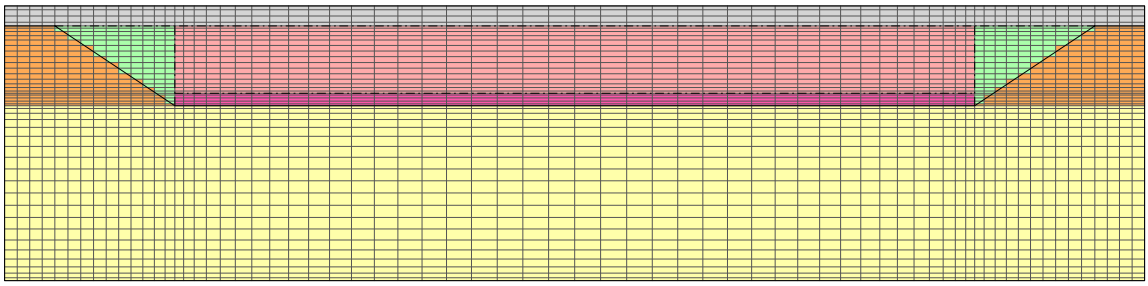

Figure 1-10. Engineered Trench Vadose Zone Model Grid

Temporally, the flow model was implemented by simulating steady-state flow fields for each of the steady-state time periods identified in Section 1.6.3.2. The velocity fields associated with each of these periods were then used to simulate transient transport for the generic radionuclides and special wasteforms analyzed in this investigation.

The upper boundary of each steady-state flow model was established as a specified flux boundary with the flux defined as the infiltration rate associated with that period. Within the transport models, this boundary was established as no-flux (C=0) with respect to the contaminant transport. The side boundaries were established as no-flux boundaries with respect to both advection and contaminant flux (F=0, C=0). The lower boundary was assigned a prescribed pressure, P = 0, with respect to advection and was permitted to calculate contaminant flux by advection and diffusion.

This model domain was populated with material properties and infiltration rates as well as transport properties that reflected each the 4 simulation scenarios described Section 1.6.4. Specific flow and transport properties are presented in Sections 1.6.3.2 and 1.6.3.4.

In the transport simulations, each parent radionuclide and its progeny were simulated individually. One mole of parent was introduced uniformly throughout the Upper and Lower Waste Zones and the sloped-sides waste zones. After the Operations Control period (when trench compaction occurs), all of the contaminant mass in the Upper Waste Zone and sloped-sides waste zones was transferred to the Lower Waste Zone. Flow and transport properties were changed for the Soil Fill, Upper and Lower Waste zones and sloped-sides waste zones at this point to reflect those of compacted backfill material.

Each of the 4 bounding scenarios described in Section 1.6.4 was evaluated. Output flux files were created for each radionuclide for each of the four scenarios. The resulting mass flux files include mass flux for both parent and progeny. For each radionuclide and its progeny, the total output mass for 2 individual Engineered Trenches was then combined to produce the source term input files for the aquifer model.

1.6.4.2 Saturated Zone Flow and Transport Models

Two PORFLOW-based 3-D aquifer transport models were created to represent the saturated regions beneath the Slit and Engineered Trenches, respectively. The flow fields were extracted from an already existing GSA flow solution based on PORFLOW; therefore, only 3-D transport simulations were required. More detailed descriptions of these models are provided below.

Taking into account the general aquifer flow direction and required 100-m compliance boundary surrounding the Slit and Engineered Trenches, the domains for two aquifer models were established. Both models were extracted from a baseline aquifer (flow only) model that extends over the entire General Separation Area (GSA); see Flach (2004).

The domain of the first of these aquifer models is shown in Figure 1-11. This model was used to perform simulations for the western grouping of Slit Trench Units, indicated by blue dots within the Slit Trench Unit outlines, and the central grouping of Slit Trench Units, indicated by green dots within the Slit Trench Unit outlines. The domain of the second aquifer model is shown in Figure 1-12. This model was used to perform simulations for the Engineered Trenches, indicated by blue dots within Engineered Trench outlines, and the eastern grouping of Slit Trench Units, indicated by red dots within the Slit Trench Unit outlines. Elements with brown diamonds indicate the position of the 100-m buffer used to evaluate peak groundwater concentration in this PA.

The general GSA flow model has a uniform horizontal grid spacing of 200 ft in both directions, which is indicated in Figure 1-11 and Figure 1-12 by the coarser hachure marks around the perimeter of each domain. The cut-out sub domains utilized in this investigation have a range of horizontal extent measuring 3,600 ft by 2,800 ft and 2,400 ft by 4,000 ft, respectively. In this investigation the horizontal mesh spacing was reduced to a grid of smaller elements, each measuring 50 ft by 50 ft.

The grid mesh was refined for several reasons, primarily to minimize artificial spreading of contaminants in grid elements, both at the location of the introduction of the source term and at the 100-m well where concentrations were recorded. The finer mesh allowed source nodes to more accurately approximate the outline of trench units and allowed distinguishing the concentrations at a point 100 m from the facility without having to average over a 200-foot grid.

These grid elements are represented in PORFLOW with an array of nodes 74 by 58 by 18 for the model shown in Figure 1-11 and an array of nodes 50 by 82 by 18 for the model shown in Figure 1-12. The vertical mesh spacing of the baseline GSA model was retained for the Slit and Engineered Trenches aquifer models. A representative vertical configuration of model elements is shown for the central grouping of Slit Trenches in the cross-section illustrated in Figure 1-13.

The location of the cross-section with respect to the trench units is indicated by the solid green line (A-A') in the plan view of the model. The pink lines represent the boundary lines between model elements, the "yellow" zones represent sandy aquifer units and the "brown" elements represent clayey confining units. Travel time along groundwater pathlines is indicated by 5-year markers.

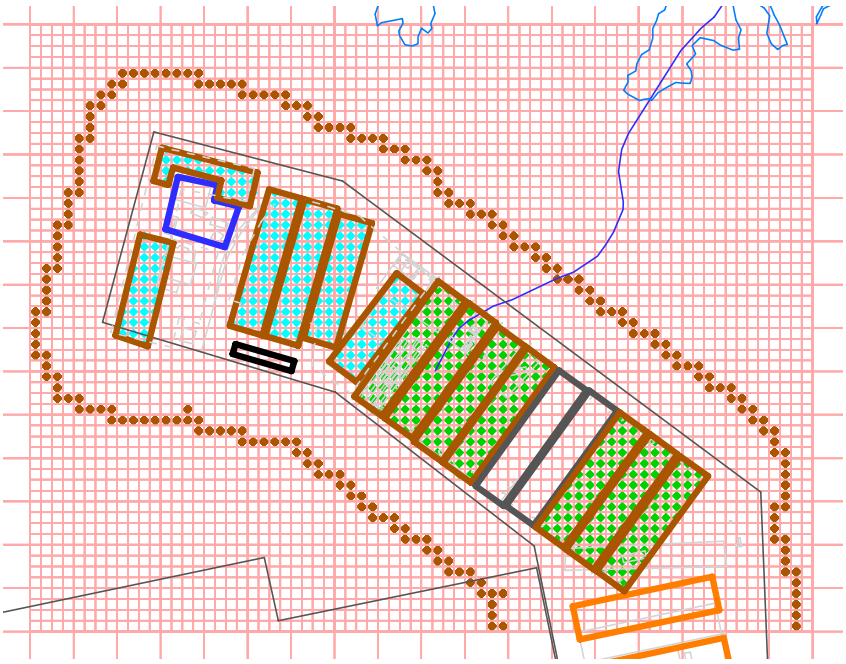

Figure 1-11. Aquifer model grid in plan view for SLITw and SLITc units

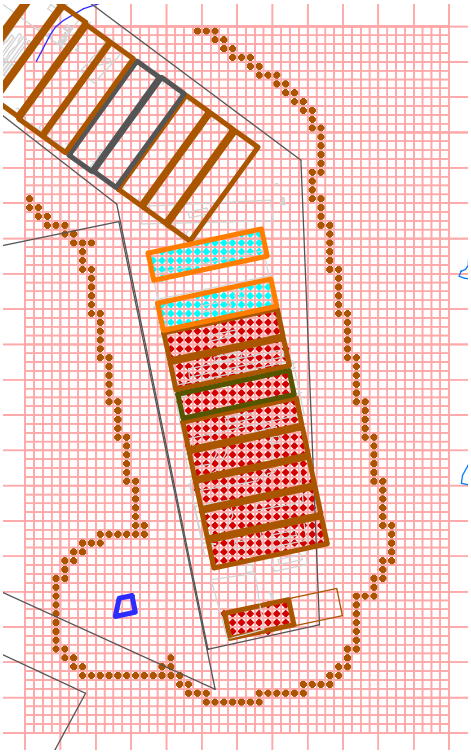

Figure 1-12. Aquifer model grid in plan view for SLITe and ET units

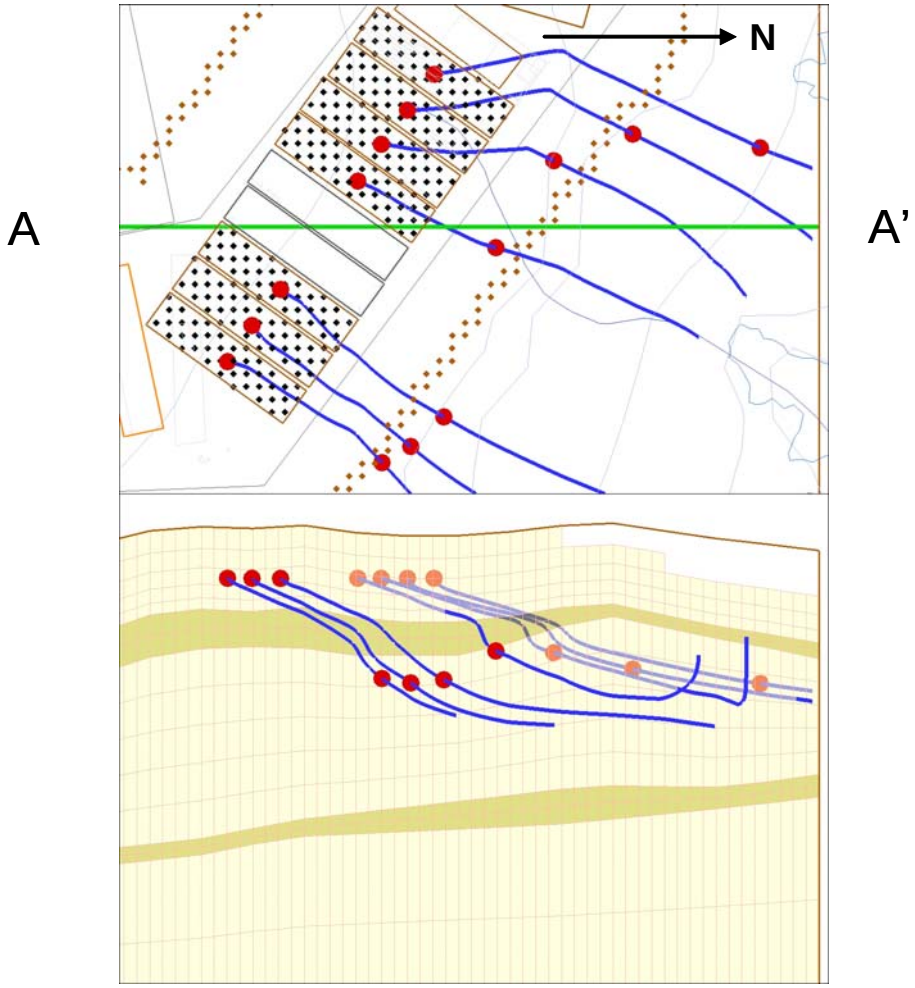

Figure 1-13. Plan view and vertical cross-section of the groundwater model for the central group of Slit Trenches.

From top to bottom, the aquifers are the upper UTR aquifer zone, the lower UTR aquifer, and the Gordon aquifer unit. The boundaries between units are established based on actual field measurements. The solid line extending from the left side across the mesh and on to the right represents the water table, or upper surface of the saturated zone.

The blue stream lines indicate the pattern of groundwater movement in the vertical plane. The solid red "dots" from which the streamlines emanate are the model elements within which the contaminant flux source term (output from the vadose zone transport model) is introduced into the aquifer model. The location of these source elements is also indicated in the plan view by the prominent dots beneath the trace of trench units. Farther along the blue groundwater flow lines, the set of red "dots" below the upper clay zone indicates 5-year travel times.

The Slit and Engineered Trench aquifer models were used only for transport simulations, where the flow fields were input from an interpolated flow field taken from the baseline GSA flow model. Amongst the 50 ft by 50 ft model elements, those located more than 100 meters (328.1 ft) distance from the perimeter of the Slit and Engineered Trenches are indicated with a solid symbol in the center of the element in the upper (plan view) illustration. Internal PORFLOW processing locates the maximum concentration of each species at all locations outside its 100 meter buffer region at every time step. Post-processing of specific PORFLOW output files was then performed to locate the overall maximum (peak) concentration in time for each disposed parent radionuclide.

The sandy aquifer units are a heterogeneous material that is primarily sandy with local clayey sediments distributed throughout. From a purely transport advection viewpoint (i.e., pore velocity), its effective porosity is significantly lower than its total porosity. Here the clayey sediments behave like small hydraulic barriers forcing the groundwater to navigate past them. Based on engineering judgment and available in-the-field tritium measurements in neighboring sites on SRS, its effective porosity is assumed to be ~25%. To account for the faster pore velocity, the aquifer transport analyses were performed where the porosity was set to 0.25. Similarly, the effective sandy aquifer unit density was set to 1.39 g/cm^3.

The Slit and Engineered Trenches aquifer transport models are impacted by surface boundary conditions and internal source nodes. At the outer surfaces (i.e., the x, y, and z domain faces) incoming versus outgoing boundary conditions are handled differently. At an incoming face, the radionuclide species of interest is assumed to have a zero concentration. At an outgoing face, the diffusive flux of the radionuclide species of interest is assumed to have a value of zero. Here the outgoing faces are sufficiently far from the regions of interest that this method has negligible impact on the upstream concentration profiles.

The aquifer transport models were used to evaluate the 4 bounding cases for 4 groupings of disposal Units identified in Section 1.6.4 in a series of simulations. The bounding cases refer to the presence of non-crushable waste within 10% of the trench area and the presence or absence of CDP products within the trench waste zones. The 4 groupings of disposal units include the western, central and eastern Slit Trench Units and the Engineered Trench Units. Each grouping of Units has been evaluated individually for all 4 of the bounding cases.

The aquifer model source terms for all radionuclides of interest and special wasteforms were introduced at the source nodes identified for each grouping of Trenches. The source term for each simulation was derived from the PORFLOW output files obtained from the vadose zone models for each parent and its progeny. The source nodes were established beneath the footprint of each grouping of units and are indicated in Figure 1-11 for the western and central groupings of Slit Trench Units and in Figure 1-12 for the eastern grouping of Slit Trench Units and the Engineered Trench Units.

Different source term files were generated for each of the four cases evaluated, for both the Slit and Engineered Trenches. The appropriate source term for Case 01, the case where the waste is assumed to be 100% crushable material, was taken directly from output files generated by PORFLOW for both the CDP present and absent scenarios. Since vadose zone simulations were also performed for the case where the trench closure cap was assumed to collapse after the loss of institutional control, the output had to be blended with the output files from the former case to produce the appropriate input files for the aquifer model. This blending was implemented in the proportion of 9:1 to capture the assumption that only 10% of the trench area contains non-crushable waste material which resulted in damage to the closure cap. Blended source term files were generated for both the CDP present and absent scenarios.

1.6.5 Groundwater Transport Deterministic Model Results

The concentration output for each parent radionuclide from the PORFLOW aquifer model was utilized to calculate Beta-Gamma, Gross Alpha, Radium and Uranium peak concentrations within the 1000-year compliance period. The peak concentrations were determined by evaluating the concentration through time for a group of model elements that were determined to be greater than 100 meters from the Slit and Engineered Trench Units. These elements are indicated in Figure 1-11 and Figure 1-12 as the elements with a prominent dot in the middle. At any given time the maximum concentration was determined to be the maximum concentration in any of these model elements. The PORFLOW concentration output files were converted into input for the all-pathways program (Koffman 2006a) using the IdealFileMaker program (Taylor 2006). The disposal limits for each trench unit were then calculated for each of the groundwater protection performance objectives in the automated all-pathways program.

Using the results from the all-pathways program, the groundwater activity or concentration calculated for Beta-Gamma, Gross Alpha, Radium and Uranium were used to derive the Slit and Engineered Trench groundwater pathway limits for each radionuclide evaluated. The performance measures for each are 4 mrem/yr, 15 pCi/L, 5 pCi/L and 30 μg/L for beta-gamma, gross alpha, radium and uranium, respectively as identified in Wilhite (2005). The established activity or concentration limit for each of these, divided by the activity or concentration calculated in the all-pathways analysis for each from the disposal of 1 Ci of parent is proportional to the trench unit groundwater limit, in Ci, divided by the source term of 1 Ci, for each radionuclide.

Radionuclide disposal limits in this section are derived without considering the impact of groundwater contaminant plume interactions with nearby disposal units (e.g., CIG Trenches) and are therefore presented as preliminary information. The results of plume interaction are presented in Chapter 6, Integrated Facility Analysis. Final limits will be adjusted as needed to account for plume interaction and the results of sensitivity and/or uncertainty analyses and presented in Chapter 7, Integration and Interpretation.

Two factors were included in the development of Slit and Engineered Trench models. These factors were the presence or absence of non-crushable containers and the presence or absence of CDPs. The term "non-crushable" refers to waste containers that have not collapsed by the time the final cover system is placed over E-Area. These containers are expected to withstand corrosion during the operational and institutional control periods and subsidence treatment (e.g., dynamic compaction) prior to final cover installation, but then collapse at some later time, leading to post institutional closure waste subsidence. Waste and cap layer subsidence would lead to an increase in rainwater infiltration, which changes the speed at which the waste releases and is carried to the aquifer.

The second factor included in the development of the Engineered and Trench models was the presence or absence of cellulose (e.g. wood, cardboard, paper) and associated degradation products. Cellulose degradation products (CDP) have been shown to significantly affect the distribution coefficients (K_ds) of a number of radionuclides (Kaplan 2006). These K_ds are one of the prime factors affecting the transport velocity of the nuclides. When cellulose is assumed to be co-disposed with waste, the original distribution coefficient is modified by a CDP multiplier (Kaplan 2006).

To cover a range of possible waste disposal patterns, models were developed for each of four generic disposal cases (i.e., 0% non-crushable containers with no cellulose degradation products, 0% non-crushable containers with cellulose degradation products, 10% non-crushable containers with no cellulose degradation products, and 10% non-crushable containers with cellulose degradation products) for each of four sets of trenches (i.e., Engineered Trenches, Center Slit Trenches, East Slit Trenches and West Slit Trenches). Groundwater and all-pathways limits were produced using the all-pathways application for each of the four cases. The minimum limit produced by each of the four cases becomes the base limit for the nuclide. This selection allows for operational flexibility within the bounds of all four cases.

In addition to a range of generic disposal conditions, several special wasteforms were explicitly analyzed. These analyses account for improved geochemical conditions and/or container integrity characteristic of particular waste streams. These scenarios are represented in the model by a larger K_d and/or delayed or hindered waste release to surrounding trench backfill.

For certain waste disposals, conditions can be constrained to a specific non-crushable container percentage and CDP environment. Such was the case for Ra-226 and Th-230 in 211-F Cooling Tower D&D waste disposed to Slit Trench #6. The vast majority of this waste is in the form of wood from the 211-F Cooling Tower. In the case of Ra-226 and Th-230, the case when CDPs are considered gives a larger limit. Since the waste is largely wood, which is a form of cellulose, it follows that consideration of CDPs for this waste is an acceptable assumption. So, special wasteform versions of Ra-226 and Th-230 in cooling tower waste are given separately in the table.

Another special wasteform limit was developed for tritium embedded in concrete, by adjusting the limit for the generic nuclide disposal. The adjustment was developed from a preliminary Closure Analysis for Slit Trenches #1 and #2 (Flach et al. 2005). The 2005 analysis considered tritium release from generic and concrete wasteforms for conditions specific to those trenches, such as burial locations and times, ground cover and slope, and soil type. For generic disposals, tritium was assumed to be present as soil contamination. For tritium embedded in concrete, the analysis considered the impact on impervious concrete rubble on trench water flow and diffusive release of tritium from concrete chunks of varying sizes.

The distribution of concrete rubble size was defined from photographs of 232-F building demolition, from which the burials came, and a more recent comparable demolition in A-Area. The peak water table flux for tritium-in-concrete was predicted to be 42.9% of that for generic tritium disposal (Flach et al. 2005, Figure 2.5- 6), with all other conditions being equal in the two simulations. The lower flux was a result of slow (diffusional) release of tritium from concrete to soil pore water and a reduced effective trench hydraulic conductivity from the presence of impervious concrete. Compared to the 2005 analysis, the current PA analysis for generic tritium burials embodies several updates, such refined estimates of soil properties. For these conditions, the relative impact of concrete rubble versus generic tritium disposal is expected to be very similar to the 2005 preliminary closure analysis. Thus, the tritium-in-concrete limit was derived by dividing the generic limit by 0.429.

The resulting disposal limits are listed in Table 1-16 through Table 1-19 for the East Slit Trenches, Center Slit Trenches, West Slit Trenches and Engineered Trenches, respectively. The results of the Slit and Engineered Trench Base Case evaluations are presented as graphs of concentration (pCi/L) versus time in Appendix A1.

Table 1-16. Preliminary Groundwater Protection Limits for East Slit Trenches

	Beta-Gamma Limit (Ci/Disposal Unit)			Gross Alpha Limit (Ci/Disposal Unit)			Radium Limit (Ci/Disposal Unit)			Uranium Limit (Ci/Disposal Unit)
Parent Nuclide	**0-12 yrs**	**12-100 yrs**	**100-1130 yrs**	**0-1000 yrs**	**1000-1120 yrs**	**1120-1130 yrs**	**0-1000 yrs**	**1000-1120 yrs**	**1120-1130 yrs**	
Am-241	2.4E+10	2.1E+06	7.8E+03	3.9E+02	4.6E+02	4.6E+02	---	---	---	1.2E+12
Am-243	---	4.8E+16	2.9E+03	5.5E+02	1.6E+02	1.5E+02	---	---	---	1.1E+13
C-14	3.1E-01	2.6E-01	6.0E+00	---	---	---	---	---	---	---
C-14_NR.Pump	---	---	1.8E+00	---	---	---	---	---	---	---
Cf-249	7.6E+17	3.9E+12	1.4E+05	2.4E+03	8.4E+02	7.8E+02	---	---	---	6.5E+13
Cf-251	---	---	1.0E+09	1.1E+03	3.4E+02	3.2E+02	---	---	---	6.8E+18
Cl-36	1.1E-01	9.2E-02	2.1E+00	---	---	---	---	---	---	---
Cm-244	---	---	7.8E+18	2.9E+12	3.2E+11	2.7E+11	1.4E+19	1.1E+19	1.1E+19	3.7E+19
Cm-245	1.0E+14	1.3E+09	4.3E+03	1.9E+02	7.5E+01	6.9E+01	---	---	---	1.2E+12
Cm-246	---	---	6.8E+15	5.8E+02	1.7E+02	1.6E+02	1.3E+16	4.7E+15	4.3E+15	1.7E+14
Cm-247	---	---	2.2E+04	4.6E+02	1.3E+02	1.2E+02	---	---	---	1.2E+14
Cm-248	---	---	2.3E+10	5.5E+02	1.6E+02	1.4E+02	---	---	---	2.9E+18
H-3	6.1E+00	5.7E+00	1.6E+04	---	---	---	---	---	---	---
H-3_ETF.Carbon	---	---	6.7E+04	---	---	---	---	---	---	---
I-129	2.1E-04	1.4E-04	4.2E-03	---	---	---	---	---	---	---
I-129_ETF.Carbon	---	---	1.2E-01	---	---	---	---	---	---	---
I-129_ETF.GT.73	1.6E+00	4.2E-01	1.6E-01	---	---	---	---	---	---	---
I-129_F.Carbon	2.1E+01	5.6E+00	2.1E+00	---	---	---	---	---	---	---
I-129_F.CG.8	8.1E-03	2.1E-03	2.9E-03	---	---	---	---	---	---	---
I-129_F.Dowex.21K	1.1E+00	2.9E-01	1.1E-01	---	---	---	---	---	---	---
I-129_F.Filtercake	9.2E-03	2.4E-03	3.1E-03	---	---	---	---	---	---	---
I-129_H.Carbon	9.3E+00	2.5E+00	9.3E-01	---	---	---	---	---	---	---
I-129_H.CG.8	6.1E-02	1.6E-02	1.0E-02	---	---	---	---	---	---	---
I-129_H.Dowex.21K	2.5E+00	6.6E-01	2.5E-01	---	---	---	---	---	---	---
I-129_H.Filtercake	1.0E-01	2.8E-02	1.5E-02	---	---	---	---	---	---	---
K-40	1.6E-01	1.1E-01	1.1E+00	---	---	---	---	---	---	---
Mo-93	2.4E-01	1.9E-01	2.4E+00	---	---	---	---	---	---	---
Nb-94	1.2E-01	1.0E-01	2.3E+00	---	---	---	---	---	---	---
Ni-59	---	1.1E+10	7.1E+00	---	---	---	---	---	---	---

Table 1-16. Preliminary Groundwater Protection Limits for East Slit Trenches - continued

	Beta-Gamma Limit (Ci/Disposal Unit)			Gross Alpha Limit (Ci/Disposal Unit)			Radium Limit (Ci/Disposal Unit)			Uranium Limit (Ci/Disposal Unit)
Parent Nuclide	**0-12 yrs**	**12-100 yrs**	**100-1130 yrs**	**0-1000 yrs**	**1000-1120 yrs**	**1120-1130 yrs**	**0-1000 yrs**	**1000-1120 yrs**	**1120-1130 yrs**	
Np-237	1.4E+04	4.5E+00	1.2E+00	6.1E-02	1.0E-01	2.2E-01	---	---	---	1.8E+08
Pd-107	---	1.3E+12	8.6E+02	---	---	---	---	---	---	---
Pu-238	---	---	1.3E+07	4.6E+05	1.5E+05	1.4E+05	4.6E+05	1.5E+05	1.4E+05	8.3E+18
Pu-239	5.9E+18	6.2E+12	7.3E+06	6.6E+06	5.7E+06	5.7E+06	---	---	---	1.3E+17
Pu-240	---	---	2.0E+16	1.1E+10	1.2E+09	1.0E+09	3.6E+16	2.8E+16	2.7E+16	1.4E+17
Pu-241	9.1E+12	3.0E+08	2.4E+05	1.2E+04	1.4E+04	1.4E+04	---	---	---	3.5E+13
Pu-242	---	---	1.3E+14	1.0E+10	1.1E+09	8.8E+08	4.3E+12	1.5E+12	1.4E+12	1.2E+17
Pu-244	---	---	7.5E+10	9.4E+09	9.4E+08	7.9E+08	1.5E+18	1.1E+18	1.0E+18	1.2E+18
Ra-226	6.4E+18	6.5E+07	3.1E+00	9.3E-02	3.8E-02	3.7E-02	9.3E-02	3.8E-02	3.7E-02	---
Se-79	---	---	---	---	---	---	---	---	---	---
Sn-126	---	---	---	---	---	---	---	---	---	---
Sr-90	2.8E+16	9.1E+06	1.8E+02	---	---	---	---	---	---	---
Tc-99	3.1E-01	1.4E-01	3.1E+00	---	---	---	---	---	---	---
Th-230	---	5.2E+10	1.1E+01	4.6E-01	1.3E-01	1.2E-01	4.6E-01	1.3E-01	1.2E-01	---
Th-232	1.8E+18	3.9E+10	2.2E+04	2.3E+04	5.2E+04	6.7E+04	3.0E+04	6.9E+04	8.9E+04	---
U-233	---	---	2.1E+13	5.7E+13	5.3E+12	4.5E+12	---	---	---	6.9E+14
U-234	---	2.0E+15	3.2E+03	1.2E+02	3.8E+01	3.5E+01	1.2E+02	3.8E+01	3.5E+01	2.1E+15
U-235	1.1E+10	2.8E+04	4.4E+00	3.4E+00	3.5E+00	4.0E+00	---	---	---	1.1E+12
U-236	---	---	2.0E+11	2.6E+11	2.1E+11	2.1E+11	3.5E+11	2.8E+11	2.8E+11	2.2E+13
U-238	---	---	4.2E+06	1.5E+05	5.0E+04	4.6E+04	1.5E+05	5.0E+04	4.6E+04	1.1E+11
Zr-93	2.3E+00	5.4E-01	6.2E-01	---	---	---	---	---	---	---

Note: Limits reported as "---" indicate that there is no limit or that the limit $\geq$ 1E+20.

Note: Groundwater limits in this table are to be considered preliminary. Adjustments are made in the groundwater limits as appropriate based on consideration of plume overlap effects from adjacent units in Chapter 6 and interpretation of sensitivity and uncertainty analyses in Chapter 7. Final limits are to be found in results tables in Chapter 7.

Table 1-17. Preliminary Groundwater Protection Limits for Center Slit Trenches

	Beta-Gamma Limit			Gross Alpha Limit			Radium Limit			Uranium Limit
	(Ci/Disposal Unit)			(Ci/Disposal Unit)			(Ci/Disposal Unit)			(Ci/Disposal Unit)
Parent Nuclide	**0-12 yrs**	**12-100 yrs**	**100-1130 yrs**	**0-1000 yrs**	**1000-1120 yrs**	**1120-1130 yrs**	**0-1000 yrs**	**1000-1120 yrs**	**1120-1130 yrs**	
Am-241	4.6E+09	2.1E+06	1.3E+04	2.6E+02	1.5E+02	1.4E+02	---	---	---	1.9E+12
Am-243	---	6.2E+16	5.6E+02	7.8E+01	3.0E+01	2.8E+01	---	---	---	1.4E+12
C-14	2.9E-01	2.9E-01	1.0E+01	---	---	---	---	---	---	---
C-14_NR.Pump	---	---	2.9E+00	---	---	---	---	---	---	---
Cf-249	1.4E+17	3.7E+12	3.8E+04	3.7E+02	1.6E+02	1.5E+02	---	---	---	1.1E+14
Cf-251	---	---	2.0E+08	1.5E+02	6.5E+01	6.1E+01	---	---	---	9.5E+17
Cl-36	1.0E-01	1.0E-01	3.5E+00	---	---	---	---	---	---	---
Cm-244	---	---	1.0E+18	8.2E+10	1.1E+10	9.3E+09	1.9E+18	1.5E+18	1.4E+18	1.2E+18
Cm-245	2.0E+13	1.2E+09	1.4E+03	4.2E+01	1.6E+01	1.5E+01	---	---	---	2.1E+12
Cm-246	---	---	9.1E+14	8.2E+01	3.2E+01	3.0E+01	1.3E+16	4.3E+15	3.9E+15	2.3E+13
Cm-247	---	---	4.2E+03	6.5E+01	2.5E+01	2.3E+01	---	---	---	1.6E+13
Cm-248	---	---	3.7E+09	7.7E+01	3.0E+01	2.8E+01	---	---	---	3.4E+17
H-3	5.5E+00	5.6E+00	2.7E+04	---	---	---	---	---	---	---
H-3_Concrete	1.3E+01	1.3E+01	6.3E+04	---	---	---	---	---	---	---
H-3_ETF.Carbon	---	---	6.6E+04	---	---	---	---	---	---	---
I-129	1.7E-04	1.6E-04	7.4E-03	---	---	---	---	---	---	---
I-129_ETF.Carbon	---	---	2.0E-01	---	---	---	---	---	---	---
I-129_ETF.GT.73	1.4E+00	6.8E-01	2.7E-01	---	---	---	---	---	---	---
I-129_F.Carbon	1.8E+01	9.1E+00	3.5E+00	---	---	---	---	---	---	---
I-129_F.CG.8	6.9E-03	3.5E-03	4.2E-03	---	---	---	---	---	---	---
I-129_F.Dowex.21K	9.3E-01	4.7E-01	1.9E-01	---	---	---	---	---	---	---
I-129_F.Filtercake	7.8E-03	3.9E-03	4.4E-03	---	---	---	---	---	---	---
I-129_H.Carbon	7.9E+00	4.0E+00	1.6E+00	---	---	---	---	---	---	---
I-129_H.CG.8	5.2E-02	2.6E-02	1.7E-02	---	---	---	---	---	---	---
I-129_H.Dowex.21K	2.1E+00	1.1E+00	4.2E-01	---	---	---	---	---	---	---
I-129_H.Filtercake	8.9E-02	4.5E-02	2.6E-02	---	---	---	---	---	---	---
I-129_Mk50A	4.2E+00	1.7E+00	4.6E-01	---	---	---	---	---	---	---
K-40	2.2E-01	1.6E-01	1.9E+00	---	---	---	---	---	---	---
Mo-93	2.2E-01	2.2E-01	4.1E+00	---	---	---	---	---	---	---
Nb-94	1.1E-01	1.1E-01	3.9E+00	---	---	---	---	---	---	---
Ni-59	6.8E+19	4.0E+09	4.8E+00	---	---	---	---	---	---	---
Np-237	2.8E+03	4. 6E+00	2.0E+00	1.0E-01	1.9E-01	4.5E-01	---	---	---	2.5E+08

Table 1-17. Preliminary Groundwater Protection Limits for Center Slit Trenches – continued

	Beta-Gamma Limit			Gross Alpha Limit			Radium Limit			Uranium Limit
	(Ci/Disposal Unit)			(Ci/Disposal Unit)			(Ci/Disposal Unit)			(Ci/Disposal Unit)
Parent Nuclide	**0-12 yrs**	**12-100 yrs**	**100-1130 yrs**	**0-1000 yrs**	**1000-1120 yrs**	**1120-1130 yrs**	**0-1000 yrs**	**1000-1120 yrs**	**1120-1130 yrs**	
Pd-107	---	4.9E+11	5. 8E+02	---	---	---	---	---	---	---
Pu-238	---	---	1.2E+07	4.4E+05	1.4E+05	1.3E+05	4.4E+05	1.4E+05	1.3E+05	1.8E+17
Pu-239	1.1E+18	7.9E+12	1.3E+07	1.1E+07	7.9E+06	7.7E+06	---	---	---	3.9E+15
Pu-240	---	---	2.7E+15	3.1E+08	3.8E+07	3.3E+07	4.9E+15	3.8E+15	3.6E+15	4.2E+15
Pu-241	1.7E+12	2.9E+08	3.9E+05	7.7E+03	4.4E+03	4.2E+03	---	---	---	5.9E+13
Pu-242	---	---	1.2E+14	2.8E+08	3.4E+07	2.9E+07	4.4E+12	1.4E+12	1.3E+12	3.8E+15
Pu-244	---	---	2.5E+09	2.6E+08	3.1E+07	2.6E+07	2.0E+17	1.5E+17	1.4E+17	3.6E+16
Ra-226	2.7E+17	3.0E+07	3.5E+00	7.5E-02	4.6E-02	4.6E-02	7.5E-02	4.6E-02	4.6E-02	---
Ra-226_Cooling.Tower	---	1.4E+12	1.6E+01	2.6E-01	1.2E+00	9.8E-01	2.7E-01	1.2E+00	9.8E-01	---
Se-79	---	---	3.8E+19	---	---	---	---	---	---	---
Sn-126	---	---	---	---	---	---	---	---	---	---
Sr-90	1.2E+15	4.0E+06	8.4E+01	---	---	---	---	---	---	---
Sr-90_Mk50A	1.6E+18	3.8E+09	4.7E+04	---	---	---	---	---	---	---
Tc-99	1.9E-01	1.6E-01	5.3E+00	---	---	---	---	---	---	---
Tc-99_Mk50A	6.2E+03	1.5E+03	4.0E+02	---	---	---	---	---	---	---
Th-230	---	2.4E+10	1.0E+01	3.7E-01	1.3E-01	1.2E-01	3.7E-01	1.3E-01	1.2E-01	---
Th-230_Cooling.Tower	---	1.2E+15	1.2E+02	2.3E+00	2.1E+00	2.0E+00	2.3E+00	2.1E+00	2.0E+00	---
Th-232	7.1E+16	4.5E+09	3.1E+03	3.2E+03	7.4E+03	9.4E+03	4.2E+03	9.9E+03	1.2E+04	---
U-233	---	---	5.5E+11	1.4E+12	1.4E+11	1.2E+11	---	---	---	1.9E+13
U-234	---	8.9E+14	3.0E+03	1.1E+02	3.6E+01	3.4E+01	1.1E+02	3.6E+01	3.4E+01	4.5E+13
U-234_MGlass	---	1.3E+18	1.2E+06	4.3E+04	1.5E+04	1.4E+04	4.3E+04	1.5E+04	1.4E+04	2.6E+16
U-235	2.0E+09	3.5E+04	7.3E+00	5.7E+00	5.9E+00	7.0E+00	---	---	---	1.5E+10
U-235_MGlass	2.7E+12	2.0E+07	2.9E+03	2.4E+03	2.2E+03	2.3E+03	---	---	---	9.0E+12
U-235_Paducah.Cask	6.6E+13	4.8E+08	3.1E+04	2.7E+04	2.4E+04	2.4E+04	---	---	---	9.9E+13
U-236	---	2.7E+19	2.7E+10	3.6E+10	2.9E+10	2.8E+10	4.8E+10	3.9E+10	3.7E+10	4.6E+11
U-236_MGlass	---	---	1.9E+13	2.5E+13	2.0E+13	1.9E+13	3.3E+13	2.7E+13	2.6E+13	2.7E+14
U-238	---	---	3.9E+06	1.5E+05	4.6E+04	4.3E+04	1.5E+05	4.6E+04	4.3E+04	2.4E+09
U-238_MGlass	---	---	1.5E+09	5.6E+07	1.8E+07	1.7E+07	5.6E+07	1.8E+07	1.7E+07	1.4E+12
Zr-93	1.7E+00	7.5E-01	8.8E-01	---	---	---	---	---	---	---

Note: Limits reported as "---" indicate that there is no limit or that the limit $\geq$ 1E+20.

Note: Groundwater limits in this table are to be considered preliminary. Adjustments are made in the groundwater limits as appropriate based on consideration of plume overlap effects from adjacent units in Chapter 6 and interpretation of sensitivity and uncertainty analyses in Chapter 7. Final limits are to be found in results tables in Chapter 7.

Table 1-18. Preliminary Groundwater Protection Limits for West Slit Trenches

	Beta-Gamma Limit			Gross Alpha Limit			Radium Limit			Uranium Limit
	(Ci/Disposal Unit)			(Ci/Disposal Unit)			(Ci/Disposal Unit)			(Ci/Disposal Unit)
Parent Nuclide	**0-12 yrs**	**12-100 yrs**	**100-1130 yrs**	**0-1000 yrs**	**1000-1120 yrs**	**1120-1130 yrs**	**0-1000 yrs**	**1000-1120 yrs**	**1120-1130 yrs**	
Am-241	1.5E+09	2.4E+06	1.7E+04	1.0E+02	6.8E+01	6.7E+01	---	---	---	2.6E+12
Am-243	---	7.9E+16	2.5E+02	2.5E+01	1.3E+01	1.2E+01	---	---	---	4.1E+11
C-14	3.7E-01	3.8E-01	1.6E+01	---	---	---	---	---	---	---
C-14_NR.Pump	---	---	4.2E+00	---	---	---	---	---	---	---
Cf-249	4.1E+16	4.2E+12	1.7E+04	1.2E+02	7.0E+01	6.8E+01	---	---	---	1.5E+14
Cf-251	---	---	8.7E+07	4.9E+01	2.8E+01	2.7E+01	---	---	---	2.9E+17
Cl-36	1.3E-01	1.3E-01	5.4E+00	---	---	---	---	---	---	---
Cm-244	---	---	2.7E+17	6.1E+09	9.2E+08	8.0E+08	5.0E+17	3.8E+17	3.7E+17	9.3E+16
Cm-245	5.9E+12	1.4E+09	6.4E+02	1.4E+01	7.0E+00	6.7E+00	---	---	---	2.8E+12
Cm-246	---	---	2.6E+14	2.6E+01	1.4E+01	1.3E+01	1.7E+16	5.1E+15	4.7E+15	6.6E+12
Cm-247	---	---	1.9E+03	2.1E+01	1.1E+01	1.0E+01	---	---	---	4.8E+12
Cm-248	---	---	1.3E+09	2.5E+01	1.3E+01	1.2E+01	---	---	---	8.6E+16
H-3	6.7E+00	7.4E+00	4.2E+04	---	---	---	---	---	---	---
H-3_ETF.Carbon	---	---	5.6E+01	---	---	---	---	---	---	---
I-129	2.1E-04	2.1E-04	9.4E-03	---	---	---	---	---	---	---
I-129_ETF.Carbon	---	---	3.0E-01	---	---	---	---	---	---	---
I-129_ETF.GT.73	1.7E+00	1.0E+00	4.0E-01	---	---	---	---	---	---	---
I-129_F.Carbon	2.3E+01	1.3E+01	5.2E+00	---	---	---	---	---	---	---
I-129_F.CG.8	8.7E-03	5.1E-03	5.9E-03	---	---	---	---	---	---	---
I-129_F.Dowex.21K	1.2E+00	6.9E-01	2.8E-01	---	---	---	---	---	---	---
I-129_F.Filtercake	9.8E-03	5.8E-03	6.3E-03	---	---	---	---	---	---	---
I-129_H.Carbon	9.9E+00	5.9E+00	2.3E+00	---	---	---	---	---	---	---
I-129_H.CG.8	6.5E-02	3.8E-02	2.5E-02	---	---	---	---	---	---	---
I-129_H.Dowex.21K	2.7E+00	1.6E+00	6.2E-01	---	---	---	---	---	---	---
I-129_H.Filtercake	1.1E-01	6.6E-02	3.8E-02	---	---	---	---	---	---	---
K-40	3.2E-01	2.4E-01	2.6E+00	---	---	---	---	---	---	---
Mo-93	2.9E-01	2.9E-01	6.4E+00	---	---	---	---	---	---	---
Nb-94	1.4E-01	1.5E-01	5.9E+00	---	---	---	---	---	---	---
Ni-59	9.5E+17	3.8E+09	5.3E+00	---	---	---	---	---	---	---
Np-237	1.0E+03	5.E+00	2.73E+00	1.4E-01	2.6E-01	6.1E-01	---	---	---	4.1E+08

Table 1-18. Preliminary Groundwater Protection Limits for West Slit Trenches – continued

	Beta-Gamma Limit			Gross Alpha Limit			Radium Limit			Uranium Limit
	(Ci/Disposal Unit)			(Ci/Disposal Unit)			(Ci/Disposal Unit)			(Ci/Disposal Unit)
Parent Nuclide	**0-12 yrs**	**12-100 yrs**	**100-1130 yrs**	**0-1000 yrs**	**1000-1120 yrs**	**1120-1130 yrs**	**0-1000 yrs**	**1000-1120 yrs**	**1120-1130 yrs**	
Pd-107	---	4.6E+11	6.5E+02	---	---	---	---	---	---	---
Pu-238	---	---	1.4E+07	5.2E+05	1.7E+05	1.6E+05	5.2E+05	1.7E+05	1.6E+05	1.0E+16
Pu-239	3.4E+17	1.0E+13	1.7E+07	8.9E+06	2.4E+06	2.1E+06	---	---	---	3.1E+14
Pu-240	---	---	6.9E+14	2.2E+07	3.2E+06	2.8E+06	1.3E+15	9.7E+14	9.4E+14	3.3E+14
Pu-241	5.3E+11	3.3E+08	5.3E+05	3.1E+03	2.0E+03	2.0E+03	---	---	---	7.8E+13
Pu-242	---	---	1.4E+14	2.0E+07	2.8E+06	2.4E+06	5.4E+12	1.7E+12	1.5E+12	2.9E+14
Pu-244	---	---	2.1E+08	1.8E+07	2.5E+06	2.2E+06	5.2E+16	3.8E+16	3.6E+16	2.8E+15
Ra-226	6.8E+15	3.0E+07	4.6E+00	8.9E-02	6.1E-02	6.2E-02	8.9E-02	6.1E-02	6.2E-02	---
Se-79	---	---	6.8E+17	---	---	---	---	---	---	---
Sn-126	---	---	---	---	---	---	---	---	---	---
Sr-90	2.9E+13	2.2E+06	5.9E+01	---	---	---	---	---	---	---
Tc-99	2.2E-01	2.0E-01	7.4E+00	---	---	---	---	---	---	---
Th-230	1.1E+19	2.4E+10	1.3E+01	4.2E-01	1.6E-01	1.5E-01	4.2E-01	1.6E-01	1.5E-01	---
Th-232	1.5E+15	9.4E+08	8.3E+02	8.4E+02	2.0E+03	2.5E+03	1.1E+03	2.7E+03	3.3E+03	---
U-233	---	---	3.0E+10	6.5E+10	7.6E+09	6.4E+09	---	---	---	1.1E+12
U-234	---	8.8E+14	3.7E+03	1.3E+02	4.4E+01	4.2E+01	1.3E+02	4.4E+01	4.2E+01	2.6E+12
U-235	6.2E+08	4.4E+04	9.8E+00	7.6E+00	7.9E+00	9.4E+00	---	---	---	9.1E+08
U-236	---	5.6E+18	7.1E+09	9.5E+09	7.5E+09	7.2E+09	1.3E+10	1.0E+10	9.6E+09	2.7E+10
U-238	---	---	4.7E+06	1.8E+05	5.6E+04	5.2E+04	1.8E+05	5.6E+04	5.2E+04	1.4E+08
Zr-93	2.1E+00	1.1E+00	1.2E+00	---	---	---	---	---	---	---

Note: Limits reported as "---" indicate that there is no limit or that the limit ≥ 1E+20.
Note: Groundwater limits in this table are to be considered preliminary. Adjustments are made in the groundwater limits as appropriate based on consideration of plume overlap effects from adjacent units in Chapter 6 and interpretation of sensitivity and uncertainty analyses in Chapter 7. Final limits are to be found in results tables in Chapter 7.

Table 1-19. Preliminary Groundwater Protection Limits for Engineered Trenches

	Beta-Gamma Limit (Ci/Disposal Unit)			Gross Alpha Limit (Ci/Disposal Unit)			Radium Limit (Ci/Disposal Unit)			Uranium Limit (Ci/Disposal Unit)
Parent Nuclide	**0-12 yrs**	**12-100 yrs**	**100-1130 yrs**	**0-1000 yrs**	**1000-1120 yrs**	**1120-1130 yrs**	**0-1000 yrs**	**1000-1120 yrs**	**1120-1130 yrs**	
Am-241	2.5E+11	1.4E+07	2.8E+04	1.4E+03	1.4E+03	1.4E+03	---	---	---	3.4E+12
Am-243	---	5.1E+17	2.3E+04	5.2E+03	1.3E+03	1.1E+03	---	---	---	1.0E+14
C-14	1.1E+00	6.5E-01	1.5E+01	---	---	---	---	---	---	---
Cf-249	9.0E+18	2.9E+13	7.6E+05	2.0E+04	6.3E+03	5.8E+03	---	---	---	2.2E+14
Cf-251	---	---	7.8E+09	1.0E+04	2.7E+03	2.4E+03	---	---	---	6.3E+19
Cl-36	3.9E-01	2.3E-01	5.2E+00	---	---	---	---	---	---	---
Cm-244	---	---	5.8E+19	8.6E+13	8.3E+12	7.0E+12	9.9E+19	8.1E+19	7.8E+19	---
Cm-245	1.2E+15	9.3E+09	2.0E+04	1.2E+03	4.8E+02	4.4E+02	---	---	---	4.1E+12
Cm-246	---	---	6.4E+16	5.5E+03	1.3E+03	1.2E+03	3.8E+16	1.6E+16	1.5E+16	1.6E+15
Cm-247	---	---	1.7E+05	4.3E+03	1.0E+03	9.2E+02	---	---	---	1.1E+15
Cm-248	---	---	2.0E+11	5.1E+03	1.2E+03	1.1E+03	---	---	---	3.0E+19
H-3	2.2E+01	1.6E+01	4.1E+04	---	---	---	---	---	---	---
H-3_ETF.Carbon	---	---	1.8E+05	---	---	---	---	---	---	---
I-129	1.0E-03	3.9E-04	1.1E-02	---	---	---	---	---	---	---
I-129_ETF.Carbon	---	---	5.9E-01	---	---	---	---	---	---	---
I-129_ETF.GT.73	6.8E+00	2.1E+00	8.0E-01	---	---	---	---	---	---	---
I-129_F.Carbon	9.1E+01	2.7E+01	1.0E+01	---	---	---	---	---	---	---
I-129_F.CG.8	3.5E-02	1.1E-02	1.1E-02	---	---	---	---	---	---	---
I-129_F.Dowex.21K	4.7E+00	1.4E+00	5.4E-01	---	---	---	---	---	---	---
I-129_F.Filtercake	3.9E-02	1.2E-02	1.2E-02	---	---	---	---	---	---	---
I-129_H.Carbon	4.0E+01	1.2E+01	4.6E+00	---	---	---	---	---	---	---
I-129_H.CG.8	2.6E-01	7.9E-02	4.4E-02	---	---	---	---	---	---	---
I-129_H.Dowex.21K	1.1E+01	3.2E+00	1.2E+00	---	---	---	---	---	---	---
I-129_H.Filtercake	4.5E-01	1.3E-01	7.3E-02	---	---	---	---	---	---	---
K-40	5.3E-01	3.2E-01	3.0E+00	---	---	---	---	---	---	---
Mo-93	8.5E-01	4.4E-01	6.2E+00	---	---	---	---	---	---	---
Nb-94	4.3E-01	2.5E-01	5.8E+00	---	---	---	---	---	---	---
Ni-59	---	3.8E+11	2.2E+01	---	---	---	---	---	---	---
Np-237	1.5E+05	2.7E+01	4.6E+00	2.3E-01	2.8E-01	3.3E-01	---	---	---	4.8E+08
Pd-107	---	4.7E+13	2.7E+03	---	---	---	---	---	---	---

Table 1-19. Preliminary Groundwater Protection Limits for Engineered Trenches – continued

	Beta-Gamma Limit (Ci/Disposal Unit)			Gross Alpha Limit (Ci/Disposal Unit)			Radium Limit (Ci/Disposal Unit)			Uranium Limit (Ci/Disposal Unit)
Parent Nuclide	**0-12 yrs**	**12-100 yrs**	**100-1130 yrs**	**0-1000 yrs**	**1000-1120 yrs**	**1120-1130 yrs**	**0-1000 yrs**	**1000-1120 yrs**	**1120-1130 yrs**	
Pu-238	---	---	4.8E+07	1.6E+06	5.6E+05	5.1E+05	1.6E+06	5.6E+05	5.1E+05	---
Pu-239	6.9E+19	6.2E+13	2.6E+07	2.0E+07	1.8E+07	1.8E+07	---	---	---	3.5E+18
Pu-240	---	---	1.5E+17	3.4E+11	3.1E+10	2.6E+10	2.5E+17	2.1E+17	2.0E+17	3.8E+18
Pu-241	9.8E+13	2.0E+09	8.4E+05	4.2E+04	4.3E+04	4.3E+04	---	---	---	1.1E+14
Pu-242	---	---	4.5E+14	3.1E+11	2.7E+10	2.3E+10	1.3E+13	5.3E+12	4.9E+12	3.3E+18
Pu-244	---	---	1.9E+12	2.8E+11	2.5E+10	2.0E+10	1.1E+19	8.2E+18	7.9E+18	3.1E+19
Ra-226	---	1.9E+09	1.1E+01	3.1E-01	1.3E-01	1.2E-01	3.1E-01	1.3E-01	1.2E-01	---
Se-79	---	---	---	---	---	---	---	---	---	---
Sn-126	---	---	---	---	---	---	---	---	---	---
Sr-90	2.6E+18	2.7E+08	5.7E+02	---	---	---	---	---	---	---
Tc-99	1.6E+00	3.6E-01	7.7E+00	---	---	---	---	---	---	---
Th-230	---	1.6E+12	4.4E+01	2.0E+00	5.0E-01	4.6E-01	2.0E+00	5.0E-01	4.6E-01	---
Th-232	---	1.2E+12	1.5E+05	1.5E+05	3.9E+05	5.2E+05	2.0E+05	5.2E+05	6.9E+05	---
U-233	---	---	7.8E+14	2.4E+15	2.0E+14	1.7E+14	---	---	---	2.4E+16
U-234	---	6.1E+16	1.2E+04	4.4E+02	1.4E+02	1.3E+02	4.4E+02	1.4E+02	1.3E+02	8.2E+16
U-235	1.1E+11	2.6E+05	1.4E+01	1.0E+01	1.1E+01	1.1E+01	---	---	---	2.8E+13
U-236	---	---	1.5E+12	1.8E+12	1.6E+12	1.5E+12	2.4E+12	2.1E+12	2.0E+12	8.5E+14
U-238	---	---	1.6E+07	4.7E+05	1.8E+05	1.7E+05	4.7E+05	1.8E+05	1.7E+05	4.4E+12
Zr-93	8.2E+00	1.5E+00	1.7E+00	---	---	---	---	---	---	---

Note: Limits reported as "---" indicate that there is no limit or that the limit $\geq$ 1E+20.
Note: Groundwater limits in this table are to be considered preliminary. Adjustments are made in the groundwater limits as appropriate based on consideration of plume overlap effects from adjacent units in Chapter 6 and interpretation of sensitivity and uncertainty analyses in Chapter 7. Final limits are to be found in results tables in Chapter 7.

1.6.6 Groundwater Transport Uncertainty Analysis

This section discusses the results of the uncertainty analysis for the Slit Trenches and Engineered Trenches. The Slit Trench 5 analysis was run using both PORFLOW and GoldSim and its results will be discussed in more detail than the other seven trenches. All trenches behaved similarly. The significant differences are discussed.

The results for each trench are presented in terms of the mean value, the median value, and the 95^{th} percentile value for each of the performance objectives. The values are based on 1000 realizations. The plots are for the 100-m well point of assessment.

The uncertainty results are expressed in terms of the groundwater protection and all-pathways performance measures and use estimated final inventories for the Slit Trenches (no special wasteforms were considered). The estimate made on June 12, 2007 is used, and is given in Table 1-20. This inventory was regarded as adequate for performing the uncertainty analysis; however, the estimated final inventory was later refined slightly and is presented in Appendix C.

The probabilistic uncertainty analysis was done using the GoldSim computer program. The parameters that were varied were the future land use scenario, infiltration rate through the closure cap, the time at which institutional control ceases, final waste zone thickness, dry bulk density, particle density and water content, and K_d. Details of the analysis and parameter distributions are presented in Appendix F.

Table 1-20. Estimated Final Inventories for Slit Trenches 1 – 8 (Ci) (June 12, 2007 Estimate)

Parent Nuclide	Slit 1	Slit 2	Slit 3	Slit 4	Slit 5	Slit 6	Slit 7	Slit 8
Am-241	3.7E-02	1.6E-01	1.6E-01	2.1E-01	2.0E-01	1.4E+00	2.7E-01	4.8E-01
Am-243	6.1E-05	1.7E-03	2.8E-03	1.3E-03	6.2E-03	1.4E-01	8.6E-04	2.1E-01
C-14	8.9E-03	4.0E-02	1.8E-02	1.6E-02	3.7E-02	4.5E-03	3.9E-02	3.5E-03
C-14_NR.Pump	5.2E-02	8.2E-02	1.0E-02	3.7E-02	5.0E-03	5.0E-04	4.1E-02	5.0E-03
Cf-249	6.7E-06	6.2E-04	4.3E-04	1.9E-04	1.1E-02	2.8E-01	3.2E-03	4.2E-01
Cf-251	6.6E-05	6.7E-04	4.4E-04	2.5E-04	1.1E-02	2.5E-01	2.6E-03	3.8E-01
Cl-36	0.0E+00	0.0E+00	1.0E-05	1.0E-05	2.3E-06	1.0E-03	1.0E-06	1.0E-06
Cm-244	3.8E-02	1.1E-01	2.0E-01	7.8E-01	1.2E+00	1.1E+01	4.2E-02	1.5E+01
Cm-245	2.7E-07	2.9E-06	2.3E-04	3.5E-04	3.4E-04	3.6E-03	2.7E-04	7.3E-03
Cm-246	1.4E-06	2.2E-05	7.5E-04	9.6E-04	3.2E-04	9.6E-04	6.5E-04	9.6E-06
Cm-247	1.5E-06	2.5E-09	6.6E-05	9.0E-04	7.2E-05	3.6E-03	2.7E-04	1.6E-02
Cm-248	1.4E-06	2.6E-05	8.1E-05	2.9E-07	2.7E-05	5.4E-05	1.2E-04	3.0E-05
H-3	8.5E-01	1.1E+00	9.0E-01	4.5E-01	4.0E-01	2.0E-01	3.5E-01	5.0E-01
H-3_concrete	3.9E+00	0.0E+00	0.0E+00	0.0E+00	0.0E+00	0.0E+00	0.0E+00	0.0E+00
H-3_ETF.Carbon	0.0E+00	0.0E+00	4.0E-01	0.0E+00	0.0E+00	0.0E+00	1.5E-01	1.2E-04
I-129	2.0E-05	2.0E-05	2.2E-05	4.4E-05	4.9E-05	8.3E-05	2.9E-05	0.0E+00
I-129_ETF.Carbon	0.0E+00	0.0E+00	2.2E-02	0.0E+00	0.0E+00	0.0E+00	1.3E-02	0.0E+00
I-129_ETF.GT.73	0.0E+00	8.6E-05	5.4E-05	9.3E-05	0.0E+00	0.0E+00	0.0E+00	0.0E+00
I-129_F.Carbon	0.0E+00	0.0E+00	0.0E+00	0.0E+00	0.0E+00	0.0E+00	0.0E+00	0.0E+00
I-129_F.CG.8	0.0E+00	5.2E-05	0.0E+00	0.0E+00	0.0E+00	0.0E+00	0.0E+00	0.0E+00
I-129_F.Dowex.21K	0.0E+00	4.4E-03	0.0E+00	0.0E+00	0.0E+00	0.0E+00	0.0E+00	0.0E+00
I-129_F.Filtercake	8.1E-05	3.4E-04	1.6E-05	0.0E+00	7.6E-07	0.0E+00	7.8E-07	0.0E+00
I-129_H.Carbon	0.0E+00	0.0E+00	0.0E+00	0.0E+00	0.0E+00	0.0E+00	0.0E+00	0.0E+00

Table 1-20. Estimated Final Inventories for Slit Trenches 1 – 8 (Ci) (June 12, 2007 Estimate) - continued

Parent Nuclide	Slit 1	Slit 2	Slit 3	Slit 4	Slit 5	Slit 6	Slit 7	Slit 8
I-129_H.CG.8	0.0E+00	1.2E-04	0.0E+00	0.0E+00	0.0E+00	0.0E+00	0.0E+00	0.0E+00
I-129_H.Dowex.21K	0.0E+00	0.0E+00	0.0E+00	0.0E+00	0.0E+00	0.0E+00	0.0E+00	0.0E+00
I-129_H.Filtercake	2.8E-07	0.0E+00	0.0E+00	0.0E+00	0.0E+00	0.0E+00	0.0E+00	0.0E+00
I-129_Mk50A	0.0E+00	0.0E+00	0.0E+00	0.0E+00	8.2E-06	0.0E+00	0.0E+00	0.0E+00
K-40	4.1E-03	3.2E-06	1.0E-03	9.9E-06	2.9E-04	1.0E-03	1.0E-06	1.0E-06
Mo-93	1.1E-05	3.4E-07	1.0E-05	1.0E-05	0.0E+00	1.5E-03	1.0E-06	1.0E-06
Nb-94	1.1E-03	2.3E-03	8.1E-04	9.9E-04	8.7E-04	1.0E-04	1.3E-03	1.0E-03
Ni-59	2.2E-02	3.6E-02	8.9E-03	1.2E-02	1.1E-02	2.5E-02	3.9E-02	5.1E-05
Np-237	1.1E-03	2.0E-03	2.0E-02	2.5E-03	5.4E-03	2.4E-03	2.0E-02	4.6E-04
Pd-107	1.1E-07	1.8E-10	1.0E-07	1.0E-07	0.0E+00	1.0E-07	1.0E-06	1.0E-06
Pu-238	2.4E-01	5.9E-01	2.4E+00	2.4E+00	1.8E+00	8.8E+00	4.9E+00	9.9E+00
Pu-239	2.5E-02	2.0E-01	6.2E-01	8.2E-01	8.2E-01	2.5E+00	1.1E+00	3.1E+00
Pu-240	6.8E-03	7.6E-02	1.8E-01	2.2E-01	2.6E-01	6.7E-01	2.7E-01	9.3E-01
Pu-241	2.1E-01	2.2E+00	7.0E+00	4.5E+00	5.4E+00	1.3E+01	6.7E+00	9.4E+00
Pu-242	1.1E-04	1.0E-03	1.9E-03	2.3E-02	5.0E-03	4.4E-02	2.5E-02	5.9E-01
Pu-244	2.4E-15	5.1E-15	3.5E-16	1.7E-15	1.5E-15	1.0E-15	2.8E-15	1.0E-15
Ra-226	3.2E-03	6.5E-06	3.0E-05	4.2E-05	3.6E-04	9.8E-04	6.0E-08	1.0E-04
Ra-226_Cooling.Tower	0.0E+00	0.0E+00	0.0E+00	0.0E+00	0.0E+00	4.0E-02	0.0E+00	0.0E+00
Se-79	2.0E-04	5.4E-04	1.7E-04	3.2E-05	4.0E-04	2.9E-02	1.4E-03	4.1E-05
Sn-126	0.0E+00	2.1E-06	1.5E-04	1.0E-04	3.2E-05	1.2E-08	1.2E-05	6.0E-08
Sr-90	3.2E+00	4.7E+00	1.6E+01	3.7E+00	1.2E+01	1.5E+01	1.1E+01	4.1E+00
Sr-90_Mk50A	0.0E+00	0.0E+00	0.0E+00	0.0E+00	7.4E+00	0.0E+00	0.0E+00	0.0E+00
Tc-99	5.3E-03	2.0E-02	6.7E-02	6.1E-02	4.2E-02	3.5E-02	1.2E-02	1.8E-02
Tc-99_Mk50A	0.0E+00	0.0E+00	0.0E+00	0.0E+00	1.8E-03	0.0E+00	0.0E+00	0.0E+00

Table 1-20. Estimated Final Inventories for Slit Trenches 1 – 8 (Ci) (June 12, 2007 Estimate) - continued

Parent Nuclide	Slit 1	Slit 2	Slit 3	Slit 4	Slit 5	Slit 6	Slit 7	Slit 8
Th-230	2.9E-04	0.0E+00	3.0E-05	2.5E-06	3.9E-04	8.9E-04	1.2E-07	1.0E-04
Th-230_Cooling.Tower	0.0E+00	0.0E+00	0.0E+00	0.0E+00	0.0E+00	4.0E-02	0.0E+00	0.0E+00
Th-232	2.3E-03	3.5E-06	4.6E-05	4.1E-06	3.7E-05	3.5E-02	1.8E-08	5.7E-08
U-233	6.2E-03	2.7E-02	3.0E-02	5.9E-03	2.0E+00	7.9E-03	8.6E-02	8.3E-01
U-234	7.7E-02	3.6E-01	1.5E+00	2.6E+00	1.8E+00	2.2E-01	2.9E+00	6.2E-01
U-234_MGlass	0.0E+00	2.8E+00	0.0E+00	0.0E+00	0.0E+00	0.0E+00	0.0E+00	0.0E+00
U-235	6.1E-03	3.2E-02	4.9E-02	5.6E-02	3.9E-02	4.8E-03	9.3E-02	2.5E-04
U-235_MGlass	0.0E+00	1.9E-01	0.0E+00	0.0E+00	0.0E+00	0.0E+00	0.0E+00	0.0E+00
U-235_Paducah.Cask	0.0E+00	0.0E+00	0.0E+00	0.0E+00	3.9E-01	0.0E+00	0.0E+00	0.0E+00
U-236	3.3E-03	1.1E-02	3.3E-02	1.4E-02	2.6E-02	6.2E-03	1.3E-02	1.7E-06
U-236_MGlass	0.0E+00	1.4E-01	0.0E+00	0.0E+00	0.0E+00	0.0E+00	0.0E+00	0.0E+00
U-238	1.5E-01	1.4E+00	1.8E+00	3.6E-01	3.3E+00	3.5E-01	1.2E-01	2.9E-01
U-238_MGlass	0.0E+00	1.1E+01	0.0E+00	0.0E+00	0.0E+00	0.0E+00	0.0E+00	0.0E+00
Zr-93	2.7E-05	2.3E-05	1.6E-06	7.4E-06	6.6E-06	1.0E-05	1.2E-05	1.0E-05

1.6.6.1 Slit Trench 5 Uncertainty Analysis

An explicit Slit Trench 5 performance objective case was run with PORFLOW in order to compare results with the GoldSim analysis. When PORFLOW results are referred to, what is implied is the Automated All-Pathways analysis which used PORFLOW generated concentrations. Slit Trench 5 was chosen because it is full and is effectively closed.

All-Pathways Dose Performance Measure

The all-pathways dose assessment begins at 130 years, the time of loss of institutional control. Before this time it is not credible for a member of the public to use water from the vicinity of the ELLWF because the area will be under institutional control. The result is shown in Figure 1-14. The timing of the PORFLOW and GoldSim peaks is different due to the different manners which the codes use to calculate the effect of the distribution coefficients.

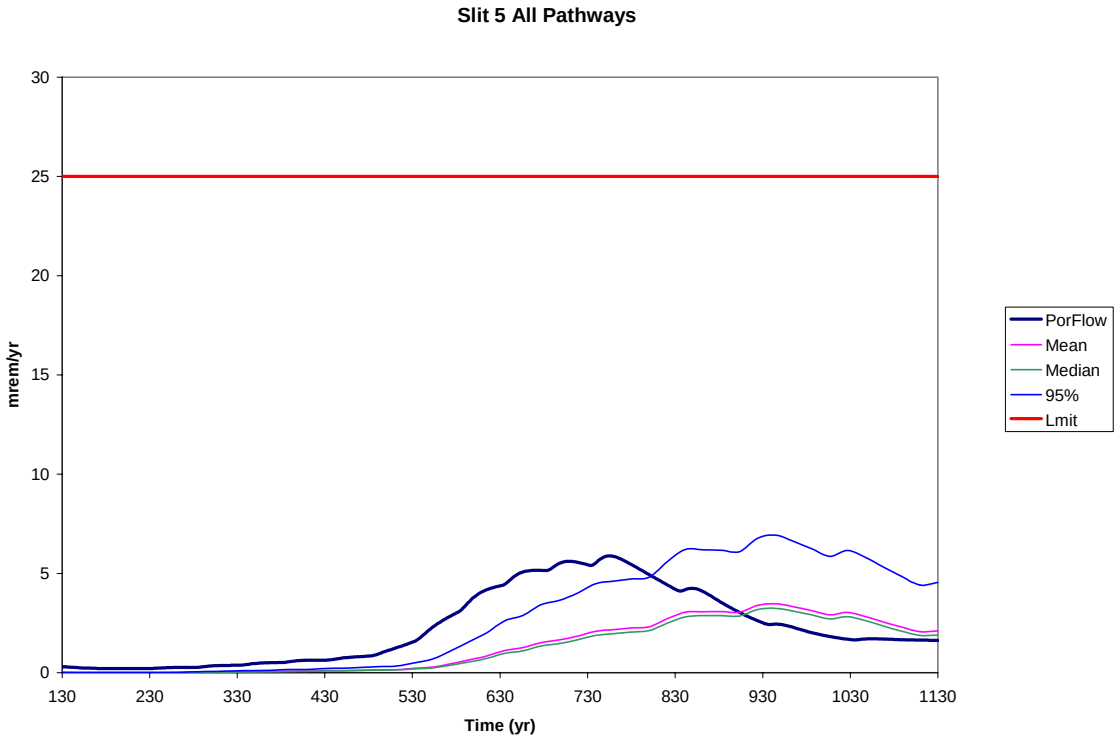

Figure 1-14. Slit Trench 5 All-Pathways Dose Uncertainties

Figure 1-15 shows the major contributors to the all-pathways dose. Np-237 is the major contributor with Pa-231 being the second largest. Both these are long lived, mobile species. Np-237 is present in the initial inventory and also as a decay product. Pa-231 appears as an in-growth decay product of U-235. Both are alpha emitters and figure in the alpha concentration performance limit. Note that Figure 1-15 shows only one realization.

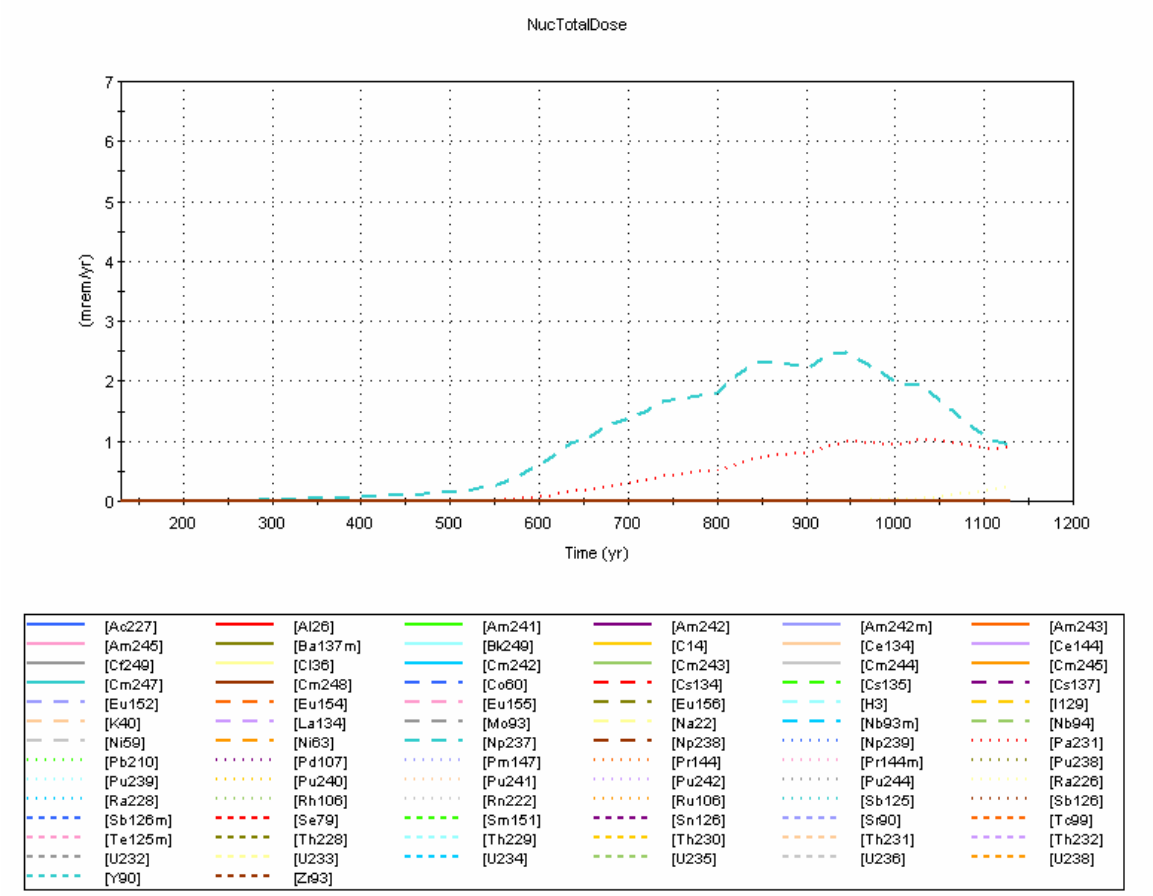

Figure 1-15. Slit Trench 5 Major Contributors to All-Pathways Dose

Beta-Gamma Performance Measure

As can be seen in Figure 1-16, all the beta-gamma dose occurs within the first 50 years of the analysis. Figure 1-17 shows the beta-gamma dose comparison for only the first 50 years. This dose comes from short lived, mobile species. The PORFLOW curve shows one peak because it has a more dispersive calculation than GoldSim and the PORFLOW model is set up in two and three dimensions so that radionuclides are released over the length of each trench along the flow paths, which tends to smear the early peaks into a single one.

The first GoldSim peak is caused by those radionuclides which have a K_d of 0 mL/g, C-14, H-3, I-129 and Nb-94. In this case the major contributors are C-14 and Nb-94. The second peak is caused by Tc-99 which has a K_d of 0.1 mL/g.

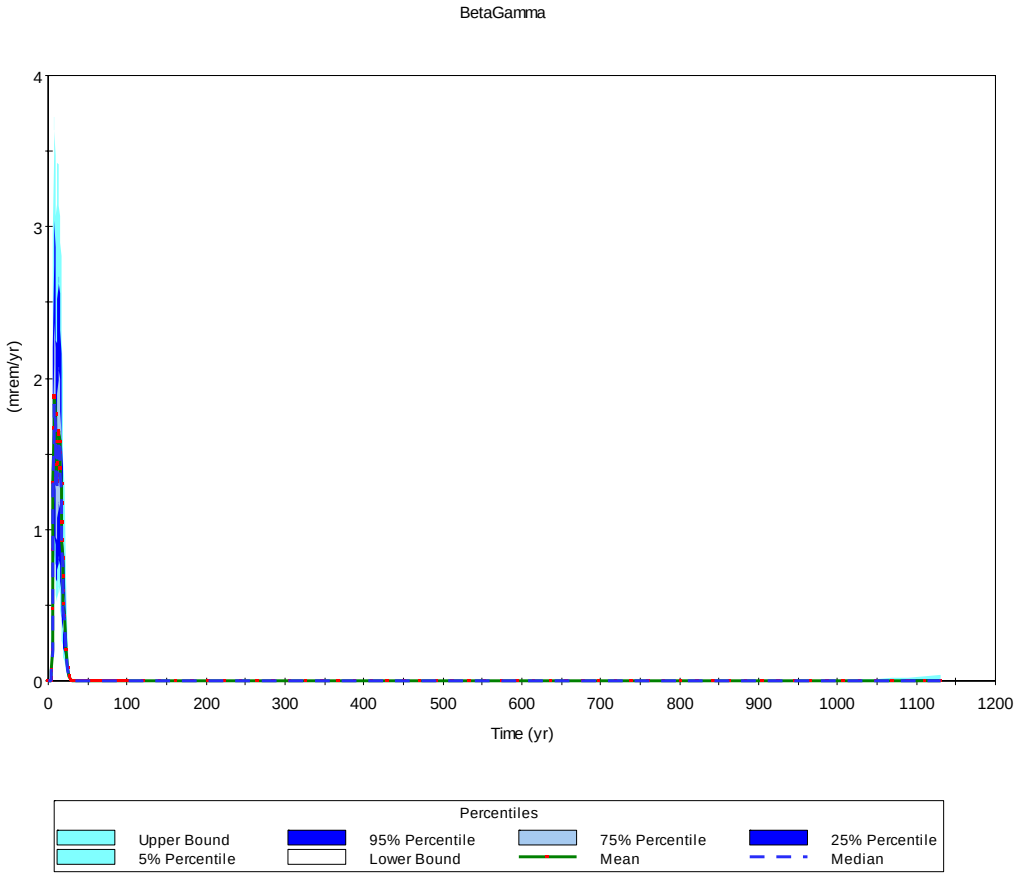

Figure 1-16. GoldSim Beta-Gamma Uncertainty

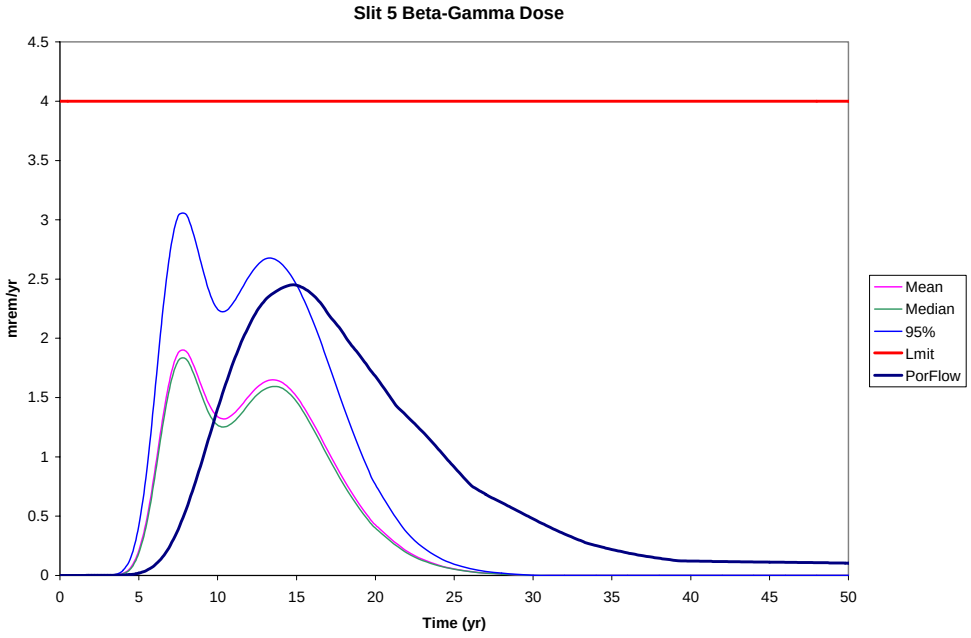

Figure 1-17. Slit Trench 5 Beta-Gamma Uncertainty

Alpha Performance Measure

The major contributors in Figure 1-18 are Np-237 for both the early and late concentrations and Pa-231 for the late concentration. The late concentration was discussed in the all-pathways section. The early concentration is due to the mobility of Np-237 (K_d = 0.6 mL/g) and the fact that the closure cap is not in place for 130 years.

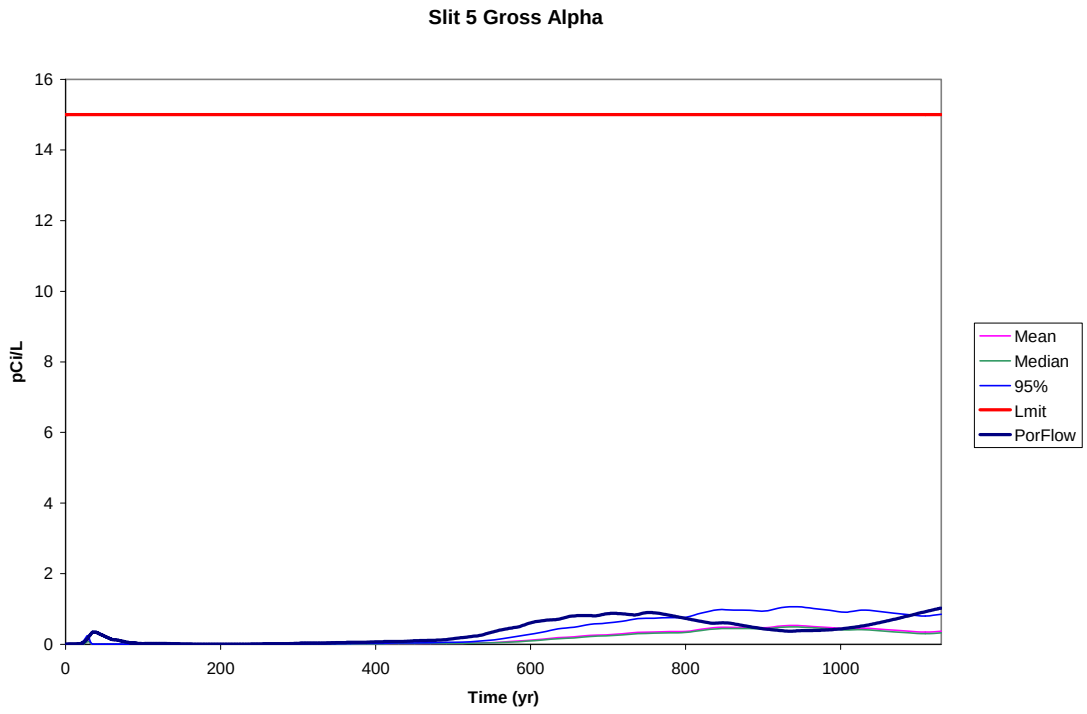

Figure 1-18. Slit Trench 5 Alpha Uncertainty

Uranium Performance Measure

The uranium concentration, as seen in Figure 1-19 is about 10 orders of magnitude below the performance measure of 30 µg/L.

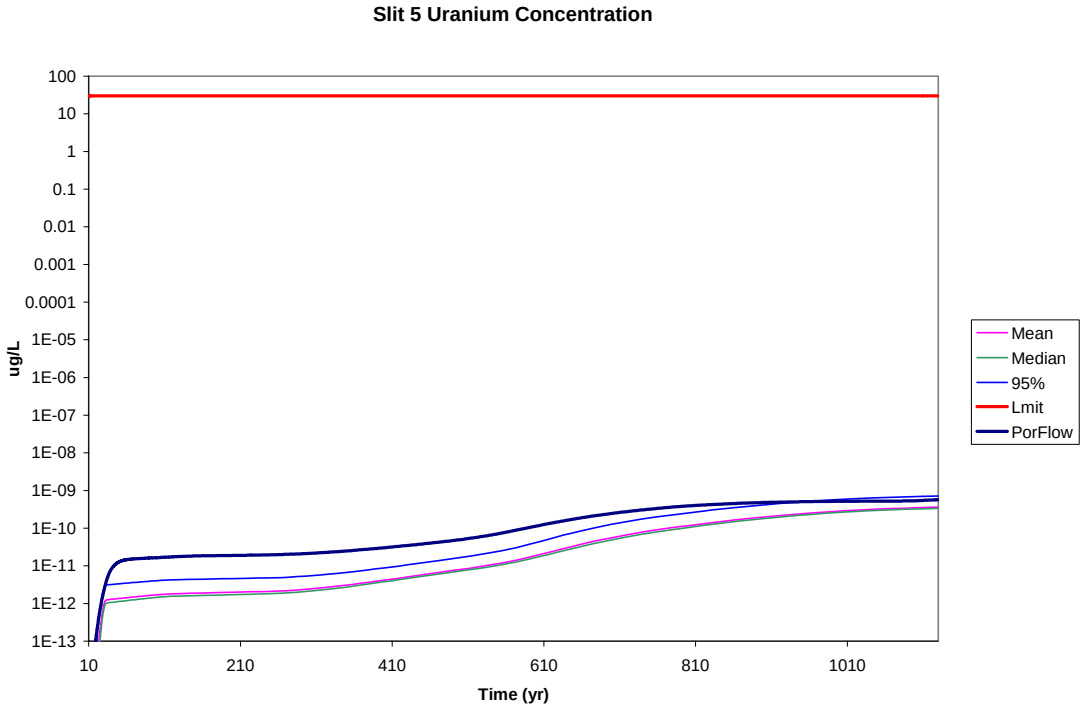

Figure 1-19. Uranium Performance Objective Uncertainty

Radium Performance Measure

Radium is a daughter of relatively slow moving radionuclides that has a K_d of 5 mL/g and does not appear at the compliance point until near the end of the period of concern. Its concentrations remain well below the performance objective (Figure 1-20). A K_d of 5 mL/g appears to be about the highest a radionuclide can have and appear at the 100-m well within the 1100-year period of assessment.

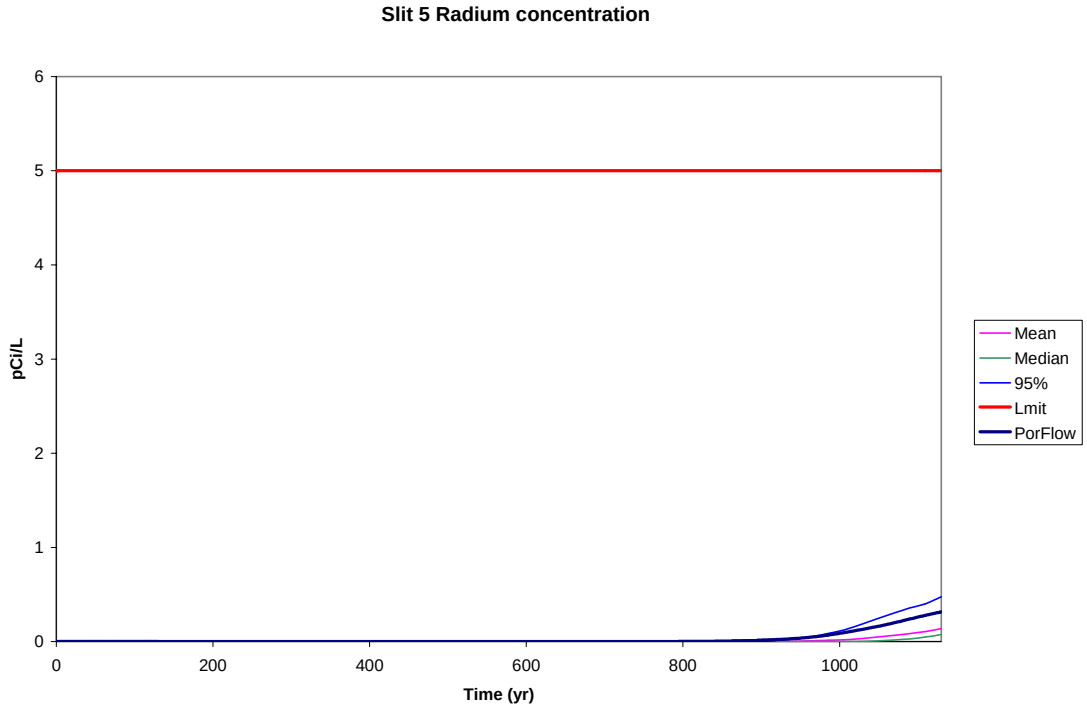

Figure 1-20. Radium Performance Objective Uncertainty

1.6.6.2 Slit Trench 1 Uncertainty Analysis

Slit Trench 1 uncertainties are shown in Figure 1-21. The beta-gamma performance objective does not exhibit the double peak as the inventory of Tc-99 is much lower than that of Slit Trench 5.

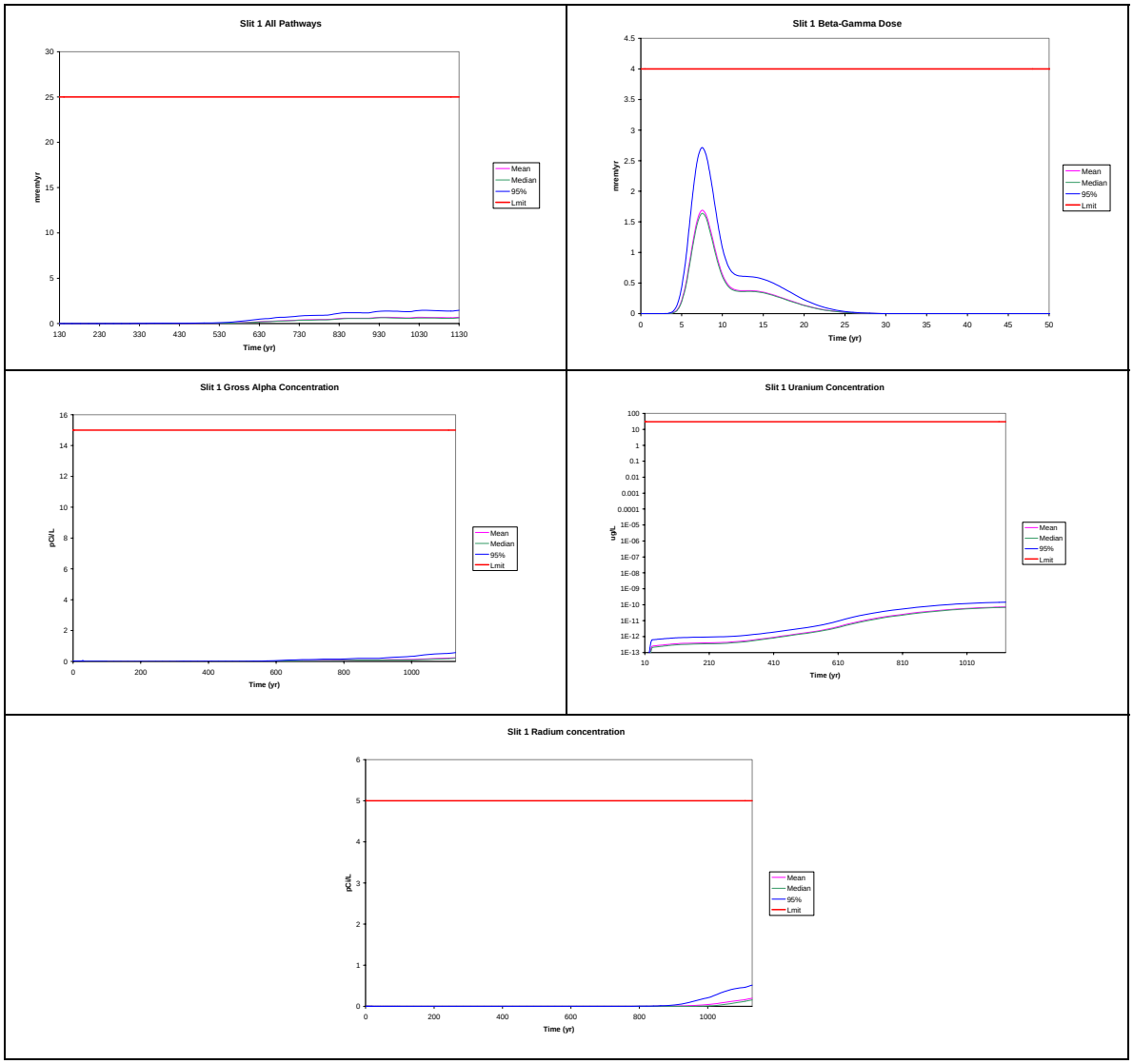

Figure 1-21. Slit Trench 1 Uncertainty Analyses

1.6.6.3 Slit Trench 2 Uncertainty analysis

Slit Trench 2 uncertainties are shown in Figure 1-22. The 95th percentile of the beta-gamma dose exceeds the performance objective. However, the mean and median doses are 2.7 and 2.8 mrem/yr respectively. From these results it appears that the trench contains short –lived, mobile radionuclides as there is no appreciable late dose (see all-pathways dose).

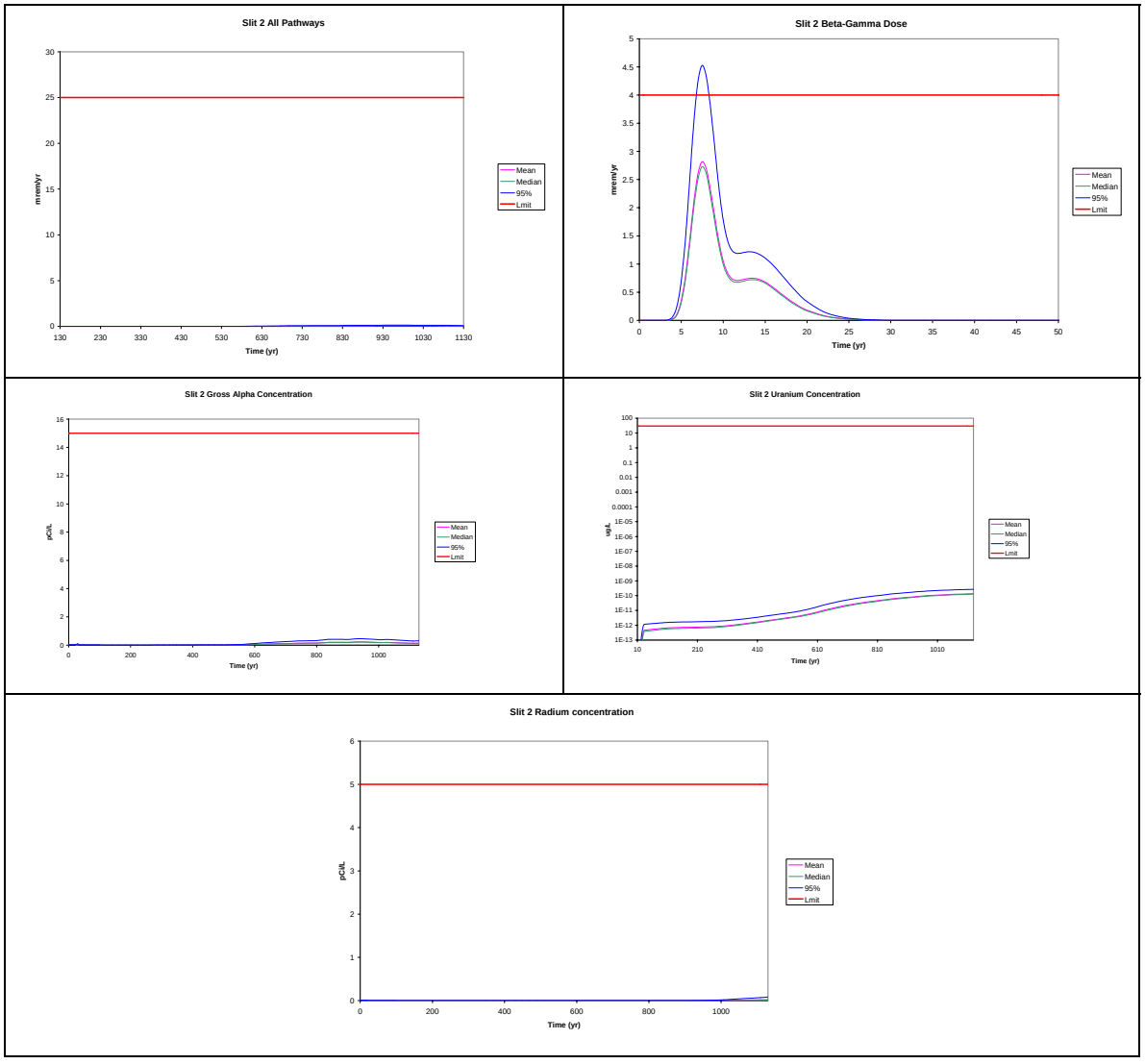

Figure 1-22. Slit Trench 2 Uncertainty Analyses

1.6.6.4 Slit Trench 3 Uncertainty Analysis

Slit Trench 3 (Figure 1-23) gives the second highest alpha concentration of the eight trenches, 3.6 pCi/L at the 95th percentile, but is still well below the performance measure of 15 pCi/L.

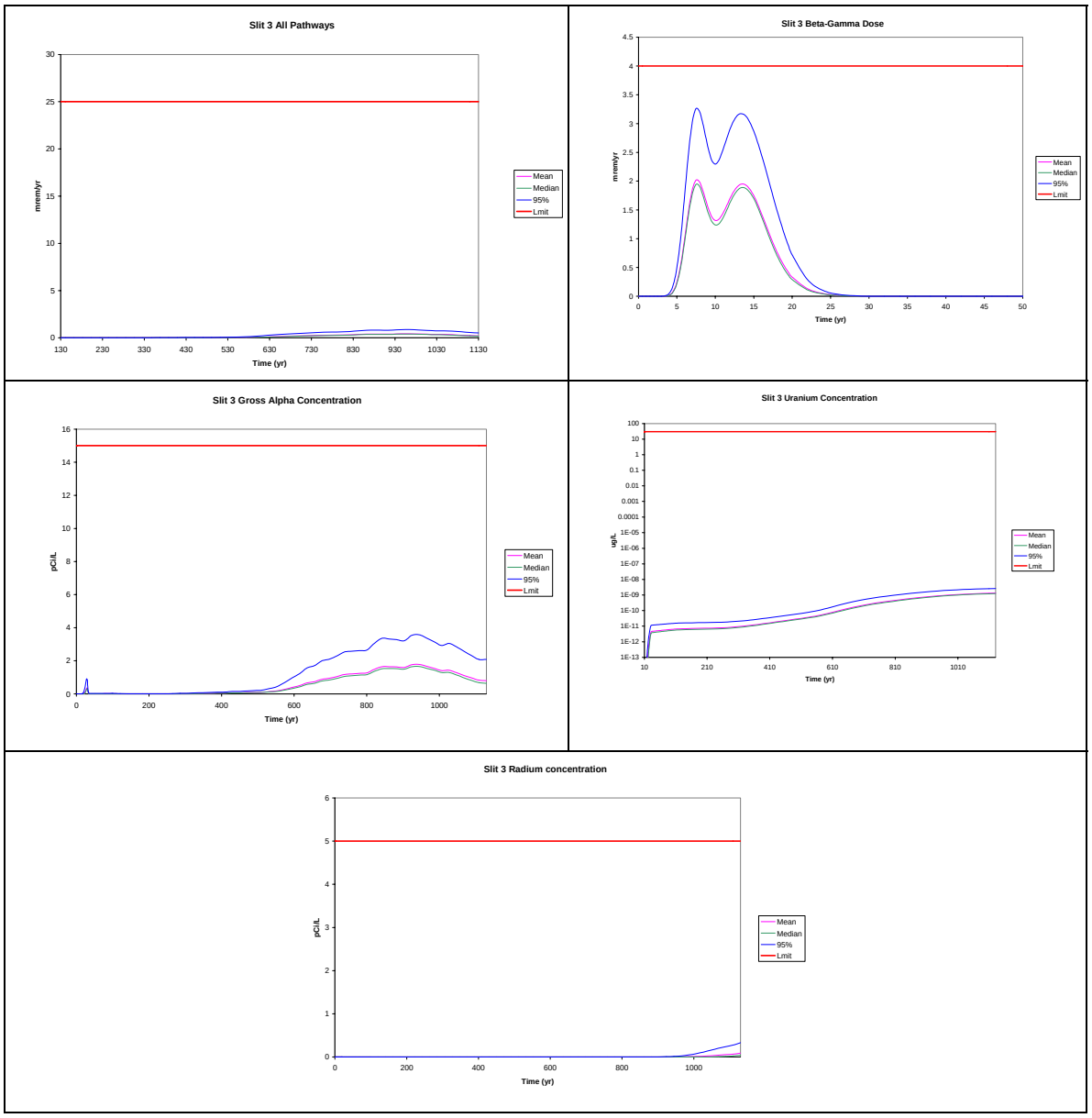

Figure 1-23. Slit Trench 3 Uncertainty Analyses

1.6.6.5 Slit Trench 4 Uncertainty Analysis

Slit Trench 4 uncertainty analyses (Figure 1-24) provided no challenge to any of the performance objectives.

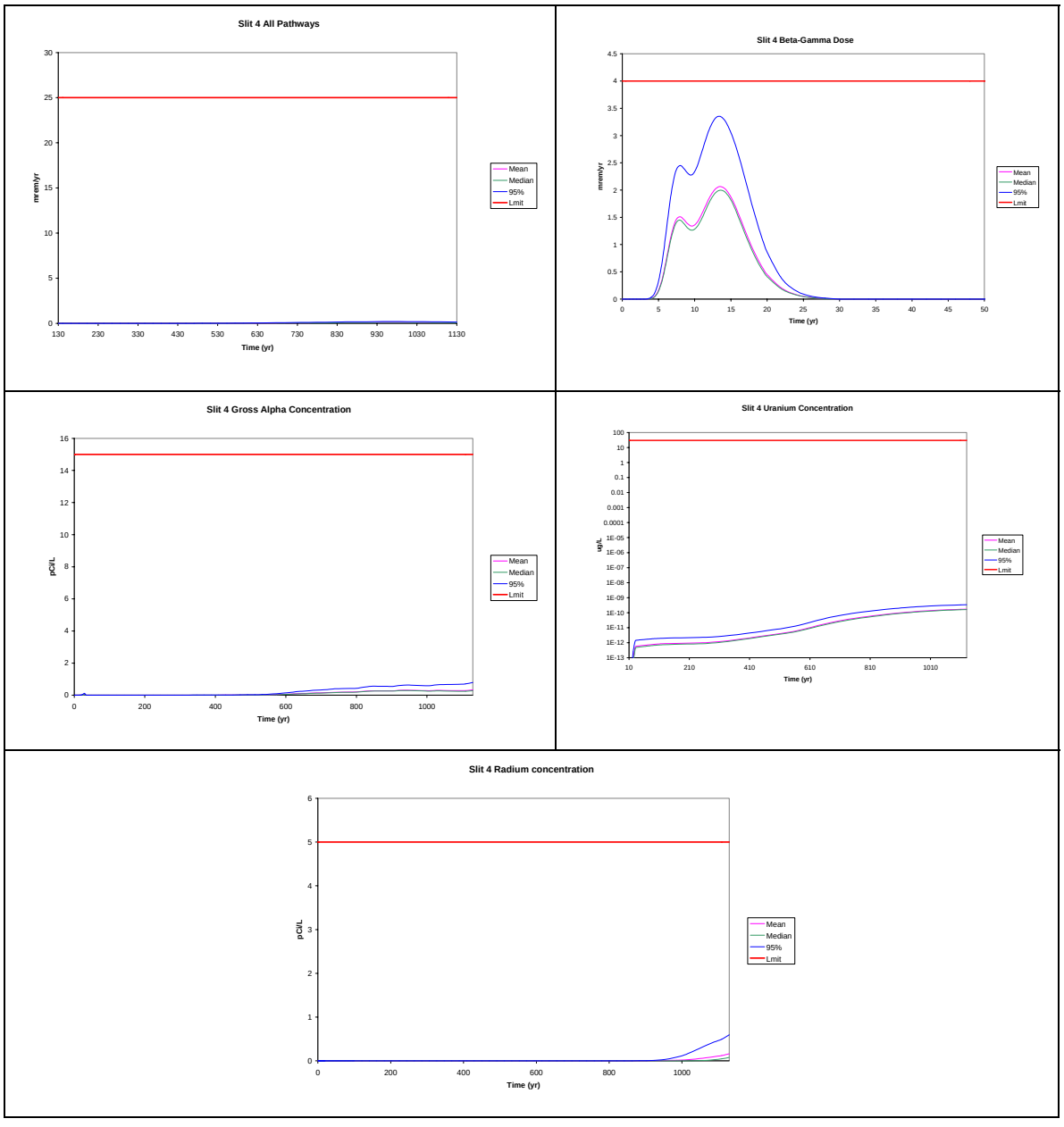

Figure 1-24. Slit Trench 4 Uncertainty Analyses

1.6.6.6 Slit Trench 6 Uncertainty Analysis

Slit Trench 6 uncertainty analyses (Figure 1-25) provided no challenge to any of the performance objectives.

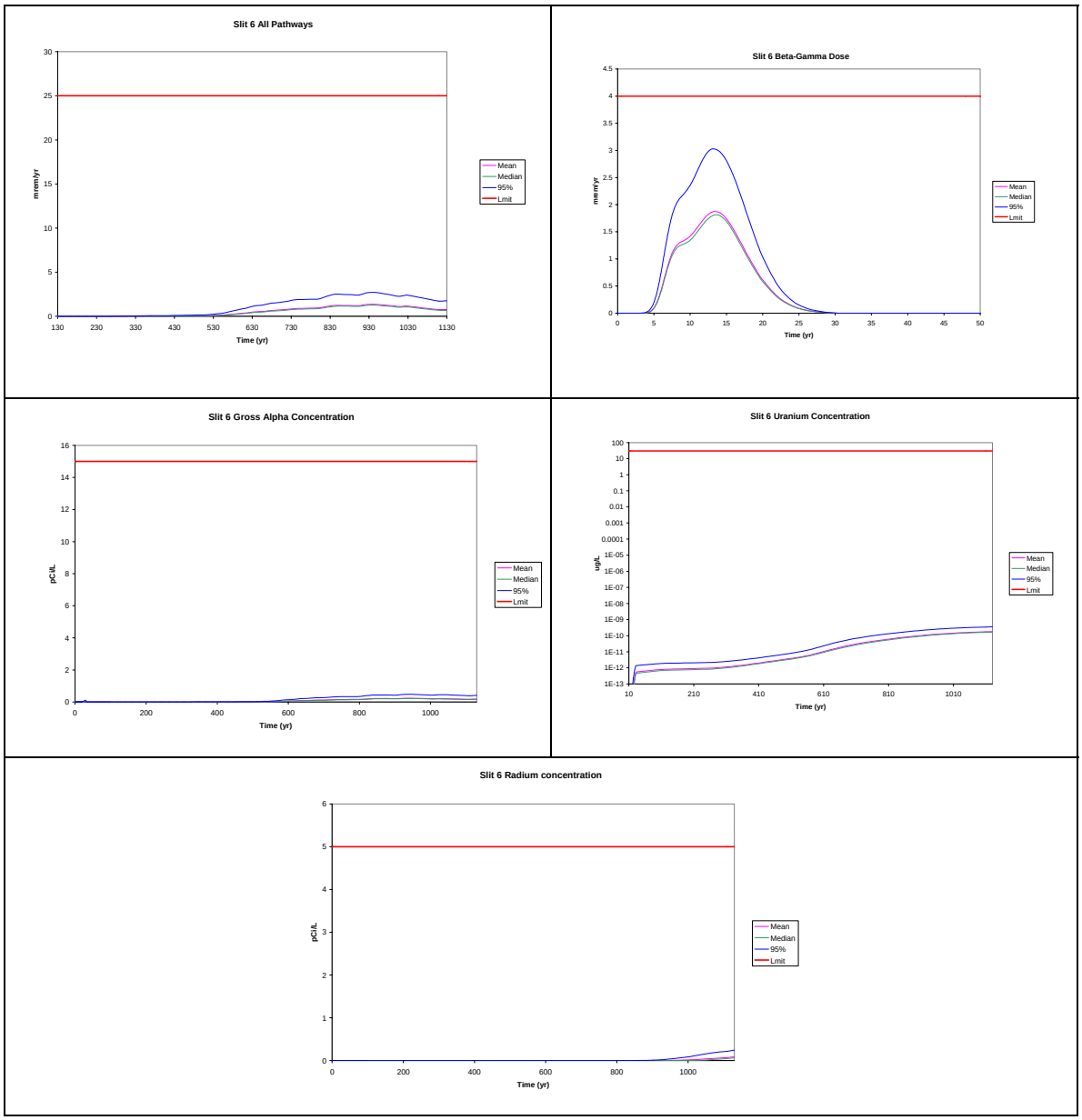

Figure 1-25. Slit Trench 6 Uncertainty Analyses

1.6.6.7 Slit Trench 7 Uncertainty Analysis

Slit Trench 7 uncertainties are shown in Figure 1-26. Slit Trench 7 gives the highest all-pathways dose and alpha concentration at the 95th percentile of all eight Slit Trenches. Both of these are due to Np-237 and Pa-231, alpha emitters.

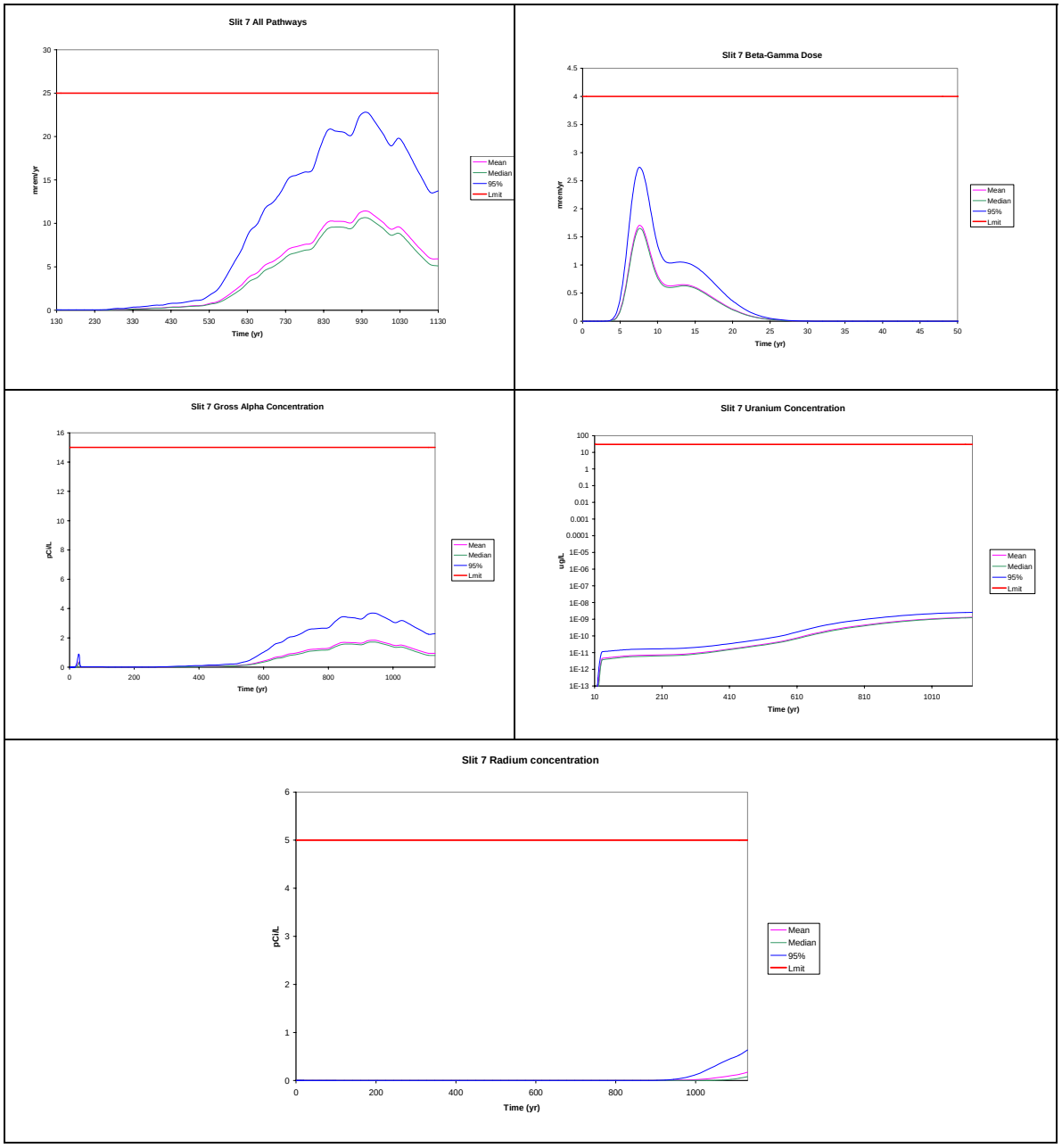

Figure 1-26. Slit Trench 7 Uncertainty Analyses

1.6.6.8 Slit Trench 8 Uncertainty Analysis

Slit Trench 8 uncertainty analyses (Figure 1-27) provide no challenge to the performance objectives.

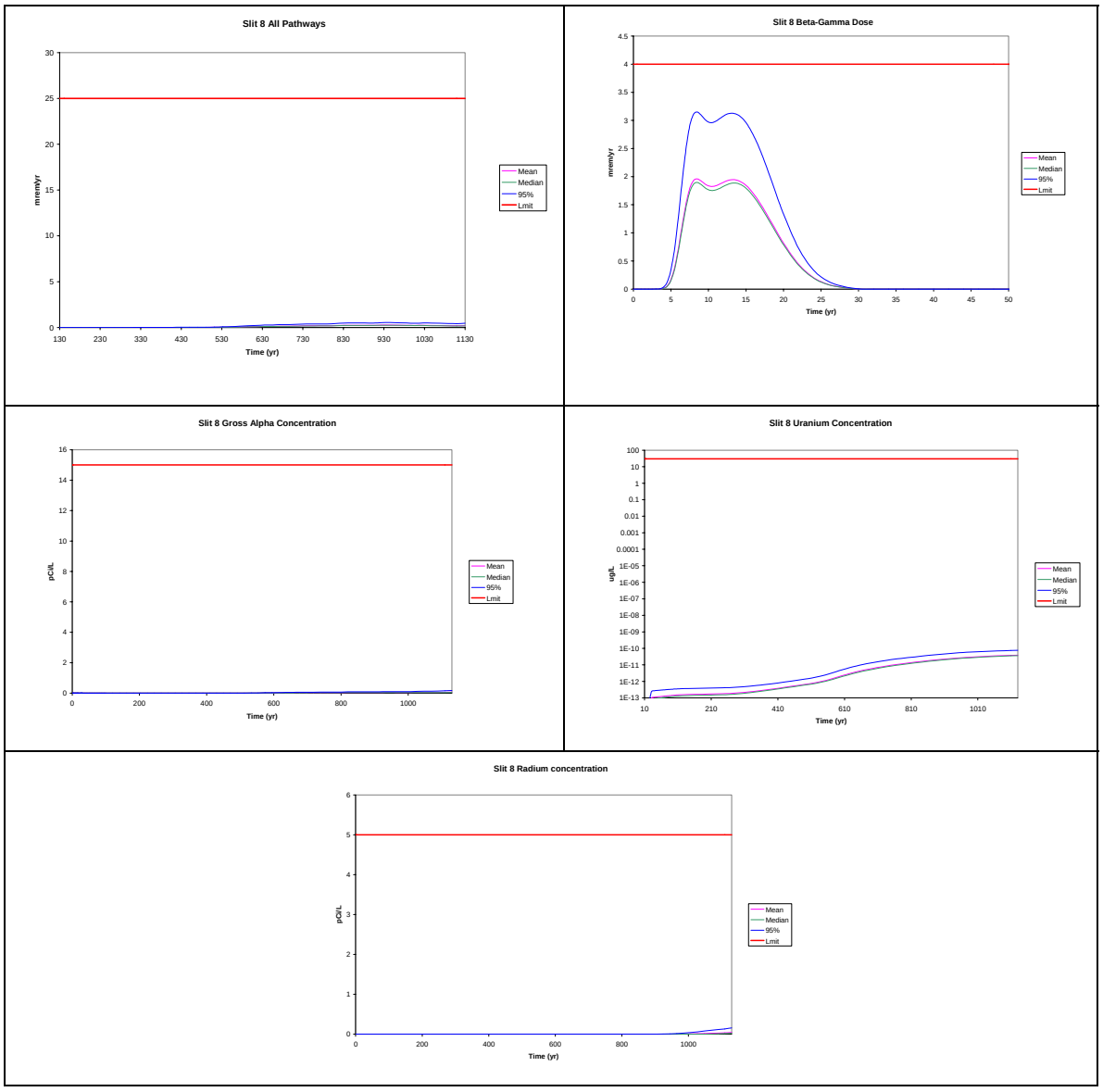

Figure 1-27. Slit Trench 8 Uncertainty Analyses

1.6.6.9 Summary of Slit Trench Uncertainty Analysis Results

Table 1-21 is a summary of the uncertainty results. It shows that the mean and median values do not exceed any of the performance objectives for any of the trenches. The all-pathways dose, the alpha, uranium, and radium concentration limits were not exceeded at the 95th percentile for any trench. The beta-gamma limit of 4 mrem/yr was exceeded at the 95th percentile in Trench 2 with a value of 4.5 mrem/yr. It should be noted that this "exceedance" occurs during a period when institutional control is still in effect.

Only radionuclides with very low K_d values (C-14, H-3, I-129, Np-237, Pa-231, Ra-226 and Tc-99) were a significant factor in the analysis. Of these, Ra-226 has the largest K_d with a best estimate K_d of 5 mL/g. Radionuclides with a K_d greater than 5 mL/g do not get to the point of assessment within the time of compliance.

Table 1-21. Summary of Slit Trench Uncertainty Results

		Slit 1			Slit 2			Slit 3		
Performance measure	**limit**	**mean**	**median**	**95%**	**mean**	**median**	**95%**	**mean**	**median**	**95%**
All pathways, mr/yr	25.0	0.7	0.6	1.5	6.7	6.5	10.8	10.9	10.6	20.8
βγ, mrem/yr	4.0	1.7	1.6	2.7	2.8	2.7	4.5	2.0	1.9	3.3
α, pCi/L	15.0	0.2	0.2	0.6	0.2	0.2	0.5	1.8	1.7	3.6
Uranium, µg/L	30	7.29E-11	6.83E-11	1.44E-10	1.35E-10	1.27E-10	2.68E-10	1.32E-09	1.24E-09	2.62E-09
Radium, pCi/L	5.00	0.20	0.16	0.52	0.02	0.01	0.08	0.09	0.04	0.33
		Slit 4			**Slit 5**			**Slit 6**		
Performance measure	**limit**	**mean**	**median**	**95%**	**mean**	**median**	**95%**	**mean**	**median**	**95%**
All pathways, mr/yr	25.0	2.6	2.4	5.2	3.5	3.2	6.9	1.4	1.3	2.7
βγ, mrem/yr	4.0	2.1	2.0	3.4	1.9	1.8	3.0	1.9	1.8	3.0
α, pCi/L	15.0	0.3	0.3	0.8	0.5	0.5	1.1	0.2	0.2	0.5
Uranium, µg/L	30	1.7E-10	1.59E-10	3.36E-10	3.6E-10	3.37E-10	7.13E-10	1.78E-10	1.67E-10	3.52E-10
Radium, pCi/L	5.00	0.16	0.08	0.59	0.14	0.08	0.48	0.09	0.07	0.24
		Slit 7			**Slit 8**					
Performance measure	**limit**	**mean**	**median**	**95%**	**mean**	**median**	**95%**			
All pathways, mr/yr	25.0	11.4	10.6	22.8	0.3	0.2	0.5			
βγ, mrem/yr	4.0	1.7	1.6	2.7	2.0	1.9	3.1			
α, pCi/L	15.0	1.8	1.7	3.7	0.1	0.1	0.2			
Uranium, µg/L	30	1.31E-09	1.22E-09	2.59E-09	3.85E-11	3.61E-11	7.6E-11			
Radium, pCi/L	5.00	0.17	0.08	0.64	0.04	0.02	0.16			

1.6.6.10 Engineered Trench Uncertainty

Figure 1-28 and Figure 1-29 show the uncertainty analysis of the two Engineered Trenches. The trenches were modeled in the same way as the Slit Trenches. The only differences were the inventories used (see Table 1-22) and the flow rate through the vadose zone. That flow rate was calibrated to the PORFLOW Engineered Trench model similar to the Slit Trenches.

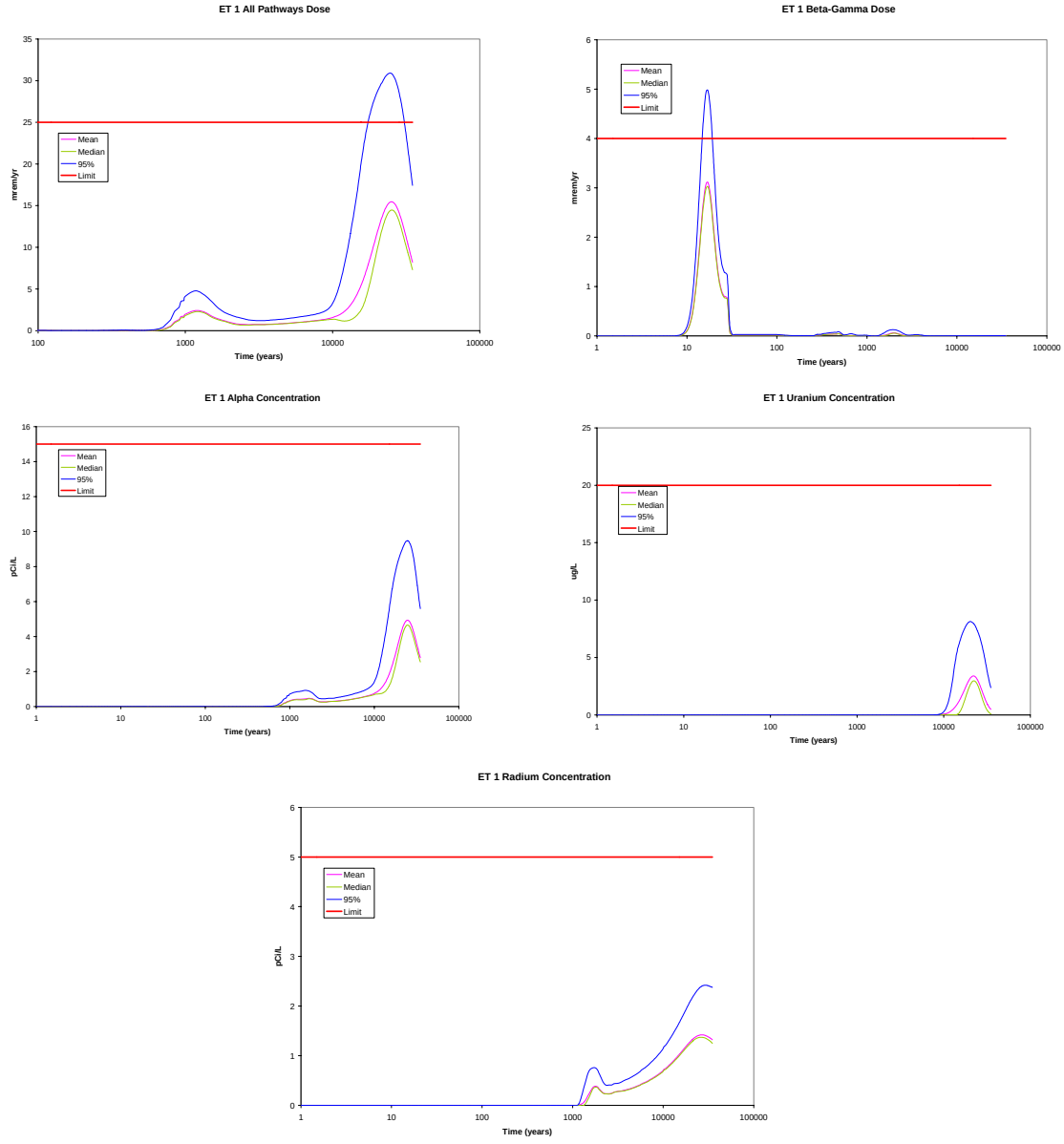

Figure 1-28. Engineered Trench 1 Uncertainty Analysis

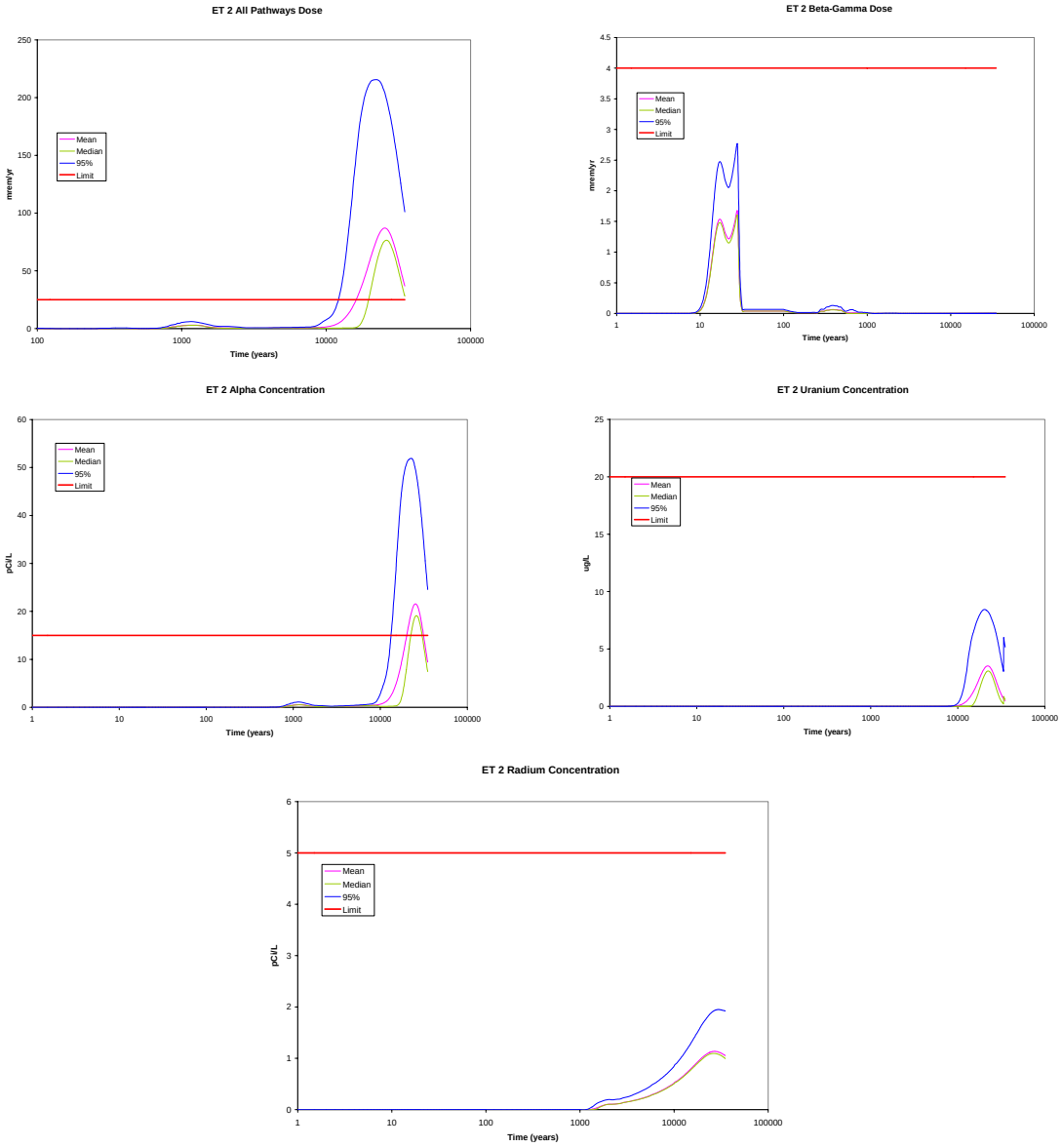

Figure 1-29. Engineered Trench 2 Uncertainty Analysis

Table 1-22. Estimated Final Inventories for Engineered Trenches (Ci) (June 12, 2007 Estimate)

Parent Radionuclide	Engineered Trench 1	Engineered Trench 2
Am-241	6.84E-01	3.62E+00
Am-243	1.55E-03	6.84E-02
C-14	1.75E-01	5.00E-02
Cf-249	9.74E-06	7.69E-02
Cl-36	8.98E-05	1.00E-05
Cm-244	6.38E-01	5.80E+00
Cm-245	3.67E-04	1.43E-03
Cm-247	4.09E-11	7.59E-04
Cm-248	1.02E-14	3.55E-15
H-3	1.90E+00	1.50E+00
I-129	1.27E-04	1.10E-04
K-40	1.68E-04	5.56E-05
Mo-93	2.66E-03	1.00E-03
Nb-94	2.73E-03	2.98E-05
Ni-59	9.08E-02	2.16E-03
Np-237	7.00E-03	9.02E-03
Pd-107	1.00E-05	1.00E-05
Pu-238	2.40E+00	6.13E+00
Pu-239	1.62E+00	1.81E+01
Pu-240	4.32E-01	3.95E+00
Pu-241	9.77E+00	7.26E+01
Pu-242	6.36E-03	1.12E-01
Pu-244	5.10E-15	8.41E-18
Ra-226	5.14E-03	6.58E-05
Se-79	9.63E-03	2.84E-04
Sn-126	6.38E-05	5.11E-05
Sr-90	2.17E+01	7.79E+01
Tc-99	1.00E-02	1.10E-01
Th-230	8.46E-03	1.30E-03
Th-232	5.43E-03	1.42E-03
U-233	2.28E+00	2.16E+00
U-234	5.11E-01	4.28E-01
U-235	1.72E-02	8.97E-03
U-236	3.21E-02	2.46E-03
U-238	4.33E-01	4.51E-01
Z-r93	2.18E-05	1.15E-07

Note that the two figures show the performance indicators out to the time past their peaks. The calculation was run to 35,000 years and the time axis is shown on a logarithmic scale.

Performance criteria are not exceeded during the 1,000-year compliance period by either the mean or median. The 95th percentile exceeds the beta-gamma performance criterion for Engineered Trench 1 during the 1,000 year compliance period. This dose is driven by H-3 and Tc-99. The 95th percentile exceeds the all-pathways performance criterion for Engineered Trench 1 around 10,000 years. This dose is driven by Th-229, U-233, and Pu-239. While the gross alpha performance limit is not exceeded, this particular combination of radionuclides with high ingestion dose conversion factors leads to a high all-pathways dose.

The median all-pathways dose for Engineered Trench 2 exceeds the performance criterion at about 24,000 years. Unlike Engineered Trench 1 where the dose is attributable to a combination of radionuclides, for Engineered Trench 2 this dose is driven by the Pu-239 contribution (2 orders of magnitude greater than either U-233 or Th-229).

1.6.6.11 Summary of Engineered Trenches Uncertainty Analysis Results

Neither mean nor median exceeded the performance measures for the Engineered Trenches during the 1,000-year compliance period. The all-pathways dose was exceeded by Engineered Trench 2 at about 10,000 years. Several of the performance measures were exceeded by the 95th percentile during the compliance period. Table 1-23 shows the maximum values during the compliance period while Table 1-24 shows the maximum values during the entire 35,000 years of the simulation.

Table 1-23. Summary of Results 0 – 1,000 years

		Engineered Trench 1				Engineered Trench 2		
Performance measure	**limit**	**mean**	**median**	**95%**		**mean**	**median**	**95%**
All pathways, mrem/yr	25.0	2.4	2.3	4.8		3.1	2.9	6.1
βγ, mrem/yr	4.0	3.1	3.0	5.0		1.5	1.5	2.5
Alpha, pCi/L	15.0	0.4	0.4	0.8		0.6	0.5	1.1
Uranium, µg/L	30	2.3E-10	2.1E-10	4.9E-10		3.2E-10	3.0E-10	1.0E-09
Radium, pCi/L	5.00	0.005	1.6E-10	0.03		5.0E-4	1.6E-12	0.003

Table 1-24. Summary of Results 0 - 35,000 years

		Engineered Trench 1				Engineered Trench 2		
Performance measure	**limit**	**mean**	**median**	**95%**		**mean**	**median**	**95%**
All pathways, mrem/yr	25.0	15.0	15.0	31.0		87.0	76.0	205.0
βγ, mrem/yr	4.0	3.1	3.0	5.0		1.5	1.5	2.5
Alpha, pCi/L	15.0	4.9	4.7	9.5		22.0	19.0	50.0
Uranium, µg/L	30	3.9	3.0	8.0		3.5	3.1	8.3
Radium, pCi/L	5.00	1.40	1.40	2.40		1.10	1.10	1.90

1.6.7 Groundwater Transport Sensitivity Analysis

The groundwater transport sensitivity analysis consisted of four principal components. First a deterministic sensitivity analysis was conducted in which additional percentages of non-crushable waste was assumed to be present. Second, a sum-of-fractions (SOF) analysis was conducted for 4 highly mobile, high-impact radionuclides using the projected closure inventory for the Central Slit Trench Unit. Only the Central Slit Trench Unit was selected for this investigation because the sensitivity derived for this Unit should also represent the other Slit Trench Units and the Engineered Trenches. Third, the SOF analysis was expanded to include all 58 radionuclides and their progeny. Finally, a probabilistic sensitivity analysis was conducted for the Slit and Engineered Trenches using the probabilistic GoldSim code. These analyses are documented in Sections 1.6.7.1, 1.6.7.2, 1.6.7.3, and 1.6.7.4, respectively.

1.6.7.1 Deterministic Sensitivity Analysis

A deterministic sensitivity analysis was conducted to evaluate varying amounts of non-crushable waste that might be incorporated within the Slit and Engineered Trench waste zones. The PORFLOW model was utilized for this evaluation, as it was for the evaluation of the two base cases, 0% and 10% non-crushable waste material. The sensitivity study evaluated the additional cases where 5% and 15% non-crushable waste was assumed to exist, examining both the CDP-on and CDP-off scenarios for each PORFLOW simulation. These sensitivity simulations were conducted for only the vadose zone flux to the water table, since an evaluation of relative sensitivity could be achieved without carrying the calculations any further because the peak aquifer concentration is largely proportional to peak water table flux. The evaluation was made by comparing the peak contaminant fluxes exiting the vadose zone for each radionuclide under each of the non-crushable waste scenarios.

Results were generated for each parent radionuclide and its progeny. An example of the contaminant mass flux to the water table for one particular radionuclide, Cf-249, is shown in Figure 1-30. Fluxes are presented for the full PA period of compliance.

In Figure 1-30, the curves for each radionuclide are color coded as indicated in the legend. Lines of different weights and patterns represent the cases simulated, 0%, 5%, 10% and 15% non-crushable material in the waste zone. All radionuclides exhibit identical fluxes for the first 130 years, then a divergence after the collapse of the closure cap. The divergences in fluxes under the scenarios of 0%, 5%, 10% and 15% non-crushable material in the waste zone can readily be seen for Np-237, U-233, and Th-229. The radionuclides indicate a clear progression of increasing flux as the percentage of non-crushable material in the waste zone increases.

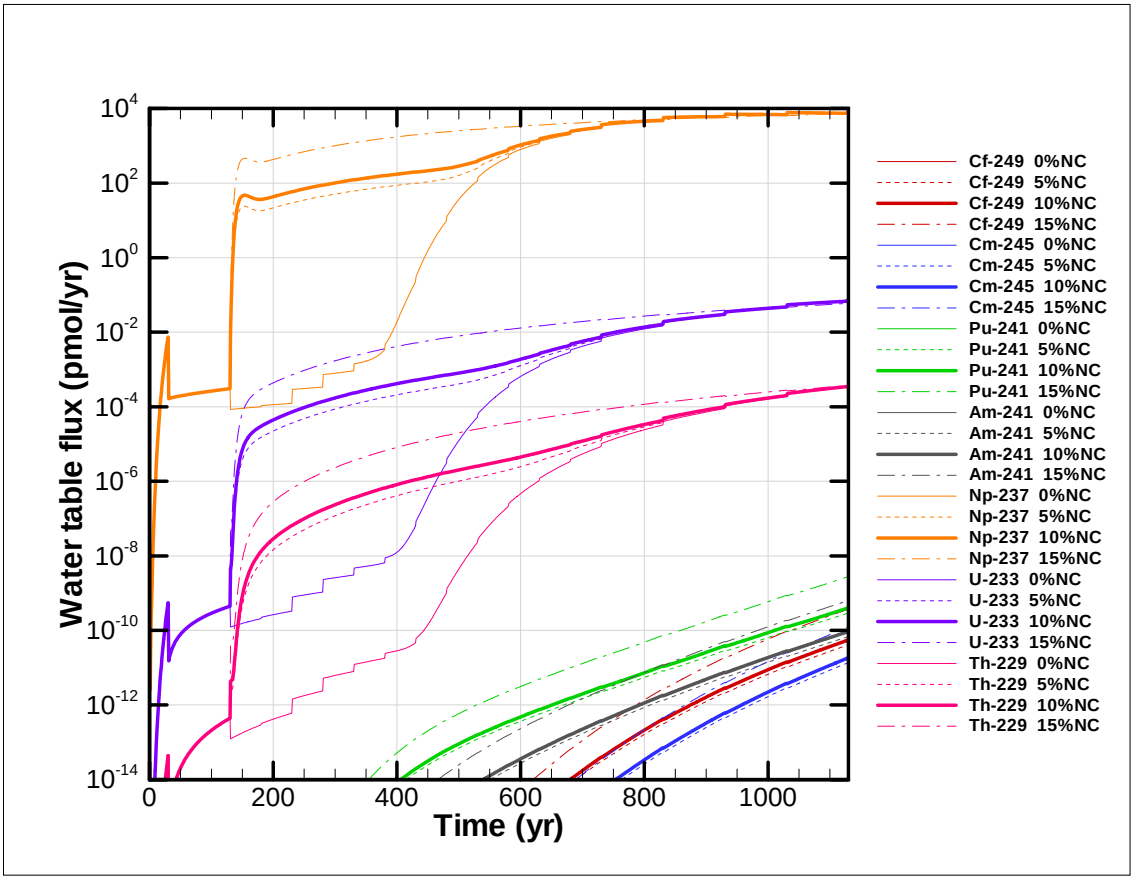

Figure 1-30. Contaminant molar flux to the water table for Cf-249 and progeny

The relative sensitivity of molar flux (picomoles/yr, or pmol/yr) exiting the vadose zone for each radionuclide under the scenarios of 0%, 5%, 10% and 15% non-crushable material is indicated in Table 1-25. To facilitate a determination of the sensitivity, the peak molar flux was selected from two different groups of cases that were analyzed. The first group included the peak fluxes for the 0% non-crushable material (a base case), 5% non-crushable material (a sensitivity case) and 10% non-crushable material (base case) with both the CDP on and CDP off case for each. The second group included the same cases as the first group with the addition of the two 15% non-crushable material scenarios, i.e., with both CDP on and CDP off. Peak values selected from the first group are presented in columns 2 and 6 in Table 1-25, while peaks selected from the second group are presented in columns 3 and 7 in Table 1-25. This method of selecting peak values allowed a determination of how much higher the peak values of contaminant flux under the 15% non-crushable case were, with and without the presence of CDPs.

Table 1-25. Sensitivity of molar flux from vadose zone to % non-crushable waste

Parent	Peak of 0, 5, 10% with CDP off & on, pmol/yr	Peak of 0, 5, 10, 15% with CDP off & on, pmol/yr	ratio	Parent	Peak of 0, 5, 10% with CDP off & on, pmol/yr	Peak of 0, 5, 10, 15% with CDP off & on, pmol/yr	ratio
Am-241	2.69E+07	3.77E+07	1.40	Th-230	2.18E-02	2.29E-02	1.05
Am-243	1.21E+08	1.75E+08	1.45	Th-232	2.20E-02	2.32E-02	1.05
C-14	1.91E+11	1.91E+11	1.00	U-233	2.69E+04	3.12E+04	1.16
Cf-249	1.91E+07	2.68E+07	1.40	U-234	1.55E+04	1.77E+04	1.14
Cf-251	6.00E+07	8.69E+07	1.45	U-235	1.55E+04	1.77E+04	1.14
Cl-36	1.91E+11	1.91E+11	1.00	U-236	1.55E+04	1.77E+04	1.14
Cm-244	1.52E-02	1.71E-02	1.12	U-238	1.55E+04	1.77E+04	1.14
Cm-245	1.22E+08	1.77E+08	1.45	Zr-93	1.00E+08	1.42E+08	1.42
Cm-246	1.14E+08	1.66E+08	1.45	H-3_ETF.Carbon	1.21E+07	1.78E+07	1.47
Cm-247	1.33E+08	1.93E+08	1.45	I-129_ETF.Carbon	9.46E+07	1.07E+08	1.13
Cm-248	1.33E+08	1.92E+08	1.45	I-129_ETF.GT.73	7.09E+07	8.06E+07	1.14
H-3	1.25E+11	1.25E+11	1.00	I-129_F.Carbon	5.39E+06	6.14E+06	1.14
I-129	1.52E+11	1.52E+11	1.00	I-129_F.CG.8	5.47E+09	7.53E+09	1.38
K-40	3.94E+10	3.94E+10	1.00	I-129_F.Dowex.21K	1.02E+08	1.16E+08	1.13
Mo-93	1.91E+11	1.91E+11	1.00	I-129_F.Filtercake	4.83E+09	6.95E+09	1.44
Nb-94	1.91E+11	1.91E+11	1.00	I-129_H.Carbon	1.23E+07	1.40E+07	1.14
Ni-59	2.74E+09	2.74E+09	1.00	I-129_H.Carbon	1.16E+09	1.31E+09	1.13
Np-237	3.47E+09	5.09E+09	1.47	I-129_H.CG.8	4.57E+07	5.21E+07	1.14
Pd-107	2.77E+09	2.77E+09	1.00	I-129_H.Dowex.21K	7.47E+08	7.73E+08	1.04
Pu-238	1.61E+01	1.93E+01	1.20	U-234_MGlass	2.10E+01	2.45E+01	1.17
Pu-239	1.22E+05	1.46E+05	1.20	U-235_MGlass	2.11E+01	2.46E+01	1.17
Pu-240	1.12E+05	1.34E+05	1.20	U-236_MGlass	2.11E+01	2.46E+01	1.17
Pu-241	5.31E-11	5.40E-11	1.02	U-238_MGlass	2.11E+01	2.46E+01	1.17
Pu-242	1.26E+05	1.51E+05	1.20	C-14_NR.Pump	1.93E+10	2.86E+10	1.48
Pu-244	1.26E+05	1.51E+05	1.20	Sr-90_Mk50A	2.74E+04	3.89E+04	1.42
Ra-226	2.53E+09	2.53E+09	1.00	Tc-99_Mk50A	4.47E+07	4.47E+07	1.00
Se-79	3.13E-02	3.30E-02	1.05	I-129_Mk50A	4.14E+07	4.14E+07	1.00
Sn-126	4.92E-14	4.92E-14	1.00	U-235_Paducah	1.92E+00	2.24E+00	1.17
Sr-90	1.55E+07	2.20E+07	1.42	Sr-90_Cask	1.32E+07	1.88E+07	1.42
Tc-99	1.58E+11	1.58E+11	1.00				

The ratio of the two peak values for each radionuclide is indicated in the fourth and eighth columns of Table 1-25, and range from 1 to 1.48. This ratio can be thought of as an indicator of the sensitivity of the increase in peak value that would occur if an increase of the percentage of non-crushable material to 15% were permitted. A ratio of 1.0 indicates that the overall peak value for a given radionuclide did not originate with either of the two 15% non-crushable material scenarios. These correspond to the most mobile radionuclides which realize their peaks fluxes prior to installation of the final closure cap. Conversely, those contaminants whose ratios exceed 1.0 reach peak values after final in-trench waste compaction and cover installation. For some contaminants, notably iodine-129, variable ratios above 1.0 for different special wasteforms indicate their influence on release and migration processes.

The results underlying Table 1-25 also show that, in every case, the peak fluxes of parents and associated progeny for 5% non-crushable content are bounded by the 0 and 10% results. That is, inventory limits based on 0 and 10% results are also protective with respect to the 5% results. The 15% results illustrate the importance of controlling the non-crushable content to 10% or less through administrative controls.

Table 1-25 was generated from Slit Trench simulations. Similar relative sensitivities are expected for Engineered Trenches, because the two trench models share nearly all key dimensions and properties. The primary difference is trench width. Slit Trenches exhibit slightly higher average Darcy flow because the narrow (20 ft wide), higher conductivity, trench cross-section draws in surrounding soil moisture. Conversely, average flow through the much wider Engineered Trenches is essentially the surface infiltration rate.

1.6.7.2 Sum-of-Fractions sensitivity analysis for high-impact radionuclides in the Central Slit Trenches

Two factors were included in the development of Slit and Engineered Trench models. These factors were the presence or absence of non-crushable containers and the presence or absence of cellulose degradation products (CDPs). The term “non-crushable” refers to waste containers that have not collapsed by the time the final cover system is placed on E Area. These containers are expected to withstand corrosion during the operational and institutional control periods and subsidence treatment (e.g., dynamic compaction) prior to final cover installation, but then collapse at some later time, leading to post closure waste subsidence. Waste and cap layer subsidence would lead to an increase in rainwater infiltration which changes the speed at which radionuclides are released from the waste and carried to the aquifer.

The second factor included in the development of the Engineered and Slit Trench models was the presence or absence of cellulose (e.g., wood, cardboard, paper) and associated degradation products. CDPs have been shown to significantly affect the distribution coefficients (K_ds) of a number of radionuclides (Kaplan, 2006). These K_ds are one of the prime factors affecting the transport velocity of the nuclides. When cellulose is assumed to be co-disposed with waste, the original distribution coefficient is modified by a CDP multiplier (Kaplan 2006).

To cover a range of possible waste disposal patterns, models were developed for each of four generic disposal cases (i.e., 0% non-crushable containers with no CDPs, 0% non-crushable containers with CDPs, 10% non-crushable containers with no CDPs and 10% non-crushable containers with CDPs) for each of the fours sets of trenches (i.e., Engineered Trenches, Center Slit Trenches, East Slit Trenches and West Slit Trenches). Groundwater and all-pathways limits were produced using the all-pathways application for each of the four cases for each of the four trench disposal unit types. The minimum limit (i.e., the most restrictive) produced by each of the four cases became the base limit for the nuclide. This selection allows for operational flexibility within the bounds of all four cases.

For the purposes of this discussion, four highly mobile, high-impact radionuclides were selected, C-14, H-3, I-129 and Tc-99, and the fraction of the limit was calculated for all four cases for each and its special wasteforms using the predicted closure inventory for Center Slit Trench units (see Appendix C), for example. A sum-of-fractions (SOF - sum of the fractions of limits for all the radionuclides considered) was generated for each case for each applicable ground water protection (only the beta-gamma limit was applicable for the chosen isotopes) and all-pathways limit. These SOFs are presented in Table 1-26 along with the base case SOFs for the Center Slit Trench units. As should be the case, the SOF for each individual case is equal to or less than the SOF for the base case.

With the exception of the all-pathways fractions in the 130-200-year time frame, the two factors, CDP and crushable versus non-crushable waste, make relatively little difference (i.e., less than a factor of 2) in the total SOFs for these highly mobile radionuclides. For the all-pathways between 130-200 years, the CDP seemed to make little difference for the same fraction of non-crushable containers, but the addition of non-crushable waste for the same CDP condition (off versus on) changed the SOFs by a factor of about 5. Therefore, it can be concluded that for these radionuclides the SOFs are not very sensitive to the CDPs or the amount of non-crushable material in most cases.

Table 1-26. SOFs for High Impact Radionuclides for the Four Groundwater Analysis Cases for the Center Slit Trench Units

	Sums of Fractions for all 4 high-impact radionuclides					
	All-Pathways			Groundwater Protection Beta-Gamma		
Case	**130-200 yrs**	**200-1000 yrs**	**1000-1300 yrs**	**0-12 yrs**	**12-100 yrs**	**100-1130 yrs**
No Non-crushable - CDP off	6.72E-03	3.92E-02	8.43E-03	5.72E-01	7.86E-01	1.12E-01
No Non-crushable - CDP on	7.54E-03	4.08E-02	9.97E-03	7.93E-01	8.98E-01	1.66E-01
10% Non-crushable - CDP off	3.48E-02	3.64E-02	8.66E-03	5.72E-01	7.86E-01	1.32E-01
10% Non-crushable - CDP on	3.63E-02	3.82E-02	1.05E-02	7.93E-01	8.98E-01	2.09E-01
Base Case (Worst Limit)	3.63E-02	4.14E-02	1.05E-02	8.13E-01	9.19E-01	2.14E-01
Max/Base	100%	98.6%	100%	97.5%	97.7%	97.7%

1.6.7.3 Sum-of-Fractions sensitivity analysis for all radionuclides in the Central Slit Trenches

Eight separate sensitivity analysis cases for different assumptions on the fraction of non-crushable containers and the distribution coefficients were created for the Center Slit Trench limits. Table 1-27 is a summary of those cases with a distinction between the cases that were included in the PA for developing the limits and the cases that were added for the purposes of the sensitivity analysis. The no non-crushable and the 10% non-crushable cases with and without K_d adjustments for the presence of cellulose degradation products (CDP) were used in the derivation of the limits for the Center Slit Trenches. The 5% and 15% non-crushable cases with and without K_d adjustments for the presence of CDP were derived later to consider the sensitivity of results to different amounts of non-crushable material added to the Slit Trenches.

Table 1-27. Center Slit Trench Cases Considered

Fraction Non-Crushable	K_ds Adjusted for Cellulose Degradation Products	
	No	Yes
0%	Basis for Limits in PA	Basis for Limits in PA
5%	Additional Case	Additional Case
10%	Basis for Limits in PA	Basis for Limits in PA
15%	Additional Case	Additional Case

Concentrations of the isotopes of interest for the eight cases were generated at the hypothesized 100-m well using the PORFLOW code. The files containing the isotope concentrations with respect to time at the 100-m well were then used, along with an EXCEL file containing the anticipated closure inventories of the isotopes of interest, to run the all-pathways application in the Maximum Dose mode. Multiplication of the total dose from all-pathways by the plume interaction factor gives the total impacts for each time frame run. From each of these impacts, an SOF was calculated by dividing the total impact by the performance measure limit. This represents the maximum SOF for each time frame for the all-pathways, groundwater beta-gamma, groundwater alpha, groundwater radium and groundwater uranium performance measures for all 58 radionuclides and their progeny (including the designated special wasteforms). Since the SOFs for the groundwater alpha, groundwater radium and groundwater uranium performance measures were generally not significant, only the SOFs for the all-pathways and groundwater beta-gamma performance measures are considered further.

The SOFs for the All-Pathways and groundwater beta-gamma performance measures for each of the eight cases and three timeframes are given in Table 1-28. None of the SOFs calculated exceeds one. The SOFs were also compared against Table 1-26. Table 1-26 contains the SOFs for All-Pathways and beta-gamma performance measures for the four initial cases using only H-3, C-14, Tc-99 and I-129, instead of the entire suite of radionuclides that did not screen out. As expected, the SOFs from Table 1-26 are less than the SOFs given in Table 1-28. For the All-Pathways performance measure, the difference in SOFs is significant. For the groundwater beta-gamma performance measure, it is generally relatively small. This is to be expected, since the radionuclides used in Table 1-26 comprise a significant portion of the dose from beta-gamma emitting isotopes analyzed in the PA.

Table 1-28. Center Slit Trenches Worst Case Sum of Fractions - Plume Interaction Included

Case	All-Pathways - Limit 25 mrem/yr			Beta-Gamma - Limit 4 mrem/yr		
	130-200 yrs	200-1000 yrs	1000-1300 yrs	0-12 yrs	12-100 yrs	100-1130 yrs
15% Non-crushable - CDP off	4.94E-01	3.89E-01	1.35E-01	5.80E-01	7.95E-01	4.19E-01
15% Non-crushable - CDP on	3.54E-01	3.65E-01	2.48E-01	8.00E-01	9.05E-01	2.83E-01
10% Non-crushable - CDP off	3.37E-01	4.04E-01	1.39E-01	5.80E-01	7.95E-01	3.13E-01
10% Non-crushable - CDP on	2.42E-01	3.46E-01	2.47E-01	8.00E-01	9.05E-01	2.31E-01
5% Non-crushable - CDP off	1.75E-01	4.18E-01	1.43E-01	5.80E-01	7.95E-01	2.21E-01
5% Non-crushable - CDP on	1.27E-01	3.54E-01	2.43E-01	8.00E-01	9.05E-01	1.96E-01
0% Non-crushable - CDP off	1.48E-02	4.32E-01	1.47E-01	5.80E-01	7.95E-01	1.27E-01
0% Non-crushable - CDP on	1.01E-02	3.59E-01	2.37E-01	8.00E-01	9.05E-01	1.76E-01

Individual isotopic contributions were compared for four cases to gain some insight into the SOFs. The following two cases were considered for the groundwater beta-gamma performance measure: the 0% non-crushable case with CDP included for 12 – 100 year time frame and the 10% non-crushable case with CDP not included for the 100 – 1130 time frame. The 0% non-crushable case gave results similar to most of the beta-gamma cases. Only the four nuclides named above contributed significantly (>5%) to the total dose. However, for one beta-gamma case (10% non-crushable with CDP not included), Sr-90 was also a significant contributor (~70% of the dose).

Looking at Table 1-28, one can see that the beta-gamma SOFs do not change at all with the addition of non-crushable material in the first two time periods. This is to be expected since the effect of non-crushable material only becomes apparent after the dynamic compaction step at the end of institutional control. Since the worst beta-gamma offenders (H-3, C-13, Tc-99 and I-129) are highly mobile in the SRS environment, the SOFs for beta-gamma increase rapidly, and the peak occurs relatively quickly in the 12 – 100 year period. The absence or presence of CDP makes relatively little difference. The presence increases the SOF during the first two time periods, but can change the SOFs in either direction in the third time period, probably due largely to the transition in SOF domination to a different set of less soluble mobile radionuclides.

For the All-Pathways performance measure patterns of change in relative levels of groundwater contamination indicated by SOF value changes (Table 1-28) involve more radionuclides and are more complex. These changes occur because the suite of radionuclides dominating groundwater contamination changes over time. Such changes are attributed to variations in travel time induced by differing levels of inherent radionuclide-specific chemical reactivity and, in these cases, additional influences from non-crushability and CDP assumptions. Comparison of two cases demonstrates this point, one being the 0% non-crushable case with CDP not considered for the 130 – 200-year time frame and the other being the 10% non-crushable with CDP considered for the 1000 – 1130-year time frame.

For the 0% non-crushable case C-14 was a significant contributor at 6%, and Tc-99 contributed about 40% to the total dose, but the other significant contributor was Np-237 at about 50%. For the 10% non-crushable case, Am-241 (5%), Np-237 (62%) and U-235 (25%) were the significant contributors. Clearly, the relatively strong influence of mobile radionuclides on groundwater contamination in the early time frame diminishes to inconsequential levels and yields to the dominant influence of less mobile radionuclides on groundwater contamination. Note that the suite of radionuclides contaminating groundwater are generally most effective (maximum SOF values) in the 200-1000 year time frame for a given case condition. The relatively greater groundwater contamination impact in this time period is enhanced as decreasing non-crushable container fractions are assumed.

Again looking at Table 1-28, the effect of non-crushable materials is present for all the time periods for the All-Pathways limits. This is because the All-Pathways limits only become pertinent after dynamic compaction and the end of institutional control. Even so, the effect of non-crushable materials is relatively small except for going from 0% non-crushable to 5% non-crushable during the first time period (130 – 200 yrs). At greater non-crushable fractions in this first time period, SOF values continue to increase but to a lesser extent. This relationship between SOF values and fraction of non-crushable containers does not occur in the later time periods and generally reverses in the 1000-1130-year time period. As with the beta-gamma limits, the absence or presence of CDP seems to make only a small difference with respect to the All-Pathways limits. The addition of CDP reduces the All-Pathways SOF during the 130 – 200-year and 200 – 1000-year time frames, but the change is in the other direction for the 1000- 1130-year time frame.

1.6.7.4 Probabilistic Sensitivity Analysis

The draft GoldSim model used for this sensitivity analysis has the file name "E-Area Slit Trench SA v1.0 InvAvg r5000.gsm". This is a copy of v1.0 of the model, set to perform 5000 realizations, with Latin Hypercube Sampling enabled and a seed value of 1. The model run assumed a single trench, with an inventory that is an average mix of all the 8 slit trenches. The model ran for 1130 years, the period of performance. A detailed description of the global sensitivity analysis approach appears in Appendix F.

The sensitivity analysis is limited principally by the uncertainty incorporated in the input parameters. For example, the values of soil/water distribution coefficients (K_ds) are defined stochastically, reflecting the uncertainty of the parameter. The influence of these variables on various results (called endpoints, like groundwater concentrations or future doses) can be properly assessed in the sensitivity analysis.

For some other input parameters, a stochastic distribution of values was not developed in such a robust manner, and the input distribution is more *ad hoc*, relying on professional judgment, or in some cases simply applying a rough range just to see if the parameter would even register with the sensitivity analysis. An example of this type of placeholder distribution is the saturated thickness of the aquifer. As it turns out, this was the single most influential modeling parameter in most of the E-Area analyses, among those parameters given a distribution. Much of the uncertainty in the model results can be attributed to this parameter, suggesting that more work go into a defensible assessment of its value.

Some parameters, which may or may not be influential, were provided no uncertainty. For example, the inventory, which would normally be expected to dominate uncertainty as it does at other radioactive waste sites, was populated with only deterministic values. The distributions that would reflect the state of knowledge regarding uncertainty in the inventory have yet to be developed. Given this limitation, the sensitivity analysis presented for this edition of the E-Area PA is preliminary, and is limited to those model parameters that were defined stochastically.

Results

The results of the sensitivity analysis for the Slit Trenches are discussed in detail in Appendix F, complete with graphs depicting the range over which each parameter exhibits its influence on the endpoint of interest. For the Slit Trenches, the endpoints identified for sensitivity analysis are:

- the maximum potential all-pathways dose to a member of the public (based on use of groundwater at a well 100 meters downstream of the facility) within the period of performance
- the maximum gross alpha concentration in groundwater at the well within the period of performance
- the maximum dose from beta and gamma emitters in groundwater at the well within the period of performance

For each endpoint, a global sensitivity analysis was performed in order to identify which stochastic model parameters are most significant in determining the value of that endpoint. The top four parameters are ranked by a value called the sensitivity index. The sum of all sensitivity indices for all parameters equals 100. These results are summarized in Table 1-29. Discussion is limited to those parameters showing a sensitivity index greater than 1. The R^2 factor is the Coefficient of Determination computed in GoldSim for this sensitivity determination.

Table 1-29. Identification of the Most Sensitive Parameters for the Slit Trench Endpoints of Interest

Endpoint	SI rank	input parameter	Sensitivity Index	R^2
Max. Total Dose (Early)	1	saturated thickness of aquifer	94.7	99%
	2	Tc K_d in clayey soil (and the waste)	3.69	
	3	Tc K_d in sandy soil	1.04	
	4	longitudinal dispersivity ratio	0.21*	
Max. Total Dose (Late)	1	saturated thickness of aquifer	72.9	55%
	2	final subsided waste thickness	4.23	
	3	Np K_d in clayey soil (and the waste)	1.88	
	4	Fr K_d in reducing (young) concrete	0.79*	
Max. Alpha Concentration	1	saturated thickness of aquifer	45.8	84%
	2	final subsided waste thickness	2.67	
	3	Np K_d in clayey soil (and the waste)	2.03	
	4	Ra K_d in sandy soil	0.58*	
Maximum Beta+Gamma Dose	1	saturated thickness of aquifer	98.9	99%
	2	longitudinal dispersivity ratio	0.25*	
	3	transverse/longitudinal dispersivity ratio	0.21*	
	4	particle density of sandy soil	0.21*	

*Note that SI values below 1 are probably spurious.

By far, the most significant parameter for all endpoints is the saturated thickness of the aquifer. This value defines the vertical dimension of the compartments (or Cells, as they are called in GoldSim) used to model lateral waterborne advective transport from beneath the waste zone to the exposure point, a water well located 100 meters directly downstream of the border of the modeled slit trench. Since these Cells assume instantaneous mixing throughout, the vertical dimension is effectively the depth over which the plume of contamination is mixed, effectively the volume of water that dilutes the contaminated recharge as it gets extracted by the well. The saturated thickness input distribution was set to be uniform, from 5 to 15 meters, as reflected in the green background. (This particular distribution was chosen simply in order to determine if the parameter had any significance in the model.) Since the same mass of radionuclide contaminants is introduced into the aquifer regardless of its thickness, their concentration is inversely proportional to the thickness. The potential dose through water-related pathways is also a generally linear response to concentration, since few of the dose calculation parameters are defined stochastically. Hence, the strong dependence of dose on saturated thickness is not surprising. Clearly, a refinement of the probabilistic distribution representing well hydraulics is indicated.

Another common sensitive parameter type is the K_d. Generally, the K_d of that radionuclide contributing most to the dose is identified. For the Slit Trenches, early doses are dominated by Tc, and later doses by Np. A good bit of work has already been put into the definitions of K_d for the E-Area models, and continuing investigations will serve to refine the input distributions with evermore defensible values.

The final subsided waste thickness is also influential, and has a uniform "placeholder" distribution of 2.5 to 4.0 meters. This is the estimated thickness of the waste layer after all subsidence is complete and all void space in the waste is gone, and higher doses are correlated with smaller values of final thickness. This is an example of how the later doses are influenced by parameters different from those influencing early doses: Waste subsidence does not occur until later time, and so could not possibly influence the early doses. The influence on later doses may come from the concentrating of contaminants in the waste layer from having the same mass of waste in a smaller volume. This is also an effect worthy of further investigation.

1.6.7.5 Summary of Sensitivity Analysis for the Engineered Trenches

A sensitivity analysis for the E-Area Engineered Trenches (ETs) was also performed in support of the E-Area PA Maintenance Program. Like the Slit Trenches, a GoldSim model was developed for performing the sensitivity analysis. The GoldSim model that was run for this sensitivity analysis has the file name "E-Area Engd Trench SA v1.1 et1 r2000.gsm". This is a copy of version 1.1 of the model, set to use one of the two engineered trench inventories and 2000 realizations, with Latin Hypercube Sampling enabled. The exporting of results is done the same way as for the Slit Trenches (see Section 1.6.7.4). The inventory used is the closed/projected inventory for Engineered Trench #2. See the caveats regarding the sensitivity analysis described in Section 1.6.7.4.

The following ET model endpoints were selected for sensitivity analysis. A modification in endpoints was made between the running of the Slit Trench sensitivity analysis and this analysis. Specifically, the model duration was extended to 20,000 years in order to capture the peak all-pathways dose, though the concentrations of radium, uranium, and alpha emitters, as well as the dose from beta-gamma emitters, was restricted to those maxima occurring within the period of performance. The endpoints are:

- the maximum potential all-pathways dose to a member of the public (based on use of groundwater at a well 100 meters downstream of the facility) within the period of performance (divided into early and midtime peaks)
- the maximum potential all-pathways dose to a member of the public for all (late) time
- the maximum gross alpha concentration in groundwater at the well within the period of performance
- the maximum dose from beta and gamma emitters in groundwater at the well within the period of performance
- the maximum radium concentration in groundwater at the well within the period of performance
- the maximum uranium concentration in groundwater at the well within the period of performance

The ET sensitivity analysis results are summarized in Table 1-30. Again, discussion is limited to those parameters showing a sensitivity index greater than one.

As was found for the Slit Trenches, the results of the sensitivity analysis indicate that the most significant stochastic parameter in the model for most of the above endpoints is the assumed thickness of the saturated zone, or aquifer. Other less significant sensitive parameters include soil/water partition coefficients for dose-significant (or concentration-significant) radionuclides, aquifer dispersivity ratios (also related to mixing), the rate of natural compaction and final thickness of the waste after subsidence, and parameters influencing the infiltration through the closure cap.

The poor showing of radium in well water indicates that radium is nowhere near its groundwater MCL within the period of performance. So, few concentration values were obtained, even with 2000 realizations, that no reasonable sensitivity analysis could be done.

Table 1-30. Identification of the most sensitive parameters for the Engineered Trench #2 endpoints of interest

Endpoint	SI rank	input parameter	Sensitivity Index	R^2
max. dose early (within period of performance) (mrem/yr)	1	saturated thickness of aquifer	75.9	98%
	2	Tc K_d in sandy soil	16.6	
	3	Tc K_d in clayey soil (and the waste)	7.4	
max. dose – midtime (mrem/yr)	1	saturated thickness of aquifer	75.5	82%
	2	final subsided waste thickness	7.61	
	3	Np K_d in clayey soil (and the waste)	7.36	
	4	post-compaction subsidence rate	1.17	
max. dose – late time (mrem/yr)	1	Pu K_d in sandy soil	44.3	76%
	2	saturated thickness of aquifer	12.0	
	3	Pu K_d in clayey soil (and the waste)	1.61	
max. alpha conc. at well (pCi/L)	1	saturated thickness of aquifer	29.5	84%
	2	Np K_d in clayey soil (and the waste)	7.82	
	3	final subsided waste thickness	5.67	
	4	post-compaction subsidence rate	5.14	
max. beta + gamma dose at well (mrem/yr)	1	saturated thickness of aquifer	92.2	99%
	2	Tc K_d in sandy soil	4.34	
	3	Tc K_d in clayey soil (and the waste)	2.58	
max. radium conc. at well		insufficient information		49%
max. uranium conc. at well (μg/L)	1	saturated thickness of aquifer	24.9	88%
	2	infiltration rate timing warp factor	13.1	
	3	U K_d in sandy soil	8.24	
	4	Np K_d in clayey soil (and the waste)	5.98	

1.7 SLIT AND ENGINEERED TRENCH AIR-PATHWAY ANALYSIS

1.7.1 Overview of Air-Pathway Analysis

This section describes the investigation conducted to evaluate the potential magnitude of gaseous release of radionuclides from the Slit and Engineered Trenches to the point-of-compliance over the nominal 25-year operational period[2], 100-year institutional control period, and 1000-year post-closure compliance period versus the atmospheric pathway exposure maximum dose to a representative member of the public of 10 mrem/yr.

A screening analysis was conducted to produce a list of radionuclides requiring a more thorough analysis to derive disposal limits for the Slit and Engineered Trenches based on the atmospheric pathway. This study, described in Crapse and Cook (2006) used a methodology developed by the National Council on Radiation Protection and Measurements, professional judgment and process knowledge to determine this list. The list of potential radionuclides includes C-14, Cl-36, H-3, I-129, S-35, Sb-124, Sb-125, Se-75, Se-79, Sn-113, Sn-119m, Sn-121, Sn-121m, Sn-123, and Sn-126.

This analysis considers diffusion of these gaseous radionuclides upward from the trenches through the overlying soil materials to the ground surface and subsequent atmospheric transport to the point-of-compliance. The flux of gaseous radionuclides from the trenches to the ground surface and transport to the point-of-compliance was evaluated for two separate time periods: 1) 0 to 125 years (25-year operational and 100-year institutional control periods), and 2) 125 to 1125 years (1000-year post-closure compliance period). During the first time period evaluated a minimum 4-foot operational soil cover overlies the waste. Although the presence of the interim runoff cover in the second time period would likely inhibit the upward diffusion of gaseous radionuclides, it was not explicitly incorporated into the analysis and therefore no credit has been taken for its impact.

The second time period occurs after subsidence treatment and final closure cap installation has been conducted. During the operational and institutional control period this maximum dose is applicable at the SRS boundary, due to active institutional controls. During the post-closure compliance period this maximum dose is applicable at 100 m from the disposal unit boundary, due to the assumed loss of active institutional controls. Because of the similarity of the Slit and Engineered Trenches, a single model will be used to estimate gaseous radionuclide flux at the ground surface for these disposal units.

The analysis presented here uses accepted computer programs for chemical interactions (MINTEQ), diffusion (PORFLOW), and atmospheric transport and dose calculations (CAP88).

[2] The air-pathway analysis was performed for all disposal units using a 25-year operational period. Since, for the Slit and Engineered Trenches, the maximum flux to the disposal unit surface is within the first year or so, this assumption is not inconsistent with the 30-year operational period assumed in the groundwater analysis.

1.7.2 Key Air-Pathway Assumptions

The key air-pathway analysis assumptions associated with the Slit and Engineered Trenches are presented in Appendix B.

1.7.3 Slit and Engineered Trench Closure Considerations

The concepts for closure of the Slit and Engineered Trenches disposal units are relevant to the determination of the gaseous flux at the land surface for all gaseous radionuclides. Trench construction specifics and closure concept are described by Phifer et al. (2006). For the purposes of this investigation, it is assumed that during the operational and institutional control periods (0 to 125 years) there is only a four-foot operational soil cover above a 16-foot waste zone. Therefore, during this time period, the top of the operation soil cover (as described by Phifer et al. 2006) is the point where the gaseous flux was evaluated.

For the post-closure compliance period (125 to 1125 years), subsidence treatment (i.e., static surcharge and/or dynamic compaction) and final closure cap installation will have occurred for the Slit and Engineered Trenches. As outlined in Sections 1.3.1 and 1.3.2, it is assumed that this subsidence treatment essentially eliminates future subsidence potential except in those areas designated not to undergo dynamic compaction or containing non-crushable containers with significant void space. However, areas designated not to undergo dynamic compaction or containing non-crushable containers with significant void space may result in limited subsidence damage to the final closure cap, some time during the 1000-year post-closure compliance period during which no closure cap maintenance is assumed be performed. These areas represent the worse case basis for the gaseous radionuclide flux from the Slit and Engineered Trenches during the 1000-year post-closure compliance period.

For purposes of this investigation, modeling of the 1000-year post-closure compliance period will be based upon a trench cross-section containing non-crushable containers overlain by the operational soil cover and final closure cap as shown in Figure 1-3. It will be assumed that the waste zone containing non-crushable containers collapses from a 16-foot thickness to 2.5 feet (Phifer et al. 2006) at the beginning of the 1000-year post-closure compliance period, when no closure cap maintenance is assumed to be performed. This results in subsidence of the closure cap and destruction of the individual layers of the closure cap. It will further be assumed that all closure cap materials above the erosion barrier are gone prior to waste collapse and closure cap subsidence. These assumptions result in 10.33 ft of clean material (i.e., operational soil cover and final closure cap through the erosion barrier) above the 2.5-foot waste zone for gaseous radionuclides to diffuse through to the point which the flux was evaluated. See Figure 1-3 for a cross-section of the operational soil cover and final closure cap (the 48-inch clean layer in the figure represents the operational soil cover). Materials are indicated with the associated thickness of each component in feet (Table 1-31).

Table 1-31. Vertical Layer Sequence and Thickness for Slit and Engineered Trench Profiles during the Pre- and Post-Closure Compliance Period

Layer	Vertical Thicknesses 125-Year Operations Period (ft)	Vertical Thicknesses 1000-Year Post-Operations Period (ft)
Final Closure Cap (through the Erosion Barrier)	---	6.33
Operational Soil Cover	4	4
Waste Layer	16	2.5

SOURCE: Adapted from Phifer et al. (2006)

1.7.4 Slit and Engineered Trench Air-Pathway Conceptual Model

The flux of the radioactive gasses at the land surface above the Slit and Engineered Trenches was evaluated for its specific closure configuration. Gaseous radionuclides introduced within the waste zone diffuse outward from this zone into the air-filled soil pores surrounding the trenches, eventually resulting in some of the radionuclides emanating at the land surface. As such, air is the medium through which they diffuse. It is assumed that fluctuations in atmospheric pressure at the land surface that could induce small pulses of air movement into and out of the shallow soil profile over relatively short periods of time will have a zero net effect when averaged over longer time periods. Thus, advective transport of these radionuclides in air-filled soil pores is not considered to be a significant process when compared to the rate of air diffusion.

The radionuclides present as gases are those identified in the screening process described in Crapse and Cook (2006). Certain gaseous radionuclides will not likely remain in the monatomic elemental form but combine with other gaseous elements or form diatomic molecules. The state of existence of each of these radionuclides in the gaseous phase is important in evaluating their transport to the land surface because the diffusion coefficient associated with each is related to its molecular weight.

In this investigation it is assumed that:

- C-14 exists as part of the CO_2 molecule
- Cl-36, H-3 and I-129 exist as diatomic gasses
- S-35, Sb-124, Sb-125, Se-75, Se-79, Sn-113, Sn-119m, Sn-121, Sn-121m, Sn-123, and Sn-126 exist as monatomic gasses.

1.7.5 Slit and Engineered Trench Air-Pathway Numerical Model

The mathematical model utilized in this report is provided by the PORFLOW simulation package (ACRI 2004). PC-based PORFLOW Version 5.97.0 was used to conduct a series of simulations. PORFLOW is developed and marketed by Analytic & Computational Research, Inc. to solve problems involving transient and steady-state fluid flow, heat and mass transport in multi-phase, variably saturated, porous or fractured media with dynamic phase change. PORFLOW has been widely used at the SRS and in the DOE complex to address major issues related to the groundwater and nuclear waste management.

The governing equation for mass transport of species *k* in the fluid phase is given by

$$\frac{\partial C_k}{\partial t} + \frac{\partial}{\partial x_i}(V_i C_k) = \frac{\partial}{\partial x_i}(D_{ij}\frac{\partial C_k}{\partial x_j}) + \gamma_k \qquad \text{Eq 1-1}$$

Where

C_k	concentration of species *k*, Ci/m^3
V_i	fluid velocity in the ith direction, m/yr
D_{ij}	effective diffusion coefficient for the species, m^2/yr
γ_k	net decay of species *k*, Ci/m^3 yr
i, j	direction index
t	time, yr
x	distance coordinate, m

(Boundary and initial conditions are discussed in Section 1.6.5.1)

This equation is solved within PORFLOW to evaluate transient radionuclide transport above the Slit and Engineered Trenches and to determine gaseous radionuclide flux at the land surface over time. Since source radionuclides exist as gases, air was taken to be the medium within which transport occurs. The flow field was assumed to be isobaric and isothermal. The impact of naturally occurring fluctuations in atmospheric pressure at the land surface that could induce small pulses of air movement into and out of the shallow soil profile over relatively short periods of time will have a zero net effect when averaged over longer time periods. Therefore, for the relatively long periods of time evaluated in this investigation, air diffusion was the only transport mechanism simulated in the model and advective air-transport was assumed to be negligible, so the advection term was disabled within PORFLOW and only the diffusive and net decay terms were evaluated.

1.7.5.1 Slit and Engineered Trench Air-Pathway Model Development and Assumptions

The numerical representation of the conceptual model is as a 1-dimensional vertical stack of elements configured to represent the thickness of the Slit and Engineered Trench waste zone and anticipated operational soil cover and final closure cap, appropriate to the time frame under consideration.

Since source radionuclides exist as gasses, air was taken to be the medium within which transport occurs. The flow field was assumed to be isobaric and isothermal. The impact of naturally occurring fluctuations in atmospheric pressure at the land surface that could induce small pulses of air movement into and out of the shallow soil profile over relatively short periods of time will have a zero net effect when averaged over longer time periods. Therefore, for the relatively long periods of time evaluated in this investigation, air-diffusion was the only transport mechanism simulated in the model and advective air-transport was assumed to be negligible.

A small percentage of the radionuclides dissolve in residual pore water, but since diffusion proceeds more slowly in water than in air, air-diffusion is regarded as the only transport process by which they can reach the land surface from the Slit and Engineered Trenches waste zone. This assertion is substantiated in Nielson et al. (1984). The radon effective diffusion coefficient, D_{eff}, for soil is reported to range from the open-air diffusion coefficient of 1.0E-05 m^2/sec to that of fully saturated soil, 1.0E-09 m^2/sec (Nielson et al. 1984).

This 4-order of magnitude difference is consistent with the comparison of water diffusion coefficients to air diffusion coefficients of other common molecular compounds and reported in many references, for example Bolz and Tuve (1973). Thus, the larger volume of water-filled pore space compared to air-filled pore space (maximum of 2 orders of magnitude difference) is inconsequential. The ability of water-dissolved compounds to diffuse through water-filled pores is negligible compared to the ability of the same compounds to diffuse as gas in the vapor-filled pore spaces. Furthermore, there is vertical downward movement of the pore water which acts to offset or overcome any vertical upward diffusion of dissolved constituents. Consequently, in this investigation, radionuclide transport was allowed to proceed only through air-filled pore space and, therefore, residual pore water was treated as if it was part of the solid matrix material within the flow field. No accounting was made of the partitioning of the gaseous radionuclides into the pore water as diffusive vapor transport proceeded from the waste zone to the land surface. By ignoring this mechanism, diffusive fluxes at the land surface were slightly overestimated.

The boundary conditions imposed on the model domain included:

- No-flux specified for all radionuclides along sides and bottom
  ($\partial C/\partial X = 0$ at x_{min}, x_{max} and $\partial C/\partial Y = 0$ at y_{min})
- Species concentration set to 0 at land surface (top of erosion barrier)
  ($C = 0$ at y_{max})

where $x_{min} = 0$, $x_{max}= 1$m, $y_{min}= 0$m and $y_{max}= 6.1$m

The initial condition imposed on the domain included:

- Species concentration set to 0 for the entire model domain at time = 0
  ($C=0$ for $0 \leq x \leq 1$ at $t=0$ and $C=0$ for $0 \leq y \leq y_{max}$ at $t=0$)

The initial conditions for the model also assumed a 1 Ci inventory of each radionuclide uniformly spread over the waste zone.

These boundary conditions force all of the gaseous radionuclides to move upward from the waste disposal zone to the land surface. In reality, some lateral and downward diffusion occurs in the air-filled pores surrounding the waste zone; hence ignoring this lateral and downward movement has the effect of increasing the flux at the land surface, thus introducing a significant measure of conservatism in the calculated results. Simulations were conducted in transient mode for diffusive transport in air, with results being obtained over 1,125 years.

A summary of the radionuclides and compounds of interest in this investigation are summarized in Table 1-32.

Table 1-32. Radionuclides and Compounds of Interest

Radionuclide	Half-life (yrs)	Atomic Wt.	Molecular form in gaseous state	Molecular Wt.
C-14	5.730E+03	14	CO_2	46
Cl-36	3.010E+05	36	Cl_2	72
H-3	12.333	3	H_2	6
I-129	1.570E+07	129	I_2	258
S-35	2.394E-01	35	S	35
Sb-124	1.649E-01	124	Sb	124
Sb-125	2.759	125	Sb	125
Se-75	3.270E-01	75	Se	75
Se-79	2.950E+05	79	Se	79
Sn-113	3.153E-01	113	Sn	113
Sn-119m	8.020E-01	119	Sn	119
Sn-121	3.089E-03	121	Sn	121
Sn-121m	44.1	121	Sn	121
Sn-123	3.550E-01	123	Sn	123
Sn-126	2.300E+05	126	Sn	126

1.7.5.2 Measures Implemented to Ensure Conservative Results

In this analysis, several conditions introduce a significant measure of conservatism into the calculations. These include:

- The use of boundary conditions that force all of the gaseous radionuclides to move upward from the waste disposal zone to the land surface. In reality, some of the gaseous radionuclides diffuse sideways and downward in the air-filled pores surrounding the waste zone; hence ignoring this has the effect of increasing the gaseous radionuclide flux at the land surface.
- Not taking credit for the removal of the gaseous radionuclides by pore water moving vertically downward through the model domain. This mechanism would likely remove some dissolved gaseous radionuclides, and therefore its omission has the effect of increasing the estimate of instantaneous gaseous radionuclide flux at the land surface.
- Use of the top of the erosion layer in the soil cover as the land surface for the purpose of calculating gaseous radionuclide flux during the 125 to 1125 year post-closure compliance period. No credit is taken for the additional distance the gaseous radionuclides must migrate above the erosion barrier prior to that portion of the soil cover eroding away.
- During the 125 to 1125 year post-closure compliance period the modeling is based upon a trench cross-section containing a non-crushable container waste zone which has collapsed to 2.5 feet. This both concentrates the radionuclide inventory in a thinner waste zone and minimizes the amount of clean material through which the gaseous radionuclides must diffuse.
- Ignoring the presence of the GCL within the final closure cap. The GCL should be near 100 percent saturation; therefore it will contain very little air-filled porosity within which gaseous radionuclide transport could occur.
- The assignment of E-Area operational soil cover prior to dynamic compaction (Phifer et al. 2006) properties to the closure cap following collapse of the non-crushable waste (125 to 1125 years). Some of the closure cap is likely to remain intact and retain its original material properties.

1.7.5.3 Grid Construction

The model grid was constructed as a node mesh 3 nodes wide by 55 nodes high. This mesh creates the vertical stack of 53 model elements. Figure 1-31 shows a schematic of the PORFLOW model grid. The grid extends from the bottom of the waste layer upward to the top of the erosion barrier. Extending the grid only to the top of the erosion barrier results in the minimum possible cover thickness over the waste that could exist during the 125 to 1,125 year period. A set of consistent units was employed in the simulations for length, mass and time, these being meters, grams and years, respectively.

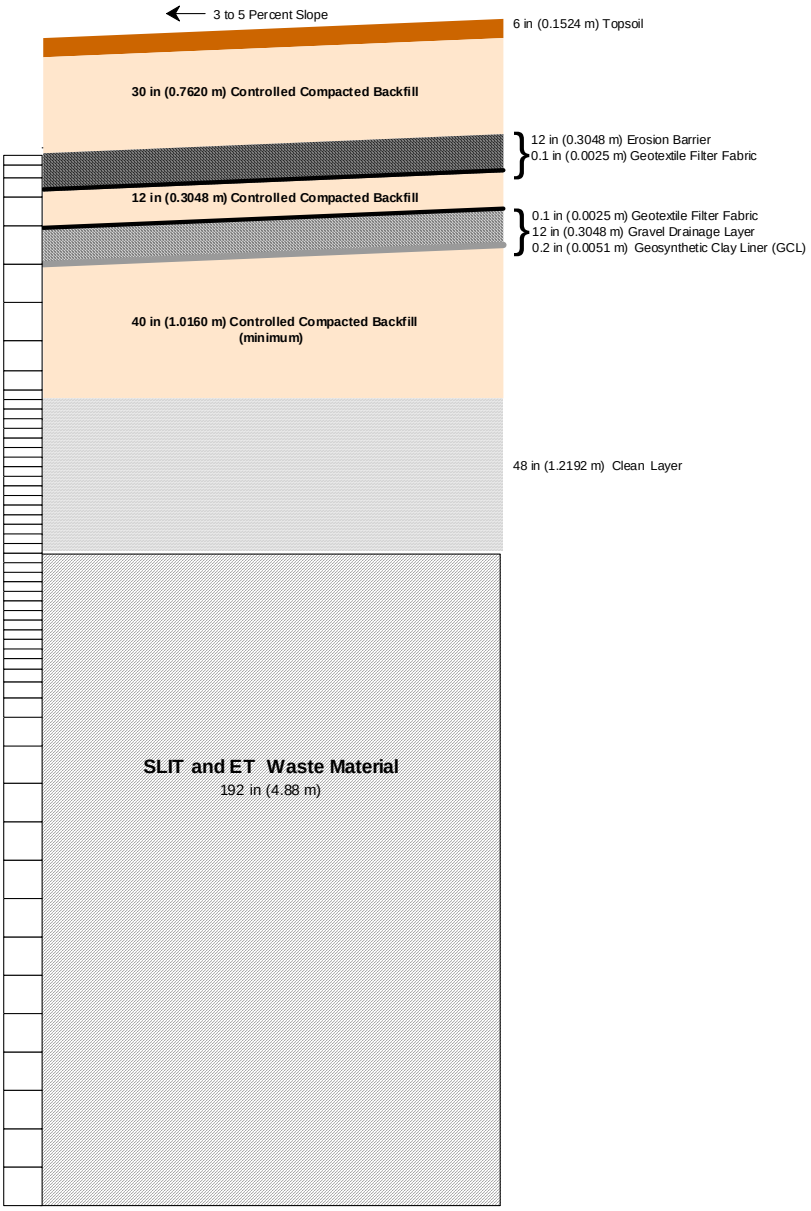

Figure 1-31. PORFLOW Model Grid for Air and Radon Pathway Analysis

1.7.5.4 Material Zones

The model domain was divided into the following four material zones: the lower waste zone (13.5 ft [4.11 m]); upper waste zone (2.5 ft); operational soil cover (4 ft); and final closure cap (6.33 ft). The model elements were scaled to correspond to the geometry of these zones. Table 1-33 and Table 1-34 list the individual components of the Slit and Engineered Trench model for the 125-year operational and institutional control period and the 1000-year post-closure compliance period, respectively.

During the operational and institutional control periods (0 to 125 years), the land surface where the gaseous radionuclide flux is determined is taken as the top of the operational soil cover. During the post-closure compliance period (125 to 1125 years), the waste zone is reduced to 2.5 ft and overlain by the operational soil cover and the final closure cap through the erosion barrier. During the post-closure compliance period, the land surface where the gaseous radionuclide flux is determined is taken as the top of the erosion barrier. The properties assigned to the various zones of the model domain during the two time periods were chosen to correspond to the above configurations.

1.7.5.5 Material Zone Properties and Other Input Parameters

Material properties utilized within the 1-D numerical model were specified for the four material zones defined within the model domain for each of the time periods. Each material zone was assigned values of particle density, total porosity, average saturation, air-filled porosity, air density, and an effective air-diffusion coefficient for each source element or compound. With the use of an effective air-diffusion coefficient, tortuosity was assigned a unit value in each material zone during both periods. An air fluid density of 1.24E+03 g/m^3 was used for each material zone during both periods. This air fluid density was obtained from the Bolz and Tuve (1973), *CRC Handbook of Tables for Applied Engineering Science* and represents that of standard atmospheric conditions.

During the 125-year operational and institutional control period the trenches consist only of the 16-foot waste layer and the 4-foot operational soil cover (see Table 1-33). Although the interim runoff cover, utilized during the first 125 years (see discussion in Section 2.3), includes the potential use of up to an additional 2-foot of soil to establish necessary grades to promote runoff, this soil was not included in the model during this time period. This soil was not included since it is only used as necessary and its thickness will be highly variable. Since the closure cap does not exist during this time period, the closure cap material zone of the model domain was assigned a total and air-filled porosity of one, which makes it have the properties of air. Since the Slit and Engineered Trench waste layers contain significant soil, the operational soil cover and both waste zones of the model domain are assigned the particle density and total porosity properties of the E-Area operational soil cover prior to dynamic compaction as specified by Phifer et al. (2006). The E-Area operational soil cover prior to dynamic compaction soil represents relatively loose soil with a significant air-filled porosity through which gaseous radionuclide diffusion can occur. E-Area vadose zone field pore pressure measurements indicate average suction levels in the approximate range of 50 to 200 cm (Nichols et al. 2000). A value of 200 cm represents the upper end of the range which will have a greater air-filled porosity. The average saturation for the operational soil cover and both waste zones were taken as the value of saturation at a suction head of approximately 200 cm from the characteristic curves for the E-Area operational soil cover prior to dynamic compaction (Phifer et al. 2006) in order to be consistent with field measurements. The air-filled porosity was calculated from the average saturation and total porosity as shown in Table 1-33**.** The particle density, total porosity, average saturation, air-filled porosity values utilized for each model domain material zone during the 125-year operational and institutional control period are summarized in Table 1-33**.**

Table 1-33. Material Properties utilized for the 0 to 125 Year Operational and Institutional Control Period.

Layer	Layer Thickness (ft)	Particle Density (g/cm^3)	Total Porosity (fraction)	Average Saturation (fraction)	Air-filled Porosity [4] (fraction)
Final Closure Cap [1]	6.33	na	1	0	1
Operational Soil Cover	4	2.65 [2]	0.46 [2]	0.825 [3]	0.081
Upper Waste Zone	2.5	2.65 [2]	0.46 [2]	0.825 [3]	0.081
Lower Waste Zone	13.5	2.65 [2]	0.46 [2]	0.825 [3]	0.081

na = not applicable

[1] During the first 125 years of the simulation, the closure cap is assigned a total porosity of 1, and an average saturation of 0

[2] E-Area operational soil cover prior to dynamic compaction property values assigned from Phifer et al. (2006)

[3] Average saturation taken from the E-Area operational soil cover prior to dynamic compaction characteristic curve from Phifer et al. (2006) at a suction head (matrix potential) of 195 cm

[4] Air-filled Porosity = (1 – Average Saturation) × Total Porosity

At the beginning of the 1000-year post-closure compliance period, it is assumed that the waste zone containing non-crushable containers collapses from a 16 foot thickness to 2.5 feet (Phifer et al. 2006), when no closure cap maintenance is assumed to be performed. This results in subsidence of the closure cap and destruction of the individual layers of the closure cap. This reduction in waste layer thickness is handled utilizing the same model grid used for the prior time period (i.e., 0 to 125 years) by reassigning the radionuclide inventory of the lower 13.5 feet of the waste zone to the upper 2.5 feet of the waste zone and assigning a porosity of 0 to the lower 13.5 feet of the waste zone. While this is not necessarily intuitive, it is appropriate, since the migration of interest is upward rather than downward and since it results in no additional material through which upward diffusion has to occur. For this time period, the particle density and total porosity values for all layers, other than the lower waste zone, were assigned those of the E-Area operational soil cover prior to dynamic compaction (Phifer et al. 2006).

The E-Area operational soil cover prior to dynamic compaction soil represents relatively loose soil consistent with conditions resulting from subsidence that has a significant air-filled porosity through which gaseous radionuclide diffusion can occur. The average saturation for the final closure cap, operational soil cover, and upper waste zone was taken as the value of saturation at a suction head of approximately 200 cm from the characteristic curves for the E-Area operational soil cover prior to dynamic compaction (Nichols et al. 2000; Phifer et al. 2006). The air-filled porosity was calculated from the average saturation and total porosity as shown in Table 1-34. The particle density, total porosity, average saturation, air-filled porosity values utilized for each model domain material zone during the 1000-year post-closure compliance period are summarized in Table 1-34.

Table 1-34. Material Properties utilized for the 125 to 1,125 Year Post-Closure Compliance Period.

Layer	Layer Thickness (ft)	Particle Density (g/cm^3)	Total Porosity (fraction)	Average Saturation (fraction)	Air-filled Porosity [3] (fraction)
Final Closure Cap	6.33	2.65 [1]	0.46 [1]	0.825 [2]	0.081
Operational Soil Cover	4	2.65 [1]	0.46 [1]	0.825 [2]	0.081
Upper Waste Zone	2.5	2.65 [1]	0.46 [1]	0.825 [2]	0.081
Lower Waste Zone [4]	13.5	na	0	na	0

na = not applicable

[1] E-Area operational soil cover prior to dynamic compaction property values assigned from Phifer et al. (2006)

[2] Average saturation taken from the E-Area operational soil cover prior to dynamic compaction characteristic curve from Phifer et al. (2006) at a suction head (matrix potential) of 195 cm

[3] Air-filled Porosity = (1 – Average Saturation) × Total Porosity

[4] During years 125 to 1,125 of the simulation, the lower waste zone is assigned a total porosity of 0

The molecular diffusion coefficient of Rn-222 in open air is 347 m^2/yr (Nielson et al. 1984). Nielson et al. (1984) established a relationship between moisture saturation and the radon effective air-diffusion coefficient for various pore sizes of earthen materials. Using this method, a radon effective air-diffusion coefficient was determined for each material type based upon the average moisture saturation for the material. Subsequently, using Graham's Law, the effective air-diffusion coefficient of each radionuclide or compound evaluated was determined for each material type based on the radon effective air-diffusion coefficient using the following relationship:

$$D = D' \sqrt{\frac{MWT'}{MWT}} \qquad \text{Eq 1-2}$$

Where:

D = the diffusion coefficient of the radionuclide of interest (m^2/yr)
D' = the diffusion coefficient of the reference radionuclide (Rn-222) (m^2/yr)
MWT' = the molecular weight of the reference radionuclide (Rn-222)
MWT = the molecular weight of the element or compound of interest

A summary of the radon effective air-diffusion coefficients and the calculated effective air-diffusion coefficients for each radionuclide/compound by material zone are presented in Table 1-35 and Table 1-36 for the 0 to 125 year operational and institutional control period and 125 to 1,125 year post-closure compliance period, respectively.

1.7.6 Air-Pathway Model Results

1.7.6.1 Slit and Engineered Trench Air Flux to Ground Surface

Model simulations were conducted to evaluate the peak flux of each radionuclide emanating from the top of the domain. A unit inventory of 1 Ci was assigned to the Slit and Engineered Trenches waste zone for each radionuclide considered in the analysis. Results were output in Ci/yr, consistent with the set of units employed in the model, and are presented for each radionuclide in Figure 1-32 through Figure 1-34. The peak fluxes emanating at the land surface are presented for each time period in Table 1-37. The results are reported in this way to facilitate calculation of human exposure at the SRS boundary and at the 100-m boundary due to the Slit and Engineered Trenches. Flux behavior is based primarily on the closure considerations discussed in Section 1.7.3 and the half-life of the particular radionuclide as provided in Table 1-32.

Table 1-35. Effective Air-Diffusion Coefficients for Each Radionuclide/Compound, by Material for the 0 to 125 Year Operational and Institutional Control Period

Radionuclide	Effective Air-Diffusion Coefficients for Each Material (m^2/yr)[1]			
	Lower Waste Zone	Upper Waste Zone	Operational Soil Cover	Final Closure Cap
Rn-222	1.262E+00	1.262E+00	1.262E+00	3.470E+02
C-14	2.773E+00	2.773E+00	2.773E+00	7.623E+02
Cl-36	2.217E+00	2.217E+00	2.217E+00	6.093E+02
H-3	7.678E+00	7.678E+00	7.678E+00	2.111E+03
I-129	1.171E+00	1.171E+00	1.171E+00	3.219E+02
S-35	3.179E+00	3.179E+00	3.179E+00	8.739E+02
Sb-124	1.689E+00	1.689E+00	1.689E+00	4.643E+02
Sb-125	1.682E+00	1.682E+00	1.682E+00	4.624E+02
Se-75	2.172E+00	2.172E+00	2.172E+00	5.970E+02
Se-79	2.116E+00	2.116E+00	2.116E+00	5.817E+02
Sn-113	1.769E+00	1.769E+00	1.769E+00	4.864E+02
Sn-119m	1.724E+00	1.724E+00	1.724E+00	4.739E+02
Sn-121	1.710E+00	1.710E+00	1.710E+00	4.700E+02
Sn-121m	1.710E+00	1.710E+00	1.710E+00	4.700E+02
Sn-123	1.696E+00	1.696E+00	1.696E+00	4.662E+02
Sn-126	1.676E+00	1.676E+00	1.676E+00	4.606E+02

[1] The effective diffusion coefficient for ^{222}Rn was used to determine the effective air diffusion coefficient of each radionuclide/compound based on Graham's law.

Table 1-36. Effective Air-Diffusion Coefficients for Each Radionuclide/Compound, by Material for the 125 to 1,125 Year Post-Closure Compliance Period

Radionuclide	Effective Air-Diffusion Coefficients for Each Material (m^2/yr)[1]			
	Lower Waste Zone	Upper Waste Zone	Operational Soil Cover	Final Closure Cap
Rn-222	na	1.262E+00	1.262E+00	1.260E+00
C-14	0.000E+00	2.773E+00	2.773E+00	2.773E+00
Cl-36	0.000E+00	2.217E+00	2.217E+00	2.217E+00
H-3	0.000E+00	7.678E+00	7.678E+00	7.678E+00
I-129	0.000E+00	1.171E+00	1.171E+00	1.171E+00
S-35	0.000E+00	3.179E+00	3.179E+00	3.179E+00
Sb-124	0.000E+00	1.689E+00	1.689E+00	1.689E+00
Sb-125	0.000E+00	1.682E+00	1.682E+00	1.682E+00
Se-75	0.000E+00	2.172E+00	2.172E+00	2.172E+00
Se-79	0.000E+00	2.116E+00	2.116E+00	2.116E+00
Sn-113	0.000E+00	1.769E+00	1.769E+00	1.769E+00
Sn-119m	0.000E+00	1.724E+00	1.724E+00	1.724E+00
Sn-121	0.000E+00	1.710E+00	1.710E+00	1.710E+00
Sn-121m	0.000E+00	1.710E+00	1.710E+00	1.710E+00
Sn-123	0.000E+00	1.696E+00	1.696E+00	1.696E+00
Sn-126	0.000E+00	1.676E+00	1.676E+00	1.676E+00

na = not applicable

[1] The effective diffusion coefficient for ^{222}Rn was used to determine the effective air diffusion coefficient of each radionuclide/compound based on Graham's law.

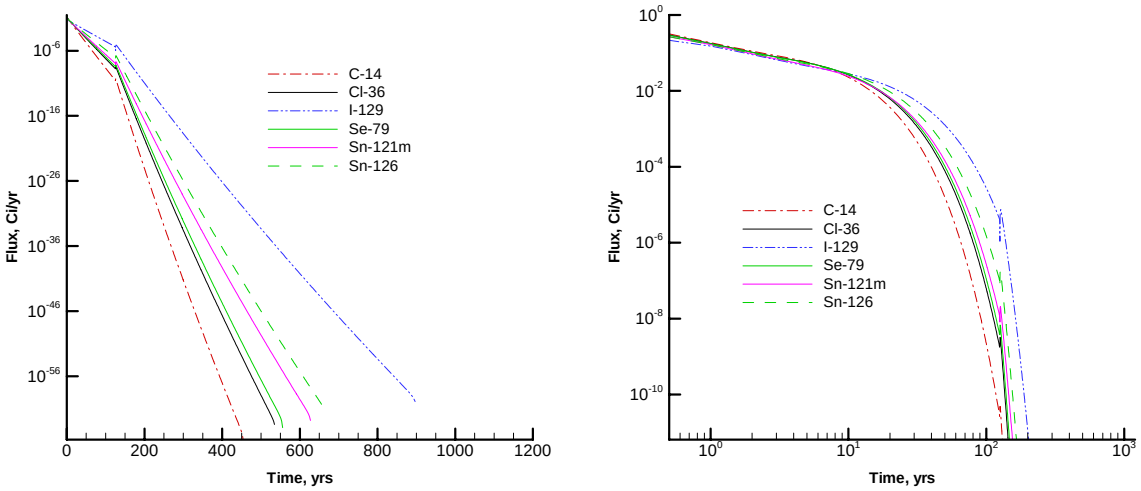

Figure 1-32. Flux Rate at Land Surface for C-14, Cl-36, I-129, Se-79, Sn-121m, and Sn-126 on a (a) semi-log and (b) log-log scale

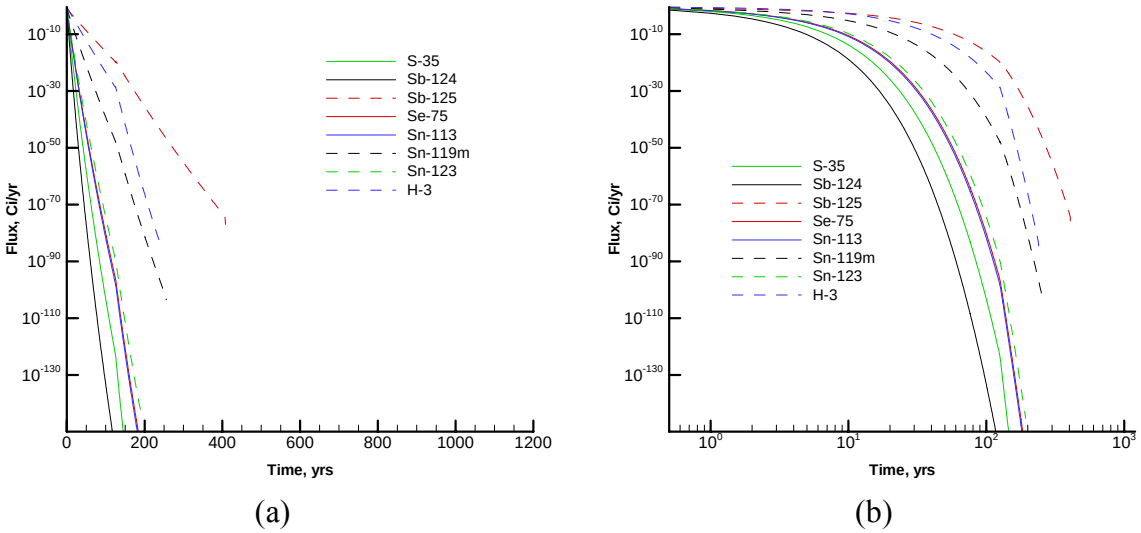

Figure 1-33. Flux Rate at Land Surface for S-35, Sb-124, Sb-125, Se-75, Sn-113, Sn-119m, Sn123, and H-3 on a (a) semi-log and (b) log-log scale.

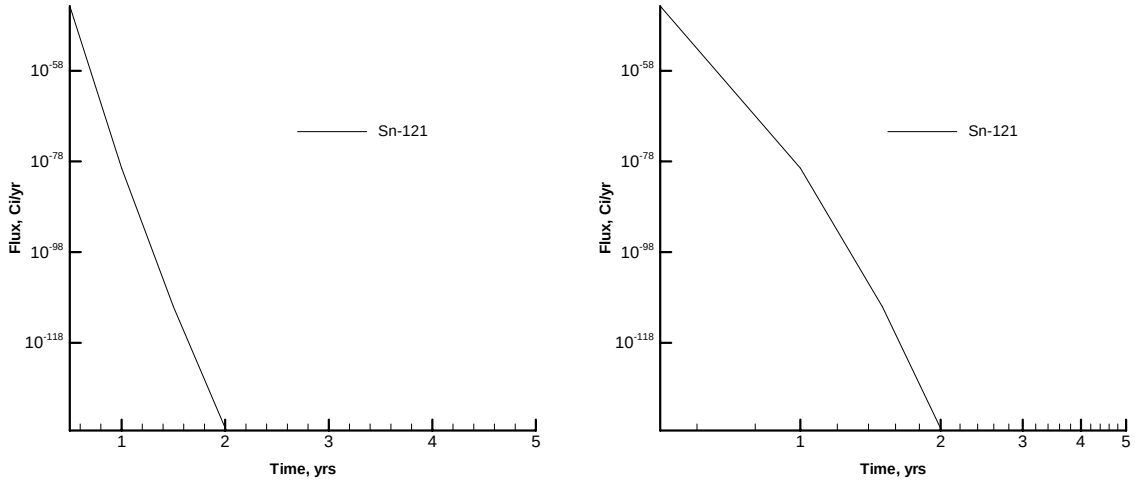

(a) (b)

Figure 1-34. Flux Rate at Land Surface for Sn-121 on a (a) semi-log and (b) log-log scale

Table 1-37. Summary of the Peak Flux Rates for Each Radionuclide

		Max. Flux (Ci/yr)	
Radionuclide	**Activity in Waste (Ci)**	**0 - 125 Years**	**125 – 1125 years**
C-14	1.0	3.19E-01	4.87E-11
Cl-36	1.0	2.97E-01	3.20E-09
H-3	1.0	3.92E-01	2.70E-29
I-129	1.0	2.15E-01	7.45E-06
S-35	1.0	7.80E-02	5.03E-124
Sb-124	1.0	3.28E-02	5.02E-159
Sb-125	1.0	2.35E-01	2.30E-20
Se-75	1.0	1.03E-01	2.81E-97
Se-79	1.0	2.93E-01	6.76E-09
Sn-113	1.0	9.09E-02	2.74E-99
Sn-119m	1.0	1.75E-01	1.30E-48
Sn-121	1.0	1.90E-44	0.00E+00
Sn-121m	1.0	2.66E-01	2.08E-08
Sn-123	1.0	1.01E-01	1.05E-90
Sn-126	1.0	2.66E-01	1.82E-07

1.7.7 Slit and Engineered Trench Air-Pathway Dose Calculations

An evaluation was conducted to assess the potential dose to a maximally exposed individual (MEI) located at both the SRS boundary and at the 100-m locations (Lee 2006). During the 125-year operational and institutional control period, the SRS boundary is the compliance point for the dose calculations. Therefore, the peak flux during this time period was used to assess the dose to the MEI. For the remainder of the time period, the 100-m boundary is the compliance point. Thus, the peak flux between 125 and 1125 years was used for these calculations. Dose-release factors (DRF) were calculated for each radionuclide potentially released from the Slit and Engineered Trenches disposal units using CAP88, the EPA model for National Emissions Standards for Hazardous Air Pollutants (NESHAPs) (see Beres 1990). The DRFs represent the dose to the receptor exposed to 1 Ci of the specified radionuclide being released to the atmosphere. For the receptor located at the SRS boundary the distance from the Slit and Engineered Trenches is sufficient for an assumption of a point source. However, the DRFs for the 100-m receptor require evaluation of an area source because of the close proximity of the Slit and Engineered Trenches disposal units to the 100-m receptor. For radionuclides not contained within the CAP88 library (Se-75, Se-79, Sn-119m, and Sn-121m) atmospheric transport was estimated by assigning surrogates with similar radiological properties (Lee 2006). Doses for these four radionuclides were estimated by applying their dosimetric properties to the surrogate's relative air concentrations estimated by the model.

Specific SRS Boundary DRFs, the calculated exposure levels for the 0 to 125 year MEI at the SRS boundary, and the resulting 0 to 125 year Slit and Engineered Trench disposal limits are presented in Table 1-38. Specific SRS 100-m DRFs, the calculated exposure levels for the 125 to 1125 year MEI at 100 meters, and the resulting 125 to 1125-year Slit and Engineered Trench disposal limits are presented in Table 1-39. See Lee (2006) for details on the estimation of all DRFs in Table 1-38 and Table 1-39. The Slit and Engineered Trench disposal unit limits were calculated by dividing the maximum permissible exposure level (10 mrem/yr, DOE 1999) by the highest dose received by the MEI from the 1 Ci source during each of the two time periods. Table 1-40 provides a comparison of the limits derived for these two time periods (i.e., 0 – 125 and 125 – 1125 years) and the resulting overall Slit and Engineered Trench air-pathway disposal limits. These disposal limits are applicable for each radionuclide for each Slit and Engineered Trench footprint separately.

Table 1-38. SRS Boundary Dose Release Factors and 0 – 125 Year Slit and Engineered Trench Disposal Limits

Radionuclide	0 - 125 Year Peak Flux (Ci/yr/Ci)	SRS Boundary Dose Release Factor[1] (mrem/Ci)	0 – 125 Year Dose to MEI at SRS Boundary [2] (mrem/yr/Ci)	0 - 125 Year Trench Disposal Limits [3] (Ci)
C-14	3.19E-01	1.1E-04	3.4E-05	2.9E+05
Cl-36	2.97E-01	2.3E-04	6.8E-05	1.5E+05
H-3	3.92E-01	2.2E-06	8.8E-07	1.1E+07
I-129	2.15E-01	4.9E-02	1.0E-02	9.5E+02
S-35	7.80E-02	2.8E-05	2.2E-06	4.5E+06
Sb-124	3.28E-02	2.0E-03	6.7E-05	1.5E+05
Sb-125	2.35E-01	6.5E-03	1.5E-03	6.6E+03
Se-75	1.03E-01	1.1E-03	1.1E-04	9.0E+04
Se-79	2.93E-01	6.3E-04	1.8E-04	5.5E+04
Sn-113	9.09E-02	2.3E-04	2.1E-05	4.8E+05
Sn-119m	1.75E-01	1.0E-04	1.8E-05	5.6E+05
Sn-121	1.90E-44	4.2E-05	8.0E-49	---
Sn-121m	2.66E-01	6.5E-04	1.7E-04	5.8E+04
Sn-123	1.01E-01	1.3E-05	1.3E-06	7.8E+06
Sn-126	2.66E-01	3.0E-01	7.9E-02	1.3E+02

[1]From (Lee 2006)
[2] Dose to MEI at SRS Boundary = Peak Flux × Dose Release Factor
[3] Disposal Limit = 10 mrem/yr / Dose to MEI at SRS Boundary per Year per Ci
Note: Limits reported as "---" indicate that there is no limit or that the limit $\geq$ 1E+20.
Note: Limits for special wasteforms (e.g., Ra-226 and Th-230 Cooling Tower) are the same as the generic radionuclide.

Table 1-39. 100-m Dose Release Factors and 125 - 1125 Year Slit and Engineered Trench Disposal Limits

Radionuclide	125 –1125 Year Peak Flux (Ci/yr/Ci)	100-m Dose Release Factor [1] (mrem/Ci)	125 –1125 Year Dose to MEI at 100 m^2 (mrem/yr/Ci)	125 –1125 Year Trench Disposal Limits [3] (Ci)
C-14	4.87E-11	5.90E-02	2.9E-12	3.5E+12
Cl-36	3.20E-09	9.30E-02	3.0E-10	3.4E+10
H-3	2.70E-29	1.20E-03	3.2E-32	---
I-129	7.45E-06	8.60E+01	6.4E-04	1.6E+04
S-35	5.03E-124	7.70E-03	3.9E-126	---
Sb-124	5.02E-159	5.70E-01	2.9E-159	---
Sb-125	2.30E-20	1.70E+00	3.9E-20	---
Se-75	2.81E-97	3.10E-01	8.7E-98	---
Se-79	6.76E-09	1.80E-01	1.2E-09	8.2E+09
Sn-113	2.74E-99	7.70E-02	2.1E-100	---
Sn-119m	1.30E-48	3.30E-02	4.3E-50	---
Sn-121	0.00E+00	1.20E-02	0.0E+00	---
Sn-121m	2.08E-08	1.80E-01	3.7E-09	2.7E+09
Sn-123	1.05E-90	3.30E-03	3.5E-93	---
Sn-126	1.82E-07	7.70E+01	1.4E-05	7.1E+05

[1] From (Lee 2006)
[2] Dose to MEI at SRS Boundary = Peak Flux × Dose Release Factor
[3] Disposal Limit = 10 mrem/yr / Dose to MEI at SRS Boundary per Year per Ci
Note: Limits reported as "---" indicate that there is no limit or that the limit $\geq$ 1E+20.
Note: Limits for special wasteforms (e.g., Ra-226 and Th-230 Cooling Tower) are the same as the generic radionuclide.

Table 1-40. Overall Slit and Engineered Trench Air-Pathway Disposal Limit

Radionuclide	0 - 125 Year Trench Disposal Limits[1] (Ci)	125 –1125 Year Trench Disposal Limits[2] (Ci)	Overall Trench Air-Pathway Disposal Limit (Ci)
C-14	2.9E+05	3.5E+12	2.9E+05
Cl-36	1.5E+05	3.4E+10	1.5E+05
H-3	1.1E+07	---	1.1E+07
I-129	9.5E+02	1.6E+04	9.5E+02
S-35	4.5E+06	---	4.5E+06
Sb-124	1.5E+05	---	1.5E+05
Sb-125	6.6E+03	---	6.6E+03
Se-75	9.0E+04	---	9.0E+04
Se-79	5.5E+04	8.2E+09	5.5E+04
Sn-113	4.8E+05	---	4.8E+05
Sn-119m	5.6E+05	---	5.6E+05
Sn-121	---	---	---
Sn-121m	5.8E+04	2.7E+09	5.8E+04
Sn-123	7.8E+06	---	7.8E+06
Sn-126	1.3E+02	7.1E+05	1.3E+02

[1]From Table 1-38
[2]From Table 1-39
Note: Limits reported as "---" indicate that there is no limit or that the limit $\geq$ 1E+20.
Note: Limits for special wasteforms (e.g., Ra-226 and Th-230 Cooling Tower) are the same as the generic radionuclide.

1.8 ALL-PATHWAYS ANALYSIS

This section documents the development of preliminary all-pathways limits for the Slit and Engineered Trenches. The limits developed within this section are considered preliminary, since they do not take into consideration the effects of plume overlap from adjacent units or the results of sensitivity and uncertainty analyses. The effects of plume overlap are considered in Chapter 6 and the interpretation of sensitivity and uncertainty analyses is conducted in Chapter 7. Final limits are provided in Chapter 7.

1.8.1 Overview of All-Pathways Analysis

This section describes the investigation conducted to evaluate the potential magnitude of the all-pathways dose from the each of the Engineered and Slit Trench disposal units over the 30-year operational period, 100-year institutional control period, and 1000-year post-closure compliance period.

The permissible all-pathways dose for DOE LLW disposal facilities is addressed in DOE M 435.1, IV.P.(1)(a) (DOE 1999). This requirement is that dose to representative members of the public shall not exceed 25 mrem (0.25 mSv) in a year total effective dose equivalent from all exposure pathways, excluding the dose from radon and its progeny in air.

Although the all-pathways performance objective includes not only all exposure pathways, but also all transport pathways, in this PA, the air pathway is evaluated separately. The all-pathways dose evaluated here includes only the groundwater transport pathway because the receptors for the groundwater and air pathways will likely be at different locations and the maximum doses from the two pathways will occur at different times.

The all-pathways analysis uses the groundwater concentrations developed in Section 1.6. The concentrations as a function of time are input into the all-pathways application (Koffman 2006a), which calculates dose to humans from direct ingestion of contaminated groundwater and consumption of locally grown leafy vegetables, produce, mild, and meat, which are contaminated with radionuclides from use of the groundwater for irrigation and direct consumption by the cattle (Section 4.5.1 of the Part C Background Chapter).

Two factors were included in the development of the models to be used for generation of the various Slit and Engineered Trench models. These factors were the presence or absence of non-crushable containers and the presence or absence of CDPs, leading to four generic disposal scenarios. Models were developed for each of the four cases (i.e., no non-crushable containers with no accounting for CDPs, no non-crushable containers with accounting for CDPs, 10% non-crushable containers with no accounting for CDPs and 10% non-crushable containers with accounting for CDPs) for each of four sets of trenches (i.e., Engineered Trenches, Center Slit Trenches, East Slit Trenches and West Slit Trenches). Groundwater and all-pathways limits were produced using the all-pathways application for each of the four cases.

The minimum limit produced by each of the four cases becomes the base limit for the nuclide. This bounds all four cases and allows for operational flexibility.

A number of special wasteforms were considered in additional to generic wasteforms. Separate disposal limits were generated for these.

Finally, after all the initial limits were generated using the all-pathways application (Koffman 2006a) with the three adjustments for special wasteforms, an adjustment was made to account for plume overlap between the various disposal units. The plume overlap adjustments were generated separately for each of the sets of trenches (Flach 2007). The adjustments were applied as multipliers to the initial limits.

1.8.2 Slit and Engineered Trench Summary of Key All-Pathways Analysis Assumptions

The key all-pathways analysis assumption(s) associated with the Engineered and Slit Trenches are presented in Appendix B.

1.8.3 Slit and Engineered Trenches All-Pathways Analysis

Radionuclide disposal limits for the East, West and Center Slit Trench Units and the Engineered Trench Units over the 1,000-year post-closure compliance period were calculated using the all-pathways application (Koffman 2006a). The application uses the results of the PORFLOW program to calculate the dose to a hypothetical individual from using the groundwater at the point of assessment (location of the maximum concentration of each radionuclide outside of a 100 m buffer zone) for all credible purposes (drinking, irrigation of crops and ingestion of the crops and the meat and milk of animals fed on the crops and groundwater). Table 1-41 through Table 1-44 present the preliminary disposal limits for the East Slit Trenches, Center Slit Trenches, West Slit Trenches and Engineered Trenches, respectively, based on the all-pathways analysis.

Table 1-41. Preliminary All-Pathways Radionuclide Disposal Limits for East Slit Trenches

	(Ci/Disposal Unit)		
Parent Nuclide	**130 - 200 yrs**	**200-1000 yrs**	**1000-1130 yrs**
Am-241	6.0E+02	1.2E+02	1.5E+02
Am-243	2.3E+10	2.1E+02	5.6E+01
C-14	7.7E+00	7.7E+00	7.7E+00
C-14_NR.Pump	3.2E+00	1.9E+00	5.5E+02
Cf-249	1.4E+06	7.4E+02	2.5E+02
Cf-251	3.2E+18	3.1E+02	9.0E+01
Cl-36	1.3E+00	1.3E+00	1.3E+00
Cm-244	---	1.1E+12	1.1E+11
Cm-245	5.9E+03	6.6E+01	2.5E+01
Cm-246	---	2.2E+02	5.8E+01
Cm-247	5.2E+12	1.8E+02	4.8E+01
Cm-248	---	5.1E+01	1.3E+01
H-3	2.7E+06	2.7E+06	2.7E+06
H-3_ETF.Carbon	1.8E+06	8.5E+08	---
I-129	3.2E-01	3.2E-01	3.2E-01
I-129_ETF.Carbon	1.4E+01	7.4E+00	7.0E+00
I-129_ETF.GT.73	2.0E+01	1.0E+01	9.7E+00
I-129_F.Carbon	2.6E+02	1.4E+02	1.3E+02
I-129_F.CG.8	1.8E-01	2.5E-01	8.8E-01
I-129_F.Dowex.21K	1.3E+01	7.1E+00	6.7E+00
I-129_F.Filtercake	1.9E-01	2.6E-01	8.4E-01
I-129_H.Carbon	1.1E+02	5.9E+01	5.6E+01
I-129_H.CG.8	7.7E-01	6.4E-01	6.1E-01
I-129_H.Dowex.21K	3.1E+01	1.6E+01	1.5E+01
I-129_H.Filtercake	1.3E+00	1.0E+00	9.3E-01
K-40	3.0E+00	3.9E+00	5.8E+01
Mo-93	1.4E+01	1.4E+01	1.4E+01
Nb-94	1.6E+00	1.6E+00	1.6E+00
Ni-59	1.4E+07	2.6E+03	1.8E+03
Np-237	2.7E-02	1.9E-02	3.1E-02
Pd-107	2.1E+07	4.1E+03	2.7E+03
Pu-238	2.3E+10	1.4E+06	4.0E+05
Pu-239	3.9E+07	7.9E+05	7.2E+05
Pu-240	1.8E+19	4.5E+09	3.9E+08
Pu-241	2.1E+04	3.7E+03	4.5E+03
Pu-242	3.2E+18	4.2E+09	3.6E+08
Pu-244	---	3.9E+09	3.3E+08
Ra-226	4.0E+01	2.7E-01	1.1E-01

Table 1-41. Preliminary All-Pathways Radionuclide Disposal Limits for East Slit Trenches – continued

	(Ci/Disposal Unit)		
Parent Nuclide	**130 - 200 yrs**	**200-1000 yrs**	**1000-1130 yrs**
Se-79	---	---	---
Sn-126	---	---	---
Sr-90	4.8E+04	3.4E+03	3.6E+10
Tc-99	5.3E+00	5.3E+00	5.3E+00
Th-230	1.3E+03	1.3E+00	3.6E-01
Th-232	2.3E+05	6.1E+04	1.4E+05
U-233	---	1.8E+12	1.6E+11
U-234	2.3E+06	3.6E+02	1.0E+02
U-235	3.1E+00	4.2E-01	4.3E-01
U-236	3.5E+13	6.6E+11	3.3E+11
U-238	1.7E+10	4.3E+05	1.3E+05
Zr-93	1.0E+01	4.0E+00	3.7E+00

Note: Limits reported as "---" indicate that there is no limit or that the limit $\geq$ 1E+20.
Note: All-pathways limits in this table are to be considered preliminary. Adjustments are made in the all-pathways limits as appropriate based on consideration of plume overlap effects from adjacent units in Chapter 6 and interpretation of sensitivity and uncertainty analyses in Chapter 7. Final limits are to be found in results tables in Chapter 7.

Table 1-42. Preliminary All-Pathways Radionuclide Disposal Limits for Center Slit Trenches

	(Ci/Disposal Unit)		
Parent Nuclide	**130 - 200 yrs**	**200-1000 yrs**	**1000-1130 yrs**
Am-241	7.4E+02	9.3E+01	5.3E+01
Am-243	3.4E+10	2.9E+01	1.1E+01
C-14	1.3E+01	1.3E+01	1.3E+01
C-14_NR.Pump	3.5E+00	3.1E+00	1.2E+02
Cf-249	2.2E+06	1.1E+02	4.9E+01
Cf-251	4.2E+18	4.4E+01	1.7E+01
Cl-36	2.3E+00	2.3E+00	2.3E+00
Cm-244	---	3.2E+10	3.6E+09
Cm-245	7.7E+03	1.5E+01	5.6E+00
Cm-246	---	3.0E+01	1.1E+01
Cm-247	7.4E+12	2.6E+01	9.2E+00
Cm-248	2.8E+19	7.2E+00	2.6E+00
H-3	4.8E+06	4.8E+06	4.8E+06
H-3_Concrete	1.1E+07	1.1E+07	1.1E+07
H-3_ETF.Carbon	1.7E+06	1.3E+09	---
I-129	5.3E-01	5.3E-01	5.3E-01
I-129_ETF.Carbon	2.5E+01	1.3E+01	1.2E+01
I-129_ETF.GT.73	3.3E+01	1.7E+01	1.6E+01
I-129_F.Carbon	4.4E+02	2.3E+02	2.1E+02
I-129_F.CG.8	2.5E-01	4.1E-01	1.3E+00
I-129_F.Dowex.21K	2.2E+01	1.2E+01	1.1E+01
I-129_F.Filtercake	2.7E-01	4.4E-01	1.3E+00
I-129_H.Carbon	1.9E+02	1.0E+02	9.4E+01
I-129_H.CG.8	1.3E+00	1.1E+00	1.0E+00
I-129_H.Dowex.21K	5.1E+01	2.7E+01	2.5E+01
I-129_H.Filtercake	2.2E+00	1.7E+00	1.6E+00
I-129_Mk50	7.6E+01	2.8E+01	8.9E+01
K-40	4.9E+00	6.1E+00	3.0E+01
Mo-93	2.5E+01	2.5E+01	2.5E+01
Nb-94	2.7E+00	2.7E+00	2.7E+00
Ni-59	1.1E+06	2.5E+03	1.2E+03
Np-237	3.3E-02	3.1E-02	5.9E-02
Pd-107	1.8E+06	3.9E+03	1.8E+03
Pu-238	2.7E+09	1.3E+06	3.8E+05
Pu-239	5.1E+07	1.4E+06	1.2E+06
Pu-240	1.5E+18	1.2E+08	1.3E+07
Pu-241	2.6E+04	2.8E+03	1.6E+03
Pu-242	3.9E+17	1.2E+08	1.2E+07
Pu-244	---	1.1E+08	1.1E+07

Table 1-42. Preliminary All-Pathways Radionuclide Disposal Limits for Center Slit Trenches - continued

	(Ci/Disposal Unit)		
Parent Nuclide	**130 - 200 yrs**	**200-1000 yrs**	**1000-1130 yrs**
Ra-226	6.2E+00	2.2E-01	1.3E-01
Ra-226_Cooling.Tower	1.2E+04	7.7E-01	2.9E+00
Se-79	---	---	4.0E+19
Sn-126	---	---	---
Sr-90	7.1E+03	1.6E+03	2.8E+10
Sr-90_Mk50	3.6E+06	9.1E+05	3.9E+12
Tc-99	9.0E+00	9.0E+00	9.0E+00
Tc-99_Mk50	1.9E+03	6.0E+02	2.0E+03
Th-230	1.7E+02	1.1E+00	3.6E-01
Th-230_Cooling.Tower	5.8E+05	6.6E+00	5.7E+00
Th-232	2.0E+04	8.4E+03	2.0E+04
U-233	---	4.5E+10	4.5E+09
U-234	2.8E+05	3.3E+02	9.9E+01
U-234_MGlass	4.6E+08	1.3E+05	4.1E+04
U-235	3.8E+00	6.9E-01	7.4E-01
U-235_MGlass	8.8E+03	3.1E+02	2.8E+02
U-235_Paducah.Cask	1.2E+05	3.3E+03	3.0E+03
U-236	2.9E+12	6.9E+10	1.4E+10
U-236_MGlass	3.9E+15	4.3E+13	8.7E+12
U-238	2.1E+09	4.3E+05	1.2E+05
U-238_MGlass	3.5E+12	1.6E+08	4.8E+07
Zr-93	1.1E+01	5.7E+00	5.2E+00

Note: Limits reported as "---" indicate that there is no limit or that the limit $\geq$ 1E+20.
Note: All-pathways limits in this table are to be considered preliminary. Adjustments are made in the all-pathways limits as appropriate based on consideration of plume overlap effects from adjacent units in Chapter 6 and interpretation of sensitivity and uncertainty analyses in Chapter 7. Final limits are to be found in results tables in Chapter 7.

Table 1-43. Preliminary All-Pathways Radionuclide Disposal Limits for West Slit Trenches

	(Ci/Disposal Unit)		
Parent Nuclide	**130 - 200 yrs**	**200-1000 yrs**	**1000-1130 yrs**
Am-241	9.5E+02	3.9E+01	2.5E+01
Am-243	4.6E+10	9.4E+00	4.7E+00
C-14	1.8E+01	1.8E+01	1.8E+01
C-14_NR.Pump	4.6E+00	4.4E+00	2.1E+02
Cf-249	2.9E+06	3.7E+01	2.1E+01
Cf-251	9.2E+17	1.4E+01	7.7E+00
Cl-36	3.2E+00	3.2E+00	3.2E+00
Cm-244	---	2.4E+09	3.1E+08
Cm-245	1.0E+04	5.1E+00	2.5E+00
Cm-246	1.2E+18	9.8E+00	4.9E+00
Cm-247	9.8E+12	8.3E+00	4.1E+00
Cm-248	3.1E+17	2.3E+00	1.1E+00
H-3	6.5E+06	6.5E+06	6.5E+06
H-3_ETF.Carbon	1.5E+03	1.2E+06	---
I-129	6.6E-01	6.6E-01	6.6E-01
I-129_ETF.Carbon	3.6E+01	1.9E+01	1.8E+01
I-129_ETF.GT.73	4.9E+01	2.5E+01	2.4E+01
I-129_F.Carbon	6.5E+02	3.4E+02	3.2E+02
I-129_F.CG.8	3.6E-01	6.1E-01	1.6E+00
I-129_F.Dowex.21K	3.3E+01	1.8E+01	1.7E+01
I-129_F.Filtercake	3.8E-01	6.4E-01	1.6E+00
I-129_H.Carbon	2.8E+02	1.5E+02	1.4E+02
I-129_H.CG.8	1.9E+00	1.6E+00	1.5E+00
I-129_H.Dowex.21K	7.6E+01	4.0E+01	3.7E+01
I-129_H.Filtercake	3.2E+00	2.6E+00	2.3E+00
K-40	6.6E+00	8.7E+00	4.5E+01
Mo-93	3.4E+01	3.4E+01	3.4E+01
Nb-94	3.7E+00	3.7E+00	3.7E+00
Ni-59	2.0E+05	2.8E+03	1.3E+03
Np-237	4.2E-02	4.2E-02	8.0E-02
Pd-107	3.0E+05	4.3E+03	2.0E+03
Pu-238	7.2E+08	1.5E+06	4.6E+05
Pu-239	6.7E+07	1.6E+06	6.3E+05
Pu-240	2.6E+17	8.8E+06	1.1E+06
Pu-241	3.3E+04	1.1E+03	7.4E+02
Pu-242	1.0E+17	8.3E+06	1.0E+06
Pu-244	5.3E+19	7.6E+06	9.1E+05
Ra-226	2.0E+00	2.6E-01	1.8E-01

Table 1-43. Preliminary All-Pathways Radionuclide Disposal Limits for West Slit Trenches - continued

	(Ci/Disposal Unit)		
Parent Nuclide	**130 - 200 yrs**	**200-1000 yrs**	**1000-1130 yrs**
Se-79	---	9.7E+18	7.2E+17
Sn-126	---	---	---
Sr-90	2.2E+03	1.1E+03	3.3E+10
Tc-99	1.4E+01	1.4E+01	1.4E+01
Th-230	4.6E+01	1.2E+00	4.5E-01
Th-232	3.6E+03	2.2E+03	5.3E+03
U-233	---	2.2E+09	2.6E+08
U-234	7.3E+04	3.8E+02	1.2E+02
U-235	4.9E+00	9.2E-01	1.0E+00
U-236	5.3E+11	8.4E+09	1.0E+09
U-238	5.5E+08	5.2E+05	1.5E+05
Zr-93	1.3E+01	8.0E+00	7.4E+00

Note: Limits reported as "---" indicate that there is no limit or that the limit $\geq$ 1E+20.
Note: All-pathways limits in this table are to be considered preliminary. Adjustments are made in the all-pathways limits as appropriate based on consideration of plume overlap effects from adjacent units in Chapter 6 and interpretation of sensitivity and uncertainty analyses in Chapter 7. Final limits are to be found in results tables in Chapter 7.

Table 1-44. Preliminary All-Pathways Radionuclide Disposal Limits for Engineered Trenches

	(Ci/Disposal Unit)		
Parent Nuclide	**130 - 200 yrs**	**200-1000 yrs**	**1000-1130 yrs**
Am-241	1.8E+03	4.3E+02	4.7E+02
Am-243	6.7E+10	2.0E+03	4.3E+02
C-14	2.1E+01	2.1E+01	2.1E+01
Cf-249	4.2E+06	6.2E+03	1.8E+03
Cf-251	1.0E+19	2.9E+03	7.0E+02
Cl-36	3.6E+00	3.6E+00	3.6E+00
Cm-244	---	3.4E+13	2.7E+12
Cm-245	1.7E+04	3.9E+02	1.6E+02
Cm-246	---	2.0E+03	4.5E+02
Cm-247	1.6E+13	1.7E+03	3.7E+02
Cm-248	---	4.8E+02	1.0E+02
H-3	7.4E+06	7.4E+06	7.4E+06
H-3_ETF.Carbon	4.7E+06	2.1E+09	---
I-129	7.7E-01	7.7E-01	7.7E-01
I-129_ETF.Carbon	7.5E+01	3.8E+01	3.6E+01
I-129_ETF.GT.73	1.0E+02	5.2E+01	4.8E+01
I-129_F.Carbon	1.3E+03	6.8E+02	6.3E+02
I-129_F.CG.8	6.5E-01	9.0E-01	1.5E+00
I-129_F.Dowex.21K	6.9E+01	3.5E+01	3.3E+01
I-129_F.Filtercake	7.2E-01	9.2E-01	1.4E+00
I-129_H.Carbon	5.9E+02	3.0E+02	2.8E+02
I-129_H.CG.8	3.9E+00	3.0E+00	2.6E+00
I-129_H.Dowex.21K	1.6E+02	8.0E+01	7.5E+01
I-129_H.Filtercake	6.7E+00	5.1E+00	4.4E+00
K-40	7.9E+00	9.9E+00	1.7E+02
Mo-93	3.8E+01	3.8E+01	3.8E+01
Nb-94	4.2E+00	4.2E+00	4.2E+00
Ni-59	1.6E+08	5.6E+03	1.0E+04
Np-237	8.3E-02	7.1E-02	8.7E-02
Pd-107	2.4E+08	8.5E+03	1.6E+04
Pu-238	1.9E+11	4.7E+06	1.5E+06
Pu-239	1.1E+08	2.4E+06	2.1E+06
Pu-240	---	1.3E+11	1.0E+10
Pu-241	6.3E+04	1.3E+04	1.4E+04
Pu-242	2.7E+19	1.3E+11	9.3E+09
Pu-244	---	1.2E+11	8.4E+09
Ra-226	3.3E+02	9.1E-01	3.5E-01
Se-79	---	---	---
Sn-126	---	---	---
Sr-90	4.0E+05	1.1E+04	1.9E+11

Table 1-44. Preliminary All-Pathways Radionuclide Disposal Limits for Engineered Trenches - continued

	(Ci/Disposal Unit)		
Parent Nuclide	**130 - 200 yrs**	**200-1000 yrs**	**1000-1130 yrs**
Tc-99	1.3E+01	1.3E+01	1.3E+01
Th-230	1.1E+04	5.9E+00	1.3E+00
Th-232	2.4E+06	4.1E+05	1.0E+06
U-233	---	7.4E+13	5.8E+12
U-234	1.9E+07	1.3E+03	3.8E+02
U-235	9.3E+00	1.2E+00	1.3E+00
U-236	3.6E+14	4.9E+12	3.6E+12
U-238	1.4E+11	1.4E+06	4.9E+05
Zr-93	2.7E+01	1.1E+01	1.0E+01

Note: Limits reported as "---" indicate that there is no limit or that the limit $\geq$ 1E+20.
Note: All-pathways limits in this table are to be considered preliminary. Adjustments are made in the all-pathways limits as appropriate based on consideration of plume overlap effects from adjacent units in Chapter 6 and interpretation of sensitivity and uncertainty analyses in Chapter 7. Final limits are to be found in results tables in Chapter 7.

1.9 INADVERTENT INTRUDER ANALYSIS

The inadvertent intruder analysis considers the radiological impacts to hypothetical persons who are assumed to intrude into the Slit Trench disposal units at the EALLWF after institutional control ceases 100 years after facility closure. Descriptions of intruder scenarios are provided in the Background Chapter in Part C of this PA. The analysis was carried out using an automated computer application developed at SRNL (Koffman 2006b), which implements equations calculating dose per unit intake documented in Lee (2004). One important functional requirement of the application is that it computes a “no leaching” case in which the full decay chain is determined and the activities are calculated at specified times using the Bateman equation. This means that the intruder calculations are completely independent from the PORFLOW calculations. In the intruder analysis, no credit is taken for the more robust packaging of the “special” wasteforms containing H-3, C-14, Tc-99 and I-129.

1.9.1 Slit and Engineered Trench Specific Parameters

The final closure system for the EALLWF includes a 12-inch thick erosion barrier near the top of the cap. Because the erosion barrier is assumed to never erode and all the layers between the waste and the erosion barrier always remain in place at their design thickness, approximately 10.37 ft of material always exists above the waste. The erosion barrier has been shown to be effective for at least 10,000 years (Phifer and Nelson 2003) so that all the layers between the waste and the erosion barrier always remain in place at their design thickness, approximately 10.37 ft of material always exists above the waste. Because the thickness from the top of the erosion barrier to the waste is greater than the depth of a typical basement (10 ft), the agriculture scenario can never occur as it relies on a basement extending into the waste zone. The resident and post-drilling scenarios are credible for the slit and Engineered Trench units after the institutional control period of 100 years.

The parameters specific to the Slit Trench and Engineered Trench Disposal Units used in the intruder analysis are given in Table 1-45 and Table 1-46 respectively. The geometry factors and erosion rate are documented in McDowell-Boyer et al. (2000). The waste volumes for these disposal units are consistent with those presented in Section 1.5.2.3.

1.9.2 Results

The agriculture scenario was not evaluated because implementation of an erosion barrier during closure eliminates the potential for contact with the waste via this scenario. Results of the resident intruder analyses for Slit Trench disposal units for the time period of 100 – 1,000 years are provided in Table 1-47. Results of the post-drilling intruder analyses for the Slit Trench disposal units for the time period of 100 – 1,000 years are provided in Table 1-48. Results of the resident intruder analyses for Engineered Trench disposal units for the time period of 100 – 1,000 years are provided in Table 1-49. Results of the post-drilling intruder analyses for the Engineered Trench disposal units for the time period of 100 – 1,000 years are provided in Table 1-50. The entry "---" in the Time of Limit column means that the dose calculation is always zero so there is no limit.

For cases where there is a time given, there may be an entry "---" in one or both of the limit columns. In this case the entry "---"indicates a limit value greater than or equal to the threshold value of 1E+20. Additional details are provided in Part C Background, Section 4.4. Because the automated method applies a transient analysis, it calculates the lowest inventory limit for the entire time period, regardless of when it occurs.

Table 1-45. Intruder Parameters for the Slit Trench Disposal Units

Facility	E-Area
Disposal Unit Name	Slit Trenches
Abbreviated Name	Slit Trenches
Agriculture Geometry Factor	0.637
Resident Geometry Factor	0.637
Post-Drilling Geometry Factor	1
Waste Volume (ft^3)	1,040,000

Transient Layer Model (Surface to Top of Waste)

Layer	Thickness (ft)	Description	Erosion Rate (mm/yr)	Erosion Earliest Start (yr)
1	3	Soil cover	1.4	
2	1	Erosion barrier	1.4	1E+10
3	9.37	Soil backfill	1.4	

Table 1-46. Intruder Parameters for the Engineered Trench Disposal Units

Facility	E-Area
Disposal Unit Name	Engineered Trenches
Abbreviated Name	EngrTrenches
Agriculture Geometry Factor	1
Resident Geometry Factor	1
Post-Drilling Geometry Factor	1
Waste Volume (ft^3)	1,080,000

Transient Layer Model (Surface to Top of Waste)

Layer	Thickness (inches)	Description	Erosion Rate (mm/yr)	Erosion Earliest Start (yr)
1	3	Soil cover	1.4	
2	1	Erosion barrier	1.4	1E+10
3	9.37	Soil backfill	1.4	

Table 1-47. Intruder-Based Radionuclide Disposal Limits for Slit Trenches – Resident Scenario with Transient Calculation for 1000 Years

Radionuclide	Time of Limit (Years)	Concentration Limit (µCi/m^3)	Inventory Limit (Ci/Unit)
Ac-227	100	1.05E+09	3.1E+07
Ag-108m	760	1.24E+03	3.6E+01
Al-26	760	1.33E+02	3.9E+00
Am-241	760	2.10E+07	6.2E+05
Am-242m	760	5.50E+06	1.6E+05
Am-243	760	1.33E+04	3.9E+02
Ar-39	---	---	---
Ba-133	100	1.46E+11	4.3E+09
Bi-207	100	3.37E+06	9.9E+04
Bk-249	760	4.82E+06	1.4E+05
C-14	---	---	---
Ca-41	---	---	---
Cd-113m	---	---	---
Cf-249	760	1.25E+04	3.7E+02
Cf-250	1000	1.28E+15	3.8E+13
Cf-251	760	4.64E+04	1.4E+03
Cf-252	1000	2.55E+13	7.5E+11
Cl-36	---	---	---
Cm-242	1000	9.00E+10	2.6E+09
Cm-243	760	1.38E+09	4.1E+07
Cm-244	760	1.48E+13	4.4E+11
Cm-245	760	7.98E+04	2.4E+03
Cm-246	1000	3.51E+12	1.0E+11
Cm-247	1000	2.67E+03	7.9E+01
Cm-248	1000	1.87E+08	5.5E+06
Co-60	100	6.86E+10	2.0E+09
Cs-134	100	---	1.5E+19
Cs-135	---	---	---
Cs-137	100	7.19E+07	2.1E+06
Eu-152	100	7.70E+07	2.3E+06
Eu-154	100	1.38E+09	4.1E+07
Eu-155	100	---	4.0E+18
H-3	---	---	---
I-129	760	2.48E+11	7.3E+09
K-40	760	2.27E+03	6.7E+01
Kr-85	100	3.36E+12	9.9E+10
Mo-93	760	---	---
Na-22	100	9.25E+16	2.7E+15
Nb-93m	760	---	---

Table 1-47. Intruder-Based Radionuclide Disposal Limits for Slit Trenches – Resident Scenario with Transient Calculation for 1000 Years - continued

Radionuclide	Time of Limit (Years)	Concentration Limit ($\mu Ci/m^3$)	Inventory Limit (Ci/Unit)
Nb-94	760	3.26E+02	9.6E+00
Ni-59	---	---	---
Ni-63	---	---	---
Np-237	1000	5.66E+03	1.7E+02
Pa-231	760	2.75E+03	8.1E+01
Pb-210	100	4.77E+12	1.4E+11
Pd-107	---	---	---
Pu-238	1000	4.57E+08	1.3E+07
Pu-239	760	1.29E+08	3.8E+06
Pu-240	760	4.09E+10	1.2E+09
Pu-241	760	6.31E+08	1.9E+07
Pu-242	1000	2.35E+10	6.9E+08
Pu-244	760	1.49E+03	4.4E+01
Ra-226	760	3.10E+02	9.1E+00
Ra-228	100	4.44E+09	1.3E+08
Rb-87	---	---	---
S-35	---	---	---
Sb-125	100	1.69E+18	5.0E+16
Sc-46	100	---	---
Se-79	---	---	---
Sm-151	760	---	---
Sn-121m	---	---	---
Sn-126	760	2.94E+02	8.7E+00
Sr-90	---	---	---
Tc-99	760	3.54E+10	1.0E+09
Th-228	100	---	6.6E+18
Th-229	760	3.05E+03	9.0E+01
Th-230	1000	6.37E+02	1.9E+01
Th-232	760	1.49E+02	4.4E+00
U-232	100	1.08E+05	3.2E+03
U-233	1000	3.16E+04	9.3E+02
U-234	1000	1.29E+05	3.8E+03
U-235	1000	1.71E+04	5.0E+02
U-236	1000	9.43E+08	2.8E+07
U-238	1000	3.30E+04	9.7E+02
W-181	100	---	---
W-185	100	---	---
W-188	100	---	---
Zr-93	760	---	---

Note: Intruder limits for special wasteforms (e.g., Mk50A or Cooling Tower) are identical to the generic radionuclide associated with each one.

Note: Limits reported as "---" indicate that there is no limit or that the limit $\geq$ 1E+20.

Table 1-48. Intruder-Based Radionuclide Disposal Limits for Slit Trenches – Post-Drilling Scenario with Transient Calculation for 1000 Years

Radionuclide	Time of Limit (Years)	Concentration Limit ($\mu Ci/m^3$)	Inventory Limit (Ci/Unit)
Ac-227	100	1.42E+05	4.2E+03
Ag-108m	100	7.79E+04	2.3E+03
Al-26	100	5.42E+04	1.6E+03
Am-241	100	4.73E+04	1.4E+03
Am-242m	100	4.70E+04	1.4E+03
Am-243	100	3.88E+04	1.1E+03
Ar-39	100	1.22E+09	3.6E+07
Ba-133	100	2.78E+08	8.2E+06
Bi-207	100	7.97E+05	2.3E+04
Bk-249	100	1.66E+07	4.9E+05
C-14	100	6.72E+04	2.0E+03
Ca-41	100	4.05E+05	1.2E+04
Cd-113m	100	1.01E+06	3.0E+04
Cf-249	100	4.28E+04	1.3E+03
Cf-250	100	8.80E+06	2.6E+05
Cf-251	100	3.95E+04	1.2E+03
Cf-252	100	1.81E+09	5.3E+07
Cl-36	100	8.54E+02	2.5E+01
Cm-242	100	2.37E+07	7.0E+05
Cm-243	100	7.33E+05	2.2E+04
Cm-244	100	3.38E+06	1.0E+05
Cm-245	1000	2.60E+04	7.7E+02
Cm-246	100	4.98E+04	1.5E+03
Cm-247	1000	4.28E+04	1.3E+03
Cm-248	100	1.34E+04	3.9E+02
Co-60	100	2.81E+10	8.3E+08
Cs-134	100	1.64E+19	4.8E+17
Cs-135	100	8.26E+05	2.4E+04
Cs-137	100	8.15E+05	2.4E+04
Eu-152	100	2.20E+07	6.5E+05
Eu-154	100	3.77E+08	1.1E+07
Eu-155	100	7.99E+12	2.4E+11
H-3	100	7.03E+07	2.1E+06
I-129	100	1.29E+04	3.8E+02
K-40	100	1.73E+04	5.1E+02
Kr-85	100	3.92E+10	1.2E+09
Mo-93	100	1.61E+07	4.7E+05
Na-22	100	2.01E+16	5.9E+14
Nb-93m	100	4.24E+09	1.2E+08
Nb-94	100	9.28E+04	2.7E+03

Table 1-48. Intruder-Based Radionuclide Disposal Limits for Slit Trenches – Post-Drilling Scenario with Transient Calculation for 1000 Years - continued

Radionuclide	Time of Limit (Years)	Concentration Limit ($\mu Ci/m^3$)	Inventory Limit (Ci/Unit)
Ni-59	100	1.41E+07	4.2E+05
Ni-63	100	1.03E+07	3.0E+05
Np-237	100	3.69E+03	1.1E+02
Pa-231	220	4.14E+03	1.2E+02
Pb-210	100	7.31E+04	2.2E+03
Pd-107	100	2.96E+07	8.7E+05
Pu-238	100	1.21E+05	3.6E+03
Pu-239	100	4.99E+04	1.5E+03
Pu-240	100	5.03E+04	1.5E+03
Pu-241	100	1.39E+06	4.1E+04
Pu-242	100	5.25E+04	1.5E+03
Pu-244	1000	4.31E+04	1.3E+03
Ra-226	130	2.42E+03	7.1E+01
Ra-228	100	8.38E+08	2.5E+07
Rb-87	100	5.18E+05	1.5E+04
S-35	100	---	---
Sb-125	100	2.50E+16	7.4E+14
Sc-46	100	---	---
Se-79	100	8.01E+05	2.4E+04
Sm-151	100	2.02E+08	5.9E+06
Sn-121m	100	5.47E+07	1.6E+06
Sn-126	100	7.03E+04	2.1E+03
Sr-90	100	5.57E+04	1.6E+03
Tc-99	100	8.26E+04	2.4E+03
Th-228	100	---	3.4E+18
Th-229	100	1.70E+04	5.0E+02
Th-230	1000	6.49E+03	1.9E+02
Th-232	180	5.03E+03	1.5E+02
U-232	100	3.19E+04	9.4E+02
U-233	1000	7.47E+04	2.2E+03
U-234	1000	1.16E+05	3.4E+03
U-235	1000	7.50E+04	2.2E+03
U-236	100	1.33E+05	3.9E+03
U-238	1000	1.36E+05	4.0E+03
W-181	100	---	---
W-185	100	---	---
W-188	100	---	---
Zr-93	250	3.22E+07	9.5E+05

Note: Intruder limits for special wasteforms (e.g., Mk50A or Cooling Tower) are identical to the generic radionuclide associated with each one.

Note: Limits reported as "---" indicate that there is no limit or that the limit $\geq$ 1E+20.

Table 1-49. Intruder-Based Radionuclide Disposal Limits for Engineered Trenches – Resident Scenario with Transient Calculation for 1000 Years

Radionuclide	Time of Limit (Years)	Concentration Limit ($\mu Ci/m^3$)	Inventory Limit (Ci/Unit)
Ac-227	100	6.69E+08	2.0E+07
Ag-108m	760	7.88E+02	2.4E+01
Al-26	760	8.47E+01	2.6E+00
Am-241	760	1.34E+07	4.1E+05
Am-242m	760	3.50E+06	1.1E+05
Am-243	760	8.46E+03	2.6E+02
Ar-39	---	---	---
Ba-133	100	9.30E+10	2.8E+09
Bi-207	100	2.15E+06	6.6E+04
Bk-249	760	3.07E+06	9.4E+04
C-14	---	---	---
Ca-41	---	---	---
Cd-113m	---	---	---
Cf-249	760	7.93E+03	2.4E+02
Cf-250	1000	8.16E+14	2.5E+13
Cf-251	760	2.95E+04	9.0E+02
Cf-252	1000	1.62E+13	5.0E+11
Cl-36	---	---	---
Cm-242	1000	5.73E+10	1.8E+09
Cm-243	760	8.77E+08	2.7E+07
Cm-244	760	9.41E+12	2.9E+11
Cm-245	760	5.09E+04	1.6E+03
Cm-246	1000	2.23E+12	6.8E+10
Cm-247	1000	1.70E+03	5.2E+01
Cm-248	1000	1.19E+08	3.6E+06
Co-60	100	4.37E+10	1.3E+09
Cs-134	100	---	9.9E+18
Cs-135	---	---	---
Cs-137	100	4.58E+07	1.4E+06
Eu-152	100	4.91E+07	1.5E+06
Eu-154	100	8.78E+08	2.7E+07
Eu-155	100	8.72E+19	2.7E+18
H-3	---	---	---
I-129	760	1.58E+11	4.8E+09
K-40	760	1.45E+03	4.4E+01
Kr-85	100	2.14E+12	6.5E+10
Mo-93	760	---	---
Na-22	100	5.89E+16	1.8E+15
Nb-93m	760	---	---

Table 1-49. Intruder-Based Radionuclide Disposal Limits for Engineered Trenches – Resident Scenario with Transient Calculation for 1000 Years - continued

Radionuclide	Time of Limit (Years)	Concentration Limit ($\mu Ci/m^3$)	Inventory Limit (Ci/Unit)
Nb-94	760	2.08E+02	6.4E+00
Ni-59	---	---	---
Ni-63	---	---	---
Np-237	1000	3.60E+03	1.1E+02
Pa-231	760	1.75E+03	5.4E+01
Pb-210	100	3.04E+12	9.3E+10
Pd-107	---	---	---
Pu-238	1000	2.91E+08	8.9E+06
Pu-239	760	8.19E+07	2.5E+06
Pu-240	760	2.60E+10	8.0E+08
Pu-241	760	4.02E+08	1.2E+07
Pu-242	1000	1.50E+10	4.6E+08
Pu-244	760	9.49E+02	2.9E+01
Ra-226	760	1.97E+02	6.0E+00
Ra-228	100	2.83E+09	8.7E+07
Rb-87	---	---	---
S-35	---	---	---
Sb-125	100	1.07E+18	3.3E+16
Sc-46	100	---	---
Se-79	---	---	---
Sm-151	760	---	---
Sn-121m	---	---	---
Sn-126	760	1.88E+02	5.7E+00
Sr-90	---	---	---
Tc-99	760	2.26E+10	6.9E+08
Th-228	100	---	4.4E+18
Th-229	760	1.95E+03	6.0E+01
Th-230	1000	4.06E+02	1.2E+01
Th-232	760	9.48E+01	2.9E+00
U-232	100	6.85E+04	2.1E+03
U-233	1000	2.01E+04	6.2E+02
U-234	1000	8.21E+04	2.5E+03
U-235	1000	1.09E+04	3.3E+02
U-236	1000	6.01E+08	1.8E+07
U-238	1000	2.10E+04	6.4E+02
W-181	100	---	---
W-185	100	---	---
W-188	100	---	---
Zr-93	760	---	---

Note: Intruder limits for special wasteforms (e.g., Mk50A or Cooling Tower) are identical to the generic radionuclide associated with each one.

Note: Limits reported as "---" indicate that there is no limit or that the limit $\geq$ 1E+20.

Table 1-50. Intruder-Based Radionuclide Disposal Limits for Engineered Trenches – Post-Drilling Scenario with Transient Calculation for 1000 Years

Radionuclide	Time of Limit (Years)	Concentration Limit ($\mu Ci/m^3$)	Inventory Limit (Ci/Unit)
Ac-227	100	1.42E+05	4.3E+03
Ag-108m	100	7.79E+04	2.4E+03
Al-26	100	5.42E+04	1.7E+03
Am-241	100	4.73E+04	1.4E+03
Am-242m	100	4.70E+04	1.4E+03
Am-243	100	3.88E+04	1.2E+03
Ar-39	100	1.22E+09	3.7E+07
Ba-133	100	2.78E+08	8.5E+06
Bi-207	100	7.97E+05	2.4E+04
Bk-249	100	1.66E+07	5.1E+05
C-14	100	6.72E+04	2.1E+03
Ca-41	100	4.05E+05	1.2E+04
Cd-113m	100	1.01E+06	3.1E+04
Cf-249	100	4.28E+04	1.3E+03
Cf-250	100	8.80E+06	2.7E+05
Cf-251	100	3.95E+04	1.2E+03
Cf-252	100	1.81E+09	5.5E+07
Cl-36	100	8.54E+02	2.6E+01
Cm-242	100	2.37E+07	7.3E+05
Cm-243	100	7.33E+05	2.2E+04
Cm-244	100	3.38E+06	1.0E+05
Cm-245	1000	2.60E+04	7.9E+02
Cm-246	100	4.98E+04	1.5E+03
Cm-247	1000	4.28E+04	1.3E+03
Cm-248	100	1.34E+04	4.1E+02
Co-60	100	2.81E+10	8.6E+08
Cs-134	100	1.64E+19	5.0E+17
Cs-135	100	8.26E+05	2.5E+04
Cs-137	100	8.15E+05	2.5E+04
Eu-152	100	2.20E+07	6.7E+05
Eu-154	100	3.77E+08	1.2E+07
Eu-155	100	7.99E+12	2.4E+11
H-3	100	7.03E+07	2.1E+06
I-129	100	1.29E+04	3.9E+02
K-40	100	1.73E+04	5.3E+02
Kr-85	100	3.92E+10	1.2E+09
Mo-93	100	1.61E+07	4.9E+05
Na-22	100	2.01E+16	6.2E+14
Nb-93m	100	4.24E+09	1.3E+08

Table 1-50. Intruder-Based Radionuclide Disposal Limits for Engineered Trenches – Post-Drilling Scenario with Transient Calculation for 1000 Years - continued

Radionuclide	Time of Limit (Years)	Concentration Limit ($\mu Ci/m^3$)	Inventory Limit (Ci/Unit)
Nb-94	100	9.28E+04	2.8E+03
Ni-59	100	1.41E+07	4.3E+05
Ni-63	100	1.03E+07	3.1E+05
Np-237	100	3.69E+03	1.1E+02
Pa-231	220	4.14E+03	1.3E+02
Pb-210	100	7.31E+04	2.2E+03
Pd-107	100	2.96E+07	9.1E+05
Pu-238	100	1.21E+05	3.7E+03
Pu-239	100	4.99E+04	1.5E+03
Pu-240	100	5.03E+04	1.5E+03
Pu-241	100	1.39E+06	4.2E+04
Pu-242	100	5.25E+04	1.6E+03
Pu-244	1000	4.31E+04	1.3E+03
Ra-226	130	2.42E+03	7.4E+01
Ra-228	100	8.38E+08	2.6E+07
Rb-87	100	5.18E+05	1.6E+04
S-35	100	---	---
Sb-125	100	2.50E+16	7.7E+14
Sc-46	100	---	---
Se-79	100	8.01E+05	2.5E+04
Sm-151	100	2.02E+08	6.2E+06
Sn-121m	100	5.47E+07	1.7E+06
Sn-126	100	7.03E+04	2.1E+03
Sr-90	100	5.57E+04	1.7E+03
Tc-99	100	8.26E+04	2.5E+03
Th-228	100	---	3.6E+18
Th-229	100	1.70E+04	5.2E+02
Th-230	1000	6.49E+03	2.0E+02
Th-232	180	5.03E+03	1.5E+02
U-232	100	3.19E+04	9.7E+02
U-233	1000	7.47E+04	2.3E+03
U-234	1000	1.16E+05	3.5E+03
U-235	1000	7.50E+04	2.3E+03
U-236	100	1.33E+05	4.1E+03
U-238	1000	1.36E+05	4.2E+03
W-181	100	---	---
W-185	100	---	---
W-188	100	---	---
Zr-93	250	3.22E+07	9.8E+05

Note: Intruder limits for special wasteforms (e.g., Mk50A or Cooling Tower) are identical to the generic radionuclide associated with each one.

Note: Limits reported as "---" indicate that there is no limit or that the limit > 1E+20.

1.10 SLIT AND ENGINEERED TRENCH RADON ANALYSIS

1.10.1 Overview of Radon Analysis

This section describes the investigation conducted to evaluate the potential magnitude of radon release from the Slit and Engineered Trenches over the 25-year operational period, 100-year institutional control period, and 1000-year post-closure compliance period.

Because of the similarity of the Slit and Engineered Trenches, a single model was used to estimate the radon flux at the ground surface for these disposal units. The flux of Rn-222 from the Slit and Engineered Trenches was evaluated for two separate time periods: 1) 0 to 125 years, and 2) 125 to 1125 years. The first time period evaluated covers the operational and institutional control periods, during which a minimum 4-foot operational soil cover overlies the waste. The second time period evaluated covers the post-closure compliance period, after subsidence treatment and final closure cap installation.

The permissible radon flux for DOE facilities is addressed in DOE M 435.1-1 Chapter IV, P.(1)(c) (DOE 1999). Specifically, Section IV. P.(c) states the radon flux limitations associated with the development of a disposal facility, maintenance of a performance assessment, and the closure of the disposal facility. This requirement is that the release of radon shall be less than an average flux of 20 $pCi/m^2/sec$ at the surface of the disposal facility. The requirements analysis states that this standard was adopted from the uranium mill tailings requirements in 40 CFR Part 192 and 10 CFR Part 40. 10 CFR Part 40 discusses both Rn-222 from uranium and Rn-220 from thorium, therefore the performance objective refers only to radon, and the correct species must be analyzed depending on the characteristics of the waste stream.

This guidance forms the basis for the investigation to evaluate radon flux above the Slit and Engineered Trenches. The scope of the investigation involved defining a decay chain of parent radionuclides to evaluate with a 1-D, vertical, numerical model. This analysis applies the capability of the standard SRS groundwater simulation program (PORFLOW) to model gas phase transport through partially saturated porous media to the ground surface. The model was customized to represent the vertical dimension of the Slit and Engineered Trench waste zone and the anticipated operational soil cover and final closure cap. The instantaneous Rn-222 flux at the land surface was evaluated for the two time periods previously mentioned and the maximum flux was then compared to the USDOE performance objective.

This investigation addresses only Rn-222, since the short half-life of Rn-220 (55.6 s) makes it unlikely to escape the Slit and Engineered Trenches and migrate to the land surface via air-diffusion before it is transformed by radioactive decay. The potential parent radionuclides that can contribute to the creation of Rn-222 are illustrated in Figure 1-35. The diagram indicates the specific decay chains that lead to the formation of Rn-222, as well as the half-lives for each radionuclide. The extremely long half-life of U-238 (4.468E+9 years) cause the other radionuclides higher up on the chain of parents to be of little concern with regard to their potential to contribute significantly to the Rn-222 flux at the land surface over the period of interest.

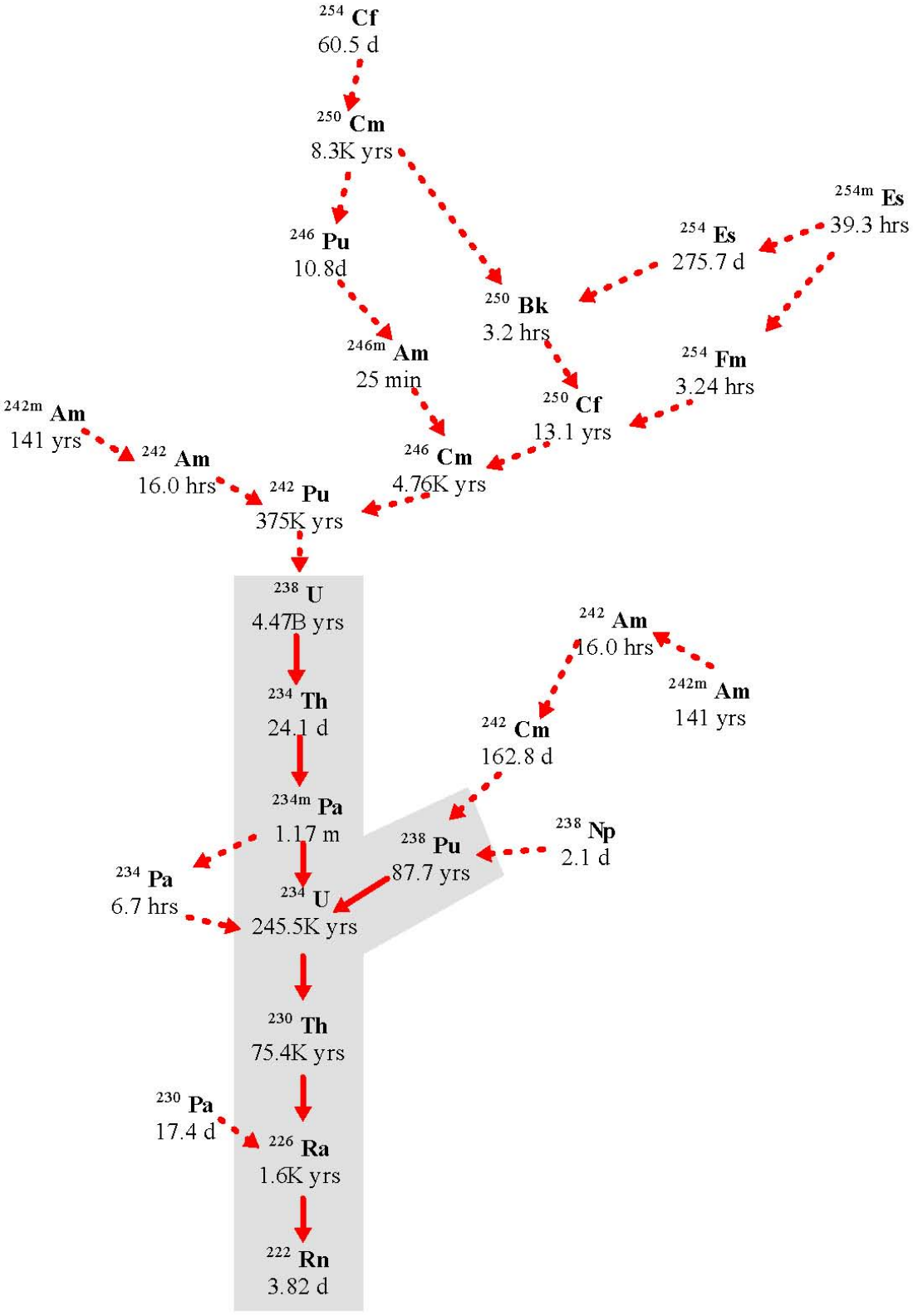

Figure 1-35. Radioactive Decay Chains Leading to Rn-222

1.10.2 Summary of Key Radon Analysis Assumptions for the Slit and Engineered Trenches

The key radon analysis assumptions associated with the Slit and Engineered Trenches are presented in Appendix B.

1.10.3 Slit and Engineered Trench Radon Analysis Conceptual Model

1.10.3.1 Slit and Engineered Trench Closure Considerations

The concepts for closure of the Slit and Engineered Trench are relevant to the determination of the radon flux at the land surface. The Slit Trench and Engineered Trench construction specifics and closure concept are described by Phifer et al. (2006). For the purposes of this investigation, it is assumed that during the operational and institutional control periods (0 to 125 years) there is only a four-foot operational soil cover above a 16-foot waste zone. Therefore, during this time period, the top of the operation soil cover (as described by Phifer et al. 2006) is the point where the Rn-222 flux was evaluated.

For the post-closure compliance period (125 to 1125 years), subsidence treatment (i.e., static surcharge and/or dynamic compaction) and final closure cap installation will have occurred for the Slit and Engineered Trenches. As outlined in Sections 1.3.1 and 1.3.2, it is assumed that this subsidence treatment essentially eliminates future subsidence potential except in those areas designated not to undergo dynamic compaction or containing non-crushable containers with significant void space. However, areas designated not to undergo dynamic compaction or containing non-crushable containers with significant void space may result in limited subsidence damage to the final closure cap, some time during the 1000-year post-closure compliance period during which no closure cap maintenance is assumed be performed. These areas represent the worse case basis for the radon flux from the Slit and Engineered Trenches during the 1000-year post-closure compliance period.

For purposes of this investigation, modeling of the 1000-year post-closure compliance period will be based upon a trench cross-section containing non-crushable containers overlain by the operational soil cover and final closure cap as shown in Figure 1-3. It will be assumed that the waste zone containing non-crushable containers collapses from a 16 foot thickness to 2.5 feet (Phifer et al. 2006) at the beginning of the 1000-year post-closure compliance period, when no closure cap maintenance is assumed be performed. This results in subsidence of the closure cap and destruction of the individual layers of the closure cap. It will further be assumed that all closure cap materials above the erosion barrier are gone prior to waste collapse and closure cap subsidence. These assumptions result in 10.33 ft of clean material (i.e., operational soil cover and final closure cap through the erosion barrier) above the 2.5-foot waste zone for radon to diffuse through to the point which the Rn-222 flux was evaluated. See Figure 1-3 for a cross-section of the operational soil cover and final closure cap (the 48-inch clean layer in the figure represents the operational soil cover).

Materials are indicated with the associated thickness of each component in feet (Table 1-51).

Table 1-51. Vertical Layer Sequence and Thickness for Slit and Engineered Trench Profiles during the Pre- and Post-Closure Compliance Period

Layer	Vertical Thicknesses 125-Year Operations Period (ft)	Vertical Thicknesses 1000-Year Post-Operations Period (ft)
Final Closure Cap (through the Erosion Barrier)	---	6.33
Operational Soil Cover	4	4
Waste Layer	16	2.5

SOURCE: Adapted from Phifer et al. (2006)

1.10.3.2 Conceptual Model

The Rn-222 flux at the land surface above the Slit and Engineered Trenches was evaluated for the specific closure configurations discussed above. Rn-222 is generated within the waste zone by radioactive decay of different parent radionuclides following along the decay chains that lead to the formation of Rn-222. The decay chains for all possible parent radionuclides of Rn-222 are shown in Figure 1-35. In this figure, the parent radionuclides that were individually evaluated are indicated with the gray shaded area (i.e., beginning with Pu-238 and U-238). Rn-222 generated within the waste zone is in the gaseous phase and diffuses outward from this zone into the air-filled soil pores surrounding the Slit and Engineered Trenches, eventually resulting in some of the radon emanating at the land surface. As such, air is the fluid through which Rn-222 diffuses, although some Rn-222 may dissolve in residual pore water. It is assumed that fluctuations in atmospheric pressure at the land surface that could induce small pulses of air movement into and out of the shallow soil column will have a zero net effect over the long-term period of evaluation in this study, thus advective transport of Rn-222 in air-filled soil pores is not considered to be a significant process when compared to air diffusion.

The parent radionuclides exist in the solid phase and therefore do not migrate upward through the air-filled pore space, although they could be leached and transported downward from the waste zone by pore water movement. This potential downward migration of the parent radionuclides was neglected in the radon analysis.

The flux of Rn-222 from the Slit and Engineered Trenches was evaluated for two separate time periods: 1) 0 to 125 years, and 2) 125 to 1125 years. The first time period evaluated covers the operational and institutional control periods, during which a minimum 4-foot operational soil cover overlies the waste. The second time period evaluated covers the post-closure compliance period, after subsidence treatment and final closure cap installation.

1.10.4 Slit and Engineered Trench Radon Analysis Numerical Model

The mathematical model utilized in this report is provided by the PORFLOW simulation package. PC-based PORFLOW Version 5.97.0 was used to conduct a series of simulations. PORFLOW is developed and marketed by Analytic & Computational Research, Inc. to solve problems involving transient and steady-state fluid flow, heat and mass transport in multi-phase, variably saturated, porous or fractured media with dynamic phase change. PORFLOW has been widely used at the SRS and in the DOE complex to address major issues related to the groundwater and nuclear waste management.

The governing equation for mass transport of species k in the fluid phase is given by

$$\frac{\partial C_k}{\partial t} + \frac{\partial}{\partial x_i}(V_i C_k) = \frac{\partial}{\partial x_i}(D_{ij}\frac{\partial C_k}{\partial x_j}) + \gamma_k \qquad \text{Eq 1-3}$$

Where

C_k	concentration of species *k* , Ci/m^3
V_i	fluid velocity in the ith direction, m/yr
D_{ij}	effective diffusion coefficient for the species, m^2/yr
γ_k	net decay of species *k* , Ci/m^3 yr
i, j	direction index
t	time, yr
x	distance coordinate, m

(Boundary and initial conditions are discussed in Section 1.10.4.1)

This equation is solved using PORFLOW to evaluate transient Rn-222 transport above the Slit and Engineered Trenches and subsequent Rn-222 flux at the land surface over time. As explained, advection is not considered to be a significant process when compared to air diffusion, so the advection term was disabled within PORFLOW and only the diffusive and net decay terms were evaluated.

1.10.4.1 Model Development and Assumptions

The numerical representation of the conceptual model is as a 1-dimensional vertical stack of elements configured to represent the thickness of the Slit and Engineered Trench waste zone and anticipated operational soil cover and final closure cap, appropriate to the time frame under consideration.

Decay chains evaluated were U-238→Th-234→Pa-234m→U-234→Th-230→ Ra-226→Rn-222 and Pu-238 →U-234→Th-230→Ra-226→Rn-222. Each parent in these chains, except Th-234 and Pa-234m, were simulated separately as the starting point of the decay chain. Th-234 and Pa-234m have extremely short half-lives compared to the other parent radionuclides in these chains, and they were therefore not simulated separately as the starting point of the decay chain.

Only a fraction of the Rn-222 generated by the decay of each parent is available for migration away from its source and into open pore space. Since the Rn-222 parent radionuclides exist as oxides or in other crystalline forms, only a fraction of Rn-222 generated by decay of Ra-226 has sufficient energy to migrate away from its original location into adjacent pore space before further decay occurs (3.82 day half-life for Rn-222).

The emanation coefficient is generally defined as the fraction of the total amount of Rn-222 produced by radium decay that escapes from soil particles and enters the pore space of the medium. This is the fraction of the Rn-222 that is available for transport. In the case of the LAW Vault, the parent radionuclides are not embedded in soil but are contained within wastes of varying types stored within varying types of containers. Literature values for the Rn-222 emanation factor for these conditions are not available.

Studies have shown the emanation factor to vary between 0.02 and 0.7 for various soil types depending primarily on moisture content. Generally, higher emanation factors are associated with higher moisture contents.

RESRAD is a model used to estimate radiation dose and risk from residual radioactive materials. This US DOE and NRC approved code, assumes an emanation factor of 0.25 for Rn-222 which is representative of a silty loam soil with a low moisture content. For the LAW Vault radon pathway analysis, the RESRAD default emanation factor of 0.25 was chosen recognizing that literature values for wastes similar to the LAW Vault are not available. The use of 0.25 should be conservative since the waste is assumed to be dry and emanation factors reported in the literature for drier soils are much lower (Yu et al. 2001). To account for the emanation factor in the model, an effective source term of 0.25 Ci of parent radionuclide was utilized as the source term for each Ci disposed within the facility.

At 125 years, the waste zone is assumed to collapse thereby reducing the thickness of the waste zone from 16 ft to 2.5 ft. To account for this in the model, at 125 years, the remaining inventory of parent radionuclide in the lower portion of the waste zone was transferred to the upper 2.5 ft., as opposed to the lower 2.5 ft., as a conservative measure. The porosity of the lower half of the waste zone was set to zero essentially removing it from the model.

Since Rn-222 exists as a gas, air was assumed to be the medium within which radon transport occurs. The flow field was assumed to be isobaric and isothermal. The impact of naturally occurring fluctuations of atmospheric pressure is likely to have a zero net effect. Therefore, for the relatively long periods of time evaluated in this investigation, air-diffusion was the only transport mechanism simulated in the model and advective air-transport was assumed to be negligible.

Some radon dissolves in pore water but since diffusion proceeds more slowly in that fluid, air diffusion is the only transport process by which Rn-222 can reach the land surface from the Slit and Engineered Trenches. This assertion is substantiated in Yu, et al. 2001. In that report the D_{eff} for soil is reported to range from the radon open air diffusion coefficient of 1.0E-5 m^2/sec to that of fully saturated soil, 1.0E-10 m^2/sec. This 4-order of magnitude difference is consistent with the comparison of water diffusion coefficients to air diffusion coefficients of other common molecular compounds (Bolz and Tuve 1973).

Thus, the larger volume of water-filled pore space compared to air-filled pore space (maximum of 1 order of magnitude difference) is inconsequential, in terms of the ability of water-dissolved radon to diffuse through water-filled pores as compared to the ability of the same compounds to diffuse as gas in the vapor-filled pore spaces. In this investigation, transport was allowed to proceed only through air-filled pore space and, therefore, residual pore water was treated as if it was part of the solid matrix material within the flow field.

No credit was taken for airborne radon dissolving in pore water as it proceeds from the waste trenches to the land surface although it has been observed to partition between air and water in the ratio of 4 to 1, respectively, at 20° C (Nazaroff and Nero 1988).

The boundary conditions imposed on the domain included:

- No-flux specified for all radionuclides along sides and bottom
  ($\partial C/\partial X = 0$ at x_{min}, x_{max} and $\partial C/\partial Y = 0$ at y_{min})
- Species concentration set to 0 at land surface (top of erosion barrier)
  ($C = 0$ at y_{max})

where $x_{min} = 0$, $x_{max} = 1$m, $y_{min} = 0$m and $y_{max} = 6.1$m

The initial condition imposed on the domain included:

- Rn-222 concentration set to 0 for the entire model domain at time = 0
  ($C=0$ for $0 \leq x \leq 1$ at $t=0$ and $C=0$ for $0 \leq y \leq y_{max}$ at $t=0$)

The initial conditions for the model also assumed a 1 Ci inventory (prior to application of the emanation factor) of each parent radionuclide uniformly spread over the waste zone. The model does not account for an initial inventory of Rn-222 since it would readily migrate out of the waste containers prior to disposal operations and has a half-life of 3.8 days.

Simulations were conducted in transient mode for diffusive transport in air, with results being obtained over 1,125 years.

1.10.4.2 Measures Implemented to Ensure Conservative Results

In this analysis, several conditions introduce a significant measure of conservatism into the calculations. These include:

- The use of boundary conditions that force all of the Rn-222 to move upward from the waste disposal zone to the land surface. In reality, some of the Rn-222 diffuses sideways and downward in the air-filled pores surrounding the waste zone; hence ignoring this has the effect of increasing the radon flux at the land surface.
- Not taking credit for the removal of either Rn-222 or of the parent radionuclides by pore water moving vertically downward through the model domain. This mechanism would likely remove some dissolved Rn-222 in addition to the parent radionuclides, and therefore its omission has the effect of increasing the estimate of instantaneous Rn-222 flux at the land surface.
- The addition of an extra 125 years to the required 1,000-year evaluation period to account for any Rn-222 generated during the operational and institutional control period, thus incrementally increasing the instantaneous Rn-222 flux.
- Use of the top of the erosion layer in the soil cover as the land surface for the purpose of calculating Rn-222 flux during the 125- to 1125-year post-closure compliance period. No credit is taken for the additional distance Rn-222 must migrate above the erosion barrier prior to that portion of the soil cover eroding away.
- During the 125- to 1125-year post-closure compliance period the modeling is based upon a trench cross-section containing a non-crushable container waste zone which has collapsed to 2.5 feet. This both concentrates the radionuclide inventory in a thinner waste zone and minimizes the amount of clean material through which the radon must diffuse.
- Ignoring the presence of the GCL within the final closure cap. The GCL should be near 100 percent saturation; therefore it will contain very little air-filled porosity within which radon transport could occur.
- The assignment of E-Area operational soil cover prior to dynamic compaction (Phifer et al. 2006) properties to the closure cap following collapse of the non-crushable waste (125 to 1125 years). Some of the closure cap is likely to remain intact and retain its original material properties.

1.10.4.3 Grid Construction

The model grid was constructed as a node mesh 3 nodes wide by 55 nodes high. This mesh creates the vertical stack of 53 model elements. Figure 1-31 shows a schematic of the PORFLOW model grid. The grid extends from the bottom of the waste layer upward to the top of the erosion barrier. Extending the grid only to the top of the erosion barrier results in the minimum possible cover thickness over the waste that could exist during the 125 to 1,125 year period. A set of consistent units was employed in the simulations for length, mass and time, these being meters, grams and years, respectively.

1.10.4.4 Material Zones

The model domain was divided into the following four material zones: the lower waste zone (13.5 ft [4.11 m]); upper waste zone (2.5 ft (0.76 m)); operational soil cover (4 ft); and final closure cap (6.33 ft). The elements were scaled to correspond to the geometry of these zones. Table 1-52 and Table 1-53 list the individual components of the Slit and Engineered Trench model for the 125-year operational and institutional control period and the 1000-year post-closure compliance period, respectively. During the operational and institutional control periods (0 to 125 years), the land surface where the radon flux is determined is taken as the top of the operational soil cover. During the post-closure compliance period (125 to 1125 years), the waste zone is reduced to 2.5 ft and overlain by the operational soil cover and the final closure cap through the erosion barrier. During the post-closure compliance period, the land surface where the radon flux is determined is taken as the top of the erosion barrier. The properties assigned to the various zones of the model domain during the two time periods were chosen to correspond to the above configurations.

1.10.4.5 Material Zone Properties and Other Input Parameters

Material properties utilized within the 1-D numerical model were specified for the four material zones defined within the model domain for each of the time periods. Each material zone was assigned values of particle density, total porosity, average saturation, air-filled porosity, air density, and an effective air-diffusion coefficient for Rn-222. With the use of an effective radon air-diffusion coefficient, tortuosity was assigned a unit value in each material zone during both periods. An air fluid density of 1.24E+03 g/m^3 was used for each material zone during both periods. This air fluid density was obtained from the Bolz and Tuve (1973), *CRC Handbook of Tables for Applied Engineering Science*, and represents that of standard atmospheric conditions.

Table 1-52. Material Properties Utilized for the 0 to 125 Year Operational and Institutional Control Period.

Layer	Layer Thickness (ft)	Particle Density (g/cm^3)	Total Porosity (fraction)	Average Saturation (fraction)	Air-filled Porosity [4] (fraction)	Effective Radon Air-Diffusion Coefficient [5] (m^2/yr)
Final Closure Cap [1]	6.33	na	1	0	1	347 [6]
Operational Soil Cover	4	2.65 [2]	0.46 [2]	0.825 [3]	0.081	1.26
Upper Waste Zone	2.5	2.65 [2]	0.46 [2]	0.825 [3]	0.081	1.26
Lower Waste Zone	13.5	2.65 [2]	0.46 [2]	0.825 [3]	0.081	1.26

na = not applicable

[1] During the first 125 years of the simulation, the closure cap is assigned a total porosity of 1, an average saturation of 0, and a diffusion coefficient of radon in open air (347 m^2/yr)

[2] E-Area operational soil cover prior to dynamic compaction property values assigned from Phifer et al. (2006)

[3] Average saturation taken from the E-Area operational soil cover prior to dynamic compaction characteristic curve from Phifer et al. (2006) at a suction head (matrix potential) of 195 cm

[4] Air-filled Porosity = (1 – Average Saturation) × Total Porosity

[5] Determined from methodology developed by Nielson et al. (1984)

[6] Yu et al. (2001)

Table 1-53. Material Properties utilized for the 125 to 1,125 Year Post-Closure Compliance Period.

Layer	Layer Thickness (ft)	Particle Density (g/cm^3)	Total Porosity (fraction)	Average Saturation (fraction)	Air-filled Porosity [3] (fraction)	Effective Air-Diffusion Coefficient [4] (m^2/yr)
Final Closure Cap	6.33	2.65 [1]	0.46 [1]	0.825 [2]	0.081	1.26
Operational Soil Cover	4	2.65 [1]	0.46 [1]	0.825 [2]	0.081	1.26
Upper Waste Zone	2.5	2.65 [1]	0.46 [1]	0.825 [2]	0.081	1.26
Lower Waste Zone	13.5	na	0 [5]	na	0	na

na = not applicable

[1] E-Area operational soil cover prior to dynamic compaction property values assigned from Phifer et al. (2006)

[2] Average saturation taken from the E-Area operational soil cover prior to dynamic compaction characteristic curve from Phifer et al. (2006) at a suction head (matrix potential) of 195 cm

[3] Air-filled Porosity = (1 – Average Saturation) × Total Porosity

[4] Determined from methodology developed by Nielson et al. (1984)

[5] During years 125 to 1,125 of the simulation, the lower waste zone is assigned a total porosity of 0

During the 125-year operational and institutional control period the trenches consist only of the 16-foot waste layer and the 4-foot operational soil cover (see Table 1-52). Although the interim runoff cover, utilized during the first 125 years (see discussion in Section 2.3), includes the potential use of up to an additional 2-foot of soil to establish necessary grades to promote runoff, this soil was not included in the model during this time period. This soil was not included since it is only used as necessary and its thickness will be highly variable. Since the closure cap does not exist during this time period, the closure cap material zone of the model domain was assigned a total and air-filled porosity of one, which makes it have the properties of air.

Since the Slit and Engineered Trench waste layers contain significant soil, the operational soil cover and both waste zones of the model domain are assigned the particle density and total porosity properties of the E-Area operational soil cover prior to dynamic compaction as specified by Phifer et al. (2006). The E-Area operational soil cover prior to dynamic compaction soil represents relatively loose soil with a significant air-filled porosity through which radon diffusion can occur. E-Area vadose zone field pore pressure measurements indicate average suction levels in the approximate range of 50 to 200 cm (Nichols et al. 2000). A value of 200 cm represents the upper end of the range which will have a greater air-filled porosity. The average saturation for the operational soil cover and both waste zones were taken as the value of saturation at a suction head of approximately 200 cm from the characteristic curves for the E-Area operational soil cover prior to dynamic compaction (Phifer et al. 2006) in order to be consistent with field measurements. The air-filled porosity was calculated from the average saturation and total porosity as shown in Table 1-52. The particle density, total porosity, average saturation, air-filled porosity values utilized for each model domain material zone during the 125-year operational and institutional control period are summarized in Table 1-52.

At the beginning of the 1000-year post-closure compliance period, it is assumed that the waste zone containing non-crushable containers collapses from a 16 foot (4.88 m) thickness to 2.5 feet (0.76 m) (Phifer et al. 2006), when no closure cap maintenance is assumed to be performed. This results in subsidence of the closure cap and destruction of the individual layers of the closure cap. This reduction in waste layer thickness is handled utilizing the same model grid used for the prior time period (i.e., 0 to 125 years) by reassigning the radionuclide inventory of the lower 13.5 feet of the waste zone to the upper 2.5 feet of the waste zone and assigning a porosity of 0 to the lower 13.5 feet of the waste zone. While this is not necessarily intuitive, it is appropriate, since the migration of interest is upward rather than downward and since it results in no additional material through which upward diffusion has to occur. For this time period, the particle density and total porosity values for all layers, other than the lower waste zone, were assigned those of the E-Area operational soil cover prior to dynamic compaction (Phifer et al., 2006). The E-Area operational soil cover prior to dynamic compaction soil represents relatively loose soil consistent with conditions resulting from subsidence that has a significant air-filled porosity through which radon diffusion can occur. The average saturation for the final closure cap, operational soil cover, and upper waste zone was taken as the value of saturation at a suction head of approximately 200 cm from the characteristic curves for the E-Area operational soil cover prior to dynamic compaction (Nichols et al. 2000 and Phifer et al. 2006). The air-filled porosity was calculated from the average saturation and total porosity as shown in Table 1-53. The particle density, total porosity, average saturation, air-filled porosity values utilized for each model domain material zone during the 1000-year post-closure compliance period are summarized in Table 1-53.

The molecular diffusion coefficient of Rn-222 in open air is 347 m^2/yr (Nielson et al. 1984). Nielson et al. (1984) established a relationship between moisture saturation and the radon effective air-diffusion coefficient for various pore sizes of earthen materials. Using this method, a radon effective air-diffusion coefficient was determined for each material type based upon the average moisture saturation for the material. With the use of an effective air diffusion coefficient, tortuosity was assigned a unit value in each material zone. A summary of the radon effective air-diffusion coefficients by material zone are presented in Table 1-52 and Table 1-53, respectively for the 125-year operational and institutional control period and the 1000-year post-closure compliance period.

1.10.5 Model Results

Model simulations were conducted to evaluate the peak instantaneous Rn-222 flux at the land surface for the two time periods of interest. These time periods include 0 to 125 years and 125 to 1125 years. Model results were output in Ci/m^2/yr, consistent with the set of units employed in the model. A graph of these results is shown in Figure 1-36, although the units are converted to (pCi/m^2/sec) / (Ci/m^2), which are the units used to define the regulatory flux limit in DOE G 435.1-1. Figure 1-36 shows a sharp flux discontinuity at 125 years which results from the installation of the closure cap.

The maximum fluxes represent the peak Rn-222 flux per square meter at the land surface as defined for each simulation period and are listed in Table 1-54. The land surface for the 0- to 125-year time period was taken to be the top of the operational soil cover. For the 125- to 1125-year simulation period, the land surface was taken to be the top of the erosion barrier.

The calculated disposal limits per unit area and the disposal limits for the Slit and Engineered Trenches are presented in Table 1-55 for each of the 5 parent radionuclides. The unit-area disposal limit was calculated as follows:

> Disposal Limit per unit area (Ci/m^2) = Regulatory limit (20 pCi/m^2/s) / Maximum Inst. flux per unit area per unit inventory of parent radionuclide per unit area ([pCi/m^2/s]/Ci/m^2]).

The unit area limits for each of the 5 parent radionuclides were calculated using the maximum Rn-222 flux that occurred over the two time periods. For each radionuclide, the maximum flux of Rn-222 was observed during the initial 125-year simulation period prior to installation of the closure cap. Therefore, the peak flux of Rn-222 during the initial 125 year period was used to calculate the unit area limits for each radionuclide. The unit area limits for each of the 5 parent radionuclides were converted to Slit and Engineered Trench-specific disposal limits by multiplying the unit area limit for each by the maximum area utilized for disposal within the Slit and Engineered Trench footprints.

For the Engineered Trenches, the maximum area utilized for disposal used to determine the disposal limits is the smaller area of the two trenches in order to be conservative. The maximum area utilized for disposal within a Slit Trench footprint is 6098 m^2 (5 trenches/footprint × 20-foot wide × 656-foot long = 65,600 ft^2 / footprint). The maximum area utilized for disposal within an Engineered Trench footprint is 9063 m^2 (150-foot wide × 650-foot long = 97,500 ft^2 / footprint). The disposal limit results are presented in Table 1-55.

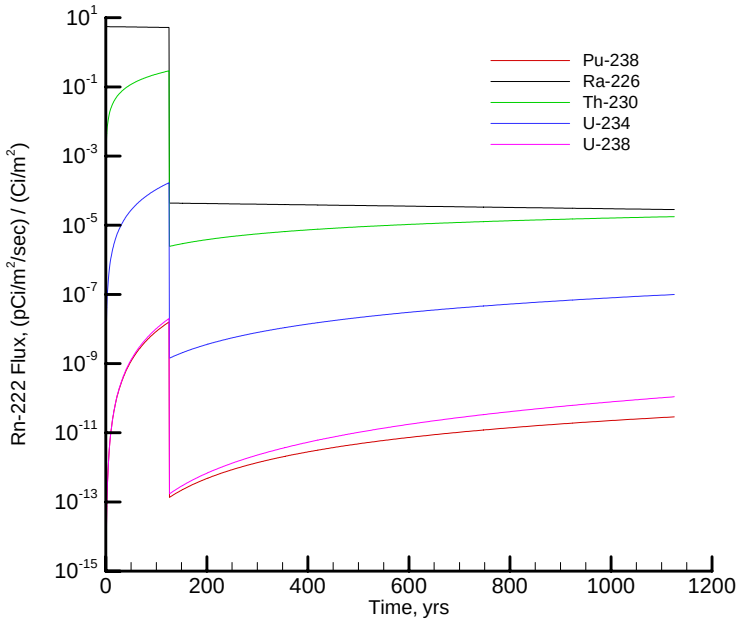

Figure 1-36. Rn-222 Flux at Land Surface Resulting from Unit Source Term

Table 1-54. Simulated Maximum Instantaneous Rn-222 Flux over 1,125-Years at the Land Surface

	Maximum Instantaneous Rn-222 flux at Land Surface ($pCi/m^2/s$)/(Ci/m^2)*	
Parent Source	**0-125 years**	**125-1125 years**
Pu-238	1.59E-08	2.88E-11
Ra-226	5.52E+00	4.38E-05
Th-230	2.91E-01	1.77E-05
U-234	1.69E-04	9.94E-08
U-238	2.00E-08	1.10E-10

*Flux resulting from unit source spread over unit area of trench (Ci/m^2)

Table 1-55. Slit and Engineered Trenches Disposal Limits for Parent Radionuclides

Parent Source	Maximum Instantaneous Rn-222 flux at Land Surface ($pCi/m^2/s$)/(Ci/m^2) [1]	Time to Max (years)	Disposal Limit Per Unit Area (Ci/m^2) [2]	Slit Trench Disposal Limit[3] (Ci/SLT)	Engineered Trench Disposal Limit[4] (Ci/ET)
Pu-238	1.59E-08	125	1.26E+09	7.7E+12	1.1E+13
Ra-226	5.52E+00	1	3.62E+00	2.2E+04	3.3E+04
Th-230	2.91E-01	125	6.88E+01	4.2E+05	6.2E+05
U-234	1.69E-04	125	1.18E+05	7.2E+08	1.1E+09
U-238	2.00E-08	125	1.00E+09	6.1E+12	9.1E+12

[1] Flux resulting from unit source term spread over unit area of trench (Ci/m^2).
[2] Disposal Limit per unit area (Ci/m^2) = 20 $pCi/m^2/s$ / Maximum Instantaneous Rn-222 flux at Land Surface
[3] Slit Trench Disposal Limit = Disposal Limit per unit area (Ci/m^2) × 6098 m^2
[4] Engineered Trench Disposal Limit = Disposal Limit per unit area (Ci/m^2) × 9063 m^2

1.11 REFERENCES

ACRI (Analytical & Computational Research, Inc.). 2004. *PORFLOW Version 5.0 User's Manual*, Revision 5, Analytical & Computational Research, Inc., Los Angeles, California.

Beres, D.A. 1990. *The Clean Air Act Assessment package-1988 (CAP-88) A dose and Risk Assessment Methodology for Radionuclide Emissions to Air.* U.S. Environmental Protection Agency Contract No. 68-D9-0170, Washington, DC.

Bolz, R.E. and G.L. Tuve, (Editors), 1973. *Handbook of tables for APPLIED ENGINEERING SCIENCE, 2'nd Edition*. CRC Press, 18901 Cranwood Parkway, Cleveland, OH.

Crapse, K.P. and J.R. Cook, 2006. *Atmospheric Pathway Screening Analysis for the E-Area Low Level Waste Facility*, WSRC-STI-2006-00159, Washington Savannah River Company, Aiken, SC 29808. 09/05/2006.

Collard, L.B. 2001. *Special Analysis for Disposal of High-Concentration I-129 Waste in Slit Trenches at the E-Area Low-Level Waste Facility*. WSRC-TR-2001-00021. Westinghouse Savannah River Company, Aiken, SC 29808.

Collard, L.B. and R.A. Hiergesell. *2004. SPECIAL ANALYSIS: 2004 General Revision of Slit and Engineered Trench Limits*. WSRC-TR-2004-00300, Rev. 0. Westinghouse Savannah River Company, Aiken, SC 29808. June 14, 2004.

Cook, J.R., and A.D. Yu. 2002. *SPECIAL ANALYSIS: Disposal of M-Area Glass in Trenches*. WSRC-TR-2002-00337, Rev. 1. Westinghouse Savannah River Company, Aiken, SC 29808. August 21, 2002.

Cook, J. R., Phifer, M. A., Wilhite, E. L., Young, K. E., and Jones, W. E. 2004. *Closure Plan for the E-Area Low-Level Waste Facility*, Revision 4, WSRC-RP-2000-00425. Westinghouse Savannah River Company, Aiken, South Carolina. May, 2004.

DOE 1999. Implementation Guide for use with DOE M 435.1-1. DOE G 435.1-1. U. S. Department of Energy, July 9, 1999.

Flach, G.P. 2004. *Groundwater Flow Model of the General Separations Area Using PORFLOW*. WSCR-TR-2004-00106. Westinghouse Savannah River Company, Aiken, SC 29808.

Flach, G.P., L.B. Collard, M.A. Phifer, K.P. Crapse, K.L. Dixon, L.D. Koffman, and E.L. Wilhite. 2005. Preliminary Closure Analysis for Slit Trenches #1 and #2. WSRC-TR-2005-00093. Westinghouse Savannah River Company, Aiken, SC 29808.

Hang, T., Collard, L. B., and Phifer, M. A. 2005. Unreviewed Disposal Question Evaluation: Subsidence Study for Non-Crushable Containers in Slit Trenches (U), Revision 0, WSRC-TR-2005-00104. Westinghouse Savannah River Company, Aiken, South Carolina. March 15, 2005.

Hiergesell, R.A. and W.E. Jones. 2003. *An Updated Regional Water Table of the Savannah River Site and Related Coverages*. WSRC-TR-2003-00250, Revision 0. Westinghouse Savannah River Company, Aiken, SC 29808.

Jones, W. E. and Phifer, M. A. 2002. Corrosion and Potential Subsidence Scenarios for Buried B-25 Waste Containers (U), WSRC-TR-2002-00354. Westinghouse Savannah River Company, Aiken, South Carolina. September 2002.

Kaplan, D.I. 2006. *Geochemical Data Package for Performance Assessment Calculations Related to the Savannah River Site (U*). WSRC-TR-2006-00004, Revision 0. Washington Savannah River Company, Aiken, SC 29808.

Koffman, L.D. 2006a. *SRNL All-Pathways Application*, WSRC-STI-2006-00179, Rev. 0. SRNL, Washington Savannah River Company, Aiken, SC 29808.

Koffman, Larry D. 2006b. *Automated Inadvertent Intruder Application, Version 2*. WSRC-TR-2006-00037. Savannah River National Laboratory, Aiken, SC. September 2006.

Lee, P. 2004. *Inadvertent Intruder Analysis Input for Radiological Performance Assessments,* WSRC-TR-2004-00295, Westinghouse Savannah River Company, Aiken, SC 29808.

Lee, P. 2006. *Atmospheric Dose Modeling for the E-Area Low Level Waste Facility at the Savannah River Site,* WSRC-STI-2006-00262, Washington Savannah River Company, Aiken, SC 29808.

McDowell-Boyer, L., Yu, A. D., Cook, J. R., Kocher, D. C., Wilhite, E. L., Holmes-Burns, H., and Young, K. E. 2000. *Radiological Performance Assessment for the E-Area Low-Level Waste Facility,* Revision 1, WSRC-RP-94-218. Westinghouse Savannah River Company, Aiken, South Carolina. January 31, 2000.

Nazaroff, W.W., and A.V. Nero (editors), 1998, *Radon and its Decay Products in Indoor Air*, John Wiley & Sons, New York, N.Y.

NCRP 1996. "Screening Models for Releases of Radionuclides to Atmosphere, Surface Water and Ground," NCRP report No. 123, National Council on Radiation Protection and Measurements, Bethesda, Maryland, Jan. 22, 1996.

Nichols, R. L., Looney, B. B., Flach, G. P., and Rossabi, J. 2000. Recommendations for Phase II Vadose Zone Characterization and Monitoring at the E-Area Disposal "Slit" Trenches and Mega-Trench (U), WSRC-TR-2000-00059. Westinghouse Savannah River Company, Aiken, South Carolina. February 2000.

Nielson, K.K., V.C. Rogers and G.W. Gee, 1984. *Diffusion of Radon through Soils: A pore distribution Model*, Soil Science Society of America, J. 48:482-487.

Phifer, M.A. 2003. *Saltstone Disposal Facility Mechanically Stabilized Earth Vault Closure Cap Degradation Base Case: Institutional Control to Pine Forest Scenario (U).* WSRC-TR-2003-00523. Westinghouse Savannah River Company, Aiken, South Carolina. December 18, 2003.

Phifer, M.A. 2006. *Software Quality Assurance Plan for the Hydrologic Evaluation of Landfill Performance (HELP) Model*. Q-SQA-A-00005, Rev. 0.

Phifer, M. A. and Wilhite, E. L. 2001. Waste Subsidence Potential versus Supercompaction, WSRC-RP-2001-00613. Westinghouse Savannah River Company, Aiken, South Carolina. September 27, 2001.

Phifer, M. A. and Nelson, E. A. 2003. *Saltstone Disposal Facility Closure Cap Configuration and Degradation Base Case: Institutional Control to Pine Forest Scenario (U)*, Revision 0, WSRC-TR-2003-00436. Westinghouse Savannah River Company, Aiken, South Carolina, September 22, 2003.

Phifer, M. A., 2004. Preliminary E-Area Trench Closure Cap Closure Sequence, Infiltration, and Waste Thickness (U), WSRC-TR-2004-00119. Westinghouse Savannah River Company, Aiken, South Carolina. March 2004.

Phifer, M. A., Millings, M. R., and Flach, G. P. 2006. Hydraulic Property Data Package for the E-Area And Z-Area Vadose Zone Soils, Cementitious Materials, and Waste Zones, WSRC-STI-2006-00198. Washington Savannah River Company, Aiken, South Carolina. September 2006

Swingle, R. F. and Phifer, M. A. 2006. Unreviewed Disposal Question Evaluation: Increased Disposal Volume in Slit and Engineered Trenches, Revision 0, WSRC-TR-2006-00186. Washington Savannah River Company, Aiken, South Carolina.

Taylor, G.A. 2006. *Software Quality Assurance Plan for Ideal Filemaker: An Application to Translate PORFLOW Output to All-Pathways Input*. G-SQP-A-00010, Rev. 0.

Taylor, G.A. and L.B. Collard. 2005. *Automated Groundwater Screening*. WSRC-TR-2005-00203, Rev. 0. SRNL, Washington Savannah River Company, Aiken, SC.

WSRC 2006. *SRS Waste Acceptance Criteria Manual,* Procedure Manual 1S. Washington Savannah River Company, Aiken, South Carolina. January 19, 2006.

Yu, C., A.J. Zielen, J.J. Cheng, D.J. LePoire, E. Gnanapragasam, S. Kamboj, J. Arnish, A. Wallo III, W.A. Williams, and H. Peterson, 2001. *Users Manual for RESRAD Version 6*, Environmental Assessment Division, Argonne National Laboratory. Chicago, Illinois.

This page intentionally left blank.

CHAPTER 2

COMPONENT-IN-GROUT TRENCHES

This page intentionally left blank.

2.0 COMPONENT-IN-GROUT TRENCHES

LIST OF FIGURES

LIST OF TABLES

2.0 COMPONENT-IN-GROUT TRENCHES

2.1 EXECUTIVE SUMMARY

Component-In-Grout disposal units are below-grade earthen trenches, which have essentially vertical side slopes and contain grout encapsulated waste components. Two such CIG Trench units or footprints [157-foot-wide by 656-foot-long], designated CIG-1 and CIG- 2, are anticipated. Each CIG footprint is divided into five, nominally 20-foot-wide by 650-foot-long trenches separated by a nominal 10 feet of undisturbed soil. Components to be disposed within the CIG Trenches consist of large radioactively contaminated equipment and other smaller wasteforms such as B-25 boxes to fill the space around and above the large equipment. The waste components are surrounded by a minimum one foot of grout.

Estimated CIG Trench disposal limits through the 1,000-year compliance period have been developed for the following pathways: groundwater protection, air, all-pathways, inadvertent intruder (resident scenario and post-drilling scenario), and radon. Table 2-1, Table 2-2, and Table 2-3 provide these estimated CIG Trench disposal limits. All instances of groundwater protection and all-pathways "limits" in this chapter refer to "preliminary limits" only, because they do not account for plume interaction or uncertainties. Trigger values for radionuclides that did not screen out of the groundwater and air analyses and were not specifically analyzed are given in Tables 4-4 and 4-5, respectively, in the Part C Background chapter. The trigger values were developed using very conservative screening methodologies and can be used as surrogate disposal unit limits should any of the listed radionuclides be proposed for disposal.

Table 2-1. Preliminary Groundwater Protection and All-Pathways Trench Disposal Limits for the CIG-1 Trench

Parent Radionuclide	CIG-1 Preliminary Inventory Limit 0-125 year (Ci)					CIG-1 Preliminary Inventory Limit 125-1,125 year (Ci)				
	Groundwater Protection				All-Pathways	Groundwater Protection				All-Pathways
	Beta-Gamma	Gross Alpha	Radium	Uranium		Beta-Gamma	Gross Alpha	Radium	Uranium	
Am-241	---	---	---	---	---	1.0E+04	5.0E+02	---	1.3E+12	1.5E+02
Am-243	---	---	---	---	---	1.9E+05	9.6E+03	---	5.4E+15	3.6E+03
C-14	4.4E+09	---	---	---	4.6E+09	5.0E-01	---	---	---	4.9E-01
C-14_K	5.7E+10	---	---	---	6.0E+10	4.7E+00	---	---	---	4.9E+00
Cl-36	9.9E+04	---	---	---	5.2E+04	1.3E-01	---	---	---	7.3E-02
Cm-244	---	---	---	---	---	---	---	---	---	---
Cm-245	---	---	---	---	---	7.5E+03	3.6E+02	---	9.8E+11	1.1E+02
Cm-247	---	---	---	---	---	1.4E+06	7.8E+03	---	5.1E+16	3.1E+03
Cm-248	---	---	---	---	---	4.4E+12	9.4E+03	---	---	8.6E+02
H-3 [1]	2.2E+05	---	---	---	1.0E+07	1.4E+05	---	---	---	3.7E+06
I-129	4.0E+04	---	---	---	2.4E+06	1.4E-04	---	---	---	8.2E-03
I-129_C	5.2E+06	---	---	---	3.2E+08	8.2E-03	---	---	---	5.0E-01
I-129_K	3.2E+07	---	---	---	1.9E+09	5.1E-02	---	---	---	3.0E+00
K-40	---	---	---	---	---	6.1E+07	---	---	---	1.3E+08
Mo-93	6.8E+02	---	---	---	3.3E+03	3.8E-01	---	---	---	1.8E+00
Nb-94	5.5E+18	---	---	---	3.1E+18	8.9E+00	---	---	---	5.0E+00
Ni-59	---	---	---	---	---	7.8E+00	---	---	---	1.9E+03
Np-237	---	---	---	---	---	2.2E+00	1.1E-01	---	3.0E+08	3.3E-02
Pd-107	---	---	---	---	---	9.4E+02	---	---	---	2.9E+03
Pu-238	---	---	---	---	---	3.4E+06	4.1E+04	5.5E+04	---	1.6E+05
Pu-239	---	---	---	---	---	5.0E+06	3.8E+06	---	---	4.8E+05
Pu-240	---	---	---	---	---	---	3.0E+18	---	---	1.2E+18
Pu-241	---	---	---	---	---	3.0E+05	1.5E+04	---	3.9E+13	4.6E+03

Table 2-1. Preliminary Groundwater Protection and All-Pathways Trench Disposal Limits for the CIG-1 Trench - continued

Parent Radionuclide	CIG-1 Preliminary Inventory Limit 0-125 year (Ci)					CIG-1 Preliminary Inventory Limit 125-1,125 year (Ci)				
	Groundwater Protection				All-Pathways	Groundwater Protection				All-Pathways
	Beta-Gamma	Gross Alpha	Radium	Uranium		Beta-Gamma	Gross Alpha	Radium	Uranium	
Pu-242	---	---	---	---	---	2.9E+13	3.3E+11	4.4E+11	---	1.3E+12
Pu-244	---	---	---	---	---	---	2.5E+18	---	---	1.0E+18
Ra-226	---	---	---	---	---	1.5E+00	1.9E-02	2.6E-02	---	7.4E-02
Se-79	---	---	---	---	---	---	---	---	---	---
Sn-126	---	---	---	---	---	---	---	---	---	---
Sr-90	---	---	---	---	---	1.4E+04	---	---	---	2.8E+05
Tc-99	3.3E+03	---	---	---	4.9E+03	4.4E-01	---	---	---	6.5E-01
Tc-99_K	5.7E+06	---	---	---	8.6E+06	1.3E+01	---	---	---	2.0E+01
Th-230	---	---	---	---	---	4.2E+00	5.5E-02	7.3E-02	---	2.1E-01
Th-232	---	---	---	---	---	9.3E+07	9.4E+07	1.3E+08	---	2.5E+08
U-233	---	---	---	---	---	---	---	---	---	---
U-234	---	---	---	---	---	9.5E+02	1.2E+01	1.6E+01	---	4.5E+01
U-235	---	---	---	---	---	3.7E+00	2.8E+00	---	---	3.6E-01
U-236	---	---	---	---	---	1.3E+15	1.3E+15	1.8E+15	---	3.5E+15
U-238	---	---	---	---	---	1.1E+06	1.2E+04	1.6E+04	---	4.7E+04
Zr-93	5.0E+18	---	---	---	3.0E+19	2.4E-01	---	---	---	1.4E+00

Note: Limits reported as "---" indicate that there is no limit or that the limit $\geq$ 5.41E+19 Ci
Note: Groundwater and all-pathways limits in this table are to be considered preliminary. Adjustments are made in the groundwater and all-pathways limits as appropriate based on consideration of plume overlap effects from adjacent unites in Chapter 6 and interpretation of sensitivity and uncertainty analyses in Chapter 7. Final limits are to be found in results tables in Chapter 7.

[1] H-3 Preliminary Inventory Limit values reduced by a factor of 10 to account for uncertainty associated with H-3 release from 232-F stainless steel process equipment

Table 2-2. Preliminary Groundwater Protection and All-Pathways Trench Disposal Limits for the CIG-2 Trench

Parent Radionuclide	CIG-2 Preliminary Inventory Limit 0-125 year (Ci)					CIG-2 Preliminary Inventory Limit 125-1,125 year (Ci)				
	Groundwater Protection				All-Pathways	Groundwater Protection				All-Pathways
	Beta-Gamma	Gross Alpha	Radium	Uranium		Beta-Gamma	Gross Alpha	Radium	Uranium	
Am-241	---	---	---	---	---	1.2E+04	6.0E+02	---	1.5E+12	1.8E+02
Am-243	---	---	---	---	---	2.3E+05	1.1E+04	---	6.3E+15	4.2E+03
C-14	5.2E+09	---	---	---	5.4E+09	5.4E-01	---	---	---	5.8E-01
C-14_K	6.8E+10	---	---	---	7.0E+10	5.4E+00	---	---	---	5.7E+00
Cl-36	1.2E+05	---	---	---	6.2E+04	1.6E-01	---	---	---	8.5E-02
Cm-244	---	---	---	---	---	---	---	---	---	---
Cm-245	---	---	---	---	---	8.9E+03	4.2E+02	---	1.2E+12	1.3E+02
Cm-247	---	---	---	---	---	1.7E+06	9.2E+03	---	6.1E+16	3.6E+03
Cm-248	---	---	---	---	---	5.2E+12	1.1E+04	---	---	1.0E+03
H-3 [1]	2.6E+05	---	---	---	1.2E+07	1.7E+05	---	---	---	4.4E+06
I-129	4.8E+04	---	---	---	2.9E+06	1.5E-04	---	---	---	9.6E-03
I-129_C	6.1E+06	---	---	---	3.7E+08	9.7E-03	---	---	---	5.8E-01
I-129_K	3.8E+07	---	---	---	2.3E+09	6.0E-02	---	---	---	3.6E+00
K-40	---	---	---	---	---	7.1E+07	---	---	---	1.6E+08
Mo-93	8.1E+02	---	---	---	3.9E+03	4.4E-01	---	---	---	2.1E+00
Nb-94	6.4E+18	---	---	---	3.7E+18	1.0E+01	---	---	---	5.8E+00
Ni-59	---	---	---	---	---	9.1E+00	---	---	---	2.3E+03
Np-237	---	---	---	---	---	2.6E+00	1.3E-01	---	3.5E+08	3.9E-02
Pd-107	---	---	---	---	---	1.1E+03	---	---	---	3.5E+03
Pu-238	---	---	---	---	---	4.0E+06	4.8E+04	6.5E+04	---	1.9E+05
Pu-239	---	---	---	---	---	6.0E+06	4.5E+06	---	---	5.7E+05
Pu-240	---	---	---	---	---	---	3.5E+18	---	---	1.4E+18
Pu-241	---	---	---	---	---	3.6E+05	1.8E+04	---	4.6E+13	5.5E+03

Table 2-2. Preliminary Groundwater Protection and All-Pathways Trench Disposal Limits for the CIG-2 Trench - continued

Parent Radionuclide	CIG-2 Preliminary Inventory Limit 0-125 year (Ci)					CIG-2 Preliminary Inventory Limit 125-1,125 year (Ci)				
	Groundwater Protection				All-Pathways	Groundwater Protection				All-Pathways
	Beta-Gamma	Gross Alpha	Radium	Uranium		Beta-Gamma	Gross Alpha	Radium	Uranium	
Pu-242	---	---	---	---	---	3.5E+13	3.9E+11	5.2E+11	---	1.5E+12
Pu-244	---	---	---	---	---	---	2.9E+18	---	---	1.2E+18
Ra-226	---	---	---	---	---	1.8E+00	2.3E-02	3.1E-02	---	8.8E-02
Se-79	---	---	---	---	---	---	---	---	---	---
Sn-126	---	---	---	---	---	---	---	---	---	---
Sr-90	---	---	---	---	---	1.7E+04	---	---	---	3.3E+05
Tc-99	3.9E+03	---	---	---	5.8E+03	5.1E-01	---	---	---	7.7E-01
Tc-99_K	6.8E+06	---	---	---	1.0E+07	1.5E+01	---	---	---	2.3E+01
Th-230	---	---	---	---	---	5.0E+00	6.4E-02	8.7E-02	---	2.5E-01
Th-232	---	---	---	---	---	1.1E+08	1.1E+08	1.5E+08	---	2.9E+08
U-233	---	---	---	---	---	---	---	---	---	---
U-234	---	---	---	---	---	1.1E+03	1.4E+01	1.8E+01	---	5.2E+01
U-235	---	---	---	---	---	4.3E+00	3.3E+00	---	---	4.2E-01
U-236	---	---	---	---	---	1.6E+15	1.6E+15	2.1E+15	---	4.1E+15
U-238	---	---	---	---	---	1.2E+06	1.4E+04	1.9E+04	---	5.6E+04
Zr-93	6.0E+18	---	---	---	3.6E+19	2.9E-01	---	---	---	1.7E+00

Note: Limits reported as "---" indicate that there is no limit or that the limit $\geq$ 5.41E+19 Ci
Note: Groundwater and all-pathways limits in this table are to be considered preliminary. Adjustments are made in the groundwater and all-pathways limits as appropriate based on consideration of plume overlap effects from adjacent unites in Chapter 6 and interpretation of sensitivity and uncertainty analyses in Chapter 7. Final limits are to be found in results tables in Chapter 7.

[1] H-3 Preliminary Inventory Limit values reduced by a factor of 10 to account for uncertainty associated with H-3 release from 232-F stainless steel process equipment

Table 2-3. CIG Trench Disposal Limits for Air, Intruder Scenarios, and Radon (for one CIG)

Parent Radionuclide	Air Pathway Disposal Limit (Ci) [1,2]	Resident Intruder Scenario Disposal Limit (Ci) [2,3]	Post-Drilling Intruder Scenario Disposal Limit (Ci) [2,3]	Radon Analysis Disposal Limit (Ci)[2]
Ac-227	---	1.9E+07	1.9E+06	---
Ag-108m	---	1.0E+01	2.5E+03	---
Al-26	---	1.6E+00	1.3E+03	---
Am-241	---	2.2E+04	1.5E+03	---
Am-242m	---	3.5E+04	2.1E+03	---
Am-243	---	6.9E+01	9.1E+02	---
Ar-39	---	---	4.7E+07	---
Ba-133	---	2.5E+09	3.4E+12	---
Bi-207	---	6.5E+04	1.2E+06	---
Bk-249	---	3.2E+04	5.6E+05	---
C-14	1.7E+06	---	1.6E+03	---
Ca-41	---	---	9.4E+03	---
Cd-113m	---	---	4.4E+08	---
Cf-249	---	8.2E+01	1.4E+03	---
Cf-250	---	4.3E+10	4.3E+05	---
Cf-251	---	2.1E+02	1.1E+03	---
Cf-252	---	2.2E+11	4.2E+07	---
Cl-36	1.0E+06	---	2.0E+01	---
Cm-242	---	1.0E+09	2.7E+06	---
Cm-243	---	7.1E+06	6.5E+05	---
Cm-244	---	3.7E+09	4.3E+05	---
Cm-245	---	2.7E+02	6.0E+02	---
Cm-246	---	1.2E+08	1.2E+03	---
Cm-247	---	1.8E+01	9.9E+02	---
Cm-248	---	1.6E+06	3.1E+02	---
Co-60	---	1.4E+09	---	---
Cs-134	---	9.5E+18	---	---
Cs-135	---	---	1.9E+04	---
Cs-137	---	1.3E+06	1.9E+06	---
Eu-152	---	1.5E+06	1.5E+10	---
Eu-154	---	2.7E+07	8.9E+13	---
Eu-155	---	1.8E+18	---	---
H-3	3.1E+07	---	1.3E+11	---
I-129	1.7E+02	1.2E+06	3.0E+02	---
K-40	---	2.6E+01	4.0E+02	---
Kr-85	---	6.0E+10	3.7E+14	---
Mo-93	---	---	3.8E+05	---
Na-22	---	1.8E+15	---	---
Nb-93m	---	---	5.3E+11	---
Nb-94	---	3.0E+00	2.2E+03	---

Table 2-3. CIG Trench Disposal Limits for Air, Intruder Scenarios, and Radon (for one CIG) - continued

Parent Radionuclide	Air Pathway Disposal Limit (Ci) [1,2]	Resident Intruder Scenario Disposal Limit (Ci) [2,3]	Post-Drilling Intruder Scenario Disposal Limit (Ci) [2,3]	Radon Analysis Disposal Limit (Ci)[2]
Ni-59	---	---	3.3E+05	---
Ni-63	---	---	9.5E+05	---
Np-237	---	3.4E+01	8.6E+01	---
Pa-231	---	1.8E+01	9.6E+01	---
Pb-210	---	9.0E+10	8.7E+05	---
Pd-107	---	---	6.9E+05	---
Pu-238	---	5.1E+06	1.4E+04	4.6E+14
Pu-239	---	3.6E+05	1.2E+03	---
Pu-240	---	1.0E+07	1.2E+03	---
Pu-241	---	6.6E+05	4.4E+04	---
Pu-242	---	8.5E+06	1.2E+03	---
Pu-244	---	1.5E+01	1.0E+03	---
Ra-226	---	3.5E+00	6.0E+01	1.3E+06
Ra-228	---	9.2E+07	5.7E+17	---
Rb-87	---	---	1.2E+04	---
S-35	2.4E+07	---	---	---
Sb-124	1.3E+06	---	---	---
Sb-125	5.7E+04	3.1E+16	---	---
Sc-46	---	---	---	---
Se-75	6.3E+05	---	---	---
Se-79	3.8E+05	---	1.9E+04	---
Sm-151	---	---	2.2E+07	---
Sn-113	4.0E+06	---	---	---
Sn-119m	4.8E+06	---	---	---
Sn-121	---	---	---	---
Sn-121m	4.6E+05	---	3.0E+07	---
Sn-123	6.7E+07	---	---	---
Sn-126	8.2E+02	2.5E+00	1.6E+03	---
Sr-90	---	---	1.6E+05	---
Tc-99	---	6.6E+07	1.9E+03	---
Th-228	---	4.7E+18	---	---
Th-229	---	2.5E+01	4.0E+02	---
Th-230	---	7.1E+00	1.5E+02	2.5E+07
Th-232	---	1.8E+00	1.2E+02	---
U-232	---	2.2E+03	5.5E+03	---
U-233	---	2.6E+02	1.7E+03	---
U-234	---	1.4E+03	2.7E+03	4.3E+10
U-235	---	7.2E+01	1.7E+03	---
U-236	---	1.1E+06	3.1E+03	---
U-238	---	3.1E+02	3.1E+03	3.6E+14

Table 2-3. CIG Trench Disposal Limits for Air, Intruder Scenarios, and Radon (for one CIG)- continued

Parent Radionuclide	Air Pathway Disposal Limit (Ci) [1,2]	Resident Intruder Scenario Disposal Limit (Ci) [2,3]	Post-Drilling Intruder Scenario Disposal Limit (Ci) [2,3]	Radon Analysis Disposal Limit (Ci)[2]
W-181	---	---	---	---
W-185	---	---	---	---
W-188	---	---	---	---
Zr-93	---	---	7.5E+05	---

[1] The disposal limit for two footprints would be greater than that for one, but less than twice that of two footprints.
[2] Intruder-based radionuclide disposal limits for a CIG Trench unit with a transient calculation for 1000 years.
Note: Limits reported as "---" indicate that there is no limit or that the limit $\geq$ 1E+20 Ci.
Note: Limits for special wasteforms (e.g. Mk50A, Cooling Tower) are the same as the limit for generic radionuclide.

2.2 INTRODUCTION AND GENERAL APPROACH

Component-In-Grout disposal units are below-grade earthen trenches, which have essentially vertical side slopes and contain grout encapsulated waste components. Two such CIG Trench units or footprints (157-foot-wide by 656-foot-long), designated CIG-1 and CIG- 2, are anticipated. Each CIG footprint is divided into five, nominally 20-foot-wide by 650-foot-long trenches separated by a nominal 10 feet of undisturbed soil. Components to be disposed within the CIG Trenches consist of large radioactively contaminated equipment and other smaller wasteforms such as B-25 boxes to fill the space around and above the large equipment. The waste components are surrounded by a minimum one foot of grout.

Estimated CIG Trench disposal limits through the 1,000-year compliance period have been developed for the following pathways: groundwater protection, air, all-pathways, inadvertent intruder (resident scenario and post-drilling scenario), and radon. All instances of groundwater protection and all-pathways "limits" in this chapter refer to "preliminary limits" only, because they do not account for plume interaction or uncertainties.

A groundwater transport analysis has been conducted to determine maximum well concentrations (as a function of time) within a 100-m buffer zone surrounding both CIG footprints. The main analysis tool employed was the PORFLOW code, which handles both flow and transport of radionuclide chains (i.e., parents and daughters) in porous media. Two-dimensional flow and transport analyses were conducted to describe in detail the migration of species from the CIG Trench units through the vadose zone to the underlying water table. The results from these 2-D vadose zone simulations (treated as source terms) were then input into a 3-D aquifer transport model to compute maximum groundwater concentrations of radionuclides within the 100-m buffer zone. Preliminary groundwater protection disposal limits over the 1,000-year compliance period for the each of the two CIG units (CIG-1 and CIG-2) were developed from the computed maximum groundwater concentrations using the Future Limits feature of the all-pathways application (Koffman 2006a). Additionally preliminary all-pathways disposal limits over the 1,000-year compliance period for each of the two CIG units were also developed from the computed maximum groundwater concentrations using the all-pathways application (Koffman 2006a).

An air pathway analysis has been conducted to determine air pathway disposal limits for 15 potentially volatile radionuclides over the 1,000 year compliance period for a single CIG Trench unit. The PORFLOW code was utilized for diffusional transport of radionuclides out of the CIG Trench unit to the ground surface and the CAP88 code was utilized for subsequent atmospheric transport and dose calculations. A one-dimensional PORFLOW diffusional transport analysis was conducted to determine the flux of species to the ground surface from the CIG Trench unit. The atmospheric transport and dose calculation results obtained using CAP88 were combined with the flux of species at the ground surface to develop air pathway disposal limits.

An inadvertent intruder analysis has been conducted to determine inadvertent intruder disposal limits over the 1,000 year compliance period for a single CIG Trench unit. The analysis was conducted using an automated inadvertent intruder computer application developed at SRNL (Koffman 2006b) for the resident and post-drilling inadvertent intruder scenarios.

A radon pathway analysis has been conducted to determine radon pathway disposal limits for 5 radon-producing parent radionuclides over the 1,000 year compliance period for each of the CIG Trench units. A one-dimensional PORFLOW diffusional transport analysis was conducted to determine the flux of radon to the ground surface from the CIG Trench units.

Within Chapter 7, Integration and Interpretation, the various CIG Trench disposal limits developed herein will be adjusted in consideration of the results of the CIG Trench uncertainty analyses reported in this chapter and the plume interaction analysis reported in Chapter 6, Integrated Facility Analysis.

2.3 GENERAL FACILITY DESCRIPTION AND LIFECYCLE

Figure 2-1 provides the layout of the two CIG Trench footprints relative to other E-Area LLWF disposal unit types. Each CIG footprint is divided into five, nominally 20-foot-wide by 650-foot-long trenches separated by a nominal 10 feet of undisturbed soil.

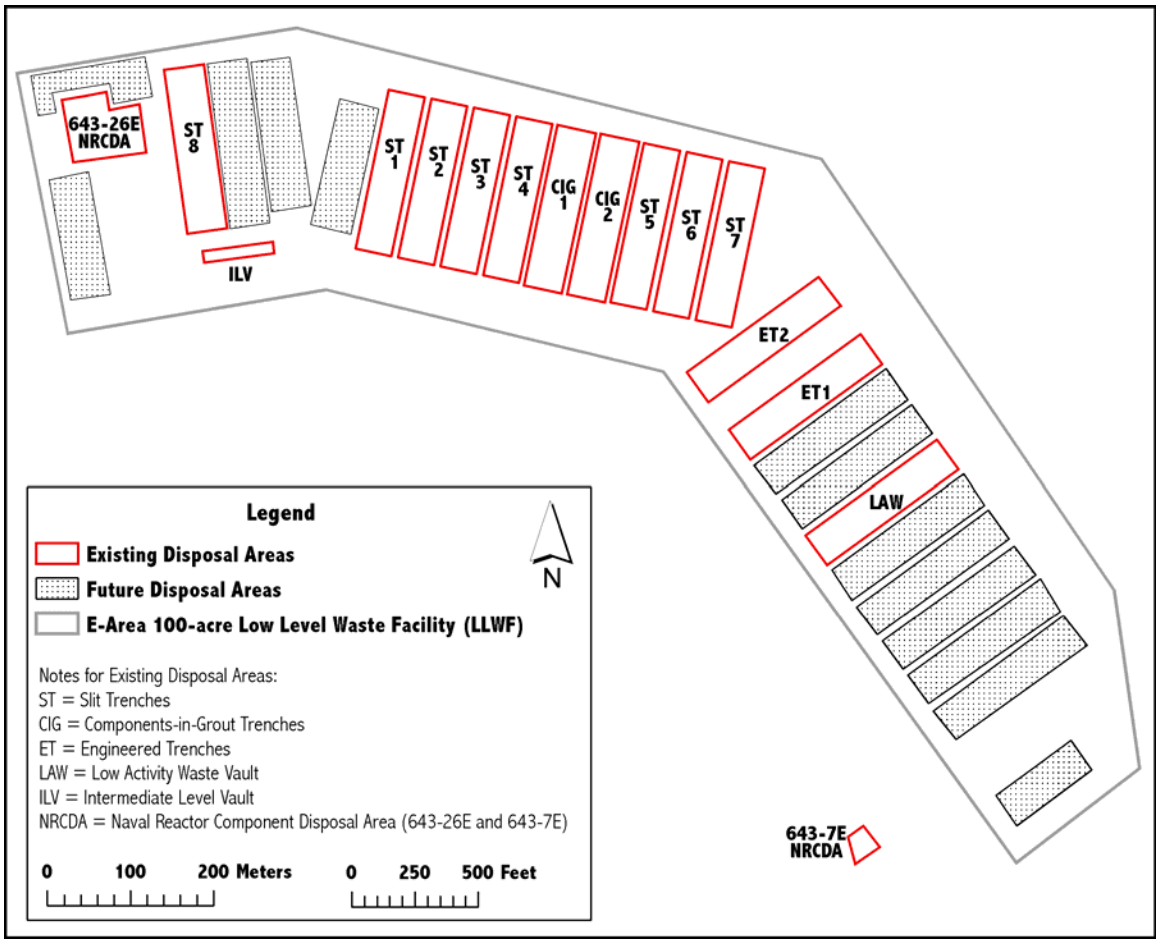

Figure 2-1. Location of CIG Trenches associated with the E-Area LLWF

Components to be disposed within the CIG Trenches consist of large radioactively contaminated equipment and other smaller wasteforms such as B-25 boxes to fill the space around and above the large equipment. Components to date consist of tankers, radioactive sources in a concrete culvert filled with grout, SeaLands, B-25s, B-12s, flatbed trailers, tanks, high integrity containers, columns, etc.

During the 25-year operational period, trench excavation is conducted on an as-needed basis and only to that depth, width, and length (i.e., trench segment) required for disposal of a particular component(s) to minimize the area of open trench, the time the trench section is open, and to minimize grout costs. The depth and width of each segment can vary greatly depending upon the size of the component(s) being disposed. The segments within a CIG Trench footprint are numbered in order of placement. The excavated soil is stockpiled for later use. Operational practice results in a nominal 6 feet of undisturbed soil separating each segment within an individual trench.

The bottom of a segment is filled with high flow grout to a minimum one-foot thickness, and the grout is allowed to solidify. The component(s) are then placed on the one-foot base grout layer with a crane and the grout is poured around, between, and over the component(s) in order to encapsulate the component(s). Additional layers of component(s) and grout may be placed on top of previous layers until a trench segment height of approximately 16 feet is filled up with component(s) and grout. The operation is conducted so that a minimum one foot of grout is between the component(s) and the surrounding soil at the bottom and sides of the trench segment and so that a minimum one foot of grout is over the top of the upper most component(s).

In order to ensure structural integrity for 300 years after disposal, components are filled with grout or CLSM, determined to be in and of themselves structurally sound for 300 years after burial, or overlaid with an 20-inch steel-reinforced 3000 psi concrete mat with CLSM between the top of the grout and bottom of the concrete mat. A 20-inch thick concrete mat is capable of supporting a 12.5-foot soil overburden from the final closure cap. Due to these stabilization options and component variability, the subsidence potential of CIG Trench segments is highly variable. The subsidence potential ranges from zero for segments 1-3, containing component(s) filled with grout or CLSM, to an estimated maximum of 10 feet for segments containing component(s) that are not filled or containing predominately B-25 boxes with low density waste. (Jones et al. 2004; Phifer 2004b; Peregoy 2006)

After the top grout has solidified, a 4-foot-thick clean layer of material is placed over the grout-encapsulated waste components. The 4-foot-thick clean layer includes an overlying soil, which is graded to provide positive drainage off and away from the CIG Trenches. This process continues until the entire trench is filled and completely covered with 4 feet of clean material.

The 4-foot-thick clean layer consists of one of the following:

- A minimum 4-foot layer of clean soil from the excavation stockpile placed in a single lift with a bulldozer (i.e., operational soil cover), or
- A combination from bottom to top of a nominal 1.33-foot layer of CLSM, a minimum 20-inch-thick concrete mat, and a nominal 1-foot layer of clean soil from the excavation stockpile is placed over the grout encapsulated waste components for a minimum 4-foot thickness. The reinforced concrete mat utilizes minimum 3000 psi concrete, is a minimum 20-inch thick, extends 1 foot beyond the aerial dimensions of the grout on all sides, includes #8 rebar at 6-inch spacing across the width of the trench and #4 rebar at 6-inch spacing along the length of the trench tied to the #8 rebar, and the rebar is placed at the bottom of the mat and has a minimum concrete cover of 3-inches. (Peregoy 2006)

In addition to this 4-foot soil cover, an interim runoff cover will be installed within 3 months after each CIG Segment has been emplaced. The interim runoff cover will be maintained during both the 25-year operational period and the following 100-year institutional control period. The interim runoff cover will involve the placement of up to an additional 2-foot of soil over the CIG Segments, that is graded to promote even greater drainage off the Segment. The interim runoff cover will consist of the surface application of a HDPE geomembrane or geotextile fabric with spray on asphalt emulsion or some other water-shedding material. It will extend a minimum of 10 feet beyond the edge of all sides of each segment (Phifer et al. 2006).

At the end of the 25-year operational period, a second interim runoff cover will be placed over the first. The difference between these two covers is that the second will be placed over an entire CIG Trench (operations will have ceased), and graded appropriately to facilitate drainage. Otherwise, the two interim runoff covers are similarly constructed.

Final closure of the CIG Trenches will take place at final closure of the entire E-Area LLWF, at the end of the 100-year institutional control period. Dynamic compaction of the CIG Trenches will not be conducted. Final closure will consist of the installation of an integrated closure system designed to minimize moisture contact with the waste and to provide an intruder deterrent. The integrated closure system will consist of one or more closure caps installed over all the disposal units and a drainage system Figure 2-2 provides the anticipated CIG Trench closure cap configuration and Figure 2-3 provides a cross-section of the closure cap over a 157-foot-wide CIG Trench footprint (McDowell-Boyer et al. 2000; Cook et al. 2004; Phifer et al. 2006).

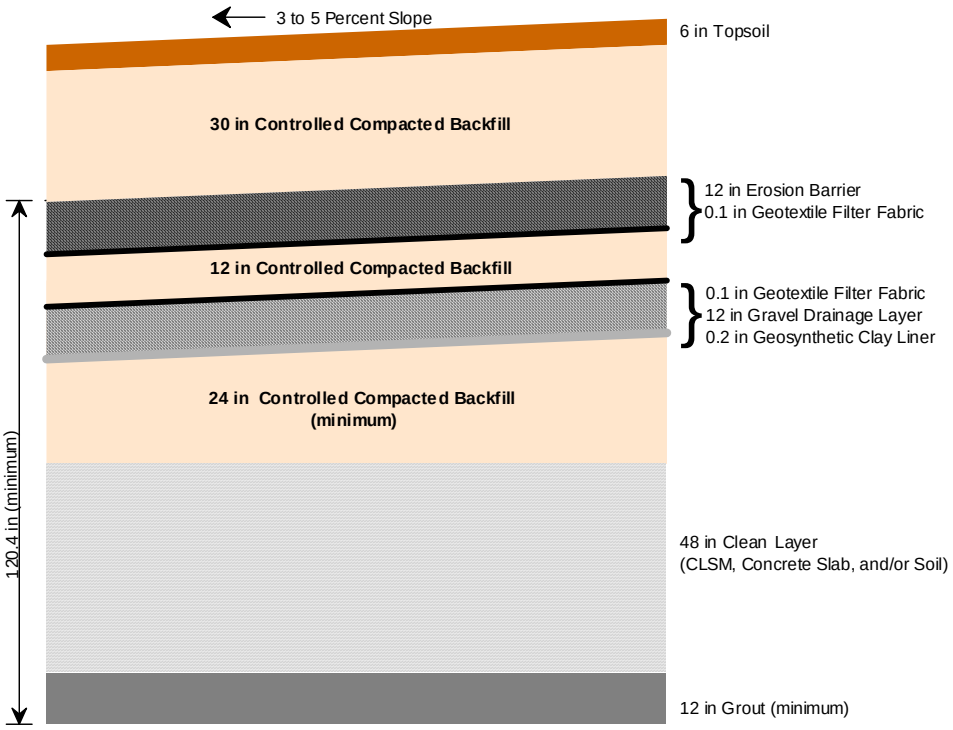

Figure 2-2. CIG Trench Closure Cap Configuration

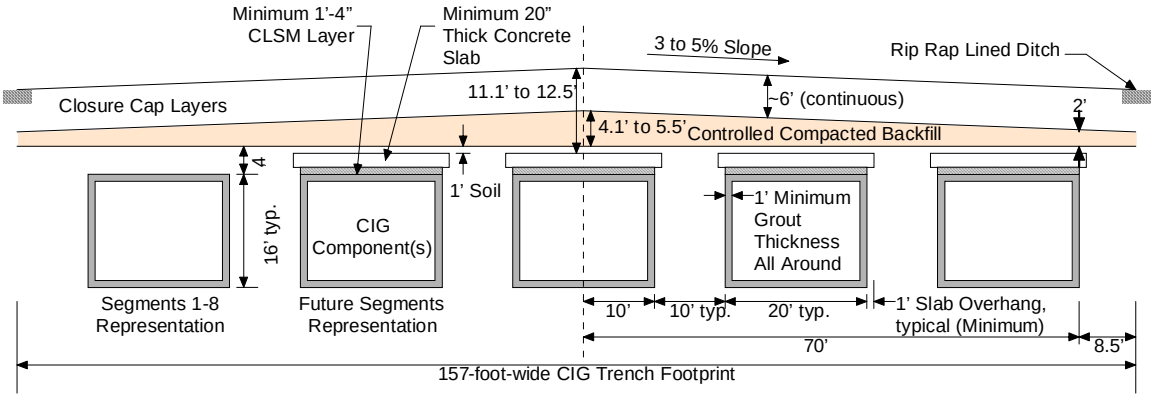

Figure 2-3. CIG Trench Closure Cap Cross-Section

Currently waste has been placed within CIG Trench footprint CIG-1 within Segments 1 through 8. The following provides information on these existing segments:

- CIG-1 Segments 1 through 3: The interiors of the components within segments 1 through 3 were filled with grout or CLSM; therefore there is essentially no significant void space within these segments. These segments are covered with an interim runoff cover.
- CIG-1 Segments 4 through 7: Many of the components and other wastes within segments 4, 5, 6, and 7 consist of low strength containers such as B-25 boxes, Tankers, and SeaLands with significant interior void space. These segments are covered with an interim runoff cover. Installation of a reinforced concrete mat over these segments is planned prior to installation of the E-Area LLWF final closure cap over these segments at the end of the 100-year institutional control period (the timing of this installation is yet to be determined).
- CIG-1 Segment 8: This segment has been overlaid with CLSM, an 18-inch thick reinforced concrete mat, and clean soil. This 18-inch thick concrete mat is capable of supporting an 11.4-foot soil overburden from the final closure cap (Peregoy 2006). This segment is covered with an interim runoff cover.

Figure 2-4 provides photographs of the placement sequence for existing CIG-1 Segment 6.

Emplacement of Bottom Foot of Grout

Component Emplacement

Grouting Sides of Segment

Initial Waste Layer Encapsulated

Top of Grout

4-Foot of Clean Soil Cover

Figure 2-4. CIG-1 Segment 6 Placement Sequence

2.4 CIG TRENCH PRINCIPAL DESIGN FEATURES

2.4.1 CIG Trench Structural Stability and Cover Integrity

Structural stability of the CIG Trenches is ensured for a minimum 300 years after disposal by filling components with grout or CLSM, determining that components are in and of themselves structurally sound for 300 years after burial, or overlaying segments with an 20-inch steel-reinforced 3000 psi concrete mat with CLSM between the top of the grout and bottom of the concrete mat. A 20-inch thick concrete mat is capable of supporting a 12.5-foot soil overburden from the final closure cap. Due to these stabilization options and component variability, the subsidence potential of CIG Trench segments is highly variable. The subsidence potential ranges from zero for segments containing component(s) filled with grout or CLSM to an estimated maximum of 10 feet for segments containing component(s) that are not filled or containing predominately B-25 boxes with low density waste (Jones et al. 2004; Phifer 2004b; Peregoy 2006).

Since steps have been taken to ensure CIG Trench segment structural stability for a minimum of 300 years, it is not anticipated that the integrity of the interim runoff cover will be impacted by subsidence.

The final E-Area LLWF closure cap will be installed at the end of the 100-year institutional control period (Phifer 2004a). After installation it is assumed that no closure cap maintenance will be performed other than that required for establishment of the vegetative cover. Therefore it is assumed that the hydraulic properties of the closure cap will immediately begin to degrade after construction due to the following (Phifer and Nelson 2003; Phifer 2004a):

- Formation of holes in the upper GCL by pine forest succession,
- Reduction in the saturated hydraulic conductivity of the drainage layers due to colloidal clay migration into the layers, and
- Erosion of layers that provide water storage for the promotion of evapotranspiration.

After 300 years it is assumed that subsidence of CIG Trench segments could occur and affect the integrity of the final E-Area LLWF closure cap. It is anticipated that such subsidence will be highly variable due to the stabilization option utilized and component variability.

2.4.2 CIG Trench Water Infiltration

During the 25-year operational period and 100-year institutional control period, water infiltration through the waste, is minimized by minimizing the area of open trench, minimizing the time a trench segment is open, encapsulating the components in grout, and placement of an interim runoff cover (Cook et al. 2000, Rev. 4) over each CIG Segment within 3 months after the given CIG Segment's grouting activities are completed. The interim runoff cover will be maintained during both the operational period and the following institutional control period. The interim runoff cover will involve the placement of up to an additional 2-foot of soil over the CIG Segments, that is graded to promote even greater drainage off the Segment. The interim runoff cover will consist of the surface application of a HDPE geomembrane or geotextile fabric with spray on asphalt emulsion or some other water-shedding material. It will extend a minimum of 10 feet beyond the edge of all sides of each segment. The interim runoff cover minimizes infiltration into the soil column overlying the waste while the grout encapsulation diverts water around the waste (Phifer et al. 2006).

The final closure cap minimizes infiltration through the waste during the post-institutional control period. However after installation, as outlined above, it is assumed that no cap maintenance will be performed other than that required for establishment of the vegetative cover. Therefore the hydraulic properties of the cap are assumed to degrade resulting in increased infiltration through the cap over time. Additionally, as outlined above, after 300 years it is assumed that subsidence of CIG Trench segments could occur, affect the integrity of the final E-Area LLWF closure cap, and result in increased infiltration.

2.4.3 CIG Trench Inadvertent Intruder Barrier

Inadvertent intrusion into CIG Trench waste is not considered feasible during the operational and institutional control periods, due to facility security during these periods. However it is assumed that inadvertent intrusion could occur during the post-institutional control period. During the 300 year period of wasteform structural stability, the grout encapsulation is assumed to provide a barrier to normal residential construction and well drilling equipment used in the vicinity of the SRS, since it is not capable of penetrating the grout (McDowell-Boyer et al. 2000).

Additionally the closure cap (Figure 2-2) includes an erosion barrier designed to maintain a minimum of 10 ft of clean material above the waste. This distance above the waste provides a barrier to excavation into the waste, since it is assumed that excavations for residential construction do not exceed 10 ft (McDowell-Boyer et al. 2000). Although it is constructed of large cobbles, the erosion barrier is not assumed to provide a barrier to drilling into the waste.

2.5 CIG TRENCH WASTE CHARACTERISTICS

2.5.1 Waste Type/Chemical and Physical Form

CIG waste is predominantly large equipment, tanks, and containerized waste contaminated with radioactive materials. Multiple components, large equipment, or containers can be disposed in a single CIG segment. The smaller wasteforms, such as B-25 boxes, are used to fill in the space around and above the larger equipment. Components to date consist of tankers, radioactive sources in a concrete culvert filled with grout, SeaLand containers, B-25s, B-12s, flat bed trailers, tanks, high integrity containers, columns, etc.

2.5.2 Radionuclide Inventory

The existing inventory for the cement-stabilized encapsulated waste is given in Appendix C.

2.5.3 Waste Volume

CIG Trenches are contained within 157-foot-wide by 656-foot-long footprints. Two CIG Trench footprints, designated CIG-1 and CIG- 2, are anticipated. Each CIG footprint is laid out into five, nominally 20-foot-wide by 650-foot-long trenches separated by a nominal 10 to 14 feet of undisturbed soil. Trench width and depth can vary based on component size. A CIG footprint, which includes five trenches, has slightly less waste volume capacity than a Slit Trench footprint, due to surrounding the waste with a minimum 1-foot of grout on the bottom, top, and sides (i.e., 5 times 650 ft L x 18 ft W x 14 ft D, or 819,000 ft^3 .

2.5.4 Packaging Criteria

Packaging criteria are described in the WAC in the SRS 1S Manual, Waste Acceptance Criteria (WSRC 2006). Generators follow WAC requirements for packaging and shipping waste to applicable waste disposal facilities in E-Area. The PA process sets many of the criteria that are the basis for the WAC.

2.5.5 Pre-Disposal Treatment Methods

Some items with large void spaces (such as tanks) have been filled with either grout or CLSM prior to disposal. Some containers with a small amount of liquids (water) are solidified/stabilized prior to disposal. In some rare occurrences, significant amounts of liquid are solidified/stabilized. Waste placed in these trenches is encapsulated by a cementitious grout as an alternative to vault disposal. The PA process sets many of the criteria that are the basis for the WAC.

2.5.6 Waste Acceptance Restrictions

Waste acceptance for disposal in the CIG Trenches must conform to criteria put forth in the SRS WAC (WSRC 2006). The PA process sets many of the criteria that are the basis for the WAC.

2.6 GROUNDWATER TRANSPORT ANALYSIS

Within this section the details associated with computing CIG preliminary groundwater limits for groundwater protection and all pathways are presented. The limits developed within this section are considered preliminary, since they do not take into consideration the effects of plume overlap from adjacent units or the results of sensitivity and uncertainty analyses. The effects of plume overlap are considered in Chapter 6, and the interpretation of sensitivity and uncertainty analyses is conducted in Chapter 7. Final limits are provided in Chapter 7.

The methodology employed and the key aspects of the analyses performed are discussed. To establish CIG inventory limits for all radionuclides of interest, maximum well concentrations (as a function of time) within a 100-m buffer zone surrounding both CIG units are required. A summary (in tabular form) of estimated CIG maximum well concentrations within a 100-m buffer zone is provided with graphical results in Appendix A2.

The overall methodology chosen is a hybrid approach where most parameters were set to their best estimate values (i.e., based on available site-specific measurements, literature, or engineering judgment), while other parameters were set to conservative/bounding values. The conceptual flow and transport PORFLOW models selected have imbedded within them modeling biases that are intended to be conservative where possible. These settings and conceptual models establish the baseline case (i.e., sometimes referred to as the nominal case).

2.6.1 Relation of Current Analysis to Previous Analyses

The current analysis approach employed for CIG performance assessment is different than prior approaches. For example, to list a few of the key differences:

- New material flow and transport properties are used for all materials considered (i.e., both cementitious and non-cementitious materials such as grout and soils, respectively)
- A new K_d database was used where CDP effects were incorporated into the baseline set of analyses
- Refined meshes for both the aquifer and vadose zone models (i.e., in some cases one order in magnitude refinement was employed)
- Initially only a Soil Covers are in place followed by an Interim Runoff Covers employed within the 25 year operational period
- New infiltration rate boundary conditions were employed
- New trench designs to incorporate concrete slabs that mitigate risks of early subsidence potential
- Reassessment of H-3 existing inventories at time of burial to take credit for certain special wasteforms and available process knowledge

- Existing radionuclide inventories addressed uniquely (i.e., both spatially and temporally) and separate from future disposal inventories that are handed by the standard burial approach (i.e., all buried simultaneously and spatially uniform)
- All species were contained within special waste containers (e.g., B-25 boxes) whose hydraulic properties went from sealed and intact to leaking after 40 years of burial
- Some species were addressed as volatile components whose diffusion coefficients were large within their special waste containers
- Depth of water table to grout chamber increased from 25 ft to 35 ft (see Millings and Phifer (2007))

As such, the set of CIG analyses contained within this Performance Assessment document supersedes all prior performance assessments and special analyses to date with regard to CIG inventory limits.

2.6.2 Overview of Groundwater Transport Analysis

The approach taken focuses primarily on a baseline scenario where nominal settings for many of the input parameters have been conservatively chosen. The main analysis tool employed is the PORFLOW code which handles both flow and transport of radionuclide chains (i.e., parents and daughters) in porous media. Two-dimensional flow and transport analyses are used to describe in more detail the migration of species from buried CIG Trench segments to the underlying water table. The results from these 2-D Vadose Zone simulations (treated as source terms) are then input into a 3-D transport only aquifer (saturated zone) model to compute maximum well concentrations of radionuclides within a 100-m buffer zone. These aquifer analyses are performed where both CIG units are being considered together in establishing inventory limits.

To accommodate the methodology used to arrive at inventory limits for future disposals and address the sum –of-fraction method, the all-pathways method, and plume interaction studies, for each potential radionuclide to be buried within a CIG segment two sets of aquifer transport runs are necessary:

- One set of analyses was performed where all existing inventories (within Segments 1 through 8) were applied as source terms for those buried radionuclide parents who were provided within the WITS database for these existing segments.
- Another set of analyses was performed where all future inventories were applied uniformly over available trench regions in both CIG units (i.e., those regions not already occupied by existing segments) as source terms for those radionuclide parents who are potentially going to be buried in future CIG disposals.

By making use of the linearity assumption of the saturated groundwater transport equation, these two aquifer cases above can be used to arrive at combined contributions each contributing to a maximum well concentration within the 100-m buffer zone. The first set of analyses above is based on a known amount of buried parents (in gmoles or Curies) in the 8 existing segments of CIG-1. In the second set of analyses above, one unit of each buried parent (in gmoles or Curies) is considered. In arriving at the composite effect in the 100-m buffer zone for each trench, the existing inventory establishes a remaining margin to a required criterion (e.g., an MCL) for CIG-1. This remaining margin represents the remaining quantity (i.e., amount of future inventory) that can be placed in CIG-1 while still meeting the specified criterion. Some degree of conservatism occurs here since the maximum well concentration for each case will most likely occur at different spatial and temporal points within the 100-m buffer zone.

2.6.3 Summary of Key Groundwater Transport Assumptions

The following section (2.6.3.1) summarizes key inputs and assumptions with implications for design and operation of this disposal unit (see also Appendix B). Section 2.6.3.2 summarizes other important modeling inputs and assumptions that do not necessarily need to be operationally protected.

2.6.3.1 Key Design and Operational Assumptions

For CIG groundwater transport analysis purposes, time zero was set to the date 7/17/2001 (i.e., the calendar date when Segment 2 was placed into operation). For computational purposes Segments 1, 2, and 3 were combined and the burial date of Segment 2 was chosen as the mid-point. As such, the 25 year operational window ends, and the start of the institutional control period begins, on 7/17/2026. The end of institutional control occurs on 7/18/2126.

Rainfall infiltration rates can have a significant impact on the migration rates of radionuclides within subsurface vadose zone region. Various operational assumptions have been made in controlling these infiltration rates imposed on the segments within each CIG unit. The key assumptions made in the analyses are listed in Table 2-4 (infiltration values from Phifer et al. [2006]).

Table 2-4. E-Area CIG Trench Infiltration Barrier Hydraulic Requirements

Calendar Date	Modeling Year	Period	Layer Employed to Provide Infiltration Control	Infiltration Requirement (in/yr)
7/17/2001	0.0	Operations without a Runoff Cover over any portion of the CIG units	Operational Soil Covers	12.70
4/1/2006	4.7	Operations using a Runoff Cover with a 10 ft overhang for the 8 existing segments of CIG Unit 1	Maintained Interim Runoff Cover where runoff handled using appropriate drainage systems	0.36
4/1/2007 and beyond	5.7 and beyond	Operations using a Runoff Cover with a 10 ft overhang for future segments of CIG Units 1 and 2	Maintained Interim Runoff Cover where runoff handled using appropriate drainage systems	0.36
7/17/2026	25.0	Operations using a Runoff Cover covering entire CIG Units 1 and 2	Maintained Interim Runoff Cover where runoff handled using appropriate drainage systems	0.36
7/18/2126	125.0	Closure Cap covering entire CIG Units 1 and 2	GCL covering entire CIG Units 1 and 2 where runoff handled using appropriate drainage systems	0.41

Based on earlier scoping analyses, that evaluated the existing tritium inventories buried in Segments 1 through 8, a recommendation to place Interim Runoff Covers with a minimum of 10 ft overhang was made. Emplacement of these Interim Runoff Covers for Segments 1 through 8 was incorporated into disposal operations by 4/1/2006. It is also required that the runoff from these Interim Runoff Covers be handled by a drainage system designed to remove these flows. It is assumed that all runoff is entirely removed from the CIG region and does not impact either the local Vadose Zone or Aquifer flow fields. Emplacement of similar Interim Runoff Covers are required for all future segments within 3 months of their creation.

In the groundwater flow and transport analyses it is assumed that subsidence does not occur until after 325 years (i.e., 200 years beyond the 25 years of operation plus 100 years of institutional control). It is assumed that during the first 125 years subsidence surveillance and maintenance will be performed. Beyond this 125-year period, reliance must be made on existing engineered design features. Twenty-inch-thick, rebar reinforcement, concrete slabs above the grout chambers are planned for all future CIG segments. The existing Segment 8 has an 18-inch-thick, rebar reinforcement, concrete slab. Segments 1 through 7 have only soil backfill over their grout chambers.

A structural calculation (Peregoy 2006) conducted for the CIG Trenches demonstrates that Segments 1, 2, and 3 (with grout-filled components) can support interim and final closure cap loads. Future segments which contain only grout-filled components will also be able to support interim and final closure cap loads. Segments 4, 5, 6, and 7 can support interim loads, but a 20-inch thick cover slab will be required to support final closure cap loads (maximum of 12.5 feet of soil overburden). The slab must be emplaced prior to the end of the 100-year institutional control period and installation of the final closure cap. The 18-inch thick cover slab over segment 8 is capable of supporting interim loads and an 11.4-foot thick soil overburden associated with the final closure cap. This restriction will be considered in the design of the final closure cap. Future segments will require a 10-inch thick cover slab to support the final closure cap loads (maximum 12.5-foot thick soil overburden). The slabs on future segments will be emplaced immediately following disposal. Peregoy (2006) determined that all CIG segments conforming to the above will maintain structural stability for at least 300 years.

Based on hydraulic measurements (and subsequent "limited" performance analyses) of the existing grout formulations used for Segments 1 through 8, it has been determined that future CIG segments should have better hydraulic barrier performance. Basically, to achieve desired CIG inventory limits improved grout chambers for future segments is required.

As such, all future CIG segments are to be created using a new grout or concrete formulation and implementation procedure. Table 2-5 shows some selected hydraulic values used in describing the future grout performance employed in these analyses. Criteria values below a water saturation of 0.8 are not provided since analysis to date indicates that these cementitious materials generally have higher water saturation values (see Figure 2-29 through Figure 2-33).

Table 2-5. Minimum Hydraulic Conductivity Requirement for Future Grout Barrier Formulations for First 325 Years

Water Saturation (-)	Relative Permeability (-)	Unsaturated Hydraulic Conductivity [a] (cm/s)
1.00	1.0000	1.000E-08
0.95	0.1544	1.544E-09
0.90	0.0748	7.480E-10
0.85	0.0401	4.014E-10
0.80	0.0221	2.207E-10

a Unsaturated hydraulic conductivity calculated by multiplying saturated hydraulic conductivity of 1.0E-08 cm/s by relative permeability.

For the engineered grout barrier no degradation of the hydraulic properties are assumed throughout the first 325-year time period (e.g., no account is taken for potential cracking of aging grout walls and internal regions). However, simple hydraulic analysis of the grout chamber indicates that through-wall cracks covering less than ~1% of its surface area would be acceptable. Based upon no evidence of significant cracking associated with test pours, calculations demonstrating structural stability (Peregoy 2006), and engineering judgment, it is assumed that through-wall cracking greater than 1% is highly unlikely for the first 325 years.

At 325 years (200 years beyond institutional control) subsidence is assumed to have occurred (refer to Sect. 2.4.1). At this point in time it is further assumed that complete hydraulic failure occurs for the engineered grout barriers. Their hydraulic properties are replaced with those for the soil residing above the grout chamber (i.e., Operational Soil Cover whose properties are consistent with the local Upper Vadose Zone material).

For the first 40 years the wasteform containers are assumed to be hydraulically intact with a low fixed hydraulic conductivity value of 10^{-12} cm/s (waste containers are typically constructed of carbon steel, which has a permeability of 0, but in order to produce a stable model a low permeability of 1.0E-12 cm/s was assigned). After 40 years, through-wall pitting of the waste containers (e.g., B-25 boxes) is assumed to occur. Field data indicate through-wall pitting would require greater than 40 years, especially in a high pH environment encountered within a caustic grout chamber (Dunn 2002; Jones and Phifer 2002).

Complete hydraulic failure is assumed to occur for the waste containers at 40 years. Their hydraulic properties are replaced with those for the soil residing above the grout chamber (i.e., Operational Soil Cover). Their transport properties are assumed to remain consistent with the chemical nature of the wasteform being considered.

2.6.3.2 Other Key Assumptions

The calculated inventory limits presented within this chapter are based on the following (see also Appendix B):

- For each of the existing segments the radionuclide parent inventories are modeled explicitly in their segment location and time of burial.
- All future burials are assumed to occur in 1/1/2007 and have 10 ft interim runoff covers in place within 3 months of their creation.
- For all future radionuclide parents, their inventories are distributed uniformly over the remaining territory available within CIG Units 1 and 2. This is a simplifying assumption that is based on the fact that there are criteria in place to limit the level to which radionuclides may be concentrated in one location.
- No explicit account is being taken for actual plume dispersion. Numerical dispersion is occurring to the degree consistent with the mesh spacings being employed.
- For all future burials the CIG grout chambers are nominally 20 ft by 20 ft with a minimum grout wall thickness of 1 ft.
- For all future burials the CIG grout chamber's bottom is not placed closer than 35 ft to the time-averaged water table elevation (Phifer and Millings 2007).
- Subsidence does not occur for all future segments until 325 years and that those existing segments that have a subsidence potential be structurally improved by the end of the institutional control period.
- Structural credit to reduce the risk of subsidence is achieved by the addition of a concrete slab placed over the segments. Based on the structural analyses supporting this it is assumed that the open span across the trench does not exceed 18 ft (i.e., 20-ft wide unit with 1-ft minimum grout wall thickness).
- The aquifer flow pattern does not change over the entire time period on interest (e.g., at facility closure the various units will have closure caps with runoff drainage systems and these surface changes are assumed to have negligible impact on the underlying aquifer flows).

2.6.4 Aquifer Groundwater Transport Model

In E-Area a variety of solid waste disposal units currently exist as shown in Figure 2-1. These units are used to store and/or dispose of various forms of radioactive solid waste materials contained within various wasteforms. The various disposal units highlighted in Figure 2-1.

The majority of these units have geometric footprints consistent with an original LAW vault footprint concept (i.e., 157 ft wide by 656 ft long). The two CIG Units are referred to as CIG Unit 1 (or CIG-1) and CIG Unit 2 (or CIG-2). Both CIG units reside within the E-Area footprint as shown in Figure 2-1. Both units are designed to handle five trenches per unit and are sandwiched in between neighboring slit trench units SLIT#4 and SLIT#5.

2.6.4.1 Transport Model

A PORFLOW based CIG aquifer transport model was created. This 3-D aquifer model represents the saturated region beneath the CIG units. The flow field was extracted from an already existing GSA flow solution based on PORFLOW; therefore, only 3-D transport simulations were required. A more detailed description of this model is provided below.

2.6.4.2 CIG Unit Description

Taking into account the general aquifer flow direction and required 100-m compliance boundary surrounding both CIG units, the domain of a CIG aquifer model was established. This CIG aquifer model was extracted from a general baseline aquifer (flow only) model that extends over the entire GSA (Flach 2004). The domain of the chosen CIG aquifer model is shown in Figure 2-5, along with a series of 3D streamtraces in the region of interest. The streamtraces were created using the flow field solution taken from the general baseline GSA model. As illustrated in Figure 2-5, the two CIG units are fairly inline with the aquifer flow direction underneath them.

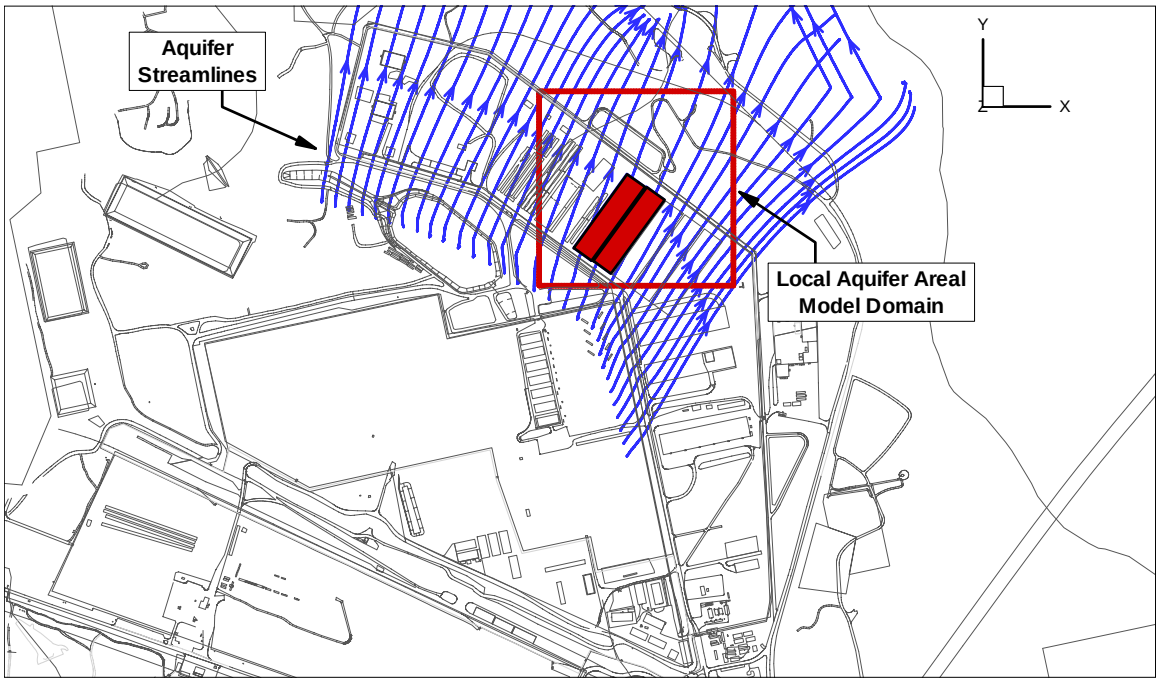

Figure 2-5. 3-D streamtraces Generated from the General Baseline GSA Model and Used to Help Establish the Location of the CIG Aquifer Model Domain

The outer domain of the CIG aquifer model coincides with specific grid surfaces of the general baseline GSA flow model. The GSA flow model has a uniform horizontal grid spacing of 200 ft in both directions. As shown in Figure 2-6, the CIG aquifer model overlaps 7 by 7 cells of the GSA flow model. Thus, the CIG aquifer model's horizontal range is 1,400 ft by 1,400 ft.

For reducing PORFLOW numerical dispersion during transport simulations to be performed using the CIG aquifer model, its horizontal mesh spacing was reduced by one order in magnitude to 20 ft by 20 ft. The vertical mesh spacing of the baseline GSA model was retained for the CIG aquifer model. The CIG aquifer model was used only for transport simulations where its flow field was input from an interpolated flow field taken from the baseline GSA flow model. A close-up of the CIG aquifer model horizontal mesh footprint is shown in Figure 2-7. Also highlighted in Figure 2-7 (in red) is the 100-m compliance boundary that surrounds the composite of CIG Units 1 and 2.

Internal PORFLOW processing locates the spatially maximum concentration of each species between the 100-m buffer zone and the modeling grid boundary. Post-processing of specific PORFLOW output files was performed to locate the maximum (peak) concentration in time of each buried parent radionuclide.

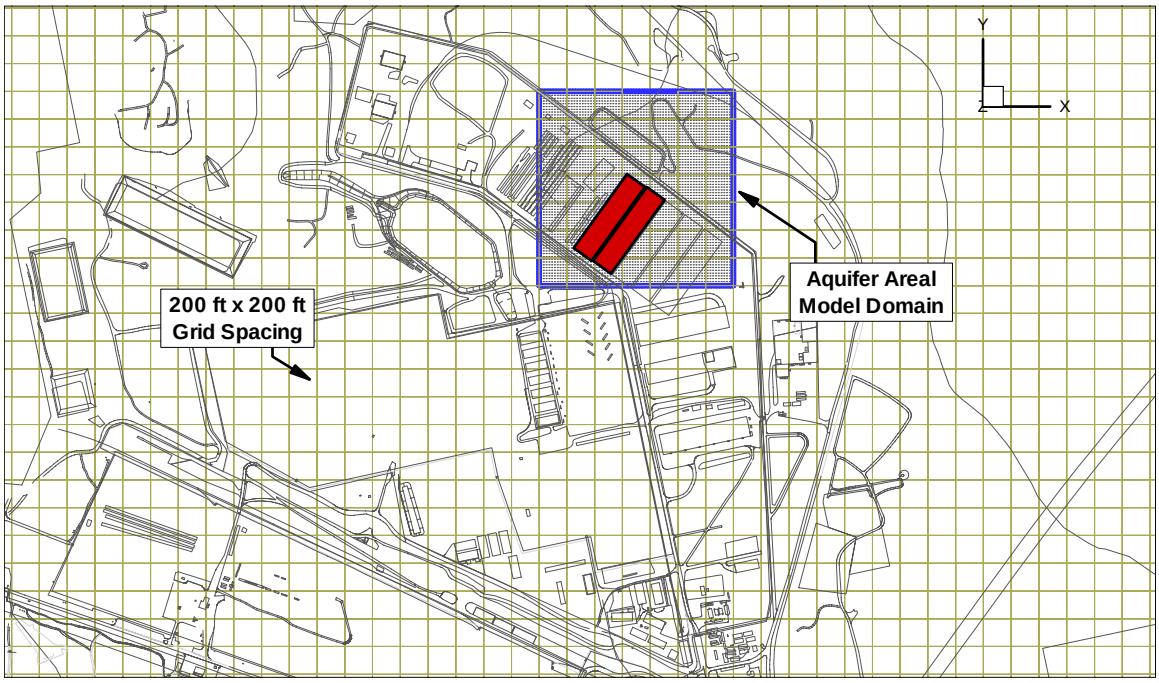

Figure 2-6. The Outer Domain of the CIG Aquifer Model Showing Its Alignment with Specific Grid Surfaces of the General Baseline GSA Model (i.e., 200 ft by 200 ft Horizontal Mesh)

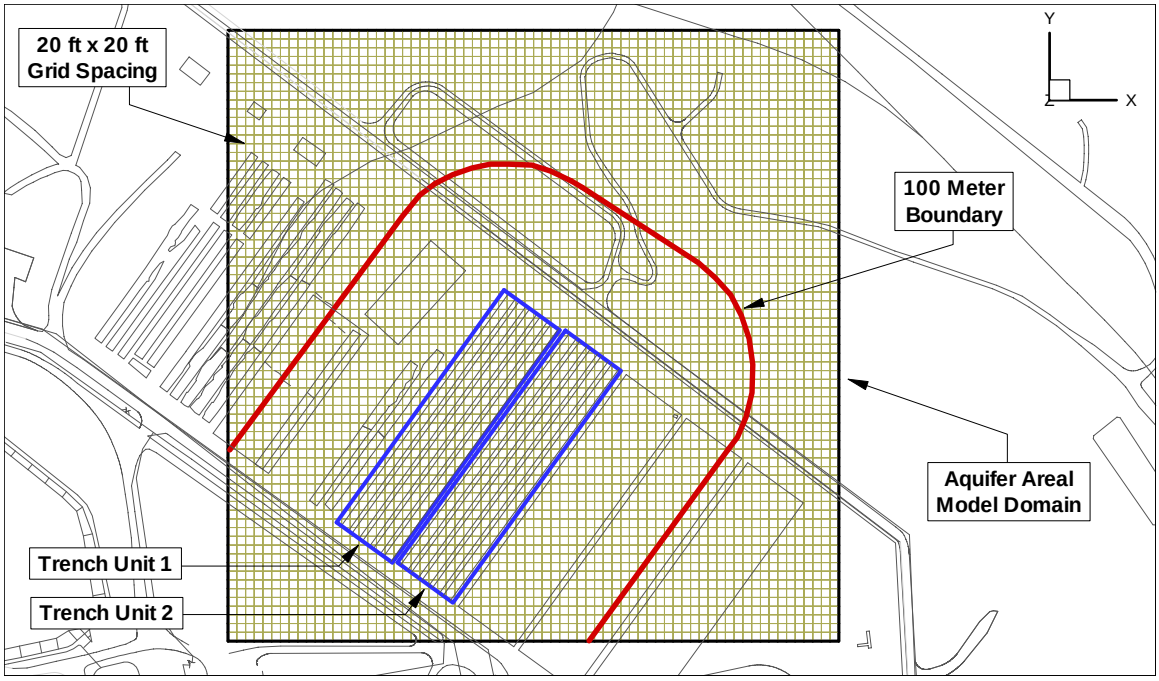

Figure 2-7. The Horizontal Mesh of the CIG Aquifer Transport Model Showing the Locations of the Trench Units and the 100-m Compliance Boundary

Each CIG Unit contains 5 planed trenches that run parallel with the long leg of an LAW vault footprint. Each trench is envisioned to be approximately 20 ft wide by 656 ft long. The first segment put into service was created within CIG Unit 1 on August 29th of 2000 and is referred to as "Segment 1." Since that date a total of 8 segments have been created. A close-up view of both CIG units along with the actual locations and burial dates for the 8 existing segments is shown in Figure 2-8. Segments 1, 2, and 3 were combined for computational purposes only and are referred to as Segment 1-2-3 in further details.

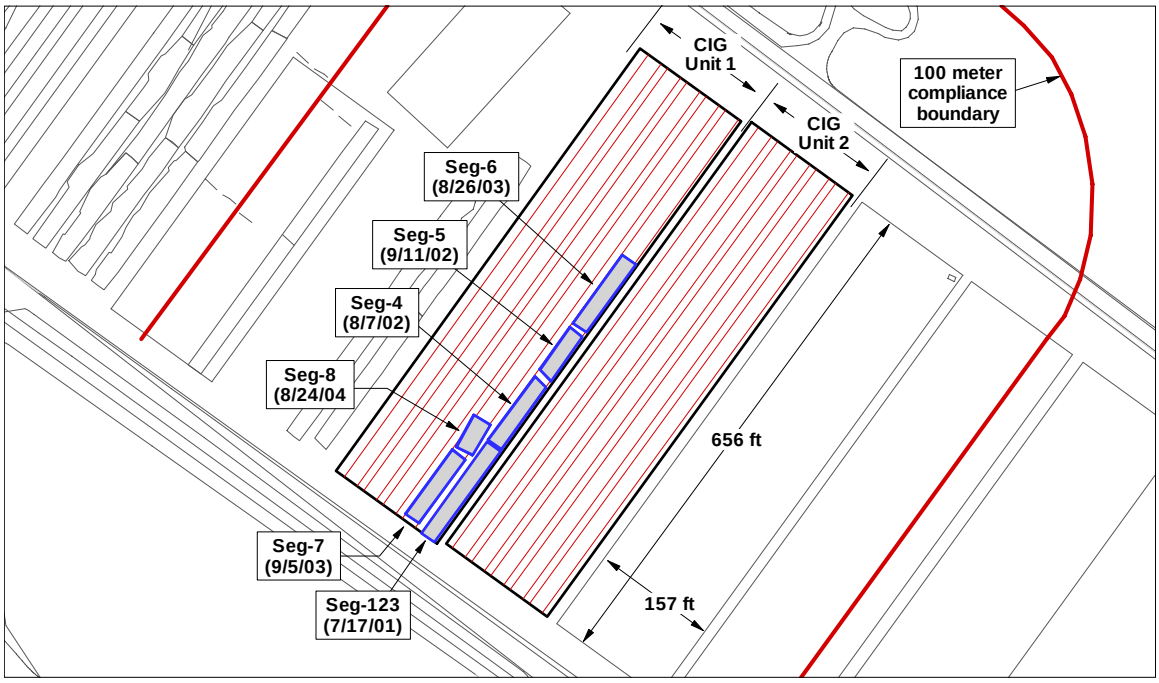

Figure 2-8. Close-up View of the Two CIG Units Showing the Trench Layout and Location of the 8 Existing Segments Along With Their Burial Dates

In principle, future disposals can be placed into segments of arbitrary lengths located within any of the 10 trenches that the current 8 existing segments do not occupy. In Figure 2-9 streamtraces were placed directly underneath the ten trench paths starting at the water table surface. As shown in Figure 2-9, these streamtraces follow a common path. The maximum well location lies near the 100-m circle (in red), where the PORFLOW output for the model cells on the 100-m boundary indicates the cell with the greatest concentration of each radionuclide over time.

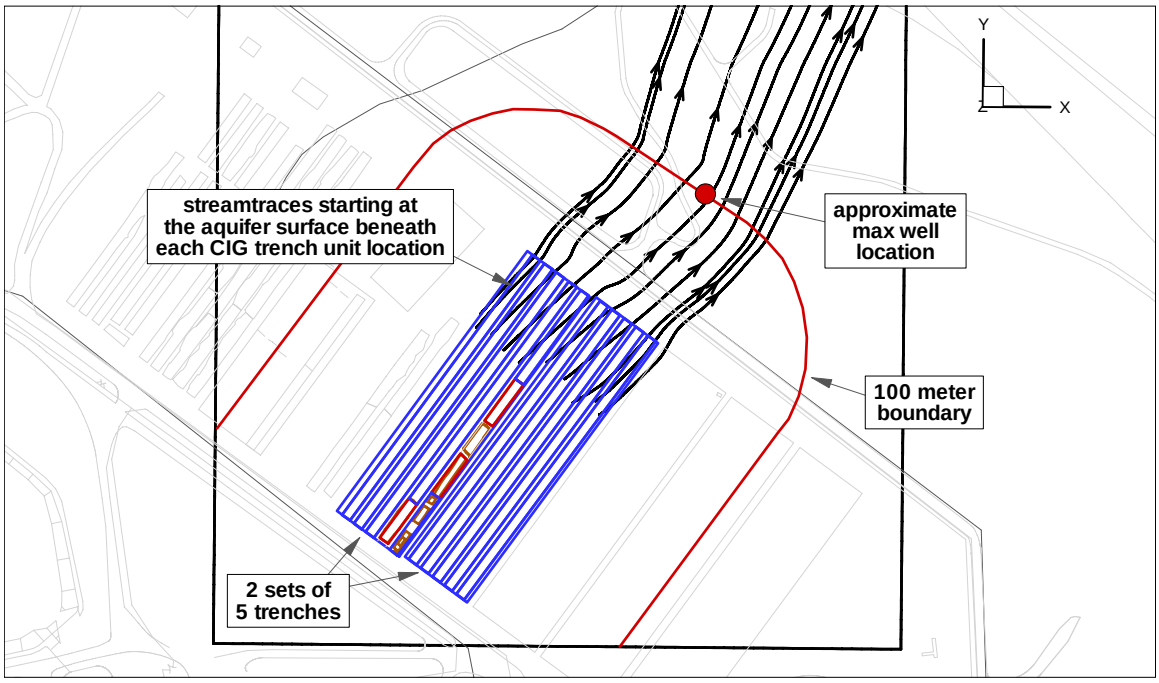

Figure 2-9. 3-D Streamtraces Starting Underneath the Two CIG Units Illustrating the General Locations where Contaminant from the Trenches Cross the 100-m Compliance Boundary

2.6.4.3 Transport Model Boundary Conditions

The CIG aquifer transport model is impacted by surface boundary conditions and internal source nodes. At the outer surfaces (i.e., the x, y, and z domain faces) incoming versus outgoing boundary conditions are handled differently. At an incoming face the radionuclide species of interest is assumed to have a zero concentration. Here we are assuming no plume interactions are taking place (i.e., no upstream source plume is being addressed or plume interactions with neighboring Slit Trench units). At an outgoing face the diffusive flux of the radionuclide species of interest is assumed to have a value of zero. Here we are placing the outgoing faces far enough from the regions of interest where this assumption has negligible impact on its upstream concentration profiles.

The inventories for the radionuclide of interest were injected into the CIG aquifer transport model by way of source nodes that resided in the top layers of the model where the water table exists. For existing trench segments with known inventories, those inventories were uniformly (i.e., on a volume basis) placed within each specified segment. For current purposes there are 8 existing segments (i.e., Segments 1 through 8). In coming up with an overall CIG Unit inventory limit, the remaining amount of inventory (minus the known values) was uniformly (volume based) distributed to the remaining unused trench paths available in each CIG Unit.

These source node locations were determined by knowing the footprint of each trench (10 in total) and any potential existing segments that might be residing within that trench. A search algorithm taking the geometric center of each node cell checked to determine which regions (i.e., unused trench or segment) the node cell center resided within. The majority of node cells reside outside of the CIG units. A typical overlay of source node locations relative to cell node centers is provided in Figure 2-10. Due to the actual small foot print of Segments 1, 2, and 3 (as well as their radionuclide inventory lists), these three segments were combined for modeling purposes and the combined segments are referred to as Segment 1-2-3.

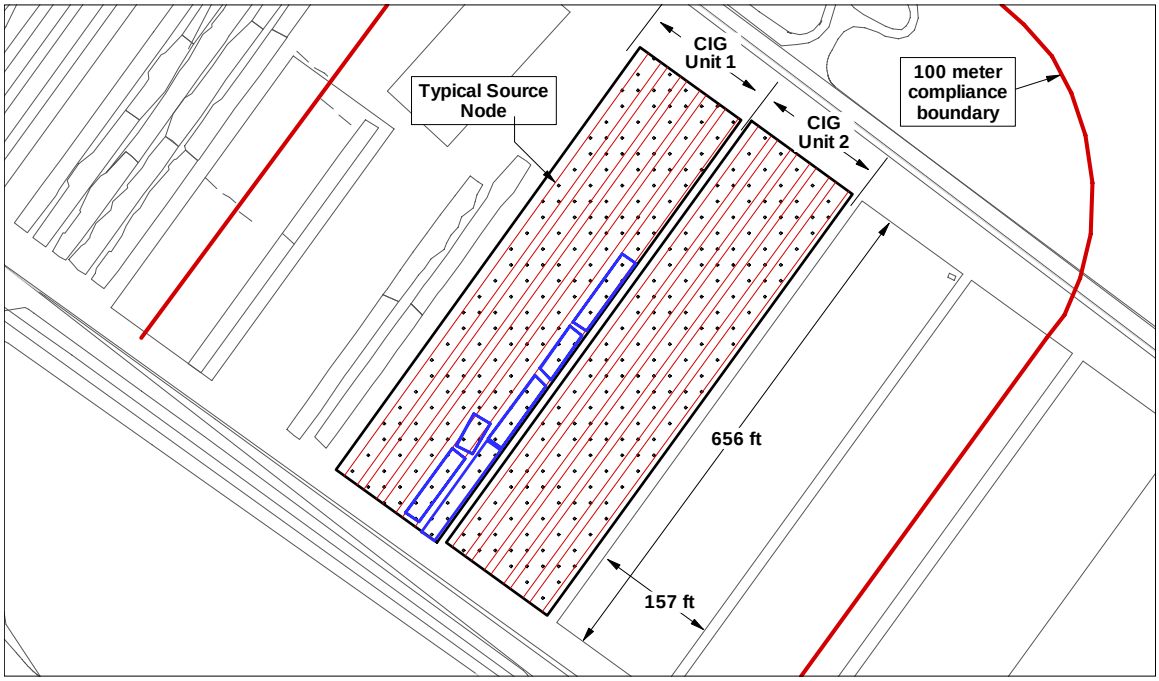

Figure 2-10. Overlay of the Various Unused Trenches, Existing Segments, and Remaining Partially Unused Trenches versus Cell (Source) Node Centers

In total, 16 unique regions were generated each containing a subset of source nodes:

- 6 regions in CIG Unit 1 representing existing segments (Segments 1-2-3, 4, 5, 6, 7, and 8)
- 2 regions in CIG Unit 1 representing the remaining trench area not occupied by existing segments
- 3 regions in CIG Unit 1 representing unused trenches
- 5 regions in CIG Unit 2 representing unused trenches

2.6.4.4 Transport Property Assumptions

For PORFLOW transport analyses the following properties are required:

- Effective, total, and diffusive porosities (assumed to be equal)
- Particle density
- Molecular diffusivity (assumed to apply to all elements)
- Sorption K_d values (these are also element specific)
- Longitudinal and transverse dispersivity coefficients (assumed to be zero)

The effective, total, and diffusive porosities are set equal resulting in PORFLOW transport simulations being based on a single porosity formulation approach. Sorption K_d values are discussed below under the section for Vadose Zone transport property assumptions. For the Lower Vadose Zone material the values associated with the first three bullets above (from Phifer et al. [2006]) are:

- Effective, total, and diffusive porosities = 0.39
- Particle density = 2.66 g/ml
- Molecular diffusivity = 0.18 ft^2/yr

The CIG aquifer transport model resides within a single aquifer unit whose material is consistent with the Lower Vadose Zone material defined for Vadose Zone modeling (i.e., a sandy native soil).

This aquifer unit is a heterogeneous aquifer primarily sandy with local clayey sediments distributed throughout. From a purely transport advection viewpoint (i.e., pore velocity) its effective porosity is significantly lower than its total porosity. Here the clayey sediments behave like small hydraulic barriers forcing the groundwater to navigate past them. Based on information presented in Flach and Harris (1996), Flach (2004), and Phifer et al. (2006), the effective porosity of this unit is assumed to be ~25%. To account for the faster pore velocity, the aquifer transport analyses were performed where all three porosities were set to 0.25.

The primary velocity of interest is the retarded pore velocity that is obtained based on the retardation coefficient defined for a saturated porous media as:

$$v_R = \frac{v}{R} \quad \text{where} \quad R = 1 + \frac{\rho_s (1-\phi) K_d}{\phi} \qquad \text{Equation 2-1}$$

where, v_R = retarded pore velocity (m/s)
v = pore velocity (m/s)
R = retardation coefficient (unitless)
ρ_s = particle density (g/ml)
ϕ = porosity (unitless)
K_d = distribution coefficient (mL/g)

Since PORFLOW is not being used in a dual porosity formulation manner, by changing its porosity from 39% to 25% we also are changing its effective retardation coefficient. In order to maintain an effective retardation coefficient the effective particle density (ρ_s^{eff} , in g/ml) was changed using the following formula (based on an equivalent R value):

$$\rho_s^{eff} = \rho_s \left(\frac{\phi_{eff}}{\phi_{tot}} \right) \left(\frac{1-\phi_{tot}}{1-\phi_{eff}} \right) \qquad \text{Equation 2-2}$$

where, ϕ_{eff} = effective porosity (unitless)

ϕ_{tot} = total porosity (unitless)

The computed effective particle density now becomes 1.39 g/ml.

Aquifer transport analyses were performed for a variety of the radionuclides of interest to ensure that this effective property approach resulted in peak well concentrations that exceeded those based on the original property approach.

2.6.5 Vadose Zone Flow and Transport Models

A single version of the PORFLOW code, 5.97, was used in prior scoping analyses and in the actual modeling for this report. A revision of the existing software QA plan and verification testing for this version of PORFLOW is essentially complete. No problems requiring changes to the code were identified as a result of this testing. The following are a few of the aspects that have been considered in determining an acceptable Vadose Zone model:

- To determine if, when, and to what extent operational infiltration barriers are required.
- Mesh and time-step sizes to achieve acceptable numerical accuracy.
- To determine if unique Center, Middle, and Edge trench models (or a combination of trenches) are required or if one single representative model is acceptable.
- To determine how to handle the changing geometry associate with ground surface during and after the operational period.

Based on these prior scoping studies, two PORFLOW-based CIG Vadose Zone flow and transport models were chosen and created. These 2-D Vadose Zone models represent perpendicular vertical slices through two CIG Trench segment designs (i.e., Existing Segments and Future Segments). These models extend vertically from the water table up to ground surface (or near ground surface where appropriate infiltration rate boundary conditions apply). A series of steady-state flow fields were computed and used in a stepwise fashion during the transient transport simulations. The computed transient flow rates of radionuclides (sometimes referred to as water table fluxes) leaving the model domain at the water table were stored and used in subsequent CIG aquifer transient transport analyses. More detailed descriptions of these models are provided.

2.6.5.1 CIG Unit Descriptions

The typical size of a CIG footprint is 656 ft long by 157 ft wide. Looking more specifically (from overhead) at the general layout of a CIG unit, within its footprint we see five parallel trench positions as shown in more detail in Figure 2-11. From a geometrical perspective we can see three distinct types of trenches (i.e., 1 center trench, 2 middle trenches, and 2 edge trenches). Initial trench cover will include either a minimum 4-foot thick layer of clean soil, or a combination of a nominal 1.33-foot thick layer of CLSM, a minimum 20-inch thick concrete mat, and a nominal 1-foot thick layer of clean soil for a minimum 4-foot thickness. An interim runoff cover will be maintained for the 25-year operational and 100-year institutional control periods. The interim runoff cover will include up to two additional feet of soil and application of an HDPE geomembrane or geotextile fabric with spray-on asphalt emulsion or other type water resistant material. Each trench path is assumed to be 20 ft wide with a 10 foot wide distance of undisturbed soil residing between neighboring trench paths. There is also an additional 10 foot wide distance between neighboring units (CIG footprint).

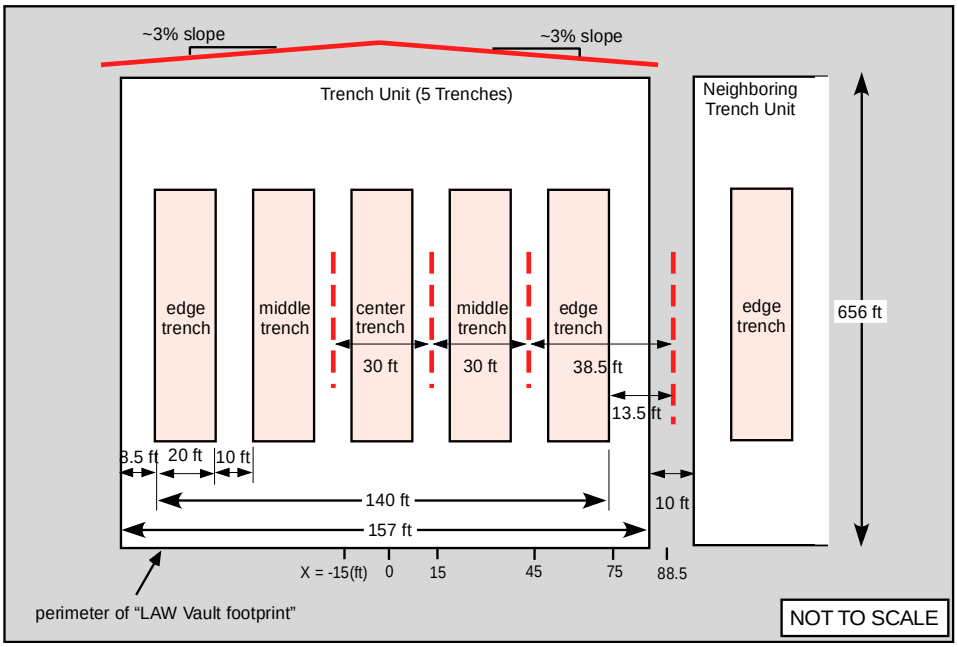

Figure 2-11. Basic Schematic of a CIG Unit Showing the Geometric Locations of Each Trench Path within its CIG Footprint

A typical cross-sectional cut (vertical and perpendicular to the trench length) through a section of a CIG Trench is 20 ft by 20 ft. Note that some of the early-on existing segments have cross-sectional areas that are less than the generic 20 ft by 20 ft dimensions; however, all existing segments have grout walls that are greater than the minimum allowed 1 ft thick requirement. The total trench path length is 656 ft. For computational purposes given the type of aspect ratios observed thus far it is believed that a 2-dimensional representation of a CIG Trench segment is acceptable (i.e., slightly conservative in respect to the contaminant flux delivered to the water table below. Based on ground survey and water table elevations, a minimum of 35 ft is required within the Vadose Zone from the bottom of a CIG segment to the surface of the water table beneath it. This minimum distance was obtained by looking at local groundwater elevations (in MSL) measured over the last few decades. Prior CIG analysis had employed a domain depth of 25 ft; however, based on available water table data a 35 ft estimate is closer to the best estimate of its minimum value.

By making the 2-D assumption for the CIG segment and surrounding Vadose Zone, separate flow and transport simulations are performed for the contaminant transport within the Vadose Zone. The contaminant flux leaving the CIG Vadose Zone model then becomes a forcing function (i.e., source nodes) to the CIG aquifer transport model. Only limited numbers of CIG Vadose Zone model simulations have to be performed based on symmetry and bounding arguments.

Under conditions where the CIG units have been filled and the interim cap has been placed, a cross-sectional view of one region of one unit would look similar to the cartoon shown in Figure 2-12. Lines of symmetry exist between each trench and neighboring CIG unit.

It is required that there be a minimum of 35 ft between the water table and the bottom of each CIG segment. Each segment is generally created by digging a 20 ft by 20 ft trench with some required trench length based on the volume of wasteforms being disposed of. At the cross-sectional level there is to be a minimum of 1 ft of grout walls surrounding the disposed waste. Prior to Segment 8 only 4 ft of clean backfill was used to bring the unit up to its original ground level. For Segment 8, due to the awareness of the potential for future subsidence, an 18-inch concrete slab was placed between the top surface of grout and ground level.

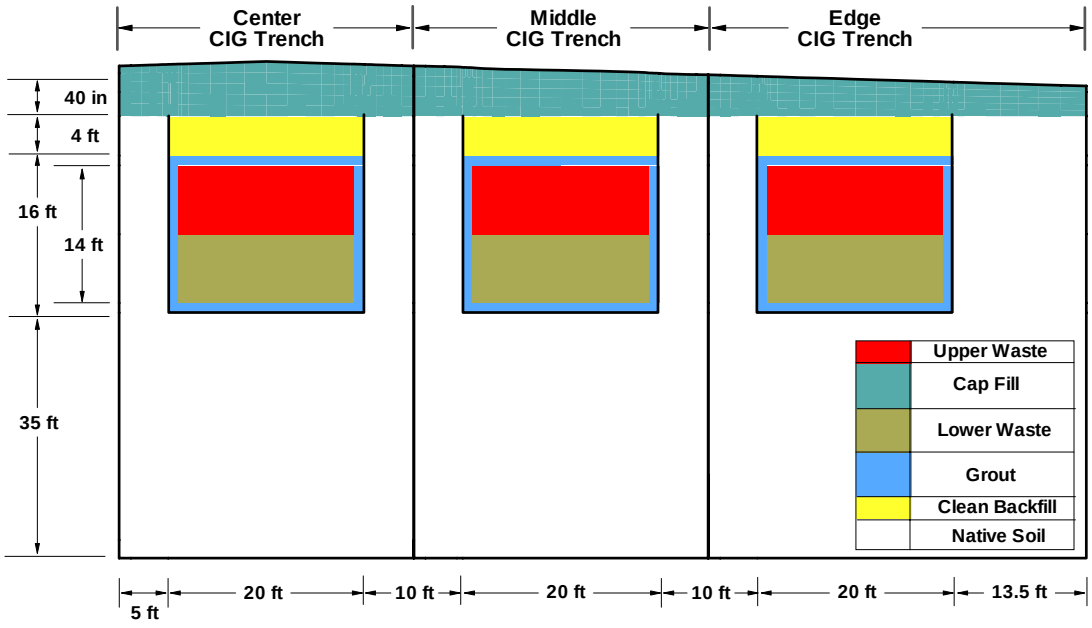

Figure 2-12. Cross-Sectional View Through a Portion of a CIG Unit Starting From The Ground Surface Down to the Water Table after the Interim Runoff Cover has been Placed

In order to take into account the impact of possible subsidence during transport simulations, the waste region (i.e., a 14 ft by 14 ft zone surrounded by a 1 ft of grout barrier) was divided into separate zones (i.e., upper 7 ft waste zone and a lower 7 ft waste zone). During a subsidence event it is assumed that the upper waste zone collapses into the lower waste zone, ultimately moving its contaminant contents into the lower waste zone at the point of subsidence. Local native top soil (i.e., Upper Vadose Zone soil) is assumed to refill the collapsed section of earth.

At the end of the operational period (~25 years) the start of an institutional control period begins and lasts ~100 years. At the end of the operational period the CIG units will have interim runoff covers placed over them that extend over the entire footprint of each CIG unit. These covers will have locally disturbed soil used for mounding (i.e., Cap Fill soil referred to as Operational Soil Cover). The rain runoff from these covers is assumed to be removed from the region through appropriately designed drainage systems.

2.6.5.2 Flow Property Assumptions

From a material's hydraulic perspective, there are potentially 8 different material types present in the CIG segment models:

- **Lower Vadose Zone soil** (lower half of the Vadose Zone that's more sandy in nature and consistent with the properties of the saturated portion of the aquifer model).
- **Upper Vadose Zone soil** (upper half of the Vadose Zone that's more clayey in content and undisturbed soil sometimes referred to as Native soil).
- **Operational Soil Cover** (referred to as Operational Soil Cover Prior to Dynamic Compaction in Phifer et al. [2006], comprises Upper Vadose Zone soil that has been disturbed during digging/filling activities and sometimes used as Clean Backfill, Cap Fill Sides, and/or Cap Fill Center).
- **Existing Grout** (a cement mixture with small sized aggregate used as the primary migration barrier based on the existing formulation used for Segments 1 through 8).
- **Future Grout** (low quality concrete mixture with small sized aggregate used as the primary migration barrier based on the new formulation used for future segments).
- **Waste** (here in reality numerous forms of waste exist spanning a very large range; however, the conceptual model assumes all the wasteforms behave similar to the properties of a hydraulically competent intact container for the first 40 years then as Backfill thereafter).
- **CLSM** (controlled low strength material used to separate the grout chamber from a concrete slab used to mitigate the potential of subsidence).
- **Concrete Slab** (medium quality reinforced concrete used to mitigate the potential of subsidence).

Clean Backfill is locally disturbed soil use to bring the trench back up to its original ground level. Cap Fill (for the sides and center) is locally disturbed soil use to establish the ~3% slope mound over the CIG units.

Table 2-6 lists the material types employed in the CIG Vadose Zone models (i.e., their material ID numbers, terminology used, and some of their attributes). In Table 2-7 the key hydraulic properties for the various material zones employed in the CIG Vadose Zone models are listed. Within the Vadose Zone there are two basic regions referred to as the UVZ and LVZ materials.

These two regions are undisturbed native soils whose anisotropic nature is being addressed using the anisotropic ratios provided in Table 2-7. The UVZ region is a more clayey material than the LVZ region with lower saturated hydraulic conductivity values. For the CIG Vadose Zone models it is assumed that the bottom of the grout chamber resides at the interface of these two Vadose Zone regions. Available stratigraphic information indicates that this interface should be fairly close to the elevation where the bottom of the grout chamber is located (Phifer et al. 2006).

The key hydraulic properties provided in Table 2-7 correspond to un-degraded materials. Over certain time periods hydraulic events occur that change these properties resulting in material degradation and/or alteration. A brief summary of the three time periods where hydraulic degradation impacts are addressed is provided in Table 2-8. As provided in Table 2-8 these 3 time periods are:

- **0-40 years** (all materials within the CIG Vadose Zone models are at their initial hydraulically un-degraded values).
- **40-325 years** (hydraulically degraded waste containers with all other materials remaining at their initial hydraulically un-degraded values).
- **Beyond 325 years** (all cementitious materials hydraulically degraded with all other non-cementitious materials remaining at their initial hydraulically un-degraded values).

The vertical hydraulic conductivity variations associated with the various time periods discussed above can be seen in Figure 2-13 (a detailed discussion of materials properties can be found in Phifer et al. [2006]). As seen in Figure 2-13, significant changes occur at the 40 and 325 year time points for the waste material and grout material, respectively.

Table 2-6. Material Types Employed in the CIG Vadose Zone Unit Flow Analyses

Material Number	Material Zone Name	Description	Material Type	Moisture Characteristic Curves
1	**LVZ**	Lower Vadose Zone (below 264 ft-msl)	<25 wt% silt + clay[a]	E-Area LVZ
2	**UVZ**	Upper Vadose Zone (above 264 ft-msl)	>25 wt% silt + clay	E-Area UVZ
3	**Backfill**	Operational Soil Cover	>25 wt% silt + clay	OSC_NDC
4	**Cap Sides**	Operational Soil Cover	>25 wt% silt + clay	OSC_NDC
5	**Cap Center**	Operational Soil Cover	>25 wt% silt + clay	OSC_NDC
6	**Existing Grout**	Grout used for Segments 1 through 8	Cementitious	Existing E-Area Grout
6	**Future* Grout**	Grout to be used for all future segments	Cementitious	Low Quality Concrete
7	**Waste**	Waste	0-40 yr: intact containers 40+ yr: >25 wt% silt + clay	OSC_NDC (after 40 yr)
8	**CLSM***	Controlled low strength material	Cementitious	E-Area CLSM
9	**Concrete slab**	Reinforced concrete slab	Cementitious	Low Quality Concrete

[a] Predominant material type
[b] See Phifer et al. (2006) for detailed information

Table 2-7. Hydraulic Properties for the Various Materials Contained within the CIG Vadose Zone Unit Required to Perform Flow Analysis (from Phifer et al. 2006)

Material Zone Name	Particle Density (ρ) (g/ml)	Porosity (ϕ) (-)	Non-degraded Horizontal Saturated Hydraulic Conductivity (cm/s)	Non-degraded Vertical Saturated Hydraulic Conductivity (cm/s)	Anisotropic Ratio [a] (-)
LVZ[a]	2.66	0.390	3.30E-04	9.10E-05	3.6
UVZ[a]	2.70	0.390	6.20E-05	8.70E-06	7.1
Backfill	2.65	0.460	1.20E-04	1.20E-04	1.0
Cap Sides	2.65	0.460	1.20E-04	1.20E-04	1.0
Cap Center	2.65	0.460	1.20E-04	1.20E-04	1.0
Existing Grout	2.41	0.235[b]	6.00E-04	6.00E-04	1.0
Future Grout	2.61	0.211	1.00E-08	1.00E-08	1.0
Waste	2.65	0.500	1.00E-12	1.00E-12	1.0
CLSM	2.67	0.330	1.00E-08	1.00E-08	1.0
Concrete slab	2.61	0.211	1.00E-08	1.00E-08	1.0

a Only the anisotropic (unequal vertical compared to horizontal hydraulic conductivity) nature of the native soils (upper and lower Vadose Zone soils) were accounted for.

b A porosity value of 0.235 was employed for Vadose Zone transport analyses since an updated database became available. A porosity value of 0.224 was used in earlier flow runs prior to this new information being available. However, the value of this parameter does not impact flow results when steady-state flow fields are being used.

Table 2-8. Hydraulic Property Changes due to Assumed Degradation for the Various Materials Contained within the CIG Vadose Zone Unit

Material Number	Non-degraded Material (0-40 yrs)	Degraded Material (40-325 yrs)	Degraded Material (325+ yrs)
1	**LVZ**	**-**	**-**
2	**UVZ**	**-**	**-**
3	**Backfill**	**-**	**-**
4	**Cap Sides**	**-**	**-**
5	**Cap Center**	**-**	**-**
6	**Existing Grout**	**-**	**Backfill**
6	**Future Grout**	**-**	**Backfill**
7	**Waste**	**Backfill**	**Backfill**
8	**CLSM**	**-**	**Backfill**
9	**Concrete slab**	**-**	**Backfill**

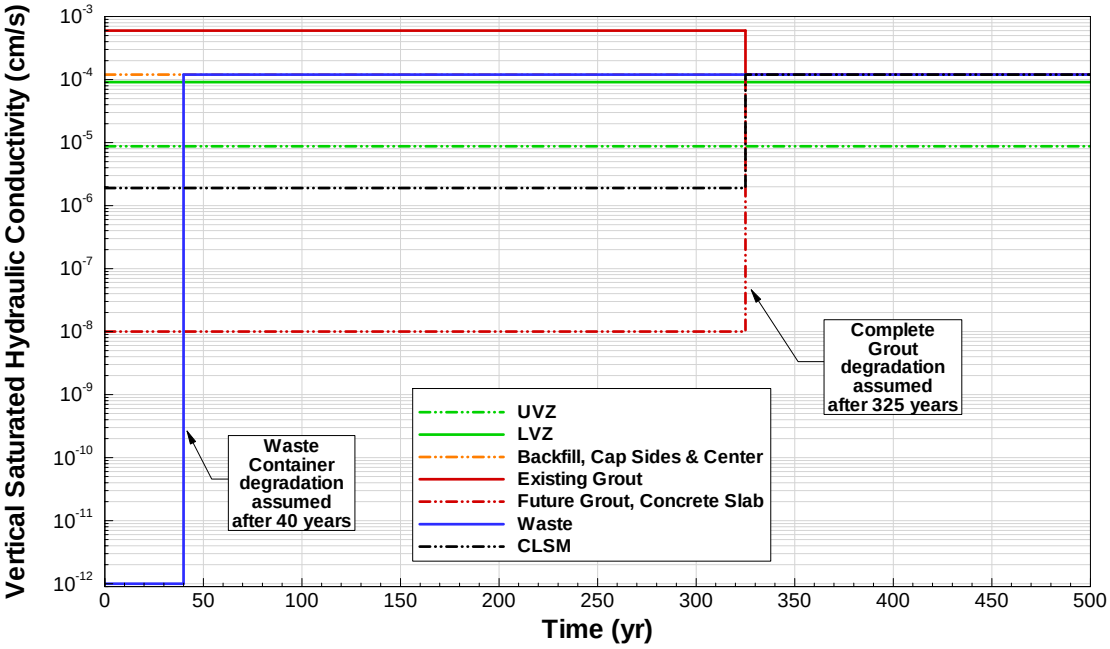

Figure 2-13. Assumed Hydraulic Degradation Behavior of the Various Material Used in the CIG Vadose Zone Model when Performing Flow Simulations

The grout material is being employed as one of the main engineered barriers to radionuclide transport into the environment and its hydraulic performance is a key parameter (see Appendix B). A literature survey of concrete formulations (i.e., cement-to-water ratios) provided a range of saturated hydraulic conductivity values to be expected for grout performance. Based on this survey a nominal value (i.e., considered to be a best estimate value) of $1x10^{-8}$ cm/s was expected, with a lower bound of approximately $1x10^{-7}$ cm/s.

Saturated and unsaturated hydraulic conductivity measurements were made on grout specimens created (in-the-field efforts) consistent with the formulation and procedures employed in the creation of the grout used for the existing segments (i.e., Segments 1 through 8). A special set of experiments were performed to establish the hydraulic character of the existing grout segments (Phifer et al. 2006). As can be seen in Figure 2-14, a large variability exists within the database due to the level of difficulty in the creation of small representative measurement samples and in their measurement as well. Based on the available data a conservative upper bound curve for existing grout hydraulic conductivity was created. A comparison of this bounding curve versus the available database is also shown in Figure 2-14. Due to the very large range of saturated hydraulic conductivity values measured and their associated uncertainties, the upper bound estimate was used instead of using a best estimate value.

Based on the performance observed in the existing grout formulation and pouring process, an improved grout formulation is under development for future CIG segments. It is expected that an improved formulation can be achieved that results in a hydraulic performance barrier better than medium quality concrete. For analysis purposes the future grout hydraulic behavior is assumed to be better than medium quality concrete, and is characterized by the theoretical hydraulic conductivity curve shown in Figure 2-14, labeled as "Future Grout" (see discussion in Section 2.6.3.1).

Four concrete/grout mixes were recently tested for use in future CIG disposals (Butcher et al. 2007). Preliminary hydraulic conductivity results from core samples of concrete and grout mixes poured in test trenches indicated the lowest average saturated conductivity was approximately 4E-08 cm/s, which is four times higher than the theoretical "Future Grout" saturated hydraulic conductivity shown in Figure 2-14, and used in simulations represented here. However, a subsequent analysis of the moisture retention data acquired for the grout (hereafter called the "new grout" in this discussion) with the lowest measured saturated hydraulic conductivity (Wilhite and Flach 2007) indicated that this new grout shows a more rapid drop in unsaturated hydraulic conductivity as it becomes unsaturated than represented in the "Future Grout" curve in Figure 2-14. Wilhite and Flach (2007) indicate that because the new grout will be predominantly exposed to negative pressure heads in the vadose zone, it is projected to exhibit conductivities lower than assumed in the modeling based on the future grout.

To perform flow analysis within a Vadose zone also requires moisture characteristic curves (i.e., relative permeability and suction head versus water saturation) to address the unsaturated aspects of the Vadose zone. For the Existing Grout material it is assumed that at low saturation values the grout will perform at least as well as saturated medium quality concrete. As such, the unsaturated hydraulic conductivity curve for the Existing Grout was established to bound the available data and to reduce to $1x10^{-8}$ cm/s for water saturation values below 80%. This curve is shown in Figure 2-14, labeled as "Existing Grout." The unsaturated hydraulic conductivity curve for medium quality concrete was assumed to be valid for the Future Grout material as shown in Figure 2-14.

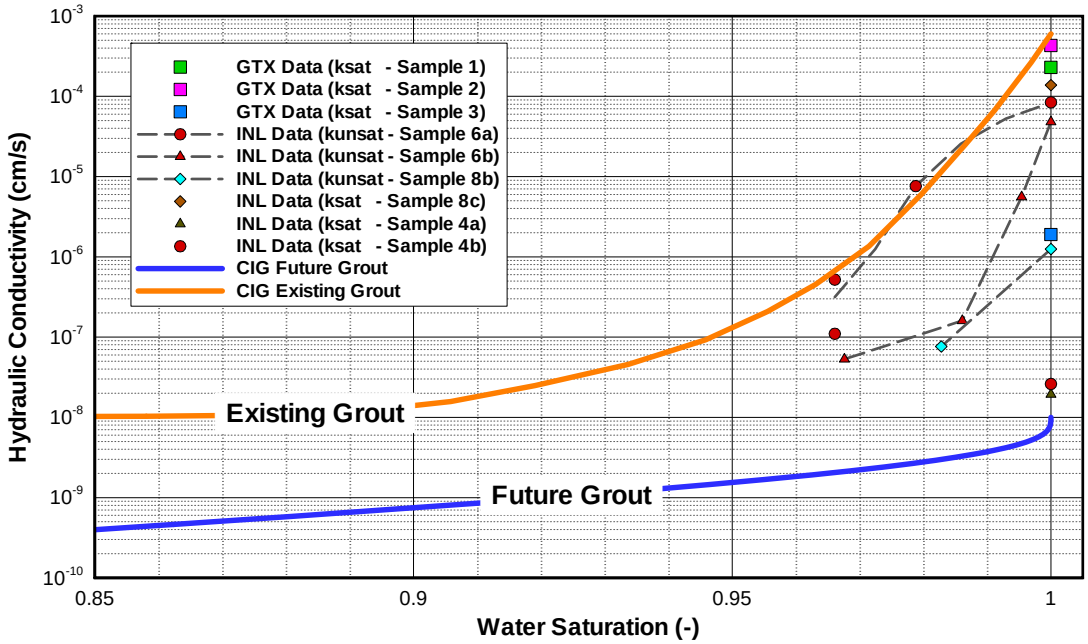

Figure 2-14. Comparison of Bounding Hydraulic Conductivity Curve for Existing Grout to Available Test Data and to Proposed Future Grout Formulation

A variety of cementitious materials is being used in the vadose zone flow modeling. The moisture characteristic curves (i.e., suction head and relative permeability) for these materials are shown in Figure 2-15. Throughout the various time periods where vadose zone flow fields are computed, water saturation levels were always higher than 95% for cementitious materials. In Figure 2-15 the moisture characteristic curves have been plotted from 60 to 100% for comparison purposes to those shown for the non-cementitious materials. The moisture characteristic curves for the Future Grout and the Concrete Slab are identical and relate to the moisture characteristic curves of a medium quality concrete formulation. The moisture characteristic curves for the Waste Zone shown were designed to address intact waste containers (e.g., B-25 boxes) during the first 40 years of operation (note: the Waste Permeability curve lies along the right axis, since the B-25 saturation was set to unity for modeling purposes). After 40 years of operation the Waste Zone hydraulic properties are set to those for Operational Soil Cover material.

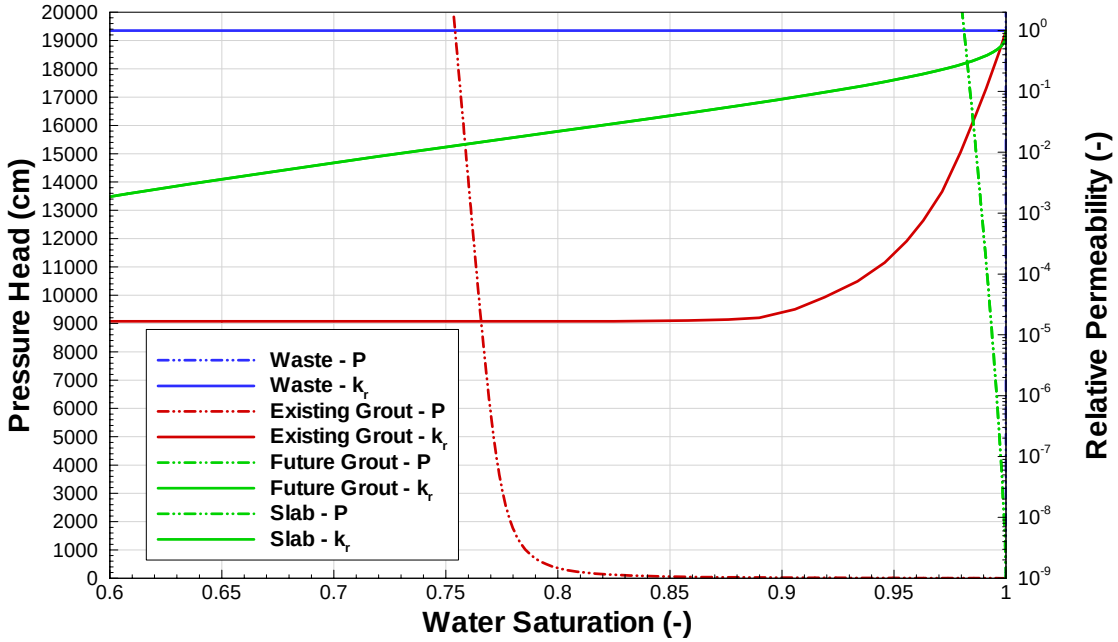

Figure 2-15. Moisture Characteristic Curves for the Cementitious Materials (Phifer et al. 2006).

A variety of non-cementitious materials (soil-like) is being used in the vadose zone flow modeling. The moisture characteristic curves (i.e., suction head and relative permeability) for these materials are shown in Figure 2-16. Throughout the various time periods where vadose zone flow fields are computed, water saturation levels were always higher than 60% for non-cementitious materials. In Figure 2-16 the moisture characteristic curves have been plotted from 60 to 100% for comparison purposes. The relative permeability curves for the UVZ and the OSC_NDC are identical.

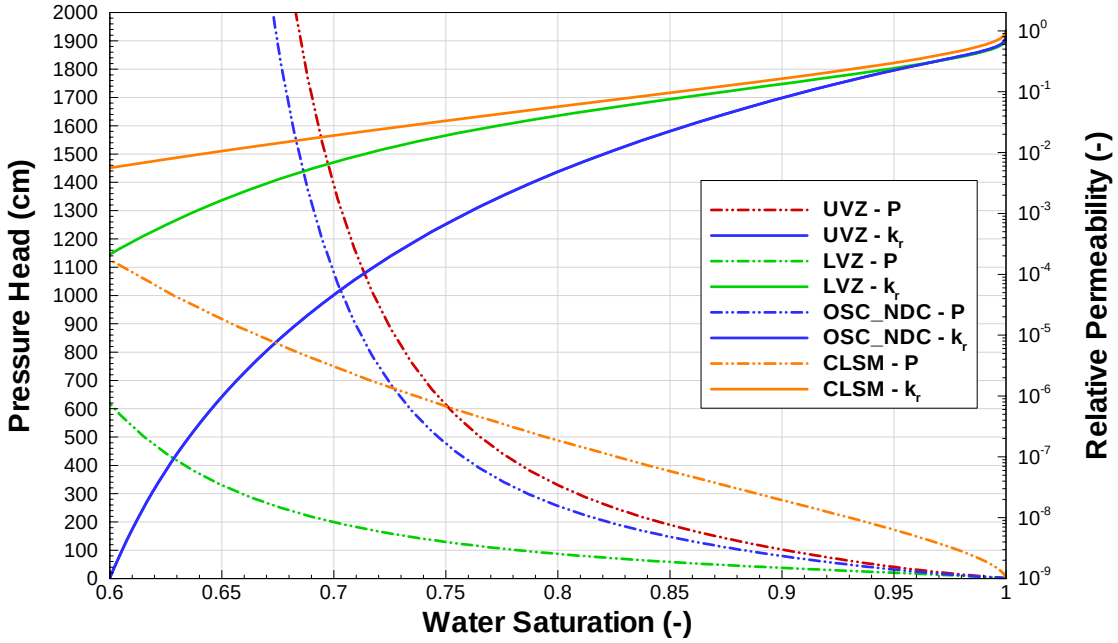

Figure 2-16. Moisture Characteristic Curves for the Non-Cementitious Materials (Phifer et al. 2006).

2.6.5.3 Infiltration Rate Boundary Conditions

As shown in Figure 2-12, there are three distinctly different CIG Trenches (i.e., Center, Middle, and Edge trenches). Right after the creation of a CIG segment it resides under what is referred to as an "Operational Soil Cover" where the local rainfall infiltration rate is approximately 12.7 in/yr (Phifer et al. 2006). Once an "Interim Runoff Cover" spanning the entire trench width has been placed and remains intact, the infiltration rate to all three trench types is significantly reduced and is practically identical. The infiltration rate remains constant (~0.36 in/yr) during the 100 year period of institutional control resulting from periodic maintenance efforts (Phifer et al. 2006). Beyond the period of institutional control if one of these trench types experiences a local subsidence event the infiltration rates to one or more of the neighboring trench types may change (i.e., a significant increase of 20 to 40 in/yr depending on the scenario of interest). The impact of subsidence on infiltration rate increases when going from considering the event to occur on a Center trench versus a Middle trench versus an Edge trench. Basically, the runoff from the upper trenches will increase the infiltration rate into the locally subsided downhill trench. After a subsidence event gradual hydraulic improvements will occur due to runoff deposits (silting) that gradually reduce local infiltration rates.

A variety of scenarios looking at various trench types experiencing a subsidence event has been analyzed using the HELP code (Phifer et al. 2006; Hang et al. 2005). For the flow simulations performed only one of these scenario types was employed here. It is assumed that subsidence occurs 325 years into operation and that all segments within both CIG units subside at the same point in time. This provides an upper estimate of the total amount of infiltration to the entire CIG units and represents a generic (Best Estimate) infiltration rate scenario. However, other scenarios could be envisioned such that limited subsidence would yield locally larger infiltration rates but a smaller total amount of infiltration to the entire CIG units would result.

As shown in Figure 2-17 four time periods of interest have been highlighted:

- **Operational Soil Cover Period** (This represents the initial period right after disposal within the 25 year operational window where both CIG units are being used for waste disposal. For current purposes time zero was set to 7/17/2001 which corresponds closely to the time when Segment 2 was created. During the 25 year period operational covers [Interim Runoff Covers with a limited width of 10 ft overhang] are placed over certain segments soon after they are created. Otherwise, high infiltration rates would be occurring.)
- **Interim Runoff Cover Period** (The limited extent Interim Runoff Covers are maintained from their placement until the end of the 25 year operational period. At the end of 25 years of operation an interim runoff cover is placed over each entire CIG unit. Hydraulically these covers are to reduce infiltration rates to 0.36 in/yr or less over the entire CIG units. During the 100 year institutional period these covers are also to be maintained such that their hydraulic criteria are not exceeded and any runoff is removed through appropriately designed drainage systems.)
- **Final Cover Period** (At the end of the interim runoff cover period a final cap will be placed over each CIG unit where no longer will there be further institutional maintenance performed. Gradual hydraulic [e.g., vegetation impacts] degradation will occur resulting in a gradual increase in infiltration rates and this is shown as the red curve in Figure 2-17.)
- **Subsidence Period** (At 325 years no further structural credit for the concrete slabs is taken to eliminate subsidence. Subsidence is assumed to occur at every location within both CIG units [the generic infiltration scenario]. Gradual hydraulic [e.g., silting and runoff deposits] improvement will occur resulting in a gradual decrease in infiltration rates and this is shown as the green curve in Figure 2-17.)

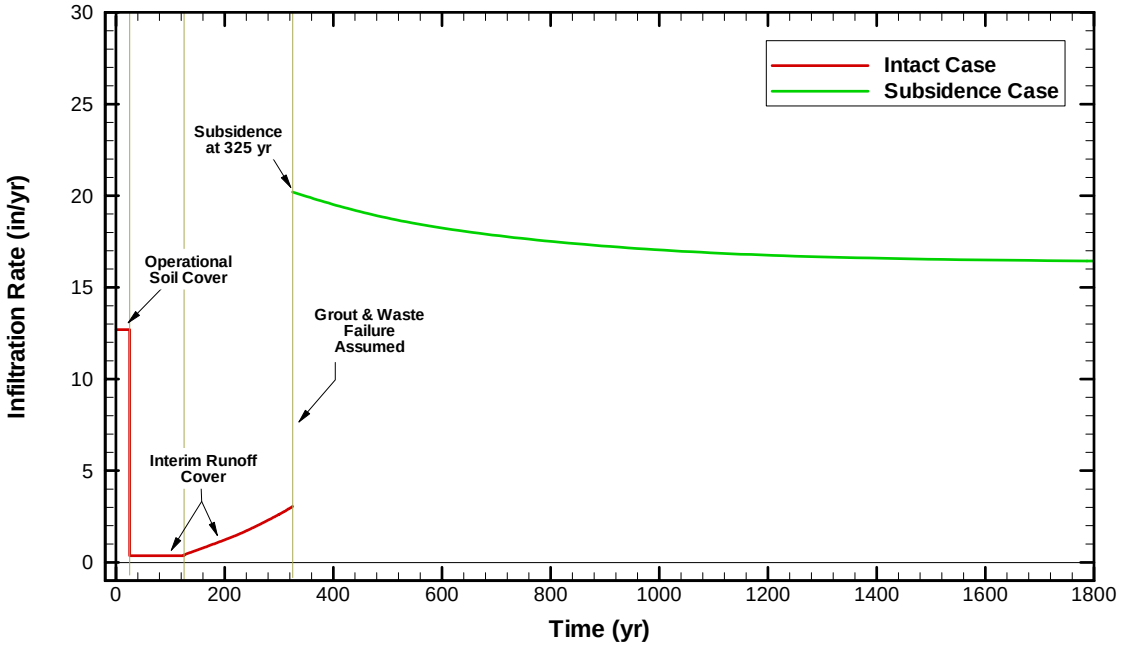

Figure 2-17. Computed (HELP Code) Infiltration Rates to a Generic CIG Trench Segment During the Operational (Soil Cover), Maintenance (Interim Runoff Cover), and Subsidence Periods

A series of steady-state flow analyses followed by a transient transport simulation was chosen as the computational strategy to address contaminant transport within the Vadose Zone. To perform transient transport simulations using PORFLOW, a series of steady-state flow fields were computed to approximate the dynamic behavior of the infiltration rate boundary conditions discussed above. A total of 18 time periods were chosen. Some time periods were required due to hydraulic property changes within the domain, others were required to account for the gradual shifting (up or down) of the infiltration rate over time, and others to account for abrupt changes in surface coverings. The 18 time periods chosen are listed in Table 2-9 along with average infiltration rates imposed over each time period. For each time interval given the infiltration value represents the integral average value over that time interval. A graphical close-up of the first 500 years, showing the infiltration rate boundary conditions employed in PORFLOW, is provided in Figure 2-18. Overlaid on the infiltration rate curves is a thick dashed line (blue in color) representing the average infiltration rate values used to generate the 18 unique flow fields for each CIG segment type (i.e., Existing or Future).

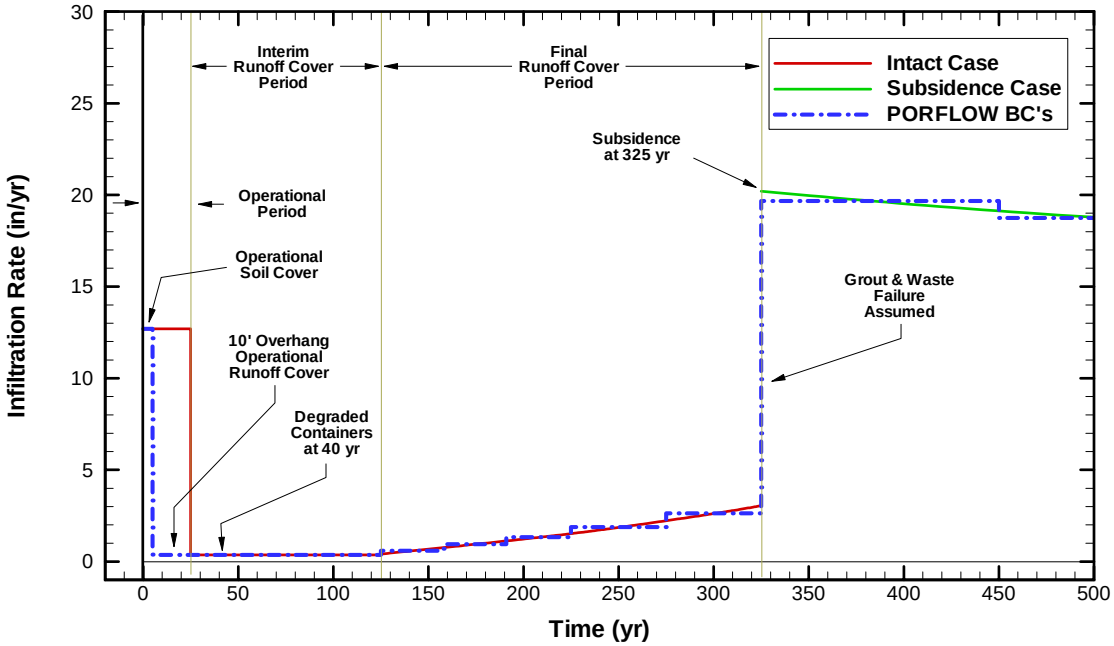

Figure 2-18. Close-up Comparison of Computed Infiltration Rates versus PORFLOW Boundary Conditions Employed During the First 500 Years of Simulation

Table 2-9. Infiltration Rate Boundary Conditions Used In PORFLOW for the Various Unique Time Period of Interest

Time Period	Cover Status	Starting Time (yr)	Ending Time (yr)	Infiltration Rate (in/yr)
1	soil cover	0	segment specific	12.7
2	Maintained interim runoff cover with 10 ft overhang	segment specific	25	0.36
3	Maintained interim runoff cover over entire CIG units and intact waste containers	25	40	0.36
4	Maintained interim runoff cover over entire CIG units and leaking waste containers	40	125	0.36
5	Degrading final runoff cover over entire CIG units and leaking waste containers	125	158	0.59
6	Degrading final runoff cover over entire CIG units and leaking waste containers	158	191	0.95
7	Degrading final runoff cover over entire CIG units and leaking waste containers	191	225	1.33
8	Degrading final runoff cover over entire CIG units and leaking waste containers	225	275	1.88
9	Degrading final runoff cover over entire CIG units and leaking waste containers	275	325	2.64
10	Subsidence on entire CIG units with grout and waste failure assumed along with silting	325	450	19.67
11	Subsidence on entire CIG units with grout and waste failure assumed along with silting	450	575	18.75
12	Subsidence on entire CIG units with grout and waste failure assumed along with silting	575	800	17.94
13	Subsidence on entire CIG units with grout and waste failure assumed along with silting	800	1,025	17.26
14	Subsidence on entire CIG units with grout and waste failure assumed along with silting	1,025	1,450	16.78
15	Subsidence on entire CIG units with grout and waste failure assumed along with silting	1,450	1,825	16.50
16	Subsidence on entire CIG units with grout and waste failure assumed along with silting	1,825	3,425	16.34
17	Subsidence on entire CIG units with grout and waste failure assumed along with silting	3,425	5,625	16.19
18	Subsidence on entire CIG units with grout and waste failure assumed along with silting	5,625	and beyond	16.14

For each existing segment and future segments, their specific time of burial and subsequent placement of the 10 ft overhang interim runoff cover differ. Table 2-10 provides for each segment the unique dates and modeling times employed in the Vadose Zone transport simulations. As listed in Table 2-10, the duration of having only an operational soil cover differs between segments. The 10 ft overhang interim runoff cover for the existing 8 segments was made operational by 4/1/2006. For all future segments it is assumed that their burial date is 1/1/2007 and within a 3-month period they have a 10-ft overhang interim runoff cover in place.

Table 2-10. Timing When Interim Runoff Cover with a 10-Ft Overhang was Placed Over CIG Existing and Future Segments

Segment Number	Comments	Burial Date for Modeling	Cover Date for Modeling	Time in Modeling Terms (yr)	Duration of Soil Cover Only (yr)
1,2,3	All 3 existing segments combined for analysis purposes (time zero set to 7/17/2001)	7/17/2001	4/1/2006	0.24	4.47
4	Existing segment	8/7/2002	4/1/2006	1.06	3.65
5	Existing segment	9/11/2002	4/1/2006	1.15	3.55
6	Existing segment	8/26/2003	4/1/2006	2.11	2.60
7	Existing segment	9/5/2003	4/1/2006	2.13	2.57
8	Existing segment	8/24/2004	4/1/2006	3.10	1.60
Future	All future segments assumed to be buried at the same time with a 3 month duration for placement of the interim runoff cover with a 10 ft overhang	1/1/2007	4/1/2007	5.46	0.25

2.6.5.4 Operational Cover Requirements

Early on, H-3 transport analyses strongly indicated that operational covers were needed during the 25-year operational period. In order to specify its hydraulic specifications the following items had to be considered:

- The degree of extent (i.e., overhang) beyond the CIG Trench.
- The amount of time after disposal that is available.
- The infiltration rate limit required.
- The removal of rainfall runoff.

An infiltration rate limit of 0.36 in/yr was chosen based on the value being imposed on the interim runoff cover that is to be in place after the 25-year operational period. It is assumed that some sort of drainage system is in place to completely remove rainfall runoff during this operational period, just as required during the 100 years. The timing and extent specifications required making numerous H-3 transport simulations to arrive at a reasonable balance between the various factors of importance. The discussion to follow is only those simulations that eventually established the most optimal setting for each parameter (i.e., cover timing and extent).

When looking at the H-3 fractional flux profiles generated, the impact of an operational cover is quite apparent. There are two extreme cases of interest: (1) no operational cover during the 0-25 year period and (2) an operational cover the entire 0-25 year period (i.e., the assumption used in prior PA analysis efforts). A 5-order change in H-3 flux magnitude exists between these two extremes. These H-3 transport scoping analyses performed in FY2006 strongly indicated the need for replacing the operational soil cover with an interim runoff cover as soon as practicable. This was determined through numerous test runs varying both the extent of the overhang of the interim runoff cover as well as the time of replacement itself. Placement of the interim runoff covers was completed in 4/1/2006. Three overhang values were considered (i.e., 5 ft, 10 ft, and 15 ft). An acceptable overhang value of 10 ft was established based on scoping analyses, as well.

Additional analyses indicated that the time delay from a future segment's creation to its placement of an interim runoff cover significantly impacts the allowable total inventory of H-3 that can be disposed of in the CIG units. These analyses indicated that a 3 month window for placement would provide acceptable H-3 inventory limits when grout hydraulic properties for the future segments met those values discussed earlier.

2.6.5.5 Structural Design Reducing Risk of Local Subsidence

As discussed earlier, local subsidence of a CIG Trench segment, operating with an interim runoff cover, can change the local infiltration rate substantially (e.g., ~0.36 in/yr for an intact trench to ~28 in/yr for an Edge-trench-only scenario). Infiltration rate increases of this potential magnitude have very profound impacts on the migration rates for species with low K_d values (i.e., a mobile radionuclide such as H-3). No special design efforts were engineered into the first existing segments (i.e., Segments 1 through 7). Once the issue of subsidence was considered plausible design efforts were employed to mitigate the potential of subsidence in future disposals. To mitigate the subsidence potential an additional 18 inch reinforced concrete slab was added to the design to sit directly over the top of the grout chamber. This new subsidence resistance design was first employed in-the-field for Segment 8. It was believed that this new design would greatly reduce the risk of local subsidence for future disposals. An improved subsidence resistance design has now been established for all future segments (i.e., Segment 9 and beyond) which consists of a 20 inch reinforced concrete slab sitting above the top of the grout chamber with 16 inches of CLSM material sandwiched in between.

Structural credit for the existing Segment 8 design and the future improved design is being taken out to 325 years. At 325 years, the degradation is being assumed to be abrupt and not gradual over any actual time period. All concrete, grout, CLSM, and waste structural and hydraulic properties are considered to remain un-degraded up to 325 years and then to degrade completely at that point in time. There appears to be only marginal inventory limit improvements to be gained by attempting to extend the structural failure point beyond the 325 year point in time.

The new CIG Trench designs address Segment 8 and all future disposal segments; however, the subsidence issue remains for the earlier Segments 1 through 7. Some of the earlier segments have low risks to local subsidence resulting from the particular wasteforms contained within them (i.e., they have components that have no low density regions housed within the grout chambers). Others unfortunately have containers, such as B-25 boxes that have very low densities when compared to the Native soil density. A six inch local surface subsidence, or greater, can result in the increased infiltration rates mentions above. During the operational and institutional control periods (i.e., the first 125 years), a local subsidence event can be repaired with grout fill-in and cap patching. Beyond the institutionally controlled period local subsidence will persist after the event happens.

For future segments engineered designed slabs are being relied upon, while some earlier existing segments will have local subsidence potential. Existing trench Segments 1-3 have no subsidence potential since the components were filled with grout or CLSM. Existing segments 4-7 will have an overlying 20-inch thick reinforced concrete mat slab installed prior to the construction of the final closure cap, as discussed in Section 2.3. To assess the impact of potential subsidence on existing segments, H-3 scoping transport analyses were performed for those existing segments not specifically designed to reduce subsidence risk. Three points in time for local subsidence were considered (i.e., 125, 225, 325 years). The earliest time when local subsidence could occur without damage repair is right after the end of the institutional control period (i.e., 125 years). Peak H-3 concentration values exceeded the H-3 MCL value for the first two cases indicating that subsidence during the 125-to-325 year period needed to be addressed. These analyses indicated that structural improvements were required to existing segments 4 through 7 to reduce the risk of local subsidence after the 125 year institutional control period has ended. Until the 125 year institutional control period end-date, proper maintenance of operational covers where necessary is sufficient.

2.6.5.6 Model Domain Description

Note that during the period of 25 years of operation neighboring CIG Trenches may not exist sometimes and then show up as new segments when created. Also, the fully extended interim runoff cover containing a minimum of 40 inches of soil cover and a GCL will not be present until the end of this 25 year operational period. To address these aspects of CIG operation and their potential impact on radionuclide burial limits, a variety of Vadose Zone conceptual models were considered where flow and transport simulations were performed to help minimize the computational efforts and to establish one unique Vadose Zone conceptual model that would provide acceptably conservative results.

During the scoping phase, modeling efforts for the CIG Trenches were first based on three separate models as shown connected together in Figure 2-19. Separate models for the Center CIG Trench, the Middle CIG Trench, and the Edge CIG Trench were created. Each of these models generated flux values (for each radionuclide of interest) at the water table to be supplied as source nodes to the CIG Aquifer transport model. During the scoping effort only a 25-foot distance was employed between the bottom of the CIG grout base and the water table (later a 35 foot distance was determined to be acceptable). As mentioned earlier the flux results from all three trench types proved to be very similar in value.

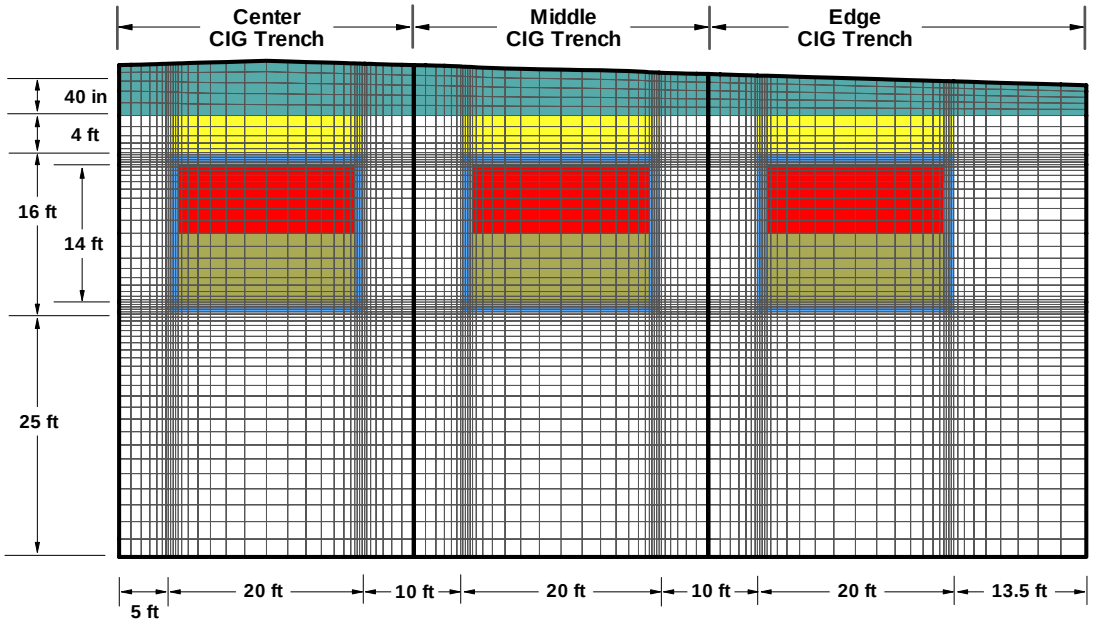

Figure 2-19. View of the Initial CIG Trench Vadose Zone Conceptual Models for the Center, Middle, and Edge Trenches

For the complete set of performance assessment analyses it was considered acceptable to choose just one of the trench types and impose a composite infiltration rate boundary condition (as mentioned above). Of the three possible trench types, the Middle trench model was chosen as highlighted in Figure 2-20. All of the prior scoping analyses mentioned earlier were performed using the model presented in Figure 2-20.

The modeling is designed to approximate the CIG operation–and-closure sequence described in Section 2.3. Deviations from the sequence are conservative, with some sequence steps modified to facilitate modeling runs. The sequence can be broken up in the four time frames of interest, as put forth in Section 2.6.5.3:

- **Operational Soil Cover Period** (This represents the initial period right after disposal within the 25 year operational window where both CIG units are being used for waste disposal. Limited-extent Interim Runoff Covers with a limited width of 10 ft overhang are placed over certain segments soon after they are created, and are maintained until the end of the 25-year operational period.)
- **Interim Runoff Cover Period** (At the end of 25 years of operation an interim runoff cover is placed over each entire CIG unit. These covers are maintained during the 100 year institutional period.)
- **Final Cover Period** (At the end of the interim runoff cover period a final cap will be placed over each CIG unit where no longer will there be further institutional maintenance performed.)
- **Subsidence Period** (At 325 years no further structural credit for the concrete slabs is taken to eliminate subsidence. Subsidence is assumed to occur at every location within both CIG units.)

Based on the scenario being analyzed the model domain residing above the original ground level does not exist for the first 25 years (during the operational soil cover period). At the start of the interim runoff cover period (at 25 years) the cap fill and cap are placed over each entire CIG unit. To handle this domain change within the PORFLOW environment the following two types of approaches were considered and also verified:

1. The entire model domain as shown in Figure 2-20 was present throughout the entire simulation period. For the first 25 years the horizontal hydraulic conductivity was set to zero and the vertical value was set to a very large value within the Cap Fill zone. From 25 years and beyond the horizontal and vertical hydraulic conductivity of the Cap Fill was set to their actual values provide in Table 2-7. This is a conservative approach, given that each CIG segment has the 4 ft + 2 ft soil, plus impermeable cover placed within 3 months of segment emplacement.
2. The model domain associated with the Cap Fill region as shown in Figure 2-20 was made a uniform layer of 1 foot thickness. This Cap Fill layer remained in place throughout the entire simulation period without any hydraulic property changes being applied.

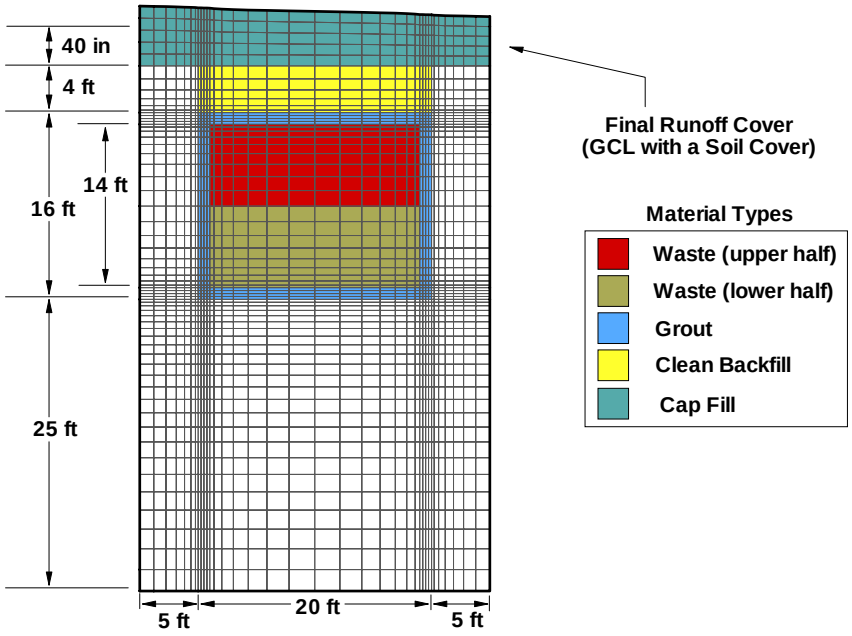

Figure 2-20. View of the Initial CIG Trench Vadose Zone Conceptual Model for a Middle Trench

Sensitivity calculations indicated that both approaches gave results within 1% of each other. The second approach is much simpler to implement and was chosen over the first approach. As mentioned earlier, based on this conceptual model early H-3 analyses strongly indicated that operational covers would be necessary during some portion of the 25-year operational period. To address the aspects of using operational covers of limited extent, a new revised Middle trench model had to be developed. The new model required extending the vertical boundaries of the initial model to allow consideration of covers with only finite extent beyond the CIG Trench itself (i.e., runoff covers with some degree of overhang beyond the edges of each segment). The new extended Middle trench model is shown conceptually in Figure 2-21 for existing segments (i.e., Segments 1 through 8) and in Figure 2-22 for future segments. The main difference between the conceptual model for existing versus new segments is the addition of a 20-inch slab above the CIG grout trench to be used in future segments to reduce the risk of subsidence. This new model also incorporated the 35-ft estimated depth to water table considered to be the best estimate of its minimum value (Section 2.6.5.1).

Segments 1 through 7 do not have a slab present as represented in Figure 2-21. However, for Segment 8 an 18-inch slab was placed over the trench. Sensitivity calculations unique to that geometry were made indicating that the conceptual model shown in Figure 2-21 was adequately conservative to be used to represent Segment 8 as well.

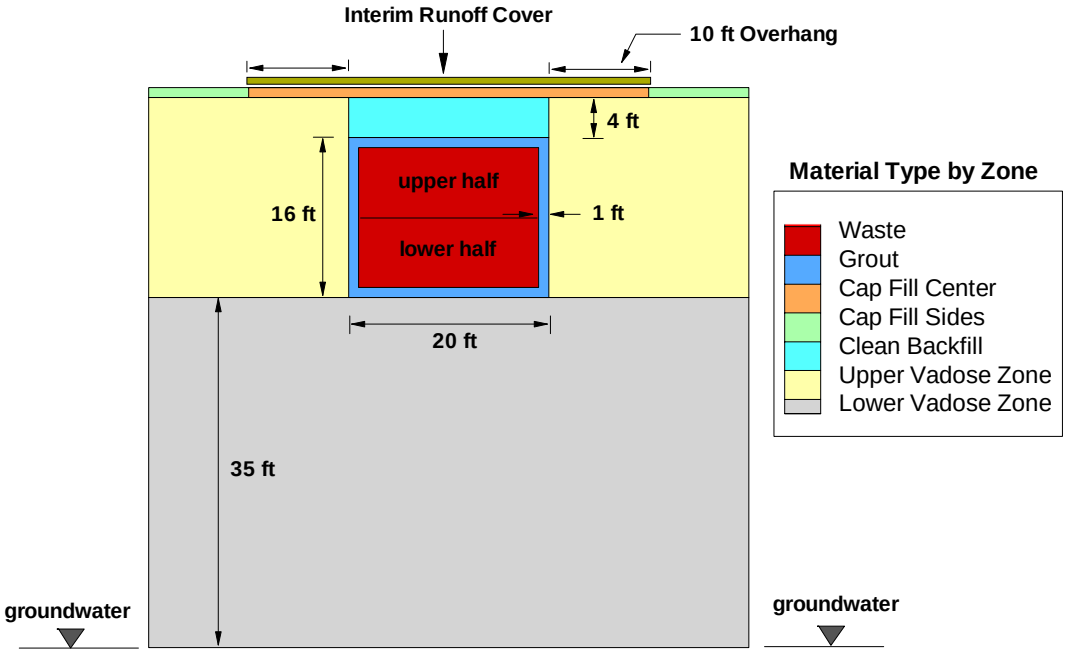

Figure 2-21. Cross-Sectional View Through the Existing Segment Model of a CIG Middle Trench Starting from the Ground Surface Down to the Water Table Showing the Interim Runoff Cover

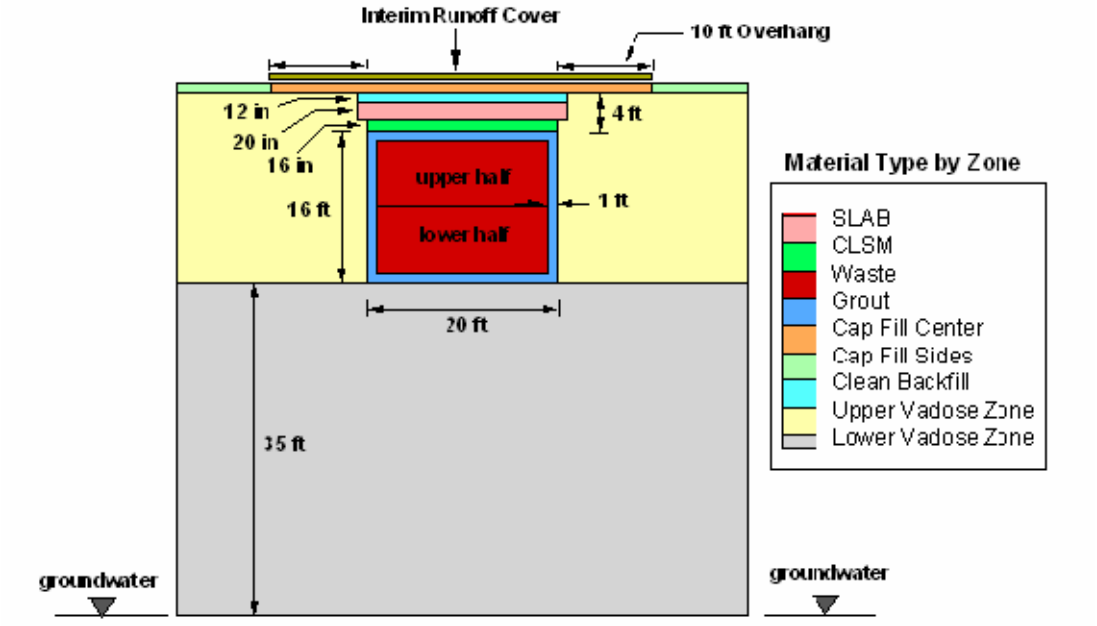

Figure 2-22. Cross-Sectional View Through the Future Segment Model of a CIG Middle Trench Starting from the Ground Surface Down to the Water Table Showing the Interim Runoff Cover

The initial Middle trench model extended only 5 ft to each side of the CIG grout chamber. To address operational covers that might extend as far as 15 ft beyond each side of the CIG grout chamber, 15 ft more model domain was provided (i.e., now 20 ft to each side of the CIG grout chamber). Based on prior sensitivity runs the geometrical impact of the Cap Fill zone was shown to have a small impact on overall results. For the new extended Middle trench model a uniformly thick 1 ft Cap Fill zone was provided. That portion of the interim runoff cover that extends beyond the CIG Trench is referred to within this report as overhang. The actual extended model showing its mesh is shown in Figure 2-23 for the existing segments and in Figure 2-24 for future segments. Along the top surface of this model regions were created allowing the variation in infiltration rate boundary condition values for simulating a partial cover (i.e., the limited extent interim runoff cover). Overhang options of 5, 10, 15, and 20 ft were analyzed for H-3 transport to determine the minimum overhang required to provide acceptable infiltration relief. A 20-ft overhang corresponds to a complete cover over the entire top surface. Rainfall runoff from these covers was always assumed to be removed from the segment of the CIG unit by some form of drainage systems.

The larger the overhang the greater the benefit achieved in reducing infiltration into the Grout chamber. However, the larger the overhang the more difficult it becomes to create neighboring CIG segments without disturbance of prior covers. Note that only a 10-ft distance exists between neighboring trenches. An Interim Runoff Cover with a 10-ft overhang was determined to be the acceptable design with respect to reduced infiltration, operational placement, and reduced disturbance to neighboring segments.

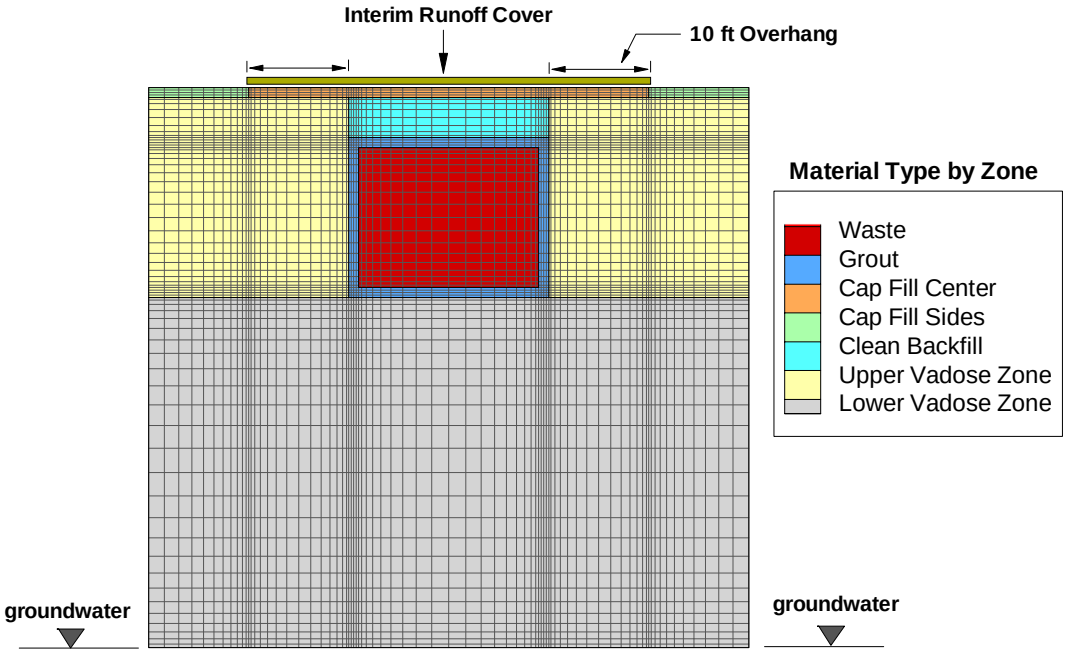

Figure 2-23. Cross-Sectional View through the Existing Segment Model of a CIG Middle Trench Showing the PORFLOW Mesh Used

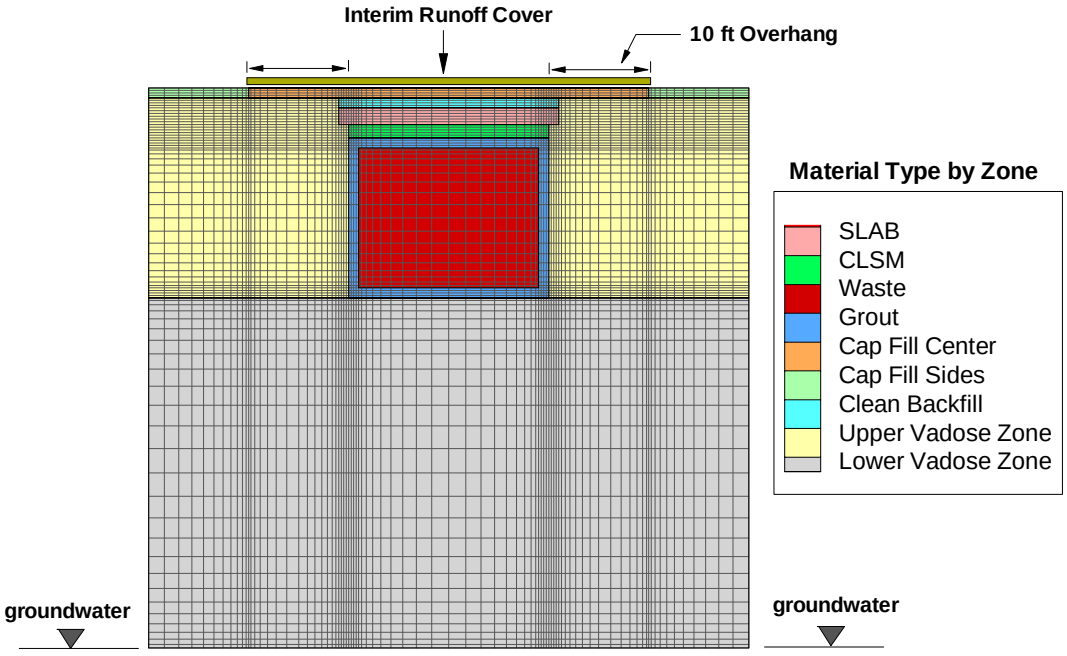

Figure 2-24. Cross-Sectional View through the Future Segment Model of a CIG Middle Trench Showing the PORFLOW Mesh Used

For both conceptual meshes shown in Figure 2-23 and Figure 2-24, mesh refinement studies were performed (using H-3 transport as the radionuclide of choice) to establish adequate meshes whose fluxes to the water table were within 1%. Mesh refinement at differing material interfaces was a key aspect to achieve numerical accuracy. For example, to adequately model the engineered grout walls, a minimum of 4 cells was required to capture the concentration gradients across this barrier.

2.6.5.7 Transport Property Assumptions

The following key assumptions (see also Appendix B) are being made for CIG transport analyses:

- Subsidence affects hydraulic properties and transport properties (however K_d values remain constant).
- Subsidence results in translation of upper half of Waste Zone radionuclide inventories to bottom half of Waste Zone (i.e., abrupt transfer at 325 years).
- Young, Middle, Old, and then Gone (i.e., cement properties become those for neighboring soil properties) are time markers for step changes in K_d values for those materials that are cementitious.
- Oxidizing cement beyond Old (i.e., Gone) takes on non-cement transport properties consistent with those for the Upper Vadose Zone Clayey soil.
- CDPs (i.e., at a concentration level of 95 mg/L of carbon) are assumed to be present as the baseline scenario; except for special resin based wasteforms.
- Special resin based wasteforms remain chemically intact and their K_d values remain constant throughout the entire simulation period.
- Stepwise steady-state flow fields are used to approximate the transient behavior occurring at the surface due to infiltration rate boundary condition changes (e.g., no account taken for the impact due to storage/drainage of pore water during the transition resulting from the surface change from starting with a Soil Cover and then replacing that with an Interim Runoff Cover).
- Hydraulic and transport properties for non-cementitious (e.g., Upper and Lower Vadose Zone soils) are considered to be invariant throughout the simulations.

Cementitious Material Environmental Impacts

The sorption characteristics of radionuclides onto cementitious materials are impacted by the physiochemical environment that the material is exposed to, as well as to the type of cement considered. For CIG segments the following material types are considered to be an oxidizing cementitious solid:

- Existing and Future Grout Formulations
- Waste Zone (noting however the added aspect of Waste containers such as B-25 boxes)
- CLSM
- Concrete Slabs

Of primary importance to radionuclide groundwater transport is their chemical changes (i.e., expressed in terms of K_d value [surface-to-aqueous concentration ratio] changes). K_d values are surface to aqueous-phase concentration ratios that represent the chord of a sorption isotherm. We assume a constant ground temperature and that the K_d values are constant over the range of species concentration considered (i.e., generally a valid assumption at very low aqueous-phase concentration levels and under conditions where a solubility limit is unlikely to be reached).

For the transport analyses within this report the following two environmental factors are being addressed:

- Cellulose Degradation Products – CDPs are released from wood, cardboard, and paper products that are present within the wasteforms disposed of in CIG segments. These carbon-based products can either improve or degrade sorption capacity in cementitious materials when in their presence and the degree of change is related to the concentration of CDPs within the local groundwater. For CIG transport analyses we assume a baseline amount of CDPs at a carbon concentration level of 95 mg/L.
- Aging – Cementitious materials age under chemical attack from a variety of chemicals present within neighboring groundwater. One of the key aqueous parameters used to identify aging is pH. Three stages (i.e., 1st Stage, 2nd Stage, and 3rd Stage) of the aging process has been established (i.e., referred to as "Young", "Middle", and "Old", respectively). The duration of each stage is controlled by how much pore water passes through the cement of interest, thereby promoting cement degradation. Ultimately the cementitious material losses all of its unique chemical sorption capability and then resorts back to the behavior of neighboring soils (i.e., referred to as "Gone").

See Kaplan (2006) for further details on the above impacts to sorption characteristics of radionuclides onto cementitious materials.

Cellulose degradation product factors represent the ratio of K_d values with CDPs present to those without. At carbon concentration levels of 95 mg/L, CDP factors (Kaplan 2006) range from values as low as 0.08 for Zr to values as high as 1.89 for Ra and U. Except for special resin based wasteforms, CDP's are assumed to be present throughout the entire Vadose and Aquifer Zones at the carbon concentration levels of 95 mg/L.
For establishing the three aging stages of cement the concept of exchange cycles (i.e., pore volumes) has been employed by Kaplan (2006). For E-Area purposes these stages are defined as:

- Stage 1 ("Young") - 0 to 50 pore volumes
- Stage 2 ("Middle") - 50 to 500 pore volumes
- Stage 3 ("Old") - 500 to 7,000 pore volumes
- Beyond ("Gone") – greater than 7,000 pore volumes

Degradation of cement, and thus the time duration of each stage, is affected by how much pore water passes through the cement (Kaplan 2006). In order to estimate the time duration of each stage of a unique CIG grout chamber, the cumulative amount of pore water passing through a segment must be determined by time integration of the flow field (i.e., based on step changes of the various computed steady-state flow fields). At each point in time the net throughput volume of water passing through the walls of the grout chamber (i.e., the water volume to which the grout cement is exposed) was determined for both the existing segments and for the future segments. The cumulative amount of pore water passing through each of the CIG segment types is plotted in Figure 2-25, along with the water volumes defining each stage associated with the grout walls of each segment type. Cement material whose age exceeds Stage 3 is assumed to have completely lost its unique chemical properties and takes on those of the surrounding Upper Vadose Zone soil.

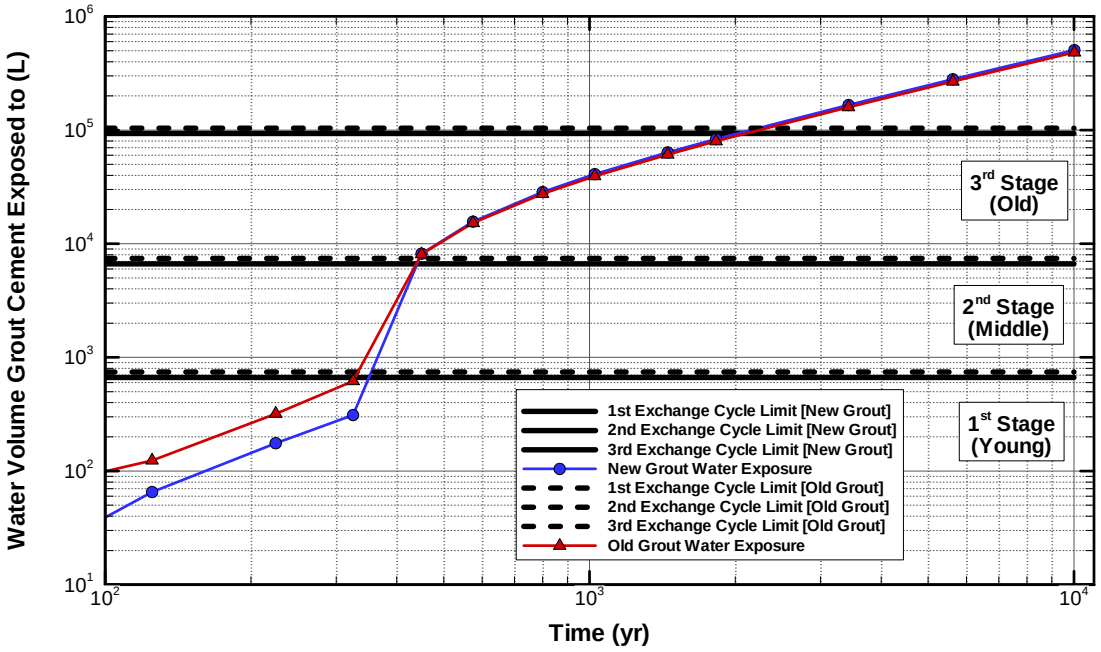

Figure 2-25. Estimated Amount of Pore Water Passing Through the CIG Grout Chambers for Both the Existing and Future Grout Formulations versus Aging Criteria

The intersection of the estimated amount of cumulative water throughput versus the water volumes defining cement's age provides the time durations for each segment type. The resulting time durations are provided in Table 2-11.

Table 2-11. Summary of CIG Cement Aging Time Periods

Case	Time Period (yr)	Young [Stage 1] (yr)	Middle [Stage 2] (yr)	Old [Stage 3] (yr)	Local Soil (yr)
Existing Grout	start	0	334	443	2223
	end	334	443	2223	and beyond
Future Grout	start	0	350	441	2078
	end	350	441	2078	and beyond

Vadose Zone Transport Properties

Within each of the Vadose zone flow and transport models (i.e., existing and future models), physical and chemical property changes are taken into account based on a specific time line of assumed events. For PORFLOW transport analyses the following properties are required for each material used within the vadose zone models:

- Effective, total, and diffusive porosities (-) [assumed to be equal]
- Particle density (g/ml)
- Molecular diffusivity (cm^2/yr) [assumed to apply to all elements]
- Sorption K_d values (ml/g) [these are also element specific]
- Longitudinal and transverse dispersivity coefficients (-) [assumed to be zero]

Effective, total, and diffusive porosities were set equal to the estimated value for a material's total porosity. For the Waste Zone a 50% total gas volume was assumed prior to subsidence.

The particle density was set to available measured values.

Molecular diffusivities were estimated values that were applied to each material and not made uniquely element dependent. However, within the Waste Zone molecular diffusivity values were set based on two different categories (i.e., radionuclides that are non-volatile and those that could potentially be volatile within the air space of waste containers such as B-25 boxes). The list of potentially volatile species is C-14, Cl-36, H-3, I-129, Se-79, and Sn-126. Gas-phase diffusion coefficients are much larger than their counterpart liquid-phase values. For example, a generic liquid-phase diffusion coefficient value of 59.33 cm^2/yr is used for non-volatile elements, while the binary gas-phase diffusion coefficient value for H-3 in air is ~0.5 cm^2/s (i.e., ~1.6×10^7 cm^2/yr). In scoping PORFLOW transport simulations a Waste Zone employing a diffusion coefficient value of ~1.6×10^7 cm^2/yr for volatile elements required excessively small time steps in order to maintain numerical accuracy (i.e., conserve mass balances).

To compromise between the need to have a large diffusion coefficient for volatile elements and reasonable time step sizes, a value of 1,578.0 cm^2/yr was found acceptable. For volatile elements the gas-phase transport is only required within the Waste Zone for the first 40 years and at that point in time the waste containers hydraulically leak and are assumed to transport elements primarily through the pore water. For this diffusion coefficient value accuracy was maintainable for time steps of 0.01 year in value. This large diffusion coefficient value also maintained a fairly uniform element concentration throughout the Waste Zone regions as needed.

Sorption K_d values for the baseline case were based on best estimate values (i.e., experimental values where available) with CDPs and cement aging taken into account (Section 2.6.9, Kaplan 2006). Sorption K_d values are element, but not isotope, dependent. In several cases an element K_d value was not experimentally available and was set equal to its chemical group value.

The longitudinal and transverse dispersivity coefficients were set to zero in an attempt to minimize the total computed dispersion that occurs (i.e., only numerical dispersion present). To further reduce the magnitude of numerical dispersion mesh refinement was employed, especially in the neighborhood of material boundaries.

Table 2-12 and Table 2-13 list the attributes associated with the vadose zone transport time line for the existing and future segments, respectively.

Table 2-12. Timeline for Vadose Zone Transport Simulations Showing Time Periods Where Transport Properties Change for Existing Segments

Flow Period (yr)	Flow State	Cement Age (stages)	Waste Container State [b]	Grout Chamber State	Physical Property State
Burial [a] to 4.47	Soil Cover	Young	Intact / Cement K_d / Cement D_{eff}	Intact / Cement K_d / Cement D_{eff}	Waste / Grout
4.47 to 25	10 ft Interim Runoff Cover	Young	Intact / Cement K_d / Cement D_{eff}	Intact / Cement K_d / Cement D_{eff}	Waste / Grout
25 to 40	Interim Runoff Cover	Young	Intact / Cement K_d / Cement D_{eff}	Intact / Cement K_d / Cement D_{eff}	Waste / Grout
40 to 125	Interim Runoff Cover	Young	Leaking / Cement K_d / Cement D_{eff}	Intact / Cement K_d / Cement D_{eff}	Waste to Soil / Grout
125 to 325	Final runoff cover	Young	Leaking / Cement K_d / Cement D_{eff}	Intact / Cement K_d / Cement D_{eff}	Soil / Grout
325 to 334	subsidence	Young	Leaking / Cement K_d / Soil D_{eff}	Leaking / Cement K_d / Soil D_{eff}	Soil / Grout to Soil
334 to 443	subsidence	Middle	Leaking / Cement K_d / Soil D_{eff}	Leaking / Cement K_d / Soil D_{eff}	Soil / Soil
443 to 2,223	subsidence	Old	Leaking / Cement K_d / Soil D_{eff}	Leaking / Cement K_d / Soil D_{eff}	Soil / Soil
2,223 & Beyond	subsidence	UVZ Soil	Leaking / Soil K_d / Soil D_{eff}	Leaking / Soil K_d / Soil D_{eff}	Soil / Soil

a Burial times are: 0.0 yr for Segment 123, 1.06 yr for Segment 4, 1.15 yr for Segment 5, 2.11 yr for Segment 6, 2.13 yr for Segment 7, and 3.10 yr for Segment 8.

b Within the Waste Containers there are two types of species (i.e., potentially volatile and non-volatile). The potentially volatile species are C-14, Cl-36, H-3, I-129, and Se-126) while the non-volatile are the remaining radionuclides considered. Volatile species have very large (gas-phase like; 1578 cm^2/yr) effective diffusion coefficients within their Waste Containers until the containers begin leaking after 40 years.

Table 2-13. Timeline for Vadose Zone Transport Simulations Showing Time Periods Where Transport Properties Change for All Future Segments

Flow Period (yr)	Flow State	Cement Age (stages)	Waste Container State [b]	Grout Chamber State	Physical Property State
5.46 to 5.70 [a]	Soil Cover	Young	Intact / Cement K_d / Cement D_{eff}	Intact / Cement K_d / Cement D_{eff}	Waste / Grout
5.70 to 25	10 ft Interim Runoff Cover	Young	Intact / Cement K_d / Cement D_{eff}	Intact / Cement K_d / Cement D_{eff}	Waste / Grout
25 to 40	Interim Runoff Cover	Young	Intact / Cement K_d / Cement D_{eff}	Intact / Cement K_d / Cement D_{eff}	Waste / Grout
40 to 125	Interim Runoff Cover	Young	Leaking / Cement K_d / Cement D_{eff}	Intact / Cement K_d / Cement D_{eff}	Waste to Soil / Grout
125 to 325	Final runoff cover	Young	Leaking / Cement K_d / Cement D_{eff}	Intact / Cement K_d / Cement D_{eff}	Soil / Grout
325 to 350	subsidence	Young	Leaking / Cement K_d / Soil D_{eff}	Leaking / Cement K_d / Soil D_{eff}	Soil / Grout to Soil
350 to 441	subsidence	Middle	Leaking / Cement K_d / Soil D_{eff}	Leaking / Cement K_d / Soil D_{eff}	Soil / Soil
441 to 2,078	subsidence	Old	Leaking / Cement K_d / Soil D_{eff}	Leaking / Cement K_d / Soil D_{eff}	Soil / Soil
2,078 & Beyond	subsidence	UVZ Soil	Leaking / Soil K_d / Soil D_{eff}	Leaking / Soil K_d / Soil D_{eff}	Soil / Soil

a Burial times are assumed to be identical for future segments that ultimately fill up all ten trenches within both CIG units.

b Within the Waste Containers there are two types of species (i.e., potentially volatile and non-volatile). The potentially volatile species are C-14, Cl-36, H-3, I-129, and Se-126) while the non-volatile are the remaining radionuclides considered. Volatile species have very large (gas-phase like; 1578 cm^2/yr) effective diffusion coefficients within their Waste Containers until the containers begin leaking after 40 years.

2.6.6 Radionuclide Parents and Wasteforms Considered for Transport Analysis

The results provided in this Chapter represent the flow and transport analyses in support of establishing radionuclide inventory limits for operation of CIG Units 1 and 2. The flow and transport analyses were limited to the 35 radionuclide parents that were obtained from the groundwater screening process, briefly described in the Background Chapter, and documented in Cook (2007). From an overall exposure concern (i.e., groundwater only pathway) these 35 radionuclide parents represent an adequate list of existing and potential nuclides that might be buried within one of the E-Area facilities. Further approximations were made by reducing the radionuclide chains associated with each of these parents to what is referred to as "abbreviated chains." These abbreviated chains were established by assuming that all nuclides with half-life's less than 5 years are in secular equilibrium with their nearest parent within the full chain.

For each parent PORFLOW transport analyses were performed where only those radionuclides existing within each abbreviated chain were explicitly accounted for. The exposure contributions associated with the omitted radionuclides of each chain were accounted for in separate post-processing (see in Section 8.3).

To better illustrate the approach taken, an example comparison is provided in Table 2-14 for the radionuclide parent Thorium-232. As shown in Table 2-14 the full chain, and its branching, consists of a total of 11 radionuclides. By applying a less than 5 year half-life cutoff criterion for nuclides considered to be in secular equilibrium, the abbreviated chain consists of 2 radionuclides. For this case PORFLOW transport analyses were performed for the abbreviated chain Th-232 decaying to Ra-228, while post-processing established the concentration levels of the remaining 9 radionuclides assuming them to be in secular equilibrium.

Table 2-14. Example Comparison of Full Chain versus Abbreviated Chain Used in PORFLOW Transport Analysis for the Nuclide Parent Thorium-232 (Th-232)

Nuclide (half-life in years)	Full Chain	Full Chain Branch	Abbreviated Chain	Abbreviated Chain Branch
Parent Buried	Th-232 (1.405E+10)		Th-232 (1.405E+10)	
Daughter	Ra-228 (5.750E+00)		Ra-228 (5.750E+00)	
Daughter	Ac-228 (7.021E-04)		Secular Equilibrium	
Daughter	Th-228 (1.912E+00)		Secular Equilibrium	
Daughter	Ra-224 (1.003E-02)		Secular Equilibrium	
Daughter	Rn-220 (1.763E-06)		Secular Equilibrium	
Daughter	Po-216 (4.598E-09)		Secular Equilibrium	
Daughter	Pb-212 (1.215E-03)		Secular Equilibrium	
Daughter & Branch	Bi-212 (1.152E-04)	Bi-212 (1.152E-04)	Secular Equilibrium	Secular Equilibrium
Daughters	Po-212 (9.481E-15)	Tl-208 (5.809E-06)	Secular Equilibrium	Secular Equilibrium

Within the 35 radionuclide parents to be addressed, for CIG operation four unique wasteforms are being handled based on past burials and anticipated future burials. The following wasteform categories are being addressed:

- **Generic Wasteform** – Used for standard nuclides where their release mechanisms are assumed to be instantaneous within the CIG waste zone (default case where all 35 radionuclide parents are handled). One typical example would be general job control waste such as cotton rags.

- **K & L Basin Resin Wasteform** – Used for a portion of the nuclides C-14, I-129, and Tc-99 that was buried within several segments of CIG Unit 1. Their release mechanisms are assumed to be instantaneous within the CIG waste zone, but have significantly different transport K_d values. This wasteform represents organic ion-exchange resins used in the K & L Reactor Basins. These special radionuclide parents are denoted as C-14_K, I-129_K, and Tc-99_K, respectively.
- **ETF Activated Carbon Wasteform** – Used for a portion of nuclide I-129 that will potentially be buried within segments of CIG Units 1 or 2. Its release mechanism is assumed to be instantaneous within the CIG waste zone, but has a significantly different transport K_d value. This wasteform represents carbon activated ion-exchange resins used in the Effluent Treatment Facility. This special radionuclide parent is denoted as I-129_C.
- **232-F Facility Metal Components Wasteform** – Used for a portion of the nuclide H-3 that was buried within Segment 6 of CIG Unit 1 on 8/21/2003. Its release mechanism is assumed to be a rate limited diffusional process from the buried 232-F metal components into its neighboring CIG waste zone. This wasteform represents metal components initially containing H-3 atoms bound in the stainless steel solid matrix. This special radionuclide parent is denoted as H-3_M.

In summary, PORFLOW transport analyses were performed for a total of 40 radionuclide parents and their daughters from their abbreviated chains (i.e., the 35 radionuclide parents [Cook 2007]in their generic wasteform and 5 radionuclide parents in special wasteforms; see tables in Section 2.6.6.1 for a listing).

2.6.6.1 Existing Radionuclide Parent Inventories Considered for Transport Analysis

Currently 8 segments exist within CIG Unit 1, while CIG Unit 2 has not been utilized. Within the WITS inventory database, the inventories (activity levels in terms of Curies) by segment number are provided for a variety of radionuclides that were obtained during waste assay analyses some time prior to their storage and ultimate disposal. Within this database the inventories of many of the 35 radionuclide parents and some of the special wasteforms discussed above are available. The WITS database does not perform radioactive decay corrections within its database to account for the time duration between a particular waste inventories assay to the time in which it is buried.

For CIG operations a multitude of waste types can potentially be disposed of within a given segment. For example, within a given segment job control waste, process equipment, miscellaneous equipment, piping, valves, spent resin beds, building materials can all reside typically separated by grout during the pouring process. The creation of a given segment, from the initial disposal item to the last disposal item and final placement of the interim soil cover, can occur over a 1-2 week time period. For the current 8 existing segments in CIG Unit 1, the range of dates for waste assays and burial are provided in Table 2-15. Based on the WITS database the average assay date, average burial date, and average time difference were computed and are also provided in Table 2-15.

Table 2-15. Summary of CIG Unit #1 Assay and Burial Dates by Existing Segment

Existing Segment Number	Date of Initial Assay	Date of Final Assay	Average Assay Date	Date of Initial Burial	Date of Final Burial	Average Burial Date	Average Assay to Burial Time (yr)
Segment 1	8/15/2000	8/15/2000	8/15/2000	8/29/2000	8/29/2000	8/29/2000	0.04
Segment 2	4/26/2001	4/26/2001	4/26/2001	7/17/2001	7/17/2001	7/17/2001	0.22
Segment 3 [a]	NA	NA	NA	NA	NA	NA	NA
Segment 4	7/3/2002	7/23/2002	7/16/2002	8/7/2002	8/7/2002	8/7/2002	0.06
Segment 5	7/16/1995	1/29/2002	4/19/1999	9/10/2002	9/11/2002	9/10/2002	3.40
Segment 6	4/26/1995	8/5/2003	7/1/1999	8/21/2003	8/28/2003	8/25/2003	4.15
Segment 7	4/5/1995	8/4/2003	1/22/1998	8/21/2003	9/5/2003	9/3/2003	5.61
Segment 8	10/30/2003	7/19/2004	6/15/2004	8/18/2004	8/18/2004	8/18/2004	0.18

a None of the 35 radionuclide parents was disposed of in Segment 3.

The available WITS radionuclide inventories are only the assay values. The WITS database does not allow one to perform any radioactive decay calculations internally. For the performance assessment transport analyses presented within this report, decay corrected inventory values were performed only for H-3. For all other radionuclide parents the WITS inventories were used directly as the existing inventories for burial in each segment. Also, none of the 35 radionuclide parent inventories were altered to account for the potential of being generated as a daughter from some other radionuclide that was originally contained within a waste item. For example, for Segment 6 generation of Cm-248 from Cf-252 (with a half-life of 2.65 years) was not considered.

As mentioned above H-3 WITS inventories were decay corrected and also broken out into two types of wasteforms. H-3 is a very special radionuclide that's very mobile (K_d values near zero in most porous media, volatile, rapid isotopic exchange with H-1, large Fickian diffusion coefficients within carbon steel and most other solid materials, etc.) and a half-life of 12.32 years. H-3 readily diffuses through job control waste such as cloth materials and carbon steel containers (e.g., B-25 boxes). On the other hand its diffusion rates through stainless steels such as 304L are much slower. Realizing that H-3 diffusion rates are much slower out of 304L based components, a special wasteform denoted as H-3_M was created. The details associated with the unique waste from (only contained within Segment 6 to date) are addressed within the next section.

For H-3 the WITS uncorrected inventory and decay corrected inventory values are provided in Table 2-16. Significant H-3 inventory reductions were achieved for Segments 6 and 7 when decay corrections and process knowledge are used to address the waste on a more detailed basis. For example, the total H-3 inventory for all 8 segments from WITS is 4,145 Ci assayed, while the corrected amount at time of burial was estimated to be 1,684 Ci. Of this estimated 1,684 Ci buried, 495 Ci is confined within 304L components with a slow diffusional release mechanism.

For the PORFLOW transport analyses performed for the CIG performance assessment, the existing radionuclide parents used in terms of activities are given in Table 2-17 and in terms of gmoles buried in Table 2-18. To properly handle the decay chain aspects within PORFLOW, the transport analyses (both vadose and aquifer zones) were performed based on a gmole basis. Activity based concentrations were computed on a post-processing basis. All values given are uncorrected assay values taken directly from WITS except for H-3 which was decay corrected as mentioned above and discussed in further detail in the next section. Of the possible 40 parents, 10 of them were not buried in the existing 8 segments (i.e., Cl-36, I-129_C, K-40, Mo-93, Nb-94, Pu-244, Ra-226, Th-230, Th-232, and Zr-93). PORFLOW transport analyses for these 10 parents were only performed for future burial consideration.

Table 2-16. Summary of CIG Unit #1 H-3 Inventory Values (Activities in Ci) Uncorrected from WITS and Decay Corrected (from Time of Assay to Time of Burial) by Segment and Wasteform Type

Existing Segment Number	Wasteform Category	Average Assay Date	Assay Inventory (Ci)	Average Burial Date	Burial Date for Modeling	Burial Inventory [a] (Ci)
Segment 1	generic	8/15/2000	5.296E-04	8/29/2000	7/17/2001	5.285E-04
Segment 2 [b]	generic	4/26/2001	7.280E+00	7/17/2001	7/17/2001	7.189E+00
Segment 3 [d]	generic	NA	0	NA	NA	0
Segment 4	generic	7/16/2002	2.369E+01	8/7/2002	8/7/2002	2.361E+01
Segment 5	generic	4/19/1999	2.503E+02	9/10/2002	9/11/2002	2.497E+02
Segment 6 [e]	generic	10/29/1999	4.956E+02	8/25/2003	8/26/2003	3.876E+02
Segment 6 [c]	metal	NA	2.555E+03	8/21/2003	8/21/2003	4.951E+02
Segment 7	generic	1/22/1998	8.123E+02	9/3/2003	9/5/2003	5.202E+02
Segment 8	generic	6/15/2004	9.354E-01	8/18/2004	8/24/2004	9.256E-01
Total (generic)			4.145E+3			1.189E+03
Total (metal)			NA			4.951E+02
Grand Total			4.145E+3			1.684E+03

a Inventory value has been decay corrected from time of assay to time of burial. Each burial item was uniquely decayed and the value provided represents the sum of all decay corrected items buried within each specified segment.
b Segments 1, 2, and 3 were combined as source terms within the vadose zone transport model. The time of burial was set to Segment 2's burial date such that the modeling time of zero corresponds to the date 7/17/2001.
c Two types of wasteforms (i.e., generic and metal) are being used in the vadose zone transport modeling. Generic wasteforms assume release mechanisms are instantaneous within the CIG waste zone, while metal wasteforms (i.e., 232-F metal) assume a release mechanism based on a 1-dimensional (cylindrical) transient solid-phase transport model.
d None of the 35 radionuclide parents was disposed of in Segment 3.
e Within WITS for Segment 6 all H-3 waste was categorized as generic waste. Post-processing of the entire contents contained within Segment 6 broke out the waste into two wasteforms (i.e., generic and metal). The average times for assay and burial are different for the 2 wasteforms.

Table 2-17. Summary of Existing CIG Unit #1 Inventory Values (in Curies) by Segment for the Abbreviated List of Parent Nuclides under Consideration (from Clark 2007 and SRS WITS database)

Species (nuclide & form) [a]	Existing Segment 1 (Ci)	Existing Segment 2 (Ci)	Existing Segment 3 (Ci)[b]	Existing Segment 4 (Ci)	Existing Segment 5 (Ci)	Existing Segment 6 (Ci)	Existing Segment 7 (Ci)	Existing Segment 8 (Ci)
Am-241	6.630E-03				7.988E-03	1.814E-02	2.794E-03	4.551E-03
Am-243	7.423E-04				6.137E-06	1.319E-07		1.105E-06
C-14	1.810E-06			1.724E-03	1.978E-02	8.476E-03	5.804E-03	5.388E-03
C-14_K[c]						4.680E-02	7.378E-03	1.187E-02
Cl-36								
Cm-244	1.952E-01				5.278E-04	3.928E-08	3.430E-06	6.501E-07
Cm-245	1.543E-05				3.837E-10	5.427E-10		4.546E-09
Cm-247	8.757E-05					8.766E-15		7.345E-14
Cm-248	8.757E-05							
H-3[d]	5.285E-04	7.189E+00		2.361E+01	2.497E+02	3.876E+02	5.202E+02	9.256E-01
H-3_M[e]						4.951E+02		
I-129	6.297E-07	3.764E-11		3.198E-06	3.340E-07	1.374E-06	4.236E-06	2.305E-06
I-129_C[f]								
I-129_K[c]						5.921E-05	5.249E-06	1.069E-05
K-40								
Mo-93								
Nb-94								
Ni-59	2.890E-04				3.115E-05	4.257E-04	2.252E-04	5.167E-06
Np-237	5.421E-06			8.622E-07	4.930E-04	2.511E-04	8.882E-05	6.245E-05
Pd-107	6.755E-06							
Pu-238	7.089E-02			4.406E-06	3.874E-02	4.429E-02	2.929E-02	1.066E-02
Pu-239	1.297E-02			1.663E-05	2.946E-02	1.560E-01	2.329E-02	4.708E-02
Pu-240	8.924E-03			1.663E-05	7.723E-03	5.260E-04	6.351E-03	2.814E-03
Pu-241	5.630E-02				1.423E-01	3.896E-01	1.108E-01	1.109E-01
Pu-242	2.072E-06				2.914E-05	5.118E-08	1.157E-06	1.380E-06
Pu-244								
Ra-226								
Se-79	3.369E-05				2.980E-04	8.043E-06	1.739E-06	2.368E-09
Sn-126	1.076E-05				4.771E-06	8.569E-10	2.700E-06	3.003E-10
Sr-90	2.072E-02				5.050E-01	2.222E+00	2.309E+00	2.479E+00
Tc-99	1.347E-05	1.747E-07		5.401E-05	1.433E-04	5.088E-03	7.074E-04	2.692E-04
Tc-99_K[c]						9.113E-03	1.328E-04	3.331E-05
Th-230								
Th-232								
U-233	1.768E-06			7.627E-06	4.327E-05	1.521E-02	2.369E-01	1.668E-08
U-234	8.924E-06	3.764E-10		6.538E-08	1.064E-03	2.972E-02	4.280E-04	2.624E-03
U-235	1.810E-07				2.250E-05	8.027E-04	5.649E-06	4.523E-05
U-236	2.356E-07				5.304E-05	2.389E-04	6.431E-06	2.298E-04
U-238	1.660E-05				6.217E-04	1.374E-01	9.618E-05	6.706E-04
Zr-93	1.017E-03							

a Generic wasteforms for the standard nuclides where their release mechanisms are assumed to be instantaneous within the CIG waste zone.

b None of the 35 radionuclide parents was disposed of in Segment 3.

c K refers to a special wasteform termed "K & L Basin Resins" employed for nuclides C-14, I-129, and Tc-99 affecting their transport K_d values within the CIG wasteform only.

d H-3 inventory value was decay corrected from time of assay to time of burial.

e M refers to a special wasteform termed "232-F Facility Metal Components" for nuclide H-3 affecting how its release mechanism within the CIG waste zone is addressed by using a 1-dimensional (cylindrical) transient solid-phase transport model. Inventory value was also decay corrected from time of assay to time of burial.

f _C refers to a special wasteform termed "ETF Activated Carbon" employed for nuclide I-129 affecting its transport K_d value within the CIG wasteform only.

Table 2-18. Summary of Existing CIG Unit #1 Inventory Values (in gmoles) by Segments Modeled for the Abbreviated List of Parent Nuclides under Consideration

Species (nuclide & form) [a]	Half-life (year)	Existing Segments 1-2-3 [b] (gmole)[c]	Existing Segment 4 (gmole)[c]	Existing Segment 5 (gmole)[c]	Existing Segment 6 (gmole)[c]	Existing Segment 7 (gmole)[c]	Existing Segment 8 (gmole)[c]
Am-241	4.322E+02	8.015E-06		9.656E-06	2.193E-05	3.377E-06	5.501E-06
Am-243	7.370E+03	1.530E-05		1.265E-07	2.718E-09		2.277E-08
C-14	5.730E+03	2.901E-08	2.764E-05	3.169E-04	1.358E-04	9.302E-05	8.636E-05
C-14_K$_d$	5.730E+03				7.501E-04	1.182E-04	1.903E-04
Cl-36	3.010E+05						
Cm-244	1.810E+01	9.880E-06		2.672E-08	1.988E-12	1.737E-10	3.291E-11
Cm-245	8.500E+03	3.668E-07		9.124E-12	1.290E-11		1.081E-10
Cm-247	1.560E+07	3.821E-03			3.825E-13		3.205E-12
Cm-248	3.480E+05	8.524E-05					
H-3[e]	1.233E+01	2.479E-04	8.141E-04	8.611E-03	1.337E-02	1.795E-02	3.192E-05
H-3_M[f]	1.233E+01				1.506E-04		
I-129	1.570E+07	2.765E-05	1.404E-04	1.467E-05	6.035E-05	1.860E-04	1.012E-04
I-129_C[g]	1.570E+07						
I-129_K$_d$	1.570E+07				2.600E-03	2.305E-04	4.694E-04
K-40	1.277E+09						
Mo-93	4.000E+03						
Nb-94	2.030E+04						
Ni-59	7.600E+04	6.143E-05		6.622E-06	9.049E-05	4.786E-05	1.098E-06
Np-237	2.144E+06	3.251E-05	5.171E-06	2.957E-03	1.506E-03	5.326E-04	3.745E-04
Pd-107	6.500E+06	1.228E-04					
Pu-238	8.770E+01	1.739E-05	1.081E-09	9.503E-06	1.086E-05	7.185E-06	2.616E-06
Pu-239	2.411E+04	8.746E-04	1.121E-06	1.987E-03	1.052E-02	1.571E-03	3.175E-03
Pu-240	6.564E+03	1.638E-04	3.053E-07	1.418E-04	9.657E-06	1.166E-04	5.167E-05
Pu-241	1.429E+01	2.250E-06		5.688E-06	1.557E-05	4.430E-06	4.431E-06
Pu-242	3.733E+05	2.164E-06		3.042E-05	5.344E-08	1.209E-06	1.441E-06
Pu-244	8.000E+07						
Ra-226	1.600E+03						
Se-79	1.100E+06	1.037E-04		9.168E-04	2.475E-05	5.350E-06	7.285E-09
Sn-126	1.000E+05	3.009E-06		1.335E-06	2.397E-10	7.551E-07	8.401E-11
Sr-90	2.879E+01	1.669E-06		4.067E-05	1.789E-04	1.859E-04	1.996E-04
Tc-99	2.111E+05	8.056E-06	3.189E-05	8.464E-05	3.004E-03	4.177E-04	1.589E-04
Tc-99_K$_d$	2.111E+05				5.381E-03	7.841E-05	1.967E-05
Th-230	7.538E+04						
Th-232	1.405E+10						
U-233	1.592E+05	7.873E-07	3.396E-06	1.927E-05	6.771E-03	1.055E-01	7.426E-09
U-234	2.455E+05	6.128E-06	4.489E-08	7.304E-04	2.041E-02	2.939E-04	1.802E-03
U-235	7.038E+08	3.563E-04		4.429E-02	1.580E+00	1.112E-02	8.903E-02
U-236	2.342E+07	1.543E-05		3.475E-03	1.565E-02	4.212E-04	1.505E-02
U-238	4.468E+09	2.074E-01		7.770E+00	1.717E+03	1.202E+00	8.381E+00
Zr-93	1.530E+06	4.354E-03					

a Generic wasteforms for the standard nuclides where their release mechanisms are assumed to be instantaneous within the CIG waste zone

b For modeling purposes segments 1, 2, and 3 inventories were combined in the vadose zone transport modeling. This was done in order to have an adequate number of source nodes for these segments within the aquifer modeling analyses.

c g/mole = (Ci)/(Ci/g)/M

d _K refers to a special wasteform termed "K & L Basin Resins" employed for nuclides C-14, I-129, and Tc-99 affecting their transport K_d values within the CIG wasteform only.

e H-3 inventory value was decay corrected from time of assay to time of burial.

f M refers to a special wasteform termed "232-F Facility Metal Components" for nuclide H-3 affecting how its release mechanism within the CIG waste zone is addressed by using a 1-dimensional (cylindrical) transient solid-phase transport model. Inventory value was also decay corrected from time of assay to time of burial.

g C refers to a special wasteform termed "ETF Activated Carbon" employed for nuclide I-129 affecting its transport K_d value within the CIG wasteform only.

2.6.6.2 Special Considerations for H-3 within Segment 6 for Transport Analysis

As mentioned above, H-3 (referred to here as T) WITS inventories were decay corrected and also broken out into two types of wasteforms. This was done in recognition of the unique aspects of hydrogen migration (i.e., H-1[H], H-2[D], and H-3[T]) through most materials (gas, liquid, and solid phases). Due to the rapid isotopic exchange mechanisms between T and H in all three phases, T residing within job control waste in the form of THO water quickly establishes a vapor-liquid equilibrium with the gaseous phase present now containing TH molecules. On contact with the carbon-steel container walls (e.g., B-25 boxes), isotopic exchange between the gaseous HT molecules and atomic H and T on the surface of the walls occurs. The diffusion rate of T through carbon-steel containers is relatively fast. The results of application of a simple 1-dimensional analysis of the Fickian diffusion rate of T through a flat plate of carbon-steel is presented in Figure 2-26 (consistent with the properties of a B-25 container typically used to store tritiated job control waste). Clark (2007) documents the equation and solution method used to generate the curves in Figure 2-26. The B-25 walls was initially uniformly loaded with 1, 10, and 100 Ci of atomic tritium and then allowed to diffuse out of the outside surface of the walls.

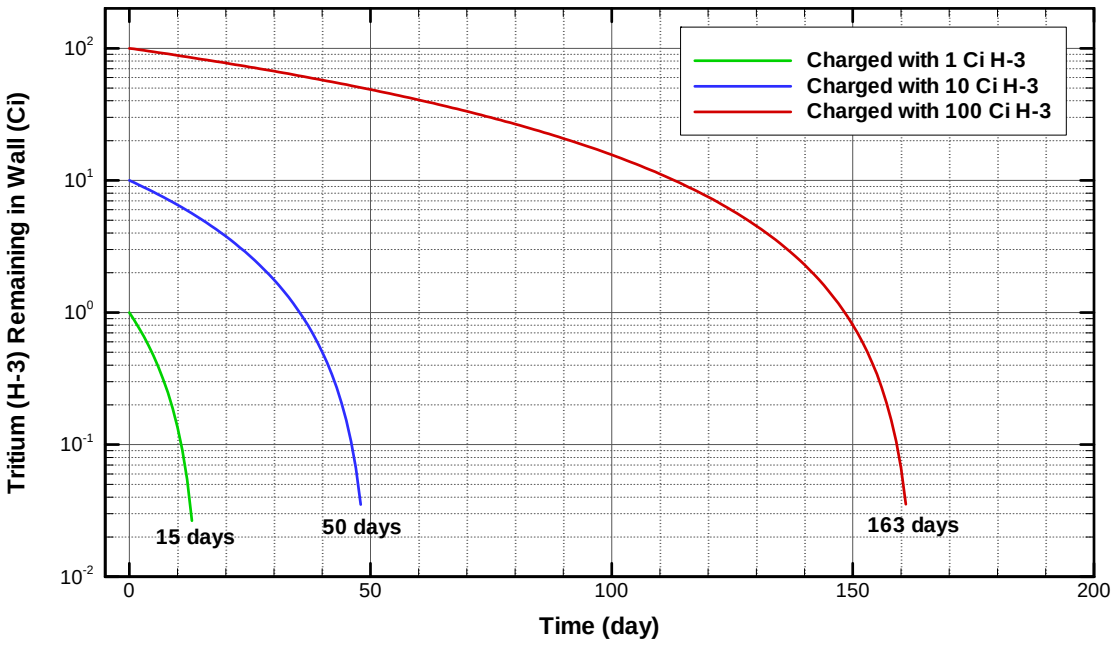

Figure 2-26. Illustrative Examples of the Diffusive Rate (permeation) of Atomic Tritium (H-3) out of Carbon-Steel Based B-25 Containers

As illustrated in Figure 2-26, the permeation (or diffusive) rate of atomic tritium out of carbon-steel materials is relatively high when compared to the time scales of interest in CIG performance assessments. Tritium passes through B-25 walls on the order of months not years. Therefore, for H-3 wasteforms whose release mechanisms are rapid, such as tritiated job control waste, the assumption that the buried H-3 waste is instantaneously available for migration into the surrounding grout is warranted. For these types of wasteforms, the wasteform category "Generic" was defined. Under these set of conditions the migration rates for release from the wasteforms (e.g., rags) and the migration rates through the liquid and solid phases are assumed to be infinite (i.e., no credit is taken for finite release rates for diffusion out of their solid forms). For PORFLOW numerical purposes the migration rates within the gas phase were reduced using a molecular diffusivity value that allowed acceptable time step sizes but also provided very high diffusion rates (i.e., a molecular diffusivity value D_{eff} = 1578.00 cm^2/yr was applied). For conservatism the above large molecular diffusivity value was also employed for all radionuclides that had a potential of becoming volatile within their storage containers (i.e., C-14, Cl-36, H-3, I-129, Se-79, and Sn-126). All other radionuclide parents were considered to be nonvolatile species whose molecular diffusivity value was set to D_{eff} = 59.33 cm^2/yr (Phifer et al. 2006).

A second type of wasteform category was defined for wasteforms where credit for finite diffusion rates out of the solid material was taken into account. This category is termed "Metal." Figure 2-27 provides a simple cartoon highlighting the basic aspects of the two wasteform categories (1) Generic and (2) Metal. It should be noted that the liquid phase portrayed in the simple cartoon represents only the presence of moisture within the wasteform, not free liquid.

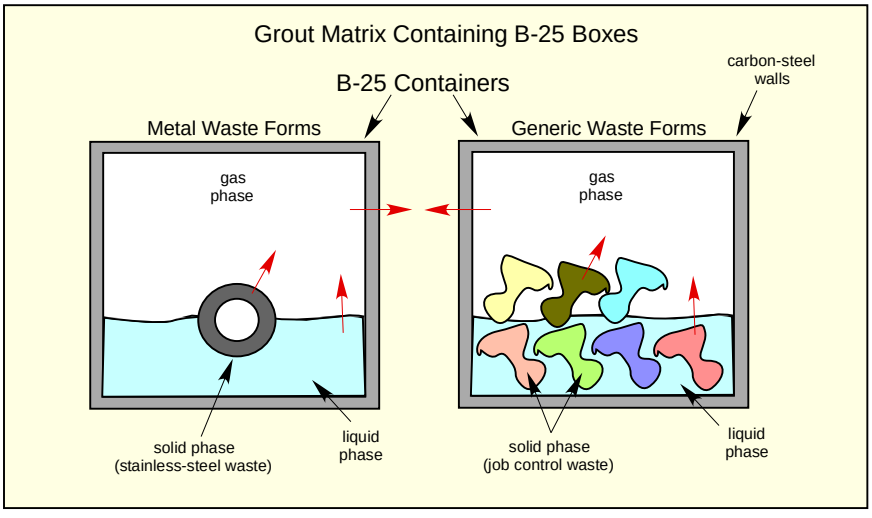

Figure 2-27. Simple Schematic Illustrating the Two Different Wasteform Types Being Applied for H-3

The migration (diffusional) rate of atomic tritium through stainless-steel 304L is much slower than through carbon-steel components. In the existing CIG Unit 1 inventory the dominant amount of H-3 buried, based on the uncorrected WITS database, is in the Metal wasteform category. From this WITS database a total of 4,145 Ci of H-3 was buried within the 8 segments (see Table 2-6 for detail segment breakdown). Of that inventory, 2,555 Ci (~62% of total) was reported to reside within stainless-steel components disposed of from 232-F facility operations within the time period of 1955 to 1958 (Roddy 2007, Table 4). However, it was realized that the amount of H-3 in the metal wasteform was actually smaller due to off gas and decay not taken credit for in the calculation of the 2,555 Ci value (Roddy 2007).

It has long been recognized that assay measurements for H-3 through surface smears can have modest to high levels of uncertainty, especially with regard to assaying of tritiated metal components (standardized internal-to-surface concentration ratio factors are employed; typical factors of 10 to 100). For tritiated metal components a more preferred approach is the estimation of remaining H-3 within a component be estimated using a facility's processing history and the component history after operation and during its storage period waiting disposal. Fortunately, for metal waste components in the 232-F facility such process knowledge and storage history were available.

The 232-F facility was in operation during the time period of 1955 to 1958 (~3 years). The process equipment employed that contained tritium gas was made of 304L stainless-steel. Within WITS the weights of all 232-F equipment was registered; however, the sizes and geometry of the disposed equipment was not. For calculational purposes (thought to be conservative) all of the 232-F equipment was assumed to be in the form of a cylindrical pipe with a wall thickness of 0.109 inches. A 1-dimensional transient Fickian diffusion model was used to model both the initial phase of tritium charging and subsequence out-gassing. Sievert's Law was assumed to address the gas-solid equilibrium interface at the outer surface of the pipe wall. When a hydrogen molecule dissolves, it dissociates into two atoms, which are then incorporated into the bulk solid by diffusion. For modest gas-phase pressures of hydrogen gas Sievert's Law (based on ideal solution behavior) is applicable since non-idealities are small. A zero flux boundary condition was imposed on the inner surface of the pipe wall at the end of operation (Clark 2007).

The total volume of 304L pipe was determined based on the total WITS weight for the 232-F equipment. For the ~3 years of operation (1955 to 1958), a 1 atmosphere pressure of T_2 gas at 25 C was applied (in this calculation) to the inner surface of the pipe and a zero flux boundary condition to the outer surface. At the end of operation, an atomic tritium concentration profile was established within the pipe. Beyond the end of operation, a zero flux boundary condition was applied at the inner surface with a zero partial pressure of tritiated gas outside the pipe. Throughout the calculational period the pipe was assumed to be at 25 C. The calculated H-3 inventory with in pipe and its flux rate are provided in Figure 2-28 (Clark 2007).

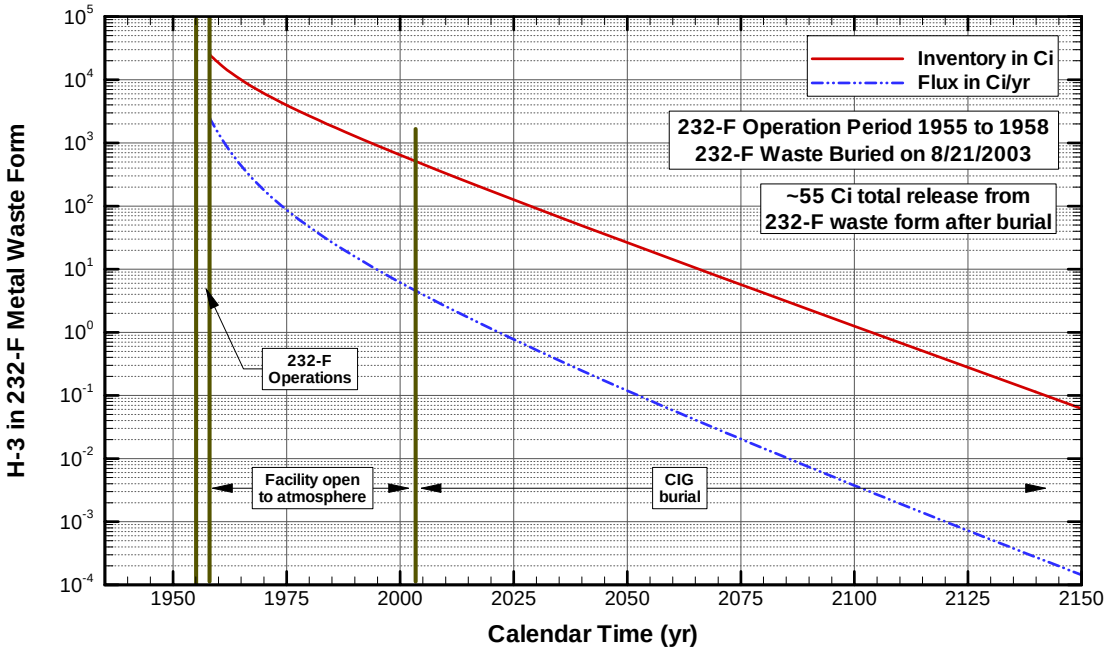

Figure 2-28. H-3 Inventory and Release Rate from 232-F Metal Waste that was ultimately buried in Segment 6 of CIG Unit #1 on August 21st 2003. Analysis based on process knowledge during facility operation and wasteform environment up to the point of burial.

As illustrated in Figure 2-28, by accounting for the decay and diffusional process of H-3 release from the Metal wasteform a significant reduction in the total amount of H-3 released into the grout is achieved. The Segment 6 inventory of H-3 in this Metal wasteform was initially reported to be 2,555 Ci based on information in the WITS database. By accounting for both its decay and rate limited release not accounted for in that database, the total amount buried becomes 495 Ci (Clark 2007), of which only ~55 Ci is ultimately released outside the Metal wasteform (Roddy 2007). In summary, the updating of the existing H-3 inventory in all 8 segments results in a significant reduction in the estimated amount buried.

2.6.7 Vadose Zone Flow Results

To perform the transient Vadose Zone transport simulations a series of steady-state flow profiles were created using PORFLOW. For each model (i.e., existing and future segments) a total of 18 flow periods were considered. Some of these flow periods were required to accommodate significant alterations to infiltration rates resulting from changes being made at the ground surface (e.g., 10 ft overhang interim runoff cover replacing existing soil cover). Others were required to address the gradual degradation of an existing un-maintained cover after the 100 year institutional control period (e.g., performance loss associated with the final runoff cover). Also, to investigate the impact that partially extended operational covers would have on inventory limits, a series of special scoping steady-state flow profiles were created as well. Overhang lengths of 5, 10, and 15 ft were considered, where from an operational perspective the 10 ft overhang option appeared to be optimal.

Of the 18 steady-state flow fields generated, the following five unique ones are highlighted and discussed below:

- **Time period 1** (i.e., burial to limited runoff cover) where only the soil cover is present.
- **Time period 2** (i.e., limited runoff cover to 25 year) where 10 overhang interim runoff cover is in operation.
- **Time period 3** (i.e., 25 to 40 year) where interim runoff cover over entire unit is in operation and all waste containers are still hydraulically intact.
- **Time period 4 through 9** (i.e., 40 to 125 year with interim runoff cover; and 125 through 325 year) with final closure cap which is degrading over time where interim runoff cover and final closure cap are over entire unit and all waste containers are hydraulically leaking.
- **Time period 9 through 18** (i.e., 325 year and beyond) where subsidence has occurred.

For the five time periods above, the steady-state flow only simulations performed using PORFLOW are shown in Figures 2-26 through 2-30, (where each figure contains plots a, b, c, and d). In plots (a) and (b) the saturation profile is provided where a cutoff value of 0.65 in water saturation was chosen (i.e., any region shown in white has a saturation value less than 0.65). Streamtraces showing the basic flow pattern have also been overlaid on the saturation profiles. Time markers at appropriate time intervals have also been provided. These time markers are based on pore (phasic) velocities that represent mass-averaged migration rates (i.e., advection only, no dispersion impacts). In plots (c) and (d) the corresponding pressure profile is provided. Plots (a) and (c) are for existing segments, while plots (b) and (d) are for future segments.

In Figure 2-29, the impact of having a high infiltration rate of 12.7 in/yr passing over a grout chamber, that encapsulates an intact wasteform, is shown. As shown, the majority of rainfall infiltration is diverted around the grout chamber with a transport travel time from ground surface to the water table on the order of 14 years. Also, as expected the grout chamber and its contents are nearly saturated.

To significantly reduce the amount of infiltration water passing through the grout chamber region, a 10 ft overhang interim runoff cover placed over the existing soil cover reduces the local infiltration rate to 0.36 in/yr. As shown in Figure 2-30, averaged transport travel times are now on the order of 100 to 150 years.

By extending the interim runoff cover to the entire surface domain, a further reduction in averaged transport travel times is achieved. As shown in Figure 2-31, the averaged transport travel times are now on the order of 400 to 500 years. Here the Waste Zone containers are still being modeled as intact units and the majority of rainfall infiltration is bypassing the grout chamber region.

At 40 years it is assumed that these waste containers are no longer hydraulically intact and the resulting impact is shown in Figure 2-32. Even though the averaged transport travel times are similar, we now see a hydraulic preference for the rainfall infiltration to migrate through the grout chamber region.

After 325 years it is assumed that complete hydraulic degradation of the Grout and Waste and local subsidence have occurred. During the early subsidence time period of 325 to 450 years the average infiltration rate is estimated to be 19.67 in/yr. Also, the most hydraulically favorable path is through the grout chamber region. The results during this period are shown in Figure 2-33 where the averaged transport travel times are now on the order of 8 to 10 years.

As shown in these five sets of figures, the impact of surface covers and Grout/Waste materials can clearly be seen. Significant changes are observed in transport times and preferred flow paths. The remaining 13 time (flow) periods show similar behavior to their appropriate counterparts and as such are not presented here graphically.

These 18 steady-state flow results for each segment design are inputted into PORFLOW where Vadose Zone transient transport simulations are performed.

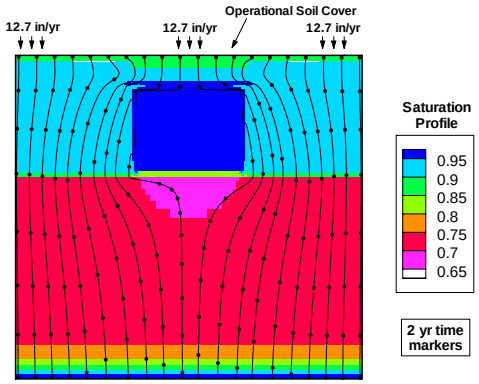

(a) Saturation Profile for Existing Segments

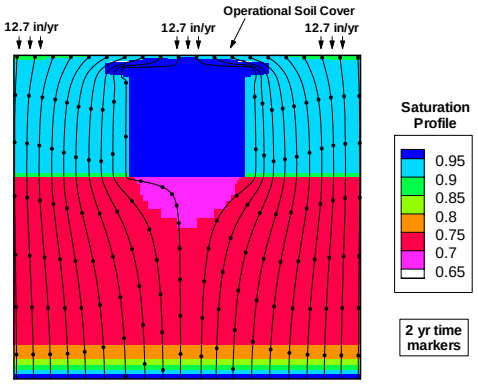

(b) Saturation Profile for Future Segments

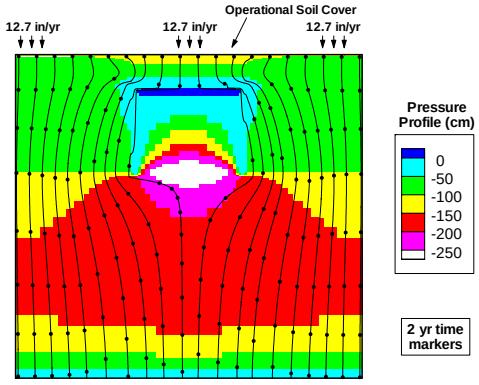

(c) Pressure Profile for Existing Segments

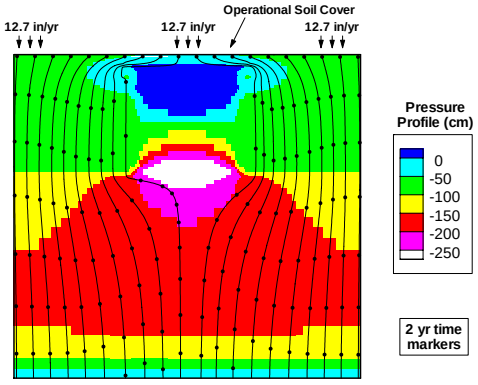

(d) Pressure Profile for Future Segments

Figure 2-29. Saturation and Pressure Profiles for Existing and Future CIG Middle Trench Models Showing Streamtraces with Time Markers (based on the time period where only an operational soil cover is present)

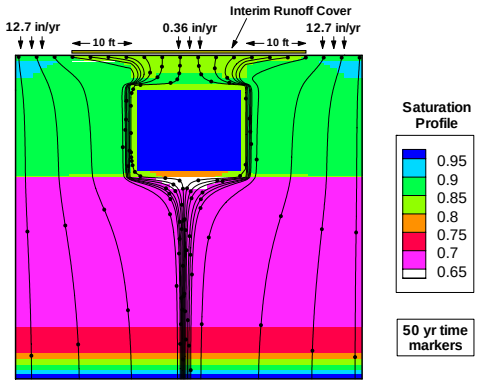

(a) Saturation Profile for Existing Segments

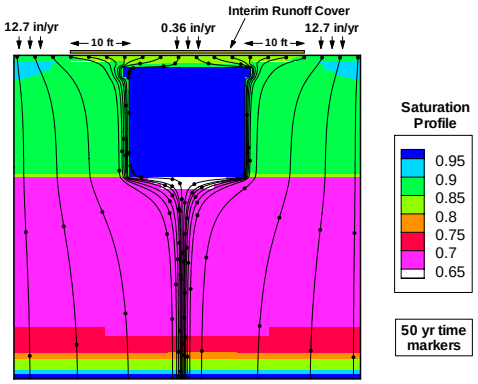

(b) Saturation Profile for Future Segments

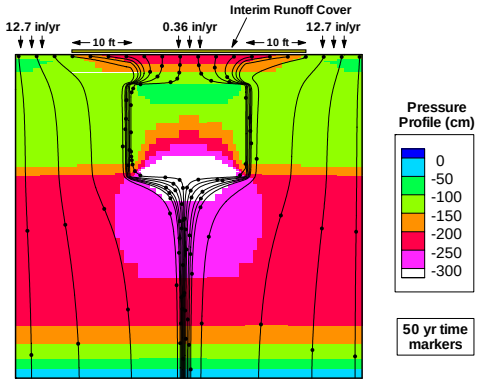

(c) Pressure Profile for Existing Segments

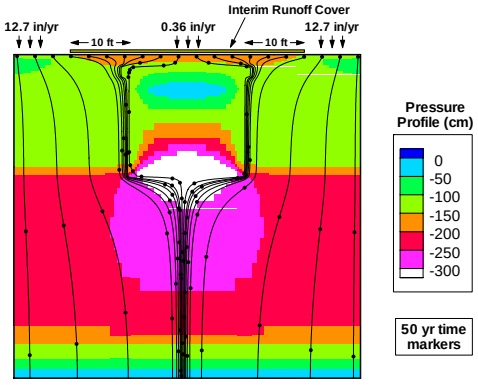

(d) Pressure Profile for Future Segments

Figure 2-30. Saturation and Pressure Profiles for Existing and Future CIG Middle Trench Models Showing Streamtraces with Time Markers (based on the time period where an interim runoff cover with a 10 ft overhang is present)

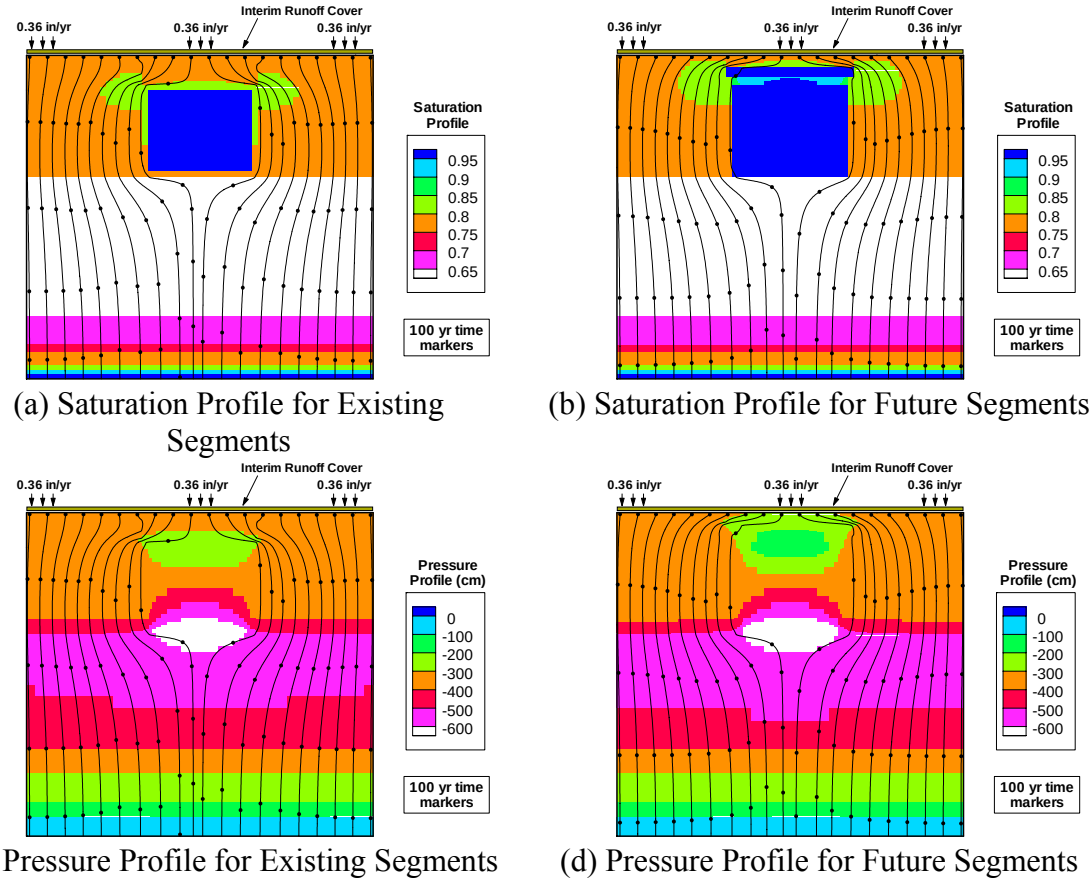

(a) Saturation Profile for Existing Segments

(b) Saturation Profile for Future Segments

(c) Pressure Profile for Existing Segments

(d) Pressure Profile for Future Segments

Figure 2-31. Saturation and Pressure Profiles for Existing and Future CIG Middle Trench Models Showing Streamtraces With Time Markers (25-40 year time period where an interim runoff cover over the entire unit is present and waste containers are hydraulically intact)

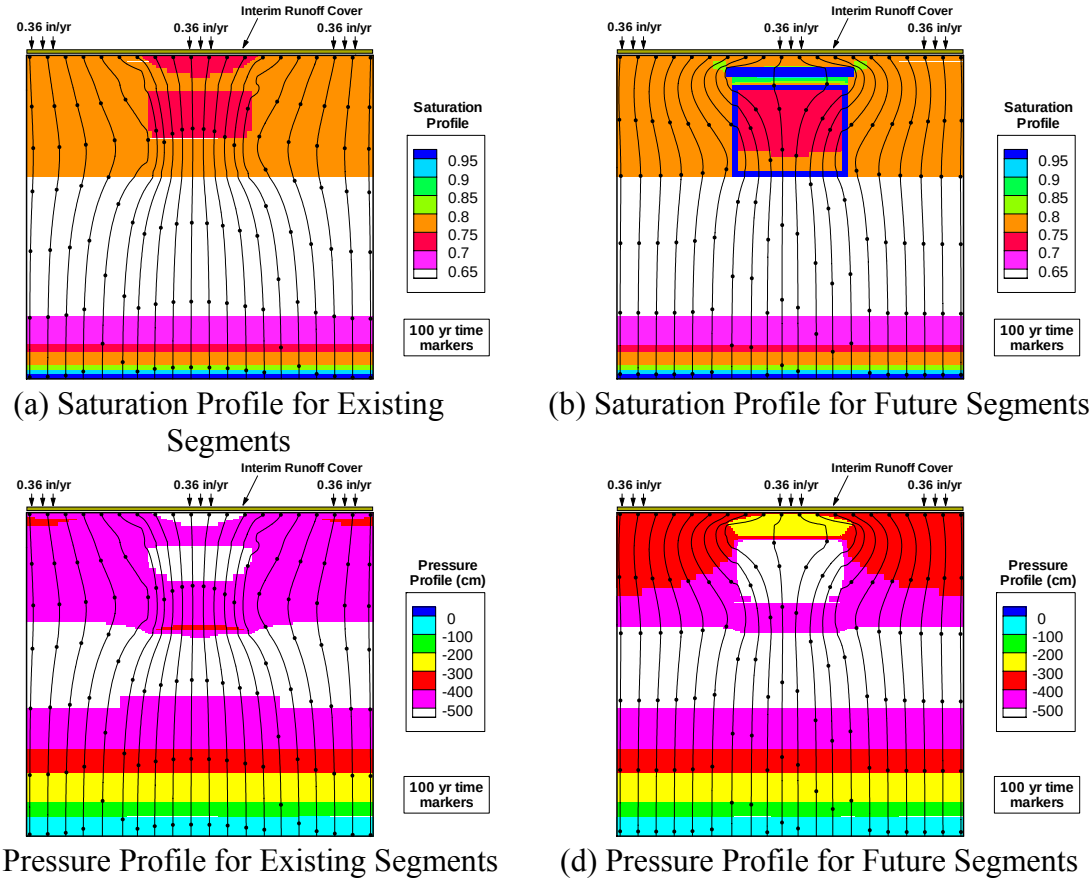

(a) Saturation Profile for Existing Segments

(b) Saturation Profile for Future Segments

(c) Pressure Profile for Existing Segments

(d) Pressure Profile for Future Segments

Figure 2-32. Saturation and Pressure Profiles for Existing and Future CIG Middle Trench Models Showing Streamtraces With Time Markers (40-125 year time period where an interim runoff cover with a 10 ft overhang is present and waste containers are assumed to be leaking)

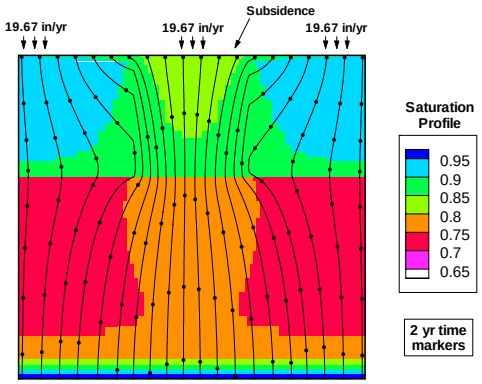

(a) Saturation Profile for Existing Segments

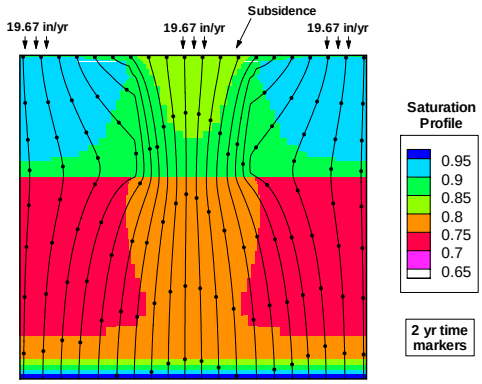

(b) Saturation Profile for Future Segments

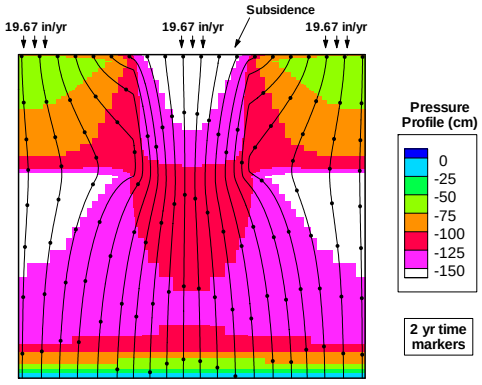

(c) Pressure Profile for Existing Segments

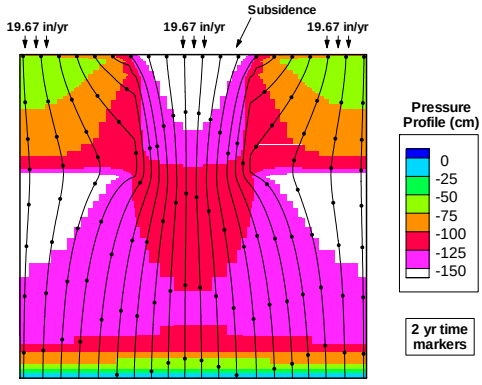

(d) Pressure Profile for Future Segments

Figure 2-33. Saturation and Pressure Profiles for Existing and Future CIG Middle Trench Models Showing Streamtraces with Time Markers (325-450 year time period where subsidence has been assumed to have occurred)

2.6.8 Groundwater Transport Deterministic Model Results

Within this section the results from the Vadose Zone transport analysis and subsequent Aquifer transport analysis runs are discussed for the Baseline case. The Vadose Zone transport analysis provides radionuclide source terms at the water table for subsequent Aquifer transport analysis. These Aquifer transport analyses are performed to determine maximum well concentrations within the 100-m buffer zone surrounding each of the CIG units (i.e., CIG-1 and CIG-2). The maximum well concentrations as a function of time are then used to determine inventory limits for CIG-1 and CIG-2 based on a variety of exposure criteria.

For the CIG Vadose and Aquifer Zone transport analyses it is assumed that no solubility limits are reached and that radionuclide concentrations remain low enough that the sorption isotherms can be addressed using constant K_d values (i.e., linear isotherms). Under these assumptions the unsaturated and saturated transport equations are linear. Based on the linearity assumption for these transport equations, a linear combination of well concentration contributions resulting from upstream sources can be employed. This allows us to separate out existing versus future disposal inventories in a variety ways. The existing inventories (i.e., Segments 1 through 8) are fixed quantities, while the future inventories are unknown and their limits are related to the margin between the inventory limits (e.g., based on groundwater Beta-Gamma pathway MCLs) and the impact resulting from existing inventories.

Based on the methodology being employed to establish inventory limits, the above super-positioning approach provides some degree of conservatism due to how maximum well concentrations within the 100-m buffer zone is employed. For example, at each point in time a maximum well concentration resulting from existing segments might not be co-located with the maximum value resulting from future segments.

In order to compute CIG inventory limits, a separate set of aquifer transport analyses were performed. Of the many possible ways to combine individual segment contributions to obtain a composite maximum well concentration, one particular choice appeared most appropriate. The following approach based on two separate sets of aquifer analyses was chosen:

- The existing Segments 1 through 8 are simulated in a single aquifer run where the water table flux for each radionuclide (per gmole of parent) is based on the known burial time and inventory amount for each radionuclide in each existing segment. For each segment, its existing inventory was uniformly distributed throughout its segment's Waste Zone volume.
- All future segments are simulated in a single aquifer run from fluxes (per gmole of parent) at the water table derived under the following assumptions: 1) radionuclides are buried in all future segments simultaneously, and 2) The buried inventory (i.e., one gmole of each radionuclide) is uniformly distributed over the trench areas not occupied by existing segments.

Prior to performing the two sets of aquifer transport runs mentioned above, a series of Vadose Zone transport runs are required. These runs provide the source terms (i.e., fluxes at the water table) employed in the aquifer analyses and are discussed below.

2.6.8.1 Vadose Zone Transport Results

Baseline Vadose Zone transport analyses were performed for all 6 unique existing segments (i.e., Segment 123, 4, 5, 6, 7, and 8) and for a generic future segment. For the Existing Segments only those radionuclide parents actually buried, and provided in the WITS database, were considered. The existing inventory values were discussed in an earlier section where special consideration was given to the radionuclide H-3. For the Future Segments all of the abbreviated radionuclide parents were considered.

For each buried radionuclide parent considered, Vadose Zone transport runs were made to generate the appropriate species fluxes (i.e., source nodes to aquifer model) at the water table. In each case one gram-mole (i.e., gmole) of the radionuclide parent was uniformly distributed throughout the defined Waste Zone volume. The computed transient fluxes at the water table are in units of gmoles of radionuclide per year per gmole of parent buried. The results for all radionuclides (parents and its progeny) are graphically presented in Appendix A2 where their units have been converted to pCi/yr per Ci of parent buried. In Appendix A2 a set of plots are provided for each unique segment modeled. Each plot contains the flux at the water table for the buried parent and any potential progeny consistent with the screening process used to arrive at the abbreviated chains discussed earlier.

A total of 40 radionuclides (parents and progeny) are being explicitly addressed within the PORFLOW transport simulations. The transport properties “radioactive half-life” and “sorption K_d value” play a prominent role in the migration behavior of these radionuclides. Within this set of radionuclides their half-life values range from 5.74 years to 1.405×10^{10} years. Also, there is a significant variation in sorption K_d values based on chemical element and porous material type/age. For example, for the sandy soil used for the Lower Vadose Zone and Aquifer regions the range is 0.0 to 2820 g/ml and for the waste zone region for Young cementitious material the range is 0.0 to 3700 g/ml. These sorption K_d values listed are best estimate values with CDP factors applied (i.e., the baseline case).

For a quick graphical perspective of the range of property variations being addressed see Figure 2-34 for the Lower Vadose Zone and Aquifer soils and Figure 2-35 for the cementitious materials (e.g., Waste and Grout materials). For a quick reference, a select number of the radionuclides are labeled in each figure.

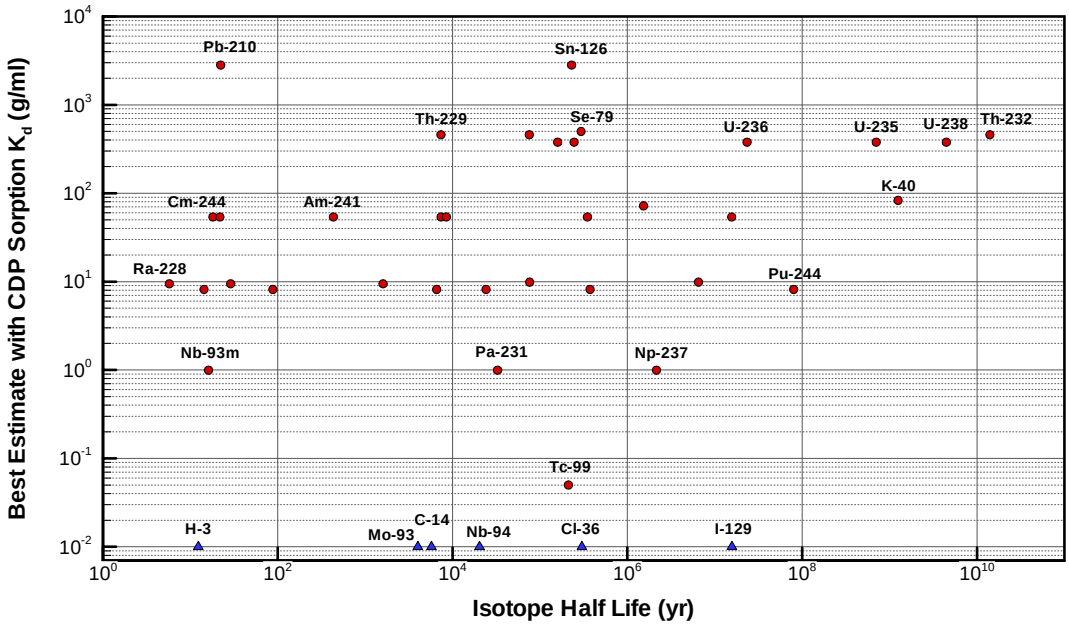

Figure 2-34. Comparison of Each Nuclide's Half-life versus Its Sorption K_d Value in Sandy Soil (i.e., Lower Vadose Zone and Aquifer soils)*

*Triangles indicate mobile species; Circles indicate other species.

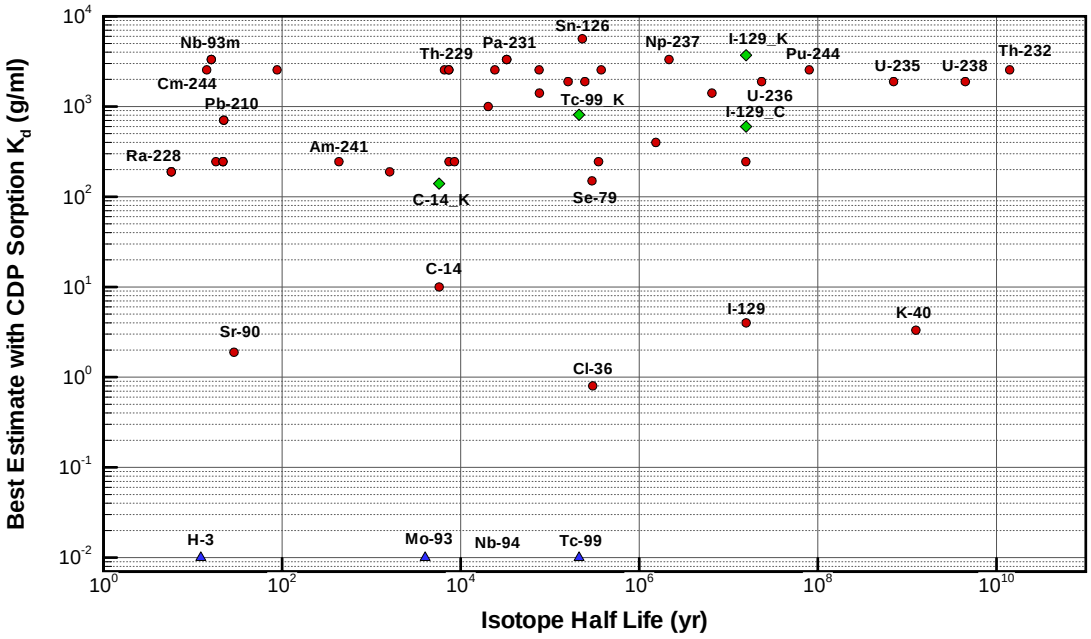

Figure 2-35. Comparison of each Nuclide's half-life versus its Sorption K_d Value in Cementitious Material (i.e., Waste and Grout zones).*

*Triangles indicate mobile species; Diamonds indicate special wasteforms (only in waste); Circles indicate other species.

As mentioned, sorption K_d values are both element, material type, and material age dependent. The cementitious materials are primarily designed as engineered hydraulic barriers to greatly reduce infiltration rates passing through the grout chamber or for subsidence risk reduction. The formulations for these materials were not altered to enhance chemical sorption properties. As such, for some of the radionuclides considered we find that their sorption K_d values can be larger in the native non-cementitious soils than in the cementitious materials within the grout chamber. Figure 2-36 highlights those elements whose sandy values are larger than their cementitious materials values. During subsidence and aging conditions these elements can experience increased retardation effects within the grout chamber as the cementitious materials age. See Kaplan (2006) for details regarding age-related K_d effects.

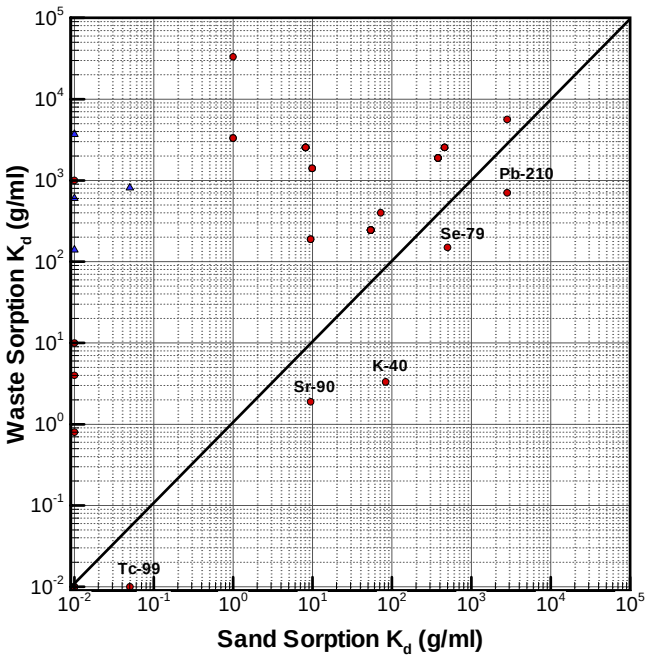

Figure 2-36. Comparison of Each Nuclide's Sandy versus "Young" Cementitious Material Sorption K_d values*

*Triangles indicate mobile species; Circles indicate other species.

The resulting transport behavior for all of the 40 parents buried (and their associated progeny) is graphically shown in Appendix A2. Within this chapter only four of the buried parents are discussed. These are:

- **H-3** (a very mobile contaminant with a K_d value of ~0 ml/g in all materials and a relatively short half-life of 12.32 yrs. This particular radionuclide required special considerations due to its mobility and was the primary reason for the need for interim covers during the 25 year operational period.)
- **I-129_K** (a very highly retarded contaminant with a K_d value of ~3700 ml/g within its special resin wasteform, a very mobile contaminant with a K_d value of ~1 ml/g in all other materials, and a long half-life of $1.57x10^7$ yrs. This particular radionuclide is unique in that its retardation is only significant while residing within the Waste Zone.)
- **Am-241** (a highly retarded contaminant with a K_d value of ~245 ml/g within its wasteform and a modest half-life of 432.2 yrs. This particular radionuclide is a typical parent where 3 daughters in its chain are also being tracked [i.e., Np-237, U-233, and Th-229].)
- **Zr-93** (a highly retarded contaminant with a K_d value of ~400 ml/g within its wasteform and a long half-life of $1.53x10^6$ yrs. This particular radionuclide is a typical parent where 1 daughter in its chain is also being tracked [i.e., Nb-93m]. Both of these radionuclides are only beta-gamma emitters allowing us to perform a simple exposure calculation for their composite impact to one of the groundwater pathways.)

H-3 Results

The H-3 (in its generic wasteform) fluxes to the water table as shown in Figure 2-37 are for two different segments (i.e., Existing Segment 6 and a Future Segment). More detailed information relevant to the timing of burial and closure operations noted in this figure are provided in Table 2-7, 2-8, and 2-13. Both curves shown in Figure 2-37 are consistently normalized by one initial Curie of H-3 buried. The two cases shown clearly illustrate how much impact the new grout formulation has on peak flux values prior to placement of the interim runoff cover that extents over the entire CIG units (i.e., at 25 years). The ultimate magnitude in this early time peak (i.e., around year 29) is quite sensitive to the timing chosen for the placement of the limited in extent interim runoff cover and its overhang length. For the existing segments this operational cover was put into operation as soon as possible (4/1/2006) and for future segments within 3 months of their creation. As stated early, an optimal overhang of 10 feet was chosen.

The later local peaking (observed for both segments) that occurs around 205 years reflects a balance between the gradual increase occurring in infiltration rates after institutional control has stop and the radioactive decay of H-3 occurring (i.e., 12.3 yr half-life). Marginal peaks can be observed near 325 years due to the assumption of subsidence.

Note that the two peaks for future segments are close in magnitude indicating that to some degree a balance has been achieved between the grout chamber's hydraulic performance, timing of placement of the interim runoff cover, and the hydraulic performance of the cover. For the existing segments the poorer grout performance and longer time period prior to a cover results in a significant increase in peak value at the 29th year.

The details associated with the interim runoff cover (i.e., timing and extent of overhang) and grout chamber hydraulic performance appears to have minimal impact on peak behavior beyond 200 years. As such, for Future Segments the combined performance of the covers and grout only has to be sufficient to maintain the early time peak (i.e., ~29 years) from exceeding the ~205 year value.

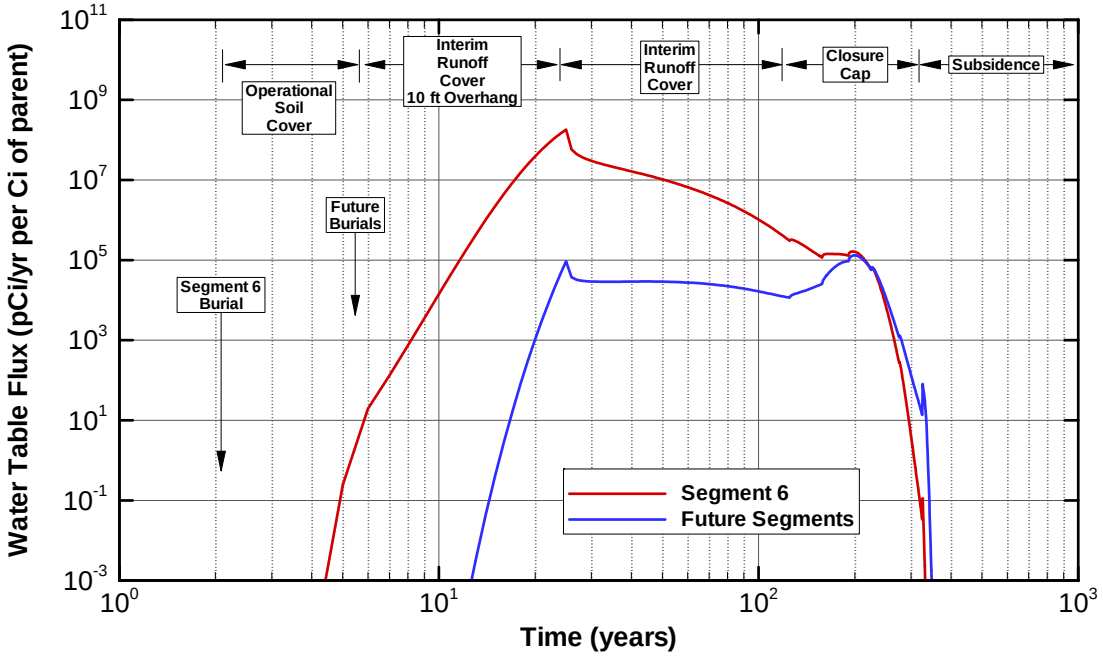

Figure 2-37. Comparison of Fluxes of H-3 in its Generic Wasteform at the Water Table for Segment 6 and All Future Segments

For the generic wasteform of H-3 within Segment 6 a series of contour plots are shown in Figure 2-38. In Figure 2-38 a series of time shots are shown. For each time shot the H-3 concentration profile (in pCi/L units) is shown along with the outline of the grout barrier. Note that regions with H-3 concentrations below its groundwater Beta-Gamma pathway MCL (i.e., 20,000 pCi/L) are shown in white. In modeling time Segment 6 was buried in at the 2.1 yr point and operated with a soil cover for 2.6 years until the time 4.7 yr when the 10 ft overhang interim runoff cover was established. Groundwater with H-3 concentrations above its MCL value reached the water table in ~13 years and then dropped below its MCL by ~121 years. Several of the time shots shown are associated with key points in time during the scenario of interest:

- 3 year: shows initial release of H-3 through grout barrier prior to 10 ft interim cover
- 6 years: shows profile slightly over one year after placement of 10 ft interim cover
- 25 years: shows profile just prior to placement of the 25 year interim cover
- 40 years: shows profile just prior to hydraulic leaking of waste containers
- 121 years: shows profile just when plume existing Vadose Zone under MCL value
- 165 years: shows profile just when plume exiting grout chamber under MCL value

As pointed out in earlier sections, H-3 was buried in several existing segments over a range of operation. Each subsequent existing segment had an operational soil cover for a smaller duration of time. For Segment 6 two wasteforms for H-3 were established (i.e., the "Generic" form and the special "Metal" form based on 232-F process equipment). The computed fluxes of H-3 to the water table for all existing segments and wasteforms are shown in Figure 2-39 for comparative purposes. The fluxes shown have incorporated into them the actual amount of H-3 buried initially, such that a consistent comparison can be made in terms of Ci/yr. For the Generic wasteform the entire amount of H-3 buried is immediately available for transport within the model domain, while for the special Metal wasteform its contents are metered into the model domain based on a separate diffusional model. For the Metal wasteform initially ~495 Ci was buried in Segment 6 and over the entire simulation period only ~55 Ci of H-3 actually escapes the Metal waste from entering into the model domain.

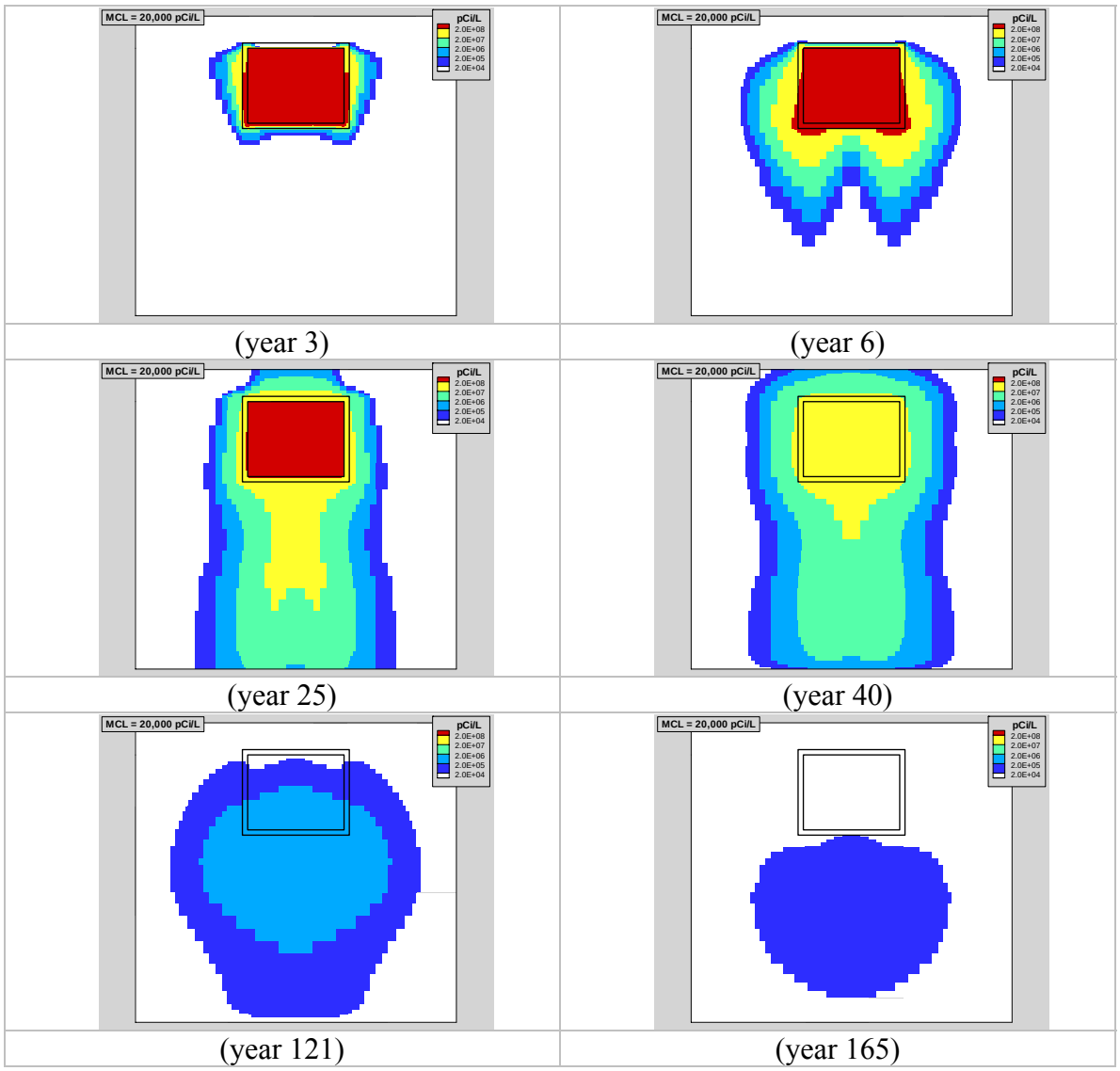

Figure 2-38. Selected Vertical Cross-Sectional Concentration Profile Views (in pCi/L) of H-3 in its Generic Wasteform Released from CIG Segment 6 to the Water Table

As shown in Figure 2-39, the ultimate peaks for all cases occur around 25 years with minor local peaking around 200 years. Segments 5, 6 (Generic only), and 7 provide the dominant contributions to the aquifer. The total amount of H-3 entering the aquifer is represented by the areas under each curve. By integrating the areas under each curve, total H-3 contributions to the aquifer are calculated to be:

- ~2 Ci for Segments 5, 6 (Generic only), and 7 (initially buried ~1,158 Ci)
- ~0.1 Ci for Segments 1-2-3 and 4 (initially buried ~31 Ci)
- ~0.0005 Ci for Segments 8 and 6 (Metal only) (initially buried ~496 Ci)

Thus, for the initial total buried amount of ~1,685 Ci, only ~2.1 Ci (i.e., ~0.12%) enters the underlying aquifer unit. The rest is held up in its wasteform, grout chamber, or in transit to the water table and decays away prior to reaching the aquifer unit.

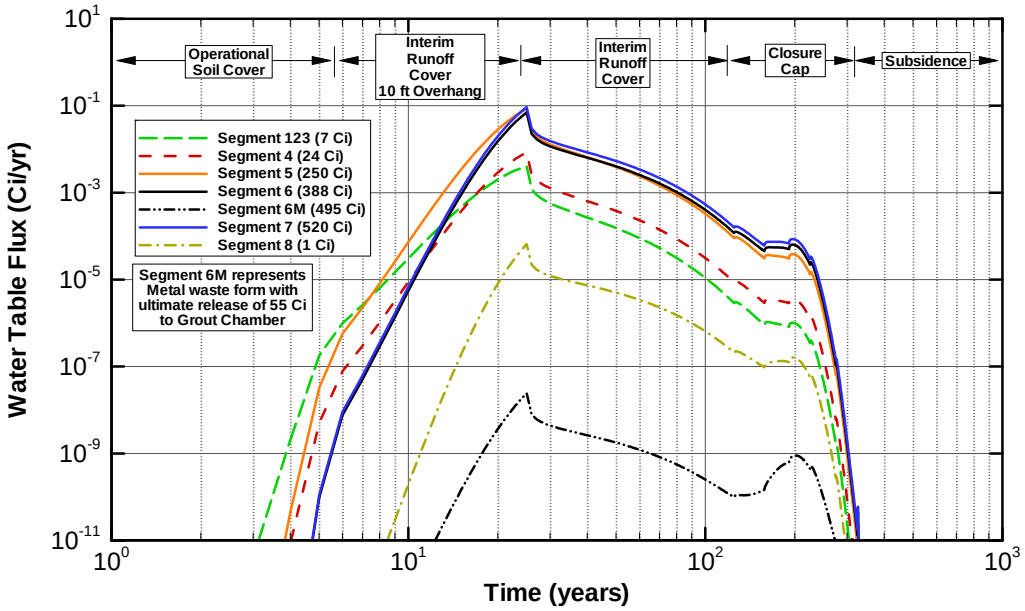

Figure 2-39. Comparison of Fluxes (in terms of Ci/yr which incorporates actual amounts buried) of H-3 at the Water Table for All Existing Segments

I-129_K Results

I-129 was buried in the existing segments in two wasteforms referred to as "I-129" and "I-129_K". The species I-129_K referred to I-129 contained within K and L reactor resin bed material. For calculational purposes the only difference between these two species is the sorption K_d value employed while the radionuclide is within the Waste Zone. For I-129 the sorption K_d value ranges from 0 to 20 ml/g (depending upon concrete aging) and for I-129_K it is fixed to the value 3,700 ml/g. I-129 has a long half-life of 1.57×10^7 yrs. I-129_K is particularly unique in that its retardation is only significant while residing within the Waste Zone.

For the radionuclide I-129 (in its generic wasteform and in its K&L Basin wasteform) fluxes to the water table are shown in Figure 2-40 for Segment 6. Both curves shown are consistently normalized by one initial Curie of I-129 buried. Given its long half-life, essentially all of the buried radionuclide ultimately enters the aquifer at the water table for both wasteforms. Since species I-129 is less retarded its flux curve raises faster and has a higher peak than for the species I-129_K. At the point of subsidence the species I-129 is quickly flushed through the Vadose Zone, while for species I-129_K its high sorption K_d value in the Waste Zone only allows a small metered amount to be released (i.e., note that the areas under the curves as shown in Figure 2-40 are approximately equal except for the very small amount of decay occurring).

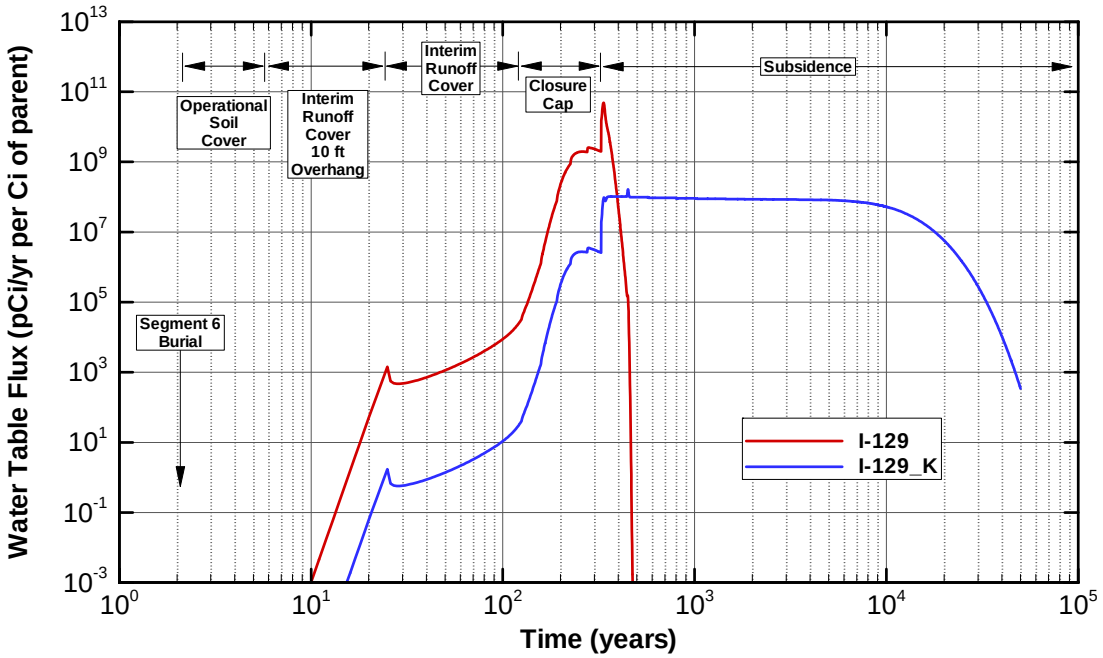

Figure 2-40. Comparison of Fluxes of I-129 in its Generic and K&L Basin Wasteforms at the Water Table for Segment 6

For I-129_K within Segment 6 a series of contour plots are shown in Figure 2-41. In Figure 2-41 a series of time shots are shown. For each time shot the I-129_K concentration profile (in pCi/L units) is shown along with the outline of the grout barrier. Note that radionuclide I-129 has a groundwater Beta-Gamma pathway MCL equal to 1 pCi/L). For Segment 6 only a small amount of I-129_K was buried (i.e., 5.92×10^{-5} Ci or 2.60×10^{-3} gmoles) and groundwater concentrations never exceeded its MCL value. For graphical purposes concentrations below 5×10^{-5} pCi/L are shown in white. Several of the time shots shown are associated with key points in time during the scenario of interest:

- 3 year: shows initial release of I-129_K through waste zone prior to 10 ft interim cover
- 125 years: shows profile slightly just prior to end of institutional control
- 326 years: shows profile just after subsidence has occurred
- 1,000 years: shows profile whose shape remains relatively stable for a significant time period
- 20,008 years: shows profile beginning to drop within the lower half of the waste zone
- 30,008 years: shows profile just when plume exiting waste zone

Between the time interval of 325 to 10,000 years the concentration profile remains relatively constant resulting from the slow release of I-129_K from its wasteform.

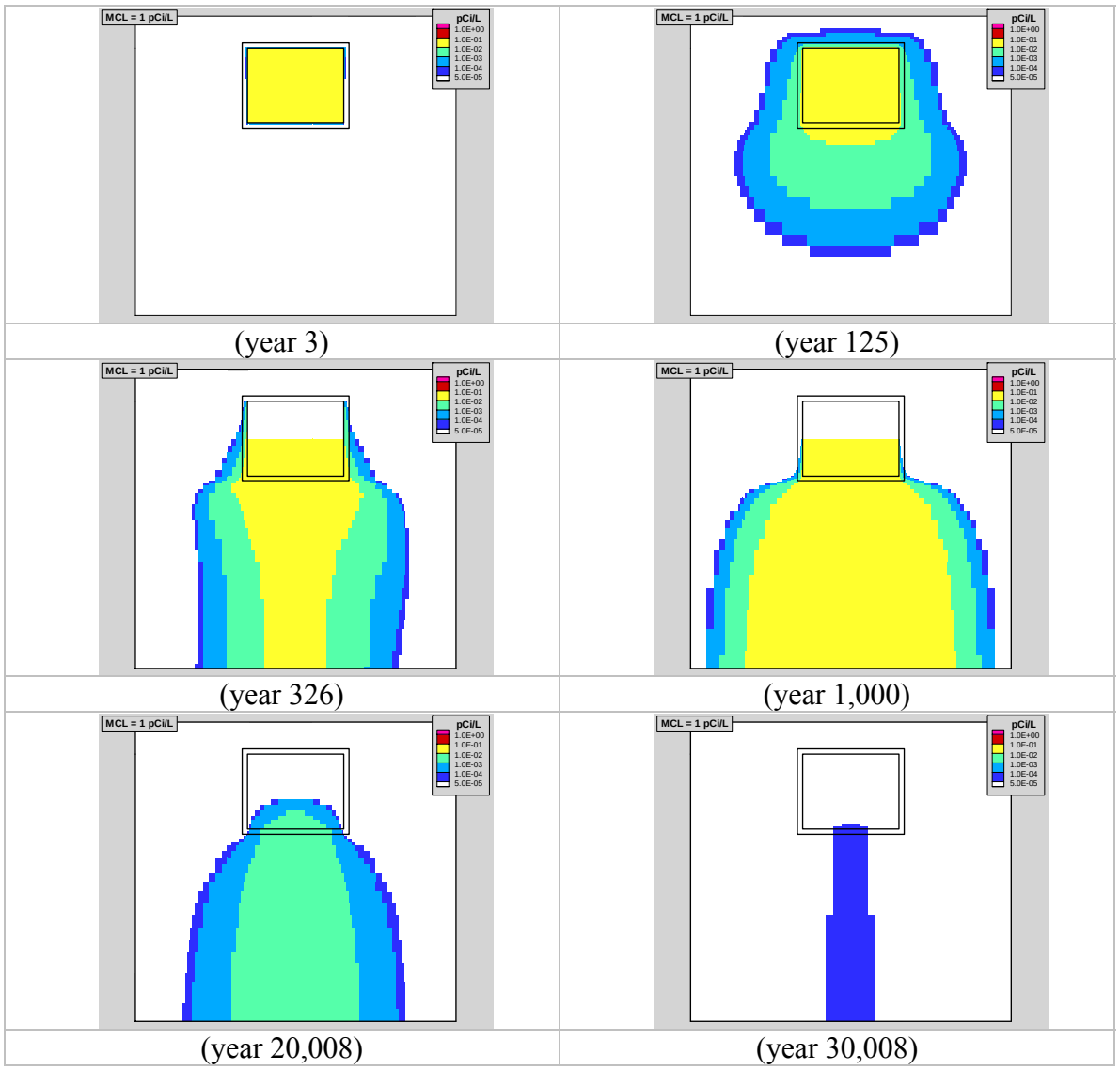

Figure 2-41. Selected Vertical Cross-Sectional Concentration Profile Views (in pCi/L) of I-129_K Released from CIG Segment 6 to the Water Table

Am-241 Results

As one representative sample of a buried parent having progeny, the species Am-241 was chosen. The fluxes to the water table for the parent Am-241 buried in Segment 6 and its progeny (i.e., Np-237 going to U-233 going to Th-229) are shown in Figure 2-42. The fluxes plotted are in terms of pCi/yr per Curie of parent buried. The flux curves reflect the radiological decay rates of Am-241 and progeny, and element-specific sorption coefficients (K_ds) of all species in the decay chain, resulting in different flux profiles over time. All four of these flux curves are used as source terms for Segment 6 when performing the Aquifer analyses for Am-241 for the case of addressing Existing Segment impact on maximum well concentration contributions.

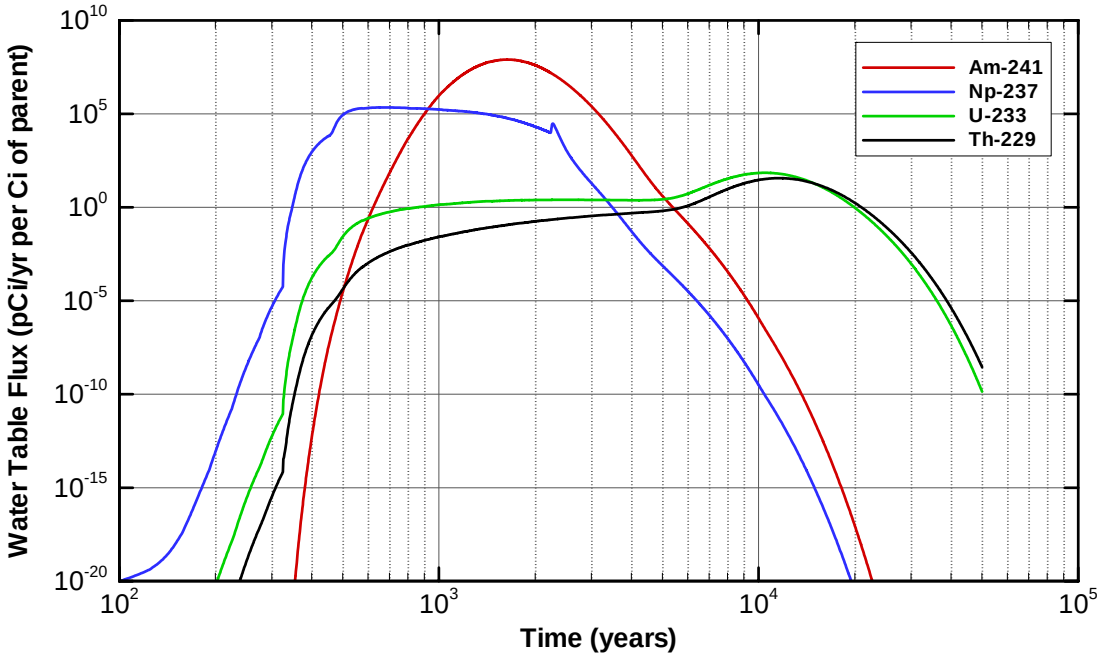

Figure 2-42. Comparison of Fluxes of Am-241 (parent) and its Progeny (Np-237, U-233, and Th-229) at the Water Table for Segment 6

Zr-93 Results

As one simple sample of a buried parent having one daughter, the species Zr-93 was chosen. The fluxes to the water table for the parent Zr-93 buried in Segment 6 and its daughter (Nb-93m) are shown in Figure 2-43. Again, the two flux curves reflect the radiological decay rates of Zr-93 and Nb-93m, and element-specific sorption coefficients (K_ds) of both species, resulting in different flux profiles over time. The fluxes plotted are in terms of pCi/yr per Curie of parent buried. Both of these flux curves are used as source terms for Segment 6 when performing the Aquifer analyses for Zr-93 for the case of addressing Existing Segment impact on maximum well concentration contributions.

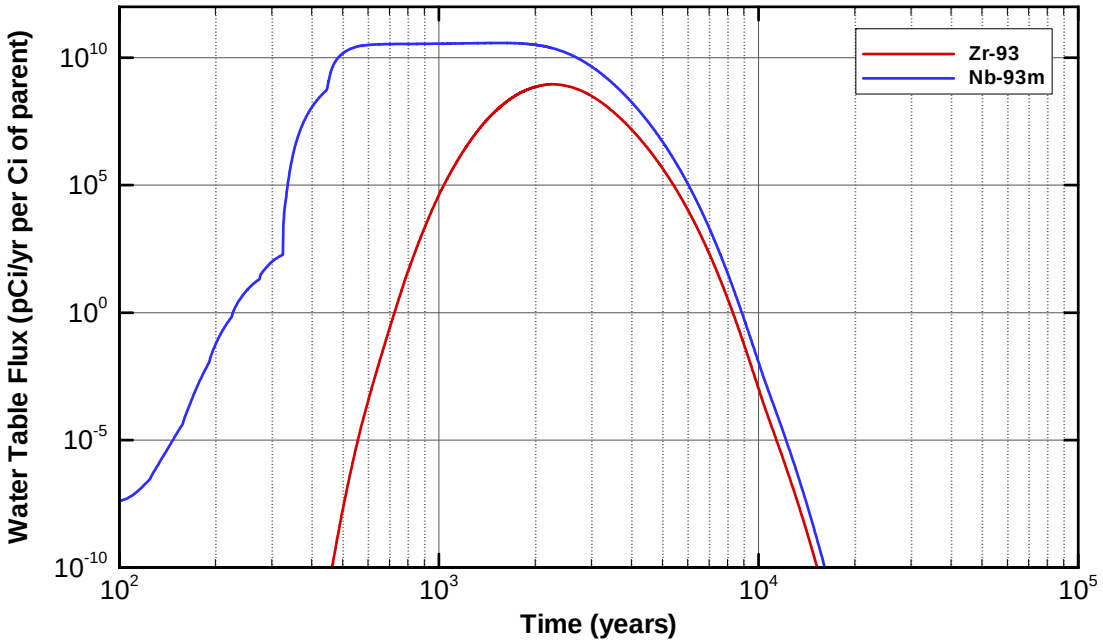

Figure 2-43. Comparison of Fluxes of Zr-93 (parent) and its Progeny (Nb-93m) at the Water Table for Segment 6

2.6.8.2 Aquifer Transport Results

As stated earlier for each buried parent two Aquifer analysis runs were performed: (1) addressing contributions from all Existing Segments and (2) addressing contributions from all Future Segments. A discussion of the set of species follows.

H-3 Results

For the two cases defined above, the resulting H-3 maximum well concentrations within the 100-m compliance boundary are shown in Figure 2-44. The maximum well concentration curve for the Existing Segments shows the early time peak around 29 years with a significantly lower in magnitude local peak around 205 years. For the Existing Segments analysis the H-3 inventories (~1250 Ci) were pre-known. This pre-known inventory represents the approximate total H-3 inventory buried (1690 Ci) less the 440Ci estimated to remain in the Metal waste (i.e., 495 Ci minus the 55 Ci which escapes) throughout the simulation period (Clark 2007). For the Future Segments analysis the H-3 inventories were set to ~3.13×10^6 Ci buried simultaneously and uniformly over the available unused portions of the two CIG units. This value of total future inventory produces a maximum well concentration curve that just meets the groundwater pathway MCL of 20,000 pCi/L value at approximately 205 years. Tritium inventory for future trench segments was purposely selected to produce a groundwater peak that just reaches the MCL to illustrate how much additional inventory capacity is remaining.

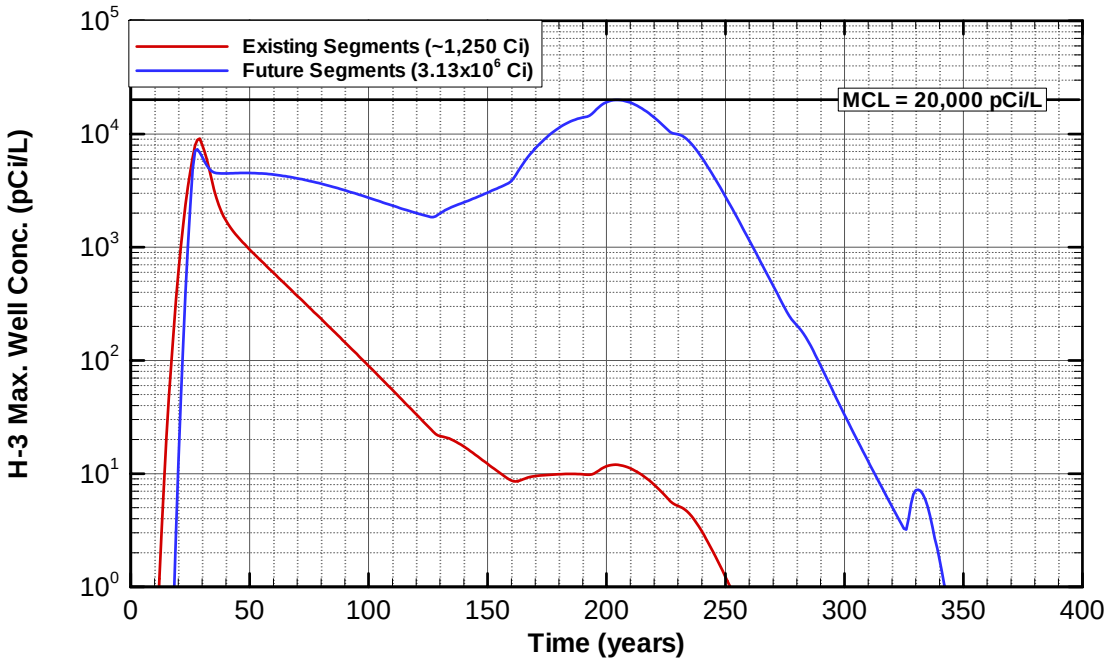

Figure 2-44. Comparison of H-3 Maximum Well Concentration within the Buffer zone for all the Existing versus Future Segments (future inventory set to value that trims the MCL value of 20,000 pCi/L)

For the two cases defined above, the H-3 concentration profiles for two selected horizontal cross-sections are plotted in Figure 2-45 (Existing Segment inventory) and in Figure 2-46 (Future Segment inventory set to 3.13×10^6 Ci).

For the Existing Segment case four snapshots in time are shown (i.e., 20, 29, 40, and 50 years). The left column contains a horizontal cross-section near the water table surface and the right column contains a horizontal cross-section deeper into the aquifer near where the peak well concentration occurs. The elevation of the peak well concentration is approximately 20 ft below the water table in these figures. Concentrations exceeding the Beta-Gamma MCL for H-3 are shown in red. The peak well concentration within the 100-m buffer zone occurs around 29 years.

For the Future Segment case four snapshots in time are shown also (i.e., 30, 120, 205, and 250 years). The peak well concentration within the 100-m buffer zone occurs around 205 years. This peak value can be seen in the right column of Figure 2-46 for the time 205 yr. The leading edge of the H-3 plume is just touching the 100-m boundary line shown in red.

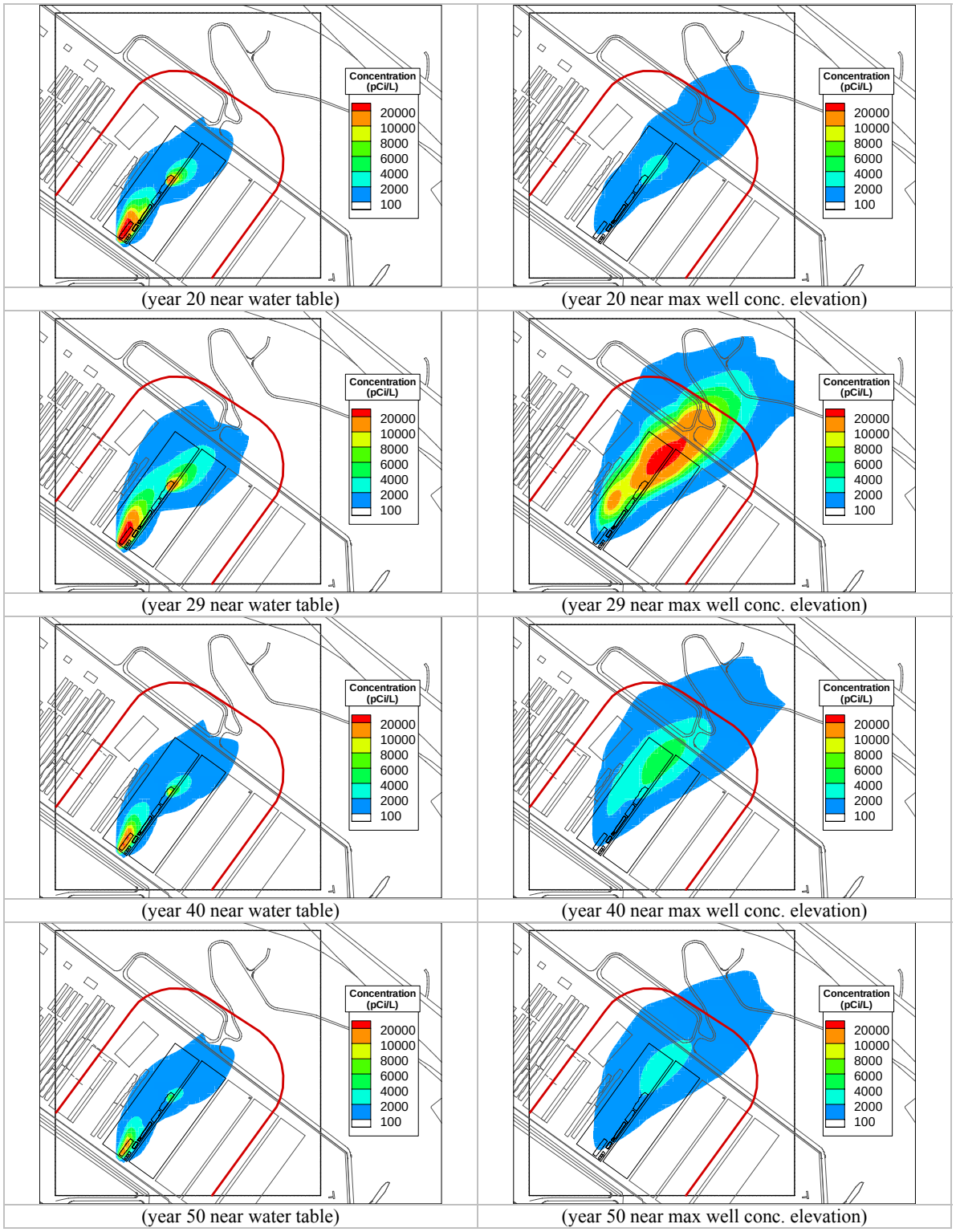

Figure 2-45. Selected Aquifer Horizontal Cross-Sectional Concentration Profile Views (in pCi/L) of H-3 Released from Existing CIG Segments 1 through 8 (maximum well concentration elevation approximately 20 ft below the water table).

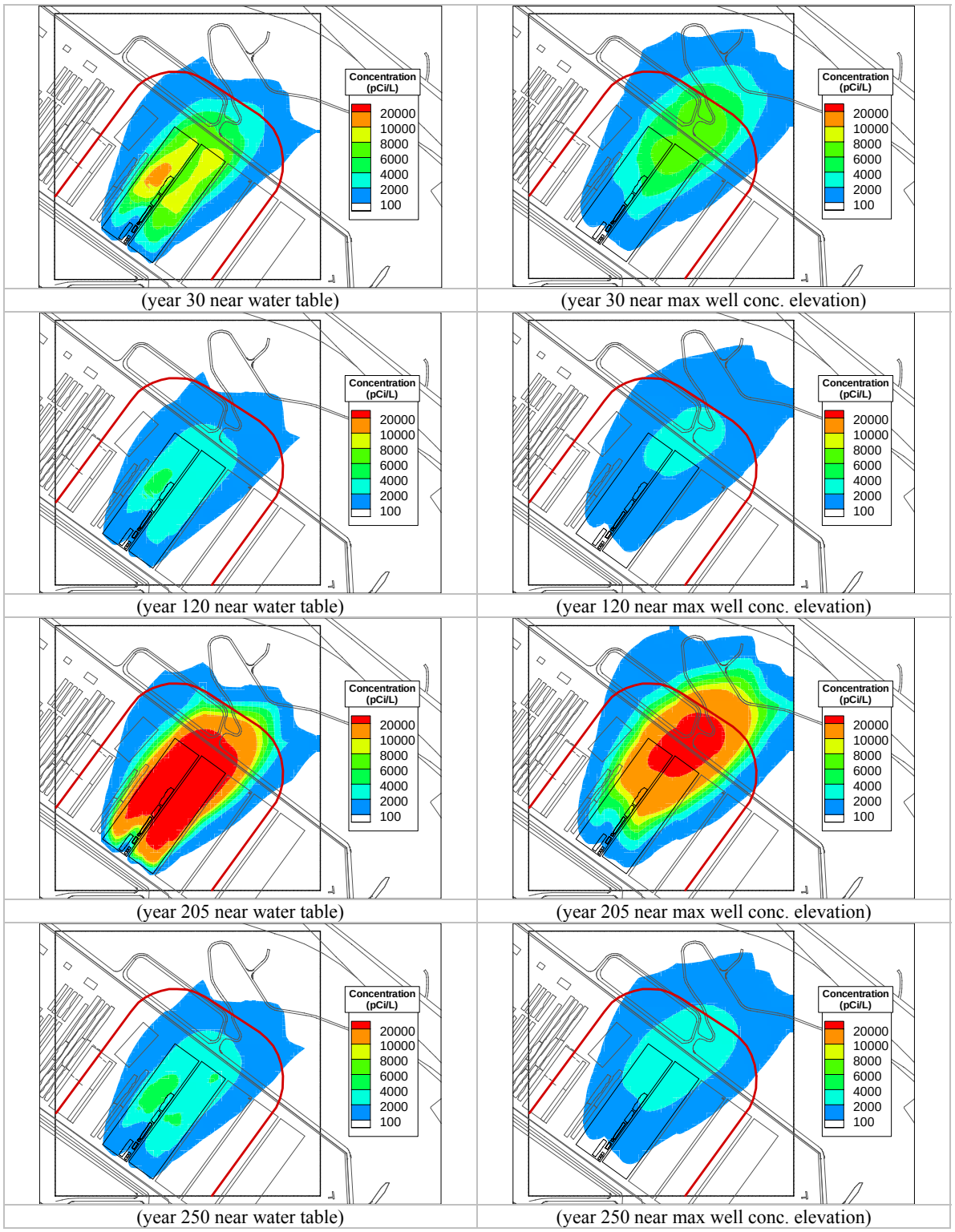

Figure 2-46. Selected Aquifer Horizontal Cross-Sectional Concentration Profile Views (in pCi/L) of 3.13×10^6 Ci of H-3 uniformly buried in Future CIG Segments (maximum well concentration elevation approximately 20 ft below the water table).

Note that dispersivity values are set to zero for the Baseline scenarios and that lateral dispersion shown in Figure 2-45 and Figure 2-46 reflects numerical dispersion not actual mechanical dispersion. Also note the degree of potential plume interactions that could occur with neighboring disposals units (i.e., Slit Trenches 4 and 5).

I-129_K Results

For species I-129 in its Generic and Resin wasteforms, the resulting maximum well concentrations within the 100-m compliance boundary are shown in Figure 2-47 for the composite behavior of the Existing Segments. The maximum well concentration curve for the Existing Segments shows a time peak around 341 years for I-129 (Generic form) and 454 years for I-129_K (Resin form). The peak concentration contributions due to Existing Segment disposals result in peak values significantly below the beta-gamma MCL value of I-129 (i.e., 1.0 pCi/L).

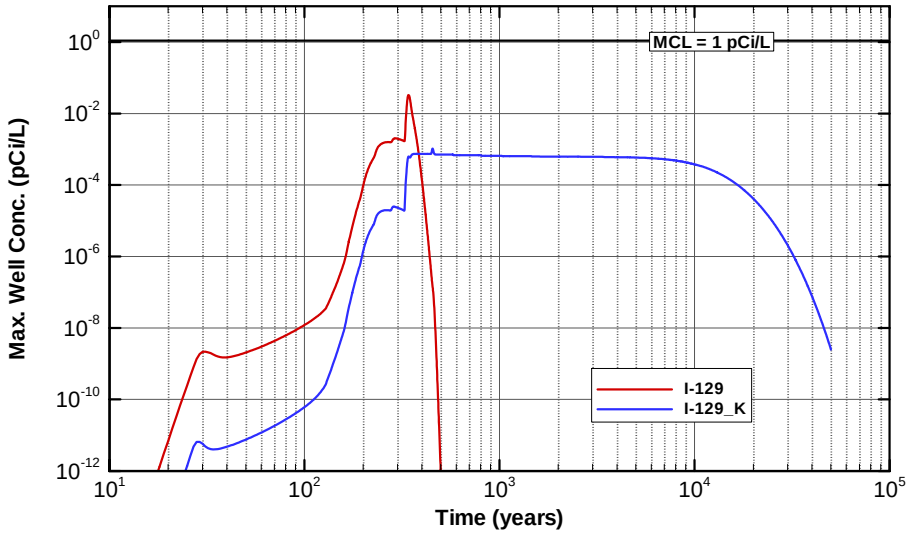

Figure 2-47. Maximum Well Concentration within the Buffer zone for I-129 in its Generic versus K&L Basin Wasteforms for the Existing Segments

For I-129_K (Resin form) its concentration profiles for two selected horizontal cross-sections are plotted in Figure 2-48 (based on Existing Segment inventory). Four snapshots in time are shown (i.e., 200, 300, 454, and 1,125 years). The left column contains a horizontal cross-section near the water table surface and the right column contains a horizontal cross-section deeper into the aquifer near where the peak well concentration occurs. The elevation of the peak well concentration is approximately 20 ft below the water table. The upper contour level shown (i.e., 0.001 pCi/L) corresponds to its peak well concentration value within the 100-m buffer zone occurring around 454 years. This peak value can be seen in the right column of Figure 2-48 for the time 454 yr. The leading edge of the I-129_K plume is just touching the 100-m boundary line shown in red.

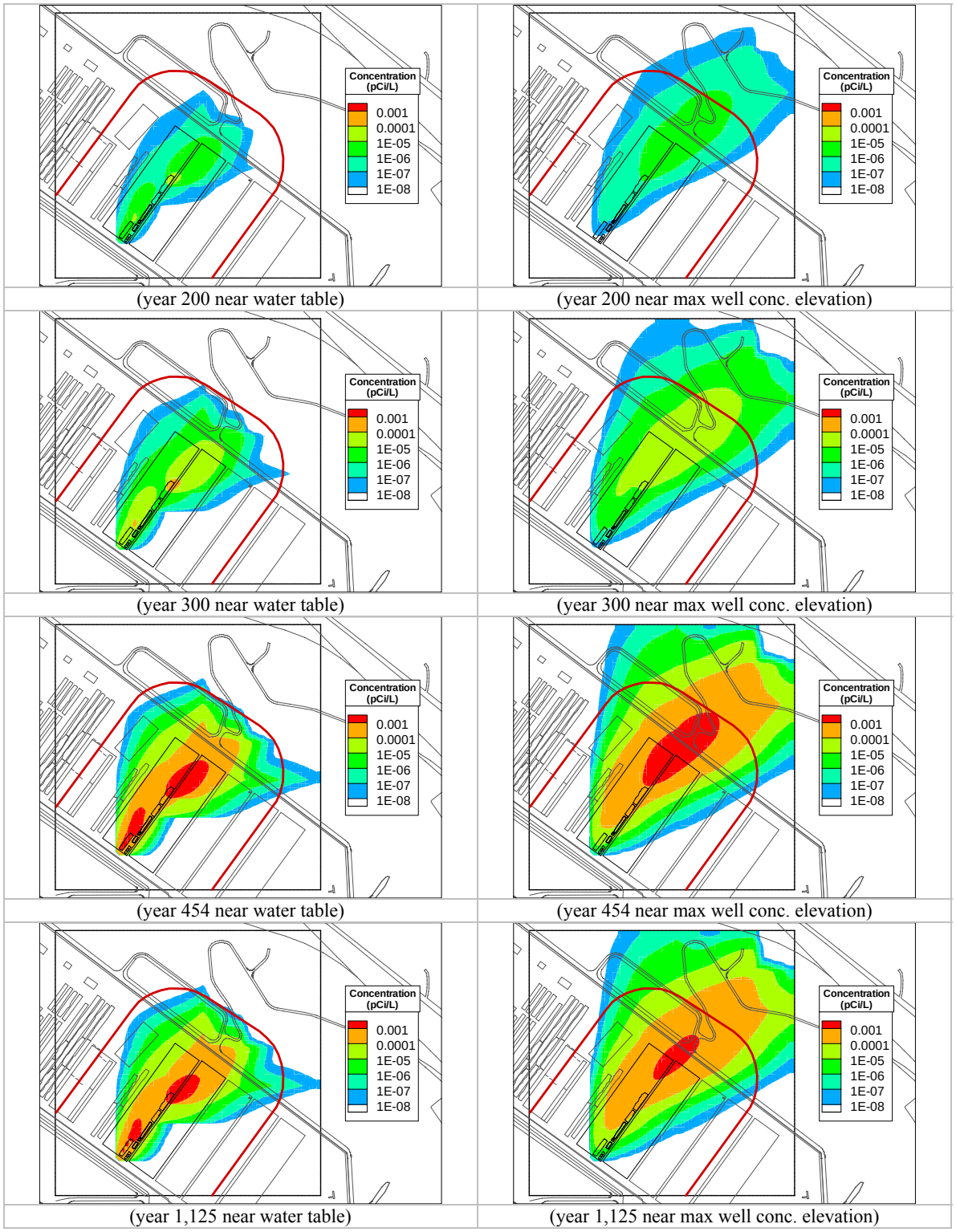

Figure 2-48. Selected Aquifer Horizontal Cross-Sectional Concentration Profile Views (in pCi/L) of I-129_K Released from Existing CIG Segments 1 through 8 (maximum well concentration elevation approximately 20 ft below the water table).

As mentioned earlier for I-129_K its K_d value is very large (i.e., 3,700 ml/g) within its waste zone and remains fixed over the entire simulation period. The long term slow release of this species leads to a quasi-steady state behavior for a long period of time where lateral dispersion ends up being greater than that experienced by a species with a more pulse like injection into the aquifer. As shown in Figure 2-48, the plume spreads out at almost a 45 degree angle with respect to the aquifer flow direction.

Am-241 Results

For species Am-241 (parent) in its Generic wasteform and its progeny (i.e., Np-237 going to U-233 going to Th-229), the resulting maximum well concentrations within the 100-m compliance boundary are shown in Figure 2-49 for the composite behavior of the Existing Segments. The maximum well concentration curves for the Existing Segments show peak times of 2403, 701, 17808, and 19308 years for Am-241, Np-237, U-233, and Th-229, respectively. These concentrations curves, along with a similar set for Future Segments on a per-Curie-of–parent-buried basis, are used in computing Am-241 inventory limits. Comparisons with drinking water MCLs are provided in Section 6.8.4.

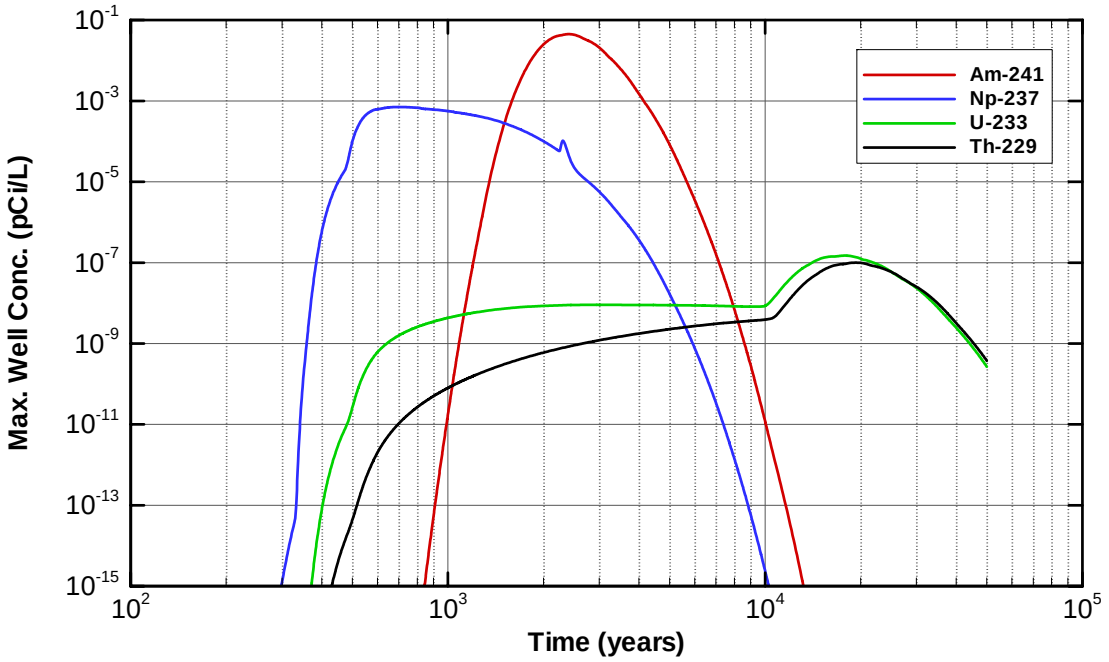

Figure 2-49. Maximum Well Concentration within the Buffer zone for Am-241 (parent) and Progeny (Np-237, U-233, and Th-229) for Existing Segments

Zr-93 Results

For species Zr-93 (parent) in its Generic wasteform and its only daughter (i.e., Nb-93m), the resulting maximum well concentrations within the 100-m compliance boundary are shown in Figure 2-50 for the composite behavior of the Existing Segments. The maximum well concentration curves for the Existing Segments show peak times of 4593 and 3813 years for Zr-93 and Nb-93m, respectively. These concentrations curves, along with a similar set for Future Segments on a per-Curie–of-parent-buried basis, are used in computing Zr-93 inventory limits. Comparisons with drinking water MCLs are provided in Section 6.8.4.

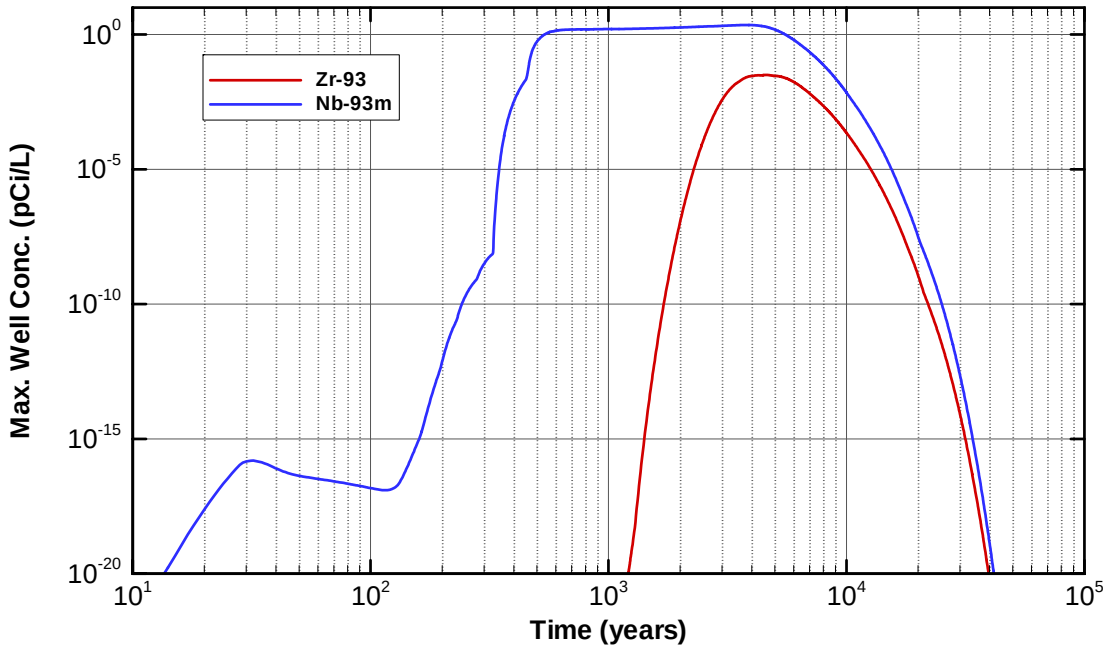

Figure 2-50. Maximum Well Concentration within the Buffer zone for Zr-93 (parent) and its Daughter (Nb-93m) for the Existing Segments

2.6.8.3 Baseline Case Peak Concentration Summary for Radionuclides

The following summary of results is for the Baseline case. For all of the existing radionuclide species (i.e., parents and their progeny) that were listed within WITS, the computed peak well concentrations within the 100-m buffer zone for the aquifer analyses based on Existing Segments are listed in Table 2-19 along with the timing of their peak values. Two time windows of interest were considered. Peak values within the first 1,125 years (operations, institutional control, and compliance periods) and peak values beyond this 1,125-year period. If the global peak concentration value occurs within the first 1,125 years no values are supplied for the second time period. For the Existing Segment results listed in Table 2-19, the entire existing inventory (shown in Table 2-16) was used and the peak values are in terms of pCi/L at the well. A similar listing is provided in Table 2-20 for the aquifer analyses based on Future Segments. For the Future Segments analyses, all 40 species were addressed (i.e., this included all of the abbreviated parents and their progeny, as well as currently expected future special wasteforms). The additional radionuclides addressed for the Future Segments included Cl-36, I-129_C, K-40, Mo-93, Nb-94, Pu-244, Ra-226, Th-230, and Th-232. For the Future Segment results listed in Table 2-20, the future inventory was based on a per-Curie of parent buried and the peak values are in terms of pCi/L at the well per Curie of parent buried.

Table 2-19. Baseline Case Maximum Concentrations of the Radionuclide Parent and Progeny Resulting from the Existing 8 Segments within 100-m Compliance Zone[a]

Parent	Daughters	Time of Peak (0-1125 yrs)	Peak Concentration (pCi/L)	Time of Ultimate Peak (1125+ yrs)	Ultimate Peak Concentration (pCi/L)
Am-241		1,125	5.72E-09	2,403	4.49E-02
	Np-237	701	7.05E-04		
	U-233	1,125	5.24E-09	17,808	1.49E-07
	Th-229	1,125	1.25E-10	19,308	1.00E-07
Am-243		1,125	3.61E-13	3,493	2.26E-02
	Pu-239	1,125	1.50E-16	6,603	6.39E-04
	U-235	1,125	1.36E-24	11,808	1.58E-09
	Pa-231	1,125	1.68E-11	8,773	4.16E-10
	Ac-227	1,125	3.60E-13	8,743	9.37E-12
C-14		350	1.39E+02		
C-14_K		347	1.83E+01		
Cm-244		1,125	1.27E-30	1,266	2.80E-30
	Pu-240	1,125	4.57E-32	8,123	3.52E-03
	U-236	1,125	2.63E-38	21,308	3.85E-07
	Th-232	1,125	4.83E-47	25,608	3.17E-13
	Ra-228	1,125	6.94E-29	25,308	1.48E-11
Cm-245		1,125	9.97E-16	3,503	4.84E-04
	Pu-241	1,125	2.57E-16	3,513	1.90E-04
	Am-241	1,125	6.06E-16	3,513	5.08E-04
	Np-237	1,125	2.99E-07	1,453	3.06E-07
	U-233	1,125	2.13E-12	22,308	1.34E-11
	Th-229	1,125	4.38E-14	23,908	9.71E-12
Cm-247		1,125	1.99E-17	3,523	3.66E-03
	Am-243	1,125	2.08E-18	3,593	1.04E-03
	Pu-239	1,125	6.36E-22	5,313	2.37E-05
	U-235	1,125	4.31E-30	9,533	3.37E-11
	Pa-231	1,125	6.33E-14	7,673	6.58E-12
	Ac-227	1,125	1.32E-15	7,653	1.47E-13
Cm-248		1,125	1.99E-17	3,523	3.63E-03
	Pu-244	1,125	1.71E-24	6,513	2.91E-08
	Pu-240	1,125	4.84E-27	8,293	1.30E-08
	U-236	1,125	9.74E-34	11,808	7.37E-13
	Th-232	1,125	6.98E-43	18,108	2.20E-19
	Ra-228	1,125	9.83E-36	17,908	1.01E-17
H-3		29	9.11E+03		
I-129		341	3.29E-02		
I-129_K		454	1.05E-03		
Ni-59		1,125	1.67E-02	2,723	8.38E-02
Np-237		814	7.60E-02		
	U-233	1,125	5.26E-07	17,908	3.94E-05
	Th-229	1,125	1.05E-08	19,308	2.64E-05
Pd-107		1,125	5.60E-05	2,843	4.68E-04
Pu-238		1,125	3.21E-32	3,333	2.20E-15
	U-234	1,125	8.72E-37	18,608	4.56E-04
	Th-230	1,125	1.52E-40	23,008	6.46E-05
	Ra-226	1,125	6.65E-06	18,208	2.65E-04
	Pb-210	1,125	2.01E-08	18,308	9.07E-07
Pu-239		1,125	1.14E-27	7,033	6.01E+00
	U-235	1,125	9.07E-36	14,308	1.21E-05
	Pa-231	1,125	6.06E-07	7,743	2.92E-06
	Ac-227	1,125	1.34E-08	7,693	6.60E-08

[a]maximum based on first 1,000 years and its ultimate peak if beyond 1,000 years

Table 2-19. Baseline Case Maximum Concentrations of the Radionuclide Parent and Progeny Resulting from the Existing 8 Segments within 100-m Compliance Zone[a] - continued

Parent	Daughters	Time of Peak (0-1125 yrs)	Peak Concentration (pCi/L)	Time of Ultimate Peak (1125+ yrs)	Ultimate Peak Concentration (pCi/L)
Pu-240		1,125	3.51E-30	7,713	1.99E-01
	U-236	1,125	8.41E-37	18,308	2.06E-05
	Th-232	1,125	6.77E-46	22,208	1.46E-11
	Ra-228	1,125	5.88E-25	21,908	6.78E-10
Pu-241		1,125	1.88E-51	1,423	6.06E-50
	Am-241	1,125	4.18E-09	2,403	3.19E-02
	Np-237	695	4.80E-04		
	U-233	1,125	3.56E-09	17,808	9.71E-08
	Th-229	1,125	8.55E-11	19,208	6.51E-08
Pu-242		1,125	3.91E-34	7,793	8.23E-04
	U-238	1,125	4.89E-43	15,208	2.61E-10
	U-234	1,125	3.00E-47	18,208	9.83E-12
	Th-230	1,125	4.42E-51	21,108	6.41E-13
	Ra-226	1,125	1.38E-16	17,808	1.84E-12
	Pb-210	1,125	3.90E-19	17,808	6.28E-15
Se-79		1,125	1.88E-57	25,208	2.25E-03
Sn-126		1,125	1.36E-108	165,408	9.03E-06
Sr-90		597	4.89E-04		
Tc-99		240	1.14E+01		
Tc-99_K		385	4.64E-01		
U-233		1,125	2.08E-51	20,908	1.35E+00
	Th-229	1,125	1.27E-53	22,408	9.56E-01
U-234		1,125	4.08E-51	17,008	4.16E-01
	Th-230	1,125	2.44E-54	19,208	5.31E-02
	Ra-226	1,125	7.84E-03	15,108	1.66E-01
	Pb-210	1,125	2.44E-05	15,208	5.66E-04
U-235		1,125	1.11E-52	17,008	1.16E-02
	Pa-231	1,033	3.17E-03		
	Ac-227	1,042	7.21E-05		
U-236		1,125	3.29E-53	17,908	5.02E-03
	Th-232	1,125	1.06E-61	20,408	3.90E-09
	Ra-228	1,125	9.00E-21	20,108	1.81E-07
U-238		1,125	1.89E-50	16,508	1.93E+00
	U-234	1,125	6.27E-53	17,408	9.07E-02
	Th-230	1,125	3.51E-56	19,108	6.30E-03
	Ra-226	1,125	3.17E-05	16,008	1.53E-02
	Pb-210	1,125	9.44E-08	16,008	5.24E-05
Zr-93		1,125	9.79E-23	4,593	3.20E-02
	Nb-93m	1,125	1.62E+00	3,813	2.28E+00

[a]maximum based on first 1,000 years and its ultimate peak if beyond 1,000 years

Table 2-20. Baseline Case Maximum Concentrations (per Ci of parent buried) of Radionuclide Parent and Progeny Resulting From All Future Inventories Within the 100-m Compliance Zone[a]

Parent	Daughters	Time of Peak (0-1125 yrs)	Peak Concentration (pCi/L-Ci$_{parent}$)	Time of Ultimate Peak (1125+ yrs)	Ultimate Peak Concentration (pCi/L-Ci$_{parent}$)
Am-241		1,125	1.28E-04	2,123	1.25E+00
	Np-237	695	1.36E-02		
	U-233	1,125	1.02E-07	15,108	2.78E-06
	Th-229	1,125	2.46E-09	17,508	1.80E-06
Am-243		1,125	7.13E-04	2,433	3.89E+01
	Pu-239	1,125	4.31E-07	4,353	8.71E-01
	U-235	1,125	5.52E-15	8,223	1.46E-06
	Pa-231	1,125	2.19E-08	6,103	2.61E-07
	Ac-227	1,125	4.71E-10	6,073	5.84E-09
C-14		347	1.81E+03		
C-14_K		362	1.90E+02		
Cl-36		335	2.31E+03		
Cm-244		1,028	2.68E-22		
	Pu-240	1,125	6.79E-21	6,033	2.67E-02
	U-236	1,125	2.44E-27	13,508	2.07E-06
	Th-232	1,125	3.19E-36	17,308	1.10E-12
	Ra-228	1,125	5.67E-23	17,008	5.10E-11
Cm-245		1,125	7.24E-04	2,433	4.01E+01
	Pu-241	1,125	2.08E-04	2,443	1.58E+01
	Am-241	1,125	4.82E-04	2,453	4.12E+01
	Np-237	1,125	1.80E-02	1,433	1.84E-02
	U-233	1,125	1.35E-07	15,908	9.71E-07
	Th-229	1,125	2.92E-09	17,408	6.26E-07
Cm-247		1,125	7.94E-04	2,453	4.89E+01
	Am-243	1,125	8.08E-05	2,733	1.07E+01
	Pu-239	1,125	4.66E-08	3,703	1.83E-01
	U-235	1,125	5.81E-16	6,593	1.78E-07
	Pa-231	1,125	7.22E-10	6,153	2.72E-08
	Ac-227	1,125	1.51E-11	6,143	6.05E-10
Cm-248		1,125	7.92E-04	2,453	4.87E+01
	Pu-244	1,125	1.31E-10	4,323	3.05E-04
	Pu-240	1,125	6.92E-13	5,813	1.01E-04
	U-236	1,125	2.52E-19	8,333	4.05E-09
	Th-232	1,125	3.18E-28	14,408	9.19E-16
	Ra-228	1,125	3.16E-25	14,308	4.18E-14
H-3		205	6.39E-03		
I-129		340	3.25E+03		
I-129_C		451	5.54E+01		
I-129_K		451	9.02E+00		
K-40		1,125	2.22E-06	3,353	3.19E+01
Mo-93		236	9.69E+02		
	Nb-93m	236	9.61E+02		
Nb-94		800	3.96E+01	2,093	6.24E+02
Ni-59		1,125	1.77E+01	2,533	8.62E+01
Np-237		807	6.30E+01		
	U-233	1,125	4.44E-04	15,108	3.24E-02
	Th-229	1,125	9.11E-06	17,508	2.10E-02
Pd-107		1,125	1.79E+01	2,533	8.82E+01
Pu-238		1,125	2.76E-22	2,813	1.23E-12
	U-234	1,125	1.08E-26	14,908	2.37E-03
	Th-230	1,125	2.63E-30	18,708	2.90E-04
	Ra-226	1,125	4.15E-05	14,508	9.86E-04
	Pb-210	1,125	1.29E-07	14,508	3.37E-06

[a]maximum based on first 1,000 years and its ultimate peak if beyond 1,000 years

Table 2-20. Baseline Case Maximum Concentrations (per Ci of parent buried) of Radionuclide Parent and Progeny Resulting From All Future Inventories Within the 100-m Compliance Zone[a] - continued

Parent	Daughters	Time of Peak (0-1125 yrs)	Peak Concentration (pCi/L-Ci$_{parent}$)	Time of Ultimate Peak (1125+ yrs)	Ultimate Peak Concentration (pCi/L-Ci$_{parent}$)
Pu-239		1,125	2.40E-18	6,133	1.54E+01
	U-235	1,125	2.57E-26	13,008	3.19E-05
	Pa-231	1,125	1.62E-06	7,433	7.37E-06
	Ac-227	1,125	3.57E-08	7,383	1.67E-07
Pu-240		1,125	2.20E-18	6,033	9.66E+00
	U-236	1,125	7.09E-25	13,608	7.53E-04
	Th-232	1,125	7.59E-34	17,308	4.03E-10
	Ra-228	1,125	2.15E-20	17,008	1.86E-08
Pu-241		1,125	3.86E-42	1,195	4.72E-42
	Am-241	1,125	4.36E-06	2,123	4.26E-02
	Np-237	690	4.53E-04		
	U-233	1,125	3.38E-09	15,108	8.78E-08
	Th-229	1,125	8.20E-11	17,508	5.68E-08
Pu-242		1,125	2.48E-18	6,503	1.83E+01
	U-238	1,125	4.17E-27	12,508	5.54E-06
	U-234	1,125	3.41E-31	15,508	1.71E-07
	Th-230	1,125	6.59E-35	17,908	9.55E-09
	Ra-226	1,125	5.17E-12	17,408	2.67E-08
	Pb-210	1,125	1.49E-14	17,508	9.14E-11
Pu-244		1,125	2.48E-18	6,503	1.85E+01
	Pu-240	1,125	2.86E-19	6,843	9.27E+00
	U-236	1,125	8.99E-26	9,703	4.19E-04
	Th-232	1,125	9.41E-35	14,808	1.17E-10
	Ra-228	1,125	8.76E-22	14,508	5.33E-09
Ra-226		933	8.80E+01		
	Pb-210	968	2.96E-01		
Se-79		1,125	2.04E-37	19,408	4.99E+00
Sn-126		1,125	1.31E-75	119,908	6.09E-01
Sr-90		563	2.22E-04		
Tc-99		245	9.43E+02		
Tc-99_K		382	2.91E+01		
Th-230		1,125	1.85E-39	18,208	4.79E+00
	Ra-226	1,125	3.12E+01	1,160	3.12E+01
	Pb-210	1,125	1.05E-01	1,201	1.06E-01
Th-232		1,125	1.87E-39	19,508	5.67E+00
	Ra-228	1,125	1.81E-08	19,108	2.67E+02
U-233		1,125	2.99E-35	14,908	6.49E+00
	Th-229	1,125	2.17E-37	17,308	4.24E+00
U-234		1,125	3.00E-35	14,908	6.64E+00
	Th-230	1,125	2.14E-38	18,708	8.17E-01
	Ra-226	1,125	1.47E-01	14,508	2.78E+00
	Pb-210	1,125	4.66E-04	14,508	9.52E-03
U-235		1,125	3.01E-35	15,008	6.93E+00
	Pa-231	1,030	2.16E+00		
	Ac-227	1,040	4.90E-02		
U-236		1,125	3.01E-35	15,008	6.93E+00
	Th-232	1,125	1.15E-43	18,908	4.91E-06
	Ra-228	1,125	1.27E-15	18,608	2.28E-04
U-238		1,125	3.01E-35	15,008	6.93E+00
	U-234	1,125	9.87E-38	17,108	3.13E-01
	Th-230	1,125	6.43E-41	19,108	2.18E-02
	Ra-226	1,125	1.39E-04	15,808	5.84E-02
	Pb-210	1,125	4.19E-07	15,908	2.00E-04
Zr-93		1,125	2.98E-07	3,163	3.66E+01
	Nb-93m	1,125	1.88E+03	2,463	2.21E+03

[a]maximum based on first 1,000 years and its ultimate peak if beyond 1,000 years

2.6.8.4 Groundwater Protection

The maximum groundwater concentrations from the current radionuclide inventory in CIG-1 through the 1,000-year post closure compliance period were compared with the MCLs (Cook 2007) using the all-pathways application (Koffman 2006a). Table 2-21 shows the results.

The results of the groundwater protection analysis for the current inventory in CIG-1 are low compared to the MCLs. The maximum total beta-gamma dose is about 46 percent of the MCL, the maximum total gross alpha concentration is 0.6% of the MCL, the maximum total radium concentration is about 0.2% of the MCL, and the maximum total uranium concentration is about 12 orders of magnitude less than the MCL.

Groundwater protection disposal limits for each of the two CIGs were developed from the calculated maximum groundwater concentrations, including impacts from the current inventory, using the Future Limits feature of the All-Pathways application (Koffman 2006a). Groundwater protection disposal limits in this section are derived without considering the impact of groundwater contaminant plume interaction with nearby disposal units (e.g., Slit Trenches) and are therefore presented as preliminary information. The results of plume interaction are presented in Chapter 6.0, Integrated Facility Analysis. Final limits will be adjusted as needed to account for plume interaction and the results of sensitivity and/or uncertainty analyses and present in Chapter 7.0, Integration and interpretation. The preliminary limits are shown in Table 2-22.

Table 2-21. Groundwater Protection Impacts from Current CIG Inventory

Time Period	0 – 1125 Years Post-Closure
Beta-Gamma MCL, mrem/yr	4
Maximum Total Dose, mrem/yr	1.82
Time of Maximum, year	29
Parent Nuclide	% of Max Dose
H-3	1.00E+02
Tc-99	9.94E-03
Gross Alpha MCL, pCi/L	15
Maximum Gross Alpha Concentration, pCi/L	0.10
Time of Maximum, year	1125
Parent Nuclide	% of Max Concentration
Np-237	6.49E+01
U-234	3.07E+01
U-235	3.41E+00
Am-241	4.75E-01
Pu-241	3.20E-01
U-238	1.24E-01
Radium MCL, pCi/L	5
Maximum Radium Concentration, pCi/L	0.01
Time of Maximum, year	1125
Parent Nuclide	% of Max Concentration
U-234	9.95E+01
U-238	4.02E-01
Pu-238	8.44E-02
Uranium MCL, µg/L	30
Maximum Uranium Concentration, µg/L	5.50E-11
Time of Maximum, year	1125
Parent Nuclide	% of Max Concentration
Np-237	9.84E+01
Am-241	9.79E-01
Pu-241	6.66E-01

Table 2-22. Preliminary Groundwater Protection Limits for CIG-1 and CIG-2

Parent Radionuclide	CIG-1 Preliminary Inventory Limit 0-125 year (Ci)				CIG-1 Preliminary Inventory Limit 125-1,125 year (Ci)			
	Beta-Gamma	Gross Alpha	Radium	Uranium	Beta-Gamma	Gross Alpha	Radium	Uranium
Am-241	---	---	---	---	1.0E+04	5.0E+02	---	1.3E+12
Am-243	---	---	---	---	1.9E+05	9.6E+03	---	5.4E+15
C-14	4.4E+09	---	---	---	5.0E-01	---	---	---
C-14_K	5.7E+10	---	---	---	4.7E+00	---	---	---
Cl-36	9.9E+04	---	---	---	1.3E-01	---	---	---
Cm-244	---	---	---	---	---	---	---	---
Cm-245	---	---	---	---	7.5E+03	3.6E+02	---	9.8E+11
Cm-247	---	---	---	---	1.4E+06	7.8E+03	---	5.1E+16
Cm-248	---	---	---	---	4.4E+12	9.4E+03	---	---
H-3 [1]	2.2E+05	---	---	---	1.4E+05	---	---	---
I-129	4.0E+04	---	---	---	1.4E-04	---	---	---
I-129_C	5.2E+06	---	---	---	8.2E-03	---	---	---
I-129_K	3.2E+07	---	---	---	5.1E-02	---	---	---
K-40	---	---	---	---	6.1E+07	---	---	---
Mo-93	6.8E+02	---	---	---	3.8E-01	---	---	---
Nb-94	5.5E+18	---	---	---	8.9E+00	---	---	---
Ni-59	---	---	---	---	7.8E+00	---	---	---
Np-237	---	---	---	---	2.2E+00	1.1E-01	---	3.0E+08
Pd-107	---	---	---	---	9.4E+02	---	---	---
Pu-238	---	---	---	---	3.4E+06	4.1E+04	5.5E+04	---
Pu-239	---	---	---	---	5.0E+06	3.8E+06	---	---
Pu-240	---	---	---	---	---	3.0E+18	---	---
Pu-241	---	---	---	---	3.0E+05	1.5E+04	---	3.9E+13
Pu-242	---	---	---	---	2.9E+13	3.3E+11	4.4E+11	---
Pu-244	---	---	---	---	---	2.5E+18	---	---
Ra-226	---	---	---	---	1.5E+00	1.9E-02	2.6E-02	---
Se-79	---	---	---	---	---	---	---	---
Sn-126	---	---	---	---	---	---	---	---
Sr-90	---	---	---	---	1.4E+04	---	---	---
Tc-99	3.3E+03	---	---	---	4.4E-01	---	---	---
Tc-99_K	5.7E+06	---	---	---	1.3E+01	---	---	---
Th-230	---	---	---	---	4.2E+00	5.5E-02	7.3E-02	---
Th-232	---	---	---	---	9.3E+07	9.4E+07	1.3E+08	---
U-233	---	---	---	---	---	---	---	---
U-234	---	---	---	---	9.5E+02	1.2E+01	1.6E+01	---
U-235	---	---	---	---	3.7E+00	2.8E+00	---	---
U-236	---	---	---	---	1.3E+15	1.3E+15	1.8E+15	---
U-238	---	---	---	---	1.1E+06	1.2E+04	1.6E+04	---
Zr-93	5.0E+18	---	---	---	2.4E-01	---	---	---

Note: Limits reported as "---" indicate that there is no limit or that the limit $\geq$ 4.59E+19 Ci
NA = this radionuclide was screened out in the screening process for this pathway
[1] H-3 Preliminary Inventory Limit values reduced by a factor of 10 to account for uncertainty associated with H-3 release from 232-F stainless steel process equipment.

Table 2-22. Preliminary Groundwater Protection Limits for CIG-1 and CIG-2 - continued

Parent Radionuclide	CIG-2 Preliminary Inventory Limit 0-125 year (Ci)				CIG-2 Preliminary Inventory Limit 125-1,125 year (Ci)			
	Beta-Gamma	Gross Alpha	Radium	Uranium	Beta-Gamma	Gross Alpha	Radium	Uranium
Am-241	---	---	---	---	1.2E+04	6.0E+02	---	1.5E+12
Am-243	---	---	---	---	2.3E+05	1.1E+04	---	6.3E+15
C-14	5.2E+09	---	---	---	5.4E-01	---	---	---
C-14_K	6.8E+10	---	---	---	5.4E+00	---	---	---
Cl-36	1.2E+05	---	---	---	1.6E-01	---	---	---
Cm-244	---	---	---	---	---	---	---	---
Cm-245	---	---	---	---	8.9E+03	4.2E+02	---	1.2E+12
Cm-247	---	---	---	---	1.7E+06	9.2E+03	---	6.1E+16
Cm-248	---	---	---	---	5.2E+12	1.1E+04	---	---
H-3 [1]	2.6E+05	---	---	---	1.7E+05	---	---	---
I-129	4.8E+04	---	---	---	1.5E-04	---	---	---
I-129_C	6.1E+06	---	---	---	9.7E-03	---	---	---
I-129_K	3.8E+07	---	---	---	6.0E-02	---	---	---
K-40	---	---	---	---	7.1E+07	---	---	---
Mo-93	8.1E+02	---	---	---	4.4E-01	---	---	---
Nb-94	6.4E+18	---	---	---	1.0E+01	---	---	---
Ni-59	---	---	---	---	9.1E+00	---	---	---
Np-237	---	---	---	---	2.6E+00	1.3E-01	---	3.5E+08
Pd-107	---	---	---	---	1.1E+03	---	---	---
Pu-238	---	---	---	---	4.0E+06	4.8E+04	6.5E+04	---
Pu-239	---	---	---	---	6.0E+06	4.5E+06	---	---
Pu-240	---	---	---	---	---	3.5E+18	---	---
Pu-241	---	---	---	---	3.6E+05	1.8E+04	---	4.6E+13
Pu-242	---	---	---	---	3.5E+13	3.9E+11	5.2E+11	---
Pu-244	---	---	---	---	---	2.9E+18	---	---
Ra-226	---	---	---	---	1.8E+00	2.3E-02	3.1E-02	---
Se-79	---	---	---	---	---	---	---	---
Sn-126	---	---	---	---	---	---	---	---
Sr-90	---	---	---	---	1.7E+04	---	---	---
Tc-99	3.9E+03	---	---	---	5.1E-01	---	---	---
Tc-99_K	6.8E+06	---	---	---	1.5E+01	---	---	---
Th-230	---	---	---	---	5.0E+00	6.4E-02	8.7E-02	---
Th-232	---	---	---	---	1.1E+08	1.1E+08	1.5E+08	---
U-233	---	---	---	---	---	---	---	---
U-234	---	---	---	---	1.1E+03	1.4E+01	1.8E+01	---
U-235	---	---	---	---	4.3E+00	3.3E+00	---	---
U-236	---	---	---	---	1.6E+15	1.6E+15	2.1E+15	---
U-238	---	---	---	---	1.2E+06	1.4E+04	1.9E+04	---
Zr-93	6.0E+18	---	---	---	2.9E-01	---	---	---

Note: Limits reported as "---" indicate that there is no limit or that the limit ≥ 5.41E+19 Ci.
[1] H-3 Preliminary Inventory Limit values reduced by a factor of 10 to account for uncertainty associated with H-3 release from 232-F stainless steel process equipment

2.6.9 Groundwater Transport Uncertainty Analysis

The draft E-Area Components-in-Grout (CIG) Trenches Sensitivity Analysis Model is very similar in layout, operation, and execution to the Slit and Engineered Trench models, though it differs a great deal in the treatment of the contaminant transport in the near field—that is, in the region near the trenches themselves. The principal differences are necessary in order to perform detailed modeling of the contaminant transport within the concrete that surrounds the radioactive materials. Details of the model and its uncertainty analyses and sensitivity analyses appear in Appendix F. All results are preliminary.

As for the deterministic analysis described earlier in this chapter, two different cases of the CIG Model were run for the uncertainty and sensitivity analyses: one with the full inventory anticipated to be present in both trenches (CIG #1 and CIG #2) at the time of closure, and the other with just that inventory buried in Segments 1 through 8. This is done in order to better assess the limits on what may be disposed in the future. In both cases, all contaminated water flowing out of the trenches into the aquifer is assumed to be directly upstream of the observation well.

The following CIG model endpoints were selected for uncertainty and sensitivity analysis, which is based on 2000 realizations. Like for the Engineered Trenches, the model duration was set to 20,000 years in order to capture the peak all-pathways dose, and the concentrations of radium, uranium, and alpha emitters, as well as the dose from beta-gamma emitters, was restricted to those maxima occurring within the period of performance (assumed to be 1130 years, which roughly corresponds to the 1125 years used in the PORFLOW analyses). The endpoints are

- the maximum potential all-pathways dose to a member of the public (based on use of groundwater at a well 100 meters downstream of the facility) within the period of performance (divided into early and midtime peaks)
- the maximum potential all-pathways dose to a member of the public for all (late) time
- the maximum gross alpha concentration in groundwater at the well within the period of performance
- the maximum dose from beta and gamma emitters in groundwater at the well within the period of performance
- the maximum radium concentration in groundwater at the well within the period of performance
- the maximum uranium concentration in groundwater at the well within the period of performance

2.6.9.1 Summary of Uncertainty Analysis with Estimated Closure Inventory

The closure inventory was provided by the site operator as a radionuclide-specific inventory that is the same for both CIG 1 and CIG 2. The summary statistics for a point in groundwater 100 m downstream of the facilities is provided in Table 2-23.

Table 2-23. Summary statistics from 2000 realizations for the CIG Trenches endpoints of interest (full projected inventory)

Endpoint	Mean	Standard Deviation	Min	1st Qtr.	Median (2nd Qtr.)	3rd Qtr.	Max
max. dose in period of performance (mrem/yr)	3.2	1.3	1.1	2.2	2.9	3.6	12
max. dose – all time (mrem/yr)	50	24	11	33	44	61	210
max. alpha concentration at well within period of performance (pCi/L)	0.52	0.21	0.18	0.36	0.47	0.63	2.0
max. beta - gamma dose at well within period of performance (mrem/yr)	0.69	0.60	0.14	0.30	0.50	0.87	5.7
max. radium concentration at well within period of performance (pCi/L)	0.034	0.011	0.017	0.025	0.031	0.041	0.067
max. uranium concentration at well within period of performance (μg/L)	1.6E-08	3.6E-07	1.1E-10	3.2E-10	4.4E-10	6.3E-10	1.5E-05

1 mrem = 10 μSv
27 pCi = 1 Bq

The maximum dose within the period of performance occurs at about 900 years after the model begins calculations (which corresponds to the time of disposal of the first CIG Segment). This dose is caused primarily by Np-237. Earlier dose peaks are the result of H-3, Tc-99, and C-14. Later doses, peaking at about 9000 years, are from Pu-239. These patterns of radionuclide appearances at the well can be seen in the detailed graphs in Appendix F.

2.6.9.2 Summary of Uncertainty Analysis with Currently Disposed Inventory

A similar analysis was performed for CIG Segments 1 through 8, all of which exist in CIG 1. (At the time of this analysis, Segment 9 was still considered to be part of the future inventory.) Summary statistics are provided in Table 2-24.

In the case of Segments 1-8, the maximum dose achieved during the period of performance is not driven by Np-237. Dose contributors within the period of performance are H-3, Tc-99, and C-14, appearing sequentially in time. Late dose is again dominated by Pu-239 at around 9000 years.

2.6.10 Groundwater Transport Sensitivity Analysis

The groundwater transport sensitivity analysis consisted of two principal components. First, a probabilistic sensitivity analysis was conducted for the CIG Trenches using the same CIG GoldSim model and endpoints used for the uncertainty analysis (summarized in Section 2.6.9 and described more completely in Appendix F). Second, a deterministic sensitivity analysis was conducted in PORFLOW evaluating four sensitivity cases. These cases are described in section 2.6.10.2.

2.6.10.1 Probabilistic Groundwater Transport Sensitivity Analysis

The same CIG model and endpoints used for the uncertainty analysis (summarized in Section 2.6.9 and described more completely in Appendix F) are used for the sensitivity analysis. Again, the two different inventory assumptions were examined separately, one with the inventory at closure and one with the inventory from only Segments 1 through 8. Each is summarized in this section. See the caveats regarding the sensitivity analysis described in Section 1.6.7.

2.6.10.1.1 Summary of Sensitivity Analysis with Estimated Closure Inventory

Each of the modeling endpoints discussed in section 2.6.9 was analyzed to identify those stochastic parameters having the most influence on that endpoint (Table 2-25.)

The most sensitive parameters for the CIG doses and concentrations assuming the full disposed inventory are the saturated thickness of the aquifer and the infiltration multiplier, a parameter unique to the CIG model. The CIG Trenches do not share the infiltration model arising from the closure cap modeling that is used for the Slit and Engineered Trenches - rather the CIG model uses the infiltration calculated by PORFLOW, assuming the presence of a concrete slab over the CIG segments.

The infiltration multiplier is an *ad hoc* value (uniform 0.75 to 1.25) designed to artificially add uncertainty to the value of infiltration, in order to determine whether it is sensitive in the model. Indeed it is. Other significant parameters are the K_ds for the elements whose isotopes contribute to dose, and to a minor degree the porosities of sandy soil and of future waste.

Table 2-24. Summary statistics from 2000 realizations for the CIG Trenches endpoints of interest (segments 1 through 8 inventory)

Endpoint	Mean	Standard Deviation	Min	1st Qtr.	Median 2nd Qtr.	3rd Qtr.	Max
max. dose in period of performance (mrem/yr)	0.22	0.12	0.098	0.14	0.19	0.22	1.4
max. dose – all time (mrem/yr)	4.8	2.2	1.1	3.2	4.3	5.9	19
max. alpha conccentration at well within period of performance (pCi/L)	3.1E-03	1.0E-03	1.7E-03	2.3E-03	2.9E-03	3.8E-03	5.9E-03
max. beta - gamma dose at well within period of performance (mrem/yr)	0.23	0.33	0.016	0.045	0.11	0.28	3.2
max. radium concentration at well within period of performance (pCi/L)	2.4E-03	8.0E-04	1.3E-03	1.8E-03	2.2E-03	3.0E-03	4.7E-03
max. uranium concentration at well within period of performance (μg/L)	7.5E-10	2.0E-08	7.0E-14	2.1E-13	3.1E-13	5.7E-13	8.4E-07

1 mrem = 10 μSv
27 pCi = 1 Bq

Table 2-25. Identification of the most sensitive parameters for the CIG Trenches endpoints of interest (full projected inventory)

Endpoint	SI rank	input parameter	Sensitivity Index	R^2
max. dose within period of performance (mrem/yr)	1	saturated thickness of aquifer	65	99%
	2	Np K_d in oxidized old concrete	17	
	3	infiltration multiplier	13	
	4	porosity of future waste	4.1	
max. dose – late time (mrem/yr)	1	saturated thickness of aquifer	50	98%
	2	infiltration multiplier	22	
	3	Pu K_d in sandy soil	20	
	4	Pu K_d in oxidized old concrete	3.1	
max. alpha concentration at well (pCi/L)	1	saturated thickness of aquifer	63	99%
	2	Np K_d in oxidized old concrete	18	
	3	infiltration multiplier	13	
	4	porosity of future waste	4.8	
max. beta - gamma dose at well (mrem/yr)	1	infiltration multiplier	33	96%
	2	Sr K_d in sandy soil	26	
	3	saturated thickness of aquifer	18	
	4	porosity of sandy soil	15	
max. radium concentration at well (pCi/L)	1	saturated thickness of aquifer	97	99%
	2	infiltration multiplier	1.1	
	3	Ra K_d in sandy soil	1.1	
	4	porosity of sandy soil	0.22	
maximum uranium concentration at well		insufficient information		

For the maximum dose achieved within the period of performance, the thickness of the aquifer and the K_d of Np in oxidized old concrete, which is consistent with neptunium's domination of midtime doses, are the two most important parameters. Following this is the infiltration multiplier. The fourth-ranked parameter is the porosity of future waste.

Similarly for peak doses occurring in later time, the thickness of the aquifer and the infiltration multiplier dominate the sensitivity. These are followed by Pu K_d, in both sandy soil and in oxidized old concrete, consistent with Pu-239's domination of doses in later time.

The sensitive parameters identified for the maximum gross alpha concentration are identical to those selected for the maximum dose within the period of performance, which is dominated by neptunium. Even the SI values are essentially the same. The timing of the maximum alpha concentration is here constrained to be that maximum achieved within the period of performance, so alpha-emitters occurring later (e.g., plutonium) are not seen. If we were to examine the maximum alpha concentration in late time, it would be expected to mimic the sensitivities for the dose in late time.

In addition to the familiar infiltration multiplier and saturated aquifer thickness, we see a new parameter for sensitivity of dose from beta-gamma emitters: The K_d of Sr in sandy soil exhibits the typical behavior for K_d, being most sensitive at low values (see the sensitivity index graphs in Appendix F). The dependence on sandy soil porosity does not appear to make much sense, however, showing (in the graphs) some sensitivity at the higher values as well as strong sensitivities at low values.

The concentration of radium in well water is completely dominated by the saturated thickness of the aquifer. A distant second to that is the infiltration multiplier, the K_d for Ra, and sandy soil porosity.

The sensitivity analysis for uranium concentrations in well water within the period of performance was problematic, since very few non-zero data were available for examination. Within the period of performance, very little U escapes to the well. The sensitivity indices, therefore, are not well founded, despite the high R^2 of the fit of the statistical model to the GoldSim. This situation is perhaps acceptable, since apparently the water concentration of U from the CIG Trenches is not a matter of grave concern.

2.6.10.1.2 Summary of Sensitivity Analysis with Currently Disposed Inventory

Much of what can be concluded from the full closure inventory of the CIG Trenches can be said of the limited inventory of Segments 1 through 8. Table 2-26 summarizes the Sensitivity Analysis results.

Table 2-26. Identification of the most sensitive parameters for the CIG Trenches endpoints of interest (segments 1 through 8 inventory)

Endpoint	SI rank	input parameter	Sensitivity Index	R^2
max. dose within period of performance (mrem/yr)	1	porosity of sandy soil	35	97%
	2	saturated thickness of aquifer	35	
	3	infiltration multiplier	19	
	4	molecular diffusivity in water	3.0	
max. dose – all time (mrem/yr)	1	saturated thickness of aquifer	51	98%
	2	infiltration multiplier	21	
	3	Pu K_d in sandy soil	21	
	4	Pu K_d in oxidized old concrete	2.7	
max. alpha concentration at well (pCi/L)	1	saturated thickness of aquifer	99	99%
	2	Ra K_d in sandy soil	0.59	
	3	porosity of sandy soil	0.18	
	4	infiltration multiplier	0.15	
max. beta - gamma dose at well (mrem/yr)	1	porosity of sandy soil	46	98%
	2	infiltration multiplier	37	
	3	saturated thickness of aquifer	9.1	
	4	molecular diffusivity in water	3.5	
max. radium concentration at well (pCi/L)	1	saturated thickness of aquifer	98	99%
	2	infiltration multiplier	0.92	
	3	Ra K_d in sandy soil	0.90	
	4	porosity of sandy soil	0.20	
maximum uranium concentration at well		insufficient information		

The maximum all-pathways (water use) dose within the period of performance for the CIG Segments 1-8 is most sensitive to the porosity of sandy soil, but this is closely followed by the saturated thickness. The last two parameters are also water-related: infiltration multiplier, a parameter discussed in Section 2.6.10.1, and the molecular diffusivity D_m in water, which is the same for all radionuclides.

For peak dose in all time, the thickness of the aquifer dominates the sensitivity, followed by the infiltration multiplier and Pu K_d in sandy soil. Fourth is the Pu K_d in oxidized old concrete, consistent with Pu-239's domination of doses in later time.

Note that although U and Pu are the major alpha contributors in later time, they play a minor role in the concentration of gross alpha during the period of performance. The gross alpha concentration is here completely dominated by the saturated thickness of the aquifer, to the exclusion of any other significant explanatory variables.

The sensitivity of dose within the period of performance from beta-gamma emitters for Segments 1 through 8 is explained entirely by the same water-related variables that predict dose: porosity of sandy soil, the infiltration multiplier, the saturated thickness, and the molecular diffusivity in water. No partition coefficients played a significant role. The parallels between beta-gamma dose and water use dose within the period of performance occur since the water dose is dominated by beta and gamma emitters within the period of performance.

The maximum concentration of Ra in well water during the period of performance is, like the alpha concentration, dominated by the saturated thickness of the aquifer to the exclusion of any other significant explanatory variables.

Again, as with the full closure CIG inventory, uranium well water concentrations are rarely non-zero within the period of performance. The few occurrences are insufficient for a reliable sensitivity analysis.

2.6.10.2 Deterministic Groundwater Transport Sensitivity Analysis

Four sensitivity cases were analyzed in this PA for the CIG Trenches using PORFLOW, all of which address the sensitivity of the groundwater model results to properties affecting transport. Based on prior sensitivity studies, it is known that the wasteform model used to address H-3 release from 232-F process equipment has a very high impact on H-3 inventory limits. This model was not a subject of the current sensitivity study. As such, H-3 inventory limits for CIG operations within this PA should be reduced by a factor of 10 to account for the uncertainty resulting from this sensitivity.

A list of the four sensitivity cases, and the parameters varied in the resulting evaluations, are presented in Table 2-27. All four cases address transport properties where the flow fields, geometrical meshes, material property zones, etc., are unaltered.

Table 2-27. Preliminary Sensitivity Cases Considered within this PA

Sensitivity Case ID	Parameter of Interest	Nominal Setting	Sensitivity Case Setting
A	**Sorption Coefficients (K_d values)**	Best Estimate values [a] with CDP factors applied	Best Estimate [a] values without CDP factors applied
B	**Sorption Coefficients (K_d values)**	Best Estimate values [a] with CDP factors applied	Conservative Estimate [a] values with CDP factors applied
C	**Timing of Cementitious Material Aging**	For Existing Segments 334 yr for Young-to-Middle transition and 443 yr for Middle-to-Old transition. 350 and 441 yrs transition points for Future Segments.	Omit Middle age and transition Young-to-Old at 325 yr for both Existing and Future Segments.
D	**Effective Diffusion Coefficient of Grout Barrier and other Cementitious Materials**	Mean value for Existing Grout, Future Grout, and other Cementitious Materials.	Mean value plus 3-sigma for Existing Grout, Future Grout, and other Cementitious Materials.

A summary of the results for each of the four cases highlighted in Table 2-27 is discussed where a comparison to the "nominal" Baseline Case is provided. The primary impact of interest is how radionuclide inventory limits are affected (i.e., the mrem dose level at the 100-m compliance well). Before discussing a direct comparison of the inventory limit impacts associated with the chosen sensitivity cases, the various inventory limits associated with the Baseline case for reference to the four selected sensitivity cases are presented. For the sensitivity comparisons, the focus is on the beta-gamma pathway results.

Baseline Case Summary

The following summary of results is for the Baseline case. The computed peak well concentrations within the 100-m compliance region for the Existing and Future Segments are listed in Table 2-19 and Table 2-20**.** For comparison purposes to sensitivity cases, peak concentration comparisons are only consistent with dose comparisons for radionuclides without any progeny. Since the majority of radionuclides considered have progeny, the comparisons are based on dose quantities. However, for completeness, the peak well concentrations within the 100-m compliance region for each sensitivity case studied are also provided.

To provide a brief connection between well concentrations and their associated dose values, the following discussion explains the transformation from well concentration in terms of pCi/L to beta-gamma dose in terms of mrem/yr. The linearity assumption for the transport equations is used to additively compute a composite maximum well concentration that accounts for both existing as well as future disposals.

For example, the maximum well concentration for a particular species as a function of time can be estimated from its existing and future inventory contributions using:

$$C_{well}^{max}(t) = C_{ES}^{max}(t) + \eta_{FS}\hat{C}_{FS}^{max}(t) \qquad \text{Equation 2-3}$$

where $C_{well}^{max}(t)$ - composite maximum well concentration (pCi/L)

$C_{ES}^{max}(t)$ - Existing Segment inventory maximum well concentration (pCi/L)

$\hat{C}_{FS}^{max}(t)$ - Future Segment inventory maximum well concentration (pCi/L-Ci)

η_{FS} - Future Segment inventory of parent buried (Ci)

t - time (yr)

Equation 2-3 applies for every radionuclide parent buried and its progeny. To assist in establishing a groundwater beta-gamma pathway inventory limit, the above equation can be used only for those radionuclides without a decay chain (i.e., no significant exposure contributions from progeny). Following are two examples where only the buried radionuclide is considered (i.e., H-3 and I-129_K).

Application of the above equation to the radionuclide H-3 yields a Future Segment inventory of ~3.13×10^6 Ci, when the beta-gamma MCL of 20,000 pCi/L is chosen as the concentration limit of interest. The H-3 maximum well concentration for the Existing Segments compared to its value for the composite value is shown in Figure 2-51 (i.e., here the Future Segment inventory was set to 3.13×10^6 Ci). As shown in Figure 2-51, the MCL was trimmed at ~205 years.

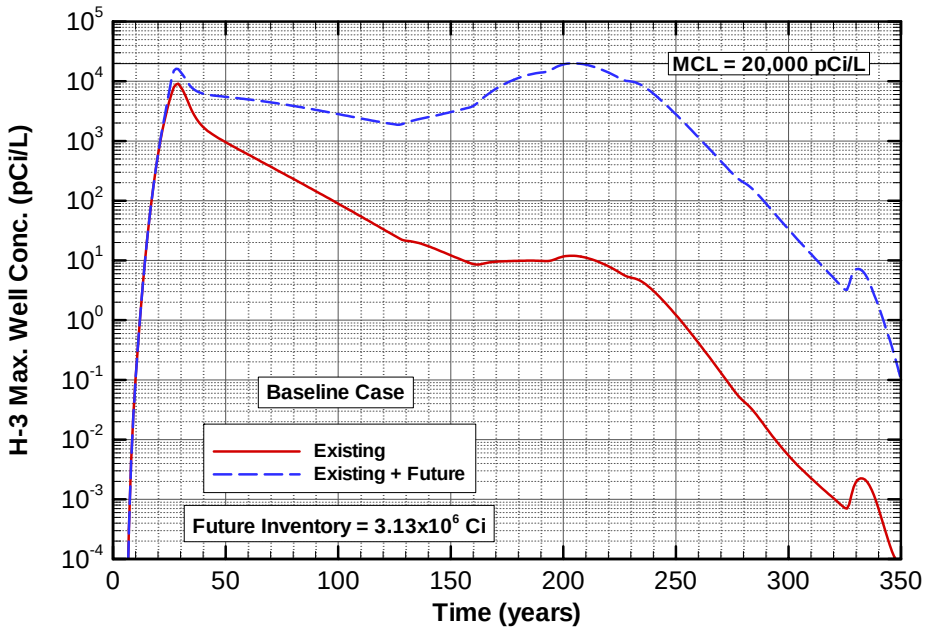

Figure 2-51. Maximum Well Concentration for H-3 within the 100-m Compliance Region (based on Existing Segment Inventory and the Composite Inventory)

Application of the above equation to the radionuclide I-129_K (i.e., in its K&L Basin resin form) yields a Future Segment inventory of ~0.11 Ci, when the beta-gamma MCL of 1 pCi/L is chosen as the concentration limit of interest. The I-129_K maximum well concentration for the Existing Segments compared to its value for the composite value is shown in Figure 2-52 (i.e., here the Future Segment inventory was set to 0.11 Ci). As shown in Figure 2-52, the MCL was trimmed at ~451 years.

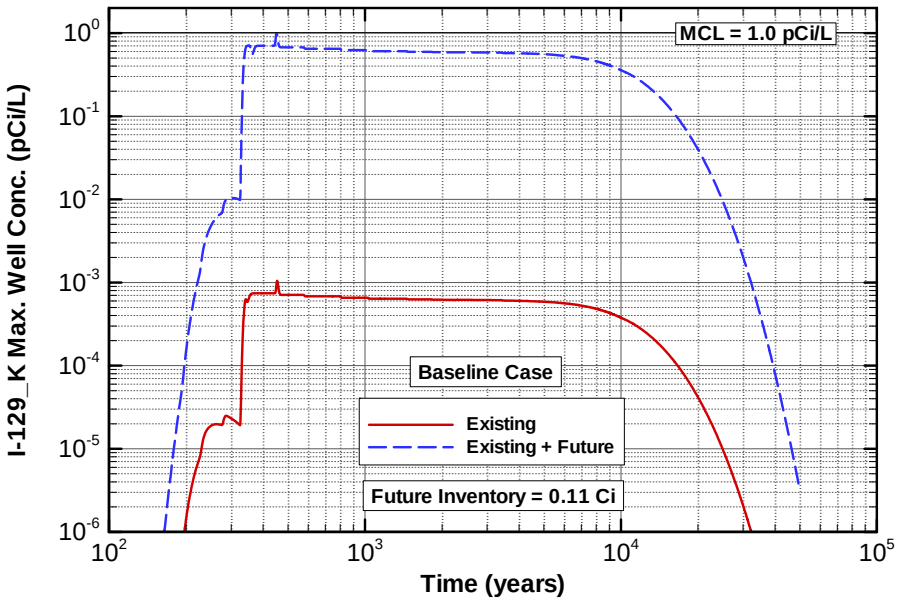

Figure 2-52. Maximum Well Concentration for I-129_K within the 100-m Compliance Region (based on Existing Segment Inventory and the Composite Inventory)

To address buried radionuclide parents with decay chain contributions, the following equation can be used to determine the composite exposure associated with the groundwater beta-gamma pathway:

$$E_{\beta\gamma}(t) = 4.0 * \sum_{j=1}^{nchain} \left[\frac{C_{ES}^{max}(t,j) + \eta_{FS}\hat{C}_{FS}^{max}(t,j)}{C_{MCL}(j)} \right] \qquad \text{Equation 2-4}$$

where

$E_{\beta\gamma}(t)$ - composite maximum well beta-gamma exposure (mrem/yr)

$C_{ES}^{max}(t,j)$ - Existing Segment maximum well concentration for j^{th} isotope (pCi/L)

$\hat{C}_{FS}^{max}(t,j)$ - Future Segment maximum well concentration for j^{th} isotope (pCi/L-Ci)

$C_{MCL}(j)$ - Beta-Gamma MCL for j^{th} isotope (pCi/L)

t - time (yr)

Application of the above equation to the radionuclide Zr-93 (i.e., which has one daughter Nb-93m) yields a Future Segment inventory limit of ~0.532 Ci when the time frame of interest is 125 to 1,125 years (peak occurs at 1,125 yrs). The limit drops to ~0.451 Ci when the time frame of interest is over all times where the ultimate peak occurs at 2,493 years. These results are shown in Figure 2-53. Note that the beta-gamma MCL for Zr-93 is 2,000 pCi/L and for Nb-93m it is 1,000 pCi/L. The beta-gamma groundwater exposure limit is 4.0 mrem/yr total.

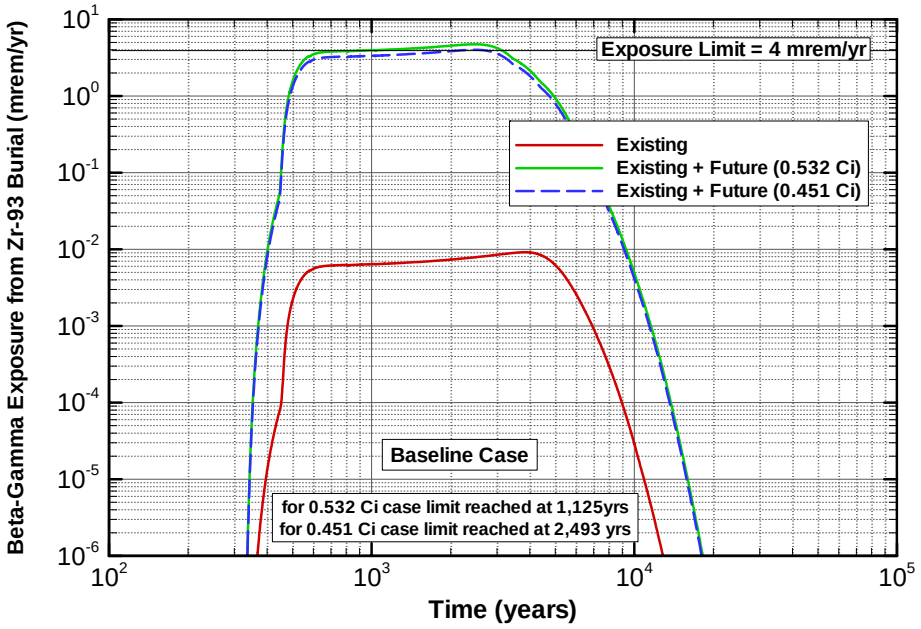

Figure 2-53. Beta-gamma Exposure (mrem/yr) for buried Zr-93 (based on Existing Segment Inventory and the Composite Inventories)

Calculations similar to the examples provided above are performed to derive inventory limits for all potential future disposal species (note that these calculations also handle the contributions associated with those radionuclides assumed to be in secular equilibrium within each parents decay chain). The abbreviated chains are expanded up to their full chains using an application named "IdealFileMaker" (Taylor 2006) where those species assumed to be in secular equilibrium with their own parent are addressed. Then, inventory limits (based on a sum-of-fractions [SOF] and maximum dose in time approaches) associated with other pathways are provided:

- LADTAP – all-pathways exposure limit criterion of 25 mrem/yr
- Beta-Gamma – beta/gamma emitter exposure limit criterion of 4 mrem/yr
- Gross-Alpha – alpha emitter combined concentration limit criterion of 15 pCi/L
- Radium – Ra-226 and Ra-228 combined concentration limit criterion of 5 pCi/L
- Uranium – all uranium isotopes combined concentration limit criterion of 30 µg/L

All of these inventory calculations are performed using Visual Basic based applications named "All-Pathways.exe" and "FutureLimits.exe" (Koffman, 2006).

The CIG units are somewhat unique in this E-Area LLWF PA in that existing inventories are being handled separately from future inventories within the PORFLOW transport analyses. In order to accommodate this unique aspect, the "FutureLimits.exe" application was created. As such, future disposal inventory limits are computed in terms of Ci of parent radionuclide buried for the five pathways listed above. Since CIG Unit #1 contains existing inventory segments, the future disposal limits for each CIG unit differ in value. However, the results from the application "FutureLimits.exe" only provides the total allowable future disposal limit for the combined set of CIG units.

In order to establish the future inventory limits for each CIG unit separately, an allocation factor must be applied to this total (combined) value. This allocation factor is based on the amount of unused trench length currently available within each CIG unit. Each CIG unit contains five 656-ft trenches for a total of 3,280 ft of trenches per unit. For CIG Unit #1, a total of 493.4 ft of trench space has been already used (i.e., 144.3 ft for Segments 123, 97.7 ft for Segment 4, 40.8 ft for Segment 5, 105.6 ft for Segment 6, 59.8 ft for Segment 7, and 45.2 ft for Segment 8), leaving 2,786.6 ft unused. For CIG Unit #2, all 3,280 ft is unused. Given this, the allocation factor required for each CIG unit becomes:

- 45.9% for CIG Unit #1
- 54.1% for CIG Unit #2

The inventory results are scaled down by these factors to arrive at individual CIG unit inventory limits. For CIG Unit #1, which contains existing inventory, its total inventory limit becomes the sum of its existing inventory plus the above allocated amount of future inventory.

From the original SOF approach, maximum well concentrations for each species in time were used to compute exposure limit contributions. Time intervals were established (e.g., first 100 years, next 1,000 years) whereby inventory limits were computed for those time intervals. Within the All-Pathways.exe application this type of analysis remains available; however, a more detailed approach of computing the maximum dose as a function of time is also provided. By way of an example, for the existing CIG inventory the beta-gamma dose as a function of time is shown in Figure 2-54 based on output from the All-Pathways.exe application (based on the time interval 0 to 1,125 years). The total dose and some of its major contributors are provided (i.e., C-14, C-14_K, H-3, I-129, and Tc-99). The total peak dose is 1.82 mrem/yr, occurring at approximately 29 years. By summing up the peak doses from each species, the SOF dose is 2.34 mrem/yr.

For the same time period of interest the LADTAP exposure doses are shown in Figure 2-55. Here the maximum dose is 1.89 mrem/yr, occurring at approximately 350 years with a SOF total dose of 3.03 mrem/yr.

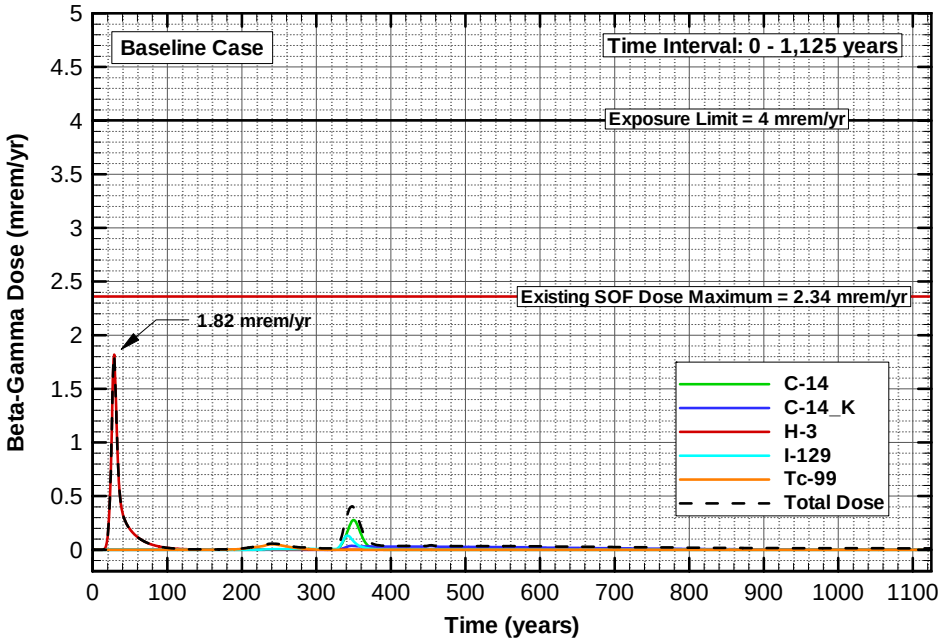

Figure 2-54. Computed beta-gamma exposures (total and major contributors) from the "AllPathways.exe" application for the Existing Segment inventory (0 - 1,125 years)

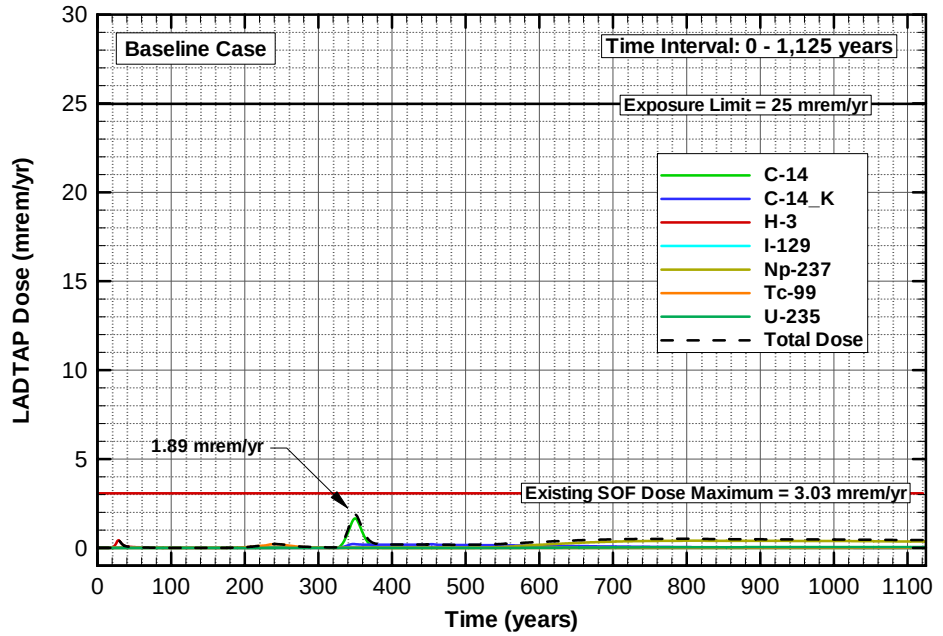

Figure 2-55. Computed LADTAP exposures (total and major contributors) from the "AllPathways.exe" application for the Existing Segment inventory (0 - 1,125 years)

For a longer time period of interest (i.e., 0 to 10,125 years) the LADTAP exposure doses are shown in Figure 2-56. Here the maximum dose is 26.62 mrem/yr, occurring at approximately 7,033 years with a SOF total dose of 30.34 mrem/yr. The main contributor in the later years is Pu-239 buried in Segment 6.

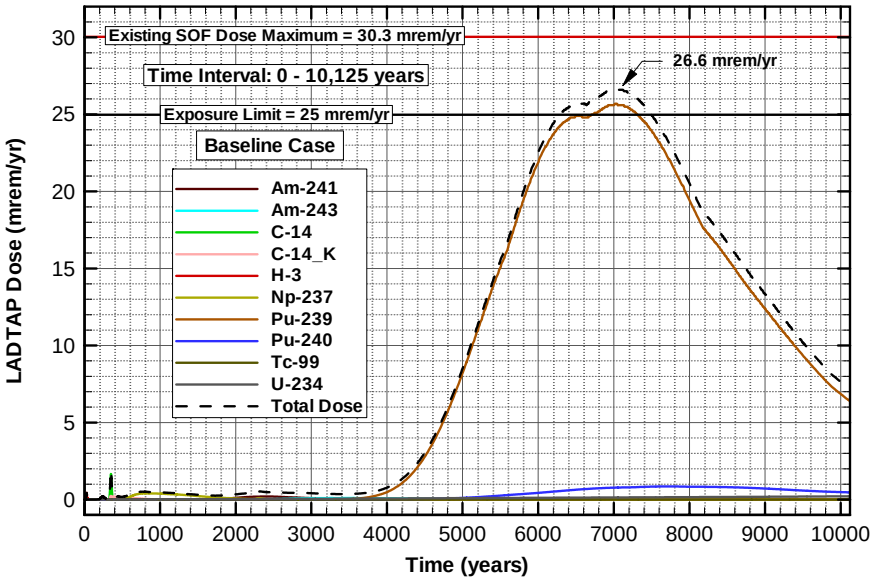

Figure 2-56. Computed LADTAP exposures (total and major contributors) from the "AllPathways.exe" application for the Existing Segment inventory (0 - 10,125 years)

For the Baseline Case the overall inventory limits for beta-gamma exposure (i.e., a total of 4.0 mrem/yr) are listed in Table 2-28 for the 39 potential radionuclide parents of interest. These dose calculations were arrived at using the All-Pathways.exe code for the Existing and Future Segment Contributions, which were then input into the FutureLimits.exe code to estimate the overall future inventory limit values. These are approximate limits since their exposure values were slightly under 4.0 (i.e., typically around 3.99 mrem/yr values). The inventory limits listed are shown for three time periods (0 to 125 yrs, 125 to 1125 yrs, and 1125 to 10125 yrs). For comparison purposes the inventory values in Table 2-28 for Zr-93 are 0.530 Ci in the 125 to 1,125 yr time period and 0.449 Ci for the 1,125 to 10,125 yr time period. These values are very close to the hand calculated values discussed above (0.532 and 0.451 Ci, respectively), providing some degree of verification of the All-Pathways.exe and FutureLimits.exe methodology employed.

Using this All-Pathways.exe and FutureLimits.exe methodology the future total inventory limits for both units combined were computed for beta-gamma, LADTAP, gross alpha, radium, and uranium exposures. For the Baseline Case these total inventory limit values are listed in Table 2-28 through Table 2-32. Note that only those parent chains that contribute to a specified exposure path are listed for each category.

Table 2-28. Baseline Case future total inventory limits[a] (per Ci initially buried) for beta-gamma exposure from radionuclide parents

Parent Buried	0 - 125 year Inventory Limit (Ci)	125 - 1,125 year Inventory Limit (Ci)	1,125 - 10,125 year Inventory Limit (Ci)
Am-241	---	2.20E+04	3.22E+04
Am-243	---	4.19E+05	7.68E+00
C-14	9.56E+09	9.91E-01	---
C-14_K	1.25E+11	1.00E+01	5.98E+02
Cl-36	2.15E+05	2.90E-01	---
Cm-244	---	---	2.00E+11
Cm-245	---	1.64E+04	1.62E+01
Cm-247	---	3.14E+06	2.59E+01
Cm-248	---	9.66E+12	4.16E+06
H-3	4.75E+06	3.12E+06	---
I-129	8.79E+04	2.83E-04	---
I-129_C	1.13E+07	1.79E-02	3.16E-02
I-129_K	6.98E+07	1.10E-01	1.81E-01
K-40	---	1.32E+08	9.23E+00
Mo-93	1.49E+03	8.21E-01	1.06E+18
Nb-94	1.19E+19	1.93E+01	1.23E+00
Ni-59	---	1.69E+01	3.47E+00
Np-237	---	4.74E+00	5.48E+00
Pd-107	---	2.04E+03	4.14E+02
Pu-238	---	7.41E+06	3.75E+05
Pu-239	---	1.10E+07	2.34E+06
Pu-240	---	---	5.51E+08
Pu-241	---	6.59E+05	9.79E+05
Pu-242	---	6.40E+13	7.51E+07
Pu-244	---	---	6.91E+01
Ra-226	---	3.26E+00	4.22E+00
Se-79	---	---	9.30E+03
Sn-126	---	---	---
Sr-90	---	3.15E+04	1.34E+11
Tc-99	7.14E+03	9.41E-01	---
Tc-99_K	1.25E+07	2.81E+01	3.69E+01
Th-230	---	9.16E+00	9.05E+00
Th-232	---	2.03E+08	3.42E-01
U-233	---	---	3.56E+01
U-234	---	2.06E+03	1.33E+02
U-235	---	8.02E+00	8.10E+00
U-236	---	2.88E+15	1.90E+05
U-238	---	2.29E+06	2.54E+02
Zr-93	1.10E+19	5.30E-01	4.49E-01

a – These are future inventory limits that represent disposal limits for both CIG units combined. To arrive at the individual limits on a per unit basis, these values must be multiplied by 0.459 for CIG Unit #1 and 0.541 for CIG Unit #2. Total inventory limit estimates greater than $1x10^{20}$ Ci are not shown.

Table 2-29. Baseline Case future total inventory limits[a] (per Ci initially buried) for LADTAP exposure from radionuclide parents

Parent Buried	0 - 125 year Inventory Limit (Ci)	125 - 1,125 year Inventory Limit (Ci)	1,125 - 10,125 year Inventory Limit [b] (Ci)
Am-241	---	3.36E+02	NA
Am-243	---	7.84E+03	NA
C-14	9.98E+09	1.07E+00	NA
C-14_K	1.30E+11	1.06E+01	NA
Cl-36	1.14E+05	1.58E-01	NA
Cm-244	---	---	NA
Cm-245	---	2.41E+02	NA
Cm-247	---	6.74E+03	NA
Cm-248	---	1.88E+03	NA
H-3	2.19E+08	8.14E+07	NA
I-129	5.32E+06	1.78E-02	NA
I-129_C	6.87E+08	1.08E+00	NA
I-129_K	4.22E+09	6.64E+00	NA
K-40	---	2.87E+08	NA
Mo-93	7.15E+03	3.95E+00	NA
Nb-94	6.77E+18	1.08E+01	NA
Ni-59	---	4.18E+03	NA
Np-237	---	7.22E-02	NA
Pd-107	---	6.39E+03	NA
Pu-238	---	3.44E+05	NA
Pu-239	---	1.05E+06	NA
Pu-240	---	2.61E+18	NA
Pu-241	---	1.01E+04	NA
Pu-242	---	2.77E+12	NA
Pu-244	---	2.20E+18	NA
Ra-226	---	1.62E-01	NA
Se-79	---	---	NA
Sn-126	---	---	NA
Sr-90	---	6.05E+05	NA
Tc-99	1.07E+04	1.42E+00	NA
Tc-99_K	1.87E+07	4.31E+01	NA
Th-230	---	4.58E-01	NA
Th-232	---	5.39E+08	NA
U-233	---	---	NA
U-234	---	9.70E+01	NA
U-235	---	7.85E-01	NA
U-236	---	7.67E+15	NA
U-238	---	1.03E+05	NA
Zr-93	6.58E+19	3.11E+00	NA

a – These are future inventory limits that represent disposal limits for both CIG units combined. To arrive at the individual limits on a per unit basis, these values must be multiplied by 0.459 for CIG Unit #1 and 0.541 for CIG Unit #2. Total inventory limit estimates greater than $1x10^{20}$ Ci are not shown.
b – Existing inventory exceeds LADTAP criterion of 25 mrem/yr for the time range from 1,125 to 10,125 years; therefore, zero future inventory would be allowed.

Table 2-30. Baseline Case future total inventory limits[a] (per Ci initially buried) for Gross Alpha exposure from radionuclide parents

Parent Buried	0 - 125 year Inventory Limit (Ci)	125 - 1,125 year Inventory Limit (Ci)	1,125 - 10,125 year Inventory Limit (Ci)
Am-241	---	1.10E+03	1.19E+01
Am-243	---	2.09E+04	3.77E-01
Cm-244	---	---	3.38E+02
Cm-245	---	7.77E+02	1.82E-01
Cm-247	---	1.70E+04	2.49E-01
Cm-248	---	2.05E+04	3.32E-01
Np-237	---	2.37E-01	2.73E-01
Pu-238	---	8.95E+04	4.06E+03
Pu-239	---	8.29E+06	5.68E-01
Pu-240	---	6.53E+18	9.34E-01
Pu-241	---	3.30E+04	3.48E+02
Pu-242	---	7.19E+11	4.77E-01
Pu-244	---	5.38E+18	3.13E-01
Ra-226	---	4.23E-02	6.17E-02
Th-230	---	1.19E-01	9.38E-02
Th-232	---	2.05E+08	2.97E-01
U-233	---	---	6.45E+00
U-234	---	2.53E+01	1.43E+00
U-235	---	6.19E+00	5.77E+00
U-236	---	2.92E+15	1.65E+05
U-238	---	2.67E+04	1.04E+02

a – These are future inventory limits that represent disposal limits for both CIG units combined. To arrive at the individual limits on a per unit basis, these values must be multiplied by 0.459 for CIG Unit #1 and 0.541 for CIG Unit #2. Total inventory limit estimates greater than $1x10^{20}$ Ci are not shown.

Table 2-31. Baseline Case future total inventory limits[a] (per Ci initially buried) for radium exposure from radionuclide parents

Parent Buried	0 - 125 year Inventory Limit (Ci)	125 - 1,125 year Inventory Limit (Ci)	1,125 - 10,125 year Inventory Limit (Ci)
Cm-244	---	---	2.64E+11
Cm-248	---	---	1.46E+14
Pu-238	---	1.20E+05	6.45E+03
Pu-240	---	---	7.29E+08
Pu-242	---	9.64E+11	3.49E+08
Pu-244	---	---	1.44E+09
Ra-226	---	5.68E-02	8.27E-02
Th-230	---	1.60E-01	1.60E-01
Th-232	---	2.75E+08	4.51E-01
U-234	---	3.39E+01	2.28E+00
U-236	---	3.91E+15	2.51E+05
U-238	---	3.58E+04	1.59E+02

a – These are future inventory limits that represent disposal limits for both CIG units combined. To arrive at the individual limits on a per unit basis, these values must be multiplied by 0.459 for CIG Unit #1 and 0.541 for CIG Unit #2. Total inventory limit estimates greater than $1x10^{20}$ Ci are not shown.

Table 2-32. Baseline Case future total inventory limits[a] (per Ci initially buried) for uranium exposure from radionuclide parents

Parent Buried	0 - 125 year Inventory Limit (Ci)	125 - 1,125 year Inventory Limit (Ci)	1,125 - 10,125 year Inventory Limit (Ci)
Am-241	---	2.84E+12	4.86E+11
Am-243	---	1.17E+16	4.45E+07
Cm-244	---	---	1.12E+09
Cm-245	---	2.14E+12	1.25E+11
Cm-247	---	1.12E+17	3.63E+08
Cm-248	---	---	4.77E+11
Np-237	---	6.49E+08	4.33E+07
Pu-238	---	---	3.47E+08
Pu-239	---	---	2.17E+06
Pu-240	---	---	3.09E+06
Pu-241	---	8.55E+13	1.53E+13
Pu-242	---	---	1.88E+06
Pu-244	---	---	4.61E+06
U-233	---	---	1.95E+05
U-234	---	---	1.24E+05
U-235	---	---	4.19E+01
U-236	---	---	1.25E+03
U-238	---	---	6.51E+00

a – These are future inventory limits that represent disposal limits for both CIG units combined. To arrive at the individual limits on a per unit basis, these values must be multiplied by 0.459 for CIG Unit #1 and 0.541 for CIG Unit #2. Total inventory limit estimates greater than $1x10^{20}$ Ci are not shown.

The future total inventory limit values provided in Table 2-28 represent Baseline values for beta-gamma exposure (i.e., limits derived from the conceptual model using "nominal" parameter settings). In the context of the selected sensitivity cases, these "nominal" inventory limit values are compared to similarly estimated values where some of the parameter settings (or modeling assumptions) are altered in the PORFLOW analyses (i.e., sensitivity studies).

Sensitivity Analysis Case Study A

For case study A, sorption K_d values for all the vadose and aquifer material zones are altered. The Baseline (nominal) case used best estimate values where CDP factors were also applied (i.e., assuming an organic carbon concentration of 95 mg/L). For case study A, the best estimate values are used directly (i.e., no application of CDP factors, such that an organic carbon concentration of 0 mg/L is assumed). All other modeling and parameter settings remain unaltered. For case study A the sorption K_d values employed are listed in Table 2-33 for the non-cementitious materials and in Table 2-34 for the cementitious materials. In both tables the corresponding values employed in the Baseline case are provided for a direct comparison.

In Table 2-33, the CDP factors used in the Baseline case are also provided by element. These factors are based on the assumptions that a pH environment of 5.5 exists with a pore water content of 95 mg/L organic carbon present. A significant variation in CDP factors by element can be seen (i.e., factors ranging from 0.049 up to 1.89). CDP factors are also dependent upon the level of organic carbon present within the groundwater as shown in Figure 2-57 where the CDP factor curves are unique within their element grouping. As illustrated in Figure 2-57 when viewing Baseline versus Case A CDP factors:

- First group of elements (i.e., Cl, H, and Nb) are independent of aqueous CDP levels.
- Next 3 groups of elements (i.e., [Ni, Pb, Sn, Pd], [Np, Pa, K], and [U, Sr, Ra]) have higher K_d values under Baseline settings than under Case A (and are shown as solid lines).
- Next 3 groups of elements (i.e., [Ac, Am, Cm], [Pu, Th], and [Zr]) have lower K_d values under Baseline settings than under Case A (and are shown as dashed lines).

Table 2-33. List of best estimate sorption K_d values with and without CDP applied for the non-cementitious materials[a]

Case	Case A	Case A	-	Nominal	Nominal
Element	Sand Material Best Estimate K_d (ml/g)	Clay Material Best Estimate K_d (ml/g)	CDP factor[b] (-)	Sand Material Best Estimate K_d with CDP (ml/g)	Clay Material Best Estimate K_d with CDP (ml/g)
Ac	1100	8500	0.049	53.9	416.5
Am	1100	8500	0.049	53.9	416.5
C	0	0	0.5	0	0
Cl	0	0	1	0	0
Cm	1100	8500	0.049	53.9	416.5
H	0	0	1.0	0	0
I	0	0.6	0.5	0	0.3
K	50	250	1.66	83	415
Mo	0	0	0.5	0	0
Nb	0	0	1	0	0
Ni	7	30	1.41	9.87	42.3
Np	0.6	35	1.66	0.996	58.1
Pa	0.6	35	1.66	0.996	58.1
Pb	2000	5000	1.41	2820	7050
Pd	7	30	1.41	9.87	42.3
Pu	270	5900	0.51	137.7	3009
Ra	5	17	1.89	9.45	32.13
Se	1000	1000	0.5	500	500
Sn	2000	5000	1.41	2820	7050
Sr	5	17	1.89	9.45	32.13
Tc	0.1	0.2	0.5	0.05	0.1
Th	900	2000	0.51	459	1020
U	200	300	1.89	378	567
Zr	900	2000	0.08	72	160
C-14_K	NA[c]	NA	1	NA	NA
I-129_C	NA	NA	1	NA	NA
I-129_K	NA	NA	1	NA	NA
Tc-99_K	NA	NA	1	NA	NA

a – For sand LVZ and Aquifer zones. For clay UVZ, Backfill, Cap Sides, and Cap Center zones.
b – The CDP factors employed assume a pH of 5.5 environment with a 95 mg/L organic carbon present.
c - NA – Not Applicable; special wasteforms only exist in the waste zone, where they do not contact non-cementitious materials

Table 2-34. List of best estimate sorption K_d values with and without CDP applied for the cementitious materials[a] in an oxidizing environment

Case	Case A	Case A	Case A	Nominal	Nominal	Nominal
Element	"Young" Best Est. K_d (ml/g)	"Middle" Best Est. K_d (ml/g)	"Old" Best Estimate K_d (ml/g)	"Young" Best Est. K_d with CDP (ml/g)	"Middle" Best Est. K_d with CDP (ml/g)	"Old" Best Est. K_d with CDP (ml/g)
Ac	5000	5000	500	245	245	24.5
Am	5000	5000	500	245	245	24.5
C	20	10	0	10	5	0
Cl	0.8	2	0	0.8	2	0
Cm	5000	5000	500	245	245	24.5
H	0	0	0	0	0	0
I	8	20	0	4	10	0
K	2	4	2	3.32	6.64	3.32
Mo	0	0	0	0	0	0
Nb	1000	1000	500	1000	1000	500
Ni	1000	1000	500	1410	1410	705
Np	2000	2000	200	3320	3320	332
Pa	2000	2000	200	3320	3320	332
Pb	500	500	250	705	705	352.5
Pd	1000	1000	500	1410	1410	705
Pu	5000	5000	500	2550	2550	255
Ra	100	100	70	189	189	132.3
Se	300	300	150	150	150	75
Sn	4000	4000	2000	5640	5640	2820
Sr	1	1	0.8	1.89	1.89	1.51
Tc	0	0	0	0	0	0
Th	5000	5000	500	2550	2550	255
U	1000	1000	70	1890	1890	132.3
Zr	5000	5000	500	400	400	40
C-14_K [b]	140	140	140	140	140	140
I-129_C [b]	600	600	600	600	600	600
I-129_K [b]	3700	3700	3700	3700	3700	3700
Tc-99_K [b]	810	810	810	810	810	810

a – For Grout, Waste, CLSM, and Concrete Slab zones
b – Special wasteforms are characterized by K_d values fixed at their lowest values over the exposed pH range.

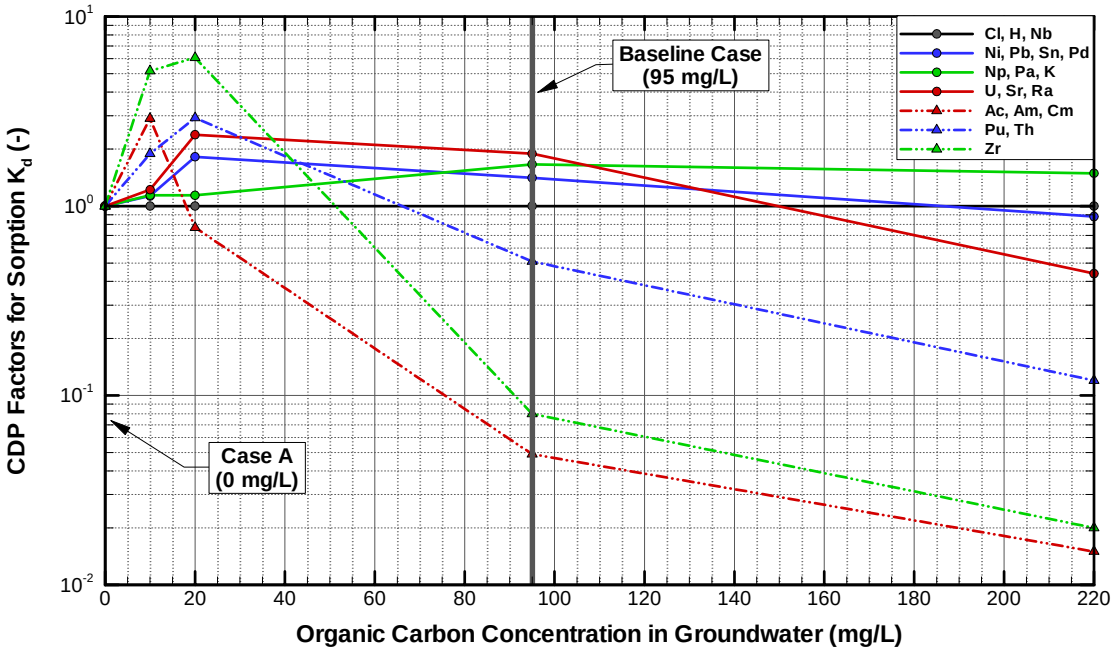

Figure 2-57. CDP Factors for sorption K_d values versus groundwater concentration of organic carbon by element group

For the four special wasteforms (i.e., C-14_K, I-129_C, I-129_K, and Tc-99_K) their K_d values have been fixed to their lowest recorded values over their available pH database range (Table 2-34). Here the chosen K_d values represent their lowest available value over the entire expected pH exposure range.

The following summary of results is for the Case A sensitivity study. Peak well concentrations for Existing and Future Segments are provided in Table 2-35 and Table 2-36, respectively. The total future inventory limits for beta-gamma exposure (i.e., a total of 4.0 mrem/yr) are listed in Table 2-37 and comparison ratios (inventory limit for Case A versus Baseline) are listed in Table 2-38. The shaded values shown in Table 2-38 indicate ratios less than unity.

Table 2-35. Case A maximum concentrations (in terms of pCi/L) of the radionuclide parent and progeny resulting from the existing 8 segments within the 100-m compliance zone[a]

Parent	Daughters	Time of Peak (0-1125 yrs)	Peak Concentration (pCi/L)	Time of Ultimate Peak (1125+ yrs)	Ultimate Peak Concentration (pCi/L)
Am-241		1,125	7.32E-79	18,708	2.09E-20
	Np-237	806	7.79E-04		
	U-233	1,125	7.30E-09	9,713	2.78E-07
	Th-229	1,125	4.41E-11	12,708	2.22E-08
Am-243		1,125	3.15E-83	50,025	8.22E-06
	Pu-239	1,125	8.54E-53	20,308	5.58E-04
	U-235	1,125	2.34E-49	20,008	1.20E-08
	Pa-231	1,125	1.67E-11	16,008	1.65E-09
	Ac-227	1,125	1.21E-14	16,008	1.26E-12
C-14		355	9.62E+01		
C-14_K		454	2.10E+01		
Cm-244		1,125	4.66E-102	1,873	6.49E-97
	Pu-240	1,125	1.01E-52	14,508	7.35E-04
	U-236	1,125	2.30E-48	14,208	1.06E-06
	Th-232	1,125	4.86E-58	26,308	1.14E-13
	Ra-228	1,125	8.81E-23	25,808	1.93E-11
Cm-245		1,125	1.32E-85	50,025	3.13E-07
	Pu-241	1,125	9.67E-67	50,025	1.29E-06
	Am-241	1,125	2.01E-68	50,025	3.33E-07
	Np-237	1,125	2.87E-07	2,303	4.40E-07
	U-233	1,125	1.93E-12	12,708	1.02E-10
	Th-229	1,125	8.99E-15	18,108	1.17E-11
Cm-247		1,125	5.24E-89	50,025	1.07E-04
	Am-243	1,125	5.52E-90	50,025	1.06E-04
	Pu-239	1,125	4.27E-59	50,025	1.66E-04
	U-235	1,125	1.28E-56	35,108	1.97E-09
	Pa-231	1,125	6.23E-14	27,508	2.32E-10
	Ac-227	1,125	4.34E-17	27,608	1.78E-13
Cm-248		1,125	5.23E-89	50,025	9.69E-05
	Pu-244	1,125	5.26E-61	33,908	5.93E-08
	Pu-240	1,125	4.94E-62	29,608	4.59E-08
	U-236	1,125	1.19E-58	25,908	1.45E-11
	Th-232	1,125	2.43E-68	40,108	2.60E-18
	Ra-228	1,125	7.71E-31	39,408	4.20E-16
H-3		29	9.11E+03		
I-129		343	2.18E-02		
I-129_K		454	1.36E-03		
Ni-59		1,125	4.26E-02	2,573	4.94E-02
Np-237		702	1.27E-01		
	U-233	1,125	1.12E-06	9,623	5.86E-05
	Th-229	1,125	7.47E-09	13,508	4.49E-06
Pd-107		1,125	2.23E-04	1,493	2.85E-04
Pu-238		1,125	2.05E-49	4,583	6.40E-24
	U-234	1,125	1.28E-38	9,993	8.96E-04
	Th-230	1,125	4.64E-43	18,508	1.13E-05
	Ra-226	1,125	1.26E-05	13,108	1.82E-04
	Pb-210	1,125	3.14E-08	13,208	4.74E-07

Table 2-35. Case A maximum concentrations (in terms of pCi/L) of the radionuclide parent and progeny resulting from the existing 8 segments within the 100-m compliance zonea - continued

Parent	Daughters	Time of Peak (0-1125 yrs)	Peak Concentration (pCi/L)	Time of Ultimate Peak (1125+ yrs)	Ultimate Peak Concentration (pCi/L)
Pu-239		1,125	7.29E-45	13,308	2.26E+00
	U-235	1,125	4.97E-41	11,708	4.03E-05
	Pa-231	1,125	5.76E-07	8,993	3.48E-06
	Ac-227	1,125	4.33E-10	9,013	2.66E-09
Pu-240		1,125	2.25E-47	14,408	4.32E-02
	U-236	1,125	4.96E-42	13,508	5.66E-05
	Th-232	1,125	9.53E-52	22,708	5.48E-12
	Ra-228	1,125	1.11E-19	22,208	9.26E-10
Pu-241		1,125	1.20E-68	1,583	6.84E-66
	Am-241	1,125	3.70E-70	18,708	1.53E-20
	Np-237	806	5.21E-04		
	U-233	1,125	4.88E-09	9,693	1.84E-07
	Th-229	1,125	2.94E-11	12,608	1.46E-08
Pu-242		1,125	2.48E-51	14,908	3.66E-04
	U-238	1,125	2.58E-48	13,308	9.29E-10
	U-234	1,125	7.17E-51	13,008	1.65E-11
	Th-230	1,125	2.53E-55	19,108	2.20E-13
	Ra-226	1,125	4.88E-16	16,308	1.50E-12
	Pb-210	1,125	1.14E-18	16,408	3.91E-15
Se-79		1,125	1.80E-74	50,025	1.07E-03
Sn-126		1,125	1.72E-99	118,808	1.47E-05
Sr-90		481	2.41E-02		
Tc-99		251	1.02E+01		
Tc-99_K		388	4.64E-01		
U-233		1,125	1.35E-35	11,208	2.72E+00
	Th-229	1,125	5.03E-39	17,008	2.26E-01
U-234		1,125	2.64E-35	9,143	8.21E-01
	Th-230	1,125	9.60E-40	14,608	8.24E-03
	Ra-226	1,125	1.14E-02	10,665	1.10E-01
	Pb-210	1,125	2.88E-05	10,739	2.87E-04
U-235		1,125	7.16E-37	9,123	2.24E-02
	Pa-231	773	3.74E-03		
	Ac-227	807	2.84E-06		
U-236		1,125	2.13E-37	9,613	9.68E-03
	Th-232	1,125	4.15E-47	20,008	6.10E-10
	Ra-228	1,125	9.44E-16	19,308	1.05E-07
U-238		1,125	1.23E-34	8,863	3.73E+00
	U-234	1,125	4.07E-37	9,343	9.54E-02
	Th-230	1,125	1.46E-41	13,208	8.43E-04
	Ra-226	1,125	6.22E-05	10,910	6.28E-03
	Pb-210	1,125	1.52E-07	11,008	1.64E-05
Zr-93		1,125	4.92E-83	49,608	2.39E-03
	Nb-93m	1,125	4.89E-01	43,608	2.22E+00

[a]maximum based on first 1,000 years and its ultimate peak if beyond 1,000 years

Table 2-36. Case A maximum concentrations (pCi/L per Ci of parent buried) of the radionuclide parent and progeny resulting from all future inventories within the 100-m compliance zone

Parent	Daughters	Time of Peak (0-1125 yrs)	Peak Concentration (pCi/L-Ci$_{parent}$)	Time of Ultimate Peak (1125+ yrs)	Ultimate Peak Concentration (pCi/L-Ci$_{parent}$)
Am-241		1,125	3.45E-57	15,008	3.08E-16
	Np-237	803	1.50E-02		
	U-233	1,125	1.41E-07	8,773	5.13E-06
	Th-229	1,125	8.60E-10	11,808	4.18E-07
Am-243		1,125	2.00E-56	35,808	5.19E-02
	Pu-239	1,125	8.68E-33	15,408	8.88E-01
	U-235	1,125	1.37E-31	14,308	1.21E-05
	Pa-231	1,125	2.13E-08	11,508	1.15E-06
	Ac-227	1,125	1.54E-11	11,508	8.76E-10
C-14		365	1.65E+03		
C-14_K		451	2.18E+02		
Cl-36		335	2.31E+03		
Cm-244		1,125	2.18E-75	1,553	1.68E-73
	Pu-240	1,125	1.54E-33	11,108	6.75E-03
	U-236	1,125	1.72E-30	10,481	5.55E-06
	Th-232	1,125	4.38E-40	18,208	4.52E-13
	Ra-228	1,125	7.88E-19	17,708	7.57E-11
Cm-245		1,125	2.03E-56	36,408	8.16E-02
	Pu-241	1,125	1.05E-43	36,408	3.35E-01
	Am-241	1,125	3.33E-45	36,408	8.65E-02
	Np-237	1,125	1.75E-02	2,133	3.13E-02
	U-233	1,125	1.22E-07	9,233	6.70E-06
	Th-229	1,125	5.85E-10	13,108	6.18E-07
Cm-247		1,125	2.23E-56	46,808	2.21E+00
	Am-243	1,125	2.32E-57	46,908	2.18E+00
	Pu-239	1,125	2.09E-34	35,608	1.78E+00
	U-235	1,125	1.87E-33	25,608	1.29E-05
	Pa-231	1,125	6.90E-10	22,908	1.08E-06
	Ac-227	1,125	4.81E-13	23,008	8.24E-10
Cm-248		1,125	2.23E-56	46,608	2.02E+00
	Pu-244	1,125	2.51E-36	25,908	6.35E-04
	Pu-240	1,125	2.30E-37	20,408	3.93E-04
	U-236	1,125	1.74E-35	18,108	7.97E-08
	Th-232	1,125	4.40E-45	32,608	1.11E-14
	Ra-228	1,125	1.89E-23	32,008	1.77E-12
H-3		205	6.39E-03		
I-129		345	2.23E+03		
I-129_C		451	7.19E+01		
I-129_K		451	1.17E+01		
K-40		1,125	1.56E-01	2,113	5.29E+01
Mo-93		236	9.69E+02		
	Nb-93m	236	9.61E+02		
Nb-94		800	3.96E+01	2,093	6.24E+02
Ni-59		1,125	3.81E+01	2,393	5.68E+01
Np-237		694	1.05E+02		
	U-233	1,125	9.36E-04	8,163	4.75E-02
	Th-229	1,125	6.35E-06	11,708	3.81E-03

Table 2-36. Case A maximum concentrations (pCi/L per Ci of parent buried) of the radionuclide parent and progeny resulting from all future inventories within the 100-m compliance zone – continued

Parent	Daughters	Time of Peak (0-1125 yrs)	Peak Concentration (pCi/L-Ci$_{parent}$)	Time of Ultimate Peak (1125+ yrs)	Ultimate Peak Concentration (pCi/L-Ci$_{parent}$)
Nb-94		800	3.96E+01	2,093	6.24E+02
Pd-107		1,125	3.85E+01	2,393	5.80E+01
Pu-238		1,125	6.66E-35	3,723	1.30E-19
	U-234	1,125	1.87E-26	8,063	4.62E-03
	Th-230	1,125	8.91E-31	14,908	5.26E-05
	Ra-226	1,125	6.31E-05	10,739	6.74E-04
	Pb-210	1,125	1.58E-07	10,739	1.76E-06
Pu-239		1,125	6.08E-31	11,508	5.81E+00
	U-235	1,125	2.25E-29	11,208	9.69E-05
	Pa-231	1,125	1.53E-06	8,473	8.67E-06
	Ac-227	1,125	1.15E-09	8,503	6.63E-09
Pu-240		1,125	5.56E-31	11,108	2.44E+00
	U-236	1,125	6.66E-28	10,481	2.01E-03
	Th-232	1,125	1.69E-37	18,208	1.64E-10
	Ra-228	1,125	2.99E-16	17,708	2.75E-08
Pu-241		1,125	7.31E-55	1,305	2.35E-54
	Am-241	1,125	4.54E-56	15,008	1.05E-17
	Np-237	804	4.89E-04		
	U-233	1,125	4.61E-09	8,783	1.65E-07
	Th-229	1,125	2.80E-11	11,808	1.34E-08
Pu-242		1,125	6.28E-31	12,308	7.95E+00
	U-238	1,125	3.56E-30	11,408	1.77E-05
	U-234	1,125	9.50E-33	11,308	2.73E-07
	Th-230	1,125	4.41E-37	19,408	3.35E-09
	Ra-226	1,125	1.22E-11	16,608	2.29E-08
	Pb-210	1,125	2.88E-14	16,608	5.96E-11
Pu-244		1,125	6.29E-31	12,308	8.13E+00
	Pu-240	1,125	7.28E-32	12,608	5.95E+00
	U-236	1,125	1.51E-29	12,308	1.57E-03
	Th-232	1,125	3.84E-39	18,908	1.24E-10
	Ra-228	1,125	1.03E-17	18,508	2.00E-08
Ra-226		673	1.79E+02		
	Pb-210	704	4.46E-01		
Se-79		1,125	8.86E-51	38,408	2.40E+00
Sn-126		1,125	1.93E-68	84,808	9.55E-01
Sr-90		463	7.16E-03		
Tc-99		258	8.41E+02		
Tc-99_K		384	2.91E+01		
Th-230		1,125	1.08E-52	35,508	2.06E+00
	Ra-226	724	4.10E+01		
	Pb-210	760	1.04E-01		
Th-232		1,125	1.09E-52	38,208	2.87E+00
	Ra-228	1,057	7.94E-05	36,908	4.87E+02
U-233		1,125	5.47E-23	8,053	1.28E+01
	Th-229	1,125	2.67E-26	11,708	1.01E+00
U-234		1,125	5.48E-23	8,053	1.29E+01
	Th-230	1,125	2.61E-27	14,908	1.47E-01
	Ra-226	1,125	2.06E-01	10,665	1.91E+00
	Pb-210	1,125	5.20E-04	10,739	4.99E-03

Table 2-36. Case A maximum concentrations (pCi/L per Ci of parent buried) of the radionuclide parent and progeny resulting from all future inventories within the 100-m compliance zone – continued

Parent	Daughters	Time of Peak (0-1125 yrs)	Peak Concentration (pCi/L-Ci$_{parent}$)	Time of Ultimate Peak (1125+ yrs)	Ultimate Peak Concentration (pCi/L-Ci$_{parent}$)
U-235		1,125	5.50E-23	8,063	1.32E+01
	Pa-231	771	2.54E+00		
	Ac-227	805	1.93E-03		
U-236		1,125	5.50E-23	8,063	1.32E+01
	Th-232	1,125	1.41E-32	19,008	8.72E-07
	Ra-228	1,125	1.79E-11	18,208	1.49E-04
U-238		1,125	5.50E-23	8,063	1.32E+01
	U-234	1,125	1.80E-25	9,183	3.26E-01
	Th-230	1,125	8.41E-30	13,708	3.36E-03
	Ra-226	1,125	2.62E-04	13,108	2.54E-02
	Pb-210	1,125	6.39E-07	13,108	6.62E-05
Zr-93		1,125	1.09E-52	38,208	2.82E+00
	Nb-93m	1,125	5.73E+02	26,808	2.16E+03

[a]maximum based on first 1,000 years and its ultimate peak if beyond 1,000 years

Table 2-37. Case A future total inventory limits[a] (Ci initially buried) for beta-gamma exposure from radionuclide parents

Parent Buried	0 - 125 year Inventory Limit (Ci)	125 - 1,125 year Inventory Limit (Ci)	1,125 - 10,125 year Inventory Limit (Ci)
Am-241	---	2.00E+04	2.83E+04
Am-243	---	2.56E+10	2.49E+08
C-14	2.49E+11	1.14E+00	---
C-14_K	1.68E+12	8.74E+00	5.88E+02
Cl-36	2.15E+05	2.97E-01	---
Cm-244	---	4.67E+18	1.01E+11
Cm-245	---	1.72E+04	9.59E+03
Cm-247	---	8.19E+11	8.37E+08
Cm-248	---	---	7.40E+06
H-3	4.75E+06	3.13E+06	---
I-129	1.78E+06	4.21E-04	---
I-129_C	1.22E+08	1.37E-02	3.17E-02
I-129_K	7.52E+08	8.43E-02	1.81E-01
K-40	---	1.89E+03	5.57E+00
Mo-93	1.49E+03	8.25E-01	1.06E+18
Nb-94	1.19E+19	1.93E+01	1.23E+00
Ni-59	---	7.85E+00	5.27E+00
Np-237	---	2.83E+00	6.45E+00
Pd-107	---	9.49E+02	6.30E+02
Pu-238	---	5.99E+06	5.36E+05
Pu-239	---	3.43E+08	2.61E+07
Pu-240	---	1.23E+16	2.77E+08
Pu-241	---	6.13E+05	8.53E+05
Pu-242	---	3.28E+13	2.41E+07
Pu-244	---	3.58E+17	1.95E+02
Ra-226	---	2.13E+00	7.71E+01
Se-79	---	---	3.96E+10
Sn-126	---	---	---
Sr-90	---	9.74E+02	1.34E+13
Tc-99	2.94E+04	1.06E+00	---
Tc-99_K	5.13E+07	2.88E+01	3.69E+01
Th-230	---	9.13E+00	1.41E+01
Th-232	---	4.63E+04	4.92E+01
U-233	---	---	1.51E+01
U-234	---	1.83E+03	1.89E+02
U-235	---	2.04E+02	1.88E+02
U-236	---	2.05E+11	3.15E+04
U-238	---	1.48E+06	2.99E+01
Zr-93	---	1.74E+00	4.93E-01

a – These are future inventory limits that represent disposal limits for both CIG units combined. To arrive at the individual limits on a per unit basis, these values must be multiplied by 0.459 for CIG Unit #1 and 0.541 for CIG Unit #2. Total inventory limit estimates greater than $1x10^{20}$ pCi/L are not shown.

Table 2-38. Case A versus Baseline total future inventory limit ratios[a] for beta-gamma exposure from radionuclide parents (values less than one are shaded)

Parent Buried	0 - 125 year Inventory Limit Ratio (-)	125 - 1,125 year Inventory Limit Ratio (-)	1,125 - 10,125 year Inventory Limit Ratio (-)
Am-241	1	9.12E-01	8.80E-01
Am-243	1	6.11E+04	3.25E+07
C-14	2.60E+01	1.15E+00	1
C-14_K	1.34E+01	8.71E-01	9.84E-01
Cl-36	1	1.03E+00	1
Cm-244	1	4.67E-02	5.05E-01
Cm-245	1	1.05E+00	5.93E+02
Cm-247	1	2.61E+05	3.24E+07
Cm-248	1	1.03E+07	1.78E+00
H-3	1	1	1
I-129	2.03E+01	1.48E+00	1
I-129_C	1.08E+01	7.69E-01	1
I-129_K	1.08E+01	7.69E-01	1
K-40	1	1.42E-05	6.03E-01
Mo-93	1	1	1
Nb-94	1	1	1
Ni-59	1	4.64E-01	1.52E+00
Np-237	1	5.98E-01	1.18E+00
Pd-107	1	4.64E-01	1.52E+00
Pu-238	1	8.08E-01	1.43E+00
Pu-239	1	3.11E+01	1.11E+01
Pu-240	1	1.23E-04	5.02E-01
Pu-241	1	9.29E-01	8.71E-01
Pu-242	1	5.13E-01	3.21E-01
Pu-244	1	3.58E-03	2.82E+00
Ra-226	1	6.52E-01	1.83E+01
Se-79	1	1	4.25E+06
Sn-126	1	1	1
Sr-90	1	3.10E-02	9.99E+01
Tc-99	4.12E+00	1.12E+00	1
Tc-99_K	4.12E+00	1.03E+00	1
Th-230	1	9.97E-01	1.56E+00
Th-232	1	2.29E-04	1.44E+02
U-233	1	1	4.23E-01
U-234	1	8.86E-01	1.43E+00
U-235	1	2.54E+01	2.32E+01
U-236	1	7.12E-05	1.66E-01
U-238	1	6.49E-01	1.17E-01
Zr-93	9.07E+00	3.28E+00	1.10E+00

a - Inventory limit ratios that are nearly unity (i.e., no change) are shown as 1.

As highlighted in Table 2-38 by shading, various parent radionuclide inventory limits are reduced as a result of removing the CDP factors. Some have significant reduction factors. For example, the limit ratio for radionuclide K-40 is 1.42×10^{-5} for the time period 125 to 1,125 years, but its only 6.03×10^{-1} for the time period beyond 1,125 years. As shown in Table 2-33, the cementitious material K_d values for K-40 are decreased (i.e., $f_{CDP} = 1.66$) when going from the Baseline Case to Case A. This ~66% change in K_d values resulted in a significant decrease in inventory limit for one time period and a modest amount within another period. This can be easily understood when looking at the maximum well concentration curves for both cases and noting that for K-40 there is no decay chain. As shown in Figure 2-58, the maximum concentrations for the 125 to 1,125-year period occur at the end of the time period, at which point a 10^5 ratio in concentration values occurs. For the 1,125 to 10,125-year time period both cases exhibit their ultimate peaks in maximum well concentrations and the ratio is on the order of 2. The significant impact to inventory limit for the 125 to 1,125-year period occurs due to the steep rise occurring up to the ultimate peaks.

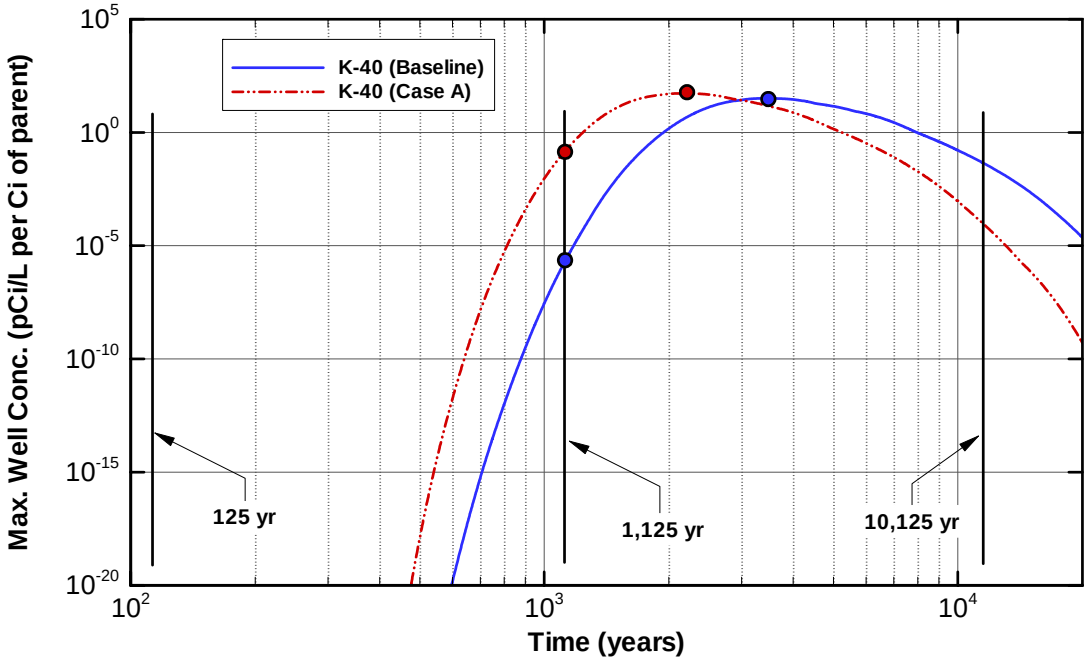

Figure 2-58. Baseline versus Case A comparison of maximum well concentrations within the 100-m compliance region for K-40 (based on a Future Segment inventory of 1.0 Ci)

For the various wasteforms of I-129 (i.e., I-129, I-129_C, and I-129_K), the maximum well concentration curves for Case A are compared to Baseline results in Figure 2-59. The K_d values for I-129 increase from the Baseline Case to Case A (i.e., $f_{CDP} = 0.5$). Throughout the simulations the K_d values for the special wasteforms I-129_C and I-129_K remain fixed (both are ion exchange resins). I-129 nuclide has no decay chain and, for the three wasteforms, its peak concentration values are reduced when going from the Baseline Case to Case A. Migration of I-129 outside of the special wasteforms is more retarded under Case A K_d values. For I-129_C and I-129_K their peak values occur near 451 years where a step reduction in infiltration rate occurs. This short-lived spiking can be seen in Figure 2-59. Further refinement of the infiltration-rate-based steady-state flow fields would result in a slight reduction in their peak values (i.e., and a corresponding increase in their inventory limits); however, since this results in a slight conservatism no refinement in flow fields is addressed within this PA effort.

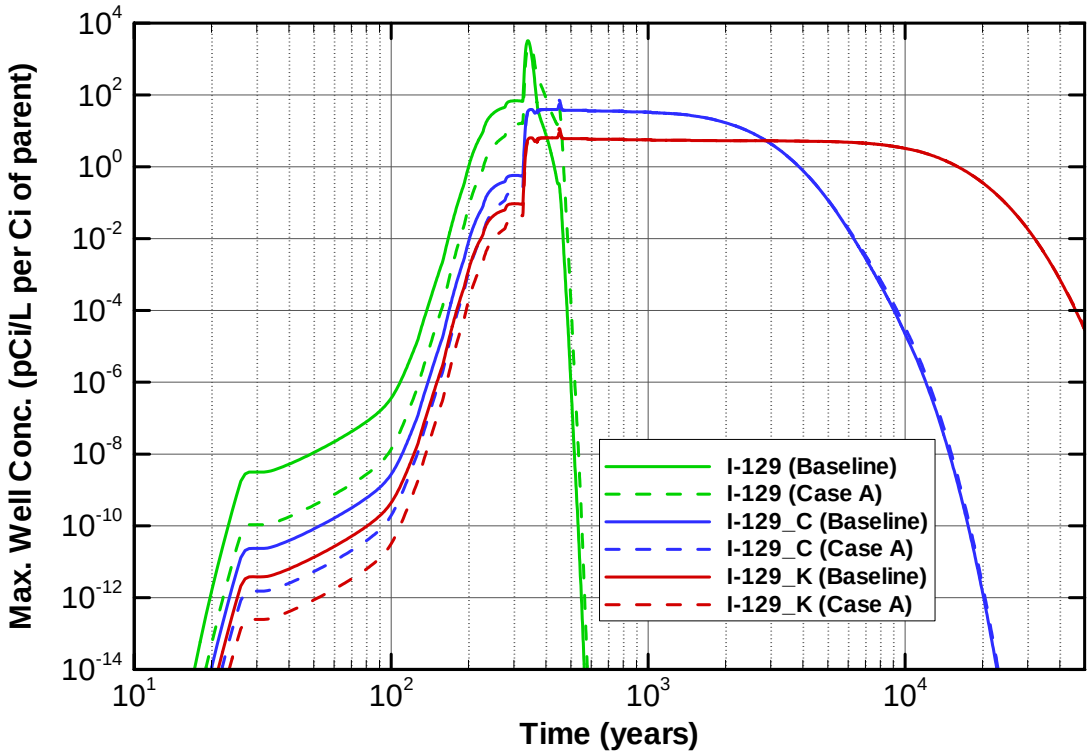

Figure 2-59. Baseline versus Case A comparison of maximum well concentrations within the 100-m compliance region for I-129, I-129_C, and I-129_K (based on a Future Segment inventory of 1.0 Ci)

Sensitivity Analysis Case Study B

For case study B, sorption K_d values for all the vadose and aquifer material zones are altered. The Baseline (nominal) case used best estimate values (considered to be median values that correspond to their 50% expectation values) with CDP factors applied. Generally, inventory limits are reduced when sorption K_d values are lowered. The sorption K_d values are assumed to be random variables, distributed log-normally. Conservative estimates of K_d (at a 97.5% expectation value; close to a 2-sigma level) for all elements are used in Case B, with the CDP factors applied prior to estimating the conservative estimates. Specifically, for each element, its median K_d value was first multiplied by its appropriate CDP factor (i.e., $f_{CDP}*K_d$) and then its conservative value was computed from this product using the following logic:

- If the product ($f_{CDP}*K_d$) is less than 1000 ml/g, then divide product by 1.4.
- If the product ($f_{CDP}*K_d$) is greater than or equal to 1000 ml/g, then divide product by 3.4.

All other modeling and parameter settings remain unaltered. For case study B the sorption K_d values employed are listed in Table 2-39 for the non-cementitious materials and in Table 2-40 for the cementitious materials. In both tables the corresponding values employed in the Baseline case are provided for a direct comparison. As stated in the Case A sensitivity discussion, special wasteforms are characterized by K_d values that are their lowest value over their available database pH range.

Table 2-39. Best estimate sorption K_d values with CDP applied and conservative estimate values with CDP applied for the non-cementitious materials[a]

Case	Case B	Case B	-	Nominal	Nominal
Element	Sand Material Conservative Estimate K_d with CDP (ml/g)	Clay Material Conservative Estimate K_d with CDP (ml/g)	CDP factor[b] (-)	Sand Material Best Estimate K_d with CDP (ml/g)	Clay Material Best Estimate K_d with CDP (ml/g)
Ac	38.5	297.5	0.049	53.9	416.5
Am	38.5	297.5	0.049	53.9	416.5
C	0	0	0.5	0	0
Cl	0	0	1	0	0
Cm	38.5	297.5	0.049	53.9	416.5
H	0	0	1.0	0	0
I	0	0.21	0.5	0	0.3
K	59.29	296.43	1.66	83	415
Mo	0	0	0.5	0	0
Nb	0	0	1	0	0
Ni	7.05	30.21	1.41	9.87	42.3
Np	0.71	41.50	1.66	0.996	58.1
Pa	0.71	41.50	1.66	0.996	58.1
Pb	829.39	2073.48	1.41	2820	7050
Pd	7.05	30.21	1.41	9.87	42.3
Pu	98.36	884.98	0.51	137.7	3009
Ra	6.75	22.95	1.89	9.45	32.13
Se	357.14	357.14	0.5	500	500
Sn	829.39	2073.48	1.41	2820	7050
Sr	6.75	22.95	1.89	9.45	32.13
Tc	0.04	0.07	0.5	0.05	0.1
Th	327.86	299.99	0.51	459	1020
U	270	405	1.89	378	567
Zr	51.43	114.28	0.08	72	160
C-14_K	NA[c]	NA	1	NA	NA
I-129_C	NA	NA	1	NA	NA
I-129_K	NA	NA	1	NA	NA
Tc-99_K	NA	NA	1	NA	NA

a – For sand LVZ and Aquifer zones. For clay UVZ, Backfill, Cap Sides, and Cap Center zones.
b – The CDP factors employed assume a pH of 5.5 environment with a 95 mg/L organic carbon present.
c - NA – Not Applicable; special wasteforms only exist in the waste zone, where they do not contact non-cementitious materials

Table 2-40. Best estimate sorption K_d values with CDP applied and conservative estimate values with CDP applied for the cementitious materials[a] in an oxidizing environment

Case	Case B	Case B	Case B	Nominal	Nominal	Nominal
Element	"Young" Conservative Estimate K_d with CDP (ml/g)	"Middle" Conservative Estimate K_d with CDP (ml/g)	"Old" Conservative Estimate K_d with CDP (ml/g)	"Young" Best Estimate K_d with CDP (ml/g)	"Middle" Best Estimate K_d with CDP (ml/g)	"Old" Best Estimate K_d with CDP (ml/g)
Ac	175	175	17.5	245	245	24.5
Am	175	175	17.5	245	245	24.5
C	7.14	3.57	0	10	5	0
Cl	0.57	1.43	0	0.8	2	0
Cm	175	175	17.5	245	245	24.5
H	0	0	0	0	0	0
I	2.86	7.14	0	4	10	0
K	2.37	4.74	2.37	3.32	6.64	3.32
Mo	0	0	0	0	0	0
Nb	294.11	294.11	357.14	1000	1000	500
Ni	414.7	414.7	503.57	1410	1410	705
Np	976.45	976.45	237.14	3320	3320	332
Pa	976.45	976.45	237.14	3320	3320	332
Pb	503.57	503.57	251.78	705	705	352.5
Pd	414.7	414.7	503.57	1410	1410	705
Pu	749.98	749.98	182.14	2550	2550	255
Ra	135	135	94.5	189	189	132.3
Se	107.14	107.14	53.57	150	150	75
Sn	1658.78	1658.78	829.39	5640	5640	2820
Sr	1.35	1.35	1.08	1.89	1.89	1.51
Tc	0	0	0	0	0	0
Th	749.98	749.98	182.14	2550	2550	255
U	555.87	555.87	94.5	1890	1890	132.3
Zr	285.71	285.71	28.57	400	400	40
C-14_K [b]	140	140	140	140	140	140
I-129_C [b]	600	600	600	600	600	600
I-129_K [b]	3700	3700	3700	3700	3700	3700
Tc-99_K [b]	810	810	810	810	810	810

a – For Grout, Waste CLSM, and Concrete Slab zones.
b – Special wasteforms with K_d values fixed at their lowest values over exposed pH range.

The following summary of results is for the Case B sensitivity study. Peak well concentrations for Existing and Future Segments are provided in Table 2-41 and Table 2-42, respectively. The total future inventory limits for beta-gamma exposure (i.e., a total of 4.0 mrem/yr) are listed in Table 2-43 and comparison ratios (inventory limit for Case B versus Baseline) are listed in Table 2-44. The shaded values shown in Table 2-44 indicate ratio values less than unity.

Table 2-41. Case B maximum concentrations of the radionuclide parent and its progeny resulting from the existing 8 segments within the 100-m compliance zone[a]

Parent	Daughters	Time of Peak (0-1125 yrs)	Peak Concentration (pCi/L)	Time of Ultimate Peak (1125+ yrs)	Ultimate Peak Concentration (pCi/L)
Am-241		1,125	1.16E-04	1,863	1.60E-01
	Np-237	637	8.82E-04		
	U-233	1,125	6.91E-09	12,808	1.61E-07
	Th-229	1,125	1.81E-10	14,008	9.26E-08
Am-243		1,125	1.73E-08	2,613	3.41E-02
	Pu-239	1,125	9.11E-12	4,953	7.01E-04
	U-235	1,125	1.03E-19	8,693	1.27E-09
	Pa-231	1,125	1.76E-11	6,473	2.41E-10
	Ac-227	1,125	4.10E-13	6,443	5.81E-12
C-14		348	1.48E+02		
C-14_K		347	1.77E+01		
Cm-244		1,121	1.99E-25		
	Pu-240	1,125	6.31E-26	5,913	6.24E-03
	U-236	1,125	4.09E-32	15,008	4.34E-07
	Th-232	1,125	8.63E-41	18,308	2.49E-13
	Ra-228	1,125	3.85E-25	18,008	1.14E-11
Cm-245		1,125	2.98E-11	2,613	7.23E-04
	Pu-241	1,125	8.15E-12	2,623	2.84E-04
	Am-241	1,125	1.90E-11	2,633	7.47E-04
	Np-237	1,041	2.98E-07		
	U-233	1,125	2.54E-12	16,108	1.31E-11
	Th-229	1,125	5.61E-14	17,408	8.42E-12
Cm-247		1,125	7.14E-11	2,623	5.08E-03
	Am-243	1,125	7.40E-12	2,673	1.12E-03
	Pu-239	1,125	2.84E-15	3,933	1.87E-05
	U-235	1,125	2.39E-23	7,043	1.95E-11
	Pa-231	1,125	6.76E-14	5,673	2.78E-12
	Ac-227	1,125	1.53E-15	5,653	6.64E-14
Cm-248		1,125	7.13E-11	2,623	5.05E-03
	Pu-244	1,125	7.75E-18	4,863	2.92E-08
	Pu-240	1,125	2.74E-20	6,213	1.07E-08
	U-236	1,125	6.81E-27	8,733	4.43E-13
	Th-232	1,125	5.96E-36	13,208	9.55E-20
	Ra-228	1,125	2.89E-31	13,008	4.29E-18
H-3		340	3.39E-02		
I-129		454	9.57E-04		
I-129_K		1,125	4.43E-02	1,134	4.43E-02
Ni-59		732	1.07E-01		
Np-237		1,125	8.41E-07	12,808	4.53E-05
	U-233	1,125	2.00E-08	14,008	2.61E-05
	Th-229	1,125	2.55E-04	1,363	2.83E-04
Pd-107		1,125	1.40E-23	2,773	4.50E-12
Pu-238		1,125	4.92E-28	13,308	6.48E-04
	U-234	1,125	1.09E-31	16,508	6.71E-05
	Th-230	1,125	1.18E-05	13,108	2.00E-04
	Ra-226	1,125	9.36E-08	13,108	1.68E-06
	Pb-210	1,125	4.73E-19	5,113	8.89E+00

Table 2-41. Case B maximum concentrations of the radionuclide parent and its progeny resulting from the existing 8 segments within the 100-m compliance zone[a] - continued

Parent	Daughters	Time of Peak (0-1125 yrs)	Peak Concentration (pCi/L)	Time of Ultimate Peak (1125+ yrs)	Ultimate Peak Concentration (pCi/L)
Pu-239		1,125	4.65E-27	10,384	1.26E-05
	U-235	1,125	6.02E-07	5,613	2.18E-06
	Pa-231	1,125	1.45E-08	5,573	5.27E-08
	Ac-227	1,125	1.47E-21	5,623	3.49E-01
Pu-240		1,125	4.33E-28	12,908	2.31E-05
	U-236	1,125	4.28E-37	15,908	1.15E-11
	Th-232	1,125	1.25E-21	15,608	5.23E-10
	Ra-228	1,125	1.06E-42	1,276	2.49E-42
Pu-241		1,125	8.50E-05	1,863	1.14E-01
	Am-241	635	5.97E-04		
	Np-237	1,125	4.67E-09	12,708	1.04E-07
	U-233	1,125	1.22E-10	14,008	5.98E-08
	Th-229	1,125	1.95E-25	5,653	1.16E-03
Pu-242		1,125	2.96E-34	11,208	2.64E-10
	U-238	1,125	2.19E-38	13,108	7.27E-12
	U-234	1,125	3.89E-42	14,908	3.46E-13
	Th-230	1,125	3.52E-16	12,808	7.19E-13
	Ra-226	1,125	2.57E-18	12,808	6.01E-15
	Pb-210	1,125	1.85E-49	18,108	3.20E-03
Se-79		1,125	1.69E-76	48,708	4.41E-05
Sn-126		528	4.83E-03		
Sr-90		239	1.15E+01		
Tc-99		385	4.64E-01		
Tc-99_K		1,125	4.37E-42	15,008	1.93E+00
U-233		1,125	2.74E-44	16,308	1.21E+00
	Th-229	1,125	8.56E-42	11,908	5.95E-01
U-234		1,125	5.25E-45	13,808	5.53E-02
	Th-230	1,125	1.15E-02	10,910	1.25E-01
	Ra-226	1,125	9.33E-05	11,008	1.04E-03
	Pb-210	1,125	2.32E-43	11,808	1.64E-02
U-235		807	3.47E-03		
	Pa-231	891	8.40E-05		
	Ac-227	1,125	6.90E-44	12,808	7.05E-03
U-236		1,125	2.27E-52	14,608	3.92E-09
	Th-232	1,125	1.26E-17	14,308	1.79E-07
	Ra-228	1,125	3.97E-41	11,808	2.73E+00
U-238		1,125	1.32E-43	12,508	9.25E-02
	U-234	1,125	7.58E-47	13,708	4.67E-03
	Th-230	1,125	5.47E-05	11,508	8.24E-03
	Ra-226	1,125	4.24E-07	11,508	6.89E-05
	Pb-210	1,125	1.26E-15	3,393	4.44E-02
Zr-93		1,125	1.69E+00	2,833	2.27E+00
	Nb-93m	1,125	4.89E-01	43,608	2.22E+00

[a]maximum based on first 1,000 years and its ultimate peak if beyond 1,000 years

Table 2-42. Case B maximum concentrations (pCi/L per Ci of parent buried) of radionuclide parent and progeny resulting from all future inventories within the 100-m compliance zone [a]

Parent	Daughters	Time of Peak (0-1125 yrs)	Peak Concentration (pCi/L-Ci$_{parent}$)	Time of Ultimate Peak (1125+ yrs)	Ultimate Peak Concentration (pCi/L-Ci$_{parent}$)
Am-241		1,125	9.29E-02	1,723	3.96E+00
	Np-237	634	1.70E-02		
	U-233	1,125	1.34E-07	10,820	3.01E-06
	Th-229	1,125	3.52E-09	12,708	1.65E-06
Am-243		1,125	5.14E-01	1,843	5.76E+01
	Pu-239	1,125	4.31E-04	3,373	9.28E-01
	U-235	1,125	7.36E-12	6,103	1.17E-06
	Pa-231	1,125	2.24E-08	4,553	1.53E-07
	Ac-227	1,125	5.23E-10	4,523	3.65E-09
C-14		344	2.32E+03		
C-14_K		361	1.82E+02		
Cl-36		335	1.75E+03		
Cm-244		925	1.09E-18		
	Pu-240	1,125	6.08E-15	4,413	4.46E-02
	U-236	1,125	2.36E-21	9,683	2.29E-06
	Th-232	1,125	3.02E-30	12,408	8.62E-13
	Ra-228	1,125	2.69E-20	12,108	3.90E-11
Cm-245		1,125	5.21E-01	1,843	5.89E+01
	Pu-241	1,125	1.64E-01	1,863	2.32E+01
	Am-241	1,125	3.72E-01	1,873	5.82E+01
	Np-237	1,028	1.78E-02		
	U-233	1,125	1.58E-07	11,408	9.66E-07
	Th-229	1,125	3.62E-09	12,608	5.27E-07
Cm-247		1,125	5.72E-01	1,853	6.85E+01
	Am-243	1,125	5.78E-02	2,053	1.16E+01
	Pu-239	1,125	4.56E-05	2,763	1.45E-01
	U-235	1,125	7.51E-13	4,933	1.05E-07
	Pa-231	1,125	7.51E-10	4,573	1.17E-08
	Ac-227	1,125	1.70E-11	4,563	2.76E-10
Cm-248		1,125	5.71E-01	1,853	6.83E+01
	Pu-244	1,125	1.31E-07	3,323	3.06E-04
	Pu-240	1,125	9.19E-10	4,393	8.39E-05
	U-236	1,125	4.32E-16	6,183	2.46E-09
	Th-232	1,125	6.88E-25	10,598	4.05E-16
	Ra-228	1,125	1.97E-22	10,430	1.80E-14
H-3		205	6.39E-03		
I-129		339	3.52E+03		
I-129_C		451	5.08E+01		
I-129_K		451	8.27E+00		
K-40		1,125	6.41E-03	2,463	4.45E+01
Mo-93		236	9.69E+02		
	Nb-93m	236	9.61E+02		
Nb-94		696	5.74E+01	2,093	1.26E+02
Ni-59		1,106	3.91E+01	2,393	4.92E+01
Np-237		723	8.88E+01		
	U-233	1,125	7.04E-04	10,820	3.75E-02
	Th-229	1,125	1.70E-05	12,708	2.05E-02

[a]maximum based on first 1,000 years and its ultimate peak if beyond 1,000 years

Table 2-42. Case B maximum concentrations (pCi/L per Ci of parent buried) of radionuclide parent and progeny resulting from all future inventories within the 100-m compliance zone [a] - continued

Parent	Daughters	Time of Peak (0-1125 yrs)	Peak Concentration (pCi/L-Ci_{parent})	Time of Ultimate Peak (1125+ yrs)	Ultimate Peak Concentration (pCi/L-Ci_{parent})
Pd-107		1,108	3.95E+01	2,393	5.03E+01
Pu-238		1,125	2.82E-16	2,383	7.58E-10
	U-234	1,125	1.39E-20	10,739	3.40E-03
	Th-230	1,125	4.20E-24	13,508	3.01E-04
	Ra-226	1,125	6.16E-05	10,537	7.37E-04
	Pb-210	1,125	4.96E-07	10,537	6.18E-06
Pu-239		1,125	2.37E-12	4,473	2.27E+01
	U-235	1,125	3.04E-20	9,473	3.33E-05
	Pa-231	1,125	1.60E-06	5,393	5.50E-06
	Ac-227	1,125	3.86E-08	5,343	1.33E-07
Pu-240		1,125	2.17E-12	4,413	1.61E+01
	U-236	1,125	8.37E-19	9,713	8.35E-04
	Th-232	1,125	1.07E-27	12,408	3.15E-10
	Ra-228	1,125	1.01E-17	12,108	1.43E-08
Pu-241		1,088	4.96E-36		
	Am-241	1,125	3.18E-03	1,723	1.35E-01
	Np-237	632	5.63E-04		
	U-233	1,125	4.41E-09	10,820	9.47E-08
	Th-229	1,125	1.17E-10	12,708	5.17E-08
Pu-242		1,125	2.45E-12	4,723	2.57E+01
	U-238	1,125	4.92E-21	9,193	5.62E-06
	U-234	1,125	4.78E-25	11,108	1.27E-07
	Th-230	1,125	1.10E-28	12,908	5.16E-09
	Ra-226	1,125	9.72E-12	12,508	1.04E-08
	Pb-210	1,125	7.29E-14	12,608	8.72E-11
Pu-244		1,125	2.45E-12	4,733	2.59E+01
	Pu-240	1,125	2.81E-13	4,983	1.03E+01
	U-236	1,125	1.05E-19	7,003	3.31E-04
	Th-232	1,125	1.30E-28	10,598	6.55E-11
	Ra-228	1,125	4.81E-19	10,384	2.92E-09
Ra-226		779	1.31E+02		
	Pb-210	811	1.07E+00		
Se-79		1,125	6.92E-31	13,908	7.11E+00
Sn-126		1,125	2.14E-50	36,508	2.71E+00
Sr-90		503	1.70E-03		
Tc-99		242	9.64E+02		
Tc-99_K		381	2.91E+01		
Th-230		1,125	4.69E-32	13,108	7.08E+00
	Ra-226	881	3.84E+01		
	Pb-210	921	3.18E-01		
Th-232		1,125	4.74E-32	13,208	7.98E+00
	Ra-228	1,125	7.86E-06	12,808	3.72E+02
U-233		1,125	5.75E-28	10,739	9.35E+00
	Th-229	1,125	4.66E-30	12,608	5.19E+00

[a]maximum based on first 1,000 years and its ultimate peak if beyond 1,000 years

Table 2-42. Case B maximum concentrations (pCi/L per Ci of parent buried) of radionuclide parent and progeny resulting from all future inventories within the 100-m compliance zone [a] - continued

Parent	Daughters	Time of Peak (0-1125 yrs)	Peak Concentration (pCi/L-Ci_{parent})	Time of Ultimate Peak (1125+ yrs)	Ultimate Peak Concentration (pCi/L-Ci_{parent})
U-234		1,125	5.76E-28	10,739	9.50E+00
	Th-230	1,125	4.59E-31	13,508	8.49E-01
	Ra-226	1,125	2.07E-01	10,481	2.09E+00
	Pb-210	1,125	1.69E-03	10,537	1.75E-02
U-235		1,125	5.78E-28	10,739	9.80E+00
	Pa-231	805	2.36E+00		
	Ac-227	889	5.71E-02		
U-236		1,125	5.78E-28	10,739	9.79E+00
	Th-232	1,125	2.47E-36	13,608	4.94E-06
	Ra-228	1,125	5.27E-13	13,208	2.25E-04
U-238		1,125	5.78E-28	10,739	9.80E+00
	U-234	1,125	1.89E-30	12,208	3.18E-01
	Th-230	1,125	1.38E-33	13,708	1.61E-02
	Ra-226	1,125	2.31E-04	11,408	3.13E-02
	Pb-210	1,125	1.80E-06	11,408	2.62E-04
Zr-93		1,125	1.72E-03	2,363	5.12E+01
	Nb-93m	1,125	1.96E+03	1,863	2.21E+03

[a]maximum based on first 1,000 years and its ultimate peak if beyond 1,000 years

Table 2-43. Case B future total inventory limits[a] per Ci buried) for beta-gamma exposure from radionuclide parents

Parent Buried	0 - 125 year Inventory Limit (Ci)	125 - 1,125 year Inventory Limit (Ci)	1,125 - 10,125 year Inventory Limit (Ci)
Am-241	---	1.75E+04	3.41E+04
Am-243	---	5.82E+02	5.19E+00
C-14	2.07E+09	7.72E-01	---
C-14_K	3.72E+10	1.07E+01	6.02E+02
Cl-36	8.80E+04	3.80E-01	---
Cm-244	---	---	1.09E+11
Cm-245	---	1.43E+03	1.10E+01
Cm-247	---	4.38E+03	2.33E+01
Cm-248	---	9.67E+09	4.15E+06
H-3	4.75E+06	3.12E+06	---
I-129	2.28E+04	2.61E-04	---
I-129_C	3.95E+06	1.95E-02	3.16E-02
I-129_K	2.43E+07	1.20E-01	1.81E-01
K-40	---	4.59E+04	6.60E+00
Mo-93	1.49E+03	8.20E-01	9.71E+17
Nb-94	2.67E+16	1.33E+01	6.07E+00
Ni-59	---	7.65E+00	6.08E+00
Np-237	---	3.36E+00	5.67E+00
Pd-107	---	9.25E+02	7.27E+02
Pu-238	---	2.00E+06	1.59E+05
Pu-239	---	1.02E+07	2.92E+06
Pu-240	---	3.63E+17	3.00E+08
Pu-241	---	5.30E+05	1.04E+06
Pu-242	---	1.35E+13	7.03E+07
Pu-244	---	5.20E+14	4.93E+01
Ra-226	---	9.26E-01	4.23E+00
Se-79	---	---	2.19E+02
Sn-126	---	---	6.91E+08
Sr-90	---	4.11E+03	1.13E+12
Tc-99	5.25E+03	9.19E-01	---
Tc-99_K	9.17E+06	2.81E+01	3.69E+01
Th-230	---	3.11E+00	3.64E+00
Th-232	---	4.67E+05	1.58E-02
U-233	---	---	3.69E+00
U-234	---	5.87E+02	5.63E+01
U-235	---	6.88E+00	7.94E+00
U-236	---	6.97E+12	2.36E+04
U-238	---	5.50E+05	4.15E+01
Zr-93	8.92E+17	5.07E-01	4.47E-01

a – These are future inventory limits that represent disposal limits for both CIG units combined. To arrive at the individual limits on a per unit basis, these values must be multiplied by 0.459 for CIG Unit #1 and 0.541 for CIG Unit #2. Total inventory limit estimates greater than $1x10^{20}$ pCi/L are not shown.

Table 2-44. Case B versus Baseline total future inventory limit ratios[a] for beta-gamma exposure from radionuclide parents (values less than one are shaded)

Parent Buried	0 - 125 year Inventory Limit Ratio (-)	125 - 1,125 year Inventory Limit Ratio (-)	1,125 - 10,125 year Inventory Limit Ratio (-)
Am-241	1	7.99E-01	1.06E+00
Am-243	1	1.39E-03	6.76E-01
C-14	2.17E-01	7.78E-01	1
C-14_K	2.97E-01	1.06E+00	1.01E+00
Cl-36	4.10E-01	1.31E+00	1
Cm-244	1	1	5.47E-01
Cm-245	1	8.69E-02	6.81E-01
Cm-247	1	1.40E-03	9.03E-01
Cm-248	1	1.00E-03	9.97E-01
H-3	1	9.99E-01	1
I-129	2.59E-01	9.20E-01	1
I-129_C	3.48E-01	1.09E+00	1.00E+00
I-129_K	3.48E-01	1.09E+00	1.00E+00
K-40	1	3.46E-04	7.15E-01
Mo-93	1.00E+00	9.98E-01	9.17E-01
Nb-94	2.23E-03	6.88E-01	4.95E+00
Ni-59	1	4.53E-01	1.75E+00
Np-237	1	7.09E-01	1.04E+00
Pd-107	1	4.53E-01	1.75E+00
Pu-238	1	2.69E-01	4.25E-01
Pu-239	1	9.24E-01	1.25E+00
Pu-240	1	3.63E-03	5.44E-01
Pu-241	1	8.04E-01	1.06E+00
Pu-242	1	2.12E-01	9.36E-01
Pu-244	1	5.20E-06	7.13E-01
Ra-226	1	2.84E-01	1
Se-79	1	1	2.35E-02
Sn-126	1	1	6.91E-12
Sr-90	1	1.31E-01	8.45E+00
Tc-99	7.36E-01	9.76E-01	1
Tc-99_K	7.36E-01	1.00E+00	1.00E+00
Th-230	1	3.40E-01	4.02E-01
Th-232	1	2.31E-03	4.62E-02
U-233	1	1	1.04E-01
U-234	1	2.85E-01	4.25E-01
U-235	1	8.58E-01	9.80E-01
U-236	1	2.42E-03	1.25E-01
U-238	1	2.41E-01	1.63E-01
Zr-93	8.09E-02	9.58E-01	9.96E-01

a - Inventory limit ratios that are nearly unity (i.e., no change) are shown as 1.

As shown in Table 2-44, effects due to using conservative estimate K_d values with CDP applied are seen throughout the three periods. As highlighted in Table 2-44 by shading, various parent radionuclide inventory limits are reduced. Some have significant reduction factors. For example, the limit ratio for radionuclide K-40 is $3.46x10^{-4}$ for the time period 125 to 1,125 years and then $7.15x10^{-1}$ for the time period 1,125 to 10,125 years (i.e., similar behavior as observed for Case A).

Sensitivity Analysis Case Study C

Cement chemical aging has been established based on the amount of throughput of rainfall that infiltrates through the grout chamber. Hydraulic performance has been established based on the point where subsidence is assumed to occur. As shown in Figure 2-25, right after subsidence the rate of water exposure experienced by the existing and future grout chambers increases significantly and ultimately becomes very similar over time. To address the cement aging aspects of the grout chambers, the Case C sensitivity study increases the aging process by removing the time period where the grout chambers are in Stage 2 ("Middle" age) and moving to an earlier time the "old" age transition to the point of subsidence (i.e., 325 years). For Case C the new resulting time durations are provided in Table 2-45. For comparison purposes, the time durations employed in the Baseline Case are also provided.

Table 2-45. Baseline versus Case C comparison of CIG cement accelerated aging time periods

Case	Segment	Time Period (yr)	Young [Stage 1] (yr)	Middle [Stage 2] (yr)	Old [Stage 3] (yr)	Local Soil (yr)
Baseline	**Existing**	start	0	334	443	2223
		end	334	443	2223	and beyond
	Future	start	0	350	441	2078
		end	350	441	2078	and beyond
Case C	**Existing**	start	0	NA[a]	325	2223
		end	325	NA	2223	and beyond
	Future	start	0	NA	325	2078
		end	325	NA	2078	and beyond

a – NA – Not Applicable; "Middle" age removed for Case C study

The following summary of results is for the Case C sensitivity study. Peak well concentrations for Existing and Future Segments are provided in Table 2-46 and Table 2-47, respectively. The total future inventory limits for beta-gamma exposure (i.e., a total of 4.0 mrem/yr) are listed in Table 2-48 and comparison ratios (inventory limit for Case C versus Baseline) are listed in Table 2-49. The shaded values shown in Table 2-49 indicate ratio values less than unity.

Table 2-46. Case C maximum concentrations of the radionuclide parent and progeny resulting from the existing 8 segments within the 100-m compliance zone [a]

Parent	Daughters	Time of Peak (0-1125 yrs)	Peak Concentration (pCi/L)	Time of Ultimate Peak (1125+ yrs)	Ultimate Peak Concentration (pCi/L)
Am-241		1,125	3.31E-07	2,283	5.49E-02
	Np-237	574	7.39E-04		
	U-233	1,125	6.01E-09	17,708	1.16E-07
	Th-229	1,125	1.75E-10	19,208	7.80E-08
Am-243		1,125	2.40E-11	3,363	2.29E-02
	Pu-239	1,125	1.12E-14	6,333	6.43E-04
	U-235	1,125	1.13E-22	11,508	1.53E-09
	Pa-231	1,125	1.66E-11	8,533	3.93E-10
	Ac-227	1,125	3.57E-13	8,503	8.85E-12
C-14		337	2.86E+02		
C-14_K		341	1.66E+01		
Cm-244		1,125	1.21E-28	1,194	1.48E-28
	Pu-240	1,125	8.36E-30	7,993	3.58E-03
	U-236	1,125	5.09E-36	21,008	3.82E-07
	Th-232	1,125	9.88E-45	25,308	3.11E-13
	Ra-228	1,125	1.27E-28	25,008	1.45E-11
Cm-245		1,125	5.77E-14	3,373	4.90E-04
	Pu-241	1,125	1.56E-14	3,383	1.92E-04
	Am-241	1,125	3.62E-14	3,393	5.13E-04
	Np-237	1,125	2.83E-07	1,703	2.97E-07
	U-233	1,125	2.29E-12	4,733	1.28E-11
	Th-229	1,125	5.41E-14	23,608	6.11E-12
Cm-247		1,125	2.95E-15	3,393	3.66E-03
	Am-243	1,125	3.07E-16	3,473	1.01E-03
	Pu-239	1,125	9.94E-20	5,173	2.28E-05
	U-235	1,125	7.10E-28	9,273	3.18E-11
	Pa-231	1,125	6.33E-14	7,483	6.04E-12
	Ac-227	1,125	1.32E-15	7,463	1.35E-13
Cm-248		1,125	2.94E-15	3,393	3.64E-03
	Pu-244	1,125	2.68E-22	6,273	2.90E-08
	Pu-240	1,125	8.02E-25	8,023	1.25E-08
	U-236	1,125	1.70E-31	11,508	6.94E-13
	Th-232	1,125	1.27E-40	17,608	2.02E-19
	Ra-228	1,125	1.86E-34	17,508	9.25E-18
H-3		29	9.11E+03		
I-129		338	5.87E-02		
I-129_K		344	7.48E-04		
Ni-59		1,125	2.10E-02	2,723	7.86E-02
Np-237		760	7.67E-02		
	U-233	1,125	6.37E-07	17,808	3.54E-05
	Th-229	1,125	1.58E-08	19,208	2.37E-05
Pd-107		1,125	7.72E-05	2,843	4.39E-04
Pu-238		1,125	7.55E-29	3,203	5.98E-15
	U-234	1,125	2.46E-33	18,408	4.56E-04
	Th-230	1,125	5.07E-37	22,908	6.43E-05
	Ra-226	1,125	7.70E-06	18,108	2.63E-04
	Pb-210	1,125	2.38E-08	18,108	9.00E-07

[a]maximum based on first 1,000 years and its ultimate peak if beyond 1,000 years

Table 2-46. Case C maximum concentrations of the radionuclide parent and progeny resulting from the existing 8 segments within the 100-m compliance zone [a] - continued

Parent	Daughters	Time of Peak (0-1125 yrs)	Peak Concentration (pCi/L)	Time of Ultimate Peak (1125+ yrs)	Ultimate Peak Concentration (pCi/L)
Pu-239		1,125	2.64E-24	6,903	6.04E+00
	U-235	1,125	2.44E-32	13,908	1.19E-05
	Pa-231	1,125	5.82E-07	7,613	2.87E-06
	Ac-227	1,125	1.29E-08	7,563	6.49E-08
Pu-240		1,125	8.13E-27	7,583	2.02E-01
	U-236	1,125	2.26E-33	18,008	2.04E-05
	Th-232	1,125	2.11E-42	21,908	1.43E-11
	Ra-228	1,125	1.08E-24	21,608	6.62E-10
Pu-241		1,125	4.79E-48	1,313	1.83E-47
	Am-241	1,125	2.43E-07	2,273	3.91E-02
	Np-237	567	5.04E-04		
	U-233	1,125	4.08E-09	17,708	7.46E-08
	Th-229	1,125	1.20E-10	19,108	5.00E-08
Pu-242		1,125	9.20E-31	7,663	8.24E-04
	U-238	1,125	1.33E-39	14,708	2.59E-10
	U-234	1,125	9.45E-44	18,008	9.54E-12
	Th-230	1,125	1.60E-47	20,908	6.17E-13
	Ra-226	1,125	1.63E-16	17,608	1.76E-12
	Pb-210	1,125	4.75E-19	17,608	6.02E-15
Se-79		1,125	9.77E-57	25,108	2.25E-03
Sn-126		1,125	2.95E-107	165,208	9.03E-06
Sr-90		597	4.91E-04		
Tc-99		240	1.14E+01		
Tc-99_K		385	4.64E-01		
U-233		1,125	7.45E-48	20,808	1.35E+00
	Th-229	1,125	5.17E-50	22,308	9.56E-01
U-234		1,125	1.46E-47	16,908	4.17E-01
	Th-230	1,125	9.94E-51	19,108	5.28E-02
	Ra-226	1,125	8.58E-03	15,008	1.64E-01
	Pb-210	1,125	2.73E-05	15,008	5.61E-04
U-235		1,125	3.95E-49	16,808	1.16E-02
	Pa-231	944	2.97E-03		
	Ac-227	979	6.77E-05		
U-236		1,125	1.18E-49	17,808	5.03E-03
	Th-232	1,125	4.30E-58	20,208	3.88E-09
	Ra-228	1,125	1.48E-20	19,908	1.80E-07
U-238		1,125	6.77E-47	16,308	1.93E+00
	U-234	1,125	2.24E-49	17,308	9.01E-02
	Th-230	1,125	1.41E-52	18,908	6.22E-03
	Ra-226	1,125	3.55E-05	15,908	1.51E-02
	Pb-210	1,125	1.09E-07	15,908	5.16E-05
Zr-93		1,125	2.66E-20	4,473	3.20E-02
	Nb-93m	1,125	1.65E+00	3,693	2.28E+00

[a]maximum based on first 1,000 years and its ultimate peak if beyond 1,000 years

Table 2-47. Case C maximum concentrations (per Ci of parent buried) of radionuclide parent and progeny resulting from all future inventories within the 100-m compliance zone [a]

Parent	Daughters	Time of Peak (0-1125 yrs)	Peak Concentration ($pCi/L\text{-}Ci_{parent}$)	Time of Ultimate Peak (1125+ yrs)	Ultimate Peak Concentration ($pCi/L\text{-}Ci_{parent}$)
Am-241		1125	2.34E-03	1993	1.52E+00
	Np-237	570	1.43E-02		
	U-233	1125	1.16E-07	15008	2.17E-06
	Th-229	1125	3.42E-09	17408	1.40E-06
Am-243		1125	1.31E-02	2303	3.95E+01
	Pu-239	1125	9.81E-06	4123	8.72E-01
	U-235	1125	1.53E-13	7923	1.39E-06
	Pa-231	1125	2.16E-08	5883	2.40E-07
	Ac-227	1125	4.66E-10	5853	5.37E-09
C-14		336	6.23E+03		
C-14_K		341	1.66E+02		
Cl-36		335	2.64E+03		
Cm-244		952	1.43E-20		
	Pu-240	1125	1.84E-18	5903	2.71E-02
	U-236	1125	7.53E-25	13308	2.05E-06
	Th-232	1125	1.06E-33	17108	1.07E-12
	Ra-228	1125	1.05E-22	16808	4.95E-11
Cm-245		1125	1.32E-02	2313	4.07E+01
	Pu-241	1125	4.04E-03	2323	1.60E+01
	Am-241	1125	9.13E-03	2333	4.15E+01
	Np-237	1125	1.71E-02	1573	1.78E-02
	U-233	1125	1.44E-07	15608	5.99E-07
	Th-229	1125	3.54E-09	17108	3.85E-07
Cm-247		1125	1.45E-02	2323	4.91E+01
	Am-243	1125	1.47E-03	2613	1.03E+01
	Pu-239	1125	1.05E-06	3563	1.74E-01
	U-235	1125	1.58E-14	6343	1.64E-07
	Pa-231	1125	7.20E-10	5973	2.44E-08
	Ac-227	1125	1.51E-11	5963	5.42E-10
Cm-248		1125	1.45E-02	2323	4.89E+01
	Pu-244	1125	2.99E-09	4113	3.02E-04
	Pu-240	1125	1.92E-11	5563	9.44E-05
	U-236	1125	8.33E-18	8073	3.71E-09
	Th-232	1125	1.24E-26	14008	8.27E-16
	Ra-228	1125	5.04E-24	13908	3.75E-14
H-3		205	6.39E-03		
I-129		336	5.90E+03		
I-129_C		345	3.94E+01		
I-129_K		345	6.42E+00		
K-40		1125	2.22E-06	3353	3.19E+01
Mo-93		236	9.69E+02		
	Nb-93m	236	9.61E+02		
Nb-94		800	4.06E+01	2093	5.52E+02
Ni-59		1125	2.09E+01	2523	8.12E+01
Np-237		750	6.35E+01		
	U-233	1125	5.34E-04	15008	2.92E-02
	Th-229	1125	1.34E-05	17408	1.89E-02

[a]maximum based on first 1,000 years and its ultimate peak if beyond 1,000 years

Table 2-47. Case C maximum concentrations (per Ci of parent buried) of radionuclide parent and progeny resulting from all future inventories within the 100-m compliance zone [a] - continued

Parent	Daughters	Time of Peak (0-1125 yrs)	Peak Concentration ($pCi/L\text{-}Ci_{parent}$)	Time of Ultimate Peak (1125+ yrs)	Ultimate Peak Concentration ($pCi/L\text{-}Ci_{parent}$)
Pd-107		1125	2.11E+01	2523	8.31E+01
Pu-238		1125	7.89E-20	2683	3.28E-12
	U-234	1125	3.91E-24	14808	2.38E-03
	Th-230	1125	1.18E-27	18608	2.88E-04
	Ra-226	1125	4.51E-05	14408	9.77E-04
	Pb-210	1125	1.43E-07	14408	3.34E-06
Pu-239		1125	6.77E-16	6003	1.55E+01
	U-235	1125	8.69E-24	12708	3.15E-05
	Pa-231	1125	1.55E-06	7303	7.24E-06
	Ac-227	1125	3.44E-08	7253	1.64E-07
Pu-240		1125	6.19E-16	5903	9.81E+00
	U-236	1125	2.40E-22	13308	7.44E-04
	Th-232	1125	3.06E-31	17108	3.91E-10
	Ra-228	1125	3.94E-20	16808	1.81E-08
Pu-241		1084	1.27E-39		
	Am-241	1125	8.02E-05	1993	5.20E-02
	Np-237	564	4.75E-04		
	U-233	1125	3.86E-09	15008	6.77E-08
	Th-229	1125	1.14E-10	17408	4.37E-08
Pu-242		1125	6.98E-16	6373	1.83E+01
	U-238	1125	1.41E-24	12108	5.49E-06
	U-234	1125	1.37E-28	15308	1.65E-07
	Th-230	1125	3.15E-32	17708	9.15E-09
	Ra-226	1125	5.82E-12	17308	2.56E-08
	Pb-210	1125	1.73E-14	17308	8.76E-11
Pu-244		1125	7.00E-16	6383	1.85E+01
	Pu-240	1125	8.04E-17	6723	9.18E+00
	U-236	1125	3.02E-23	9553	4.12E-04
	Th-232	1125	3.75E-32	14508	1.12E-10
	Ra-228	1125	1.87E-21	14308	5.12E-09
Ra-226		892	9.10E+01		
	Pb-210	927	3.05E-01		
Se-79		1125	1.01E-36	19308	4.99E+00
Sn-126		1125	2.70E-74	119808	6.09E-01
Sr-90		562	2.25E-04		
Tc-99		245	9.43E+02		
Tc-99_K		382	2.91E+01		
Th-230		1125	1.04E-36	18108	4.80E+00
	Ra-226	1104	3.13E+01		
	Pb-210	1124	1.07E-01	1137	1.07E-01
Th-232		1125	1.05E-36	19308	5.67E+00
	Ra-228	1089	2.70E-08	19008	2.68E+02
U-233		1125	2.96E-32	14808	6.50E+00
	Th-229	1125	2.46E-34	17208	4.23E+00
U-234		1125	2.97E-32	14808	6.65E+00
	Th-230	1125	2.42E-35	18608	8.12E-01
	Ra-226	1125	1.59E-01	14308	2.76E+00
	Pb-210	1125	5.10E-04	14408	9.43E-03

[a]maximum based on first 1,000 years and its ultimate peak if beyond 1,000 years

Table 2-47. Case C maximum concentrations (per Ci of parent buried) of radionuclide parent and progeny resulting from all future inventories within the 100-m compliance zone [a] - continued

Parent	Daughters	Time of Peak (0-1125 yrs)	Peak Concentration ($pCi/L\text{-}Ci_{parent}$)	Time of Ultimate Peak (1125+ yrs)	Ultimate Peak Concentration ($pCi/L\text{-}Ci_{parent}$)
U-235		1125	2.98E-32	14808	6.93E+00
	Pa-231	943	2.02E+00		
	Ac-227	978	4.61E-02		
U-236		1125	2.98E-32	14808	6.93E+00
	Th-232	1125	1.30E-40	18808	4.88E-06
	Ra-228	1125	2.05E-15	18408	2.26E-04
U-238		1125	2.98E-32	14808	6.93E+00
	U-234	1125	9.77E-35	17008	3.11E-01
	Th-230	1125	7.25E-38	18908	2.15E-02
	Ra-226	1125	1.54E-04	15708	5.75E-02
	Pb-210	1125	4.76E-07	15808	1.96E-04
Zr-93		1125	1.39E-05	3043	3.67E+01
	Nb-93m	1,125	1.91E+03	2,333	2.21E+03

[a]maximum based on first 1,000 years and its ultimate peak if beyond 1,000 years

Table 2-48. Case C total future inventory limits[a] (per Ci initially buried) for beta-gamma exposure from radionuclide parents

Parent Buried	0 - 125 year Inventory Limit (Ci)	125 - 1,125 year Inventory Limit (Ci)	1,125 - 10,125 year Inventory Limit (Ci)
Am-241	---	2.09E+04	3.80E+04
Am-243	---	2.29E+04	7.57E+00
C-14	9.56E+09	2.56E-01	---
C-14_K	1.25E+11	9.70E+00	5.98E+02
Cl-36	2.15E+05	2.17E-01	---
Cm-244	---	---	1.91E+11
Cm-245	---	1.37E+04	1.60E+01
Cm-247	---	1.72E+05	2.68E+01
Cm-248	---	4.24E+11	4.20E+06
H-3	4.75E+06	3.12E+06	---
I-129	8.79E+04	1.35E-04	---
I-129_C	1.13E+07	2.13E-02	3.16E-02
I-129_K	6.98E+07	1.31E-01	1.81E-01
K-40	---	1.32E+08	9.23E+00
Mo-93	1.49E+03	8.21E-01	1.09E+18
Nb-94	1.19E+19	1.88E+01	1.39E+00
Ni-59	---	1.43E+01	3.68E+00
Np-237	---	4.69E+00	6.09E+00
Pd-107	---	1.73E+03	4.40E+02
Pu-238	---	6.72E+06	3.75E+05
Pu-239	---	1.14E+07	2.38E+06
Pu-240	---	9.32E+19	5.27E+08
Pu-241	---	6.27E+05	1.16E+06
Pu-242	---	5.54E+13	7.49E+07
Pu-244	---	1.82E+18	6.89E+01
Ra-226	---	3.16E+00	4.75E+00
Se-79	---	---	8.49E+03
Sn-126	---	---	---
Sr-90	---	3.11E+04	1.34E+11
Tc-99	7.14E+03	9.41E-01	---
Tc-99_K	1.25E+07	2.99E+01	3.69E+01
Th-230	---	9.03E+00	9.03E+00
Th-232	---	1.36E+08	2.96E-01
U-233	---	---	3.12E+01
U-234	---	1.88E+03	1.32E+02
U-235	---	8.54E+00	8.90E+00
U-236	---	1.79E+15	1.68E+05
U-238	---	2.02E+06	2.29E+02
Zr-93	1.10E+19	5.21E-01	4.49E-01

a – These are future inventory limits that represent disposal limits for both CIG units combined. To arrive at the individual limits on a per unit basis, these values must be multiplied by 0.459 for CIG Unit #1 and 0.541 for CIG Unit #2. Total inventory limit estimates greater than $1x10^{20}$ pCi/L are not shown.

Table 2-49. Case C versus Baseline total future inventory limit ratios[a] for beta-gamma exposure from radionuclide parents (values less than one are shaded

Parent Buried	0 - 125 year Inventory Limit Ratio (-)	125 - 1,125 year Inventory Limit Ratio (-)	1,125 - 10,125 year Inventory Limit Ratio (-)
Am-241	1	9.52E-01	1.18E+00
Am-243	1	5.47E-02	9.86E-01
C-14	1	2.59E-01	1
C-14_K	1	9.67E-01	1
Cl-36	1	7.49E-01	1
Cm-244	1	1	9.55E-01
Cm-245	1	8.37E-01	9.87E-01
Cm-247	1	5.48E-02	1.04E+00
Cm-248	1	4.39E-02	1.01E+00
H-3	1	1	1
I-129	1	4.78E-01	1
I-129_C	1	1.19E+00	1
I-129_K	1	1.19E+00	1
K-40	1	9.99E-01	1
Mo-93	1	1	1.03E+00
Nb-94	1	9.74E-01	1.13E+00
Ni-59	1	8.46E-01	1.06E+00
Np-237	1	9.91E-01	1.11E+00
Pd-107	1	8.46E-01	1.06E+00
Pu-238	1	9.07E-01	9.99E-01
Pu-239	1	1.04E+00	1.02E+00
Pu-240	1	9.32E-01	9.55E-01
Pu-241	1	9.51E-01	1.18E+00
Pu-242	1	8.66E-01	9.97E-01
Pu-244	1	1.82E-02	9.98E-01
Ra-226	1	9.68E-01	1.13E+00
Se-79	1	1	9.12E-01
Sn-126	1	1	1
Sr-90	1	9.89E-01	1
Tc-99	1	1	1
Tc-99_K	1	1.07E+00	1
Th-230	1	9.86E-01	9.97E-01
Th-232	1	6.71E-01	8.67E-01
U-233	1	1	8.77E-01
U-234	1	9.14E-01	9.98E-01
U-235	1	1.06E+00	1.10E+00
U-236	1	6.22E-01	8.88E-01
U-238	1	8.82E-01	9.01E-01
Zr-93	1	9.83E-01	9.99E-01

Aging effects were addressed beyond 325 years; therefore, as shown in Table 2-49 the limit ratio values are all unity for the 0 to 125 yr time period. As highlighted in Table 2-49 by shading, various parent inventory limits are reduced. Some have modest reduction factors. For example, the limit ratio for radionuclide Pu-244 is 1.82×10^{-2} for the time period 125 to 1,125 years.

Sensitivity Analysis Case Study D

For case study D, saturated "effective" molecular diffusion coefficient (D_{eff}) values for all the cementitious material zones are altered (i.e., the values for the non-cementitious material zones are unaltered). Note that for the waste zone, its value for the first 40 years depends upon the species type (i.e., volatile or not). For non-volatile species and for all species beyond 40 years its value is set to the greater value between old and new grout numbers regardless of which segment is being considered. The Baseline (nominal) case used best estimate values as listed in Table 2-50. For case study D, upper bound values were estimated and used (i.e., best estimate plus 3-sigma values). All other modeling and parameter settings remain unaltered. For case study D, the upper bound estimate values employed are also listed in Table 2-50.

Table 2-50. Mean and upper bound estimates of saturated "effective" molecular diffusion coefficient for cementitious materials employed in CIG Vadose zone modeling

Material Type	Nominal Setting (mean value) (cm^2/yr)	Sensitivity Case Setting (mean value + 3-sigma) (cm^2/yr)
Existing Grout	59.33	85.56
Future Grout	25.25	107.69
CLSM	126.23	182.03
Concrete Slab	25.25	107.69
Waste (less than 40 yrs and volatile species)	1578.00	1578.00
Waste (non-volatile species or volatile species beyond 40 yrs)	59.33	107.69

The following summary of results is for the Case D sensitivity study. Peak well concentrations for Existing and Future Segments are provided in Table 2-51 and Table 2-52, respectively. The total future inventory limits for beta-gamma exposure (i.e., a total of 4.0 mrem/yr) are listed in Table 2-53 and comparison ratios (inventory limit for Case D versus Baseline) are listed in Table 2-54. The shaded values shown in Table 2-54 indicate ratio values less than unity.

Table 2-51. Case D maximum concentrations of radionuclide parent and progeny resulting from the existing 8 segments within the 100-m compliance zone[a]

Parent	Daughters	Time of Peak (0-1125 yrs)	Peak Concentration (pCi/L)	Time of Ultimate Peak (1125+ yrs)	Ultimate Peak Concentration (pCi/L)
Am-241		1,125	5.86E-09	2,403	4.48E-02
	Np-237	702	7.04E-04		
	U-233	1,125	5.23E-09	17,808	1.50E-07
	Th-229	1,125	1.25E-10	19,308	1.01E-07
Am-243		1,125	3.72E-13	3,493	2.25E-02
	Pu-239	1,125	1.55E-16	6,603	6.39E-04
	U-235	1,125	1.41E-24	11,808	1.58E-09
	Pa-231	1,125	1.68E-11	8,773	4.16E-10
	Ac-227	1,125	3.59E-13	8,743	9.37E-12
C-14		350	1.37E+02		
C-14_K		347	1.83E+01		
Cm-244		1,125	1.32E-30	1,266	2.84E-30
	Pu-240	1,125	4.91E-32	8,123	3.52E-03
	U-236	1,125	2.84E-38	21,308	3.85E-07
	Th-232	1,125	5.23E-47	25,608	3.17E-13
	Ra-228	1,125	6.94E-29	25,308	1.48E-11
Cm-245		1,125	1.02E-15	3,503	4.84E-04
	Pu-241	1,125	2.64E-16	3,513	1.90E-04
	Am-241	1,125	6.22E-16	3,513	5.08E-04
	Np-237	1,125	2.99E-07	1,453	3.06E-07
	U-233	1,125	2.13E-12	22,308	1.34E-11
	Th-229	1,125	4.37E-14	23,908	9.74E-12
Cm-247		1,125	2.12E-17	3,523	3.66E-03
	Am-243	1,125	2.22E-18	3,593	1.04E-03
	Pu-239	1,125	6.80E-22	5,313	2.37E-05
	U-235	1,125	4.62E-30	9,533	3.37E-11
	Pa-231	1,125	6.33E-14	7,673	6.58E-12
	Ac-227	1,125	1.32E-15	7,663	1.47E-13
Cm-248		1,125	2.11E-17	3,523	3.63E-03
	Pu-244	1,125	1.82E-24	6,513	2.91E-08
	Pu-240	1,125	5.19E-27	8,293	1.30E-08
	U-236	1,125	1.05E-33	11,808	7.37E-13
	Th-232	1,125	7.54E-43	18,108	2.20E-19
	Ra-228	1,125	9.89E-36	17,908	1.01E-17
H-3		29	1.15E+04		
I-129		341	3.25E-02		
I-129_K		454	1.05E-03		
Ni-59		1,125	1.67E-02	2,723	8.39E-02
Np-237		814	7.59E-02		
	U-233	1,125	5.26E-07	17,908	3.94E-05
	Th-229	1,125	1.05E-08	19,308	2.64E-05
Pd-107		1,125	5.60E-05	2,843	4.68E-04
Pu-238		1,125	3.31E-32	3,333	2.20E-15
	U-234	1,125	9.04E-37	18,608	4.56E-04
	Th-230	1,125	1.58E-40	23,008	6.46E-05
	Ra-226	1,125	6.64E-06	18,208	2.65E-04
	Pb-210	1,125	2.01E-08	18,308	9.07E-07

[a]maximum based on first 1,000 years and its ultimate peak if beyond 1,000 years

Table 2-51. Case D maximum concentrations of radionuclide parent and progeny resulting from the existing 8 segments within the 100-m compliance zone[a] - continued

Parent	Daughters	Time of Peak (0-1125 yrs)	Peak Concentration (pCi/L)	Time of Ultimate Peak (1125+ yrs)	Ultimate Peak Concentration (pCi/L)
Pu-239		1,125	1.17E-27	7,033	6.01E+00
	U-235	1,125	9.39E-36	14,308	1.21E-05
	Pa-231	1,125	6.06E-07	7,743	2.92E-06
	Ac-227	1,125	1.34E-08	7,693	6.60E-08
Pu-240		1,125	3.62E-30	7,713	1.99E-01
	U-236	1,125	8.71E-37	18,308	2.06E-05
	Th-232	1,125	7.04E-46	22,208	1.46E-11
	Ra-228	1,125	5.88E-25	21,908	6.78E-10
Pu-241		1,125	1.94E-51	1,423	6.11E-50
	Am-241	1,125	4.28E-09	2,403	3.19E-02
	Np-237	695	4.79E-04		
	U-233	1,125	3.56E-09	17,808	9.73E-08
	Th-229	1,125	8.54E-11	19,308	6.52E-08
Pu-242		1,125	4.04E-34	7,793	8.23E-04
	U-238	1,125	5.06E-43	15,208	2.61E-10
	U-234	1,125	3.12E-47	18,208	9.83E-12
	Th-230	1,125	4.62E-51	21,108	6.41E-13
	Ra-226	1,125	1.38E-16	17,808	1.84E-12
	Pb-210	1,125	3.90E-19	17,808	6.29E-15
Se-79		1,125	2.00E-57	25,208	2.25E-03
Sn-126		1,125	1.57E-108	165,408	9.03E-06
Sr-90		597	4.78E-04		
Tc-99		240	1.09E+01		
Tc-99_K		377	4.64E-01		
U-233		1,125	2.13E-51	20,908	1.35E+00
	Th-229	1,125	1.30E-53	22,408	9.56E-01
U-234		1,125	4.17E-51	17,008	4.16E-01
	Th-230	1,125	2.50E-54	19,208	5.31E-02
	Ra-226	1,125	7.83E-03	15,108	1.66E-01
	Pb-210	1,125	2.44E-05	15,208	5.66E-04
U-235		1,125	1.13E-52	17,008	1.16E-02
	Pa-231	1,033	3.17E-03		
	Ac-227	1,042	7.21E-05		
U-236		1,125	3.36E-53	17,908	5.02E-03
	Th-232	1,125	1.08E-61	20,408	3.90E-09
	Ra-228	1,125	8.99E-21	20,108	1.81E-07
U-238		1,125	1.93E-50	16,508	1.93E+00
	U-234	1,125	6.41E-53	17,408	9.07E-02
	Th-230	1,125	3.60E-56	19,108	6.30E-03
	Ra-226	1,125	3.17E-05	16,008	1.53E-02
	Pb-210	1,125	9.43E-08	16,008	5.24E-05
Zr-93		1,125	1.03E-22	4,593	3.20E-02
	Nb-93m	1,125	1.62E+00	3,813	2.28E+00

[a]maximum based on first 1,000 years and its ultimate peak if beyond 1,000 years

Table 2-52. Case D maximum concentrations (per Ci of parent buried) of radionuclide parent and progeny resulting from all future inventories within the 100-m compliance zone[a]

Parent	Daughters	Time of Peak (0-1125 yrs)	Peak Concentration (pCi/L-Ci$_{parent}$)	Time of Ultimate Peak (1125+ yrs)	Ultimate Peak Concentration (pCi/L-Ci$_{parent}$)
Am-241		1,125	1.29E-04	2,123	1.24E+00
	Np-237	697	1.35E-02		
	U-233	1,125	1.01E-07	15,208	2.80E-06
	Th-229	1,125	2.45E-09	17,508	1.81E-06
Am-243		1,125	7.22E-04	2,433	3.89E+01
	Pu-239	1,125	4.38E-07	4,353	8.71E-01
	U-235	1,125	5.65E-15	8,223	1.46E-06
	Pa-231	1,125	2.19E-08	6,103	2.61E-07
	Ac-227	1,125	4.70E-10	6,083	5.85E-09
C-14		347	1.71E+03		
C-14_K		362	1.89E+02		
Cl-36		336	2.18E+03		
Cm-244		1,025	2.78E-22		
	Pu-240	1,125	7.15E-21	6,033	2.67E-02
	U-236	1,125	2.61E-27	13,608	2.07E-06
	Th-232	1,125	3.49E-36	17,308	1.10E-12
	Ra-228	1,125	5.66E-23	17,008	5.10E-11
Cm-245		1,125	7.32E-04	2,433	4.01E+01
	Pu-241	1,125	2.11E-04	2,443	1.57E+01
	Am-241	1,125	4.88E-04	2,453	4.12E+01
	Np-237	1,125	1.80E-02	1,443	1.84E-02
	U-233	1,125	1.35E-07	15,908	9.80E-07
	Th-229	1,125	2.91E-09	17,408	6.32E-07
Cm-247		1,125	8.04E-04	2,453	4.89E+01
	Am-243	1,125	8.18E-05	2,733	1.07E+01
	Pu-239	1,125	4.74E-08	3,703	1.83E-01
	U-235	1,125	5.94E-16	6,593	1.79E-07
	Pa-231	1,125	7.21E-10	6,163	2.72E-08
	Ac-227	1,125	1.51E-11	6,143	6.06E-10
Cm-248		1,125	8.02E-04	2,453	4.87E+01
	Pu-244	1,125	1.34E-10	4,323	3.05E-04
	Pu-240	1,125	7.08E-13	5,813	1.01E-04
	U-236	1,125	2.59E-19	8,333	4.05E-09
	Th-232	1,125	3.29E-28	14,408	9.20E-16
	Ra-228	1,125	3.19E-25	14,308	4.18E-14
H-3		28	4.60E-02		
I-129		341	3.01E+03		
I-129_C		451	5.53E+01		
I-129_K		451	9.01E+00		
K-40		1,125	2.17E-06	3,363	3.11E+01
Mo-93		236	9.12E+02		
	Nb-93m	236	9.04E+02		
Nb-94		800	3.94E+01	2,093	6.33E+02
Ni-59		1,125	1.76E+01	2,533	8.62E+01
Np-237		807	6.30E+01		
	U-233	1,125	4.44E-04	15,108	3.24E-02
	Th-229	1,125	9.10E-06	17,508	2.10E-02
Pd-107		1,125	1.78E+01	2,533	8.82E+01

[a]maximum based on first 1,000 years and its ultimate peak if beyond 1,000 years

Table 2-52. Case D maximum concentrations (per Ci of parent buried) of radionuclide parent and progeny resulting from all future inventories within the 100-m compliance zone[a] - continued

Parent	Daughters	Time of Peak (0-1125 yrs)	Peak Concentration (pCi/L-Ci$_{parent}$)	Time of Ultimate Peak (1125+ yrs)	Ultimate Peak Concentration (pCi/L-Ci$_{parent}$)
Pu-238		1,125	2.82E-22	2,813	1.23E-12
	U-234	1,125	1.11E-26	14,908	2.37E-03
	Th-230	1,125	2.70E-30	18,708	2.90E-04
	Ra-226	1,125	4.15E-05	14,508	9.86E-04
	Pb-210	1,125	1.29E-07	14,508	3.37E-06
Pu-239		1,125	2.45E-18	6,133	1.54E+01
	U-235	1,125	2.64E-26	13,008	3.19E-05
	Pa-231	1,125	1.61E-06	7,433	7.38E-06
	Ac-227	1,125	3.57E-08	7,383	1.67E-07
Pu-240		1,125	2.24E-18	6,033	9.65E+00
	U-236	1,125	7.26E-25	13,608	7.53E-04
	Th-232	1,125	7.79E-34	17,308	4.03E-10
	Ra-228	1,125	2.14E-20	17,008	1.86E-08
Pu-241		1,125	3.95E-42	1,194	4.80E-42
	Am-241	1,125	4.41E-06	2,123	4.25E-02
	Np-237	691	4.51E-04		
	U-233	1,125	3.37E-09	15,208	8.83E-08
	Th-229	1,125	8.17E-11	17,508	5.71E-08
Pu-242		1,125	2.53E-18	6,503	1.82E+01
	U-238	1,125	4.27E-27	12,508	5.54E-06
	U-234	1,125	3.50E-31	15,508	1.71E-07
	Th-230	1,125	6.77E-35	17,908	9.55E-09
	Ra-226	1,125	5.16E-12	17,508	2.68E-08
	Pb-210	1,125	1.49E-14	17,508	9.14E-11
Pu-244		1,125	2.54E-18	6,503	1.85E+01
	Pu-240	1,125	2.92E-19	6,843	9.27E+00
	U-236	1,125	9.20E-26	9,703	4.19E-04
	Th-232	1,125	9.65E-35	14,808	1.17E-10
	Ra-228	1,125	8.75E-22	14,508	5.33E-09
Ra-226		934	8.70E+01		
	Pb-210	969	2.93E-01		
Se-79		1,125	2.27E-37	19,408	4.98E+00
Sn-126		1,125	1.73E-75	120,008	6.09E-01
Sr-90		563	2.13E-04		
Tc-99		244	8.93E+02		
Tc-99_K		400	2.91E+01		
Th-230		1,125	1.91E-39	18,208	4.79E+00
	Ra-226	1,125	3.11E+01	1,162	3.12E+01
	Pb-210	1,125	1.05E-01	1,203	1.06E-01
Th-232		1,125	1.93E-39	19,508	5.67E+00
	Ra-228	1,125	1.81E-08	19,108	2.67E+02
U-233		1,125	3.06E-35	14,908	6.49E+00
	Th-229	1,125	2.21E-37	17,308	4.24E+00
U-234		1,125	3.06E-35	14,908	6.64E+00
	Th-230	1,125	2.17E-38	18,808	8.17E-01
	Ra-226	1,125	1.47E-01	14,508	2.78E+00
	Pb-210	1,125	4.65E-04	14,508	9.52E-03

[a]maximum based on first 1,000 years and its ultimate peak if beyond 1,000 years

Table 2-52. Case D maximum concentrations (per Ci of parent buried) of radionuclide parent and progeny resulting from all future inventories within the 100-m compliance zonea [a] - continued

Parent	Daughters	Time of Peak (0-1125 yrs)	Peak Concentration (pCi/L-Ci_{parent})	Time of Ultimate Peak (1125+ yrs)	Ultimate Peak Concentration (pCi/L-Ci_{parent})
U-235		1,125	3.07E-35	15,008	6.93E+00
	Pa-231	1,030	2.16E+00		
	Ac-227	1,040	4.90E-02		
U-236		1,125	3.07E-35	15,008	6.93E+00
	Th-232	1,125	1.17E-43	18,908	4.91E-06
	Ra-228	1,125	1.27E-15	18,608	2.28E-04
U-238		1,125	3.07E-35	15,008	6.93E+00
	U-234	1,125	1.01E-37	17,108	3.13E-01
	Th-230	1,125	6.54E-41	19,108	2.18E-02
	Ra-226	1,125	1.39E-04	15,808	5.84E-02
	Pb-210	1,125	4.19E-07	15,908	2.00E-04
Zr-93		1,125	3.05E-07	3,173	3.66E+01
	Nb-93m	1,125	1.88E+03	2,463	2.21E+03

[a]maximum based on first 1,000 years and its ultimate peak if beyond 1,000 years

Table 2-53. Case D total future inventory limits[a] (in terms of Ci initially buried) for beta-gamma exposure from radionuclide parents

Parent Buried	0 - 125 year Inventory Limit (Ci)	125 - 1,125 year Inventory Limit (Ci)	1,125 - 10,125 year Inventory Limit (Ci)
Am-241	---	2.21E+04	3.23E+04
Am-243	---	4.14E+05	7.69E+00
C-14	6.78E+07	1.05E+00	---
C-14_K	8.35E+08	1.01E+01	5.61E+02
Cl-36	6.18E+03	3.07E-01	---
Cm-244	---	---	2.00E+11
Cm-245	---	1.64E+04	1.62E+01
Cm-247	---	3.10E+06	2.59E+01
Cm-248	---	9.50E+12	4.16E+06
H-3	2.42E+05	2.89E+06	---
I-129	1.22E+03	3.06E-04	---
I-129_C	1.45E+05	1.79E-02	3.17E-02
I-129_K	8.87E+05	1.10E-01	1.81E-01
K-40	---	1.35E+08	9.47E+00
Mo-93	2.64E+02	8.74E-01	7.67E+17
Nb-94	5.36E+16	1.94E+01	1.21E+00
Ni-59	---	1.69E+01	3.47E+00
Np-237	---	4.74E+00	5.48E+00
Pd-107	---	2.05E+03	4.14E+02
Pu-238	---	7.43E+06	3.75E+05
Pu-239	---	1.10E+07	2.34E+06
Pu-240	---	---	5.52E+08
Pu-241	---	6.62E+05	9.82E+05
Pu-242	---	6.40E+13	7.51E+07
Pu-244	---	---	6.91E+01
Ra-226	---	3.29E+00	4.25E+00
Se-79	---	---	9.36E+03
Sn-126	---	---	---
Sr-90	---	3.28E+04	1.22E+11
Tc-99	1.06E+03	9.94E-01	---
Tc-99_K	1.61E+06	2.81E+01	3.69E+01
Th-230	---	9.18E+00	9.07E+00
Th-232	---	2.03E+08	3.42E-01
U-233	---	---	3.56E+01
U-234	---	2.07E+03	1.33E+02
U-235	---	8.03E+00	8.11E+00
U-236	---	2.89E+15	1.90E+05
U-238	---	2.29E+06	2.55E+02
Zr-93	5.57E+16	5.30E-01	4.49E-01

a – These are future inventory limits that represent disposal limits for both CIG units combined. To arrive at the individual limits on a per unit basis, these values must be multiplied by 0.459 for CIG Unit #1 and 0.541 for CIG Unit #2. Total inventory limit estimates greater than $1x10^{20}$ pCi/L are not shown.

Table 2-54. Case D versus Baseline total future inventory limit ratios[a] for beta-gamma exposure from radionuclide parents (values less than one are shaded)

Parent Buried	0 - 125 year Inventory Limit Ratio (-)	125 - 1,125 year Inventory Limit Ratio (-)	1,125 - 10,125 year Inventory Limit Ratio (-)
Am-241	1	1	1
Am-243	1	9.88E-01	1
C-14	7.09E-03	1.06E+00	1
C-14_K	6.68E-03	1.01E+00	9.39E-01
Cl-36	2.88E-02	1.06E+00	1
Cm-244	1	1	1
Cm-245	1	1	1
Cm-247	1	9.88E-01	1
Cm-248	1	9.83E-01	1
H-3	5.09E-02	9.27E-01	1
I-129	1.39E-02	1.08E+00	1
I-129_C	1.27E-02	1	1
I-129_K	1.27E-02	1	1
K-40	1	1.02E+00	1.03E+00
Mo-93	1.77E-01	1.06E+00	7.24E-01
Nb-94	4.49E-03	1	9.86E-01
Ni-59	1	1	1
Np-237	1	1	1
Pd-107	1	1	1
Pu-238	1	1	1
Pu-239	1	1	1
Pu-240	1	1	1
Pu-241	1	1	1
Pu-242	1	1	1
Pu-244	1	1	1
Ra-226	1	1	1.01E+00
Se-79	1	1	1.01E+00
Sn-126	1	1	1.00E+00
Sr-90	1	1	9.13E-01
Tc-99	1.48E-01	1	1
Tc-99_K	1.29E-01	1	1
Th-230	1	1	1
Th-232	1	1	1
U-233	1	1	1
U-234	1	1	1
U-235	1	1	1
U-236	1	1	1
U-238	1	1	1
Zr-93	5.05E-03	1	1

a - Inventory limit ratios that are nearly unity (i.e., no change) are shown as 1.

As shown in Table 2-54, effects due to increased diffusion within the grout chamber are seen in the early time period (i.e., 0 to 125 years) as well as later periods. As highlighted in Table 2-54 by shading, various parent inventory limits are reduced. Some have modest reduction factors. For example, the limit ratio for radionuclide Nb-94 is 4.49×10^{-3} for the time period 0 to 125 years.

Sensitivity Analysis Summary

Above, the transport results for the Baseline case and four sensitivity cases have been presented. Peak maximum well concentrations and beta-gamma dose inventory limits for each radionuclide have been provided in tabular form. In Table 2-55, an overall summary of the Baseline total future inventory limit for beta-gamma exposure versus the minimum value among the five cases considered (i.e., four sensitivity cases plus the Baseline case) is provided for the 125 to 1125 time period. The minimum inventory limit computed within the set of five cases is shaded.

Minimum to Baseline inventory ratios are provided in Table 2-56 for the first two time periods. In many cases the minimum value is the Baseline case and a 1.0 value is obtained. Inventory limits that are less than 1% of their Baseline values are shaded.

Table 2-55. Total future inventory limits[a] for beta-gamma exposure from radionuclide parents for all cases studied (for 125 to 1,125 year time period)

	Baseline Case	Case A	Case B	Case C	Case D
Parent Buried	**Inventory Limit (Ci)**	**Inventory Limit (Ci)**	**Inventory Limit (Ci)**	**Inventory Limit (Ci)**	**Inventory Limit (Ci)**
Am-241	2.20E+04	2.00E+04	1.75E+04	2.09E+04	2.21E+04
Am-243	4.19E+05	2.56E+10	5.82E+02	2.29E+04	4.14E+05
C-14	9.91E-01	1.14E+00	7.72E-01	2.56E-01	1.05E+00
C-14_K	1.00E+01	8.74E+00	1.07E+01	9.70E+00	1.01E+01
Cl-36	2.90E-01	2.97E-01	3.80E-01	2.17E-01	3.07E-01
Cm-244	1.00E+20	4.67E+18	1.00E+20	1.00E+20	1.00E+20
Cm-245	1.64E+04	1.72E+04	1.43E+03	1.37E+04	1.64E+04
Cm-247	3.14E+06	8.19E+11	4.38E+03	1.72E+05	3.10E+06
Cm-248	9.66E+12	1.00E+20	9.67E+09	4.24E+11	9.50E+12
H-3	3.12E+06	3.13E+06	3.12E+06	3.12E+06	2.89E+06
I-129	2.83E-04	4.21E-04	2.61E-04	1.35E-04	3.06E-04
I-129_C	1.79E-02	1.37E-02	1.95E-02	2.13E-02	1.79E-02
I-129_K	1.10E-01	8.43E-02	1.20E-01	1.31E-01	1.10E-01
K-40	1.32E+08	1.89E+03	4.59E+04	1.32E+08	1.35E+08
Mo-93	8.21E-01	8.25E-01	8.20E-01	8.21E-01	8.74E-01
Nb-94	1.93E+01	1.93E+01	1.33E+01	1.88E+01	1.94E+01
Ni-59	1.69E+01	7.85E+00	7.65E+00	1.43E+01	1.69E+01
Np-237	4.74E+00	2.83E+00	3.36E+00	4.69E+00	4.74E+00
Pd-107	2.04E+03	9.49E+02	9.25E+02	1.73E+03	2.05E+03
Pu-238	7.41E+06	5.99E+06	2.00E+06	6.72E+06	7.43E+06
Pu-239	1.10E+07	3.43E+08	1.02E+07	1.14E+07	1.10E+07
Pu-240	1.00E+20	1.23E+16	3.63E+17	9.32E+19	1.00E+20
Pu-241	6.59E+05	6.13E+05	5.30E+05	6.27E+05	6.62E+05
Pu-242	6.40E+13	3.28E+13	1.35E+13	5.54E+13	6.40E+13
Pu-244	1.00E+20	3.58E+17	5.20E+14	1.82E+18	1.00E+20
Ra-226	3.26E+00	2.13E+00	9.26E-01	3.16E+00	3.29E+00
Se-79	1.00E+20	1.00E+20	1.00E+20	1.00E+20	1.00E+20
Sn-126	1.00E+20	1.00E+20	1.00E+20	1.00E+20	1.00E+20
Sr-90	3.15E+04	9.74E+02	4.11E+03	3.11E+04	3.28E+04
Tc-99	9.41E-01	1.06E+00	9.19E-01	9.41E-01	9.94E-01
Tc-99_K	2.81E+01	2.88E+01	2.81E+01	2.99E+01	2.81E+01
Th-230	9.16E+00	9.13E+00	3.11E+00	9.03E+00	9.18E+00
Th-232	2.03E+08	4.63E+04	4.67E+05	1.36E+08	2.03E+08
U-233	1.00E+20	1.00E+20	1.00E+20	1.00E+20	1.00E+20
U-234	2.06E+03	1.83E+03	5.87E+02	1.88E+03	2.07E+03
U-235	8.02E+00	2.04E+02	6.88E+00	8.54E+00	8.03E+00
U-236	2.88E+15	2.05E+11	6.97E+12	1.79E+15	2.89E+15
U-238	2.29E+06	1.48E+06	5.50E+05	2.02E+06	2.29E+06
Zr-93	5.30E-01	1.74E+00	5.07E-01	5.21E-01	5.30E-01

a – The minimum inventory limit value for each radionuclide is shaded.

Table 2-56. Comparison of Minimum to Baseline total future inventory limit ratios[a] for beta-gamma exposure from radionuclide parents

Parent Buried	Baseline Case 0 - 125 year Inventory Limit (Ci)	Baseline Case 125 - 1,125 year Inventory Limit (Ci)	Minimum/Baseline 0 - 125 year Inventory Limit Ratio (-)	Minimum/Baseline 125 - 1,125 year Inventory Limit Ratio (-)
Am-241	---	2.20E+04	1	7.99E-01
Am-243	---	4.19E+05	1	1.39E-03
C-14	9.56E+09	9.91E-01	7.09E-03	2.59E-01
C-14_K	1.25E+11	1.00E+01	6.68E-03	8.71E-01
Cl-36	2.15E+05	2.90E-01	2.88E-02	7.49E-01
Cm-244	---	---	1	4.67E-02
Cm-245	---	1.64E+04	1	8.69E-02
Cm-247	---	3.14E+06	1	1.40E-03
Cm-248	---	9.66E+12	1	1.00E-03
H-3	4.75E+06	3.12E+06	4.01E-02	9.27E-01
I-129	8.79E+04	2.83E-04	1.39E-02	4.78E-01
I-129_C	1.13E+07	1.79E-02	1.27E-02	7.69E-01
I-129_K	6.98E+07	1.10E-01	1.27E-02	7.69E-01
K-40	---	1.32E+08	1	1.42E-05
Mo-93	1.49E+03	8.21E-01	1.77E-01	9.98E-01
Nb-94	1.19E+19	1.93E+01	2.23E-03	6.88E-01
Ni-59	---	1.69E+01	1	4.53E-01
Np-237	---	4.74E+00	1	5.98E-01
Pd-107	---	2.04E+03	1	4.53E-01
Pu-238	---	7.41E+06	1	2.69E-01
Pu-239	---	1.10E+07	1	9.24E-01
Pu-240	---	1.00E+20	1	1.23E-04
Pu-241	---	6.59E+05	1	8.04E-01
Pu-242	---	6.40E+13	1	2.12E-01
Pu-244	---	1.00E+20	1	5.20E-06
Ra-226	---	3.26E+00	1	2.84E-01
Se-79	---	---	1	1.00E+00
Sn-126	---	---	1	1.00E+00
Sr-90	---	3.15E+04	1	3.10E-02
Tc-99	7.14E+03	9.41E-01	1.48E-01	9.76E-01
Tc-99_K	1.25E+07	2.81E+01	1.29E-01	1.00E+00
Th-230	---	9.16E+00	1	3.40E-01
Th-232	---	2.03E+08	1	2.29E-04
U-233	---	---	1	1.00E+00
U-234	---	2.06E+03	1	2.85E-01
U-235	---	8.02E+00	1	8.58E-01
U-236	---	2.88E+15	1	7.12E-05
U-238	---	2.29E+06	1	2.41E-01
Zr-93	1.10E+19	5.30E-01	5.05E-03	9.58E-01

a - Inventory limit ratios that are nearly unity (i.e., no change) are shown as 1 and values significantly less than 1 are shaded.

In several cases the inventory ratio is significantly less than one and are shaded (i.e., ratio values less than 1%). These radionuclide parents with their abbreviated chains are:

- Am-243 > Pu-239 > U-235 > Pa-231 > Ac-227
- C-14
- C-14_K
- Cm-247 > Am-243 > Pu-239 > U-235 > Pa-231 > Ac-227
- Cm-248 > Pu-244 > Pu-240 > U-236 > Th-232 > Ra-228
- K-40
- Nb-94
- Pu-240 > U-236 > Th-232 > Ra-228
- Pu-244 > Pu-240 > U-236 > Th-232 > Ra-228
- Th-232 > Ra-228
- U-236 > Th-232 > Ra-228
- Zr-93 > Nb-93m

The significant reductions in inventory limit can better be understood by looking at the Future Segment beta-gamma dose curves (per Ci of parent buried) for all twelve cases considered, as shown in Figure 2-60 through Figure 2-71.

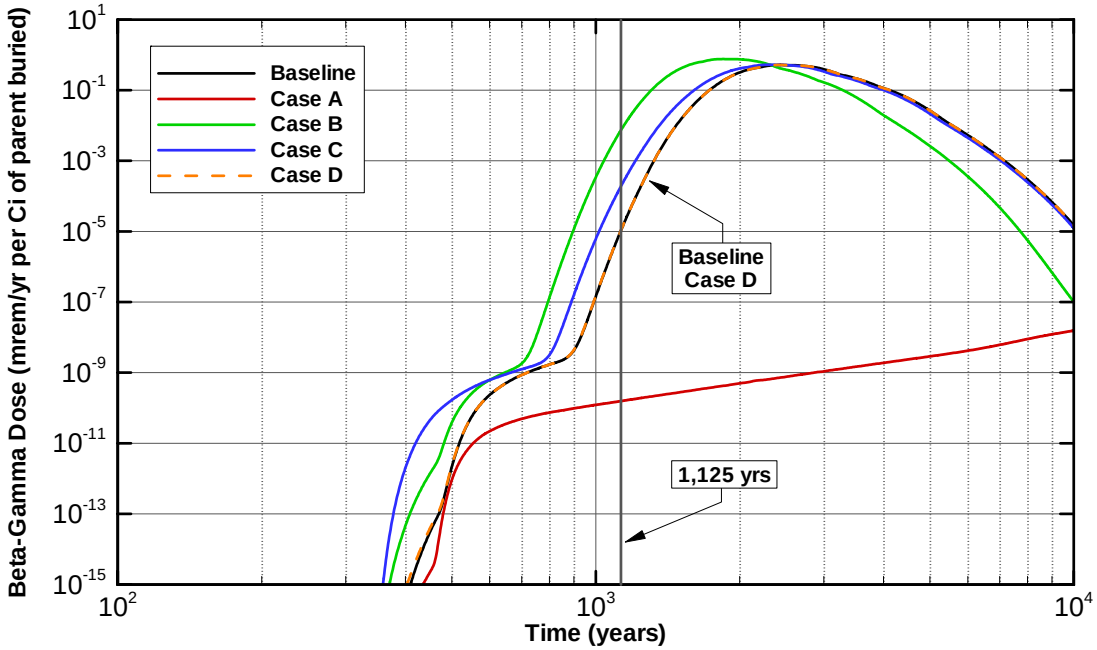

Figure 2-60. Maximum well concentrations within the 100-m compliance region for Am-243 case studies based on a Future Segment inventory of 1.0 Ci

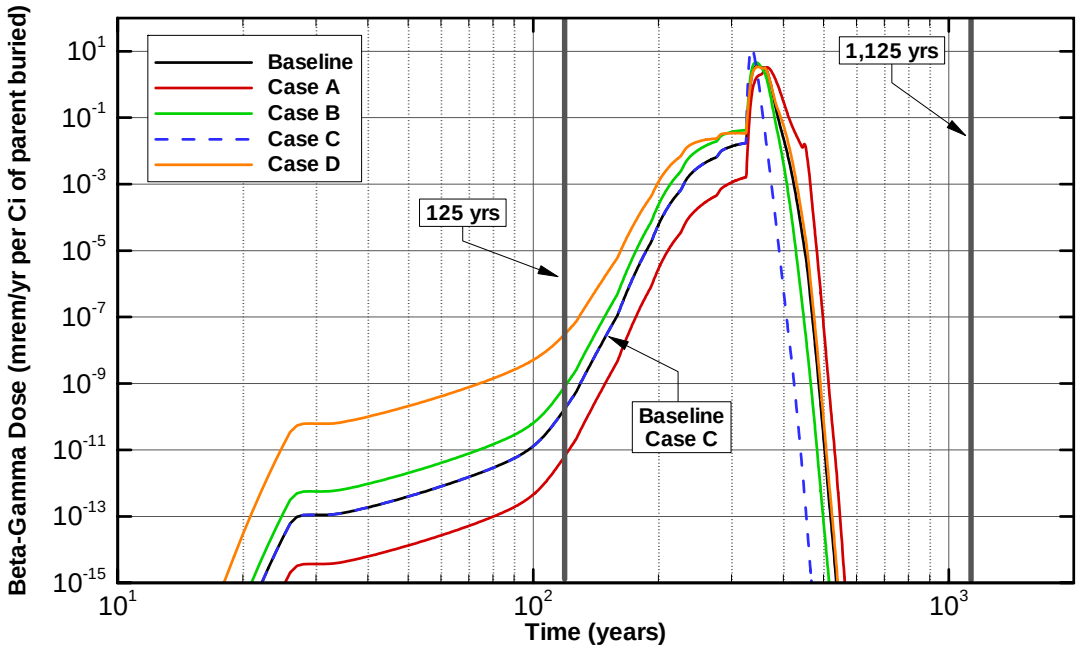

Figure 2-61. Maximum well concentrations within the 100-m compliance region for C-14 case studies based on a Future Segment inventory of 1.0 Ci

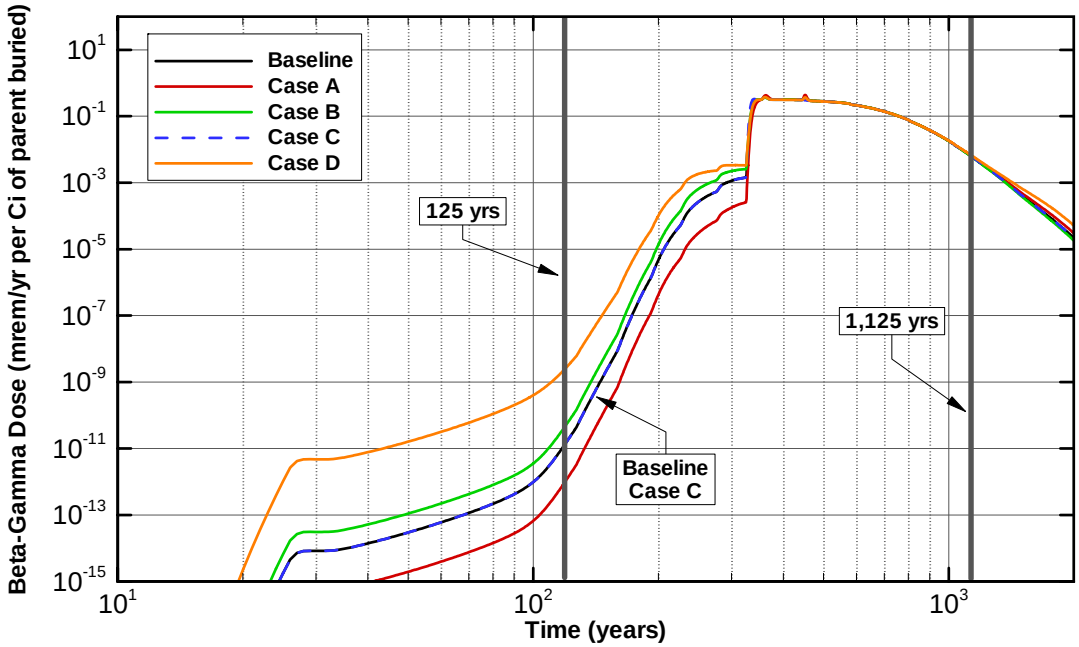

Figure 2-62. Maximum well concentrations within the 100-m compliance region for C-14_K case studies based on a Future Segment inventory of 1.0 Ci

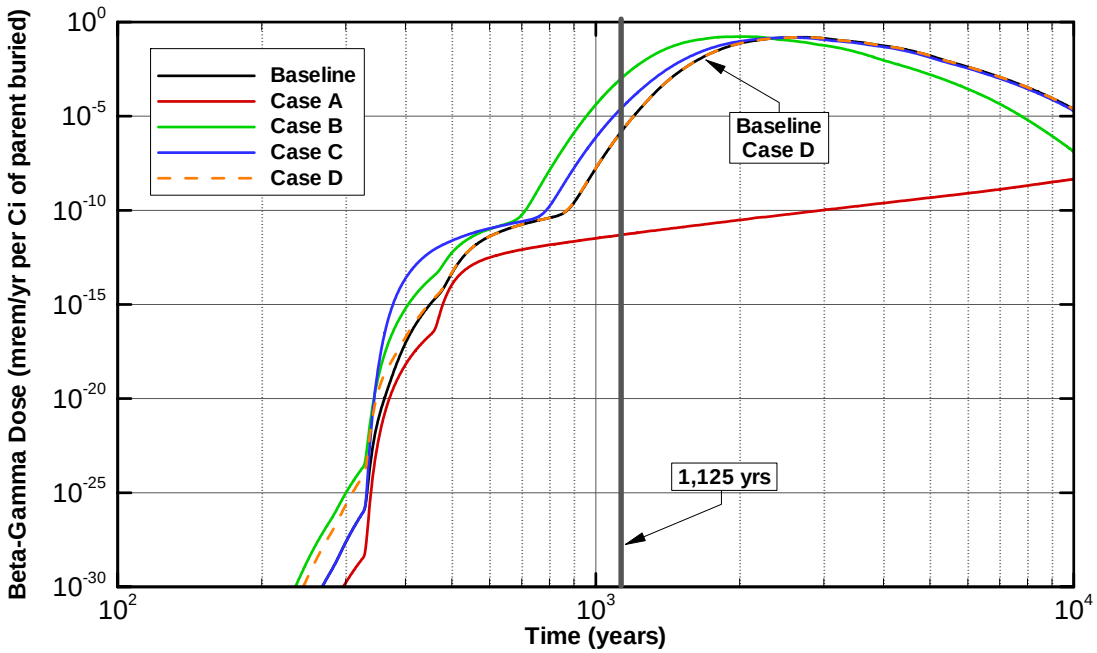

Figure 2-63. Maximum well concentrations within the 100-m compliance region for Cm-247 case studies based on a Future Segment inventory of 1.0 Ci

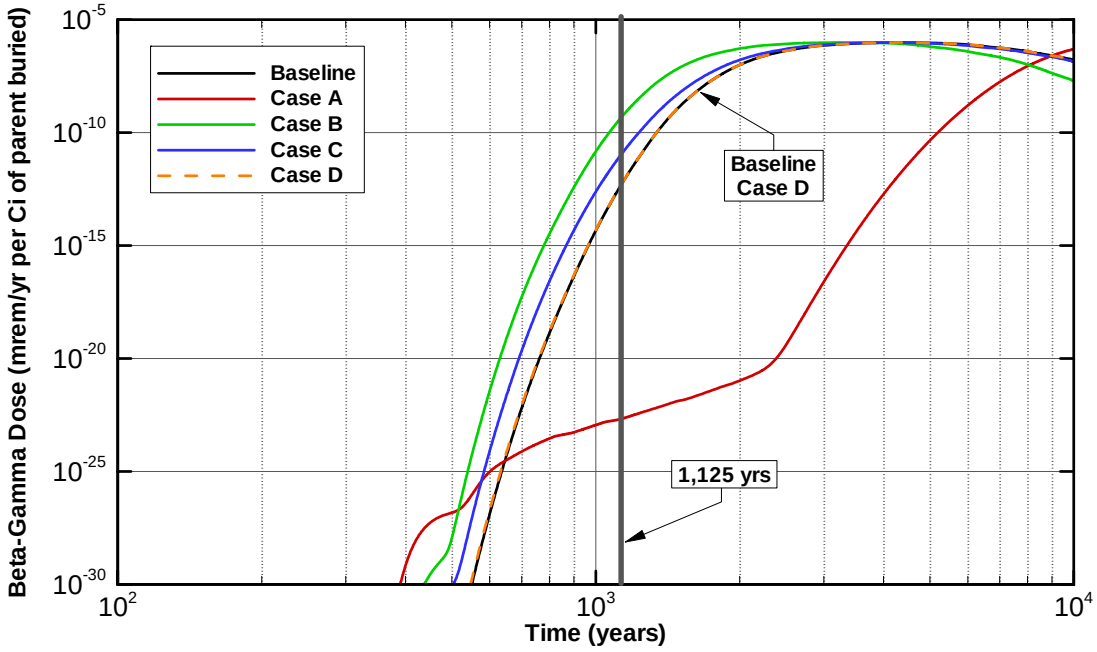

Figure 2-64. Maximum well concentrations within the 100-m compliance region for Cm-248 case studies based on a Future Segment inventory of 1.0 Ci

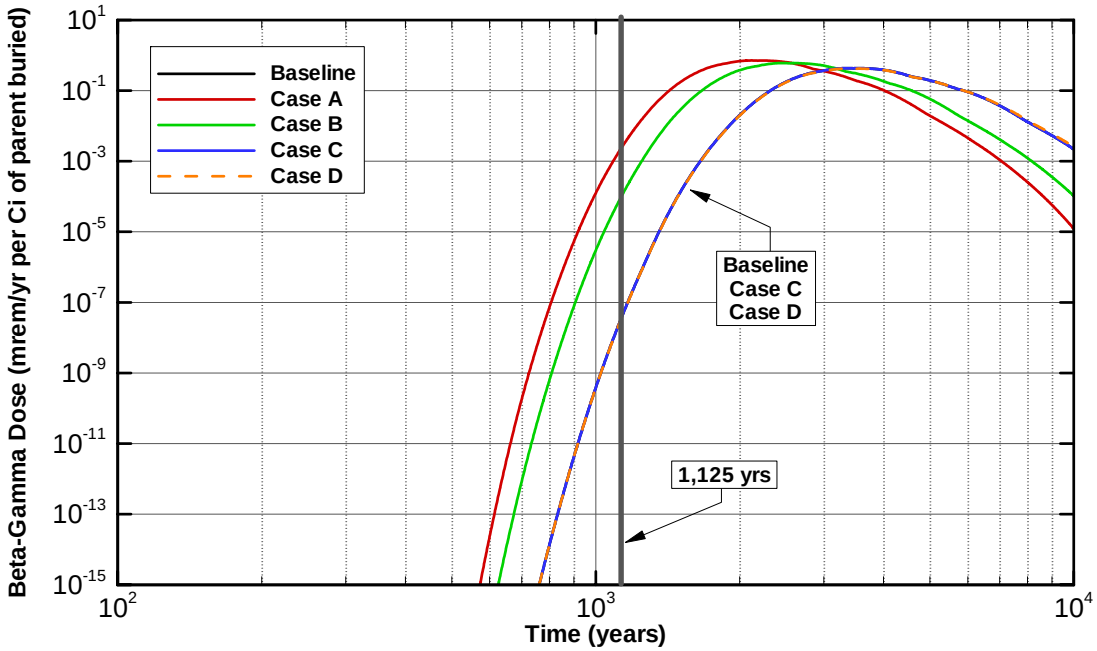

Figure 2-65. Maximum well concentrations within the 100-m compliance region for K-40 case studies based on a Future Segment inventory of 1.0 Ci

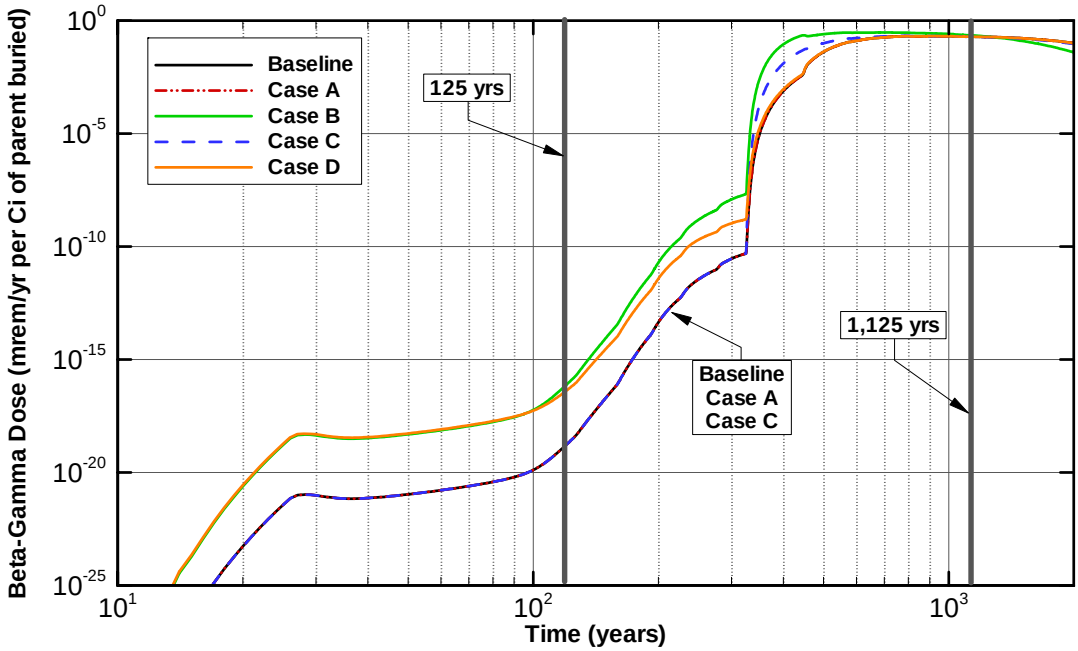

Figure 2-66. Maximum well concentrations within the 100-m compliance region for Nb-94 case studies based on a Future Segment inventory of 1.0 Ci

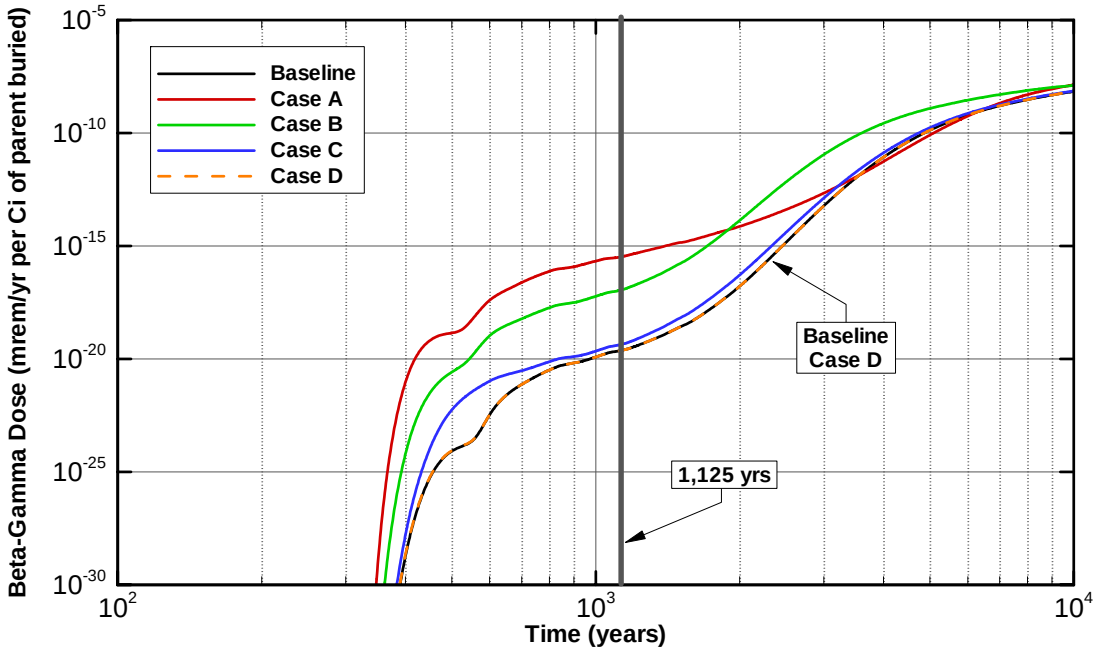

Figure 2-67. Maximum well concentrations within the 100-m compliance region for Pu-240 case studies based on a Future Segment inventory of 1.0 Ci

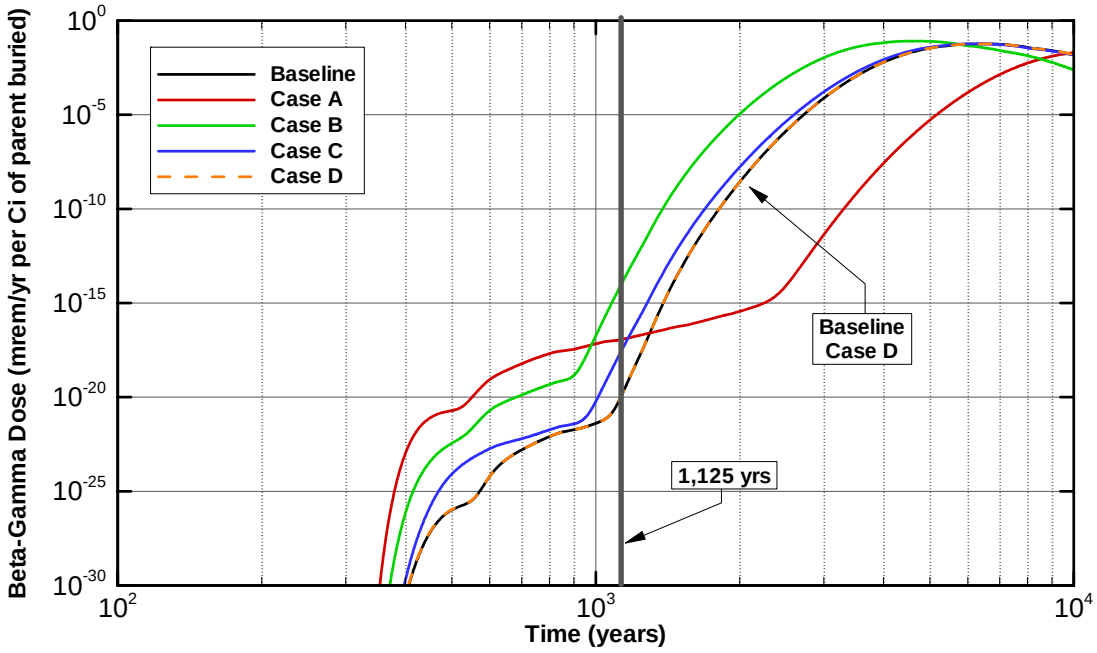

Figure 2-68. Maximum well concentrations within the 100-m compliance region for Pu-244 case studies based on a Future Segment inventory of 1.0 Ci

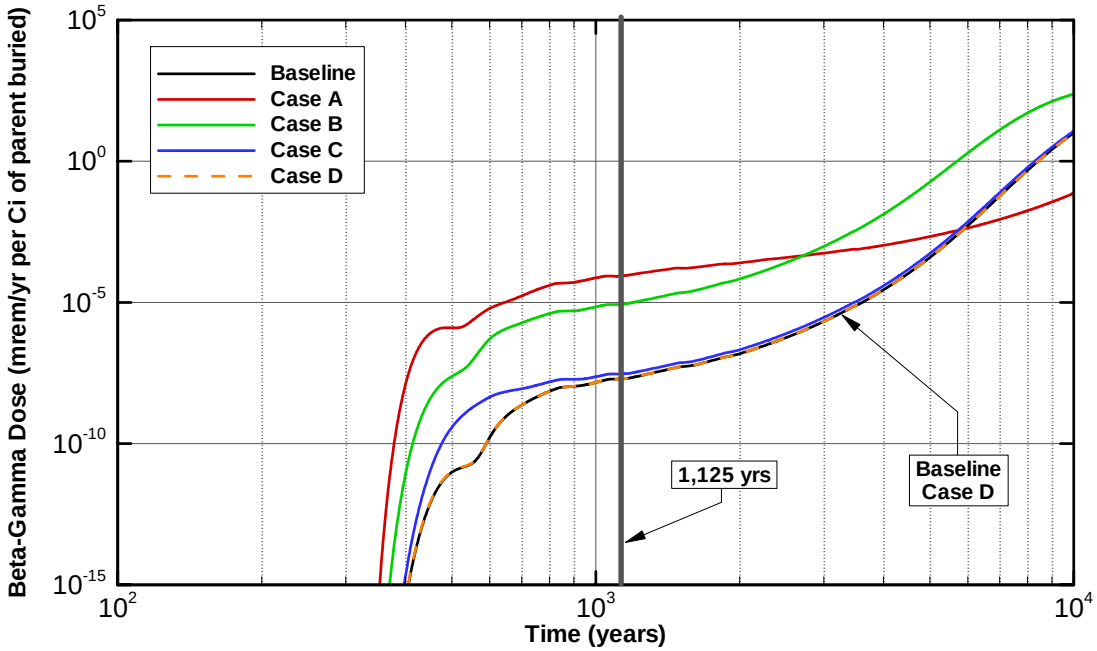

Figure 2-69. Maximum well concentrations within the 100-m compliance region for Th-232 case studies based on a Future Segment inventory of 1.0 Ci

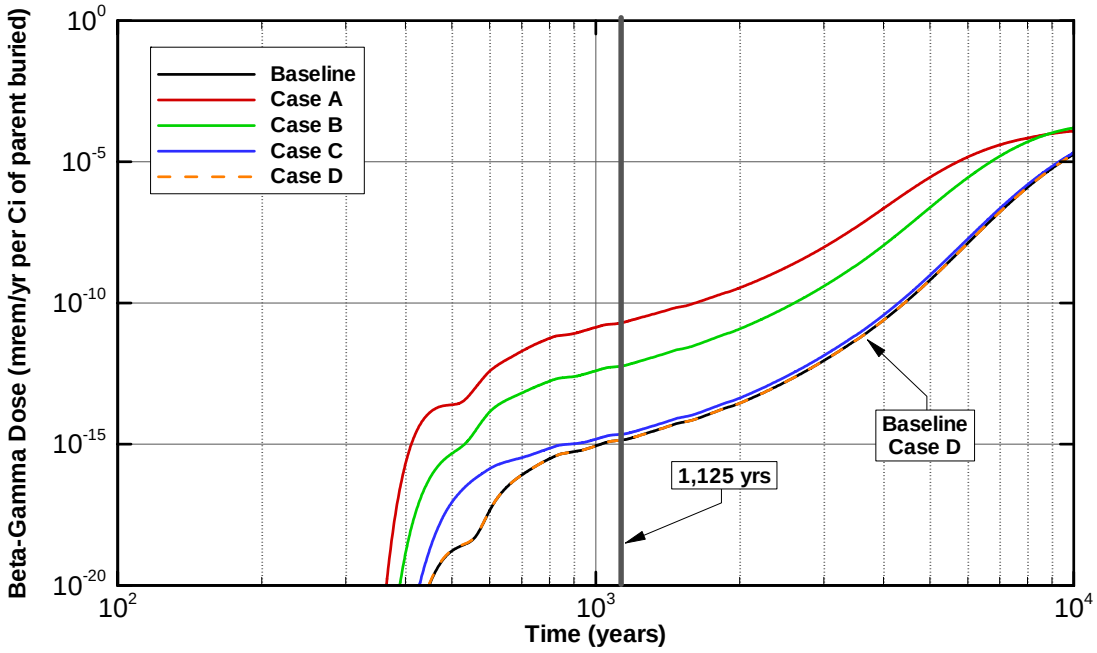

Figure 2-70. Maximum well concentrations within the 100-m compliance region for U-236 case studies based on a Future Segment inventory of 1.0 Ci

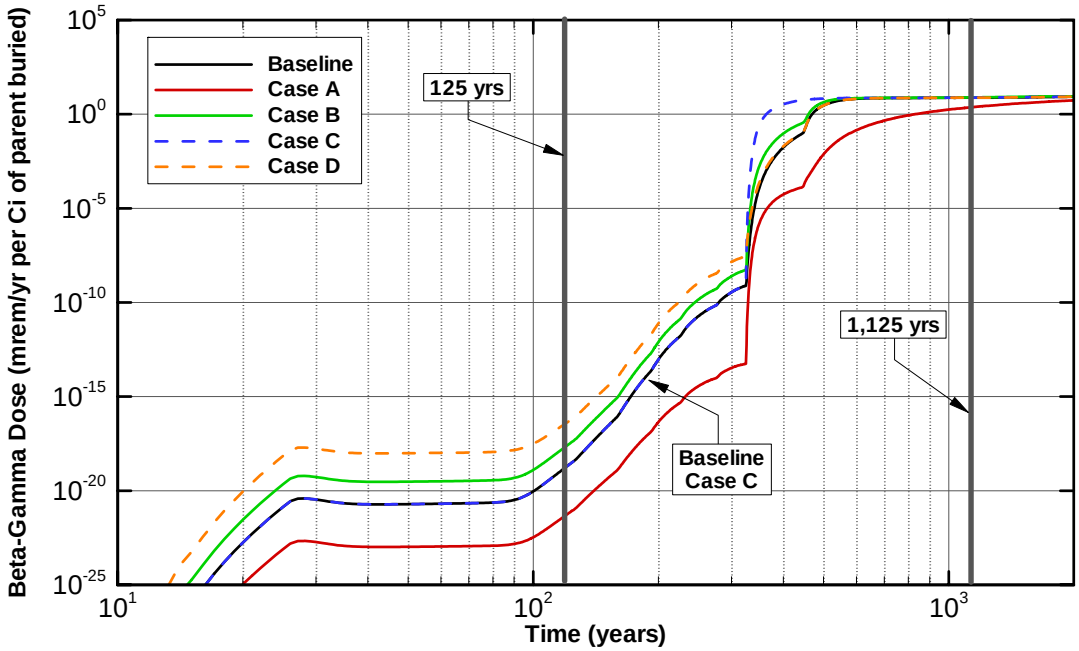

Figure 2-71. Maximum well concentrations within the 100-m compliance region for Zr-93 case studies based on a Future Segment inventory of 1.0 Ci

The higher the beta-gamma dose per Ci buried, the lower its allowable inventory limit will be. In the majority of cases, these significant inventory limit shifts are the direct result of the compliance window chosen. When looking at inventory limits associated with the ultimate concentration peaks, significant differences between the various sensitivity cases versus the Baseline Case are not apparent.

From the 12 cases presented, the following general observations are made:

- For the first time period (i.e., 0 to 125 years), the effects of increased diffusion (Case D) have a more dominant impact.
- For the second time period (i.e., 125 to 1125 years), the effects of decreased sorption K_d values (Case A or Case B) have a more dominant impact.

For completeness the total future inventory limits (in the 125 to 1,125 year time period) for LADTAP, beta-gamma, gross-alpha, radium, and uranium exposures are summarized for all five cases considered in Table 2-57 through Table 2-61, respectively. The minimum inventory values are shaded in gray and the percentage of each minimum versus its Baseline value is provided in the farthermost column to the right in each table. Minimums that are less that 1% of the Baseline values are shaded in yellow; those that are less than 0.01% of Baseline value are shaded in red.

Table 2-57. Total future inventory limits[a] for LADTAP exposure from radionuclide parents for all cases studied (for 125 to 1,125 year time period)

	Baseline Case	Case A	Case B	Case C	Case D	% of Baseline
Parent Buried	**Inventory Limit (Ci)**	**Inventory Limit (Ci)**	**Inventory Limit (Ci)**	**Inventory Limit (Ci)**	**Inventory Limit (Ci)**	**(%)**
Am-241	3.36E+02	3.02E+02	5.38E+01	3.20E+02	3.37E+02	16.0
Am-243	7.84E+03	8.19E+07	1.09E+01	4.29E+02	7.75E+03	0.14
C-14	1.07E+00	1.21E+00	8.35E-01	2.88E-01	1.13E+00	27.0
C-14_K	1.06E+01	9.24E+00	1.12E+01	1.09E+01	1.06E+01	87.5
Cl-36	1.58E-01	1.60E-01	2.07E-01	1.23E-01	1.67E-01	77.9
Cm-244	1.00E+20	1.24E+19	9.46E+14	3.12E+18	1.00E+20	0.0009
Cm-245	2.41E+02	2.63E+02	5.98E+00	1.28E+02	2.41E+02	2.5
Cm-247	6.74E+03	2.53E+09	9.37E+00	3.69E+02	6.66E+03	0.14
Cm-248	1.88E+03	1.00E+20	2.61E+00	1.03E+02	1.86E+03	0.14
H-3	8.14E+07	8.16E+07	8.14E+07	8.14E+07	7.55E+07	92.7
I-129	1.78E-02	2.61E-02	1.64E-02	8.80E-03	1.92E-02	49.5
I-129_C	1.08E+00	8.33E-01	1.18E+00	1.38E+00	1.08E+00	77.1
I-129_K	6.64E+00	5.12E+00	7.25E+00	8.47E+00	6.65E+00	77.0
K-40	2.87E+08	4.09E+03	9.93E+04	2.87E+08	2.93E+08	0.0014
Mo-93	3.95E+00	3.96E+00	3.95E+00	3.95E+00	4.20E+00	100
Nb-94	1.08E+01	1.06E+01	7.35E+00	1.05E+01	1.08E+01	68.3
Ni-59	4.18E+03	1.95E+03	1.89E+03	3.54E+03	4.20E+03	45.2
Np-237	7.22E-02	4.26E-02	5.08E-02	7.16E-02	7.23E-02	59.0
Pd-107	6.39E+03	2.97E+03	2.89E+03	5.41E+03	6.41E+03	45.3
Pu-238	3.44E+05	2.28E+05	2.26E+05	3.17E+05	3.44E+05	65.8
Pu-239	1.05E+06	1.14E+06	1.06E+06	1.10E+06	1.05E+06	100
Pu-240	2.61E+18	3.28E+16	2.65E+12	9.31E+15	2.55E+18	0.00010
Pu-241	1.01E+04	9.23E+03	1.58E+03	9.59E+03	1.01E+04	15.7
Pu-242	2.77E+12	1.18E+12	9.09E+11	2.46E+12	2.77E+12	32.9
Pu-244	2.20E+18	9.53E+17	2.23E+12	7.82E+15	2.15E+18	0.00010
Ra-226	1.62E-01	7.88E-02	1.05E-01	1.57E-01	1.64E-01	48.6
Se-79	1.00E+20	1.00E+20	1.00E+20	1.00E+20	1.00E+20	100
Sn-126	1.00E+20	1.00E+20	1.00E+20	1.00E+20	1.00E+20	100
Sr-90	6.05E+05	1.88E+04	7.90E+04	5.92E+05	6.31E+05	3.1
Tc-99	1.42E+00	1.59E+00	1.39E+00	1.42E+00	1.50E+00	98
Tc-99_K	4.31E+01	4.39E+01	4.31E+01	4.58E+01	4.32E+01	100
Th-230	4.58E-01	3.44E-01	3.59E-01	4.56E-01	4.58E-01	75.2
Th-232	5.39E+08	1.23E+05	1.24E+06	3.62E+08	5.39E+08	0.023
U-233	1.00E+20	1.00E+20	1.00E+20	1.00E+20	1.00E+20	100
U-234	9.70E+01	6.98E+01	6.72E+01	8.98E+01	9.72E+01	69.3
U-235	7.85E-01	6.75E-01	7.11E-01	8.39E-01	7.86E-01	86.1
U-236	7.67E+15	5.46E+11	1.85E+13	4.78E+15	7.68E+15	0.0071
U-238	1.03E+05	5.49E+04	6.04E+04	9.28E+04	1.03E+05	53.5
Zr-93	3.11E+00	1.02E+01	2.98E+00	3.06E+00	3.11E+00	95.8

a – The minimum inventory limit value for each radionuclide is shaded.

Table 2-58. Total future inventory limits[a] for beta-gamma exposure from radionuclide parents for all cases studied (for 125 to 1,125 year time period)

	Baseline Case	Case A	Case B	Case C	Case D	% of Baseline
Parent Buried	**Inventory Limit (Ci)**	**Inventory Limit (Ci)**	**Inventory Limit (Ci)**	**Inventory Limit (Ci)**	**Inventory Limit (Ci)**	**(%)**
Am-241	2.20E+04	2.00E+04	1.75E+04	2.09E+04	2.21E+04	79.9
Am-243	4.19E+05	2.56E+10	5.82E+02	2.29E+04	4.14E+05	0.14
C-14	9.91E-01	1.14E+00	7.72E-01	2.56E-01	1.05E+00	25.9
C-14_K	1.00E+01	8.74E+00	1.07E+01	9.70E+00	1.01E+01	87.1
Cl-36	2.90E-01	2.97E-01	3.80E-01	2.17E-01	3.07E-01	74.9
Cm-244	1.00E+20	4.67E+18	1.00E+20	1.00E+20	1.00E+20	4.7
Cm-245	1.64E+04	1.72E+04	1.43E+03	1.37E+04	1.64E+04	8.7
Cm-247	3.14E+06	8.19E+11	4.38E+03	1.72E+05	3.10E+06	0.14
Cm-248	9.66E+12	1.00E+20	9.67E+09	4.24E+11	9.50E+12	0.10
H-3	3.12E+06	3.13E+06	3.12E+06	3.12E+06	2.89E+06	92.7
I-129	2.83E-04	4.21E-04	2.61E-04	1.35E-04	3.06E-04	47.8
I-129_C	1.79E-02	1.37E-02	1.95E-02	2.13E-02	1.79E-02	76.9
I-129_K	1.10E-01	8.43E-02	1.20E-01	1.31E-01	1.10E-01	76.9
K-40	1.32E+08	1.89E+03	4.59E+04	1.32E+08	1.35E+08	0.0014
Mo-93	8.21E-01	8.25E-01	8.20E-01	8.21E-01	8.74E-01	99.8
Nb-94	1.93E+01	1.93E+01	1.33E+01	1.88E+01	1.94E+01	68.8
Ni-59	1.69E+01	7.85E+00	7.65E+00	1.43E+01	1.69E+01	45.3
Np-237	4.74E+00	2.83E+00	3.36E+00	4.69E+00	4.74E+00	59.8
Pd-107	2.04E+03	9.49E+02	9.25E+02	1.73E+03	2.05E+03	45.3
Pu-238	7.41E+06	5.99E+06	2.00E+06	6.72E+06	7.43E+06	26.9
Pu-239	1.10E+07	3.43E+08	1.02E+07	1.14E+07	1.10E+07	92.4
Pu-240	1.00E+20	1.23E+16	3.63E+17	9.32E+19	1.00E+20	0.012
Pu-241	6.59E+05	6.13E+05	5.30E+05	6.27E+05	6.62E+05	80.4
Pu-242	6.40E+13	3.28E+13	1.35E+13	5.54E+13	6.40E+13	21.2
Pu-244	1.00E+20	3.58E+17	5.20E+14	1.82E+18	1.00E+20	0.00052
Ra-226	3.26E+00	2.13E+00	9.26E-01	3.16E+00	3.29E+00	28.4
Se-79	1.00E+20	1.00E+20	1.00E+20	1.00E+20	1.00E+20	100
Sn-126	1.00E+20	1.00E+20	1.00E+20	1.00E+20	1.00E+20	100
Sr-90	3.15E+04	9.74E+02	4.11E+03	3.11E+04	3.28E+04	3.1
Tc-99	9.41E-01	1.06E+00	9.19E-01	9.41E-01	9.94E-01	97.6
Tc-99_K	2.81E+01	2.88E+01	2.81E+01	2.99E+01	2.81E+01	100
Th-230	9.16E+00	9.13E+00	3.11E+00	9.03E+00	9.18E+00	34.0
Th-232	2.03E+08	4.63E+04	4.67E+05	1.36E+08	2.03E+08	0.023
U-233	1.00E+20	1.00E+20	1.00E+20	1.00E+20	1.00E+20	100
U-234	2.06E+03	1.83E+03	5.87E+02	1.88E+03	2.07E+03	28.5
U-235	8.02E+00	2.04E+02	6.88E+00	8.54E+00	8.03E+00	85.8
U-236	2.88E+15	2.05E+11	6.97E+12	1.79E+15	2.89E+15	0.0071
U-238	2.29E+06	1.48E+06	5.50E+05	2.02E+06	2.29E+06	24.1
Zr-93	5.30E-01	1.74E+00	5.07E-01	5.21E-01	5.30E-01	95.8

a – The minimum inventory limit value for each radionuclide is shaded.

Table 2-59. Total future inventory limits[a] for gross-alpha exposure from radionuclide parents for all cases studied (for 125 to 1,125 year time period)

	Baseline Case	Case A	Case B	Case C	Case D	% of Baseline
Parent Buried	**Inventory Limit (Ci)**	**Inventory Limit (Ci)**	**Inventory Limit (Ci)**	**Inventory Limit (Ci)**	**Inventory Limit (Ci)**	**(%)**
Am-241	1.10E+03	9.94E+02	1.46E+02	1.05E+03	1.10E+03	13.31
Am-243	2.09E+04	6.95E+08	2.89E+01	1.14E+03	2.06E+04	0.14
Cm-244	1.00E+20	4.72E+18	2.45E+15	8.06E+18	1.00E+20	0.002
Cm-245	7.77E+02	8.55E+02	1.63E+01	3.78E+02	7.77E+02	2.10
Cm-247	1.70E+04	2.15E+10	2.36E+01	9.31E+02	1.68E+04	0.14
Cm-248	2.05E+04	1.00E+20	2.85E+01	1.12E+03	2.03E+04	0.14
Np-237	2.37E-01	1.41E-01	1.68E-01	2.35E-01	2.37E-01	59.58
Pu-238	8.95E+04	5.89E+04	6.02E+04	8.24E+04	8.96E+04	65.87
Pu-239	8.29E+06	9.66E+06	8.29E+06	8.63E+06	8.30E+06	99.93
Pu-240	6.53E+18	1.24E+16	6.86E+12	2.41E+16	6.39E+18	0.00011
Pu-241	3.30E+04	3.04E+04	4.29E+03	3.15E+04	3.32E+04	13.0
Pu-242	7.19E+11	3.05E+11	3.59E+11	6.38E+11	7.20E+11	42.4
Pu-244	5.38E+18	3.62E+17	5.45E+12	1.91E+16	5.26E+18	0.00010
Ra-226	4.23E-02	2.07E-02	2.82E-02	4.09E-02	4.28E-02	48.9
Th-230	1.19E-01	9.03E-02	9.65E-02	1.19E-01	1.19E-01	75.8
Th-232	2.05E+08	4.68E+04	4.73E+05	1.38E+08	2.05E+08	0.023
U-233	1.00E+20	1.00E+20	1.00E+20	1.00E+20	1.00E+20	100
U-234	2.53E+01	1.81E+01	1.79E+01	2.33E+01	2.53E+01	70.9
U-235	6.19E+00	5.81E+00	5.62E+00	6.61E+00	6.20E+00	90.9
U-236	2.92E+15	2.07E+11	7.05E+12	1.81E+15	2.92E+15	0.0071
U-238	2.67E+04	1.42E+04	1.61E+04	2.41E+04	2.67E+04	53.3

a – The minimum inventory limit value for each radionuclide is shaded.

Table 2-60. Total future inventory limits[a] for radium exposure from radionuclide parents for all cases studied (for 125 to 1,125 year time period)

	Baseline Case	Case A	Case B	Case C	Case D	% of Baseline
Parent Buried	**Inventory Limit (Ci)**	**Inventory Limit (Ci)**	**Inventory Limit (Ci)**	**Inventory Limit (Ci)**	**Inventory Limit (Ci)**	**(%)**
Cm-244	1.00E+20	6.32E+18	1.00E+20	1.00E+20	1.00E+20	6.3
Cm-248	1.00E+20	1.00E+20	1.00E+20	1.00E+20	1.00E+20	100
Pu-238	1.20E+05	7.90E+04	8.09E+04	1.11E+05	1.20E+05	65.8
Pu-240	1.00E+20	1.67E+16	4.93E+17	1.00E+20	1.00E+20	0.017
Pu-242	9.64E+11	4.08E+11	5.12E+11	8.56E+11	9.66E+11	42.4
Pu-244	1.00E+20	4.85E+17	1.04E+19	1.00E+20	1.00E+20	0.48
Ra-226	5.68E-02	2.79E-02	3.80E-02	5.49E-02	5.74E-02	49.1
Th-230	1.60E-01	1.22E-01	1.30E-01	1.59E-01	1.60E-01	76.1
Th-232	2.75E+08	6.27E+04	6.34E+05	1.84E+08	2.75E+08	0.023
U-234	3.39E+01	2.42E+01	2.41E+01	3.13E+01	3.39E+01	71.0
U-236	3.91E+15	2.78E+11	9.45E+12	2.43E+15	3.92E+15	0.007
U-238	3.58E+04	1.91E+04	2.16E+04	3.23E+04	3.58E+04	53.2

a – The minimum inventory limit value for each radionuclide is shaded.

Table 2-61. Total future inventory limits[a] for uranium exposure from radionuclide parents for all cases studied (for 125 to 1,125 year time period)

	Baseline Case	Case A	Case B	Case C	Case D	% of Baseline
Parent Buried	**Inventory Limit (Ci)**	**Inventory Limit (Ci)**	**Inventory Limit (Ci)**	**Inventory Limit (Ci)**	**Inventory Limit (Ci)**	**(%)**
Am-241	2.84E+12	2.05E+12	2.16E+12	2.49E+12	2.85E+12	72.1
Am-243	1.17E+16	1.00E+20	8.81E+12	4.23E+14	1.15E+16	0.075
Cm-244	1.00E+20	1.00E+20	1.00E+20	1.00E+20	1.00E+20	100
Cm-245	2.14E+12	2.38E+12	1.63E+12	2.00E+12	2.14E+12	76.3
Cm-247	1.12E+17	1.00E+20	8.63E+13	4.10E+15	1.09E+17	0.077
Cm-248	1.00E+20	1.00E+20	4.39E+18	1.00E+20	1.00E+20	4.4
Np-237	6.49E+08	3.08E+08	4.10E+08	5.40E+08	6.49E+08	47.5
Pu-238	1.00E+20	1.00E+20	1.00E+20	1.00E+20	1.00E+20	100
Pu-239	1.00E+20	1.00E+20	1.00E+20	1.00E+20	1.00E+20	100
Pu-240	1.00E+20	1.00E+20	1.00E+20	1.00E+20	1.00E+20	100
Pu-241	8.55E+13	6.27E+13	6.54E+13	7.49E+13	8.58E+13	73.3
Pu-242	1.00E+20	1.00E+20	1.00E+20	1.00E+20	1.00E+20	100
Pu-244	1.00E+20	1.00E+20	1.00E+20	1.00E+20	1.00E+20	100
U-233	1.00E+20	1.00E+20	1.00E+20	1.00E+20	1.00E+20	100
U-234	1.00E+20	1.00E+20	1.00E+20	1.00E+20	1.00E+20	100
U-235	1.00E+20	1.00E+20	1.00E+20	1.00E+20	1.00E+20	100
U-236	1.00E+20	1.00E+20	1.00E+20	1.00E+20	1.00E+20	100
U-238	1.00E+20	1.00E+20	1.00E+20	1.00E+20	1.00E+20	100

a – The minimum inventory limit value for each radionuclide is shaded.

Perhaps a more important view of the sensitivity impacts is comparing the minimum Baseline inventory limit (i.e., sometimes referred to as the controlling value) to the minimum value obtain for each of the four sensitivity cases. Here the minimum values are obtained by selecting the inventory value over the 5 different dose categories for each case considered. The results are listed in Table 2-62 where shading of differing colors has been used:

- Red for percentage inventory estimates less than 0.01% of the controlling Baseline value;
- Yellow for percentage inventory estimates between 0.01% to 1% of the controlling Baseline value;
- Cyan for percentage inventory estimates between 1% to 10% of the controlling Baseline value;
- Orange for percentage inventory estimates between 10% to 50% of the controlling Baseline value;
- Green for percentage inventory estimates between 50% to 100% of the controlling Baseline value; and
- Gray for percentage inventory estimates equal to the controlling Baseline value.

Also the list of radionuclides has been sorted based on the degree of impact observed versus the Baseline Case.

Table 2-62. Minimum total future inventory limits[a] over the five different exposure categories from radionuclide parents for all cases studied (for 125 to 1,125 year time period)

	Baseline Case	Case A	Case B	Case C	Case D	% of Baseline
Parent Buried	**Minimum Inventory Limit (Ci)**	**Minimum Inventory Limit (Ci)**	**Minimum Inventory Limit (Ci)**	**Minimum Inventory Limit (Ci)**	**Minimum Inventory Limit (Ci)**	**(%)**
Pu-244	2.20E+18	3.58E+17	2.23E+12	7.82E+15	2.15E+18	0.00010
Pu-240	2.61E+18	1.23E+16	2.65E+12	9.31E+15	2.55E+18	0.00010
Cm-244	1.00E+20	4.67E+18	9.46E+14	3.12E+18	1.00E+20	0.00095
K-40	1.32E+08	1.89E+03	4.59E+04	1.32E+08	1.35E+08	0.0014
U-236	2.88E+15	2.05E+11	6.97E+12	1.79E+15	2.89E+15	0.0071
Th-232	2.03E+08	4.63E+04	4.67E+05	1.36E+08	2.03E+08	0.023
Am-243	7.84E+03	8.19E+07	1.09E+01	4.29E+02	7.75E+03	0.14
Cm-248	1.88E+03	1.00E+20	2.61E+00	1.03E+02	1.86E+03	0.14
Cm-247	6.74E+03	2.53E+09	9.37E+00	3.69E+02	6.66E+03	0.14
Cm-245	2.41E+02	2.63E+02	5.98E+00	1.28E+02	2.41E+02	2.5
Sr-90	3.15E+04	9.74E+02	4.11E+03	3.11E+04	3.28E+04	3.1
Pu-241	1.01E+04	9.23E+03	1.58E+03	9.59E+03	1.01E+04	15.7
Am-241	3.36E+02	3.02E+02	5.38E+01	3.20E+02	3.37E+02	16.0
C-14	9.91E-01	1.14E+00	7.72E-01	2.56E-01	1.05E+00	25.9
Pu-242	7.19E+11	3.05E+11	3.59E+11	6.38E+11	7.20E+11	42.4
Ni-59	1.69E+01	7.85E+00	7.65E+00	1.43E+01	1.69E+01	45.3
Pd-107	2.04E+03	9.49E+02	9.25E+02	1.73E+03	2.05E+03	45.3
I-129	2.83E-04	4.21E-04	2.61E-04	1.35E-04	3.06E-04	47.8
Ra-226	4.23E-02	2.07E-02	2.82E-02	4.09E-02	4.28E-02	48.9
U-238	2.67E+04	1.42E+04	1.61E+04	2.41E+04	2.67E+04	53.3
Np-237	7.22E-02	4.26E-02	5.08E-02	7.16E-02	7.23E-02	59.0
Pu-238	8.95E+04	5.89E+04	6.02E+04	8.24E+04	8.96E+04	65.9
Nb-94	1.08E+01	1.06E+01	7.35E+00	1.05E+01	1.08E+01	68.3
U-234	2.53E+01	1.81E+01	1.79E+01	2.33E+01	2.53E+01	70.9
Th-230	1.19E-01	9.03E-02	9.65E-02	1.19E-01	1.19E-01	75.8
I-129_K	1.10E-01	8.43E-02	1.20E-01	1.31E-01	1.10E-01	76.9
I-129_C	1.79E-02	1.37E-02	1.95E-02	2.13E-02	1.79E-02	76.9
Cl-36	1.58E-01	1.60E-01	2.07E-01	1.23E-01	1.67E-01	77.9
U-235	7.85E-01	6.75E-01	7.11E-01	8.39E-01	7.86E-01	86.1
C-14_K	1.00E+01	8.74E+00	1.07E+01	9.70E+00	1.01E+01	87.1
H-3	3.12E+06	3.13E+06	3.12E+06	3.12E+06	2.89E+06	92.7
Zr-93	5.30E-01	1.74E+00	5.07E-01	5.21E-01	5.30E-01	95.8
Tc-99	9.41E-01	1.06E+00	9.19E-01	9.41E-01	9.94E-01	97.6
Mo-93	8.21E-01	8.25E-01	8.20E-01	8.21E-01	8.74E-01	99.8
Tc-99_K	2.81E+01	2.88E+01	2.81E+01	2.99E+01	2.81E+01	99.95
Pu-239	1.05E+06	1.14E+06	1.06E+06	1.10E+06	1.05E+06	100.0
Se-79	1.00E+20	1.00E+20	1.00E+20	1.00E+20	1.00E+20	100.0
Sn-126	1.00E+20	1.00E+20	1.00E+20	1.00E+20	1.00E+20	100.0
U-233	1.00E+20	1.00E+20	1.00E+20	1.00E+20	1.00E+20	100.0

a – The minimum inventory limit value for each radionuclide is shaded using different colors depending upon its percentage value relative to the Baseline minimum value [gray for 100%; green for 50 to 100%; orange for 10 to 50%; cyan for 1 to 10%; yellow for 0.01 to 1%; and red for less than 0.01%].

2.7 CIG TRENCH AIR-PATHWAY ANALYSIS

2.7.1 Overview of Air-Pathway Analysis

This section describes the investigation conducted to evaluate the potential magnitude of gaseous release of radionuclides from the CIG Trenches over the 25-year operational period, 100-year institutional control period, and 1000-year post-closure compliance period versus the atmospheric pathway exposure maximum dose to a representative member of the public of 10 mrem/yr. The CIG Trenches are contained within two footprints of equal area (~103,000 ft^2 [9570 m^2]) and are designated as CIG-1 and CIG-2. These earthen trenches contain grout encapsulated waste including large radioactively contaminated equipment and other smaller wasteforms such as B-25 boxes to fill in the space around and above the large equipment (Phifer et al. 2006).

A screening analysis was conducted to produce a list of radionuclides requiring a more thorough analysis to derive disposal limits for the CIG disposal unit based on the atmospheric pathway. This study, described in Crapse and Cook (2006), used a methodology developed by the National Council on Radiation Protection and Measurements, professional judgment and process knowledge to determine this list. The list of potential radionuclides includes C-14, Cl-36, H-3, I-129, S-35, Sb-124, Sb-125, Se-75, Se-79, Sn-113, Sn-119m, Sn-121, Sn-121m, Sn-123, and Sn-126.

During the 25-year operational period and 100-year institutional control period this maximum atmospheric dose is applicable at the SRS boundary, due to active institutional controls. During the 1000-year post-closure compliance period this maximum atmospheric dose is applicable at 100 m from the disposal unit boundary, due to the assumed loss of active institutional controls. The atmospheric dose from the CIG Trenches was evaluated for three separate time periods: 1) 0 to 125 years, 2) 125 to 325 years, and 3) 325 to 1125 years. The first time period evaluated covers the operational and institutional control period. During this time period, the final closure cap does not cover the trenches. During the second time period, 125 to 325 years, a final closure cap is in place over the trenches. For the third time period, 325 to 1125 years, it is assumed that the grout structure encapsulating the waste collapses resulting in settlement of the waste and final closure cap.

The analysis presented here uses accepted computer programs for diffusion (PORFLOW) and atmospheric transport and dose calculations (CAP88).

2.7.2 Air-Pathway Assumptions

Key assumptions and inputs used in the air-pathway analysis are presented in Appendix B.

2.7.3 CIG Trench Closure Considerations

The concepts for closure of the CIG Trenches are relevant to the determination of the gaseous flux at the land surface for all gaseous radionuclides. The CIG construction specifics and closure concept are described by Phifer et al. (2006). The waste placed in the CIG Trenches during the operational and institutional control period (0 to 125 years), is overlain with a minimum of 5 ft of clean materials (i.e., minimum 1 ft of grout and 4 ft of a combination of CLSM, concrete slab, and/or soil) but not the final closure cap. Therefore, the ground surface where the gaseous flux was evaluated during this time period is the top of the 5 ft of clean materials.

For the 125 to 325 year time period, a closure cap is assumed to be in place over the waste trenches. A conceptual drawing of the closure cap over the CIG Trenches is shown in Figure 2-2 and the vertical section over which gaseous radionuclide diffusion was evaluated is indicated. For the 325 to 1125 year time period, it is assumed that the grout structure encapsulating the waste collapses. This results in settlement of the waste zone and destruction of the closure cap structure. For this time period, the material properties of the closure cap were re-assigned to represent the bulk properties of E-Area Operational Soil Cover (Phifer et al. 2006), and the overall thickness of this material over the waste was assumed to remain the same as that for the intact closure cap.

The closure cap utilized in this analysis includes all materials, as constructed and placed over the CIG Trenches at the end of the 100-year institutional control period. The components of concern for the long-term air-pathway performance calculation are those that have no potential to erode during the 200-year period between cap placement and grout collapse. These components are situated below the top of the erosion barrier. The composite thickness of the non-waste material below the top of the erosion barrier is approximately 10 ft. Table 2-63 lists the individual components of the CIG Trenches and closure cap (excluding the layers overlying the erosion control barrier). Materials are indicated with the associated thickness of each component in feet.

Table 2-63. Vertical Layer Sequence and Associated Thickness for CIG Cover Material

Layer	Thickness (ft)
Erosion barrier	1
Middle backfill layer	1
Gravel drainage layer	1
Lower backfill layer	2
Clean soil	4
CIG grout top	1
CIG waste layer	14
CIG waste layer after collapse at 325 years	7

SOURCE: Adapted from Phifer et al. (2006)

2.7.4 CIG Trench Air-Pathway Conceptual Model

The flux of the radioactive gasses at the land surface above the CIG Trenches was evaluated for its specific closure configuration. Gaseous radionuclides introduced within the waste zone diffuse outward from this zone into the air-filled grout and/or soil pores surrounding the trenches, eventually resulting in some of the radionuclides emanating at the land surface. As such, air is the medium through which they diffuse. It is assumed that fluctuations in atmospheric pressure at the land surface that could induce small pulses of air movement into and out of the shallow soil profile over relatively short periods of time will have a zero net effect when averaged over longer time periods. Thus, advective transport of these radionuclides in air-filled soil pores is not considered to be a significant process when compared to the rate of air diffusion.

The radionuclides present as gasses are those identified in the screening process described in Crapse and Cook (2006). Certain gaseous radionuclides will not likely remain in the monatomic elemental form but combine with other gaseous elements or form diatomic molecules. The state of existence of each of these radionuclides in the gaseous phase is important in evaluating their transport to the land surface because the diffusion coefficient associated with each is related to its molecular weight.

In this investigation it is assumed that:

- C-14 exists as part of the CO_2 molecule
- Cl-36, H-3 and I-129 exist as diatomic gasses
- S-35, Sb-124, Sb-125, Se-75, Se-79, Sn-113, Sn-119m, Sn-121, Sn-121m, Sn-123, and Sn-126 exist as monatomic gasses.

2.7.5 CIG Trench Air-Pathway Numerical Model

The mathematical model utilized in this report is provided by the PORFLOW (ACRI 2004) simulation package. PC-based PORFLOW Version 5.97.0 was used to conduct a series of simulations. PORFLOW is developed and marketed by Analytic & Computational Research, Inc., to solve problems involving transient and steady-state fluid flow, heat and mass transport in multi-phase, variably saturated, porous or fractured media with dynamic phase change. PORFLOW has been widely used at the SRS and in the DOE complex to address major issues related to the groundwater and nuclear waste management.

The governing equation for mass transport of species *k* in the fluid phase is given by

$$\frac{\partial C_k}{\partial t} + \frac{\partial}{\partial x_i}(V_i C_k) = \frac{\partial}{\partial x_i}(D_{ij}\frac{\partial C_k}{\partial x_j}) + \gamma_k \qquad \text{Equation 2-5}$$

Where

C_k	concentration of species *k* (Ci/cm^3)
V_i	fluid velocity in the i^{th} direction (cm/yr)
D_{ij}	effective diffusion coefficient for the species (cm^2/yr)
γ_k	net decay of species *k* ($Ci/cm^3/yr$)
i, j	direction index (unitless)
t	time (yr)
x	distance coordinate (cm)

The equation is solved within PORFLOW to evaluate transient radionuclide transport above the CIG Trenches and to determine gaseous radionuclide flux at the land surface over time. Since source radionuclides exist as gases, air was taken to be the medium within which transport occurs. The flow field was assumed to be isobaric and isothermal. The impact of naturally occurring fluctuations in atmospheric pressure at the land surface that could induce small pulses of air movement into and out of the shallow soil profile over relatively short periods of time will have a zero net effect when averaged over longer time periods. Therefore, for the relatively long periods of time evaluated in this investigation, air diffusion was the only transport mechanism simulated in the model and advective air-transport was assumed to be negligible, so the advection term was disabled within PORFLOW and only the diffusive and net decay terms were evaluated.

The boundary conditions imposed on the model domain included:

- No-flux specified for all radionuclides along sides and bottom ($\partial C/\partial X = 0$ at x=0, x=1 and $\partial C/\partial Y = 0$ at y=0)
- Species concentration set to 0 at land surface (top of erosion barrier) ($C = 0$ at $y=y_{max}$)

The initial condition imposed on the domain included:

- Species concentration set to 0 for the entire model domain at time = 0 ($C=0$ for $0 \leq x \leq 1$ at $t=0$ and $C=0$ for $0 \leq y \leq y_{max}$ at $t=0$)

The initial conditions for the model also assumed a 1 Ci inventory of each radionuclide uniformly spread over the waste zone.

These boundary conditions force all of the gaseous radionuclides to move upward from the waste disposal zone to the land surface. In reality, some lateral and downward diffusion occurs in the air-filled pores surrounding the waste zone; hence ignoring this lateral and downward movement has the effect of increasing the flux at the land surface. This should introduce some conservatism in the calculated results. Simulations were conducted in transient mode for diffusive transport in air, with results being obtained over 1,125 years.

2.7.5.1 CIG Trench Air-Pathway Model Development and Assumptions

The numerical representation of the conceptual model is as a 1-dimensional vertical stack of elements configured to represent the thickness of the CIG waste and overlying materials.

The radionuclides evaluated are C-14, Cl-36, H-3, I-129, S-35, Sb-124, Sb-125, Se-75, Se-79, Sn-113, Sn-119m, Sn-121, Sn-121m, Sn-123, and Sn-126.

Since source radionuclides exist as gases, air was taken to be the medium within which transport occurs. The flow field was assumed to be isobaric and isothermal. The impact of naturally occurring fluctuations in atmospheric pressure at the land surface that could induce small pulses of air movement into and out of the shallow soil profile over relatively short periods of time will have a zero net effect when averaged over longer time periods. Therefore, for the relatively long periods of time evaluated in this investigation, air-diffusion was the only transport mechanism simulated in the model and advective air-transport was assumed to be negligible.

A small percentage of the radionuclides dissolve in residual pore water, but since diffusion proceeds more slowly in water than in air, air-diffusion is regarded as the only transport process by which they can reach the land surface from the CIG waste zone. This assertion is substantiated in Nielson et al. (1984). The radon effective diffusion coefficient, D_{eff}, for soil is reported to range from the open-air diffusion coefficient of 1.0E-05 m^2/s to that of fully saturated soil, 1.0E-09 m^2/s (Nielson et al. 1984).

This 4-order of magnitude difference is consistent with the comparison of water diffusion coefficients to air diffusion coefficients of other common molecular compounds and reported in many references. Thus, the larger volume of water-filled pore space compared to air-filled pore space (maximum of 2 orders of magnitude difference) is inconsequential. The ability of water-dissolved compounds to diffuse through water-filled pores is negligible compared to the ability of the same compounds to diffuse as gas in the vapor-filled pore spaces.

Furthermore, there is vertical downward movement of the pore water which acts to offset or overcome any vertical upward diffusion of dissolved constituents. Consequently, in this investigation radionuclide transport was allowed to proceed only through air-filled pore space and, therefore, residual pore water was treated as if it was part of the solid matrix material within the flow field. No accounting was made of the partitioning of the gaseous radionuclides into the pore water as diffusive vapor transport proceeded from the waste zone to the land surface. By ignoring this mechanism, diffusive fluxes at the land surface were slightly overestimated.

The boundary conditions imposed on the model domain included:

- No-flux specified for all radionuclides along sides and bottom
- Radionuclide concentrations set to 0 at land surface.

These boundary conditions force all of the gaseous radionuclides to move upward from the waste disposal zone to the land surface. In reality, some lateral and downward diffusion occurs in the air-filled pores surrounding the waste zone; hence ignoring this lateral and downward movement has the effect of increasing the flux at the land surface, thus introducing a significant measure of conservatism in the calculated results. Simulations were conducted in transient mode for diffusive transport in air, with results being obtained over 1,125 years.

A summary of the radionuclides and compounds of interest in this investigation are summarized in Table 2-64.

Table 2-64. Radionuclides and Compounds of Interest

Radionuclide	Half-life (yrs)	Atomic Wt.	Molecular form in gaseous state	Molecular Wt.
C-14	5.730E+03	14	CO_2	46
Cl-36	3.010E+05	36	Cl_2	72
H-3	1.2333E+01	3	H_2	6
I-129	1.570E+07	129	I_2	258
S-35	2.394E-01	35	S	35
Sb-124	1.649E-01	124	Sb	124
Sb-125	2.759E+00	125	Sb	125
Se-75	3.270E-01	75	Se	75
Se-79	2.950E+05	79	Se	79
Sn-113	3.153E-01	113	Sn	113
Sn-119m	8.020E-01	119	Sn	119
Sn-121	3.089E-03	121	Sn	121
Sn-121m	4.41E+01	121	Sn	121
Sn-123	3.550E-01	123	Sn	123
Sn-126	2.300E+05	126	Sn	126

2.7.5.2 Measures Implemented to Ensure Conservative Results

In this analysis, several conditions introduce a significant measure of conservatism into the calculations. These include:

- The use of boundary conditions that force all of the gaseous radionuclides to move upward from the waste disposal zone to the land surface. In reality, some of the gaseous radionuclides diffuse sideways and downward in the air-filled pores surrounding the waste zone; hence ignoring this has the effect of increasing the radon flux at the land surface.
- Not taking credit for the removal of the gaseous radionuclides by pore water moving vertically downward through the model domain once the cask is breached. This mechanism would likely remove some dissolved gaseous radionuclides, and therefore its omission has the effect of increasing the estimate of instantaneous radionuclide flux at the land surface in simulations conducted as a part of this investigation.
- Use of the top of the erosion layer in the soil cover as the land surface for the purpose of calculating radionuclide flux during the 125 to 325 year time period. No credit is taken for the additional distance the gaseous radionuclides must migrate above the erosion layer prior to that portion of the Soil Cover Zone eroding away.
- Ignoring the presence of the GCL within the final closure cap. The GCL should be near 100 percent saturation; therefore it will contain very little air-filled porosity within which radon transport could occur.

- The assignment of E-Area Operational Soil Cover (Phifer et al. 2006) properties to the closure cap following collapse of the grout structure (325 to 1125 years). Some of the closure cap is likely to remain intact and retain its original material properties.

2.7.5.3 Grid Construction

The model grid was constructed as a node mesh 3 nodes wide by 54 nodes high. This mesh creates the vertical stack of 52 model elements. Figure 2-72 shows a schematic of the PORFLOW model grid. The grid extends upward only as far as the erosion barrier, since this is the minimum possible cover thickness that could exist during the 1,125-year evaluation period. A set of consistent units was employed in the simulations for length, mass and time, consisting of meters, grams, and years, respectively.

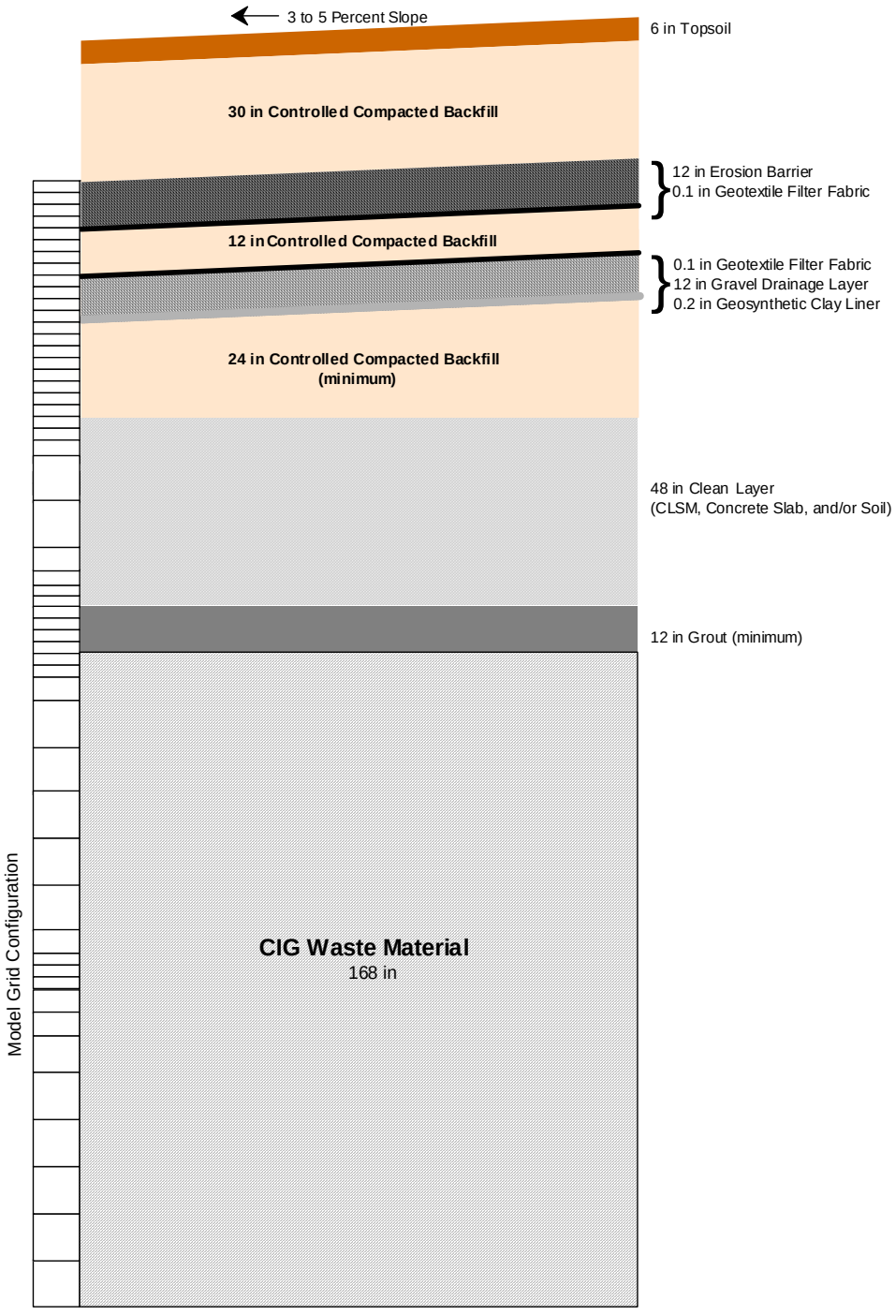

Figure 2-72. PORFLOW Model Grid for Air-Pathway Analysis

2.7.5.4 Material Zones

The model domain was divided into two primary zones, the CIG waste zone occupying the lower 14 ft of the domain and the cover zone (including the grout top), extending approximately 10 ft above the waste zone to the top of the domain. The cover zone includes the grout top as well as the different closure cap layers. The upper model elements were scaled to correspond to the geometry of the closure cap thickness while the lower model elements were scaled to correspond to the CIG waste zone.

During the first 125 years of simulation, the land surface is assumed to be the top of the soil layer placed over the grout top. For the 125 to 325 years simulation period, the land surface is assumed to be the top of the erosion barrier, within the closure cap, and no credit is taken for the compacted backfill and topsoil above that layer. For the 325 to 1125 year simulation period, the thickness of the waste zone is reduced by 7 ft and the overlying 10 ft of material is assigned the properties of the E-Area Operational Soil Cover (Phifer et al. 2006). The top of this layer is taken as the ground surface.

2.7.5.5 Material Zone Properties and Other Input Parameters

Material properties utilized within the 1-D numerical model were specified for eight material zones defined within the model domain. Each material zone was assigned values of particle density, total porosity, average saturation, air-filled porosity, air density, and an effective air-diffusion coefficient for each source element or compound. With the use of an effective air-diffusion coefficient, tortuosity was assigned a unit value in each material zone. An air fluid density of 1.24E+03 g/m^3 was used. This air fluid density was obtained from the *CRC Handbook of Tables for Applied Engineering Science* (Bolz and Tuve 1973) and represents that of standard atmospheric conditions.

During the first 125 years the layers associated with the CIG Trench consist only of the CIG waste layer, CIG grout, and clean soil (see Figure 2-2). Although the interim runoff cover, utilized during the first 125 years (see discussion in Section 2.3), includes the potential use of up to an additional 2-foot of soil to establish necessary grades to promote runoff, this soil was not included in the model during this time period. This soil was not included, since it is only used as necessary and its thickness will be highly variable. The total porosity for the CIG waste zone was taken to be 0.5 and it was assumed that the waste was dry and that the air filled porosity would equal the total porosity for this zone (Phifer et al. 2006). The particle density and total porosity for the CIG grout and clean soil were taken from the recommended values for the existing E-Area CIG grout and E-Area Operational Soil Cover, respectively (Phifer et al. 2006). The average saturation for the CIG grout and clean soil were taken as the value of saturation at a suction head of approximately 200 cm from the characteristic curves for the existing E-Area CIG grout and E-Area Operational Soil Cover, respectively (Phifer et al. 2006).

E-Area vadose zone field pore pressure measurements indicate average suction levels in the approximate range of 50 to 200 cm (Nichols et al. 2000). A value of 200 cm represents the upper end of the range which will have a greater air-filled porosity. The air-filled porosity of the CIG grout and clean soil were calculated from the total porosity and average saturation. While the model includes all the layers from the CIG waste layer to the erosion barrier, during the first 125 years of simulation, the closure cap materials (i.e., the lower backfill on up) are assigned a porosity of 1.0. This has the effect of making these layers equivalent to air. Table 2-65 provides the values of particle density, total porosity, average saturation, and air-filled porosity utilized for the CIG waste layer, CIG grout, and clean soil during the first 125 years.

For the 125 to 325 year time period the layers associated with the CIG Trench consist of all layers from the CIG waste layer to the erosion barrier (see Figure 2-2). The CIG waste layer, CIG grout, and clean soil retain the same properties as utilized for the first 125 years. The particle density of the lower backfill, gravel drainage layer, middle backfill, and erosion barrier (these materials collectively are considered the closure cap layers) was taken as 2.65 g/cm^3. This is based on the density of quartz sand and is regarded as representative of most SRS soils. Values for total porosity and long-term average moisture content for the closure cap materials were taken from Phifer (2003). Phifer (2003) evaluated infiltration through a closure cap over time as the closure cap degraded using the HELP model. The porosity and average moisture content values for a 10,000 year degraded closure cap were utilized, since this represented the greatest air filled porosity in which a gas could diffuse (values from earlier time periods were saturated, therefore choosing a period having unsaturated conditions was deliberately conservative). Average saturation and air-filled porosity values were calculated from the total porosity and long-term average moisture content. Table 2-65 also provides the values of particle density, total porosity, average saturation, and air-filled porosity utilized for all the layers (i.e., CIG waste layer to the erosion barrier) for the 125 to 325-year time period.

For the 325 to 1125 year time period, it is assumed that the grout structure encapsulating the waste collapses, resulting in settlement of the waste zone and destruction of the closure cap structure. From Phifer et al. (2006), it is assumed that the waste layer collapses from 14 to 7 feet at year 325 (see Table 2-63). This reduction in waste layer thickness is handled utilizing the same model grid used for prior years by reassigning the radionuclide inventory of the lower 7 feet of the waste zone to the upper 7 feet of the waste zone and assigning a porosity of 0 to the lower 7 feet of the waste zone.

While this is not necessary intuitive, it is appropriate for two reasons: 1) the migration pathway of interest is upward rather than downward, and 2) no additional material is added to the migration pathway. For this time period, the material properties for all the layers (i.e., CIG waste layer to the erosion barrier) cap were assigned the properties of the E-Area Operational Soil Cover (Phifer et al. 2006). This is identical to the properties of the clean soil from Table 2-65 as described.

Table 2-66 provides the values of particle density, total porosity, average saturation, and air-filled porosity utilized for all the layers (i.e., CIG waste layer to the erosion barrier) for the 325 to 1125 year time period.

Table 2-65. Particle Density, Porosity, Average Saturation, and Air-filled Porosity Values for the 0 to 125 Year and 125 to 325 Year Time Periods

Layer	Particle Density (g/cm^3)	Total Porosity (fraction)	Long Term Average Moisture Content (vol/vol)	Average Saturation (fraction)	Air-filled Porosity (fraction)
Erosion barrier [1, 3]	2.65	0.088	0.0726	0.825 [4]	0.015 [5]
Middle backfill [1, 3]	2.65	0.375	0.2435	0.649 [4]	0.132 [5]
Gravel drainage layer [1, 3]	2.65	0.375	0.1967	0.525 [4]	0.178 [5]
Lower backfill [1, 3]	2.65	0.370	0.2710	0.732 [4]	0.099 [5]
Clean soil [2]	2.65	0.460	na[6]	0.825	0.081 [5]
CIG grout [2]	2.31	0.224	na[6]	0.812	0.042 [5]
CIG waste layer [2]	2.65	0.5	na[6]	0	0.5

[1] During the first 125 years of simulation, the materials comprising the closure cap were assigned a porosity of 1.0 and a diffusion coefficient equivalent to the molecular diffusion coefficient of the specific radionuclide in air.

[2] Values for particle density, total porosity, and average saturation taken from Phifer et al. (2006)

[3] Values for total porosity and long term average moisture content taken from Phifer (2003). Particle density taken as 2.65, which is based on the density of quartz and regarded as fairly representative of most SRS soils

[4] Average Saturation =Long Term Average Moisture Content / Total Porosity

[5] Air-filled Porosity = (1 – Average Saturation) × Total Porosity

[6] Not applicable

Table 2-66. Particle Density, Porosity, Average Saturation, and Air-filled Porosity Values for the 325 to 1125 Year Time Period

Layer	Particle Density (g/cm^3)	Total Porosity (fraction)	Average Saturation (fraction)	Air-filled Porosity [1] (fraction)
Erosion barrier	2.65	0.46	0.825	0.081
Middle backfill	2.65	0.46	0.825	0.081
Gravel drainage layer	2.65	0.46	0.825	0.081
Lower backfill	2.65	0.46	0.825	0.081
Clean soil	2.65	0.46	0.825	0.081
CIG grout	2.65	0.46	0.825	0.081
CIG waste layer	2.65	0.46	0.825	0.081

Note: The values of particle density, total porosity, and average saturation for all layers was taken as that of the E-Area Operational Soil Cover Prior to Dynamic Compaction (Phifer et al. 2006)
[1]Air-filled Porosity = (1 – Average Saturation) × Total Porosity

The molecular diffusion coefficient of Rn-222 in open air is 347 m^2/yr (Nielson et al. 1984). Nielson et al. (1984) established a relationship between moisture saturation and the radon effective air-diffusion coefficient for various pore sizes of earthen materials. Using this method, a radon effective air-diffusion coefficient was determined for each material type based upon the average moisture saturation for the material. Subsequently, using Graham's Law, the effective air-diffusion coefficient of each radionuclide or compound evaluated was determined for each material type based on the radon effective air-diffusion coefficient using the following relationship:

$$D = D' \sqrt{\frac{MWT'}{MWT}} \qquad \text{Equation 2-6}$$

Where:

D = the diffusion coefficient of the radionuclide of interest (m^2/yr)
D' = the diffusion coefficient of the reference radionuclide (Rn-222) (m^2/yr)
MWT' = the molecular weight of the reference radionuclide (Rn-222)
MWT = the molecular weight of the element or compound of interest

A summary of the radon effective air-diffusion coefficients and the calculated effective air-diffusion coefficients for each radionuclide/compound by material zone and simulation period, are presented in Table 2-67 through Table 2-69.

Table 2-67. Effective Air-Diffusion Coefficients for Each Radionuclide/Compound, by Material for the 0 to 125 Year Time Period

Radionuclide[1]	CIG Waste (m2/yr)	Grout and Soil (m2/yr)	Lower Backfill (m2/yr)	Gravel Drainage Layer (m2/yr)	Middle Backfill (m2/yr)	Erosion Barrier (m2/yr)
Rn-222[2]	3.470E+02	1.262E+00	3.470E+02	3.470E+02	3.470E+02	3.470E+02
C-14	7.623E+02	2.773E+00	7.623E+02	7.623E+02	7.623E+02	7.623E+02
Cl-36	6.093E+02	2.217E+00	6.093E+02	6.093E+02	6.093E+02	6.093E+02
H-3	2.111E+03	7.678E+00	2.111E+03	2.111E+03	2.111E+03	2.111E+03
I-129	3.219E+02	1.171E+00	3.219E+02	3.219E+02	3.219E+02	3.219E+02
S-35	8.739E+02	3.179E+00	8.739E+02	8.739E+02	8.739E+02	8.739E+02
Sb-124	4.643E+02	1.689E+00	4.643E+02	4.643E+02	4.643E+02	4.643E+02
Sb-125	4.624E+02	1.682E+00	4.624E+02	4.624E+02	4.624E+02	4.624E+02
Se-75	5.970E+02	2.172E+00	5.970E+02	5.970E+02	5.970E+02	5.970E+02
Se-79	5.817E+02	2.116E+00	5.817E+02	5.817E+02	5.817E+02	5.817E+02
Sn-113	4.864E+02	1.769E+00	4.864E+02	4.864E+02	4.864E+02	4.864E+02
Sn-119m	4.739E+02	1.724E+00	4.739E+02	4.739E+02	4.739E+02	4.739E+02
Sn-121	4.700E+02	1.710E+00	4.700E+02	4.700E+02	4.700E+02	4.700E+02
Sn-121m	4.700E+02	1.710E+00	4.700E+02	4.700E+02	4.700E+02	4.700E+02
Sn-123	4.662E+02	1.696E+00	4.662E+02	4.662E+02	4.662E+02	4.662E+02
Sn-126	4.606E+02	1.676E+00	4.606E+02	4.606E+02	4.606E+02	4.606E+02

[1] See Table 2-64 for molecular form in gaseous state
[2]The effective diffusion coefficient for ^{222}Rn was used to determine the effective air diffusion coefficient of each radionuclide/compound based on Graham's law (Nielson et al. 1984).

Table 2-68. Effective Air-Diffusion Coefficients for Each Radionuclide/Compound, by Material for the 125 to 325 Year Time Period

Radionuclide[1]	CIG Waste (m2/yr)	Grout and Soil (m2/yr)	Lower Backfill (m2/yr)	Gravel Drainage Layer (m2/yr)	Middle Backfill (m2/yr)	Erosion Barrier (m2/yr)
Rn-222[2]	3.470E+02	1.262E+00	2.840E+00	4.734E+00	4.734E+00	7.889E-01
C-14	7.623E+02	2.773E+00	6.239E+00	1.040E+01	1.040E+01	1.733E+00
Cl-36	6.093E+02	2.217E+00	4.987E+00	8.312E+00	8.312E+00	1.385E+00
H-3	2.111E+03	7.678E+00	1.728E+01	2.879E+01	2.879E+01	4.799E+00
I-129	3.219E+02	1.171E+00	2.635E+00	4.391E+00	4.391E+00	7.318E-01
S-35	8.739E+02	3.179E+00	7.153E+00	1.192E+01	1.192E+01	1.987E+00
Sb-124	4.643E+02	1.689E+00	3.800E+00	6.334E+00	6.334E+00	1.056E+00
Sb-125	4.624E+02	1.682E+00	3.785E+00	6.308E+00	6.308E+00	1.051E+00
Se-75	5.970E+02	2.172E+00	4.886E+00	8.144E+00	8.144E+00	1.357E+00
Se—79	5.817E+02	2.116E+00	4.761E+00	7.935E+00	7.935E+00	1.323E+00
Sn-113	4.864E+02	1.769E+00	3.981E+00	6.635E+00	6.635E+00	1.106E+00
Sn-119m	4.739E+02	1.724E+00	3.879E+00	6.465E+00	6.465E+00	1.078E+00
Sn-121	4.700E+02	1.710E+00	3.847E+00	6.412E+00	6.412E+00	1.069E+00
Sn-121m	4.700E+02	1.710E+00	3.847E+00	6.412E+00	6.412E+00	1.069E+00
Sn-123	4.662E+02	1.696E+00	3.816E+00	6.359E+00	6.359E+00	1.060E+00
Sn-126	4.606E+02	1.676E+00	3.770E+00	6.283E+00	6.283E+00	1.047E+00

[1] See Table 2-64 for molecular form in gaseous state

[2]The effective diffusion coefficient for ^{222}Rn was used to determine the effective air diffusion coefficient of each radionuclide/compound based on Graham's law (Nielson et al. 1984).

Table 2-69. Effective Air-Diffusion Coefficients for Each Radionuclide/Compound, by Material for the 325 to 1125 Year Time Period

Radionuclide[1]	CIG Waste (m2/yr)	Grout and Soil (m2/yr)	Lower Backfill (m2/yr)	Gravel Drainage Layer (m2/yr)	Middle Backfill (m2/yr)	Erosion Barrier (m2/yr)
Rn-222[2]	1.262E+00	1.262E+00	1.262E+00	1.262E+00	1.262E+00	1.262E+00
C-14	2.773E+00	2.773E+00	2.773E+00	2.773E+00	2.773E+00	2.773E+00
Cl-36	2.217E+00	2.217E+00	2.217E+00	2.217E+00	2.217E+00	2.217E+00
H-3	7.678E+00	7.678E+00	7.678E+00	7.678E+00	7.678E+00	7.678E+00
I-129	1.171E+00	1.171E+00	1.171E+00	1.171E+00	1.171E+00	1.171E+00
S-35	3.179E+00	3.179E+00	3.179E+00	3.179E+00	3.179E+00	3.179E+00
Sb-124	1.689E+00	1.689E+00	1.689E+00	1.689E+00	1.689E+00	1.689E+00
Sb-125	1.682E+00	1.682E+00	1.682E+00	1.682E+00	1.682E+00	1.682E+00
Se-75	2.172E+00	2.172E+00	2.172E+00	2.172E+00	2.172E+00	2.172E+00
Se—79	2.116E+00	2.116E+00	2.116E+00	2.116E+00	2.116E+00	2.116E+00
Sn-113	1.769E+00	1.769E+00	1.769E+00	1.769E+00	1.769E+00	1.769E+00
Sn-119m	1.724E+00	1.724E+00	1.724E+00	1.724E+00	1.724E+00	1.724E+00
Sn-121	1.710E+00	1.710E+00	1.710E+00	1.710E+00	1.710E+00	1.710E+00
Sn-121m	1.710E+00	1.710E+00	1.710E+00	1.710E+00	1.710E+00	1.710E+00
Sn-123	1.696E+00	1.696E+00	1.696E+00	1.696E+00	1.696E+00	1.696E+00
Sn-126	1.676E+00	1.676E+00	1.676E+00	1.676E+00	1.676E+00	1.676E+00

[1] See Table 2-64 for molecular form in gaseous state
[2]The effective diffusion coefficient for ^{222}Rn was used to determine the effective air diffusion coefficient of each radionuclide/compound based on Graham's law (Nielson et al. 1984).

2.7.6 Air-Pathway Model Results

2.7.6.1 CIG Trench Flux to Ground Surface

Model simulations were conducted to evaluate the peak flux of each radionuclide emanating from the top of the domain. A unit inventory of 1 Ci was assigned to the CIG waste zone for each radionuclide considered in the analysis. Results were output in Ci/yr, consistent with the set of units employed in the model, and are presented for each radionuclide in Figure 2-73 through Figure 2-75. The peak fluxes emanating at the land surface are presented for each time period in Table 2-70. The results are reported in this way to facilitate calculation of human exposure at the SRS boundary and at the 100-m boundary due to the CIG Trenches. Flux behavior is based primarily on the closure considerations discussed in Section 2.7.3 and the half-life of the particular radionuclide as provided in Table 2-64.

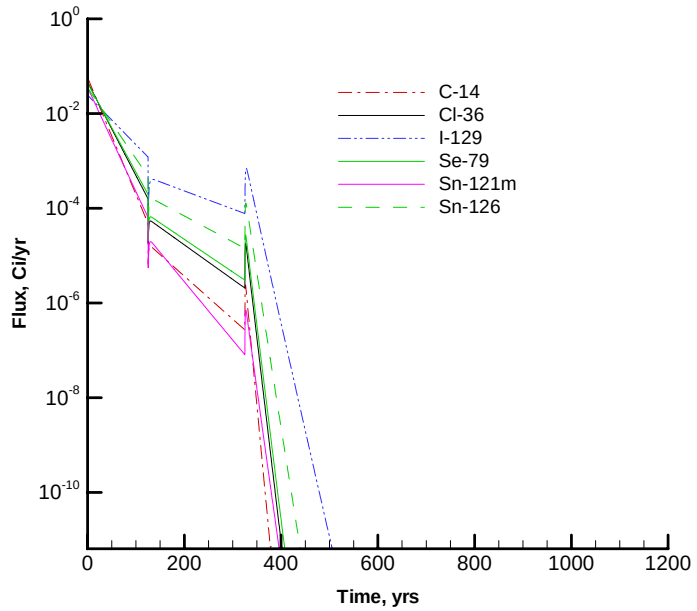

Figure 2-73. Flux Rate at Land Surface for C-14, Cl-36, I-129, Se-79, Sn-121m, and Sn-126

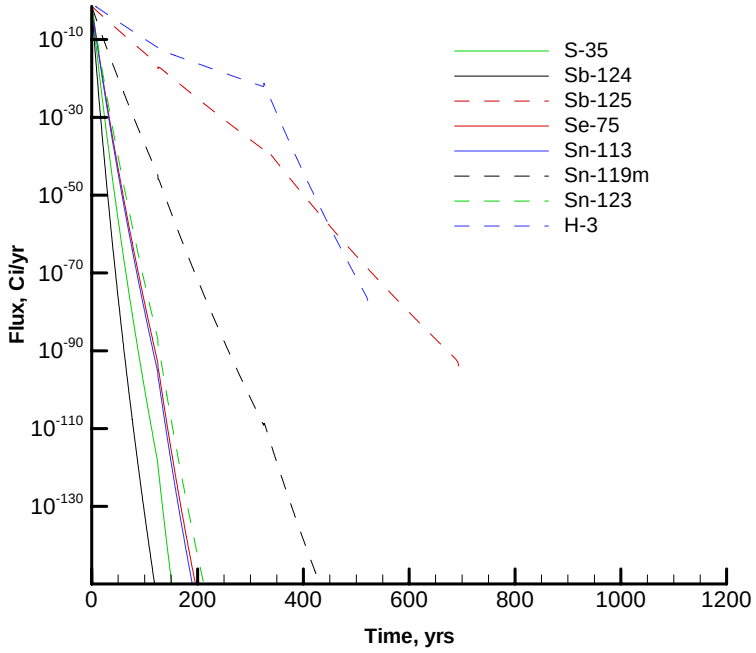

Figure 2-74. Flux Rate at Land Surface for S-35, Sb-124, Sb-125, Se-75, Sn-113, Sn-119m, Sn-123, and H-3.

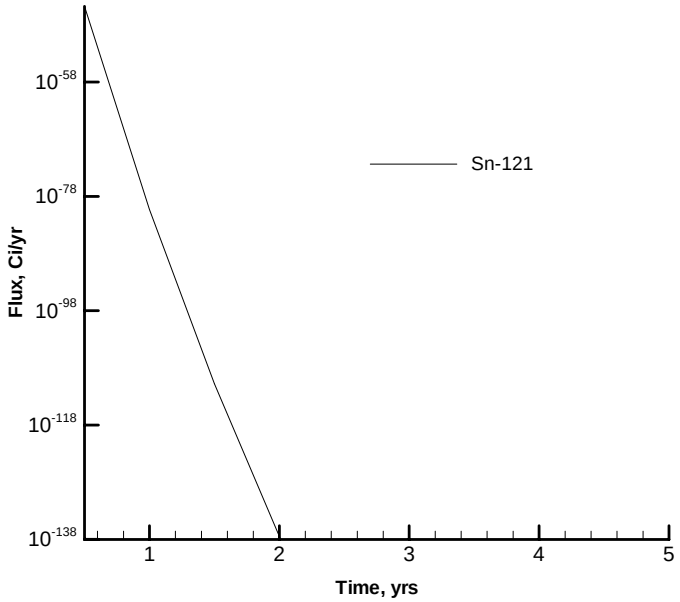

Figure 2-75. Flux Rate at Land Surface for Sn-121

Table 2-70. Summary of the Peak Flux Rates for Each Radionuclide

Radionuclide	Activity in Waste (Ci)	Peak Flux (Ci/yr/Ci)		
		0 - 125 Years	125 – 325 Years	325 – 1125 Years
C-14	1.0	5.51E-02	1.60E-05	2.41E-06
Cl-36	1.0	4.40E-02	5.38E-05	1.85E-05
H-3	1.0	1.44E-01	2.61E-13	6.20E-22
I-129	1.0	2.34E-02	4.06E-04	6.96E-04
S-35	1.0	1.49E-02	5.31E-121	3.62E-285
Sb-124	1.0	3.78E-03	2.85E-158	0.00E+00
Sb-125	1.0	2.71E-02	7.04E-18	2.76E-38
Se-75	1.0	1.46E-02	2.88E-95	2.35E-225
Se-79	1.0	4.21E-02	6.58E-05	2.73E-05
Sn-113	1.0	1.09E-02	7.27E-98	1.94E-231
Sn-119m	1.0	2.06E-02	1.20E-46	2.24E-109
Sn-121	1.0	1.81E-45	0.00E+00	0.00E+00
Sn-121m	1.0	3.36E-02	1.97E-05	7.10E-07
Sn-123	1.0	1.17E-02	2.83E-89	2.90E-211
Sn-126	1.0	3.35E-02	1.60E-04	1.29E-04

2.7.7 CIG Trench Air-Pathway Dose Calculations

An evaluation was conducted to assess the potential dose to a MEI located at both the SRS boundary and at the 100-m locations (Lee 2006). During the 125-year operational and institutional control period, the SRS boundary is the compliance point for the dose calculations. Therefore, the peak flux during this time period was used to assess the dose to the MEI. For the remainder of the time period, the 100-m boundary is the compliance point. Thus, the peak flux between 125 and 1125 years was used for these calculations. Dose-release factors were calculated for each radionuclide potentially released from the CIG disposal unit using CAP88, the EPA model for NESHAPs. The DRFs represent the dose to the receptor exposed to 1 Ci of the specified radionuclide being released to the atmosphere. For the receptor located at the SRS boundary the distance from the CIG Trenches is sufficient for an assumption of a point source. However, the DRFs for the 100-m receptor require evaluation of an area source because of the close proximity of the CIG disposal unit to the 100-m receptor. For radionuclides not contained within the CAP88 library (Se-75, Se-79, Sn-119m, and Sn-121m) atmospheric transport was estimated by assigning surrogates with similar radiological properties. Doses for these four radionuclides were estimated by applying their dosimetric properties to the surrogate's relative air concentrations estimated by the model.

Specific SRS Boundary DRFs, the calculated exposure levels for the 0-to-125 year MEI at the SRS boundary, and the resulting 0-to-125 year CIG disposal limits are presented in Table 2-71. Specific SRS 100-m DRFs, the calculated exposure levels for the 125-to-1125 year MEI at 100 m, and the resulting 125-to-1125 year CIG disposal limits are presented in Table 2-72. See Lee (2006) for details on the estimation of all DRFs in Table 2-71 and Table 2-72. The CIG disposal unit limits were calculated by dividing the maximum permissible exposure level (10 mrem/yr, DOE 1999) by the highest dose received by the MEI from the 1 Ci source during each of the two time periods. Table 2-73 provides a comparison of the limits derived for these two time periods (i.e., 0 – 125 and 125 – 1125 years) and the resulting overall CIG Trench air-pathway disposal limits. These disposal limits are applicable for each radionuclide for each CIG Trench footprint separately.

Table 2-71. SRS Boundary Dose Release Factors and 0-125 Year CIG Trench Disposal Limits

Radionuclide	0 - 125 Year Peak Flux (Ci/yr/Ci)	SRS Boundary Dose Release Factor[1] (mrem/Ci)	0 – 125 Year Dose to MEI at SRS Boundary[2] (mrem/yr/Ci)	0 - 125 Year CIG Disposal Limits[3] (Ci)
C-14	5.51E-02	1.1E-04	5.9E-06	1.7E+06
Cl-36	4.40E-02	2.3E-04	1.0E-05	1.0E+06
H-3	1.44E-01	2.2E-06	3.2E-07	3.1E+07
I-129	2.34E-02	4.9E-02	1.1E-03	8.8E+03
S-35	1.49E-02	2.8E-05	4.2E-07	2.4E+07
Sb-124	3.78E-03	2.0E-03	7.7E-06	1.3E+06
Sb-125	2.71E-02	6.5E-03	1.7E-04	5.7E+04
Se-75	1.46E-02	1.1E-03	1.6E-05	6.3E+05
Se-79	4.21E-02	6.3E-04	2.6E-05	3.8E+05
Sn-113	1.09E-02	2.3E-04	2.5E-06	4.0E+06
Sn-119m	2.06E-02	1.0E-04	2.1E-06	4.8E+06
Sn-121	1.81E-45	4.2E-05	7.6E-50	1.3E+50
Sn-121m	3.36E-02	6.5E-04	2.2E-05	4.6E+05
Sn-123	1.17E-02	1.3E-05	1.5E-07	6.7E+07
Sn-126	3.35E-02	3.0E-01	9.9E-03	1.0E+03

[1]From Lee (2006)
[2]Dose to MEI at SRS Boundary = Peak Flux × Dose Release Factor
[3] Disposal Limit = 10 mrem/yr / Dose to MEI at SRS Boundary per year per Ci
Note: Limits for special wasteforms (e.g. Mk50A, Cooling Tower) are the same as the limit for generic radionuclide.

Table 2-72. 100-m Dose Release Factors and 125 - 1125 Year CIG Trench Disposal Limits

Radionuclide	125 –1125 Year Peak Flux (Ci/yr/Ci)	100-m Dose Release Factor[1] (mrem/Ci)	125 –1125 Year Dose to MEI at 100 m[2] (mrem/yr/Ci)	125 –1125 Year CIG Disposal Limits[3] (Ci)
C-14	1.60E-05	5.9E-02	9.4E-07	1.1E+07
Cl-36	5.38E-05	9.3E-02	5.0E-06	2.0E+06
H-3	2.61E-13	1.2E-03	3.2E-16	3.2E+16
I-129	6.96E-04	8.6E+01	6.0E-02	1.7E+02
S-35	5.31E-121	7.7E-03	4.1E-123	---
Sb-124	2.85E-158	5.7E-01	1.6E-158	---
Sb-125	7.04E-18	1.7E+00	1.2E-17	8.4E+17
Se-75	2.88E-95	3.1E-01	8.8E-96	---
Se-79	6.58E-05	1.8E-01	1.2E-05	8.3E+05
Sn-113	7.27E-98	7.7E-02	5.6E-99	---
Sn-119m	1.20E-46	3.3E-02	4.0E-48	---
Sn-121	0.00E+00	1.2E-02	0.0E+00	---
Sn-121m	1.97E-05	1.8E-01	3.6E-06	2.8E+06
Sn-123	2.83E-89	3.3E-03	9.3E-92	---
Sn-126	1.60E-04	7.7E+01	1.2E-02	8.2E+02

[1]From Lee (2006)
[2]Dose to MEI at 100 m = Peak Flux × Dose Release Factor
[3] Disposal Limit = 10 mrem/yr / Dose to MEI at 100 m
NL = No limit
Note: Limits reported as "---" indicate that there is no limit or that the limit $\geq$ 1E+20.
Note: Limits for special wasteforms (e.g., Mk50A, Cooling Tower) are the same as the limit for generic radionuclide.

Table 2-73. Overall CIG Trench Air-Pathway Disposal Limit

Radionuclide	0 - 125 Year CIG Disposal Limits [1] (Ci)	125 –1125 Year CIG Disposal Limits[2] (Ci)	Overall CIG Trench Air-Pathway Disposal Limit (Ci)
C-14	1.7E+06	1.1E+07	1.7E+06
Cl-36	1.0E+06	2.0E+06	1.0E+06
H-3	3.1E+07	3.2E+16	3.1E+07
I-129	8.8E+03	1.7E+02	1.7E+02
S-35	2.4E+07	---	2.4E+07
Sb-124	1.3E+06	---	1.3E+06
Sb-125	5.7E+04	8.4E+17	5.7E+04
Se-75	6.3E+05	---	6.3E+05
Se-79	3.8E+05	8.3E+05	3.8E+05
Sn-113	4.0E+06	---	4.0E+06
Sn-119m	4.8E+06	---	4.8E+06
Sn-121	---	---	---
Sn-121m	4.6E+05	2.8E+06	4.6E+05
Sn-123	6.7E+07	---	6.7E+07
Sn-126	1.0E+03	8.2E+02	8.2E+02

[1]From Table 2-71.
[2]From Table 2-72
NL = No limit
Note: Limits reported as " --- " signify a number >1E+20.
Note: Limits for Special Wasteforms (e.g., Mk50A, Cooling Tower) are the same as the limit for the generic radionuclide.

2.8 CIG ALL-PATHWAYS ANALYSIS

This section documents the development of preliminary all-pathways limits for the CIG Trenches. The limits developed within this section are considered preliminary, since they do not take into consideration the effects of plume overlap from adjacent units or the results of sensitivity and uncertainty analyses. The effects of plume overlap are considered in Chapter 6 and the interpretation of sensitivity and uncertainty analyses is conducted in Chapter 7. Final limits are provided in Chapter 7.

2.8.1 Overview of All-Pathways Analysis

This section describes the investigation conducted to evaluate the potential magnitude of the all-pathways dose from the CIG over the 25-year operational period, 100-year institutional control period, and 1000-year post-closure compliance period. The CIG disposal units are used for a variety of wastes containing more radioactive material than that allowed in the slit and engineered trenches.

The permissible all-pathways dose for DOE LLW disposal facilities is addressed in DOE M 435.1, IV.P.(1)(a) (DOE 1999). This requirement is that dose to representative members of the public shall not exceed 25 mrem (0.25 mSv) in a year total effective dose equivalent from all exposure pathways, excluding the dose from radon and its progeny in air.

Although the all-pathways performance objective includes not only all exposure pathways, but also all transport pathways, in this PA, the air pathway is evaluated separately. The all-pathways dose evaluated here includes only the groundwater transport pathway because the receptors for the groundwater and air pathways will likely be at different locations and the maximum doses from the two pathways will occur at different times.

The all-pathways analysis uses the groundwater concentrations developed in Section 2.6. The concentrations as a function of time are input into the all-pathways application (Koffman 2006a), which calculates dose to humans from direct ingestion of contaminated groundwater and consumption of locally grown leafy vegetables, produce, milk, and meat, which are contaminated with radionuclides from use of the groundwater for irrigation and direct consumption by the cattle (Section C.4.5.1).

2.8.2 CIG Summary of Key All-Pathways Analysis Assumptions

Key assumptions and inputs used in the all-pathways analysis are presented in Appendix B.

2.8.3 CIG All-Pathways Analysis

The maximum all-pathways doses from the existing inventory in CIG-1 over the 1,000-year post closure compliance period were calculated using the all-pathways application (Koffman 2006a) and the current inventory (Table 2-17). The application uses the results of the PORFLOW program to calculate the dose to a hypothetical individual from using the groundwater at the point of assessment (location of the maximum concentration of each radionuclide outside of a 100-m buffer zone) for all credible purposes (drinking, irrigation of crops and ingestion of the crops and the meat and milk of animals fed on the crops and groundwater). Table 2-74 summarizes the results.

Table 2-74. All Pathways Dose from CIG-1, Considering only the Current Inventory

Time Period	125 – 1125 Years Post-Closure
Maximum Total Dose, mrem/yr	1.89
Performance Measure, mrem/yr	25
Nuclide	% of Max Dose
C-14	8.79E+01
C-14_K	1.13E+01
I-129	4.24E-01
I-129_K	1.34E-02
Tc-99_K	4.51E-01

The doses from the existing inventory are very low, less than eight percent of the performance measure of 25 mrem/yr. The dose is dominated by C-14, which represents about 88% of the total maximum dose.

Radionuclide disposal limits for the CIG-1 (accounting for existing inventory) and CIG-2 were developed from the PORFLOW results, considering the effects of the currently disposed inventory. The limits are shown in Table 2-75.

Table 2-75. Preliminary All-Pathways Radionuclide Disposal Limits for CIG-1 and CIG-2

Parent Radionuclide	CIG Preliminary All-Pathways Inventory Limit (Ci)			
	CIG-1 0-125 year	CIG-1 125-1,125 year	CIG-2 0-125 year	CIG-2 125-1,125 year
Am-241	---	1.5E+02	---	1.8E+02
Am-243	---	3.6E+03	---	4.2E+03
C-14	4.6E+09	4.9E-01	5.4E+09	5.8E-01
C-14_K	6.0E+10	4.9E+00	7.0E+10	5.7E+00
Cl-36	5.2E+04	7.3E-02	6.2E+04	8.5E-02
Cm-244	---	---	---	---
Cm-245	---	1.1E+02	---	1.3E+02
Cm-247	---	3.1E+03	---	3.6E+03
Cm-248	---	8.6E+02	---	1.0E+03
H-3 [1]	1.0E+07	3.7E+06	1.2E+07	4.4E+06
I-129	2.4E+06	8.2E-03	2.9E+06	9.6E-03
I-129_C	3.2E+08	5.0E-01	3.7E+08	5.8E-01
I-129_K	1.9E+09	3.0E+00	2.3E+09	3.6E+00
K-40	---	1.3E+08	---	1.6E+08
Mo-93	3.3E+03	1.8E+00	3.9E+03	2.1E+00
Nb-94	3.1E+18	5.0E+00	3.7E+18	5.8E+00
Ni-59	---	1.9E+03	---	2.3E+03
Np-237	---	3.3E-02	---	3.9E-02
Pd-107	---	2.9E+03	---	3.5E+03
Pu-238	---	1.6E+05	---	1.9E+05
Pu-239	---	4.8E+05	---	5.7E+05
Pu-240	---	1.2E+18	---	1.4E+18
Pu-241	---	4.6E+03	---	5.5E+03
Pu-242	---	1.3E+12	---	1.5E+12
Pu-244	---	1.0E+18	---	1.2E+18
Ra-226	---	7.4E-02	---	8.8E-02
Se-79	---	---	---	---
Sn-126	---	---	---	---
Sr-90	---	2.8E+05	---	3.3E+05
Tc-99	4.9E+03	6.5E-01	5.8E+03	7.7E-01
Tc-99_K	8.6E+06	2.0E+01	1.0E+07	2.3E+01
Th-230	---	2.1E-01	---	2.5E-01
Th-232	---	2.5E+08	---	2.9E+08
U-233	---	---	---	---
U-234	---	4.5E+01	---	5.2E+01
U-235	---	3.6E-01	---	4.2E-01
U-236	---	3.5E+15	---	4.1E+15
U-238	---	4.7E+04	---	5.6E+04
Zr-93	3.0E+19	1.4E+00	3.6E+19	1.7E+00

Note: Limits reported as "---" indicate that there is no limit or that the limit $\geq$ 4.59E+19 Ci for CIG-1 and $\geq$ 5.41E+19 Ci for CIG-2

[1] H-3 Preliminary Inventory Limit values reduced by a factor of 10 to account for uncertainty associated with H-3 release from 232-F stainless steel process equipment

2.9 INADVERTENT INTRUDER ANALYSIS

The inadvertent intruder analysis considers the radiological impacts to hypothetical persons who are assumed to inadvertently intrude into the Components in Grout Trench disposal units at the EALLWF after institutional control ceases 100 years after facility closure. Descriptions of intruder scenarios are provided in the Background Chapter in Part C of this PA. The analysis was carried out using an automated computer application developed at SRNL (Koffman 2006b), which implements equations calculating dose per unit intake documented in Lee (2004). One important functional requirement of the application is that it computes a "no leaching" case in which the full decay chain is determined and the activities are calculated at specified times using the Bateman equation. This means that the intruder calculations are completely independent from the PORFLOW calculations.

2.9.1 CIG Trench-Specific Parameters

The final closure system for the EALLWF includes a 12-inch thick erosion barrier near the top of the cap. The erosion barrier has been shown to be effective for at least 10,000 years (Phifer and Nelson 2003) so that all the layers between the waste and the erosion barrier remain in place at their design thickness, approximately 10 ft of material always exists above the waste. Because the thickness from the top of the erosion barrier to the waste is the same as the depth of a typical basement (10 ft), the agriculture scenario can never occur as it relies on a basement extending into the waste zone. The combination of the reinforced concrete mat and the cementitious encapsulation of the wasteforms in the components in grout disposal system are assumed to preclude the post-drilling scenario for 200 years following the 100-year institutional control period. The resident scenario is credible for the Components in Grout units after the institutional control period of 100 years.

The parameters specific to the Components in Grout Trench Disposal Units used in the intruder analysis are given in Table 2-76. The geometry factors and erosion rate are documented in McDowell-Boyer et al. (2000). The waste volume for the CIG is consistent with that presented in Section 2.5.3. The "degradation duration" of 300 years reflects the fact that structural stability of the CIG grout can be assumed for that period of time (see discussion in Section 2.6.3.1).

2.9.2 Results

The agriculture scenario was not evaluated because implementation of an erosion barrier during closure eliminates the potential for contact with the waste via this scenario. Results of the resident intruder analyses for Components in Grout Trench disposal units for the time period of 1,000 years after closure are provided in Table 2-77. Results of the post-drilling intruder analyses for the Components in Grout Trench disposal units for the time period of 1,000 years after closure are provided in Table 2-78. The entry "---" in the Time of Limit column means that the dose calculation is always zero so there is no limit.

For cases where there is a time given, there may be an entry "---"in one or both of the limit columns. In this case the entry "---"indicates a limit value greater than or equal to the threshold value of 1E+20. Because the automated method applies a transient analysis, it calculates the lowest inventory limit for the entire time period, regardless of when it occurs.

Table 2-76. Intruder Parameters for the Components in Grout Trench Disposal Units

Facility	E-Area
Disposal Unit Name	Components in Grout
Abbreviated Name	CIG
Agriculture Geometry Factor	0.6
Resident Geometry Factor	0.6
Post-Drilling Geometry Factor	1
Waste Volume (ft3)	819000

Transient Layer Model (Surface to Top of Waste)

Layer	Thickness (inches)	Description	Erosion Rate (mm/yr)	Erosion Earliest Start (yr)	Degradation Duration (yr)	Degradation Start (yr)
1	36	Soil cover	1.4			
2	12	Erosion barrier	1.4	1.00E+10		
3	96.4	Soil backfill	1.4			
4	12	Grout	1.4		300	0

Table 2-77. Intruder-Based Radionuclide Disposal Limits for Components in Grout – Resident Scenario with Transient Calculation for 1000 Years

Radionuclide	Time of Limit (Years)	Concentration Limit ($\mu Ci/m^3$)	Inventory Limit (Ci/Unit)
Ac-227	100	8.36E+08	1.9E+07
Ag-108m	760	4.45E+02	1.0E+01
Al-26	760	6.78E+01	1.6E+00
Am-241	760	9.63E+05	2.2E+04
Am-242m	760	1.50E+06	3.5E+04
Am-243	760	2.97E+03	6.9E+01
Ar-39	760	---	---
Ba-133	100	1.08E+11	2.5E+09
Bi-207	100	2.82E+06	6.5E+04
Bk-249	760	1.37E+06	3.2E+04
C-14	760	---	---
Ca-41	760	---	---
Cd-113m	760	---	---
Cf-249	760	3.53E+03	8.2E+01
Cf-250	760	1.87E+12	4.3E+10
Cf-251	760	9.11E+03	2.1E+02
Cf-252	1000	9.56E+12	2.2E+11
Cl-36	760	---	---
Cm-242	1000	4.33E+10	1.0E+09
Cm-243	760	3.05E+08	7.1E+06
Cm-244	760	1.58E+11	3.7E+09
Cm-245	760	1.17E+04	2.7E+02
Cm-246	760	5.14E+09	1.2E+08
Cm-247	1000	7.70E+02	1.8E+01
Cm-248	1000	7.02E+07	1.6E+06
Co-60	100	5.84E+10	1.4E+09
Cs-134	100	---	9.5E+18
Cs-135	760	---	---
Cs-137	100	5.71E+07	1.3E+06
Eu-152	100	6.49E+07	1.5E+06
Eu-154	100	1.16E+09	2.7E+07
Eu-155	100	7.72E+19	1.8E+18
H-3	760	---	---
I-129	760	5.13E+07	1.2E+06
K-40	760	1.12E+03	2.6E+01
Kr-85	100	2.59E+12	6.0E+10
Mo-93	760	---	---
Na-22	100	7.77E+16	1.8E+15
Nb-93m	760	---	---
Nb-94	760	1.29E+02	3.0E+00

* --- means that the calculated limit was ≥ 1E+20 Ci

Table 2-77. Intruder-Based Radionuclide Disposal Limits for Components in Grout – Resident Scenario with Transient Calculation for 1000 Years - continued

Radionuclide	Time of Limit (Years)	Concentration Limit ($\mu Ci/m^3$)	Inventory Limit (Ci/Unit)
Ni-59	760	---	---
Ni-63	760	---	---
Np-237	1000	1.48E+03	3.4E+01
Pa-231	760	7.83E+02	1.8E+01
Pb-210	100	3.87E+12	9.0E+10
Pd-107	760	---	---
Pu-238	1000	2.20E+08	5.1E+06
Pu-239	760	1.54E+07	3.6E+05
Pu-240	760	4.36E+08	1.0E+07
Pu-241	760	2.83E+07	6.6E+05
Pu-242	1000	3.65E+08	8.5E+06
Pu-244	760	6.26E+02	1.5E+01
Ra-226	760	1.50E+02	3.5E+00
Ra-228	100	3.97E+09	9.2E+07
Rb-87	760	---	---
S-35	---	---	---
Sb-125	100	1.31E+18	3.0E+16
Sc-46	100	---	---
Se-79	760	---	---
Sm-151	760	---	---
Sn-121m	760	---	---
Sn-126	760	1.08E+02	2.5E+00
Sr-90	760	---	---
Tc-99	760	2.85E+09	6.6E+07
Th-228	100	---	4.7E+18
Th-229	760	1.07E+03	2.5E+01
Th-230	1000	3.08E+02	7.1E+00
Th-232	760	7.57E+01	1.8E+00
U-232	100	9.65E+04	2.2E+03
U-233	1000	1.10E+04	2.6E+02
U-234	1000	6.21E+04	1.4E+03
U-235	1000	3.08E+03	7.2E+01
U-236	1000	4.76E+07	1.1E+06
U-238	1000	1.33E+04	3.1E+02
W-181	100	---	---
W-185	100	---	---
W-188	100	---	---
Zr-93	760	---	---

Note: Limits reported as "---" indicate that there is no limit or that the limit $\geq$ 1E+20.
Note: Limits for special wasteforms (e.g., Mk50A, Cooling Tower) are the same as the limit for generic radionuclide.

Table 2-78. Intruder-Based Radionuclide Disposal Limits for Components in Grout – Post-Drilling Scenario with Transient Calculation for 1000 Years

Radionuclide	Time of Limit (Years)	Concentration Limit ($\mu Ci/m^3$)	Inventory Limit (Ci/Unit)
Ac-227	300	8.25E+07	1.9E+06
Ag-108m	300	1.07E+05	2.5E+03
Al-26	300	5.42E+04	1.3E+03
Am-241	300	6.51E+04	1.5E+03
Am-242m	300	9.07E+04	2.1E+03
Am-243	300	3.94E+04	9.1E+02
Ar-39	300	2.04E+09	4.7E+07
Ba-133	300	1.46E+14	3.4E+12
Bi-207	300	5.39E+07	1.2E+06
Bk-249	300	2.40E+07	5.6E+05
C-14	300	6.89E+04	1.6E+03
Ca-41	300	4.06E+05	9.4E+03
Cd-113m	300	1.88E+10	4.4E+08
Cf-249	300	6.21E+04	1.4E+03
Cf-250	300	1.86E+07	4.3E+05
Cf-251	300	4.61E+04	1.1E+03
Cf-252	300	1.81E+09	4.2E+07
Cl-36	300	8.54E+02	2.0E+01
Cm-242	300	1.15E+08	2.7E+06
Cm-243	300	2.80E+07	6.5E+05
Cm-244	300	1.85E+07	4.3E+05
Cm-245	1000	2.60E+04	6.0E+02
Cm-246	300	5.12E+04	1.2E+03
Cm-247	1000	4.28E+04	9.9E+02
Cm-248	300	1.34E+04	3.1E+02
Co-60	300	---	---
Cs-134	300	---	---
Cs-135	300	8.26E+05	1.9E+04
Cs-137	300	8.24E+07	1.9E+06
Eu-152	300	6.31E+11	1.5E+10
Eu-154	300	3.84E+15	8.9E+13
Eu-155	300	---	---
H-3	300	5.42E+12	1.3E+11
I-129	300	1.29E+04	3.0E+02
K-40	300	1.73E+04	4.0E+02
Kr-85	300	1.60E+16	3.7E+14
Mo-93	300	1.66E+07	3.8E+05
Na-22	300	---	---
Nb-93m	300	2.29E+13	5.3E+11
Nb-94	300	9.34E+04	2.2E+03

Table 2-78. Intruder-Based Radionuclide Disposal Limits for Components in Grout – Post-Drilling Scenario with Transient Calculation for 1000 Years - continued

Radionuclide	Time of Limit (Years)	Concentration Limit ($\mu Ci/m^3$)	Inventory Limit (Ci/Unit)
Ni-59	300	1.42E+07	3.3E+05
Ni-63	300	4.11E+07	9.5E+05
Np-237	300	3.69E+03	8.6E+01
Pa-231	300	4.15E+03	9.6E+01
Pb-210	300	3.77E+07	8.7E+05
Pd-107	300	2.96E+07	6.9E+05
Pu-238	300	5.89E+05	1.4E+04
Pu-239	300	5.02E+04	1.2E+03
Pu-240	300	5.14E+04	1.2E+03
Pu-241	300	1.90E+06	4.4E+04
Pu-242	300	5.25E+04	1.2E+03
Pu-244	1000	4.31E+04	1.0E+03
Ra-226	300	2.57E+03	6.0E+01
Ra-228	300	2.48E+19	5.7E+17
Rb-87	300	5.18E+05	1.2E+04
S-35	---	---	---
Sb-125	300	---	---
Sc-46	---	---	---
Se-79	300	8.02E+05	1.9E+04
Sm-151	300	9.43E+08	2.2E+07
Sn-121m	300	1.29E+09	3.0E+07
Sn-126	300	7.03E+04	1.6E+03
Sr-90	300	6.75E+06	1.6E+05
Tc-99	300	8.26E+04	1.9E+03
Th-228	300	---	---
Th-229	300	1.73E+04	4.0E+02
Th-230	1000	6.49E+03	1.5E+02
Th-232	300	5.03E+03	1.2E+02
U-232	300	2.38E+05	5.5E+03
U-233	1000	7.47E+04	1.7E+03
U-234	1000	1.16E+05	2.7E+03
U-235	1000	7.50E+04	1.7E+03
U-236	300	1.33E+05	3.1E+03
U-238	1000	1.36E+05	3.1E+03
W-181	300	---	---
W-185	---	---	---
W-188	---	---	---
Zr-93	300	3.22E+07	7.5E+05

Note: Limits reported as "---" indicate that there is no limit or that the limit $\geq$ 1E+20.
Note: Limits for special wasteforms (e.g. Mk50A, Cooling Tower) are the same as the limit for generic radionuclide.

2.10 CIG TRENCH RADON ANALYSIS

2.10.1 Overview of Radon Analysis

This section describes the investigation conducted to evaluate the potential magnitude of radon release from the CIG Trenches over the 25-year operational period, 100-year institutional control period, and 1000-year post-closure compliance period. The CIG Trenches are contained within two footprints of equal area (~103,000 ft^2) and are designated as CIG-1 and CIG-2. These earthen trenches contain grout encapsulated waste including large radioactively contaminated equipment and other smaller wasteforms such as B-25 boxes to fill in the space around and above the large equipment (Phifer et al. 2006).

The flux of Rn-222 from the CIG Trenches was evaluated for three separate time periods: 1) 0 to 125 years, 2) 125 to 325 years, and 3) 325 to 1125 years. The first time period evaluated covers the operational and institutional control period. During this time period, the final closure cap does not cover the trenches. During the second time period, 125 to 325 years, a final closure cap is in place over the trenches. For the third time period, 325 to 1125 years, it is assumed that the grout structure encapsulating the waste collapses resulting in settlement of the waste and final closure cap.

The permissible radon flux for DOE facilities is addressed in DOE M 435.1-1 Chapter IV (DOE 1999). Specifically, Section IV. P(1)(c) states the radon flux limitations associated with the development of a disposal facility and maintenance of a performance assessment and the closure of the disposal facility. This requirement is that the release of radon shall be less than an average flux of 20 $pCi/m^2/s$ at the surface of the disposal facility. The requirements analysis states that this standard was adopted from the uranium mill tailings requirements in 40 CFR Part 192 and 10 CFR Part 40. 10 CFR Part 40 discusses both Rn-222 from uranium and Rn-220 from thorium, therefore the performance objective refers only to radon, and the correct species must be analyzed depending on the characteristics of the waste stream.

This guidance forms the basis for the investigation to evaluate radon flux above the CIG Trenches. The scope of the investigation involved defining a decay chain of parent radionuclides to evaluate with a 1-D, vertical, numerical model. This analysis applies the capability of the standard SRS groundwater simulation program (PORFLOW) to model gas phase transport through partially saturated porous media to the ground surface. The model was customized to represent the vertical dimension of CIG Trenches and the anticipated cover material. The instantaneous Rn-222 flux at the land surface was evaluated for the three time periods previously mentioned and the maximum flux was then compared to the DOE performance objective.

This investigation addresses only Rn-222, since the short half-life of Rn-220 (55.6 seconds) makes it unlikely to escape the CIG Trenches and migrate to the land surface via air-diffusion before it is transformed by radioactive decay.

The potential parent radionuclides that can contribute to the creation of Rn-222 are illustrated in Figure 2-76. The diagram indicates the specific decay chains that lead to the formation of Rn-222, as well as the half-lives for each radionuclide. The extremely long half-life of U-238 (4.468E+09 years) cause the other radionuclides higher up on the chain of parents to be of little concern with regard to their potential to contribute significantly to the Rn-222 flux at the land surface over the period of interest.

2.10.2 CIG Summary of Key Radon Analysis Assumptions

Key assumptions and inputs used in the radon analysis are presented in Appendix B.

2.10.3 CIG Radon Analysis Conceptual Model

2.10.3.1 CIG Closure Considerations

The concepts for closure of the CIG Trenches are relevant to the determination of the radon flux at the land surface. The CIG Trench construction specifics and closure concept are described by Phifer et al. (2006). For the purposes of this investigation, it is assumed that during the 25-year operational period and 100-year institutional control period that the final closure cap does not overlie the trenches. Therefore, the ground surface during this time period is the top of the 48 inch clean soil from Table 2-63 and this is the point where the Rn-222 flux was evaluated. For the 125 to 325-year time period, a final closure cap is assumed to be in place over the waste trenches.

A conceptual drawing of the closure cap over the CIG Trenches is shown in Figure 2-2 and the vertical section over which Rn-222 diffusion was evaluated is indicated. For the 325 to 1125 year time period, it is assumed that the grout structure encapsulating the waste collapses. This results in settlement of the waste zone and destruction of the closure cap. For this time period, the material properties of the closure cap were re-assigned to represent the bulk properties of E-Area Operational Soil Cover (Phifer et al. 2006), and the overall thickness of this material over the waste was assumed to remain the same as that for the intact closure cap.

The closure cap utilized in this analysis includes all materials, as constructed and placed over the CIG Trenches at the end of the 100-year institutional control period. The components of concern for the long-term radon performance calculation are those that have no potential to erode during the 200-year period between cap placement and grout collapse. These components are situated below the top of the erosion barrier. The composite thickness of the non-waste material below the top of the erosion barrier is approximately 10 ft. Table 2-63 lists the individual components of the CIG Trenches and closure cap (excluding the layers overlying the erosion control barrier). Materials are indicated with the associated thickness of each component in feet.

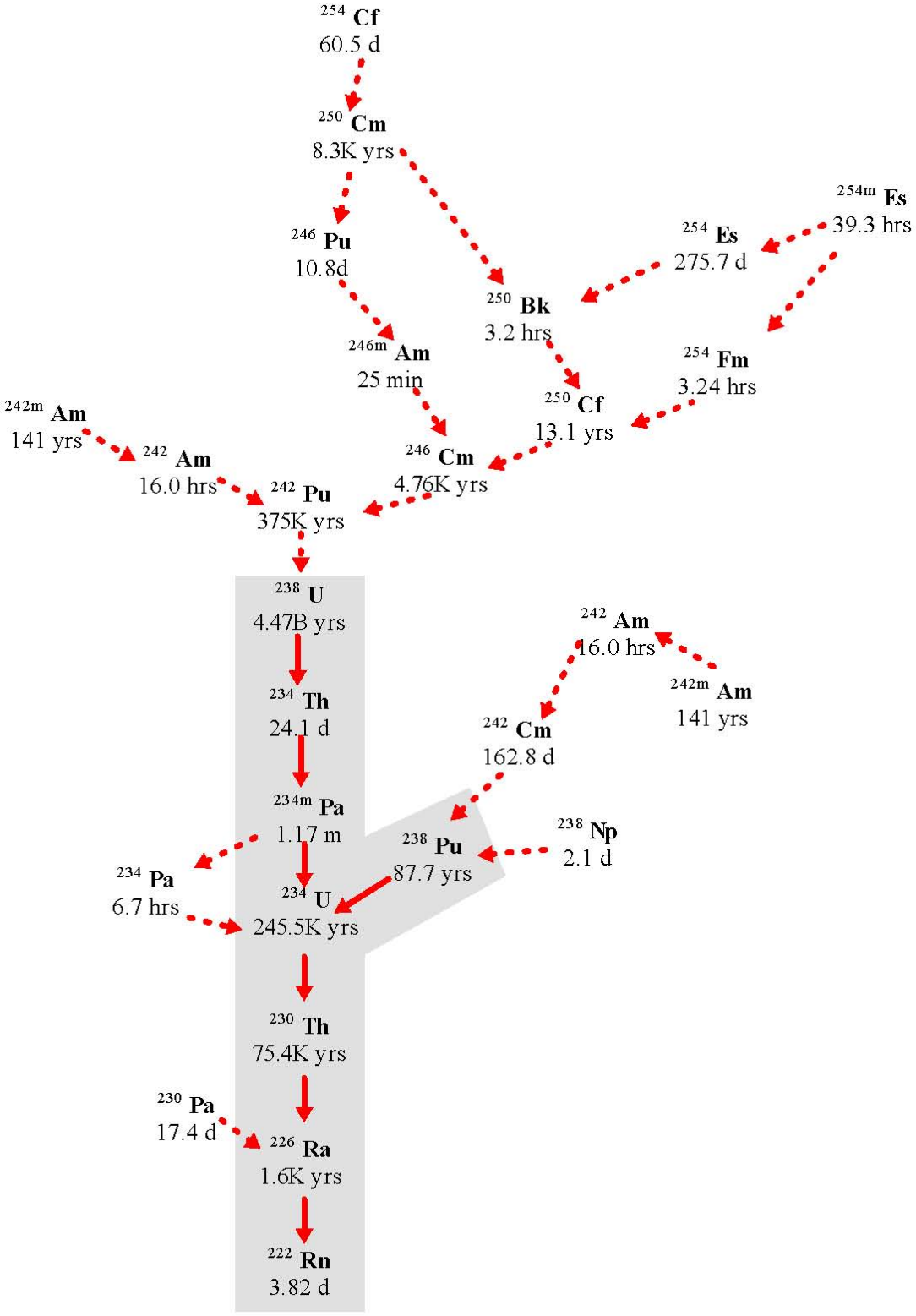

Figure 2-76. Radioactive Decay Chains Leading to Rn-222

2.10.3.2 Conceptual Model

The Rn-222 flux at the land surface above the CIG Trenches was evaluated for its specific closure configuration discussed above. Rn-222 is generated within the waste zone by radioactive decay of different parent radionuclides following along the decay chains that lead to the formation of Rn-222. The decay chains for all possible parent radionuclides of Rn-222 are shown in Figure 2-76. In Figure 2-76, the parent radionuclides that were individually evaluated are indicated with the gray shaded area (i.e., beginning with Pu-238 and U-238). Rn-222 generated within the waste zone is in the gaseous phase and diffuses outward from this zone into the air-filled soil pores surrounding the CIG Trenches, eventually resulting in some of the radon emanating at the land surface.

As such, air is the fluid through which Rn-222 diffuses, although some Rn-222 may dissolve in residual pore water. It is assumed that fluctuations in atmospheric pressure at the land surface that could induce small pulses of air movement into and out of the shallow soil column will have a zero net effect over the long-term period of evaluation in this study, thus advective transport of Rn-222 in air-filled soil pores is not considered to be a significant process when compared to air diffusion.

The parent radionuclides exist in the solid phase and therefore do not migrate upward through the air-filled pore space, although they could be leached and transported downward from the waste zone by pore water movement. This potential downward migration of the parent radionuclides was neglected in the radon analysis.

The flux of Rn-222 from the CIG Trenches was evaluated for three separate time periods: 1) 0 to 125 years, 2) 125 to 325 years, and 3) 325 to 1125 years. The first time period evaluated covers the operational and institutional control period. During this time period, the final closure cap does not overlie the trenches. During the second time period, 125 to 325 years, the final closure cap is in place over the trenches. For the third time period, 325 to 1125 years, it is assumed that the grout structure encapsulating the waste collapses resulting in subsidence of the waste and closure cap.

2.10.4 CIG Radon Analysis Numerical Model

The mathematical model utilized in this report is provided by the PORFLOW simulation package. PC-based PORFLOW Version 5.97.0 was used to conduct a series of simulations. PORFLOW is developed and marketed by Analytic & Computational Research, Inc. to solve problems involving transient and steady-state fluid flow, heat and mass transport in multi-phase, variably saturated, porous or fractured media with dynamic phase change. PORFLOW has been widely used at the SRS and in the DOE complex to address major issues related to the groundwater and nuclear waste management.

The governing equation for mass transport of species k in the fluid phase is given by

$$\frac{\partial C_k}{\partial t} + \frac{\partial}{\partial x_i}(V_i C_k) = \frac{\partial}{\partial x_i}(D_{ij}\frac{\partial C_k}{\partial x_j}) + \gamma_k$$

Equation 2-7

Where

C_k	concentration of species k (Ci/cm^3)
V_i	fluid velocity in the ith direction (cm/yr)
D_{ij}	effective diffusion coefficient for the species (cm^2/yr)
γ_k	net decay of species k ($Ci/cm^3/yr$)
i, j	direction index (unitless)
t	time (yr)
x	distance coordinate (cm)

This equation is solved using PORFLOW to evaluate transient Rn-222 transport above the CIG Trenches to evaluate Rn-222 flux at the land surface over time. As explained, advection is not considered to be a significant process when compared to air diffusion, so the advection term was disabled within PORFLOW and only the diffusive and net decay terms were evaluated.

The boundary conditions imposed on the model domain included:

- No-flux specified for all radionuclides along sides and bottom ($\partial C/\partial X = 0$ at x=0, x=1 and $\partial C/\partial Y = 0$ at y=0)
- Species concentration set to 0 at land surface (top of erosion barrier) ($C = 0$ at $y=y_{max}$)

The initial condition imposed on the domain included:

- Species concentration set to 0 for the entire model domain at time = 0 ($C=0$ for $0 \le x \le 1$ at t=0 and $C=0$ for $0 \le y \le y_{max}$ at t=0)

The initial conditions for the model also assumed a 1 Ci inventory of each radionuclide uniformly spread over the waste zone.

These boundary conditions force all of the gaseous radionuclides to move upward from the waste disposal zone to the land surface. In reality, some lateral and downward diffusion occurs in the air-filled pores surrounding the waste zone; hence ignoring this lateral and downward movement has the effect of increasing the flux at the land surface. This should introduce some conservatism in the calculated results. Simulations were conducted in transient mode for diffusive transport in air, with results being obtained over 1,125 years.

2.10.4.1 Model Development and Assumptions

The numerical representation of the conceptual model is as a 1-dimensional vertical stack of elements configured to represent the thickness of the CIG Trenches and overlying cover material appropriate to the time frame under consideration.

Decay chains evaluated were U-238→Th-234→Pa-234m→U-234→Th-230→Ra-226→Rn-222 and Pu-238 →U-234→Th-230→Ra-226→Rn-222. Each parent in these chains, except Th-234 and Pa-234m, were simulated separately as the starting point of the decay chain. Th-234 and Pa-234m have extremely short half-lives compared to the other parent radionuclides in these chains. Only a fraction of the Rn-222 generated by the decay of each parent is available for migration away from its source and into open pore space. Since the Rn-222 parent radionuclides exist as oxides or in other crystalline forms, only a fraction of Rn-222 generated by decay of Ra-226 has sufficient energy to migrate away from its original location into adjacent pore space before further decay occurs (3.82 day half-life for Rn-222).

The fraction of radon escaping its source and migrating into adjacent pore space is approximated by the use of a radon emanation coefficient. This coefficient has been shown to vary between 0.02 and 0.7 in soils but is typically 0.25 (Yu et al. 2001). This value is taken as the default factor value for the RESRAD program, developed for the DOE. To account for this effect in the model, an effective source term of 0.25 Ci of parent radionuclide was utilized as the source term for each Ci disposed within the facility. The 0.25 Ci inventory was applied over the waste zone during the first 325 years of simulation.

At 325 years, the waste zone is assumed to collapse thereby reducing the thickness of the waste zone from 14 ft to 7 ft. To account for this in the model, at 325 years, the remaining inventory of parent radionuclide in the lower half of the waste zone was transferred to the upper half. The porosity of the lower half of the waste zone was set to zero essentially removing it from the model.

Since Rn-222 exists as a gas, air was assumed to be the medium within which radon transport occurs. The flow field was assumed to be isobaric and isothermal. The impact of naturally occurring fluctuations of atmospheric pressure is likely to have a zero net effect. Therefore, for the relatively long periods of time evaluated in this investigation, air-diffusion was the only transport mechanism simulated in the model and advective air-transport was assumed to be negligible.

Some radon dissolves in pore water but since diffusion proceeds more slowly in that fluid, air diffusion is the only transport process by which Rn-222 can reach the land surface from the CIG Trenches. This assertion is substantiated in Yu et al. (2001). In that report the D_{eff} for soil is reported to range from the radon open air diffusion coefficient of 1.0E-06 m^2/s to that of fully saturated soil, 1.0E-10 m^2/s.

Thus, the larger volume of water-filled pore space compared to air-filled pore space (maximum of 1 order of magnitude difference) is inconsequential, in terms of the ability of water-dissolved radon to diffuse through water-filled pores as compared to the ability of the same compounds to diffuse as gas in the vapor-filled pore spaces. In this investigation, transport was allowed to proceed only through air-filled pore space and, therefore, residual pore water was treated as if it was part of the solid matrix material within the flow field. No credit was taken for airborne radon dissolving in pore water as it proceeds from the waste trenches to the land surface although it has been observed to partition between air and water in the ratio of 4 to 1, respectively, at 20° C (Nazaroff and Nero 1988).

The boundary conditions imposed on the domain included:

- No-flux specified for all parent radionuclides at perimeter of the domain
- No-flux specified for Rn-222 along sides and bottom
- Rn-222 concentration set to 0 at land surface.

Simulations were conducted in transient mode for diffusive transport in air, with results being obtained over 1,125 years.

2.10.4.2 Measures Implemented to Ensure Conservative Results

In this analysis, several conditions introduce a significant measure of conservatism into the calculations. These include:

- The use of boundary conditions that force all of the Rn-222 to move upward from the waste disposal zone to the land surface. In reality, some of the Rn-222 diffuses sideways and downward in the air-filled pores surrounding the waste zone; hence ignoring this has the effect of increasing the radon flux at the land surface.
- Not taking credit for the removal of either Rn-222 or of the parent radionuclides by pore water moving vertically downward through the model domain. This mechanism would likely remove some dissolved Rn-222 in addition to the parent radionuclides, and therefore its omission has the effect of increasing the estimate of instantaneous Rn-222 flux at the land surface in simulations conducted as a part of this investigation.
- The addition of an extra 125 years to the required 1,000-year evaluation period to account for any Rn-222 generated during the operations and institutional control period, thus incrementally increasing the instantaneous Rn-222 flux.
- Use of the top of the erosion layer in the soil cover as the land surface for the purpose of calculating Rn-222 flux during the 125 to 1125 year time period. No credit is taken for the additional distance Rn-222 must migrate above the erosion barrier prior to that portion of the soil cover eroding away. This assumption impacts only Ra-226 (due to its relatively short half life).
- Ignoring the presence of the GCL within the final closure cap. The GCL should be near 100 percent saturation; therefore it will contain very little air-filled porosity within which radon transport could occur.

- The assignment of E-Area Operational Soil Cover (Phifer et al. 2006) properties to the closure cap following collapse of the grout structure (325 to 1125 years). Some of the closure cap is likely to remain in-tact and retain its original material properties.

2.10.4.3 Grid Construction

The model grid was constructed as a node mesh 3 nodes wide by 54 nodes high. This mesh creates the vertical stack of 52 model elements. Figure 2-72 shows a schematic of the PORFLOW model grid. The grid extends upward only as far as the erosion barrier, since this is the minimum possible cover thickness that could exist during the 1,125-year evaluation period. A set of consistent units was employed in the simulations for length, mass and time, these being meters, grams and years, respectively.

2.10.4.4 Material Zones

The model domain was divided into two primary zones, the CIG waste zone occupying the lower 14 ft of the domain and the cover zone (including the grout top), extending 10 ft above the waste zone to the top of the domain. The cover zone includes the grout top as well as the different closure cap layers (see Table 2-63 and Figure 2-2). The upper model elements were scaled to correspond to the geometry of the closure cap thickness while the lower model elements were scaled to correspond to the CIG waste zone.

During the first 125 years of simulation, the land surface is assumed to be the top of the 48 inch clean soil layer placed over the grout top, which results in a total of 5 ft of clean material above the waste. For the 125 to 325 years simulation period, the land surface is assumed to be the top of the erosion barrier, which results in a total of 10 ft of clean material above the waste. No credit is taken for the compacted backfill and topsoil above the erosion barrier. For the 325 to 1125 year simulation period, the thickness of the waste zone is reduced by 7 ft, but the clean material above the waste to the ground surface remains at 10 ft. However, the overlying soil cover material is assigned the properties of E-Area Operational Soil Cover (Phifer et al. 2006).

2.10.4.5 Material Zone Properties and Other Input Parameters

Material properties utilized within the 1-D numerical model were specified for eight material zones defined within the model domain. Each material zone was assigned values of particle density, total porosity, average saturation, air-filled porosity, air density, and an effective air-diffusion coefficient for each source element or compound. With the use of an effective air-diffusion coefficient, tortuosity was assigned a unit value in each material zone. An air fluid density of 1.24E+03 g/m^3 was used. This air fluid density was obtained from the *CRC Handbook of Tables for Applied Engineering Science* (Bolz and Tuve 1973) and represents that of standard atmospheric conditions.

During the first 125 years the layers associated with the CIG Trench consist only of the CIG waste layer, CIG grout, and clean soil (see Figure 2-2). Although the interim runoff cover, utilized during the first 125 years (see discussion in Section 3), includes the potential use of up to an additional 2-foot of soil to establish necessary grades to promote runoff, this soil was not included in the model during this time period. This soil was not included, since it is only used as necessary and its thickness will be highly variable. The total porosity for the CIG waste zone was taken to be 0.5 and it was assumed that the waste was dry and that the air filled porosity would equal the total porosity for this zone (Phifer et al. 2006). The particle density and total porosity for the CIG grout and clean soil were taken from the recommended values for the existing E-Area CIG grout and E-Area Operational Soil Cover, respectively (Phifer et al. 2006). The average saturation for the CIG grout and clean soil were taken as the value of saturation at a suction head of approximately 200 cm from the characteristic curves for the existing E-Area CIG grout and E-Area Operational Soil Cover, respectively (Phifer et al. 2006).

E-Area vadose zone field pore pressure measurements indicate average suction levels in the approximate range of 50 to 200 cm (Nichols et al. 2000). A value of 200 cm represents the upper end of the range which will have a greater air-filled porosity. The air-filled porosity of the CIG grout and clean soil were calculated from the total porosity and average saturation. While the model includes all the layers from the CIG waste layer to the erosion barrier, during the first 125 years of simulation, the closure cap materials (i.e. the lower backfill on up) are assigned a porosity of 1.0. This has the effect of making these layers equivalent to air. Table 2-79 provides the values of particle density, total porosity, average saturation, and air-filled porosity utilized for the CIG waste layer, CIG grout, and clean soil during the first 125 years.

For the 125 to 325 year time period the layers associated with the CIG Trench consist of all layers from the CIG waste layer to the erosion barrier (see Figure 2-2). The CIG waste layer, CIG grout, and clean soil retain the same properties as utilized for the first 125 years. The particle density of the lower backfill, gravel drainage layer, middle backfill, and erosion barrier (these materials collectively are considered the closure cap layers) was taken as 2.65 g/cm^3. This is based on the density of quartz and is regarded as representative of most SRS soils.

Values for total porosity and long-term average moisture content for the closure cap materials were taken from Phifer (2003). Phifer (2003) evaluated infiltration through a closure cap over time as the closure cap degraded using the HELP model. The porosity and average moisture content values for a 10,000 year degraded closure cap were utilized, since this represented the greatest air filled porosity in which a gas could diffuse. Average saturation and air-filled porosity values were calculated from the total porosity and long-term average moisture content. Table 2-79 provides the values of particle density, total porosity, average saturation, and air-filled porosity utilized for all the layers (i.e., CIG waste layer to the erosion barrier) for the 125 to 325 year time period.

For the 325 to 1125 year time period, it is assumed that the grout structure encapsulating the waste collapses, resulting in settlement of the waste zone and destruction of the closure cap structure. From Phifer et al. 2006, it is assumed that the waste layer collapses from 14 to 7 feet at year 325 (see Table 2-63). This reduction in waste layer thickness is handled utilizing the same model grid used for prior years by reassigning the radionuclide inventory of the lower 7 feet of the waste zone to the upper 7 feet of the waste zone and assigning a porosity of 0 to the lower 7 feet of the waste zone. While this is not necessary intuitive, it is appropriate, since the migration of interest is upward rather than downward and since it results in no additional material through which upward diffusion has to occur. For this time period, the material properties for all layers (i.e., CIG waste layer to the erosion barrier) cap were assigned the properties of the E-Area Operational Soil Cover (Phifer et al. 2006). This is identical to the properties of the clean soil from Table 2-79 as described above. Table 2-80 provides the values of particle density, total porosity, average saturation, and air-filled porosity utilized for all the layers (i.e., CIG waste layer to the erosion barrier) for the 325 to 1125 year time period.

The molecular diffusion coefficient of Rn-222 in open air is 347 m^2/yr (Nielson et al. 1984). Nielson et al. (1984) established a relationship between moisture saturation and the radon effective air-diffusion coefficient for various pore sizes of earthen materials. Using this method, a radon effective air-diffusion coefficient was determined for each material type based upon the average moisture saturation for the material. With the use of an effective air diffusion coefficient, tortuosity was assigned a unit value in each material zone. A summary of the radon effective air-diffusion coefficients by material zone and simulation period, are presented in Table 2-81.

Table 2-79. Particle Density, Porosity, Average Saturation, and Air-filled Porosity Values for the 0 to 125 Year and 125 to 325 Year Time Periods

Layer	Particle Density (g/cm^3)	Total Porosity (fraction)	Long Term Average Moisture Content (vol/vol)	Average Saturation (fraction)	Air-filled Porosity (fraction)
Erosion barrier [1, 3]	2.65	0.088	0.0726	0.825 [4]	0.015 [5]
Middle backfill [1, 3]	2.65	0.375	0.2435	0.649 [4]	0.132 [5]
Gravel drainage layer [1, 3]	2.65	0.375	0.1967	0.525 [4]	0.178 [5]
Lower backfill [1, 3]	2.65	0.370	0.2710	0.732 [4]	0.099 [5]
Clean soil [2]	2.65	0.460		0.825	0.081 [5]
CIG grout [2]	2.31	0.224		0.812	0.042 [5]
CIG waste layer [2]	2.65	0.5		0	0.5

[1] During the first 125 years of simulation, the materials comprising the closure cap were assigned a porosity of 1.0 and a diffusion coefficient equivalent to the molecular diffusion coefficient of the specific radionuclide in air.

[2] Values for particle density, total porosity, and average saturation taken from Phifer et al. 2006

[3] Values for total porosity and long term average moisture content taken from Phifer 2003. Particle density taken as 2.65, which is based on the density of quartz and regarded as fairly representative of most SRS soils

[4] Average Saturation = Long Term Average Moisture Content / Total Porosity

[5] Air-filled Porosity = (1 – Average Saturation) × Total Porosity

Table 2-80. Particle Density, Porosity, Average Saturation, and Air-filled Porosity Values for the 325 to 1125 Year Time Period

Layer	Particle Density (g/cm^3)	Total Porosity (fraction)	Average Saturation (fraction)	Air-filled Porosity [1] (fraction)
Erosion barrier	2.65	0.46	0.825	0.081
Middle backfill	2.65	0.46	0.825	0.081
Gravel drainage layer	2.65	0.46	0.825	0.081
Lower backfill	2.65	0.46	0.825	0.081
Clean soil	2.65	0.46	0.825	0.081
CIG grout	2.65	0.46	0.825	0.081
CIG waste layer	2.65	0.46	0.825	0.081

Note: The values of particle density, total porosity, and average saturation for all layers was taken as that of the E-Area Operational Soil Cover Prior to Dynamic Compaction (Phifer et al. 2006)

[1] Air-filled Porosity = (1 – Average Saturation) × Total Porosity

Table 2-81. Effective Air-Diffusion Coefficient

Layer	Effective Air Diffusion Coefficient (m^2/yr)		
	Operational and Institutional Control Periods (First 125 Years)	Post Closure Period (125 to 325 Years)	Post Collapse Period (325 to 1125 Years)
Erosion barrier layer	347	0.79	1.26
Middle backfill	347	4.73	1.26
Gravel drainage layer	347	4.73	1.26
Lower backfill	347	2.84	1.26
Clean Soil	1.26	1.26	1.26
CIG Grout Top	1.26	1.26	1.26
CIG waste layer	347	347	1.26

2.10.5 Model Results

Model simulations were conducted to evaluate the peak instantaneous Rn-222 flux at the land surface for the three periods of interest. These time periods include: 1) 0 to 125 years, 2) 125 to 325 years, and 3) 325 to 1125 years. Model results were output in $Ci/m^2/yr$, consistent with the set of units employed in the model. A graph of these results is shown in Figure 2-77**,** although the units are converted to $pCi/m^2/sec$, which are the units used to define the regulatory flux limit in DOE M 435.1-1.

The peak fluxes represent the peak Rn-222 flux per square meter at the land surface as defined for each simulation period and are listed below in Table 2-82. The land surface for the 0 to 125 year time period was taken to be the top of the clean soil layer used to cover the trenches. For the 125 to 325 year simulation period, the land surface was taken to be the top of the erosion barrier. For the 325 to 1125 year simulation period, the land surface is taken to be the top of the erosion barrier following settlement of the waste zone.

The calculated disposal limits per unit area and the disposal limits for the each CIG disposal unit are presented in Table 2-83 for each of the 5 parent radionuclides. The unit-area disposal limit was calculated as follows:

> Disposal Limit per unit area (Ci/m^2) = Regulatory limit (20 $pCi/m^2/s$) / Peak Inst. flux per unit area per unit inventory of parent radionuclide per unit area ($[pCi/m^2/s]/Ci/m^2]$)).

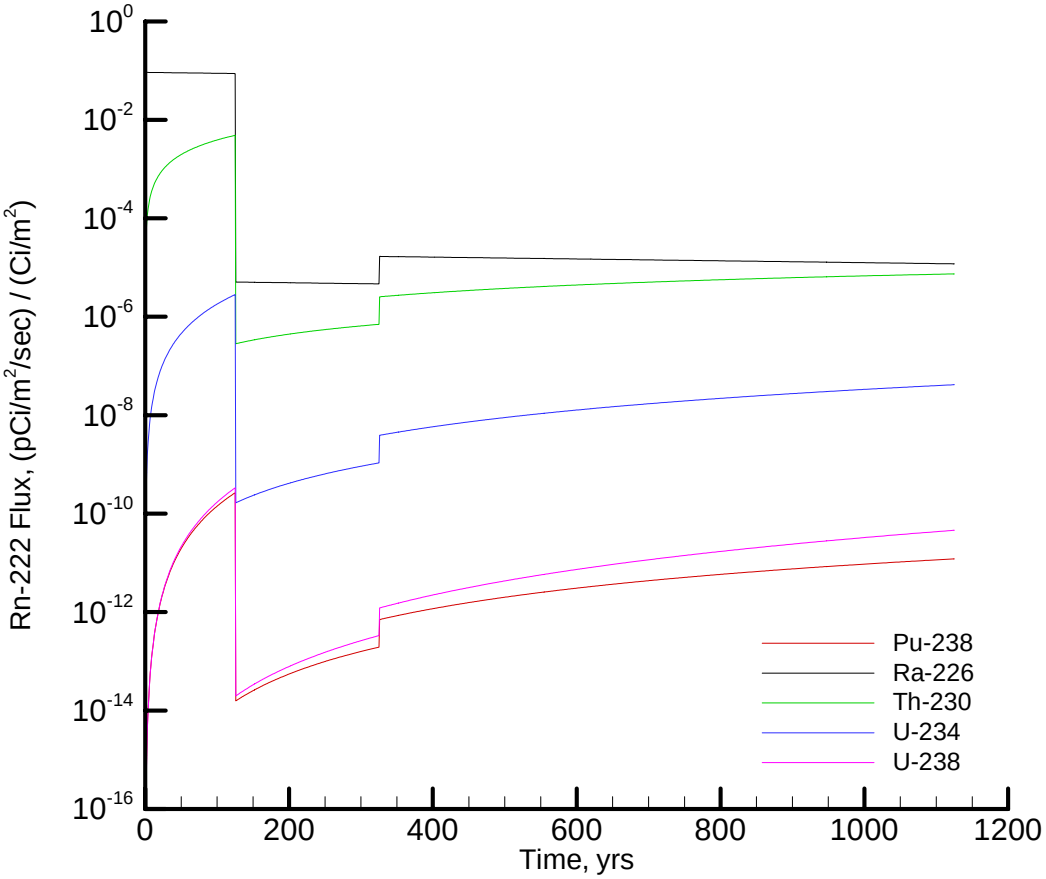

Figure 2-77. Rn-222 Flux at Land Surface Resulting from Unit Source Term Spread over Unit Area of Trench

Table 2-82. Simulated Peak Instantaneous Rn-222 Flux over 1,125-Years at the Land Surface

	Peak Instantaneous Rn-222 flux at Land Surface ($pCi/m^2/sec$)/(Ci/m^2)*		
Parent Source	**0-125 years**	**125-325 years**	**325-1125 years**
Pu-238	2.65E-10	1.94E-13	1.20E-11
U-238	3.34E-10	3.33E-13	4.59E-11
U-234	2.82E-06	1.07E-09	4.16E-08
Th-230	4.85E-03	7.01E-07	7.42E-06
Ra-226	9.21E-02	5.06E-06	1.68E-05

* Flux resulting from unit source term spread over unit area of trench (Ci/m^2).

The unit area limits for each of the 5 parent radionuclides were calculated using the maximum Rn-222 flux of the three time periods. For each radionuclide, the maximum flux of Rn-222 was observed during the initial 125 year simulation period when a closure cap was not present. Therefore, the peak flux of Rn-222 during the initial 125-year period (i.e. maximum flux) was used to calculate the unit area limits for each radionuclide. The unit area limits for each of the 5 parent radionuclides were converted to CIG-specific disposal limits by multiplying the unit area limit for each by the maximum area utilized for disposal (65,000 ft^2) within a CIG footprint (9570 m^2). As discussed within Section 2.5.3 the maximum area utilized for disposal within a CIG footprint consists of 5 trenches that are 20-foot wide by 650-foot long (65,000 ft^2). The results are presented in Table 2-83.

Table 2-83. CIG Trenches Disposal Limits for Parent Radionuclides

Parent Source	Maximum Instantaneous Rn-222 flux at Land Surface ($pCi/m^2/sec$)/(Ci/m^2)[1]	Time to Max (yrs)	Disposal Limit Per Unit Area [2] (Ci/m^2)	CIG-1 Disposal Limit [3] (Ci)	CIG-2 Disposal Limit [3] (Ci)
Pu-238	2.65E-10	125	7.5E+10	4.6E+14	4.6E+14
U-238	3.34E-10	125	6.0E+10	3.6E+14	3.6E+14
U-234	2.82E-06	125	7.1E+06	4.3E+10	4.3E+10
Th-230	4.85E-03	125	4.1E+03	2.5E+07	2.5E+07
Ra-226	9.21E-02	1	2.2E+02	1.3E+06	1.3E+06

[1] Flux resulting from unit source term spread over unit area of trench (Ci/m^2).
[2] Disposal Limit per unit area (Ci/m^2) = 20 $pCi/m^2/s$ / Maximum Instantaneous Rn-222 flux at Land Surface
[3] CIG-1 and CIG-2 Preliminary Disposal Limit = Disposal Limit per unit area (Ci/m^2) × 6042 m^2

2.11 REFERENCES

ACRI (Analytical & Computational Research, Inc.). 2004. *PORFLOW Version 5.0 User's Manual*, Revision 5, Analytical & Computational Research, Inc., Los Angeles, California.

Bolz, R.E. and G.L. Tuve, (Editors), 1973. *Handbook of tables for APPLIED ENGINEERING SCIENCE, 2'nd Edition*. CRC Press, 18901 Cranwood Parkway, Cleveland, OH.

Butcher, B. T., Wilhite, E. L., Phifer, M. A., and Dixon, K. L. 2007. "Future CIG Grout Recommendation", Memorandum to Don Sink, April 10, 2007, SRNL-ESD-2007-00049, Savannah River National Laboratory, Washington Savannah River Company, Aiken, SC.

Clark, E.A. 2007. *Calculation of Tritium Retention and Release from Components in Grout- Segment 6 Metallic Waste from Demolished building 232-F*, WSRC-STI-2007-00051, Washington Savannah River Company, Aiken, SC 29808. February 2007.

Cook, J. R. 2007. *Radionuclide Data Package for Performance Assessment Calculations Related to the E-Area Low-Level Waste Facility at the Savannah River Site (U)*, WSRC-STI-2006-00162, Savannah River National Laboratory, Washington Savannah River Company, Aiken, SC.

Cook, J. R., Phifer, M. A., Wilhite, E. L., Young, K. E., and Jones, W. E. 2004. *Closure Plan for the E-Area Low-Level Waste Facility*, Revision 4, WSRC-RP-2000-00425. Westinghouse Savannah River Company, Aiken, SC. May, 2004.

Crapse, K.P. and J.R. Cook, 2006. *Atmospheric Pathway Screening Analysis for the E-Area Low Level Waste Facility*, WSRC-STI-2006-00159, Washington Savannah River Company, Aiken, SC 29808. 09/05/2006.

DOE 1999. *Radioactive Waste Management Manual*, DOE M 435.1-1, Change 1: 6-19-01, U. S. Department of Energy, Approved July 9, 1999.

Dunn, K. A. 2002. B-25 Corrosion Evaluation Summary Report (U), WSRC-TR-2001-00587. Westinghouse Savannah River Company, Aiken, SC. January 2002.

Flach, G.P. 2004. *Groundwater Flow Model of the General Separations Area Using Porflow (U)*, WSRC-TR-2004-00106, Washington Savannah River Company, Aiken, SC 29808. July 15, 2004.

Flach, G. P. and Harris, M. K. 1996. *Integrated Hydrogeological Modeling of the General Separations Area, Volume 2, Groundwater Flow Model (U)*, WSRC-TR-96-0399, Rev. 1. Westinghouse Savannah River Company, Aiken SC. April 1999.

Hang, T., Collard, L. B., and Phifer, M. A. 2005. *Unreviewed Disposal Question Evaluation: Subsidence Study for non-Crushable Containers in Slit Trenches (U)*, WSRC-TR-2005-00104, Revision 0, Savannah River National Laboratory, Westinghouse Savannah River Company, Aiken, SC, March.

Jones, W. E. and Phifer, M. A. 2002. Corrosion and Potential Subsidence Scenarios for Buried B-25 Waste Containers (U), WSRC-TR-2002-00354. Westinghouse Savannah River Company, Aiken, SC. September 2002.

Jones, W. E., Phifer, M. A., and Kukreja, J. 2004. Unreviewed Disposal Question Evaluation: Components-In-grout Options for Structural Stability – Component Filling, Component Stability, or Concrete Mat Cover, WSRC-TR-2004-00039, Westinghouse Savannah River Company, Aiken, SC. February 2004.

Kaplan, D.I., 2006. *Geochemical Data Package for Performance Assessment Calculations Related to the Savannah River Site (U)*, WSRC-TR-2006-00004, Rev. 0. Washington Savannah River Company, Aiken SC. February 2006.

Koffman, Larry D. 2006a. *SRNL All-Pathways Application*, WSRC-STI-2006-00179. Rev. 0, Savannah River National Laboratory, Aiken, SC. September 2006.

Koffman, Larry D. 2006b. *Automated Inadvertent Intruder Application, Version 2*. WSRC-TR-2006-00037. Savannah River National Laboratory, Aiken, SC. September 2006.

Lee, P. L. 2004. Inadvertent *Intruder Analysis Input for Radiological Performance Assessments*, WSRC-TR-2004-00295, Westinghouse Savannah River Company, Aiken, SC.

Lee, P. L. 2006. *Air Pathway Dose Modeling for the E-Area Low-Level Waste Facility* WSRC-STI-2006-00262, Rev. 0, Washington Savannah River Company, Aiken, SC. May, 2004.

McDowell-Boyer, L., Yu, A. D., Cook, J. R., Kocher, D. C., Wilhite, E. L., Holmes-Burns, H., and Young, K. E. 2000. *Radiological Performance Assessment for the E-Area Low-Level Waste Facility,* Revision 1, WSRC-RP-94-218. Westinghouse Savannah River Company, Aiken, SC. January 31, 2000.

Millings, M. R. and Phifer, M. A. 2007. Evaluation of Water Table Elevation and Vadose Zone Thickness at the Components-in-Grout (CIG) Trenches, WSRC-STI-2007-00132, Rev. 0, Washington Savannah River Company, Aiken, SC. (Draft)

Nazaroff, W.W., and A.V. Nero (editors), 1988, *Radon and its Decay Products in Indoor Air*, John Wiley & Sons, New York, N.Y.

Nichols, R. L., B. B. Looney, G. P. Flach and J. Rossabi, 2000, Recommendations for Phase II Vadose Zone Characterization and Monitoring at the E-Area Disposal "Slit" Trenches and Mega-Trench (U), WSRC-TR-2000-00059.

Nielson, K.K., V.C. Rogers and G.W. Gee, 1984. *Diffusion of Radon through Soils: A pore distribution Model*, Soil Science Society of America, J. 48:482-487.

Peregoy, W. 2006. Structural Evaluation of Component-in-Grout Trenches, T-CLC-E-00026, Rev. 0. Washington Savannah River Company, Aiken, SC. August 3, 2006.

Phifer, M.A. 2003. *Saltstone Disposal Facility Mechanically Stabilized Earth Vault Closure Cap Degradation Base Case: Institutional Control to Pine Forest Scenario (U).* WSRC-TR-2003-00523. Westinghouse Savannah River Company, Aiken, SC. December 18, 2003.

Phifer, M. A., 2004a. Preliminary E-Area Trench Closure Cap Closure Sequence, Infiltration, and Waste Thickness (U), WSRC-TR-2004-00119, Westinghouse Savannah River Company, Aiken, SC. March 2004.

Phifer, M. A., 2004b. Unreviewed Disposal Question Evaluation: Low Strength Containers with Compressible Waste in Component-In-Grout Trenches, WSRC-TR-2004-00475, Westinghouse Savannah River Company, Aiken, SC. September 21, 2004.

Phifer, M. A., Millings, M. R., and Flach, G. P. 2006. Hydraulic Property Data Package for the E-Area and Z-Area Soils, Cementitious Materials, and Waste Zones, WSRC-STI-2006-00198, Revision 0. Washington Savannah River Company, Aiken, SC. September 2006.

Phifer, M. A. and Nelson, E. A. 2003. *Saltstone Disposal Facility Closure Cap Configuration and Degradation Base Case: Institutional Control to Pine Forest Scenario (U), Rev. 0*, WSRC-TR-2003-00436, Westinghouse Savannah River Company, Aiken, SC. September 22, 2003.

Roddy, N. S., 2007. *Tritium Decay in Components in Grout Location in E Area,* G-CLC-E-00109, Washington Savannah River Company, Aiken, SC. March 21, 2007.

Taylor, G.A. 2006. *Software Quality Assurance Plan for Ideal Filemaker: An Application to Translate PORFLOW Output to All-Pathways Input*. G-SQP-A-00010, Rev. 0.

Wilhite, E. L., and Flach, G. P. 2007. *Evaluation of Proposed New Low-Level Waste Disposal Activity: Disposal of D-Area Waste Into Component-In-Grout Trenches Using Higher Hydraulic Conductivity Grout*, WSRC-TR-2007-00142, Revision 1, Savannah River National Laboratory, Washington Savannah River Company, Aiken, SC, May.

WSRC 2006. *SRS Waste Acceptance Criteria Manual, Procedure Manual 1S*, Washington Savannah River Company, Aiken, SC. January 19, 2006.

Yu, C., A.J. Zielen, J.J. Cheng, D.J. LePoire, E. Gnanapragasam, S. Kamboj, J. Arnish, A. Wallo III, W.A. Williams, and H. Peterson, 2001. *Users Manual for RESRAD Version 6*, Environmental Assessment Division, Argonne National Laboratory. Chicago, IL.

CHAPTER 3

LOW-ACTIVITY WASTE VAULT (LAWV)

This page intentionally left blank.

3.0 LOW-ACTIVITY WASTE VAULT (LAWV)

LIST OF FIGURES

LIST OF TABLES

This page intentionally left blank.

3.0 LOW-ACTIVITY WASTE VAULT (LAWV)

3.1 EXECUTIVE SUMMARY

The LAWV disposal unit is an above-grade reinforced concrete structure, which contains containerized waste components. Ultimately the LAWV will be closed by placing a closure cap over the structure. The LAWV is used to dispose of waste containers that exceed the radiological dose and radionuclide concentration limits of the more cost effective Slit Trench disposal units. Additionally, LAWV waste containers are mined and some are subsequently relocated to other disposal units such as Slit Trenches. The existing vault is the only one anticipated to be needed over the lifetime of 643-26E (the E-Area LLW Facility).

LAWV disposal limits through the 1,000 year compliance period have been developed for the following pathways: groundwater protection, air, all-pathways, inadvertent intruder (resident scenario and post-drilling scenario), and radon. All instances of groundwater protection and all-pathways "limits" in this chapter refer to "preliminary limits" only, because they do not account for plume interaction or uncertainties. Table 3-1 provides these disposal limits. In Chapter 7 these limits will be adjusted in consideration of the result of the LAWV sensitivity analyses reported in this chapter and the plume interaction analysis reported in Chapter 6. Trigger values for radionuclides that did not screen out of the groundwater and air analyses and were not specifically analyzed are given in Tables 4-4 and 4-5, respectively, in the Part C Background chapter. The trigger values were developed using very conservative screening methodologies and can be used as surrogate disposal unit limits should any of the listed radionuclides be proposed for disposal.

Table 3-1. Preliminary Groundwater Protection and All-Pathways Disposal Limits and Intruder, Air, and Radon Disposal Limits for the LAWV[1]

Isotope	Beta - gamma (Ci)	Gross alpha (Ci)	Radium (Ci)	Uranium (Ci)	All pathways (Ci)	Intruder (Ci)	Air (Ci)	Radon (Ci)
Ac-227	---	---	---	---	---	3.6E+04	---	---
Ag-108m	---	---	---	---	---	1.5E+02	---	---
Al-26	---	---	---	---	---	1.9E+01	---	---
Am-241	1.5E+10	7.6E+08	---	1.4E+19	2.4E+08	2.5E+07	---	---
Am-242m	---	---	---	---	---	5.9E+04	---	---
Am-243	3.1E+16	1.7E+16	---	---	2.1E+15	1.3E+04	---	---
Ar-39	---	---	---	---	---	---	---	---
Ba-133	---	---	---	---	---	1.4E+06	---	---
Bi-207	---	---	---	---	---	4.9E+02	---	---
Bk-249	---	---	---	---	---	7.8E+05	---	---
C-14	8.8E+00	---	---	---	9.2E+00	---	3.3E+03	---
Ca-41	---	---	---	---	---	---	---	---
Cd-113m	---	---	---	---	---	---	---	---
Cf-249	---	---	---	---	---	2.0E+03	---	---
Cf-250	---	---	---	---	---	1.2E+13	---	---
Cf-251	---	---	---	---	---	4.1E+04	---	---
Cf-252	---	---	---	---	---	5.9E+12	---	---
Cl-36	2.6E+00	---	---	---	1.4E+00	---	2.0E+03	
Cm-242	---	---	---	---	---	1.4E+10	---	---
Cm-243	---	---	---	---	---	2.1E+05	---	---
Cm-244	---	---	---	---	---	1.3E+15	---	---
Cm-245	1.1E+10	5.3E+08	---	1.1E+19	1.7E+08	2.1E+05	---	---
Cm-246	---	---	---	---	---	5.5E+13	---	---
Cm-247	6.5E+17	3.5E+17	---	---	4.3E+16	1.5E+03	---	---
Cm-248	---	---	---	---	---	4.3E+07	---	---
Co-60	---	---	---	---	---	1.4E+07	---	---
Cs-134	---	---	---	---	---	3.5E+16	---	---
Cs-135	---	---	---	---	---	---	---	---
Cs-137	---	---	---	---	---	3.3E+03	---	---
Eu-152	---	---	---	---	---	1.3E+04	---	---
Eu-154	---	---	---	---	---	2.2E+05	---	---
Eu-155	---	---	---	---	---	3.8E+12	---	---
H-3	6.3E+08	---	---	---	5.5E+10	---	1.1E+08[3]	---
I-129	4.7E-03	---	---	---	2.9E-01	6.1E+18	1.7E+01	---
I-129_H[2]	1.1E-01	---	---	---	6.9E+00	6.1E+18	1.7E+01	---
I-129_J[2]	2.1E-02	---	---	---	1.2E+00	6.1E+18	1.7E+01	---
K-40	---	---	---	---	---	3.6E+02	---	---
Kr-85	---	---	---	---	---	8.4E+07	---	---
Mo-93	3.1E+00	---	---	---	1.5E+01	---	---	---
Na-22	---	---	---	---	---	1.4E+13	---	---

Table 3-1. Preliminary Groundwater Protection and All-Pathways Disposal Limits and Intruder, Air, and Radon Disposal Limits for the LAWV - continued

Isotope	Beta - gamma (Ci)	Gross alpha (Ci)	Radium (Ci)	Uranium (Ci)	All pathways (Ci)	Intruder (Ci)	Air (Ci)	Radon (Ci)
Nb-93m	---	---	---	---	---	---	---	---
Nb-94	4.8E+01	---	---	---	2.7E+01	8.6E+01	---	---
Ni-59	1.4E+10	---	---	---	3.6E+12	---	---	---
Ni-63	---	---	---	---	---	---	---	---
Np-237	2.4E+07	1.2E+06	---	2.4E+16	3.7E+05	4.1E+03	---	---
Pa-231	---	---	---	---	---	1.4E+03	---	---
Pb-210	---	---	---	---	---	3.5E+08	---	---
Pd-107	1.7E+12	---	---	---	5.5E+12	---	---	---
Pu-238	9.4E+14	6.8E+12	9.1E+12	---	2.7E+13	7.2E+07	---	8.4E+10
Pu-239	1.3E+15	7.3E+14	---	---	9.2E+13	6.1E+08	---	---
Pu-240	---	---	---	---	---	2.1E+13	---	---
Pu-241	4.5E+11	2.2E+10	---	---	7.0E+09	7.7E+08	---	---
Pu-242	---	---	---	---	---	4.9E+10	---	---
Pu-244	---	---	---	---	---	3.4E+02	---	---
Ra-226	3.9E+07	2.9E+05	3.8E+05	---	1.1E+06	3.6E+01	---	2.4E+00
Ra-228	---	---	---	---	---	2.4E+06	---	---
Rb-87	---	---	---	---	---	---	---	---
S-35	---	---	---	---	---	---	1.1E+04	---
Sb-124	---	---	---	---	---	---	3.0E+02	---
Sb-125	---	---	---	---	---	5.2E+13	9.2E+01	---
Sc-46	---	---	---	---	---	---	---	---
Se-75	---	---	---	---	---	---	---	---
Se-79	---	---	---	---	---	---	7.5E+02	---
Sm-151	---	---	---	---	---	---	---	---
Sn-113	---	---	---	---	---	---	2.5E+03	---
Sn-119m	---	---	---	---	---	---	5.7E+03	---
Sn-121	---	---	---	---	---	---	3.1E+04	---
Sn-121m	---	---	---	---	---	---	8.9E+02	---
Sn-123	---	---	---	---	---	---	4.7E+04	---
Sn-126	---	---	---	---	---	9.3E+01	2.0E+00	---
Sr-90	3.4E+15	---	---	---	6.6E+16	---	---	---
Tc-99	5.2E+02	---	---	---	7.8E+02	4.5E+11	---	---
Th-228	---	---	---	---	---	1.4E+17	---	---
Th-229	---	---	---	---	---	7.8E+02	---	---
Th-230	2.8E+08	2.1E+06	2.8E+06	---	8.1E+06	1.0E+02	---	2.2E+02
Th-232	---	---	---	---	---	2.0E+01	---	

Table 3-1. Preliminary Groundwater Protection and All-Pathways Disposal Limits and Intruder, Air, and Radon Disposal Limits for the LAWV - continued

Isotope	Beta - gamma (Ci)	Gross alpha (Ci)	Radium (Ci)	Uranium (Ci)	All pathways (Ci)	Intruder (Ci)	Air (Ci)	Radon (Ci)
U-232	---	---	---	---	---	6.7E+01	---	
U-233	---	---	---	---	---	8.6E+03	---	
U-234	1.8E+11	1.3E+09	1.7E+09	---	5.1E+09	2.0E+04	---	1.9E+06
U-235	2.7E+08	1.5E+08	---	---	1.9E+07	2.5E+04	---	
U-236	---	---	---	---	---	4.1E+08	---	
U-238	5.0E+14	3.6E+12	4.8E+12	---	1.4E+13	7.6E+03	---	8.1E+10
W-181	---	---	---	---	---	---	---	---
W-185	---	---	---	---	---	---	---	---
W-188	---	---	---	---	---	---	---	---
Zr-93	1.5E+02	---	---	---	8.8E+02	---	---	---

[1]--- represents limits > 1E20 Ci; blank represents nuclides not analyzed
[2]I-129 special waste forms were not specifically analyzed for air and intruder pathways, but limits are equivalent. I-129_H is H-Area CG-8. I-129_J is F-Area filtercake
[3]In addition to the total inventory limits shown in this table, there is a maximum permissible annual disposal limit of 4.5E+06 Ci for tritium

3.2 INTRODUCTION AND GENERAL APPROACH

The LAWV disposal unit is an above-grade reinforced concrete structure, which contains waste components in B-25 boxes, 55-gallon drums and other containers. Ultimately the LAWV will be closed by placing a closure cap over the structure. The LAWV is used to dispose of waste containers that exceed the radiological dose and radionuclide concentration limits of the more cost effective Slit Trench disposal units. Additionally, LAWV waste containers are mined and some are subsequently relocated to other disposal units such as Slit Trenches. The existing vault is the only one anticipated to be needed over the lifetime of 643-26E (the E-Area LLW Facility).

LAWV disposal limits through the 1,000 year compliance period have been developed for the following pathways: groundwater protection, air, all-pathways, inadvertent intruder (resident scenario and post-drilling scenario), and radon. All instances of groundwater protection and all-pathways "limits" in this chapter refer to "preliminary limits" only, because they do not account for plume interaction or uncertainties. A groundwater transport analysis has been conducted to determine maximum well concentrations (as a function of time) within a 100-m compliance region surrounding the LAWV. The main analysis tool employed was the PORFLOW (ACRI 2004) code, which handles both flow and transport of radionuclide chains (i.e., parents and daughters) in porous media. Two-dimensional flow and transport analyses were conducted to describe in detail the migration of species from the LAWV through the vadose zone to the underlying water table.

The results from these 2-D vadose zone simulations (treated as source terms) were then input into a 3-D aquifer transport model to compute maximum groundwater concentrations of radionuclides within the 100-m compliance region. Preliminary groundwater protection disposal limits over the 1,000-year compliance period for the LAWV were developed from the computed maximum groundwater concentrations using the all-pathways application (Koffman 2006). Additionally preliminary all-pathways disposal limits over the 1,000 year compliance period for LAWV were developed from the computed maximum groundwater concentrations using the all-pathways application (Koffman 2006).

An air-pathway analysis has been conducted to determine air-pathway disposal limits for 15 potentially volatile radionuclides over the 1,000 year compliance period for the LAWV. The PORFLOW code was utilized for diffusional transport of radionuclides out of the LAWV to the ground surface and the CAP88 (Beres 1990) code was utilized for subsequent atmospheric transport and dose calculations. A one-dimensional PORFLOW diffusional transport analysis was conducted to determine the flux of species to the ground surface from the LAWV. The atmospheric transport and dose calculation results obtained using CAP88 were combined with the flux of species at the ground surface to develop air-pathway disposal limits.

An inadvertent intruder analysis has been conducted to determine inadvertent intruder disposal limits over the 1,000 year compliance period for the LAWV. The analysis was conducted using an automated inadvertent intruder computer application developed at SRNL (Koffman 2006) for the resident and post-drilling inadvertent intruder scenarios.

A radon pathway analysis has been conducted to determine radon pathway disposal limits for 5 radon-producing parent radionuclides over the 1,000-year compliance period for the LAWV. A one-dimensional PORFLOW diffusional transport analysis was conducted to determine the flux of radon to the ground surface from the LAWV.

Within Chapter 7, Integration and Interpretation, the individual LAWV disposal limits developed in this chapter will be adjusted in consideration of the result of the LAWV sensitivity analyses reported in this chapter and the plume interaction analysis reported in Chapter 6, Integrated Facility Analysis.

3.3 LAW VAULT GENERAL DESCRIPTION AND LIFECYCLE

The LAW Vault is an above-grade, reinforced concrete vault. Figure 3-1 provides the layout of the LAW Vault relative to other ELLWF disposal unit types. It is approximately 643 feet (196 m) long, 145 feet (44.2 m) wide, and 27 feet (8.2 m) high at the roof crest. It is divided into 3 modules along its length, which are approximately 214 feet (65 m) long and contain 4 cells each. The modules share a common footer but have a 2-inch (5.08 cm) gap between their adjacent walls. The 12-cell total is designed to contain more than 12,000 B-25 boxes of waste. Figure 3-2 provides photographs of the LAW Vault and Figure 3-3 provides a cross-sectional view (A-A′).

LAW VAULT

The LAW Vault consists of the following:

- Controlled compacted backfill soil base
- Geotextile Filter Fabric
- 1-foot 3-inch (0.38 m) graded stone sub-drainage system to collect water from under and around the vault and route it to manhole drains
- Crusher run stone base
- 30-inch (0.76 m) continuous footer under all interior and exterior walls
- 1-foot (0.3 m) thick, cast-in-place, reinforced concrete floor slab sloped to an interior collection trench, which drains to an external sump
- 2-foot (0.6 m) thick, cast-in-place, reinforced, interior and exterior concrete walls that are structurally mated to the footer (the exterior end walls of modules 1 and 3 are 2-foot 6-inches thick (0.76 m))
- Exterior and interior personnel openings with doors, 36 inch (0.9 m) square exterior fan openings, and exterior forklift access openings
- AASHTO Type IV bridge beams to support the concrete roof
- 3-½ inch (9 cm) thick precast deck panels overlain by 12-½ inch (31.7 cm) thick cast-in-place, reinforced concrete slab for a total 16 inch (40.6 cm) thick concrete roof.
- A bonded-in-place layer of fiberboard insulation and a layer of waterproof membrane roofing on top of the roof slab
- A gutter/downspout system to drain the roof

During the 25-year operational period low-activity waste contained within metal boxes (predominately B-25 boxes and B-12 boxes), drums, concrete containers, and other containers are stacked by forklift within the vault. B-25 (approximately 4-foot high by 6-foot long by 4-foot wide) and/or equivalent pairs of B-12 (approximately 2-foot high by 6-foot long by 4-foot wide) boxes are stacked four high. The waste within the containers typically includes job control waste, scrap metal, and contaminated soil and rubble. Job control waste consists of potentially contaminated protective clothing (plastic suits, shoe covers, lab coats, etc.), plastic sheeting, etc. The scrap metal consists of contaminated tools, process equipment and piping, and laboratory equipment. Soil and rubble is generated from demolition activities. The average waste density within the containers has been estimated at 0.1785 g/cm^3 (Phifer and Wilhite 2001). The waste zone (if B-25 boxes) can subside from about 17.3 ft thick originally to about 2.5 ft thick, or about 14.8 ft. Because there is a void space of about 6.2 ft over a stack of B-25 boxes, the roof can potentially drop about 21 feet (Jones and Phifer 2006).

Operational closure of the LAW Vault will be conducted in stages. Individual cells will be closed as they are filled with stacks of containerized waste (metal and/or concrete containers) and the entire vault will be closed after it is filled. Such operational closure includes filling the interior collection trench and exterior sump with grout and sealing exterior vault openings, including those between modules, with reinforced concrete equivalent to that utilized within the vault floor, walls and roof. The reinforcing steel will be tied into the reinforcing steel of the vault itself, forming a unified structure with continuous walls. No additional closure actions are anticipated beyond that of operational closure for the LAW Vault during the 100-year institutional control period (i.e., interim closure).

Final closure of the LAW Vault will take place at final closure of the entire ELLWF, at the end of the 100-year institutional control period. Final closure will consist of the installation of an integrated closure system designed to minimize moisture contact with the waste and to provide an intruder deterrent. The integrated closure system will consist of one or more closure caps installed over all the disposal units and a drainage system. Figure 3-4 provides the anticipated LAW Vault closure cap configuration. The apex of the closure cap will extend the length of the vault and be approximately centered over the vault, in order to minimize the overburden loads on the vault and maximize runoff and lateral drainage from the overlying closure cap. (McDowell-Boyer et al. 2000; Cook et al. 2004; Phifer et al. 2006)

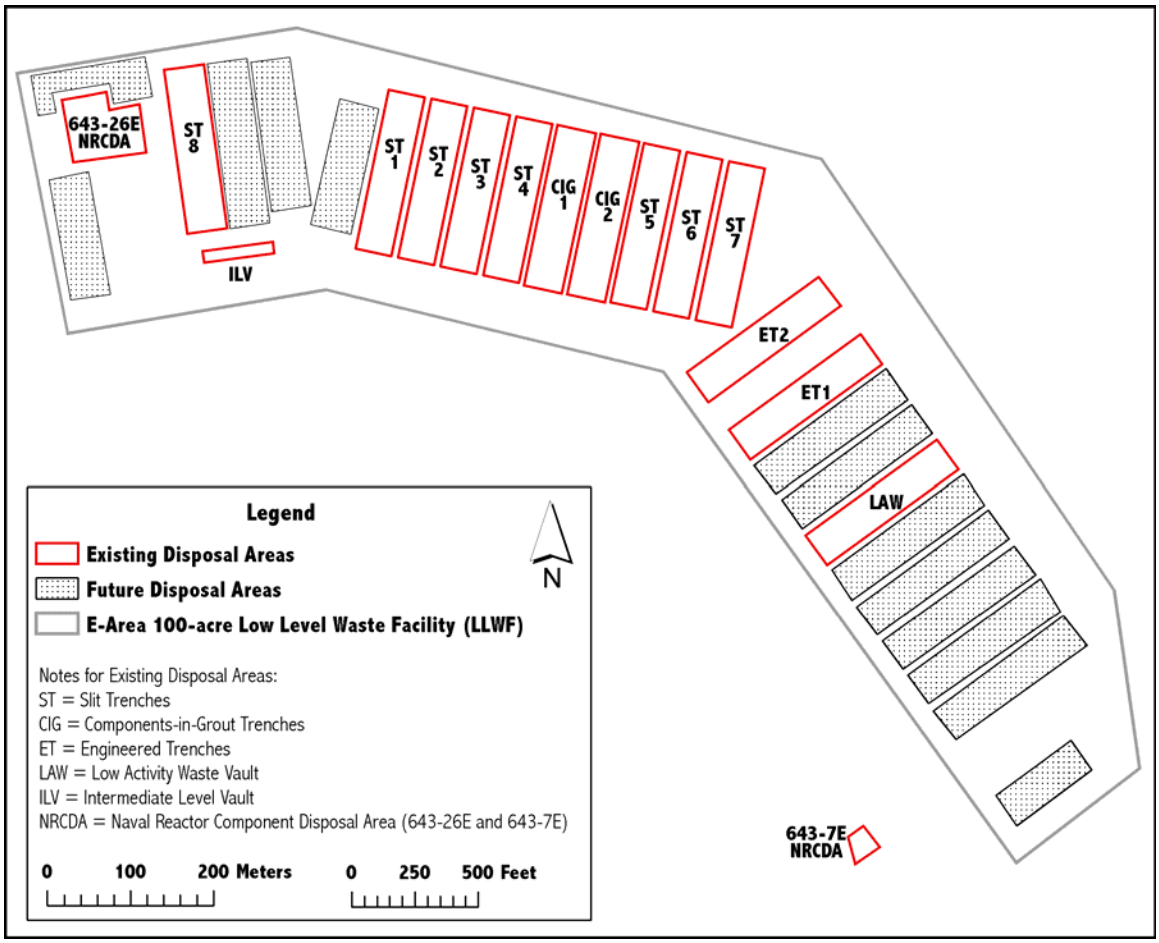

Figure 3-1. Location of the LAW Vault within the ELLWF

Exterior View

Interior View

Figure 3-2. LAW Vault Photographs

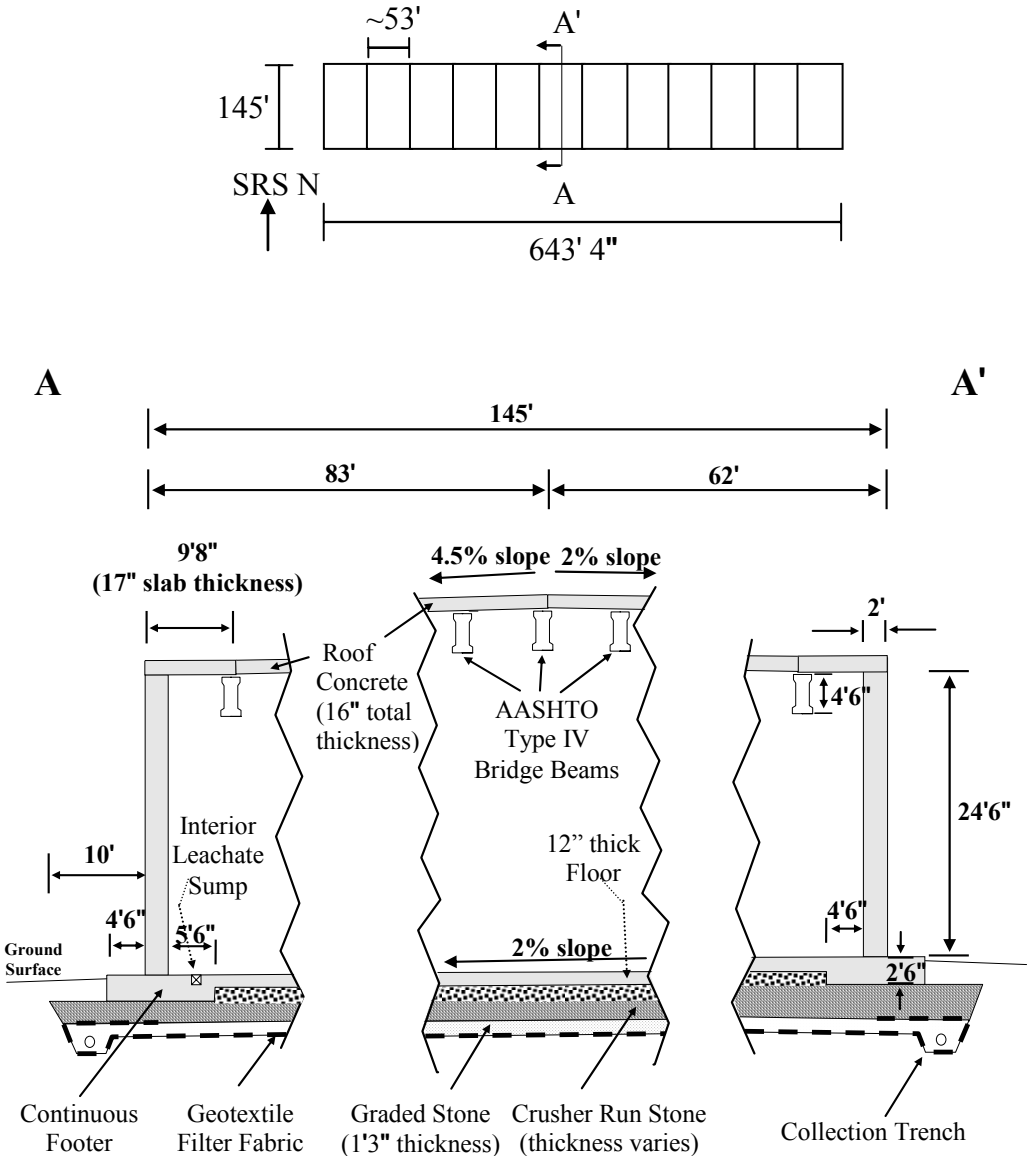

Figure 3-3. LAW Vault Cross-Sectional View (A-A′)

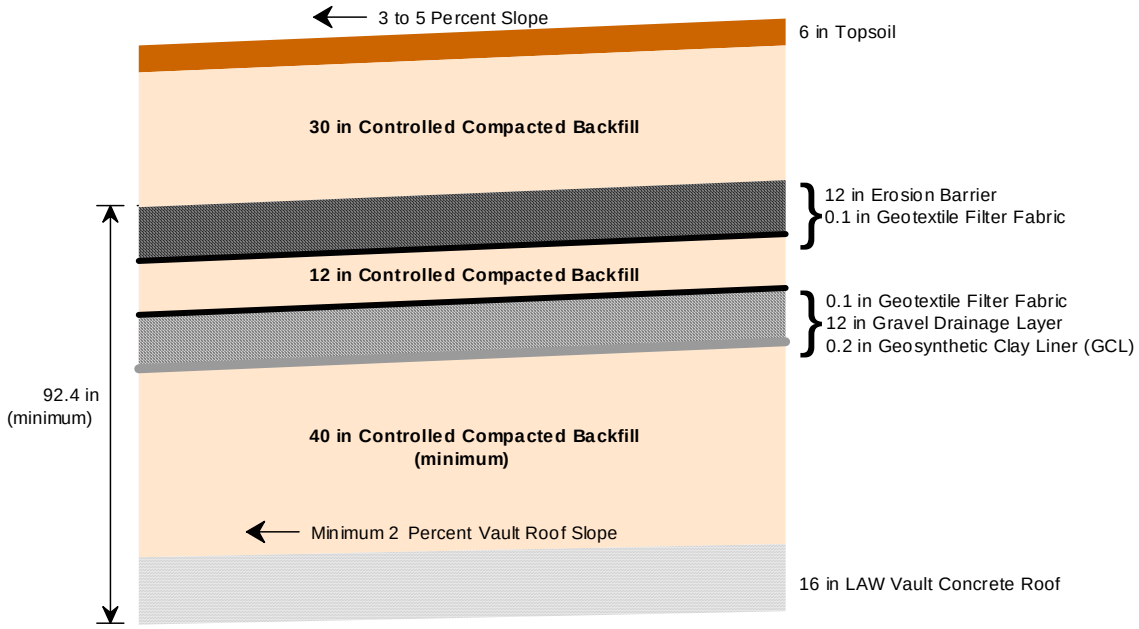

Figure 3-4. LAW Vault Closure Cap Configuration

3.4 LAW VAULT PRINCIPAL DESIGN FEATURES

3.4.1 LAW Vault Structural Stability and Cover Integrity

The LAW Vault is designed to withstand Design Basis Accident loads (as specified in Project S2889) that ensure continued structural stability during its anticipated life. Carey (2006) conducted a structural degradation prediction analysis and documented the following significant degradation points in the life of the LAW Vault:

- Upon placement of the closure cap overburden over the LAW Vault, non-through-slab static cracking of the roof slab will occur and remain fairly constant over time.
- Upon placement of the closure cap overburden over the LAW Vault, non-through-wall static cracking of the exterior side walls will occur and increase slightly over time.
- It is anticipated that the LAW Vault roof slab will collapse due to closure cap and seismic loading and rebar corrosion at a mean time of 2805 years with a standard deviation of 920 years.
- It is anticipated that the LAW Vault exterior side walls will collapse due to closure cap and seismic loading and rebar corrosion at a mean time of 9415 years with a standard deviation of 2290 years.
- It is anticipated that differential settlement due to seismic loading could result in side wall through-wall cracking that opens into the roof slab. The probability of such an event occurring over a 1000 year period has been determined to be 0.8%.
- It is anticipated that differential settlement due to seismic loading could result in side wall through-wall cracking that opens into the footer. The probability of such an event occurring over a 1000 year period has been determined to be 1.2%.
- Within 50 to 100 years after placement of the closure cap overburden over the LAW Vault, it is anticipated that differential settlement between the footers and floor slab will occur due to static (i.e. closure cap) loading differences between the two. This will result in a separation between the footers and floor slab.
- It is anticipated that differential settlement beneath the floor slab due to seismic loading could result in flexural cracking of the floor slab. The probability of such an event occurring over a 1000 year period has been estimated to be 50%.

It has also been estimated that a full LAW Vault has a subsidence potential of approximately 21 feet (Jones and Phifer 2006). This subsidence potential does not impact the structural stability of the LAW Vaults until the time of anticipated roof structural failure (i.e., 2805 years). At the time of roof structural failure, it is assumed that the LAW Vault roof will collapse into the vault itself and that subsidence of the overlying closure cap will occur.

The final ELLWF closure cap will be installed at the end of the 100-year institutional control period (Phifer 2004). After installation it is assumed that no closure cap maintenance will be performed other than that required for establishment of the vegetative cover. Therefore it is assumed that the hydraulic properties of the closure cap will immediately begin to degrade after construction due to the following (Phifer and Nelson 2003; Phifer 2004):

- Formation of holes in the upper GCL by pine forest succession
- Reduction in the saturated hydraulic conductivity of the drainage layers due to colloidal clay migration into the layers
- Erosion of layers that provide water storage for the promotion of evapotranspiration

The hydraulic properties of the closure cap are provided in Jones and Phifer 2006.

As outlined, it has been estimated that the LAW Vault roof will structurally fail at a mean of 2,805 years. At that point it is assumed that the LAW Vault roof will collapse into the vault itself and that subsidence of the overlying closure cap will occur. This will lead to further degradation of the hydraulic properties of that portion of the closure cap overlying the LAW Vault.

3.4.2 LAW Vault Water Infiltration

During the operational period, water entrance into the LAW Vault is minimized through the crushed stone sub-drainage system, doors on external personnel openings, the waterproof membrane roofing, and the gutter/downspout system. Any water that does enter the LAW Vault during operations is collected in a sump, which is appropriately monitored, sampled, and pumped out as necessary. During the 100-year institutional control period after the LAW Vault has been operationally closed, water infiltration into the vault is minimized through the crushed stone sub-drainage system, continuous concrete walls to seal all openings, and the waterproof membrane roofing.

During the post-institutional control period prior to vault structural failure, the final closure cap, along with the structurally intact concrete vault structure, minimize infiltration into the vault. During this period the hydraulic properties of the closure cap are assumed to degrade resulting in increased infiltration through the closure cap over time. At structural failure of the LAW Vault roof (i.e. mean time of 2,805 years) it is assumed that the roof will collapse into the vault itself, that subsidence of the overlying closure cap will occur, and that increased infiltration will occur through that portion of the closure cap overlying the collapsed LAW Vault.

3.4.3 LAW Vault Inadvertent Intruder Barrier

Inadvertent intrusion into the LAW Vault waste is not considered feasible during the operational and institutional control periods, due to facility security during these periods. However it is assumed that inadvertent intrusion could occur during the post-institutional control period. The roof slab and pre-cast beams ensure structural stability for an estimated mean of 2,805 years. They also provide a barrier to intrusion for this time period because normal residential construction and well drilling equipment used in the vicinity of the SRS is not capable of penetrating the roof structure (McDowell-Boyer et al. 2000).

3.5 LAW VAULT WASTE CHARACTERISTICS

3.5.1 Waste Type/Chemical and Physical Form

During the 25-year operational period, low-activity waste contained within metal boxes (predominately B-25 boxes and B-12 boxes), drums and/or concrete containers is stacked by forklift within the vault. B-25 (approximately 4-ft high by 6-ft long by 4-ft wide) and/or equivalent pairs of B-12 (approximately 2-ft high by 6-ft long by 4-ft wide) boxes are stacked four high.

The waste within the containers typically includes job control waste, scrap metal, and contaminated soil and rubble. Job control waste consists of potentially contaminated protective clothing (plastic suits, shoe covers, lab coats, etc.), plastic sheeting, etc. The scrap metal consists of contaminated tools, process equipment and piping, and laboratory equipment. Soil and rubble is generated from demolition activities.

The average waste density within the containers has been estimated at 0.1785 g/cm^3 (Phifer and Wilhite 2001), which along with the vault dimensions results in a subsidence potential of approximately 21 feet (6.4 m; Jones and Phifer 2006). Historically, the majority of the waste disposed in the LAW Vault has been generated by the Tank Farms, Canyons, Tritium Facilities, Savannah River National Laboratory, and Naval Reactors waste received from offsite.

3.5.2 Radionuclide Inventory

The radiation dose rate measured at 5 cm from the surface of an unshielded container is less than 200 mR/hr for containers destined for the LAW Vault. The 20-year projected inventory is given in Appendix C.

3.5.3 Waste Volume

The LAW Vault is an above grade, reinforced concrete vault. It is approximately 643 ft (196 m) long, 145 ft (44.2 m) wide, and 27 ft (8.2 m) high at the roof crest. It is divided into 3 modules along its length, which are approximately 214 ft (65 m) long and contain 4 cells each. The 12 cell total is designed to contain more than 12,000 B-25 boxes of waste (i.e., approximately 1.1E+06 ft^3 [3.1E+04 m^3] of waste).

Because of SRS waste minimization and volume reduction programs, and increased trench disposal options, it is estimated that one LAW Vault will be required for low-level radioactive disposal over the 25-year operational period.

3.5.4 Packaging Criteria

All LAW Vault waste is subject to packaging requirements of the SRS WAC (WSRC 2006). The PA process sets many of the criteria that are the basis for the WAC.

3.5.5 Pre-Disposal Treatment Methods

Generators follow WAC (WSRC 2006) requirements for predisposal treatment methods. The PA process sets many of the criteria that are the basis for the WAC.

3.5.6 Waste Acceptance Restrictions

Waste acceptance for disposal in the LAW Vault must conform to criteria put forth in the SRS WAC (WSRC 2006). The PA process sets many of the criteria that are the basis for the WAC.

3.5.7 Security Classification of Wastes

A very small (insignificant) fraction of disposed LLW contains classified material. The security issues related to the disposal of this material are addressed in the SRS/SWMF security program. However, no classified material can be disposed into the LAW Vault due to accessibility issues.

3.6 GROUNDWATER TRANSPORT ANALYSIS

This section documents the development of preliminary groundwater protection limits for the LAW Vault. The limits developed within this section are considered preliminary, since they do not take into consideration the effects of plume overlap from adjacent units or the results of sensitivity and uncertainty analyses. The effects of plume overlap are considered in Chapter 6, and the interpretation of sensitivity and uncertainty analyses is conducted in Chapter 7. Final limits are provided in Chapter 7.

This section discusses analyses for the groundwater transport scenario and other related material. The analyses start from the conceptual models, continue through the numerical implementation and finish with the results. Analyses are subdivided into a series of steady-state vadose zone flow models that feed into the vadose zone transport models, which in turn generate contaminant fluxes at the water table. The contaminant fluxes at the water table from the vadose zone models are combined with a single steady-state aquifer flow model to ultimately produce contaminant concentrations at a hypothetical 100-m well.

3.6.1 Relation of Current Analysis to Previous Analyses

The current analysis approach employed for the LAW Vault performance assessment is significantly different than prior approaches. For example, some of the key differences are as follows;

- New material flow and transport properties are used for all materials considered (i.e., both cementitious and non-cementitious materials such as concrete and soils, respectively).
- A new K_d database was used where CDP effects were incorporated into the baseline set of analyses
- Refined meshes for both the aquifer and vadose zone models were employed
- New infiltration rate boundary conditions were employed
- Depth to the water table below the bottom of the vault was increased from 25 ft to 40.5 ft
- The waste zone was considered hydraulically to be CLSM rather than concrete
- A new structural analysis was performed that shows that cracking will commence immediately upon burial
- A new method for considering cracking and its hydraulic effects was implemented
- Floor separation from footers was incorporated
- Limits for the "groundwater all-pathways" was implemented
- K_ds as a function of pore volume flow through the vault were implemented

3.6.2 Overview of Groundwater Transport Analysis

The approach taken focuses primarily on a baseline scenario using a combination of "best estimate" values and some values that are intended to be conservative. Limited sensitivity cases are also provided for further insight into the transport aspects resulting from the parameter choices made. The main analysis tool employed is the PORFLOW code which handles both flow and transport of radionuclide chains (i.e., parents and daughters) in porous media. 2-Dimensional flow and transport analyses are used to describe in more detail the migration of species from the LAW Vault to the underlying water table. The results from these 2-D vadose zone simulations (treated as source terms) are then input into a 3-D transport only aquifer (saturated zone) model to compute maximum well concentrations of radionuclides within a 100-m compliance region (i.e., beyond a 100-m buffer surrounding the LAW Vault).

A pair of vadose zone analyses was performed for each parent radionuclide. The first analysis was for a "typical" cross-section of the LAW Vault that represented most of the sidewall length. The second analysis was for a "cracked" cross-section of the LAW Vault that contained seismically-induced cracks that were estimated via a stochastic structural analysis. Sidewall settlement can produce through-wall cracking that is open at the top and that extends into the roof, typically to the nearest joint. Similarly sidewall settlement can produce through-wall cracking that is open at the bottom and that extends into the floor, typically to the nearest joint. Section 3.4.1 and section 3.6.4.2 provide more details on cracking and its application.

Both the "typical" and "cracked" cross-sections contained some cracking induced by the original cap placement. The "typical" cross-section is also referred to as the "uncracked" or "intact" section later in this report.

- It is anticipated that differential settlement due to seismic loading could result in side wall through-wall cracking that opens into the roof slab. That cracking was modeled although the probability of such an event occurring over a 1000 year period has been determined to be 0.8%.
- It is anticipated that differential settlement due to seismic loading could result in side wall through-wall cracking that opens into the footer. That cracking was modeled although the probability of such an event occurring over a 1000 year period has been determined to be 1.2%.
- Within 50 to 100 years after placement of the closure cap overburden over the LAW Vault, it is anticipated that differential settlement between the footers and floor slab will occur due to static (i.e., closure cap) loading differences between the two. This will result in a separation between the footers and floor slab.

After both vadose zone analyses were completed, they were combined via scaling factors to produce a single aquifer analysis. Each scaling factor was merely the length of sidewall represented by the particular analysis divided by the overall length of the sidewall.

3.6.3 Summary of Key Groundwater Transport Assumptions

This section includes assumptions deemed to be significant in development of a base case conceptual model. The first subsection covers those assumptions regarding design and operation, while the second subsection covers other assumptions. For the first set of assumptions, the justification is that operations personnel ensure that expectations are not violated.

Where the phrase "is adequate" appears, it means that the assumption is required if limits are established without consideration for uncertainties, because the values are not known. Limits established using appropriate uncertainty results do not need to include the assumptions. Therefore, Chapter 7 which includes the effects of uncertainties should remove the need for these types of assumptions.

3.6.3.1 Key Design and Operational Assumptions

1. 25-year operation duration starting in 1995
2. All openings and penetrations are sealed with material that provides a saturated hydraulic conductivity (Ksat) that is not greater than 1E-12 cm/s and that does not exceed that level for 1800 years. Said material must have material characteristic curves similar to that of the LAW Vault concrete, especially in producing an unsaturated hydraulic conductivity curve with values equal to or lower than those for the concrete.
3. Inventories are uniformly distributed throughout the LAW Vault.
4. The time lag between characterization and disposal is short enough that decay to potentially more problematic daughters during the time lag can be ignored.
5. Only contaminants/waste forms that are properly screened out and/or analyzed are disposed.
6. Burial/capping occurs 125 years after start of disposal operations in 1995 (in 2120).
7. Cap is properly maintained for 100 years after placement – until 2220.
8. Intact LAW Vault materials have a saturated hydraulic conductivity that does not exceed 1E-12 cm/s until the time of collapse, i.e., for 1800 years after burial.
9. In-cell sump collection systems are grouted during vault closure process.
10. Cap contains lower drainage layer. The LAWV model does not include a high-density polyethylene (HDPE) layer directly over the vault. Such an HDPE layer should reduce the infiltration, which tends to be conservative for the time period that it properly functions. Subsequent peaks could be higher after a sudden failure, such as roof collapse, because the residual waste inventory would be higher.

3.6.3.2 Other Key Assumptions

1. Depth to water table (of 40.5 ft) does not diminish from the base case value.
2. Major climate change does not occur.
3. No contamination enters the aquifer within the model domain from sources other than the LAWV.
4. Material properties for waste zone are adequate. For example, hydraulic properties for CLSM were assigned to the waste zone. If testing is performed, the material properties likely will change.
5. Material properties for all other zones are adequate. For example, anisotropy has been introduced since the latest published analysis. Field testing could modify those properties.

6. Cracking has no effect on hydraulic properties other than to change Ksat in the manner assumed. The cracking pattern, extent of cracking, roughness, and crack widths and depths are uncertain. This key assumption follows the National Institute of Standards and Technology approach (Snyder 2003). No crack healing or infilling is assumed. Infilling will reduce the Ksat for the crack, which typically will produce slower water movement and slower transport of contaminants.
7. Future cracking is confined to "cracked" sections.
8. Cellulose degradation products are present forever at the concentration levels assumed in the K_d report.
9. Method of assuming secular equilibrium for decay chain members with half-lives of less than 5 years is adequate. Detailed analyses may produce some short-lived daughters that do not attain secular equilibrium because they are transported more quickly than their precursors.
10. Two-dimensional cross-section representation of LAW Vault in vadose zone is adequate.
11. Numerical dispersion is insignificant.
12. Time step sizes and mesh sizes are adequate. A more refined aquifer model with accompanying smaller time steps would improve the accuracy of results.
13. One dimensional infiltration analysis is adequate. A multi-dimensional analysis with the sloping concrete roof has not been evaluated.
14. Series of steady-state flow fields, rather than transient flow analysis is adequate. In some cases steady-state may require many years to attain.
15. Use of K_d values from similar elements is adequate. In many cases specific K_d measurements do not exist.
16. Bias in conceptual model is insignificant. Other base cases that are equally likely would produce different results.
17. Hydraulic CLSM properties were assumed for the waste zone, because the waste zone properties have not directly been measured

Some of the above assumptions will be addressed when an uncertainty analysis is performed or other studies are completed.

3.6.4 Groundwater Transport Conceptual Model

This section covers the operation, closure, and degradation time frames. Separately derived information from structural analyses and infiltration analyses are inputs for the numerical models and are included in the discussion in this section. Special considerations include time intervals and treatment of the waste zone, which has not been tested or studied, except for special waste forms. The various material zones and their properties are discussed in the final subsections. The vadose zone models and aquifer models are presented separately.

3.6.4.1 Operation and Closure

The operation period for the LAWV commenced in 1995 and is assumed to continue for 25 years. Waste has been disposed in the LAWV and some has been retrieved for disposal elsewhere, such as in trenches, consequently the rate of waste filling is dynamic. However, for modeling purposes a constant rate of filling over the operational period of 25 years was assumed.

At least four simplified concepts exist to represent filling operations as shown in Figure 3-5. Possibly the worst case is to apply the full waste volume at the start of operations as shown in the "initial full" concept below. The best representation of the assumption is the "constant fill rate" concept, which is to apply a constant rate of waste filling for the first 25 years. However, this concept is more difficult to implement in the model. A slightly easier concept to implement is the "initial half-full" concept, which is to apply half the waste volume initially, hold the volume constant for the 25 years, then to increase to the full waste volume instantaneously. The final concept is the "full at half-time" concept, which is to apply the full waste volume at the mid-point of the operational period. This "full at half-time" concept was implemented in the model, because it is the easiest concept to apply.

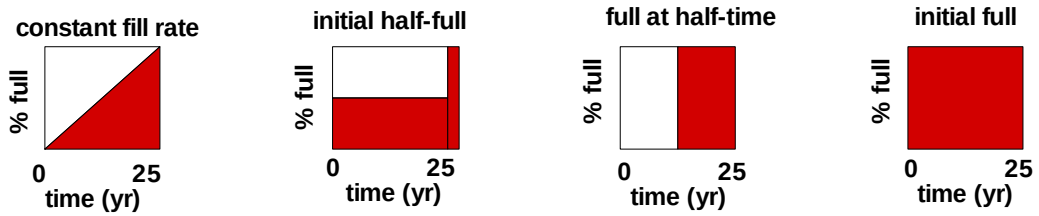

Figure 3-5. Four Concepts of Filling Operations

3.6.4.2 Structural Modeling Incorporation

Previous structural modeling (Carey 2006) provided estimates of crack sizes, locations, and timing for each major structural component of the LAWV. Crack information was input to an algorithm to adjust the saturated hydraulic conductivity (Ksat) as described below in the section "Specific implementation of crack information to adjust Ksat." The Ksat for uncracked LAWV concrete was 1.0E-12 cm/s (Phifer et al. 2006, page 195).

Structural modeling also provided estimates of the time for roof collapse. Crack and collapse information was included on a time basis for each major structural component of the LAW Vault. Because a 2-dimensional cross-section was modeled, interior walls were ignored.

Independent Intact and Cracked Section Method

Structural modeling results were incorporated in the vadose-zone groundwater flow and transport modeling by assuming that two LAW Vault cross-sections existed; one cross-section that remained intact without any cracking, while the second cross-section contained all the cracking, with one exception. The exception (discussed below) was that any cracking that had a probability of unity of occurring was incorporated in both sections.

Each of the assumed sections was independently analyzed in separate vadose zone models. Vadose zone results (in terms of contaminant flux to the water table) from each cross-section were subsequently combined in the aquifer transport analyses by applying length-weighting factors based on the length of each section relative to the overall length of one LAW Vault module.

For wall cracks, the length of the assumed cracked section was twice the width of the wall. For roof cracks, any previously perched water over the crack would be drained by the crack. The zone of influence that the crack would drain was assumed to extend upward at a 45 degree angle from the vertical. Because the drained section extends on both sides of the vertical (for a two-dimensional analysis) a 1 ft tall drained section would extend 2 ft horizontally. The length of roof below the zone of influence was considered to be the length of the drained section. Note that the structural analysis indicated that typically there would only be one sidewall crack for a LAWV module.

The length of the cracked section was selected as the maximum applicable value from the following alternatives:

1. for wall cracks, assume twice the width of the wall or 2 * 2 ft = 4 ft
2. for the roof if an overlying horizontal drainage layer is not used, assume twice the height of the cap or 2 * 40 inches = 80 inches (6.67 ft)
3. for the roof if an overlying horizontal drainage layer is used, assume twice the height of the drainage layer or 2 * 1 ft = 2 ft.

For a base case, no overlying horizontal drainage layer was considered hence Alternative 2 was included, while Alternative 3 was excluded. The maximum value used for the assumed cracked section length thus was 80 inches (6.666 ft).

Because the overall length of one LAW Vault module is 214 feet, the cracked section was assigned a length-weighting factor of 6.666 ft / 214 ft or 0.03115. The uncracked section was assigned a length-weighting factor of 1 – 0.03115 or 0.96885.

Cracking categories

Crack information from the structural modeling analyses were assessed for each of the categories shown in Table 3-2 (from Carey 2006).

Table 3-2. Cracking Categories, Probabilities, and Applicable Cross-sections

Vault component	Category	Probability	Applicable cross-sections[1]
Side wall	Collapse – initial	1	Both
Side wall	Collapse – over time	1	Both
Side wall	Settlement from seismic	<1	"cracked"
Roof	Collapse – initial	1	Both
Roof	Collapse – over time	1	Both
Roof	Settlement from seismic	<1	"cracked"
Floor	Settlement from seismic	1	Both

[1]Both refers to intact and "cracked" sections

"Collapse" is terminology from the structural analysis that refers to the cap loading only, with no consideration of seismic activity. "Initial" refers to cracking that occurs from the initial cap placement, while "over time" refers to subsequent cracking, that ultimately leads to true collapse.

The initial collapse analyses estimated early cracking that would occur due to the initial loading from cap placement. The collapse analyses over time estimated crack development from initial and seismic loading in combination with degradation of the vault, ultimately causing failure and roof collapse.

All collapse results were applied to both the cracked and intact sections from time zero, because the probability was assumed to be unity. As a consequence, both the cracked and intact sections were failed when collapse was predicted to occur. The floor settlement had its first significant impact at 1000 years and those results were applied to both sections. All other cracking categories had a probability of less than one and their impacts were applied only to the cracked section.

Specific implementation of crack information to adjust Ksat

Ksat for concrete is calculated as $Ksat = k\rho g/\mu$
where

k = intrinsic permeability, cm^2
ρ = dry bulk density, g/cm^3
μ = dynamic viscosity, $g/(cm\ s)$
g = gravitational acceleration, cm/s^2

Ksat for cracked concrete is calculated as $Ksat = k_b\rho g/\mu$
where

k_b = bulk intrinsic permeability for a concrete block, cm^2

The general method to calculate the bulk permeability (k_b) for cracked concrete, based on the permeability for uncracked concrete (k_0) and crack thickness and frequency was presented in Phifer et al. (2006). That method involves lumping the cracks together in the region where the permeability for the lumped cracks (k_c) applies as shown in Figure 3-6. That depth of the cracks is αh and lumped width of the cracks is mw.

The calculation involves two steps. In Step 1 parallel flow is assumed through the hashed area and a k_p is calculated. In Step 2 serial flow is assumed through the entire block and the combined effects of k_o and k_p produce a bulk permeability k_b.

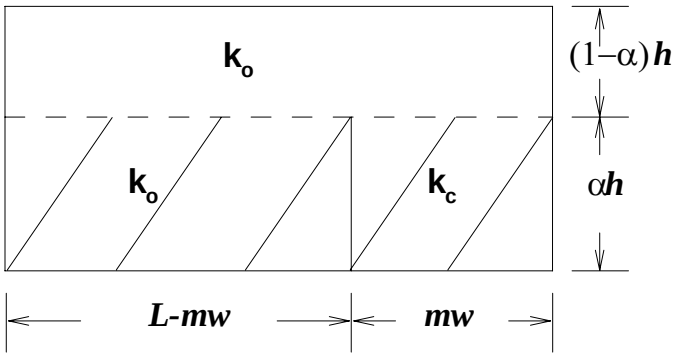

Figure 3-6. Crack Model Schematic after Snyder 2003

For the current model, cracking was only used to adjust Ksat values, because no approved method was available to adjust porosities or other hydraulic or transport parameters. Infilling of cracks was ignored, which likely produced higher Ksat values with an undetermined effect on K_d values and other transport parameters. Application of crack information for each of the cracking categories is discussed below.

1. Side wall collapse: initial and over time (cracked and intact sections)
Top, middle and bottom bands (two feet high) along the walls were predicted to occur, with cracking increasing over time. Cracks created only slight increases in Ksat, hence the maximum crack at the end of the earliest period after roof collapse (0 to 3000) years was used to calculate a Ksat of 3.2000E-11 cm/s. This value was assigned directly to the wall of the intact section (because the probability was unity). This value was the starting value to determine the adjusted Ksat for the wall of the cracked section when other cracks were included.

2. Side wall settlement (intact section)

Seismic events would create differential side wall settlement resulting in through-wall cracking with the crack sizes increasing over time. Cracks open at the top would extend into the roof and be closed at the bottom. Cracks open at the bottom would extend into the floor and be closed at the top. Both the top-wall cracking and the bottom-wall cracking were assumed to occur only in the same 80-inch long cracked section. Side wall cracking vs. time is provided in Table 3-3.

Table 3-3. Side wall cracking vs. time (after Carey 2006)

	Average Crack Depth (in)			Average Crack Spacing (in)			Average Crack Width (in)		
Time (yrs)	Top	Middle	Bottom	Top	Middle	Bottom	Top	Middle	Bottom
50	20.17	0.41	17.94	9.36	12.40	7.01	0.041	0.0001	0.007
100	20.35	0.75	17.95	9.31	12.37	7.02	0.044	0.0002	0.007
500	21.22	3.65	18.08	8.55	12.10	7.11	0.082	0.0008	0.008
1000	22.10	6.38	18.25	7.29	11.69	7.24	0.154	0.0015	0.008
3000	23.25	14.14	18.98	5.96	10.42	7.91	0.314	0.0037	0.013
5000	23.45	17.39	20.90	5.95	10.05	7.42	0.465	0.0064	0.074
7500	23.64	18.84	22.58	5.95	10.25	6.29	0.784	0.0123	0.180
10000	23.73	19.09	22.90	5.96	10.41	6.11	1.061	0.0154	0.216

The general method (described above) of increasing the Ksat for cracked concrete based on crack sizes was applied. However, one change was made, namely the intrinsic permeability for uncracked concrete (k_0) was replaced by the maximum intrinsic permeability calculated for the side-wall collapse analysis that corresponded to a Ksat of 3.20E-11 cm/s. Because the top and bottom cracks were assumed to occur in the same cracked section, the sum of both crack widths was applied simultaneously to obtain a net Ksat. Linear interpolation was applied to produce Ksats for key infiltration and analysis times. The net Ksat values and their corresponding time ranges are provided in Table 3-4.

Table 3-4. Side wall settlement net Ksat values[1]

After burial Start year	After burial End year	Modeled Start year	Modeled End year	Avg Ksat (cm/yr)	Avg Ksat (cm/sec)
0	10	112.5	122.5	8.81367E-01	2.79E-08
10	100	122.5	212.5	1.00267E+02	3.18E-06
100	300	212.5	412.5	4.20508E+02	1.33E-05
300	550	412.5	662.5	9.17434E+02	2.91E-05
550	1000	662.5	1112.5	1.69043E+03	5.36E-05
1000	1800	1112.5	1912.5	1.86537E+04	5.91E-04

[1]For all tables, where many of digits are presented for values the precision typically is only one to three digits. The excess digits are presented because the values are copied directly from references or they are calculated values that are applied as shown as model inputs.

3. Roof collapse - initial (cracked and intact sections)

This section and the following section on roof collapse over time determine when the roof collapse is likely to occur and provide cracking conditions prior to that time. All structural information is based on the structural analysis (Carey 2006). The section titles are borrowed from the structural analysis.

All these cracks were assumed to occur when the LAW Vault is buried, i.e., at 112.5 years. Cracks over interior roof beams had an average spacing of six inches spread over 5 feet resulting in 11 cracks. Cracks over exterior roof beams had an average spacing of six inches spread over 2.5 feet resulting in 6 cracks.

Starting from an assumed intact concrete saturated hydraulic conductivity (Ksat) of 1E-12 cm/s, cracking increased that value to 3.3E-08 cm/s for both sets (interior and exterior) of beams. This increased Ksat for the cracked-beam fraction was weighted with the uncracked fraction (0.96885) of the roof, producing a net Ksat of 3.12E-9 cm/s to be applied to the entire roof. The net Ksat was applied directly for to the intact section and was used as a starting value for the intact section when considering additional cracking of the roof near the walls as described below in the “roof settlement” section.

4. Roof collapse – over time (cracked and intact sections)

The structural analysis stated “since significant cracking is expected at the beginning of the analysis, the depth, spacing and width of the cracks is not expected to change significantly over time” (Carey 2006). Thus, later roof collapse results were used to adjust the initial Ksat values, but they were assumed not to cause any changes in the hydraulic conductivity over time after the initial impact. The mean time to collapse for the roof was estimated to be 2805 years with a standard deviation of 920 years. As discussed below, roof collapse was modeled as occurring at 1800 years to reduce the number of time intervals requiring steady-state flow fields.

5. Roof settlement caused by side wall differential settlement (intact section)
Cracking at the top of side walls (see Table 3-3) caused by differential settlement was assumed to extend to the roof and crack information was provided from the structural analysis. Resulting roof cracks were assumed to extend from the outside walls in a distance of 9 feet to the first set of joints. Based on recommendations from the structural analyst, linear interpolation was applied to produce Ksats for key infiltration times. The starting Ksat value was that calculated for the roof collapse cracks, 3.12E-9 cm/s rather than the 1E-12 cm/s value for intact concrete. Results are provided in Table 3-5. These results were only applied to the cracked section.

Table 3-5. Ksat Values and Times for Cracked Roof Section from Settlement Analysis

After burial Start year	After burial End year	Modeled Start year	Modeled End year	Avg Ksat (cm/yr)	Avg Ksat (cm/sec)
0	10	112.5	122.5	9.83389E-02	3.12E-09
10	100	122.5	212.5	7.67670E+01	2.43E-06
100	300	212.5	412.5	3.23810E+02	1.03E-05
300	550	412.5	662.5	7.07154E+02	2.24E-05
550	1000	662.5	1112.5	1.30347E+03	4.13E-05
1000	1800	1112.5	1912.5	1.38061E+04	4.37E-04

6. Floor settlement (cracked and intact sections)
Based on the structural engineering report which stated "it is recommended the permeability of the entire floor slab be increased after 1000 years" (Carey 2006) the Ksat of the floor was increased by an order of magnitude 1000 years after burial. Given the high Ksat (1.9E-6 cm/sec) that was applied to the floor area under and adjacent to the walls, a similarly high Ksat for the rest of floor would be required to significantly affect results. In the absence of specific crack sizes and location, a high Ksat for the rest of the floor was not deemed to be warranted, thus a change of one order of magnitude was assumed.

7. Sump (intact section)
The floor slab of the LAW Vault rests on the footers, but is not attached to the footers. Thus part of the footer forms part of the overall floor.

The cap will transmit forces through the walls to the footer, causing the footers to settle and separate from the rest of the unattached floor. Additionally at the south end a sump exists that will be filled with grout prior to closure. The portion of the floor below and adjacent to the south wall was assigned the same hydraulic properties as the waste zone.

8. Floor/wall gap at north end (intact section)
At the north end of the wall, separation will also occur between the floor slab and the footer, creating a small gap. Similar to the south end, the portion of the floor below and adjacent to the north wall was assigned the same hydraulic properties as the waste zone.

3.6.4.3 Infiltration Boundary Condition

Infiltration boundary conditions were established based on HELP model results (Phifer et al. 2006). Infiltration rates calculated by the HELP model were provided for discrete points in time. Those time points were used to establish endpoints for time intervals. The infiltration rates at the endpoints were averaged to be applied for the time interval. One exception was that collapse and failure were assumed to occur at 1800 years after burial (1912.5 model years), so the final infiltration rates for 2800 years to 10,000 (2917.5 to 10112.5 model years) were applied from the time of collapse onward. Additionally, an infiltration rate of zero caused numerical problems, so the initial infiltration above the vault was changed from zero to a value slightly less than the Ksat for the intact concrete (<1E-12 cm/s). Infiltration rates for the area above the vault and to both sides (off-vault) are provided in Table 3-6 for each time interval and are shown in Figure 3-7.

Table 3-6. Infiltration rates

	Infiltration Data		Model			
Description	**Start year**	**End year**	**Start year**	**End year**	**Above vault (in/yr)**	**Off vault (in/yr)**
½ operation period, uncovered	-112.5	-100	0	12.5	1.18E-05	15.74800
Institutional control, uncovered	-100	0	12.5	112.5	0.00041	15.74800
Start of burial, maintained cap	0	100	112.5	212.5	0.06350	0.06700
Start of cap degradation	100	300	212.5	412.5	0.51400	0.60850
Next step in cap degradation	300	550	412.5	662.5	1.65150	1.97700
End at time-of-compliance	550	1000	662.5	1112.5	4.01650	4.76350
End at time-of-collapse	1000	1800	1112.5	1912.5	8.34450	9.45000
Post-collapse	1800+		1912.5+		15.93000	13.72600

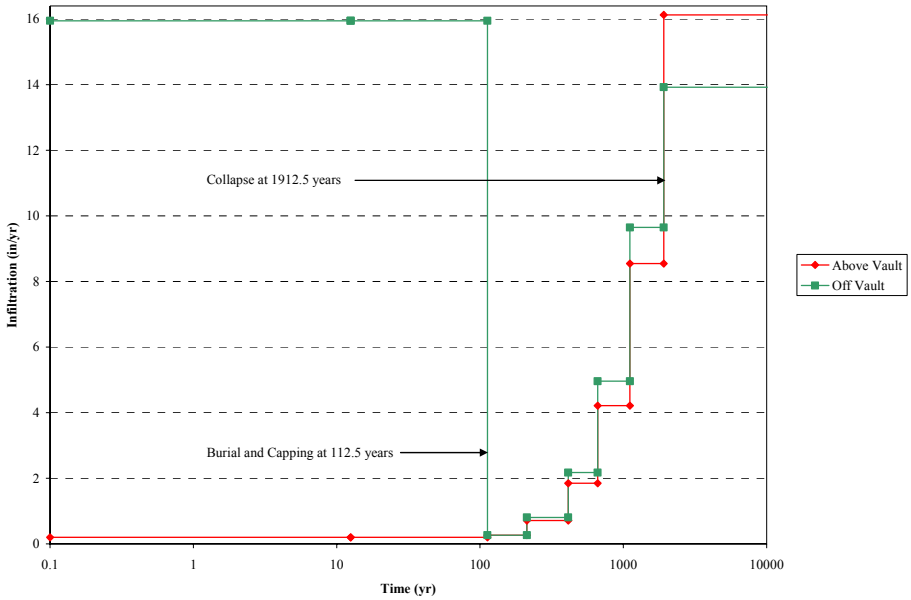

Figure 3-7. Infiltration rates

3.6.4.4 Special Considerations

Time ranges

Crack information was reviewed to select significant changes and their respective times. Significant changes in infiltration rates were reviewed to select significant changes and their respective times. The union of the key times from both the cracking and infiltration as shown in Table 3-7 was used to establish the set of times required for a LAW Vault base case model.

Waste zone representation challenges

Because the waste is highly variable its performance is very poorly understood. Rather than specifically measuring properties for a "representative sample" of waste, other materials were used as surrogates. The initial surrogate was gravel, because it has a high porosity similar to that of the waste. However, flow convergence could not reasonably be attained, especially when a gravel material was placed adjacent to a very low conductivity concrete. A second effort was attempted using sand as a surrogate for the waste with the same results. Finally, changes in the geometry, e.g., ignoring the presence of footers below portions of the floor, in combination with using Controlled Low Strength Material (CLSM) as a surrogate produced converged flow solutions. CLSM has a higher total porosity that gravel, even though porosity has no effect on steady-state flow solutions. The other flow properties for CLSM are likely closer to those of the waste than are gravel. The original surrogate of gravel was agreed upon in a meeting of PA modelers and others, but it was also stated at that meeting that gravel may cause convergence problems and that it may not be the best choice.

Openings and penetrations in external vault concrete members

All openings and penetrations in external vault concrete members are assumed to be filled with material that will provide performance that is equivalent to or better than intact concrete, which was modeled with a saturated hydraulic conductivity of 1E-12 cm/s until the time of collapse. These openings and penetrations include such items as exterior forklift access openings and exterior fan openings, doors between modules, but they do not include the two-inch separation between the LAWV modules. All these openings contain exposed rebar to allow a tie-in between future sealing material and the existing concrete.

Table 3-7. Combined Time Intervals for Analyses

		Infiltration Data		Model	
Cracking Description	**Infiltration Description**	**Start year**	**End year**	**Start year**	**End year**
Uncovered, only intact section applied	½ operation period, uncovered	-112.5	-100	0	12.5
Uncovered, only intact section applied	Institutional control, uncovered	-100	0	12.5	112.5
Covered, all initial cracks apply to both intact and cracked sections	Start of Burial, maintained cap	0	10	112.5	122.5
Start of new cracking applied only to cracked section	Maintained cap	10	100	122.5	212.5
No significant further cracking	Start of cap degradation	100	300	212.5	412.5
	Next step in cap degradation	300	550	412.5	662.5
	End at time-of-compliance	550	1000	662.5	1112.5
	End at time-of-collapse	1000	1800	1112.5	1912.5
Failure applied to both intact and cracked sections	Post-collapse	1800+		1912.5+	

3.6.4.5 Waste and Vadose Zone Flow and Transport

Materials for the vadose zone model are depicted in Figure 3-8. The model extends from the water table upward to the bottom of the geosynthetic clay liner (GCL). Thirteen material zones were selected for the model as follows:

1. Lower vadose zone
2. Upper vadose zone
3. Floor: center portion away from footers
4. Bottom waste zone: representing thickness of waste after collapse
5. Top waste zone: in combination with bottom waste zone represents initial thickness of waste zone
6. Void: void over waste
7. Roof: center portion not influenced by side wall cracking
8. Horizontal drainage zone: identification of layer for possible sensitivity analyses. For a base case this zone was treated as part of the cap.
9. Cap
10. Wall
11. Compacted fill: ultimate fill outside the perimeter of the vault to the base of the cap or horizontal drainage zone
12. Cracked roof: edge of roof subject to cracking from extension of side wall cracks
13. Floor leak: floor near edges subject to separation from main floor slab when initial cap forces footers to subside.

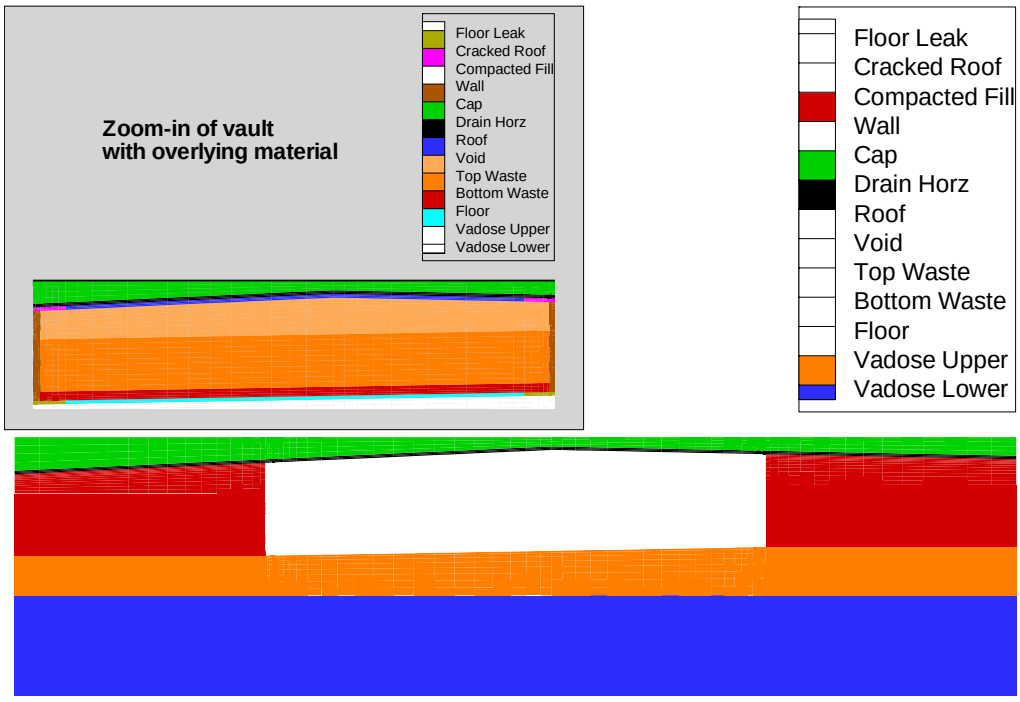

Figure 3-8. Materials for Vadose Zone Model

Key vault geometries are depicted in Figure 3-9, which is exaggerated in the vertical direction. Slopes and lengths are shown for the floor and roof. Heights of the walls and elevations for the floor and the water table at the base of the model are shown. The elevation of the water table was provided by Greg Flach in an email (Flach 2006). Thicknesses of the waste zones (2.5 ft for the lower and 14.5 ft for the upper) and the various structural members of the vault are indicated.

Flow model properties

For the flow model, the entire waste zone prior to collapse ultimately was modeled as being Controlled Low Strength Material (CLSM). Additionally, the floor leak was treated similarly. All concrete was assigned High-quality-concrete properties, except that cracking from the structural model was used to adjust the Ksat values. After collapse the lower vadose zone, upper vadose zone and compacted backfill remained the same, while all other materials were considered to be Operational Soil Cover (OSC) before Dynamic Compaction (DC).

General flow analogs for all the material zones are shown in Table 3-8 and selected material property values are provided in Table 3-9 and Table 3-10 for uncracked and cracked sections, respectively. Only collapse affects the choice of material analogs for the flow cases.

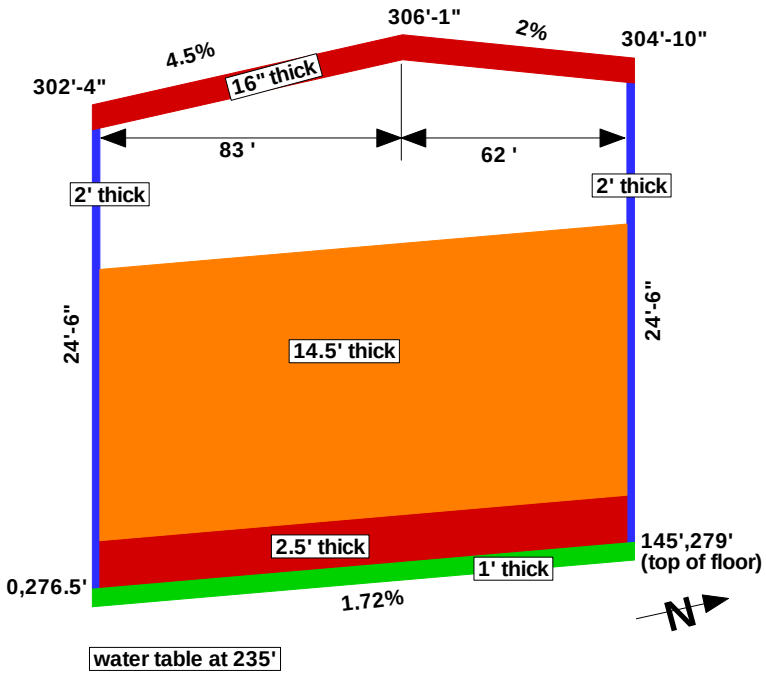

Figure 3-9. Key vault geometries

Table 3-8. Vadose Zone Material Zone Analogs for Flow Model

Id	Model material	Pre-collapse properties	Post-collapse properties
1	Lower vadose zone	Lower vadose zone	Lower vadose zone
2	Upper vadose zone	Upper vadose zone	Upper vadose zone
3	Floor center	High quality concrete	OSC prior to DC
4	Bottom waste zone	CLSM	OSC prior to DC
5	Upper waste zone	CLSM	OSC prior to DC
6	Void	CLSM	OSC prior to DC
7	Roof center	High quality concrete	OSC prior to DC
8	Horizontal drain	Compacted backfill	OSC prior to DC
9	Cap	Compacted backfill	OSC prior to DC
10	Wall	High quality concrete	OSC prior to DC
11	Compacted fill	Compacted backfill	Compacted backfill
12	Cracked roof	High quality concrete	OSC prior to DC
13	Floor leak	CLSM	OSC prior to DC

Table 3-9. Selected material properties for uncracked flow analysis vs. time

	Time Stage (years)						
Material Zone	**0 to 112.5 (uncovered)**	**112.5 to 212.5**	**212.5 to 412.5**	**412.5 to 662.5**	**662.5 to 1112.5**	**1112.5 to 1912.5**	**1912.5+ (collapsed)**
LVZ							
Ksat-V (cm/yr)	2.87E3	2.87E3	2.87E3	2.87E3	2.87E3	2.87E3	2.87E3
Ksat-H (cm/yr)	1.04E4	1.04E4	1.04E4	1.04E4	1.04E4	1.04E4	1.04E4
Porosity (-)	0.39	0.39	0.39	0.39	0.39	0.39	0.39
UVZ							
Ksat-V (cm/yr)	2.75E2	2.75E2	2.75E2	2.75E2	2.75E2	2.75E2	2.75E2
Ksat-H (cm/yr)	1.96E3	1.96E3	1.96E3	1.96E3	1.96E3	1.96E3	1.96E3
Porosity (-)	0.39	0.39	0.39	0.39	0.39	0.39	0.39
Floor center							
Ksat-V (cm/yr)	3.16E-5	3.16E-5	3.16E-5	3.16E-5	3.16E-5	3.16E-5	3.79E+3
Ksat-H (cm/yr)	3.16E-5	3.16E-5	3.16E-5	3.16E-5	3.16E-5	3.16E-5	3.79E+3
Porosity (-)	0.184	0.184	0.184	0.184	0.184	0.184	0.46
Bottom waste zone							
Ksat-V (cm/yr)	6.00E1	6.00E1	6.00E1	6.00E1	6.00E1	6.00E1	3.79E+3
Ksat-H (cm/yr)	6.00E1	6.00E1	6.00E1	6.00E1	6.00E1	6.00E1	3.79E+3
Porosity (-)	0.33	0.33	0.33	0.33	0.33	0.33	0.46
Upper waste zone							
Ksat-V (cm/yr)	6.00E1	6.00E1	6.00E1	6.00E1	6.00E1	6.00E1	3.79E+3
Ksat-H (cm/yr)	6.00E1	6.00E1	6.00E1	6.00E1	6.00E1	6.00E1	3.79E+3
Porosity (-)	0.33	0.33	0.33	0.33	0.33	0.33	0.46
Void							
Ksat-V (cm/yr)	6.00E1	6.00E1	6.00E1	6.00E1	6.00E1	6.00E1	3.79E+3
Ksat-H (cm/yr)	6.00E1	6.00E1	6.00E1	6.00E1	6.00E1	6.00E1	3.79E+3
Porosity (-)	0.33	0.33	0.33	0.33	0.33	0.33	0.46
Roof center							
Ksat-V (cm/yr)	3.16E-5	9.83E-2	9.83E-2	9.83E-2	9.83E-2	9.83E-2	3.79E+3
Ksat-H (cm/yr)	3.16E-5	9.83E-2	9.83E-2	9.83E-2	9.83E-2	9.83E-2	3.79E+3
Porosity (-)	0.184	0.184	0.184	0.184	0.184	0.184	0.46

Table 3-9. Selected material properties for uncracked flow analysis vs. time - continued

	Time Stage (years)						
Material Zone	**0 to 112.5 (uncovered)**	**112.5 to 212.5**	**212.5 to 412.5**	**412.5 to 662.5**	**662.5 to 1112.5**	**1112.5 to 1912.5**	**1912.5+ (collapsed)**
Horizontal drain							
Ksat-V (cm/yr)	1.29E+03	1.29E+03	1.29E+03	1.29E+03	1.29E+03	1.29E+03	3.79E+3
Ksat-H (cm/yr)	0	2.40E3	2.40E3	2.40E3	2.40E3	2.40E3	3.79E+3
Porosity (-)	0.35	0.35	0.35	0.35	0.35	0.35	0.46
Cap							
Ksat-V (cm/yr)	1.29E+03	1.29E+03	1.29E+03	1.29E+03	1.29E+03	1.29E+03	3.79E+3
Ksat-H (cm/yr)	0	2.40E3	2.40E3	2.40E3	2.40E3	2.40E3	3.79E+3
Porosity (-)	0.35	0.35	0.35	0.35	0.35	0.35	0.46
Wall							
Ksat-V (cm/yr)	3.16E-5	1.01E-3	1.01E-3	1.01E-3	1.01E-3	1.01E-3	3.79E+3
Ksat-H (cm/yr)	3.16E-5	1.01E-3	1.01E-3	1.01E-3	1.01E-3	1.01E-3	3.79E+3
Porosity (-)	0.184	0.184	0.184	0.184	0.184	0.184	0.46
Compacted backfill							
Ksat-V (cm/yr)	1.29E+03	1.29E+03	1.29E+03	1.29E+03	1.29E+03	1.29E+03	1.29E+03
Ksat-H (cm/yr)	0	2.40E3	2.40E3	2.40E3	2.40E3	2.40E3	2.40E3
Porosity (-)	0.35	0.35	0.35	0.35	0.35	0.35	0.35
Cracked roof							
Ksat-V (cm/yr)	3.16E-5	9.83E-2	9.83E-2	9.83E-2	9.83E-2	9.83E-2	3.79E+3
Ksat-H (cm/yr)	3.16E-5	9.83E-2	9.83E-2	9.83E-2	9.83E-2	9.83E-2	3.79E+3
Porosity (-)	0.184	0.184	0.184	0.184	0.184	0.184	0.46
Floor leak							
Ksat-V (cm/yr)	3.16E-5	6.00E1	6.00E1	6.00E1	6.00E1	6.00E1	3.79E+3
Ksat-H (cm/yr)	3.16E-5	6.00E1	6.00E1	6.00E1	6.00E1	6.00E1	3.79E+3
Porosity (-)	0.184	0.33	0.33	0.33	0.33	0.33	0.46

Table 3-10. Selected material properties for cracked flow analysis vs. time

	Time Stage (years)							
Material Zone	**0 to 112.5 (uncovered)**	**112.5 to 122.5 (uncracked)**	**122.5 to 212.5**	**212.5 to 412.5**	**412.5 to 662.5**	**662.5 to 1112.5**	**1112.5 to 1912.5**	**1912.5+ (collapsed)**
LVZ								
Ksat-V (cm/yr)	2.87E3	2.87E3	2.87E3	2.87E3	2.87E3	2.87E3	2.87E3	2.87E3
Ksat-H (cm/yr)	1.04E4	1.04E4	1.04E4	1.04E4	1.04E4	1.04E4	1.04E4	1.04E4
Porosity (-)	0.39	0.39	0.39	0.39	0.39	0.39	0.39	0.39
UVZ								
Ksat-V (cm/yr)	2.75E2	2.75E2	2.75E2	2.75E2	2.75E2	2.75E2	2.75E2	2.75E2
Ksat-H (cm/yr)	1.96E3	1.96E3	1.96E3	1.96E3	1.96E3	1.96E3	1.96E3	1.96E3
Porosity (-)	0.39	0.39	0.39	0.39	0.39	0.39	0.39	0.39
Floor center								
Ksat-V (cm/yr)	3.16E-5	3.16E-5	3.16E-5	3.16E-5	3.16E-5	3.16E-5	3.16E-5	3.79E+3
Ksat-H (cm/yr)	3.16E-5	3.16E-5	3.16E-5	3.16E-5	3.16E-5	3.16E-5	3.16E-5	3.79E+3
Porosity (-)	0.184	0.184	0.184	0.184	0.184	0.184	0.184	0.46
Bottom waste zone								
Ksat-V (cm/yr)	6.00E1	6.00E1	6.00E1	6.00E1	6.00E1	6.00E1	6.00E1	3.79E+3
Ksat-H (cm/yr)	6.00E1	6.00E1	6.00E1	6.00E1	6.00E1	6.00E1	6.00E1	3.79E+3
Porosity (-)	0.33	0.33	0.33	0.33	0.33	0.33	0.33	0.46
Upper waste zone								
Ksat-V (cm/yr)	6.00E1	6.00E1	6.00E1	6.00E1	6.00E1	6.00E1	6.00E1	3.79E+3
Ksat-H (cm/yr)	6.00E1	6.00E1	6.00E1	6.00E1	6.00E1	6.00E1	6.00E1	3.79E+3
Porosity (-)	0.33	0.33	0.33	0.33	0.33	0.33	0.33	0.46
Void								
Ksat-V (cm/yr)	6.00E1	6.00E1	6.00E1	6.00E1	6.00E1	6.00E1	6.00E1	3.79E+3
Ksat-H (cm/yr)	6.00E1	6.00E1	6.00E1	6.00E1	6.00E1	6.00E1	6.00E1	3.79E+3
Porosity (-)	0.33	0.33	0.33	0.33	0.33	0.33	0.33	0.46
Roof center								
Ksat-V (cm/yr)	3.16E-5	9.83E-2	9.83E-2	9.83E-2	9.83E-2	9.83E-2	9.83E-2	3.79E+3
Ksat-H (cm/yr)	3.16E-5	9.83E-2	9.83E-2	9.83E-2	9.83E-2	9.83E-2	9.83E-2	3.79E+3
Porosity (-)	0.184	0.184	0.184	0.184	0.184	0.184	0.184	0.46

Table 3-10. Selected material properties for cracked flow analysis vs. time - continued

	Time Stage (years)							
Material Zone	**0 to 112.5 (uncovered)**	**112.5 to 122.5 (uncracked)**	**122.5 to 212.5**	**212.5 to 412.5**	**412.5 to 662.5**	**662.5 to 1112.5**	**1112.5 to 1912.5**	**1912.5+ (collapsed)**
Horizontal drain								
Ksat-V (cm/yr)	1.29E+03	1.29E+03	1.29E+03	1.29E+03	1.29E+03	1.29E+03	1.29E+03	3.79E+3
Ksat-H (cm/yr)	0	2.40E3	2.40E3	2.40E3	2.40E3	2.40E3	2.40E3	3.79E+3
Porosity (-)	0.35	0.35	0.35	0.35	0.35	0.35	0.35	0.46
Cap								
Ksat-V (cm/yr)	1.29E+03	1.29E+03	1.29E+03	1.29E+03	1.29E+03	1.29E+03	1.29E+03	3.79E+3
Ksat-H (cm/yr)	0	2.40E3	2.40E3	2.40E3	2.40E3	2.40E3	2.40E3	3.79E+3
Porosity (-)	0.35	0.35	0.35	0.35	0.35	0.35	0.35	0.46
Wall								
Ksat-V (cm/yr)	3.16E-5	1.01E-3	1.00E+2	4.21E+2	9.17E+2	1.69E+3	1.87E+4	3.79E+3
Ksat-H (cm/yr)	3.16E-5	1.01E-3	1.00E+2	4.21E+2	9.17E+2	1.69E+3	1.87E+4	3.79E+3
Porosity (-)	0.184	0.184	0.184	0.184	0.184	0.184	0.184	0.46
Compacted backfill								
Ksat-V (cm/yr)	1.29E+03	1.29E+03	1.29E+03	1.29E+03	1.29E+03	1.29E+03	1.29E+03	1.29E+03
Ksat-H (cm/yr)	0	2.40E3	2.40E3	2.40E3	2.40E3	2.40E3	2.40E3	2.40E3
Porosity (-)	0.35	0.35	0.35	0.35	0.35	0.35	0.35	0.35
Cracked roof								
Ksat-V (cm/yr)	3.16E-5	9.83E-2	7.68E+1	3.24E+2	7.07E+2	1.30E+3	1.38E+4	3.79E+3
Ksat-H (cm/yr)	3.16E-5	9.83E-2	7.68E+1	3.24E+2	7.07E+2	1.30E+3	1.38E+4	3.79E+3
Porosity (-)	0.184	0.184	0.184	0.184	0.184	0.184	0.184	0.46
Floor leak								
Ksat-V (cm/yr)	3.16E-5	6.00E1	6.00E1	6.00E1	6.00E1	6.00E1	6.00E1	3.79E+3
Ksat-H (cm/yr)	3.16E-5	6.00E1	6.00E1	6.00E1	6.00E1	6.00E1	6.00E1	3.79E+3
Porosity (-)	0.184	0.33	0.33	0.33	0.33	0.33	0.33	0.46

Figure 3-10 presents a more detailed graphical view that includes flow and transport analogs and concrete time eras. In Figure 3-10 the analogs for the flow model are depicted in the left-hand column for each material. Five time eras are depicted. The first four time eras (moving up from the lower left in Figure 3-10) represent the degradation and depletion of concrete (which apply only to the transport model). The fifth time era represents post-collapse, which can occur during any of the concrete stages.

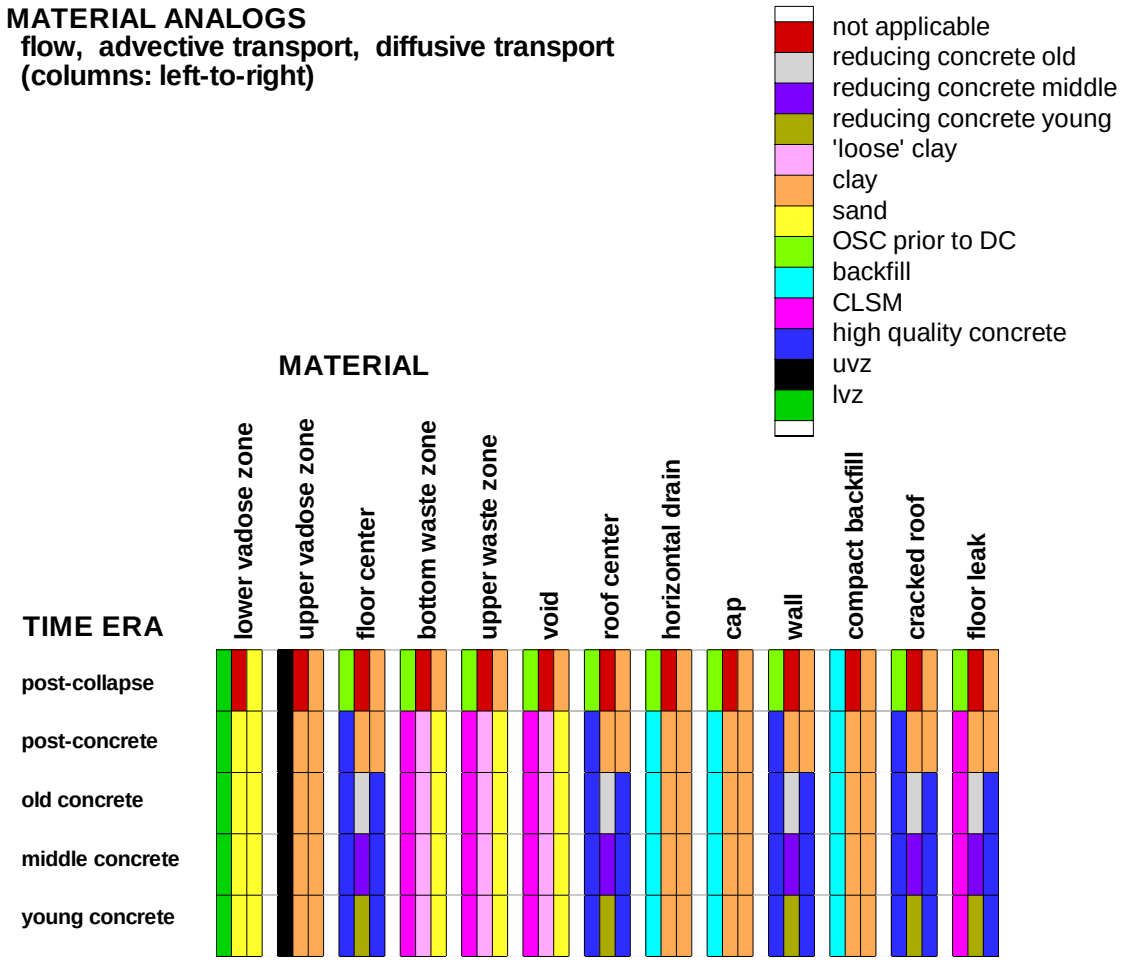

Figure 3-10. Material Analogs for Flow and Transport Models

As stated by Kaplan and Myers (2001), the concrete time eras represent quantities of water (expressed in terms of pore volumes) flushing through the vault, which change the pH of the concrete, because the groundwater is acidic. Figure 3-11 shows a plot of the pore volumes versus time estimated to flush through the LAW Vault. This figure shows the times when the various concrete stages are entered and ended.

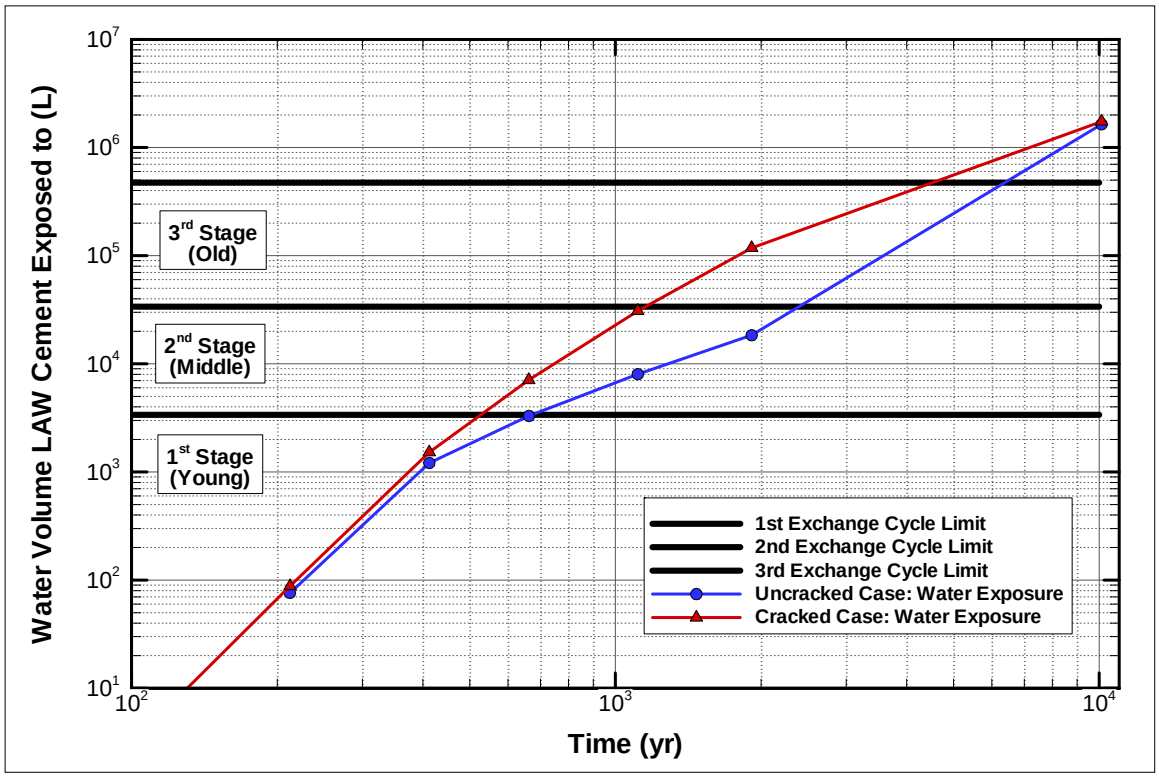

Figure 3-11. Pore Volumes Used to Estimate Timing for Concrete Stages

The Post-collapse time era from Table 3-8 was assumed to occur at 1800 years to reduce the number of flow time intervals to model. The start of collapse was actually estimated at 2700 years by the structural modeling. However, inventory limits are established only for the time up to the time-of-compliance, which was assumed to be 1000 years after closure. Because subsequent modeling was only performed to estimate peaks (for those radionuclides that did not peak earlier), a more accurate representation was not required. The earlier collapse that was assumed tends to increase the flow through the waste, increasing contaminant fluxes at the water table, and subsequently peak concentrations at the 100-m well.

Table 3-11 shows the graphical results for the concrete time eras that are derived from Figure 3-11. Based on this table and the assumed collapse at 1800 years, the collapse occurs during the middle concrete era for uncracked concrete and during the old concrete era for the cracked concrete.

Table 3-11. Concrete Time Eras

Case	Model Time Period	Young (yr)	Middle (yr)	Old (yr)	Gone (yr)
Uncracked	Start	112.5	790.5	2539.5	6569.5
	End	790.5	2539.5	6569.5	and beyond
Cracked	Start	112.5	640.5	1267.5	4689.5
	End	640.5	1267.5	4689.5	and beyond

Actual model values for porosity, particle density, saturated hydraulic conductivity, and matrix compressibility can be found in Phifer et al. 2006. Tables of moisture characteristic curves, including suction head as a function of relative saturation and relative permeability as a function of relative saturation can be found in Phifer et al. 2006.

Vadose zone transport model properties

Transport model properties include the following:

1. selection of subset of nuclides to analyze
2. flow velocities and saturations
3. physical and chemical information for radionuclides
4. physical and chemical information for sediments
5. boundary and initial conditions

1. Selection of subset of nuclides to analyze

The selection of the subset of nuclides to analyze was based on prior screening analyses. Those screening analyses considered a simplified trench-like model that was assumed to apply to all disposal units. The screening model applied general flow velocities, a 10,000,000 Ci inventory, and literature dose ingestion factors. Because the analysis was conducted prior to Kaplan's report on K_d values, the screening K_d values were based on literature values (with some SRS experimentally determined values) that did not include the effects of cellulose degradation products.

Initially, a highly simplified spreadsheet analysis was performed (Cook and Wilhite 2004) only for parents and any peak dose that was less than 0.04 mrem/yr (0.01 of the beta-gamma limit) was screened out and not included in a list for more detailed analysis with PORFLOW. No tests for the groundwater all-pathways or other analyses were conducted during the screening analysis. Subsequent improvements (Taylor and Collard 2005) included an automated analysis that included doses from the entire decay chain, assigning different K_d values for each member of the chain, and examining multiple time intervals. A discussion on groundwater screening methodology is found in the Background Chapter, Section 4.1.1.

Two special waste forms were also analyzed that were not previously considered for disposal in the LAW Vault. Those special waste forms and their descriptions are:

I-129_H: H-Area CG-8 resin
I-129_J: F-Area filtercake.

These special waste forms exist in limited quantities in the LAW Vault. However, because neither the geometries nor the locations were known, each special waste form was analyzed as though it occupied an entire cross-section of the LAW Vault. This approach is likely to estimate peak concentrations that are too low because the concentrated waste is diluted spatially throughout the entire cross-section. The peak concentration estimates are also likely to be too low because the high K_d for the waste form itself is assigned throughout the entire cross-section. Refining the model to account for the relatively small volumes of these special wasteforms would be an improvement; however, the special I-129 inventories of these wastes in the LAW Vault are orders of magnitude below the preliminary limits calculated in this analysis.

2. Flow velocities and saturations

Flow information is produced by the vadose zone flow model. Darcy velocities and Darcy volumetric water fluxes across each cell face are inputs for mechanical dispersion and advection, respectively. Saturations provide information to determine the amount of solids that can participate in retardation, because flow only moves through the wetted portion of the vadose zone.

3. Physical and chemical information for radionuclides

Physical and chemical information for radionuclides include decay, sorption and diffusion properties.

For decay purposes abbreviated decay chains were selected by a group to be modeled. This approach is the same as in previous PA work where no rationale was provided. For the current PA the rationale is to not model any radionuclide with a half-life that is less than 5 years. Improving on previous PA work, the shorter-lived progeny were included by assuming that they were in secular equilibrium with their immediate longer-lived precursor that was modeled.

For transport, the advective component was governed by the distribution coefficient (K_d), while the diffusive component was governed by the effective diffusion coefficient (D_{eff}). Analogs for each of these transport components were selected by a consensus. The selections for the flow analog, advective analog and diffusive analog were often independent, e.g., for the initial waste zone the flow analog was CLSM, the advective analog was “loose” clay and the diffusive analog was sand.

4. Physical and chemical information for sediments

For the transport model, the porosities and densities were those from the material analogs provided in Table 3-12 and shown graphically as part of Figure 3-10, except for the volume inside the vault. For the waste zones and the void, the porosity was increased to 90 percent and the density was significantly reduced, because the waste initially is in a very loose state. Using the lower porosity and higher density from the flow model would have artificially produced a higher volume of solids and unduly increased the retardation.

Table 3-12 shows the material analogs for the transport model. No effects on porosity or density are affected by this table except for the "loose" clay for the waste zone and void. In Table 3-12 "initial" refers to the time interval when cementitious materials would be in their young stage. Cementitious material properties will change as the material ages and more pore volumes of groundwater flush through the LAW Vault. The property values for reducing cement apply to these changes, which are the "young," "middle" and "old" stages. Note that the CLSM which is cementitious was only used as an analog for the flow model, not for the transport model. "Post-concrete" refers to the time interval when the cementitious materials would cease to be cementitious, presented as the "gone" stage in Table 3-11. "Post-collapse" in Table 3-12 is self-explanatory.

Table 3-12. Vadose Zone Material Zone Analogs for Transport Model Properties Not Common to Flow Model

		Advection	Diffusion
Model number	**Model material**	**Initial/post-concrete/ post-collapse**	**Initial/post-concrete/ post-collapse**
1	Lower vadose zone	Sand/sand/NA	Sand/sand/sand
2	Upper vadose zone	Clay/clay/NA	Clay/clay/clay
3	Floor center	Reducing concrete/clay/NA	High-quality-concrete/clay/clay
4	Bottom waste zone	"loose" clay/"loose" clay/NA	Sand/sand/clay
5	Upper waste zone	"loose" clay/"loose" clay/NA	Sand/sand/clay
6	Void	"loose" clay/"loose" clay/NA	Sand/sand/clay
7	Roof center	Reducing concrete/clay/NA	High-quality-concrete/clay/clay
8	Horizontal drain	Clay/clay/NA	Clay/clay/clay
9	Cap	Clay/clay/NA	Clay/clay/clay
10	Wall	Reducing concrete/clay/NA	High-quality-concrete/clay/clay
11	Compacted fill	Clay/clay/NA	Clay/clay/clay
12	Cracked roof	Reducing concrete/clay/NA	High-quality-concrete/clay/clay
13	Floor leak	Reducing concrete/clay/NA	High-quality-concrete/clay/clay

As stated in the "Flow Model Properties" section, Table 3-11 shows that post-collapse (after 1800 years) starts during the middle concrete era for uncracked concrete and during the old concrete era for cracked concrete. Collapse is not assumed to affect the chemical adsorption portion of advection, because the K_d is assumed only to be a chemical property. However, the density and porosity for the replacement analog material after collapse can affect the overall retardation. When collapse occurs, it immediately changes diffusion for the rest of the analysis as major degradation is assumed or actual movement of materials via subsidence, with replacement from above.

All K_d values were set to those for the case where cellulose degradation products are available. Some K_d values increased and some K_d values decreased relative to the case where cellulose degradation products are not available.

Actual model values for porosity, particle density, effective diffusion coefficients and distribution coefficients (K_ds) can be found in Phifer et al. (2006) and Kaplan (2006). K_d values are presented in the following tables:

- Table 3-13. Cementitious K_d values (ml/g) vs. time for vault concrete
- Table 3-14. Non-cementitious K_d values (ml/g) that are constant over time
- Table 3-15. Non-cementitious K_d values (ml/g) in waste zone that vary over time

All mechanical dispersivities were set to zero, which generally will tend to increase fluxes and concentrations, because plume spreading will be reduced.

Table 3-13. Cementitious K_d values (ml/g) vs. time for vault concrete

Element	Young	Middle	Old	Gone
Ac	245	245	24.5	53.9
Am	245	245	24.5	53.9
C	10	5	0	0
Cl	0.8	2	0	0
Cm	245	245	24.5	53.9
H	0	0	0	0
I	4	10	0	0
K	3.32	6.64	3.32	83
Mo	0	0	0	0
Nb	1000	1000	500	0
Ni	1410	1410	705	9.87
Np	3320	3320	332	0.996
Pa	3320	3320	332	0.996
Pb	705	705	352.5	2820
Pd	1410	1410	705	9.87
Pu	2550	2550	255	137.7
Ra	189	189	132.3	9.45
Se	150	150	75	500
Sn	5640	5640	2820	2820
Sr	1.89	1.89	1.512	9.45
Tc	2500	2500	2500	0.05
Th	2550	2550	255	459
U	9450	9450	9450	378
Zr	400	400	40	72

Type of section	Time era (years)			
Uncracked	0 to 790.5	790.5 to 2539.5	2539.5 to 6569.5	6569.5 and beyond
Cracked	0 to 640.5	640.5 to 1267.5	1267.5 to 4689.5	4689.5 and beyond

Table 3-14. Non-cementitious K_d values (ml/g) that are constant over time

Element	Lower vadose zone (Sand)	All areas outside vault that are above the LVZ (Clay)
Ac	53.9	416.5
Am	53.9	416.5
C	0	0
Cl	0	0
Cm	53.9	416.5
H	0	0
I	0	0.3
K	83	415
Mo	0	0
Nb	0	0
Ni	9.87	42.3
Np	0.996	58.1
Pa	0.996	58.1
Pb	2820	7050
Pd	9.87	42.3
Pu	137.7	3009
Ra	9.45	32.13
Se	500	500
Sn	2820	7050
Sr	9.45	32.13
Tc	0.05	0.1
Th	459	1020
U	378	567
Zr	72	160

Table 3-15. Non-cementitious K_d values (ml/g) in waste zone that vary over time

Isotope	Concrete present	Concrete gone (acidic conditions)
I-129_H	190	50
I-129_J	28.35	6.95

Type of section	Time era1 (years)	Time era2 (years)
Uncracked	0 to 6569.5	6569.5 and beyond
Cracked	0 to 4689.5	4689.5 and beyond

5. Boundary and initial conditions
Boundary conditions were to set fluxes at the side and top boundaries to zero, while setting a concentration of zero at the water table representing the base of the model. Initial conditions were to set the overall inventory in the waste zone to 1 gram-mole of parent. Distribution was assumed to be uniform on a volumetric basis.

3.6.4.6 Saturated Zone Flow and Transport

The saturated zone flow model is a refined subset of the overall General Separations Area (GSA) flow model described in Flach (2004). The LAW Vault model mesh was established by using a "cookie cutter" program that first extracted a vertical chunk from the overall model, starting from the surface and extending to the base of the upper aquifer. Subsequently each original 200-ft by 200-ft cell was replaced by sixteen 50-ft by 50-ft cells to reduce numerical dilution and dispersion. Flows and saturations from the overall model parent cell were duplicated for the smaller cells in the final model. Flow information was captured as Darcy velocities and Darcy volumetric fluxes across each cell face.

The saturated zone transport model consisted only of the sandy portion of the sediments that contained the Lower Vadose Zone, because that is where the model was terminated. Contrary to the vadose zone model, the porosity and density base values were adjusted for the Lower Vadose Zone transport materials. The saturated Lower Vadose Zone was assumed to consist of horizontal sand layers and horizontal clay layers with flow only moving through the sand. The model's porosity was reduced from the total vadose zone value of 0.39 to an effective value of 0.25. This change by itself effectively creates more solids to that could retard the contaminants. Therefore, the particle density was reduced from 39% to 25% in order to maintain the same retardation as in the vadose zone model if saturated conditions were present. Alternatively, an artificially lower saturation could have been selected because only the solids in the wetted region participate in retardation.

3.6.5 Groundwater Transport Deterministic Model Description

This section only discusses the model discretizations for the vadose zone and aquifer models.

3.6.5.1 Waste and Vadose Zone Flow and Transport Model Discretization

The modeling orthogonal mesh for the vadose zone is depicted in Figure 3-12. The overall mesh size is 75 nodes wide by 60 nodes tall, or 73 elements wide by 58 elements tall. The same mesh is used for both the flow and transport models.

The mesh captures the slope of the floor and both sides of the roof. The slopes are continued to the lateral boundaries. The slopes are gradually reduced as one moves vertically away from the floor or roof.

The mesh is refined near material interfaces, especially where a large contrast in hydraulic conductivities exists, such as between concrete and any other material. The mesh then becomes coarser as one moves away from the material intersection. The aspect ratio for each element generally does not exceed 8:1, but some exceptions exist for very narrow elements.

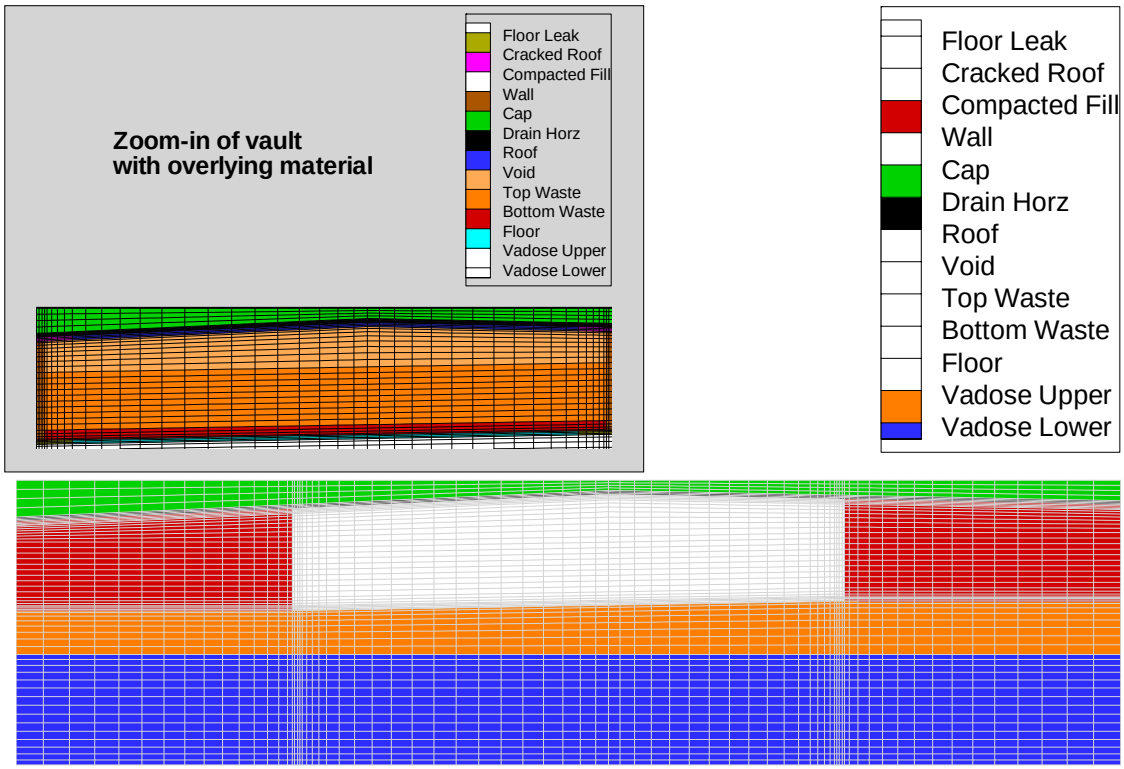

Figure 3-12. Vadose Zone Mesh with Material Types

3.6.5.2 Saturated Zone Flow and Transport Model Discretization

Figure 3-13 depicts a portion of the General Separations Area (GSA) aquifer model that shows the E-Area disposal units. The GSA model was described in Flach (2004).

Figure 3-13 shows the LAW Vault model outlined by the blue double line. The cutout view is expanded in Figure 3-14. The horizontal grid spacing was reduced from 200 ft by 200 ft in the GSA model to 50 ft by 50 ft in the LAW Vault model.

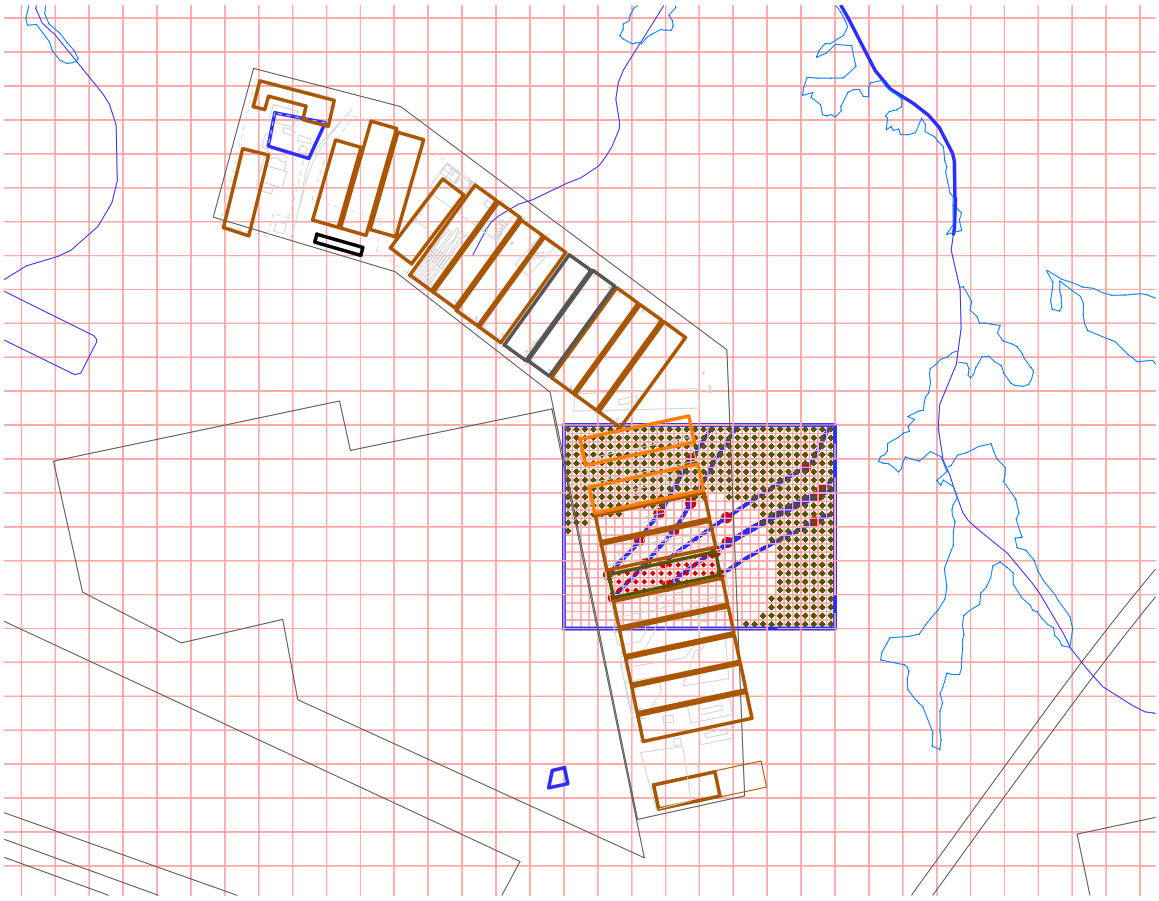

Figure 3-13. LAWV Aquifer Mesh – Portion of GSA

In Figure 3-14, red diamonds indicate columns selected for sources based on LAW Vault coordinates. Each source cell was the cell in the source column that contained the water table.

Green diamonds indicate the columns located beyond the 100-m buffer that could contain the hypothetical well with the peak concentration at any point in time. These cells helped define the model footprint as they extended in the primary flow direction. The blue lines are stream traces representing the path of water particles released from the four corners of the LAW Vault footprint (at the water table) and from two releases halfway between each set of corner nodes along a long edge. The red dots on the blue lines are five-year time markers for pore velocities. The flow pattern indicates a divergence for the water particles started at the upstream edge of the LAW Vault footprint versus the other four starting locations. This divergence indicates that contaminant plumes should show significant spreading and interaction with other disposal units (at least on a spatial basis).

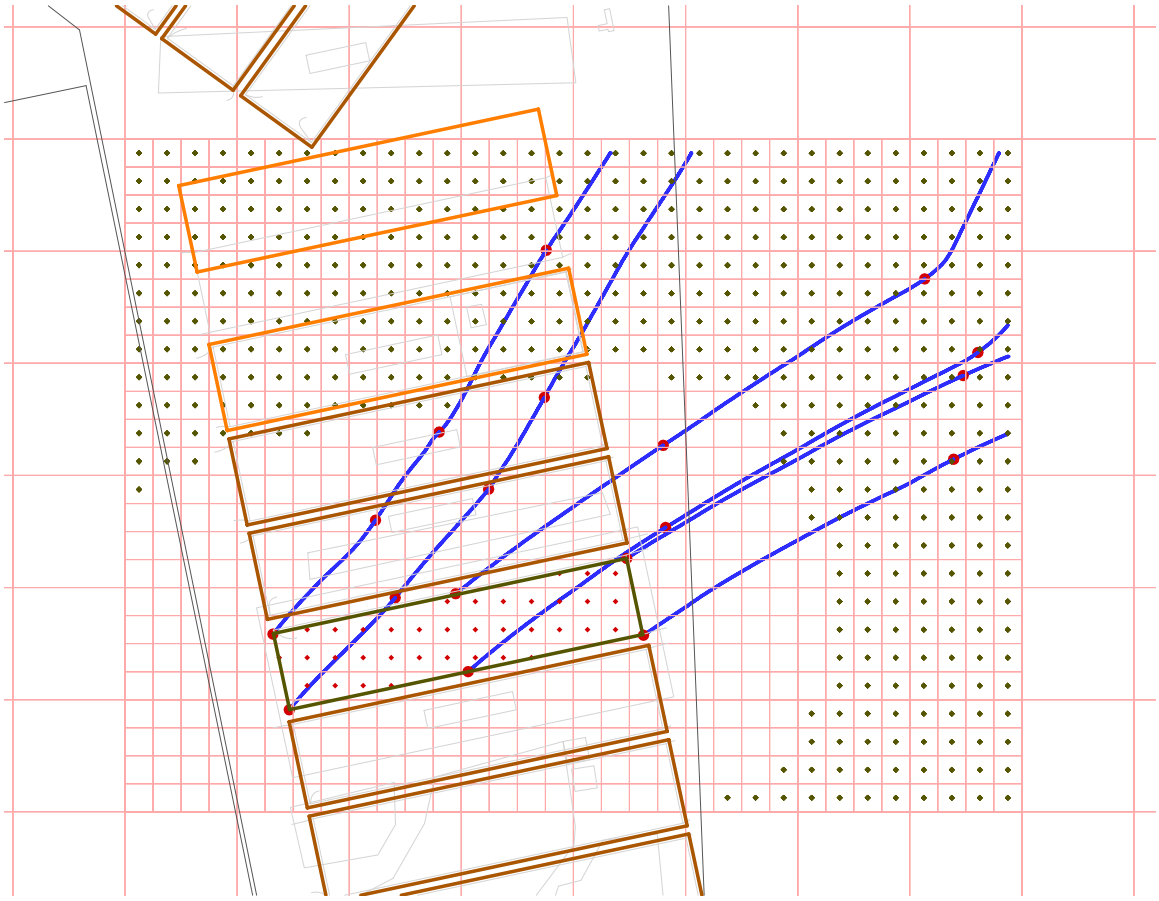

Figure 3-14. LAWV Aquifer Mesh - Model

3.6.6 Groundwater Transport Deterministic Model Results

This section discusses the transport results for both the vadose zone and aquifer models.

3.6.6.1 Waste and Vadose Zone Flow and Transport Model Results

Vadose zone flow

The primary outputs for the vadose zone flow model are the saturations and velocity information that are fed to the vadose zone transport model. Because the approach is to establish multiple steady-state flow fields, each flow field must be converged to produce meaningful results.

Plots of pressures and saturations are shown in Figure 3-15 through Figure 3-19 for several time intervals of interest as follows:

Figure	Section	Start time (yr)	End time (yr)	Description
Figure 3-15	All	0	112.5	Before burial
Figure 3-16	Uncracked	212.5	412.5	100 to 300 years after burial
Figure 3-17	Cracked	212.5	412.5	100 to 300 years after burial
Figure 3-18	Cracked	1112.5	1912.5	1000+ yrs after burial to collapse
Figure 3-19	All	1912.5	Beyond	After collapse

The first pair of plots (Figure 3-15) covers one-half of the operation period and the 100 years of institutional control and applies to both the cracked and the uncracked sections. Infiltration is essentially zero over the vault and about 16 inches/year beside it. During this time interval the vault is not actually buried, so the model was specified so that the infiltrating water could only move vertically until it reached the elevation at the bottom of the floor. This approach means that the small amount of contaminant diffusion from the walls and roof during this time period would be released to points within the model, rather than into the air. The saturation profile shown in the right-hand figure indicates that the vault concrete essentially stays saturated. A dry region forms below the vault resulting in extremely long travel times in that region.

The next two pairs of figures (Figure 3-16 and Figure 3-17) are presented to compare results for the cracked and uncracked sections from 100 to 300 years after burial. The right-hand figure for each of these cases has 50-year time markers based on pore velocities with extra stream traces being placed in the vicinity of the walls. For the cracked section the stream traces converge at the walls and follow down the walls before spreading out beneath the floor. This effectively short-circuits some of the flow from the roof, keeping it away from the waste. Also, the travel distance is increased because the water particles in the upper outside edges of the waste must bend more to reach the wall rather than flowing downward to the floor leak areas. For the uncracked section the stream traces demonstrate a much different behavior. Outside the wall, water particles travel essentially vertically downward parallel with the wall until they bend away starting at the floor level. Inside the wall, in the waste, water particles bend toward the floor leaks located near the base of the walls.

The fourth pair of figures (Figure 3-18) chronicles the years starting from 1000 years after burial for the cracked section. The flow across the upper boundary is fairly uniform, varying from 9.45 inches at the edges to 8.34 inches over the vault. Additional cracking has occurred from the initial period and cap degradation has occurred, which both affect the flow field. Water perches both over the floor and over the center of the roof. Cracking along the roof edges prevents perching there. Flows through the vault are very slow relative to flows elsewhere. Flows at the outer edges are slower than for the initial case, because the infiltration rates at the edges are lower.

The final pair of figures (Figure 3-19) shows conditions after collapse. Infiltration rates are fairly constant, but the overall rates are slightly higher than the initial infiltration rates and the rates are higher over the vault than over the native soil beside it. The fairly constant infiltration rates produce flow fields that are close to vertical.

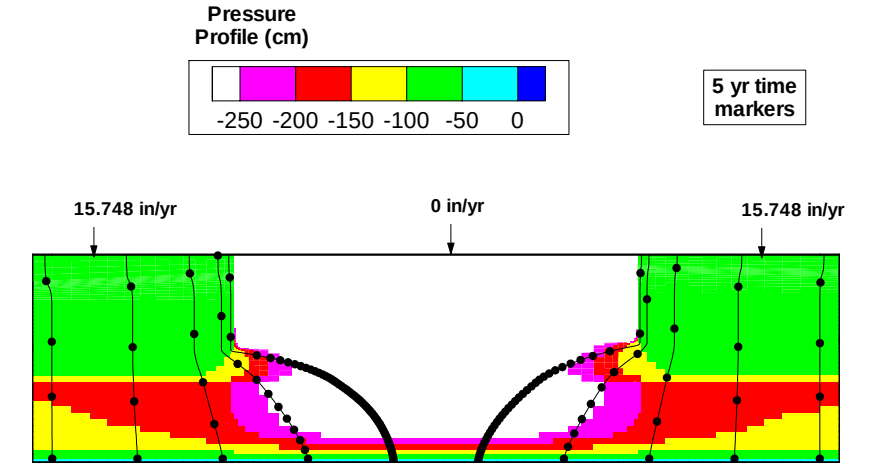

(a) Pressure Profile

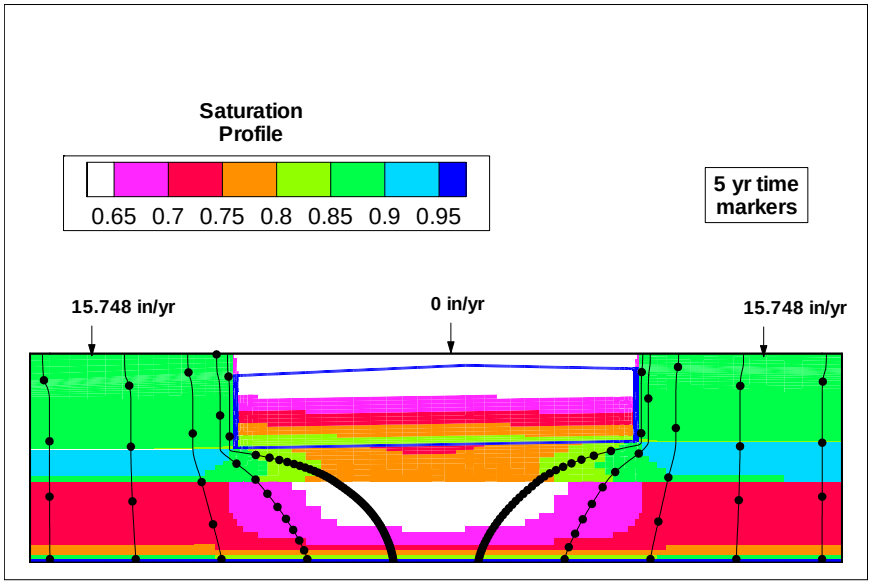

(b) Saturation Profile

Figure 3-15. Law Vault Pressure profile (a) and Saturation Profile (b) for All Sections from 0 to 112.5 Years - Before Burial with No Cracking

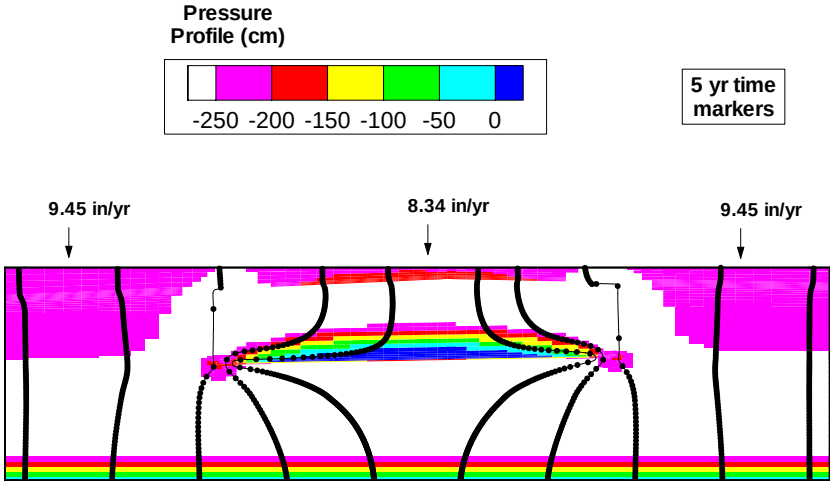

(a) Pressure Profile

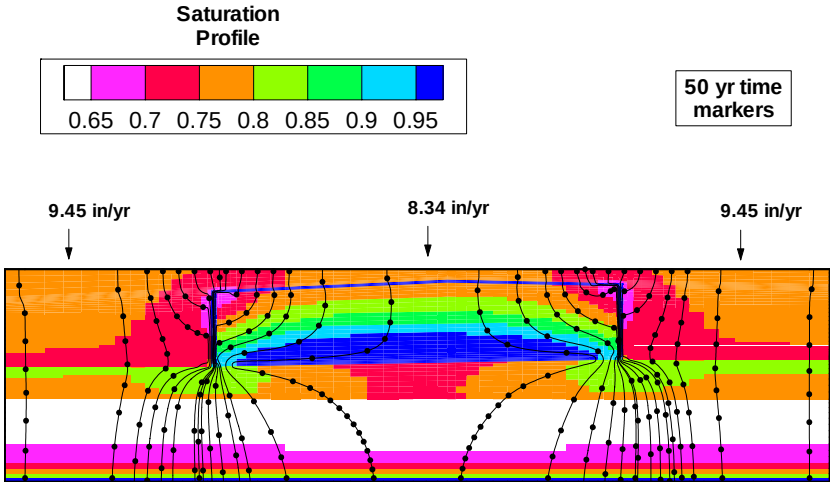

(b) Saturation Profile

Figure 3-16. LAW Vault Pressure Profile (a) and Saturation Profile (b) for Cracked Section from 212.5 to 412.5 Years

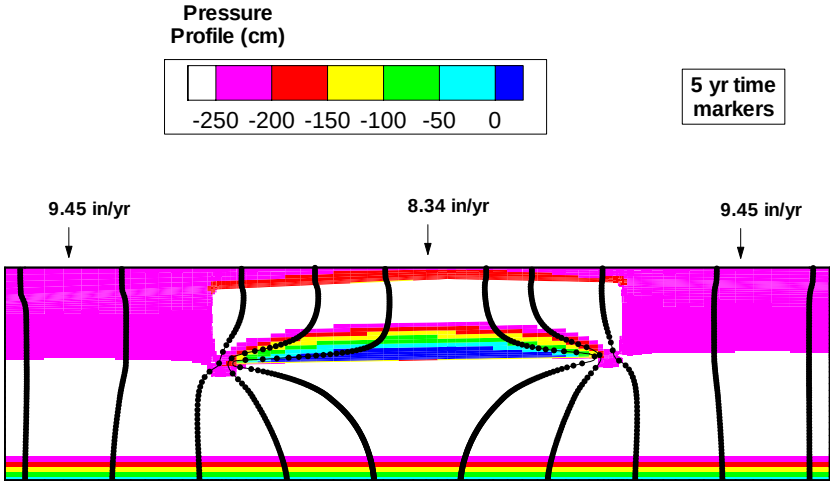

(a) Pressure Profile

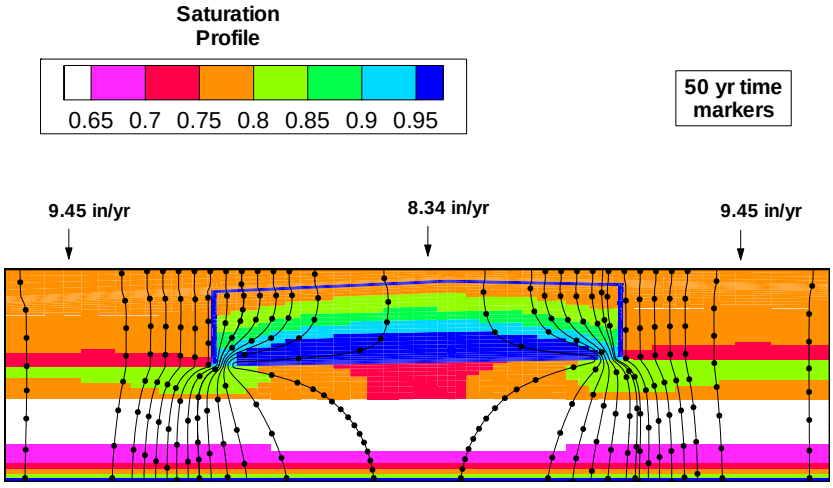

(b) Saturation Profile

Figure 3-17. LAW Vault Pressure Profile (a) and Saturation Profile (b) for Uncracked Section from 212.5 to 412.5 Years

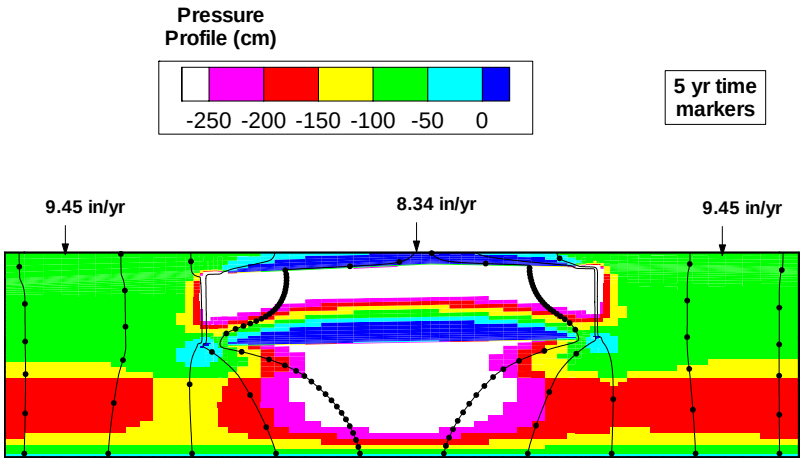

(a) Pressure Profile

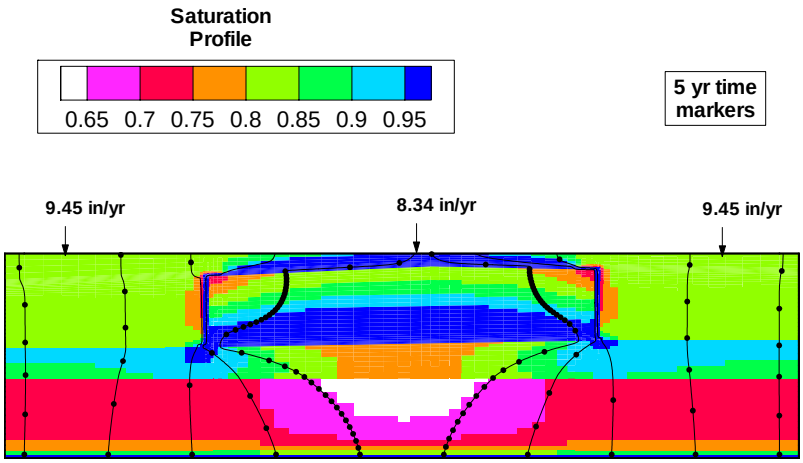

(b) Saturation Profile

Figure 3-18. LAW Vault Pressure Profile (a) and Saturation Profile (b) for Cracked Section from 1112.5 to 1912.5 Years

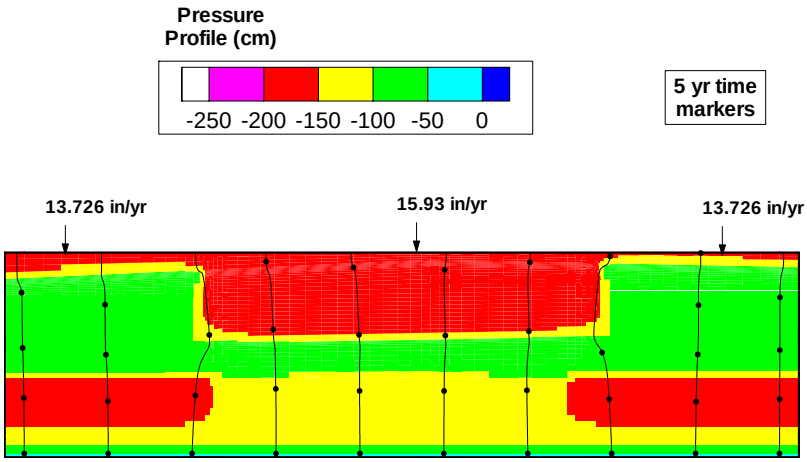

(a) Pressure Profile

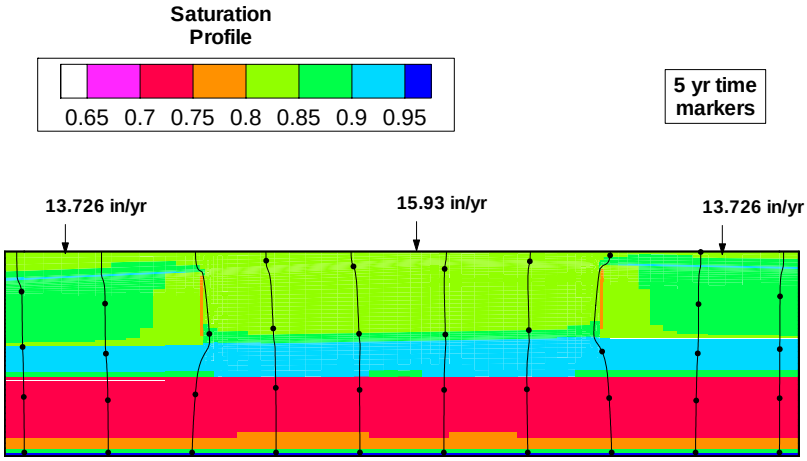

(b) Saturation Profile

Figure 3-19. LAW Vault Pressure Profile (a) and Saturation Profile (b) for All Sections from 1912.5+ Years - After Collapse

Vadose zone transport

The primary outputs of the vadose zone transport model are contaminant fluxes at the water table. For the LAW Vault those fluxes were separated into the section that contained common cracks ("uncracked section") and the cracked section. Peak results are presented in Table 3-16, where fluxes for daughters are indented for each decay chain.

Table 3-16. Peak Fluxes and Times for Cracked Section versus Uncracked Section

	Cracked		Uncracked		Cracked-Uncracked
Nuclide	Time (year)	Peak Flux (pCi/yr/Ci)	Time (year)	Peak Flux (pCi/yr/Ci)	Change (%) (-)
Am-241	5517.8	3.08E+03	5777.8	2.34E+03	3.18E+01
Np-237	2963.5	1.82E+05	3487.8	2.11E+05	-1.37E+01
U-233	20896	1.50E+02	22796	1.80E+02	-1.65E+01
Th-229	22596	9.86E+01	24496	1.21E+02	-1.85E+01
Am-243	8517.8	7.63E+07	8627.8	7.63E+07	6.90E-02
Pu-239	10472	3.45E+06	10568.5	3.44E+06	4.44E-01
U-235	26296	1.32E+02	26496	1.38E+02	-4.02E+00
Pa-231	20296	3.78E+01	20496	3.87E+01	-2.45E+00
Ac-227	20196	8.55E-01	20396	8.77E-01	-2.48E+00
C-14	673.5	2.54E+09	436.5	3.53E+09	-2.80E+01
Cl-36	437.5	3.85E+09	429.5	4.22E+09	-8.85E+00
Cm-244	1329.5	9.26E-28	1327.5	1.42E-30	6.52E+04
Pu-240	31996	1.13E+03	31496	1.20E+03	-6.13E+00
U-236	23896	4.94E+01	24896	5.24E+01	-5.80E+00
Th-232	27696	3.82E-05	28496	4.12E-05	-7.31E+00
Ra-228	27396	1.78E-03	28196	1.92E-03	-7.35E+00
Cm-245	8567.8	8.49E+07	8677.8	8.50E+07	-7.77E-02
Pu-241	8577.8	3.34E+07	8697.8	3.34E+07	-7.76E-02
Am-241	8577.8	8.95E+07	8697.8	8.95E+07	-7.80E-02
Np-237	3145.5	5.80E+05	3567.8	7.69E+05	-2.46E+01
U-233	18596	5.43E+02	19796	5.62E+02	-3.32E+00
Th-229	20396	3.36E+02	21796	3.58E+02	-6.19E+00
Cm-247	8917.8	1.73E+08	9027.8	1.75E+08	-1.00E+00
Am-243	9247.8	9.94E+07	9347.8	1.01E+08	-1.71E+00
Pu-239	11196	4.02E+06	11296	4.08E+06	-1.62E+00
U-235	26096	5.78E+01	26196	5.96E+01	-3.03E+00
Pa-231	20496	1.53E+01	20596	1.57E+01	-2.56E+00
Ac-227	20396	3.45E-01	20496	3.54E-01	-2.58E+00
Cm-248	8907.8	1.70E+08	9017.8	1.72E+08	-9.80E-01
Pu-244	10997.5	2.16E+03	11096	2.18E+03	-6.46E-01
Pu-240	35796	1.25E+03	35896	1.28E+03	-2.88E+00
U-236	36396	1.43E+00	36296	1.46E+00	-1.85E+00
Th-232	39496	9.57E-07	39296	9.74E-07	-1.78E+00
Ra-228	39096	4.42E-05	38996	4.50E-05	-1.77E+00
H-3	86.4	6.80E+02	86.4	6.80E+02	0.00E+00

Table 3-16. Peak Fluxes and Times for Cracked Section versus Uncracked Section - continued

	Cracked		Uncracked		Cracked-Uncracked
Nuclide	Time (year)	Peak Flux (pCi/yr/Ci)	Time (year)	Peak Flux (pCi/yr/Ci)	Change (%) (-)
I-129	462.5	2.76E+09	443.5	3.29E+09	-1.60E+01
K-40	9677.8	1.70E+08	9697.8	1.70E+08	-4.72E-01
Mo-93	433.5	3.66E+09	428.5	4.03E+09	-9.21E+00
Nb-93m	432.5	3.59E+09	427.5	4.00E+09	-1.01E+01
Nb-94	1918.5	2.84E+09	1918.5	2.40E+09	1.85E+01
Ni-59	3149.5	7.35E+08	3507.8	7.88E+08	-6.73E+00
Np-237	2932.5	8.93E+08	3477.8	1.06E+09	-1.55E+01
U-233	21296	9.40E+05	22996	1.10E+06	-1.48E+01
Th-229	22996	6.20E+05	24696	7.44E+05	-1.67E+01
Pd-107	3151.5	7.56E+08	3517.8	8.13E+08	-7.03E+00
Pu-238	3014.5	1.68E-17	3577.8	2.08E-20	8.08E+04
U-234	22196	3.16E+04	23796	3.12E+04	1.39E+00
Th-230	25496	4.40E+03	27096	4.65E+03	-5.42E+00
Ra-226	20196	2.09E+04	21496	2.22E+04	-6.08E+00
Pb-210	20196	7.14E+01	21496	7.60E+01	-6.08E+00
Pu-239	41996	6.78E+06	41396	6.90E+06	-1.78E+00
U-235	25896	9.50E+02	26396	1.03E+03	-7.65E+00
Pa-231	19796	2.88E+02	20396	2.98E+02	-3.23E+00
Ac-227	19696	6.54E+00	20196	6.76E+00	-3.28E+00
Pu-240	31996	4.09E+05	31496	4.36E+05	-6.14E+00
U-236	23896	1.79E+04	24896	1.90E+04	-5.79E+00
Th-232	27696	1.39E-02	28496	1.50E-02	-7.32E+00
Ra-228	27396	6.45E-01	28196	6.97E-01	-7.35E+00
Pu-241	1308.5	3.22E-48	1275.5	7.45E-52	4.33E+05
Am-241	5517.8	1.05E+02	5777.8	8.00E+01	3.18E+01
Np-237	2964.5	6.03E+03	3487.8	6.98E+03	-1.37E+01
U-233	20896	4.92E+00	22796	5.90E+00	-1.65E+01
Th-229	22596	3.23E+00	24496	3.97E+00	-1.85E+01

Table 3-16. Peak Fluxes and Times for Cracked Section versus Uncracked Section - continued

	Cracked		Uncracked		Cracked-Uncracked
Nuclide	Time (year)	Peak Flux (pCi/yr/Ci)	Time (year)	Peak Flux (pCi/yr/Ci)	Change (%) (-)
Pu-242	47496	2.25E+07	46896	2.25E+07	-1.39E-01
U-238	28796	1.90E+02	27896	2.04E+02	-6.70E+00
U-234	27796	9.20E+00	27696	1.01E+01	-9.01E+00
Th-230	30396	7.23E-01	30196	7.99E-01	-9.45E+00
Ra-226	26396	2.37E+00	26396	2.62E+00	-9.41E+00
Pb-210	26496	8.11E-03	26396	8.96E-03	-9.41E+00
Pu-244	47896	2.46E+07	47296	2.46E+07	-2.73E-02
Pu-240	48096	2.44E+07	47496	2.44E+07	1.46E-02
U-236	40196	3.17E+04	39696	3.16E+04	4.05E-01
Th-232	41096	2.35E-02	40596	2.35E-02	3.49E-01
Ra-228	40796	1.09E+00	40296	1.09E+00	3.49E-01
Ra-226	2638.5	3.94E+08	2628	4.05E+08	-2.88E+00
Pb-210	2668.5	1.34E+06	2657.8	1.38E+06	-2.96E+00
Se-79	22096	8.10E+07	22096	8.11E+07	-1.94E-01
Sn-126	175947.2	5.30E+06	174947.2	5.30E+06	3.31E-02
Sr-90	977.5	1.80E-05	1152.5	2.21E-06	7.15E+02
Tc-99	4703.1	1.14E+10	6583.1	1.17E+09	8.72E+02
Th-230	28196	4.64E+07	28196	4.69E+07	-9.30E-01
Ra-226	2730.5	7.54E+08	2767.8	7.13E+08	5.69E+00
Pb-210	2763.5	2.56E+06	2797.8	2.42E+06	5.73E+00
Th-232	28496	6.02E+07	28496	6.08E+07	-9.41E-01
Ra-228	28096	2.85E+09	28196	2.87E+09	-9.39E-01
U-233	22196	8.54E+07	23796	8.40E+07	1.61E+00
Th-229	23896	5.68E+07	25496	5.72E+07	-5.71E-01
U-234	22196	8.83E+07	23796	8.72E+07	1.36E+00
Th-230	25596	1.23E+07	27096	1.31E+07	-5.46E+00
Ra-226	20196	5.88E+07	21496	6.26E+07	-6.03E+00
Pb-210	20196	2.01E+05	21496	2.14E+05	-6.02E+00
U-235	22196	9.41E+07	23896	9.32E+07	8.81E-01
Pa-231	3076.5	4.65E+07	3567.8	6.20E+07	-2.49E+01
Ac-227	3108.5	1.06E+06	3597.8	1.41E+06	-2.48E+01

Table 3-16. Peak Fluxes and Times for Cracked Section versus Uncracked Section - continued

	Cracked		Uncracked		Cracked-Uncracked
Nuclide	Time (year)	Peak Flux (pCi/yr/Ci)	Time (year)	Peak Flux (pCi/yr/Ci)	Change (%) (-)
U-236	22196	9.40E+07	23896	9.32E+07	8.86E-01
Th-232	25796	7.69E+01	27396	8.22E+01	-6.39E+00
Ra-228	25496	3.58E+03	27096	3.83E+03	-6.46E+00
U-238	22196	9.41E+07	23896	9.32E+07	8.81E-01
U-234	22896	5.80E+06	24596	6.15E+06	-5.67E+00
Th-230	25296	4.87E+05	26996	5.43E+05	-1.04E+01
Ra-226	21396	1.71E+06	22796	1.96E+06	-1.30E+01
Pb-210	21396	5.83E+03	22896	6.70E+03	-1.30E+01
Zr-93	5997.8	3.72E+08	6277.8	3.73E+08	-2.75E-01
Nb-93m	4700.9	3.36E+10	4837.8	3.23E+10	3.97E+00
I-129_H	1971.5	1.96E+09	1976.5	1.97E+09	-3.40E-03
I-129_J	1939.5	6.16E+09	1949.5	5.96E+09	1.29E-01

For contaminants that are not highly mobile, peak results are mixed. In some cases the cracked section produced higher peaks, while in other cases the uncracked section produced higher peaks. Results in most cases are similar with most large percentage differences occurring when the peak values have very low magnitudes.

Meanwhile, peak fluxes for mobile contaminants, e.g., I-129, are lower for the cracked section than for the uncracked section, and occur later. These results occur, because the concrete properties that were modeled for the cracked section turn the walls into preferential pathways. Infiltrating water that starts above the outer edges of the waste only passes through an upper corner of the waste as it heads for the wall, providing no driving advective force for the waste near the outer edges at greater depths. Infiltrating water nearer the center of the waste bends around, seeking to find the wall rather than the floor leak areas, thus taking a longer and slower path relative to water in the uncracked section.

Figure 3-20 shows the effects of this behavior on the C-14 fluxes at the water table. The flux for the uncracked section climbs above that for the cracked section until its inventory is sufficiently depleted (around 460 years), when it falls below that of the cracked section. Both sections exhibit surges after 412.5 years and 662.5 years when new steady-state flow fields are applied for each section.

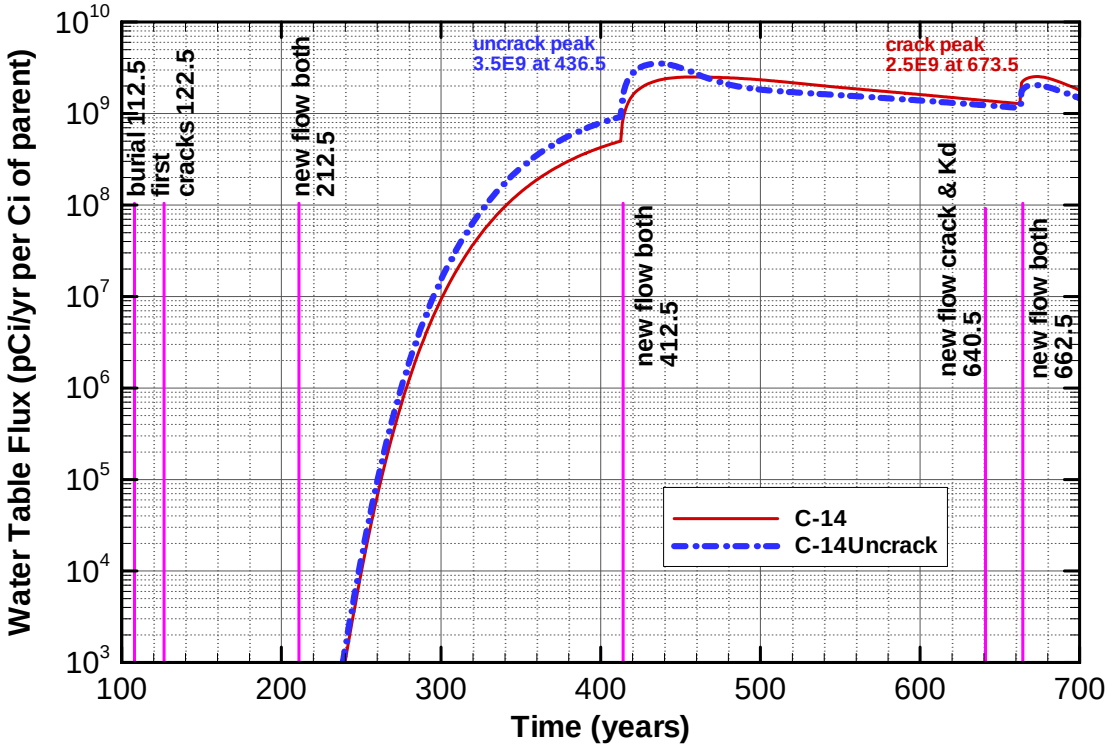

Figure 3-20. C-14 Flux at the Water Table for Cracked and Uncracked Sections

Figure 3-21 shows C-14 contours at selected times for the vadose zone containing the cracked section. Results are very similar to those for the uncracked section shown in Figure 3-22, although some times are different. Results show that for early times higher concentrations are restricted to the waste zone and vault. Soon after burial, contaminants start escaping through the floor leaks near the walls. These leaks grow in size until they merge at least by 420 years. Because of the relatively dry section below the center of the vault, the concentrations in the dry section never reach the same levels as for those sections directly below the floor leaks. After the contours merge, the concentration levels decrease over time as the inventory is depleted. At the time of the peak, the residual inventory is significantly less than the original. The extent of the highest concentration lobes is greater for the uncracked section at both 420 years and about 660 years, while the lateral spreading is less relative to the cracked section.

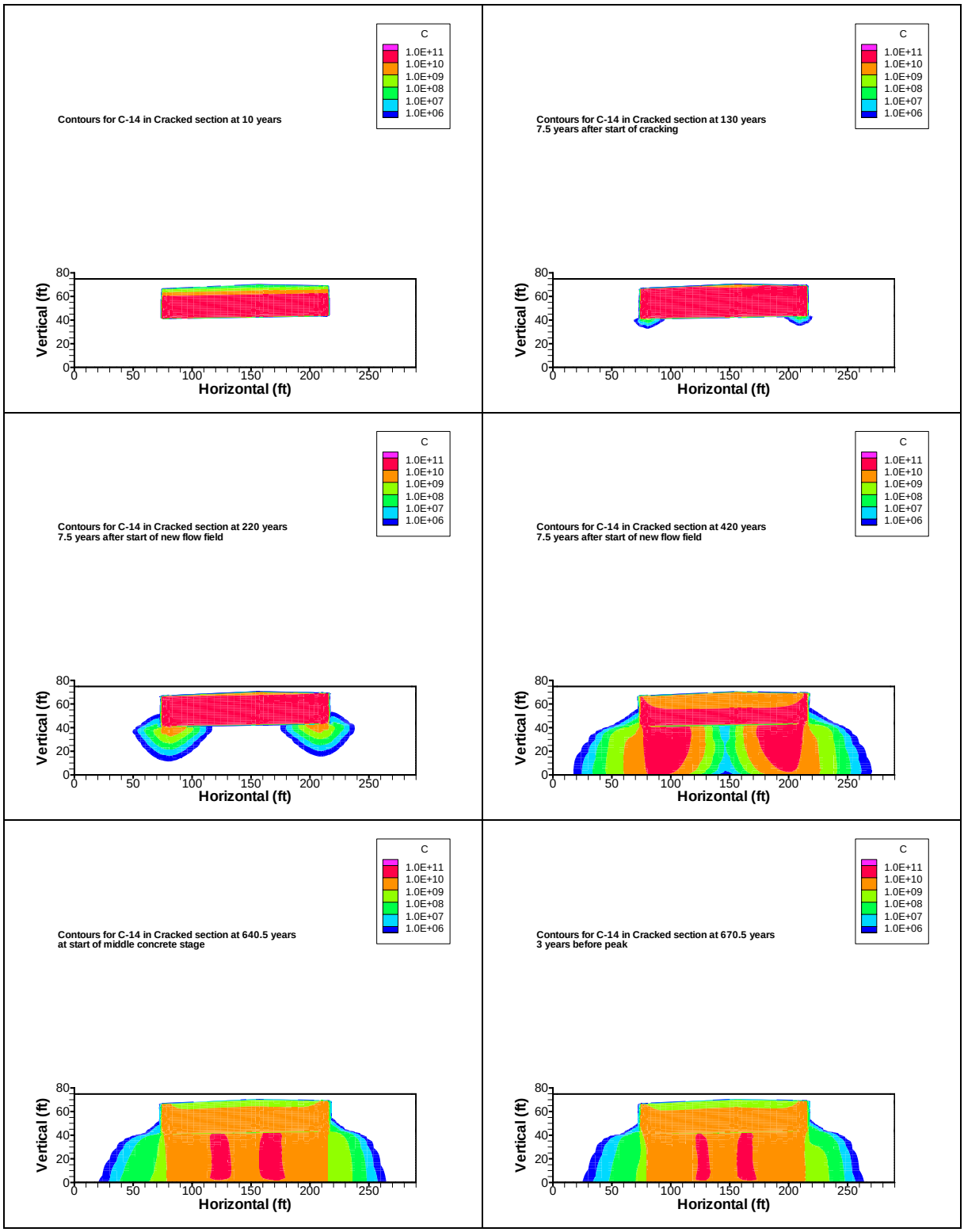

Figure 3-21. C-14 Concentration (pCi/L) Contours in Vadose Zone for Cracked Section at Key Times

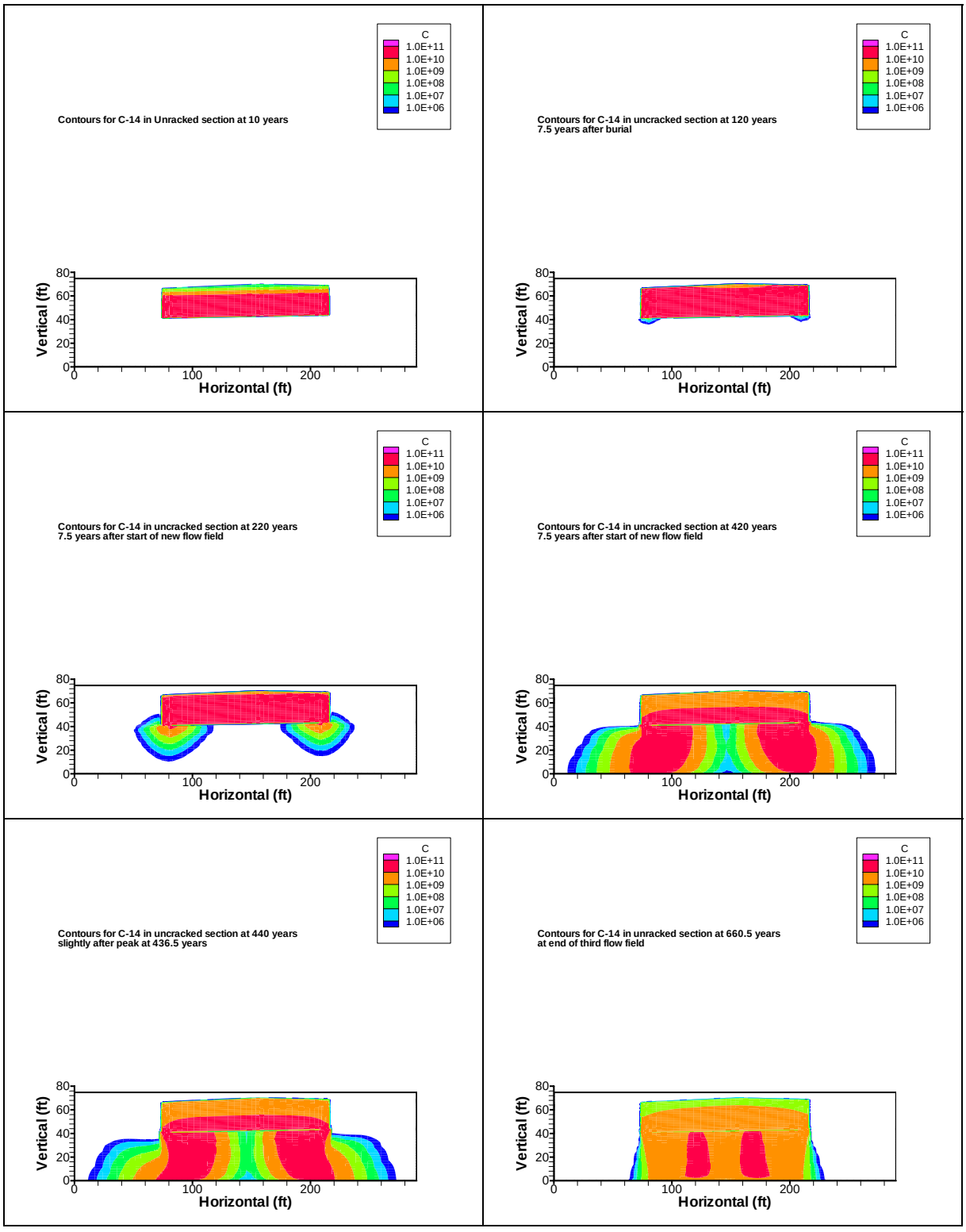

Figure 3-22. C-14 Concentration (pCi/L) Contours in Vadose Zone for Uncracked Section at Key Times

Plots of contaminant fluxes at the water table are presented in Appendix A3 for the cracked sections and uncracked sections. The legend for each figure shows the decay chain that was modeled starting from the parent at the top and followed by each progeny in turn moving down the legend.

Rather than discussing each figure in turn, general points will be presented citing specific examples and any peculiar results. The discussion will focus only on the cracked section, because a general comparison of results for cracked sections and uncracked sections was described above.

The radionuclides can be grouped into three categories based on K_d values for their elements in sand as shown in Table 3-17. The general behavior for the nuclides with a very low K_d in sand is that they typically are rapidly flushed from the system soon after a major system change. Most of the exodus occurs from 400 to 600 years when new flow fields appear. H-3 disappears earlier due to decay. Nb-94 stays until soon after collapse. Tc-99 remains until after 4700 years, because the gone concrete era is entered at 4689.5 years when the K_d in the vault decreases from 2500 to 0.1 ml/g. Np-237 remains until 2932 years and does not flush rapidly because its K_d in the concrete is 3320 ml/g and that controls until after collapse.

The general behavior for the nuclides with a low K_d in sand is that their peak develops more slowly and occurs after 1000 years. The subsequent decline from the peak is at a slower rate than for the very low K_d nuclides.

The general behavior for the nuclides with a high K_d in sand is that their peak develops very slowly and typically occurs after 10,000 years, which is followed by a gentle decline. Exceptions occur when the half-life is short and decay forces an earlier peak, such as for the following:

- Cm-244 (18.1 year half-life)
- Pu-238 (87.8 year half-life)
- Pu-241 (14.3 year half-life)

Those nuclides with high K_ds that are parents typically produce progeny that also have peaks that occur very late, especially because the parent continues to produce the progeny even while the parent is in transit.

Table 3-17. Sand K_d by Element

Very low K_d		Low K_d		High K_d	
Element	Sand K_d (ml/g)	Element	Sand K_d (ml/g)	Element	Sand K_d (ml/g)
C	**0**	**Ra**	5	**K**	50
Cl	**0**	**Sr**	5	**U**	200
H	**0**	**Ni**	7	**Pu**	270
I	**0**	**Pd**	7	**Th**	900
Mo	**0**			**Zr**	900
Nb	**0**			**Se**	1000
Tc	**0.1**			**Am**	1100
Np	**0.6**			**Cm**	1100
				Sn	2000

3.6.6.2 Saturated Zone Flow and Transport Model Results

Aquifer flow model results

The aquifer flow model was depicted in Figure 3-13 and Figure 3-14. A discussion of results depicted by those figures was presented in Section 3.6.5.2. The primary outputs from the aquifer flow model are the Darcy velocities and the Darcy volumetric flows across each face. Because it is a saturated zone model, the saturations are unity.

Aquifer transport model results

Analyses were performed for each of the radionuclides that survived the screening process. Results were the concentrations at a hypothetical 100-m well (beyond the 100-m buffer) versus time for each parent and daughter that were modeled. Modeling was accomplished in gram-mole units, but results were converted to pCi/L per Ci of parent buried for presentation in Table 3-18 for the peaks and their associated times. The table provides information for two time periods: the first includes the time up until the time-of-compliance specified as 1000 years after final closure, while the second period is for all time after that to be able to portray the peak if it occurred after 1112.5 years. In the table, modeled daughters are indented. Peaks for the special waste forms I-129_H and I-129_J are shown at the end of the table. Concentration curves are provided in Appendix A3.

Table 3-18. Peak Aquifer Concentrations and Times

	period1 (0-1112.5 yrs)		period2 (1112.5+ yrs)	
Nuclide	max time1 (years)	max conc1 (pCi/L per Ci buried)	max time2 (years)	max conc2 (pCi/L per Ci buried)
Am-241	1113	1.29E-27	6768	2.29E-05
Np-237	1113	1.66E-08	3511	1.36E-02
U-233	1113	1.74E-14	31596	9.40E-06
Th-229	1113	8.38E-17	33296	7.23E-06
Am-243	1113	7.24E-27	9978	4.28E+00
Pu-239	1113	2.61E-30	12796	2.89E-01
U-235	1113	2.05E-38	36696	8.55E-06
Pa-231	1113	6.68E-16	31896	3.48E-06
Ac-227	1113	1.05E-17	31696	7.95E-08
C-14	443	2.26E+02		
Cl-36	437	2.73E+02		
Cm-244	1113	1.76E-45	1526	2.83E-43
Pu-240	1113	4.68E-47	34896	5.49E-05
U-236	1113	2.46E-53	34496	2.85E-06
Th-232	1113	4.14E-62	38996	3.42E-12
Ra-228	1113	1.86E-40	38696	1.60E-10
Cm-245	1113	7.35E-27	10028	4.85E+00
Pu-241	1113	1.77E-27	10048	1.91E+00
Am-241	1113	4.34E-27	10048	5.12E+00
Np-237	1113	2.36E-08	3602	4.97E-02
U-233	1113	2.30E-14	29096	3.07E-05
Th-229	1113	1.05E-16	30896	2.32E-05
Cm-247	1113	8.06E-27	10392	1.11E+01
Am-243	1113	8.22E-28	10624	7.00E+00
Pu-239	1113	2.88E-31	14696	4.05E-01
U-235	1113	2.22E-39	35896	3.80E-06
Pa-231	1113	3.22E-17	29796	1.54E-06
Ac-227	1113	4.98E-19	29696	3.51E-08
Cm-248	1113	8.05E-27	10358	1.09E+01
Pu-244	1113	7.96E-34	14896	2.08E-04
Pu-240	1113	2.58E-36	18296	9.42E-05
U-236	1113	5.99E-43	46096	1.01E-07
Th-232	1113	4.94E-52	63947	1.17E-13
Ra-228	1113	1.75E-44	63947	5.50E-12
H-3	92	3.19E-05		
I-129	451	2.12E+02		
K-40	1113	7.79E-29	11796	1.05E+01
Mo-93	436	2.60E+02		
Nb-93m	436	2.58E+02		
Nb-94	1113	9.22E+00	1926	1.37E+02
Ni-59	1113	1.44E-08	3759	4.99E+01
Np-237	1113	1.04E-05	3501	6.78E+01
U-233	1113	1.02E-11	31896	5.70E-02

Table 3-18. Peak Aquifer Concentrations and Times continued

	period1 (0-1112.5 yrs)		period2 (1112.5+ yrs)	
Nuclide	max time1 (years)	max conc1 (pCi/L per Ci buried)	max time2 (years)	max conc2 (pCi/L per Ci buried)
Th-229	1113	4.73E-14	33696	4.39E-02
Pd-107	1113	1.46E-08	3761	5.16E+01
Pu-238	1113	1.00E-49	3811	4.16E-31
U-234	1113	4.60E-54	32996	1.55E-03
Th-230	1113	1.54E-57	37096	3.28E-04
Ra-226	1113	3.89E-13	34696	1.92E-03
Pb-210	1113	6.90E-16	34696	6.55E-06
Pu-239	1113	7.94E-46	44796	4.07E-01
U-235	1113	8.09E-54	36896	6.08E-05
Pa-231	1113	1.56E-14	28396	2.47E-05
Ac-227	1113	2.50E-16	28196	5.65E-07
Pu-240	1113	7.27E-46	34896	1.99E-02
U-236	1113	2.23E-52	34496	1.04E-03
Th-232	1113	2.27E-61	38996	1.24E-09
Ra-228	1113	7.23E-38	38596	5.80E-08
Pu-241	1113	2.30E-69	1479	1.01E-67
Am-241	1113	4.41E-29	6768	7.82E-07
Np-237	1113	5.66E-10	3512	4.48E-04
U-233	1113	5.90E-16	31596	3.09E-07
Th-229	1113	2.85E-18	33296	2.37E-07
Pu-242	1113	8.18E-46	50323	1.46E+00
U-238	1113	1.31E-54	40296	1.30E-05
U-234	1113	1.03E-58	48096	9.43E-07
Th-230	1113	1.93E-62	59947	1.41E-07
Ra-226	1113	1.15E-20	52565	8.73E-07
Pb-210	1113	2.00E-23	52565	2.98E-09
Pu-244	1113	8.20E-46	50723	1.60E+00
Pu-240	1113	9.34E-47	50884	1.59E+00
U-236	1113	2.80E-53	49896	2.17E-03
Th-232	1113	2.79E-62	66947	2.70E-09
Ra-228	1113	1.96E-39	66947	1.27E-07
Ra-226	1113	9.42E-06	2860	2.30E+01
Pb-210	1113	1.71E-08	2891	7.83E-02
Se-79	1113	5.76E-49	34196	3.75E+00
Sn-126	1113	5.19E-81	243947	2.42E-01
Sr-90	1113	2.06E-15	1281	2.54E-15
Tc-99	1113	1.01E+00	6588	3.83E+01
Th-230	1113	7.53E-54	39496	2.32E+00
Ra-226	1113	1.30E-06	3010	4.03E+01
Pb-210	1113	2.34E-09	3043	1.37E-01
Th-232	1113	7.61E-54	39996	3.34E+00
Ra-228	1113	1.75E-25	39596	1.58E+02
U-233	1113	2.43E-51	32996	4.13E+00
Th-229	1113	1.91E-53	34796	3.18E+00

Table 3-18. Peak Aquifer Concentrations and Times - continued

	period1 (0-1112.5 yrs)		period2 (1112.5+ yrs)	
Nuclide	max time1 (years)	max conc1 (pCi/L per Ci buried)	max time2 (years)	max conc2 (pCi/L per Ci buried)
U-234	1113	2.43E-51	32996	4.34E+00
Th-230	1113	1.88E-54	37196	9.21E-01
Ra-226	1113	2.06E-09	34696	5.38E+00
Pb-210	1113	3.67E-12	34696	1.84E-02
U-235	1113	2.44E-51	33096	4.77E+00
Pa-231	1113	7.75E-08	3595	3.99E+00
Ac-227	1113	1.26E-09	3627	9.13E-02
U-236	1113	2.44E-51	33096	4.76E+00
Th-232	1113	1.01E-59	37596	6.15E-06
Ra-228	1113	6.95E-33	37296	2.88E-04
U-238	1113	2.44E-51	33096	4.77E+00
U-234	1113	7.89E-54	33896	4.29E-01
Th-230	1113	5.51E-57	36896	5.31E-02
Ra-226	1113	7.29E-13	41896	3.05E-01
Pb-210	1113	1.29E-15	41896	1.04E-03
Zr-93	1113	1.42E-26	8058	2.07E+01
Nb-93m	1113	2.81E+00	6418	2.02E+03
I-129_H	682	8.81E+00	1984	1.28E+02
I-129_J	682	4.87E+01	1956	3.55E+02

Similar to the vadose zone transport model results, rather than discussing each figure in turn, general points will be presented citing specific examples and any peculiar results. All of the aquifer transport responses mimicked the vadose zone transport results. Plots for the aquifer transport results only cover 30 orders of magnitude rather than the 80 orders of magnitude shown for the vadose zone transport results, so some nuclides with extremely low concentrations do not appear in the aquifer transport plots and the curve shapes are not identical. Because the uncracked and cracked contaminant fluxes were weighted and combined before being fed to the aquifer transport model, the aquifer transport model only has a single set of results to consider.

The same radionuclide groupings based on K_d values for their elements in sand are considered for the aquifer as shown above in Table 3-17. The general behavior for the nuclides with a very low K_d in sand is that they typically are rapidly flushed from the system soon after a major system change. Most of the exodus occurs from 400 to 600 years when new flow fields appear. H-3 disappears earlier due to decay. Nb-94 stays until soon after collapse. Tc-99 remains until after 4700 years, because the gone concrete era is entered at 4689.5 years when the K_d in the vault decreases from 2500 to 0.1 ml/g. Np-237 peaks at 3501 years (versus 2932 years in the vadose zone model) and does not flush rapidly because its K_d in the concrete is 3320 ml/g and that controls until after collapse.

The general behavior based on the K_d in sand is similar to the behavior displayed in the vadose zone. Each nuclide with a low K_d in sand develops its peak concentration more slowly and occurs after 1000 years. The subsequent decline from the peak is at a slower rate than for the very low K_d nuclides.

The general behavior for the nuclides with a high K_d in sand is similar to the behavior displayed in the vadose zone. Each nuclide with a high K_d in sand develops its peak concentration very slowly and typically occurs after 10,000 years, which is followed by a gentle decline. Exceptions occur when the half-life is short and decay forces an earlier peak where the parents typically do not even show on the plot, such as for the following:

- Cm-244 (18.1 year half-life)
- Pu-238 (87.8 year half-life)
- Pu-241 (14.3 year half-life)

Those nuclides with high K_ds that are parents typically produce progeny that also have peaks that occur very late, especially because the parent continues to produce the progeny even while the parent is in transit.

Figure 3-23 shows plan-view contour plots for C-14 in the aquifer at key times. The timing was set to be similar to those in Figure 3-21 for the vadose zone. The aquifer plots show that the concentrations initially are very low and delay until well after 227 years to start approaching the peak values.

In Figure 3-23 two black perimeters appear. The inner perimeter describes the aquifer source cell columns projected down to the horizontal plane that is displayed. The outer perimeter similarly describes the 100-m buffer. Additionally, the pink circle outlined by black indicates the location where the peak occurred for the time plotted.

3.6.6.3 Groundwater Protection

Groundwater protection radionuclide disposal limits for the LAWV were developed using the all-pathways application (Koffman 2006) from the maximum groundwater concentrations per curie of each radionuclide, as calculated using PORFLOW. The disposal limits are determined by calculating the inventory that would cause the peak groundwater concentration to match the groundwater concentration limit, based on the following equations:

$$L_D = CL_{gw} / C_{gw} * I_m \qquad \text{Eq. 3-1}$$

where

L_D is the disposal limit (Ci)
CL_{gw} is the concentration limit for groundwater (pCi/L)
C_{gw} is the peak concentration for groundwater (pCi/L) and
I_m is the modeled inventory (Ci)

Because the modeled inventory was 1 mole, that inventory was first converted to its Ci content.

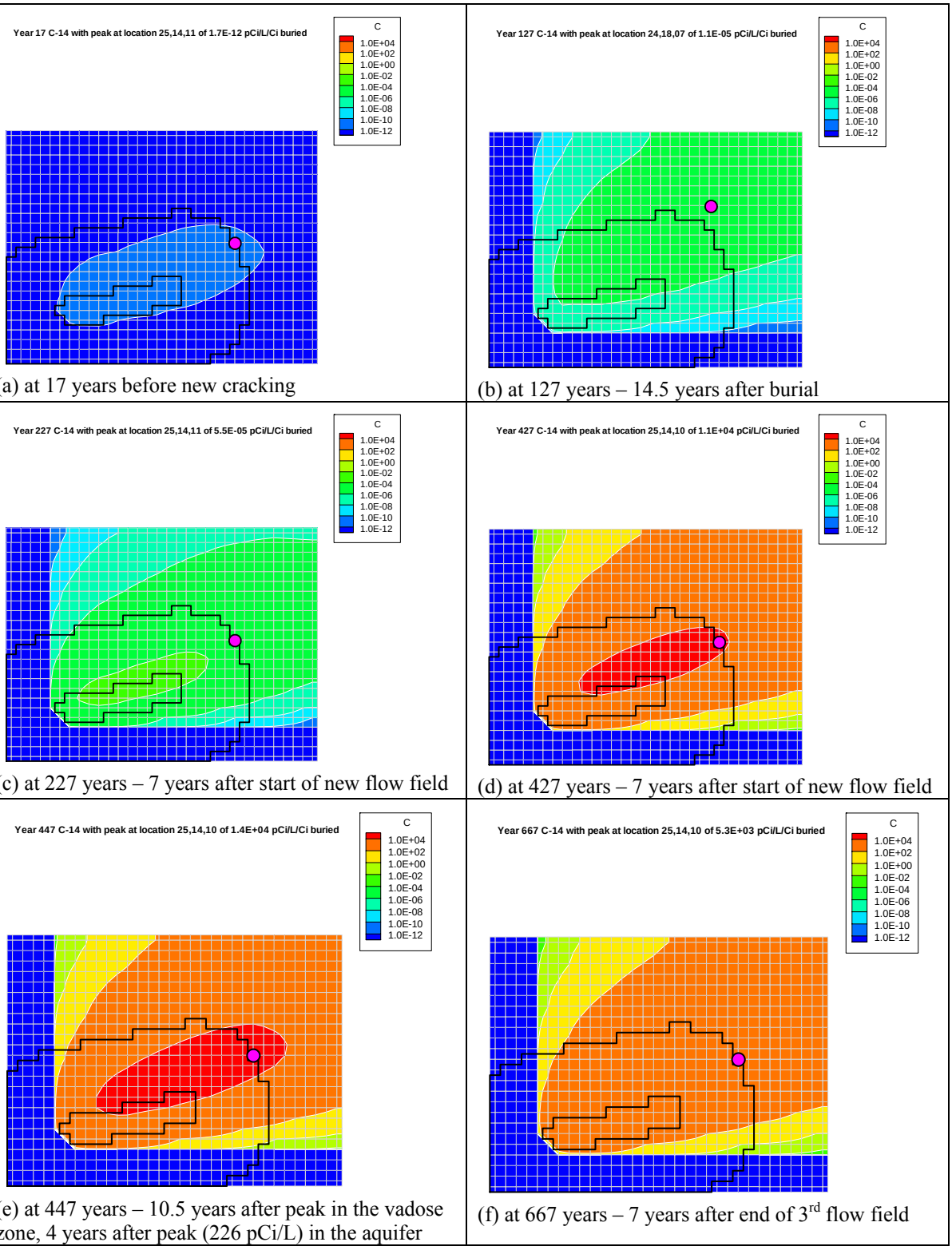

(a) at 17 years before new cracking

(b) at 127 years – 14.5 years after burial

(c) at 227 years – 7 years after start of new flow field

(d) at 427 years – 7 years after start of new flow field

(e) at 447 years – 10.5 years after peak in the vadose zone, 4 years after peak (226 pCi/L) in the aquifer

(f) at 667 years – 7 years after end of 3rd flow field

Figure 3-23. Plan View - Contour Plots for C-14 at a Sequence of Times

The groundwater concentration limits are 4 mrem/yr, 15 pCi/L, 5 pCi/L and 30 μg/L for beta-gamma, gross alpha, radium and uranium, respectively. The disposal limits are shown in Table 3-19.

Radionuclide disposal limits in this section are derived without considering the impact of groundwater contaminant plume interaction with nearby disposal units (e.g., Slit Trenches) and are therefore presented as preliminary information. The results of plume interaction are presented in Chapter 6.0, Integrated Facility Analysis. Final limits will be adjusted as needed to account for plume interaction and the results of sensitivity and/or uncertainty analyses and presented in Chapter 7.0, Integration and Interpretation.

3.6.7 Groundwater Transport Sensitivity Analysis

3.6.7.1 Description of sensitivity cases

Four sensitivity cases were performed for the LAWV groundwater analysis. Those cases covered the following topics:

1. more mobile contaminants
2. absence of CDPs
3. greater diffusion through the vault concrete
4. greater portion of wall length being cracked

No sensitivity cases were conducted at this time that involved changes in flow fields.

Sensitivity Case 1: More mobile contaminants

For this case the distribution coefficient (K_d) for each contaminant was set at a value that was two standard deviations below the base case values. Originally the conservative values from Kaplan's report (Kaplan 2006) were planned to be used. However, some of the values were as much as seven standard deviations below the base case values and extended beyond the realm of typical sensitivity studies. Hence, all K_ds were lowered by subtracting two standard deviations from the base case value. The set of K_ds for the base case and the first two sensitivity cases is provided in Table 3-20 for cementitious materials and in Table 3-21 for sand and clay materials.

Two special waste forms I-129_H (H-Area CG-8 resin) and I-129_J (F-Area filtercake) were included in Table 3-21 only. Their special properties are only applied to the waste form itself, which is assumed to occupy the entire waste zone. Their properties were not assumed to change with time, except that when the concrete entered the gone era (i.e. all cement-like effects ceased to exist), the properties reverted to those specific to the special waste in an acidic environment. This change was invoked because the groundwater is acidic.

Table 3-19. Groundwater Protection Limits for Low-Activity Waste Vault

	Disposal Limits, Ci per Low Activity Waste Vault[1]			
Parent Radionuclide	**Beta-Gamma**	**Gross Alpha**	**Radium**	**Uranium**
Am-241	1.5E+10	7.6E+08	---[2]	1.4E+19
Am-243	3.1E+16	1.7E+16	---	---
C-14	8.8E+00	---	---	---
Cl-36	2.6E+00	---	---	---
Cm-244	---	---	---	---
Cm-245	1.1E+10	5.3E+08	---	1.1E+19
Cm-247	6.5E+17	3.5E+17	---	---
Cm-248	---	---	---	---
H-3	6.3E+08	---	---	---
I-129	4.7E-03	---	---	---
I-129_H	1.1E-01	---	---	---
I-129_J	2.1E-02	---	---	---
K-40	---	---	---	---
Mo-93	3.1E+00	---	---	---
Nb-94	4.8E+01	---	---	---
Ni-59	1.4E+10	---	---	---
Np-237	2.4E+07	1.2E+06	---	2.4E+16
Pd-107	1.7E+12	---	---	---
Pu-238	9.4E+14	6.8E+12	9.1E+12	---
Pu-239	1.3E+15	7.3E+14	---	---
Pu-240	---	---	---	---
Pu-241	4.5E+11	2.2E+10	---	---
Pu-242	---	---	---	---
Pu-244	---	---	---	---
Ra-226	3.9E+07	2.9E+05	3.8E+05	---
Se-79	---	---	---	---
Sn-126	---	---	---	---
Sr-90	3.4E+15	---	---	---
Tc-99	5.2E+02	---	---	---
Th-230	2.8E+08	2.1E+06	2.8E+06	---
Th-232	---	---	---	---
U-233	---	---	---	---
U-234	1.8E+11	1.3E+09	1.7E+09	---
U-235	2.7E+08	1.5E+08	---	---
U-236	---	---	---	---
U-238	5.0E+14	3.6E+12	4.9E+12	---
Zr-93	1.5E+02	---	---	---

[1] Limits calculated per Koffman (2006)
[2] --- means that the calculated limit was ≥ 1E+20 Ci

Table 3-20. Cementitious K_d values for base case and first two sensitivity cases

	CDP[a]			No CDP			CDP -2Sigma		
Element	**Young**	**Middle**	**Old**	**Young**	**Middle**	**Old**	**Young**	**Middle**	**Old**
Ac	245	245	24.5	5000	5000	500	175	175	17.5
Am	245	245	24.5	5000	5000	500	175	175	17.5
C	10	5	0	20	10	0	7.14	3.57	0
Cl	0.8	2	0	0.8	2	0	0.571	1.43	0
Cm	245	245	24.5	5000	5000	500	175	175	17.5
H	0	0	0	0	0	0	0	0	0
I	4	10	0	8	20	0	2.86	7.14	0
K	3.32	6.64	3.32	2	4	2	2.37	4.74	2.37
Mo	0	0	0	0	0	0	0	0	0
Nb	1000	1000	500	1000	1000	500	294	294	357
Ni	1410	1410	705	1000	1000	500	415	415	504
Np	3320	3320	332	2000	2000	200	976	976	237
Pa	3320	3320	332	2000	2000	200	976	976	237
Pb	705	705	352.5	500	500	250	504	504	252
Pd	1410	1410	705	1000	1000	500	415	415	504
Pu	2550	2550	255	5000	5000	500	750	750	182
Ra	189	189	132.3	100	100	70	135	135	94.5
Se	150	150	75	300	300	150	107	107	53.6
Sn	5640	5640	2820	4000	4000	2000	1660	1660	829
Sr	1.89	1.89	1.512	1	1	0.8	1.35	1.35	1.08
Tc	2500	2500	2500	5000	5000	5000	735	735	735
Th	2550	2550	255	5000	5000	500	750	750	182
U	9450	9450	9450	5000	5000	5000	2780	2780	2780
Zr	400	400	40	5000	5000	500	286	286	28.6

[a]The CDP factors are based on an assumption of a pH of 5.5 with organic carbon present at a concentration of 95 mg/L

Table 3-21. Sand and Clay K_d values for base case and first two sensitivity cases

	CDP[a]		No CDP		CDP -2Sigma	
	Sand	Clay	Sand	Clay	Sand	Clay
Ac	53.9	416.5	1100	8500	38.5	298
Am	53.9	416.5	1100	8500	38.5	298
C	0	0	0	0	0	0
Cl	0	0	0	0	0	0
Cm	53.9	416.5	1100	8500	38.5	298
H	0	0	0	0	0	0
I	0	0.3	0	0.6	0	0.214
K	83	415	50	250	59.3	296
Mo	0	0	0	0	0	0
Nb	0	0	0	0	0	0
Ni	9.87	42.3	7	30	7.05	30.2
Np	0.996	58.1	0.6	35	0.711	41.5
Pa	0.996	58.1	0.6	35	0.711	41.5
Pb	2820	7050	2000	5000	829	2070
Pd	9.87	42.3	7	30	7.05	30.2
Pu	137.7	3009	270	5900	98.4	885
Ra	9.45	32.13	5	17	6.75	23
Se	500	500	1000	1000	357	357
Sn	2820	7050	2000	5000	829	2070
Sr	9.45	32.13	5	17	6.75	23
Tc	0.05	0.1	0.1	0.2	0.0357	0.0714
Th	459	1020	900	2000	328	300
U	378	567	200	300	270	405
Zr	72	160	900	2000	51.4	114

	CDP Basecase		**CDP -2Sigma**		**No CDP Basecase**	
	Waste	**Acidic**	**Waste**	**Acidic**	**Waste**	**Acidic**
I-129_H	190	50	35.7	136	380	100
I-129_J	28.35	6.95	4.96	20.3	56.7	13.9

[a]The CDP factors are based on an assumption of a pH of 5.5 with organic carbon present at a concentration of 95 mg/L

Sensitivity Case 2: Absence of Cellulose Degradation Products (CDPs)

For this case the distribution coefficient (K_d) for each contaminant was set at a value that did not include the presence of CDP. Much of the waste in the LAWV likely does not contain CDP, thus the level of CDP assumed (95 mg/L) would not be present throughout the waste. The K_d for the sensitivity case can be calculated from the K_d for the base case by dividing by the CDP factor (f_{CDP}) provided in Table 3-22, which is reproduced from Kaplan (2006). The f_{CDP} values range from 0.049 to 1.89, meaning that the K_ds for the sensitivity case will range from 20.4 times the base case to 0.529 times the base case. The K_d values for this sensitivity case are provided in Table 3-20 and Table 3-21.

Table 3-22. CDP factors from Kaplan 2006

Radionuclides	Analog	f_{CDP} [(a)]
Kr, Ar, Rn, ^{3}H, Nb, Cl,	N/A	N/A
Ac, Am, Bk, Cf Cm, Eu, Gd, Sm	Ce & Eu	0.049
C	None	0.5[(b)]
Cs, Rb , Fr	Cs	1.66
I, At, Se, Te, Tc, Re,	None	0.5[(b)]
Ni	Ni	1.41
Np, Pa	Cs	1.66
Pb, Po	Ni	1.41
Pu	Th	0.51
Sn	Ni	1.41
Sr, Ba, Ra	Sr	1.89
Th	Th	0.51
U	Sr[(c)]	1.89
Zr	Zr	0.08

[(a)] CDP correction Factor at pH 5.5 and 95 mg/L organic C from CDP (defined in Equation 1).
[(b)] Estimated value based on professional opinion. It is believed that these radionuclides would sorb rather weakly (compared to tetravalent or trivalent metals). So a conservative value of 0.5 was selected.
[(c)] U is expected to exist most of the time as UO_2^{2+}, similar to Sr^{2+} (under reducing conditions U exists as U^{4+}).

Sensitivity Case 3: Greater diffusion through the vault concrete

For this case the effective diffusion coefficient of the vault concrete was increased by a factor of three standard deviations, which would allow contaminants to more easily diffuse through the containing vault. The changes in values for this sensitivity case are reflected in Table 3-23. The values in Table 3-23 were obtained from WSRC-STI-2006-00198 (Phifer et al. 2006, Table 6-59). The values used in the calculation were as follows:

Log Nominal = -7.30 (cm^2/s)
Log Mean Maximum (3 sigma) = -7.22 (cm^2/s)
Mean Maximum (3 sigma) = 6.0256E-8 (cm^2/s).

The increased diffusion coefficient was only applied during the time period when cementitious properties were applicable. Afterwards, the vault concrete was assumed to morph into material similar to that of the Upper Vadose Zone and the effective diffusion coefficient (5.3E-6 cm^2/s) for the Upper Vadose Zone was applied

Table 3-23. Sensitivity Case 3: Changes to the effective diffusion coefficient

	Basecase			Sensitivity: Mean +3Sigma	
Concrete State	cm^2/s	cm^2/yr		cm^2/s	cm^2/yr
Start	5.0E-8	1.57788		6.0256E-8	1.90153
Gone	5.3E-6	167.25		5.3E-6	167.25

Sensitivity Case 4: Greater portion of wall length being cracked

As discussed in Section 3.6.4.2, the length of the wall influenced by cracking was assumed to be defined by the base of an isosceles triangle that stood 80 inches tall as shown in the left-hand side of Figure 3-24. For the base case, the unique angle at the top of the triangle was assumed to be 90 degrees, representing spreading along both sides at an angle of 45 degrees from vertical. For the sensitivity cases, the unique top angle was assumed to have a deviation from vertical of 7.5 degrees.

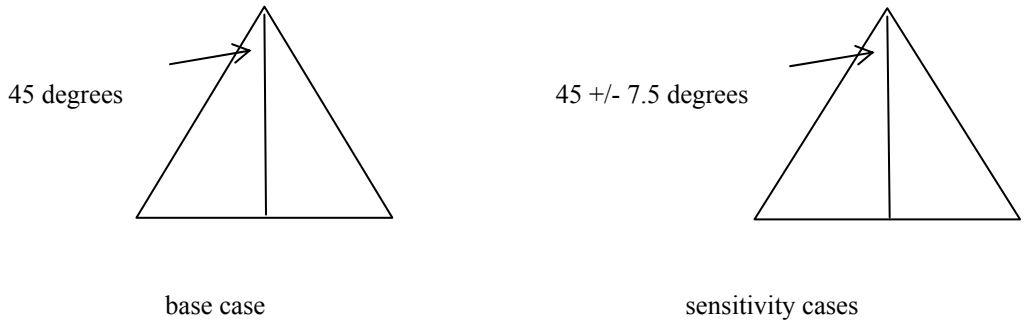

Figure 3-24. Isosceles triangle with base representing wall length of cracked section

The length of the base is calculated as L=2*H*tan(angle), where the angle is ½ of the top angle of the triangle. The wall length of the cracked section is shown in Table 3-24. Based on a total wall length of 214 ft, the fractions of the total wall length assigned to the cracked and intact section are shown in the same table.

Table 3-24. Wall length of cracked section and fractions for cracked and intact sections

description	H (in)	angle (degrees)	1/2 base (in)	base (in)	fraction cracked	fraction intact
basecase	40	45	40	80	0.03115	0.96885
sensitivity1	40	52.5	52.1	104.3	0.04060	0.95940
sensitivity2	40	37.5	30.7	61.4	0.02390	0.97610

3.6.7.2 Results

The ultimate impact of each sensitivity case is determined by the change in the peak of the total dose for the entire decay chain. The inventory limits are simply calculated by dividing the limit for the well dose by the peak total dose for the chain that was evaluated for 1 Ci of the parent.

Intermediate values, such as peak fluxes at the water table or peak well concentrations for individual isotopes and the associated times provide hints and can subsequently be examined to develop explanations of impacts, but the modeling results must be integrated over time and combined with dose conversion factors, before the full impact is realized. Therefore, the results presented in this section are the total dose for each decay chain for the base case and each of the sensitivity cases.

Results are presented for several exposure scenarios as follow:

1. LADTAP
2. Beta-Gamma
3. Gross alpha
4. Radium
5. Uranium

LADTAP stand for "Liquid Annual Doses To All Persons." The original LADTAP performs environmental dose analyses for releases of liquid effluents from light-water nuclear power plants into surface waters during routine operation. The analyses estimate radiation doses to individuals, population groups, and biota from ingestion (aquatic foods, water, and terrestrial irrigated foods) and external exposure (shoreline, swimming, and boating) pathways. The original LADTAP was written by US NRC Radiological Assessment Branch staff, but has been revised for use with the PA (Jannik and Dixon 2006).

LADTAP is executed independently of the PA by applying a unit pCi/L concentration for each parent radionuclide and including the resulting output factors per unit pCi/L in the PA post-processing software used to establish total doses versus time. For the PA, the only exposure pathways from LADTAP that are activated are as follow:

1. water ingestion
2. vegetable consumption
3. milk consumption
4. meat consumption

The pathway from pond water in which fish are raised and recreational activities occur was deactivated.

Tables are provided for the base case and each sensitivity case that show the peak total doses for each of the exposure scenarios listed above (from LADTAP to uranium) as follows:

1. Table 3-25. Base case: total dose by decay chain for multiple exposure scenarios
2. Table 3-26. Sensitivity 1, more mobile contaminants: total dose by decay chain for multiple exposure scenarios
3. Table 3-27. Sensitivity 2, absence of CDP: total dose by decay chain for multiple exposure scenarios
4. Table 3-28. Sensitivity 3, higher diffusion through vault concrete: total dose by decay chain for multiple exposure scenarios
5. Table 3-29. Sensitivity 4, longer wall cracked section: total dose by decay chain for multiple exposure scenarios
6. Table 3-30. Sensitivity 5, shorter wall cracked section: total dose by decay chain for multiple exposure scenarios

Subsequently Table 3-31 compares all the cases for the water ingestion exposure scenario that is represented by the total Beta/Gamma results. Finally Table 3-32 provides the same comparison as Table 3-31, except that the results are relative to the base case results. In Table 3-32 grey highlighted results are greater than base case results; amber highlighted results are greater than base case results by a factor of at least 1,000; and red highlighted results are greater than base case results by a factor of at least 1,000,000.

Table 3-25. Base case: total dose by decay chain for multiple exposure scenarios

	Alpha		Beta/Gamma		LADTAP		Radium		Uranium	
Nuclide	**Year**	**pCi/L**	**Year**	**mrem/yr**	**Year**	**mrem/yr**	**Year**	**pCi/L**	**Year**	**µg/L**
Am-241	1112.5	1.66E-08	1112.5	1.57E-10	1112.5	8.93E-08			1112.5	1.80E-18
Am-243	1112.5	7.21E-16	1112.5	7.27E-17	1112.5	9.59E-15			1112.5	9.48E-39
C-14			443.5	4.35E-01	442.5	2.71E+00				
Cl-36			434.5	1.58E+00	436.5	1.83E+01				
Cm-244	1112.5	7.44E-40	1112.5	1.32E-40	1112.5	4.67E-40	1112.5	1.86E-40	1112.5	3.80E-55
Cm-245	1112.5	2.35E-08	1112.5	2.26E-10	1112.5	1.27E-07			1112.5	2.39E-18
Cm-247	1112.5	3.48E-17	1112.5	3.52E-18	1112.5	4.63E-16			1112.5	1.03E-39
Cm-248	1112.5	7.37E-27	1112.5	1.72E-36	1112.5	1.33E-25	1112.5	1.76E-44	1112.5	1.01E-44
H-3			94.4	4.62E-09	92.4	1.53E-09				
I-129			451.5	8.36E+02	450.5	8.78E+01				
I-129_H			680.5	3.57E+01	681.5	3.64E+00				
I-129_J			680.5	1.98E+02	681.5	2.01E+01				
K-40			1112.5	1.04E-30	1112.5	3.01E-30				
Mo-93			433.5	1.31E+00	435.5	1.69E+00				
Nb-94			1112.5	3.38E-02	1112.5	5.31E-01				
Ni-59			1112.5	1.21E-10	1112.5	4.79E-12				
Np-237	1112.5	1.04E-05	1112.5	8.62E-08	1112.5	5.59E-05			1112.5	1.06E-15
Pd-107			1112.5	9.97E-13	1112.5	3.14E-12				
Pu-238	1112.5	1.56E-12	1112.5	2.12E-15	1112.5	6.64E-13	1112.5	3.89E-13	1112.5	7.40E-58
Pu-239	1112.5	1.69E-14	1112.5	1.57E-15	1112.5	2.24E-13			1112.5	3.74E-54
Pu-240	1112.5	2.89E-37	1112.5	5.15E-38	1112.5	1.82E-37	1112.5	7.23E-38	1112.5	3.45E-54
Pu-241	1112.5	5.65E-10	1112.5	5.33E-12	1112.5	3.04E-09			1112.5	6.13E-20
Pu-242	1112.5	4.59E-20	1112.5	6.15E-23	1112.5	1.96E-20	1112.5	1.15E-20	1112.5	3.90E-54
Pu-244	1112.5	7.84E-39	1112.5	1.39E-39	1112.5	4.92E-39	1112.5	1.96E-39	1112.5	4.33E-55
Ra-226	1112.5	3.77E-05	1112.5	5.23E-08	1112.5	1.61E-05	1112.5	9.42E-06		
Se-79			1112.5	2.63E-51	1112.5	2.17E-50				
Sn-126			1112.5	6.99E-83	1112.5	3.68E-82				
Sr-90			1112.5	1.16E-15	1112.5	3.79E-16				
Tc-99			1112.5	2.88E-03	1112.5	1.87E-02				
Th-230	1112.5	5.21E-06	1112.5	7.18E-09	1112.5	2.22E-06	1112.5	1.30E-06		
Th-232	1112.5	7.01E-25	1112.5	1.26E-25	1112.5	4.40E-25	1112.5	1.75E-25		
U-233	1112.5	9.51E-53	1112.5	3.25E-54	1112.5	9.54E-52			1112.5	2.52E-55
U-234	1112.5	8.24E-09	1112.5	1.13E-11	1112.5	3.51E-09	1112.5	2.06E-09	1112.5	3.91E-55
U-235	1112.5	8.40E-08	1112.5	7.93E-09	1112.5	1.11E-06			1112.5	1.13E-51
U-236	1112.5	2.78E-32	1112.5	4.97E-33	1112.5	1.75E-32	1112.5	6.96E-33	1112.5	3.78E-53
U-238	1112.5	2.92E-12	1112.5	3.95E-15	1112.5	1.24E-12	1112.5	7.29E-13	1112.5	7.27E-51
Zr-93			1112.5	8.48E-03	1112.5	1.18E-02				

Table 3-26. Sensitivity 1, more mobile contaminants: total dose by decay chain for multiple exposure scenarios

	Alpha		Beta/Gamma		LADTAP		Radium		Uranium	
Nuclide	**Year**	**pCi/L**	**Year**	**mrem/yr**	**Year**	**mrem/yr**	**Year**	**pCi/L**	**Year**	**µg/L**
Am-241	1112.5	3.24E-07	1112.5	4.31E-09	1112.5	1.74E-06			1112.5	4.30E-17
Am-243	1112.5	2.43E-14	1112.5	3.97E-15	1112.5	3.21E-13			1112.5	2.65E-34
C-14			441.5	4.69E-01	441.5	2.81E+00				
Cl-36			434.5	1.59E+00	434.5	1.87E+01				
Cm-244	1112.5	6.27E-35	1112.5	1.70E-35	1112.5	3.93E-35	1112.5	1.57E-35	1112.5	1.54E-47
Cm-245	1112.5	3.42E-07	1112.5	4.55E-09	1112.5	1.84E-06			1112.5	4.27E-17
Cm-247	1112.5	7.77E-16	1112.5	1.25E-16	1112.5	1.03E-14			1112.5	2.86E-35
Cm-248	1112.5	1.87E-22	1112.5	6.67E-32	1112.5	3.37E-21	1112.5	4.87E-40	1112.5	2.89E-40
H-3			94.4	4.62E-09	94.4	1.11E-09				
I-129			445.5	9.22E+02	445.5	9.53E+01				
I-129_H			680.5	1.67E+02	680.5	1.72E+01				
I-129_J			447.5	5.22E+02	447.5	5.39E+01				
K-40			1112.5	2.64E-26	1112.5	7.51E-26				
Mo-93			433.5	1.31E+00	433.5	1.71E+00				
Nb-94			1112.5	2.26E-01	1112.5	2.50E+00				
Ni-59			1112.5	5.47E-07	1112.5	1.36E-08				
Np-237	1112.5	1.45E-03	1112.5	1.93E-05	1112.5	7.81E-03			1112.5	1.89E-13
Pd-107			1112.5	4.53E-09	1112.5	8.92E-09				
Pu-238	1112.5	3.03E-10	1112.5	1.50E-12	1112.5	1.31E-10	1112.5	7.57E-11	1112.5	9.67E-49
Pu-239	1112.5	2.54E-12	1112.5	4.25E-13	1112.5	3.35E-11			1112.5	6.00E-45
Pu-240	1112.5	2.46E-32	1112.5	6.67E-33	1112.5	1.55E-32	1112.5	6.16E-33	1112.5	5.53E-45
Pu-241	1112.5	1.07E-08	1112.5	1.43E-10	1112.5	5.78E-08			1112.5	1.43E-18
Pu-242	1112.5	9.47E-18	1112.5	4.61E-20	1112.5	4.10E-18	1112.5	2.36E-18	1112.5	6.26E-45
Pu-244	1112.5	6.42E-34	1112.5	1.74E-34	1112.5	4.08E-34	1112.5	1.60E-34	1112.5	6.93E-46
Ra-226	1112.5	6.57E-03	1112.5	3.35E-05	1112.5	2.85E-03	1112.5	1.64E-03		
Se-79			1112.5	2.43E-46	1112.5	1.44E-45				
Sn-126			1112.5	6.14E-64	1112.5	1.97E-63				
Sr-90			1029.5	1.69E-13	1029.5	5.49E-14				
Tc-99			1112.5	5.30E-02	1112.5	2.21E-01				
Th-230	1112.5	9.55E-04	1112.5	4.82E-06	1112.5	4.13E-04	1112.5	2.38E-04		
Th-232	1112.5	9.84E-20	1112.5	2.66E-20	1112.5	6.17E-20	1112.5	2.46E-20		
U-233	1112.5	2.16E-45	1112.5	1.22E-46	1112.5	2.89E-45			1112.5	2.56E-49
U-234	1112.5	1.57E-06	1112.5	7.85E-09	1112.5	6.80E-07	1112.5	3.92E-07	1112.5	3.97E-49
U-235	1112.5	1.21E-05	1112.5	2.05E-06	1112.5	1.59E-04			1112.5	1.15E-45
U-236	1112.5	2.70E-27	1112.5	7.31E-28	1112.5	1.69E-27	1112.5	6.75E-28	1112.5	3.83E-47
U-238	1112.5	5.78E-10	1112.5	2.85E-12	1112.5	2.50E-10	1112.5	1.44E-10	1112.5	7.37E-45
Zr-93			1112.5	2.11E-02	1112.5	2.21E-02				

Table 3-27. Sensitivity 2, absence of CDP: total dose by decay chain for multiple exposure scenarios

	Alpha		Beta/Gamma		LADTAP		Radium		Uranium	
Nuclide	Year	pCi/L	Year	mrem/yr	Year	mrem/yr	Year	pCi/L	Year	ug/L
Am-241	1112.5	4.41E-08	1112.5	5.87E-10	1112.5	2.37E-07			1112.5	6.93E-18
Am-243	1112.5	3.58E-15	1112.5	2.00E-17	1112.5	5.02E-14			1112.5	3.92E-51
C-14			678.5	3.24E-01	678.5	1.94E+00				
Cl-36			434.5	1.58E+00	434.5	1.86E+01				
Cm-244	1112.5	1.14E-33	1112.5	3.09E-34	1112.5	7.16E-34	1112.5	2.85E-34	1112.5	1.99E-51
Cm-245	1112.5	1.34E-08	1112.5	1.78E-10	1112.5	7.20E-08			1112.5	1.99E-18
Cm-247	1112.5	4.18E-17	1112.5	2.29E-19	1112.5	5.87E-16			1112.5	4.74E-53
Cm-248	1112.5	2.07E-38	1112.5	5.61E-39	1112.5	1.30E-38	1112.5	5.18E-39	1112.5	1.52E-56
H-3			94.4	4.62E-09	94.4	1.11E-09				
I-129			678.5	6.21E+02	678.5	6.42E+01				
I-129_H			680.5	1.76E+01	680.5	1.82E+00				
I-129_J			680.5	1.06E+02	680.5	1.09E+01				
K-40			1112.5	4.24E-24	1112.5	1.21E-23				
Mo-93			433.5	1.31E+00	433.5	1.71E+00				
Nb-94			1112.5	3.38E-02	1112.5	3.73E-01				
Ni-59			1112.5	6.21E-08	1112.5	1.55E-09				
Np-237	1112.5	5.29E-04	1112.5	7.05E-06	1112.5	2.85E-03			1112.5	8.58E-14
Pd-107			1112.5	5.14E-10	1112.5	1.01E-09				
Pu-238	1112.5	1.43E-08	1112.5	2.61E-11	1112.5	6.11E-09	1112.5	3.58E-09	1112.5	2.86E-49
Pu-239	1112.5	8.32E-13	1112.5	4.73E-15	1112.5	1.17E-11			1112.5	7.96E-49
Pu-240	1112.5	4.40E-31	1112.5	1.19E-31	1112.5	2.76E-31	1112.5	1.10E-31	1112.5	7.89E-49
Pu-241	1112.5	1.39E-09	1112.5	1.85E-11	1112.5	7.46E-09			1112.5	2.18E-19
Pu-242	1112.5	4.69E-16	1112.5	8.36E-19	1112.5	2.00E-16	1112.5	1.17E-16	1112.5	8.10E-49
Pu-244	1112.5	1.26E-32	1112.5	3.41E-33	1112.5	7.91E-33	1112.5	3.15E-33	1112.5	1.47E-50
Ra-226	1112.5	2.97E-01	1112.5	5.61E-04	1112.5	1.26E-01	1112.5	7.41E-02		
Se-79			1112.5	1.08E-61	1112.5	6.39E-61				
Sn-126			1112.5	1.51E-77	1112.5	4.84E-77				
Sr-90			958.5	7.93E-12	958.5	2.57E-12				
Tc-99			1112.5	3.88E-04	1112.5	1.62E-03				
Th-230	1112.5	4.38E-02	1112.5	8.16E-05	1112.5	1.87E-02	1112.5	1.09E-02		
Th-232	1112.5	4.38E-19	1112.5	1.18E-19	1112.5	2.74E-19	1112.5	1.09E-19		
U-233	1112.5	1.39E-44	1112.5	7.80E-46	1112.5	2.04E-42			1112.5	5.89E-46
U-234	1112.5	7.35E-05	1112.5	1.35E-07	1112.5	3.13E-05	1112.5	1.84E-05	1112.5	9.14E-46
U-235	1112.5	4.12E-06	1112.5	2.38E-08	1112.5	5.78E-05			1112.5	2.64E-42
U-236	1112.5	3.62E-26	1112.5	9.81E-27	1112.5	2.27E-26	1112.5	9.05E-27	1112.5	8.83E-44
U-238	1112.5	2.78E-08	1112.5	5.03E-11	1112.5	1.18E-08	1112.5	6.95E-09	1112.5	1.70E-41
Zr-93			1112.5	4.49E-06	1112.5	4.71E-06				

Table 3-28. Sensitivity 3, higher diffusion through vault concrete: total dose by decay chain for multiple exposure scenarios

	Alpha		Beta/Gamma		LADTAP		Radium		Uranium	
Nuclide	Year	pCi/L	Year	mrem/yr	Year	mrem/yr	Year	pCi/L	Year	µg/L
Am-241	1112.5	1.17E-08	1112.5	1.57E-10	1112.5	6.32E-08			1112.5	1.26E-18
Am-243	1112.5	4.97E-16	1112.5	7.28E-17	1112.5	6.60E-15			1112.5	6.50E-39
C-14			443.5	4.30E-01	443.5	2.58E+00				
Cl-36			434.5	1.57E+00	434.5	1.85E+01				
Cm-244	1112.5	4.89E-40	1112.5	1.32E-40	1112.5	3.07E-40	1112.5	1.22E-40	1112.5	2.55E-55
Cm-245	1112.5	1.70E-08	1112.5	2.26E-10	1112.5	9.13E-08			1112.5	1.70E-18
Cm-247	1112.5	2.44E-17	1112.5	3.53E-18	1112.5	3.25E-16			1112.5	7.05E-40
Cm-248	1112.5	5.08E-27	1112.5	1.72E-36	1112.5	9.15E-26	1112.5	1.26E-44	1112.5	6.96E-45
H-3			92.4	8.12E-09	92.4	1.95E-09				
I-129			451.5	8.28E+02	451.5	8.56E+01				
I-129_H			680.5	3.57E+01	680.5	3.69E+00				
I-129_J			680.5	1.97E+02	680.5	2.04E+01				
K-40			1112.5	1.04E-30	1112.5	2.96E-30				
Mo-93			433.5	1.31E+00	433.5	1.71E+00				
Nb-94			1112.5	3.33E-02	1112.5	3.67E-01				
Ni-59			1112.5	1.21E-10	1112.5	3.00E-12				
Np-237	1112.5	6.46E-06	1112.5	8.61E-08	1112.5	3.48E-05			1112.5	6.60E-16
Pd-107			1112.5	9.97E-13	1112.5	1.96E-12				
Pu-238	1112.5	1.11E-12	1112.5	2.12E-15	1112.5	4.73E-13	1112.5	2.77E-13	1112.5	4.54E-58
Pu-239	1112.5	1.05E-14	1112.5	1.57E-15	1112.5	1.39E-13			1112.5	2.30E-54
Pu-240	1112.5	1.90E-37	1112.5	5.15E-38	1112.5	1.19E-37	1112.5	4.76E-38	1112.5	2.12E-54
Pu-241	1112.5	4.00E-10	1112.5	5.34E-12	1112.5	2.15E-09			1112.5	4.31E-20
Pu-242	1112.5	3.27E-20	1112.5	6.15E-23	1112.5	1.39E-20	1112.5	8.16E-21	1112.5	2.40E-54
Pu-244	1112.5	5.15E-39	1112.5	1.39E-39	1112.5	3.23E-39	1112.5	1.29E-39	1112.5	2.66E-55
Ra-226	1112.5	2.68E-05	1112.5	5.23E-08	1112.5	1.14E-05	1112.5	6.70E-06		
Se-79			1112.5	2.64E-51	1112.5	1.56E-50				
Sn-126			1112.5	7.00E-83	1112.5	2.24E-82				
Sr-90			1112.5	1.16E-15	1112.5	3.75E-16				
Tc-99			1112.5	2.84E-03	1112.5	1.18E-02				
Th-230	1112.5	3.71E-06	1112.5	7.17E-09	1112.5	1.58E-06	1112.5	9.27E-07		
Th-232	1112.5	4.64E-25	1112.5	1.26E-25	1112.5	2.91E-25	1112.5	1.16E-25		
U-233	1112.5	5.78E-53	1112.5	3.25E-54	1112.5	5.79E-52			1112.5	1.53E-55
U-234	1112.5	5.87E-09	1112.5	1.12E-11	1112.5	2.50E-09	1112.5	1.47E-09	1112.5	2.38E-55
U-235	1112.5	5.22E-08	1112.5	7.93E-09	1112.5	6.93E-07			1112.5	6.86E-52
U-236	1112.5	1.83E-32	1112.5	4.97E-33	1112.5	1.15E-32	1112.5	4.59E-33	1112.5	2.29E-53
U-238	1112.5	2.08E-12	1112.5	3.95E-15	1112.5	8.85E-13	1112.5	5.19E-13	1112.5	4.41E-51
Zr-93			1112.5	8.47E-03	1112.5	8.89E-03				

Table 3-29. Sensitivity 4, longer wall cracked section: total dose by decay chain for multiple exposure scenarios

	Alpha		Beta/Gamma		LADTAP		Radium		Uranium	
Nuclide	Year	pCi/L	Year	mrem/yr	Year	mrem/yr	Year	pCi/L	Year	ug/L
Am-241	1112.5	1.88E-08	1112.5	2.50E-10	1112.5	1.01E-07			1112.5	2.05E-18
Am-243	1112.5	8.32E-16	1112.5	1.22E-16	1112.5	1.11E-14			1112.5	1.21E-38
C-14			442.5	4.51E-01	442.5	2.70E+00				
Cl-36			436.5	1.56E+00	436.5	1.83E+01				
Cm-244	1112.5	9.69E-40	1112.5	2.62E-40	1112.5	6.08E-40	1112.5	2.42E-40	1112.5	4.81E-55
Cm-245	1112.5	2.69E-08	1112.5	3.59E-10	1112.5	1.45E-07			1112.5	2.75E-18
Cm-247	1112.5	4.02E-17	1112.5	5.83E-18	1112.5	5.34E-16			1112.5	1.31E-39
Cm-248	1112.5	9.41E-27	1112.5	3.19E-36	1112.5	1.69E-25	1112.5	2.27E-44	1112.5	1.29E-44
H-3			92.4	6.39E-09	92.4	1.53E-09				
I-129			450.5	8.48E+02	450.5	8.76E+01				
I-129_H			680.5	3.57E+01	680.5	3.69E+00				
I-129_J			680.5	1.97E+02	680.5	2.04E+01				
K-40			1112.5	1.29E-30	1112.5	3.67E-30				
Mo-93			435.5	1.29E+00	435.5	1.68E+00				
Nb-94			1112.5	4.86E-02	1112.5	5.37E-01				
Ni-59			1112.5	2.36E-10	1112.5	5.88E-12				
Np-237	1112.5	1.22E-05	1112.5	1.63E-07	1112.5	6.57E-05			1112.5	1.25E-15
Pd-107			1112.5	1.95E-12	1112.5	3.85E-12				
Pu-238	1112.5	1.86E-12	1112.5	3.56E-15	1112.5	7.93E-13	1112.5	4.65E-13	1112.5	9.55E-58
Pu-239	1112.5	2.03E-14	1112.5	3.05E-15	1112.5	2.70E-13			1112.5	4.84E-54
Pu-240	1112.5	3.77E-37	1112.5	1.02E-37	1112.5	2.36E-37	1112.5	9.42E-38	1112.5	4.46E-54
Pu-241	1112.5	6.39E-10	1112.5	8.52E-12	1112.5	3.44E-09			1112.5	6.97E-20
Pu-242	1112.5	5.58E-20	1112.5	1.05E-22	1112.5	2.38E-20	1112.5	1.39E-20	1112.5	5.05E-54
Pu-244	1112.5	1.02E-38	1112.5	2.77E-39	1112.5	6.41E-39	1112.5	2.55E-39	1112.5	5.60E-55
Ra-226	1112.5	4.37E-05	1112.5	8.55E-08	1112.5	1.86E-05	1112.5	1.09E-05		
Se-79			1112.5	4.66E-51	1112.5	2.76E-50				
Sn-126			1112.5	1.49E-82	1112.5	4.76E-82				
Sr-90			1112.5	1.26E-15	1112.5	4.08E-16				
Tc-99			1112.5	4.55E-03	1112.5	1.90E-02				
Th-230	1112.5	6.11E-06	1112.5	1.19E-08	1112.5	2.61E-06	1112.5	1.53E-06		
Th-232	1112.5	9.12E-25	1112.5	2.47E-25	1112.5	5.72E-25	1112.5	2.28E-25		
U-233	1112.5	1.23E-52	1112.5	6.90E-54	1112.5	1.23E-51			1112.5	3.25E-55
U-234	1112.5	9.79E-09	1112.5	1.88E-11	1112.5	4.17E-09	1112.5	2.45E-09	1112.5	5.04E-55
U-235	1112.5	9.98E-08	1112.5	1.52E-08	1112.5	1.32E-06			1112.5	1.46E-51
U-236	1112.5	3.62E-32	1112.5	9.81E-33	1112.5	2.27E-32	1112.5	9.06E-33	1112.5	4.87E-53
U-238	1112.5	3.51E-12	1112.5	6.68E-15	1112.5	1.49E-12	1112.5	8.76E-13	1112.5	9.37E-51
Zr-93			1112.5	1.15E-02	1112.5	1.21E-02				

Table 3-30. Sensitivity 5, shorter wall cracked section: total dose by decay chain for multiple exposure scenarios

	Alpha		Beta/Gamma		LADTAP		Radium		Uranium	
Nuclide	**Year**	**pCi/L**	**Year**	**mrem/yr**	**Year**	**mrem/yr**	**Year**	**pCi/L**	**Year**	**ug/L**
Am-241	1112.5	1.49E-08	1112.5	1.99E-10	1112.5	8.03E-08			1112.5	1.61E-18
Am-243	1112.5	6.37E-16	1112.5	9.35E-17	1112.5	8.47E-15			1112.5	7.48E-39
C-14			442.5	4.54E-01	442.5	2.72E+00				
Cl-36			436.5	1.56E+00	436.5	1.84E+01				
Cm-244	1112.5	5.72E-40	1112.5	1.55E-40	1112.5	3.59E-40	1112.5	1.43E-40	1112.5	3.03E-55
Cm-245	1112.5	2.09E-08	1112.5	2.79E-10	1112.5	1.12E-07			1112.5	2.11E-18
Cm-247	1112.5	3.06E-17	1112.5	4.44E-18	1112.5	4.08E-16			1112.5	8.11E-40
Cm-248	1112.5	5.81E-27	1112.5	1.97E-36	1112.5	1.05E-25	1112.5	1.37E-44	1112.5	8.02E-45
H-3			92.4	6.39E-09	92.4	1.53E-09				
I-129			450.5	8.51E+02	450.5	8.80E+01				
I-129_H			680.5	3.57E+01	680.5	3.69E+00				
I-129_J			680.5	1.98E+02	680.5	2.04E+01				
K-40			1112.5	8.79E-31	1112.5	2.50E-30				
Mo-93			435.5	1.29E+00	435.5	1.69E+00				
Nb-94			1112.5	4.77E-02	1112.5	5.26E-01				
Ni-59			1112.5	1.59E-10	1112.5	3.95E-12				
Np-237	1112.5	9.00E-06	1112.5	1.20E-07	1112.5	4.84E-05			1112.5	9.21E-16
Pd-107			1112.5	1.31E-12	1112.5	2.59E-12				
Pu-238	1112.5	1.32E-12	1112.5	2.53E-15	1112.5	5.64E-13	1112.5	3.31E-13	1112.5	5.74E-58
Pu-239	1112.5	1.42E-14	1112.5	2.14E-15	1112.5	1.89E-13			1112.5	2.90E-54
Pu-240	1112.5	2.22E-37	1112.5	6.02E-38	1112.5	1.40E-37	1112.5	5.56E-38	1112.5	2.67E-54
Pu-241	1112.5	5.08E-10	1112.5	6.77E-12	1112.5	2.73E-09			1112.5	5.48E-20
Pu-242	1112.5	3.84E-20	1112.5	7.23E-23	1112.5	1.63E-20	1112.5	9.58E-21	1112.5	3.03E-54
Pu-244	1112.5	6.03E-39	1112.5	1.63E-39	1112.5	3.78E-39	1112.5	1.51E-39	1112.5	3.36E-55
Ra-226	1112.5	3.31E-05	1112.5	6.46E-08	1112.5	1.41E-05	1112.5	8.27E-06		
Se-79			1112.5	2.89E-51	1112.5	1.71E-50				
Sn-126			1112.5	8.89E-83	1112.5	2.85E-82				
Sr-90			1112.5	1.10E-15	1112.5	3.56E-16				
Tc-99			1112.5	4.42E-03	1112.5	1.84E-02				
Th-230	1112.5	4.52E-06	1112.5	8.74E-09	1112.5	1.93E-06	1112.5	1.13E-06		
Th-232	1112.5	5.39E-25	1112.5	1.46E-25	1112.5	3.38E-25	1112.5	1.35E-25		
U-233	1112.5	7.41E-53	1112.5	4.17E-54	1112.5	7.43E-52			1112.5	1.96E-55
U-234	1112.5	7.05E-09	1112.5	1.35E-11	1112.5	3.00E-09	1112.5	1.76E-09	1112.5	3.04E-55
U-235	1112.5	7.18E-08	1112.5	1.09E-08	1112.5	9.53E-07			1112.5	8.80E-52
U-236	1112.5	2.14E-32	1112.5	5.79E-33	1112.5	1.34E-32	1112.5	5.35E-33	1112.5	2.94E-53
U-238	1112.5	2.47E-12	1112.5	4.69E-15	1112.5	1.05E-12	1112.5	6.16E-13	1112.5	5.65E-51
Zr-93			1112.5	1.10E-02	1112.5	1.16E-02				

Table 3-31. Sensitivity comparison: total dose by decay chain for water ingestion (beta/gamma)

	Cdp		Cdp-2Sigma		Cdp+3SigmaDe		CdpCrackNarrow		CdpCrackWide		CdpOff	
Nuclide	**Year**	**mrem/yr**	**Year**	**mrem/yr**	**Year**	**mrem/yr**	**Year**	**mrem/yr**	**Year**	**mrem/yr**	**Year**	**mrem/yr**
Am-241	1112.5	1.57E-10	1112.5	4.31E-09	1112.5	1.57E-10	1112.5	1.99E-10	1112.5	2.50E-10	1112.5	5.87E-10
Am-243	1112.5	7.27E-17	1112.5	3.97E-15	1112.5	7.28E-17	1112.5	9.35E-17	1112.5	1.22E-16	1112.5	2.00E-17
C-14	443.5	4.35E-01	441.5	4.69E-01	443.5	4.30E-01	442.5	4.54E-01	442.5	4.51E-01	678.5	3.24E-01
Cl-36	434.5	1.58E+00	434.5	1.59E+00	434.5	1.57E+00	436.5	1.56E+00	436.5	1.56E+00	434.5	1.58E+00
Cm-244	1112.5	1.32E-40	1112.5	1.70E-35	1112.5	1.32E-40	1112.5	1.55E-40	1112.5	2.62E-40	1112.5	3.09E-34
Cm-245	1112.5	2.26E-10	1112.5	4.55E-09	1112.5	2.26E-10	1112.5	2.79E-10	1112.5	3.59E-10	1112.5	1.78E-10
Cm-247	1112.5	3.52E-18	1112.5	1.25E-16	1112.5	3.53E-18	1112.5	4.44E-18	1112.5	5.83E-18	1112.5	2.29E-19
Cm-248	1112.5	1.72E-36	1112.5	6.67E-32	1112.5	1.72E-36	1112.5	1.97E-36	1112.5	3.19E-36	1112.5	5.61E-39
H-3	94.4	4.62E-09	94.4	4.62E-09	92.4	8.12E-09	92.4	6.39E-09	92.4	6.39E-09	94.4	4.62E-09
I-129	451.5	8.36E+02	445.5	9.22E+02	451.5	8.28E+02	450.5	8.51E+02	450.5	8.48E+02	678.5	6.21E+02
I-129_H	680.5	3.57E+01	680.5	1.67E+02	680.5	3.57E+01	680.5	3.57E+01	680.5	3.57E+01	680.5	1.76E+01
I-129_J	680.5	1.98E+02	447.5	5.22E+02	680.5	1.97E+02	680.5	1.98E+02	680.5	1.97E+02	680.5	1.06E+02
K-40	1112.5	1.04E-30	1112.5	2.64E-26	1112.5	1.04E-30	1112.5	8.79E-31	1112.5	1.29E-30	1112.5	4.24E-24
Mo-93	433.5	1.31E+00	433.5	1.31E+00	433.5	1.31E+00	435.5	1.29E+00	435.5	1.29E+00	433.5	1.31E+00
Nb-94	1112.5	3.38E-02	1112.5	2.26E-01	1112.5	3.33E-02	1112.5	4.77E-02	1112.5	4.86E-02	1112.5	3.38E-02
Ni-59	1112.5	1.21E-10	1112.5	5.47E-07	1112.5	1.21E-10	1112.5	1.59E-10	1112.5	2.36E-10	1112.5	6.21E-08
Np-237	1112.5	8.62E-08	1112.5	1.93E-05	1112.5	8.61E-08	1112.5	1.20E-07	1112.5	1.63E-07	1112.5	7.05E-06
Pd-107	1112.5	9.97E-13	1112.5	4.53E-09	1112.5	9.97E-13	1112.5	1.31E-12	1112.5	1.95E-12	1112.5	5.14E-10
Pu-238	1112.5	2.12E-15	1112.5	1.50E-12	1112.5	2.12E-15	1112.5	2.53E-15	1112.5	3.56E-15	1112.5	2.61E-11
Pu-239	1112.5	1.57E-15	1112.5	4.25E-13	1112.5	1.57E-15	1112.5	2.14E-15	1112.5	3.05E-15	1112.5	4.73E-15
Pu-240	1112.5	5.15E-38	1112.5	6.67E-33	1112.5	5.15E-38	1112.5	6.02E-38	1112.5	1.02E-37	1112.5	1.19E-31
Pu-241	1112.5	5.33E-12	1112.5	1.43E-10	1112.5	5.34E-12	1112.5	6.77E-12	1112.5	8.52E-12	1112.5	1.85E-11
Pu-242	1112.5	6.15E-23	1112.5	4.61E-20	1112.5	6.15E-23	1112.5	7.23E-23	1112.5	1.05E-22	1112.5	8.36E-19
Pu-244	1112.5	1.39E-39	1112.5	1.74E-34	1112.5	1.39E-39	1112.5	1.63E-39	1112.5	2.77E-39	1112.5	3.41E-33
Ra-226	1112.5	5.23E-08	1112.5	3.35E-05	1112.5	5.23E-08	1112.5	6.46E-08	1112.5	8.55E-08	1112.5	5.61E-04
Se-79	1112.5	2.63E-51	1112.5	2.43E-46	1112.5	2.64E-51	1112.5	2.89E-51	1112.5	4.66E-51	1112.5	1.08E-61
Sn-126	1112.5	6.99E-83	1112.5	6.14E-64	1112.5	7.00E-83	1112.5	8.89E-83	1112.5	1.49E-82	1112.5	1.51E-77
Sr-90	1112.5	1.16E-15	1029.5	1.69E-13	1112.5	1.16E-15	1112.5	1.10E-15	1112.5	1.26E-15	958.5	7.93E-12

Table 3-31. Sensitivity comparison: total dose by decay chain for water ingestion (beta/gamma) - continued

	Cdp		Cdp-2Sigma		Cdp+3SigmaDe		CdpCrackNarrow		CdpCrackWide		CdpOff	
Nuclide	**Year**	**mrem/yr**	**Year**	**mrem/yr**	**Year**	**mrem/yr**	**Year**	**mrem/yr**	**Year**	**mrem/yr**	**Year**	**mrem/yr**
Tc-99	1112.5	2.88E-03	1112.5	5.30E-02	1112.5	2.84E-03	1112.5	4.42E-03	1112.5	4.55E-03	1112.5	3.88E-04
Th-230	1112.5	7.18E-09	1112.5	4.82E-06	1112.5	7.17E-09	1112.5	8.74E-09	1112.5	1.19E-08	1112.5	8.16E-05
Th-232	1112.5	1.26E-25	1112.5	2.66E-20	1112.5	1.26E-25	1112.5	1.46E-25	1112.5	2.47E-25	1112.5	1.18E-19
U-233	1112.5	3.25E-54	1112.5	1.22E-46	1112.5	3.25E-54	1112.5	4.17E-54	1112.5	6.90E-54	1112.5	7.80E-46
U-234	1112.5	1.13E-11	1112.5	7.85E-09	1112.5	1.12E-11	1112.5	1.35E-11	1112.5	1.88E-11	1112.5	1.35E-07
U-235	1112.5	7.93E-09	1112.5	2.05E-06	1112.5	7.93E-09	1112.5	1.09E-08	1112.5	1.52E-08	1112.5	2.38E-08
U-236	1112.5	4.97E-33	1112.5	7.31E-28	1112.5	4.97E-33	1112.5	5.79E-33	1112.5	9.81E-33	1112.5	9.81E-27
U-238	1112.5	3.95E-15	1112.5	2.85E-12	1112.5	3.95E-15	1112.5	4.69E-15	1112.5	6.68E-15	1112.5	5.03E-11
Zr-93	1112.5	8.48E-03	1112.5	2.11E-02	1112.5	8.47E-03	1112.5	1.10E-02	1112.5	1.15E-02	1112.5	4.49E-06

Table 3-32. Sensitivity comparison: relative total dose by decay chain for water ingestion (beta/gamma)

	Cdp		Cdp-2Sigma		Cdp+3SigmaDe		CdpCrackNarrow		CdpCrackWide		CdpOff	
Nuclide	**Year**	**rel. dose**	**Year**	**rel. dose**	**Year**	**rel. dose**	**Year**	**rel. dose**	**Year**	**rel. dose**	**Year**	**rel. dose**
Am-241	1112.5	1.00E+00	1112.5	2.76E+01	1112.5	1.00E+00	1112.5	1.27E+00	1112.5	1.60E+00	1112.5	3.75E+00
Am-243	1112.5	1.00E+00	1112.5	5.46E+01	1112.5	1.00E+00	1112.5	1.29E+00	1112.5	1.68E+00	1112.5	2.75E-01
C-14	443.5	1.00E+00	441.5	1.08E+00	443.5	9.89E-01	442.5	1.04E+00	442.5	1.04E+00	678.5	7.45E-01
Cl-36	434.5	1.00E+00	434.5	1.00E+00	434.5	9.95E-01	436.5	9.88E-01	436.5	9.88E-01	434.5	1.00E+00
Cm-244	1112.5	1.00E+00	1112.5	1.28E+05	1112.5	9.97E-01	1112.5	1.17E+00	1112.5	1.98E+00	1112.5	2.33E+06
Cm-245	1112.5	1.00E+00	1112.5	2.02E+01	1112.5	1.00E+00	1112.5	1.23E+00	1112.5	1.59E+00	1112.5	7.87E-01
Cm-247	1112.5	1.00E+00	1112.5	3.54E+01	1112.5	1.00E+00	1112.5	1.26E+00	1112.5	1.65E+00	1112.5	6.50E-02
Cm-248	1112.5	1.00E+00	1112.5	3.89E+04	1112.5	1.00E+00	1112.5	1.15E+00	1112.5	1.86E+00	1112.5	3.27E-03
H-3	94.4	1.00E+00	94.4	1.00E+00	92.4	1.76E+00	92.4	1.38E+00	92.4	1.38E+00	94.4	1.00E+00
I-129	451.5	1.00E+00	445.5	1.10E+00	451.5	9.91E-01	450.5	1.02E+00	450.5	1.01E+00	678.5	7.43E-01
I-129_H	680.5	1.00E+00	680.5	4.66E+00	680.5	1.00E+00	680.5	1.00E+00	680.5	1.00E+00	680.5	4.93E-01
I-129_J	680.5	1.00E+00	447.5	2.64E+00	680.5	9.97E-01	680.5	1.00E+00	680.5	9.97E-01	680.5	5.37E-01
K-40	1112.5	1.00E+00	1112.5	2.54E+04	1112.5	1.00E+00	1112.5	8.48E-01	1112.5	1.24E+00	1112.5	4.09E+06
Mo-93	433.5	1.00E+00	433.5	1.00E+00	433.5	1.00E+00	435.5	9.84E-01	435.5	9.84E-01	433.5	1.00E+00
Nb-94	1112.5	1.00E+00	1112.5	6.70E+00	1112.5	9.85E-01	1112.5	1.41E+00	1112.5	1.44E+00	1112.5	1.00E+00
Ni-59	1112.5	1.00E+00	1112.5	4.54E+03	1112.5	1.00E+00	1112.5	1.32E+00	1112.5	1.96E+00	1112.5	5.15E+02
Np-237	1112.5	1.00E+00	1112.5	2.25E+02	1112.5	9.99E-01	1112.5	1.39E+00	1112.5	1.89E+00	1112.5	8.18E+01
Pd-107	1112.5	1.00E+00	1112.5	4.54E+03	1112.5	1.00E+00	1112.5	1.31E+00	1112.5	1.96E+00	1112.5	5.15E+02
Pu-238	1112.5	1.00E+00	1112.5	7.10E+02	1112.5	1.00E+00	1112.5	1.19E+00	1112.5	1.68E+00	1112.5	1.23E+04
Pu-239	1112.5	1.00E+00	1112.5	2.70E+02	1112.5	9.98E-01	1112.5	1.36E+00	1112.5	1.94E+00	1112.5	3.01E+00
Pu-240	1112.5	1.00E+00	1112.5	1.29E+05	1112.5	9.99E-01	1112.5	1.17E+00	1112.5	1.98E+00	1112.5	2.31E+06
Pu-241	1112.5	1.00E+00	1112.5	2.68E+01	1112.5	1.00E+00	1112.5	1.27E+00	1112.5	1.60E+00	1112.5	3.47E+00
Pu-242	1112.5	1.00E+00	1112.5	7.50E+02	1112.5	1.00E+00	1112.5	1.18E+00	1112.5	1.71E+00	1112.5	1.36E+04
Pu-244	1112.5	1.00E+00	1112.5	1.24E+05	1112.5	9.97E-01	1112.5	1.17E+00	1112.5	1.99E+00	1112.5	2.45E+06
Ra-226	1112.5	1.00E+00	1112.5	6.40E+02	1112.5	1.00E+00	1112.5	1.24E+00	1112.5	1.64E+00	1112.5	1.07E+04
Se-79	1112.5	1.00E+00	1112.5	9.23E+04	1112.5	1.00E+00	1112.5	1.10E+00	1112.5	1.77E+00	1112.5	4.10E-11
Sn-126	1112.5	1.00E+00	1112.5	8.78E+18	1112.5	1.00E+00	1112.5	1.27E+00	1112.5	2.13E+00	1112.5	2.16E+05
Sr-90	1112.5	1.00E+00	1056.5	1.46E+02	1112.5	1.00E+00	1112.5	9.50E-01	1112.5	1.09E+00	958.5	6.85E+03

Table 3-32. Sensitivity comparison: relative total dose by decay chain for water ingestion (beta/gamma) - continued

	Cdp		Cdp-2Sigma		Cdp+3SigmaDe		CdpCrackNarrow		CdpCrackWide		CdpOff	
Nuclide	**Year**	**rel. dose**	**Year**	**rel. dose**	**Year**	**rel. dose**	**Year**	**rel. dose**	**Year**	**rel. dose**	**Year**	**rel. dose**
Tc-99	1112.5	1.00E+00	1112.5	1.84E+01	1112.5	9.85E-01	1112.5	1.53E+00	1112.5	1.58E+00	1112.5	1.35E-01
Th-230	1112.5	1.00E+00	1112.5	6.72E+02	1112.5	9.99E-01	1112.5	1.22E+00	1112.5	1.66E+00	1112.5	1.14E+04
Th-232	1112.5	1.00E+00	1112.5	2.12E+05	1112.5	1.00E+00	1112.5	1.16E+00	1112.5	1.97E+00	1112.5	9.40E+05
U-233	1112.5	1.00E+00	1112.5	3.75E+07	1112.5	1.00E+00	1112.5	1.28E+00	1112.5	2.12E+00	1112.5	2.40E+08
U-234	1112.5	1.00E+00	1112.5	6.97E+02	1112.5	9.95E-01	1112.5	1.20E+00	1112.5	1.67E+00	1112.5	1.20E+04
U-235	1112.5	1.00E+00	1112.5	2.58E+02	1112.5	1.00E+00	1112.5	1.37E+00	1112.5	1.92E+00	1112.5	3.00E+00
U-236	1112.5	1.00E+00	1112.5	1.47E+05	1112.5	1.00E+00	1112.5	1.17E+00	1112.5	1.98E+00	1112.5	1.98E+06
U-238	1112.5	1.00E+00	1112.5	7.22E+02	1112.5	1.00E+00	1112.5	1.19E+00	1112.5	1.69E+00	1112.5	1.27E+04
Zr-93	1112.5	1.00E+00	1112.5	2.48E+00	1112.5	9.99E-01	1112.5	1.30E+00	1112.5	1.36E+00	1112.5	5.29E-04

3.6.7.3 Discussion

The first part of the discussion is restricted to examining results on a parent-by-parent basis only for the base case. The second part of the discussion provides a comparison of water ingestion results among all the sensitivity cases and the base case. This discussion section is not intended to be exhaustive, but to focus on presenting a general overall understanding, then specifically discussing extreme results and presenting additional subject material as needed.

1. Base case alpha

For the alpha analysis, all chains that produce alpha emissions are included. The sum of the alpha concentrations for all isotopes in the chain is evaluated over time and the peak is reported for each sensitivity case. For the base case Np-237 and Ra-226 produce the highest alpha concentrations (1.04E-5 pCi/L and 3.77E-5 pCi/L, respectively) if the initial inventory is 1 Ci of the parent. Np-237 has a K_d (see Table 3-21) of about 1 ml/g in sand, thus it is highly mobile which helps explain its high alpha concentration. Ra-226 has a relatively low K_d of about 9 ml/g in sand, which in combination with a lower half-life (1600 years) relative to Np-237 (2.15E6 years) produces and even higher alpha concentration.

All peak alpha concentrations occur at 1112.5 years, the end of the time of compliance, indicating that they are all rising and their global peaks will occur later in time.

2. Base case water ingestion

For the water ingestion analysis, the beta/gamma contribution for each radionuclide chain is summed for all isotopes in the chain and the peak sum is presented in the tables. All chains produce beta/gamma contributions. The biggest beta/gamma doses based on an initial inventory of 1 Ci occur for the following parents:

Parent	Peak dose (mrem/yr)
I-129	8.36E+02
I-129_J	1.98E+02
I-129_H	3.6E+01
Mo-93	1.3E+00
C-14	4.0E-02

I-129 is not retarded in sand which produces a high peak dose. The two special waste forms of I-129 have waste zone K_ds of 28 ml/g (I-129_J) and 190 ml/g (I-129_H), but once they have escaped the waste zone, they move rapidly producing relatively high doses.

Mo-93 and C-14 are also not retarded in the sand, with long half-lives as shown.

Parent	Half-life (years)
I-129	1.57E+07
Mo-93	4.0E+03
C-14	5.73E+03

However, the dose conversion factor for I-129 is about 2000 times that for C-14 and about 4000 times that for Mo-93, which explains the relative differences in their results. Mo not being retarded anywhere, while C-14 has a K_d of 10 ml/g in the young concrete which slows its migration and reduces its peak beta/gamma dose.

All peak beta/gamma doses for nuclides other than the highly mobile parents occur at 1112.5 years, the end of the time of compliance, indicating that they are all rising and their global peaks will occur later in time.

3. Base case LADTAP

The relative LADTAP results are similar to those for the Water Ingestion results, except that Cl-36 appears near the top of the list.

Parent	Peak dose (mrem/yr)
I-129	8.78E+01
I-129_J	2.01E+01
Cl-36	1.83E+01
I-129_H	3.64E+00
C-14	2.71E+00
Mo-93	1.69E+00

Cl-36 is not retarded in sand and has a very low K_d of 0.8 ml/g in young concrete that increases to 2 ml/g for middle-aged concrete. The Cl-36 dose from consuming vegetables, milk and meat that are produced from contaminated irrigation water drive its Ladtap results.

All peak LADTAP doses for nuclides other than the highly mobile parents occur at 1112.5 years, the end of the time of compliance, indicating that they are all rising and their global peaks will occur later in time.

4. Base case radium

The radium analysis only considers Ra-226 and Ra-228. The two parents with the highest peak radium concentrations are Ra-226 and Th-230, its precursor. Th-232 and Ra-228 are not high-performance parents because of their half-lives as follows:

Parent	Half-life (years)
Th-230	7.55E+04
Ra-226	1.6E+03
Th-232	1.4E+10
Ra-228	5.74E+00

Th-232 produces smaller quantities of Ra-228 relative to Th-230 producing Ra-226. The half-life of Ra-228 is so short that as a parent, most of it decays before reaching the hypothetical well.

All peak radium concentrations for parents occur at 1112.5 years, the end of the time of compliance, indicating that they are all rising and their global peaks will occur later in time.

5. Base case uranium

The three top producers of U mass concentrations are as follows:

Parent	Peak mass concentration (µg/L)
Np-237	1.1E-15
Cm-245	2.4E-18
Am-241	1.8E-18

All of these chains produce U-233. However, U-233 as a parent does not appear on the list above. The reason is that U-233 is highly retarded with a K_d of 378 ml/g in sand, while Np-237, its precursor, is highly mobile in sand with a K_d of 1 ml/g. The Np-237 is rapidly transported to a location near the well, where it decays to produce the U-233 at the well, whereas U-233 by itself barely reaches the well.

All peak uranium mass concentrations for parents occur at 1112.5 years, the end of the time of compliance, indicating that they are all rising and their global peaks will occur later in time.

6. Water ingestion results among all cases

Water ingestion results are presented in terms of beta/gamma doses for the base case (CDP) and all the sensitivity cases. The first major observation is that the biggest sensitivities occur when the K_ds are reduced by two standard deviations (CDP-2Sigma) and when no CDP is present (CDPOff). The sensitivity cases of lesser importance will be discussed first.

a) Increased diffusion coefficient for vault concrete (CDP+3SigmaDe)
Increasing the diffusion coefficient has minimal impact, except for H-3, which increased by a factor of 1.76 (76%) versus the base case. No other peak beta/gamma dose increased by even 1%. Apparently, the small rate of increase in the diffusion coefficient from 1.58 cm^2/yr to 1.90 cm^2/yr was less important than other effects, such as the effects of cracks, except for H-3. H-3 has a short half-life of 12.3 years, which means that enhanced releases will be more important than for other nuclides that tend to survive longer when later increases in cracking may be more important.

b) Reducing the length of wall that is assumed to be cracked (CdpCrackNarrow)
Reducing the length of wall that is assumed to be cracked produced peak doses that were mainly less than those for the base case as was expected. Four parents exhibited increased peak doses that were no more than 4 percent higher than for the base case. Those parents included C-14 and I-129 with its special waste forms. These results indicate that the cracked section is slightly less important than the "intact" section for these four parents. Although the specific cause is unknown, the small change does not warrant further investigation.

c) Increasing the length of wall that is assumed to be cracked (CDPCrackWide)
Increasing the length of wall that is assumed to be cracked produced peak doses that mainly were greater than those for the base case as was expected. Four parents produced slightly lower peak doses that did not decrease by more than 2 percent. Those parents exhibiting the highest increased peak doses (about 100 to 110 percent) are as follows:

- Cm-244
- Pu-240
- Pu-244
- Sn-126
- Th-232
- U-233
- U-236.

These parents also exhibited the highest decrease in peak doses when the length of the cracked section was decreased (CdpCrackNarrow). The parents share a common portion of an abbreviated decay chain (except for Sn-126 and U-233) as follows:

Cm-244 → Pu-240 → U-236 → Th-232 → Ra-228
Pu-244 → Pu-240 → U-236 → Th-232 → Ra-228.

The last two isotopes in common have two key properties as follow:

Isotope	K_d in sand with CDP (ml/g)	Half-life (years)
Th-232	459	1.405+E10
Ra-228	9.45	5.74E+00

Apparently for the cracked section, the Ra-228 escapes faster (versus the "intact" section) and has a relatively high mobility that combined with a sufficiently long half-life can reach the 100-m well before decaying away.

Sn-126 has a very high K_d of 2820 ml/g, which produces a peak total dose of only 1.49E-82 mrem/yr at 1112.5 years. Therefore, even though it displays a high relative increase in dose, the absolute dose is tiny and does not warrant further investigation.

U-233 is similar to Sn-126 in that U-233 and its progeny Th-229 have high K_ds of 378 ml/g and 459 ml/g, respectively. U-233 produces a peak total dose of only 6.90E-54 mrem/yr at 1112.5 years. Therefore, even though it displays a high relative increase in dose, the absolute dose is tiny and does not warrant further investigation.

d) Decreased distribution coefficient (Cdp-2Sigma)
Decreasing the distribution coefficient significantly increased the peak beta/gamma dose, with one increase by a factor of 3.75E7 (U-233) and another by a factor of 8.78E18 (Sn-126). However, both of those increases only produce tiny peak total doses of 1.22E-46 mrem/yr and 6.14E-64 mrem/yr for U-233 and Sn-126, respectively and do not warrant further investigation. Two of the parents that increase the peak dose by a factor of more than 1000 and that produce appreciable doses are as follow:

- Ni-59 with an increase factor of 4.54E3 and a total peak dose of 5.47E-7 mrem/yr
- Pd-107 with an increase factor of 4.54E3 and a total peak dose of 4.53E-9 mrem/yr

Both of these nuclides share the same K_d factors for all materials, so the same relative change in the peak dose for the sensitivity case is expected. For explanation, only results for Ni-59 need to be examined. A plot comparing well concentration results for Ni-59 versus its base case is presented in Figure 3-25. While the peak concentrations are similar over 10,000 years, imposing a 1000-year time-of-compliance (indicated by the vertical green line) significantly changes the peak during the shorter duration.

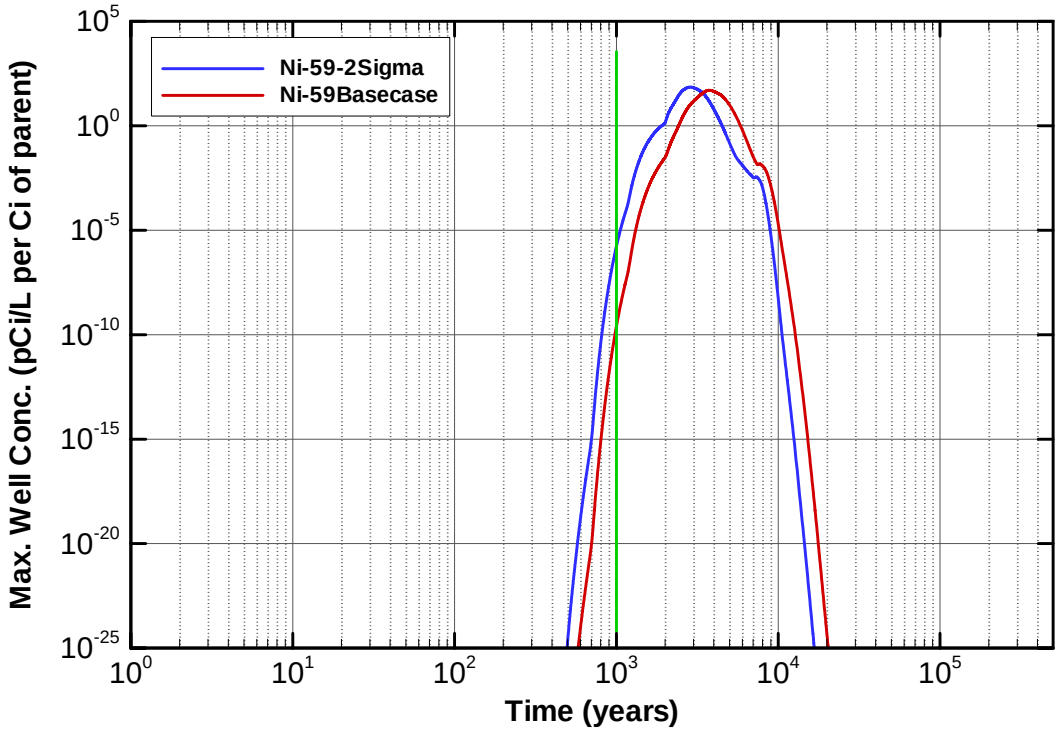

Figure 3-25. Comparison of Ni-59 for increased mobility versus base case

e) Absence of CDP (CdpOff)
When the case with no CDP is analyzed, wide swings in results occur. The maximum increase is by a factor of 2.40E8 for U-233, while the maximum decrease is by a factor of 4.10E-11 for Se-79.

The largest increases by a factor of more than 1E6 still only produce tiny total doses with the greatest change producing the lowest factor of 4E-24 for K-40. A set of five parents have increases by a factor of more than 1000 and a significant total dose as follows:

1.	Pu-238	1.23E4	2.61E-11
2.	Sr-90	6.85E3	7.93E-12
3.	Th-230	1.14E4	8.16E-5
4.	U-234	1.20E4	1.35E-7
5.	U-238	1.27E4	5.03E-11.

Examining the decay chains four of the five parents share common elements as follows:

Pu-238 → U-234 → Th-230 → Ra-226 → Pb-210
U-238 → U-234 → Th-230 → Ra-226 → Pb-210

Examining Th-230 (which also had the largest relative change) will shed some light on four of these parents, while Sr-90 needs to be examined independently. For Th-230, by the end of the 1000-year time-of-compliance, only the daughters (Ra-226 and Pb-210) have reached the well at any significant level (see Figure 3-26). The K_d values in sand for the sensitivity case and the base case are as follows:

Isotope	Basecase	No Cdp
Th-230	459	900
Ra-226	9.45	5
Pb-210	2820	2000

Even though the Th-230 is more retarded when no CDP is present, the daughters are more mobile when no CDP is present, with Ra-226 moving almost twice as fast as for the base case, which results in the significantly higher doses when the 1000-year time of compliance is enforced.

Sr-90 is not modeled with any daughters, so only its own K_d is important. That K_d is 9.45 for the base case but reduces to 5 when CDP is not present. The lower K_d for the non-CDP case creates a peak at 959 years, while the base case does not peak until 1281 years, thus the time-of-compliance at 1000 years magnifies the relative differences (Figure 3-27).

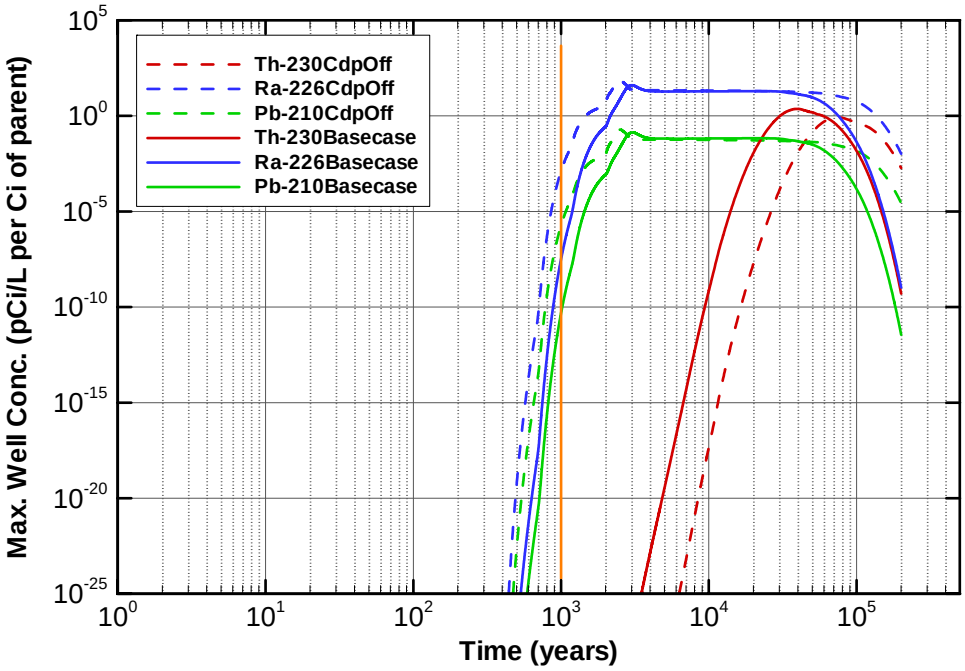

Figure 3-26. Comparison of Th-230 for absence of CDP versus base case

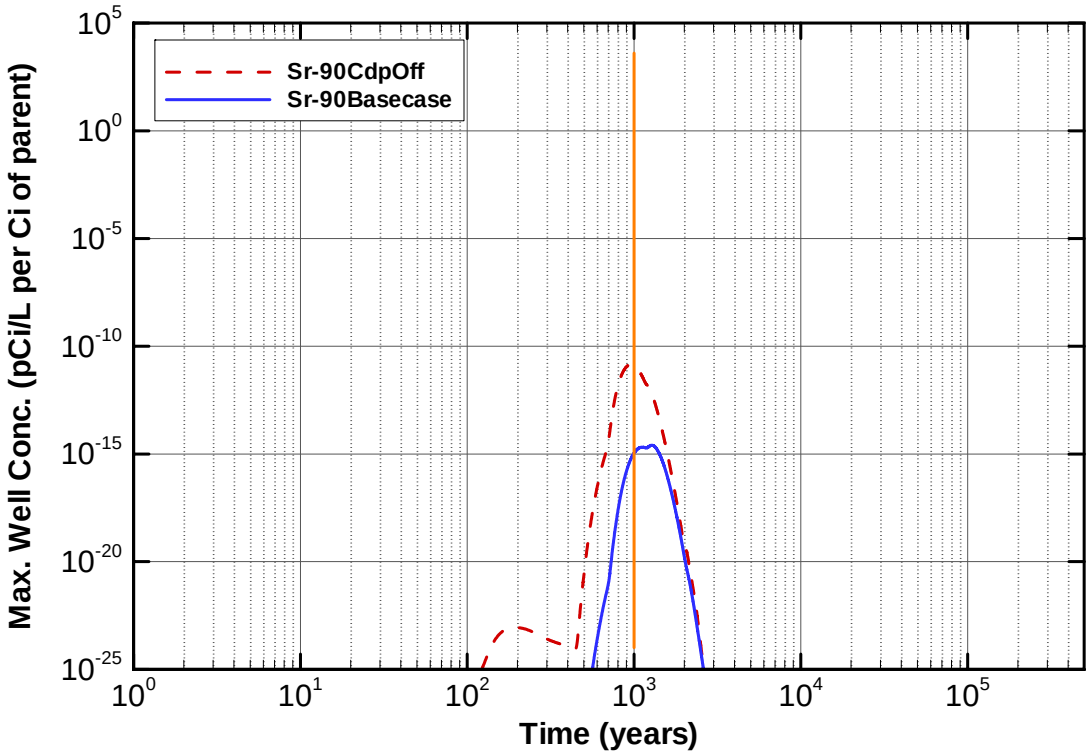

Figure 3-27. Comparison of Sr-90 for absence of CDP versus base case

For the base case and each sensitivity case, the maximum value of the desired metric has been presented by pathway analysis (alpha, beta/gamma, etc.) for each parent, where the metric includes the contributions of all members of the parent's decay chain. The beta/gamma results were compared across all the cases. General results were presented and specifics for some extreme results were explained. One common factor is the significance of the 1000-year time-of-compliance, because most peaks do not occur until after the specified time limit.

3.7 LAW VAULT AIR-PATHWAY ANALYSIS

3.7.1 Overview of Air-Pathway Analysis

This section describes the investigation conducted to evaluate the potential magnitude of gaseous release of radionuclides from the LAW Vault over the 25-year operational period, 100-year institutional control period, and 1000-year post-closure compliance period versus the atmospheric pathway exposure maximum dose to a representative member of the public of 10 mrem/yr.

A screening analysis was conducted to produce a list of radionuclides requiring a more thorough analysis to derive disposal limits for the LAW Vault disposal unit based on the atmospheric pathway. This study, described in Crapse and Cook (2006), used a methodology developed by the National Council on Radiation Protection and Measurements, professional judgment, and process knowledge to determine this list. The list of potential radionuclides includes C-14, Cl-36, H-3, I-129, S-35, Sb-124, Sb-125, Se-75, Se-79, Sn-113, Sn-119m, Sn-121, Sn-121m, Sn-123, and Sn-126. . Because tritium readily diffuses through carbon steel, it is assumed to be entirely released from the waste containers over a 1-year timeframe.

This analysis considers the following two cases:

- Diffusion of tritium through the waste containers over a 1-year time frame and subsequent transport to the SRS boundary (during the operational period).
- Diffusion of the other radionuclides upward from the LAW Vault through the overlying soil material (anticipated closure cap) and subsequent transport to the SRS boundary during the operational and institutional control period and to the 100-m boundary during the post closure compliance period.

During the 25-year operational period and 100-year institutional control period the maximum atmospheric dose is applicable at the SRS boundary, due to active institutional controls. During the 1000-year post-closure compliance period, the maximum atmospheric dose is applicable at 100 m from the disposal unit boundary, due to the assumed loss of active institutional controls. The atmospheric dose from the LAW Vault was evaluated for three separate time periods: 1) 0 to 25 years, 2) 25 to 125 years, and 3) 125 to 1125 years. The first time period evaluated covers the operational period. During this time period, waste containers are placed in the vault and the vault is open to the atmosphere. The second time period covers the institutional control period. During this time period, the exterior vault openings are sealed with reinforced concrete. The final time period covers the post-closure compliance monitoring period. During this time period, a closure cap is placed over the vault (Phifer et al. 2006).

The analysis presented here uses accepted computer programs for diffusion (PORFLOW) and atmospheric transport and dose calculations (CAP88).

3.7.2 Air-Pathway Assumptions

Key assumptions and inputs used in the air-pathway analysis are presented in Appendix B.

3.7.3 LAW Vault Closure Considerations

The concepts for closure of the LAW Vault are relevant to the determination of the gaseous flux at the land surface for all gaseous radionuclides except tritium. The LAW Vault construction specifics and closure concepts are described by Phifer et al. (2006). For the purposes of this investigation, it is assumed that during the operational time period, waste containers are placed in the vault and the vault is open to the atmosphere. Therefore, during this time period, the gaseous flux is evaluated immediately outside the waste containers. During the institutional control time period, the exterior vault openings are sealed with reinforced concrete. For this time period, the gaseous flux was evaluated at the top of the vault roof. For the post-closure compliance period, the vault is covered with a closure cap. For this time period, gaseous flux was evaluated at the top of the erosion barrier. A conceptual drawing of the closure cap over the LAW Vault is shown in Figure 3-4 and the vertical section over which gaseous radionuclide diffusion was evaluated is indicated.

The closure cap utilized in this analysis includes all materials as constructed and placed over the LAW Vault. The components of concern for the long-term air-pathway performance calculation are those that are assumed to have no potential to erode during the 1000-year post-closure compliance period. These components are situated below the top of the erosion barrier. For this analysis, the closure cap is assumed to remain intact over the 1000 year post closure monitoring period. The composite thickness of the non-waste material below the top of the closure cap is 7.67 ft (2.34 m) during the post closure compliance period. Table 3-33 lists the individual components of the LAW Vault and closure cap (excluding the layers overlying the erosion barrier. Materials are indicated with the associated thickness of each component, in inches, feet, and meters.

Table 3-33. Vertical Layer Sequence and Associated Thickness for the LAW Vault and Cover Material

Layer	Thickness (inches)	Thickness (ft)	Thickness (m)
Erosion barrier	12	1	0.30
Middle backfill layer	12	1	0.30
Gravel drainage layer	12	1	0.30
Lower backfill layer	40	3.33	1.02
LAW Vault Roof	16	1.33	0.41
LAW Vault Waste Layer	294	24.5	7.47

SOURCE: Adapted from Phifer et al. (2006).

3.7.4 LAW Vault Air-Pathway Conceptual Model

All tritium within the waste containers is assumed to diffuse through the containers over a 1-year time frame and be subsequently transported to the SRS boundary.

The flux of all other radioactive gasses at the land surface above the LAW Vault was evaluated for its specific closure configuration. Gaseous radionuclides introduced within the waste zone diffuse outward from this zone into the air-filled pore space of the materials surrounding the vault, eventually resulting in some of the radionuclides emanating at the land surface. As such, air is the medium through which they diffuse. It is assumed that fluctuations in atmospheric pressure at the land surface that could induce small pulses of air movement into and out of the shallow soil profile over relatively short periods of time will have a zero net effect when averaged over longer time periods. Thus, advective transport of these radionuclides in air-filled soil pores is not considered to be a significant process when compared to the rate of air diffusion.

The radionuclides present as gasses are those identified in the screening process described in Crapse and Cook (2006). Certain gaseous radionuclides will not likely remain in the monatomic elemental form but combine with other gaseous elements or form diatomic molecules. The state of existence of each of these radionuclides in the gaseous phase is important in evaluating their transport to the land surface because the diffusion coefficient associated with each is related to its molecular weight.

In this investigation it is assumed that:

- C-14 exists as part of the CO_2 molecule
- Cl-36, H-3 and I-129 exist as diatomic gasses
- S-35, Sb-124, Sb-125, Se-75, Se-79, Sn-113, Sn-119m, Sn-121, Sn-121m, Sn-123, and Sn-126 exist as monatomic gasses.

3.7.5 LAW Vault Air-Pathway Numerical Model

The mathematical model utilized in this report is provided by the PORFLOW simulation package (ACRI 2004). PC-based PORFLOW Version 5.97.0 was used to conduct a series of simulations. PORFLOW is developed and marketed by Analytic & Computational Research, Inc. to solve problems involving transient and steady-state fluid flow, heat and mass transport in multi-phase, variably saturated, porous or fractured media with dynamic phase change. PORFLOW has been widely used at the SRS and in the DOE complex to address major issues related to the groundwater and nuclear waste management.

The governing equation for mass transport of species *k* in the fluid phase is given by

$$\frac{\partial C_k}{\partial t} + \frac{\partial}{\partial x_i}(V_i C_k) = \frac{\partial}{\partial x_i}(D_{ij}\frac{\partial C_k}{\partial x_j}) + \gamma_k \qquad \text{Eq. 3-2}$$

Where

C_k	concentration of species *k*, Ci/m^3
V_i	fluid velocity in the ith direction, m/yr
D_{ij}	effective diffusion coefficient for the species, m^2/yr
γ_k	net decay of species *k*, Ci/m^{3}yr
i, j	direction index
t	time, yr
x	distance coordinate, m

This equation is solved within PORFLOW to evaluate transient radionuclide transport above the LAW Vault and to determine gaseous radionuclide flux at the land surface over time. Since source radionuclides exist as gases, air was taken to be the medium within which transport occurs. The flow field was assumed to be isobaric and isothermal. The impact of naturally occurring fluctuations in atmospheric pressure at the land surface that could induce small pulses of air movement into and out of the shallow soil profile over relatively short periods of time will have a zero net effect when averaged over longer time periods. Therefore, for the relatively long periods of time evaluated in this investigation, air diffusion was the only transport mechanism simulated in the model and advective air-transport was assumed to be negligible, so the advection term was disabled within PORFLOW and only the diffusive and net decay terms were evaluated.

3.7.5.1 LAW Vault Air-Pathway Model Development and Assumptions

The numerical representation of the conceptual model is as a 1-dimensional vertical stack of elements configured to represent the thickness of the LAW Vault and overlying materials.

The radionuclides evaluated are C-14, Cl-36, H-3, I-129, S-35, Sb-124, Sb-125, Se-75, Se-79, Sn-113, Sn-119m, Sn-121, Sn-121m, Sn-123, and Sn-126.

Since source radionuclides exist as gases, air was taken to be the medium within which transport occurs. The flow field was assumed to be isobaric and isothermal. The impact of naturally occurring fluctuations in atmospheric pressure at the land surface that could induce small pulses of air movement into and out of the shallow soil profile over relatively short periods of time is assumed to have a zero net effect when averaged over longer time periods. Therefore, for the relatively long periods of time evaluated in this investigation, air-diffusion was the only transport mechanism simulated in the model and advective air-transport was assumed to be negligible.

Once the gaseous radionuclides diffuse into the overlying cover material, a small percentage of the radionuclides dissolve in residual pore water; however, diffusion proceeds more slowly in water than in air. Therefore, air-diffusion is assumed to be the dominant transport process by which contaminants reach the land surface from the LAW Vault waste zone. This assumption is substantiated by Nielson et al. (1984) where it was found that the effective radon diffusion coefficient decreased with increasing moisture content. The radon effective diffusion coefficient, D_{eff}, for soil was reported to range from the open-air diffusion coefficient of 1.1E-05 m^2/s to that of fully saturated soil, 1.0E-09 m^2/s (Nielson et al. 1984).

This four-order of magnitude difference is consistent with the comparison of water diffusion coefficients to air diffusion coefficients of other common molecular compounds and reported in many references such as Bolz and Tuve (1973). Thus, the larger volume of water-filled pore space compared to air-filled pore space (maximum of 2 orders of magnitude difference) is inconsequential. The ability of water-dissolved compounds to diffuse through water-filled pores is negligible compared to the ability of the same compounds to diffuse as gas in the vapor-filled pore spaces. Furthermore, there is vertical downward movement of the pore water which acts to offset or overcome any vertical upward diffusion of dissolved constituents. Consequently, in this investigation radionuclide transport was allowed to proceed only through air-filled pore space and, therefore, residual pore water was treated as if it was part of the solid matrix material within the flow field. No accounting was made of the partitioning of the gaseous radionuclides into the pore water as diffusive vapor transport proceeded from the waste zone to the land surface. By ignoring this mechanism, diffusive fluxes at the land surface were slightly overestimated.

The boundary conditions imposed on the model domain included:

- No-flux specified for all radionuclides along sides and bottom
  ($dC/dX = 0$ at $x=0$, $x=1$ and $dC/dY = 0$ at $y=0$)
- Species concentration set to 0 at land surface (top of erosion barrier)
  ($C = 0$ at $y=y_{max}$)

The initial condition imposed on the domain included:

- Species concentration set to 0 for the entire model domain at time = 0
  ($C=0$ for $0 \leq x \leq 1$ at $t=0$ and $C=0$ for $0 \leq y \leq y_{max}$ at $t=0$)

The initial conditions for the model also assumed a 1 Ci inventory of each radionuclide uniformly spread over the waste zone.

These boundary conditions force all of the gaseous radionuclides to move upward from the waste disposal zone to the land surface. In reality, some lateral and downward diffusion occurs in the air-filled pores surrounding the waste zone; hence ignoring this lateral and downward movement has the effect of increasing the flux at the land surface. This should introduce some conservatism in the calculated results. Simulations were conducted in transient mode for diffusive transport in air, with results being obtained over 1,125 years.

A summary of the radionuclides and compounds of interest in this investigation is shown in Table 3-34.

Table 3-34. Radionuclides and Compounds of Interest

Radionuclide	Half-life (yrs)	Approximate Atomic Wt.	Molecular form in gaseous state	Molecular Wt.
C-14	5.730E+03	14	CO_2	46
Cl-36	3.010E+05	36	Cl_2	72
H-3	12.33E+00	3	H_2	6
I-129	1.570E+07	129	I_2	258
Rn-222	1.047E-02	222	Rn	222
S-35	2.394E-01	35	S	35
Sb-124	1.649E-01	124	Sb	124
Sb-125	2.759E+00	125	Sb	125
Se-75	3.270E-01	75	Se	75
Se-79	2.950E+05	79	Se	79
Sn-113	3.153E-01	113	Sn	113
Sn-119m	8.020E-01	119	Sn	119
Sn-121	3.089E-03	121	Sn	121
Sn-121m	44.10E+00	121	Sn	121
Sn-123	3.550E-01	123	Sn	123
Sn-126	2.300E+05	126	Sn	126

3.7.5.2 Measures Implemented to Ensure Conservative Results

In this analysis, several conditions introduce conservatism into the calculations. These include:

- The use of boundary conditions that force all of the gaseous radionuclides to move upward from the waste disposal zone to the land surface. In reality, some of the gaseous radionuclides diffuse sideways and downward in the air-filled pores surrounding the waste zone; hence ignoring this has the effect of increasing the flux at the land surface.
- Not taking credit for the removal of radionuclides by pore water moving vertically downward through the model domain. This mechanism would likely remove some dissolved radionuclides, and therefore its omission has the effect of increasing the estimate of instantaneous radionuclide flux at the land surface in simulations conducted as a part of this investigation.
- The addition of an extra 125 years to the required 1,000-year evaluation period to account for any gaseous radionuclide flux generated during the operational and institutional control period, thus incrementally increasing the instantaneous radionuclide flux.
- Not taking credit for the waste being stored in steel containers. For the first 25 years of simulation, the vault is open to the atmosphere and radionuclides are allowed to diffuse directly from the waste. In reality, the steel containers will slow diffusion until the containers are breached by corrosion.
- Use of the top of the erosion layer in the soil cover as the land surface for the purpose of calculating the gaseous radionuclide flux during the 125 to 1125 year time period. No credit is taken for the additional distance gaseous radionuclides must migrate above the erosion barrier prior to that portion of the closure cap eroding away.
- Ignoring the presence of the GCL within the final closure cap. The GCL should be near 100 percent saturation. Therefore, it will contain very little air-filled porosity within which gaseous transport could occur.
- During the post-closure time period (125 to 1125 years) assigning the concrete roof a low saturation associated with concrete rubble exposed to the atmosphere rather than a high saturation associated with buried concrete (i.e. the vault is overlain with a closure cap during the post-closure time period).

3.7.5.3 Grid Construction

The model grid was constructed as a node mesh 3 nodes wide by 54 nodes high. This mesh creates the vertical stack of 52 model elements, as shown in Figure 3-28. The grid extends upward to the top of the erosion barrier, since this is the minimum possible cover thickness that could exist during the 1,125-year evaluation period. A set of consistent units was employed in the simulations for length, mass and time, these being meters, grams and years, respectively.

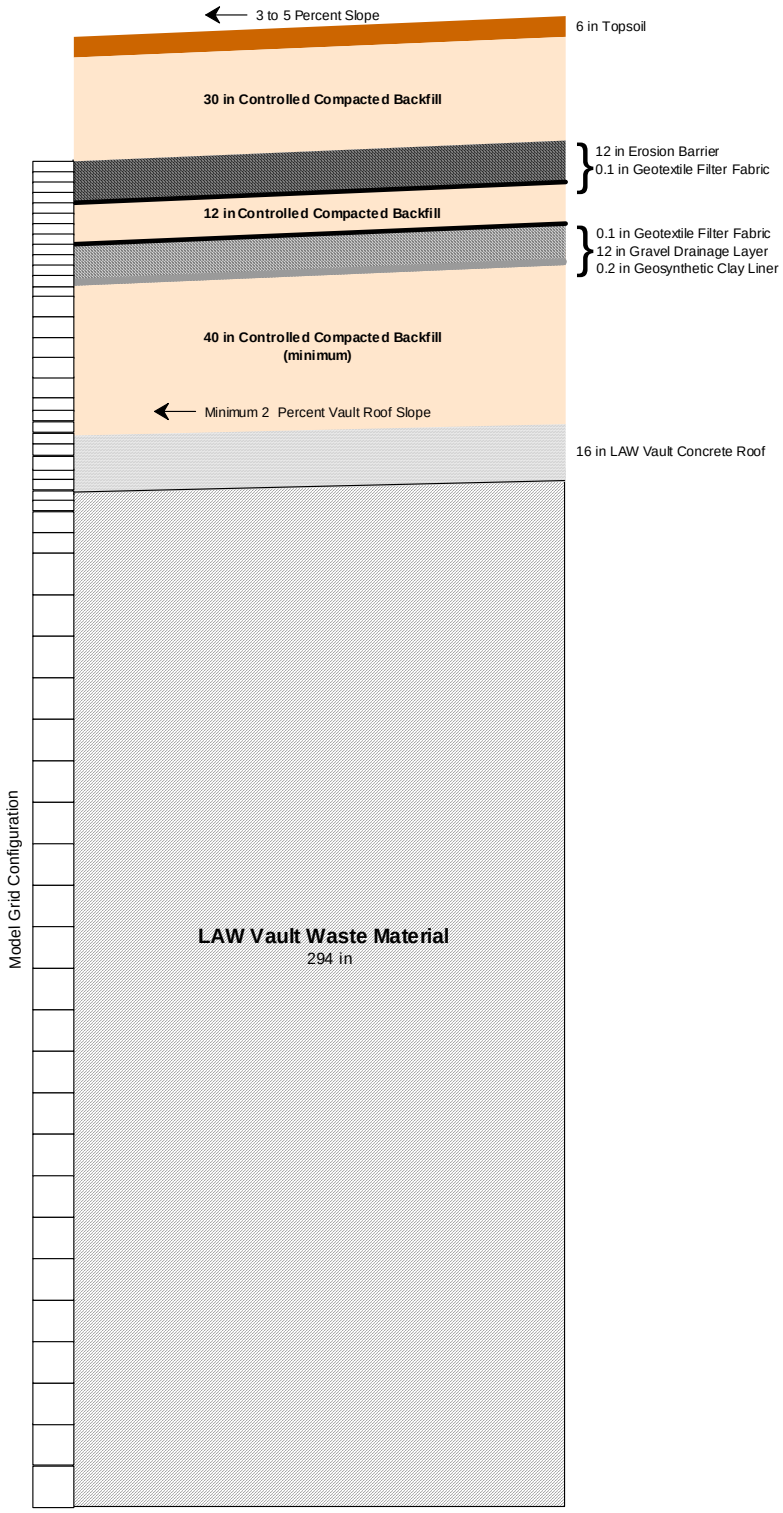

Figure 3-28. LAW Vault Air and Radon Model Grid Configuration

3.7.5.4 Material Zones

The model domain was divided into two primary zones, the LAW Vault waste zone occupying the lower 24.5 ft (7.47 m) of the domain and the cover zone extending 7.67 ft. (2.34 m) above the waste zone to the top of the domain. The waste zone was taken as the thickness of a LAW Vault waste cell. The upper model elements were scaled to correspond to the geometry of the closure cap thickness while the lower model elements were scaled to correspond to the Law Vault waste zone.

During the operational period (0 to 25 years) the vault is open to the atmosphere. During the institutional control period (25 to 125 years) the exterior vault openings are sealed with reinforced concrete. Thus, during this time period, the land surface is assumed to be the top of the vault roof. During the post-closure compliance time period (125 to 1125 years), the land surface is taken as top of the erosion resistant layer, within the closure cap, and no credit is taken for the compacted backfill and topsoil above that layer.

3.7.5.5 Material Zone Properties and Other Input Parameters

Material properties utilized within the 1-D numerical model were specified for 6 material zones defined within the model domain. Each material zone was assigned values of particle density, total porosity, average saturation, air-filled porosity, air density, and an effective air-diffusion coefficient for each source element or compound. With the use of an effective air-diffusion coefficient, tortuosity was assigned a unit value in each material zone. An air fluid density of 1.24E+03 g/m^3 was used. This air fluid density was obtained from the Bolz and Tuve (1973), *CRC Handbook of Tables for Applied Engineering Science* and represents that of standard atmospheric conditions.

During the operational period (0 to 25 years) the vault is open to the atmosphere. The layers associated with the LAW Vault during this period consist only of the waste layer. The LAW Vault waste zone was assigned a total porosity of 0.5 and particle density of 2.65 g/cm^3 assuming the waste is half air space.

The LAW Vault Waste Zone is comprised of stacked B-25 boxes, B-12 boxes, drums, and other metal and/or concrete containers (WSRC 2006). This is similar to the CIG waste form, and waste zone properties for the LAW Vault air-pathway analysis were based on those assumed for the CIG disposal unit (WSRC 2006). For the groundwater pathway (Section 3.6.4.5), the waste zone was assumed to have a porosity of 0.9 in order not to over-estimate the retardation of radionuclides (Phifer et al. 2006). For the air-pathway analysis, retardation of the radionuclides was not a factor.

It was assumed the waste was dry and therefore the air filled porosity would equal the total porosity for this zone. While the model includes all the layers from the LAW Vault waste layer to the erosion barrier, during the first 25 years of simulation, the concrete roof and all overlying materials were assigned a porosity of 1.0 and a saturation of 0. This has the effect of making these layers equivalent to air. Table 3-35 provides the values of particle density, total porosity, average saturation, and air-filled porosity utilized for the LAW Vault layers for the first 25 years.

Table 3-35. Operational Period (First 25 Years) Layer Particle Density, Total Porosity, Average Saturation, and Air-Filled Porosity

Layer	Particle Density (g/cm^3)	Total Porosity (fraction)	Average Saturation (fraction)	Air-filled Porosity [3] (fraction)
Erosion barrier layer [1]	0	1	0	1
Middle backfill [1]	0	1	0	1
Gravel drainage layer [1]	0	1	0	1
Lower backfill [1]	0	1	0	1
LAW Vault concrete roof [1]	0	1	0	1
LAW Vault waste layer [2]	2.65	0.500	0	0.500

[1] During the first 25 years of simulation, the concrete roof and materials comprising the closure cap were assigned a porosity of 1.0 and an average saturation of 0 in order to represent air.

[2] The waste is assumed to be dry (i.e. saturation of 0) resulting in the air-filled porosity equaling the total porosity.

[3] Air-filled Porosity = (1 – Average Saturation) × Total Porosity

During the institutional control period (25 to 125 years), the vault openings are sealed with reinforced concrete. The layers associated with the LAW Vault during this period consist of the waste layer and the concrete vault roof. The waste layer retains the properties from the operational period. The particle density and total porosity for the LAW Vault reinforced concrete roof was taken from Phifer et al. (2006). The properties of the LAW Vault roof were assumed to be similar to concrete exposed to the atmosphere as described by Sappington and Phifer (2005). The average saturation for the LAW Vault roof was calculated by dividing the in-field moisture content (0.096) by the saturated moisture content (0.132) as reported by Sappington and Phifer (2005). This yielded an average saturation of 0.73 for the LAW Vault reinforced concrete roof. As with the operational period, the model includes all the layers from the LAW Vault waste layer to the erosion barrier. However, during the 25 to 125 year time period, the closure cap materials were assigned a porosity of 1.0 and a saturation of 0. This has the effect of making these layers equivalent to air. Table 3-36 provides the values of particle density, total porosity, average saturation, and air-filled porosity utilized for the LAW Vault layers for the 25 to 125 year time period.

Table 3-36. Institutional Control Period (25 to 125 Years) Layer Particle Density, Total Porosity, Average Saturation, and Air-Filled Porosity

Layer	Particle Density (g/cm^3)	Total Porosity (fraction)	Average Saturation [5] (fraction)	Air-filled Porosity [6] (fraction)
Erosion barrier layer [1]	0	1	0	1
Middle backfill [1]	0	1	0	1
Gravel drainage layer [1]	0	1	0	1
Lower backfill [1]	0	1	0	1
LAW Vault concrete roof [2, 4]	2.59	0.184	0.730	0.050
LAW Vault waste layer [3]	2.65	0.500	0	0.500

[1] During the first 25 years of simulation, the materials comprising the closure cap were assigned a porosity of 1.0 and an average saturation of 0 in order to represent air.

[2] Waste layer and concrete roof particle density and total porosity taken from Phifer et al. (2006).

[3] The waste is assumed to be dry (i.e. saturation of 0) resulting in the air-filled porosity equaling the total porosity.

[4] Average saturation for the LAW Vault roof was calculated by dividing the in-field moisture content (0.096) by the saturated moisture content (0.132) as reported by Sappington and Phifer (2005).

[5] Average Saturation = Long Term Average Moisture Content / Total Porosity

[6] Air-filled Porosity = (1 – Average Saturation) × Total Porosity

During the post-closure time period (125 to 1125 years) the layers associated with the LAW Vault consist of all layers from the waste layer to the erosion barrier. The waste layer and concrete roof retain the same properties as utilized for the 25 to 125-year period. The particle density of the lower backfill, gravel drainage layer, middle backfill, and erosion barrier (these materials collectively are considered the closure cap layers) was taken as 2.65 g/cm^3. This is based on the density of quartz and is regarded as representative of most SRS soils. Values for total porosity and long-term average moisture content for the closure cap materials were taken from Phifer (2003). Phifer (2003) evaluated infiltration through a closure cap over time as the closure cap degraded using the HELP model. The porosity and average moisture content values for a 10,000-year degraded closure cap were utilized, since this represented the greatest air filled porosity in which a gas could diffuse. Average saturation and air-filled porosity values were calculated from the total porosity and long-term average moisture content. Table 3-37 provides the values of particle density, total porosity, average saturation, and air-filled porosity utilized for all the layers (i.e., waste layer to the erosion barrier) for the 125 to 1125-year time period.

Table 3-37. Post Closure Period (125 to 1125 Years) Layer Particle Density, Total Porosity, Long-Term Average Moisture Content, Average Saturation, and Air-Filled Porosity

Layer	Particle Density (g/cm^3)	Total Porosity (fraction)	Long-Term Average Moisture Content	Average Saturation (fraction)	Air-filled Porosity [6] (fraction)
Erosion barrier layer [1]	2.65	0.088	0.0726	0.825 [5]	0.015
Middle backfill [1]	2.65	0.375	0.2435	0.649 [5]	0.132
Gravel drainage layer[1]	2.65	0.375	0.1967	0.525 [5]	0.178
Lower backfill [1]	2.65	0.370	0.2710	0.732 [5]	0.099
LAW Vault Roof [2]	2.59	0.184	N/A[4]	0.730 [4]	0.050
LAW Vault waste layer [3]	2.65	0.500	0.000[3]	0.000	0.500

[1] Values for total porosity and long term average moisture content taken from Phifer (2003). Particle density taken as 2.65, which is based on the density of quartz and regarded as fairly representative of most SRS soils.

[2] Concrete roof particle density and total porosity taken from Phifer et al. (2006).

[3] The waste is assumed to be dry (i.e. saturation of 0) resulting in the air-filled porosity equaling the total porosity.

[4] Average saturation for the LAW Vault roof was calculated by dividing the in-field moisture content (0.096) by the saturated moisture content (0.132) as reported by Sappington and Phifer (2005).

[5] Average Saturation = Long Term Average Moisture Content / Total Porosity

[6] Air-filled Porosity = (1 – Average Saturation) × Total Porosity

The molecular diffusion coefficient of Rn-222 in open air is 347 m^2/yr (Nielson et al. 1984). Nielson et al. (1984) established a relationship between moisture saturation and the radon effective air-diffusion coefficient for various pore sizes of earthen materials. Using this method, a radon effective air-diffusion coefficient was determined for each material type based upon the average moisture saturation for the material. Subsequently, using Graham's Law, the effective air-diffusion coefficient of each radionuclide or compound evaluated was determined for each material type based on the radon effective air-diffusion coefficient using the following relationship:

$$D = D' \sqrt{\frac{MWT'}{MWT}}$$

Where:

D = the diffusion coefficient of the radionuclide of interest (m^2/yr)
D' = the diffusion coefficient of the reference radionuclide (Rn-222) (m^2/yr)
MWT' = the molecular weight of the reference radionuclide (Rn-222)
MWT = the molecular weight of the element or compound of interest

A summary of the radon effective air-diffusion coefficients and the calculated effective air-diffusion coefficients for each radionuclide/compound by material zone and simulation period, are presented in Table 3-38 through Table 3-40.

Table 3-38. Effective Air-Diffusion Coefficients for Each Radionuclide/Compound, by Material for the 0 to 25-Year Time Period

Radionuclide	LAW Vault Waste (m^2/yr)	LAW Vault Roof (m^2/yr)	Lower Backfill (m^2/yr)	Gravel Drainage Layer (m^2/yr)	Middle Backfill (m^2/yr)	Erosion Barrier (m^2/yr)
Rn-222[1]	3.470E+02	3.470E+02	3.470E+02	3.470E+02	3.470E+02	3.470E+02
C-14	7.623E+02	7.623E+02	7.623E+02	7.623E+02	7.623E+02	7.623E+02
Cl-36	6.093E+02	6.093E+02	6.093E+02	6.093E+02	6.093E+02	6.093E+02
I-129	3.219E+02	3.219E+02	3.219E+02	3.219E+02	3.219E+02	3.219E+02
S-35	8.739E+02	8.739E+02	8.739E+02	8.739E+02	8.739E+02	8.739E+02
Sb-124	4.643E+02	4.643E+02	4.643E+02	4.643E+02	4.643E+02	4.643E+02
Sb-125	4.624E+02	4.624E+02	4.624E+02	4.624E+02	4.624E+02	4.624E+02
Se75	5.970E+02	5.970E+02	5.970E+02	5.970E+02	5.970E+02	5.970E+02
Se79	5.817E+02	5.817E+02	5.817E+02	5.817E+02	5.817E+02	5.817E+02
Sn113	4.864E+02	4.864E+02	4.864E+02	4.864E+02	4.864E+02	4.864E+02
Sn-119m	4.739E+02	4.739E+02	4.739E+02	4.739E+02	4.739E+02	4.739E+02
Sn-121	4.700E+02	4.700E+02	4.700E+02	4.700E+02	4.700E+02	4.700E+02
Sn-121m	4.700E+02	4.700E+02	4.700E+02	4.700E+02	4.700E+02	4.700E+02
Sn-123	4.662E+02	4.662E+02	4.662E+02	4.662E+02	4.662E+02	4.662E+02
Sn-126	4.606E+02	4.606E+02	4.606E+02	4.606E+02	4.606E+02	4.606E+02

[1]The effective diffusion coefficient for ^{222}Rn was used to determine the effective air diffusion coefficient of each radionuclide/compound based on Graham's law.

Table 3-39. Effective Air-Diffusion Coefficients for Each Radionuclide/Compound, by Material for the 25 to 125-Year Time Period

Radionuclide	LAW Vault Waste (m^2/yr)	LAW Vault Roof (m^2/yr)	Lower Backfill (m^2/yr)	Gravel Drainage Layer (m^2/yr)	Middle Backfill (m^2/yr)	Erosion Barrier (m^{2-}/yr)
Rn-222[1]	3.470E+02	2.840E+00	3.470E+02	3.470E+02	3.470E+02	3.470E+02
C-14	7.623E+02	6.239E+00	7.623E+02	7.623E+02	7.623E+02	7.623E+02
Cl-36	6.093E+02	4.987E+00	6.093E+02	6.093E+02	6.093E+02	6.093E+02
I-129	3.219E+02	2.635E+00	3.219E+02	3.219E+02	3.219E+02	3.219E+02
S-35	8.739E+02	7.153E+00	8.739E+02	8.739E+02	8.739E+02	8.739E+02
Sb-124	4.643E+02	3.800E+00	4.643E+02	4.643E+02	4.643E+02	4.643E+02
Sb-125	4.624E+02	3.785E+00	4.624E+02	4.624E+02	4.624E+02	4.624E+02
Se75	5.970E+02	4.886E+00	5.970E+02	5.970E+02	5.970E+02	5.970E+02
Se79	5.817E+02	4.761E+00	5.817E+02	5.817E+02	5.817E+02	5.817E+02
Sn113	4.864E+02	3.981E+00	4.864E+02	4.864E+02	4.864E+02	4.864E+02
Sn-119m	4.739E+02	3.879E+00	4.739E+02	4.739E+02	4.739E+02	4.739E+02
Sn-121	4.700E+02	3.847E+00	4.700E+02	4.700E+02	4.700E+02	4.700E+02
Sn-121m	4.700E+02	3.847E+00	4.700E+02	4.700E+02	4.700E+02	4.700E+02
Sn-123	4.662E+02	3.816E+00	4.662E+02	4.662E+02	4.662E+02	4.662E+02
Sn-126	4.606E+02	3.770E+00	4.606E+02	4.606E+02	4.606E+02	4.606E+02

[1]The effective diffusion coefficient for ^{222}Rn was used to determine the effective air diffusion coefficient of each radionuclide/compound based on Graham's law.

Table 3-40. Effective Air-Diffusion Coefficients for Each Radionuclide/Compound, by Material for the 125 to 1125-Year Time Period

Radionuclide	LAW Vault Waste (m^2/yr)	LAW Vault Roof ($m^2$2/yr)	Lower Backfill (m^2/yr)	Gravel Drainage Layer (m^2/yr)	Middle Backfill (m^2/yr)	Erosion Barrier (m^2/yr)
Rn-222[1]	3.470E+02	2.840E+00	2.840E+00	4.734E+00	4.734E+00	7.889E-01
C-14	7.623E+02	6.239E+00	6.239E+00	1.040E+01	1.040E+01	1.733E+00
Cl-36	6.093E+02	4.987E+00	4.987E+00	8.312E+00	8.312E+00	1.385E+00
I-129	3.219E+02	2.635E+00	2.635E+00	4.391E+00	4.391E+00	7.318E-01
S-35	8.739E+02	7.153E+00	7.153E+00	1.192E+01	1.192E+01	1.987E+00
Sb-124	4.643E+02	3.800E+00	3.800E+00	6.334E+00	6.334E+00	1.056E+00
Sb-125	4.624E+02	3.785E+00	3.785E+00	6.308E+00	6.308E+00	1.051E+00
Se75	5.970E+02	4.886E+00	4.886E+00	8.144E+00	8.144E+00	1.357E+00
Se79	5.817E+02	4.761E+00	4.761E+00	7.935E+00	7.935E+00	1.323E+00
Sn113	4.864E+02	3.981E+00	3.981E+00	6.635E+00	6.635E+00	1.106E+00
Sn-119m	4.739E+02	3.879E+00	3.879E+00	6.465E+00	6.465E+00	1.078E+00
Sn-121	4.700E+02	3.847E+00	3.847E+00	6.412E+00	6.412E+00	1.069E+00
Sn-121m	4.700E+02	3.847E+00	3.847E+00	6.412E+00	6.412E+00	1.069E+00
Sn-123	4.662E+02	3.816E+00	3.816E+00	6.359E+00	6.359E+00	1.060E+00
Sn-126	4.606E+02	3.770E+00	3.770E+00	6.283E+00	6.283E+00	1.047E+00

[1]The effective diffusion coefficient for Rn-222 was used to determine the effective air diffusion coefficient of each radionuclide/compound based on Graham's law.

3.7.6 Air-Pathway Model Results

3.7.6.1 LAW Vault Flux to Ground Surface

Model simulations were conducted to evaluate the peak flux of each radionuclide emanating from the top of the domain. A unit inventory of 1 Ci was assigned to the LAW Vault waste zone for each radionuclide considered in the analysis. Results were output in Ci/yr, consistent with the set of units employed in the model, and are presented for each radionuclide in Figure 3-29 and Figure 3-30. The peak fluxes emanating at the land surface are presented for each time period in Table 3-41. The results are reported in this way to facilitate calculation of human exposure at the SRS boundary and at the 100-m boundary due to the LAW Vault. Flux behavior is based primarily on the closure considerations discussed in Section 3.7.3 and the half-life of the particular radionuclide as provided in Table 3-34.

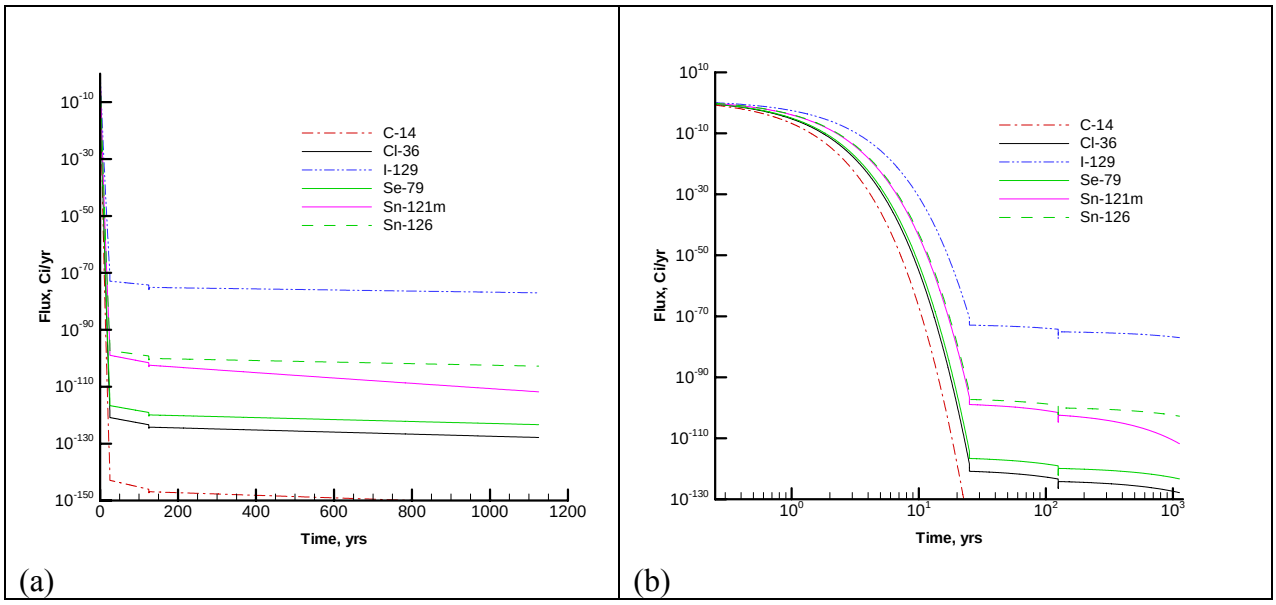

Figure 3-29. Flux Rate at Land Surface for C-14, Cl-36, I-129, Se-79, Sn-121m, and Sn-126 on a (a) Semi-log and (b) Log-log Scale

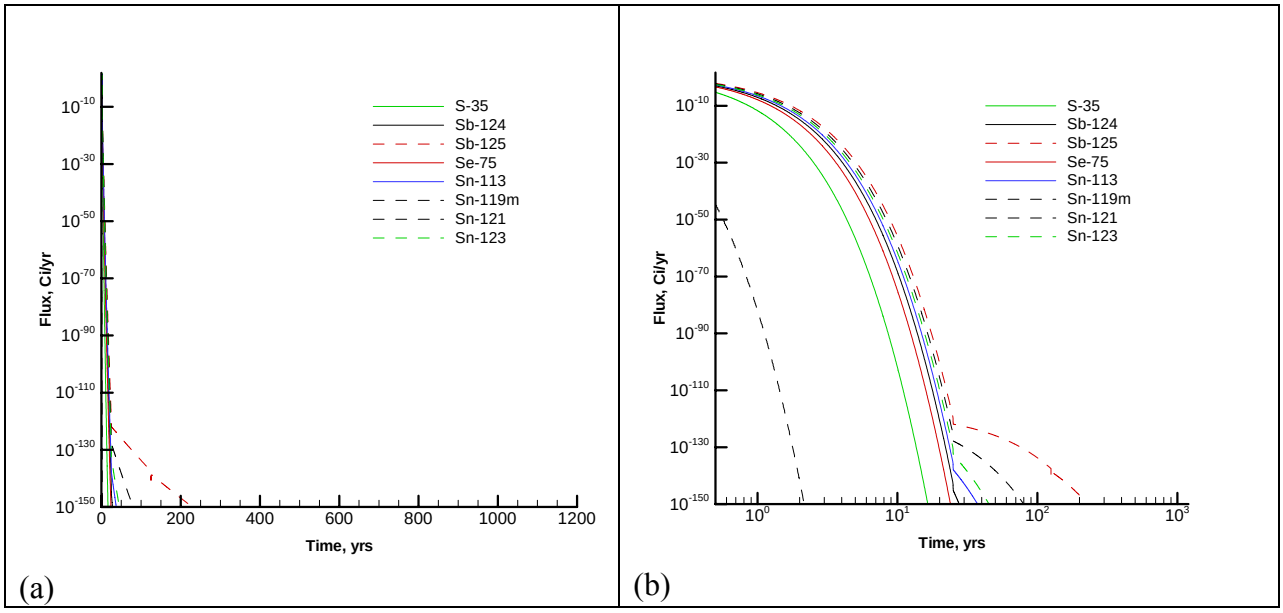

Figure 3-30. Flux Rate at Land Surface for S-35, Sb-124, Sb-125, Se-75, Sn-113, Sn-119m, Sn-121, and Sn123 on a (a) semi-log and (b) log-log scale

Table 3-41. Summary of the Peak Flux Rates for Each Radionuclide

Radionuclide	Activity in Waste (Ci)	Peak Flux (Ci/yr/Ci)		
		0 - 25 Years	25 – 125 years	125 – 1125 years
C-14	1.0	2.79E+01	2.36E-172	3.13E-184
Cl-36	1.0	2.23E+01	1.60E-146	1.10E-156
I-129	1.0	1.18E+01	2.65E-89	3.19E-96
S-35	1.0	3.17E+01	8.12E-203	7.840E-310
Sb-124	1.0	1.66E+01	9.69E-144	1.13E-280
Sb-125	1.0	1.69E+01	1.68E-120	1.69E-139
Se75	1.0	2.17E+01	9.42E-156	2.20E-239
Se79	1.0	2.13E+01	1.43E-141	1.98E-151
Sn113	1.0	1.76E+01	1.61E-136	1.15E-221
Sn-119m	1.0	1.73E+01	2.03E-126	9.88E-169
Sn-121	1.0	7.72E+00	0.00E+00	0.00E+00
Sn-121m	1.0	1.72E+01	1.44E-120	7.53E-130
Sn-123	1.0	1.69E+01	2.45E-131	4.41E-209
Sn-126	1.0	1.69E+01	1.30E-118	4.16E-127

3.7.7 LAW Vault Air-Pathway Dose Calculations

An evaluation was conducted to assess the potential dose to a maximally exposed individual (MEI) located at both the SRS boundary and at the 100-m locations (Lee 2006). During the 125-year operational and institutional control period, the SRS boundary is the compliance point for the dose calculations. Therefore, the peak flux during this time period was used to assess the dose to the MEI. For the remainder of the time period, the 100-m boundary is the compliance point based on DOE Order 435.1. Thus, the peak flux between 125 and 1125 years was used for these calculations. Dose-release factors (DRF) were calculated for each radionuclide potentially released from the LAW Vault disposal unit using CAP88, the EPA model for National Emissions Standards for Hazardous Air Pollutants (NESHAPs). The DRFs represent the dose to the receptor exposed to 1 Ci of the specified radionuclide being released to the atmosphere. For the receptor located at the SRS boundary the distance from the LAW Vault is sufficient for an assumption of a point source. However, the DRFs for the 100-m receptor require evaluation of an area source because of the close proximity of the LAW Vault disposal unit to the 100-m receptor. For radionuclides not contained within the CAP88 library (Se-75, Se-79, Sn-119m, and Sn-121m) atmospheric transport was estimated by assigning surrogates with similar radiological properties (Lee 2006). Doses for these four radionuclides were estimated by applying their dosimetric properties to the surrogate's relative air concentrations estimated by the model.

Tritium within the LAW Vault waste containers is assumed to diffuse through the waste containers over a 1-year time frame and be subsequently transported to the SRS boundary. During the 25-year operational period, when the tritium is assumed to be entirely released from the waste containers over a 1-year timeframe, the SRS boundary is the compliance point for the dose calculation. Therefore, the maximum permissible annual inventory is determined based on the DRF for tritium at the site boundary and an annual flux of 1 Ci/yr. The maximum permissible total inventory is then determined by multiplying the annual inventory by the length of the operational period (25 yrs). The results of these calculations are presented in Table 3-42.

Table 3-42. Projected Maximum Tritium Dose at the SRS Boundary and Permissible Inventory

Unit Curie Tritium Inventory (Ci)	SRS Boundary DRF (mrem/Ci)	Unit Curie Projected Maximum Dose (mrem/yr/Ci)	Maximum Permissible Exposure Level (mrem/yr)	Maximum Permissible Annual Inventory (Ci)	Maximum Permissible Total Inventory (Ci)
1 [a]	2.2E-06	2.2E-06[b]	10	4.5E06[c]	1.1E08[d]

[a]Unit Curie Inventory
[b]Unit Cure Projected maximum dose = Unit Curie Tritium Inventory * SRS Boundary DRF
[c]Maximum Permissible Annual Inventory = Maximum Permissible Exposure Level / Unit Curie Projected Maximum Dose
[d]Maximum Permissible Total Inventory = Maximum Permissible Annual Inventory * 25 yrs of operation.

Specific SRS Boundary DRFs (Lee 2006), the calculated exposure levels for the 0 to 125 year MEI at the SRS boundary, and the resulting 0 to 125 year LAW Vault disposal limits are presented in Table 3-43 (except tritium). Specific SRS 100-m DRFs, the calculated exposure levels for the 125 to 1125 year MEI at 100 m, and the resulting 125 to 1125 year LAW Vault disposal limits are presented in Table 3-44 (except tritium). See Lee (2006) for details on the estimation of all DRFs in Table 3-43 and Table 3-44. The LAW Vault disposal unit limits were calculated by dividing the maximum permissible exposure level (10 mrem/yr, DOE 1999) by the highest dose received by the MEI from the 1 Ci source during each of the two time periods. Table 3-45 provides a comparison of the limits derived for these two time periods (i.e., 0 – 125 and 125 – 1125 years) and the resulting overall LAW Vault air-pathway disposal limits.

Table 3-43. SRS Boundary Dose Release Factors and 0 – 125 Year LAW Vault Disposal Limits

Radionuclide	0 - 125 Year Peak Flux (Ci/yr/Ci)	SRS Boundary Dose Release Factor[1] (mrem/Ci)	0 – 125 Year Dose to MEI at SRS Boundary[2] (mrem/yr/Ci)	0 - 125 Year LAW Vault Disposal Limits[3] (Ci)
C-14 as CO_2	2.79E+01	1.1E-04	3.0E-03	3.3E+03
Cl-36 as Cl_2	2.23E+01	2.3E-04	5.1E-03	2.0E+03
I-129 as I_2	1.18E+01	4.9E-02	5.7E-01	1.7E+01
S-35	3.17E+01	2.8E-05	8.9E-04	1.1E+04
Sb-124	1.66E+01	2.0E-03	3.4E-02	3.0E+02
Sb-125	1.69E+01	6.5E-03	1.1E-01	9.2E+01
Se-75	2.17E+01	1.1E-03	2.4E-02	4.3E+02
Se-79	2.13E+01	6.3E-04	1.3E-02	7.5E+02
Sn113	1.76E+01	2.3E-04	4.0E-03	2.5E+03
Sn-119m	1.73E+01	1.0E-04	1.8E-03	5.7E+03
Sn-121	7.72E+00	4.2E-05	3.3E-04	3.1E+04
Sn-121m	1.72E+01	6.5E-04	1.1E-02	8.9E+02
Sn-123	1.69E+01	1.3E-05	2.1E-04	4.7E+04
Sn-126	1.69E+01	3.0E-01	5.0E+00	2.0E+00

[1] From Lee (2006)
[2] Dose to MEI at SRS Boundary = Peak Flux × Dose Release Factor
[3] Disposal Limit = 10 mrem/yr / Dose to MEI at SRS Boundary per yr per Ci

Table 3-44. 100-m Dose Release Factors and 125 – 1125 Year LAW Vault Disposal Limits

Radionuclide	125 –1125 Year Peak Flux (Ci/yr/Ci)	100-m Dose Release Factor[1] (mrem/Ci)	125 –1125 Year Dose to MEI at 100-m[2] (mrem/yr/Ci)	125 –1125 Year LAW Vault Disposal Limits[3] (Ci)
C-14 as CO_2	3.13E-184	5.90E-02	1.8E-185	---
Cl-36 as Cl_2	1.10E-156	9.30E-02	1.0E-157	---
I-129 as I_2	3.19E-96	8.60E+01	2.7E-94	---
S-35	7.840E-310	7.70E-03	0.0E+00	No Limit
Sb-124	1.13E-280	5.70E-01	6.4E-281	---
Sb-125	1.69E-139	1.70E+00	2.9E-139	---
Se-75	2.20E-239	3.10E-01	6.8E-240	---
Se-79	1.98E-151	1.80E-01	3.6E-152	---
Sn113	1.15E-221	7.70E-02	8.9E-223	---
Sn-119m	9.88E-169	3.30E-02	3.3E-170	---
Sn-121	0.00E+00	1.20E-02	0.0E+00	No Limit
Sn-121m	7.53E-130	1.80E-01	1.4E-130	---
Sn-123	4.41E-209	3.30E-03	1.5E-211	---
Sn-126	4.16E-127	7.70E+01	3.2E-125	---

[1] From Lee (2006)
[2] Dose to MEI at 100 m = Peak Flux × Dose Release Factor
[3] Disposal Limit = 10 mrem/yr / Dose to MEI at 100 m per year per Ci
--- represents llimits >1E20 Ci

Table 3-45. Overall LAW Vault Air-Pathway Disposal Limit

Radionuclide	0 - 125-Year LAW Vault Disposal Limits[1] (Ci)	125 –1125-Year LAW Vault Disposal Limits[2] (Ci)	Overall LAW Vault Air-Pathway Disposal Limit (Ci)
C-14 as CO_2	3.3E+03	---	3.3E+03
Cl-36 as Cl_2	2.0E+03	---	2.0E+03
I-129 as I_2	1.7E+01	---	1.7E+01
S-35	1.1E+04	NL	1.1E+04
Sb-124	3.0E+02	---	3.0E+02
Sb-125	9.2E+01	---	9.2E+01
Se-75	4.3E+02	---	4.3E+02
Se-79	7.5E+02	---	7.5E+02
Sn113	2.5E+03	---	2.5E+03
Sn-119m	5.7E+03	---	5.7E+03
Sn-121	3.1E+04	NL	3.1E+04
Sn-121m	8.9E+02	---	8.9E+02
Sn-123	4.7E+04	---	4.7E+04
Sn-126	2.0E+00	---	2.0E+00
H-3[3]	Maximum Permissible Annual Inventory		4.5E+06
H-3[3]	Maximum Permissible Total Inventory over 25-year Operational Period		1.1E+08

[1] From Table 3-43 except for Tritium
[2] From Table 3-44 except for Tritium
[3] From Table 3-42 for Tritium
NL = No Limit
Note: Limits reported as "---" signify a number >1E+20
Note: Limits for special waste forms (i.e., I-129_H and I-129_J) are the same as for the generic radionuclide.

3.8 LAW VAULT ALL-PATHWAYS ANALYSIS

This section documents the development of preliminary all-pathways limits for the LAW Vault. The limits developed within this section are considered preliminary, since they do not take into consideration the effects of plume overlap from adjacent units or the results of sensitivity and uncertainty analyses. The effects of plume overlap are considered in Chapter 6 and the interpretation of sensitivity and uncertainty analyses is conducted in Chapter 7. Final limits are provided in Chapter 7.

3.8.1 Overview of All-Pathways Analysis

This section describes the investigation conducted to evaluate the potential magnitude of the all-pathways dose from the LAWV over the 25-year operational period, 100-year institutional control period, and 1000-year post-closure compliance period. The permissible all-pathways dose for DOE LLW disposal facilities is addressed in DOE M 435.1, IV.P.(1)(a) (DOE 1999). This requirement is that dose to representative members of the public shall not exceed 25 mrem (0.25 mSv) in a year total effective dose equivalent from all exposure pathways, excluding the dose from radon and its progeny in air.

Although the all-pathways performance objective includes not only all exposure pathways, but also all transport pathways. In this PA, the air pathway is evaluated separately. The all-pathways dose evaluated here includes only the groundwater transport pathway because the receptors for the groundwater and air pathways will likely be at different locations and the maximum doses from the two pathways will occur at different times.

The all-pathways analysis uses the groundwater concentrations developed in Section 2.6. The concentrations as a function of time are input into the all-pathways application (Koffman 2006), which calculates dose to humans from direct ingestion of contaminated groundwater and consumption of locally grown leafy vegetables, produce, milk, and meat, which are contaminated with radionuclides from use of the groundwater for irrigation and direct consumption by the cattle (Section C.4.5).

3.8.2 All-Pathways Assumptions

Key assumptions and inputs used in the all-pathways analysis are presented in Appendix B.

3.8.3 LAW Vault All-Pathways Analysis

Radionuclide disposal limits for the LAWV were developed from the PORFLOW results, using the all-pathways application (Koffman 2006). The application uses the results of the PORFLOW program to calculate the dose to a hypothetical individual from using the groundwater at the point of assessment (location of the maximum concentration of each radionuclide outside of a 100-m buffer zone) for all credible purposes (drinking, irrigation of crops and ingestion of the crops and the meat and milk of animals fed on the crops and groundwater). The preliminary limits are shown in Table 3-46.

Table 3-46. Preliminary All-pathways Radionuclide Disposal Limits for the LAW Vault

Parent Radionuclide	Inventory Limit, Ci
Am-241	2.4E+08
Am-243	2.1E+15
C-14	9.2E+00
Cl-36	1.4E+00
Cm-244	---
Cm-245	1.7E+08
Cm-247	4.3E+16
Cm-248	---
H-3	5.5E+10
I-129	2.9E-01
I-129_H	6.9E+00
I-129_J	1.2E+00
K-40	---
Mo-93	1.5E+01
Nb-94	2.7E+01
Ni-59	3.6E+12
Np-237	3.7E+05
Pd-107	5.5E+12
Pu-238	2.7E+13
Pu-239	9.2E+13
Pu-240	---
Pu-241	7.0E+09
Pu-242	---
Pu-244	---
Ra-226	1.1E+06
Se-79	---
Sn-126	---
Sr-90	6.6E+16
Tc-99	7.8E+02
Th-230	8.1E+06
Th-232	---
U-233	---
U-234	5.1E+09
U-235	1.9E+07
U-236	---
U-238	1.4E+13
Zr-93	8.8E+02

3.9 INADVERTENT INTRUDER ANALYSIS

The inadvertent intruder analysis considers the radiological impacts to hypothetical persons who are assumed to intrude into the Low-Activity Waste Vault (LAWV) disposal units at the EALLWF after institutional control ceases 100 years after facility closure. Descriptions of intruder scenarios are provided in the Background chapter in Part C of this PA. The analysis was carried out using an automated computer application developed at SRNL (Koffman 2006), which implements equations calculating dose per unit intake documented in Lee (2004). One important functional requirement of the application is that it computes a "no leaching" case in which the full decay chain is determined and the activities are calculated at specified times using the Bateman equation. This means that the intruder calculations are completely independent from the PORFLOW calculations.

3.9.1 LAW Vault Intruder Analysis Key Assumptions

These are intruder analysis key assumptions and inputs specific to the LAW Vault (see also Appendix B).

Intruder Pathway

1. Reinforced concrete roof prevents excavation and drilling into the disposed waste for at least 1,000 years, which makes intrusive intruder scenarios – agriculture and post-drilling – not credible.
2. Erosion barrier in closure cap, as described in Phifer and Nelson (2003), will prevent erosion below the top of the erosion barrier over 10,000 years thus maintaining a minimum of 7.7 feet of clean material over the top of the disposed waste. This includes the following thicknesses of materials:

Thickness (inches)	Description
36	Soil cover
12	Erosion barrier
64.4	Backfill to bottom of Erosion Barrier
16	Vault roof (16")

3. The volume of disposed waste will be approximately 1,080,000 ft^3.

Factors Affecting Operations

4. Final Closure - The final closure of the entire ELLWF at the end of the 100-year Institutional Control period will be done using the Final Closure system conceptual design and installation measures described in the E-Area Closure Plan (Cook et al. 2004).
5. The layout of the LAW Vault and any future adjacent disposal units will be such that the actual area taken up by the LAW Vault (i.e., 145' by 643.33') takes up 80% of the area assigned to the vault (i.e., ~116,600 ft^2).

3.9.2 LAW Vault Specific Parameters

The LAW Vault reinforced concrete roof prevents excavation and drilling into the exposed waste for at least 1,000 years (structural failure has been projected to occur at 2805 years (Carey 2006)). Therefore, the intrusive intruder scenarios (i.e., agricultural and post-drilling) are not credible. The final closure system for the ELLWF includes a 12-inch thick erosion barrier near the top of the cap. Because the erosion barrier is assumed to never erode and all the layers between the waste and the erosion barrier always remain in place at their design thickness, approximately 7.7 ft of material always exists above the waste. The erosion barrier has been shown to be effective for at least 10,000 years (Phifer and Nelson 2003) so that all the layers between the waste and the erosion barrier always remain in place at their design thickness, approximately 7.7 ft of material always exists above the waste. The resident scenario is credible for the LAW Vaults after the institutional control period of 100 years.

The parameters specific to the LAW Vault Disposal Units used in the intruder analysis are given in Table 3-47. The geometry factors and erosion rate are documented in McDowell-Boyer et al. (2000). The waste volume for the LAW Vault is consistent with that presented in Section 3.5.3. The "degradation duration" of 1800 years reflects the fact that structural stability of the LAW Vault can be assumed for that period of time (see discussion in Section 3.6.3.1).

Table 3-47. Intruder Parameters for the LAW Vault Disposal Units

Facility	E-Area
Disposal Unit Name	Low Activity Waste Vaults
Abbreviated Name	LAW Vaults
Agriculture Geometry Factor	0.8
Resident Geometry Factor	0.8
Post-Drilling Geometry Factor	1
Waste Volume (ft3)	1080000

Transient Layer Model (Surface to Top of Waste)

Layer	Thickness (inches)	Description	Erosion Rate (mm/yr)	Erosion Earliest Start (yr)	Degradation Duration (yr)	Degradation Start (yr)
1	36	Soil cover	1.4			
2	12	Erosion barrier	1.4	1.00E+10		
3	64.4	Soil backfill	1.4			
4	16	Vault roof	1.4		1800	0

3.9.3 Results

Performance measures for intruders are 100 mrem/yr for chronic exposure and 500 mrem/yr for acute exposure for total effective dose equivalent excluding radon in air. Performance measures are used to establish the intruder disposal limits.

Results of the resident intruder analyses for LAW Vault disposal units for the time period of 1,000 years are provided in Table 3-48. The entry "---" in the Time of Limit column means that the dose calculation is always zero so there is no limit. For cases where there is a time given, there may be an entry "---" in one or both of the limit columns. In this case the entry "---" indicates a limit value greater than or equal to the threshold value of 1E+20. Additional details are provided in Part C Background, Section 4.4. Because the automated method applies a transient analysis, it calculates the lowest inventory limit for the entire time period, regardless of when it occurs.

Table 3-48. Intruder-Based Radionuclide Disposal Limits for Low Activity Waste Vaults – Resident Scenario with Transient Calculation for 1000 Years

		Concentration	Inventory
	Time of Limit	Limit	Limit
Radionuclide	(Years)	($\mu Ci/m^3$)	(Ci/Unit)[1]
Ac-227	100	1.17E+06	3.6E+04
Ag-108m	100	4.79E+03	1.5E+02
Al-26	100	6.27E+02	1.9E+01
Am-241	1000	8.27E+08	2.5E+07
Am-242m	100	1.95E+06	5.9E+04
Am-243	100	4.10E+05	1.3E+04
Ar-39	---	---	---
Ba-133	100	4.45E+07	1.4E+06
Bi-207	100	1.61E+04	4.9E+02
Bk-249	100	2.55E+07	7.8E+05
C-14	---	---	---
Ca-41	---	---	---
Cd-113m	---	---	---
Cf-249	100	6.58E+04	2.0E+03
Cf-250	100	4.00E+14	1.2E+13
Cf-251	100	1.33E+06	4.1E+04
Cf-252	1000	1.93E+14	5.9E+12
Cl-36	---	---	---
Cm-242	1000	4.62E+11	1.4E+10
Cm-243	100	6.80E+06	2.1E+05
Cm-244	100	4.39E+16	1.3E+15
Cm-245	100	7.01E+06	2.1E+05
Cm-246	1000	1.81E+15	5.5E+13
Cm-247	1000	5.00E+04	1.5E+03
Cm-248	1000	1.41E+09	4.3E+07
Co-60	100	4.53E+08	1.4E+07
Cs-134	100	1.15E+18	3.5E+16
Cs-135	---	---	---
Cs-137	100	1.10E+05	3.3E+06
Eu-152	100	4.14E+05	1.3E+04
Eu-154	100	7.14E+06	2.2E+05
Eu-155	100	1.23E+14	3.8E+12
H-3	---	---	---
I-129	100	---	6.1E+18
K-40	100	1.17E+04	3.6E+02
Kr-85	100	2.74E+09	8.4E+07
Mo-93	---	---	---
Na-22	100	4.74E+14	1.4E+13
Nb-93m	---	---	---
Nb-94	100	2.80E+03	8.6E+01
Ni-59	---	---	---
Ni-63	---	---	---
Np-237	1000	1.33E+05	4.1E+03
Pa-231	230	4.68E+04	1.4E+03
Pb-210	100	1.16E+10	3.5E+08
Pd-107	---	---	---

Table 3-48. Intruder-Based Radionuclide Disposal Limits for Low Activity Waste Vaults – Resident Scenario with Transient Calculation for 1000 Years - continued

Radionuclide	Time of Limit (Years)	Concentration Limit ($\mu Ci/m^3$)	Inventory Limit (Ci/Unit)[1]
Pu-238	1000	2.35E+09	7.2E+07
Pu-239	100	2.00E+10	6.1E+08
Pu-240	1000	6.70E+14	2.1E+13
Pu-241	1000	2.52E+10	7.7E+08
Pu-242	1000	1.60E+12	4.9E+10
Pu-244	100	1.12E+04	3.4E+02
Ra-226	100	1.19E+03	3.6E+01
Ra-228	100	8.00E+07	2.4E+06
Rb-87	---	---	---
S-35	---	---	---
Sb-125	100	1.69E+15	5.2E+13
Sc-46	100	---	---
Se-79	---	---	---
Sm-151	---	---	---
Sn-121m	---	---	---
Sn-126	100	3.05E+03	9.3E+01
Sr-90	---	---	---
Tc-99	100	1.48E+13	4.5E+11
Th-228	100	4.57E+18	1.4E+17
Th-229	100	2.54E+04	7.8E+02
Th-230	1000	3.27E+03	1.0E+02
Th-232	180	6.50E+02	2.0E+01
U-232	100	2.18E+03	6.7E+01
U-233	1000	2.80E+05	8.6E+03
U-234	1000	6.62E+05	2.0E+04
U-235	1000	8.34E+05	2.5E+04
U-236	1000	1.33E+10	4.1E+08
U-238	1000	2.48E+05	7.6E+03
W-181	100	---	---
W-185	100	---	---
W-188	100	---	---
Zr-93	---	---	---

[1]Unit refers to LAW Vault

3.10 LOW-ACTIVITY WASTE VAULT RADON ANALYSIS

3.10.1 Overview of Radon Analysis

This section describes the investigation conducted to evaluate the potential magnitude of radon release from the LAW Vault over the 25-year operational period, 100-year institutional control period, and 1000-year post-closure compliance period.

The flux of Rn-222 from the LAW Vault was evaluated for three separate time periods: 1) 0 to 25 years, 2) 25 to 125 years, and 3) 125 to 1125 years. The first time period evaluated covers the operational period. During this time period, waste containers are placed in the vault and the vault is open to the atmosphere. The second time period covers the institutional control period. During this time period, the vaults are sealed with reinforced concrete. The final time period covers the post-closure compliance monitoring period. During this time period, a closure cap is placed over the vault (Phifer et al. 2006).

The permissible radon flux for DOE facilities is addressed in DOE M 435.1-1 Chapter IV (DOE 1999). Specifically, Section IV. P(1)(c) states the radon flux limitations associated with the development of a disposal facility and maintenance of a performance assessment and the closure of the disposal facility. This requirement is that the release of radon shall be less than an average flux of 20 $pCi/m^2/s$ at the surface of the disposal facility. The requirements analysis states that this standard was adopted from the uranium mill tailings requirements in 40 CFR Part 192 and 10 CFR Part 40. 10 CFR Part 40 discusses both Rn-222 from uranium and Rn-220 from thorium, therefore the performance objective refers only to radon, and the correct species must be analyzed depending on the characteristics of the waste stream.

This guidance forms the basis for the investigation to evaluate radon flux from the LAW Vault. The scope of the investigation involved defining a decay chain of parent radionuclides to evaluate with a 1-D, vertical, numerical model. This analysis applies the capability of the standard SRS groundwater simulation program (PORFLOW) to model gas phase transport through partially saturated porous media to the ground surface. The model was customized to represent the vertical dimension of the LAW Vault and the anticipated cover material. The instantaneous Rn-222 flux at the land surface was evaluated for the three time periods previously mentioned and the maximum flux was then compared to the DOE performance objective.

This investigation addresses only Rn-222 from uranium. It is assumed that the short half-life of Rn-220 (55.6 seconds) renders it unable to escape the waste containers and LAW Vault and migrate to the land surface via air-diffusion before it is transformed by radioactive decay.

The potential parent radionuclides that can contribute to the creation of Rn-222 are illustrated in Figure 3-31. The diagram indicates the specific decay chains that lead to the formation of Rn-222, as well as the half-lives for each radionuclide. The extremely long half-life of U-238 (4.468E+9 years) cause the other radionuclides higher up on the chain of parents to be of little concern with regard to their potential to contribute significantly to the Rn-222 flux at the land surface over the period of interest.

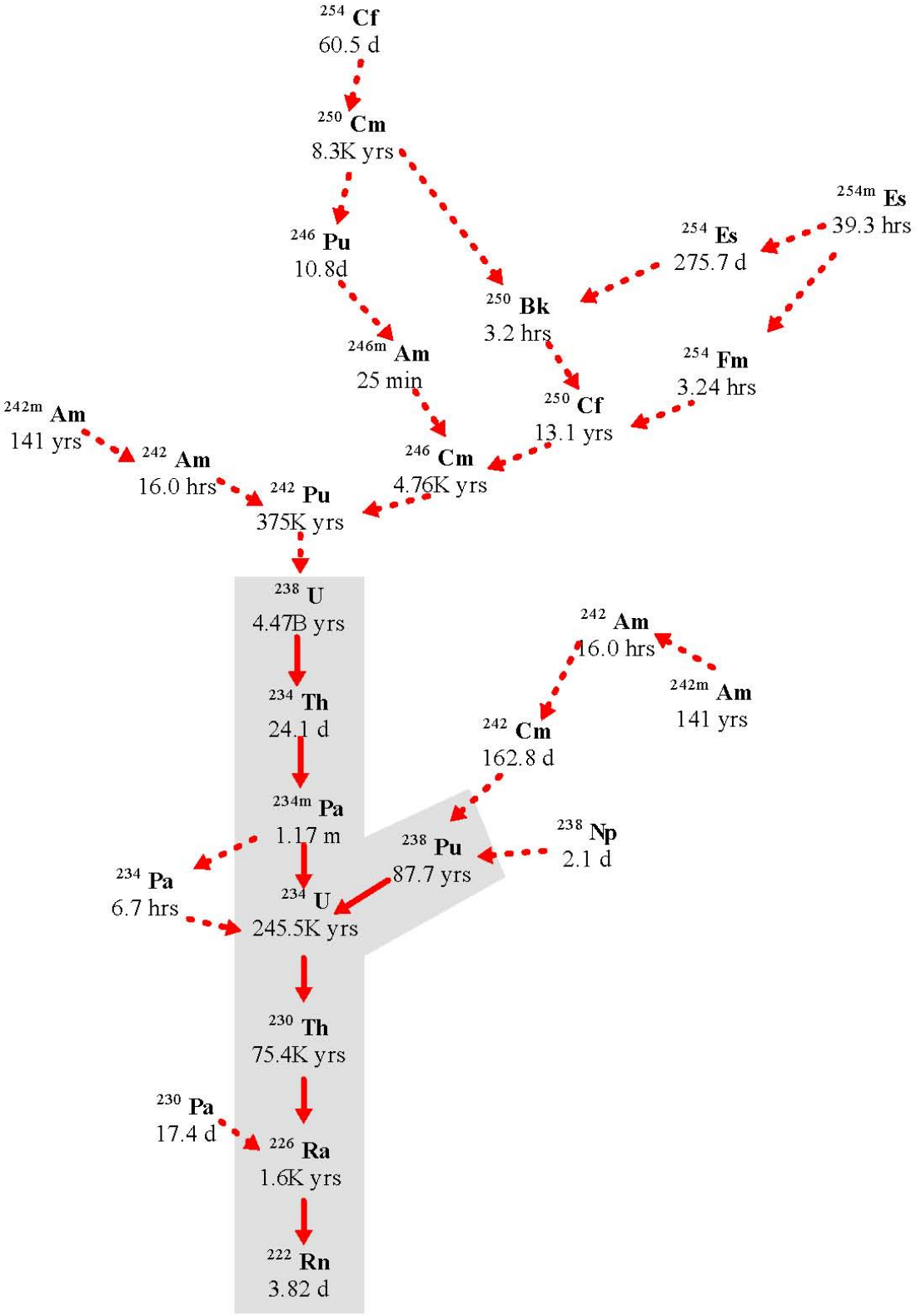

Figure 3-31. Radioactive Decay Chains Leading to Rn-222

3.10.2 Radon Analysis Assumptions

Key assumptions and inputs used in the radon analysis are presented in Appendix B.

3.10.3 LAW Vault Radon Analysis Conceptual Model

3.10.3.1 LAW Vault Closure Considerations

The concepts for closure of the LAW Vault are relevant to the determination of the radon flux at the land surface. The LAW Vault construction specifics and closure concept are described by Phifer et al. (2006). For the purposes of this investigation, it is assumed that during the operational time period, waste containers are placed in the vault and the vault is open to the atmosphere. Therefore, during this time period, the Rn-222 flux is evaluated immediately outside the waste containers. During the institutional control time period, the vault openings are sealed with reinforced concrete and the Rn-222 flux was evaluated at the top of the roof. For the post-closure compliance period, a closure cap is placed over the vault. A conceptual drawing of the closure cap over the waste vault is shown in Figure 3-28 and the vertical section over which Rn-222 was evaluated is indicated.

The closure cap utilized in this analysis includes all materials, as constructed and placed over the LAW Vault. The components of concern for the long-term radon performance calculation are those that have no potential to erode during the 1000-year post-closure compliance period. These components are situated below the top of the erosion barrier. For this analysis, the closure cap is assumed to remain intact over the 1000 year post closure monitoring period. The composite thickness of the non-waste material below the top of the closure cap is 7.67 ft (2.34 m) during the post closure compliance period. Table 3-49 lists the individual components of the LAW Vault and closure cap (excluding the layers overlying the erosion barrier). Materials are indicated with the associated thickness of each component, in inches, feet, and meters.

The closure cap utilized in this analysis includes all materials, as constructed and placed over the LAW Vault. The components of concern for the long-term radon performance calculation are those that have no potential to erode during the 1000-year post-closure compliance period. For this analysis, the closure cap is assumed to remain intact over the 1000 year post closure monitoring period. The composite thickness of the non-waste material below the top of the closure cap is 7.67 ft (2.34 m) during the post closure compliance period. Table 3-49 lists the individual components of the LAW Vault and closure cap. Materials are indicated with the associated thickness of each component, in inches, feet, and meters.

Table 3-49. Vertical Layer Sequence and Associated Thickness for the LAW Vault Cover Material and Waste

Layer	Thickness (inches)	Thickness (ft)	Thickness (m)
Erosion barrier	12	1	0.30
Middle backfill layer	12	1	0.30
Gravel drainage layer	12	1	0.30
Lower backfill layer	40	3.33	1.02
LAW Vault Roof	16	1.33	0.41
LAW Vault Waste Layer	294	24.5	7.47

SOURCE: Adapted from Phifer et al. (2006)

3.10.3.2 Conceptual Model

The Rn-222 flux at the land surface above the LAW Vault was evaluated for its specific closure configuration discussed above. Rn-222 is generated within the waste zone by radioactive decay of different parent radionuclides following along the decay chains that lead to the formation of Rn-222. The decay chains for all possible parent radionuclides of Rn-222 are shown in Figure 3-31. In this figure, the parent radionuclides that were individually evaluated are indicated with the gray shaded area (i.e., beginning with Pu-238 and U-238). Rn-222 generated within the waste zone is in the gaseous phase and diffuses outward from this zone into the air-filled soil pores surrounding the LAW Vault, eventually resulting in some of the radon emanating at the land surface. As such, air is the fluid through which Rn-222 diffuses, although some Rn-222 may dissolve in residual pore water. It is assumed that fluctuations in atmospheric pressure at the land surface that could induce small pulses of air movement into and out of the shallow soil column will have a zero net effect over the long-term period of evaluation in this study, thus advective transport of Rn-222 in air-filled soil pores is not considered to be a significant process when compared to air diffusion.

The parent radionuclides are assumed to exist in the solid phase and therefore do not migrate upward through the air-filled pore space, although they could be leached and transported downward from the waste zone by pore water movement. This potential downward migration of the parent radionuclides was not considered in the radon analysis.

The flux of Rn-222 from the LAW Vault was evaluated for three separate time periods: 1) 0 to 25 years, 2) 25 to 125 years, and 3) 125 to 1125 years. The first time period evaluated covers the operational period. During this time period, waste containers are placed in the vault and the vault is open to the atmosphere. The second time period covers institutional control period. During this time period the vaults are sealed with reinforced concrete. The final time period covers the post-closure compliance monitoring period. During this time period, a closure cap is placed over the vault (Phifer et al. 2006).

3.10.4 LAW Vault Radon Analysis Numerical Model

The mathematical model utilized in this report is provided by the PORFLOW simulation package. PC-based PORFLOW Version 5.97.0 was used to conduct a series of simulations. PORFLOW is developed and marketed by Analytic & Computational Research, Inc. to solve problems involving transient and steady-state fluid flow, heat and mass transport in multi-phase, variably saturated, porous or fractured media with dynamic phase change. PORFLOW has been widely used at the SRS and in the DOE complex to address major issues related to the groundwater and nuclear waste management.

The governing equation for mass transport of species k in the fluid phase is given by

$$\frac{\partial C_k}{\partial t} + \frac{\partial}{\partial x_i}(V_i C_k) = \frac{\partial}{\partial x_i}(D_{ij}\frac{\partial C_k}{\partial x_j}) + \gamma_k \qquad \text{Eq. 3-3}$$

Where

C_k	concentration of species k, Ci/m^3
V_i	fluid velocity in the i^{th} direction, m/yr
D_{ij}	effective diffusion coefficient for the species, m^2/yr
γ_k	net decay of species k, Ci/m^3yr
i, j	direction index
t	time, yr
x	distance coordinate, m

This equation is solved using PORFLOW to evaluate transient Rn-222 transport above the LAW Vault to evaluate Rn-222 flux at the land surface over time. As explained, advection is not considered to be a significant process when compared to air diffusion, so the advection term was disabled within PORFLOW and only the diffusive and net decay terms were evaluated.

3.10.4.1 Model Development and Assumptions

The numerical representation of the conceptual model is as a 1-dimensional vertical stack of elements configured to represent the thickness of the LAW Vault and overlying cover material associated with final closure.

Decay chains evaluated were U-238→Th-234→Pa-234m→U-234→Th-230→ Ra-226→Rn-222 and Pu-238 →U-234→Th-230→Ra-226→Rn-222. Each parent in these chains, except Th-234 and Pa-234m, were simulated separately as the starting point of the decay chain. Th-234 and Pa-234m have extremely short half-lives compared to the other parent radionuclides in these chains. Only a fraction of the Rn-222 generated by the decay of each parent is available for migration away from its source and into open pore space. Since the Rn-222 parent radionuclides exist as oxides or in other crystalline forms, only a fraction of Rn-222 generated by decay of Ra-226 has sufficient energy to migrate away from its original location into adjacent pore space before further decay occurs (3.82 day half-life for Rn-222).

The fraction of radon escaping its source and migrating into adjacent pore space is approximated by the use of a radon emanation coefficient. This coefficient has been shown to vary between 0.02 and 0.7 in soils but is typically 0.25 (Yu et al. 2001). This value is taken as the default factor value for the RESRAD program, developed for the US DOE. To account for this effect in the model, an effective source term of 0.25 Ci of parent radionuclide was utilized as the source term for each Ci disposed within the facility.

Since Rn-222 exists as a gas, air was assumed to be the medium within which radon transport occurs. The flow field was assumed to be isobaric and isothermal. The impact of naturally occurring fluctuations of atmospheric pressure is likely to have a zero net effect. Therefore, for the relatively long periods of time evaluated in this investigation, air-diffusion was the only transport mechanism simulated in the model and advective air-transport was assumed to be negligible.

For the first 25 years of simulation, the vault is open to the atmosphere. During this period, radon was allowed to diffuse from the waste zone based upon the open air diffusion coefficient for radon. For the 100 year institutional control period and the 1000 year post-compliance monitoring period, radon was allowed to diffuse through the air filled porosity of each material type. Some radon dissolves in pore water but since diffusion proceeds more slowly in that fluid, air diffusion was the only transport process by which Rn-222 was allowed to reach the land surface from the LAW Vault. This assertion is substantiated in Yu et al. (2001). In that report the D_{eff} for soil is reported to range from the radon open air diffusion coefficient of 1.0E-6 m^2/sec to that of fully saturated soil, 1.0E-10 m^2/sec. This 4-order of magnitude difference is consistent with the comparison of water diffusion coefficients to air diffusion coefficients of other common molecular compounds and reported in many references. Thus, the larger volume of water-filled pore space compared to air-filled pore space (maximum of 1 order of magnitude difference) is inconsequential, in terms of the ability of water-dissolved radon to diffuse through water-filled pores as compared to the ability of the same compounds to diffuse as gas in the vapor-filled pore spaces.

In this investigation, transport was allowed to proceed only through air-filled pore space and, therefore, residual pore water was treated as if it was part of the solid matrix material within the flow field. No credit was taken for airborne radon dissolving in pore water as it proceeds from the vault to the land surface although it has been observed to partition between air and water in the ratio of 4 to 1, respectively, at 20° C (Nazaroff and Nero 1988).

The boundary conditions imposed on the domain included:

- No-flux specified for all parent radionuclides at perimeter of the domain ($\partial C/\partial X = 0$ at x=0, x=1 and $\partial C/\partial Y = 0$ at y=0, $y=y_{max}$)
- No-flux specified for Rn-222 along sides and bottom ($\partial C/\partial X = 0$ at x=0, x=1 and $\partial C/\partial Y = 0$ at y=0)
- Rn-222 concentration set to 0 at land surface (top of erosion barrier) ($C = 0$ at $y=y_{max}$)

The initial condition imposed on the domain included:

- Rn-222 concentration set to 0 for the entire model domain at time = 0 ($C=0$ for $0 \leq x \leq 1$ at t=0 and $C=0$ for $0 \leq y \leq y_{max}$ at t=0)

The initial conditions for the model also assumed a 1 Ci inventory (prior to application of the emanation factor) of each parent radionuclide uniformly spread over the waste zone. The model does not account for an initial inventory of Rn-222 since it would readily migrate out of the waste containers prior to disposal operations and has a half-life of 3.8 days.

Simulations were conducted in transient mode for diffusive transport in air, with results being obtained over 1,125 years.

3.10.4.2 Measures Implemented to Ensure Conservative Results

In this analysis, several conditions introduce conservatism into the calculations. These include:

- The use of boundary conditions that force all of the Rn-222 to move upward from the waste disposal zone to the land surface. In reality, some of the Rn-222 diffuses sideways and downward in the air-filled pores surrounding the waste zone; hence ignoring this has the effect of increasing the radon flux at the land surface.
- Not taking credit for the removal of either Rn-222 or of the parent radionuclides by pore water moving vertically downward through the model domain. This mechanism would likely remove some dissolved Rn-222 in addition to the parent radionuclides, and therefore its omission has the effect of increasing the estimate of instantaneous Rn-222 flux at the land surface in simulations conducted as a part of this investigation.

- The addition of an extra 125 years to the required 1,000-year evaluation period to account for any Rn-222 generated during the operational and institutional control period, thus incrementally increasing the instantaneous Rn-222 flux.
- Not taking credit for the waste being stored in steel containers. For the first 25 years of simulation, the vault is open to the atmosphere and radon is allowed to diffuse directly from the waste. In reality, the steel containers will slow diffusion until the containers are breached by corrosion.
- Use of the top of the erosion layer in the soil cover as the land surface for the purpose of calculating the Rn-222 flux during the 125 to 1125 year time period. No credit is taken for the additional distance Rn-222 must migrate above the erosion barrier prior to that portion of the closure cap eroding away. This assumption impacts only Ra-226 (due to its relatively short half life).
- Ignoring the presence of the GCL within the final closure cap. The GCL should be near 100 percent saturation. Therefore, it will contain very little air-filled porosity within which radon transport could occur.
- During the post-closure time period (125 to 1125 years) assigning the concrete roof a low saturation associated with concrete rubble exposed to the atmosphere rather than a high saturation associated with buried concrete (i.e. the vault is overlain with a closure cap during the post-closure time period).

3.10.4.3 Grid Construction

The model grid was constructed as a node mesh 3 nodes wide by 54 nodes high. This mesh creates the vertical stack of 52 model elements, as shown in Figure 3-28. The grid extends upward to the top of the soil cover, since this is the minimum possible cover thickness that could exist during the 1,125-year evaluation period. A set of consistent units was employed in the simulations for length, mass and time, these being meters, grams and years, respectively.

3.10.4.4 Material Zones

The model domain was divided into two primary zones, the LAW Vault waste zone occupying the lower 24.5 ft (7.47 m) of the domain and the cover zone extending 7.67 ft. (2.34 m) above the waste zone to the top of the domain. The upper model elements were scaled to correspond to the geometry of the closure cap thickness while the lower model elements were scaled to correspond to the LAW Vault waste zone.

During the operational period (0 to 25 years) the vault is open to the atmosphere. During the institutional control period (25 to 125 years) the vault openings are sealed with reinforced concrete. Thus, during this time period, the land surface is assumed to be the top of the vault. During the post-closure time period (125 to 1125 years), the land surface is taken as top of the erosion resistant layer, within the closure cap, and no credit is taken for the compacted backfill and topsoil above that layer.

3.10.4.5 Material Zone Properties and Other Input Parameters

Material properties utilized within the 1-D numerical model were specified for six material zones defined within the model domain. Each material zone was assigned values of total porosity, long term average saturation, air-filled porosity, matrix density, air density, and an effective air-diffusion coefficient for Rn-222. An air fluid density of 1.24E+03 g/m^3 was used for all material zones. This air fluid density was obtained from the Bolz and Tuve (1973), *CRC Handbook of Tables for Applied Engineering Science* and represents that of standard atmospheric conditions.

During the operational period (0 to 25 years) the vault is open to the atmosphere. The layers associated with the LAW Vault during this period consist only of the waste layer. The LAW Vault waste zone was assigned a total porosity of 0.5 and particle density of 2.65 g/cm^3 assuming the waste is half air space. It was assumed the waste was dry and therefore the air filled porosity would equal the total porosity for this zone. While the model includes all the layers from the LAW Vault waste layer to the erosion barrier, during the first 25 years of simulation, the concrete roof and all overlying materials were assigned a porosity of 1.0 and a saturation of 0.

This has the effect of making these layers equivalent to air. Table 3-50 provides the values of particle density, total porosity, average saturation, and air-filled porosity utilized for the LAW Vault layers for the first 25 years.

During the institutional control period (25 to 125 years), the vault openings are sealed with reinforced concrete. The layers associated with the LAW Vault during this period consist of the waste layer and the concrete vault roof. The waste layer retains the properties from the operational period. The particle density and total porosity for the LAW Vault reinforced concrete roof was taken from Phifer et al. (2006). The properties of the LAW Vault roof were assumed to be similar to concrete exposed to the atmosphere as described by Sappington and Phifer (2005). The average saturation for the LAW Vault roof was calculated by dividing the in-field moisture content (0.096) by the saturated moisture content (0.132) as reported by Sappington and Phifer (2005). This yielded an average saturation of 0.73 for the LAW Vault reinforced concrete roof. As with the operational period, the model includes all the layers from the LAW Vault waste layer to the erosion barrier. However, during the 25 to 125 year time period, the closure cap materials were assigned a porosity of 1.0 and a saturation of 0. This has the effect of making these layers equivalent to air. Table 3-51 provides the values of particle density, total porosity, average saturation, and air-filled porosity utilized for the LAW Vault layers for the 25 to 125 year time period.

During the post-closure time period (125 to 1125 years) the layers associated with the LAW Vault consist of all layers from the waste layer to the erosion barrier. The waste layer and concrete roof retain the same properties as utilized for the 25 to 125 year period. The particle density of the lower backfill, gravel drainage layer, middle backfill, and erosion barrier (these materials collectively are considered the closure cap layers) was taken as 2.65 g/cm^3. This is based on the density of quartz and is regarded as representative of most SRS soils.

Table 3-50. Operational Period (First 25 Years) Layer Particle Density, Total Porosity, Average Saturation, and Air-Filled Porosity

Layer	Particle Density (g/cm^3)	Total Porosity (fraction)	Average Saturation (fraction)	Air-filled Porosity [3] (fraction)
Erosion barrier layer [1]	0	1	0	1
Middle backfill [1]	0	1	0	1
Gravel drainage layer [1]	0	1	0	1
Lower backfill [1]	0	1	0	1
LAW Vault concrete roof [1]	0	1	0	1
LAW Vault waste layer [2]	2.65	0.500	0	0.500

[1] During the first 25 years of simulation, the concrete roof and materials comprising the closure cap were assigned a porosity of 1.0 and an average saturation of 0 in order to represent air.

[2] The waste is assumed to be dry (i.e. saturation of 0) resulting in the air-filled porosity equaling the total porosity.

[3] Air-filled Porosity = (1 – Average Saturation) × Total Porosity

Table 3-51. Institutional Control Period (25 to 125 Years) Layer Particle Density, Total Porosity, Average Saturation, and Air-Filled Porosity

Layer	Particle Density (g/cm^3)	Total Porosity (fraction)	Average Saturation (fraction)	Air-filled Porosity [5] (fraction)
Erosion barrier layer [1]	0	1	0	1
Middle backfill [1]	0	1	0	1
Gravel drainage layer [1]	0	1	0	1
Lower backfill [1]	0	1	0	1
LAW Vault concrete roof [2, 4]	2.59	0.184	0.730	0.050
LAW Vault waste layer [3]	2.65	0.500	0	0.500

[1] During the first 25 years of simulation, the materials comprising the closure cap were assigned a porosity of 1.0 and an average saturation of 0 in order to represent air.

[2] Concrete roof particle density and total porosity taken from Phifer et al. (2006).

[3] The waste is assumed to be dry (i.e. saturation of 0) resulting in the air-filled porosity equaling the total porosity.

[4] Average saturation for the LAW Vault roof was calculated by dividing the in-field moisture content (0.096) by the saturated moisture content (0.132) as reported by Sappington and Phifer (2005).

[5] Air-filled Porosity = (1 – Average Saturation) × Total Porosity

Values for total porosity and long-term average moisture content for the closure cap materials were taken from Phifer (2003). Phifer (2003) evaluated infiltration through a closure cap over time as the closure cap degraded using the HELP model. The porosity and average moisture content values for a 10,000 year degraded closure cap were utilized, since this represented the greatest air filled porosity in which a gas could diffuse (values from earlier time periods were saturated, therefore choosing a period having unsaturated conditions was deliberately conservative). Average saturation and air-filled porosity values were calculated from the total porosity and long-term average moisture content. Table 3-52 provides the values of particle density, total porosity, average saturation, and air-filled porosity utilized for all the layers (i.e., waste layer to the erosion barrier) for the 125 to 1125-year time period.

The molecular diffusion coefficient of Rn-222 in open air is 347 m^2/yr (Nielson et al. 1984). Nielson et al. (1984) established a relationship between moisture saturation and the radon effective air-diffusion coefficient for various pore sizes of earthen materials. Using this method, a radon effective air-diffusion coefficient was determined for each material type based upon the average moisture saturation for the material. With the use of an effective air diffusion coefficient, tortuosity was assigned a unit value in each material zone. A summary of the radon effective air-diffusion coefficients by material zone and simulation period, are presented in Table 3-53.

Table 3-52. Post Closure Period (125 to 1125 Years) Layer Particle Density, Total Porosity, Long-Term Average Moisture Content, Average Saturation, and Air-Filled Porosity

Layer	Particle Density (g/cm^3)	Total Porosity (fraction)	Long-Term Average Moisture Content	Average Saturation (fraction)	Air-filled Porosity [6] (fraction)
Erosion barrier layer [1]	2.65	0.088	0.0726	0.825 [5]	0.015
Middle backfill [1]	2.65	0.375	0.2435	0.649 [5]	0.132
Gravel drainage layer[1]	2.65	0.375	0.1967	0.525 [5]	0.178
Lower backfill [1]	2.65	0.370	0.2710	0.732 [5]	0.099
LAW Vault Roof [2]	2.59	0.184	N/A[4]	0.730 [4]	0.050
LAW Vault waste layer [3]	2.65	0.500	0.000[3]	0.000	0.500

[1] Values for total porosity and long term average moisture content taken from Phifer (2003). Particle density is taken as 2.65, which is based on the density of quartz and regarded as fairly representative of most SRS soils.

[2] Concrete roof particle density and total porosity taken from Phifer et al. (2006).

[3] The waste is assumed to be dry (i.e. saturation of 0) resulting in the air-filled porosity equaling the total porosity.

[4] Average saturation for the LAW Vault roof was calculated by dividing the in-field moisture content (0.096) by the saturated moisture content (0.132) as reported by Sappington and Phifer (2005).

[5] Average Saturation = Long Term Average Moisture Content / Total Porosity

[6] Air-filled Porosity = (1 – Average Saturation) × Total Porosity

Table 3-53. Effective Air-Diffusion Coefficient

Layer	Effective Air-Diffusion Coefficient (m^2/yr)		
	Operational Period (First 25 Years)	Institutional Control Period (25 to 125 Years)	Post Closure Period (125 to 1125 Years)
Erosion barrier layer	347	347	0.79
Middle backfill	347	347	4.73
Gravel drainage layer	347	347	4.73
Lower backfill	347	347	2.84
LAW Vault Roof	347	2.84	2.84
LAW Vault waste layer	347	347	347

3.10.5 Model Results

Model simulations were conducted to evaluate the peak instantaneous Rn-222 flux at the land surface for the three periods of interest. These time periods include 0 to 25 years, 25 to 125 years, and 125 to 1125 years. Model results were output in $Ci/m^2/yr$, consistent with the set of units employed in the model. A graph of these results is shown in Figure 3-32, although the units are converted to $(pCi/m^2/sec)/(Ci/m^2)$, which are the units used to define the regulatory flux limit in DOE G 435.1-1. Figure 3-32 shows a sharp flux discontinuity at 125 years which results from the installation of the close cap.

The peak fluxes represent the peak Rn-222 flux per square meter at the land surface as defined for each simulation period and are listed below in Table 3-54. For the first 25 years of simulation, the vault is open to the atmosphere. During this period, radon was allowed to diffuse from the waste zone based upon the open air diffusion coefficient for radon. The land surface was taken as the top of the waste zone. The land surface for the 25 to 125 year time period was taken as the top of the reinforced concrete vault roof. The land surface for the 125 to 1125 year time period was taken as the top of the erosion control layer within the closure cap.

The calculated disposal limits per unit area and the disposal limits for the LAW Vault is presented in Table 3-55 for each of the 5 parent radionuclides. The unit-area disposal limit was calculated as follows:

Disposal Limit per unit area (Ci/m^2) = Regulatory limit (20 $pCi/m^2/s$) / Peak Inst. flux per unit area per unit inventory of parent radionuclide per unit area ($[pCi/m^2/s]/[Ci/m^2]$).

The unit area limits for each of the 5 parent radionuclides were calculated using the maximum Rn-222 flux for the three time periods. For each radionuclide, the maximum flux of Rn-222 was observed during the initial 25 year simulation period when there was no reinforced concrete roof or closure cap present. Therefore, the peak flux of Rn-222 during the initial 25 year period was used to calculate the unit area limits for each radionuclide. The unit area limits for each of the 5 parent radionuclides were converted to LAW Vault-specific radon disposal limits by multiplying the unit area limit for each by the area of the LAW Vault footprint (8666 m^2).

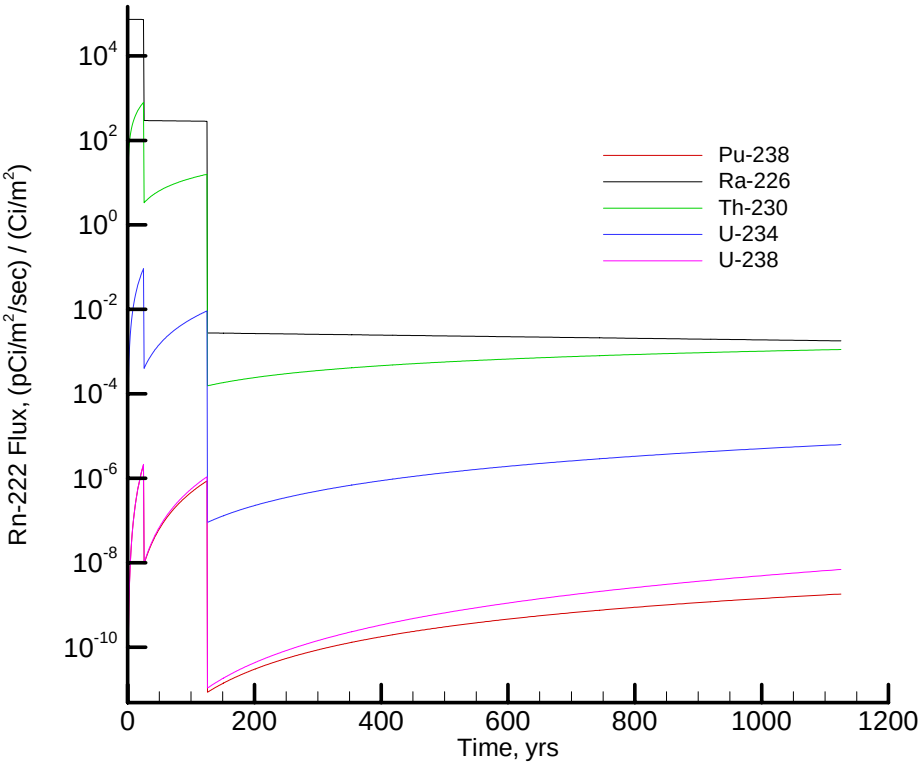

Figure 3-32. Rn-222 Flux at Land Surface Resulting from Unit Source Term

Table 3-54. Simulated Peak Instantaneous Rn-222 Flux over 1,125-Years at the Land Surface

	Peak Instantaneous Rn-222 flux at Land Surface ($pCi/m^2/sec$)/(Ci/m^2)*		
Parent Source	**0-25 years**	**25-125 years**	**125-1125 years**
Pu-238	2.06E-06	8.63E-07	1.82E-09
U-238	2.14E-06	1.08E-06	6.95E-09
U-234	9.16E-02	9.17E-03	6.28E-06
Th-230	7.94E+02	1.58E+01	1.12E-03
Ra-226	7.37E+04	2.96E+02	2.77E-03

* Flux resulting from unit source spread over unit area of trench (Ci/m^2)

Table 3-55. LAW Vault Disposal Limits for Parent Radionuclides

Parent Source	Peak Instantaneous Rn-222 flux at Land Surface (pCi/m2/sec)/(Ci/m^2)[1]	Time to Max (years)	Disposal Limit Per Unit Area[2] (Ci/m2)	LAW Vault Radon Disposal Limit[3] (Ci/LAW)
Pu-238	2.06E-06	25	9.70E+06	8.4E+10
U-238	2.14E-06	25	9.34E+06	8.1E+10
U-234	9.16E-02	25	2.18E+02	1.9E+06
Th-230	7.94E+02	25	2.52E-02	2.2E+02
Ra-226	7.37E+04	25	2.71E-04	2.4E+00

[1] Flux resulting from unit source term spread over unit area of trench (Ci/m^2).
[2] Preliminary Disposal Limit per unit area (Ci/m^2) = 20 pCi/m^2/s / Maximum Instantaneous Rn-222 flux at Land Surface
[3]LAW Vault Preliminary Radon Disposal Limit = Preliminary Disposal Limit per unit area (Ci/m^2) x 8666 m^2.

3.11 REFERENCES

Bolz, R.E. and G.L. Tuve, (Editors), 1973. *Handbook of tables for APPLIED ENGINEERING SCIENCE, 2'nd Edition*. CRC Press, 18901 Cranwood Parkway, Cleveland, OH.

Carey, S. 2005. Low Activity Waste (LAW) Vault Structural Degradation Prediction, T-CLC-E-00018, Rev. 0. Westinghouse Savannah River Company, Aiken, South Carolina. October 27, 2005.

Cook, J. R., Phifer, M. A., Wilhite, E. L., Young, K. E., and Jones, W. E. 2004. *Closure Plan for the E-Area Low-Level Waste Facility*, Revision 4, WSRC-RP-2000-00425. Westinghouse Savannah River Company, Aiken, South Carolina. May, 2004.

Cook, J.R. and Wilhite, E.L., 2004, Special Analysis: Radionuclide Screening Analysis for E-Area, WSRC-TR-2004-00294, June 1, 2004.

Crapse, K.P. and J.R. Cook, 2006. *Atmospheric Pathway Screening Analysis for the E-Area Low Level Waste Facility*, WSRC-STI-2006-00159, Washington Savannah River Company, Aiken, SC 29808. 09/05/2006.

Lee, P. 2006. *Atmospheric Dose Modeling for the E-Area Low Level Waste Facility at the Savannah River Site,* WSRC-STI-2006-00262, Washington Savannah River Company, Aiken, SC 29808.

DOE 1999. *Radioactive Waste Management Manual,* DOE M 435.1-1, Change 1:6-19-01, U.S. Department of Energy, Approved July 9, 1999.

Jannik, G. T. and Dixon, K. L, 2006. *LADTAP-PA: A Spreadsheet for Estimating Dose Resulting from E-Area Groundwater Contamination at the Savannah River Site*, WSRC-STI-2006-00123, Savannah River National Laboratory, Aiken, SC.

Jones, W. E. and Phifer, M. A. 2006. E-Area Low-Activity Waste Vault Subsidence Potential and Closure Cap Performance (U), WSRC-TR-2005-00405. Westinghouse Savannah River Company, Aiken, South Carolina. September 2006.

Kaplan, D.I. and J.L. Myers 2001, *Long-Term Dynamics of Lead Solubility in a Cementitious Groundwater Environment*, WSRC-TR-2000-00416, September 28, 2001.

Kaplan, D.I., 2006, *Geochemical Data Package for Performance Assessment Calculations Related to the Savannah River Site*, WSRC-TR-2006, 00004, February 28, 2006.

Koffman, Larry D. 2006. *SRNL All-Pathways Application,* WSRC-STI-2006-00179, Rev. 0, Savannah River National Laboratory, Aiken, SC 29808.

Lee, P. 2004. *Inadvertent Intruder Analysis Input for Radiological Performance Assessments,* WSRC-TR-2004-00295, Westinghouse Savannah River Company, Aiken, SC 29808.

Lee, P. 2006. *Atmospheric Dose Modeling for the E-Area Low Level Waste Facility at the Savannah River Site,* WSRC-STI-2006-00262, Washington Savannah River Company, Aiken, SC 29808.

McDowell-Boyer, L., Yu, A. D., Cook, J. R., Kocher, D. C., Wilhite, E. L., Holmes-Burns, H., and Young, K. E. 2000. *Radiological Performance Assessment for the E-Area Low-Level Waste Facility,* Revision 1, WSRC-RP-94-218. Westinghouse Savannah River Company, Aiken, South Carolina. January 31, 2000.

Nazaroff, W.W., and A.V. Nero (editors), 1998, *Radon and its Decay Products in Indoor Air*, John Wiley & Sons, New York, N.Y.

Nielson, K.K., V.C. Rogers and G.W. Gee, 1984. *Diffusion of Radon through Soils: A pore distribution Model*, Soil Science Society of America, J. 48:482-487.

Phifer, M. A. and Wilhite, E. L. 2001. Waste Subsidence Potential versus Supercompaction. WSRC-RP-2001-00613, Westinghouse Savannah River Company, Aiken, South Carolina. October 5, 2001,

Phifer, M. A. and Nelson, E. A. 2003. *Saltstone Disposal Facility Closure Cap Configuration and Degradation Base Case: Institutional Control to Pine Forest Scenario (U)*, Revision 0, WSRC-TR-2003-00436. Westinghouse Savannah River Company, Aiken, South Carolina, September 22, 2003.

Phifer, M.A. 2003. *Saltstone Disposal Facility Mechanically Stabilized Earth Vault Closure Cap Degradation Base Case: Institutional Control to Pine Forest Scenario (U).* WSRC-TR-2003-00523. Westinghouse Savannah River Company, Aiken, South Carolina. December 18, 2003.

Phifer, M. A., 2004. Preliminary E-Area Trench Closure Cap Closure Sequence, Infiltration, and Waste Thickness (U), WSRC-TR-2004-00119, Westinghouse Savannah River Company, Aiken, South Carolina. March 2004.

Phifer, M.A., M. A. Millings, G. P. Flach, 2006. *Hydraulic Property Estimation for the E-Area and Z-Area Vadose Zone Soils, Cementitious Materials, and Waste Zones (U).* WSRC-STI-2006-00198. Westinghouse Savannah River Company, Aiken, South Carolina. September 2003.

Sappington, F. C. and M. A. Phifer. 2005. *Moisture Content and Porosity of Concrete Rubble Study (U).* WSRC-TR-2005-00054, Rev. 0. Westinghouse Savannah River Company, Aiken, South Carolina. October, 2005.

Taylor, G. A. and L. B. Collard, 2005, *Automated Groundwater Screening*, WSRC-TR-2005-00203, October 31, 2005.

WSRC 2006. *SRS Waste Acceptance Criteria Manual,* Procedure Manual 1S, Washington Savannah River Company, Aiken, South Carolina. January 19, 2006.

Yu, C., A. J. Zielen, J. J. Cheng, D. J. LePoire, E. Gnanapragasam, S. Kamboj, J. Arnish, A. Wallo III, W. A. Williams, and H. Peterson, 2001. *Users Manual for RESRAD Version 6*, Environmental Assessment Division, Argonne National Laboratory. Chicago, Illinois.

This page intentionally left blank.

CHAPTER 4

INTERMEDIATE LEVEL VAULT (ILV)

This page intentionally left blank.

4.0 INTERMEDIATE LEVEL VAULT (ILV)

LIST OF FIGURES

LIST OF TABLES

4.0 INTERMEDIATE LEVEL VAULT

4.1 EXECUTIVE SUMMARY

The ILV disposal unit is a robust below-grade reinforced concrete structure, which contains grout encapsulated waste containers. The existing vault is the only one anticipated to be needed over the lifetime of 643-26E (WMAP 2006). The ILV is used to dispose of waste containers exceeding radiological dose and radionuclide concentration limits of the other, more cost effective, LLW disposal facilities, (e.g., trenches and LAWV).

ILV disposal limits through the 1,000 year compliance period have been developed for the following pathways: groundwater protection, air, all-pathways, inadvertent intruder (resident scenario), and radon. All instances of groundwater protection and all-pathways "limits" in this chapter refer to "preliminary limits" only, because they do not account for plume interaction or uncertainties. Table 4-1 provides these disposal limits. In Chapter 7 these limits will be adjusted in consideration of the result of the ILV sensitivity analyses reported in this chapter and the plume interaction analysis reported in Chapter 6. Trigger values for radionuclides that did not screen out of the groundwater and air analyses and were not specifically analyzed are given in Tables 4-4 and 4-5, respectively, in the Part C Background chapter. The trigger values were developed using very conservative screening methodologies and can be used as surrogate disposal unit limits should any of the listed radionuclides be proposed for disposal.

Table 4-1. Preliminary Groundwater Protection and All-Pathways Disposal Limits and Intruder, Air, and Radon Disposal Limits for the ILV

Limits Based on Years 0 - 200

Radionuclide	Beta-Gamma Limit (Ci)	Gross Alpha Limit (Ci)	Radium Limit (Ci)	Uranium Limit (Ci)	All-Pathways Limit (Ci)	Intruder Limit[1] (Ci)	Air-Pathway Limit[3] (Ci)	Radon Limit[4] (Ci)
Ac-227	---	---	---	---	---	4.2E+05	---	---
Ag-108m	---	---	---	---	---	1.4E+03	---	---
Al-26	---	---	---	---	---	6.8E+01	---	---
Am-241	---	---	---	---	---	5.5E+08	---	---
Am-242m	---	---	---	---	---	3.5E+05	---	---
Am-243	---	---	---	---	---	3.9E+05	---	---
Ar-39	---	---	---	---	---	---	---	---
Ba-133	---	---	---	---	---	2.6E+07	---	---
Bi-207	---	---	---	---	---	2.6E+03	---	---
Bk-249	---	---	---	---	---	1.4E+07	---	---
C-14	5.4E+16	--	---	---	5.6E+16	---	2.2E+05	---
C-14_KB[2]	8.6E+17	---	---	---	9.0E+17	---	2.2E+05	---
Ca-41	---	---	---	---	---	---	---	---
Cd-113m	---	---	---	---	---	---	---	---
Cf-249	---	---	---	---	---	3.6E+04	---	---
Cf-250	---	---	---	---	---	2.1E+16	---	---
Cf-251	---	---	---	---	---	2.0E+06	---	---
Cf-252	---	---	---	---	---	3.6E+13	---	---
Cl-36	1.9E+08	---	---	---	9.9E+07	---	1.3E+05	---
Cm-242	---	---	---	---	---	5.4E+10	---	---

Table 4-1. Preliminary Groundwater Protection and All-Pathways Disposal Limits and Intruder, Air, and Radon Disposal Limits for the ILV – continued

Limits Based on Years 0 - 200

Radionuclide	Beta-Gamma Limit (Ci)	Gross Alpha Limit (Ci)	Radium Limit (Ci)	Uranium Limit (Ci)	All-Pathways Limit (Ci)	Intruder Limit[1] (Ci)	Air-Pathway Limit[3] (Ci)	Radon Limit[4] (Ci)
Cm-243	---	---	---	---	---	7.5E+06	---	---
Cm-244	---	---	---	---	---	3.3E+16	---	---
Cm-245	---	---	---	---	---	2.2E+07	---	---
Cm-246	---	---	---	---	---	3.3E+14	---	---
Cm-247	---	---	---	---	---	2.6E+04	---	---
Cm-248	---	---	---	---	---	2.6E+08	---	---
Co-60	---	---	---	---	---	6.3E+07	---	---
Cs-134	---	---	---	---	---	2.6E+17	---	---
Cs-137	---	---	---	---	---	3.0E+04	---	---
Eu-152	---	---	---	---	---	6.3E+04	---	---
Eu-154	---	---	---	---	---	1.1E+06	---	---
Eu-155	---	---	---	---	---	1.1E+15	---	---
H-3	1.4E+08	---	---	---	3.8E+09	---	3.8E+06	---
H-3_TPBAR	2.4E+08	---	---	---	6.2E+09	---	9.4E+10	---
I-129	5.9E+10	---	---	---	3.5E+12	---	1.1E+03	---
I-129_ETF	3.9E+12	---	---	---	2.3E+14	---	1.1E+03	---
I-129_KB	2.1E+14	---	---	---	1.3E+16	---	1.1E+03	---
K-40	---	---	---	---	---	1.4E+03	---	---
Kr-85	---	---	---	---	---	1.0E+09	---	---
Mo-93	1.2E+04	---	---	---	5.4E+04	---	---	---
Na-22	---	---	---	---	---	7.4E+13	---	---

Table 4-1. Preliminary Groundwater Protection and All-Pathways Disposal Limits and Intruder, Air, and Radon Disposal Limits for the ILV – continued

Limits Based on Years 0 - 200

Radionuclide	Beta-Gamma Limit (Ci)	Gross Alpha Limit (Ci)	Radium Limit (Ci)	Uranium Limit (Ci)	All-Pathways Limit (Ci)	Intruder Limit[1] (Ci)	Air-Pathway Limit[3] (Ci)	Radon Limit[4] (Ci)
Nb-94	---	---	---	---	---	6.2E+02	---	---
Np-237	---	---	---	---	---	8.9E+04	---	---
Pa-231	---	---	---	---	---	1.7E+04	---	---
Pb-210	---	---	---	---	---	2.6E+09	---	---
Pu-238	---	---	---	---	---	2.7E+08	---	2.3E+11
Pu-239	---	---	---	---	---	1.1E+11	---	---
Pu-240	---	---	---	---	---	8.6E+13	---	---
Pu-241	---	---	---	---	---	1.7E+10	---	---
Pu-242	---	---	---	---	---	2.9E+11	---	---
Pu-244	---	---	---	---	---	2.1E+03	---	---
Ra-226	---	---	---	---	---	1.4E+02	---	2.0E+01
Ra-228	---	---	---	---	---	7.1E+06	---	---
S-35	---	---	---	---	---	---	7.6E+05	---
Sb-124	---	---	---	---	---	---	2.1E+04	---
Sb-125	---	---	---	---	---	5.7E+14	6.1E+03	---
Se-75	---	---	---	---	---	---	2.9E+04	---
Se-79	---	---	---	---	---	---	4.9E+04	---
Sn-113	---	---	---	---	---	---	1.7E+05	---
Sn-119m	---	---	---	---	---	---	3.8E+05	---
Sn-121	---	---	---	---	---	---	5.5E+06	---
Sn-121m	---	---	---	---	---	---	5.9E+04	---

Table 4-1. Preliminary Groundwater Protection and All-Pathways Disposal Limits and Intruder, Air, and Radon Disposal Limits for the ILV – continued

Limits Based on Years 0 - 200

Radionuclide	Beta-Gamma Limit (Ci)	Gross Alpha Limit (Ci)	Radium Limit (Ci)	Uranium Limit (Ci)	All-Pathways Limit (Ci)	Intruder Limit[1] (Ci)	Air-Pathway Limit[3] (Ci)	Radon Limit[4] (Ci)
Sn-123	---	---	---	---	---	---	3.2E+06	---
Sn-126	---	---	---	---	---	8.1E+02	1.3E+02	---
Sr-90	1.6E+15	---	---	---	3.0E+16	---	---	---
Tc-99	---	---	---	---	---	2.6E+14	---	---
Tc-99KB	---	---	---	---	---	2.6E+14	---	---
Th-228	---	---	---	---	---	3.8E+17	---	---
Th-229	---	---	---	---	---	4.2E+03	---	---
Th-230	---	---	---	---	---	3.8E+02	---	1.8E+03
Th-232	---	---	---	---	---	5.9E+01	---	---
U-232	---	---	---	---	---	1.8E+02	---	---
U-233	---	---	---	---	---	4.6E+04	---	---
U-234	---	---	---	---	---	7.7E+04	---	1.6E+07
U-235	---	---	---	---	---	6.5E+05	---	---
U-236	---	---	---	---	---	1.2E+09	---	---
U-238	---	---	---	---	---	4.5E+04	---	1.8E+11
W-181	---	---	---	---	---	---	---	---
W-185	---	---	---	---	---	---	---	---
W-188	---	---	---	---	---	---	---	---
Zr-93	---	---	---	---	---	---	---	---

Table 4-1. Preliminary Groundwater Protection and All-Pathways Disposal Limits and Intruder, Air, and Radon Disposal Limits for the ILV – continued

Limits Based on Years 200 - 1100

Radionuclide	Beta-Gamma Limit (Ci)	Gross Alpha Limit (Ci)	Radium Limit (Ci)	Uranium Limit (Ci)	All-Pathways Limit (Ci)	Intruder Limit[1] (Ci)	Air-Pathway Limit[3] (Ci)	Radon Limit[4] (Ci)
Ac-227	---	---	---	---	---	4.2E+05	---	---
Ag-108m	---	---	---	---	---	1.4E+03	---	---
Al-26	---	---	---	---	---	6.8E+01	---	---
Am-241	3.7E+10	1.8E+09	---	2.3E+19	5.7E+08	5.5E+08	---	---
Am-242m	---	---	---	---	---	3.5E+05	---	---
Am-243	1.9E+17	4.0E+15	---	---	4.7E+14	3.9E+05	---	---
Ar-39	---	---	---	---	---	---	---	---
Ba-133	---	---	---	---	---	2.6E+07	---	---
Bi-207	---	---	---	---	---	2.6E+03	---	---
Bk-249	---	---	---	---	---	1.4E+07	---	---
C-14	5.7E+02	--	---	---	5.9E+02	---	2.2E+05	---
C-14_KB[2]	1.0E+13	---	---	---	1.1E+13	---	2.2E+05	---
Ca-41	---	---	---	---	---	---	---	---
Cd-113m	---	---	---	---	---	---	---	---
Cf-249	---	---	---	---	---	3.6E+04	---	---
Cf-250	---	---	---	---	---	2.1E+16	---	---
Cf-251	---	---	---	---	---	2.0E+06	---	---
Cf-252	---	---	---	---	---	3.6E+13	---	---
Cl-36	8.8E+00	---	---	---	4.7E+00	---	1.3E+05	---

Table 4-1. Preliminary Groundwater Protection and All-Pathways Disposal Limits and Intruder, Air, and Radon Disposal Limits for the ILV – continued

Limits Based on Years 200 - 1100

Radionuclide	Beta-Gamma Limit (Ci)	Gross Alpha Limit (Ci)	Radium Limit (Ci)	Uranium Limit (Ci)	All-Pathways Limit (Ci)	Intruder Limit[1] (Ci)	Air-Pathway Limit[3] (Ci)	Radon Limit[4] (Ci)
Cm-242	---	---	---	---	---	5.4E+10	---	---
Cm-243	---	---	---	---	---	7.5E+06	---	---
Cm-244	---	---	---	---	---	3.3E+16	---	---
Cm-245	6.1E+10	3.0E+09	---	3.9E+19	9.4E+08	2.2E+07	---	---
Cm-246	---	---	---	---	---	3.3E+14	---	---
Cm-247	1.0E+19	2.2E+17	---	---	2.6E+16	2.6E+04	---	---
Cm-248	---	---	---	---	---	2.6E+08	---	---
Co-60	---	---	---	---	---	6.3E+07	---	---
Cs-134	---	---	---	---	---	2.6E+17	---	---
Cs-135	---	---	---	---	---	---	---	---
Cs-137	---	---	---	---	---	3.0E+04	---	---
Eu-152	---	---	---	---	---	6.3E+04	---	---
Eu-154	---	---	---	---	---	1.1E+06	---	---
Eu-155	---	---	---	---	---	1.1E+15	---	---
H-3	6.0E+11	---	---	---	1.6E+13	---	3.8E+06	---
H-3_TPBAR	3.2E+11	---	---	---	8.2E+12	---	9.4E+10	---
I-129	2.1E-02	---	---	---	1.3E+00	---	1.1E+03	---
I-129_ETF	7.5E-01	---	---	---	4.6E+01	---	1.1E+03	---
I-129_KB	4.5E+00	---	---	---	2.7E+02	---	1.1E+03	---
K-40	2.3E+13	---	---	---	5.1E+13	1.4E+03	---	---
Kr-85	---	---	---	---	---	1.0E+09	---	---

Table 4-1. Preliminary Groundwater Protection and All-Pathways Disposal Limits and Intruder, Air, and Radon Disposal Limits for the ILV – continued

Limits Based on Years 200 - 1100

Radionuclide	Beta-Gamma Limit (Ci)	Gross Alpha Limit (Ci)	Radium Limit (Ci)	Uranium Limit (Ci)	All-Pathways Limit (Ci)	Intruder Limit[1] (Ci)	Air-Pathway Limit[3] (Ci)	Radon Limit[4] (Ci)
Mo-93	8.1E+00	---	---	---	3.8E+01	---	---	---
Na-22	---	---	---	---	---	7.4E+13	---	---
Nb-93m	---	---	---	---	---	---	---	---
Nb-94	2.2E+05	---	---	---	1.2E+05	6.2E+02	---	---
Ni-59	2.1E+08	---	---	---	5.4E+10	---	---	---
Ni-63	---	---	---	---	---	---	---	---
Np-237	4.8E+06	2.4E+05	---	2.9E+15	7.4E+04	8.9E+04	---	---
Pa-231	---	---	---	---	---	1.7E+04	---	---
Pb-210	---	---	---	---	---	2.6E+09	---	---
Pd-107	2.6E+10	---	---	---	8.2E+10	---	---	---
Pu-238	1.9E+10	1.4E+08	1.8E+08	---	5.4E+08	2.7E+08	---	2.3E+11
Pu-239	1.4E+15	3.0E+13	---	---	3.5E+12	1.1E+11	---	---
Pu-240	---	---	---	---	---	8.6E+13	---	---
Pu-241	1.1E+12	5.7E+10	---	---	1.8E+10	1.7E+10	---	---
Pu-242	3.3E+17	2.3E+15	3.1E+15	---	9.0E+15	2.9E+11	---	---
Pu-244	---	---	---	---	---	2.1E+03	---	---
Ra-226	3.4E+03	2.5E+01	3.4E+01	---	9.9E+01	1.4E+02	---	2.0E+01
Ra-228	---	---	---	---	---	7.1E+06	---	---
Rb-87	---	---	---	---	---	---	---	---
S-35	---	---	---	---	---	---	7.6E+05	---
Sb-124	---	---	---	---	---		2.1E+04	---

Table 4-1. Preliminary Groundwater Protection and All-Pathways Disposal Limits and Intruder, Air, and Radon Disposal Limits for the ILV – continued

Limits Based on Years 200 - 1100

Radionuclide	Beta-Gamma Limit (Ci)	Gross Alpha Limit (Ci)	Radium Limit (Ci)	Uranium Limit (Ci)	All-Pathways Limit (Ci)	Intruder Limit[1] (Ci)	Air-Pathway Limit[3] (Ci)	Radon Limit[4] (Ci)
Sb-125	---	---	---	---	---	5.7E+14	6.1E+03	---
Sc-46	---	---	---	---	---	---	---	---
Se-75	---	---	---	---	---	---	2.9E+04	---
Se-79	---	---	---	---	---	---	4.9E+04	---
Sm-151	---	---	---	---	---	---	---	---
Sn-113	---	---	---	---	---	---	1.7E+05	---
Sn-119m	---	---	---	---	---	---	3.8E+05	---
Sn-121	---	---	---	---	---	---	5.5E+06	---
Sn-121m	---	---	---	---	---	---	5.9E+04	---
Sn-123	---	---	---	---	---	---	3.2E+06	---
Sn-126	---	---	---	---	---	8.1E+02	1.3E+02	---
Sr-90	1.5E+10	---	---	---	2.9E+11	---	---	---
Tc-99	2.0E+07	---	---	---	3.0E+07	2.6E+14	---	---
Tc-99_KB	2.8E+08	---	---	---	4.2E+08	2.6E+14	---	---
Th-228	---	---	---	---	---	3.8E+17	---	---
Th-229	---	---	---	---	---	4.2E+03	---	---
Th-230	1.2E+04	9.2E+01	1.2E+02	---	3.6E+02	3.8E+02	---	1.8E+03
Th-232	2.1E+15	2.1E+15	2.9E+15	---	5.7E+15	5.9E+01	---	---

Table 4-1. Preliminary Groundwater Protection and All-Pathways Disposal Limits and Intruder, Air, and Radon Disposal Limits for the ILV – continued

Limits Based on Years 200 - 1100

Radionuclide	Beta-Gamma Limit (Ci)	Gross Alpha Limit (Ci)	Radium Limit (Ci)	Uranium Limit (Ci)	All-Pathways Limit (Ci)	Intruder Limit[1] (Ci)	Air-Pathway Limit[3] (Ci)	Radon Limit[4] (Ci)
U-232	---	---	---	---	---	1.8E+02	---	---
U-233	---	---	---	---	---	4.6E+04	---	---
U-234	4.5E+06	3.3E+04	4.4E+04	---	1.3E+05	7.7E+04	---	1.6E+07
U-235	5.5E+08	1.2E+07	---	---	1.4E+06	6.5E+05	---	---
U-236	---	---	---	---	---	1.2E+09	---	---
U-238	7.9E+09	5.7E+07	7.5E+07	---	2.2E+08	4.5E+04	---	1.8E+11
W-181	---	---	---	---	---	---	---	---
W-185	---	---	---	---	---	---	---	---
W-188	---	---	---	---	---	---	---	---
Zr-93	2.6E+08	---	---	---	1.5E+09	---	---	---

[1] Special wasteforms for radionuclides C-14, H-3, I-129 and Tc-99 were not explicitly evaluated in the intruder analysis, however their intruder limit is assumed to be the same as that of the generic radionuclide. One intruder analysis was done over the period of performance; therefore the limits are the same for 0 to 200 years and 200 to 1100 years

[2] Waste containing C-14_KB is assumed to not be in Cell #4.

[3] Initial air-pathway modeling derived limits for 0-125 years and 125-1,125 years. However, a final overall conservative limit was derived to cover all time periods. This limit is included for both time frames (i.e., 0-200 years and 200-1100 years) given in Table 4-1.

[4] The initial modeling for Radon pathway examined three separate time periods (i.e., 0-25 years, 25-125 years, and 125-1,125 years). A single overall conservative limit was derived and is given for both time frames in Table 4-1.

4.2 INTRODUCTION AND GENERAL APPROACH

The Intermediate Level Vault disposal unit is a robust below-grade reinforced concrete structure, which contains grout encapsulated waste containers. The existing vault is the only one anticipated to be needed over the lifetime of 643-26E. The ILV is used to dispose of waste containers exceeding radiological dose and radionuclide concentration limits of the other, more cost effective, LLW disposal facilities, (e.g., trenches and LAWV).

ILV disposal limits through the 1,000 year compliance period have been developed for the following pathways: groundwater protection, air, all-pathways, inadvertent intruder (resident scenario and post-drilling scenario), and radon. All instances of groundwater protection and all-pathways "limits" in this chapter refer to "preliminary limits" only, because they do not account for plume interaction or uncertainties. A groundwater transport analysis has been conducted to determine maximum well concentrations (as a function of time) within a 100-m compliance region surrounding the ILV. The main analysis tool employed was the PORFLOW code (ACRI 2004), which handles both flow and transport of radionuclide chains (i.e., parents and daughters) in porous media. Two-dimensional flow and transport analyses were conducted to describe in detail the migration of radionuclides from the ILV through the vadose zone to the underlying water table. The results from these 2-D vadose zone simulations (treated as source terms) were then input into a 3-D aquifer transport model to compute maximum groundwater concentrations of radionuclides within the 100-m compliance region. Preliminary groundwater protection disposal limits over the 1,000 year compliance period for the ILV were developed from the computed maximum groundwater concentrations using the of the All-Pathways application (Koffman 2006a).

An air-pathway analysis has been conducted to determine air-pathway disposal limits for 15 potentially volatile radionuclides over the 1,000 year compliance period for the ILV. The PORFLOW code was utilized for diffusional transport of radionuclides out of the ILV to the ground surface and the CAP88 code was utilized for subsequent atmospheric transport and dose calculations. A one-dimensional PORFLOW diffusional transport analysis was conducted to determine the flux of radionuclides to the ground surface from the ILV. The atmospheric transport and dose calculation results obtained using CAP88 were combined with the flux of species at the ground surface to develop air-pathway disposal limits.

An inadvertent intruder analysis has been conducted to determine inadvertent intruder disposal limits over the 1,000 year compliance period for the ILV. The analysis was conducted using an automated inadvertent intruder computer application developed at SRNL (Koffman 2006b) for the resident and post-drilling inadvertent intruder scenarios.

A radon pathway analysis has been conducted to determine radon pathway disposal limits for 5 radon-producing parent radionuclides over the 1,000-year compliance period for the ILV. A one-dimensional PORFLOW diffusional transport analysis was conducted to determine the flux of radon to the ground surface from the ILV.

Within Chapter 7, Integration and Interpretation, the individual ILV disposal limits developed herein will be adjusted in consideration of the result of the ILV sensitivity analyses reported in this chapter and the plume interaction analysis reported in Chapter 6, Integrated Facility Analysis.

Plots of flux to the water table versus time and concentration versus time at the point of assessment for each radionuclide in the groundwater analysis are in Appendix A. A listing of the key inputs and assumptions used in the ILV assessment is given in Appendix B.

4.3 ILV GENERAL FACILITY DESCRIPTION AND LIFECYCLE

The IL Vault is a below-grade, reinforced concrete vault. It consists of two modules, which together encompass a 278.83-foot by 48.5-foot area. Figure 4-1 provides the layout of the ILV relative to other ELLWF disposal unit types. The ILT module contains two cells, whose inside dimensions are 25-foot by 44-foot 6-inches by 26-foot deep. ILT Cell #1 contains 144, 20-inch diameter by 20-foot long vertical silos. The ILNT module contains seven identical cells, whose inside dimensions are 25-foot by 44-foot 6-inches by 28-foot 5-inches deep. The area between the two modules provides manhole access to the subdrain system. Figure 4-2 provides photographs of the ILV exterior, Figure 4-3 shows the ILV interior, Figure 4-4 provides a plan view of the operational vault, and Figure 4-5 provides a cross-section of the operationally closed vault. The ILV consists of the following:

- Controlled compacted backfill soil base
- Graded stone sub-drainage system to collect and drain any water under the vault to a dry well
- Crusher Run stone base
- 30-inch thick, reinforced concrete, base slab, which extends 2 feet beyond the exterior walls
- Floors of each cell sloped to a drain which runs to a sump in the base slab of each cell, and is overlain by a minimum 14-inch (0.36 m) graded stone drainage layer
- 30-inch thick, reinforced concrete, exterior end walls and 24-inch thick, reinforced concrete, exterior side walls; and 18-inch thick, reinforced concrete, interior walls; all of which are structurally mated to the base slab and have no horizontal joints
- Exterior wall surfaces coated with a tar-based waterproofing and interior wall surfaces with a drainage net attached.

- Continuous waterstop seals at all concrete joints
- 1.5-foot thick, reinforced concrete, shielding tees available when necessary for radiation shielding over all bulk cells (the silo cell utilizes individual shielding plugs for each silo)
- Sloped rain covers, consisting of a roofing membrane on metal deck on steel framing installed over each cell, to direct rainwater onto the ground for runoff (used during operations only and will be replaced with a permanent concrete roof after cessation of operations)

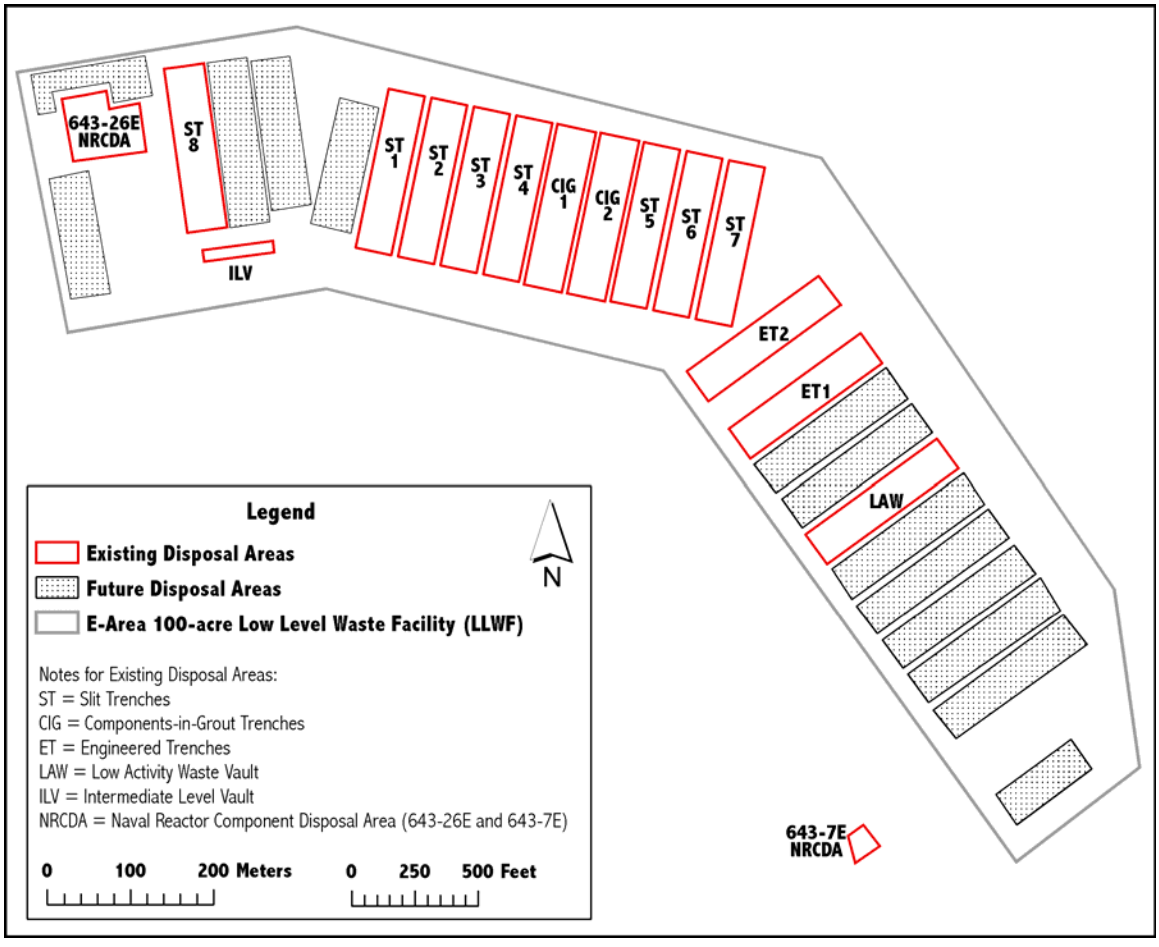

Figure 4-1. Location of the IL Vault within the ELLWF

Figure 4-2. ILV Overhead View

Figure 4-3. ILV Interior Views

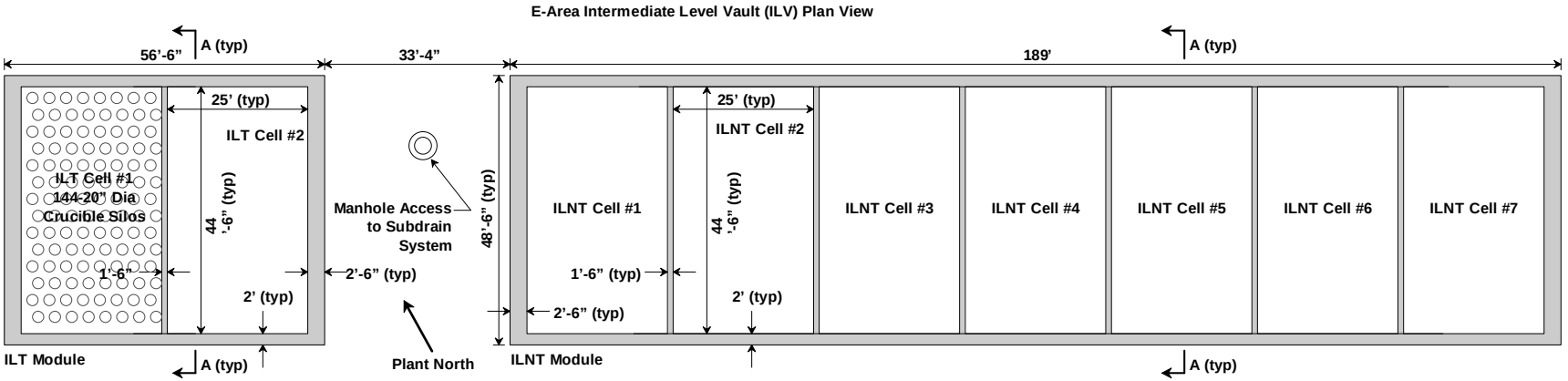

Note:
- RC Base Slab, which extends 2 feet beyond the eterior walls all around is not shown
- The top of the interior ILT wall is 2'-6" lower than exterior ILT walls
- The top of interior INLT walls are 1'-3" lower than exterior INLT walls

Figure 4-4. E-Area ILV Plan View

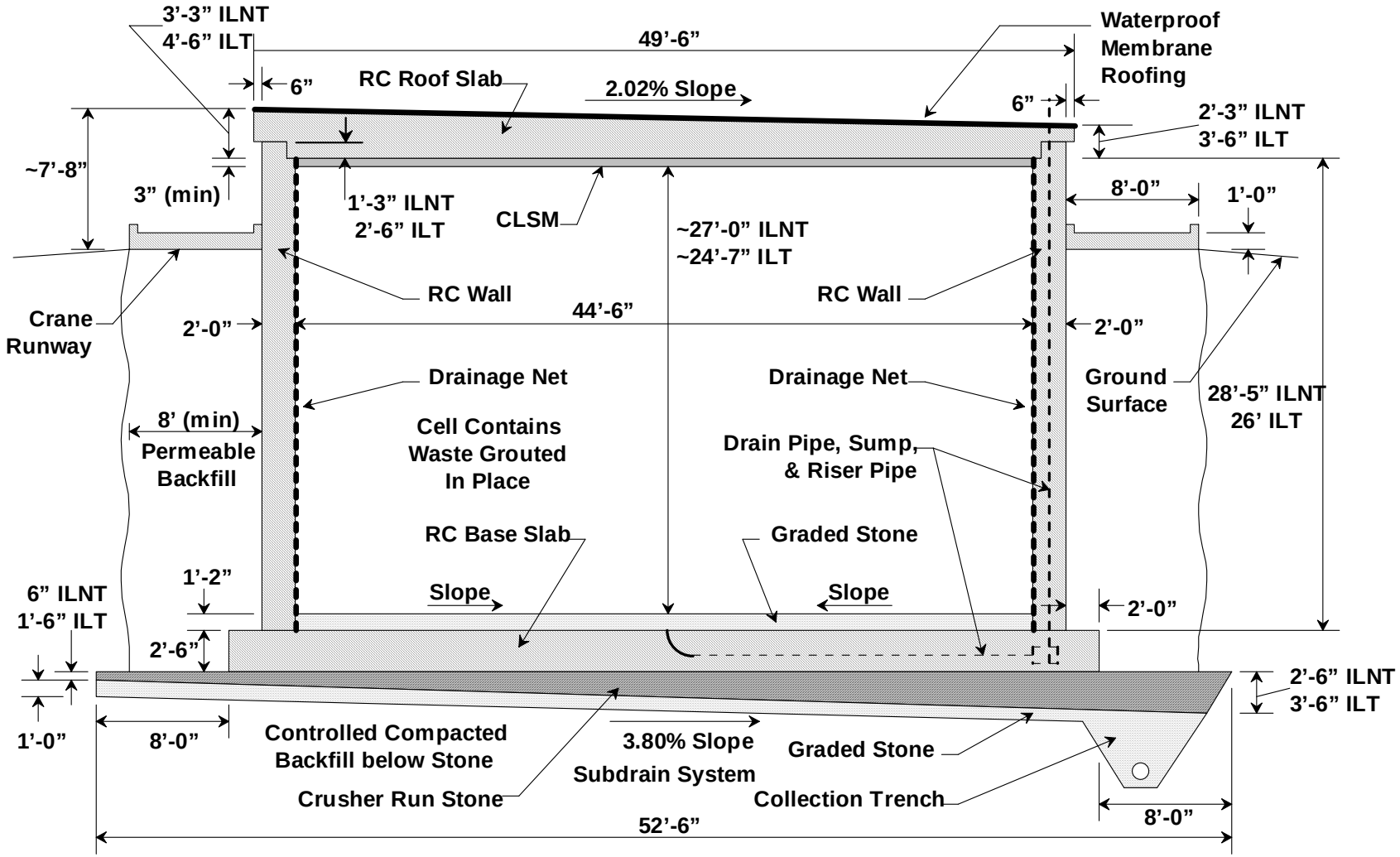

Figure 4-5. E-Area ILV Section A-A

Notes to Figure 4-5:

- Crucible Silos in ILT Cell #1 not shown
- Permeable backfill is sand with a maximum of 10% passing through a #200 sieve compacted to 90% minimum Proctor density
- Interior graded stone is ASTM D488-88 No. 57 and it is 1'-2" thick at walls and 1'-5" thick in cell center at drain; the top 6" of the stone is underlain by a geotextile fabric to prevent intrusion of grout into the bottom 8" of the stone
- Reinforced concrete base slab is 2'-6" at walls and 2'-3" in cell center at drain
- Crusher run stone is Georgia 25
- Exterior graded stone is ASTM D488-88 No. 57 or 67

During the 25-year operational period, tritium crucibles (or other compatible wasteforms) are placed in ILT Cell #1 as follows:

- The waste is placed in individual silos.
- A shielding plug is placed over each silo containing waste.

During the 25- year operational period, intermediate-activity waste is placed in ILT Cell #2 and ILNT Cells #1 through #7 as follows:

- The first layer of waste is placed within each cell directly on top of the graded stone drainage layer.
- The first layer of waste is encapsulated in grout which forms the surface for the placement of the next layer of waste.
- Subsequent layers of waste are placed directly on top of the previous encapsulated waste; however subsequent layers may be encapsulated with CLSM rather than grout.

The waste placed within ILT Cell #2 and ILNT Cells #1 through #7 typically consists of job control waste, scrap hardware, and contaminated soil and rubble, which is contained within metal or concrete containers. Containers predominately include drums, B-12 boxes, B-25 boxes, other metal containers, and concrete containers. Job control waste primarily consists of highly contaminated protective clothing (plastic suits, shoe covers, lab coats, etc.), plastic sheeting, etc. The scrap hardware consists of reactor hardware, jumpers, and used canyon and tank farm equipment. Soil and rubble is generated from demolition or remediation activities. Average waste density within the ILV containers has not been estimated; however with the assumption that the waste has a density similar to that of waste within the LAW Vault (i.e., 0.1785 g/cm^3) (Phifer and Wilhite 2001), a maximum subsidence potential of 19 feet is estimated.

Operational closure of the ILV will be conducted in stages. ILT Cell #1 will be operationally closed by placing a final layer of grout level with the top of the interior vault wall, with silo shielding plugs remaining in place within the final grout layer. ILT Cell #2 and ILNT Cells #1 through #7 will be operationally closed as they are filled with waste by removing any shielding tees and placing a final layer of grout or CLSM level with the top of the interior vault walls. The final layer over the ILT cells will have a minimum of 3 in of clean grout or CLSM above all waste material. After the entire ILT module has been filled, it will be operationally closed, by installing a 3-foot 6-inch to 4-foot 6-inch permanent reinforced concrete roof slab and overlying bonded-in-place fiberboard insulation and waterproof membrane roofing over the entire module. After the entire ILNT module has been filled, it will be operationally closed, by installing a 2-foot 3-inch to 3-foot 3-inch permanent reinforced concrete roof slab and overlying bonded-in-place fiberboard insulation and waterproof membrane roofing over the entire module. The rain covers and shielding tees will no longer be required after installation of the permanent roof slab. No additional closure actions are anticipated beyond that of operational closure for the ILV during the 100-year institutional control period (i.e. interim closure).

Final closure of the ILV will take place at final closure of the entire ELLWF, at the end of the 100-year institutional control period. Final closure will consist of the installation of an integrated closure system designed to minimize moisture contact with the waste and to provide an intruder deterrent. The integrated closure system will consist of one or more closure caps installed over all the disposal units and a drainage system. Figure 4-6 provides the ILV closure cap configuration. The apex of the closure cap will extend the length of the vault and be approximately centered over the vault, in order to minimize the overburden loads on the vault and maximize runoff and lateral drainage from the overlying closure cap.

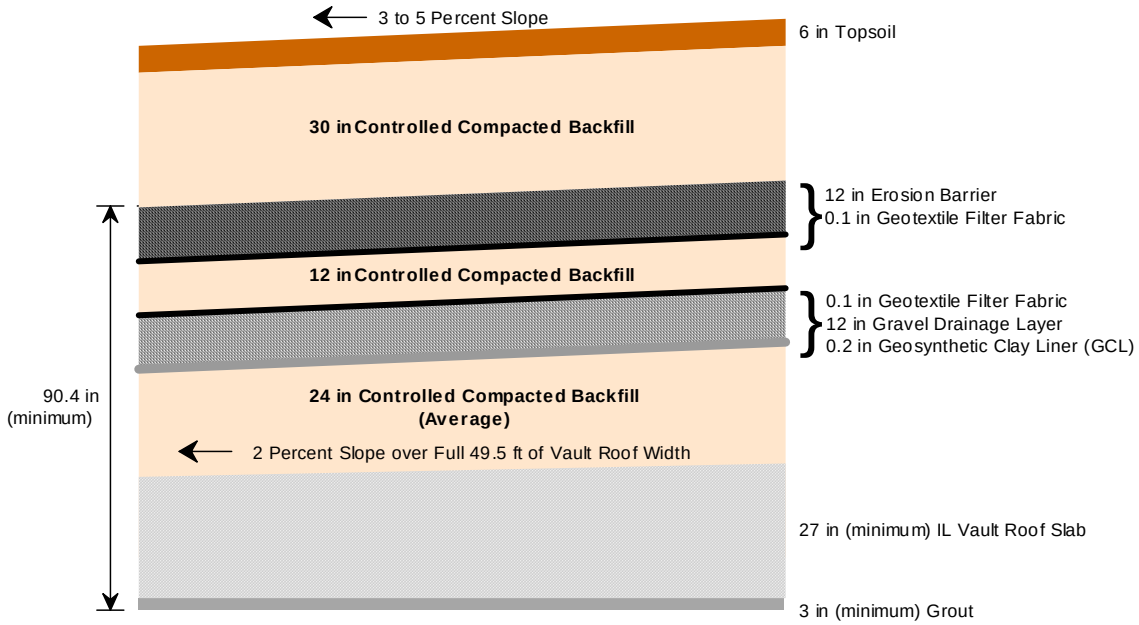

Figure 4-6. ILV Closure Cap Configuration

4.4 ILV PRINCIPAL DESIGN FEATURES

4.4.1 ILV Structural Stability and Cover Integrity

The ILV is designed to withstand Design Basis Accident loads (as specified in Project S2889) that ensure continued structural stability during its anticipated life. Peregoy (2006) conducted a structural degradation prediction analysis and documented the following significant degradation points in the life of the ILV:

- Upon placement of the closure cap overburden over the ILV, non-through-slab static cracking of the roof slab will occur and increase slightly over time.
- Upon placement of the closure cap overburden over the ILV, non-through-wall static cracking of the exterior side and end walls will occur and increase slightly over time.
- It is anticipated that the ILV roof slab will collapse due to closure cap and seismic loading and rebar corrosion at a mean time of 6703 years with a standard deviation of 1976 years.

- It is anticipated that the ILV roof slab will collapse due to rebar corrosion and a beyond Performance Category 4 (PC-4) earthquake event, if the PC-4 earthquake occurs at 5985 years or after. A PC-4 earthquake is one with a recurrence interval of 10,000 years at the facility location (DOE 2002). The probability of a beyond-PC-4 earthquake is 3% over a 1,000 year period.
- It is anticipated that the ILV exterior side and end walls will collapse due to closure cap and seismic loading and rebar corrosion at a mean time of 9427 years with a standard deviation of 2795 years.
- It is anticipated that differential settlement due to PC-4 seismic loading or greater will result in cracking of the INLT Cell #4 floor slab construction and control joints and extend a limited distance up the associated exterior wall vertical construction and control joints. The probability of a PC-4 earthquake is 9.5% over a 1,000 year period.

Average waste density within the ILV containers has not been estimated; however with the assumption that the waste has a density similar to that of waste within the LAW Vault (i.e., 0.1785 g/cm^3) (Phifer and Wilhite 2001), a maximum subsidence potential of 19 feet is estimated. This maximum subsidence potential will not impact the calculated structural stability of the ILVs until after both the time of anticipated roof structural failure (i.e. mean time of 6703 years) and the time of waste container collapse (not currently estimated) because no credit was taken for the wasteforms or backfill in the structural stability calculations. To be conservative it is assumed that the ILV roof will collapse into the vault itself and that subsidence of the overlying closure cap will occur at the time of roof structural failure.

The final ELLWF closure cap will be installed at the end of the 100-year institutional control period (Phifer 2004). After installation it is assumed that no closure cap maintenance will be performed other than that required for establishment of the vegetative cover. Therefore it is assumed that the hydraulic properties of the closure cap will immediately begin to degrade after construction due to the following (Phifer and Nelson 2003; Phifer 2004):

- Formation of holes in the upper GCL by pine forest succession
- Reduction in the saturated hydraulic conductivity of the drainage layers due to colloidal clay migration into the layers
- Erosion of layers that provide water storage for the promotion of evapotranspiration

As outlined above it has been estimated the ILV roof slab will structurally fail at a mean of 6703 years. At that point it is conservatively assumed that the ILV roof will collapse into the vault itself and that subsidence of the overlying closure cap will occur. This will lead to further degradation of the hydraulic properties of that portion of the closure cap overlying the ILV.

4.4.2 ILV Water Infiltration

During the operational period water entrance into the ILV is minimized through the stone sub-drainage system, the 30-inch thick waterproofed concrete walls, and the cell rain covers. Any water that does enter the ILV during operations or results from the grout installation is collected in a sump, which is appropriately monitored and pumped out as necessary. During the 100-year institutional control period after the ILV has been operationally closed, water infiltration into the vault is minimized through the stone sub-drainage system, the 30-inch thick waterproofed concrete walls, and permanent reinforced concrete roof slab and overlying bonded-in-place fiberboard insulation and waterproof membrane roofing.

During the post-institutional control period prior to vault structural failure, the final closure cap, along with the structurally intact concrete vault structure, minimize infiltration into the vault. During this period the hydraulic properties of the closure cap are assumed to degrade resulting in increased infiltration through the closure cap over time. At structural failure of the ILV roof (i.e., mean time of 6703 years) it is conservatively assumed that the roof will collapse into the vault itself, that subsidence of the overlying closure cap will occur, and that increased infiltration will occur through that portion of the closure cap overlying the collapsed ILV.

4.4.3 ILV Inadvertent Intruder Barrier

Inadvertent intrusion into the ILV waste is not considered feasible during the operational and institutional control periods, due to facility security during these periods. However it is assumed that inadvertent intrusion could occur during the post-institutional control period. The roof slab ensures structural stability for an estimated mean of 6703 years after final closure. It also provides a barrier to intrusion for this time period because normal residential construction and well drilling equipment used in the vicinity of the SRS is not capable of penetrating the roof structure (McDowell-Boyer et al. 2000).

4.5 ILV WASTE CHARACTERISTICS

4.5.1 Waste Type/ Chemical and Physical Form

The ILV is used to dispose of waste containers exceeding radiological dose and radionuclide concentration limits of the other, more cost effective, LLW disposal facilities, (e.g., trenches and LAWV), which typically includes job control waste, scrap metal, and contaminated soil and rubble. Job control waste consists of potentially contaminated protective clothing (plastic suits, shoe covers, lab coats, etc.), plastic sheeting, etc. The scrap metal consists of contaminated tools, process equipment and piping, and laboratory equipment. Soil and rubble are generated from demolition or remediation activities.

ILV waste will be packaged in engineered metal or concrete containers or consist of metal process equipment that have been approved by WMAP. The waste is placed into the vault in layers, grouted in place to provide better waste isolation, reduce dose to operators, and improve stacking of subsequent layers.

The ILT portion of the vault consists of two cells. The silo cell is specially designed with vertical silos to receive waste. The other ILT cell is used for bulk waste containers.

The ILNT portion of the vault contains seven bulk cells, similar to the ILT bulk cell.

The large majority of radioactivity in ILV waste will be tritium.

4.5.2 Radionuclide Inventory

Waste is disposed in the ILV if the radiation dose rate or radionuclide activity levels exceed trench and LAW Vault limits. The closure inventory estimate for the ILV is provided in Appendix C.

4.5.3 Waste Volume

A description of the ILV, including all relevant dimensions, is presented in Section 4.3. Two parts of the ILV are described as the ILT section (2 different waste cells) and an ILNT section (seven identical waste cells). The total waste disposal volume associated with ILT Cell #1 (144 vertical silos) is 6,340 ft^3. The waste volume associated with ILT Cell #2 is approximately 28,900 ft^3. In the ILNT section the total volume of the 7 cells is approximately 221,300 ft^3.

Because of SRS waste minimization and volume reduction programs and increased trench disposal options, only one ILV is estimated to be needed for low-level radioactive disposal over the next 25 years (WMAP 2006).

4.5.4 Packaging Criteria

All ILV waste is subject to the packaging requirements of the SRS WAC (WSRC 2006). The PA process sets many of the criteria that are the basis for the WAC.

4.5.5 Pre-Disposal Treatment Methods

Generators follow the SRS WAC (WSRC 2006) requirements for predisposal treatment methods. The PA process sets many of the criteria that are the basis for the WAC.

4.5.6 Waste Acceptance Restrictions

Waste acceptance for disposal in the ILV must conform to criteria put forth in the SRS WAC (WSRC 2006). The PA process sets many of the criteria that are the basis for the WAC.

4.5.7 Security Classification of Wastes

A very small (insignificant) fraction of disposed LLW at SRS contains classified material.

4.6 ILV GROUNDWATER TRANSPORT ANALYSIS

This section documents the development of preliminary groundwater protection limits for the IL Vault. The limits developed within this section are considered preliminary, since they do not take into consideration the effects of plume overlap from adjacent units or the results of sensitivity and uncertainty analyses. The effects of plume overlap are considered in Chapter 6, and the interpretation of sensitivity and uncertainty analyses is conducted in Chapter 7. Final limits are provided in Chapter 7.

4.6.1 Relation of Current Analysis to Previous Analyses

In this Performance Assessment a re-evaluation of the groundwater transport was required for all radionuclides that could not be screened out due to numerous improvements made to the conceptual model of the ILV which were embodied within the deterministic model. This includes the findings of previous SAs and UDQEs that have not yet been superseded by subsequent documents.

The key aspects of the new groundwater transport analysis include the following:

- Entirely new conceptual and deterministic models of the vadose zone for the ILV were developed for this analysis and the aquifer model was extensively revised, though still based on the calibrated GSA flow model (Flach 2004). These changes are described below.
- As a part of these models, revised flow and transport properties for different materials were developed (Phifer et al. 2006).
- Updated estimates of infiltration with respect to time were developed (Phifer et al. 2006) and used as the basis for establishing new steady-state flow period in the vadose zone model..
- Certain radionuclides were screened out and are no longer of concern. (Cook 2007)
- Carbon-14 in generic waste was simulated using a solubility release model in the waste zone and the concrete vault; C-14_KB waste was simulated using a K_d release model in the waste zone and a solubility release model in the concrete vault (Kaplan 2006). The C-14_KB waste was assumed to be in all cells except Cell #4.

Due to the improvement of the conceptual and deterministic models, several special case radionuclides from previous investigations also had to be re-evaluated, which include:

- Radionuclides in special wasteforms, including high-concentration activated carbon I-129 vessels from ETF (Effluent Treatment Facility), K and L Basin resins containing radionuclides of interest C-14, Tc-99 and I-129 (Flach and Hiergesell 2004).
- H-3 associated with disposing the first 17 TPBAR disposal containers within the ILV (Hiergesell 2006).

4.6.2 Overview of Groundwater Transport Analysis

Groundwater transport analysis incorporates two separate models: a cross-sectional, 2-D, model of the vadose zone, and a 3-D model of the aquifer in the vicinity of the ILV. The vadose zone flow model was configured to be consistent with the latest E-Area Closure Plan (Phifer 2004) and incorporates the different materials (e.g., backfill materials, concrete, and natural sediments) described in this plan. Several features were incorporated to improve the previous analysis (Flach and Hiergesell 2004), including the use of a model domain that incorporated the full-width of the ILV and improved estimates of physical and hydraulic properties of the materials within this domain. Also, infiltration estimates were refined, as described in Phifer et al. (2006). Contaminant transport simulations were performed for those radionuclides that could not be screened out with respect to possibly causing adverse exposure to human beings, as described in Taylor and Collard (2005). The mass fluxes of radionuclides exiting the vadose zone model domain were used as input to the aquifer (saturated zone) model, which was then employed to determine groundwater concentrations with respect to time at the hypothetical 100-m well such that the timing and magnitude of the peak concentrations could be determined. CDP is not considered in this analysis since very little cellulose containing waste has been disposed within the ILV.

4.6.3 Groundwater Transport Conceptual Model

In this section, a discussion of the scenarios and conceptual models developed for evaluating subsurface transport of radionuclides released from the ILV over time is provided. Key inputs and assumptions associated with implementation of these models are provided in Appendix B.

4.6.3.1 Operations, Closure, and Degradation Scenario

Operational period assumed to last for 25 years, after which there is a 100-year period of institutional control, during which no cover is placed over the ILV. After this a permanent closure cap is to be emplaced. A detailed description of the ILV facility, its operations and closure, are provided in Section 4.3.

Physical degradation, with respect to the cementitious floor, walls and roof of the ILV, does not occur until they are cracked by static-loading or from differential settlement induced by seismic events (Peregoy 2006). Degradation, with respect to chemical properties of cementitious materials, is described in Kaplan (2006). The closure cap placed over the ILV is progressively invaded by pine roots, which allow an increasing quantity of infiltration to occur. At the time of collapse, estimated to occur at year 6703 (see Section 4.6.3.2), infiltration reaches the long-term rate calculated for SRS soils.

4.6.3.2 Incorporation of Structural Analysis

Peregoy (2006) performed structural degradation prediction analyses for the ILV, including collapse analyses, static crack analyses, and differential settlement analyses, which provided input to the PA PORFLOW modeling effort for the ILV. These structural analyses calculated either cracking or collapse of ILV concrete members which will impact the associated flow and transport modeling.

Peregoy (2006) identified the following cracking and collapse scenarios for the ILV:

- Roof collapse due to closure cap and seismic loading and rebar corrosion. The roof will collapse (100% probability at some time) and two different methods were utilized to determine when such a collapse would occur:
  - A Monte Carlo analysis determined a collapse mean time of 6703 years ± an 885-year standard deviation, and
  - A structural analysis determined that if a beyond-PC-4 event were to occur at 5985 years or beyond the roof would collapse
- Wall collapse due to degradation of the walls and closure cap and seismic loading (100% probability of occurrence at a mean time of 9427 years ± a 2795-year standard deviation)
- Roof slab static cracking due to closure cap loading (100% probability of non-through-slab cracks occurring immediately at placement of closure cap, with cracks increasing slightly in size over time)
- Side and end wall static cracking due to the closure cap loading (100% probability of non-through-wall cracks occurring immediately at placement of closure cap, with cracks increasing slightly in size over time)
- Differential settlement due to PC-4 seismic loading or greater resulting in potential cracking at construction and control joints (such cracking is projected to most likely occur in Cell 4 [i.e., center cell] of the ILV, due to the two parallel transverse joints within that cell [other cells only have one such joint])

These findings have implications for how material properties were assigned within the Waste/Vadose Zone model. The methods by which these findings were accommodated are described in Table 4-2.

4.6.3.3 Infiltration Boundary Conditions

Infiltration rates for the ILV and adjacent soil were calculated using the HELP model (Phifer et al. 2006), and are summarized in Table 4-3. Initially, during the operations period (25-years) and during the institutional control period there is no closure cap over the facility; hence there is a high infiltration rate through the soil material adjacent to the ILV while there is little, if any infiltration into the ILV due to the presence of roof material. After the institutional control period, a closure cap is placed over the entire facility, limiting infiltration. The closure cap is centered over the ILV, which results in somewhat higher infiltration in the down-slope direction off the vault because of development of higher hydraulic head. Gradually, as pine roots encroach into the closure cap, infiltration gradually increases. The results in Table 4-3 were obtained from an investigation documented in Phifer et al. (2006).

Table 4-2. Proposed ILV Base Case Realization - Vault Cracking and Collapse

Peregoy 2006 ILV Cracking and Collapse	Method of Handling within Waste/Vadose zone model
Roof collapse	Although the mean time of roof collapse was determined to be approximately 6000 years, the roof collapse was assigned at 1900 years to facilitate flow modeling. This treatment is justified based upon the following: Inventory limits are set based on the 1,000-year time-of-compliance hence analyses beyond 1,000 years are solely to estimate peaks. Earlier roof collapse combined with an earlier cap failure) should lead to somewhat higher well concentrations after 1,000 years. Long-lived contaminants will exhibit a spike due to roof collapse, regardless of whether it is near 1,000 years or much later. When the time of collapse is varied at times after 1,000 years, the peak contaminant concentrations for long-lived radionuclides will be lower, but the difference will be small if the time difference is small relative to the radionuclide half-life. The selected time of roof collapse (i.e., 1900 years) is significantly beyond 1,000 years such that the limit will not be affected. At the time of roof collapse all concrete was assigned the properties of operational soil cover prior to dynamic compaction.
Wall collapse	The time of wall collapse (mean of 9427 years) was assigned to coincide with the time of roof collapse (i.e. walls assumed to collapse when roof assumed to fail at 1900 years). At the time of roof collapse all concrete was assigned the physical properties of operational soil cover prior to dynamic compaction.
Roof slab static cracking	Although static load cracks are realized within the roof slab as soon as the closure cap is emplaced, the cracks increase slowly with time. The cracks estimated to exist at 5000 years were utilized to calculate roof slab equivalent saturated hydraulic conductivity, which was then incorporated in the model, beginning at time zero. The method for calculating this parameter is described in Snyder (2003).
Side and end wall static cracking	This is accounted for by implementing static load cracks realized at 5000 years to produce an equivalent saturated hydraulic conductivity for the side and end wall concrete, beginning at the time of closure cap placement. The method for calculating this parameter is described in Snyder (2003).
Through-cracking at construction joints in Cell 4	A separate simulation of Cell 4 (i.e., center cell) was conducted. Through cracking due to a PC-4 seismic event is assumed to occur at 400 years and the wall and floor concrete assigned gravel properties at that time. Through cracking causes a significant increase in equivalent effective hydraulic conductivity; hence a separate simulation was required for Cell 4.

Table 4-3. ILV Infiltration and Lower Drainage Layer Infiltration from HELP Model Analysis

Year	Period	Layer through which Infiltration Estimated	Infiltration Estimate *Over Vault* (cm/year)	Infiltration Estimate *Off-Vault* (cm/year)
-125 to -100	Operational	Vault Concrete Roof	0.00	40.00
-100 to 0	Institutional Control	Vault Concrete Roof	0.00104	40.00
0	Closure Cap	GCL	0.156	0.167
100	Closure Cap	GCL	0.168	0.172
300	Closure Cap	GCL	2.444	2.917
550	Closure Cap	GCL	5.947	7.124
1,000	Closure Cap	GCL	14.457	17.075
1,800	Closure Cap	GCL	27.932	30.933
2,740	Closure Cap	GCL	33.669	34.834
2,805	Closure Cap	GCL	33.726	34.864
3,400	Closure Cap	GCL	34.071	35.060
5,600	Closure Cap	GCL	34.753	35.367
7,000	Closure Cap	GCL	34.930	35.427
7,000+	Vault Roof Collapse	Collapsed Cap	40.462	34.86

Note: 7000 years was based on an early estimate of the time of vault roof collapse, later the time was refined to 6000 years; ultimately an "early-time" vault roof collapse at 1900 years was implemented which set the infiltration rate to 40.46 cm/yr at year 1900.

The vadose zone flow simulations were performed by defining a series of time-periods during which steady, average conditions were assumed to prevail. The specific periods were defined based on conditions that relate to closure (e.g. operations period, institutional control period) as well as the different calculated water infiltration rates through the closure cap. These time periods are defined as years 0-25, 25-125, 125-225, 225-425, 425-675, 675-1,125, 1,125-1,925 and 1,925 to 10,000 years. The steady-state infiltration rates for all of the period are indicated in Figure 4-7. The time periods are bracketed by "step" changes in rates, which coincide with measurement points. The steady-state time periods were established as the time periods between points in time when infiltration estimates were obtained from HELP and the steady, average infiltration rate was calculated by taking the average of the infiltration rate estimates determined for the beginning and ending of each time-period. It is assumed this is the most valid way to represent the rate of infiltration within the vadose zone mode.

Throughout the remainder of this chapter, time zero (0) is regarded to be the end of facility operations (a 25-year period). The convention used to refer to steady-state time intervals are is -25-0, 0-100, 100-200, 200-400, 400-650, 650-1100, 1100-1900 and 1900-10,000 years.

The HELP model was used to calculate infiltration rates up until the time of ILV roof collapse. While this was calculated to occur at approximately Year 6000, an early collapse was assumed to occur at Year 1900 (see Table 4-3); hence the infiltration rate was set at 40.46 cm/year from this point forward to the end of the simulation period. Although the graph in Figure 4-7 truncates at 2000 years, the recharge rates after this time are assumed to remain constant, both over the vault and over the adjacent soil.

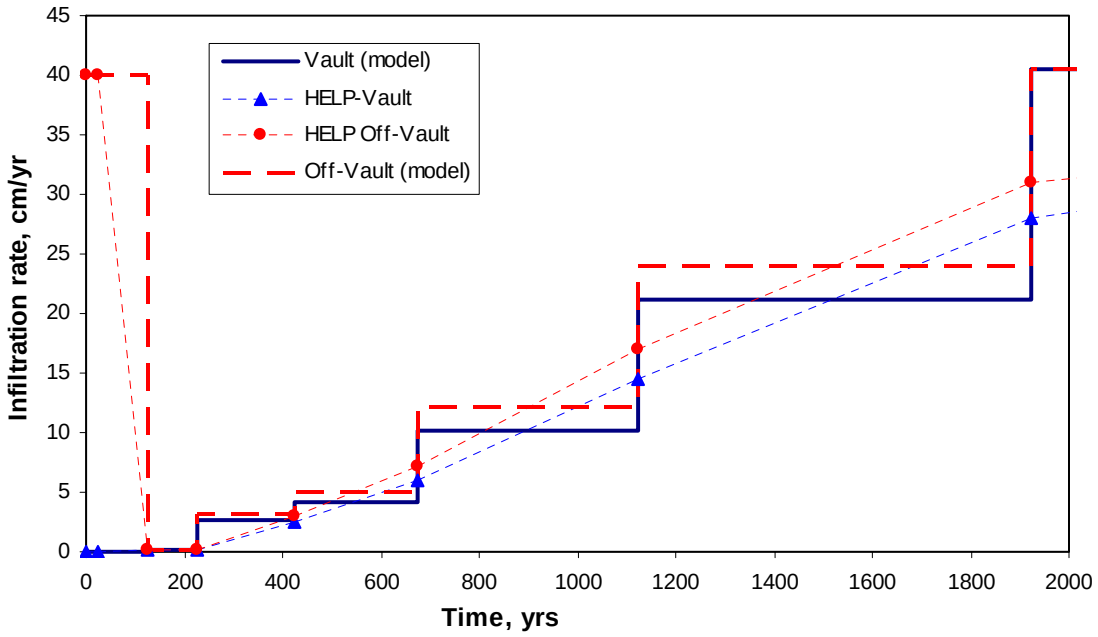

Figure 4-7. Infiltration Rates over Vault and Off-Vault Parts of Model

4.6.3.4 Existing Inventories and Special Wasteforms

SRS has been actively disposing of waste material within the ILV since September 1995. Several special wasteforms were evaluated in this investigation. The C-14, Tc-99, and I-129 associated with resins used in reactor deionizer vessels (i.e., C-14_KB, Tc-99_KB, and I-129_KB) and I-129 associated with the ETF carbon filters (i.e., I-129_ETF) required separate treatment owing to different release rates from the specific wasteform than for the generic radionuclides.

Similarly, H-3 associated with the TPBARs (i.e., H-3_TPBARS) was treated separately from generic H-3. TPBARs are expected to be disposed within the ILV in large carbon steel containers that are welded shut. These containers are modeled as a separate sub-zone within the Waste disposal zone since they are essentially impermeable until such time that the steel corrodes. Tritium enclosed within the container can, however, diffuse through the welds and container walls and must be accounted for.

4.6.3.5 Waste and Vadose Zone Flow and Transport Conceptual Model

A conceptual model of the ILV and surrounding materials in the vadose zone was developed to provide a basis for developing a deterministic numerical model for evaluation of flow and contaminant transport. This conceptual model is described as a 2-dimensional view of the ILV in its closure configuration and is illustrated in Figure 4-8. In this figure, the different materials were made to correspond to exact dimensions of the ILV and the anticipated closure design, as described in the general ILV description presented in Section 4.3.

In Figure 4-8 the interior (waste disposal zone) of an individual ILV cell is outlined in the orange material. It is surrounded by a yellow-green zone which represents E-Area Vault Concrete. The dark red rectangular zones within the waste disposal zone represent TPBAR disposal containers. Surrounding that, in light green, is a permeable backfill material, referred to as ILV Permeable Backfill, which is obtained by mixing up Lower Vadose zone material. Above the ILV is Controlled Compacted Backfill, as specified in Phifer (2004). This material is to be placed immediately underneath the final closure cap. The dark blue zone in the lower portion of the cross-section is the Lower Vadose Zone while the pale blue zone immediately above that is the Upper Vadose Zone. These zones are distinguished due to slightly different material properties and have an interface that occurs at 264 ft. above msl in the vicinity of the ILV. The flow properties, including porosity, bulk density, particle density, saturated hydraulic conductivity, characteristics curves (saturation/suction head/relative permeability), and effective diffusion coefficients of these materials are discussed in detail in a separate report, Phifer, et al. (2006). Likewise, the transport properties, distribution coefficients, K_ds, and solubility-concentration limits are discussed in detail in a separate report, Kaplan (2006). The properties of individual materials are discussed below.

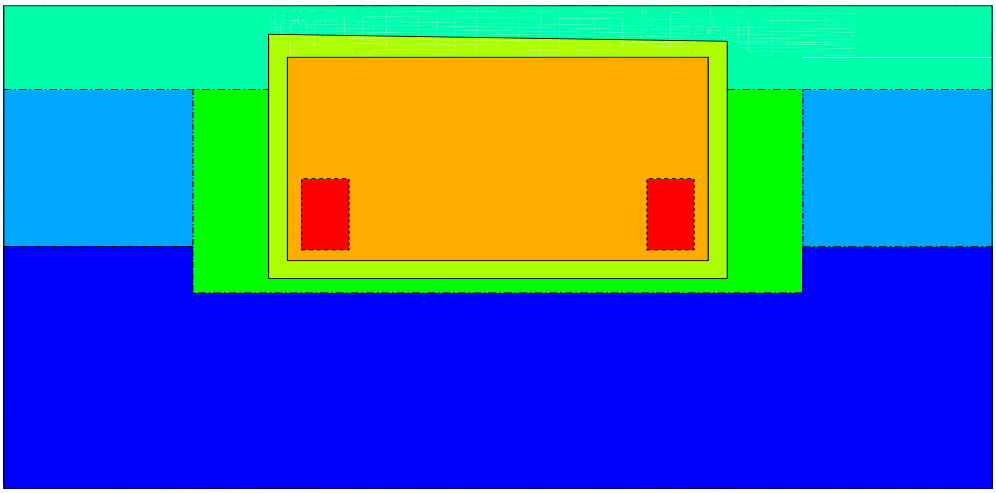

Figure 4-8. Vadose Zone Conceptual Model

Control Compacted Backfill

Control Compacted Backfill is the backfill material to be placed immediately above the ILV roof and beneath the lower drainage layer of the closure cap, as shown in Figure 4-8. At the sides of the ILV, it will be used to fill all the way down to the current land surface, shown in blue-green in Figure 4-8 as the top of the ILV Permeable Backfill and the Upper Vadose Zone Material. The effective porosity of this material is 0.35, dry bulk density is 1.71 g/cm^3, particle density is 2.63 g/cm^3, saturated hydraulic conductivity is 1.3E+03 cm/yr and the effective diffusion coefficient is 167.25 cm^2/yr. Prior to the time of placement of the closure cap the horizontal hydraulic conductivity of this material was set to zero to permit direct transfer of infiltrating water to the top of the ILV, the Permeable backfill material adjacent to the ILV and the Upper Vadose Zone material. The upper surface of the latter two constitute the current land surface. The K_ds for each simulated radionuclide are established as those that occur in "Clay" material.

ILV Permeable Backfill

ILV Permeable Backfill is the backfill material that was placed immediately around the sides of the ILV (below current land surface) and below the base of the facility, shown as green in Figure 4-8. The effective porosity of this material is 0.41, dry bulk density is 1.56 g/cm^3, particle density is 2.64 g/cm^3, saturated hydraulic conductivity is 2.4E+04 cm/yr and the effective diffusion coefficient is 252.46 cm^2/yr. The K_ds for each simulated radionuclide are established as those that occur in "Sand" material.

E-Area High Quality Concrete

E-Area Vault Concrete is the material used to build the ILV cell walls, flooring and roof. In Figure 4-8 it is represented by the yellow-green "box" that surrounds the interior waste disposal zone. The effective porosity of this material is 0.184, dry bulk density is 2.11 g/cm^3, particle density is 2.59 g/cm^3, saturated hydraulic conductivity is 3.2E-05 cm/yr and the effective diffusion coefficient is 1.58 cm^2/yr. The K_ds for each simulated radionuclide are described in Kaplan (2006, Table 14) for reducing cementitious solids. It should be noted that K_d values were adjusted per the guidance in Table 14 with regard to the pH of the cementitious solid. Cement is classified as "Young" Cement (pH~12.5), "Moderately Aged" Cement (pH~10.5) and "Aged" Cement (pH~5.5). The basis for transitioning between phases is the number of pore volume flushes. The transition from "Young" to "Moderately Aged" cement is 50 pore volume flushes while the transition from "Moderately Aged" to "Aged" cement is 500 pore volume flushes (see Kaplan [2006]). At the time that the ILV is predicted to collapse the physical properties are assumed to convert into those of Operational Soil Cover - Pre-Compaction (OSC) although the transport properties remain as "Aged" cement. The timing of this collapse is discussed later in this chapter.

The extent of cracking in the ILV concrete due to the added weight of the closure cap was addressed in the structural analysis of the ILV in Peregoy (2006), and discussed in Section 4.6.3.2. Only partially penetrating cracks developed in the roof and walls as a result of the added load and only have a minor effect in increasing the effective K_{sat} of the ILV. Although static load cracks are realized within the roof slab as soon as the closure cap is emplaced, the cracks increase slowly with time. Therefore, the cracks estimated to exist at 5000 years were utilized to calculate roof slab equivalent saturated hydraulic conductivity, which was then incorporated in the model, beginning at the time of closure cap placement. The method used to perform this calculation is described in Snyder (2003). Values were calculated for both the roof and side walls and the higher of the two was used for all ILV concrete (roof, walls and floor). The effective K_{sat} calculated for ILV concrete is 5.37E-05 cm/yr.

Gravel (waste zone)

Gravel was selected as the most representative material for the waste disposal zone. This is shown in orange in Figure 4-8. The effective porosity of this material is 0.30, dry bulk density is 1.82 g/cm^3, particle density is 2.60 g/cm^3, saturated hydraulic conductivity is 4.7E+06 cm/yr and the effective diffusion coefficient is 296.63 cm^2/yr. The K_ds for each simulated radionuclide in gravel are those assumed to occur in "Sand" material. For transport simulations prior to ILV collapse the effective porosity was assigned a value of 0.736 and a particle density of 2.32 g/cm^3 to insure that migration of radionuclides away from the waste zone was not under estimated.

Operational Soil Cover, pre-compaction (OSC)
Operational Soil Cover, pre-compaction (OSC) is the material that E-Area Vault Concrete and the material within the ILV waste disposal zone is projected to become similar to after the collapse of the facility. The effective porosity of this material is 0.46, dry bulk density is 1.44 g/cm^3, particle density is 2.65 g/cm^3, saturated hydraulic conductivity is 3.8E+03 cm/yr and the effective diffusion coefficient is 167.25 cm^2/yr. The K_ds for each simulated radionuclide are established as those that occur in "Clay" material. The timing of this collapse is discussed later in this chapter.

Upper Vadose Zone
The Upper Vadose Zone is the naturally occurring material immediately outside the Permeable Backfill surrounding the ILV, extending from an elevation of 264 ft-msl to the current grade. It is the pale blue zone in Figure 4-8. Elevation 264 ft-msl occurs slightly above the concrete floor. This material has effective porosity of 0.39, dry bulk density is 1.65 g/cm^3, particle density is 2.7 g/cm^3, saturated hydraulic conductivity is 2.0E+03 cm/yr and the effective diffusion coefficient is 167.25 cm^2/yr. The K_ds for each simulated radionuclide are established as those that occur in "Clay" material.

Lower Vadose Zone
The Lower Zone is the naturally occurring material immediately below the Permeable Backfill surrounding the ILV, extending up to the elevation of 264 ft-msl, which occurs slightly above the concrete floor. It is the dark blue zone depicted in Figure 4-8. This material has effective porosity of 0.39, dry bulk density is 1.62 g/cm^3, particle density is 2.66 g/cm^3, saturated hydraulic conductivity is 1.0E+04 cm/yr and the effective diffusion coefficient is 167.25 cm^2/yr. The K_ds for each simulated radionuclide are established as those that occur in "Sand" material.

TPBAR disposal containers
Individual ILV cells (except Cell 4) are expected to have up to 4 TPBAR disposal containers disposed within them. Cell 4 has already been filled with waste and will be unable to receive any TPBAR disposal containers. These containers are approximately 1.5 m by 1.5 m by 5.8 m and are constructed of carbon steel. Their walls are 13-inches thick with which are welded shut, the welds having a minimum thickness of 0.5-inches. Disposal within individual cells will be in stacks of two containers, each cell containing two stacks located near the outer walls, with the long axis parallel to the exterior cell walls. Within the model domain, these containers are depicted looking into the long axis, near the base of the cell, and are indicated as the red rectangles imbedded within the waste material in Figure 4-8. The containers will have a minimum distance of 12 in. from the cell wall and are positioned within the model domain as having the same distance above the cell floor. The disposal of these containers within the ILV is discussed in more detail in Hiergesell (2006).

TPBAR containers are regarded to be impermeable to water until the time when concrete degradation readily allows water to move into the waste zone and corrosion degrades the containers. The material properties assigned to these containers prior to ILV collapse do not effect the calculations. The values assigned in order for the model to run were an effective porosity of 4.2E-05, a "particle" density of 100 g/cm^3, an effective diffusion coefficient of 1 cm2/yr and K_d of 1.0E+4 ml/g. At the time of ILV collapse these containers are assumed to acquire the characteristics of the waste material.

The durability of TPBAR disposal containers within the ILV disposal environment and their ability to prevent the release of non-tritium radionuclides during the 1000-year period of compliance has been documented in previous analyses (see Hiergesell 2005 and Vinson et al. 2004). Tritium is able to diffuse through the carbon steel walls and welds of the disposal container whereas the other radionuclides in the TPBARS cannot escape the container until it fails, either mechanically or chemically (as by corrosion). Hence, only the release of H-3 is considered in this analysis.

An unclassified estimate of the flux of H-3 from a single TPBAR disposal container over a 26-year period was calculated by investigators at Pacific Northwest National Laboratory. Gaseous transport of H-3 from the TPBAR containers was not attempted. Rather, the flux emanating from the disposal containers was introduced into the elements immediately outside the TPBAR containers. This zone forms "halo" zone of elements immediately outside the TPBAR container sub-domains. The source term is a rate of introduction which peaks and then diminishes to 0 after 26 years as shown in Table 4-4. Once introduced into this source zone, the H-3 is transported through the larger domain. While separate H-3 limits were calculated in a previous SA (Hiergesell 2005), this analysis updates those limits because material properties within the vadose zone and aquifer models were updated in this analysis.

Table 4-4. Calculated Flux from TPBARS

Time (yrs)	H-3 Source (moles/yr)
0.5	0.238578926
1.5	0.397631544
2.5	0.525147866
3.5	0.589591599
4.5	0.606045318
25.5	0.303022659
26	0

Typical Cell and Cell 4 flow fields

The results of the structural analysis (Peregoy 2006) indicate a key difference in one of the ILV cells, Cell 4. This cell is different in that it has 2 construction joints in the walls and flooring which make it more prone to develop through-cracks as a result of seismic events. Through cracking due to a PC-4 seismic event is assumed to occur at 400 years causing a significant increase in equivalent effective hydraulic conductivity of the ILV floor and walls. At that time the material properties of the floor and walls of Cell 4 are assumed to change to those of gravel. This change in properties and the fact that no TPBAR disposal containers will be disposed within Cell 4 necessitated a separate simulation to be conducted of those conditions. In the remainder of this chapter these two types of cells are referred to as the "Typical Cell" and "Cell 4". The position of these cross-sectional models of the ILV can be seen in Figure 4-9, where cross-sections B-B' represents the middle cell, Cell 4, and cross-section A-A' represents one of the other vault cells. In the analysis these two cross-sectional models are used to calculate the mass flux from each cell of the ILV to the subsurface. In determining the mass flux from the entire facility at the water table, the flux output from 6 typical cells plus the flux output from the middle cell (Cell 4) is divided by 7 to obtain the mass flux from the entire facility per unit source term (i.e., 1 mole of each radionuclide) over time.

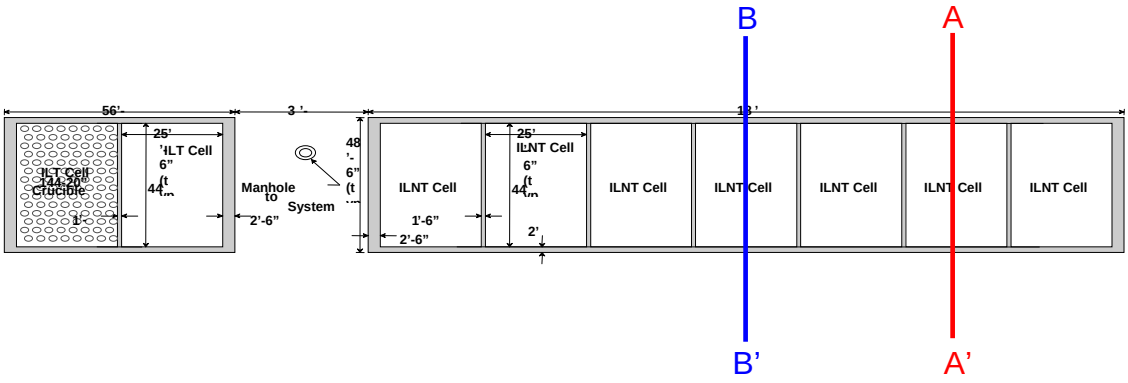

Figure 4-9. Position of Cross-Section Models

The main changes to material properties of the ILV through time are graphically presented as timelines for a Typical Cell in Figure 4-10 and for Cell 4 in Figure 4-11. With the exception of the presence of TPBAR disposal containers, both types of cells have identical material property conditions through the period of institutional control, when the facility and adjacent soil are open to the atmosphere and there is a roof over the ILV. No TPBAR disposal containers can be placed in Cell 4 because it is nearly filled at the present time and insufficient space remains for such a disposal.

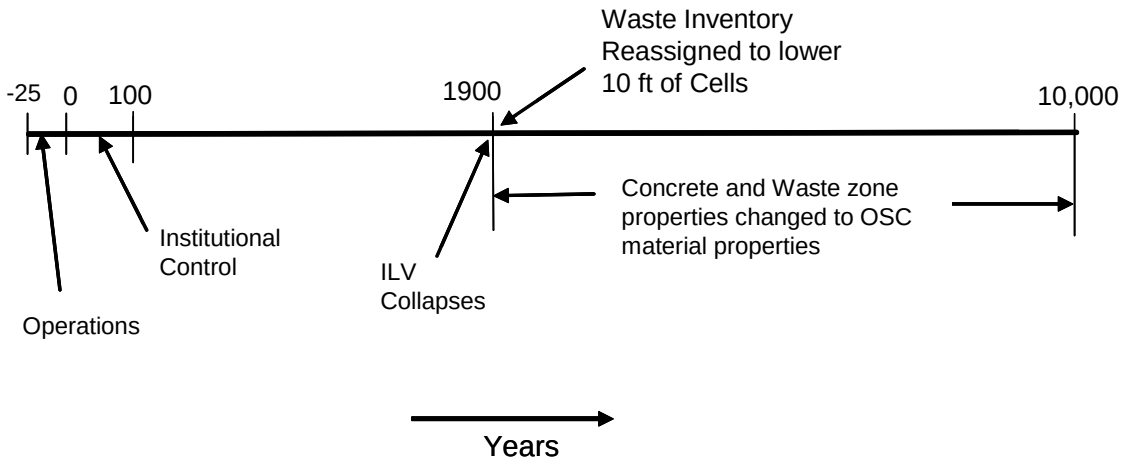

Figure 4-10. Timeline for Typical Cell

After year 100 the final closure cap is set in place, restricting the amount of infiltration that reaches the ILV and adjacent soil. At year 1900 the entire ILV is assumed to collapse, as was explained in Table 4-2. At the time of collapse, the concrete material and waste zone material are assumed to acquire the physical properties (K_{sat}, characteristic curves, porosity, bulk density, particle density and effective diffusion coefficient) of OSC pre-compaction and the radionuclide inventory from the entire waste zone is assumed to concentrate in the lower 10 ft. of the waste zone. These conditions remain constant for the duration of the period of simulation.

The timeline for material property changes for Cell 4 are similar to the Typical Cell and are illustrated in Figure 4-11. The principal difference is that at year 400 the concrete walls and floor are assumed to acquire the physical properties of gravel, due to the development of through-cracks. The properties that change are the same as those listed for the Typical Cell. Later, the concrete walls, floor and roof, as well as the waste zone, acquire the physical properties of OSC pre-compaction when the ILV collapses at year 1900.

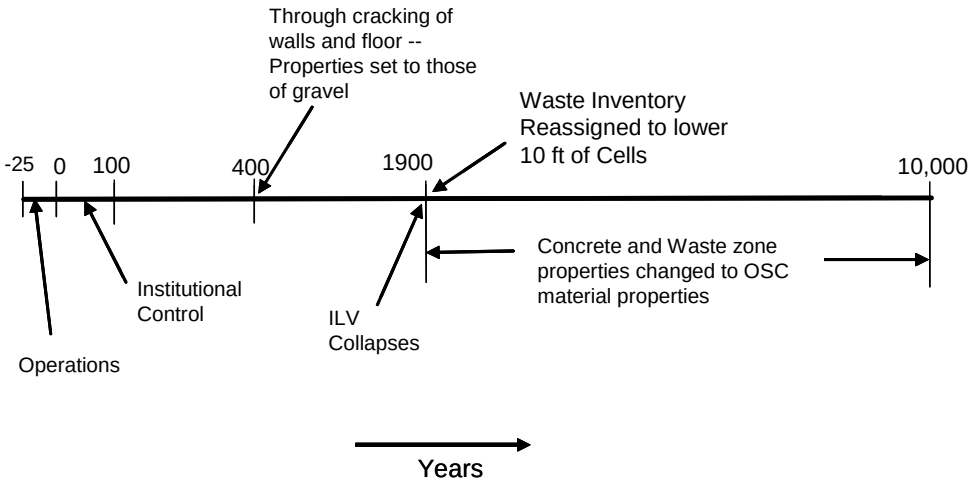

Figure 4-11. Timeline for Cell 4

Transport properties

The K_ds and solubility concentration limits were established for each of the 40 radionuclides anticipated to be disposed within the ILV (35 radionuclides that did not screen out plus 5 special wasteforms). The basis for selecting values for these properties is related to the environmental settings (e.g., clayey sediment, sandy sediment, or cementitious material) the migrating contaminant plume encounters in the subsurface. The rationale for selecting values used in the modeling involves the establishment of a "best" estimate and a "reasonably conservative" estimate for both K_d and solubility limits. The "best estimates" are based primarily on some central value of the literature, SRS site-specific environmental data or on expert judgment (Kaplan 2006). The "reasonably conservative" values were based on the lower limit of multiple K_d value measurements or the upper limit of solubility measurements (Kaplan 2006). For the base case evaluation in this investigation the "best estimate" values were utilized.

For the purposes of assigning K_d values and solubility limits, subsurface sediments (i.e., non-cementitious materials) were simplified to be considered either "clayey" or "sandy". Amongst the materials in the vadose zone, described in Section 4.6.3.5, this classification is as presented in Table 4-5.

Table 4-5. Assignment of K_d by Material Type

	"Sand" K_ds	"Clay" K_ds
ILV Permeable Backfill, pre-compaction	X	
Controlled Compacted Backfill		X
Operational Soil Cover (OSC)		X
Gravel	X	
Upper Vadose Zone		X
Lower Vadose Zone	X	

The conceptual model for establishing K_d values for the radionuclides simulated in this investigation is described in Kaplan (2006). The basis of this model is the identification of 3 stages through which all cementitious materials progress as they age. Each stage has unique physical, mineralogical and chemical properties which result in unique K_d and/or concentration solubility limits. The basis for distinguishing the 1st stage from the 2nd stage is the passing of 50 pore volumes of water through the material while the basis for distinguishing 2nd stage from 3rd stage is the passing of 500 pore volumes of water.

To make the determination of when the transitions from 1st to 2nd to 3rd stage occurred, water flux from the zones of cementitious material was evaluated using the numerical model PORFLOW. The results of this analysis are shown in Figure 4-12 and Figure 4-13 for the Typical Cell and for Cell 4, respectively. While a slight difference in timing of the occurrence of 50 and 500 pore volumes is noted for the ILV concrete and the Waste zone (gravel properties), they were both implemented at the same point in time for both the Typical Cell and Cell 4 configurations. The threshold times for 50 and 500 pore volumes occur at 1600 years and 3800 years, respectively, for the Typical Cell and at 800 years and 1900 years, respectively, for Cell 4. It should be pointed out, once again, that these transport properties are retained throughout the duration of the simulations, despite the changes in physical properties at the time of through-crack development and roof collapse.

Pore volume information was extracted from PORFLOW flow field simulations using the assigned porosity values to make the determination. Prior to 1900 years porosities of intact concrete and the waste zone material were used, after 1900 years the porosity of OSC was used in this calculation. No consideration was given to the impact of cracking with respect to changes in porosity, although increased fluxes from changing K_{sat} values were accounted for.

The upper boundary conditions of this domain consist of a prescribed infiltration surface, the amount of which varies with respect to time as described in Section 4.6.3.3. This surface is regarded as a no-flux contaminant mass boundary. The lateral boundaries are assumed to be no-flux with respect to both groundwater flow and transport. This assumption is reasonable since the domain was set to extend out more than a meter farther on either side of the ILV concrete walls than was done in previous simulations of the ILV vadose zone (see Flach and Hiergesell 2004) and since the backfill material on either side of the ILV transmits the majority of water deflected around the Vault. The lower boundary is the water table, has a prescribed pressure of $P = 0$, and allows contaminant flux to occur by advection and diffusion.

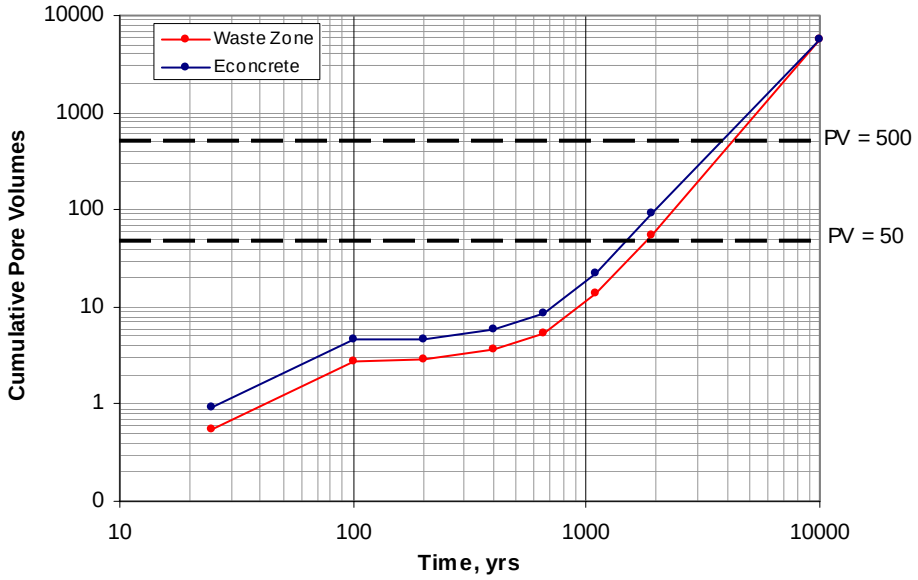

Figure 4-12. Pore Flushes in ILV Cementitious Material vs. Time for a Typical Cell

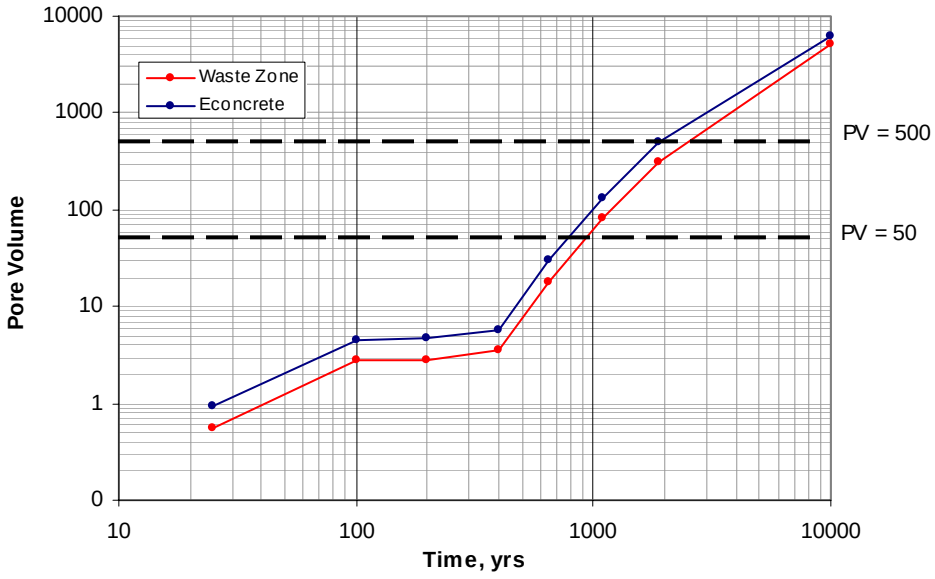

Figure 4-13. Pore Flushes in ILV Cementitious Material vs. Time for Cell 4

4.6.3.6 Saturated Zone Flow and Transport

The aquifers of primary interest for ILV are the Upper Three Runs and Gordon aquifers. Potential contamination from the IL will not enter the deeper Crouch Branch aquifer because an upward gradient exists between the Crouch Branch and Gordon aquifers near Upper Three Runs stream. Figure 4-14 is a cross-sectional schematic representation of groundwater flow patterns in the Upper Three Runs and Gordon aquifers (the underlying Crouch Branch aquifer is not shown in this figure) along a north-south cross-section running through the center of the study area, shown with significant vertical exaggeration. Although not indicated on this diagram, the ILV is situated at the land surface on the Upper Three Runs side of the groundwater divide.

Groundwater flow in the Upper Three Runs aquifer is driven by recharge, with nearby streams intercepting flow from higher elevations. The underlying Gordon aquifer is strongly influenced by discharge to Upper Three Runs stream, and is recharged from both the overlying Upper Three Runs and underlying Crouch Branch Aquifer. Therefore the predominant flow pattern within the Gordon Aquifer is in the horizontal direction toward the discharge zone adjacent to, and beneath, Upper Three Runs stream. Flow across the Meyers Branch Confining Unit is a small fraction of total recharge to the Gordon aquifer, and can be neglected in comparison to recharge from the Upper Three Runs aquifer.

Groundwater flow in the Upper Three Runs Aquifer is predominantly horizontal with a smaller, vertically-downward component. Near groundwater divides located between surface water drainages, the vertical component of groundwater flow is stronger and downward due to the decreasing hydraulic head with increasing depth. In areas along Fourmile Branch, shallow groundwater moves generally in a horizontal direction and deeper groundwater has vertically upward potential to the shallow aquifers. In these areas, hydraulic heads increase with depth. Due to the position of the ILV on the Upper Three Runs side of the groundwater divide, horizontal groundwater movement within the Upper Three Runs Aquifer beneath the ILV is entirely toward Upper Three Runs stream.

A more complete description of these units is presented in the Background Section of Part C of this report. The saturated hydraulic conductivity field is heterogeneous within hydro geologic units and reflects variations present in the characterization data. The average horizontal conductivities in the saturated “upper” Upper Three Runs aquifer zone, “lower” Upper Three Runs aquifer zone, and Gordon aquifer unit are approximately 10, 13, and 38 ft/d, respectively. The average vertical conductivities for the “tan clay” confining zone and the Gordon confining unit are 6E-03 and 1E-05 ft/d, respectively. Particle density and porosity values were assigned based on classifying the aquifer materials as either “sandy” or “clayey”. Sandy materials associated with aquifers are estimated to have a particle density of 2.66 g/cm^3 and porosity of 0.38, while clayey materials are estimated to have a particle density of 2.67 g/cm^3 and porosity of 0.43. Material property values are taken from Flach (2004).

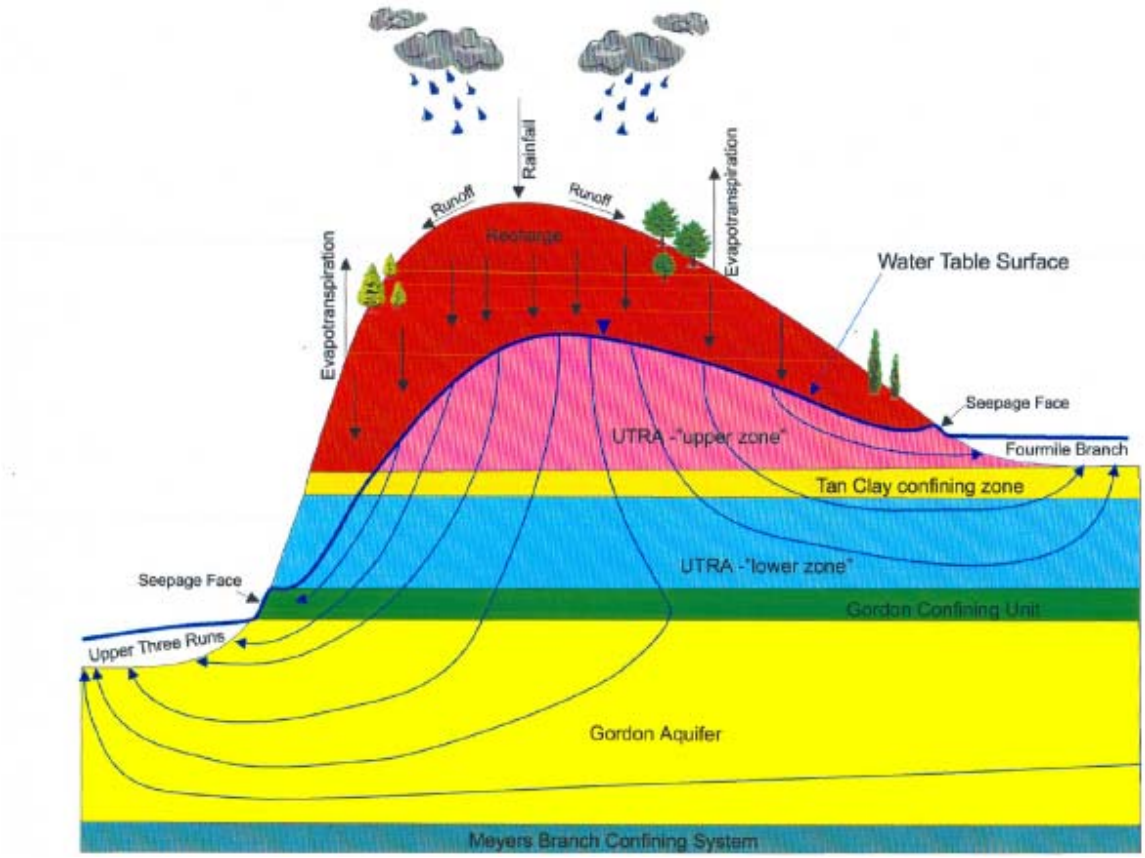

Figure 4-14. Generalized Hydro Geologic Cross-Section near E-Area

Transport properties in the saturated zone were also assigned based on the distinction between "sandy" and "clayey" materials. Effective dispersivity values of 0.18 and 0.14 were assigned for nodes representing sandy and clayey sediments, respectively. Likewise, K_d values for transport calculations were assigned based upon the "sandy" versus "clayey" distinction (aquifers vs. confining units) with specific values being selected as recommended in Kaplan (2006).

4.6.4 Groundwater Transport Deterministic Model Description

4.6.4.1 Waste and Vadose Zone Flow and Transport Models

The Waste/Vadose zone model is a 2-dimensional cross-section of the ILV as described in the conceptual model section, Section 4.6.3.5. A full-width model was necessitated due to the presence of a roof that slopes continuously from one side to the other and which tends to deflect more recharge water to one side of the ILV compared to the other.

The model domain extends from the base of the closure cap to the water table. Laterally, the domain was extended 28 ft on either side of the ILV, a distance judged sufficient to assure that flow along the lateral model boundaries is vertical. The closure cap extends a considerably greater distance laterally than the model domain, as described in Phifer (2006). The vertical distance from the base of the ILV was established at 29.5 ft to represent the actual depth to the long-term average regional water table. The regional water table configuration is based on the elevation of the long-term median water table, as recorded in wells in the vicinity of the ILV. A depiction of the regional water table at SRS, including the E-Area, and the method of how it was determined is presented in Hiergesell and Jones (2003).

The model grid was constructed to implement the conceptual model of the vadose zone, as described in Section 4.6.3.5. Figure 4-15 illustrates the configuration of this grid and the different materials, which are color coded, and which were identified in Section 4.6.3.5.

The domain consists of a 76 by 67 array of nodes spaced to allow accurate representation of the ILV cell dimensions as well as those of the major material types identified in the ILV Closure Plan (see Phifer 2004). Grid spacing was implemented to accommodate more refinement near interfaces of materials having contrasting hydraulic properties. Conversely, larger spacing was incorporated in parts of the domain that were less important (i.e., removed from locations of significant contaminant mass) to reduce computational requirements. The general rule for transitioning from wide to narrow nodes at material interfaces was applied in construction of the grid to insure that no element was more than twice the x or y dimension of its neighboring elements. Similarly, the general rule with regard to the aspect ratio of the x and y dimensions of model elements (ratio < 8:1) was applied throughout the domain. Virtually all of the elements do not exceed this guideline however, due to the necessity of incorporating mesh refinement near material interfaces, a few elements in certain parts of the domain exceeded this guidance slightly. The impact of these few elements is not thought to be significant in terms of the model results.

The ILV roof has a slope of 2%, from left to right, which was preserved within the grid mesh. This was accomplished by allowing the element layers that represent the roof cement to thin from left to right, which preserved the number of element layers and matched the slope.

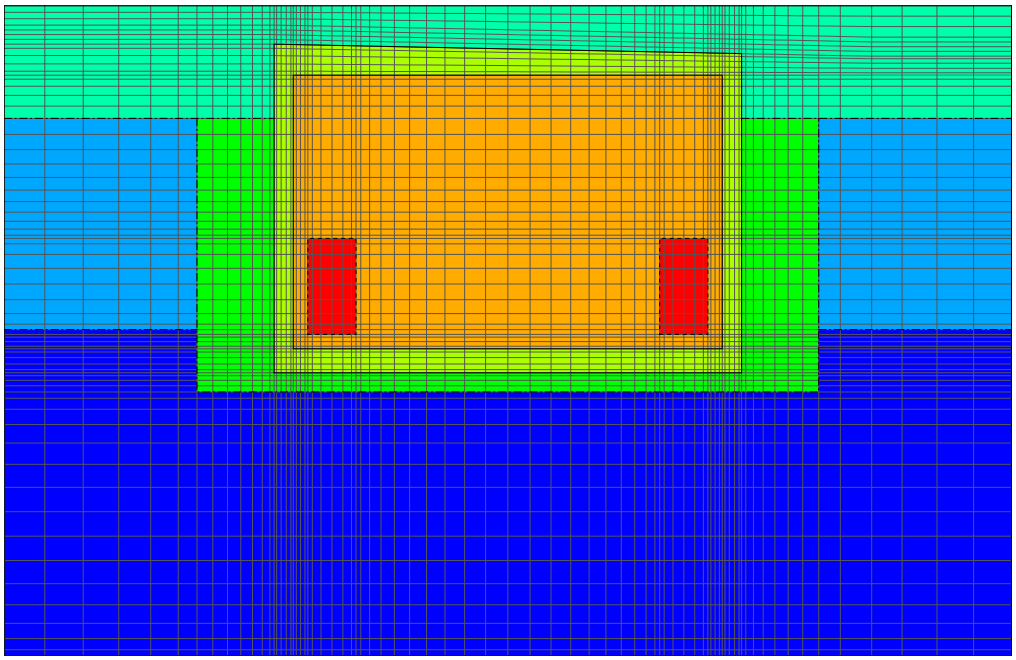

Figure 4-15. Vadose Zone model grid mesh and material zones

Temporally, the flow model was implemented by simulating steady-state flow fields for each of the steady-state time periods identified in Section 4.6.3.3. The velocity fields associated with each of these periods were used to simulate transient transport for the radionuclides and special wasteforms analyzed in this investigation.

The upper boundary was defined with two separate zones such that differentiation of recharge rates that occur over the ILV itself and the adjacent soil material could be achieved. This was necessary for application of different recharge rates during the 25-year operations period and the 100-year institutional control period during which there is not closure cap in place, but a roof is still maintained above the ILV. The contaminant flux was established as C = 0 for the entire upper boundary. Lateral boundaries were simulated as no-flux boundaries with respect to both groundwater flow (F = 0) and contaminant transport (C = 0). The lower boundary was assigned a prescribed pressure, P = 0, with respect to advection and was permitted to calculate contaminant flux by advection and diffusion.

In the process of calibrating the individual steady-state flow period models, three criteria were applied to determine if an acceptable degree of convergence to the steady-state solution had been achieved. These are summarized as: 1) Global mass balance error 2) Local mass balance error in the regions with insignificant contaminant mass, and 3) Local mass balance error in regions with significant contaminant mass. Tolerances for these criteria were established as < 1E-03, < 1E-01 and < 1E-02, respectively. While mass balance errors were usually significantly less than these tolerances, they define the maximum mass balance error permitted for any simulation. A strength of this approach is that the convergence measures are defined directly in terms of readily available flow simulation outputs. A weakness is ambiguity in the mass balance tolerances.

The transport simulations were conducted using a source term of 1 mole within the waste zone (excluding the impermeable TPBAR subdomain) and allowing transport to proceed through the velocity field for each steady-state time period. Output flux files were created for each parent radionuclide (or special wasteform) for each of the ILV cell types (Typical Cell and Cell 4). The resulting mass flux files include mass flux for both parent and progeny. For each radionuclide and its progeny, the total mass for six Typical Cells and one Cell 4 were combined to produce the composite source term to be incorporated into the aquifer model.

4.6.4.2 Saturated Zone flow and Transport Models

A PORFLOW-based ILV 3-D aquifer transport model was created which represents the saturated region beneath the ILV. The flow field was extracted from an already existing GSA flow solution based on PORFLOW; therefore, only 3-D transport simulations were required. A more detailed description of this model is provided below.

Taking into account the general aquifer flow direction and required 100-m compliance boundary surrounding the ILV, the domain of an ILV aquifer model was established. This model was extracted from a general baseline aquifer (flow only) model that extends over the entire GSA (see Flach 2004). The domain of the chosen ILV aquifer model is shown in the upper illustration in Figure 4-16 in which the coarser mesh of the General E-Area regional model is also illustrated. Flow directions are indicated by particle streamlines originating at either end of the ILV and from a central position. The outer domain of the ILV aquifer model coincides with specific grid surfaces of the general baseline GSA flow model. The GSA flow model has a uniform horizontal grid spacing of 200 ft in both directions. As shown in Figure 4-16, the ILV aquifer model overlaps a 5 by 5 cell region of the GSA flow model; thus, the ILV aquifer model's horizontal range is 1,000 ft by 1,000 ft. The horizontal mesh spacing was reduced to a grid of smaller elements, each measuring 50 ft by 50 ft. The grid mesh was refined for several reasons, primarily to minimize artificial spreading of contaminants in grid elements, both at the location of the introduction of the source term and at the 100-m well where concentrations were recorded. The finer mesh allowed source nodes to more accurately approximate the outline of trench units and allowed distinguishing the concentrations at a point 100 m from the facility without having to average over a 200-ft grid. The resulting grid mesh is a 22 by 22 by 16 array of nodes.

The vertical mesh spacing of the baseline GSA model was retained for the ILV aquifer model. Vertical configuration of model elements are shown in the cross-section illustrated in the lower part of Figure 4-16. The location of the cross-section with respect to the ILV is indicated by the solid red line (A-A') in the plan view of the model. The pink lines represent the boundary lines between model elements, the "yellow" zones represent sandy aquifer units and the "brown" elements represent clayey confining units.

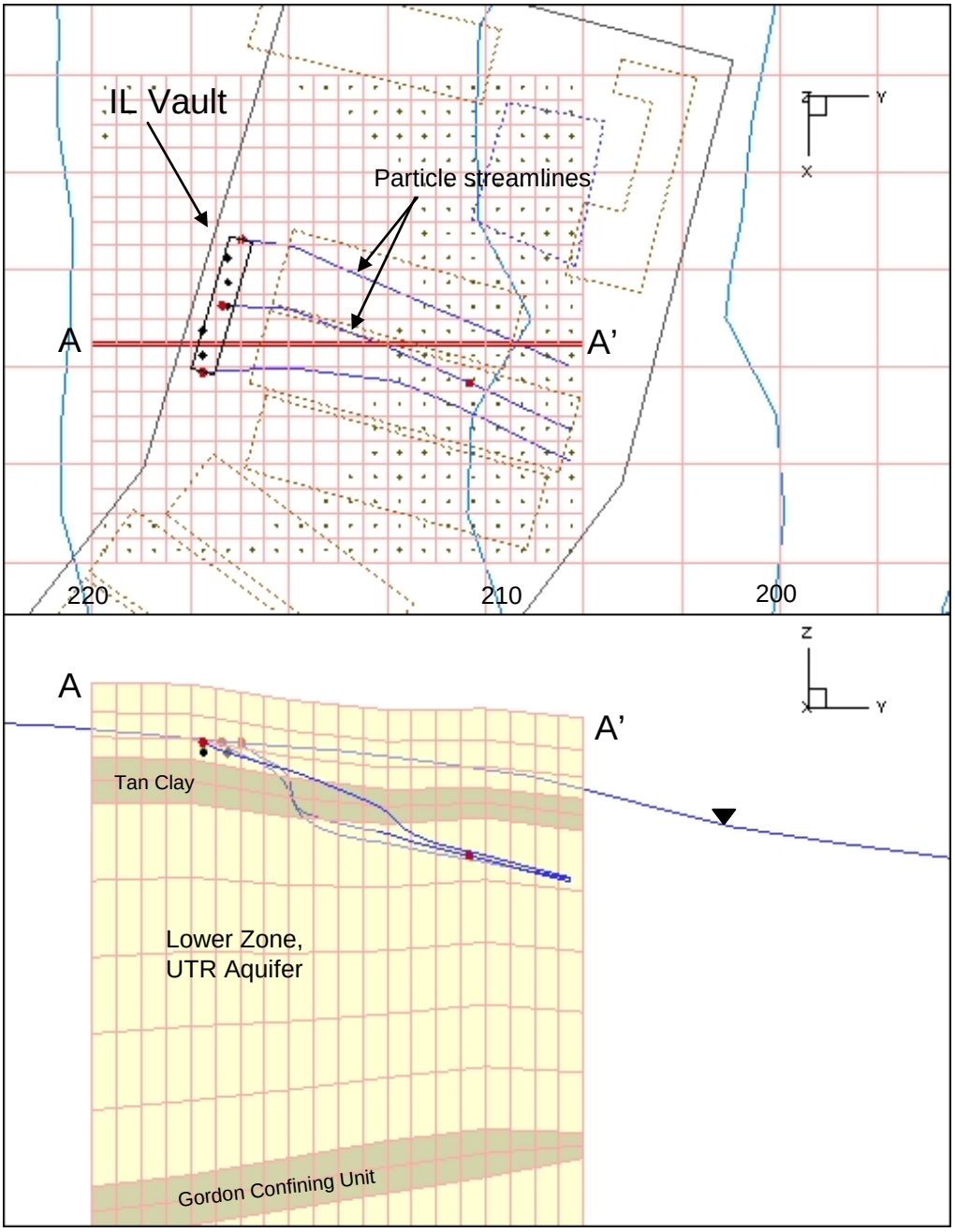

Figure 4-16. Aquifer model grid in plan view and cross-section

Each of the aquifer units is labeled. The boundaries between units established based on actual field measurements. The solid line extending from the left side across the mesh and on to the right represents the water table, or upper surface of the saturated zone.

Another feature of the cross-section is the blue streamlines, which indicate the pattern of groundwater movement in the vertical plane. The solid "dots" from which the streamlines emanate are the model elements within which the contaminant flux source term (output from the vadose zone transport model) is introduced into the aquifer model. The location of these source elements is also indicated in the plan view by the prominent dots beneath the trace of the ILV.

The ILV aquifer model was used only for transport simulations where its flow field was input from an interpolated flow field taken from the baseline GSA flow model. Amongst the 50 ft by 50 ft model elements, those located more than 100 meters from the perimeter of the ILV are indicated with a solid symbol in the center of the element. Internal PORFLOW processing locates the spatially maximum concentration of each species outside its 100-m buffer region. Post-processing of specific PORFLOW output files was performed to locate the maximum (peak) concentration in time for each disposed parent radionuclide.

The sandy aquifer units are a heterogeneous material that is primarily sandy with local clayey sediments distributed throughout. From a purely transport advection viewpoint (i.e., pore velocity) the effective porosity of these units is significantly lower than the total porosity. Here the clayey sediments behave like small hydraulic barriers forcing the groundwater to navigate past them. Based on engineering judgment and available in-the-field tritium measurements in neighboring sites on SRS, the effective porosity is assumed to be ~25%. To account for the faster pore velocity, the aquifer transport analyses were performed where the porosity was set to 0.25. Similarly, the sandy aquifer unit density was set to 1.39.

The ILV aquifer transport model is impacted by surface boundary conditions and internal source nodes. At the outer surfaces (i.e., the x, y, and z domain faces) incoming versus outgoing boundary conditions are handled differently. At an incoming face the radionuclide species of interest is assumed to have a zero concentration. At an outgoing face the diffusive flux of the radionuclide species of interest is assumed to have a value of zero. Here the outgoing faces are sufficiently far from the regions of interest that this method has negligible impact on its upstream concentration profiles.

Source terms at the water table were derived from the PORFLOW Flux.out files from the vadose zone models of the Typical Cells and Cell 4. These output fluxes were combined in the ratio of 6:1, or as 6X the Typical Cell mass flux plus the mass flux from Cell 4. Since the source term for the vadose zone models was 1 mole, the model results were divided by 7 to provide concentrations per 1 mole disposed in the entire ILV.

The source terms for all radionuclide of interest and special wasteforms were introduced within the ILV aquifer transport model by way of 5 source nodes that resided in the top layers of the model where the water table exists and are indicated in the upper diagram of Figure 4-16. Model (i,j,k) indices associated with these source nodes are (9, 7,13), (10, 7,13), (11, 7,13), (12, 6,13), and (13, 6,13).

4.6.5 Groundwater Transport Deterministic Model Results

The concentration output for each parent radionuclide from the PORFLOW aquifer model was utilized to calculate beta-gamma, gross alpha, radium and uranium peak concentrations within the 1,000-year compliance period. The peak concentrations were determined by evaluating the concentration through time for a group of model elements that were determined to be greater than 100 meters from the ILV. These elements are indicated in Figure 4-16 as the elements with a prominent dot in the middle. At any given time the maximum concentration was determined to be the maximum concentration in any of these model elements. The PORFLOW concentration output files were converted into input for the All-Pathways program (Koffman 2006a) using the Ideal Filemaker program (Taylor 2006). The peak activities and concentrations were then calculated for the groundwater pathway in the automated All-Pathways program. Plots of flux to the water table and concentration at the point of assessment for each radionuclide are in Appendix A4.

Using the results from the All-Pathways program, the groundwater activity or concentrations calculated for beta-gamma, gross alpha, radium and uranium were used to derive the ILV groundwater pathway limits for each radionuclide evaluated. The limits for each are 4 mrem/yr, 15 pCi/L, 5 pCi/L and 30 μg/L for beta-gamma, gross alpha, radium and uranium, respectively. The established activity or concentration limit for each of these, divided by the activity or concentration calculated in the All-Pathways analysis for each from the disposal of 1 Ci of parent is proportional to ILV groundwater limit, in Ci, divided by the source term of 1 Ci, for each radionuclide. The results of each are presented Table 4-6.

Radionuclide disposal limits in this section are derived without considering the impact of groundwater contaminant plume interaction with nearby disposal units (e.g., Slit Trenches) and are therefore presented as preliminary information. The results of plume interaction are presented in Chapter 6, Integrated Facility Analysis. Final limits will be adjusted as needed to account for plume interaction and the results of sensitivity and/or uncertainty analyses and presented in Chapter 7, Integration and Interpretation.

Table 4-6. Preliminary Groundwater Protection Limits

Based on Years 0 - 200				
Radionuclide	**Beta-Gamma Limit**	**Gross Alpha Limit**	**Radium Limit**	**Uranium Limit**
	Ci	**Ci**	**Ci**	**Ci**
Am-241	---	---	---	---
Am-243	---	---	---	---
C-14	5.4E+16	---	---	---
C-14_KB*	8.6E+17	---	---	---
Cl-36	1.9E+08	---	---	---
Cm-244	---	---	---	---
Cm-245	---	---	---	---
Cm-247	---	---	---	---
Cm-248	---	---	---	---
H-3	1.4E+08	---	---	---
H-3_TPBAR	2.4E+08	---	---	---
I-129	5.9E+10	---	---	---
I-129_ETF	3.9E+12	---	---	---
I-129_KB	2.1E+14	---	---	---
K-40	---	---	---	---
Mo-93	1.2E+04	---	---	---
Nb-94	---	---	---	---
Ni-59	---	---	---	---
Np-237	---	---	---	---
Pd-107	---	---	---	---
Pu-238	---	---	---	---
Pu-239	---	---	---	---
Pu-240	---	---	---	---
Pu-241	---	---	---	---
Pu-242	---	---	---	---
Pu-244	---	---	---	---
Ra-226	---	---	---	---
Se-79	---	---	---	---
Sn-126	---	---	---	---
Sr-90	1.6E+15	---	---	---
Tc-99	---	---	---	---
Tc-99_KB	---	---	---	---
Th-230	---	---	---	---
Th-232	---	---	---	---
U-233	---	---	---	---
U-234	---	---	---	---
U-235	---	---	---	---
U-236	---	---	---	---
U-238	---	---	---	---
Zr-93	---	---	---	---

Table 4-6. Preliminary Groundwater Protection Limits - continued

Based on Years 200 - 1100				
Radionuclide	**Beta-Gamma Limit**	**Gross Alpha Limit**	**Radium Limit**	**Uranium Limit**
	Ci	**Ci**	**Ci**	**Ci**
Am-241	3.7E+10	1.8E+09	---	2.3E+19
Am-243	1.9E+17	4.0E+15	---	---
C-14	5.7E+02	---	---	---
C-14_KB*	1.0E+13	---	---	---
Cl-36	8.8E+00	---	---	---
Cm-244	---	---	---	---
Cm-245	6.1E+10	3.0E+09	---	3.9E+19
Cm-247	1.0E+19	2.2E+17	---	---
Cm-248	---	---	---	---
H-3	6.0E+11	---	---	---
H-3_TPBAR	3.2E+11	---	---	---
I-129	2.1E-02	---	---	---
I-129_ETF	7.5E-01	---	---	---
I-129_KB	4.5E+00	---	---	---
K-40	2.3E+13	---	---	---
Mo-93	8.1E+00	---	---	---
Nb-94	2.2E+05	---	---	---
Ni-59	2.1E+08	---	---	---
Np-237	4.8E+06	2.4E+05	---	2.9E+15
Pd-107	2.6E+10	---	---	---
Pu-238	1.9E+10	1.4E+08	1.8E+08	---
Pu-239	1.4E+15	3.0E+13	---	---
Pu-240	---	---	---	---
Pu-241	1.1E+12	5.7E+10	---	---
Pu-242	3.3E+17	2.3E+15	3.1E+15	---
Pu-244	---	---	---	---
Ra-226	3.4E+03	2.5E+01	3.4E+01	---
Se-79	---	---	---	---
Sn-126	---	---	---	---
Sr-90	1.5E+10	---	---	---
Tc-99	2.0E+07	---	---	---
Tc-99_KB	2.8E+08	---	---	---
Th-230	1.2E+04	9.2E+01	1.2E+02	---
Th-232	2.1E+15	2.1E+15	2.9E+15	---
U-233	---	---	---	---
U-234	4.5E+06	3.3E+04	4.4E+04	---
U-235	5.5E+08	1.2E+07	---	---
U-236	---	---	---	---
U-238	7.9E+09	5.7E+07	7.5E+07	---
Zr-93	2.6E+08	---	---	---

Note: Limits reported as "---" indicate that there is no limit or that the limit $\geq$ 1E+20.
* Waste containing C-14_KB is assumed to not be in Cell #4.

The results of the ILV Base Case evaluation are presented as graphs of concentration (pCi/L) versus time in Appendix A4.

4.6.6 Groundwater Transport Sensitivity Analysis

Sensitivity analyses for the ILV focused exclusively on two transport parameters: the saturated effective diffusion coefficient and partition coefficients. The mean and standard deviations for saturated effective diffusion coefficients for each material were taken from Phifer et al. (2006). Only the case where the saturated effective diffusion coefficients were increased by two standard deviations was considered. A single PORFLOW run was made for each generic and special wasteform radionuclide using the greater value for each material in the model. The D_{eff} values used in the base case and the sensitivity run are shown in Table 4-7.

The base case K_d values were taken from Kaplan (2006). A statistical analysis was performed to determine an appropriate distribution for each radionuclide and to define the base case minus two standard deviations value for use in the sensitivity run (Shine 2007). A single PORFLOW run was made for each generic and special wasteform radionuclide using the smaller value for each radionuclide in the model. Carbon-14 and C-14 in K and L basin resins were simulated using a K_d release model, instead of a solubility release model, to assess sensitivity to K_d. In this simulation, the C-14_KB waste was assumed to be in all of the ILV cells. The K_d values used in the base case and the sensitivity run are shown in Table 4-8, Table 4-9, and Table 4-10. No consideration was given to evaluating the impact of CDP since there is not projected to be any waste that would contain significant quantities of these products in the ILV.

Table 4-7. D_{eff} Values used in Sensitivity Analysis

Material	Saturated Effective Diffusion Coefficient, (cm^2/yr)	+2 sigma Sat. Eff. Diffusion Coefficient, (cm^2/yr)
E-Area Vault Concrete	1.6E+00	1.77E+00
E-Area CLSM	1.3E+02	1.61E+02
Upper Vadose Zone	1.7E+02	2.33E+02
Lower Vadose Zone	1.7E+02	2.33E+02
E-Area Operational Soil Cover Prior to Dynamic Compaction	1.7E+02	2.33E+02
Control Compacted Backfill	1.7E+02	2.33E+02
IL Vault Permeable Backfill	2.5E+02	4.39E+02
Gravel	3.0E+02	5.15E+02
Sand	2.5E+02	4.39E+02
Clay	1.3E+02	1.61E+02
Clay_Sand	1.7E+02	2.33E+02

Table 4-8. K_d Values used in Sensitivity Analysis for Oxidizing Cementitious Material

Radionuclide	Young Cement (mL/g)		Moderately Aged Cement (mL/g)		Old Cement (mL/g)	
	Median	2σ	Median	2σ	Median	2σ
Ac	5.00E+03	1.47E+03	5.00E+03	1.47E+03	5.00E+02	3.57E+02
Am	5.00E+03	1.47E+03	5.00E+03	1.47E+03	5.00E+02	3.57E+02
Ar	0.00E+00	0.00E+00	0.00E+00	0.00E+00	0.00E+00	0.00E+00
At	8.00E+00	5.71E+00	2.00E+01	1.43E+01	0.00E+00	0.00E+00
Ba	1.00E+02	7.14E+01	1.00E+02	7.14E+01	7.00E+01	5.00E+01
Bk	5.00E+03	1.47E+03	5.00E+03	1.47E+03	5.00E+02	3.57E+02
C	2.00E+01	1.43E+01	1.00E+01	7.14E+00	0.00E+00	0.00E+00
Cf	5.00E+03	1.47E+03	5.00E+03	1.47E+03	5.00E+02	3.57E+02
Cl	8.00E-01	5.71E-01	2.00E+00	1.43E+00	0.00E+00	0.00E+00
Cm	5.00E+03	1.47E+03	5.00E+03	1.47E+03	5.00E+02	3.57E+02
Co	1.00E+03	2.94E+02	1.00E+03	2.94E+02	5.00E+02	3.57E+02
Cs	2.00E+00	1.43E+00	4.00E+00	2.86E+00	2.00E+00	1.43E+00
Eu	5.00E+03	1.47E+03	5.00E+03	1.47E+03	5.00E+02	3.57E+02
Fr	2.00E+00	1.43E+00	4.00E+00	2.86E+00	2.00E+00	1.43E+00
Gd	5.00E+03	1.47E+03	5.00E+03	1.47E+03	5.00E+02	3.57E+02
H	0.00E+00	0.00E+00	0.00E+00	0.00E+00	0.00E+00	0.00E+00
I	8.00E+00	5.71E+00	2.00E+01	1.43E+01	0.00E+00	0.00E+00
Kr	0.00E+00	0.00E+00	0.00E+00	0.00E+00	0.00E+00	0.00E+00
Nb	1.00E+03	2.94E+02	1.00E+03	2.94E+02	5.00E+02	3.57E+02
Ni	1.00E+03	2.94E+02	1.00E+03	2.94E+02	5.00E+02	3.57E+02
Np	2.00E+03	5.88E+02	2.00E+03	5.88E+02	2.00E+02	1.43E+02
Pa	2.00E+03	5.88E+02	2.00E+03	5.88E+02	2.00E+02	1.43E+02
Pb	5.00E+02	3.57E+02	5.00E+02	3.57E+02	2.50E+02	1.79E+02
Po	5.00E+02	3.57E+02	5.00E+02	3.57E+02	2.50E+02	1.79E+02
Pu	5.00E+03	1.47E+03	5.00E+03	1.47E+03	5.00E+02	3.57E+02
Pu_4	5.00E+03	1.47E+03	5.00E+03	1.47E+03	5.00E+02	3.57E+02
Pu_5	5.00E+03	1.47E+03	5.00E+03	1.47E+03	5.00E+02	3.57E+02
Ra	1.00E+02	7.14E+01	1.00E+02	7.14E+01	7.00E+01	5.00E+01
Rb	2.00E+00	1.43E+00	4.00E+00	2.86E+00	2.00E+00	1.43E+00
Re	0.00E+00	0.00E+00	0.00E+00	0.00E+00	0.00E+00	0.00E+00
Rn	0.00E+00	0.00E+00	0.00E+00	0.00E+00	0.00E+00	0.00E+00
Se	3.00E+02	2.14E+02	3.00E+02	2.14E+02	1.50E+02	1.07E+02
Sm	5.00E+03	1.47E+03	5.00E+03	1.47E+03	5.00E+02	3.57E+02
Sn	4.00E+03	1.18E+03	4.00E+03	1.18E+03	2.00E+03	5.88E+02
Sr	1.00E+00	7.14E-01	1.00E+00	7.14E-01	8.00E-01	5.71E-01
Tc	0.00E+00	0.00E+00	0.00E+00	0.00E+00	0.00E+00	0.00E+00
Te	3.00E+02	2.14E+02	3.00E+02	2.14E+02	1.50E+02	1.07E+02
Th	5.00E+03	1.47E+03	5.00E+03	1.47E+03	5.00E+02	3.57E+02
U	1.00E+03	2.94E+02	1.00E+03	2.94E+02	7.00E+01	5.00E+01
Zr	5.00E+03	1.47E+03	5.00E+03	1.47E+03	5.00E+02	3.57E+02

Table 4-8. Kd Values used in Sensitivity Analysis for Oxidizing Cementitious Material - continued

Radionuclide	Young Cement (mL/g)		Moderately Aged Cement (mL/g)		Old Cement (mL/g)	
	Median	2σ	Median	2σ	Median	2σ
Ag	0.00E+00	0.00E+00	0.00E+00	0.00E+00	0.00E+00	0.00E+00
Al	0.00E+00	0.00E+00	0.00E+00	0.00E+00	0.00E+00	0.00E+00
Be	1.00E+00	7.14E-01	1.00E+00	7.14E-01	8.00E-01	5.71E-01
Bi	0.00E+00	0.00E+00	0.00E+00	0.00E+00	0.00E+00	0.00E+00
Ca	1.00E+00	7.14E-01	1.00E+00	7.14E-01	8.00E-01	5.71E-01
Cd	1.00E+03	2.94E+02	1.00E+03	2.94E+02	5.00E+02	3.57E+02
Es	0.00E+00	0.00E+00	0.00E+00	0.00E+00	0.00E+00	0.00E+00
Fe	1.00E+03	2.94E+02	1.00E+03	2.94E+02	5.00E+02	3.57E+02
Ge	5.00E+03	1.47E+03	5.00E+03	1.47E+03	5.00E+02	3.57E+02
Hf	5.00E+03	1.47E+03	5.00E+03	1.47E+03	5.00E+02	3.57E+02
Hg	0.00E+00	0.00E+00	0.00E+00	0.00E+00	0.00E+00	0.00E+00
Ho	5.00E+03	1.47E+03	5.00E+03	1.47E+03	5.00E+02	3.57E+02
In	5.00E+03	1.47E+03	5.00E+03	1.47E+03	5.00E+02	3.57E+02
Ir	0.00E+00	0.00E+00	0.00E+00	0.00E+00	0.00E+00	0.00E+00
K	2.00E+00	1.43E+00	4.00E+00	2.86E+00	2.00E+00	1.43E+00
La	5.00E+03	1.47E+03	5.00E+03	1.47E+03	5.00E+02	3.57E+02
Lu	5.00E+03	1.47E+03	5.00E+03	1.47E+03	5.00E+02	3.57E+02
Mn	0.00E+00	0.00E+00	0.00E+00	0.00E+00	0.00E+00	0.00E+00
Mo	0.00E+00	0.00E+00	0.00E+00	0.00E+00	0.00E+00	0.00E+00
P	0.00E+00	0.00E+00	0.00E+00	0.00E+00	0.00E+00	0.00E+00
Pd	1.00E+03	2.94E+02	1.00E+03	2.94E+02	5.00E+02	3.57E+02
Pt	5.00E+03	1.47E+03	5.00E+03	1.47E+03	5.00E+02	3.57E+02
Ru	0.00E+00	0.00E+00	0.00E+00	0.00E+00	0.00E+00	0.00E+00
Si	0.00E+00	0.00E+00	0.00E+00	0.00E+00	0.00E+00	0.00E+00
Ta	8.00E-01	5.71E-01	2.00E+00	1.43E+00	0.00E+00	0.00E+00
Ti	5.00E+03	1.47E+03	5.00E+03	1.47E+03	5.00E+02	3.57E+02
V	0.00E+00	0.00E+00	0.00E+00	0.00E+00	0.00E+00	0.00E+00
C-14_KB	1.40E+02	1.00E+02	1.40E+02	1.00E+02	1.40E+02	1.00E+02
I-129_ETFCarbon	6.00E+02	4.29E+02	6.00E+02	4.29E+02	6.00E+02	4.29E+02
I-129_KB	3.70E+03	1.09E+03	3.70E+03	1.09E+03	3.70E+03	1.09E+03
Tc-99_KB	8.10E+02	5.79E+02	8.10E+02	5.79E+02	8.10E+02	5.79E+02

Table 4-9. K_d Values used in Sensitivity Analysis for Reducing Cementitious Material

Radionuclide	Young Cement (mL/g)		Moderately Aged Cement (mL/g)		Old Cement (mL/g)	
	Median	2σ	Median	2σ	Median	2σ
Ac	5.00E+03	1.47E+03	5.00E+03	1.47E+03	5.00E+02	3.57E+02
Am	5.00E+03	1.47E+03	5.00E+03	1.47E+03	5.00E+02	3.57E+02
Ar	0.00E+00	0.00E+00	0.00E+00	0.00E+00	0.00E+00	0.00E+00
At	8.00E+00	5.71E+00	2.00E+01	1.43E+01	0.00E+00	0.00E+00
Ba	1.00E+02	7.14E+01	1.00E+02	7.14E+01	7.00E+01	5.00E+01
Bk	5.00E+03	1.47E+03	5.00E+03	1.47E+03	5.00E+02	3.57E+02
C	2.00E+01	1.43E+01	1.00E+01	7.14E+00	0.00E+00	0.00E+00
Cf	5.00E+03	1.47E+03	5.00E+03	1.47E+03	5.00E+02	3.57E+02
Cl	8.00E-01	5.71E-01	2.00E+00	1.43E+00	0.00E+00	0.00E+00
Cm	5.00E+03	1.47E+03	5.00E+03	1.47E+03	5.00E+02	3.57E+02
Co	1.00E+03	2.94E+02	1.00E+03	2.94E+02	5.00E+02	3.57E+02
Cs	2.00E+00	1.43E+00	4.00E+00	2.86E+00	2.00E+00	1.43E+00
Eu	5.00E+03	1.47E+03	5.00E+03	1.47E+03	5.00E+02	3.57E+02
Fr	2.00E+00	1.43E+00	4.00E+00	2.86E+00	2.00E+00	1.43E+00
Gd	5.00E+03	1.47E+03	5.00E+03	1.47E+03	5.00E+02	3.57E+02
H	0.00E+00	0.00E+00	0.00E+00	0.00E+00	0.00E+00	0.00E+00
I	8.00E+00	5.71E+00	2.00E+01	1.43E+01	0.00E+00	0.00E+00
Kr	0.00E+00	0.00E+00	0.00E+00	0.00E+00	0.00E+00	0.00E+00
Nb	1.00E+03	2.94E+02	1.00E+03	2.94E+02	5.00E+02	3.57E+02
Ni	1.00E+03	2.94E+02	1.00E+03	2.94E+02	5.00E+02	3.57E+02
Np	2.00E+03	5.88E+02	2.00E+03	5.88E+02	2.00E+02	1.43E+02
Pa	2.00E+03	5.88E+02	2.00E+03	5.88E+02	2.00E+02	1.43E+02
Pb	5.00E+02	3.57E+02	5.00E+02	3.57E+02	2.50E+02	1.79E+02
Po	5.00E+02	3.57E+02	5.00E+02	3.57E+02	2.50E+02	1.79E+02
Pu	5.00E+03	1.47E+03	5.00E+03	1.47E+03	5.00E+02	3.57E+02
Pu_4	5.00E+03	1.47E+03	5.00E+03	1.47E+03	5.00E+02	3.57E+02
Pu_5	5.00E+03	1.47E+03	5.00E+03	1.47E+03	5.00E+02	3.57E+02
Ra	1.00E+02	7.14E+01	1.00E+02	7.14E+01	7.00E+01	5.00E+01
Rb	2.00E+00	1.43E+00	4.00E+00	2.86E+00	2.00E+00	1.43E+00
Re	5.00E+03	1.47E+03	5.00E+03	1.47E+03	5.00E+03	1.47E+03
Rn	0.00E+00	0.00E+00	0.00E+00	0.00E+00	0.00E+00	0.00E+00
Se	3.00E+02	2.14E+02	3.00E+02	2.14E+02	1.50E+02	1.07E+02
Sm	5.00E+03	1.47E+03	5.00E+03	1.47E+03	5.00E+02	3.57E+02
Sn	4.00E+03	1.18E+03	4.00E+03	1.18E+03	2.00E+03	5.88E+02
Sr	1.00E+00	7.14E-01	1.00E+00	7.14E-01	8.00E-01	5.71E-01
Tc	5.00E+03	1.47E+03	5.00E+03	1.47E+03	5.00E+03	1.47E+03
Te	3.00E+02	2.14E+02	3.00E+02	2.14E+02	1.50E+02	1.07E+02
Th	5.00E+03	1.47E+03	5.00E+03	1.47E+03	5.00E+02	3.57E+02
U	5.00E+03	1.47E+03	5.00E+03	1.47E+03	5.00E+03	1.47E+03
Zr	5.00E+03	1.47E+03	5.00E+03	1.47E+03	5.00E+02	3.57E+02

Table 4-9. Kd Values used in Sensitivity Analysis for Reducing Cementitious Material - continued

Radionuclide	Young Cement (mL/g)		Moderately Aged Cement (mL/g)		Old Cement (mL/g)	
	Median	2σ	Median	2σ	Median	2σ
Ag	0.00E+00	0.00E+00	0.00E+00	0.00E+00	0.00E+00	0.00E+00
Al	0.00E+00	0.00E+00	0.00E+00	0.00E+00	0.00E+00	0.00E+00
Be	1.00E+00	7.14E-01	1.00E+00	7.14E-01	8.00E-01	5.71E-01
Bi	0.00E+00	0.00E+00	0.00E+00	0.00E+00	0.00E+00	0.00E+00
Ca	1.00E+00	7.14E-01	1.00E+00	7.14E-01	8.00E-01	5.71E-01
Cd	1.00E+03	2.94E+02	1.00E+03	2.94E+02	5.00E+02	3.57E+02
Es	0.00E+00	0.00E+00	0.00E+00	0.00E+00	0.00E+00	0.00E+00
Fe	1.00E+03	2.94E+02	1.00E+03	2.94E+02	5.00E+02	3.57E+02
Ge	5.00E+03	1.47E+03	5.00E+03	1.47E+03	5.00E+02	3.57E+02
Hf	5.00E+03	1.47E+03	5.00E+03	1.47E+03	5.00E+02	3.57E+02
Hg	0.00E+00	0.00E+00	0.00E+00	0.00E+00	0.00E+00	0.00E+00
Ho	5.00E+03	1.47E+03	5.00E+03	1.47E+03	5.00E+02	3.57E+02
In	5.00E+03	1.47E+03	5.00E+03	1.47E+03	5.00E+02	3.57E+02
Ir	0.00E+00	0.00E+00	0.00E+00	0.00E+00	0.00E+00	0.00E+00
K	2.00E+00	1.43E+00	4.00E+00	2.86E+00	2.00E+00	1.43E+00
La	5.00E+03	1.47E+03	5.00E+03	1.47E+03	5.00E+02	3.57E+02
Lu	5.00E+03	1.47E+03	5.00E+03	1.47E+03	5.00E+02	3.57E+02
Mn	0.00E+00	0.00E+00	0.00E+00	0.00E+00	0.00E+00	0.00E+00
Mo	0.00E+00	0.00E+00	0.00E+00	0.00E+00	0.00E+00	0.00E+00
P	0.00E+00	0.00E+00	0.00E+00	0.00E+00	0.00E+00	0.00E+00
Pd	1.00E+03	2.94E+02	1.00E+03	2.94E+02	5.00E+02	3.57E+02
Pt	5.00E+03	1.47E+03	5.00E+03	1.47E+03	5.00E+02	3.57E+02
Ru	0.00E+00	0.00E+00	0.00E+00	0.00E+00	0.00E+00	0.00E+00
Si	0.00E+00	0.00E+00	0.00E+00	0.00E+00	0.00E+00	0.00E+00
Ta	8.00E-01	5.71E-01	2.00E+00	1.43E+00	0.00E+00	0.00E+00
Ti	5.00E+03	1.47E+03	5.00E+03	1.47E+03	5.00E+02	3.57E+02
V	0.00E+00	0.00E+00	0.00E+00	0.00E+00	0.00E+00	0.00E+00

Table 4-10. K_d Values used in Sensitivity Analysis for Sand and Clay

	Sand(mL/g)		Clay (mL/g)	
Radionuclide	**Median**	**2σ**	**Median**	**2σ**
Ac	1.10E+03	3.24E+02	8.50E+03	2.50E+03
Am	1.10E+03	3.24E+02	8.50E+03	2.50E+03
Ar	0.00E+00	0.00E+00	0.00E+00	0.00E+00
At	0.00E+00	0.00E+00	6.00E-01	4.29E-01
Ba	5.00E+00	3.57E+00	1.70E+01	1.21E+01
Bk	1.10E+03	3.24E+02	8.50E+03	2.50E+03
C	0.00E+00	0.00E+00	0.00E+00	0.00E+00
Cf	1.10E+03	3.24E+02	8.50E+03	2.50E+03
Cl	0.00E+00	0.00E+00	0.00E+00	0.00E+00
Cm	1.10E+03	3.24E+02	8.50E+03	2.50E+03
Co	7.00E+00	5.00E+00	3.00E+01	2.14E+01
Cs	5.00E+01	3.57E+01	2.50E+02	1.79E+02
Eu	1.10E+03	3.24E+02	8.50E+03	2.50E+03
Fr	5.00E+01	3.57E+01	2.50E+02	1.79E+02
Gd	1.10E+03	3.24E+02	8.50E+03	2.50E+03
H	0.00E+00	0.00E+00	0.00E+00	0.00E+00
I	0.00E+00	0.00E+00	6.00E-01	4.29E-01
Kr	0.00E+00	0.00E+00	0.00E+00	0.00E+00
Nb	0.00E+00	0.00E+00	0.00E+00	0.00E+00
Ni	7.00E+00	5.00E+00	3.00E+01	2.14E+01
Np	6.00E-01	4.29E-01	3.50E+01	2.50E+01
Pa	6.00E-01	4.29E-01	3.50E+01	2.50E+01
Pb	2.00E+03	5.88E+02	5.00E+03	1.47E+03
Po	2.00E+03	5.88E+02	5.00E+03	1.47E+03
Pu	2.70E+02	1.93E+02	5.90E+03	1.74E+03
Pu_4	3.00E+02	2.14E+02	6.00E+03	1.76E+03
Pu_5	1.60E+01	1.14E+01	5.00E+03	1.47E+03
Ra	5.00E+00	3.57E+00	1.70E+01	1.21E+01
Rb	5.00E+01	3.57E+01	2.50E+02	1.79E+02
Re	1.00E-01	7.14E-02	2.00E-01	1.43E-01
Rn	0.00E+00	0.00E+00	0.00E+00	0.00E+00
Se	1.00E+03	2.94E+02	1.00E+03	2.94E+02
Sm	1.10E+03	3.24E+02	8.50E+03	2.50E+03
Sn	2.00E+03	5.88E+02	5.00E+03	1.47E+03
Sr	5.00E+00	3.57E+00	1.70E+01	1.21E+01
Tc	1.00E-01	7.14E-02	2.00E-01	1.43E-01
Te	1.00E+03	2.94E+02	1.00E+03	2.94E+02
Th	9.00E+02	6.43E+02	2.00E+03	5.88E+02
U	2.00E+02	1.43E+02	3.00E+02	2.14E+02
Zr	9.00E+02	6.43E+02	2.00E+03	5.88E+02

Table 4-10. Kd Values used in Sensitivity Analysis for Sand and Clay - continued

Radionuclide	Sand(mL/g)		Clay (mL/g)	
	Median	2σ	Median	2σ
Ag	0.00E+00	0.00E+00	0.00E+00	0.00E+00
Al	0.00E+00	0.00E+00	0.00E+00	0.00E+00
Be	5.00E+00	3.57E+00	1.70E+01	1.21E+01
Bi	0.00E+00	0.00E+00	0.00E+00	0.00E+00
Ca	5.00E+00	3.57E+00	1.70E+01	1.21E+01
Cd	7.00E+00	5.00E+00	3.00E+01	2.14E+01
Es	0.00E+00	0.00E+00	0.00E+00	0.00E+00
Fe	7.00E+00	5.00E+00	3.00E+01	2.14E+01
Ge	9.00E+02	6.43E+02	2.00E+03	5.88E+02
Hf	9.00E+02	6.43E+02	2.00E+03	5.88E+02
Hg	0.00E+00	0.00E+00	0.00E+00	0.00E+00
Ho	1.10E+03	3.24E+02	8.50E+03	2.50E+03
In	1.10E+03	3.24E+02	8.50E+03	2.50E+03
Ir	0.00E+00	0.00E+00	0.00E+00	0.00E+00
K	5.00E+01	3.57E+01	2.50E+02	1.79E+02
La	1.10E+03	3.24E+02	8.50E+03	2.50E+03
Lu	1.10E+03	3.24E+02	8.50E+03	2.50E+03
Mn	0.00E+00	0.00E+00	0.00E+00	0.00E+00
Mo	0.00E+00	0.00E+00	0.00E+00	0.00E+00
P	0.00E+00	0.00E+00	0.00E+00	0.00E+00
Pd	7.00E+00	5.00E+00	3.00E+01	2.14E+01
Pt	9.00E+02	6.43E+02	2.00E+03	5.88E+02
Ru	0.00E+00	0.00E+00	0.00E+00	0.00E+00
Si	0.00E+00	0.00E+00	0.00E+00	0.00E+00
Ta	0.00E+00	0.00E+00	0.00E+00	0.00E+00
Ti	9.00E+02	6.43E+02	2.00E+03	5.88E+02
V	0.00E+00	0.00E+00	0.00E+00	0.00E+00

4.6.7 Results of Sensitivity Analysis

The sensitivity analysis was done using the groundwater pathways. The results are presented in terms of ILV disposal unit limits for each of the five groundwater-based performance objectives – beta-gamma, gross alpha, radium, uranium and all pathways and for the two time periods used in the base case, 0 - 200 years and 200 - 1100 years. These results are given in Table 4-11 through Table 4-20. A blank entry in the limit column indicates that the calculated limit was greater than 1E+20 Ci.

The overall finding of the sensitivity analysis is that the distribution of the saturated effective diffusion coefficient is relatively tight, so that the two standard deviation change is rather small. The resulting change in disposal limits is also quite small. The results are far more sensitive to changes in K_ds. The two standard deviation change makes a difference of about 25% in the value entered into the model. The change in the disposal limits ranges from none for radionuclides which have a base case K_d of 0 mL/g, to three orders of magnitude (e.g., Th-232, beta-gamma performance objective, 200 – 1100 year time frame).

4.6.8 Groundwater Transport Uncertainty Analysis

An ILV uncertainty analysis will be conducted later as a part of PA Maintenance and not in the current PA revision.

Table 4-11. Sensitivity Results for the 0-200 Year Period Beta-Gamma Cases

	Base Case		2 σ D_{eff} Case		2 σ K_d Case	
Parent	**Peak Year**	**Limit (Ci)**	**Peak Year**	**Limit (Ci)**	**Peak Year**	**Limit (Ci)**
Am-241	110		110		110	
Am-243	120		120		120	
C-14	101	2.5E+16	101	1.2E+16	101	3.5E+15
C-14_KB	102		101	7.7E+16	101	2.2E+16
Cl-36	101	1.9E+08	101	9.0E+07	101	4.1E+07
Cm-244	120		120		120	
Cm-245	110		110		110	
Cm-247	120		120		120	
Cm-248	120		120		120	
H-3	63	1.4E+08	61	7.8E+07	63	1.4E+08
H-3_TPBAR	96	2.4E+08	93	1.3E+08		
I-129	101	5.9E+10	101	2.8E+10	101	8.6E+09
I-129_ETF	101	3.9E+12	101	1.8E+12	101	5.1E+11
I-129_KB	102	2.1E+14	101	1.1E+13	101	1.3E+12
K-40	200		200		200	
Mo-93	101	1.2E+04	101	4.9E+03	101	8.5E+03
Nb-94	101		101		101	
Ni-59	200		200		200	
Np-237	110		110		110	
Pd-107	200		200		200	
Pu-238	200		200		200	
Pu-239	120		120		120	
Pu-240	120		120		120	
Pu-241	110		110		110	
Pu-242	200		200		200	
Pu-244	120		120		120	
Ra-226	200		200		200	
Se-79	200		200		200	
Sn-126	200		200		200	
Sr-90	130	1.6E+15	140	4.4E+14	130	1.1E+13
Tc-99	102		102		102	
Tc-99_KB	102		102		102	
Th-230	200		200		200	
Th-232	120		120		120	
U-233	200		200		200	
U-234	200		200		200	
U-235	120		120		120	
U-236	120		120		120	
U-238	200		200		200	
Zr-93	100		100		100	

Note: Blank entries in the Limit columns indicate the limit is > 1E+20Ci.

Table 4-12. Sensitivity Results for the 200-1100 Year Period Beta-Gamma Cases

	Base Case		2 σ D_{eff} Case		2 σ K_d Case	
Parent	**Peak Year**	**Limit (Ci)**	**Peak Year**	**Limit (Ci)**	**Peak Year**	**Limit (Ci)**
Am-241	1100	3.7E+10	1100	3.3E+10	1100	7.7E+07
Am-243	1100	1.9E+17	1100	1.7E+17	1100	3.4E+14
C-14	849	8.4E+01	848	8.4E+01	661	8.0E+01
C-14_KB	1100	5.8E+02	845	3.8E+02	844	2.9E+02
Cl-36	499	8.8E+00	494	8.5E+00	495	8.1E+00
Cm-244	1100		1100		1100	
Cm-245	1100	6.1E+10	1100	5.4E+10	1100	1.2E+08
Cm-247	1100	1.0E+19	1100	9.5E+18	1100	1.8E+16
Cm-248	1100		1100		1100	
H-3	260	6.0E+11	255	1.1E+11	260	6.0E+11
H-3_TPBAR	261	3.2E+11	253	9.3E+12		
I-129	658	2.1E-02	659	2.2E-02	658	1.9E-02
I-129_ETF	725	7.5E-01	661	6.6E-01	659	4.7E-01
I-129_KB	737	4.5E+00	661	3.8E+00	659	1.1E+00
K-40	1100	2.3E+13	1100	9.5E+12	1100	1.5E+11
Mo-93	486	8.1E+00	481	7.3E+00	485	7.6E+00
Nb-94	1100	2.2E+05	1100	2.0E+05	1100	2.1E+03
Ni-59	1100	2.1E+08	1100	1.6E+08	1100	6.7E+04
Np-237	1100	4.8E+06	1100	4.2E+06	1100	1.0E+04
Pd-107	1100	2.6E+10	1100	2.0E+10	1100	8.1E+06
Pu-238	1100	1.9E+10	1100	1.8E+10	1100	2.4E+09
Pu-239	1100	1.4E+15	1100	1.2E+15	1100	2.6E+12
Pu-240	1100		1100		1100	
Pu-241	1100	1.1E+12	1100	1.0E+12	1100	2.4E+09
Pu-242	1100	3.3E+17	1100	3.0E+17	1100	3.5E+16
Pu-244	1100		1100		1100	
Ra-226	1100	3.4E+03	1100	3.1E+03	1100	5.4E+02
Se-79	1100		1100		1100	
Sn-126	1100		1100		1100	
Sr-90	870	1.5E+10	840	1.0E+10	810	1.7E+09
Tc-99	1100	2.0E+07	1100	1.8E+07	1100	7.4E+04
Tc-99_KB	1100	2.8E+08	1100	2.6E+08	1100	7.9E+05
Th-230	1100	1.2E+04	1100	1.2E+04	1100	1.8E+03
Th-232	1100	2.1E+15	1100	1.6E+15	1100	2.3E+12
U-233	1100		1100		1100	
U-234	1100	4.5E+06	1100	4.2E+06	1100	6.0E+05
U-235	1100	5.5E+08	1100	4.9E+08	1100	1.1E+06
U-236	1100		1100		1100	2.4E+19
U-238	1100	7.9E+09	1100	7.3E+09	1100	9.4E+08
Zr-93	1100	2.6E+08	1100	2.2E+08	1100	3.4E+05

Note: Blank entries in the Limit columns indicate the limit is > 1E+20Ci.

Table 4-13. Sensitivity Results for the 0-200 Year Period Alpha Cases

	Base Case		2 σ D_{eff} Case		2 σ K_d Case	
Parent	**Peak Year**	**Limit (Ci)**	**Peak Year**	**Limit (Ci)**	**Peak Year**	**Limit (Ci)**
Am-241	110		110		110	
Am-243	110		110		110	
Cm-244	120		120		120	
Cm-245	110		110		110	
Cm-247	110		110		110	
Cm-248	120		120		120	
Np-237	110		110		110	
Pu-238	200		200		170	
Pu-239	110		110		110	
Pu-240	120		120		120	
Pu-241	110		110		110	
Pu-242	200		200		180	
Pu-244	120		120		120	
Ra-226	170		200		170	
Th-230	180		200		170	
Th-232	120		120		120	
U-233	200		200		200	
U-234	180		200		170	
U-235	110		110		110	
U-236	120		120		120	
U-238	200		200		170	

Note: Blank entries in the Limit columns indicate the limit is > 1E+20Ci.

Table 4-14. Sensitivity Results for the 200-1100 Year Period Alpha Cases

	Base Case		2 σ D_{eff} Case		2 σ K_d Case	
Parent	**Peak Year**	**Limit (Ci)**	**Peak Year**	**Limit (Ci)**	**Peak Year**	**Limit (Ci)**
Am-241	1100	1.8E+09	1100	1.6E+09	1100	3.8E+06
Am-243	1100	4.0E+15	1100	3.6E+15	1100	7.7E+12
Cm-244	1100		1100		1100	
Cm-245	1100	3.0E+09	1100	2.7E+09	1100	5.8E+06
Cm-247	1100	2.2E+17	1100	2.0E+17	1100	3.9E+14
Cm-248	1100		1100		1100	
Np-237	1100	2.4E+05	1100	2.1E+05	1100	5.2E+02
Pu-238	1100	1.4E+08	1100	1.3E+08	1100	1.9E+07
Pu-239	1100	3.0E+13	1100	2.7E+13	1100	6.0E+10
Pu-240	1100		1100		1100	
Pu-241	1100	5.7E+10	1100	5.0E+10	1100	1.2E+08
Pu-242	1100	2.3E+15	1100	2.1E+15	1100	2.7E+14
Pu-244	1100		1100		1100	
Ra-226	1100	2.5E+01	1100	2.4E+01	1100	4.6E+00
Th-230	1100	9.2E+01	1100	8.6E+01	1100	1.5E+01
Th-232	1100	2.1E+15	1100	1.6E+15	1100	2.3E+12
U-233	1100		1100		1100	
U-234	1100	3.3E+04	1100	3.1E+04	1100	4.8E+03
U-235	1100	1.2E+07	1100	1.1E+07	1100	2.5E+04
U-236	1100		1100		1100	2.5E+19
U-238	1100	5.7E+07	1100	5.3E+07	1100	7.4E+06

Note: Blank entries in the Limit columns indicate the limit is > 1E+20Ci.

Table 4-15. Sensitivity Results for the 0-200 Year Period Radium Cases

	Base Case		2 σ D_{eff} Case		2 σ K_d Case	
Parent	**Peak Year**	**Limit (Ci)**	**Peak Year**	**Limit (Ci)**	**Peak Year**	**Limit (Ci)**
Cm-244	120		120		120	
Cm-248	120		120		120	
Pu-238	200		200		170	
Pu-240	120		120		120	
Pu-242	200		200		180	
Pu-244	120		120		120	
Ra-226	170		200		170	
Th-230	180		200		170	
Th-232	120		120		120	
U-234	180		200		170	
U-236	120		120		120	
U-238	200		200		170	

Note: Blank entries in the Limit columns indicate the limit is > 1E+20Ci.

Table 4-16. Sensitivity Results for the 200-1100 Year Period Radium Cases

	Base Case		2 σ D_{eff} Case		2 σ K_d Case	
Parent	**Peak Year**	**Limit (Ci)**	**Peak Year**	**Limit (Ci)**	**Peak Year**	**Limit (Ci)**
Cm-244	1100		1100		1100	
Cm-248	1100		1100		1100	
Pu-238	1100	1.8E+08	1100	1.7E+08	1100	2.6E+07
Pu-240	1100		1100		1100	
Pu-242	1100	3.1E+15	1100	2.9E+15	1100	3.6E+14
Pu-244	1100		1100		1100	
Ra-226	1100	3.4E+01	1100	3.2E+01	1100	6.1E+00
Th-230	1100	1.2E+02	1100	1.1E+02	1100	2.0E+01
Th-232	1100	2.9E+15	1100	2.2E+15	1100	3.0E+12
U-234	1100	4.4E+04	1100	4.1E+04	1100	6.4E+03
U-236	1100		1100		1100	3.3E+19
U-238	1100	7.5E+07	1100	7.0E+07	1100	9.9E+06

Note: Blank entries in the Limit columns indicate the limit is > 1E+20Ci.

Table 4-17. Sensitivity Results for the 0-200 Year Period Uranium Cases

	Base Case		2 σ D_{eff} Case		2 σ K_d Case	
Parent	**Peak Year**	**Limit (Ci)**	**Peak Year**	**Limit (Ci)**	**Peak Year**	**Limit (Ci)**
Am-241	200		200		200	
Am-243	200		200		200	
Cm-244	200		200		200	
Cm-245	200		200		200	
Cm-247	200		200		200	
Cm-248	200		200		200	
Np-237	200		200		200	
Pu-238	200		200		200	
Pu-239	200		200		200	
Pu-240	200		200		200	
Pu-241	200		200		200	
Pu-242	200		200		200	
Pu-244	200		200		200	
U-233	200		200		200	
U-234	200		200		200	
U-235	200		200		200	
U-236	200		200		200	
U-238	200		200		200	

Note: Blank entries in the Limit columns indicate the limit is > 1E+20Ci.

Table 4-18. Sensitivity Results for the 200-1100 Year Period Uranium Cases

	Base Case		2 σ D_{eff} Case		2 σ K_d Case	
Parent	**Peak Year**	**Limit (Ci)**	**Peak Year**	**Limit (Ci)**	**Peak Year**	**Limit (Ci)**
Am-241	1100	2.3E+19	1100	1.9E+19	1100	3.8E+16
Am-243	1100		1100		1100	
Cm-244	1100		1100		1100	
Cm-245	1100	3.9E+19	1100	3.4E+19	1100	6.1E+16
Cm-247	1100		1100		1100	
Cm-248	1100		1100		1100	
Np-237	1100	2.9E+15	1100	2.5E+15	1100	4.9E+12
Pu-238	1100		1100		1100	
Pu-239	1100		1100		1100	
Pu-240	1100		1100		1100	
Pu-241	1100		1100		1100	1.2E+18
Pu-242	1100		1100		1100	
Pu-244	1100		1100		1100	
U-233	1100		1100		1100	
U-234	1100		1100		1100	
U-235	1100		1100		1100	
U-236	1100		1100		1100	
U-238	1100		1100		1100	

Note: Blank entries in the Limit columns indicate the limit is > 1E+20Ci.

Table 4-19. Sensitivity Results for the 0-200 Year Period All-Pathways Cases

	Base Case		2 σ D_{eff} Case		2 σ K_d Case	
Parent	Peak Year	Limit (Ci)	Peak Year	Limit (Ci)	Peak Year	Limit (Ci)
Am-241	110		110		110	
Am-243	110		110		110	
C-14	101	2.6E+16	101	1.2E+16	101	3.6E+15
C-14_KB	102		101	8.1E+16	101	2.3E+16
Cl-36	101	9.9E+07	101	4.8E+07	101	2.2E+07
Cm-244	120		120		120	
Cm-245	110		110		110	
Cm-247	110		110		110	
Cm-248	120		120		120	
H-3	63	3.8E+09	61	2.0E+09	63	3.8E+09
H-3_TPBAR	96	6.2E+09	93	3.4E+09		
I-129	101	3.5E+12	101	1.7E+12	101	5.2E+11
I-129_ETF	101	2.3E+14	101	1.1E+14	101	3.1E+13
I-129_KB	102	1.3E+16	101	6.6E+14	101	7.9E+13
K-40	200		200		200	
Mo-93	101	5.4E+04	101	2.4E+04	101	4.1E+04
Nb-94	101		101		101	
Ni-59	200		200		200	
Np-237	110		110		110	
Pd-107	200		200		200	
Pu-238	200		200		170	
Pu-239	110		110		110	
Pu-240	120		120		120	
Pu-241	110		110		110	
Pu-242	200		200		180	
Pu-244	120		120		120	
Ra-226	170		200		170	
Se-79	200		200		200	
Sn-126	200		200		200	
Sr-90	130	3.0E+16	140	8.5E+15	130	2.2E+14
Tc-99	102		102		102	
Tc-99_KB	102		102		102	
Th-230	180		200		170	
Th-232	120		120		120	
U-233	200		200		200	
U-234	180		200		170	
U-235	110		110		110	
U-236	120		120		120	
U-238	200		200		170	
Zr-93	100		100		100	

Note: Blank entries in the Limit columns indicate the limit is > 1E+20Ci.

Table 4-20. Sensitivity Results for the 200-1100 Year Period All-Pathways Cases

	Base Case		2 σ D_{eff} Case		2 σ K_d Case	
Parent	**Peak Year**	**Limit (Ci)**	**Peak Year**	**Limit (Ci)**	**Peak Year**	**Limit (Ci)**
Am-241	1100	5.7E+08	1100	5.0E+08	1100	1.2E+06
Am-243	1100	4.7E+14	1100	4.3E+14	1100	9.1E+11
C-14	849	8.7E+01	848	8.7E+01	661	8.3E+01
C-14_KB	1100	6.1E+02	845	3.9E+02	844	3.0E+02
Cl-36	499	4.7E+00	494	4.5E+00	495	4.3E+00
Cm-244	1100		1100		1100	
Cm-245	1100	9.4E+08	1100	8.3E+08	1100	1.8E+06
Cm-247	1100	2.6E+16	1100	2.4E+16	1100	4.7E+13
Cm-248	1100		1100		1100	
H-3	260	1.6E+13	255	6.3E+12	260	1.6E+13
H-3_TPBAR	261	8.2E+12	253	2.8E+12		
I-129	658	1.3E+00	659	1.3E+00	658	1.1E+00
I-129_ETF	725	4.6E+01	661	4.0E+01	659	2.9E+01
I-129_KB	737	2.7E+02	661	2.3E+02	659	6.9E+01
K-40	1100	5.1E+13	1100	2.1E+13	1100	3.2E+11
Mo-93	486	3.8E+01	481	3.5E+01	485	3.7E+01
Nb-94	1100	1.2E+05	1100	1.1E+05	1100	1.2E+03
Ni-59	1100	5.4E+10	1100	4.1E+10	1100	1.7E+07
Np-237	1100	7.4E+04	1100	6.5E+04	1100	1.6E+02
Pd-107	1100	8.2E+10	1100	6.3E+10	1100	2.6E+07
Pu-238	1100	5.4E+08	1100	5.0E+08	1100	7.6E+07
Pu-239	1100	3.5E+12	1100	3.2E+12	1100	7.2E+09
Pu-240	1100		1100		1100	
Pu-241	1100	1.8E+10	1100	1.6E+10	1100	3.7E+07
Pu-242	1100	9.0E+15	1100	8.4E+15	1100	1.1E+15
Pu-244	1100		1100		1100	
Ra-226	1100	9.9E+01	1100	9.3E+01	1100	1.8E+01
Se-79	1100		1100		1100	
Sn-126	1100		1100		1100	
Sr-90	870	2.9E+11	840	2.0E+11	810	3.4E+10
Tc-99	1100	3.0E+07	1100	2.7E+07	1100	1.1E+05
Tc-99_KB	1100	4.2E+08	1100	3.9E+08	1100	1.2E+06
Th-230	1100	3.6E+02	1100	3.4E+02	1100	5.9E+01
Th-232	1100	5.7E+15	1100	4.4E+15	1100	6.1E+12
U-233	1100		1100		1100	
U-234	1100	1.3E+05	1100	1.2E+05	1100	1.9E+04
U-235	1100	1.4E+06	1100	1.3E+06	1100	3.0E+03
U-236	1100		1100		1100	6.6E+19
U-238	1100	2.2E+08	1100	2.1E+08	1100	2.9E+07
Zr-93	1100	1.5E+09	1100	1.3E+09	1100	2.1E+06

Note: Blank entries in the Limit columns indicate the limit is > 1E+20Ci.

4.7 AIR-PATHWAY ANALYSIS

4.7.1 Overview of Air-Pathway Analysis

This section describes the investigation conducted to evaluate the potential magnitude of gaseous release of radionuclides from the ILV disposal unit over the 25-year operational period, 100-year institutional control period, and 1,000-year post-closure compliance period versus the atmospheric pathway performance objective of the public of 10 mrem/yr to a representative member. The ILV is a below grade, reinforced concrete vault which consists of two modules that together encompass a 278.83-ft by 48.5-ft area (Phifer et al. 2006). Waste stored in the ILV is typically placed in concrete or metal containers and subsequently encapsulated in CLSM. The waste is placed in the vaults in layers with the grout surface forming the foundation for the next layer.

A screening analysis was conducted to produce a list of radionuclides requiring a more thorough analysis to derive disposal limits for the ILV disposal unit based on the atmospheric pathway. This study, described in Crapse and Cook (2006), used a methodology developed by the National Council on Radiation Protection and Measurements (NCRP 1996), professional judgment and process knowledge to determine this list. The list of potential radionuclides is C-14, Cl-36, H-3, I-129, S-35, Sb-124, Sb-125, Se-75, Se-79, Sn-113, Sn-119m, Sn-121, Sn-121m, Sn-123, and Sn-126.

During the 25-year operational period and 100-year institutional control period, the 10-mrem/yr performance objective is applicable at the SRS boundary, due to active institutional controls. During the 1,000-year post-closure compliance period, this performance objective is applicable at 100 m from the disposal unit boundary, due to the assumed loss of active institutional controls. The atmospheric dose from the ILV was evaluated for three separate time periods: 1) 0 to 25 years, 2) 25 to 125 years, and 3) 125 to 1,125 years. The first time period evaluated covers the operational period. Since the exact mode of vault filling cannot be built into the model, it was assumed that the Typical Cell is fully loaded at time 0. For the 0-25 year time period, the model incorporates a three-inch thick layer of CLSM covering the waste contained within the vault. The second time period evaluated covers the institutional control period. During this time period, the waste is covered by the CLSM layer and a reinforced concrete roof. Finally, for the post-closure time period (125 to 1,125 years), a closure cap is placed over the ILV.

The analysis presented here uses accepted computer programs for diffusion (PORFLOW [ACRI 2004]) and atmospheric transport and dose calculations (CAP88 [Beres 1990]). This analysis considers diffusion of the radionuclides upward from the ILV waste through the overlying materials and subsequent transport either to the SRS boundary or to 100 m from the disposal unit boundary, as appropriate.

4.7.2 Summary of Key Air-Pathway Assumptions

Key assumptions and inputs used in the air-pathway analysis are presented in Appendix B.

4.7.3 ILV Closure Considerations

The concepts for closure of the ILV disposal unit are relevant to the determination of the gaseous radionuclide flux at the land surface. The ILV construction specifics and closure concept are described by Phifer et al. (2006). For the purposes of this investigation, it is assumed that during the 25-year operational time period there is a three-inch-thick layer of CLSM covering the waste. Therefore, during this time period, the top of the CLSM layer is the point where gaseous flux was evaluated. During the 100-year institutional control period, the waste is covered by the CLSM and a reinforced concrete roof. For this time period, the gaseous flux was evaluated at the top of the reinforced concrete roof. For the post-closure compliance period (125 to 1,125 years), a closure cap is assumed to be in place over the ILV disposal unit. A conceptual drawing of the closure cap over the ILV disposal unit is shown in Figure 4-6 and the vertical section over which the gaseous radionuclide diffusion was evaluated is indicated.

The closure cap utilized in this analysis includes all materials as constructed and placed over the ILV disposal unit at the end of the 100-year institutional control period. The components of concern for the long-term air-pathway performance calculation are those that have no potential to erode during the 1,000-year post-closure compliance period. These components are situated below the top of the erosion barrier. The composite thickness of the non-waste material below the top of the erosion barrier is 7.5 ft. Table 4-21 lists the individual components of the ILV disposal unit and closure cap (excluding the layers overlying the erosion control barrier). Materials are indicated with the associated thickness of each component, in inches, feet, and meters. The minimum thicknesses of the ILV reinforced concrete roof provided by Phifer et al. (2006) was utilized in the modeling effort since the minimum thickness represents a shorter diffusion path and is therefore conservative relative to the flux to the ground surface.

Table 4-21. Vertical Layer Sequence and Associated Thickness for ILV Cover Material and Waste

Layer	Thickness (inches)	Thickness (ft)	Thickness (m)
Erosion barrier	12	1	0.30
Middle backfill layer	12	1	0.30
Gravel drainage layer	12	1	0.30
Lower backfill layer	24	2	0.61
Reinforced concrete roof	27	2.25	0.69
CLSM	3	0.25	0.08
ILV waste layer	324	27.25	8.31

4.7.4 ILV Air-Pathway Conceptual Model

The flux of radioactive gasses at the land surface above the ILV was evaluated for its specific closure configuration. Gaseous radionuclides introduced within the waste zone diffuse outward from this zone into the air-filled soil pores surrounding the ILV, eventually resulting in some of the radionuclides emanating at the land surface. As such, air is the medium through which they diffuse. It is assumed that fluctuations in atmospheric pressure at the land surface that could induce small pulses of air movement into and out of the shallow soil profile over relatively short periods of time will have a zero net effect when averaged over longer time periods. Thus, advective transport of these radionuclides in air-filled soil pores is not considered to be a significant process when compared to the rate of air diffusion.

The radionuclides present as gasses are those identified in the screening process described in Crapse and Cook (2006). Certain gaseous radionuclides will not likely remain in the monatomic elemental form but combine with other gaseous elements or form diatomic molecules. The state of existence of each of these radionuclides in the gaseous phase is important in evaluating their transport to the land surface because the diffusion coefficient associated with each is related to its molecular weight.

In this investigation, based on thermodynamic stability considerations, it is assumed that:

- C-14 exists as part of the CO_2 molecule
- Cl-36, H-3 and I-129 exist as diatomic gasses
- S-35, Sb-124, Sb-125, Se-75, Se-79, Sn-113, Sn-119m, Sn-121, Sn-121m, Sn-123, and Sn-126 exist as monatomic gases.

4.7.5 ILV Air-Pathway Numerical Model

The mathematical model utilized in this report is provided by the PORFLOW (ACRI 2004) simulation package. PC-based PORFLOW Version 5.97.0 was used to conduct a series of simulations. PORFLOW is developed and marketed by Analytic & Computational Research, Inc. to solve problems involving transient and steady-state fluid flow, heat and mass transport in multi-phase, variably saturated, porous or fractured media with dynamic phase change. PORFLOW has been widely used at the SRS and in the DOE complex to address major issues related to the groundwater and nuclear waste management.

The governing equation for mass transport of species *k* in the fluid phase is given by

$$\frac{\partial C_k}{\partial t} + \frac{\partial}{\partial x_i}(V_i C_k) = \frac{\partial}{\partial x_i}(D_{ij}\frac{\partial C_k}{\partial x_j}) + \gamma_k \qquad \text{Eq 4-1}$$

Where

C_k	concentration of species *k* (g/m^3)
V_i	fluid velocity in the i^{th} direction (m/yr)
D_{ij}	effective diffusion coefficient for the species (m^2/yr)
γ_k	net decay of species *k* (g/m^3-yr)
i, j	direction index
t	time (yr)
x	distance coordinate (m)

This equation is solved within PORFLOW to evaluate transient radionuclide transport above the ILV and to determine gaseous radionuclide flux at the land surface over time.

4.7.5.1 ILV Air-Pathway Model Development and Assumptions

The numerical representation of the conceptual model is as a 1-dimensional vertical stack of elements configured to represent the thickness of the ILV and overlying cover material associated with final closure.

The radionuclides evaluated are C-14, Cl-36, H-3, I-129, S-35, Sb-124, Sb-125, Se-75, Se-79, Sn-113, Sn-119m, Sn-121, Sn-121m, Sn-123, and Sn-126.

Since source radionuclides exist as gases, air was taken to be the medium within which transport occurs. The flow field was assumed to be isobaric and isothermal. The impact of naturally occurring fluctuations in atmospheric pressure at the land surface that could induce small pulses of air movement into and out of the shallow soil profile over relatively short periods of time will have a zero net effect when averaged over longer time periods. Therefore, for the relatively long periods of time evaluated in this investigation, air diffusion was the only transport mechanism simulated in the model and advective air-transport was assumed to be negligible, so the advection term was disabled within PORFLOW and only the diffusive and net decay terms were evaluated.

A small percentage of the radionuclides dissolve in residual pore water, but since diffusion proceeds more slowly in water than in air, air diffusion is regarded as the only transport process by which they can reach the land surface from the ILV. This assertion is substantiated in Yu et al. (2001). In that report the radon effective diffusion coefficient for soil is reported to range from the open-air diffusion coefficient of 1.0E-05 m^2/s to that of fully saturated soil, 1.0E-9 m^2/s.

This 4-order of magnitude difference is consistent with the comparison of water diffusion coefficients to air diffusion coefficients of other common molecular compounds and reported in many references: for example Bolz and Tuve (1973). Thus, the larger volume of water-filled pore space compared to air-filled pore space (maximum of 2 orders of magnitude difference) is inconsequential. The ability of water-dissolved compounds to diffuse through water-filled pores is negligible compared to the ability of the same compounds to diffuse as gas in the vapor-filled pore spaces. Furthermore, there is vertical downward movement of the pore water which acts to offset or overcome any vertical upward diffusion of dissolved constituents. Consequently, in this investigation, radionuclide transport was allowed to proceed only through air-filled pore space and, therefore, residual pore water was treated as if it was part of the solid matrix material within the flow field. No accounting was made of the partitioning of the gaseous radionuclides into the pore water as diffusive vapor transport proceeded from the waste zone to the land surface. By ignoring this mechanism, diffusive fluxes at the land surface were slightly overestimated.

The boundary conditions imposed on the model domain included:

- No-flux specified for all radionuclides along sides and bottom
  ($dC/dX = 0$ at $x=0$, $x=1$ and $dC/dY = 0$ at $y=0$)
- Species concentration set to 0 at land surface (top of erosion barrier)
  ($C = 0$ at $y=y_{max}$)

The initial condition imposed on the domain included:

- Species concentration set to 0 for the entire model domain at time = 0
  ($C=0$ for $0 \leq x \leq 1$ at $t=0$ and $C=0$ for $0 \leq y \leq y_{max}$ at $t=0$)

The initial conditions for the model also assumed a 1 Ci inventory of each radionuclide uniformly spread over the waste zone.

These boundary conditions force all of the gaseous radionuclides to move upward from the waste disposal zone to the land surface. In reality, some lateral and downward diffusion occurs in the air-filled pores surrounding the waste zone; hence ignoring this lateral and downward movement has the effect of increasing the flux at the land surface, thus introducing a significant measure of conservatism in the calculated results. Simulations were conducted in transient mode for diffusive transport in air, with results being obtained over 1,125 years.

A summary of the radionuclides and compounds of interest in this investigation are summarized in Table 4-22.

Table 4-22. Radionuclides of Interest

Radionuclide	Half-life (yrs)	Atomic Wt.	Molecular form in gaseous state	Molecular Wt.
C-14	5.730E+03	14	CO_2	46
Cl-36	3.010E+05	36	Cl_2	72
H-3	1.2333E+01	3	H_2	6
I-129	1.570E+07	129	I_2	258
S-35	2.394E-01	35	S	35
Sb-124	1.649E-01	124	Sb	124
Sb-125	2.759E+00	125	Sb	125
Se-75	3.270E-01	75	Se	75
Se-79	2.950E+05	79	Se	79
Sn-113	3.153E-01	113	Sn	113
Sn-119m	8.020E-01	119	Sn	119
Sn-121	3.089E-03	121	Sn	121
Sn-121m	4.41E+01	121	Sn	121
Sn-123	3.550E-01	123	Sn	123
Sn-126	2.300E+05	126	Sn	126

4.7.5.2 Measures Implemented to Ensure Conservative Results

In this analysis, several conditions introduce a significant measure of conservatism into the calculations. These include:

- The use of boundary conditions that force all of the gaseous radionuclides to move upward from the waste disposal zone to the land surface. In reality, some of the gaseous radionuclides diffuse sideways and downward in the air-filled pores surrounding the waste zone; hence ignoring this has the effect of increasing the radon flux at the land surface.
- Not taking credit for the removal of the gaseous radionuclides by pore water moving vertically downward through the model domain. This mechanism would likely remove some dissolved gaseous radionuclides, and therefore its omission has the effect of increasing the estimate of instantaneous radionuclide flux at the land surface in simulations conducted as a part of this investigation.
- Use of the top of the erosion layer in the soil cover as the land surface for the purpose of calculating radionuclide flux during the 125 to 1,125 year time period. No credit is taken for the additional distance the gaseous radionuclides must migrate above the erosion barrier prior to that portion of the closure cap eroding away.

- Ignoring the presence of the GCL within the final closure cap. The GCL should be near 100 percent saturation; therefore it will contain very little air-filled porosity within which radon transport could occur.
- During the post-closure time period (125 to 1,125 years) assigning the concrete roof a low saturation associated with concrete rubble exposed to the atmosphere rather than a high saturation associated with buried concrete (i.e., the vault is overlain with a closure cap during the post-closure time period).

4.7.5.3 Grid Construction

The model grid was constructed as a node mesh 3 nodes wide by 50 nodes high. This mesh creates the vertical stack of 48 model elements, as shown in Figure 4-17. The grid extends upward only as far as the erosion barrier, since this is the minimum possible cover thickness that could exist during the 1,125-year evaluation period. A set of consistent units was employed in the simulations for length, mass and time, these being meters, grams and years, respectively.

4.7.5.4 Material Zones

The model domain was divided into two primary zones, the ILV waste zone occupying the lower 27 ft (8.23 m) of the domain and the cover zone (CLSM layer, reinforced concrete roof and closure cap layers), extending 7.5 ft. (2.29 m) above the waste zone to the top of the domain. The upper model elements were scaled to correspond to the geometry of the closure cap thickness while the lower model elements were scaled to correspond to the ILV waste zone.

During the operational time period, the waste contained within the vault is covered by a three-inch-thick layer of CLSM. Therefore the land surface is assumed to be the top of the CLSM layer. During the institutional control period, the ground surface is taken as the top of the reinforced concrete roof. During the post-closure time period (125 to 1,125 years), the ground surface is taken as the top of the closure cap erosion barrier placed over the ILV.

4.7.5.5 Material Zone Properties and Other Input Parameters

Material properties utilized within the 1-D numerical model were specified for 7 material zones defined within the model domain. Each material zone was assigned values of particle density, total porosity, average saturation, air-filled porosity, air density, and an effective air diffusion coefficient for each source element or compound. With the use of an effective air diffusion coefficient, tortuosity was assigned a unit value in each material zone. An air fluid density of 1.24E+03 g/m^3 was used. This air fluid density was obtained from the Bolz and Tuve (1973) and represents that of standard atmospheric conditions.

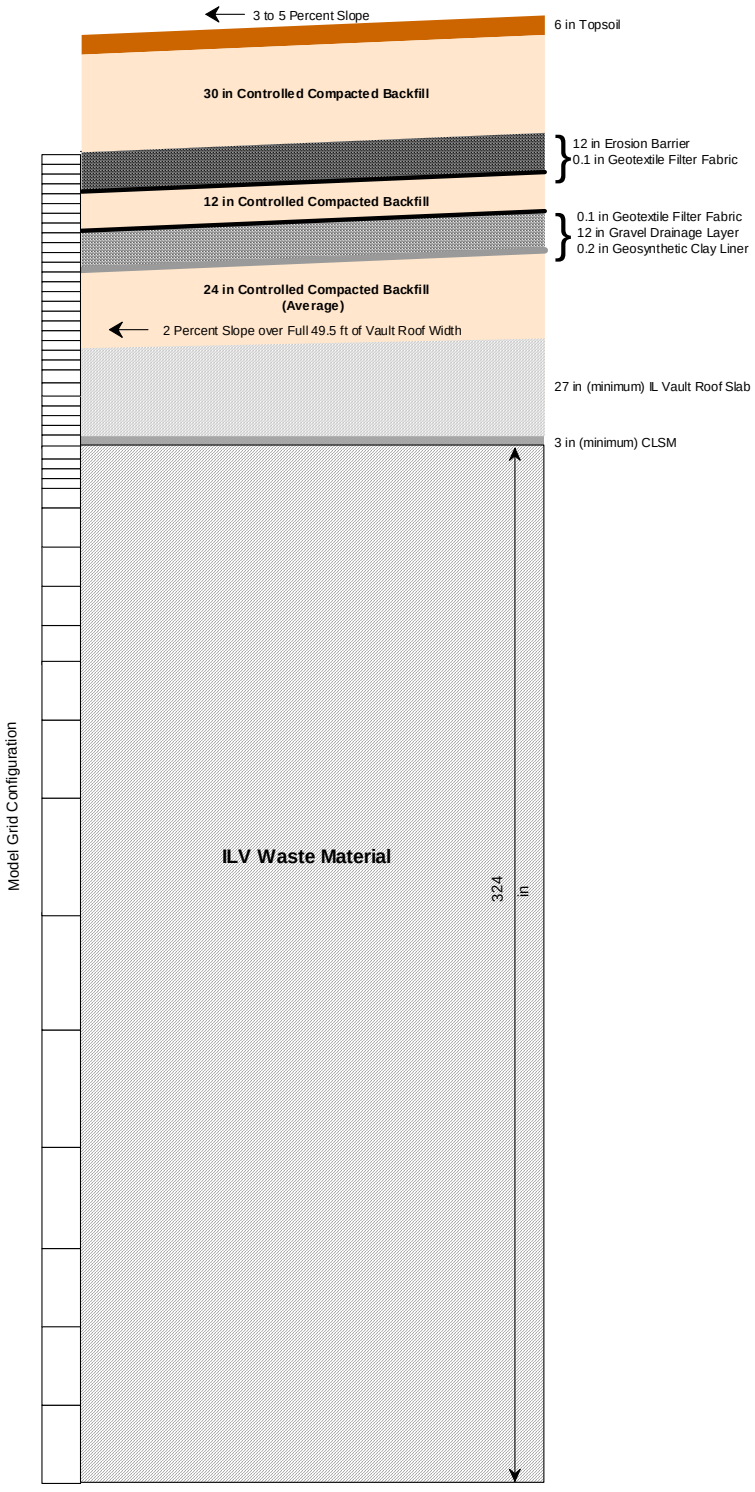

Figure 4-17. PORFLOW Model Grid for Air-Pathway and Radon Analysis

During the operational period (0 to 25 years) the layers associated with the ILV consist of the waste layer and CLSM layer (see Figure 4-5 and Figure 4-6). An ILV waste zone total porosity of 0.736 and particle density of 2.32 g/cm^3 (i.e., the ILV waste zone representation prior to vault collapse) were taken from Phifer et al. (2006). It was assumed that the waste was dry and therefore the air-filled porosity would equal the total porosity for this zone. A total porosity of 0.46 and a particle density of 2.65 g/cm^3 were assigned to the CLSM layer as given by Phifer et al. (2006). The average saturation for the CLSM was taken as the value of saturation at a suction head of approximately 200 cm from the characteristic curves for the existing E-Area operational soil cover prior to dynamic compaction (Phifer et al., 2006). E-Area vadose zone field pore pressure measurements indicate average suction levels in the approximate range of 50 to 200 cm (Nichols et al., 2000). A value of 200 cm represents the upper end of the range which will have a greater air-filled porosity. The air-filled porosity of the CLSM was calculated from the total porosity and average saturation.

While the model includes all the layers from the ILV waste layer to the erosion barrier, during the first 25 years of simulation, the concrete roof and all overlying materials were assigned a porosity of 1.0 and a saturation of 0. This has the effect of making these layers equivalent to air. Table 4-23 provides the values of particle density, total porosity, average saturation, and air-filled porosity utilized for the ILV layers for the first 25 years.

During the institutional control period (25 to 125 years) the layers associated with the ILV consist of the waste layer, the CLSM, and reinforced concrete roof (see Figure 4-5 and Figure 4-6). The waste layer and CLSM retain the same properties as utilized for the first 25 years. The particle density and total porosity for the concrete roof was taken from the recommended values for the E-Area Vault Concrete (Phifer et al. 2006). The average saturation for the concrete roof was taken as the average saturation derived from moisture content measurements of concrete rubble exposed to the atmosphere performed by Sappington and Phifer (2005). The air-filled porosity of the concrete roof was calculated from the total porosity and average saturation. All materials overlying the concrete roof retain a porosity of 1.0 and a saturation of 0, making these layers equivalent to air. Table 4-24 provides the values of particle density, total porosity, average saturation, and air-filled porosity utilized for the ILV layers for the 25 to 125 year period.

During the post-closure time period (125 to 1,125 years) the layers associated with the ILV consist of all layers from the waste layer to the erosion barrier (see Figure 4-5 and Figure 4-6). The waste layer, the CLSM layer, and the concrete roof retain the same properties as utilized for the 25 to 125 year period. The particle density of the lower backfill, gravel drainage layer, middle backfill, and erosion barrier (these materials collectively are considered the closure cap layers) was taken as 2.65 g/cm^3. This is based on the density of quartz and is regarded as representative of most SRS soils. Values for total porosity and long-term average moisture content for the closure cap materials were taken from Phifer (2003).

Phifer (2003) evaluated infiltration through a closure cap over time as the closure cap degraded using the HELP model. The porosity and average moisture content values for a 10,000 year degraded closure cap were utilized, since this represented the greatest air-filled porosity in which a gas could diffuse (values from earlier time periods were saturated, therefore choosing a period having unsaturated conditions was deliberately conservative). Average saturation and air-filled porosity values were calculated from the total porosity and long-term average moisture content. Table 4-25 provides the values of particle density, total porosity, average saturation, and air-filled porosity utilized for all the layers (i.e., waste layer to the erosion barrier) for the 125 to 1,125 year time period. Average saturation values for the vault roof for this time period was taken from Sappington and Phifer (2005).

Table 4-23. Operational Period (First 25 Years) Layer Particle Density, Total Porosity, Average Saturation, and Air-Filled Porosity

Layer	Particle Density (g/cm^3)	Total Porosity (fraction)	Average Saturation (fraction)	Air-Filled Porosity [4] (fraction)
Erosion barrier layer [1]	0	1	0	1
Upper backfill [1]	0	1	0	1
Gravel drainage layer [1]	0	1	0	1
Lower backfill [1]	0	1	0	1
ILV concrete roof [1]	0	1	0	1
CLSM[2]	2.65	0.460	0.825	0.081
ILV waste layer [2, 3]	2.32	0.736	0	0.736

[1] During the first 25 years of simulation, the concrete roof and materials comprising the closure cap were assigned a porosity of 1.0 and an average saturation of 0 in order to represent air.

[2] Waste layer and CLSM particle density and total porosity taken from Phifer et al. (2006).

[3] The waste is assumed to be dry (i.e., saturation of 0) resulting in the air-filled porosity equaling the total porosity.

[4] Air-filled Porosity = (1 – Average Saturation) × Total Porosity

Table 4-24. Institutional Control Period (25 to 125 Years) Layer Particle Density, Total Porosity, Average Saturation, and Air-Filled Porosity

Layer	Particle Density (g/cm^3)	Total Porosity (fraction)	Average Saturation (fraction)	Air-Filled Porosity [4] (fraction)
Erosion barrier layer [1]	0	1	0	1
Upper backfill [1]	0	1	0	1
Gravel drainage layer [1]	0	1	0	1
Lower backfill [1]	0	1	0	1
ILV concrete roof [2, 4]	2.59	0.184	0.73	0.050
CLSM[2]	2.65	0.460	0.825	0.081
ILV waste layer [2, 3]	2.32	0.736	0	0.736

[1] During the first 25 years of simulation, the materials comprising the closure cap were assigned a porosity of 1.0 and an average saturation of 0 in order to represent air.

[2] Waste layer, CLSM, and concrete roof particle density and total porosity taken from Phifer et al. (2006).

[3] The waste is assumed to be dry (i.e. saturation of 0) resulting in the air-filled porosity equaling the total porosity.

[4] Air-filled Porosity = (1 – Average Saturation) × Total Porosity

Table 4-25. Post-Closure Period (125 to 1,125 Years) Layer Particle Density, Total Porosity, Long-Term Average Moisture Content, Average Saturation, and Air-Filled Porosity

Layer	Particle Density (g/cm^3)	Total Porosity (fraction)	Long-Term Average Moisture Content	Average Saturation (fraction)	Air-Filled Porosity[6] (fraction)
Erosion barrier layer	2.65[1]	0.088[1]	0.0726[1]	0.825[5]	0.015
Upper backfill	2.65[1]	0.375[1]	0.2435[1]	0.649[5]	0.132
Gravel drainage layer	2.65[1]	0.375[1]	0.1967[1]	0.525[5]	0.178
Lower backfill	2.65[1]	0.370[1]	0.2710[1]	0.732[5]	0.099
ILV Roof	2.59[2]	0.184[2]	na[1]	0.730[4]	0.050
CLSM	2.65[2]	0.460	na[1]	0.825	0.081
ILV waste layer	2.32[2]	0.736[2]	na[1]	0.000[3]	0.736

[1] Values for total porosity and long term average moisture content taken from Phifer (2003). Particle density is taken as 2.65, which is based on the density of quartz and regarded as fairly representative of most SRS soils.

[2] Waste layer, CLSM, and concrete roof particle density and total porosity taken from Phifer et al. (2006).

[3] The waste is assumed to be dry (i.e., saturation of 0) resulting in the air-filled porosity equaling the total porosity.

[4] Average saturation for the ILV roof was calculated by dividing the in-field moisture content (0.096) by the saturated moisture content (0.132) as reported by Sappington and Phifer (2005).

[5] Average Saturation = Long Term Average Moisture Content / Total Porosity

[6] Air-filled Porosity = (1 – Average Saturation) × Total Porosity

The molecular diffusion coefficient of Rn-222 in open air is 347 m^2/yr (Nielson et al. 1984). Nielson et al. (1984) established a relationship between moisture saturation and the radon effective air diffusion coefficient for various pore sizes of earthen materials. Using this method, a radon effective air diffusion coefficient was determined for each material type based upon the average moisture saturation for the material.

Subsequently, using Graham's Law, the effective air diffusion coefficient of each radionuclide or compound evaluated was determined for each material type based on the radon effective air diffusion coefficient using the following relationship:

$$D = D'\sqrt{\frac{MWT'}{MWT}} \qquad \text{Eq 4-2}$$

Where:

D = the diffusion coefficient of the radionuclide of interest (m^2/yr)
D' = the diffusion coefficient of the reference radionuclide (Rn-222) (m^2/yr)
MWT' = the molecular weight of the reference radionuclide (Rn-222)
MWT = the molecular weight of the element or compound of interest

A summary of the radon effective air diffusion coefficients and the calculated effective air diffusion coefficients for each radionuclide/compound by material zone and simulation period, are presented in Table 4-26 through Table 4-28.

Table 4-26. Effective Air Diffusion Coefficients for Each Radionuclide/Compound, by Material for the 0 to 25 Year Time Period

Radionuclide	ILV Waste (m2/yr)	CLSM (m2/yr)	ILV Roof (m2/yr)	Lower Backfill (m2/yr)	Gravel Drainage Layer (m2/yr)	Upper Backfill (m2/yr)	Erosion Barrier (m2/yr)
^{222}Rn [1]	3.470E+02	1.262E+00	3.470E+02	3.470E+02	3.470E+02	3.470E+02	3.470E+02
C-14 as $^{14}CO_2$	7.623E+02	2.773E+00	7.623E+02	7.623E+02	7.623E+02	7.623E+02	7.623E+02
Cl-36 as $^{36}Cl_2$	6.093E+02	2.217E+00	6.093E+02	6.093E+02	6.093E+02	6.093E+02	6.093E+02
$^{3}H_2$	2.111E+03	7.678E+00	2.111E+03	2.111E+03	2.111E+03	2.111E+03	2.111E+03
I-129 as $^{129}I_2$	3.219E+02	1.171E+00	3.219E+02	3.219E+02	3.219E+02	3.219E+02	3.219E+02
S-35	8.739E+02	3.179E+00	8.739E+02	8.739E+02	8.739E+02	8.739E+02	8.739E+02
Sb-124	4.643E+02	1.689E+00	4.643E+02	4.643E+02	4.643E+02	4.643E+02	4.643E+02
Sb-125	4.624E+02	1.682E+00	4.624E+02	4.624E+02	4.624E+02	4.624E+02	4.624E+02
Se-75	5.970E+02	2.172E+00	5.970E+02	5.970E+02	5.970E+02	5.970E+02	5.970E+02
Se-79	5.817E+02	2.116E+00	5.817E+02	5.817E+02	5.817E+02	5.817E+02	5.817E+02
Sn-113	4.864E+02	1.769E+00	4.864E+02	4.864E+02	4.864E+02	4.864E+02	4.864E+02
Sn-119m	4.739E+02	1.724E+00	4.739E+02	4.739E+02	4.739E+02	4.739E+02	4.739E+02
Sn-121	4.700E+02	1.710E+00	4.700E+02	4.700E+02	4.700E+02	4.700E+02	4.700E+02
Sn-121m	4.700E+02	1.710E+00	4.700E+02	4.700E+02	4.700E+02	4.700E+02	4.700E+02
Sn-123	4.662E+02	1.696E+00	4.662E+02	4.662E+02	4.662E+02	4.662E+02	4.662E+02
Sn-126	4.606E+02	1.676E+00	4.606E+02	4.606E+02	4.606E+02	4.606E+02	4.606E+02

[1] The effective diffusion coefficient for ^{222}Rn was used to determine the effective air diffusion coefficient of each radionuclide/compound based on Graham's law.

Table 4-27. Effective Air Diffusion Coefficients for Each Radionuclide/Compound, by Material for the 25 to 125 Year Time Period

Radionuclide	ILV Waste (m2/yr)	CLSM (m2/yr)	ILV Roof (m2/yr)	Lower Backfill (m2/yr)	Gravel Drainage Layer (m2/yr)	Upper Backfill (m2/yr)	Erosion Barrier (m2/yr)
^{222}Rn [1]	3.470E+02	1.262E+00	2.840E+00	3.470E+02	3.470E+02	3.470E+02	3.470E+02
C-14 as $^{14}CO_2$	7.623E+02	2.773E+00	6.239E+00	7.623E+02	7.623E+02	7.623E+02	7.623E+02
Cl-36 as $^{36}Cl_2$	6.093E+02	2.217E+00	4.987E+00	6.093E+02	6.093E+02	6.093E+02	6.093E+02
$^{3}H_2$	2.111E+03	7.678E+00	1.728E+01	2.111E+03	2.111E+03	2.111E+03	2.111E+03
I-129 as $^{129}I_2$	3.219E+02	1.171E+00	2.635E+00	3.219E+02	3.219E+02	3.219E+02	3.219E+02
S-35	8.739E+02	3.179E+00	7.153E+00	8.739E+02	8.739E+02	8.739E+02	8.739E+02
Sb-124	4.643E+02	1.689E+00	3.800E+00	4.643E+02	4.643E+02	4.643E+02	4.643E+02
Sb-125	4.624E+02	1.682E+00	3.785E+00	4.624E+02	4.624E+02	4.624E+02	4.624E+02
Se-75	5.970E+02	2.172E+00	4.886E+00	5.970E+02	5.970E+02	5.970E+02	5.970E+02
Se-79	5.817E+02	2.116E+00	4.761E+00	5.817E+02	5.817E+02	5.817E+02	5.817E+02
Sn-113	4.864E+02	1.769E+00	3.981E+00	4.864E+02	4.864E+02	4.864E+02	4.864E+02
Sn-119m	4.739E+02	1.724E+00	3.879E+00	4.739E+02	4.739E+02	4.739E+02	4.739E+02
Sn-121	4.700E+02	1.710E+00	3.847E+00	4.700E+02	4.700E+02	4.700E+02	4.700E+02
Sn-121m	4.700E+02	1.710E+00	3.847E+00	4.700E+02	4.700E+02	4.700E+02	4.700E+02
Sn-123	4.662E+02	1.696E+00	3.816E+00	4.662E+02	4.662E+02	4.662E+02	4.662E+02
Sn-126	4.606E+02	1.676E+00	3.770E+00	4.606E+02	4.606E+02	4.606E+02	4.606E+02

[1] The effective diffusion coefficient for ^{222}Rn was used to determine the effective air diffusion coefficient of each radionuclide/compound based on Graham's law.

Table 4-28. Effective Air Diffusion Coefficients for Each Radionuclide/Compound, by Material for the 125 to 1,125 Year Time Period

Radionuclide	ILV Waste (m2/yr)	CLSM (m2/yr)	ILV Roof (m2/yr)	Lower Backfill (m2/yr)	Gravel Drainage Layer (m2/yr)	Upper Backfill (m2/yr)	Erosion Barrier (m2/yr)
^{222}Rn [1]	3.470E+02	1.262E+00	2.840E+00	2.840E+00	4.734E+00	4.734E+00	7.889E-01
C-14 as $^{14}CO_2$	7.623E+02	2.773E+00	6.239E+00	6.239E+00	1.040E+01	1.040E+01	1.733E+00
Cl-36 as $^{36}Cl_2$	6.093E+02	2.217E+00	4.987E+00	4.987E+00	8.312E+00	8.312E+00	1.385E+00
$^{3}H_2$	2.111E+03	7.678E+00	1.728E+01	1.728E+01	2.879E+01	2.879E+01	4.799E+00
I-129 as $^{129}I_2$	3.219E+02	1.171E+00	2.635E+00	2.635E+00	4.391E+00	4.391E+00	7.318E-01
S-35	8.739E+02	3.179E+00	7.153E+00	7.153E+00	1.192E+01	1.192E+01	1.987E+00
Sb-124	4.643E+02	1.689E+00	3.800E+00	3.800E+00	6.334E+00	6.334E+00	1.056E+00
Sb-125	4.624E+02	1.682E+00	3.785E+00	3.785E+00	6.308E+00	6.308E+00	1.051E+00
Se-75	5.970E+02	2.172E+00	4.886E+00	4.886E+00	8.144E+00	8.144E+00	1.357E+00
Se-79	5.817E+02	2.116E+00	4.761E+00	4.761E+00	7.935E+00	7.935E+00	1.323E+00
Sn-113	4.864E+02	1.769E+00	3.981E+00	3.981E+00	6.635E+00	6.635E+00	1.106E+00
Sn-119m	4.739E+02	1.724E+00	3.879E+00	3.879E+00	6.465E+00	6.465E+00	1.078E+00
Sn-121	4.700E+02	1.710E+00	3.847E+00	3.847E+00	6.412E+00	6.412E+00	1.069E+00
Sn-121m	4.700E+02	1.710E+00	3.847E+00	3.847E+00	6.412E+00	6.412E+00	1.069E+00
Sn-123	4.662E+02	1.696E+00	3.816E+00	3.816E+00	6.359E+00	6.359E+00	1.060E+00
Sn-126	4.606E+02	1.676E+00	3.770E+00	3.770E+00	6.283E+00	6.283E+00	1.047E+00

[1] The effective diffusion coefficient for ^{222}Rn was used to determine the effective air diffusion coefficient of each radionuclide/compound based on Graham's law.

4.7.6 Air-Pathway Model Results

4.7.6.1 ILV Flux to Ground Surface

Model simulations were conducted to evaluate the peak flux of each radionuclide emanating from the top of the domain. A unit inventory of 1 Ci was assigned to the ILV waste zone for each radionuclide considered in the analysis. Results were output in Ci/yr through a 1 m^2 area, consistent with the set of units employed in the model, and are presented for each radionuclide in Figure 4-18 through Figure 4-20, respectively. The peak fluxes emanating at the land surface are presented for each time period in Table 4-29. The results are reported in this way to facilitate calculation of human exposure at the SRS boundary and at the 100-m boundary due to the ILV disposal unit. Flux behavior is based primarily on the closure considerations discussed in Section 4.7.3 and the half-life of the particular radionuclide as provided in Table 4-22.

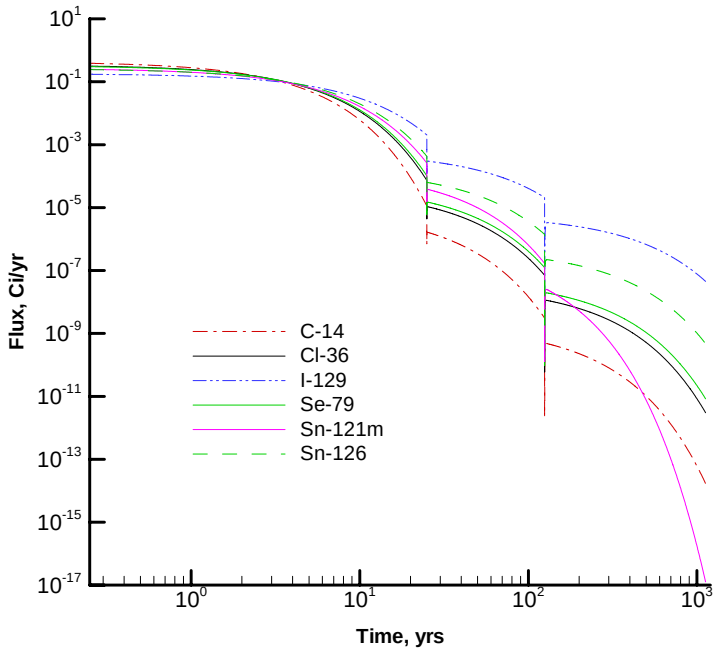

Figure 4-18. Flux Rate at Land Surface for C-14, Cl-36, I-129, Se-79, Sn-121m, and Sn-126

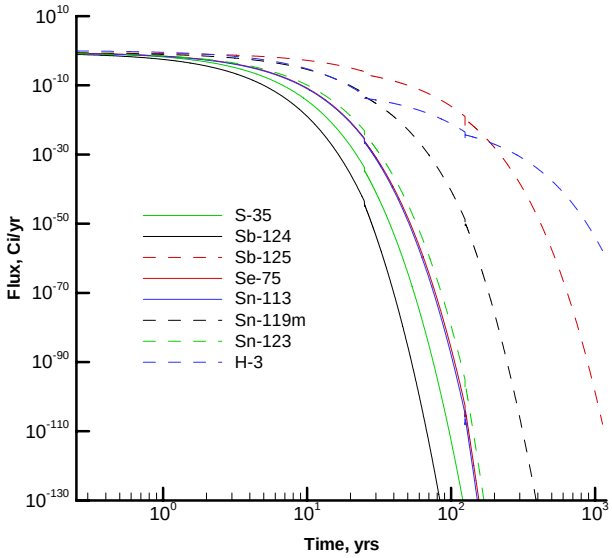

Figure 4-19. Flux Rate at Land Surface for S-35, Sb-124, Sb-125, Se-75, Sn-113, Sn-119m, Sn-123, and H-3

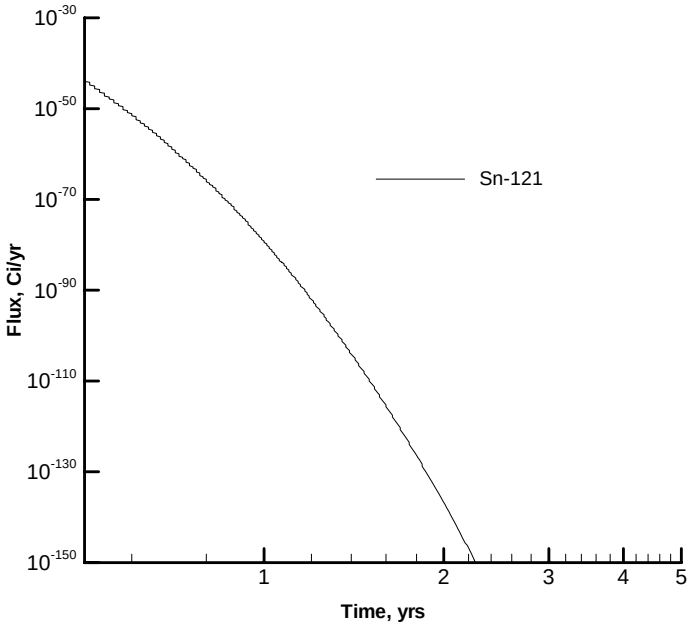

Figure 4-20. Flux Rate at Land Surface for Sn-121

Table 4-29. Summary of the Peak Flux Rates for Each Radionuclide

Radionuclide	Activity in Waste (Ci)	Max. Flux (Ci/yr/Ci)		
		0 - 25 Years	25 – 125 years	125 – 1,125 years
C-14	1.0	4.25E-01	1.12E-05	4.83E-10
Cl-36	1.0	3.40E-01	7.30E-05	1.11E-08
H-3	1.0	1.18E+00	1.27E-13	4.60E-25
I-129	1.0	1.79E-01	2.04E-03	3.32E-06
S-35	1.0	4.68E-01	1.65E-34	1.08E-135
Sb-124	1.0	2.36E-01	2.54E-44	1.13E-177
Sb-125	1.0	2.56E-01	9.07E-07	9.19E-21
Se-75	1.0	3.19E-01	4.73E-26	6.79E-105
Se-79	1.0	3.24E-01	1.02E-04	1.95E-08
Sn-113	1.0	2.57E-01	2.68E-26	2.88E-107
Sn-119m	1.0	2.58E-01	3.65E-13	8.46E-51
Sn-121	1.0	4.33E-02	0.00E+00	0.00E+00
Sn-121m	1.0	2.62E-01	2.60E-04	2.51E-08
Sn-123	1.0	2.48E-01	7.25E-24	1.84E-97
Sn-126	1.0	2.57E-01	4.27E-04	2.22E-07

4.7.7 ILV Air-Pathway Dose Calculations

An evaluation was conducted to assess the potential dose to a MEI located at both the SRS boundary and at the 100-m locations (Lee 2006). During the 125-year operational and institutional control period, the SRS boundary is the compliance point for the dose calculations. Therefore, the peak flux during this time period was used to assess the dose to the MEI. For the remainder of the time period, the 100-m boundary is the compliance point. Thus, the peak flux between 125 and 1,125 years was used for these calculations. DRFs were calculated for each radionuclide potentially released from the ILV using CAP88 (Beres 1990), the EPA model for National Emissions Standards for Hazardous Air Pollutants. DRFs represent the dose to the receptor exposed to 1 Ci of the specified radionuclide being released to the atmosphere. For the receptor located at the SRS boundary the distance from the ILV is sufficient for an assumption of a point source. However, the DRFs for the 100-m receptor require evaluation as an area source because of the close proximity of the ILV to the 100-m receptor. For radionuclides not contained within the CAP88 library (Se-75, Se-79, Sn-119m, and Sn-121m) atmospheric transport was estimated by assigning surrogates with similar radiological properties (Sn-113 for Se-75, Sn-126 for Se-79, Sn-113 for Sn-119m and Sn-126 for Sn-121m). Doses for these four radionuclides were estimated by applying their dosimetric properties to the surrogate's relative air concentrations estimated by the model.

Specific SRS Boundary DRFs, the calculated exposure levels for the 0 to 125 year MEI at the SRS boundary, and the resulting 0 to 125 year ILV disposal limits are presented in Table 4-30. Specific SRS 100-meter DRFs, the calculated exposure levels for the 125 to 1,125 year MEI at 100 meters, and the resulting 125 to 1,125 year ILV disposal limits are presented in Table 4-31. See Lee (2006) for details on the estimation of DRFs. The ILV disposal unit limits were calculated by dividing the maximum permissible exposure level (10 mrem/yr, DOE 1999) by the highest dose received by the MEI from the 1 Ci source during each of the two time periods.

Table 4-32 provides a comparison of the limits derived for these two time periods (i.e., 0-125 and 125-1,125 years) and the resulting overall IL Vault air-pathway disposal limits.

Table 4-30. SRS Boundary Dose Release Factors and 0-125 Year ILV Disposal Limits

Radionuclide	0 - 125 Year Peak Flux (Ci/yr/Ci)	SRS Boundary Dose Release Factor[1] (mrem/Ci)	0 – 125 Year Dose to MEI at SRS Boundary[2] (mrem/yr/Ci)	0 - 125 Year ILV Disposal Limits[3] (Ci)
C-14	4.25E-01	1.1E-04	4.6E-05	2.2E+05
Cl-36	3.40E-01	2.3E-04	7.7E-05	1.3E+05
H-3	1.18E+00	2.2E-06	2.6E-06	3.8E+06
I-129	1.79E-01	4.9E-02	8.7E-03	1.1E+03
S-35	4.68E-01	2.8E-05	1.3E-05	7.6E+05
Sb-124	2.36E-01	2.0E-03	4.8E-04	2.1E+04
Sb-125	2.56E-01	6.5E-03	1.6E-03	6.1E+03
Se-75	3.19E-01	1.1E-03	3.5E-04	2.9E+04
Se-79	3.24E-01	6.3E-04	2.0E-04	4.9E+04
Sn-113	2.57E-01	2.3E-04	5.9E-05	1.7E+05
Sn-119m	2.58E-01	1.0E-04	2.6E-05	3.8E+05
Sn-121	4.33E-02	4.2E-05	1.8E-06	5.5E+06
Sn-121m	2.62E-01	6.5E-04	1.7E-04	5.9E+04
Sn-123	2.48E-01	1.3E-05	3.1E-06	3.2E+06
Sn-126	2.57E-01	3.0E-01	7.6E-02	1.3E+02

[1] From Lee (2006)
[2] Dose to MEI at SRS Boundary = Peak Flux × Dose Release Factor
[3] Disposal Limit = 10 mrem/yr / Dose to MEI at SRS Boundary per year per curie

Table 4-31. 100-meter Dose Release Factors and 125 - 1,125 Year ILV Disposal Limits

Radionuclide	125 –1,125 Year Peak Flux (Ci/yr/Ci)	100-meter Dose Release Factor (mrem/Ci)	125 –1,125 Year Dose to MEI at 100-meters[1] (mrem/yr/Ci)	125 –1,125 Year ILV Disposal Limits[2] (Ci)
C-14	4.83E-10	3.5E-01	1.7E-10	5.9E+10
Cl-36	1.11E-08	5.6E-01	6.2E-09	1.6E+09
H-3	4.60E-25	7.3E-03	3.4E-27	3.0E+27
I-129	3.32E-06	5.2E+02	1.7E-03	5.8E+03
S-35	1.08E-135	4.6E-02	5.0E-137	2.0E+137
Sb-124	1.13E-177	3.4E+00	3.8E-177	2.6E+177
Sb-125	9.19E-21	1.0E+01	9.3E-20	1.1E+20
Se-75	6.79E-105	1.8E+00	1.3E-104	8.0E+104
Se-79	1.95E-08	1.1E+00	2.1E-08	4.7E+08
Sn-113	2.88E-107	4.6E-01	1.3E-107	7.6E+107
Sn-119m	8.46E-51	2.0E-01	1.7E-51	6.0E+51
Sn-121	0.00E+00	7.1E-02	0.0E+00	NL
Sn-121m	2.51E-08	1.1E+00	2.7E-08	3.6E+08
Sn-123	1.84E-97	2.0E-02	3.6E-99	2.7E+99
Sn-126	2.22E-07	4.6E+02	1.0E-04	9.8E+04

[1] Dose to MEI at 100-meters = Peak Flux × Dose Release Factor
[2] Disposal Limit = 10 mrem/yr / Dose to MEI at 100-meters
NL = No limit

Table 4-32. Overall ILV Air-Pathway Disposal Limits

Radionuclide	0 - 125 Year ILV Disposal Limits[1] (Ci)	125 –1,125 Year ILV Disposal Limits[2] (Ci)	Overall ILV Air-pathway Disposal Limit (Ci)
C-14	2.2E+05	5.9E+10	2.2E+05
C-14_KB	2.2E+05	5.9E+10	2.2E+05
Cl-36	1.3E+05	1.6E+09	1.3E+05
H-3	3.8E+06	---	3.8E+06
H-3_TPBAR	9.4E+10	---	9.4E+10
I-129	1.1E+03	5.8E+03	1.1E+03
I-129_ETF	1.1E+03	5.8E+03	1.1E+03
I-129_KB	1.1E+03	5.8E+03	1.1E+03
S-35	7.6E+05	---	7.6E+05
Sb-124	2.1E+04	---	2.1E+04
Sb-125	6.1E+03	---	6.1E+03
Se-75	2.9E+04	---	2.9E+04
Se-79	4.9E+04	4.7E+08	4.9E+04
Sn-113	1.7E+05	---	1.7E+05
Sn-119m	3.8E+05	---	3.8E+05
Sn-121	5.5E+06	NL	5.5E+06
Sn-121m	5.9E+04	3.6E+08	5.9E+04
Sn-123	3.2E+06	---	3.2E+06
Sn-126	1.3E+02	9.8E+04	1.3E+02

[1] From Table 4-30
[2] From Table 4-31
NL = No limit
Note: Limits reported as "--- " signify a number >1E+20

4.8 ILV ALL-PATHWAYS ANALYSIS

This section documents the development of preliminary all-pathways limits for the IL Vault. The limits developed within this section are considered preliminary, since they do not take into consideration the effects of plume overlap from adjacent units or the results of sensitivity and uncertainty analyses. The effects of plume overlap are considered in Chapter 6 and the interpretation of sensitivity and uncertainty analyses is conducted in Chapter 7. Final limits are provided in Chapter 7.

4.8.1 Overview of All-Pathways Analysis

This section describes the investigation conducted to evaluate the potential magnitude of the all-pathways dose from the ILV over the 25-year operational period, 100-year institutional control period, and 1,000-year post-closure compliance period.

The permissible all-pathways dose for DOE LLW disposal facilities is addressed in DOE M 435.1, IV.P.(1)(a) (DOE 1999). This requirement is that dose to representative members of the public shall not exceed 25 mrem (0.25 mSv) in a year total effective dose equivalent from all exposure pathways, excluding the dose from radon and its progeny in air.

Although the all-pathways performance objective includes not only all exposure pathways, but also all transport pathways, in this PA, the air pathway is evaluated separately. The all-pathways dose evaluated here includes only the groundwater transport pathway. Doses from the air pathway are considered in Section 4.7.

The all-pathways analysis uses the groundwater concentrations developed in Section 4.6. The concentrations as a function of time are input into the all-pathways application (Koffman 2006a), which calculates dose to humans from direct ingestion of contaminated groundwater and consumption of locally grown leafy vegetables, produce, milk, and meat, which are contaminated with radionuclides from use of the groundwater for irrigation and direct consumption by the cattle (Section C.4.5.1).

4.8.2 ILV Summary of Key All-Pathways Analysis Assumptions

Key assumptions and inputs used in the all-pathways analysis are presented in Appendix B.

4.8.3 ILV All-Pathways Analysis

The maximum all-pathways doses from the ILV disposal unit over the 1,000-year post-closure compliance period were calculated using the all-pathways application (Koffman 2006a). The application uses the results of the PORFLOW program to calculate the dose to a hypothetical individual from using the groundwater at the point of assessment (location of the maximum concentration of each radionuclide outside of a 100-m buffer zone) for all credible purposes (drinking, irrigation of crops and ingestion of the crops and the meat and milk of animals fed on the crops and groundwater). Table 4-33 presents the preliminary disposal limits for the ILV based on the all-pathways analysis.

Table 4-33. Preliminary All-Pathways Radionuclide Disposal Limits for the ILV

Limits Based on Years 0 - 200	
Radionuclide	**All-pathways Limit (Ci/Vault)**
Am-241	---
Am-243	---
C-14	5.6E+16
C-14_KB*	9.0E+17
Cl-36	9.9E+07
Cm-244	---
Cm-245	---
Cm-247	---
Cm-248	---
H-3	3.8E+09
H-3_TPBAR	6.2E+09
I-129	3.5E+12
I-129_ETF	2.3E+14
I-129_KB	1.3E+16
K-40	---
Mo-93	5.4E+04
Nb-94	---
Ni-59	---
Np-237	---
Pd-107	---
Pu-238	---
Pu-239	---
Pu-240	---
Pu-241	---
Pu-242	---
Pu-244	---
Ra-226	---
Se-79	---
Sn-126	---
Sr-90	3.0E+16
Tc-99	---
Tc-99_KB	---
Th-230	---
Th-232	---
U-233	---
U-234	---
U-235	---
U-236	---
U-238	---
Zr-93	---

Table 4-33. Preliminary All-Pathways Radionuclide Disposal Limits for the ILV - continued

Limits Based on Years 200 - 1100	
Radionuclide	**All-pathways Limit (Ci/Vault)**
Am-241	5.7E+08
Am-243	4.7E+14
C-14	5.9E+02
C-14_KB*	1.1E+13
Cl-36	4.7E+00
Cm-244	---
Cm-245	9.4E+08
Cm-247	2.6E+16
Cm-248	---
H-3	1.6E+13
H-3_TPBAR	8.2E+12
I-129	1.3E+00
I-129_ETF	4.6E+01
I-129_KB	2.7E+02
K-40	5.1E+13
Mo-93	3.8E+01
Nb-94	1.2E+05
Ni-59	5.4E+10
Np-237	7.4E+04
Pd-107	8.2E+10
Pu-238	5.4E+08
Pu-239	3.5E+12
Pu-240	---
Pu-241	1.8E+10
Pu-242	9.0E+15
Pu-244	---
Ra-226	9.9E+01
Se-79	---
Sn-126	---
Sr-90	2.9E+11
Tc-99	3.0E+07
Tc-99_KB	4.2E+08
Th-230	3.6E+02
Th-232	5.7E+15
U-233	---
U-234	1.3E+05
U-235	1.4E+06
U-236	---
U-238	2.2E+08
Zr-93	1.5E+09

Note: Limits reported as "---" indicate that there is no limit or that the limit $\geq$ 1E+20.
* Waste containing C-14_KB is assumed to not be in Cell #4.

4.9 INADVERTENT INTRUDER ANALYSIS

The inadvertent intruder analysis considers the radiological impacts to hypothetical persons who are assumed to intrude into the ILV disposal units at the ELLWF after institutional control ceases 100 years after facility closure. Descriptions of intruder scenarios are provided in the Background Chapter in Part C of this PA. The analysis was carried out using an automated computer application developed at SRNL (Koffman 2006b), which implements equations calculating dose per unit intake documented in Lee (2004). One important functional requirement of the application is that it computes a "no leaching" case in which the full decay chain is determined and the activities are calculated at specified times using the Bateman equation. This means that the intruder calculations are completely independent from the PORFLOW calculations. In the intruder analysis, no credit is taken for the more robust packaging of the "special" wasteforms containing H-3, C-14, Tc-99 and I-129.

4.9.1 ILV Specific Parameters

The IL Vault reinforced concrete roof prevents excavation and drilling into the disposed waste for at least 1000 years (structural failure has been projected to occur at 6703 years [Peregoy 2006]). Therefore, the intrusive intruder scenarios (i.e., agricultural and post-drilling) are not credible. The final closure system for the ELLWF includes a 12-inch thick erosion barrier near the top of the cap. Because the erosion barrier is assumed to never erode and all the layers between the waste and the erosion barrier always remain in place at their design thickness, approximately 8.6 ft of material always exists above the waste. The erosion barrier has been shown to be effective for at least 10,000 years (Phifer and Nelson 2003) so that all the layers between the waste and the erosion barrier always remain in place at their design thickness, approximately 8.6 ft of material always exists above the waste. The resident scenario is credible for the ILV after the institutional control period of 100 years.

The parameters specific to the ILV disposal unit used in the intruder analysis are given in Table 4-34. The geometry factors and erosion rate are documented in McDowell-Boyer et al. (2000). The waste volume for the ILV is consistent with that presented in Section 4.5.3. The "degradation duration" of 7000 years reflects the fact that structural stability of the ILV can be assumed for that period of time (see discussion in Section 4.6.3.1).

4.9.2 Results

Results of the resident intruder analyses for ILV disposal unit for the time period of 1,000 years are provided in Table 4-35. The entry "---" in the Time of Limit column means that the dose calculation is always zero so there is no limit. For cases where there is a time given, there may be an entry "---" in one or both of the limit columns. In this case the entry "---"indicates a limit value greater than or equal to the threshold value of 1E+20. Additional details are provided in C.4.4. Because the automated method applies a transient analysis, it calculates the lowest inventory limit for the entire time period, regardless of when it occurs.

Table 4-34. Intruder Parameters for the ILV Disposal Units

Facility	E-Area
Disposal Unit Name	Intermediate-Level Vaults
Abbreviated Name	ILVs
Agriculture Geometry Factor [1]	0.4
Resident Geometry Factor [1]	0.4
Post-Drilling Geometry Factor	1
Waste Volume (ft3)	256540

[1] The layout of the IL Vault and any future adjacent disposal units will be such that the actual area taken up by the IL Vault (i.e., 48.5 ft by 278.83 ft) takes up 40% of the area assigned to the vault (i.e., ~33,810 ft^2).

Transient Layer Model (Surface to Top of Waste)

Layer	Thickness (inches)	Description	Erosion Rate (mm/yr)	Erosion Earliest Start (yr)	Degradation Duration (yr)	Degradation Start (yr)
1	36	Soil cover	1.4			
2	12	Erosion barrier	1.4	1.00E+10		
3	48.4	Soil backfill	1.4			
4	27	Vault roof	1.4		7000	0

Table 4-35. Intruder-Based Radionuclide Disposal Limits for Intermediate-Level Vaults – Resident Scenario with Transient Calculation for 1,000 Years

Radionuclide[1]	Time of Limit (Years)	Concentration Limit ($\mu Ci/m^3$)	Inventory Limit (Ci/Unit)
Ac-227	100	5.78E+07	4.2E+05
Ag-108m	100	1.87E+05	1.4E+03
Al-26	100	9.41E+03	6.8E+01
Am-241	1,000	7.60E+10	5.5E+08
Am-242m	100	4.75E+07	3.5E+05
Am-243	100	5.42E+07	3.9E+05
Ar-39	---	---	---
Ba-133	100	3.61E+09	2.6E+07
Bi-207	100	3.58E+05	2.6E+03
Bk-249	100	1.89E+09	1.4E+07
C-14	---	---	---
Ca-41	---	---	---
Cd-113m	---	---	---
Cf-249	100	4.89E+06	3.6E+04
Cf-250	100	2.87E+18	2.1E+16
Cf-251	100	2.76E+08	2.0E+06
Cf-252	1,000	4.91E+15	3.6E+13
Cl-36	---	---	---
Cm-242	1,000	7.38E+12	5.4E+10
Cm-243	100	1.03E+09	7.5E+06
Cm-244	1,000	4.53E+18	3.3E+16
Cm-245	100	3.05E+09	2.2E+07
Cm-246	1,000	4.54E+16	3.3E+14
Cm-247	1,000	3.55E+06	2.6E+04
Cm-248	1,000	3.60E+10	2.6E+08
Co-60	100	8.65E+09	6.3E+07
Cs-134	100	3.63E+19	2.6E+17
Cs-135	---	---	---
Cs-137	100	4.17E+06	3.0E+04
Eu-152	100	8.71E+06	6.3E+04
Eu-154	100	1.53E+08	1.1E+06
Eu-155	100	1.55E+17	1.1E+15
H-3	---	---	---
H-3 TPBAR	---	---	---
I-129	100	---	---
I-129 ETF	100	---	---
I-129 KB	100	---	---
K-40	100	1.94E+05	1.4E+03
Kr-85	100	1.40E+11	1.0E+09
Mo-93	---	---	---
Na-22	100	1.02E+16	7.4E+13
Nb-93m	---	---	---
Nb-94	100	8.50E+04	6.2E+02

Table 4-35. Intruder-Based Radionuclide Disposal Limits for Intermediate-Level Vaults – Resident Scenario with Transient Calculation for 1,000 Years - continued

Radionuclide[1]	Time of Limit (Years)	Concentration Limit (µCi/m^3)	Inventory Limit (Ci/Unit)
Ni-59	---	---	---
Ni-63	---	---	---
Np-237	1,000	1.22E+07	8.9E+04
Pa-231	230	2.36E+06	1.7E+04
Pb-210	100	3.54E+11	2.6E+09
Pd-107	---	---	---
Pu-238	1,000	3.75E+10	2.7E+08
Pu-239	1,000	1.49E+13	1.1E+11
Pu-240	1,000	1.19E+16	8.6E+13
Pu-241	1,000	2.32E+12	1.7E+10
Pu-242	1,000	4.00E+13	2.9E+11
Pu-244	100	2.86E+05	2.1E+03
Ra-226	100	1.90E+04	1.4E+02
Ra-228	100	9.76E+08	7.1E+06
Rb-87	---	---	---
S-35	---	---	---
Sb-125	100	7.83E+16	5.7E+14
Sc-46	100	---	---
Se-79	---	---	---
Sm-151	---	---	---
Sn-121m	---	---	---
Sn-126	100	1.11E+05	8.1E+02
Sr-90	---	---	---
Tc-99	100	3.58E+16	2.6E+14
Tc-99 KB	100	3.58E+16	2.6E+14
Th-228	100	5.17E+19	3.8E+17
Th-229	100	5.76E+05	4.2E+03
Th-230	1,000	5.21E+04	3.8E+02
Th-232	180	8.18E+03	5.9E+01
U-232	100	2.47E+04	1.8E+02
U-233	1,000	6.35E+06	4.6E+04
U-234	1,000	1.06E+07	7.7E+04
U-235	1,000	8.95E+07	6.5E+05
U-236	1,000	1.68E+11	1.2E+09
U-238	1,000	6.20E+06	4.5E+04
W-181	100	---	---
W-185	100	---	---
W-188	100	---	---
Zr-93	---	---	---

[1] Special wasteforms for radionuclides C-14, H-3, I-129 and Tc-99 were not explicitly evaluated in the intruder analysis, however their intruder limit is assumed to be the same as that of the generic radionuclide.
Note: Limits reported as "---" indicate that there is no limit or that the limit > 1E+20.

4.10 ILV RADON ANALYSIS

4.10.1 Overview of Radon Analysis

This section describes the investigation conducted to evaluate the potential magnitude of radon release from the ILV over the 25-year operational period, 100-year institutional control period, and 1,000-year post-closure compliance period. The ILV is a below grade, reinforced concrete vault which consists of two modules that together encompass a 278.83-ft by 48.5-ft area (Phifer et al. 2006). Waste disposed in the ILV is typically placed in concrete or metal containers and subsequently encapsulated in grout and/or CLSM. The waste is placed in the vaults in layers with the grout and/or CLSM surface forming the foundation for the next layer.

The flux of Rn-222 from the ILV was evaluated for three separate time periods: 1) 0 to 25 years, 2) 25 to 125 years, and 3) 125 to 1,125 years. The first time period evaluated covers the operational period. During this time period, there is a three-inch-thick layer of CLSM covering the waste contained within the vault. The second time period evaluated covers the institutional control period. During this time period, the waste is covered by the CLSM layer and a reinforced concrete roof. Finally, for the post-closure time period (125 to 1,125 years), a closure cap is placed over the ILV.

The permissible radon flux for DOE facilities is addressed in DOE M 435.1 Chapter IV, P(1)(c) (DOE 1999), which states the radon flux limitations associated with the development of a disposal facility and maintenance of a performance assessment and the closure of the disposal facility. This requirement is that the release of radon shall be less than an average flux of 20 $pCi/m^2/s$ at the surface of the disposal facility. The requirements analysis states that this standard was adopted from the uranium mill tailings requirements in 40 CFR Part 192 and 10 CFR Part 40. 10 CFR Part 40 discusses both Rn-222 from uranium and Rn-220 from thorium, therefore the performance objective refers only to radon, and the correct species must be analyzed depending on the characteristics of the waste stream.

This guidance forms the basis for the investigation to evaluate radon flux above the ILV. The scope of the investigation involved defining a decay chain of parent radionuclides to evaluate with a 1-D, vertical, numerical model. This analysis applies the capability of the standard SRS groundwater simulation program (PORFLOW) to model gas phase transport through partially saturated porous media to the ground surface. The model was customized to represent the vertical dimension of the ILV and the anticipated cover material. The instantaneous Rn-222 flux at the land surface was evaluated for the three time periods previously mentioned and the maximum flux was then compared to the DOE performance objective.

This investigation addresses only Rn-222, since the short half-life of Rn-220 (55.6 s) makes it unlikely to escape the ILV and migrate to the land surface via air diffusion before it is transformed by radioactive decay.

The potential parent radionuclides that can contribute to the creation of Rn-222 are illustrated in Figure 4-21. The diagram indicates the specific decay chains that lead to the formation of Rn-222, as well as the half-lives for each radionuclide. The extremely long half-life of U-238 (4.468E+09 years) cause the other radionuclides higher up on the chain of parents to be of little concern with regard to their potential to contribute significantly to the Rn-222 flux at the land surface over the period of interest.

4.10.2 ILV Summary of Key Radon Analysis Assumptions

Key assumptions and inputs used in the radon analysis are presented in Appendix B.

4.10.3 ILV Radon Analysis Conceptual Model

4.10.3.1 ILV Closure Considerations

The concepts for closure of the ILV disposal unit are relevant to the determination of the radon flux at the land surface. The ILV disposal unit construction specifics and closure concept are described by Phifer et al. (2006). For the purposes of this investigation, it is assumed that during the 25 year operational time period there is a three inch thick layer of CLSM covering the waste. Therefore, during this time period, the top of the CLSM layer is the point where Rn-222 flux was evaluated. During the 100-year institutional control period, the waste is covered by the CLSM and a reinforced concrete roof. For this time period, the Rn-222 flux was evaluated at the top of the reinforced concrete roof. For the post-closure compliance period (125 to 1,125 years), a closure cap is assumed to be in place over the ILV disposal unit. A conceptual drawing of the closure cap over the ILV disposal unit is shown in Figure 4-17 and the vertical section over which Rn-222 diffusion was evaluated is indicated.

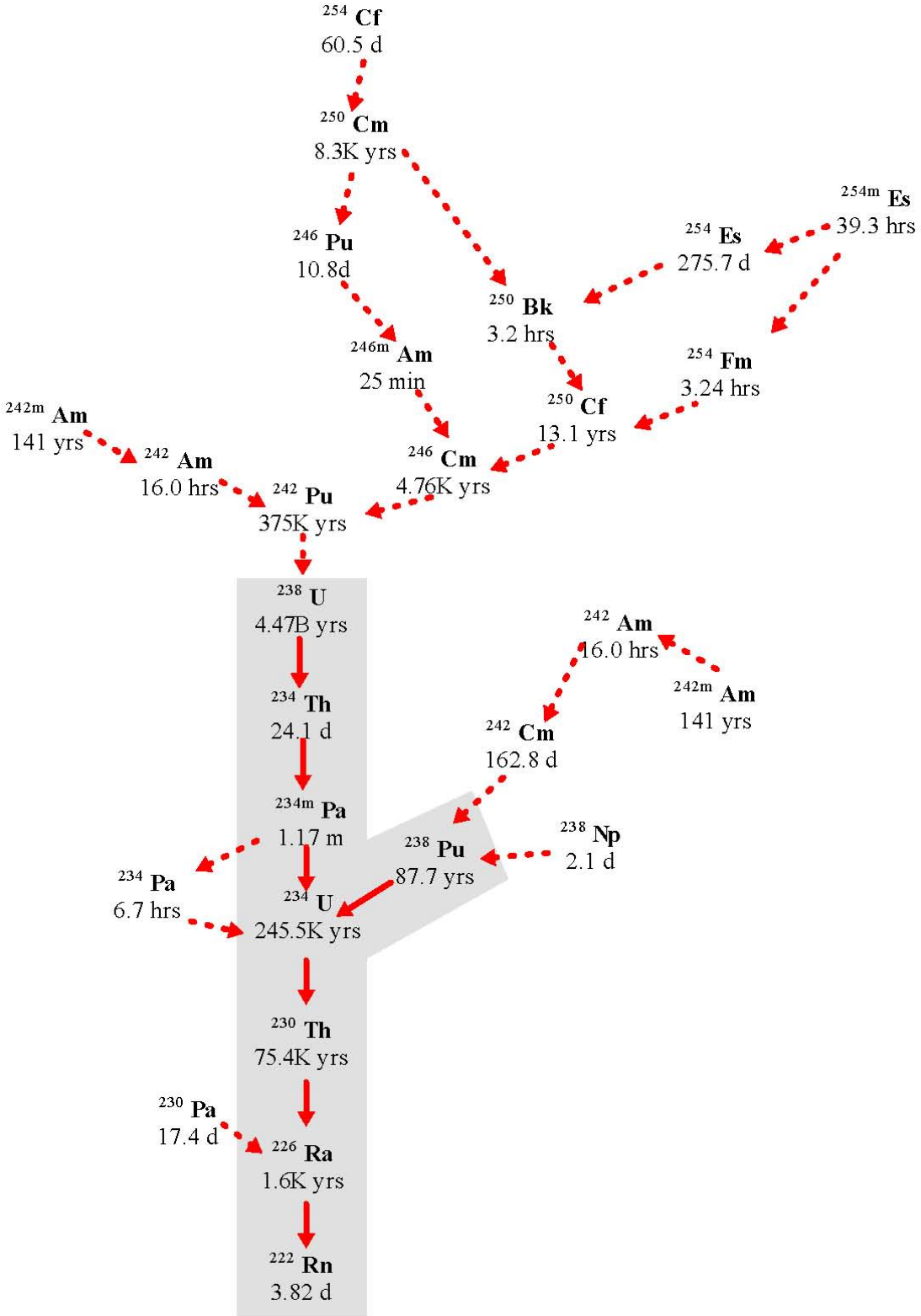

Figure 4-21. Radioactive Decay Chains Leading to Rn-222

The closure cap utilized in this analysis includes all materials, as constructed and placed over the ILV disposal unit at the end of the 100-year institutional control period. The components of concern for the long-term radon performance calculation are those that have no potential to erode during the 1,000-year post-closure compliance period. These components are situated below the top of the erosion barrier. The composite thickness of the non-waste material below the top of the erosion barrier is 7.5 ft. Table 4-36 lists the individual components of the ILV disposal unit and closure cap (excluding the layers overlying the erosion control barrier). Materials are indicated with the associated thickness of each component, in inches, feet, and meters. The minimum thicknesses of the ILV reinforced concrete roof provided by Phifer et al. (2006) were utilized in the modeling effort since the minimum thickness represents a shorter diffusion path and is therefore conservative relative to the flux to the ground surface.

Table 4-36. Vertical Layer Sequence and Associated Thickness for ILV Cover Material and Waste

Layer	Thickness (inches)	Thickness (ft)	Thickness (m)
Erosion barrier	12	1	0.30
Middle backfill layer	12	1	0.30
Gravel drainage layer	12	1	0.30
Lower backfill layer	24	2	0.61
Reinforced concrete roof	27	2.25	0.69
CLSM	3	0.25	0.08
ILV waste layer	327	27.25	8.31

SOURCE: Adapted from Phifer et al., 2006.

4.10.3.2 Conceptual Model

The Rn-222 flux at the land surface above the ILV disposal unit was evaluated for the specific closure configurations discussed above. Rn-222 is generated within the waste zone by radioactive decay of different parent radionuclides following along the decay chains that lead to the formation of Rn-222. The decay chains for all possible parent radionuclides of Rn-222 are shown in Figure 4-21. In this figure, the parent radionuclides that were individually evaluated are indicated with the gray shaded area (i.e., beginning with Pu-238 and U-238). Rn-222 generated within the waste zone is in the gaseous phase and diffuses outward from this zone into the air-filled soil pores surrounding the ILV disposal unit, eventually resulting in some of the radon emanating at the land surface.

As such, air is the fluid through which Rn-222 diffuses, although some Rn-222 may dissolve in residual pore water. It is assumed that fluctuations in atmospheric pressure at the land surface that could induce small pulses of air movement into and out of the shallow soil column will have a zero net effect over the long-term period of evaluation in this study, thus advective transport of Rn-222 in air-filled soil pores is not considered to be a significant process when compared to air diffusion.

The parent radionuclides exist in the solid phase and therefore do not migrate upward through the air-filled pore space, although they could be leached and transported downward from the waste zone by pore water movement. This potential downward migration of the parent radionuclides was neglected in the radon analysis.

The flux of Rn-222 from the ILV disposal unit was evaluated for three separate time periods: 1) 0 to 25 years, 2) 25 to 125 years, and 3) 125 to 1,125 years. The first time period evaluated covers the operational period. During this time period, the waste contained within the vault is covered by a three inch thick layer of CLSM. The second time period evaluated covers the institutional control period. During this time period, the waste is covered by a three inch thick layer of CLSM and a reinforced concrete roof. Finally, for the post-closure time period (125 to 1,125 years), a closure cap is placed over the ILV disposal unit.

4.10.4 ILV Radon Analysis Numerical Model

The mathematical model utilized in this report is provided by the PORFLOW simulation package. PC-based PORFLOW Version 5.97.0 was used to conduct a series of simulations. PORFLOW is developed and marketed by Analytic & Computational Research, Inc. to solve problems involving transient and steady-state fluid flow, heat and mass transport in multi-phase, variably saturated, porous or fractured media with dynamic phase change. PORFLOW has been widely used at the SRS and in the DOE complex to address major issues related to the groundwater and nuclear waste management.

The governing equation for mass transport of species k in the fluid phase is given by

$$\frac{\partial C_k}{\partial t} + \frac{\partial}{\partial x_i}(V_i C_k) = \frac{\partial}{\partial x_i}(D_{ij}\frac{\partial C_k}{\partial x_j}) + \gamma_k \qquad \text{Eq 4-3}$$

Where

C_k	concentration of species *k* (g/m^3)
V_i	fluid velocity in the i^{th} direction (m/yr)
D_{ij}	effective diffusion coefficient for the species (m^2/yr)
γ_k	net decay of species *k* (g/m^3-yr)
i, j	direction index
t	time (yr)
x	distance coordinate (m)

This equation is solved using PORFLOW to evaluate transient Rn-222 transport above the ILV disposal unit to evaluate Rn-222 flux at the land surface over time. As explained, advection is not considered to be a significant process when compared to air diffusion so the advection term was disabled within PORFLOW and only the diffusive and net decay terms were evaluated.

4.10.4.1 Model Development and Assumptions

The numerical representation of the conceptual model is as a 1-dimensional vertical stack of elements configured to represent the thickness of the ILV and overlying cover material associated with final closure.

Decay chains evaluated were U-238→Th-234→Pa-234m→U-234→Th-230→ Ra-226→Rn-222 and Pu-238 →U-234→Th-230→Ra-226→Rn-222. Each parent in these chains, except Th-234 and Pa-234m, were simulated separately as the starting point of the decay chain. Th-234 and Pa-234m have extremely short half-lives compared to the other parent radionuclides in these chains

Since the Rn-222 parent radionuclides exist as oxides or in other crystalline forms, only a fraction of Rn-222 generated by decay of Ra-226 has sufficient energy to migrate away from its original location into adjacent pore space before further decay occurs (3.82-day half-life for Rn-222). The fraction of radon escaping its source and migrating into adjacent pore space is approximated by the use of a radon emanation coefficient. This coefficient has been shown to vary between 0.02 and 0.7 in soils but is typically 0.25 (Yu et al. 2001). This value is taken as the default factor value for the RESRAD program, developed for the DOE. To account for this effect in the model, an effective source term of 0.25 Ci of parent radionuclide was utilized as the source term for each Ci disposed within the facility.

Since Rn-222 exists as a gas, air was assumed to be the medium within which radon transport occurs. The flow field was assumed to be isobaric and isothermal. The impact of naturally occurring fluctuations of atmospheric pressure is likely to have a zero net effect. Therefore, for the relatively long periods of time evaluated in this investigation, air diffusion was the only transport mechanism simulated in the model and advective air-transport was assumed to be negligible.

Some radon dissolves in pore water but since diffusion proceeds more slowly in that fluid, air diffusion is the only transport process by which Rn-222 can reach the land surface from the ILV disposal unit. This assertion is substantiated in Yu et al. (2001). In that report the D_{eff} for soil is reported to range from the radon open air diffusion coefficient of 1.0E-5 m^2/s to that of fully saturated soil, 1.0E-9 m^2/s. This 4-order of magnitude difference is consistent with the comparison of water diffusion coefficients to air diffusion coefficients of other common molecular compounds and reported in many references.

Thus, the larger volume of water-filled pore space compared to air-filled pore space (maximum of 1 order of magnitude difference) is inconsequential, in terms of the ability of water-dissolved radon to diffuse through water-filled pores as compared to the ability of the same compounds to diffuse as gas in the vapor-filled pore spaces. In this investigation, transport was allowed to proceed only through air-filled pore space and, therefore, residual pore water was treated as if it was part of the solid matrix material within the flow field. No credit was taken for airborne radon dissolving in pore water as it proceeds from the waste zone to the land surface although it has been observed to partition between air and water in the ratio of 4 to 1, respectively, at 20° C (Nazaroff and Nero 1988).

The boundary conditions imposed on the domain included:

- No-flux specified for all parent radionuclides at perimeter of the domain ($dC/dX = 0$ at $x=0$, $x=1$ and $dC/dY = 0$ at $y=0$, $y=y_{max}$)
- No-flux specified for Rn-222 along sides and bottom ($dC/dX = 0$ at $x=0$, $x=1$ and $dC/dY = 0$ at $y=0$)
- Rn-222 concentration set to 0 at land surface (top of erosion barrier) ($C = 0$ at $y=y_{max}$)

The initial condition imposed on the domain included:

- Species concentration set to 0 for the entire model domain at time = 0 ($C=0$ for $0 \leq x \leq 1$ at $t=0$ and $C=0$ for $0 \leq y \leq y_{max}$ at $t=0$)

The initial conditions for the model also assumed a 1 Ci inventory of each radionuclide uniformly spread over the waste zone.

Simulations were conducted in transient mode for diffusive transport in air, with results being obtained over 1,125 years.

4.10.4.2 Measures Implemented to Ensure Conservative Results

In this analysis, several conditions introduce a significant measure of conservatism into the calculations. These include:

- The use of boundary conditions that force all of the Rn-222 to move upward from the waste disposal zone to the land surface. In reality, some of the Rn-222 diffuses sideways and downward in the air-filled pores surrounding the waste zone; hence ignoring this has the effect of increasing the radon flux at the land surface.
- Not taking credit for the removal of either Rn-222 or of the parent radionuclides by pore water moving vertically downward through the model domain. This mechanism would likely remove some dissolved Rn-222 in addition to the parent radionuclides, and therefore its omission has the effect of increasing the estimate of instantaneous Rn-222 flux at the land surface in simulations conducted as a part of this investigation.

- The addition of an extra 125 years to the required 1,000-year evaluation period to account for any Rn-222 generated during the operational and institutional control period, thus incrementally increasing the instantaneous Rn-222 flux.
- Use of the top of the erosion layer in the soil cover as the land surface for the purpose of calculating Rn-222 flux during the 125 to 1,125 year time period. No credit is taken for the additional distance Rn-222 must migrate above the erosion barrier prior to that portion of the closure cap eroding away. This assumption impacts only Ra-226 (due to its relatively short half-life).
- Ignoring the presence of the GCL within the final closure cap. The GCL should be near 100 percent saturation; therefore it will contain very little air-filled porosity within which radon transport could occur.
- During the post-closure time period (125 to 1,125 years) assigning the concrete roof a low saturation associated with concrete rubble exposed to the atmosphere rather than a high saturation associated with buried concrete (i.e., the vault is overlain with a closure cap during the post-closure time period).

4.10.4.3 Grid Construction

The model grid was constructed as a node mesh 3 nodes wide by 50 nodes high. This mesh creates the vertical stack of 48 model elements. The grid extends upward only as far as the erosion barrier, since this is the minimum possible cover thickness that could exist during the 1,125-year evaluation period. A set of consistent units was employed in the simulations for length, mass and time, these being meters, grams and years, respectively. The grid is shown in Figure 4-17.

4.10.4.4 Material Zones

The model domain was divided into two primary zones, the ILV waste zone (including the top grout) occupying the lower 27 ft of the domain and the cover zone (including the CLSM, the reinforced concrete roof and the closure cap layers), extending 7.5 ft above the waste zone to the top of the domain. The upper model elements were scaled to correspond to the geometry of the closure cap thickness while the lower model elements were scaled to correspond to the ILV waste zone.

During the operational time period, the waste contained within the vault is covered by a three inch thick layer of CLSM. Therefore the land surface is assumed to be the top of the CLSM layer. During the institutional control period, the ground surface is taken as the top of the reinforced concrete roof. During the post-closure time period (125 to 1,125 years), the ground surface is taken as the top of the closure cap erosion barrier placed over the ILV.

4.10.4.5 Material Zone Properties and Other Input Parameters

Material properties utilized within the 1-D numerical model were specified for 6 material zones defined within the model domain. Each material zone was assigned values of particle density, total porosity, average saturation, air-filled porosity, air density, and an effective air diffusion coefficient for Rn-222. An air fluid density of 1.24E+03 g/m^3 was used for all material zones. This air fluid density was obtained from Bolz and Tuve (1973) and represents that of standard atmospheric conditions.

During the operational period (0 to 25 years) the layers associated with the ILV consist of the waste layer and CLSM layer (see Figure 4-17). An ILV waste zone total porosity of 0.736 and particle density of 2.32 g/cm^3 were taken from Phifer et al. (2006) (i.e., the ILV waste zone representation prior to vault collapse). It was assumed that the waste was dry and therefore the air-filled porosity would equal the total porosity for this zone. A total porosity of 0.46 and a particle density of 2.65 g/cm^3 were assigned to the CLSM layer as given by Phifer et al. (2006). The average saturation for the CLSM was taken as the value of saturation at a suction head of approximately 200 cm from the characteristic curves for the existing E-Area operational soil cover prior to dynamic compaction (Phifer et al. 2006). E-Area vadose zone field pore pressure measurements indicate average suction levels in the approximate range of 50 to 200 cm (Nichols et al. 2000). A value of 200 cm represents the upper end of the range which will have a greater air-filled porosity. The air-filled porosity of the CLSM was calculated from the total porosity and average saturation.

While the model includes all the layers from the ILV waste layer to the erosion barrier, during the first 25 years of simulation, the concrete roof and all overlying materials were assigned a porosity of 1.0 and a saturation of 0. This has the effect of making these layers equivalent to air. Table 4-37 provides the values of particle density, total porosity, average saturation, and air-filled porosity utilized for the ILV layers for the first 25 years.

Table 4-37. Operational Period (First 25 Years) Layer Particle Density, Total Porosity, Average Saturation, and Air-Filled Porosity

Layer	Particle Density (g/cm^3)	Total Porosity (fraction)	Average Saturation (fraction)	Air-Filled Porosity [4] (fraction)
Erosion barrier layer [1]	0	1	0	1
Upper backfill [1]	0	1	0	1
Gravel drainage layer [1]	0	1	0	1
Lower backfill [1]	0	1	0	1
ILV concrete roof [1]	0	1	0	1
CLSM[2]	2.65	0.460	0.825	0.081
ILV waste layer [2, 3]	2.32	0.736	0	0.736

[1] During the first 25 years of simulation, the concrete roof and materials comprising the closure cap were assigned a porosity of 1.0 and an average saturation of 0 in order to represent air.

[2] Waste layer and CLSM particle density and total porosity taken from Phifer et al. (2006).

[3] The waste is assumed to be dry (i.e., saturation of 0) resulting in the air-filled porosity equaling the total porosity.

[4] Air-Filled Porosity = (1 – Average Saturation) × Total Porosity

During the institutional control period (25 to 125 years) the layers associated with the ILV consist of the waste layer, the CLSM layer, and the reinforced concrete roof. The waste layer and CLSM layer retain the same properties as utilized for the first 25 years. The particle density and total porosity for the concrete roof was taken from the recommended values for the E-Area Vault Concrete (Phifer et al. 2006). The average saturation for the concrete roof was taken as the average saturation derived from moisture content measurements of concrete rubble exposed to the atmosphere performed by Sappington and Phifer (2005). The air-filled porosity of the concrete roof was calculated from the total porosity and average saturation. All materials overlying the concrete roof retain a porosity of 1.0 and a saturation of 0, making these layers equivalent to air. Table 4-38 provides the values of particle density, total porosity, average saturation, and air-filled porosity utilized for the ILV layers for the 25 to 125 year period.

During the post-closure time period (125 to 1,125 years) the layers associated with the ILV consist of all layers from the waste layer to the erosion barrier (see Figure 4-17). The waste layer, the CLSM layer, and the concrete roof retain the same properties as utilized for the 25 to 125 year period. The particle density of the lower backfill, gravel drainage layer, middle backfill, and erosion barrier (these materials collectively are considered the closure cap layers) was taken as 2.65 g/cm^3. This is based on the density of quartz and is regarded as representative of most SRS soils since quartz sand is the predominant material in SRS soil. Values for total porosity and long-term average moisture content for the closure cap materials were taken from Phifer (2003). Phifer (2003) evaluated infiltration through a closure cap over time as the closure cap degraded using the HELP model. The porosity and average moisture content values for a 10,000 year degraded closure cap were utilized, since this represented the greatest air-filled porosity in which a gas could diffuse. Average saturation and air-filled porosity values were calculated from the total porosity and long-term average moisture content. Table 4-39 provides the values of particle density, total porosity, average saturation, and air-filled porosity utilized for all the layers (i.e., waste layer to the erosion barrier) for the 125 to 1,125 year time period. Average saturation values for the vault roof for this time period was taken from Sappington and Phifer (2005).

The molecular diffusion coefficient of Rn-222 in open air is 347 m^2/yr (Nielson et al. 1984). Nielson et al. (1984) established a relationship between moisture saturation and the radon effective air diffusion coefficient for various pore sizes of earthen materials. Using this method, a radon effective air diffusion coefficient was determined for each material type based upon the average moisture saturation for the material. With the use of an effective air diffusion coefficient, tortuosity was assigned a unit value in each material zone. A summary of the radon effective air diffusion coefficients by material zone and simulation period, are presented in Table 4-40.

Table 4-38. Institutional Control Period (25 to 125 Years) Layer Particle Density, Total Porosity, Average Saturation, and Air-Filled Porosity

Layer	Particle Density (g/cm^3)	Total Porosity (fraction)	Average Saturation (fraction)	Air-Filled Porosity [4] (fraction)
Erosion barrier layer [1]	0	1	0	1
Upper backfill [1]	0	1	0	1
Gravel drainage layer [1]	0	1	0	1
Lower backfill [1]	0	1	0	1
ILV concrete roof [2, 4]	2.59	0.184	0.73	0.050
CLSM[2]	2.65	0.460	0.825	0.081
ILV waste layer [2, 3]	2.32	0.736	0	0.736

[1] During the first 125 years of simulation, the materials comprising the closure cap were assigned a porosity of 1.0 and an average saturation of 0 in order to represent air.

[2] Waste layer, CLSM, and concrete roof particle density and total porosity taken from Phifer et al. (2006).

[3] The waste is assumed to be dry (i.e. saturation of 0) resulting in the air-filled porosity equaling the total porosity.

[4] Air-Filled Porosity = (1 – Average Saturation) × Total Porosity

Table 4-39. Post-Closure Period (125 to 1,125 Years) Layer Particle Density, Total Porosity, Long-Term Average Moisture Content, Average Saturation, and Air-Filled Porosity

Layer	Particle Density (g/cm^3)	Total Porosity (fraction)	Long-Term Average Moisture Content	Average Saturation (fraction)	Air-Filled Porosity[6] (fraction)
Erosion barrier layer	2.65[1]	0.088[1]	0.0726[1]	0.825[5]	0.015
Upper backfill	2.65[1]	0.375[1]	0.2435[1]	0.649[5]	0.132
Gravel drainage layer	2.65[1]	0.375[1]	0.1967[1]	0.525[5]	0.178
Lower backfill	2.65[1]	0.370[1]	0.2710[1]	0.732[5]	0.099
ILV Roof	2.59[2]	0.184[2]	na[1]	0.730[4]	0.050
CLSM	2.65[2]	0.460	na[1]	0.825	0.081
ILV waste layer	2.32[2]	0.736[2]	na[1]	0.000[3]	0.736

[1] Values for total porosity and long term average moisture content taken from Phifer (2003). Particle density is taken as 2.65, which is based on the density of quartz and regarded as fairly representative of most SRS soils.

[2] Waste layer, CLSM, and concrete roof particle density and total porosity taken from Phifer et al. (2006).

[3] The waste is assumed to be dry (i.e., saturation of 0) resulting in the air-filled porosity equaling the total porosity.

[4] Average saturation for the ILV roof was calculated by dividing the in-field moisture content (0.096) by the saturated moisture content (0.132) as reported by Sappington and Phifer (2005).

[5] Average Saturation = Long Term Average Moisture Content / Total Porosity

[6] Air-Filled Porosity = (1 – Average Saturation) × Total Porosity

Table 4-40. Effective Air Diffusion Coefficient

Layer	Effective Air Diffusion coefficient (m^2/yr)		
	Operational Period (First 25 Years)	Institutional Control Period (25 to 125 Years)	Post-Closure Period (125 to 1,125 Years)
Erosion barrier layer	347	347	0.79
Upper backfill	347	347	4.73
Gravel drainage layer	347	347	4.73
Lower backfill	347	347	2.84
ILV Roof	347	2.84	2.84
CLSM	1.26	1.26	1.26
ILV waste layer	347	347	347

4.10.5 Model Results

Model simulations were conducted to evaluate the peak instantaneous Rn-222 flux at the land surface for the three periods of interest. These time periods include: 1) 0 to 25 years, 2) 25 to 125 years, and 3) 125 to 1,125 years. Model results were output in $Ci/m^2/yr$, consistent with the set of units employed in the model. A graph of these results is shown in Figure 4-22, although the units are converted to $(pCi/m^2/s)/(Ci/m^2)$, which are the units used to define the regulatory flux limit in DOE G 435.1-1. Figure 4-22 shows a sharp flux discontinuity at 125 years which results from the installation of the closure cap.

The peak fluxes represent the peak Rn-222 flux per square meter at the land surface as defined for each simulation period and are listed below in Table 4-41. The land surface for the 0 to 25 year time period was taken to be the top of the grout layer. For the 25 to 125 year simulation period, the land surface was taken to be the top of the reinforced concrete roof. For the 125 to 1,125 year simulation period, the land surface is taken to be the top of the closure cap erosion barrier.

The calculated disposal limits per unit area and the disposal limits for the ILV disposal unit are presented in Table 4-42 for each of the five parent radionuclides. The unit-area disposal limit was calculated as follows:

> Disposal Limit per unit area (Ci/m^2) = Regulatory limit (20 $pCi/m^2/s$) / Maximum Instantaneous Rn-222 flux at land surface per unit inventory of parent radionuclide per unit area ($[pCi/m^2/s]/[Ci/m^2]$).

The unit area limits for each of the 5 parent radionuclides were calculated using the maximum Rn-222 flux of the three time periods. For each radionuclide, the maximum flux of Rn-222 was observed either during the initial 25 year or 25 to 125 year simulation periods when a closure cap was not present. This maximum flux of Rn-222 was used to calculate the unit area limits for each radionuclide. The unit area limits for each of the 5 parent radionuclides were converted to ILV-specific radon disposal limits by multiplying the unit area limit for each by the maximum area utilized for disposal within the ILV footprint (1258 m^2). As discussed within Section 4.3, the maximum area utilized for disposal in the ILV footprint consists of nine disposal cells that are each 25-foot by 44-foot 6-inches (i.e., 10,013 ft^2).

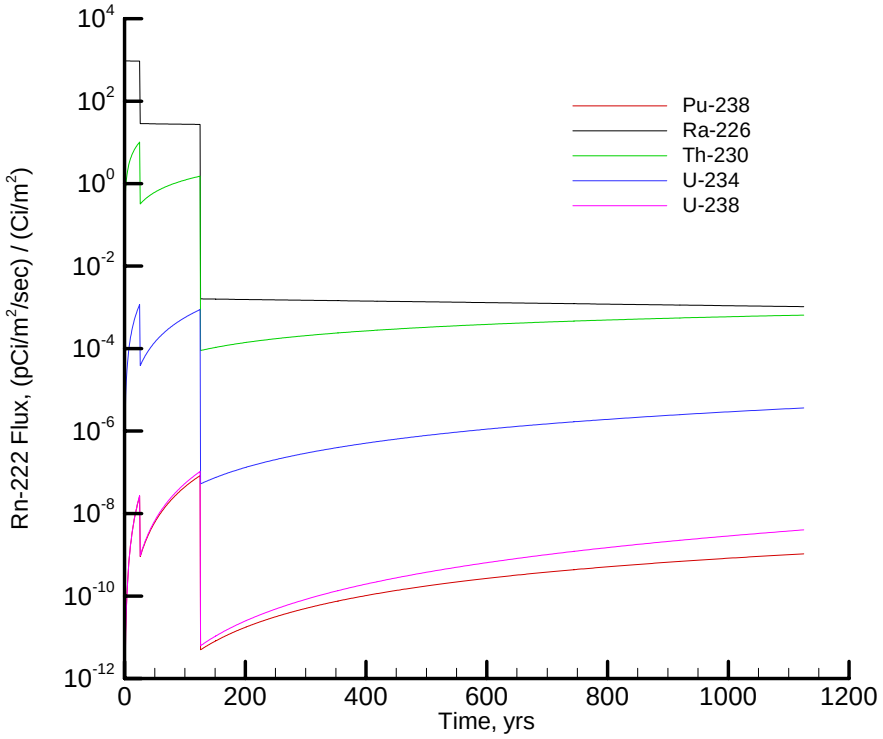

Figure 4-22. Rn-222 Flux at Land Surface Resulting from Unit Source Term

Table 4-41. Simulated Peak Instantaneous Rn-222 Flux over 1,125-Years at the Land Surface

Parent Source	Peak Instantaneous Rn-222 flux at Land Surface $(pCi/m^2/s)/(Ci/m^2)$*		
	0-25 years	25-125 years	125-1,125 years
Pu-238	2.64E-08	8.29E-08	1.05E-09
U-238	2.74E-08	1.04E-07	4.02E-09
U-234	1.17E-03	8.81E-04	3.64E-06
Th-230	1.02E+01	1.52E+00	6.49E-04
Ra-226	9.45E+02	2.85E+01	1.60E-03

* Flux resulting from unit source spread over unit area of trench (Ci/m^2)

Table 4-42. Radon-Pathway Disposal Limits for the ILV

Parent Source (1 Ci/m^2)	Maximum Instantaneous Rn-222 flux at Land Surface (pCi/m^2/s) / (Ci/m^2)	Time to Max (years)	Disposal Limit Per Unit Area [1] (Ci/m^2)	ILV Radon Disposal Limit [2] (Ci)
Pu-238	8.29E-08	125	2.41E+08	2.3E+11
Ra-226	9.45E+02	25	2.12E-02	2.0E+01
Th-230	1.02E+01	25	1.97E+00	1.8E+03
U-234	1.17E-03	25	1.71E+04	1.6E+07
U-238	1.04E-07	125	1.92E+08	1.8E+11

[1] Disposal Limit per unit area (Ci/m^2) = 20 pCi/m^2/s / Maximum Instantaneous Rn-222 flux at Land Surface

[2] ILV Radon Disposal Limit = Disposal Limit per unit area (Ci/m^2) × 931 m^2

4.11 REFERENCES

ACRI. 2004. *PORFLOW Version 5.0 User's Manual*, Revision 5, Analytical & Computational Research, Inc., Los Angeles, California.

Beres, D.A. 1990. *The Clean Air Act Assessment package-1988 (CAP-88) A dose and Risk Assessment Methodology for Radionuclide Emissions to Air.* U.S. Environmental Protection Agency Contract No. 68-D9-0170, Washington, DC.

Bolz, R.E. and G.L. Tuve, (Editors), 1973. *Handbook of Tables for Applied Engineering Science, 2nd Edition*. CRC Press, 18901 Cranwood Parkway, Cleveland, OH.

Cook, J. R. 2007. *Radionuclide Data Package*, WSRC-STI-2006-00-162. Westinghouse Savannah River Company, Aiken, South Carolina. March 20, 2007

Cook, J. R., Phifer, M. A., Wilhite, E. L., Young, K. E., and Jones, W. E. 2004. *Closure Plan for the E-Area Low-Level Waste Facility*, Revision 4, WSRC-RP-2000-00425. Westinghouse Savannah River Company, Aiken, South Carolina. May, 2004.

Crapse, K.P. and J.R. Cook, 2006. *Atmospheric Pathway Screening Analysis for the E-Area Low Level Waste Facility*, WSRC-STI-2006-00159, Washington Savannah River Company, Aiken, SC 29808. 09/05/2006.

DOE 2002. *Natural Phenomena Hazards Design and Evaluation Criteria for Department of Energy Facilities*. DOE-STD-1020-2002. U. S. Department of Energy, Washington DC.

DOE 1999. Implementation Guide for use with DOE M 435.1-1. DOE G 435.1-1. Department of Energy, July 9, 1999.

Flach, G.P. 2004. *Groundwater Flow Model of the General Separations Area Using PORFLOW*. WSCR-TR-2004-00106. Westinghouse Savannah River Company, Aiken, SC 29808.

Flach, G.P. and R.A. Hiergesell. 2004. *Special Analysis: Revision of Intermediate Level Vault Disposal Limits (U)*. WSRC-TR-2004-00346, Revision 0. Westinghouse Savannah River Company. Aiken, SC 29808.

Hiergesell, R.A. 2005. Special Analysis: *Production TPBAR Waste Container Disposal Within the Intermediate Level Vault. WSRC-TR-00531, Revision 0*. Westinghouse Savannah River Company, Aiken, SC 29808.

Hiergesell, R.A. and W.E. Jones. 2003. *An Updated Regional Water Table of the Savannah River Site and Related Coverages*. WSRC-TR-2003-00250, Revision 0. Westinghouse Savannah River Company, Aiken, SC 29808.

Kaplan, D.I. 2006. *Geochemical Data Package for Performance Assessment Calculations Related to the Savannah River Site (U*). WSRC-TR-2006-00004, Revision 0. Washington Savannah River Company, Aiken, SC 29808.

Koffman, L. D. 2006b. *Automated Inadvertent Intruder Application, Version 2*. WSRC-TR-2006-00037. Savannah River National Laboratory, Aiken, SC. September 2006.

Koffman, L.D. 2006a. *SRNL All-Pathways Application*, WSRC-STI-2006-00179, Rev. 0. SRNL, Washington Savannah River Company, Aiken, SC 29808.

Lee, P. 2004. *Inadvertent Intruder Analysis Input for Radiological Performance Assessments,* WSRC-TR-2004-00295, Westinghouse Savannah River Company, Aiken, SC 29808.

Lee, P. 2006. *Atmospheric Dose Modeling for the E-Area Low Level Waste Facility at the Savannah River Site,* WSRC-STI-2006-00262, Washington Savannah River Company, Aiken, SC 29808.

McDowell-Boyer, L., Yu, A. D., Cook, J. R., Kocher, D. C., Wilhite, E. L., Holmes-Burns, H., and Young, K. E. 2000. *Radiological Performance Assessment for the E-Area Low-Level Waste Facility,* Revision 1, WSRC-RP-94-218. Westinghouse Savannah River Company, Aiken, South Carolina. January 31, 2000.

Nazaroff, W.W., and A.V. Nero (editors), 1988, *Radon and its Decay Products in Indoor Air*, John Wiley & Sons, New York, N.Y.

NCRP 1996. "Screening Models for Releases of Radionuclides to Atmosphere, Surface Water and Ground," NCRP report No. 123, National Council on Radiation Protection and Measurements, Bethesda, Maryland, Jan. 22, 1996.

Nielson, K.K., V.C. Rogers and G.W. Gee, 1984. *Diffusion of Radon through Soils: A pore distribution Model*, Soil Science Society of America, J. 48:482-487.

Nichols, R. L., B. B. Looney, G. P. Flach and J. Rossabi, 2000, Recommendations for Phase II Vadose Zone Characterization and Monitoring at the E-Area Disposal "Slit" Trenches and Mega-Trench (U), WSRC-TR-2000-00059.

Peregoy, W. 2006. Structural Evaluation of Intermediate Level Waste Disposal Vaults for Long-Term Behavior, T-CLC-E-00024, Rev. 0. Washington Savannah River Company, Aiken, South Carolina. June 27, 2006.

Phifer, M.A., M. A. Millings, G. P. Flach, 2006. *Hydraulic Property Data Package for the E-Area and Z-Area Vadose Zone Soils, Cementitious Materials, and Waste Zones (U).* WSRC-STI-2006-00198. Washington Savannah River Company, Aiken, South Carolina. September 2006.

Phifer, M. A., 2004. Preliminary E-Area Trench Closure Cap Closure Sequence, Infiltration, and Waste Thickness (U), WSRC-TR-2004-00119, Westinghouse Savannah River Company, Aiken, South Carolina. March 2004.

Phifer, M.A. 2003. *Saltstone Disposal Facility Mechanically Stabilized Earth Vault Closure Cap Degradation Base Case: Institutional Control to Pine Forest Scenario (U).* WSRC-TR-2003-00523. Westinghouse Savannah River Company, Aiken, South Carolina. December 18, 2003.

Phifer, M.A. 2006. *Software Quality Assurance Plan for the Hydrologic Evaluation of Landfill Performance (HELP) Model*. Q-SQA-A-00005, Rev. 0.

Phifer, M. A. and Nelson, E. A. 2003. *Saltstone Disposal Facility Closure Cap Configuration and Degradation Base Case: Institutional Control to Pine Forest Scenario (U), Rev. 0*, WSRC-TR-2003-00436, Westinghouse Savannah River Company, Aiken, South Carolina. September 22, 2003.

Phifer, M. A. and Wilhite, E. L. 2001. Waste Subsidence Potential versus Supercompaction. WSRC-RP-2001-00613, Westinghouse Savannah River Company, Aiken, South Carolina. October 5, 2001.

Sappington and Phifer 2005. Moisture Content and Porosity of Concrete Rubble Study (U). WSRC-TR-2005-00054. Westinghouse Savannah River Company, Aiken, South Carolina. October 7, 2005.

Shine, E. P. 2007. *Memorandum to B. T. Butcher and R. A. Hiergesell*, SRNL-SCS-2007-00011.

Snyder, K. A. 2003. *Condition Assessment of Concrete Nuclear Structures Considered for Entombment*, National Institute of Standards and Technology (NIST), NISTIR 7026. July 14, 2003.

Taylor, G.A. 2006. *Software Quality Assurance Plan for Ideal Filemaker: An Application to Translate PORFLOW Output to All-Pathways Input*. G-SQP-A-00010, Rev. 0.

Taylor, G.A. and L.B. Collard. 2005. *Automated Groundwater Screening*. WSRC-TR-2005-00203, Rev. 0. SRNL, Washington Savannah River Company, Aiken, SC.

Vinson, D.W., Subramanian, K.H. and Clark, E.A. 2004. *Containment Material Performance for TPBAR Disposal*. WSRC-TR-2004-00374. Washington Savannah River Company, Aiken, SC. July 2004.

WMAP 2006. *System Plan For Solid Waste Management*, WSRC-RP-99-01092, Volumes I and II, Revision 9.

WSRC 2006. *SRS Waste Acceptance Criteria Manual,* Procedure Manual 1S, Washington Savannah River Company, Aiken, South Carolina. January 19, 2006.

Yu, C., A.J. Zielen, J.J. Cheng, D.J. LePoire, E. Gnanapragasam, S. Kamboj, J. Arnish, A. Wallo III, W.A. Williams, and H. Peterson, 2001. *Users Manual for RESRAD Version 6*, Environmental Assessment Division, Argonne National Laboratory. Chicago, Illinois.

This page intentionally left blank.

CHAPTER 5

NAVAL REACTOR COMPONENT DISPOSAL AREA

This page intentionally left blank.

5.0 NAVAL REACTOR COMPONENT DISPOSAL AREA

LIST OF FIGURES

LIST OF TABLES

5.0 NAVAL REACTOR COMPONENT DISPOSAL AREAS

5.1 EXECUTIVE SUMMARY

Disposal at two NRCDAs has been assessed versus the DOE performance measures. The results of the analysis show that none of the performance measures are expected to be exceeded. The analysis results have also been used to develop radionuclide disposal limits to ensure that performance measures will not be exceeded due to continued disposal at the 643-26E NRCDA (Table 5-1). NRCDA disposal limits through the 1,000-year compliance period have been developed for the following pathways: groundwater protection, air, all-pathways, inadvertent intruder (resident scenario), and radon. All instances of groundwater protection and all-pathways "limits" in this chapter refer to "preliminary limits" only, because they do not take into account consideration of uncertainty discussed in Chapter 7, Integration and Interpretation. The NRCDAs were excluded from the plume interaction analysis in Chapter 6, Integrated Facility Analysis, because of their very low impact in the groundwater analysis.

For the groundwater all-pathways dose, a quantitative sensitivity and uncertainty analysis has been performed. The sensitivity analysis shows that the failure time of the disposal cask welds and the aquifer cross-sectional area are the parameters to which the all-pathways dose is most sensitive. The uncertainty analysis shows that the mean all-pathways dose is about 0.5 mrem/year, the 95^{th} percentile interval dose is about 2.4 mrem/year and the upper bound dose is about 6.2 mrem/year. These results firmly demonstrate that the all-pathways dose limit will not be exceeded due to disposal of the NR components.

Trigger values for radionuclides that did not screen out of the groundwater and air analyses and were not specifically analyzed are given in Tables 4-4 and 4-5, respectively, in the Part C Background chapter. The trigger values were developed using conservative screening methodologies and can be used as surrogate disposal unit limits should any of the listed radionuclides be proposed for disposal.

Table 5-1. Preliminary Groundwater Protection and All-Pathways Disposal Limits and Intruder, Air, and Radon Disposal Limits for the 643-26E and 643-7E NRCDAs[1]

Radionuclide	Beta-Gamma Limit	Gross Alpha Limit	Radium Limit	Uranium Limit	All-Pathways Limit	643-26E Air-Pathway Limit	643-7E Air-Pathway Limit	643-26E Radon Limit	643-7E Radon Limit
	Ci	Ci	Ci	Ci	Ci	Ci	Ci	Ci	Ci
C-14	1.3E+04	---	---	---	1.4E+04	2.6E+03	5.3E+02	---	---
Cl-36	---	---	---	---	---	1.9E+03	3.7E+02	---	---
H-3	---	---	---	---	---	4.5E+06	4.5E+06	---	---
I-129	1.5E-02	---	---	---	9.1E-01	3.9E+00	7.7E-01	---	---
Nb-94	1.6E+03	---	---	---	8.8E+02	---	---	---	---
Ni-59	9.7E+04	---	---	---	2.4E+07	---	---	---	---
Pu-238	---	-----	---	---	---	---	---	1.1E+12	2.4E+11
Pu-239	6.5E+09	4.5E+07	---	---	2.3E+07	---	---	---	---
Ra-226	---	---	---	---	---	---	---	9.9E+05	2.1E+05
Se-79	---	---	---	---	---	1.0E+03	2.0E+02	---	---
Sn-121m	---	---	---	---	---	1.4E+08	2.9E+07	---	---
Sn-126	---	---	---	---	---	3.1E+00	6.1E-01	---	---
Tc-99	6.2E+02	---	---	---	9.3E+02	---	---	---	---
Th-230	---	---	---	---	---	---	---	1.9E+06	3.9E+05
U-234	---	---	---	---	---	---	---	3.3E+08	7.0E+07
U-238	---	---	---	---	---	---	---	3.0E+11	6.4E+10

[1] It is demonstrated in Section 5.9 that the 100 mrem/yr performance objective for intrusion cannot be exceeded. Therefore, no intruder limits were calculated.

Note: Limits reported as "---" indicate that there is no limit or that limit >1E20.

5.2 INTRODUCTION AND GENERAL APPROACH

Two separate areas within E Area have recently been used for disposal of reactor components from the US Navy. The characteristics of the two areas and the materials disposed at them are similar enough that one set of analyses can be used to show that there is reasonable assurance that each will meet the performance objectives of DOE Order 435.1. (DOE 1999)

Two general types of waste forms are described in this analysis, highly radioactive components consisting of activated corrosion-resistant metal alloy contained within thick steel casks, and auxiliary equipment primarily contaminated with activated corrosion products (crud) at low levels and contained within thinner-walled casks. The inventories for the two types of waste were combined and conceptually placed in a representative heavily shielded cask. Section 5.11 describes the treatment of the other waste types disposed in the NRCDAs.

The waste forms disposed on the NRCDAs are robust. The outer containers consist of approximately 1 foot of steel with welds at least 1.25 inches thick. The actual waste inside the casks consists of activated metal, either as intact metal components or as loose corrosion products known as crud. Corrosion analysis of the casks indicates that it is possible for small holes to develop in the welds in approximately 750 years, which could allow release of contamination in the gas phase and flow of water into and out of the cask. A one-dimensional model was developed to examine the gas phase transport of a few radioactive gasses which were not screened out. A similar model was developed to look at generation of radon within the casks and transport of the gas to the ground surface. A simplified methodology was used to analyze releases to the groundwater pathway. A screening-level analysis showed that no intruder scenarios were credible over the 1,000-year compliance period.

5.3 NRCDA GENERAL DESCRIPTION AND LIFECYCLE

NRCDAs are above-grade gravel pads for the disposal of shipping/disposal casks containing waste NR components. Two NRCDAs are associated with the ELLWF. The 643-7E NRCDA contains 41 casks, is a trapezoidal area consisting of approximately 0.3 acres, and is closed to future receipts. It has an interim soil cover in place. The 643-26E NRCDA is currently in operation, is an irregularly shaped area consisting of approximately 1.4 acres, and is expected to receive up to 100 casks for disposal.

Figure 5-1 provides the layout of the two NRCDAs relative to other ELLWF disposal unit types.

During the operational period, waste NR components contained within casks are placed on the NRCDA. The steel casks have thick walls, are closed with a gasket or welds, and are considered water and air-tight. Figure 5-2 provides an operational photograph of the 643-26E NRCDA that shows the offloading of a cask. Figure 5-3 provides a diagram of a typical cask.

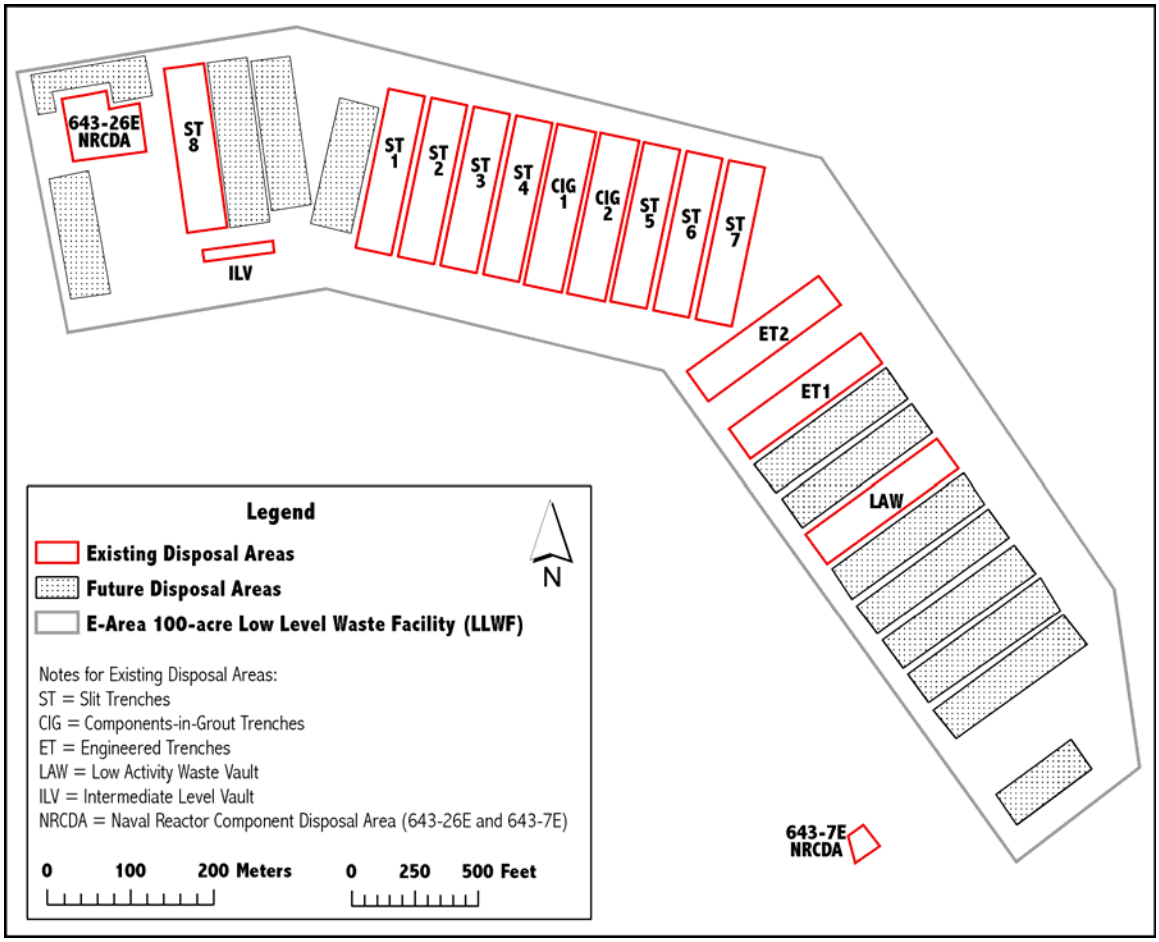

Figure 5-1. Location of NRCDAs associated with the ELLWF

Figure 5-2. Operational NRCDA Photograph

No additional operational closure or interim closure beyond simply placing the casks on the NRCDAs is necessitated due to the water and air-tight nature of the casks. However, if radiation shielding is required for personnel protection during the operational or institutional-control period, the casks may be surrounded with a structurally suitable material that will be capable of supporting the final closure cap without resulting in differential subsidence at the time the cap is installed.

Final closure of the NRCDAs will take place at final closure of the entire ELLWF, at the end of the 100-year institutional control period. Prior to final closure, the space around, between, and over the casks will have to be filled with a structurally suitable material that will be capable of supporting the final closure cap without resulting in differential subsidence. Dynamic compaction of the NRCDAs will not be conducted.

Final closure will consist of installation of an integrated closure system designed to minimize moisture contact with the waste and to provide an intruder deterrent. The integrated closure system will consist of one or more closure caps installed over all the disposal units and a drainage system. Figure 5-4 provides the anticipated NRCDA closure cap configuration.

This discussion is drawn from McDowell-Boyer et al. (2000) and Cook et al. (2004).

5.4 NRCDA PRINCIPAL DESIGN FEATURES

5.4.1 NRCDA Structural Stability and Cover Integrity

As shown in Figure 5-3, the NR Waste Shipping/Disposal Casks have a minimum wall thickness of 13.8 in and consist of corrosion-resistant steel. "Using a corrosion rate of 4E-03 cm/yr for carbon steel a 13.8 in wall can be assumed to be completely corroded through in 8750 years." (Cook et al. 2002) However, the cask will not remain structurally stable until it is completely corroded through. If it is assumed that the 13.8-in thick casks will remain structurally stable until the wall thickness has been reduced to 1.18 in due to a corrosion rate of 4E-03 cm/yr, then the casks will remain structurally stable for 8,000 years. It has been assumed that the air-filled porosity within a cask is approximately 20%.

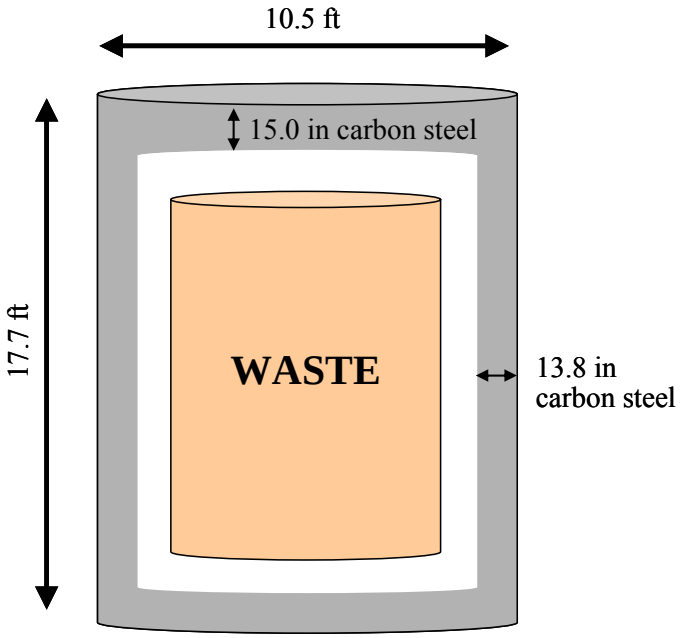

Volume = 43 m^3
Minimum weld thickness = 1.25 inches (~3 cm)
Note that cask dimensions may vary depending on type of shipping/disposal cask
(Figure not to scale)

Figure 5-3. Example of NR Waste Shipping/Disposal Cask

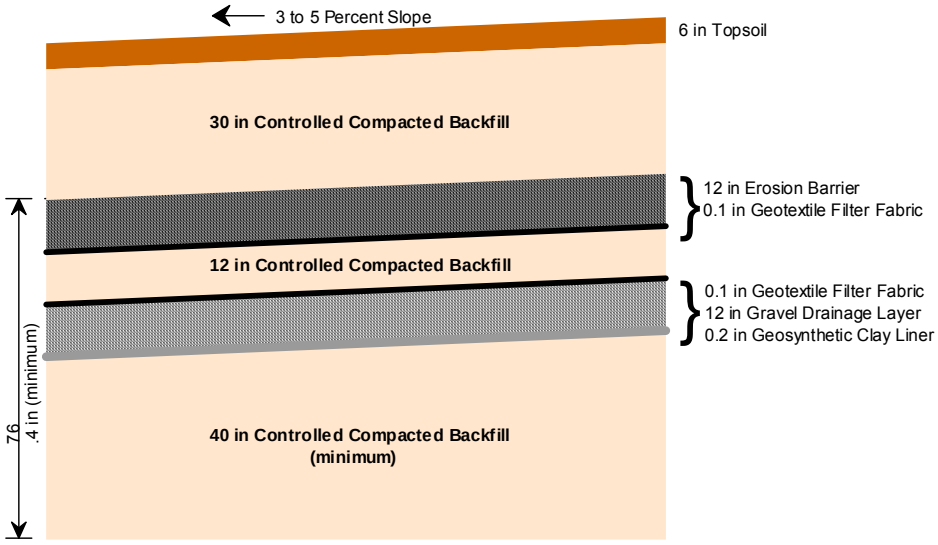

Figure 5-4. NRCDA Closure Cap Configuration

The final ELLWF closure cap will be installed at the end of the 100-year institutional control period (Phifer 2004). After installation it is assumed that no closure cap maintenance will be performed other than that required for establishment of the vegetative cover. Therefore, it is assumed that the hydraulic properties of the closure cap will immediately begin to degrade after construction due to the following (Phifer and Nelson 2003; Phifer 2004):

- Formation of holes in the upper GCL by pine forest succession
- Reduction in the saturated hydraulic conductivity of the drainage layers due to colloidal clay migration into the layers
- Erosion of layers that provide water storage for the promotion of evapotranspiration

Since it is anticipated that the casks will maintain structural stability for 8,000 years after placement on the pad, it is not anticipated that the integrity of the final closure cap could be impacted by subsidence until that time. Due to the limited porosity (20%) within the casks and the fact that steel corrosion products take up more volume than the original steel, it is anticipated that loss of cask structural stability will not result in any significant subsidence damage to the closure cap.

5.4.2 NRCDA Water Infiltration

As noted, the steel casks have thick walls, are closed with a gasket or welds, and are considered water and air-tight. Additionally, it has been estimated that the casks will remain watertight for 750 years after placement on the pads. (McDowell-Boyer et al. 2000). Therefore, no water infiltration through the contained waste is anticipated during the operational period, the 100-year institutional control period, and during the post-institutional control period prior to cask hydraulic failure at 750 years. The final closure cap, in addition, will minimize infiltration to the casks. However after installation it is assumed that no cap maintenance will be performed other than that required for establishment of the vegetative cover. Therefore the hydraulic properties of the cap are assumed to degrade resulting in increased infiltration through the cap over time.

5.4.3 NRCDA Inadvertent Intruder Barrier

Inadvertent intrusion into the NRCDA waste is not considered feasible during the operational and institutional control periods, due to the existence of facility security during these periods. However, it is assumed that inadvertent intrusion could occur during the post-institutional control period. Since the casks are assumed to be structurally stable for 8,000 years after placement on the pads, they also provide a barrier to intrusion for this time period. Normal residential construction and well drilling equipment used in the vicinity of the SRS is not capable of penetrating a structurally intact cask (McDowell-Boyer et al. 2000).

5.5 NRCDA WASTE CHARACTERISTICS

Heavily shielded shipping/disposal casks containing waste NR components are disposed at the NRCDAs. The 643-7E NRCDA contains 41 components and is closed to future receipts. It has an interim soil cover in place.

The 643-26E NRCDA is currently in operation and is expected to receive up to 100 components for disposal. Large quantities of activation products are associated with the metal matrix of the waste forms within the disposal containers. Lesser amounts of radioactive contaminants are present in corrosion products.

5.5.1 Waste Type/ Chemical and Physical Form

Waste NR components consist of a variety of activated metal forms. These components include CB/TS adapter flanges, closure heads, HD barrels, pumps and other similar equipment. Some components are also surface-contaminated with corrosion products known as crud. The shielded shipping/disposal casks reduce the safety risks involved in the handling, transportation and disposal of waste NR components.

The containers that are disposed of on the NRCDA contain almost no cellulosic material. What little there is consists of wood blocks used as chocking to stabilize equipment inside of casks and an occasional sheet of plywood as part of a closure system. This amount of cellulosic material is assumed to be too small to make consideration of the effect on K_d necessary for this disposal unit evaluation (effect on K_d is, however, considered for some of the other disposal areas in the ELLWF).

5.5.2 Radionuclide Inventory

The NR program provided radionuclide inventories of the two representative types of NR waste components, the KAPL CB/TS and the KAPL Head units, shown in Table 5-2. The activity listed for each radionuclide in this table is considered a general upper bound case by KAPL personnel, suitable for use in this PA. A representative activity for the "average" component is about one-half the value listed in Table 5-2, according to NR personnel. The listed curie inventories of 66 contaminants are further characterized as either "Activation" or "Crud" waste. Activation waste contains activation product radionuclides intimately dispersed in the metal matrix, which are released only as the metal is corroded. In contrast, crud waste resides in a thin surface coating and is more readily leached once containers are breached. Table 5-2 shows that the upper bound activity of a KAPL CB/TS cask is about 80,000 Ci of activation waste and 9 Ci of crud waste. The upper bound activity of a KAPL Head cask is about 0.02 Ci of activation waste and 40 Ci of crud waste. Thus, essentially all activation waste radionuclides reside in KAPL CB/TS casks. By contrast, the activity of crud waste radionuclides in KAPL Head casks is somewhat greater than the activity of crud-associated radionuclides in KAPL CB/TS casks.

Table 5-2 shows upper-bound activities per representative disposal cask. The NR estimates that of the 100 casks destined for disposal at E Area, about one-half, or 50, are best represented by the CB/TS waste components, while the remaining 50 are best represented by the Head components. In order to project a representative total inventory of NR waste, the upper-bound values in Table 5-2 are first halved to obtain average activities in the two representative types of waste. Next, these halved values are multiplied by 50 to obtain total inventories for each representative waste component (i.e., CB/TS or Head), since there are assumed to be 50 of each type of component. To obtain the total inventory of each radionuclide in activation or crud waste, the total inventories for each of the two types of representative waste components are then added together, keeping activation and crud waste categories separate. The final results of these operations are listed in Table 5-3. The inventory listed in Table 5-3 is the total projected inventory for the NR waste components used in this assessment.

Table 5-2. Radionuclide Inventory in Representative NR Waste Component Casks to be Shipped to the NRCDA

Radionuclide	KAPL CB/TS		KAPL Head	
	Activation [Curies]	Crud [Curies]	Activation [Curies]	Crud [Curies]
Am-241	3.52E-02	9.22E-06	---	1.58E-05
Am-242m	---	2.24E-07	---	9.02E-08
Am-243	2.41E-04	8.40E-08	---	1.35E-07
Ba-137m	5.17E-01	1.10E-03	---	1.80E-03
C-14	1.35E+01	2.80E-02	7.92E-08	4.51E-02
Ce-144	4.93E-01	---	---	---
Cf-249	1.24E-11	1.40E-14	---	2.26E-14
Cf-251	2.64E-13	5.59E-16	---	9.02E-16
Cm-242	5.22E-01	5.78E-05	---	2.93E-04
Cm-243	---	7.00E-08	---	1.13E-07
Cm-244	1.92E-02	9.50E-07	---	1.58E-05
Cm-245	1.02E-06	7.01E-10	---	1.13E-09
Cm-246	3.93E-07	2.80E-10	---	4.51E-10
Cm-247	7.90E-13	8.40E-16	---	1.35E-15
Cm-248	1.86E-12	2.66E-15	---	4.29E-15
Co-58	2.03E+03	8.00E-01	3.09E-05	1.8E+01
Co-60	9.82E+03	2.54E+00	1.34E-03	4.51E+00
Cr-51	7.49E+02	8.16E-04	3.64E-03	1.13E+00
Cs-135	3.47E-06	---	---	---
Cs-137	5.17E-01	1.10E-03	---	1.80E-03
Eu-154	6.75E-03	---	---	---
Eu-155	3.84E-03	---	---	---
Fe-55	8.98E+03	4.63E+00	1.49E-02	9.02E+00
Fe-59	7.49E+02	1.05E-02	9.27E-04	1.13E+00
H-3	1.35E+01	6.35E-05	2.02E-05	---
Hf-181	7.49E+02	3.39E-03	---	4.51E-01
I-129	8.50E-08	1.12E-07	---	1.80E-07
In-113m	4.89E+02	---	---	---
Mn-54	1.37E+02	1.54E-01	2.75E-05	4.51E-01
Mo-93	1.44E-01	---	---	---
Nb-93m	7.49E+02	4.06E-02	---	6.76E-02
Nb-94	6.50E-01	5.60E-04	1.01E-07	9.02E-04
Nb-95	1.31E+04	3.24E-02	---	9.7E-01
Nb-95m	1.31E+02	1.28E-04	---	---

Table 5-2. Radionuclide Inventory in Representative NR Waste Component Casks to be Shipped to the NRCDA - continued

Radionuclide	KAPL CB/TS		KAPL Head	
	Activation [Curies]	Crud [Curies]	Activation [Curies]	Crud [Curies]
Ni-59	1.56E+02	8.4E-03	1.22E-06	1.35E-02
Ni-63	1.8E+04	8.36E-01	1.49E-04	1.35E+00
Np-237	4.03E-07	8.40E-10	---	1.35E-10
Pm-147	2.98E-01	---	---	---
Pu-238	2.69E-02	7.01E-06	---	1.13E-05
Pu-239	1.24E-02	1.12E-06	---	1.80E-06
Pu-240	1.11E-02	7.01E-07	---	1.13E-06
Pu-241	3.41E+00	2.80E-04	---	4.51E-04
Pu-242	4.07E-05	8.40E-09	---	1.35E-08
Pu-244	2.77E-12	1.26E-15	---	2.03E-15
Ru-106	4.20E-02	---	---	---
Sb-125	4.08E+03	2.32E-02	---	4.51E-02
Se-79	1.23E-04	4.20E-09	3.93E-14	6.77E-09
Sm-151	5.40E-03	---	---	---
Sn-113	4.89E+02	---	---	---
Sn-119m	8.11E+03	---	---	---
Sn-123	2.36E+02	---	---	---
Sn-126	7.18E-05	1.26E-06	---	2.03E-06
Sr-90	5.27E-01	1.10E-03	---	1.80E-03
Ta-182	1.77E+03	---	2.55E-03	---
Tc-99	1.43E-02	2.8E-05	7.04E-09	4.51E-05
Te-125m	2.55E+03	6.45E-03	---	1.04E-02
Th-232	2.20E-16	2.66E-12	---	4.29E-12
U-232	2.06E-09	4.15E-08	---	6.77E-08
U-234	2.78E-05	---	---	---
U-235	2.06E-08	---	---	---
U-236	4.22E-05	---	---	---
U-238	2.33E-06	---	---	---
Y-90	5.27E-01	1.10E-03	---	1.80E-03
Zr-93	7.49E+02	5.59E-06	---	9.02E-06
Zr-95	6.18E+03	1.51E-02	---	4.51E-01
Total	8.00E+04	9.13E+00	2.36E-02	3.77E+01

Table 5-3. Total Projected Inventory for 643-26E NRCDA (100 Disposal Casks)

Radionuclide	Total Activation [Curies]	Total Crud [Curies]
Am-241	8.8E-01	6.3E-04
Am-242m	---	7.9E-06
Am-243	6.0E-03	5.5E-06
Ba-137m	1.3E+01	7.3E-02
C-14	3.4E+02	1.8E+00
Ce-144	1.2E+01	---
Cf-249	3.1E-10	9.2E-13
Cf-251	6.6E-12	3.7E-14
Cm-242	1.3E+01	8.8E-03
Cm-243	---	4.6E-06
Cm-244	4.8E-01	4.2E-04
Cm-245	2.6E-05	4.6E-08
Cm-246	9.8E-06	1.8E-08
Cm-247	2.0E-11	5.5E-14
Cm-248	4.7E-11	1.7E-13
Co-58	5.1E+04	4.7E+02
Co-60	2.5E+05	1.8E+02
Cr-51	1.9E+04	2.8E+01
Cs-135	8.7E-05	---
Cs-137	1.3E+01	7.3E-02
Eu-154	1.7E-01	---
Eu-155	9.6E-02	---
Fe-55	2.2E+05	3.4E+02
Fe-59	1.9E+04	2.9E+01
H-3	3.4E+02	1.6E-03
Hf-181	1.9E+04	1.1E+01
I-129	2.1E-06	7.3E-06
In-113m	1.2E+04	---
Mn-54	3.4E+03	1.5E+01
Mo-93	3.6E+00	---
Nb-93m	1.9E+04	2.7E+00
Nb-94	1.6E+01	3.7E-02
Nb-95	3.3E+05	2.5E+01
Nb-95m	3.3E+03	3.2E-03
Ni-59	3.9E+03	5.5E-01
Ni-63	4.5E+05	5.5E+01

Table 5-3. Total Projected Inventory for 643-26E NRCDA (100 Disposal Casks) - continued

Radionuclide	Total Activation [Curies]	Total Crud [Curies]
Np-237	1.0E-05	2.4E-08
Pm-147	7.5E+00	---
Pu-238	6.7E-01	4.6E-04
Pu-239	3.1E-01	7.3E-05
Pu-240	2.8E-01	4.6E-05
Pu-241	8.5E+01	1.8E-02
Pu-242	1.0E-03	5.5E-07
Pu-244	6.9E-11	8.2E-14
Ru-106	1.1E+00	---
Sb-125	1.0E+05	1.7E+00
Se-79	3.1E-03	2.7E-07
Sm-151	1.4E-01	---
Sn-113	1.2E+04	---
Sn-119m	2.0E+05	---
Sn-123	5.9E+03	---
Sn-126	1.8E-03	8.2E-05
Sr-90	1.3E+01	7.3E-02
Ta-182	4.4E+04	---
Tc-99	3.6E-01	1.8E-03
Te-125m	6.4E+04	4.2E-01
Th-232	5.5E-15	1.7E-10
U-232	5.2E-08	2.7E-06
U-234	7.0E-04	---
U-235	5.2E-07	---
U-236	1.1E-03	---
U-238	5.8E-05	---
Y-90	1.3E+01	7.3E-02
Zr-93	1.9E+04	3.7E-04
Zr-95	1.5E+05	1.2E+01

The inventory of radionuclides in the 41 components disposed in the 643-7E NRCDA is listed in Table 5-4.

5.5.3 Waste Volume

Approximately 41 NR components are disposed in casks on a gravel pad in the ELLWF (643-7E). Up to 100 NR components are to be disposed in casks on a gravel pad in the 643-26E NRCDA.

5.5.4 Packaging Criteria

No standard NR waste shipping/disposal cask exists due to the variety of waste components. The actual cask configuration, thickness, material of construction, and closure method may be tailored to the characteristics of the NR waste component at the time of disposal.

Table 5-5 shows that the planned or proposed casks for NR waste disposal are mostly composed of carbon steel or low-alloy steel and closed by a gasket or a weld. A simplified cross-section of a typical NR cask is illustrated in Figure 5-3, showing the outside dimensions of 10.5 ft in diameter and 17.7 ft in height. The thickness of the cask is based on estimated shielding requirements for a bounding CB/TS radionuclide inventory. The life expectancy and shielding capacity of the casks are determined by the specifications of the containers.

5.5.5 Pre-Disposal Treatment Methods

The offsite generator is responsible for any pre-disposal treatment methods prior to shipment to SRS.

5.5.6 Waste Acceptance Restrictions

Waste acceptance for disposal on the NRCDA must conform to criteria put forth in the SRS WAC (WSRC 2006). The PA process sets many of the criteria that are the basis for the WAC.

5.5.7 Security Classification of Wastes

Detailed descriptions of the configurations of the NR waste components are not available because of the classified nature of this information.

Table 5-4. Radionuclide Inventory for the 643-7E NRCDA

Radionuclide	Total Ci
Am-241	3.52E-01
Am-242m	8.03E-06
Am-43	2.41E-03
Ba-137m	5.28E+00
C-14	1.39E+02
Ca-45	1.34E-04
Ce-144	5.14E+00
Cf-249	1.25E-10
Cf-251	2.70E-12
Cl-36	1.80E-05
Cm-242	5.22E+00
Cm-243	7.90E-06
Cm-244	1.92E-01
Cm-245	1.02E-05
Cm-246	3.95E-06
Cm-247	7.96E-12
Cm-248	1.89E-11
Co-58	2.07E+04
Co-60	9.85E+04
Cr-51	7.47E+03
Cs-134	5.33E-02
Cs-135	3.45E-05
Cs-137	5.29E+00
Eu-154	6.72E-02
Eu-155	3.83E-02
Fe-55	9.03E+04
Fe-59	7.48E+03
H-3	1.34E+02
Hf-181	7.46E+03
I-129	1.48E-05
In-113m	4.87E+03
Kr-85	5.71E-03
Mn-54	1.39E+03
Mo-93	1.43E+00
Nb-93m	7.46E+03
Nb-94	6.54E+00
Nb-95	1.31E+05
Nb-95m	1.31E+03
Ni-59	1.55E+03
Ni-63	1.80E+05

Table 5-4. Radionuclide Inventory for the 643-7E NRCDA - continued

Radionuclide	Total Ci
Np-237	4.03E-06
Pm-147	3.05E+00
Pr-144	2.20E-01
Pu-238	2.69E-01
Pu-239	1.23E-01
Pu-240	1.11E-01
Pu-241	3.40E+01
Pu-242	4.07E-04
Pu-244	2.77E-11
Ru-106	6.60E-01
S-35	3.09E-03
Sb-125	4.07E+04
Sc-46	3.26E-03
Se-79	1.22E-03
Sm-151	5.38E-02
Sn-113	4.87E+03
Sn-119m	8.08E+04
Sn-123	2.35E+03
Sn-126	8.59E-06
Sr-90	5.39E+00
Ta-182	1.76E+04
Tc-99	1.46E-01
Te-125m	2.54E+04
Th-232	3.02E-10
U-232	4.77E-06
U-233	7.83E-07
U-234	3.64E-06
U-235	2.06E-07
U-236	4.21E-06
U-238	2.32E-05
Y-90	5.39E+00
Zn-65	1.13E+01
Zr-93	7.46E+03
Zr-95	6.16E+04

Table 5-5. Forecast of NR Waste Components for Disposal at the NRCDA (Anderson 2007)

Description:	Bettis CB/TS	Bettis HD Barrels	Bettis Head/CP	Bettis Adapter Flange	Bettis Shrouds	Bettis Pump	Bettis Barrel	KAPL CB/TS	KAPL Head
Number of Units	8	8	2	10	2	2	1	16	16
Gross Weight (lb.)	241,000	159,070	152,600	87,710	26,090	111,350	290,065	360,000	78,000
Component:									
Component Weight (lb.)	61,000	59,710	121,920	42,910	18,090	90,130	60,065	72,000	47,000
Component Volume (ft^3)	125	122	249	86	37	184	123	147	96
Component Alloy [1]	304 s.s.	Inconel	Carbon Steel	Carbon Steel	Inconel	Carbon Steel	Inconel	Inconel/ Zircaloy	Inconel clad c. Steel
Max Water (gals)	1	5	13.5	0.4	1.5	8	8	3.5	0
Cask:									
Cask Weight (lb.)	180,000	99,360	30,680	44,800	8,000	21,220	230,000	288,000	31,000
Thinnest Thickness of Cask (in) [2]	5.2	4	0	0	0	0	1.25	1.64	0
Cask Alloy	Carbon Steel	HY-80[3]	Carbon Steel	Carbon Steel	Carbon Steel	Carbon Steel	Carbon Steel	Carbon Steel	Carbon Steel
Type of Cask Closure	Full Pen Weld	Full Pen Weld	Gasket	Gasket	Gasket	Gasket	Full Pen Weld	Full Pen Weld	Gasket

Notes:
[1] Alloy shown is major alloy of construction.
[2] Zero indicates gasketed and bolted closure.
[3] HY-80 is a high yield strength (minimum of 80 ksi), low carbon, low alloy steel with nickel, molybdenum and chromium. It has excellent weldability and notch toughness along with good ductility even in welded sections.

5.6 NRCDA GROUNDWATER TRANSPORT ANALYSIS

5.6.1 Relation of Current Analysis to Previous Analyses

Disposal at the NRCDA has previously been analyzed in the 1994 and 2000 versions of the E-Area PA (MMES 1994 and McDowell-Boyer et al. 2000, respectively). In each case the conceptual model concluded that after 750 years water could enter the disposal casks via small holes corroded in the welds. The water would leach any remaining radioactivity from the crud fraction of the waste quickly. Intact activated stainless steel components, which would contain the major portion of the radioactive contamination, would begin to release contamination at a rate equal to the low corrosion rate of the steel. In the current analysis, this same conceptual model has been implemented using a combination of screening methodologies and analytical models.

5.6.2 Overview of NRCDA Groundwater Transport Analysis

The NRCDA analysis is unique in that there is an agreement between the USDOD and the SRS as to the total radionuclide inventory which can be shipped to the site for disposal. With this knowledge, an enhanced groundwater screening was performed based on NCRP methodology (NCRP 1996). A screening limit of 0.04 mrem/yr (1% of the MCL for beta-gamma emitting radionuclides) was selected. For those radionuclides whose screening limit was exceeded, a simple model using the GOLDSIM® code was used to calculate the radionuclide concentration at the 100-m well. The model assumes that the radionuclides released from the casks are directly injected into the saturated zone (i.e., the model does not represent flow and transport in the vadose zone). A plume function was then used to represent flow and transport in the saturated zone in order to determine the 100-m well concentrations versus time for each radionuclide of interest.

5.6.3 Summary of Key Groundwater Pathway Assumptions

The key assumption in the groundwater pathway analysis is that the nature of the waste materials sent to SRS for disposal on the NRCDA remains the same, i.e., activated metal components within robust casks. Specific assumptions follow:

1. Operational and Interim Closure - NR waste shipping containers / disposal casks are considered watertight requiring no operational closure measures. However, if radiation shielding is required for personnel protection during the operational or institutional control period, the NRCDA or a portion of it could be operationally closed per Section 4.2.6 of the E-Area Closure Plan (Cook et al. 2004) which allows for filling the space around, between and over the casks with structurally suitable material.
2. Final Closure - The final closure of the entire ELLWF at the end of the 100-year institutional control period will be done using the Final Closure system conceptual design and installation measures described in the E-Area Closure Plan (Cook et al. 2004).

3. Welds of material and thickness such that no less than 0.39 in. of the material remains after 500 years. A 1.25 inch weld on the representative carbon-steel container meets this minimum requirement.
4. Casks and wasteforms of material and thickness such that complete corrosion will not occur until after 9,500 years.
5. Thickness of top of waste disposal container must be at least 15.0 in. thick.
6. Thickness of sides of waste disposal container must be at least 13.8 in. thick.
7. Surface-contaminated auxiliary equipment such as pumps and closure heads may be disposed on the NR Pad without meeting the aforementioned requirements.

5.6.4 Groundwater Transport Conceptual Model

5.6.4.1 Operations and Closure Scenarios

The key assumption in the groundwater pathway analysis is that the nature of the waste materials sent to SRS for disposal at the NRCDA remains the same, i.e., activated metal components within robust casks.

The simplified conceptual model employed in this analysis applied any radionuclides released from the waste directly into the water table aquifer. No infiltration boundary condition is imposed with this approach.

5.6.4.2 Existing Inventories

Consideration of the existing inventory on the 643-26E NRCDA is not necessary in this analysis because of the long time delay until any releases are predicted to occur.

5.6.4.3 Structural Modeling Incorporation

No structural modeling has been performed on the disposal casks. The robust nature of the casks ensures structural integrity over the period of compliance.

5.6.4.4 Waste and Vadose Zone Flow and Transport

5.6.4.4.1 <u>All Radionuclides except Tritium</u>

The waste zone consists of two components, activation products and crud. The crud component is assumed to be instantaneously released when the cask is breached. The activation products component is discussed below. Its release rate is based on the corrosion rate of the steel and the radioactive decay of the radionuclides. The total projected inventory for the 643-26E NRCDA disposal unit is given in Table 5-3.

The corrosion rate is given as constant; therefore Equation 5-5-1 shows the rate of change of the activated metal volume as a constant. The rate is given as cm/yr so to convert to a volumetric rate an area must be applied. The area chosen is that of the inside cylinder of the shipping cask.

Equation 5-5-2 shows the rate of change of the number of atoms. The first term on the RHS is the rate due to radioactive decay. The second RHS term accounts for the number of atoms in the volume removed by corrosion.

$$\frac{dV}{dt} = -k \qquad \text{Equation 5-5-1}$$

$$\frac{dN}{dt} = -\lambda N - \frac{N}{V}k \qquad \text{Equation 5-5-2}$$

where N = number of atoms
λ = radioactive decay constant (1/yr)
V = volume (cm^3)
k = volumetric corrosion rate (cm^3/yr)

Equation 5-5-2 is valid for a single isotope. In this case of decay chains, a term is needed for the ingrowth of an isotope. The first term on the RHS of Equation 5-5-3 accounts for isotope ingrowth. The second and third terms are the same as in Equation 5-5-2. Therefore, for the i^{th} member of a chain

$$\frac{dN_i}{dt} = \lambda_{i-1}N_{i-1} - \lambda_i N_i - \frac{N_i}{V}k \qquad \text{Equation 5-5-3}$$

When solving for a chain, one has a set of coupled differential equations. The Aspen Custom Modeler software package (Aspentech 2004) was used to generate a source term table for each radionuclide in the chain. Aspen Custom Modeler is a powerful DAE solver which has been extensively used by the SRNL.

A time-dependant solution for a 10,000-year simulation was run. The solution of the coupled ordinary differential equations gives an activation source in Ci/yr for each radionuclide in the chain as a function of time. The maximum rate was chosen for each radionuclide, whether it be by corrosion over time or release from crud in one year, and is shown in Table 5-6.

Table 5-6. Maximum Release Rates

Radionuclide	Ci/yr
C-14	9.74E-05
I-129	1.66E-11
Mo-93	8.83E-08
Nb-93	3.44E-10
Nb-93m	5.99E-04
Nb-94	4.91E-06
Ni-59	1.22E-03
Np-237	3.15E-12
Pa-231	3.14E-14
Pu-239	9.56E-08
Pu-240	8.12E-08
Pu-242	3.15E-10
Ra-226	3.15E-10
Sn-126	4.49E-10
Tc-99	1.14E-07
Th-229	1.58E-16
Th-230	2.01E-19
Th-232	2.79E-15
U-233	9.98E-15
U-234	6.81E-18
U-235	8.51E-13
U-236	3.55E-14
U-238	4.93E-16
Zr-93	5.99E-04

5.6.4.4.2 Tritium

Tritium was considered separately from the other radionuclides as its behavior is quite different. There are two cases to consider: 1) tritium in gaseous form and 2) tritium in liquid form. If the tritium is in its liquid form, it will not be able to migrate out of the shipping cask until the cask is breached. The cask is assumed to breach at 750 years, or about 60 half-lives for the tritium. It can safely be assumed that no tritium will exist in its liquid form when the casks are breached.

In its gaseous form tritium can readily migrate through steel. An analysis was performed to assess the rate at which the tritium escapes the shipping cask. The methodology used was the same as that used to assess the tritium migration through steel in the TPBARs SA (Hiergesell 2005). The analysis showed that tritium would permeate the walls and weld of a shipping cask at a rate that would deplete the tritium in less than one year.

In adapting the Hiergesell (2005) methodology to the NR casks, the following additional key assumptions were used:

1. 340 Ci tritium total (Table 5-3)
2. 50 casks containing tritium (Section 5.5.2, 50 casks contain almost all of the tritium)
3. Cask walls and ends 13.8 in. thick (Section 5.4.1)
4. Cask free vapor volume = 20% of total interior volume (Section 5.4.1)
5. Weld is nominally 1.6 in. thick and no less than 1.25 in. thick (Section 5.4.1)

Several simple modifications were made to the methodology used in Hiergesell (2005). These modifications were made to address the different geometry of the NR shipping cask from the TPBAR shipping cask.

Steady-state permeation rates of 24 Ci/yr and 4 Ci/yr for the cask walls and welds respectively were calculated. As each cask contains 6.8 Ci of tritium it can be safely assumed that the tritium will not be a significant source to the groundwater.

5.6.4.5 Saturated Zone Flow and Transport

With its known final inventory of radionuclides, an enhanced groundwater screening was run. All 826 radionuclides in NCRP 1996 were used. A starting inventory of 10,000,000 Ci for each of the 826 radionuclides considered in the NCRP screening methodology (NCRP 1996) was used. If 10,000,000 Ci resulted in a screening dose of less than 0.04 mrem/yr for the groundwater pathway, it was then assumed that the inventories shown in Table 5-2, all of which are considerably less than 10,000,000 Ci, would not exceed the screening limit. Table 5-7 shows those radionuclides that produced a calculated dose exceeding 0.04 mrem/yr with the projected inventory shown in Table 5-2. The radionuclides shown in Table 5-7 were subjected to more rigorous analysis described in Section 5.6.5.

For those radionuclides that exceeded the screening criterion, the next step in their assessment was determining a source term. The crud radionuclides were considered to be released instantaneously. The activation radionuclides were released at the corrosion rate. Additional detail is provided below. A source term, in Ci/yr, and its implied dose, was then compared to the Curies required to exceed the screening criterion.

If the dose still exceeded the screening criterion, then a simple transport model was employed. For this simple model, it was assumed that the entire inventory of a radionuclide was instantaneously dumped into the aquifer. The GOLDSIM® code was used to estimate the concentration at the 100-m point of compliance for each radionuclide for which the dose exceeded the screening criterion. Specifically, the GOLDSIM® Pipe Pathway application and *Plume function* were used in estimating the 100-m concentrations (GTG 2005). The model included retardation and radioactive decay with generation of progeny.

The Pipe Pathway application of GOLDSIM® uses a Laplace transform approach to provide analytical solutions to advectively-dominated transport processes involving one-dimensional advection, longitudinal dispersion (and diffusion), retardation, and decay and ingrowth. The pathway is defined by specifying a length, cross-sectional area, and perimeter of a fluid conduit, which is applied to an aquifer simulation by specifying the porosity. Mass enters at one end, advects, disperses, diffuses, decays and partitions within the mobile zone of the Pipe, and then exits the other end. The flow rate was specified for Pipe pathway by choosing a representative velocity in the flow field from the GSA groundwater model, in the vicinity of the 643-26E NRCDA. The mass (or source) is introduced in the pipe as an initial condition (i.e., when the entire inventory of radionuclides is assumed to be dumped into the aquifer).

Concentration at the output of the designated Pipe is computed in the Pipe Pathway application of GOLDSIM®. However, use of the *Plume function* in this code returns a correction factor, taking into account horizontal and vertical dispersivity, the size of the source, and other aspects of the aquifer geometry, which can be multiplied by the Pipe's concentration output in order to compute the concentration at an observation point 100-m from the specified source. A diagram of the plume function from the GOLDSIM® user's manual is reproduced in Figure 5-5. The resulting correction factor derived from this function was then used to estimate the concentration 100 m downgradient of the source.

The centerline of the plume was chosen as the sampling point as it is assumed this is where the maximum concentration occurs. GOLDSIM® assumes an average, i.e., flat, concentration profile across the face of a cell (or pipe). The plume function accounts for a more realistic shape. In fact, the plume function can give higher concentrations at the plume centerline than the cell calculated average concentration. That is the case in this analysis.

Stochastic elements were used to provide reasonable assurance that the resulting concentrations were below applicable limits. Stochastic elements were used for dispersion factors used in the plume function, distribution coefficients, aquifer cross-sectional area, aquifer velocity, soil porosity, and time of weld breakthrough.

The following diagram illustrates the various input arguments required by the Plume function.

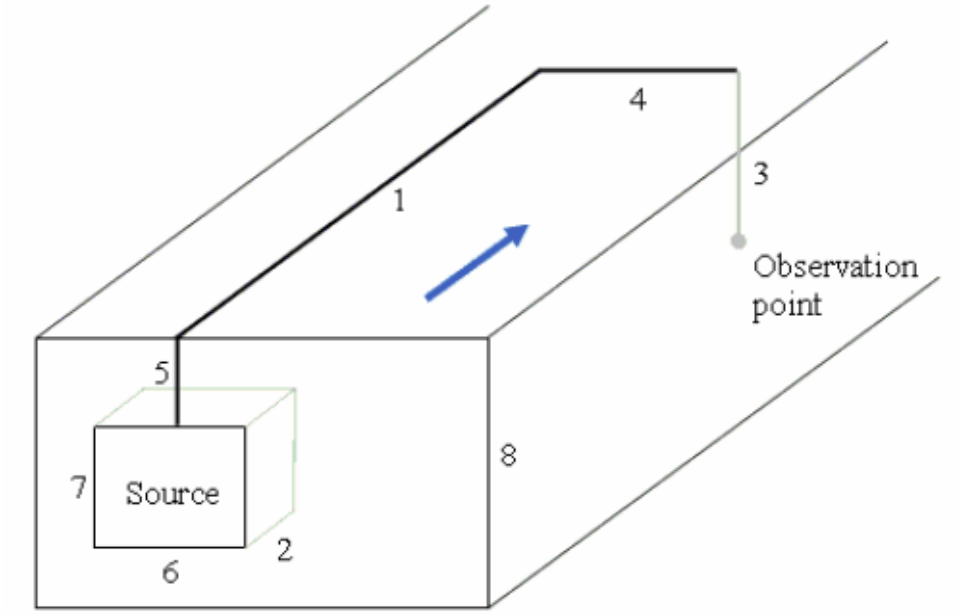

The arguments are as follows (the numbers reference lengths in the figure above):

- Pipe Length (1)
- Pipe cross-sectional Area
- Source Length (2)
- Depth (vertical distance) from the ground surface (or top of the flowing zone) to the observation point (3)
- Horizontal (transverse) distance from the source center to the observation point (4)
- Depth of the top of the source (5)
- Width of the source (6)
- Vertical thickness of the source (7)
- Total thickness of the aquifer or river being simulated (8)
- Horizontal dispersivity
- Vertical dispersivity

Figure 5-5. The Plume Function from the GOLDSIM® Model (from GTG 2005)

Table 5-7. Screening Dose for Radionuclides Not Screened Out

Radionuclide	Total NRCDA Activation Inventory (Ci)	Total NRCDA Crud Inventory (Ci)	Ci to give 0.04 mrem/yr
Am-243	6.0E-3	5.5E-6	4.26E-4
C-14	3.4E2	1.8E0	7.37E-5
I-129	2.1E-6	7.3E-6	1.21E-7
Mo-93	3.6E0	-	4.80E-4
Nb-94	1.6E1	3.7E-2	1.59E-3
Ni-59	3.9E3	5.5E-1	1.27E-1
Np-237	1.0E-5	2.4E-8	1.53E-7
Pu-239	3.1E-1	7.3E-5	1.24E-5
Pu-240	2.8E-1	4.6E-5	2.22E-5
Pu-242	1.0E-3	5.5E-7	1.07E-5
Se-79	3.1E-3	2.7E-7	1.89E-3
Sn-126	1.8E-3	8.2E-5	3.54E-4
Tc-99	3.6E-1	1.8E-3	1.58E-5
U-234	7.0E-4	-	5.15E-4
U-235	5.2E-7	-	2.52E-4
U-236	1.1E-3	-	5.62E-4
U-238	5.8E-5		4.81E-4
Zr-93	1.9E4	3.7E-4	2.29E-2

5.6.5 Groundwater Pathway Deterministic Model Description

5.6.5.1 Use of 643-26E NRCDA Groundwater Model to simulate the 643-7E NRCDA

The groundwater flow and transport model discussed above was developed to simulate the release of radionuclides from the 643-26E NRCDA and their transport to the 100-m well. This model assumes that the waste is a combination of crud and activated metal as discussed above. It also assumes that the waste is contained in a durable steel container. The groundwater model assumes that radionuclides released from the disposal container are immediately transported to the saturated zone and concentrations at the downgradient 100-m well location are estimated using the GOLDSIM® Plume function described in Section 5.6.4.5.

To use the results of the 643-26E NRCDA model to represent the 643-7E NRCDA, the important elements of the analysis must be shown to be the same as, or no worse than, the conditions at the 643-7E NRCDA. These elements are discussed below.

Waste Type

The types of waste, both irradiated metal and crud, in the components stored at the 643-7E NRCDA are the same as those in the 643-26E NRCDA and the ratio of the irradiated metal and crud is the same (KAPL 2004).

Waste Containers
The waste containers for the components stored at the 643-7E NRCDA are bounded by the representative container (i.e., provide at least the same degree of confinement) analyzed in the 643-26E NRCDA analysis (KAPL 2004).

Hydrology
The hydrologic regime of the 643-7E NRCDA was compared with that of the 643-26E NRCDA using the GSA groundwater model (Flach 2004). The results are shown in Table 5-8.

Table 5-8. NRCDA Hydrologic Regime

	NRCDA Location	
Parameter	**643-7E**	**643-26E**
Ground elevation	291 ft[a]	274 ft[a]
Water table elevation	237 ft[a]	214 ft[a]
Depth to water table	54 ft	60 ft
Unsaturated zone travel time to water table	12 years[b]	13 years[c]
Saturated zone travel time to 100-m well (Figure 5-6)	20 years[a]	2 years[a]
Total travel time	32 years	15 years

a. From Flach (2004)
b. Calculated from unsaturated zone travel time for 643-26E NRCDA and difference in depth to groundwater
c. From McDowell-Boyer et al. 2000

Although the depth to the water table is about 10% less at the 643-7E NRCDA than at the 643-26E NRCDA, the total travel time to the 100-m compliance point, which is the most important element of the disposal unit hydrology, is approximately twice as long for the 643-7E NRCDA than for the 643-26E NRCDA. The difference in saturated zone travel time is shown in Figure 5-6. This difference is explained by the position of the two disposal units relative to a groundwater divide between Upper Three Runs and Fourmile Branch (see Background chapter Part C Section 3.1.5 for a general discussion of the hydrology in E Area). The 643-7E NRCDA is located near the divide, where the horizontal hydraulic head gradient is small. Hence, lateral groundwater movement away from this location is slow. In contrast, the 643-26E NRCDA is located midway between the groundwater divide and Upper Three Runs where the horizontal hydraulic head gradients and groundwater velocities are relatively large.

The longer travel time for the 643-7E NRCDA makes the analysis for the 643-26E NRCDA obviously conservative when applied to the 643-7E NRCDA for radionuclides without significant (i.e., in terms of PA impact) long-lived daughters. Since the travel time for the 643-7E NRCDA is longer than that in the analysis, it will take radionuclides longer to reach the 100-m compliance well; therefore, more of the radionuclide will actually decay than is shown in the analysis. Thus, the concentration in the 100-m well would be less than stated in the analysis and the 643-26E NRCDA analysis is conservative for the 643-7E NRCDA.

However, for radionuclides with longer-lived daughters that could potentially impact the PA performance measures, the short travel time used in the analysis may not be conservative when applied to the 643-7E NRCDA. For example, a parent radionuclide with a significant long-lived daughter, when represented with the shorter, 15-year travel time, might migrate past the point of compliance before producing a significant amount of the daughter. If the longer, 32-year travel time had been used, enough of the daughter to significantly impact the calculated disposal limit might have been produced. In the 643-26E analysis, however, the disposal containers delay the release of radionuclides for 750 years. During this delay time, the radioactive daughters are building up prior to the release from the disposal container. This delay and the fact that the difference in travel times is small (approximately a factor of two) should mitigate the potential non-conservatism in using the shorter travel time to represent the 643-7E NRCDA.

Since the waste on the 643-7E NRCDA is the same as that analyzed in the 643-26E NRCDA, the waste containers on the 643-7E NRCDA are bounded by the assumptions in the 643-26E NRCDA analysis. In addition, the hydrology at the 643-7E NRCDA is more favorable than that at the 643-26E NRCDA, thereby also making the 643-26E NRCDA analysis a bounding analysis for the 643-7E NRCDA.

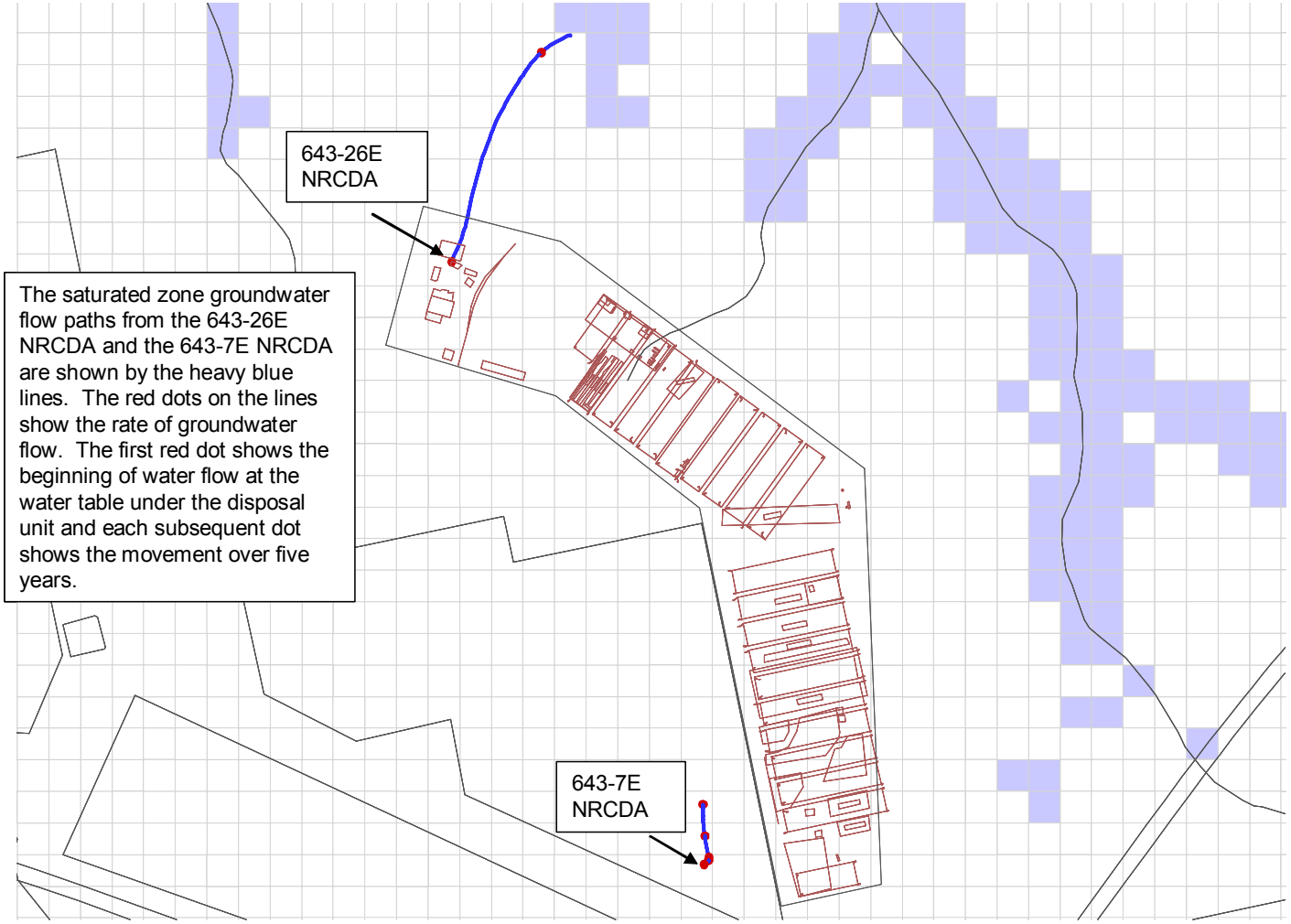

Figure 5-6. Saturated Zone Groundwater Travel Times – 5-Year Markers to 20 Years

5.6.5.2 Groundwater Protection

The maximum groundwater concentrations from the two NRCDAs over the 1,000-year post closure compliance period were compared with MCLs (EPA 2004) using the all-pathways application (Koffman 2006a). Table 5-9 and Table 5-10 show the results.

Table 5-9. Groundwater Protection Impacts from the 643-26E NRCDA

Radionuclide	Beta-Gamma mrem/yr	Gross Alpha pCi/L	Radium pCi/L	Uranium µg/L
C-14	1.05E-01	0	0	0
I-129	2.50E-03	0	0	0
Nb-94	4.15E-02	0	0	0
Ni-59	1.62E-01	0	0	0
Pu-239	1.92E-10	1.04E-07	0	1.14E-23
Pu-240	4.48E-24	7.84E-21	4.23E-24	5.19E-22
Tc-99	2.34E-03	0	0	0
Total	3.13E-01	1.04E-07	4.23E-24	5.30E-22
MCL	4	15	5	30
Total as fraction of MCL*	7.82E-02	6.92E-09	8.46E-25	1.77E-23

* Assuming the maximum impact for each radionuclide occurs at the same time

Table 5-10. Groundwater Protection Impacts from the 643-7E NRCDA

Radionuclide	Beta-Gamma mrem/yr	Gross Alpha pCi/L	Radium pCi/L	Uranium µg/L
C-14	4.27E-02	0	0	0
I-129	3.93E-03	0	0	0
Nb-94	1.69E-02	0	0	0
Ni-59	6.43E-02	0	0	0
Pu-239	7.63E-11	4.12E-08	0	4.51E-24
Pu-240	1.77E-24	3.11E-21	1.68E-24	2.06E-22
Tc-99	9.45E-04	0	0	0
Total	1.29E-01	4.12E-08	1.68E-24	2.10E-22
MCL	4	15	5	30
Total as fraction of MCL*	3.22E-02	2.75E-09	3.35E-25	7.00E-24

* Assuming the maximum impact for each radionuclide occurs at the same time

The results of the groundwater protection analysis are low compared to the MCLs. For the 643-23E NRCDA, the total beta-gamma dose (assuming that the maximum dose for each radionuclide occurs at the same time) is approximately eight percent of the MCL, the total gross alpha concentration is more than eight orders of magnitude less than the MCL and the total radium and uranium concentrations are more than 20 orders of magnitude less than the MCL.

For the 643-7E NRCDA, the total beta-gamma dose (assuming that the maximum dose for each radionuclide occurs at the same time) is approximately three percent of the MCL, the total gross alpha concentration is approximately nine orders of magnitude less than the MCL and the total radium and uranium concentrations are more than 20 orders of magnitude less than the MCL.

Radionuclide disposal limits for the NRCDA were developed from the results shown. These limits are presented as preliminary because they are derived without considering the sensitivity and uncertainty analyses results. Limits will be adjusted as needed to account for these results, and final limits will be presented in chapter 7, Integration and Interpretation. The preliminary limits are shown in Table 5-11.

Table 5-11. Preliminary Groundwater Protection Radionuclide Disposal Limits for the NRCDA

	Disposal Limit, Ci/Pad			
Radionuclide	**Beta-Gamma**	**Gross Alpha**	**Radium**	**Uranium**
C-14	1.3E+04	>1.00E+20	>1.00E+20	>1.00E+20
I-129	1.5E-02	>1.00E+20	>1.00E+20	>1.00E+20
Nb-94	1.6E+03	>1.00E+20	>1.00E+20	>1.00E+20
Ni-59	9.7E+04	>1.00E+20	>1.00E+20	>1.00E+20
Pu-239	6.5E+09	4.5E+07	>1.00E+20	>1.00E+20
Pu-240	>1.00E+20	>1.00E+20	>1.00E+20	>1.00E+20
Tc-99	6.2E+02	>1.00E+20	>1.00E+20	>1.00E+20

5.6.6 Groundwater Pathway Sensitivity Analysis

A multivariate sensitivity analysis was performed on the groundwater pathway model using the GoldSim platform. The sensitivity of the total dose with respect to each of the parameters with a stochastic distribution was determined. The Pearson correlation coefficients and the Importance Measures found are given in Table 5-12. The Pearson correlation coefficient varies between -1 and 1 and is an expression of the extent to which there is a linear relationship between the total dose and each variable. The Importance Measure varies between 0 and 1 and represents the fraction of the overall variance in the total dose that is explained by each variable. This measure is useful in identifying non-linear, non-monotonic relationships between an input variable and the result which the Pearson correlation coefficients may not reveal. The results in Table 5-12 have been sorted by descending Importance Measure.

Table 5-12. Results of Sensitivity Analysis

Variable	Correlation Coefficient	Importance Measure
Time of Through-Weld Failure	-0.369	0.163
Aquifer Cross-Sectional Area	-0.343	0.116
Soil Porosity	-0.017	0.044
Tc K_d	-0.112	0.039
Transverse to Lateral Dispersivity Ratio	-0.028	0.027
Aquifer Velocity	0.066	0.026
I K_d	0.008	0.022
Pu Sandy Soil K_d	-0.007	0.021
Lateral Dispersivity	-0.078	0.017
C K_d	0.027	0.009
Zr K_d	0	0.007
Pu Soil K_d	0.059	0.001
Nb K_d	0	0
Ni K_d	0.029	0

The results in Table 5-12 show that the time of failure for the welds and the size of the aquifer cross section used in the model are clearly the parameters to which the total dose is most sensitive.

5.6.7 Groundwater Pathway Uncertainty Analysis for the NRCDAs

5.6.7.1 Introduction

Many of the features, events, and processes that control the behavior of contaminant transport are not known or understood with certainty. The uncertainties can be considered to be of four types, parameter uncertainty, uncertainty regarding future events, conceptual model uncertainty, and numerical uncertainty. Incorporating these uncertainties into the predictions of system behavior is called probabilistic performance assessment. Probabilistic analysis consists of explicitly representing the uncertainty in the parameters, process, and events and propagating those uncertainties through the system such that the uncertainty in the results (i.e., predicted future performance) can be quantified. This type of analysis produces results in terms of a distribution of values. As the uncertainty in the input parameters is decreased with increasing knowledge of the overall system, the uncertainty in results also decreases.

The uncertainty analysis for the NRCDAs is limited to those radionuclides that failed to screen out in the groundwater analysis. Those radionuclides are C-14, I-129, Nb-94, Ni-59, Pu-239, Pu-240, and Tc-99. The GOLDSIM® model that was used to produce the deterministic results is identical to that used to produce the stochastic results. For the deterministic analysis, mean values were chosen for appropriate parameters. For the stochastic analysis, a Monte Carlo simulation was run where the parameters were varied about the mean. The simulation consisted of 500 realizations.

5.6.7.2 Parametric Variations for Uncertainty Analysis

Table 5-13 shows the parameters that were varied for the uncertainty analysis. The parameters with the major effect on the calculation are the aquifer K_ds, the aquifer area, and the aquifer velocity. The model assumes that the radionuclides released from the casks are directly injected into the aquifer (i.e., the model does not simulate flow and transport in the vadose zone); therefore, these are the only parameters that will affect the aquifer flow and transport in the model. The time of weld breakthrough will affect the time at which the radionuclides are released to the environment along with the length of time they decay in-place.

Table 5-13. Parameters Varied

Parameter	Distribution	Range
K_d	Normal if K_d<1,000 ml/g	Factor of 2 about the mean*
K_d	Log-normal if $K_d \geq$1,000 ml/g	Factor of 10 about the mean*
Aquifer area	Normal	9,500-10,500 m^2
Aquifer velocity	Uniform	2-6 ft/yr
Time of weld breakthrough	Uniform	600-900 yrs

* from Kaplan and Millings (2006)

5.6.7.3 Uncertainty Analysis

The radionuclides in the crud and corrosion products in the shipping casks are released at the time of weld break through. The crud is released as an instantaneous source and the corrosion products are released at a constant rate, based on the corrosion rate of the metal waste form.

Figure 5-7 shows the uncertainty in total dose (i.e., dose from direct ingestion of groundwater plus dose from use of groundwater for irrigation for all of the radionuclides that did not screen out).

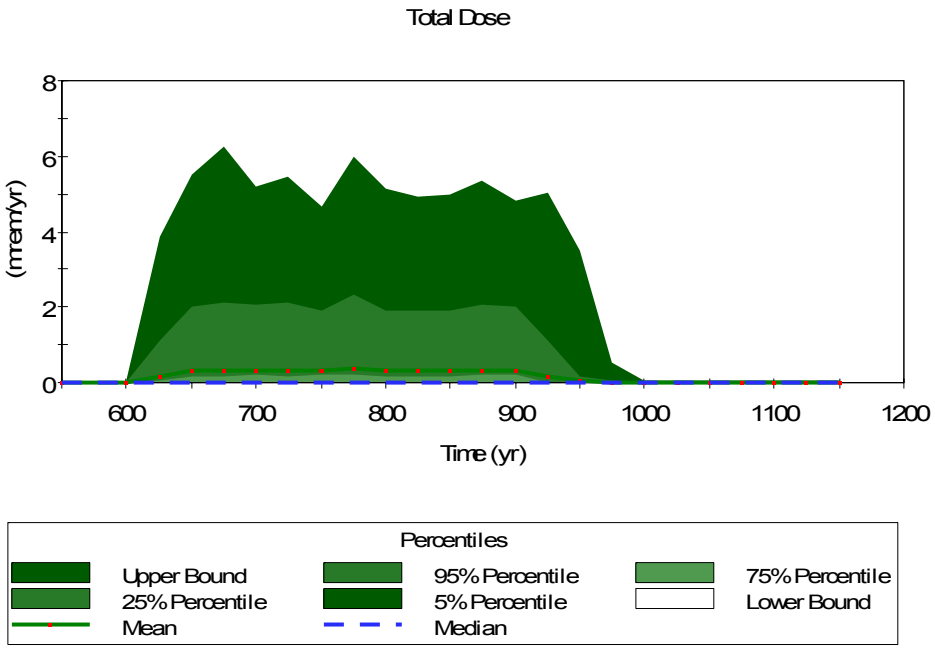

Figure 5-7. Total Dose

The mean dose is approximately 0.5 mrem/year, which is approximately 2 percent of the 25 mrem/year all-pathways limit. This is about one half of the deterministic all-pathways dose (see Section 5.8), which reflects the conservative selection of some parameter values in the deterministic analysis. The 95th percentile interval dose is approximately 2.4 mrem/year and the upper bound dose is approximately 6.2 mrem/year. These results show that there is great confidence in the all-pathways dose limit not being exceeded due to disposal of the NR components.

Figure 5-8 shows the two major contributors to the crud dose (C-14 and Nb-94), which is the dominant portion of the dose from the NRCDAs.

5.7 AIR-PATHWAY ANALYSIS

5.7.1 Overview of Air-Pathway Analysis

This section describes the investigation conducted to evaluate the potential magnitude of gaseous release of radionuclides from the NRCDAs over the 25-year operational period, 100-year institutional control period, and 1,000-year post-closure compliance period versus the atmospheric pathway performance objective of 10 mrem/yr to a representative member of the public (DOE 1999). During the 25-year operational period and 100-year institutional control period this performance objective is applicable at the SRS boundary, due to active institutional controls. During the 1000-year post-closure compliance period the performance objective is applicable at 100 m from the disposal unit boundary, due to the assumed loss of active institutional controls.

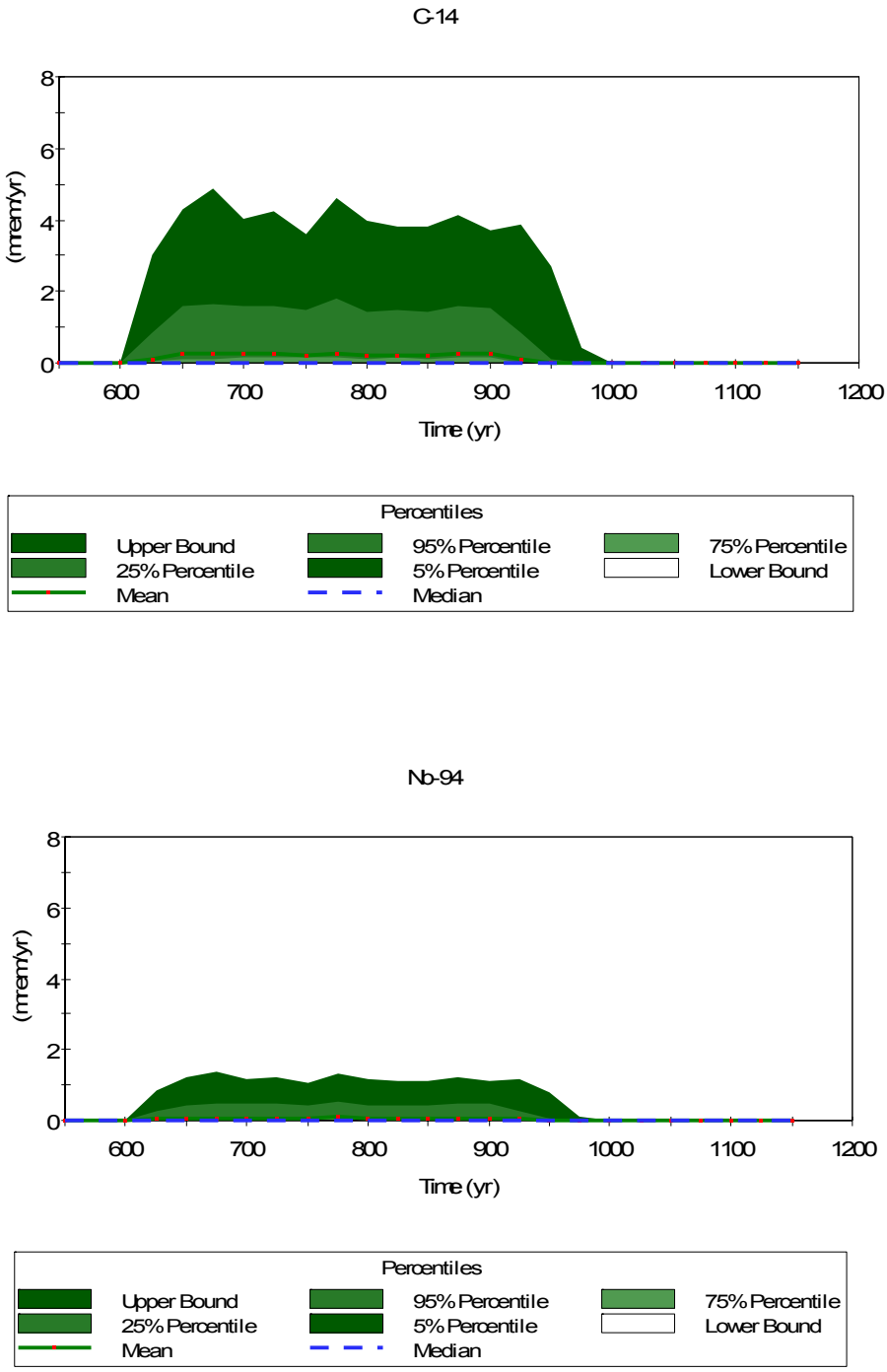

Figure 5-8. Major Crud Dose Contributors

These above-grade gravel pads are used as the disposal location for NR Waste Shipping/Disposal Casks, which are assumed to remain water and air-tight to all gases except for tritium for a period of 750 years. Therefore, gaseous flux of all gases except for tritium from the NRCDAs does not occur during the 25-year operational or 100-year institutional control periods, but only during the 1,000-year post-closure compliance period, after the casks have been breached. However tritium, which readily diffuses through carbon steel, is assumed to be entirely released from the casks over a 1-year time frame prior to the end of the 100-year institutional control period.

A screening analysis was conducted to produce a list of radionuclides requiring a more thorough analysis to derive disposal limits for the NRCDAs based on the atmospheric pathway. This study, described in Crapse and Cook (2006) used a methodology developed by the NCRP (NCRP 1996), professional judgment, and process knowledge to determine this list.

The list of potential radionuclides includes C-14, Cl-36, H-3, I-129, S-35, Sb-124, Sb-125, Se-75, Se-79, Sn-113, Sn-119m, Sn-121, Sn-121m, Sn-123, and Sn-126. This analysis considers the following two cases:

- Diffusion of tritium through the casks over a 1-year time frame and subsequent transport to the SRS boundary.
- Diffusion of the other radionuclides upward from the NRCDAs through the overlying soil material (anticipated closure cap) and subsequent transport 100 m from the disposal unit boundary.

The analysis presented here uses accepted computer programs for diffusion (PORFLOW) [ACRI 2004] and atmospheric transport and dose calculations (CAP88) (Beres 1990).

5.7.2 Summary of Key Air-Pathway Assumptions

Key assumptions and inputs used in the air-pathway analysis are presented in Appendix B.

5.7.3 NRCDA Closure Considerations

The concepts for closure of the NRCDAs are relevant to the determination of the gaseous flux at the land surface for all gaseous radionuclides except for tritium. The NRCDAs construction specifics and closure concept are described by Phifer et al. (2006). For the purposes of this investigation, it is assumed that the flux of these gaseous radionuclides only occurs during the 1,000-year post-closure compliance period, after the casks have been breached. The final closure cap will exist during the 1000-year post-closure compliance period and is the configuration that must be considered in evaluating the long-term gaseous release at the land surface. A conceptual drawing of the closure cap over the NR casks is shown in Figure 5-4 and the vertical section over which gaseous radionuclide diffusion was evaluated is indicated.

The closure configuration utilized in this analysis includes all materials, as constructed, including the final closure cap placed over NRCDAs at the end of the 100-year institutional control period. The components of concern for the long-term air-pathway performance calculation are those that have no potential to erode during the 1,000-year post-closure compliance period. These components are situated below the top of the erosion barrier. The composite thickness of the non-waste material below the top of the erosion barrier is 76 inches. Table 5-14 lists the individual components of the NRCDA closure cap (excluding the layers overlying the erosion control barrier).

Table 5-14. Vertical Layer Sequence and Associated Thickness for NRCDA Cover Material

Layer	Thickness (inches)
Erosion barrier	12
Middle backfill layer	12
Gravel drainage layer	12
Lower backfill layer	40
Stainless Steel Top	14
Waste Layer	184

SOURCE: Adapted from Phifer et al. (2006)

5.7.4 NRCDA Air-Pathway Conceptual Model

All tritium within the casks is assumed to diffuse through the casks over a 1-year time frame and be subsequently transported to the SRS boundary prior to the end of the 100-year institutional control period.

The flux of the other radioactive gasses at the land surface above the NRCDAs was evaluated for its specific closure configuration. Gaseous radionuclides introduced within the waste zone diffuse outward from this zone into the air-filled soil pores surrounding the pads, eventually resulting in some of the radionuclides emanating at the land surface. As such, air is the medium through which they diffuse. It is assumed that fluctuations in atmospheric pressure at the land surface that could induce small pulses of air movement into and out of the shallow soil profile over relatively short periods of time will have a zero net effect when averaged over longer time periods. Thus, advective transport of these radionuclides in air-filled soil pores is not considered to be a significant process when compared to the rate of air diffusion.

The radionuclides present as gasses are those identified in the screening process described in Crapse and Cook (2006). Certain gaseous radionuclides will not likely remain in the monatomic elemental form but combine with other gaseous elements or form diatomic molecules. The state of existence of each of these radionuclides in the gaseous phase is important in evaluating their transport to the land surface because the diffusion coefficient associated with each is related to its molecular weight.

In this investigation it is assumed that:

- C-14 exists as part of the CO_2 molecule
- Cl-36, H-3 and I-129 exist as diatomic gasses
- S-35, Sb-124, Sb-125, Se-75, Se-79, Sn-113, Sn-119m, Sn-121, Sn-121m, Sn-123, and Sn-126 exist as monatomic gasses.

5.7.5 NRCDA Air-Pathway Numerical Model

The mathematical model utilized in this report is provided by the PORFLOW (ACRI 2004) simulation package. PC-based PORFLOW Version 5.97.0 was used to conduct a series of simulations. PORFLOW is developed and marketed by Analytic & Computational Research, Inc. to solve problems involving transient and steady-state fluid flow, heat and mass transport in multi-phase, variably saturated, porous or fractured media with dynamic phase change. PORFLOW has been widely used at the SRS and in the DOE complex to address major issues related to the groundwater and nuclear waste management.

The governing equation for mass transport of species *k* in the fluid phase is given by

$$\frac{\partial C_k}{\partial t} + \frac{\partial}{\partial x_i}(V_i C_k) = \frac{\partial}{\partial x_i}(D_{ij}\frac{\partial C_k}{\partial x_j}) + \gamma_k \qquad \text{Equation 5-4}$$

Where

C_k	concentration of species *k*, Ci/m^3
V_i	fluid velocity in the i^{th} direction, m/yr
D_{ij}	effective diffusion coefficient for the species, m^2/yr
γ_k	net decay of species *k*, Ci/m^3 yr
i, j	direction index
t	time, yr
x	distance coordinate, m

This equation is solved within PORFLOW to evaluate transient radionuclide transport through the soil cover above NRCDAs and to determine gaseous radionuclide flux at the land surface over time. Since source radionuclides exist as gases, air was taken to be the medium within which transport occurs. The flow field was assumed to be isobaric and isothermal. The impact of naturally occurring fluctuations in atmospheric pressure at the land surface that could induce small pulses of air movement into and out of the shallow soil profile over relatively short periods of time will have a zero net effect when averaged over longer time periods. Therefore, for the relatively long periods of time evaluated in this investigation, air diffusion was the only transport mechanism simulated in the model and advective air-transport was assumed to be negligible, so the advection term was disabled within PORFLOW and only the diffusive and net decay terms were evaluated.

5.7.5.1 NRCDA Air-Pathway Model Development and Assumptions

The numerical representation of the conceptual model is as a 1-dimensional vertical stack of elements configured to represent the thickness of the NR Waste Shipping/Disposal Casks and overlying cover material associated with final closure. This conceptual model is equally valid for both the 643-26E and the 643-7E NRCDAs

The radionuclides evaluated are C-14, Cl-36, H-3, I-129, S-35, Sb-124, Sb-125, Se-75, Se-79, Sn-113, Sn-119m, Sn-121, Sn-121m, Sn-123, and Sn-126.

Since source radionuclides exist as gases, air was taken to be the medium within which transport occurs. The flow field was assumed to be isobaric and isothermal. The impact of naturally occurring fluctuations in atmospheric pressure at the land surface that could induce small pulses of air movement into and out of the shallow soil profile over relatively short periods of time will have a zero net effect when averaged over longer time periods. Therefore, for the relatively long periods of time evaluated in this investigation, air diffusion was the only transport mechanism simulated in the model and advective air transport was assumed to be negligible.

A small percentage of the radionuclides dissolve in residual pore water, but since diffusion proceeds more slowly in water than in air, air diffusion is regarded as the only transport process by which they can reach the land surface from the NRCDA waste zone. This assertion is substantiated in Yu et al. (2001). In that report the radon effective diffusion coefficient, D_{eff}, for soil is reported to range from the open-air diffusion coefficient of 1.0E-05 m^2/s to that of fully saturated soil, 1.0E-09 m^2/s.

This four order of magnitude difference is consistent with the comparison of water diffusion coefficients to air diffusion coefficients of other common molecular compounds and reported in many references; for example see Tables 5-45 and 5-47 in Bolz and Tuve (1973). Thus, the larger volume of water-filled pore space compared to air-filled pore space (maximum of 2 orders of magnitude difference) is inconsequential. The ability of water-dissolved compounds to diffuse through water-filled pores is negligible compared to the ability of the same compounds to diffuse as gas in the vapor-filled pore spaces.

Furthermore, there is vertical downward movement of the pore water which acts to offset or overcome any vertical upward diffusion of dissolved constituents. Consequently, in this investigation radionuclide transport was allowed to proceed only through air-filled pore space and, therefore, residual pore water was treated as if it was part of the solid matrix material within the flow field. No accounting was made of the partitioning of the gaseous radionuclides into the pore water as diffusive vapor transport proceeded from the waste zone to the land surface. By ignoring this mechanism, diffusive fluxes at the land surface were slightly overestimated.

The boundary conditions imposed on the model domain included:

- No-flux specified for all radionuclides along sides and bottom
  ($\partial C/\partial X = 0$ at x=0, x=1 and $\partial C/\partial Y = 0$ at y=0)
- Species concentration set to 0 at land surface (top of erosion barrier)
  ($C = 0$ at $y=y_{max}$)

The initial condition imposed on the domain included:

- Species concentration set to 0 for the entire model domain at time = 0
  ($C=0$ for $0 \leq x \leq 1$ at t=0 and $C=0$ for $0 \leq y \leq y_{max}$ at t=0)

The initial conditions for the model also assumed a 1 Ci inventory of each radionuclide uniformly spread over the waste zone.

These boundary conditions force all of the gaseous radionuclides to move upward from the waste disposal zone to the land surface. In reality, some lateral and downward diffusion occurs in the air-filled pores surrounding the waste zone; hence ignoring this lateral and downward movement has the effect of increasing the flux at the land surface. This should introduce some conservatism in the calculated results. Simulations were conducted in transient mode for diffusive transport in air, with results being obtained over 1,125 years.

A summary of the radionuclides and compounds of interest in this investigation are summarized in Table 5-15.

5.7.5.2 Measures Implemented to Ensure Conservative Results

In this analysis, several conditions introduce a significant measure of conservatism into the calculations. These include:

- The use of boundary conditions that force all of the gaseous radionuclides to move upward from the waste disposal zone to the land surface. In reality, some of the gaseous radionuclides diffuse sideways and downward in the air-filled pores surrounding the waste zone; hence ignoring this has the effect of increasing the gaseous radionuclide flux at the land surface.
- Not taking credit for the removal of the gaseous radionuclides by pore water moving vertically downward through the model domain once the cask is breached. This mechanism would likely remove some dissolved gaseous radionuclides, and therefore its omission has the effect of increasing the estimate of instantaneous gaseous radionuclide flux at the land surface in simulations conducted as a part of this investigation.

Use of the top of the erosion layer in the soil cover as the land surface for the purpose of calculating gaseous radionuclide flux. No credit is taken for the additional distance the gaseous radionuclides must migrate above the erosion layer prior to that portion of the Soil Cover Zone eroding away.

Table 5-15. Radionuclides and Compounds of Interest

Radionuclide	Half-life (yrs)	Approximate Atomic Weight	Molecular form in gaseous state	Molecular Weight
C-14	5.730E+03	14	CO_2	46
Cl-36	3.010E+05	36	Cl_2	72
I-129	1.570E+07	129	I_2	258
Rn-222[1]	1.047E-02	222	Rn	222
S-35	2.394E-01	35	S	35
Sb-124	1.649E-01	124	Sb	124
Sb-125	2.759E+00	125	Sb	125
Se-75	3.270E-01	75	Se	75
Se-79	2.950E+05	79	Se	79
Sn-113	3.153E-01	113	Sn	113
Sn-119m	8.020E-01	119	Sn	119
Sn-121	3.089E-03	121	Sn	121
Sn-121m	44.10E+00	121	Sn	121
Sn-123	3.550E-01	123	Sn	123
Sn-126	2.300E+05	126	Sn	126

[1] Rn-222 molecular weight is needed to compute diffusion coefficients using Equation 5-5.

5.7.5.3 Grid Construction

The model grid was constructed as a node mesh 3 nodes wide by 42 nodes high. This mesh creates the vertical stack of 40 model elements. Figure 5-9 shows a schematic of the PORFLOW model grid. The grid extends upward only as far as the erosion barrier, since this is the minimum possible cover thickness that could exist during the 1,125-year evaluation period. A set of consistent units was employed in the simulations for length, mass and time, consisting of meters, grams, and years, respectively.

5.7.5.4 Material Zones

The model domain was divided into two primary zones, the NRCDA waste zone occupying the lower 15.3 ft of the domain and the cover zone (including the cask top), extending ~7.5 ft. above the waste zone to the top of the domain. The cover zone includes the cask top as well as the different closure cap layers. The upper model elements were scaled to correspond to the geometry of the closure cap thickness while the lower model elements were scaled to correspond to the NRCDA waste zone. The land surface for the evaluation period of interest is assumed to be the top of the erosion resistant layer, within the closure cap, and no credit is taken for the compacted soil and topsoil above that layer.

5.7.5.5 Material Zone Properties and Other Input Parameters

Material properties utilized within the 1-D numerical model were specified for 6 material zones defined within the model domain. Each material zone was assigned values of particle density, total porosity, average saturation, air-filled porosity, air density, and an effective air diffusion coefficient for each source element or compound. With the use of an effective air diffusion coefficient, tortuosity was assigned a unit value in each material zone. An air fluid density of 1.24E+03 g/m^3 was used. This air fluid density was obtained from Bolz and Tuve (1973) and represents that of standard atmospheric conditions.

The total porosity for the NRCDA waste zone was taken to be 0.2. It was assumed that the waste was dry and that the air-filled porosity would equal the total porosity for this zone. For the cask top, the steel was assumed to have a total porosity of 0.0 for the first 750 years of the simulation. This essentially prevents any transport from the cask during this time period. At 750 years, the steel is reassigned a porosity of 0.2 to represent pitting thereby allowing flux from the cask over the remaining 375 years of the simulation period.

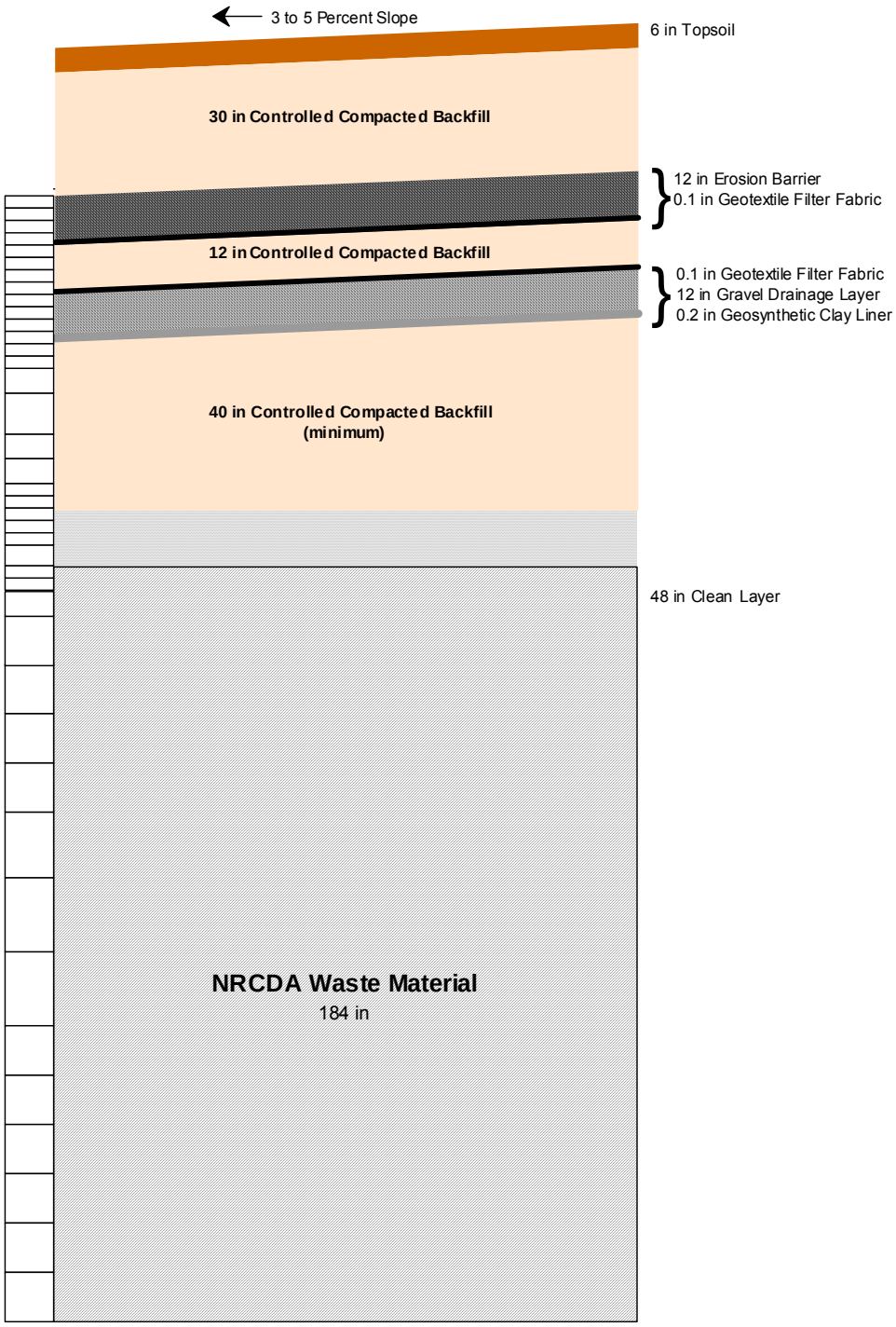

Figure 5-9. PORFLOW Model Grid for Air and Radon Pathway Analysis

The particle density of the lower backfill, gravel drainage layer, middle backfill, and erosion barrier (these materials collectively are considered the closure cap layers) was taken as 2.65 g/cm^3. This is based on the density of quartz and is regarded as representative of most SRS soils. Values for total porosity and long-term average moisture content for the closure cap materials were taken from Phifer (2003).

Using the HELP model, Phifer (2003) evaluated infiltration through a closure cap over time as the closure cap degraded. The porosity and average moisture content values for a 10,000-year degraded closure cap were utilized, since this represented the greatest air-filled porosity in which a gas could diffuse. Average saturation and air-filled porosity values were calculated from the total porosity and long-term average moisture content. Table 5-16 provides the values of particle density, total porosity, average saturation, and air-filled porosity utilized for all the layers (i.e., waste layer to the erosion barrier) for the 125- to 325-year time period.

Table 5-16. Porosity, Average Saturation, and Air-filled Porosity Values

Layer	Particle Density (g/cm^3)	Total Porosity (fraction)	Long-term Average Moisture Content (vol/vol)	Average Saturation[5] (fraction)	Air-filled Porosity [6] (fraction)
Erosion barrier layer	2.65 [1]	0.088 [1]	0.073 [1]	0.825	0.015
Upper backfill	2.65 [1]	0.375 [1]	0.244 [1]	0.649	0.132
Gravel drainage layer	2.65 [1]	0.375 [1]	0.197 [1]	0.525	0.178
Lower backfill	2.65 [1]	0.370 [1]	0.271 [1]	0.732	0.099
Stainless Steel Top	8.03	0.200 [3]	0.000 [4]	0.000	0.200
Waste Layer	2.65	0.200 [2]	0.000 [4]	0.000	0.200

[1] Values for total porosity and long-term average moisture content taken from Phifer (2003). Particle density is taken as 2.65, which is based on the density of quartz and regarded as fairly representative of most SRS soils.

[2] The waste layer is assumed to have a total porosity of 0.2.

[3] The stainless steel top is assumed to have a total porosity of 0 for the first 750 years and of 0.2 for the remaining duration of the simulation

[4] The waste and stainless steel top are assumed to be dry (i.e., saturation of 0) resulting in the air-filled porosity equaling the total porosity.

[5] Average Saturation = Long-term Average Moisture Content / Total Porosity

[6] Air-filled Porosity = (1 – Average Saturation) × Total Porosity

The molecular diffusion coefficient of Rn-222 in open air is 347 m^2/yr (Nielson et al. 1984). Nielson et al. (1984) established a relationship between moisture saturation and the radon effective air diffusion coefficient for various pore sizes of earthen materials. Using this method, a radon effective air diffusion coefficient was determined for each material type based upon the average moisture saturation for the material.

Subsequently, using Graham's Law, the effective air diffusion coefficient of each radionuclide or compound evaluated was determined for each material type based on the radon effective air diffusion coefficient using the following relationship:

$$D = D' \sqrt{\frac{MWT'}{MWT}} \qquad \text{Equation 5-5}$$

Where:

D = the diffusion coefficient of the radionuclide of interest (m^2/yr)
D' = the diffusion coefficient of the reference radionuclide (Rn-222) (m^2/yr)
MWT' = the molecular weight of the reference radionuclide (Rn-222)
MWT = the molecular weight of the element or compound of interest

A summary of the radon effective air diffusion coefficients and the calculated effective air diffusion coefficients for each radionuclide/compound by material zone is presented in Table 5-17.

5.7.6 Air-Pathway Model Results

5.7.6.1 Flux to Ground Surface

Model simulations were conducted to evaluate the peak flux of each radionuclide emanating from the top of the domain. A unit inventory of 1 Ci was assigned to the NRCDA waste zone for each radionuclide considered in the analysis. Results were output in Ci/yr through a 1 m^2 area, consistent with the set of units employed in the model, and are presented for C-14 Cl-36, I-129, Se-79, Sn-121m, Sn-126, S-35, and Sb-124 in Figure 5-10 and Figure 5-11. The peak fluxes emanating at the land surface are presented for the 1125-year period in Table 5-18. The results are reported in this way to facilitate calculation of human exposure at the SRS boundary and at the 100-m boundary due to the NRCDA. Flux behavior is based primarily on the closure considerations discussed in Section 5.7.3 and the half-life of the particular radionuclide as provided in Table 5-15. Graphs showing the flux rates at the land surface for Sb-125, Se-75, Sn-113, Sn-119m, and Sn-123 are not shown because these radionuclides produced either extraordinarily low flux or no flux at the land surface due to their short half-lives.

Table 5-17. Effective Air Diffusion Coefficients for Each Radionuclide/Compound, by Material

Radionuclide	NRCDAs Waste and Steel Top (m^2/yr)	Lower Backfill (m^2/yr)	Gravel Drainage Layer (m^2/yr)	Upper Backfill (m^2/yr)	Erosion Barrier (m^2/yr)
Rn-222 [1]	3.470E+02	2.840E+00	4.730E+00	4.730E+00	7.890E-01
C-14	7.623E+02	6.239E+00	1.040E+01	1.040E+01	1.733E+00
Cl-36	6.093E+02	4.987E+00	8.312E+00	8.312E+00	1.385E+00
I-129	3.219E+02	2.635E+00	4.391E+00	4.391E+00	7.318E-01
S-35	8.739E+02	7.153E+00	1.192E+01	1.192E+01	1.987E+00
Sb-124	4.643E+02	3.800E+00	6.334E+00	6.334E+00	1.056E+00
Sb-125	4.624E+02	3.785E+00	6.308E+00	6.308E+00	1.051E+00
Se-75	5.970E+02	4.886E+00	8.144E+00	8.144E+00	1.357E+00
Se-79	5.817E+02	4.761E+00	7.935E+00	7.935E+00	1.323E+00
Sn-113	4.864E+02	3.981E+00	6.635E+00	6.635E+00	1.106E+00
Sn-119m	4.739E+02	3.879E+00	6.465E+00	6.465E+00	1.078E+00
Sn-121	4.700E+02	3.847E+00	6.412E+00	6.412E+00	1.069E+00
Sn-121m	4.700E+02	3.847E+00	6.412E+00	6.412E+00	1.069E+00
Sn-123	4.662E+02	3.816E+00	6.359E+00	6.359E+00	1.060E+00
Sn-126	4.606E+02	3.770E+00	6.283E+00	6.283E+00	1.047E+00

[1] The effective diffusion coefficient for ^{222}Rn was used to determine the effective air diffusion coefficient of each radionuclide/compound based on Graham's Law.

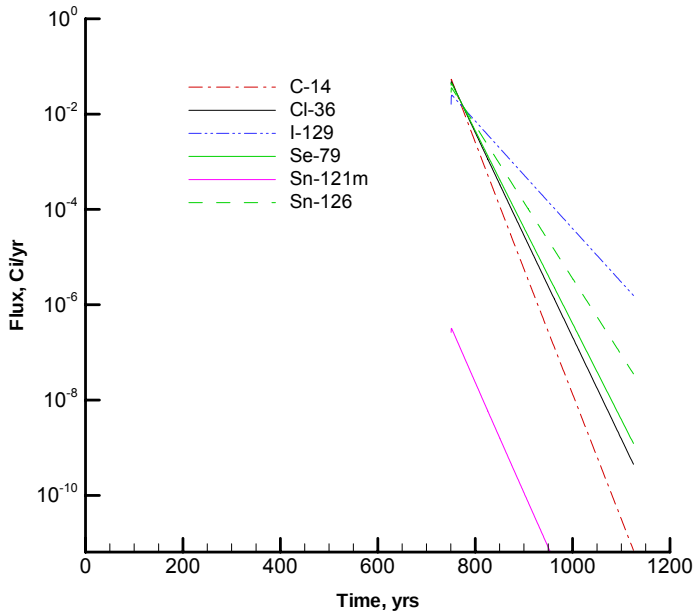

Figure 5-10. Flux Rate at Land Surface for C-14, Cl-36, I-129, Se-79, Sn-121m, and Sn-126

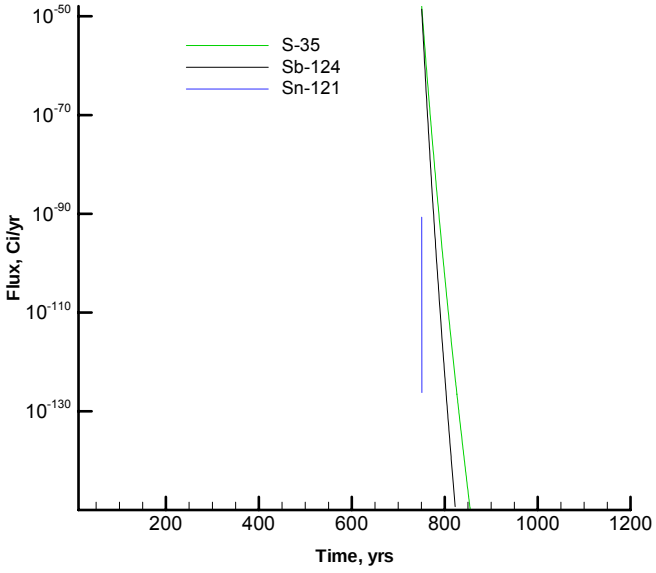

Figure 5-11. Flux Rate at Land Surface for S-35, Sb-124, and Sn-121

Table 5-18. Peak Flux Rates for Each Radionuclide for both NRCDAs

Radionuclide	Activity in Waste (Ci)	Max. Flux (Ci/yr/Ci)	Time of Peak (yr)
C-14	1.0	5.38E-02	751.0
Cl-36	1.0	4.78E-02	751.0
I-129	1.0	2.50E-02	752.0
S-35	1.0	1.14E-48	750.5
Sb-124	1.0	2.64E-49	750.5
Sb-125	1.0	0.00E+00	0.0
Se-75	1.0	0.00E+00	0.0
Se-79	1.0	4.50E-02	751.0
Sn-113	1.0	0.00E+00	0.0
Sn-119m	1.0	0.00E+00	0.0
Sn-121	1.0	2.13E-91	750.5
Sn-121m	1.0	3.20E-07	751.5
Sn-123	1.0	0.00E+00	0.0
Sn-126	1.0	3.56E-02	751.5

5.7.7 NRCDA Air-Pathway Dose Calculations

An evaluation was conducted to assess the potential dose to an MEI located at both the SRS boundary and at the 100-m locations (Lee 2006). During the 125-year operational and institutional control period, when the tritium is assumed to be entirely released over a 1-year time frame, the SRS boundary is the compliance point for the dose calculation. For the remainder of time, the 100-m boundary is the compliance point. The DRFs were calculated for each radionuclide potentially released from the 643-26E and 643-7E NRCDAs using CAP88 (Beres 1990), the EPA model for NESHAP. The DRFs represent the dose to the receptor exposed to 1 Ci of the specified radionuclide being released to the atmosphere. For the receptor located at the SRS boundary, the distance from each release location is sufficient for an assumption of a point source, so that the DRFs for both release locations are the same. However, separate DRFs must be calculated for the 100-m receptor. The distance from the 643-7E NRCDA to the 100-m receptor is sufficient for a point source. However, the close proximity of the 643-26E NRCDA to the 100-m receptor requires evaluation of an area source. For radionuclides not contained within the CAP88 library (Se-75, Se-79, Sn-119m, and Sn-121m) atmospheric transport was estimated by assigning surrogates with similar radiological properties. Doses for these four radionuclides were estimated by applying their dosimetric properties to the surrogate's relative air concentrations estimated by the model. Specific DRFs applicable to the NRCDAs are presented in Table 5-19. See Lee (2006) for details on the estimation of all DRFs.

Table 5-19. DRFs for the NRCDAs

Radionuclide	SRS Boundary Dose Release Factor[1] (mrem/Ci)	643-26E NRCDA 100-m Dose Release Factor (mrem/Ci)	643-7E NRCDA 100-m Dose Release Factor (mrem/Ci)
C-14	1.1E-04	7.0E-02	3.5E-01
Cl-36	2.3E-04	1.1E-01	5.6E-01
I-129	4.9E-02	1.0E+02	5.2E+02
S-35	2.8E-05	9.3E-03	4.6E-02
Sb-124	2.0E-03	6.8E-01	3.4E+00
Sb-125	6.5E-03	2.0E+00	1.0E+01
Se-75	1.1E-03	3.7E-01	1.8E+00
Se-79	6.3E-04	2.2E-01	1.1E+00
Sn-113	2.3E-04	9.2E-02	4.6E-01
Sn-119m	1.0E-04	4.0E-02	2.0E-01
Sn-121	4.2E-05	1.4E-02	7.1E-02
Sn-121m	6.5E-04	2.2E-01	1.1E+00
Sn-123	1.3E-05	4.0E-03	2.0E-02
Sn-126	3.0E-01	9.2E+01	4.6E+02

[1]From (Lee, 2006)

Disposal limits for both NRCDAs were calculated for each of the radionuclides associated with the atmospheric pathway and are presented in Table 5-20 and Table 5-21 for the 643-26E and 643-7E NRCDAs, respectively. The NRCDA limits were calculated by dividing the maximum permissible exposure level (10 mrem/yr, DOE 1999) by the highest dose received by the MEI from the 1 Ci source during the 1,125-year period.

Table 5-22 presents the inventories of the 643-26E NRCDA and 643-7E NRCDA versus their respective disposal limits. As seen the inventories of each radionuclide are well below their respective disposal limits. Table 5-23 presents the maximum projected dose occurring in years 750 and 751 resulting from the 643-26E NRCDA and 643-7E NRCDA inventories. As seen the maximum projected doses from 643-26E NRCDA and 643-7E NRCDA are 1.3 and 2.7 mrem/yr, respectively, versus a maximum permissible exposure level of 10 mrem/yr.

As stated previously, tritium readily diffuses through carbon steel, therefore for the purposes of this calculation, all the tritium is assumed to diffuse through the casks over a 1-year time frame and be subsequently transported to the SRS boundary prior to the end of the 100-year institutional control period. Based upon these assumptions a limit for tritium has been calculated. The assumption that all the tritium diffuses through the casks over a 1-yr time frame results in a peak flux of 1 Ci/yr/Ci of tritium disposed. Table 5-24 provides the resulting tritium limit based upon these assumptions. Table 5-25 presents the dose to the MEI at SRS boundary from the entire inventory of each NRCDA. As shown in Table 5-25, the projected dose is orders of magnitude below the maximum permissible exposure level (10 mrem/yr).

Table 5-20. Disposal Limits for the 643-26E NRCDA

Radionuclide	643-26E Peak Flux (Ci/yr/Ci)	643-26E 100-m DRF[1] (mrem/Ci)	643-26E Dose to MEI at 100-m[2] (mrem/yr/Ci)	643-26E Disposal Limits[3] (Ci)
C-14	5.38E-02	7.0E-02	3.8E-03	2.6E+03
Cl-36	4.78E-02	1.1E-01	5.3E-03	1.9E+03
I-129	2.50E-02	1.0E+02	2.5E+00	3.9E+00
S-35	1.14E-48	9.3E-03	1.1E-50	---
Sb-124	2.64E-49	6.8E-01	1.8E-49	---
Sb-125	0.00E+00	2.0E+00	0.0E+00	NL
Se-75	0.00E+00	3.7E-01	0.0E+00	NL
Se-79	4.50E-02	2.2E-01	9.9E-03	1.0E+03
Sn-113	0.00E+00	9.2E-02	0.0E+00	NL
Sn-119m	0.00E+00	4.0E-02	0.0E+00	NL
Sn-121	2.13E-91	1.4E-02	3.0E-93	---
Sn-121m	3.20E-07	2.2E-01	7.0E-08	1.4E+08
Sn-123	0.00E+00	4.0E-03	0.0E+00	NL
Sn-126	3.56E-02	9.2E+01	3.3E+00	3.1E+00

[1]From (Lee 2006)
[2] Dose to MEI at 100 meters = Peak Flux × DRF
[3] Disposal Limit = 10 mrem/yr / Dose to MEI at 100
NL = No limit
"---" indicates limit >1E20

Table 5-21. Disposal Limits for the 643-7E NRCDA

Radionuclide	643-7E Peak Flux (Ci/yr/Ci)	643-7E 100-m DRF[1] (mrem/Ci)	643-7E Dose to MEI at 100-m[2] (mrem/yr/Ci)	643-7E Disposal Limits[3] (Ci)
C-14	5.38E-02	3.5E-01	1.9E-02	5.3E+02
Cl-36	4.78E-02	5.6E-01	2.7E-02	3.7E+02
I-129	2.50E-02	5.2E+02	1.3E+01	7.7E-01
S-35	1.14E-48	4.6E-02	5.3E-50	---
Sb-124	2.64E-49	3.4E+00	9.0E-49	---
Sb-125	0.00E+00	1.0E+01	0.0E+00	NL
Se-75	0.00E+00	1.8E+00	0.0E+00	NL
Se-79	4.50E-02	1.1E+00	4.9E-02	2.0E+02
Sn-113	0.00E+00	4.6E-01	0.0E+00	NL
Sn-119m	0.00E+00	2.0E-01	0.0E+00	NL
Sn-121	2.13E-91	7.1E-02	1.5E-92	---
Sn-121m	3.20E-07	1.1E+00	3.5E-07	2.9E+07
Sn-123	0.00E+00	2.0E-02	0.0E+00	NL
Sn-126	3.56E-02	4.6E+02	1.6E+01	6.1E-01

[1]From Lee (2006)
[2] Dose to MEI at 100 meters = Peak Flux × DRF
[3] Disposal Limit = 10 mrem/yr / Dose to MEI at 100 m
NL = No limit
"---" indicates limit >1E20

Table 5-22. Limits versus Inventories

Radionuclide	643-26E NRCDA		643-7E NRCDA	
	Projected Inventory [1] (Ci)	Disposal Limit (Ci)	Bounding Inventory [2] (Ci)	Disposal Limit (Ci)
C-14	3.42E+02	2.6E+03	1.4E+02	5.3E+02
Cl-36	None	1.9E+03	1.8E-05	3.7E+02
I-129	9.4E-06	3.9E+00	1.5E-05	7.7E-01
S-35	None	---	3.1E-03	---
Sb-124	None	---	None	---
Sb-125	1.0E+05	NL	4.1E+04	NL
Se-75	None	NL	None	NL
Se-79	3.1E-03	1.0E+03	1.2E-03	2.0E+02
Sn-113	1.2E+04	NL	4.9E+03	NL
Sn-119m	2.0E+05	NL	8.1E+04	NL
Sn-121	None	---	None	---
Sn-121m	None	1.4E+08	None	2.9E+07
Sn-123	5.9E+03	NL	2.4E+03	NL
Sn-126	1.88E-03	3.1E+00	8.6E-06	6.1E-01

[1] Projected inventory for a maximum 100 casks
[2] Bounding inventory for existing 41 casks from WMAP (2002)
NL = no limit
"---" indicates limit >1E20

Table 5-23. Maximum Projected Air-Pathway Dose from Inventory

Radionuclide	643-26E NRCDA		
	Dose to MEI at 100 meters from 1 Ci Source at Years 750/751 (mrem/yr)	Projected Inventory (Ci)	Calculated Dose to MEI at 100 meters from Inventory at Years 750/751 (mrem/yr)
C-14	3.8E-03	3.4E+02	1.3E+00
Cl-36	5.3E-03	0	0
I-129	2.6E+00	9.4E-06	2.4E-05
S-35	1.1E-50	0	0
Sb-124	1.8E-49	0	0
Sb-125	0	1.0E+05	0
Se-75	0	0	0
Se-79	9.8E-03	3.1E-03	3.0E-05
Sn-113	0	1.2E+04	0
Sn-119m	0	2.0E+05	0
Sn-121	3.0E-93	0	0
Sn-121m	7.0E-08	0	0
Sn-123	0	5.9E+03	0
Sn-126	3.3E+00	1.9E-03	6.2E-03
		Total	1.3
Radionuclide	**643-7E NRCDA**		
	Dose to MEI at 100 meters from 1 Ci Source Years 750/751 (mrem/yr)	**Bounding Inventory (Ci)**	**Calculated Dose to MEI at 100 meters from Inventory at Years 750/751 (mrem/yr)**
C-14	1.9E-02	1.4E+02	2.7E00
Cl-36	2.7E-02	1.8E-05	4.9E-07
I-129	1.3E+01	1.5E-05	2.0E-04
S-35	5.3E-50	3.1E-03	1.6E-52
Sb-124	9.0E-49	0	0
Sb-125	0	4.1E+04	0
Se-75	0	0	0
Se-79	4.9E-02	1.2E-03	5.9E-05
Sn-113	0	4.9E+03	0
Sn-119m	0	8.1E+04	0
Sn-121	1.5E-92	0	0
Sn-121m	3.5E-07	0	0
Sn-123	0	2.4E+03	0
Sn-126	1.6E+01	8.6E-06	1.4E-04
		Total	2.7

Table 5-24. Tritium Disposal Limits for 643-26E and 643-7E NRCDA

Radionuclide	643-26E and 643-7E Tritium Peak Flux (Ci/yr/Ci)	SRS Boundary DRF [1] (mrem/Ci)	Tritium Dose to MEI at SRS Boundary [2] (mrem/yr/Ci)	643-26E and 643-7E Tritium Disposal Limit [3] (Ci)
H-3	1	2.2E-06	2.2E-06	4.5E+06

[1] From Lee (2006)
[2] Dose to MEI at SRS Boundary = Peak Flux × DRF
[3] Disposal Limit = 10 mrem/yr / Dose to MEI at SRS Boundary per yr per Ci

Table 5-25. Projected Maximum Tritium Dose at the SRS Boundary

NRCDA	Tritium Inventory (Ci)	SRS Boundary DRF [3] (mrem/Ci)	Projected Maximum Dose (mrem/yr)	Maximum Permissible Exposure Level (mrem/yr)
643-26E NRCDA	340 [1]	2.2E-06	7.5E-04	10
643-7E NRCDA	134 [2]	2.2E-06	2.9E-04	10

[1] Projected inventory for a maximum 100 casks from Table 5-3
[2] Bounding inventory for existing 41 casks from Table 5-4
[3] From Lee (2006)

5.8 NRCDA ALL-PATHWAYS ANALYSIS

This section documents the development of preliminary all-pathways limits for the NRCDAs. The limits developed within this section are considered preliminary since they do not take into consideration the results of sensitivity and uncertainty analyses. Interpretation of sensitivity and uncertainty analyses is conducted in Chapter 7, and final limits are provided there.

5.8.1 Overview of All-Pathways Analysis

This section describes the investigation conducted to evaluate the potential magnitude of the all-pathways dose from the NRCDA over the 25-year operational period, 100-year institutional control period, and 1000-year post-closure compliance period. These above-grade gravel pads are used as the disposal location for NR Waste Shipping/Disposal Casks, which are assumed to remain water and air-tight for a period of 750 years.

The permissible all-pathways dose for DOE LLW disposal facilities is addressed in DOE M 435.1, IV.P.(1)(a) (DOE 1999). This requirement is that dose to representative members of the public shall not exceed 25 mrem (0.25 mSv) in a year total effective dose equivalent from all exposure pathways, excluding the dose from radon and its progeny in air.

Although the all-pathways performance objective includes not only all exposure pathways, but also all transport pathways, in this PA, the air pathway is evaluated separately. The all-pathways dose evaluated here includes only the groundwater transport pathway because doses from the air pathway are low compared with those from the groundwater pathway.

The all-pathways analysis uses the groundwater concentrations developed in Section 5.6. The concentrations as a function of time are input into the all-pathways application (Koffman 2006a), which calculates dose to humans from direct ingestion of contaminated groundwater and consumption of locally grown leafy vegetables, produce, milk, and meat, which are contaminated with radionuclides from use of the groundwater for irrigation and direct consumption by the cattle (Section 4.5.1 of Part C, Background Chapter).

5.8.2 All-Pathways Assumptions

Key assumptions and inputs used in the all-pathway analysis are presented in Appendix B.

5.8.3 NRCDA All-Pathways Analysis

The maximum all-pathways doses from the two NRCDAs over the 1,000-year post closure compliance period were calculated using the all-pathways application (Koffman 2006a). The application uses the results of the PORFLOW program to calculate the dose to a hypothetical individual from using the groundwater at the point of assessment (location of the maximum concentration of each radionuclide outside of a 100-m buffer zone) for all credible purposes (drinking, irrigation of crops and ingestion of the crops and the meat and milk of animals fed on the crops and groundwater). Table 5-26 shows the results of the all-pathways analysis for the 643-26E NRCDA based on the projected inventory given in Table 5-3. Table 5-27 shows the all-pathways analysis results for the 643-7E NRCDA based on existing inventory given in Table 5-4. Table 5-28 presents the preliminary disposal limits for the 643-26E NRCDA based on the all-pathways analysis.

Table 5-26. All-Pathways Dose from the 643-26E NRCDA

Nuclide	All-pathways Dose, mrem/yr
C-14	6.29E-01
I-129	2.58E-04
Nb-94	4.58E-01
Ni-59	4.02E-03
Pu-239	3.35E-07
Pu-240	4.44E-20
Tc-99	9.76E-03
Total	1.10E+00
Total as fraction of dose limit	4.40E-02

Table 5-27. All-Pathways Dose from the 643-7E NRCDA

Nuclide	All-pathways Dose, mrem/yr
C-14	8.89E-02
I-129	1.57E-04
Nb-94	6.54E-02
Ni-59	5.62E-04
Pu-239	4.66E-08
Pu-240	6.12E-21
Tc-99	1.38E-03
Total	1.56E-01
Total as fraction of dose limit	6.26E-03

Table 5-28. Preliminary All-Pathways Radionuclide Disposal Limits for the NRCDA

Nuclide	Limit, Ci per Pad All-pathways
C-14	1.4E+04
I-129	9.1E-01
Nb-94	8.8E+02
Ni-59	2.4E+07
Pu-239	2.3E+07
Pu-240	---
Tc-99	9.3E+02

"---" indicates limit >1E20

The doses from the two NRCDAs are low. The dose from the 643-26E NRCDA is about four percent of the 25 mrem/year performance objective and the dose from the 643-7E NRCDA is about one-half of a percent of the performance objective.

5.9 INADVERTENT INTRUDERS

As described in the Part C Background chapter, Section 4.4, disposal of low-level radioactive waste in the ELLWF must meet a performance measure for protection of inadvertent intruders onto the disposal site. In particular, after loss of active institutional control at 100 years after facility closure, the EDE to an intruder should not exceed 100 mrem per year for scenarios involving continuous exposure or 500 mrem for scenarios involving a single acute exposure. These dose limits apply to the sum of dose equivalents from all exposure pathways that are assumed to occur in a given exposure scenario for an inadvertent intruder. The time period covered by the intruder analysis for this PA for the NRCDA extends to 1,000 years after loss of institutional control.

Inadvertent intruder exposure scenarios selected for analysis are summarized in Section 5.9.1. The selection of scenarios is based on a review of the intruder scenarios described in McDowell-Boyer et al. (2000). This review indicates that the dominant scenarios for an at-grade NRCDA Pad are the same as those for a below-grade pad due to the fact that the planned cover depth and design is identical for both modes of disposal. The below-grade pad was evaluated in McDowell-Boyer et al. (2000). Access to the NR disposal casks by an inadvertent intruder is not expected to occur earlier than in the present analysis.

Screening of the list of radionuclides projected for disposal in the NRCDA is described in Section 5.9.2. Screening allows for selection of radionuclides of potential significance to estimate inadvertent intruder dose. Radionuclides not considered potentially significant are those that decay to insignificant levels before human exposures may occur.

Additionally, in Section 5.9.2, analysis of dose to inadvertent intruders for the potentially significant scenarios and radionuclides is described. Results of the dose calculations are also presented in that section.

5.9.1 Exposure Scenarios for Inadvertent Intruders

The focus in development of exposure scenarios for inadvertent intruders is on selecting reasonable events that may occur, giving consideration to regional customs and construction practices. An important assumption in all scenarios is that an intruder has no prior knowledge of the existence of a waste disposal facility at the site. Therefore, after active institutional control ceases, certain exposure scenarios are assumed to be precluded only by the physical state of the disposal facility, i.e., the integrity of the engineered barriers used in facility construction. Passive institutional controls, such as permanent marker systems at the disposal site and public records of prior land use, also could prevent inadvertent intrusion after active institutional control ceases, but the use of passive institutional controls is not assumed in this analysis.

Intruder exposure scenarios described below do not include consumption of groundwater and crop irrigation with groundwater because impacts associated with these exposure routes are evaluated separately in the water resource protection analysis. Pathways of exposure to volatile forms of fifteen radionuclides are considered separately in the air-pathway analysis (Section 5.7).

Several chronic and acute exposure scenarios for inadvertent intruders were initially considered for use in the PA (Part C, Background chapter, Section 4.4). However, analyses of how these scenarios would apply to the ELLWF indicated that only three chronic exposure scenarios need to be included in the PA:

- an agriculture scenario involving direct intrusion into disposal units at times after the engineered barriers above the waste have lost their structural and physical integrity and can be penetrated by the types of excavation procedures normally used at the SRS;
- a resident scenario involving permanent residence in a home located either on top of an intact concrete roof or other engineered barrier, which first could occur upon loss of active institutional control at 100 years after facility closure, or on top of intact but essentially exposed waste at times after the engineered barriers have lost their integrity; and
- a post-drilling scenario involving exhumation of waste from a disposal unit at times after drilling through a disposal unit becomes credible.

In Part C, Background chapter, Section 4.4, it is indicated that the post-drilling scenario is potentially relevant for any disposal unit for which drilling into the waste may occur before the agriculture scenario becomes credible. Previous analyses of the agriculture and post-drilling scenarios have shown that the dose to an intruder per unit concentration of radionuclides in excavated material should be considerably greater for the agriculture scenario than for the post-drilling scenario, provided the assumptions for the exposure pathways in the two scenarios are reasonably consistent.

The principal reasons for the greater doses in the agriculture scenario are 1) the greater volume of waste exhumed during construction of a foundation for a home compared with the volume of waste exhumed during drilling of a well, which results in greater concentrations of radionuclides in contaminated soil in the intruder's vegetable garden, and 2) the doses from external and inhalation exposure while residing in a home on the disposal site, which contribute to the dose for the agriculture scenario but are not relevant for the post-drilling scenario. For the NRCDA, there is no reason to believe that drilling may occur before the agriculture scenario becomes credible; thus, the post-drilling scenario is not relevant for this analysis.

5.9.2 Dose Analysis for Inadvertent Intruders

In this section of the NRCDA analysis, radionuclide-specific doses to inadvertent intruders and inventory limits for chronic exposures are calculated. Acute exposure scenarios are not evaluated since chronic exposure scenarios as shown in Part C, Background chapter, Section 4.4 are the dose-limiting scenarios for all ELLWF disposal facilities. Dose calculations are based on the total projected inventory given in Table 5-1. Inventory limits are based on the EDE limit of 100 mrem/yr, as required for compliance with the performance measure for protection of inadvertent intruders (Part C, Section 4.4). By comparing radionuclide-specific doses to the 100-mrem/yr limit, or inventory limits to projected inventory for the NRCDA, compliance with the performance measure can be determined. As described in Part C, Background chapter, Section 4.4, compliance with the performance measure for protection of inadvertent intruders is assumed to be required for 1,000 years after disposal.

In this section it is established that the two exposure scenarios of potential concern for this analysis are the resident scenario and the agriculture scenario. The agriculture scenario involves direct intrusion into disposal units at any time after the disposal casks and any other engineered barriers above the waste have lost their structural and physical integrity and excavation into the waste becomes credible. The resident scenario involves permanent residence in a home located immediately above an intact disposal cask or other engineered barrier at any time after loss of active institutional control. The exposure pathways of concern for these two scenarios are described in Part C, Background chapter, Section 4.4. Doses to inadvertent intruders resulting from use of contaminated groundwater obtained from a well on the disposal site are evaluated separately, in the water resource protection analysis, and are not calculated for the intruder, in accordance with the reasoning put forth in the Format and Content Guide for PAs (DOE 1996).

The models for estimating dose for the two chronic exposure scenarios for inadvertent intruders considered in this analysis are presented in Part C, Background chapter, Section 4.4. In this section, SDCFs are developed that estimate EDE per unit concentration in the waste zone.

5.9.2.1 Dose Analysis for the Agriculture Scenario

The agriculture scenario involves direct excavation into disposal units at times after the engineered barriers above the waste have lost their structural and physical integrity and can be penetrated by normal excavation procedures at SRS. At some distant time in the future, it is conceivable that the corrosion-resistant steel disposal casks will have degraded by corrosion and that the waste could be accessed by excavation, resulting in exposures of inadvertent intruders according to the agriculture scenario described in Part C, Background Chapter, Section 4.4.

On the basis of the design of the conceptual waste cask described in Section 5.3 and estimates of corrosion rates of carbon steel, excavation into the waste would not be a credible occurrence for a long time after disposal. For excavation into the waste to occur, the top of the casks would need to be degraded by corrosion. Assuming the thickness of steel on top of the disposal cask is 38 cm (Section 5.3), and using a corrosion rate of 4E-03 cm/yr for carbon steel (Sullivan et al. 1988), an estimate of the time for complete corrosion of the steel top is about 9,500 years.

The NR components are constructed of highly corrosion-resistant Inconel and Zircaloy metals and hold the vast majority of radionuclide contaminants as activation products in the metal matrices. Corrosion rates for these alloys are different. The corrosion rate for Inconel is conservatively estimated at 2.5E-05 cm/yr, and for Zircaloy, 2.5E-06 cm/yr. The corrosion rates are based on data from the Hanford site (Hanford 1993), and notification by the NR program that Zircaloy corrosion rates in similar environments would be expected to be orders of magnitude below those identified for stainless steel and Inconel. Assuming that corrosion occurs on both sides of a metal plate, effective corrosion rates for Inconel and Zircaloy are estimated at 5E-05 cm/yr and 5E-06 cm/yr, respectively. The NR Inconel and Zircaloy waste forms are expected to maintain their structural and physical integrity for 30,000 years or more. Thus, unless the corrosion rates for Inconel or Zircaloy have been underestimated by more than an order of magnitude, which is not likely, it seems reasonable to conclude that direct intrusion into the waste by excavation is not a credible occurrence for about the first 40,000 years after disposal which is well beyond the assumed time period for compliance with the performance measure for protection of inadvertent intruders (1000 years). Therefore, on the basis of the agriculture scenario, no limits on average concentrations or inventories of radionuclides in the waste casks need to be imposed to provide protection of future inadvertent intruders. This information is summarized in Table 5-29.

Table 5-29. Estimated Corrosion of Inconel and Zircaloy

Component Part	Metal	t_{eff} [inch]	Corrosion Rate [in/yr][a]	Fraction Corroded [year^{-1}]	Time till 100% corroded [years]
1	Inconel	0.543	1E-5	3.68E-05	2.72E+04
2	Inconel	0.095	1E-5	2.11E-04	4.75E+03
3	Inconel	0.714	1E-5	2.80E-05	3.57E+04
4	Inconel	0.726	1E-5	2.76E-05	3.63E+04
5	Zircaloy	0.375	1E-6	5.33E-06	1.88E+05
6	Zircaloy	0.150	1E-6	1.33E-05	7.50E+04

[a] Hanford (1993)

5.9.2.2 Dose Analysis for the Resident Scenario

In the intruder-resident scenario, the intruder is assumed to reside in a home located immediately on top of an intact concrete roof or other engineered barrier above a disposal unit, and the scenario is assumed to be credible immediately following loss of active institutional control at 100 years after disposal. The intruder is assumed not to excavate into the waste itself, as this is not credible at this time for the NRCDA, given the corrosion resistance of the disposal containers. Thus, the only pathway of concern for this scenario is external exposure to photon-emitting radionuclides in the waste while residing in the home.

The NR components are encased in high-strength, low-alloy, corrosion-resistant steel waste disposal containers, or casks, which are closed by a weld (Section 5.3). These casks are disposed in the NRCDA, which may ultimately contain 100 casks. There is no standard disposal container due to the variety of components stored in the containers; therefore, precisely accounting for shielding afforded by the waste form or cask is not possible.

Before a detailed analysis of potential dose to a resident intruder was made, the list of radionuclides from Table 5-3 was further screened for potential significance by calculating external dose arising from exposure to radionuclides in unshielded waste. While this is not a credible scenario, it is useful in limiting the number of radionuclides for which a more detailed analysis is required. The intruder application (Koffman 2006b) was used to calculate screening limits by assuming that no shielding was provided by the disposal casks. The results are presented in Table 5-30. The results of this screening analysis indicate that even under these assumptions of no shielding, only the projected inventory of Nb-94 exceeds the screening-level inventory limit (i.e., ratio of limit to projected inventory is less than one), and thus needs further analysis. The screening-level inventory limits for all other radionuclides exceed the projected inventory, under the conservative conditions assumed.

Table 5-30. Screening-Level Disposal Limits for the NRCDA Resident Scenario at 100 Years with No Shielding

(Used for screening only – scenario not credible because no shielding of the waste is assumed)

Radionuclide	Inventory Limit (Ci/Pad)	Projected Inventory (Ci/Pad)[a]	Ratio of Inventory Limit to Projected Inventory
Am-241	4.09E+02	8.8E-01	4.6E+02
Am-242m	3.67E+02	7.9E-06	4.6E+07
Am-243	1.72E+01	6.0E-03	2.9E+03
C-14	1.15E+06	3.4E+02	3.4E+03
Cf-249	1.00E+01	3.1E-10	3.2E+10
Cf-251	3.12E+01	6.6E-12	4.7E+12
Cm-243	2.83E+02	4.6E-06	6.1E+07
Cm-244	4.87E+06	4.8E-01	1.0E+07
Cm-245	4.45E+01	2.6E-05	1.7E+06
Cm-246	1.33E+05	9.8E-06	1.4E+10
Cm-247	8.15E+00	2.0E-11	4.1E+11
Cm-248	1.70E+05	4.7E-11	3.6E+15
Co-60	4.78E+05	2.5E+05	1.9E+00
Cs-135	3.98E+05	8.7E-05	4.6E+09
Cs-137	4.49E+01	1.3E+01	3.4E+00
Eu-154	6.34E+03	1.7E-01	3.7E+04
H-3	---	3.4E+02	
I-129	1.18E+03	9.4E-06	1.3E+08
Mo-93	2.24E+04	3.6E+00	6.2E+03
Nb-94	1.58E+00	1.6E+01	9.8E-02
Ni-59	---	3.9E+03	
Ni-63	---	4.5E+05	
Np-237	1.39E+01	1.0E-05	1.4E+06
Pu-238	2.22E+05	6.7E-01	3.3E+05
Pu-239	5.17E+04	3.1E-01	1.7E+05
Pu-240	1.05E+05	2.8E-01	3.7E+05
Pu-241	1.21E+04	8.5E+01	1.4E+02
Pu-242	1.19E+05	1.0E-03	1.2E+08
Pu-244	7.55E+00	6.9E-11	1.1E+11
Se-79	8.19E+05	3.1E-03	2.6E+08

Table 5-30. Screening-Level Disposal Limits for the NRCDA Resident Scenario at 100 Years with No Shielding - continued

Radionuclide	Inventory Limit (Ci/Pad)	Projected Inventory (Ci/Pad)[a]	Ratio of Inventory Limit to Projected Inventory
Sm-151	3.35E+07	1.4E-01	2.4E+08
Sn-126	1.29E+00	1.8E-03	7.2E+02
Sr-90	6.79E+03	1.3E+01	5.2E+02
Tc-99	1.21E+05	3.6E-01	3.4E+05
Th-232	9.42E-01	1.7E-10	5.5E+09
U-232	3.97E+00	2.8E-06	1.4E+06
U-234	2.45E+04	7.0E-04	3.5E+07
U-235	2.00E+01	5.2E-07	3.8E+07
U-236	7.09E+04	1.1E-03	6.4E+07
U-238	1.18E+02	5.8E-05	2.0E+06
Zr-93	1.49E+05	1.9E+04	7.8E+00

[a] Table 5-3

A simplified approach is used to obtain a conservative, upper-bound estimate of the external dose that could be received by an inadvertent intruder at 100 years after disposal, the presumed end of institutional control, which is the earliest time that exposures could occur. This approach is described below and will show that a container thickness sufficient to keep initial dose below 200 mrem/hr at the container surface will be adequate for residential intruder protection at the end of institutional control.

Conservative, upper-bound estimates of external dose Nb-94 at 100 years after disposal are obtained as follows. First, a conservative assumption is made that the external dose rate at the surface of a waste cask at the present time is 200 mrem/hr, which is the limit for any cask specified in 49 CFR Part 173.

Next, it is assumed that the dose rate of 200 mrem/hr is entirely due to Co-60 at the time of disposal, due to its relatively high projected inventory (2.5E+03 Ci per cask [see Table 5-3]) and high energies and intensities of the emitted photons (Kocher 1981). This assumption also is conservative (i.e., the dose rate from Co-60 is overestimated), because a fraction of the external dose at the present time is due to other photon-emitting radionuclides in the waste.

If the dose rate from Co-60 at the present time is assumed to be 200 mrem/hr, the dose rate at 100 years after disposal would be reduced by a factor of 1.95E-6, based on the known half-life of 5.27 years. Thus, a conservative, upper-bound estimate of the external dose rate from Co-60 at 100 years after disposal would be (200 mrem/hr) × (1.95E-6) = 3.9E-4 mrem/hr.

Long-term external doses from the NR disposal casks will be controlled by Nb-94, which has a 20,000-year half-life and energetic gamma radiations of 0.87 and 0.70 Mev. In order to estimate the contributions to external dose from Nb-94 at 100 years after disposal, it is assumed that the activities of Co-60 and Nb-94 in disposed waste are in the same proportions as the total activities of these radionuclides in all casks given in Table 5-3. That is, the ratio of the activities of Co-60 and Nb-94 cask are assumed to be (2.5E+5):(16) at the time of disposal. Then, taking into account the decay of Co-60 after 100 years (Nb-94 experiences negligible decay over this time), the activity ratio at 100 years would be (2.5E+5 x 1.95E-6):(16). It is then assumed that each radionuclide is a point source, in which case the dose rate per unit activity of each radionuclide calculated by Unger and Trubey (1982) can be used. The values in units of mrem/hr per Ci are 1,400 for Co-60 and 980 for Nb-94.

It is further assumed that the only shielding between the source and receptor locations is the 1.6 in. minimum carbon-steel container thickness and the transmission curves for iron in Figure 13 of NCRP (1976) are used to estimate the reduction in dose rate due to shielding. The latter assumption provides conservative overestimates of dose rate (i.e., underestimates of shielding) for Nb-94, because the actual amount of shielding will be greater than 1.6 in. and the transmission of photons from Nb-94 relative to the transmission of photons from Co-60 decreases as the amount of shielding increases. The transmission (shielding) factor for Co-60 for 1.6 in. of iron is obtained directly from Figure 13 of NCRP (1976) as 0.4, respectively, and the value for Nb-94 is estimated by interpolation, based on the known photon spectrum for this radionuclide, as 0.32. With the information on dose rate per unit activity and transmission through 1.6 in. of iron, a conservative, upper-bound estimate of the external dose rate from Nb-94 can be obtained from the previous upper-bound estimate of the dose rate from Co-60 of 3.9E-4 mrem/hr as (3.9E-4) × (16/0.48) × (980/1,400) × (0.32/0.4) = 7.3E-3 mrem/hr.

Thus, a conservative, upper-bound estimate of external dose rate next to a waste cask at 100 years after disposal is 7.7E-3 mrem/hr (3.9E-4 plus 7.3E-3 mrem/hr), which is due mostly to Nb-94. This estimate is conservative because (1) the dose rate from Co-60 alone is likely overestimated, based on the acceptance criterion on external dose rate for the waste casks of 200 mrem/hr and measured dose rates for casks at the present time of less than 15 mrem/hr, and (2) the transmission of photons from Nb-94 through all shielding materials relative to the transmission for Co-60 have been overestimated. The analysis would provide an underestimate of the dose rate only if the activity of Nb-94 in the waste relative to the activity of Co-60 has been greatly underestimated.

The conservative, upper-bound estimate of external dose rate obtained above corresponds to a dose from continuous exposure of 67 mrem per year. If an inadvertent intruder were located next to an “average” waste cask continuously throughout the year, with no additional shielding assumed, the conservative, upper-bound estimate of the external dose rate indicates that the dose received from external exposure would be considerably less than the dose limit of 100 mrem per year in the assessment requirement for protection of inadvertent intruders.

Thus, although the foregoing analysis is not intended to provide an exact estimate of external dose at future times, the analysis clearly shows that the external dose to an inadvertent intruder due to exposure to intact waste casks at the end of institutional control should not be of concern in regard to meeting the performance measures for disposal of the NR wastes if the dose rate at the surface of the casks is less than 200 mR/hr. External dose to an inadvertent intruder could be of concern only if the container thickness fails to provide adequate shielding at the start of institutional control.

5.10 NRCDA RADON ANALYSIS

5.10.1 Overview of Radon Analysis

This section describes the investigation conducted to evaluate the potential magnitude of radon release from the NRCDAs over the 25-year operational period, 100-year institutional control period, and 1000-year post-closure compliance period. These above-grade gravel pads are used as the disposal location for NR Waste Shipping/Disposal Casks, which are assumed to remain water and air-tight for a period of 750 years. Therefore radon flux from the NRCDAs does not occur during the 25-year operational or 100-year institutional control periods, but only during the 1000-year post-closure compliance period, after the casks have been breached.

The permissible radon flux for DOE facilities is addressed in DOE M 435.1-1 Chapter IV (DOE 1999). In this Appendix, Section IV. P(1)(c) states the radon flux limitations associated with the development of a disposal facility and maintenance of a PA and the closure of the disposal facility. This requirement is that the release of radon shall be less than an average flux of 20 $pCi/m^2/s$ at the surface of the disposal facility. The requirements analysis states that this standard was adopted from the uranium mill tailings requirements in 40 CFR Part 192 and 10 CFR Part 40. 10 CFR Part 40 discusses both Rn-222 from uranium and Rn-220 from thorium, therefore the performance objective refers only to radon, and the correct species must be analyzed depending on the characteristics of the waste stream.

This guidance forms the basis for the investigation to evaluate radon flux above the NRCDAs. The scope of the investigation involved defining a decay chain of parent radionuclides to evaluate with a 1-D, vertical, numerical model. The model was customized to represent the vertical dimension of NRCDAs waste disposal unit and the anticipated cover material. The instantaneous Rn-222 flux at the land surface was evaluated for the PA 1000-year post-closure compliance period, after the casks have been breached and this flux was then compared to the DOE performance objective.

This investigation addresses only Rn-222 from uranium because screening calculations, using the numerical model developed in this analysis, indicate that the short half-life of Rn-220 (55.6 s) renders it unable to escape the NRCDAs waste unit and migrate to the land surface via air diffusion before it is transformed by radioactive decay.

The potential parent radionuclides that can contribute to the creation of Rn-222 are illustrated in Figure 5-12. The diagram indicates the specific decay chains that lead to the formation of Rn-222, as well as the half-lives for each radionuclide. The long half-life of U-238 (4.468E+9 years) causes the other radionuclides higher up on the chain of parents to be of little concern with regard to their potential to contribute significantly to the Rn-222 flux at the land surface over the period of interest.

5.10.2 NRCDA Summary of Key Radon Analysis Assumptions

Key assumptions and inputs used in the radon analysis are presented in Appendix B.

5.10.3 NRCDA Radon Analysis Conceptual Model

5.10.3.1 NRCDAs Closure Considerations

The concepts for closure of the NRCDAs are relevant to the determination of the radon flux at the land surface. The NRCDAs construction specifics and closure concept are described by Phifer et al. (2006). For the purposes of this investigation, it is assumed that radon flux only occurs during the 1000-year post-closure compliance period, after the casks have been breached. The final closure cap will exist during the 1000-year post-closure compliance period and is the configuration that must be considered in evaluating the long-term radon release at the land surface. A conceptual drawing of the closure cap over the NR casks is shown in Figure 5-8 and the vertical section over which Rn-222 diffusion was evaluated is indicated.

The closure configuration utilized in this analysis includes all materials, as constructed, including the final closure cap placed over NRCDAs at the end of the 100-year institutional control period. The components of concern for the long-term radon performance calculation are those that have no potential to erode during the 1000-year post-closure compliance period. These components are situated below the top of the erosion barrier. The composite thickness of the non-waste material below the top of the erosion barrier is 78 inches. Table 5-31 lists the individual components of the NRCDAs and closure cap (excluding the layers overlying the erosion control barrier). Materials are indicated with the associated thickness of each component.

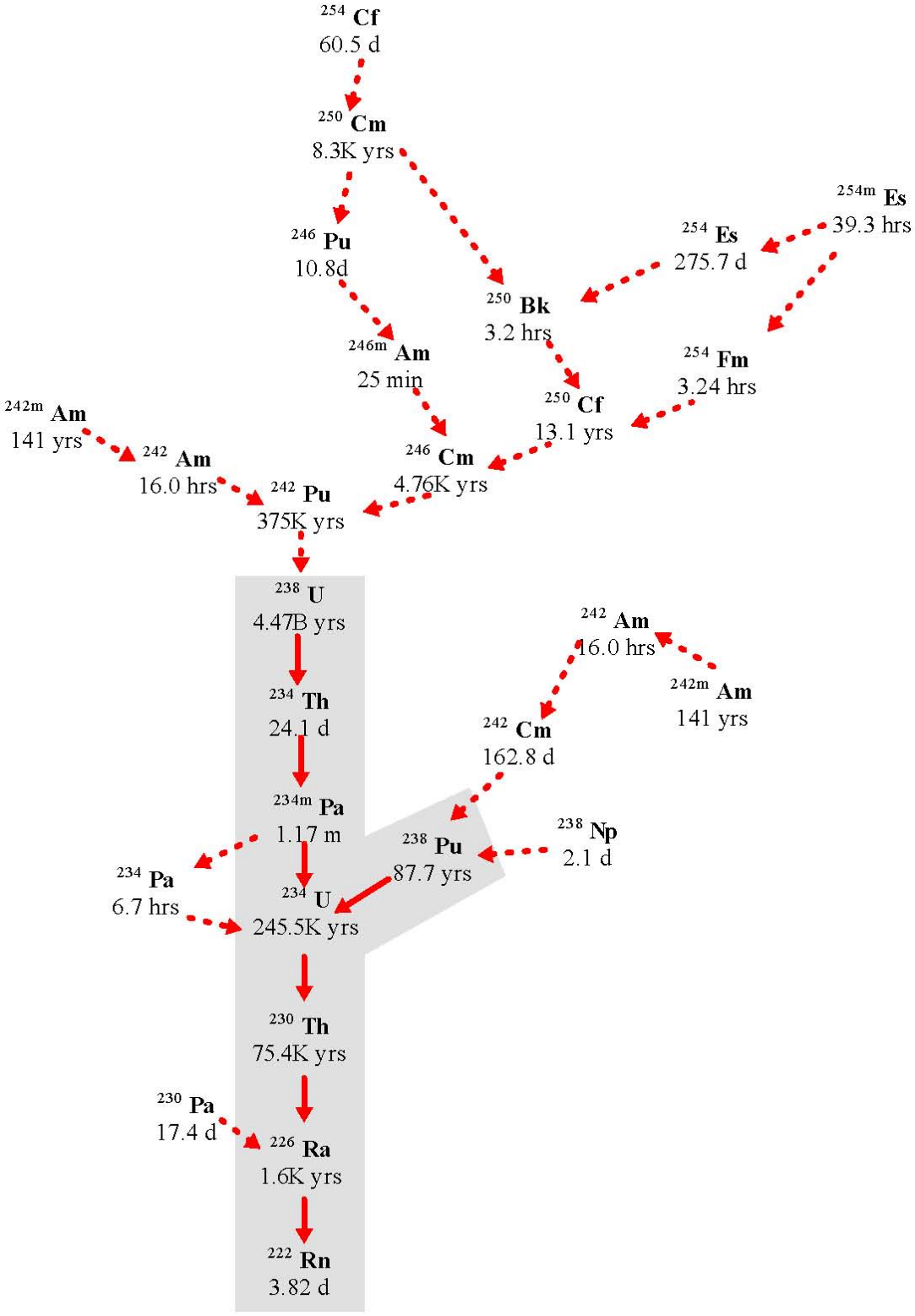

Figure 5-12. Radioactive Decay Chains Leading to Rn-222

Table 5-31. Vertical Layer Sequence and Associated Thickness for NRCDA Cover Material

Layer	Thickness (inches)
Erosion Barrier	12
Middle Backfill Layer	12
Gravel Drainage Layer	12
Lower Backfill Layer	40
Stainless Steel Top	14
Waste Layer	184

SOURCE: Adapted from Phifer et al. (2006).

5.10.3.2 Conceptual Model

The Rn-222 flux at the land surface above the NRCDAs was evaluated for its specific closure configuration discussed above. Rn-222 is generated within the waste zone by radioactive decay of different parent radionuclides following along the decay chains that lead to the formation of Rn-222. The decay chains for all possible parent radionuclides of Rn-222 are shown in Figure 5-12. In this figure, the parent radionuclides that were individually evaluated are indicated with the gray shaded area (i.e., beginning with Pu-238 and U-238). Rn-222 generated within the waste zone is in the gaseous phase and diffuses outward from this zone into the air-filled soil pores surrounding the vault, eventually resulting in some of the radon emanating at the land surface.

As such, air is the fluid through which Rn-222 diffuses, although some Rn-222 may dissolve in residual pore water. It is assumed that fluctuations in atmospheric pressure at the land surface that could induce small pulses of air movement into and out of the shallow soil column will have a zero net effect over the long-term period of evaluation in this study, thus advective transport of Rn-222 in air-filled soil pores is not considered to be a significant process when compared to air diffusion.

The parent radionuclides exist in the solid phase and therefore do not migrate upward through the air-filled pore space, although they could be leached and transported downward from the waste zone by pore water movement (assuming cask failure).

The flux of Rn-222 was evaluated for a period 1000 years beyond the operational and institutional control period (i.e., 1125 years). The NR Waste Shipping/ Disposal Casks are assumed to remain intact and watertight for a period of 750 years. No transport of Rn-222 is allowed during this time period. After 750 years, the casks are breached and flux of Rn-222 is allowed. Transport of Rn-222 is simulated from 750 years to 1125 years (totaling 375 years).

5.10.4 NRCDA Radon Analysis Numerical Model

The mathematical model utilized in this report is provided by the PORFLOW simulation package. PC-based PORFLOW Version 5.97.0 was used to conduct a series of simulations. PORFLOW is developed and marketed by Analytic & Computational Research, Inc. to solve problems involving transient and steady-state fluid flow, heat and mass transport in multi-phase, variably saturated, porous or fractured media with dynamic phase change. PORFLOW has been widely used at the SRS and in the DOE complex to address major issues related to the groundwater and nuclear waste management.

The governing equation for mass transport of species k in the fluid phase is given by

$$\frac{\partial C_k}{\partial t} + \frac{\partial}{\partial x_i}(V_i C_k) = \frac{\partial}{\partial x_i}(D_{ij}\frac{\partial C_k}{\partial x_j}) + \gamma_k \qquad \text{Eq 5-3}$$

Where

C_k	concentration of species k, Ci/m^3
V_i	fluid velocity in the i^{th} direction, m/yr
D_{ij}	effective diffusion coefficient for the species, m^2/yr
γ_k	net decay of species k, Ci/m^3yr
i, j	direction index
t	time, yr
x	distance coordinate, m

This equation is solved using PORFLOW to evaluate transient Rn-222 transport through the soil cover above the NRCDAs to evaluate Rn-222 flux at the land surface over time. As explained, advection is not considered to be a significant process when compared to air diffusion, so the advection term was disabled within PORFLOW and only the diffusive and net decay terms were evaluated.

5.10.4.1 Model Development and Assumptions

The numerical representation of the conceptual model is as a 1-dimensional vertical stack of elements configured to represent the thickness of the NR Waste Shipping/Disposal Casks and overlying cover material associated with final closure.

Decay chains evaluated were U-238→Th-234→Pa-234m→U-234→Th-230→Ra-226→Rn-222 and Pu-238 →U-234→Th-230→Ra-226→Rn-222. Each parent in these chains, except Th-234 and Pa-234m, were simulated separately as the starting point of the decay chain. Th-234 and Pa-234m have short half-lives compared to the other parent radionuclides in these chains. Only a fraction of the Rn-222 generated by the decay of each parent is available for migration away from its source and into open pore space. Since the Rn-222 parent radionuclides exist as oxides or in other crystalline forms, only a fraction of Rn-222 generated by decay of Ra-226 has sufficient energy to migrate away from its original location into adjacent pore space before further decay occurs (3.82 day half-life for Rn-222).

The emanation coefficient is generally defined as the fraction of the total amount of Ra-222 produced by radium decay that escapes from soil particles and enters the pore space of the medium. This is the fraction of the Ra-222 that is available for transport. In the case of the NRCDA, the parent radionuclides are not embedded in soil but are contained within wastes of varying types stored within stainless steel containers. Literature values for the Ra-222 emanation factor for these conditions are not available.

Studies have shown the emanation factor to vary between 0.02 and 0.7 for various soil types depending primarily on moisture content. Generally, higher emanation factors are associated with higher moisture contents.

RESRAD (Yu et al. 2001) is a model used to estimate radiation dose and risk from residual radioactive materials. This DOE and NRC approved code, assumes an emanation factor of 0.25 for radon-222 which is representative of a silty loam soil with a low moisture content. For the NRCDA radon pathway analysis, the RESRAD default emanation factor of 0.25 was chosen recognizing that literature values for wastes similar to the NRCDA are not available. The use of 0.25 should be conservative since the waste is assumed to be dry and emanation factors reported in the literature for drier soils are much lower (Yu et al. 2001). To account for the emanation factor in the model, an effective source term of 0.25 Ci of parent radionuclide was utilized as the source term for each Ci disposed within the facility.

Since Rn-222 exists as a gas, air was assumed to be the medium within which radon transport occurs. The flow field was assumed to be isobaric and isothermal. The impact of naturally occurring fluctuations of atmospheric pressure is likely to have a zero net effect. Therefore, for the relatively long periods of time evaluated in this investigation, air diffusion was the only transport mechanism simulated in the model and advective air transport was assumed to be negligible.

Some radon dissolves in pore water but since diffusion proceeds more slowly in that fluid, air diffusion is the only transport process by which Rn-222 can reach the land surface from the NRCDAs. This assertion is substantiated in Yu et al. (2001). In that report the D_{eff} for soil is reported to range from the radon open air diffusion coefficient of 1.0E-6 m^2/s to that of fully saturated soil, 1.0E-10 m^2/s. This 4-order of magnitude difference is consistent with the comparison of water diffusion coefficients to air diffusion coefficients of other common molecular compounds and reported in many references.

Thus, the larger volume of water-filled pore space compared to air-filled pore space (maximum of 1 order of magnitude difference) is inconsequential, in terms of the ability of water-dissolved radon to diffuse through water-filled pores as compared to the ability of the same compounds to diffuse as gas in the vapor-filled pore spaces. In this investigation, transport was allowed to proceed only through air-filled pore space and, therefore, residual pore water was treated as if it was part of the solid matrix material within the flow field. No credit was taken for airborne radon dissolving in pore water as it proceeds from the vault to the land surface although it has been observed to partition between air and water in the ratio of 4 to 1, respectively, at 20° C (Nazaroff and Nero 1988).
The boundary conditions imposed on the domain included:

- No-flux specified for all parent radionuclides at perimeter of the domain ($\partial C/\partial X = 0$ at $x=0$, $x=1$ and $\partial C/\partial Y = 0$ at $y=0$, $y=y_{max}$)
- No-flux specified for Rn-222 along sides and bottom ($\partial C/\partial X = 0$ at $x=0$, $x=1$ and $\partial C/\partial Y = 0$ at $y=0$)
- Rn-222 concentration set to 0 at land surface (top of erosion barrier) ($C = 0$ at $y=y_{max}$)

The initial condition imposed on the domain included:

- Rn-222 concentration set to 0 for the entire model domain at time = 0 ($C=0$ for $0 \leq x \leq 1$ at $t=0$ and $C=0$ for $0 \leq y \leq y_{max}$ at $t=0$)

The initial conditions for the model also assumed a 1 Ci inventory (prior to application of the emanation factor) of each parent radionuclide uniformly spread over the waste zone. The model does not account for an initial inventory of Rn-222 since it would readily migrate out of the waste containers prior to disposal operations and has a half-life of 3.8 days.

Simulations were conducted in transient mode for diffusive transport in air, with results being obtained over 1,125 years.

5.10.4.2 Measures Implemented to Ensure Conservative Results

In this analysis, several conditions introduce a significant measure of conservatism into the calculations. These include:

- The use of boundary conditions that force all of the Rn-222 to move upward from the waste disposal zone to the land surface. In reality, some of the Rn-222 diffuses sideways and downward in the air-filled pores surrounding the waste zone; hence ignoring this has the effect of increasing the radon flux at the land surface.
- Not taking credit for the removal of either Rn-222 or of the parent radionuclides by pore water moving vertically downward through the model domain once the cask is breached. This mechanism would likely remove some dissolved Rn-222 in addition to the parent radionuclides, and therefore its omission has the effect of increasing the estimate of instantaneous Rn-222 flux at the land surface in simulations conducted as a part of this investigation.
- The addition of an extra 125 years to the required 1,000-year evaluation period to account for any Rn-222 generated during the operations and institutional control period, thus incrementally increasing the instantaneous Rn-222 flux.
- Use of the top of the erosion layer in the soil cover as the land surface for the purpose of calculating Rn-222 flux. No credit is taken for the additional distance Rn-222 must migrate above the erosion layer prior to that portion of the Soil Cover Zone eroding away. This assumption impacts only Ra-226 (due to its relatively short half-life).

5.10.4.3 Grid Construction

The model grid was constructed as a node mesh 3 nodes wide by 42 nodes high. This mesh creates the vertical stack of 40 model elements. Figure 5-9 shows a schematic of the PORFLOW model grid. The grid extends upward only as far as the erosion barrier, since this is the minimum possible cover thickness that could exist during the 1,125-year evaluation period. A set of consistent units was employed in the simulations for length, mass and time, these being meters, grams and years, respectively.

5.10.4.4 Material Zones

The model domain was divided into two primary zones, the NRCDA waste zone occupying the lower 15.3 ft of the domain and the cover zone (including the cask top), extending ~7.5 ft. above the waste zone to the top of the domain. The cover zone includes the cask top as well as the different closure cap layers. The upper model elements were scaled to correspond to the geometry of the closure cap thickness while the lower model elements were scaled to correspond to the NRCDA waste zone. The land surface for the evaluation period of interest is assumed to be the top of the erosion resistant layer, within the closure cap, and no credit is taken for the compacted backfill and topsoil above that layer.

5.10.4.5 Material Zone Properties and Other Input Parameters

Material properties utilized within the 1-D numerical model were specified for 6 material zones defined within the model domain. Each material zone was assigned values of particle density, total porosity, average saturation, air-filled porosity, air density, and an effective air diffusion coefficient for Rn-222. Selection of effective Rn-222 diffusion coefficients was based on a soil pore size distribution model that allowed the selection of effective Rn-222 air diffusion coefficients based on the degree of residual water saturation (Nielson et al. 1984). With the use of an effective air diffusion coefficient, tortuosity was assigned a unit value in each material zone. An air fluid density of 1.24E+03 g/m^3 was used. This air fluid density was obtained from the Bolz and Tuve (1973) and represents that of standard atmospheric conditions.

The total porosity for the NRCDA waste zone was taken to be 0.2. It was assumed that the waste was dry and that the air-filled porosity would equal the total porosity for this zone. For the cask top, the steel was assumed to have a total porosity of 0.0 for the first 750 years of the simulation. This essentially prevents any Rn-222 transport from the cask during this time period. At 750 years, the steel is reassigned a porosity of 0.2 to represent pitting thereby allowing Rn-222 flux from the cask over the remaining 375 years of the simulation period.

The particle density of the lower backfill, gravel drainage layer, middle backfill, and erosion barrier (these materials collectively are considered the closure cap layers) was taken as 2.65 g/cm^3. This is based on the density of quartz and is regarded as representative of most SRS soils. Values for total porosity and long-term average moisture content for the closure cap materials were taken from Phifer (2003). Phifer (2003) evaluated infiltration through a closure cap over time as the closure cap degraded using the HELP model. The porosity and average moisture content values for a 10,000-year degraded closure cap were utilized, since this represented the greatest air-filled porosity in which a gas could diffuse. Average saturation and air-filled porosity values were calculated from the total porosity and long-term average moisture content. Table 5-32 provides the values of particle density, total porosity, average saturation, air-filled porosity, and effective Rn-222 diffusion coefficient utilized for all the layers (i.e., waste layer to the erosion barrier).

5.10.5 Model Results

Model simulations were conducted to evaluate the peak instantaneous Rn-222 flux at the land surface over the 1,125-year period. This time period includes the 25-year operations cycle, 100 years of institutional control, and the 1,000-year compliance period. However radon flux to the land surface can only occur after the casks are breached at 750 years. Model results were output in $Ci/m^2/yr$, consistent with the set of units employed in the model. A graph of these results is shown in Figure 5-13, although the units are converted to $(pCi/m^2/s)/(Ci/m^2)$, which are the units used to define the regulatory flux limit in DOE M 435.1-1.

Table 5-32. Porosity, Average Saturation, and Air-filled Porosity Values

Layer	Particle Density (g/cm^3)	Total Porosity (fraction)	Long-term Average Moisture Content (vol/vol)	Average Saturation [5] (fraction)	Air-filled Porosity [6] (fraction)	Effective Diffusion Coefficient (m^2/yr)
Erosion Barrier Layer	2.65 [1]	0.088 [1]	0.073 [1]	0.825	0.015	0.789
Upper Backfill	2.65 [1]	0.375 [1]	0.244 [1]	0.649	0.132	4.73
Gravel Drainage Layer	2.65 [1]	0.375 [1]	0.197 [1]	0.525	0.178	4.73
Lower Backfill	2.65 [1]	0.370 [1]	0.271 [1]	0.732	0.099	2.84
Stainless Steel Top	8.03	0.200 [2]	0.000 [4]	0.000	0.200	347
Waste Layer	2.65	0.200 [3]	0.000 [4]	0.000	0.200	347

[1] Values for total porosity and long-term average moisture content taken from Phifer (2003). Particle density is taken as 2.65, which is based on the density of quartz and regarded as fairly representative of most SRS soils.

[2] The stainless steel top is assumed to have a total porosity of 0.0 for the first 750 years and of 0.2 for the remaining duration of the simulation

[3] The waste layer is assumed to have a total porosity of 0.2

[4] The waste and stainless steel top are assumed to be dry (i.e., saturation of 0) resulting in the air-filled porosity equaling the total porosity.

[5] Average Saturation = Long-term Average Moisture Content / Total Porosity

[6] Air-filled Porosity = (1 – Average Saturation) × Total Porosity

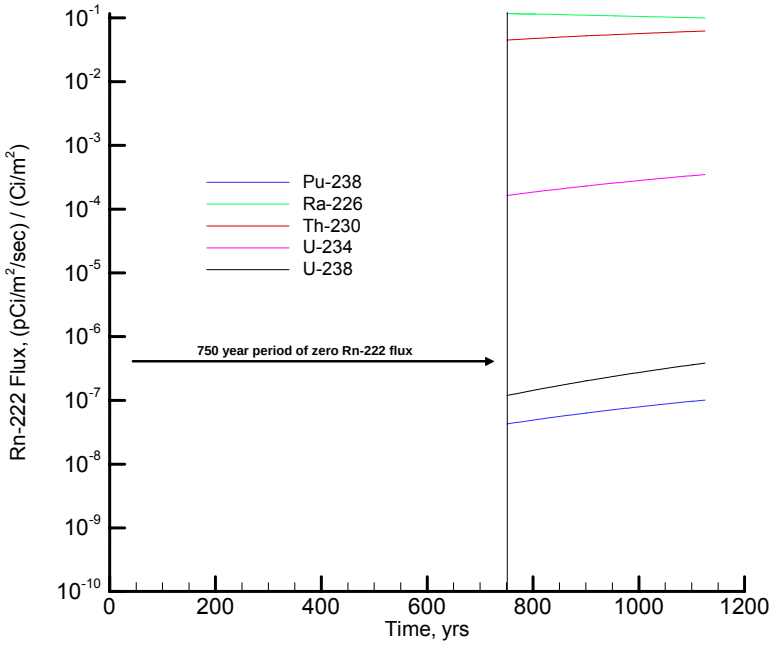

Figure 5-13. Rn-222 Flux at Land Surface Resulting from Unit Source Term

The peak fluxes represent the peak Rn-222 flux per square meter at the top of the closure cap erosion barrier and are listed below in Table 5-33. The top of the erosion barrier is conservatively assumed to represent the land surface throughout the 1,125-year simulation. Also shown in Table 5-33, for each of the 5 parent radionuclides, are the calculated disposal limits per unit area and the disposal limits for the existing and proposed NRCDAs. The unit-area disposal limit was calculated as follows:

Disposal Limit per unit area (Ci/m^2) = Regulatory limit (20 $pCi/m^2/s$) / Maximum Instantaneous Rn-222 flux at land surface per unit area per unit inventory of parent radionuclide per unit area ($[pCi/m^2/s]/[Ci/m^2]$)).

The unit area limits for each of the 5 parent radionuclides were converted to NRCDA-specific disposal limits by multiplying the unit area limit for each by the area of the existing NRCDA footprint. The area of the 643-26E NRCDA is 5762 m^2 and the area of the 643-7E NRCDA is 1227 m^2. The disposal limits for each of the NRCDAs based on the radon flux performance objective of 20 pCi/m^2-s are shown in Table 5-33.
Table 5-34 presents the inventories of the 643-26E NRCDA and 643-7E NRCDA versus their respective disposal limits. As seen the inventories of each parent are well below their radon disposal limits. Table 5-35 presents the maximum projected radon flux to the ground surface resulting from the 643-26E NRCDA and 643-7E NRCDA inventories. As seen the maximum projected fluxes from 643-26E NRCDA and 643-7E NRCDA are 3E-07 and 3E-08 $pCi/m^2/s$, respectively, versus the maximum permissible flux of 20 $pCi/m^2/s$.

Table 5-33. Land Surface and Associated Disposal Limits for Parent Radionuclides

Parent Radionuclide	Peak Instantaneous Rn-22 Flux at Land Surface ($pCi/m^2/s$)/(Ci/m^2)	Disposal Limit Per Unit Area (Ci/m^2)	Disposal Limit for 643-26E NRCDA (Ci)	Disposal Limit for 643-7E NRCDA (Ci)
Pu-238	1.01E-07	1.98E+08	1.1E+12	2.4E+11
U-238	3.84E-07	5.21E+07	3.0E+11	6.4E+10
U-234	3.48E-04	5.75E+04	3.3E+08	7.0E+07
Th-230	6.22E-02	3.22E+02	1.9E+06	3.9E+05
Ra-226	1.17E-01	1.71E+02	9.9E+05	2.1E+05

Table 5-34. Limits versus Inventories

Parent Radionuclide	643-26E NRCDA Projected Inventory [1] (Ci)	Disposal Limit for 643-26E NRCDA (Ci)	643-7E NRCDA Bounding Inventory [2] (Ci)	Disposal Limit for 643-7E NRCDA (Ci)
Pu-238	6.7E-01	1.1E+12	2.69E-01	2.4E+11
U-238	5.8E-05	3.0E+11	2.32E-05	6.4E+10
U-234	7.0E-04	3.3E+08	3.64E-06	7.0E+07
Th-230	None	1.9E+06	None	3.9E+05
Ra-226	None	9.9E+05	None	2.1E+05

[1] Projected inventory for a maximum 100 casks from Table 5-3
[2] Bounding inventory for existing 41 casks from Table 5-4

Table 5-35. Maximum Projected Radon Flux from Inventory

Parent Radionuclide	Peak Instantaneous Rn-222 Flux at Land Surface ($pCi/m^2/s$)/(Ci/m^2)	643-26E NRCDA		643-7E NRCDA	
		Projected Inventory [1] (Ci)	Maximum Projected Flux ($pCi/m^2/s$)	Bounding Inventory [2] (Ci)	Maximum Projected Flux ($pCi/m^2/s$)
Pu-238	1.0E-07	6.7E-01	6.8E-08	2.7E-01	2.7E-08
U-238	3.8E-07	5.8E-05	2.2E-11	2.3E-05	8.7E-12
U-234	3.5E-04	7.0E-04	2.4E-07	3.6E-06	1.3E-09
Th-230	6.2E-02	0	0	0	0
Ra-226	1.2E-01	0	0	0	0
		Total	3.1E-07	Total	2.8E-08

[1] Projected inventory for a maximum 100 casks from Table 5-3
[2] Bounding inventory for existing 41 casks from Table 5-4

5.11 CONSIDERATION OF OTHER NR WASTEFORMS

Two general types of wasteforms are described in the analysis, highly radioactive components consisting of activated corrosion-resistant metal alloy contained within thick steel casks, and auxiliary equipment primarily contaminated with activated corrosion products (crud) at low levels and contained within thinner-walled casks. In the analysis, the inventories for the two types of waste were combined and conceptually placed in a representative heavily shielded cask, shown in Figure 5-3. The justification for not conducting separate analyses for the auxiliary equipment is given below.

Screening analysis shows that a number of radionuclides in the equipment inventory are potentially significant by the groundwater pathway. In Section 5.6, the radionuclide inventory of the auxiliary equipment was added to that of the reactor components. In effect, this analyzed the case where the component casks and the equipment containers failed at the same time. For the radionuclides not screened out, all of which have relatively long half-lives, this is a conservative assumption, because the contributions from the two sources will peak at exactly the same time. If the containers fail at different times, which they will, because the equipment containers are not as robust as those for the components and the containers are sealed with gaskets rather than welds, there will be separate peaks. In this case, each individual peak, as well as the sum of the individual contributions will always be less than if the peaks were to coincide. Thus the groundwater pathway analysis for the NRCDA is conservative for both the auxiliary equipment and the reactor components.

The intruder screening analysis indicates that Nb-94 is of potential concern. The screening-level disposal for Nb-94 from Table 5-30 is 1.6 Ci. The total inventory estimated for Nb-94 in the auxiliary equipment is 2.3E-2 Ci (9.02E-4 Ci [Table 5-2] *50 / 2). Since the screening-level intruder limit is a factor of 70 greater than the total inventory estimate, the conclusion that no disposal limits based on intruder considerations need be implemented for the NRCDA is valid for the auxiliary equipment as well as the disposal casks.

5.12 REFERENCES

ACRI (Analytical & Computational Research, Inc.). 2004. *PORFLOW Version 5.0 User's Manual*, Revision 5, Analytical & Computational Research, Inc., Los Angeles, California.

Anderson, Michael, 2006. *Fax to Kevin Tempel.* Knowles Atomic Power Laboratory. August 22, 2007.

Aspentech 2004. *Aspen Custom Modeler PB177.*

Beres, D.A. 1990. *The Clean Air Act Assessment package-1988 (CAP-88) A Dose and Risk Assessment Methodology for Radionuclide Emissions to Air.* U.S. Environmental Protection Agency Contract No. 68-D9-0170, Washington, DC.

Bolz, R.E. and G.L. Tuve, (Editors), 1973. *Handbook of Tables for Applied Engineering Science, 2nd Edition*. CRC Press, 18901 Cranwood Parkway, Cleveland, OH.

Cook, J.R., D.C. Kocher, L. McDowell-Boyer and E.L. Wilhite, 2002. Special Analysis: Reevaluation of the Inadvertent Intruder, Groundwater, Air, and Radon Analyses for the Saltstone Disposal Facility, WSRC-TR-2002-00456. Westinghouse Savannah River Company, Aiken, South Carolina. 10/23/2002.

Cook, J. R., Phifer, M. A., Wilhite, E. L., Young, K. E., and Jones, W. E. 2004. *Closure Plan for the E-Area Low-Level Waste Facility*, Revision 4, WSRC-RP-2000-00425. Westinghouse Savannah River Company, Aiken, South Carolina. May, 2004.

Cook, J.R. 2006. Radionuclide Data Package for Performance Assessment Calculations Related to the E-Area Low-Level Waste Facility at the Savannah River Site, WSRC-STI-2006-00162, Savannah River National Laboratory, Aiken, SC.

Crapse, K.P. and J.R. Cook, 2006. *Atmospheric Pathway Screening Analysis for the E-Area Low Level Waste Facility*, WSRC-STI-2006-00159, Washington Savannah River Company, Aiken, SC 29808. 09/05/2006.

DOE 1999. *Radioactive Waste Management Manual*, DOE M 435.1-1, Change 1:6-19-01, Department of Energy, Approved July 9, 1999.

DOE. 1996. *Interim Format and Content Guide and Standard Review Plan for U.S. Department of Energy Low-Level Waste Disposal Facility Performance Assessments.* October 1996. Department of Energy. Washington, DC.

EPA 2004. *National Primary Drinking Water Regulations*, 40 CFR Part 141.

Flach, G. P. 2004 *Groundwater Flow Model Of The General Separations Area Using PORFLOW*, WSRC-TR-2004-00106, Savannah River National Laboratory, July 15 2004.

GTG (GoldSim Technology Group LLC). 2005. *GOLDSIM User's Guide*, Version 9.0, GoldSim Technology Group LLC, available at www.goldsim.com, May.

Hanford. 1993. *Corrosion Behavior of HY-80 Steel, Type 304 Stainless Steel, and Inconel Alloy 500 at 218-E-12B Burial Ground, Hanford, WA.* Hanford report no. TR-2001-SHR, Hanford, Washington.

Hiergesell, R.A.. 2005. Special Analysis: Production TPBAR Waste Container Disposal Within the Intermediate Level Vault, WSRC-TR-2005-00531.

KAPL 2004 *Radiological Inventory on 643-7E Naval Reactors Component Storage Area (643-7E Area*), OEH-61310-MJA-04-033, Knolls Atomic Power Laboratory, April 21, 2004.

Kaplan, D.I. 2006. *Geochemical Data Package for Performance Assessment Calculations Related to the Savannah River Site*, WSRC-TR-2006-00004, Savannah River National Laboratory, February 28, 2006.

Kaplan, D.I. and M. R. Millings. 2006. *Early Guidance for Assigning Distribution Parameters to Geochemical Input Terms to Stochastic Transport Models*, WSRC-STI-2006-00019, Savannah River National Laboratory, June 30, 2006.

Kocher, D. C. 1981. *Radioactive Decay Data Tables.* DOE/TIC-11026. Technical Information Center, U.S. Department of Energy, Oak Ridge, Tennessee.

Koffman, L.D. 2006a. *SRNL All-Pathways Application*, WSRC-STI-2006-00179, Rev. 0. SRNL, Washington Savannah River Company, Aiken, SC 29808.

Koffman, L. D. 2006b. *Automated Inadvertent Intruder Application, Version 2*. WSRC-TR-2006-00037. Savannah River National Laboratory, Aiken, SC. September 2006.

Lee, P. 2006. *Atmospheric Dose Modeling for the E-Area Low Level Waste Facility at the Savannah River Site,* WSRC-STI-2006-00262, Washington Savannah River Company, Aiken, SC 29808.

McDowell-Boyer, L., Yu, A. D., Cook, J. R., Kocher, D. C., Wilhite, E. L., Holmes-Burns, H., and Young, K. E. 2000. *Radiological Performance Assessment for the E-Area Low-Level Waste Facility,* Revision 1, WSRC-RP-94-218. Westinghouse Savannah River Company, Aiken, South Carolina. January 31, 2000.

MMES (Martin Marietta Energy Systems, Inc), EG&G Idaho, Inc., and Westinghouse Savannah River Company. 1994. *Radiological Performance Assessment for the E-Area Vaults Disposal Facility (U),* WSRC-RP-94-218, Westinghouse Savannah River Company, Aiken, SC.

Nazaroff, W.W., and A.V. Nero (editors), 1988, Radon and its Decay Products in Indoor Air, John Wiley & Sons, New York, N.Y.

NCRP. 1976. *Structural Shielding Design and Evaluation for Medical Use of X Rays and Gamma Rays of Energies up to 10 MeV.* NCRP Report No. 49. National Council on Radiation Protection and Measurements, Bethesda, Maryland.

NCRP 1996. "Screening Models for Releases of Radionuclides to Atmosphere, Surface Water and Ground," NCRP report No. 123, National Council on Radiation Protection and Measurements, Bethesda, Maryland, Jan. 22, 1996.

Nielson, K.K., V.C. Rogers and G.W. Gee, 1984. *Diffusion of Radon through Soils: A Pore Distribution Model*, Soil Science Society of America, J. 48:482-487.

Phifer, M.A. 2003. Saltstone Disposal Facility Mechanically Stabilized Earth Vault Closure Cap Degradation Base Case: Institutional Control to Pine Forest Scenario (U). WSRC-TR-2003-00523. Westinghouse Savannah River Company, Aiken, South Carolina. December 18, 2003.

Phifer, M. A. and Nelson, E. A. 2003. *Saltstone Disposal Facility Closure Cap Configuration and Degradation Base Case: Institutional Control to Pine Forest Scenario (U)*, Revision 0, WSRC-TR-2003-00436. Westinghouse Savannah River Company, Aiken, South Carolina, September 22, 2003.

Phifer, M. A. 2004. *Preliminary E-Area Trench Closure Cap Closure Sequence, Infiltration, and Waste Thickness (U)*, WSRC-TR-2004-00119. Westinghouse Savannah River Company, Aiken, South Carolina, March 12, 2004.

Phifer, M. A., Millings, M. R., and Flach, G. P. 2006. *Hydraulic Property Data Package for the E-Area And Z-Area Vadose Zone Soils, Cementitious Materials, and Waste Zones*, WSRC-STI-2006-00198. Washington Savannah River Company, Aiken, South Carolina. September 2006.

Sullivan, T. M., C. R. Kempf, C. J. Suen, and S. M. Mughabghab. 1988. *Low-Level Radioactive Waste Source Term Model Development and Testing.* NUREG/CR-5204, BNL-NUREG-52160. Brookhaven National Laboratory, Upton, NY.

Taylor, G. A. and Collard, L. B. 2005. *Automated Groundwater Screening,* WSCR-TR-2005-00203, Revision 0, May 2, 2005

Unger, L. M. and D. K. Trubey. 1982. *Specific Gamma-Ray Dose Constants for Nuclides Important to Dosimetry and Radiological Assessment.* ORNL/TSIC-45/R1. Oak Ridge National Laboratory, Oak Ridge, Tennessee.

WMAP 2002. *Radionuclide Inventory Calculation for 643-7E Naval Reactor Component Storage Area*, N-CLC-E-00085, Rev. 0. October 16, 2002.

WSRC 2006. *SRS Waste Acceptance Criteria Manual,* Procedure Manual 1S, Washington Savannah River Company, Aiken, South Carolina. January 19, 2006.

Yu, C., A.J. Zielen, J.J. Cheng, D.J. LePoire, E. Gnanapragasam, S. Kamboj, J. Arnish, A. Wallo III, W.A. Williams, and H. Peterson, 2001. *Users Manual for RESRAD Version 6*, Environmental Assessment Division, Argonne National Laboratory. Chicago, Illinois.

This page intentionally left blank.

CHAPTER 6

INTEGRATED FACILITY ANALYSIS FOR THE GROUNDWATER PATHWAY

This page intentionally left blank.

6.0 INTEGRATED FACILITY ANALYSIS FOR THE GROUNDWATER PATHWAY

LIST OF FIGURES

LIST OF TABLES

6.0 INTEGRATED FACILITY ANALYSIS FOR THE GROUNDWATER PATHWAY

6.1 EXECUTIVE SUMMARY

The groundwater analyses of the individual waste disposal units (i.e., Slit and Engineered Trenches, Component-In-Grout Trenches, Low Activity Waste Vault, Intermediate Level Vault, and the Naval Reactor Component Disposal Area) did not attempt to account for any co-mingling of plumes from adjacent units. Therefore, the potential for overlap of radionuclide plumes from the various disposal units in the ELLWF is considered in this section. An explicit analysis of the effect of overlapping atmospheric plumes was not performed for the air pathway (see Section 6.9).

6.2 INTRODUCTION AND GENERAL APPROACH

Performance Assessments of selected disposal units (e.g., individual, pair, more) do not account for possible groundwater plume interaction with other nearby units. The potential for plume intermingling depends on several factors, such as facility proximity and orientation, groundwater flow direction, and the relative timing of peak releases (i.e., peak flux rates to the water table from individual disposal units). The purpose of this analysis is to develop disposal limit reduction factors, ranging between 0 and 1, that account for these influences. The fractional plume interaction factors are intended to be a multiplier to initial disposal limits based on an isolated unit or group of units.

The general approach was to place a non-depleting, non-decaying, non-sorbing, tracer source in the aquifer beneath each group of disposal units. The selected groupings (Figure 6-1 and Figure 6-2) include:

- Central Slit Trenches, SLITc (7 units, ST 1 through ST 7 in Figure 6-1)
- Western Slit Trenches, SLITw (6 units, ST 8 plus the five “future disposal areas” west of ST 1 in Figure 6-1)
- Eastern Slit Trenches, SLITe (8 units, the “future disposal areas” east of ST 7 in Figure 6-1)
- Engineered Trenches, ET (2 units)
- Component-In-Grout Trenches, CIG (2 units)
- Intermediate Level Vault, ILV (1 unit)
- Low Activity Waste Vault, LAWV (1 unit)

where the number of disposal units by area is noted in parentheses[1]. These groupings align with E-Area PA analyses for each type of disposal unit. The choice of a continuous tracer species precludes the possibility of plume separation in time, which introduces a significant conservatism with respect to plume overlap in many instances.

[1] The NRCDAs were excluded from the plume interaction analysis because of their very low impact in the groundwater analysis.

Simulations of the tracer migration in the aquifer were carried out using PORFLOW (ACRI 2004), based on the same flow field incorporated in the transport runs for the individual units (Chapters 1 through 5). Comparisons of peak tracer concentrations at 100-m points of compliance were made for model runs assuming an isolated source below each of the groups/units listed above and for model runs with sources below all groups/units simultaneously, in order to evaluate potential plume overlap. Plume interaction factors are intended to reduce the disposal limits for each unit when the potential for plume overlap exists.

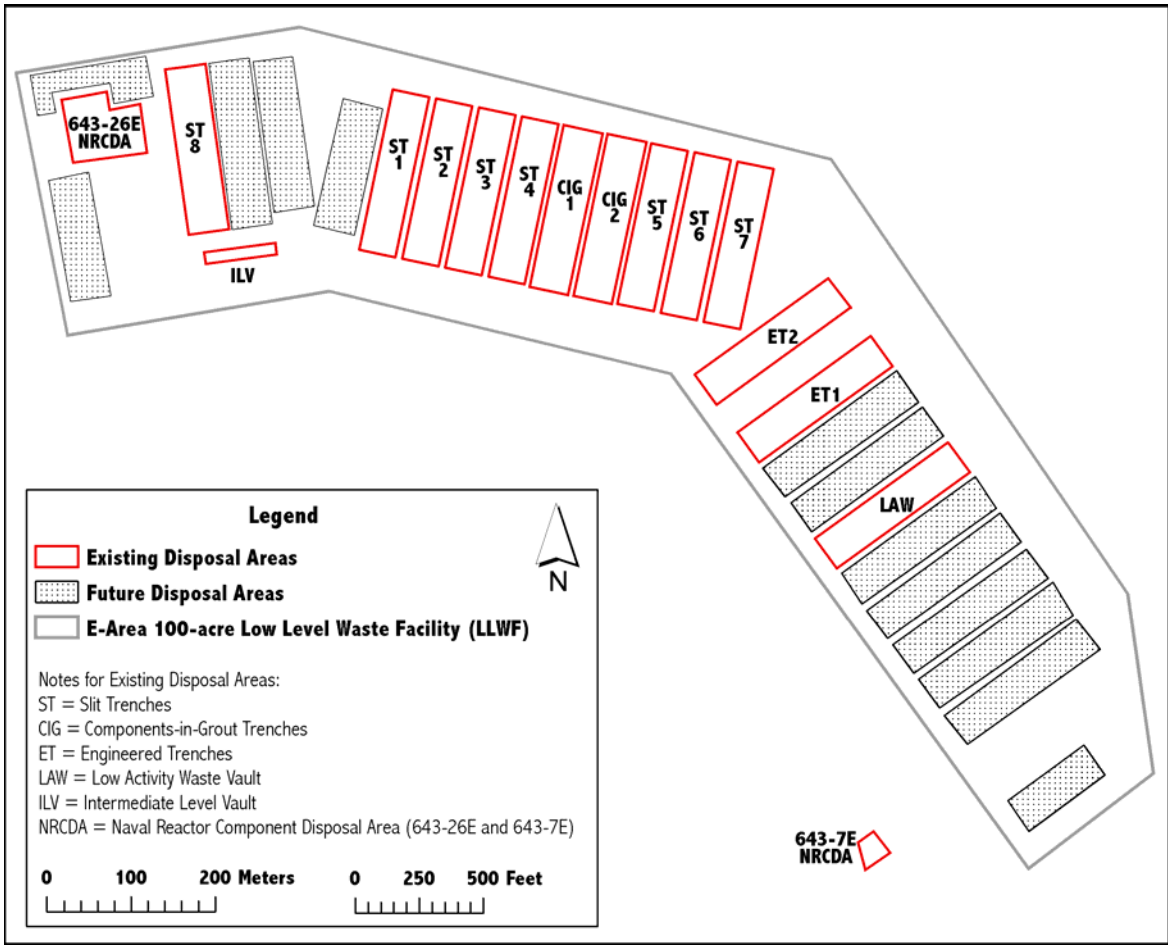

Figure 6-1. E-Area Facility Layout - Existing and Future Disposal Areas

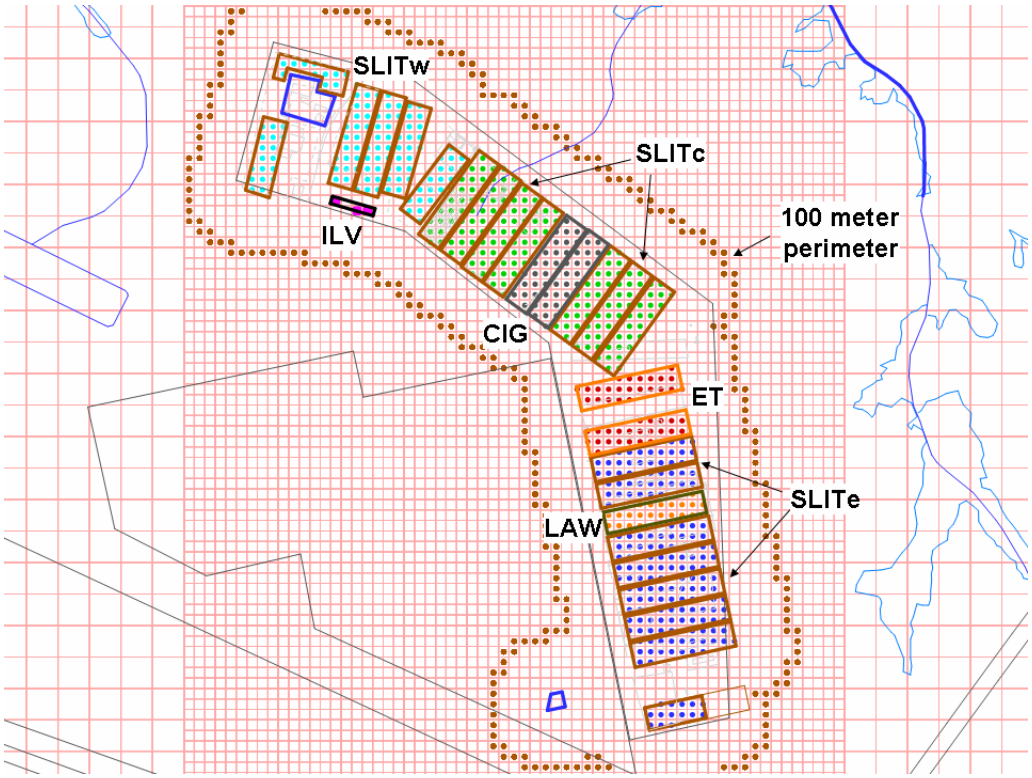

Figure 6-2. E-Area Facility Layout - Source Nodes as Defined in Plume Interaction Model

6.3 CALIBRATION

The source strength for each disposal unit group was adjusted to achieve the same peak concentration (1.E-8 mol/L) at the 100-m boundary surrounding E-Area (depicted in Figure 6-2 as a dotted line around the waste disposal units). The value of 1.E-8 mol/L corresponds approximately to the 100-m concentration resulting from a unit continuous (i.e., one mole per year) source term in the aquifer, and was chosen as the arbitrary "MCL" for the tracer. This choice implies that each disposal unit has been filled to the radionuclide limit, because the source was adjusted for each group of disposal units to achieve this "MCL". This will not typically be the case for all nuclides in all types of disposal units, and introduces another general conservatism to the analysis (in addition to the continuous source specification). This choice implies that each disposal unit has been filled to the radionuclide limit. The location of the peak concentration down-gradient of each group was also identified in the course of calibrating the sources. Figure 6-3 shows the peak 100-m concentration for each disposal unit group after calibration. The figure also shows the peak concentration along the 100-m E-Area boundary when all seven disposal unit groupings are releasing a tracer. Because of plume interaction, the resulting concentration is nearly twice as large as that from SLITc, SLITw, SLITe, ET, CIG, ILV or LAW individually.

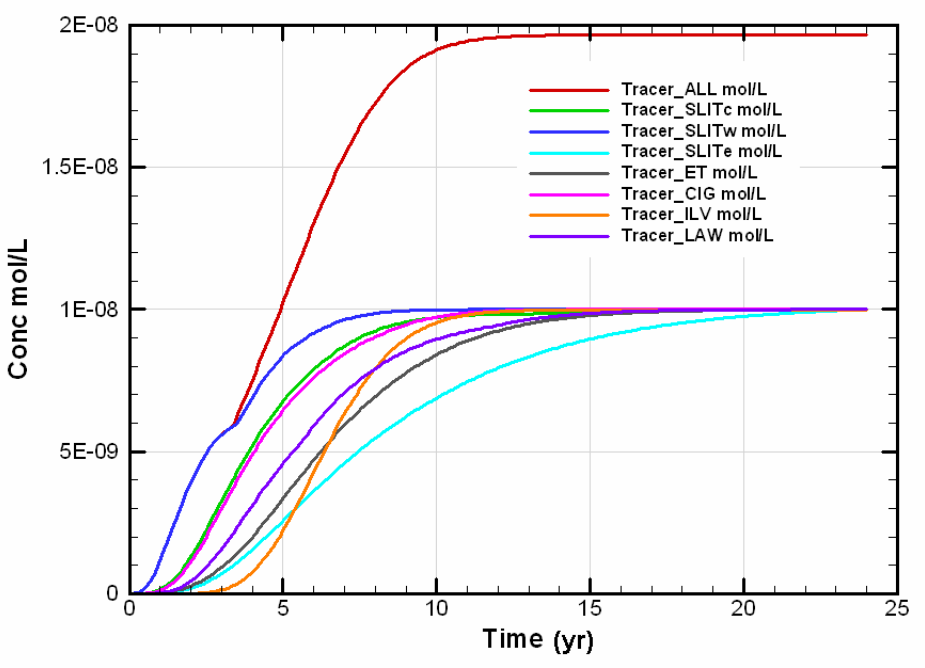

Figure 6-3. Peak 100-m Concentrations after Initial Tracer Source Calibration

6.4 INITIAL GENERIC PLUME INTERACTION FACTORS

The next step was to compare peak concentrations for individual disposal unit types/locations, to the concentration observed at the same locations when all disposal units are emitting the tracer. The results are shown in Figure 6-4 through Figure 6-10. In each of these figures, the time-dependent tracer concentration associated with the disposal group of interest (e.g., SLITc in Figure 6-4), at its 100-m compliance point, is plotted along with the concentration at that same location taking into account the contribution to tracer concentration by plumes associated with all disposal groups. In cases where there is obvious plume interaction between two or more groups, the tracer concentration profile for the disposal groups contributing most significantly to that interaction is displayed (e.g., the ILV contribution at the SLITw 100-m compliance point, Figure 6-5). In Figure 6-6, the "Tracer_ALL" results are obscured by the "Tracer_SLITe" results, indicating minimal interaction of plumes at the compliance point for the SLITe group.

Plume interactions range from minimal (e.g. SLITc, SLITe) to significant (e.g. SLITW, ILV). The SLITc simulation (Figure 6-4) involves 7 disposal units (ST 1 through ST 7, Figure 6-1) in groups of three and four adjoining units. The plume overlap of the individual disposal units within this group, which is accounted for in developing limits for SLITc, is sufficiently large that additional interaction between the SLITc plume and plumes from other disposal unit groups is minimal. Conversely, SLITw and ILV lay directly down- and up-gradient of one another, and their associated plumes exhibit strong interaction (Figure 6-5).

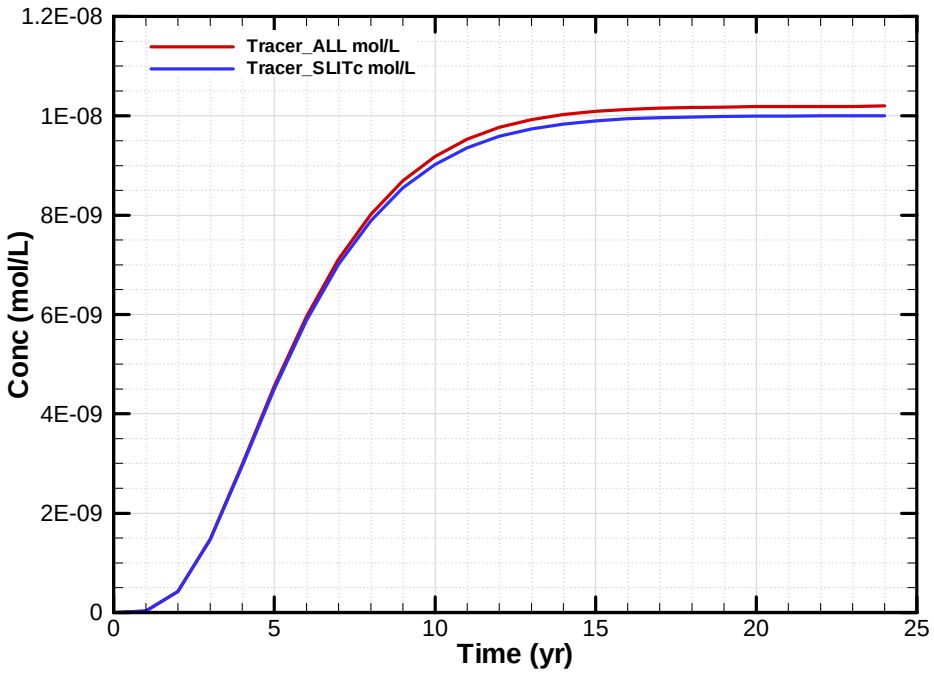

Figure 6-4. Peak 100-m Concentrations for SLITc and ALL Disposal Units

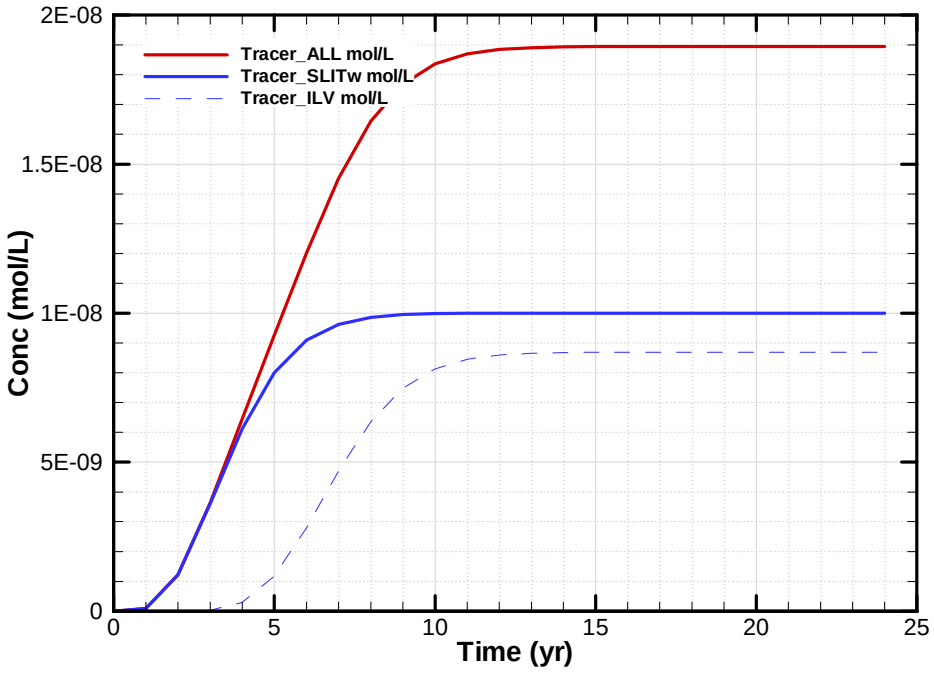

Figure 6-5. Peak 100-m Concentrations for SLITw and ALL Disposal Units

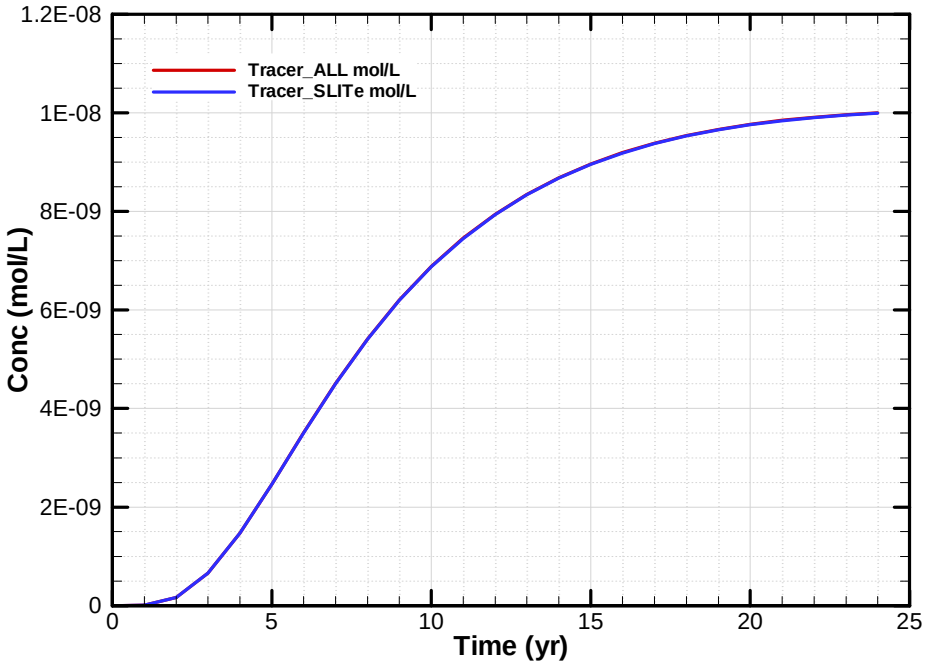

Figure 6-6. Peak 100-m Concentrations for SLITe and ALL Disposal Units (Tracer_ALL and Tracer_SLITe Overlap)

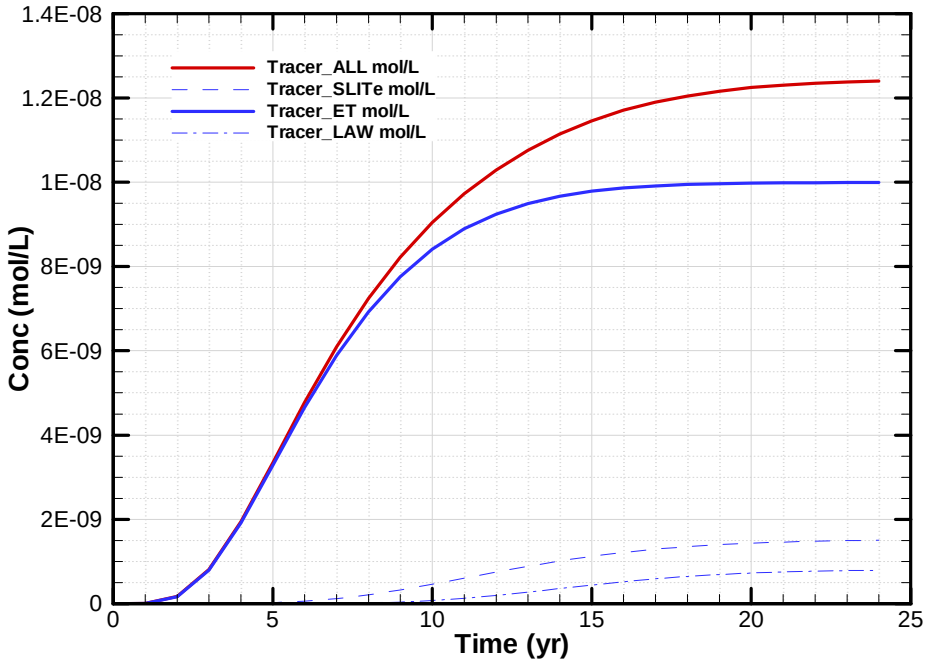

Figure 6-7. Peak 100-m Concentrations for ET and ALL Disposal Units

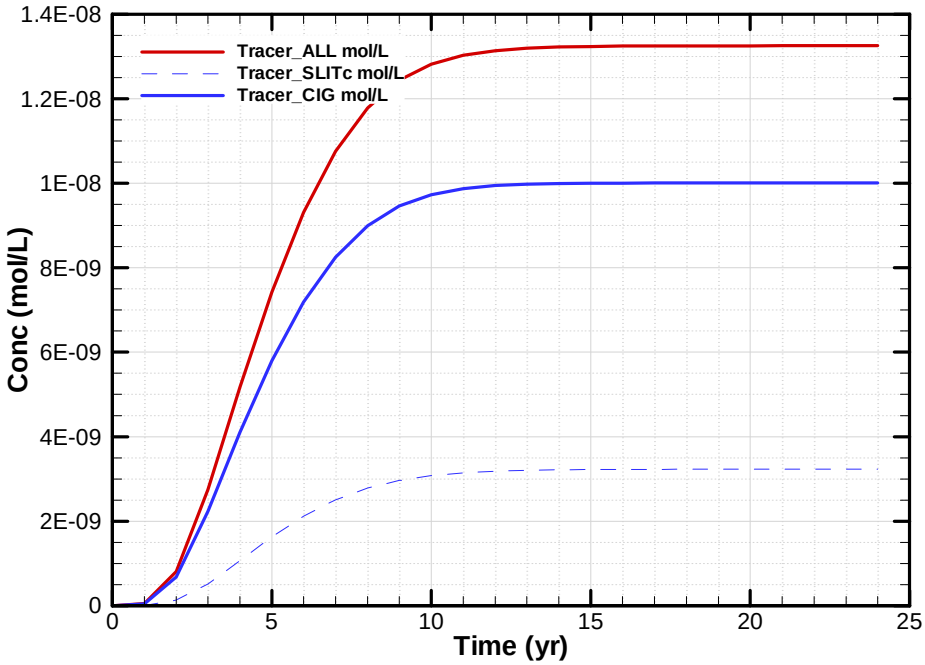

Figure 6-8. Peak 100-m Concentrations for CIG and ALL Disposal Units

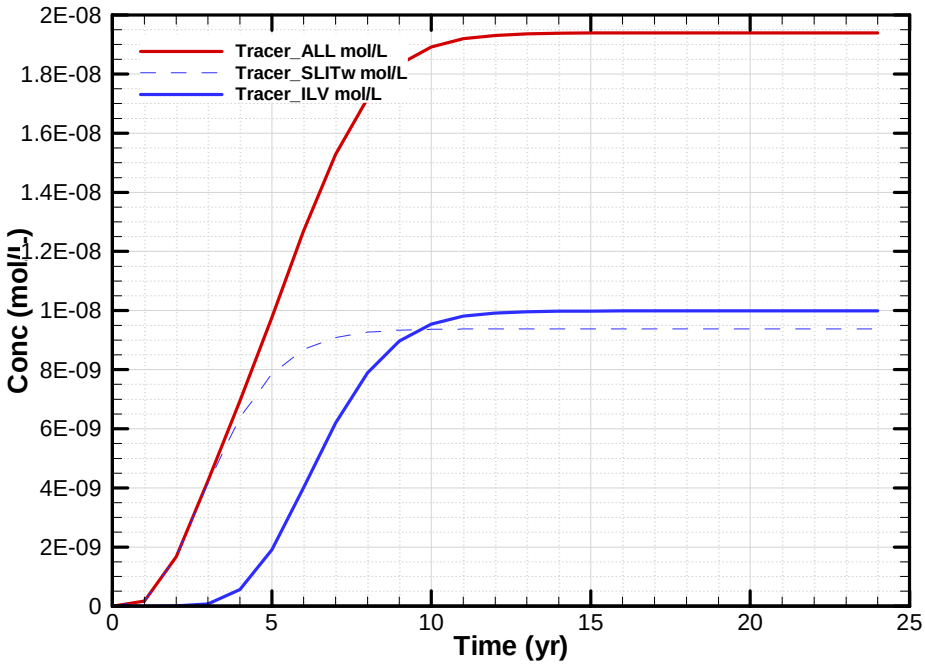

Figure 6-9. Peak 100-m Concentrations for ILV and ALL Disposal Units

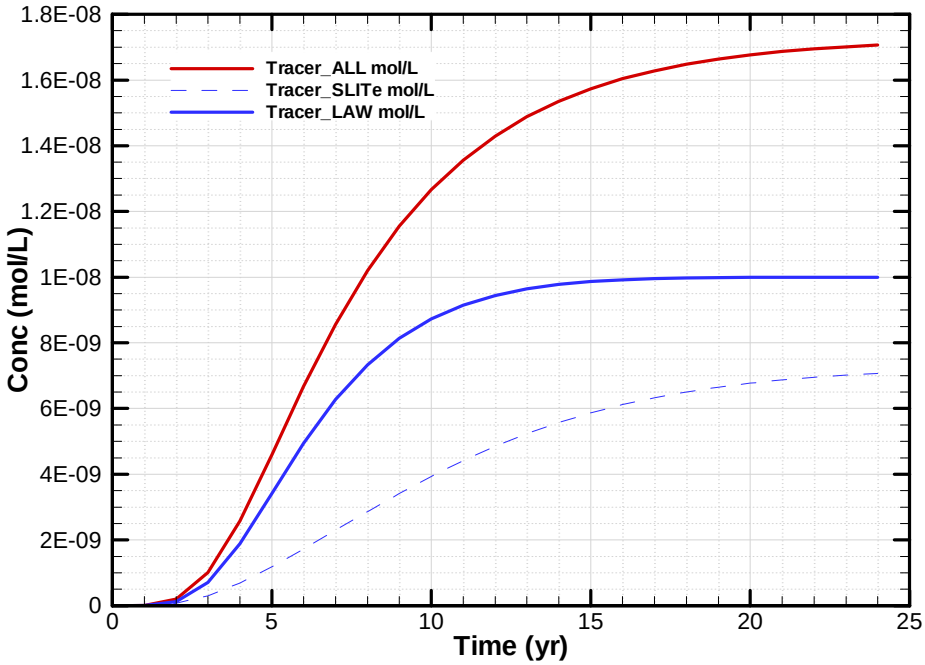

Figure 6-10. Peak 100-m Concentrations for LAW and ALL Disposal Units

Initial generic plume interaction factors were devised by taking the ratio of peak concentration from ALL disposal units in play to each individual group. The initial factors are shown in Table 6-1. The Concentration Multiplier represents this ratio for each group. The Disposal Limit Multiplier is simply the inverse of the Concentration Multiplier. The Concentration Multiplier is greatest for units, or groups of units, for which plume interactions are greatest.

Table 6-1. Initial Generic Plume Interaction Factors

Disposal Unit Group	Concentration Multiplier	Disposal Limit Multiplier
SLITc	1.02	0.98
SLITw	1.90	0.53
SLITe	1.00	1.00
ET	1.24	0.81
CIG	1.33	0.75
ILV	1.94	0.52
LAW	1.71	0.58

6.5 VALIDATION

As a validation step, the factors from Table 6-1 were used to reduce the tracer source strength. For example, the SLITw source strength was decreased by a factor of 1.90. After re-simulating plume migration (Figure 6-11), the peak 100-m concentration was compared to 1.E-8 mol/L (Figure 6-12), the pseudo-MCL selected for this study. While significantly improving compliance with the MCL, some refinement was warranted, as evidenced by the exceedence of 1.E-8 mol/L near the 100-m boundary when contributions to the peak concentration by all units are considered together (Tracer_ALL curve, Figure 6-12).

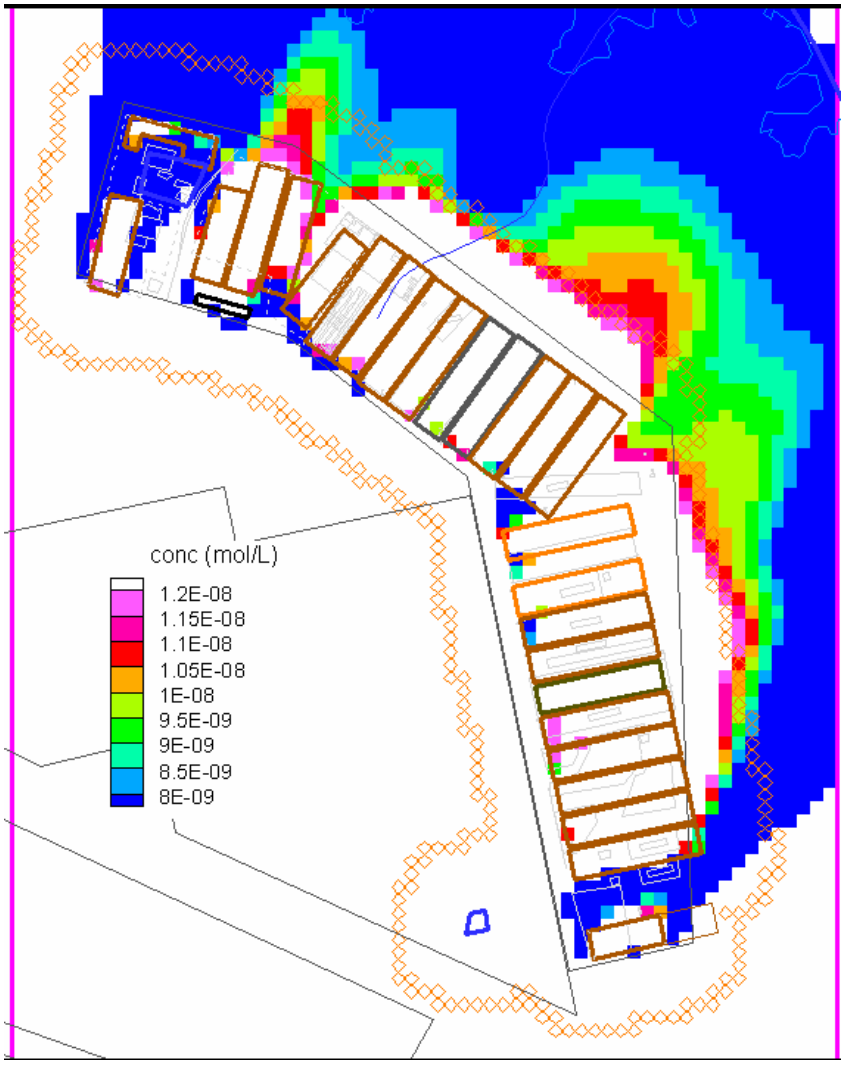

Figure 6-11. Steady-state Plume Configuration for All Disposal Units Emitting a Continuous Tracer After Application of the Initial Generic Plume Interaction Factors from Table 6-1

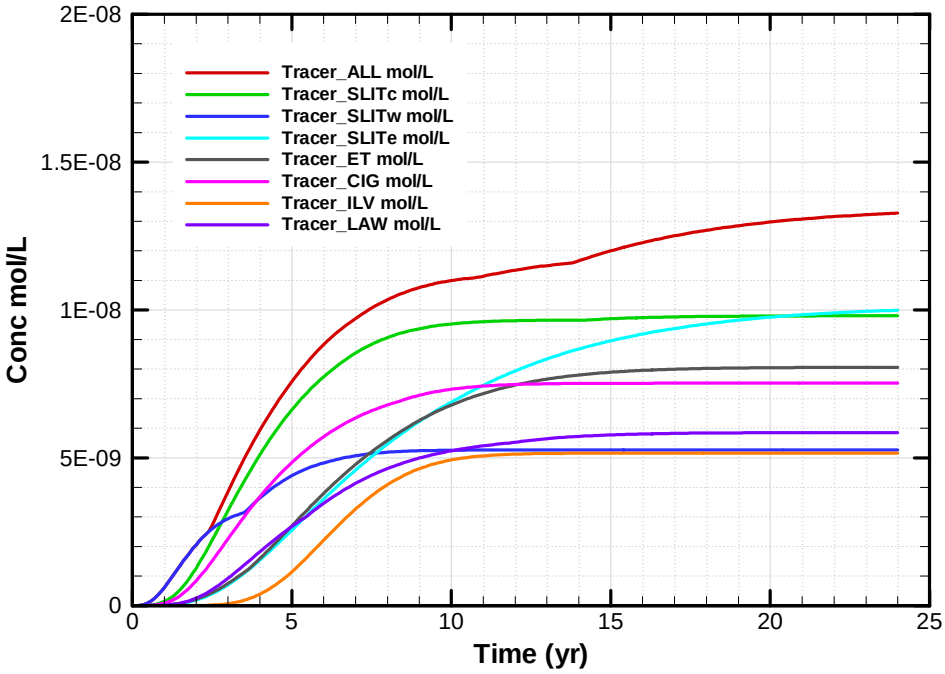

Figure 6-12. Peak 100-m Concentrations after Application of Initial Generic Plume Interaction Factors from Table 6-1

6.6 REFINING GENERIC PLUME INTERACTION FACTORS

Refinement of the plume interaction factors in Table 6-1 was necessary to adjust the disposal limits to adequately consider potential plume overlap. For the SLITw, ILV, and ET the initial plume factors were adequate because concentrations downstream of these units are at or below the pseudo-MCL. For SLITc and CIG, the initial generic plume interaction factors were adjusted such that the source strengths for these units were reduced by 13% (i.e., the Concentration Multipliers were increased by 15%). Similarly, the SLITe and LAW factors were selected such that the source strength for these units was reduced by 20%. These adjustments were done on a trial and error basis to achieve adherence to the 1.E-8 mol/L peak concentration at the 100-m boundary. The refined factors are given in Table 6-2. Figure 6-13 shows the facility plume after these adjustments are applied, and Figure 6-14 illustrates the peak 100-m facility concentration. As indicated in Figure 6-14, the total contribution from all waste units (Tracer_ALL) is essentially now in compliance with the assumed 1.E-8 mol/L MCL, thus validating the refined generic plume interaction factors given in Table 6-2. These refined plume interaction factors can be used with any radionuclide released from the E-Area LLWF to adjust disposal limits to account for plume overlap.

Table 6-2. Refined Generic Plume Interaction Factors

Disposal Unit Group	Concentration Multiplier	Disposal Limit Multiplier
SLITc	1.17	0.85
SLITw	1.90	0.53
SLITe	1.25	0.80
ET	1.24	0.81
CIG	1.53	0.65
ILV	1.94	0.52
LAW	2.14	0.47

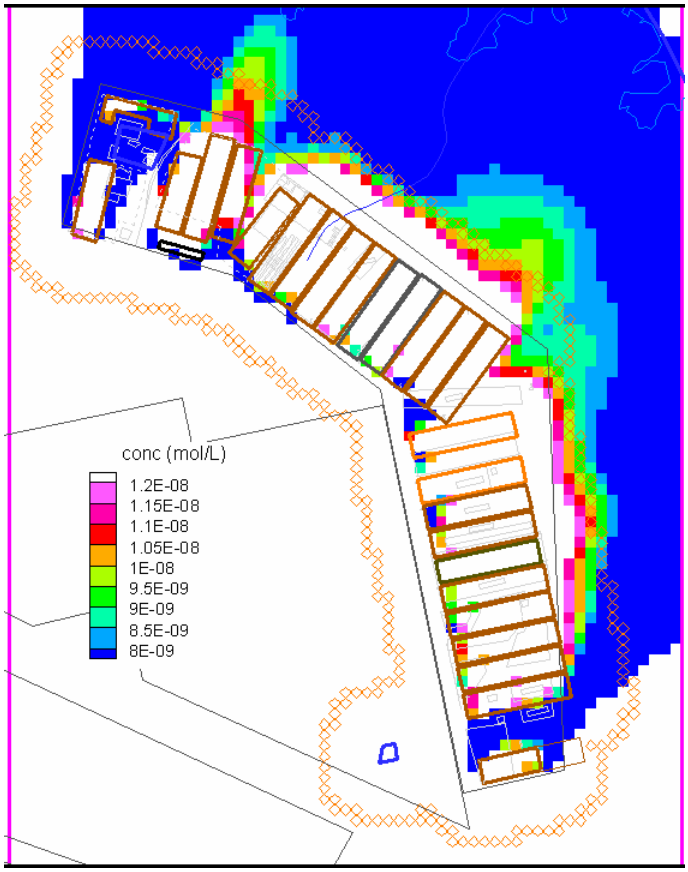

Figure 6-13. Steady-state Plume Configuration for All Disposal Units Emitting a Continuous Tracer After Application of the Refined Generic Plume Interaction Factors from Table 6-2

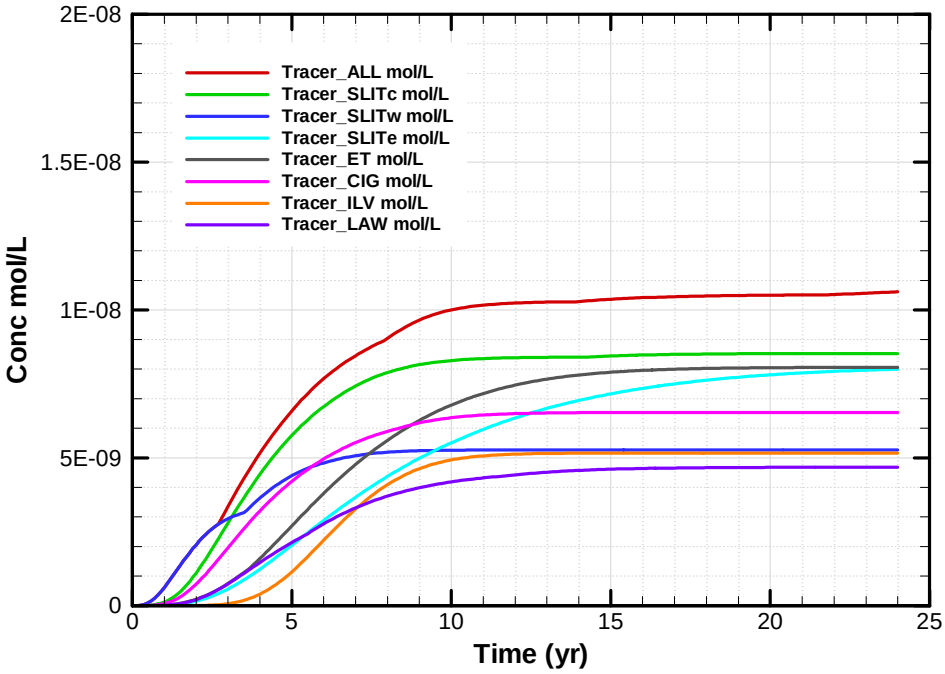

Figure 6-14. Peak 100-m Concentrations after Application of Refined Generic Plume Interaction Factors from Table 6-1

6.7 SPECIFIC PLUME INTERACTION FACTORS

The derived generic plume interaction factors (Table 6-2) are bounding estimates of plume overlap due to two assumptions: 1) a continuous source exists over time, and 2) all sources are designated at the limit to achieve the MCL at the 100-m boundary. These factors can be significantly relaxed for certain disposal units and specific nuclides. In particular, I-129 disposed in the SLITw group of trenches results in a peak concentration at the 100-m boundary within the 0-30 year operational period, while I-129 from the ILV is released much later in time (see simulation results for these disposal units in Appendix A). For this reason, an analysis specific to I-129 was conducted. In this specific analysis, the vadose model predictions for I-129 flux to the water table from the SLIT, ET and ILV disposal units are used, as opposed to assuming a continuous flux to the water table (i.e., non-depleting tracer) at both the SLITw and ILV locations. The LAWV, far from the ILV, was treated as a slit trench for convenience. The specified source strength at the water table achieves a peak concentration at the 100-m boundary of approximately 1.E-9 mol/L; thus, a value of 1.E-9 mol/L is used for adjusting the source strengths to achieve the same peak concentration at the 100-m boundary.

The result of this specific analysis for I-129 is shown in Figure 6-15. Note that plume interaction is much lower compared to a non-depleting tracer, and the SLITw and ILV peaks are essentially completely separated in time. Interaction with the adjoining SLITc group remains, although the impact is small. A specific plume interaction factor (i.e., Disposal Limit Multiplier) of 0.98 for I-129 in the SLITw is adequate to account for this effect, as confirmed by Figure 6-16, which shows 100-m peak concentrations for generic I-129 after applying plume interaction factors. To generate the curves for I-129 from its various sources in Figure 6-16, the factor of 0.98 for I-129 in SLITw and the refined generic values from Table 6-2 for the other sources of I-129 were applied. The limited impact of *generic* I-129 (that is, I-129 not associated with a special wasteform) from SLITw on the total peak concentrations allows the use of the relaxed plume interaction factor for SLITw in this specific case.

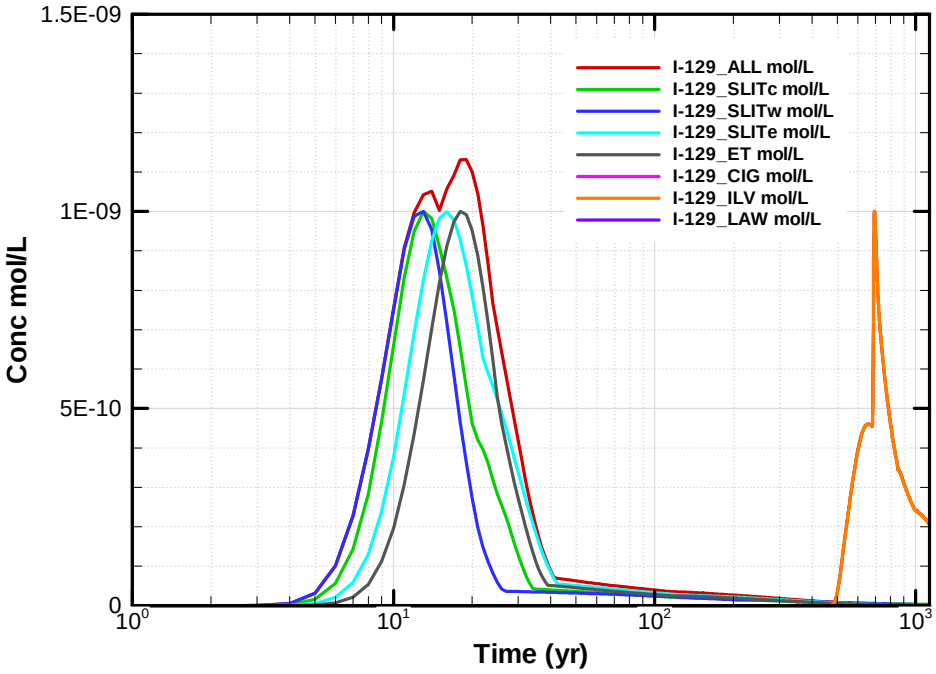

Figure 6-15. Peak 100-m Concentrations after Initial I-129 Source Calibration

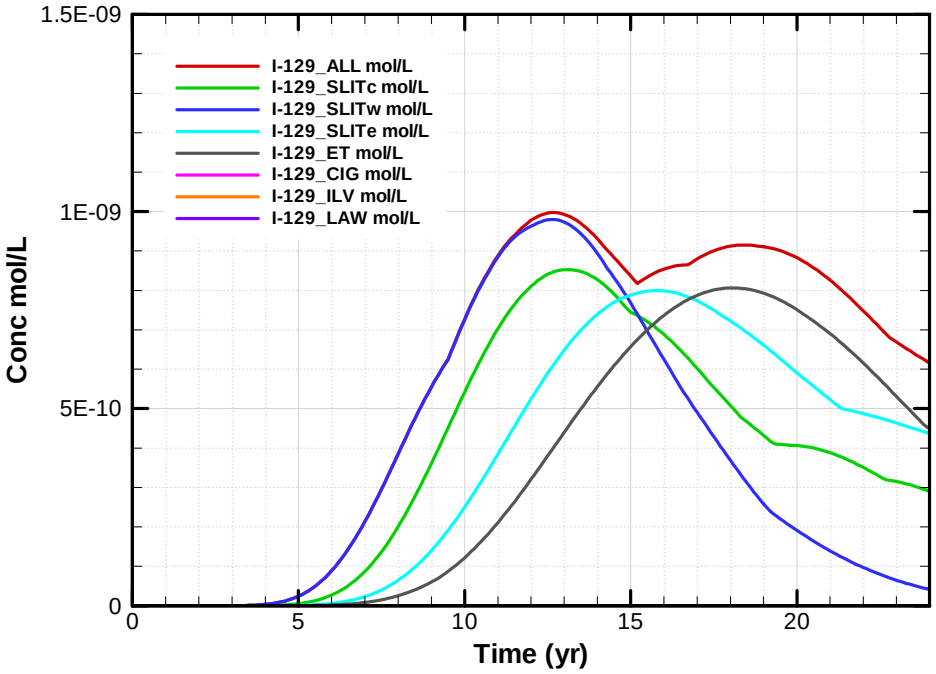

Figure 6-16. Peak 100-m Concentrations after I-129 (generic) Plume Factor of 0.98 is Applied to SLITw

6.8 APPLICATION OF PLUME INTERACTION FACTORS

The generic plume interaction factors will be used to adjust groundwater limits derived in this PA for all units except for the NRCDAs. Each groundwater limit (i.e., all-pathways, beta-gamma, gross alpha, radium, and uranium) will be multiplied by the generic plume interaction factor (Disposal Limit Multiplier) from Table 6-2 for each of the disposal units except for the NRCDAs. A special case is used for generic I-129 (in contrast to I-129 associated with special wasteforms) in SLITw, where the specific plume interaction factor of 0.98 is applied. The final groundwater limits (i.e., after adjustment for plume interaction and sensitivity/uncertainty, as appropriate) are documented in Chapter 7.

The derived generic plume interaction factors in many cases are upper bound estimates of the correction needed to address the actual effects of plume overlap because they are based on two assumptions that are often conservative. First, it is assumed that the tracer (representing each radionuclide in the disposal units) is released continuously over time, and thus that there is no depletion in the source term. As noted earlier, this continuous release assumption precludes the possibility of plume separation in time, and maximizes plume overlap potential. The specific interaction factor calculated for the I-129 in SLITw eliminates some of the conservatism added by this assumption. Second, the magnitude of the release from each disposal unit group is assumed to be at the disposal limit. This also maximizes the plume overlap potential, yet is not realistic for many radionuclides in terms of the current projected inventories (Appendix C) for the various units. It is unlikely that these factors would underestimate the effects of plume overlap.

6.9 POTENTIAL PLUME OVERLAP IN THE AIR PATHWAY

An explicit analysis of the effect of overlapping atmospheric plumes was not performed for the air pathway. However, during the LFRG review of the draft PA, one of the secondary issues noted by the LFRG review team was that there is potential for the overlap of atmospheric plumes at the SRS boundary. Air-pathway impacts are assessed at the SRS boundary during the operational and active institutional control periods. To respond to this issue, the projected closure inventory of tritium in the Intermediate Level Vault was reduced to 1.5E+06 Ci to reduce the sum-of-fractions of the air-pathway limits for the ILV to 0.4, which results in the sum of all of the air-pathway SOFs for all units to be < 1 (see Tables C-24 and C-25 in Appendix C and Table B-1 in Appendix B) (Di Sanza 2008).

6.10 REFERENCES

ACRI (Analytic & Computational Research, Inc.). 2004. *PORFLOW User's Manual*, Version 5.0, Rev: 5. Available at http://www.acricfd.com/download/papers/PORFLOW.pdf

Di Sanza 2008. Memorandum, E. Frank Di Sanza to Marty J. Letourneau, *Transmittal of the Review Team Report for the E-Area Low-Level Waste Facility DOE 435.1 Performance Assessment at the Savannah River Site*, Feb 4, 2008.

CHAPTER 7

INTEGRATION AND INTERPRETATION

This page intentionally left blank.

7.0 INTEGRATION AND INTERPRETATION

LIST OF TABLES

7.0 INTEGRATION AND INTERPRETATION

7.1 EXECUTIVE SUMMARY

Results of sensitivity analyses for the Slit Trenches, Engineered Trenches, CIG Trenches, ILV, and LAWV have been assessed. These results indicate that no reduction of radionuclide disposal limits other than for plume overlap is needed.

7.2 INTRODUCTION AND GENERAL APPROACH

Preliminary radionuclide disposal limits have been derived in this PA for each individual disposal unit (e.g., LAWV) or group of units (e.g., East Slit Trenches). The disposal limits are developed with consideration of the performance objectives and measures set forth by DOE Order 435.1 (DOE 1999). Table 7-1 summarizes the performance objectives and assessment requirements relative to the measure applied and the points of compliance assumed in this PA.

For water resources impacts, the SRS interpretation of the measure (i.e., compliance with EPA public drinking water standards) considers the hierarchical approach put forth in the Order:

- First, the DOE low-level waste disposal facility must comply with any applicable State or local law, regulation, or other legally *applicable* requirements for water resource protection.
- Second, the DOE low-level waste disposal facility must comply with any formal agreement applicable to water resource protection that is made with appropriate State or local officials.
- Third, if neither of the above conditions applies, the site needs to select assumptions for use in the performance assessment based on criteria established in the site groundwater protection management program and any formal land-use plans.
- If none of the above conditions apply, the site may select assumptions for use in the performance assessment for the protection of water resources that are consistent with the use of water as a drinking water source.

The points of compliance listed in Table 7-1 were developed with consideration of the guidance put forth in the Order and institutional controls. Although the SRS Future Use Plan (DOE 1998) indicates that the land will remain under the ownership of the federal government, consistent with the site's designation as a National Environmental Research Park, the results were evaluated at the point of highest concentration outside of the 100-m buffer zone surrounding the disposal units, with the following exceptions. For the air pathway, the point of highest concentration outside of the SRS boundary was considered the point of compliance during the operational and institutional control period. For the intruder assessment, the time period of the analysis did not commence until after the 100-year institutional control period.

Table 7-1. Performance Objectives, Assessment Requirements, and Points of Compliance

Performance Objective[a]	Measure	Point of Compliance
All pathways	≤25 mrem in a year, not including doses from radon and progeny	Point of highest projected dose or concentration beyond a 100-m buffer zone surrounding the disposed waste.
Air pathway	≤10 mrem in a year, not including doses from radon and progeny	Point of highest projected dose or concentration beyond a 100-m buffer zone surrounding the disposed waste.
Radon	an average flux of ≤ 20 pCi/m^2/s	Disposal facility surface
Assessment Requirement[b]	Measure	Point of Compliance
Hypothetical inadvertent intruder	100 mrem in a year from chronic exposure	Disposal facility
	500 mrem from a single event	Disposal facility
Impact on Water Resources	The SRS interpretation is that concentrations of radioactive contaminants should not exceed standards for public drinking water supplies established by the EPA (40 CFR Part 141).	Point of highest projected dose or concentration beyond a 100-m buffer zone surrounding the disposed waste.

a. DOE Order 435.1 requires that low-level waste disposal facilities shall be sited, designed, operated, maintained, and closed so that a reasonable expectation exists that the performance objectives will be met for waste disposed after September 26, 1988.

b. DOE Order 435.1 also requires that the performance assessment include, for purposes of establishing limits on radionuclides that may be disposed of near-surface, an assessment of the impacts on water resources and an assessment of impacts calculated for a hypothetical person assumed to inadvertently intrude for a temporary period into the low-level waste disposal facility.

The preliminary limits are reported in Chapters 1 through 5 of Part B for (in numerical chapter order) Slit and Engineered Trenches, CIG Trenches, LAWV, and ILV, and NRCDA, and do not consider potential interaction of groundwater plumes from the various units. These limits are considered preliminary because they do not consider the potential interaction of groundwater plumes, which may in effect lower the calculated unit-specific limit, and do not consider the results of the uncertainty and sensitivity analyses.

Interaction of groundwater plumes may occur due to proximity of disposal units to other nearby units. The potential for plume intermingling depends on several factors, such as facility proximity and orientation, groundwater flow direction, and the relative timing of peak releases. In Chapter 6, Integrated Facility Analysis, fractional plume interaction factors are provided to be used as multipliers with preliminary disposal limits. The interaction factors, which in effect are disposal limit reduction factors, range between 0 and 1, and account for these influences.

For the E-Area disposal units, a tiered approach for addressing uncertainty in PORFLOW-based groundwater concentration calculations was carried out, which involved adopting conservative assumptions for some portions of the groundwater pathway analysis, and conducting qualitative sensitivity analysis. For the Slit and Engineered Trenches, a sensitivity analysis was conducted in which additional percentages of non-crushable waste was assumed to be present and a sum-of-fractions (SOF) analysis was conducted for four highly-mobile radionuclides that contribute the most to the SOF as depicted in Table 7-34 and Appendix C (i.e., H-3, C-14, Tc-99, and I-129 and their special waste forms).

For the CIG, Kd values, timing of cementitious material aging and grout effective diffusivity were selected for sensitivity analysis. For the ILV, sorption coefficients and effective diffusion coefficients were judged to be the dominant contributors to radionuclide concentration uncertainty, and sensitivity runs were conducted by varying these two parameters. For the LAWV, K_d, D_{eff}, vault cracking, and infiltration were identified for sensitivity runs. Sensitivity runs were conducted by varying all except infiltration rates, since uncertainty in infiltration has not yet been defined. The results of the sensitivity analyses can be evaluated by considering the impact of independently varied parametric values on the summed fraction of each radionuclide's disposal limit for the disposal unit of interest.

In this chapter, the radionuclide disposal limits, corrected for plume interaction, are presented for each disposal unit. Implications of parametric sensitivity analyses are also evaluated. The final radionuclide disposal limits are compared with the projected radionuclide inventories (Appendix C) and the SOF of limits for all performance measures for each disposal unit are provided in Appendix C. The SOF of limits are summarized in section 7.6.

7.3 CONSIDERATION OF SENSITIVITY

7.3.1 Slit and Engineered Trenches

The deterministic groundwater sensitivity analysis for the Slit and Engineered Trenches using PORFLOW is presented in Section 1.6.7. Two sensitivity cases were considered. First, the effects of cellulose degradation products (CDP) and the presence or absence of non-crushable waste at 10% of the trench volume were considered. Second, the effects of varying the amount of non-crushable waste were considered.

7.3.1.1 CDP and Non-Crushable Waste

As indicated in Section 1.6.2, four scenarios were simulated for the Slit Trenches to represent the range of waste types expected. The scenarios account for the presence or absence of cellulose degradation products (CDP) and the presence or absence of non-crushable waste at a loading of 10% of the trench area. The preliminary disposal limits for the Slit Trenches developed in Section 1 and presented in Table 1-1, Table 1-2, and Table 1-3 are the most restrictive, for each radionuclide, of the limits developed for the four scenarios. To illustrate the conservative nature of these limits, Table 7-2 shows the sums-of-fractions for four mobile radionuclides, H-3, C-14, Tc-99, and I-129, which are the nuclides that contribute the most to the sums-of-fractions (see Table 7-34), and their special wasteforms using the predicted closure inventory for the Center Slit Trench units (see Appendix C).

Table 7-2. Sums-of-Fractions for Mobile Radionuclides for Four Groundwater Analysis Scenarios for the Center Slit Trench Units

	Sums of Fractions for Mobile Radionuclides					
	All-Pathways			Groundwater Protection Beta-Gamma		
Case	**130-200 yrs**	**200-1000 yrs**	**1000-1300 yrs**	**0-12 yrs**	**12-100 yrs**	**100-1130 yrs**
No Non-crushable - CDP off	6.72E-03	3.92E-02	8.43E-03	5.72E-01	7.86E-01	1.12E-01
No Non-crushable - CDP on	7.54E-03	4.08E-02	9.97E-03	7.93E-01	8.98E-01	1.66E-01
10% Non-crushable - CDP off	3.48E-02	3.64E-02	8.66E-03	5.72E-01	7.86E-01	1.32E-01
10% Non-crushable - CDP on	3.63E-02	3.82E-02	1.05E-02	7.93E-01	8.98E-01	2.09E-01
Base Case (Worst Limit)	3.63E-02	4.14E-02	1.05E-02	8.13E-01	9.19E-01	2.14E-01

As expected, the base case, which is the most restrictive of the limits among the four scenarios, SOF is greater than or equal to the SOFs for the individual scenarios. For the all-pathways performance measure, the base case is equal to the SOF for two of the time periods for the case with both CDP and 10% non-crushable waste; for the 200-1000 year time period, the base case SOF is larger than that for any of the four scenarios. For the Beta-Gamma groundwater protection performance measure, the base case is larger than that for any of the four scenarios. These results show the conservative nature of the limits for the Slit Trenches. The Engineered Trenches are expected to perform similarly.

7.3.1.2 Non-Crushable Waste

To assess the sensitivity of PA results to the amount of non-crushable waste in the trenches, simulations were run for the Slit Trench model using 5% and 15% non-crushable waste to complement the results in the PA for cases with 0% and 10% non-crushable waste. The results are shown in Section 1.6.7.1. These results show that the analysis using 0% and 10% non-crushable waste bound the case with 5% non-crushable. The results also show that the presence of 15% non-crushable waste can increase the radionuclide flux to the water table by up to 50%. This indicates the importance of controlling the non-crushable content to 10% or less through administrative controls.

7.3.2 Components-in-Grout Trenches

The deterministic groundwater sensitivity analysis for CIG using PORFLOW is presented in Section 2.6.10.1. Four sensitivity cases were analyzed. They are:

A. K_d values were changed to not use the CDP factors.

B. K_d values were changed to use the conservative estimate K_ds with CDP factors applied.

C. The timing of cementitious material aging was changed to omit the middle age, thus transitioning from the young age to the old age at 325 years; an unrealistic case. This change was applied to both the existing and future segments.

D. Grout D_{eff} was changed to the mean value plus 3-sigma for both the existing and future segments.

The CIG sensitivity analysis results were assessed from the perspective of the change in the sum-of-fractions (SOF) of the limits between the base case and the sensitivity cases, using the projected CIG inventory at closure (see Appendix C). The results are shown in Table 7-3.

Table 7-3. CIG Sensitivity Analysis Results

Performance Measure/Time Period (years)	Baseline	Case A	Case B	Case C	Case D
All-Pathways 0-125	1.6E-04	1.6E-04	1.6E-04	1.6E-04	3.1E-03
125-1125	6.3E-01	7.3E-01	8.0E-01	1.4E+00	6.1E-01
Beta-Gamma 0-125	7.1E-03	7.1E-03	7.1E-03	7.1E-03	1.8E-01
125-1125	8.1E-01	7.8E-01	9.4E-01	1.9E+00	7.7E-01
Gross Alpha 0-125	0.0E+00	0.0E+00	0.0E+00	0.0E+00	0.0E+00
125-1125	7.5E-02	1.2E-01	1.1E-01	7.7E-02	7.5E-02
Radium 0-125	0.0E+00	0.0E+00	0.0E+00	0.0E+00	0.0E+00
125-1125	1.4E-02	1.9E-02	1.9E-02	1.5E-02	1.4E-02
Uranium 0-125	0.0E+00	0.0E+00	0.0E+00	0.0E+00	0.0E+00
125-1125	2.0E-11	4.2E-11	3.2E-11	2.4E-11	2.0E-11

Most of the sensitivity case results are compliant with the performance measures (i.e., the SOF does not exceed one). The SOFs for the 0-125 year time period are much smaller than those for the 125-1125 year period. The early results will not be discussed further.

For the all-pathways performance measure, Case A results in a 20% increase in SOF, Case B results in a 30% increase in SOF and Case D results in a slight decrease in SOF. The SOF for Case C is about a factor of two greater than the baseline and the SOF for Case C is non-compliant, being 1.40. For the Beta-Gamma performance measure, the results are very similar; Cases A and D result in a slight decrease in SOF, Case B results in a small increase, and Case C is somewhat more than a factor of two greater than the baseline. The SOF for Case C is also non-compliant for the Beta-Gamma performance measure, being 1.9. For the Gross Alpha performance measure, the SOF for Case A is about 60% higher than the baseline, Case B is about 50% higher and Cases C and D are about the same as the baseline. For the Radium performance measure, Cases A and B result in an SOF about 40% higher than the baseline, Case C is slightly higher than the baseline and Case D is the same as the baseline. For the Uranium performance measure, the Case A SOF is slightly more than twice the baseline, Case B is 60% higher and Case C is 20% higher, with Case D being the same as the baseline.

These results show the relatively strong influence of the K_d parameter in Cases A and B and the small influence of the grout effective diffusivity in Case D. Case C gives somewhat varying results. The SOF for the all-pathways and Beta-Gamma performance measures are increased by factors of 2 and 1.9, respectively and both of these SOFs are greater than one, signifying non-compliance. The SOFs for the three other performance measures (i.e., Gross Alpha, Radium, and Uranium) are the same as, 10% greater than, and 20% greater than the baseline, respectively.

In Case C, cementitious material aging was accelerated. The age of the cementitious material affects the K_d for many radionuclides. Generally, the K_d decreases at each step in the transition from young to moderately-aged to aged cement. However, the difference in K_d between the young and moderately-aged cement is much less than the difference between the moderately-aged and aged cement (Kaplan 2006). Therefore, in sensitivity case C, where the moderately-aged state was omitted, the reduction in K_d is much greater than would be expected, as well as occurring earlier. This sensitivity case also illustrates the strong influence of the K_d parameter. The non-compliant results for the Beta-Gamma and all-pathways performance measures for Case C do not indicate that the CIG disposal limits should be decreased. Rather, they indicate that further research on the chemical transitions in cementitious materials due to leaching should be conducted to better define the transition timing.

7.3.3 Intermediate Level Vault

The groundwater sensitivity analysis for the ILV is presented in Section 4.6.6. The results show very small sensitivity to D_{eff}. For the K_d, the change in disposal limit ranges from none for radionuclides which have a base case K_d of 0 mL/g to three orders of magnitude (e.g., Th-232, beta-gamma performance objective, 200-1100 year time frame) for radionuclides with an appreciable K_d.

The sensitivity analysis results were assessed from the perspective of the change in the SOF of the limits between the base case and the 2-sigma (i.e., 95th percentile) K_d case. The projected inventory at closure was used to calculate the fraction of each radionuclide's disposal limit and the fractions were summed to determine the SOF. The results are shown in Table 7-4.

Table 7-4. ILV Sensitivity Analysis Results for K_d

Performance Measure	Base Case SOF	Kd 2 σ SOF
βγ 0 – 200 yrs	3.64E-02	2.50E-02
βγ 200 - 1100 yrs	4.95E-01	7.03E-01
Gross Alpha 0 – 200 yrs	0.00	0.00
Gross Alpha 200 – 1100 yrs	1.21E-01	6.68E-01
Radium 0 – 200 yrs	0.00	0.00
Radium 200 – 1100 yrs	9.06E-02	5.01E-01
Uranium 0 - 200 yrs	0.00	0.00
Uranium 200 – 1100 yrs	6.86E-18	4.05E-15
All Pathways 0 – 200 yrs	1.40E-03	9.60E-04
All Pathways 200 – 1100 yrs	1.11E-01	3.18E-01

The use of the 2-sigma Kd values results in the SOF being unchanged for three of the limits (i.e., those where the SOF is zero), with the others increasing, except for the beta-gamma 0 – 200 year and all pathways 0 - 200 year SOF, which decreases with the use of the 2-sigma Kd values. The greatest increase is for the uranium 200 to 1100 year limits, which is a factor of almost 600. However, the SOF for that limit is very small, only 4.05E-15 for the 2-sigma case. For the other limits, the greatest increase is a factor of 5.5 for the Gross Alpha 200 to 1100 year limits and for the radium 200 to 1100 year limits.

The greatest SOFs for the 2-sigma case are 70.3% for the Beta-Gamma 200 to 1100 year limits and 66.8% for the gross alpha 200 to 1100 year limits. Because of the potential for groundwater plume interaction, these SOFs should be multiplied by 1.94 (See Chapter 6), which results in an SOF of 136% for the 2-sigma case for the 200-1100 year Beta-Gamma limits and 130% for the Gross Alpha limits for the same time period. However, as shown in Chapter 6 when the potential plume interaction with the ILV for a specific radionuclide (i.e., I-129), was calculated, the plume interaction factor became 1.00. The Beta-Gamma SOF is dominated by C-14 and I-129, therefore applying the plume interaction factor is unnecessarily conservative. However, in the case of the Gross Alpha limits, applying the plume interaction factor is appropriate since the alpha-emitting radionuclides peak at the same time (i.e., about 1100 years). However, the 2-sigma Kd case is very conservative (i.e., Kds are selected so that, for each radionuclide, the selected Kd is at least 2 standard deviations less than the mean Kd). Thus, it is not a reasonable one to base disposal waste acceptance on; therefore, the ILV sensitivity analysis results do not indicate that the PORFLOW derived limits should be further reduced.

7.3.4 Low-Activity Waste Vault

The groundwater sensitivity analysis for the LAWV is presented in Section 3.6.7. Five sensitivity cases were run:

1. More mobile contaminants (i.e., reduced K_d)
2. Absence of Cellulose Degradation Products
3. Greater diffusion through the vault concrete
4. Greater portion of wall length being cracked
5. Lesser portion of wall length being cracked

The results in Section 3.6.7 show minimal impact from increased diffusion through the vault concrete (i.e., Case 3) except for tritium, for which the beta-gamma dose increased 76%. Case 5 produced peak doses that mainly were less than those for the base case. Case 4 generally resulted in larger doses. Case 1 resulted in very large increases in peak dose for some radionuclides; dose increases of up to 14 orders of magnitude were observed. However, the increased doses were small compared to the 4 mrem/year beta-gamma MCL. Case 2 resulted in considerable variability in the dose results. The dose for some radionuclides increased, with the maximum increase being a factor of 2E+08, while some decreased, with the maximum decrease being a factor of 4E-11.

The LAWV is currently about 42% filled volumetrically. However, plans are to remove waste from the LAWV that is suitable for trench disposal. This is expected to leave about 25% of the vault's volumetric capacity filled. Then, waste conforming to the LAWV disposal limits will be emplaced to fill the remaining capacity. The projected inventory at closure for the LAWV is presented in Appendix C.

The LAWV sensitivity analysis results were assessed from the perspective of the change in the sum-of-fractions (SOF) of the limits between the base case and the sensitivity cases, using the projected LAWV inventory at closure. The results are shown in Table 7-5.

Table 7-5. LAWV Sensitivity Analysis Results for Closure Inventory

Performance Measure	Base Case SOF	K_d -2 σ SOF	No CDP SOF	D_{eff} +3 σ SOF	Wider Crack SOF	More Narrow Crack SOF
Beta-gamma	4.21E-01	4.83E-01	3.18E-01	4.35E-01	4.40E-01	4.42E-01
Gross Alpha	2.77E-07	3.48E-05	1.00E-04	1.74E-07	3.25E-07	2.40E-07
Radium	7.31E-09	5.82E-07	6.52E-05	5.22E-09	8.69E-09	6.25E-09
Uranium	1.35E-17	2.00E-15	1.06E-15	8.43E-18	1.59E-17	1.17E-17
All Pathways	1.68E-01	1.82E-01	1.21E-01	1.60E-01	1.67E-01	1.68E-01

For the Beta-Gamma performance measure, the sensitivity cases are only slightly different than the base case; the SOF for the first sensitivity case (i.e., K_d -2 σ) is about 15% greater than that for the base case, the second sensitivity case (i.e., No CDP) is about 75% of the base case and the third, fourth and fifth sensitivity cases are three to five percent greater than the base case. For the Gross Alpha performance measure, the first sensitivity case SOF is about 130 times greater than the base case, the second case is about 360 times the base case, the third case SOF is about 60% of the base case SOF, the fourth case is about 17% greater than the base case, and the fifth case is about 87% of the base case. Even though the first and second case SOFs are hundreds of times greater than the base case, the greatest SOF, that for the second case, is only 0.0001.

For the Radium performance measure, the first sensitivity case SOF is about 80 times the base case, the second case SOF is about 9,000 times the base case, the third case SOF is about 70% of the base case, the SOF for the fourth case is about 19% greater than the base case SOF and the SOF for the fifth case is about 86% of the base case SOF. Even though the second case SOF is 9,000 times the base case, it is only 0.00006.

For the Uranium performance measure, the first sensitivity case SOF is about 150 times the base case SOF, the SOF for the second case is about 80 times that of the base case, in the third case, the SOF is about 62% that of the base case, for the fourth case, the SOF is about 18% greater than the base case and in the fifth case, the SOF is about 87% of the base case SOF. As for the Gross Alpha and Radium performance measures, even though the first case SOF is 150 times the base case, the SOF is only 2E-15.

For the All Pathways performance measure, the SOF for the first sensitivity case is about 8% greater than that for the base case, the SOFs for the second, third, and fourth cases are about 72%, 95%, and 99%, respectively, that of the base case and, for the fifth case, the SOF is the same as the base case.

These results show considerable sensitivity to the selection of Kd and the presence or absence of cellulose degradation products. However, the magnitude of the sums-of-fractions of the limits for all cases is less than one, showing compliance with all the performance measures. Therefore, the groundwater-based disposal limits for the LAWV do not need to be further reduced to account for sensitivity/uncertainty.

7.3.5 Sensitivity Analysis Conclusions

The results of the sensitivity analyses do not suggest that the PORFLOW-derived radionuclide disposal limits should be further reduced.

7.4 FINAL RADIONUCLIDE DISPOSAL LIMITS

The final radionuclide disposal limits determined in this PA are the PORFLOW-derived limits reduced to account for interaction of groundwater plumes. As shown in the individual disposal unit chapters, these limits include consideration of the physical and chemical characteristics that affect the release and transport of radionuclides. These limits are presented in the following tables. The NRCDA has no intruder limits, as discussed in Section 5.11 (Part B).

Slit and Engineered Trenches: Table 7-6 - Table 7-16

CIG: Table 7-17 - Table 7-21

LAWV: Table 7-22 - Table 7-25

ILV: Table 7-26 - Table 7-30

NRCDA: Table 7-31 - Table 7-33

Table 7-6. Final Groundwater Protection Limits for East Slit Trenches

	Beta-Gamma Limit (Ci)			Gross Alpha (Ci)			Radium (Ci)			Uranium (Ci)
Radionuclide	**0-12 yrs**	**12-100 yrs**	**100-1130 yrs**	**0-1000 yrs**	**1000-1120 yrs**	**1120-1130 yrs**	**0-1000 yrs**	**1000-1120 yrs**	**1120-1130 yrs**	**All Years**
Am-241	1.9E+10	1.7E+06	6.3E+03	3.1E+02	3.7E+02	3.6E+02	---	---	---	9.2E+11
Am-243	---	3.8E+16	2.3E+03	4.4E+02	1.3E+02	1.2E+02	---	---	---	8.6E+12
C-14	2.5E-01	2.1E-01	4.8E+00	---	---	---	---	---	---	---
C-14_NR.Pump	---	---	1.4E+00	---	---	---	---	---	---	---
Cf-249	6.1E+17	3.1E+12	1.1E+05	1.9E+03	6.7E+02	6.2E+02	---	---	---	5.2E+13
Cf-251	---	---	8.1E+08	8.7E+02	2.8E+02	2.5E+02	---	---	---	5.4E+18
Cl-36	8.6E-02	7.4E-02	1.7E+00	---	---	---	---	---	---	---
Cm-244	---	---	6.2E+18	2.3E+12	2.6E+11	2.2E+11	1.1E+19	8.7E+18	8.4E+18	2.9E+19
Cm-245	8.2E+13	1.0E+09	3.5E+03	1.5E+02	6.0E+01	5.5E+01	---	---	---	9.7E+11
Cm-246	---	---	5.5E+15	4.6E+02	1.4E+02	1.2E+02	1.1E+16	3.8E+15	3.4E+15	1.4E+14
Cm-247	---	---	1.8E+04	3.7E+02	1.0E+02	9.6E+01	---	---	---	9.3E+13
Cm-248	---	---	1.9E+10	4.4E+02	1.3E+02	1.2E+02	---	---	---	2.3E+18
H-3	4.9E+00	4.6E+00	1.3E+04	---	---	---	---	---	---	---
H-3_ETF.Carbon	---	---	5.4E+04	---	---	---	---	---	---	---
I-129	1.7E-04	1.1E-04	3.4E-03	---	---	---	---	---	---	---
I-129_ETF.Carbon	---	---	9.3E-02	---	---	---	---	---	---	---
I-129_ETF.GT.73	1.3E+00	3.4E-01	1.3E-01	---	---	---	---	---	---	---
I-129_F.Carbon	1.7E+01	4.5E+00	1.7E+00	---	---	---	---	---	---	---
I-129_F.CG.8	6.5E-03	1.7E-03	2.3E-03	---	---	---	---	---	---	---
I-129_F.Dowex.21K	8.7E-01	2.3E-01	8.9E-02	---	---	---	---	---	---	---
I-129_F.Filtercake	7.3E-03	1.9E-03	2.5E-03	---	---	---	---	---	---	---
I-129_H.Carbon	7.4E+00	2.0E+00	7.4E-01	---	---	---	---	---	---	---
I-129_H.CG.8	4.9E-02	1.3E-02	8.0E-03	---	---	---	---	---	---	---
I-129_H.Dowex.21K	2.0E+00	5.3E-01	2.0E-01	---	---	---	---	---	---	---
I-129_H.Filtercake	8.3E-02	2.2E-02	1.2E-02	---	---	---	---	---	---	---

Table 7-6. Final Groundwater Protection Limits for East Slit Trenches - continued

	Beta-Gamma Limit (Ci)			Gross Alpha (Ci)			Radium (Ci)			Uranium (Ci)
Radionuclide	**0-12 yrs**	**12-100 yrs**	**100-1130 yrs**	**0-1000 yrs**	**1000-1120 yrs**	**1120-1130 yrs**	**0-1000 yrs**	**1000-1120 yrs**	**1120-1130 yrs**	**All Years**
K-40	1.3E-01	8.7E-02	9.0E-01	---	---	---	---	---	---	---
Mo-93	1.9E-01	1.5E-01	1.9E+00	---	---	---	---	---	---	---
Nb-94	9.4E-02	8.1E-02	1.8E+00	---	---	---	---	---	---	---
Ni-59	---	8.7E+09	5.7E+00	---	---	---	---	---	---	---
Np-237	1.1E+04	3.6E+00	9.8E-01	4.9E-02	8.1E-02	1.7E-01	---	---	---	1.4E+08
Pd-107	---	1.1E+12	6.9E+02	---	---	---	---	---	---	---
Pu-238	---	---	1.0E+07	3.7E+05	1.2E+05	1.1E+05	3.7E+05	1.2E+05	1.1E+05	6.6E+18
Pu-239	4.7E+18	5.0E+12	5.9E+06	5.3E+06	4.6E+06	4.6E+06	---	---	---	1.0E+17
Pu-240	---	---	1.6E+16	9.2E+09	9.5E+08	8.0E+08	2.8E+16	2.2E+16	2.2E+16	1.1E+17
Pu-241	7.3E+12	2.4E+08	1.9E+05	9.6E+03	1.1E+04	1.1E+04	---	---	---	2.8E+13
Pu-242	---	---	1.0E+14	8.3E+09	8.4E+08	7.1E+08	3.5E+12	1.2E+12	1.1E+12	9.8E+16
Pu-244	---	---	6.0E+10	7.5E+09	7.5E+08	6.3E+08	1.2E+18	8.7E+17	8.3E+17	9.2E+17
Ra-226	5.1E+18	5.2E+07	2.5E+00	7.4E-02	3.0E-02	3.0E-02	7.4E-02	3.1E-02	3.0E-02	---
Se-79	---	---	---	---	---	---	---	---	---	---
Sn-126	---	---	---	---	---	---	---	---	---	---
Sr-90	2.2E+16	7.2E+06	1.4E+02	---	---	---	---	---	---	---
Tc-99	2.5E-01	1.1E-01	2.5E+00	---	---	---	---	---	---	---
Th-230	---	4.1E+10	9.1E+00	3.7E-01	1.1E-01	9.9E-02	3.7E-01	1.1E-01	9.9E-02	---
Th-232	1.4E+18	3.1E+10	1.8E+04	1.8E+04	4.2E+04	5.3E+04	2.4E+04	5.5E+04	7.1E+04	---
U-233	---	---	1.7E+13	4.5E+13	4.3E+12	3.6E+12	---	---	---	5.5E+14
U-234	---	1.6E+15	2.6E+03	9.8E+01	3.1E+01	2.8E+01	9.8E+01	3.1E+01	2.8E+01	1.7E+15
U-235	8.5E+09	2.2E+04	3.5E+00	2.8E+00	2.8E+00	3.2E+00	---	---	---	8.8E+11
U-236	---	---	1.6E+11	2.1E+11	1.7E+11	1.7E+11	2.8E+11	2.3E+11	2.2E+11	1.7E+13
U-238	---	---	3.4E+06	1.2E+05	4.0E+04	3.7E+04	1.2E+05	4.0E+04	3.7E+04	9.0E+10
Zr-93	1.8E+00	4.3E-01	5.0E-01	---	---	---	---	---	---	---

Limits reported as "---" indicate that there is no limit or that the limit > 1E+20

Table 7-7. Final Groundwater Protection Limits for Center Slit Trenches

	Beta-Gamma (Ci)			Gross Alpha (Ci)			Radium (Ci)			Uranium (Ci)
Radionuclide	**0-12 yrs**	**12-100 yrs**	**100-1130 yrs**	**0-1000 yrs**	**1000-1120 yrs**	**1120-1130 yrs**	**0-1000 yrs**	**1000-1120 yrs**	**1120-1130 yrs**	**All Years**
Am-241	3.9E+09	1.8E+06	1.1E+04	2.2E+02	1.3E+02	1.2E+02	---	---	---	1.6E+12
Am-243	---	5.3E+16	4.8E+02	6.6E+01	2.6E+01	2.4E+01	---	---	---	1.2E+12
C-14	2.5E-01	2.5E-01	8.6E+00	---	---	---	---	---	---	---
C-14_NR.Pump	---	---	2.5E+00	---	---	---	---	---	---	---
Cf-249	1.2E+17	3.1E+12	3.2E+04	3.1E+02	1.4E+02	1.3E+02	---	---	---	9.3E+13
Cf-251	---	---	1.7E+08	1.3E+02	5.5E+01	5.2E+01	---	---	---	8.1E+17
Cl-36	8.6E-02	8.6E-02	3.0E+00	---	---	---	---	---	---	---
Cm-244	---	---	8.9E+17	7.0E+10	9.2E+09	7.9E+09	1.6E+18	1.3E+18	1.2E+18	9.8E+17
Cm-245	1.7E+13	1.1E+09	1.2E+03	3.6E+01	1.4E+01	1.3E+01	---	---	---	1.8E+12
Cm-246	---	---	7.7E+14	7.0E+01	2.7E+01	2.5E+01	1.1E+16	3.6E+15	3.3E+15	1.9E+13
Cm-247	---	---	3.6E+03	5.5E+01	2.1E+01	2.0E+01	---	---	---	1.4E+13
Cm-248	---	---	3.1E+09	6.6E+01	2.5E+01	2.4E+01	---	---	---	2.9E+17
H-3	4.7E+00	4.8E+00	2.3E+04	---	---	---	---	---	---	---
H-3_Concrete	1.1E+01	1.1E+01	5.4E+04	---	---	---	---	---	---	---
H-3_ETF.Carbon	---	---	5.6E+04	---	---	---	---	---	---	---
I-129	1.4E-04	1.4E-04	6.3E-03	---	---	---	---	---	---	---
I-129_ETF.Carbon	---	---	1.7E-01	---	---	---	---	---	---	---
I-129_ETF.GT.73	1.2E+00	5.8E-01	2.3E-01	---	---	---	---	---	---	---
I-129_F.Carbon	1.5E+01	7.7E+00	3.0E+00	---	---	---	---	---	---	---
I-129_F.CG.8	5.9E-03	3.0E-03	3.5E-03	---	---	---	---	---	---	---
I-129_F.Dowex.21K	7.9E-01	4.0E-01	1.6E-01	---	---	---	---	---	---	---
I-129_F.Filtercake	6.6E-03	3.3E-03	3.8E-03	---	---	---	---	---	---	---
I-129_H.Carbon	6.7E+00	3.4E+00	1.3E+00	---	---	---	---	---	---	---
I-129_H.CG.8	4.4E-02	2.2E-02	1.4E-02	---	---	---	---	---	---	---
I-129_H.Dowex.21K	1.8E+00	9.1E-01	3.6E-01	---	---	---	---	---	---	---
I-129_H.Filtercake	7.5E-02	3.8E-02	2.2E-02	---	---	---	---	---	---	---
I-129_Mk50A	3.6E+00	1.4E+00	3.9E-01	---	---	---	---	---	---	---

Table 7-7. Final Groundwater Protection Limits for Center Slit Trenches - continued

	Beta-Gamma (Ci)			Gross Alpha (Ci)			Radium (Ci)			Uranium (Ci)
Radionuclide	**0-12 yrs**	**12-100 yrs**	**100-1130 yrs**	**0-1000 yrs**	**1000-1120 yrs**	**1120-1130 yrs**	**0-1000 yrs**	**1000-1120 yrs**	**1120-1130 yrs**	**All Years**
K-40	1.9E-01	1.4E-01	1.6E+00	---	---	---	---	---	---	---
Mo-93	1.9E-01	1.9E-01	3.5E+00	---	---	---	---	---	---	---
Nb-94	9.4E-02	9.4E-02	3.3E+00	---	---	---	---	---	---	---
Ni-59	5.8E+19	3.4E+09	4.1E+00	---	---	---	---	---	---	---
Np-237	2.4E+03	3.9E+00	1.7E+00	8.6E-02	1.6E-01	3.8E-01	---	---	---	2.2E+08
Pd-107	---	4.2E+11	4.9E+02	---	---	---	---	---	---	---
Pu-238	---	---	9.8E+06	3.7E+05	1.2E+05	1.1E+05	3.7E+05	1.2E+05	1.1E+05	1.5E+17
Pu-239	9.6E+17	6.7E+12	1.1E+07	9.5E+06	6.7E+06	6.5E+06	---	---	---	3.3E+15
Pu-240	---	---	2.3E+15	2.7E+08	3.3E+07	2.8E+07	4.1E+15	3.2E+15	3.1E+15	3.6E+15
Pu-241	1.4E+12	2.5E+08	3.3E+05	6.6E+03	3.7E+03	3.6E+03	---	---	---	5.0E+13
Pu-242	---	---	1.0E+14	2.4E+08	2.9E+07	2.5E+07	3.7E+12	1.2E+12	1.1E+12	3.2E+15
Pu-244	---	---	2.1E+09	2.2E+08	2.6E+07	2.2E+07	1.7E+17	1.2E+17	1.2E+17	3.0E+16
Ra-226	2.3E+17	2.5E+07	3.0E+00	6.4E-02	3.9E-02	3.9E-02	6.4E-02	3.9E-02	3.9E-02	---
Ra-226_Cooling.Tower	---	1.2E+12	1.4E+01	2.3E-01	9.8E-01	8.3E-01	2.3E-01	9.9E-01	8.3E-01	---
Se-79	---	---	3.2E+19	---	---	---	---	---	---	---
Sn-126	---	---	---	---	---	---	---	---	---	---
Sr-90	9.9E+14	3.4E+06	7.1E+01	---	---	---	---	---	---	---
Sr-90_Mk50A	1.4E+18	3.2E+09	4.0E+04	---	---	---	---	---	---	---
Tc-99	1.6E-01	1.3E-01	4.5E+00	---	---	---	---	---	---	---
Tc-99_Mk50A	5.3E+03	1.3E+03	3.4E+02	---	---	---	---	---	---	---
Th-230	---	2.0E+10	8.9E+00	3.1E-01	1.1E-01	1.0E-01	3.1E-01	1.1E-01	1.0E-01	---
Th-230_Cooling.Tower	---	1.0E+15	1.1E+02	1.9E+00	1.8E+00	1.7E+00	1.9E+00	1.8E+00	1.7E+00	---
Th-232	6.0E+16	3.8E+09	2.7E+03	2.7E+03	6.3E+03	8.0E+03	3.6E+03	8.4E+03	1.1E+04	---
U-233	---	---	4.7E+11	1.2E+12	1.2E+11	9.9E+10	---	---	---	1.6E+13
U-234	---	7.5E+14	2.6E+03	9.5E+01	3.1E+01	2.9E+01	9.5E+01	3.1E+01	2.9E+01	3.8E+13
U-234_MGlass	---	1.1E+18	1.1E+06	3.6E+04	1.3E+04	1.2E+04	3.6E+04	1.3E+04	1.2E+04	2.2E+16

Table 7-7. Final Groundwater Protection Limits for Center Slit Trenches - continued

	Beta-Gamma (Ci)			Gross Alpha (Ci)			Radium (Ci)			Uranium (Ci)
Radionuclide	**0-12 yrs**	**12-100 yrs**	**100-1130 yrs**	**0-1000 yrs**	**1000-1120 yrs**	**1120-1130 yrs**	**0-1000 yrs**	**1000-1120 yrs**	**1120-1130 yrs**	**All Years**
U-235	1.7E+09	3.0E+04	6.2E+00	4.8E+00	5.0E+00	6.0E+00	---	---	---	1.3E+10
U-235_MGlass	2.3E+12	1.7E+07	2.4E+03	2.1E+03	1.9E+03	1.9E+03	---	---	---	7.7E+12
U-235_Paducah.Cask	5.6E+13	4.1E+08	2.6E+04	2.3E+04	2.1E+04	2.1E+04	---	---	---	8.4E+13
U-236	---	2.3E+19	2.3E+10	3.1E+10	2.5E+10	2.4E+10	4.1E+10	3.3E+10	3.2E+10	3.9E+11
U-236_MGlass	---	---	1.6E+13	2.1E+13	1.7E+13	1.6E+13	2.8E+13	2.3E+13	2.2E+13	2.3E+14
U-238	---	---	3.3E+06	1.2E+05	3.9E+04	3.6E+04	1.3E+05	3.9E+04	3.6E+04	2.0E+09
U-238_MGlass	---	---	1.3E+09	4.7E+07	1.5E+07	1.4E+07	4.7E+07	1.5E+07	1.4E+07	1.2E+12
Zr-93	1.5E+00	6.4E-01	7.4E-01	---	---	---	---	---	---	---

Limits reported as "---" indicate that there is no limit or that the limit > 1E+20

Table 7-8. Final Groundwater Protection Limits for West Slit Trenches

	Beta-Gamma (Ci)			Gross Alpha (Ci)			Radium (Ci)			Uranium (Ci)
Radionuclide	0-12 yrs	12-100 yrs	100-1130 yrs	0-1000 yrs	1000-1120 yrs	1120-1130 yrs	0-1000 yrs	1000-1120 yrs	1120-1130 yrs	All Years
Am-241	8.2E+08	1.3E+06	9.2E+03	5.5E+01	3.6E+01	3.5E+01	---	---	---	1.4E+12
Am-243	---	4.2E+16	1.3E+02	1.3E+01	6.9E+00	6.6E+00	---	---	---	2.2E+11
C-14	1.9E-01	2.0E-01	8.3E+00	---	---	---	---	---	---	---
C-14_NR.Pump	---	---	2.2E+00	---	---	---	---	---	---	---
Cf-249	2.2E+16	2.2E+12	9.0E+03	6.3E+01	3.7E+01	3.6E+01	---	---	---	7.8E+13
Cf-251	---	---	4.6E+07	2.6E+01	1.5E+01	1.4E+01	---	---	---	1.6E+17
Cl-36	6.8E-02	7.0E-02	2.9E+00	---	---	---	---	---	---	---
Cm-244	---	---	1.4E+17	3.2E+09	4.9E+08	4.2E+08	2.6E+17	2.0E+17	1.9E+17	4.9E+16
Cm-245	3.1E+12	7.5E+08	3.4E+02	7.4E+00	3.7E+00	3.6E+00	---	---	---	1.5E+12
Cm-246	---	---	1.4E+14	1.4E+01	7.3E+00	7.0E+00	8.8E+15	2.7E+15	2.5E+15	3.5E+12
Cm-247	---	---	9.9E+02	1.1E+01	5.6E+00	5.4E+00	---	---	---	2.5E+12
Cm-248	---	---	6.7E+08	1.3E+01	6.8E+00	6.5E+00	---	---	---	4.6E+16
H-3	3.6E+00	3.9E+00	2.2E+04	---	---	---	---	---	---	---
H-3_ETF.Carbon	---	---	3.0E+01	---	---	---	---	---	---	---
I-129	2.0E-04	2.0E-04	9.2E-03	---	---	---	---	---	---	---
I-129_ETF.Carbon	---	---	1.6E-01	---	---	---	---	---	---	---
I-129_ETF.GT.73	9.1E-01	5.4E-01	2.1E-01	---	---	---	---	---	---	---
I-129_F.Carbon	1.2E+01	7.1E+00	2.8E+00	---	---	---	---	---	---	---
I-129_F.CG.8	4.6E-03	2.7E-03	3.1E-03	---	---	---	---	---	---	---
I-129_F.Dowex.21K	6.2E-01	3.6E-01	1.5E-01	---	---	---	---	---	---	---
I-129_F.Filtercake	5.2E-03	3.1E-03	3.4E-03	---	---	---	---	---	---	---
I-129_H.Carbon	5.3E+00	3.1E+00	1.2E+00	---	---	---	---	---	---	---
I-129_H.CG.8	3.5E-02	2.0E-02	1.3E-02	---	---	---	---	---	---	---
I-129_H.Dowex.21K	1.4E+00	8.4E-01	3.3E-01	---	---	---	---	---	---	---
I-129_H.Filtercake	5.9E-02	3.5E-02	2.0E-02	---	---	---	---	---	---	---
K-40	1.7E-01	1.3E-01	1.4E+00	---	---	---	---	---	---	---

Table 7-8. Final Groundwater Protection Limits for West Slit Trenches - continued

	Beta-Gamma (Ci)			Gross Alpha (Ci)			Radium (Ci)			Uranium (Ci)
Radionuclide	0-12 yrs	12-100 yrs	100-1130 yrs	0-1000 yrs	1000-1120 yrs	1120-1130 yrs	0-1000 yrs	1000-1120 yrs	1120-1130 yrs	All Years
Mo-93	1.5E-01	1.6E-01	3.4E+00	---	---	---	---	---	---	---
Nb-94	7.4E-02	7.7E-02	3.1E+00	---	---	---	---	---	---	---
Ni-59	5.0E+17	2.0E+09	2.8E+00	---	---	---	---	---	---	---
Np-237	5.4E+02	2.8E+00	1.4E+00	7.2E-02	1.4E-01	3.2E-01	---	---	---	2.2E+08
Pd-107	---	2.4E+11	3.4E+02	---	---	---	---	---	---	---
Pu-238	---	---	7.5E+06	2.7E+05	8.9E+04	8.4E+04	2.8E+05	8.9E+04	8.4E+04	5.5E+15
Pu-239	1.8E+17	5.3E+12	9.0E+06	4.7E+06	1.3E+06	1.1E+06	---	---	---	1.6E+14
Pu-240	---	---	3.7E+14	1.2E+07	1.7E+06	1.5E+06	6.7E+14	5.2E+14	5.0E+14	1.8E+14
Pu-241	2.8E+11	1.8E+08	2.8E+05	1.6E+03	1.1E+03	1.0E+03	---	---	---	4.2E+13
Pu-242	---	---	7.5E+13	1.1E+07	1.5E+06	1.3E+06	2.8E+12	8.8E+11	8.1E+11	1.6E+14
Pu-244	---	---	1.1E+08	9.7E+06	1.3E+06	1.2E+06	2.8E+16	2.0E+16	1.9E+16	1.5E+15
Ra-226	3.6E+15	1.6E+07	2.5E+00	4.7E-02	3.2E-02	3.3E-02	4.7E-02	3.2E-02	3.3E-02	---
Se-79	---	---	3.6E+17	---	---	---	---	---	---	---
Sn-126	---	---	---	---	---	---	---	---	---	---
Sr-90	1.5E+13	1.2E+06	3.2E+01	---	---	---	---	---	---	---
Tc-99	1.2E-01	1.1E-01	3.9E+00	---	---	---	---	---	---	---
Th-230	5.6E+18	1.3E+10	6.8E+00	2.2E-01	8.4E-02	8.2E-02	2.2E-01	8.4E-02	8.2E-02	---
Th-232	8.0E+14	5.0E+08	4.4E+02	4.5E+02	1.1E+03	1.3E+03	5.9E+02	1.4E+03	1.8E+03	---
U-233	---	---	1.6E+10	3.4E+10	4.0E+09	3.4E+09	---	---	---	5.8E+11
U-234	---	4.7E+14	2.0E+03	6.9E+01	2.3E+01	2.2E+01	6.9E+01	2.4E+01	2.2E+01	1.4E+12
U-235	3.3E+08	2.3E+04	5.2E+00	4.0E+00	4.2E+00	5.0E+00	---	---	---	4.8E+08
U-236	---	3.0E+18	3.8E+09	5.0E+09	4.0E+09	3.8E+09	6.7E+09	5.3E+09	5.1E+09	1.4E+10
U-238	---	---	2.5E+06	9.4E+04	3.0E+04	2.8E+04	9.4E+04	3.0E+04	2.8E+04	7.5E+07
Zr-93	1.1E+00	5.6E-01	6.6E-01	---	---	---	---	---	---	---

Limits reported as "---" indicate that there is no limit or that the limit > 1E+20

Table 7-9. Final Groundwater Protection Limits for Engineered Trenches

	Beta-Gamma (Ci)			Gross Alpha (Ci)			Radium (Ci)			Uranium (Ci)
Radionuclide	**0-12 yrs**	**12-100 yrs**	**100-1130 yrs**	**0-1000 yrs**	**1000-1120 yrs**	**1120-1130 yrs**	**0-1000 yrs**	**1000-1120 yrs**	**1120-1130 yrs**	**All Years**
Am-241	2.1E+11	1.1E+07	2.2E+04	1.1E+03	1.2E+03	1.2E+03	---	---	---	2.8E+12
Am-243	---	4.2E+17	1.8E+04	4.2E+03	1.0E+03	9.1E+02	---	---	---	8.3E+13
C-14	9.0E-01	5.3E-01	1.2E+01	---	---	---	---	---	---	---
Cf-249	7.3E+18	2.4E+13	6.1E+05	1.6E+04	5.1E+03	4.7E+03	---	---	---	1.8E+14
Cf-251	---	---	6.3E+09	8.3E+03	2.2E+03	2.0E+03	---	---	---	5.1E+19
Cl-36	3.2E-01	1.9E-01	4.3E+00	---	---	---	---	---	---	---
Cm-244	---	---	4.7E+19	7.0E+13	6.7E+12	5.6E+12	8.0E+19	6.5E+19	6.3E+19	---
Cm-245	9.7E+14	7.6E+09	1.6E+04	9.4E+02	3.9E+02	3.6E+02	---	---	---	3.3E+12
Cm-246	---	---	5.2E+16	4.4E+03	1.1E+03	9.7E+02	3.1E+16	1.3E+16	1.2E+16	1.3E+15
Cm-247	---	---	1.4E+05	3.5E+03	8.3E+02	7.5E+02	---	---	---	8.8E+14
Cm-248	---	---	1.6E+11	4.2E+03	1.0E+03	9.0E+02	---	---	---	2.4E+19
H-3	1.8E+01	1.3E+01	3.3E+04	---	---	---	---	---	---	---
H-3_ETF.Carbon	---	---	1.5E+05	---	---	---	---	---	---	---
I-129	8.1E-04	3.2E-04	9.0E-03	---	---	---	---	---	---	---
I-129_ETF.Carbon	---	---	4.8E-01	---	---	---	---	---	---	---
I-129_ETF.GT.73	5.5E+00	1.7E+00	6.4E-01	---	---	---	---	---	---	---
I-129_F.Carbon	7.3E+01	2.2E+01	8.5E+00	---	---	---	---	---	---	---
I-129_F.CG.8	2.8E-02	8.6E-03	8.8E-03	---	---	---	---	---	---	---
I-129_F.Dowex.21K	3.8E+00	1.1E+00	4.4E-01	---	---	---	---	---	---	---
I-129_F.Filtercake	3.2E-02	9.7E-03	9.6E-03	---	---	---	---	---	---	---
I-129_H.Carbon	3.2E+01	9.7E+00	3.7E+00	---	---	---	---	---	---	---
I-129_H.CG.8	2.1E-01	6.4E-02	3.5E-02	---	---	---	---	---	---	---
I-129_H.Dowex.21K	8.6E+00	2.6E+00	1.0E+00	---	---	---	---	---	---	---
I-129_H.Filtercake	3.6E-01	1.1E-01	5.9E-02	---	---	---	---	---	---	---
K-40	4.3E-01	2.6E-01	2.4E+00	---	---	---	---	---	---	---
Mo-93	6.9E-01	3.5E-01	5.0E+00	---	---	---	---	---	---	---
Nb-94	3.5E-01	2.0E-01	4.7E+00	---	---	---	---	---	---	---

Table 7-9. Final Groundwater Protection Limits for Engineered Trenches - continued

	Beta-Gamma (Ci)			Gross Alpha (Ci)			Radium (Ci)			Uranium (Ci)
Radionuclide	**0-12 yrs**	**12-100 yrs**	**100-1130 yrs**	**0-1000 yrs**	**1000-1120 yrs**	**1120-1130 yrs**	**0-1000 yrs**	**1000-1120 yrs**	**1120-1130 yrs**	**All Years**
Ni-59	---	3.1E+11	1.8E+01	---	---	---	---	---	---	---
Np-237	1.2E+05	2.2E+01	3.7E+00	1.8E-01	2.3E-01	2.6E-01	---	---	---	3.9E+08
Pd-107	---	3.8E+13	2.2E+03	---	---	---	---	---	---	---
Pu-238	---	---	3.9E+07	1.3E+06	4.5E+05	4.1E+05	1.3E+06	4.5E+05	4.1E+05	---
Pu-239	5.6E+19	5.0E+13	2.1E+07	1.6E+07	1.4E+07	1.4E+07	---	---	---	2.8E+18
Pu-240	---	---	1.2E+17	2.8E+11	2.5E+10	2.1E+10	2.0E+17	1.7E+17	1.6E+17	3.1E+18
Pu-241	7.9E+13	1.6E+09	6.8E+05	3.4E+04	3.5E+04	3.5E+04	---	---	---	8.5E+13
Pu-242	---	---	3.6E+14	2.5E+11	2.2E+10	1.8E+10	1.0E+13	4.3E+12	4.0E+12	2.7E+18
Pu-244	---	---	1.6E+12	2.3E+11	2.0E+10	1.6E+10	8.6E+18	6.6E+18	6.4E+18	2.5E+19
Ra-226	---	1.6E+09	8.8E+00	2.5E-01	1.0E-01	9.8E-02	2.5E-01	1.0E-01	9.8E-02	---
Se-79	---	---	---	---	---	---	---	---	---	---
Sn-126	---	---	---	---	---	---	---	---	---	---
Sr-90	2.1E+18	2.2E+08	4.6E+02	---	---	---	---	---	---	---
Tc-99	1.3E+00	2.9E-01	6.2E+00	---	---	---	---	---	---	---
Th-230	---	1.3E+12	3.5E+01	1.6E+00	4.1E-01	3.7E-01	1.6E+00	4.1E-01	3.7E-01	---
Th-232	---	9.3E+11	1.2E+05	1.2E+05	3.1E+05	4.2E+05	1.7E+05	4.2E+05	5.6E+05	---
U-233	---	---	6.3E+14	2.0E+15	1.6E+14	1.3E+14	---	---	---	2.0E+16
U-234	---	5.0E+16	1.0E+04	3.6E+02	1.2E+02	1.1E+02	3.6E+02	1.2E+02	1.1E+02	6.6E+16
U-235	9.3E+10	2.1E+05	1.1E+01	8.5E+00	8.7E+00	8.7E+00	---	---	---	2.3E+13
U-236	---	---	1.2E+12	1.5E+12	1.3E+12	1.2E+12	2.0E+12	1.7E+12	1.6E+12	6.9E+14
U-238	---	---	1.3E+07	3.8E+05	1.5E+05	1.4E+05	3.8E+05	1.5E+05	1.4E+05	3.6E+12
Zr-93	6.6E+00	1.2E+00	1.4E+00	---	---	---	---	---	---	---

Limits reported as "---" indicate that there is no limit or that the limit > 1E+20.

Table 7-10. Final All-Pathways Radionuclide Disposal Limits for East Slit Trenches

Radionuclide	Limit (Ci)		
	130 - 200 yrs	200-1000 yrs	1000-1130 yrs
Am-241	4.8E+02	9.7E+01	1.2E+02
Am-243	1.8E+10	1.7E+02	4.5E+01
C-14	6.1E+00	6.1E+00	6.1E+00
C-14_NR.Pump	2.5E+00	1.5E+00	4.3E+02
Cf-249	1.1E+06	5.9E+02	2.0E+02
Cf-251	2.6E+18	2.5E+02	7.2E+01
Cl-36	1.1E+00	1.1E+00	1.1E+00
Cm-244	---	9.1E+11	8.5E+10
Cm-245	4.7E+03	5.3E+01	2.0E+01
Cm-246	---	1.7E+02	4.6E+01
Cm-247	4.1E+12	1.5E+02	3.8E+01
Cm-248	---	4.1E+01	1.1E+01
H-3	2.2E+06	2.2E+06	2.2E+06
H-3_ETF.Carbon	1.4E+06	6.8E+08	---
I-129	2.5E-01	2.5E-01	2.5E-01
I-129_ETF.Carbon	1.1E+01	5.9E+00	5.6E+00
I-129_ETF.GT.73	1.6E+01	8.2E+00	7.8E+00
I-129_F.Carbon	2.1E+02	1.1E+02	1.0E+02
I-129_F.CG.8	1.4E-01	2.0E-01	7.0E-01
I-129_F.Dowex.21K	1.1E+01	5.7E+00	5.4E+00
I-129_F.Filtercake	1.5E-01	2.1E-01	6.7E-01
I-129_H.Carbon	9.1E+01	4.8E+01	4.5E+01
I-129_H.CG.8	6.2E-01	5.1E-01	4.8E-01
I-129_H.Dowex.21K	2.4E+01	1.3E+01	1.2E+01
I-129_H.Filtercake	1.0E+00	8.3E-01	7.4E-01
K-40	2.4E+00	3.1E+00	4.7E+01
Mo-93	1.1E+01	1.1E+01	1.1E+01
Nb-94	1.3E+00	1.3E+00	1.3E+00
Ni-59	1.1E+07	2.1E+03	1.4E+03
Np-237	2.1E-02	1.5E-02	2.5E-02
Pd-107	1.7E+07	3.3E+03	2.2E+03
Pu-238	1.8E+10	1.1E+06	3.2E+05
Pu-239	3.1E+07	6.3E+05	5.8E+05
Pu-240	1.4E+19	3.6E+09	3.1E+08
Pu-241	1.7E+04	3.0E+03	3.6E+03
Pu-242	2.6E+18	3.4E+09	2.9E+08
Pu-244	---	3.1E+09	2.6E+08
Ra-226	3.2E+01	2.2E-01	8.6E-02
Se-79	---	---	---

Table 7-10. Final All-Pathways Radionuclide Disposal Limits for East Slit Trenches - continued

Radionuclide	Limit (Ci)		
	130 - 200 yrs	**200-1000 yrs**	**1000-1130 yrs**
Sn-126	---	---	---
Sr-90	3.9E+04	2.7E+03	2.9E+10
Tc-99	4.3E+00	4.3E+00	4.3E+00
Th-230	1.1E+03	1.1E+00	2.9E-01
Th-232	1.8E+05	4.8E+04	1.1E+05
U-233	---	1.4E+12	1.3E+11
U-234	1.8E+06	2.9E+02	8.3E+01
U-235	2.5E+00	3.3E-01	3.5E-01
U-236	2.8E+13	5.3E+11	2.7E+11
U-238	1.4E+10	3.5E+05	1.1E+05
Zr-93	8.0E+00	3.2E+00	3.0E+00

Limits reported as "---" indicate that there is no limit or that the limit > 1E+20.

Table 7-11. Final All-Pathways Radionuclide Disposal Limits for Center Slit Trenches

Radionuclide	Limit (Ci)		
	130 - 200 yrs	200-1000 yrs	1000-1130 yrs
Am-241	6.3E+02	7.9E+01	4.5E+01
Am-243	2.9E+10	2.5E+01	9.1E+00
C-14	1.1E+01	1.1E+01	1.1E+01
C-14_NR.Pump	3.0E+00	2.6E+00	1.0E+02
Cf-249	1.8E+06	9.7E+01	4.1E+01
Cf-251	3.6E+18	3.7E+01	1.5E+01
Cl-36	2.0E+00	2.0E+00	2.0E+00
Cm-244	---	2.7E+10	3.1E+09
Cm-245	6.6E+03	1.3E+01	4.8E+00
Cm-246	---	2.6E+01	9.4E+00
Cm-247	6.3E+12	2.2E+01	7.8E+00
Cm-248	2.3E+19	6.1E+00	2.2E+00
H-3	4.1E+06	4.1E+06	4.1E+06
H-3_Concrete	9.4E+06	9.4E+06	9.4E+06
H-3_ETF.Carbon	1.5E+06	1.1E+09	---
I-129	4.5E-01	4.5E-01	4.5E-01
I-129_ETF.Carbon	2.1E+01	1.1E+01	1.0E+01
I-129_ETF.GT.73	2.8E+01	1.5E+01	1.4E+01
I-129_F.Carbon	3.7E+02	1.9E+02	1.8E+02
I-129_F.CG.8	2.1E-01	3.5E-01	1.1E+00
I-129_F.Dowex.21K	1.9E+01	1.0E+01	9.6E+00
I-129_F.Filtercake	2.3E-01	3.7E-01	1.0E+00
I-129_H.Carbon	1.6E+02	8.5E+01	8.0E+01
I-129_H.CG.8	1.1E+00	9.1E-01	8.6E-01
I-129_H.Dowex.21K	4.4E+01	2.3E+01	2.1E+01
I-129_H.Filtercake	1.8E+00	1.5E+00	1.3E+00
I-129_Mk50A	6.4E+01	2.4E+01	7.6E+01
K-40	4.2E+00	5.2E+00	2.6E+01
Mo-93	2.1E+01	2.1E+01	2.1E+01
Nb-94	2.3E+00	2.3E+00	2.3E+00
Ni-59	9.8E+05	2.2E+03	1.0E+03
Np-237	2.8E-02	2.7E-02	5.0E-02
Pd-107	1.5E+06	3.3E+03	1.6E+03
Pu-238	2.3E+09	1.1E+06	3.2E+05
Pu-239	4.3E+07	1.2E+06	9.9E+05
Pu-240	1.3E+18	1.0E+08	1.1E+07
Pu-241	2.2E+04	2.4E+03	1.3E+03
Pu-242	3.3E+17	9.9E+07	1.0E+07
Pu-244	---	9.0E+07	9.2E+06

Table 7-11. Final All-Pathways Radionuclide Disposal Limits for Center Slit Trenches - continued

Radionuclide	Limit (Ci)		
	130 - 200 yrs	200-1000 yrs	1000-1130 yrs
Ra-226	5.2E+00	1.9E-01	1.1E-01
Ra-226_Cooling.Tower	1.0E+04	6.6E-01	2.4E+00
Se-79	---	---	3.4E+19
Sn-126	---	---	---
Sr-90	6.0E+03	1.4E+03	2.4E+10
Sr-90_Mk50A	3.1E+06	7.7E+05	3.3E+12
Tc-99	7.7E+00	7.7E+00	7.7E+00
Tc-99_Mk50A	1.6E+03	5.1E+02	1.7E+03
Th-230	1.4E+02	9.2E-01	3.0E-01
Th-230_Cooling.Tower	4.9E+05	5.6E+00	4.9E+00
Th-232	1.7E+04	7.2E+03	1.7E+04
U-233	---	3.8E+10	3.8E+09
U-234	2.3E+05	2.8E+02	8.4E+01
U-234_MGlass	3.9E+08	1.1E+05	3.5E+04
U-235	3.2E+00	5.8E-01	6.3E-01
U-235_MGlass	7.5E+03	2.6E+02	2.4E+02
U-235_Paducah.Cask	1.0E+05	2.8E+03	2.6E+03
U-236	2.5E+12	5.9E+10	1.2E+10
U-236_MGlass	3.3E+15	3.7E+13	7.4E+12
U-238	1.8E+09	3.7E+05	1.1E+05
U-238_MGlass	3.0E+12	1.4E+08	4.1E+07
Zr-93	8.9E+00	4.8E+00	4.4E+00

Limits reported as "---" indicate that there is no limit or that the limit > 1E+20.

Table 7-12. Final All-Pathways Radionuclide Disposal Limits for West Slit Trenches

	Limit (Ci)		
Radionuclide	**130 - 200 yrs**	**200-1000 yrs**	**1000-1130 yrs**
Am-241	5.0E+02	2.1E+01	1.3E+01
Am-243	2.4E+10	5.0E+00	2.5E+00
C-14	9.6E+00	9.6E+00	9.6E+00
C-14_NR.Pump	2.4E+00	2.3E+00	1.1E+02
Cf-249	1.5E+06	1.9E+01	1.1E+01
Cf-251	4.9E+17	7.4E+00	4.1E+00
Cl-36	1.7E+00	1.7E+00	1.7E+00
Cm-244	---	1.3E+09	1.6E+08
Cm-245	5.4E+03	2.7E+00	1.3E+00
Cm-246	6.3E+17	5.2E+00	2.6E+00
Cm-247	5.2E+12	4.4E+00	2.2E+00
Cm-248	1.6E+17	1.2E+00	6.0E-01
H-3	3.5E+06	3.5E+06	3.5E+06
H-3_ETF.Carbon	7.8E+02	6.2E+05	---
I-129	6.4E-01	6.4E-01	6.4E-01
I-129_ETF.Carbon	1.9E+01	1.0E+01	9.6E+00
I-129_ETF.GT.73	2.6E+01	1.3E+01	1.3E+01
I-129_F.Carbon	3.4E+02	1.8E+02	1.7E+02
I-129_F.CG.8	1.9E-01	3.2E-01	8.7E-01
I-129_F.Dowex.21K	1.8E+01	9.3E+00	8.9E+00
I-129_F.Filtercake	2.0E-01	3.4E-01	8.5E-01
I-129_H.Carbon	1.5E+02	7.8E+01	7.3E+01
I-129_H.CG.8	1.0E+00	8.4E-01	7.9E-01
I-129_H.Dowex.21K	4.0E+01	2.1E+01	2.0E+01
I-129_H.Filtercake	1.7E+00	1.4E+00	1.2E+00
K-40	3.5E+00	4.6E+00	2.4E+01
Mo-93	1.8E+01	1.8E+01	1.8E+01
Nb-94	2.0E+00	2.0E+00	2.0E+00
Ni-59	1.0E+05	1.5E+03	7.1E+02
Np-237	2.2E-02	2.2E-02	4.2E-02
Pd-107	1.6E+05	2.3E+03	1.1E+03
Pu-238	3.8E+08	8.1E+05	2.5E+05
Pu-239	3.5E+07	8.3E+05	3.3E+05
Pu-240	1.4E+17	4.7E+06	5.7E+05
Pu-241	1.7E+04	6.1E+02	3.9E+02
Pu-242	5.3E+16	4.4E+06	5.3E+05
Pu-244	2.8E+19	4.0E+06	4.8E+05

Table 7-12. Final All-Pathways Radionuclide Disposal Limits for West Slit Trenches - continued

	Limit (Ci)		
Radionuclide	**130 - 200 yrs**	**200-1000 yrs**	**1000-1130 yrs**
Ra-226	1.1E+00	1.4E-01	9.4E-02
Se-79	---	5.1E+18	3.8E+17
Sn-126	---	---	---
Sr-90	1.2E+03	6.1E+02	1.7E+10
Tc-99	7.3E+00	7.3E+00	7.3E+00
Th-230	2.5E+01	6.5E-01	2.4E-01
Th-232	1.9E+03	1.2E+03	2.8E+03
U-233	---	1.2E+09	1.4E+08
U-234	3.9E+04	2.0E+02	6.5E+01
U-235	2.6E+00	4.9E-01	5.3E-01
U-236	2.8E+11	4.5E+09	5.3E+08
U-238	2.9E+08	2.7E+05	8.1E+04
Zr-93	7.1E+00	4.3E+00	3.9E+00

Limits reported as "---" indicate that there is no limit or that the limit > 1E+20.

Table 7-13. Final All-Pathways Radionuclide Disposal Limits for Engineered Trenches

Radionuclide	Limit (Ci)		
	130 - 200 yrs	200-1000 yrs	1000-1130 yrs
Am-241	1.5E+03	3.5E+02	3.8E+02
Am-243	5.4E+10	1.6E+03	3.5E+02
C-14	1.7E+01	1.7E+01	1.7E+01
Cf-249	3.4E+06	5.0E+03	1.5E+03
Cf-251	8.3E+18	2.4E+03	5.7E+02
Cl-36	2.9E+00	2.9E+00	2.9E+00
Cm-244	---	2.7E+13	2.2E+12
Cm-245	1.4E+04	3.1E+02	1.3E+02
Cm-246	---	1.6E+03	3.6E+02
Cm-247	1.3E+13	1.4E+03	3.0E+02
Cm-248	---	3.9E+02	8.3E+01
H-3	6.0E+06	6.0E+06	6.0E+06
H-3_ETF.Carbon	3.8E+06	1.7E+09	---
I-129	6.2E-01	6.2E-01	6.2E-01
I-129_ETF.Carbon	6.1E+01	3.1E+01	2.9E+01
I-129_ETF.GT.73	8.2E+01	4.2E+01	3.9E+01
I-129_F.Carbon	1.1E+03	5.5E+02	5.1E+02
I-129_F.CG.8	5.3E-01	7.3E-01	1.2E+00
I-129_F.Dowex.21K	5.6E+01	2.9E+01	2.7E+01
I-129_F.Filtercake	5.8E-01	7.4E-01	1.2E+00
I-129_H.Carbon	4.8E+02	2.4E+02	2.3E+02
I-129_H.CG.8	3.2E+00	2.4E+00	2.1E+00
I-129_H.Dowex.21K	1.3E+02	6.5E+01	6.1E+01
I-129_H.Filtercake	5.4E+00	4.1E+00	3.6E+00
K-40	6.4E+00	8.0E+00	1.4E+02
Mo-93	3.1E+01	3.1E+01	3.1E+01
Nb-94	3.4E+00	3.4E+00	3.4E+00
Ni-59	1.3E+08	4.5E+03	8.2E+03
Np-237	6.8E-02	5.7E-02	7.1E-02
Pd-107	2.0E+08	6.9E+03	1.3E+04
Pu-238	1.5E+11	3.8E+06	1.2E+06
Pu-239	9.2E+07	1.9E+06	1.7E+06
Pu-240	---	1.1E+11	8.1E+09
Pu-241	5.1E+04	1.1E+04	1.1E+04
Pu-242	2.2E+19	1.0E+11	7.6E+09
Pu-244	---	9.4E+10	6.8E+09
Ra-226	2.6E+02	7.3E-01	2.9E-01

Table 7-13. Final All-Pathways Radionuclide Disposal Limits for Engineered Trenches - continued

Radionuclide	Limit (Ci)		
	130 - 200 yrs	200-1000 yrs	1000-1130 yrs
Se-79	---	---	---
Sn-126	---	---	---
Sr-90	3.3E+05	8.9E+03	1.5E+11
Tc-99	1.1E+01	1.1E+01	1.1E+01
Th-230	8.9E+03	4.8E+00	1.1E+00
Th-232	1.9E+06	3.3E+05	8.3E+05
U-233	---	6.0E+13	4.7E+12
U-234	1.5E+07	1.1E+03	3.1E+02
U-235	7.5E+00	1.0E+00	1.0E+00
U-236	2.9E+14	3.9E+12	2.9E+12
U-238	1.2E+11	1.1E+06	4.0E+05
Zr-93	2.1E+01	9.0E+00	8.3E+00

Limits reported as "---" indicate that there is no limit or that the limit > 1E+20.

Table 7-14. Final Intruder-Based Disposal Limits for Slit and Engineered Trenches - Resident and Post-drilling Scenarios

	Slit Trench Limits (Ci/Unit)		Eng. Trench Limits (Ci/Unit)	
Radionuclide	**Resident**	**Post-drilling**	**Resident**	**Post-drilling**
Ac-227	3.1E+07	4.2E+03	2.0E+07	4.3E+03
Ag-108m	3.6E+01	2.3E+03	2.4E+01	2.4E+03
Al-26	3.9E+00	1.6E+03	2.6E+00	1.7E+03
Am-241	6.2E+05	1.4E+03	4.1E+05	1.4E+03
Am-242m	1.6E+05	1.4E+03	1.1E+05	1.4E+03
Am-243	3.9E+02	1.1E+03	2.6E+02	1.2E+03
Ar-39	---	3.6E+07	---	3.7E+07
Ba-133	4.3E+09	8.2E+06	2.8E+09	8.5E+06
Bi-207	9.9E+04	2.3E+04	6.6E+04	2.4E+04
Bk-249	1.4E+05	4.9E+05	9.4E+04	5.1E+05
C-14	---	2.0E+03	---	2.1E+03
C-14_NR.Pump	---	2.0E+03	---	2.1E+03
Ca-41	---	1.2E+04	---	1.2E+04
Cd-113m	---	3.0E+04	---	3.1E+04
Cf-249	3.7E+02	1.3E+03	2.4E+02	1.3E+03
Cf-250	3.8E+13	2.6E+05	2.5E+13	2.7E+05
Cf-251	1.4E+03	1.2E+03	9.0E+02	1.2E+03
Cf-252	7.5E+11	5.3E+07	5.0E+11	5.5E+07
Cl-36	---	2.5E+01	---	2.6E+01
Cm-242	2.6E+09	7.0E+05	1.8E+09	7.3E+05
Cm-243	4.1E+07	2.2E+04	2.7E+07	2.2E+04
Cm-244	4.4E+11	1.0E+05	2.9E+11	1.0E+05
Cm-245	2.4E+03	7.7E+02	1.6E+03	7.9E+02
Cm-246	1.0E+11	1.5E+03	6.8E+10	1.5E+03
Cm-247	7.9E+01	1.3E+03	5.2E+01	1.3E+03
Cm-248	5.5E+06	3.9E+02	3.6E+06	4.1E+02
Co-60	2.0E+09	8.3E+08	1.3E+09	8.6E+08
Cs-134	1.5E+19	4.8E+17	9.9E+18	5.0E+17
Cs-135	---	2.4E+04	---	2.5E+04
Cs-137	2.1E+06	2.4E+04	1.4E+06	2.5E+04
Eu-152	2.3E+06	6.5E+05	1.5E+06	6.7E+05
Eu-154	4.1E+07	1.1E+07	2.7E+07	1.2E+07
Eu-155	4.0E+18	2.4E+11	2.7E+18	2.4E+11
H-3	---	2.1E+06	---	2.1E+06
H-3_Concrete	---	2.1E+06	---	2.1E+06
H-3_ETF. Carbon	---	2.1E+06	---	2.1E+06
I-129	7.3E+09	3.8E+02	4.8E+09	3.9E+02

Table 7-14. Final Intruder-Based Disposal Limits for Slit and Engineered Trenches - Resident and Post-drilling Scenarios - continued

	Slit Trench Limits (Ci/Unit)		Eng. Trench Limits (Ci/Unit)	
Radionuclide	**Resident**	**Post-drilling**	**Resident**	**Post-drilling**
I-129_ETF.Carbon	7.3E+09	3.8E+02	4.8E+09	3.9E+02
I-129_ETF.GT.73	7.3E+09	3.8E+02	4.8E+09	3.9E+02
I-129_F.Carbon	7.3E+09	3.8E+02	4.8E+09	3.9E+02
I-129_F.CG.8	7.3E+09	3.8E+02	4.8E+09	3.9E+02
I-129_F.Dowex.21K	7.3E+09	3.8E+02	4.8E+09	3.9E+02
I-129_F.Filtercake	7.3E+09	3.8E+02	4.8E+09	3.9E+02
I-129_H.Carbon	7.3E+09	3.8E+02	4.8E+09	3.9E+02
I-129_H.CG.8	7.3E+09	3.8E+02	4.8E+09	3.9E+02
I-129_H.Dowex.21K	7.3E+09	3.8E+02	4.8E+09	3.9E+02
I-129_H.Filtercake	7.3E+09	3.8E+02	4.8E+09	3.9E+02
I-129_Mk50A	7.3E+09	3.8E+02	4.8E+09	3.9E+02
K-40	6.7E+01	5.1E+02	4.4E+01	5.3E+02
Kr-85	9.9E+10	1.2E+09	6.5E+10	1.2E+09
Mo-93	---	4.7E+05	---	4.9E+05
Na-22	2.7E+15	5.9E+14	1.8E+15	6.2E+14
Nb-93m	---	1.2E+08	---	1.3E+08
Nb-94	9.6E+00	2.7E+03	6.4E+00	2.8E+03
Ni-59	---	4.2E+05	---	4.3E+05
Ni-63	---	3.0E+05	---	3.1E+05
Np-237	1.7E+02	1.1E+02	1.1E+02	1.1E+02
Pa-231	8.1E+01	1.2E+02	5.4E+01	1.3E+02
Pb-210	1.4E+11	2.2E+03	9.3E+10	2.2E+03
Pd-107	---	8.7E+05	---	9.1E+05
Pu-238	1.3E+07	3.6E+03	8.9E+06	3.7E+03
Pu-239	3.8E+06	1.5E+03	2.5E+06	1.5E+03
Pu-240	1.2E+09	1.5E+03	8.0E+08	1.5E+03
Pu-241	1.9E+07	4.1E+04	1.2E+07	4.2E+04
Pu-242	6.9E+08	1.5E+03	4.6E+08	1.6E+03
Pu-244	4.4E+01	1.3E+03	2.9E+01	1.3E+03
Ra-226	9.1E+00	7.1E01	6.0E+00	7.4E+01
Ra-226_Cooling.Tower	9.1E+00	7.1E01	6.0E+00	7.4E+01
Ra-228	1.3E+08	2.5E+07	8.7E+07	2.6E+07
Rb-87	---	1.5E+04	---	1.6E+04
S-35	---	---	---	---
Sb-125	5.0E+16	7.4E+14	3.3E+16	7.7E+14
Sc-46	---	---	---	---
Se-79	---	2.4E+04	---	2.5E+04
Sm-151	---	5.9E+06	---	6.2E+06

Table 7-14. Final Intruder-Based Disposal Limits for Slit and Engineered Trenches - Resident and Post-drilling Scenarios - continued

	Slit Trench Limits (Ci/Unit)		Eng. Trench Limits (Ci/Unit)	
Radionuclide	**Resident**	**Post-drilling**	**Resident**	**Post-drilling**
Sn-121m	---	1.6E+06	---	1.7E+06
Sn-126	8.7E+00	2.1E+03	5.7E+00	2.1E+03
Sr-90	---	1.6E+03	---	1.7E+03
Sr-90_Mk50A	---	1.6E+03	---	1.7E+03
Tc-99	1.0E+09	2.4E+03	6.9E+08	2.5E+03
Tc-99_Mk50A	1.0E+09	2.4E+03	6.9E+08	2.5E+03
Th-228	6.6E+18	3.4E+18	4.4E+18	3.6E+18
Th-229	9.0E+01	5.0E+02	6.0E+01	5.2E+02
Th-230	1.9E+01	1.9E+02	1.2E+01	2.0E+02
Th-230_Cooling.Tower	1.9E+01	1.9E+02	1.2E+01	2.0E+02
Th-232	4.4E+00	1.5E+02	2.9E+00	1.5E+02
U-232	3.2E+03	9.4E+02	2.1E+03	9.7E+02
U-233	9.3E+02	2.2E+03	6.2E+02	2.3E+03
U-234	3.8E+03	3.4E+03	2.5E+03	3.5E+03
U-234_MGlass	3.8E+03	3.4E+03	2.5E+03	3.5E+03
U-235	5.0E+02	2.2E+03	3.3E+02	2.3E+03
U-235_MGlass	5.0E+02	2.2E+03	3.3E+02	2.3E+03
U-235_Paducah.Cask	5.0E+02	2.2E+03	3.3E+02	2.3E+03
U-236	2.8E+07	3.9E+03	1.8E+07	4.1E+03
U-236_MGlass	2.8E+07	3.9E+03	1.8E+07	4.1E+03
U-238	9.7E+02	4.0E+03	6.4E+02	4.2E+03
U-238_MGlass	9.7E+02	4.0E+03	6.4E+02	4.2E+03
W-181	---	---	---	---
W-185	---	---	---	---
W-188	---	---	---	---
Zr-93	---	9.5E+05	---	9.8E+05

Note: Unless otherwise noted in the Table, limits for special waste forms are the same as for their generic radionuclide.

Limits reported as "---" indicate that there is no limit or that the limit > 1E+20.

Table 7-15. Final Slit and Engineered Trench Air Pathway Disposal Limits

Radionuclide	0 - 125 Year Limit (Ci)
C-14	2.9E+05
C-14_NR.Pump	2.9E+05
Cl-36	1.5E+05
H-3	1.1E+07
H-3_Concrete	1.1E+07
H-3_ETF.Carbon	1.1E+07
I-129	9.5E+02
I-129_ETF.Carbon	9.5E+02
I-129_ETF.GT.73	9.5E+02
I-129_F.Carbon	9.5E+02
I-129_F.CG.8	9.5E+02
I-129_F.Dowex.21K	9.5E+02
I-129_F.Filtercake	9.5E+02
I-129_H.Carbon	9.5E+02
I-129_H.CG.8	9.5E+02
I-129_H.Dowex.21K	9.5E+02
I-129_H.Filtercake	9.5E+02
I-129_Mk50A	9.5E+02
S-35	4.5E+06
Sb-124	1.5E+05
Sb-125	6.6E+03
Se-75	9.0E+04
Se-79	5.5E+04
Sn-113	4.8E+05
Sn-119m	5.6E+05
Sn-121	---
Sn-121m	5.8E+04
Sn-123	7.8E+06
Sn-126	1.3E+02

Note: Unless otherwise noted in the Table, limits for special waste forms are the same as for their generic radionuclide.

Limits reported as "---" indicate that there is no limit or that the limit > 1E+20.

Table 7-16. Final Slit and Engineered Trench Disposal Limits for Radon Parent Radionuclides

Radionuclide	Slit Trench Radon Pathway Disposal Limit (Ci)	Engineered Trench Radon Pathway Disposal Limit (Ci)
Pu-238	7.7E+12	1.1E+13
Ra-226	2.2E+04	3.3E+04
Ra-226_Cooling.Tower	2.2E+04	3.3E+04
Th-230	4.2E+05	6.2E+05
Th-230_Cooling.Tower	4.2E+05	6.2E+05
U-234	7.2E+08	1.1E+09
U-234_MGlass	7.2E+08	1.1E+09
U-238	6.1E+12	9.1E+12
U-238_MGlass	6.1E+12	9.1E+12

Note: Unless otherwise noted in the Table, limits for special waste forms are the same as for their generic radionuclide.

Table 7-17. Components in Grout Trench 1 Groundwater Protection and All-Pathways Limits

Parent Radionuclide	CIG-1 Inventory Limit 0-125 year (Ci)					CIG-1 Inventory Limit 125-1,125 year (Ci)				
	Groundwater Protection				All-Pathways	Groundwater Protection				All-Pathways
	Beta-Gamma	Gross Alpha	Radium	Uranium		Beta-Gamma	Gross Alpha	Radium	Uranium	
Am-241	---	---	---	---	---	6.6E+03	3.3E+02	---	8.5E+11	1.0E+02
Am-243	---	---	---	---	---	1.3E+05	6.2E+03	---	3.5E+15	2.3E+03
C-14	2.9E+09	---	---	---	3.0E+09	3.2E-01	---	---	---	3.5E-01
C-14_K	3.7E+10	---	---	---	3.9E+10	3.0E+00	---	---	---	3.2E+00
Cl-36	6.4E+04	---	---	---	3.4E+04	8.7E-02	---	---	---	4.7E-02
Cm-244	---	---	---	---	---	---	---	---	---	---
Cm-245	---	---	---	---	---	4.9E+03	2.3E+02	---	6.4E+11	7.2E+01
Cm-247	---	---	---	---	---	9.4E+05	5.1E+03	---	3.3E+16	2.0E+03
Cm-248	---	---	---	---	---	2.9E+12	6.1E+03	---	---	5.6E+02
H-3	1.4E+05	---	---	---	6.5E+06	9.3E+04	---	---	---	2.4E+06
I-129	2.6E+04	---	---	---	1.6E+06	9.2E-05	---	---	---	5.3E-03
I-129_C	3.4E+06	---	---	---	2.0E+08	5.3E-03	---	---	---	3.2E-01
I-129_K	2.1E+07	---	---	---	1.3E+09	3.3E-02	---	---	---	2.0E+00
K-40	---	---	---	---	---	4.0E+07	---	---	---	8.6E+07
Mo-93	4.4E+02	---	---	---	2.1E+03	2.4E-01	---	---	---	1.2E+00
Nb-94	3.6E+18	---	---	---	2.0E+18	5.8E+00	---	---	---	3.2E+00
Ni-59	---	---	---	---	---	5.0E+00	---	---	---	1.2E+03
Np-237	---	---	---	---	---	1.4E+00	7.1E-02	---	1.9E+08	2.2E-02
Pd-107	---	---	---	---	---	6.1E+02	---	---	---	1.9E+03
Pu-238	---	---	---	---	---	2.2E+06	2.7E+04	3.6E+04	---	1.0E+05
Pu-239	---	---	---	---	---	3.3E+06	2.5E+06	---	---	3.1E+05
Pu-240	---	---	---	---	---	---	1.9E+18	---	---	7.8E+17
Pu-241	---	---	---	---	---	2.0E+05	9.9E+03	---	2.6E+13	3.0E+03

Table 7-17. Components in Grout Trench 1 Groundwater Protection and All-Pathways Limits - continued

Parent Radionuclide	CIG-1 Inventory Limit 0-125 year (Ci)					CIG-1 Inventory Limit 125-1,125 year (Ci)				
	Groundwater Protection				All-Pathways	Groundwater Protection				All-Pathways
	Beta-Gamma	Gross Alpha	Radium	Uranium		Beta-Gamma	Gross Alpha	Radium	Uranium	
Pu-242	---	---	---	---	---	1.9E+13	2.1E+11	2.9E+11	---	8.3E+11
Pu-244	---	---	---	---	---	---	1.6E+18	---	---	6.6E+17
Ra-226	---	---	---	---	---	9.7E-01	1.3E-02	1.7E-02	---	4.8E-02
Se-79	---	---	---	---	---	---	---	---	---	---
Sn-126	---	---	---	---	---	---	---	---	---	---
Sr-90	---	---	---	---	---	9.4E+03	---	---	---	1.8E+05
Tc-99	2.1E+03	---	---	---	3.2E+03	2.8E-01	---	---	---	4.3E-01
Tc-99_K	3.7E+06	---	---	---	5.6E+06	8.4E+00	---	---	---	1.3E+01
Th-230	---	---	---	---	---	2.7E+00	3.6E-02	4.8E-02	---	1.4E-01
Th-232	---	---	---	---	---	6.0E+07	6.1E+07	8.2E+07	---	1.6E+08
U-233	---	---	---	---	---	---	---	---	---	---
U-234	---	---	---	---	---	6.2E+02	7.6E+00	1.0E+01	---	2.9E+01
U-235	---	---	---	---	---	2.4E+00	1.8E+00	---	---	2.3E-01
U-236	---	---	---	---	---	8.6E+14	8.7E+14	1.2E+15	---	2.3E+15
U-238	---	---	---	---	---	6.8E+05	8.0E+03	1.1E+04	---	3.1E+04
Zr-93	3.3E+18	---	---	---	2.0E+19	1.6E-01	---	---	---	9.3E-01

Limits reported as "---" indicate that there is no limit or that the limit > 1E+20.

Table 7-18. Components in Grout Trench 2 Groundwater Protection and All-Pathways Limits

Parent Radionuclide	CIG-2 Inventory Limit 0-125 year (Ci)					CIG-2 Inventory Limit 125-1,125 year (Ci)				
	Groundwater Protection				All-Pathways	Groundwater Protection				All-Pathways
	Beta-Gamma	Gross Alpha	Radium	Uranium		Beta-Gamma	Gross Alpha	Radium	Uranium	
Am-241	---	---	---	---	---	7.7E+03	3.9E+02	---	1.0E+12	1.2E+02
Am-243	---	---	---	---	---	1.5E+05	7.3E+03	---	4.1E+15	2.8E+03
C-14	3.4E+09	---	---	---	3.5E+09	3.5E-01	---	---	---	3.8E-01
C-14_K	4.4E+10	---	---	---	4.6E+10	3.5E+00	---	---	---	3.7E+00
Cl-36	7.6E+04	---	---	---	4.0E+04	1.0E-01	---	---	---	5.5E-02
Cm-244	---	---	---	---	---	---	---	---	---	---
Cm-245	---	---	---	---	---	5.8E+03	2.7E+02	---	7.5E+11	8.5E+01
Cm-247	---	---	---	---	---	1.1E+06	6.0E+03	---	3.9E+16	2.4E+03
Cm-248	---	---	---	---	---	3.4E+12	7.2E+03	---	---	6.6E+02
H-3	1.7E+05	---	---	---	7.7E+06	1.1E+05	---	---	---	2.9E+06
I-129	3.1E+04	---	---	---	1.9E+06	1.0E-04	---	---	---	6.3E-03
I-129_C	4.0E+06	---	---	---	2.4E+08	6.3E-03	---	---	---	3.8E-01
I-129_K	2.5E+07	---	---	---	1.5E+09	3.9E-02	---	---	---	2.3E+00
K-40	---	---	---	---	---	4.6E+07	---	---	---	1.0E+08
Mo-93	5.2E+02	---	---	---	2.5E+03	2.9E-01	---	---	---	1.4E+00
Nb-94	4.2E+18	---	---	---	2.4E+18	6.8E+00	---	---	---	3.8E+00
Ni-59	---	---	---	---	---	5.9E+00	---	---	---	1.5E+03
Np-237	---	---	---	---	---	1.7E+00	8.3E-02	---	2.3E+08	2.5E-02
Pd-107	---	---	---	---	---	7.2E+02	---	---	---	2.2E+03
Pu-238	---	---	---	---	---	2.6E+06	3.1E+04	4.2E+04	---	1.2E+05
Pu-239	---	---	---	---	---	3.9E+06	2.9E+06	---	---	3.7E+05
Pu-240	---	---	---	---	---	---	2.3E+18	---	---	9.2E+17
Pu-241	---	---	---	---	---	2.3E+05	1.2E+04	---	3.0E+13	3.6E+03

Table 7-18. Components in Grout Trench 2 Groundwater Protection and All-Pathways Limits - continued

Parent Radionuclide	CIG-2 Inventory Limit 0-125 year (Ci)					CIG-2 Inventory Limit 125-1,125 year (Ci)				
	Groundwater Protection				All-Pathways	Groundwater Protection				All-Pathways
	Beta-Gamma	Gross Alpha	Radium	Uranium		Beta-Gamma	Gross Alpha	Radium	Uranium	
Pu-242	---	---	---	---	---	2.3E+13	2.5E+11	3.4E+11	---	9.7E+11
Pu-244	---	---	---	---	---	---	1.9E+18	---	---	7.7E+17
Ra-226	---	---	---	---	---	1.1E+00	1.5E-02	2.0E-02	---	5.7E-02
Se-79	---	---	---	---	---	---	---	---	---	---
Sn-126	---	---	---	---	---	---	---	---	---	---
Sr-90	---	---	---	---	---	1.1E+04	---	---	---	2.1E+05
Tc-99	2.5E+03	---	---	---	3.8E+03	3.3E-01	---	---	---	5.0E-01
Tc-99_K	4.4E+06	---	---	---	6.6E+06	9.9E+00	---	---	---	1.5E+01
Th-230	---	---	---	---	---	3.2E+00	4.2E-02	5.6E-02	---	1.6E-01
Th-232	---	---	---	---	---	7.1E+07	7.2E+07	9.7E+07	---	1.9E+08
U-233	---	---	---	---	---	---	---	---	---	---
U-234	---	---	---	---	---	7.2E+02	8.9E+00	1.2E+01	---	3.4E+01
U-235	---	---	---	---	---	2.8E+00	2.2E+00		---	2.8E-01
U-236	---	---	---	---	---	1.0E+15	1.0E+15	1.4E+15	---	2.7E+15
U-238	---	---	---	---	---	8.0E+05	9.4E+03	1.3E+04	---	3.6E+04
Zr-93	3.9E+18	---	---	---	2.3E+19	1.9E-01	---	---	---	1.1E+00

Limits reported as "---" indicate that there is no limit or that the limit > 1E+20.

Table 7-19. Final CIG Intruder Limits

Radionuclide	Resident (Ci)	Post Drilling (Ci)
Ac-227	1.9E+07	1.9E+06
Ag-108m	1.0E+01	2.5E+03
Al-26	1.6E+00	1.3E+03
Am-241	2.2E+04	1.5E+03
Am-242m	3.5E+04	2.1E+03
Am-243	6.9E+01	9.1E+02
Ar-39	---	4.7E+07
Ba-133	2.5E+09	3.4E+12
Bi-207	6.5E+04	1.2E+06
Bk-249	3.2E+04	5.6E+05
C-14	---	1.6E+03
C-14_K	---	1.6E+03
Ca-41	---	9.4E+03
Cd-113m	---	4.4E+08
Cf-249	8.2E+01	1.4E+03
Cf-250	4.3E+10	4.3E+05
Cf-251	2.1E+02	1.1E+03
Cf-252	2.2E+11	4.2E+07
Cl-36	---	2.0E+01
Cm-242	1.0E+09	2.7E+06
Cm-243	7.1E+06	6.5E+05
Cm-244	3.7E+09	4.3E+05
Cm-245	2.7E+02	6.0E+02
Cm-246	1.2E+08	1.2E+03
Cm-247	1.8E+01	9.9E+02
Cm-248	1.6E+06	3.1E+02
Co-60	1.4E+09	---
Cs-134	9.5E+18	---
Cs-135	---	1.9E+04
Cs-137	1.3E+06	1.9E+06
Eu-152	1.5E+06	1.5E+10
Eu-154	2.7E+07	8.9E+13
Eu-155	1.8E+18	---
H-3	---	1.3E+11
I-129	1.2E+06	3.0E+02
I-129_C	1.2E+06	3.0E+02
I-129_K	1.2E+06	3.0E+02
K-40	2.6E+01	4.0E+02
Kr-85	6.0E+10	3.7E+14
Mo-93	---	3.8E+05
Na-22	1.8E+15	---
Nb-93m	---	5.3E+11
Nb-94	3.0E+00	2.2E+03

Table 7-19. Final CIG Intruder Limits - continued

Radionuclide	Resident (Ci)	Post Drilling (Ci)
Ni-59	---	3.3E+05
Ni-63	---	9.5E+05
Np-237	3.4E+01	8.6E+01
Pa-231	1.8E+01	9.6E+01
Pb-210	9.0E+10	8.7E+05
Pd-107	---	6.9E+05
Pu-238	5.1E+06	1.4E+04
Pu-239	3.6E+05	1.2E+03
Pu-240	1.0E+07	1.2E+03
Pu-241	6.6E+05	4.4E+04
Pu-242	8.5E+06	1.2E+03
Pu-244	1.5E+01	1.0E+03
Ra-226	3.5E+00	6.0E+01
Ra-228	9.2E+07	5.7E+17
Rb-87	---	1.2E+04
S-35	---	---
Sb-125	3.0E+16	---
Sc-46	---	---
Se-79	---	1.9E+04
Sm-151	---	2.2E+07
Sn-121m	---	3.0E+07
Sn-126	2.5E+00	1.6E+03
Sr-90	---	1.6E+05
Tc-99	6.6E+07	1.9E+03
Tc-99_K	6.6E+07	1.9E+03
Th-228	4.7E+18	---
Th-229	2.5E+01	4.0E+02
Th-230	7.1E+00	1.5E+02
Th-232	1.8E+00	1.2E+02
U-232	2.2E+03	5.5E+03
U-233	2.6E+02	1.7E+03
U-234	1.4E+03	2.7E+03
U-235	7.2E+01	1.7E+03
U-236	1.1E+06	3.1E+03
U-238	3.1E+02	3.1E+03
W-181	---	---
W-185	---	---
W-188	---	---
Zr-93	---	7.5E+05

Note: Unless otherwise noted in the Table, limits for special waste forms are the same as for their generic radionuclide.

Limits reported as "---" indicate that there is no limit or that the limit > 1E+20.

Table 7-20. Final CIG Air Pathway Disposal Limits

Radionuclide	CIG-1 and CIG-2 Trench Air Pathway
	Disposal Limit (Ci)
C-14	1.7E+06
C-14_K	1.7E+06
Cl-36	1.0E+06
H-3	3.1E+07
I-129	1.7E+02
I-129_C	1.7E+02
I-129_K	1.7E+02
S-35	2.4E+07
Sb-124	1.3E+06
Sb-125	5.7E+04
Se-75	6.3E+05
Se-79	3.8E+05
Sn-113	4.0E+06
Sn-119m	4.8E+06
Sn-121	---
Sn-121m	4.6E+05
Sn-123	6.7E+07
Sn-126	8.2E+02

Note: Unless otherwise noted in the Table, limits for special waste forms are the same as for their generic radionuclide.
Limits reported as "---" indicate that there is no limit or that the limit > 1E+20.

Table 7-21. Final CIG Disposal Limits for Radon Parent Radionuclides

Radionuclide	Limit (Ci)
Pu-238	4.6E+14
Ra-226	1.3E+06
Th-230	2.5E+07
U-234	4.3E+10
U-238	3.6E+14

Note: Unless otherwise noted in the Table, limits for special waste forms are the same as for their generic radionuclide.

Table 7-22. Final LAWV Groundwater Protection and All-Pathways Limits

Radionuclide	Beta-Gamma (Ci)	Gross Alpha (Ci)	Radium (Ci)	Uranium (Ci)	All-Pathways (Ci)
Am-241	7.2E+09	3.6E+08	---	6.6E+18	1.1E+08
Am-243	1.5E+16	7.9E+15	---	---	9.9E+14
C-14	4.2E+00	---	---	---	4.3E+00
Cl-36	1.2E+00	---	---	---	6.4E-01
Cm-244	---	---	---	---	---
Cm-245	5.0E+09	2.5E+08	---	4.9E+18	7.8E+07
Cm-247	3.1E+17	1.6E+17	---	---	2.0E+16
Cm-248	---	---	---	---	---
H-3	2.9E+08	---	---	---	2.6E+10
I-129	2.2E-03	---	---	---	1.3E-01
I-129_H	5.3E-02	---	---	---	3.2E+00
I-129_J	9.7E-03	---	---	---	5.8E-01
K-40	---	---	---	---	---
Mo-93	1.5E+00	---	---	---	7.0E+00
Nb-94	2.3E+01	---	---	---	1.3E+01
Ni-59	6.7E+09	---	---	---	1.7E+12
Np-237	1.1E+07	5.7E+05	---	1.1E+16	1.8E+05
Pd-107	8.1E+11	---	---	---	2.6E+12
Pu-238	4.4E+14	3.2E+12	4.3E+12	---	1.3E+13
Pu-239	6.2E+14	3.4E+14	---	---	4.3E+13
Pu-240	---	---	---	---	---
Pu-241	2.1E+11	1.1E+10	---	---	3.3E+09
Pu-242	---	---	---	---	---
Pu-244	---	---	---	---	---

Table 7-22. Final LAWV Groundwater Protection and All-Pathways Limits - continued

Radionuclide	Beta-Gamma (Ci)	Gross Alpha (Ci)	Radium (Ci)	Uranium (Ci)	All-Pathways (Ci)
Ra-226	1.8E+07	1.3E+05	1.8E+05	---	5.3E+05
Se-79	---	---	---	---	---
Sn-126	---	---	---	---	---
Sr-90	1.6E+15	---	---	---	3.1E+16
Tc-99	2.4E+02	---	---	---	3.6E+02
Th-230	1.3E+08	9.7E+05	1.3E+06	---	3.8E+06
Th-232	---	---	---	---	---
U-233	---	---	---	---	---
U-234	8.3E+10	6.1E+08	8.1E+08	---	2.4E+09
U-235	1.2E+08	7.0E+07	---	---	8.7E+06
U-236	---	---	---	---	---
U-238	2.4E+14	1.7E+12	2.3E+12	---	6.7E+12
Zr-93	6.9E+01	---	---	---	4.1E+02

Limits reported as "---" indicate that there is no limit or that the limit > 1E+20.

Table 7-23. Final LAWV Resident Intruder Limits

Radionuclide	Limit (Ci)
Ac-227	3.6E+04
Ag-108m	1.5E+02
Al-26	1.9E+01
Am-241	2.5E+07
Am-242m	5.9E+04
Am-243	1.3E+04
Ar-39	---
Ba-133	1.4E+06
Bi-207	4.9E+02
Bk-249	7.8E+05
C-14	---
Ca-41	---
Cd-113m	---
Cf-249	2.0E+03
Cf-250	1.2E+13
Cf-251	4.1E+04
Cf-252	5.9E+12
Cl-36	---
Cm-242	1.4E+10
Cm-243	2.1E+05
Cm-244	1.3E+15
Cm-245	2.1E+05
Cm-246	5.5E+13
Cm-247	1.5E+03
Cm-248	4.3E+07
Co-60	1.4E+07
Cs-134	3.5E+16
Cs-135	---
Cs-137	3.3E+03
Eu-152	1.3E+04
Eu-154	2.2E+05
Eu-155	3.8E+12
H-3	---
I-129	6.1E+18
I-129_H	6.1E+18
I-129_J	6.1E+18
K-40	3.6E+02
Kr-85	8.4E+07
Mo-93	---
Na-22	1.4E+13
Nb-93m	---
Nb-94	8.6E+01
Ni-59	---

Table 7-23. Final LAWV Resident Intruder Limits - continued

Radionuclide	Limit (Ci)
Ni-63	---
Np-237	4.1E+03
Pa-231	1.4E+03
Pb-210	3.5E+08
Pd-107	---
Pu-238	7.2E+07
Pu-239	6.1E+08
Pu-240	2.1E+13
Pu-241	7.7E+08
Pu-242	4.9E+10
Pu-244	3.4E+02
Ra-226	3.6E+01
Ra-228	2.4E+06
Rb-87	---
S-35	---
Sb-125	5.2E+13
Sc-46	---
Se-79	---
Sm-151	---
Sn-121m	---
Sn-126	9.3E+01
Sr-90	---
Tc-99	4.5E+11
Th-228	1.4E+17
Th-229	7.8E+02
Th-230	1.0E+02
Th-232	2.0E+01
U-232	6.7E+01
U-233	8.6E+03
U-234	2.0E+04
U-235	2.5E+04
U-236	4.1E+08
U-238	7.6E+03
W-181	---
W-185	---
W-188	---
Zr-93	---

Limits reported as "---" indicate that there is no limit or that the limit > 1E+20.

Table 7-24. Final LAWV Air Pathway Disposal Limits

Radionuclide	Limit (Ci)
C-14	3.3E+03
Cl-36	2.0E+03
H-3 *	1.1E+08
H-3 #	4.5E+06
I-129	1.7E+01
I-129_H	1.7E+01
I-129_J	1.7E+01
S-35	1.1E+04
Sb-124	3.0E+02
Sb-125	9.2E+01
Se-75	4.3E+02
Se-79	7.5E+02
Sn-113	2.5E+03
Sn-119m	5.7E+03
Sn-121	3.1E+04
Sn-121m	8.9E+02
Sn-123	4.7E+04
Sn-126	2.0E+00

* Maximum permissible Total Inventory over 25-year operational period.
# Maximum permissible Annual Inventory

Table 7-25. Final LAWV Disposal Limits for Radon Parent Radionuclides

Radionuclide	Limit (Ci)
Pu-238	8.4E+10
Ra-226	2.4E+00
Th-230	2.2E+02
U-234	1.9E+06
U-238	8.1E+10

Note: Unless otherwise noted in the Table, limits for special waste forms are the same as for their generic radionuclide.

Table 7-26. Final Intermediate Level Vault Groundwater Protection Limits

	Beta-Gamma (Ci)		Gross Alpha (Ci)		Radium (Ci)		Uranium	
Radionuclide	**0-200 yrs**	**200-1100 yrs**	**0-200 yrs**	**200-1100 yrs**	**0-200 yrs**	**200-1100 yrs**	**0-200 yrs**	**200-1100 yrs**
Am-241	---	1.9E+10	---	9.6E+08	---	---	---	1.2E+19
Am-243	---	9.9E+16	---	2.1E+15	---	---	---	---
C-14	2.8E+16	2.9E+02	---	---	---	---	---	---
C-14_KB*	4.5E+17	5.3E+12	---	---	---	---	---	---
Cl-36	9.7E+07	4.6E+00	---	---	---	---	---	---
Cm-244	---	---	---	---	---	---	---	---
Cm-245	---	3.1E+10	---	1.6E+09	---	---	---	2.0E+19
Cm-247	---	5.4E+18	---	1.1E+17	---	---	---	---
Cm-248	---	---	---	---	---	---	---	---
H-3	7.5E+07	3.1E+11	---	---	---	---	---	---
H-3_TPBAR	1.2E+08	1.6E+11	---	---	---	---	---	---
I-129	3.0E+10	1.1E-02	---	---	---	---	---	---
I-129_ETF	2.0E+12	3.9E-01	---	---	---	---	---	---
I-129_KB	1.1E+14	2.3E+00	---	---	---	---	---	---
K-40	---	1.2E+13	---	---	---	---	---	---
Mo-93	6.3E+03	4.2E+00	---	---	---	---	---	---
Nb-94	---	1.1E+05	---	---	---	---	---	---
Ni-59	---	1.1E+08	---	---	---	---	---	---
Np-237	---	2.5E+06	---	1.2E+05	---	---	---	1.5E+15
Pd-107	---	1.3E+10	---	---	---	---	---	---
Pu-238	---	9.9E+09	---	7.1E+07	---	9.5E+07	---	---
Pu-239	---	7.2E+14	---	1.5E+13	---	---	---	---
Pu-240	---	---	---	---	---	---	---	---
Pu-241	---	5.9E+11	---	3.0E+10	---	---	---	---
Pu-242	---	1.7E+17	---	1.2E+15	---	1.6E+15	---	---
Pu-244	---	---	---	---	---	---	---	---
Ra-226	---	1.8E+03	---	1.3E+01	---	1.8E+01	---	---

Table 7-26. Final Intermediate Level Vault Groundwater Protection Limits - continued

	Beta-Gamma (Ci)		Gross Alpha (Ci)		Radium (Ci)		Uranium	
Radionuclide	**0-200 yrs**	**200-1100 yrs**	**0-200 yrs**	**200-1100 yrs**	**0-200 yrs**	**200-1100 yrs**	**0-200 yrs**	**200-1100 yrs**
Se-79	---	---	---	---	---	---	---	---
Sn-126	---	---	---	---	---	---	---	---
Sr-90	8.2E+14	8.0E+09	---	---	---	---	---	---
Tc-99	---	1.1E+07	---	---	---	---	---	---
Tc-99_KB	---	1.4E+08	---	---	---	---	---	---
Th-230	---	6.5E+03	---	4.8E+01	---	6.4E+01	---	---
Th-232	---	1.1E+15	---	1.1E+15	---	1.5E+15	---	---
U-233	---	---	---	---	---	---	---	---
U-234	---	2.4E+06	---	1.7E+04	---	2.3E+04	---	---
U-235	---	2.9E+08	---	6.2E+06	---	---	---	---
U-236	---	---	---	---	---	---	---	---
U-238	---	4.1E+09	---	2.9E+07	---	3.9E+07	---	---
Zr-93	---	1.3E+08	---	---	---	---	---	---

Limits reported as "---" indicate that there is no limit or that the limit > 1E+20.
* Waste containing C-14_KB is assumed to not be in Cell #4.

Table 7-27. Final Intermediate Level Vault All-Pathways Limits

Radionuclide	0-200 yrs (Ci)	200-1100 yrs (Ci)
Am-241	---	3.0E+08
Am-243	---	2.5E+14
C-14	2.9E+16	3.1E+02
C-14_KB*	4.7E+17	5.6E+12
Cl-36	5.1E+07	2.4E+00
Cm-244	---	---
Cm-245	---	4.9E+08
Cm-247	---	1.3E+16
Cm-248	---	---
H-3	2.0E+09	8.2E+12
H-3_TPBAR	3.2E+09	4.3E+12
I-129	1.8E+12	6.7E-01
I-129_ETF	1.2E+14	2.4E+01
I-129_KB	6.5E+15	1.4E+02
K-40	---	2.7E+13
Mo-93	2.8E+04	2.0E+01
Nb-94	---	6.3E+04
Ni-59	---	2.8E+10
Np-237	---	3.9E+04
Pd-107	---	4.3E+10
Pu-238	---	2.8E+08
Pu-239	---	1.8E+12
Pu-240	---	---
Pu-241	---	9.2E+09
Pu-242	---	4.7E+15
Pu-244	---	---
Ra-226	---	5.2E+01
Se-79	---	---
Sn-126	---	---
Sr-90	1.6E+16	1.5E+11
Tc-99	---	1.6E+07
Tc-99_KB	---	2.2E+08
Th-230	---	1.9E+02
Th-232	---	3.0E+15
U-233	---	---
U-234	---	6.7E+04
U-235	---	7.4E+05
U-236	---	---
U-238	---	1.2E+08
Zr-93	---	8.0E+08

Limits reported as "---" indicate that there is no limit or that the limit > 1E+20.
* Waste containing C-14_KB is assumed to not be in Cell #4.

Table 7-28. Final ILV Resident Intruder Limits

Radionuclide	Limit (Ci)
Ac-227	4.2E+05
Ag-108m	1.4E+03
Al-26	6.8E+01
Am-241	5.5E+08
Am-242m	3.5E+05
Am-243	3.9E+05
Ar-39	---
Ba-133	2.6E+07
Bi-207	2.6E+03
Bk-249	1.4E+07
C-14	---
C-14_KB	---
Ca-41	---
Cd-113m	---
Cf-249	3.6E+04
Cf-250	2.1E+16
Cf-251	2.0E+06
Cf-252	3.6E+13
Cl-36	---
Cm-242	5.4E+10
Cm-243	7.5E+06
Cm-244	3.3E+16
Cm-245	2.2E+07
Cm-246	3.3E+14
Cm-247	2.6E+04
Cm-248	2.6E+08
Co-60	6.3E+07
Cs-134	2.6E+17
Cs-135	---
Cs-137	3.0E+04
Eu-152	6.3E+04
Eu-154	1.1E+06
Eu-155	1.1E+15
H-3	---
H-3_TPBAR	---
I-129	---
I-129_ETF	---
I-129_KB	---
K-40	1.4E+03
Kr-85	1.0E+09
Mo-93	---
Na-22	7.4E+13

Table 7-28. Final ILV Resident Intruder Limits - continued

Radionuclide	Limit (Ci)
Nb-93m	---
Nb-94	6.2E+02
Ni-59	---
Ni-63	---
Np-237	8.9E+04
Pa-231	1.7E+04
Pb-210	2.6E+09
Pd-107	---
Pu-238	2.7E+08
Pu-239	1.1E+11
Pu-240	8.6E+13
Pu-241	1.7E+10
Pu-242	2.9E+11
Pu-244	2.1E+03
Ra-226	1.4E+02
Ra-228	7.1E+06
Rb-87	---
S-35	---
Sb-125	5.7E+14
Sc-46	---
Se-79	---
Sm-151	---
Sn-121m	---
Sn-126	8.1E+02
Sr-90	---
Tc-99	2.6E+14
Tc-99_KB	2.6E+14
Th-228	3.8E+17
Th-229	4.2E+03
Th-230	3.8E+02
Th-232	5.9E+01
U-232	1.8E+02
U-233	4.6E+04
U-234	7.7E+04
U-235	6.5E+05
U-236	1.2E+09
U-238	4.5E+04
W-181	---
W-185	---
W-188	---
Zr-93	---

Limits reported as "---" indicate that there is no limit or that the limit > 1E+20.

Table 7-29. Final ILV Air Pathway Limits

Radionuclide	IL Vault Air Pathway Disposal Limit (Ci)
C-14	2.2E+05
C-14_KB	2.2E+05
Cl-36	1.3E+05
H-3	3.8E+06
H-3_TPBAR *	9.4E+10
I-129	1.1E+03
I-129_ETF	1.1E+03
I-129_KB	1.1E+03
S-35	7.6E+05
Sb-124	2.1E+04
Sb-125	6.1E+03
Se-75	2.9E+04
Se-79	4.9E+04
Sn-113	1.7E+05
Sn-119m	3.8E+05
Sn-121	5.5E+06
Sn-121m	5.9E+04
Sn-123	3.2E+06
Sn-126	1.3E+02

* TPBAR tritium limit for the ILV is taken from Hiergesell 2005 Table 4

Table 7-30. Final ILV Limits for Radon Parent Radionuclides

Radionuclide	Limits (Ci)
Pu-238	2.3E+11
Ra-226	2.0E+01
Th-230	1.8E+03
U-234	1.6E+07
U-238	1.8E+11

Note: Unless otherwise noted in the Table, limits for special waste forms are the same as for their generic radionuclide.

Table 7-31. Final NRCDA (643-26E and 643-7E) Groundwater Protection and All-Pathways Limits

Radionuclide	Beta-Gamma (Ci)	Gross Alpha (Ci)	Radium (Ci)	Uranium (Ci)	All-Pathways (Ci)
C-14	1.3E+04	---	---	---	1.4E+04
I-129	1.5E-02	---	---	---	9.1E-01
Nb-94	1.6E+03	---	---	---	8.8E+02
Ni-59	9.7E+04	---	---	---	2.4E+07
Pu-239	6.5E+09	4.5E+07	---	---	2.3E+07
Pu-240	---	---	---	---	---
Tc-99	6.2E+02	---	---	---	9.3E+02

Table 7-32. Final NRCDA Air Pathway Limits

Radionuclide	643-26E (Ci)	643-7E (Ci)
C-14	2.6E+03	5.3E+02
Cl-36	1.9E+03	3.7E+02
H-3	4.5E+06	4.5E+06
I-129	3.9E+00	7.7E-01
S-35	---	---
Sb-124	---	---
Sb-125	---	---
Se-79	1.0E+03	2.0E+02
Sn-113	---	---
Sn-119m	---	---
Sn-121m	1.4E+08	2.9E+07
Sn-123	---	---
Sn-126	3.1E+00	6.1E-01

Note: Unless otherwise noted in the Table, limits for special waste forms are the same as for their generic radionuclide.

Limits reported as "---" indicate that there is no limit or that the limit > 1E+20.

Table 7-33. Final NRCDA Radon Limits

Radionuclide	643-26E (Ci)	643-7E (Ci)
Pu-238	1.1E+12	2.4E+11
Ra-226	9.9E+05	2.1E+05
Th-230	1.9E+06	3.9E+05
U-234	3.3E+08	7.0E+07
U-238	3.0E+11	6.4E+10

Note: Unless otherwise noted in the table, limits for special waste forms are the same as for their generic radionuclide.

7.5 PERFORMANCE EVALUATION

This PA documents the projected radiological impacts associated with the disposal of LLW at the ELLWF. The projected impacts are used to demonstrate compliance with applicable radiological dose criteria of the DOE for protection of the public and the environment. This section compares the PA results to the applicable performance objectives in the context of compliance. It also considers the ALARA requirement and considers impacts to the Composite Analysis.

7.5.1 Comparison of Results to Performance Objectives

The final radionuclide disposal limits are compared with the projected radionuclide inventories of the disposal units in Appendix C. The maximum SOF for each disposal unit is shown in Table 7-34. None of the SOFs is greater than one; therefore, there is a reasonable expectation that all of the performance measures set forth in DOE O 435.1 will continue to be met throughout the life of the ELLWF.

7.5.3 ALARA Analysis

DOE's approach to radiation protection for LLW disposal is based on the performance objectives listed in the Order (DOE 1999), which specify maximum doses for various pathways, and on the ALARA principle, which requires doses to be maintained as low as reasonably achievable. The requirement is stated in DOE (1999):

> "Performance assessments shall include a determination that projected releases of radionuclide to the environment shall be maintained as low as reasonably achievable (ALARA)."

In addition to providing a reasonable expectation that the performance objectives described in DOE M 435.1-1.IV.P, the PA also needs to show that LLW disposal is being conducted in a manner that maintains releases of radionuclides to the environment ALARA. The goal of the ALARA process is attainment of the lowest practical dose level after taking into account social, technical, economic, and public policy considerations.

Table 7-34. Maximum SOF Using Projected Final Inventories

Disposal Unit	Maximum SOF	Performance Measure	Major Nuclides
ST			
East	9.3E-01	4 mrem/year beta-gamma 12-100 years	I-129, H-3, C-14
Central	9.3E-01	4 mrem/year beta-gamma 12-100 years	Tc-99, I-129, H-3
West	9.5E-01	4 mrem/year beta-gamma 0-12 years	I-129, H-3
ET	9.6E-01	4 mrem/year beta-gamma 12-100 years	Tc-99, C-14, I-129, H-3
CIG	9.6E-01	4 mrem/year beta-gamma 125-1125 years	C-14, H-3, I-129
LAWV	9.2E-01	4 mrem/year beta-gamma	I-129, C-14
ILV	8.2E-01	4 mrem/year beta-gamma 200-1100 years	I-129
NRDCA			
643-7E	2.6E-01	10 mrem/year Air	C-14
642-26E	1.3E-01	10 mrem/year Air	C-14

For the E-Area LLWF PA, the point of compliance was selected to be the point of highest calculated dose or concentration beyond a 100-m buffer zone surrounding the waste after the institutional control period. The results of groundwater and air dispersion modeling indicate this location of highest dose or concentration is very close to the 100-m distance from the waste. However, the SRS Future Use Plan (DOE 1998) indicates that the current SRS boundaries will remain unchanged. Under this Plan, the land will remain under the ownership of the federal government, consistent with the site's designation as a National Environmental Research Park. Thus, no member of the public would have unrestricted access to the E-Area LLWF. Because the ELLWF is a much greater distance from the site boundary than 100 meters, and groundwater potentially affected by releases from the ELLWF is completely intercepted by UTR creek, the PA results protect the public to a much greater degree than the performance measures require. Considerably more dispersion of any radionuclides released to groundwater or air would occur if the closest access point to the disposal facility is the SRS site boundary. Therefore, the principle of ALARA is satisfied based on these technical and public policy considerations.

7.5.4 Impact on Composite Analysis

The results of the CA for the SRS (WSRC 1997) concluded that the predominant sources of radionuclides contributing to the calculated dose at the identified points of assessment were facilities other than the E-Area waste disposal facility. The points of assessment for the CA are as follows. For the hypothetical future public individual, the points of assessment are the mouths of UTR and FMB (where creek water is undiluted by the Savannah River, but still accessible by the public), and the Savannah River at the highway 301 bridge. For the hypothetical future public population, the points of assessment are the Savannah River at the Highway 301 bridge and the water treatment plants at Beaufort-Jasper, SC and Port Wentworth, GA. These were selected based on considerations of the points of maximum concentration accessible by the public, consistent with site plans for future use and control. The primary dose limit of 100 mrem/yr and dose constraint of 30 mrem/yr are applicable to the CA. The current E-Area PA considers performance measures for groundwater and air (media by which members of the public may be exposed to radionuclides at the points of assessment) that are considerably less than these limits and constraints (4 mrem/yr beta-gamma for groundwater resource protection, 25 mrem/yr for all-pathways dose, and 10 mrem/yr for the air pathway dose). In addition, the points of assessment for the CA are far enough removed from the vicinity of E-Area that considerable dispersion and decay in transit would occur. Therefore, it is concluded that the impact of the ELLWF PA results on the CA are negligible.

7.6 REFERENCES

DOE (Department of Energy). 1998. *Savannah River Site Future Use Plan*, March 1998.

DOE (Department of Energy). 1999. *Radioactive Waste Management*, Order 435.1, U.S. Department of Energy, Washington, DC.

Hiergesell, R. A. 2005. *Special Analysis: Production TRBAR Waste Container Disposal within the Intermediate Level Vault*, WSRC-TR-2005-00531, Revision 0. Westinghouse Savannah River Company, Aiken, SC.

WSRC (Westinghouse Savannah River Company). 1997. *Composite Analysis, E-Area Vaults and Saltstone Disposal Facilities*, WSRC-RP-97-311, Rev. 0, Westinghouse Savannah River Company, Aiken, SC.

PART C

BACKGROUND

This page intentionally left blank.

BACKGROUND

LIST OF FIGURES

LIST OF TABLES

1.0 GENERAL FACILITY BACKGROUND INFORMATION

The E-Area LLWF is located in the central region of the SRS known as the GSA. Radiological operations at the E-Area LLWF began in 1994. The E-Area LLWF is comprised of 200 acres for waste disposal and a surrounding buffer zone that extends out to the 100-m point of compliance. The current E-Area LLWF area developed for disposal consists of approximately 100 acres. It is an elbow-shaped, cleared area, which curves to the northwest, situated immediately north of the MWMF. Disposal units within the footprint of the LLWF include the Slit Trenches, Engineered Trenches, CIG Trenches, the LAWV, the ILV, and the NRCDAs. The current LLWF also includes a buffer zone surrounding the 100-acre disposal area, which extends out to the 100-m point of compliance for all disposal units.

The Slit Trenches, Engineered Trenches and CIG Trenches are below-grade earthen disposal units. During the operational period, the Slit Trenches and Engineered Trenches are designed to accept low level waste consisting of soil, debris, rubble, wood, concrete, equipment, and job control waste, which may be contained within B-25 boxes, B-12 boxes, 55-gallon drums, SeaLand containers, and other metal containers. The CIG Trenches are designed to accept large radioactively contaminated equipment and other smaller wasteforms such as B-25 boxes to fill in the space around and above the large equipment. In addition, grout is poured around, between, and over the component(s) in order to encapsulate the component(s).

The LAWV is an above grade, reinforced concrete vault, which is designed to contain predominately B-25 boxes and B-12 boxes, drums and/or concrete containers. The ILV is a below-grade, reinforced concrete vault built to accommodate intermediate-activity waste including tritium crucibles, job control waste, scrap hardware, and contaminated soil and rubble. The NRCDAs are above-grade gravel pads for the disposal of Naval Reactor Waste Shipping/Disposal Casks containing NR components. During the operational period waste naval reactor components contained within casks are placed on the NRCDA as disposed in place.

Final closure of the Slit Trenches, Engineered Trenches, CIG Trenches, LAWV, ILV and NRCDAs will take place at final closure of the entire E-Area LLWF at the end of the 100-year institutional control period (WSRC, 2004a). Static surcharging and/or dynamic compaction will be conducted at the end of the 100-year institutional control period at the Slit Trenches and Engineered Trenches when the efficiency of the subsidence treatment will be greater due to container corrosion and subsequent strength loss. Dynamic compaction will not be carried out over any Slit or Engineered Trench (such as those containing M-Area glass and ETP Carbon Columns) that has been designated not to undergo such compaction (Phifer et al. 2006).

Prior to final closure of the NRCDAs, the space around, between, and over the casks will be filled with a structurally suitable material capable of supporting the final closure cap without resulting in differential subsidence. Final closure of the E-Area LLWF will consist of the installation of an integrated closure system designed to minimize moisture contact with the waste and to provide an intruder deterrent. The integrated closure system will consist of one or more closure caps installed over all the disposal units and a drainage system.

2.0 RELATED DOCUMENTS

This revised PA has been prepared within the regulatory context of LLW management per DOE Order 435.1 (DOE, 1999a) and associated *Implementation Guide* (DOE, 1999b). The DOE Order 435.1-1 *Radioactive Waste Management Manual* (DOE,1999c) and *Format and Content Guide for U.S. Department of Energy Low-Level Waste Disposal Facility Performance Assessments and Composite Analyses* (DOE, 1999d) were also relied on for guidance. The PA is influenced by and has an influence on other documents that are discussed in this section.

2.1 GROUNDWATER PROTECTION MANAGEMENT PROGRAM

The plan for protection of groundwater at SRS is documented in the SRS Groundwater Protection Management Program (WSRC, 1996). The hydrogeologic information utilized in this revision of the E-Area LLWF is consistent with that in the groundwater protection program. The groundwater protection program is focused on those activities regulated by external agencies (i.e., the State of South Carolina and the EPA). The E-Area LLWF is not regulated by the State of South Carolina or the EPA; rather, it is regulated by DOE through DOE Order 435.1 (DOE, 1999a). Additionally, the SRS had not entered into any formal agreement applicable to groundwater protection with respect to the E-Area LLWF. However, consistent with guidance for preparing the PA (DOE, 1999b), the requirement of DOE Order 435.1 to assess impacts to water resources has been interpreted as meaning that concentrations of radioactive contaminants should not exceed standards for public drinking water supplies established by the EPA. This interpretation is consistent with the SRS groundwater protection program.

2.2 LAND USE PLAN

The SRS Future Use Plan (DOE, 1998) indicates that the current SRS boundaries will remain unchanged. The land will remain under the ownership of the federal government, consistent with the site's designation as a National Environmental Research Park. Thus, no member of the public would have unrestricted access to the E-Area LLWF. Nonetheless, per the requirements of DOE 435.1, this revised PA has used the point of maximum calculated dose or concentration, outside a 100-m buffer zone surrounding the disposed waste, as the point of assessment. For the inadvertent intruder calculations, the assumed period of active institutional control was limited to 100 years.

2.3 COMPOSITE ANALYSIS

A CA (WSRC, 1997) has been completed to assess the potential impacts to hypothetical members of the public from residual radioactive material that may be left at the SRS when operations are complete. The CA concluded that the impacts of the operating low-level radioactive waste disposal facilities, the E-Area LLWF and the Saltstone facility, are negligible contributors to calculated doses. Thus, the CA will not influence WAC (WSRC, 2005a) for the E-Area LLWF. The CA will be revised, as appropriate, to incorporate relevant material from this revision of the PA.

2.4 E-AREA LOW-LEVEL WASTE FACILITY CLOSURE PLAN

The E-Area LLWF closure plan (WSRC, 2004a) was developed according to the specifications of the *Format and Content Guide for U.S. Department of Energy Low-Level Waste Disposal Facility Closure Plans* (DOE, 1999e). This plan will be updated during the operational period, to reflect the current status of the facility and to ensure compliance with applicable orders and regulations. This plan describes the technical approach to closure, and includes operational, interim, and final closure details, as well as the schedule of closure as these elements apply to each of the disposal units in the E-Area LLWF.

2.5 WASTE MANAGEMENT ENVIRONMENTAL IMPACT STATEMENT

The SRS has prepared an EIS for waste management (DOE, 1995). The EIS considered continued disposal of LLW in the 643-7E disposal facility (i.e., the former LLW burial site; disposal in this site has now ceased) and disposal in the E-Area LLWF. The analyses presented in this revised PA are consistent with the EIS.

2.6 DISPOSAL AUTHORIZATION STATEMENT

On September 28, 1999 DOE Headquarters issued the DAS for low-level waste disposal in the E-Area and Saltstone disposal facilities. The DAS serves as the "federal permit" under which SRS may dispose of low-level waste at the two disposal facilities. The performance assessments for the facilities, the composite analysis, and information developed during and subsequent to the review of these documents (e.g., addenda to the PAs and CA) form the basis for the DAS. Changes in disposal operations, such as the development of new disposal technologies, are appropriate, if the changes conform to the PA/CA maintenance requirements.

3.0 DISPOSAL FACILITY CHARACTERISTICS

3.1 SITE CHARACTERISTICS

Evaluation of radionuclide transport from the E-Area LLWF, and of human exposure resulting from release of radionuclides to the environment, requires careful consideration of factors affecting transport processes and exposure potential. Topographic features and hydrogeologic characteristics strongly affect the direction and flow of radionuclides potentially released from the disposal site. Projected land use and population distributions affect the estimation of human exposure. In this section, the relevant natural and demographic characteristics of the E-Area site and surrounding area are discussed.

3.1.1 Geography and Demography

3.1.1.1 Disposal Site Location

The SRS occupies approximately 300 mi^2 in Aiken, Barnwell, and Allendale Counties and is located on the Upper Atlantic Coastal Plain in southwestern South Carolina. The center of the SRS is approximately 22 mi southeast of Augusta, GA; 20 mi south of Aiken, SC; 100 mi from the Atlantic Coast. In addition, the site is bounded on the southwest by the Savannah River for about 20 mi. The Fall Line, which separates the Atlantic Coastal Plain physiographic province from the Piedmont physiographic province, is approximately 30 mi northwest of the central SRS (Figure 3-1).

Prominent geographic features within 30 mi of the SRS include the Savannah River and Clarks Hill Lake (also known as Thurmond Lake) (Figure 3-2). The Savannah River forms the southwest boundary of the SRS. Clarks Hill Lake is the largest nearby public recreational area. This reservoir lies on the Savannah River approximately 40 mi upstream of the center of the SRS. Within SRS boundary, prominent water features include Par Pond and L Lake (Figure 3-3). Par Pond is an 4 mi^2 former reactor cooling water impoundment that lies in the eastern sector of the SRS. L Lake is a 1.5 mi^2 former reactor cooling water impoundment that lies in the southern sector of the SRS.

The E-Area LLWF is located in the central region of the SRS known as the GSA (Figure 3-4). The current E-Area LLWF area developed for disposal consists of approximately 100 acres and a surrounding buffer zone that extends out to the 100-m point of compliance. The disposal area is an elbow-shaped, cleared area, which curves to the northwest, situated immediately north of the MWMF.

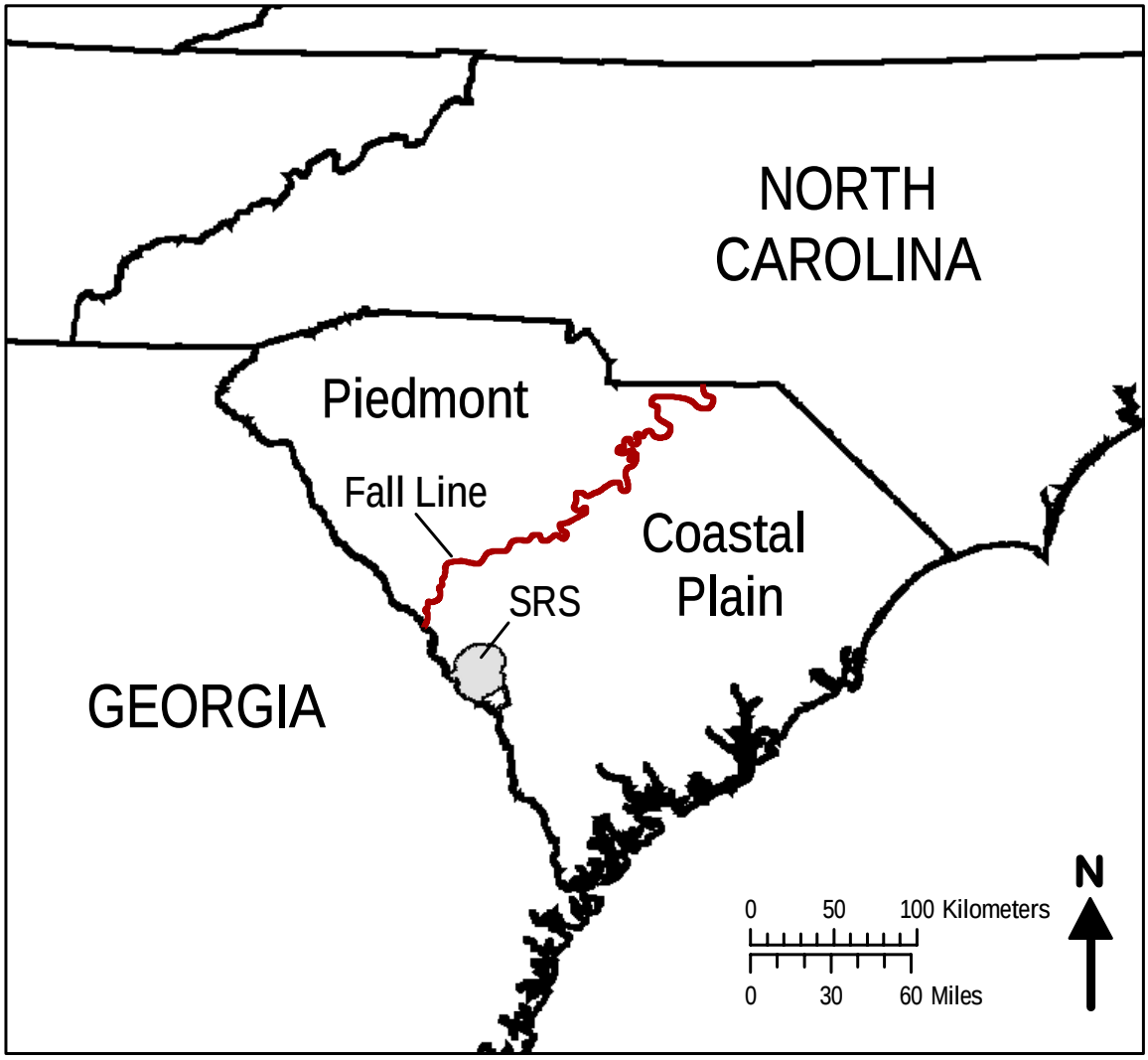

Figure 3-1. Physiographic Location of Savannah River Site

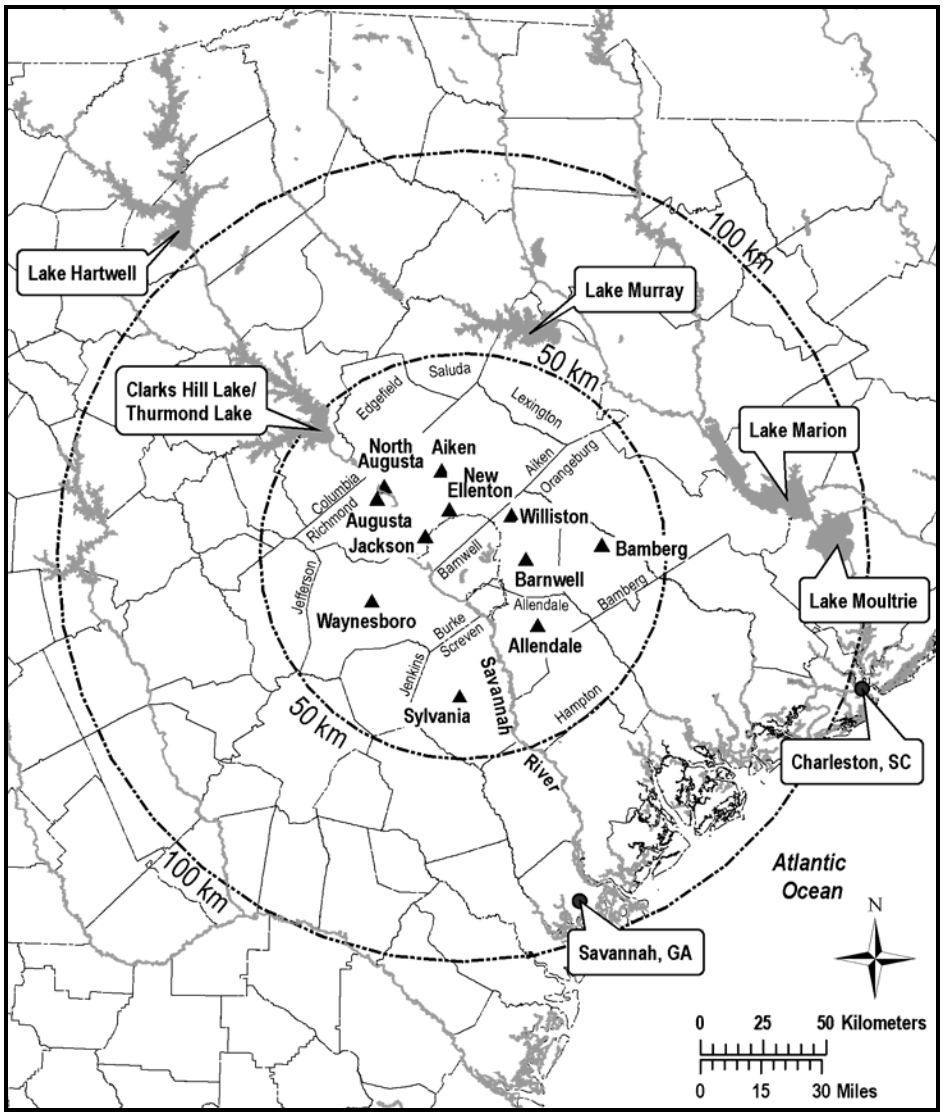

Figure 3-2. Location of Savannah River Site and Adjacent Areas

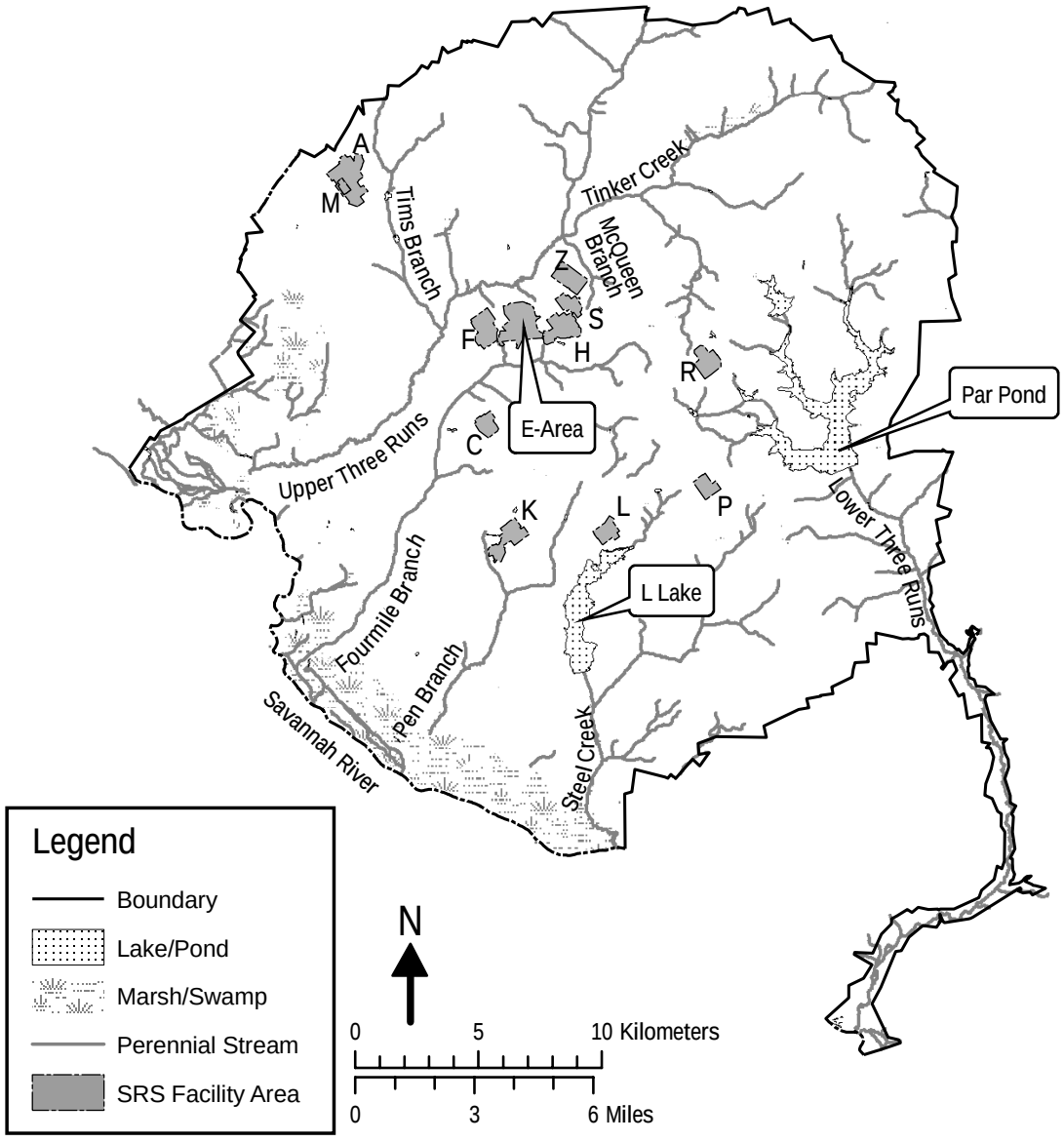

Figure 3-3. Facility Location Map of the SRS Showing Surface Drainage

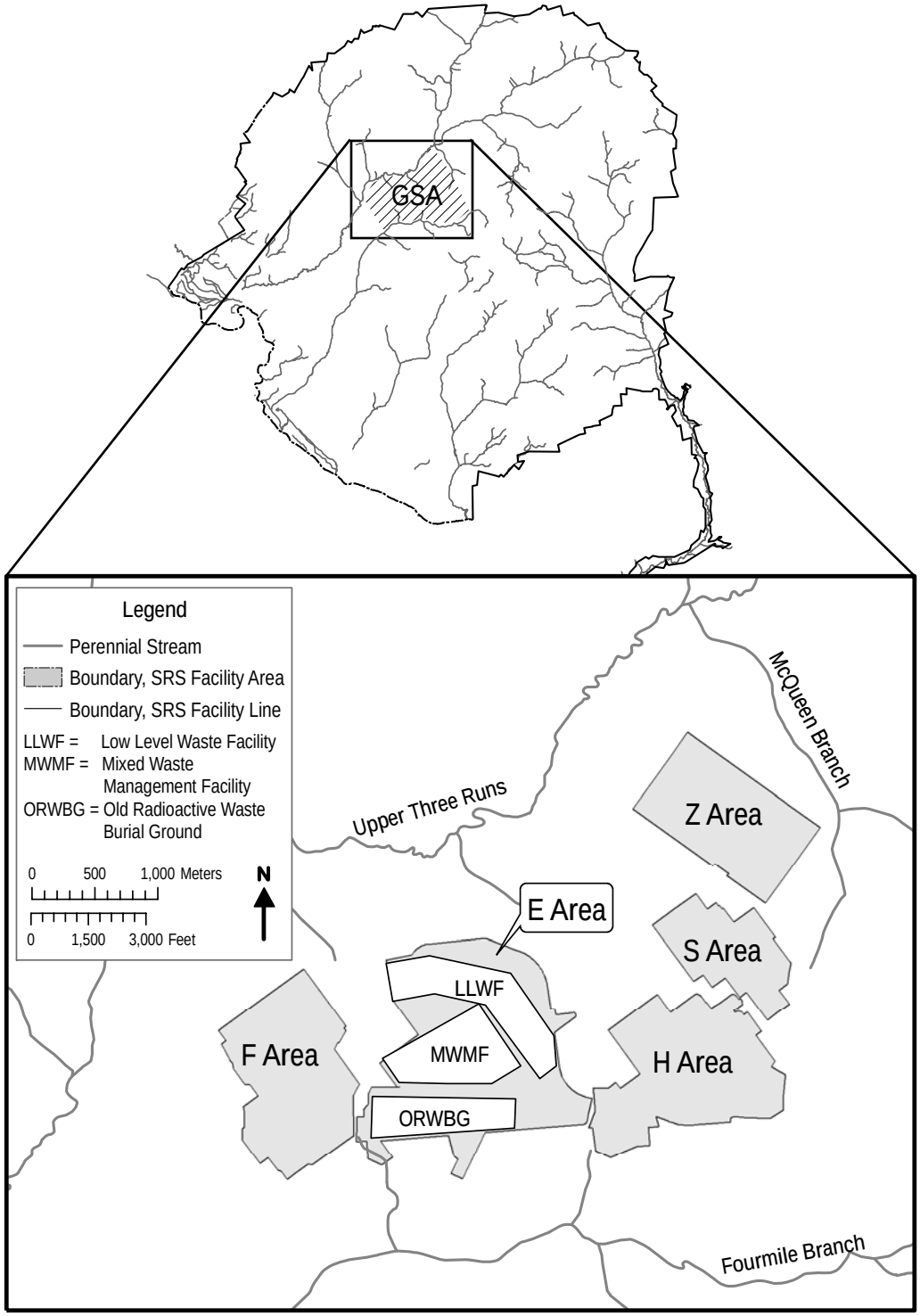

Figure 3-4. Location of the General Separations Area

3.1.1.2 Disposal Site Description

The E-Area LLWF is located on a 200-acre site immediately north of the former LLW disposal facility in an area of the SRS that is limited to industrial uses. Only 100 acres have been developed at this time. The additional 100 acres will allow for expansion of the LLW disposal capacity if needed. The LLWF also includes a buffer zone surrounding the disposal area, which extends out to the 100-m point of compliance for all disposal units. The nearest SRS boundary to the E-Area LLWF is approximately 11 km to the west. The current SRS Future Use Plan states that the entire SRS will never be released for unrestricted use. In particular, the plan states that the central portion of the SRS, which includes the E-Area LLWF, will only be used for industrial purposes (WSRC, 2005b).

E-Area is located on a topographically elevated interfluvial plateau. The plateau is located between two tributaries to the Savannah River, Upper Three Runs and Four Mile Branch, which are located to the northwest and southeast of E-Area, respectively. The underlying geology consists primarily of coastal plain sands and clays, with occasional carbonate sediments (see Section 3.1.4 for details). In the disposal area, typical depth to water table beneath natural land surface is approximately 65 to 70 ft, varying with topographic location and rainfall. Faults in the vicinity of E-Area are not "capable", i.e., have not moved at or near the ground surface within the past 35,000 years or are associated with a fault that has moved within the past 35,000 years (see Section 3.1.4.2 for details).

General E-Area vegetation ranges from managed grass-cover overlying closure caps covering buried waste to re-forested former agricultural land. Pine or pine and hardwood forests exist on higher topographic areas, while bottomland hardwood forests are typical in the lower topographic areas adjacent to streams (see Section 3.1.3 for details).

Except for three roadways near the edge of the SRS, public access to the SRS is restricted to guided tours, controlled deer hunts, and authorized environmental studies. Figure 3-3 shows the major operational areas at the SRS. Prominent operational areas, both past and present, include: Separations (F and H Areas), Waste Management Operations (E, F, and H Areas), the Reactor Areas (C, K, L, P, R), and Defense Waste Processing (S and Z Areas). Administrative and support services, SRNL, and SREL are located in A Area.

Within E-Area, the LLWF includes the Engineered Trenches, Slit Trenches, CIG Trenches, LAWV, ILV, and the NRCDAs (Figure 3-5). A brief description of the disposal units is provided in Section 3.2; more detailed descriptions are provided in Part B of the PA.

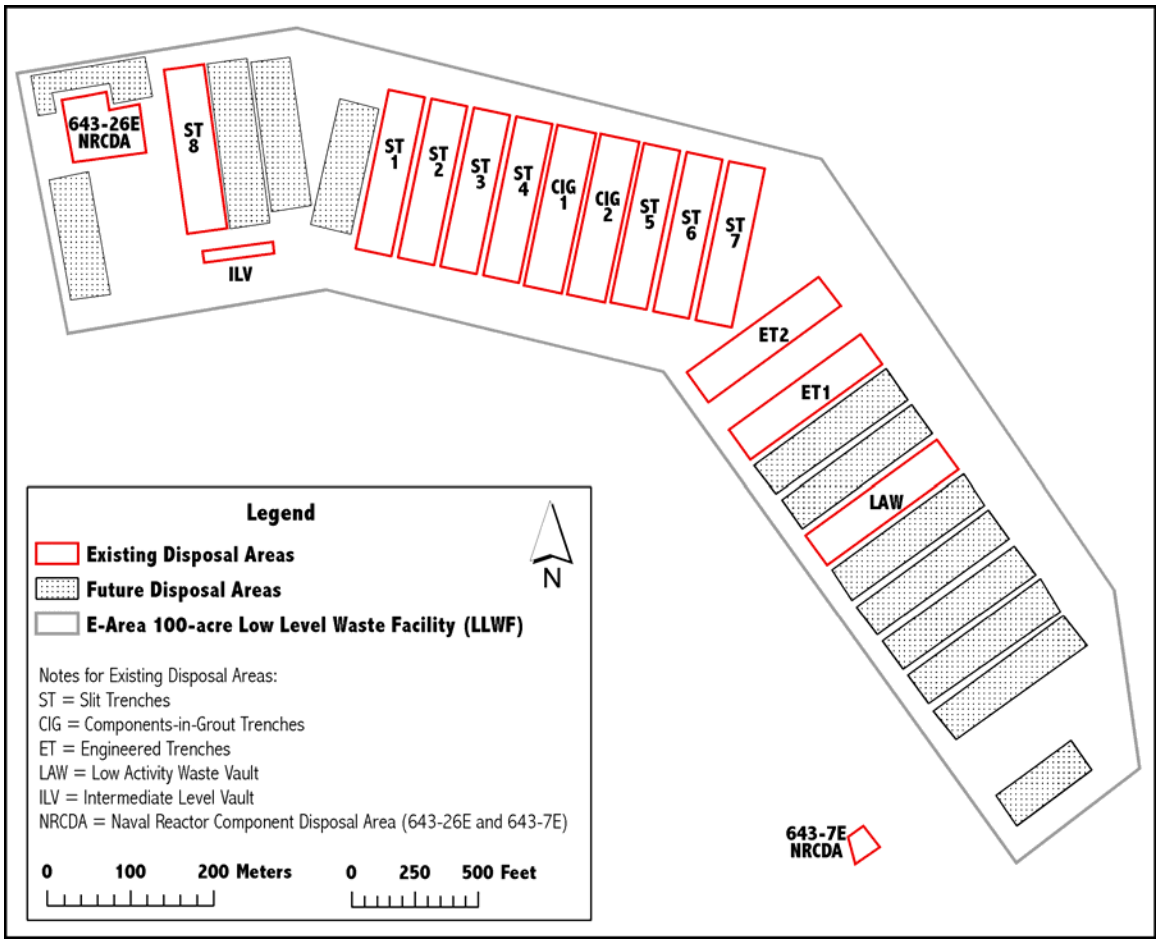

Figure 3-5. Location of Disposal Units within the E-Area LLWF (buffer zone not depicted)

3.1.1.3 Population Distribution

According to U. S. Census Bureau data, the estimated 2005 population in the six-county region of influence was 499,904. A total of 90 percent lived in the following three counties: Aiken (30.0 percent), Columbia (20.8 percent), and Richmond (39.2 percent). The remainder of the population lived in Allendale, Barnwell and Bamberg counties (Table 3-1).

From 1990 to 2000 the population in the six-county region grew 13.5 percent. This positive net immigration was consistent with population growth in Georgia and South Carolina. Columbia county had the highest growth during this period (35.2 percent) followed by Aiken (17.8 percent) and Barnwell (15.7 percent) counties. Over the same period, however, Allendale and Bamberg counties experienced a net loss of population.

From 2000 to 2005 the population in the six-county region grew an estimated 3.5 percent. Columbia County had the highest average estimated growth with 3 percent followed by Aiken County with an average estimated growth of 1 percent. Richmond, Barnwell, Allendale, and Bamberg Counties faced a net population loss.

Population projections indicate that the overall population in the region should continue to grow through 2030. Allendale and Bamberg counties are expected to have little growth or a population decline; however Aiken and Columbia Counties are predicted to have the greatest growth (Table 3-2).

Further information regarding the region of influence around the SRS can be found in "Socioeconomic Characteristics of Selected Counties and Communities Adjacent to the Savannah River Site" (HNUS, 1997) and a recent Environmental Impact Statement report (DOE, 2002).

Table 3-1. Population Distribution and Percent of Region of Influence (%ROI) for Counties and Selected Communities

Jurisdiction	2005 Population Estimate[1]	2005 %ROI
South Carolina	4,255,083	
Aiken County	150,181	30.0
Aiken, city	27,490	5.5
Jackson, town	1,644	0.3
New Ellenton, town	2,259	0.5
North Augusta, city	19,467	3.9
Allendale County	10,917	2.2
Allendale, town	3,897	0.8
Bamberg County	15,880	3.2
Bamberg, town	3,552	0.7
Barnwell County	23,345	4.7
Barnwell, city	4,874	1.0
Georgia	9,072,576	
Columbia County	103,812	20.8
Augusta/Richmond County	195,769	39.2
Six-county total	499,904	
United States	296,410,404	

[1]2005 Population estimates based on 2000 population census and are provided by the U.S. Census Bureau, Population Estimates Program (http://factfinder.census.gov/home/saff/main.html?_lang=en); data for births, deaths, and domestic and international migration were used by the U.S. Census Bureau to update the 2000 base counts.

Table 3-2: Population Projections and Percent of Region of Influence (ROI)

Jurisdiction	April 1, 2000 (Estimate Base)	ROI (%)	Projection July 1, 2010	ROI (%)	Projection July 1, 2020	ROI (%)	Projection July 1, 2030	ROI (%)
SOUTH CAROLINA	4,011,816		4,482,260		4,998,110		5,564,460	
Aiken County	142,552	29.5	159,540	30.4	179,130	31.2	200,490	31.9
Allendale County	11,211	2.3	11,300	2.2	11,590	2.0	11,800	1.9
Bamberg County	16,658	3.4	15,450	2.9	14,680	2.6	13,760	2.2
Barnwell County	23,478	4.9	24,720	4.7	26,770	4.7	28,540	4.5
GEORGIA	8,186,816		9,517,760		10,788,860		12,172,150	
Columbia County	89,288	18.5	111,170	21.2	131,530	22.9	153,280	24.4
Augusta-Richmond County	199,775	41.4	202,410	38.6	210,250	36.6	220,070	35.0
SIX COUNTY TOTAL	482,962	100.0	524,590	100.0	573,950	100.0	627,940	100.0

Note: 2005 Population estimates based on 2000 population census and are provided by the U.S. Census Bureau, Population Estimates Program (http://factfinder.census.gov/home/saff/main.html?_lang=en). Data for births, deaths, and domestic and international migration were used by the U.S. Census Bureau to update the 2000 base counts. Projections for Allendale, Bamberg and Barnwell Counties are from the SC Office of Research and Statistics, Health and Demographics Division. They are based on 2003 Census population estimates (http://www.ors2.state.sc.us/population/proj2030.asp). All other projections are from the 2005 City of North Augusta Comprehensive Plan and are based on Woods and Poole, 2005.

3.1.1.4 Use of Adjacent Lands

This section briefly describes land use patterns at and around the SRS. Land use is a classification of parcels of land relative to their suitability for or the actual presence of human activities (e.g., industry, agriculture, recreation, etc.) and natural uses. Natural resource attributes and other environmental characteristics could make one site more suitable than others for a particular land use. Changes in land use may have both beneficial and adverse effects on other resources (e.g., ecological, cultural, geological, and hydrological).

Savannah River Site Land Use

Existing land use at the SRS can be characterized in three main categories: (1) undeveloped/forest, (2) wetlands/water, and (3) developed. Approximately 73% of the SRS is undeveloped; 22% consists of wetlands, streams, and lakes; and 5% is developed (e.g., facilities, roads, and utility corridors) (DCS, 2002).

The forested areas are managed for timber production. The U.S. Forest Service, under an interagency agreement with DOE, harvests approximately 0.8 to 1.3 mi^2 out of a potential 2.8 mi^2 of timber from the SRS each year (Blake, 2005). Blake (2005) and (Barton et al., 2005) and Wike et al., (2006) provide further information regarding management practices at the SRS.

Prime farmland soils exist at the SRS, but areas of prime farmland are not identified within the SRS because the land is not available for agricultural activities. A portion of the SRS is open for fishing, as discussed below under "Off-Site Land Use" for the Crackerneck WMA. Limited hunting is allowed at the SRS to control the deer population and feral hog populations (Johns and Kilgo, 2005; Mayer, 2005).

The SRS has been designated a National Environmental Research Park by DOE. The scientific community can use the site to study past impacts of human activity on local ecosystems. Approximately 22 mi^2 of land has been set aside at the SRS for nondestructive environmental research and monitoring. The set aside areas encompass a wide range of ecological conditions including Carolina bays, major streams systems, fields, and old experimental sites (Davis and Janecek, 1997; Blake et al., 2005b; Wike et al., 2006).

As SRS transitioned from the Cold War to the post-Cold War era, the Site's missions have changed from primarily a defense mission to one that includes environmental stewardship and future operational missions not yet defined. Current activities include the development of future infrastructure and facilities in addition to decommissioning obsolete facilities. SRS is generally envisioned to be divided into three principal land use zones: Site Industrial, Site Industrial Support, and General Support. The most intensive uses will be located in the Site Industrial zone located at the Site's center in order to minimize the effect on surrounding communities, maintain controlled access, and ensure the integrity of the established safety and security buffer. The Site Industrial Support and General Support zones will accommodate uses of decreasing intensity (DOE 2000a).

Over the next 50 years, the industrial footprint is expected to shrink, consolidating toward the Site center. Site boundaries are expected to remain intact, with residential use continuing not to be allowed and site security and institutional controls maintained in all areas (SRS 2000a). Decommissioning of obsolete facilities is already well underway. Most of all obsolete outlying facilities (e.g., the Gunsites) have been disposed in addition to facilities located in D-Area, M-Area, and T-Area. Decommissioning of obsolete facilities in the reactor areas and other areas is currently underway (Mamatey 2006).

Future land use at the SRS is determined by the DOE through site development, land use, and future planning processes (DCS, 2002). The SRS Long Range Comprehensive Plan includes the construction and operation of the proposed facilities as part of the plan for its Nuclear Materials Stewardship mission (SRS, 2000a). New missions for the SRS in the 21st Century, as stated in the Savannah River Site Strategic Plan, include the construction and operation of new facilities for tritium extraction and the storage and disposal of surplus plutonium. In addition to these new facilities, the SRS plans to have an increased role in the advancement of nuclear materials protection, control, and accounting (SRS, 2000b).

Nearby facilities which could potentially contribute to migration of radionuclides in the vicinity of E-Area include the radionuclide processing facilities of F-Area and H-Area, between which E-Area is located. H-Area Tank Farms, near E-Area, is the location of 49 underground carbon steel tanks containing a total of about 36 million gallons of liquid radioactive waste (SRS 2006). Uranium and plutonium separation and purification processes were historically performed in both F-Area and H-Area (Bebbington 1990). Two other radioactive waste disposal sites, the Old Burial Ground and the Mixed Waste Management Facility are located within E-Area, near the E-Area LLWF.

Off-Site Land Use

Predominant regional land uses in the vicinity of the SRS include urban, residential, industrial, agricultural, and recreational areas. In the area adjacent to the SRS, less than 8 percent of the existing land is devoted to urban and built-up uses. Most such uses are in and around the cities of Augusta and Aiken. Agriculture accounts for about 21 percent of total land use; forests, wetlands, water bodies, and unclassified, predominantly rural, lands account for about 70 percent.

Forest and agricultural land predominantly border the SRS, with only limited urban and residential development. The nearest residences are located to the west, north, and northeast, some within 200 ft of the SRS boundary. Farming is diversified throughout the region and includes such crops as peaches, watermelon, cotton, soybeans, corn, and small grains. Incorporated and industrial areas are also present near the site, including textile mills, polystyrene foam and paper plants, chemical processing plants, and a commercial nuclear power plant (DOE, 1999f).

Open water and nonforested wetlands occur along the Savannah River Valley. The Crackerneck WMA, which includes a portion of the SRS along the Savannah River, is open to the public for fishing. It encompasses about 17 mi^2 and consists of pine, bottomland hardwood, and cypress-tupelo swamp habitats. Other recreational areas within 50 mi of the SRS include Sumter National Forest, Santee National Wildlife Refuge, and Clarks Hill/Thurmond Lake. State, county, and local parks include Redcliffe Plantation, Rivers Bridge, Barnwell and Aiken County State Parks in South Carolina, and Mistletoe State Park in Georgia (DOE, 1999f; Blake et al., 2005b).

Industry near the SRS includes Energy*Solutions* Low Level Radioactive Waste Disposal Facility in Barnwell, SC and Plant Vogtle, a nuclear power facility across the Savannah River from the SRS. Three Rivers Landfill, which is operating under a 50-year lease agreement, is a solid waste landfill located within the SRS boundary. The Three Rivers Solid Waste Authority provides waste management services to local governments in Aiken, Allendale, Bamberg, Barnwell, Calhoun, Edgefield, McCormick, Orangeburg, and Saluda counties (DOE, 2005).

The projected future land uses of the area adjacent to the SRS are similar to existing patterns. Normal growth is expected in metropolitan counties near the SRS; however the predominant land uses nearby the SRS are expected to stay the same within the next 20 years (DOE, 2005).

3.1.2 Meteorology and Climatology

3.1.2.1 Meteorology

The southeastern U.S. has a humid, subtropical climate characterized by relatively short, mild winters and long, warm, and humid summers. Summer-like weather typically lasts from May through September, when the area is subject to the persistent presence of the Atlantic subtropical anticyclone (i.e., the 'Bermuda' high). The humid conditions often result in scattered afternoon thunderstorms. Average seasonal rainfall is usually lowest during the fall. Mountains to the north and west prevent or delay the approach of many cold air masses (Blake et al., 2005b; DCS, 2002; Ruffner, 1985).

During the winter, the weather changes as mid-latitude low-pressure systems and fronts migrate through the region. Measurable snowfall is rare. Spring is characterized by a higher frequency of severe thunderstorms and sometimes tornadoes than the other seasons. During the spring, temperatures are typically mild and the humidity is relatively low (Blake et al., 2005b; DCS, 2002).

3.1.2.2 Local Climatology

Meteorological data are critical input to atmospheric transport and dose models used to estimate the effects of releases from SRS facilities. Weather stations at the SRS (e.g., in A-Area, H-Area and N-Area) and at Bush Field in Augusta, Georgia, provide meteorological data for the SRS and surrounding area. The Bush Field station is located about 15 mi northwest of E-Area. Data from this station have been summarized by the National Climatic Data Center (NOAA, 2004; NOAA, 2006).

The description of local climatology provided below is based on the summary of the Bush Field data (NOAA, 2004; NOAA, 2006) in addition to data provided by the Savannah River National Laboratory Atmospheric Technologies Group and summarized in recent reports (Blake et al., 2005b; DCS, 2002; WSRC, 2002; Hunter and Tatum, 1996; Mamatey, 2006; Ruffner 1985, Weber, 1998). The atmospheric transport and dose modeling performed for this PA comes from a 5 year average of the H-Area meteorological dataset from the period 1997 to 2001 (WSRC, 2002). This is the most recently quality-assured meteorological database for the SRS and is provided on CD accompanying the Environmental Report for 2005 (Mamatey, 2006). Table 3-3 provides a summary of local climatology data.

April, May, October and November are typically the driest months at the SRS (Blake et al., 2005b). Average annual rainfall at the SRS is approximately 122 cm and at Bush Field average annual rainfall is approximately 113 cm (Table 3-3). Average monthly precipitation at the SRS ranges from 6.6 cm in November to 13.1 cm in July. Rainfall events that are greater than 2 cm are common with an average occurrence of about 20 times a year. A rainfall event greater than 5 cm can be expected at least once a year and rainfall events greater than 10 cm in a 24-hour period can be expected every 5 to 10 years (Blake et al., 2005b).

Although annual average rainfall is 122 cm at the SRS, 1964 and 1972 were abnormally wet years with 186.6 cm falling in 1964 and 162.5 cm falling in 1972. In contrast, SRS received relatively little rainfall in 1954 (73.2 cm) and 2001-2002 (91.5 cm) (Blake et al., 2005b).

In general, the SRS receives little measurable snowfall. Annual snowfall averages approximately 3.6 cm at Bush Field in Augusta (NOAA, 2004). At the SRS, the greatest monthly snowfall on record occurred in February 1973, with 35.6 cm. Freezing rain can also be expected to occur one to three times per winter (Blake et al., 2005b; Ruffner 1985).

The average annual temperature at the SRS is 18°C (Table 3-3). January is the coldest month, with an average monthly temperature ranging from 1.7 to 12.8°C, and July the warmest, averaging 26.7 to 29.4°C. Below freezing temperatures can be expected from late October through early April, however extreme low temperatures are more typically in December and January (Blake et al., 2005b).

Data from 1964 through 2005 for Augusta, GA, show that on average December has 14 days with minimum temperature of 0°C or less. January averages 16 days and February 12 days. May through September typically have no freeze days (where temperatures are below 0°C) (NOAA, 2006).

The annual average wind speed at Bush Field is 2.9 m/s (Table 3-3). March has the highest monthly average wind speed of 3.5 m/s and August the lightest, 2.4 m/s (NOAA, 2006). A wind rose for the five-year (1997-2001) H-Area composite data set is included as Figure 3-6. The prevailing monthly wind direction is from the west-southwest. H-Area is adjacent to E-Area.

Average annual relative humidity at Bush Field ranges from 88% in the early morning to 52 % in the afternoon (Table 3-3). In July and August, the early morning relative humidity averages 90%, with afternoons averaging 55-56%. At the SRS, comparable values of 97% and 50% are recorded for August (DCS, 2002; NOAA, 2006). Heavy fog with visibility less than 0.40 km occurs on an average of about 30 days per year. Heavy fog occurs throughout the year but is most likely in the fall and winter (Blake et al., 2005b).

Table 3-3. Summary of Local Climatology Data

Climate Data	Cited in Blake et al., 2005a[1]	Used in Dose Calculations in Mamatey, 2006[2]	NOAA Data for Augusta, GA[3]
Average Rainfall	122.5 cm/yr	122.4 cm/yr	113.3 cm/yr
Average Annual Air Temperature	18 °C	17.8 °C	17.3 °C
Average Wind Speed	not reported	3.83 m/s	2.9 m/s
Range and Average Percent Relative Humidity[4]	45-90% 70%	Not reported	52-88% 70%

[1]based on SRS meteorological data from A-Area station; data from 1952-2001 for rainfall; data from 1964-2001 for temperature and % relative humidity
[2]based on SRS meteorological data from H-Area station, 1997-2001; data on CD accompanying the Savannah River Site Environmental Report for 2005
[3]based on NOAA data for Augusta, GA; data from Bush Field Airport, 1971-2000 for rainfall and temperature (www.ncdc.noaa.gov/oa/climate/normals/usnormals.html); for average wind speed and % relative humidity, data from Augusta station(s) that are active or sites comparable in exposure (http://www1.ncdc.noaa.gov/pub/data/ccd-data); data covers 1964-2000 for % relative humidity; data covers 1951-2000 for average wind speed
[4]based on monthly and annual means, minimums and maximums

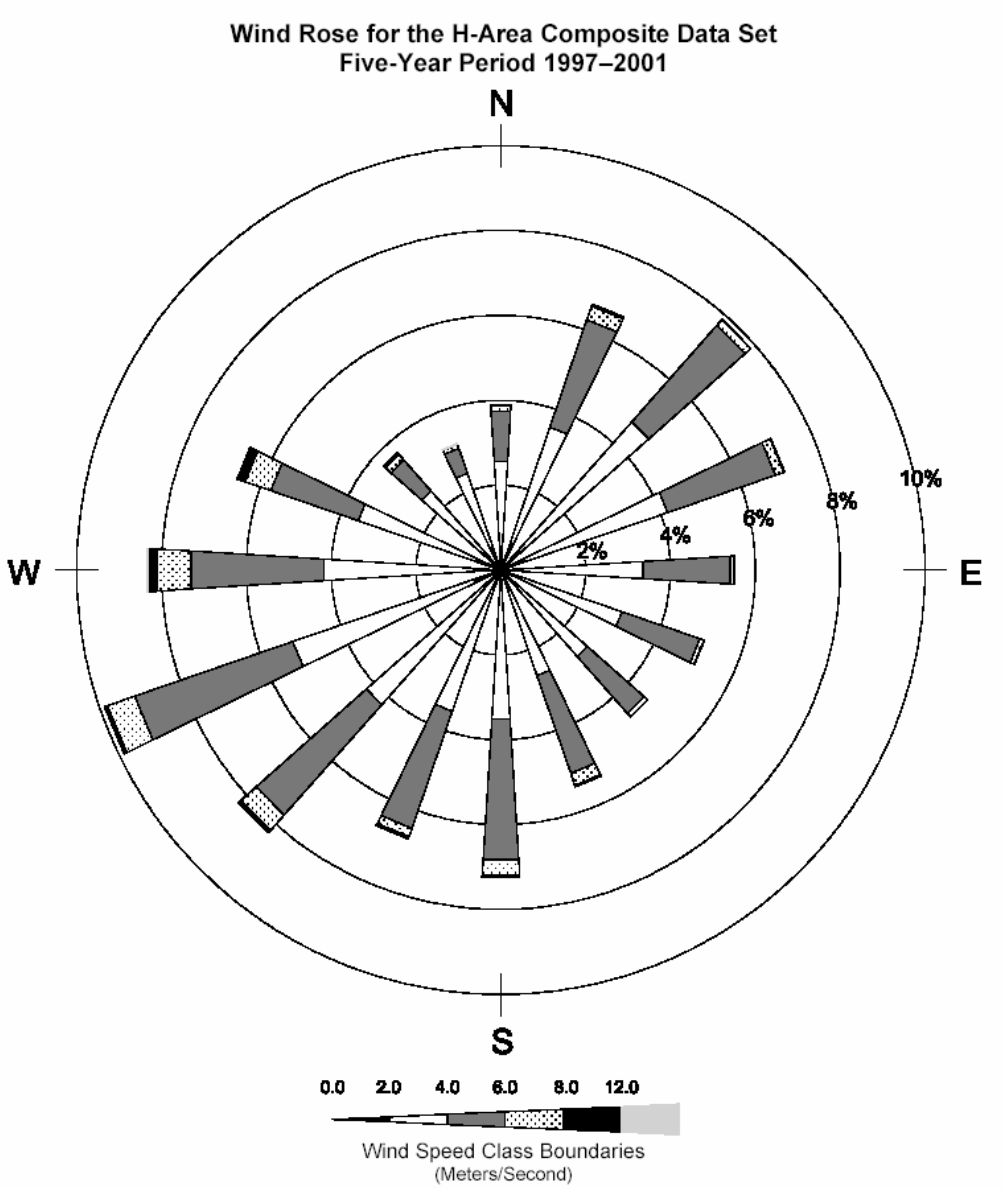

Figure 3-6. Wind Rose for H Area (adjacent to E Area)

3.1.2.3 Severe Weather

Thunderstorms, tornadoes, and hurricanes provide occasional severe weather to South Carolina (Ruffner 1985). Thunderstorms occur on an average of approximately 54 days per year at Bush Field. July averages 13 thunderstorm days, December 0.7. More than 70% of the thunderstorms occur in the four-month period from May through August. They are most common in the summer months, but the more violent storms generally occur along active cold fronts in spring (Blake et al., 2005b; Ruffner 1985). Hail with thunderstorms is infrequent and occurs about once every 2 years on the average (DCS 2002).

Tornadoes are rare in South Carolina. Most that do occur happen during the period of March through June (Blake et al., 2005b; Ruffner 1985). For the 49-year period of 1950-1998, an average of 11 tornadoes per year occurred in South Carolina (Storm Prediction Center, 1999). Between 1880 and 1995, a total of 17 significant tornadoes were reported in Aiken and Barnwell Counties, South Carolina, and Burke County, Georgia. Nine tornadoes have caused damage on the SRS, one with estimated wind speeds as high as 150 mph. None have caused damage to buildings on the SRS (DCS 2002).

Tropical storms or hurricanes affect South Carolina about once every 2 years. Most do little damage and affect only the costal areas, decreasing in intensity as they move inland. Those that do move far inland can cause considerable flooding (Ruffner 1985). Thirty-six hurricanes caused damage in South Carolina between 1700 and 1992, and the interval between them has ranged from 2 months to 27 years. About 80% have occurred in August and September. The only hurricane-force winds measured at the SRS were associated with Hurricane Gracie on September 29, 1959, when wind speeds of 75 mph were measured at F-Area (Blake et al., 2005b; DCS 2002).

3.1.3 Ecology

With the majority of the SRS undeveloped, the site sustains a variety of ecosystems. Within these ecosystems, habitat types include upland pine forests, mixed hardwood forests, bottomland hardwood forests, swamp forests, and Carolina bays. Since the early 1950s, the Site has changed from 67 percent forest and 33 percent agriculture to 94 percent forest, with the remainder in aquatic habitats and developed (facility) areas (Wike et al., 2006). The wildlife correspondingly shifted from forest farm edge species to a predominance of forest dwelling species. Currently, approximately 260 species of birds, 60 species of reptiles, 40 species of amphibians, 80 species of freshwater fish, and 50 species of mammals exist on the SRS (Mamatey, 2006).

This section describes the plant and animal resources at the SRS with particular emphasis on the biota near the GSA where the E-Area LLWF is located. Included in this section are species and special habitats protected by the federal government under the Endangered Species Act, as well as species of special concern listed by the states of South Carolina (Aiken and Barnwell counties) and Georgia (Burke County). In addition to federal and state regulations, DOE protects plants, animals, and Carolina bays in DOE Research Set-Aside Areas. Further descriptions of the ecological resources and wildlife at the SRS can be found in Davis and Janecek (1997), DCS (2002), Wike et al. (2006), Kilgo and Blake (2005), and Wike et al. (2006) in addition to environmental impact statements (DOE, 1997a; DOE, 1997b; DOE, 2002).

3.1.3.1 Ecology of General Separations Area

Ecological Communities Near E-Area LLWF

The E-Area LLWF is located within a developed, industrialized area of SRS. The immediate area provides habitat for animal species typically classified as urban wildlife. Species commonly encountered in this type of urban landscape include the Southern toad, green anole, rat snake, rock dove, European starling, house mouse, and opossum. Ground-foraging bird species (e.g., American robin, killdeer, and mourning dove) and small mammals (e.g., cotton mouse, cotton rat, and Eastern cottontail) may be present around buildings at certain times of the year, depending on the level of human activity (Mayer and Wike 1997).

Pine plantations, which occupy much of the surrounding areas, typically host a variety of wildlife including toads (i.e., the southern toad), lizards (e.g., the eastern fence lizard), snakes (e.g., the black racer), songbirds (e.g., the brown-headed nuthatch, and the pine warbler), birds of prey (e.g., the sharp-shinned hawk), and a number of mammal species (e.g., the cotton mouse), the gray squirrel, the opossum, and the white-tailed deer (DOE, 2002; Wike et al. 2006).

Several populations of rare plants have been found in undeveloped areas near E-Area. One population of Nestronia *(Nestronia umbellula)* and three populations of Oconee azalea (*Rhododendron flammeum*) were located on the steep slopes adjacent to the Upper Three Runs floodplain in an area northwest of F-Area. Populations of two additional rare plants, Elliott's croton (*Croton elliotti*) and spathulate seedbox (*Ludwigia spathulata*) were found in the pine forest southeast of H Area, approximately one-half mile from the H-Area Tank Farm (DOE, 2002).

The smooth coneflower *(Echinacea laevigata)* is the only federally listed (endangered) plant species at the SRS. In addition, it is also state endangered. Smooth coneflowers inhabit roadsides and open, sunny areas. Three populations of the smooth coneflower occur at the SRS; none of these populations are located near the E-Area LLWF. Activities near these known populations are highly restricted (Imm, 2005).

Ecological Communities at the Seeplines and Floodplain

As discussed in Section 3.1.5 Hydrology, a groundwater divide is present in the GSA. Groundwater flows from this divide and discharges at seeplines adjacent to Upper Three Runs and Fourmile Branch. These seepline areas predominantly consist of bottomland hardwood forest communities. The habitat is dominated by sweetgum (*Liquidambar styraciflua)*, red maple (*Acer rubrum*), and red bay (*Persea borbonia*). Sweet bay (*Magnolia virginiana)* is also common. The understory consists largely of saplings of these same species, as well as a herbaceous layer of greenbrier (*Smilax* sp), dog hobble (*Leucothoe axillaris*), giant cane (*Arundinaria gigantea*), poison ivy (*Rhus radicans*), chain fern (*Woodwardia virginica*), and hepatica (*Hepatica americana*). Along the upland edge, scattered American holly and white oak occur (DOE, 2002).

The floodplains of both streams provides habitat for a variety of aquatic, semi-aquatic, and terrestrial animals including amphibians (e.g., leopard frogs), reptiles (e.g., box turtles), songbirds (e.g., wood warblers), birds of prey (e.g., barred owls), semi-aquatic mammals (e.g., beaver), and terrestrial mammals (white-tailed deer). Gibbons et al. (1986), duPont (1987), Cothran et al. (1991), DOE (1997a), and Wike et al. (2006) provide detailed lists of species known or expected to occur in the riparian forests and wetlands of SRS.

No endangered or threatened fish or wildlife species have been recorded near the Upper Three Runs and Fourmile Branch seeplines (DOE, 2002). The seeplines and associated bottomland community do not provide habitat favored by endangered or threatened fish and wildlife species known to occur at SRS. The American alligator is the only federally protected species that could potentially occur in the area of the seeplines. Fourmile Branch does support a small population of American alligator in its lower reaches, where the stream enters the Savannah River swamp (Wike et al. 2006). Alligators have been infrequently observed in man-made water bodies (e.g., storm water retention basins) in the vicinity of H-Area (Mayer and Wike, 1997).

3.1.3.2 Ecology Downstream of General Separations Area

Upper Three Runs

The GSA is drained by Upper Three Runs Creek and Fourmile Branch (Figure 3-1). Upper Three Runs is characterized by unusually high measures of taxa richness and diversity. Upper Three Runs is a spring-fed stream and is colder and generally clearer than most streams in the upper Coastal Plain. As a result, species normally found in the Northern U.S. and southern Appalachians are found here along with endemic lowland (Atlantic Coastal Plain) species (Wike et al. 2006).

A 1993 study found more than 650 aquatic insect species in Upper Three Runs, including more than 100 caddisfly species. Although no threatened or endangered species have been found in Upper Three Runs, there are several environmentally sensitive species. Davis and Mulvey (Wike et al. 2006) identified a rare clam species (*Elliptio hepatica*) in this drainage. Also, in 1997 the U.S. Fish and Wildlife Service listed the American sand-burrowing mayfly (*Dolania americana*), a mayfly relatively common in Upper Three Runs, as a species of special concern (DOE, 2002). The fish community of Upper Three Runs is typical of third- and higher-order streams on SRS that have not been greatly affected by industrial operations. The stream hosts more than 60 fish species of which shiners, darters, and sunfish dominate (Wike et al. 2006; Marcy, 2005).

Fourmile Branch

Following the shutdown of C-Reactor in 1985, macroinvertebrate communities began to recover and, in some reaches of the stream, began to resemble those in nonthermal and unimpacted streams of the SRS. Surveys of macroinvertebrates in more recent years showed that some reaches of Fourmile Branch had healthy macroinvertebrate communities (high measures of taxa richness) while others had poorly developed macroinvertebrate communities (low measures of diversity or communities dominated by pollution-tolerant forms). Differences appeared to be related to variations in dissolved oxygen levels in different portions of the stream. In general, macroinvertebrate communities of Fourmile Branch show more diversity (taxa richness) in downstream reaches than upstream reaches (Wike et al. 2006).

Following the shutdown of C-Reactor in 1985, Fourmile Branch was rapidly recolonized by fish from the Savannah River swamp system. Centrarchids (sunfish) and cyprinids (minnows) were the most common taxa. To assess potential impacts of groundwater outcropping to Fourmile Branch, WSRC in 1990 surveyed fish populations in Fourmile Branch up- and downstream of F- and H-Area seepage basins (Wike et al. 2006). Upstream stations were dominated by pirate perch, creek chubsucker, yellow bullhead, and several sunfish species. Downstream stations were dominated by shiners and sunfish, with pirate perch and creek chubsucker present, but in lower numbers. Differences in species composition were believed to be due to habitat differences rather than the effect of contaminants in groundwater (DOE, 2002).

Savannah River

An extensive information base is available regarding the aquatic ecology of the Savannah River in the vicinity of SRS. Recent water quality data available from environmental monitoring conducted on the river in the vicinity of SRS and its downstream reaches can be found in Savannah River Site Environmental Data for 1998 (Arnett and Mamatey 1999b). These data demonstrate that the Savannah River is not adversely impacted by SRS wastewater discharges to its tributary streams. A full description of the ecology of the Savannah River in the vicinity of SRS can be found in the SRS Ecology Environmental Information Document (Wike et al. 2006), the Final Environmental Impact Statement for the Shutdown of the River Water System at the Savannah River Site (DOE 1997a), and the EIS for Accelerator Production of Tritium at the Savannah River Site (DOE 1997b).

3.1.4 Geology, Seismology, and Volcanology

Regional and local information on the geologic and seismic characteristics of the E-Area disposal site are presented in this section. Because the SRS is not located within a region of active plate tectonics characterized by volcanism, volcanology is not an issue of concern in this PA, and thus further discussion of this topic is omitted from the following discussion.

3.1.4.1 Regional and Site-Specific Geology/Topography

Topography

The elevation of the SRS ranges from 80 ft above msl at the Savannah River to about 400 ft above msl in the upper northwest portion of the site (USGS, 1987). The Pleistocene Coastal terraces and the Aiken Plateau comprise two distinct physiographic subregions at the SRS (McAllister et al, 1996). The Pleistocene Coastal terraces are below 270 ft above msl in elevation, with the lowest terrace constituting the present flood plain along the Savannah River and the higher terraces characterized by gently rolling terrain. The relatively flat Aiken Plateau occurs above 270 ft above msl and is dissected by local streams. The E-Area LLWF is located on an interfluvial plateau in the center of the SRS. This plateau is drained by several perennial streams, which include Upper Three Runs and Fourmile Branch (Figure 3-7).

The natural topography of the site slopes from an elevation of about 290 ft above msl in the southernmost corner to an elevation of 250 ft above msl in the northernmost corner. The site is bordered by three streams with several intermittent streams present within the area. Runoff is to the north toward Upper Three Runs Creek, to the east toward Crouch Branch, and to the west toward an unnamed branch. Upper Three Runs is approximately 2500 ft north of the facility boundary. The nearest perennial stream is approximately1200 ft northeast of the boundary.

The topography within the E-Area LLWF has changed with construction of the various disposal units; however, overall the facility remains on a topographic high relative to the natural drainage features. Storm water runoff from the LLWF is directed toward nearby constructed sedimentation basins (Figure 3-8).

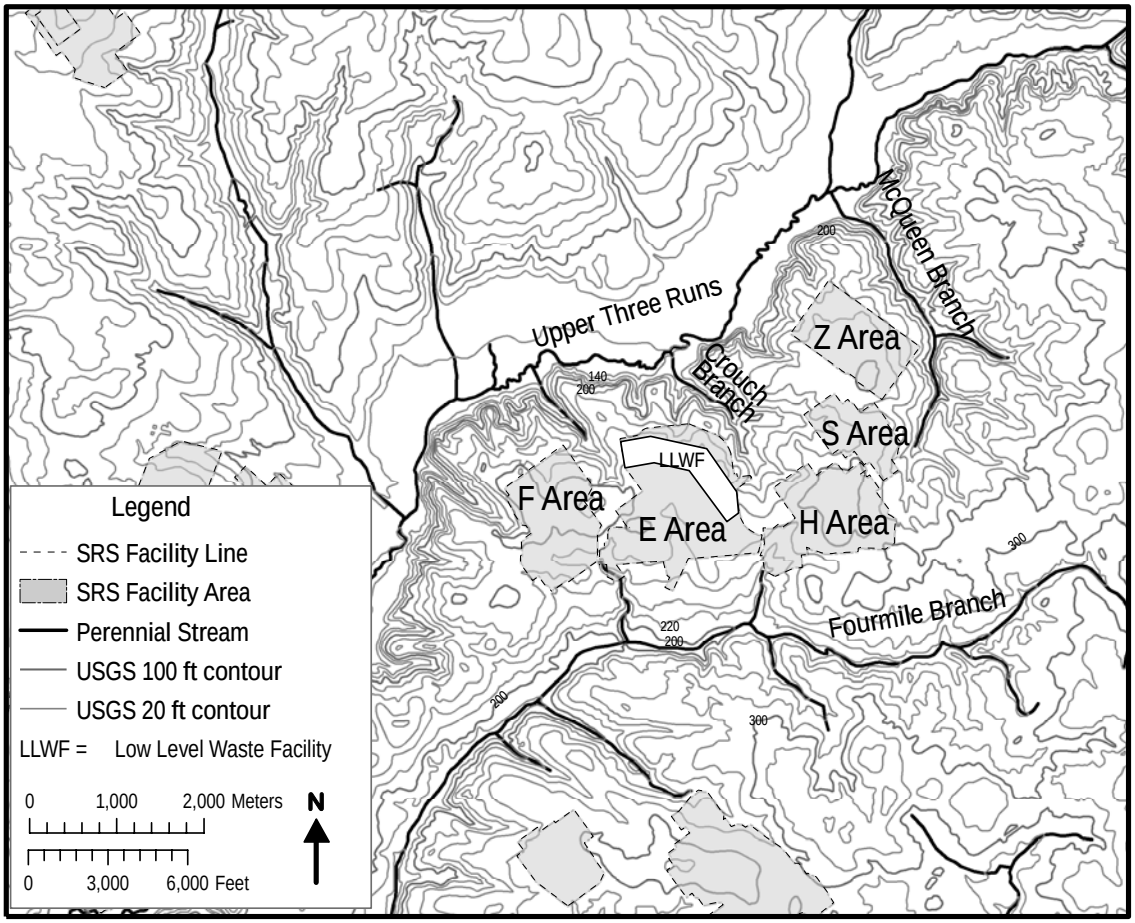

Figure 3-7. Topography of E-Area Facility in Relation to Natural Drainage Features

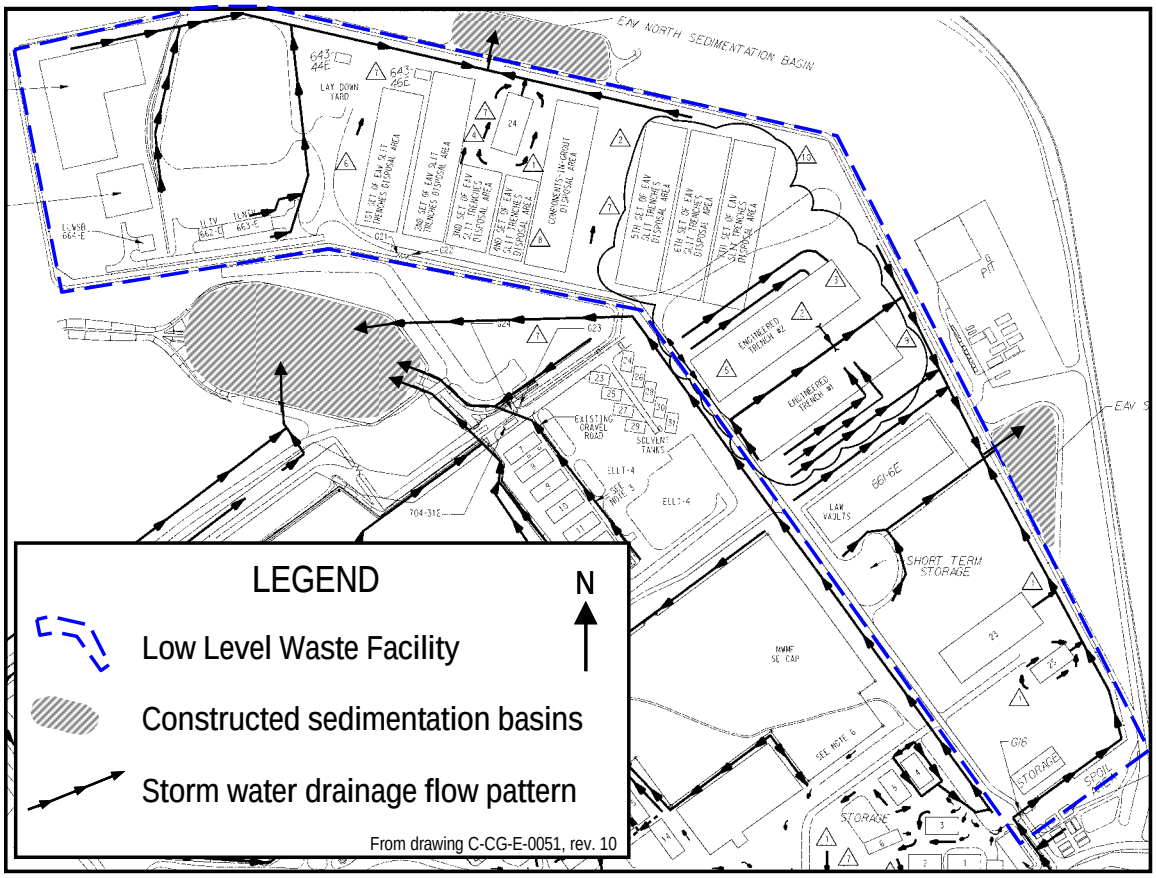

Figure 3-8. Storm Water Drainage Flow Patterns at the LLWF

Geology

The Atlantic Coastal Plain consists of a southeast-dipping wedge of unconsolidated and semi-consolidated sediments, which extends from its contact with the Piedmont Province at the Fall Line to the continental shelf edge. Sediments range in geologic age from Late Cretaceous to Recent and include sands, clays, limestones and gravels. This sedimentary sequence ranges in thickness from essentially zero at the Fall Line to more than 1,219 m at the Atlantic Coast (Siple, 1967).

The coastal plain sediments at SRS thicken from approximately 213 m at the northwestern boundary to about 430 m at the southeastern boundary of the site (Fallaw et al, 1990) and form a series of aquifers and confining or semi-confining units. Figure 3-9 shows a generalized cross section of the sedimentary strata and their corresponding depositional environments for the Upper Coastal Plain down-dip through the SRS into the Lower Coastal Plain. Figure 3-10 shows the regional lithologic units and their corresponding hydrostratigraphic units at the SRS.

Descriptions of the primary sedimentary units and surface soils are provided below. A summary of the hydrostratigraphic units is provided in Section 3.1.5, Hydrology. More detailed descriptions of the geology of the SRS and GSA can be found in several historical and recent reports (Aadland et al., 1991; Aadland et al., 1995; Colquhoun et al., 1983; Denham, 1999; Dennehy et al., 1989; Fallaw et al., 1990; Fallaw and Price, 1995; Logan and Euler, 1989; Nystrom et al., 1991; Siple, 1967; Wyatt and Harris, 2004).

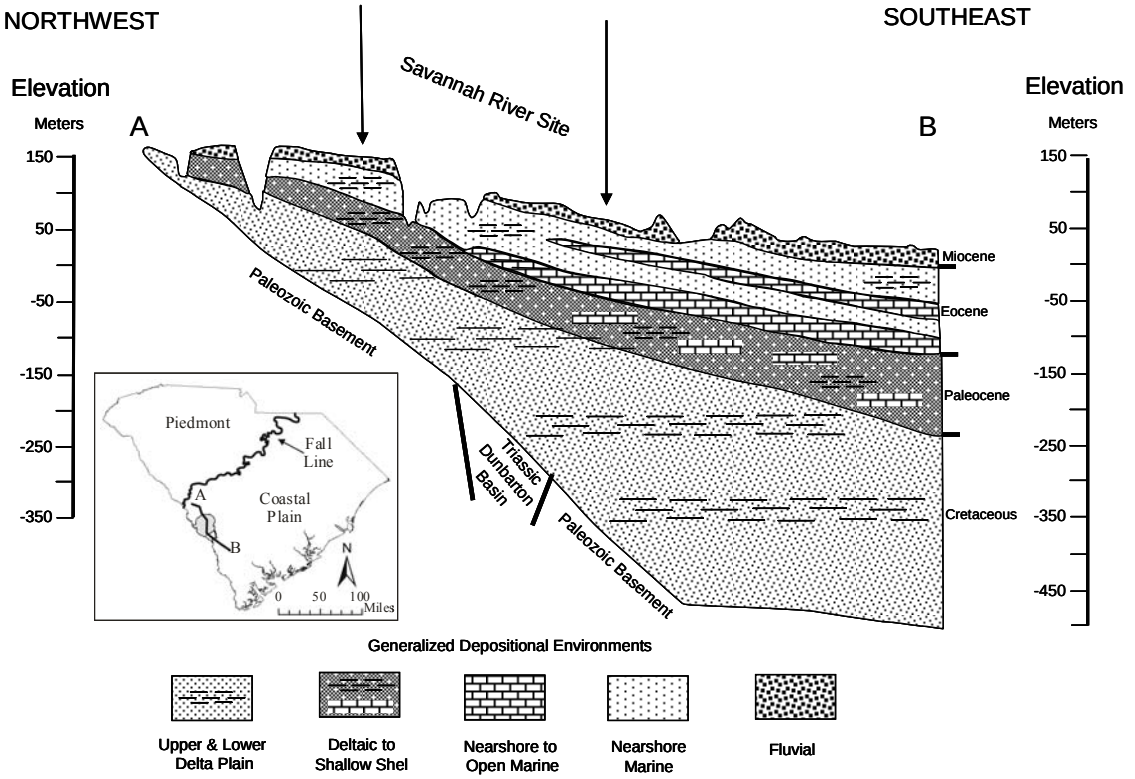

Figure 3-9. Regional NW to SE Cross-section (from Wyatt and Harris, 2004)

Late Cretaceous Sediments

The Late Cretaceous sediments include, from oldest to youngest, the Cape Fear Formation and the three formations of the Lumbee Group: the Middendorf, Black Creek, and Steel Creek Formations (Figure 3-10). These sediments are approximately 210 m thick at the center of the SRS, near E-Area. The lowermost Cape Fear Formation rests on a thin veneer of saprolite (weathered rock). It defines the surface of the Paleozoic crystalline basement rock or lies on top of weathered Triassic Basin sedimentary material of the Newark Supergroup in limited areas associated with Triassic-age basement rock faulting. This formation is composed of poorly sorted silty-to-clayey quartz sands and interbedded clays. Bedding thicknesses range from 1.5 to 6 m, with sand beds being thicker than clay beds. The formation is about 9 m thick at the northwestern boundary of the SRS, and it increases to more than 55 m near the southeastern boundary. This formation has not been observed to outcrop in the vicinity of the SRS.

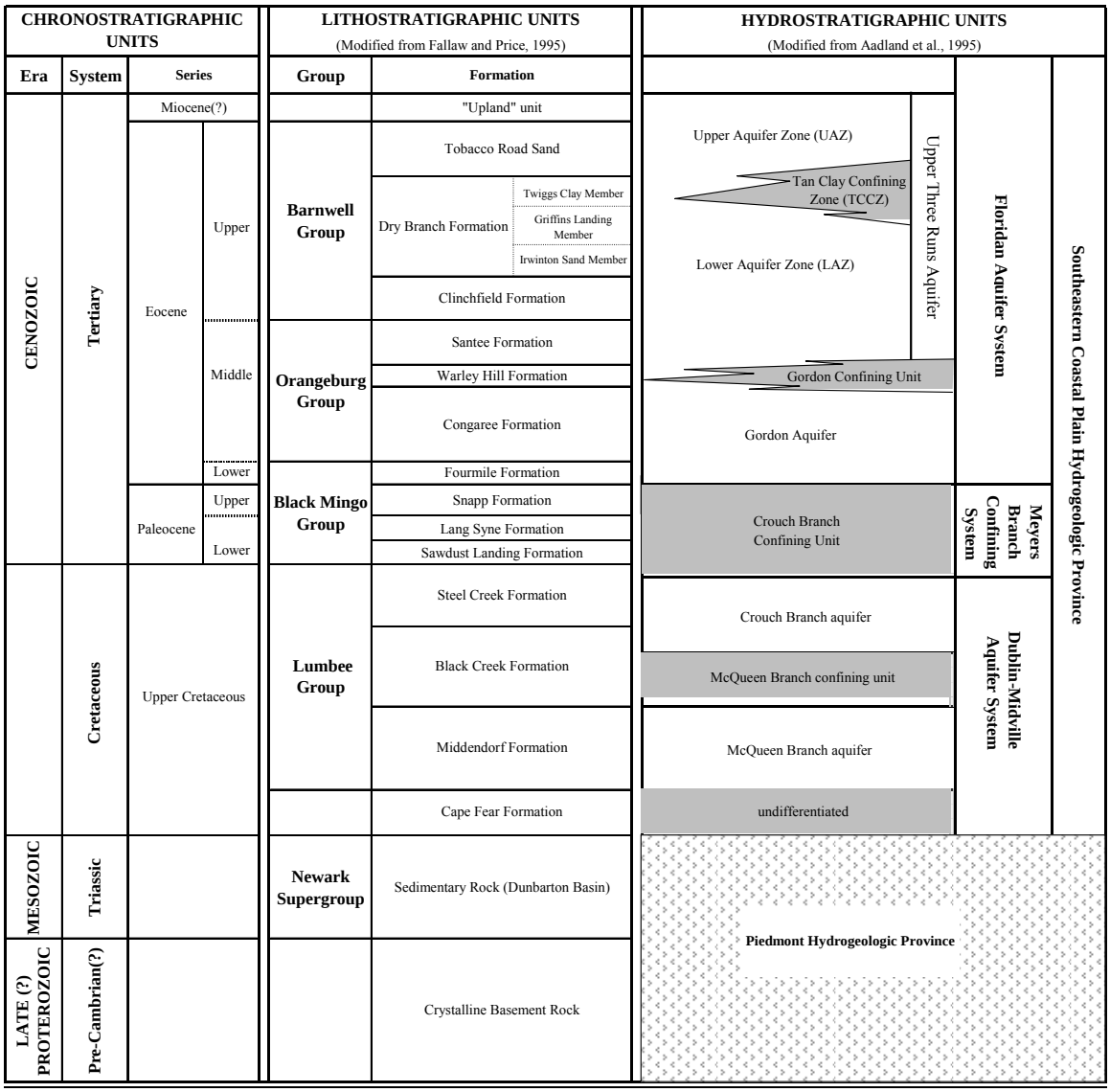

Figure 3-10. Comparison of Lithostratigraphic and Hydrostratigraphic Units at SRS

The thickness of the Lumbee Group, which overlies the Cape Fear Formation, varies across the SRS from 120 m in the northwest to more than 230 m near the southeastern boundary. The Middendorf Formation, which directly overlies the Cape Fear Formation, is composed mostly of medium and coarse quartz sand that is cleaner and less indurated than the underlying sediments. Clay casts and pebbly zones occur in several places in the Middendorf Formation. A clay zone up to 24 m thick forms the top of this formation over much of the SRS. In total, the Middendorf Formation ranges from approximately 37 to 73 m thick from the northwestern to southeastern boundary of the SRS (Wyatt and Harris 2000). Outcrops of this formation have been identified northwest of the SRS.

The Black Creek Formation consists of quartz sands, silts, and clays. The lower section consists of fine- to coarse-grained sands with layers of pebbles and clay casts. The upper section changes in composition as it crosses the SRS from northwest to southeast, from massive clay to silty sand with interbeds of clay. Thickness of the Black Creek Formation under the SRS ranges from 34 m in the northwest to 76 m in the southeast. Outcropping in the vicinity of the SRS has not been confirmed. The Black Creek is distinguished from the over-and underlying Cretaceous formations by its better sorted sand, relatively fine-grained texture, and relatively higher clay content.

The uppermost formation in the Lumbee Group is the Steel Creek Formation (previously referred to as the Peedee Formation), which consists of fine-grained sandstone and siltstone with marine fossils. This formation is comparable in age, but lithologically distinct, from the Peedee Formation in southwestern South Carolina. The lower portion of this formation consists of fine- to coarse-grained quartz sand and silty sand, with a pebble-rich zone at its base. Pebbly zones and clay casts are common throughout the lower portion of the Steel Creek Formation. The upper portion of this formation is a clay that varies from more than 15 m to less than 1 m in thickness at the SRS. The Steel Creek Formation is about 18 m thick toward the northwestern SRS boundary and about 53 m thick toward the southeastern boundary (Wyatt and Harris 2000). No nearby outcropping has been identified.

Paleocene-Eocene Black Mingo Group

Paleocene-Early Eocene sediments make up the Black Mingo Group (Figure 3-10). In E-Area, this group consists of the Early Paleocene Lang Syne/Sawdust Landing Formations, the Late Paleocene Snapp Formation, and the Early Eocene Fourmile Formation. This group is about 21 m thick at the northwestern SRS boundary, thickens to about 46 m near the southeastern boundary.

The Lang Syne/Sawdust Landing Formations together are equivalent to the lithologic unit previously referred to as the Ellenton Formation. These formations are treated as a single unit due to difficulty in mapping them separately and consist mostly of gray, poorly sorted, micaceous, lignitic, silty and clayey quartz sand interbedded with gray clays. They are approximately 12 m thick at the northwestern boundary of the SRS and thicken to about 30 m near the southeastern boundary. These formations outcrop about four miles northwest of the SRS.

The deposits near the SRS that are designated as the Snapp Formation are time-equivalent to the Williamsburg Formation. The sediments are typically silty, medium- to coarse-grained quartz sand interbedded with clay. The Snapp Formation pinches toward the northwestern SRS boundary and thickens to about 15 m near the southeastern boundary. In E-Area, the distribution of the Snapp Formation is sporadic and not continuous.

Sand immediately overlying the Snapp Formation is identified as the Fourmile Formation. The well-sorted sand of this formation is an average of 9 m in thickness. Clay beds near the middle and top of the formation are a few feet thick. In E-Area, this formation may not be continuous.

Middle Eocene Orangeburg Group

The middle Eocene sediments make up the Orangeburg Group, which in E-Area consists of the lower middle Eocene Congaree Formation, the upper middle Eocene Warley Hill Formation, and the late middle Eocene Tinker/Santee Limestone Formation (Figure 3-10). The sediments thicken from about 30 m at the northwestern SRS boundary to about 49 m near the southeastern boundary. The dip of the upper surface of this formation is about 2 m/km to the southeast across the site. The Orangeburg Group is about 100 m thick at the coast. The group outcrops at lower elevations in many places near and at the SRS.

The Congaree Formation consists of fine to coarse, well-sorted and rounded quartz sands. Thin clay laminae occur throughout, as do small pebble zones. The sand is glauconitic in places. The formation is up to 26 m thick at the center of the SRS.

The Warley Hill Formation, made up of glauconitic sand and green clay beds and thus previously referred to locally as the "green clay," overlies the Congaree Formation. This formation is generally 3 to 6 m in thickness. However, northwest of E-Area, the Warley Hill Formation is missing or very thin, such that the overlying Tinker/Santee Formation rests unconformably on the Congaree Formation.

The Tinker/Santee Formation consists of calcilutite, calcarenite, shelly limestone, calcareous sands and clays, and micritic limestone. The sands are glauconitic in places and fine- to medium-grained. The sediments comprising this formation have been referred to in the past as the Santee Limestone, McBean, and Lisbon Formations and indicate deposition in shallow marine environments. The Tinker/Santee Formation is about 12 to 15 m thick in the center of E-Area. In places where the Warley Hill Formation is absent, the Tinker/Santee Formation rests directly on the Congaree Formation.

Late Eocene Barnwell Group

The Late Eocene sediments make up the Barnwell Group, which consists of the Clinchfield, Dry Branch, and Tobacco Road Sand (Figure 3-10). The Clinchfield Formation, the oldest of the three, is made up of quartz sand, limestone, calcareous sand, and clay. It is generally identified only when the contrasting carbonates of the overlying Dry Branch and underlying Tinker/Santee Formations are present with the sand of the Clinchfield Formation sandwiched between them. It has been identified at several areas within the SRS where it is up to 8 m thick, but it is indistinguishable in the central regions of the SRS, near E-Area.

The Dry Branch Formation consists of three distinguishable members: the Twiggs Clay Member, the Griffins Landing Member, and the Irwinton Sand Member. The Twiggs Clay Member is not mapable as a continuous unit within the SRS, but lithologically similar clay is present at various levels within this formation. The tan, light gray, and brown clay of the Twiggs Clay Member has previously been referred to as the "tan clay" at the SRS. The Griffins Landing Member is up to 15 m thick in the southeastern part of the SRS. This member consists mostly of calcilutite and calcarenite, calcareous quartz sand, and slightly calcareous clay. It occurs sporadically and pinches out in the center of the SRS. The remainder of the Dry Branch Formation within the SRS is made up of the Irwinton Sand Member, which is composed of moderately sorted quartz sand with interlaminated clays, which are abundant in places. Clay beds of this member have also been referred to as the "tan clay" at the SRS. The Irwinton Sand is about 12 m thick at the northwestern SRS boundary and thickens to 21 m near the southeastern boundary. It outcrops in many places around and within the SRS.

The Tobacco Road Sand overlies the Dry Branch Formation. This formation consists of moderately to poorly sorted quartz sands, interspersed with pebble layers and clay laminae. The sediments have the characteristics of a lower Delta plain to shallow marine deposits. The upper surface of this formation is irregular due to an incision that accompanied deposition of the overlying "Upland Unit" and later erosion. The thickness is variable as a result of erosive processes, but is at least 15 m in places.

Upland Unit

The "Upland Unit" is an informal stratigraphic term applied to terrestrial deposits that occur at higher elevations in some places in the southwestern South Carolina Coastal Plain (Figure 3-10). This unit overlies the Barnwell Group in the Upper Coastal Plain of western South Carolina, on which the SRS is located. This unit occurs at the surface at higher elevations in many places around and within the SRS, but it is not present at all higher elevations. The sediments are poorly sorted, clayey-to-silty sands, with lenses and layers of conglomerates, pebbly sands, and clays. Clay casts are abundant. The "Upland Unit" is up to 21 m thick in parts of the SRS. Much of this unit corresponds to the Hawthorne Formation and the Tertiary alluvial gravels identified in previous documents (INTERA, 1986). The depositional environment is thought to be fluvial and the thickness changes abruptly due to the channeling of the underlying Tobacco Road Formation during the deposition of the "Upland Unit" and the subsequent erosion of the "Upland Unit".

Soils

Most SRS surface soils have a sand and loamy sand texture whereas subsoil textures can be classified as sandy loam or sandy clay loam (Wike et al, 2006). Approximately 28 individual soil series have been identified at the SRS (Looney et al, 1990; Wike et al, 2006). In addition, seven broad soil association groups have been identified. These groups are named and described according to the dominant soil series within the group.

The Fuquay-Blanton-Dothan Association is the primary group in the center of the General Separations Area and near the E-Area disposal units. This association consists of nearly level to sloping, well-drained soils and typically occurs on broad upland ridges except for those in the northeastern section of SRS. In general, this association is made up of 20% Fuquay soils, 20% Blanton soils, 12% Dothan soils, and 48% of other minor soils (Wike et al, 2006).

Fuquay soils are typically well-drained and have moderately thick, sandy surface and subsurface layers. The loamy subsoil contains iron-rich brittle nodules of plinthite. In comparison, Blanton soils are somewhat excessively drained. They have thick, sandy surface and subsurface layers and loamy subsoil. Dothan soils are well-drained. They have thick, sandy surface and subsurface layers. Like the Fuquay soils, they have loamy subsoil that contains iron-rich nodules of plinthite (Wike et al, 2006).

The distribution of soil types is very much influenced by the creeks on the site, with colluvial deposits on hill-tops and hillsides giving way to alluvium in valley bottoms (Dennehy et al, 1989). In addition to erosion by streams, weathering also affects soil characteristics. Soils at the SRS are typical of soils found in moderately aggressive weathering conditions such as those in the southeastern United States. The temperate climate and relatively high seasonal rainfall produce leached soils with relatively low metal concentrations. The mineralogy of the sands primarily consists of quartz with some feldspar. The mineralogy of the clays is dominated by kaolonite (an aluminum rich clay), which results from the highly weathered feldspars and muscovite (Looney et al, 1990; Nystrom et al., 1991).

3.1.4.2 Seismology

Throughout the fifty-plus year existence of SRS extensive regional and site specific geological and seismological investigations have been performed by many organizations in support of Site operations and missions. This section provides a short summary of area seismic studies. Characterization of regional seismicity is dominated by the catastrophic Charleston, SC, earthquake of August 31, 1886 (estimated magnitude of 7.3). With nearly three centuries of available historic and contemporary seismic data, the Charleston-Summerville area remains the most seismically active region of South Carolina and the most significant seismogenic region affecting the SRS. Other broad regions of South Carolina have also experienced seismic activity, but at very low levels with magnitudes or sizes generally less than or equal to 3 on the Richter scale.

Description of Nearby Seismic Zones and Earthquakes

Results obtained from seismic network data within South Carolina enabled Tarr et al. (1981) to identify two diffuse areas of seismic activity: the Lower Coastal Plain and the Piedmont/Upper Coastal Plain. Through these studies the Lower Coastal Plain area was further subdivided into three distinct clusters or zones of seismicity that include the Bowman Seismogenic Zone, the Middleton Place-Summerville Seismic Zone, and the Jedburg-Adams Run Seismogenic Zone. The most active zone is the Middleton Place-Summerville Seismic Zone, which is the only one to coincide with the meizoseismal area of the 1886 Charleston earthquake. The main two zones, the Middleton Place-Summerville Seismic Zone and the Bowman are discussed in more detail.

Lower Coastal Plain

Middleton Place-Summerville Seismic Zone:

The Charleston, SC, area, in particular the Middleton Place-Summerville Seismic Zone, is the most significant source of seismicity affecting SRS in terms of both the maximum historical site intensity and the number of earthquakes recorded at SRS. The earthquake with the greatest intensity recorded at the SRS has been estimated at a Modified Mercalli Intensity (MMI) of VI-VII (Table 3-4) and was produced by the intensity MMI X earthquake that struck Charleston, SC, on August 31, 1886, at 9:50 p.m. local time (Visvanathan, 1980). Some of the larger aftershocks of the 1886 Charleston event were also documented in the Aiken-SRS area with intensities equal to or less than MMI IV (Visvanathan, 1980)

Initially, Talwani (1985) identified the delineation of two possible intersecting faults in the Charleston area. The first was a shallow, northwest-trending fault striking parallel to the Ashley River, which was named the Ashley River fault. The second fault was labeled the Woodstock fault. The Woodstock fault trends north-northeasterly and is defined by the planar distribution of hypocenters. It intersects and appears deeper than the Ashley River fault.

Recent studies by Madabhushi and Talwani (1993) refined the earlier model by utilizing 58 additional well-recorded events in the Middleton Place-Summerville Seismic Zone from 1980 to 1991. Results of this effort demonstrated that the Ashley River and the Woodstock faults are not simple planar features, but resemble zones composed of short segments of varying strike and dip. Madabhushi and Talwani (1993) concluded that the seismicity in the Middleton Place-Summerville Seismic Zone defines the intersection of two fault zones, which they inferred to be the Ashley River fault zone and the Woodstock fault zone.

Bowman Seismic Zone:

The Bowman Seismic Zone located 95 km northeast of SRS was initially defined by Tarr et al (1981) from the location of a series of earthquakes occurring through the 1970's. The largest event occurred February 3, 1972 with a reported magnitude of 4.5 (MMI V). The SRS area is estimated to have felt this event with an intensity of MMI III-IV. The Bowman area has experienced very low level sporadic activity since that time with only four small events (magnitude less than or equal to 2.3) recorded from 1980 through 2005. The last recorded event occurred in 1997 (magnitude of 2.25).

Table 3-4. Modified Mercalli Intensity Scale of 1931

Level	Definition
I.	Not felt except by a very few under especially favorable circumstances (I Rossi-Forel Scale).
II.	Felt by only a few persons at rest, especially on upper floors of buildings. Delicately suspended objects may swing (I and II, Rossi-Forel Scale).
III.	Felt quite noticeably indoors, especially on upper floors of buildings, but many people do not recognize it as an earthquake. Standing motor cars may rock slightly. Vibration like passing truck. Duration estimated (III Rossi-Forel Scale).
IV.	During the day felt indoors by many; outdoors by few. At night some awakened. Dishes, windows, doors disturbed; walls made creaking sound. Sensation like heavy truck striking building. Standing motor cars rocked noticeably (IV to V Rossi-Forel Scale).
V.	Felt by nearly everyone; many awakened. Some dishes, windows, etc., broken, a few instances of cracked plaster, unstable objects overturned. Disturbance of trees, poles, and other tall objects sometimes noticed. Pendulum clocks may stop (V to VI Rossi-Forel Scale).
VI.	Felt by all; many are frightened and run outdoors. Some heavy furniture moved; a few instances of fallen plaster or damaged chimneys. Damage slight (VI to VII Rossi-Forel Scale).
VII.	Everybody runs outdoors. Damage negligible in buildings of good structures; considerable in poorly built or badly designed structures; some chimneys are broken. Noticed by persons driving motor cars (VIII Rossi-Forel Scale).
VIII.	Damage slight in specially designed structures; considerable in ordinary substantial buildings with partial collapse; great in poorly built structures. Panel walls thrown out of frame structures. Fall of chimneys, factory stacks, columns, monuments, and walls. Heavy furniture overturned. Sand and mud ejected in small amounts. Changes in well water. Disturbs persons driving motor cars (VIII+ to IX Rossi-Forel Scale).
IX.	Damage considerable in specially designed structures; well designed frame structures thrown out of plumb; great in substantial buildings with partial collapse. Buildings shifted off foundations. Ground cracked conspicuously. Underground pipes broken (IX+ Rossi-Forel Scale).
X	Some well built wooden structures destroyed; most masonry and frame structures destroyed with foundations, ground badly cracked. Rails bent. Landslides considerable from riverbanks and steep slopes. Shifted sand and mud. Water splashed (slopped) over banks (X Rossi-Forel Scale).
XI.	Few, if any, masonry structures remain standing. Bridges destroyed. Broad fissures in ground. Underground pipe lines completely out of service. Earth slumps and land slips in soft ground. Rails bent greatly.
XII.	Damage total. Waves seen on ground surfaces. Lines of sight and level distorted. Objects thrown upward into the air.

Source: Earthquake Intensity and Ground Motion, pp 7-8, by Frank Neumann, University of Washington Press, Seattle, WA (1954).

Piedmont/Upper Coastal Plain

The second diffuse area of seismic activity includes the Piedmont province and the Upper Coastal Plain. The Upper Coastal Plain is where the majority of the SRS is located. The structure and configuration of Upper Coastal Plain basement features have been interpreted to be the subsurface continuation of Piedmont terrain (Daniels et al., 1983). Earthquake activity occurring within this area, not associated with reservoir-induced activity, shows a lack of clustering and is best characterized by occasional small shallow events associated with strain release near small-scale faults, intrusives, and edges of metamorphic belts (Tarr et al., 1981).

Regional Earthquake Activity:

On January 1, 1913, an earthquake struck Union County, SC, approximately 100 miles north-northeast of the SRS. Outside of the Charleston area, this was the largest recorded event near the SRS. It had intensity greater than or equal to MMI VIII. In the Aiken-SRS area, this earthquake was felt with an intensity of MMI II-III (Visvanathan, 1980).

Earthquake Activity within a 50 mile radius of the SRS:

As stated above, the SRS is located within the Coastal Plain physiographic province of South Carolina. However, seismic activity associated with the SRS and the surrounding region displays characteristics more closely associated with the Piedmont province. Epicentral locations for events near the SRS (within 50 mile radius of the site) are presented in Table 3-5. Figure 3-11 shows the distribution of earthquake epicenters within 50 miles of the SRS. No damage or injury has ever been associated with any earthquake activity occurring within the 50 mile radius. The largest event in this series was the magnitude 3.7 Clarks Hill event of November 5, 1974 (event #7 on Table 3-5 and Figure 3-11). It occurred near Clarks Hill Reservoir (now Strom Thurmond Lake) and is attributed to Reservoir Induced Seismicity.

Recent Earthquake Activity at the SRS:

On June 9, 1985, an intensity MMI III earthquake with a local duration magnitude of 2.6 occurred at SRS (Talwani, et al., 1985). Duration magnitude is a method of estimating magnitudes of local earthquakes from signal duration. Workers at the western edge of the central portion of the site experienced and reported the event.

Another event occurred at the SRS on August 5, 1988. This earthquake had an intensity of MMI I-II and a local duration magnitude of 2.0. A survey of SRS personnel in 1988 indicated that it was not felt at the site (Stephenson, 1988). Neither of these earthquakes triggered SRS seismic alarms, which were set to trigger when ground accelerations equaled or exceeded 0.002 times the earth's gravitational acceleration (set point 0.002 g_o) (Stephenson et al., 1985 and Stephenson, 1988).

Table 3-5. Historic and Instrumental Earthquakes Recorded Within 50 miles of the SRS

Event #	Date	Latitude	Longitude	Depth (km)	Magnitude
1	5/6/1897	33.3	-81.2		Felt
2	5/9/1897	33.9	-81.6		Felt
3	5/24/1897	33.3	-81.2		Felt
4	5/27/1897	33.3	-81.2		Felt
5	8/14/1972	33.2	-81.4		3.2
6	10/28/1974	33.79	-81.92		3.0
7	11/5/1974	33.73	-82.22		3.7
8	9/15/1976	33.0883	-81.4480	12.0	2.4
9	6/5/1977	33.0520	-81.4120	3.50	2.7
10	2/21/1981	33.5933	-81.1476	6.61	2.0
11	1/28/1982	32.9800	-81.3900	7.00	3.4
12	6/9/1985	33.2225	-81.6842	5.81	2.6
13	2/17/1988	33.5113	-81.6966	11.73	2.5
14	8/5/1988	33.1873	-81.6290	2.26	2.0
15	7/13/1992	33.4798	-81.1920	7.60	1.9
16	10/2/1992	33.4990	-81.2020	3.00	2.4
17	12/12/1992	33.2798	-81.8328	11.80	1.2
18	6/29/1993	33.4652	-81.2210	4.90	2.2
19	8/8/1993	33.5893	-81.5852	10.18	3.2
20	8/8/1993	33.5885	-81.5812	9.22	1.6
21	9/18/1996	33.6915	-82.1248	2.38	2.8
22	5/17/1997	33.2118	-81.6765	5.44	2.5
23	10/8/2001	33.3240	-81.6650	3.90	2.6
24	10/8/2001	33.3193	-81.6733	4.19	1.0
25	10/8/2001	33.3317	-81.6762	4.15	1.4
26	10/14/2001	33.3467	-81.6627	3.14	0.7
27	10/15/2001	33.3475	-81.6938	4.67	0.8
28	12/17/2001	33.3283	-81.6745	4.13	1.1
29	12/27/2001	33.3310	-81.6652	3.76	0.1
30	3/6/2002	33.3313	-81.6792	4.61	1.4
31	1/18/2005	33.6063	-82.1631	8.76	2.5
32	1/18/2005	33.5976	-82.1681	15.4 ?	2.3
33	1/18/2005	33.5786	-82.1621	17.4 ?	2.0

Source: SEUSSN Bulletins, Virginia Tech Publication for events through December 2000; SRS unpublished data for events from January 2001 through September 20, 2006; question marks indicate depths that are estimates; numbers on the table correspond to the numbers on the map showing historical earthquakes; magnitudes are expressed in terms of the Richter scale.

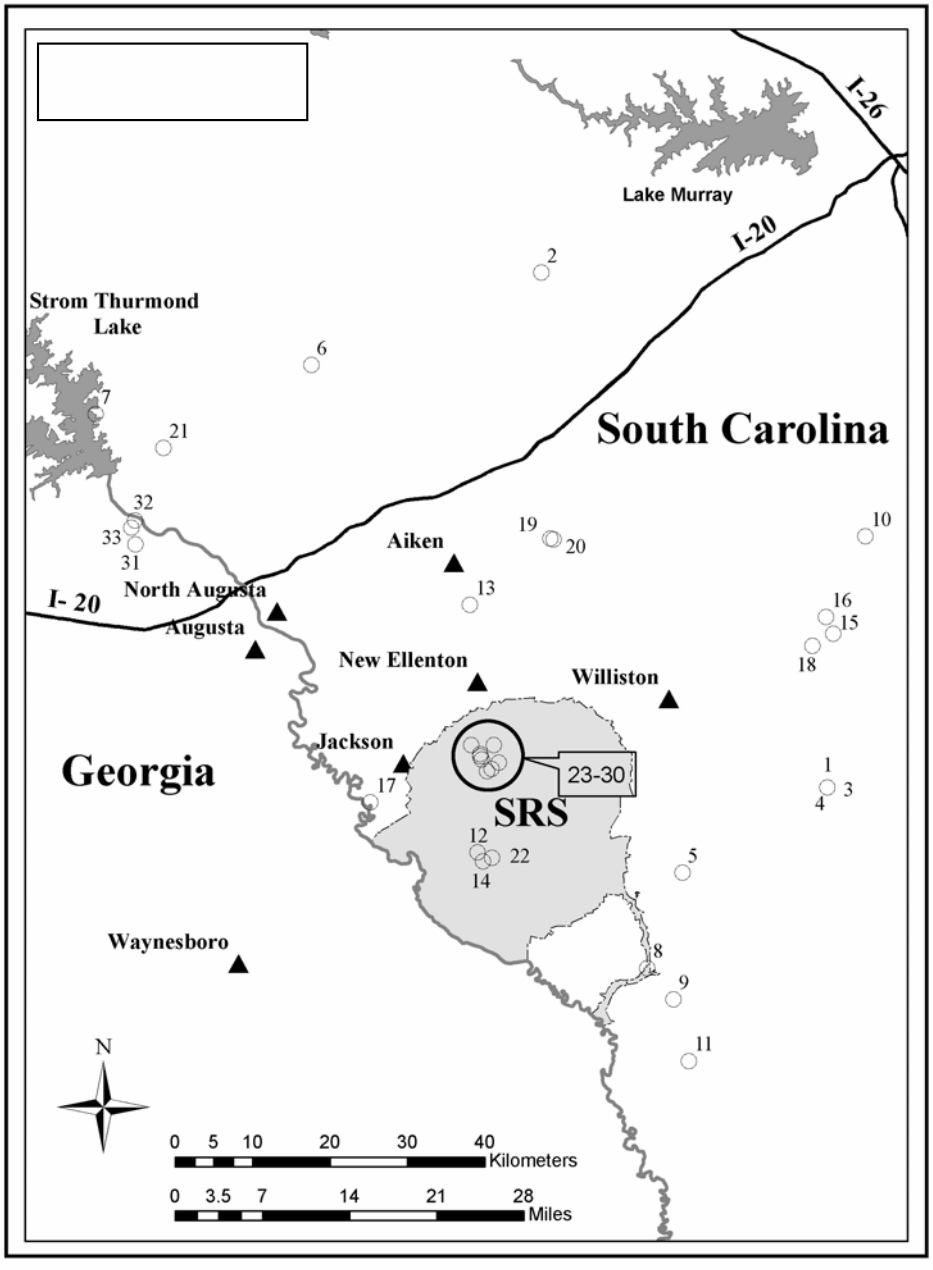

Figure 3-11. Historical Earthquakes within 50-mile Radius of the SRS

On the evening of May 17, 1997, at 23:38:38.6 UTC (7:38 pm EDST) an earthquake with a duration magnitude of approximately 2.3 occurred within the boundary of the Savannah River Site. Workers in K-Area and Wackenhut guards at a nearby barricade reported the earthquake. No strong motion accelerographs were triggered as a result of this event with the closest instrument located only 3 miles southeast of the epicenter (trigger threshold set at 0.006 g_o).

Eight small earthquakes were recorded and located between October 8, 2001 and March 6, 2002. None of these events were strong enough to trigger strong motion instrumentation installed in facilities throughout SRS. The largest earthquake occurred on October 8, 2001 with a local duration magnitude of 2.6. It was located near Upper Three Runs Creek in the north central area of the SRS. A series of seven small aftershocks followed the main event with the last one occurring March 6, 2002. Projection of hypocenters onto nearby seismic reflection line showed no apparent relationship to interpreted basement faults. Detailed analyses of collected data showed a strong relationship to a small northwest (NW-SE) trending gravity and magnetic feature (Stevenson and Talwani, 2004). This small basement feature runs counter to the regional structure (NW-SE). The shallowness, small aerial extent, and its relationship to a small basement feature running counter to the regional structure indicated that this activity was extremely localized and not related to any large scale regional feature.

Faults at the SRS:
Faults involving Coastal Plain sediments that are considered regionally significant based on their extent and amounts of offset include the ATTA, Crackerneck, Martin, Pen Branch, and Tinker Creek faults shown in Figure 3-12 (Stieve and Stephenson, 1995). The Crackerneck and Pen Branch Faults are relatively well constrained with borings. The other faults are projected only from geophysical data and their parameters are less known. DOE (2002) concludes that faults located beneath SRS are not “capable”, i.e., have not moved at or near the ground surface within the past 35,000 years or is associated with another fault that has moved within the past 35,000 years.

Of these faults the Pen Branch fault has been regarded as the primary structural feature at SRS that has the characteristics necessary to pose a potential seismic risk. As a result, the Pen Branch fault has been extensively studied in order to determine the capability of the fault to release potentially damaging seismic energy as defined by NRC regulatory guidelines, 10 CFR 100, Appendix A. Results from the Pen Branch Fault Program showed that the most recent faulting on this fault was older than 500,000 years. In a study designed to examine only the sediments with an age of 1 million years or less, no deformation of the sediments was found to exist (Hanson et al., 1993). In the end, research findings from the program indicated that the Pen Branch Fault was not capable of producing damaging earthquakes (Hanson et al., 1993; Stieve et al., 1991; Stieve et al., 1994; WSRC, 2000).

Contemporary shallow state of stress values gathered from direct in-situ measurements together with focal mechanisms of recent earthquakes have shown a consistent northeast-southwest (NE-SW) direction of maximum horizontal compressive stress (N 55-70°E) for the southeastern United States (Moos and Zoback, 1993). Overall, the state of stress for the SRS has been found to agree with these measurements (Moos and Zoback, 1992). The significance of these findings is that reactivation of the SRS's predominantly northeast striking faults would not induce potentially damaging earthquakes (Moos and Zoback, 1992; WSRC, 2000).

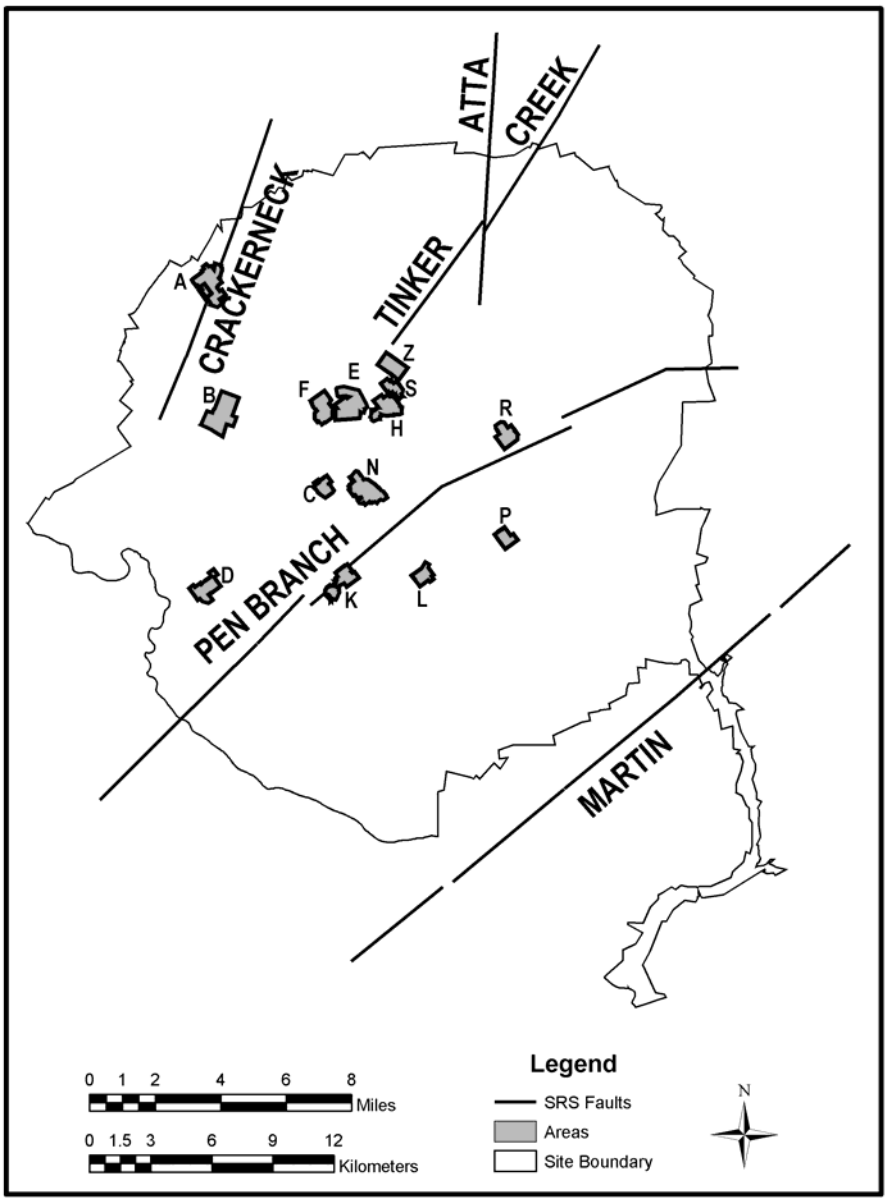

Figure 3-12. Locally Significant Faults at the SRS

Projected Recurrence of Earthquakes

Talwani and Schaeffer (2001) presented analyses of 15 years of paleoliquefaction investigations in the South Carolina Coastal Plain to arrive at an estimated recurrence interval for large earthquakes in the region. Their investigation concluded that the Charleston area had a recurrence interval for magnitude 7+ earthquakes (similar to the Charleston 1886 event) between 500 and 600 years. The recurrence of earthquakes associated with other known seismic zones in the region is not expected to be of greater intensity nor cause greater disturbance at the SRS.

3.1.5 Hydrology

3.1.5.1 Groundwater

A discussion of groundwater hydrology should consider all the aquifers and confining units that affect the subsurface distribution of contaminants potentially released from the E-Area LLWF. In the past, several hydrostratigraphic classification systems have been used at the SRS. The classification system used in this report is consistent with the system established by Aadland et al. (1995) and in Smits et al. (1997) and Denham (1999). This classification is now widely used as the standard (Mamatey, 2006). Figure 3-10 shows the regional lithologic units and their corresponding hydrostratigraphic units at the SRS. A detailed description of the lithologic units is provided in Section 3.1.4.

The hydrogeology at the SRS has several general characteristics. In general, recharge for the deeper aquifers occurs updip of the SRS, near the Fall Line (Figure 3-1). Some recharge also occurs in the northern-most fringe of the site. In contrast, recharge for the water table aquifers (e.g., Upper Three Runs Aquifer) primarily comes from local precipitation. The upper two aquifer units, the Upper Three Runs aquifer and the Gordon aquifer, discharge to local streams at the SRS in addition to recharging underlying units. Within the confining units, an abundance of clay-sized material and clay minerals helps to limit the vertical migration of contaminants. Furthermore, the presence of an upward vertical gradient or “head reversal” between the Crouch Branch aquifer and the overlying Gordon and Upper Three Runs aquifers plays a significant role in preventing the downward vertical migration of contaminants.

In the GSA, the surrounding streams influence groundwater flow. Figure 3-13 provides a cross section illustrating the GSA hydrogeology. Three streams (Upper Three Runs to the north; McQueen Branch, a tributary of Upper Three Runs to the northeast; and Fourmile Branch to the south) are natural boundaries to groundwater flow in the Upper Three Runs aquifer unit. All creeks cut into this unit, and thus groundwater is either intercepted by the creeks or recharges the underlying Gordon aquifer unit. Also important to note is a groundwater divide, which occurs in this water table unit due to the influence of these streams. Figure 3-14 shows the influence of the creeks on groundwater flow directions local to E-Area.

In this report, the discussion of groundwater hydrology is restricted to hydrostratigraphic units above the Meyers Branch confining system because units below that system are considered protected from contamination. Justification for this assumption is given in the subsection entitled "Meyers Branch Confining System". Further descriptions of the hydrogeology can be found in several recent and historical reports (Aadland et al., 1991; Aadland et al., 1995; Clarke and West, 1997; Denham, 1999; Dennehy et al., 1989; Fallaw and Price, 1995; Flach et al., 1999; Flach and Harris, 1999; Smits et al., 1997; Wyatt et al., 2000; Wyatt and Harris, 2004).

Meyers Branch Confining System

The Meyers Branch confining system overlies the Dublin-Midville aquifer system (Figure 3-10). Sediments of this Late Cretaceous-Paleocene system include the lignitic clays and interbedded sands of the Steel Creek Formation and the laminated clays and shale of the Lang Syne/Sawdust Landing and Snapp Formations. At the SRS, the Meyers Branch system consists of a single hydrostratigraphic unit, known as the Crouch Branch confining unit, which includes several thick and relatively continuous (over several miles) clay beds. The Crouch Branch confining unit ranges in thickness from 17 m to 56 m. East of E-Area, the Meyers Branch confining system is 41 m thick, 21 m of which are clay beds.

The updip limit of the Meyers Branch confining system, where the system is no longer a regional confining system, occurs north of the intersection of McQueen Branch and Upper Three Runs streams and runs approximately east to west. North of the updip limit, the Crouch Branch confining unit continues and is considered part of the Floridan-Midville aquifer system (in which all aquifer units above and including the McQueen Branch aquifer are considered layered parts of one aquifer system).

Areas of the SRS which are adjacent to the Savannah River flood plain and the Upper Three Runs drainage systems, including E-Area, exhibit an "upward" hydraulic gradient across the Crouch Branch confining unit. Hydraulic heads in the underlying Crouch Branch aquifer are higher than those in the overlying Gordon aquifer in these areas, due to the incisement of the overlying aquifer by these two river systems. This area of upward gradient encompasses all of E-Area. The magnitude of the upward gradient is about 5 meters in the vicinity of E-Area, but the low transmissivity of the Meyers Branch confining system results in a low water flux into the Gordon aquifer. Thus, in E-Area, the confining nature of the Crouch Branch confining unit along with the head-reversal phenomenon provides a natural protection of aquifers beneath the Floridan aquifer system from contamination.

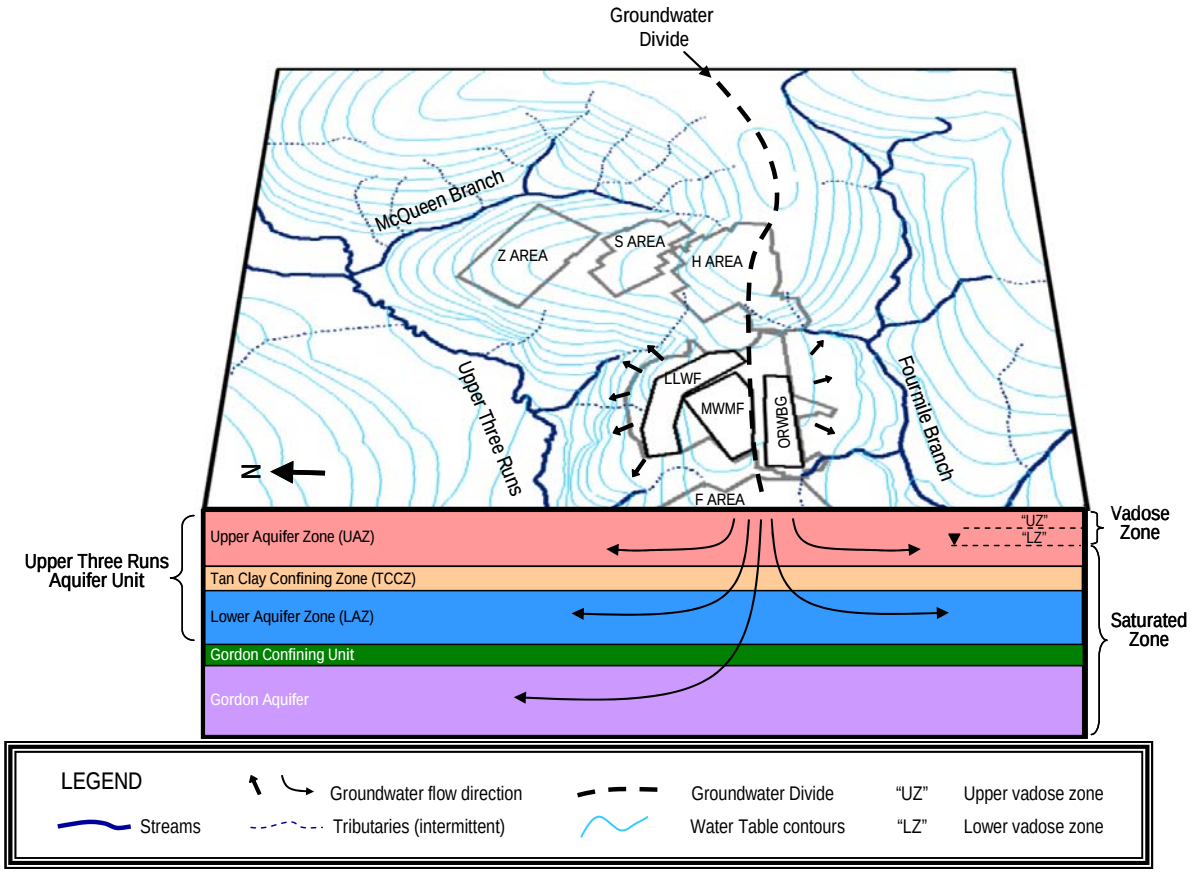

Figure 3-13. Hydrogeology at the General Separations Area

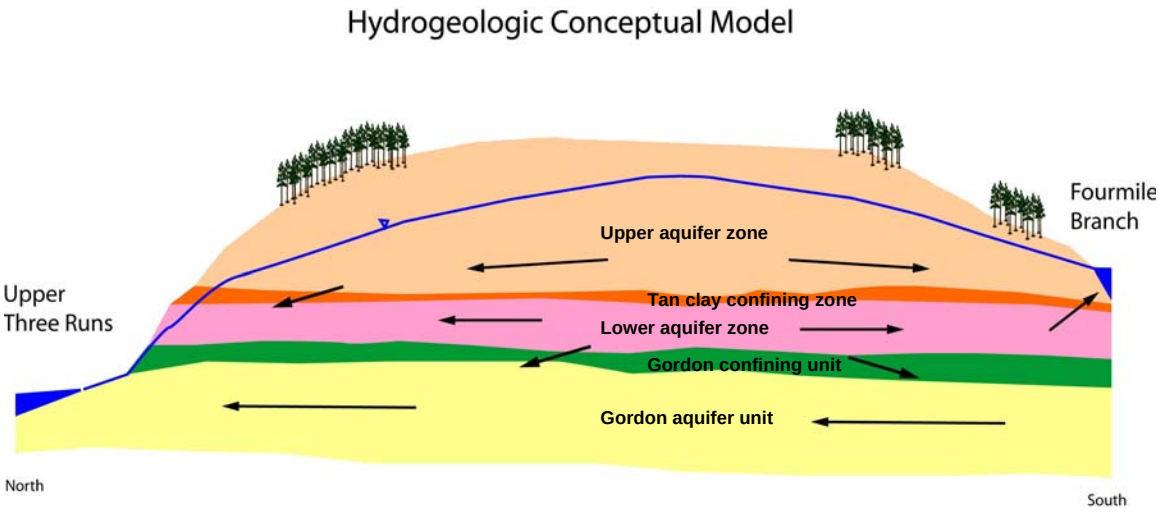

Figure 3-14. Generalized hydrogeologic cross-section near E-Area, showing Influence of Streams on Groundwater Flow

Floridan Aquifer System

Because of relative hydrologic isolation due to the Meyers Branch confining system, only the Floridan aquifer system is of interest in the performance assessment and special analysis of potential groundwater contamination from operations at E-Area. The Floridan aquifer system is comprised of the Gordon aquifer unit, the Gordon confining unit, and the uppermost Upper Three Runs aquifer unit. The Upper Three Runs aquifer unit is divided into the "lower" aquifer zone, the "tan clay" confining zone, and the "upper" aquifer zone, in which the water table occurs.

Gordon Aquifer Unit:

The Gordon aquifer unit overlies the Crouch Branch confining system and is approximately 23 m thick at E Area. The aquifer consists of sandy parts of the Late Paleocene-Early Eocene Snapp, Fourmile, and Congaree Formations. Sands and clayey sands of the Gordon aquifer unit are largely yellow to orange in color and consist of fine- to coarse-grained, subangular to subrounded quartz. The sands range from well to poorly sorted. Locally-confining clay beds are present, as are pebbly zones. The unit dips at 1.5 to 1.7 m/km to the south and southeast and thickens in the western portion of E Area and to a minor extent to the southeast.

The hydraulic gradient in the Gordon aquifer across the SRS is generally from northeast to southwest, averaging 0.9 m/km, towards the Savannah River. However, the potentiometric surface indicates considerable deflection of the contours due to incisement of aquifer sediments by Upper Three Runs such that flow from E-Area is westerly. Horizontal hydraulic conductivity for the Gordon aquifer reported from aquifer tests and modeling studies of the GSA ranges from 8.5×10^{-5} to 1.4×10^{-4} m/s (Aadland et al., 1995; Denham, 1999; Flach and Harris, 1999; Flach, 2004). According to Aadland et al. (1995) and Denham (1999), a representative horizontal hydraulic conductivity for the Gordon aquifer in the GSA is 1.2×10^{-4} m/s based on pumping test data. The horizontal hydraulic conductivity value used in the aquifer transport simulations for the E-Area PA was consistent with these previously reported values (Table 3-6).

Gordon Confining Unit:

The Gordon confining unit separates the underlying Gordon aquifer unit from the Upper Three Runs aquifer unit. This confining unit is informally known as the "green clay." It is comprised of the fine-grained glauconitic sand and clay beds of the Middle Eocene Warley Hill Formation and the micritic limestone of the Tinker/Santee Formation (Figure 3-10). Thickness of the Gordon confining unit in the vicinity of the SRS varies from 1.5 to 25 m. In the vicinity of E-Area, it is from 0.6 to 9 m thick. Recent studies indicate the unit is composed of several lenses of green and gray clays and silty sands that thicken, thin, and pinch out abruptly. Extensive carbonate sediments associated with areas of thin or truncated clay beds are present in E-Area.

Laboratory and model-derived vertical hydraulic conductivities ranging from 4.0×10^{-12} to 9.5×10^{-9} m/s have been reported for the Gordon confining unit for the GSA (Aadland et al., 1995; Flach and Harris, 1999; Flach, 2004), suggesting that the Gordon confining unit is an effective aquitard in this region.. The vertical hydraulic conductivity value used in the aquifer transport simulations for the E-Area PA falls within the range of these previously reported values (Table 3-6).

Upper Three Runs Aquifer Unit:
The Upper Three Runs aquifer unit overlies the Gordon confining unit and is the water table unit. This unit includes the sandy sediments of the Tinker/Santee Formation and all of the heterogeneous sediments in the Late Eocene Barnwell Group. In the center of the SRS, the aquifer unit is 40 m thick. In E-Area, the aquifer unit is divided into three hydrostratigraphic zones with respect to hydraulic properties (Aadland et al., 1995): a "lower" aquifer zone, a "tan clay" confining zone, and an "upper" aquifer zone in which the water table occurs (Figure 3-10).

In E-Area, the "lower" aquifer zone occurs between the overlying "tan clay" confining zone and the Gordon confining unit. It consists of sand, clayey sand, and calcareous sand of the Tinker/Santee Formation and of the lower part of the Dry Branch Formation. Groundwater that leaks across the "tan clay" confining zone recharges this zone. Most of the recharge water moves laterally toward the bounding streams that incise this zone; the remainder of the groundwater flows vertically downward across the Gordon confining unit. Hydraulic conductivity of the "lower" zone has been estimated for the E-Area vicinity by several methods including slug tests, pumping tests, and minipermeameter tests. Average values for the various methods range from 3×10^{-6} m/s to 1×10^{-4} m/s (Aadland et al., 1995). As reported by Aadland et al. (1995) and Denham (1999), the hydraulic conductivity of the "lower" aquifer zone near E-Area is on the order of 3.5×10^{-5} m/s based on pumping test data. The horizontal hydraulic conductivity value used in the aquifer transport simulations for the E-Area PA for the "lower" aquifer zone is consistent with the lower reported, field-based values (Table 3-6).

The "tan clay" confining zone is a leaky confining zone, ranging in thickness from 0 to approximately 10 m throughout the E-Area vicinity. The average thickness is about 3 m. The clay beds of this confining zone, when present, generally support a head difference (up to 5 m) in E-Area between the "upper" and "lower" aquifer zones of the Upper Three Runs aquifer unit and thus retard the movement of water downward across this zone. Laboratory analyses of undisturbed samples of the "tan clay" confining zone yielded a range of vertical hydraulic conductivities from 1.2×10^{-11} to 4.2×10^{-7} m/s (Aadland et al., 1995). The vertical hydraulic conductivity for the "tan clay" used in the aquifer transport simulations for the E-Area PA falls within this range of reported values (Table 3-6).

In E-Area, the "upper" aquifer zone consists of the silty sands of the Irwinton Sand Member of the Dry Branch Formation overlain by the clayey sands of the Tobacco Road Formation. The water table occurs in the "upper" zone. This zone overlies the "tan clay" confining zone, when present, or the "lower" aquifer zone when the confining zone is absent. Units below the "upper" aquifer zone are always saturated and therefore the "upper" aquifer is not considered a perched system. According to Aadland et al. (1995) and Denham (1999), the hydraulic conductivity of the "upper" aquifer zone near E-Area is on the order of 4.5×10^{-5} m/s based on reliable pumping test data. The horizontal hydraulic conductivity value used in the aquifer transport simulations for the E-Area PA is consistent with this reported value (Table 3-6).

Hydrogeologic Characteristics of Vadose Zone

The vadose zone, which extends from the ground surface downward to the water table, primarily consists of sediments from the Upland unit (where it is present) and the Tobacco Road formation (Figure 3-10). In general these sediments are stratified with varying amounts of clay and sand content. Phifer et al. (2006) compiled and analyzed existing characterization data for the vadose zone in E-Area. Data included grain size (sieve) analyses, hydraulic property data (laboratory measurements of vertical hydraulic conductivity and water retention), bulk property laboratory measurements, CPT data, continuous core descriptions and geophysical logs.

Using the laboratory and field data, Phifer et al. (2006) recognized two zones (an "upper" and "lower" zone) within the vadose zone ("UZ" for "upper" zone and "LZ" for "lower" zone in Figure 3-13). The "upper" zone is characterized as having a higher clay content and lower saturated hydraulic conductivity than the "lower" zone.

Table 3-6: Hydraulic Conductivity Values Used in Aquifer Transport Simulations

UNIT	Approximate Hydraulic Conductivity in Transport Simulations m/s	Cited Representative Hydraulic Conductivity Values m/s
Upper Aquifer Zone[1]	3.5×10^{-5} m/s	4.5×10^{-5} m/s[3]
Tan Clay Confining Unit[2]	2.1×10^{-8} m/s	1.2×10^{-11} to 4.2×10^{-7} m/s[4]
Lower Aquifer Zone[1]	4.6×10^{-5} m/s	3.5×10^{-5} m/s[3]
Gordon Confining Unit[2]	3.5×10^{-11} m/s	4.0×10^{-12} to 9.5×10^{-9} m/s[5]
Gordon Aquifer[1]	1.3×10^{-4} m/s	1.2×10^{-4} m/s[3]

[1]values reflect horizontal hydraulic conductivity for the aquifers
[2]values reflect vertical hydraulic conductivity for the confining zones
[3]representative value based on pumping test data from GSA as summarized in Aadland et al., 1995 and Denham, 1999
[4]range based on laboratory tests of core from the GSA as summarized in Aadland et al., 1995
[5]range based on laboratory and model-derived vertical hydraulic conductivities for the GSA as reported by Aadland et al., 1995; Flach and Harris, 1999; and Flach, 2004

Table 3-7 provides representative saturated hydraulic conductivity values based on laboratory falling head analyses for the "upper" and "lower" zones. In addition to these values, Phifer et al. (2006) also reported nominal or "best estimate" values for porosity (η), dry bulk density (ρ_b), particle density (ρ_p), saturated hydraulic conductivity (K_{sat}), characteristic curves (suction head, saturation, and relative permeability), and effective diffusion coefficient (D_{eff}) for use in the deterministic and sensitivity modeling of the E-Area PA. Moreover, they provided uncertainty estimates for the properties based on exiting laboratory data.

Both the "upper" and "lower" zones were identifiable on CPT and geophysical logs. Using these logs, the two zones were defined for the E-Area disposal units where soil property data was not available. In E-Area, the "upper zone" extends from the land surface down to approximately 111 m above msl and the "lower" zone continues from 111 m above msl to the water table, which varies from 64 to 73 m above msl near the disposal units (Phifer et al., 2006).

Table 3-7: Saturated Hydraulic Conductivity Values for the Vadose Zone

Zone	Horizontal Hydraulic Conductivity m/s	Vertical Hydraulic Conductivity m/s
Upper Vadose Zone	6.2×10^{-7} m/s	8.7×10^{-8} m/s
Lower Vadose Zone	3.3×10^{-6} m/s	9.1×10^{-7} m/s

from Phifer et al (2006)

3.1.5.2 Surface Water

Savannah River

The Savannah River forms the southwestern border of the SRS for approximately 20 mi and is approximately 140 river mi from the Atlantic Ocean. At the SRS, the river cuts a broad valley approximately 250 ft deep through the Aiken Plateau. The Savannah River Swamp, which on average is 1.5 mi wide, is located in the Savannah River flood plain (primarily along the northeastern/South Carolina side). Five tributaries discharge directly to the Savannah River from SRS. From the northwest to the southeast they are: Upper Three Runs, Beaver Dam Creek, Fourmile Branch, Steel Creek, and Lower Three Runs (Figure 3-3). A sixth stream, Pen Branch, which does not flow directly into the river, joins Steel Creek in the Savannah River floodplain swamp (particularly during swamp flooding). Each of these six streams originates on the Aiken Plateau in the Coastal Plain and descends approximately 30 to 150 ft before discharging into the river.

Near the SRS, the flow of the Savannah River has been stabilized by the construction of upstream reservoirs, which include Lake Hartwell and Clarks Hill/Thurmond Lake (Figure 3-2). Flow rate statistics for nearby USGS stations are provided in Table 3-8, and locations of these stations are shown on Figure 3-14. Based on data collected from 1940 to 2005, the mean annual flow is approximately 10,278 cfs at the point where Highway 301 crosses the river (approximately 20 km downstream of the site at the USGS surface water station #02197500). The minimum mean annual flow rate at this location was 5,124 cfs and occurred in 2002. The maximum mean annual flow rate at this location was 18,320 cfs and occurred in 1964 (USGS Water-Data Site Information for South Carolina; Cooney et al. 2006). Similar flow rates and trends are evident in the station upstream of the SRS in Augusta, GA (USGS station # 02197000).

Upstream of the SRS, the Savannah River supplies domestic and industrial water for Augusta, GA and North Augusta, SC. Approximately 130 mi downstream of the SRS, it supplies domestic and industrial water for Savannah, GA and Beaufort and Jasper counties, SC (DOE, 1995).

Table 3-8: Flow Rate Statistics for USGS and SRS Surface Water Stations

Station ID	Location Description	Time Period[1]	Annual Mean Flow Rate		
			Minimum[2] cfs	Maximum[3] cfs	Mean cfs
02197000 Source[4]	Savannah River at Augusta, GA	1940-1986; 1996-2005	4470	16580	9309
02197500 Source[4]	Savannah River at Burtons Ferry Br NR Millhaven, GA	1940-1970; 1983-1986; 1995; 1997-2003; 2004	5124	18320	10278
02197315 Source[4]	Upper Three Runs at Rd A	1975-1977; 1980-2002	130.0	320.0	234.3
U3R-4 Source[5]	Upper Three Runs at Rd A	2002-July, 2006	136.5	210.5	172.3
02197344 Source[4]	Fourmile Branch at Rd A-12.2	1986-2002[6]	10.6	63.1	31.9
FM-A7 Source[5]	Fourmile Branch at Rd A-7	1998-July, 2006	7.6	25.4	11.4

[1]Datasets are incomplete; data available only the specified years
[2]Minimum value for stations #02197000, #02197500 & #02197315 occurred in 2002; for FM-A7 in 2004
[3]Maximum value for stations #02197000 & #02197500 occurred in 1964; for #02197315 in 1993; for #02197344 in 1991
[4]data source: USGS Water-Data Site Information for South Carolina (http://waterdata.usgs.gov/nwis/) and Cooney et al., 2006
[5]data source: SRS Environmental Services Section database
[6]data shown includes years after C-Reactor shutdown

Surface Water Lakes/Ponds at the SRS

Surface water is held in artificial impoundments and natural wetlands on the Aiken Plateau. Par Pond, the largest impoundment on the SRS, is located in the eastern part of the SRS, covering about 4.2 mi^2. A second impoundment, L Lake, lies in the southern portion of SRS and covers approximately 1.5 mi^2. The waters drain from Par Pond and L Lake to the south via Lower Three Runs and Steel Creek, respectively, into the Savannah River. Lowland and upland marshes and natural and man-made basins on the SRS retain water intermittently. Neither Par Pond nor L Lake are located near the E-Area LLWF and should not be impacted by the E-Area LLWF.

Surface Water Near the E-Area LLWF

As discussed in Section 3.1.5, Hydrology, the E-Area LLWF is situated on a topographic divide separating drainage into the Upper Three Runs, to the north and Fourmile Branch, to the south (Figure 3-4 and Figure 3-13). The water table aquifer in the downslope areas of the divide outcrops at the seeplines along both Fourmile Branch and Upper Three Runs (Figure 3-14 and DOE, 2002).

Upper Three Runs

Upper Three Runs, the longest of the SRS streams, is a large blackwater stream. It drains an area of over 195 mi^2, and is approximately 25 mi long, with its lower 17 mi within the SRS (Figure 3-3). Upper Three Runs receives more water from underground sources than any other SRS stream, and is the only stream with headwaters located outside the SRS. It is the only major tributary on SRS that has not received thermal discharges. Neither Upper Three Runs nor any other SRS streams are commercial sources of water (DOE, 2002). Significant tributaries to this creek include Tinker Creek, which is a headwaters branch that connects northeast of E-Area, and Tims Branch, which connects west of E-Area (Figure 3-3).

Since the 1970s, flow rates on the Upper Three Runs have been monitored either by the U.S. Geological Survey or SRS environmental monitoring personnel. The station location at Upper Three Runs and Road A (USGS #02197315 and U3R-4) has one of the longest monitoring records of all the stations on Upper Three Runs. The station is located approximately 6 mi from the E-Area LLWF and about 2.5 mi northeast of the Savannah River (Figure 3-15). Annual mean flow rates at this location have ranged from 130 cfs to 320 cfs with the maximum occurring in 1993 and the minimum in 2002 (Table 3-8). The average annual flow rate at this location is roughly 210 cfs.

Fourmile Branch

Fourmile Branch is a blackwater stream that begins in the center of the SRS and flows southwest approximately 15 mi before discharging into the Savannah River (Wike et al., 2006) (Figure 3-3). The watershed of Fourmile Branch drains approximately 22 mi^2 inside the SRS, including areas of the GSA (DOE, 1995; DOE, 2002). Two surface water gauge locations provide historical flow rate data for this stream. One station is located approximately 4 mi from the E-Area LLWF; the other station is located further downstream approximately 8 mi from the E-Area LLWF and 3 mi northeast of the Savannah River (Figure 3-15). Data from these two stations indicate annual mean flow rates ranging from 7.6 cfs to 63.1 cfs. The maximum annual flow rate occurred in 1991, whereas the minimum annual flow was recorded in 2004 (Table 3-8).

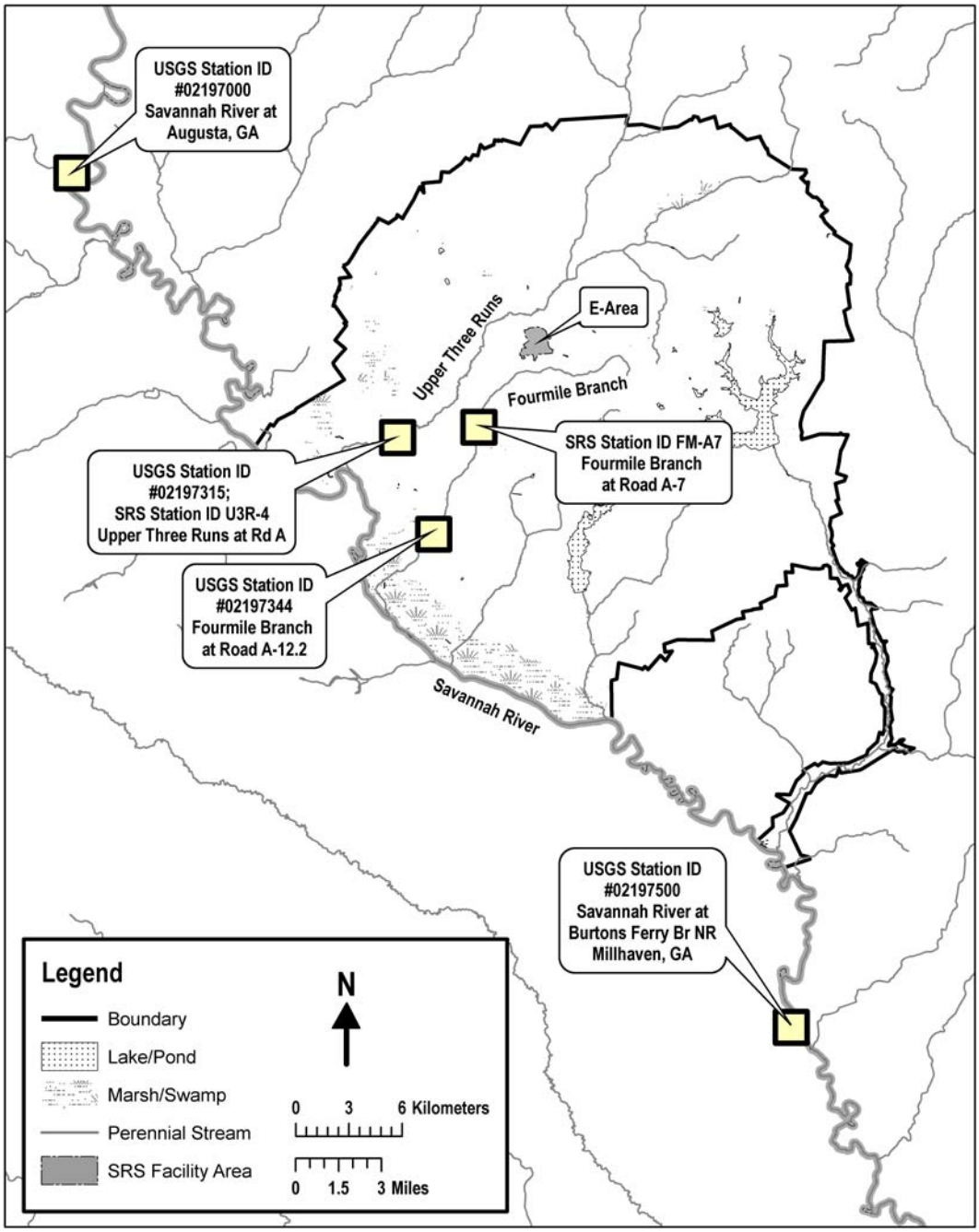

Figure 3-15. Nearby Surface Water Stations Monitored for Flow Rates

3.1.6 Geochemistry

The geochemical environment in the E-Area LLWF influences the sorptive, complexation, and solubility behavior of radionuclides in the various disposal units, and as they migrate in the subsurface strata. Kaplan (2006) is conducting a study relevant to the site-specific nature of these processes in SRS disposal areas, and recommends distribution coefficients (K_ds) and apparent solubility concentration limits for use in the transport calculations made for radionuclides migrating from the E-Area facility. The K_ds account for the influence of the different solid materials present in the waste zones as well as in the geologic strata beneath the waste units (Tables 10, 13, and 14, Kaplan 2006). The presence of CDP in both solid and dissolved phases, and their influence on speciation and mobility of radionuclides, is accounted for by the provision of a correction factor for the K_ds (Table 15, Kaplan 2006). The influence of the geochemical environment on solubility is also addressed in the transport calculations by considering the solubility limits for conditions where the concentrations of the radionuclides are believed to exceed the solubility of an assumed solubility-controlling mineral phase. In these cases, apparent solubility concentration limits (Tables 11 and 12, Kaplan 2006) are assumed for the pore concentrations.

The geochemical parameters describe transport processes for 38 elements (>90 radioisotopes) potentially occurring within six disposal unit types in the E-Area LLWF (Slit Trenches, Engineered Trenches, LAWV, ILV, NRCDAs, and the CIG Trenches). This work builds upon well-documented work from previous PA calculations (McDowell-Boyer et al. 2000). The new geochemical concepts introduced in this data package follow.

- In the past, solubility products were used only in a few conditions (element existing in a specific environmental setting). This has been expanded to >100 conditions.
- Radionuclide chemistry in cementitious environments is described through the use of both the K_d and apparent solubility concentration limit. Furthermore, the solid phase is assumed to age during the assessment period (thousands of years), resulting in three main types of controlling solid phases, each possessing a unique set of radionuclide sorption parameters (K_d and solubility concentration limit).
- A large amount of recent site-specific sorption research has been conducted since the last PA (McDowell-Boyer et al. 2000). These new data have replaced previous K_d values derived from literature values, thus reducing uncertainty and improving accuracy.

In addition to the Kaplan (2006) study, the appropriateness of using a non-zero K_d for Tc in SRS sediments was further evaluated by Kaplan (2007). This 2007 literature review was initiated in response to a PA review comment questioning the appropriateness of a non-zero K_d, and provides a more thorough consideration of the Tc K_d. Kaplan (2007) found that there have been three relevant TcO_4^- sorption studies conducted with SRS sediments (Oblath 1983, Kaplan 2003, and Kaplan and Serkiz 2006). Together these studies indicate that Tc K_d values change as a function of soil texture. The iron oxide phases associated with the clay size fraction are likely responsible for much of the TcO_4^- sorption. Site wide, SRS sediments range from 0.1 to 8 wt-% Fe, with a median of 0.8 wt-% Fe (Kaplan 2007). Sandy texture sediments also tend to have some sorption, but very little, and in some environments, especially at pH levels above background, have no Tc sorption.

In consideration of the existing clay content in the vadose zone, the most appropriate TcO_4^- K_d is approximately 0.1 mL/g for a sandy sediment, and 1 mL/g for a clayey sediment. These values are slightly higher than those recommended for transport calculations (Kaplan 2006), which implies that the transport calculations will likely overestimate the groundwater concentrations attributed to the ELLWF.

Stochastic modeling is being used in the PA program to provide a probabilistic estimate of the range of risk that buried waste may pose. Kaplan and Millings (2006) provided early guidance for the selection of the range and distribution (e.g., normal, log-normal) of distribution coefficients (K_d) and solubility values (K_{sp}) to be used in modeling subsurface radionuclide transport in E-Area at SRS. Due to the project's schedule, some modeling had to be started prior to collecting the necessary field and laboratory data needed to fully populate these models. For the interim, the project will rely on literature values and some statistical analyses of literature data as inputs. Based on statistical analyses of some literature sorption tests, the following guidance was provided:

- Set the range to an order of magnitude for radionuclides with K_d values >1000 mL/g and to a factor of two for K_d values of <1000 mL/g. This decision is based on the literature.
- Set the range to an order of magnitude for radionuclides with K_{sp} values $<10^{-6}$ *M* and to a factor of two for K_d values of $>10^{-6}$ *M*. This decision is based on the literature.
- The distribution of K_d values with a mean >1000 mL/g will be log-normally distributed. Those with a K_d value <1000 mL/g will be assigned a normal distribution. This is based on statistical analysis of non-site-specific data.

3.1.7 Natural Resources

3.1.7.1 Geologic Resources

The only material of significance as a geologic resource in the vicinity of the SRS is kaolin clay. About 90 percent of the U. S. production of kaolin at one time came from a district in Georgia and South Carolina that includes Aiken County. Commercial deposits occur as lenses in the Lang Syne Formation along the Fall Line bordering the northwestern edge of the Coastal Plain (Bates 1969).

At E Area, the Lang Syne Formation is at a depth greater than 100 m from the ground surface, making commercial exploration unlikely due to the large amount of overburden that would have to be removed to exploit a deposit.

3.1.7.2 Water Resources

SCDHEC has been delegated authority by the EPA to implement and enforce the requirements of the Clean Water Act for the State of South Carolina. SCDHEC therefore is responsible for maintaining the chemical and biological integrity of all state waters, including those on federal reservations such as SRS. It does this by enforcing a system of water quality standards and by regulating all point-source discharges through the National Pollutant Discharge Elimination System (NPDES) program. SCDHEC is the principal regulatory authority for water quality issues on the SRS.

Surface Water

The Savannah River is the principal surface water system associated with the SRS. Five of its major tributaries (Upper Three Runs, Fourmile Branch, Pen Branch, Steel Creek, and Lower Three Runs) flow through and drain the SRS (Figure 3-3). The Savannah River serves as a domestic and industrial water source for the SRS and several downstream communities (the cities of Port Wentworth and Savannah in Georgia and Beaufort and Jasper counties in South Carolina). The intakes for these downstream water systems are located at river miles 29 and 39.2, respectively. In addition, the Vogtle Electric Generating Plant, located across the river from the SRS, uses the Savannah River for cooling water, withdrawing an average of 46 cfs. Table 3-9 characterizes Savannah River water quality both up- and downstream of the SRS. Table 3-10 characterizes water quality in SRS streams.

Groundwater

Within 20 miles of the SRS, there are more than 56 major municipal, industrial, or agricultural groundwater users that consume approximately 36 million gallons of water per day (DOE, 1997a). Total SRS groundwater (domestic and process water) use ranges from 9 to 12 million gallons per day (DOE, 1997a; Arnett and Mamatey 1996). At the SRS, only the deeper aquifers (Crouch Branch and McQueen Branch) are used as groundwater sources (Figure 3-10).

Under most of the SRS, the quality of groundwater is considered to be good. The pH for SRS groundwater ranges from 4.9 to 7.7 and the water is generally soft (DOE, 1997a). Concentrations of dissolved and suspended solids are low, but iron concentrations are elevated in some of the aquifers (DOE, 1995). At the SRS, approximately 5 to 10 percent of the shallow aquifer system has been contaminated with tritium, industrial solvents, metals, and other chemicals (Arnett et al., 1993).

Table 3-9. Water Quality in the Savannah River Upstream and Downstream from SRS (Calendar Year 2005)[a,b]

Parameter	Unit of measure[c]	MCL[d,e] or DCG[f]	Upstream		Downstream	
			Minimum	Maximum[g]	Minimum	Maximum
Aluminum	mg/L	0.05-0.2[h]	0.07	0.3	0.11	0.37
Cadmium	mg/L	0.005[d]	ND	0.001	ND	0.001
Chromium	mg/L	0.1[d]	ND	ND	ND	0.002
Copper	mg/L	1.3[l]	ND	0.004	ND	0.004
Dissolved oxygen	mg/L	>5.0[m]	6.3	11.6	5.5	10.8
Gross alpha radioactivity	pCi/L	15[d]	ND	2.15	ND	1.82
Lead	mg/L	0.015[l]	ND	0.002	ND	0.004
Mercury	mg/L	0.002[d,e]	ND	0.122	ND	0.119
Nickel	mg/L	NA	ND	0.003	ND	0.002
Nitrate (as N)	mg/L	10[d]	0.18	0.34	0.19	0.42
pH	pH units	6.5-8.5[h]	5.8	6.9	6.3	6.9
Phosphate	mg/L	NA	0.045	0.14	0.045	0.16
Suspended solids	mg/L	NA	3	7	1	14
Temperature	°F	90[p]	48.4	74.3	47.1	77.2
Tritium	pCi/L	20,000[d,e]	ND	332	139	1,380
Zinc	mg/L	5[h]	ND	0.064	ND	0.079

a. Source: Mamatey (2006).

b. Parameters are those DOE routinely measures as a regulatory requirement or as part of ongoing monitoring programs.

c. mg/L = milligrams per liter (mass per unit volume; pCi/L = picocuries per liter; a picocurie is a unit of radioactivity, and is one trillionth of a curie

d. MCL, EPA National Primary Drinking Water Standards (40 CFR Part 141, EPA, 2004).

e. MCL, SCDHEC State Primary Drinking Water Regulation (SCDHEC 2003).

f. DOE DCGs for water (DOE 1999g, Order 5400.5), based on committed effective dose of 100 mrem/yr for consistency with drinking water MCL of 4 mrem/yr.

g. Minimum concentrations of samples. The maximum listed concentration is the highest single result found during one sampling event.

h. Secondary Maximum Contaminant Level. EPA National Secondary Drinking Water Regulations (40 CFR Part 143, EPA, 2002a).

i. NA = none applicable.

j. Dependent upon pH and temperature.

k. ND = none detected.

l. Action level for lead and copper.

m. WQS = water quality standard.

n. Only fecal coliform bacteria exceedances are reported.

o. Less than (<) indicates concentration below lower limit of detection.

p. Shall not exceed weekly average of 90°F after mixing nor rise more than 5°F in 1 week unless appropriate temperature criterion mixing zone has been established.

Table 3-10. Water Quality in Selected SRS Streams

Sampling location	Temperature (°F)	pH	Dissolved oxygen (mg/L)	Total suspended solids (mg/L)
Fourmile Branch (downstream)				
Mean	19.2	7	9.2	2.8
Range	48-81	6.5-7.4	7.2-11.2	1-6
Upper Three Runs (downstream)				
Mean	18.4	6.8	8.9	4
Range	48-77	5.9-7.4	7.2-10.4	1-8

a. Mamatey (2006).

3.1.8 Natural Background Radiation

All human beings are exposed to sources of ionizing radiation that include naturally occurring and man-made sources. The average dose contribution estimates from various sources to individuals were obtained from the *Savannah River Environmental Report for 1996* (Arnett and Mamatey, 1997). On average, a person living in the CSRA receives an annual radiation dose of 359 mrem. The average dose contributions from the various radiation sources to individuals in the CSRA are given in Figure 3-16.

The major source of radiation exposure to an average member of the public in the CSRA is attributed to naturally occurring radiation. This naturally occurring radiation is often referred to as natural background radiation. Natural sources of radiation include cosmic radiation from outer space, cosmogenic radionuclides formed by interaction of cosmic radiation with elements in the earth's atmosphere, terrestrial radiation from natural radioactive materials in the ground, radiation from radionuclides occurring naturally in the body, and inhaled or ingested radionuclides of natural origin. The amount of exposure individuals receive depends on their location. The average annual dose to people in the U.S. from cosmic radiation is 27 mrem per year.

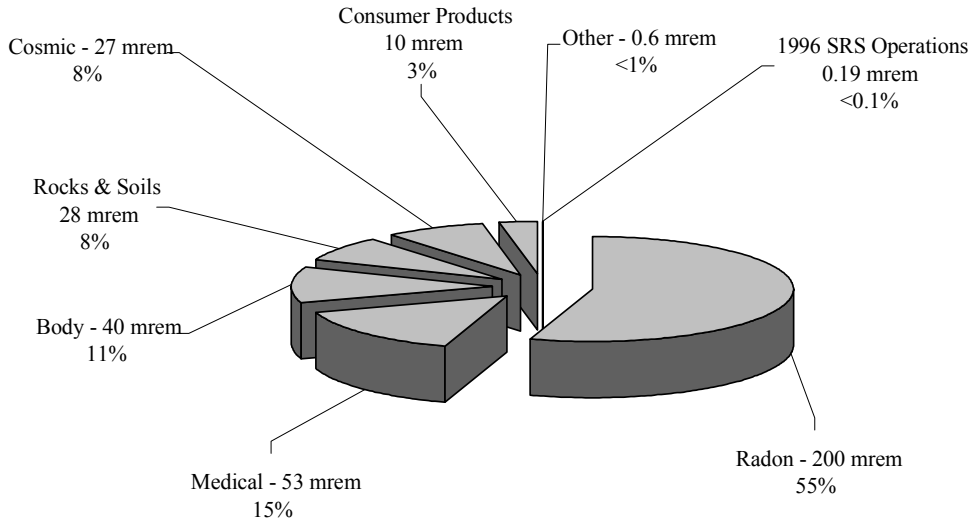

Figure 3-16. Major Sources of Radiation Exposure in the Vicinity of SRS

The major contributors to the annual EDE for internal radionuclides are the short-lived decay products of radon (mostly Rn-222), which contribute an average EDE of about 200 mrem per year. The average EDE from other internal radionuclides is about 40 mrem per year, which is predominantly attributed to the naturally occurring radioactive isotope of potassium, ^{40}K. A wide range of consumer products also contain sources of ionizing radiation. The U.S. average annual EDE to an individual from consumer products is about 10 mrem (Arnett and Mamatey, 1997). Radiation is an important tool of diagnostic medicine and cancer treatment. The average annual EDE to all individuals from all medical examinations, including diagnostic x-rays and nuclear medicine procedures, is 53 mrem.

3.2 PRINCIPAL FACILITY DESIGN FEATURES

A general description of the principal facility design features contributing to the long-term isolation of waste disposed in the E-Area LLWF is provided in this section. Some features of the disposal units themselves will serve to stabilize the wastes to limit release of radionuclides to the surrounding vadose zone. Their placement relative to the water table will also serve to limit transport of decaying radionuclides to a location where human exposures might occur as a result of ingestion of groundwater. The closure system will further minimize infiltration of water to the facility, and each unit, as well as provide a deterrent to potential inadvertent intruders (Phifer et al. 2006)

3.2.1 Characteristics of Disposal Units

The Slit Trenches are below-grade earthen disposal units which are approximately 20 feet deep, 20 feet wide, and 656 feet long. Ten to 14 feet of undisturbed soil separates each trench. A set of five Slit Trenches are grouped together, and eight groupings have currently been sited. Waste has been placed within all eight units (Figure 3-5). Low-level waste to be disposed of in the Slit Trenches contains, or will contain, soil, debris, rubble, wood, concrete, equipment, and job control waste. The waste may be disposed as bulk waste, or contained within B-25 boxes, B-12 boxes, 55-gallon drum, SeaLand containers, and other metal containers. Containerized waste and large equipment are typically placed in one end of the trench with a crane, and voids between adjacent containers and the trench wall are filled with either bulk waste or clean soil to minimize water collection prior to closure. Once a section of a Slit Trench is filled, clean soil is bulldozed over that section, which is then graded to provide drainage off and away from the disposal operation, which lessens infiltration during the operational period.

The Engineered Trenches are also below-grade earthen disposal units, which are approximately 650 to 656 feet long by 150 to 160 feet wide. Engineered Trench #1 varies in depth from 16 to 25 feet, and Engineered Trench #2 varies in depth from 14 to 23 feet. Low level waste contained within B-25 boxes, B-12 boxes, 55-gallon drums, SeaLand containers, components, and other metal containers are placed within the trenches. B-25 boxes, the predominant wasteform received, are stacked tightly within the trenches to minimize void space. A berm is constructed around the top where the local terrain slopes towards each trench, to minimize runoff into the trenches during operations. The bottom of each trench consists of compacted soil, a geotextile filter fabric, and approximately 6 inches of granite crusher run (from bottom to top), sloped to a sump (ET #1) or to a 24-inch steel pipe leading to a sump (ET #2). The sump sides and bottom are covered with concrete. The berm, permeable sloped base, steel pipe, and sump will work to minimize infiltration into the trenches, and movement of contaminants out of the base of the Engineered Trenches during the operational period.

The CIG disposal units are below-grade earthen trenches and contain grout-encapsulated waste components. Two CIG trench units are anticipated, each divided into five trenches separated by a nominal 10 feet of undisturbed soil. The unit footprint is 656 ft long by 157 ft wide. A typical cross-sectional cut (vertical and perpendicular to the trench length) through a section of a CIG trench is 20 ft by 20 ft. Waste components to be disposed in the CIG trench units consist of large radioactively-contaminated equipment and other smaller wasteforms such as B-25 boxes. Structural stability of the CIG trenches is ensured for a minimum of 300 years after disposal by filling components with grout or CLSM and by, for most trench segments, overlaying the contents with 20-inch steel-reinforced concrete mats, such that subsidence is not anticipated during that period of time (Phifer et al. 2006). This engineered aspect of the CIG units delays the increases of infiltration that would occur as a result of subsidence. Prior to subsidence of the CIG trenches, the encapsulating grout itself provides a barrier both to human intrusion, and limits infiltration of water.

The LAWV disposal unit is an above-grade reinforced concrete structure, which contains waste components in B-25 boxes, 55-gallon drums and other containers. It is approximately 643 feet long, 145 feet wide, and 27 feet high at the roof crest. The LAWV is divided into three modules, each containing four cells. The waste within the containers typically includes job control waste, and contaminated scrap metal, soil and rubble. During the operational period, water entrance into the LAWV is minimized through the sub-drainage system, doors on external personnel and forklift openings, the waterproof membrane roofing, and the gutter/downspout system. At the end of the operational period, reinforced concrete will be used to seal exterior vault openings, and those between modules, further minimizing water infiltration until failure of the roof slab, which is estimated to occur at 2,805 years. Inadvertent intrusion is prevented by the presence of the roof slab prior to structural failure.

The ILV disposal unit is a below-grade reinforced concrete structure, which contains grout-encapsulated waste components. It consists of two modules, which together encompass a 278.83-foot by 48.5-foot area. The existing vault is the only one anticipated to be needed. The ILT module, which is 26-foot deep, consists of two cells, one of which (Cell #1) will typically receive tritium crucibles. The ILNT module, which is 28-foot 5-inches deep, will consist of seven identical cells. Cell # 2 of the ILT and the seven ILNT cells will receive job control waste, scrap hardware, and contaminated soil and rubble, which are contained within metal or concrete containers. The ILV is used to dispose of waste containers for which radiological dose and radionuclide concentration limits would be exceeded if placed in more cost-effective LLW units (e.g., trenches or the LAWV). During the operational period, water entrance into the ILV is minimized through the sub-drainage system, the 30-inch thick waterproofed concrete walls, and the cell rain covers. At the end of the operational period, a permanent reinforced concrete roof slab will be placed on the vault, along with an overlying bonded-in-place fiberboard insulation and waterproof membrane roofing to further limit infiltration until structural failure of the roof, which is estimated to occur at 6,703 years. Inadvertent intrusion is prevented by the presence of the roof slab prior to structural failure.

The NRCDAs are two separate areas within E-Area which are used for disposal of reactor components from the U.S. Navy. The areas are above-grade gravel pads on which are placed waste shipping/disposal casks containing waste NR components. The 743-7E area, containing 41 casks, is approximately 0.3 acres, and the newer 643-26E area is approximately 1.4 acres, and has the capacity to receive 100 casks. Wastes within the casks consist of activated corrosion-resistant metal alloy, and auxiliary equipment primarily contaminated with activated corrosion products (crud) at low levels. The thickness of the steel outer containers varies depending on the wastes contained. For the more highly radioactive components (the activated corrosion-resistant metal alloy), the cask thickness is approximately one foot, with welds at least four inches in thickness. The auxiliary equipment requiring less shielding is contained within thinner-walled casks.

The NR casks are considered air and water tight for 750 years, at which time the welds are assumed to corrode to allow infiltration of water from the surrounding vadose zone, and release of volatile radionuclides to the air in the surrounding pore spaces. It is not anticipated that loss of cask structural stability at 8,000 years after placement on the pad will result in significant subsidence due to the limited porosity within the casks.

3.2.2 Depth to Water Table

The distance between the bottom of each disposal unit and the water table influences the ultimate flux at the water table for radionuclides that decay significantly relative to their travel time, and thus the concentration of these radionuclides at the point of compliance. Table 3-11 indicates the minimum distance to the water table for each of the E-Area LLWF disposal units, based on long-term average water table data and average disposal unit elevations.

Table 3-11. Minimum Depth to Water Table from Bottom of E-Area LLWF Disposal Units

E-Area LLWF Disposal Unit Type	Minimum Depth to Water Table
Engineered and Slit Trenches	25 ft
CIG Trenches	35 ft
LAWV	40.5 ft
ILV	29.5 ft
NRCDA	54 ft

3.2.3 Closure System

E-Area LLWF closure will be conducted in three phases: operational closure, interim closure, and final closure (Phifer et al. 2006). Operational closure will be conducted during operations as disposal units are filled; interim closure will be conducted after disposal operations have ceased; and final closure will occur at the end of the 100-year institutional control period. Both operational and interim closures are specific to each type of disposal unit. Table 3-12 summarizes the operational and interim closure aspects for the disposal unit types. No interim closure actions are anticipated beyond that of operational closure during the 100-year institutional control period for the LAWV, ILV and NRCDAs, other than monitoring and maintenance activities. Operational closure for each of these unit types is such that infiltration through the waste is already minimized to the extent practicable.

At the end of the institutional control period (100 years after cessation of operations), subsidence treatment will be performed on the Engineered Trenches and most of the Slit Trenches, to minimize the subsidence potential caused by the corrosion of B-25 boxes, or similarly corroding structural support, within the wasteforms in these trenches. Also at this time, the void space between the casks in the NRCDAs must be appropriately filled with a structurally suitable material to support the closure cap, and thus not produce differential subsidence.

Table 3-12. Operational and Interim Closure of E-Area LLWR Disposal Units[a]

Disposal Unit Type	Operational Closure	Interim Closure
Engineered/Slit Trenches	Cover with a minimum 4 ft clean soil cover graded to provide positive drainage off the trench and vegetative cover of shallow-rooted grasses	Installation of interim runoff cover to be maintained until placement of final cover
CIG Trenches	Encapsulation of components with grout and cover with a minimum 4 ft clean soil cover graded to provide positive drainage off the trench or a 4-foot combination layer of CLSM, reinforced concrete mat and soil; interim cover for each emplaced segment, with up to 2 feet of soil, graded to promote drainage, with surface application of HDPE geomembrane or geotextile fabric	Installation of interim runoff cover to be maintained during 100-year institutional control period
LAWV	Fill interior collection trench and exterior sump with grout and seal exterior vault openings with reinforced concrete	None anticipated beyond that of operational closure
ILV	·Vault: grout encapsulation of containers ·Silos: final grout layer , with silo plug remaining in place ·placement of permanent reinforced concrete roof slab with overlying fiberboard insulation and waterproof membrane roofing	None anticipated beyond that of operational closure
NRCDA	Placement of casks on gravel pad	None anticipated beyond that of operational closure

[a] From Cook et al. 2004

Final closure of the entire E-Area LLWF will consist of the installation of an integrated closure system designed to minimize water infiltration through the waste and to provide an intruder deterrent. The system will consist of one or more closure caps installed over all the disposal units, and a drainage system (Phifer et al. 2006). The closure system will be essentially the same for each disposal unit, and is intended to minimize infiltration during the post- institutional control period and provide an intruder deterrent. Because final closure of the E-Area LLWF will not occur until 100 years after operations cease, a detailed closure design has not been fully developed, but rather a closure concept has been developed. Table 3-13 indicates the closure cap layers and minimum thickness presently conceived.

In this PA, it is assumed that the hydraulic properties of the conceptual closure cap will immediately begin to degrade after construction due to the effects of pine forest succession, reduction in the effectiveness of the drainage layer due to colloidal clay migration into it, and erosion. Subsidence caused by structural failures of the wasteforms is considered to affect the integrity of the final closure cap.

Table 3-13. Closure Cap layers from Top to Bottom (Phifer et al. 2006)

Layer	Minimum Layer Thickness (inches)
Topsoil	6
Upper Backfill	30
Erosion Barrier	12
Geotextile Filter Fabric	~0.1
Middle Backfill	12
Geotextile Filter Fabric	~0.1
Drainage layer	12
Geosynthetic Clay Liner	~0.2
Lower Backfill	24 (CIG and ILV) or 40 (LAWV, NRCDA, Engineered/ Slit Trenches)

4.0 ANALYSIS OF PERFORMANCE

4.1 SOURCE TERM MODELS AND RADIONUCLIDE SCREENING

4.1.1 Source Term Models

The computer codes used in evaluating release of radionuclides from the E-Area LLWF disposal units to either groundwater or air are introduced in this section. Detailed descriptions of the mathematical models and solution methods applied in these codes are contained in the code manuals, which are cited in the following discussion. Site-specific details involved in applying these models to each unit type are discussed in the respective disposal unit chapters (Chapters 1 through 5 in Part B of this PA). The general conceptual approach in modeling source terms is described here.

Radionuclides may be released from the E-Area LLWF disposal units to the surrounding vadose zone as a result of leaching from the wasteform as water infiltrates, or as a result of diffusion of volatile radionuclides through unsaturated voids in the wasteforms. The availability of radionuclides for release is a function of their sorption, solubility, complexation, and diffusion properties. These properties are influenced by the environmental conditions the radionuclides encounter as they move from their initial location in the waste, through the vadose zone, to the interface at the water table or ground surface.

As discussed in Section 3.2, disposal units have been designed to limit release, largely by limiting infiltration of water into the waste zones. Releases from each type of disposal unit are modeled according to the disposal unit materials initially present, the cover system materials specific to each unit, and the condition of these materials through time.

4.1.1.1 Infiltration Modeling

Water infiltration rates through the various cover systems used for the E-Area LLWF disposal units (Section 3.2) are estimated in this PA with the HELP model (Schroeder et al. 1994a, 1994b). The HELP model is a quasi-two-dimensional water balance model, designed to conduct landfill water balance analyses, requiring the input of weather, soil, and design data. It is sanctioned by the EPA for its designed purpose, and verified with data from physical models and the field (WSRC 2007). It provides estimates of runoff, evapotranspiration, lateral drainage, vertical percolation (infiltration), hydraulic head, and water storage for the evaluation of various landfill designs.

Within the PA the HELP Model is used to estimate an average annual infiltration through the geosynthetic clay layer (GCL) of the E-Area closure cap. This average annual infiltration, at each time step modeled, forms the upper boundary condition for a 2-dimensional, steady-state, PORFLOW vadose zone flow model. The PORFLOW vadose zone flow model, which solves Richard's equation utilizing characteristic curves to solve variably saturated flow within the vadose zone, is then used to estimate flow through the waste and vadose zone to the water table.

Numerous water balance and infiltration studies have been conducted in and around the SRS by various organizations including the Savannah River Laboratory, the USGS, the State University of New York at Brockport, Pennsylvania State University, the University of Arizona, and the Desert Research Institute (Phifer et al. 2007). These studies included both field and modeling studies, and ranged in scale from 55-gallon drum lysimeters to entire watersheds.

The USGS (Cahill 1982) conducted a study at the Barnwell Low-Level Radioactive Waste Disposal Facility "to determine the geologic and hydrologic conditions near the burial site and to measure migration of leachates from buried waste into the surrounding unconsolidated sediments." This Barnwell Facility is located immediately to the east of the SRS. The USGS conducted another study at the Barnwell Low-Level Radioactive Waste Disposal Facility "of water movement in and adjacent to trenches excavated in the unsaturated zone and assesses the principal factors affecting this movement" (Dennehy and McMahon 1989). The State University of New York at Brockport in conjunction with the Savannah River Laboratory (Hubbard and Emslie 1984) conducted a water budget evaluation for the Savannah River Plant ORWBG, and provided an updated ORWBG water balance based on information obtained from the Defense Waste Lysimeter study (Hubbard 1986). Pennsylvania State University researchers (Parizek and Root 1986) conducted a hydrologic water budget study of the McQueen Branch watershed, located in the central portion of the SRS as part of the development of a groundwater model. The State University of New York at Brockport in conjunction with the University of Arizona (Hubbard and Englehardt 1987) utilized the Chemicals, Runoff, and Erosion from Agricultural Management Systems (CREAMS) model to produce estimated annual water balances for the SRP Burial Ground utilizing site specific weather data from 1961 to 1986.

Finally, the Desert Research Institute conducted both deterministic and probabilistic (100 Monte Carlo runs) modeling utilizing the computer code HYDRUS 2-D (finite difference model solving Richard's equation) to estimate infiltration at E-Area (Young and Pohlmann 2001). A refinement of this modeling effort was performed in 2003, to incorporate more site-specific data (Young and Pohlmann 2003). The nominal water balance and infiltration estimates arising out of these eight studies are provided in Table G-3 of Appendix G. Infiltration is seen to range from 9 to 16 in/yr with a median of the eight studies nominal values of 14.8 in/yr, or approximately 1/3 of the yearly rainfall of approximately 48 inches.

The HELP model was used in this PA to generate water infiltration estimates during operations, during the institutional control period, and after final closure, for intact and degraded states of the closure systems. The HELP model results for uncapped Slit Trenches 1 and 2, under current conditions (i.e., without topsoil, Flach et al. 2005), compare favorably with those modeled by Young and Pohlmann (2001, 2003) for E-Area trenches. The Flach et al. infiltration estimate was 11.3 in/yr, while the Young and Pohlmann estimates ranged from 9.1 and 11.7 in/yr. The Flach et al. (2005) estimate for trenches covered with a 4-ft operational soil cover and topsoil was 14.8 in/yr, which is comparable to the average infiltration estimated for various regions of the SRS and immediately adjacent, as derived from the eight studies discussed earlier.

The HELP model was also used to estimate infiltration for the scenario when the cap was fully degraded, but no subsidence had occurred, resulting in an estimated infiltration of 14.09 in/yr (Phifer et al. 2006, Table 8-7). This again is comparable to the average infiltration estimated for various regions of the SRS and immediately adjacent. Furthermore, in a study of closure cap configurations for the F-Area Tank Farm at the SRS (Phifer et al. 2007), the HELP model predicted infiltration on the order of 16.45 in/yr for a soil-only closure cap, which should be comparable, and is only slightly greater than, the infiltration estimates arising from the eight background studies. This last finding suggests the HELP model may somewhat overestimate infiltration, and thus lend conservatism to the PA results. This is consistent with findings of the National Research Council of the National Academies (NRC-NA 2007), in their study on waste barrier performance (see Phifer et al. 2007). Thus, the HELP model appears to produce reasonable and acceptable results for use in this PA.

Phifer et al. (2006) summarizes the results of the infiltration analyses for the E-Area LLWF disposal units in Tables 8-1 through 8-7 of that document, and provides references to the detailed HELP code analyses supporting these results. Infiltration estimates take into account time periods and assumed condition of the various disposal units (e.g. operational, institutional control, after closure, after subsidence, after roof collapse). Table 4-1 summarizes the references containing the HELP code parameter definitions for each condition modeled.

Table 4-1. References containing HELP model input parameter specifications for ELLWF disposal units [a]

ELLWF Disposal Unit Type	Infiltration Conditions Evaluated with HELP Code	References
Slit and Engineered Trenches	With no subsidence	Flach et al. 2005, Phifer 2003, Phifer 2004a
	With subsidence	Hang et al. 2005, Swingle and Phifer 2006
CIG Trenches	With no subsidence	Phifer and Jones 2006, Phifer 2004
	With subsidence	Hang et al. 2005
LAW Vault	Prior to vault roof collapse	Jones and Phifer 2006
IL Vault	Prior to vault roof collapse	Jones and Phifer 2006
NRCDAs	After casks fail[b]	Phifer 2003, Phifer 2004a

[a] From Phifer et al. (2006)
[b] Used infiltration analyses results for Slit and Engineered Trenches, for the condition of no subsidence

4.1.1.2 Conceptual Source Term Release Models

Once infiltrating water contacts the top of the waste disposal unit, infiltration through the containment features (concrete vaults, encapsulating concrete, casks, or clean soil covers) and transport of water and radionuclides through the waste zone and ultimately through the vadose zone is evaluated with a 2-dimensional application of the PORFLOW numerical model (ACRI 2004).

PORFLOW is a commercial computational fluid dynamics tool developed by Analytic & Computational Research, Inc. to numerically solve problems involving transient or steady state fluid flow, heat, salinity and mass transport in multi-phase, variably saturated, porous or fractured media with dynamic phase change. PORFLOW is capable of simulating first-order decay and progeny in-growth associated with radionuclide chains, and accommodates alternate fluid and media property relations and complex and arbitrary boundary conditions. Core software functions have been verified through vendor and SRNL QA testing, and SRS personnel are experienced in applying PORFLOW to performance assessments. Comparison of data derived from the VZMS in E-Area with PORFLOW vadose zone modeling results has been done, and is ongoing, showing reasonable agreement (see Appendix G).

In using PORFLOW to estimate flow of water and transport of radionuclides through the disposal unit and the surrounding vadose zone to the water table, a number of model parameters were quantified regarding the properties of the concrete, waste materials, and vadose zone that not only affect flow, but also affect the mobility of the radionuclides present. For those affecting flow, Phifer et al. (2006) provide a complete listing of, and justification for, the values of the hydraulic properties selected for the PORFLOW applications in this PA. Specifically, porosity, bulk density, particle density, saturated hydraulic conductivity, saturated intrinsic permeability, moisture characteristic curves, and saturated effective diffusivity are the properties quantified for cementitious materials, the waste zones in the different disposal units, and the soils (undisturbed vadose zone, compacted backfill, soil cover, and permeable backfill and gravel). A representation of the uncertainty associated with each parameter, with the exception of the characteristic curves, is also provided by Phifer et al. (2006).

Although the vadose and saturated zones exhibit similar physical heterogeneity, the effective porosity assumed for both zones differ (see also Section 4.3.1), because of markedly different flow conditions (Phifer et al. 2006). Vadose zone flow is predominantly perpendicular to strata, rather than parallel to layering in the aquifer. Also, unsaturated conditions in the vadose zone significantly reduce the permeability contrast between coarse- and fine-grained materials, in comparison to saturated conditions in the aquifer. For the vadose zone, the effective porosity is assumed to be equal to the total porosity. An analysis of anisotropy and the estimated effects on effective porosity is provided in Phifer et al. (2006), providing justification for the assumed equality of effective and total porosity in the vadose zone modeling.

For model parameters associated with mobility of radionuclides with respect to the water phase, Kaplan (2006) provides a listing of appropriate sorption coefficients (K_ds) to use for the various materials present in the vadose zone/ waste zone modeling domain, as well as solubility limits and K_d correction factors to account for the influence of CDPs on radionuclide migration. Best estimate values of K_ds were assumed in the base case analyses for all disposal units. The uncertainty in K_d was addressed using the parametric ranges and distributions calculated by Shine (2007) based on Kaplan and Millings (2006). For disposal units evaluated using stochastic modeling techniques, the distributions from appendices B, C, and/or D in Shine (2007) were sampled for the realizations produced in our probabilistic uncertainty analyses. For those disposal units subjected to sensitivity analysis, the -1.96 sigma values for each element from these distributions were implemented simultaneously as a sensitivity case to evaluate the effect of uncertainty in this parameter.

The conceptual source term models for the types of disposal units addressed in this PA consider both generic wasteforms (containing radionuclides identified on basis of screening analyses, Section 4.1.2.1) and special wasteforms (containing radionuclides associated with specific waste streams) for the groundwater analyses. Table 4-2 lists the number of radionuclides associated with generic and special wasteforms for each of the disposal unit types.

Special wasteform radionuclides have been referred to throughout the text, tables, and figures in the PA in either shorthand notation or using a more descriptive term (e.g., I-129_C; I-129 associated with ETF activated carbon). Table 4-2 provides a reference to the sections in the PA chapters where special wasteforms are discussed.

Table 4-2. Numbers of radionuclides analyzed for ELLWF disposal units, based on classification as associated with "generic" or "special" wasteforms

Disposal Unit Type	Number of Generic Wasteform Radionuclides Analyzed	Number of Special Wasteform Radionuclides Analyzed	Section Where Special Wasteforms Are Discussed
Slit and Engineered Trenches	38	20	1.6.3.3
CIG Trench	35	5	2.6.6
LAW Vault	35	2	3.6.4.5
IL Vault	35	5	4.6.3.4
NRCDA	--[a]	--[a]	5.6.4.4

[a] The radionuclides analyzed for the NRCDA groundwater pathway are not given a special wasteform designation. However, due to the robust containers and nature of the waste, the behavior of the radionuclides is different than the generic radionuclides in other disposal units.

For radionuclides associated with generic wasteforms, the release mechanisms are assumed to be instantaneous within the waste zone, and the K_d values are taken from Kaplan (2006). For special wasteform radionuclides, the release may or may not be assumed to be instantaneous, and K_d values may differ from those in Kaplan (2006) to account for the presence of ion-exchange resins in the wasteform, rate-limiting processes such as diffusion, dissolution, and/or corrosion.

The conceptual source term release models also address planned (e.g., closure-activity related) and unplanned (e.g., corrosion-driven) structural and chemical changes in the units that are likely to occur over time. Most of the structural changes are addressed through modeling step-wise changes in infiltration into the waste zone and hydraulic properties of cover and waste zone materials over time. However, as waste material degradation occurs, the sorption environment changes, which is addressed by selecting K_ds appropriate for each state of degradation. For example, the CDP material in the Slit and Engineered Trenches waste zone is assumed to gradually to leach away, such that the K_ds change with time. The CIG trenches are assumed to gradually become more soil-like as the grout degrades, such that soil K_ds are more appropriate in later simulation times, while grout K_ds are more appropriate in earlier times. For the LAW and IL Vaults, K_ds in concrete are assumed to change over time, as concrete degrades from young to very aged material.

A one-dimensional application of PORFLOW was used to simulate the upward diffusion of volatile radionuclides, including radon, from the waste zones to the ground surface. With the exception of radon, the conceptual model for volatile species assumes that the entire inventory of each volatile radionuclide in each disposal unit is initially present in the void space; thus ignoring the fraction that would be dissolved in the water phase within the pores. For the air pathway, fifteen radionuclides of potential concern were identified (see Section 4.1.2.2) and assessed for each disposal unit type.

Air diffusion was the only transport mechanism simulated in the model applications, because the advective air transport resulting from fluctuations in atmospheric pressure at the land surface are expected to have a zero net effect over long periods of time, and diffusion in water in partially-saturated pore spaces is relatively insignificant.. Materials within the vadose zone for each disposal unit (i.e., cementitious, soil, waste) were assigned values of particle density, total porosity, average saturation, air-filled porosity, air density and effective air-diffusion coefficient for each volatile radioactive element or compound assessed. (Tortuosity was assigned a value of unity due to the specification of an effective air-diffusion coefficient, and thus was not a variable in the simulations.) Values of particle density, total porosity and average saturation were taken from Phifer et al. (2006) for materials within the vadose zone/waste zones. A relationship between moisture saturation and the effective air diffusion coefficient for radon, established by Nielson et al. (1984) formed the basis for estimating effective diffusion coefficients for volatile radionuclides, using Graham's Law to relate the diffusion coefficient to the molecular weight of the compound or element of interest. An air fluid density of 1.24×10^3 g/m^3 was used (Bolz and Tuve 1973).

For the radon flux analyses, generation of Rn-222 is considered for the different parent radionuclides and decay chains which lead to its formation. The short half-life of Rn-220 (55.6 seconds) makes it unlikely to escape the disposal units and migrate to the land surface via air diffusion before it is transformed by radioactive decay. Rn-222 generated within the waste zone is assumed to diffuse outward from this zone into the air-filled soil pores surrounding the disposal units.

However, only a fraction of the Rn-222 generated by the decay of each parent is available for migration away from its source since the parent radionuclides exists as oxides or in other crystalline forms. The fraction of radon escaping its source and migrating into adjacent pore space is approximated by the use of a radon emanation coefficient, which is typically on the order of 0.25 (Yu et al. 2001).

The results of the two-dimensional application of PORFLOW for downward migration of waterborne radionuclides in the vadose zone, and of the one-dimension application for upward migration of volatile radionuclides within the vadose zone are expressed in terms of annual flux at either the water table or ground surface, respectively. These results are subsequently used in evaluating radionuclide concentrations in groundwater and doses to individuals due to concentrations in air or groundwater.

4.1.2 Radionuclide Screening

Before the models described above were applied for calculating releases from the E-Area LLWF disposal units, simplistic, yet conservative, screening models were implemented to identify radionuclides of potential significance with respect to the groundwater and air-pathway performance objectives. NCRP Report No. 123, Volumes 1 and 2, on screening models for releases to atmosphere, surface water and ground (NCRP 1996) forms the basis of the screening models, with adaptations where deemed necessary.

The NCRP methodology starts with 826 radionuclides (Appendix E), which are selected from among the approximately 2,800 known radioactive isotopes on the basis of their half life being long enough to be potentially significant to radiological protection of the public (Cook and Wilhite 2004). The screening analyses limit the number of radionuclides of potential significance by considering only those radionuclides that, under bounding conditions, would contribute greater than or equal to one percent of dose or concentration limits specified in applicable performance objectives for air and groundwater, not considering contributions of other radionuclides. For groundwater, this assumes the 4 mrem/yr limit for beta and photon emitters applies to all radionuclides.

4.1.2.1 Groundwater Screening

Cook and Wilhite (2004) provide a discussion of how the NCRP screening methodology for groundwater was applied for the E-Area LLWF. For the groundwater pathway, the NCRP approach in developing screening factors, which relate the dose received to the activity of each radionuclide in subsurface waste, was adapted to better represent the conditions at the SRS and at the E-Area LLWF. The rigorous application of the NCRP methodology to include radioactive progeny was automated by Taylor and Collard (2005). Conservatively assuming an initial inventory of each parent radionuclide of 10 million Ci, the dose is then calculated using the screening factor and compared to a performance criterion of 0.04 mrem/yr. This criterion represents 1% of the performance measure for beta and photon emitters in groundwater, which is 4 mrem/yr (EPA, 2000).

The Screening Factor for ingestion of groundwater, according to the NCRP methodology, (as expressed by Taylor and Collard, 2005) is given by

$$SF_{GW} = \lambda_L A_0 \frac{U_{DW}}{V} \sum_{i=1}^{n} X_i \left(DF_{ing}\right)_i$$

where

SF_{GW} = screening factor (Sv/Bq-yr)
λ_L = parent leach rate (yr^{-1})
A_0 = $e^{-\left(\lambda_o^r RT_{travel}\right)}$ = fraction of parent decayed during transport (dimensionless)
T_{travel} = time for radionuclide to travel to water table (yr)
R = retardation factor
U_{DW} = water consumption (L/yr)
V = volume dilution rate (L/yr)
DF_{ing} = ingestion dose factor (Sv/Bq)
X_i = average progeny fraction term for n progeny

The term X_i is calculated from

$$X_i = \frac{1}{T_{av}} \left[\prod_{j=1}^{k} \lambda_i^r f_j \right] \sum_{h=0}^{n} \frac{e^{-\lambda_n^r t_{delay}} \left(1 - e^{-\lambda_n^r T_{av}}\right)}{\lambda_n^r \prod_{p=0}^{k} \left(\lambda_p^r - \lambda_h^r\right)} \qquad \text{for } p \neq h$$

where

λ^r = radioactive decay constant (yr^{-1})
f_j = decay (or branching) fraction for daughter j, (unitless)
T_{av} = averaging time, typically 1 year
t_{delay} = delay time in release of parent radionuclide (yr)
subscript i = ith daughter, 0 = parent, p and h = progeny indices, and n = number of progeny.

The K_ds recommended in the documentation of the NCRP screening methodology (NCRP 1996) are used in calculating screening factors. The effect of CDP on K_ds is not accounted for in the screening. However, since the nature of the screening methodology is conservative (NCRP 1996), the variability due to the presence of CDP in certain wasteforms will not affect the results in terms of identification of radionuclides of potential significance.

For the E-Area LLWF application, no credit was taken for the delay of infiltration of water into the waste, the volume dilution rate was assumed to be 44 m^3/yr (corresponding to the smallest areal footprint of a disposal unit, to limit dilution), the waste thickness was assumed to be 0.75 m (similar to the thickness of an Engineered Trench after compaction), and a water consumption rate of 730 L/yr (Cook and Wilhite 2004).

Implementation of the automated screening method reduced the number of radionuclides requiring detailed analysis of the groundwater pathway from 826 to 86 (Taylor and Collard 2005). In other words, the remaining 740 radionuclides were calculated to contribute less than 1% of the performance criterion of 4 mrem/yr (EPA 2000), even under very conservative conditions.

The automated groundwater screening also allows calculation of "Trigger Values", or the Curie quantity that would give a dose of $1/100^{th}$ of the performance criterion, defined here to be 4 mrem. Thus, the Trigger Value is the Ci quantity of each parent radionuclide, taking into account potential dose contributions from radioactive progeny that would produce 0.04 mrem/yr EDE. These Trigger Values were used as a second level of screening in the screening analysis to further reduce the list of 86 radionuclides to include only those for which the total disposed inventory in all E-Area disposal units exceeds the Trigger Value (Cook 2007). The list of 86 radionuclides was further trimmed to the 35 parent radionuclides addressed in the groundwater transport calculations (Table 4-3).

For the 51 radionuclides that passed the second level of screening (i.e., their disposal limit did not exceed the Trigger Value based on their total E-Area inventory), referred to by footnote "c" in Table 4-3, disposal limits were set based on the screening analysis. The disposal limits assigned to these radionuclides are the Trigger Values, which are the inventories corresponding to a dose of 0.04 mrem/yr, and are shown in Table 4-4. The Trigger Values in Table 4-4, when used as disposal limits, are thus very conservative. Disposal limits can be reevaluated by a Special Analysis if necessary based on future inventory estimates.

Table 4-3. Groundwater Screening Results

Radionuclides remaining after NCRP screening[a]	Radionuclides remaining after inventory consideration[b]	Radionuclides remaining after NCRP screening[a]	Radionuclides remaining after inventory consideration[b]	Radionuclides remaining after NCRP screening[a]	Radionuclides remaining after inventory consideration[b]
Ag-108m	c	H-3	H-3	Pu-244	Pu-244
Al-26	c	Hf-182	c	Ra-226	Ra-226
Am-237	c	Hg-194	c	Rb-87	c
Am-241	Am-241	Ho-166m	c	Re-186m	c
Am-243	Am-243	I-129	I-129	Re-187	c
B3-10	c	In-115	c	Ru-97	c
Bi-210m	c	Ir-192m	c	Se-79	Se-79
Bk-247	c	K-40	K-40	Si-32	c
Bk-249	c	La-137	c	Sm-246	c
C-14	C-14	La-138	c	Sm-247	c
Ca-41	c	Lu-176	c	Sn-126	Sn-126
Cd-113	c	Mn-53	c	Sr-90	Sr-90
Cf-249	c	Mo-93	Mo-93	Ta-280	c
Cf-251	c	Nb-94	Nb-94	Tc-97	c
Cf-252	c	Ni-59	Ni-59	Tc-98	c
Cl-36	Cl-36	Np-236a	c	Tc-99	Tc-99
Cm-241	c	Np-237	Np-237	Te-123	c
Cm-242	c	Pa-230	c	Th-229	c
Cm-244	Cm-244	Pa-231	c	Th-230	Th-230
Cm-245	Cm-245	Pb-202	c	Th-232	Th-232
Cm-246	c	Pb-205	c	Ti-44	c
Cm-247	Cm-247	Pd-107	Pd-107	U-233	U-233
Cm-248	Cm-248	Pt-193	c	U-234	U-234
Cm-250	c	Pu-237	c	U-235	U-235
Cs-136	c	Pu-238	Pu-238	U-236	U-236
Es-253	c	Pu-239	Pu-239	U-238	U-238
Fe-60	c	Pu-240	Pu-240	V-49	c
Gd-152	c	Pu-241	Pu-241	Zr-93	Zr-93
Ge-68	c	Pu-242	Pu-242		

a From Taylor and Collard, 2005.
b From Cook, 2007.
c Total E-Area inventory of the radionuclide does not exceed Trigger Value calculated by Taylor and Collard (2005).

Table 4-4. Trigger Values for the Groundwater Pathway Derived from Screening Analysis

Radionuclide	Trigger Values (Ci)	Radionuclide	Trigger Values (Ci)	Radionuclide	Trigger Values (Ci)
Ag-108m	1.37E+02	Es-253	3.28E+02	Pb-205	1.47E-02
Al-26	8.03E-07	Fe-60	1.12E-04	Pt-193	4.69E+06
Am-237	2.36E+03	Gd-152	1.71E-04	Pu-237	2.63E+00
Be-10	2.64E-03	Ge-68	1.04E+17	Rb-87	8.02E-04
Bi-210m	1.24E-04	Hf-182	6.46E-04	Re-186m	1.04E-04
Bk-247	9.81E-03	Hg-194	2.40E-05	Re-187	4.43E-02
Bk-249	2.09E+01	Ho-166m	6.60E-02	Ru-97	4.74E+04
Ca-41	3.65E-04	In-115	2.25E-04	Si-32	2.98E-03
Cd-113	6.09E-05	Ir-192m	3.62E+00	Sm-146	1.33E-04
Cf-249[a]	5.22E-02	La-137	2.52E-01	Sm-147	1.46E-04
Cf-251[a]	2.53E-01	La-138	1.47E-02	Ta-180	3.50E-03
Cf-252	5.65E+00	Lu-176	7.86E-04	Tc-97	1.44E-04
Cm-241	4.55E+00	Mn-53	2.99E-02	Tc-98	5.74E-06
Cm-242	3.09E+02	Np-236a	4.17E-07	Te-123	4.08E-03
Cm-246[a]	6.25E-03	Pa-230	2.45E+03	Th-229	2.39E-01
Cm-250	9.13E-02	Pa-231	9.72E-06	Ti-44	5.47E-07
Cs-135	3.23E-03	Pb-202	5.82E-04	V-49	7.42E-03

[a] Cf-249, Cf-251, and Cm-246 were subjected to a detailed groundwater transport analysis for the Slit Trenches and Engineered Trenches; thus, the Trigger Values only apply to the other disposal units.

4.1.2.2 Atmospheric (Air) Pathway Screening

An atmospheric screening process developed and applied previously to Saltstone Disposal Facility Vault 4 (Crapse and Cook 2004) has been used to determine a list of radionuclides requiring detailed analysis to derive disposal limits for the E-Area LLWF based on the atmospheric pathway (Crapse and Cook 2006). This sequential screening process uses a methodology developed by the NCRP, professional judgment and process knowledge. Trigger values specific to the E-Area LLWF have been developed for radionuclides of potential interest to the atmospheric pathway. Using this atmospheric screening process, fifteen radionuclides have been determined to require detailed analysis. A more detailed description of this analysis follows.

The NCRP has published a report that described a methodology to screen out, or remove from further consideration, radionuclides for detailed analysis in a performance assessment (NCRP 1996). The NCRP provides a screening methodology, which uses some conservative assumptions, a few facility-specific parameters and an estimated inventory to produce a dose estimate for each radionuclide. If the estimated dose exceeds the dose criteria, then that radionuclide must undergo further analysis.

This process was implemented for the E-Area LLWF by conservatively assuming an inventory of 10,000,000 curies for each radionuclide and a dose criterion of 0.1 mrem/year. Additionally, the entire E-Area LLWF inventory was assumed to be contained within a single disposal unit. The dimensions of the disposal unit were assumed to be the unit with the smallest footprint, the ILV. When the process was applied, 10 of the 826 radionuclides considered were removed from further consideration – Ar-37, At-215, Fr-219, Hf-174, Kr-81m, Ne-19, Po-212, Po-213, Po-214, and Rn-218. The screening factors and doses are reported separately (Crapse and Cook 2006).

In order to further reduce the number of radionuclides to be considered in the detailed analysis, some fundamental principles of physics and chemistry were applied. The performance assessment only considers times after final facility closure. Once the disposal units are filled and capped, there are only two possible ways for radionuclides to be released to the atmosphere. One is by particulates produced by intrusion, which will be considered separately in the performance assessment, and the other is by release as a gas. The list of elements comprising the remaining 816 radionuclides was examined to identify those which have the potential to form a vapor phase in the disposal units. This produced the following elements: Ar, As, At, Br, C, Cl, F, Ge, H, Hg, I, Kr, N, O, P, S, Sb, Se, Sn, and Xe. Radon was not considered further because it is treated separately in the performance assessment process (DOE, 1999a). Excluding the radionuclides removed from consideration by the NCRP screening step, these elements have a total of 139 individual radionuclides. Trigger values were calculated from the screening results for these 139 remaining radionuclides using the methodology developed for E-Area (Cook and Wilhite 2004).

The current inventory for the E-Area LLWF was determined using the WITS database. Of the 139 radionuclides that could exist in the gas phase, 15 are in the inventory at levels above the calculated trigger value: C-14, Cl-36, H-3, I-129, S-35, Sb-124, Sb-125, Se-75, Se-79, Sn-113, Sn-119m, Sn-121, Sn-121m, Sn-123, and Sn-126. A detailed analysis of the atmospheric pathway for these radionuclides will be performed.

Trigger values for the remaining 124 radionuclides are reported in (Crapse and Cook 2006), and reproduced in Table 4-5. If any of the 124 other radionuclides do appear in the waste stream, the quantity can be compared to the Trigger Value. If the estimated total inventory is less than the Trigger Value, then no further analysis is needed. If the estimated total inventory exceeds the Trigger Value, a Special Analysis will be conducted.

In summary, fifteen radionuclides have been determined to require detailed analysis for the E-Area LLWF atmospheric pathway. Trigger values have been developed for other radionuclides of potential interest to the E-Area LLWF atmospheric pathway.

Table 4-5. Trigger Values for the Air Pathway Derived from Screening Analysis

Radionuclide	Trigger Values (Ci)	Radionuclide	Trigger Values (Ci)	Radionuclide	Trigger Values (Ci)
Ar-37	7.8E+06	Hg-195m	1.9E-01	Sb-120a	7.0E+01
Ar-41	8.9E+00	Hg-197	3.6E-01	Sb-120b	1.8E-03
As-69	7.4E+00	Hg-197m	4.4E-01	Sb-122	1.4E-02
As-70	1.3E+00	Hg-199m	2.4E+01	Sb-124m	1.3E+02
As-71	1.2E-01	Hg-203	7.4E-03	Sb-124n	8.3E+00
As-72	1.1E-01	I-120	1.3E+00	Sb-126	6.3E-03
As-73	4.3E-02	I-120m	9.5E-01	Sb-126m	5.1E+00
As-74	9.5E-03	I-121	2.6E+00	Sb-127	3.6E-02
As-76	2.1E-01	I-122	4.0E+01	Sb-128a	6.6E+00
As-77	6.3E-01	I-123	1.7E+00	Sb-128b	2.5E-01
As-78	2.8E+00	I-124	1.6E-03	Sb-129	8.9E-01
At-207	8.3E-01	I-125	2.6E-04	Sb-130	1.9E+00
At-211	5.5E-02	I-126	2.4E-04	Sb-131	2.3E-01
At-216	4.3E+06	I-128	6.0E+01	Se-70	1.9E+00
At-217	4.2E+04	I-130	1.9E-01	Se-73	8.3E-01
At-218	6.0E+02	I-131	4.7E-04	Se-73m	8.3E+00
Br-74	1.7E+00	I-132	1.1E+00	Se-77m	1.9E+04
Br-74m	1.4E+00	I-132m	2.1E+00	Se-81	2.3E+02
Br-75	1.1E+00	I-133	6.0E-02	Se-81m	5.1E+01
Br-76	1.6E-01	I-134	2.0E+00	Se-83	3.4E+00
Br-77	2.1E-01	I-135	5.3E-01	Sn-110	1.0E+00
Br-80	8.9E+01	Kr-74	4.2E+00	Sn-111	7.8E+00
Br-80m	8.3E+00	Kr-76	2.0E-01	Sn-117m	2.2E-02

Table 4-5. Trigger Values for the Air Pathway Derived from Screening Analysis - continued

Radionuclide	Trigger Values (Ci)	Radionuclide	Trigger Values (Ci)	Radionuclide	Trigger Values (Ci)
Br-82	5.8E-02	Kr-77	4.9E+00	Sn-123m	3.3E+01
Br-83	5.5E+01	Kr-79	4.3E+01	Sn-125	6.3E-03
Br-84	3.7E+00	Kr-81	1.0E+03	Sn-127	7.8E-01
C-11	8.9E+00	Kr-83m	1.2E+05	Sn-128	2.1E+00
Cl-38	4.0E+00	Kr-85	4.7E+03	Xe-120	3.9E+00
Cl-39	3.5E+00	Kr-85m	6.6E+01	Xe-121	3.8E+00
F-18	3.2E+00	Kr-87	1.3E+01	Xe-122	4.3E-01
Ge-66	1.1E+00	Kr-88	2.5E+00	Xe-123	7.4E+00
Ge-67	6.0E+00	N-13	1.4E+01	Xe-125	2.3E-02
Ge-68	1.0E-03	O-15	1.0E+02	Xe-127	4.0E+01
Ge-69	1.8E-01	P-30	7.0E+01	Xe-129m	4.6E+02
Ge-71	1.2E+00	P-32	1.8E-03	Xe-131m	1.2E+03
Ge-75	4.9E+01	P-33	1.4E-02	Xe-133	3.1E+02
Ge-77	4.7E-01	Sb-115	7.0E+01	Xe-133m	3.6E+02
Ge-78	3.1E+00	Sb-116	1.8E-03	Xe-135	4.4E+01
Hg-193	4.3E+00	Sb-116m	1.4E-02	Xe-135m	3.6E+01
Hg-193m	4.9E-01	Sb-117	7.0E+01	Xe-138	6.0E+00
Hg-194	2.8E-05	Sb-118m	1.8E-03		
Hg-195	2.2E+00	Sb-119	1.4E-02		

4.2 TRANSPORT AND EXPOSURE PATHWAY SCREENING

The purpose of this section is to identify potential pathways to human exposure to radionuclides potentially released from the E-Area LLWF (Sect. 4.2.1), and to justify eliminating some of these pathways from further consideration (Sect. 4.2.2). The results of this section are used in the development of models to evaluate doses potentially received as a result of releases of radionuclides from the E-Area LLWF.

4.2.1 Pathway Identification

Radionuclides released from the E-Area LLWF to the geosphere have the potential of reaching humans through numerous pathways. Potential pathways for a disposed LLW source are indicated in Figure 4-1. The pathways identified in this figure are for facilities undisturbed, from the standpoint of human intrusion. Pathways pertinent to intruder exposures are addressed separately in Section 4.4. Each pathway is briefly defined in the following list.

(1) Leaching - migration of radionuclides from the wasteform by a combination of dissolution, diffusion, and advection.
(2) Gaseous Diffusion - upward migration of gaseous radionuclides from the wasteform by diffusion through the caps and surface soils to the atmosphere.
(3) Irrigation - contamination of surface soil by radionuclides which have reached groundwater which is subsequently used for irrigation.
(4) Deposition - contamination of surface water by radionuclides which have reached the atmosphere; represents deposition of particulate associated radionuclides or gaseous species partitioning at the air-water interface.
(5) Volatilization - partitioning of volatile radionuclide species present in surface water into air above the water body.
(6) Discharge - discharge of radionuclides present in groundwater into surface water.
(7) Recharge - movement of radionuclides into the groundwater from contaminated surface water.
(8) Irrigation - contamination of surface soil by radionuclides which have reached surface water which is being subsequently used for irrigation.
(9) Washload - contamination of surface water by soil containing radionuclides as a result of erosion by rain or irrigation water.
(10) Deposition - contamination of surface soil by radionuclides which have reached the atmosphere and have become associated with airborne particulate matter.
(11) Resuspension - Resuspension of soil-associated radionuclides as a result of wind erosion.
(12) Biointrusion - contamination of surface soil by soil-associated radionuclides that are brought to the surface from the vicinity of the wasteform by burrowing animals, such as rodents or ants, or by intruding plant roots.
(13) Deposition - deposition of radionuclides in surface water that have partitioned onto suspended sediment.
(14) Resuspension - resuspension of particulate-borne radionuclides in the sediment of surface water as a result of hydrodynamic forces at the sediment-water interface.
(15) Immersion - contamination of aquatic plants by radionuclides in surface water attributable to the immersion of the plants in the contaminated water.
(16) Immersion - human exposure to radionuclides as a result of immersion in contaminated surface water.
(17) Ingestion - human exposure to radionuclides as a result of ingestion of radionuclides present in surface water.

(18) Ingestion - contamination of terrestrial animals from their ingestion of radionuclides in surface water.
(19) Ingestion - contamination of terrestrial animals from their ingestion of radionuclides in groundwater.
(20) Irrigation - contamination of terrestrial plants as a result of irrigation with surface water containing radionuclides.
(21) Irrigation - contamination of terrestrial plants as a result of irrigation with groundwater.
(22) Decomposition - contamination of surface soil as a result of decomposition of terrestrial plants in the soil.
(23) Root uptake - contamination of terrestrial plants by uptake through roots of soil water containing radionuclides.
(24) Deposition - deposition of airborne radionuclides onto terrestrial plant surfaces.
(25) Ingestion - ingestion of radionuclides by grazing animals as a result of contaminated soil ingestion.
(26) Ingestion - ingestion of radionuclide-containing vegetation by terrestrial animals.
(27) Decomposition - contamination of surface soil as a result of decomposition of terrestrial animals in the soil.
(28) Washoff - contamination of surface soil as a result of washoff of externally contaminated terrestrial animals.
(29) Resuspension - resuspension of surficial radionuclides on terrestrial animals to the atmosphere.
(30) Resuspension - resuspension of surficial radionuclides on terrestrial plants to the atmosphere.
(31) Inhalation - contamination of terrestrial animals as a result of inhalation of radionuclides in the atmosphere.
(32) Deposition - surface contamination of terrestrial animals via deposition of particulate-borne radionuclides in the atmosphere.
(33) Ingestion - contamination of terrestrial animals as a result of their ingestion of aquatic animals.
(34) Decomposition - contamination of surface water sediment as a result of decomposition of aquatic plants in the sediment.
(35) Decomposition - contamination of surface water sediment as a result of decomposition of aquatic animals in the sediment.
(36) Surface contact - surface contamination of aquatic animals as a result of contact with contaminated sediment.
(37) Root uptake - contamination of aquatic flora via radionuclide uptake through roots.
(38) Immersion - contamination of aquatic animals as a result of immersion in surface water containing radionuclides.
(39) Ingestion - contamination of aquatic animals as a result of their ingestion of aquatic plants containing radionuclides.
(40) Ingestion - human exposure to radionuclides as a result of ingestion of contaminated aquatic flora.
(41) Ingestion - human exposure to radionuclides as a result of ingestion of contaminated groundwater.

(42) Inhalation - human exposure to radionuclides as a result of inhalation of airborne radionuclides.
(43) Immersion - human exposure to radionuclides as a result of immersion in contaminated air.
(44) Ingestion - human exposure to radionuclides as a result of ingestion of contaminated terrestrial animals.
(45) Ingestion - human exposure to radionuclides as a result of ingestion of contaminated terrestrial plants.
(46) Ingestion - human exposure to radionuclides as a result of ingestion of contaminated aquatic animals containing radionuclides.
(47) Washoff - contamination of surface soil below vegetation due to rain-induced surface washoff.

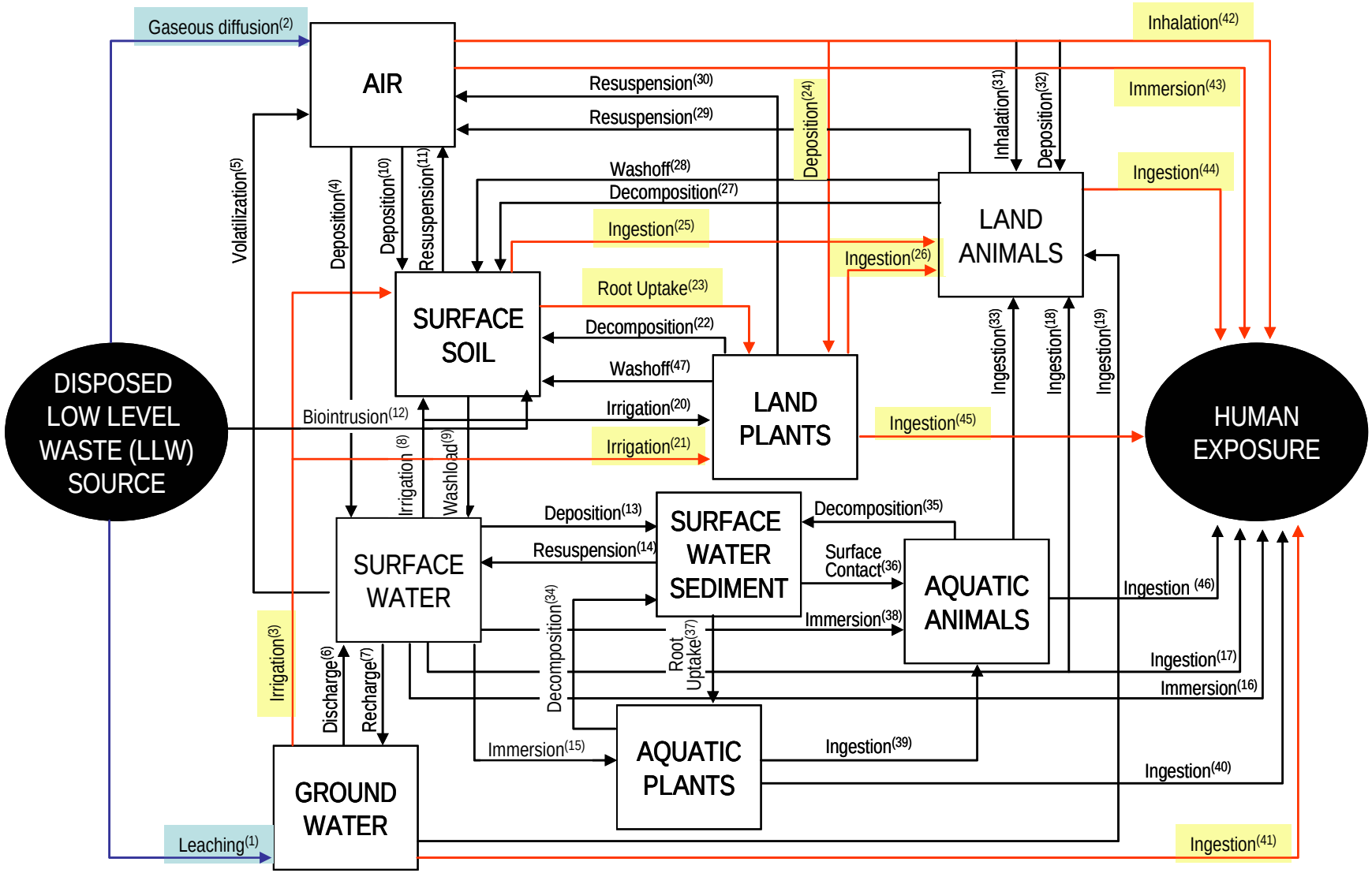

Figure 4-1. Potential Pathways to Human Exposure for Undisturbed Disposed Low-level Waste

4.2.2 Pathway Screening

The list in Sect. 4.2.1 is generic in nature, and the significance of each pathway must be evaluated on a site-specific and PA-specific basis to develop transport and exposure models. Many pathways may be removed from consideration for particular sites or PAs because of a negligible contribution to human exposure.

For the E-Area LLWF, leaching and transport of radionuclides to the groundwater (pathway (1)) is the predominant means that radionuclides may be subsequently transported in the environment. Thus, this pathway must be addressed in developing a transport model, and is addressed in this PA in the Environmental Transport of Radionuclides Section (Sect. 4.3). Use of contaminated groundwater must also be addressed in developing an exposure model, and is addressed in the Dose Analysis Section (Sect. 4.5). Other pathways which may contribute to human exposure are those tied to groundwater concentrations of contaminants. Irrigation with contaminated groundwater may lead to contamination of agricultural crops and animals (pathways (3), (21), (23), (25) and (26)).

Human exposure may occur as a result of direct human ingestion of contaminated groundwater (pathway (41)), or as a result of consumption of contaminated food supplies (pathways (44) and (45)). Direct consumption of groundwater by land animals (pathway (19)) is considered in the dose analysis, but indirect transport pathways between soil, plants and animals (pathways (22), (27), (28), and (47)) are not considered because they are judged to be insignificant. Two of these pathways involve washoff of external contamination from land animals (28) and plants (47) to surface soil. In the dose analysis, all irrigation water is assumed to be applied directly to the soil, so that none is lost by first contacting plants or animals (plants are also assumed to be exposed directly to irrigation waster to account for external contamination of plant surfaces that are then ingested by humans). The other two pathways involve transfer of radionuclides to surface soil by decomposition of plants (22) and animals (27). Allowing animal carcasses to decompose in the garden soil is not a realistic pathway. Although some parts of plants may be left in the ground to decompose, it is judged that this is a minor addition to the surface soil compared to that from irrigation.

Discharge of contaminated groundwater to surface water (pathway (6)) may result in contamination of the aquatic ecosystem including the water body itself, sediment, and aquatic plants and animals (pathways (13), (14), (15), (34), (35), (36), (37), (38), and (39)). Ingestion of contaminated surface water or aquatic animals by terrestrial animals (pathways (18) and (33)) may lead to human exposure. Human exposure may occur as a result of immersion in contaminated surface water during recreational activities such as swimming (pathway (16)) or direct ingestion of surface water (pathway (17)).

Consumption of contaminated aquatic plants (pathway (40)) was not considered because there is no indication that aquatic plants present in potentially-contaminated surface water in the vicinity of the SRS are consumed by humans. Since this PA is assessing dose to humans at a compliance point located 100-m from the disposed waste and there is no surface water near that location, and, since transport of radionuclides from groundwater to surface water will result in considerable dilution, transport to surface water and dose from uses of surface water will not be assessed. Thus, the following pathways are not considered ((4), (5), (6), (7), (8), (9), (13), (14), (15), (16), (17), (18), (20), (33), (34), (35), (36), (37), (38), (39), (40), and (46)).

For the E-Area LLWF, volatilization and transport of radionuclides in the gaseous phase to the ground surface and, subsequently, the atmosphere (pathway (2)) is another means that radionuclides may be transported in the environment. This pathway is also addressed in the Environmental Transport of Radionuclides Section (Sect. 4.3). Contamination of environmental media and foodstuffs must also be addressed in developing an exposure model, and is addressed in the Dose Analysis Section (Sect. 4.5). Radionuclides in the atmosphere may be inhaled by a human receptor (pathway (42)) and the receptor may be exposed by immersion in the contaminated air (pathway (43)). Deposition of radionuclides from the atmosphere to surface soil (pathway (10)) and resuspension of contaminated soil particles (pathway (11)) are considered in the Dose Analysis Section (Sect. 4.5) as is deposition from the atmosphere onto land plants (pathway (24)). Inhalation (pathway (31)) by and deposition (pathway (32)) onto land animals and resuspension from land plants (pathway (30)) and land animals (pathway (29)) are not considered because they are judged to be insignificant.

Finally, contamination of surface soil over the E-Area LLWF as a result of biointrusion of burrowing animals or plant roots (pathway (12)) must be addressed. It is acknowledged that biointrusion is a potentially significant pathway of contamination of surface soil over a LLW facility, as is concluded in a study by McKenzie et al. (1983). For the humid southeast, where ground surface and soil moisture limit resuspension of soil, biointrusion is likely to result in contamination of soils over the facility, but probably not significant contamination off-site. Therefore, the relative significance of biointrusion to the inadvertent intruder is the issue of concern in addressing this pathway for this PA.

Most of the burrowing animals identified as likely residents at the SRS do not burrow below 0.5 m (McKenzie et al. 1986). Only one burrower, the Florida Harvester Ant, is expected to burrow below 2 m, and then, only 5% of its burrows are expected to be that deep, resulting in very little potentially contaminated soil being moved. As the surface soil erodes, however, the significance of burrowers' activities may increase.

Furthermore, if E-Area reverts to a hardwood, pine forest sometime after loss of institutional control, it is possible that deeper roots may contact contaminated soil above, or adjacent to, the disposed waste and translocate radionuclides to other plant organs. Radionuclides may subsequently be released back to the soil as roots and leaves wither and degrade. It is, therefore, likely that biointrusion may cause some mixing of the waste components with the soil column.

The significance of biointrusion is evaluated here by considering the effect of the mixed soil column on an inadvertent intruder. An inadvertent intruder, who is assumed to dig next to, into, or above the disposal units, mixes the contaminated soil near the disposed waste with soil near the surface (Sect. 4.4). While it is not known how effective biointruders might be in causing mixing in the soil, the McKenzie et al. (1983) study of a reference humid site estimated that soil concentrations resulting from biointrusion are significantly lower than those resulting from intruder excavation activities. The effect of burrowing animals or intrusive roots, then, is not expected to enhance the inadvertent intruder's contact with contaminated soil. Thus, the biointrusion pathway is not considered further.

In summary, of the original 47 pathways identified in Figure 4-1, only two are considered to be of possible consequence for transport of radionuclides from the disposed waste into the environment. These are leaching of the wasteform resulting in contamination of groundwater local to E-Area (pathway (1)), and gaseous diffusion into the atmosphere local to E-Area (pathway (2)). These pathways are highlighted in blue on Figure 4-1. These pathways are addressed in the Environmental Transport of Radionuclides Section (Sect. 4.3). For calculating exposure to humans, pathways resulting in contamination of agricultural crops and animals as a result of irrigation with contaminated groundwater (pathways (3), (21), (23), (25), (26), (44), and (45)) and deposition or inhalation from the atmosphere (pathways (24), (42), and (43)), as well as direct ingestion of contaminated groundwater (41), are considered in the Dose Analysis Section (Sect. 4.5). These pathways are highlighted in yellow and red in Figure 4-1.

4.3 ENVIRONMENTAL TRANSPORT OF RADIONUCLIDES

The computer codes used in evaluating environmental transport of radionuclides released to the ground surface or water table from the E-Area LLWF disposal units are introduced in this section. Details describing the underlying mathematical models and methods of solution are provided in the cited references for the codes. Site-specific details involved in applying these models to each unit type are discussed in the respective PA modules.

Releases of radionuclides reaching the water table or ground surface are modeled according to the methods described in Section 4.1. Once at these interfaces, the radionuclides may be transported as a result of advective and diffusive forces to receptor locations. The receptor locations are defined for the purposes of this PA as the point of compliance, and are at the locations of maximum concentrations at the SRS site boundary, during the operational and institutional control period, and outside of the 100-m buffer zone around each disposed LLW unit, after final closure.

4.3.1 Environmental Transport in Groundwater

Transport of radionuclides reaching the water table is simulated using the flow field established for the GSA aquifer systems (Flach, 2004). The GSA/PORFLOW aquifer model uses the PORFLOW code to simulate groundwater flow within the GSA from ground surface to the bottom of the Gordon aquifer. This model was converted from the GSA/FACT aquifer model, which was used to calculate the flow field for the previous version of the E-Area LLWF PA. Flach (2004) describes how this conversion was accomplished, and the results of the subsequent validation and verification testing that was done on the resulting GSA/PORFLOW model.

The GSA is an area bounded by Fourmile Branch on the south, Upper Three Runs on the north, F-area on the west, and McQueen Branch on the east. Groundwater from the Upper Three Runs aquifer unit is assumed to discharge equally from each side of Upper Three Runs, Fourmile Branch and McQueen Branch. Therefore, these streams provide natural, no-flow boundary conditions for most of the Upper Three Runs aquifer unit. On the west side of the unit, hydraulic head values from a contour map of measured water elevations are prescribed. The Gordon aquifer is assumed to discharge equally from both sides of Upper Three Runs and a no-flow boundary condition is specified over the north face of the model. Lacking natural boundary conditions, hydraulic heads are specified over the west, south and east faces of the model within the Gordon aquifer. Areas of groundwater recharge and discharge consistent with computed hydraulic head at ground surface are computed as part of the model solution using a combined recharge/drain boundary condition applied over the entire top surface of the model. Groundwater discharges to surface water in regions where the computed head is above ground elevation. Data supporting the hydrogeologic conceptual model, as well as results of model validation studies, are provided in Appendix G.

The GSA/PORFLOW aquifer model requires a 3D application of PORFLOW. The areal resolution of the model is 200 ft square except in peripheral areas. There are 108 grid blocks along the east-west axis, and 77 blocks along the north-south axis. The vertical resolution varies depending on hydrogeologic unit and terrain/hydrostratigraphic surface variations. Each hydrostratigraphic surface is defined by numerous “picks” ranging in number from approximately 70 to 375 depending on the surface. The “upper” aquifer zone of UTR aquifer unit is represented with up to 10 finite-elements in the vertical direction. The vadose zone is included in the model. The “lower” aquifer zone contains 5 finite-elements while the “tan clay” confining zone separating the aquifer zones is modeled with 2 vertical elements.

The Gordon confining and aquifer units each contain 2 elements, for a total of 21 vertical elements from ground surface to the bottom of the Gordon aquifer. The 3D grid comprises 102,294 active cells.

Hydraulic conductivity values in the model are based on a characterization database composed of approximately 85 pumping and 481 slug test data points, 258 laboratory permeability measurements, and nearly 37,500 lithology data records. The conductivity field is heterogeneous within hydrogeologic units and reflects variations present in the characterization data. The average horizontal conductivities in the saturated "upper" Upper Three Runs aquifer zone, "lower" Upper Three Runs aquifer zone, and Gordon aquifer unit are approximately 10, 13, and 38 ft/d (Flach 2004). The average vertical conductivities for the "tan clay" confining zone and the Gordon confining unit are 6×10^{-3} and 1×10^{-5} ft/d (Flach 2004). These conductivities are consistent with measured values, the ranges of which are reported in Table 3-6 (Section 3.1.5.1).

Model calibration targets include hydraulic head, groundwater recharge and stream baseflow measurements. The overall root-mean-square difference between simulated head and approximately 639 time-averaged measurements is 3.7 ft. The root-mean-square residuals within the "upper", "lower", and Gordon aquifer zones/units are 1.7, 4.6, and 3.5 ft. The average natural recharge over the entire model domain is 14.7 in/yr compared to approximately 15 in/yr from prior groundwater budget studies (Flach, 2004). Various man-made features (e.g., basins) provide additional recharge in localized areas. The estimated discharge rates to Upper Three Runs, Fourmile Branch, McQueen Branch, and Crouch Branch within the model domain are 18.2, 2.6, 1.5, and 1.8 ft^3/s (Flach 2004); the respective simulated discharge rates are 11.4, 3.8, 2.4, and 1.7 ft^3/s. Predicted seepage faces are consistent with field observations. Simulated hydraulic heads, vertically-averaged over the entire thickness of the "upper" Upper Three Runs, "lower" Upper Three Runs, and Gordon aquifer zones, agree with potentiometric maps based on measured heads. Simulated flow directions vertically-averaged over the entire thickness of the aquifer zones agree with conceptual models of groundwater flow.

Although the GSA/PORFLOW flow field can be used directly for PORFLOW aquifer transport simulations, the application for the E-Area LLWF disposal units involves using the GSA regional flow information defined on a localized grid of smaller extent but higher resolution using the MESH3D program (Flach 2007). MESH3D is a refinement tool, which extracts a sub-region of the GSA coarse mesh, and subdivides the coarse mesh to produce a higher-resolution grid. MESH3D also transfers velocity and saturation data from the original GSA/PORFLOW grid to the refined mesh through an interpolation process. The refinement grids differ in size for the disposal unit types, and are defined within the respective modules.

In using PORFLOW to estimate transport of radionuclides through the aquifer systems under the disposal units, a number of model parameters were quantified, describing characteristics of the aquifer materials and radionuclides present. Specifically, porosity, particle density, effective diffusivity, and longitudinal and transverse dispersivity are properties of the aquifer that affect transport calculations. The properties of the more sandy lower vadose zone soils are consistent with the aquifer sediments; thus the values of porosity, particle density, and molecular diffusivity for these soils from Phifer et al. (2006) were considered in assigning values in the model. Phifer et al. (2006) provide an average total porosity and particle density of 0.39 and 2.66 g/ml, respectively, for the lower vadose zone soils. However, because of the heterogeneity of the sandy aquifer units, where the less permeable (e.g., clayey) sediments lessen the connectedness of pore spaces, the effective porosity, which determines the pore velocity, and thus the rate of migration of radionuclides, is expected to be less that the total porosity.

Based on engineering judgment and available in-the-field tritium measurements in neighboring sites on the SRS, the effective porosity is assumed to be on the order of 0.25 (Phifer et al. 2006). This required that an adjustment be made to the particle density term, to preserve the correct calculation of the retardation factor in PORFLOW, such that an effective particle density of 1.39 g/ml is assumed (Phifer et al. 2006). The longitudinal and transverse dispersivities are set to zero for the saturated zone simulations for all disposal units except Slit and Engineered Trenches. Omitting hydrodynamic dispersion tends to maximize the concentrations in the aquifer (by concentrating the plume), and thus constitute a modest conservatism in general. It should be noted that when dispersivities are set to zero, some plume spreading still occurs through numerical dispersion. For Slit and Engineered Trenches, the longitudinal and transverse dispersivities are set to 10% and 1% (Pickens and Grisak 1981) of 100 meters, the approximate plume travel distance to the compliance point. These dispersivities produce a best-estimate simulation with respect to hydrodynamic dispersion.

Geochemical parameters also affect aquifer transport. Kaplan (2006) provides a listing of appropriate K_ds to use for aquifer materials, as well as solubility limits and K_d correction factors to account for the influence of CDP on radionuclide migration. To date, work has not been done towards rigorously evaluating the uncertainty in the geochemical parameters. However, a “best” value and a “conservative” value are provided for the K_ds, which are based on the professional judgment of researchers involved in estimating this particular parameter (Kaplan 2006).

4.3.2 Environmental Transport in Air

Transport of volatile radionuclides reaching the ground surface is simulated using CAP-88 (EPA 2006). The CAP-88 model is an EPA code that uses mathematical models for assessing dose and risk due to radionuclide emissions to the air. CAP-88 was developed by the EPA and is used to demonstrate compliance with NESHAP (EPA 2002b).

CAP-88 uses a modified Gaussian plume equation to estimate the average dispersion of radionuclides released from up to six sources at the same release location with different release heights. Assessments are done for a circular grid with a radius up to 50 miles. Calculated air concentrations are averaged within each of sixteen 22.5º sectors. Plume depletion due to wet and dry deposition and radioactive decay is simulated. Special consideration is given to ^{3}H and ^{14}C. The specific activity of ^{3}H in air is calculated for an absolute humidity of 8 mg/m^3. The specific activity of ^{14}C is calculated for a carbon dioxide concentration of 330 ppm by volume. A user's manual (Beres 1990) describes the methodology implemented by CAP-88.

In applying CAP-88 to simulating transport of volatile radionuclides to a receptor for this PA, DRFs, in mrem/Ci, are estimated by calculating the ratio of the code-calculated EDEs to their annual release at specified receptor locations (Lee, 2006). Sector-averaged air concentrations were used to calculate EDEs, and thus the DRFs represent sector-averaged doses. DRFs were calculated for each disposal unit type, for two receptor locations, and for the 15 radionuclides identified in Section 4.2.2 from the atmospheric pathway screening analysis (C-14, Cl-36, H-3, I-129, S-35, Sb-124, Sb-125, Se-75, Se-79, Sn-113, Sn-119m, Sn-121, Sn-121m, Sn-123, and Sn-126). The assumed annual release of each radionuclide is 1 Ci. Receptor locations at the SRS boundary and at 100-m from each disposal unit were specified. During the operational and interim closure period, the DRFs at the SRS boundary are of interest; after final closure, the DRFs 100 m from each disposal unit is of interest. The use of DRFs in estimating air-pathway dose is discussed in Section 4.5.3. The remainder of this discussion is relevant to the environmental transport aspects of the CAP-88 simulation.

For the estimation of relative air concentrations (χ/Q) at the SRS boundary, a point source was chosen to represent ground-level releases from the E-Area LLWF. The 1997-2001 meteorological database for the closest meteorological tower, H Area (Weber and Kurzeja 2002), was used to provide wind speed, wind direction, temperature, dew point, and horizontal and vertical turbulence intensity data for CAP-88 simulations. The point source representation was deemed appropriate for doses calculated at the SRS boundary since the source-to-receptor distance/source diameter ratio was greater than 2.5 (EPA 2006).

For estimation of relative air concentrations at the 100-m location, however, the point source representation was inappropriate for most of the disposal units, since the source-to-receptor distance/source diameter ratio was less than 2.5 (EPA 2006). For these conditions (see Table 4-6), a correction factor was derived (Lee 2006), based on work by Simpkins and Lee (2006), which provides an estimate of the ratio of the CAP-88-derived point source concentration to a more appropriate concentration calculated using an area source model provided in Napier et al. (2002). For the purposes of these calculations, the disposal units were assumed to be of uniform shape with the dimensions provided in Table 4-6.

The correction factor reduced the air concentrations (χ/Qs) calculated assuming a point source for all units by a factor of 5 for the 643-26E NRCDA, and by a factor of 6 for the CIG Trench, the LAWV, and the Slit and Engineered Trenches (Lee 2006).

Four of the 15 radionuclides for which environmental transport calculations via the air pathway were required were not contained within the CAP-88 library (Se-75, Se-79, Sn-119m, and Sn-121m). For these radionuclides, surrogate radionuclides with similar radiological half-lives were selected (Lee, 2006).

Table 4-6. E-Area LLWF Disposal Unit Dimensions and Source Designation for 100-m Receptor Location (information from Lee 2006)

Disposal Unit Type	Area (m^2)	Effective Length (m)	Distance:Length	Area Source?
643-26E NRCDA[a]	5,760	76	1.3	Yes
643-7E NRCDA	1,226	35	2.9	No
CIG Trench[b]	9,568	98	1.0	Yes
LAWV	8,662	93	1.1	Yes
ILV[c]	1,256	35	2.8	No
Slit Trench[d]	9,568	98	1.0	Yes
Engineered Trench[d]	9,568	98	1.0	Yes

a Much of the assigned area does not contribute to the flux to the ground surface, as the new NR pad is scheduled to contain a total of 100 casks

b The assigned area does not exclude the area of virgin soil between individual CIG segments

c The assigned area does not exclude the non-disposal area between the ILT and ILNT sections

d The assigned area does not exclude the area of virgin soil between individual Slit Trenches

4.4 INADVERTENT INTRUDER ANALYSIS

The inadvertent intruder analysis considers the radiological impacts to hypothetical persons who are assumed to inadvertently intrude on the E-Area LLWF site after institutional control ceases 100 years after operations cease. Disposal of low-level radioactive waste in the E-Area LLWF must meet a requirement to assess impacts on such individuals, and demonstrate that the effective dose equivalent to an intruder would not likely exceed 100 mrem per year for scenarios involving continuous exposure or 500 mrem for scenarios involving a single acute exposure (DOE 1999a). These dose limits apply to the sum of dose equivalents from all exposure pathways that are assumed to occur in a given exposure scenario for an inadvertent intruder. Analytical results for the first 1,000 years after assumed loss of active institutional control are used to evaluate performance of the E-Area disposal units with respect to inadvertent intruders.

In this section, exposure scenarios considered in the E-Area LLWF PA for inadvertent intruders, and the method of dose calculation, are described. The selection of relevant scenarios and results of dose calculations for individual disposal unit types are described in the respective modules.

The focus in development of exposure scenarios for inadvertent intruders was on selecting reasonable events that may occur, giving consideration to regional customs and construction practices. An important assumption in all scenarios is that an intruder has no prior knowledge of the existence of a waste disposal facility at the site. Therefore, after active institutional control ceases, certain exposure scenarios are assumed to be precluded only by the physical state of the disposal facility, i.e., the integrity of the engineered barriers used in facility construction. Passive institutional controls, such as permanent marker systems at the disposal site and public records of prior land use, also could prevent inadvertent intrusion after active institutional control ceases, but the efficacy of passive institutional controls is not assumed in this analysis.

Intruder exposure scenarios do not include consumption of groundwater and crop irrigation with groundwater because impacts associated with these exposure routes are evaluated separately in the all-pathways analysis (Section 4.5), and are considered negligible for the intruder scenarios (Section 4.4.1). Pathways of exposure to radon and its short-lived progeny, and volatile radionuclides, are considered separately in the PA.

Screening to identify radionuclides of importance in the inadvertent intruder analysis for this PA was carried out according to a modified NCRP methodology (1996), starting with the NCRP document's list of 826 radionuclides (Cook and Wilhite 2004). The number of radionuclides requiring detailed analysis was reduced from the starting number of 826 to 78 (listed in Cook 2007) as a result of the screening process. Modifications to the NCRP methodology included omitting the groundwater pathway screening factors (as this pathway is not included in the intruder analysis here), and assuming that the radionuclides have 100 years of decay prior to possible access by intruders (rather than NCRP's 10-year period), consistent with the 100-yr institutional control period assumed for the PA. Radionuclide progeny were accounted for in the screening process (Cook and Wilhite 2004). Radionuclides with calculated Trigger Values (i.e., Ci quantities less than 10^7 Ci that result in one millirem dose under conservative screening conditions) were retained for detailed analysis (Cook and Wilhite 2004; Cook 2007).

4.4.1 Exposure Scenarios for Inadvertent Intruders

4.4.1.1 Chronic Exposure Scenarios for Inadvertent Intruders

Three distinct scenarios resulting in chronic exposure of inadvertent intruders are considered in the dose analysis for the E-Area LLWF. Two of these scenarios, which usually are referred to as the agriculture (or homesteader) and post-drilling scenarios, have often been applied in other intruder dose analyses for LLW disposal (NRC 1981; Oztunali and Roles 1986; Kennedy and Peloquin 1988; ORNL 1990). The third scenario considered in this analysis is referred to as the resident scenario. Assumptions made in defining the agriculture, resident, and post-drilling scenarios are discussed below.

Agriculture Scenario

The agriculture scenario assumes that an intruder comes onto the site after active institutional control ceases and establishes a permanent homestead, including on-site sources of water and foodstuffs. Waste in disposal units is assumed to be accessed when an intruder constructs a home directly on top of a disposal facility and the foundation of the home extends into the facility itself. All waste in the disposal facility at the time the foundation is dug is assumed to be physically indistinguishable from native soil. Direct intrusion into disposal units is assumed to be precluded during the time the thickness of the cover soil is greater than the depth of a typical basement (10 ft), or when the integrity of engineered barriers prevents it.

In the agriculture scenario, some of the waste exhumed from the disposal facility is assumed to be mixed with native soil in the intruder's vegetable garden. The following exposure pathways involving exhumed waste or waste remaining in the exposed disposal facility on which the intruder's home is located then are assumed to occur:

- internal exposure from ingestion of vegetables grown in contaminated garden soil
- internal exposure from direct ingestion of contaminated soil, primarily in conjunction with intakes of vegetables from the garden
- external exposure to contaminated soil while working in the garden or residing in the home on top of the disposal facility
- internal exposure from inhalation of radionuclides attached to soil particles that are suspended into air from contaminated soil while working in the garden or residing in the home

The agriculture scenario theoretically should also assume that the intruder's entire supply of water for domestic use is obtained from a well on the disposal site. However, doses resulting from use of contaminated groundwater obtained from a well on the disposal site are evaluated separately in the all-pathways analysis and are not calculated for the intruder, in accordance with the guidance for DOE Order 435.1 (DOE 1999a).

Resident Scenario

As in the agriculture scenario described above, the resident scenario assumes that an intruder excavates a foundation for a home on top of a disposal facility. This can occur at any time after loss of active institutional control over the disposal facility. During excavation, however, the intruder may encounter an engineered barrier, such as the roof of a concrete vault that cannot easily be penetrated by the types of excavation equipment normally used at the SRS. In these cases, the presence of intact engineered barriers, or wasteforms, or sufficient soil cover are assumed to preclude direct intrusion into the waste during excavation. Instead of abandoning the site, the intruder constructs a home directly on top of the intact barrier, wasteform, or soil cover and, thus, establishes a permanent residence at that location.

From the definition of the resident scenario, the primary exposure pathway of concern is external exposure to photon-emitting radionuclides during the time the intruder resides in the home on the disposal site. The presence of intact barriers and/or wasteforms and soil covers would preclude any ingestion exposures and most inhalation exposures.

Post-Drilling Scenario

The post-drilling scenario assumes that an intruder who resides permanently on the disposal site drills through a disposal unit in constructing a well for a domestic water supply. Following construction of the well, the contaminated material brought to the surface during drilling operations, which is assumed to be indistinguishable from native soil, is assumed to be mixed with native soil in the intruder's vegetable garden.

The exposure pathways involving ingestion of contaminated vegetables, ingestion of contaminated soil, and external and inhalation exposures while working in the garden then are the same as the pathways described previously for the agriculture scenario. In the post-drilling scenario, however, external and inhalation exposures while residing in the home on the disposal site, which are important in the agriculture scenario, are considered insignificant. All drilling waste is assumed to be mixed with native soil in the garden, which is considered to be at a sufficient distance from the home that indoor exposures are minor relative to those in the garden.

The post-drilling scenario theoretically should also assume that the intruder's entire supply of water for domestic use is obtained from a well on the disposal site. However, doses resulting from use of contaminated groundwater obtained from a well on the disposal site are evaluated separately in the all-pathways analysis and are not calculated for the intruder, in accordance with the guidance for DOE Order 435.1 (DOE 1999a).

In this analysis, as in the agriculture scenario, drilling through a disposal unit is assumed to be precluded during the time when the concrete vaults, steel containers, or cementitious wasteforms maintain their integrity. The basis for this assumption is that the types of drill bits normally used in constructing wells in the soft sand and clay soils at the SRS could not easily penetrate an intact concrete vault or other grouted wasteform or non-degraded heavy steel container. Therefore, in attempting to drill directly through a disposal facility, it seems reasonable to assume that an intruder would encounter considerable resistance and, instead of taking extraordinary measures to obtain a drill bit designed to penetrate through hard rock or heavy steel, would move the drilling operation to a different location away from the disposal facility.

4.4.1.2 Acute Exposure Scenarios for Intruders

Three distinct scenarios resulting in acute exposure of inadvertent intruders have commonly been applied to LLW disposal facilities. These scenarios usually are referred to as the construction, discovery, and drilling scenarios (NRC 1981; Oztunali and Roles 1986; Kennedy and Peloquin 1988). As noted previously, all acute exposure scenarios for inadvertent intruders are subject to a limit on EDE of 500 mrem. The following sections describe the three acute exposure scenarios and their potential importance in the intruder dose analysis for the E-Area LLWF.

Construction Scenario

The chronic agriculture scenario described is based on the assumption that an intruder builds a home on the disposal site, with the foundation extending into a disposal unit. The construction scenario considers exposures during the short period of time for digging a foundation and building a home.

During construction, the relevant exposure pathways are assumed to be inhalation of radionuclides suspended into air from an uncovered disposal unit and external exposure to photon-emitting radionuclides in the disposal unit. Ingestion exposure is assumed to be unimportant during normal work activities. The potential importance of the construction scenario arises primarily from the assumption that construction activities result in airborne concentrations of radionuclides that are substantially higher than those during normal activities while inhabiting the site, as in the agriculture scenario. The construction scenario also assumes external exposure to unshielded waste, whereas in the agriculture scenario shielding during indoor residence on the disposal site usually is taken into account.

From its definition, the construction scenario would occur at the same time as the agriculture scenario. Therefore, the dose analysis for the two scenarios would be based on the same concentrations of radionuclides. Previous calculations (Kennedy and Peloquin 1988) provide a direct comparison of doses for the two scenarios. For a few radionuclides, the dose per unit concentration could be slightly higher for the construction scenario but, for most radionuclides, the dose per unit concentration is expected to be much greater for the agriculture scenario. This result assumes a reasonable exposure time for the construction scenario and the use of a reasonably consistent set of assumptions for the exposure pathways in the two scenarios.

Therefore, since the dose limit for the acute construction scenario is a factor of 5 higher than the dose limit for the chronic agriculture scenario, the agriculture scenario always will be more restrictive and the construction scenario generally can be neglected in demonstrating compliance of the E-Area LLWF with the performance measure for inadvertent intruder analysis.

Discovery Scenario

As in the resident scenario described, the discovery scenario assumes that an intruder attempts to dig into a disposal facility while excavating a foundation for a home on the disposal site, but encounters an intact concrete roof or other engineered barrier which cannot easily be penetrated by the types of excavating equipment that normally would be used at the SRS. However, in distinction from the resident scenario, the intruder soon decides to abandon digging at that location and moves elsewhere. Since intact engineered barriers are assumed not to be breached during excavation, the primary exposure pathway for this scenario is external exposure to photon-emitting radionuclides in the disposal facility during the time the intruder digs at the site and the barriers are uncovered. The presence of intact barriers is assumed to preclude any significant inhalation or ingestion exposures.

From its definition, the discovery scenario would occur at the same time as the resident scenario. Furthermore, the relevant exposure pathway, which is external exposure to photon-emitting radionuclides in the waste, is essentially the same in the discovery and resident scenarios. Other than the exposure time, the only difference is the shielding factor during indoor residence, which is relevant only for the resident scenario. Therefore, since the exposure time for the discovery scenario presumably would be no more than 100 hr (ORNL 1990), which is considerably less than a reasonable exposure time for indoor residence in the resident scenario, and the dose limit for the discovery scenario is a factor of 5 greater than the dose limit for the resident scenario, the resident scenario always will be more restrictive and the discovery scenario generally can be neglected in demonstrating compliance of the E-Area LLWF with the performance measure for inadvertent intruder analysis.

Drilling scenario

The chronic post-drilling scenario is based on the assumption that an intruder drills a well directly through a disposal unit. The acute drilling scenario considers exposures during the short period of time for drilling and construction of the well.

During well drilling and construction, the most important exposure pathway is assumed to be external exposure to uncovered drilling wastes confined to a pile near the well. Although some radionuclides in the drilling waste could be suspended into the air and inhaled during well drilling and construction, inhalation exposures are expected to be relatively unimportant due to such factors as the initial water content of the drilling wastes, the small volume of the waste produced, and the absence of direct mechanical disturbance of the waste pile. Ingestion exposure also is assumed to be unimportant during normal drilling activities. The potential importance of the drilling scenario arises primarily from the assumption that an intruder could be located near an unshielded waste pile for a substantial period of time.

From its definition, the drilling scenario would occur at the same time as the post-drilling scenario. Therefore, the dose analyses for the two scenarios would be based on the same concentrations of radionuclides. Previous calculations (Kennedy and Peloquin 1988) provide a direct comparison of doses for the two scenarios. For all radionuclides, the dose per unit concentration for the drilling scenario is expected to be at least an order of magnitude less than the dose per unit concentration for the post-drilling scenario, provided a reasonable exposure time for the drilling scenario and a reasonably consistent set of assumptions for the exposure pathways in the two scenarios are used. Therefore, the post-drilling scenario always will be more restrictive and the drilling scenario generally can be neglected in demonstrating compliance of the E-Area LLWF with the performance measure for inadvertent intruder analysis.

Summary of Acute Exposure Scenarios

In this section, three scenarios for acute exposure of inadvertent intruders were discussed, i.e., the construction, discovery, and drilling scenarios. However, the preceding evaluation of these scenarios has shown that all three scenarios can be neglected for purposes of demonstrating compliance of the E-Area LLWF with the performance measure for inadvertent intruder analysis because the chronic agriculture, resident, and post-drilling scenarios will always be more restrictive.

4.4.1.3 Summary of Exposure Scenarios for Inadvertent Intruders

Several chronic and acute exposure scenarios for inadvertent intruders have been considered for use in the PA for the E-Area LLWF. However, on the basis of previous analyses and considerations of how these scenarios would apply to the E-Area LLWF, it is evident that only the following two chronic exposure scenarios need to be included in the PA:

- a resident scenario involving permanent residence in a home located either on top of an intact concrete roof or other engineered barrier, which first could occur upon assumed loss of active institutional control at 100 years after facility closure, or on top of intact but essentially exposed waste at times after the engineered barriers have lost their integrity
- a post-drilling scenario involving exhumation of waste from a disposal unit at times after drilling through a disposal unit becomes credible

The chronic agriculture scenario was not included because it is not credible due to the inclusion of an erosion barrier in the final closure design. The erosion barrier is considered permanent with respect to the time period of the PA analysis, eliminating the potential for contact with the waste via this scenario due to the greater depth of the cover compared to the depth to which a typical basement is excavated (10 ft).

4.4.2 Dose Analysis for the Inadvertent Intruder

The intruder analysis was performed with a software tool for automated analyses (Koffman 2004, 2006a) that calculates radionuclide-specific concentrations and inventory limits allowed in waste at the time of disposal. These values are based on dose assessments for credible exposure scenarios for the inadvertent intruder described in the PA module for each disposal unit type. The tool eliminates the historical use of complex spreadsheets that require extensive design checks. Radionuclide- and scenario-specific parameters within the software tool have been researched and independently verified (Lee, 2004). The equations implemented in the automated analysis are essentially the same equations for calculating intruder dose from the previous PA (McDowell-Boyer et al. 2000), and are also documented in the Lee (2004) report.

Effective doses and inventory limits for radionuclides within each disposal unit type for the credible exposure scenarios selected are calculated as follows (Koffman 2004, 2006a). For each exposure pathway in a scenario of interest, an EDE in rem/yr for each radionuclide in the decay chain of a parent is calculated based on published dose conversion factors (Lee 2004). These exposure pathway EDEs are summed to get an overall scenario EDE for each parent radionuclide. For a given calculational time, the activity of each radionuclide in the decay chain can be determined from the initial inventory of the parent radionuclide. The dose for each radionuclide in the decay chain is summed to yield the effective dose from the parent, based on the initial inventory of the parent. To calculate the inventory limit for that radioactive parent, the effective dose is then divided by the initial inventory of the parent, to give the effective dose per unit activity. The intruder dose limit of 0.1 rem/yr (i.e., 100 mrem/yr for chronic scenarios) is then divided by the effective dose per unit activity to obtain an inventory limit in activity (Ci) per year.

The automated analysis disregards leaching, such that radioactive decay alone determines the concentration within the waste unit for each radionuclide in the decay chain. This overestimates the radionuclide inventory in the waste and vadose zones at the time the intruder is assumed to be exposed. A transient calculation can be conducted, where the potential erosion of cover material is accounted for at the same time the decay chain calculation is being carried out. This allows an evaluation of when the maximum impact on the intruder may occur. The decay process continually changes the amount of contaminant present in the waste zone that the intruder can encounter. While the amount of parent monotonically decreases, the amount of each progeny initially increases and ultimately decreases. As the decay process takes place, sediments and engineered materials can erode and degrade as well. The transient analysis option is valid across the spectrum of disposal units and does not require extensive calculations by the analyst; rather it requires the analyst to define geometry and process inputs, and then relies on the computer model to perform pathways calculations at a specified time increment that is nominally 10 years.

4.5 DOSE ANALYSIS

In this PA, radiological dose to human receptors is analyzed in the all-pathways analysis, the inadvertent intruder analysis and the air-pathway analysis. Protection of groundwater resources and average radon flux at the surface of the facility is also addressed. The methods of calculation of dose in the all-pathways and air-pathway analyses, and evaluating groundwater resource protection and radon flux, are discussed below. Dose analysis for the inadvertent intruder analysis is addressed in Section 4.4.

4.5.1 All-Pathways Dose Calculation

The permissible all-pathways dose for DOE LLW disposal facilities is addressed in DOE M 435.1, IV.P.(1), which states the performance objectives for DOE LLW disposal facilities (DOE 1999a). This requirement, for the all-pathways dose, is stated as:

(1) **Performance Objectives** Low-level waste disposal facilities shall be sited, designed, operated, maintained, and closed so that a reasonable expectation exists that the following performance objectives will be met for waste disposed of after September 26, 1988:

(a) Dose to representative members of the public shall not exceed 25 mrem (0.25 mSv) in a year total effective dose equivalent from all exposure pathways, excluding the dose from radon and its progeny in air.

Although the all-pathways performance objective includes not only all exposure pathways, but also all transport pathways, in this PA, the air pathway is evaluated separately. The all-pathways dose evaluated here includes only the groundwater transport pathway because the receptors for the groundwater and air pathways will likely be at different locations and the maximum doses from the two pathways will occur at different times. The performance objective which applies to the air-pathways dose calculation (Section 4.5.3) is more restrictive than that which applies to the all-pathways dose calculation (Section 4.5.1) (10 mrem/yr as compared to 25 mrem/yr). Thus, the air pathway is adequately addressed in the air pathway performance objective. A screening analysis separate from that done for the groundwater pathway (Section 4.1.1) was therefore not necessary.

The methodology used to calculate the all-pathways dose is based on the methodology presented in (NRC 1977). The all-pathways scenario assumes a receptor consumes contaminated groundwater from a well located 100 meters from the disposed LLW. The receptor consumes leafy vegetables and produce that were irrigated with water from the well and milk and meat from animals that consume contaminated water and pasture grass irrigated with contaminated groundwater. The exposure pathways were selected from a larger set of potentially important pathways in Section 4.2.

The all-pathways dose is calculated from groundwater concentrations developed using the PORFLOW model. Groundwater transport modeling is discussed in Section 4.3. An All-Pathways Application (Koffman 2006b) was developed to calculate the impacts from transport of radionuclides from disposed LLW in groundwater. Two types of impact are considered. The first impact is the radiological dose from the use of contaminated groundwater, which is termed the all-pathways dose in this PA, and which is compared to the 25-mrem in a year performance objective in DOE 435.1.

The other impact is that of groundwater resource protection, where the radionuclide groundwater concentrations are compared with MCLs promulgated in the Safe Drinking Water Act (EPA, 2000; EPA, 2001). Calculation of the groundwater resource protection impacts are discussed in Section 4.5.2.

The All-Pathways Application reads PORFLOW output (i.e., groundwater concentrations over time) for all radionuclides analyzed in the groundwater analysis. Radionuclide data (e.g., half-lives, dose conversion factors, MCLs) are documented in a radionuclide data package prepared for this PA (Cook 2007). The application calculates dose to humans from direct ingestion of contaminated groundwater and consumption of locally grown leafy vegetables, produce, milk, and meat, which are contaminated with radionuclides from use of the groundwater for irrigation and direct consumption by the cattle. Exposure parameters are shown in Table 4-7. Equations used in the dose calculation are described in Koffman (2006b) and Jannik and Dixon (2006).

The All-Pathways Application facilitates calculation of disposal limits, based on an assumed unit curie disposed as well as calculation of total dose from all radionuclides disposed if a known or projected inventory at closure is available.

Table 4-7. Exposure Parameters for All-Pathway Dose Analysis

Parameter	Units	Value	Reference
Water Ingestion rate (human)	L/year	5.11E+02	Yu, et al 2001
Water Ingestion rate (beef cow)	L/d	5.00E+01	Hamby 1991
Water Ingestion rate (milk cow)	L/d	6.00E+01	Hamby 1991
Cattle Fodder Consumption rate	kg/d	5.00E+01	Hamby 1991
Meat consumption rate	kg/yr	6.30E+01	Yu, et al 2001
Milk consumption rate	L/yr	9.20E+01	Yu, et al 2001
Vegetable consumption rate	kg/yr	1.60E+02	Yu, et al 2001
Leafy vegetable consumption rate	kg/yr	1.40E+01	Yu, et al 2001
Irrigation rate	L/m^2-d	3.40E+00	Hamby 1991
Weathering constant	1/d	4.95E-02	Hamby 1991
Yield, vegetables	kg/m^2	2.00E+00	Hamby 1991
Yield, leafy vegetables	kg/m^2	2.00E+00	Hamby 1991
Yield, pasture grass	kg/m^2	2.00E+00	Hamby 1991
Surface Soil Density	kg/m^2	2.40E+02	Hamby 1991
Irrigation time for crops	d	7.00E+01	Hamby 1991
Irrigation time for pasture grass	d	3.00E+01	Hamby 1991
Buildup time in soil	d	1.82E+02	Site-specific
Washing factor (vegetables)	-	1.00E+00	Ng et al. 1979
Washing factor (leafy vegetables)	-	5.00E-01	Ng et al. 1979
Fraction of vegetables produced locally	-	5.00E-01	Yu, et al 2001
Fraction of leafy vegetables produced locally	-	5.00E-01	Yu, et al 2001
Fraction of beef produced locally	-	1.00E+00	Yu, et al 2001
Fraction of milk produced locally	-	1.00E+00	Yu, et al 2001

4.5.2 Groundwater Resource Protection

The DOE 435.1 requirement for an assessment of the protection of water resources is found in DOE M 435.1-1.IV.P.(2).(g), which states (DOE 1999a):

(g) For purposes of establishing limits on radionuclides that may be disposed of near-surface, the performance assessment shall include an assessment of impacts to water resources.

The guide for DOE 435.1 states "DOE M 435.1-1 does not specify the level of protection for water resources that should be used in a performance assessment for a specific low-level waste disposal facility. Rather, a site-specific approach, in accordance with a hierarchical set of criteria should be followed."

The hierarchy for establishing water resource protection is as follows:

- First, the DOE low-level waste disposal facility must comply with any applicable State or local law, regulation, or other legally *applicable* requirements for water resource protection.
- Second, the DOE low-level waste disposal facility must comply with any formal agreement applicable to water resource protection that is made with appropriate State or local officials.
- Third, if neither of the above conditions applies, the site needs to select assumptions for use in the performance assessment based on criteria established in the site groundwater protection management program and any formal land-use plans.

If none of the above conditions apply, the site may select assumptions for use in the performance assessment for the protection of water resources that are consistent with the use of water as a drinking water source.

At SRS, the appropriate measure for protection of water resources has been determined to be the Safe Drinking Water Act MCLs. The MCLs (EPA 2000; EPA 2001) are shown in Table 4-8.

Table 4-8. Maximum Contaminant Levels

Component	Maximum Contaminant Level
Beta-Gamma Dose	4 mrem/year
Gross Alpha	15 pCi/L
Radium	5 pCi/L
Uranium	30 μg/L

Methods for calculation of disposal limits are described below. The disposal limit calculation methods will be presented from the simplest to the most complex cases. The cases are as follows:

- Radionuclide parent without a chain
- Radionuclide parent with a chain
- Radionuclide parent with a chain combined with existing inventory

Radionuclide parent without a chain

For a radionuclide parent without a chain, disposal limits are determined for each radionuclide parent by calculating the inventory that would cause the peak groundwater concentration to match the groundwater concentration limit. The disposal limit is accomplished via the following steps:

1. Determine the fraction (f) of the groundwater limit that is consumed by the inventory that was modeled. The fraction is the peak groundwater concentration of the parent (from the PORFLOW model) divided by its groundwater limit
   $$f = \frac{C^{gw}}{CL^{gw}}$$
2. When that fraction is multiplied by the ratio of the allowable inventory divided by the modeled inventory it must not exceed the maximum allowable fraction of 1.
   Therefore $f \times \frac{I_{all}}{I_{model}} = 1$ or $I_{all} = \frac{I_{model}}{f}$

where

I_{all} is the allowable inventory (disposal limit), and
I_{model} is the modeled inventory for the parent.

Note that the modeled inventory was 1 g-mole, thus a preliminary step is needed to convert the modeled inventory to a Ci basis, but that step is not shown in the equations. Additionally, the disposal limit is calculated for each time-step that is modeled, then the lowest disposal limit is selected, but that step is not shown in the equations.

The above two steps are combined in the equation:

$$I_{all} = I_{pm} \times \frac{1}{\left(\frac{C^{gw}}{CL^{gw}}\right)}$$

where

I_{all} is the disposal limit (Ci) for the parent,
I_{pm} is the modeled inventory for the parent (Ci),
CL^{gw} is the groundwater concentration limit for the parent (pCi/L), and
C^{gw} is the groundwater concentration (calculated by PORFLOW) for the parent (pCi/L).

Radionuclide parent with a chain

The method to calculate the disposal limit for a radionuclide parent with a chain is to replace Step 1 from the method above with a sum-of-fractions, where all radionuclides in the chain are included. Thus Step 1 becomes

$$f = \sum_i \frac{C_i^{gw}}{CL_i^{gw}}$$

The combination of the revised Step 1 with Step 2 and Step 3 produces the following equation:

$$I_{all} = I_{pm} x \frac{1}{\sum_i \left(\frac{CL_i^{gw}}{C_i^{gw}} \right)}$$

where

I_{all} is the disposal limit (Ci) for the parent,

I_{pm} is the modeled inventory for the parent (Ci),

CL_i^{gw} is the groundwater concentration limit for the ith nuclide (pCi/L), and

C_i^{gw} is the groundwater concentration (calculated by PORFLOW) for the ith nuclide (pCi/L).

Radionuclide parent with a chain combined with existing inventory

To establish disposal limits where existing inventory exists and is modeled separately, which is only implemented for the CIG disposal unit, the groundwater concentration includes the contributions from the existing inventory and the future inventory for which the allowable inventory limits are being calculated. The concentration from the future inventory is scaled by the ratio of the allowable future inventory divided by the modeled inventory. The combined fraction, which cannot exceed 1, is calculated as follows:

$$\mathrm{f} = \sum_i \left[\frac{\mathrm{I}^{\mathrm{ES}}\mathrm{C}_{\mathrm{i}}^{\mathrm{ES}} + \frac{I_{all}}{I_{pm}} C_i^{FS}}{\mathrm{CL}_{\mathrm{i}}} \right] = 1$$

This equation can be rearranged to calculate the disposal limit as follows:

$$I_{all} = I_{pm} x \left[\frac{1 - I^{ES} \sum_i \left(\frac{C_i^{ES}}{CL_i} \right)}{\sum_i \left(\frac{C_i^{FS}}{CL_i} \right)} \right]$$

where

I^{ES} - Existing Segments' inventory for ith isotope,

C_i^{ES} - Existing Segments' maximum groundwater concentration for ith isotope (pCi/L-Ci),

I_{all} - allowable inventory (disposal limit Ci) for the parent,

I_{pm} - modeled inventory for the parent (Ci),

C_i^{FS} - Future Segment maximum groundwater concentration for ith isotope (pCi/L-Ci), and

CL_i - groundwater concentration limit for ith isotope (pCi/L).

For all the cases above, the calculations are performed by the All-Pathways Application (Koffman 2006b).

4.5.3 Air- Pathway Dose Calculation

The DOE 435.1 requirement for an assessment of the dose for the air pathway is found in DOE M 435.1-1.IV.P.(1).(b), which states (DOE 1999a):

(b) Dose to representative members of the public via the air pathway shall not exceed 10 mrem (0.10 mSv) in a year total effective dose equivalent, excluding the dose from radon and its progeny.

The methodology to calculate dose from the air pathway is included in the CAP-88 model. The model uses dose conversion factors which include the EDE calculated with the weighting factors in ICRP Publication Number 26, provided for ingestion and inhalation intake, ground level air immersion (plume shine), and ground surface irradiation (ground shine).

The air concentrations calculated in CAP-88 at the SRS site boundary and 100-m receptor locations (Section 4.3.2) are used within the code application to calculate pathway-specific doses to the MEI. The MEI is assumed to be located at the nearest home, farm, business, or school, and is assumed to breathe the air, as well as eat vegetables, meat, and milk produced at, that location. The MEI for the SRS boundary is located at a distance of approximately 11,800 m to the north of the E-Area LLWF (Lee 2006). An additional receptor location is assumed to be 100-m from the potential release locations (i.e., individual disposal units).

Site- and pathway-specific parameters for the SRS were taken from Lee (2001) for the air-pathway dose calculations. The DRFs, representing the ratio of the calculated EDE to the source release rate (Ci/yr), were calculated for each release point (the E-Area LLWF for the SRS boundary calculation, and the individual dose units for the 100-m calculations). The results are given in Table 4-9.

These factors are used to estimate EDE for a given release, as calculated according to the model described in Section 4.1 for estimating flux of volatile radionuclides at the ground surface. The DRFs may also be used to calculate disposal limits by considering the 10 mrem/yr performance objective.

Table 4-9. Atmospheric DRFs for E-Area LLWF Disposal Units (from Lee, 2006)

	Dose Release Factors – mrem/Ci							
	SRS Boundary	**100-m distance from disposal unit**						
Radionuclide	E-Area LLWF	643-26E NRCDA	643-7E NRCDA	CIG Trench	LAWV	ILV	Slit Trench	Engineered Trench
C-14	1.1E-04	7.0E-02	3.5E-01	5.9E-02	5.9E-02	3.5E-01	5.9E-02	5.9E-02
Cl-36	2.3E-04	1.1E-01	5.6E-01	9.3E-02	9.3E-02	5.6E-01	9.3E-02	9.3E-02
H-3	2.2E-06	1.5E-03	7.3E-03	1.2E-03	1.2E-03	7.3E-03	1.2E-03	1.2E-03
I-129	4.9E-02	1.0E+02	5.2E+02	8.6E+01	8.6E+01	5.2E+02	8.6E+01	8.6E+01
S-35	2.8E-05	9.3E-03	4.6E-02	7.7E-03	7.7E-03	4.6E-02	7.7E-03	7.7E-03
Sb-124	2.0E-03	6.8E-01	3.4E+00	5.7E-01	5.7E-01	3.4E+00	5.7E-01	5.7E-01
Sb-125	6.5E-03	2.0E+00	1.0E+01	1.7E+00	1.7E+00	1.0E+01	1.7E+00	1.7E+00
Se-75[a]	1.1E-03	3.7E-01	1.8E+00	3.1E-01	3.1E-01	1.8E+00	3.1E-01	3.1E-01
Se-79[b]	6.3E-04	2.2E-01	1.1E+00	1.8E-01	1.8E-01	1.1E+00	1.8E-01	1.8E-01
Sn-113	2.3E-04	9.2E-02	4.6E-01	7.7E-02	7.7E-02	4.6E-01	7.7E-02	7.7E-02
Sn-119m[a]	1.0E-04	4.0E-02	2.0E-01	3.3E-02	3.3E-02	2.0E-01	3.3E-02	3.3E-02
Sn-121	4.2E-05	1.4E-02	7.1E-02	1.2E-02	1.2E-02	7.1E-02	1.2E-02	1.2E-02
Sn-121m[b]	6.5E-04	2.2E-01	1.1E+00	1.8E-01	1.8E-01	1.1E+00	1.8E-01	1.8E-01
Sn-123	1.3E-05	4.0E-03	2.0E-02	3.3E-03	3.3E-03	2.0E-02	3.3E-03	3.3E-03
Sn-126[c]	3.0E-01	9.2E+01	4.6E+02	7.7E+01	7.7E+01	4.6E+02	7.7E+01	7.7E+01

a Not in CAP-88 database. DRF based on Sn-113 surrogate χ/Q.

b Not in CAP-88 database. DRF based on Sn-126 surrogate χ/Q.

c Includes progeny.

4.5.4 Radon Flux Calculation

The DOE 435.1 requirement for an assessment of the radon flux at the surface of the disposal facility is found in DOE M 435.1-1.IV.P.(1).(c), which states (DOE 1999a):

(c) Release of radon shall be less than an average flux of 20 pCi/m^2/s (0.74 Bq/m^2/s) at the surface of the disposal facility. Alternatively, a limit of 0.5 pCi/l (0.0185 Bq/l) of air may be applied at the boundary of the facility.

Radon flux was calculated according to the methodology described in Section 4.1 in evaluating flux of volatile radionuclides at the ground surface above the disposal units, using a 1D application of the PORFLOW code. The maximum flux was evaluated at different time periods for the disposal unit types, according to the degradation scenarios assumed for each type. Only Rn-222 was evaluated; the short half-life of Rn-220 (55.6 seconds) makes it unlikely to escape the E-Area LLWF disposal units and migrate to the land surface via air-diffusion through soil pores. All potential radionuclide parents within decay chains leading to formation of Rn-222 were considered.

5.0 INTERPRETATION OF RESULTS

5.1 SENSITIVITY AND UNCERTAINTY ANALYSIS

Achieving reasonable assurance that disposal units will meet DOE 435.1 performance objectives requires a thoughtful consideration of uncertainty in PA model design, model inputs, and facility operations. For this PA, uncertainties were addressed in the groundwater pathway by employing a combination of quantitative uncertainty analysis, conservative modeling assumptions, and qualitative and quantitative sensitivity analysis. Details of these analyses and results are presented in the respective PA modules.

For the Slit/Engineered trenches, CIG trenches, and NRCDAs, a probabilistic uncertainty analysis was conducted using a commercial program, GOLDSIM. GOLDSIM was developed by GoldSim Technology Group LLC (GTG 2006a), and is a user-friendly and highly graphical Windows-based program for carrying out dynamic, probabilistic simulations of complex systems to support management and decision-making. GOLDSIM utilizes the flow field outputs from PORFLOW to perform transport calculations and subsequent dose calculations for evaluation of input parameter importance and calculation uncertainties.

The baseline GOLDSIM model (using nominal input values) was calibrated to the PORFLOW model used to set disposal limits. Inputs to the GOLDSIM model for each the Slit and Engineered trenches, CIG trenches, and NRCDAs were treated as stochastic (random) variables and assigned statistical distributions based on data and/or professional judgment. The parameters selected for variable input were those which had the major effect on the calculated groundwater concentrations and dose, as determined by previous sensitivity analyses, or professional judgment. The Monte Carlo analysis performed by the GOLDSIM program generates a large number of "realizations" by randomly assigning values to each of the model inputs (according to defined statistical distributions) and computing a dose. The ensemble of Monte Carlo outputs is used to define a statistical distribution of dose. The probability of exceeding performance objectives can be defined from this distribution.

For the remaining E-Area disposal units (ILV and LAWV), a tiered approach for addressing uncertainty in PORFLOW-based dose calculations was carried out. The general approach involved the following elements:

a) Conservative assumptions: For some portions of the groundwater pathway analysis, conservative assumptions and/or parameter values were adopted in order to largely alleviate the need for subsequent uncertainty analysis for that aspect of the model. An example is assuming a worst-case (bounding) time for vault failure.

b) Qualitative sensitivity analysis: The remaining PORFLOW model inputs, by definition, are those with uncertainty on both sides of their nominal values. Nominal values are typically best estimate or mildly conservative. These inputs were qualitatively ranked, using past experience and professional judgment, with respect to anticipated contribution to overall model/dose uncertainty. Model assumptions and inputs judged to have low impact on overall uncertainty were identified and omitted from further quantitative consideration. An example input falling into this category would be radionuclide half-lives. Although radionuclide transport and dose are sensitive to half-life, the parameter is known to relatively high precision. Uncertainty in this particular parameter has a negligible contribution to overall model uncertainty.

c) Quantitative sensitivity analysis: PORFLOW sensitivity runs were performed for inputs deemed to have a significant impact on overall dose and inventory limits. For example, PORFLOW transport simulations are sensitive to K_d and this parameter often has large uncertainty. For sensitivity runs, each key input will be perturbed in the conservative direction by an amount corresponding to roughly "2-sigma" or 95th percentile.

For the ILV, sorption coefficients (K_d) and effective diffusion coefficient are judged to be the dominant contributors to dose uncertainty, and sensitivity runs were conducted by varying these two parameters. For the LAWV, K_d, diffusion coefficient, vault cracking, and infiltration were identified for sensitivity runs. Sensitivity runs were conducted by varying all except infiltration rates. Unlike the other inputs, uncertainty in infiltration has not yet been defined. Additional work is required to define the probability of the various land usage and vegetative cover scenarios, and the extent to which climate change should impact infiltration uncertainty. This additional scope is proposed for PA maintenance.

5.2 USE OF PERFORMANCE ASSESSMENT RESULTS

The primary use of the PA results is to develop radionuclide disposal limits for each of the disposal units. Limits are developed by ratio of the maximum impact (e.g., all-pathways dose) calculated for a specific time period for a unit inventory of each radionuclide to the respective performance measure (e.g., 25 mrem/year). The PA-derived limits are expressed in terms of curies per disposal unit. For the groundwater pathway, which is generally the most limiting, the time period for the analysis is sub-divided into two or three periods and limits are derived for each period. These time periods were established to separate impacts from groundwater peaks that occur at different times, which reduces the conservatism in the sum-of-fractions of limits method of assessing compliance. The time periods used in this PA are shown in Table 5-1.

Table 5-1. Time Periods for Groundwater Pathway Limits

Disposal Unit	Performance Measure	Time Periods, years
Slit & Engineered Trenches	All-Pathways Dose	130-200, 200-1000, 1000-1130
	Beta-Gamma	0-12, 12-100, 100-1130
	Gross Alpha	0-1000, 1000-1120, 1120-1130
	Radium	0-1000, 1000-1120, 1120-1130
	Uranium	0-1130
Component-In-Grout Trenches	All-Pathways Dose	0-1125
	Beta-Gamma	0-1125
	Gross Alpha	0-1125
	Radium	0-1125
	Uranium	0-1125
Low Activity Waste Vault	All-Pathways Dose	0-1125
	Beta-Gamma	0-1125
	Gross Alpha	0-1125
	Radium	0-1125
	Uranium	0-1125
Intermediate Level Vault	All-Pathways Dose	0-200, 200-1100
	Beta-Gamma	0-200, 200-1100
	Gross Alpha	0-200, 200-1100
	Radium	0-200, 200-1100
	Uranium	0-200, 200-1100
Naval Reactor Component Disposal Areas	All-Pathways Dose	0-1000
	Beta-Gamma	0-1000
	Gross Alpha	0-1000
	Radium	0-1000
	Uranium	0-1000

The inventory limits calculated in this PA are implemented through a set of WACs and managed through the SRS's computerized WITS. The operating limits for the E-Area LLWF, as documented in the SRS WAC Manual (WSRC 1997b), are derived from safety documentation and the PA. The WAC Manual is a compilation of the radionuclide limits from a DSA, criticality limits, 100 nCi/g transuranic concentration limit, and performance-based inventory limits.

As packages are received for emplacement in the various disposal units (i.e., vault or trench), their package contents are entered into WITS. Before emplacement of each package, WITS will compare the package contents with the 100 nCi/g transuranic limits, and calculate the inventory (to ensure compliance with the criticality limits) and the total disposal inventory (to ensure compliance with the PA-based limits). The DSA and PA-based limits are tracked as a sum-of-fractions of the individual radionuclide limits. A separate sum-of-fractions is calculated for the air pathway, radon pathway, each relevant intruder scenario, and separate time frames for the groundwater pathway (Collard, 2003), as appropriate. For the PA-based limits, the total disposal unit inventory for each radionuclide is divided by its corresponding limit for each of these calculations. The sum of these fractions is maintained less than one to ensure compliance with the limits and, thus, the performance measures. A similar procedure is followed to ensure compliance with the DSA limits.

The PA sensitivity and uncertainty results are also useful in determining which parameters of the disposal facility future PA maintenance activities should focus on. These activities may include development of more rigorous analytical techniques, or enhanced efforts to more accurately quantify environmental, or other physical, parameters.

5.3 PERFORMANCE EVALUATION

The purpose of this site-specific PA of the E-Area LLWF is to fulfill the DOE Order 435.1 requirement that such an assessment be prepared and maintained for any LLW disposal facility located at a DOE field site. The PA must provide reasonable assurance that the facility design and method of disposal will comply with the performance objectives of the Order, which are concerned with protection of public health and safety, limiting doses to members of the public and assessing impacts to hypothetical inadvertent intruders, and assessing impacts on water resources.

The PA results allow a comparison of projected radionuclide inventories at closure with the PA-derived radionuclide disposal limits. Compliance with performance measures is assessed by dividing the projected inventory at closure for each radionuclide in a particular disposal unit with the disposal limits determined for that unit. Summing the limit fractions for each performance measure and time period allows the sum-of-fractions to be calculated. An SOF less than one indicates compliance with the performance measure. Final radionuclide disposal limits are presented in Chapter 7. Projected inventories at closure and limit fractions are tabulated in Appendix C. The sum-of-fractions method of assessing compliance assures future compliance despite changing projected inventories.

6.0 FUTURE WORK

DOE through its Waste Management Order, DOE Order 435.1, requires the maintenance of performance assessments and composite analyses. Because the PA and CA results are in part based on technically uncertain data, conservative parameters, or both, a maintenance program has been established to provide greater confidence in the results of the analyses. The plan also identifies work needed to confirm the continued adequacy of the PA and CA in response to changes in LLW disposal practices and relevant new information and data. The plan is a 10-year forward look at potential studies needed to support near term operations, planned future PA/CA revisions and reviews, PA/CA monitoring data evaluation and program improvements, as well as long term test and research.

Preparation of this PA has identified a number of areas where further research is needed to fill data gaps, reduce uncertainty or enhance methods of analysis. Potential areas for further research include: extension of GoldSim modeling for evaluating uncertainty in the remaining disposal units, field and laboratory evaluation of geochemical parameter variability, refinement of waste zone hydraulic properties, representation of non-uniform waste emplacement, representation of flow and transport through cracked concrete, etc. These and similar studies will be considered for inclusion in the FY08 update of the PA/CA Maintenance Plan.

7.0 QUALITY ASSURANCE

7.1 SOFTWARE QA

WSRC employs an administrative system for controlling software throughout its life cycle. This administrative system is governed by and described in WSRC 1Q Manual, Procedure QAP 20-1, Software Quality Assurance (WSRC 2006a). The software life cycle is the basis for planning and implementing SQA requirements and consists of the following phases:

- Functional Requirements
- Design
- Implementation
- Verification and Validation
- Installation and Acceptance
- Operations and Maintenance
- Retirement

QAP 20-1 addresses SQA requirements for Purchased Software and Software Development. It also recognizes a third category, called Existing Software, which addresses those software applications that were not developed or acquired in accordance with this procedure. The procedure defines roles for the CTF, the CTF's Manager, and the CQF to oversee and implement the program. A set of requirements is identified and discussed in the context of the various life cycle phases. Those requirements are:

- Software Classification
- SQA Procedures / Plans
- Dedication
- Evaluation
- Requirements
- Design
- Implementation
- Testing
- User Instructions
- Acceptance Test
- Operation & Maintenance
- Configuration Control
- Error Impact
- Access Control

These QA requirements are implemented using a graded approach based on the intended use of the software and potential impacts to safety, production, cost and regulatory compliance. Software is classified and designated level A (highest) through E (lowest) based on these factors. For the purposes of the PA, software classification Level C was selected as being applicable to software used to set radionuclide disposal limits or provide direct input to other applications producing limits. This decision was based on the Level C criteria for; "software used to comply with regulatory laws, environmental permits or regulations and /or commitments to compliance" (WSRC 2006a).

Table 7-1 identifies the primary applications utilized in the development of this performance assessment, associated category and classification, use in the PA, and applicable references such as SQA Plans where the requirements for the various lifecycle phases are discussed.

Table 7-1. Primary Software Applications used in E-Area Performance Assessment

Application	Category	Level[a]	Software Use in PA Revisions	References[b]
PORFLOW version 5.97	Purchased software	C	Produced groundwater flow and transport simulations.	Hang, 2006a and 2006b; ACRI, 2004; Flach, 2004; Aleman, 2007
GoldSim version 9.0	Purchased Software	C	Carried out probabilistic simulations for evaluating uncertainty in PA model parameters.	Swingle, 2006; GTG, 2005a and 2005b
SRNL All-Pathways Application	Software Development	C	Integrated all-pathways analysis with groundwater transport and assessed impact on water resources by calculating four criteria for groundwater protection in EPA drinking water regulations. The all-pathways dose is calculated on exposure pathways used in a version of LADTAP modified for the all-pathways application.	Koffman, 2006b and 2006c; Jannik, 2006; Jannik and Dixon 2006
Automated Inadvertent Intruder Application Version 2.0	Software Development	C	Performed inadvertent intruder analyses. Includes automated groundwater screening option as part of application.	Koffman, 2006a and 2006d; Lee, 2004; Taylor and Collard, 2005
MINTEQA2 for Windows version 1.50-MS	Purchased Software	D	Used for scoping calculations to produce chemical speciation in aqueous systems.	Allison Geoscience Consultants and HydroGeoLogic, Inc., 2003
HELP version 3.07	Public Domain software	C	Calculated water balance across the closure cap to provide infiltration estimates for use in PORFLOW groundwater modeling	Phifer, 2006
CAP88 version 1.2	Purchased Software	B	Used to estimate dose to the maximally exposed individual (offsite and at 100 m from release) for numerous exposure pathways.	Jannik, 2006
RETC Version 6.0	Public Domain software	C	Analyzed the soil water retention and hydraulic conductivity functions of unsaturated soils.	Jones, 2007
ANSYS version 9.0	Purchased software	B	Evaluated impact of seismic events and long-term settling on E-Area Vaults structural integrity.	*Standard Software Quality Assurance Plan for PD&CS – Design Services Engineering Software (U)*, 2005
SCALE, version 5.0	Purchased Software	B	Performed a thermal analysis of the TEF TPBARs in the ILV.	Vinson, 2005
MESH3D	Software Development	C	Extracted a sub-region of the General Separations Area PORFLOW aquifer model and subdivided the coarse mesh to produce a higher-resolution grid for analyzing flow in the region of interest.	Flach, 2007
Idealfilemaker	Software Development	C	Extracted information from PORFLOW output files, reformatted, converted units and expanded reduced chains to produce files recognized by the SRNL All-Pathways Application (Ideal files).	Taylor, 2006

[a] From WSRC (2006a)
[b]References include software QA plans, test plans, user's manuals and other related documentation.

7.2 TECHNICAL REVIEW

Requirements for performing reviews of technical reports are established in WSRC Procedure Manual E7, 2.60, *Technical Reviews* (WSRC 2006b). The end use of data drives the level of review required. Design Verification, the highest level review, must be performed for work affecting Safety Significant/Safety Class systems. The adequacy of technical reports not subjected to Design Verification is determined by a Design Check in accordance with Manual E7, 2.60. The SRNL Technical Report Design Check Guidelines manual (WSRC 2004b) has been developed to apply a graded approach in meeting these requirements and is appropriate for use in both types of review. A good Design Check will consist of the following six elements:

- review of analytical/experimental approach
- mathematical check
- review for correct use of analytical/experimental input
- review of the justification for assumptions
- review of the reasonableness of output
- cross-check of data for accuracy of transcription

Design checks have been performed per the SRNL Design Check Guidelines for every PA analysis and supporting study. The design check instruction, reviewer responses and comment resolution are documented in writing. Upon completion of the review for the analyses contained in each Module of the PA the documentation was compiled and documented with a cover letter containing an SRNL correspondence number and placed in the E-Area PA project file. SRNL QA performed an independent assessment of many of these design check packages to ensure implementation of the technical review process.

Another component of the technical review process is customer comments. As the initial draft (Draft A) of each PA Module was completed it was sent out for review to the DOE-SR and WMAP customer representatives who were members of the E-Area PA core team. Comments were tabulated and returned for resolution to the principal investigator for each analysis. A comment reconciliation meeting was held with the customer to gain agreement on responses. These completed comment, response and resolution tables were then used to produce Draft B of each Module. Draft B was sent back out to the customer for a final review. Customer comment, response, and resolution tables were also placed in the E-Area PA project files.

8.0 LIST OF PREPARERS

Leonard B. Collard

M.S. Civil Engineering, University of Arizona
B.A., Mathematics, Duke University

Mr. Collard is a principal engineer for Washington Savannah River Company with over twenty years of experience. Recent work has focused on Performance Assessment activities. Earlier work included water and sewer planning and foundation analyses.

For this study, Mr. Collard performed the groundwater pathway analysis for the LAWV and completed a design check for the groundwater pathway analysis of the CIG trenches.

James R. Cook

M.S., Geochemistry - State University of New York at Binghamton, 1977
B.S., Geology - University of Arizona, Tucson, 1970

Jim Cook recently retired as a Senior Fellow Geologist from the Savannah River National Laboratory after working for 25 years in various aspects of low-level waste research. Research topics have included site selection, site characterization, site closure, performance assessment and probabilistic uncertainty analysis. He was the technical team lead for the earlier SRS Performance Assessments for E-Area and Saltstone disposal facilities as well as the SRS Composite Analysis.

Mr. Cook is currently a consultant.

For this Performance Assessment, Mr. Cook did the intruder analysis calculations and wrote the intruder sections for each disposal unit. He prepared the chapters on the ILV and NRCDA disposal units and contributed to the Slit and Engineered Trench, and Integration and Interpretation chapters.

Kenneth L. Dixon

M.E., Civil Engineering, University of South Carolina
M.S., Agricultural Engineering, University of Georgia
B.S., Agricultural Engineering, University of Georgia

Mr. Dixon is a Principal Engineer at the Savannah River National Laboratory (SRNL) where he has conducted research related to soil and groundwater characterization and remediation for 16 years. He has worked on pilot scale testing of innovative remedial technologies and numerical modeling of contaminant fate and transport in the vadose zone. More recently, he has been involved in projects determining the physical and hydraulic properties of cementitious materials for use in waste disposal activities at the SRS.

For this study, Mr. Dixon conducted the air and radon pathway analyses and assisted with the technical review of the Integrated Facility Analysis.

Gregory P. Flach

Ph.D., Mechanical Engineering, North Carolina State University, Raleigh, 1988
Master of Mech. Engineering, North Carolina State University, Raleigh, 1984
B.S., Mechanical Engineering, University of Kentucky, Lexington, 1983

Dr. Flach is a Fellow Engineer at Savannah River National Laboratory with 18 years of experience related to groundwater hydrology, computational simulation, and numerical code development. He has been the principal investigator on a number of groundwater modeling studies at the Savannah River Site involving regional and local scale hydrology, contaminant migration from waste sites, and evaluation of environmental cleanup alternatives. Over the last decade his efforts have focused on performance assessment and composite analysis related projects, and research involving dual-domain formulations of contaminant transport.

For this study, Dr. Flach has been one of the principal investigators, focusing on the Slit Trench, Engineered Trench, and Integrated Facility groundwater pathway modules.

L. Larry Hamm

B.S., M.S., PhD., Chemical Engineering, University of South Carolina

Dr. Hamm, with twenty-five years of experience, currently serves as a Fellow Engineer at SRNL who has been a technical contributor, technical director, and program manager on a wide variety of DOE nuclear reactor, waste management, and environmental cleanup related programs. Dr. Hamm co-authored the FACT code used for modeling subsurface contaminant transport at various DOE waste sites. Recent work has focused on Performance Assessment activities at SRS.

For this study, Dr. Hamm performed the groundwater pathway analysis for the CIG trenches and completed a design check for the groundwater pathway analysis of the LAWV.

Robert A. Hiergesell

M.S., Hydrogeology, University of Nebraska-Lincoln, 1985
B. S., Geology, Virginia Polytechnic Institute, Blacksburg, Va. 1972

Mr. Hiergesell has over 25 years of experience in the field of hydrogeology. This experience includes applications in groundwater monitoring, surface water hydrology, subsurface flow and transport simulation, environmental remediation and performance assessment for low-level radioactive waste disposal. He has been the lead technical investigator for numerous environmental restoration and waste management projects at the DOE Savannah River Site.

In this PA, Mr. Hiergesell was one of the principal investigators contributing to this investigation, including coordination, integration, design checking and documentation of the different analyses performed for the ILV and Slit and Engineered Trenches. Included in this was performing the groundwater pathway analysis for the ILV and contributing to the groundwater pathway analysis performed for the trenches.

Mary Fitzhugh Jones

M.A., Geography, University of Pittsburgh, Pittsburgh, PA, 1975
B.A., Geography, University of Oklahoma, Norman, OK, 1966

Mimi Jones is the Technical Editor for the Savannah River National Laboratory, a multi-faceted assignment. On one hand, she has sole responsibility for operation of the Division procedure program (administrative and technical procedures for all aspects of Laboratory applications). On the other hand, she edits and formats research reports for multiple projects throughout the Laboratory.

Building on her journalism background that began at the University of Oklahoma, she applied her skills to technical writing and editing. Her career started in 1981 as a technical writer at the Idaho National Laboratory. She developed a series of Process Description Manuals in support of existing and new facilities during her tenure and supported startup of three new facilities (contributing to both manuals and procedures). She transferred to the Savannah River Site in 1991 and participated in the startup of the Defense Waste Processing Facility. In 2000, she accepted a new position as Technical Editor for the Savannah River National Laboratory, where she continues her procedure and editing work.

For this project, Ms. Jones served as the principal technical editor for the Performance Assessment document.

Patricia L. Lee

Ph.D., Health Physics, Georgia Institute of Technology, Atlanta, 1998
M.S., Physics, Clark Atlanta University of California, Atlanta, 1992
B.S., Physics, Lincoln University (PA), 1987

Dr. Lee is an Environmental Health Physicist with a diverse scientific background including over 16 years of experience in Health Physics. For the past seven years, she has worked in the Savannah River National Laboratory working on and performing research associated with dose and risk assessments for a variety of Savannah River Site (SRS) projects. Her support of performance assessment activities at SRS are primarily focused on inadvertent intruder analysis, air-pathway modeling and site-specific input parameters.

For this study, Dr. Lee developed the air-pathway dose-release factors, contributed to the development of the inadvertent intruder analysis application, and participated in the document development.

Laura McDowell-Boyer

Ph.D., Civil/Environmental Engineering, University of California, Berkeley, 1989
M.S., Radiological Health Physics, Colorado State University, Fort Collins, 1976

Dr. McDowell-Boyer has 22 years experience related to radiological exposure assessment, including multi-media environmental transport models, mechanisms of subsurface contaminant migration via colloids, and groundwater flow and transport. Dr. McDowell-Boyer was the principal investigator from Oak Ridge National Laboratory on the SRS Z-Area PA, co-principal investigator on the SRS E-Area PA (Rev. 0 and Rev. 1), and was responsible for pathway and dose analysis as well as much of the documentation of the SRS CA. In addition, she has developed source terms for health risk assessments at Lawrence Livermore National Laboratory, and conducted environmental dose reconstructions for workers at the Rocky Flats Plant, Los Alamos National Laboratory, Argonne National Laboratory East facility, the Weldon Spring Plant, and Sandia National Laboratory in California.

For this study, Dr. McDowell-Boyer was the principal author of the Background Chapter, the Executive Summary and Synopsis, contributed to the final revisions of the Integrated Facility Analysis and CIG Trench Chapters, and prepared the responses to the LFRG Criteria Matrix in Appendix D.

Margaret R. Millings

M.S., Geology, University of Georgia, Athens, GA, 1997
B.S., Geology, The University of the South, Sewanee, TN, 1994

Ms. Millings is a Senior Scientist with the Savannah River National Laboratory with eight years of experience related to groundwater and surface water hydrology, coastal plain geology and geochemistry. During the last 6 years she has been involved in various subsurface characterization and monitoring studies at the Savannah River Site including: looking at the mineralogy, geochemistry, and physical characteristics of sediments from DNAPL contaminated sites; investigating naturally occurring stable isotopes of Sr, I, Cs, and Co from SRS groundwater in order to better understand the fate and transport and the remediation of their radioactive counterparts (Sr-90, I-129, Cs-137, Co-60); examining natural radium concentrations (Ra-226 and Ra-228) of coastal plain groundwater and sediments; and interpreting geology and depositional environments from core sediments, geophysical logs and piezocone penetration logs. She has also assisted in environmental restoration projects involving the injection of organics (e.g., soybean oil) into the subsurface to promote bacterial growth to remediate metal and DNAPL plumes, in addition to working on remedial alternatives for achieving regulatory compliance for metals at surface water outfalls.

For this study, Ms. Millings has been one of the principal investigators contributing to the coordination and preparation of the background sections and serving as a technical reviewer.

Mark A. Phifer

M.S., Civil Engineering (Environmental and Geotechnical) – University of Tennessee, 1993
B.S., Civil Engineering – Tennessee Tech, 1981
South Carolina Registered Professional Engineer (No. 12310)

Mr. Phifer is a Senior Fellow Engineer with the Savannah River National Laboratory. He has 23 years of environmental and geotechnical experience at the Savannah River Site. The first 10 years included environmental regulatory compliance, civil/environmental design, project engineering (closure of a mixed waste landfill and basins (80 acres)), and management (environmental remediation technology). The subsequent 13 years have been at the Savannah River National Laboratory developing, deploying, and evaluating waste site closure, groundwater remediation, and radioactive waste disposal technologies. These technologies include horizontal and vertical barrier systems, diffusion barriers, closure caps (including their degradation), waste subsidence, low-level radioactive waste disposal facilities, cementitious barriers and wasteforms, permeable reactive barriers, GeoSiphon / GeoFlow groundwater treatment systems, sulfate reduction remediation, reductive dechlorination, and vadose zone and aquifer characterization and testing. For the last 5 years Mr. Phifer has in addition worked on Performance Assessment related activities.

For this study, Mr. Phifer has been one of the principal investigators, focusing on closure cap configuration and degradation; infiltration estimates; soil and cementitious material hydraulic properties; air and radon modeling; and facility description, lifecycle, and design features.

Robert F. Swingle, II

B.S., Chemical Engineering, University of South Carolina, Columbia, 1981
B. S., Chemistry, University of South Carolina, Columbia, 1979

Mr. Swingle is a Senior Technical Advisor with the Savannah River National Laboratory, with twenty-six years of experience at the Savannah River Site. He began his career by working thirteen years with nuclear production reactor thermo-hydraulics, physics, and moderator chemistry. This was followed by ten years researching treatment and characterizing radioactive waste. For the last three years, he has been working for the Environmental Analysis and Performance Assessment Group of the Savannah River National Laboratory supporting low level radioactive waste disposal activities at the Savannah River Site.

For this study, Mr. Swingle supported groundwater pathway and intruder analysis and technical review.

John Tauxe

Ph.D., Civil Engineering, University of Texas at Austin, Austin, Texas, 1994
M.S., Civil Engineering, University of Texas at Austin, Austin, Texas, 1990
B.A., Earth Science, Wesleyan University, Middletown, Connecticut, 1984

Dr. Tauxe has been working in the earth and environmental sciences and engineering since 1981, and has developed expertise in quantitative hydrology and hydrogeology, and in computer programming, concentrating in the modeling of contaminant fate and transport in the environment. His professional experience is broad, however, including marine geology, radiolimnology, water resources assessment, hydropower systems modeling, regulatory interpretation, metrication, watershed mapping, radiological performance assessment, and training of environmental professionals. Since 1998, Dr. Tauxe has been advancing the field of probabilistic performance assessment within the Department of Energy and the Nuclear Regulatory Commission, and is an internationally recognized expert in radiological performance assessment modeling.

For this study, Dr. Tauxe has served as a lead GoldSim programmer, and advisor to probabilistic performance assessment methodology.

Glenn A. Taylor

M.S., Mechanical Engineering, University of Texas-Austin, 1979
B.S, Engineering Physics, University of Louisville, 1977

Mr. Taylor has 28 years of experience in code development, modeling, and research. His primary emphasis has been non-equilibrium thermal-hydraulics and chemical process methods development and modeling. He has been involved with PRA-type analyses since the mid-1980s. He has been doing groundwater modeling and contaminant transport modeling for the past 3 years.

For this study Mr. Taylor performed the NRCDA groundwater pathway transport and the sensitivity and uncertainty analysis for the NRCDA, Slit Trenches, and Engineered Trenches.

Elmer L. Wilhite

B.S., Chemistry, University of Missouri at Columbia, 1966
M.S., Inorganic Chemistry, Washington University, 1969

Mr. Wilhite is a Senior Advisory Scientist at the Savannah River National Laboratory. He has 38 years of experience in environmental, health physics, and waste management fields. During the past 20 years, he has focused his efforts on performance assessment projects. He was the chairman of the DOE Performance Assessment Peer Review Panel. He was also the Technical lead for DOE for the radiological assessment section of the response to the DNFSB recommendation 94-2. He continues to be a consultant to DOE Headquarters on low-level waste management.

For this study, Mr. Wilhite was the principal author of the Integration and Interpretation Section.

Karen E. Young

B.S., Environmental Resource Management, The Pennsylvania State University, 1986

Ms. Young has over 16 years of experience as an environmental scientist with expertise in regulatory compliance. She specializes in project management, regulatory agency interface/liaison services, and preparation of environmental compliance documentation. She has assisted DOE, DOD, and private industry with RCRA, CERCLA, NEPA, NRC, and DOE Order compliance and has assisted the EPA in developing RCRA regulations. Ms. Young has managed the preparations of regulatory compliance and remediation permit applications and reporting documentation for the Mixed Waste Management Facility, the Old Radioactive Waste Burial Ground, and the F- and H-Seepage Basins at the Savannah River Site as well as providing support services for preparation of the Z-Area and E-Area Low-level Waste Facility Performance Assessments, Monitoring Plans, Closure Plans and the Composite Analysis at the Savannah River Site.

For this analysis, Ms. Young assisted with documentation preparation and coordination, DOE Order compliance, and consistency, comprehensiveness, and design check review.

9.0 REFERENCES

Aadland, R. K., Harris, M. K., Lewis, C. M., Gaughan, T. F. and Westbrook, T. M. 1991. *Hydrostratigraphy of the General Separations Area, Savannah River Site (SRS), South Carolina*, WSRC-RP-91-13, Westinghouse Savannah River Company, Aiken, SC.

Aadland, R. K., Gellici, J. A. and Thayer, P. A. 1995. *Hydrogeologic Framework of West-Central South Carolina*, *Report 5*, Water Resources Division, South Carolina Department of Natural Resources, Columbia, SC.

ACRI (Analytic & Computational Research, Inc.). 2004. *PORFLOW User's Manual*, Version 5.0, Rev: 5. Available at http://www.acricfd.com/download/papers/PORFLOW.pdf

Aleman, S. E. 2007. *PORFLOW Testing and Verification Document*, WSRC-STI-2007-00150, Westinghouse Savannah River Company, Aiken, SC.

Allison Geoscience Consultants, Inc. and HydroGeoLogic, Inc. 2003. *MINTEQA2 for Windows Equilibrium Speciation Model version 1.50-MS*.

Arnett, M. W., Karapatakis, L. K. and Mamatey, A. R. 1993. *Savannah River Environmental Report for 1992*, WSRC-TR-92-0075, Westinghouse Savannah River Company, Aiken, SC.

Arnett, M. W., and Mamatey, A. R. 1996. *Savannah River Environmental Report for 1995*, WSRC-TR-96-0075, Westinghouse Savannah River Company, Aiken, SC.

Arnett, M. W., and Mamatey, A. R. 1997. *Savannah River Environmental Report for 1996*, WSRC-TR-97-0171, Westinghouse Savannah River Company, Aiken, SC.

Arnett, M. W., and Mamatey, A. R. 1999. *Savannah River Site Environmental Data for 1998*, WSRCTR-98-00314, Westinghouse Savannah River Company, Aiken, South Carolina.

Barton, C. D., Blake, J. I., and Imm, D. W. 2005. "SRS Forest Management: Ecological Restoration", in *Ecology and Management of a Forested Landscape: Fifty Years on the Savannah River Site*, J. C. Kilgo and J. I Blake eds., Island Press, Washington, DC, 479 p.

Bates, R. L. 1969. Geology of the Industrial Rock and Minerals, Dover Publications, New York, NY.

Bebbington, W. P. 1990. *History of DuPont at the Savannah River Plant*, E. I. DuPont De Nemours and Company, Wilmington, DE, 271 p.

Beres, D. A. 1990. *The Clean Air Act Assessment Package – 1988 (CAP-88). A Dose and Risk Assessment Methodology for Radionuclide Emissions to Air*, Volume 1 User's Manual, SC&A, Inc., McLean, VA, October.

Blake, J., I. 2005. "SRS Forest Management: Silviculture and Harvesting Activities", in *Ecology and Management of a Forested Landscape: Fifty Years on the Savannah River Site*, J. C. Kilgo and J. I Blake eds., Island Press, Washington, D.C. 479 p.

Blake, J. I., Hunter Jr., C. H., Bayle, B. A. 2005a. "The Physical Environment: Climate and Air Quality" in *Ecology and Management of a Forested Landscape: Fifty Years on the Savannah River Site*, J. C. Kilgo and J. I. Blake eds., Island Press, Washington, D.C. 479 p.

Blake, J. I., Mayer, J. J., and Kilgo, J. C. 2005b. "The Savannah River Site, Past and Present: Industrial Operations and Current Land Use" in *Ecology and Management of a Forested Landscape: Fifty Years on the Savannah River Site*, J. C. Kilgo and J. I Blake eds., Island Press, Washington, D.C. 479 p.

Bolz, R.E. and G.L. Tuve, (Editors), 1973. *Handbook of Tables for APPLIED ENGINEERING SCIENCE, 2'nd Edition*. CRC Press, 18901 Cranwood Parkway, Cleveland, OH

Cahill, J. M. 1982. *Hydrology of the Low-Level Radioactive-Solid-Waste Burial Site and Vicinity near Barnwell, South Carolina*, Open-File Report 82-863: Columbia, South Carolina, U. S. Geological Survey, 101 p.

Clarke, J. S. and West, C. T. 1997. *Ground-Water Levels, Predevelopment Ground-Water Flow, and Stream-Aquifer Relations in the Vicinity of the Savannah River Site, Georgia and South Carolina*, U.S. Geological Survey Water-Resources Investigations Report 974197, U.S. Geological Survey, Reston, VA.

Collard, L. B. 2003. *Special Analysis: Implementation of Sum-of-Fractions for Multiple Pathways including Select Groundwater Pathway Time Intervals*, WSRC-TR-2003-00438, Rev. 0, Westinghouse Savannah River Company, Aiken, SC.

Colquhoun, D. J., Woollen, I. D., Van Nieuwenhuise, D. S., Padgett, G. G., Oldham, R. W., Boylan, D. C., Bishop, J. W. and Howell, P. D. 1983. *Surface and Subsurface Stratigraphy, Structure and Aquifers of the South Carolina Coastal Plain*, South Carolina Department of Health and Environmental Control Report ISBN 0-9613154-0-7, 78p.

Cook, J R. and Wilhite, E. L. 2004. *Special Analysis: Radionuclide Screening Analysis for E-Area*, WSRC-TR-2004-00294. Westinghouse Savannah River Company, Aiken, SC. June 1, 2004.

Cook, J.R. 2007. *Radionuclide Data Package for Performance Assessment Calculations Related to the E-Area Low-Level Waste Facility at the Savannah River Site*, WSRC-STI-2006-00162, Rev. 0, Savannah River National Laboratory, Aiken, SC

Cooney, T. W., Drewes, P. A., Ellisor, S. W., Lanier, T. H., and Melendez, F. 2006. *Water Resources Data, South Carolina, Water Year 2005, Volume 1*, U. S. Geological Survey Water-Data Report SC-05-1, 621 p.

Cothran, E. G., Smith, M. H., Wolff, J. O., and Gentry. J. B. 1991. *Mammals of the Savannah River Site*, SRO-NERP-21, Savannah River Ecology Laboratory, Aiken, South Carolina.

Crapse, K. P. and Cook, J. R. 2004. *Atmospheric Pathway Screening Analysis for Saltstone Disposal Facility Vault 4***,** WSRC-TR-2004-00555, Rev 0**,** Westinghouse Savannah River Company, Aiken, SC.

Crapse, K. P. and Cook, J. R.. 2006. *Atmospheric Pathway Screening Analysis for the E-Area Low Level Waste Facility,* WSRC-TR-2006-00159, Rev 0**,** Westinghouse Savannah River Company, Aiken, SC.

Daniels, D.L., Zietz, I. and Popenoe, I. 1983. "Distribution of subsurface lower Mesozoic rocks in the southeastern United States, as interpreted from regional aeromagnetic and gravity maps, in studies related to the Charleston, South Carolina, earthquake of 1886 tectonics and seismicity" in *Studies Related to the Charleston, South Carolina, Earthquake of 1886--Tectonics and Seismicity*, G.S. Gohn, ed., US. Geological Survey Professional Paper 1313, KI-K24.

Davis, C. E. and Janecek, L. L. 1997. *DOE Research Set-Aside Areas of the Savannah River Site*, SRO-NERP 25, Savannah River Ecology Laboratory, Aiken, SC.

DCS (Duke Cogema Stone & Webster). 2002. *Mixed Oxide Fuel Fabrication Facility Environmental Report, Revision 1 & 2 ,* Docket Number 070-03098, Charlotte, NC. July.

Denham, M. E. 1999. *SRS Geology/Hydrogeology Environmental Information Document*, WSRC-TR-95-0046, Westinghouse Savannah River Company, Aiken, SC.

Dennehy, K. F. and McMahon, P. B. 1989. *Water Movement in the Unsaturated Zone at a Low-Level Radioactive-Waste Burial Site near Barnwell, South Carolina*, United States Geological Survey Water-Supply Paper 2345: Denver, Colorado, U. S. Geological Survey, United States Government Printing Office, 40 p.

Dennehy, K. F., Prowell, D. C., and McMahon, P. B. 1989. *Reconnaissance Hydrogeologic Investigation of the Defense Waste Processing Facility and Vicinity, Savannah River Plant, South Carolina*, U. S. Geological Survey Water Resources Investigations Report 88-4221, 74 p.

DOE (Department of Energy). 1995. *Savannah River Site Waste Management Final Environmental Impact Statement*, DOE/EIS-0217, Savannah River Operations Office, Aiken, South Carolina.

DOE (Department of Energy). 1997a. *Final Environmental Impact Statement Shutdown for the River Water System at the Savannah River Site*, DOE/EIS-0268, Savannah River Operations Office, Aiken, South Carolina.

DOE (Department of Energy). 1997b. *Draft Environmental Impact Statement, Accelerator Production of Tritium at the Savannah River Site*, DOE/EIS-0270D, Savannah River Operations Office, Aiken, South Carolina.

DOE (Department of Energy). 1998. *Savannah River Site Future Use Plan*, March 1998.

DOE (Department of Energy). 1999a. *Radioactive Waste Management*, Order 435.1, U.S. Department of Energy, Washington, DC.

DOE (Department of Energy). 1999b. Implementation Guide for use with DOE M 435.1-1, Chapter IV, Low-Level Waste Requirements, U.S. Department of Energy, Washington, DC.

DOE (Department of Energy). 1999c. *Radioactive Waste Management Manual of 7-09-99*, DOE M 435.1-1, U.S. Department of Energy, Washington, DC.

DOE (Department of Energy). 1999d. *Format and Content Guide for U.S. Department of Energy Low-Level Waste Disposal Facility Performance Assessments and Composite Analyses*, U.S. Department of Energy, Washington, DC.

DOE (Department of Energy). 1999e. *Format and Content Guide for U.S. Department of Energy Low-Level Waste Disposal Facility Closure Plans*, U.S. Department of Energy, Washington, DC.

DOE (Department of Energy). 1999f. *Surplus Plutonium Disposition Final Environmental Impact Statement*, DOE/EIS-0283, Office of Fissile Materials, Disposition, Washington, DC.

DOE (Department of Energy). 1999g, *Radiation Protection of the Public and the Environment*. DOE Order 5400.5, U. S. Department of Energy, Washington, DC.

DOE (Department of Energy). 2002. Savannah River Site High-Level Waste Tank Closure Final Environmental Impact Statement, DOE/EIS-0303, Savannah River Site, Aiken, SC.

DOE (Department of Energy). 2005. Savannah *River Site End State Vision*, July 26, 2005, Westinghouse Savannah River Company, Aiken, SC.

duPont, (E. I. du Pont de Nemours and Company, Inc.). 1987. *Comprehensive Cooling Water Study Final Report,* Volumes I - VIII, DP-1739, Savannah River Laboratory, Aiken, South Carolina.

EPA (Environmental Protection Agency). 2000. *National Primary Drinking Water Regulations; Radionuclides; Final Rule*, 40 CFR Parts 141 and 142, U. S. Environmental Protection Agency, Washington, DC.

EPA (Environmental Protection Agency). 2001. Implementation Guidance for Radionuclides, appendix I, Comparison of Derived Values of Beta and Photon Emitters, EPA 816-D-00-002, U. S. Environmental Protection Agency, Washington, DC.

EPA (Environmental Protection Agency). 2002a. *National Secondary Drinking Water Regulations*, 40 CFR Part 143.

EPA (Environmental Protection Agency). 2002b. *National Emission Standards for Hazardous Air Pollutants; Radionuclides*, 40 CFR Part 61.

EPA (Environmental Protection Agency). 2006. *CAP88-PC Version 3.0 User Guide*. Office of Radiation and Indoor Air, Washington, DC.

Fallaw, W. C., Price, V., and Thayer, P. A. 1990. "Stratigraphy of the Savannah River Site, South Carolina", in *Savannah River Region: Transition Between the Gulf and Atlantic Coastal Plains*, V. A. Zullo, W. B. Harris and V. Price, eds., Proceedings of the Second Bald Head Island Conference on Coastal Plain Geology, University of North Carolina at Wilmington, 144 p.

Fallaw, W. C. and Price, V. 1995. "Stratigraphy of the Savannah River Site and Vicinity", *Southeastern Geology*, v.35, 21-58.

Flach, G. P. and Harris, M. K. 1999. *Integrated Hydrogeological Model of the General Separations Area (U), Volume 2: Groundwater Flow Model (U)*, WSRC-TR-96-0399, Rev. 1, Westinghouse Savannah River Company, Aiken, SC.

Flach, G. P., Harris, M. K., Hiergesell, R. A., Smits, A. D., and Hawkins, K. L. 1999. *Regional Groundwater Flow Model for C, K, L, and P Reactor Areas, Savannah River Site, Aiken, South Carolina (U)*, WSRC-TR-99-00248, Rev. 0, Westinghouse Savannah River Company, Aiken, SC, 29808.

Flach, G. P. 2004. *Groundwater Flow Model of the General Separations Area Using PORFLOW (U)*, WSRC-TR-2004-00106, Rev. 0, Westinghouse Savannah River Company, Aiken, SC.

Flach, G. P., Collard, L. B., Phifer, M. A., Crapse, K. P., Dixon, K. L., Koffman, L. D. and Wilhite, E. L. 2005. *Preliminary Closure Analysis for Slit Trenches #1 and #2*, WSRC-TR-2005-00093, Westinghouse Savannah River Company, Aiken, SC, March 9, 2005.

Flach, G. P. 2007. *Software Quality Assurance Plan for Aquifer Model Refinement Tool (MESH3D)*, Q-SQP-G-00003, Rev. 0, Washington Savannah River Company, Aiken, SC.

Gibbons, J. W., McCourt, W. D., Knight, J. L., and Novak, S. S. 1986. *Semi-aquatic Mammals and Herpetefauna of the Savannah River Plant*, SREL-29, Savannah River Ecology Laboratory, Aiken, South Carolina.

GTG (GoldSim Technology Group LLC). 2005a. *GOLDSIM User's Guide*, Version 9.0, GoldSim Technology Group LLC, available at www.goldsim.com, May.

GTG (GoldSim Technology Group LLC). 2005b. *GOLDSIM Contaminant Transport Module User's Guide*, Version 3.0, available at www.goldsim.com, May.

GTG (GoldSim Technology Group LLC). 2006a. *GOLDSIM User's Guide*, Version 9.20, GoldSim Technology Group LLC, Issaquah, WA, January.

Hamby, D.M. 1991. *Land and Water-Use Characteristics in the Vicinity of the Savannah River Site*, Westinghouse Savannah River Company Report: WSRC-RP-91-17, Aiken, SC, March.

Hang, T. 2006a. *PORFLOW Software Quality Assurance Plan*, G-SQP-A-00012, Westinghouse Savannah River Company, Aiken, SC.

Hang, T. 2006b. *PORFLOW Software Test Plan*, G-STP-A-00009, Westinghouse Savannah River Company, Aiken, SC.

Hanson, K.L., Bullard T. F., Dewit, M. W., and Stieve, A. L. 1993. "Applications of Quaternary Stratigraphic, Soil-Geomorphic, and Quantitative Geomorphic Analyses to the Evaluation of Tectonic Activity and Landscape Evolution in the Upper Coastal Plain, South Carolina" in *Proceedings, 4th DOE Natural Phenomena Hazards Mitigation Conference, Atlanta, Georgia*.

HNUS (Halliburton NUS Corporation). 1997. *Socioeconomic Characteristics of Selected Counties and Communities Adjacent to the Savannah River Site*, Halliburton NUS Corporation, Aiken, SC.

Hubbard, J. E. and Emslie, R. H. 1984. *Water Budget for SRP Burial Ground Area*, DPST-83-742. E. I. du Pont de Nemours and Company, Savannah River Plant, Aiken, South Carolina, March 19, 1984.

Hubbard, J. E. 1986. *An Update on the SRP Burial Ground Area Water Balance and Hydrology*, DPST-85-958. E. I. du Pont de Nemours and Company, Savannah River Plant, Aiken, South Carolina, January 9, 1986.

Hubbard, J. E. and Englehardt M. 1987. *Calculation of Groundwater Recharge at the old SRP Burial Ground Using the CREAMS Model (1961-1986)*, State University of New York, Brockport, New York, Summer 1987 (report prepared for E. I. du Pont de Nemours and Company, Savannah River

Hunter, C. H. and Tatum, C. P. 1996. *Meteorological Annual Report for 1995 (U)*, WSRC-TR-96-0309, Westinghouse Savannah River Company, Savannah River Site, Aiken, SC.

Imm, D. W. 2005. "Threatened and Endangered Species: Smooth Purple Coneflower" in *Ecology and Management of a Forested Landscape: Fifty Years on the Savannah River Site*, J. C. Kilgo and J. I Blake eds., Island Press, Washington, D.C. 479 p.

INTERA. 1986. *Z-Area Site Assessment*, INTERA Technologies, Inc., for E. I du Pont de Nemours & Co., Inc., Savannah Research Laboratory, Aiken, SC.

Jannik, G. T. 2006. *Software Quality Assurance Plan for Environmental Dosimetry*, G-SQP-A-00002, Westinghouse Savannah River Company, Aiken, SC.

Jannik, G.T. and Dixon, K.L. 2006. *LADTAP-PA: A Spreadsheet for Estimating Dose Resulting from E-Area Groundwater Contamination at the Savannah River Site*, WSRC-STI-2006-00123, Savannah River National Laboratory, Aiken, SC.

Johns, P. E. and Kilgo, J. C. 2005. "Harvestable Natural Resources: White-Tailed Deer", in *Ecology and Management of a Forested Landscape: Fifty Years on the Savannah River Site*, J. C. Kilgo and J. I Blake eds., Island Press, Washington, D.C., 479 p.

Jones, W. E. 2007. *Software Quality Assurance Plan for the RETC (RETention Curve) Computer Code*, Q-SQP-A-00006, Westinghouse Savannah River Company, Aiken, SC.

Kaplan, D. I. 2003. "Influence of Surface Charge of an Fe-oxide and an Organic Matter Dominated Soil on Iodide and Pertechnetate Sorption." *Radiochimica Acta* 91:173-178.

Kaplan, D. I. 2006. *Geochemical Data Package for Performance Assessment Calculations Related to the Savannah River Site (U)*, WSRC-TR-2006-00004, Rev. 0, Washington Savannah River Company, Savannah River Site, Aiken, SC.

Kaplan, D. I., Millings, M. R. 2006. *Early Guidance for Assigning Distribution Parameters to Geochemical Input Terms to Stochastic Transport Models*, WSRC-STI-2006-00019, Washington Savannah River Company, Savannah River Site, Aiken, SC.

Kaplan, D. I. and S. M. Serkiz. 2006. *Influence of Dissolved Organic Carbon and pH on Iodide, Perrhenate, and Selenate Sorption to Sediment*. WSRC-STI-2006-00037. Washington Savannah River Company, Aiken, SC.

Kaplan, D. I. 2007. *A Review of Technetium Values for SRS Sediments*, WSRC-STI-2007-00698, Washington Savannah River company, Aiken, SC, December 10, 2007.

Kennedy, W. E., Jr., and R. A. Peloquin. 1988. *Intruder Scenarios for Site-Specific Low-Level Waste Classification.* DOE/LLW-71T, Idaho Operations Office, Department of Energy.

Kilgo, J. C. and Blake, J. I. eds. 2005. *Ecology and Management of a Forested Landscape: Fifty Years on the Savannah River Site*, Island Press, Washington, D.C. 479 p

Koffman, L. D. 2004. *An Automated Inadvertent Intruder Analysis Application*. WSRC-TR-2004-00293, Westinghouse Savannah River Company, Aiken, SC.

Koffman, L. D. 2006a. *An Automated Inadvertent Intruder Analysis Application, Version 2,* WSRC-TR-2006-00037, Rev. 0, Washington Savannah River Company, Aiken, SC.

Koffman, L. D. 2006b. *SRNL All-Pathways Application.* WSRC-STI-2006-000179, Rev. 0, Washington Savannah River Company, Aiken, SC

Koffman, L. D. 2006c. *Software Quality Assurance Plan for SRNL All-Pathways Application*, G-SQP-G-00012, Westinghouse Savannah River Company, Aiken, SC.

Koffman, L. D. 2006d. *Software Quality Assurance Plan for Automated Inadvertent Intruder Application*, G-SQP-00013, Westinghouse Savannah River Company, Aiken, SC.

Lee, P. L. 2004. Inadvertent *Intruder Analysis Input for Radiological Performance Assessments*, WSRC-TR-2004-00295, Westinghouse Savannah River Company, Aiken, SC.

Lee, P. L. 2006. *Air Pathway Dose Modeling for the E-Area Low level Waste Facility*, WSRC-STI-2006-00262, Rev. 0, Washington Savannah River Company, Aiken, SC.

Logan, W. R., and Euler, G. M. 1989. *Geology and Groundwater Resources of Allendale, Bamberg, and Barnwell Counties and Part of Aiken County, South Carolina*, South Carolina Water Resources Commission Report 155, 113 p.

Looney, B. B., Eddy, C. A., Ramdeen, M., Pickett, J., Rogers, V., Scott, M. T., and Shirley, P.A. 1990. *Geochemical and Physical Properties of Soils and Shallow Sediments at the Savannah River Site (U)*, WSRC-RP-90-1031, Westinghouse Savannah River Company, Aiken, SC.

McDowell-Boyer, L. A. D. Yu, J. R. Cook, D. C. Kocher, E. L. Wilhite, H. Holmes-Burns, and K. E. Young. 2000. *Radiological Performance Assessment for the E-Area Low-Level Waste Facility*, WSRC-RP-94-218, Rev. 1. Westinghouse Savannah River Company, Aiken, SC.

McKenzie, D. H., Cadwell, L. L., Eberhardt, L. E., Kennedy, Jr., W. E., Peloquin, R. A., and Simmons, M. A. 1983. *Relevance of Biotic Pathways to the Long-Term Regulation of Nuclear Waste Disposal; Topical Report on Reference Eastern Humid Low-Level Sites*, NUREG/CR-2675, PNL-4241, Vol. 3, Pacific Northwest Laboratory, Richland, Washington.

McKenzie, D. H., Cadwell, L. L., Kennedy, Jr., W. E., Prohammer, L. A., and Simmons, M. A. 1986. *Relevance of Biotic Pathways to the Long-Term Regulation of Nuclear Waste Disposal, Phase II, Final Report*, NUREG/CR-2675, PNL-4241, Vol. 6, Pacific Northwest Laboratory, Richland, Washington.

Madabhushi, S., and Talwani P. 1993. "Fault plane solutions and relocations of recent earthquakes in Middleton Place Summerville Seismic Zone near Charleston, South Carolina," *Bulletin of the Seismological Society of America,* 83, 5, 1442-1466.

Mamatey, A. R. 2006. *Savannah River Site Environmental Report for 2005*, WSRC-TR-2006-00007, Washington Savannah River Company, Savannah River Site, Aiken, SC.

Marcy, B. C. Jr. 2005. "Biotic Communities: Fishes" in *Ecology and Management of a Forested Landscape: Fifty Years on the Savannah River Site*, J. C. Kilgo and J. I Blake eds., Island Press, Washington, D.C. 479 p.

Mayer, J. J. 2005. "Harvestable Natural Resources: Wild Hog", in *Ecology and Management of a Forested Landscape: Fifty Years on the Savannah River Site*, J. C. Kilgo and J. I Blake eds., Island Press, Washington, D.C. 479 p.

Mayer, J. J. and Wike, L. D. 1997. *SRS Urban Wildlife Environmental Information Document*, WSRCTR-97-0093, Westinghouse Savannah River Company, Aiken, South Carolina.

McAllister, C., Beckert, H., Abrams, C., Bilyard, G., Cadwell, K., Friant, S., Glantz, C., Mazaika, R., and Miller, K. 1996. *Survey of Ecological Resources at Selected U. S. Department of Energy Sites*, DOE/EH-0534, PNNL, 148 p.

Moos, D. and Zoback, M.D. 1992. *In Situ Stress Measurements in the NPR Hole, Savannah River Site, South Carolina: Final Report to Westinghouse Savannah River Co., Vol. 1, Results and Interpretations*, Subcontract AA00925P, Science Applications International Corporation, Augusta, GA.

Moos, D. and Zoback, M.D. 1993. "Near Surface "Thin Skin" Reverse Faulting Stresses in the Southeastern United States," *Int. Journal of Rock Mech. Min. Sci. & Geomech.*, 30, 7, 965-971.

Napier, B. A., D. L. Strenge, J. V. Ramsdell, Jr., P. W. Eslinger, and C. Foxmire. 2002. *GENII version 2 software design document*, Washington, DC.

NCRP (National Council on Radiation Protection and Measurements). 1996. *Screening Models for Releases of Radionuclides to Atmosphere, Surface Water, and Ground*, NCRP Report No. 123, Volumes I and II, National Council on Radiation Protection and Measurements, Bethesda, MD.

Ng, Y.C., Colsher, C.S., and Thompson, S.E. 1979. *Transfer Coefficients for Terrestrial Food Chains – Their Derivation and Limitations*, UCRL-81640, Lawrence Livermore National Laboratory, Livermore, CA.

Nielson, K.K., V.C. Rogers and G.W. Gee, 1984. *Diffusion of Radon through Soils: A pore distribution Model*, Soil Science Society of America, J. 48:482-487.

NOAA (National Oceanic and Atmospheric Administration). 2004. "Climatography of the Unites States, No. 20, 1971-2000: Augusta Bush Field Ap, GA", National Climatic Data Center, Asheville, NC, (www.ncdc.noaa.gov/oa/climate/normals/usnormals.html).

NOAA (National Oceanic and Atmospheric Administration). 2006. "Comparative Climatic Data for the United States through 2005", National Climatic Data Center, Asheville, NC, (http://www1.ncdc.noaa.gov/pub/data/ccd-data).

NRC (Nuclear Regulatory Commission). 1977. *Calculation of Annual Dose to Man from Routine Releases of Reactor Effluents for the Purpose of Evaluating Compliance with 10 CFR 50*, Appendix I, Regulatory Guide 1.109, Rev. 1, Washington, DC, October.

NRC (Nuclear Regulatory Commission). 1981. Draft Environmental Impact Statement on 10 CFR Part 61 "*Licensing Requirements for Land Disposal of Radioactive Waste.*" NUREG-0782, U. S. Nuclear Regulatory Commission, Washington D. C

NRC-NA (National Research Council of the National Academies). 2007. *Assessment of the Performance of Engineered Waste Containment Barriers.* Prepublication Copy. National Research Council of the National Academies, The National Academies Press, Washington, D.C.

Nystrom, P., Widoughby, R., and Price, L. K. 1991, "Cretaceous and Tertiary Stratigraphy of the Upper Coastal Plain, South Carolina", *The Geology of the Carolinas*, Carolina Geological Society, The University of Tennessee Press.

Oblath, S. B. 1983. *Migration of TcO_4^- in SRP Soils*. April 25, 1983. Report submitted to Low-Level Waste Management Program. (this results from this report are also presented in less detail by Hoeffner, S. L. 1984. Radionuclide Sorption of SRP Burial Ground Soil: A Summary and Interpretation of Laboratory Data. DPST-84-799. E. I. Du Pont De Nemours and Company, Aiken, SC 29801.

ORNL (Oak Ridge National Laboratory). 1990. *Performance Assessment for Continuing and Future Operations at SWSA 6*, Internal draft report, Oak Ridge National Laboratory, Oak Ridge, Tenn.

Oztunali, O. I., and G. W. Roles. 1986. *Update of Part 61 Impacts Analysis Methodology*, NUREG/CR-4370, U. S. Nuclear Regulatory Commission and Envirosphere Company.

Parizek, R. R. and Root, R. W. 1986. *Development of a Ground-Water Velocity Model for the Radioactive Waste Management Facility Savannah River Plant, South Carolina*, The Pennsylvania State University, University Park, Pennsylvania, June 1986 (report prepared for E. I. du Pont de Nemours and Company, Savannah River Plant, Aiken, South Carolina and given DuPont document number DPST-86-658)

Phifer, M. A. 2006. Software Quality Assurance Plan for the Hydrologic Evaluation of Landfill Performance (HELP) Model, Q-SQA-A-00005, Westinghouse Savannah River Company, Aiken, SC.

Phifer, M. A., Millings, M. R., and Flach, G. P. 2006. Hydraulic Property Data Package for the E-Area and Z-Area Vadose Zone Soils, Cementitious Materials, and Waste Zones, WSRC-STI-2006-00198, Rev. 0, Washington Savannah River Company, Aiken, SC.

Phifer, M. A., Jones, W. E., Nelson, E. A., Denham, M. E., Lewis, M. R., and Shine, E. P. 2007. *FTF Closure Cap Concept and Infiltration Estimates*, WSRC-STI-2007-00184, Revision 2, Washington Savannah River Company, Aiken, SC, October 2007.

Pickens, J. F. and Grisak, G. E. 1981. "Modeling of scale-dependent dispersion in hydrogeologic systems", *Water Resour. Res*. 17:1701–1711.

Ruffner, J. A. 1985. *Climate of the States,* 3rd Ed, Gale Research Company, Book Tower, Detroit, MI.

SCDHEC (South Carolina Department of Health and Environmental Control). 2003. State Primary Drinking Water Regulation, R. 61-58, Columbia, SC.

Schroeder, P. R., Lloyd, C. M., Zappi, P. A., and Aziz, N. M. 1994a. *The Hydrologic Evaluation of Landfill Performance (HELP) Model User's Guide for Version 3*. EPA/600/R-94/168a. Office of Research and Development, United States Environmental Protection Agency (EPA), Cincinnati, Ohio. September 1994.

Schroeder, P. R., Dozier, T. S., Zappi, P. A., McEnroe, B. M., Sjostrom, J. W., and Peyton, R. L. 1994b. *The Hydrologic Evaluation of Landfill Performance (HELP) Engineering Documentation for Version 3*. EPA/600/R-94/168b. Office of Research and Development, United States Environmental Protection Agency (EPA), Cincinnati, Ohio. September 1994.

Siple, G. E. 1967. *Geology and Ground Water of the Savannah River Plant and Vicinity, South Carolina*, Geological Survey Water Supply Paper 1841, 113 p.

Smits, A. D., Harris, M. K., Hawkins, K. L., and Flach, G. P. 1997. *Integrated Hydrogeological Model of the General Separations Area, Volume 1: Hydrogeologic* Framework, WSRC-TR-96-0399, Rev. 0, Westinghouse Savannah River Company, Aiken, SC.

SRS (Savannah River Site). 2000a. *Savannah River Site Long Range Comprehensive Plan*, Discussion Draft, December 2000, Savannah River Site, Aiken, SC.

SRS (Savannah River Site). 2000b. *Savannah River Site Strategic Plan, 21st Century Stewards for the Nation*, March 2000, Aiken, SC.

SRS (Savannah River Site). 2006. *Facts About the Savannah River Site*, February 2006, a public fact sheet published by Washington Savannah River Site, Aiken, SC.

Standard Software Quality Assurance Plan for PD&CS – Design Services Engineering Software (U), B-SQP-G-00007, Rev. 1, March 31, 2005.

Stephenson, D.E., Talwani, P., and Rawlins, J. 1985. *Savannah River Plant Earthquake of June 1985*, DPST-85-583, E.I. du Pont de Nemours & Co., Savannah River Laboratory, Aiken, SC.

Stephenson, D.E. 1988. *Savannah River Plant Earthquake*, DPST-88-841, E.I. duPont de Nemours and Co., Savannah River Laboratory, Aiken, SC.

Stevenson, D. A., and Talwani, P. 2004. "2001-2002 Upper Three Runs Sequence of Earthquakes at the Savannah River Site, South Carolina," *Seismological Research Letters*, 75, 1, 107-116.

Stieve, A. L., Stephenson, D. E., and Aadland, R. 1991. *Pen Branch Fault Program: Consolidated Report on the Seismic Reflection Surveys and the Shallow Drilling*, WSRC-TR-91-87, Westinghouse Savannah River Company, Aiken, SC.

Stieve, A. L., Coruh, C., Costain, J. 1994. *Confirmatory Drilling Project Final Report*, WSRC-RP-94-0136, Westinghouse Savannah River Company, Aiken, SC.

Stieve, A.L. and Stephenson, D.E. 1995. "Geophysical Evidence for Post Late Cretaceous Reactivation of Basement Structures in the Central Savannah River Area," *Southeastern Geology*, 35, 1-20.

Storm Prediction Center. 1999. *Historical Tornado Data Archive, Graphs and Charts on U.S. Tornadoes: 1950-1998 Tornadoes by State*, http://www.spc.noaa.gov/archive/tornadoes/.

Swingle, R. F. 2006. *Software Quality Assurance Plan for GoldSim*, G-SQA-A-00011, Westinghouse Savannah River Company, Aiken, SC.

Talwani, P.J., Rawlins, J. and Stephenson, D. E. 1985. "The Savannah River Plant, South Carolina, Earthquake of June 9, 1985 and its Tectonic Setting," *Earthquake Notes*, 56, 4, 101-106.

Talwani, P. 1985. "An Internally Consistent Pattern of Seismicity Near Charleston, South Carolina," *Geology*, 10, 12, 654-658.

Talwani, P., and Schaeffer, W.T. 2001. "Recurrence Rates of Large Earthquakes in the South Carolina Coastal Plain Based on Paleoliquefaction Data," *Journal of Geophysical Research*, 106, B4, 6621-6642.

Tarr, A.C., Talwani, P., Rhea, S., Carver, D., and Amick D. 1981. "Results of Recent South Carolina Seismological Studies," Bu*lletin of the Seismological Society of America*, 71, 1883-1902.

Taylor, G. A. 2006. *Software Quality Assurance Plan for IdealFileMaker: An Application to Translate PORFLOW Output to All-Pathways Input*, G-SQP-A-00010, Westinghouse Savannah River Company, Aiken, SC.

Taylor, G. A. and Collard, L. B. 2005. *Automated Groundwater Screening*, WSRC-TR-2005-00203, Rev. 0, Westinghouse Savannah River Company, Aiken, SC.

USGS (U. S. Geological Survey). 1987, Digital Line Graphs from 1:24,000 Scale Maps, 10-ft intervals, United States Geological Survey.

USGS (U.S. Geological Survey) Water-Data Site Information for South Carolina. http://waterdata.usgs.gov/nwis/

Vinson, D. W. 2005. *Software Quality Assurance Plan for Scale*, N-SQP-A-00001, Westinghouse Savannah River Company, Aiken, SC.

Visvanathan, T.R. 1980. "Earthquakes in South Carolina, 1698—1975," *South Carolina Geological Survey Bulletin*, 40. 61 p.

Weber, A. H. 1998. *Tornado, Maximum Wind Gust, and Extreme Rainfall Event Recurrence Frequencies* at the Savannah River Site, WSRC-TR-98-00329, Westinghouse Savannah River Company, Aiken, SC.

Weber, A. H. and R. J. Kurzeja. 2002. *Summary of Data and Steps for Processing the SRS 1997-2001 Meteorological Database* (U), WSRC-TR-2002-00445, Westinghouse Savannah River Company, Aiken, SC.

Wike, L. D., Martin, F. D., Nelson, E. A., Halverson, N. V., Mayer, J. J., Paller, M. H., Riley, R. S., Serrato, M. G., and Specht, W. L. 2006. *SRS Ecology: Environmental Information Document*, WSRC-TR-2005-00201, Washington Savannah River Company, Aiken, SC.

WSRC (Westinghouse Savannah River Company). 1996. *Groundwater Protection Management Program*, WSRC-TR-96-0193, Westinghouse Savannah River Company, Aiken, SC.

WSRC (Westinghouse Savannah River Company). 1997. *Composite Analysis, E-Area Vaults and Saltstone Disposal Facilities*, WSRC-RP-97-311, Rev. 0, Westinghouse Savannah River Company, Aiken, SC.

WSRC (Westinghouse Savannah River Company). 2000. *Natural Phenomena Hazards (NPH) Design Criteria and Other Characterization Information for the Mixed Oxide (MOX) Fuel Fabrication Facility at Savannah River Site* (U), WSRC-TR-2000-0045, Westinghouse Savannah River Company, Aiken, SC.

WSRC (Westinghouse Savannah River Company). 2002. *Summary of Data and Steps for Processing the SRS 1997-2001 Meteorological Database (U)*, WSRC-TR-2002-00445, Westinghouse Savannah River Company, Aiken, SC.

WSRC (Westinghouse Savannah River Company). 2004a. *Closure Plan for the E-Area Low-Level Waste Facility*, Rev. 5, WSRC-RP-2000-00425, Rev. 4, May 2004, Westinghouse Savannah River Company, Aiken, SC.

WSRC (Westinghouse Savannah River Company). 2004b. *Savannah River National Laboratory Technical Report Design Check Guidelines*, WSRC-IM-2002-00011, revision 2, Westinghouse Savannah River Company, Aiken, SC.

WSRC (Westinghouse Savannah River Company). 2005a. *WSRC 1S Savannah River Site Waste Acceptance Criteria Manual,* Procedure WAC 3.17 Low Level Radioactive Waste Acceptance Criteria, Rev. 9, Westinghouse Savannah River Company, Aiken, SC.

WSRC (Westinghouse Savannah River Company). 2005b. *Savannah River Site End State Vision, July 26, 2005*, Westinghouse Savannah River Company, Aiken, SC.

WSRC (Westinghouse Savannah River Company). 2006a. WSRC 1Q Quality Assurance Manual, Procedure 20-1, *Software Quality Assurance*, Revision 8, Westinghouse Savannah River Company, Aiken, SC.

WSRC (Westinghouse Savannah River Company). 2006b. WSRC E7 Conduct of Engineering Manual, Procedure 2.60, *Technical Reviews*, Revision 9, Westinghouse Savannah River Company, Aiken, SC.

WSRC (Washington Savannah River Company). 2007. F-Area *Tank Farm Modeling Code Integration*, FTF-IP-17, Rev. 0, March 5, 2007 Predecisional Draft, Washington Savannah River Company, Aiken, SC.

Wyatt, D. E., Aadland, R. K., and Syms, F. H. 2000. "Overview of the Savannah River Site Stratigraphy, Hydrostratigraphy and Structure" in *Carolina Geological Society 2000 Field Trip Guidebook: Savannah River Site Environmental Remediation Systems in Unconsolidated Upper Coastal Plain Sediments – Stratigraphic and Structural Considerations*, D. E. Wyatt and M. K Harris eds., WSRC-MS-2000-00606, Westinghouse Savannah River Company, Aiken, SC.

Wyatt, D. E. and Harris, M. K. 2004. "Overview of the History and Geology of the Savannah River Site", *Environmental Geosciences*, v.11, no.4, 181-190.

Young, M. H. and Pohlmann, K. F. 2001. *Analysis of Vadose Zone Monitoring System: Computer Simulation of Water Flux: E-Area Disposal Trenches*, Task Order GA0074 (KG43360-0). Division of Hydrologic Sciences, Desert Research Institute, Las Vegas, NV. August 2001.

Young, M. H. and Pohlmann, K. F. 2003. *Analysis of Vadose Zone Monitoring System: Computer Simulation of Water Flux under Conditions of Variable Vegetative Cover: E-Area Disposal Trenches*, Publication No. 41188. Division of Hydrologic Sciences, Desert Research Institute, Las Vegas, NV. August 2003.

Yu, C., Zielen, A. J., Cheng, J.-J., LePoire, D. J., Gnanapragasam, E., Kamboj, S., Arnish, Wallo III, A., Williams, W. A., and H. Peterson, H. 2001. *Users Manual for RESRAD Version 6*, Argonne National Laboratory Report: ANL/EAD/4, Argonne, IL. July, 2001.

APPENDIX A1

GRAPHICS FOR GROUNDWATER AND RADON TRANSPORT

This page intentionally left blank.

TABLE OF CONTENTS

APPENDIX A1A

Vadose Zone Model

Flux to the Water Table

Pressure and Velocity Fields

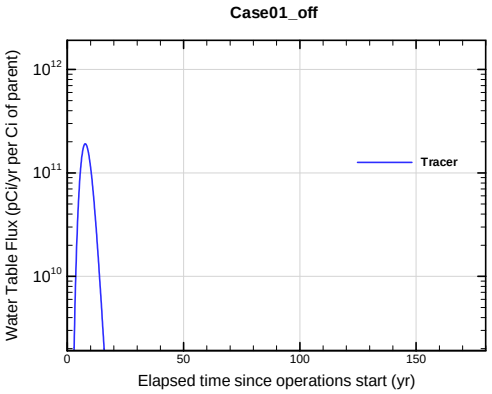

Figure A1A-1. Slit Trench water table flux for Case01_off Tracer

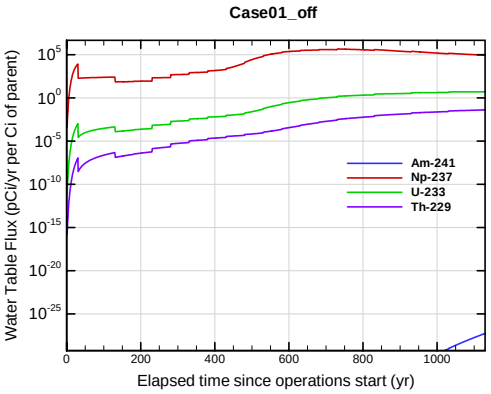

Figure A1A-2. Slit Trench water table flux for Case01_off Am-241

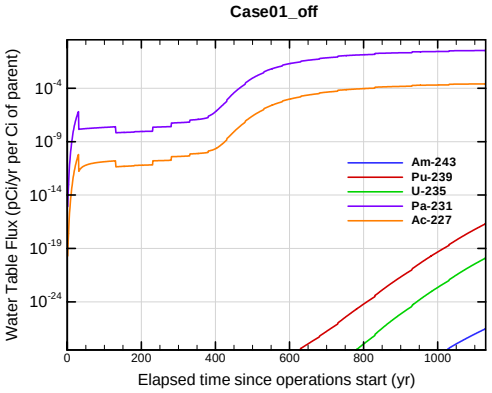

Figure A1A-3. Slit Trench water table flux for Case01_off Am-243

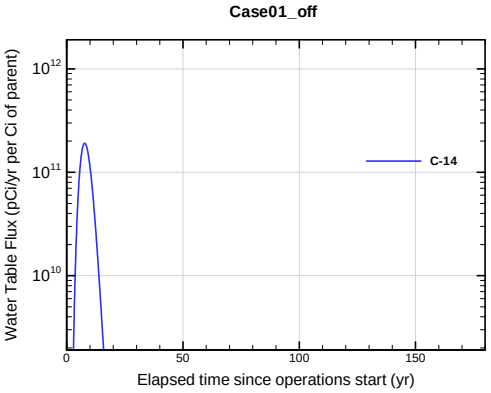

Figure A1A-4. Slit Trench water table flux for Case01_off C-14

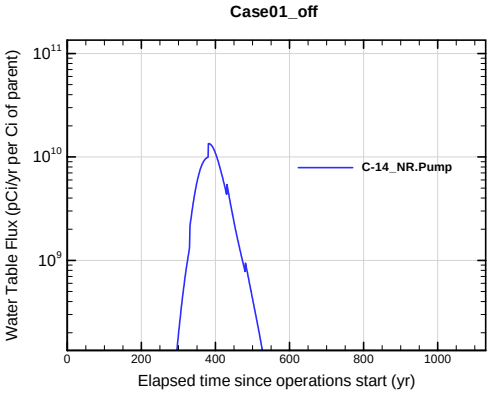

Figure A1A-5. Slit Trench water table flux for Case01_off C-14_NR.Pump

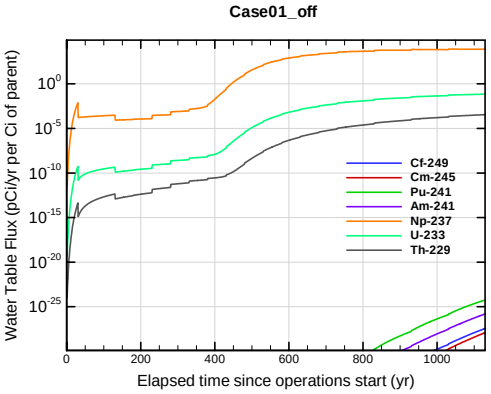

Figure A1A-6. Slit Trench water table flux for Case01_off Cf-249

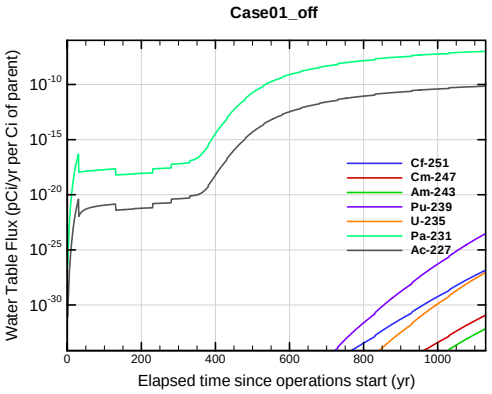

Figure A1A-7. Slit Trench water table flux for Case01_off Cf-251

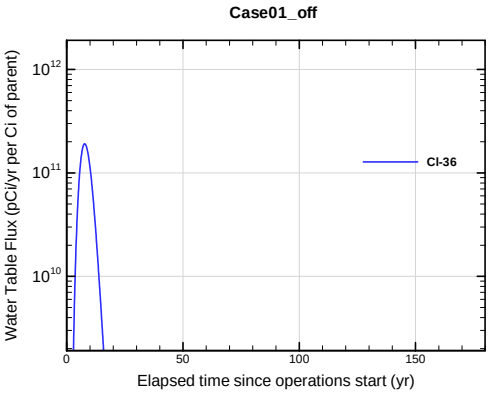

Figure A1A-8. Slit Trench water table flux for Case01_off Cl-36

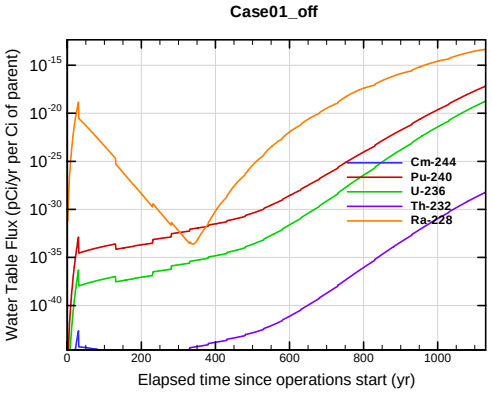

Figure A1A-9. Slit Trench water table flux for Case01_off Cm-244

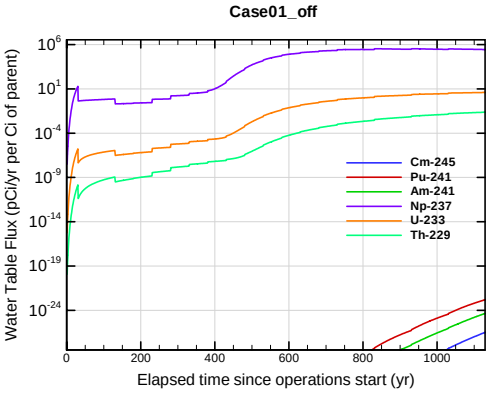

Figure A1A-10. Slit Trench water table flux for Case01_off Cm-245

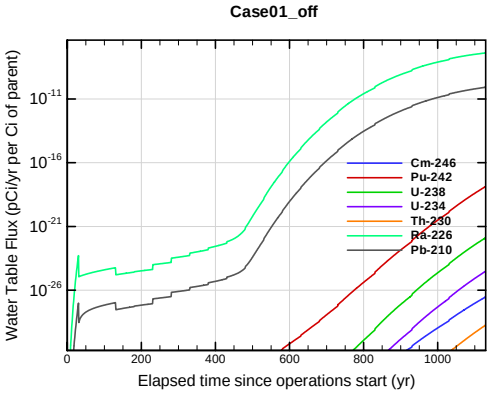

Figure A1A-11. Slit Trench water table flux for Case01_off Cm-246

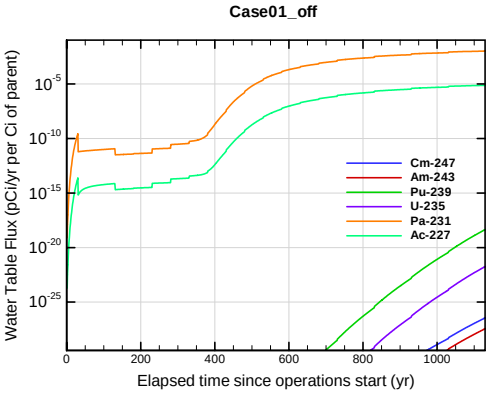

Figure A1A-12. Slit Trench water table flux for Case01_off Cm-247

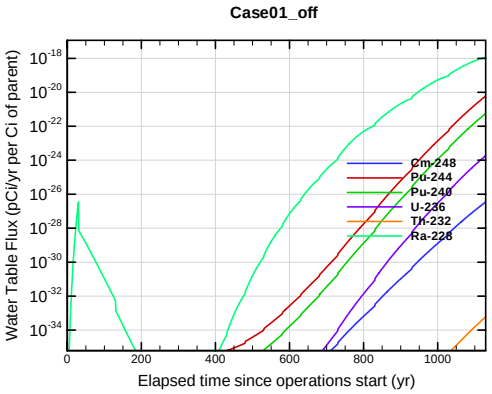

Figure A1A-13. Slit Trench water table flux for Case01_off Cm-248

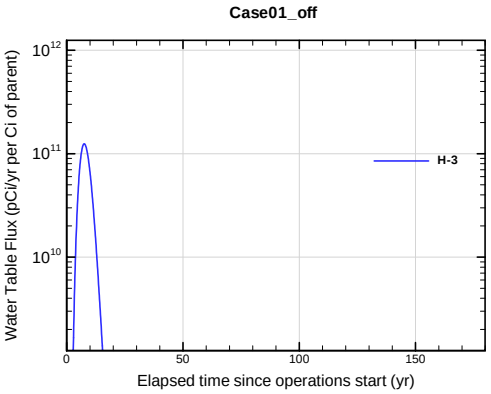

Figure A1A-14. Slit Trench water table flux for Case01_off H-3

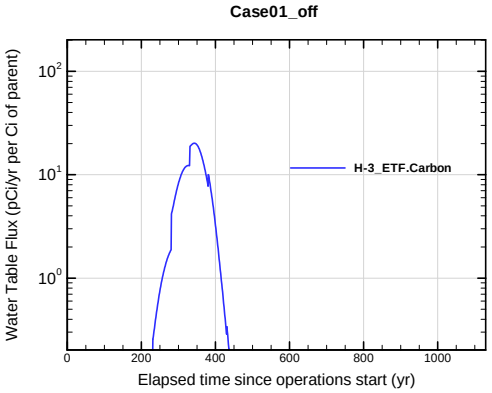

Figure A1A-15. Slit Trench water table flux for Case01_off H-3_ETF.Carbon

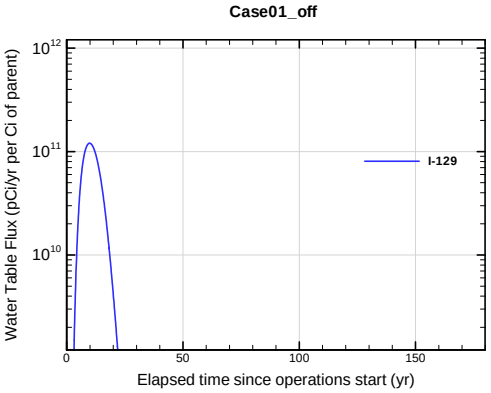

Figure A1A-16. Slit Trench water table flux for Case01_off I-129

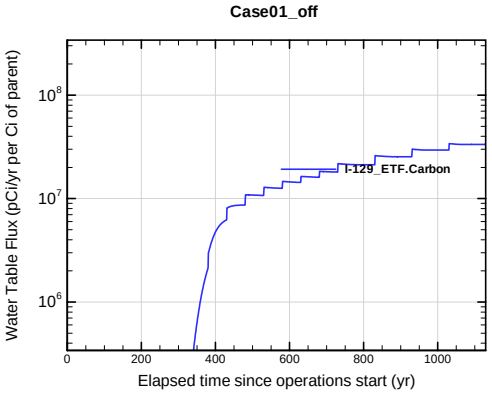

Figure A1A-17. Slit Trench water table flux for Case01_off I-129_ETF.Carbon

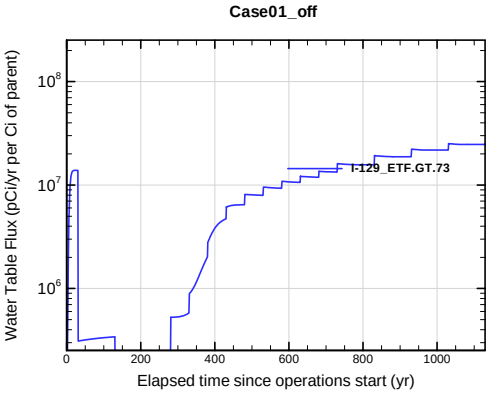

Figure A1A-18. Slit Trench water table flux for Case01_off I-129_ETF.GT.73

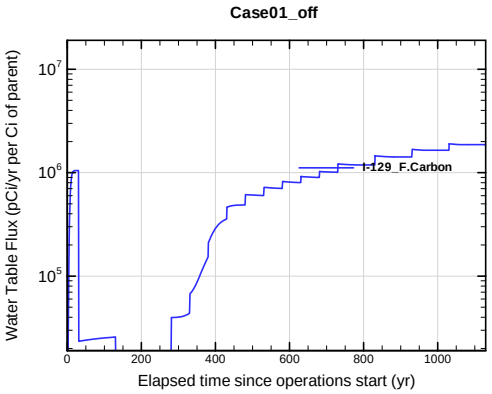

Figure A1A-19. Slit Trench water table flux for Case01_off I-129_F.Carbon

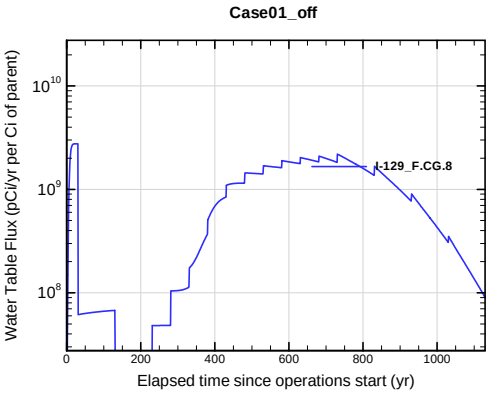

Figure A1A-20. Slit Trench water table flux for Case01_off I-129_F.CG.8

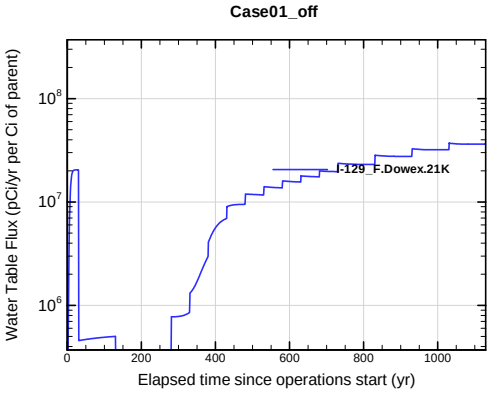

Figure A1A-21. Slit Trench water table flux for Case01_off I-129_F.Dowex.21K

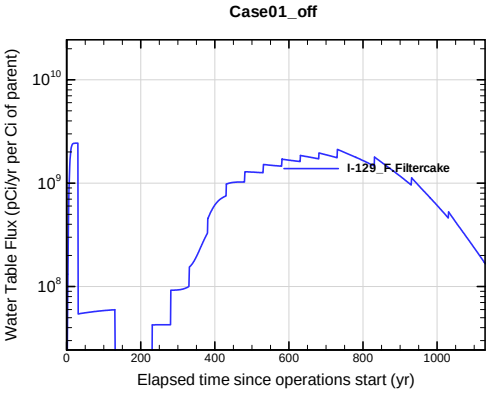

Figure A1A-22. Slit Trench water table flux for Case01_off I-129_F.Filtercake

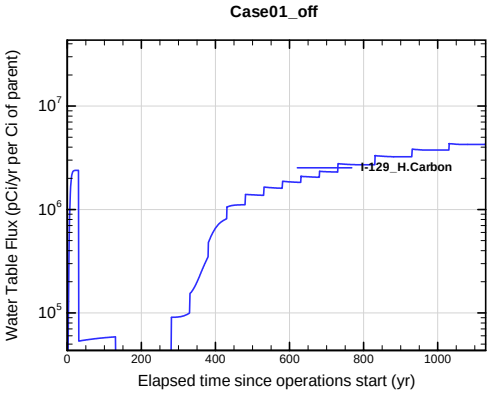

Figure A1A-23. Slit Trench water table flux for Case01_off I-129_H.Carbon

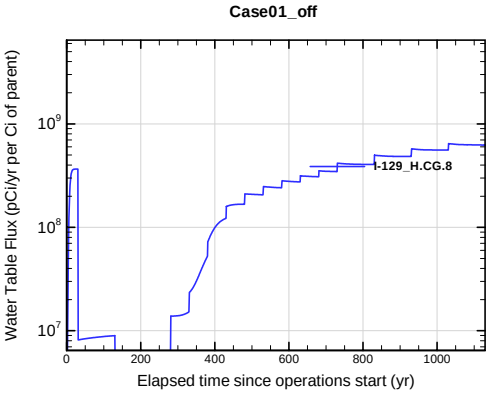

Figure A1A-24. Slit Trench water table flux for Case01_off I-129_H.CG.8

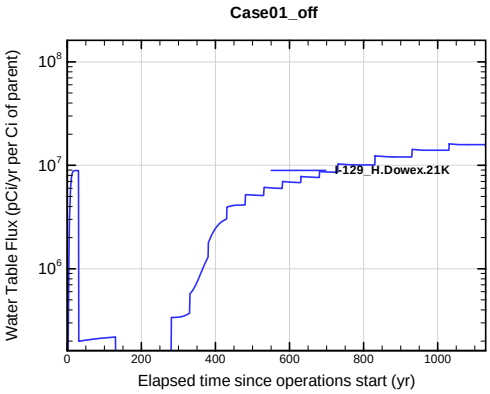

Figure A1A-25. Slit Trench water table flux for Case01_off I-129_H.Dowex.21K

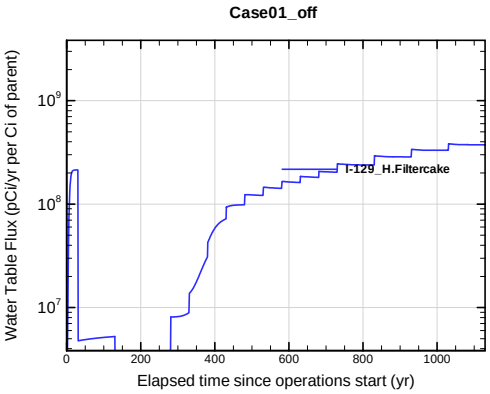

Figure A1A-26. Slit Trench water table flux for Case01_off I-129_H.Filtercake

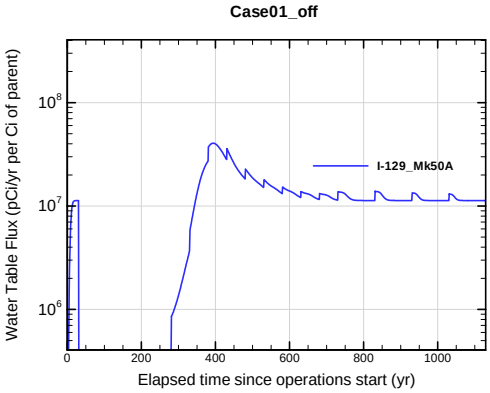

Figure A1A-27. Slit Trench water table flux for Case01_off I-129_Mk50A

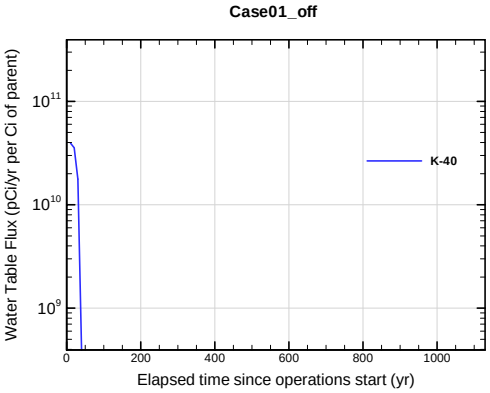

Figure A1A-28. Slit Trench water table flux for Case01_off K-40

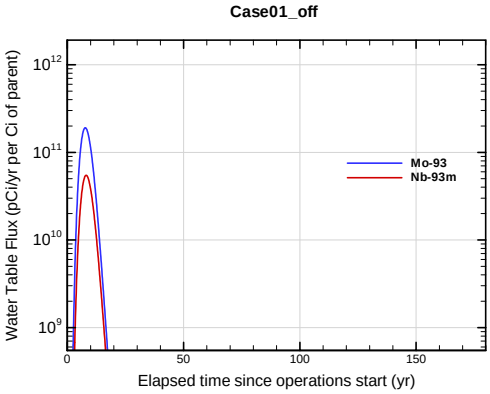

Figure A1A-29. Slit Trench water table flux for Case01_off Mo-93

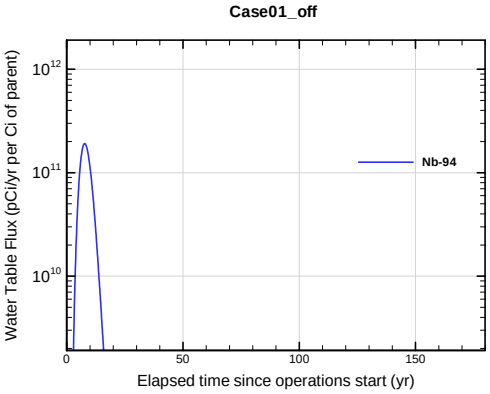

Figure A1A-30. Slit Trench water table flux for Case01_off Nb-94

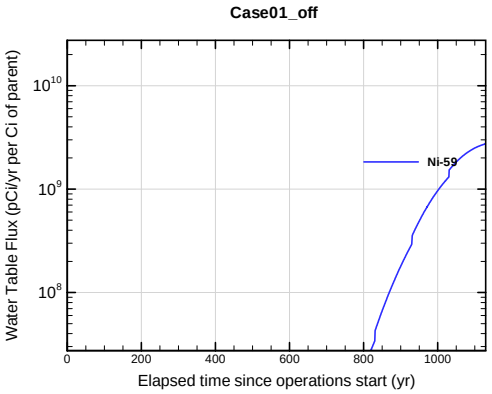

Figure A1A-31. Slit Trench water table flux for Case01_off Ni-59

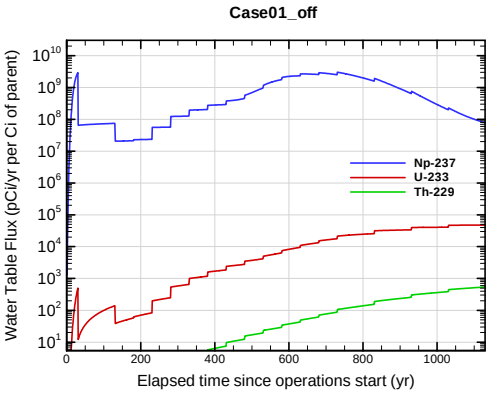

Figure A1A-32. Slit Trench water table flux for Case01_off Np-237

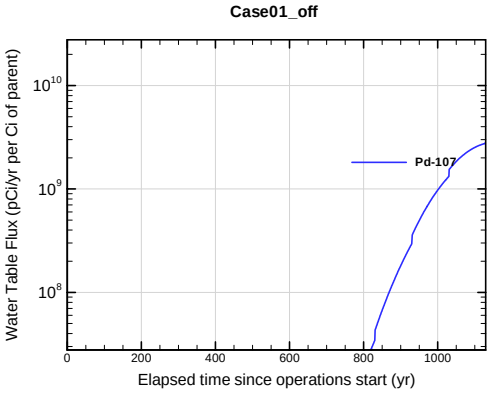

Figure A1A-33. Slit Trench water table flux for Case01_off Pd-107

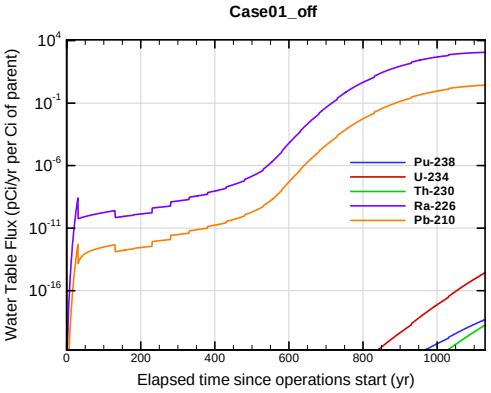

Figure A1A-34. Slit Trench water table flux for Case01_off Pu-238

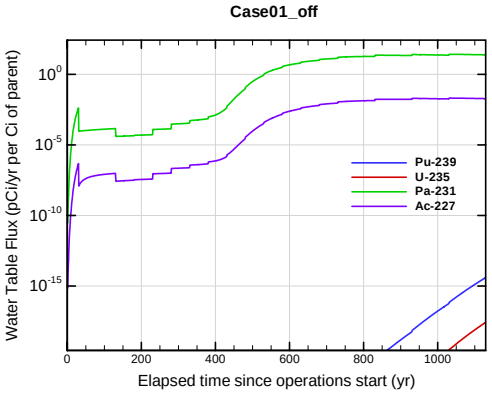

Figure A1A-35. Slit Trench water table flux for Case01_off Pu-239

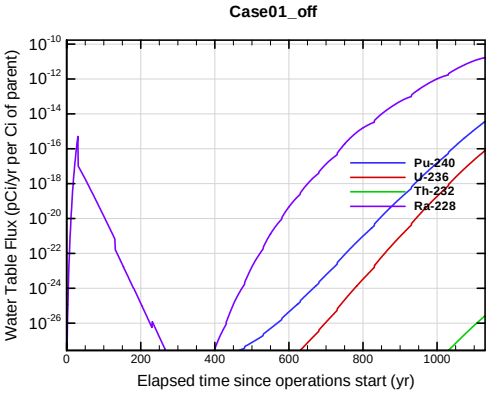

Figure A1A-36. Slit Trench water table flux for Case01_off Pu-240

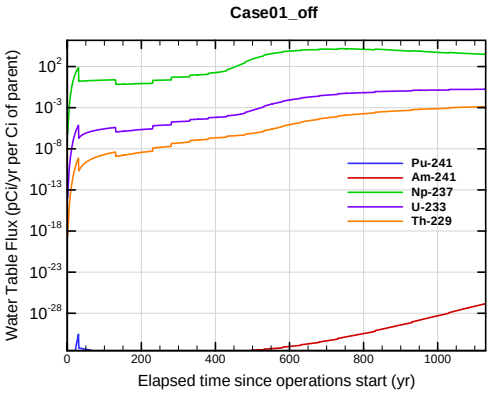

Figure A1A-37. Slit Trench water table flux for Case01_off Pu-241

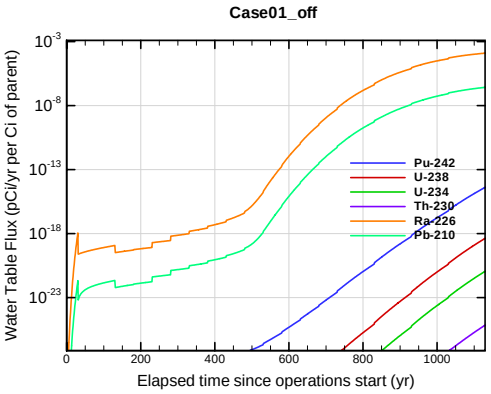

Figure A1A-38. Slit Trench water table flux for Case01_off Pu-242

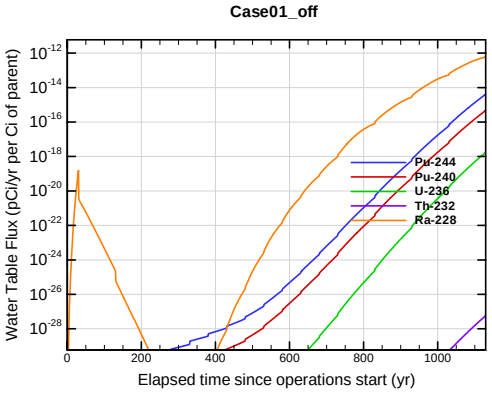

Figure A1A-39. Slit Trench water table flux for Case01_off Pu-244

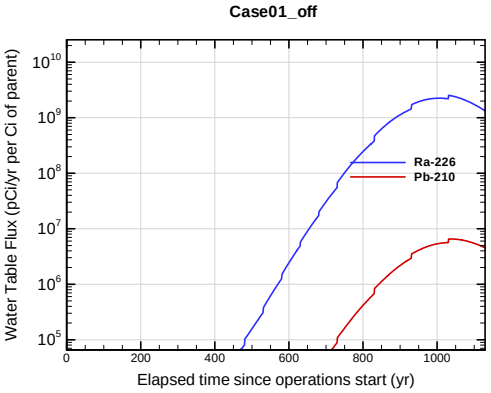

Figure A1A-40. Slit Trench water table flux for Case01_off Ra-226

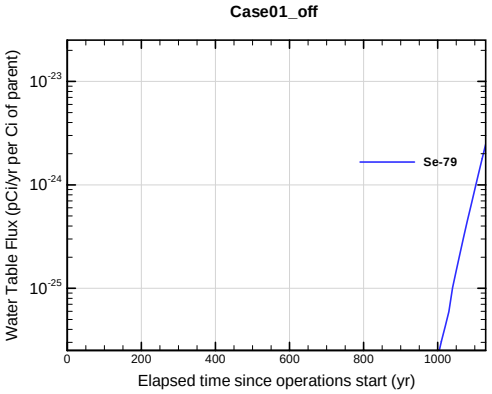

Figure A1A-41. Slit Trench water table flux for Case01_off Se-79

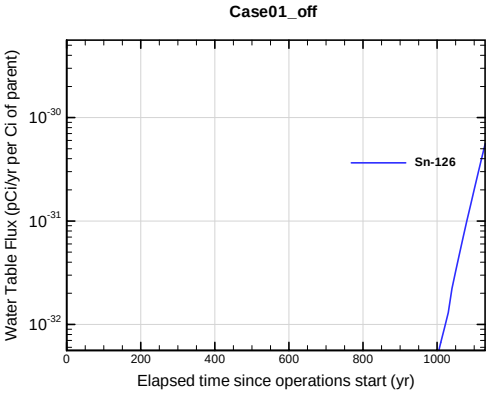

Figure A1A-42. Slit Trench water table flux for Case01_off Sn-126

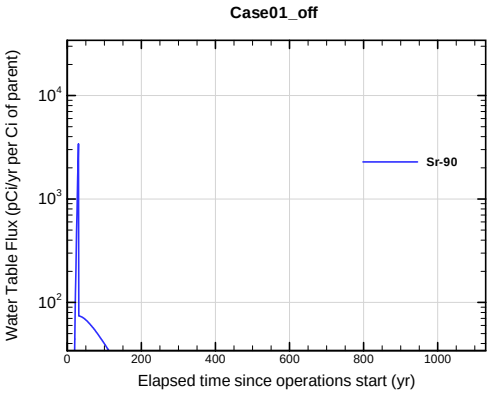

Figure A1A-43. Slit Trench water table flux for Case01_off Sr-90

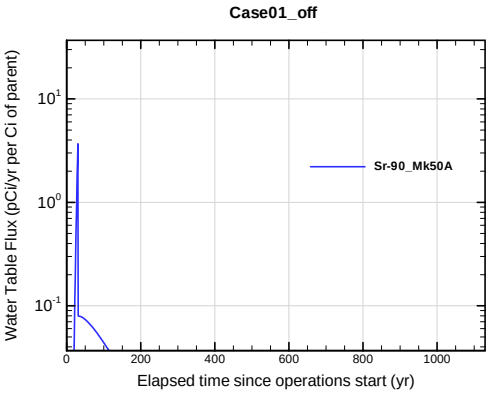

Figure A1A-44. Slit Trench water table flux for Case01_off Sr-90_Mk50A

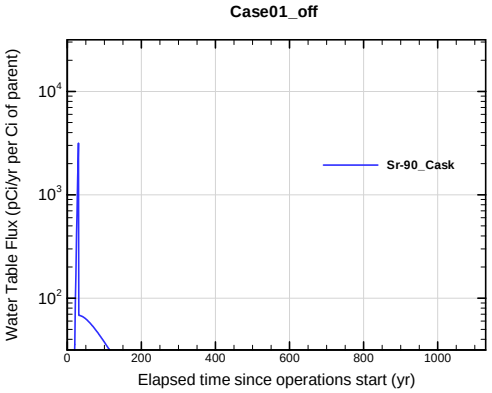

Figure A1A-45. Slit Trench water table flux for Case01_off Sr-90_Cask

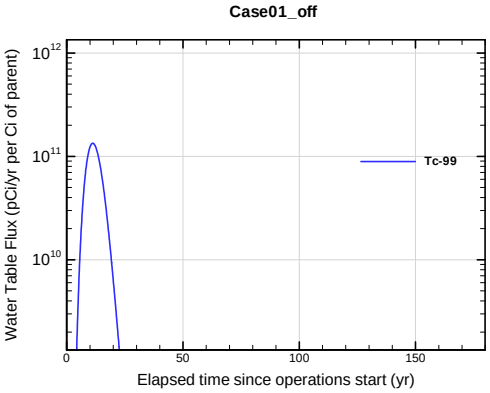

Figure A1A-46. Slit Trench water table flux for Case01_off Tc-99

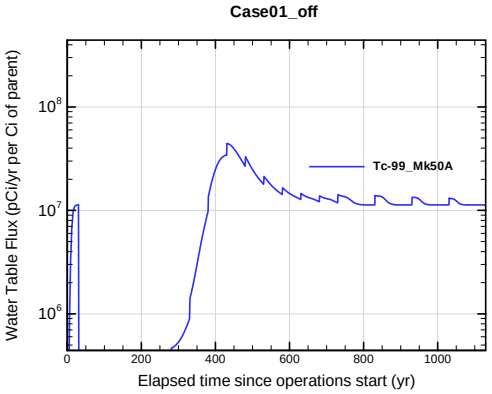

Figure A1A-47. Slit Trench water table flux for Case01_off Tc-99_Mk50A

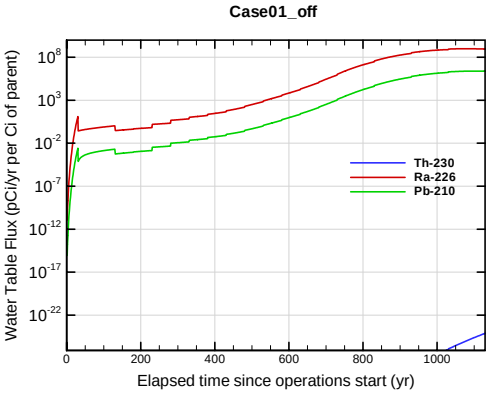

Figure A1A-48. Slit Trench water table flux for Case01_off Th-230

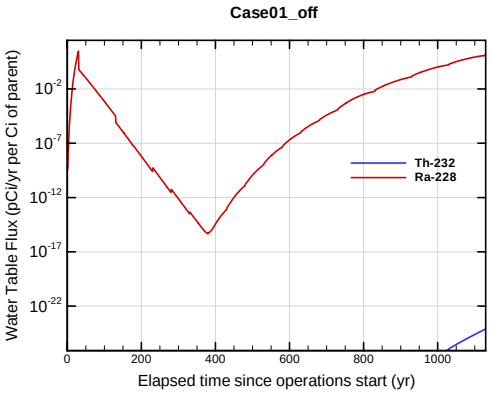

Figure A1A-49. Slit Trench water table flux for Case01_off Th-232

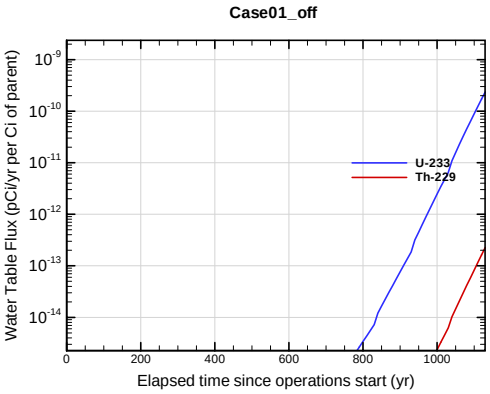

Figure A1A-50. Slit Trench water table flux for Case01_off U-233

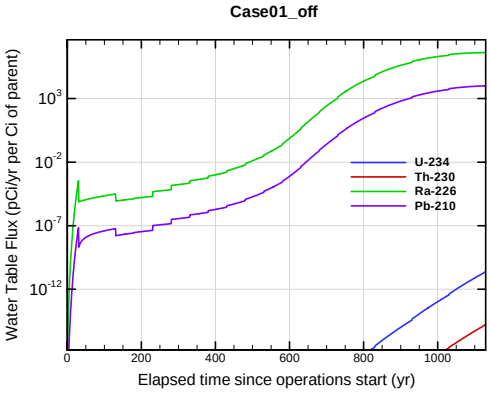

Figure A1A-51. Slit Trench water table flux for Case01_off U-234

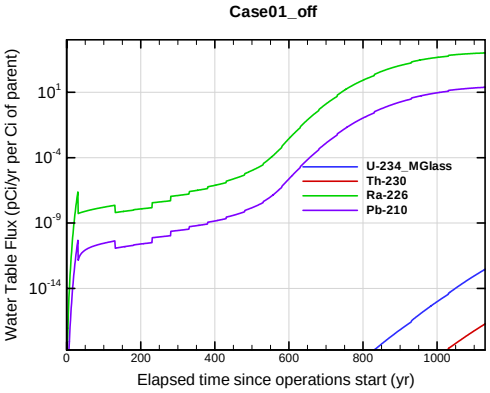

Figure A1A-52. Slit Trench water table flux for Case01_off U-234_MGlass

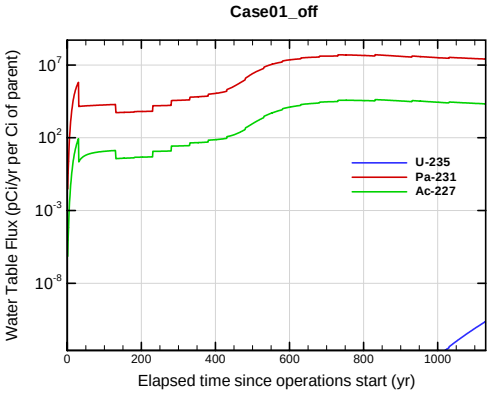

Figure A1A-53. Slit Trench water table flux for Case01_off U-235

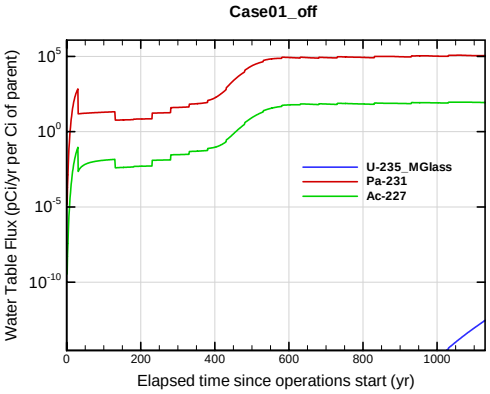

Figure A1A-54. Slit Trench water table flux for Case01_off U-235_MGlass

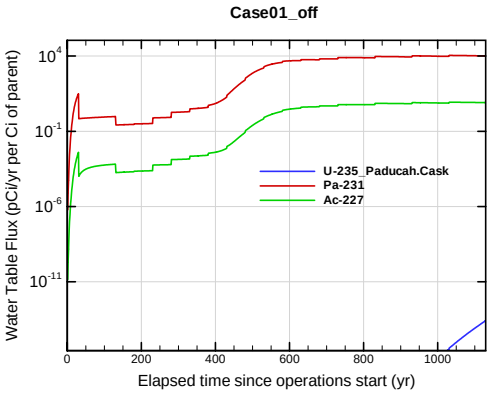

Figure A1A-55. Slit Trench water table flux for Case01_off U-235_Paducah.Cask

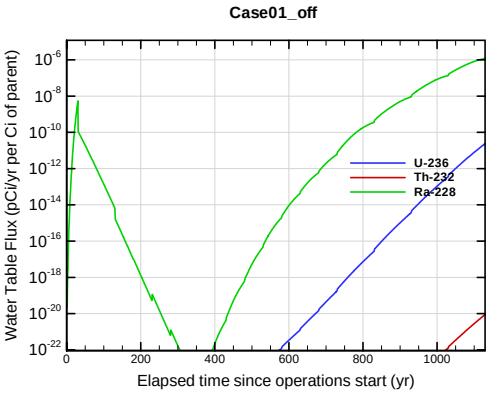

Figure A1A-56. Slit Trench water table flux for Case01_off U-236

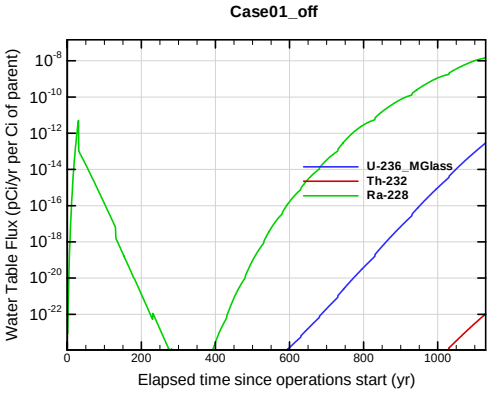

Figure A1A-57. Slit Trench water table flux for Case01_off U-236_MGlass

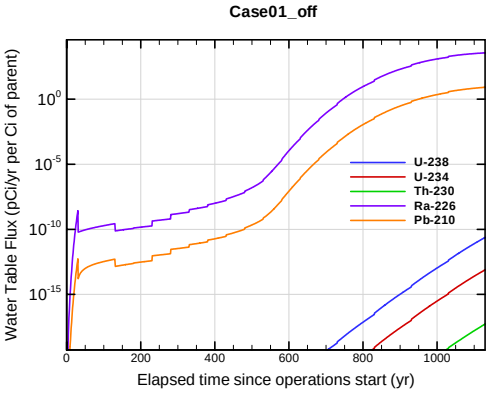

Figure A1A-58. Slit Trench water table flux for Case01_off U-238

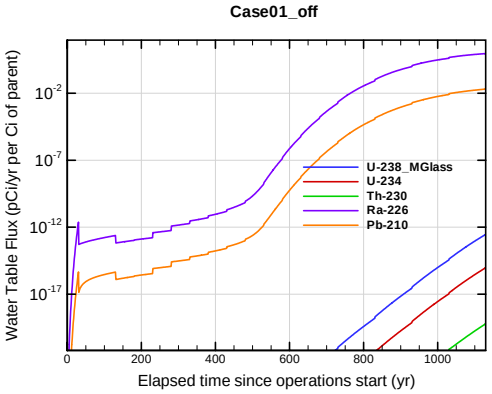

Figure A1A-59. Slit Trench water table flux for Case01_off U-238_MGlass

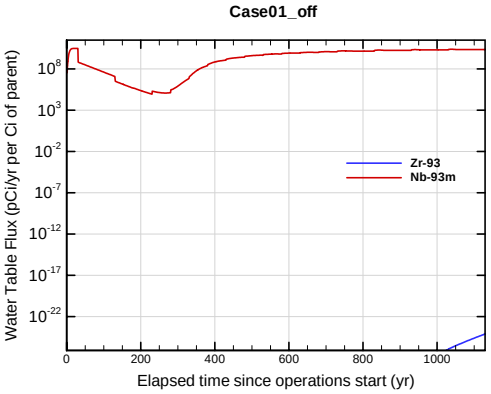

Figure A1A-60. Slit Trench water table flux for Case01_off Zr-93

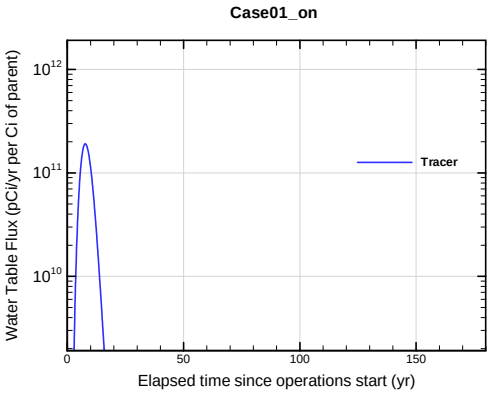

Figure A1A-61. Slit Trench water table flux for Case01_on Tracer

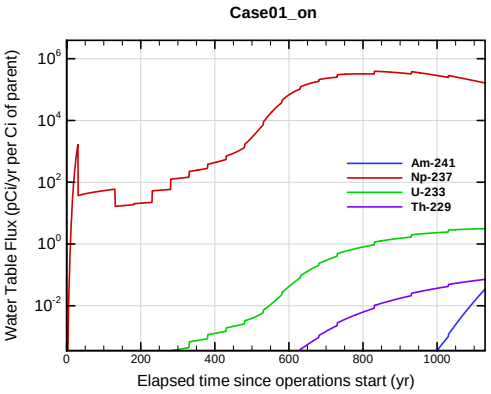

Figure A1A-62. Slit Trench water table flux for Case01_on Am-241

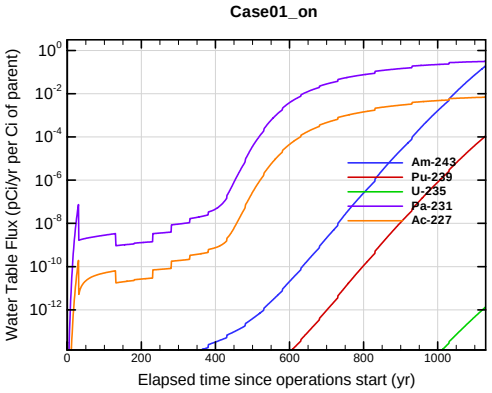

Figure A1A-63. Slit Trench water table flux for Case01_on Am-243

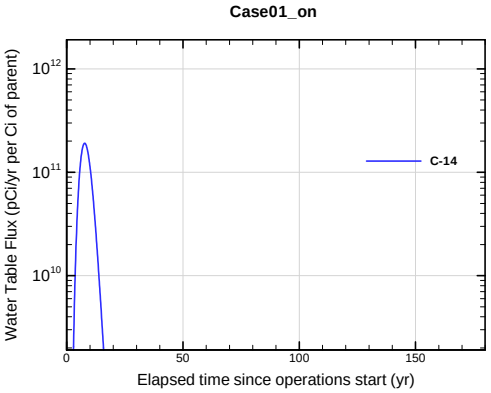

Figure A1A-64. Slit Trench water table flux for Case01_on C-14

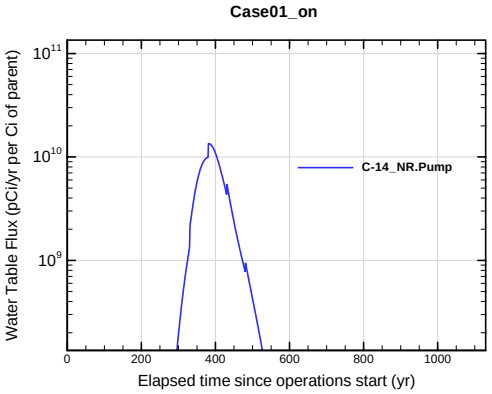

Figure A1A-65. Slit Trench water table flux for Case01_on C-14_NR.Pump

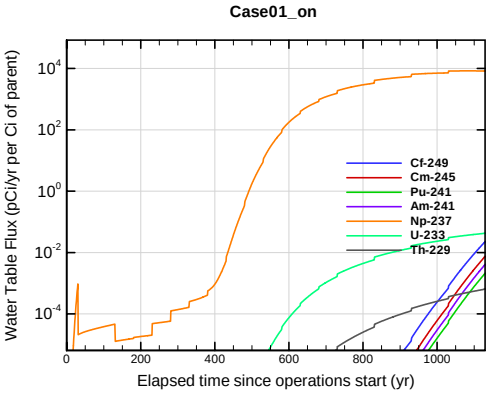

Figure A1A-66. Slit Trench water table flux for Case01_on Cf-249

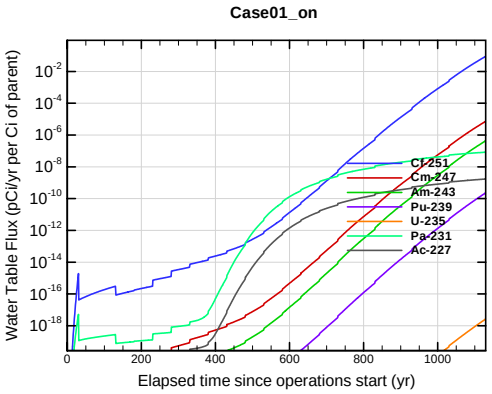

Figure A1A-67. Slit Trench water table flux for Case01_on Cf-251

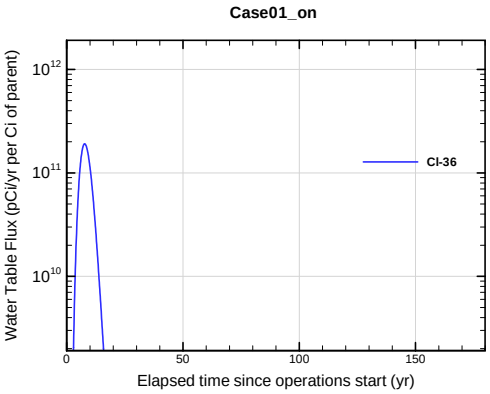

Figure A1A-68. Slit Trench water table flux for Case01_on Cl-36

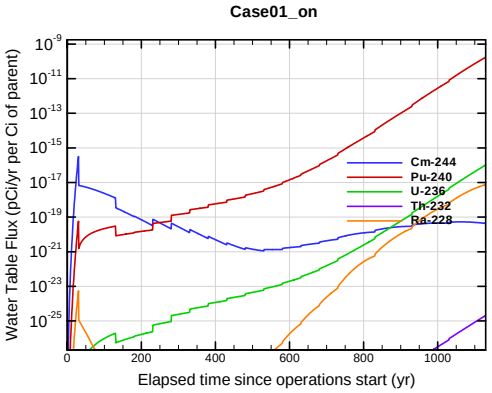

Figure A1A-69. Slit Trench water table flux for Case01_on Cm-244

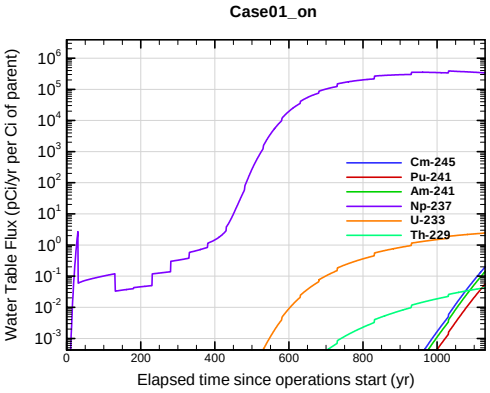

Figure A1A-70. Slit Trench water table flux for Case01_on Cm-245

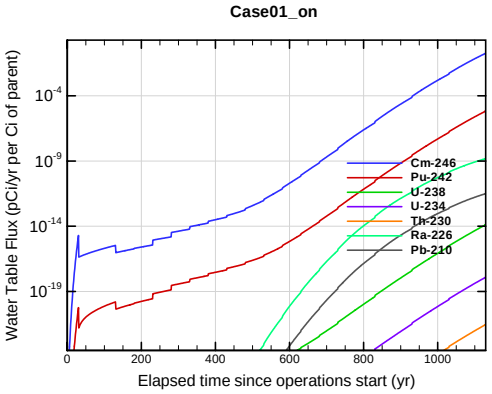

Figure A1A-71. Slit Trench water table flux for Case01_on Cm-246

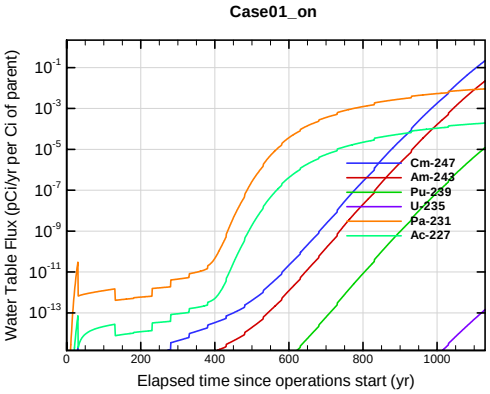

Figure A1A-72. Slit Trench water table flux for Case01_on Cm-247

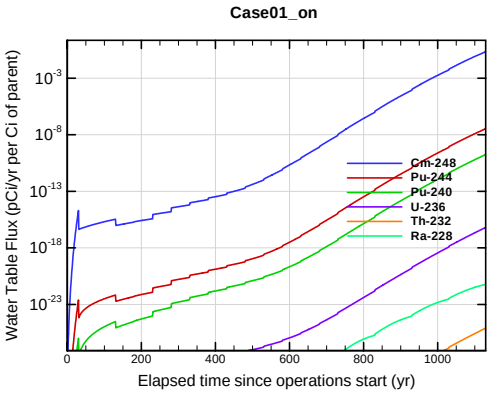

Figure A1A-73. Slit Trench water table flux for Case01_on Cm-248

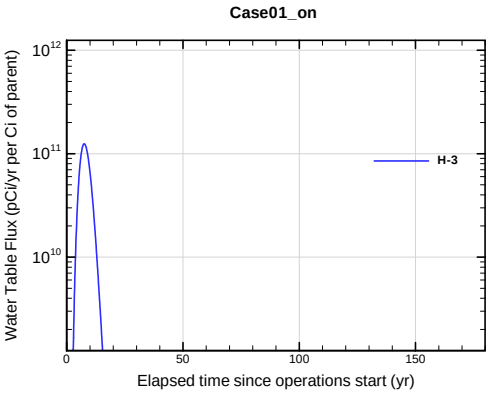

Figure A1A-74. Slit Trench water table flux for Case01_on H-3

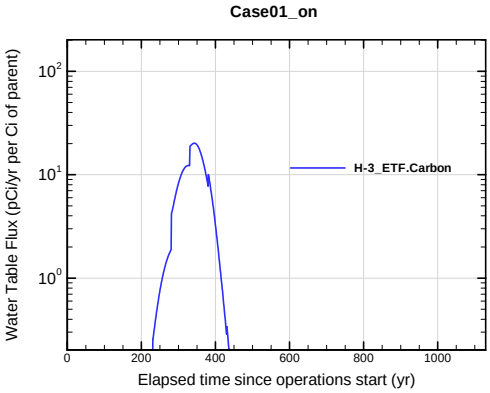

Figure A1A-75. Slit Trench water table flux for Case01_on H-3_ETF.Carbon

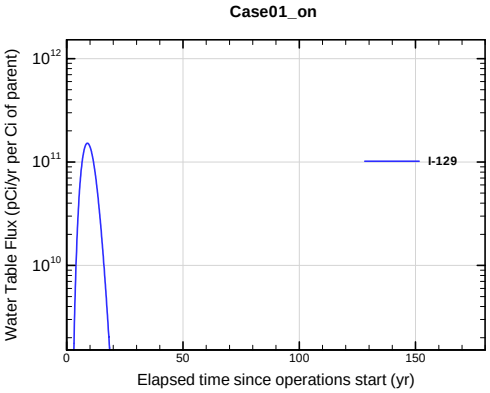

Figure A1A-76. Slit Trench water table flux for Case01_on I-129

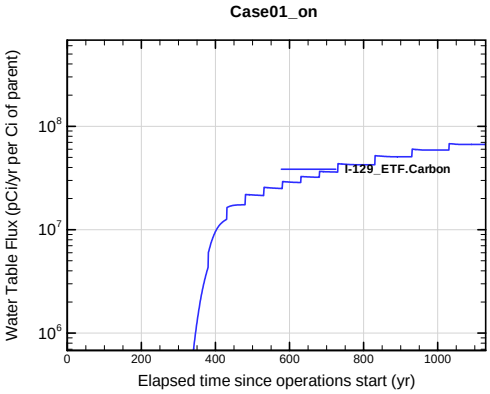

Figure A1A-77. Slit Trench water table flux for Case01_on I-129_ETF.Carbon

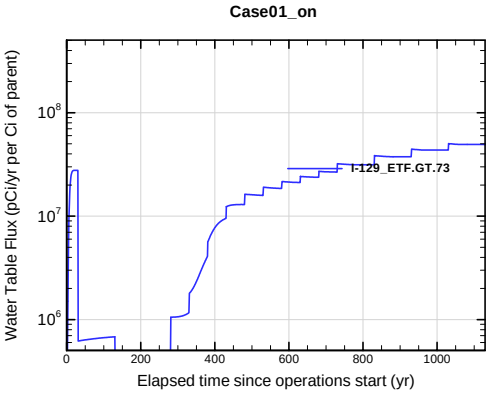

Figure A1A-78. Slit Trench water table flux for Case01_on I-129_ETF.GT.73

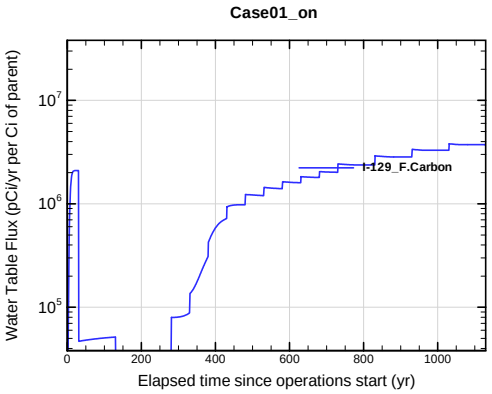

Figure A1A-79. Slit Trench water table flux for Case01_on I-129_F.Carbon

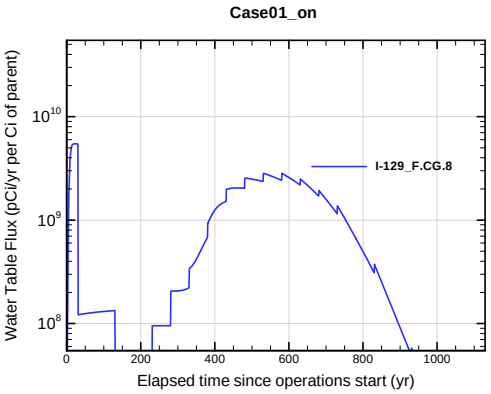

Figure A1A-80. Slit Trench water table flux for Case01_on I-129_F.CG.8

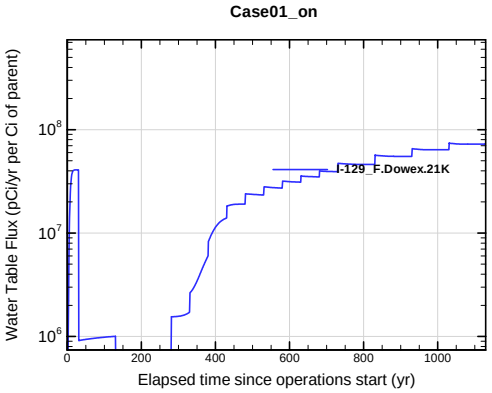

Figure A1A-81. Slit Trench water table flux for Case01_on I-129_F.Dowex.21K

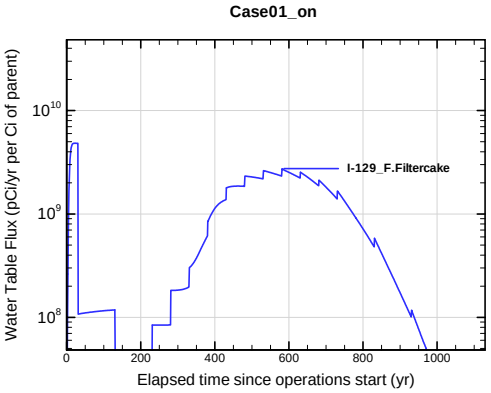

Figure A1A-82. Slit Trench water table flux for Case01_on I-129_F.Filtercake

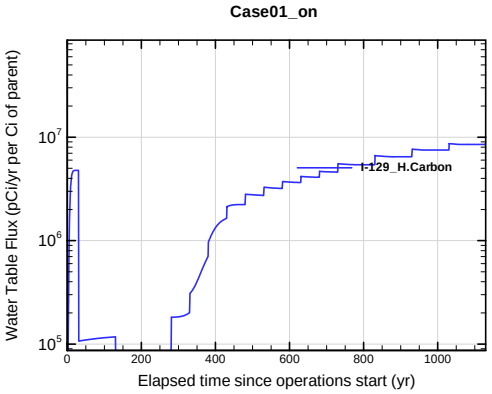

Figure A1A-83. Slit Trench water table flux for Case01_on I-129_H.Carbon

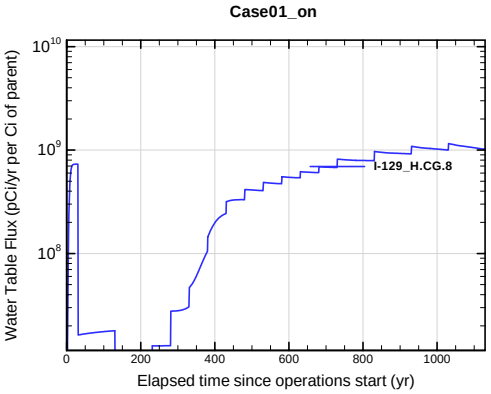

Figure A1A-84. Slit Trench water table flux for Case01_on I-129_H.CG.8

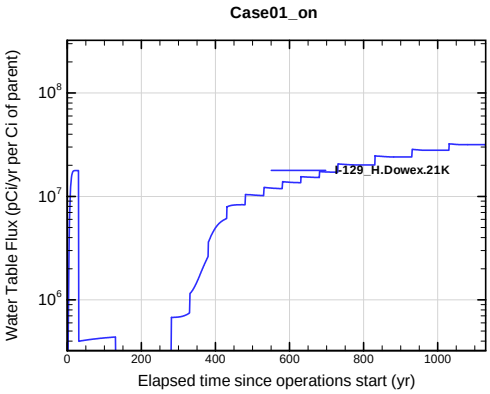

Figure A1A-85. Slit Trench water table flux for Case01_on I-129_H.Dowex.21K

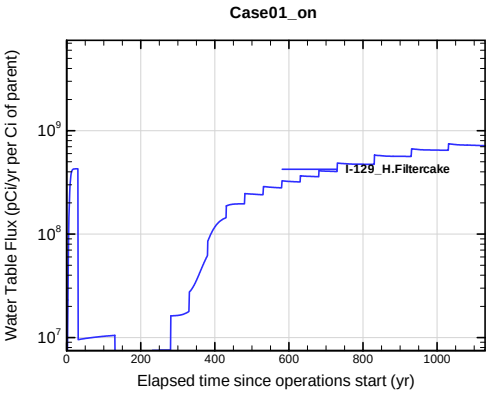

Figure A1A-86. Slit Trench water table flux for Case01_on I-129_H.Filtercake

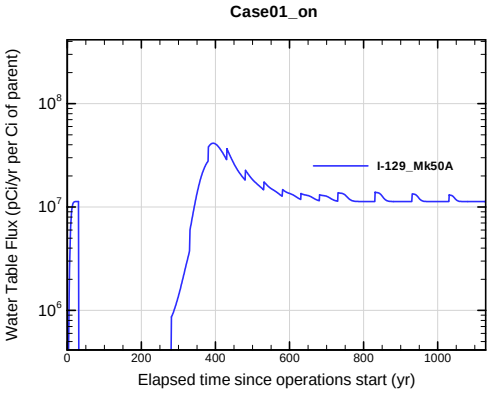

Figure A1A-87. Slit Trench water table flux for Case01_on I-129_Mk50A

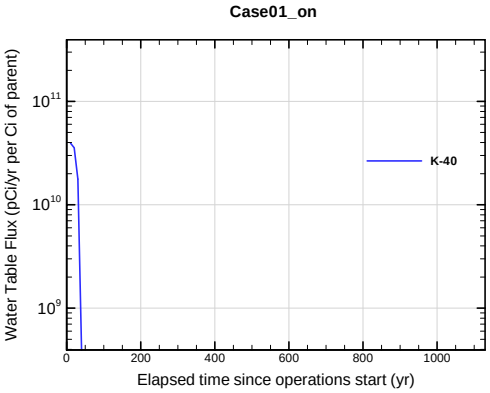

Figure A1A-88. Slit Trench water table flux for Case01_on K-40

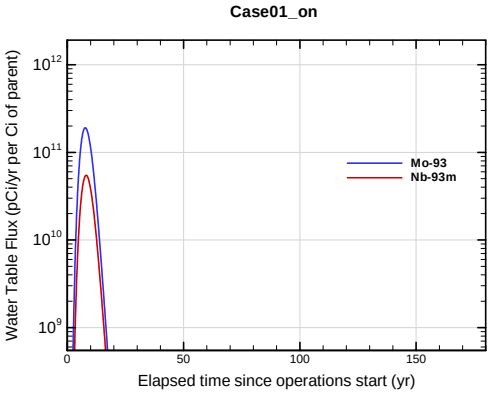

Figure A1A-89. Slit Trench water table flux for Case01_on Mo-93

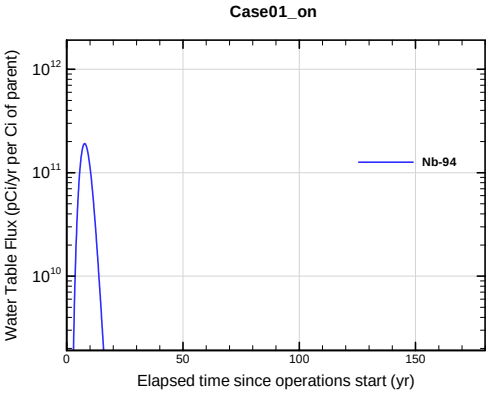

Figure A1A-90. Slit Trench water table flux for Case01_on Nb-94

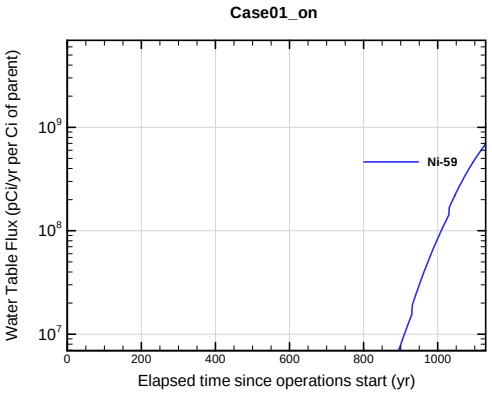

Figure A1A-91. Slit Trench water table flux for Case01_on Ni-59

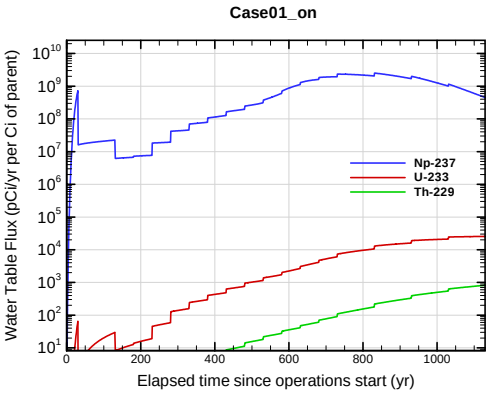

Figure A1A-92. Slit Trench water table flux for Case01_on Np-237

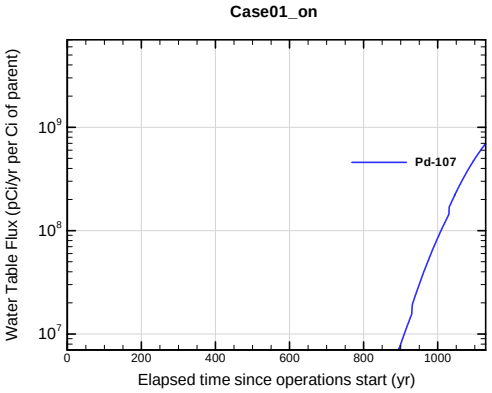

Figure A1A-93. Slit Trench water table flux for Case01_on Pd-107

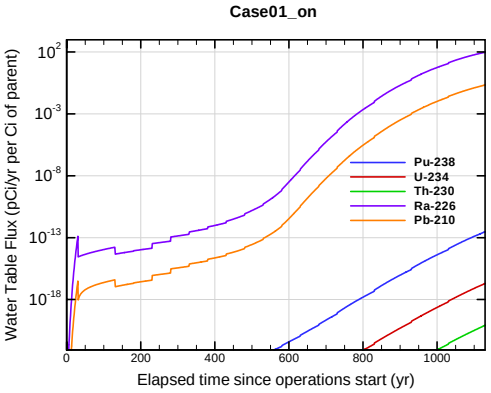

Figure A1A-94. Slit Trench water table flux for Case01_on Pu-238

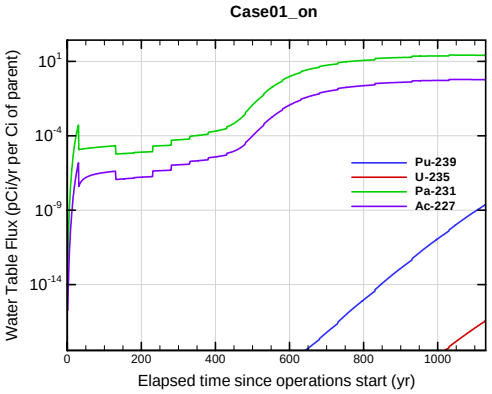

Figure A1A-95. Slit Trench water table flux for Case01_on Pu-239

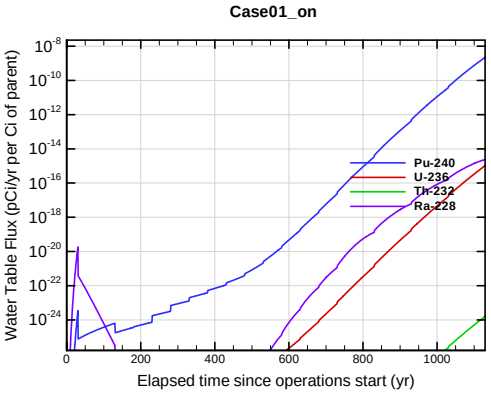

Figure A1A-96. Slit Trench water table flux for Case01_on Pu-240

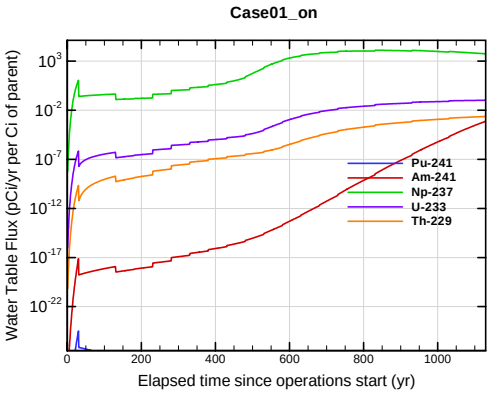

Figure A1A-97. Slit Trench water table flux for Case01_on Pu-241

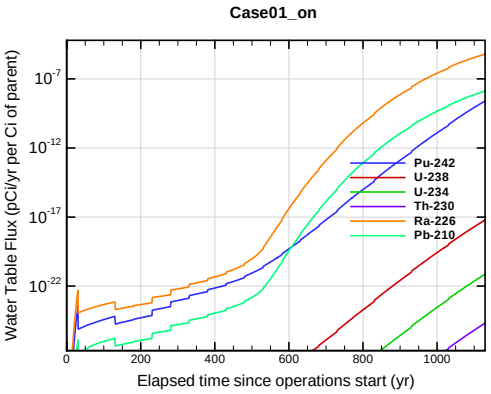

Figure A1A-98. Slit Trench water table flux for Case01_on Pu-242

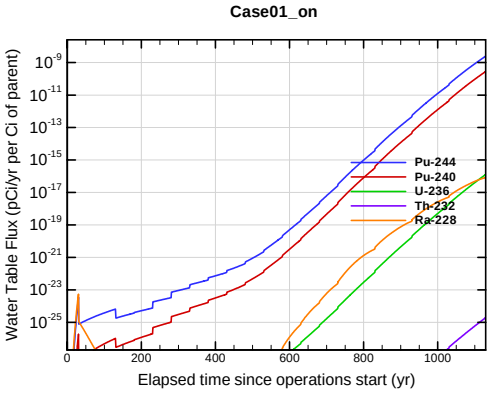

Figure A1A-99. Slit Trench water table flux for Case01_on Pu-244

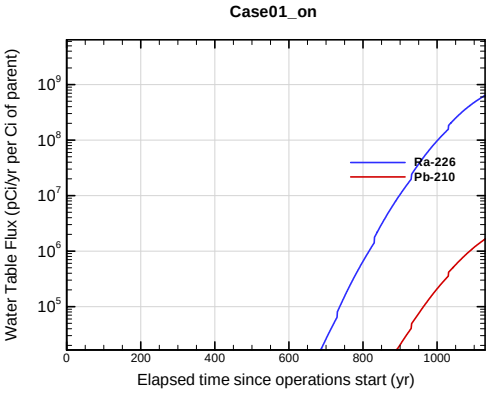

Figure A1A-100. Slit Trench water table flux for Case01_on Ra-226

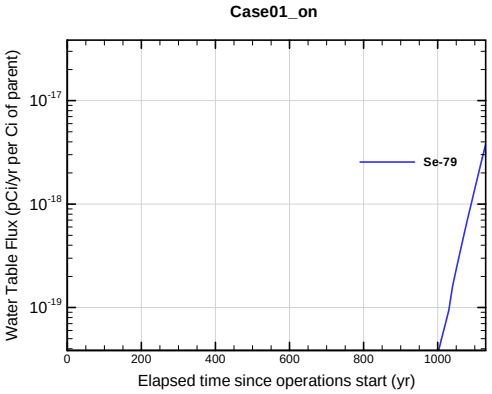

Figure A1A-101. Slit Trench water table flux for Case01_on Se-79

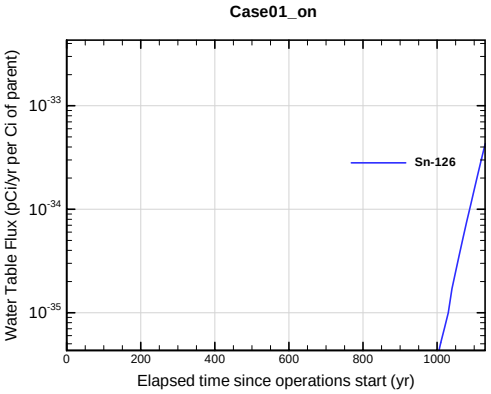

Figure A1A-102. Slit Trench water table flux for Case01_on Sn-126

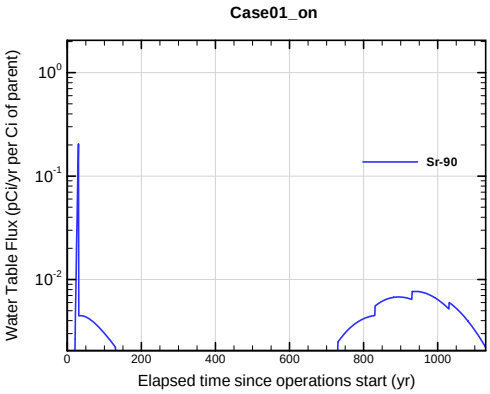

Figure A1A-103. Slit Trench water table flux for Case01_on Sr-90

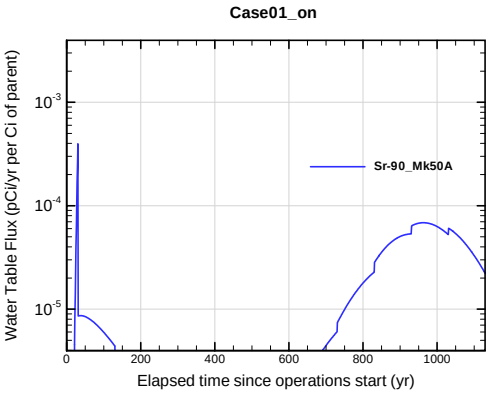

Figure A1A-104. Slit Trench water table flux for Case01_on Sr-90_Mk50A

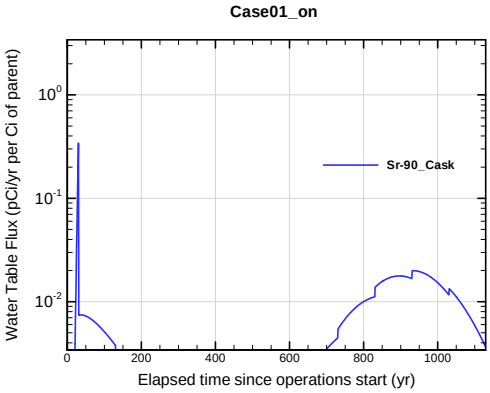

Figure A1A-105. Slit Trench water table flux for Case01_on Sr-90_Cask

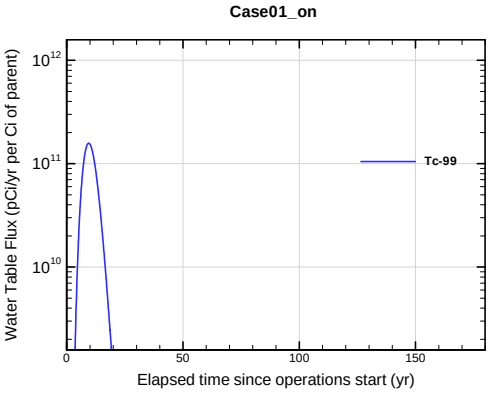

Figure A1A-106. Slit Trench water table flux for Case01_on Tc-99

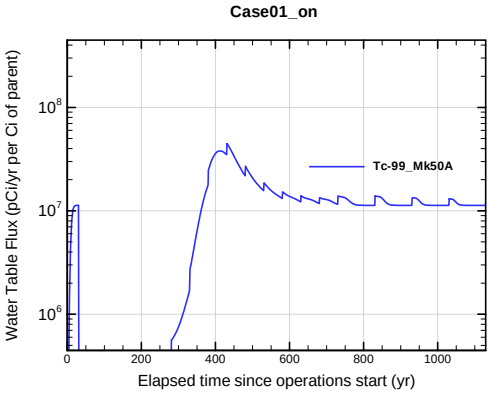

Figure A1A-107. Slit Trench water table flux for Case01_on Tc-99_Mk50A

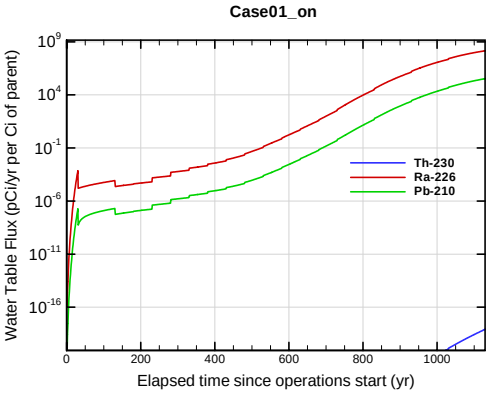

Figure A1A-108. Slit Trench water table flux for Case01_on Th-230

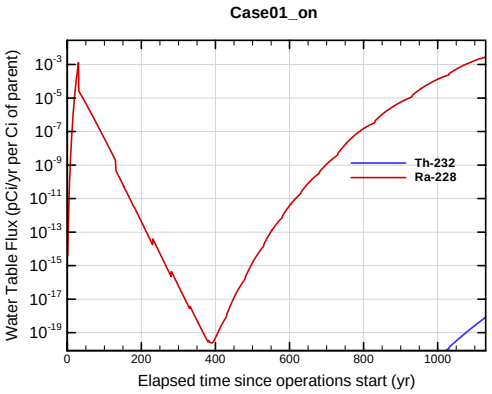

Figure A1A-109. Slit Trench water table flux for Case01_on Th-232

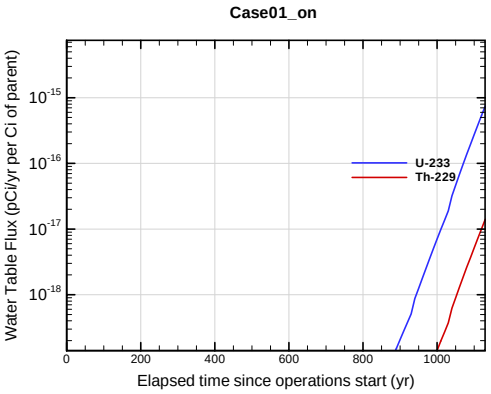

Figure A1A-110. Slit Trench water table flux for Case01_on U-233

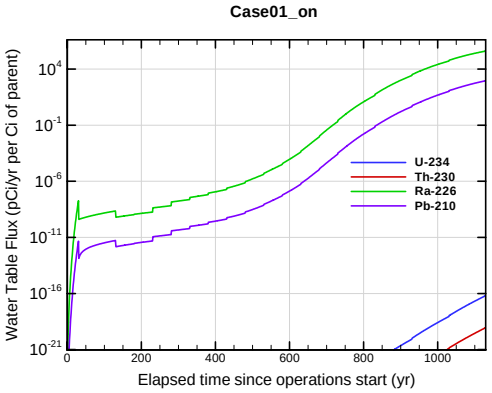

Figure A1A-111. Slit Trench water table flux for Case01_on U-234

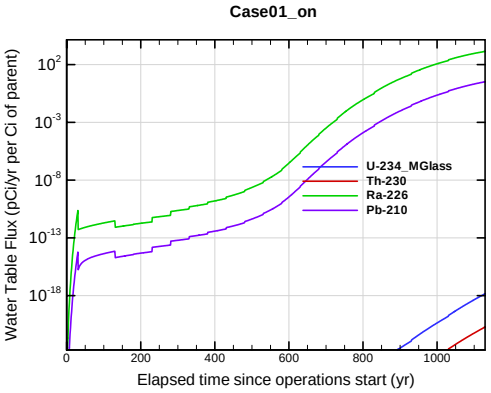

Figure A1A-112. Slit Trench water table flux for Case01_on U-234_MGlass

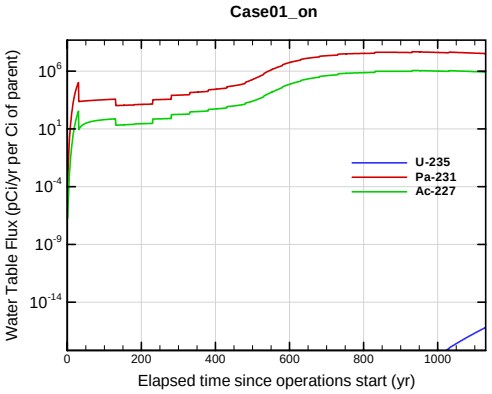

Figure A1A-113. Slit Trench water table flux for Case01_on U-235

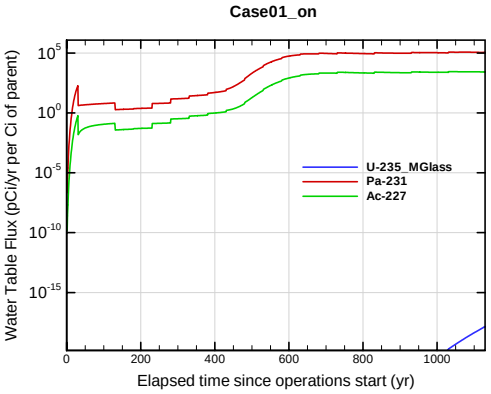

Figure A1A-114. Slit Trench water table flux for Case01_on U-235_MGlass

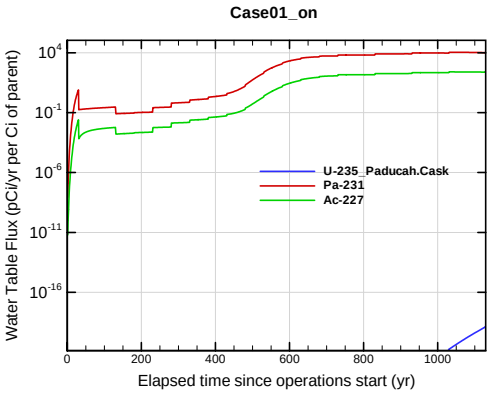

Figure A1A-115. Slit Trench water table flux for Case01_on U-235_Paducah.Cask

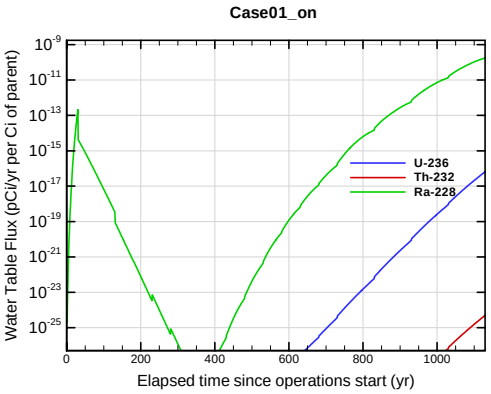

Figure A1A-116. Slit Trench water table flux for Case01_on U-236

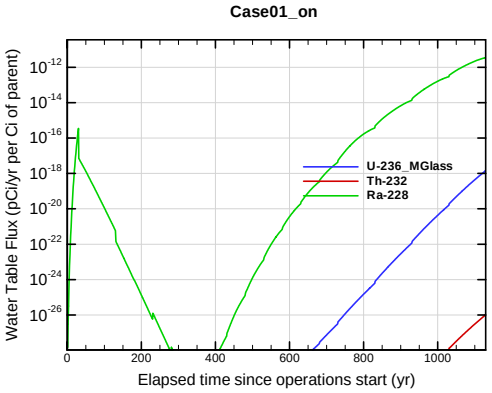

Figure A1A-117. Slit Trench water table flux for Case01_on U-236_MGlass

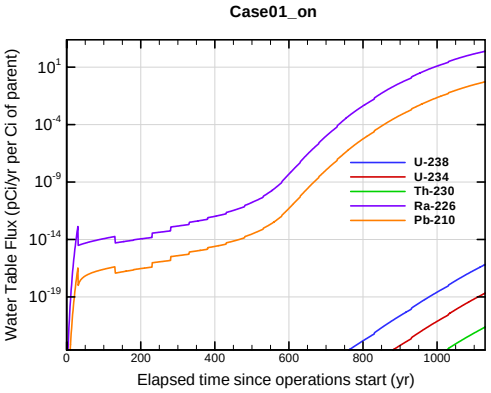

Figure A1A-118. Slit Trench water table flux for Case01_on U-238

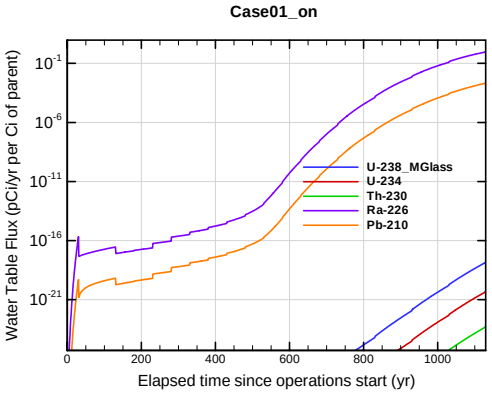

Figure A1A-119. Slit Trench water table flux for Case01_on U-238_MGlass

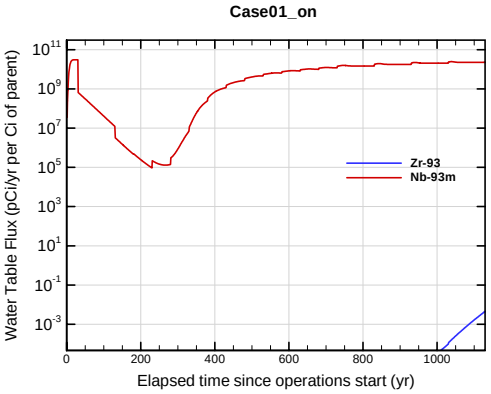

Figure A1A-120. Slit Trench water table flux for Case01_on Zr-93

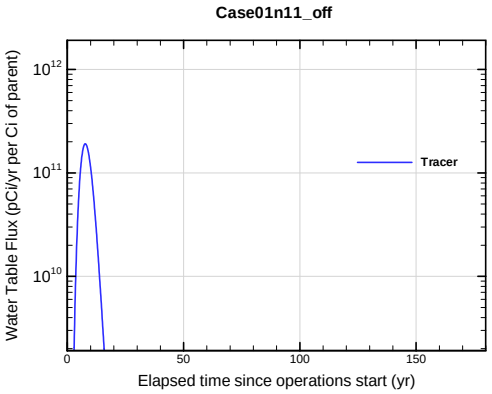

Figure A1A-121. Slit Trench water table flux for Case01n11_off Tracer

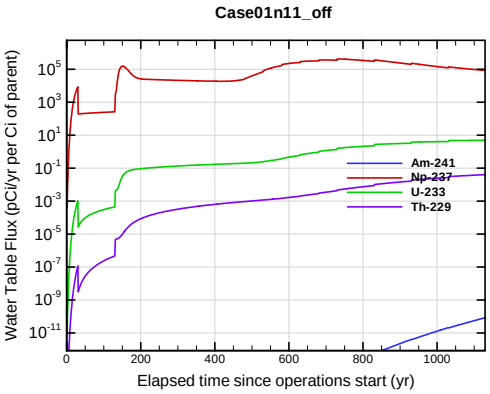

Figure A1A-122. Slit Trench water table flux for Case01n11_off Am-241

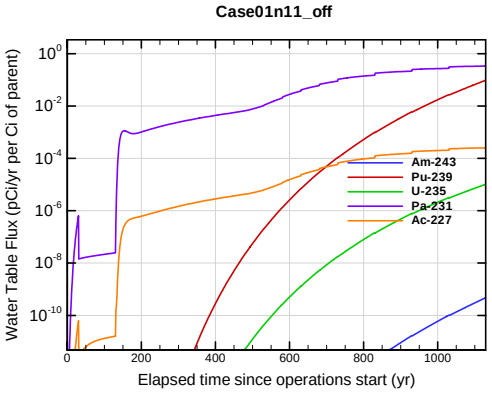

Figure A1A-123. Slit Trench water table flux for Case01n11_off Am-243

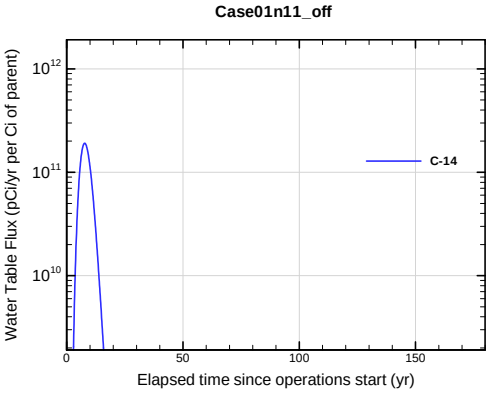

Figure A1A-124. Slit Trench water table flux for Case01n11_off C-14

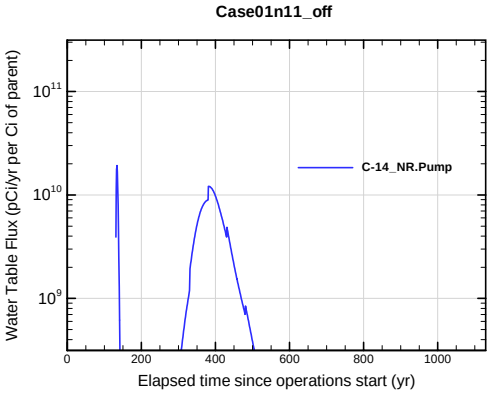

Figure A1A-125. Slit Trench water table flux for Case01n11_off C-14_NR.Pump

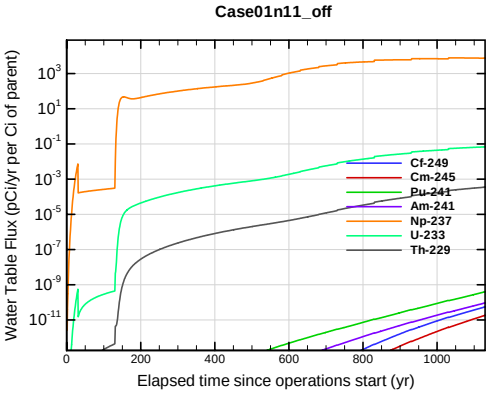

Figure A1A-126. Slit Trench water table flux for Case01n11_off Cf-249

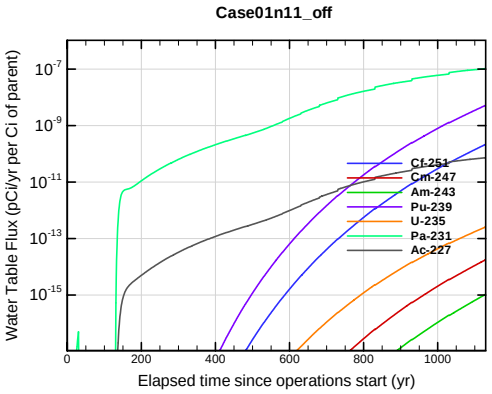

Figure A1A-127. Slit Trench water table flux for Case01n11_off Cf-251

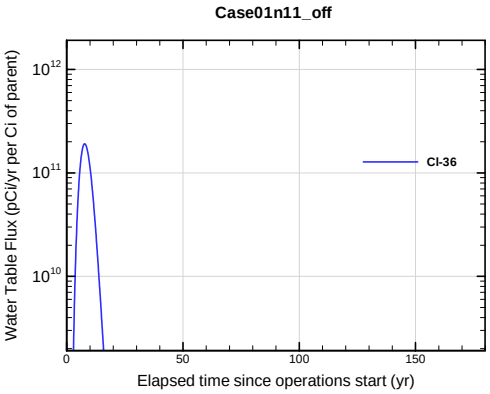

Figure A1A-128. Slit Trench water table flux for Case01n11_off Cl-36

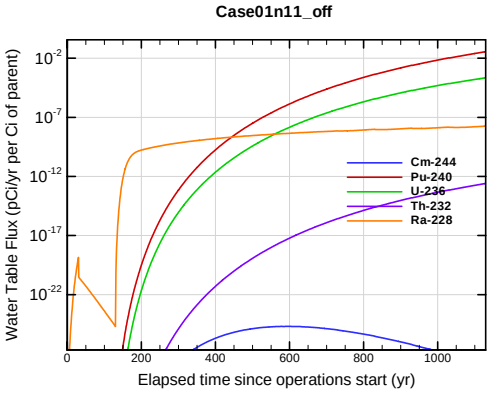

Figure A1A-129. Slit Trench water table flux for Case01n11_off Cm-244

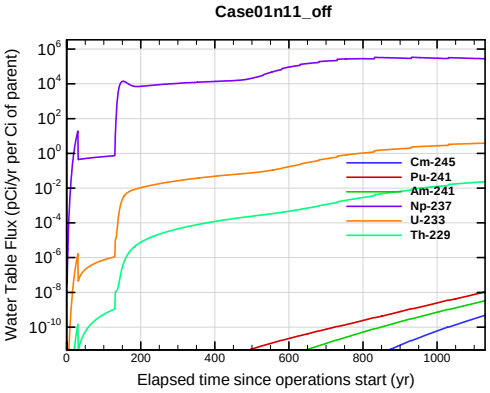

Figure A1A-130. Slit Trench water table flux for Case01n11_off Cm-245

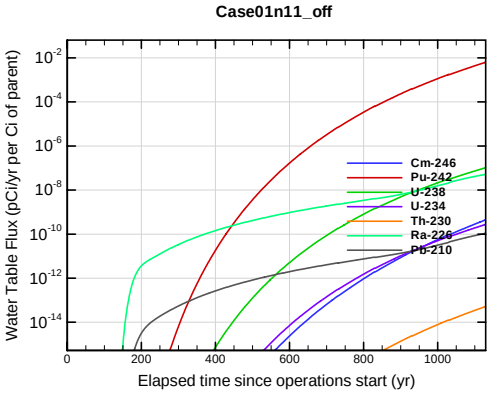

Figure A1A-131. Slit Trench water table flux for Case01n11_off Cm-246

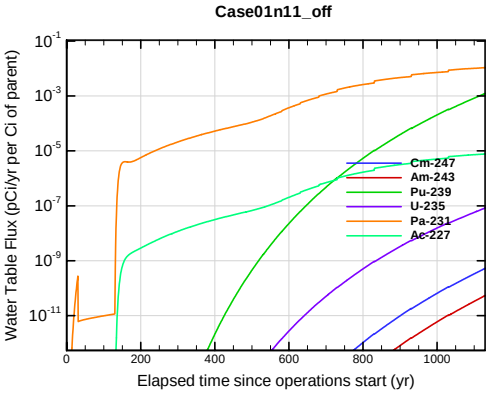

Figure A1A-132. Slit Trench water table flux for Case01n11_off Cm-247

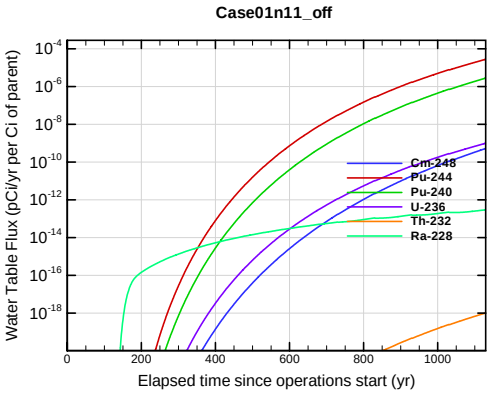

Figure A1A-133. Slit Trench water table flux for Case01n11_off Cm-248

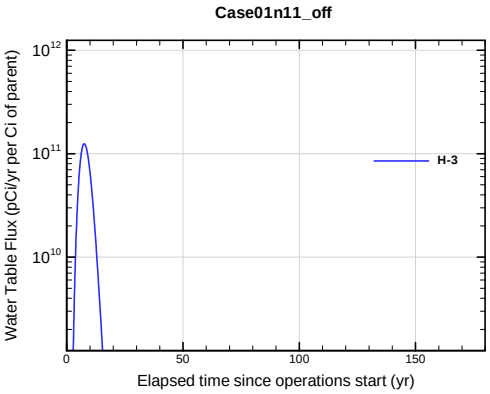

Figure A1A-134. Slit Trench water table flux for Case01n11_off H-3

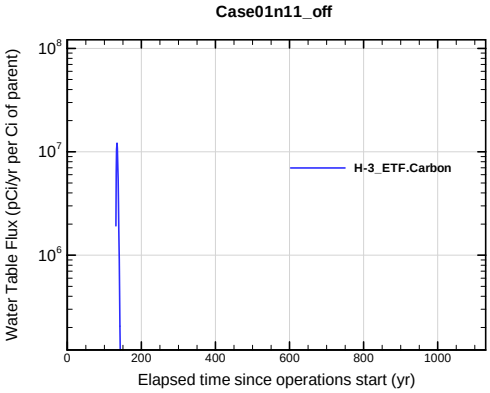

Figure A1A-135. Slit Trench water table flux for Case01n11_off H-3_ETF.Carbon

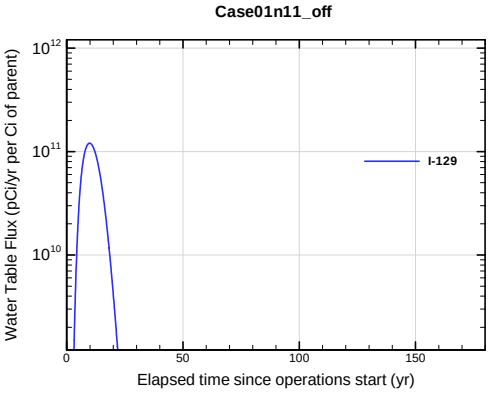

Figure A1A-136. Slit Trench water table flux for Case01n11_off I-129

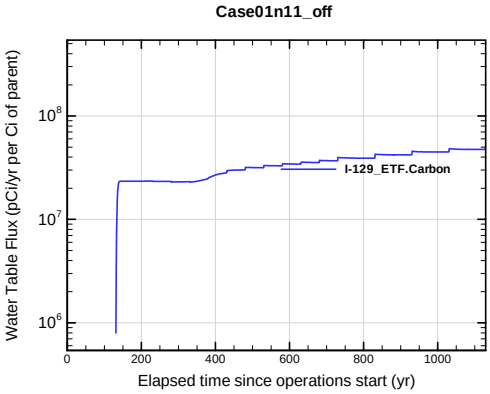

Figure A1A-137. Slit Trench water table flux for Case01n11_off I-129_ETF.Carbon

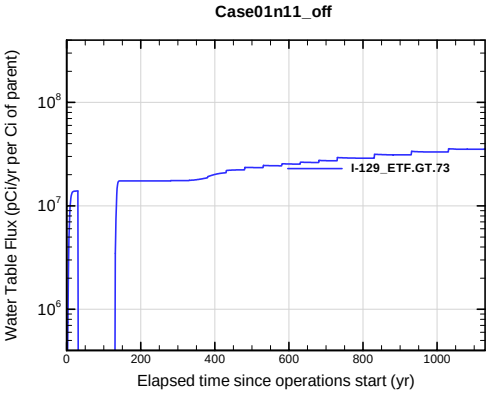

Figure A1A-138. Slit Trench water table flux for Case01n11_off I-129_ETF.GT.73

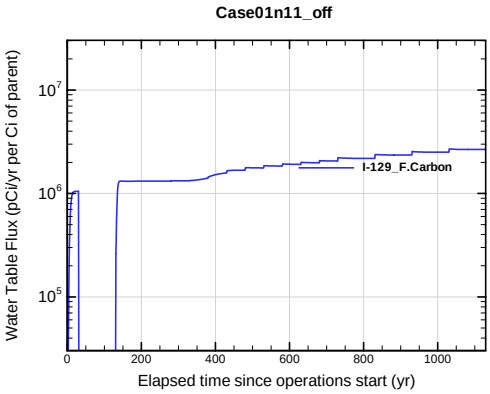

Figure A1A-139. Slit Trench water table flux for Case01n11_off I-129_F.Carbon

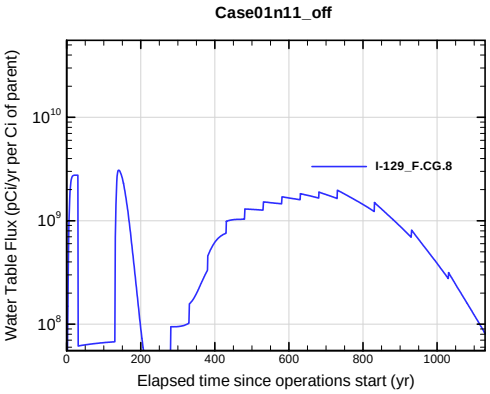

Figure A1A-140. Slit Trench water table flux for Case01n11_off I-129_F.CG.8

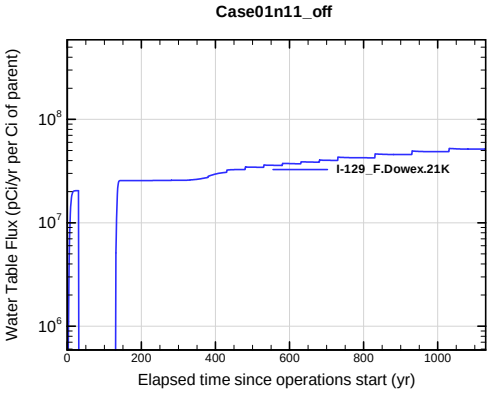

Figure A1A-141. Slit Trench water table flux for Case01n11_off I-129_F.Dowex.21K

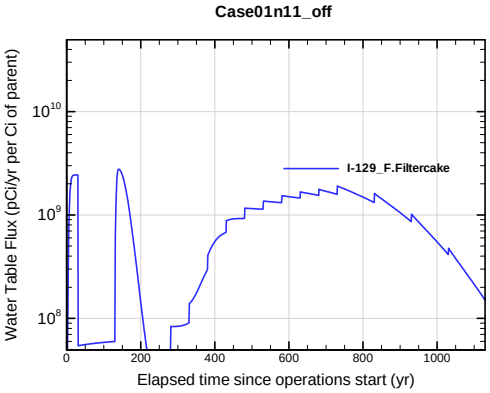

Figure A1A-142. Slit Trench water table flux for Case01n11_off I-129_F.Filtercake

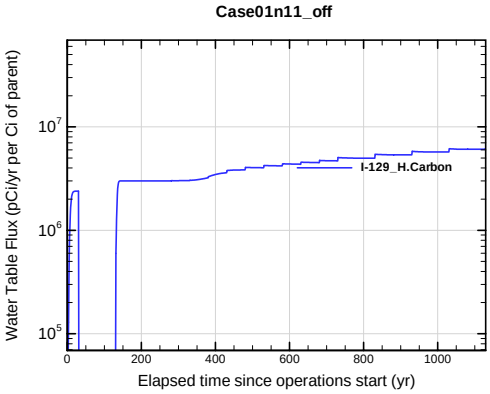

Figure A1A-143. Slit Trench water table flux for Case01n11_off I-129_H.Carbon

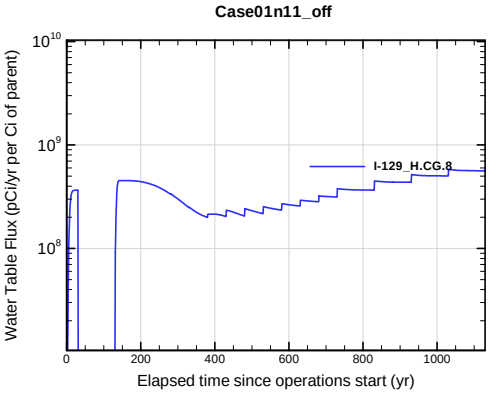

Figure A1A-144. Slit Trench water table flux for Case01n11_off I-129_H.CG.8

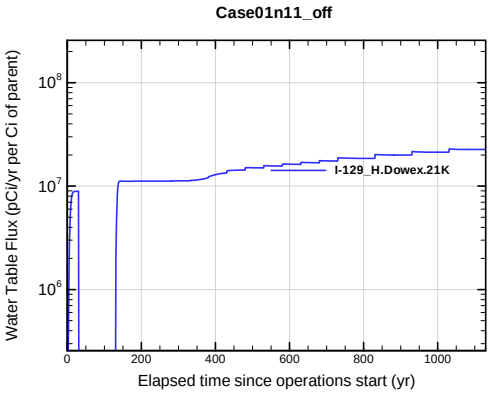

Figure A1A-145. Slit Trench water table flux for Case01n11_off I-129_H.Dowex.21K

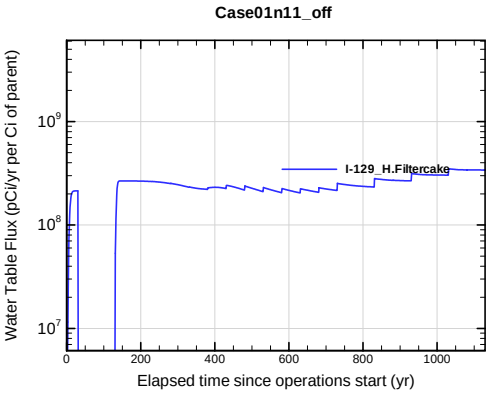

Figure A1A-146. Slit Trench water table flux for Case01n11_off I-129_H.Filtercake

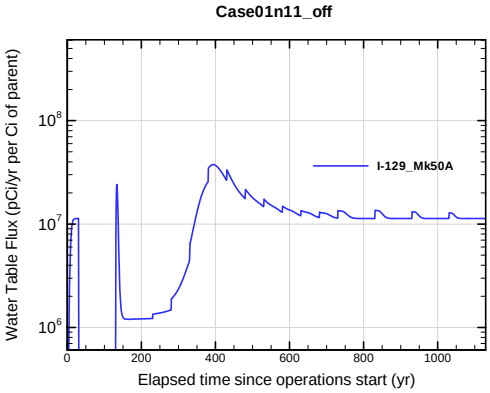

Figure A1A-147. Slit Trench water table flux for Case01n11_off I-129_Mk50A

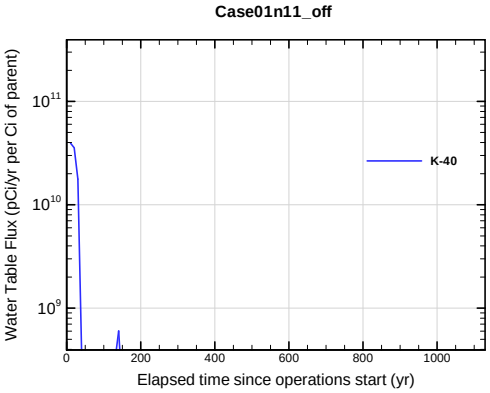

Figure A1A-148. Slit Trench water table flux for Case01n11_off K-40

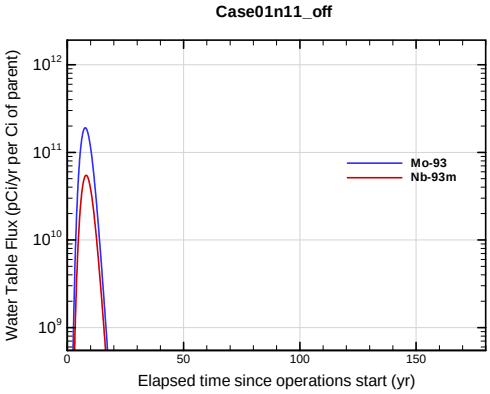

Figure A1A-149. Slit Trench water table flux for Case01n11_off Mo-93

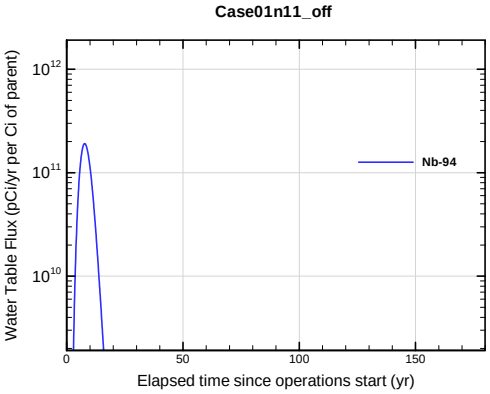

Figure A1A-150. Slit Trench water table flux for Case01n11_off Nb-94

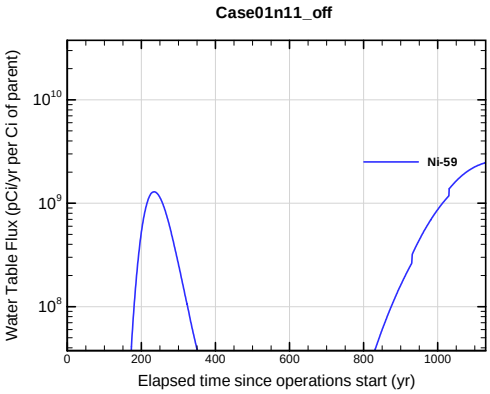

Figure A1A-151. Slit Trench water table flux for Case01n11_off Ni-59

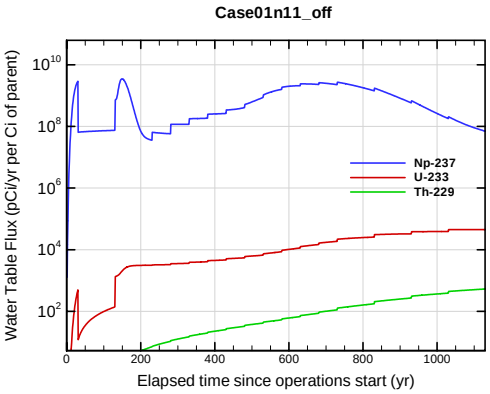

Figure A1A-152. Slit Trench water table flux for Case01n11_off Np-237

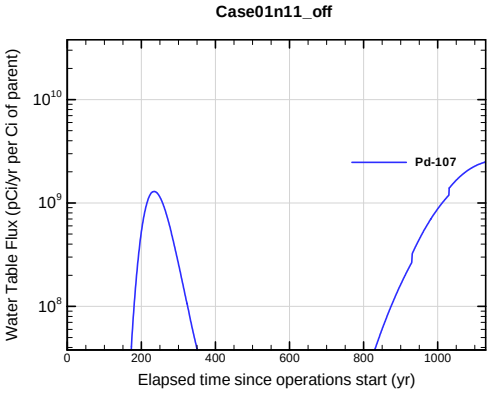

Figure A1A-153. Slit Trench water table flux for Case01n11_off Pd-107

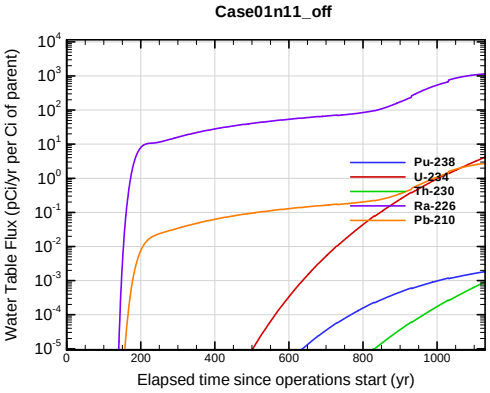

Figure A1A-154. Slit Trench water table flux for Case01n11_off Pu-238

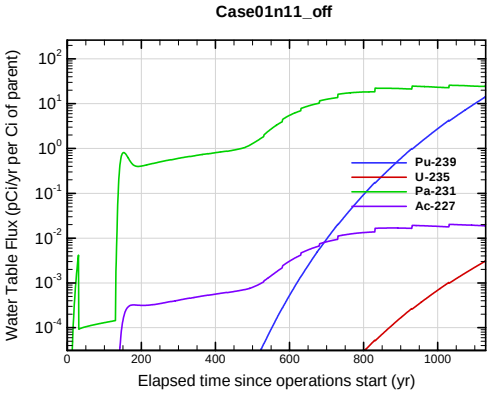

Figure A1A-155. Slit Trench water table flux for Case01n11_off Pu-239

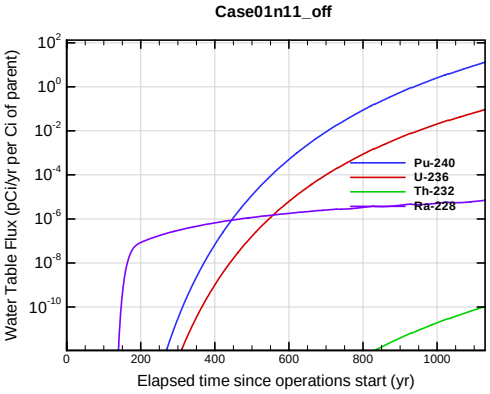

Figure A1A-156. Slit Trench water table flux for Case01n11_off Pu-240

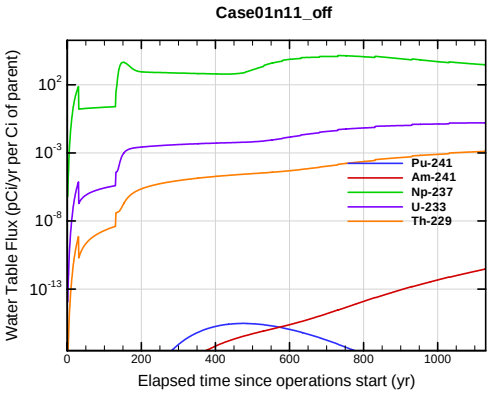

Figure A1A-157. Slit Trench water table flux for Case01n11_off Pu-241

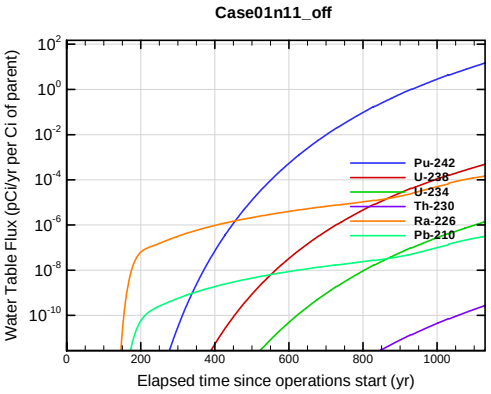

Figure A1A-158. Slit Trench water table flux for Case01n11_off Pu-242

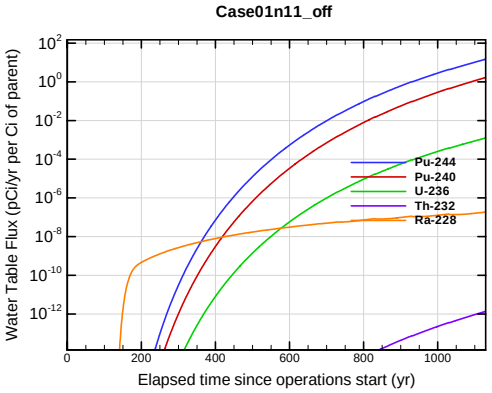

Figure A1A-159. Slit Trench water table flux for Case01n11_off Pu-244

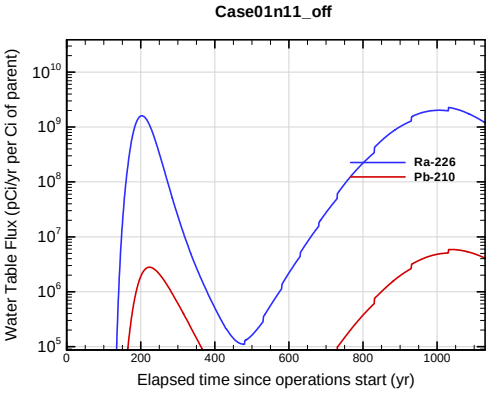

Figure A1A-160. Slit Trench water table flux for Case01n11_off Ra-226

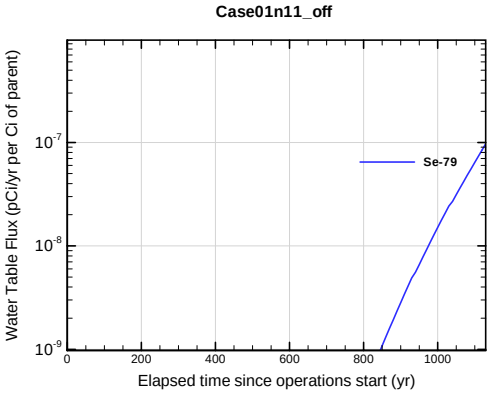

Figure A1A-161. Slit Trench water table flux for Case01n11_off Se-79

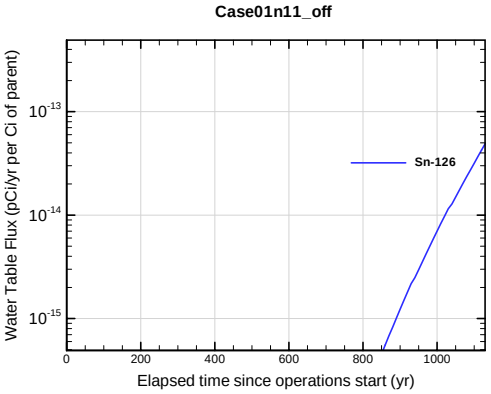

Figure A1A-162. Slit Trench water table flux for Case01n11_off Sn-126

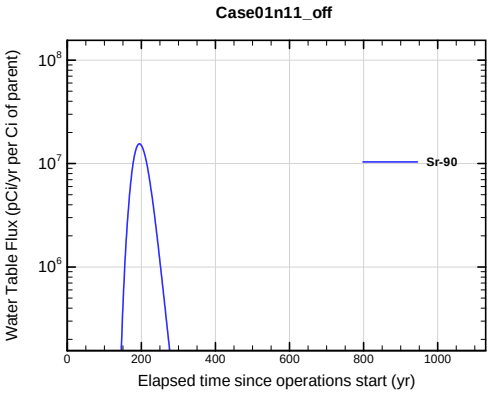

Figure A1A-163. Slit Trench water table flux for Case01n11_off Sr-90

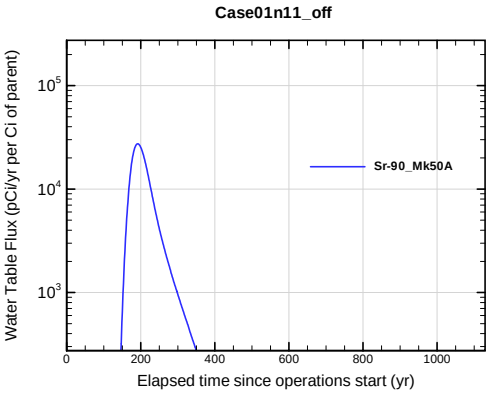

Figure A1A-164. Slit Trench water table flux for Case01n11_off Sr-90_Mk50A

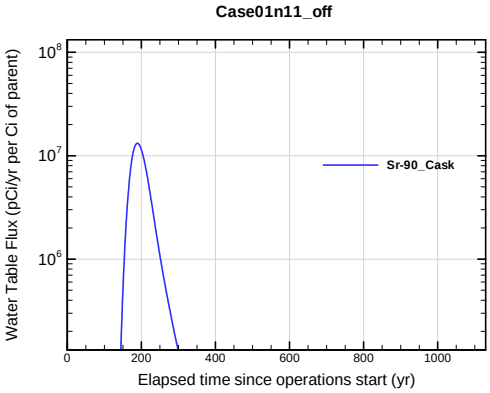

Figure A1A-165. Slit Trench water table flux for Case01n11_off Sr-90_Cask

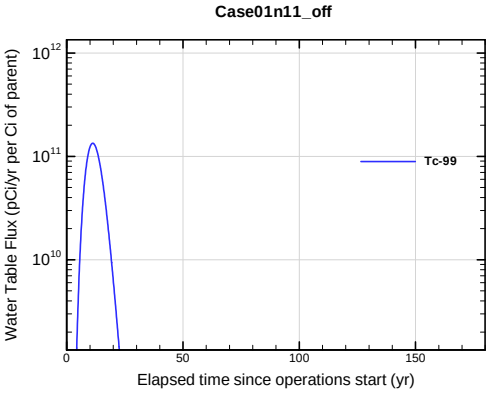

Figure A1A-166. Slit Trench water table flux for Case01n11_off Tc-99

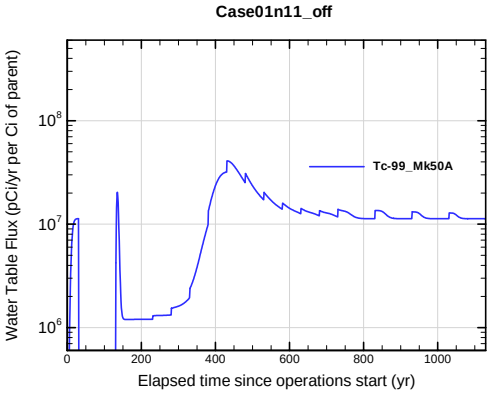

Figure A1A-167. Slit Trench water table flux for Case01n11_off Tc-99_Mk50A

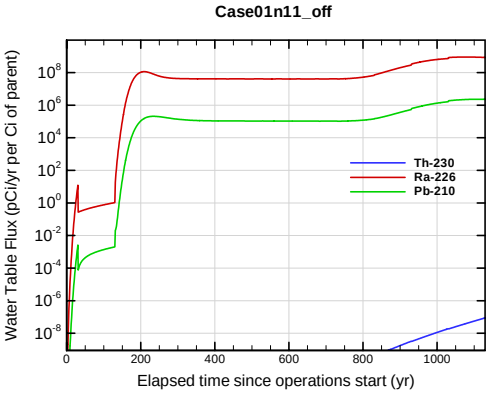

Figure A1A-168. Slit Trench water table flux for Case01n11_off Th-230

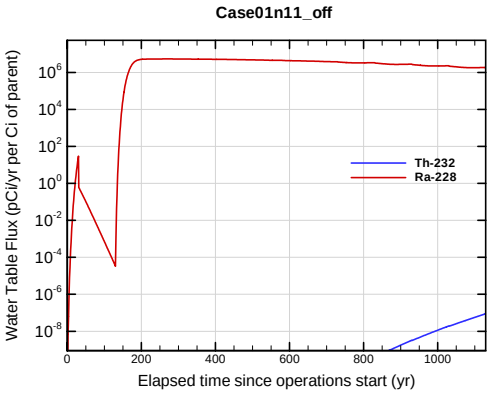

Figure A1A-169. Slit Trench water table flux for Case01n11_off Th-232

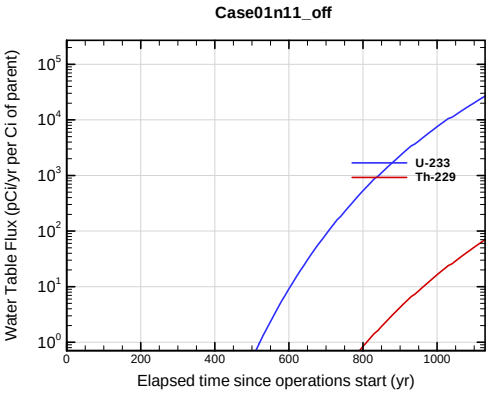

Figure A1A-170. Slit Trench water table flux for Case01n11_off U-233

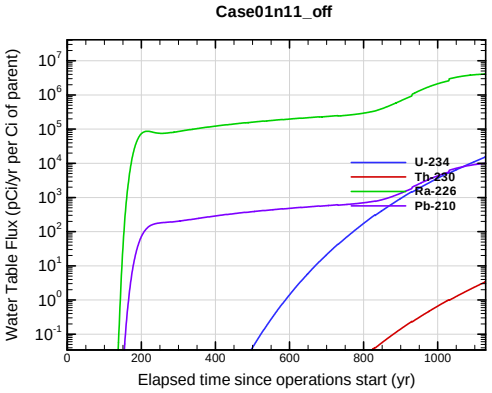

Figure A1A-171. Slit Trench water table flux for Case01n11_off U-234

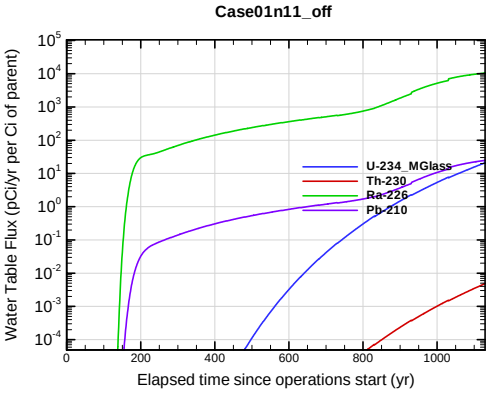

Figure A1A-172. Slit Trench water table flux for Case01n11_off U-234_MGlass

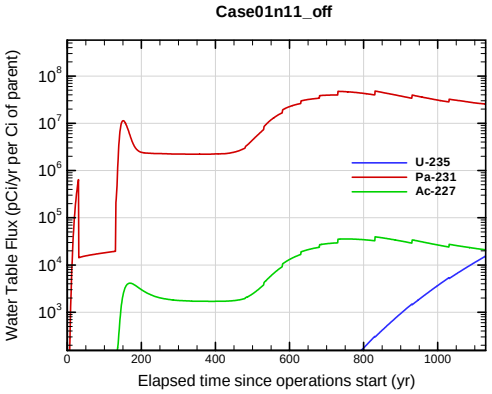

Figure A1A-173. Slit Trench water table flux for Case01n11_off U-235

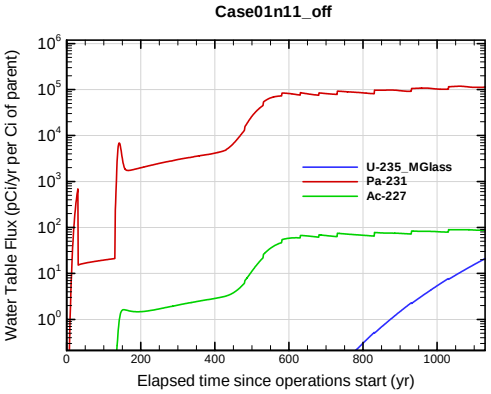

Figure A1A-174. Slit Trench water table flux for Case01n11_off U-235_MGlass

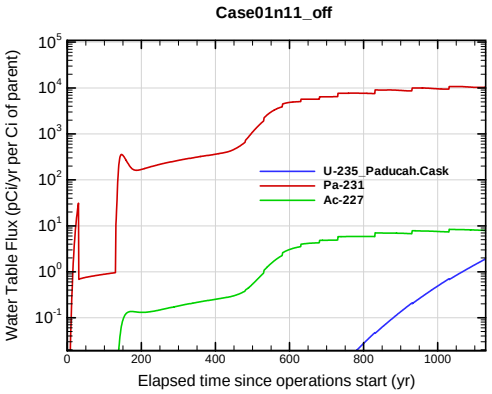

Figure A1A-175. Slit Trench water table flux for Case01n11_off U-235_Paducah.Cask

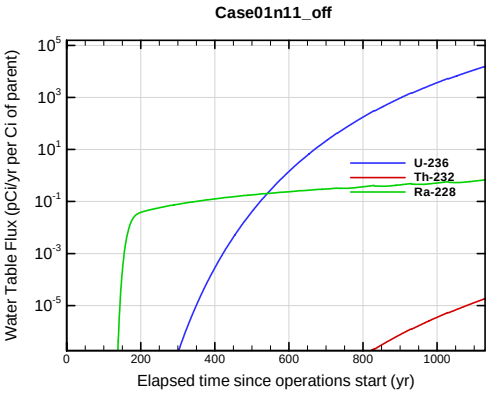

Figure A1A-176. Slit Trench water table flux for Case01n11_off U-236

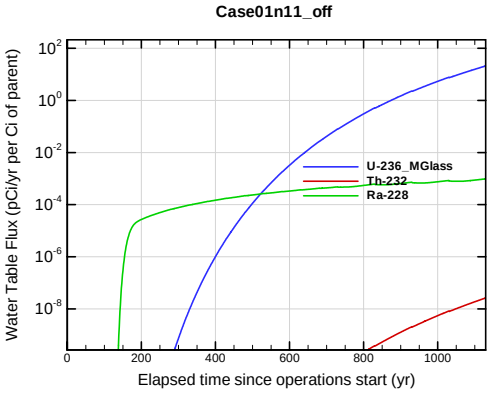

Figure A1A-177. Slit Trench water table flux for Case01n11_off U-236_MGlass

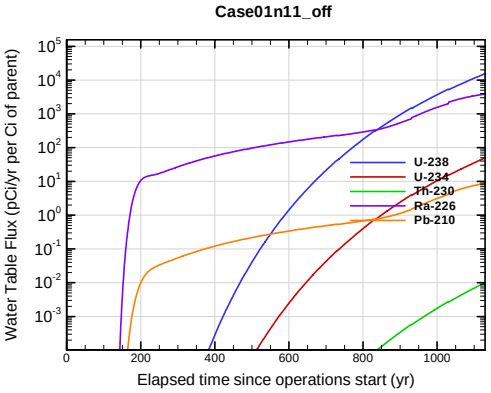

Figure A1A-178. Slit Trench water table flux for Case01n11_off U-238

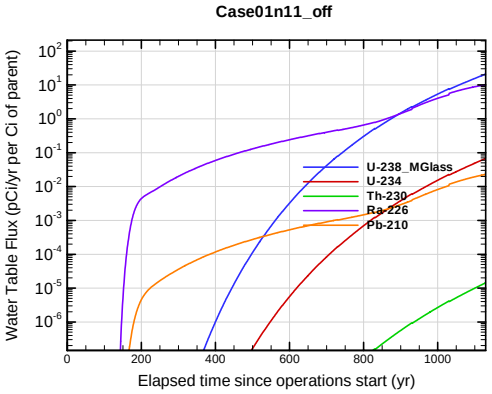

Figure A1A-179. Slit Trench water table flux for Case01n11_off U-238_MGlass

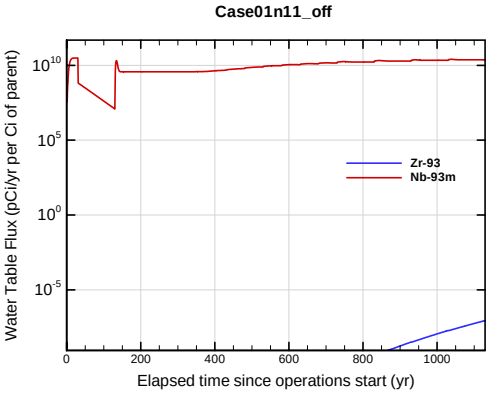

Figure A1A-180. Slit Trench water table flux for Case01n11_off Zr-93

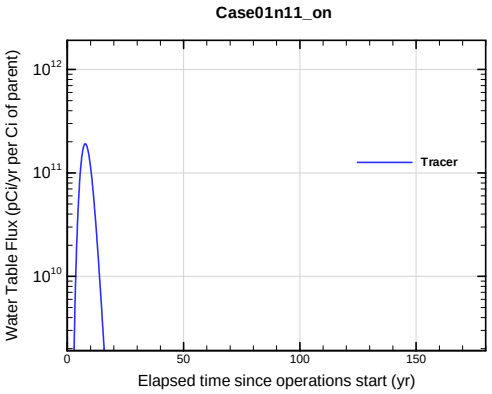

Figure A1A-181. Slit Trench water table flux for Case01n11_on Tracer

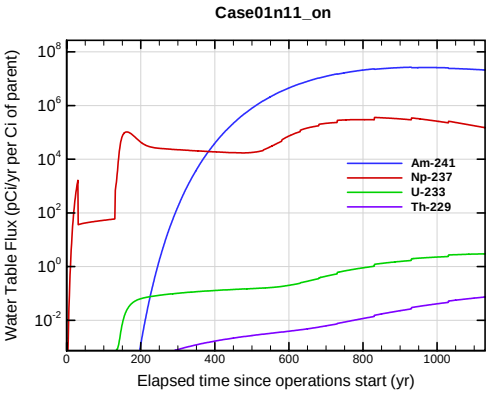

Figure A1A-182. Slit Trench water table flux for Case01n11_on Am-241

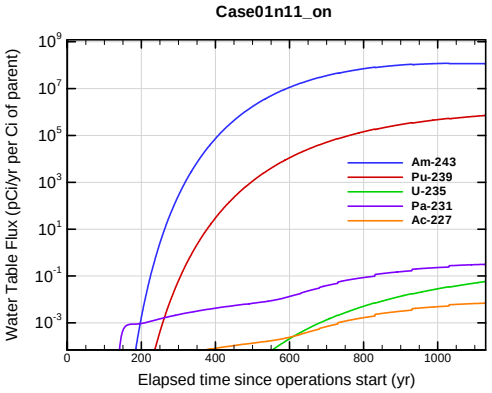

Figure A1A-183. Slit Trench water table flux for Case01n11_on Am-243

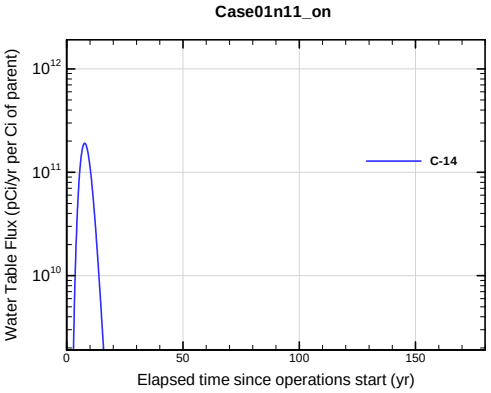

Figure A1A-184. Slit Trench water table flux for Case01n11_on C-14

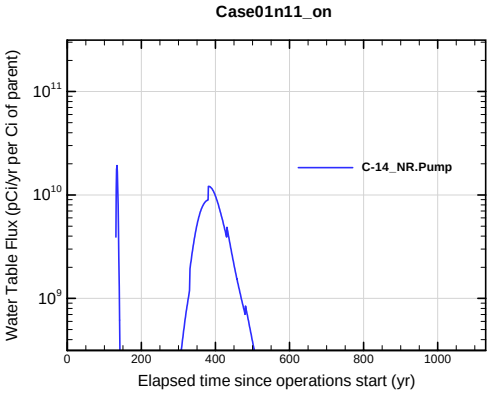

Figure A1A-185. Slit Trench water table flux for Case01n11_on C-14_NR.Pump

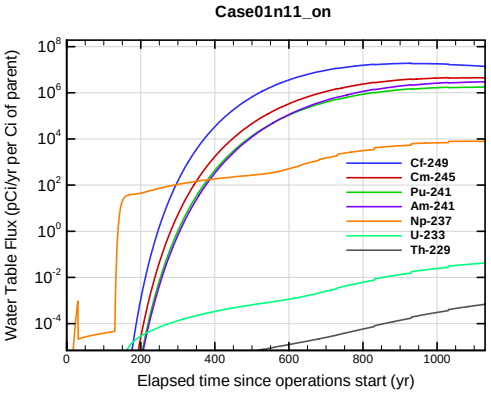

Figure A1A-186. Slit Trench water table flux for Case01n11_on Cf-249

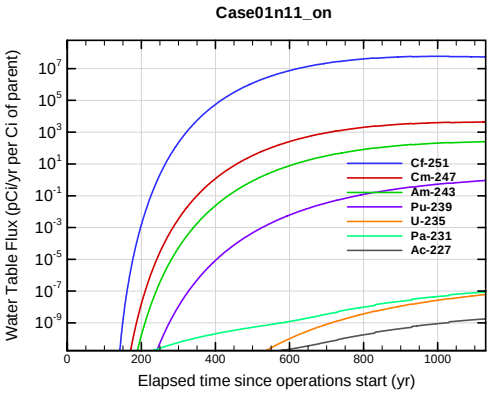

Figure A1A-187. Slit Trench water table flux for Case01n11_on Cf-251

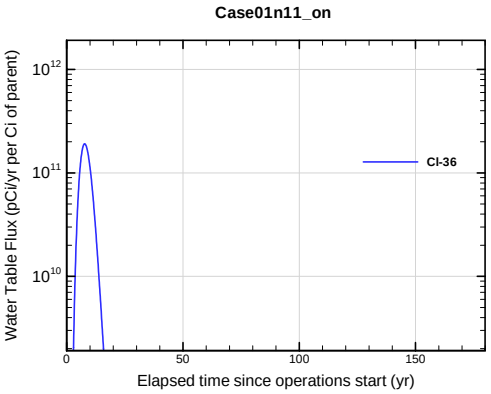

Figure A1A-188. Slit Trench water table flux for Case01n11_on Cl-36

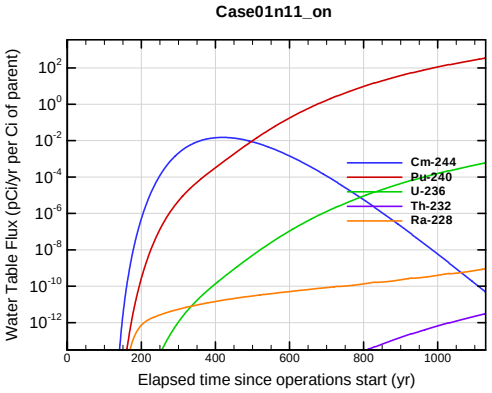

Figure A1A-189. Slit Trench water table flux for Case01n11_on Cm-244

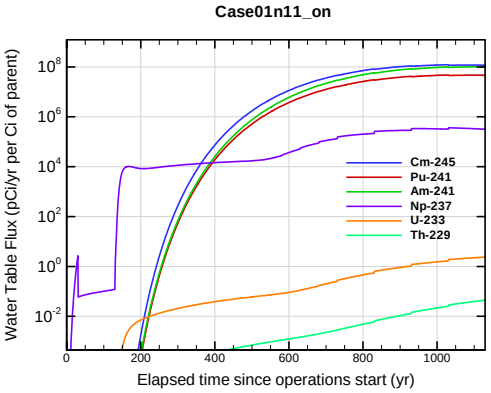

Figure A1A-190. Slit Trench water table flux for Case01n11_on Cm-245

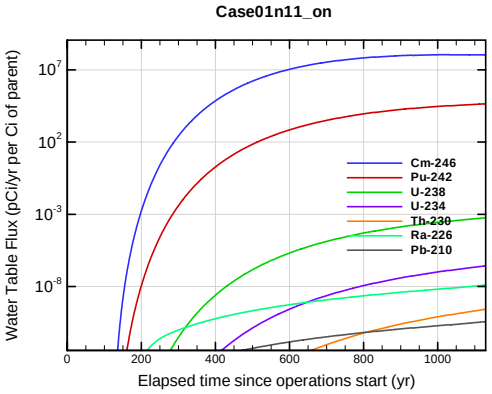

Figure A1A-191. Slit Trench water table flux for Case01n11_on Cm-246

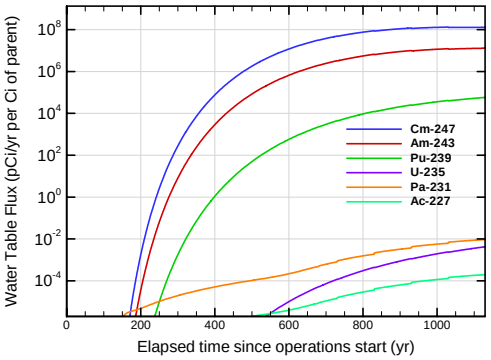

Figure A1A-192. Slit Trench water table flux for Case01n11_on Cm-247

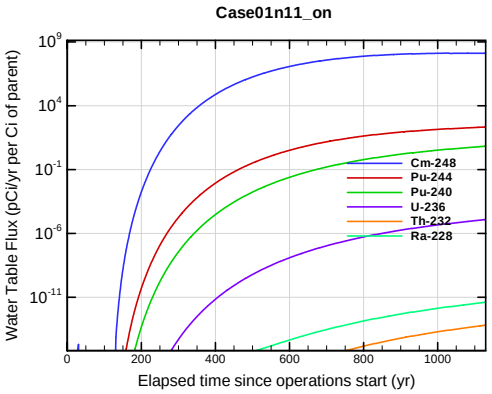

Figure A1A-193. Slit Trench water table flux for Case01n11_on Cm-248

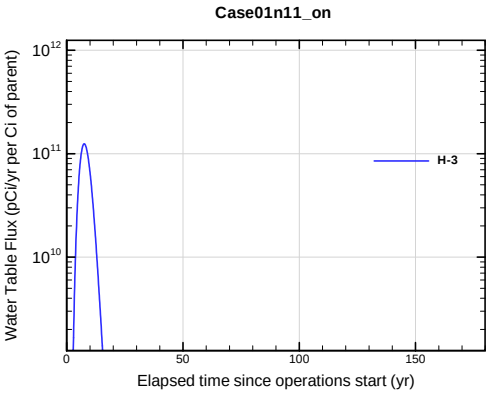

Figure A1A-194. Slit Trench water table flux for Case01n11_on H-3

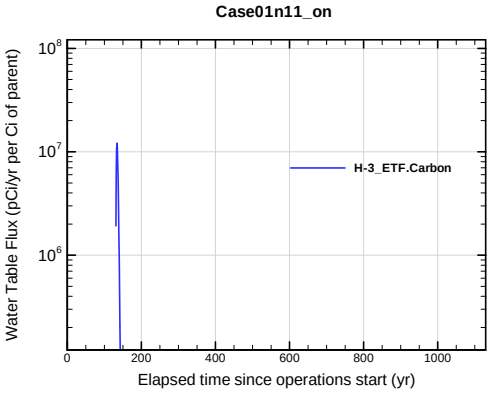

Figure A1A-195. Slit Trench water table flux for Case01n11_on H-3_ETF.Carbon

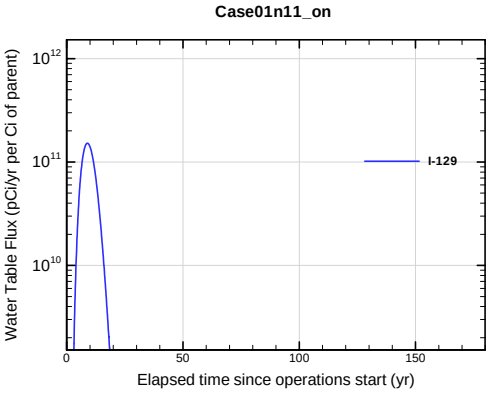

Figure A1A-196. Slit Trench water table flux for Case01n11_on I-129

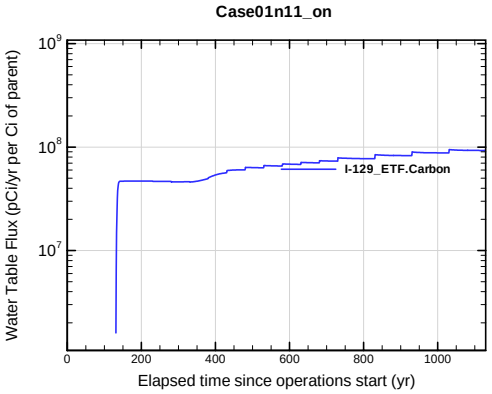

Figure A1A-197. Slit Trench water table flux for Case01n11_on I-129_ETF.Carbon

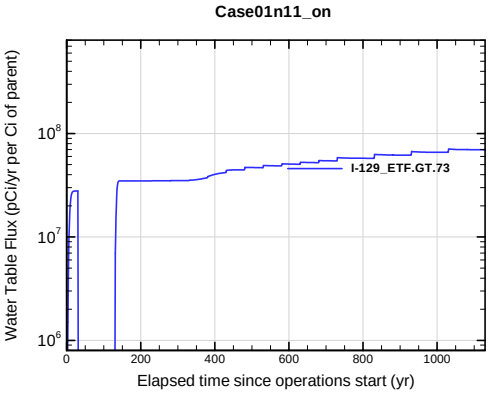

Figure A1A-198. Slit Trench water table flux for Case01n11_on I-129_ETF.GT.73

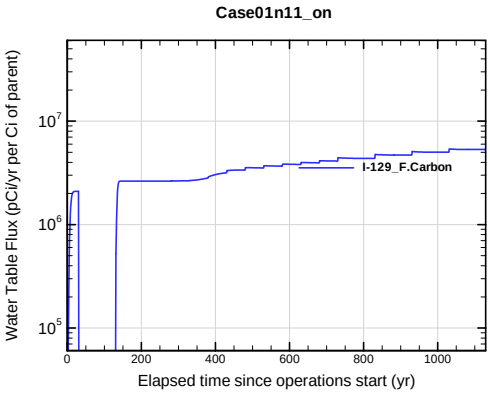

Figure A1A-199. Slit Trench water table flux for Case01n11_on I-129_F.Carbon

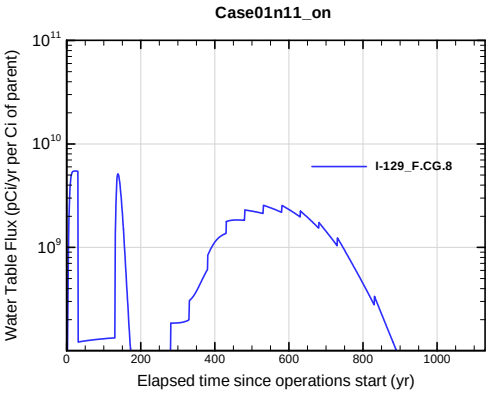

Figure A1A-200. Slit Trench water table flux for Case01n11_on I-129_F.CG.8

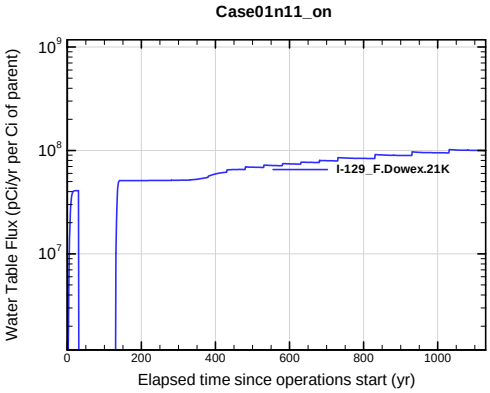

Figure A1A-201. Slit Trench water table flux for Case01n11_on I-129_F.Dowex.21K

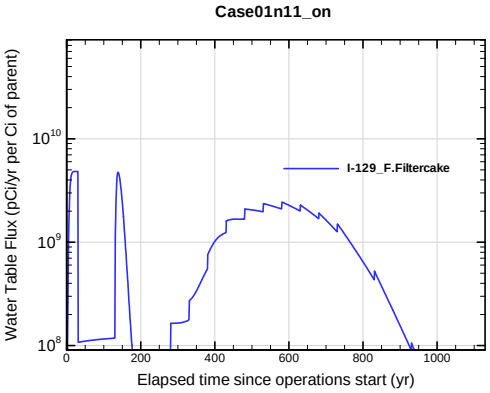

Figure A1A-202. Slit Trench water table flux for Case01n11_on I-129_F.Filtercake

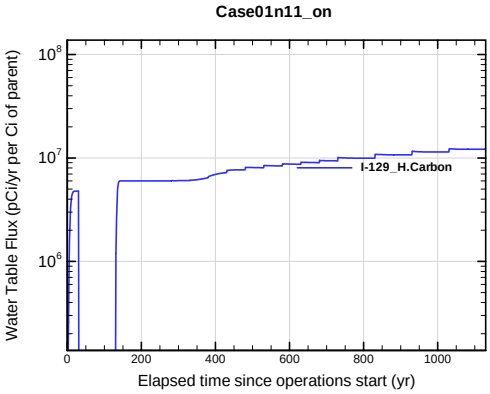

Figure A1A-203. Slit Trench water table flux for Case01n11_on I-129_H.Carbon

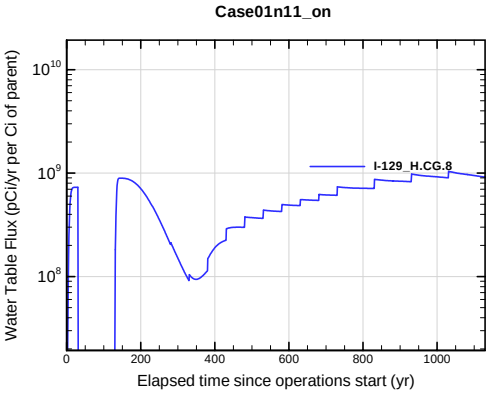

Figure A1A-204. Slit Trench water table flux for Case01n11_on I-129_H.CG.8

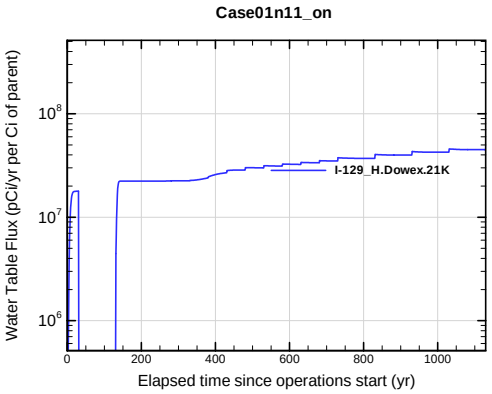

Figure A1A-205. Slit Trench water table flux for Case01n11_on I-129_H.Dowex.21K

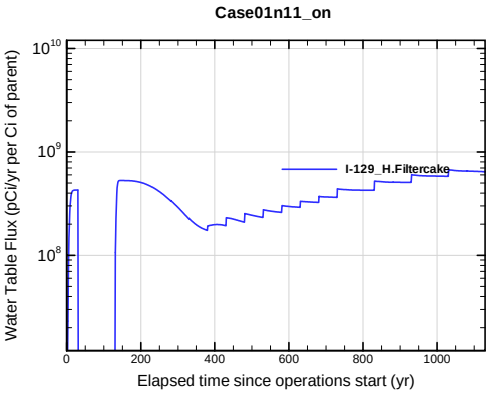

Figure A1A-206. Slit Trench water table flux for Case01n11_on I-129_H.Filtercake

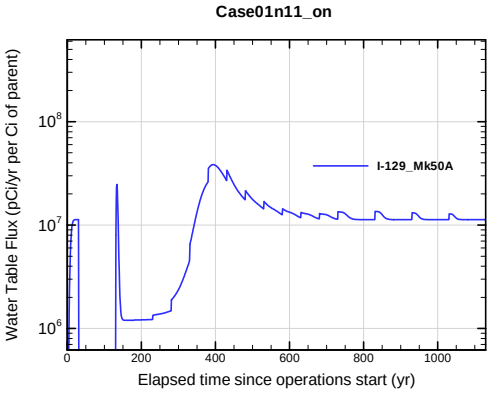

Figure A1A-207. Slit Trench water table flux for Case01n11_on I-129_Mk50A

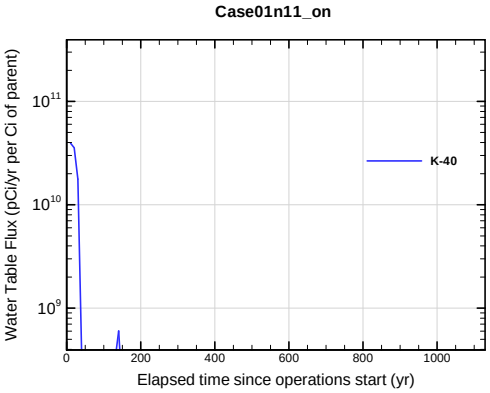

Figure A1A-208. Slit Trench water table flux for Case01n11_on K-40

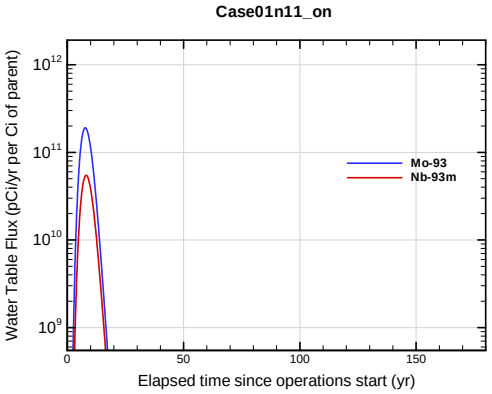

Figure A1A-209. Slit Trench water table flux for Case01n11_on Mo-93

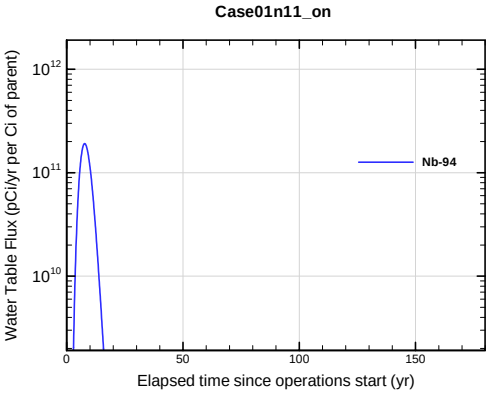

Figure A1A-210. Slit Trench water table flux for Case01n11_on Nb-94

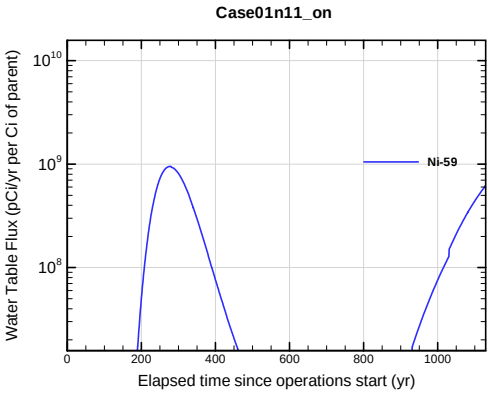

Figure A1A-211. Slit Trench water table flux for Case01n11_on Ni-59

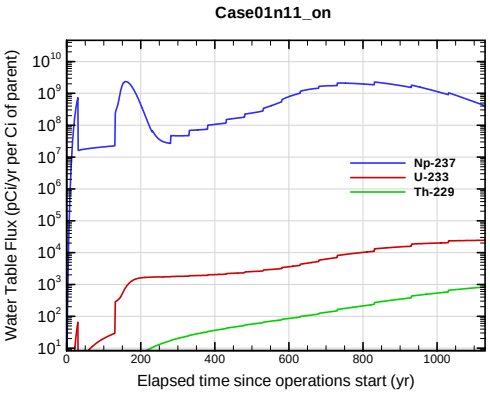

Figure A1A-212. Slit Trench water table flux for Case01n11_on Np-237

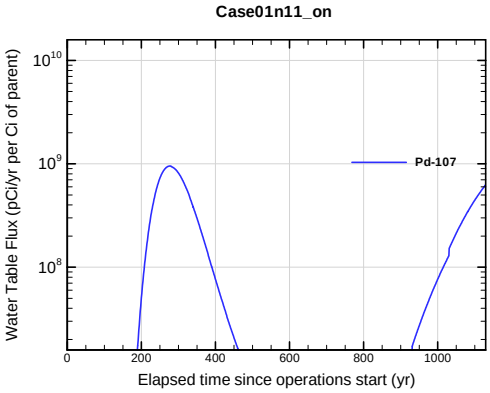

Figure A1A-213. Slit Trench water table flux for Case01n11_on Pd-107

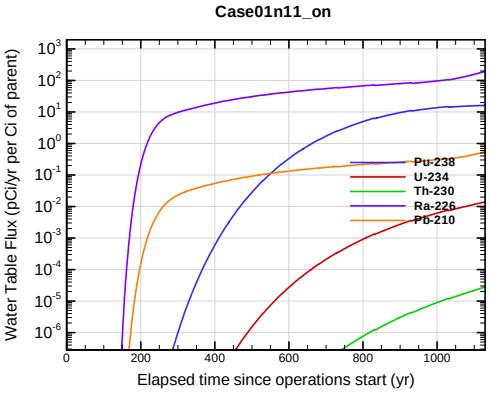

Figure A1A-214. Slit Trench water table flux for Case01n11_on Pu-238

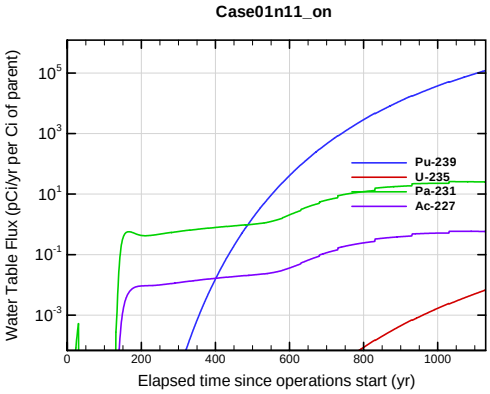

Figure A1A-215. Slit Trench water table flux for Case01n11_on Pu-239

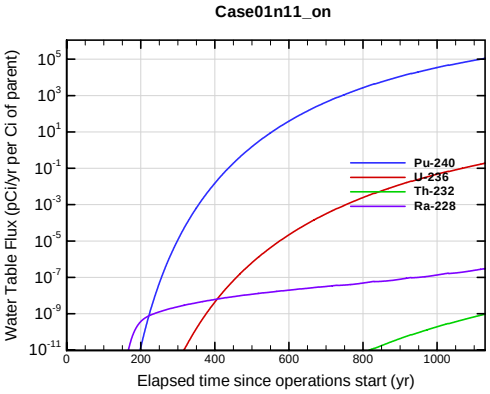

Figure A1A-216. Slit Trench water table flux for Case01n11_on Pu-240

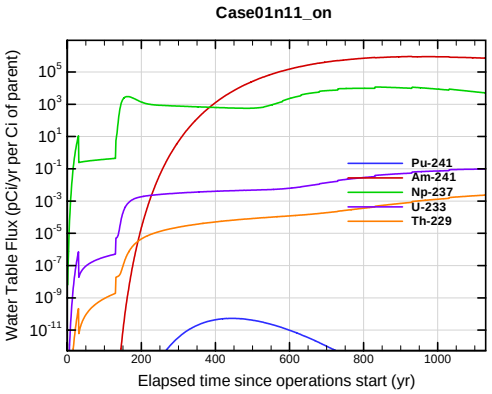

Figure A1A-217. Slit Trench water table flux for Case01n11_on Pu-241

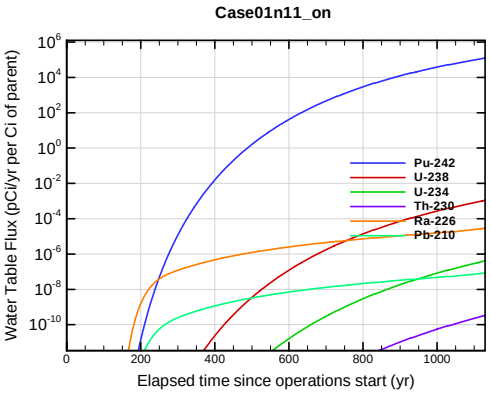

Figure A1A-218. Slit Trench water table flux for Case01n11_on Pu-242

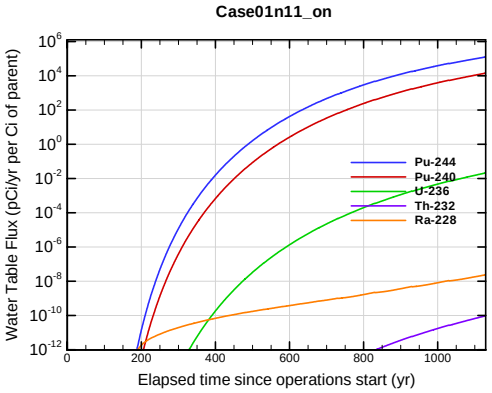

Figure A1A-219. Slit Trench water table flux for Case01n11_on Pu-244

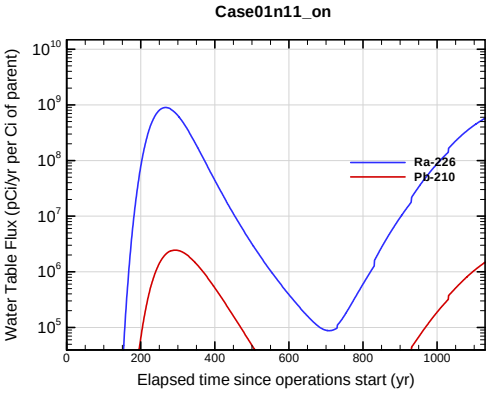

Figure A1A-220. Slit Trench water table flux for Case01n11_on Ra-226

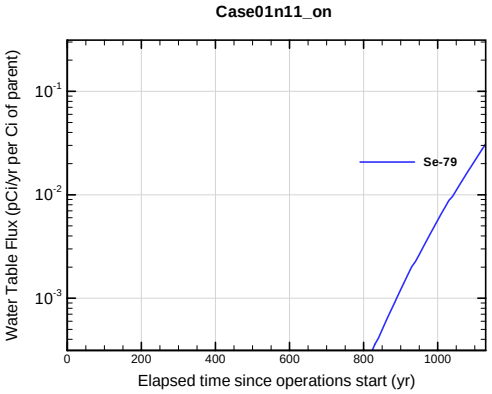

Figure A1A-221. Slit Trench water table flux for Case01n11_on Se-79

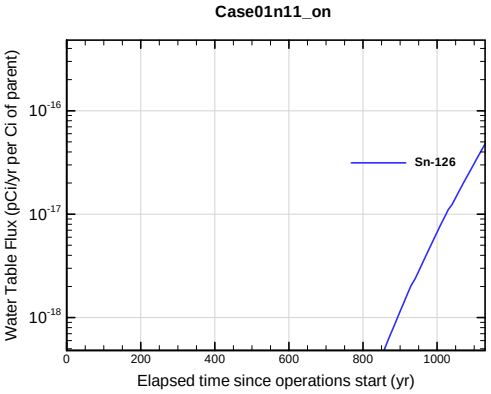

Figure A1A-222. Slit Trench water table flux for Case01n11_on Sn-126

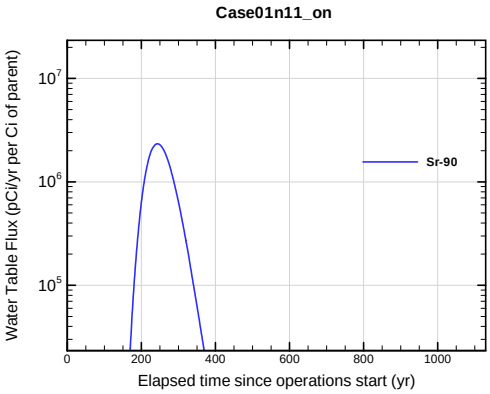

Figure A1A-223. Slit Trench water table flux for Case01n11_on Sr-90

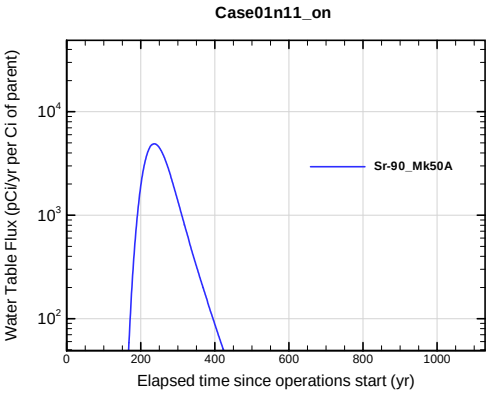

Figure A1A-224. Slit Trench water table flux for Case01n11_on Sr-90_Mk50A

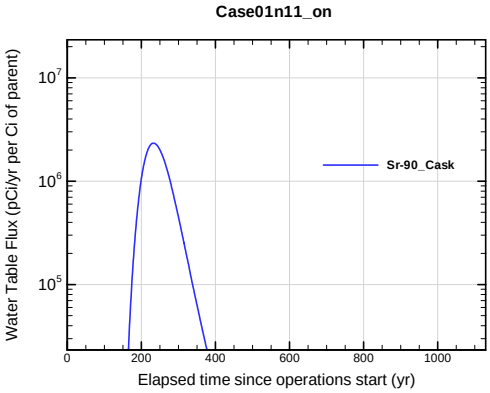

Figure A1A-225. Slit Trench water table flux for Case01n11_on Sr-90_Cask

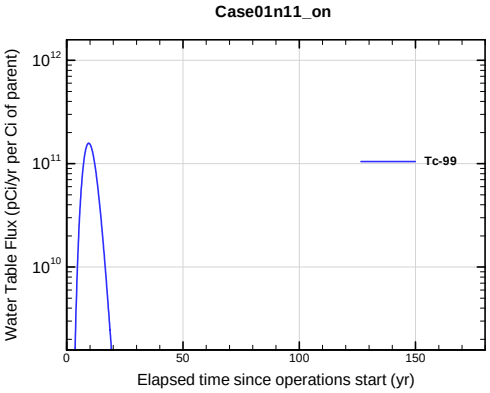

Figure A1A-226. Slit Trench water table flux for Case01n11_on Tc-99

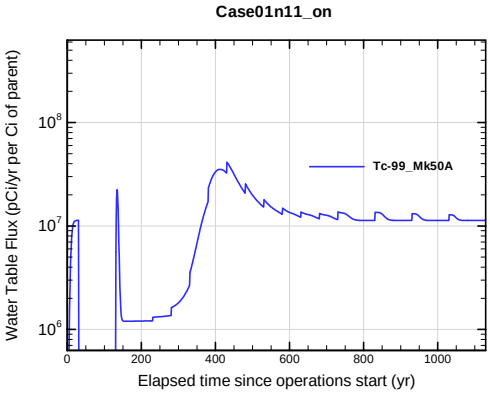

Figure A1A-227. Slit Trench water table flux for Case01n11_on Tc-99_Mk50A

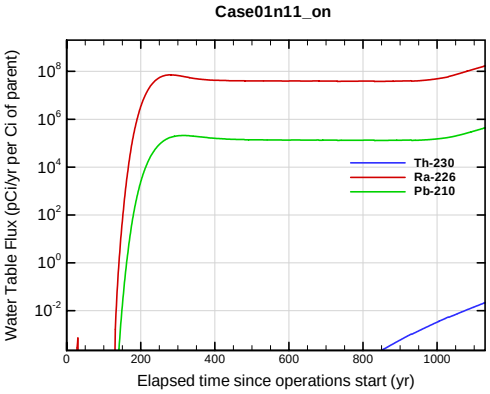

Figure A1A-228. Slit Trench water table flux for Case01n11_on Th-230

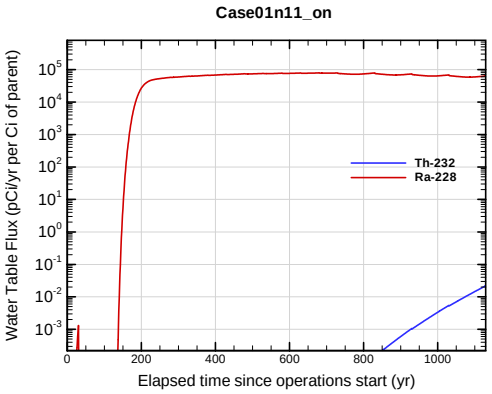

Figure A1A-229. Slit Trench water table flux for Case01n11_on Th-232

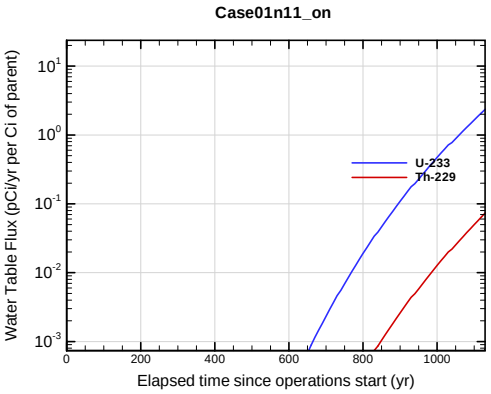

Figure A1A-230. Slit Trench water table flux for Case01n11_on U-233

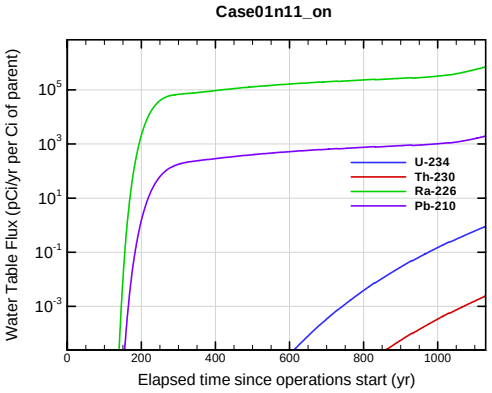

Figure A1A-231. Slit Trench water table flux for Case01n11_on U-234

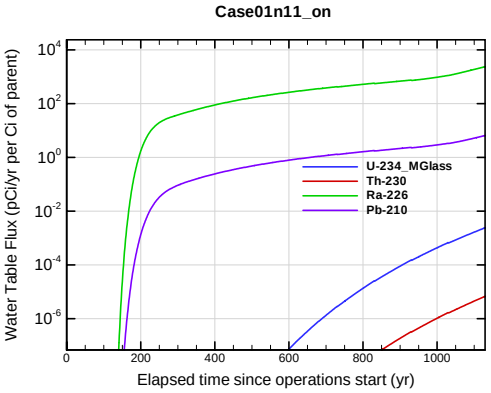

Figure A1A-232. Slit Trench water table flux for Case01n11_on U-234_MGlass

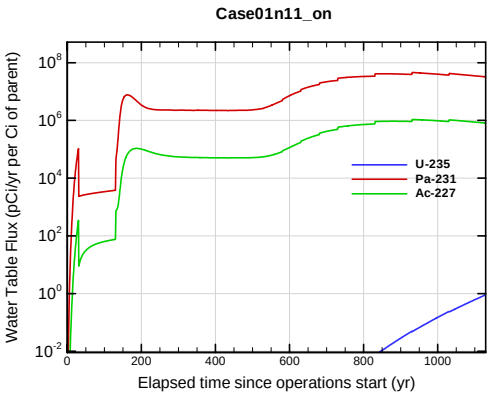

Figure A1A-233. Slit Trench water table flux for Case01n11_on U-235

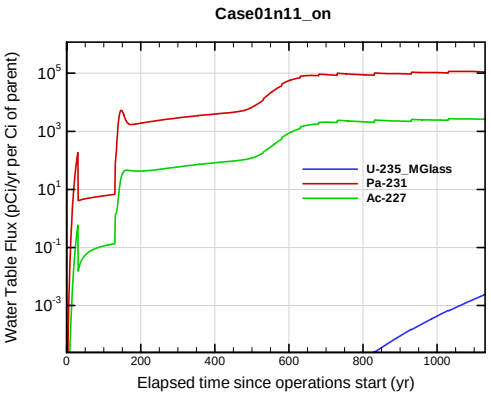

Figure A1A-234. Slit Trench water table flux for Case01n11_on U-235_MGlass

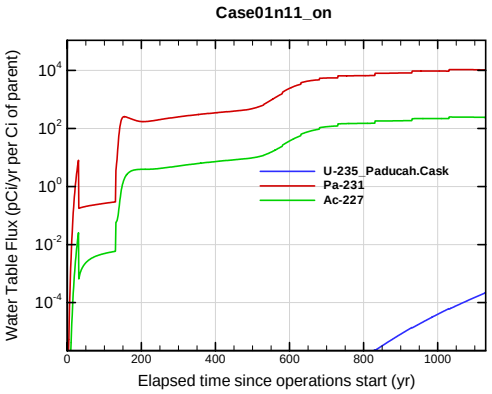

Figure A1A-235. Slit Trench water table flux for Case01n11_on U-235_Paducah.Cask

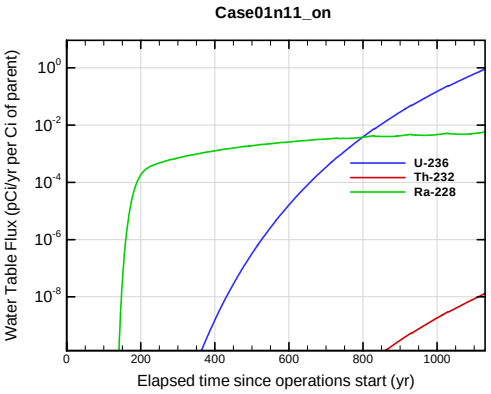

Figure A1A-236. Slit Trench water table flux for Case01n11_on U-236

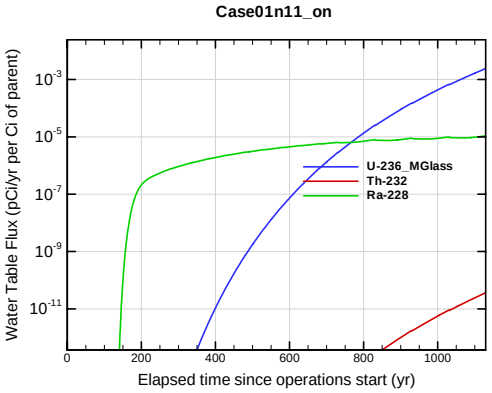

Figure A1A-237. Slit Trench water table flux for Case01n11_on U-236_MGlass

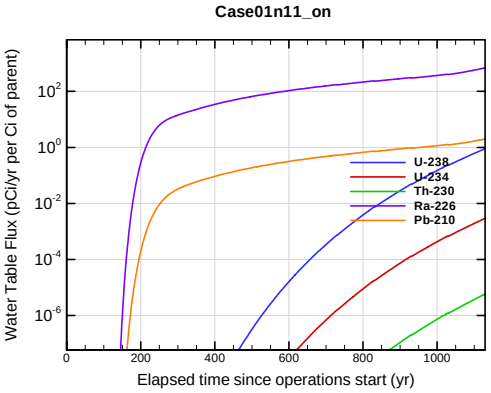

Figure A1A-238. Slit Trench water table flux for Case01n11_on U-238

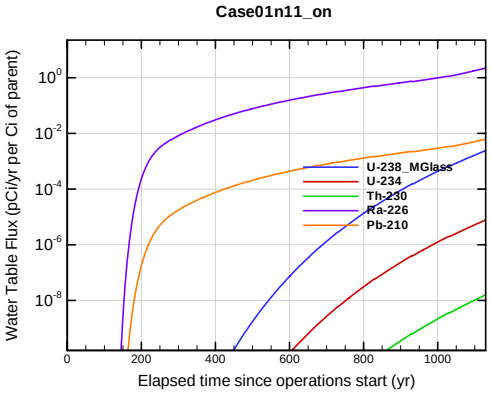

Figure A1A-239. Slit Trench water table flux for Case01n11_on U-238_MGlass

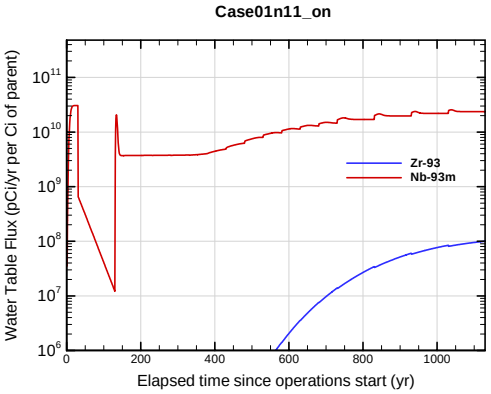

Figure A1A-240. Slit Trench water table flux for Case01n11_on Zr-93

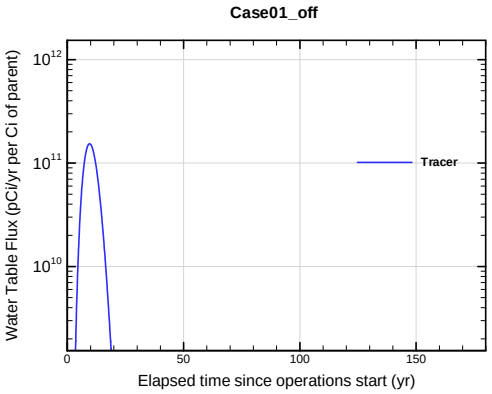

Figure A1A-241. Engineered Trench water table flux for Case01_off Tracer

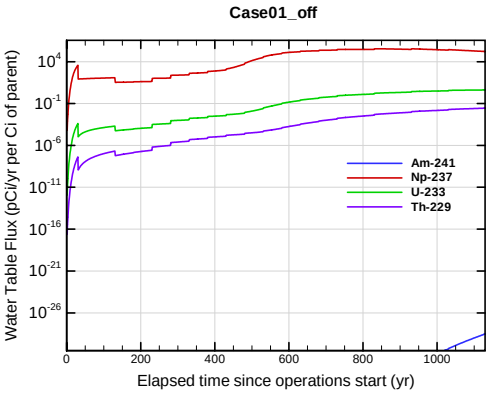

Figure A1A-242. Engineered Trench water table flux for Case01_off Am-241

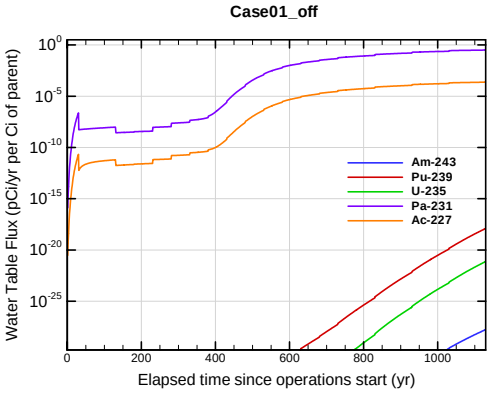

Figure A1A-243. Engineered Trench water table flux for Case01_off Am-243

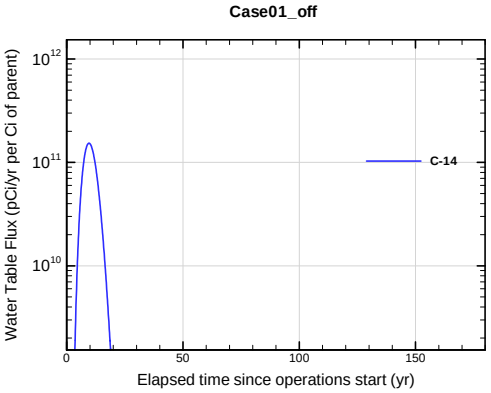

Figure A1A-244. Engineered Trench water table flux for Case01_off C-14

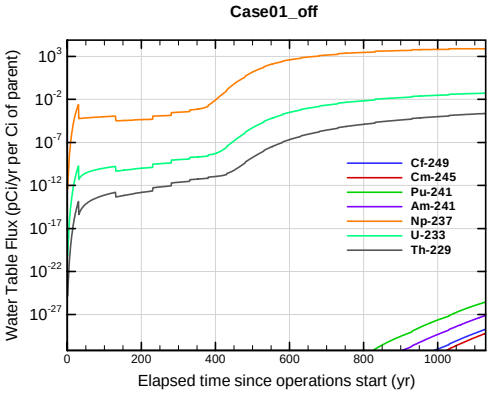

Figure A1A-245. Engineered Trench water table flux for Case01_off Cf-249

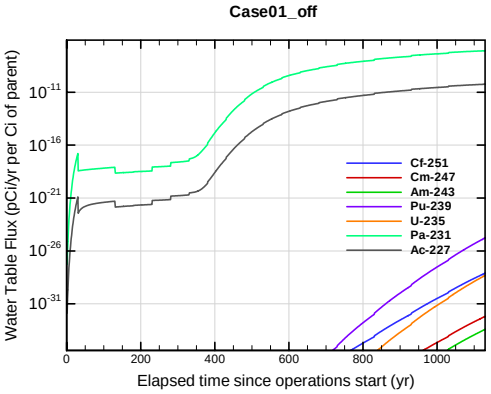

Figure A1A-246. Engineered Trench water table flux for Case01_off Cf-251

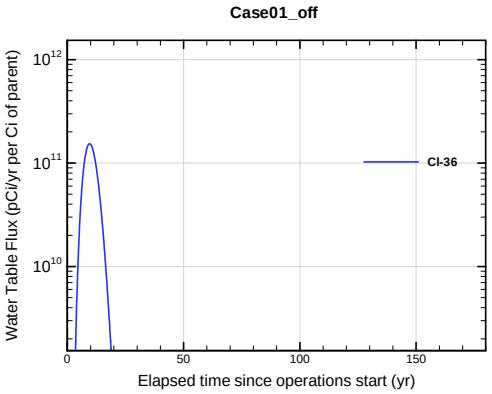

Figure A1A-247. Engineered Trench water table flux for Case01_off Cl-36

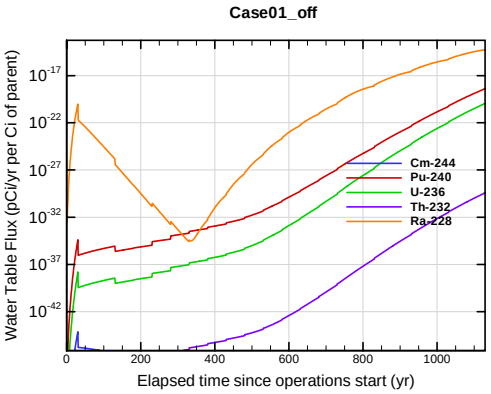

Figure A1A-248. Engineered Trench water table flux for Case01_off Cm-244

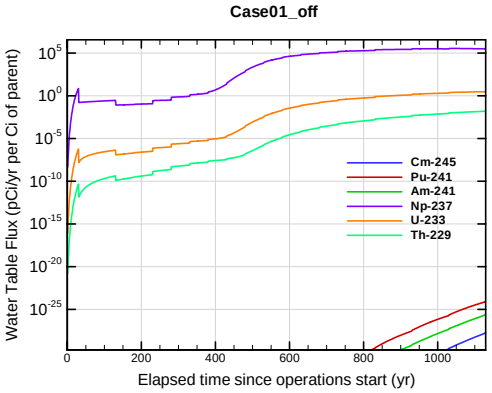

Figure A1A-249. Engineered Trench water table flux for Case01_off Cm-245

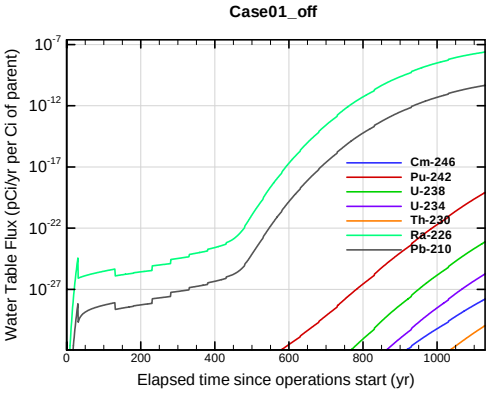

Figure A1A-250. Engineered Trench water table flux for Case01_off Cm-246

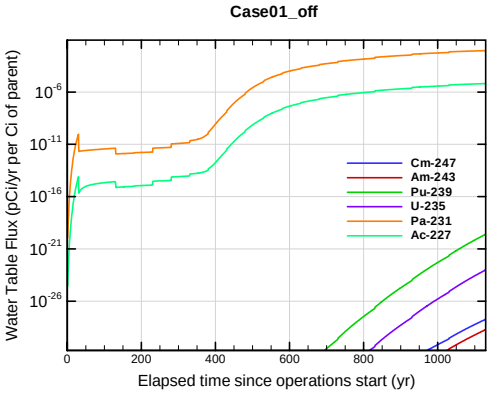

Figure A1A-251. Engineered Trench water table flux for Case01_off Cm-247

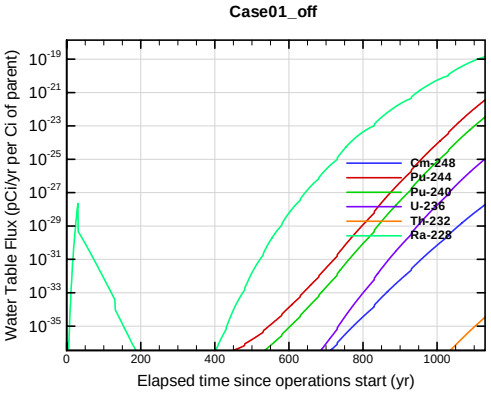

Figure A1A-252. Engineered Trench water table flux for Case01_off Cm-248

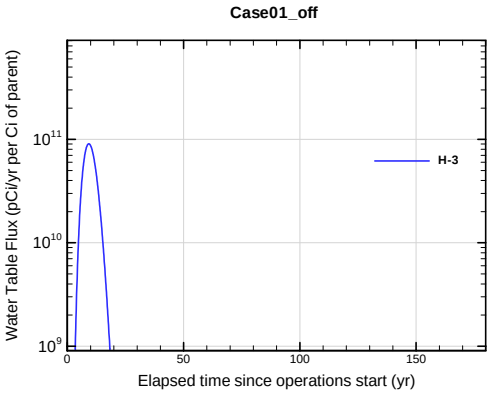

Figure A1A-253. Engineered Trench water table flux for Case01_off H-3

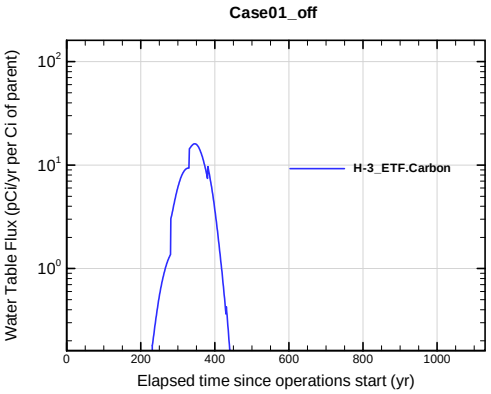

Figure A1A-254. Engineered Trench water table flux for Case01_off H-3_ETF.Carbon

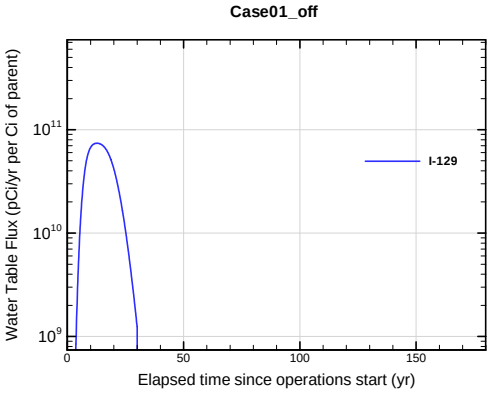

Figure A1A-255. Engineered Trench water table flux for Case01_off I-129

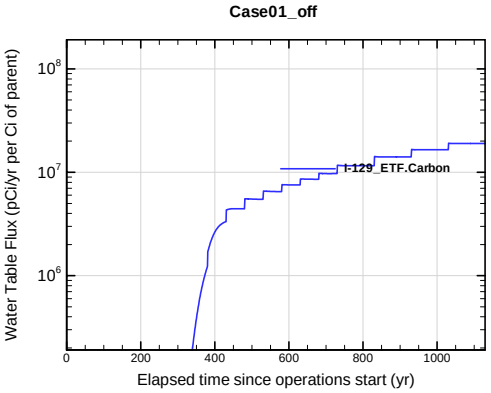

Figure A1A-256. Engineered Trench water table flux for Case01_off I-129_ETF.Carbon

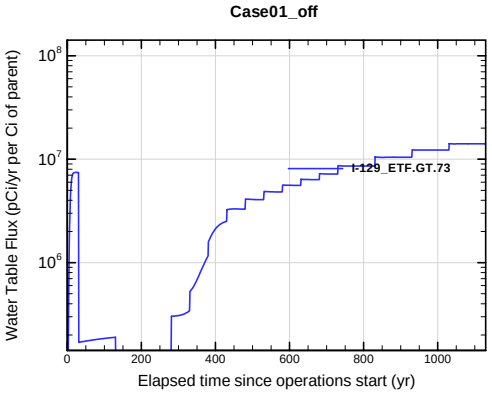

Figure A1A-257. Engineered Trench water table flux for Case01_off I-129_ETF.GT.73

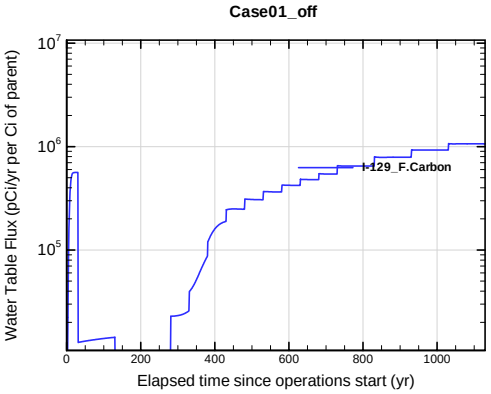

Figure A1A-258. Engineered Trench water table flux for Case01_off I-129_F.Carbon

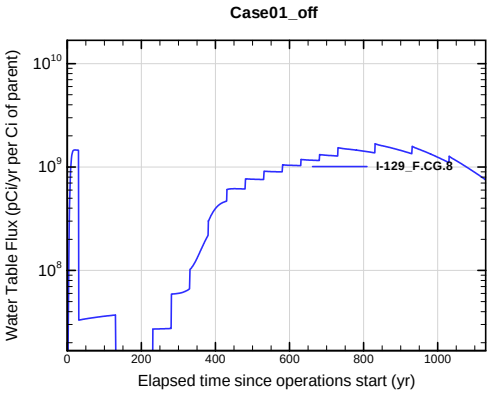

Figure A1A-259. Engineered Trench water table flux for Case01_off I-129_F.CG.8

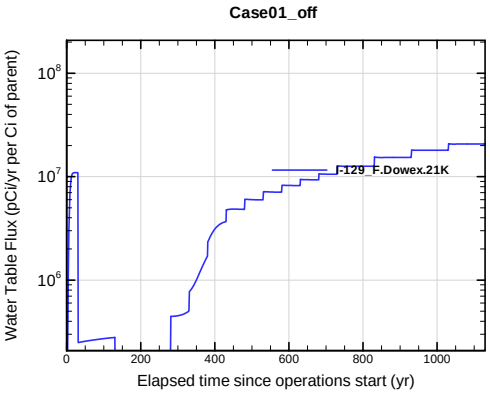

Figure A1A-260. Engineered Trench water table flux for Case01_off I-129_F.Dowex.21K

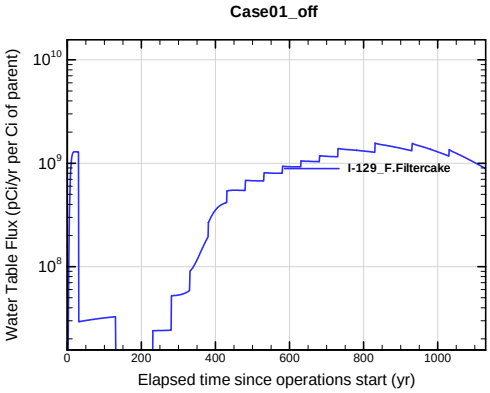

Figure A1A-261. Engineered Trench water table flux for Case01_off I-129_F.Filtercake

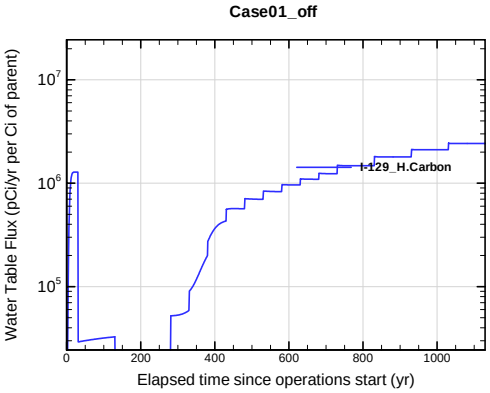

Figure A1A-262. Engineered Trench water table flux for Case01_off I-129_H.Carbon

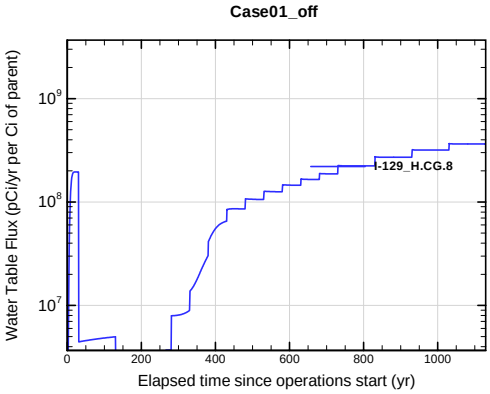

Figure A1A-263. Engineered Trench water table flux for Case01_off I-129_H.CG.8

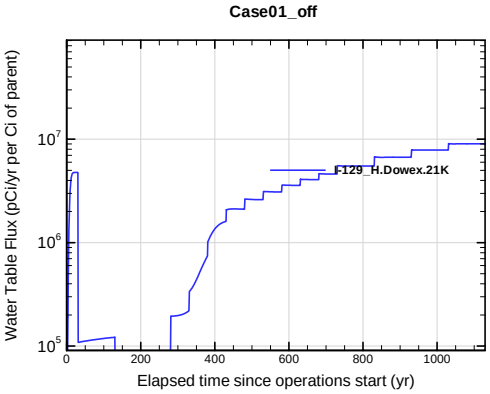

Figure A1A-264. Engineered Trench water table flux for Case01_off I-129_H.Dowex.21K

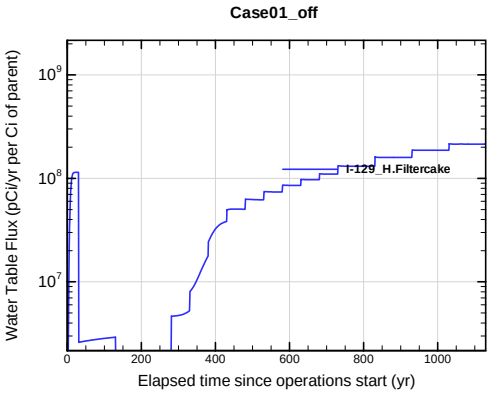

Figure A1A-265. Engineered Trench water table flux for Case01_off I-129_H.Filtercake

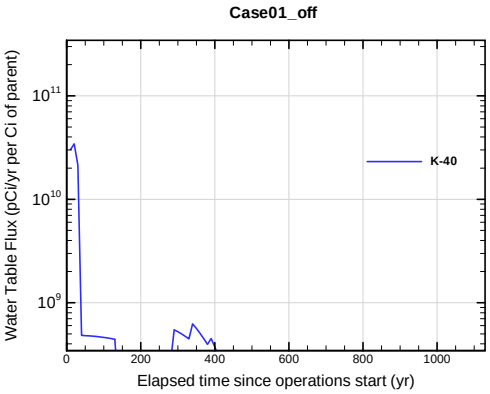

Figure A1A-266. Engineered Trench water table flux for Case01_off K-40

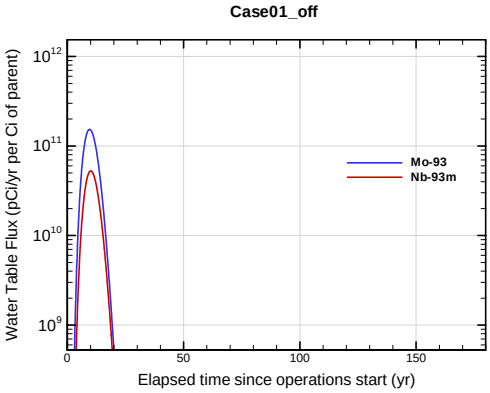

Figure A1A-267. Engineered Trench water table flux for Case01_off Mo-93

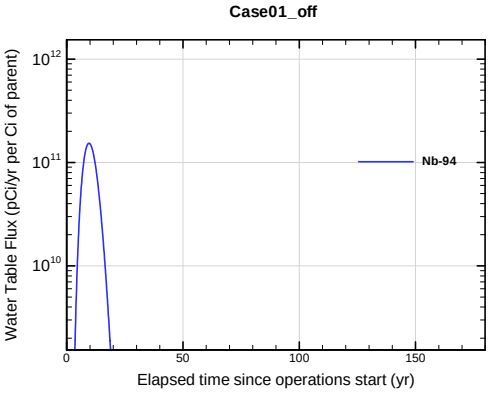

Figure A1A-268. Engineered Trench water table flux for Case01_off Nb-94

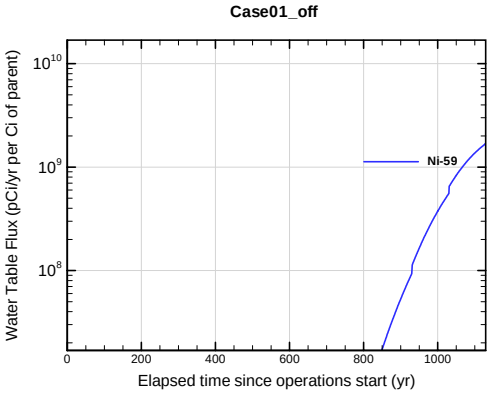

Figure A1A-269. Engineered Trench water table flux for Case01_off Ni-59

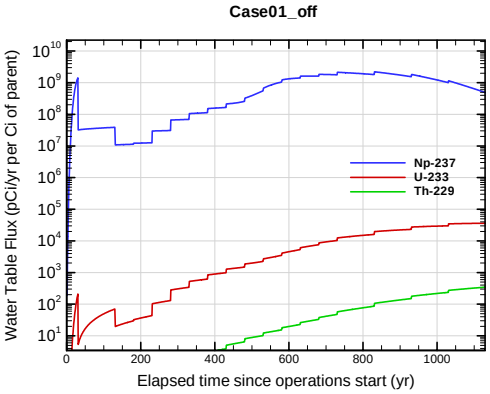

Figure A1A-270. Engineered Trench water table flux for Case01_off Np-237

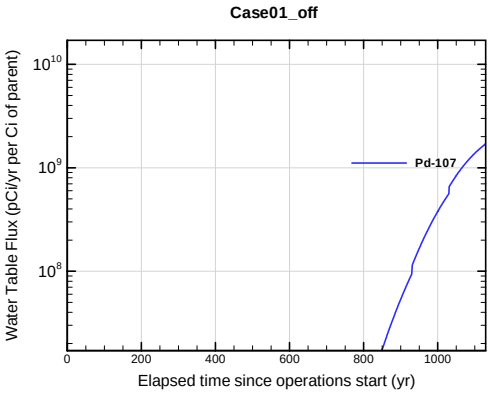

Figure A1A-271. Engineered Trench water table flux for Case01_off Pd-107

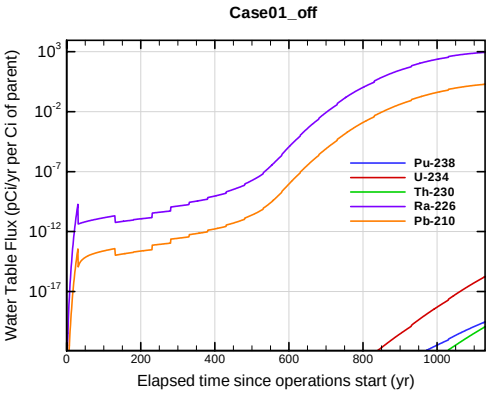

Figure A1A-272. Engineered Trench water table flux for Case01_off Pu-238

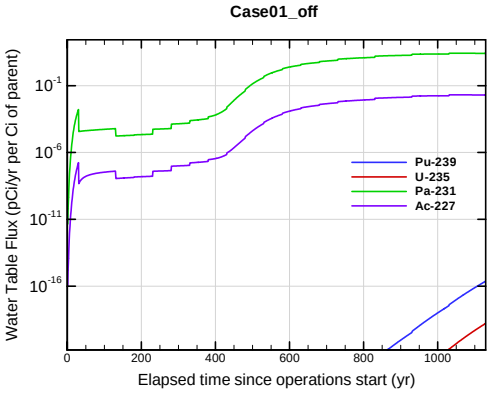

Figure A1A-273. Engineered Trench water table flux for Case01_off Pu-239

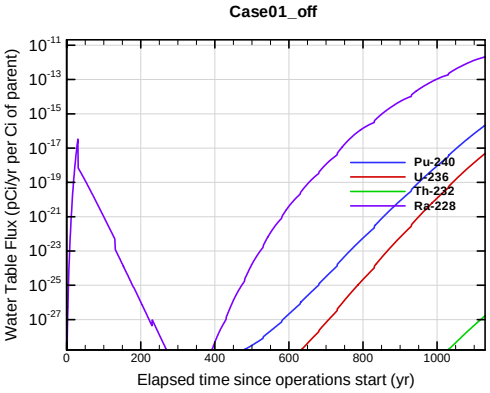

Figure A1A-274. Engineered Trench water table flux for Case01_off Pu-240

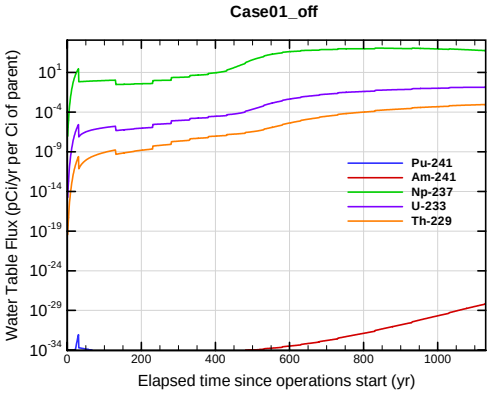

Figure A1A-275. Engineered Trench water table flux for Case01_off Pu-241

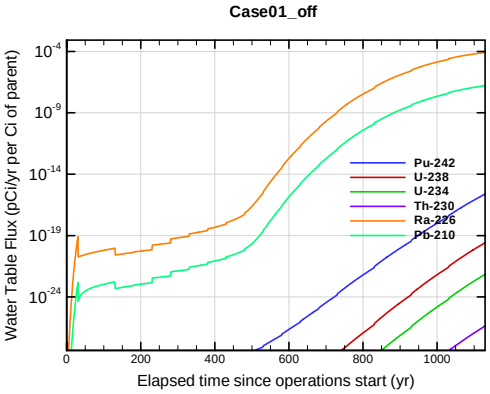

Figure A1A-276. Engineered Trench water table flux for Case01_off Pu-242

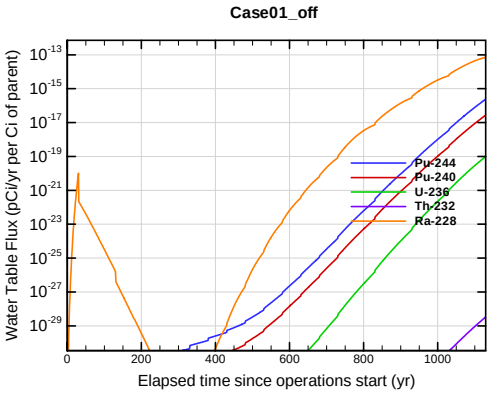

Figure A1A-277. Engineered Trench water table flux for Case01_off Pu-244

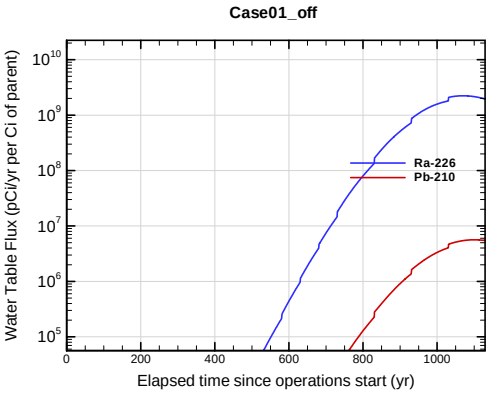

Figure A1A-278. Engineered Trench water table flux for Case01_off Ra-226

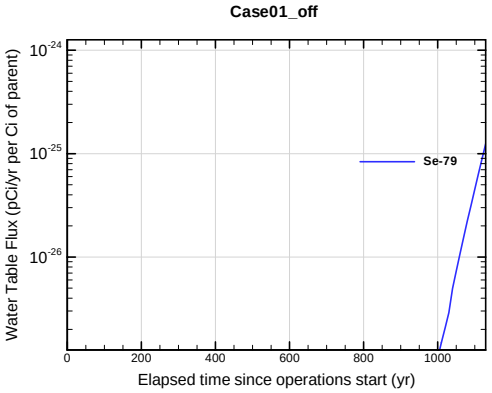

Figure A1A-279. Engineered Trench water table flux for Case01_off Se-79

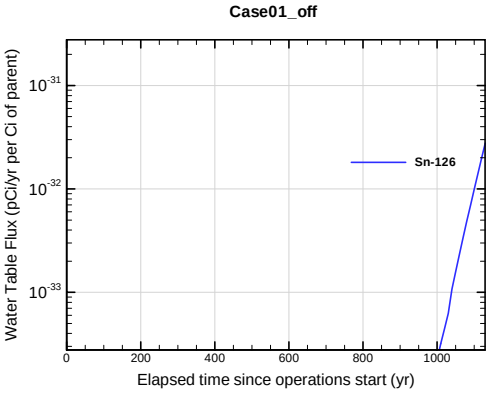

Figure A1A-280. Engineered Trench water table flux for Case01_off Sn-126

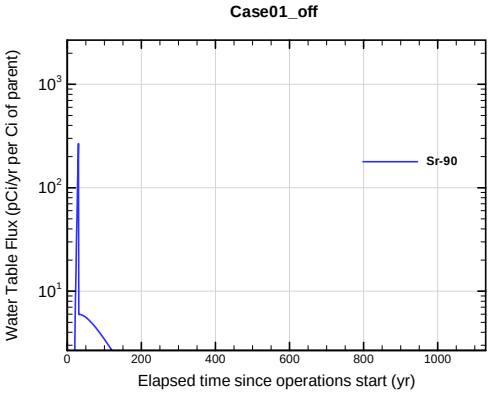

Figure A1A-281. Engineered Trench water table flux for Case01_off Sr-90

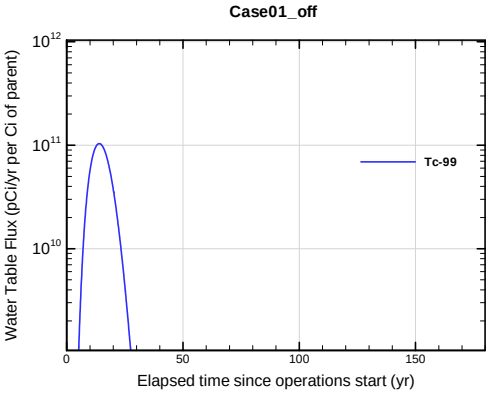

Figure A1A-282. Engineered Trench water table flux for Case01_off Tc-99

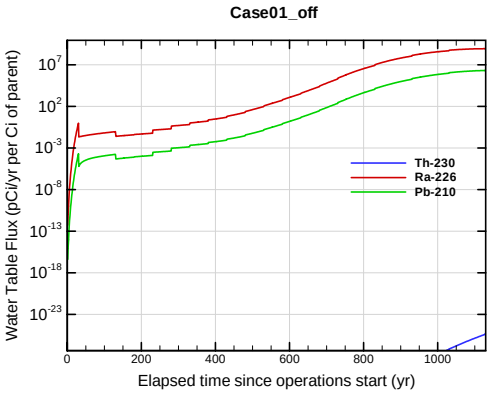

Figure A1A-283. Engineered Trench water table flux for Case01_off Th-230

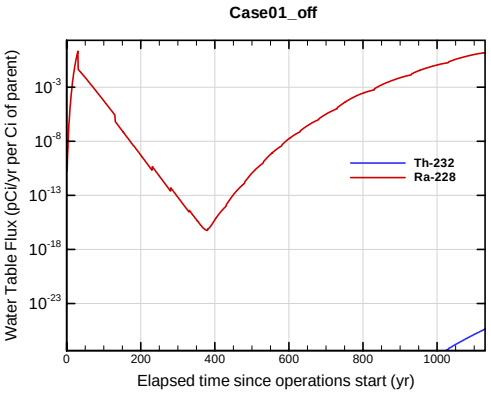

Figure A1A-284. Engineered Trench water table flux for Case01_off Th-232

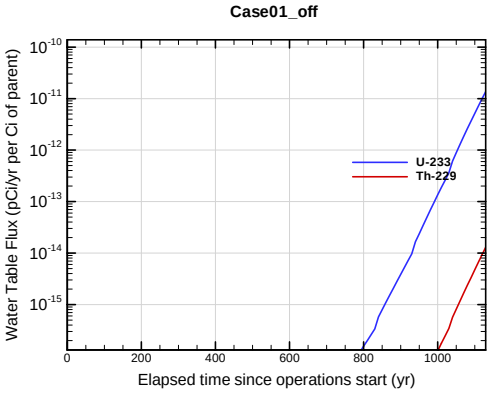

Figure A1A-285. Engineered Trench water table flux for Case01_off U-233

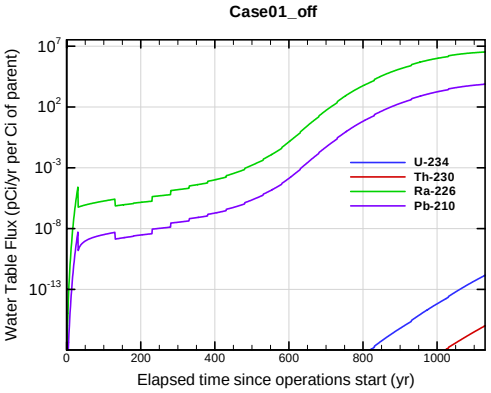

Figure A1A-286. Engineered Trench water table flux for Case01_off U-234

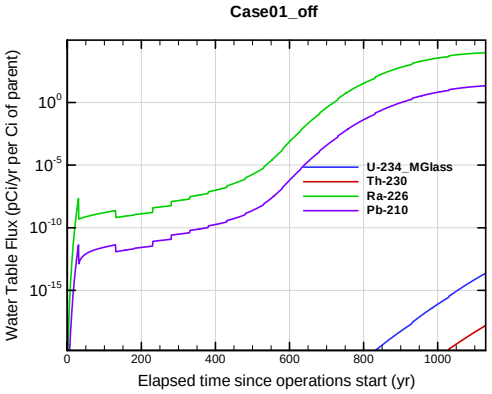

Figure A1A-287. Engineered Trench water table flux for Case01_off U-234_MGlass

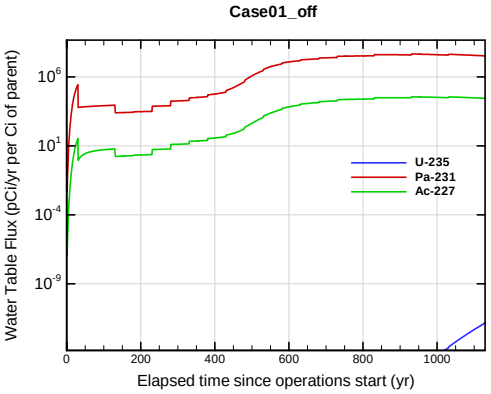

Figure A1A-288. Engineered Trench water table flux for Case01_off U-235

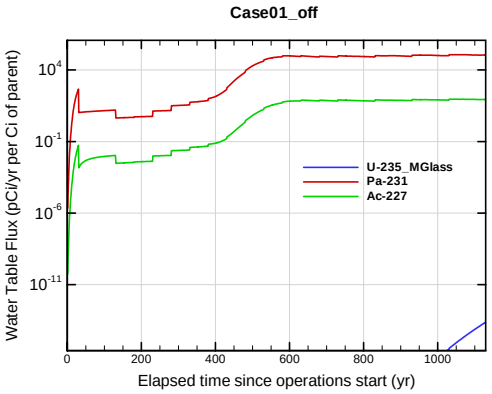

Figure A1A-289. Engineered Trench water table flux for Case01_off U-235_MGlass

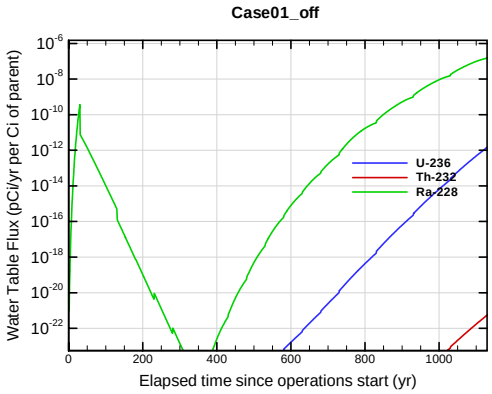

Figure A1A-290. Engineered Trench water table flux for Case01_off U-236

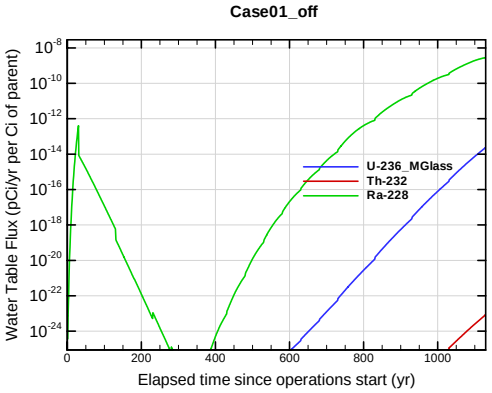

Figure A1A-291. Engineered Trench water table flux for Case01_off U-236_MGlass

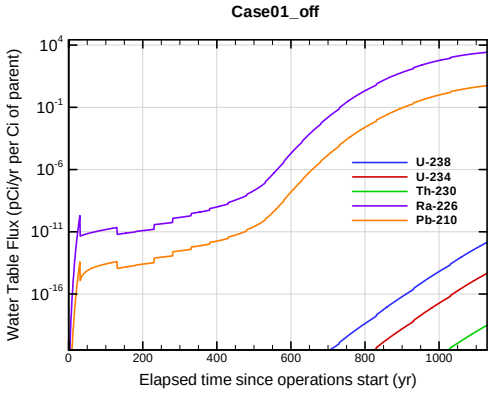

Figure A1A-292. Engineered Trench water table flux for Case01_off U-238

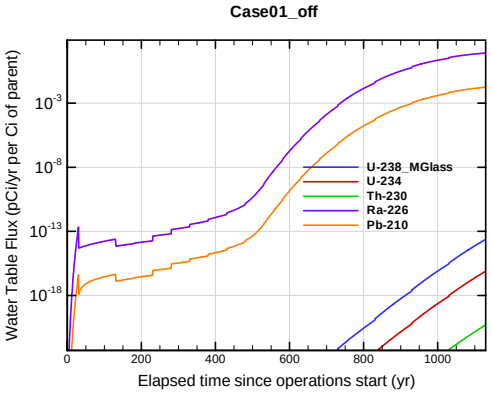

Figure A1A-293. Engineered Trench water table flux for Case01_off U-238_MGlass

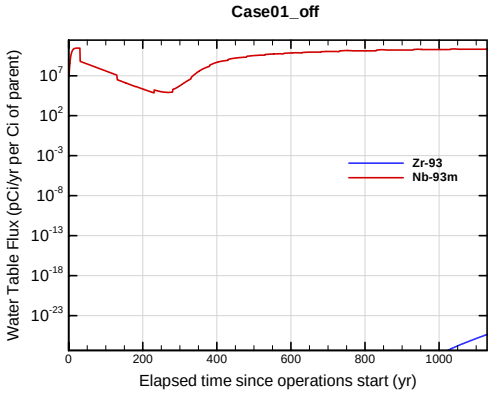

Figure A1A-294. Engineered Trench water table flux for Case01_off Zr-93

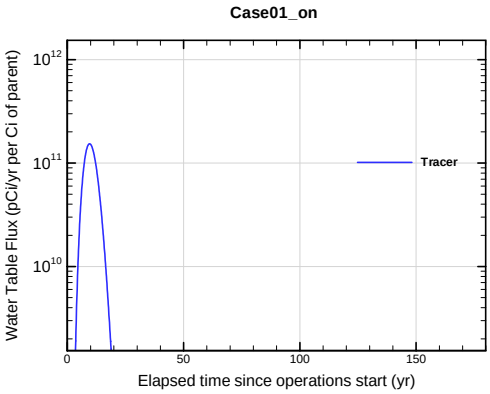

Figure A1A-295. Engineered Trench water table flux for Case01_on Tracer

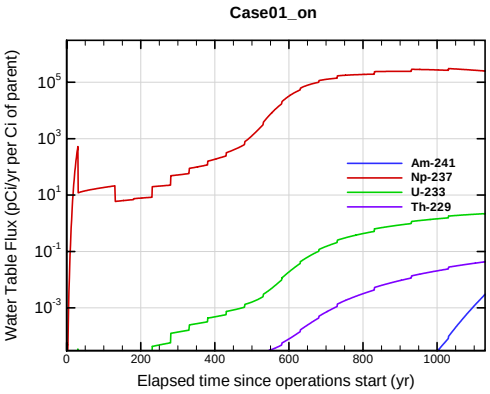

Figure A1A-296. Engineered Trench water table flux for Case01_on Am-241

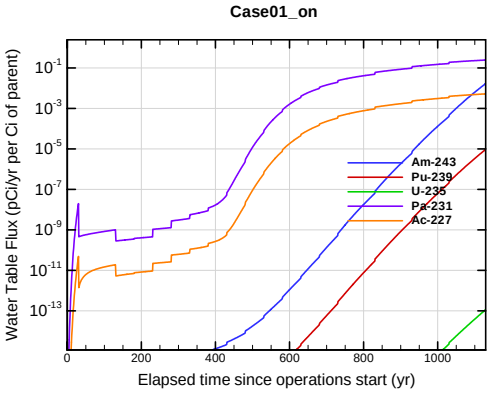

Figure A1A-297. Engineered Trench water table flux for Case01_on Am-243

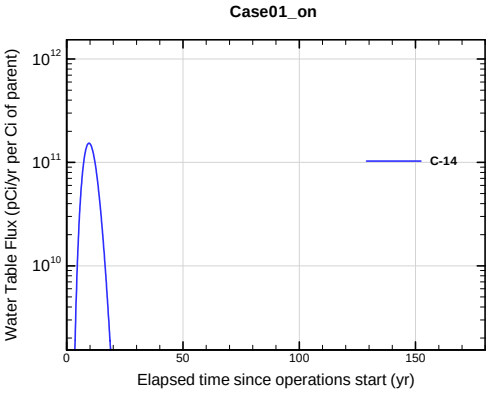

Figure A1A-298. Engineered Trench water table flux for Case01_on C-14

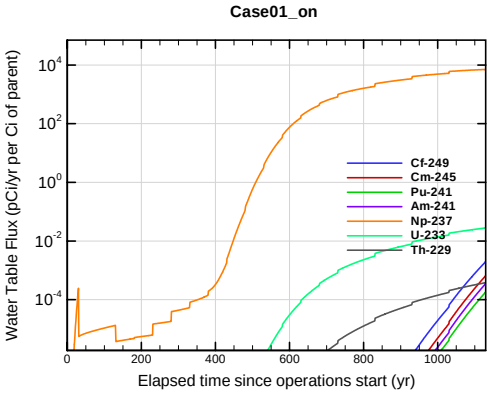

Figure A1A-299. Engineered Trench water table flux for Case01_on Cf-249

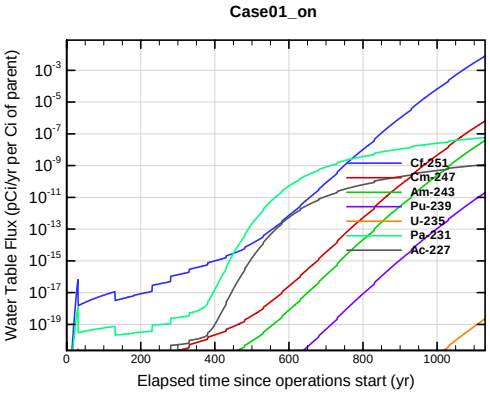

Figure A1A-300. Engineered Trench water table flux for Case01_on Cf-251

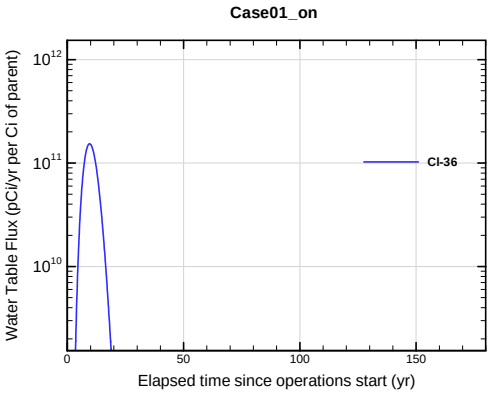

Figure A1A-301. Engineered Trench water table flux for Case01_on Cl-36

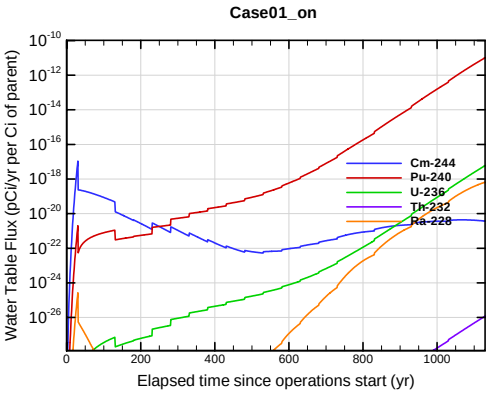

Figure A1A-302. Engineered Trench water table flux for Case01_on Cm-244

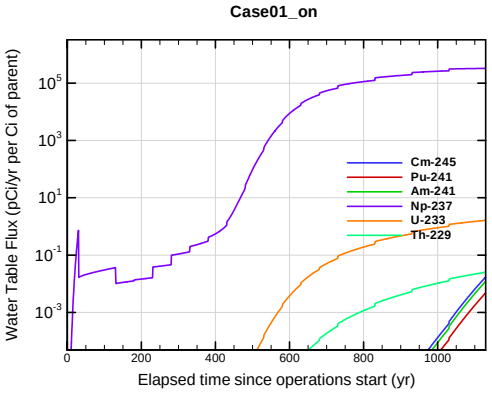

Figure A1A-303. Engineered Trench water table flux for Case01_on Cm-245

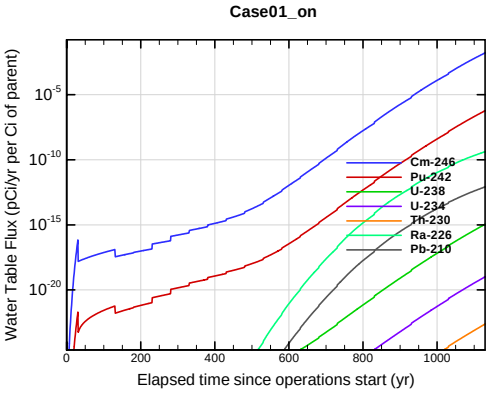

Figure A1A-304. Engineered Trench water table flux for Case01_on Cm-246

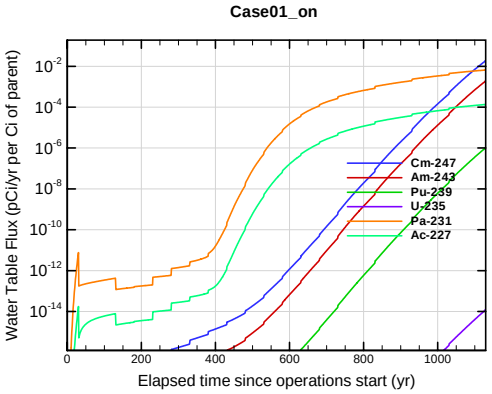

Figure A1A-305. Engineered Trench water table flux for Case01_on Cm-247

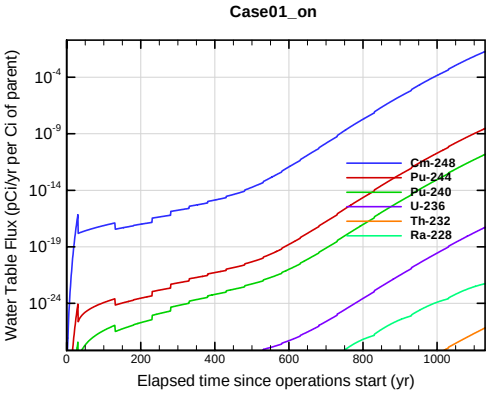

Figure A1A-306. Engineered Trench water table flux for Case01_on Cm-248

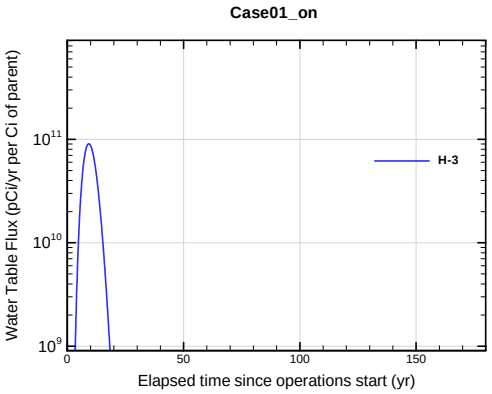

Figure A1A-307. Engineered Trench water table flux for Case01_on H-3

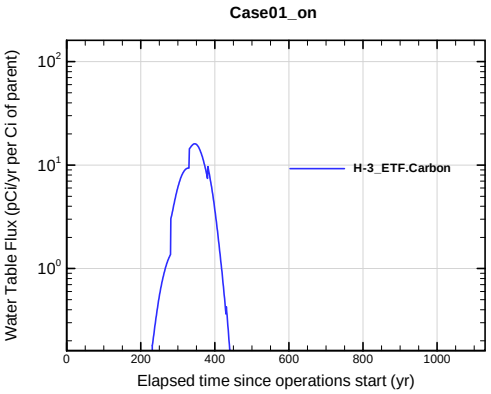

Figure A1A-308. Engineered Trench water table flux for Case01_on H-3_ETF.Carbon

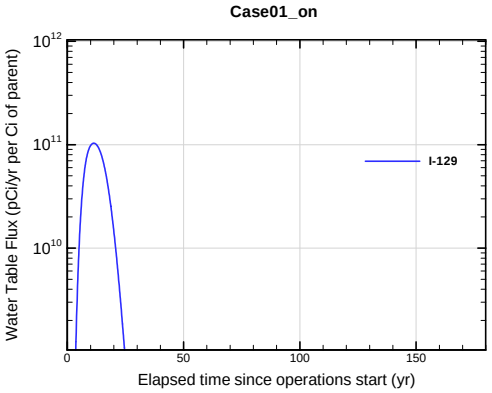

Figure A1A-309. Engineered Trench water table flux for Case01_on I-129

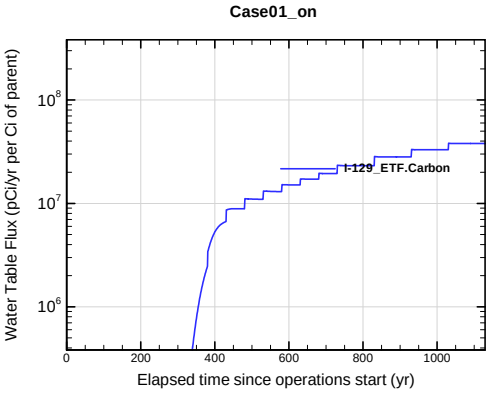

Figure A1A-310. Engineered Trench water table flux for Case01_on I-129_ETF.Carbon

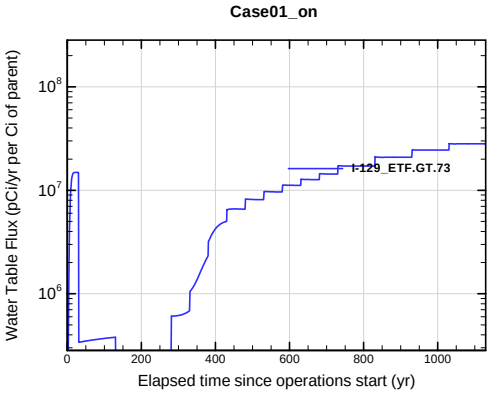

Figure A1A-311. Engineered Trench water table flux for Case01_on I-129_ETF.GT.73

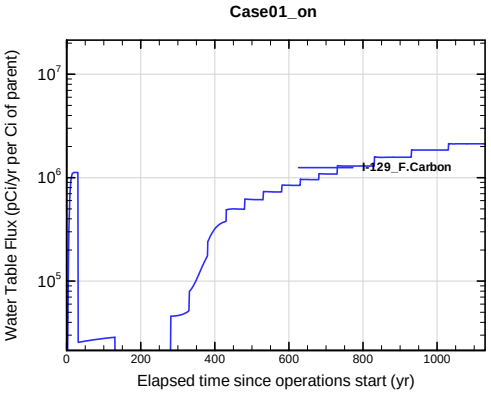

Figure A1A-312. Engineered Trench water table flux for Case01_on I-129_F.Carbon

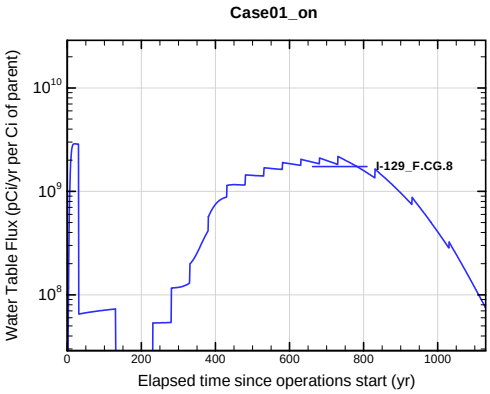

Figure A1A-313. Engineered Trench water table flux for Case01_on I-129_F.CG.8

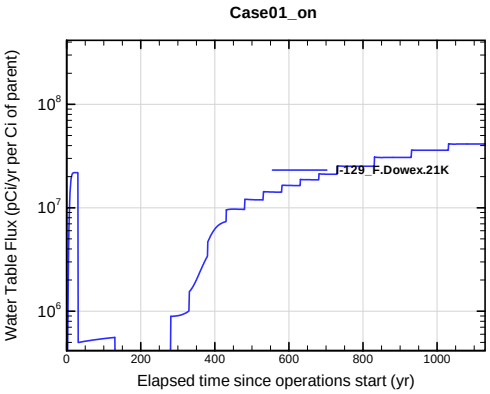

Figure A1A-314. Engineered Trench water table flux for Case01_on I-129_F.Dowex.21K

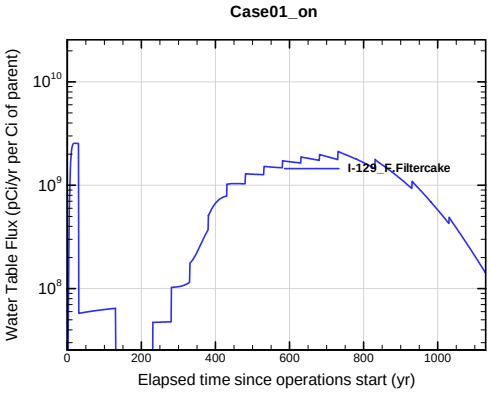

Figure A1A-315. Engineered Trench water table flux for Case01_on I-129_F.Filtercake

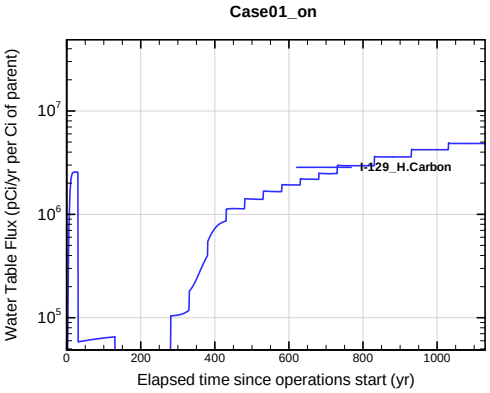

Figure A1A-316. Engineered Trench water table flux for Case01_on I-129_H.Carbon

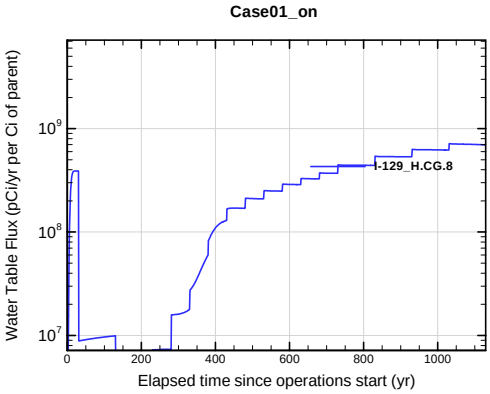

Figure A1A-317. Engineered Trench water table flux for Case01_on I-129_H.CG.8

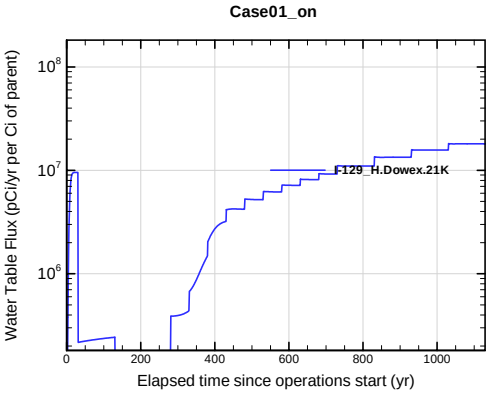

Figure A1A-318. Engineered Trench water table flux for Case01_on I-129_H.Dowex.21K

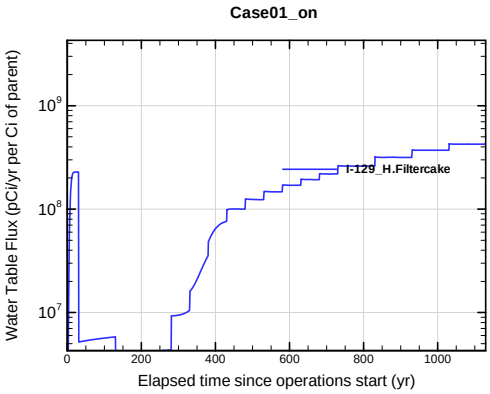

Figure A1A-319. Engineered Trench water table flux for Case01_on I-129_H.Filtercake

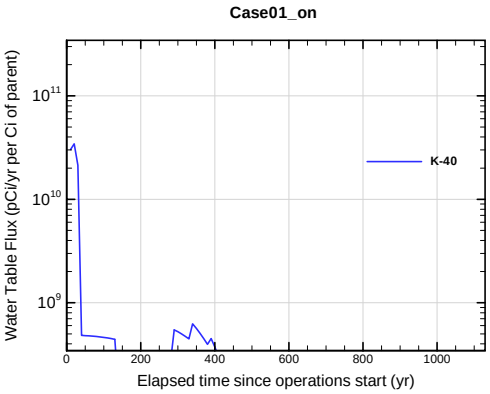

Figure A1A-320. Engineered Trench water table flux for Case01_on K-40

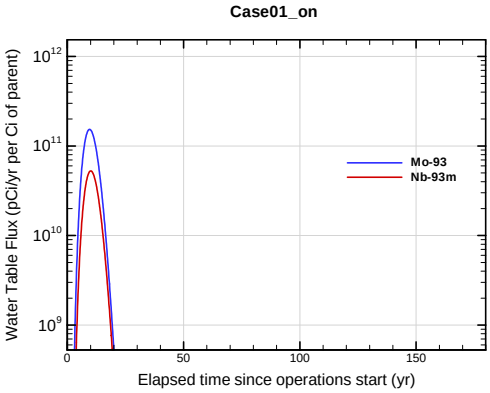

Figure A1A-321. Engineered Trench water table flux for Case01_on Mo-93

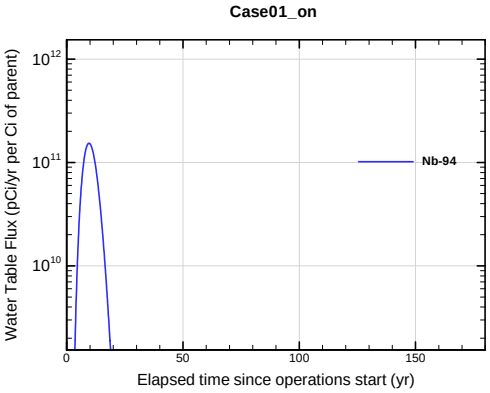

Figure A1A-322. Engineered Trench water table flux for Case01_on Nb-94

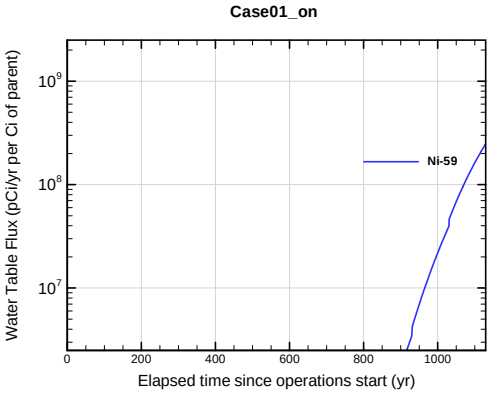

Figure A1A-323. Engineered Trench water table flux for Case01_on Ni-59

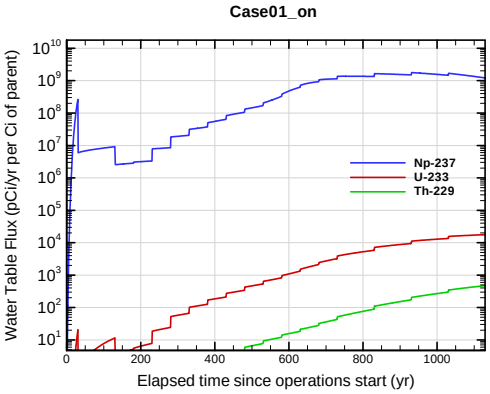

Figure A1A-324. Engineered Trench water table flux for Case01_on Np-237

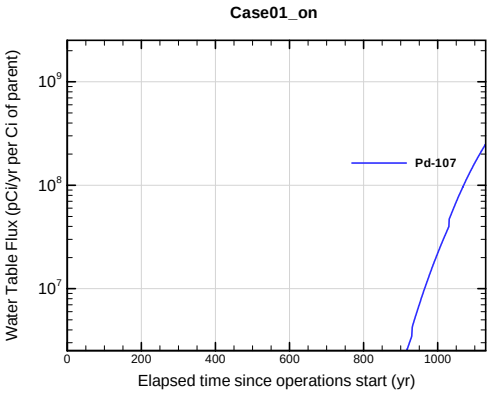

Figure A1A-325. Engineered Trench water table flux for Case01_on Pd-107

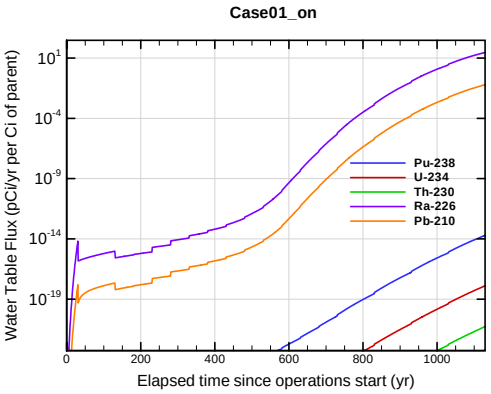

Figure A1A-326. Engineered Trench water table flux for Case01_on Pu-238

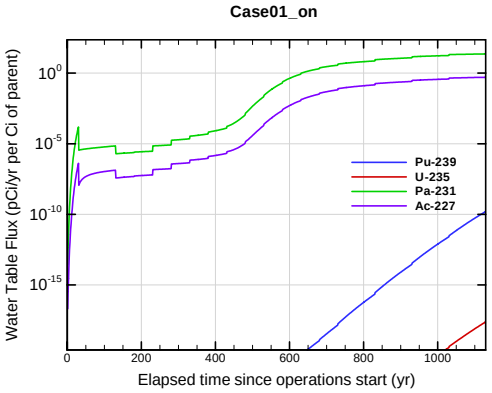

Figure A1A-327. Engineered Trench water table flux for Case01_on Pu-239

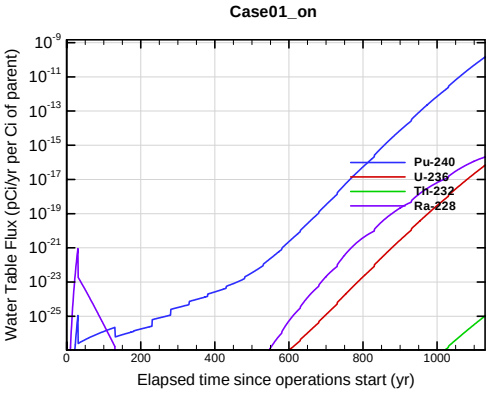

Figure A1A-328. Engineered Trench water table flux for Case01_on Pu-240

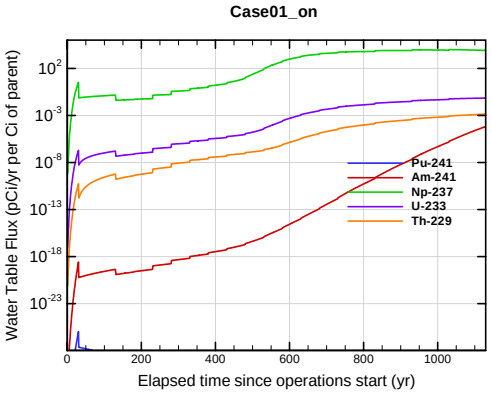

Figure A1A-329. Engineered Trench water table flux for Case01_on Pu-241

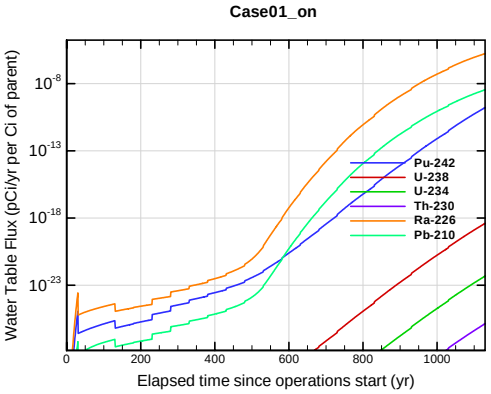

Figure A1A-330. Engineered Trench water table flux for Case01_on Pu-242

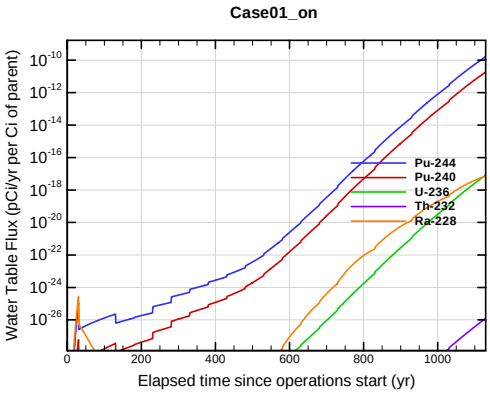

Figure A1A-331. Engineered Trench water table flux for Case01_on Pu-244

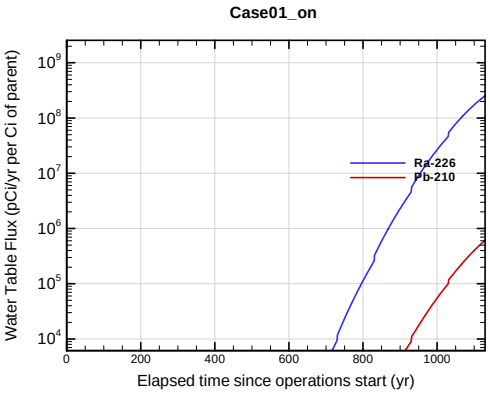

Figure A1A-332. Engineered Trench water table flux for Case01_on Ra-226

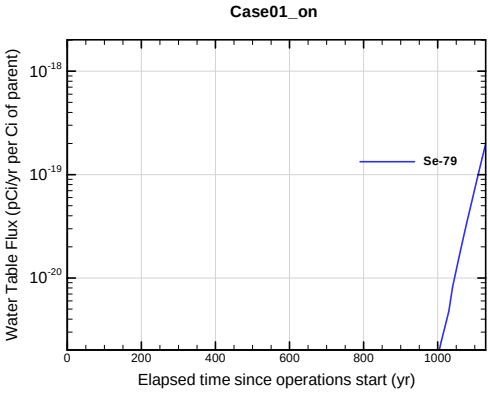

Figure A1A-333. Engineered Trench water table flux for Case01_on Se-79

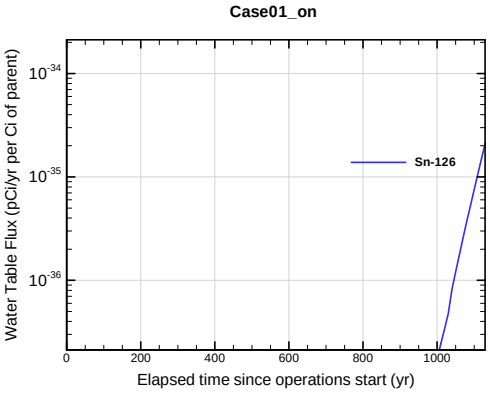

Figure A1A-334. Engineered Trench water table flux for Case01_on Sn-126

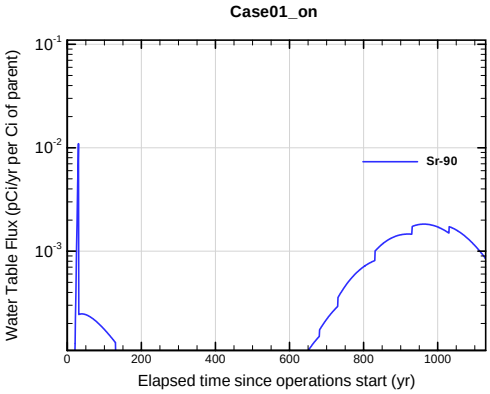

Figure A1A-335. Engineered Trench water table flux for Case01_on Sr-90

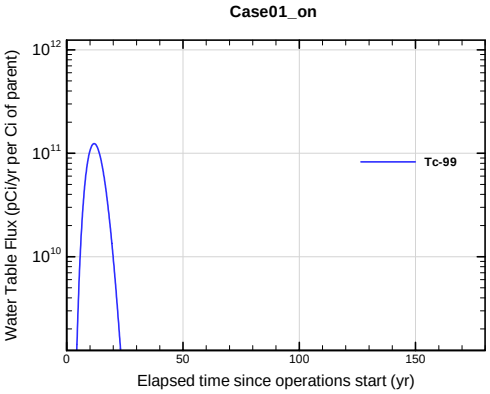

Figure A1A-336. Engineered Trench water table flux for Case01_on Tc-99

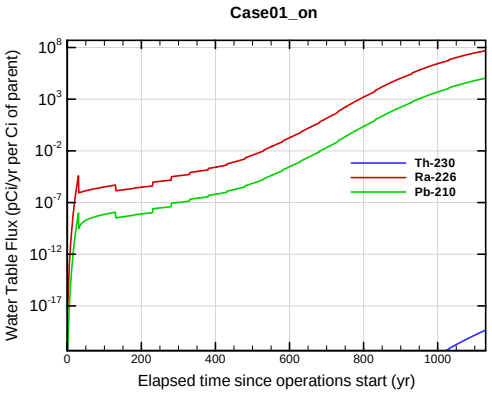

Figure A1A-337. Engineered Trench water table flux for Case01_on Th-230

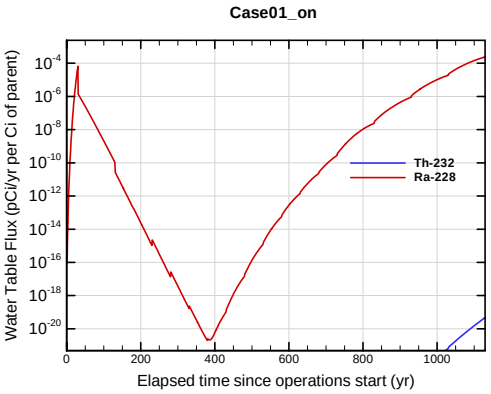

Figure A1A-338. Engineered Trench water table flux for Case01_on Th-232

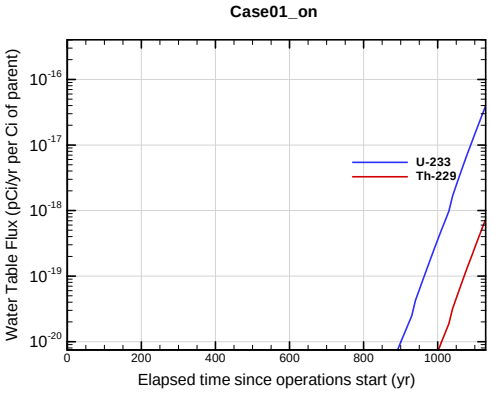

Figure A1A-339. Engineered Trench water table flux for Case01_on U-233

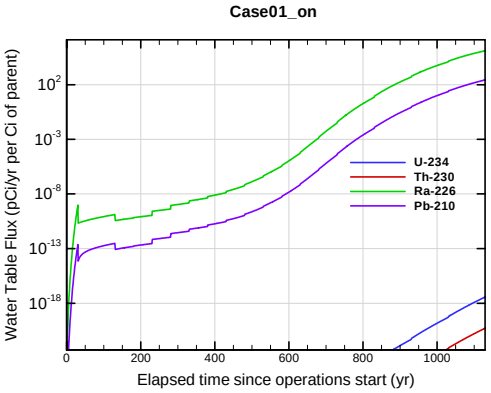

Figure A1A-340. Engineered Trench water table flux for Case01_on U-234

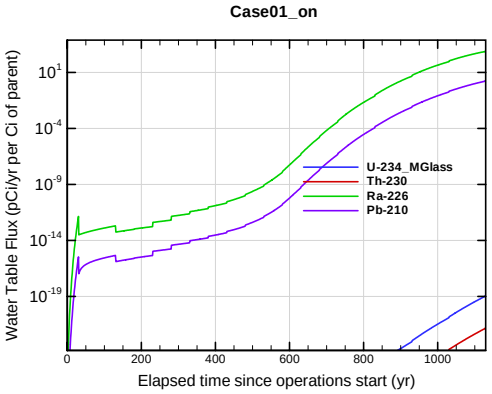

Figure A1A-341. Engineered Trench water table flux for Case01_on U-234_MGlass

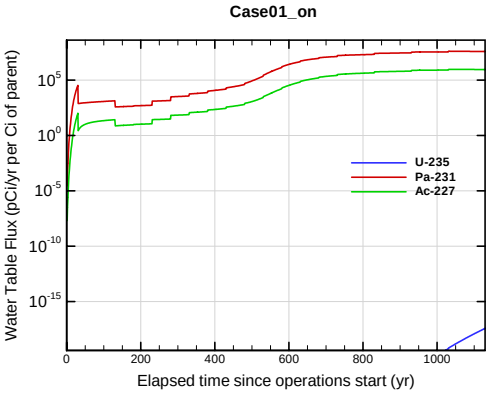

Figure A1A-342. Engineered Trench water table flux for Case01_on U-235

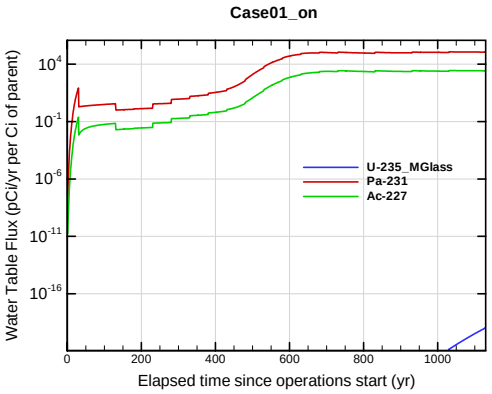

Figure A1A-343. Engineered Trench water table flux for Case01_on U-235_MGlass

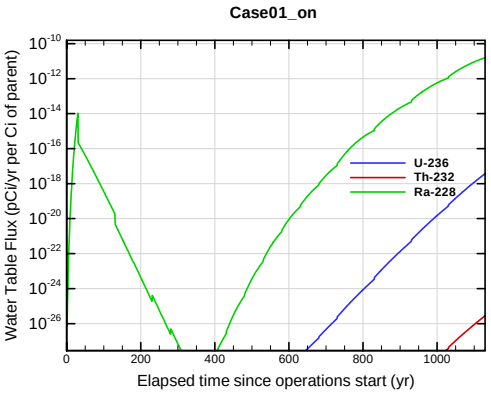

Figure A1A-344. Engineered Trench water table flux for Case01_on U-236

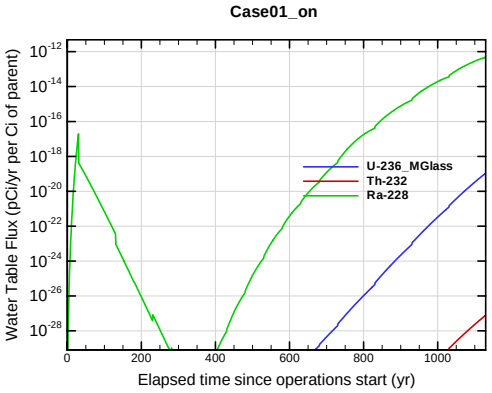

Figure A1A-345. Engineered Trench water table flux for Case01_on U-236_MGlass

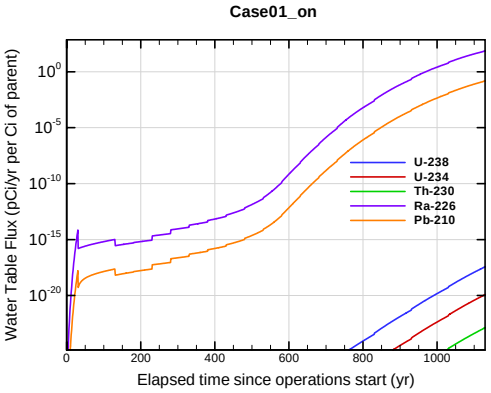

Figure A1A-346. Engineered Trench water table flux for Case01_on U-238

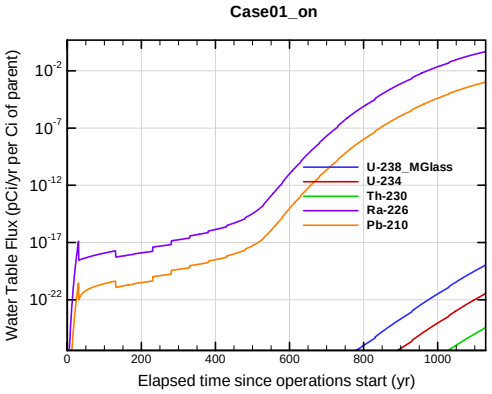

Figure A1A-347. Engineered Trench water table flux for Case01_on U-238_MGlass

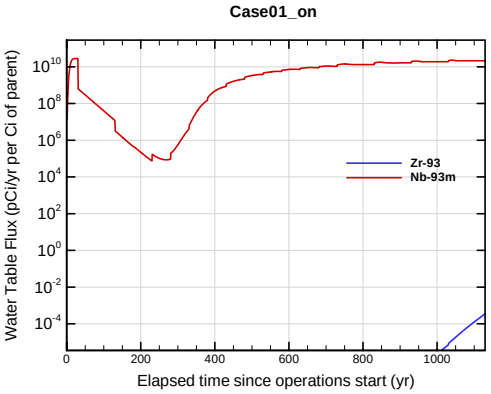

Figure A1A-348. Engineered Trench water table flux for Case01_on Zr-93

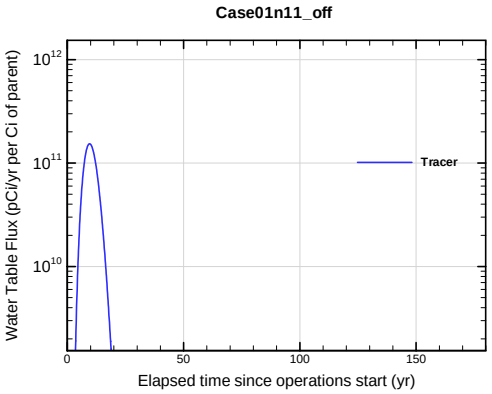

Figure A1A-349. Engineered Trench water table flux for Case01n11_off Tracer

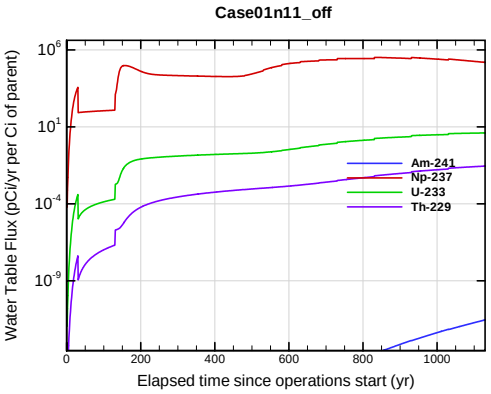

Figure A1A-350. Engineered Trench water table flux for Case01n11_off Am-241

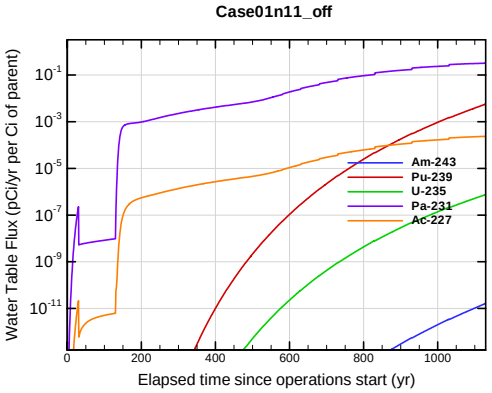

Figure A1A-351. Engineered Trench water table flux for Case01n11_off Am-243

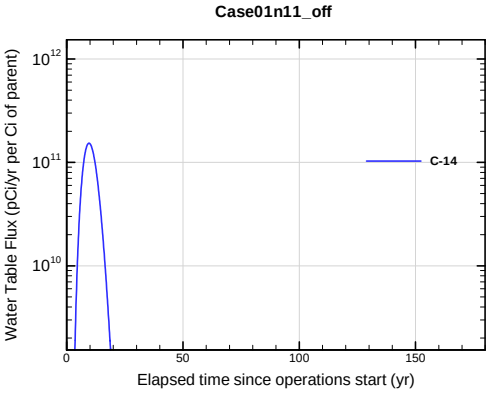

Figure A1A-352. Engineered Trench water table flux for Case01n11_off C-14

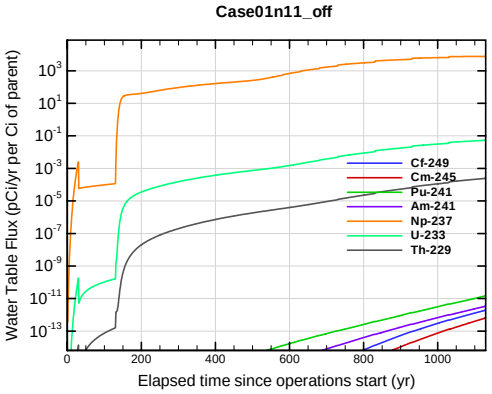

Figure A1A-353. Engineered Trench water table flux for Case01n11_off Cf-249

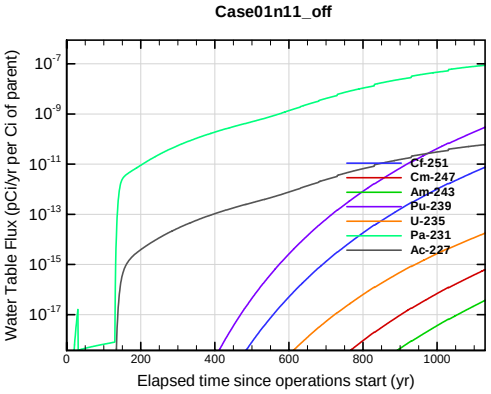

Figure A1A-354. Engineered Trench water table flux for Case01n11_off Cf-251

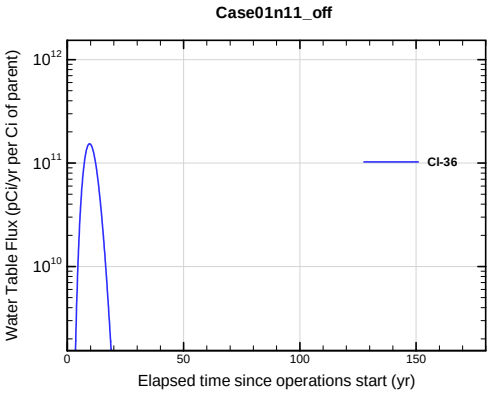

Figure A1A-355. Engineered Trench water table flux for Case01n11_off Cl-36

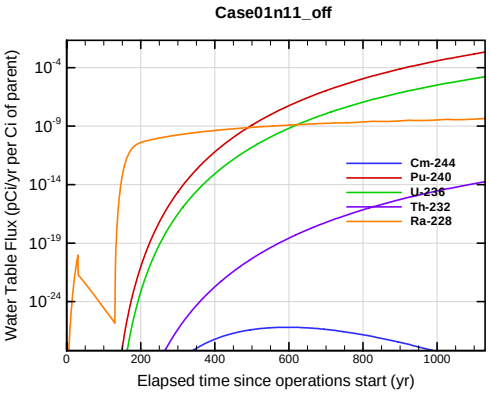

Figure A1A-356. Engineered Trench water table flux for Case01n11_off Cm-244

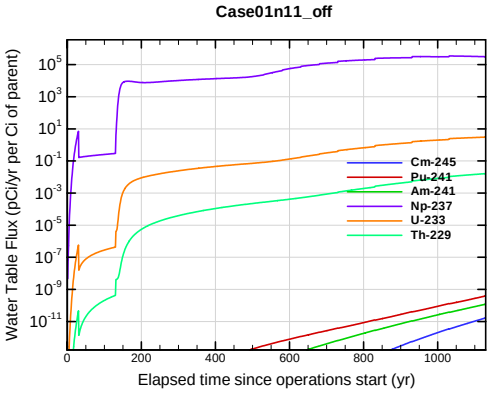

Figure A1A-357. Engineered Trench water table flux for Case01n11_off Cm-245

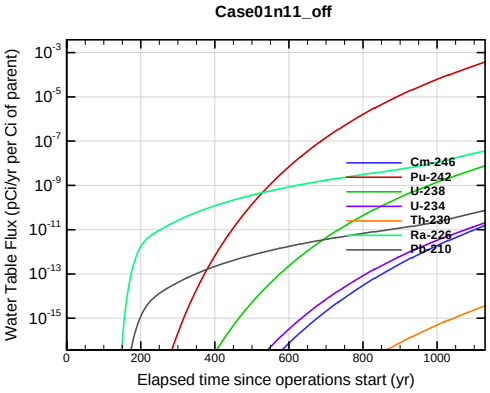

Figure A1A-358. Engineered Trench water table flux for Case01n11_off Cm-246

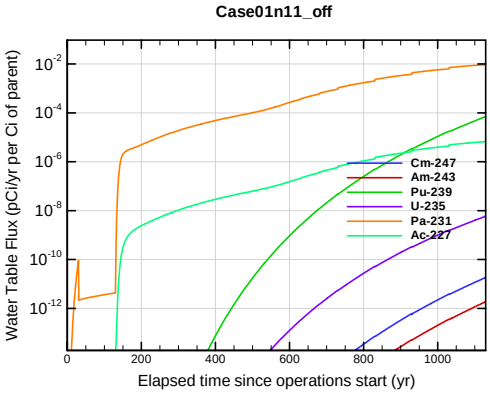

Figure A1A-359. Engineered Trench water table flux for Case01n11_off Cm-247

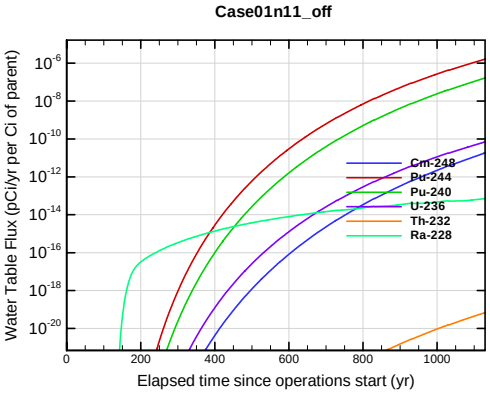

Figure A1A-360. Engineered Trench water table flux for Case01n11_off Cm-248

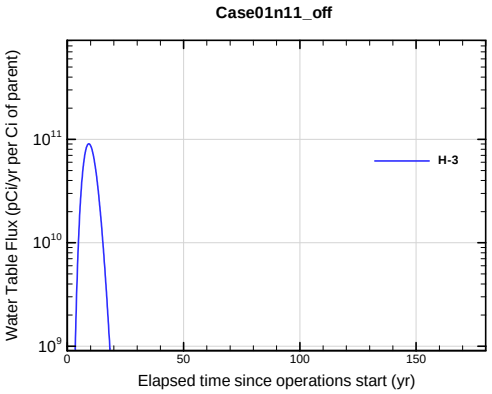

Figure A1A-361. Engineered Trench water table flux for Case01n11_off H-3

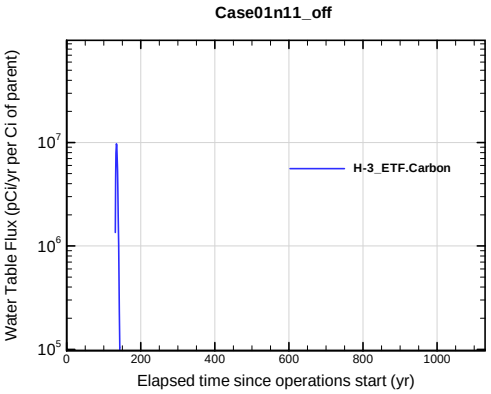

Figure A1A-362. Engineered Trench water table flux for Case01n11_off H-3_ETF.Carbon

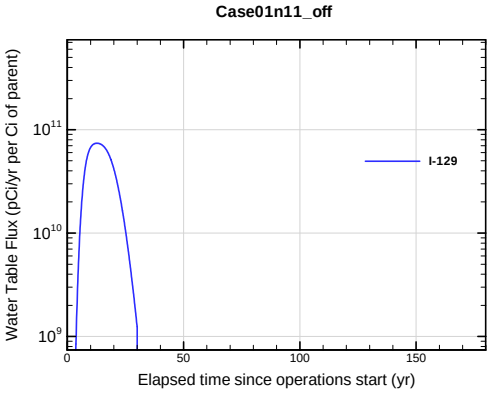

Figure A1A-363. Engineered Trench water table flux for Case01n11_off I-129

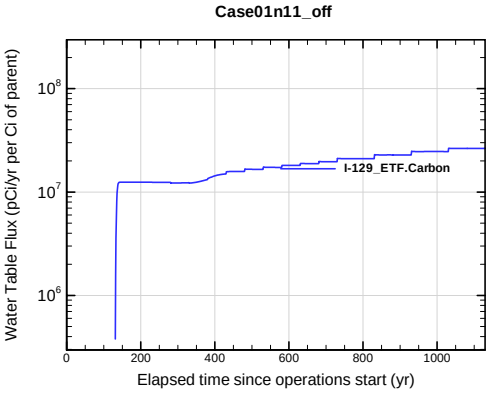

Figure A1A-364. Engineered Trench water table flux for Case01n11_off I-129_ETF.Carbon

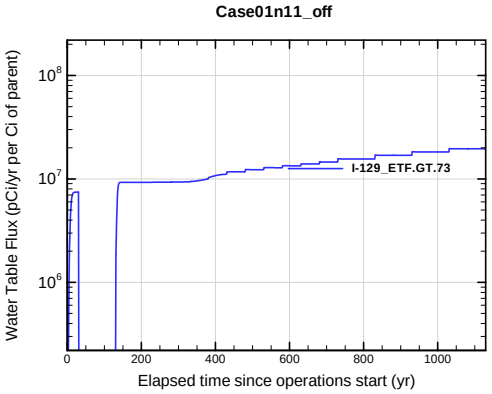

Figure A1A-365. Engineered Trench water table flux for Case01n11_off I-129_ETF.GT.73

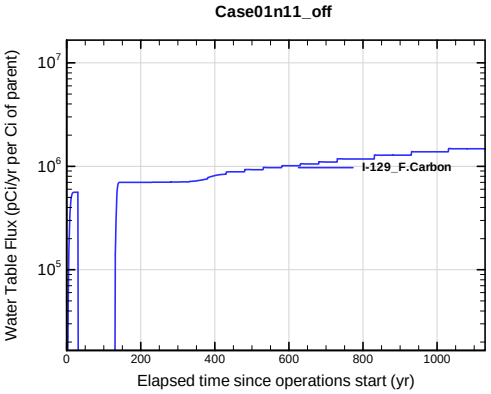

Figure A1A-366. Engineered Trench water table flux for Case01n11_off I-129_F.Carbon

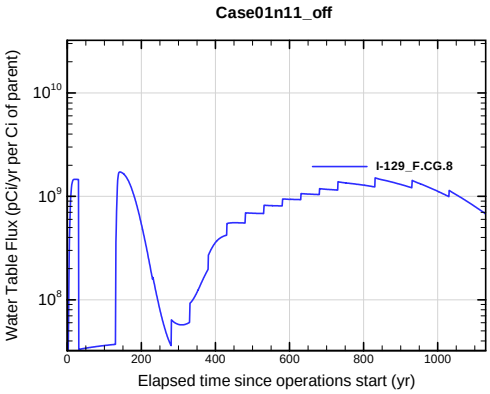

Figure A1A-367. Engineered Trench water table flux for Case01n11_off I-129_F.CG.8

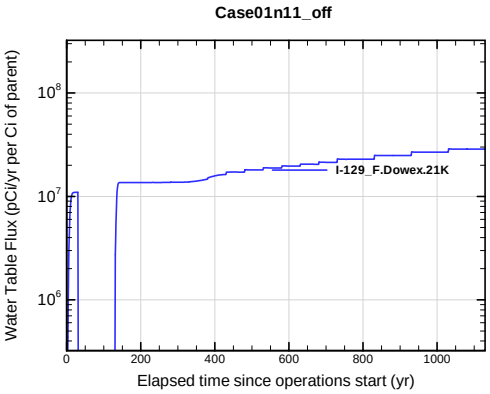

Figure A1A-368. Engineered Trench water table flux for Case01n11_off I-129_F.Dowex.21K

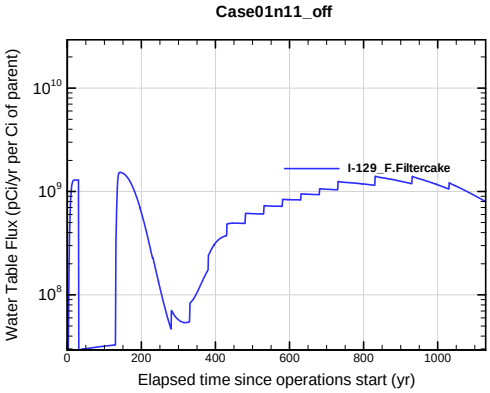

Figure A1A-369. Engineered Trench water table flux for Case01n11_off I-129_F.Filtercake

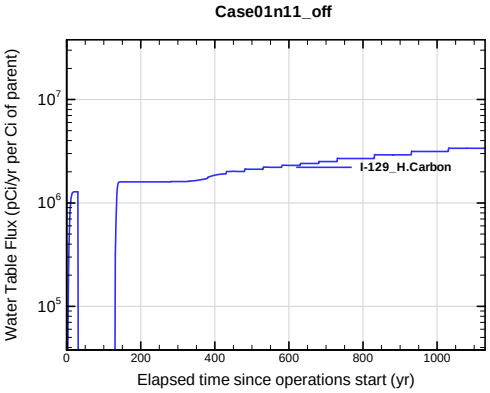

Figure A1A-370. Engineered Trench water table flux for Case01n11_off I-129_H.Carbon

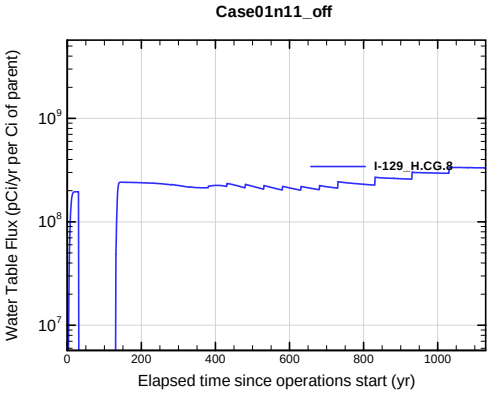

Figure A1A-371. Engineered Trench water table flux for Case01n11_off I-129_H.CG.8

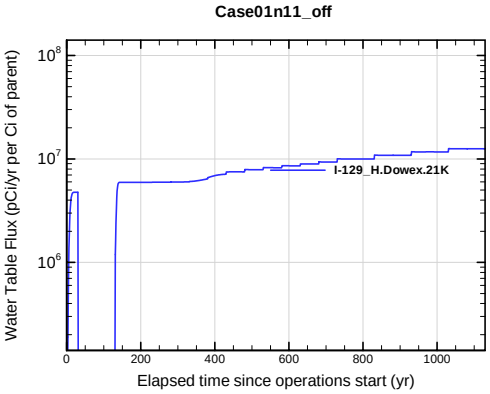

Figure A1A-372. Engineered Trench water table flux for Case01n11_off I-129_H.Dowex.21K

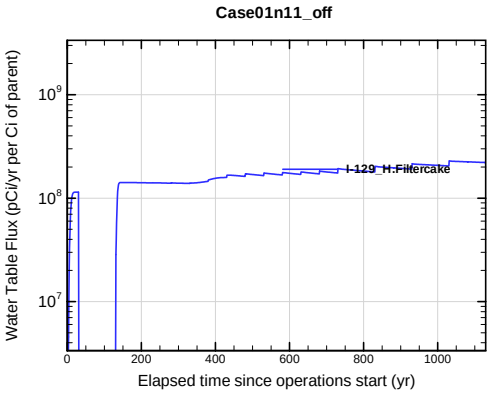

Figure A1A-373. Engineered Trench water table flux for Case01n11_off I-129_H.Filtercake

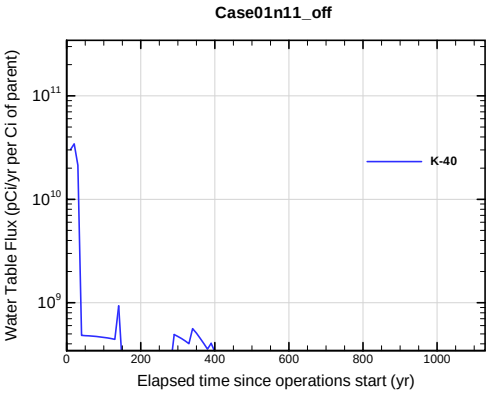

Figure A1A-374. Engineered Trench water table flux for Case01n11_off K-40

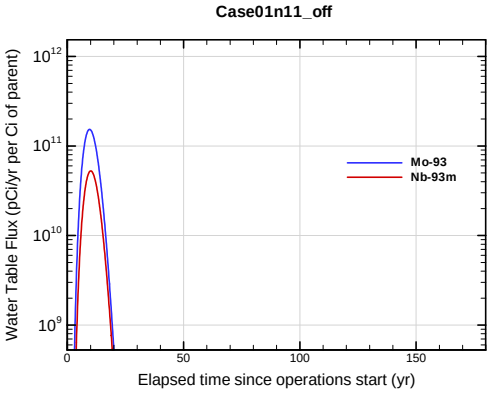

Figure A1A-375. Engineered Trench water table flux for Case01n11_off Mo-93

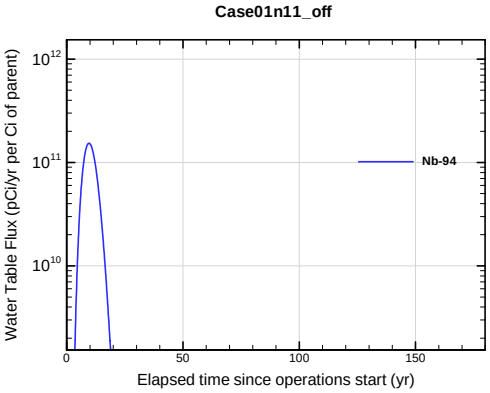

Figure A1A-376. Engineered Trench water table flux for Case01n11_off Nb-94

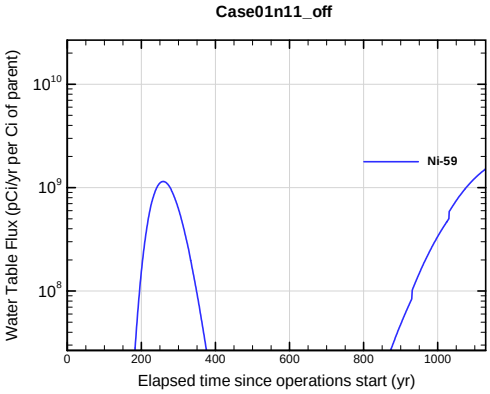

Figure A1A-377. Engineered Trench water table flux for Case01n11_off Ni-59

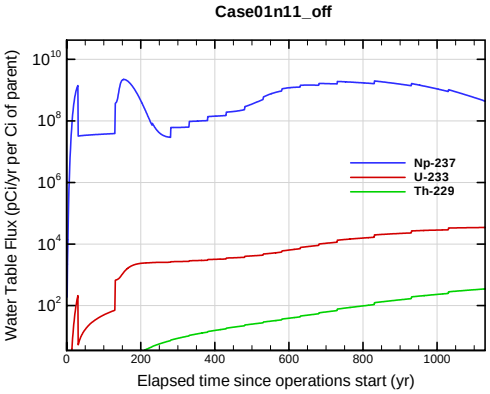

Figure A1A-378. Engineered Trench water table flux for Case01n11_off Np-237

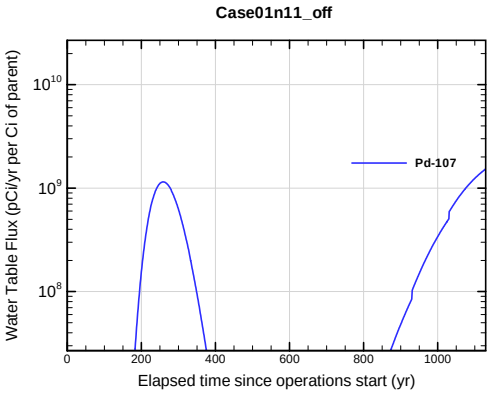

Figure A1A-379. Engineered Trench water table flux for Case01n11_off Pd-107

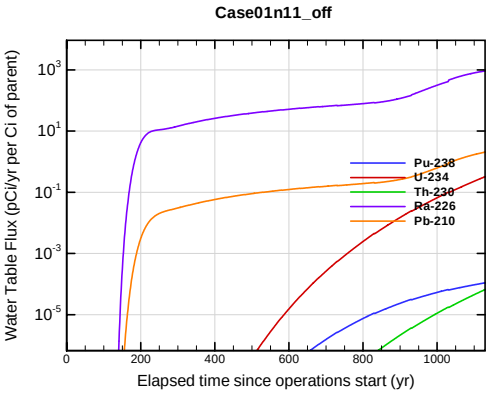

Figure A1A-380. Engineered Trench water table flux for Case01n11_off Pu-238

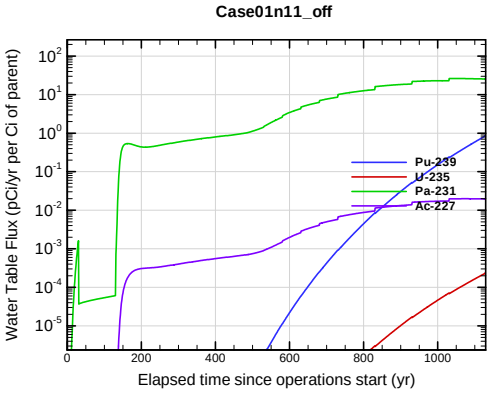

Figure A1A-381. Engineered Trench water table flux for Case01n11_off Pu-239

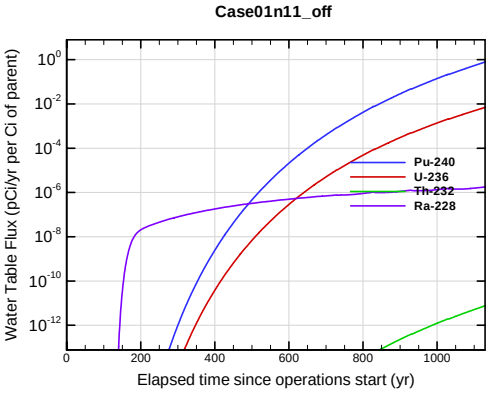

Figure A1A-382. Engineered Trench water table flux for Case01n11_off Pu-240

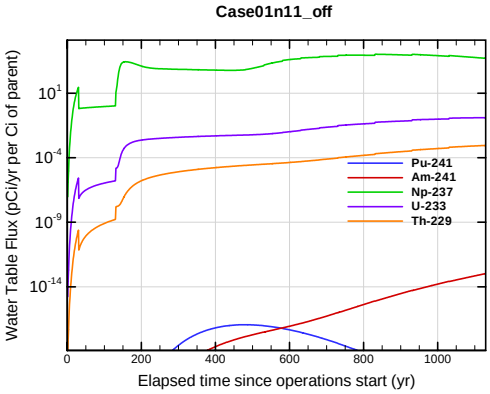

Figure A1A-383. Engineered Trench water table flux for Case01n11_off Pu-241

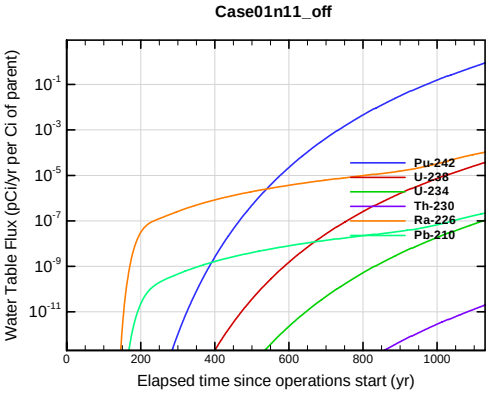

Figure A1A-384. Engineered Trench water table flux for Case01n11_off Pu-242

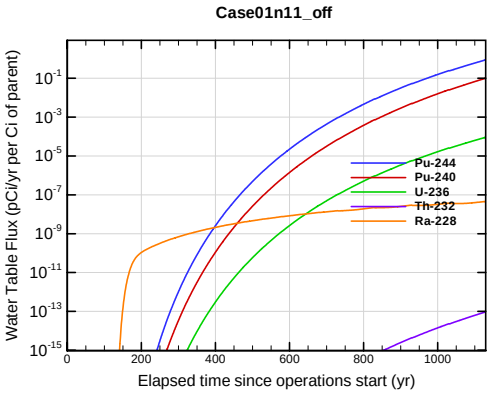

Figure A1A-385. Engineered Trench water table flux for Case01n11_off Pu-244

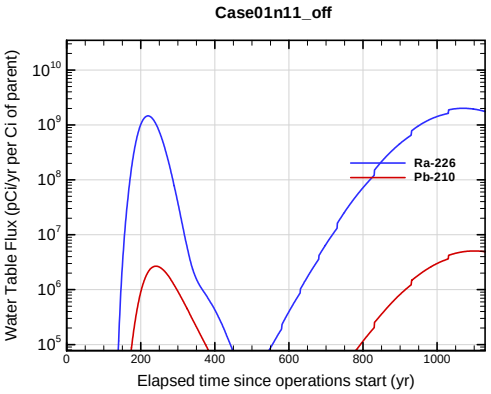

Figure A1A-386. Engineered Trench water table flux for Case01n11_off Ra-226

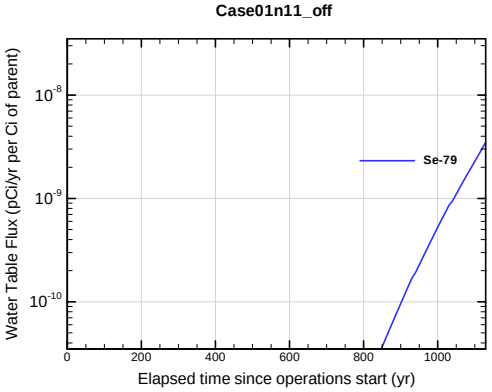

Figure A1A-387. Engineered Trench water table flux for Case01n11_off Se-79

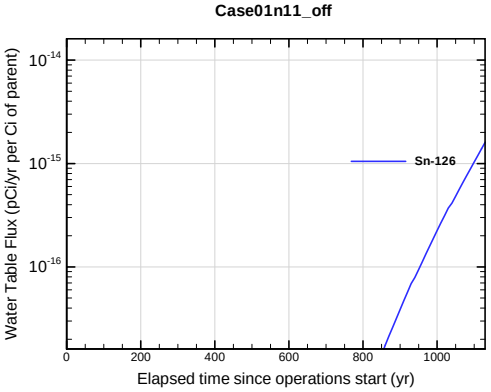

Figure A1A-388. Engineered Trench water table flux for Case01n11_off Sn-126

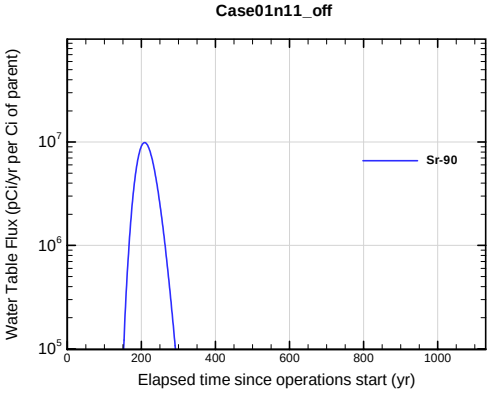

Figure A1A-389. Engineered Trench water table flux for Case01n11_off Sr-90

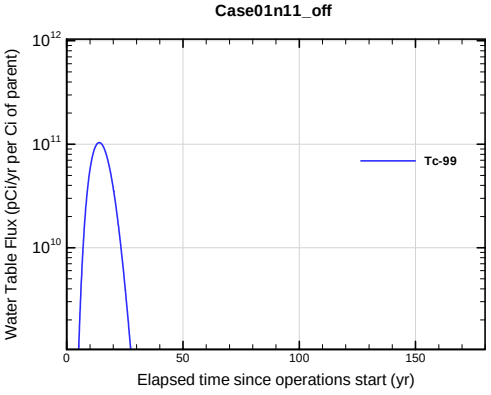

Figure A1A-390. Engineered Trench water table flux for Case01n11_off Tc-99

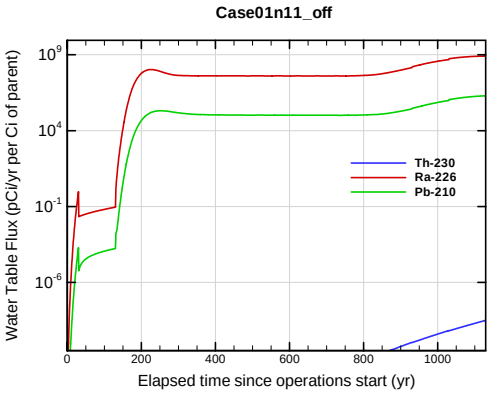

Figure A1A-391. Engineered Trench water table flux for Case01n11_off Th-230

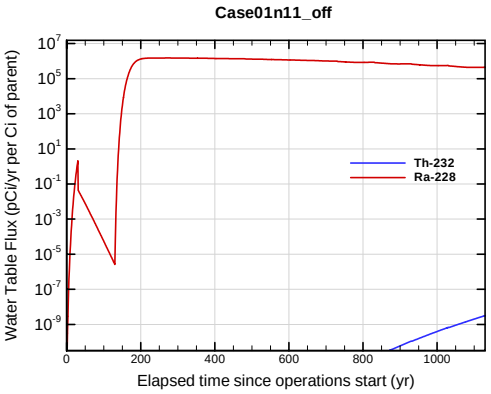

Figure A1A-392. Engineered Trench water table flux for Case01n11_off Th-232

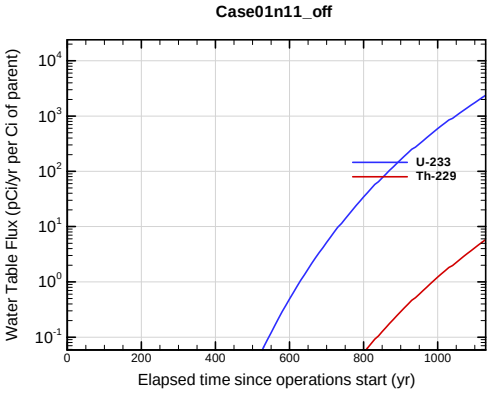

Figure A1A-393. Engineered Trench water table flux for Case01n11_off U-233

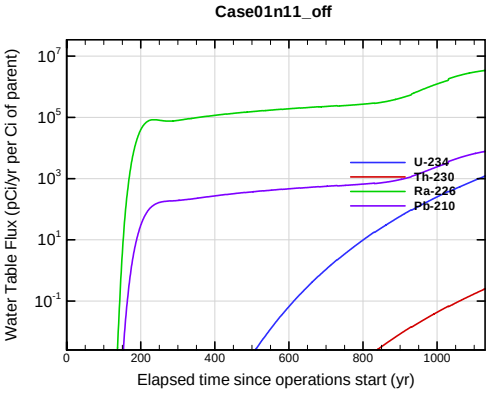

Figure A1A-394. Engineered Trench water table flux for Case01n11_off U-234

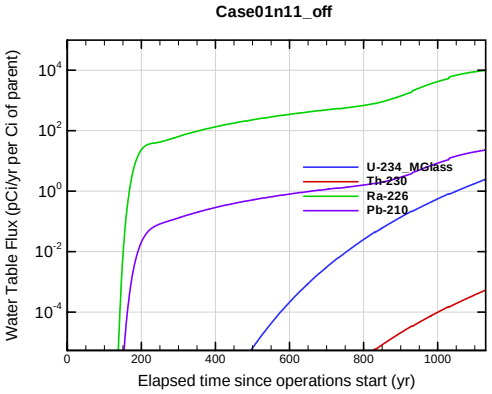

Figure A1A-395. Engineered Trench water table flux for Case01n11_off U-234_MGlass

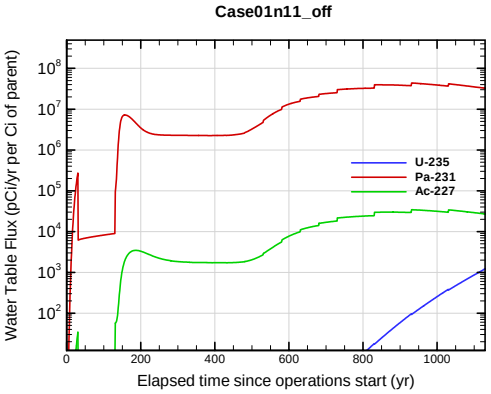

Figure A1A-396. Engineered Trench water table flux for Case01n11_off U-235

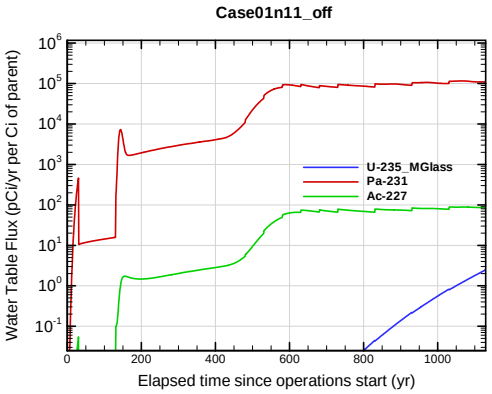

Figure A1A-397. Engineered Trench water table flux for Case01n11_off U-235_MGlass

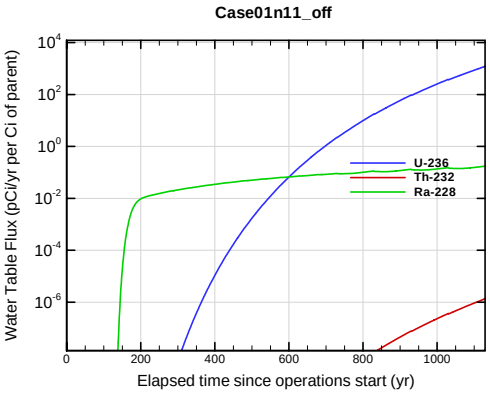

Figure A1A-398. Engineered Trench water table flux for Case01n11_off U-236

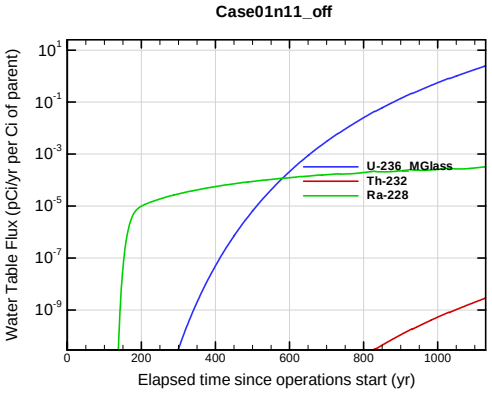

Figure A1A-399. Engineered Trench water table flux for Case01n11_off U-236_MGlass

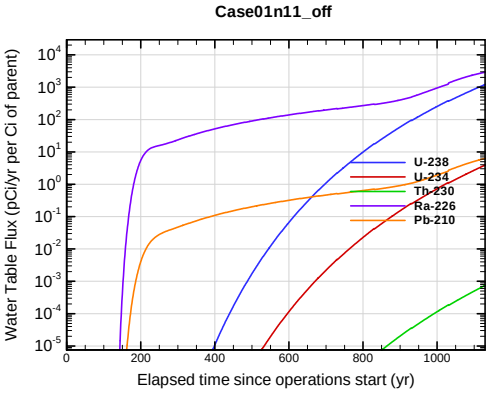

Figure A1A-400. Engineered Trench water table flux for Case01n11_off U-238

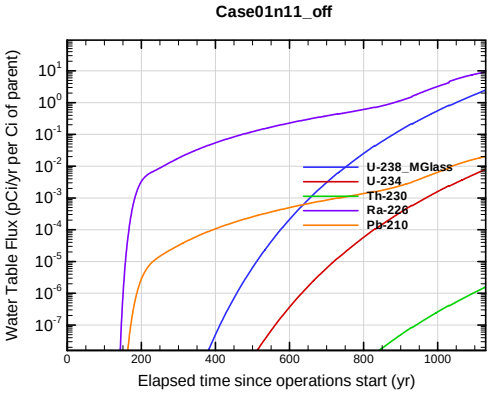

Figure A1A-401. Engineered Trench water table flux for Case01n11_off U-238_MGlass

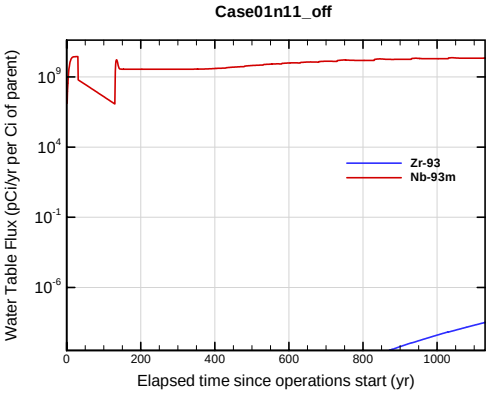

Figure A1A-402. Engineered Trench water table flux for Case01n11_off Zr-93

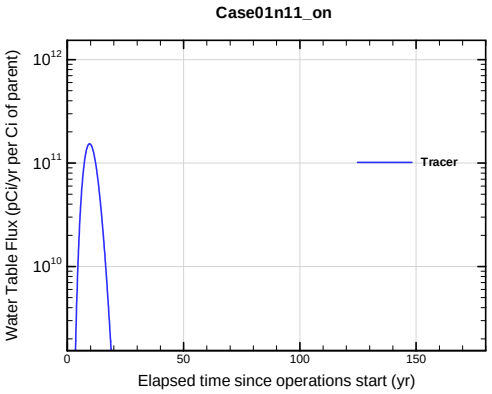

Figure A1A-403. Engineered Trench water table flux for Case01n11_on Tracer

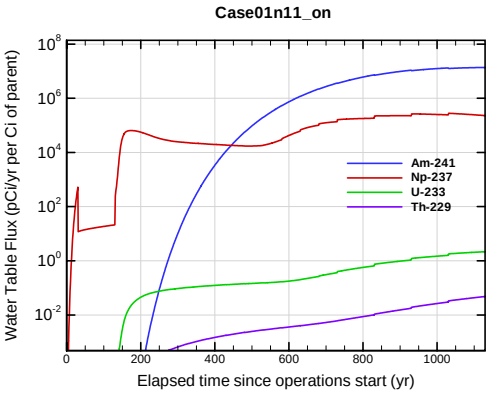

Figure A1A-404. Engineered Trench water table flux for Case01n11_on Am-241

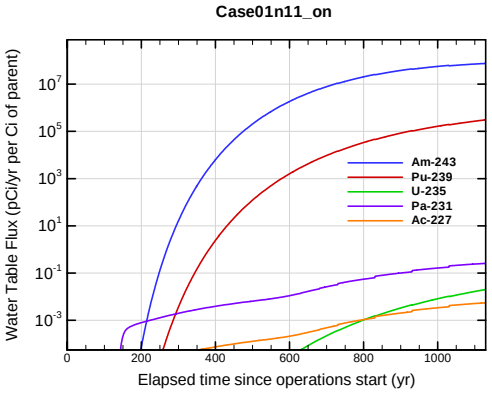

Figure A1A-405. Engineered Trench water table flux for Case01n11_on Am-243

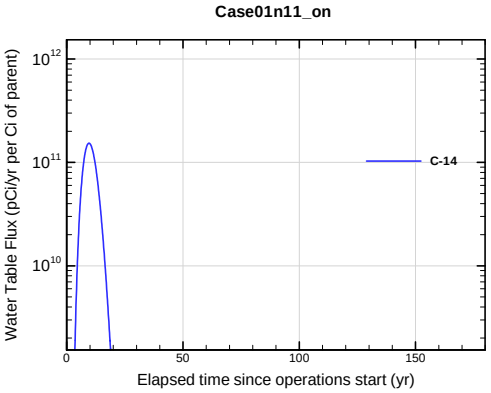

Figure A1A-406. Engineered Trench water table flux for Case01n11_on C-14

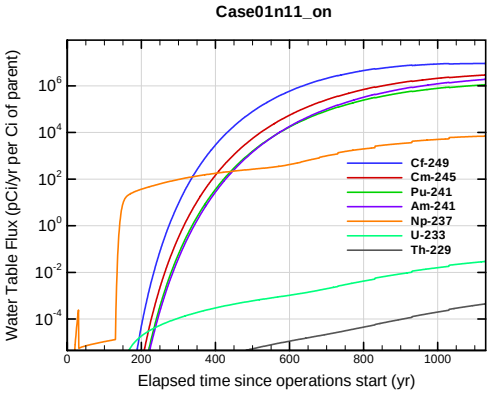

Figure A1A-407. Engineered Trench water table flux for Case01n11_on Cf-249

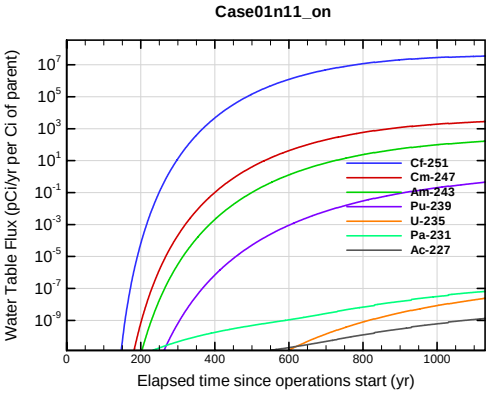

Figure A1A-408. Engineered Trench water table flux for Case01n11_on Cf-251

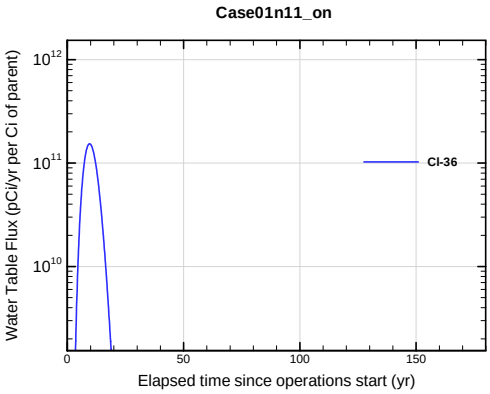

Figure A1A-409. Engineered Trench water table flux for Case01n11_on Cl-36

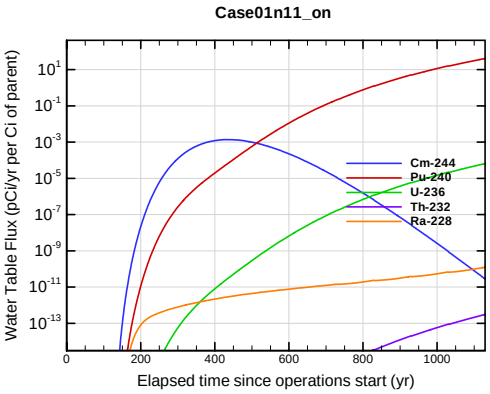

Figure A1A-410. Engineered Trench water table flux for Case01n11_on Cm-244

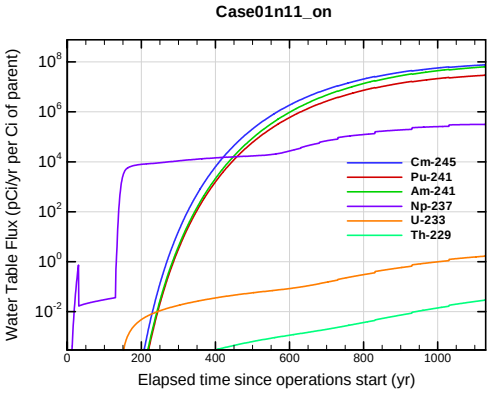

Figure A1A-411. Engineered Trench water table flux for Case01n11_on Cm-245

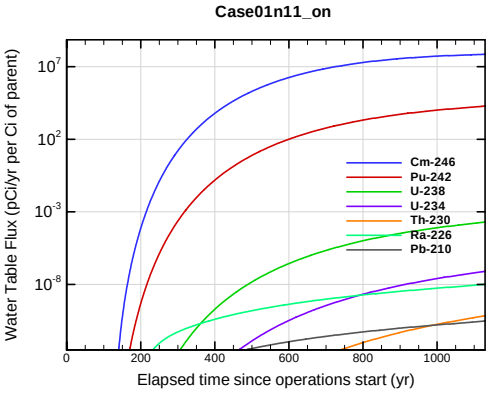

Figure A1A-412. Engineered Trench water table flux for Case01n11_on Cm-246

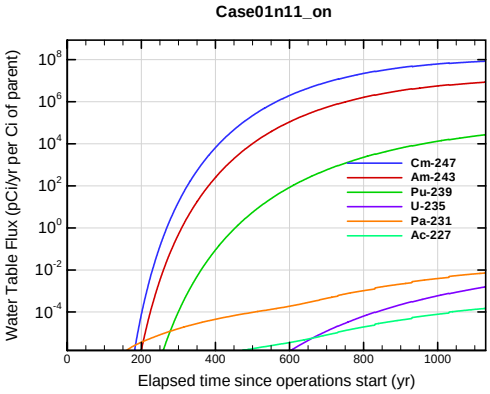

Figure A1A-413. Engineered Trench water table flux for Case01n11_on Cm-247

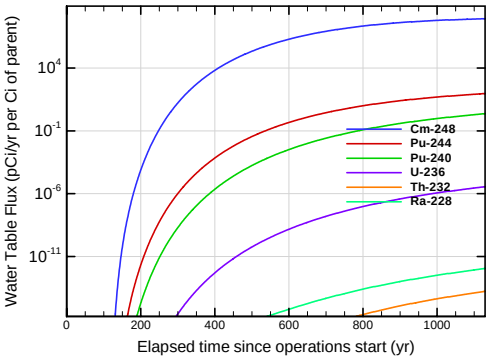

Figure A1A-414. Engineered Trench water table flux for Case01n11_on Cm-248

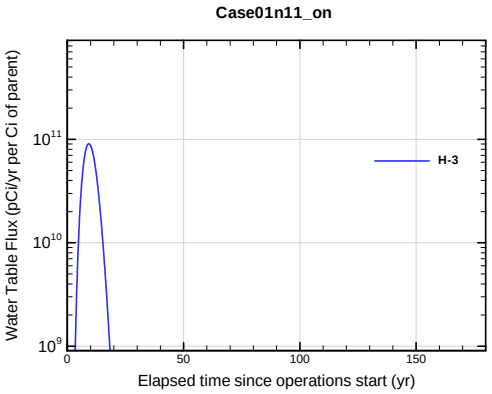

Figure A1A-415. Engineered Trench water table flux for Case01n11_on H-3

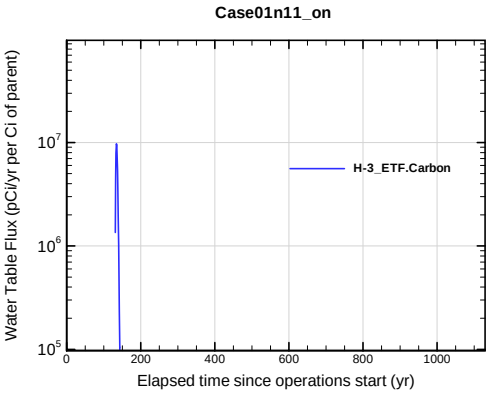

Figure A1A-416. Engineered Trench water table flux for Case01n11_on H-3_ETF.Carbon

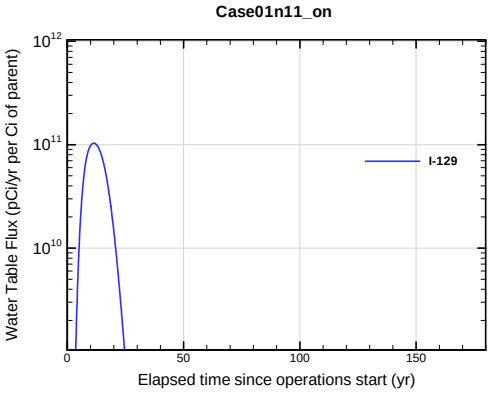

Figure A1A-417. Engineered Trench water table flux for Case01n11_on I-129

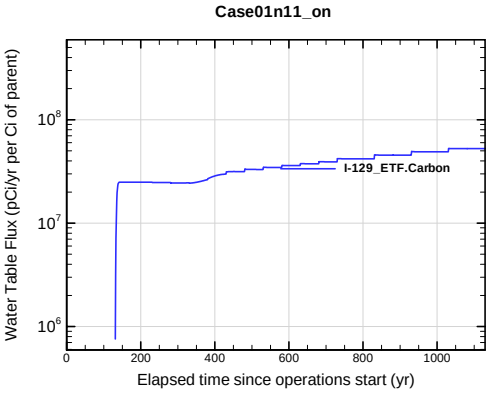

Figure A1A-418. Engineered Trench water table flux for Case01n11_on I-129_ETF.Carbon

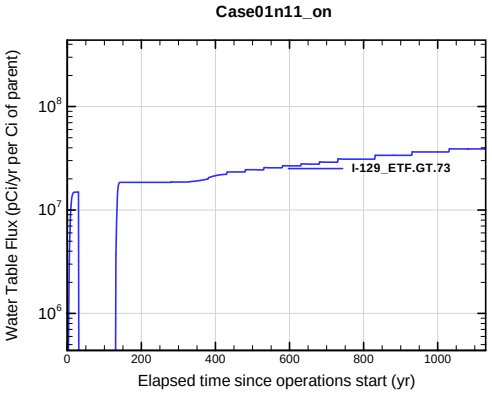

Figure A1A-419. Engineered Trench water table flux for Case01n11_on I-129_ETF.GT.73

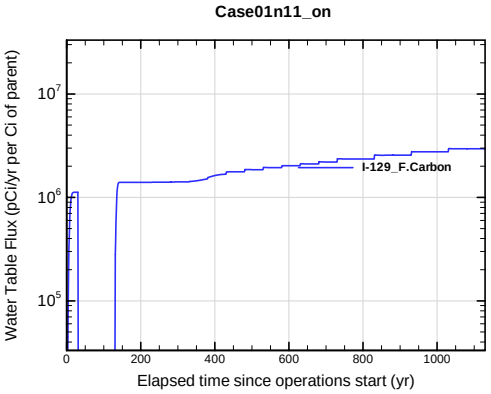

Figure A1A-420. Engineered Trench water table flux for Case01n11_on I-129_F.Carbon

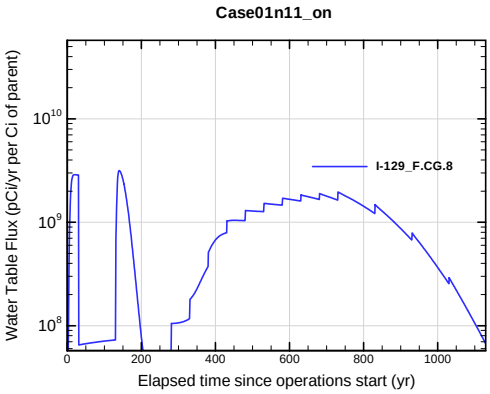

Figure A1A-421. Engineered Trench water table flux for Case01n11_on I-129_F.CG.8

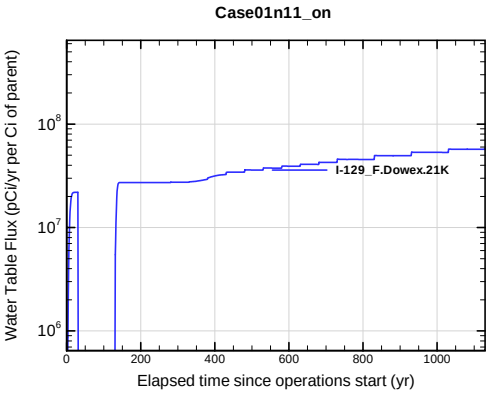

Figure A1A-422. Engineered Trench water table flux for Case01n11_on I-129_F.Dowex.21K

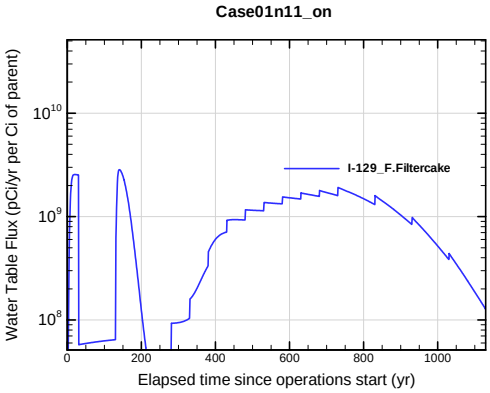

Figure A1A-423. Engineered Trench water table flux for Case01n11_on I-129_F.Filtercake

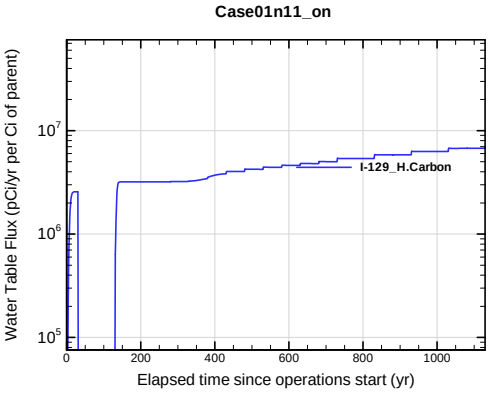

Figure A1A-424. Engineered Trench water table flux for Case01n11_on I-129_H.Carbon

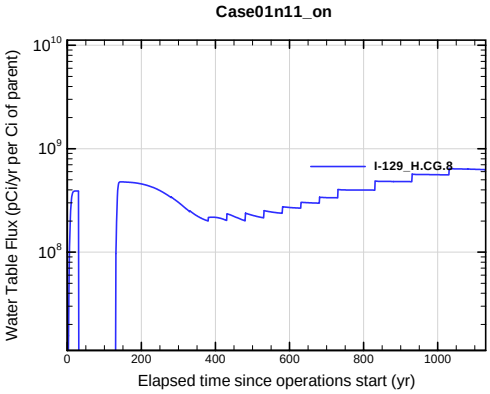

Figure A1A-425. Engineered Trench water table flux for Case01n11_on I-129_H.CG.8

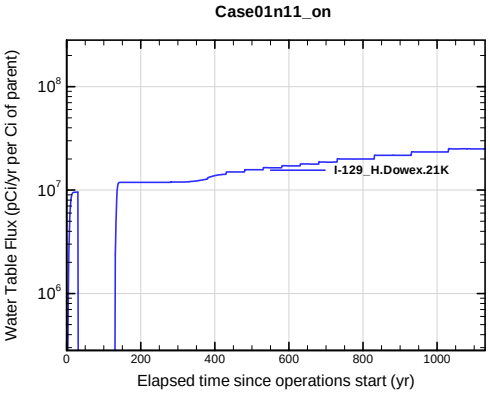

Figure A1A-426. Engineered Trench water table flux for Case01n11_on I-129_H.Dowex.21K

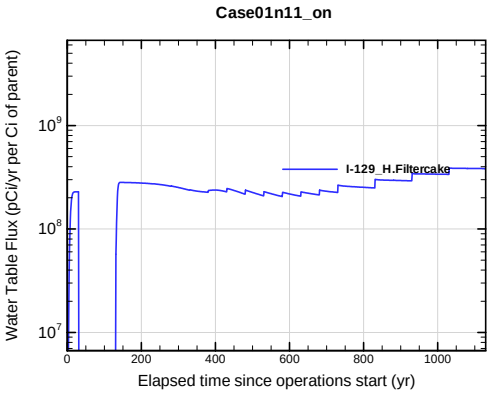

Figure A1A-427. Engineered Trench water table flux for Case01n11_on I-129_H.Filtercake

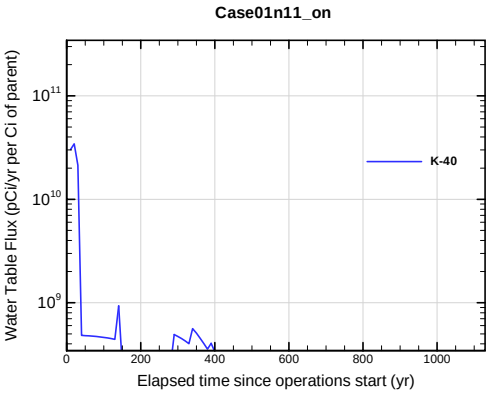

Figure A1A-428. Engineered Trench water table flux for Case01n11_on K-40

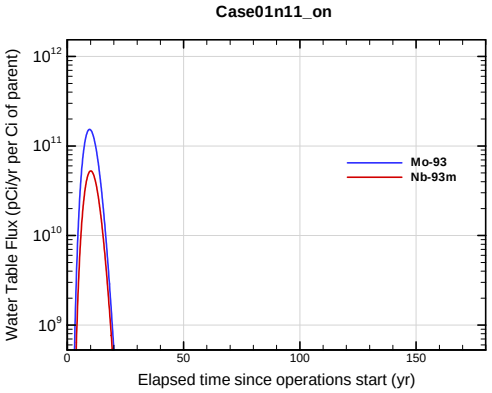

Figure A1A-429. Engineered Trench water table flux for Case01n11_on Mo-93

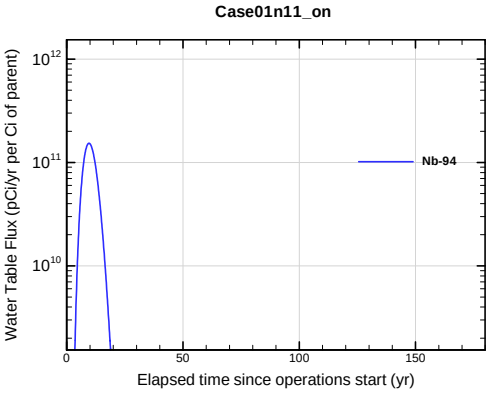

Figure A1A-430. Engineered Trench water table flux for Case01n11_on Nb-94

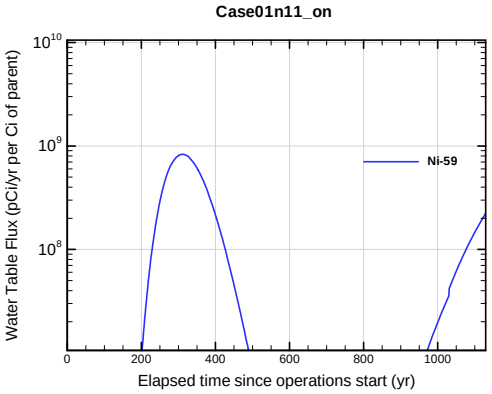

Figure A1A-431. Engineered Trench water table flux for Case01n11_on Ni-59

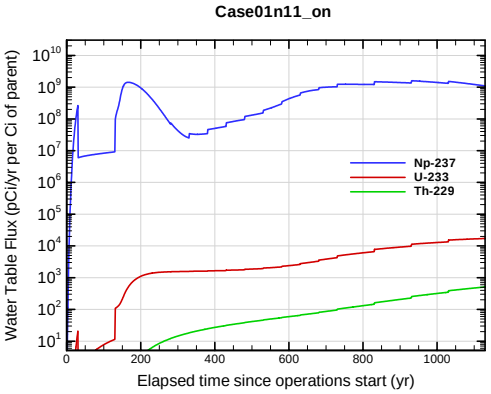

Figure A1A-432. Engineered Trench water table flux for Case01n11_on Np-237

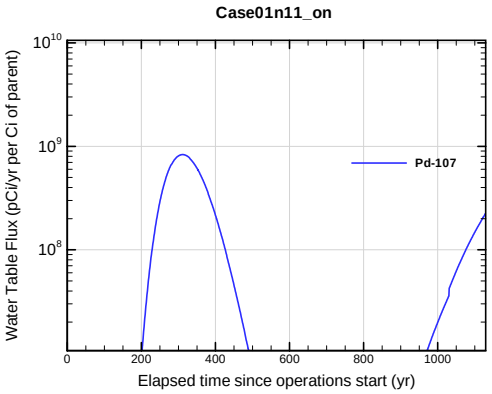

Figure A1A-433. Engineered Trench water table flux for Case01n11_on Pd-107

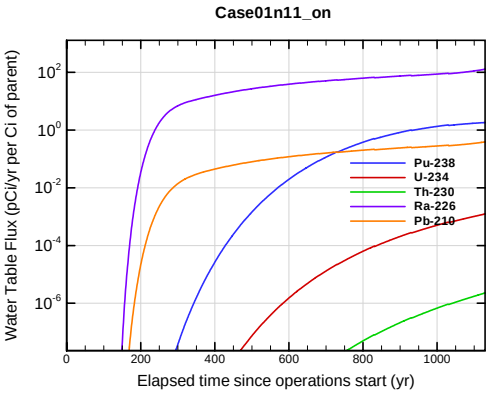

Figure A1A-434. Engineered Trench water table flux for Case01n11_on Pu-238

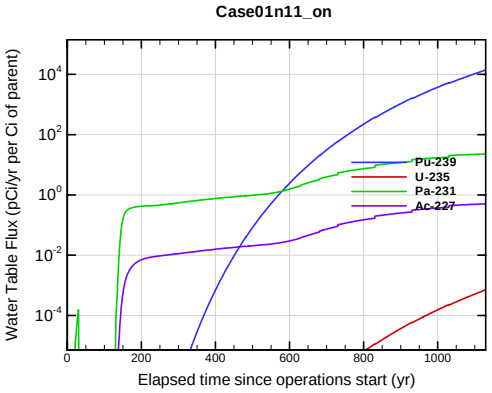

Figure A1A-435. Engineered Trench water table flux for Case01n11_on Pu-239

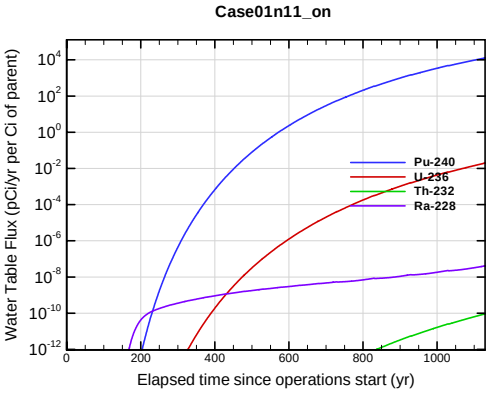

Figure A1A-436. Engineered Trench water table flux for Case01n11_on Pu-240

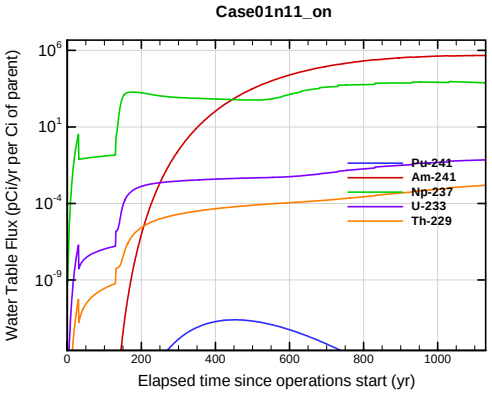

Figure A1A-437. Engineered Trench water table flux for Case01n11_on Pu-241

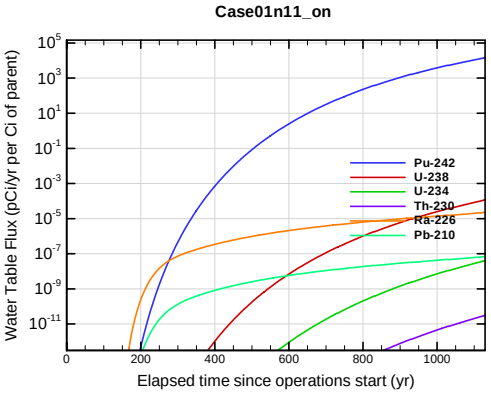

Figure A1A-438. Engineered Trench water table flux for Case01n11_on Pu-242

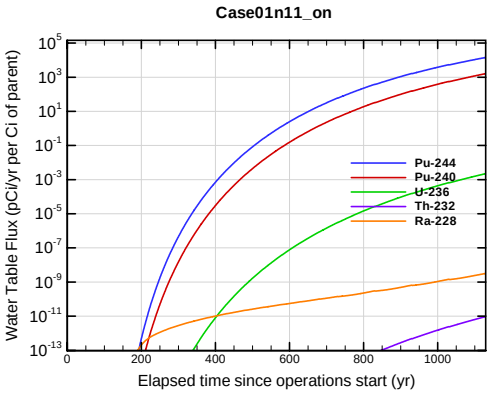

Figure A1A-439. Engineered Trench water table flux for Case01n11_on Pu-244

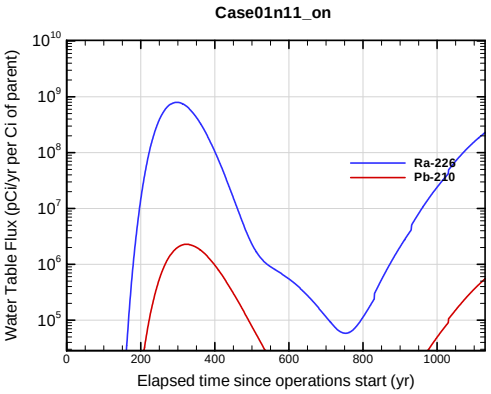

Figure A1A-440. Engineered Trench water table flux for Case01n11_on Ra-226

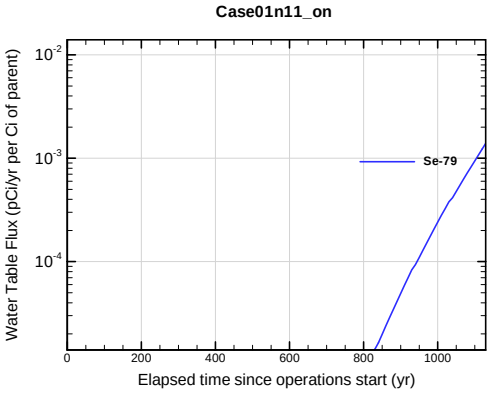

Figure A1A-441. Engineered Trench water table flux for Case01n11_on Se-79

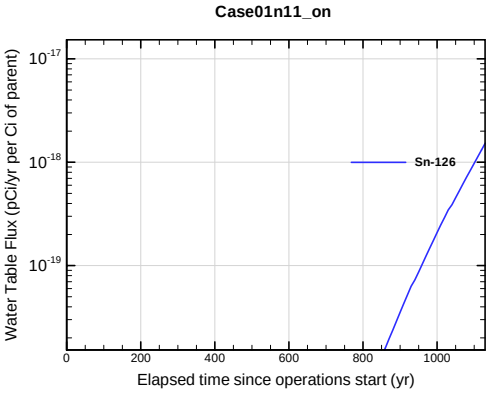

Figure A1A-442. Engineered Trench water table flux for Case01n11_on Sn-126

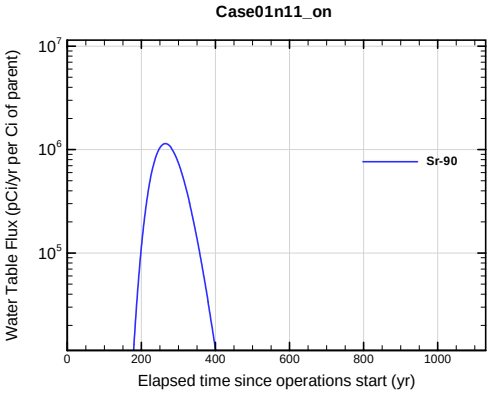

Figure A1A-443. Engineered Trench water table flux for Case01n11_on Sr-90

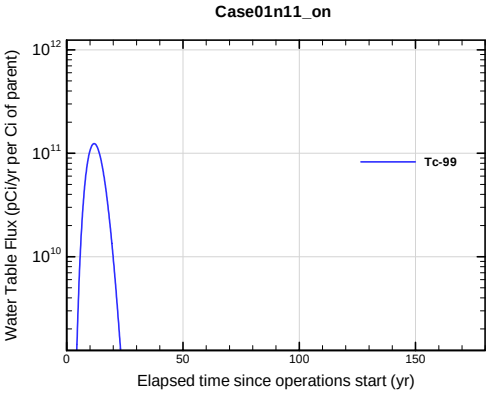

Figure A1A-444. Engineered Trench water table flux for Case01n11_on Tc-99

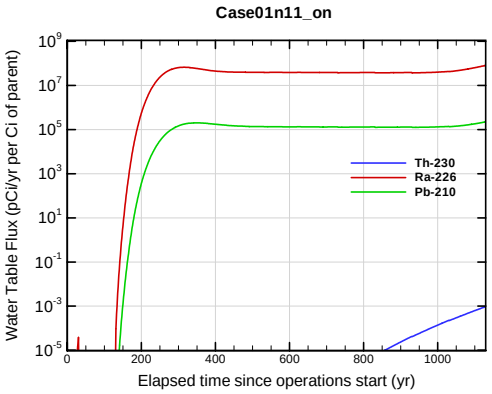

Figure A1A-445. Engineered Trench water table flux for Case01n11_on Th-230

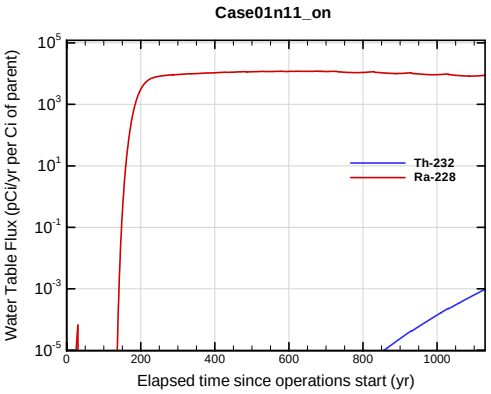

Figure A1A-446. Engineered Trench water table flux for Case01n11_on Th-232

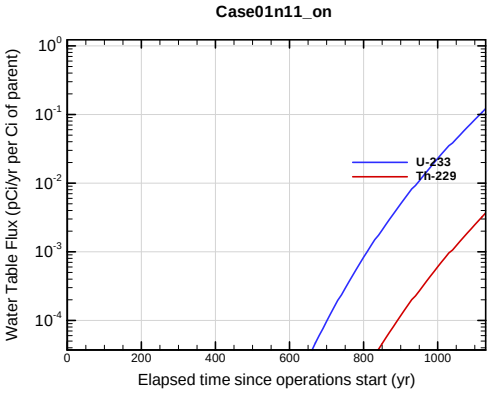

Figure A1A-447. Engineered Trench water table flux for Case01n11_on U-233

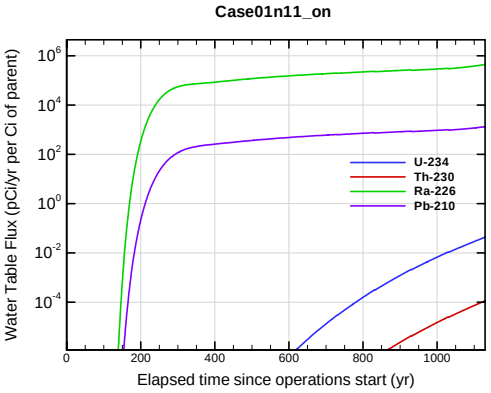

Figure A1A-448. Engineered Trench water table flux for Case01n11_on U-234

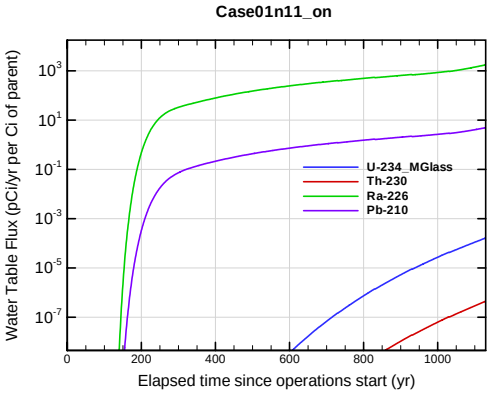

Figure A1A-449. Engineered Trench water table flux for Case01n11_on U-234_MGlass

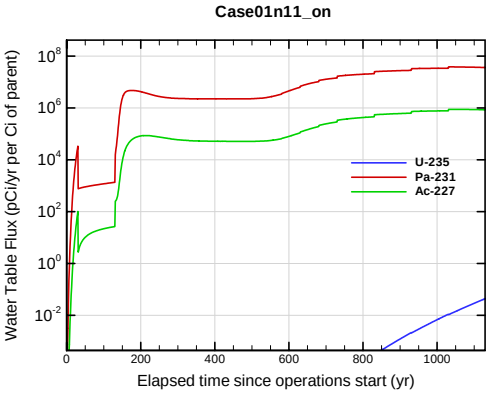

Figure A1A-450. Engineered Trench water table flux for Case01n11_on U-235

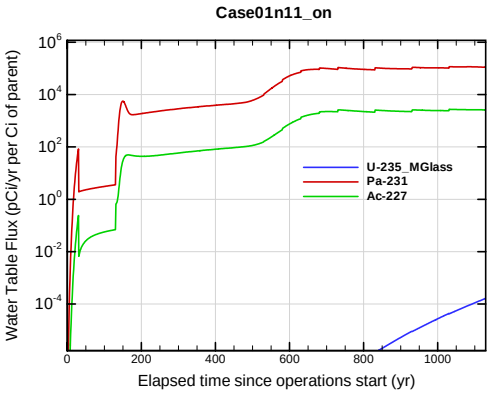

Figure A1A-451. Engineered Trench water table flux for Case01n11_on U-235_MGlass

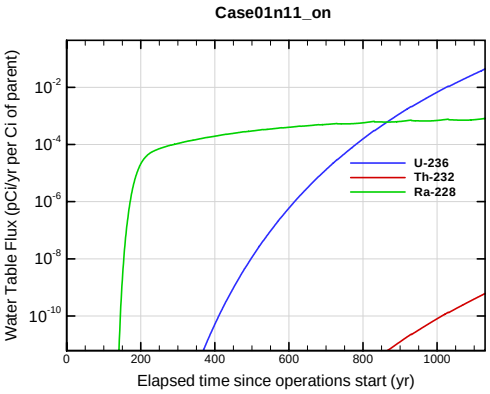

Figure A1A-452. Engineered Trench water table flux for Case01n11_on U-236

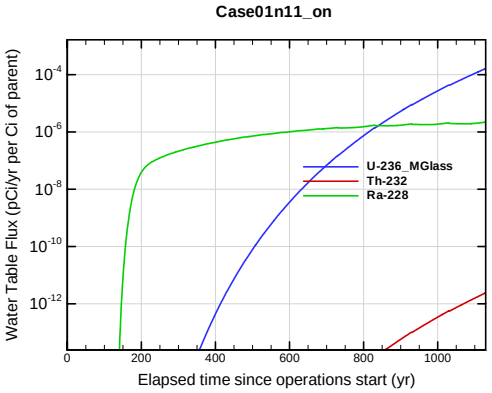

Figure A1A-453. Engineered Trench water table flux for Case01n11_on U-236_MGlass

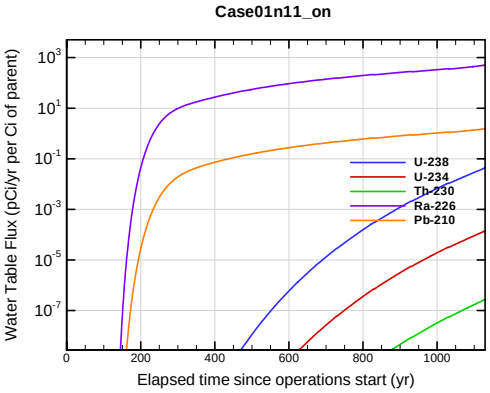

Figure A1A-454. Engineered Trench water table flux for Case01n11_on U-238

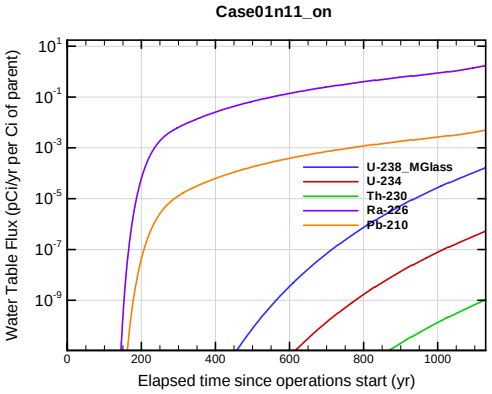

Figure A1A-455. Engineered Trench water table flux for Case01n11_on U-238_MGlass

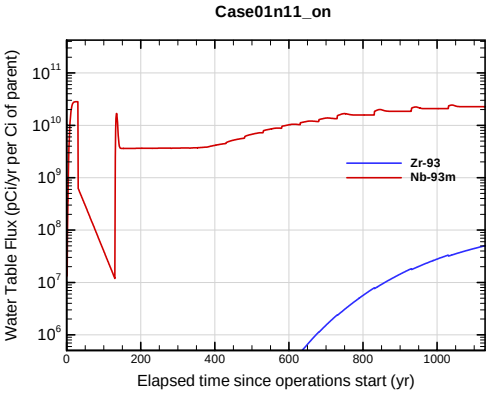

Figure A1A-456. Engineered Trench water table flux for Case01n11_on Zr-93

Vadose Zone Model
Pressure and Velocity Fields

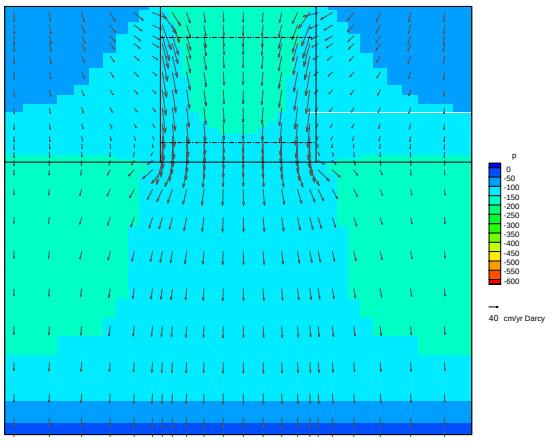

Figure A1A-457 Slit Trench during operational period

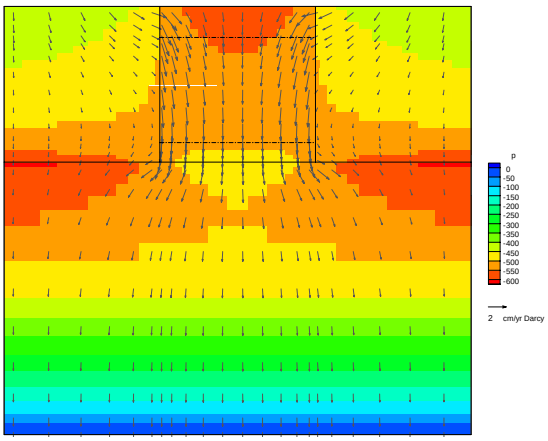

Figure A1A-458 Slit Trench during institutional control period

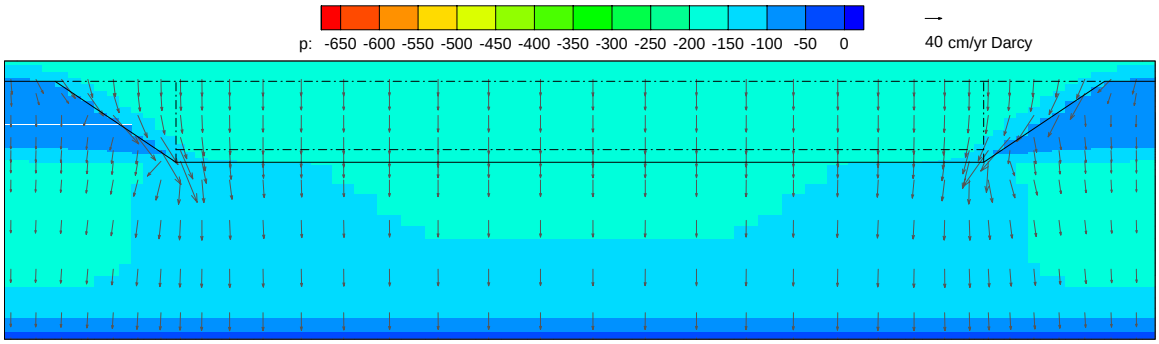

Figure A1A-459 Engineered Trench during operational period

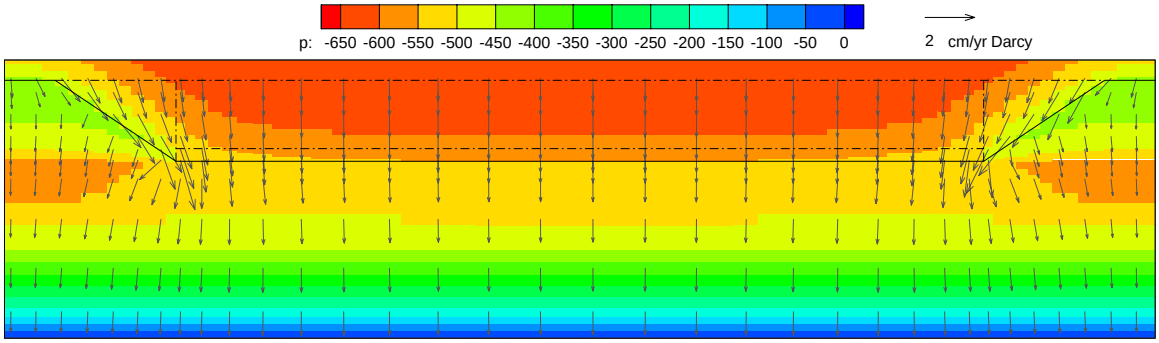

Figure A1A-460 Engineered Trench during institutional control period

APPENDIX A1B

Aquifer Model

100-m Well Concentrations

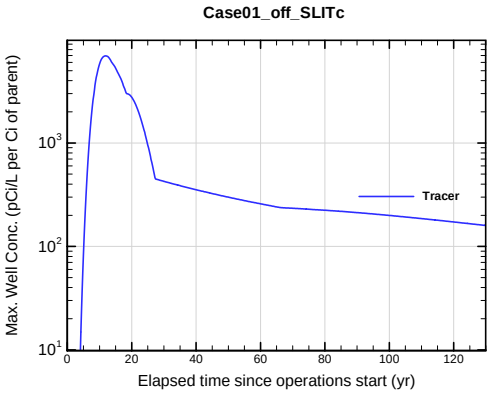

Figure A1B-1. Max. 100-m well conc. for Case01_off_SLITc Tracer

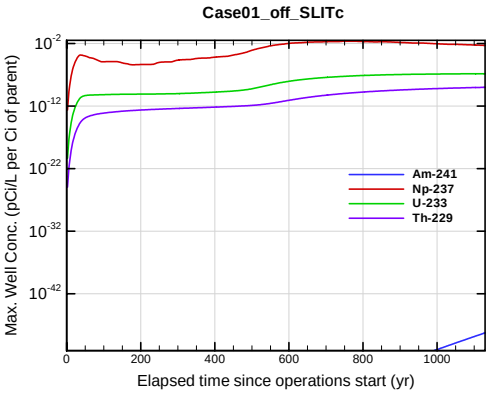

Figure A1B-2. Max. 100-m well conc. for Case01_off_SLITc Am-241

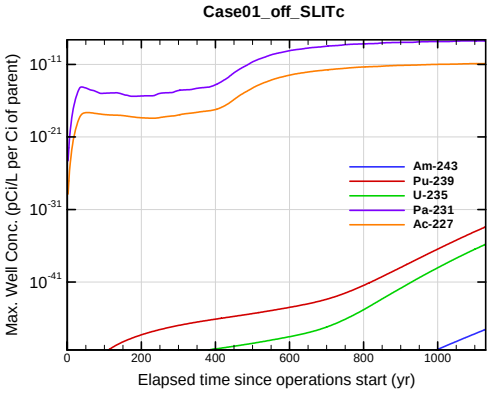

Figure A1B-3. Max. 100-m well conc. for Case01_off_SLITc Am-243

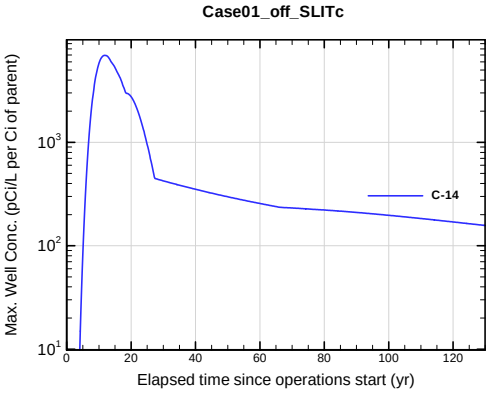

Figure A1B-4. Max. 100-m well conc. for Case01_off_SLITc C-14

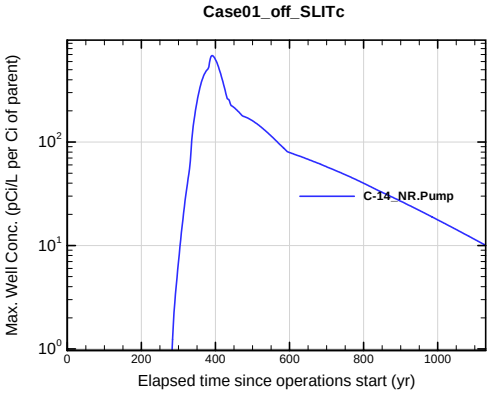

Figure A1B-5. Max. 100-m well conc. for Case01_off_SLITc C-14_NR.Pump

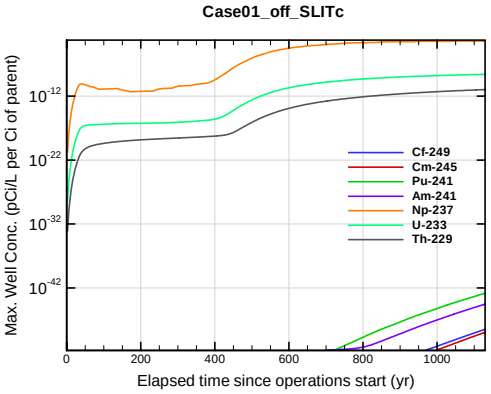

Figure A1B-6. Max. 100-m well conc. for Case01_off_SLITc Cf-249

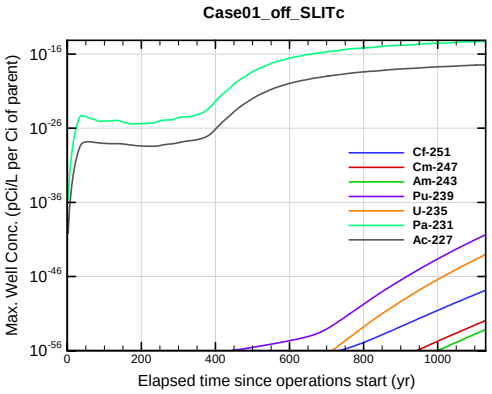

Figure A1B-7. Max. 100-m well conc. for Case01_off_SLITc Cf-251

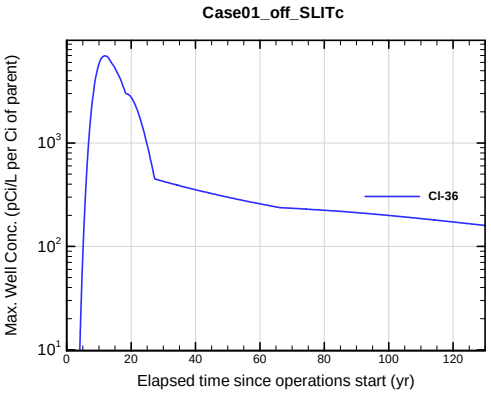

Figure A1B-8. Max. 100-m well conc. for Case01_off_SLITc Cl-36

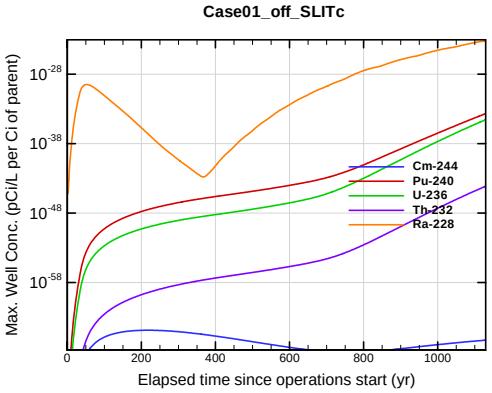

Figure A1B-9. Max. 100-m well conc. for Case01_off_SLITc Cm-244

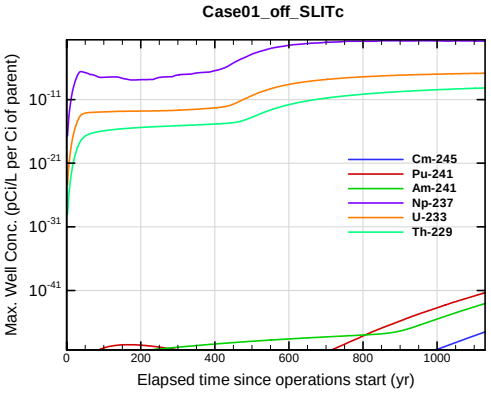

Figure A1B-10. Max. 100-m well conc. for Case01_off_SLITc Cm-245

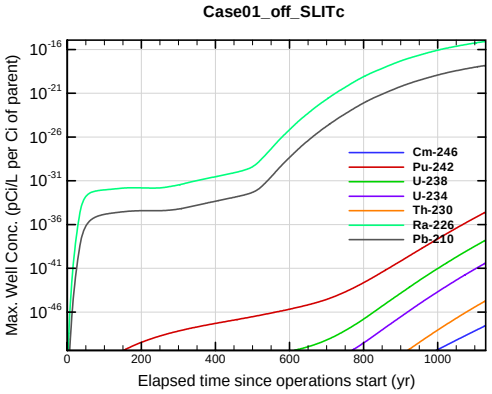

Figure A1B-11. Max. 100-m well conc. for Case01_off_SLITc Cm-246

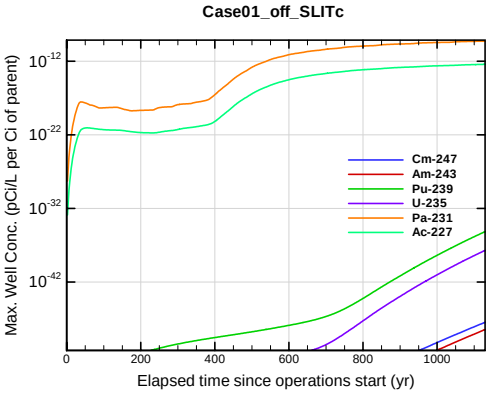

Figure A1B-12. Max. 100-m well conc. for Case01_off_SLITc Cm-247

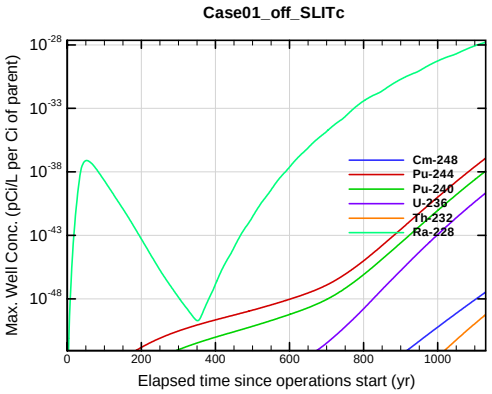

Figure A1B-13. Max. 100-m well conc. for Case01_off_SLITc Cm-248

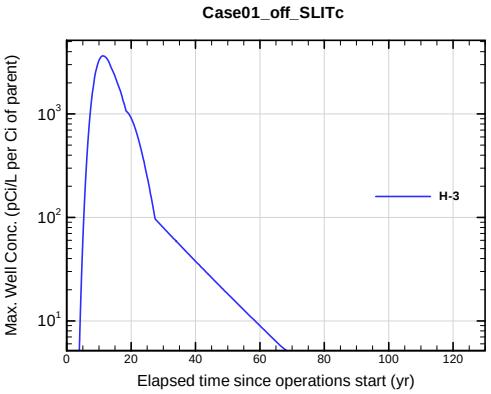

Figure A1B-14. Max. 100-m well conc. for Case01_off_SLITc H-3

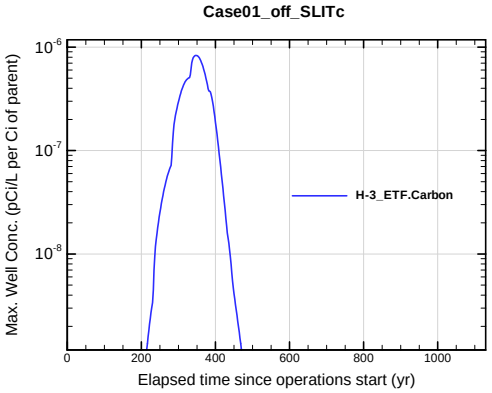

Figure A1B-15. Max. 100-m well conc. for Case01_off_SLITc H-3_ETF.Carbon

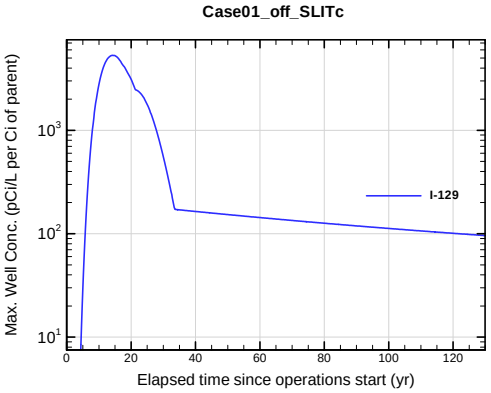

Figure A1B-16. Max. 100-m well conc. for Case01_off_SLITc I-129

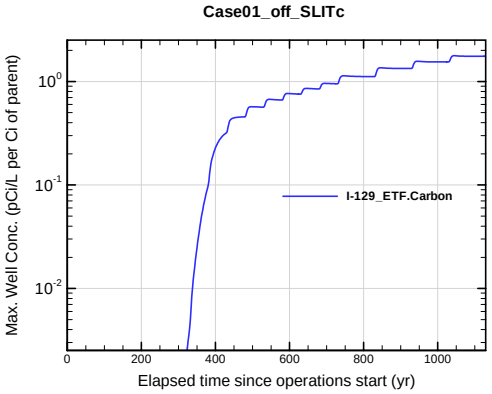

Figure A1B-17. Max. 100-m well conc. for Case01_off_SLITc I-129_ETF.Carbon

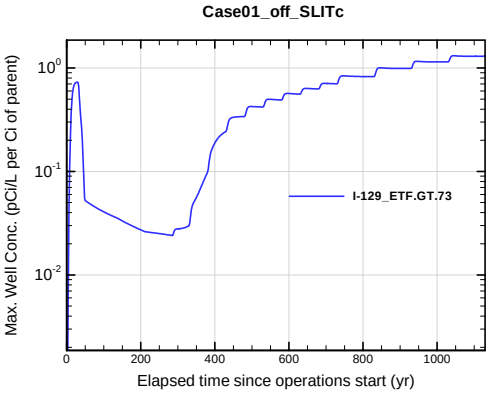

Figure A1B-18. Max. 100-m well conc. for Case01_off_SLITc I-129_ETF.GT.73

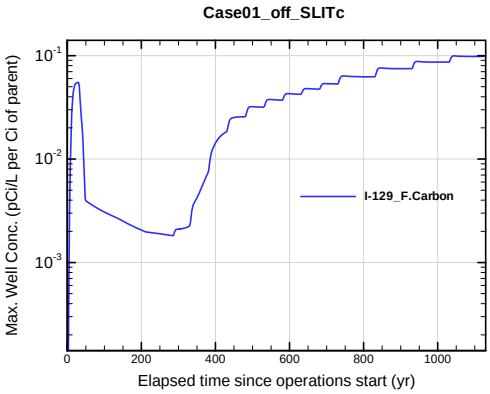

Figure A1B-19. Max. 100-m well conc. for Case01_off_SLITc I-129_F.Carbon

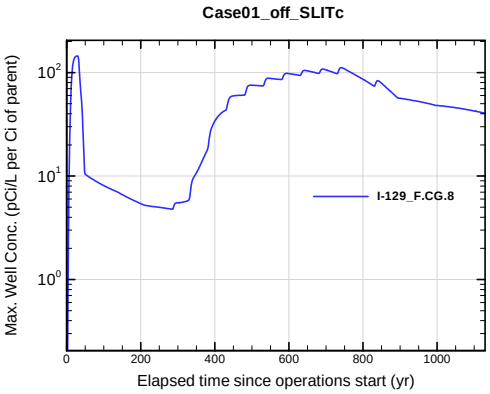

Figure A1B-20. Max. 100-m well conc. for Case01_off_SLITc I-129_F.CG.8

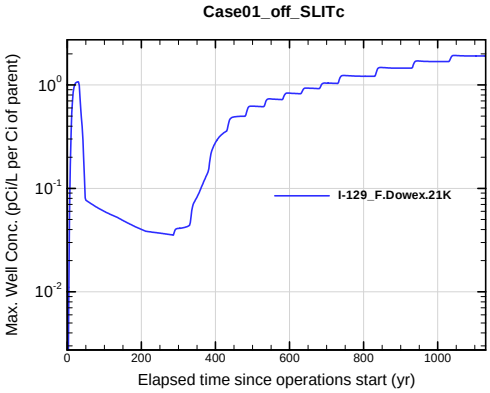

Figure A1B-21. Max. 100-m well conc. for Case01_off_SLITc I-129_F.Dowex.21K

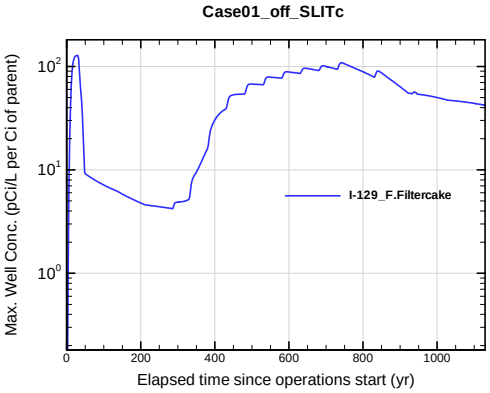

Figure A1B-22. Max. 100-m well conc. for Case01_off_SLITc I-129_F.Filtercake

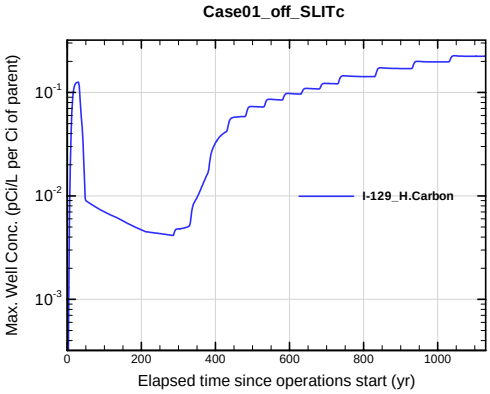

Figure A1B-23. Max. 100-m well conc. for Case01_off_SLITc I-129_H.Carbon

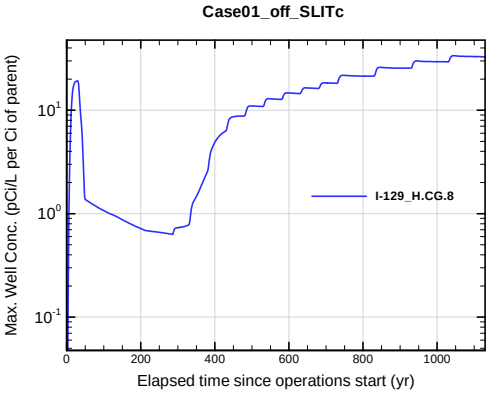

Figure A1B-24. Max. 100-m well conc. for Case01_off_SLITc I-129_H.CG.8

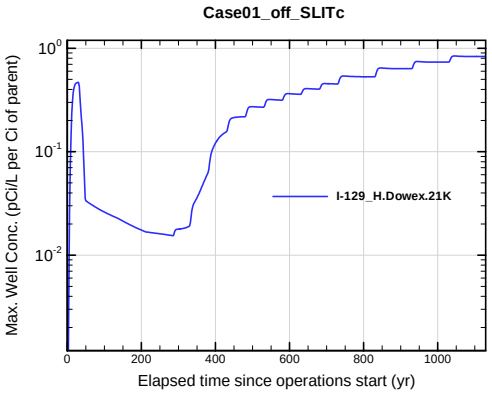

Figure A1B-25. Max. 100-m well conc. for Case01_off_SLITc I-129_H.Dowex.21K

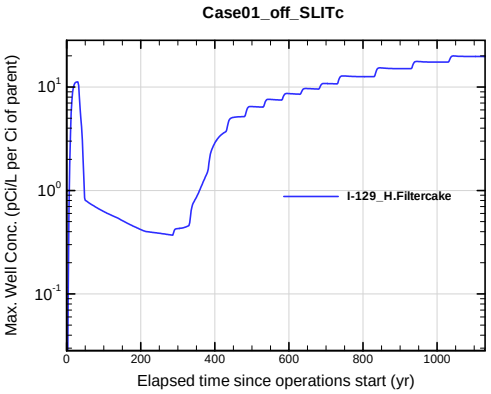

Figure A1B-26. Max. 100-m well conc. for Case01_off_SLITc I-129_H.Filtercake

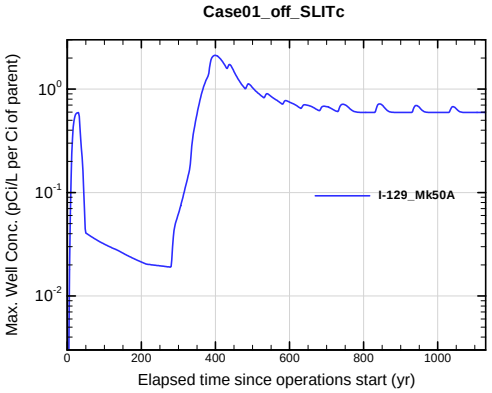

Figure A1B-27. Max. 100-m well conc. for Case01_off_SLITc I-129_Mk50A

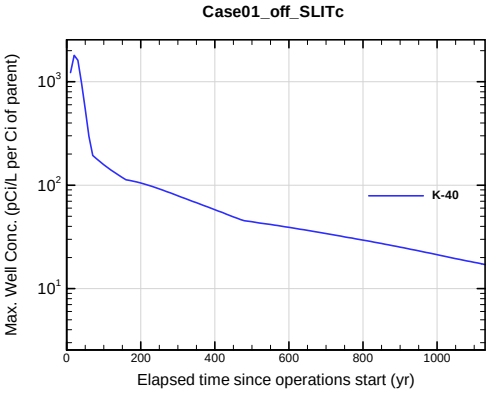

Figure A1B-28. Max. 100-m well conc. for Case01_off_SLITc K-40

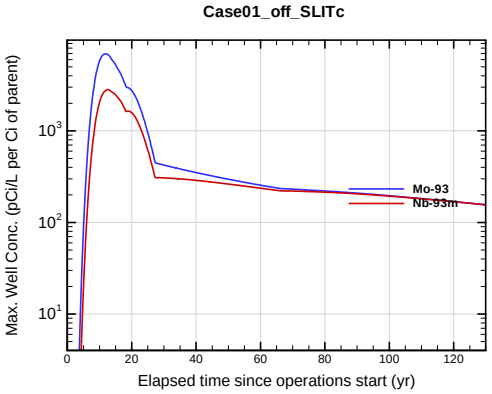

Figure A1B-29. Max. 100-m well conc. for Case01_off_SLITc Mo-93

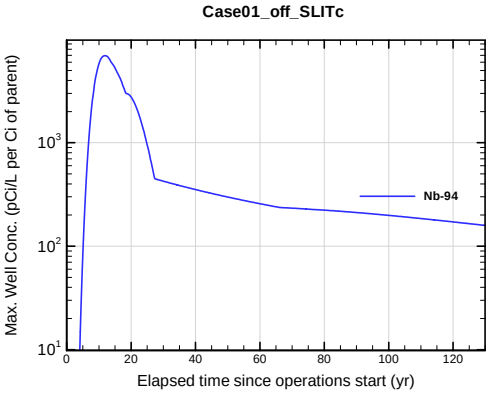

Figure A1B-30. Max. 100-m well conc. for Case01_off_SLITc Nb-94

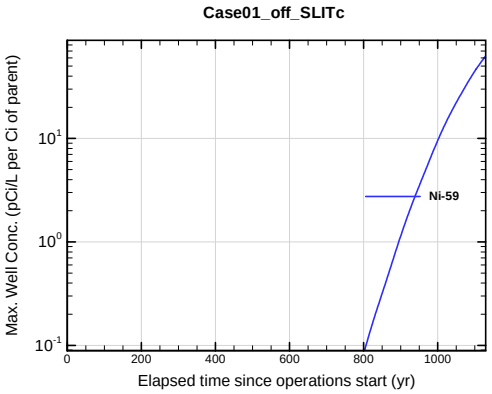

Figure A1B-31. Max. 100-m well conc. for Case01_off_SLITc Ni-59

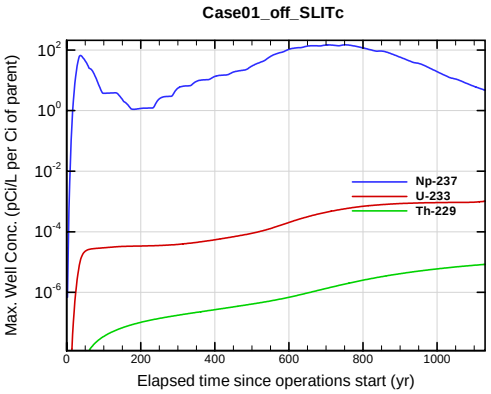

Figure A1B-32. Max. 100-m well conc. for Case01_off_SLITc Np-237

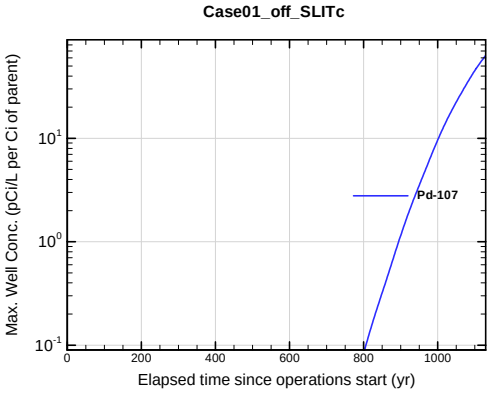

Figure A1B-33. Max. 100-m well conc. for Case01_off_SLITc Pd-107

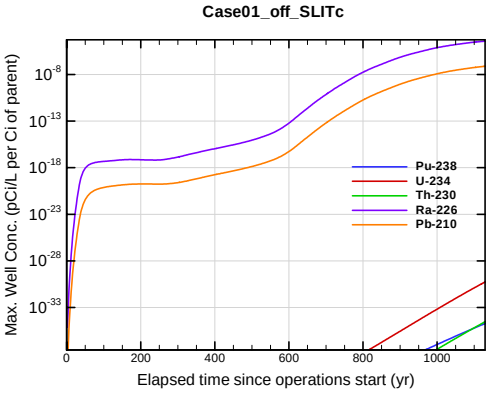

Figure A1B-34. Max. 100-m well conc. for Case01_off_SLITc Pu-238

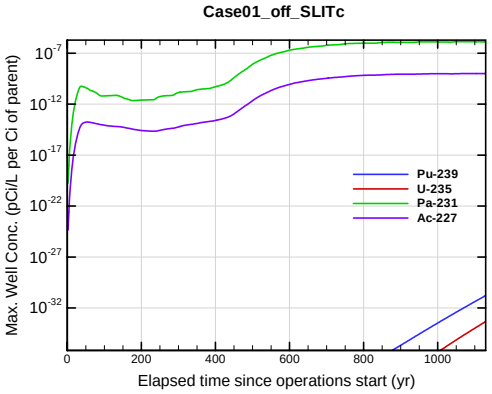

Figure A1B-35. Max. 100-m well conc. for Case01_off_SLITc Pu-239

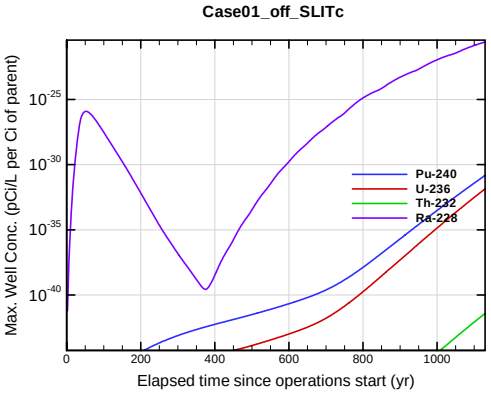

Figure A1B-36. Max. 100-m well conc. for Case01_off_SLITc Pu-240

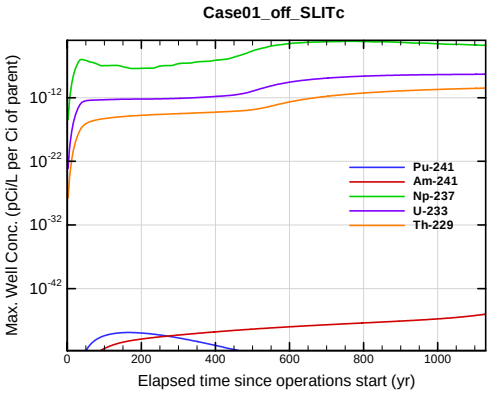

Figure A1B-37. Max. 100-m well conc. for Case01_off_SLITc Pu-241

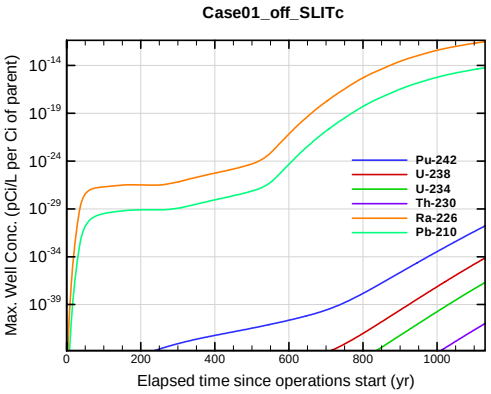

Figure A1B-38. Max. 100-m well conc. for Case01_off_SLITc Pu-242

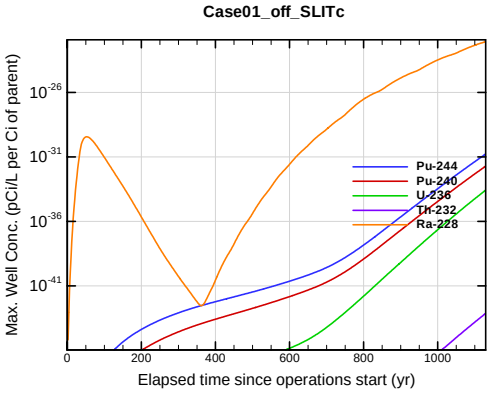

Figure A1B-39. Max. 100-m well conc. for Case01_off_SLITc Pu-244

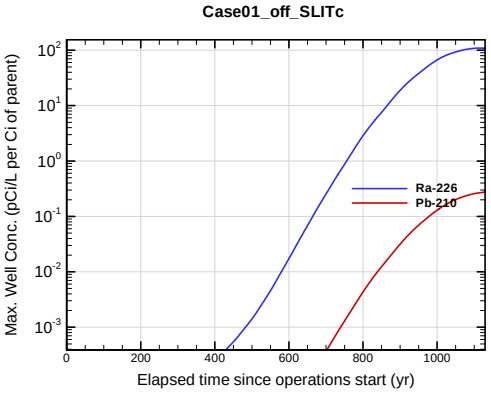

Figure A1B-40. Max. 100-m well conc. for Case01_off_SLITc Ra-226

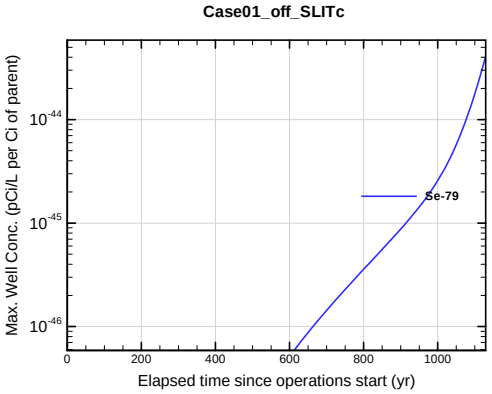

Figure A1B-41. Max. 100-m well conc. for Case01_off_SLITc Se-79

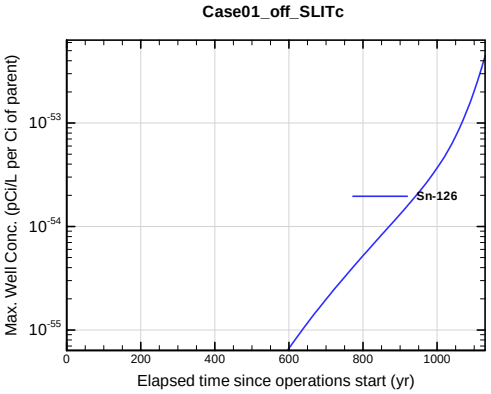

Figure A1B-42. Max. 100-m well conc. for Case01_off_SLITc Sn-126

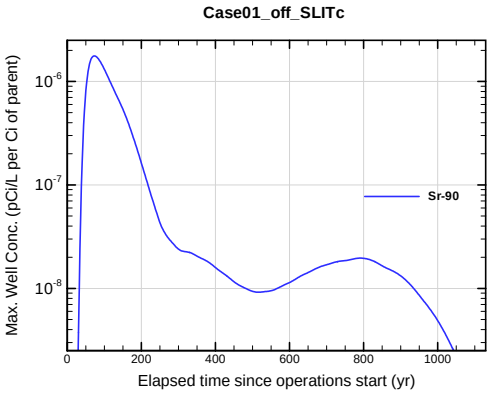

Figure A1B-43. Max. 100-m well conc. for Case01_off_SLITc Sr-90

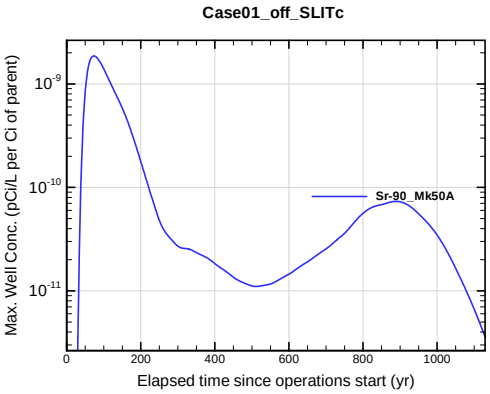

Figure A1B-44. Max. 100-m well conc. for Case01_off_SLITc Sr-90_Mk50A

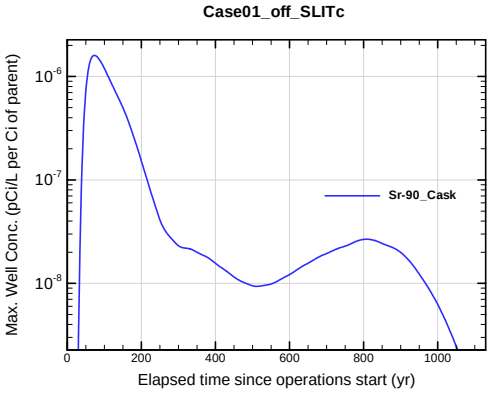

Figure A1B-45. Max. 100-m well conc. for Case01_off_SLITc Sr-90_Cask

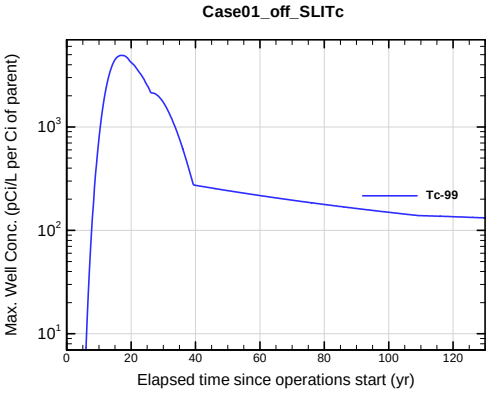

Figure A1B-46. Max. 100-m well conc. for Case01_off_SLITc Tc-99

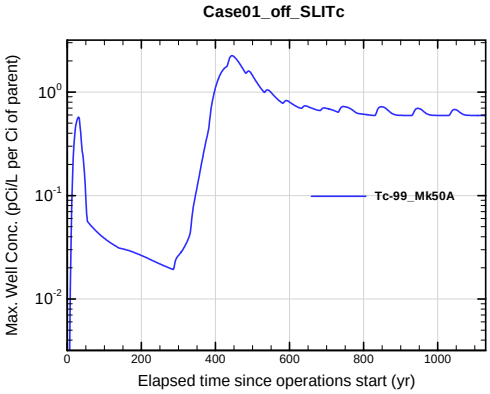

Figure A1B-47. Max. 100-m well conc. for Case01_off_SLITc Tc-99_Mk50A

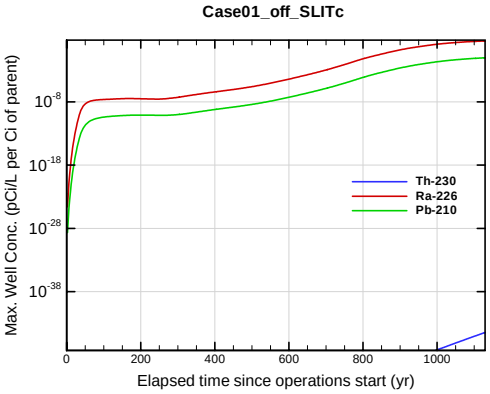

Figure A1B-48. Max. 100-m well conc. for Case01_off_SLITc Th-230

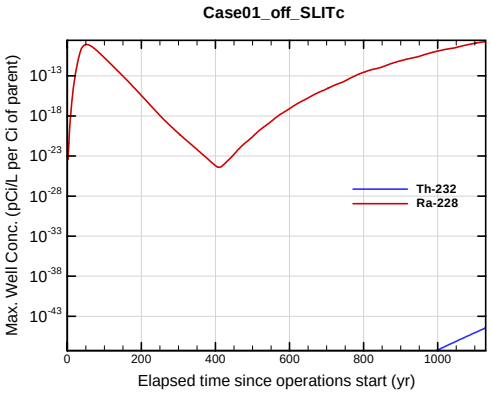

Figure A1B-49. Max. 100-m well conc. for Case01_off_SLITc Th-232

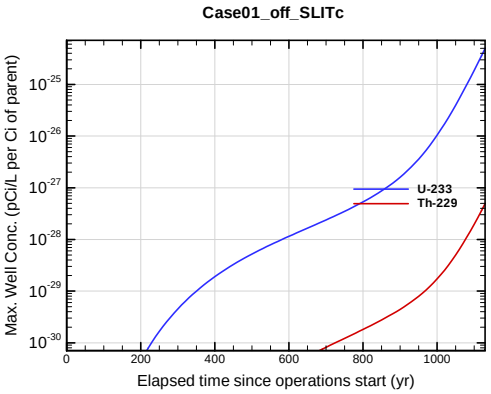

Figure A1B-50. Max. 100-m well conc. for Case01_off_SLITc U-233

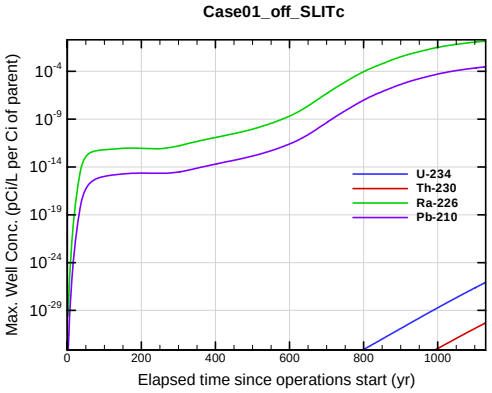

Figure A1B-51. Max. 100-m well conc. for Case01_off_SLITc U-234

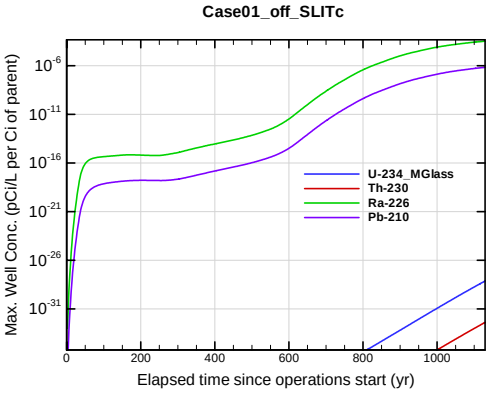

Figure A1B-52. Max. 100-m well conc. for Case01_off_SLITc U-234_MGlass

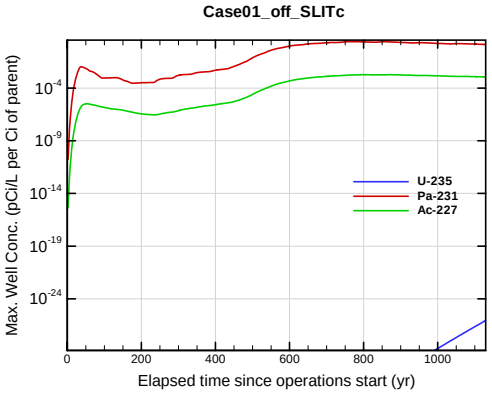

Figure A1B-53. Max. 100-m well conc. for Case01_off_SLITc U-235

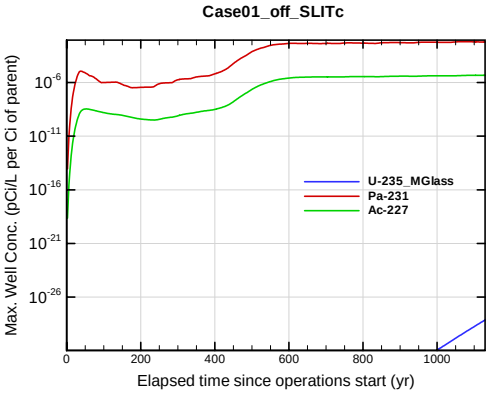

Figure A1B-54. Max. 100-m well conc. for Case01_off_SLITc U-235_MGlass

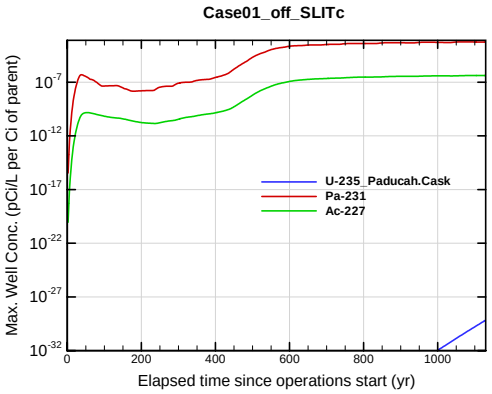

Figure A1B-55. Max. 100-m well conc. for Case01_off_SLITc U-235_Paducah.Cask

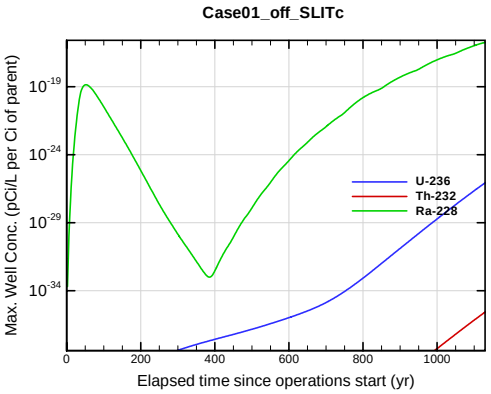

Figure A1B-56. Max. 100-m well conc. for Case01_off_SLITc U-236

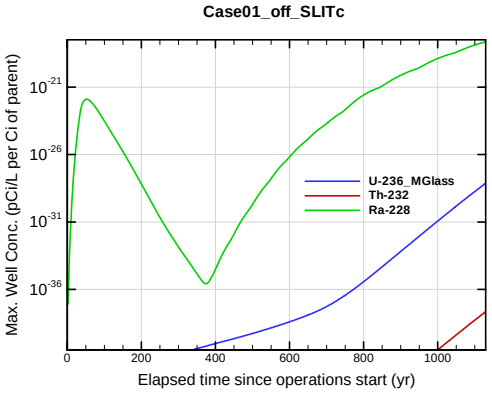

Figure A1B-57. Max. 100-m well conc. for Case01_off_SLITc U-236_MGlass

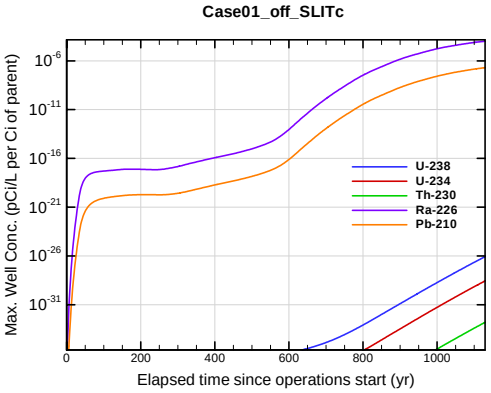

Figure A1B-58. Max. 100-m well conc. for Case01_off_SLITc U-238

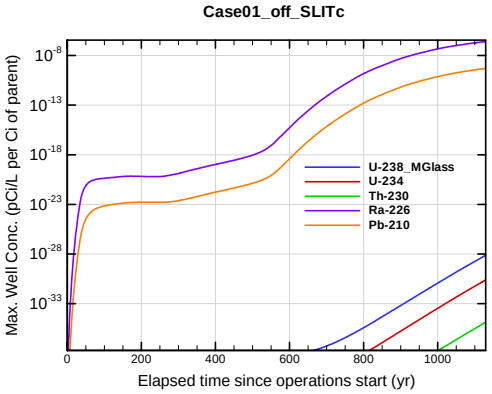

Figure A1B-59. Max. 100-m well conc. for Case01_off_SLITc U-238_MGlass

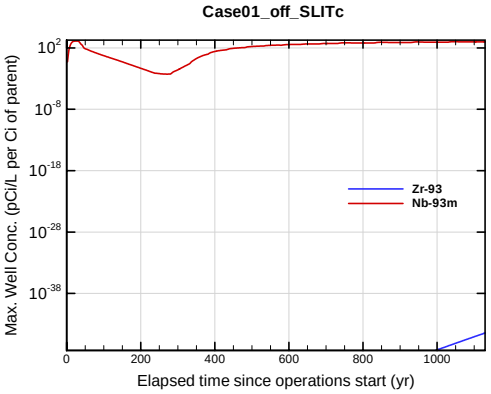

Figure A1B-60. Max. 100-m well conc. for Case01_off_SLITc Zr-93

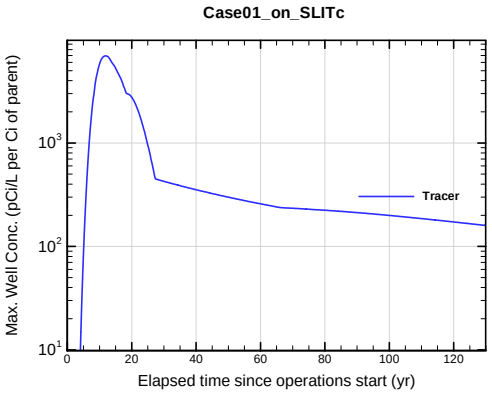

Figure A1B-61. Max. 100-m well conc. for Case01_on_SLITc Tracer

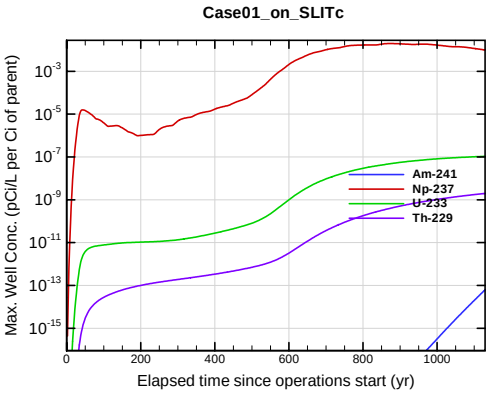

Figure A1B-62. Max. 100-m well conc. for Case01_on_SLITc Am-241

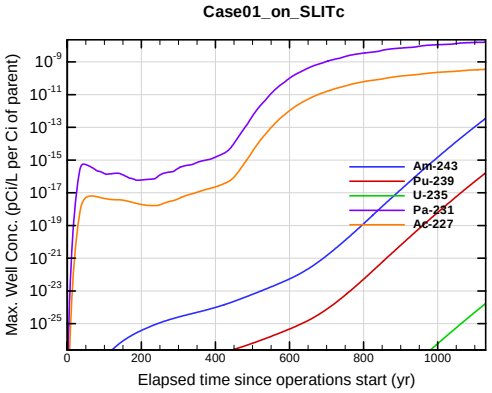

Figure A1B-63. Max. 100-m well conc. for Case01_on_SLITc Am-243

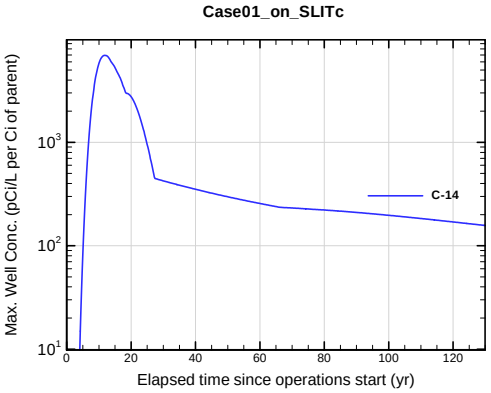

Figure A1B-64. Max. 100-m well conc. for Case01_on_SLITc C-14

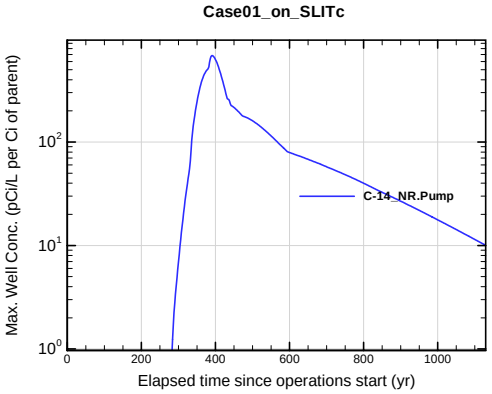

Figure A1B-65. Max. 100-m well conc. for Case01_on_SLITc C-14_NR.Pump

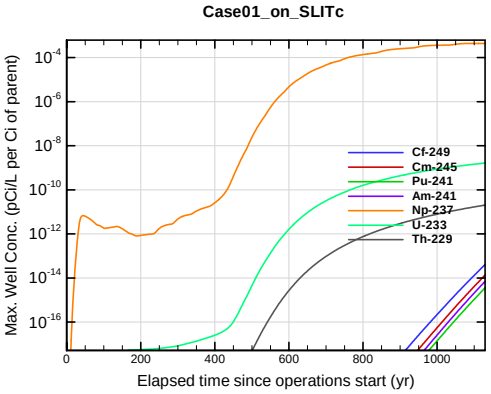

Figure A1B-66. Max. 100-m well conc. for Case01_on_SLITc Cf-249

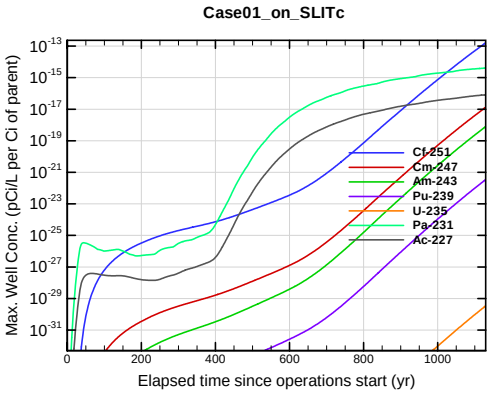

Figure A1B-67. Max. 100-m well conc. for Case01_on_SLITc Cf-251

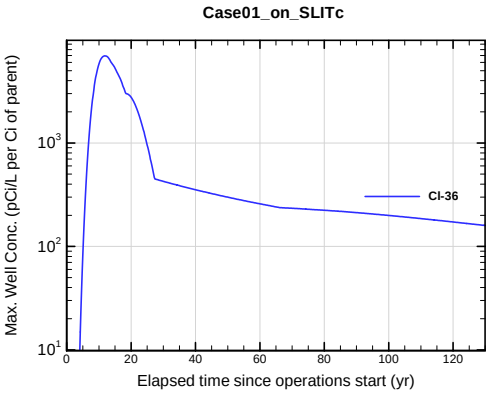

Figure A1B-68. Max. 100-m well conc. for Case01_on_SLITc Cl-36

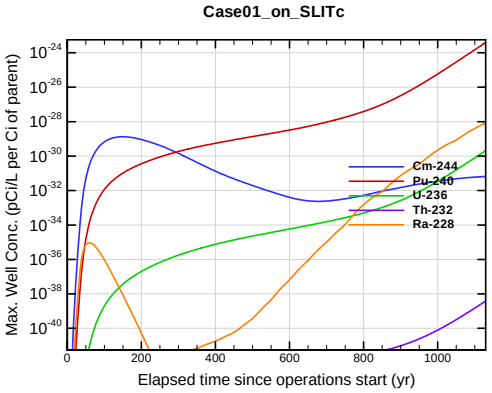

Figure A1B-69. Max. 100-m well conc. for Case01_on_SLITc Cm-244

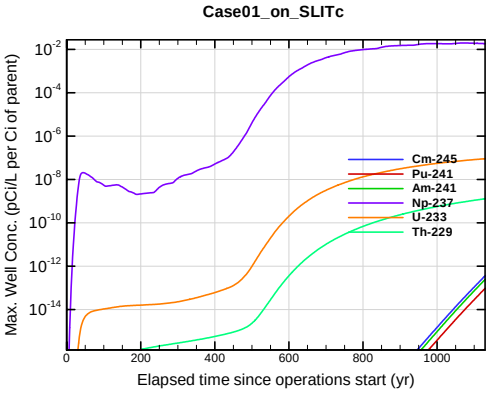

Figure A1B-70. Max. 100-m well conc. for Case01_on_SLITc Cm-245

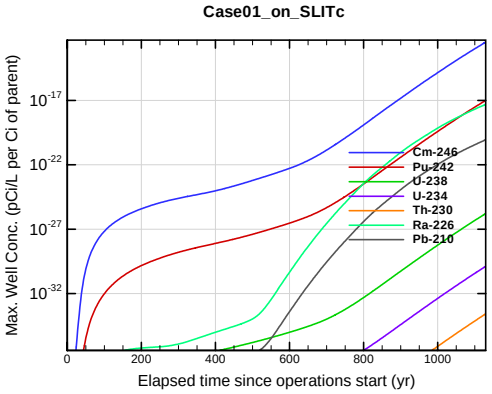

Figure A1B-71. Max. 100-m well conc. for Case01_on_SLITc Cm-246

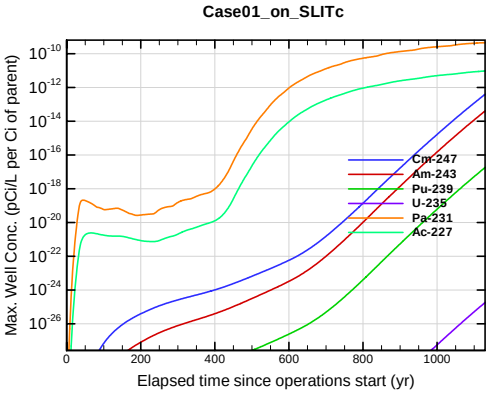

Figure A1B-72. Max. 100-m well conc. for Case01_on_SLITc Cm-247

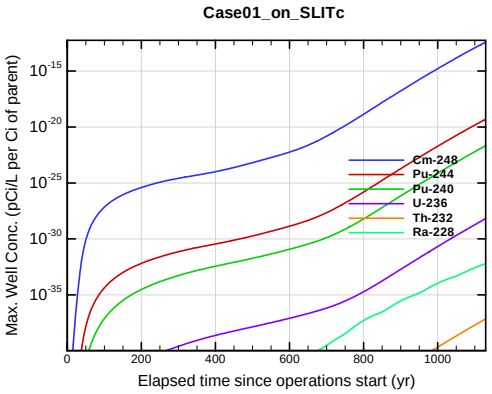

Figure A1B-73. Max. 100-m well conc. for Case01_on_SLITc Cm-248

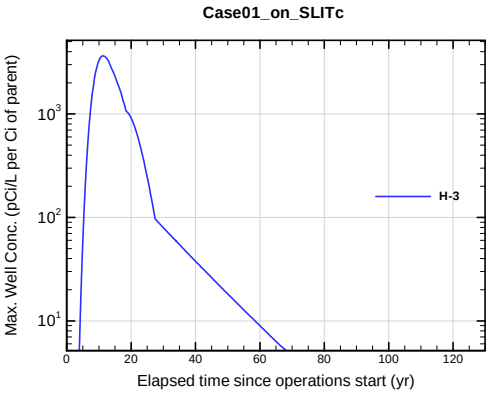

Figure A1B-74. Max. 100-m well conc. for Case01_on_SLITc H-3

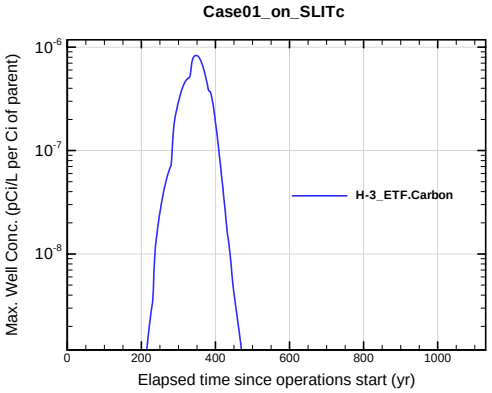

Figure A1B-75. Max. 100-m well conc. for Case01_on_SLITc H-3_ETF.Carbon

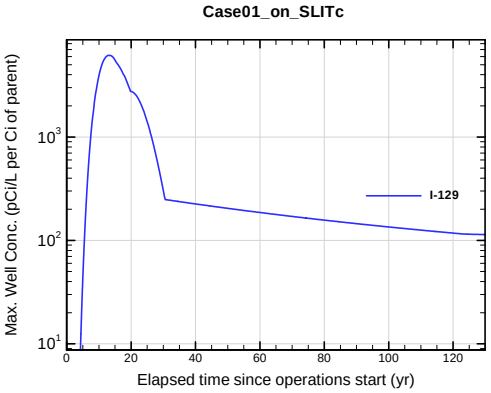

Figure A1B-76. Max. 100-m well conc. for Case01_on_SLITc I-129

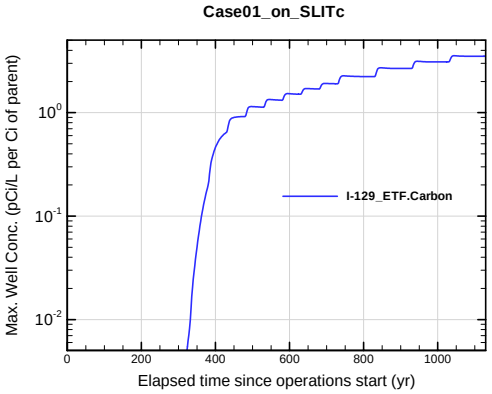

Figure A1B-77. Max. 100-m well conc. for Case01_on_SLITc I-129_ETF.Carbon

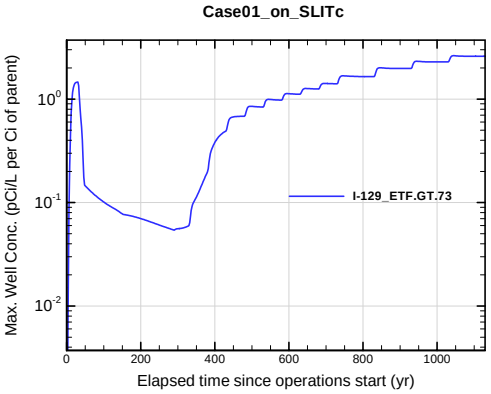

Figure A1B-78. Max. 100-m well conc. for Case01_on_SLITc I-129_ETF.GT.73

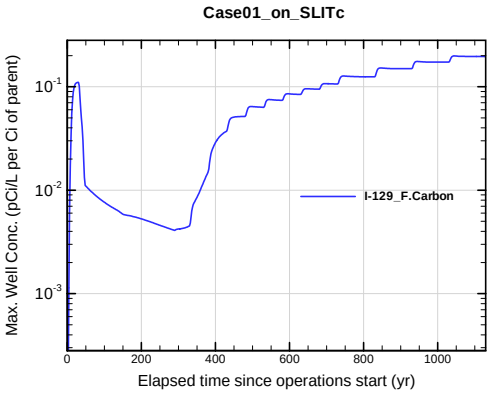

Figure A1B-79. Max. 100-m well conc. for Case01_on_SLITc I-129_F.Carbon

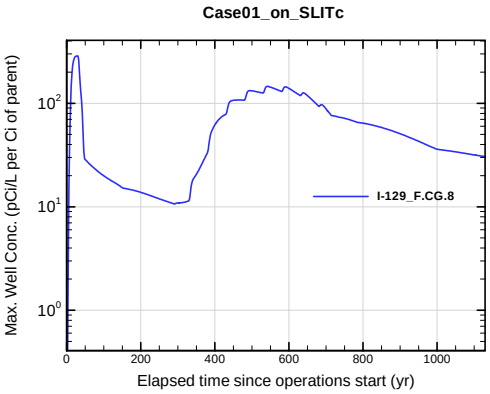

Figure A1B-80. Max. 100-m well conc. for Case01_on_SLITc I-129_F.CG.8

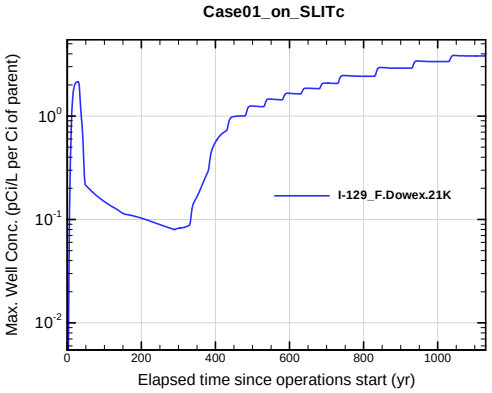

Figure A1B-81. Max. 100-m well conc. for Case01_on_SLITc I-129_F.Dowex.21K

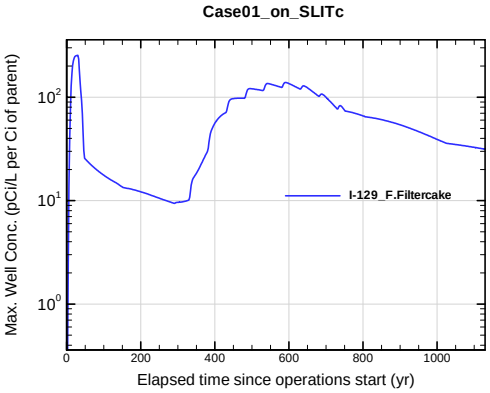

Figure A1B-82. Max. 100-m well conc. for Case01_on_SLITc I-129_F.Filtercake

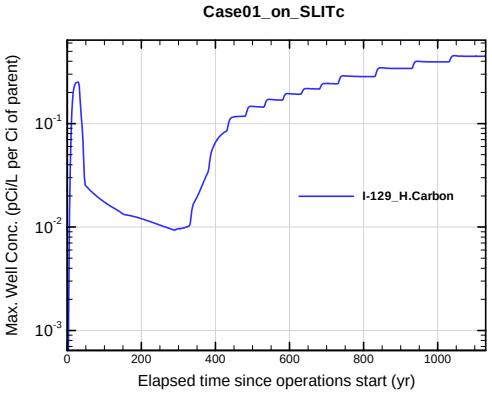

Figure A1B-83. Max. 100-m well conc. for Case01_on_SLITc I-129_H.Carbon

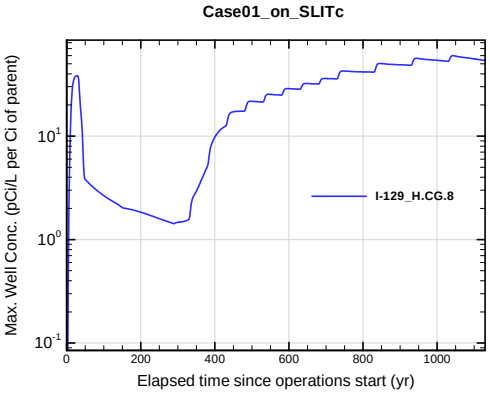

Figure A1B-84. Max. 100-m well conc. for Case01_on_SLITc I-129_H.CG.8

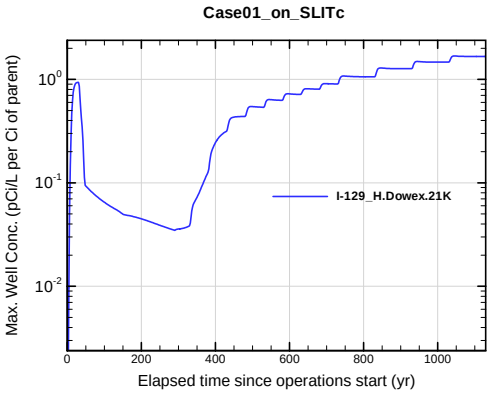

Figure A1B-85. Max. 100-m well conc. for Case01_on_SLITc I-129_H.Dowex.21K

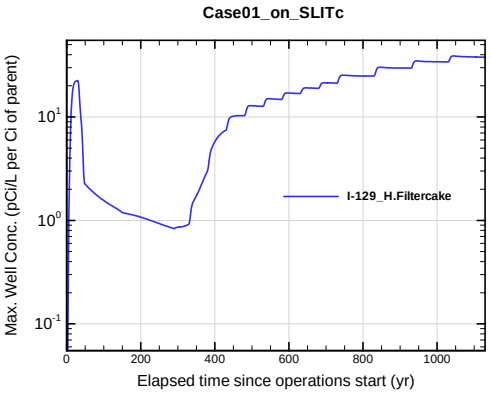

Figure A1B-86. Max. 100-m well conc. for Case01_on_SLITc I-129_H.Filtercake

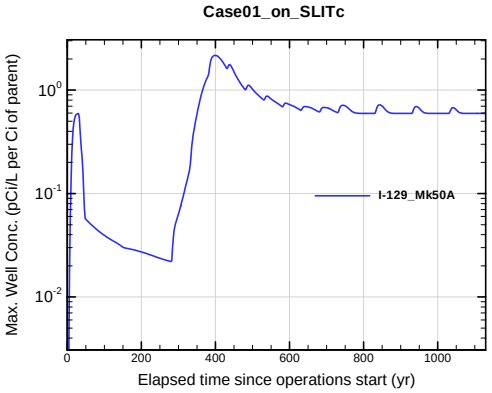

Figure A1B-87. Max. 100-m well conc. for Case01_on_SLITc I-129_Mk50A

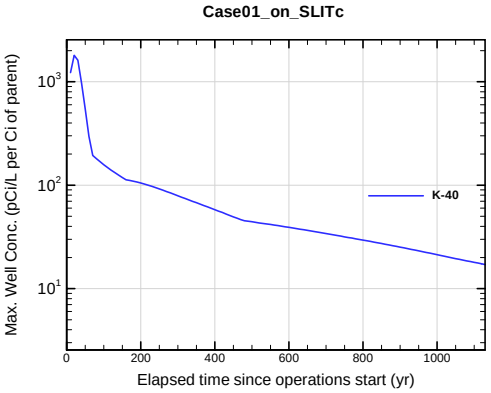

Figure A1B-88. Max. 100-m well conc. for Case01_on_SLITc K-40

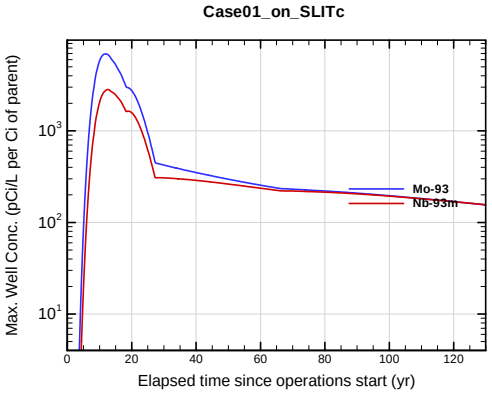

Figure A1B-89. Max. 100-m well conc. for Case01_on_SLITc Mo-93

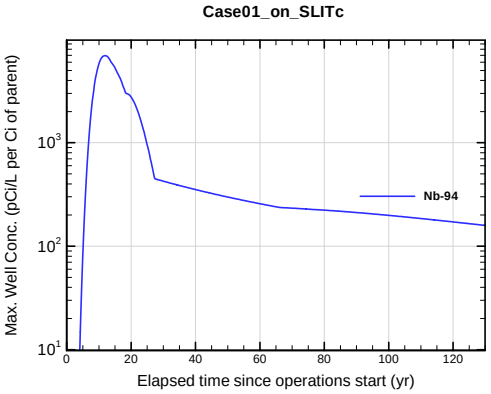

Figure A1B-90. Max. 100-m well conc. for Case01_on_SLITc Nb-94

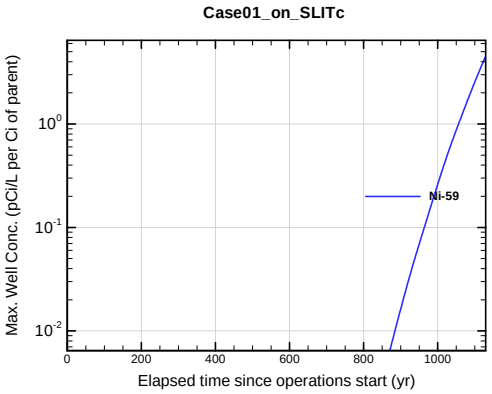

Figure A1B-91. Max. 100-m well conc. for Case01_on_SLITc Ni-59

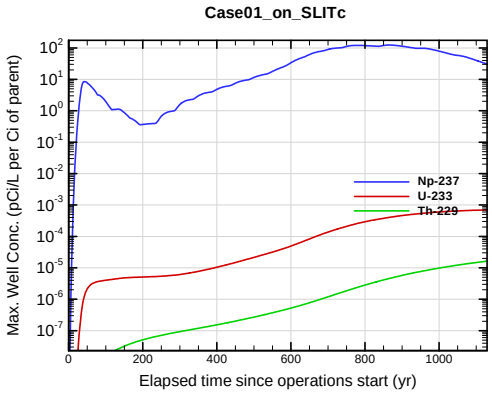

Figure A1B-92. Max. 100-m well conc. for Case01_on_SLITc Np-237

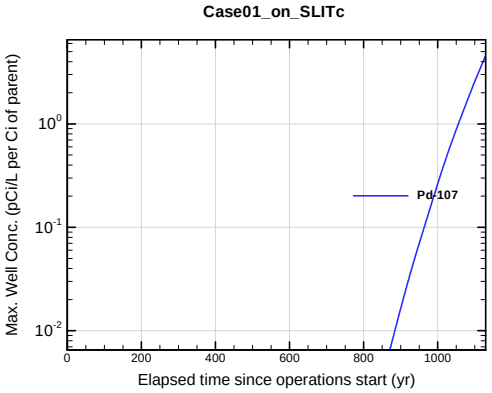

Figure A1B-93. Max. 100-m well conc. for Case01_on_SLITc Pd-107

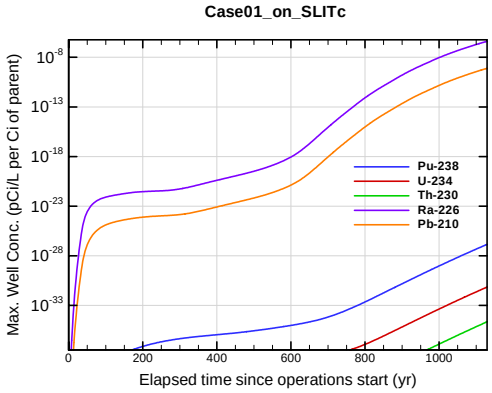

Figure A1B-94. Max. 100-m well conc. for Case01_on_SLITc Pu-238

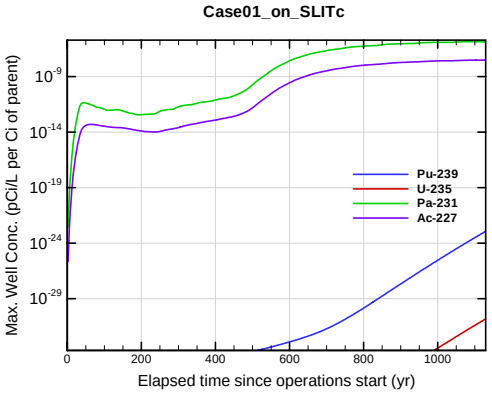

Figure A1B-95. Max. 100-m well conc. for Case01_on_SLITc Pu-239

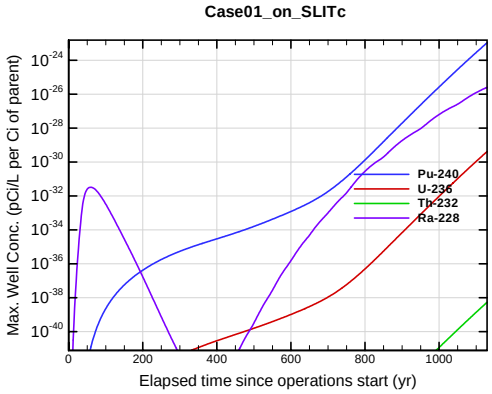

Figure A1B-96. Max. 100-m well conc. for Case01_on_SLITc Pu-240

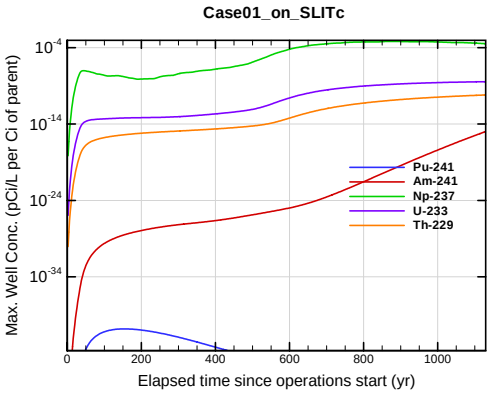

Figure A1B-97. Max. 100-m well conc. for Case01_on_SLITc Pu-241

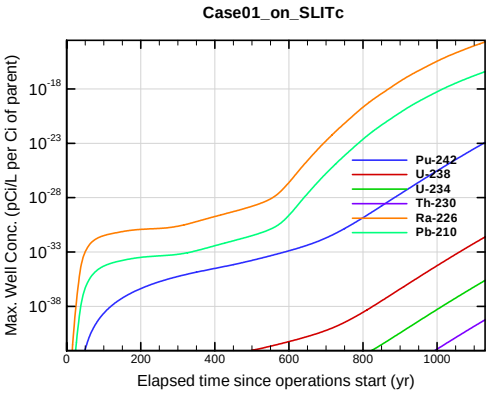

Figure A1B-98. Max. 100-m well conc. for Case01_on_SLITc Pu-242

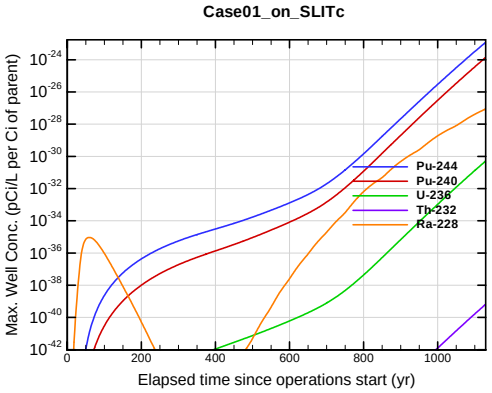

Figure A1B-99. Max. 100-m well conc. for Case01_on_SLITc Pu-244

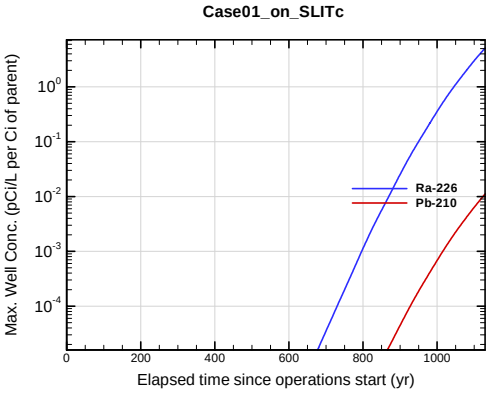

Figure A1B-100. Max. 100-m well conc. for Case01_on_SLITc Ra-226

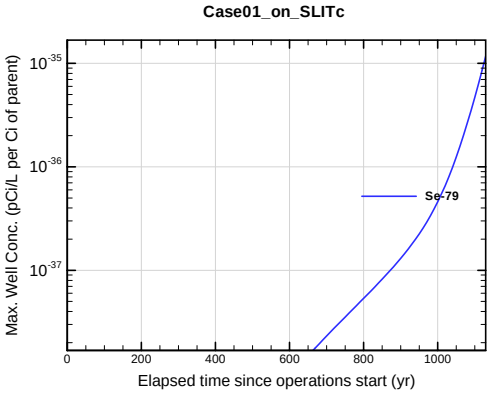

Figure A1B-101. Max. 100-m well conc. for Case01_on_SLITc Se-79

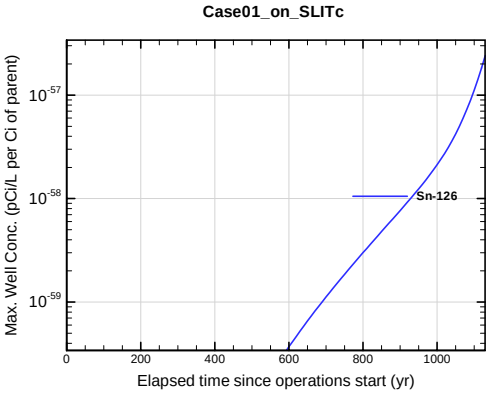

Figure A1B-102. Max. 100-m well conc. for Case01_on_SLITc Sn-126

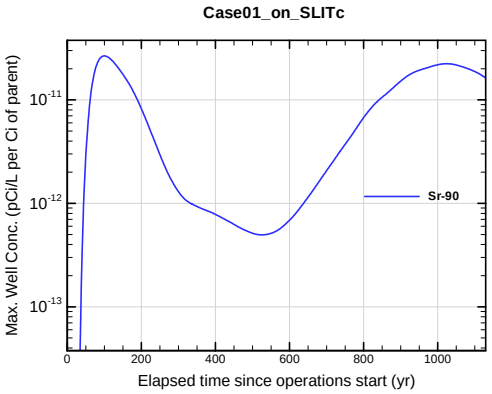

Figure A1B-103. Max. 100-m well conc. for Case01_on_SLITc Sr-90

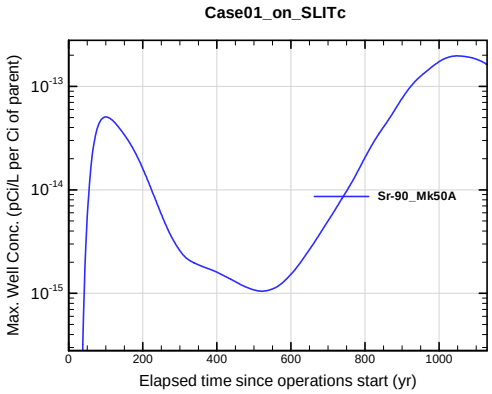

Figure A1B-104. Max. 100-m well conc. for Case01_on_SLITc Sr-90_Mk50A

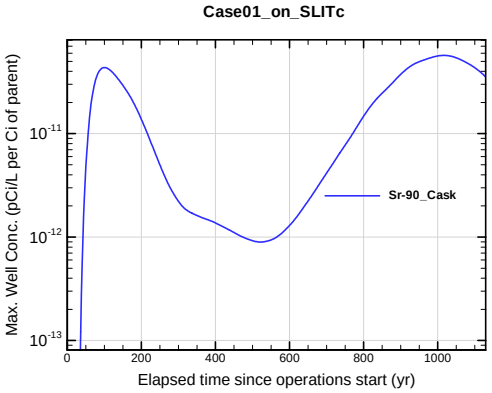

Figure A1B-105. Max. 100-m well conc. for Case01_on_SLITc Sr-90_Cask

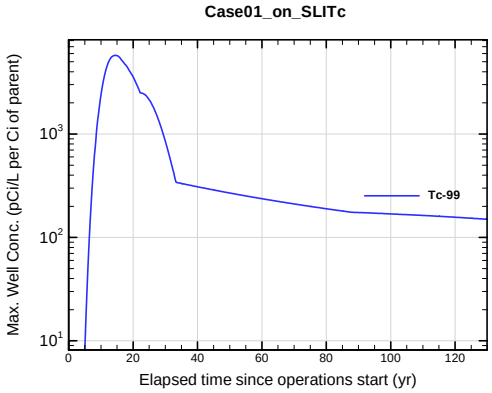

Figure A1B-106. Max. 100-m well conc. for Case01_on_SLITc Tc-99

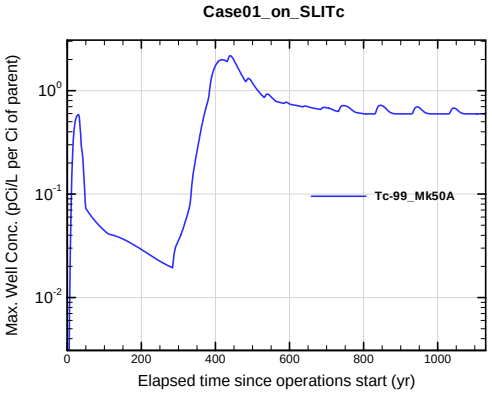

Figure A1B-107. Max. 100-m well conc. for Case01_on_SLITc Tc-99_Mk50A

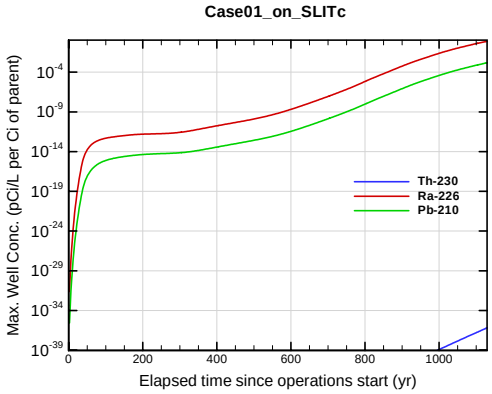

Figure A1B-108. Max. 100-m well conc. for Case01_on_SLITc Th-230

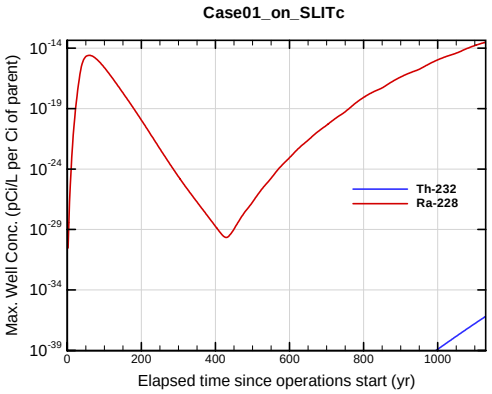

Figure A1B-109. Max. 100-m well conc. for Case01_on_SLITc Th-232

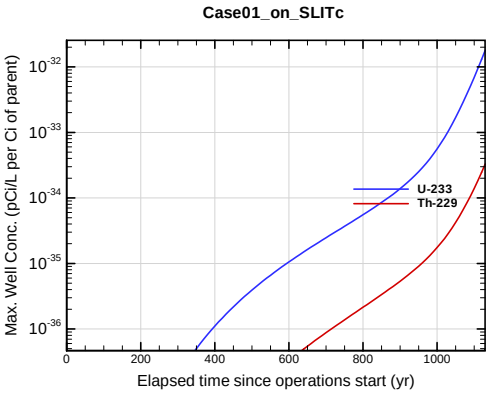

Figure A1B-110. Max. 100-m well conc. for Case01_on_SLITc U-233

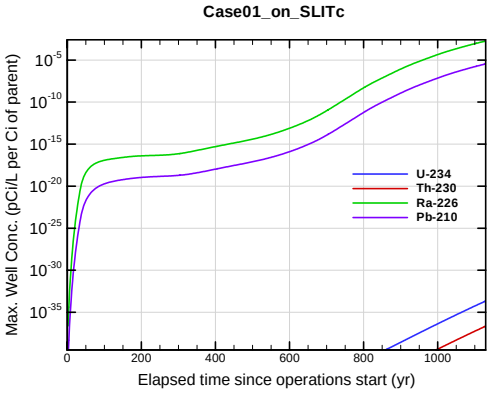

Figure A1B-111. Max. 100-m well conc. for Case01_on_SLITc U-234

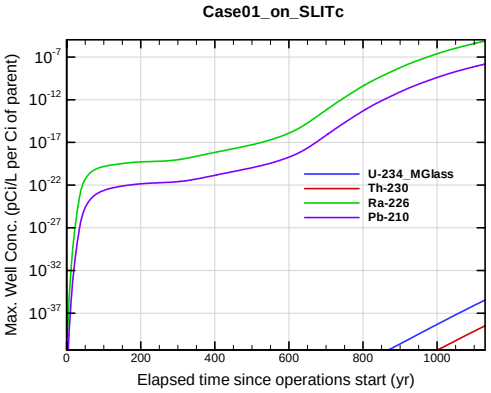

Figure A1B-112. Max. 100-m well conc. for Case01_on_SLITc U-234_MGlass

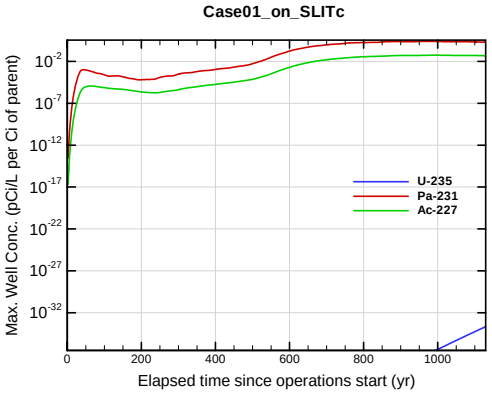

Figure A1B-113. Max. 100-m well conc. for Case01_on_SLITc U-235

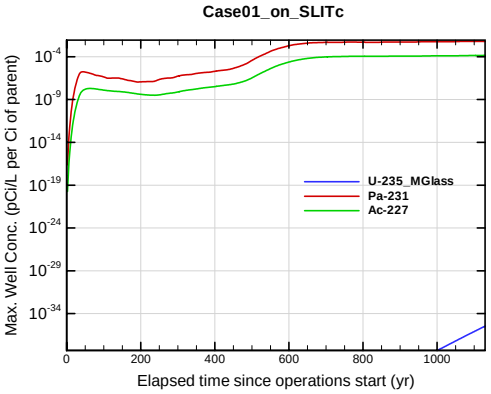

Figure A1B-114. Max. 100-m well conc. for Case01_on_SLITc U-235_MGlass

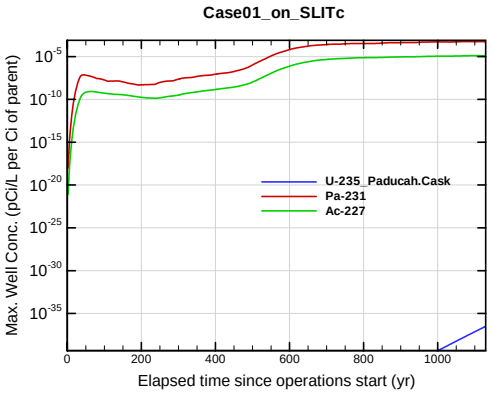

Figure A1B-115. Max. 100-m well conc. for Case01_on_SLITc U-235_Paducah.Cask

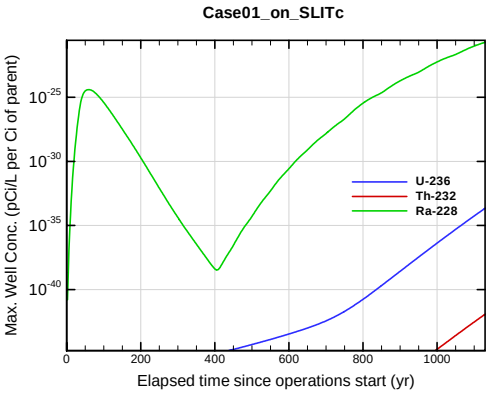

Figure A1B-116. Max. 100-m well conc. for Case01_on_SLITc U-236

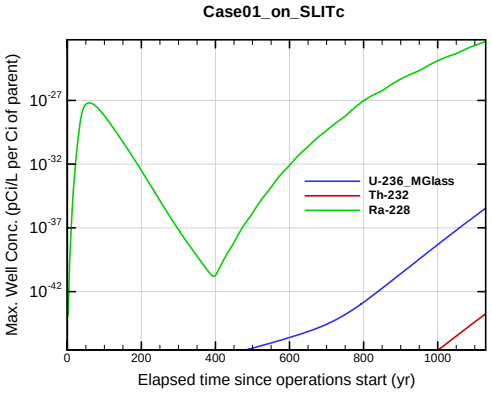

Figure A1B-117. Max. 100-m well conc. for Case01_on_SLITc U-236_MGlass

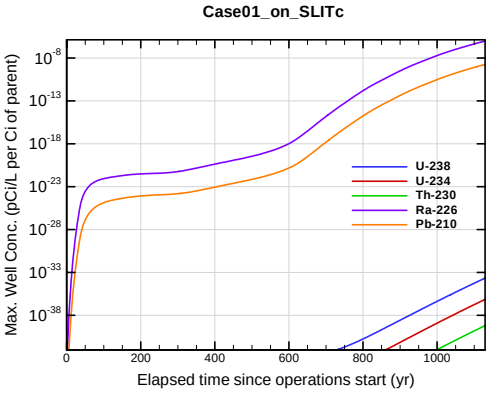

Figure A1B-118. Max. 100-m well conc. for Case01_on_SLITc U-238

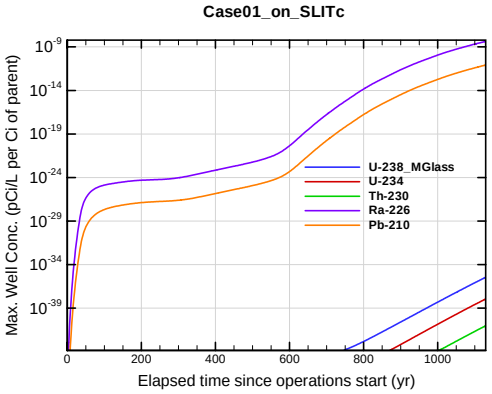

Figure A1B-119. Max. 100-m well conc. for Case01_on_SLITc U-238_MGlass

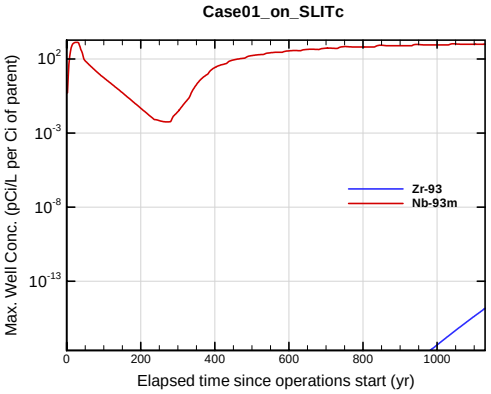

Figure A1B-120. Max. 100-m well conc. for Case01_on_SLITc Zr-93

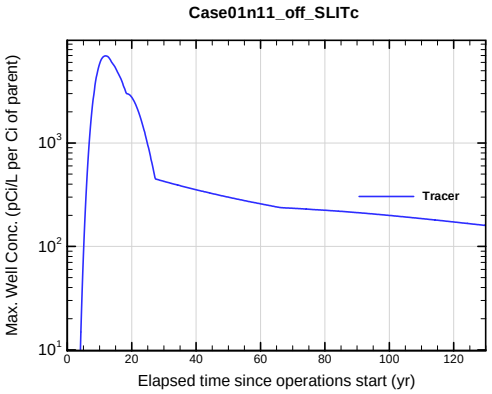

Figure A1B-121. Max. 100-m well conc. for Case01n11_off_SLITc Tracer

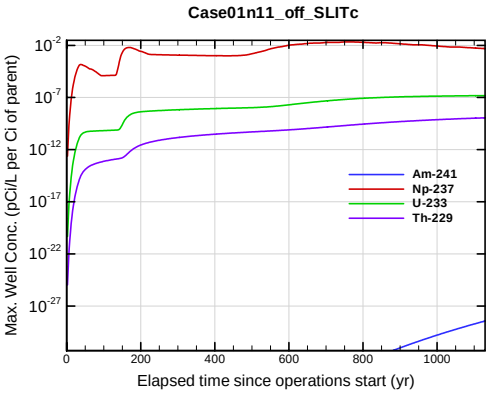

Figure A1B-122. Max. 100-m well conc. for Case01n11_off_SLITc Am-241

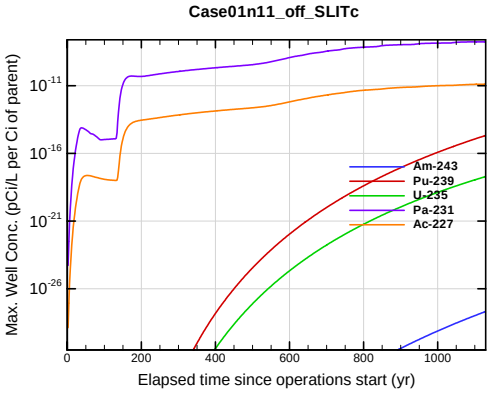

Figure A1B-123. Max. 100-m well conc. for Case01n11_off_SLITc Am-243

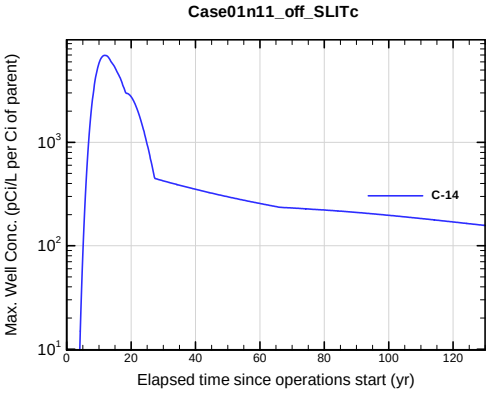

Figure A1B-124. Max. 100-m well conc. for Case01n11_off_SLITc C-14

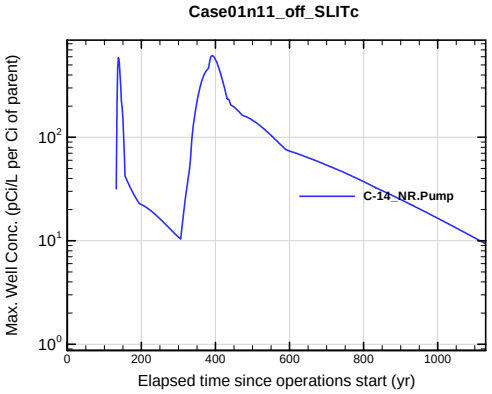

Figure A1B-125. Max. 100-m well conc. for Case01n11_off_SLITc C-14_NR.Pump

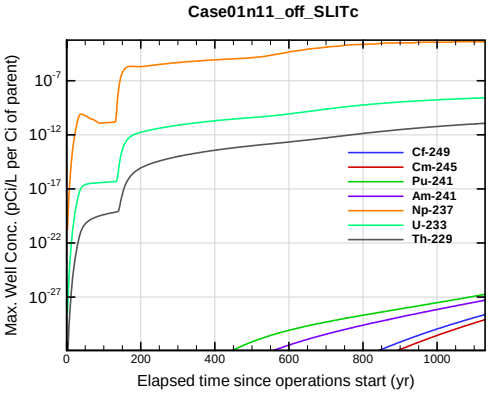

Figure A1B-126. Max. 100-m well conc. for Case01n11_off_SLITc Cf-249

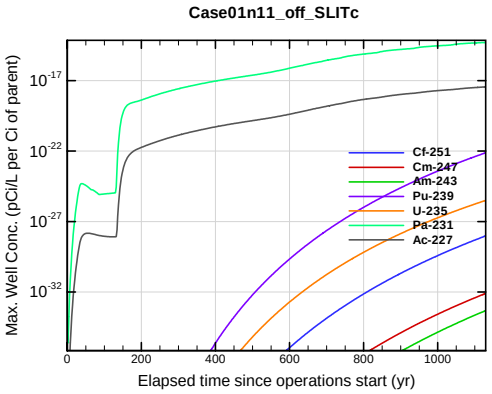

Figure A1B-127. Max. 100-m well conc. for Case01n11_off_SLITc Cf-251

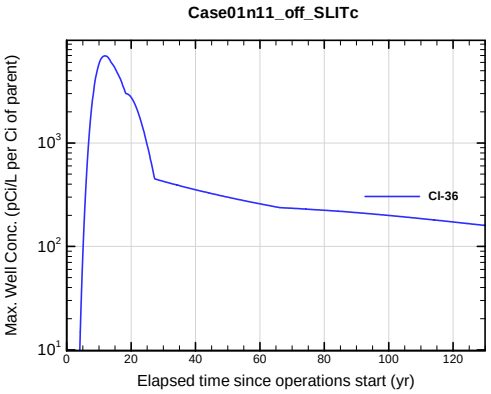

Figure A1B-128. Max. 100-m well conc. for Case01n11_off_SLITc Cl-36

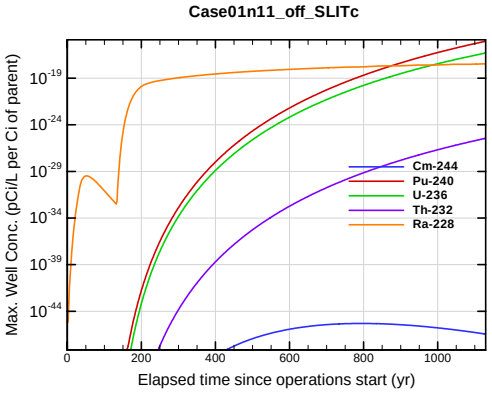

Figure A1B-129. Max. 100-m well conc. for Case01n11_off_SLITc Cm-244

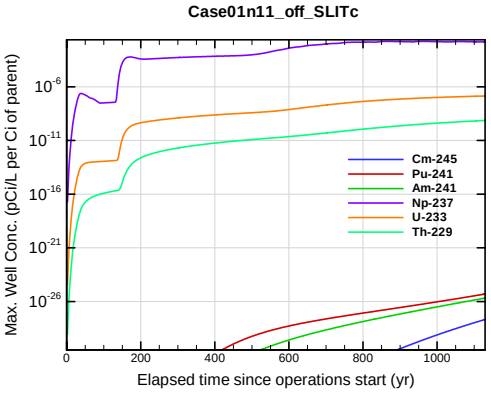

Figure A1B-130. Max. 100-m well conc. for Case01n11_off_SLITc Cm-245

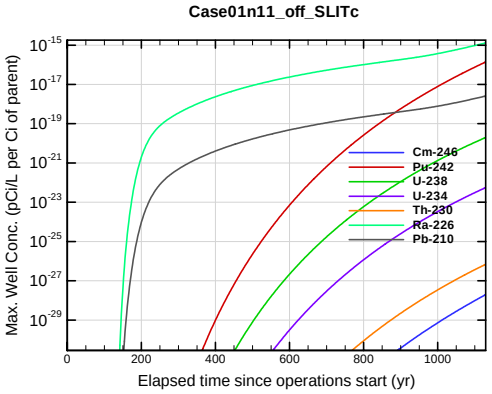

Figure A1B-131. Max. 100-m well conc. for Case01n11_off_SLITc Cm-246

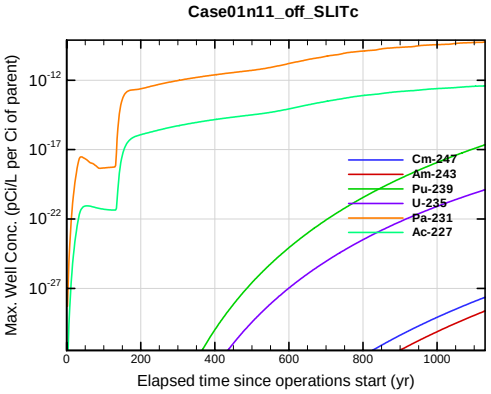

Figure A1B-132. Max. 100-m well conc. for Case01n11_off_SLITc Cm-247

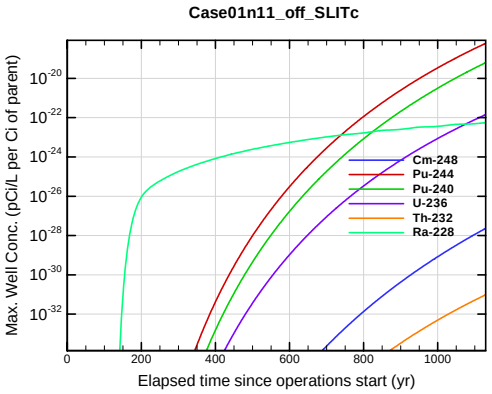

Figure A1B-133. Max. 100-m well conc. for Case01n11_off_SLITc Cm-248

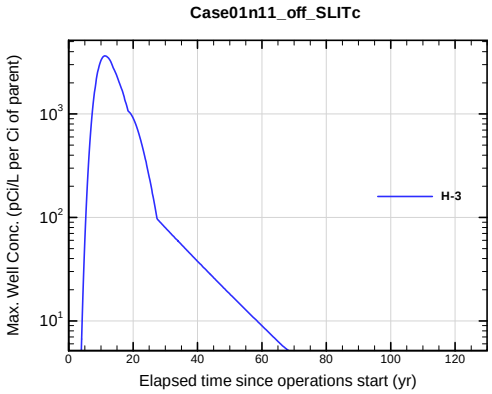

Figure A1B-134. Max. 100-m well conc. for Case01n11_off_SLITc H-3

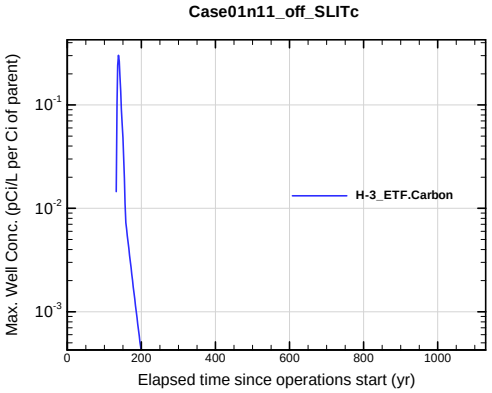

Figure A1B-135. Max. 100-m well conc. for Case01n11_off_SLITc H-3_ETF.Carbon

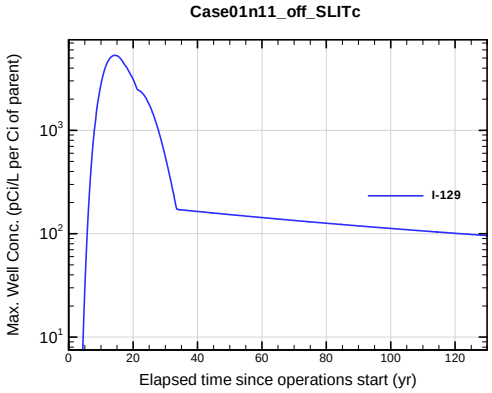

Figure A1B-136. Max. 100-m well conc. for Case01n11_off_SLITc I-129

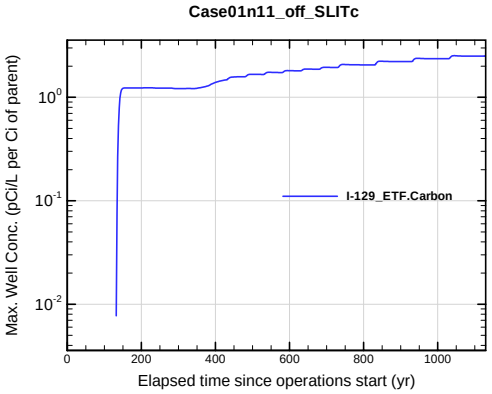

Figure A1B-137. Max. 100-m well conc. for Case01n11_off_SLITc I-129_ETF.Carbon

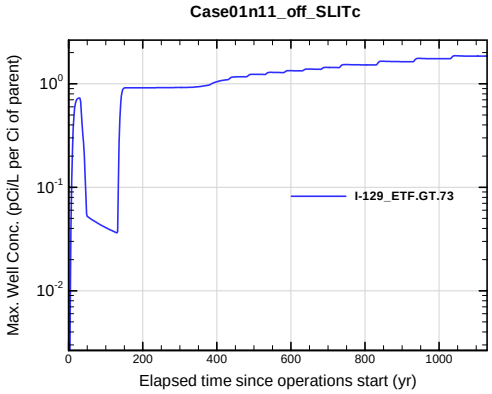

Figure A1B-138. Max. 100-m well conc. for Case01n11_off_SLITc I-129_ETF.GT.73

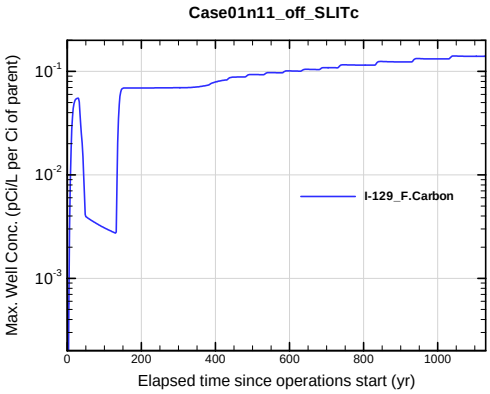

Figure A1B-139. Max. 100-m well conc. for Case01n11_off_SLITc I-129_F.Carbon

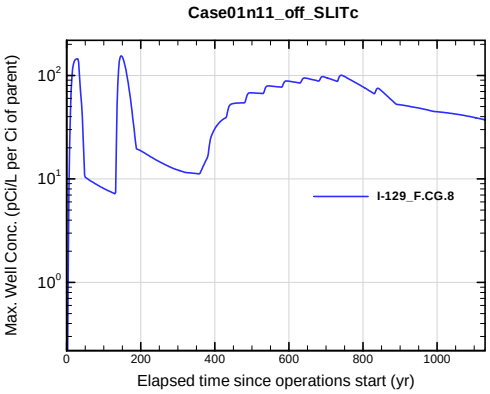

Figure A1B-140. Max. 100-m well conc. for Case01n11_off_SLITc I-129_F.CG.8

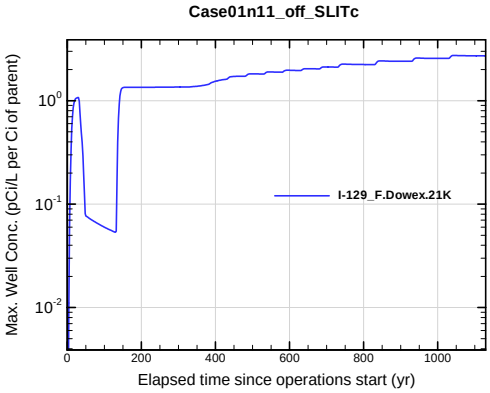

Figure A1B-141. Max. 100-m well conc. for Case01n11_off_SLITc I-129_F.Dowex.21K

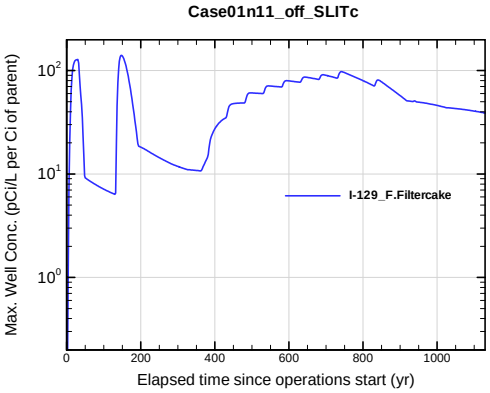

Figure A1B-142. Max. 100-m well conc. for Case01n11_off_SLITc I-129_F.Filtercake

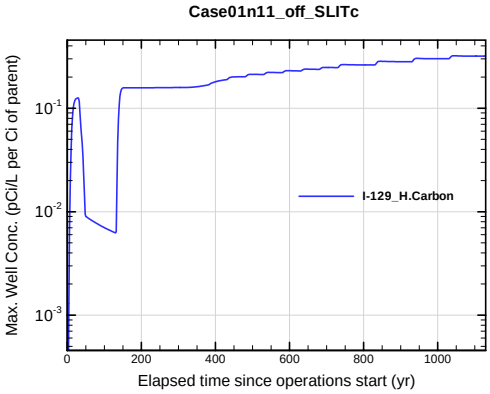

Figure A1B-143. Max. 100-m well conc. for Case01n11_off_SLITc I-129_H.Carbon

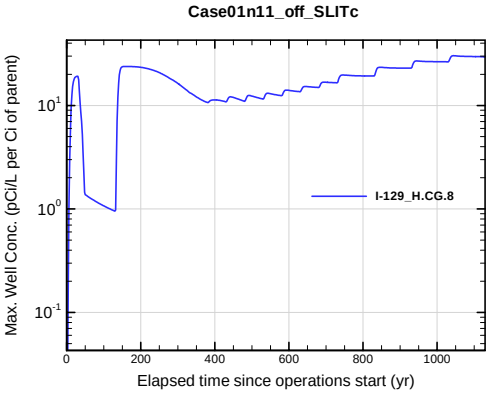

Figure A1B-144. Max. 100-m well conc. for Case01n11_off_SLITc I-129_H.CG.8

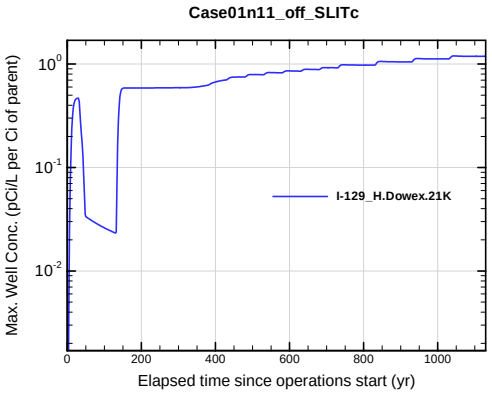

Figure A1B-145. Max. 100-m well conc. for Case01n11_off_SLITc I-129_H.Dowex.21K

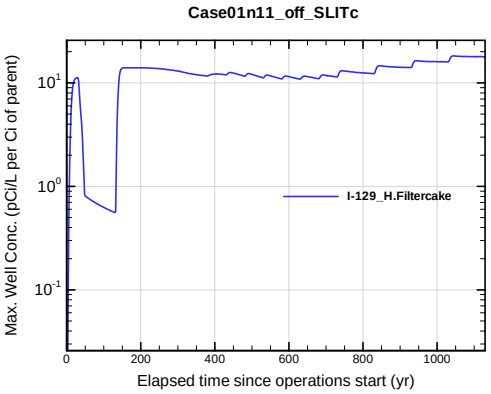

Figure A1B-146. Max. 100-m well conc. for Case01n11_off_SLITc I-129_H.Filtercake

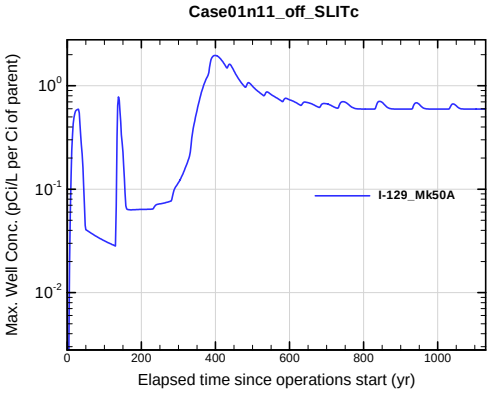

Figure A1B-147. Max. 100-m well conc. for Case01n11_off_SLITc I-129_Mk50A

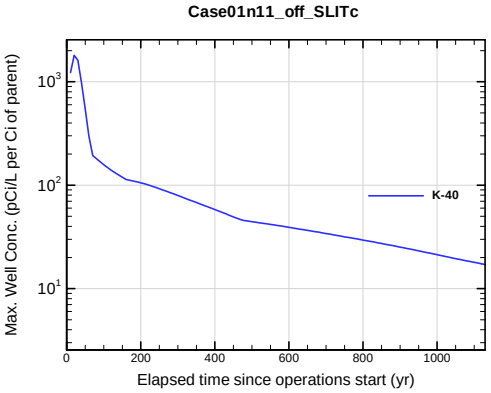

Figure A1B-148. Max. 100-m well conc. for Case01n11_off_SLITc K-40

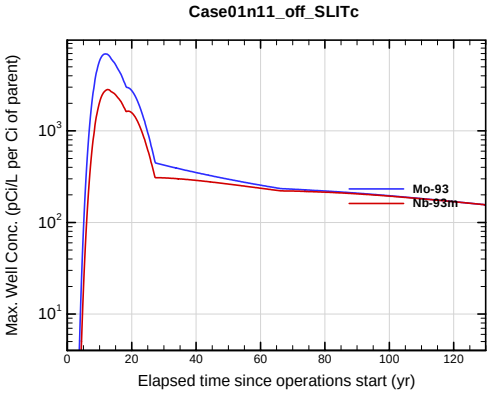

Figure A1B-149. Max. 100-m well conc. for Case01n11_off_SLITc Mo-93

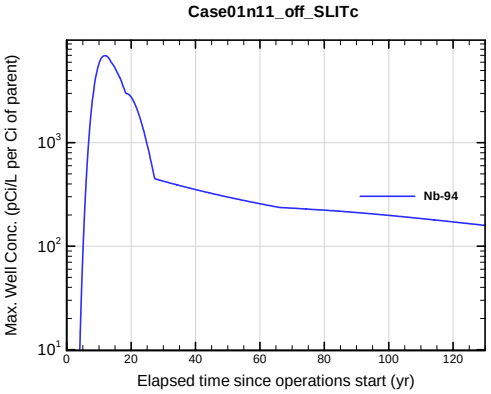

Figure A1B-150. Max. 100-m well conc. for Case01n11_off_SLITc Nb-94

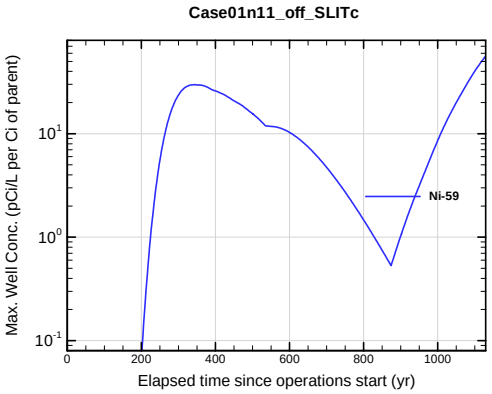

Figure A1B-151. Max. 100-m well conc. for Case01n11_off_SLITc Ni-59

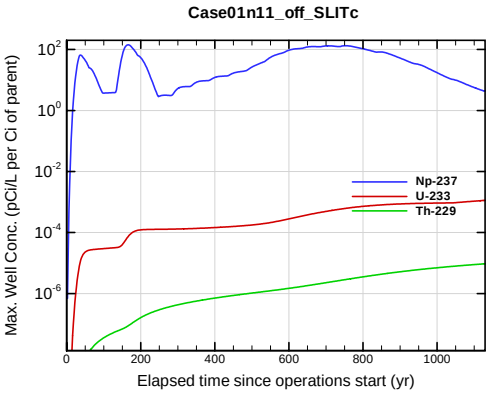

Figure A1B-152. Max. 100-m well conc. for Case01n11_off_SLITc Np-237

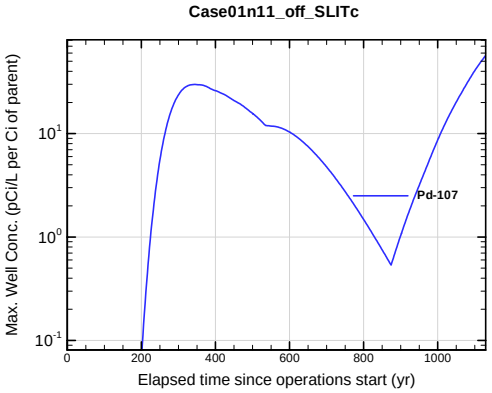

Figure A1B-153. Max. 100-m well conc. for Case01n11_off_SLITc Pd-107

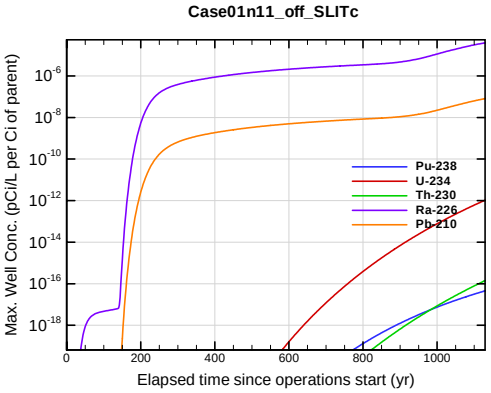

Figure A1B-154. Max. 100-m well conc. for Case01n11_off_SLITc Pu-238

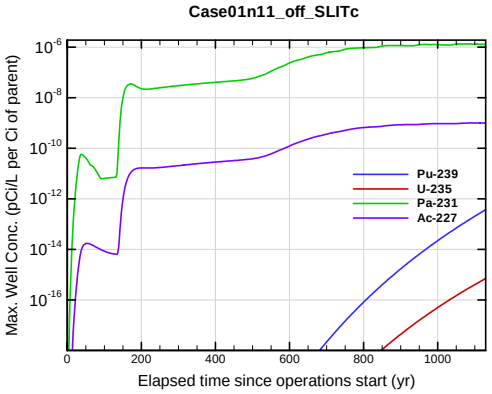

Figure A1B-155. Max. 100-m well conc. for Case01n11_off_SLITc Pu-239

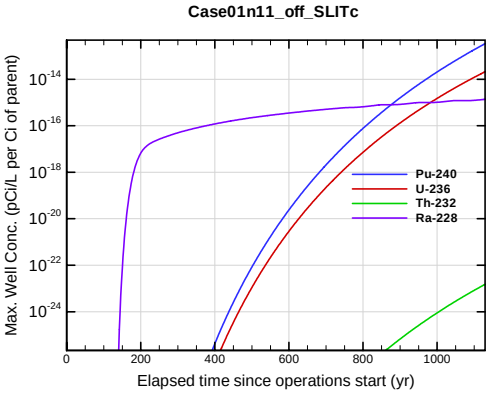

Figure A1B-156. Max. 100-m well conc. for Case01n11_off_SLITc Pu-240

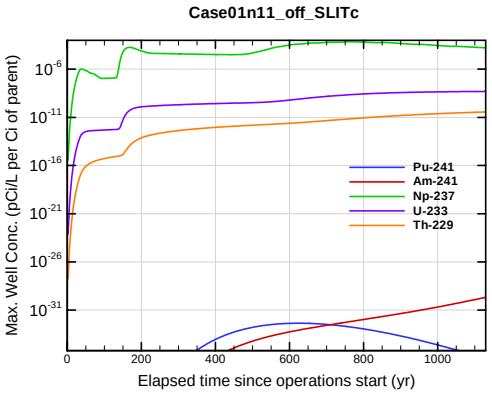

Figure A1B-157. Max. 100-m well conc. for Case01n11_off_SLITc Pu-241

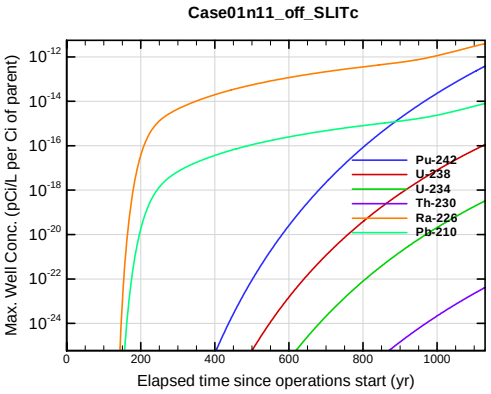

Figure A1B-158. Max. 100-m well conc. for Case01n11_off_SLITc Pu-242

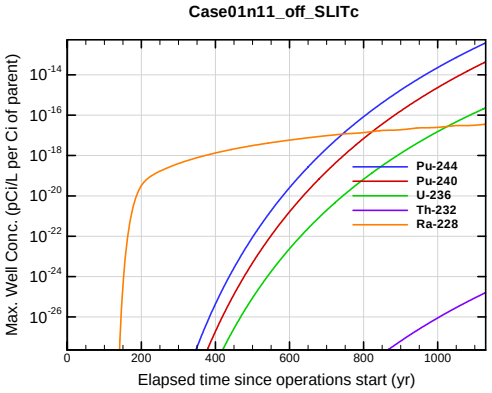

Figure A1B-159. Max. 100-m well conc. for Case01n11_off_SLITc Pu-244

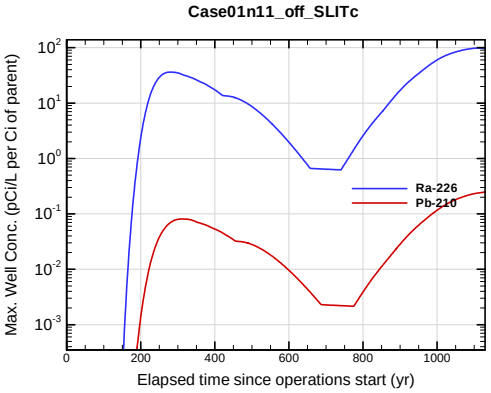

Figure A1B-160. Max. 100-m well conc. for Case01n11_off_SLITc Ra-226

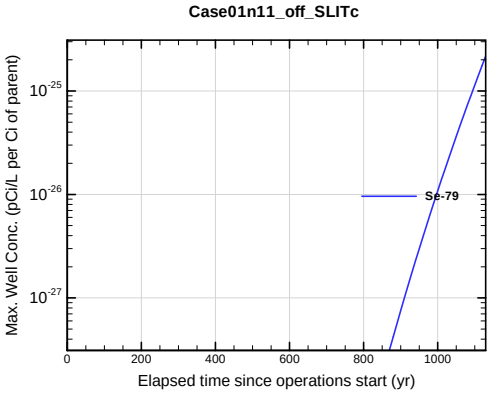

Figure A1B-161. Max. 100-m well conc. for Case01n11_off_SLITc Se-79

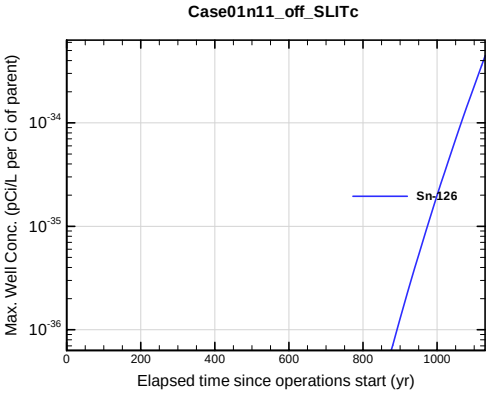

Figure A1B-162. Max. 100-m well conc. for Case01n11_off_SLITc Sn-126

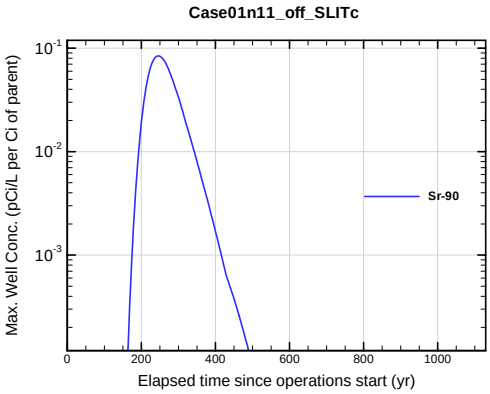

Figure A1B-163. Max. 100-m well conc. for Case01n11_off_SLITc Sr-90

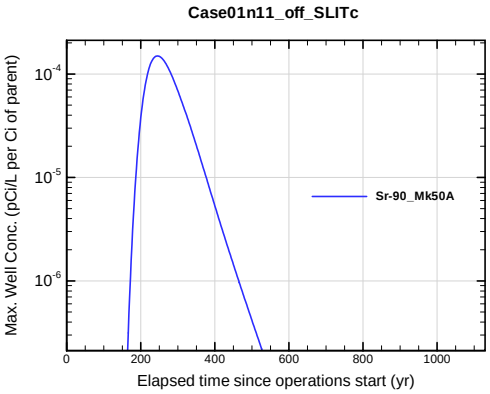

Figure A1B-164. Max. 100-m well conc. for Case01n11_off_SLITc Sr-90_Mk50A

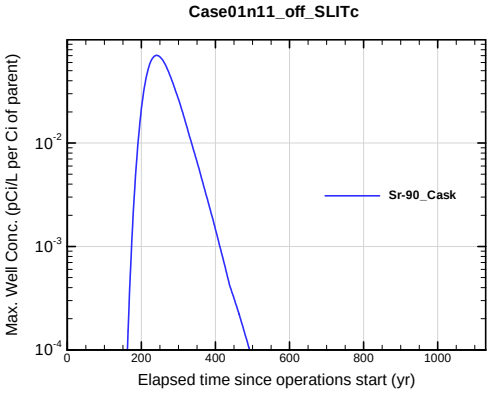

Figure A1B-165. Max. 100-m well conc. for Case01n11_off_SLITc Sr-90_Cask

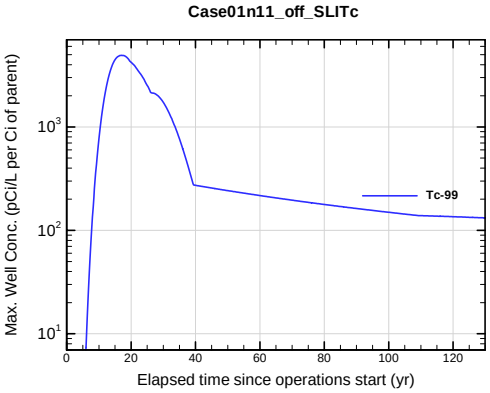

Figure A1B-166. Max. 100-m well conc. for Case01n11_off_SLITc Tc-99

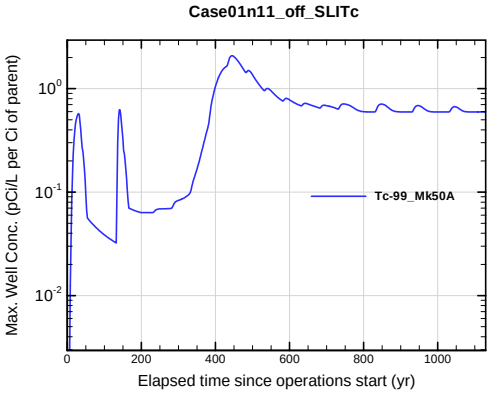

Figure A1B-167. Max. 100-m well conc. for Case01n11_off_SLITc Tc-99_Mk50A

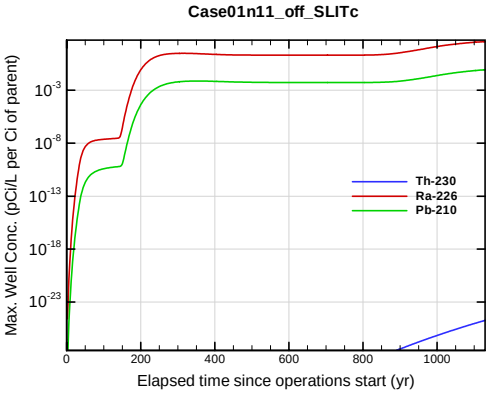

Figure A1B-168. Max. 100-m well conc. for Case01n11_off_SLITc Th-230

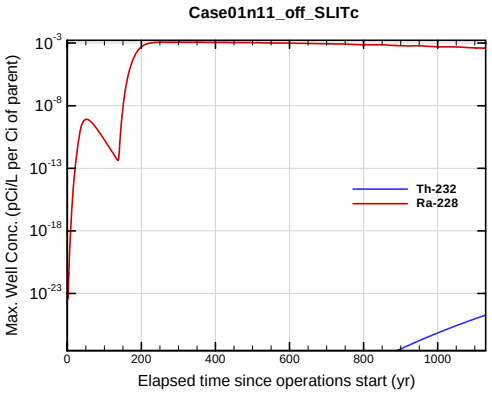

Figure A1B-169. Max. 100-m well conc. for Case01n11_off_SLITc Th-232

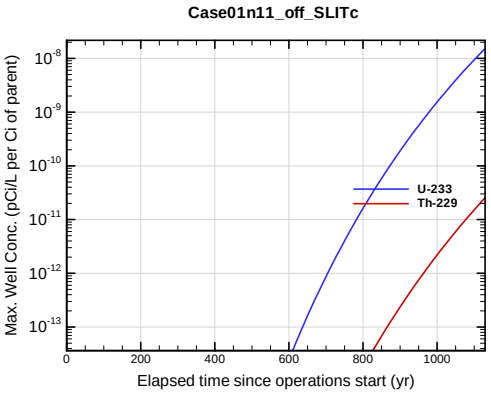

Figure A1B-170. Max. 100-m well conc. for Case01n11_off_SLITc U-233

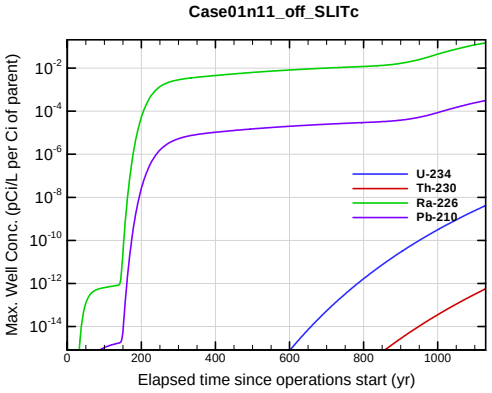

Figure A1B-171. Max. 100-m well conc. for Case01n11_off_SLITc U-234

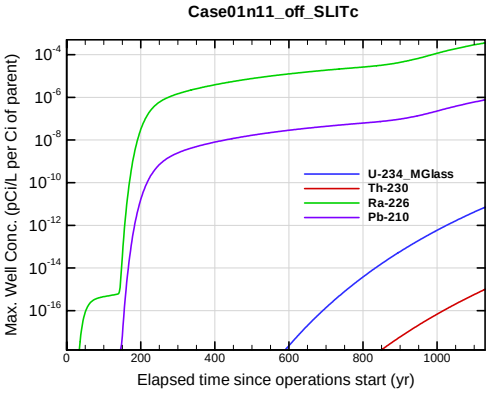

Figure A1B-172. Max. 100-m well conc. for Case01n11_off_SLITc U-234_MGlass

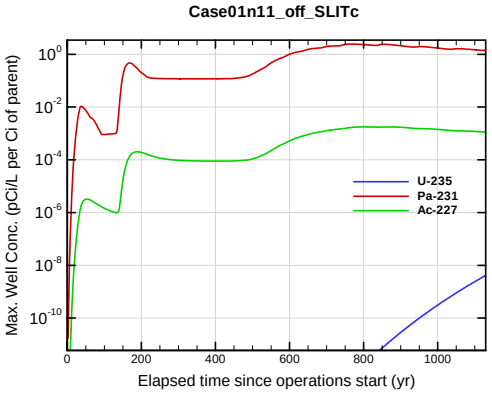

Figure A1B-173. Max. 100-m well conc. for Case01n11_off_SLITc U-235

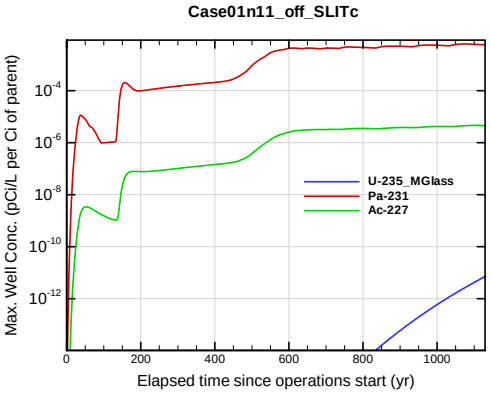

Figure A1B-174. Max. 100-m well conc. for Case01n11_off_SLITc U-235_MGlass

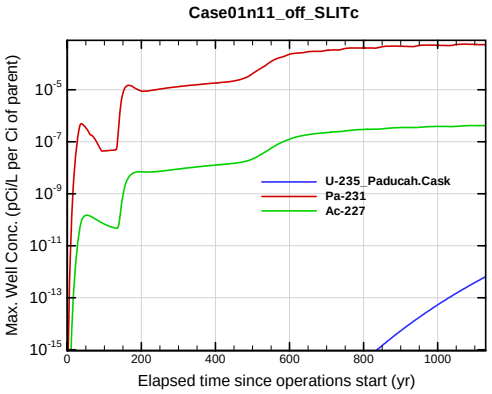

Figure A1B-175. Max. 100-m well conc. for Case01n11_off_SLITc U-235_Paducah.Cask

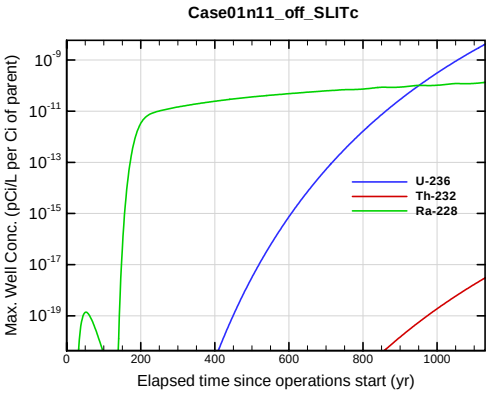

Figure A1B-176. Max. 100-m well conc. for Case01n11_off_SLITc U-236

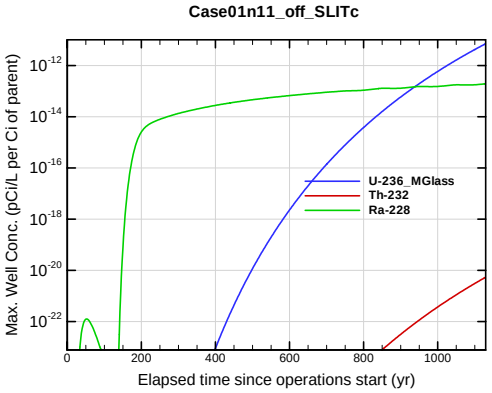

Figure A1B-177. Max. 100-m well conc. for Case01n11_off_SLITc U-236_MGlass

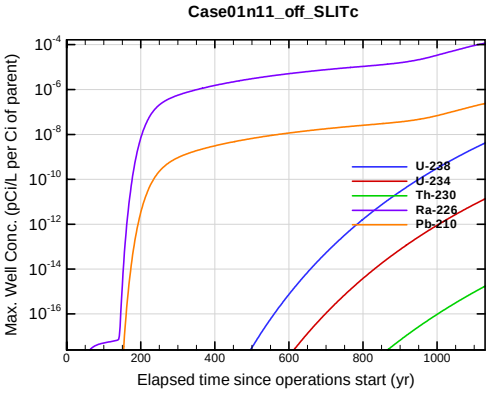

Figure A1B-178. Max. 100-m well conc. for Case01n11_off_SLITc U-238

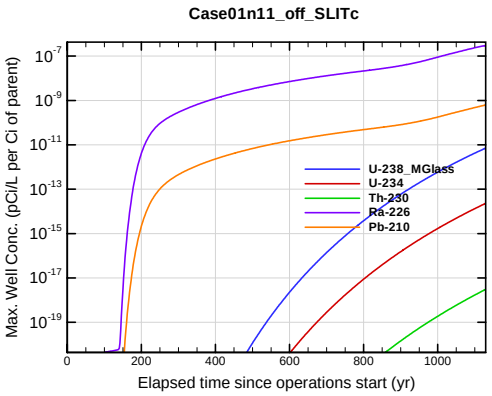

Figure A1B-179. Max. 100-m well conc. for Case01n11_off_SLITc U-238_MGlass

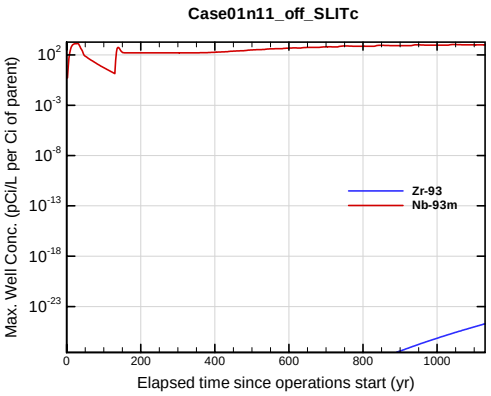

Figure A1B-180. Max. 100-m well conc. for Case01n11_off_SLITc Zr-93

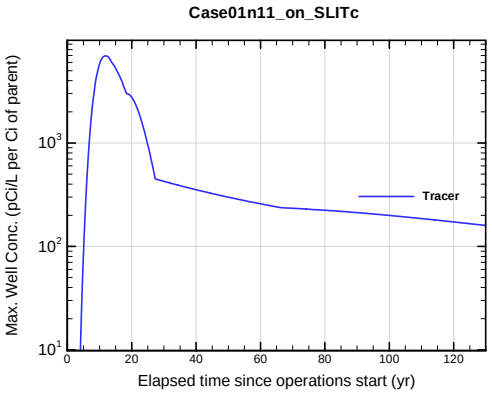

Figure A1B-181. Max. 100-m well conc. for Case01n11_on_SLITc Tracer

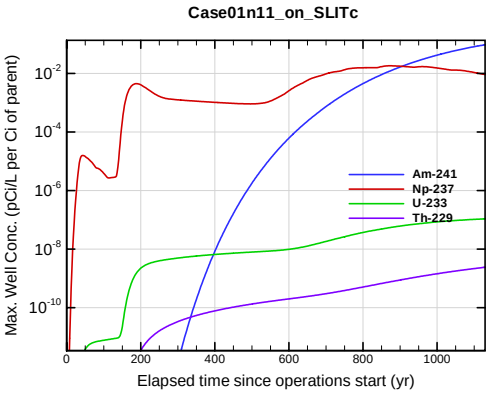

Figure A1B-182. Max. 100-m well conc. for Case01n11_on_SLITc Am-241

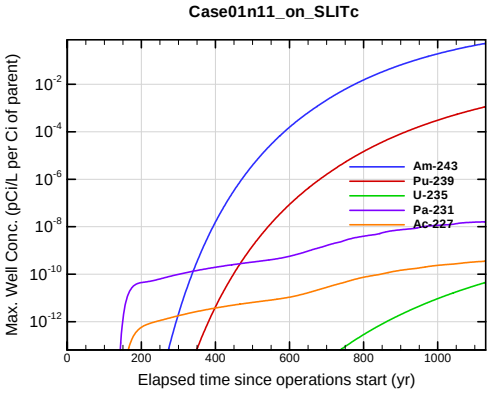

Figure A1B-183. Max. 100-m well conc. for Case01n11_on_SLITc Am-243

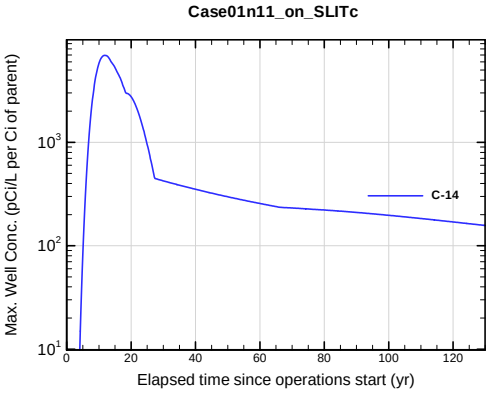

Figure A1B-184. Max. 100-m well conc. for Case01n11_on_SLITc C-14

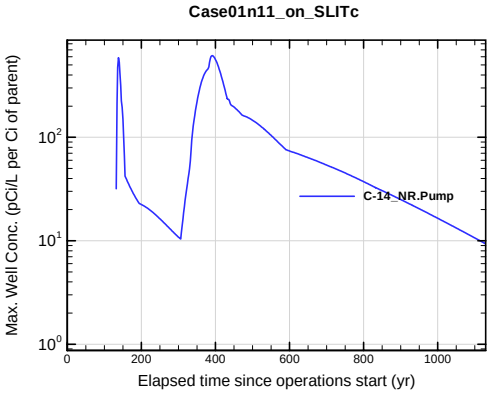

Figure A1B-185. Max. 100-m well conc. for Case01n11_on_SLITc C-14_NR.Pump

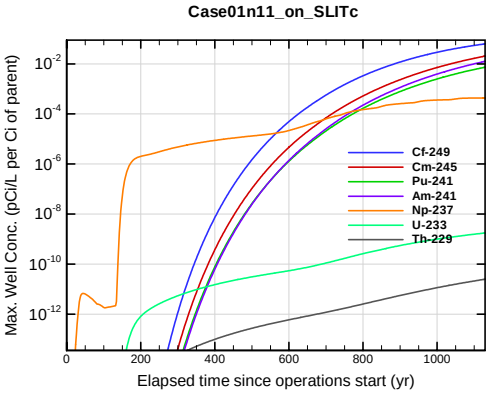

Figure A1B-186. Max. 100-m well conc. for Case01n11_on_SLITc Cf-249

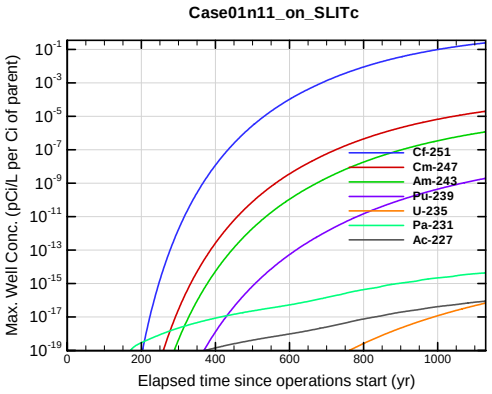

Figure A1B-187. Max. 100-m well conc. for Case01n11_on_SLITc Cf-251

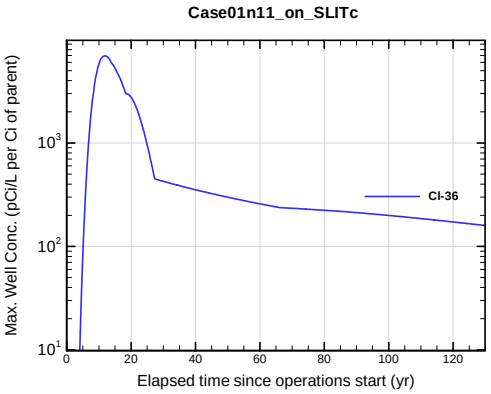

Figure A1B-188. Max. 100-m well conc. for Case01n11_on_SLITc Cl-36

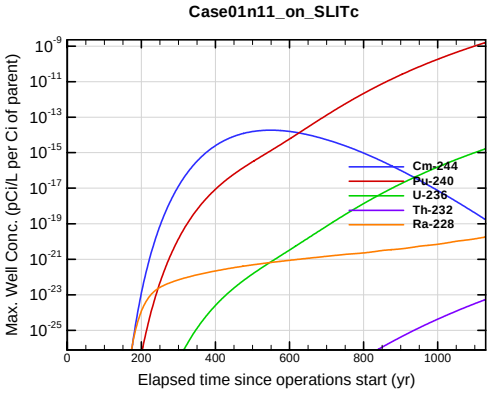

Figure A1B-189. Max. 100-m well conc. for Case01n11_on_SLITc Cm-244

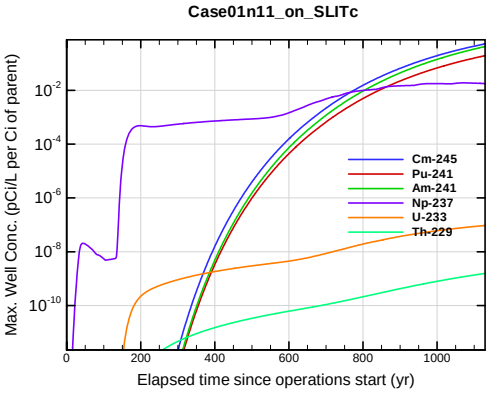

Figure A1B-190. Max. 100-m well conc. for Case01n11_on_SLITc Cm-245

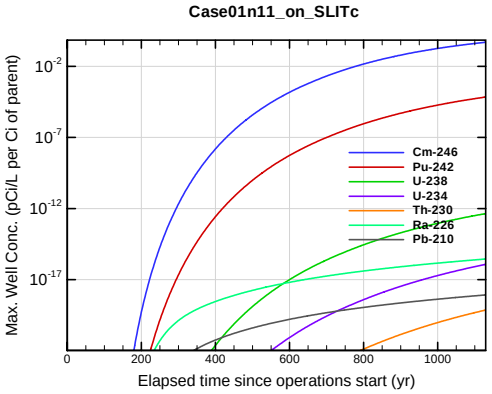

Figure A1B-191. Max. 100-m well conc. for Case01n11_on_SLITc Cm-246

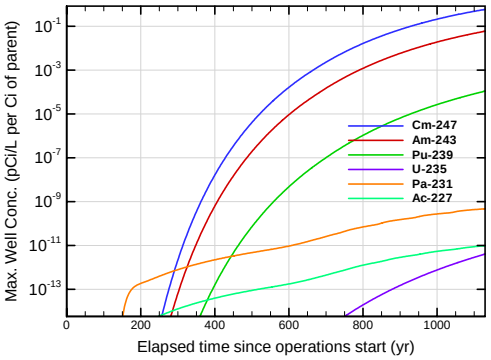

Figure A1B-192. Max. 100-m well conc. for Case01n11_on_SLITc Cm-247

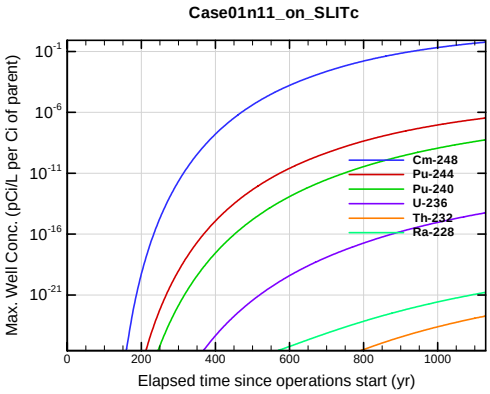

Figure A1B-193. Max. 100-m well conc. for Case01n11_on_SLITc Cm-248

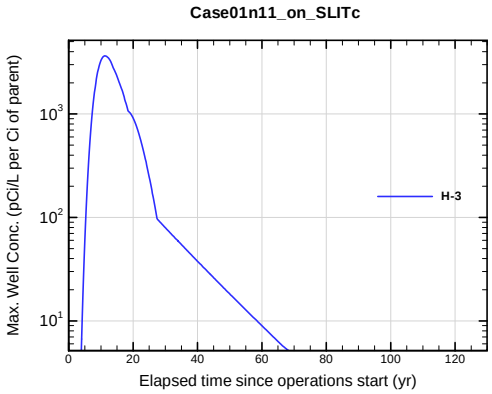

Figure A1B-194. Max. 100-m well conc. for Case01n11_on_SLITc H-3

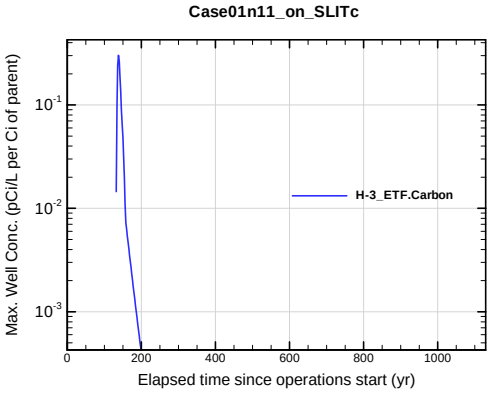

Figure A1B-195. Max. 100-m well conc. for Case01n11_on_SLITc H-3_ETF.Carbon

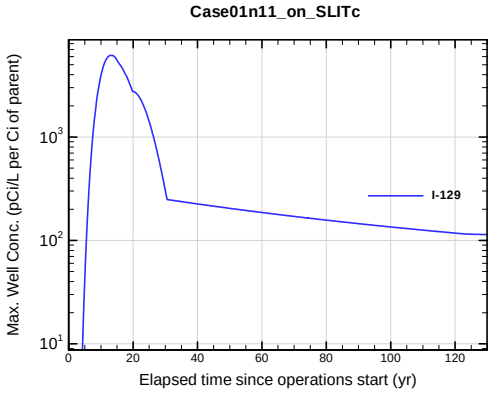

Figure A1B-196. Max. 100-m well conc. for Case01n11_on_SLITc I-129

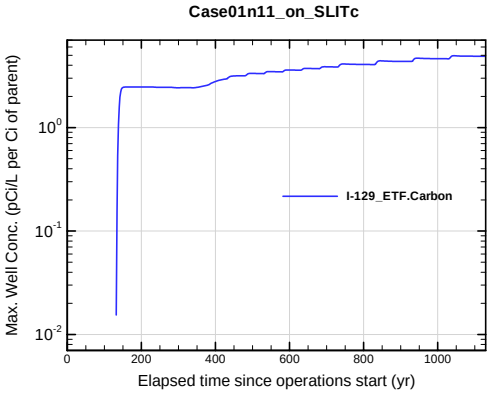

Figure A1B-197. Max. 100-m well conc. for Case01n11_on_SLITc I-129_ETF.Carbon

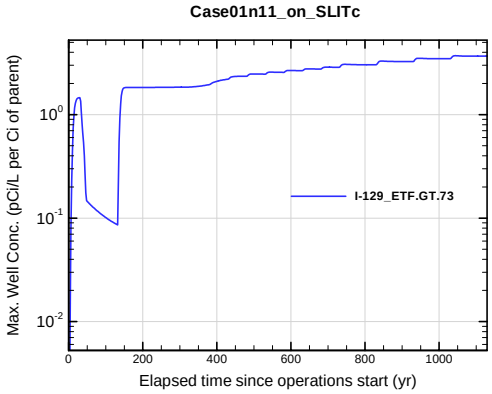

Figure A1B-198. Max. 100-m well conc. for Case01n11_on_SLITc I-129_ETF.GT.73

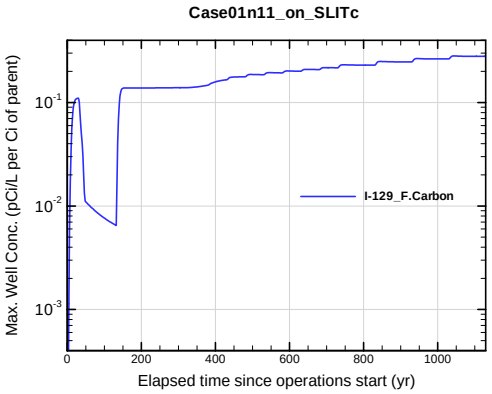

Figure A1B-199. Max. 100-m well conc. for Case01n11_on_SLITc I-129_F.Carbon

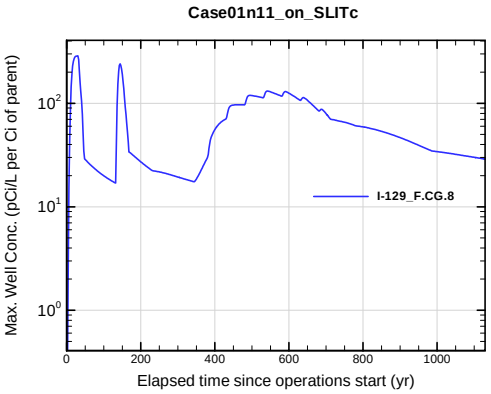

Figure A1B-200. Max. 100-m well conc. for Case01n11_on_SLITc I-129_F.CG.8

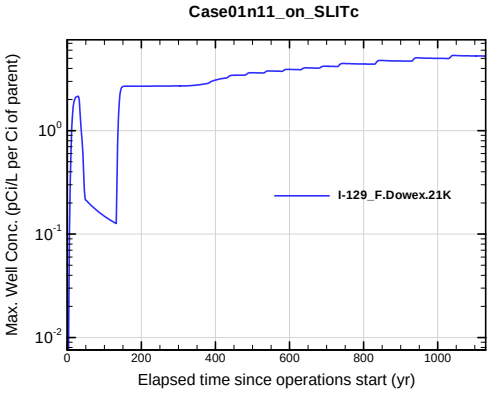

Figure A1B-201. Max. 100-m well conc. for Case01n11_on_SLITc I-129_F.Dowex.21K

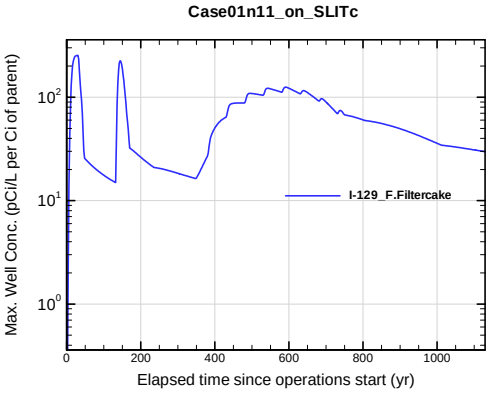

Figure A1B-202. Max. 100-m well conc. for Case01n11_on_SLITc I-129_F.Filtercake

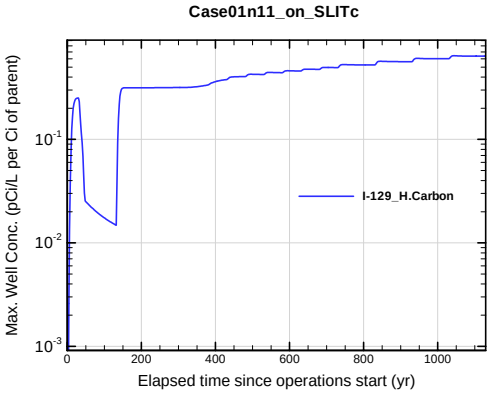

Figure A1B-203. Max. 100-m well conc. for Case01n11_on_SLITc I-129_H.Carbon

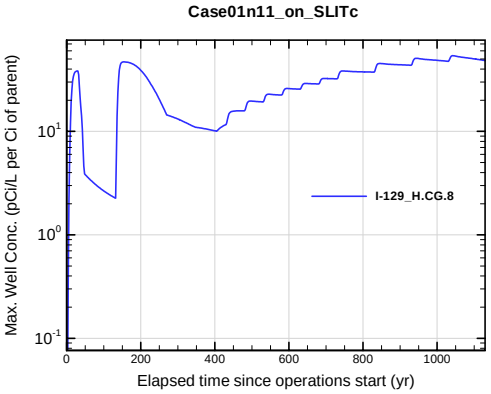

Figure A1B-204. Max. 100-m well conc. for Case01n11_on_SLITc I-129_H.CG.8

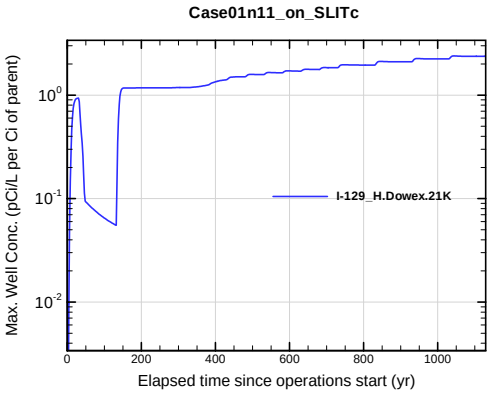

Figure A1B-205. Max. 100-m well conc. for Case01n11_on_SLITc I-129_H.Dowex.21K

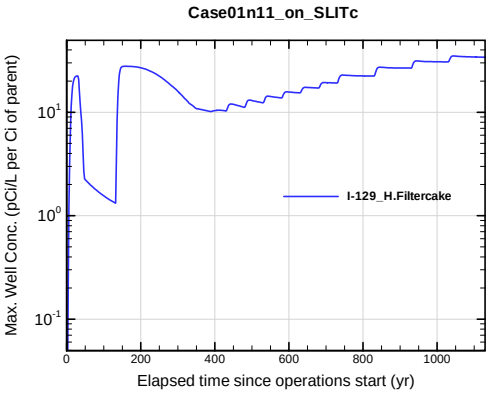

Figure A1B-206. Max. 100-m well conc. for Case01n11_on_SLITc I-129_H.Filtercake

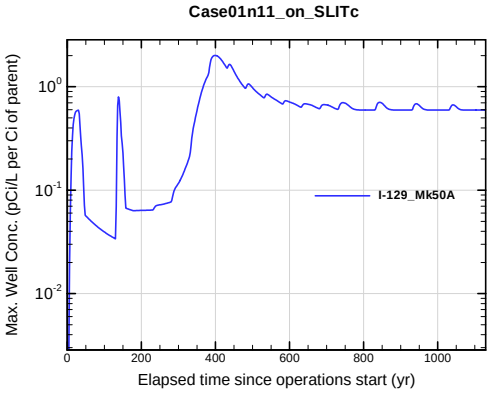

Figure A1B-207. Max. 100-m well conc. for Case01n11_on_SLITc I-129_Mk50A

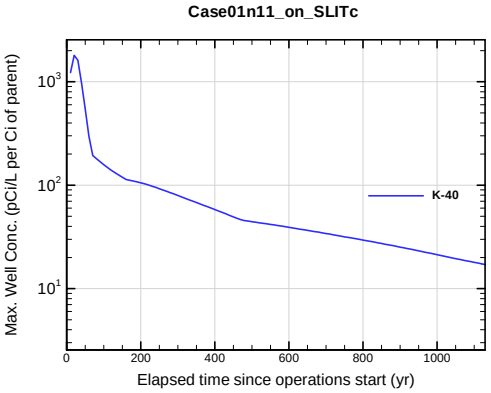

Figure A1B-208. Max. 100-m well conc. for Case01n11_on_SLITc K-40

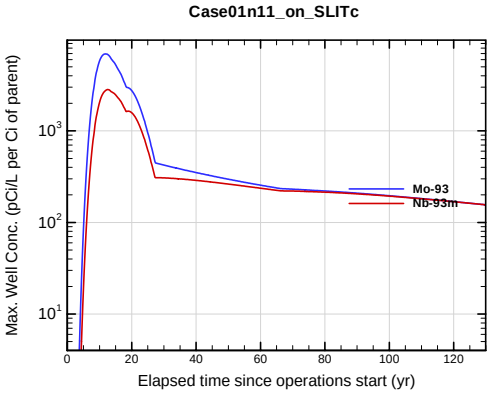

Figure A1B-209. Max. 100-m well conc. for Case01n11_on_SLITc Mo-93

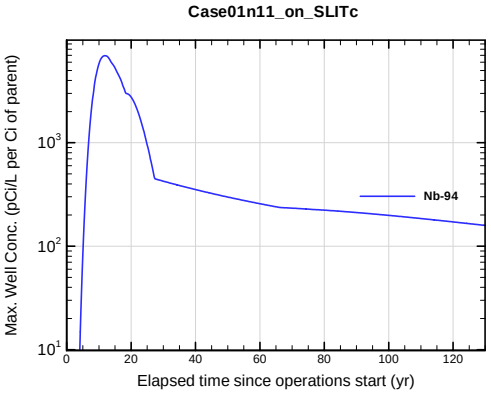

Figure A1B-210. Max. 100-m well conc. for Case01n11_on_SLITc Nb-94

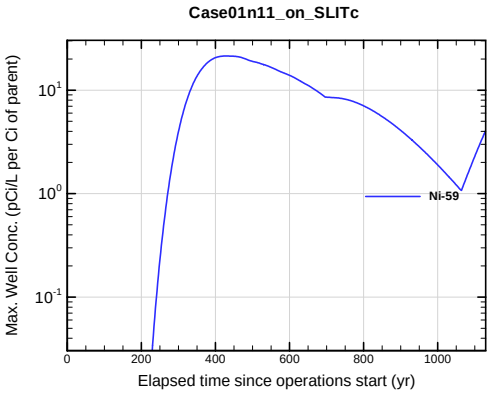

Figure A1B-211. Max. 100-m well conc. for Case01n11_on_SLITc Ni-59

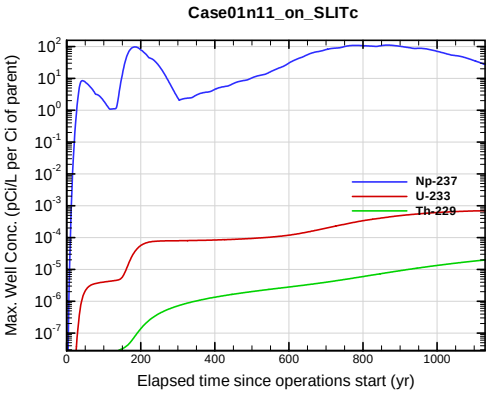

Figure A1B-212. Max. 100-m well conc. for Case01n11_on_SLITc Np-237

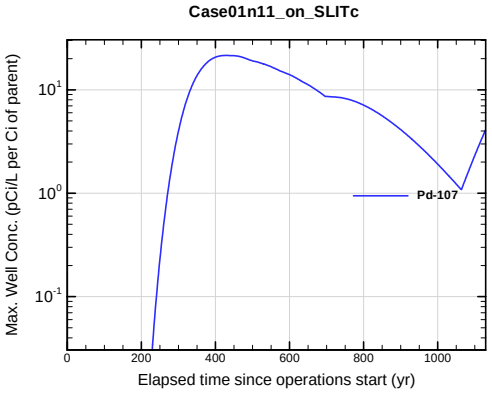

Figure A1B-213. Max. 100-m well conc. for Case01n11_on_SLITc Pd-107

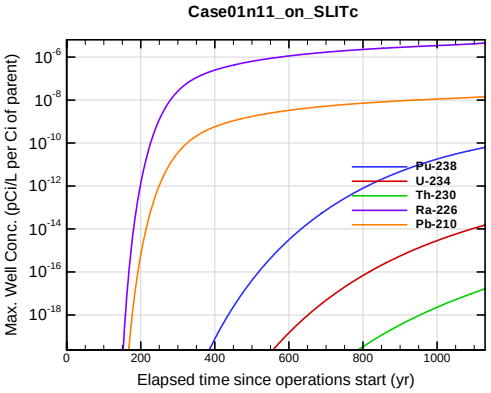

Figure A1B-214. Max. 100-m well conc. for Case01n11_on_SLITc Pu-238

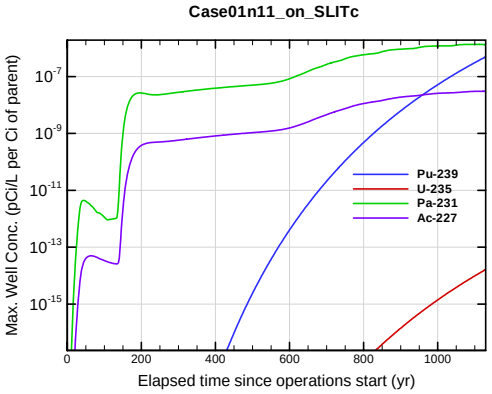

Figure A1B-215. Max. 100-m well conc. for Case01n11_on_SLITc Pu-239

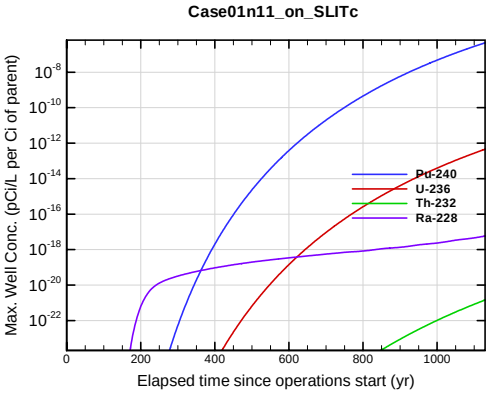

Figure A1B-216. Max. 100-m well conc. for Case01n11_on_SLITc Pu-240

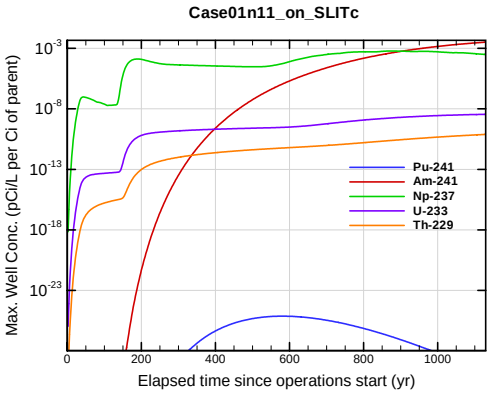

Figure A1B-217. Max. 100-m well conc. for Case01n11_on_SLITc Pu-241

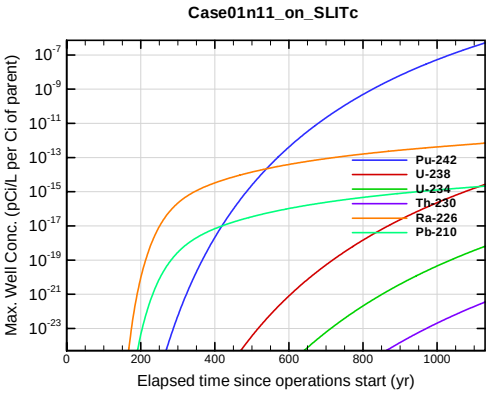

Figure A1B-218. Max. 100-m well conc. for Case01n11_on_SLITc Pu-242

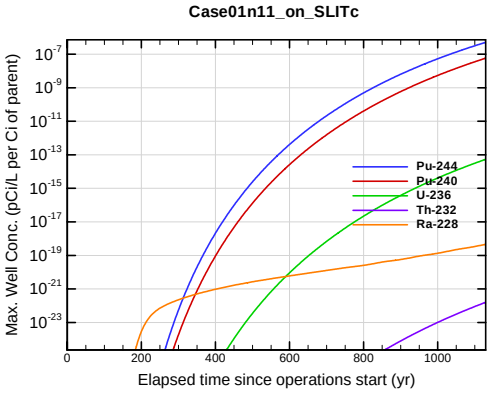

Figure A1B-219. Max. 100-m well conc. for Case01n11_on_SLITc Pu-244

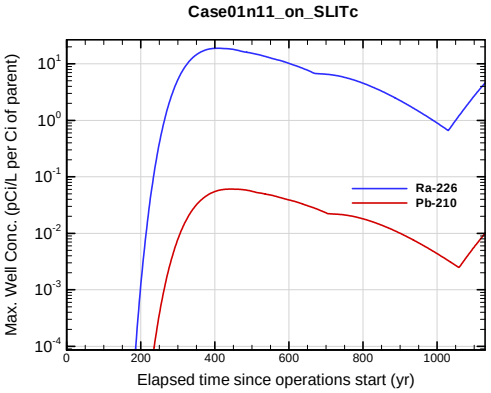

Figure A1B-220. Max. 100-m well conc. for Case01n11_on_SLITc Ra-226

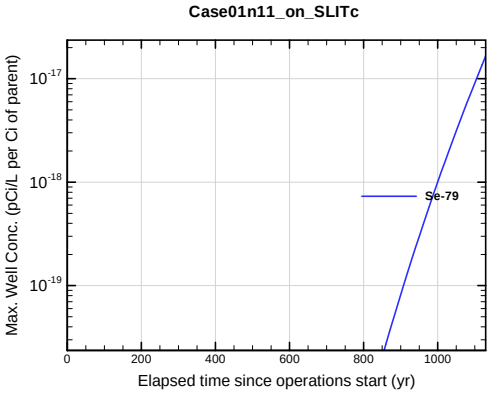

Figure A1B-221. Max. 100-m well conc. for Case01n11_on_SLITc Se-79

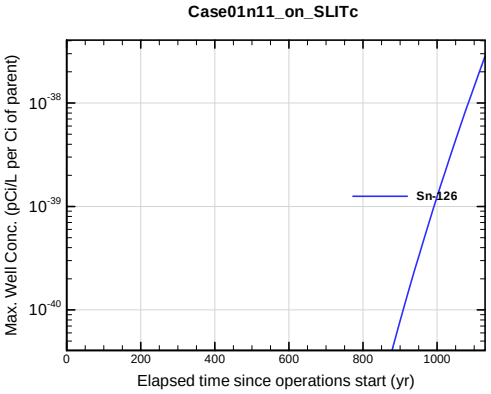

Figure A1B-222. Max. 100-m well conc. for Case01n11_on_SLITc Sn-126

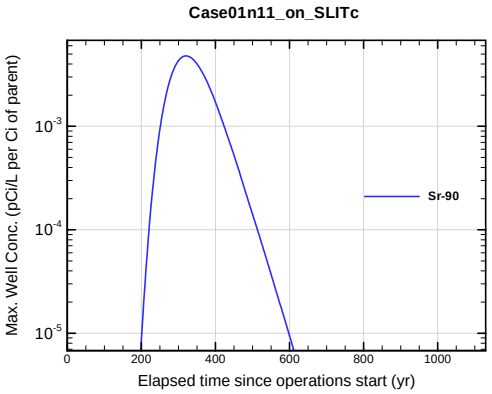

Figure A1B-223. Max. 100-m well conc. for Case01n11_on_SLITc Sr-90

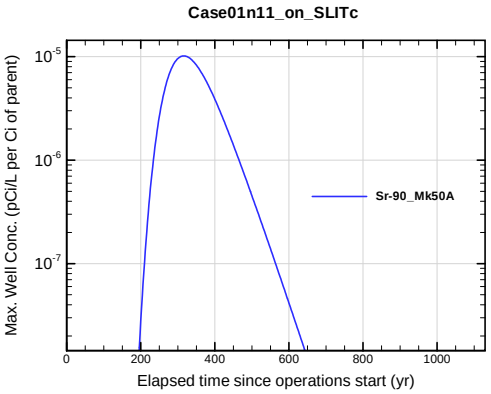

Figure A1B-224. Max. 100-m well conc. for Case01n11_on_SLITc Sr-90_Mk50A

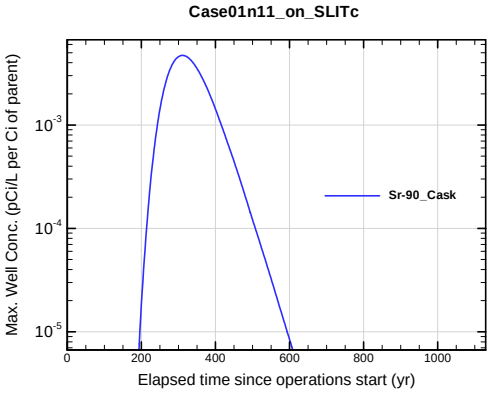

Figure A1B-225. Max. 100-m well conc. for Case01n11_on_SLITc Sr-90_Cask

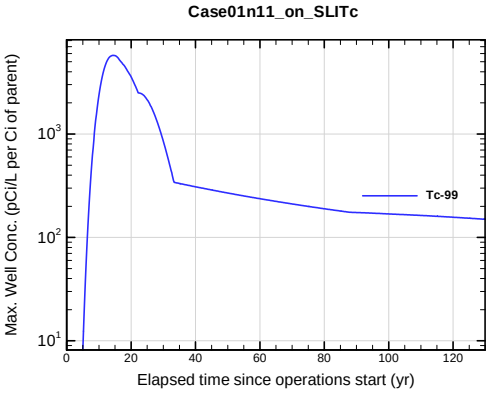

Figure A1B-226. Max. 100-m well conc. for Case01n11_on_SLITc Tc-99

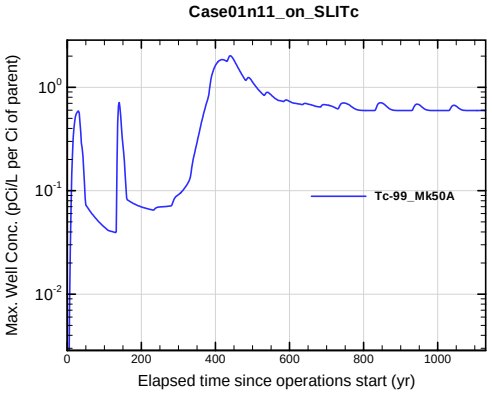

Figure A1B-227. Max. 100-m well conc. for Case01n11_on_SLITc Tc-99_Mk50A

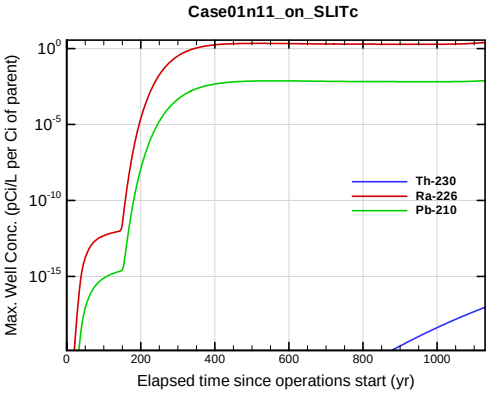

Figure A1B-228. Max. 100-m well conc. for Case01n11_on_SLITc Th-230

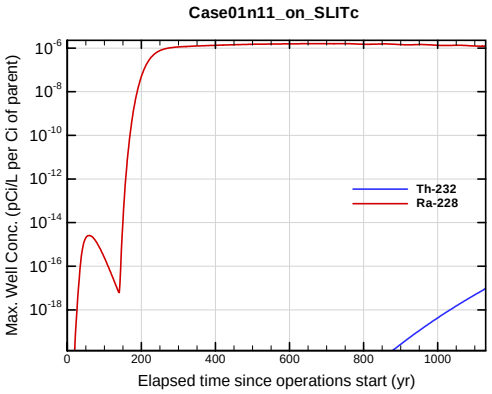

Figure A1B-229. Max. 100-m well conc. for Case01n11_on_SLITc Th-232

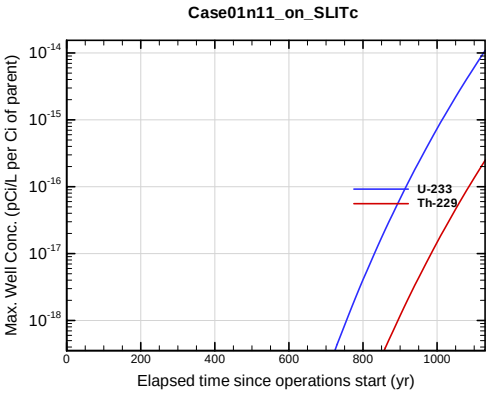

Figure A1B-230. Max. 100-m well conc. for Case01n11_on_SLITc U-233

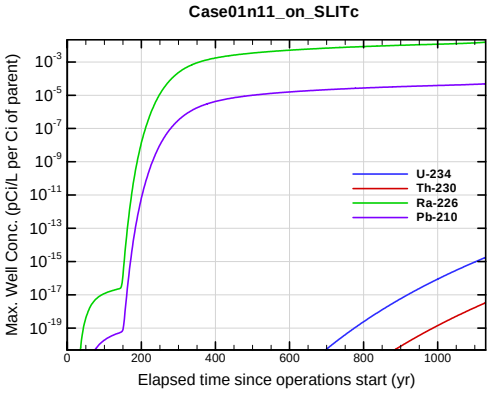

Figure A1B-231. Max. 100-m well conc. for Case01n11_on_SLITc U-234

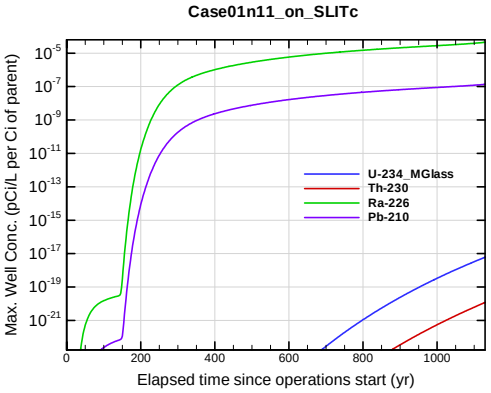

Figure A1B-232. Max. 100-m well conc. for Case01n11_on_SLITc U-234_MGlass

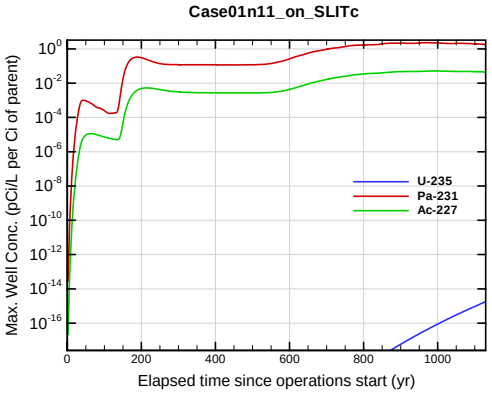

Figure A1B-233. Max. 100-m well conc. for Case01n11_on_SLITc U-235

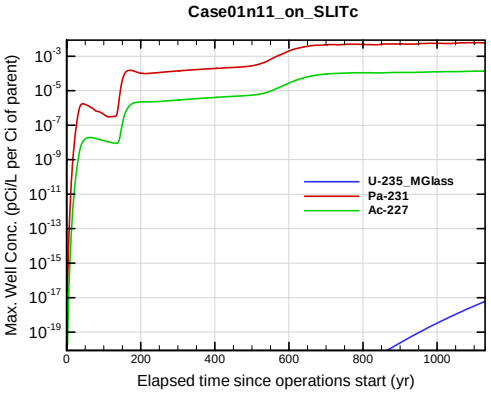

Figure A1B-234. Max. 100-m well conc. for Case01n11_on_SLITc U-235_MGlass

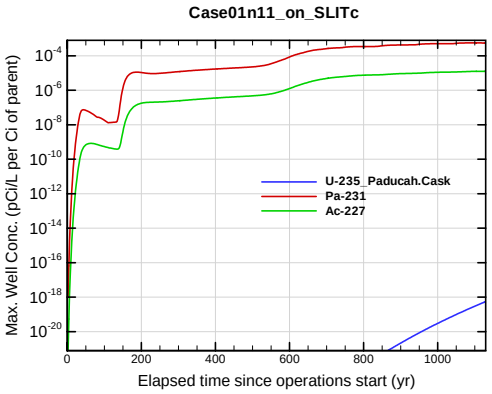

Figure A1B-235. Max. 100-m well conc. for Case01n11_on_SLITc U-235_Paducah.Cask

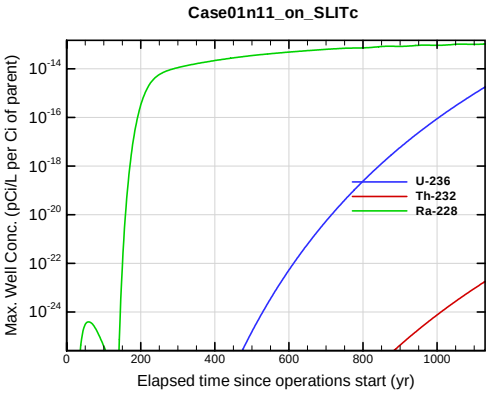

Figure A1B-236. Max. 100-m well conc. for Case01n11_on_SLITc U-236

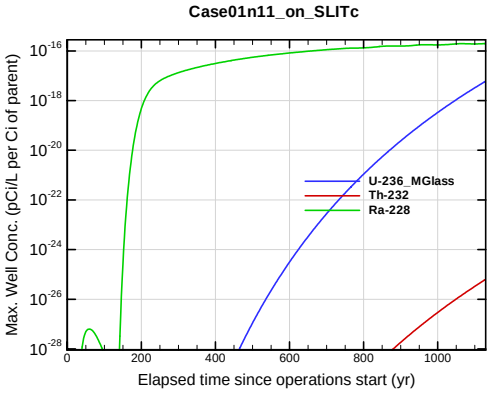

Figure A1B-237. Max. 100-m well conc. for Case01n11_on_SLITc U-236_MGlass

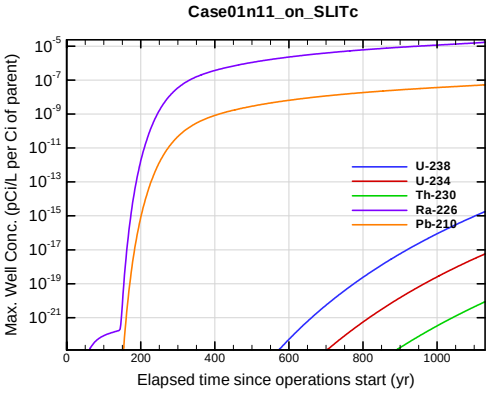

Figure A1B-238. Max. 100-m well conc. for Case01n11_on_SLITc U-238

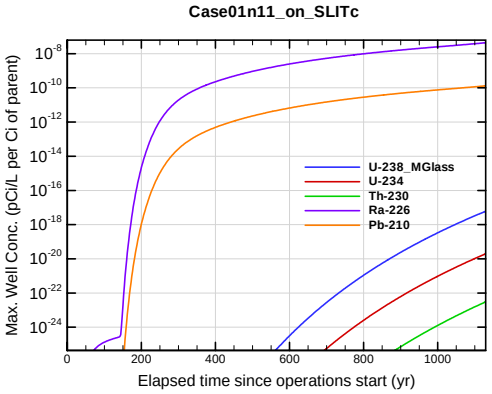

Figure A1B-239. Max. 100-m well conc. for Case01n11_on_SLITc U-238_MGlass

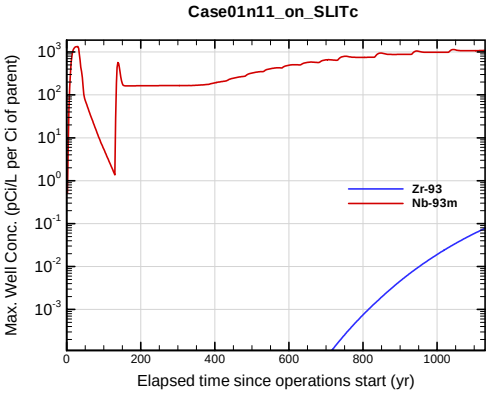

Figure A1B-240. Max. 100-m well conc. for Case01n11_on_SLITc Zr-93

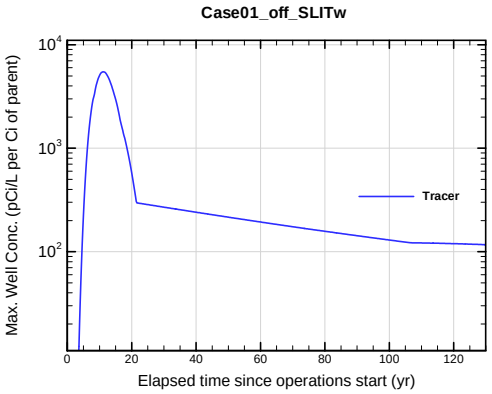

Figure A1B-241. Max. 100-m well conc. for Case01_off_SLITw Tracer

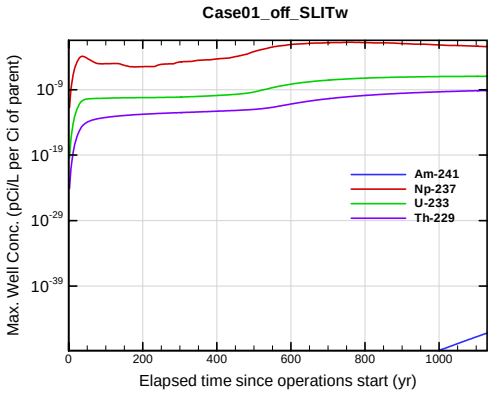

Figure A1B-242. Max. 100-m well conc. for Case01_off_SLITw Am-241

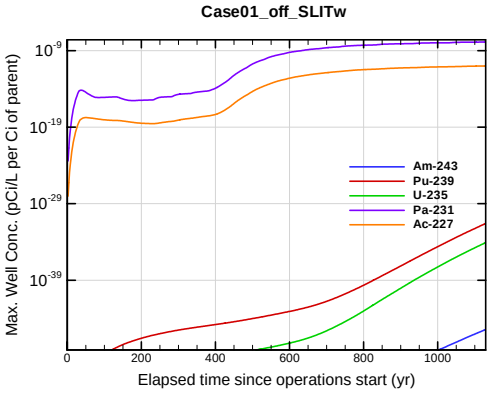

Figure A1B-243. Max. 100-m well conc. for Case01_off_SLITw Am-243

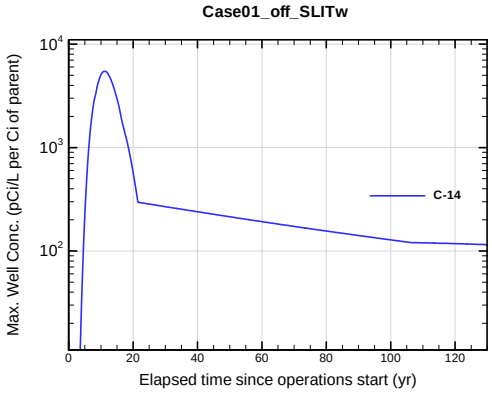

Figure A1B-244. Max. 100-m well conc. for Case01_off_SLITw C-14

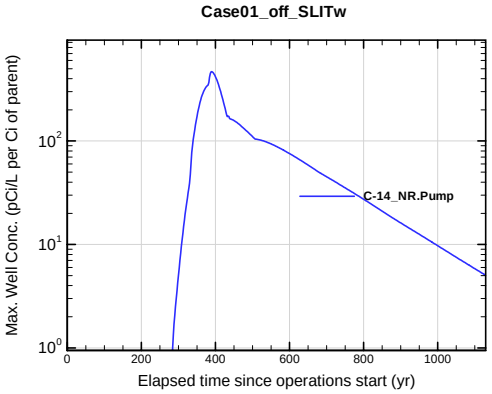

Figure A1B-245. Max. 100-m well conc. for Case01_off_SLITw C-14_NR.Pump

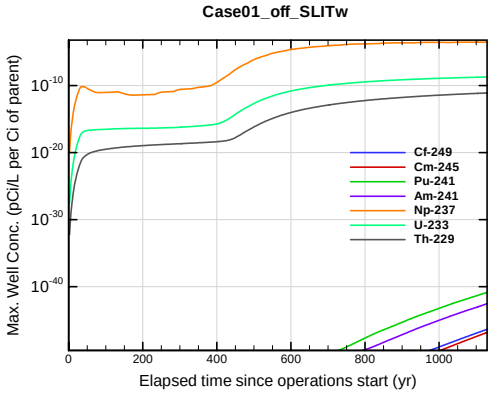

Figure A1B-246. Max. 100-m well conc. for Case01_off_SLITw Cf-249

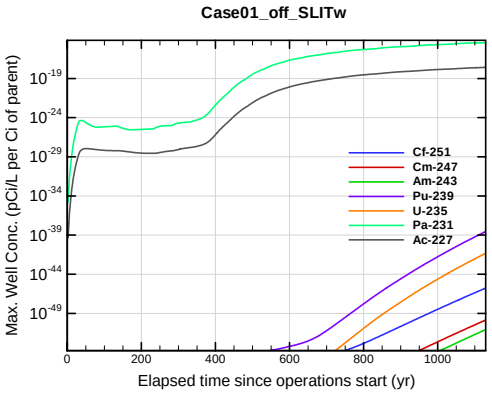

Figure A1B-247. Max. 100-m well conc. for Case01_off_SLITw Cf-251

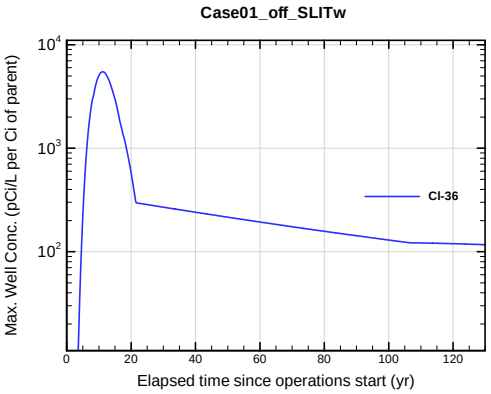

Figure A1B-248. Max. 100-m well conc. for Case01_off_SLITw Cl-36

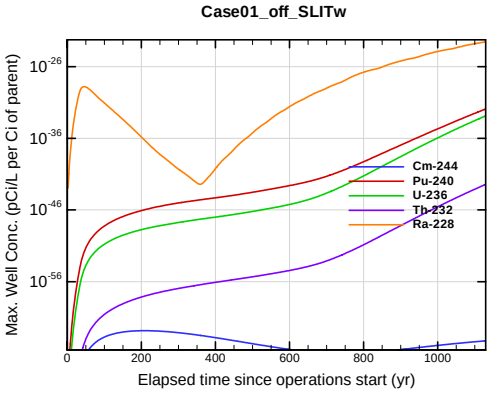

Figure A1B-249. Max. 100-m well conc. for Case01_off_SLITw Cm-244

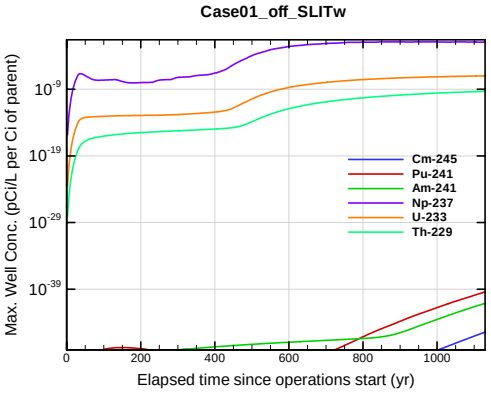

Figure A1B-250. Max. 100-m well conc. for Case01_off_SLITw Cm-245

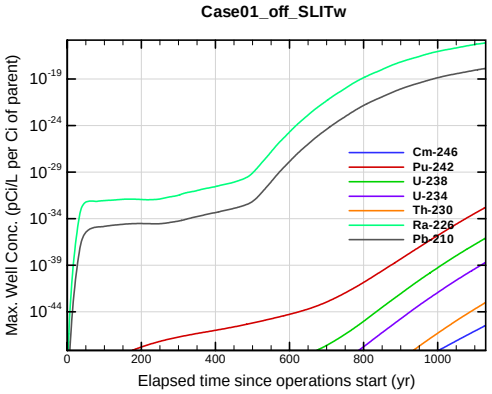

Figure A1B-251. Max. 100-m well conc. for Case01_off_SLITw Cm-246

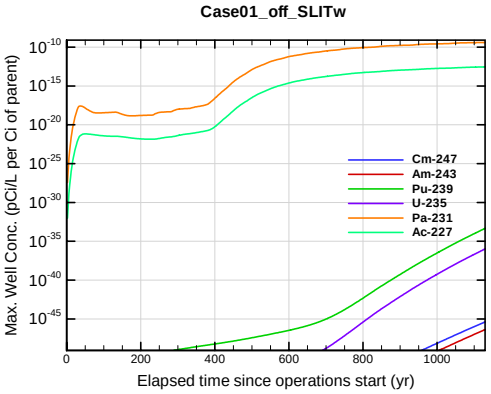

Figure A1B-252. Max. 100-m well conc. for Case01_off_SLITw Cm-247

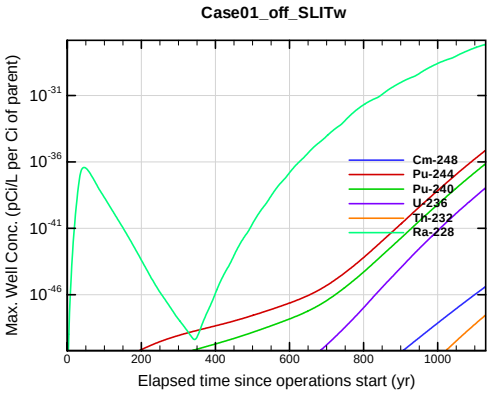

Figure A1B-253. Max. 100-m well conc. for Case01_off_SLITw Cm-248

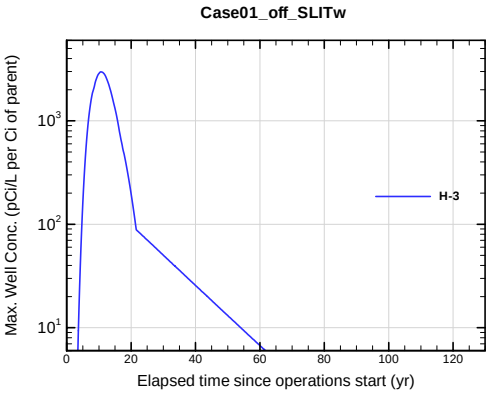

Figure A1B-254. Max. 100-m well conc. for Case01_off_SLITw H-3

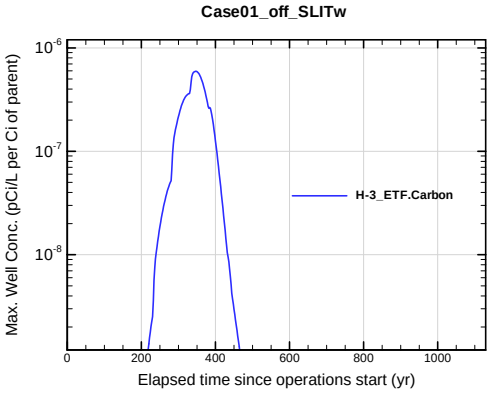

Figure A1B-255. Max. 100-m well conc. for Case01_off_SLITw H-3_ETF.Carbon

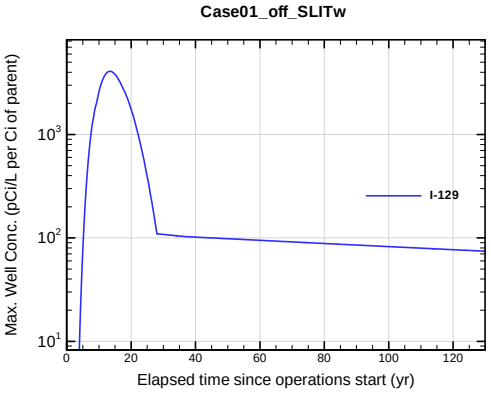

Figure A1B-256. Max. 100-m well conc. for Case01_off_SLITw I-129

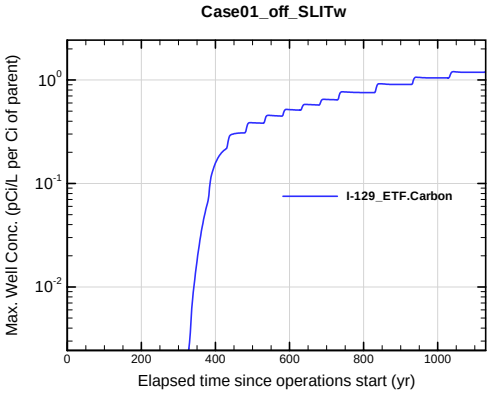

Figure A1B-257. Max. 100-m well conc. for Case01_off_SLITw I-129_ETF.Carbon

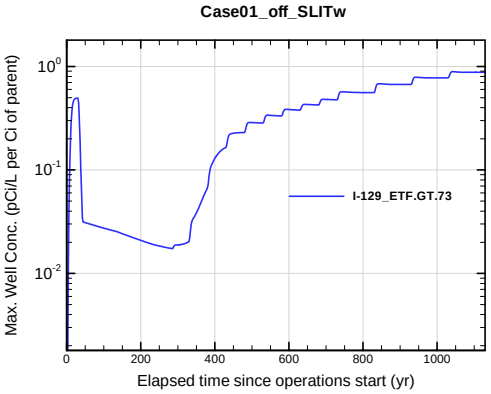

Figure A1B-258. Max. 100-m well conc. for Case01_off_SLITw I-129_ETF.GT.73

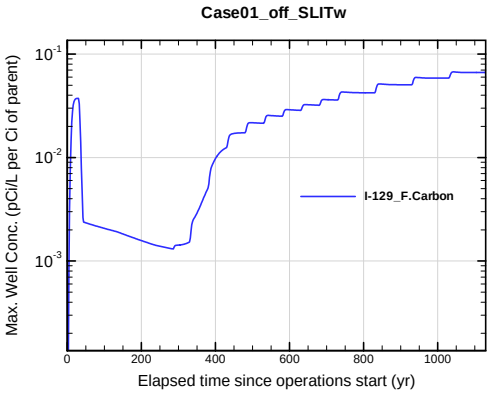

Figure A1B-259. Max. 100-m well conc. for Case01_off_SLITw I-129_F.Carbon

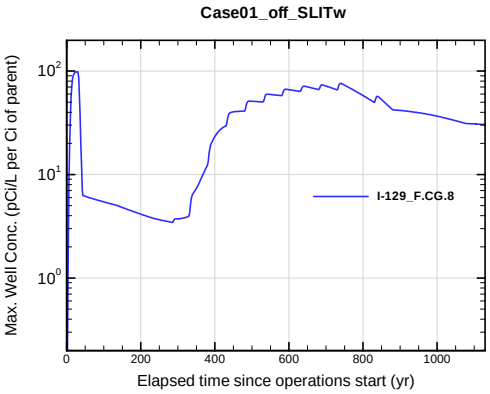

Figure A1B-260. Max. 100-m well conc. for Case01_off_SLITw I-129_F.CG.8

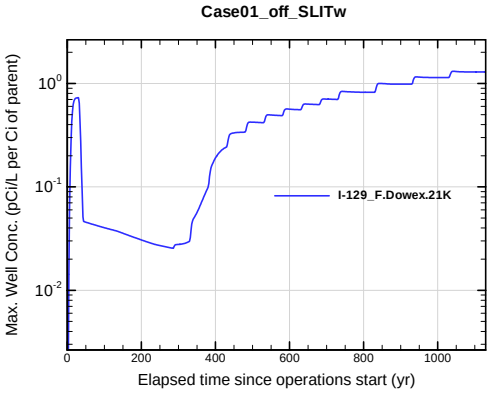

Figure A1B-261. Max. 100-m well conc. for Case01_off_SLITw I-129_F.Dowex.21K

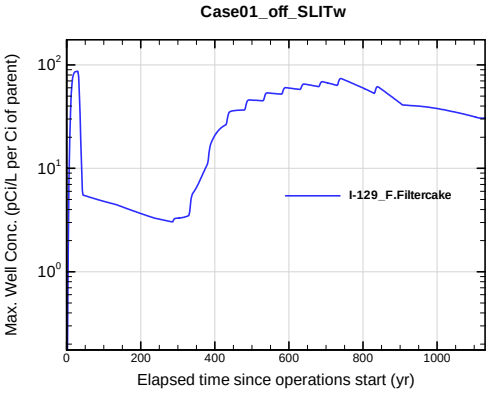

Figure A1B-262. Max. 100-m well conc. for Case01_off_SLITw I-129_F.Filtercake

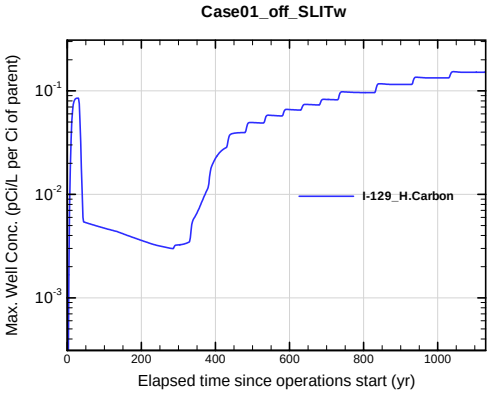

Figure A1B-263. Max. 100-m well conc. for Case01_off_SLITw I-129_H.Carbon

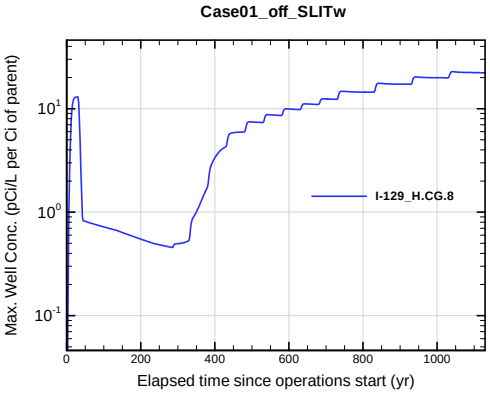

Figure A1B-264. Max. 100-m well conc. for Case01_off_SLITw I-129_H.CG.8

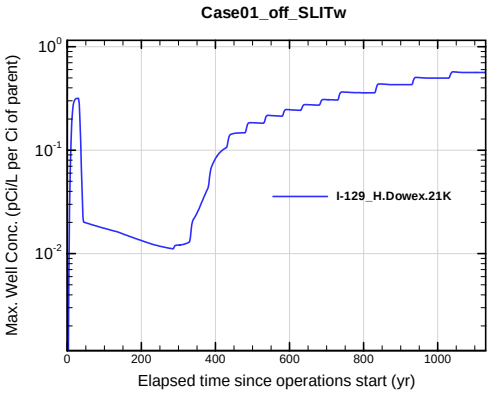

Figure A1B-265. Max. 100-m well conc. for Case01_off_SLITw I-129_H.Dowex.21K

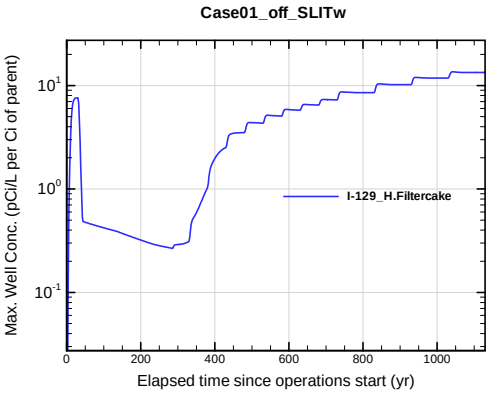

Figure A1B-266. Max. 100-m well conc. for Case01_off_SLITw I-129_H.Filtercake

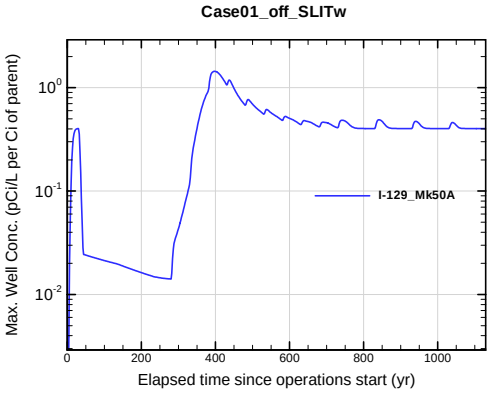

Figure A1B-267. Max. 100-m well conc. for Case01_off_SLITw I-129_Mk50A

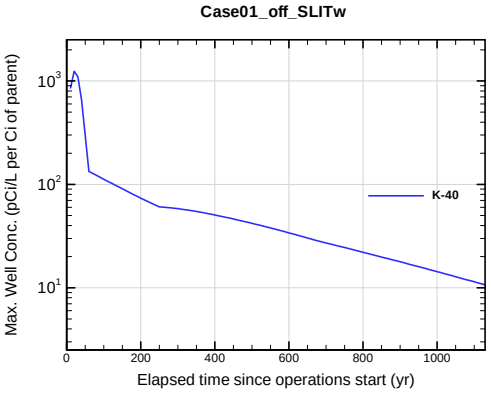

Figure A1B-268. Max. 100-m well conc. for Case01_off_SLITw K-40

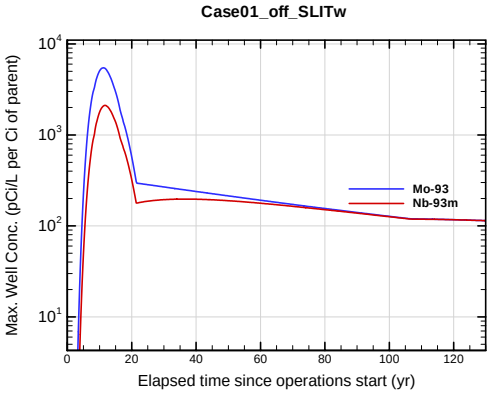

Figure A1B-269. Max. 100-m well conc. for Case01_off_SLITw Mo-93

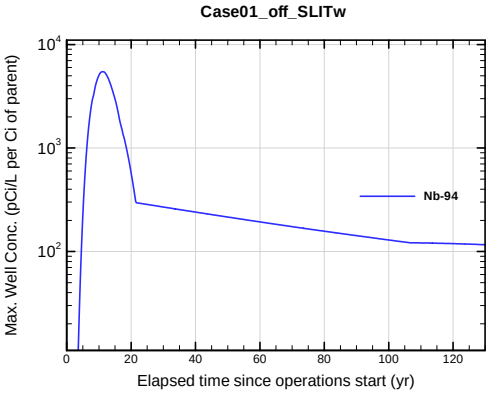

Figure A1B-270. Max. 100-m well conc. for Case01_off_SLITw Nb-94

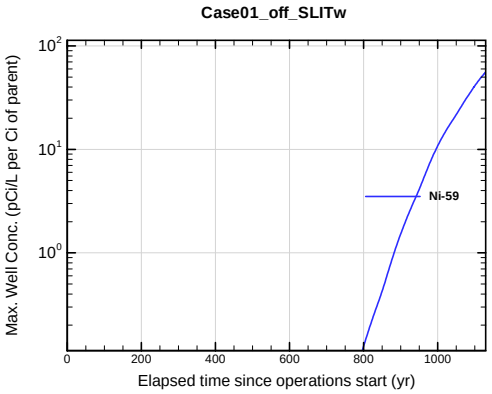

Figure A1B-271. Max. 100-m well conc. for Case01_off_SLITw Ni-59

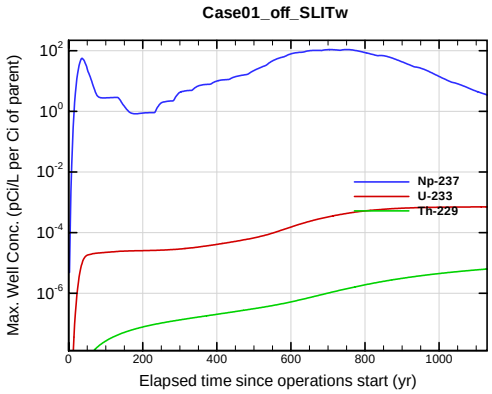

Figure A1B-272. Max. 100-m well conc. for Case01_off_SLITw Np-237

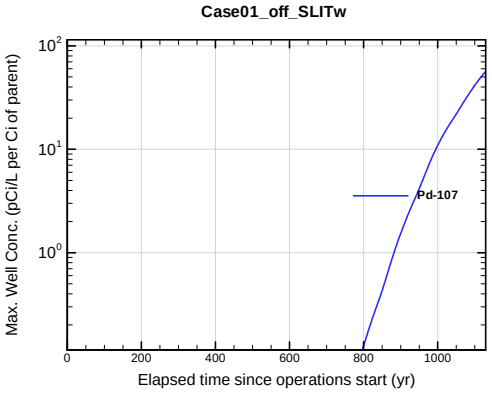

Figure A1B-273. Max. 100-m well conc. for Case01_off_SLITw Pd-107

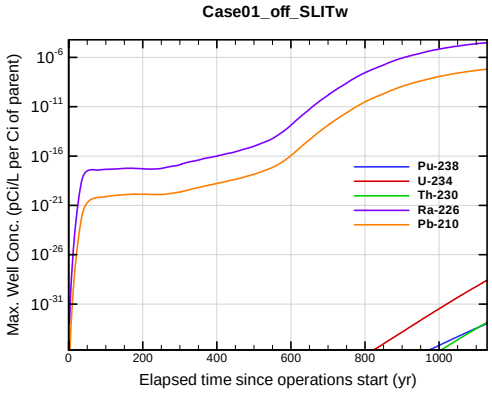

Figure A1B-274. Max. 100-m well conc. for Case01_off_SLITw Pu-238

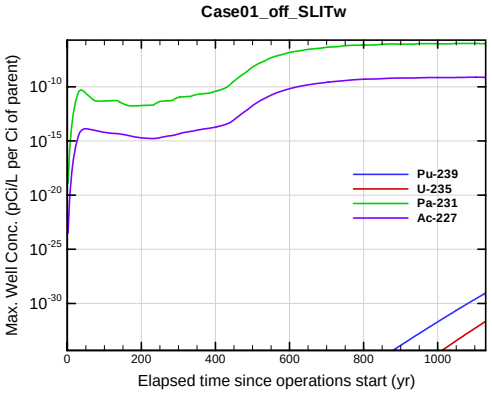

Figure A1B-275. Max. 100-m well conc. for Case01_off_SLITw Pu-239

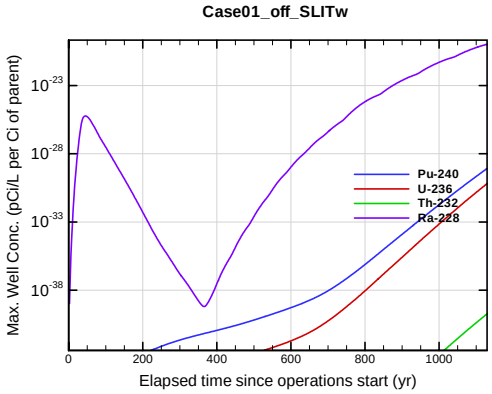

Figure A1B-276. Max. 100-m well conc. for Case01_off_SLITw Pu-240

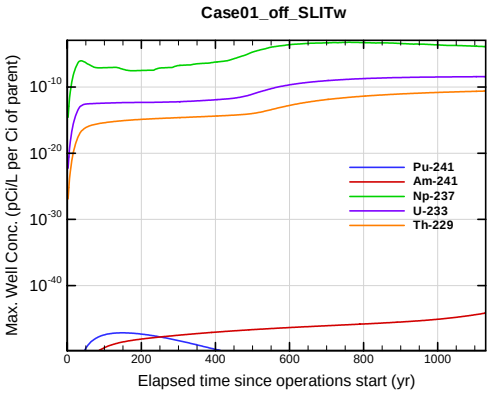

Figure A1B-277. Max. 100-m well conc. for Case01_off_SLITw Pu-241

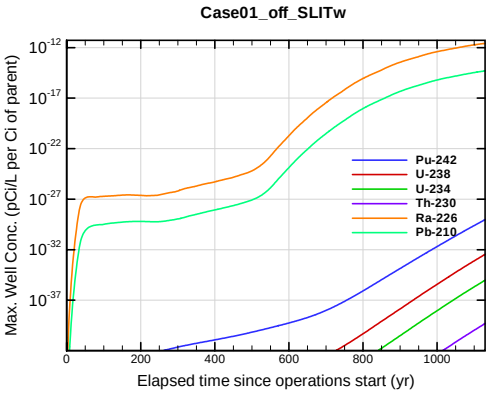

Figure A1B-278. Max. 100-m well conc. for Case01_off_SLITw Pu-242

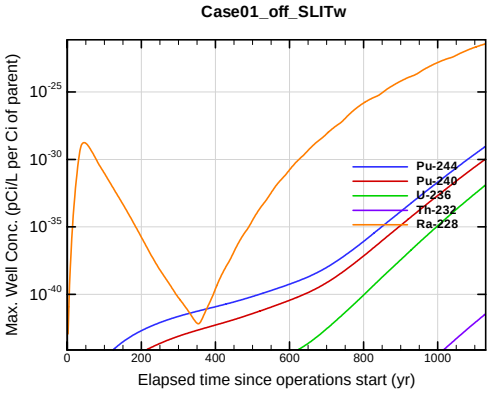

Figure A1B-279. Max. 100-m well conc. for Case01_off_SLITw Pu-244

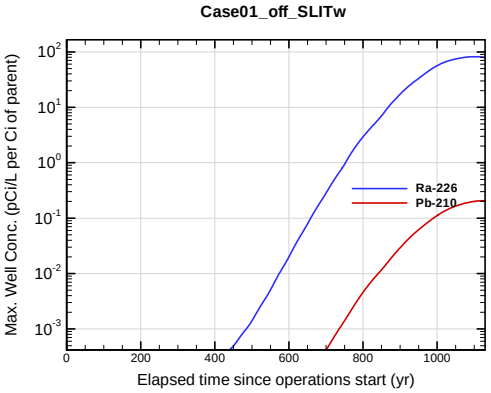

Figure A1B-280. Max. 100-m well conc. for Case01_off_SLITw Ra-226

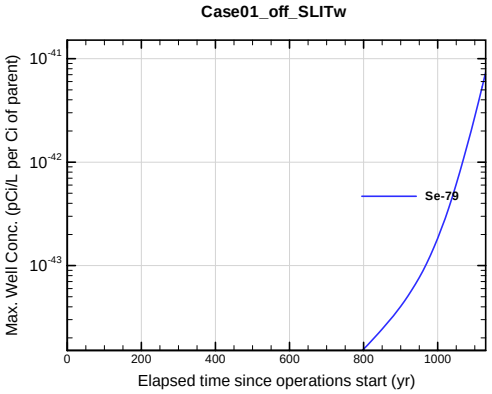

Figure A1B-281. Max. 100-m well conc. for Case01_off_SLITw Se-79

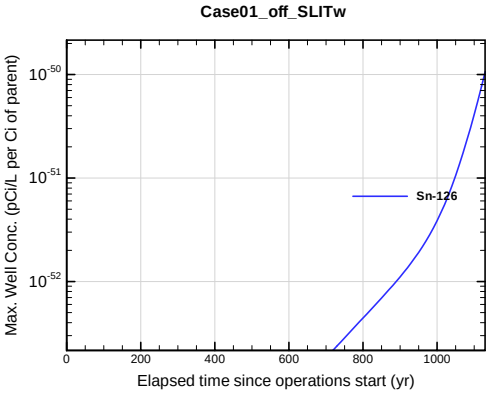

Figure A1B-282. Max. 100-m well conc. for Case01_off_SLITw Sn-126

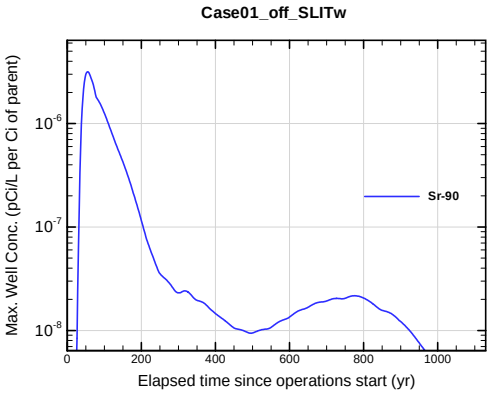

Figure A1B-283. Max. 100-m well conc. for Case01_off_SLITw Sr-90

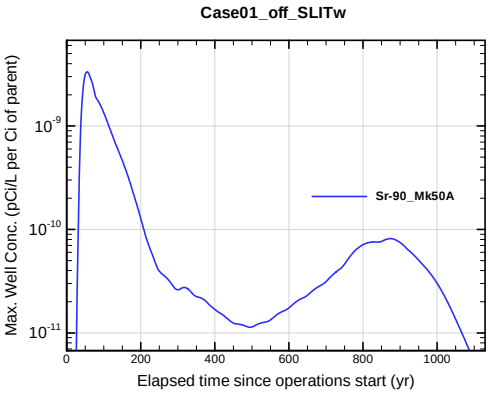

Figure A1B-284. Max. 100-m well conc. for Case01_off_SLITw Sr-90_Mk50A

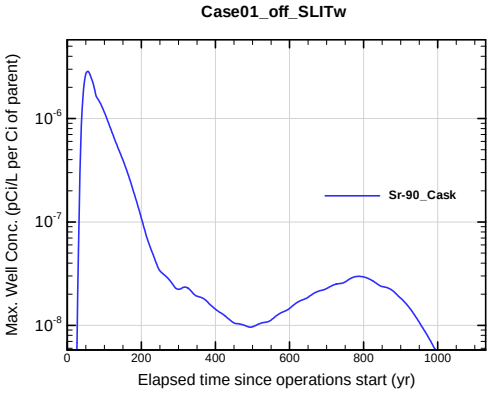

Figure A1B-285. Max. 100-m well conc. for Case01_off_SLITw Sr-90_Cask

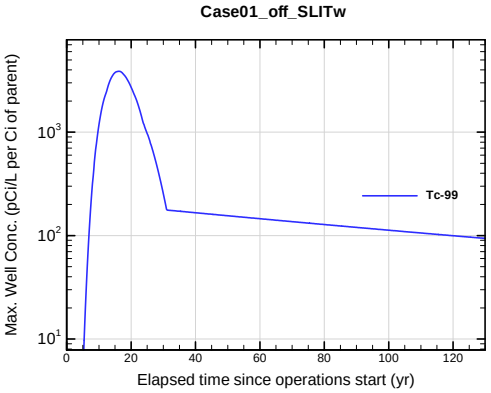

Figure A1B-286. Max. 100-m well conc. for Case01_off_SLITw Tc-99

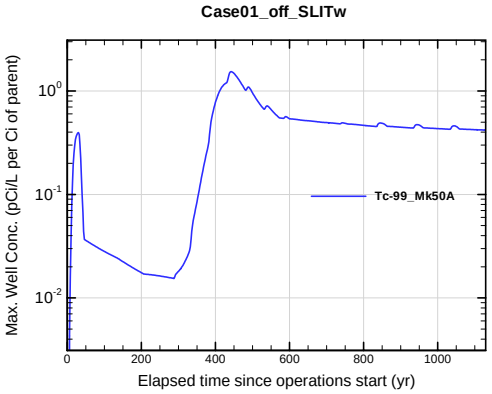

Figure A1B-287. Max. 100-m well conc. for Case01_off_SLITw Tc-99_Mk50A

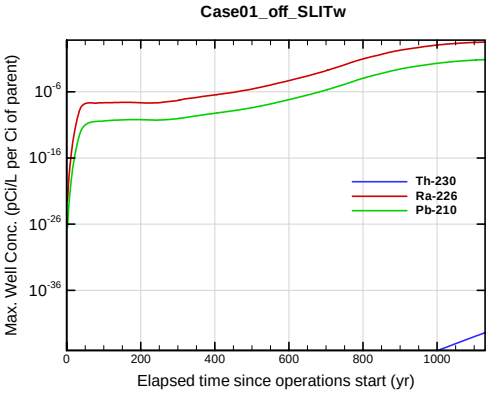

Figure A1B-288. Max. 100-m well conc. for Case01_off_SLITw Th-230

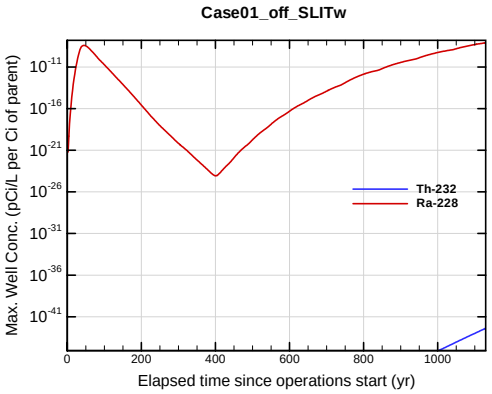

Figure A1B-289. Max. 100-m well conc. for Case01_off_SLITw Th-232

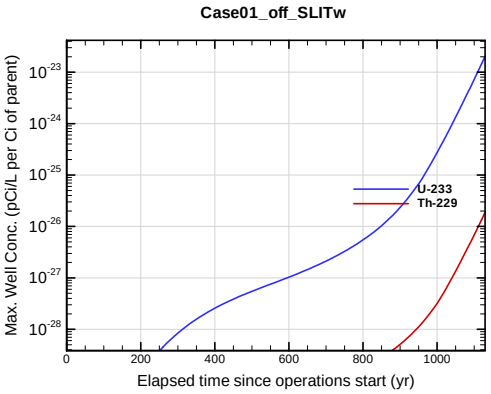

Figure A1B-290. Max. 100-m well conc. for Case01_off_SLITw U-233

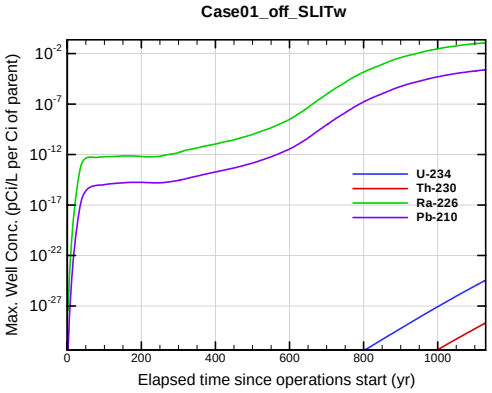

Figure A1B-291. Max. 100-m well conc. for Case01_off_SLITw U-234

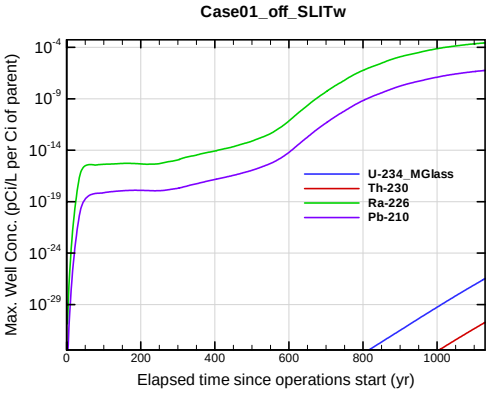

Figure A1B-292. Max. 100-m well conc. for Case01_off_SLITw U-234_MGlass

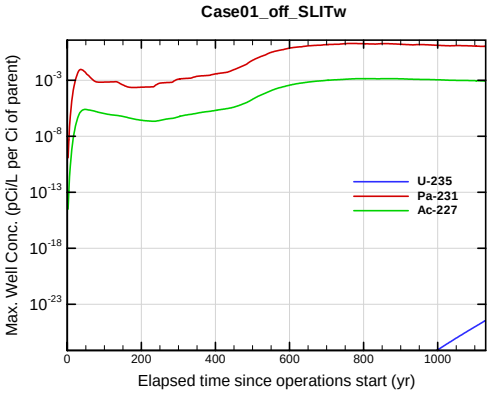

Figure A1B-293. Max. 100-m well conc. for Case01_off_SLITw U-235

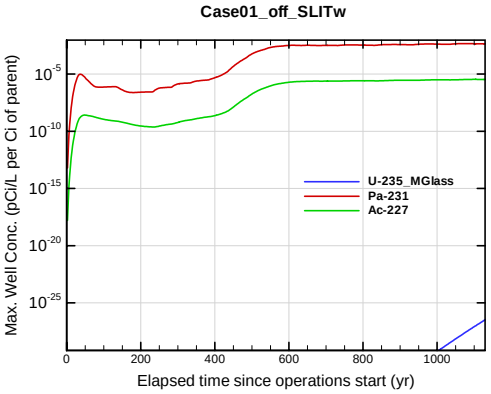

Figure A1B-294. Max. 100-m well conc. for Case01_off_SLITw U-235_MGlass

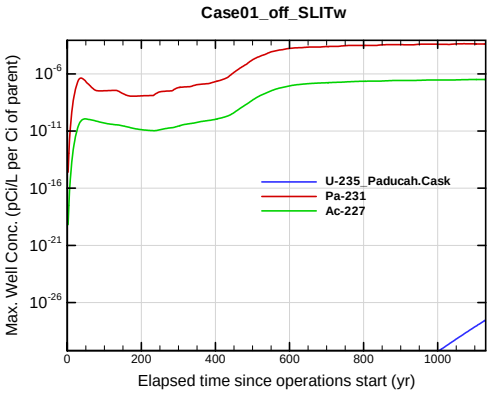

Figure A1B-295. Max. 100-m well conc. for Case01_off_SLITw U-235_Paducah.Cask

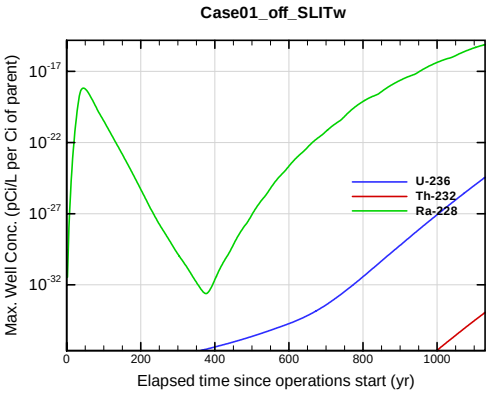

Figure A1B-296. Max. 100-m well conc. for Case01_off_SLITw U-236

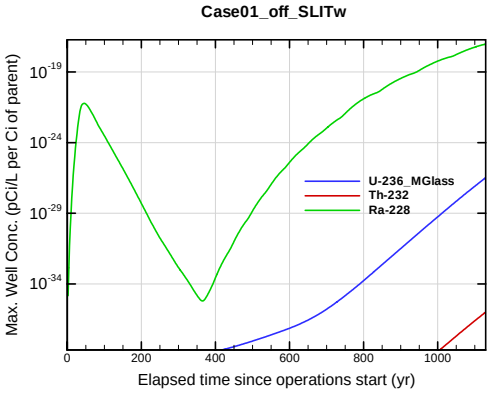

Figure A1B-297. Max. 100-m well conc. for Case01_off_SLITw U-236_MGlass

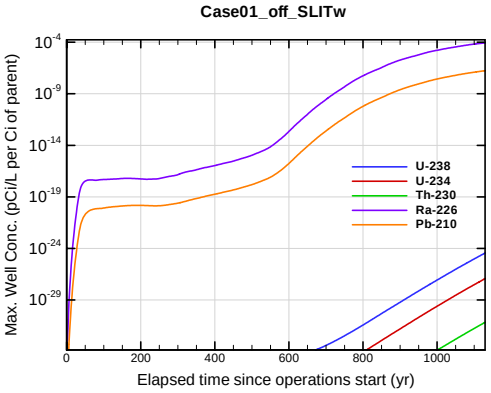

Figure A1B-298. Max. 100-m well conc. for Case01_off_SLITw U-238

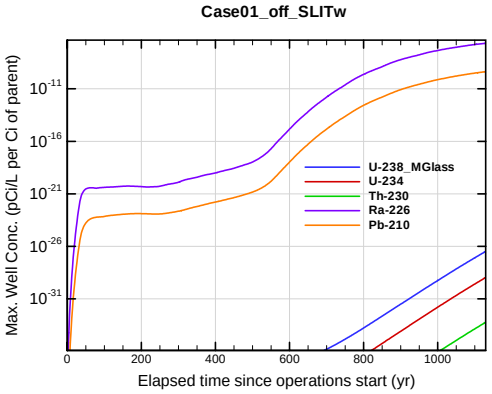

Figure A1B-299. Max. 100-m well conc. for Case01_off_SLITw U-238_MGlass

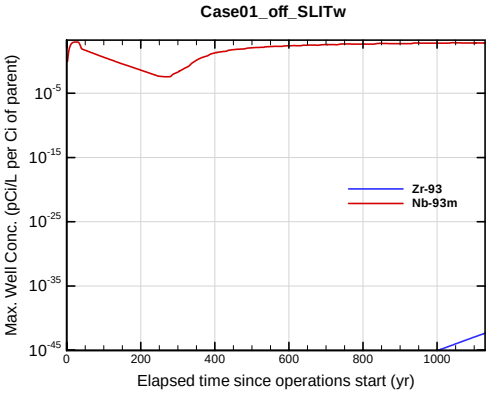

Figure A1B-300. Max. 100-m well conc. for Case01_off_SLITw Zr-93

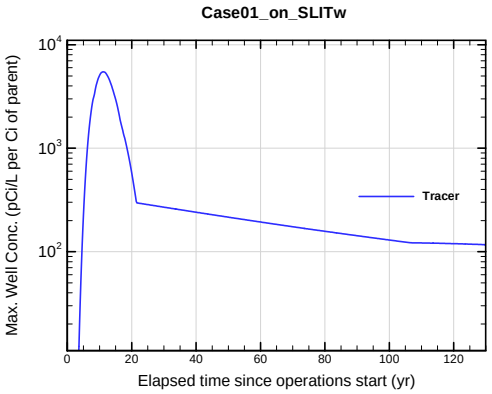

Figure A1B-301. Max. 100-m well conc. for Case01_on_SLITw Tracer

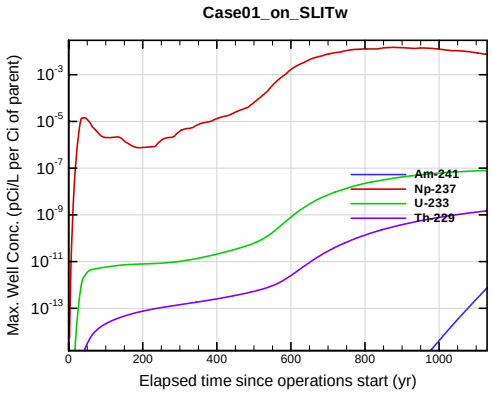

Figure A1B-302. Max. 100-m well conc. for Case01_on_SLITw Am-241

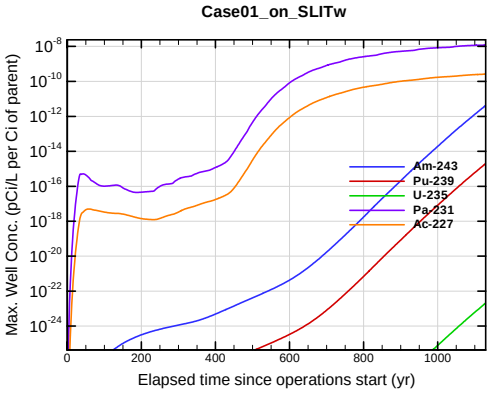

Figure A1B-303. Max. 100-m well conc. for Case01_on_SLITw Am-243

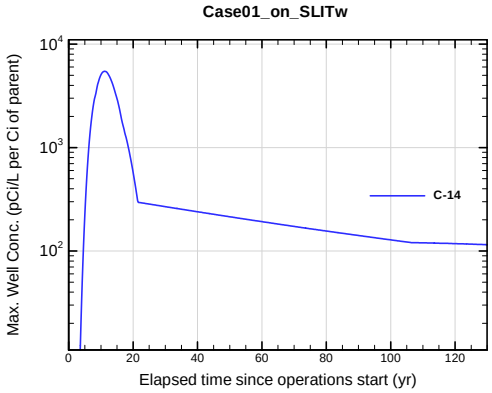

Figure A1B-304. Max. 100-m well conc. for Case01_on_SLITw C-14

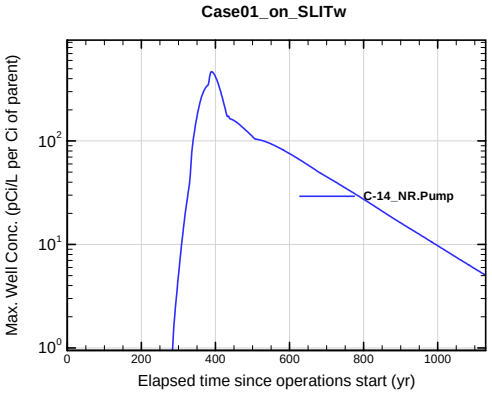

Figure A1B-305. Max. 100-m well conc. for Case01_on_SLITw C-14_NR.Pump

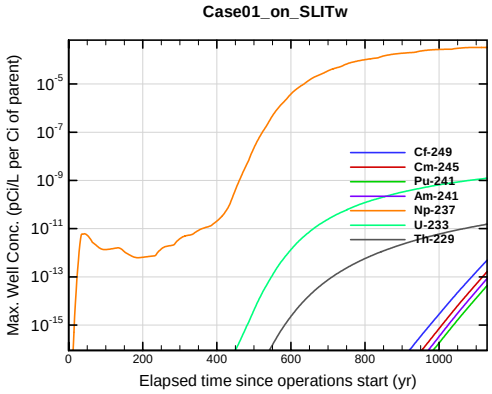

Figure A1B-306. Max. 100-m well conc. for Case01_on_SLITw Cf-249

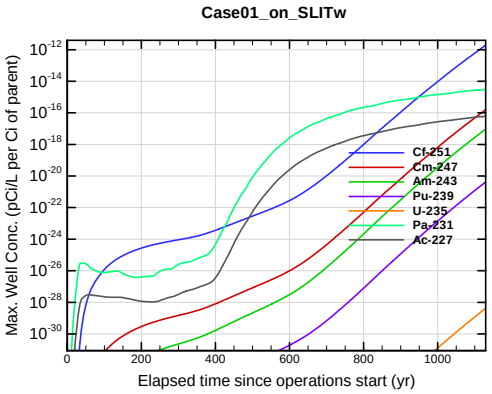

Figure A1B-307. Max. 100-m well conc. for Case01_on_SLITw Cf-251

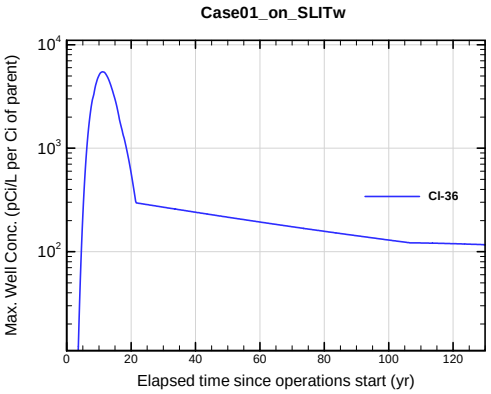

Figure A1B-308. Max. 100-m well conc. for Case01_on_SLITw Cl-36

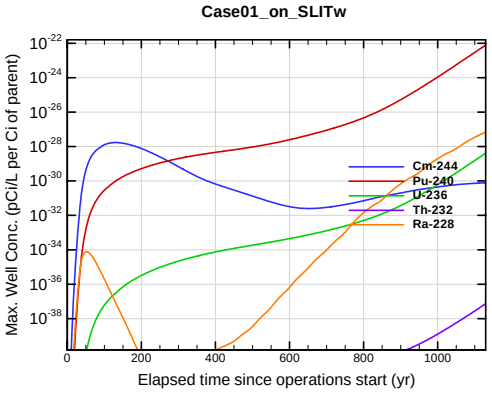

Figure A1B-309. Max. 100-m well conc. for Case01_on_SLITw Cm-244

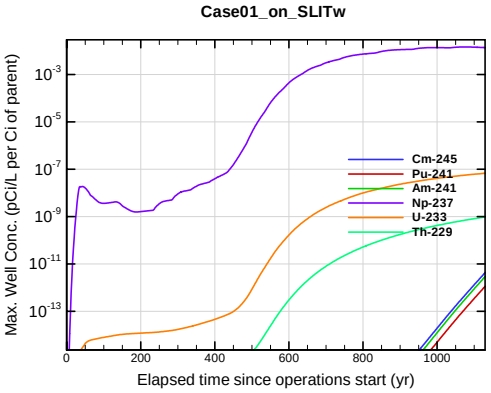

Figure A1B-310. Max. 100-m well conc. for Case01_on_SLITw Cm-245

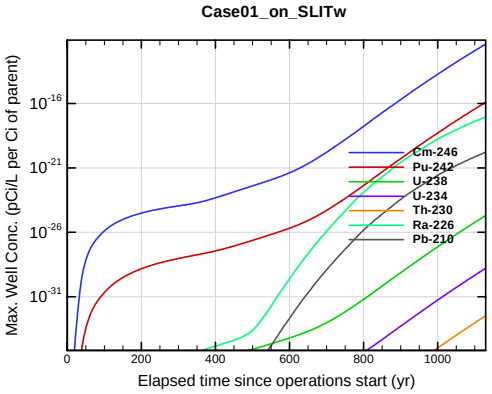

Figure A1B-311. Max. 100-m well conc. for Case01_on_SLITw Cm-246

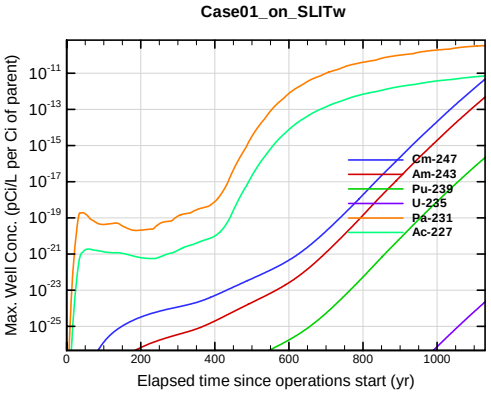

Figure A1B-312. Max. 100-m well conc. for Case01_on_SLITw Cm-247

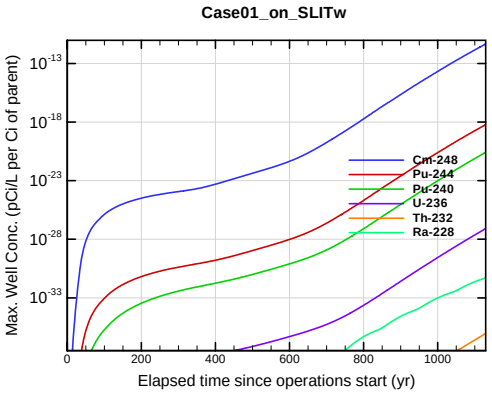

Figure A1B-313. Max. 100-m well conc. for Case01_on_SLITw Cm-248

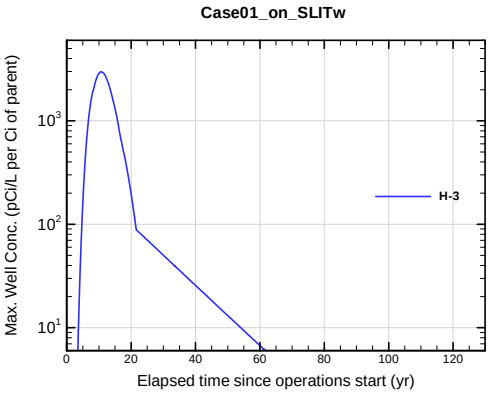

Figure A1B-314. Max. 100-m well conc. for Case01_on_SLITw H-3

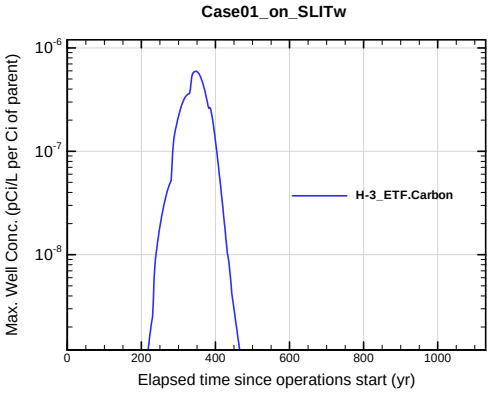

Figure A1B-315. Max. 100-m well conc. for Case01_on_SLITw H-3_ETF.Carbon

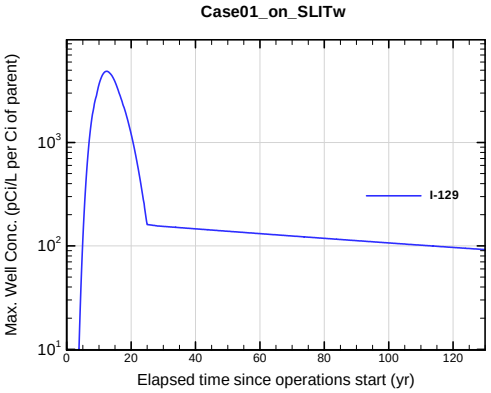

Figure A1B-316. Max. 100-m well conc. for Case01_on_SLITw I-129

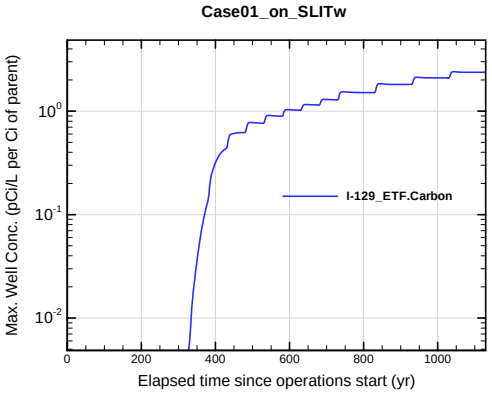

Figure A1B-317. Max. 100-m well conc. for Case01_on_SLITw I-129_ETF.Carbon

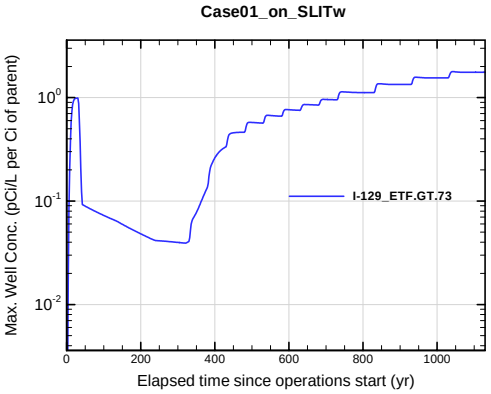

Figure A1B-318. Max. 100-m well conc. for Case01_on_SLITw I-129_ETF.GT.73

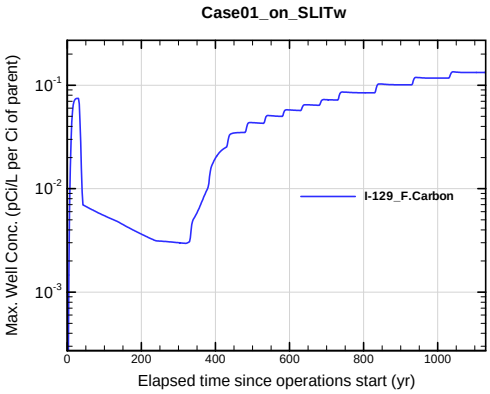

Figure A1B-319. Max. 100-m well conc. for Case01_on_SLITw I-129_F.Carbon

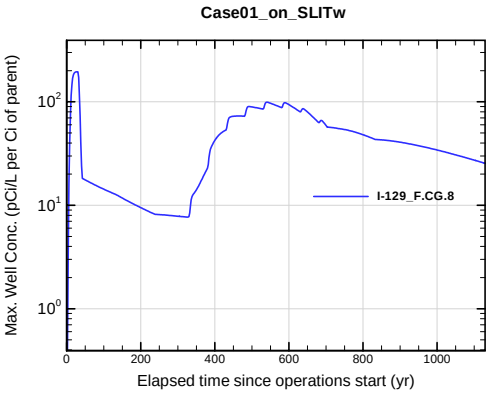

Figure A1B-320. Max. 100-m well conc. for Case01_on_SLITw I-129_F.CG.8

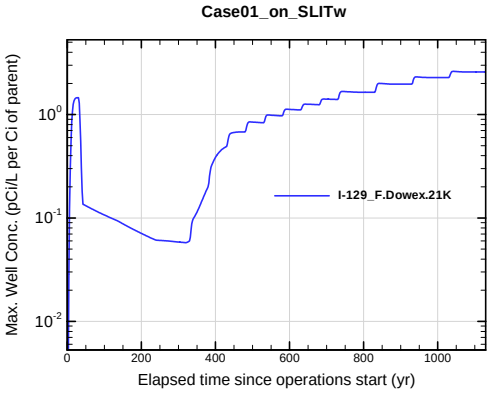

Figure A1B-321. Max. 100-m well conc. for Case01_on_SLITw I-129_F.Dowex.21K

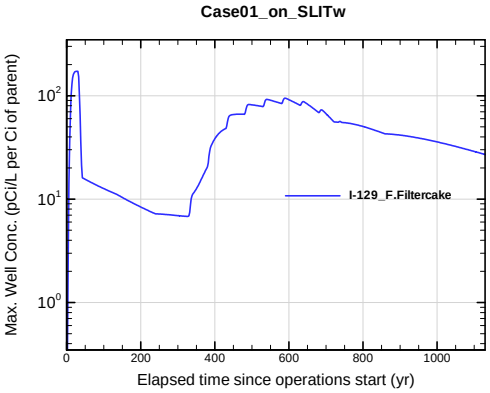

Figure A1B-322. Max. 100-m well conc. for Case01_on_SLITw I-129_F.Filtercake

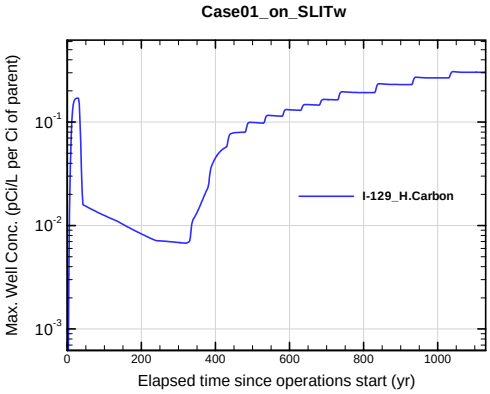

Figure A1B-323. Max. 100-m well conc. for Case01_on_SLITw I-129_H.Carbon

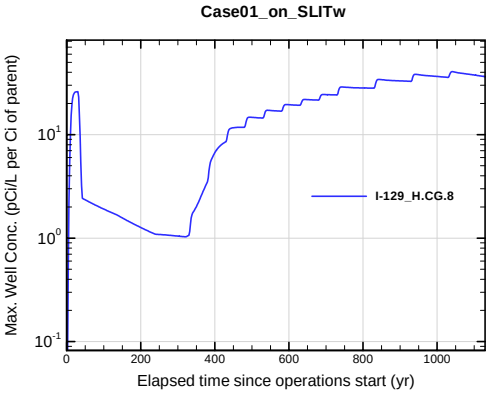

Figure A1B-324. Max. 100-m well conc. for Case01_on_SLITw I-129_H.CG.8

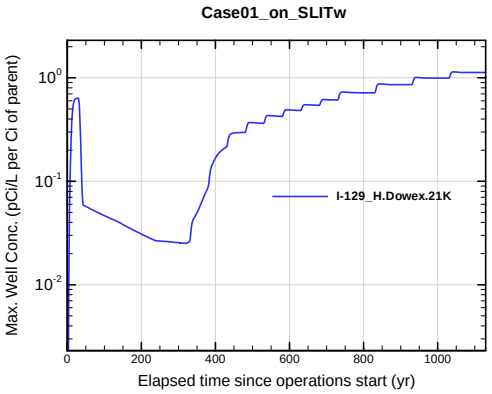

Figure A1B-325. Max. 100-m well conc. for Case01_on_SLITw I-129_H.Dowex.21K

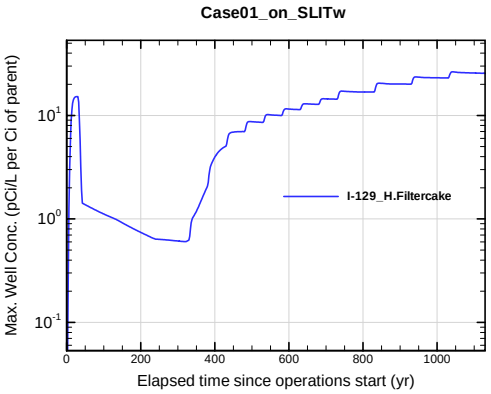

Figure A1B-326. Max. 100-m well conc. for Case01_on_SLITw I-129_H.Filtercake

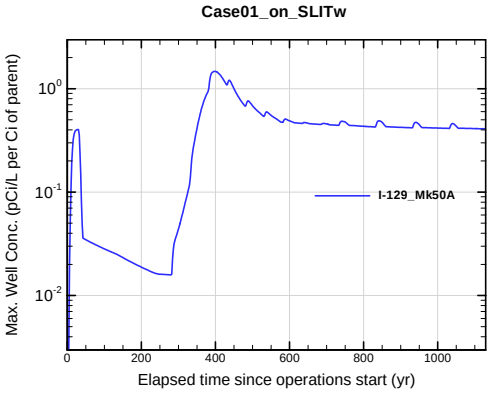

Figure A1B-327. Max. 100-m well conc. for Case01_on_SLITw I-129_Mk50A

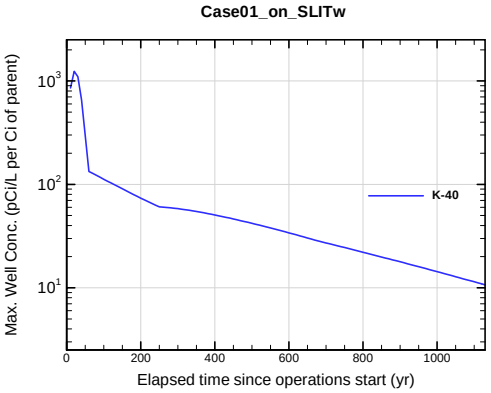

Figure A1B-328. Max. 100-m well conc. for Case01_on_SLITw K-40

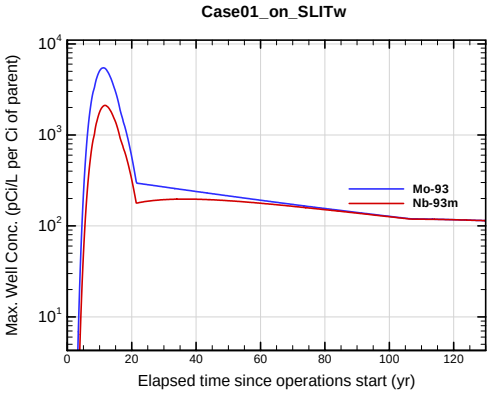

Figure A1B-329. Max. 100-m well conc. for Case01_on_SLITw Mo-93

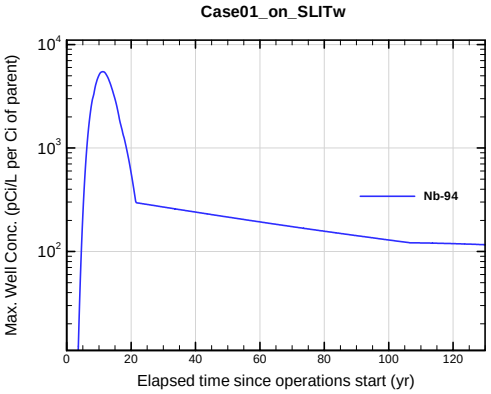

Figure A1B-330. Max. 100-m well conc. for Case01_on_SLITw Nb-94

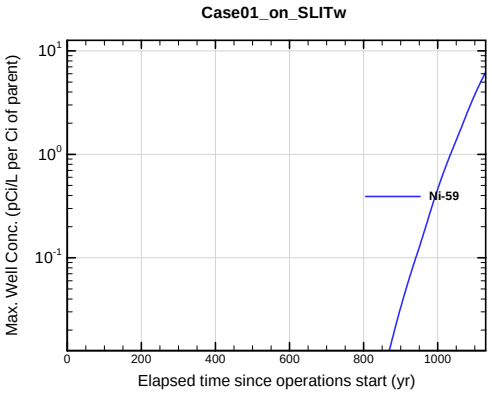

Figure A1B-331. Max. 100-m well conc. for Case01_on_SLITw Ni-59

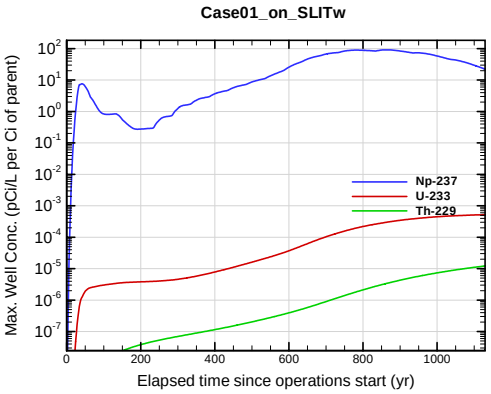

Figure A1B-332. Max. 100-m well conc. for Case01_on_SLITw Np-237

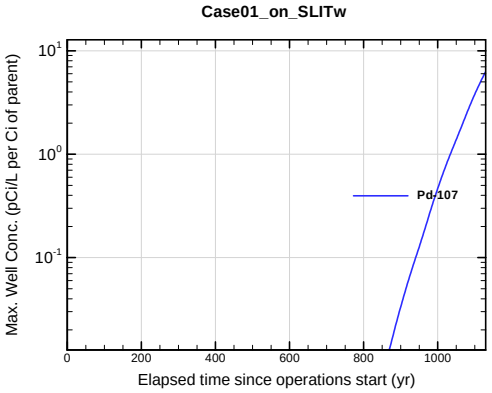

Figure A1B-333. Max. 100-m well conc. for Case01_on_SLITw Pd-107

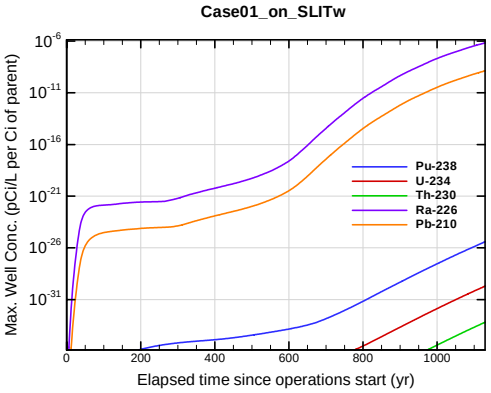

Figure A1B-334. Max. 100-m well conc. for Case01_on_SLITw Pu-238

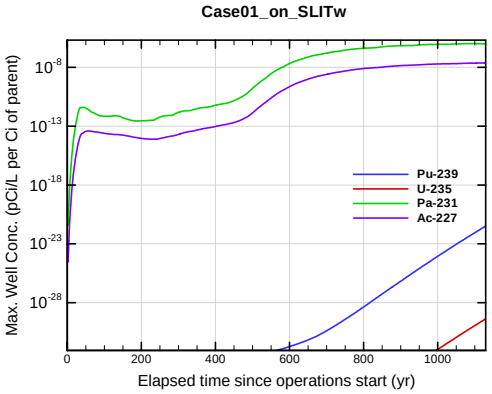

Figure A1B-335. Max. 100-m well conc. for Case01_on_SLITw Pu-239

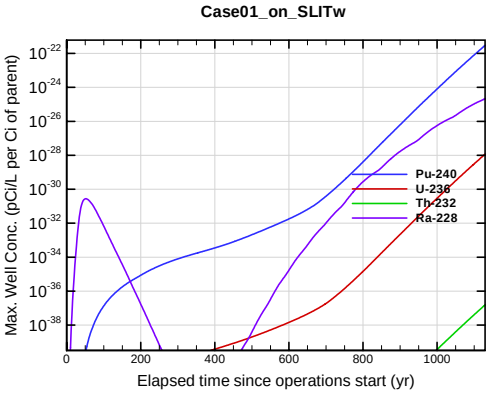

Figure A1B-336. Max. 100-m well conc. for Case01_on_SLITw Pu-240

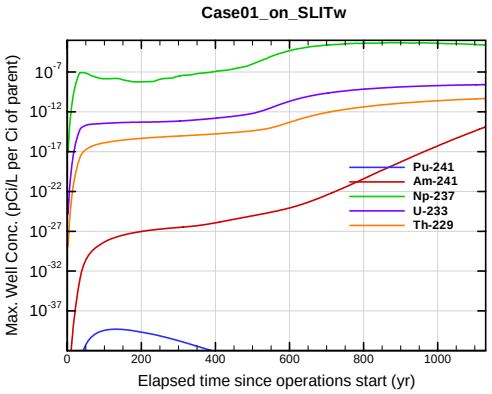

Figure A1B-337. Max. 100-m well conc. for Case01_on_SLITw Pu-241

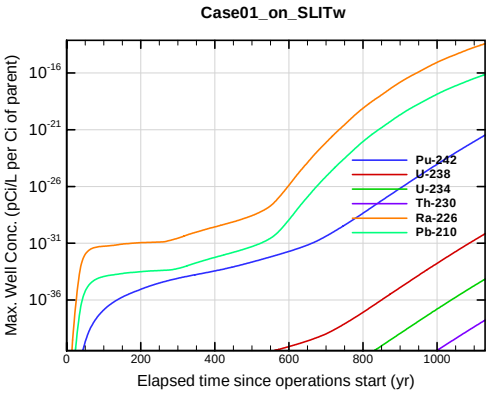

Figure A1B-338. Max. 100-m well conc. for Case01_on_SLITw Pu-242

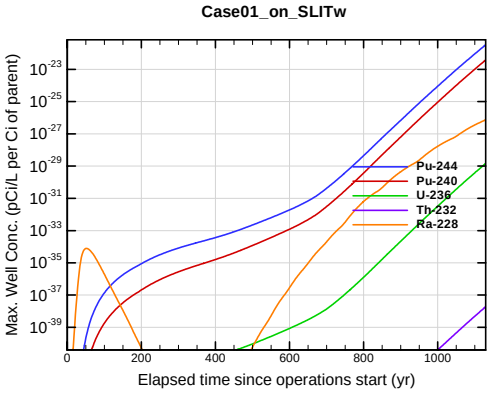

Figure A1B-339. Max. 100-m well conc. for Case01_on_SLITw Pu-244

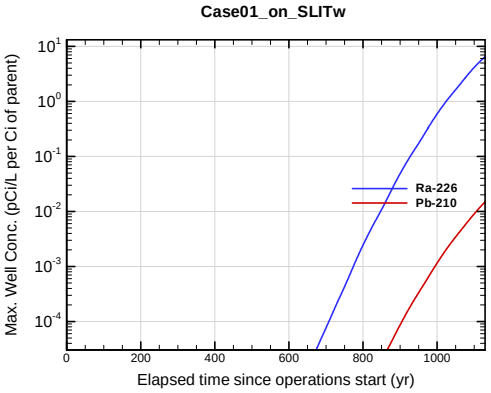

Figure A1B-340. Max. 100-m well conc. for Case01_on_SLITw Ra-226

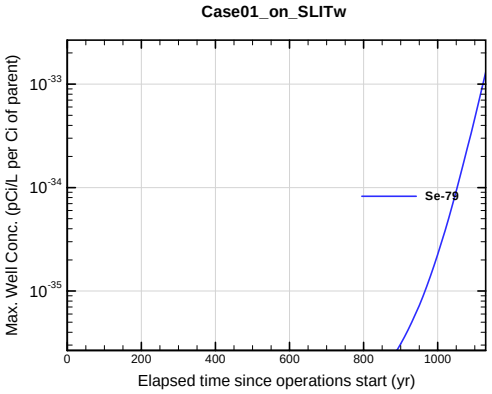

Figure A1B-341. Max. 100-m well conc. for Case01_on_SLITw Se-79

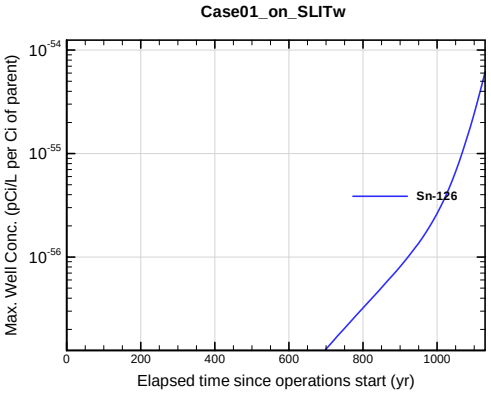

Figure A1B-342. Max. 100-m well conc. for Case01_on_SLITw Sn-126

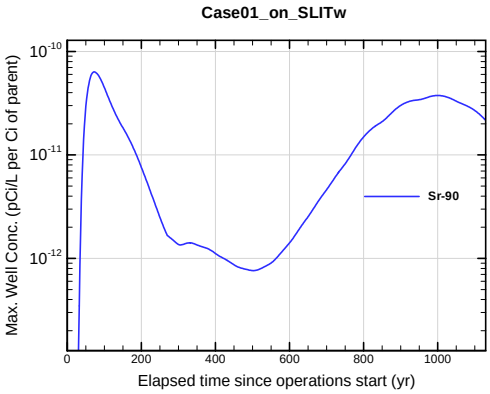

Figure A1B-343. Max. 100-m well conc. for Case01_on_SLITw Sr-90

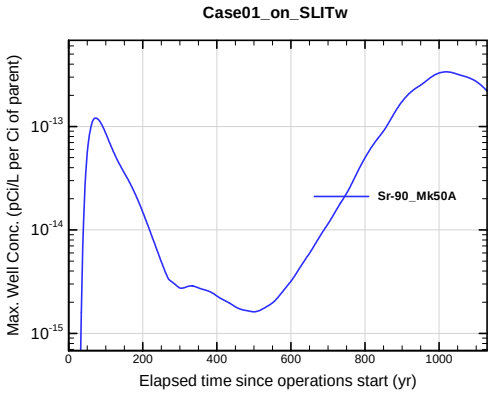

Figure A1B-344. Max. 100-m well conc. for Case01_on_SLITw Sr-90_Mk50A

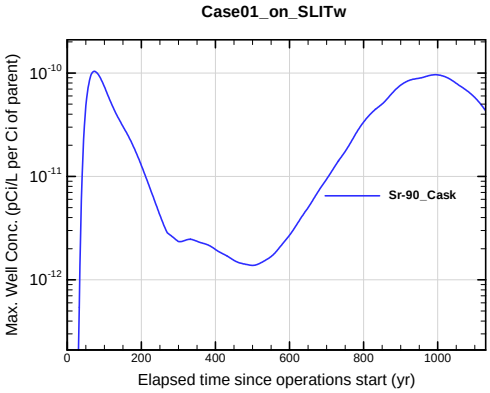

Figure A1B-345. Max. 100-m well conc. for Case01_on_SLITw Sr-90_Cask

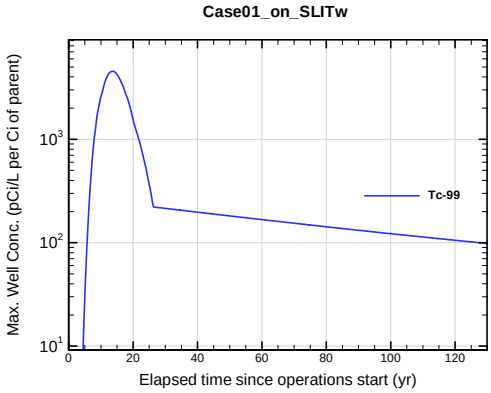

Figure A1B-346. Max. 100-m well conc. for Case01_on_SLITw Tc-99

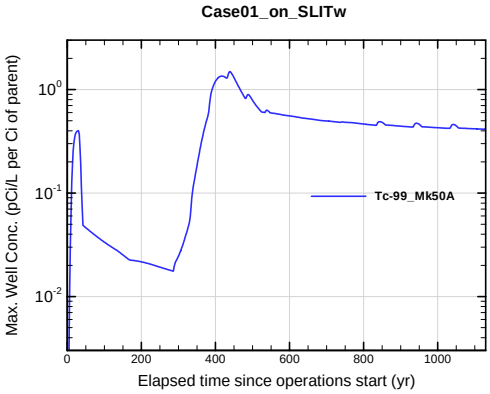

Figure A1B-347. Max. 100-m well conc. for Case01_on_SLITw Tc-99_Mk50A

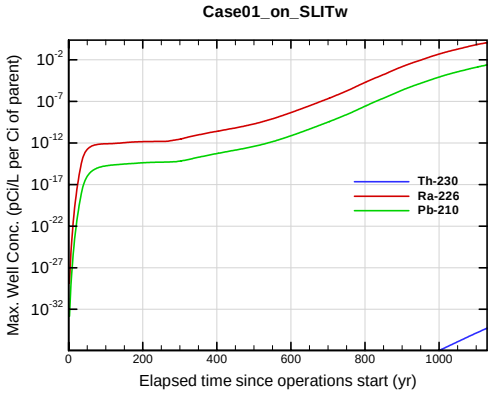

Figure A1B-348. Max. 100-m well conc. for Case01_on_SLITw Th-230

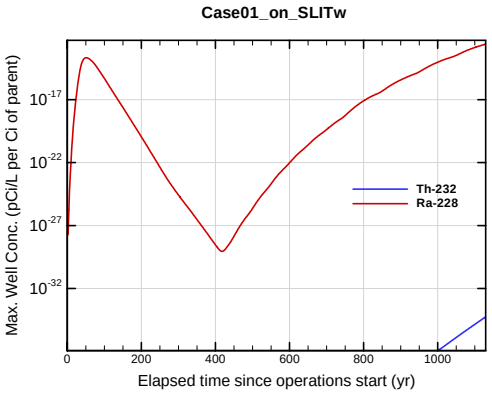

Figure A1B-349. Max. 100-m well conc. for Case01_on_SLITw Th-232

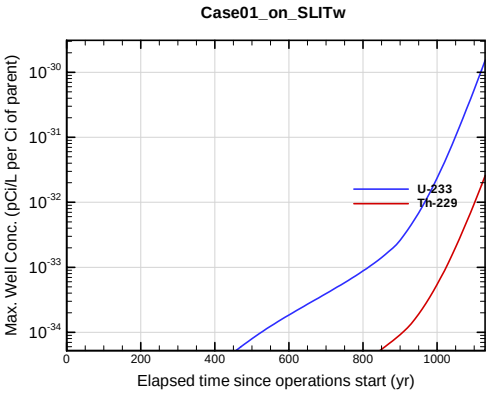

Figure A1B-350. Max. 100-m well conc. for Case01_on_SLITw U-233

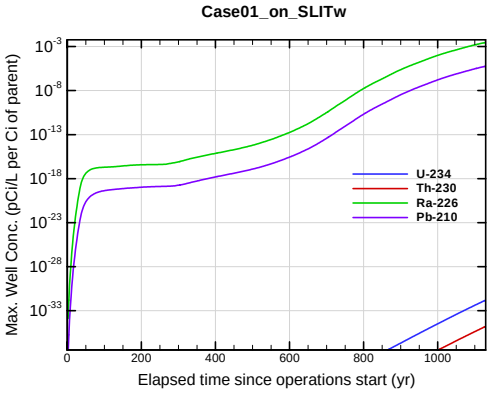

Figure A1B-351. Max. 100-m well conc. for Case01_on_SLITw U-234

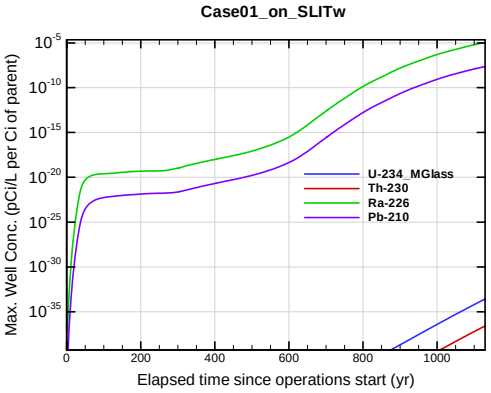

Figure A1B-352. Max. 100-m well conc. for Case01_on_SLITw U-234_MGlass

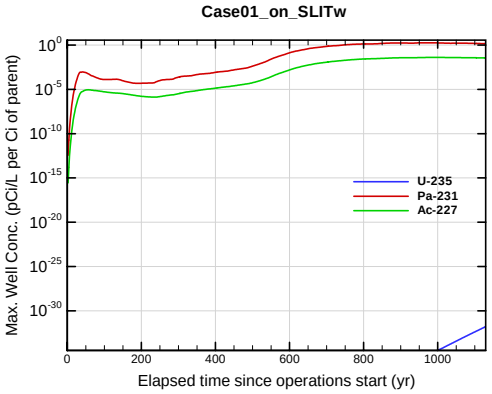

Figure A1B-353. Max. 100-m well conc. for Case01_on_SLITw U-235

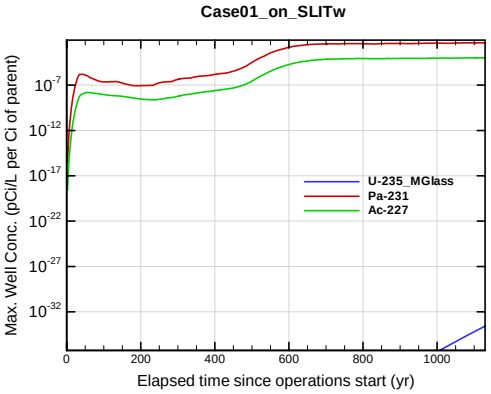

Figure A1B-354. Max. 100-m well conc. for Case01_on_SLITw U-235_MGlass

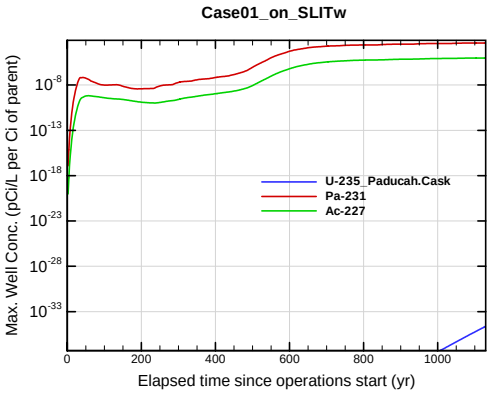

Figure A1B-355. Max. 100-m well conc. for Case01_on_SLITw U-235_Paducah.Cask

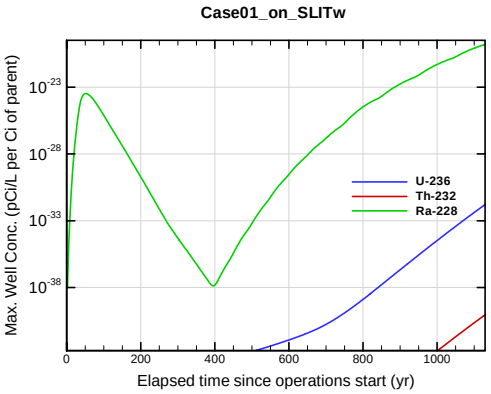

Figure A1B-356. Max. 100-m well conc. for Case01_on_SLITw U-236

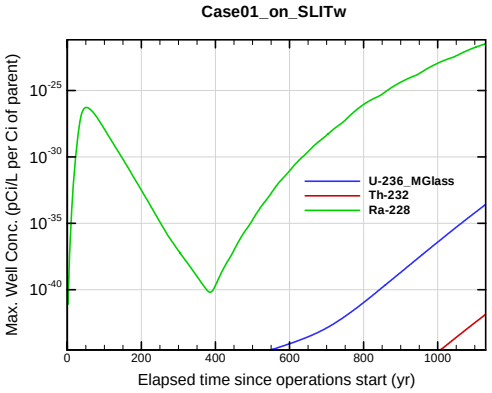

Figure A1B-357. Max. 100-m well conc. for Case01_on_SLITw U-236_MGlass

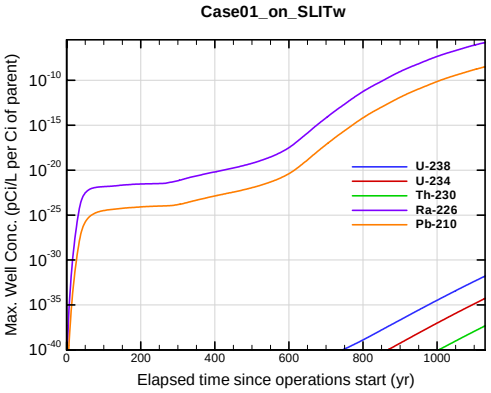

Figure A1B-358. Max. 100-m well conc. for Case01_on_SLITw U-238

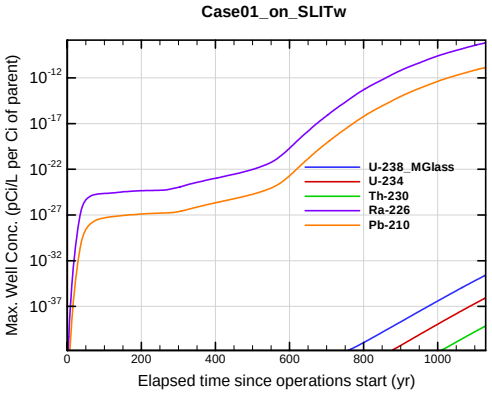

Figure A1B-359. Max. 100-m well conc. for Case01_on_SLITw U-238_MGlass

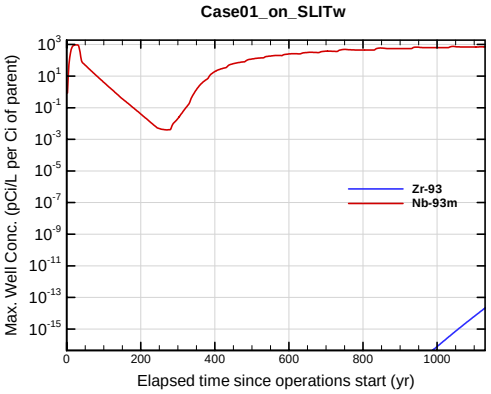

Figure A1B-360. Max. 100-m well conc. for Case01_on_SLITw Zr-93

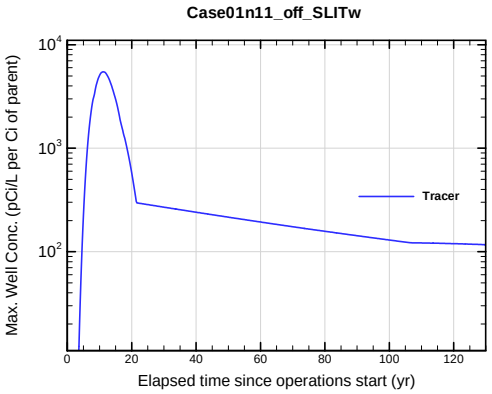

Figure A1B-361. Max. 100-m well conc. for Case01n11_off_SLITw Tracer

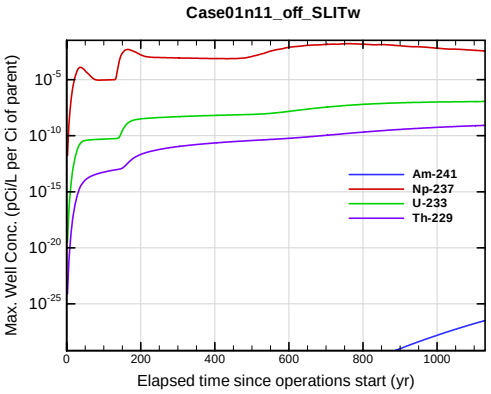

Figure A1B-362. Max. 100-m well conc. for Case01n11_off_SLITw Am-241

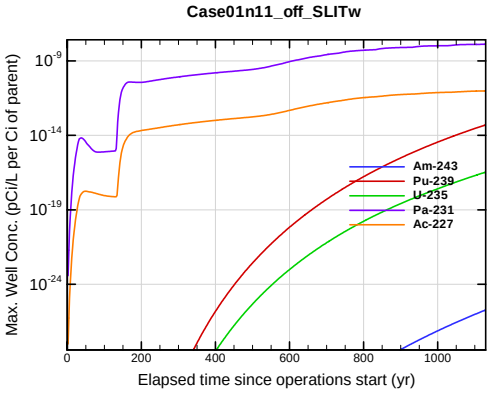

Figure A1B-363. Max. 100-m well conc. for Case01n11_off_SLITw Am-243

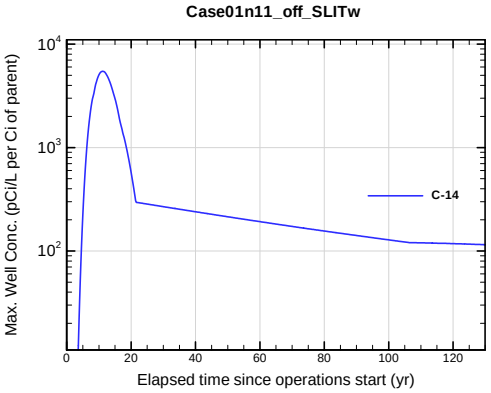

Figure A1B-364. Max. 100-m well conc. for Case01n11_off_SLITw C-14

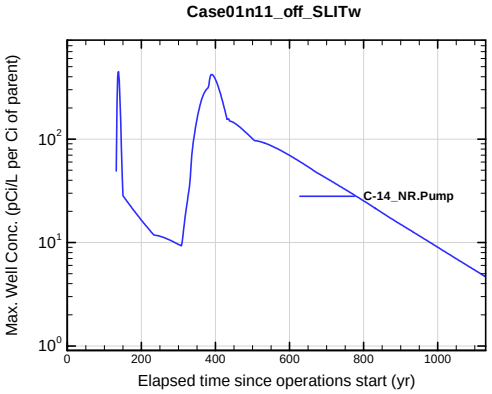

Figure A1B-365. Max. 100-m well conc. for Case01n11_off_SLITw C-14_NR.Pump

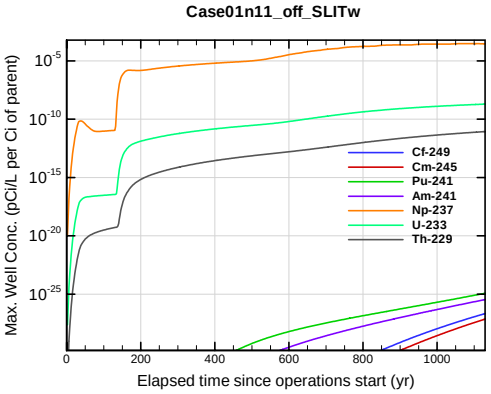

Figure A1B-366. Max. 100-m well conc. for Case01n11_off_SLITw Cf-249

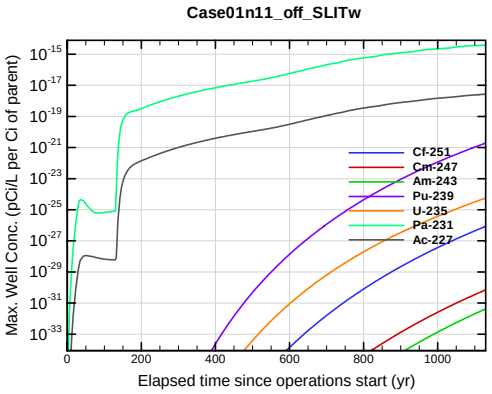

Figure A1B-367. Max. 100-m well conc. for Case01n11_off_SLITw Cf-251

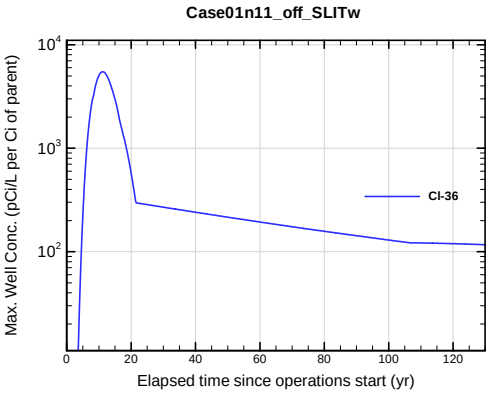

Figure A1B-368. Max. 100-m well conc. for Case01n11_off_SLITw Cl-36

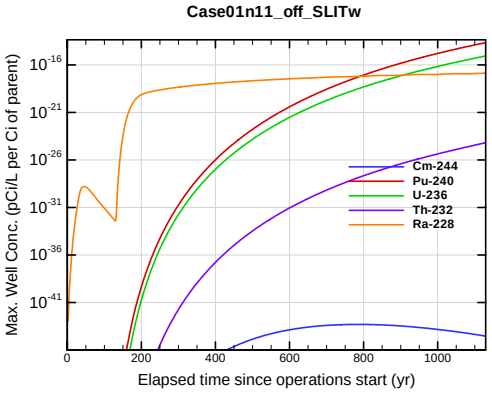

Figure A1B-369. Max. 100-m well conc. for Case01n11_off_SLITw Cm-244

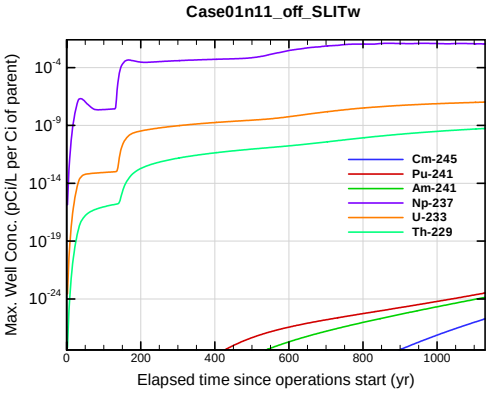

Figure A1B-370. Max. 100-m well conc. for Case01n11_off_SLITw Cm-245

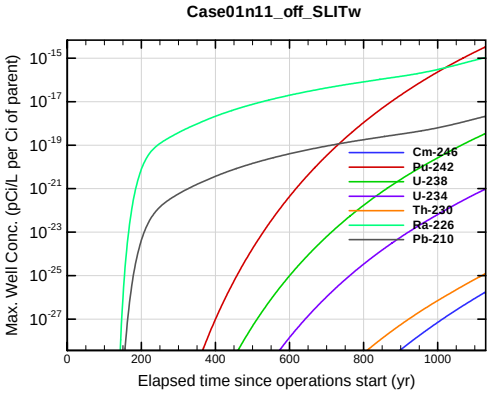

Figure A1B-371. Max. 100-m well conc. for Case01n11_off_SLITw Cm-246

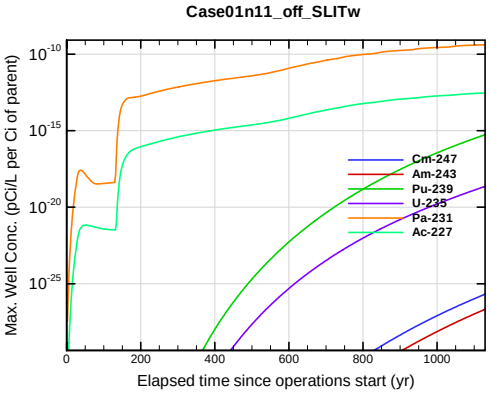

Figure A1B-372. Max. 100-m well conc. for Case01n11_off_SLITw Cm-247

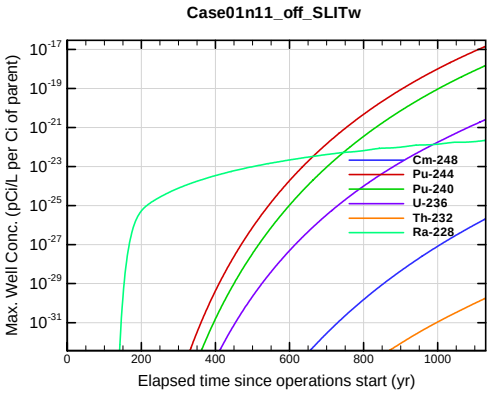

Figure A1B-373. Max. 100-m well conc. for Case01n11_off_SLITw Cm-248

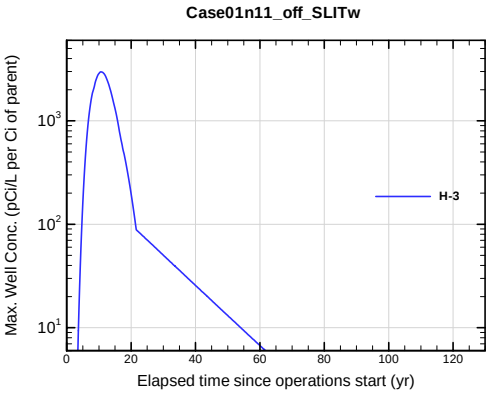

Figure A1B-374. Max. 100-m well conc. for Case01n11_off_SLITw H-3

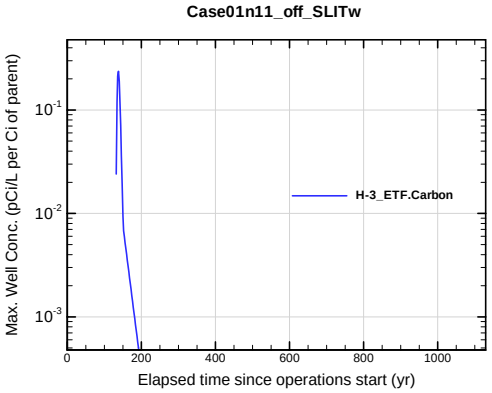

Figure A1B-375. Max. 100-m well conc. for Case01n11_off_SLITw H-3_ETF.Carbon

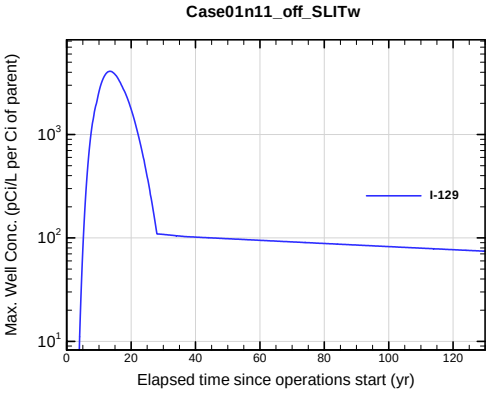

Figure A1B-376. Max. 100-m well conc. for Case01n11_off_SLITw I-129

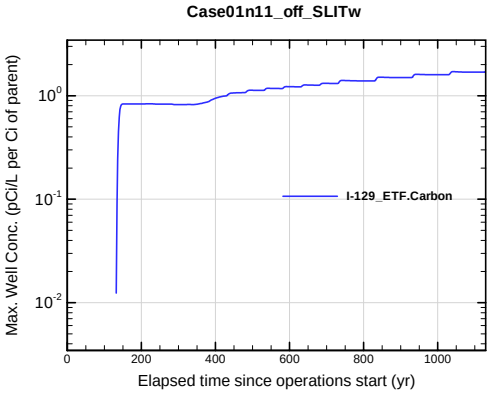

Figure A1B-377. Max. 100-m well conc. for Case01n11_off_SLITw I-129_ETF.Carbon

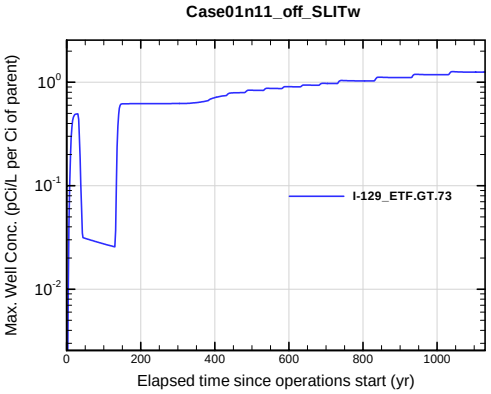

Figure A1B-378. Max. 100-m well conc. for Case01n11_off_SLITw I-129_ETF.GT.73

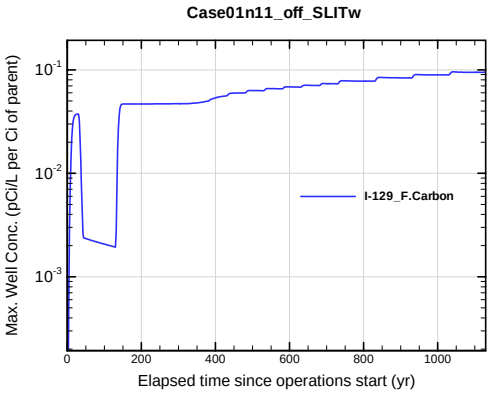

Figure A1B-379. Max. 100-m well conc. for Case01n11_off_SLITw I-129_F.Carbon

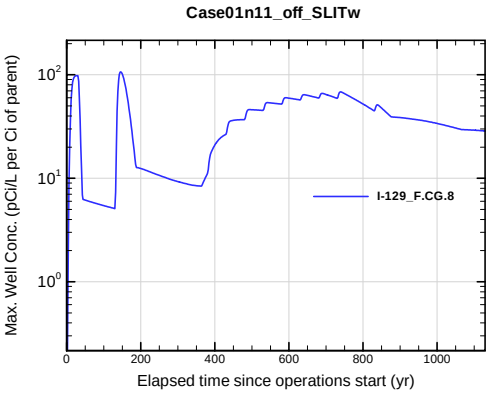

Figure A1B-380. Max. 100-m well conc. for Case01n11_off_SLITw I-129_F.CG.8

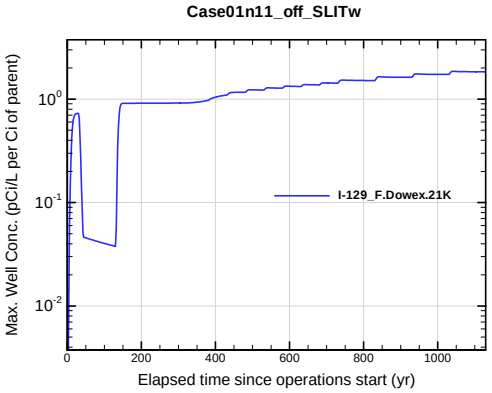

Figure A1B-381. Max. 100-m well conc. for Case01n11_off_SLITw I-129_F.Dowex.21K

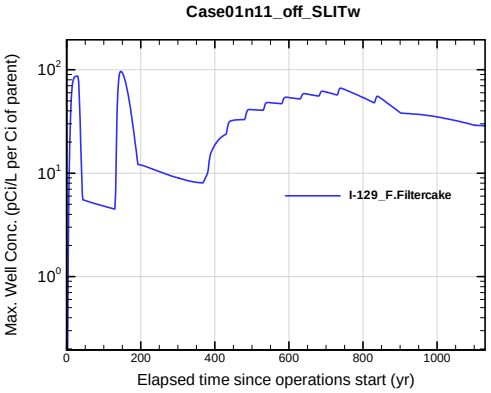

Figure A1B-382. Max. 100-m well conc. for Case01n11_off_SLITw I-129_F.Filtercake

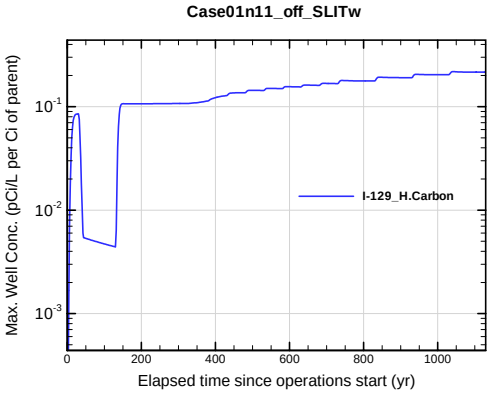

Figure A1B-383. Max. 100-m well conc. for Case01n11_off_SLITw I-129_H.Carbon

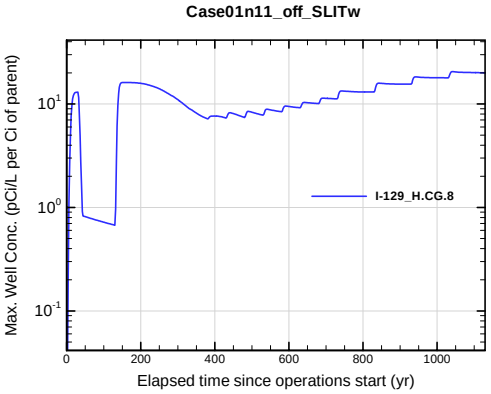

Figure A1B-384. Max. 100-m well conc. for Case01n11_off_SLITw I-129_H.CG.8

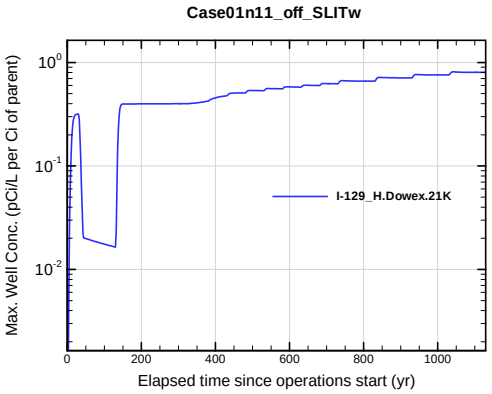

Figure A1B-385. Max. 100-m well conc. for Case01n11_off_SLITw I-129_H.Dowex.21K

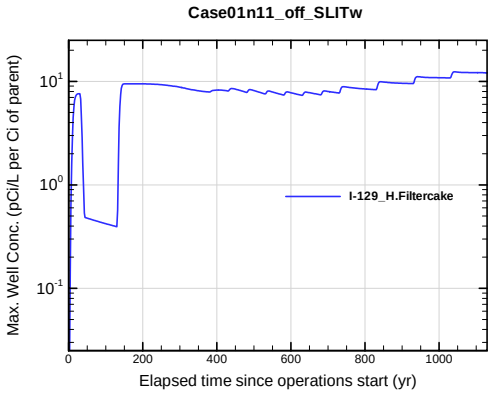

Figure A1B-386. Max. 100-m well conc. for Case01n11_off_SLITw I-129_H.Filtercake

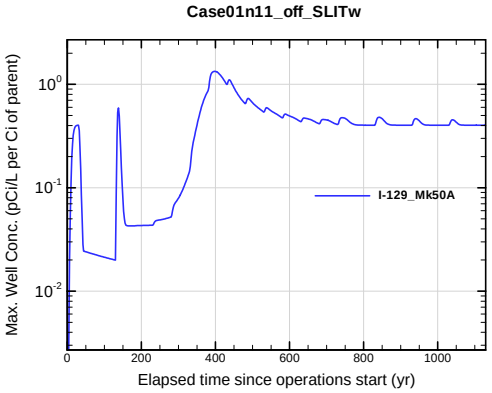

Figure A1B-387. Max. 100-m well conc. for Case01n11_off_SLITw I-129_Mk50A

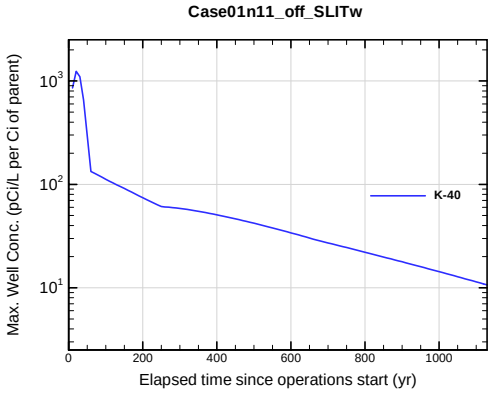

Figure A1B-388. Max. 100-m well conc. for Case01n11_off_SLITw K-40

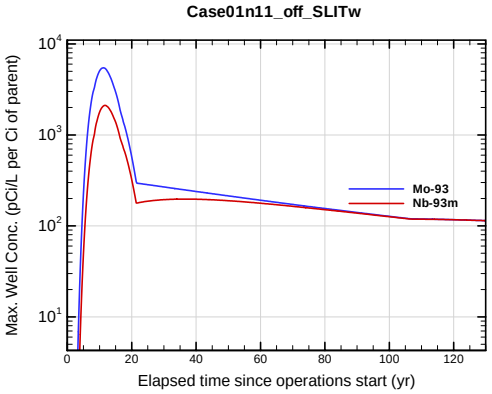

Figure A1B-389. Max. 100-m well conc. for Case01n11_off_SLITw Mo-93

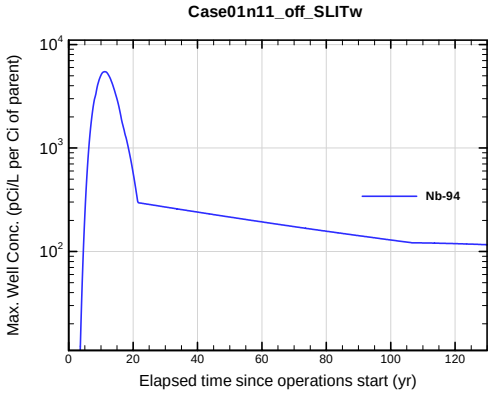

Figure A1B-390. Max. 100-m well conc. for Case01n11_off_SLITw Nb-94

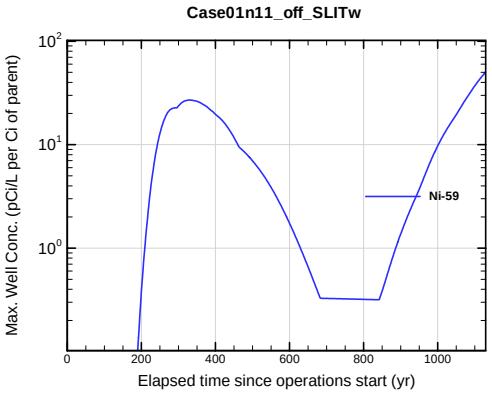

Figure A1B-391. Max. 100-m well conc. for Case01n11_off_SLITw Ni-59

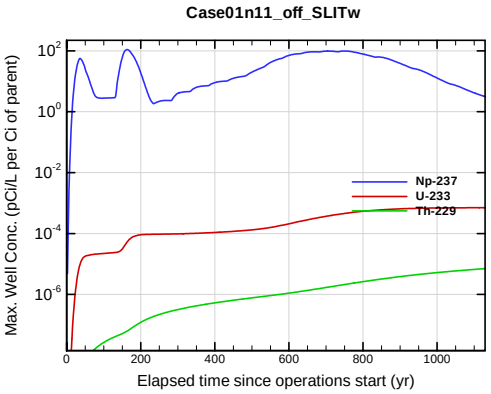

Figure A1B-392. Max. 100-m well conc. for Case01n11_off_SLITw Np-237

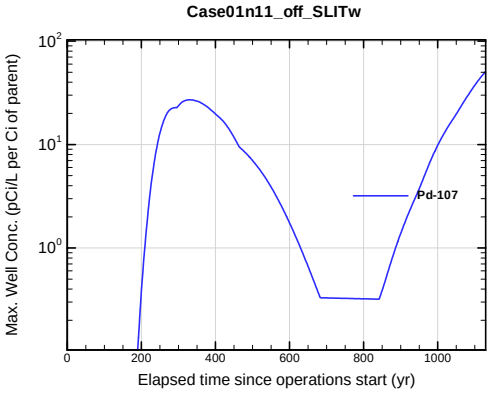

Figure A1B-393. Max. 100-m well conc. for Case01n11_off_SLITw Pd-107

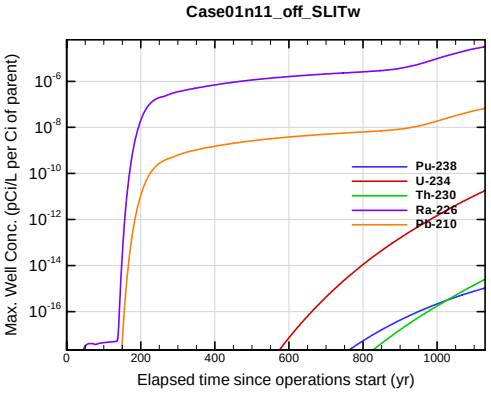

Figure A1B-394. Max. 100-m well conc. for Case01n11_off_SLITw Pu-238

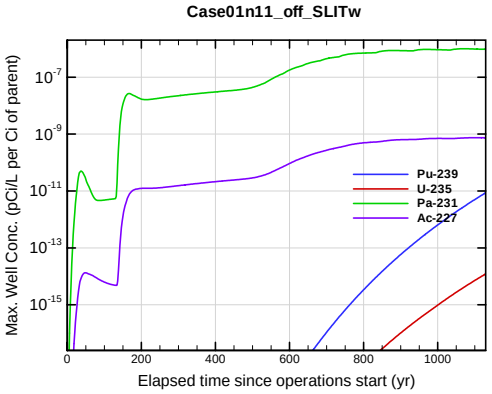

Figure A1B-395. Max. 100-m well conc. for Case01n11_off_SLITw Pu-239

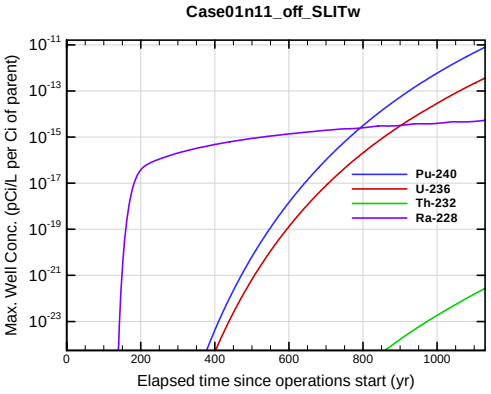

Figure A1B-396. Max. 100-m well conc. for Case01n11_off_SLITw Pu-240

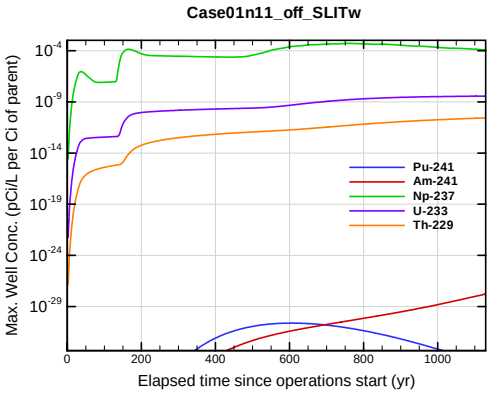

Figure A1B-397. Max. 100-m well conc. for Case01n11_off_SLITw Pu-241

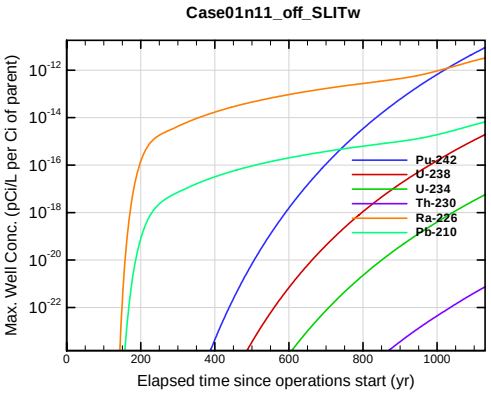

Figure A1B-398. Max. 100-m well conc. for Case01n11_off_SLITw Pu-242

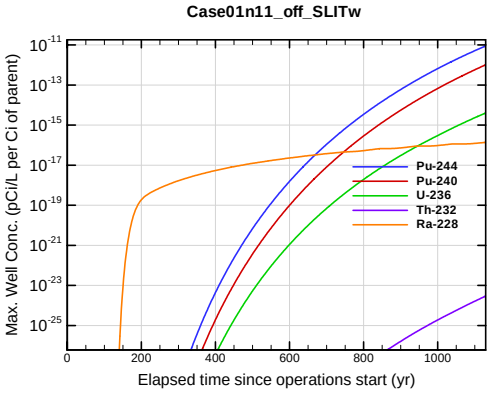

Figure A1B-399. Max. 100-m well conc. for Case01n11_off_SLITw Pu-244

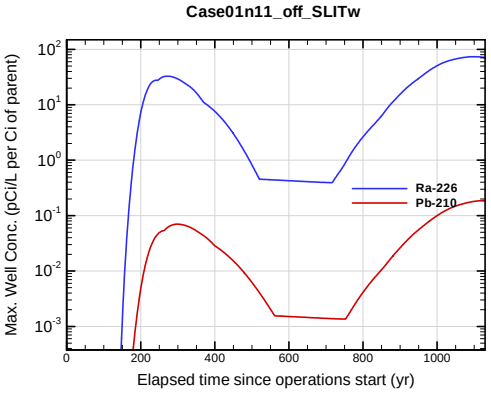

Figure A1B-400. Max. 100-m well conc. for Case01n11_off_SLITw Ra-226

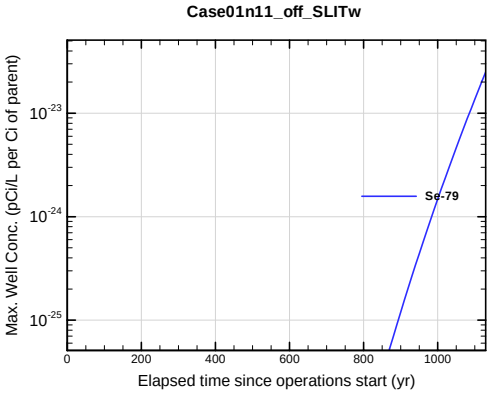

Figure A1B-401. Max. 100-m well conc. for Case01n11_off_SLITw Se-79

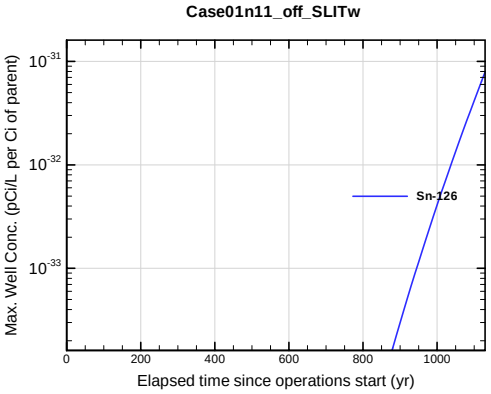

Figure A1B-402. Max. 100-m well conc. for Case01n11_off_SLITw Sn-126

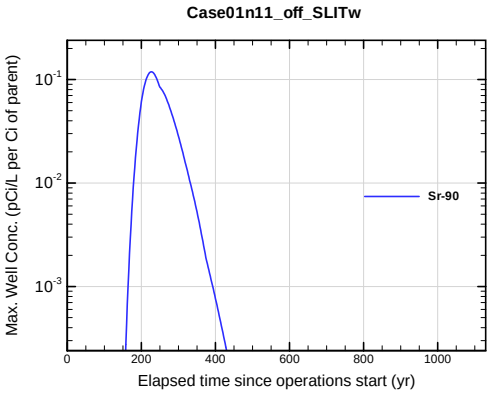

Figure A1B-403. Max. 100-m well conc. for Case01n11_off_SLITw Sr-90

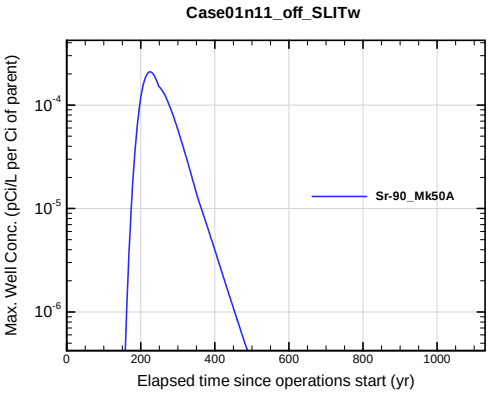

Figure A1B-404. Max. 100-m well conc. for Case01n11_off_SLITw Sr-90_Mk50A

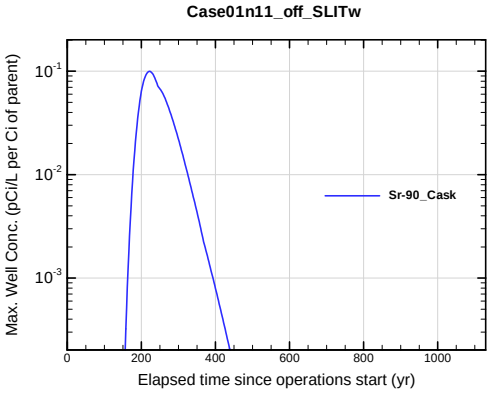

Figure A1B-405. Max. 100-m well conc. for Case01n11_off_SLITw Sr-90_Cask

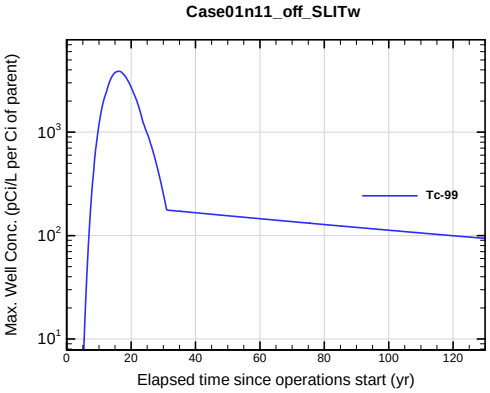

Figure A1B-406. Max. 100-m well conc. for Case01n11_off_SLITw Tc-99

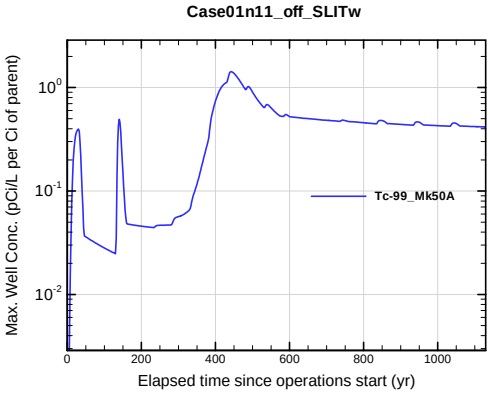

Figure A1B-407. Max. 100-m well conc. for Case01n11_off_SLITw Tc-99_Mk50A

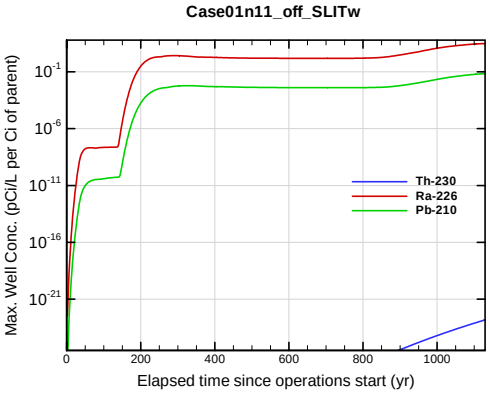

Figure A1B-408. Max. 100-m well conc. for Case01n11_off_SLITw Th-230

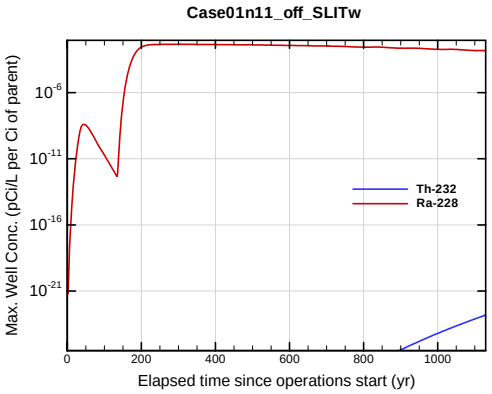

Figure A1B-409. Max. 100-m well conc. for Case01n11_off_SLITw Th-232

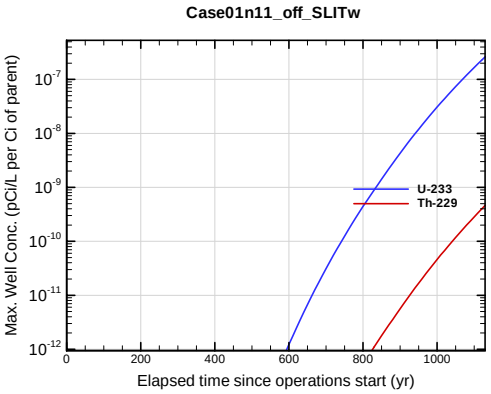

Figure A1B-410. Max. 100-m well conc. for Case01n11_off_SLITw U-233

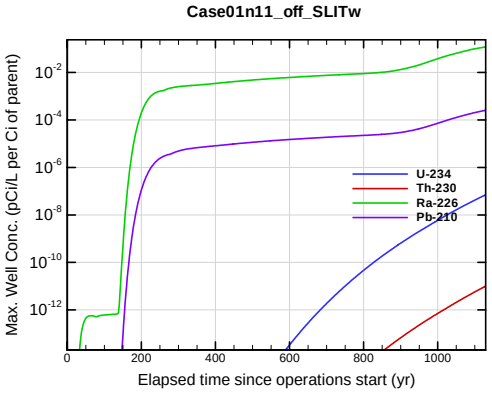

Figure A1B-411. Max. 100-m well conc. for Case01n11_off_SLITw U-234

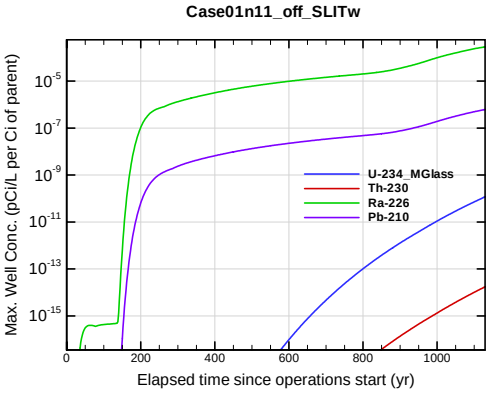

Figure A1B-412. Max. 100-m well conc. for Case01n11_off_SLITw U-234_MGlass

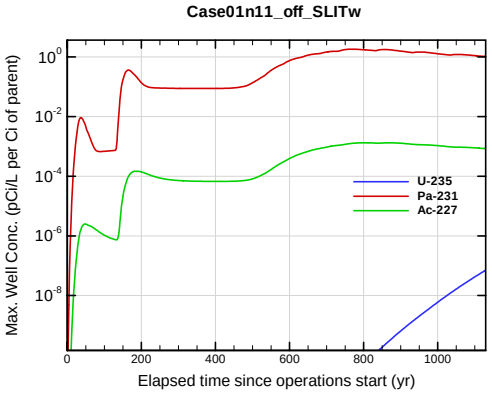

Figure A1B-413. Max. 100-m well conc. for Case01n11_off_SLITw U-235

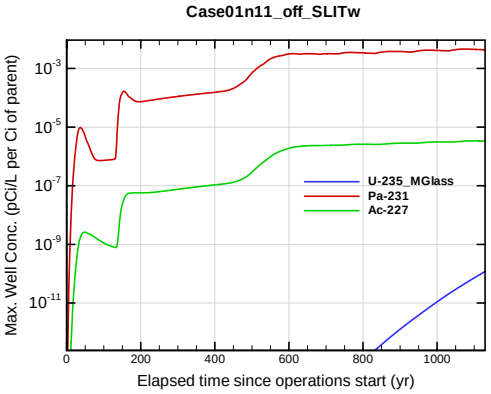

Figure A1B-414. Max. 100-m well conc. for Case01n11_off_SLITw U-235_MGlass

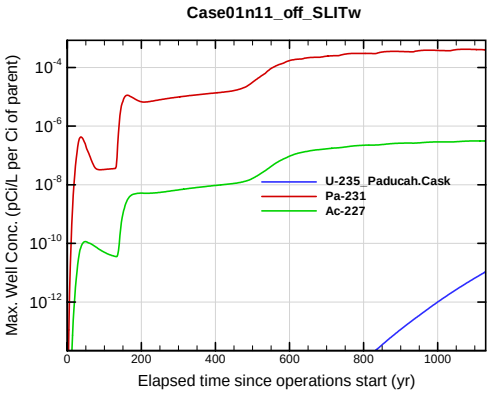

Figure A1B-415. Max. 100-m well conc. for Case01n11_off_SLITw U-235_Paducah.Cask

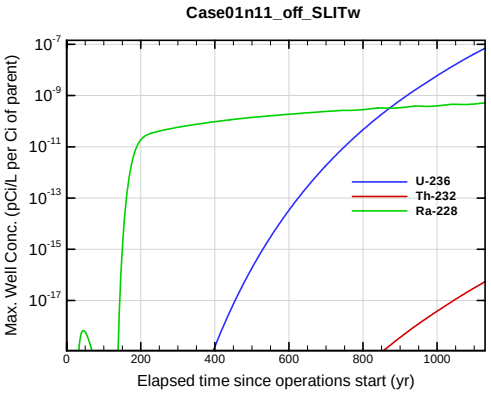

Figure A1B-416. Max. 100-m well conc. for Case01n11_off_SLITw U-236

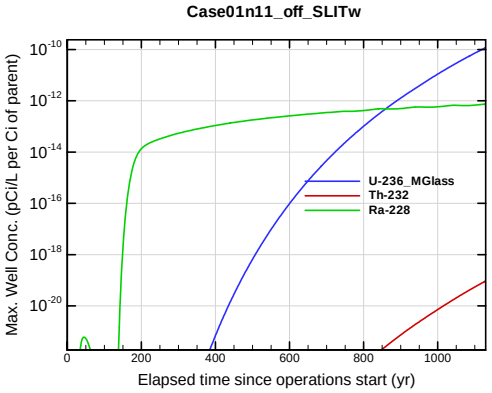

Figure A1B-417. Max. 100-m well conc. for Case01n11_off_SLITw U-236_MGlass

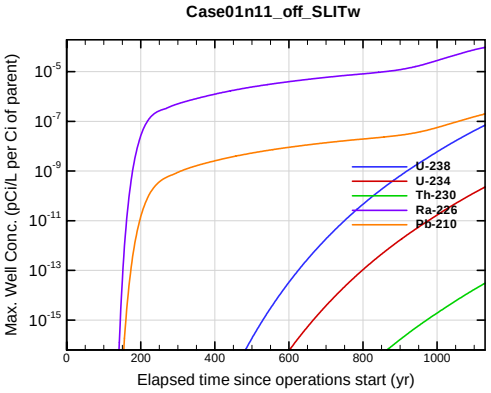

Figure A1B-418. Max. 100-m well conc. for Case01n11_off_SLITw U-238

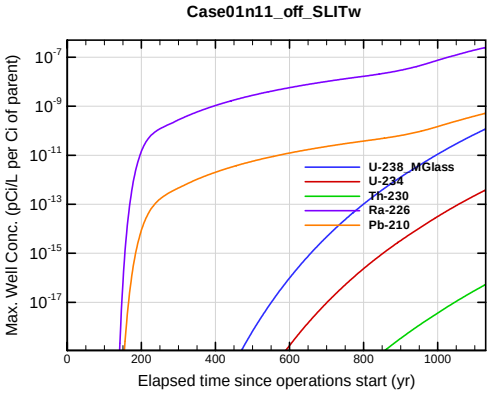

Figure A1B-419. Max. 100-m well conc. for Case01n11_off_SLITw U-238_MGlass

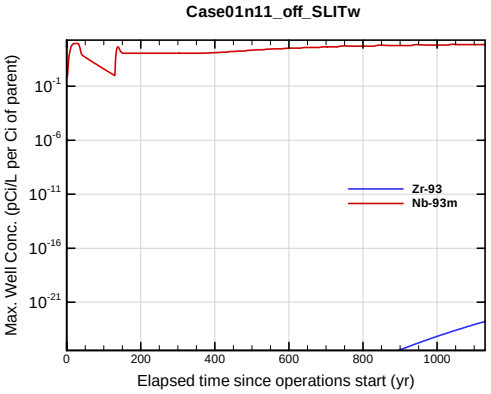

Figure A1B-420. Max. 100-m well conc. for Case01n11_off_SLITw Zr-93

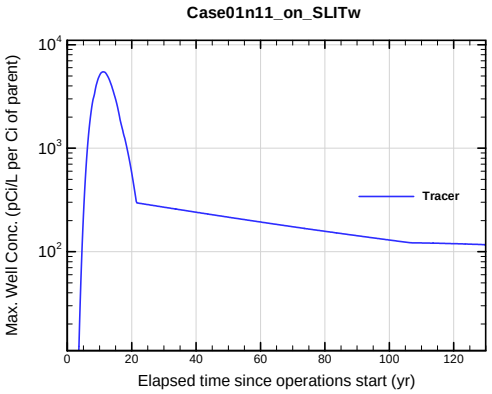

Figure A1B-421. Max. 100-m well conc. for Case01n11_on_SLITw Tracer

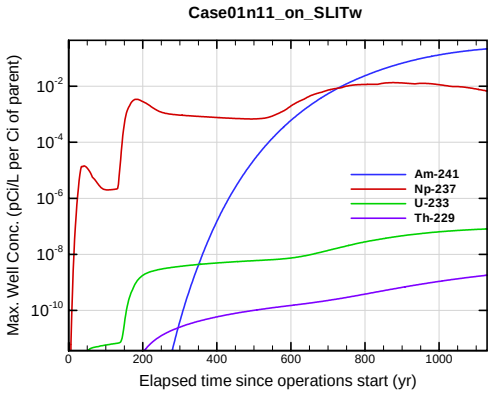

Figure A1B-422. Max. 100-m well conc. for Case01n11_on_SLITw Am-241

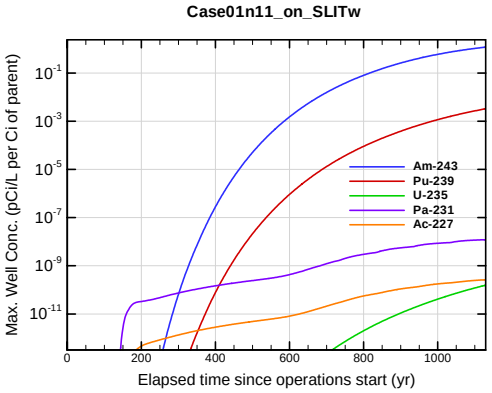

Figure A1B-423. Max. 100-m well conc. for Case01n11_on_SLITw Am-243

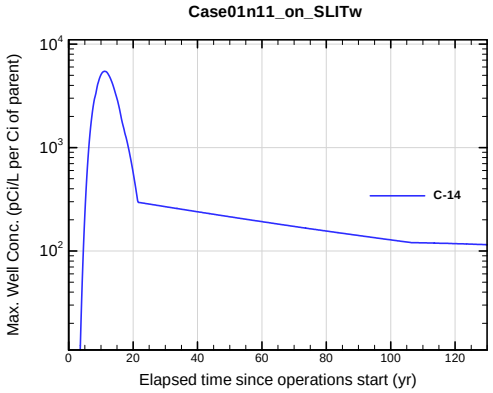

Figure A1B-424. Max. 100-m well conc. for Case01n11_on_SLITw C-14

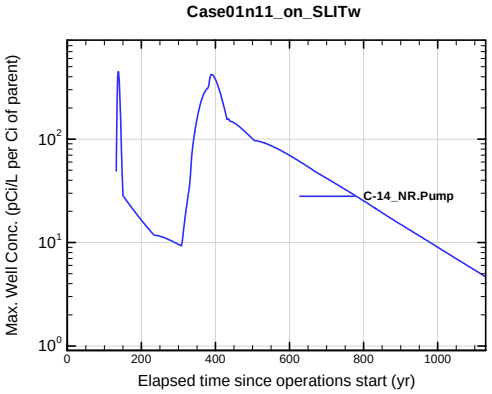

Figure A1B-425. Max. 100-m well conc. for Case01n11_on_SLITw C-14_NR.Pump

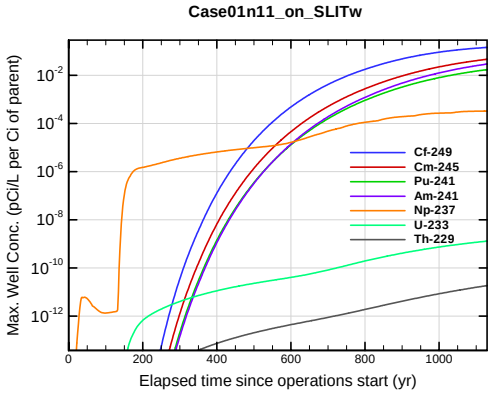

Figure A1B-426. Max. 100-m well conc. for Case01n11_on_SLITw Cf-249

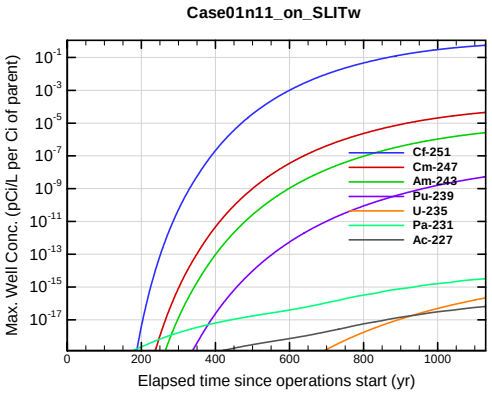

Figure A1B-427. Max. 100-m well conc. for Case01n11_on_SLITw Cf-251

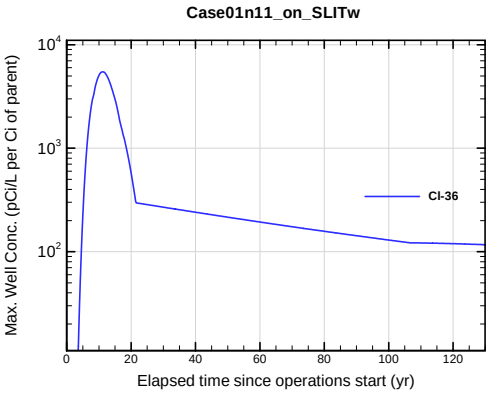

Figure A1B-428. Max. 100-m well conc. for Case01n11_on_SLITw Cl-36

Figure A1B-429. Max. 100-m well conc. for Case01n11_on_SLITw Cm-244

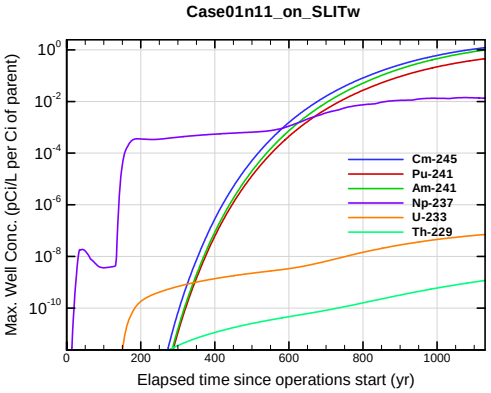

Figure A1B-430. Max. 100-m well conc. for Case01n11_on_SLITw Cm-245

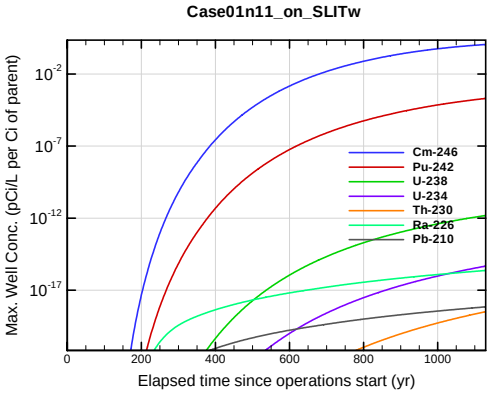

Figure A1B-431. Max. 100-m well conc. for Case01n11_on_SLITw Cm-246

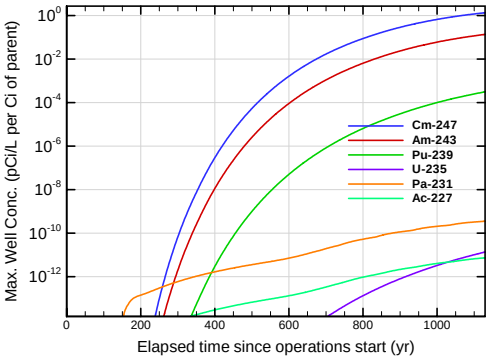

Figure A1B-432. Max. 100-m well conc. for Case01n11_on_SLITw Cm-247

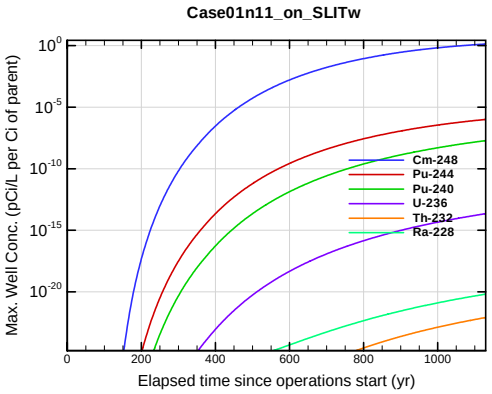

Figure A1B-433. Max. 100-m well conc. for Case01n11_on_SLITw Cm-248

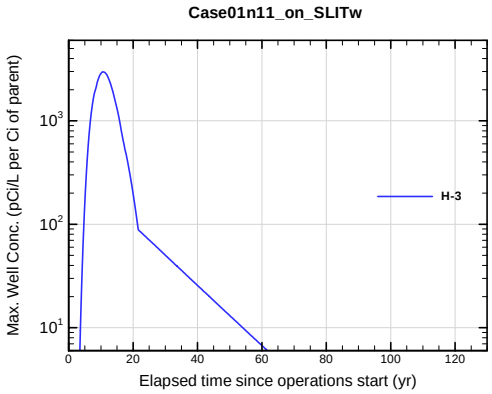

Figure A1B-434. Max. 100-m well conc. for Case01n11_on_SLITw H-3

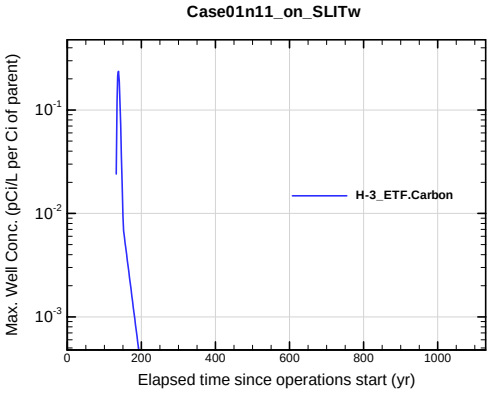

Figure A1B-435. Max. 100-m well conc. for Case01n11_on_SLITw H-3_ETF.Carbon

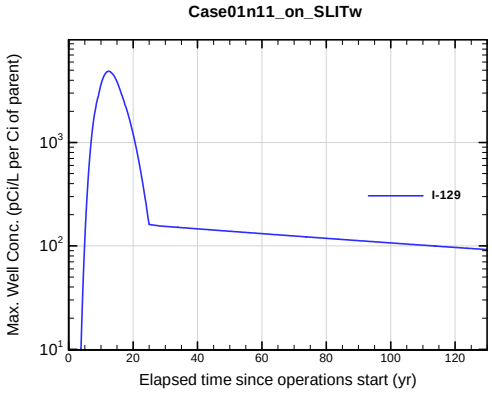

Figure A1B-436. Max. 100-m well conc. for Case01n11_on_SLITw I-129

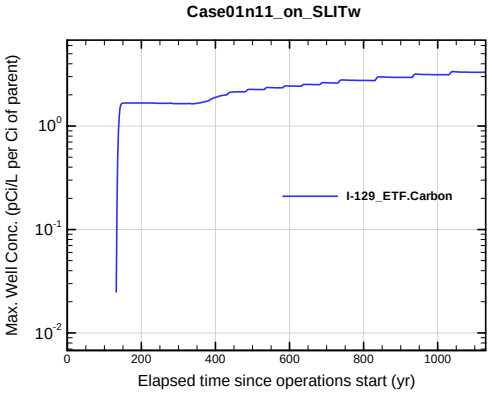

Figure A1B-437. Max. 100-m well conc. for Case01n11_on_SLITw I-129_ETF.Carbon

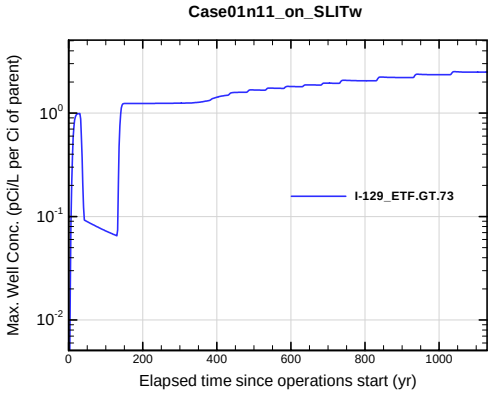

Figure A1B-438. Max. 100-m well conc. for Case01n11_on_SLITw I-129_ETF.GT.73

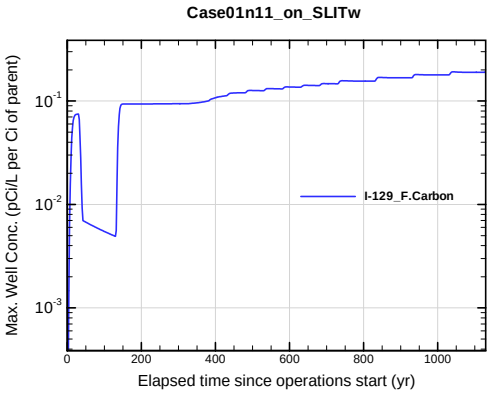

Figure A1B-439. Max. 100-m well conc. for Case01n11_on_SLITw I-129_F.Carbon

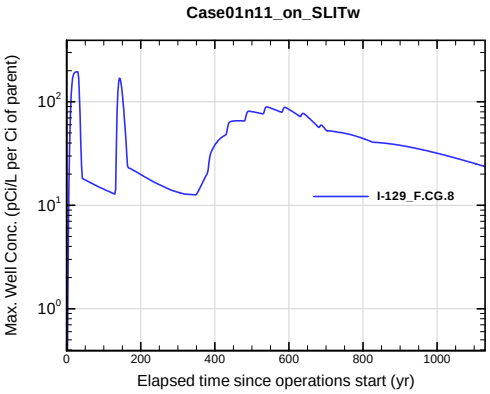

Figure A1B-440. Max. 100-m well conc. for Case01n11_on_SLITw I-129_F.CG.8

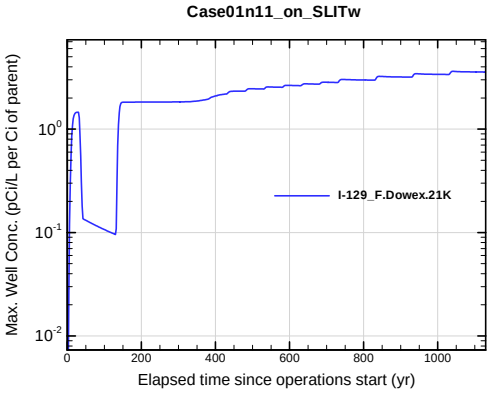

Figure A1B-441. Max. 100-m well conc. for Case01n11_on_SLITw I-129_F.Dowex.21K

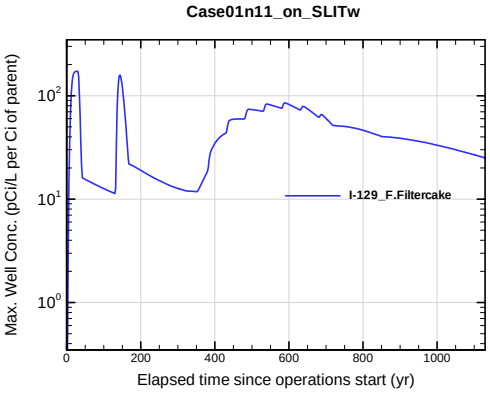

Figure A1B-442. Max. 100-m well conc. for Case01n11_on_SLITw I-129_F.Filtercake

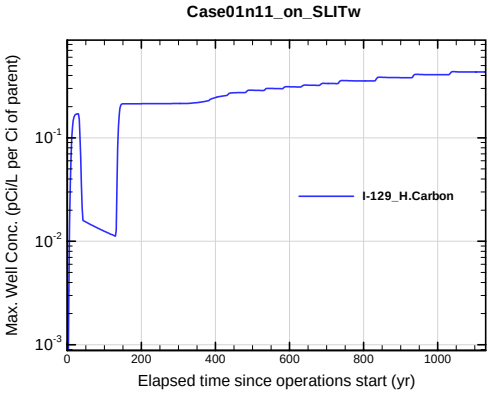

Figure A1B-443. Max. 100-m well conc. for Case01n11_on_SLITw I-129_H.Carbon

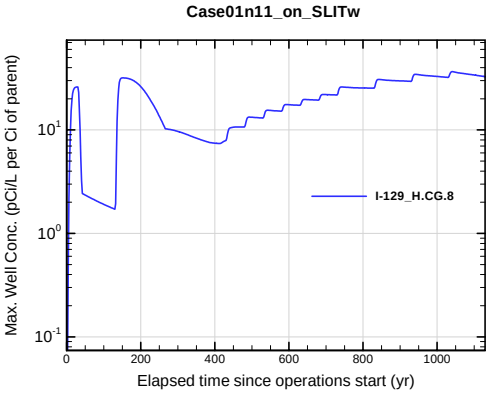

Figure A1B-444. Max. 100-m well conc. for Case01n11_on_SLITw I-129_H.CG.8

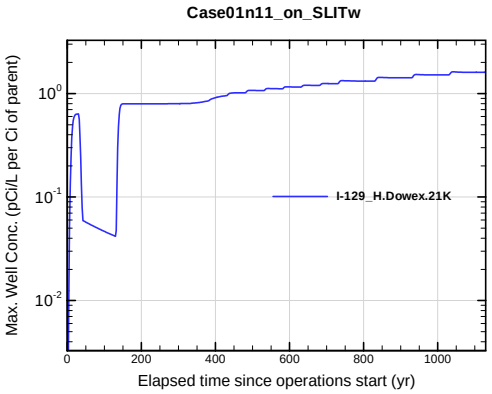

Figure A1B-445. Max. 100-m well conc. for Case01n11_on_SLITw I-129_H.Dowex.21K

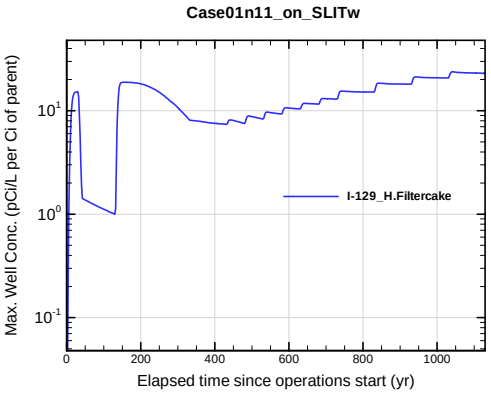

Figure A1B-446. Max. 100-m well conc. for Case01n11_on_SLITw I-129_H.Filtercake

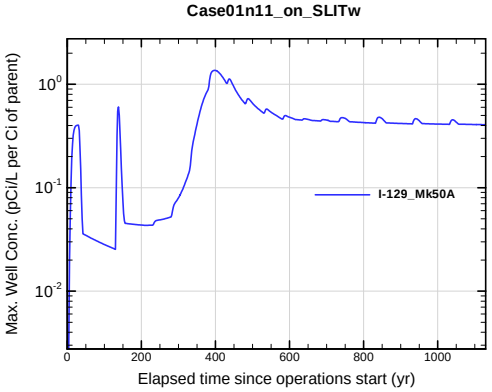

Figure A1B-447. Max. 100-m well conc. for Case01n11_on_SLITw I-129_Mk50A

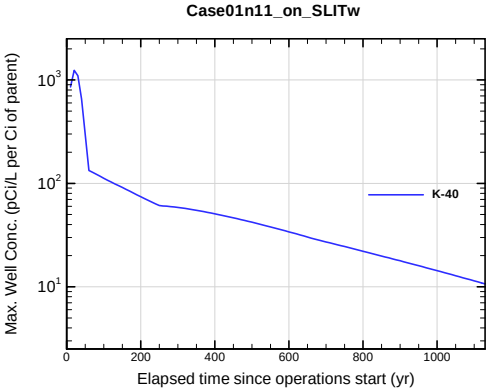

Figure A1B-448. Max. 100-m well conc. for Case01n11_on_SLITw K-40

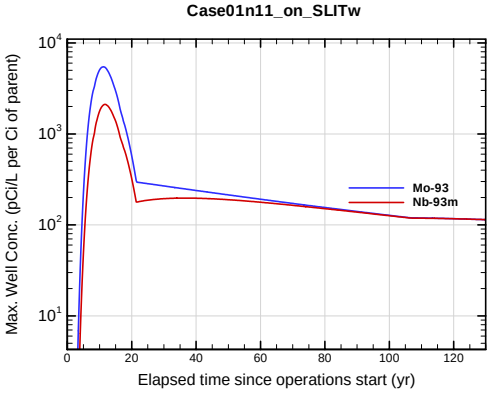

Figure A1B-449. Max. 100-m well conc. for Case01n11_on_SLITw Mo-93

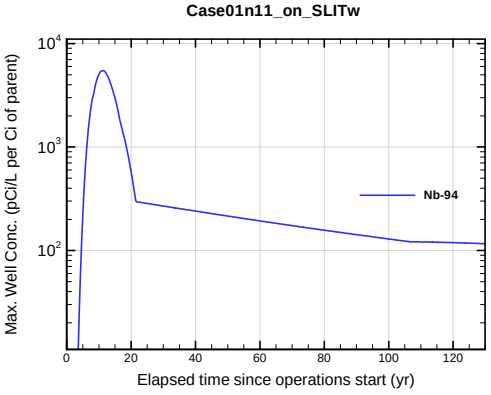

Figure A1B-450. Max. 100-m well conc. for Case01n11_on_SLITw Nb-94

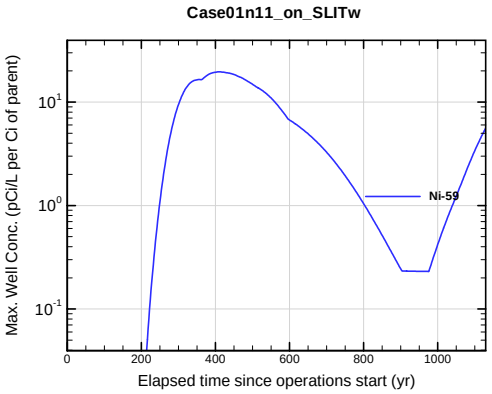

Figure A1B-451. Max. 100-m well conc. for Case01n11_on_SLITw Ni-59

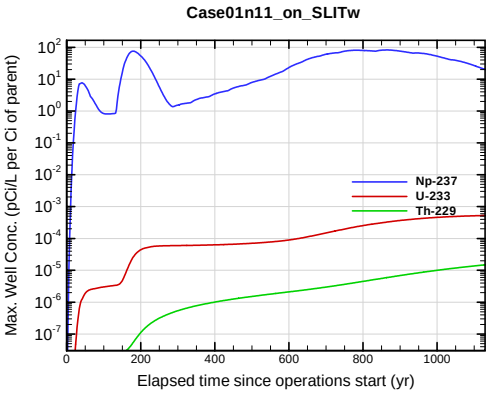

Figure A1B-452. Max. 100-m well conc. for Case01n11_on_SLITw Np-237

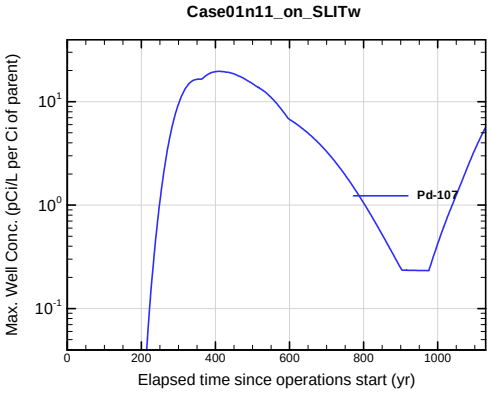

Figure A1B-453. Max. 100-m well conc. for Case01n11_on_SLITw Pd-107

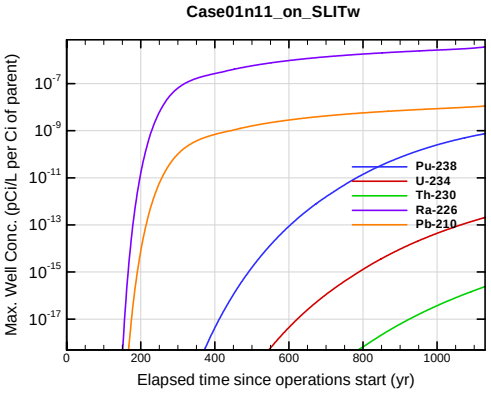

Figure A1B-454. Max. 100-m well conc. for Case01n11_on_SLITw Pu-238

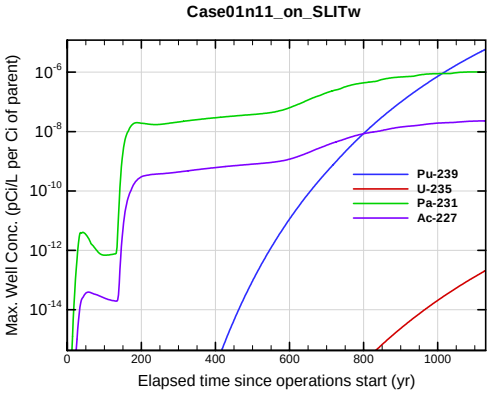

Figure A1B-455. Max. 100-m well conc. for Case01n11_on_SLITw Pu-239

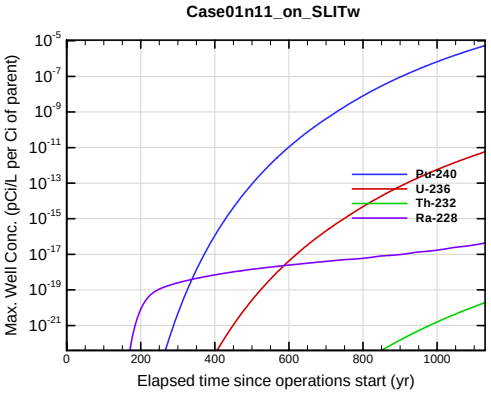

Figure A1B-456. Max. 100-m well conc. for Case01n11_on_SLITw Pu-240

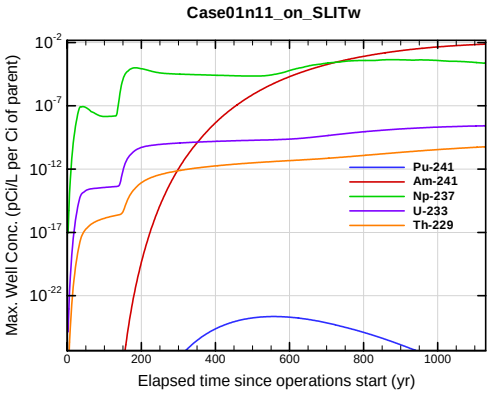

Figure A1B-457. Max. 100-m well conc. for Case01n11_on_SLITw Pu-241

Figure A1B-458. Max. 100-m well conc. for Case01n11_on_SLITw Pu-242

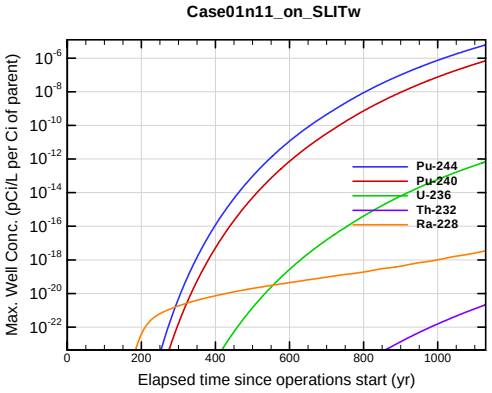

Figure A1B-459. Max. 100-m well conc. for Case01n11_on_SLITw Pu-244

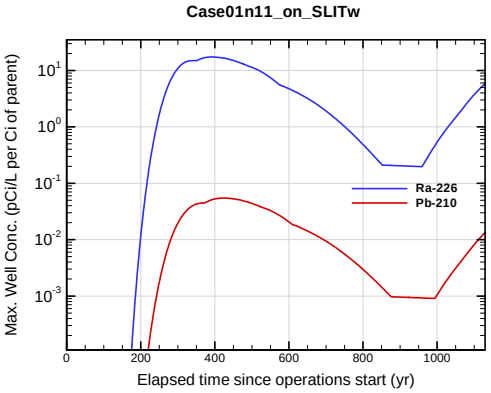

Figure A1B-460. Max. 100-m well conc. for Case01n11_on_SLITw Ra-226

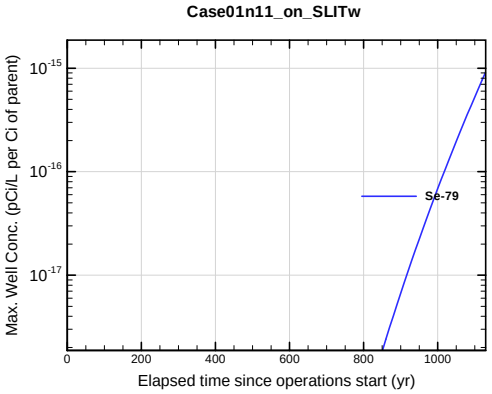

Figure A1B-461. Max. 100-m well conc. for Case01n11_on_SLITw Se-79

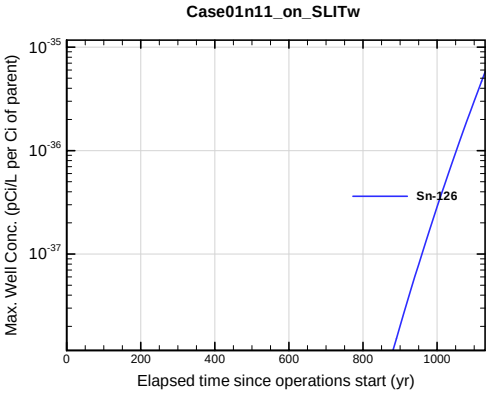

Figure A1B-462. Max. 100-m well conc. for Case01n11_on_SLITw Sn-126

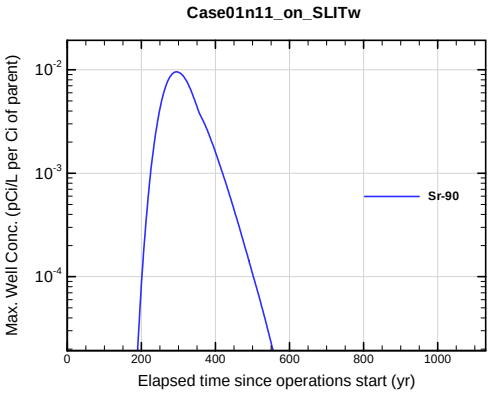

Figure A1B-463. Max. 100-m well conc. for Case01n11_on_SLITw Sr-90

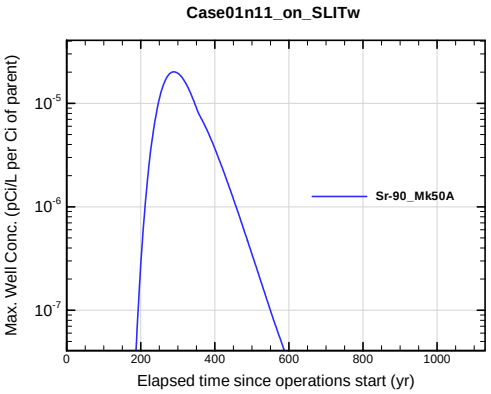

Figure A1B-464. Max. 100-m well conc. for Case01n11_on_SLITw Sr-90_Mk50A

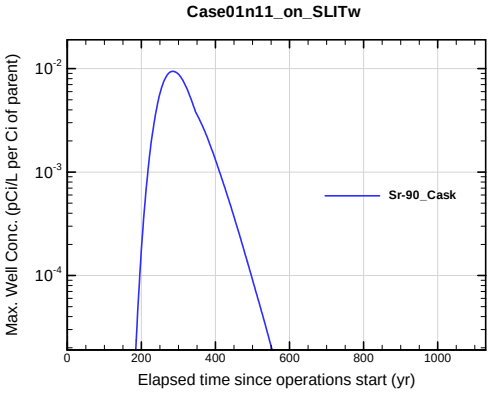

Figure A1B-465. Max. 100-m well conc. for Case01n11_on_SLITw Sr-90_Cask

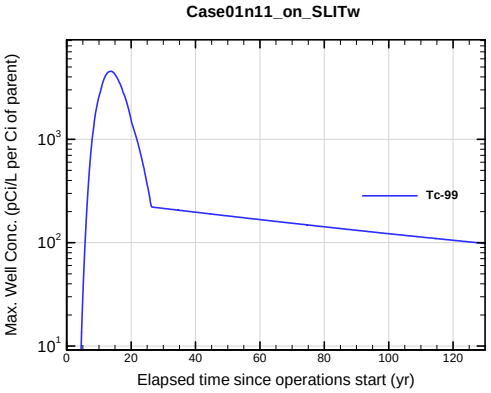

Figure A1B-466. Max. 100-m well conc. for Case01n11_on_SLITw Tc-99

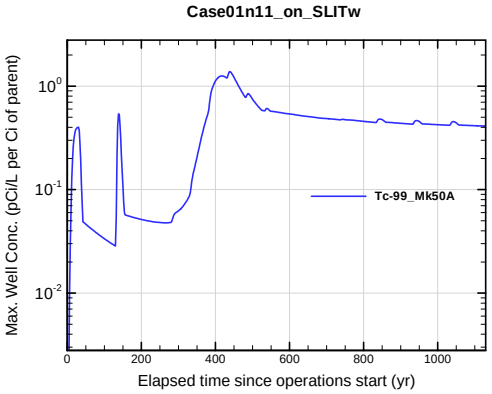

Figure A1B-467. Max. 100-m well conc. for Case01n11_on_SLITw Tc-99_Mk50A

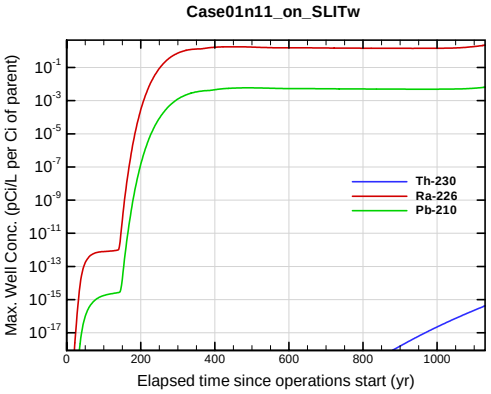

Figure A1B-468. Max. 100-m well conc. for Case01n11_on_SLITw Th-230

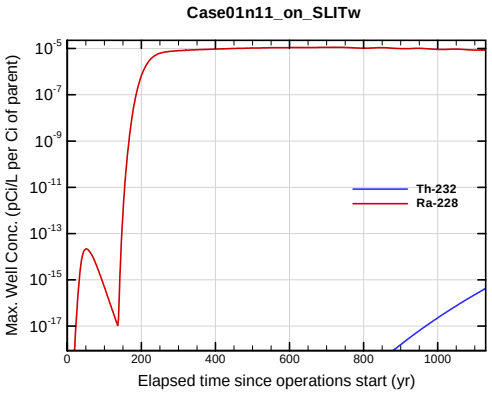

Figure A1B-469. Max. 100-m well conc. for Case01n11_on_SLITw Th-232

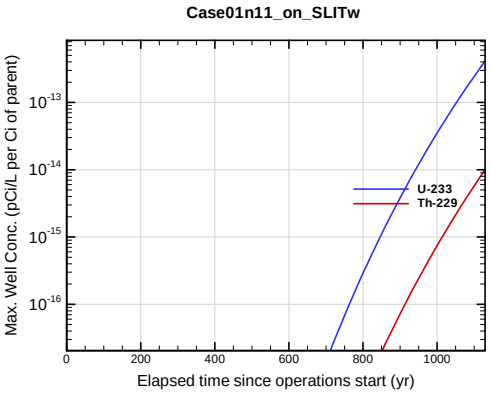

Figure A1B-470. Max. 100-m well conc. for Case01n11_on_SLITw U-233

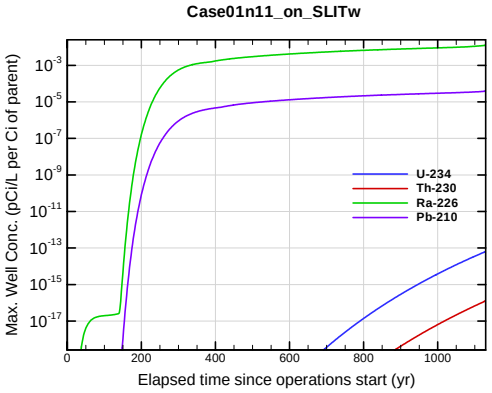

Figure A1B-471. Max. 100-m well conc. for Case01n11_on_SLITw U-234

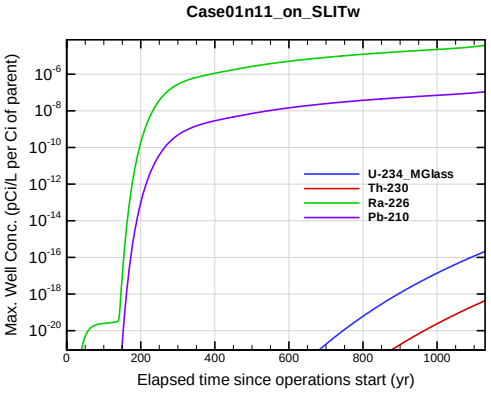

Figure A1B-472. Max. 100-m well conc. for Case01n11_on_SLITw U-234_MGlass

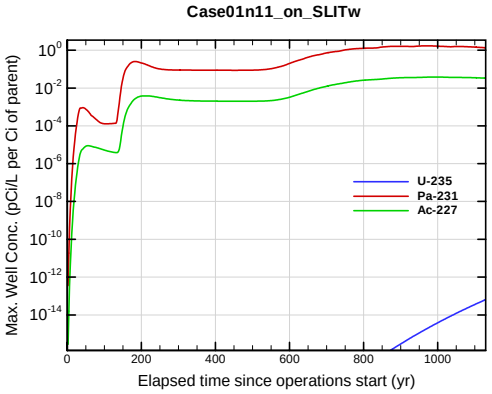

Figure A1B-473. Max. 100-m well conc. for Case01n11_on_SLITw U-235

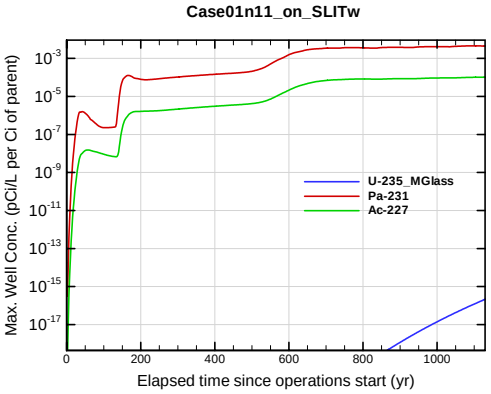

Figure A1B-474. Max. 100-m well conc. for Case01n11_on_SLITw U-235_MGlass

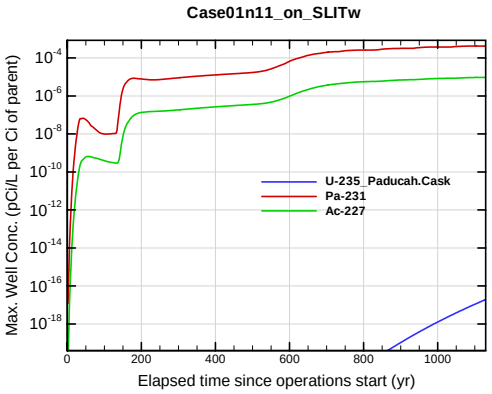

Figure A1B-475. Max. 100-m well conc. for Case01n11_on_SLITw U-235_Paducah.Cask

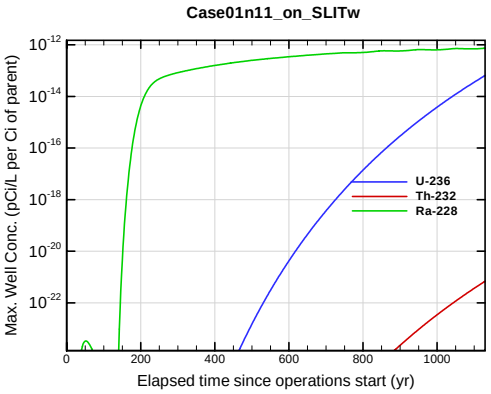

Figure A1B-476. Max. 100-m well conc. for Case01n11_on_SLITw U-236

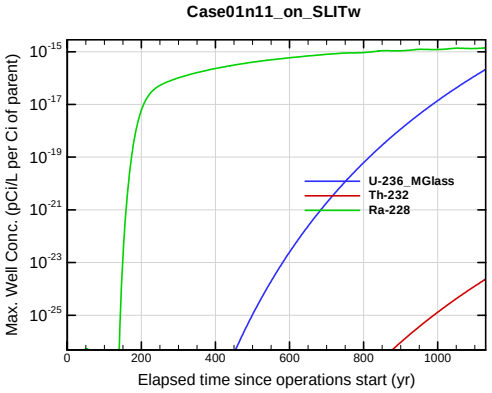

Figure A1B-477. Max. 100-m well conc. for Case01n11_on_SLITw U-236_MGlass

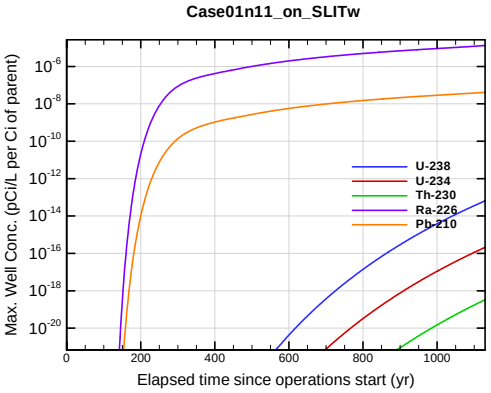

Figure A1B-478. Max. 100-m well conc. for Case01n11_on_SLITw U-238

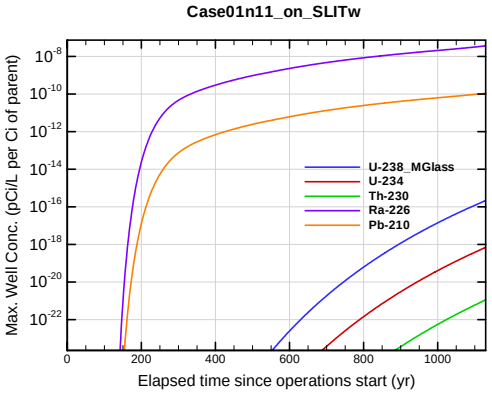

Figure A1B-479. Max. 100-m well conc. for Case01n11_on_SLITw U-238_MGlass

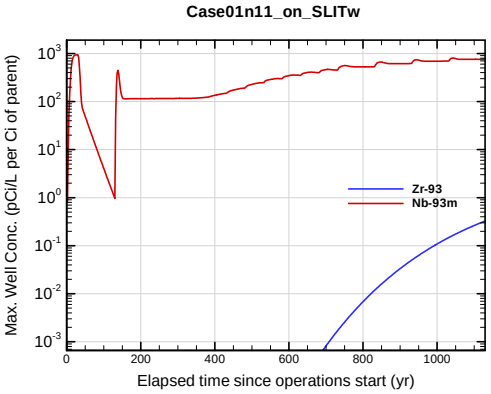

Figure A1B-480. Max. 100-m well conc. for Case01n11_on_SLITw Zr-93

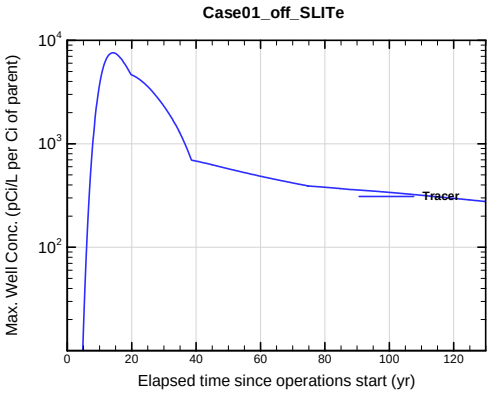

Figure A1B-481. Max. 100-m well conc. for Case01_off_SLITe Tracer

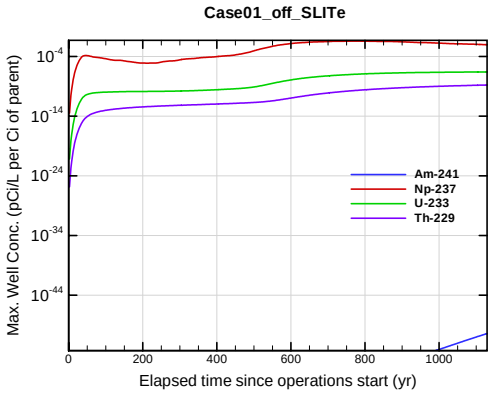

Figure A1B-482. Max. 100-m well conc. for Case01_off_SLITe Am-241

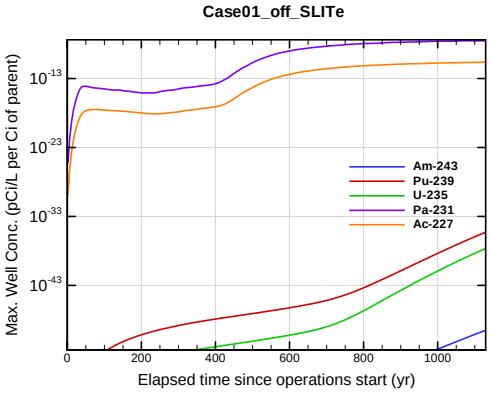

Figure A1B-483. Max. 100-m well conc. for Case01_off_SLITe Am-243

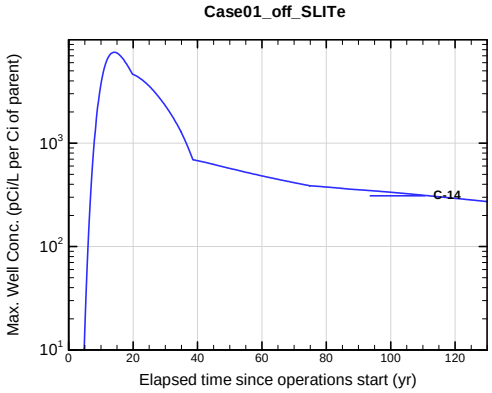

Figure A1B-484. Max. 100-m well conc. for Case01_off_SLITe C-14

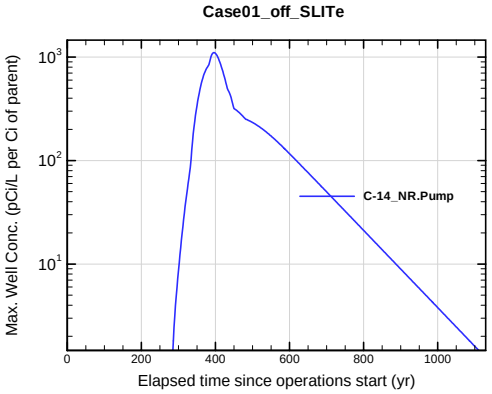

Figure A1B-485. Max. 100-m well conc. for Case01_off_SLITe C-14_NR.Pump

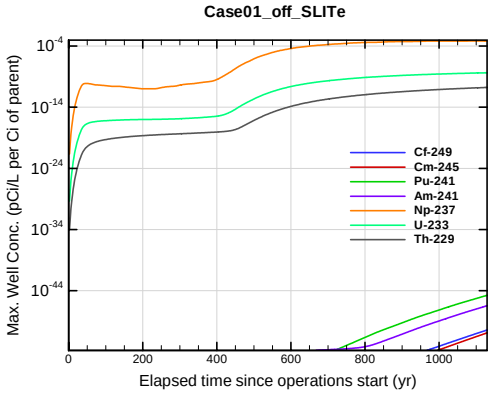

Figure A1B-486. Max. 100-m well conc. for Case01_off_SLITe Cf-249

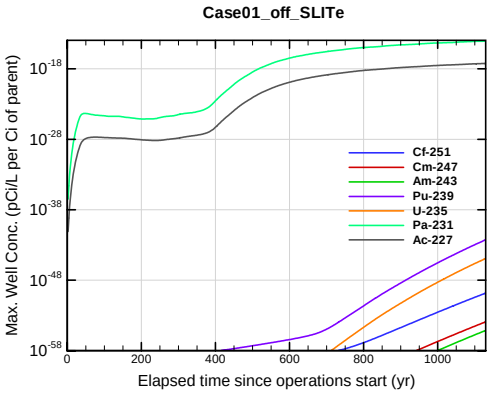

Figure A1B-487. Max. 100-m well conc. for Case01_off_SLITe Cf-251

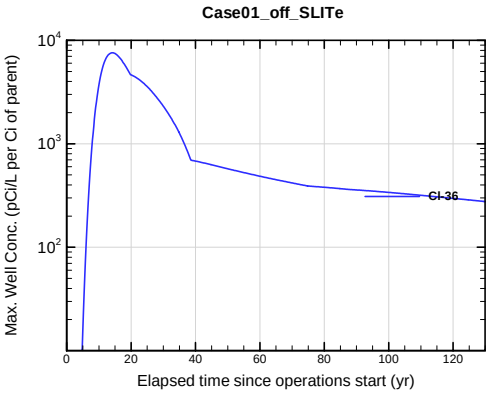

Figure A1B-488. Max. 100-m well conc. for Case01_off_SLITe Cl-36

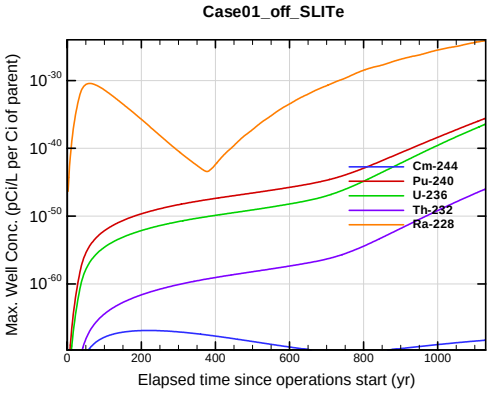

Figure A1B-489. Max. 100-m well conc. for Case01_off_SLITe Cm-244

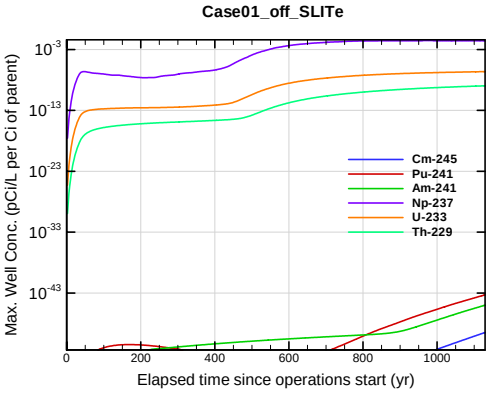

Figure A1B-490. Max. 100-m well conc. for Case01_off_SLITe Cm-245

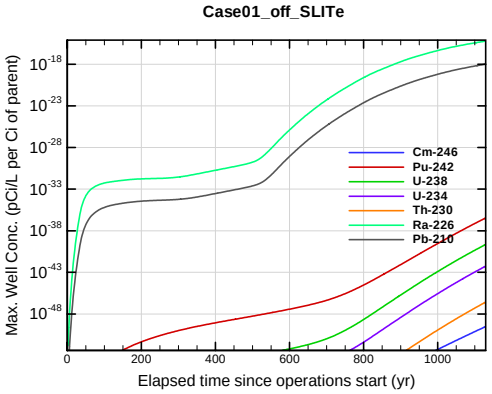

Figure A1B-491. Max. 100-m well conc. for Case01_off_SLITe Cm-246

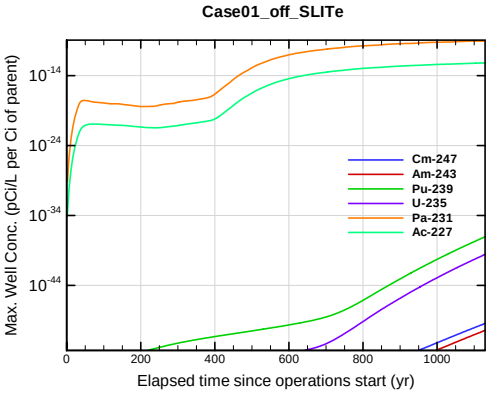

Figure A1B-492. Max. 100-m well conc. for Case01_off_SLITe Cm-247

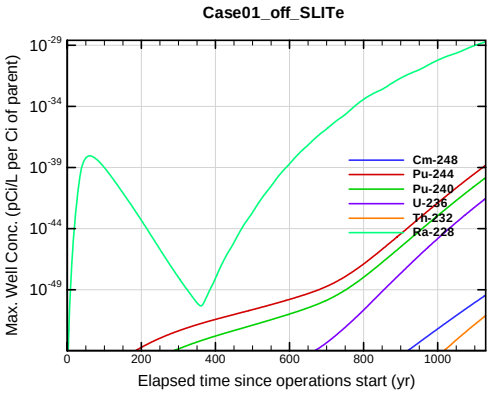

Figure A1B-493. Max. 100-m well conc. for Case01_off_SLITe Cm-248

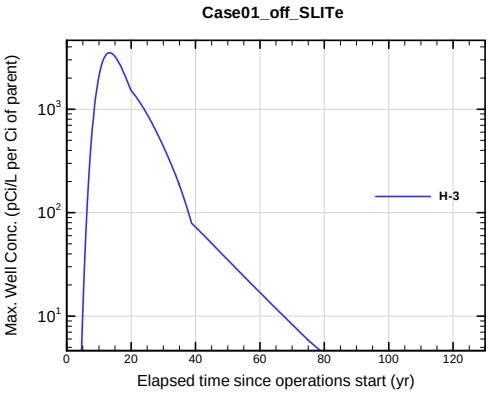

Figure A1B-494. Max. 100-m well conc. for Case01_off_SLITe H-3

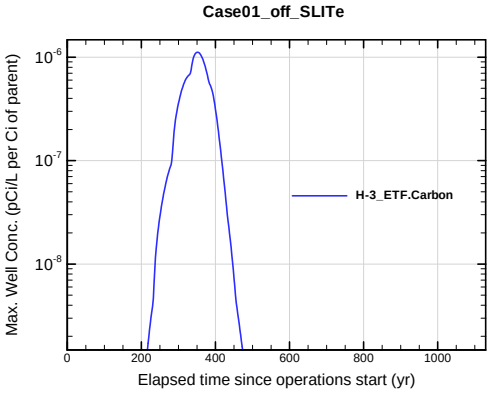

Figure A1B-495. Max. 100-m well conc. for Case01_off_SLITe H-3_ETF.Carbon

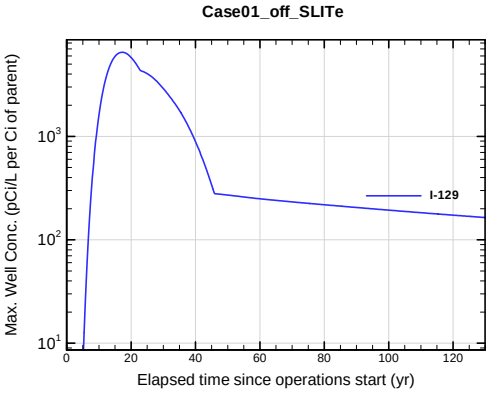

Figure A1B-496. Max. 100-m well conc. for Case01_off_SLITe I-129

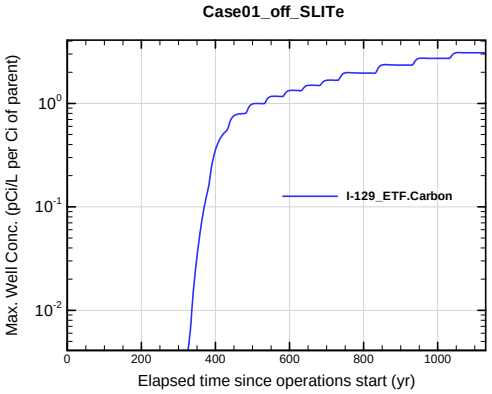

Figure A1B-497. Max. 100-m well conc. for Case01_off_SLITe I-129_ETF.Carbon

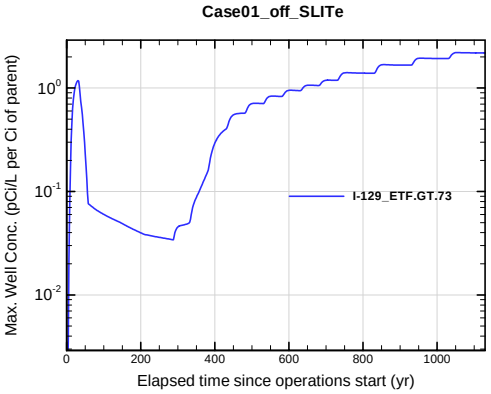

Figure A1B-498. Max. 100-m well conc. for Case01_off_SLITe I-129_ETF.GT.73

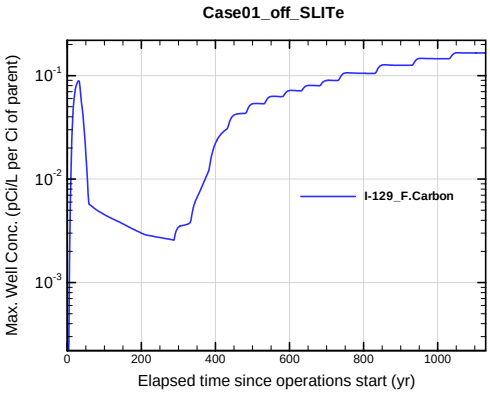

Figure A1B-499. Max. 100-m well conc. for Case01_off_SLITe I-129_F.Carbon

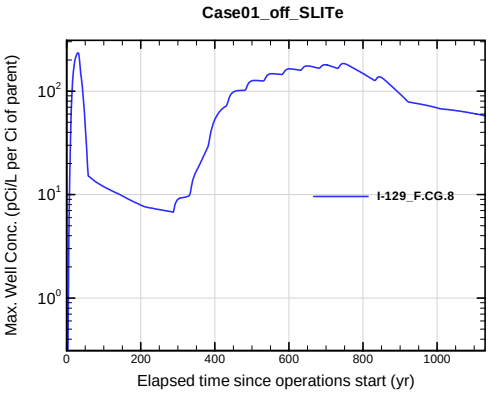

Figure A1B-500. Max. 100-m well conc. for Case01_off_SLITe I-129_F.CG.8

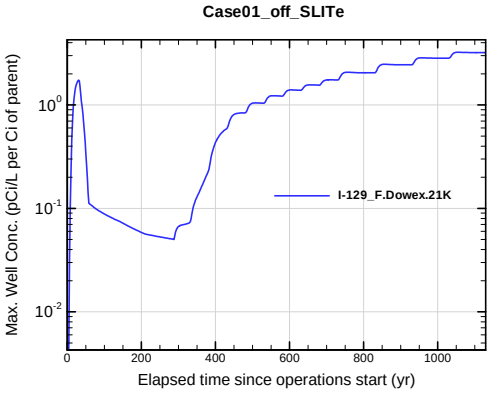

Figure A1B-501. Max. 100-m well conc. for Case01_off_SLITe I-129_F.Dowex.21K

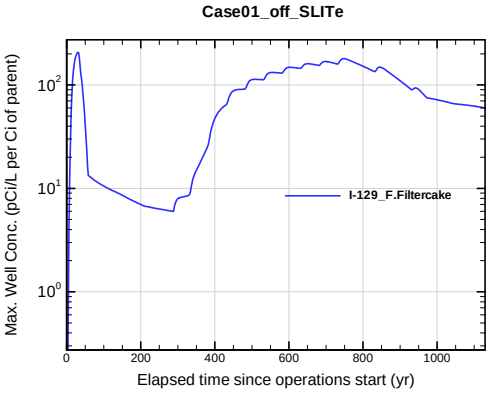

Figure A1B-502. Max. 100-m well conc. for Case01_off_SLITe I-129_F.Filtercake

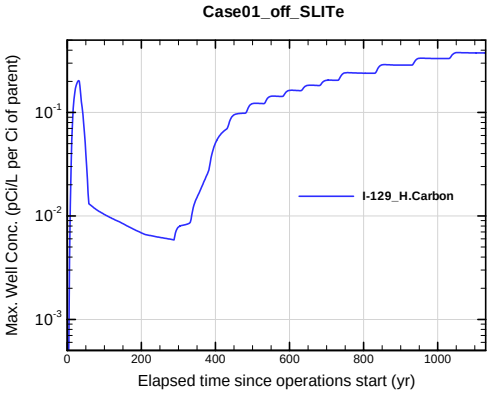

Figure A1B-503. Max. 100-m well conc. for Case01_off_SLITe I-129_H.Carbon

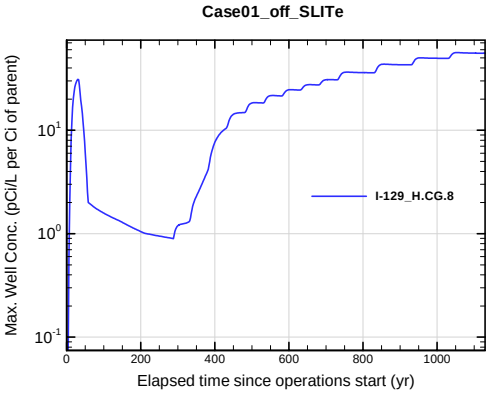

Figure A1B-504. Max. 100-m well conc. for Case01_off_SLITe I-129_H.CG.8

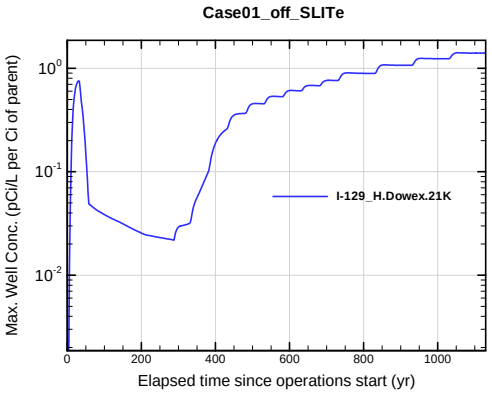

Figure A1B-505. Max. 100-m well conc. for Case01_off_SLITe I-129_H.Dowex.21K

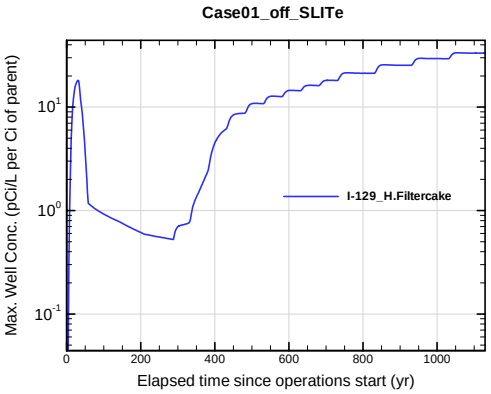

Figure A1B-506. Max. 100-m well conc. for Case01_off_SLITe I-129_H.Filtercake

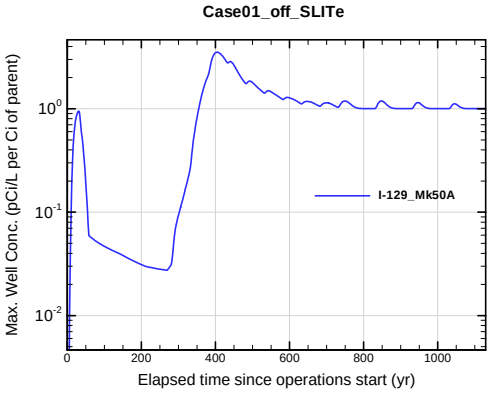

Figure A1B-507. Max. 100-m well conc. for Case01_off_SLITe I-129_Mk50A

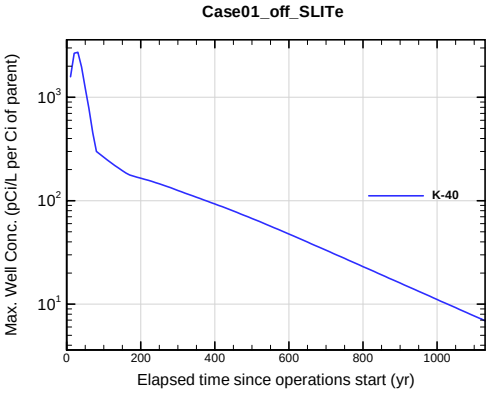

Figure A1B-508. Max. 100-m well conc. for Case01_off_SLITe K-40

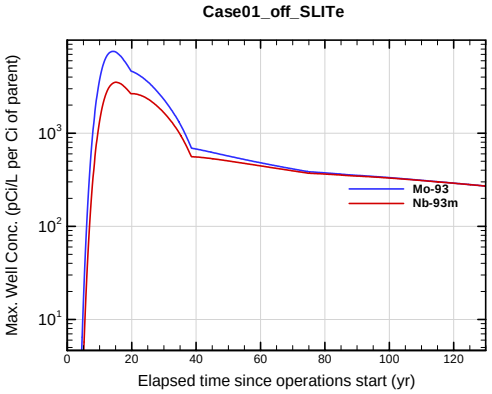

Figure A1B-509. Max. 100-m well conc. for Case01_off_SLITe Mo-93

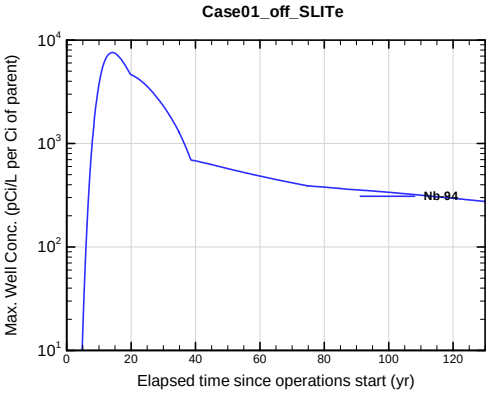

Figure A1B-510. Max. 100-m well conc. for Case01_off_SLITe Nb-94

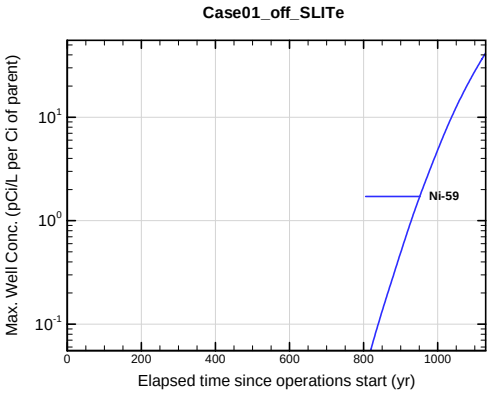

Figure A1B-511. Max. 100-m well conc. for Case01_off_SLITe Ni-59

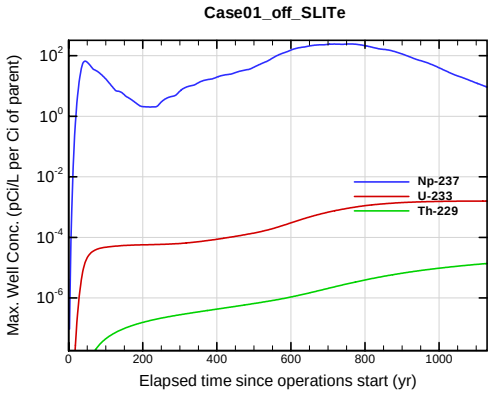

Figure A1B-512. Max. 100-m well conc. for Case01_off_SLITe Np-237

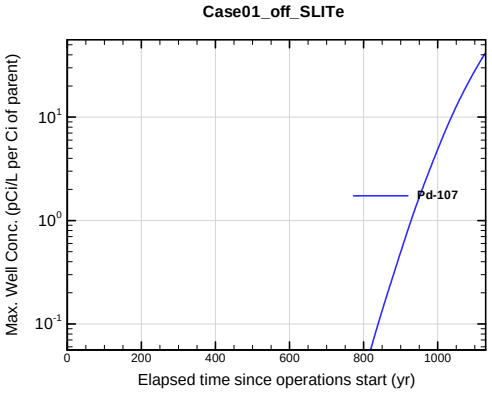

Figure A1B-513. Max. 100-m well conc. for Case01_off_SLITe Pd-107

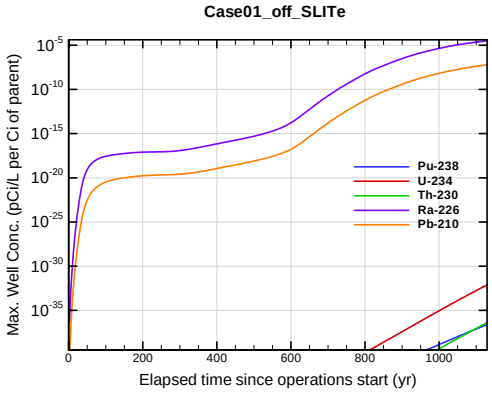

Figure A1B-514. Max. 100-m well conc. for Case01_off_SLITe Pu-238

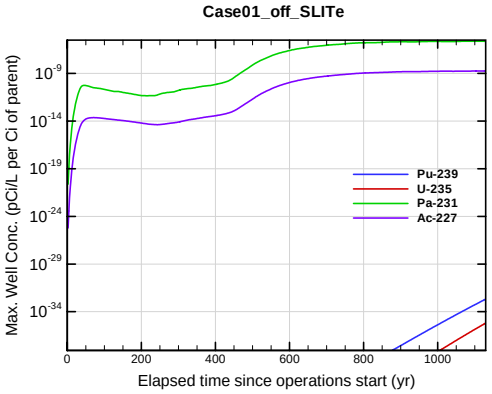

Figure A1B-515. Max. 100-m well conc. for Case01_off_SLITe Pu-239

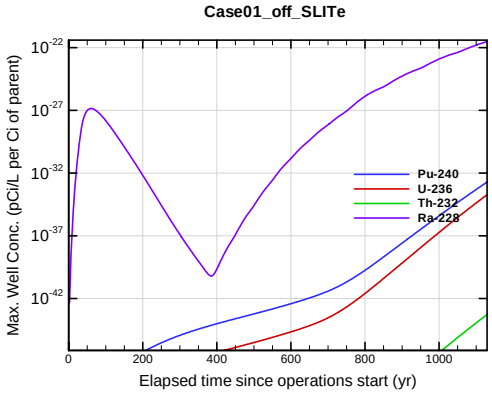

Figure A1B-516. Max. 100-m well conc. for Case01_off_SLITe Pu-240

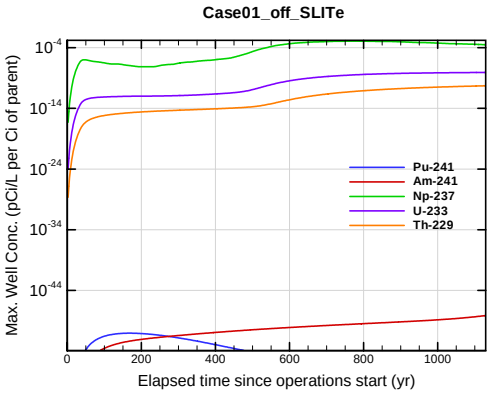

Figure A1B-517. Max. 100-m well conc. for Case01_off_SLITe Pu-241

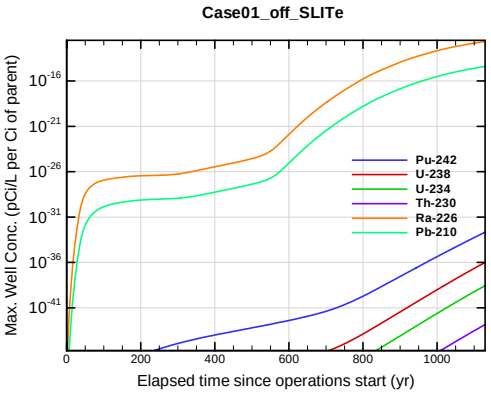

Figure A1B-518. Max. 100-m well conc. for Case01_off_SLITe Pu-242

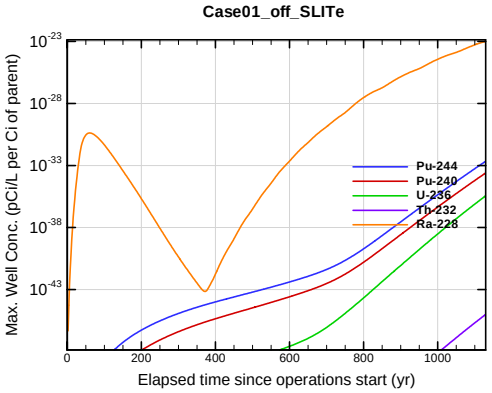

Figure A1B-519. Max. 100-m well conc. for Case01_off_SLITe Pu-244

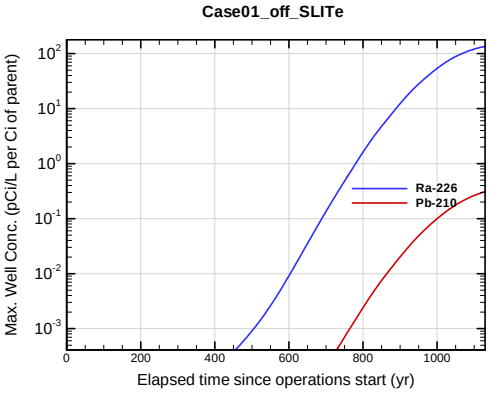

Figure A1B-520. Max. 100-m well conc. for Case01_off_SLITe Ra-226

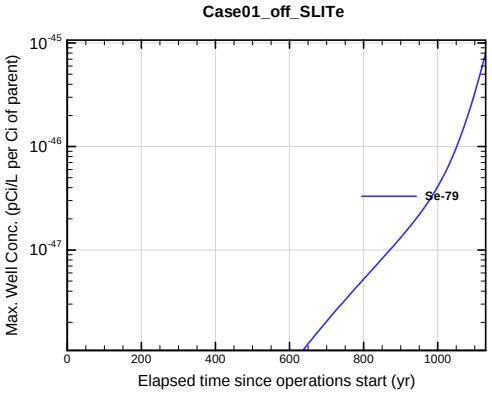

Figure A1B-521. Max. 100-m well conc. for Case01_off_SLITe Se-79

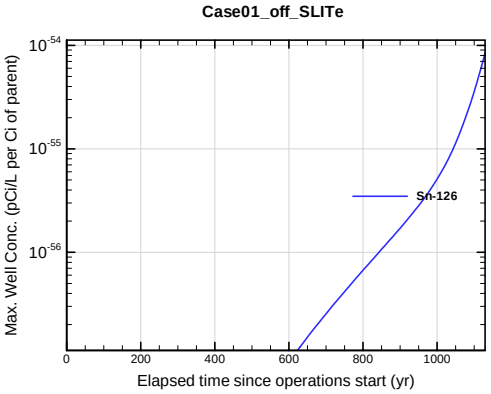

Figure A1B-522. Max. 100-m well conc. for Case01_off_SLITe Sn-126

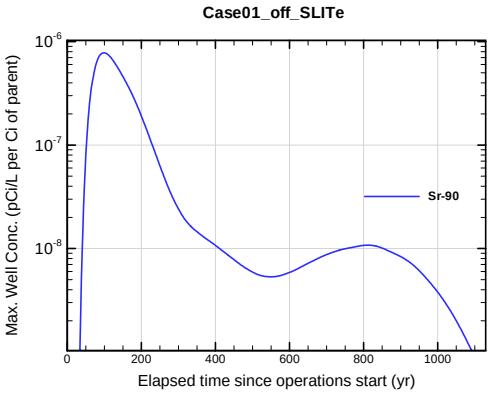

Figure A1B-523. Max. 100-m well conc. for Case01_off_SLITe Sr-90

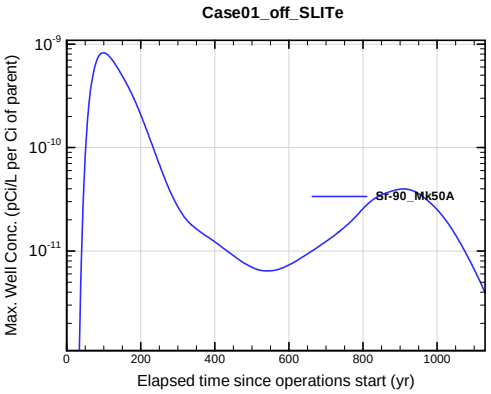

Figure A1B-524. Max. 100-m well conc. for Case01_off_SLITe Sr-90_Mk50A

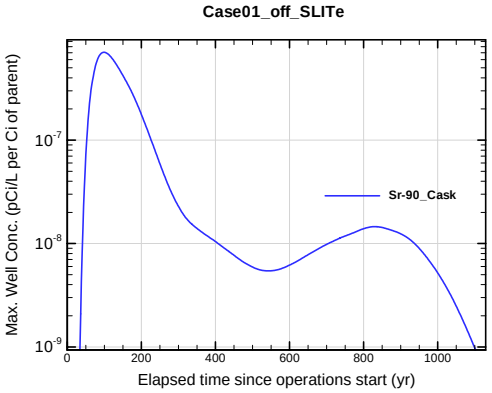

Figure A1B-525. Max. 100-m well conc. for Case01_off_SLITe Sr-90_Cask

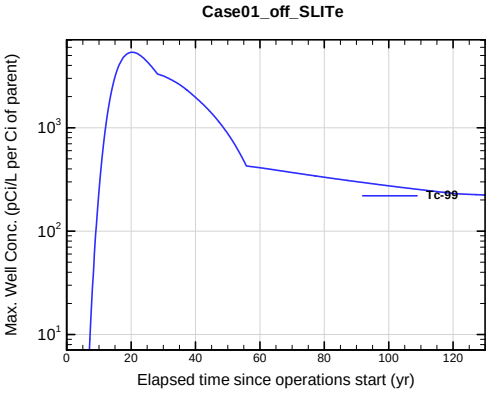

Figure A1B-526. Max. 100-m well conc. for Case01_off_SLITe Tc-99

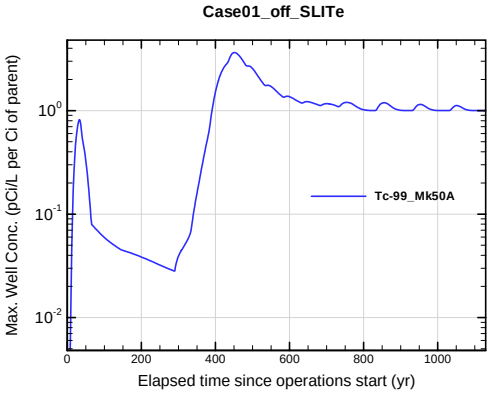

Figure A1B-527. Max. 100-m well conc. for Case01_off_SLITe Tc-99_Mk50A

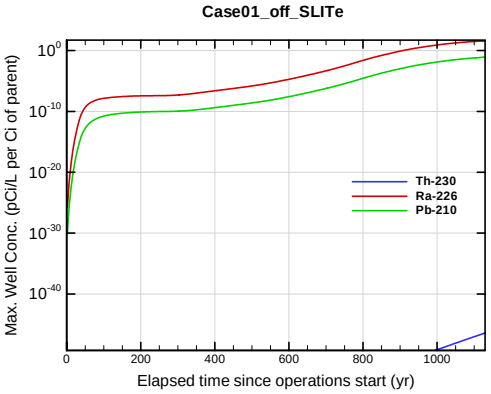

Figure A1B-528. Max. 100-m well conc. for Case01_off_SLITe Th-230

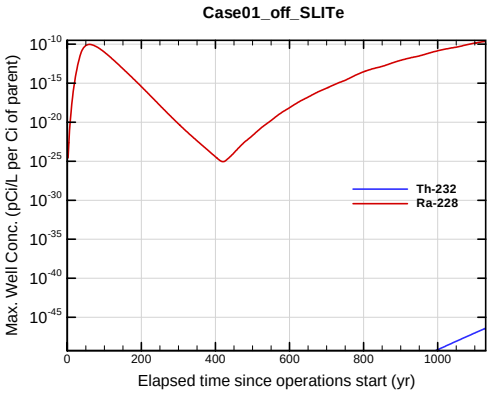

Figure A1B-529. Max. 100-m well conc. for Case01_off_SLITe Th-232

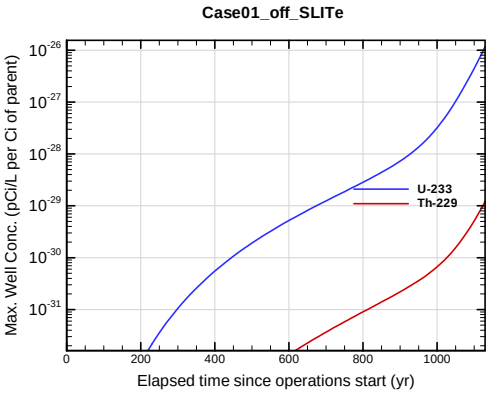

Figure A1B-530. Max. 100-m well conc. for Case01_off_SLITe U-233

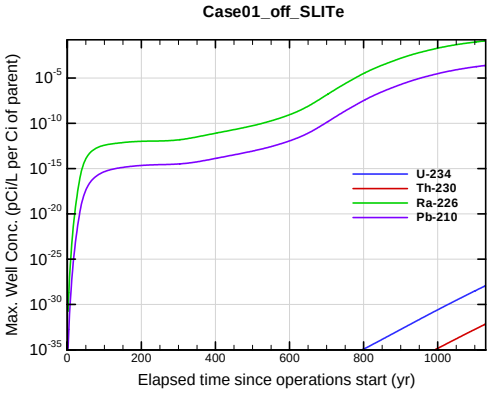

Figure A1B-531. Max. 100-m well conc. for Case01_off_SLITe U-234

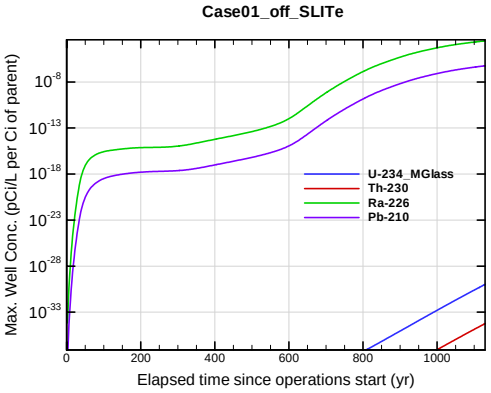

Figure A1B-532. Max. 100-m well conc. for Case01_off_SLITe U-234_MGlass

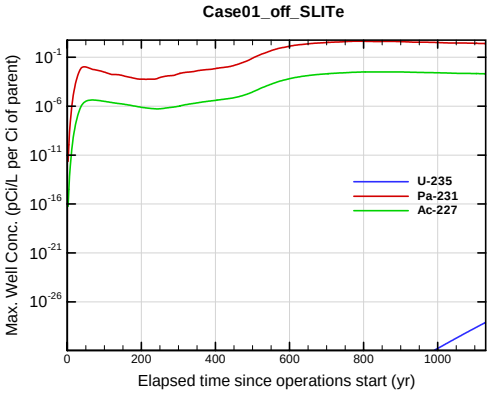

Figure A1B-533. Max. 100-m well conc. for Case01_off_SLITe U-235

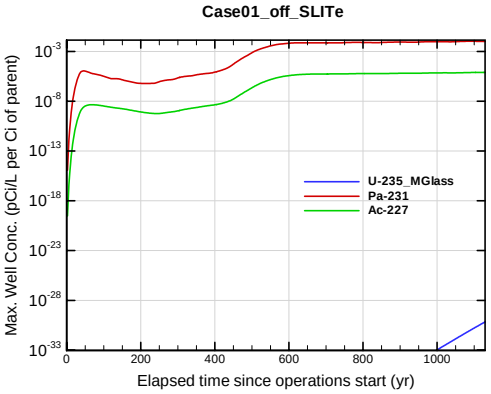

Figure A1B-534. Max. 100-m well conc. for Case01_off_SLITe U-235_MGlass

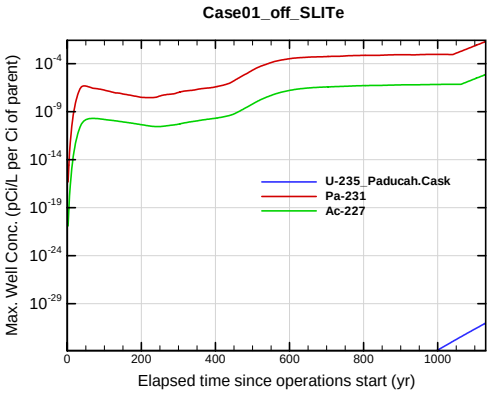

Figure A1B-535. Max. 100-m well conc. for Case01_off_SLITe U-235_Paducah.Cask

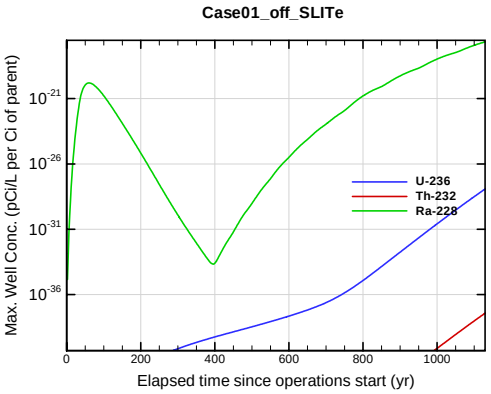

Figure A1B-536. Max. 100-m well conc. for Case01_off_SLITe U-236

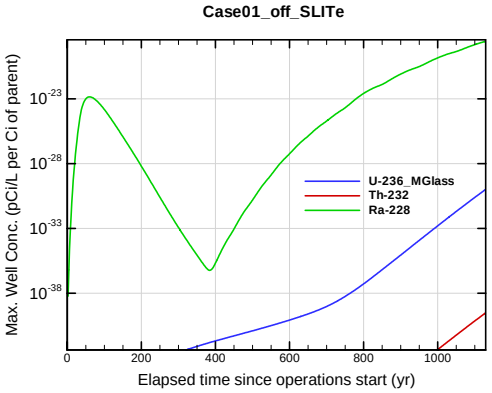

Figure A1B-537. Max. 100-m well conc. for Case01_off_SLITe U-236_MGlass

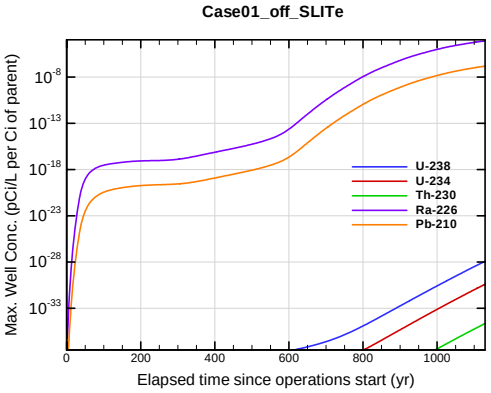

Figure A1B-538. Max. 100-m well conc. for Case01_off_SLITe U-238

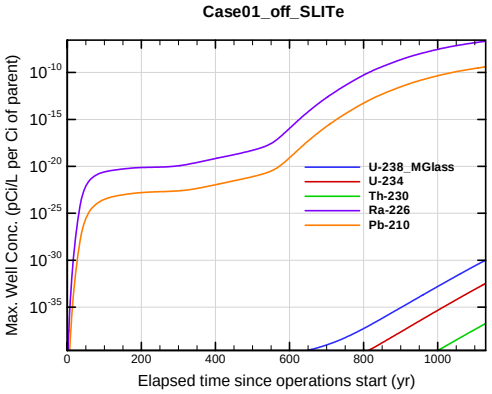

Figure A1B-539. Max. 100-m well conc. for Case01_off_SLITe U-238_MGlass

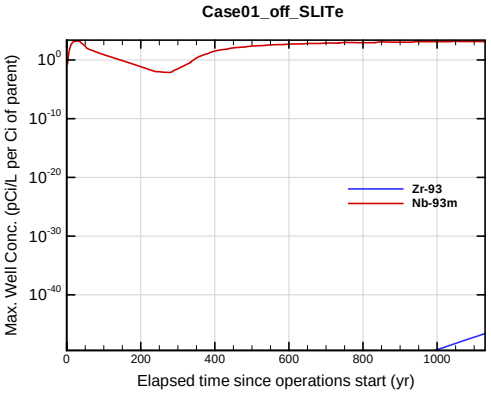

Figure A1B-540. Max. 100-m well conc. for Case01_off_SLITe Zr-93

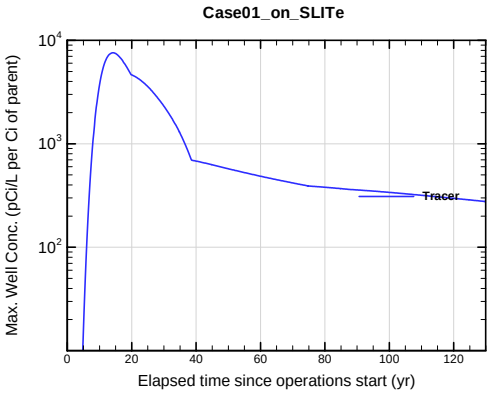

Figure A1B-541. Max. 100-m well conc. for Case01_on_SLITe Tracer

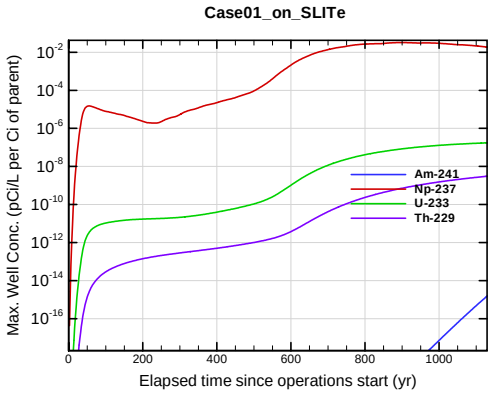

Figure A1B-542. Max. 100-m well conc. for Case01_on_SLITe Am-241

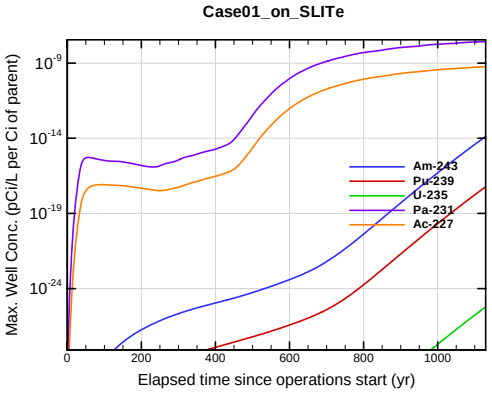

Figure A1B-543. Max. 100-m well conc. for Case01_on_SLITe Am-243

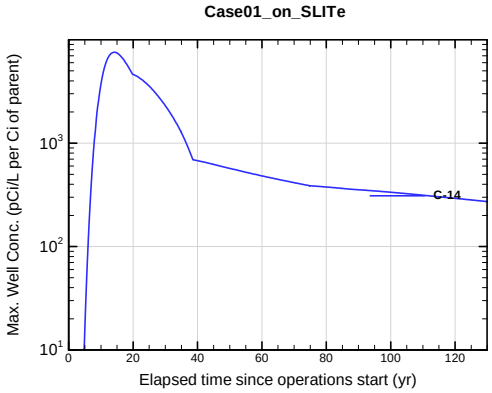

Figure A1B-544. Max. 100-m well conc. for Case01_on_SLITe C-14

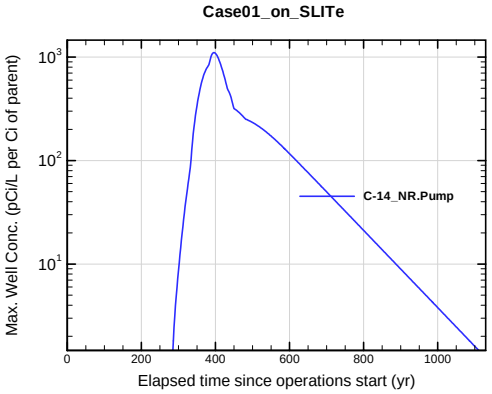

Figure A1B-545. Max. 100-m well conc. for Case01_on_SLITe C-14_NR.Pump

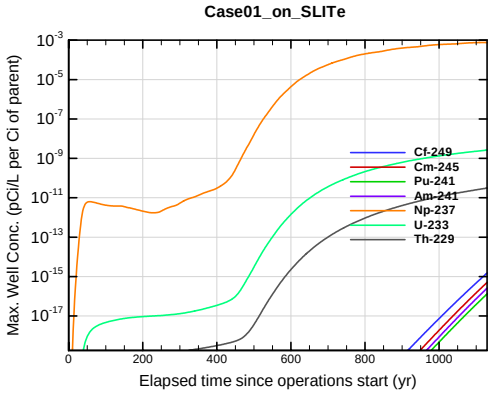

Figure A1B-546. Max. 100-m well conc. for Case01_on_SLITe Cf-249

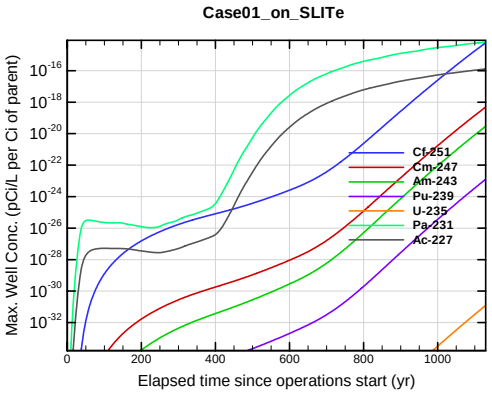

Figure A1B-547. Max. 100-m well conc. for Case01_on_SLITe Cf-251

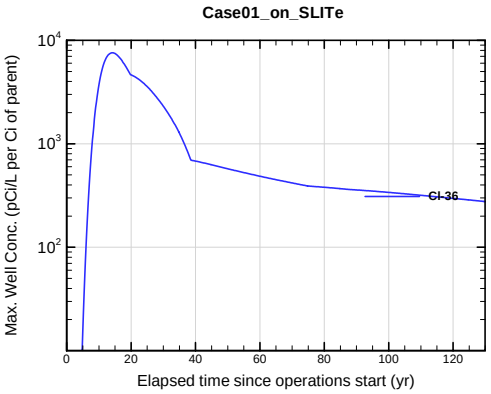

Figure A1B-548. Max. 100-m well conc. for Case01_on_SLITe Cl-36

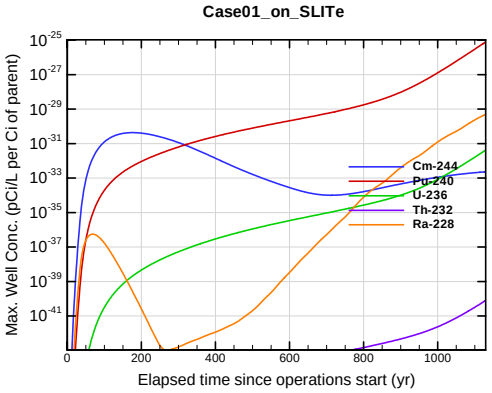

Figure A1B-549. Max. 100-m well conc. for Case01_on_SLITe Cm-244

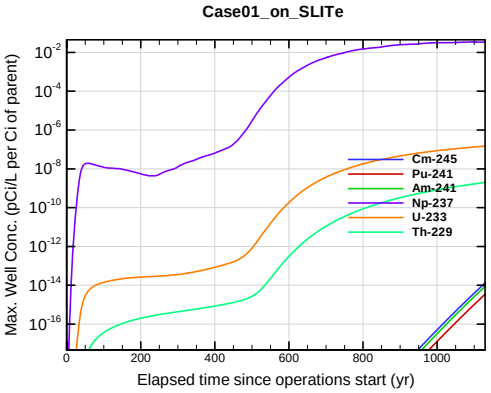

Figure A1B-550. Max. 100-m well conc. for Case01_on_SLITe Cm-245

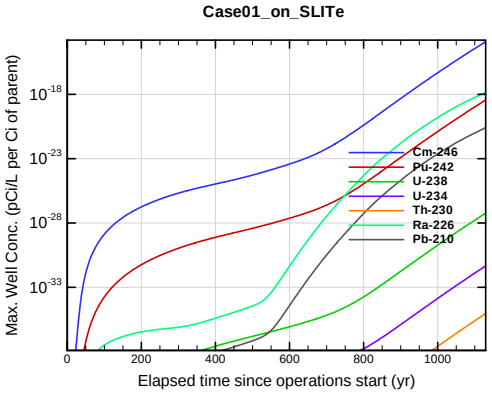

Figure A1B-551. Max. 100-m well conc. for Case01_on_SLITe Cm-246

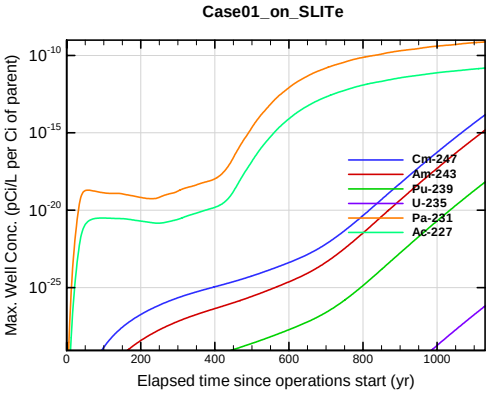

Figure A1B-552. Max. 100-m well conc. for Case01_on_SLITe Cm-247

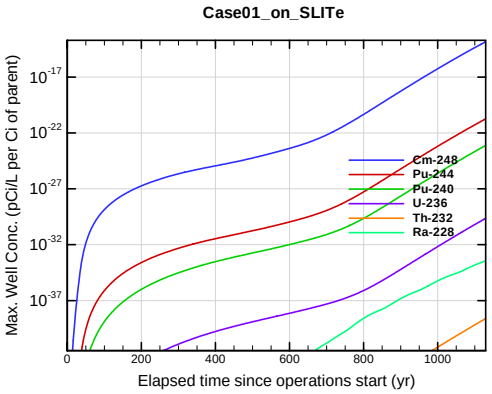

Figure A1B-553. Max. 100-m well conc. for Case01_on_SLITe Cm-248

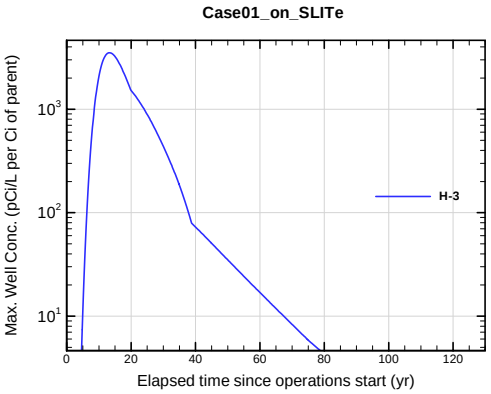

Figure A1B-554. Max. 100-m well conc. for Case01_on_SLITe H-3

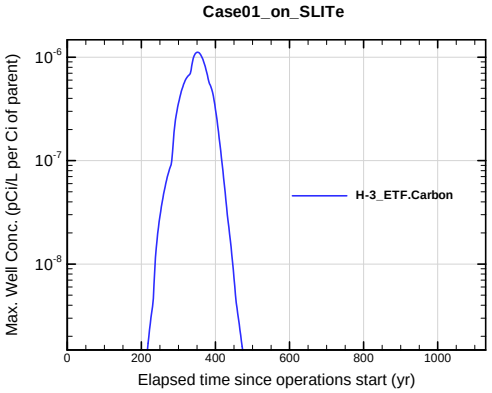

Figure A1B-555. Max. 100-m well conc. for Case01_on_SLITe H-3_ETF.Carbon

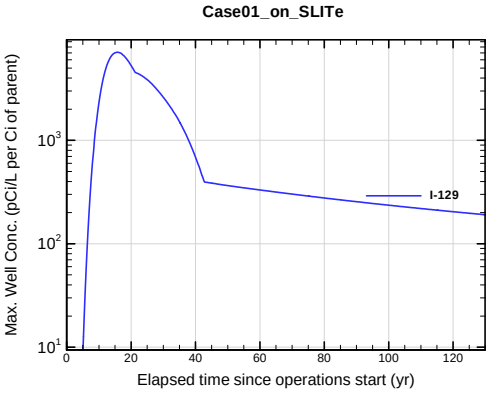

Figure A1B-556. Max. 100-m well conc. for Case01_on_SLITe I-129

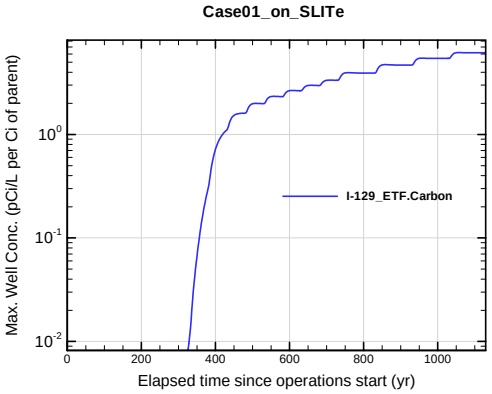

Figure A1B-557. Max. 100-m well conc. for Case01_on_SLITe I-129_ETF.Carbon

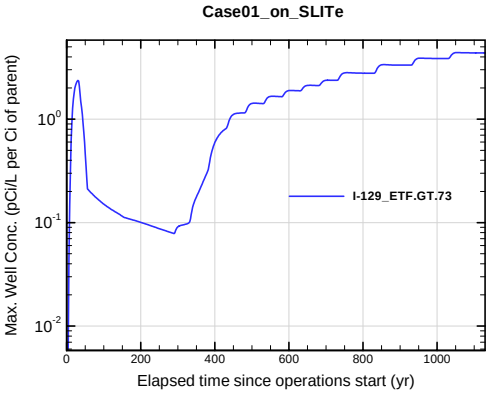

Figure A1B-558. Max. 100-m well conc. for Case01_on_SLITe I-129_ETF.GT.73

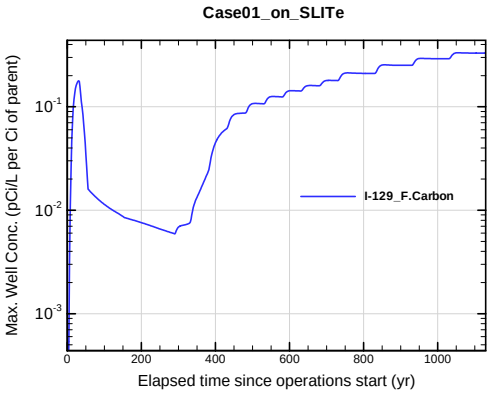

Figure A1B-559. Max. 100-m well conc. for Case01_on_SLITe I-129_F.Carbon

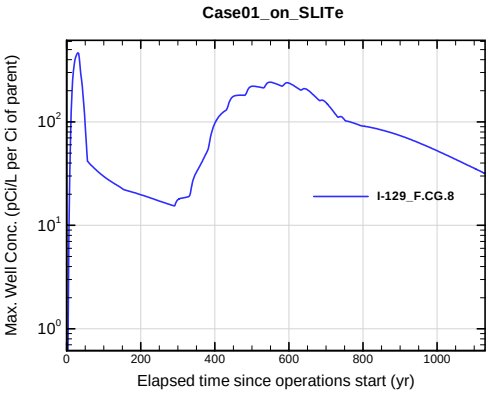

Figure A1B-560. Max. 100-m well conc. for Case01_on_SLITe I-129_F.CG.8

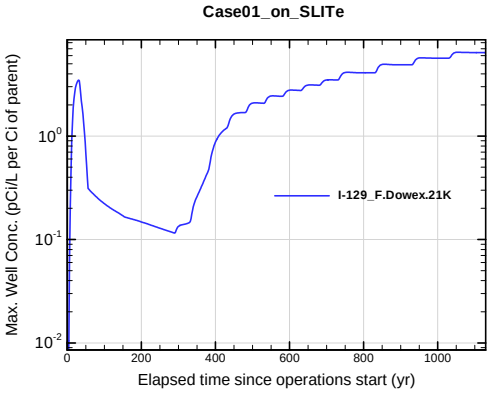

Figure A1B-561. Max. 100-m well conc. for Case01_on_SLITe I-129_F.Dowex.21K

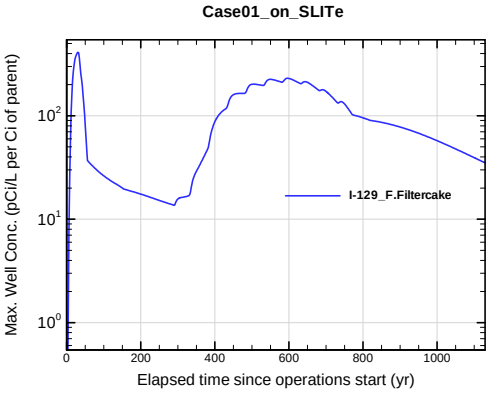

Figure A1B-562. Max. 100-m well conc. for Case01_on_SLITe I-129_F.Filtercake

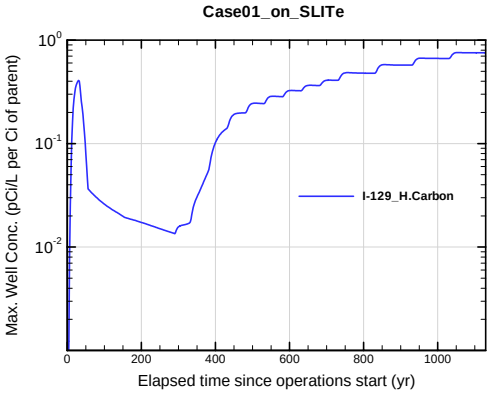

Figure A1B-563. Max. 100-m well conc. for Case01_on_SLITe I-129_H.Carbon

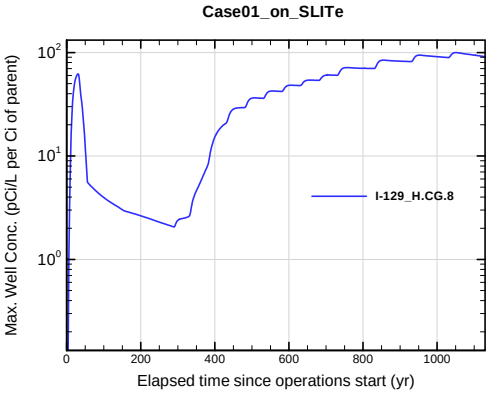

Figure A1B-564. Max. 100-m well conc. for Case01_on_SLITe I-129_H.CG.8

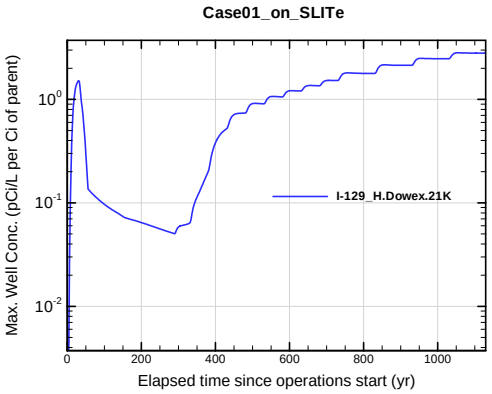

Figure A1B-565. Max. 100-m well conc. for Case01_on_SLITe I-129_H.Dowex.21K

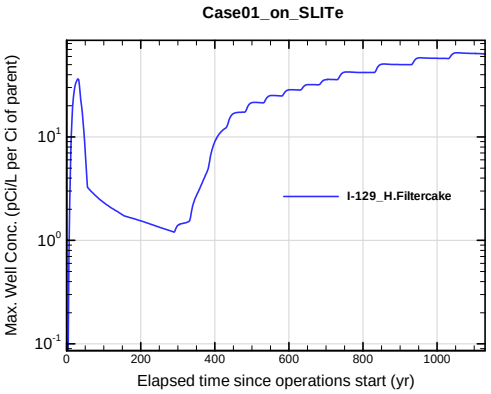

Figure A1B-566. Max. 100-m well conc. for Case01_on_SLITe I-129_H.Filtercake

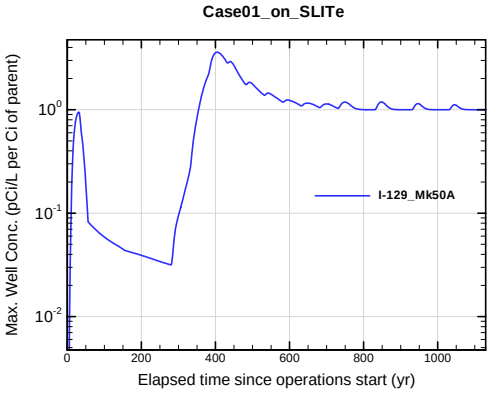

Figure A1B-567. Max. 100-m well conc. for Case01_on_SLITe I-129_Mk50A

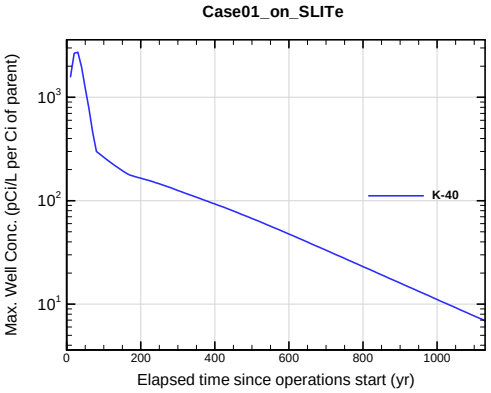

Figure A1B-568. Max. 100-m well conc. for Case01_on_SLITe K-40

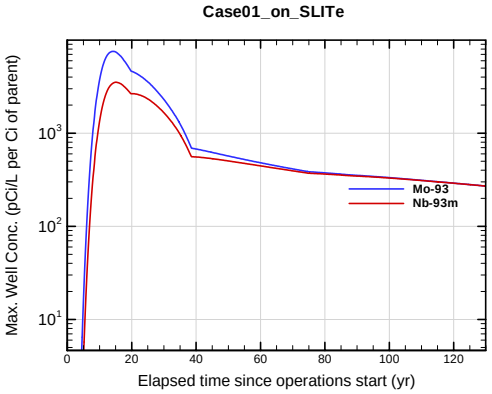

Figure A1B-569. Max. 100-m well conc. for Case01_on_SLITe Mo-93

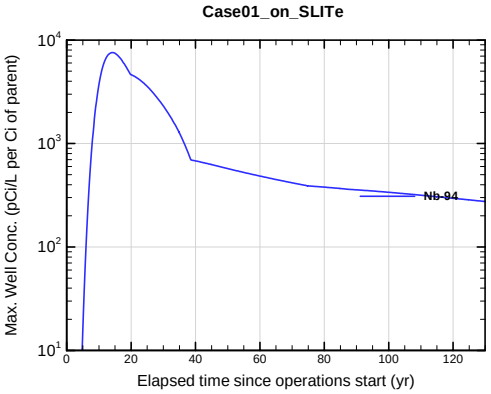

Figure A1B-570. Max. 100-m well conc. for Case01_on_SLITe Nb-94

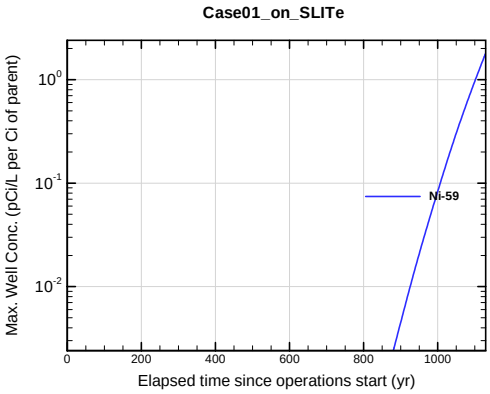

Figure A1B-571. Max. 100-m well conc. for Case01_on_SLITe Ni-59

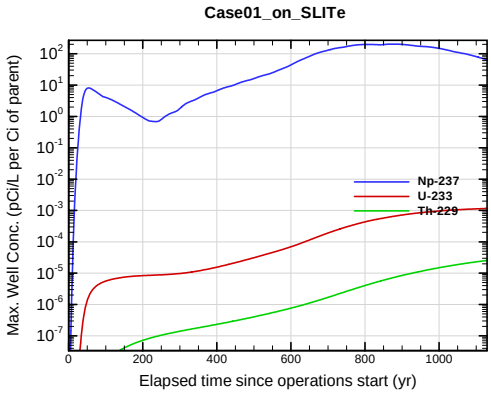

Figure A1B-572. Max. 100-m well conc. for Case01_on_SLITe Np-237

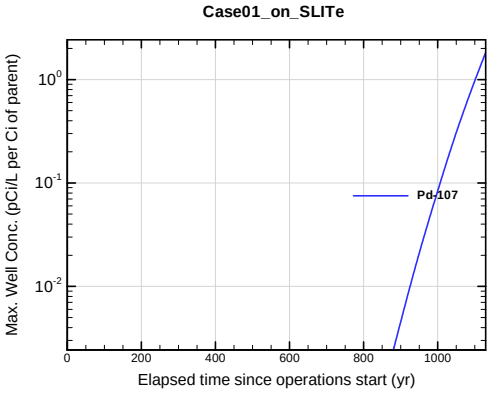

Figure A1B-573. Max. 100-m well conc. for Case01_on_SLITe Pd-107

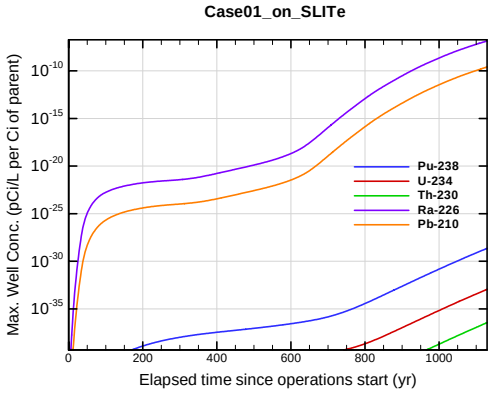

Figure A1B-574. Max. 100-m well conc. for Case01_on_SLITe Pu-238

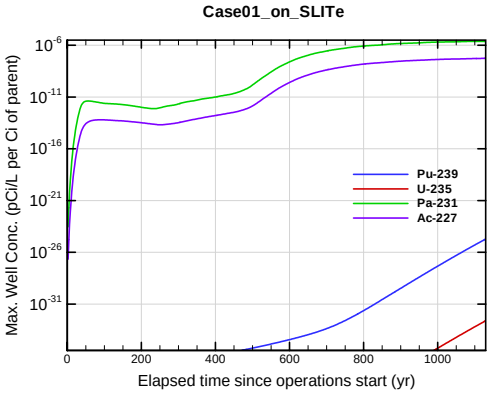

Figure A1B-575. Max. 100-m well conc. for Case01_on_SLITe Pu-239

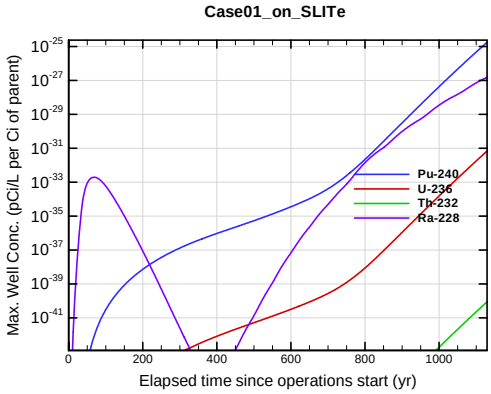

Figure A1B-576. Max. 100-m well conc. for Case01_on_SLITe Pu-240

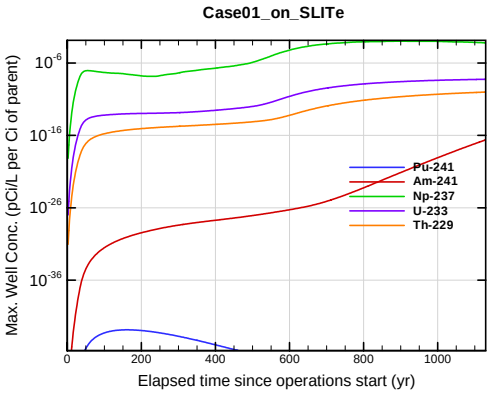

Figure A1B-577. Max. 100-m well conc. for Case01_on_SLITe Pu-241

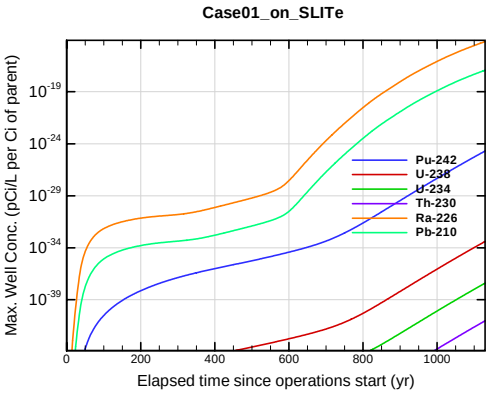

Figure A1B-578. Max. 100-m well conc. for Case01_on_SLITe Pu-242

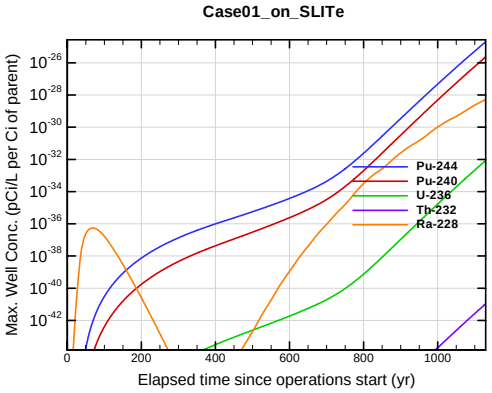

Figure A1B-579. Max. 100-m well conc. for Case01_on_SLITe Pu-244

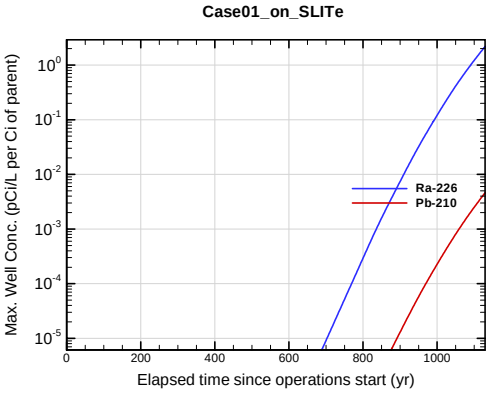

Figure A1B-580. Max. 100-m well conc. for Case01_on_SLITe Ra-226

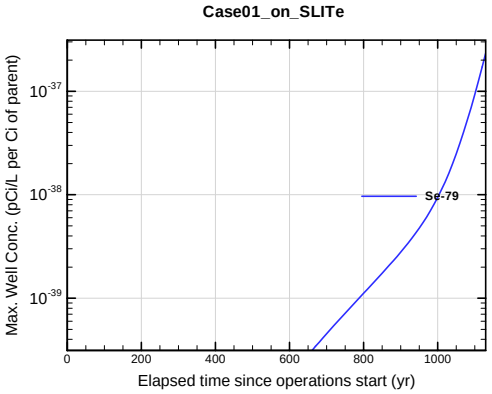

Figure A1B-581. Max. 100-m well conc. for Case01_on_SLITe Se-79

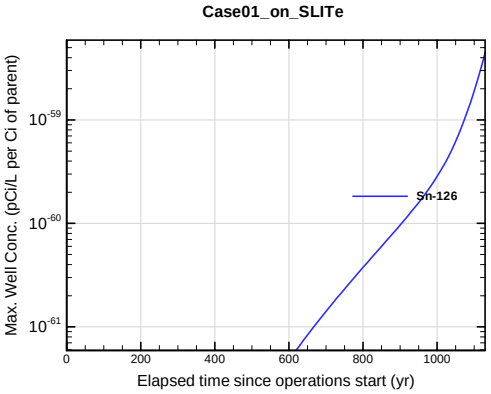

Figure A1B-582. Max. 100-m well conc. for Case01_on_SLITe Sn-126

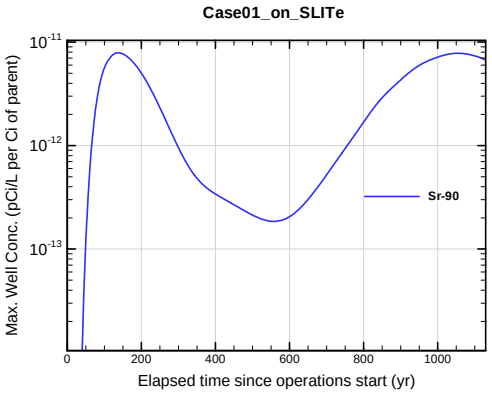

Figure A1B-583. Max. 100-m well conc. for Case01_on_SLITe Sr-90

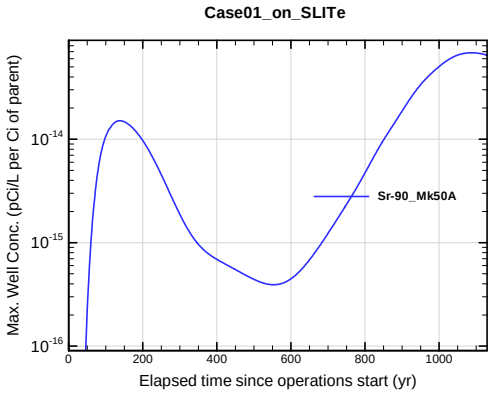

Figure A1B-584. Max. 100-m well conc. for Case01_on_SLITe Sr-90_Mk50A

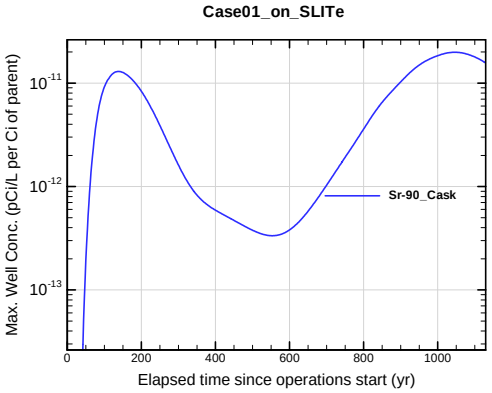

Figure A1B-585. Max. 100-m well conc. for Case01_on_SLITe Sr-90_Cask

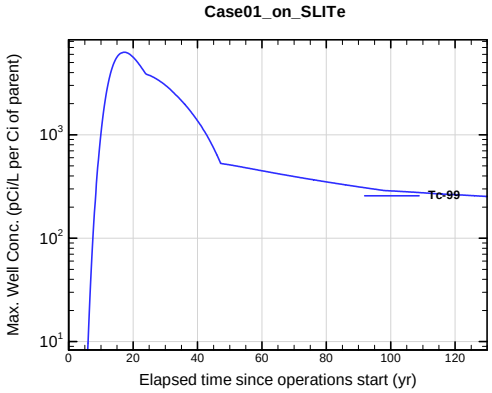

Figure A1B-586. Max. 100-m well conc. for Case01_on_SLITe Tc-99

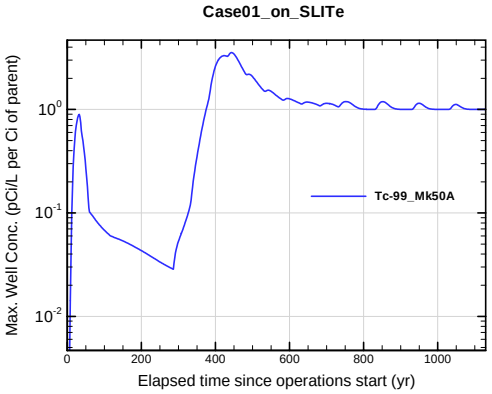

Figure A1B-587. Max. 100-m well conc. for Case01_on_SLITe Tc-99_Mk50A

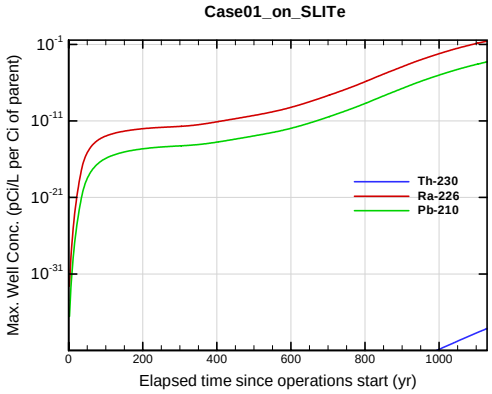

Figure A1B-588. Max. 100-m well conc. for Case01_on_SLITe Th-230

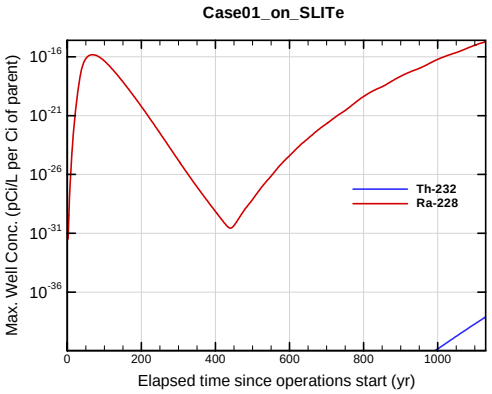

Figure A1B-589. Max. 100-m well conc. for Case01_on_SLITe Th-232

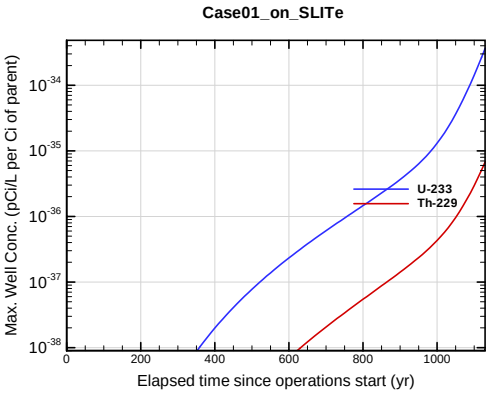

Figure A1B-590. Max. 100-m well conc. for Case01_on_SLITe U-233

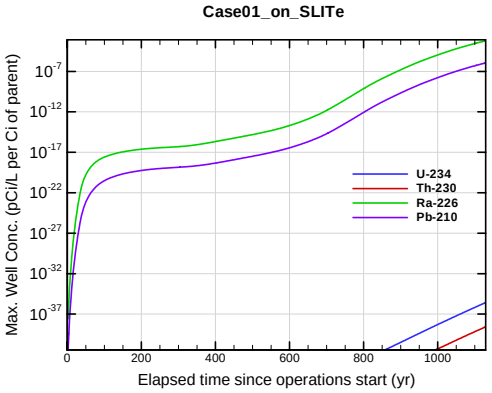

Figure A1B-591. Max. 100-m well conc. for Case01_on_SLITe U-234

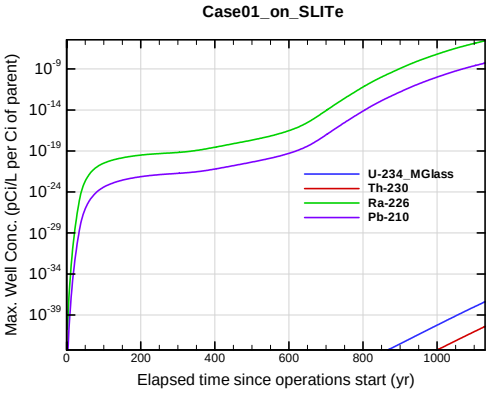

Figure A1B-592. Max. 100-m well conc. for Case01_on_SLITe U-234_MGlass

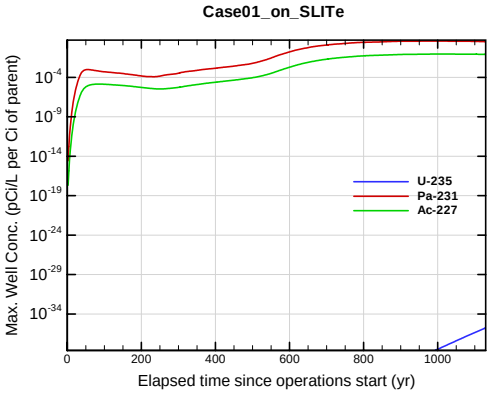

Figure A1B-593. Max. 100-m well conc. for Case01_on_SLITe U-235

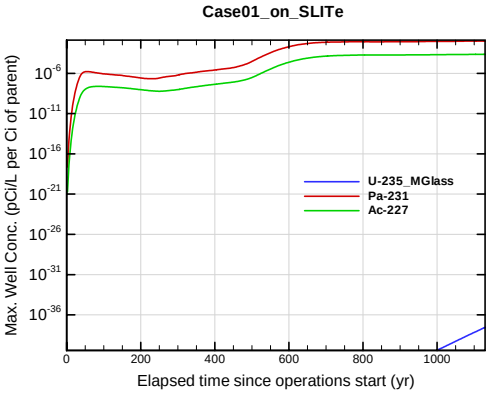

Figure A1B-594. Max. 100-m well conc. for Case01_on_SLITe U-235_MGlass

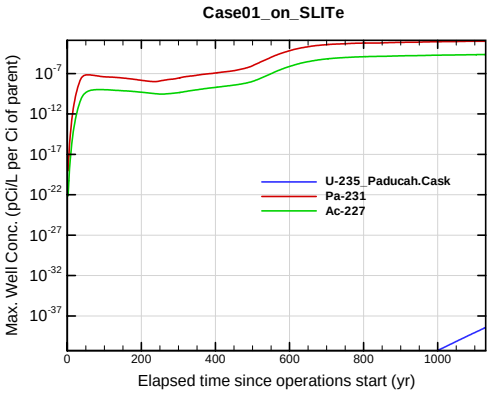

Figure A1B-595. Max. 100-m well conc. for Case01_on_SLITe U-235_Paducah.Cask

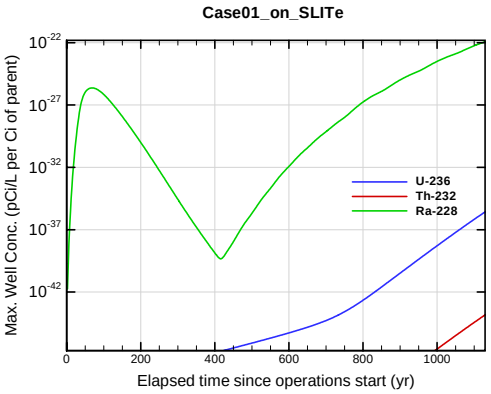

Figure A1B-596. Max. 100-m well conc. for Case01_on_SLITe U-236

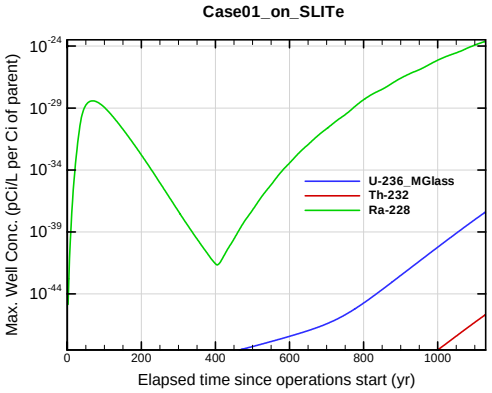

Figure A1B-597. Max. 100-m well conc. for Case01_on_SLITe U-236_MGlass

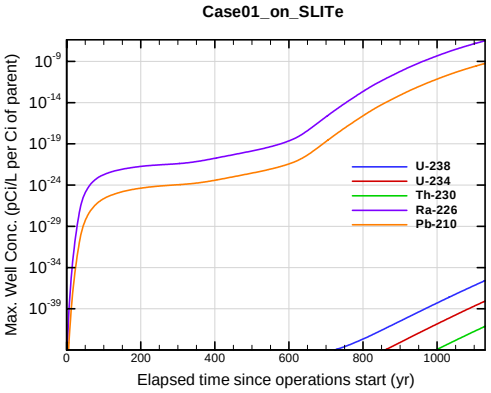

Figure A1B-598. Max. 100-m well conc. for Case01_on_SLITe U-238

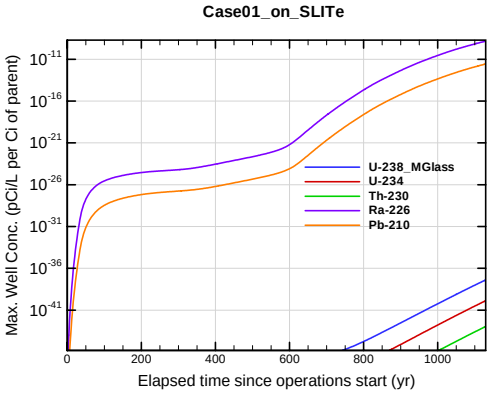

Figure A1B-599. Max. 100-m well conc. for Case01_on_SLITe U-238_MGlass

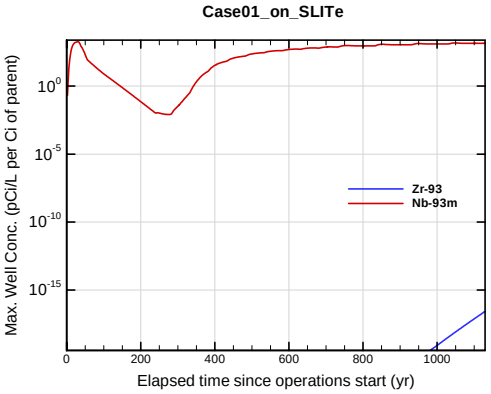

Figure A1B-600. Max. 100-m well conc. for Case01_on_SLITe Zr-93

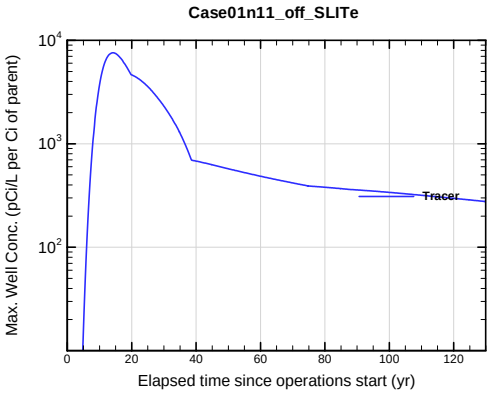

Figure A1B-601. Max. 100-m well conc. for Case01n11_off_SLITe Tracer

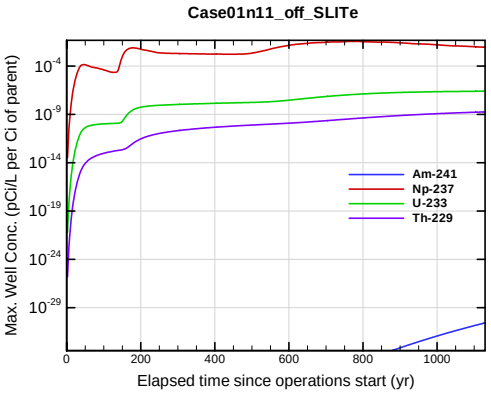

Figure A1B-602. Max. 100-m well conc. for Case01n11_off_SLITe Am-241

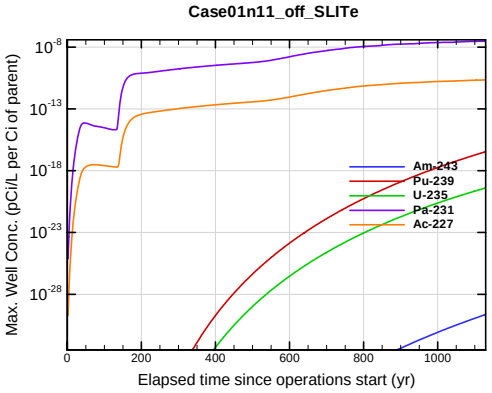

Figure A1B-603. Max. 100-m well conc. for Case01n11_off_SLITe Am-243

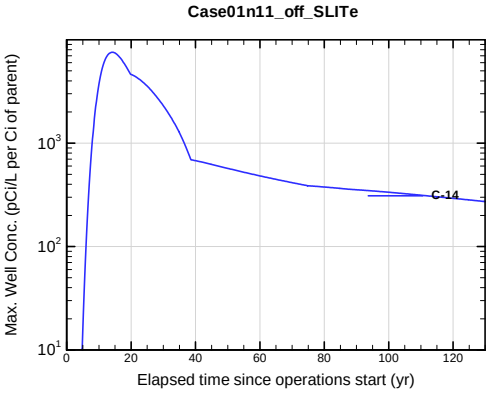

Figure A1B-604. Max. 100-m well conc. for Case01n11_off_SLITe C-14

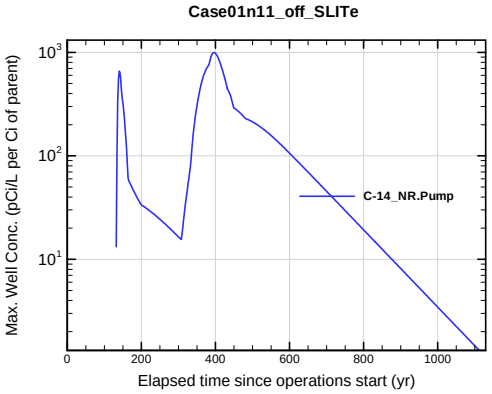

Figure A1B-605. Max. 100-m well conc. for Case01n11_off_SLITe C-14_NR.Pump

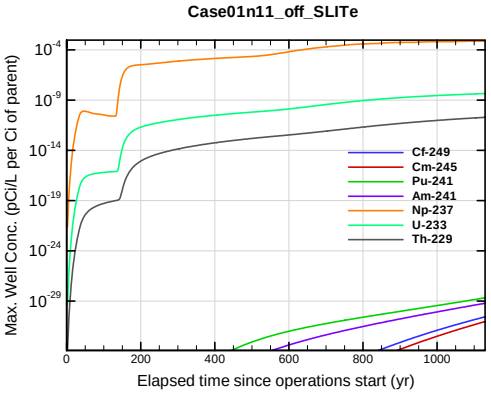

Figure A1B-606. Max. 100-m well conc. for Case01n11_off_SLITe Cf-249

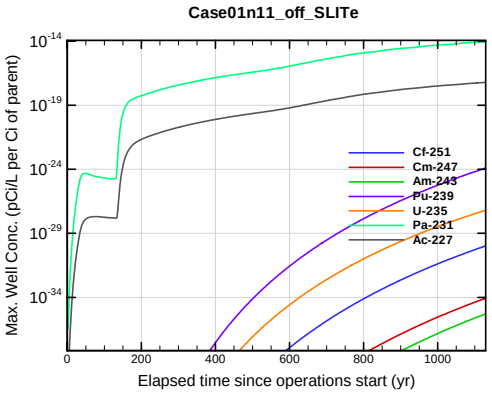

Figure A1B-607. Max. 100-m well conc. for Case01n11_off_SLITe Cf-251

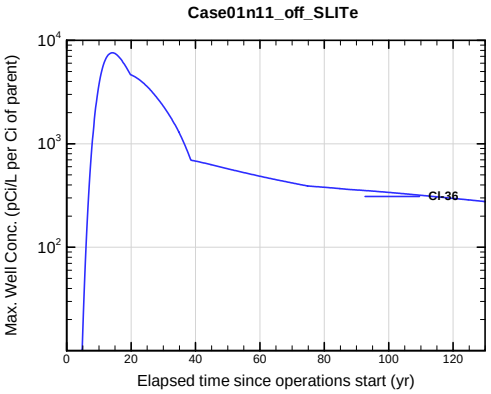

Figure A1B-608. Max. 100-m well conc. for Case01n11_off_SLITe Cl-36

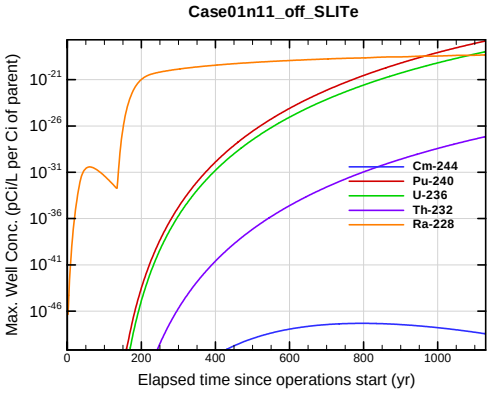

Figure A1B-609. Max. 100-m well conc. for Case01n11_off_SLITe Cm-244

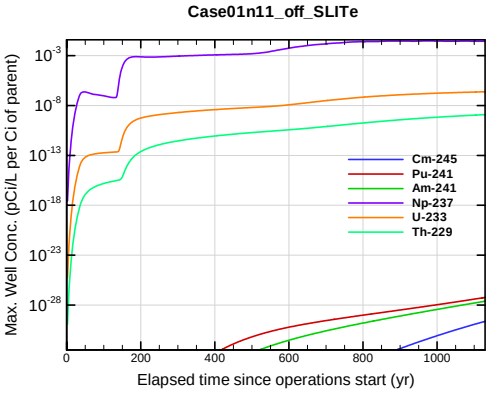

Figure A1B-610. Max. 100-m well conc. for Case01n11_off_SLITe Cm-245

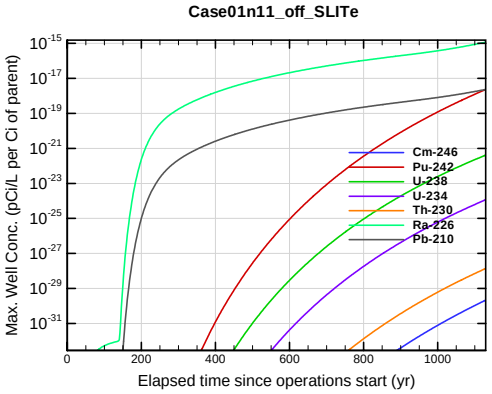

Figure A1B-611. Max. 100-m well conc. for Case01n11_off_SLITe Cm-246

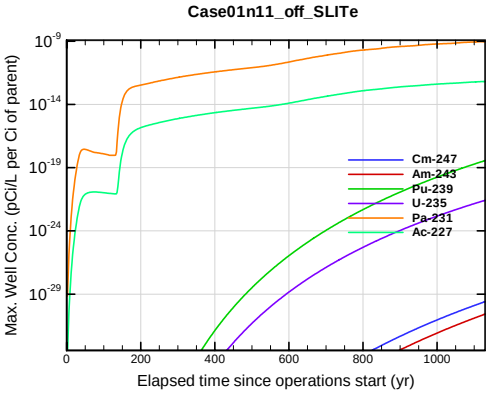

Figure A1B-612. Max. 100-m well conc. for Case01n11_off_SLITe Cm-247

Figure A1B-613. Max. 100-m well conc. for Case01n11_off_SLITe Cm-248

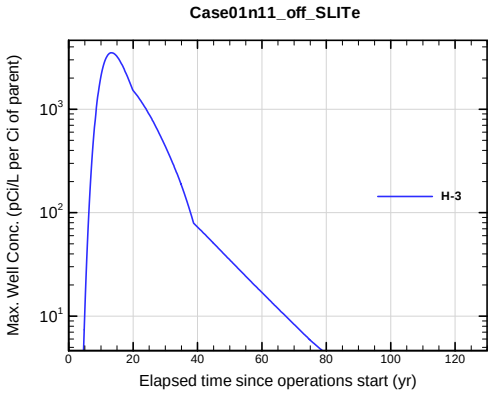

Figure A1B-614. Max. 100-m well conc. for Case01n11_off_SLITe H-3

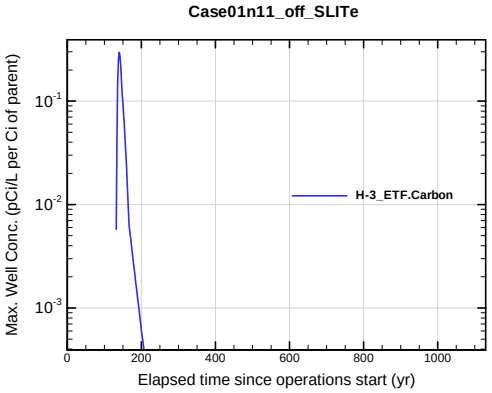

Figure A1B-615. Max. 100-m well conc. for Case01n11_off_SLITe H-3_ETF.Carbon

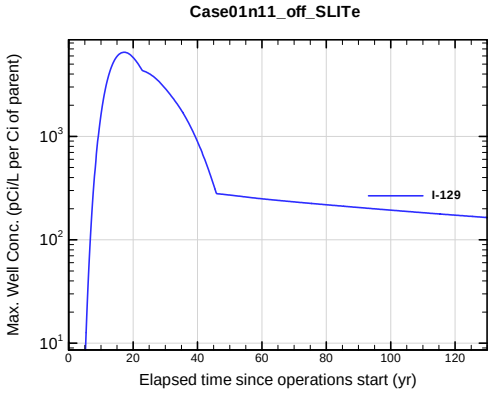

Figure A1B-616. Max. 100-m well conc. for Case01n11_off_SLITe I-129

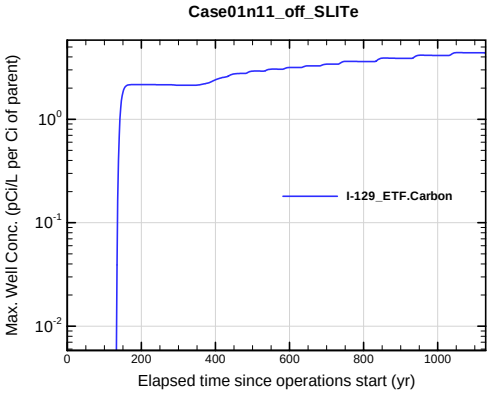

Figure A1B-617. Max. 100-m well conc. for Case01n11_off_SLITe I-129_ETF.Carbon

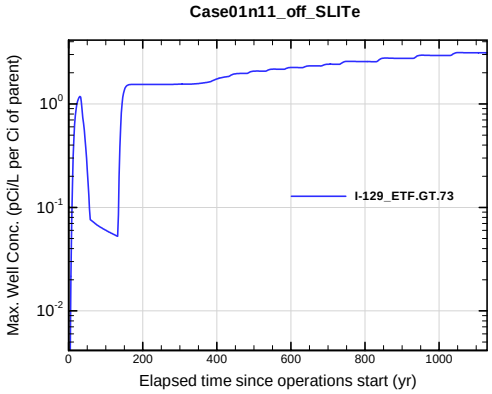

Figure A1B-618. Max. 100-m well conc. for Case01n11_off_SLITe I-129_ETF.GT.73

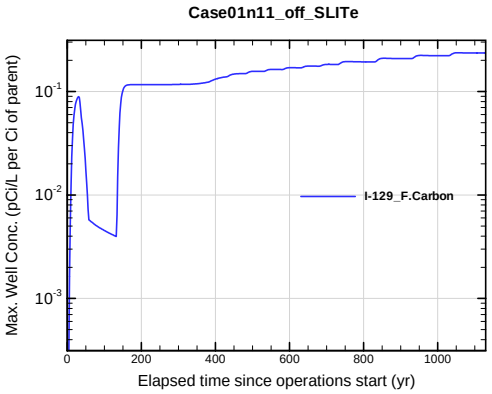

Figure A1B-619. Max. 100-m well conc. for Case01n11_off_SLITe I-129_F.Carbon

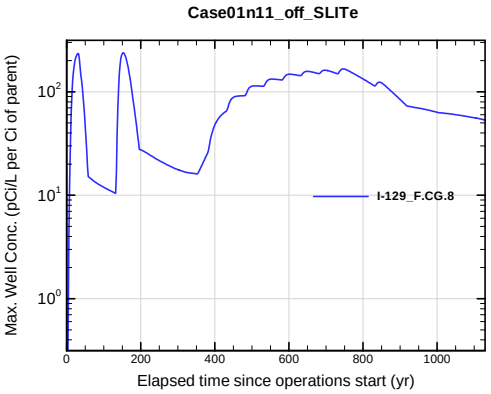

Figure A1B-620. Max. 100-m well conc. for Case01n11_off_SLITe I-129_F.CG.8

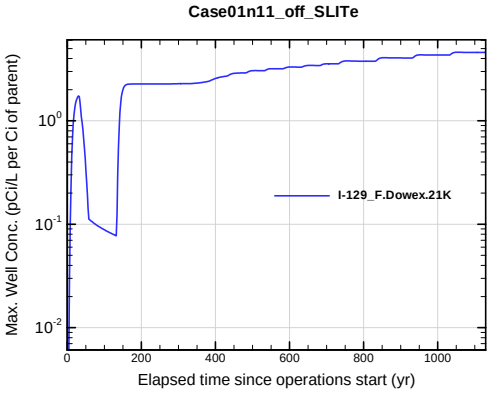

Figure A1B-621. Max. 100-m well conc. for Case01n11_off_SLITe I-129_F.Dowex.21K

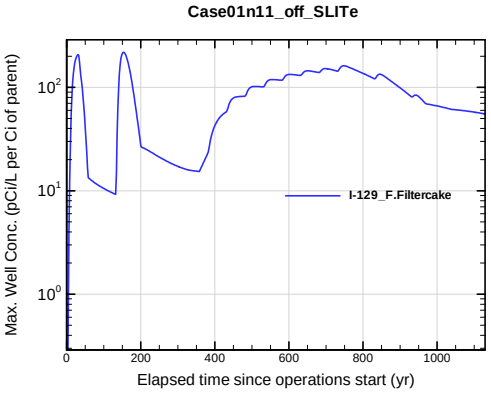

Figure A1B-622. Max. 100-m well conc. for Case01n11_off_SLITe I-129_F.Filtercake

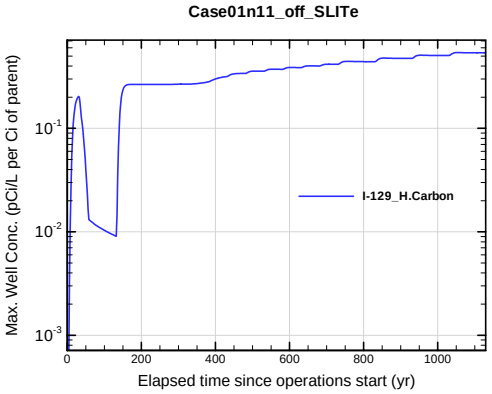

Figure A1B-623. Max. 100-m well conc. for Case01n11_off_SLITe I-129_H.Carbon

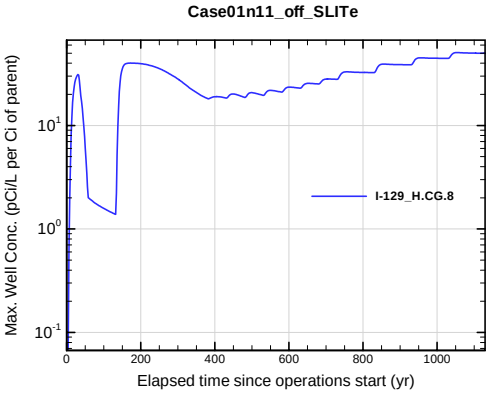

Figure A1B-624. Max. 100-m well conc. for Case01n11_off_SLITe I-129_H.CG.8

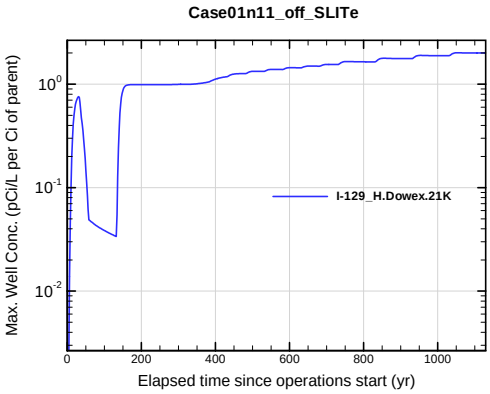

Figure A1B-625. Max. 100-m well conc. for Case01n11_off_SLITe I-129_H.Dowex.21K

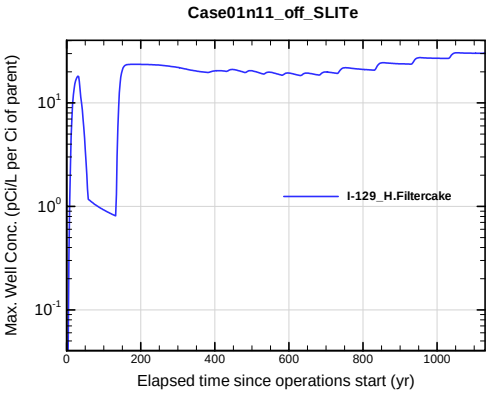

Figure A1B-626. Max. 100-m well conc. for Case01n11_off_SLITe I-129_H.Filtercake

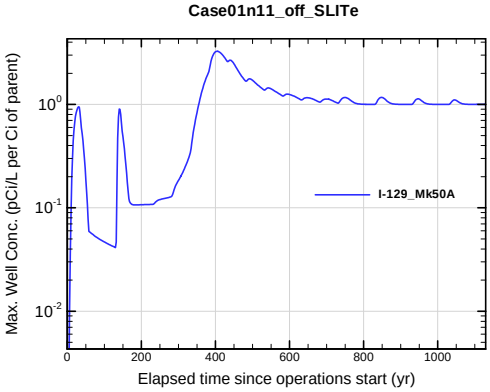

Figure A1B-627. Max. 100-m well conc. for Case01n11_off_SLITe I-129_Mk50A

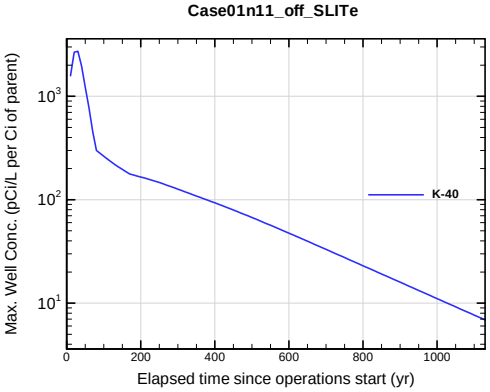

Figure A1B-628. Max. 100-m well conc. for Case01n11_off_SLITe K-40

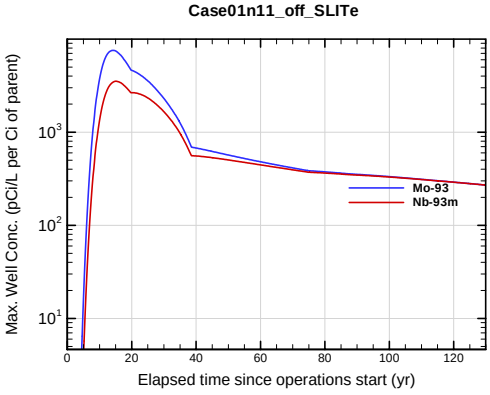

Figure A1B-629. Max. 100-m well conc. for Case01n11_off_SLITe Mo-93

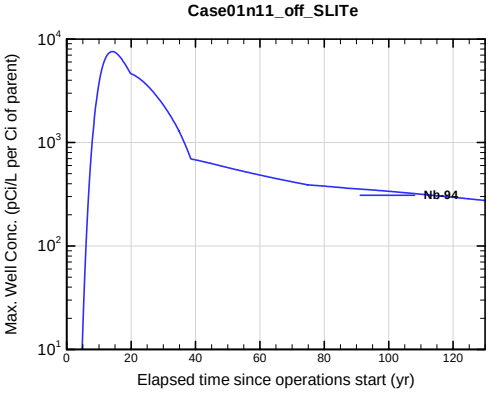

Figure A1B-630. Max. 100-m well conc. for Case01n11_off_SLITe Nb-94

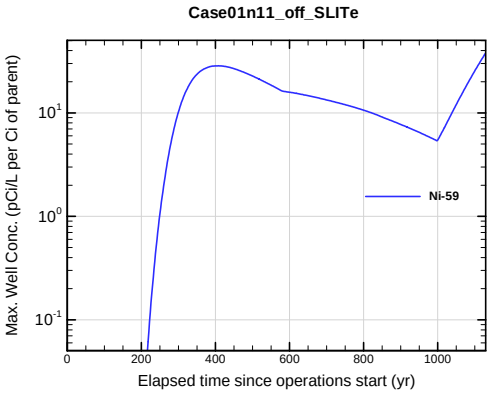

Figure A1B-631. Max. 100-m well conc. for Case01n11_off_SLITe Ni-59

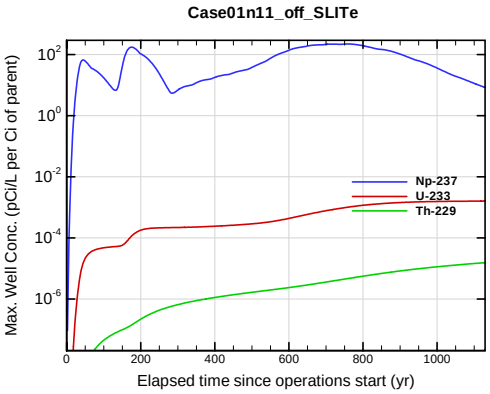

Figure A1B-632. Max. 100-m well conc. for Case01n11_off_SLITe Np-237

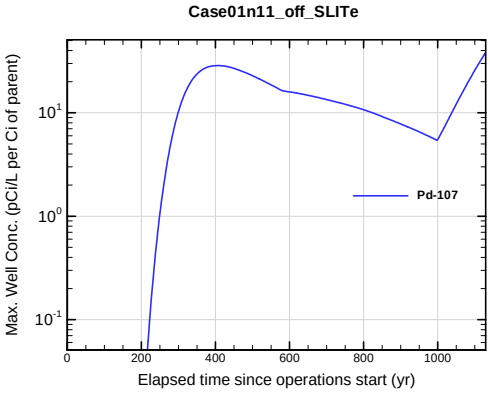

Figure A1B-633. Max. 100-m well conc. for Case01n11_off_SLITe Pd-107

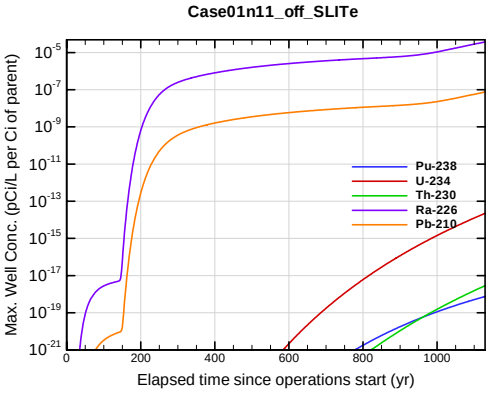

Figure A1B-634. Max. 100-m well conc. for Case01n11_off_SLITe Pu-238

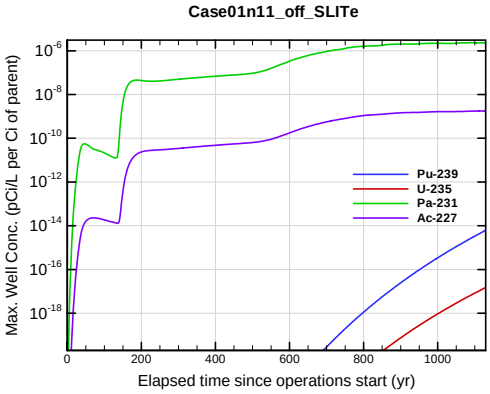

Figure A1B-635. Max. 100-m well conc. for Case01n11_off_SLITe Pu-239

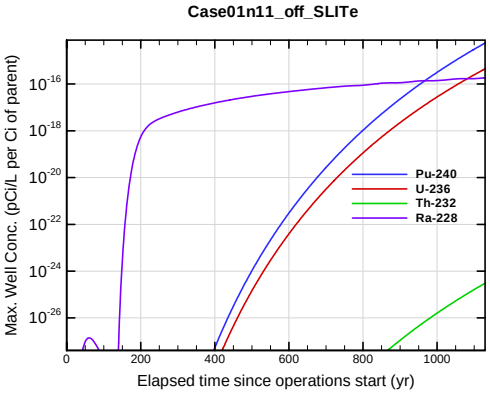

Figure A1B-636. Max. 100-m well conc. for Case01n11_off_SLITe Pu-240

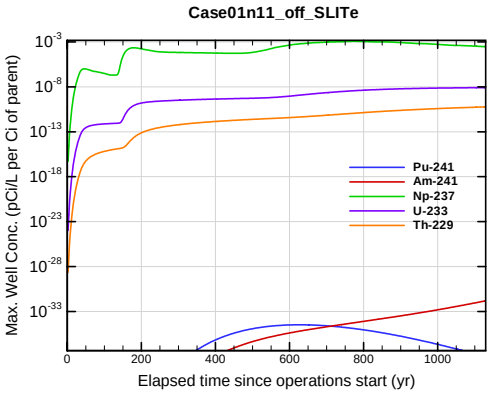

Figure A1B-637. Max. 100-m well conc. for Case01n11_off_SLITe Pu-241

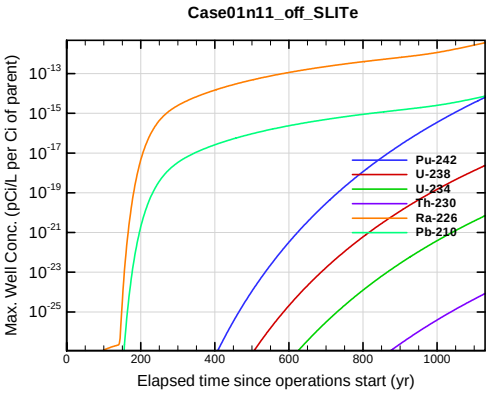

Figure A1B-638. Max. 100-m well conc. for Case01n11_off_SLITe Pu-242

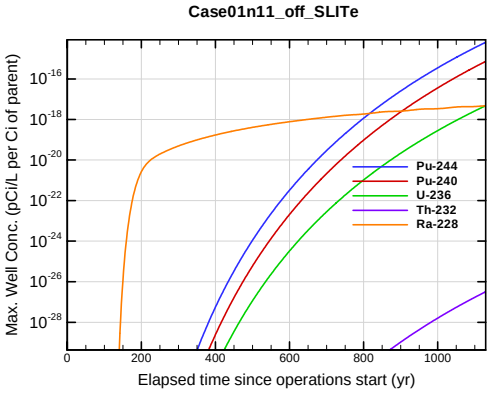

Figure A1B-639. Max. 100-m well conc. for Case01n11_off_SLITe Pu-244

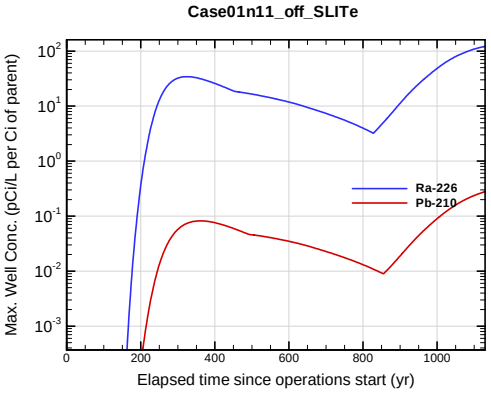

Figure A1B-640. Max. 100-m well conc. for Case01n11_off_SLITe Ra-226

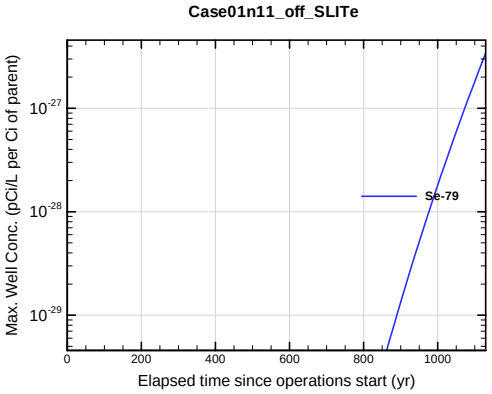

Figure A1B-641. Max. 100-m well conc. for Case01n11_off_SLITe Se-79

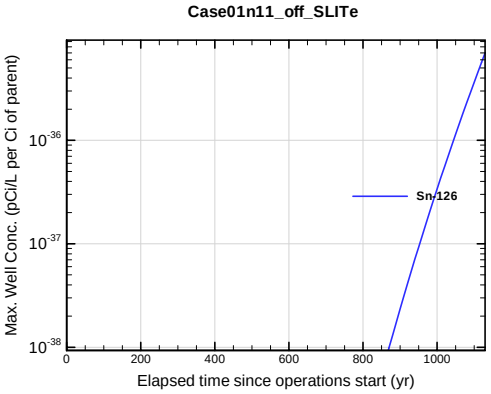

Figure A1B-642. Max. 100-m well conc. for Case01n11_off_SLITe Sn-126

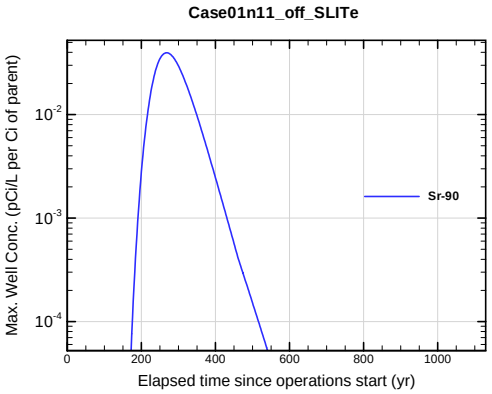

Figure A1B-643. Max. 100-m well conc. for Case01n11_off_SLITe Sr-90

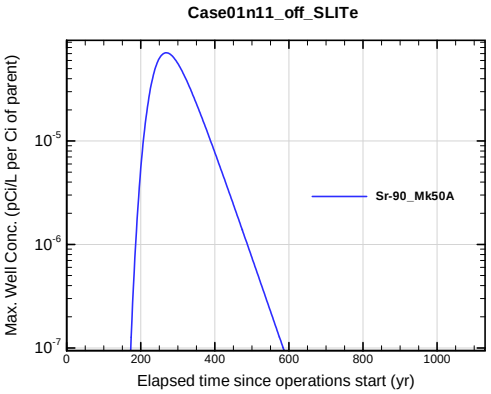

Figure A1B-644. Max. 100-m well conc. for Case01n11_off_SLITe Sr-90_Mk50A

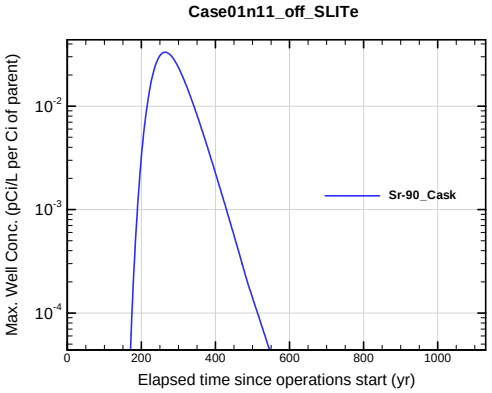

Figure A1B-645. Max. 100-m well conc. for Case01n11_off_SLITe Sr-90_Cask

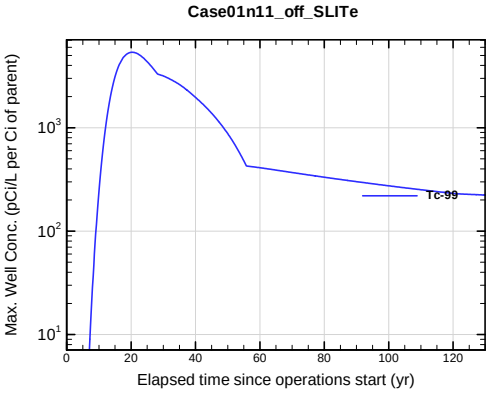

Figure A1B-646. Max. 100-m well conc. for Case01n11_off_SLITe Tc-99

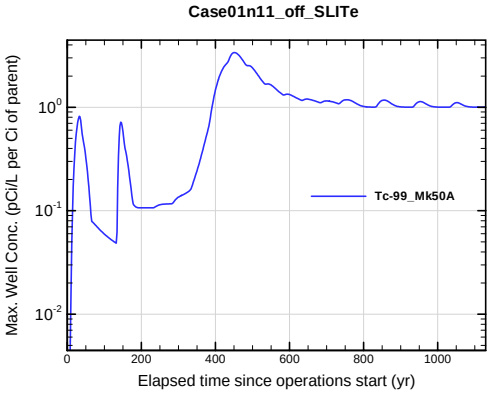

Figure A1B-647. Max. 100-m well conc. for Case01n11_off_SLITe Tc-99_Mk50A

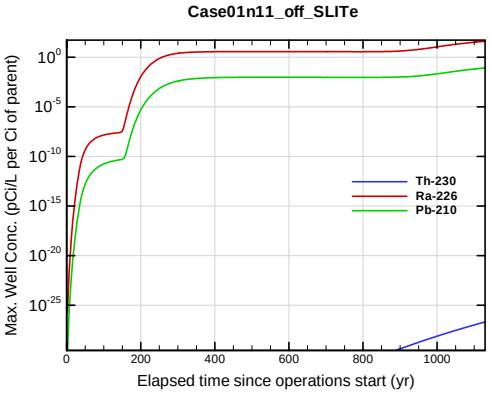

Figure A1B-648. Max. 100-m well conc. for Case01n11_off_SLITe Th-230

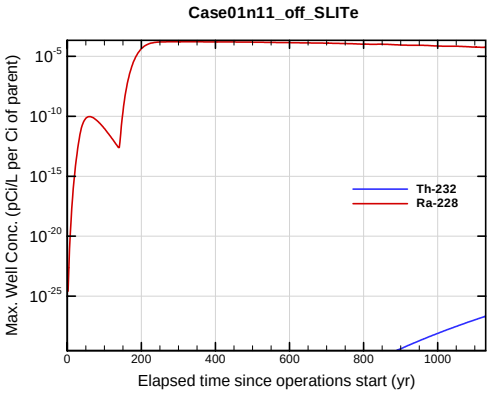

Figure A1B-649. Max. 100-m well conc. for Case01n11_off_SLITe Th-232

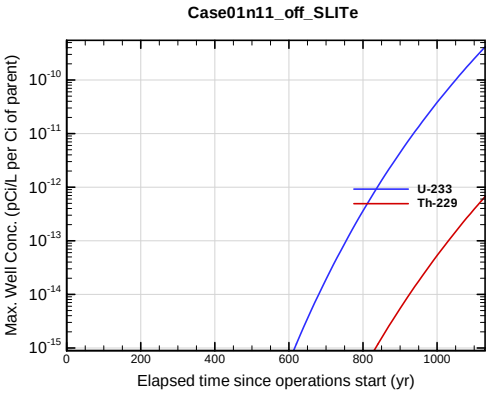

Figure A1B-650. Max. 100-m well conc. for Case01n11_off_SLITe U-233

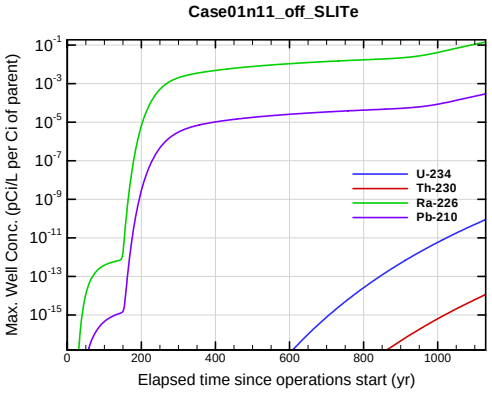

Figure A1B-651. Max. 100-m well conc. for Case01n11_off_SLITe U-234

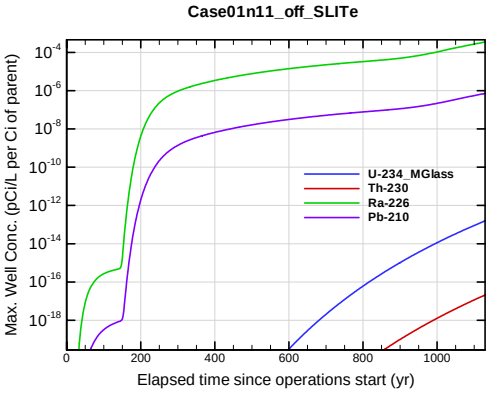

Figure A1B-652. Max. 100-m well conc. for Case01n11_off_SLITe U-234_MGlass

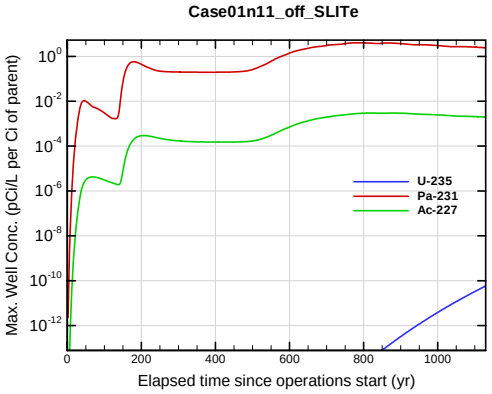

Figure A1B-653. Max. 100-m well conc. for Case01n11_off_SLITe U-235

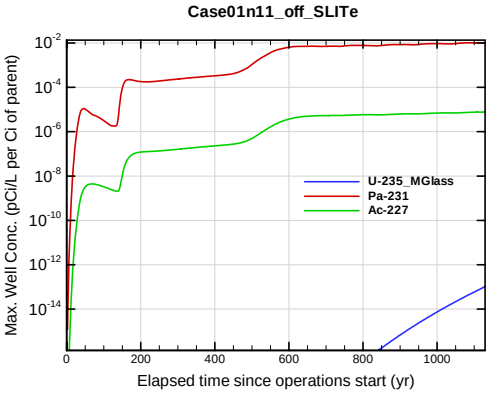

Figure A1B-654. Max. 100-m well conc. for Case01n11_off_SLITe U-235_MGlass

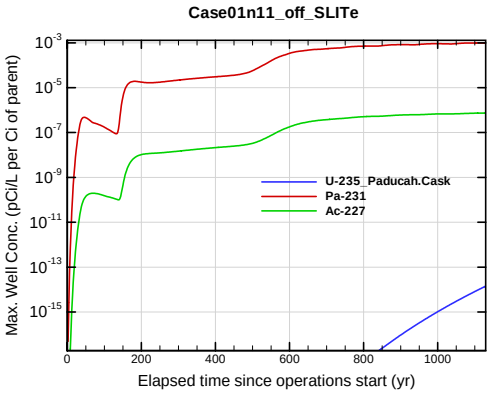

Figure A1B-655. Max. 100-m well conc. for Case01n11_off_SLITe U-235_Paducah.Cask

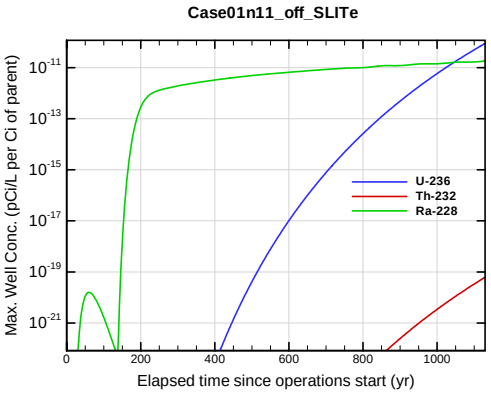

Figure A1B-656. Max. 100-m well conc. for Case01n11_off_SLITe U-236

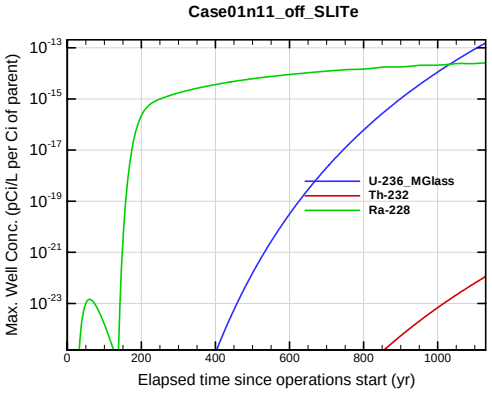

Figure A1B-657. Max. 100-m well conc. for Case01n11_off_SLITe U-236_MGlass

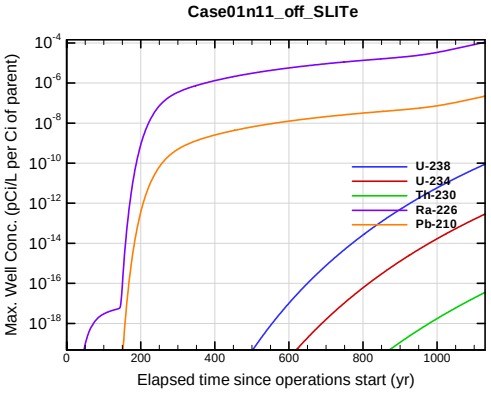

Figure A1B-658. Max. 100-m well conc. for Case01n11_off_SLITe U-238

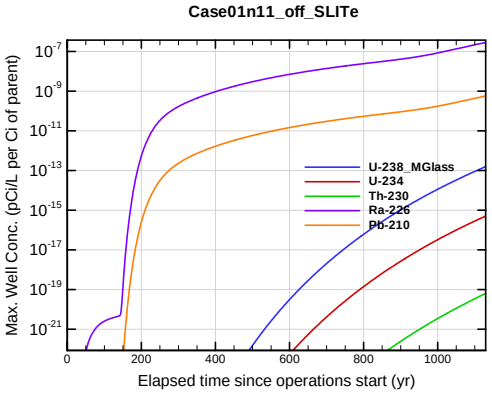

Figure A1B-659. Max. 100-m well conc. for Case01n11_off_SLITe U-238_MGlass

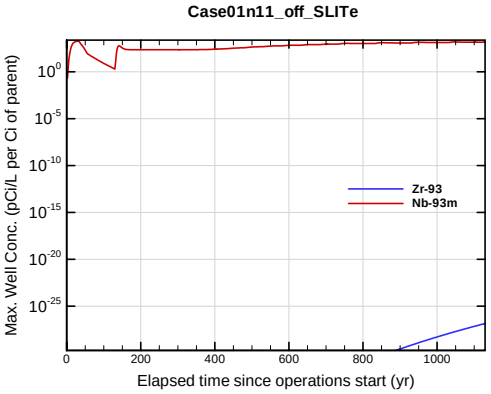

Figure A1B-660. Max. 100-m well conc. for Case01n11_off_SLITe Zr-93

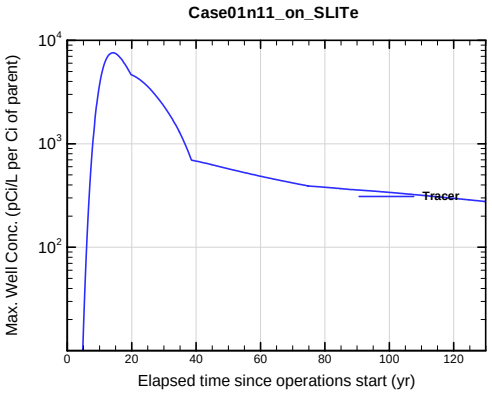

Figure A1B-661. Max. 100-m well conc. for Case01n11_on_SLITe Tracer

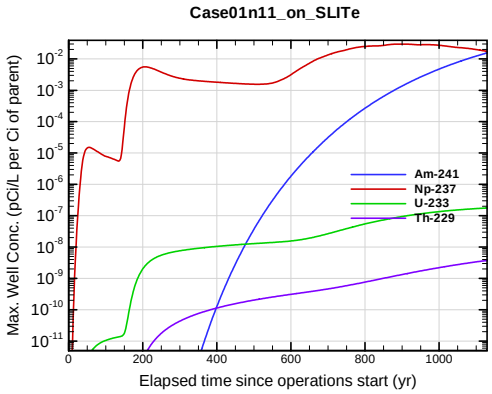

Figure A1B-662. Max. 100-m well conc. for Case01n11_on_SLITe Am-241

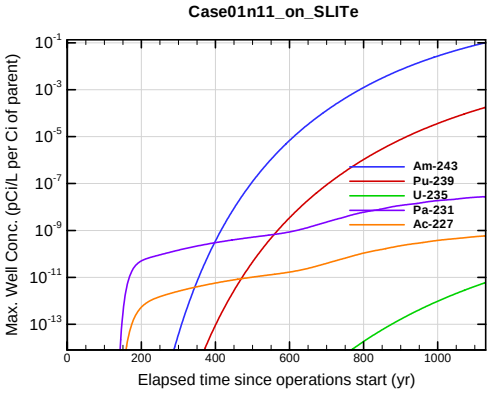

Figure A1B-663. Max. 100-m well conc. for Case01n11_on_SLITe Am-243

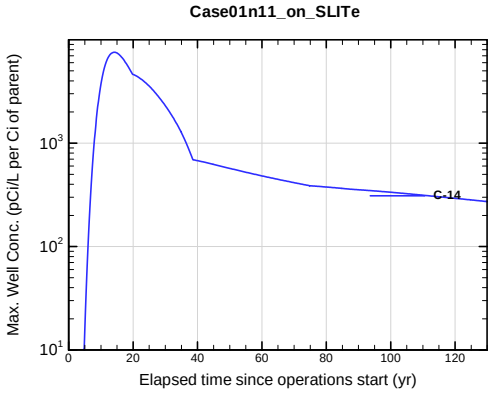

Figure A1B-664. Max. 100-m well conc. for Case01n11_on_SLITe C-14

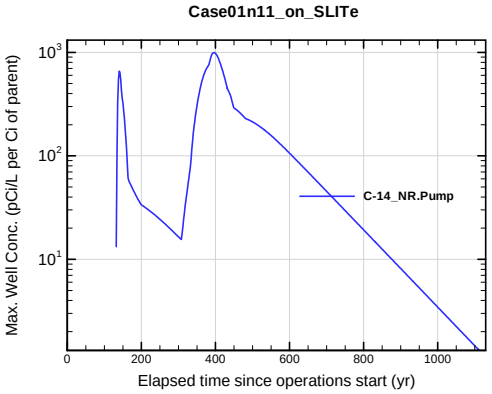

Figure A1B-665. Max. 100-m well conc. for Case01n11_on_SLITe C-14_NR.Pump

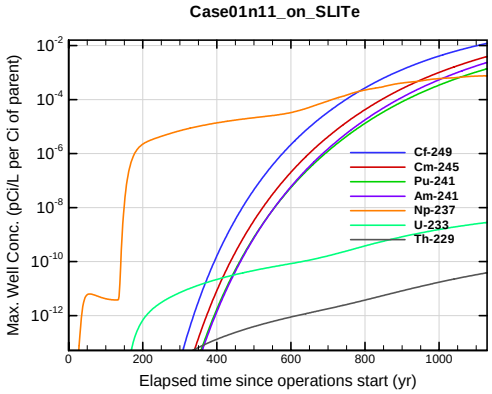

Figure A1B-666. Max. 100-m well conc. for Case01n11_on_SLITe Cf-249

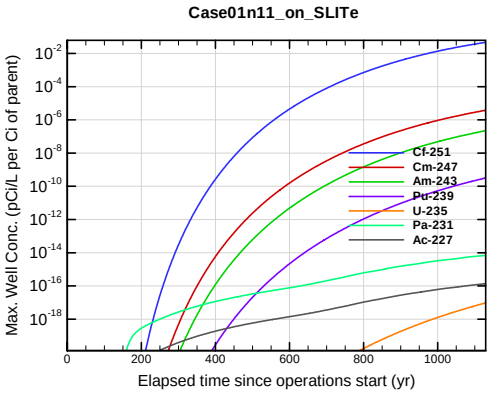

Figure A1B-667. Max. 100-m well conc. for Case01n11_on_SLITe Cf-251

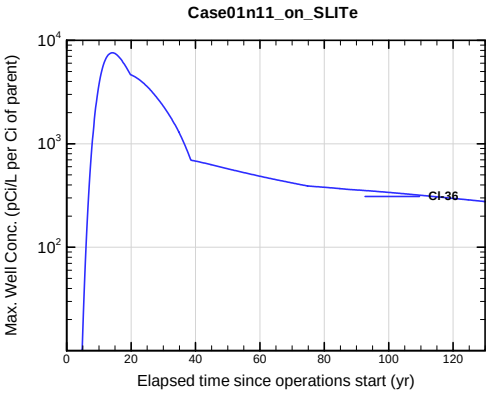

Figure A1B-668. Max. 100-m well conc. for Case01n11_on_SLITe Cl-36

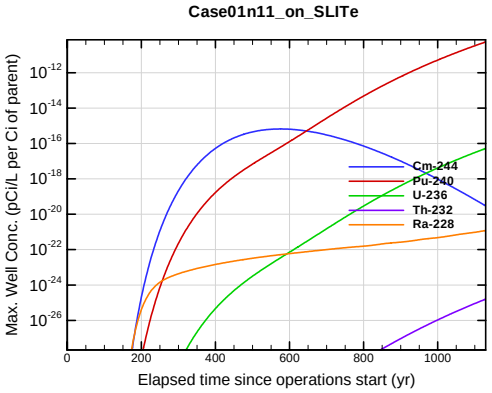

Figure A1B-669. Max. 100-m well conc. for Case01n11_on_SLITe Cm-244

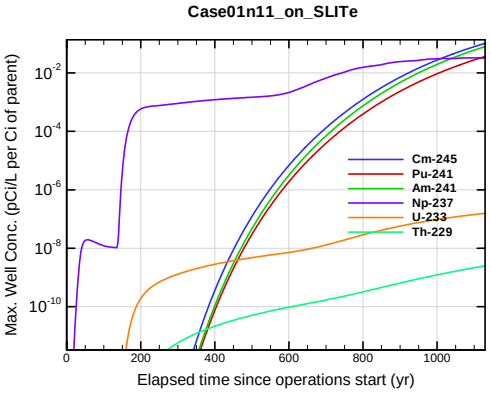

Figure A1B-670. Max. 100-m well conc. for Case01n11_on_SLITe Cm-245

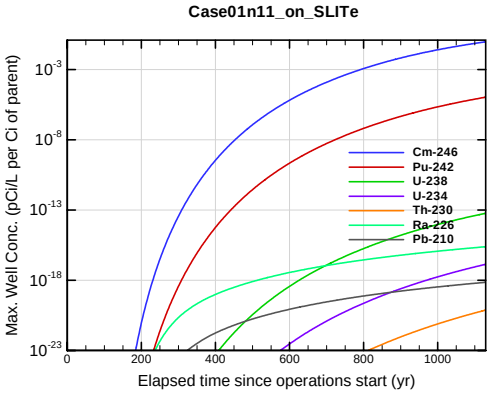

Figure A1B-671. Max. 100-m well conc. for Case01n11_on_SLITe Cm-246

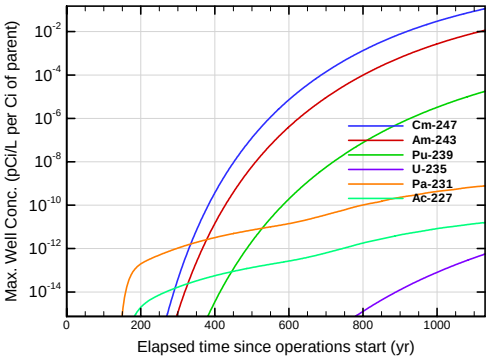

Figure A1B-672. Max. 100-m well conc. for Case01n11_on_SLITe Cm-247

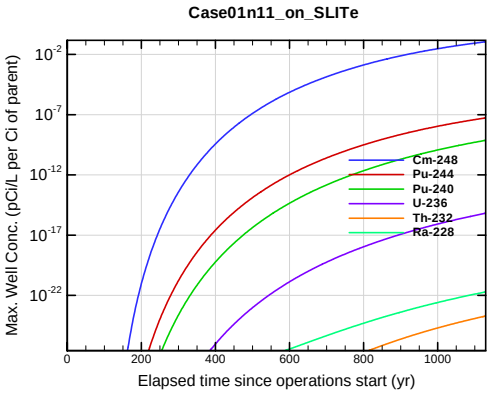

Figure A1B-673. Max. 100-m well conc. for Case01n11_on_SLITe Cm-248

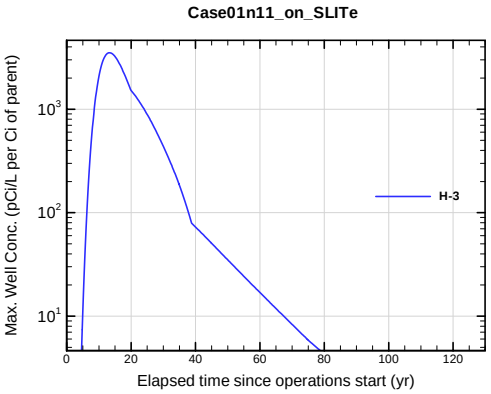

Figure A1B-674. Max. 100-m well conc. for Case01n11_on_SLITe H-3

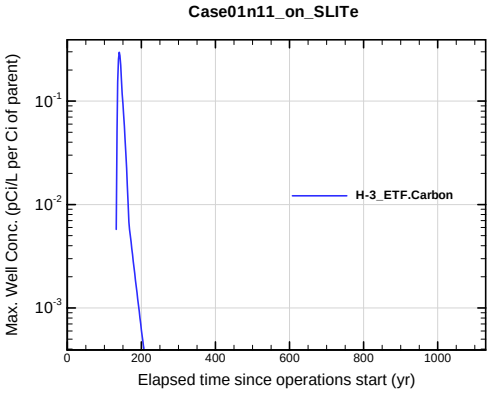

Figure A1B-675. Max. 100-m well conc. for Case01n11_on_SLITe H-3_ETF.Carbon

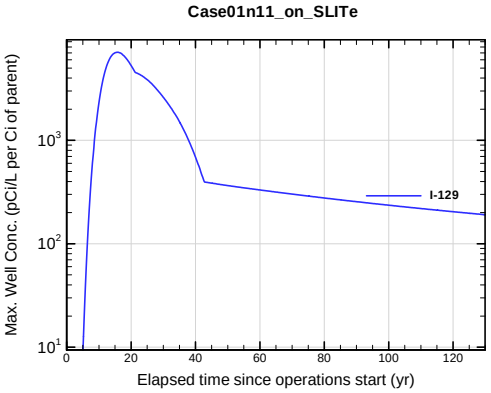

Figure A1B-676. Max. 100-m well conc. for Case01n11_on_SLITe I-129

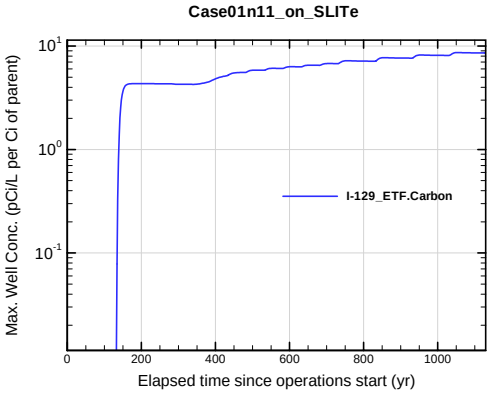

Figure A1B-677. Max. 100-m well conc. for Case01n11_on_SLITe I-129_ETF.Carbon

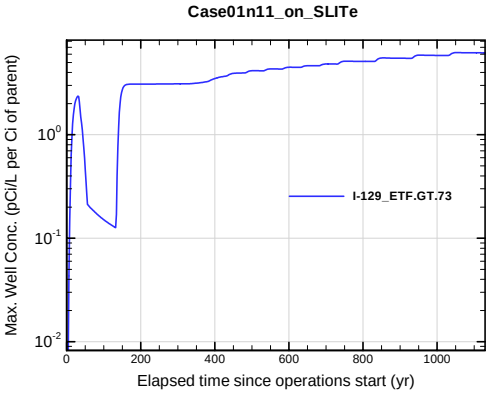

Figure A1B-678. Max. 100-m well conc. for Case01n11_on_SLITe I-129_ETF.GT.73

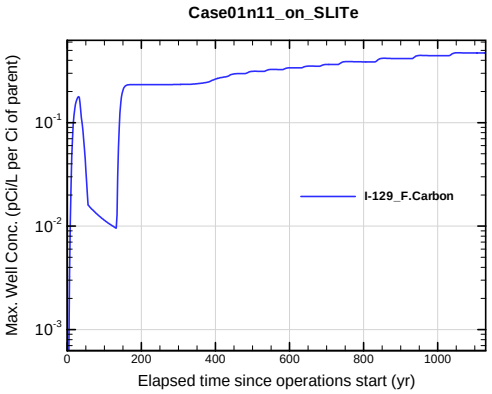

Figure A1B-679. Max. 100-m well conc. for Case01n11_on_SLITe I-129_F.Carbon

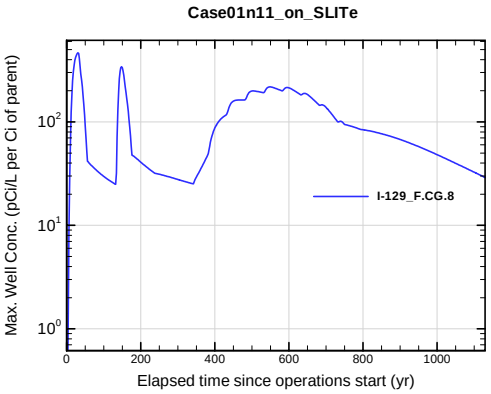

Figure A1B-680. Max. 100-m well conc. for Case01n11_on_SLITe I-129_F.CG.8

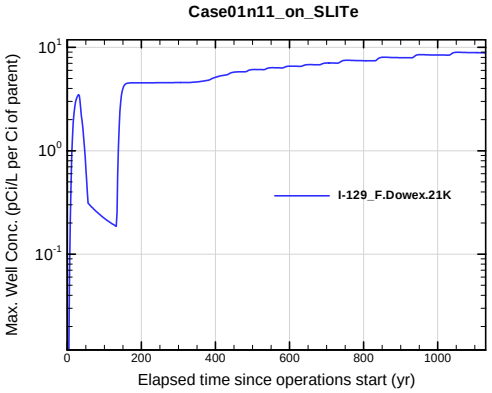

Figure A1B-681. Max. 100-m well conc. for Case01n11_on_SLITe I-129_F.Dowex.21K

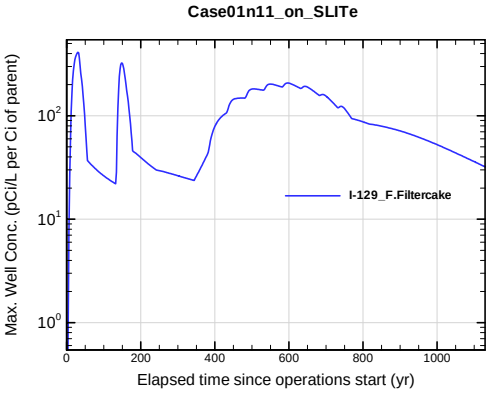

Figure A1B-682. Max. 100-m well conc. for Case01n11_on_SLITe I-129_F.Filtercake

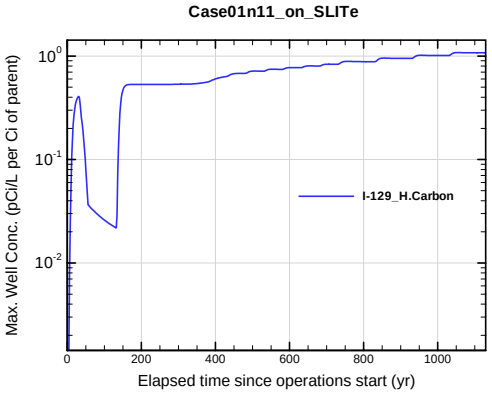

Figure A1B-683. Max. 100-m well conc. for Case01n11_on_SLITe I-129_H.Carbon

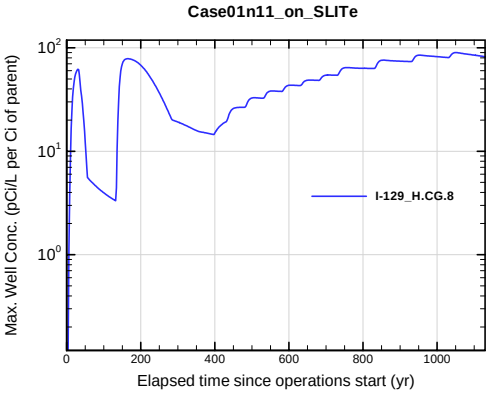

Figure A1B-684. Max. 100-m well conc. for Case01n11_on_SLITe I-129_H.CG.8

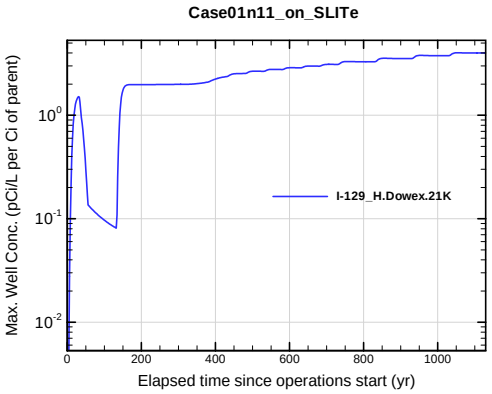

Figure A1B-685. Max. 100-m well conc. for Case01n11_on_SLITe I-129_H.Dowex.21K

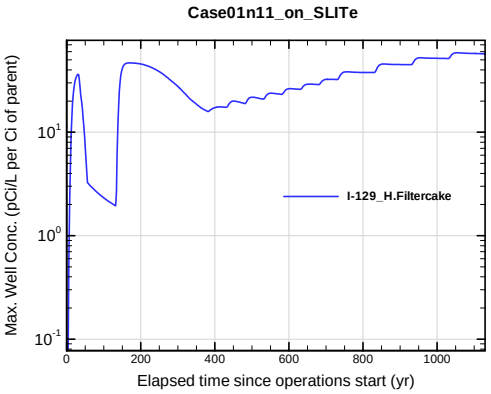

Figure A1B-686. Max. 100-m well conc. for Case01n11_on_SLITe I-129_H.Filtercake

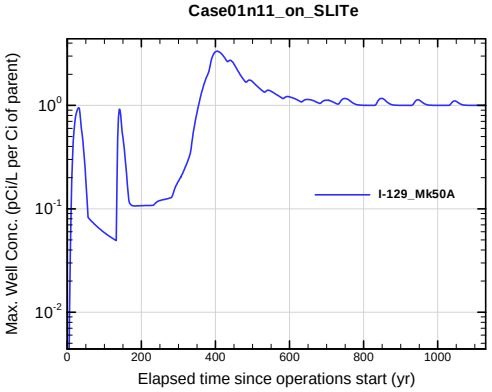

Figure A1B-687. Max. 100-m well conc. for Case01n11_on_SLITe I-129_Mk50A

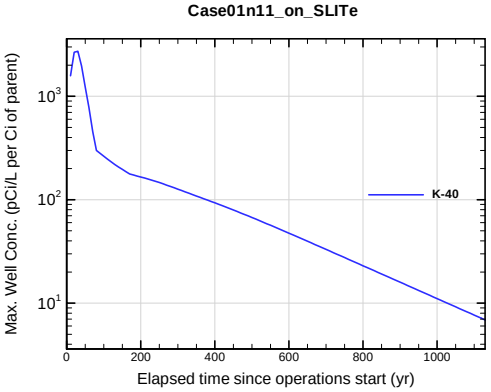

Figure A1B-688. Max. 100-m well conc. for Case01n11_on_SLITe K-40

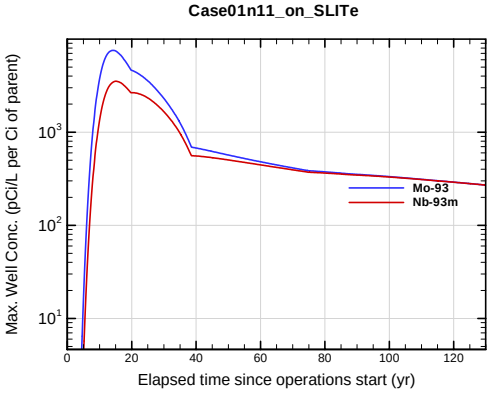

Figure A1B-689. Max. 100-m well conc. for Case01n11_on_SLITe Mo-93

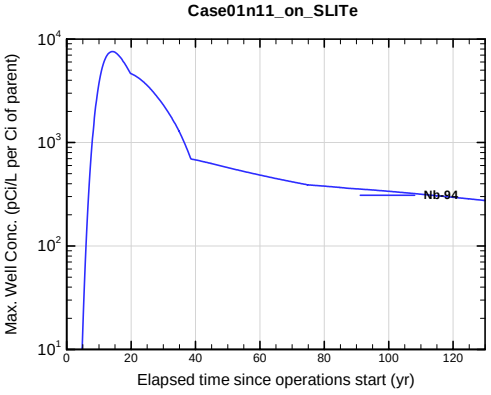

Figure A1B-690. Max. 100-m well conc. for Case01n11_on_SLITe Nb-94

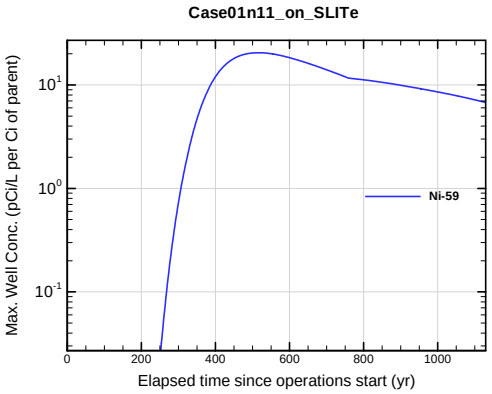

Figure A1B-691. Max. 100-m well conc. for Case01n11_on_SLITe Ni-59

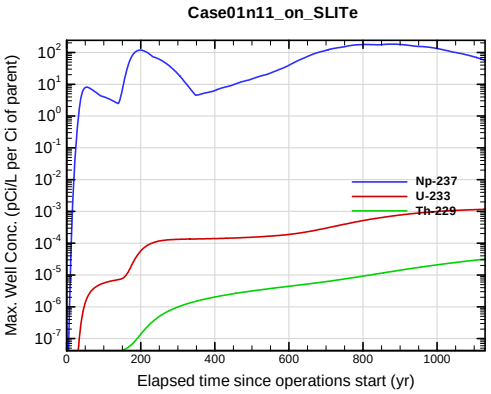

Figure A1B-692. Max. 100-m well conc. for Case01n11_on_SLITe Np-237

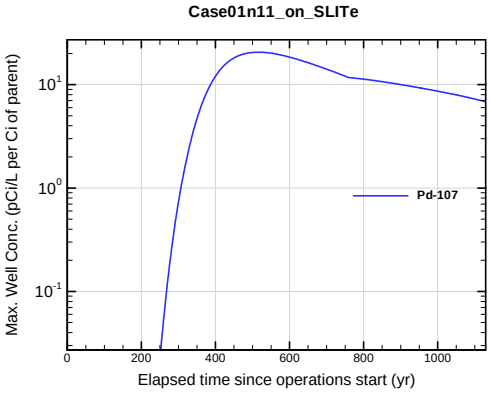

Figure A1B-693. Max. 100-m well conc. for Case01n11_on_SLITe Pd-107

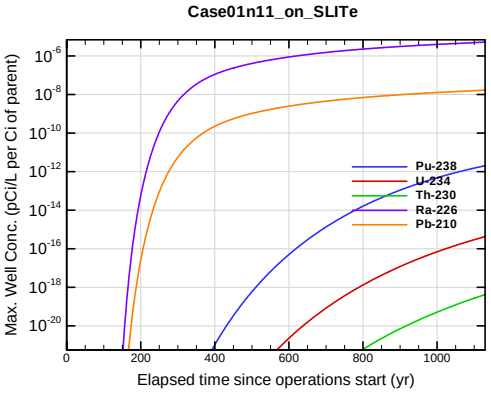

Figure A1B-694. Max. 100-m well conc. for Case01n11_on_SLITe Pu-238

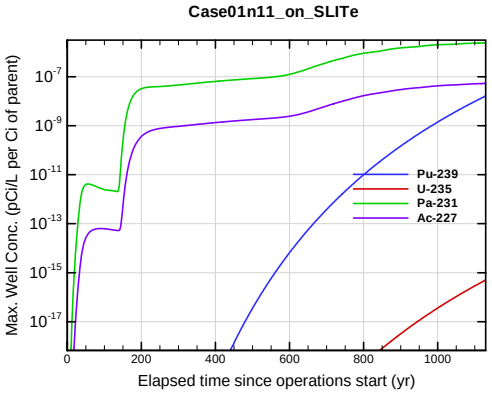

Figure A1B-695. Max. 100-m well conc. for Case01n11_on_SLITe Pu-239

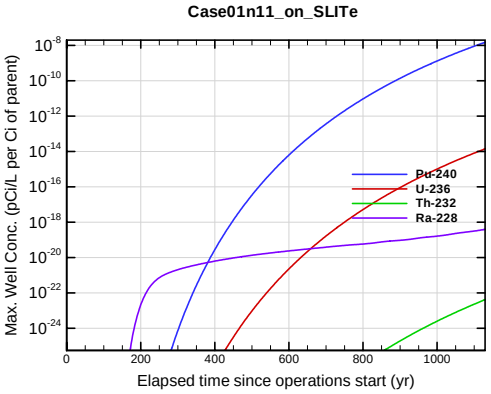

Figure A1B-696. Max. 100-m well conc. for Case01n11_on_SLITe Pu-240

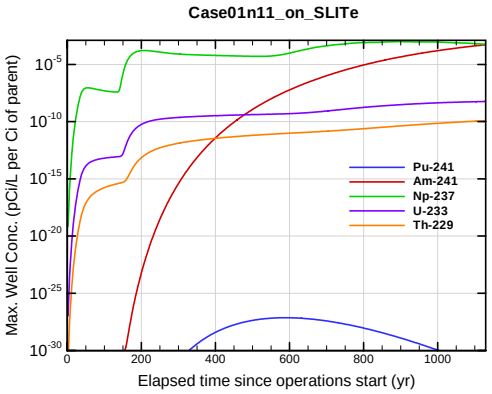

Figure A1B-697. Max. 100-m well conc. for Case01n11_on_SLITe Pu-241

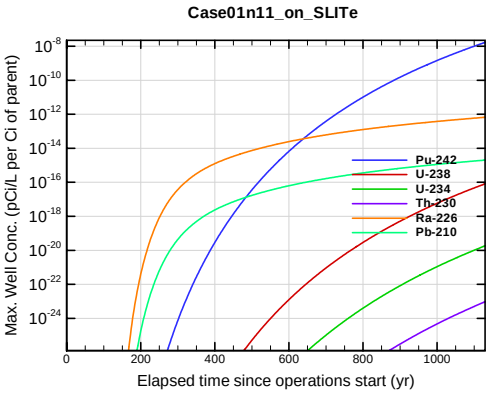

Figure A1B-698. Max. 100-m well conc. for Case01n11_on_SLITe Pu-242

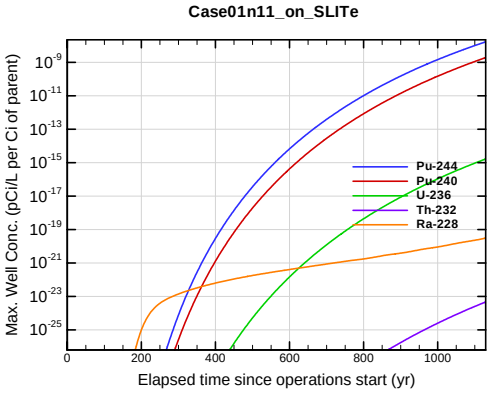

Figure A1B-699. Max. 100-m well conc. for Case01n11_on_SLITe Pu-244

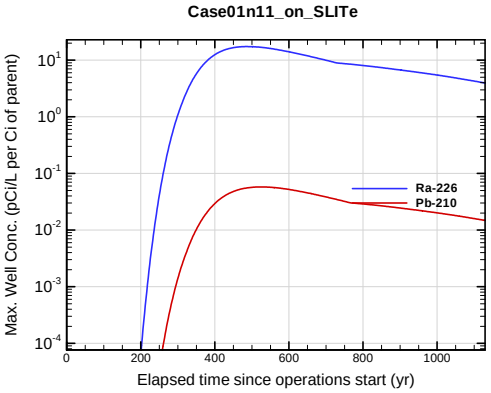

Figure A1B-700. Max. 100-m well conc. for Case01n11_on_SLITe Ra-226

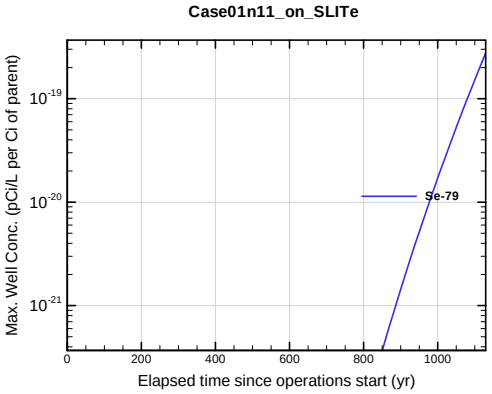

Figure A1B-701. Max. 100-m well conc. for Case01n11_on_SLITe Se-79

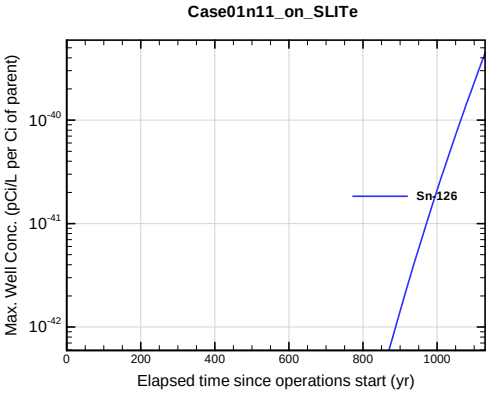

Figure A1B-702. Max. 100-m well conc. for Case01n11_on_SLITe Sn-126

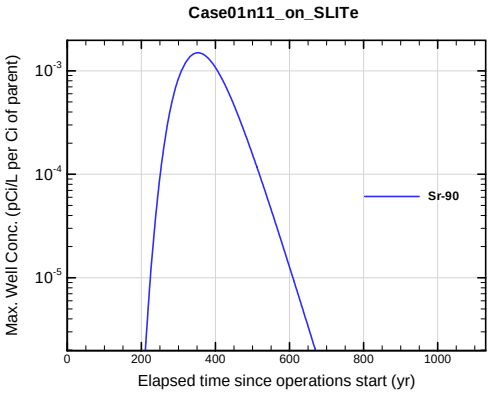

Figure A1B-703. Max. 100-m well conc. for Case01n11_on_SLITe Sr-90

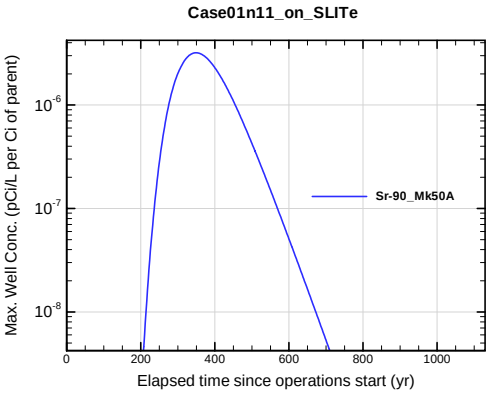

Figure A1B-704. Max. 100-m well conc. for Case01n11_on_SLITe Sr-90_Mk50A

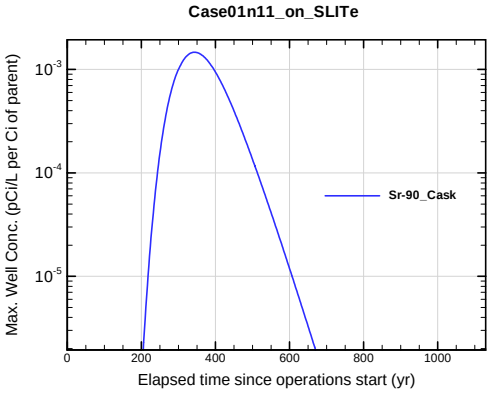

Figure A1B-705. Max. 100-m well conc. for Case01n11_on_SLITe Sr-90_Cask

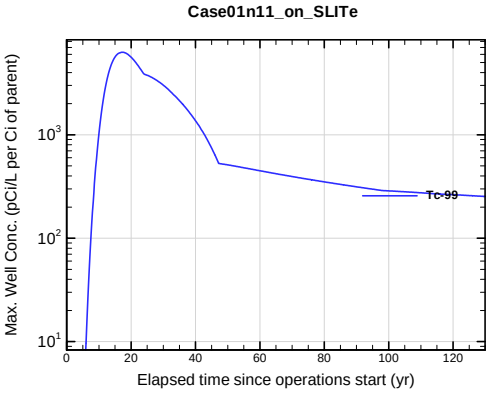

Figure A1B-706. Max. 100-m well conc. for Case01n11_on_SLITe Tc-99

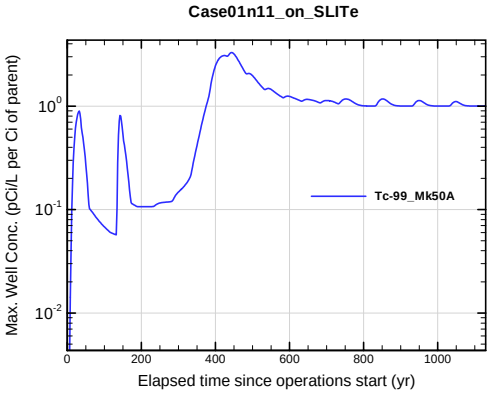

Figure A1B-707. Max. 100-m well conc. for Case01n11_on_SLITe Tc-99_Mk50A

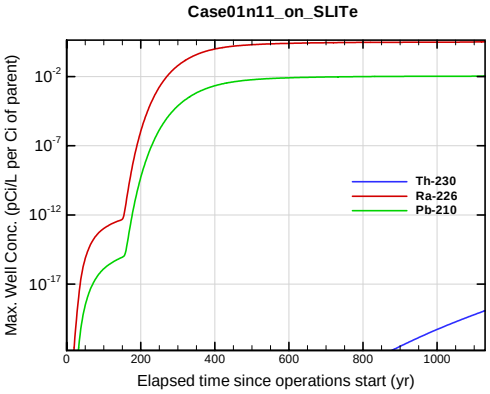

Figure A1B-708. Max. 100-m well conc. for Case01n11_on_SLITe Th-230

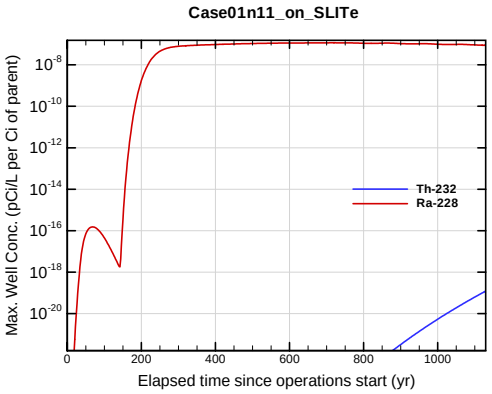

Figure A1B-709. Max. 100-m well conc. for Case01n11_on_SLITe Th-232

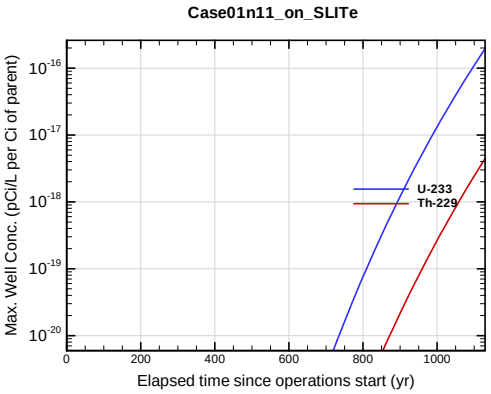

Figure A1B-710. Max. 100-m well conc. for Case01n11_on_SLITe U-233

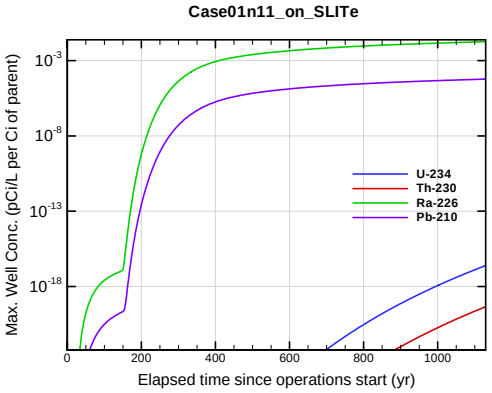

Figure A1B-711. Max. 100-m well conc. for Case01n11_on_SLITe U-234

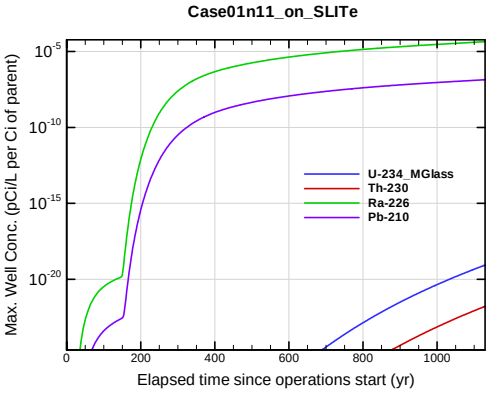

Figure A1B-712. Max. 100-m well conc. for Case01n11_on_SLITe U-234_MGlass

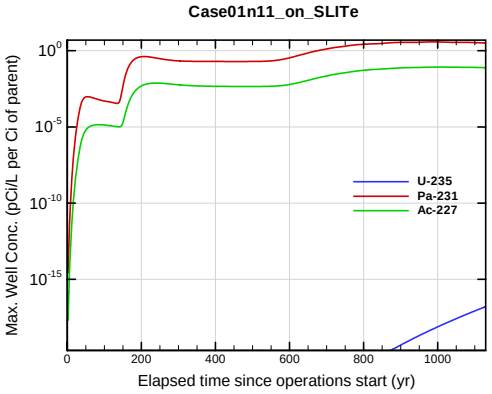

Figure A1B-713. Max. 100-m well conc. for Case01n11_on_SLITe U-235

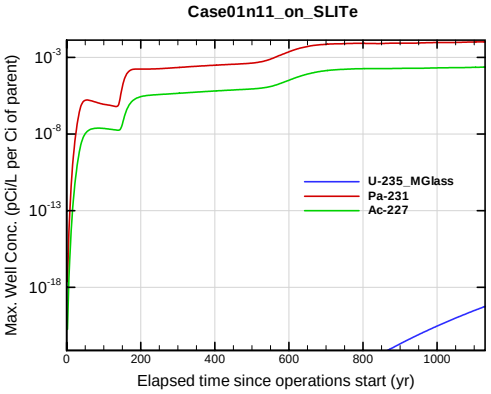

Figure A1B-714. Max. 100-m well conc. for Case01n11_on_SLITe U-235_MGlass

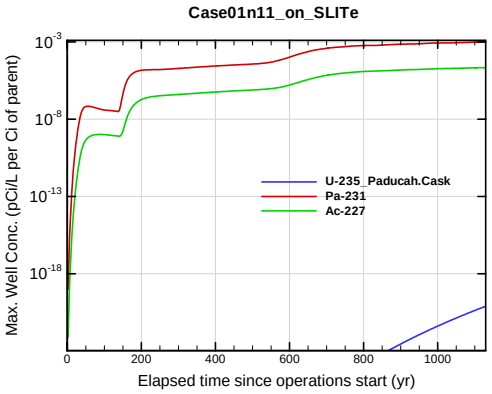

Figure A1B-715. Max. 100-m well conc. for Case01n11_on_SLITe U-235_Paducah.Cask

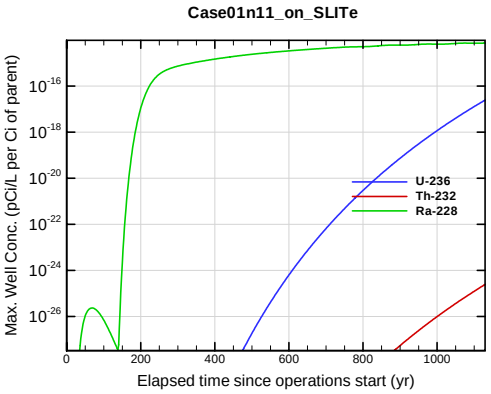

Figure A1B-716. Max. 100-m well conc. for Case01n11_on_SLITe U-236

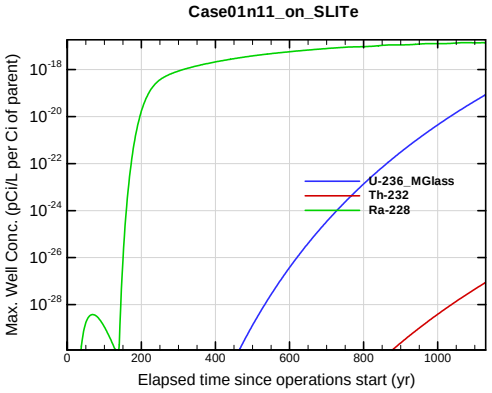

Figure A1B-717. Max. 100-m well conc. for Case01n11_on_SLITe U-236_MGlass

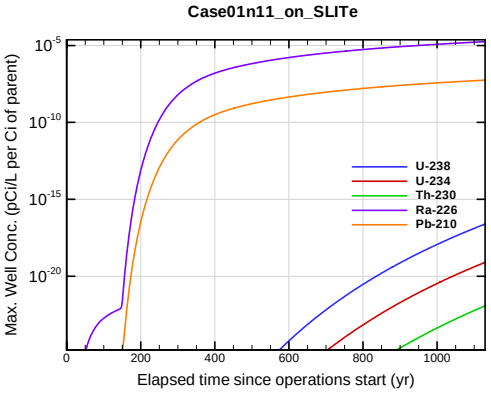

Figure A1B-718. Max. 100-m well conc. for Case01n11_on_SLITe U-238

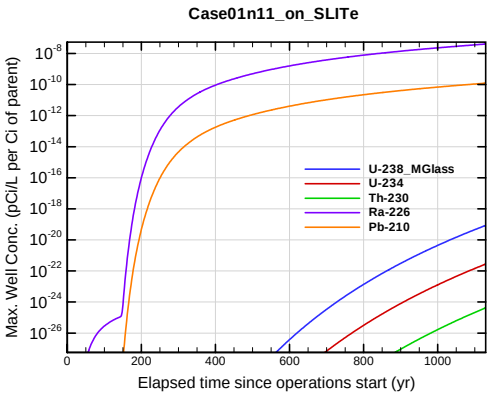

Figure A1B-719. Max. 100-m well conc. for Case01n11_on_SLITe U-238_MGlass

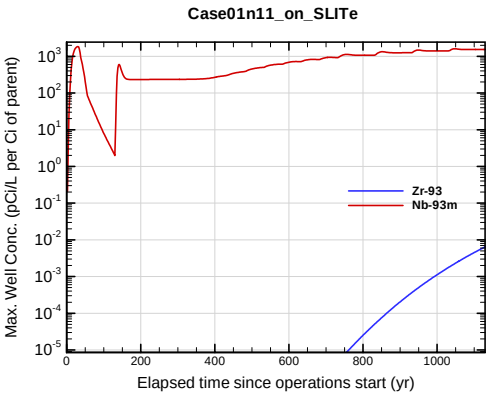

Figure A1B-720. Max. 100-m well conc. for Case01n11_on_SLITe Zr-93

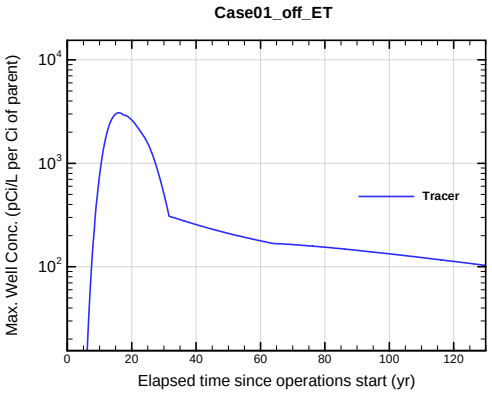

Figure A1B-721. Max. 100-m well conc. for Case01_off_ET Tracer

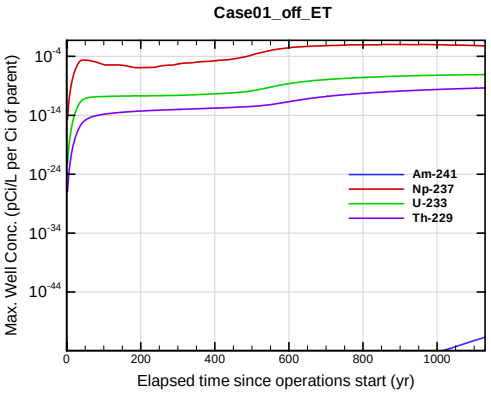

Figure A1B-722. Max. 100-m well conc. for Case01_off_ET Am-241

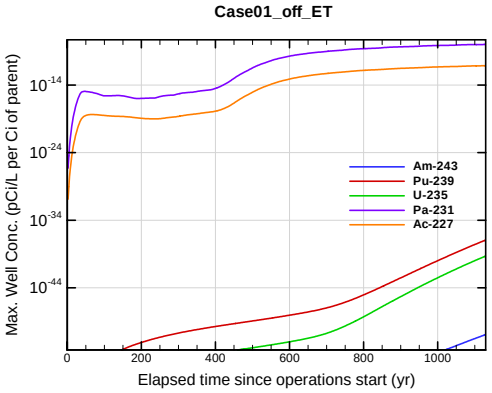

Figure A1B-723. Max. 100-m well conc. for Case01_off_ET Am-243

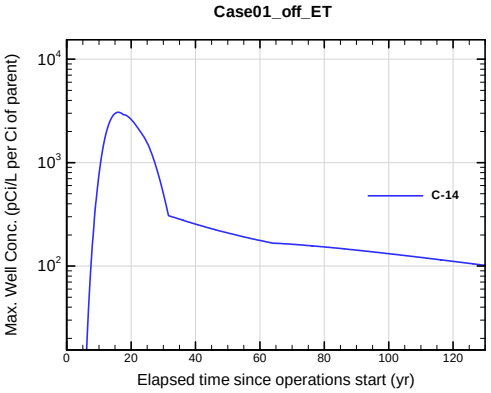

Figure A1B-724. Max. 100-m well conc. for Case01_off_ET C-14

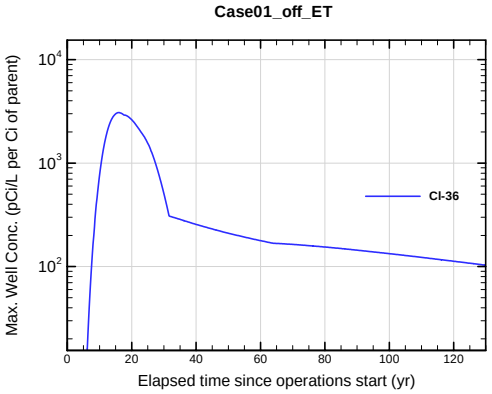

Figure A1B-725. Max. 100-m well conc. for Case01_off_ET Cl-36

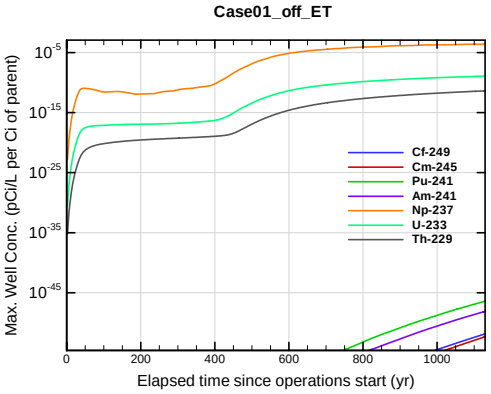

Figure A1B-726. Max. 100-m well conc. for Case01_off_ET Cf-249

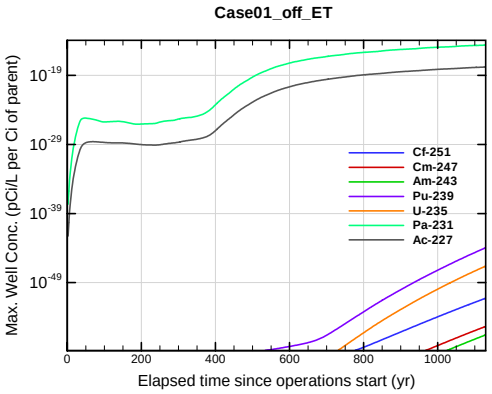

Figure A1B-727. Max. 100-m well conc. for Case01_off_ET Cf-251

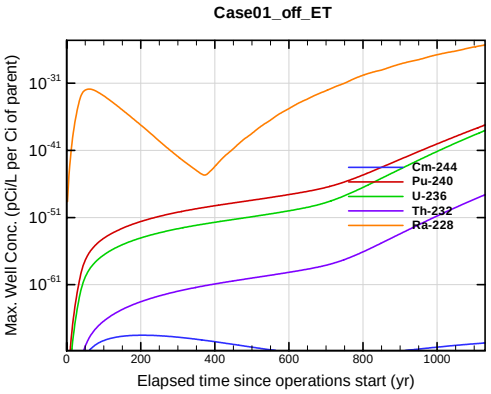

Figure A1B-728. Max. 100-m well conc. for Case01_off_ET Cm-244

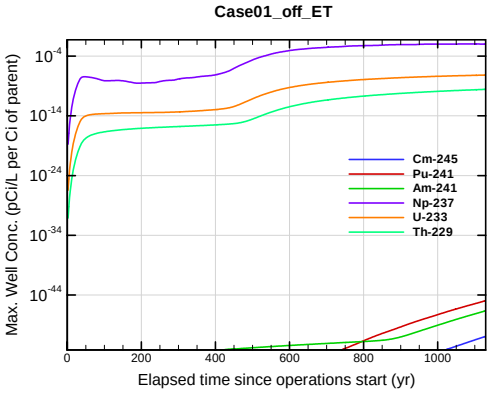

Figure A1B-729. Max. 100-m well conc. for Case01_off_ET Cm-245

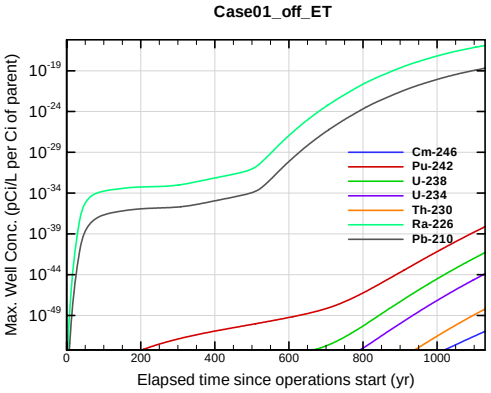

Figure A1B-730. Max. 100-m well conc. for Case01_off_ET Cm-246

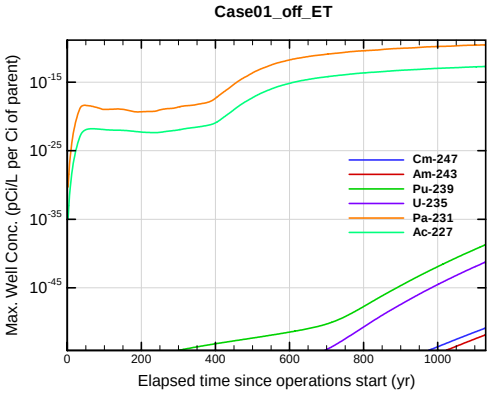

Figure A1B-731. Max. 100-m well conc. for Case01_off_ET Cm-247

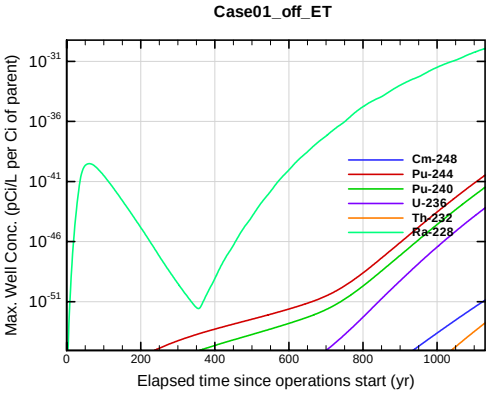

Figure A1B-732. Max. 100-m well conc. for Case01_off_ET Cm-248

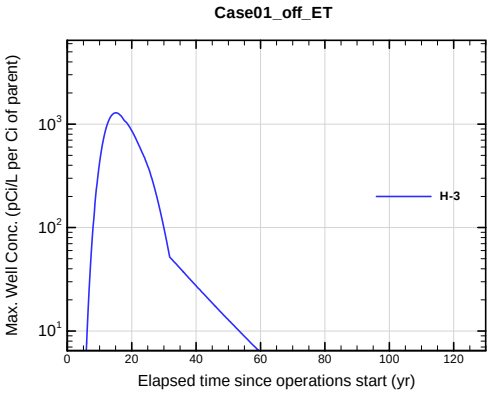

Figure A1B-733. Max. 100-m well conc. for Case01_off_ET H-3

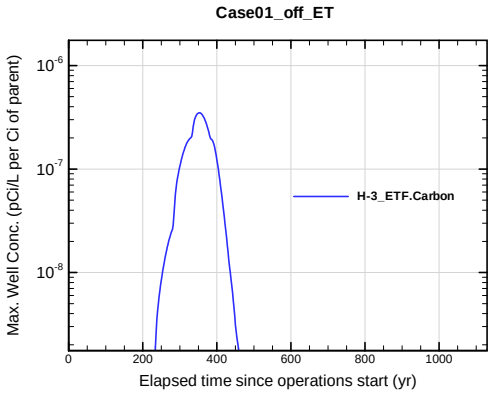

Figure A1B-734. Max. 100-m well conc. for Case01_off_ET H-3_ETF.Carbon

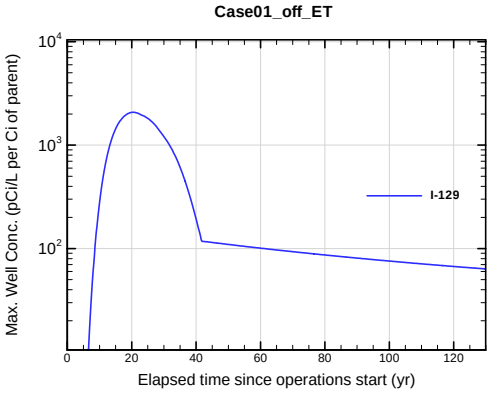

Figure A1B-735. Max. 100-m well conc. for Case01_off_ET I-129

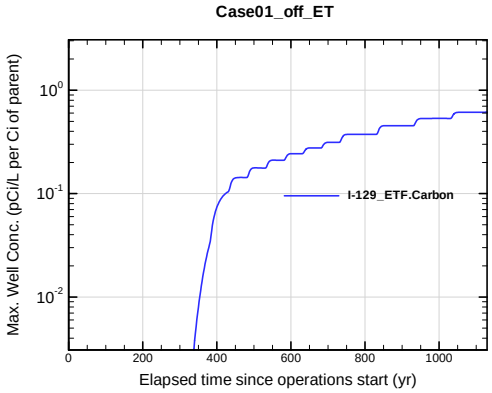

Figure A1B-736. Max. 100-m well conc. for Case01_off_ET I-129_ETF.Carbon

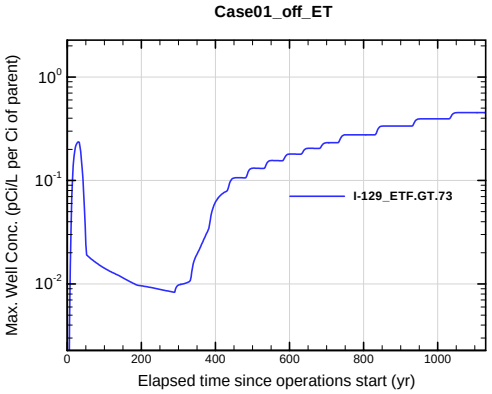

Figure A1B-737. Max. 100-m well conc. for Case01_off_ET I-129_ETF.GT.73

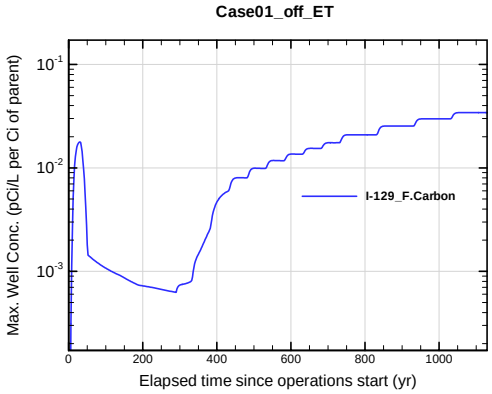

Figure A1B-738. Max. 100-m well conc. for Case01_off_ET I-129_F.Carbon

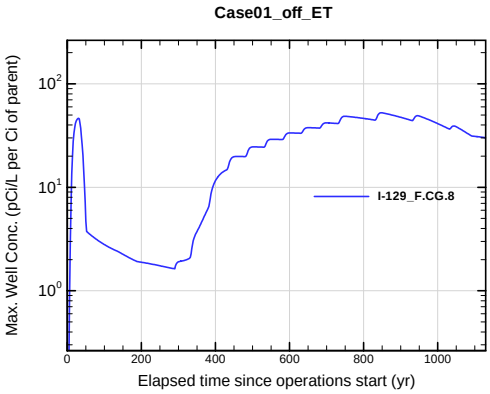

Figure A1B-739. Max. 100-m well conc. for Case01_off_ET I-129_F.CG.8

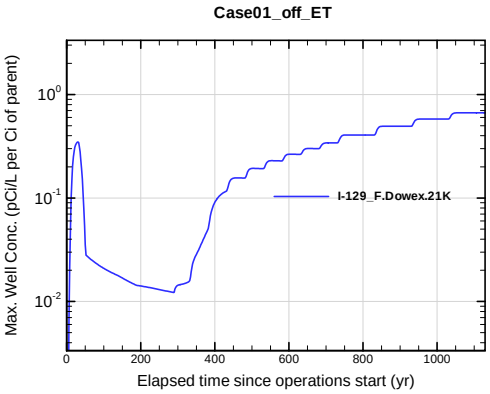

Figure A1B-740. Max. 100-m well conc. for Case01_off_ET I-129_F.Dowex.21K

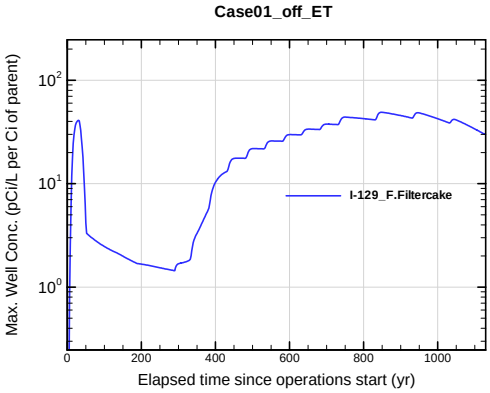

Figure A1B-741. Max. 100-m well conc. for Case01_off_ET I-129_F.Filtercake

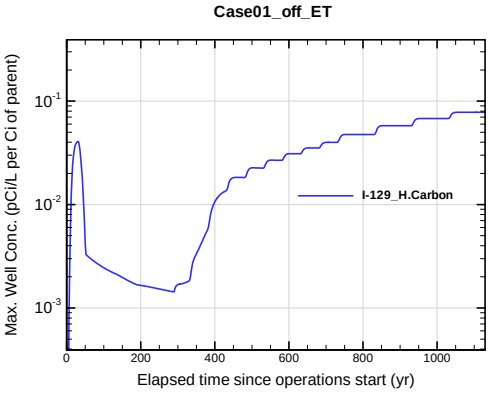

Figure A1B-742. Max. 100-m well conc. for Case01_off_ET I-129_H.Carbon

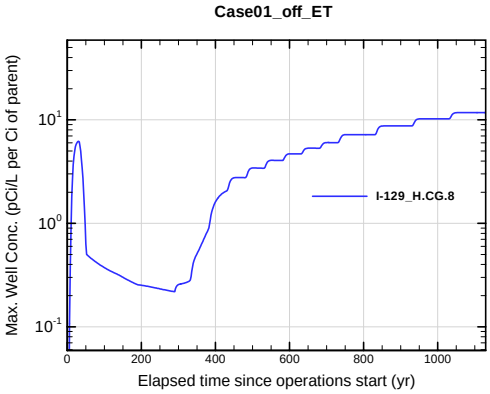

Figure A1B-743. Max. 100-m well conc. for Case01_off_ET I-129_H.CG.8

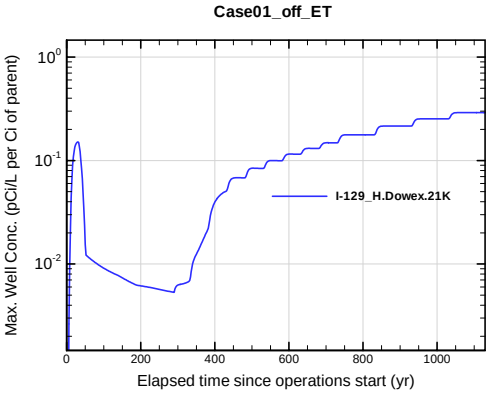

Figure A1B-744. Max. 100-m well conc. for Case01_off_ET I-129_H.Dowex.21K

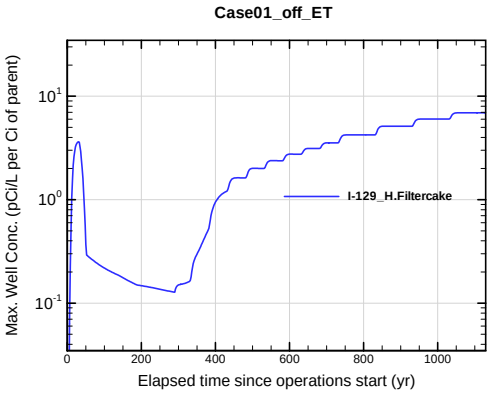

Figure A1B-745. Max. 100-m well conc. for Case01_off_ET I-129_H.Filtercake

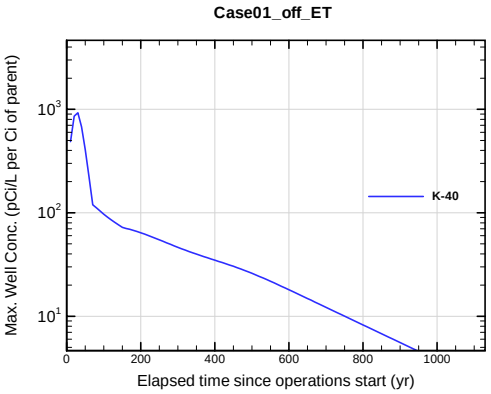

Figure A1B-746. Max. 100-m well conc. for Case01_off_ET K-40

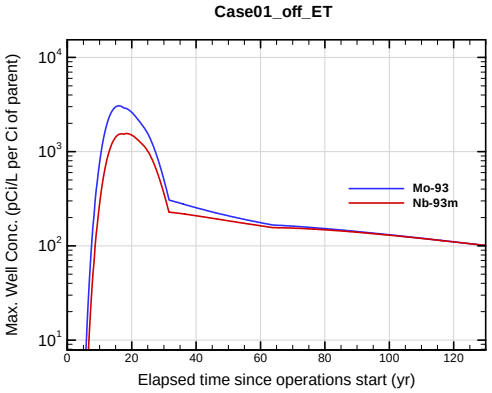

Figure A1B-747. Max. 100-m well conc. for Case01_off_ET Mo-93

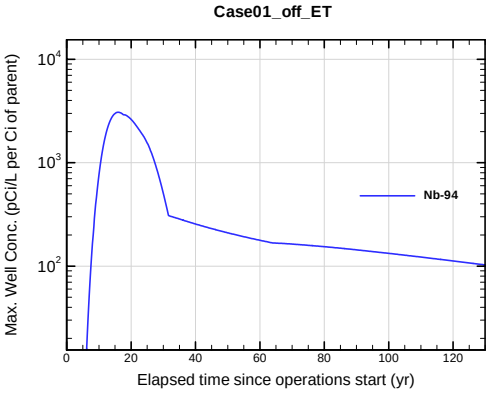

Figure A1B-748. Max. 100-m well conc. for Case01_off_ET Nb-94

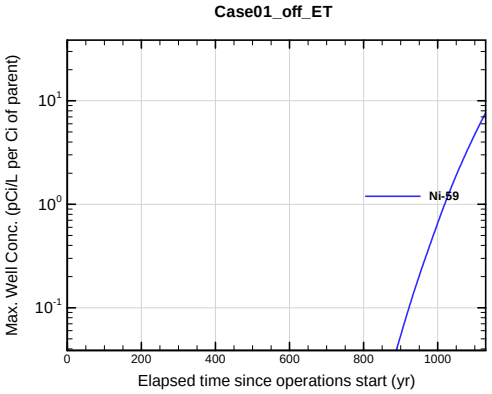

Figure A1B-749. Max. 100-m well conc. for Case01_off_ET Ni-59

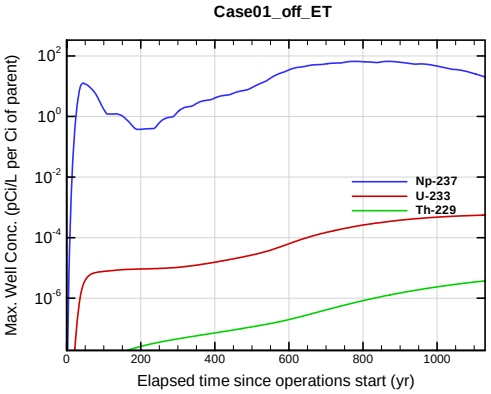

Figure A1B-750. Max. 100-m well conc. for Case01_off_ET Np-237

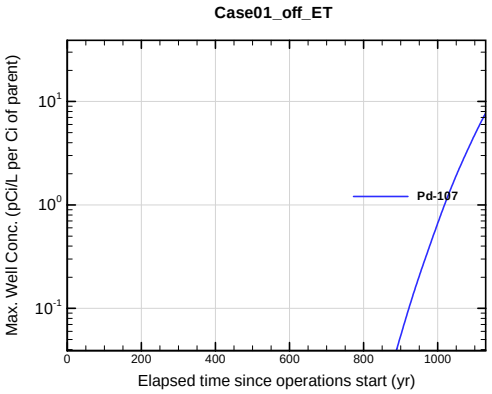

Figure A1B-751. Max. 100-m well conc. for Case01_off_ET Pd-107

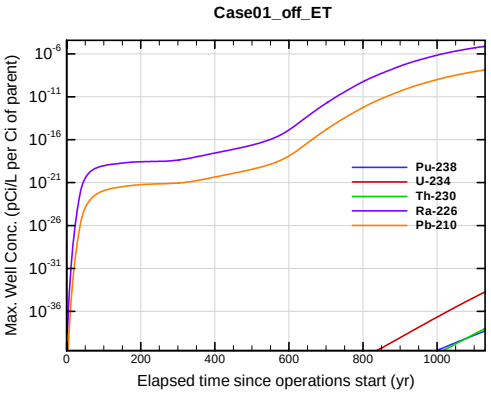

Figure A1B-752. Max. 100-m well conc. for Case01_off_ET Pu-238

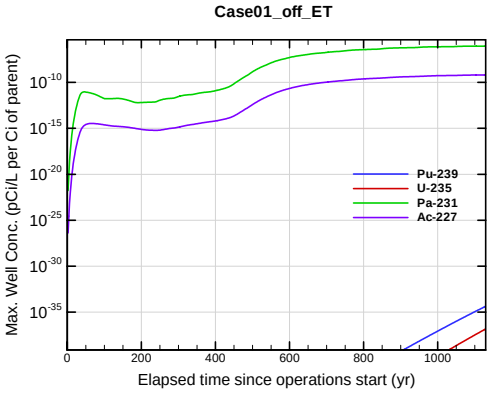

Figure A1B-753. Max. 100-m well conc. for Case01_off_ET Pu-239

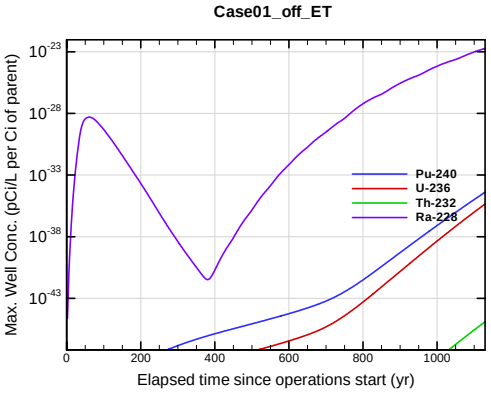

Figure A1B-754. Max. 100-m well conc. for Case01_off_ET Pu-240

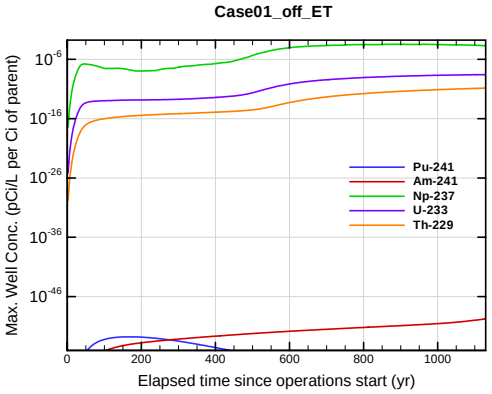

Figure A1B-755. Max. 100-m well conc. for Case01_off_ET Pu-241

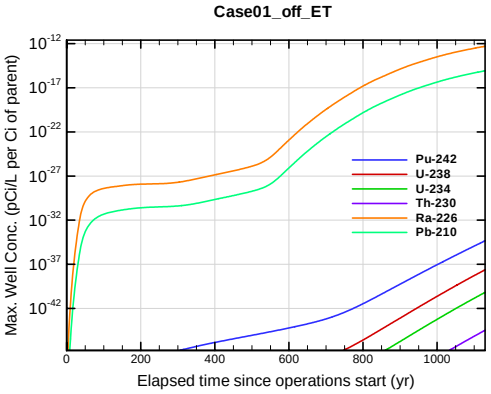

Figure A1B-756. Max. 100-m well conc. for Case01_off_ET Pu-242

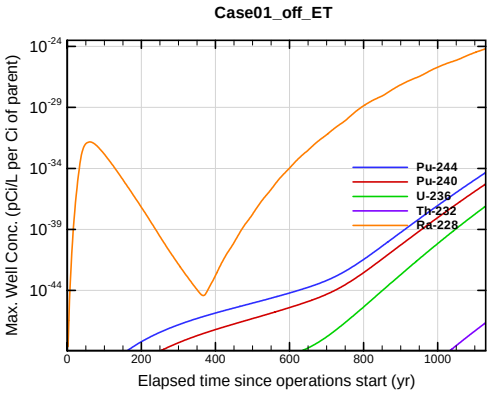

Figure A1B-757. Max. 100-m well conc. for Case01_off_ET Pu-244

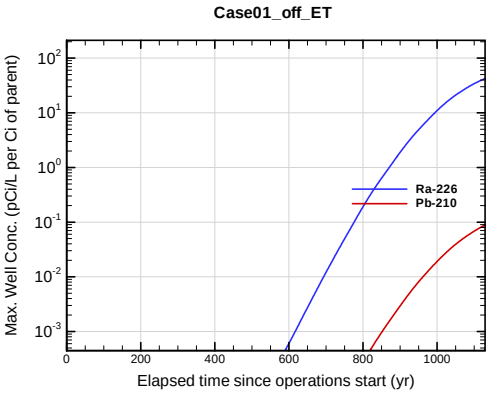

Figure A1B-758. Max. 100-m well conc. for Case01_off_ET Ra-226

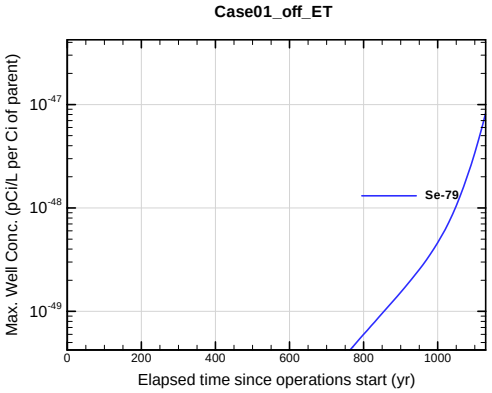

Figure A1B-759. Max. 100-m well conc. for Case01_off_ET Se-79

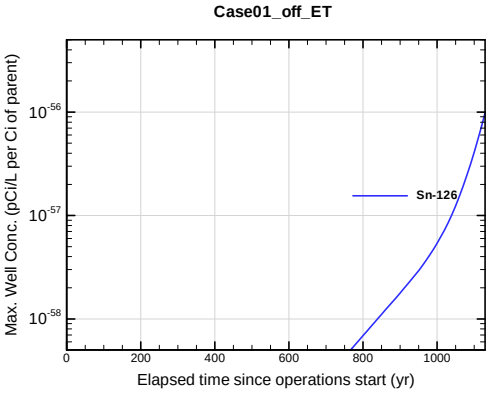

Figure A1B-760. Max. 100-m well conc. for Case01_off_ET Sn-126

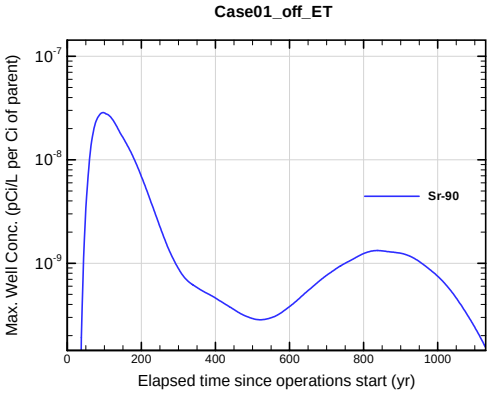

Figure A1B-761. Max. 100-m well conc. for Case01_off_ET Sr-90

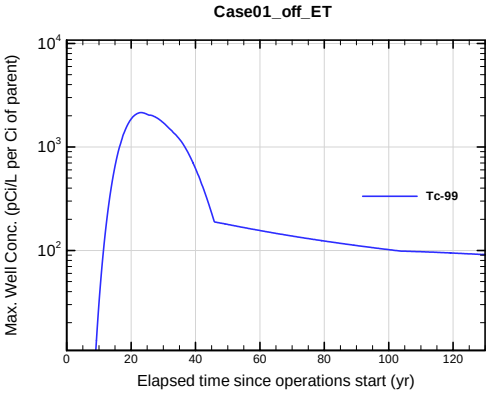

Figure A1B-762. Max. 100-m well conc. for Case01_off_ET Tc-99

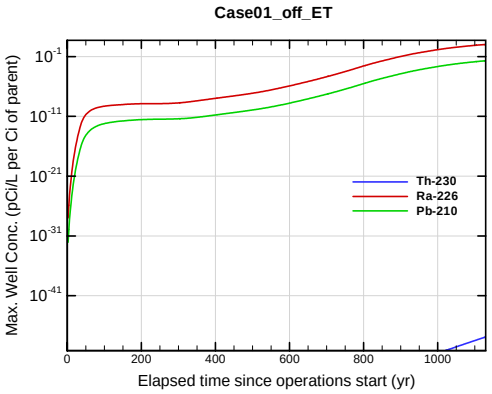

Figure A1B-763. Max. 100-m well conc. for Case01_off_ET Th-230

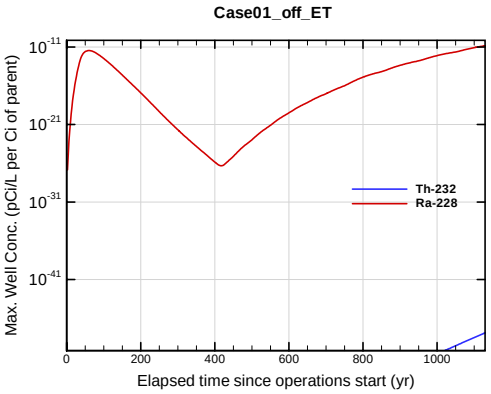

Figure A1B-764. Max. 100-m well conc. for Case01_off_ET Th-232

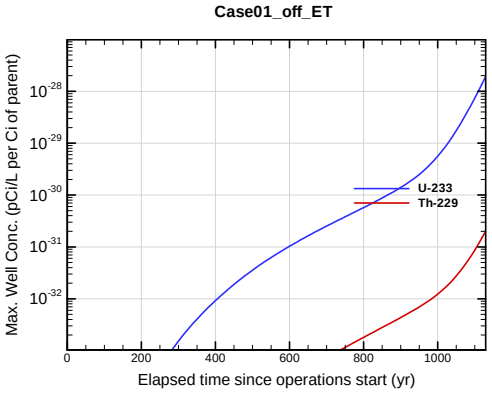

Figure A1B-765. Max. 100-m well conc. for Case01_off_ET U-233

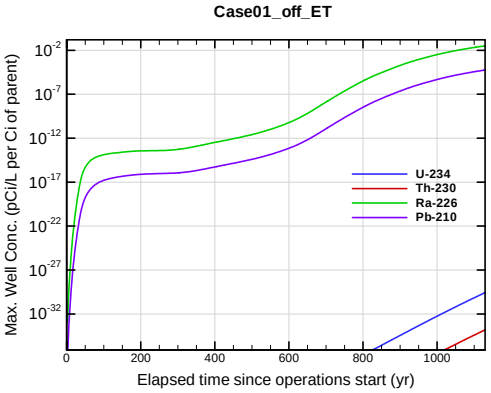

Figure A1B-766. Max. 100-m well conc. for Case01_off_ET U-234

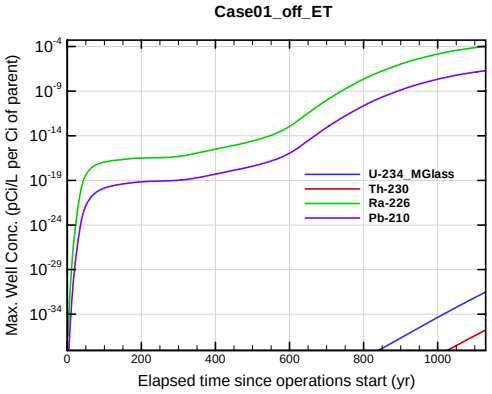

Figure A1B-767. Max. 100-m well conc. for Case01_off_ET U-234_MGlass

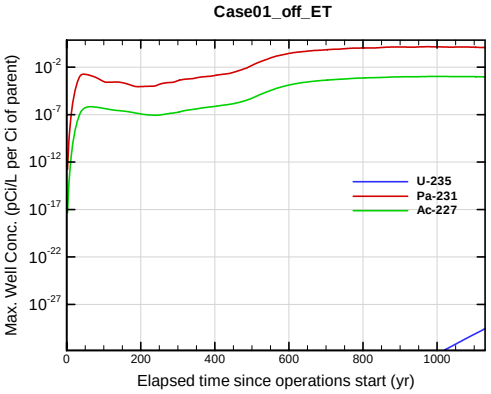

Figure A1B-768. Max. 100-m well conc. for Case01_off_ET U-235

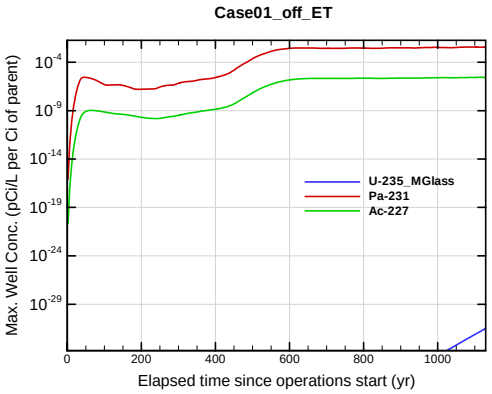

Figure A1B-769. Max. 100-m well conc. for Case01_off_ET U-235_MGlass

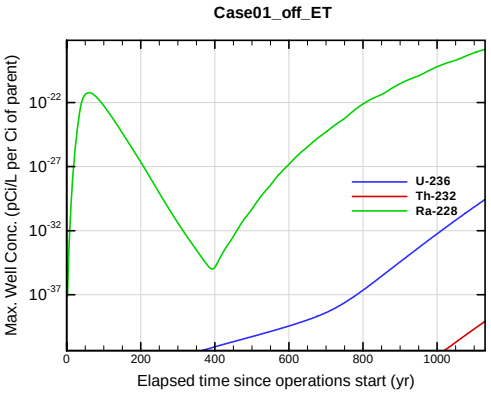

Figure A1B-770. Max. 100-m well conc. for Case01_off_ET U-236

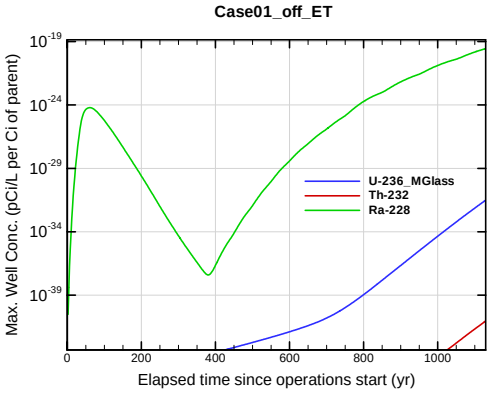

Figure A1B-771. Max. 100-m well conc. for Case01_off_ET U-236_MGlass

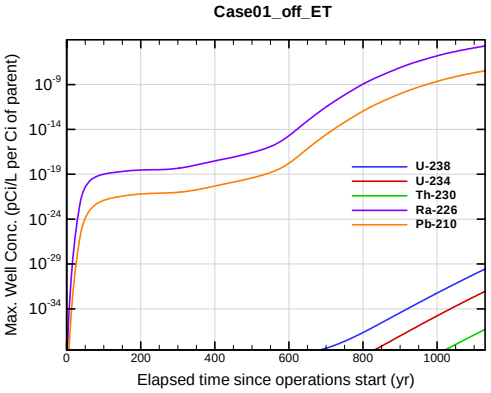

Figure A1B-772. Max. 100-m well conc. for Case01_off_ET U-238

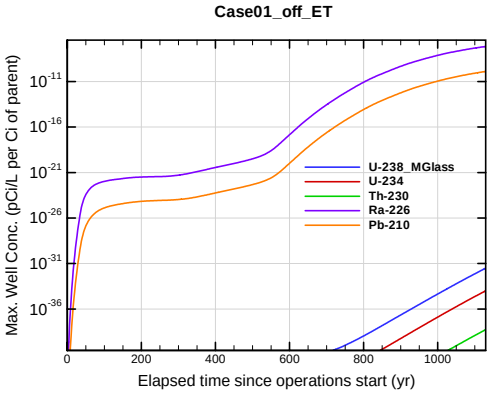

Figure A1B-773. Max. 100-m well conc. for Case01_off_ET U-238_MGlass

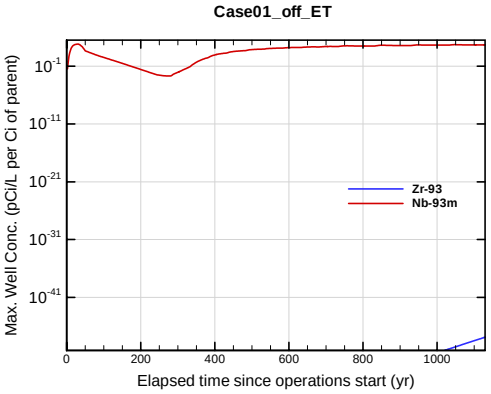

Figure A1B-774. Max. 100-m well conc. for Case01_off_ET Zr-93

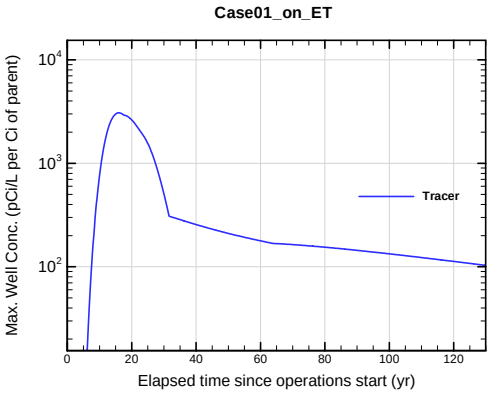

Figure A1B-775. Max. 100-m well conc. for Case01_on_ET Tracer

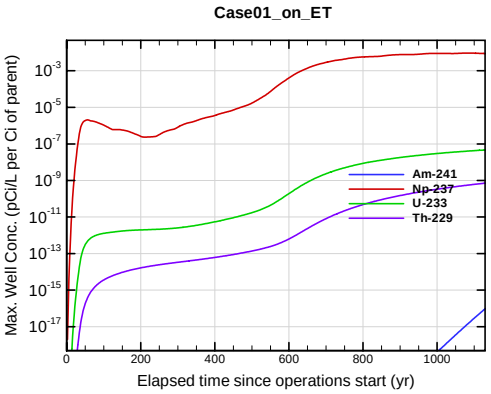

Figure A1B-776. Max. 100-m well conc. for Case01_on_ET Am-241

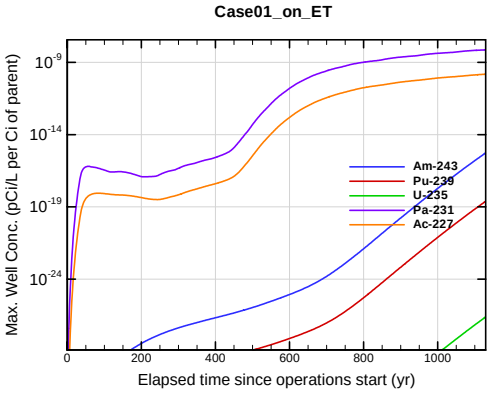

Figure A1B-777. Max. 100-m well conc. for Case01_on_ET Am-243

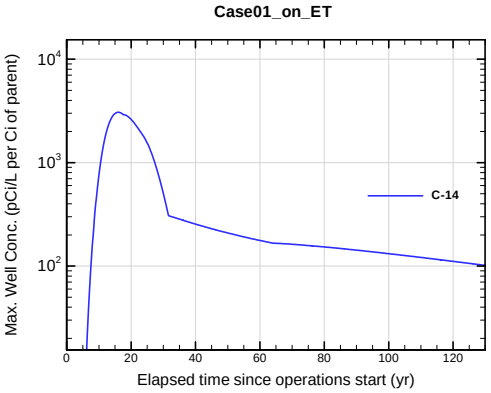

Figure A1B-778. Max. 100-m well conc. for Case01_on_ET C-14

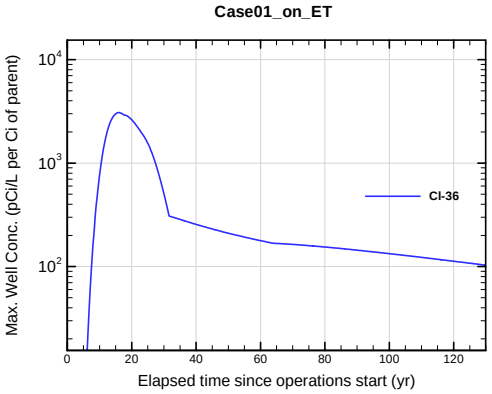

Figure A1B-779. Max. 100-m well conc. for Case01_on_ET Cl-36

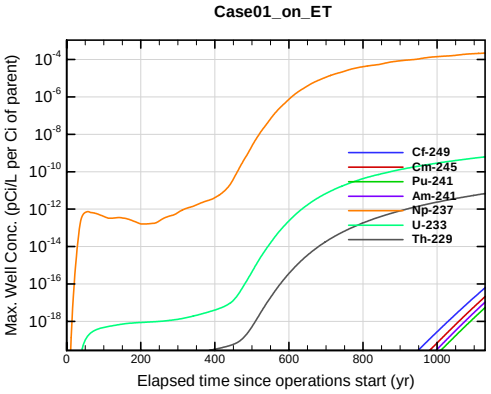

Figure A1B-780. Max. 100-m well conc. for Case01_on_ET Cf-249

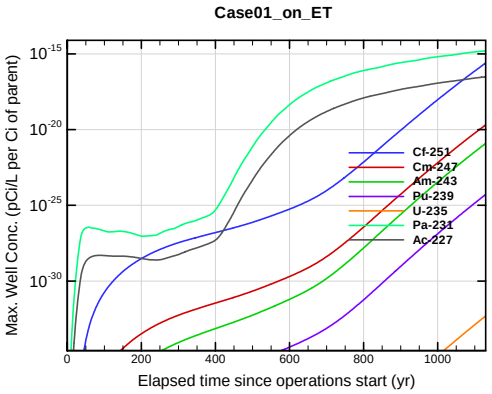

Figure A1B-781. Max. 100-m well conc. for Case01_on_ET Cf-251

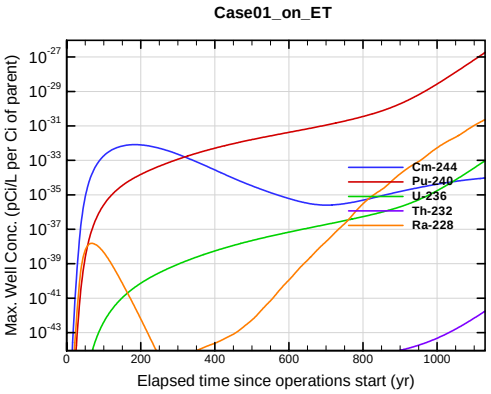

Figure A1B-782. Max. 100-m well conc. for Case01_on_ET Cm-244

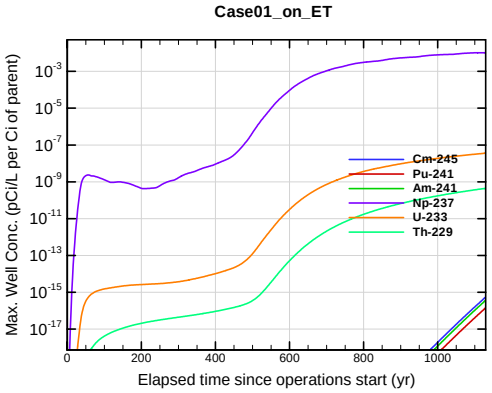

Figure A1B-783. Max. 100-m well conc. for Case01_on_ET Cm-245

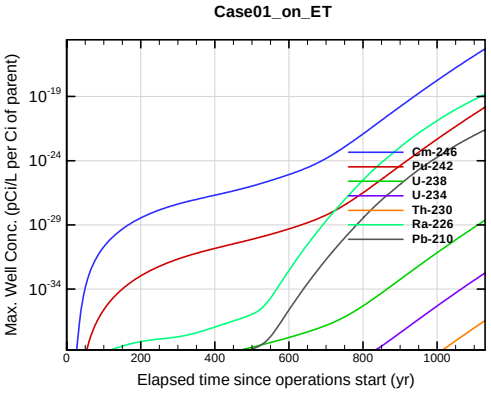

Figure A1B-784. Max. 100-m well conc. for Case01_on_ET Cm-246

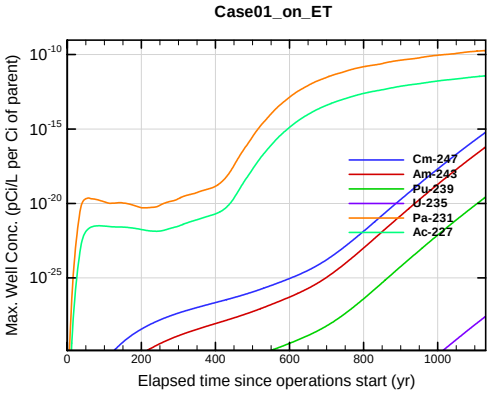

Figure A1B-785. Max. 100-m well conc. for Case01_on_ET Cm-247

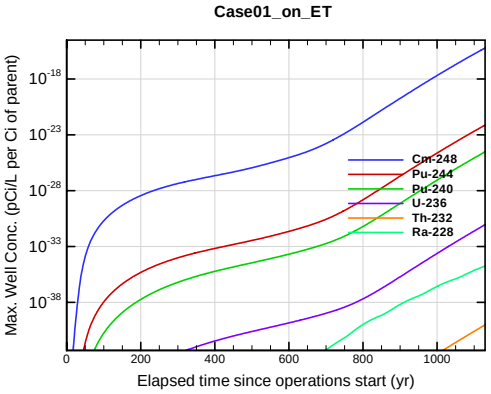

Figure A1B-786. Max. 100-m well conc. for Case01_on_ET Cm-248

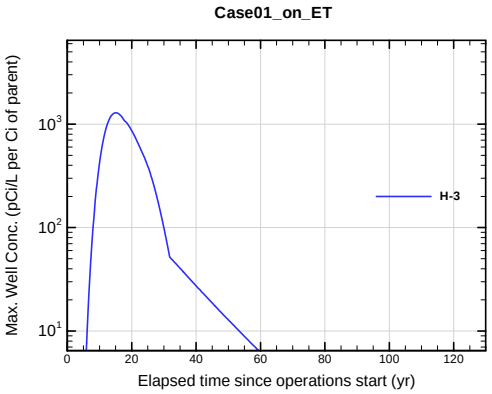

Figure A1B-787. Max. 100-m well conc. for Case01_on_ET H-3

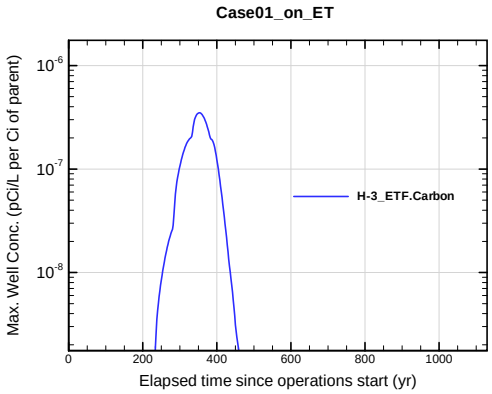

Figure A1B-788. Max. 100-m well conc. for Case01_on_ET H-3_ETF.Carbon

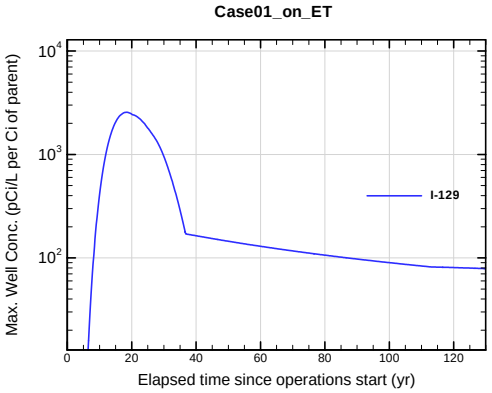

Figure A1B-789. Max. 100-m well conc. for Case01_on_ET I-129

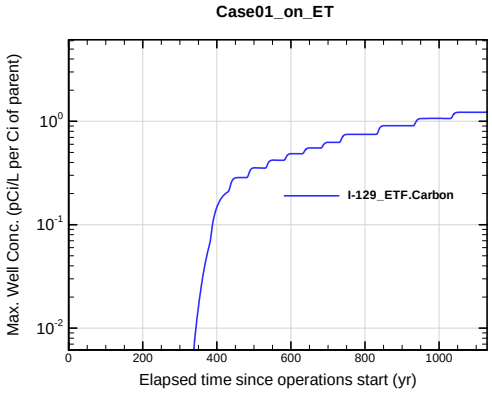

Figure A1B-790. Max. 100-m well conc. for Case01_on_ET I-129_ETF.Carbon

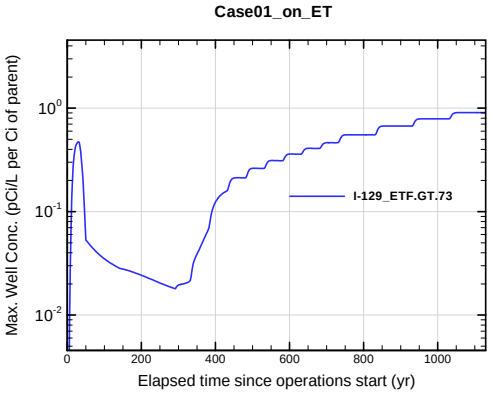

Figure A1B-791. Max. 100-m well conc. for Case01_on_ET I-129_ETF.GT.73

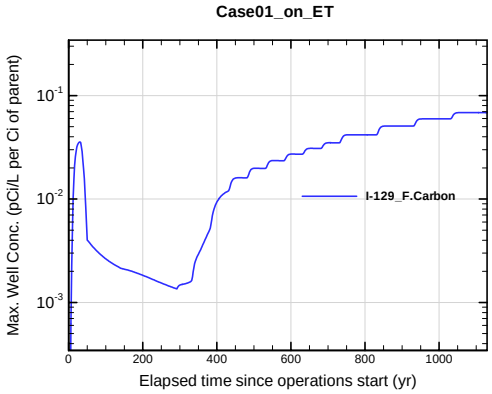

Figure A1B-792. Max. 100-m well conc. for Case01_on_ET I-129_F.Carbon

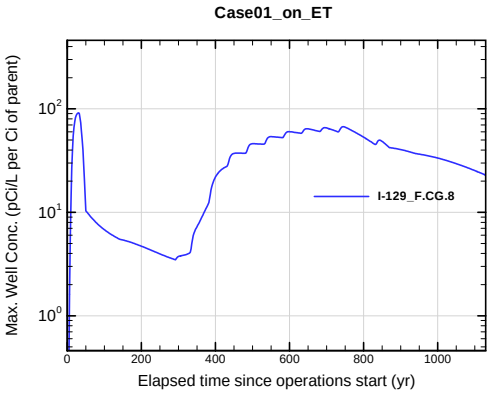

Figure A1B-793. Max. 100-m well conc. for Case01_on_ET I-129_F.CG.8

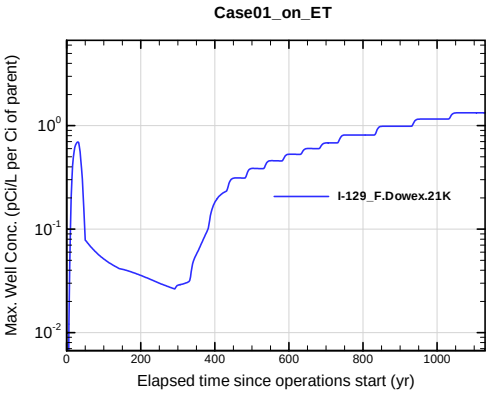

Figure A1B-794. Max. 100-m well conc. for Case01_on_ET I-129_F.Dowex.21K

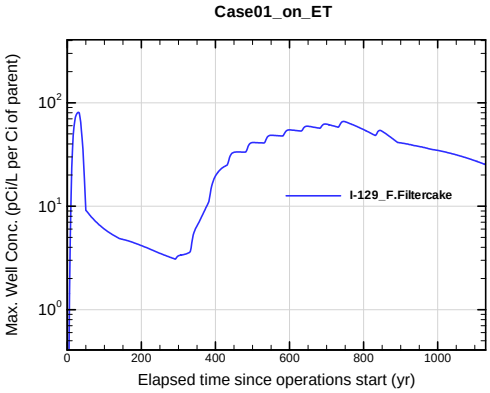

Figure A1B-795. Max. 100-m well conc. for Case01_on_ET I-129_F.Filtercake

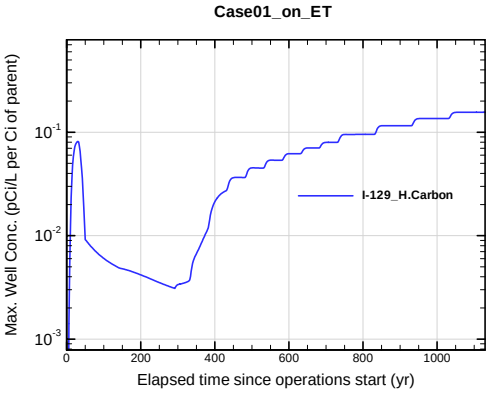

Figure A1B-796. Max. 100-m well conc. for Case01_on_ET I-129_H.Carbon

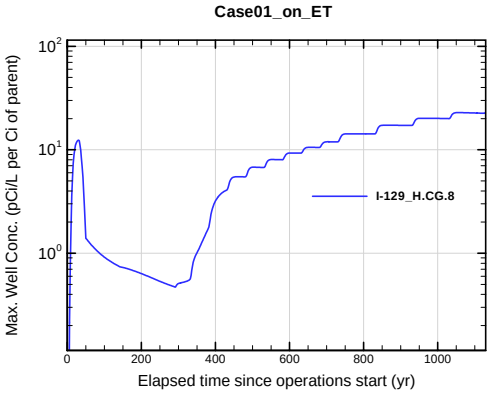

Figure A1B-797. Max. 100-m well conc. for Case01_on_ET I-129_H.CG.8

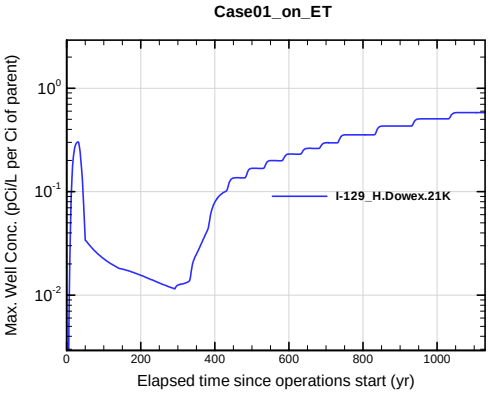

Figure A1B-798. Max. 100-m well conc. for Case01_on_ET I-129_H.Dowex.21K

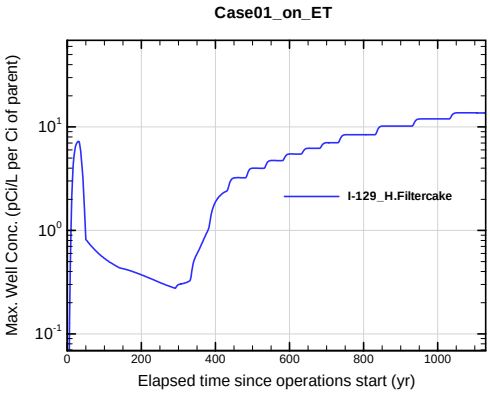

Figure A1B-799. Max. 100-m well conc. for Case01_on_ET I-129_H.Filtercake

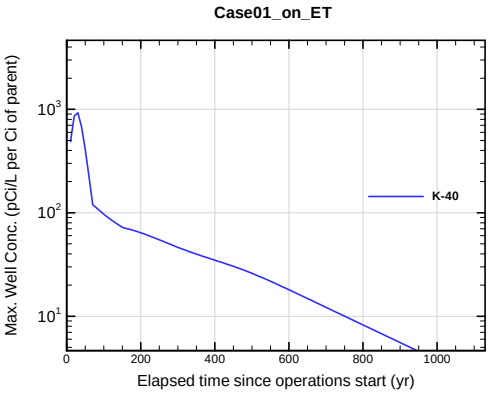

Figure A1B-800. Max. 100-m well conc. for Case01_on_ET K-40

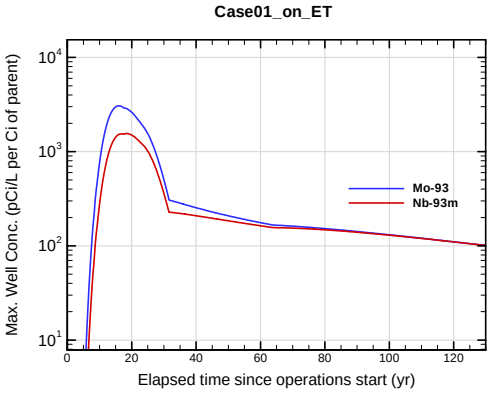

Figure A1B-801. Max. 100-m well conc. for Case01_on_ET Mo-93

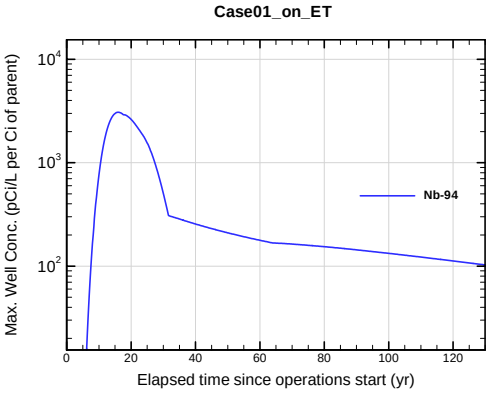

Figure A1B-802. Max. 100-m well conc. for Case01_on_ET Nb-94

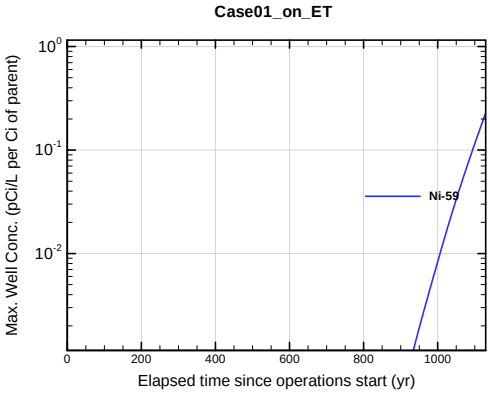

Figure A1B-803. Max. 100-m well conc. for Case01_on_ET Ni-59

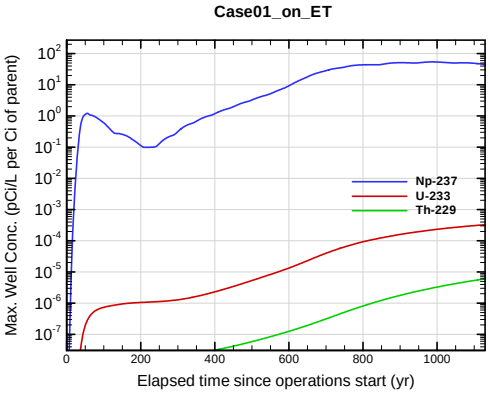

Figure A1B-804. Max. 100-m well conc. for Case01_on_ET Np-237

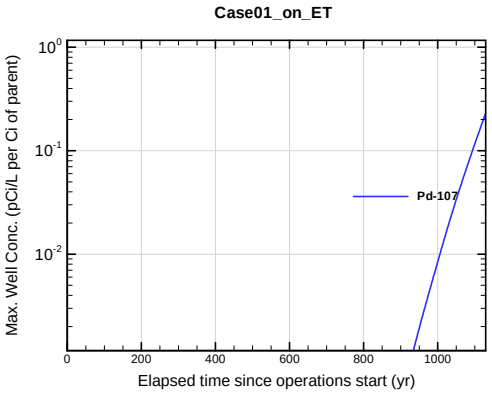

Figure A1B-805. Max. 100-m well conc. for Case01_on_ET Pd-107

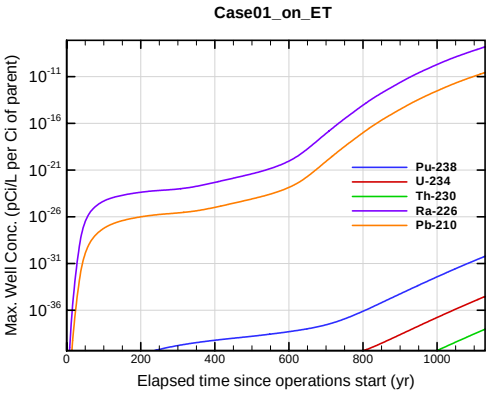

Figure A1B-806. Max. 100-m well conc. for Case01_on_ET Pu-238

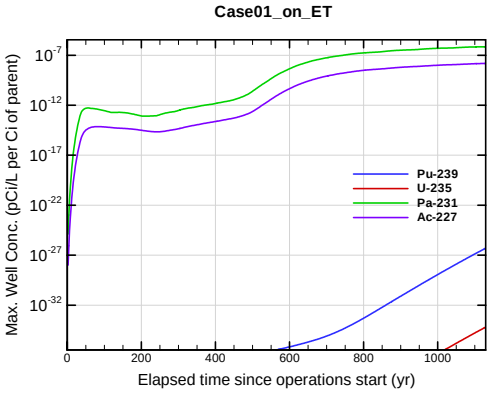

Figure A1B-807. Max. 100-m well conc. for Case01_on_ET Pu-239

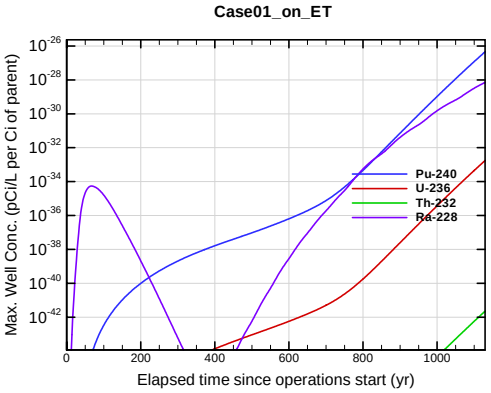

Figure A1B-808. Max. 100-m well conc. for Case01_on_ET Pu-240

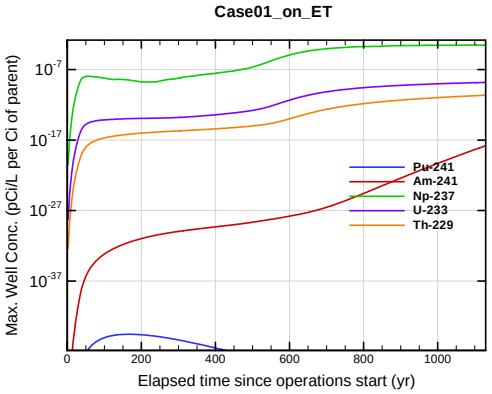

Figure A1B-809. Max. 100-m well conc. for Case01_on_ET Pu-241

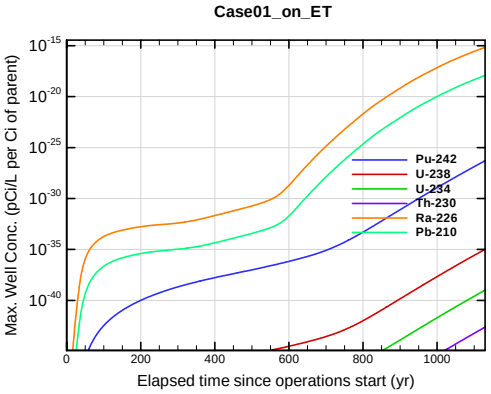

Figure A1B-810. Max. 100-m well conc. for Case01_on_ET Pu-242

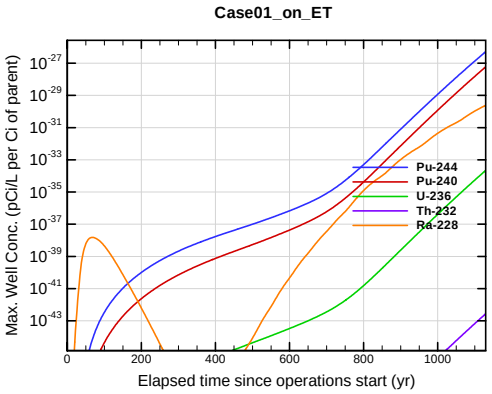

Figure A1B-811. Max. 100-m well conc. for Case01_on_ET Pu-244

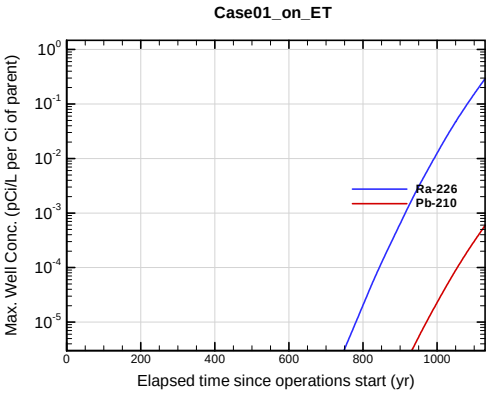

Figure A1B-812. Max. 100-m well conc. for Case01_on_ET Ra-226

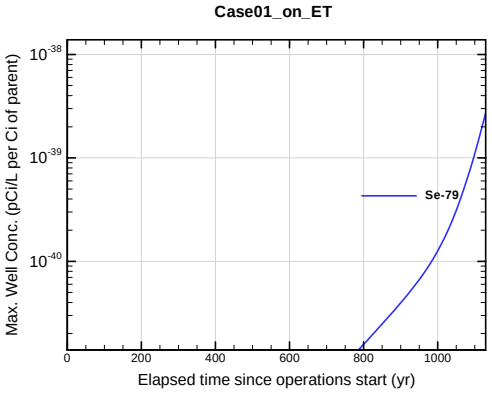

Figure A1B-813. Max. 100-m well conc. for Case01_on_ET Se-79

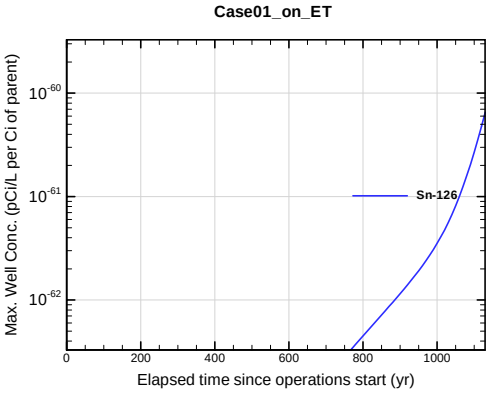

Figure A1B-814. Max. 100-m well conc. for Case01_on_ET Sn-126

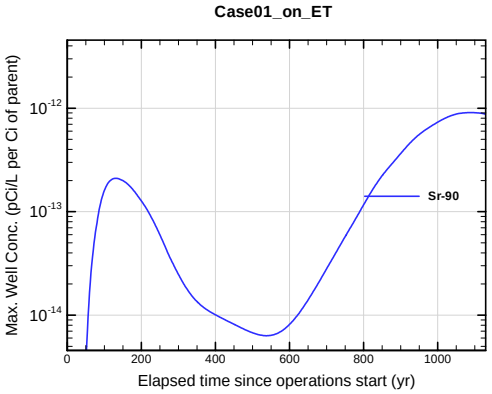

Figure A1B-815. Max. 100-m well conc. for Case01_on_ET Sr-90

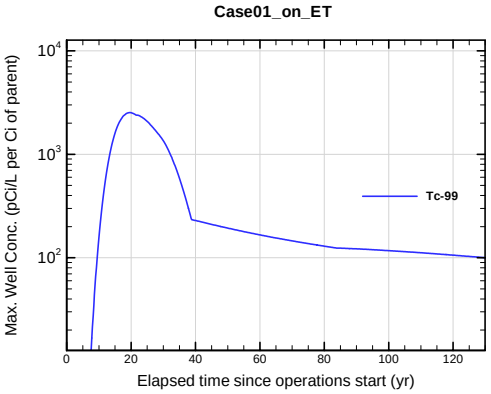

Figure A1B-816. Max. 100-m well conc. for Case01_on_ET Tc-99

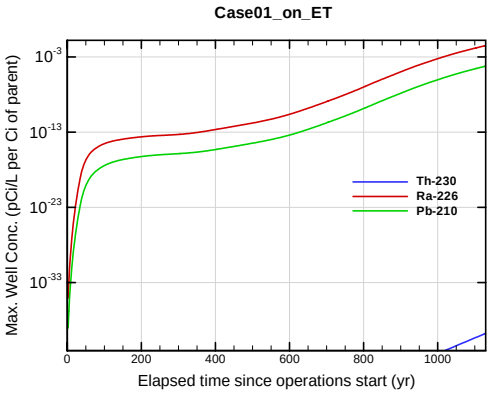

Figure A1B-817. Max. 100-m well conc. for Case01_on_ET Th-230

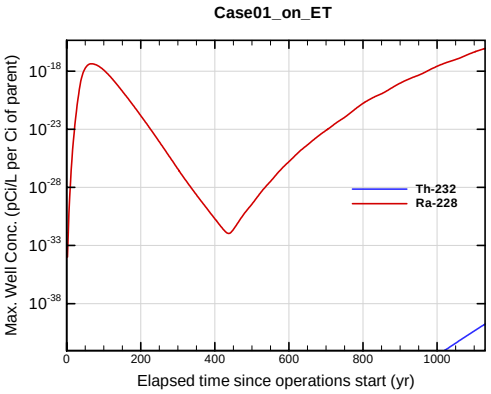

Figure A1B-818. Max. 100-m well conc. for Case01_on_ET Th-232

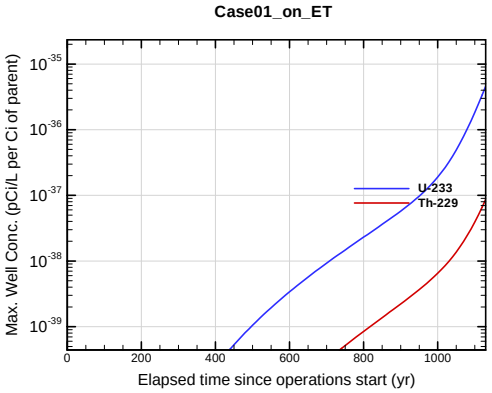

Figure A1B-819. Max. 100-m well conc. for Case01_on_ET U-233

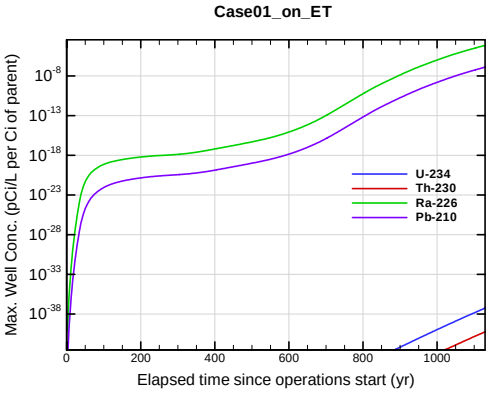

Figure A1B-820. Max. 100-m well conc. for Case01_on_ET U-234

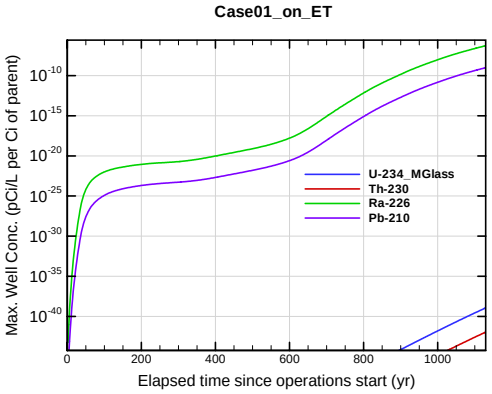

Figure A1B-821. Max. 100-m well conc. for Case01_on_ET U-234_MGlass

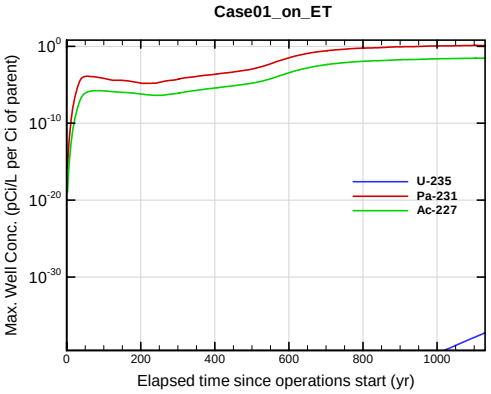

Figure A1B-822. Max. 100-m well conc. for Case01_on_ET U-235

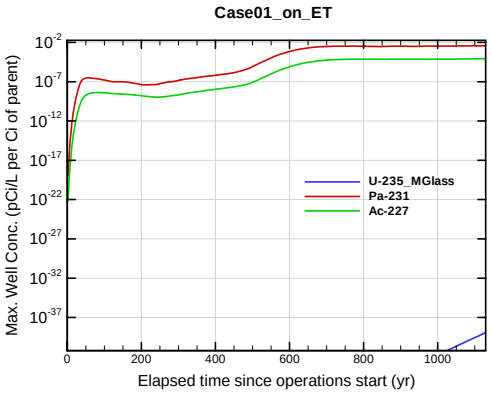

Figure A1B-823. Max. 100-m well conc. for Case01_on_ET U-235_MGlass

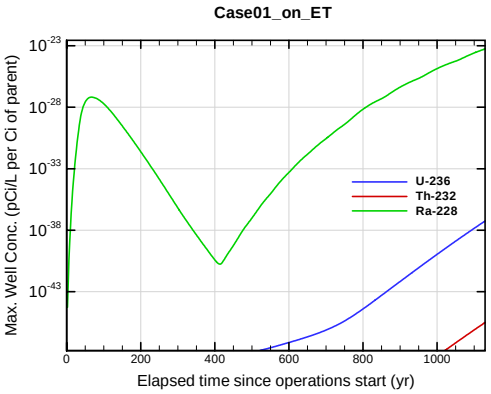

Figure A1B-824. Max. 100-m well conc. for Case01_on_ET U-236

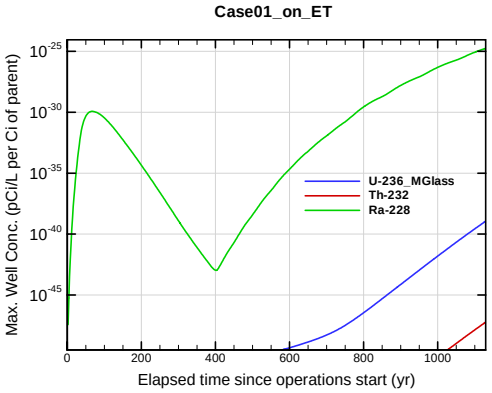

Figure A1B-825. Max. 100-m well conc. for Case01_on_ET U-236_MGlass

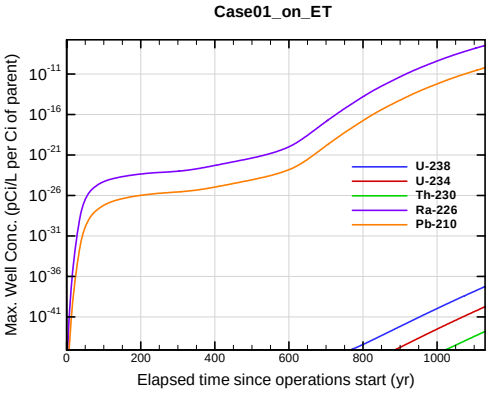

Figure A1B-826. Max. 100-m well conc. for Case01_on_ET U-238

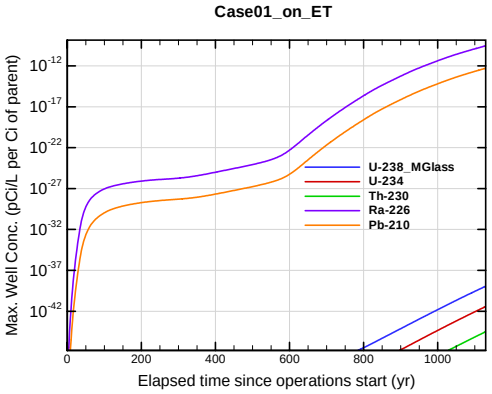

Figure A1B-827. Max. 100-m well conc. for Case01_on_ET U-238_MGlass

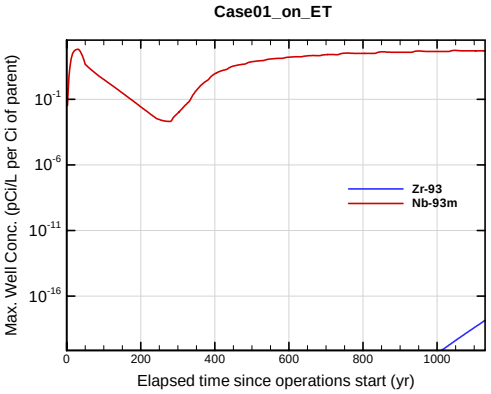

Figure A1B-828. Max. 100-m well conc. for Case01_on_ET Zr-93

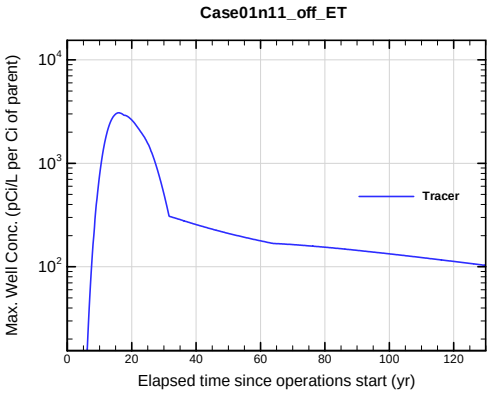

Figure A1B-829. Max. 100-m well conc. for Case01n11_off_ET Tracer

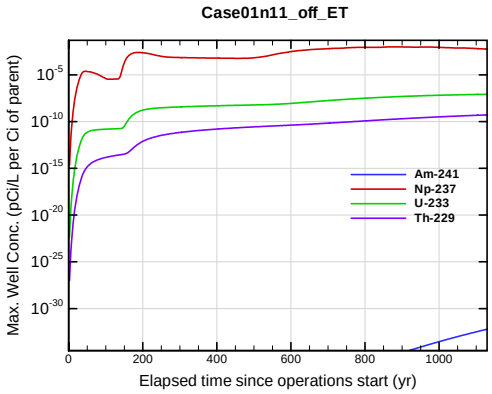

Figure A1B-830. Max. 100-m well conc. for Case01n11_off_ET Am-241

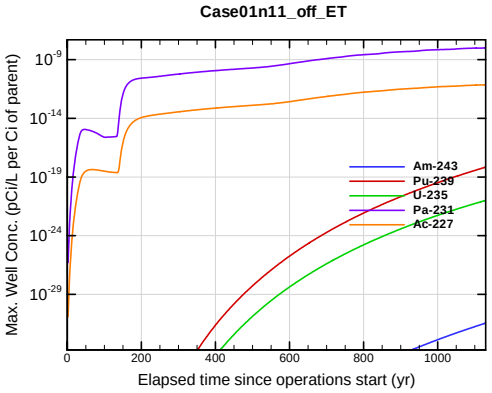

Figure A1B-831. Max. 100-m well conc. for Case01n11_off_ET Am-243

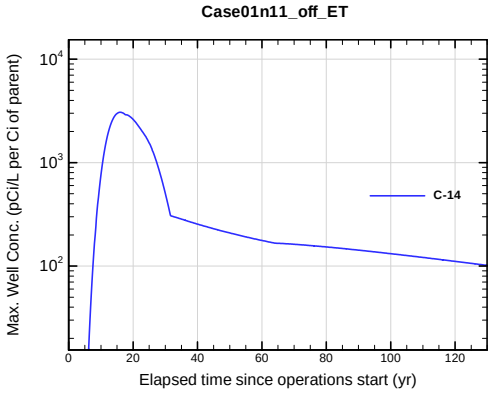

Figure A1B-832. Max. 100-m well conc. for Case01n11_off_ET C-14

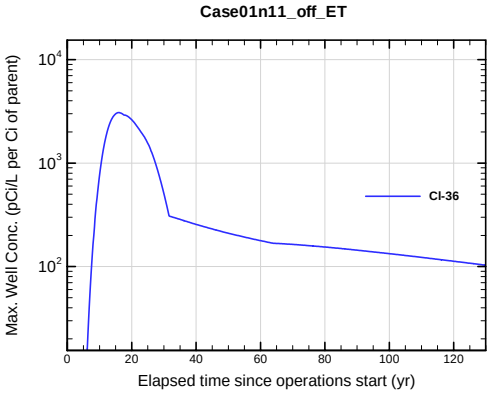

Figure A1B-833. Max. 100-m well conc. for Case01n11_off_ET Cl-36

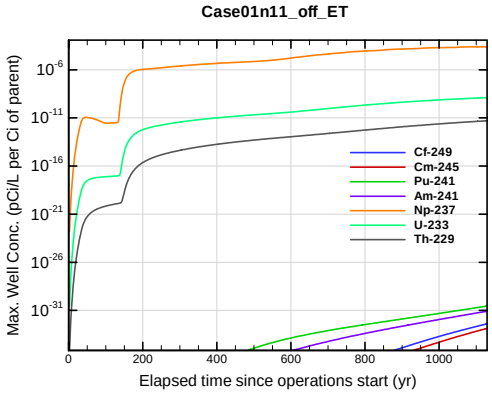

Figure A1B-834. Max. 100-m well conc. for Case01n11_off_ET Cf-249

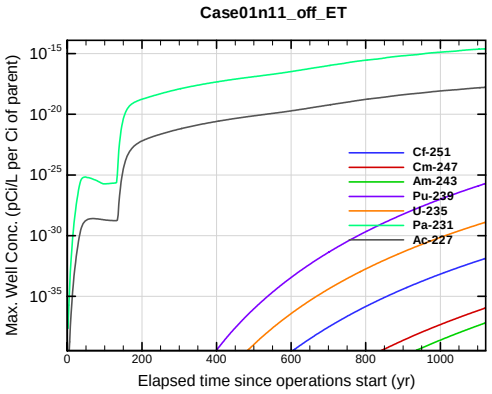

Figure A1B-835. Max. 100-m well conc. for Case01n11_off_ET Cf-251

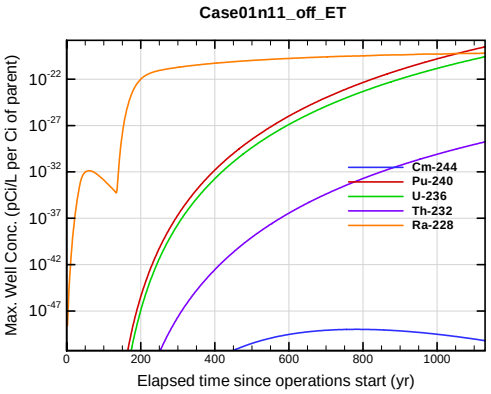

Figure A1B-836. Max. 100-m well conc. for Case01n11_off_ET Cm-244

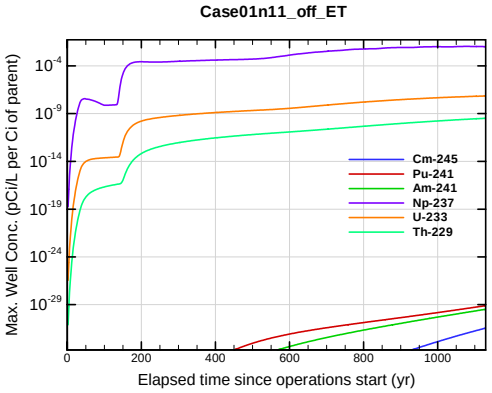

Figure A1B-837. Max. 100-m well conc. for Case01n11_off_ET Cm-245

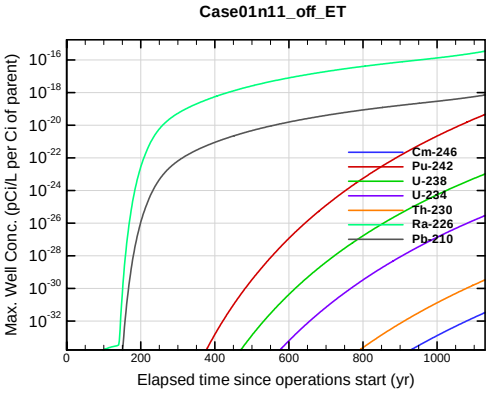

Figure A1B-838. Max. 100-m well conc. for Case01n11_off_ET Cm-246

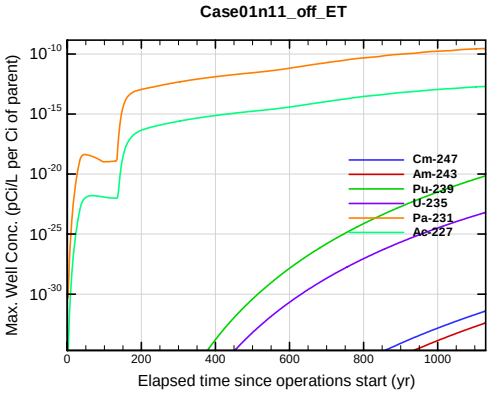

Figure A1B-839. Max. 100-m well conc. for Case01n11_off_ET Cm-247

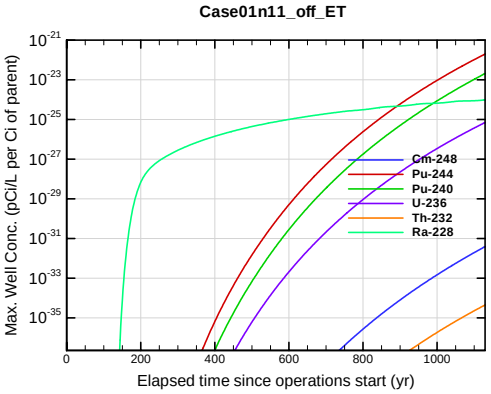

Figure A1B-840. Max. 100-m well conc. for Case01n11_off_ET Cm-248

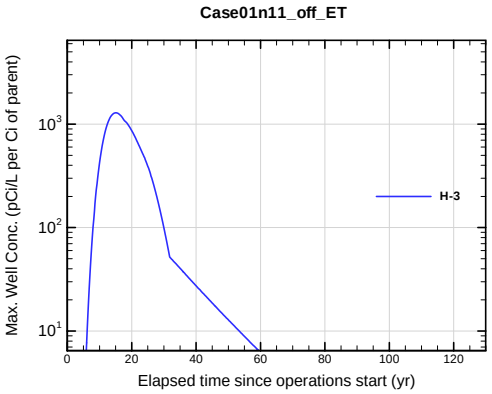

Figure A1B-841. Max. 100-m well conc. for Case01n11_off_ET H-3

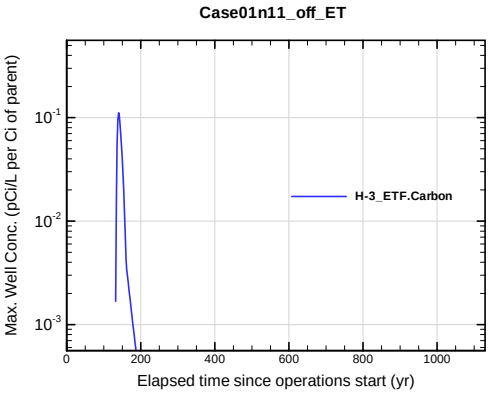

Figure A1B-842. Max. 100-m well conc. for Case01n11_off_ET H-3_ETF.Carbon

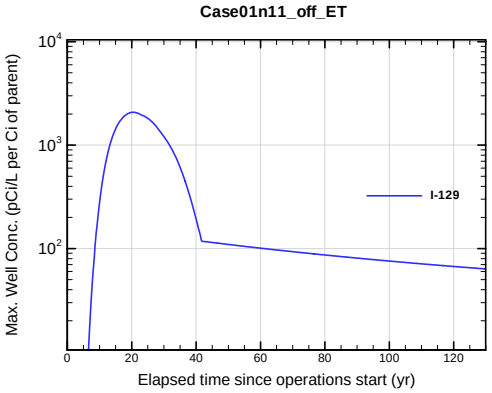

Figure A1B-843. Max. 100-m well conc. for Case01n11_off_ET I-129

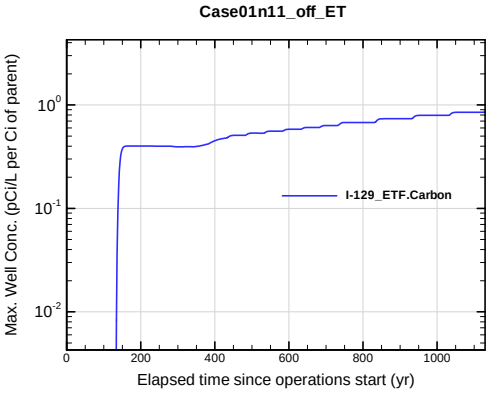

Figure A1B-844. Max. 100-m well conc. for Case01n11_off_ET I-129_ETF.Carbon

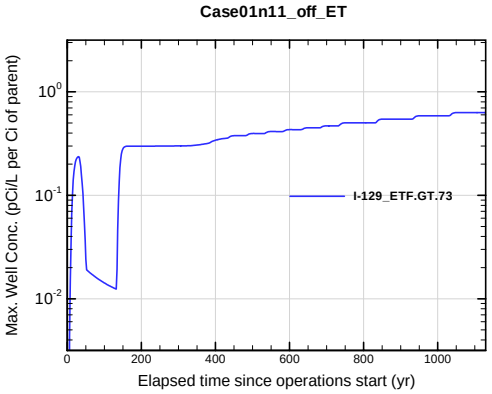

Figure A1B-845. Max. 100-m well conc. for Case01n11_off_ET I-129_ETF.GT.73

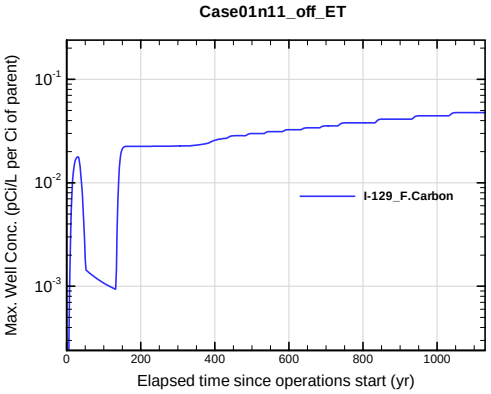

Figure A1B-846. Max. 100-m well conc. for Case01n11_off_ET I-129_F.Carbon

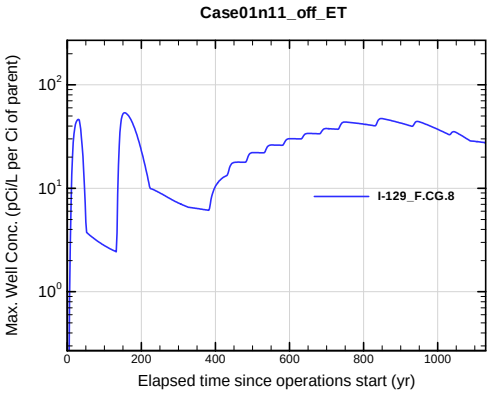

Figure A1B-847. Max. 100-m well conc. for Case01n11_off_ET I-129_F.CG.8

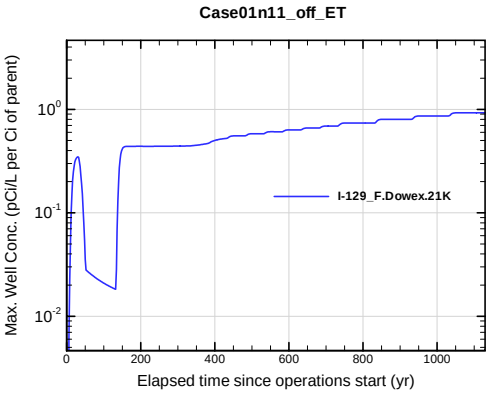

Figure A1B-848. Max. 100-m well conc. for Case01n11_off_ET I-129_F.Dowex.21K

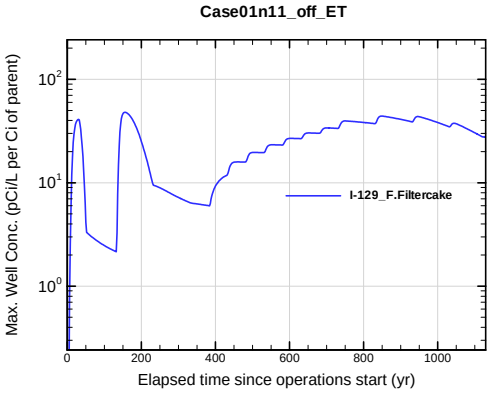

Figure A1B-849. Max. 100-m well conc. for Case01n11_off_ET I-129_F.Filtercake

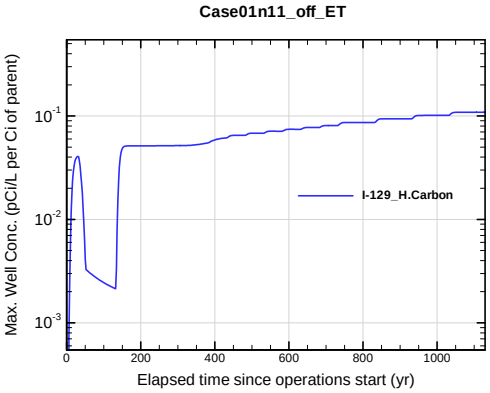

Figure A1B-850. Max. 100-m well conc. for Case01n11_off_ET I-129_H.Carbon

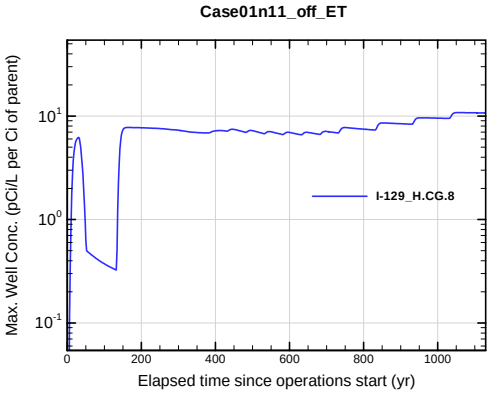

Figure A1B-851. Max. 100-m well conc. for Case01n11_off_ET I-129_H.CG.8

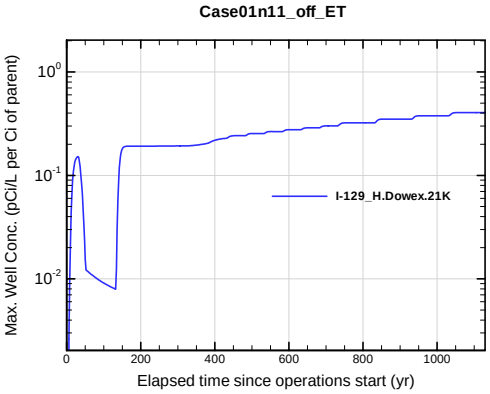

Figure A1B-852. Max. 100-m well conc. for Case01n11_off_ET I-129_H.Dowex.21K

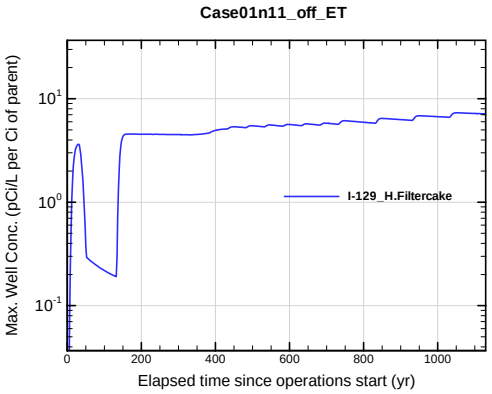

Figure A1B-853. Max. 100-m well conc. for Case01n11_off_ET I-129_H.Filtercake

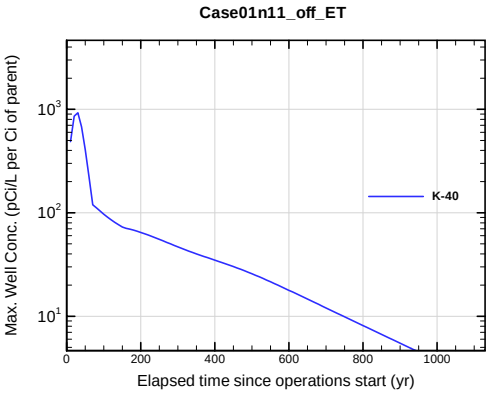

Figure A1B-854. Max. 100-m well conc. for Case01n11_off_ET K-40

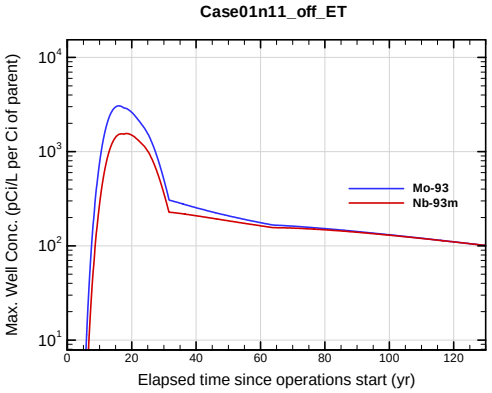

Figure A1B-855. Max. 100-m well conc. for Case01n11_off_ET Mo-93

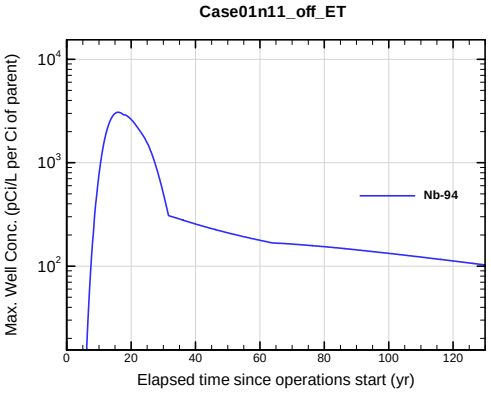

Figure A1B-856. Max. 100-m well conc. for Case01n11_off_ET Nb-94

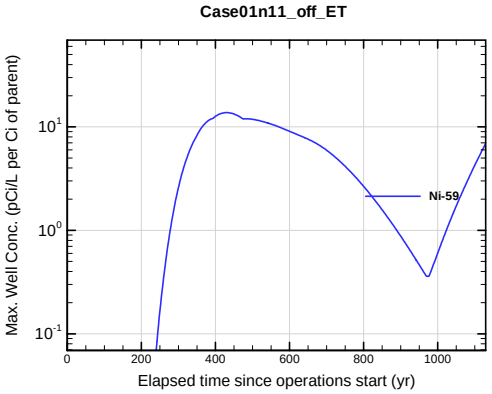

Figure A1B-857. Max. 100-m well conc. for Case01n11_off_ET Ni-59

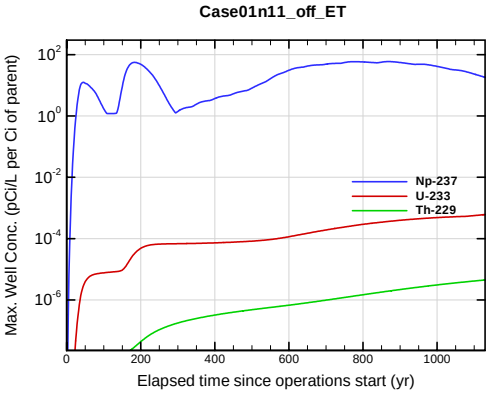

Figure A1B-858. Max. 100-m well conc. for Case01n11_off_ET Np-237

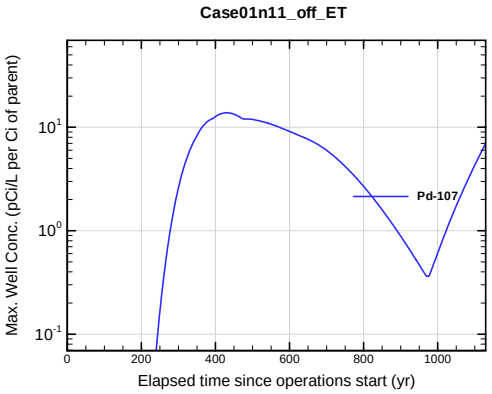

Figure A1B-859. Max. 100-m well conc. for Case01n11_off_ET Pd-107

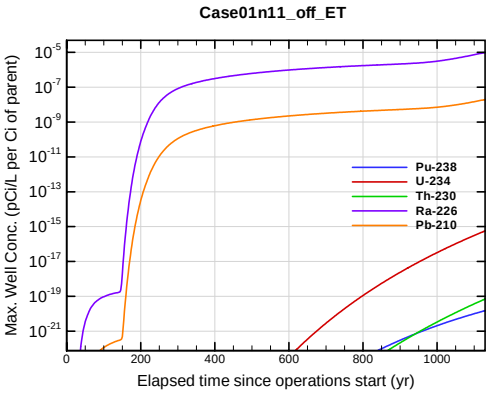

Figure A1B-860. Max. 100-m well conc. for Case01n11_off_ET Pu-238

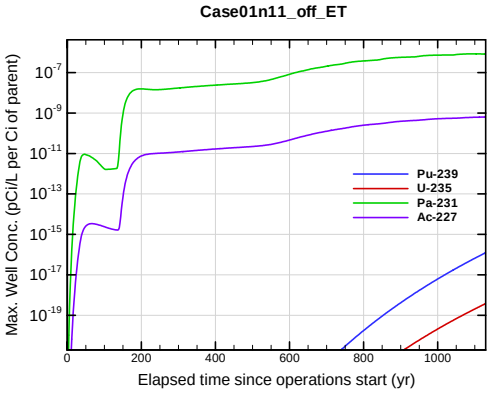

Figure A1B-861. Max. 100-m well conc. for Case01n11_off_ET Pu-239

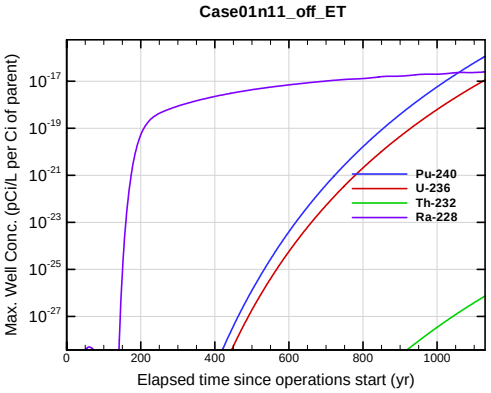

Figure A1B-862. Max. 100-m well conc. for Case01n11_off_ET Pu-240

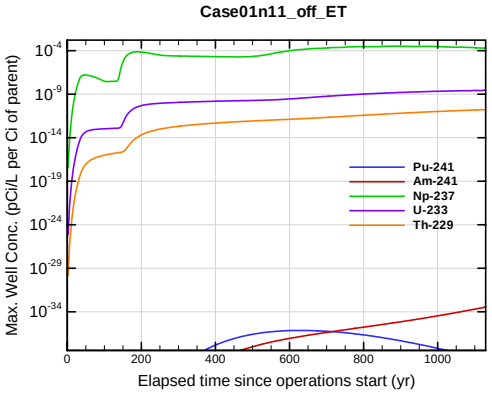

Figure A1B-863. Max. 100-m well conc. for Case01n11_off_ET Pu-241

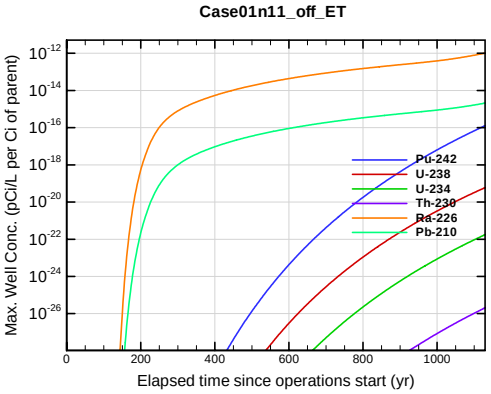

Figure A1B-864. Max. 100-m well conc. for Case01n11_off_ET Pu-242

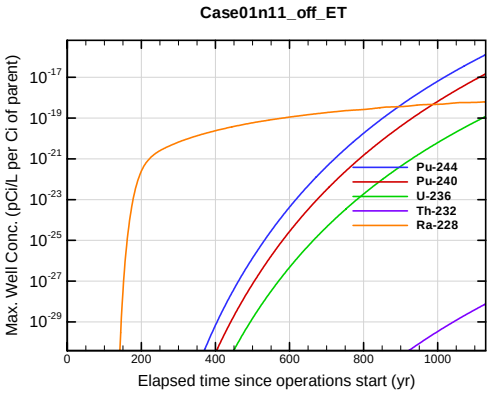

Figure A1B-865. Max. 100-m well conc. for Case01n11_off_ET Pu-244

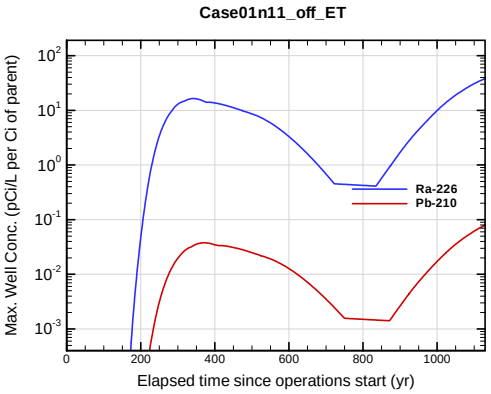

Figure A1B-866. Max. 100-m well conc. for Case01n11_off_ET Ra-226

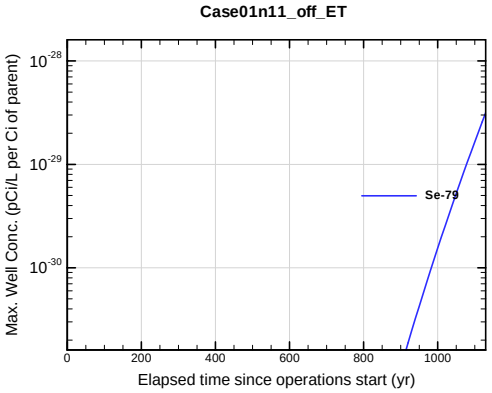

Figure A1B-867. Max. 100-m well conc. for Case01n11_off_ET Se-79

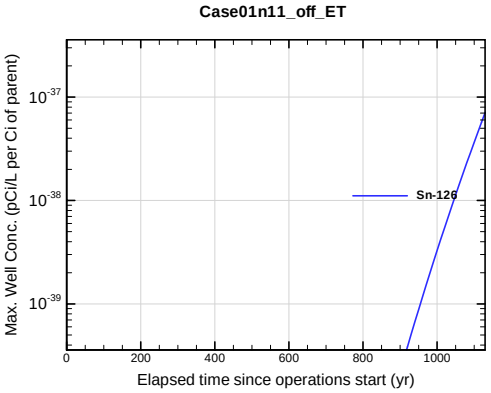

Figure A1B-868. Max. 100-m well conc. for Case01n11_off_ET Sn-126

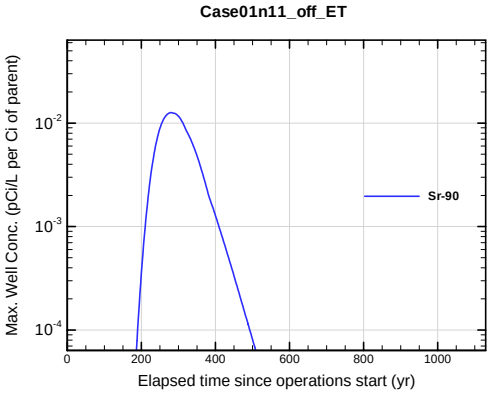

Figure A1B-869. Max. 100-m well conc. for Case01n11_off_ET Sr-90

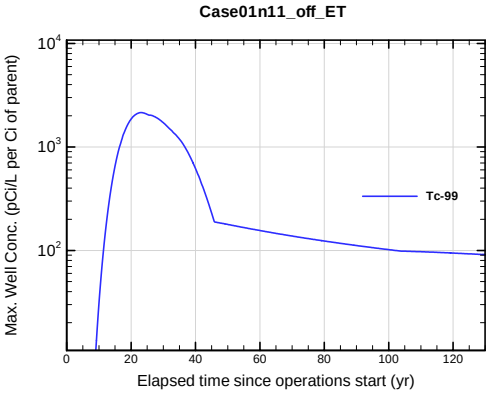

Figure A1B-870. Max. 100-m well conc. for Case01n11_off_ET Tc-99

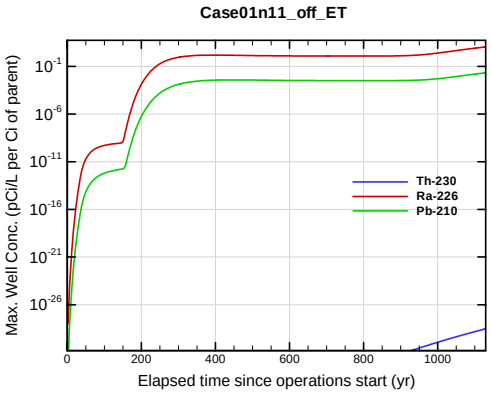

Figure A1B-871. Max. 100-m well conc. for Case01n11_off_ET Th-230

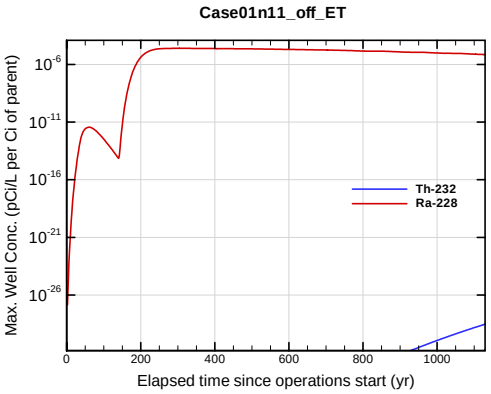

Figure A1B-872. Max. 100-m well conc. for Case01n11_off_ET Th-232

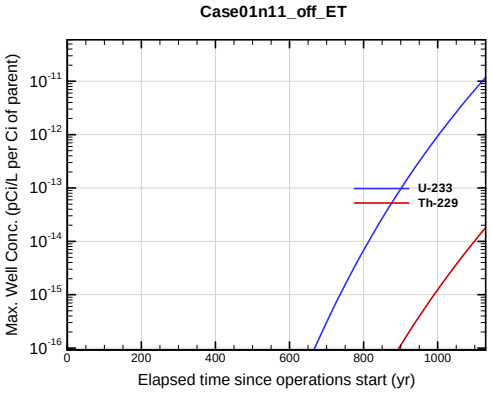

Figure A1B-873. Max. 100-m well conc. for Case01n11_off_ET U-233

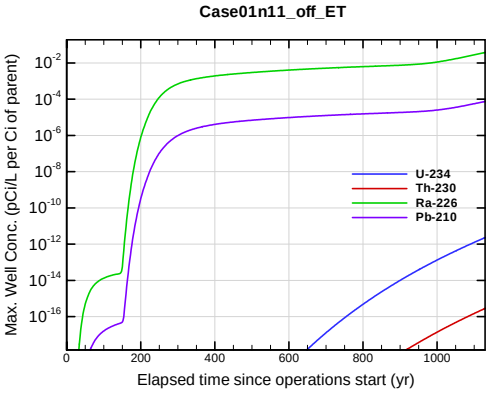

Figure A1B-874. Max. 100-m well conc. for Case01n11_off_ET U-234

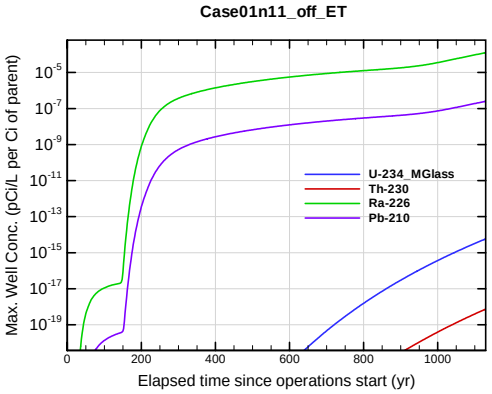

Figure A1B-875. Max. 100-m well conc. for Case01n11_off_ET U-234_MGlass

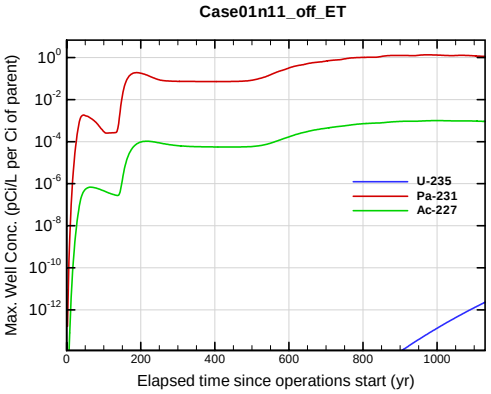

Figure A1B-876. Max. 100-m well conc. for Case01n11_off_ET U-235

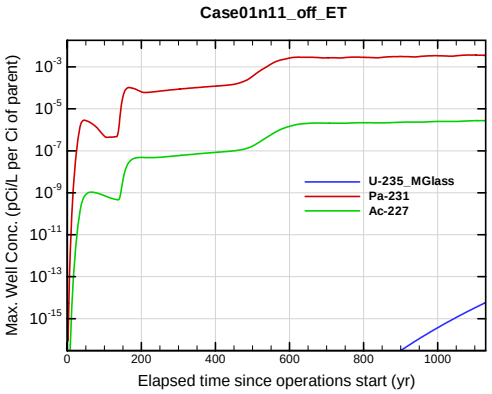

Figure A1B-877. Max. 100-m well conc. for Case01n11_off_ET U-235_MGlass

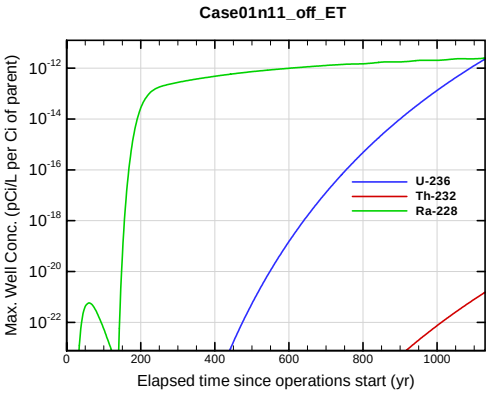

Figure A1B-878. Max. 100-m well conc. for Case01n11_off_ET U-236

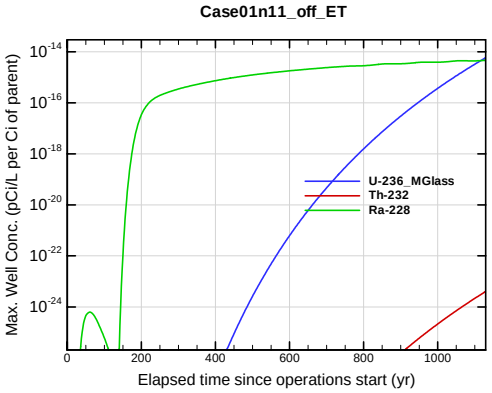

Figure A1B-879. Max. 100-m well conc. for Case01n11_off_ET U-236_MGlass

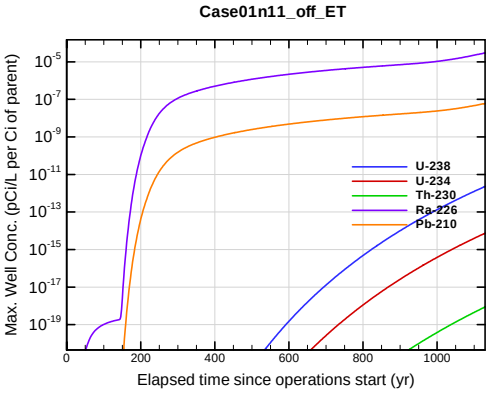

Figure A1B-880. Max. 100-m well conc. for Case01n11_off_ET U-238

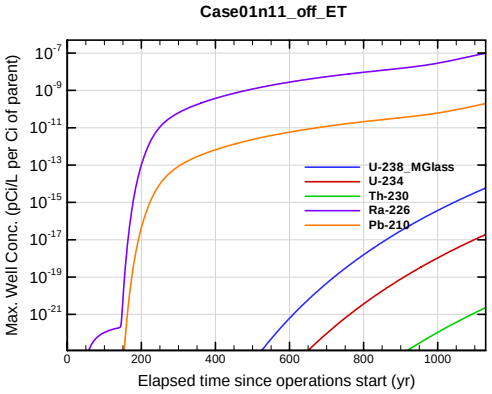

Figure A1B-881. Max. 100-m well conc. for Case01n11_off_ET U-238_MGlass

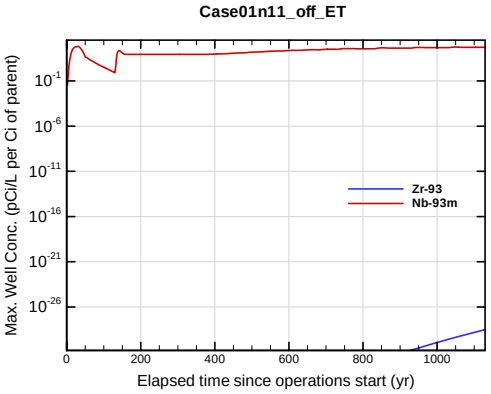

Figure A1B-882. Max. 100-m well conc. for Case01n11_off_ET Zr-93

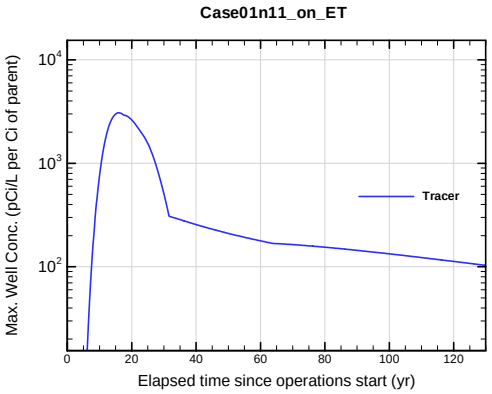

Figure A1B-883. Max. 100-m well conc. for Case01n11_on_ET Tracer

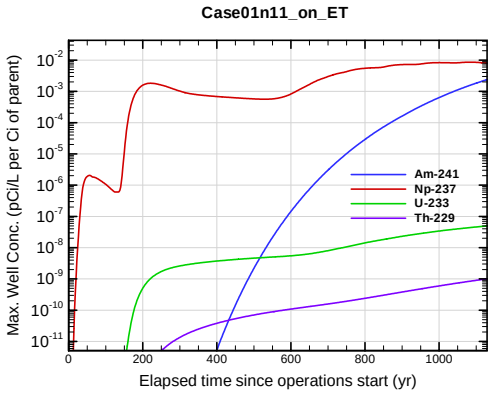

Figure A1B-884. Max. 100-m well conc. for Case01n11_on_ET Am-241

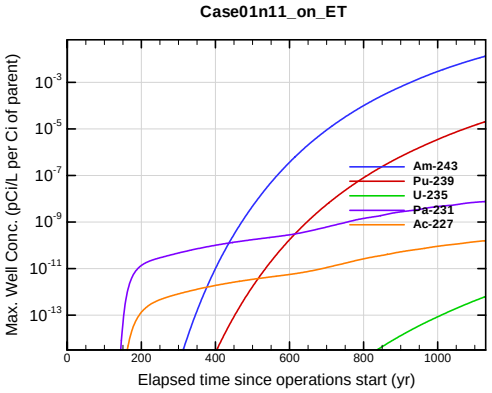

Figure A1B-885. Max. 100-m well conc. for Case01n11_on_ET Am-243

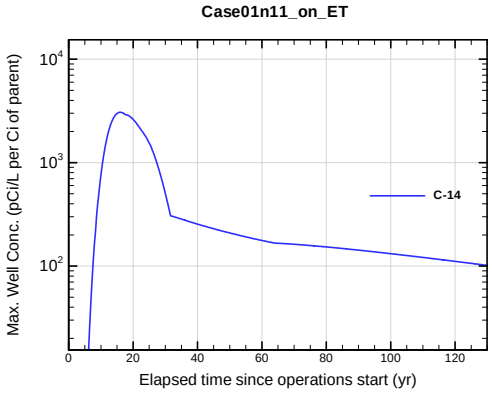

Figure A1B-886. Max. 100-m well conc. for Case01n11_on_ET C-14

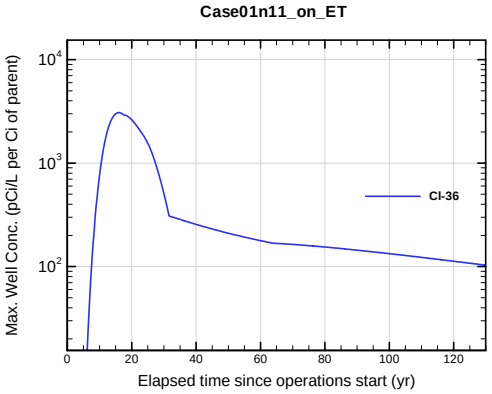

Figure A1B-887. Max. 100-m well conc. for Case01n11_on_ET Cl-36

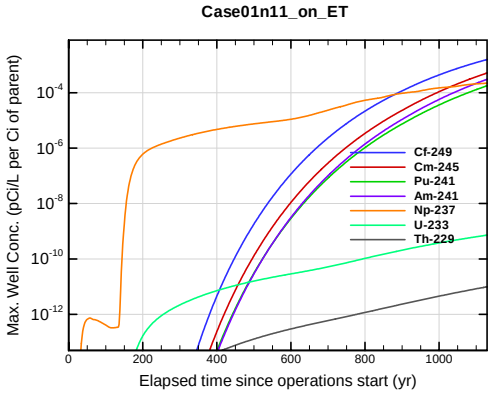

Figure A1B-888. Max. 100-m well conc. for Case01n11_on_ET Cf-249

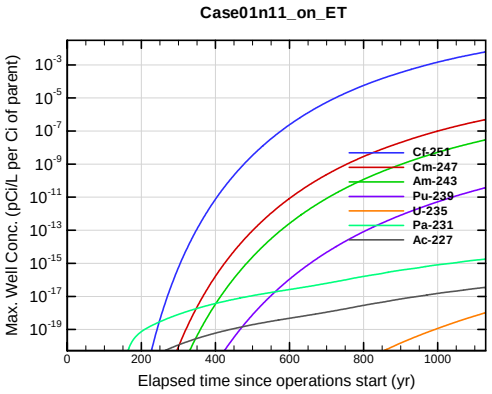

Figure A1B-889. Max. 100-m well conc. for Case01n11_on_ET Cf-251

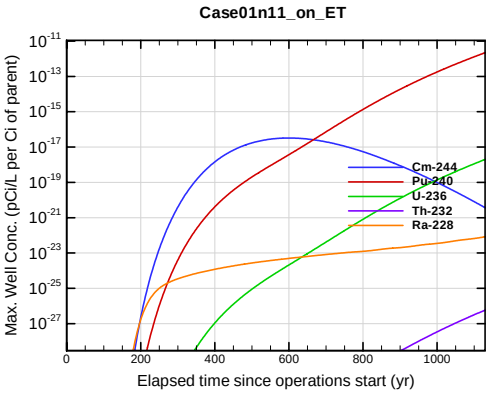

Figure A1B-890. Max. 100-m well conc. for Case01n11_on_ET Cm-244

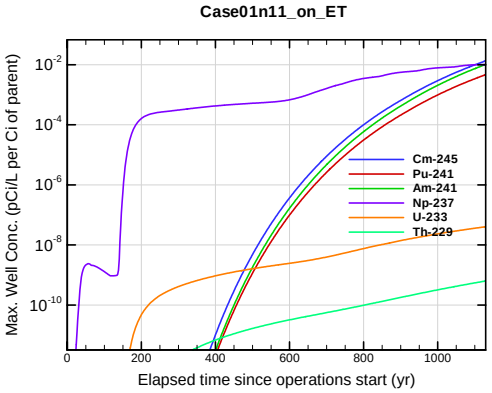

Figure A1B-891. Max. 100-m well conc. for Case01n11_on_ET Cm-245

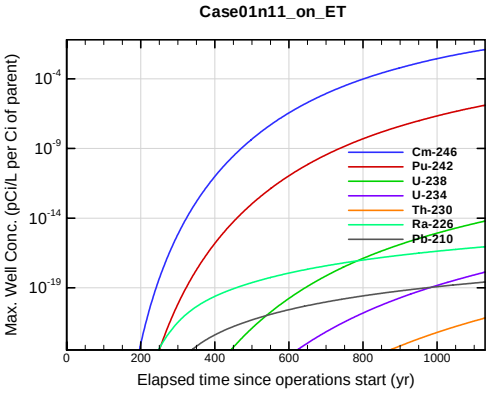

Figure A1B-892. Max. 100-m well conc. for Case01n11_on_ET Cm-246

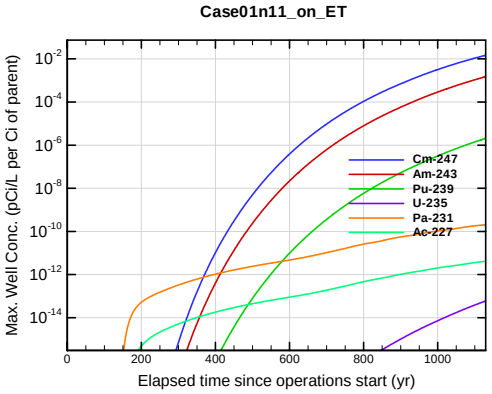

Figure A1B-893. Max. 100-m well conc. for Case01n11_on_ET Cm-247

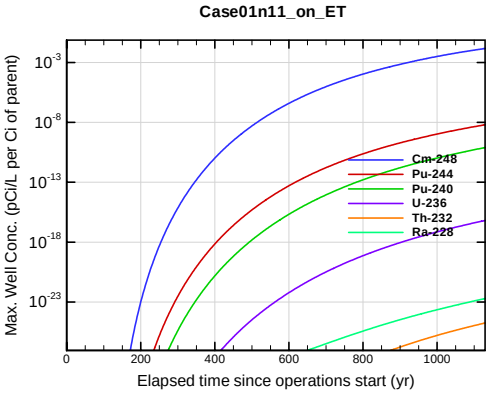

Figure A1B-894. Max. 100-m well conc. for Case01n11_on_ET Cm-248

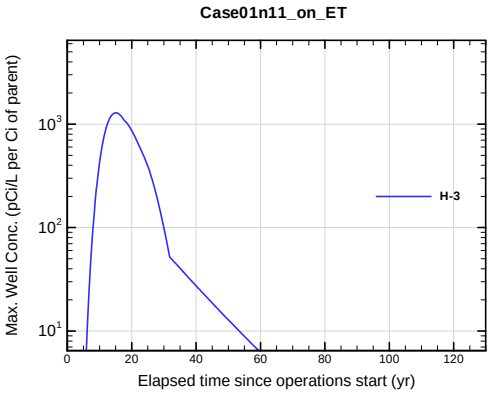

Figure A1B-895. Max. 100-m well conc. for Case01n11_on_ET H-3

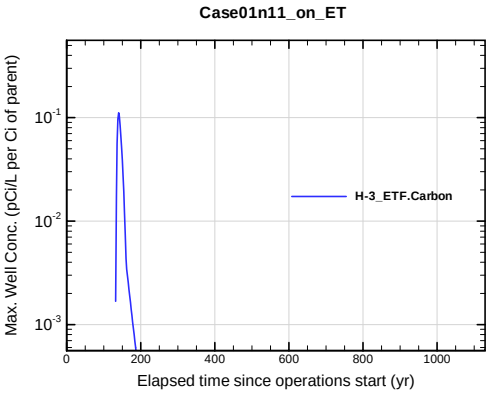

Figure A1B-896. Max. 100-m well conc. for Case01n11_on_ET H-3_ETF.Carbon

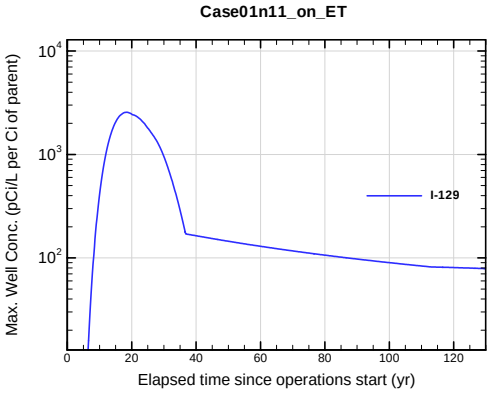

Figure A1B-897. Max. 100-m well conc. for Case01n11_on_ET I-129

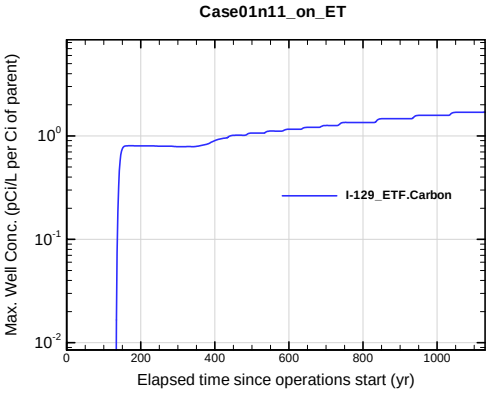

Figure A1B-898. Max. 100-m well conc. for Case01n11_on_ET I-129_ETF.Carbon

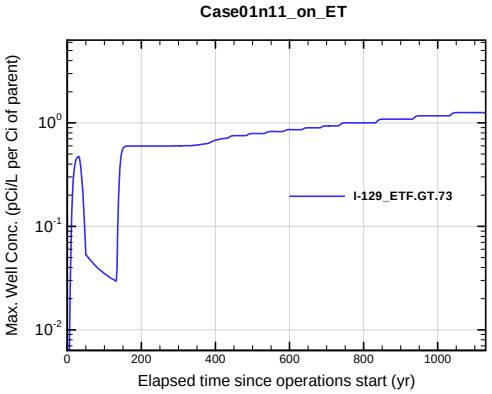

Figure A1B-899. Max. 100-m well conc. for Case01n11_on_ET I-129_ETF.GT.73

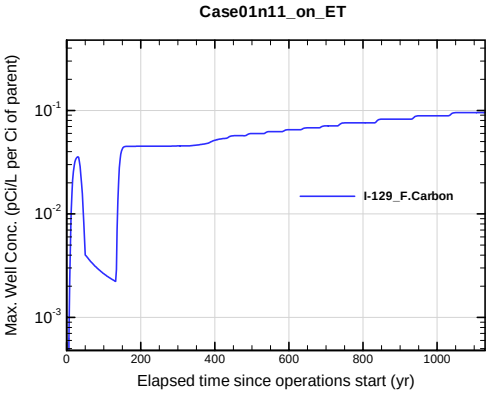

Figure A1B-900. Max. 100-m well conc. for Case01n11_on_ET I-129_F.Carbon

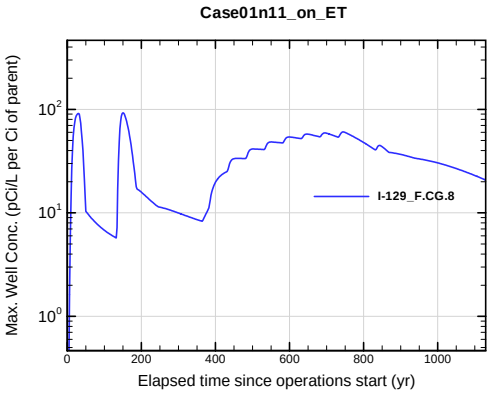

Figure A1B-901. Max. 100-m well conc. for Case01n11_on_ET I-129_F.CG.8

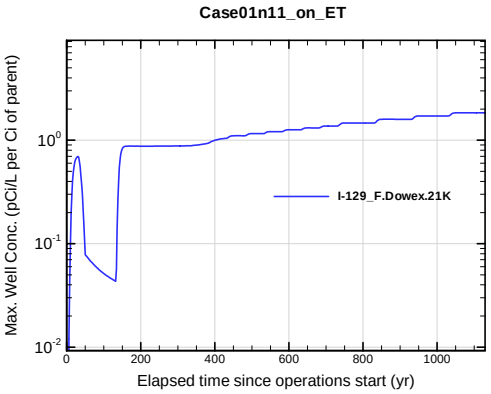

Figure A1B-902. Max. 100-m well conc. for Case01n11_on_ET I-129_F.Dowex.21K

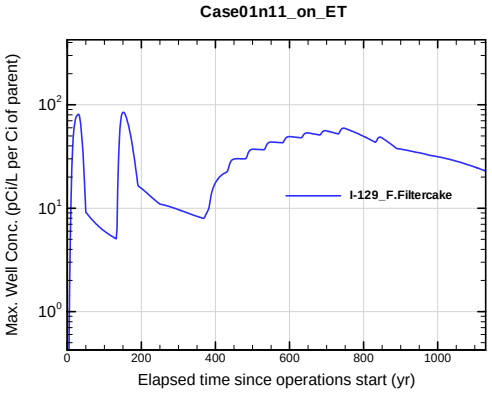

Figure A1B-903. Max. 100-m well conc. for Case01n11_on_ET I-129_F.Filtercake

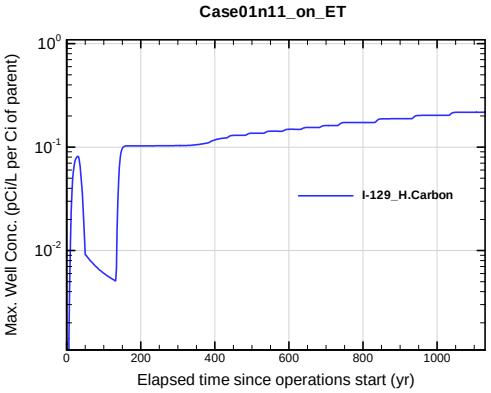

Figure A1B-904. Max. 100-m well conc. for Case01n11_on_ET I-129_H.Carbon

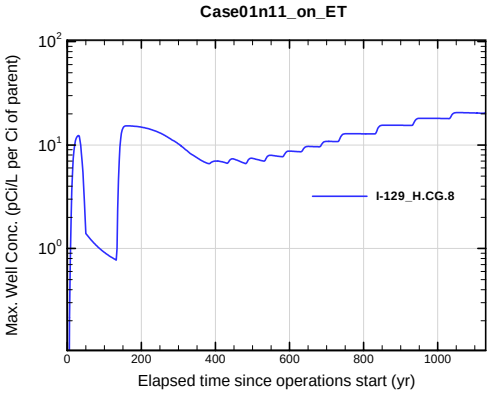

Figure A1B-905. Max. 100-m well conc. for Case01n11_on_ET I-129_H.CG.8

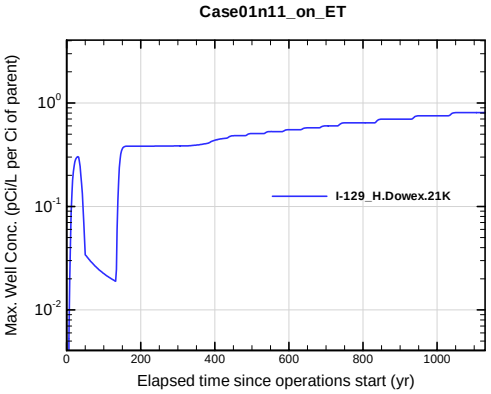

Figure A1B-906. Max. 100-m well conc. for Case01n11_on_ET I-129_H.Dowex.21K

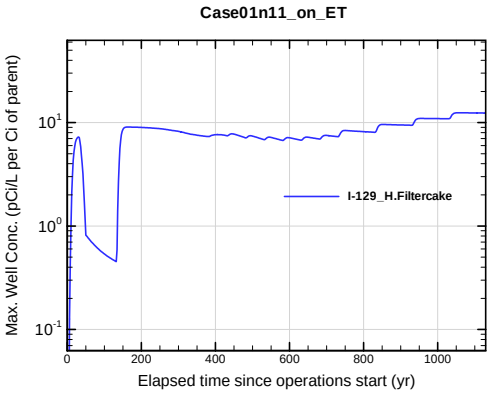

Figure A1B-907. Max. 100-m well conc. for Case01n11_on_ET I-129_H.Filtercake

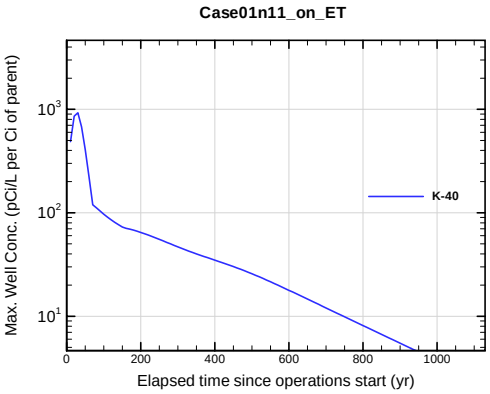

Figure A1B-908. Max. 100-m well conc. for Case01n11_on_ET K-40

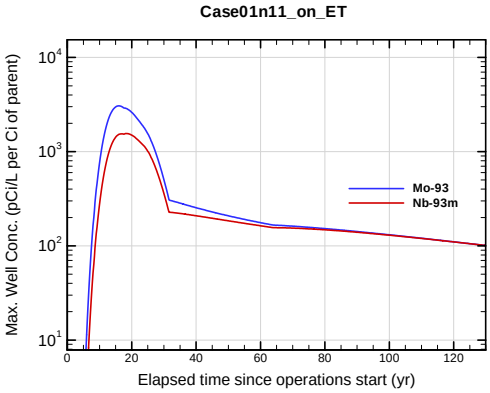

Figure A1B-909. Max. 100-m well conc. for Case01n11_on_ET Mo-93

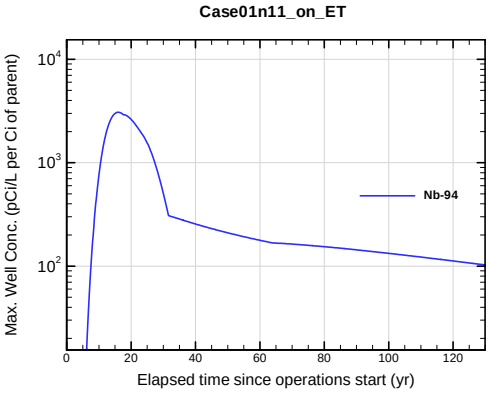

Figure A1B-910. Max. 100-m well conc. for Case01n11_on_ET Nb-94

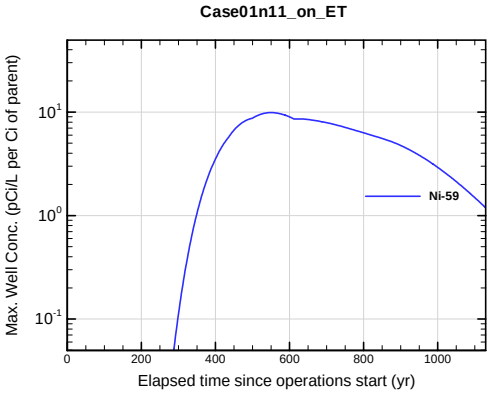

Figure A1B-911. Max. 100-m well conc. for Case01n11_on_ET Ni-59

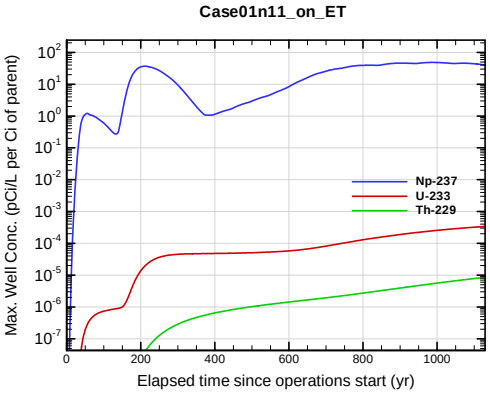

Figure A1B-912. Max. 100-m well conc. for Case01n11_on_ET Np-237

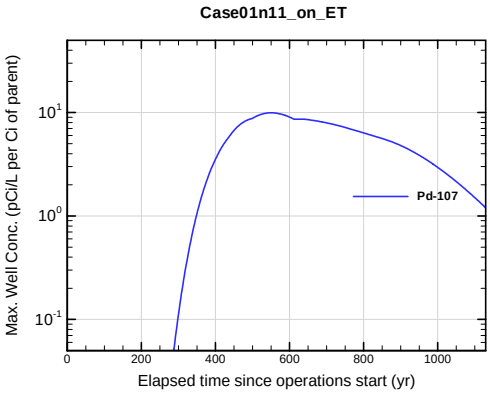

Figure A1B-913. Max. 100-m well conc. for Case01n11_on_ET Pd-107

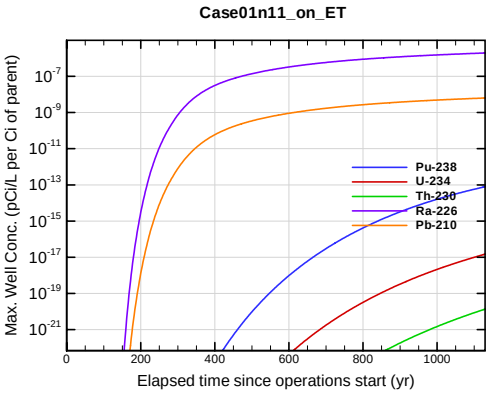

Figure A1B-914. Max. 100-m well conc. for Case01n11_on_ET Pu-238

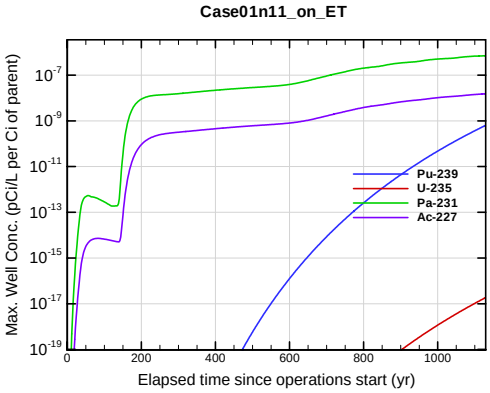

Figure A1B-915. Max. 100-m well conc. for Case01n11_on_ET Pu-239

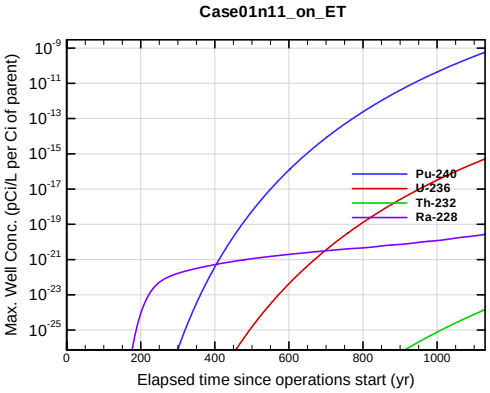

Figure A1B-916. Max. 100-m well conc. for Case01n11_on_ET Pu-240

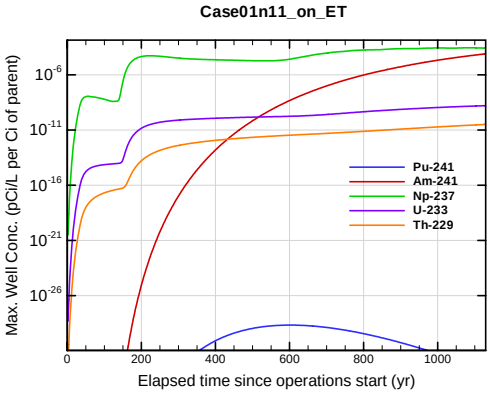

Figure A1B-917. Max. 100-m well conc. for Case01n11_on_ET Pu-241

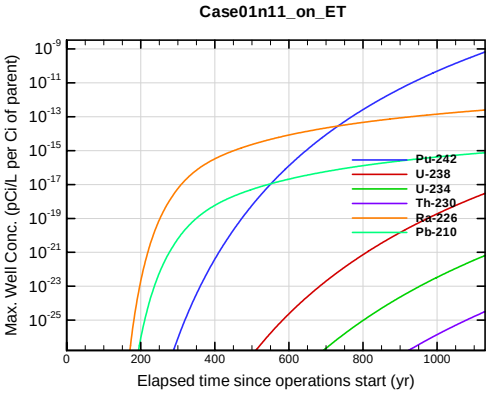

Figure A1B-918. Max. 100-m well conc. for Case01n11_on_ET Pu-242

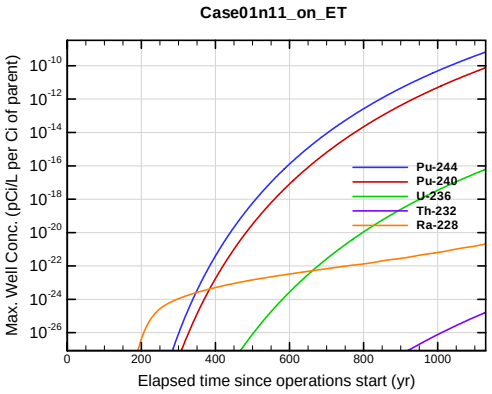

Figure A1B-919. Max. 100-m well conc. for Case01n11_on_ET Pu-244

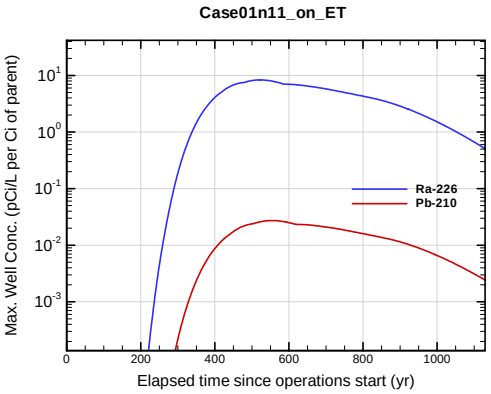

Figure A1B-920. Max. 100-m well conc. for Case01n11_on_ET Ra-226

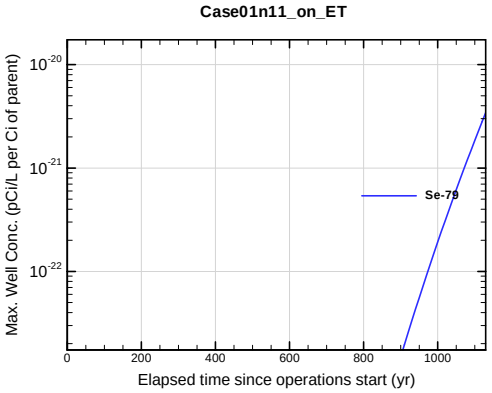

Figure A1B-921. Max. 100-m well conc. for Case01n11_on_ET Se-79

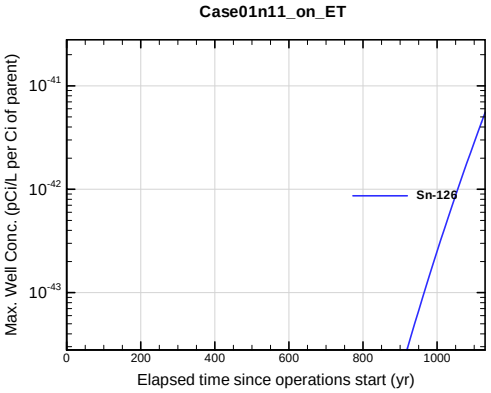

Figure A1B-922. Max. 100-m well conc. for Case01n11_on_ET Sn-126

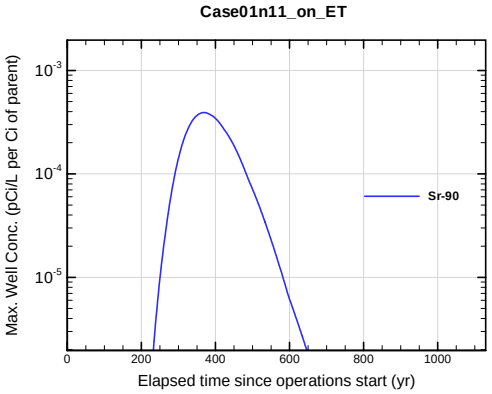

Figure A1B-923. Max. 100-m well conc. for Case01n11_on_ET Sr-90

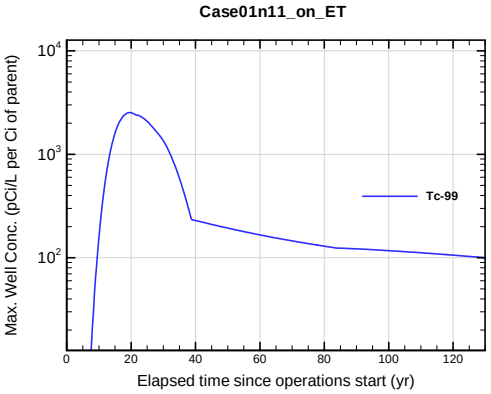

Figure A1B-924. Max. 100-m well conc. for Case01n11_on_ET Tc-99

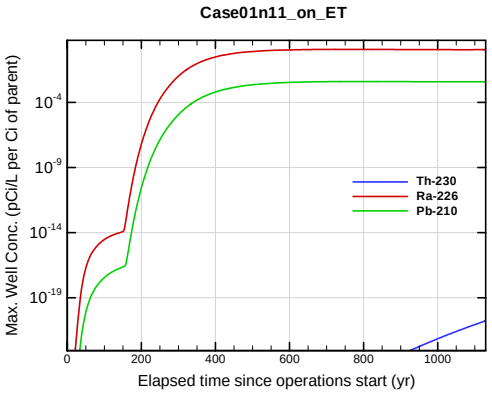

Figure A1B-925. Max. 100-m well conc. for Case01n11_on_ET Th-230

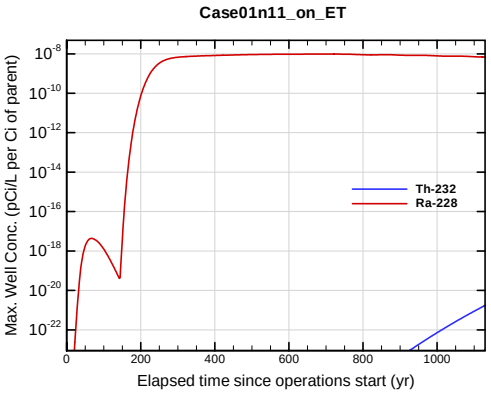

Figure A1B-926. Max. 100-m well conc. for Case01n11_on_ET Th-232

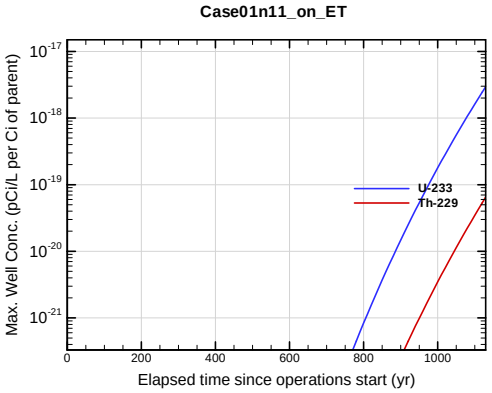

Figure A1B-927. Max. 100-m well conc. for Case01n11_on_ET U-233

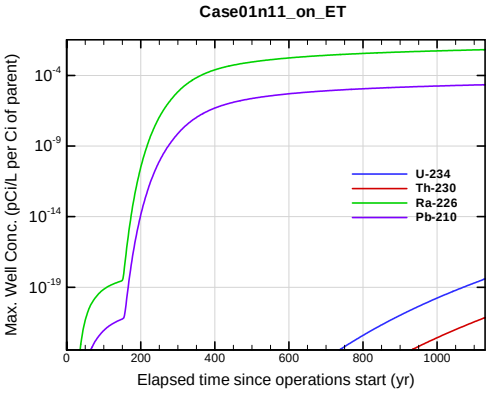

Figure A1B-928. Max. 100-m well conc. for Case01n11_on_ET U-234

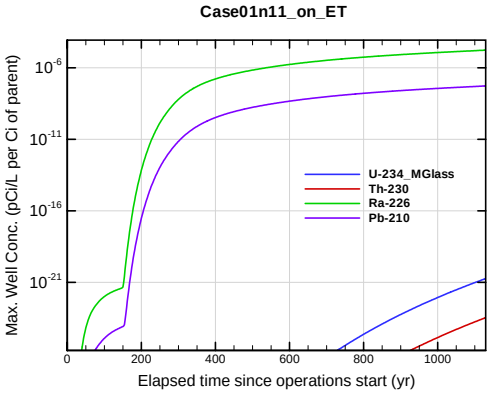

Figure A1B-929. Max. 100-m well conc. for Case01n11_on_ET U-234_MGlass

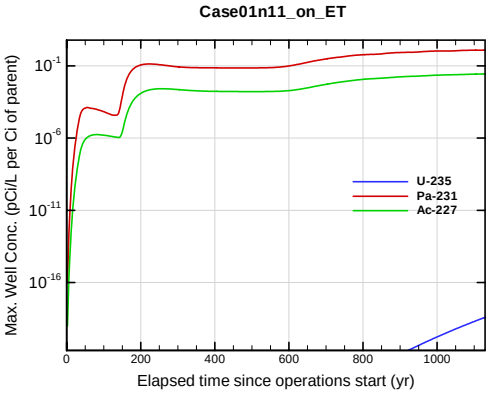

Figure A1B-930. Max. 100-m well conc. for Case01n11_on_ET U-235

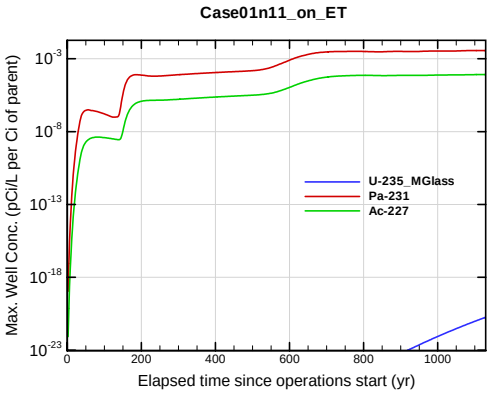

Figure A1B-931. Max. 100-m well conc. for Case01n11_on_ET U-235_MGlass

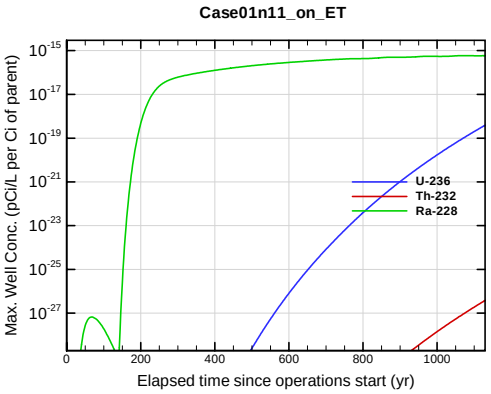

Figure A1B-932. Max. 100-m well conc. for Case01n11_on_ET U-236

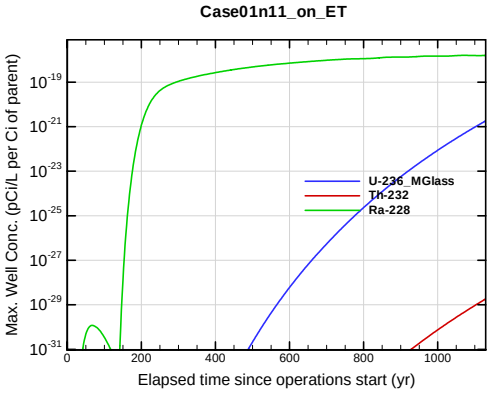

Figure A1B-933. Max. 100-m well conc. for Case01n11_on_ET U-236_MGlass

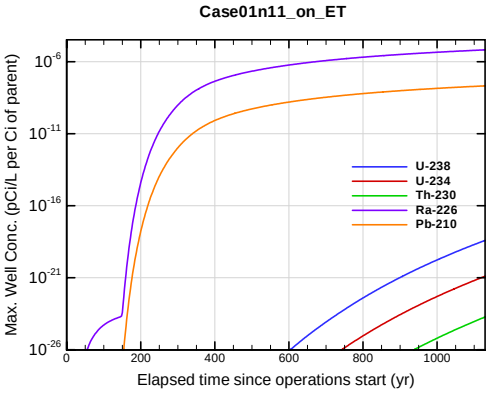

Figure A1B-934. Max. 100-m well conc. for Case01n11_on_ET U-238

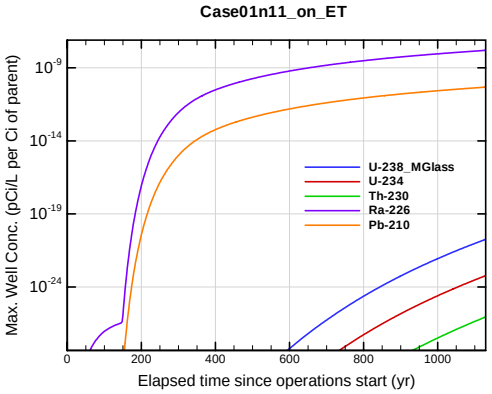

Figure A1B-935. Max. 100-m well conc. for Case01n11_on_ET U-238_MGlass

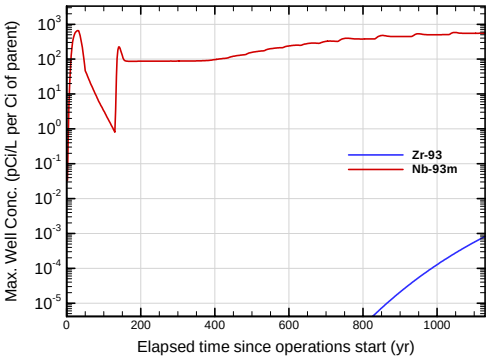

Figure A1B-936. Max. 100-m well conc. for Case01n11_on_ET Zr-93

APPENDIX A1C

Probabilistic Model

Uncertainty and Maximum Impact

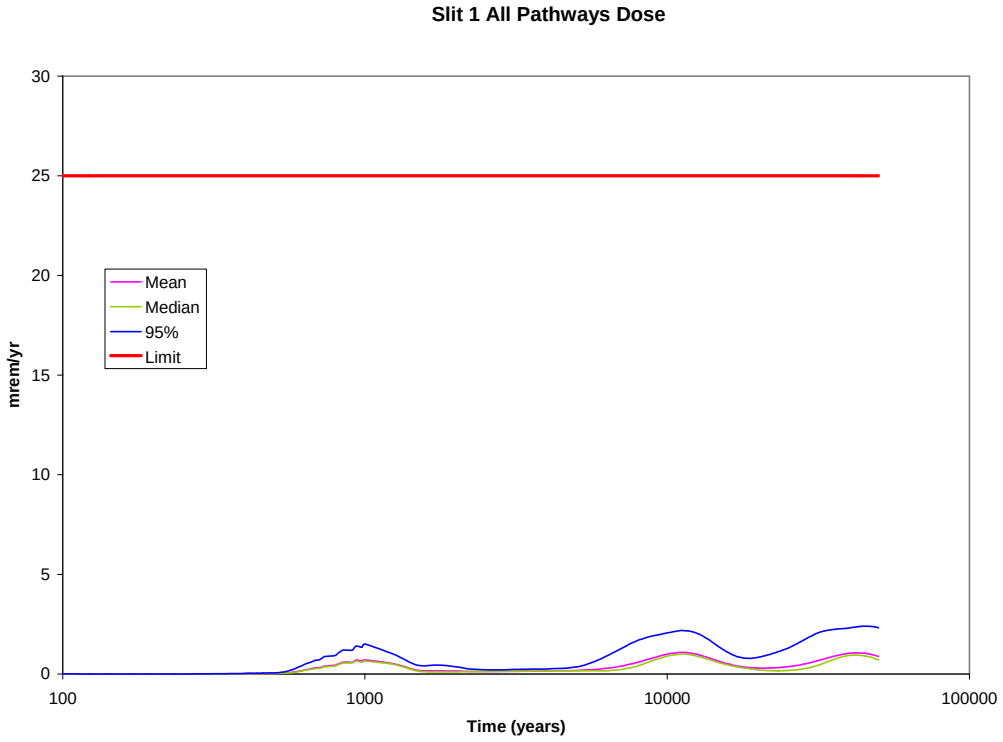

Figure A1C-1 Slit Trench 1 All Pathways Dose Uncertainty

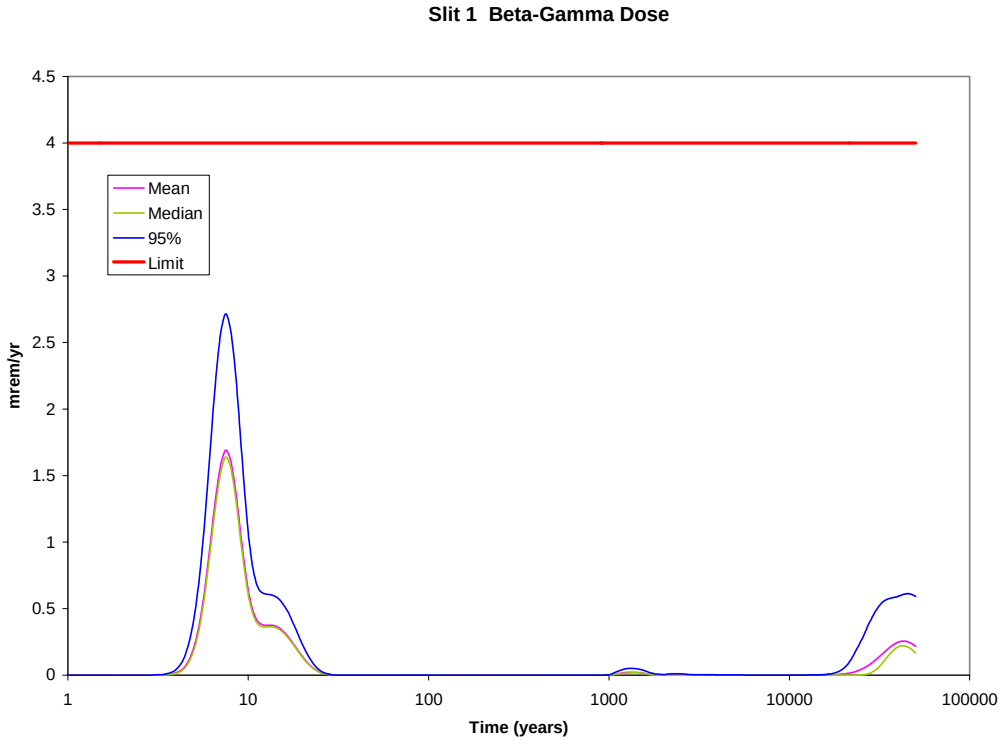

Figure A1C-2 Slit Trench 1 Beta-Gamma Dose Uncertainty

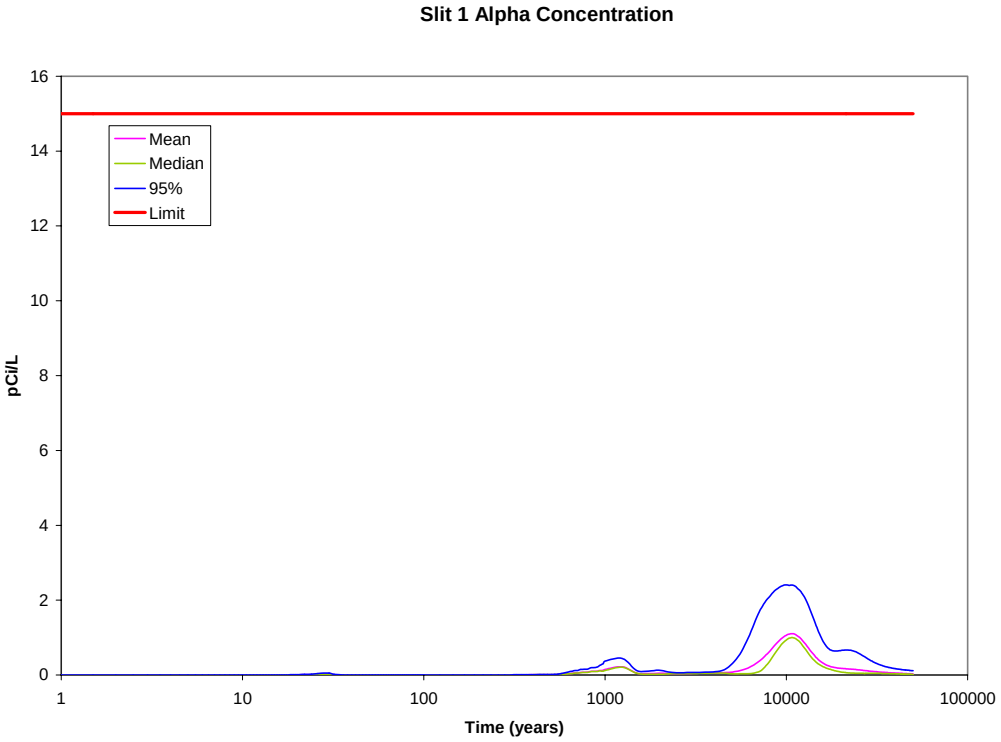

Figure A1C-3 Slit Trench 1 Gross Alpha Concentration Uncertainty

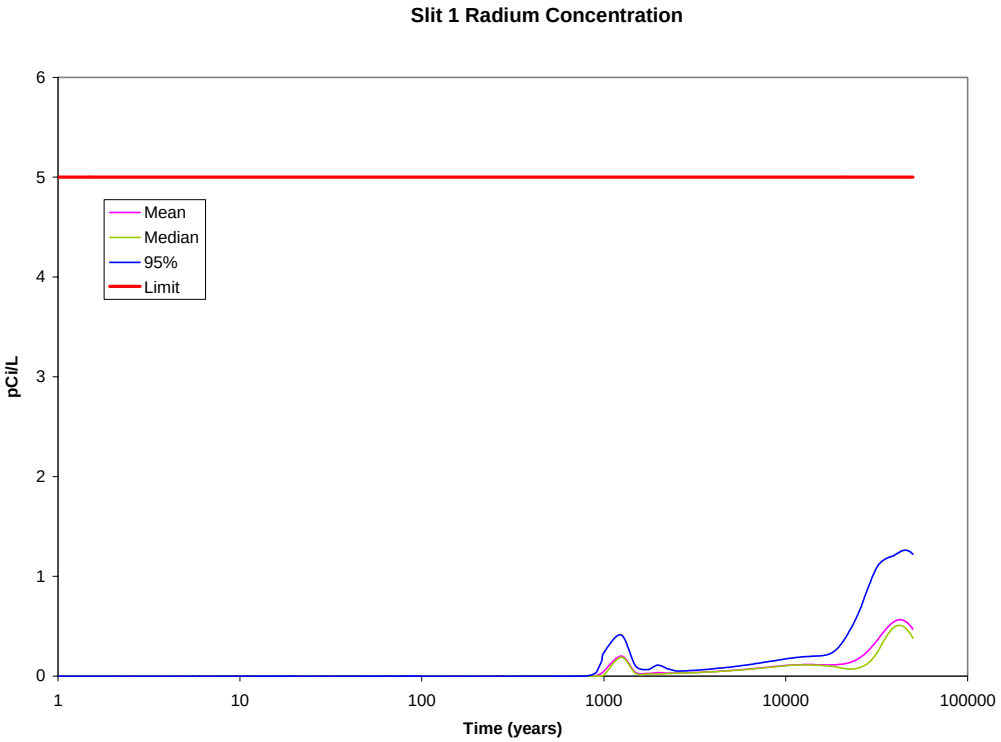

Figure A1C-4 Slit Trench 1 Radium Concentration Uncertainty

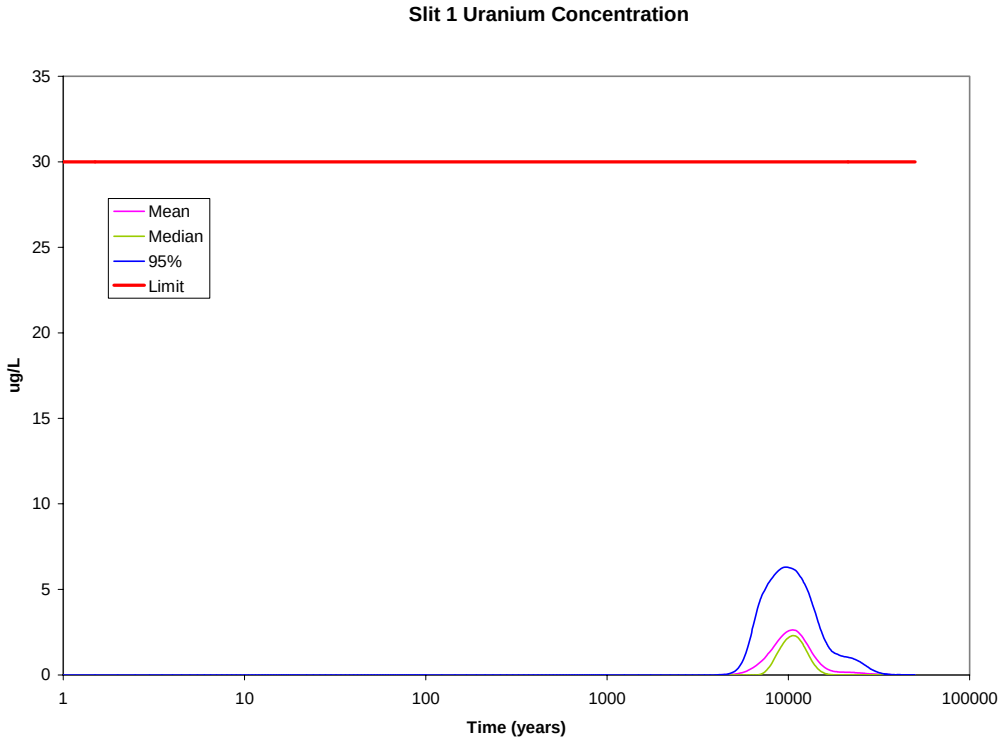

Figure A1C-5 Slit Trench 1 Uranium Concentration Uncertainty

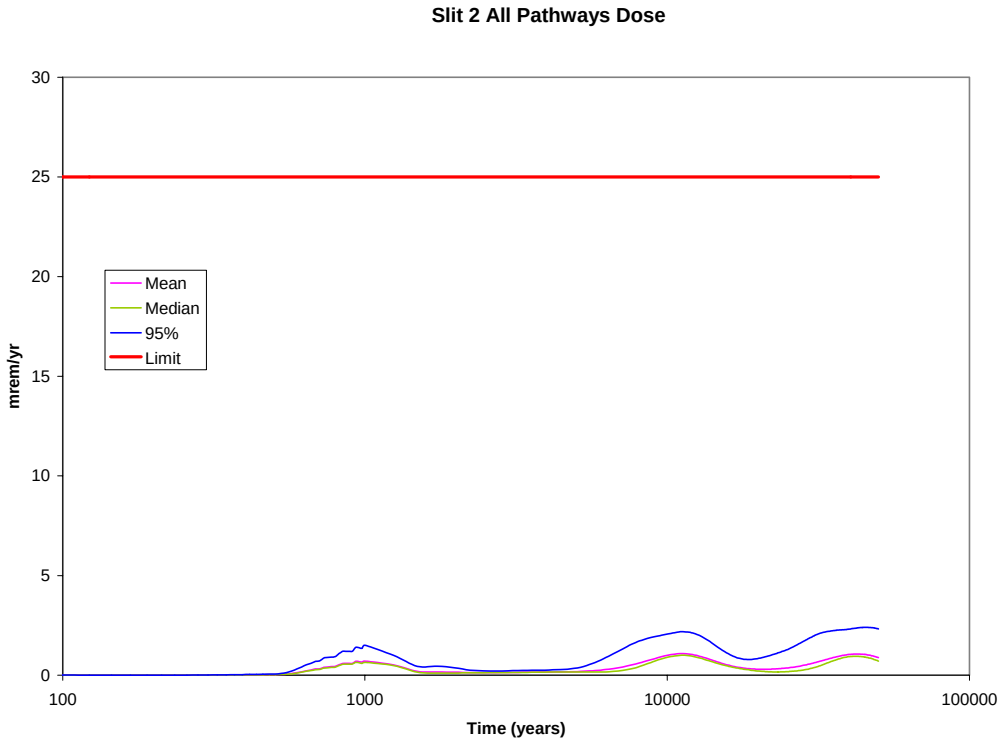

Figure A1C-6 Slit Trench 2 All Pathways Dose Uncertainty

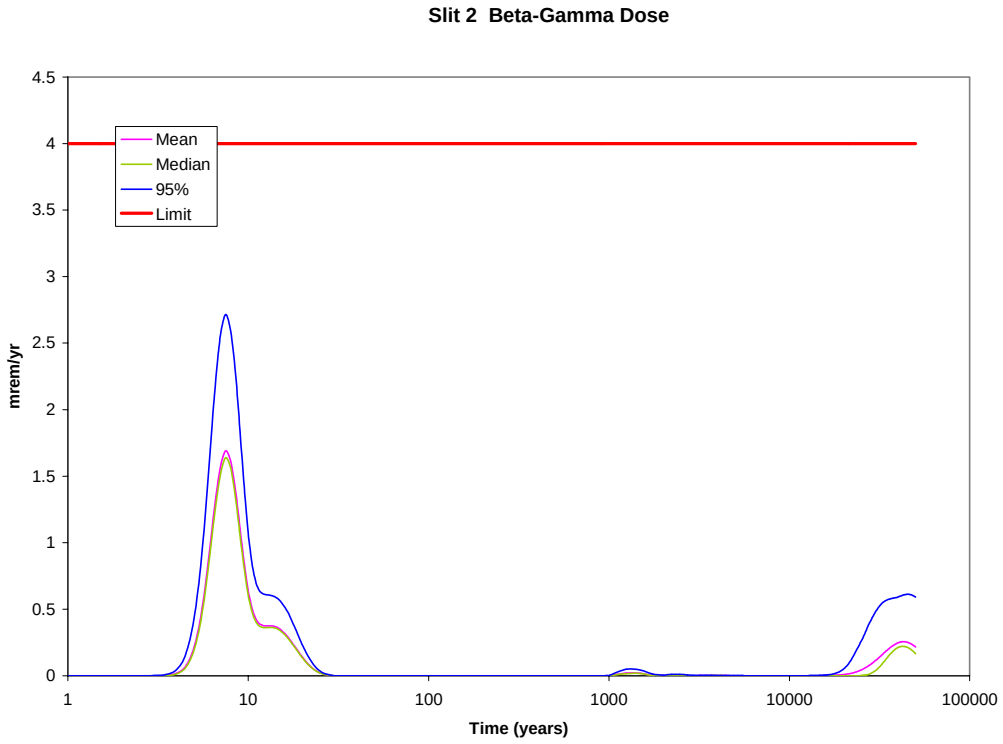

Figure A1C-7 Slit Trench 2 Beta-Gamma Dose Uncertainty

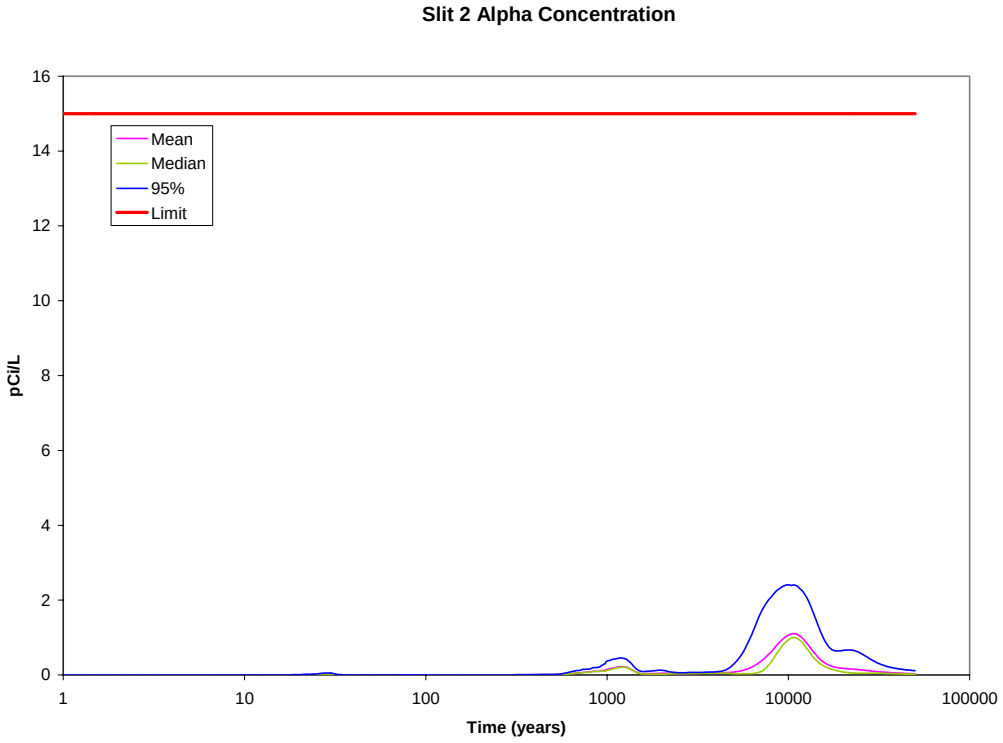

Figure A1C-8 Slit Trench 2 Gross Alpha Concentration Uncertainty

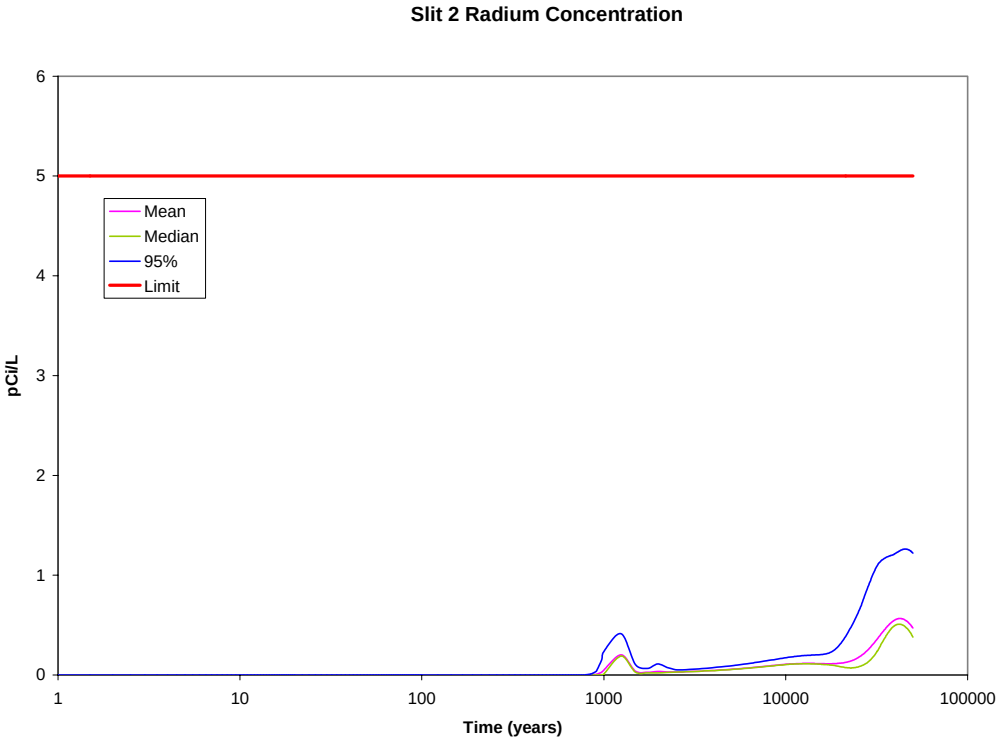

Figure A1C-9 Slit Trench 2 Radium Concentration Uncertainty

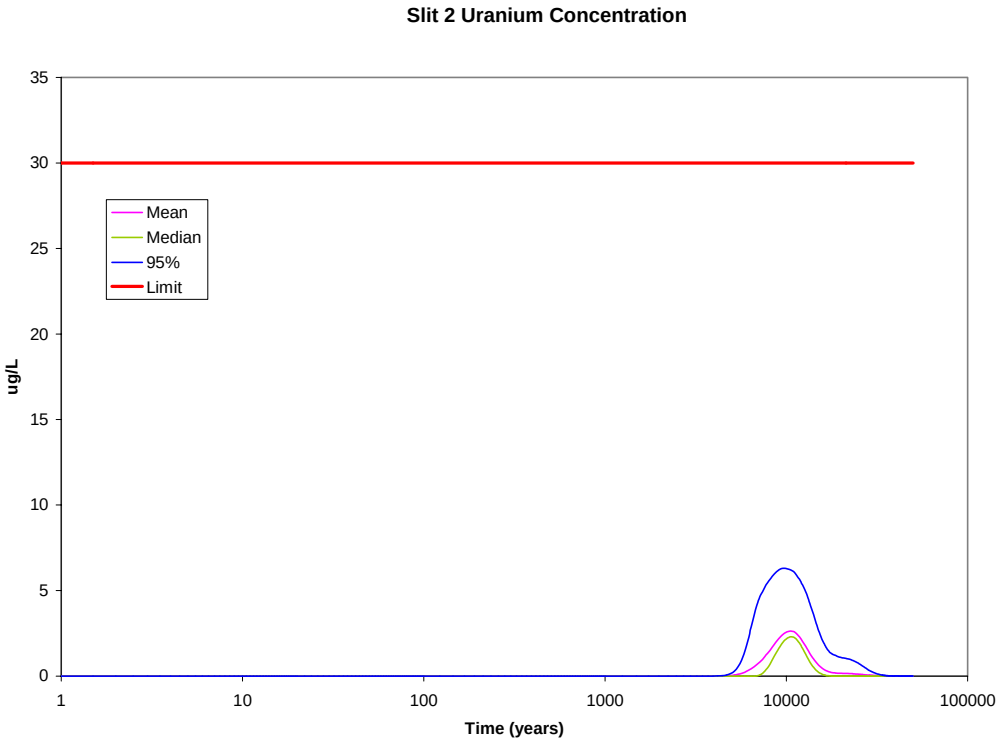

Figure A1C-10 Slit Trench 2 Uranium Concentration Uncertainty

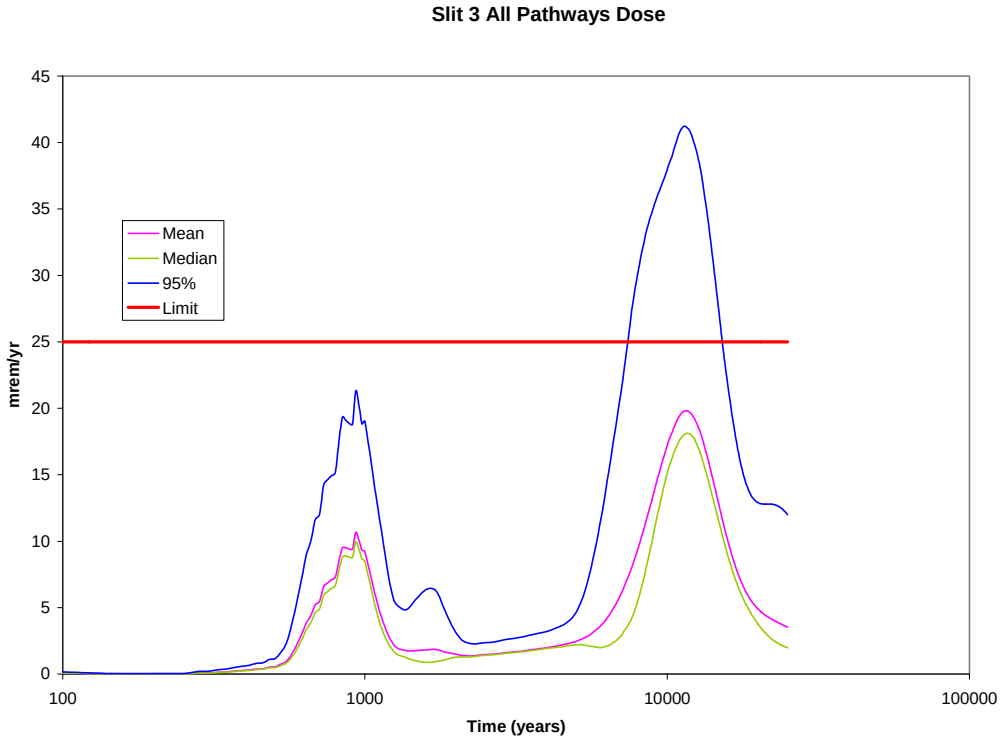

Figure A1C-11 Slit Trench 3 All Pathways Dose Uncertainty

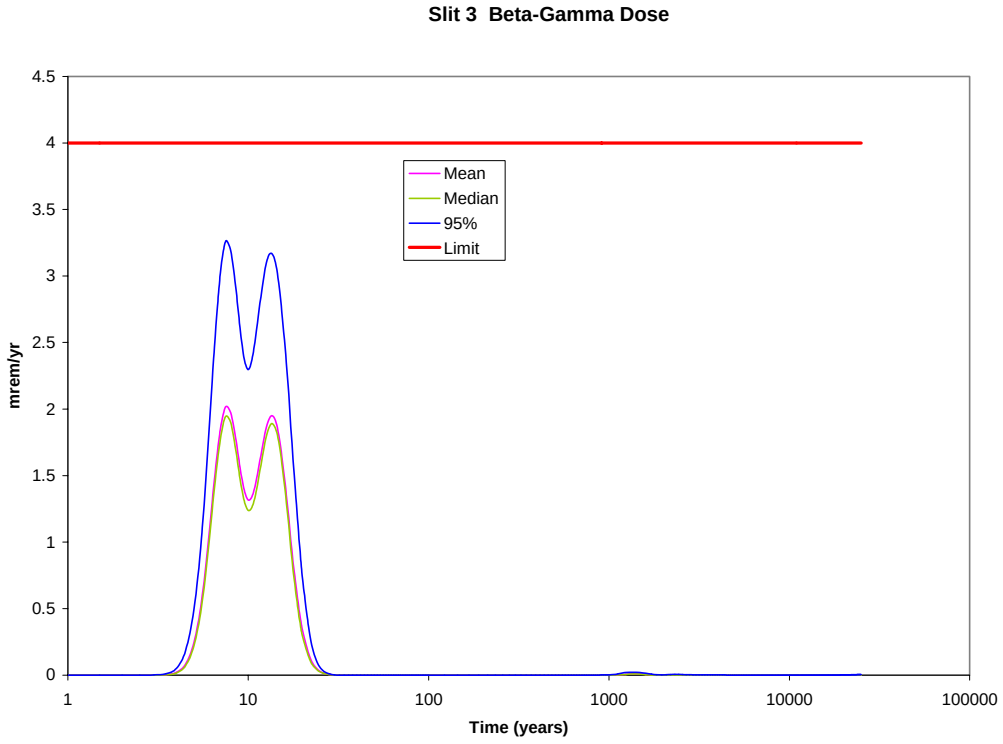

Figure A1C-12 Slit Trench 3 Beta-Gamma Dose Uncertainty

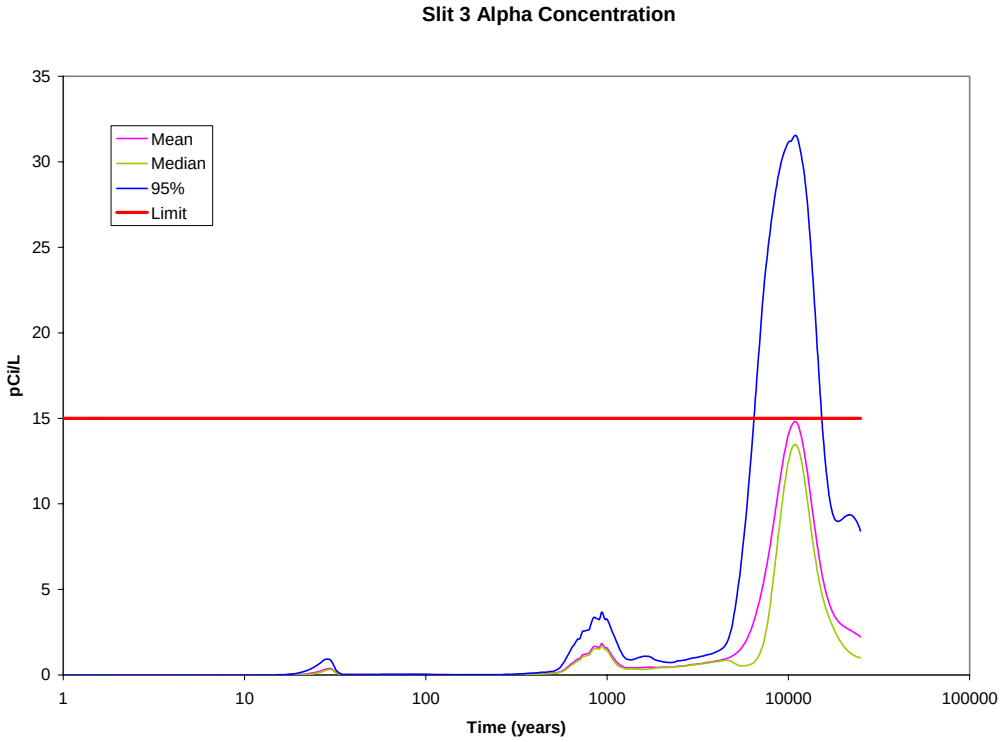

Figure A1C-13 Slit Trench 3 Gross Alpha Concentration Uncertainty

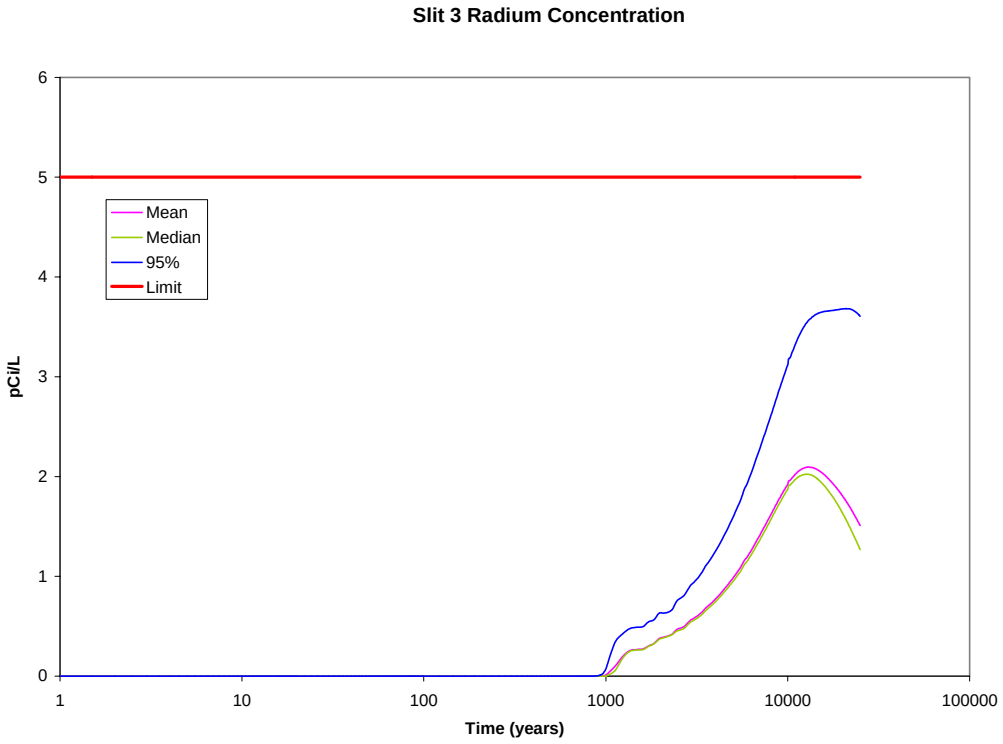

Figure A1C-14 Slit Trench 3 Radium Concentration Uncertainty

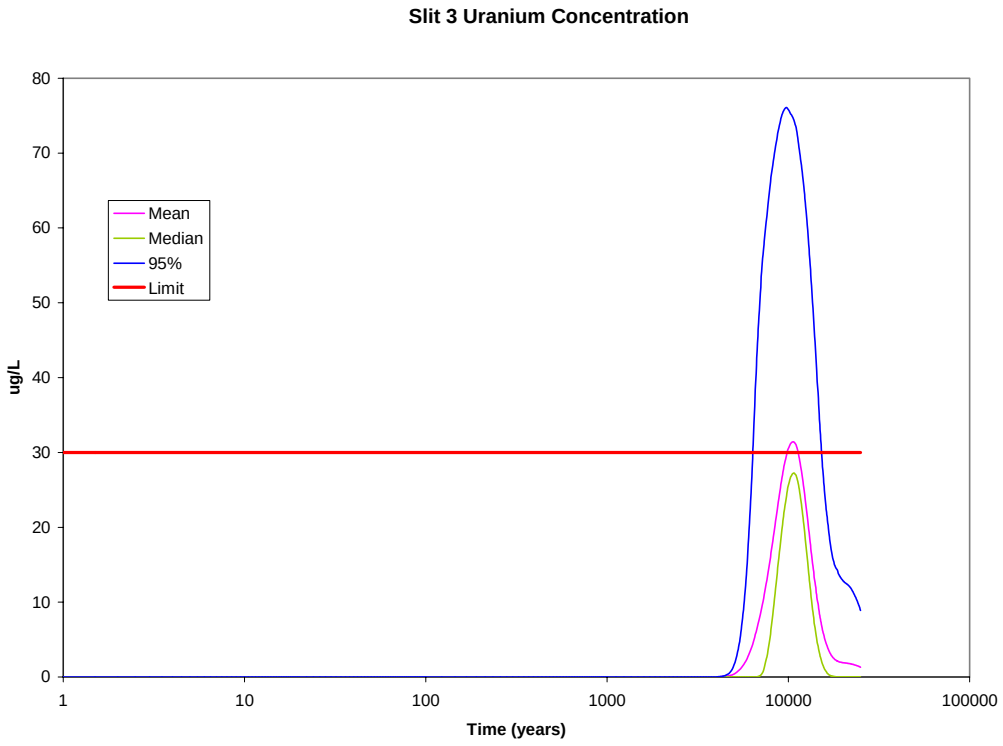

Figure A1C-15 Slit Trench 3 Uranium Concentration Uncertainty

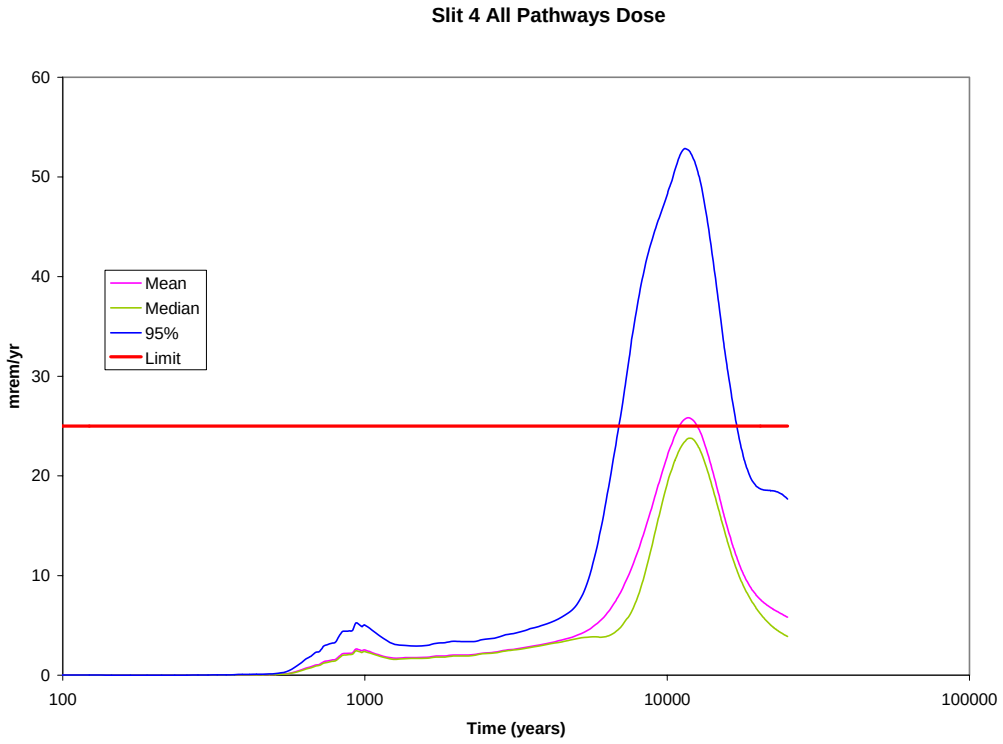

Figure A1C-16 Slit Trench 4 All Pathways Dose Uncertainty

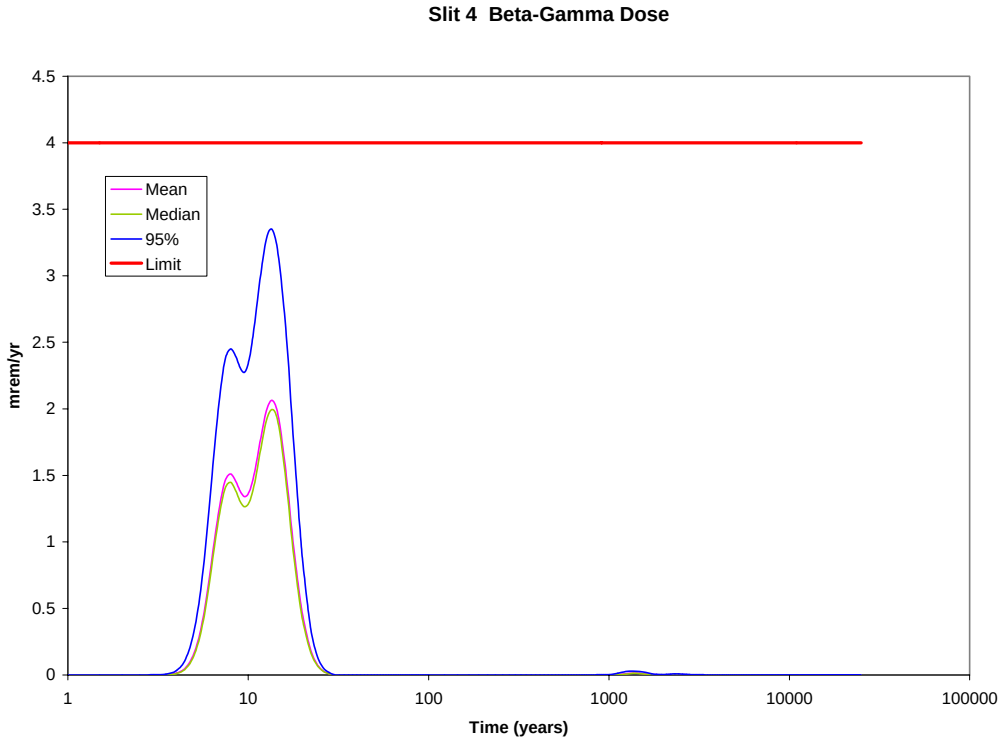

Figure A1C-17 Slit Trench 4 Beta-Gamma Dose Uncertainty

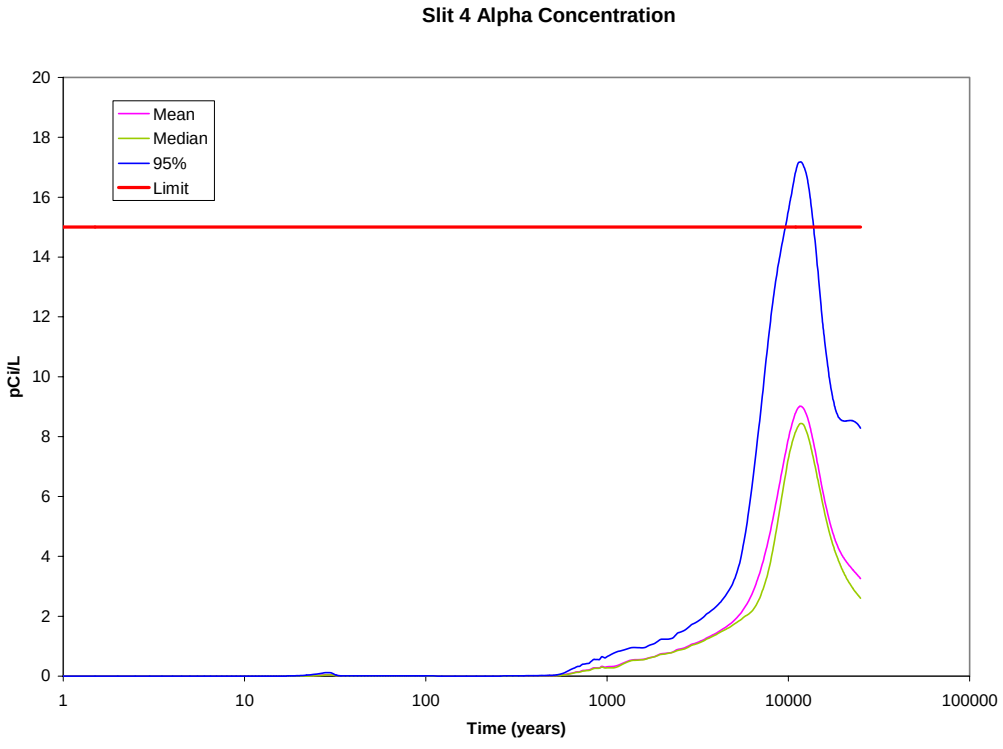

Figure A1C-18 Slit Trench 4 Gross Alpha Concentration Uncertainty

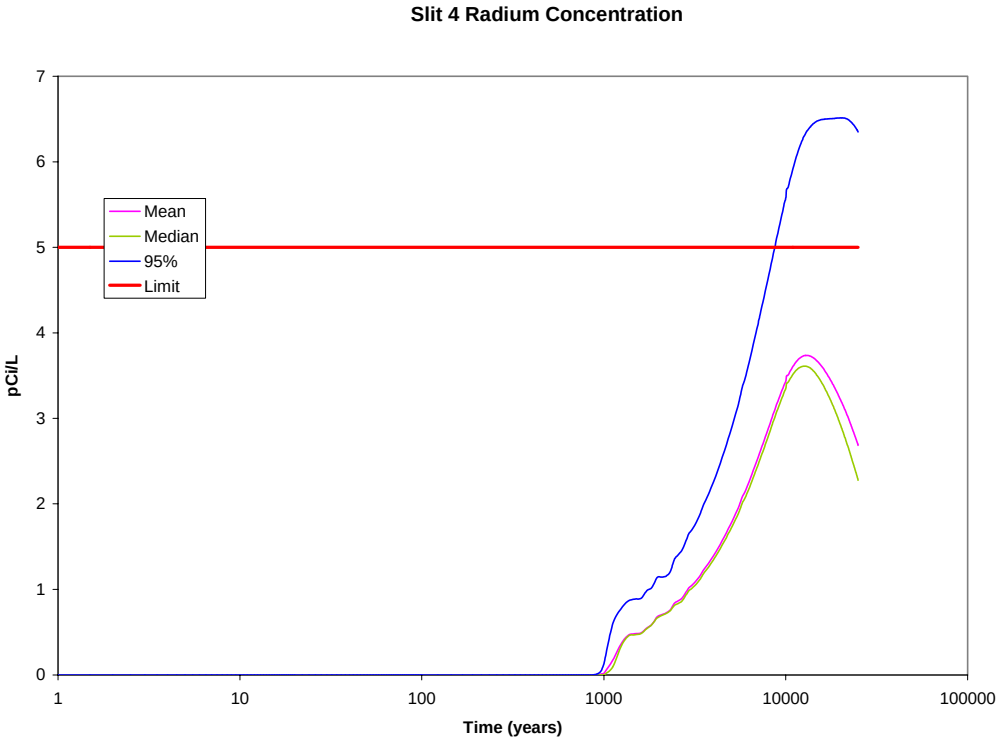

Figure A1C-19 Slit Trench 4 Radium Concentration Uncertainty

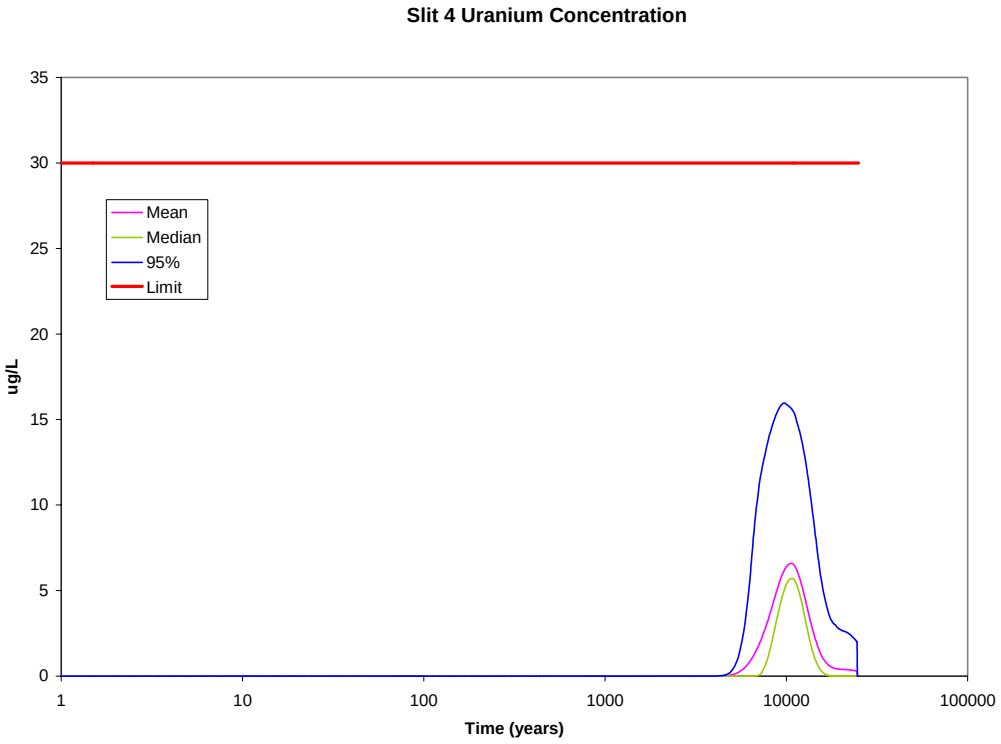

Figure A1C-20 Slit Trench 4 Uranium Concentration Uncertainty

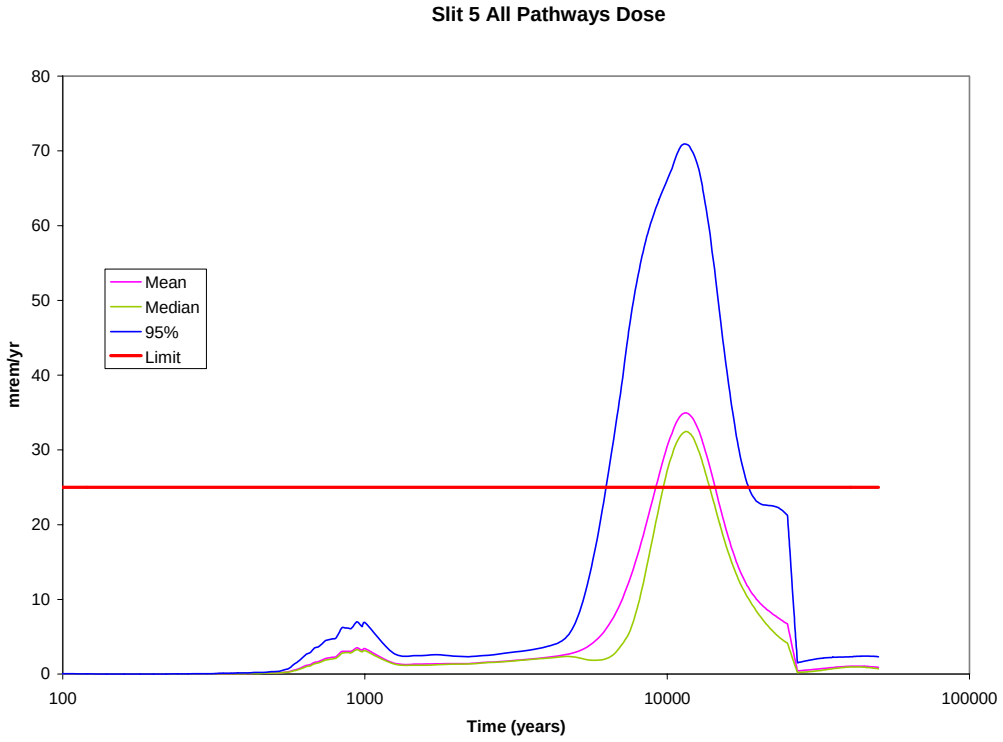

Figure A1C-21 Slit Trench 5 All Pathways Dose Uncertainty

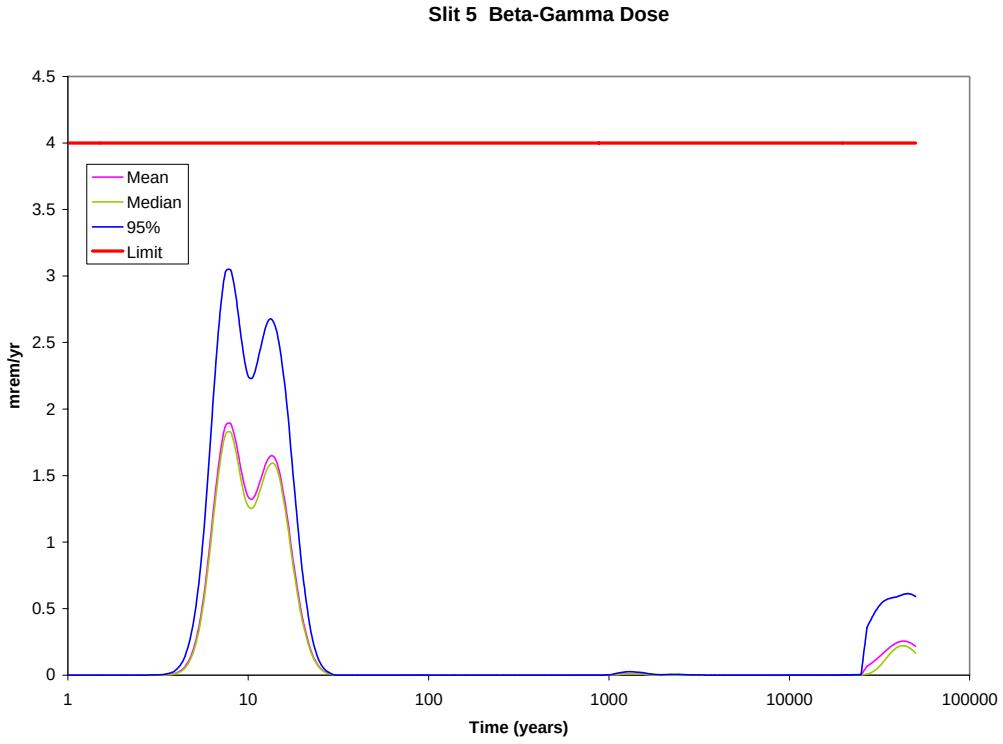

Figure A1C-22 Slit Trench 5 Beta-Gamma Dose Uncertainty

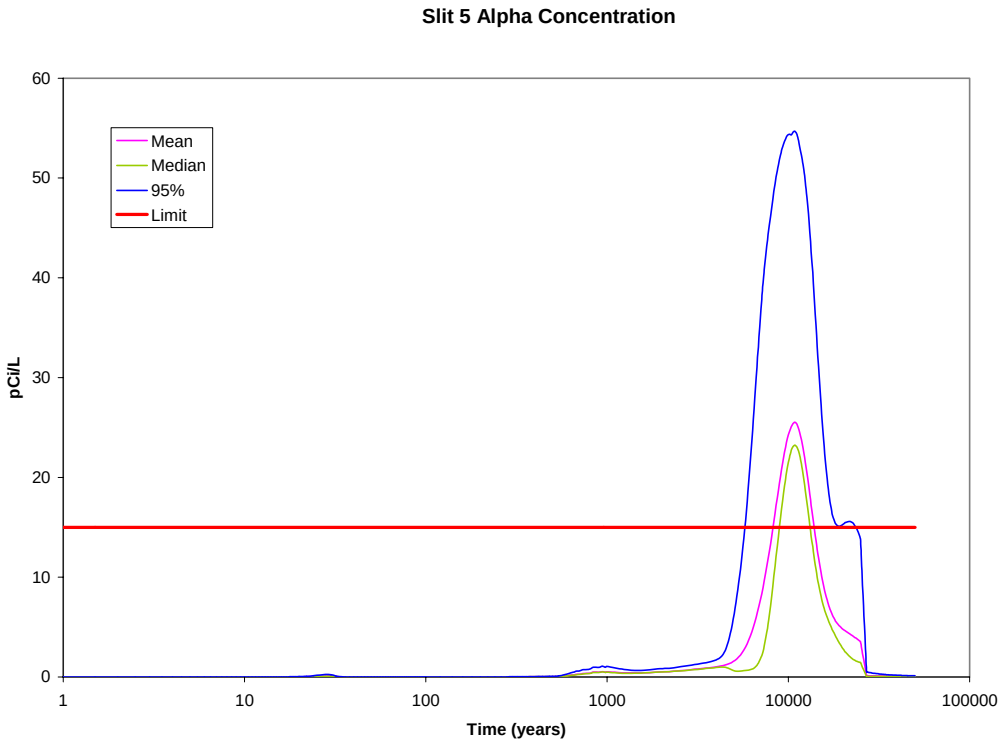

Figure A1C-23 Slit Trench 5 Gross Alpha Concentration Uncertainty

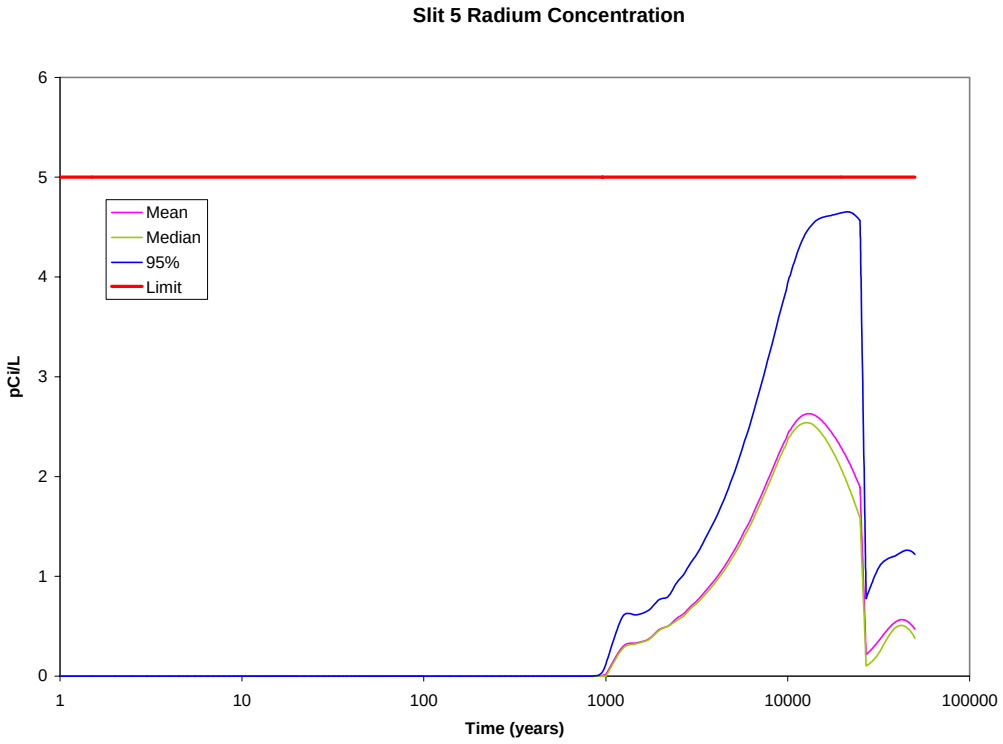

Figure A1C-24 Slit Trench 5 Radium Concentration Uncertainty

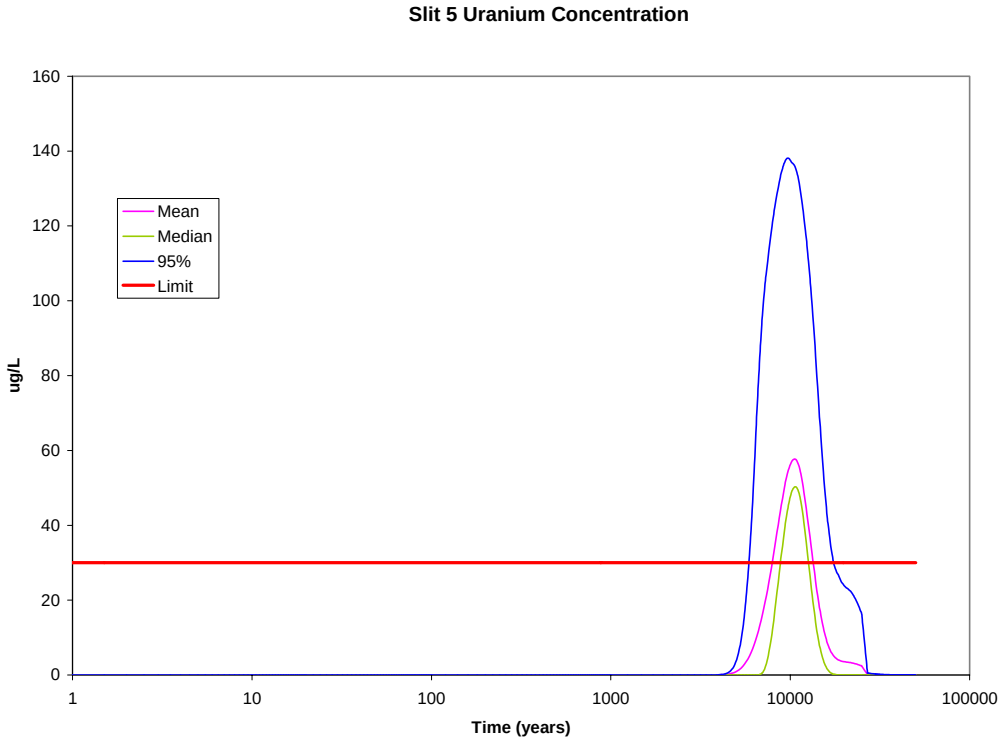

Figure A1C-25 Slit Trench 5 Uranium Concentration Uncertainty

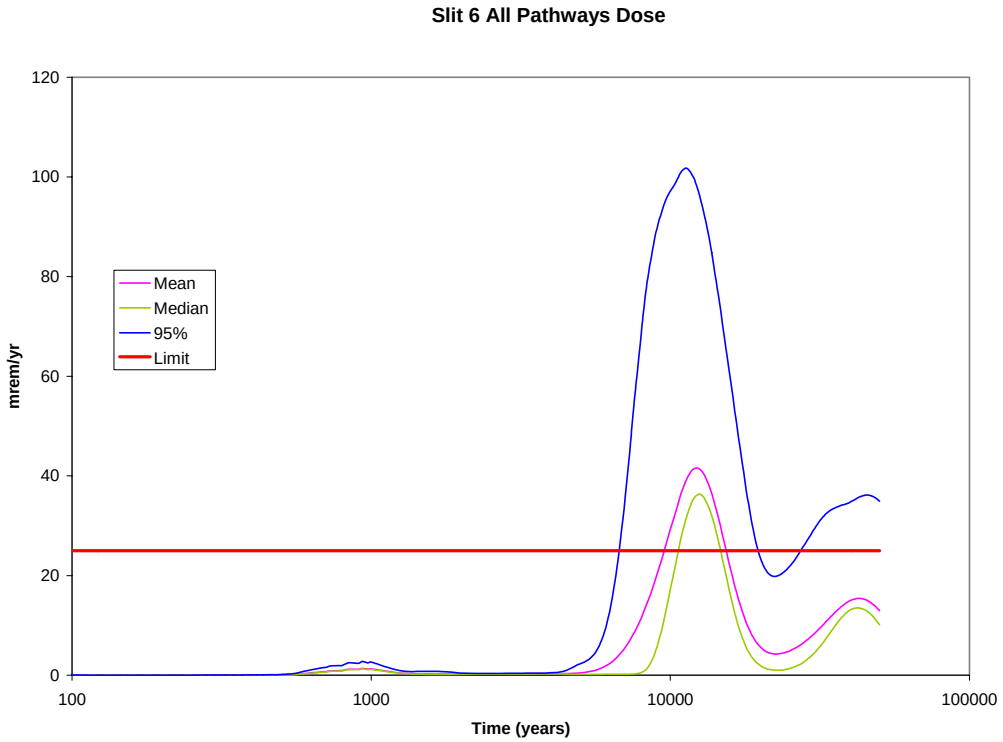

Figure A1C-26 Slit Trench 6 All Pathways Dose Uncertainty

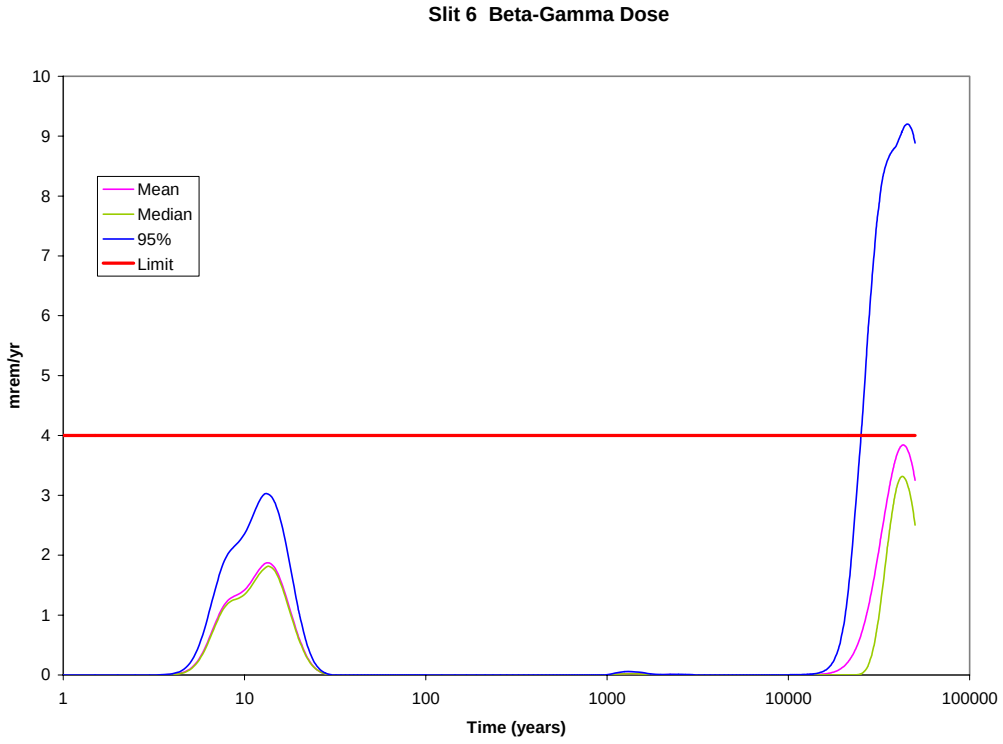

Figure A1C-27 Slit Trench 6 Beta-Gamma Dose Uncertainty

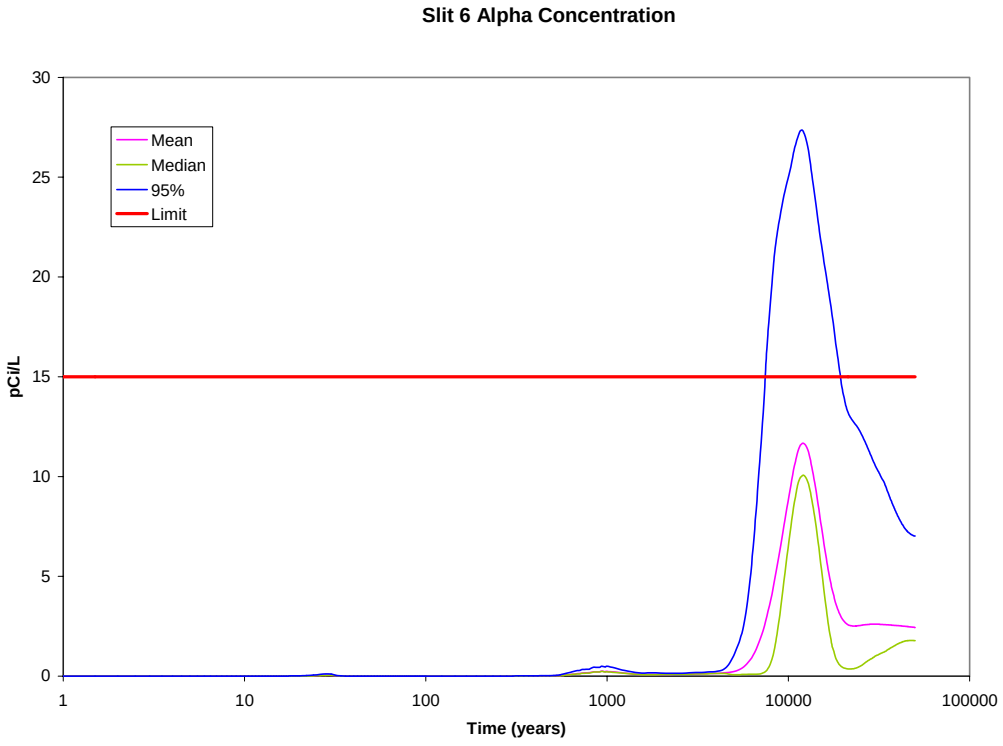

Figure A1C-28 Slit Trench 6 Gross Alpha Concentration Uncertainty

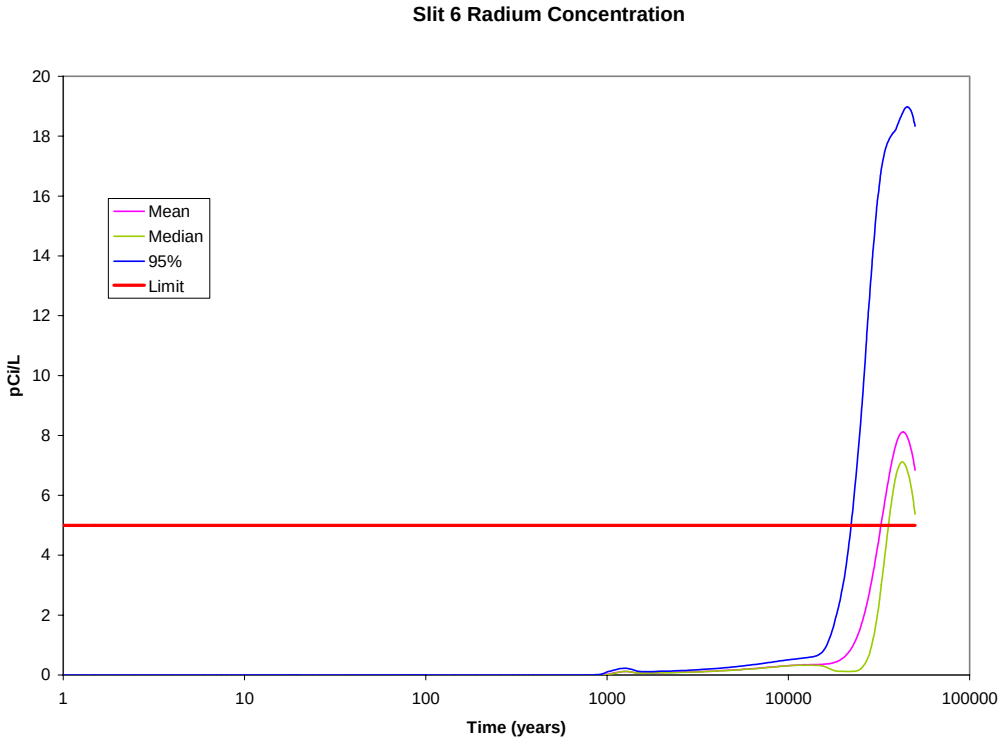

Figure A1C-29 Slit Trench 6 Radium Concentration Uncertainty

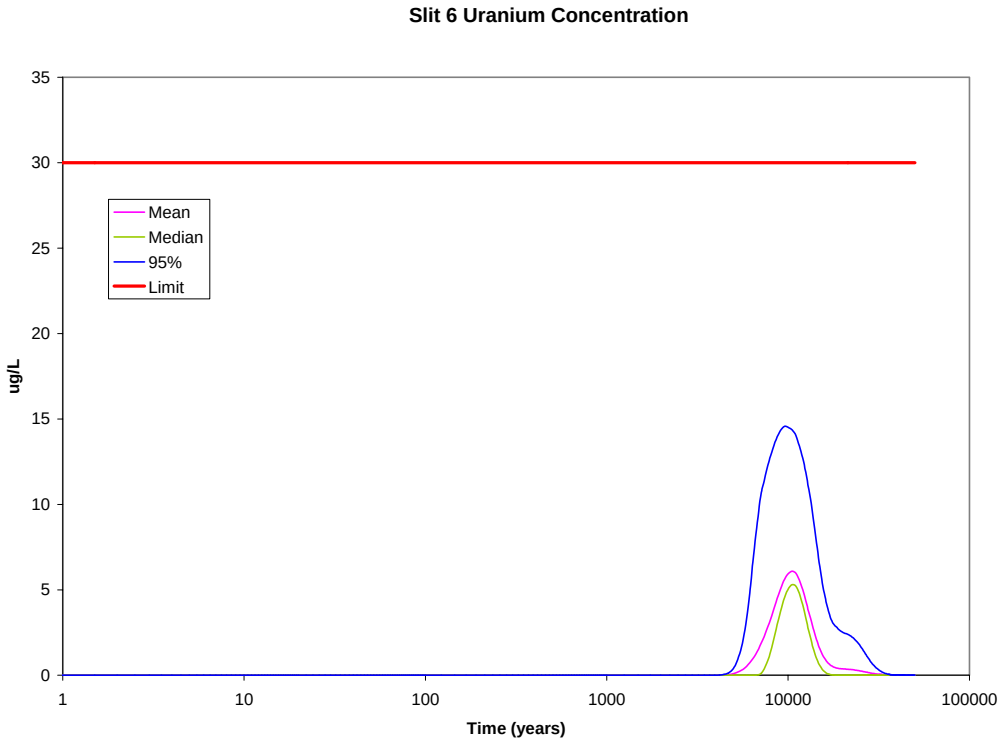

Figure A1C-30 Slit Trench 6 Uranium Concentration Uncertainty

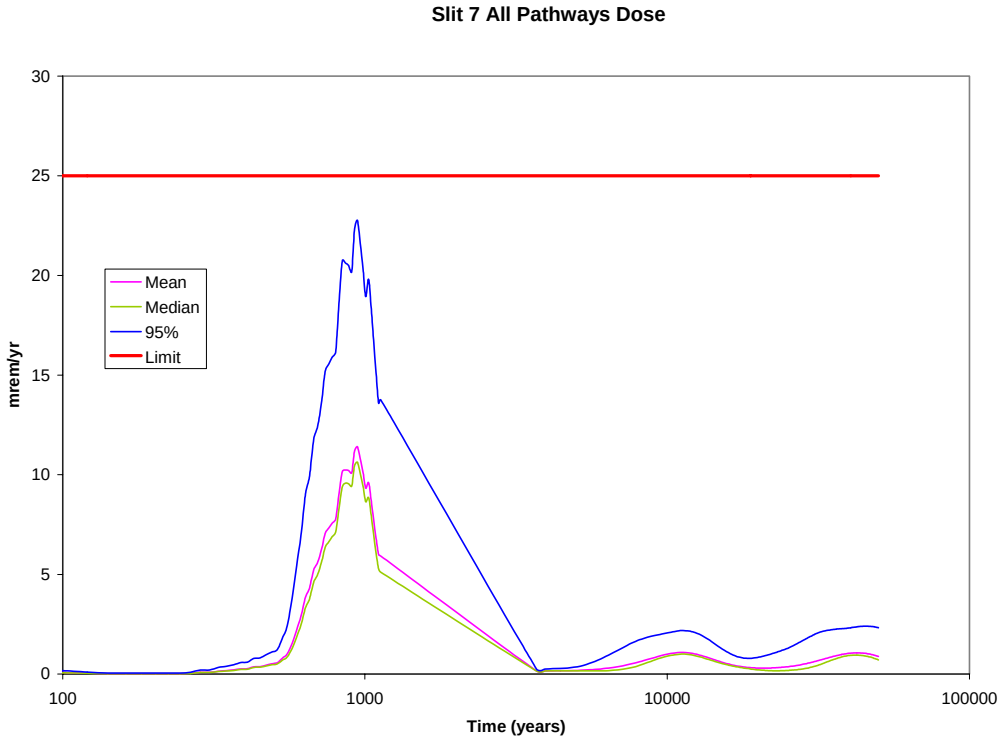

Figure A1C-31 Slit Trench 7 All Pathways Dose Uncertainty

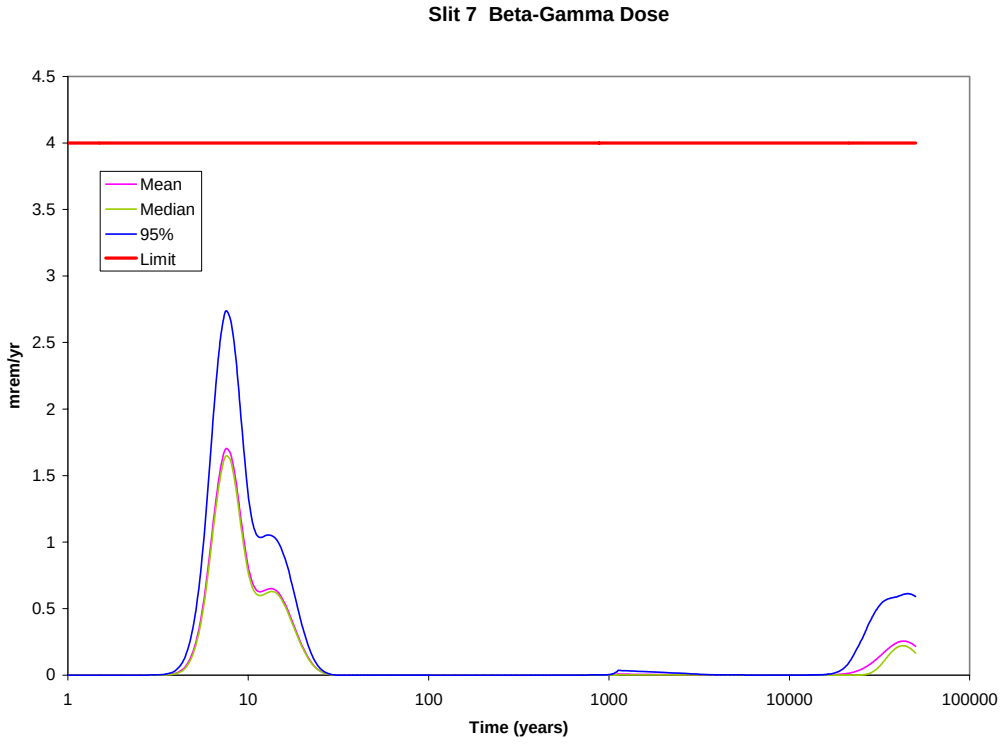

Figure A1C-32 Slit Trench 7 Beta-Gamma Dose Uncertainty

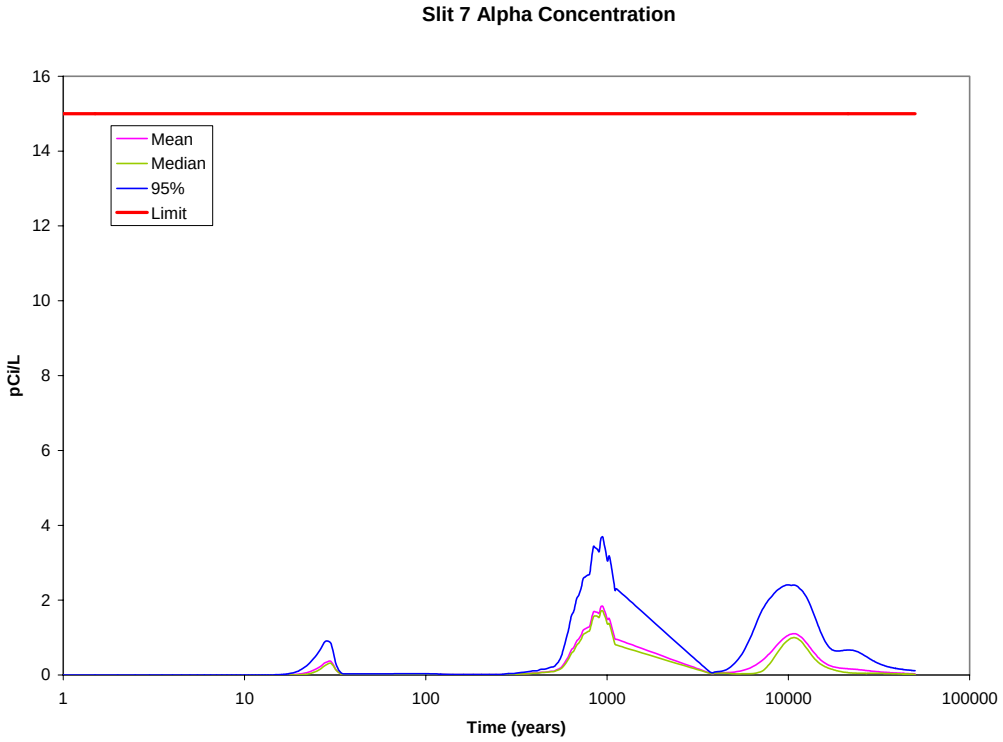

Figure A1C-33 Slit Trench 7 Gross Alpha Concentration Uncertainty

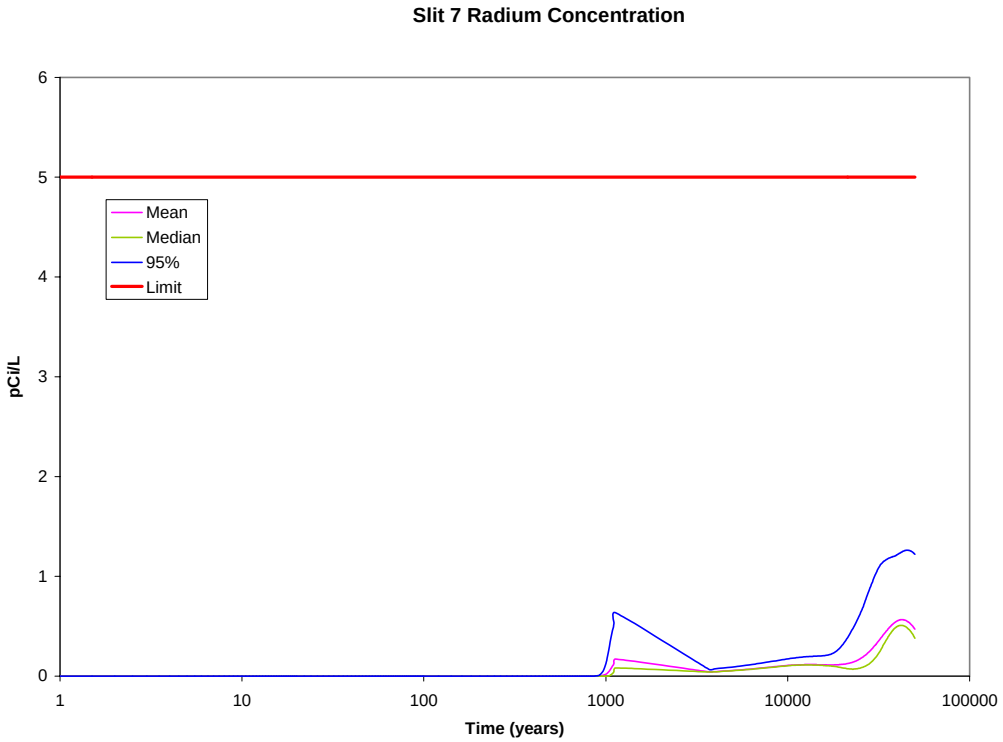

Figure A1C-34 Slit Trench 7 Radium Concentration Uncertainty

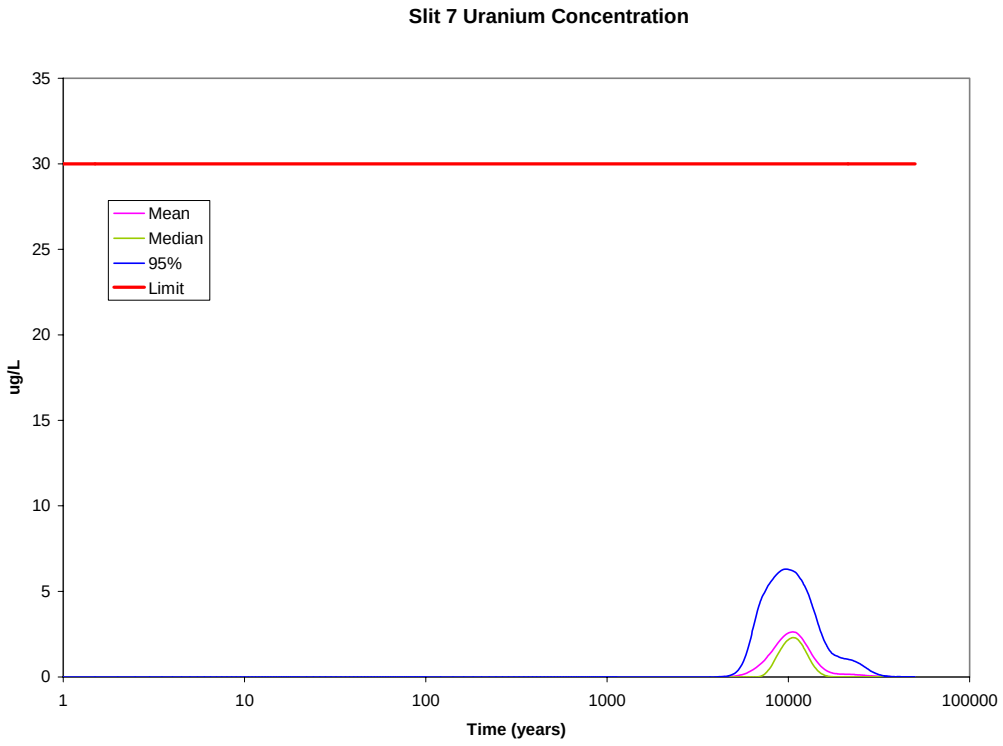

Figure A1C-35 Slit Trench 7 Uranium Concentration Uncertainty

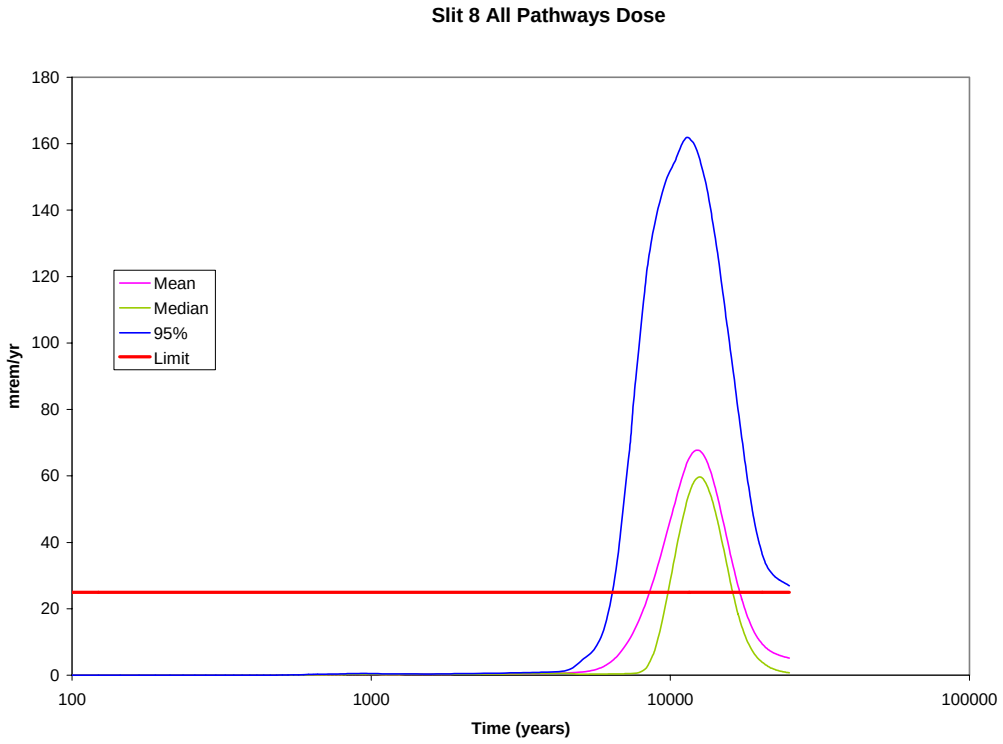

Figure A1C-36 Slit Trench 8 All Pathways Dose Uncertainty

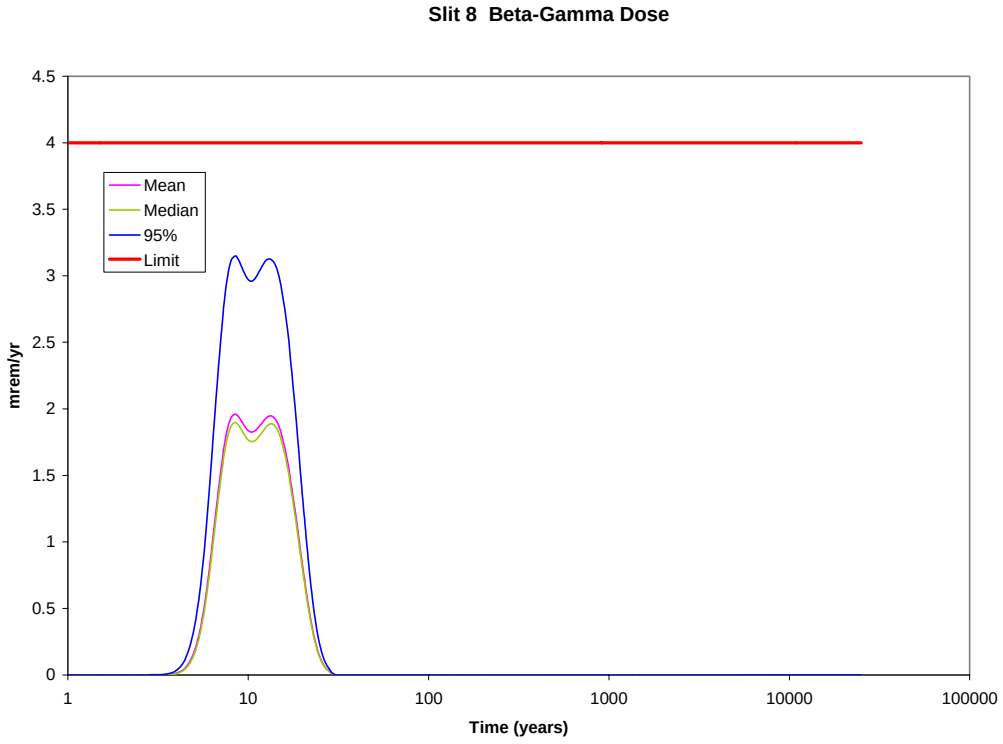

Figure A1C-37 Slit Trench 8 Beta-Gamma Dose Uncertainty

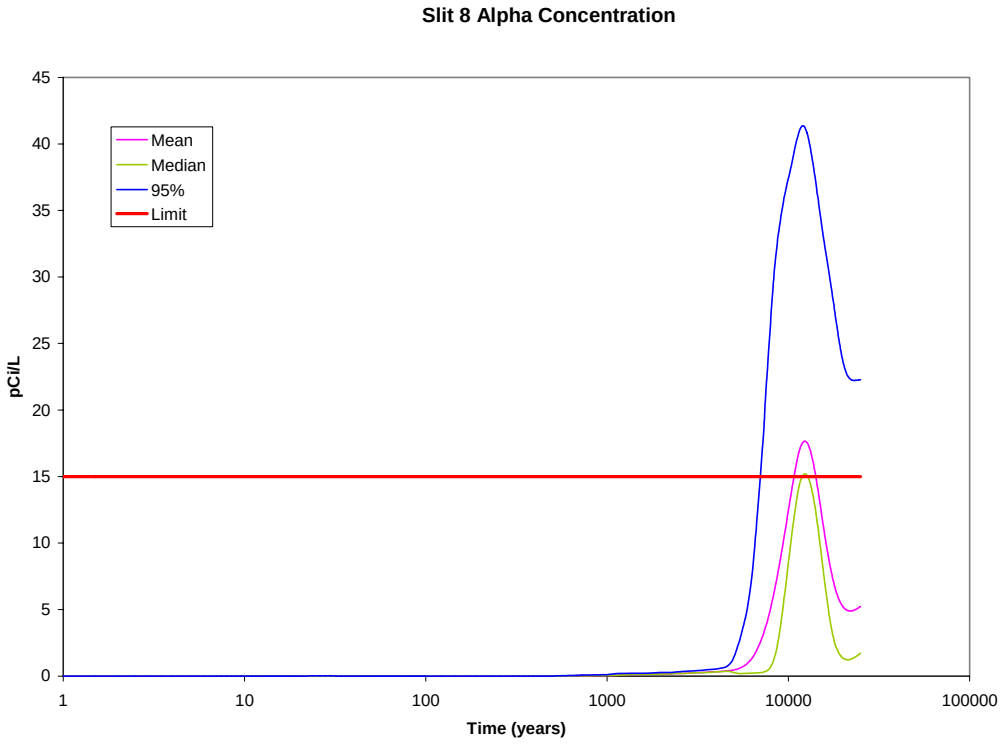

Figure A1C-38 Slit Trench 8 Gross Alpha Concentration Uncertainty

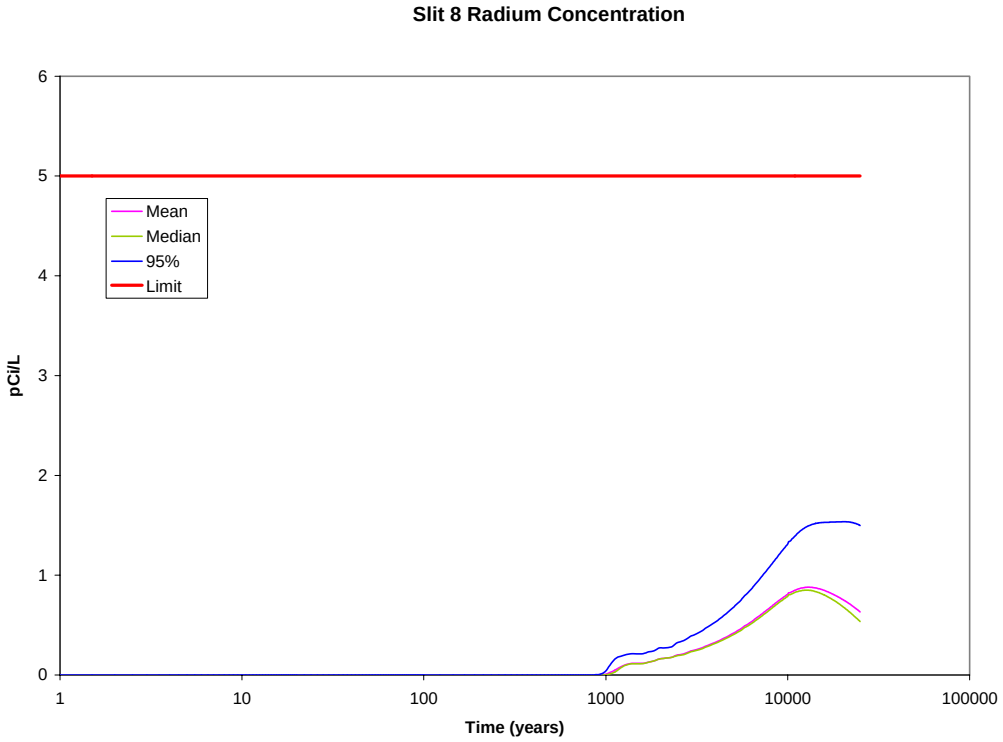

Figure A1C-39 Slit Trench 8 Radium Concentration Uncertainty

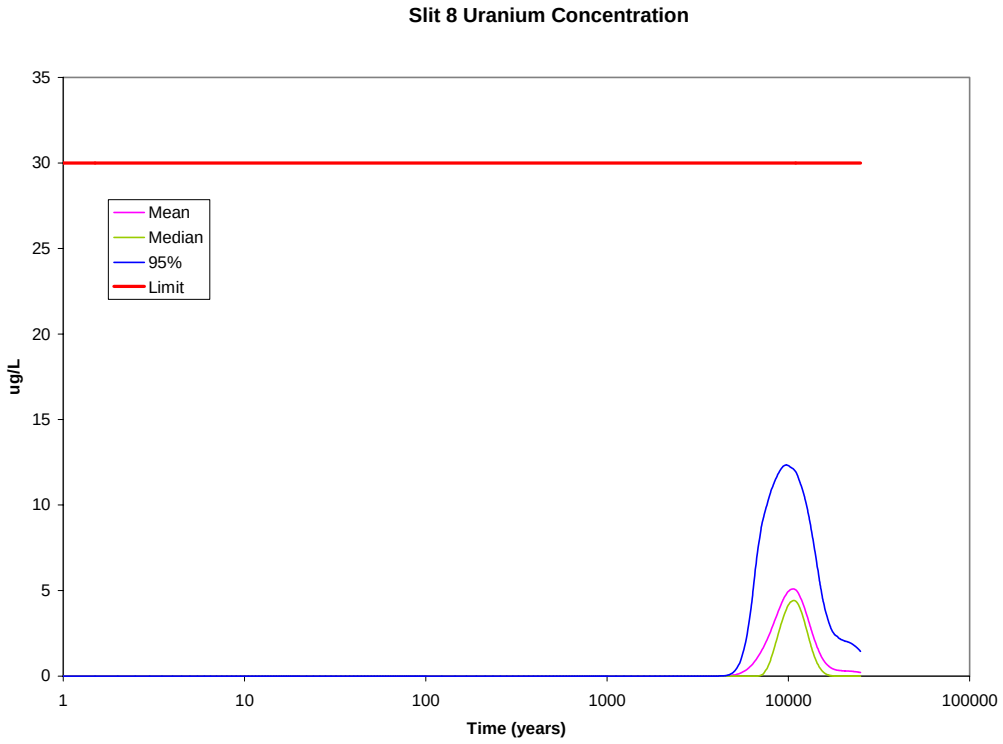

Figure A1C-40 Slit Trench 8 Uranium Concentration Uncertainty

This page intentionally left blank.

APPENDIX A1D

Radon Model

10,000-year Simulation of Rn-222 Flux at Land Surface

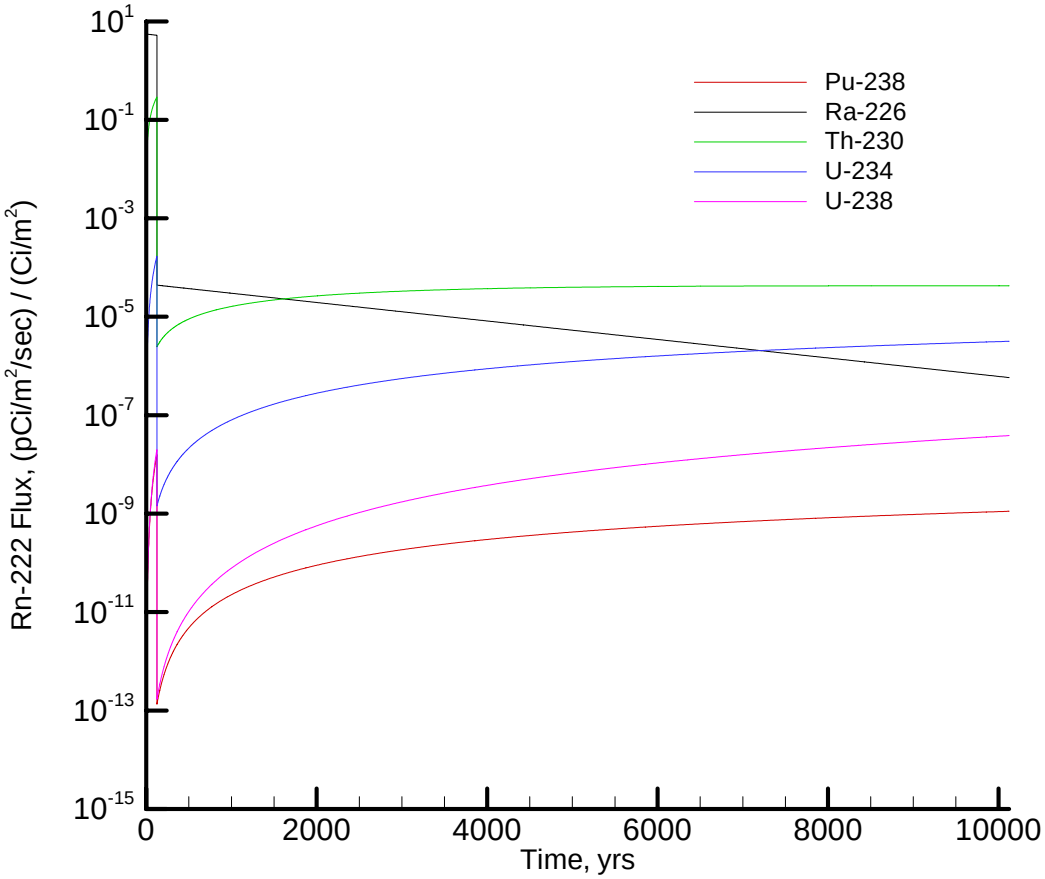

Figure A1D-1. Rn-222 Flux at Land Surface Resulting from Unit Source Term for Slit and Engineered Trenches

APPENDIX A2 - CIG TRENCHES

GRAPHICS FOR GROUNDWATER AND RADON TRANSPORT

This page intentionally left blank.

TABLE OF CONTENTS

APPENDIX A2A

Vadose Zone and Aquifer Models

Flux to the Water Table

100-m Well Concentrations

Table A2A-1. Summary of Existing CIG Unit #1 Inventory Values (in Curies) by Segment for the Abbreviated List of Parent Nuclides Under Consideration (from Clark 2007 and SRS WITS database)

Species (nuclide & form) [d]	Existing Segment 1 (Ci)	Existing Segment 2 (Ci)	Existing Segment 3 (Ci)	Existing Segment 4 (Ci)	Existing Segment 5 (Ci)	Existing Segment 6 (Ci)	Existing Segment 7 (Ci)	Existing Segment 8 (Ci)
Am-241	6.630E-03				7.988E-03	1.814E-02	2.794E-03	4.551E-03
Am-243	7.423E-04				6.137E-06	1.319E-07		1.105E-06
C-14	1.810E-06			1.724E-03	1.978E-02	8.476E-03	5.804E-03	5.388E-03
C-14_K[a]						4.680E-02	7.378E-03	1.187E-02
Cl-36								
Cm-244	1.952E-01				5.278E-04	3.928E-08	3.430E-06	6.501E-07
Cm-245	1.543E-05				3.837E-10	5.427E-10		4.546E-09
Cm-247	8.757E-05					8.766E-15		7.345E-14
Cm-248	8.757E-05							
H-3[e]	5.285E-04	7.189E+00		2.361E+01	2.497E+02	3.876E+02	5.202E+02	9.256E-01
H-3_M[c]						4.951E+02		
I-129	6.297E-07	3.764E-11		3.198E-06	3.340E-07	1.374E-06	4.236E-06	2.305E-06
I-129_C[b]								
I-129_K[a]						5.921E-05	5.249E-06	1.069E-05
K-40								
Mo-93								
Nb-94								
Ni-59	2.890E-04				3.115E-05	4.257E-04	2.252E-04	5.167E-06
Np-237	5.421E-06			8.622E-07	4.930E-04	2.511E-04	8.882E-05	6.245E-05
Pd-107	6.755E-06							
Pu-238	7.089E-02			4.406E-06	3.874E-02	4.429E-02	2.929E-02	1.066E-02
Pu-239	1.297E-02			1.663E-05	2.946E-02	1.560E-01	2.329E-02	4.708E-02
Pu-240	8.924E-03			1.663E-05	7.723E-03	5.260E-04	6.351E-03	2.814E-03
Pu-241	5.630E-02				1.423E-01	3.896E-01	1.108E-01	1.109E-01
Pu-242	2.072E-06				2.914E-05	5.118E-08	1.157E-06	1.380E-06
Pu-244								
RA226								
Se-79	3.369E-05				2.980E-04	8.043E-06	1.739E-06	2.368E-09
Sn-126	1.076E-05				4.771E-06	8.569E-10	2.700E-06	3.003E-10
Sr-90	2.072E-02				5.050E-01	2.222E+00	2.309E+00	2.479E+00
Tc-99	1.347E-05	1.747E-07		5.401E-05	1.433E-04	5.088E-03	7.074E-04	2.692E-04
Tc-99_K[a]						9.113E-03	1.328E-04	3.331E-05
Th-230								
Th-232								
U-233	1.768E-06			7.627E-06	4.327E-05	1.521E-02	2.369E-01	1.668E-08
U-234	8.924E-06	3.764E-10		6.538E-08	1.064E-03	2.972E-02	4.280E-04	2.624E-03
U-235	1.810E-07				2.250E-05	8.027E-04	5.649E-06	4.523E-05
U-236	2.356E-07				5.304E-05	2.389E-04	6.431E-06	2.298E-04
U-238	1.660E-05				6.217E-04	1.374E-01	9.618E-05	6.706E-04
Zr-93	1.017E-03							

[a] _K refers to a special waste form termed "K & L Basin Resins" employed for nuclides C-14, I-129, and Tc-99 affecting their transport K_d values within the CIG waste form only.
[b] _C refers to a special waste form termed "ETF Activated Carbon" employed for nuclide I-129 affecting its transport K_d value within the CIG waste form only.
[c] _M refers to a special waste form termed "232-F Facility Metal Components" for nuclide H-3 affecting how its release mechanism within the CIG waste zone is addressed by using a 1-dimensional (cylindrical) transient solid-phase transport model. Inventory value was also decay corrected from time of assay to time of burial.
[d] Generic waste forms for the standard nuclides where their release mechanisms are assumed to be instantaneous within the CIG waste zone.
[e] H-3 inventory value was decay corrected from time of assay to time of burial.

Flux to Water Table - Existing Inventory

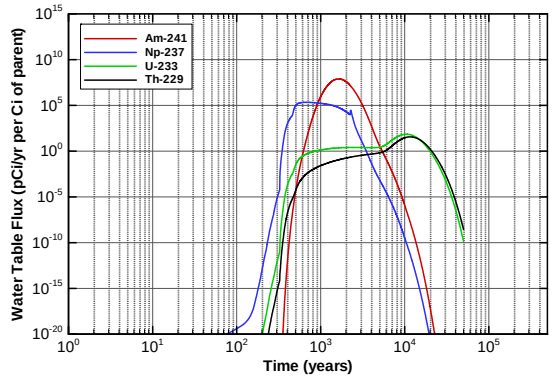

Figure A2AA-1. Baseline CIG Segment 123 Inventory Water Table Flux for Am-241

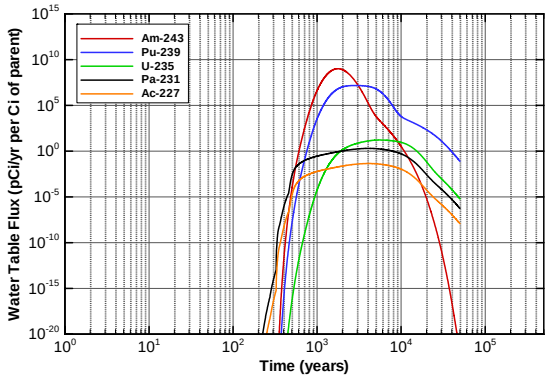

Figure A2AA-2. Baseline CIG Segment 123 Inventory Water Table Flux for Am-243

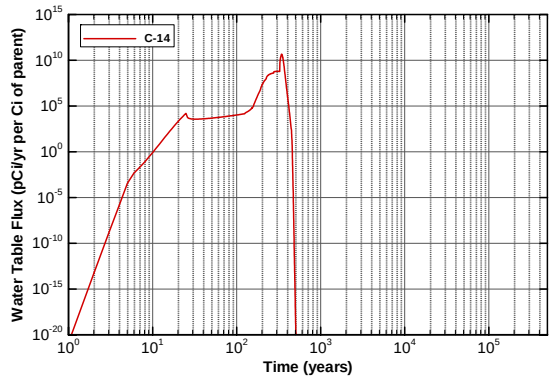

Figure A2A-3. Baseline CIG Segment 123 Inventory Water Table Flux for C-14

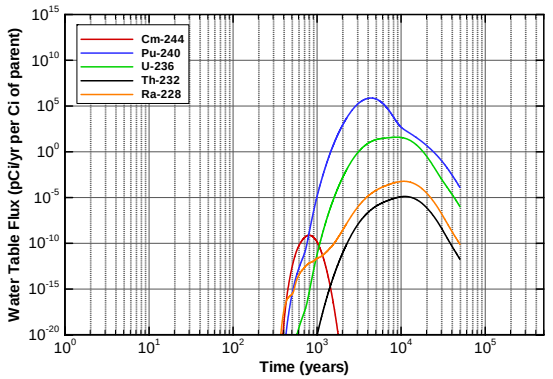

Figure A2A-4. Baseline CIG Segment 123 Inventory Water Table Flux for Cm-244

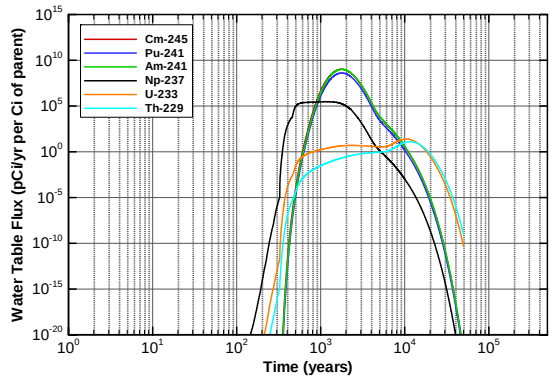

Figure A2A-5. Baseline CIG Segment 123 Inventory Water Table Flux for Cm-245

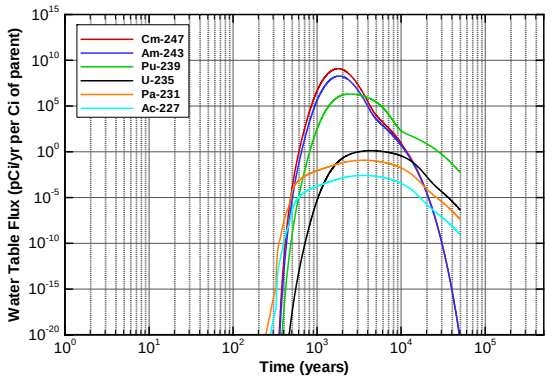

Figure A2A-6. Baseline CIG Segment 123 Inventory Water Table Flux for Cm-247

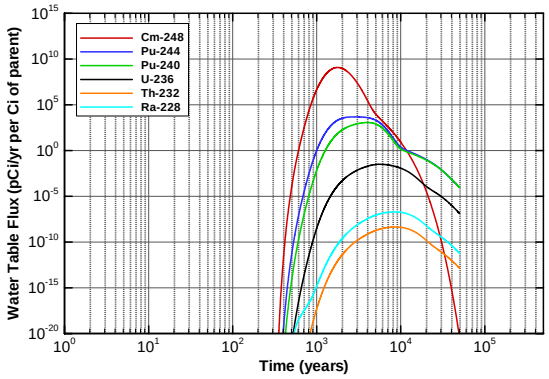

Figure A2A-7. Baseline CIG Segment 123 Inventory Water Table Flux for Cm-248

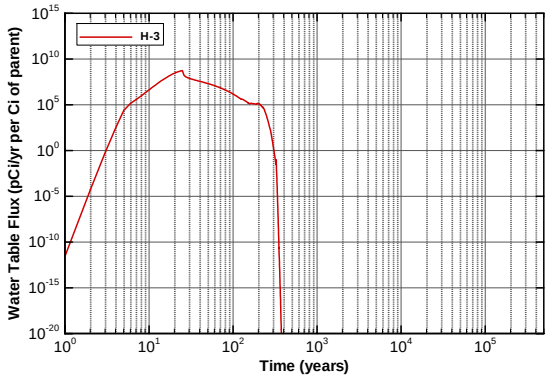

Figure A2A-8. Baseline CIG Segment 123 Inventory Water Table Flux for H-3

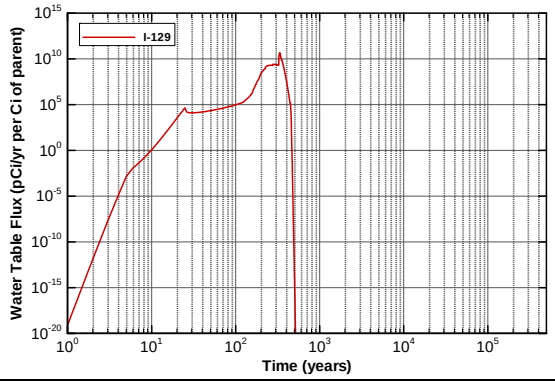

Figure A2A-9. Baseline CIG Segment 123 Inventory Water Table Flux for I-129

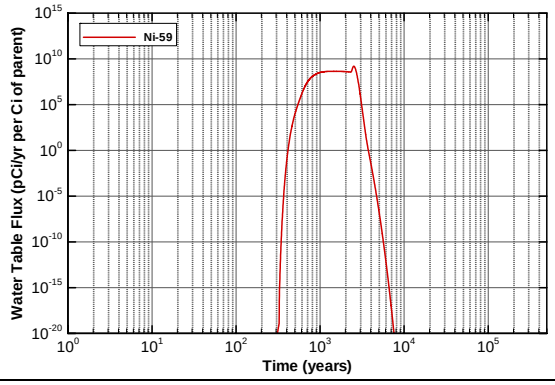

Figure A2A-10. Baseline CIG Segment 123 Inventory Water Table Flux for Ni-59

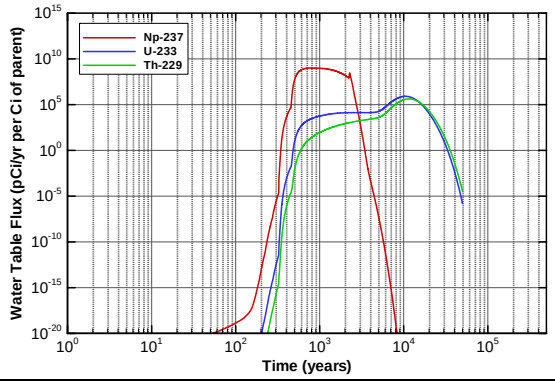

Figure A2A-11. Baseline CIG Segment 123 Inventory Water Table Flux for Np-237

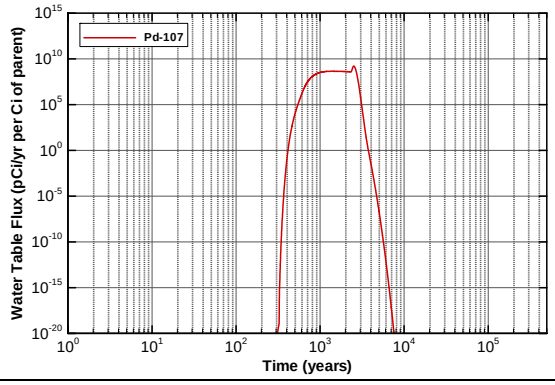

Figure A2A-12. Baseline CIG Segment 123 Inventory Water Table Flux for Pd-107

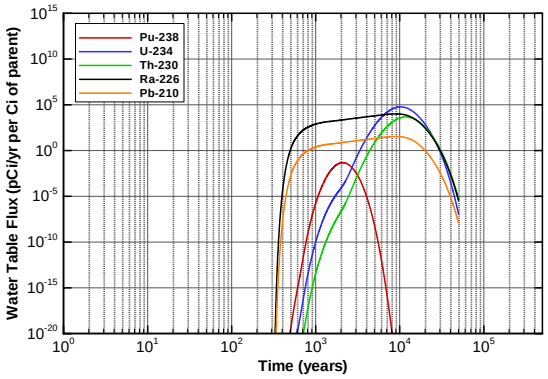

Figure A2A-13. Baseline CIG Segment 123 Inventory Water Table Flux for Pu-238

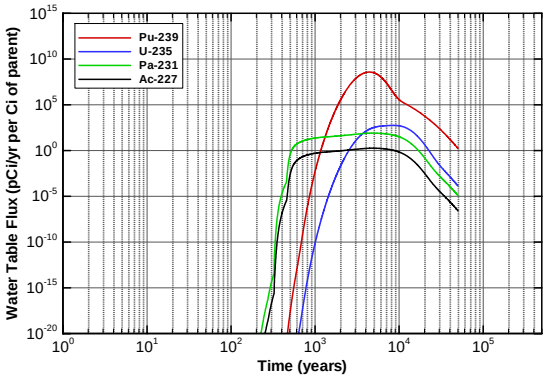

Figure A2A-14. Baseline CIG Segment 123 Inventory Water Table Flux for Pu-239

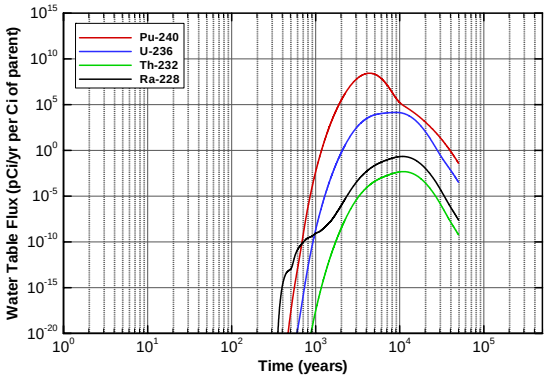

Figure A2A-15. Baseline CIG Segment 123 Inventory Water Table Flux for Pu-240

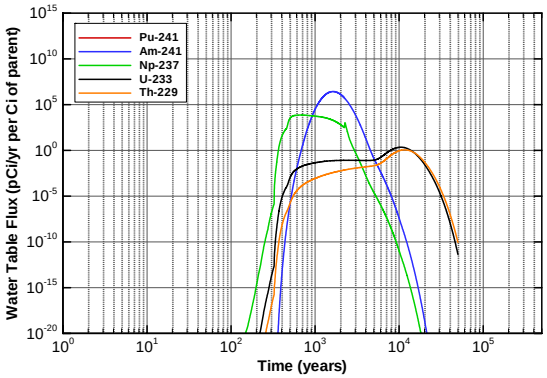

Figure A2A-16. Baseline CIG Segment 123 Inventory Water Table Flux for Pu-241

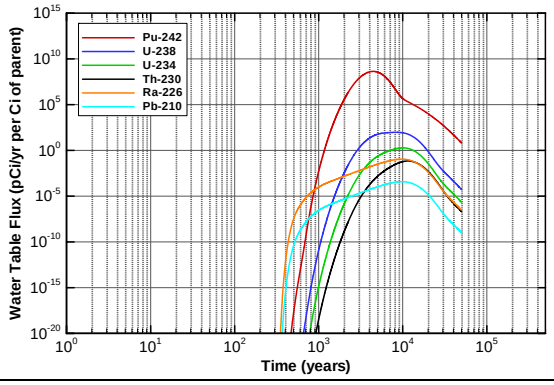

Figure A2A-17. Baseline CIG Segment 123 Inventory Water Table Flux for Pu-242

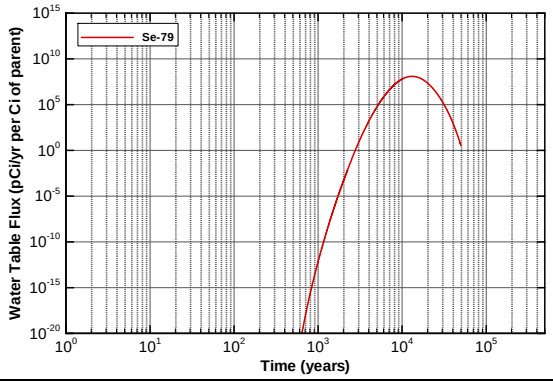

Figure A2A-18. Baseline CIG Segment 123 Inventory Water Table Flux for Se-79

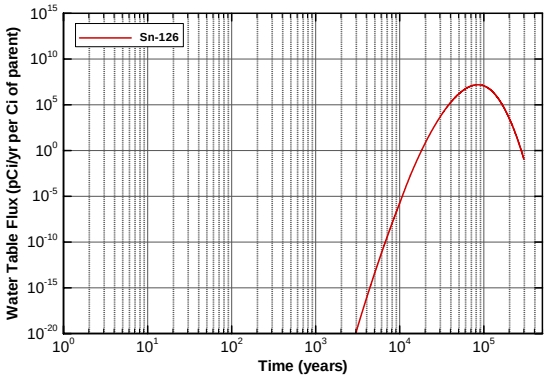

Figure A2A-19. Baseline CIG Segment 123 Inventory Water Table Flux for Sn-126

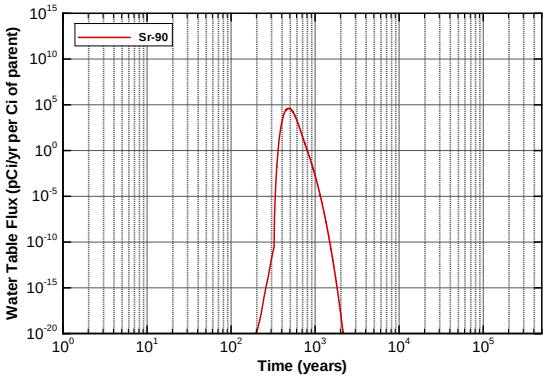

Figure A2A-20. Baseline CIG Segment 123 Inventory Water Table Flux for Sr-90

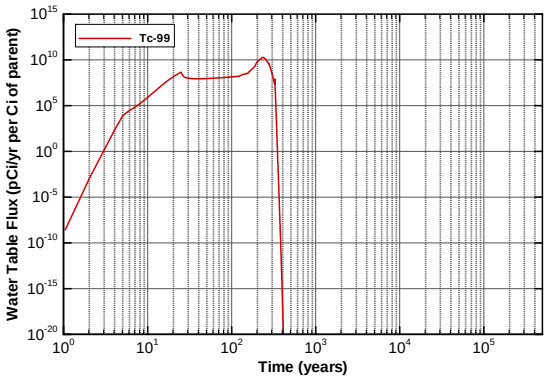

Figure A2A-21. Baseline CIG Segment 123 Inventory Water Table Flux for Tc-99

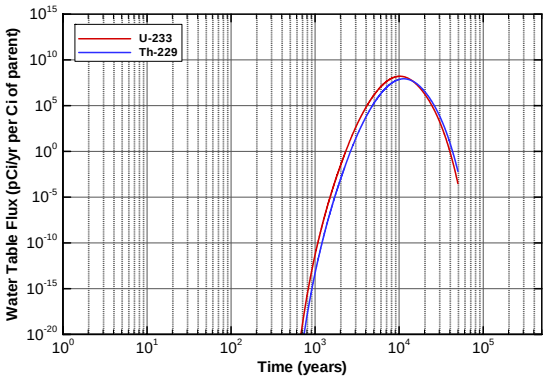

Figure A2A-22. Baseline CIG Segment 123 Inventory Water Table Flux for U-233

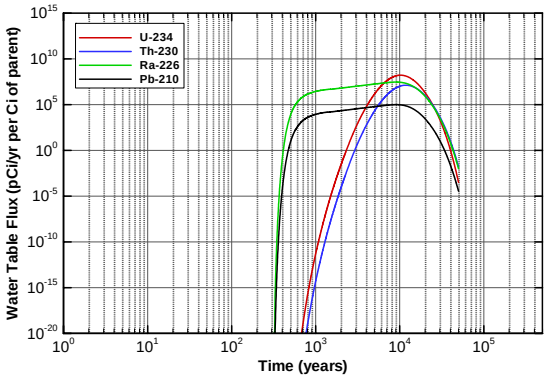

Figure A2A-23. Baseline CIG Segment 123 Inventory Water Table Flux for U-234

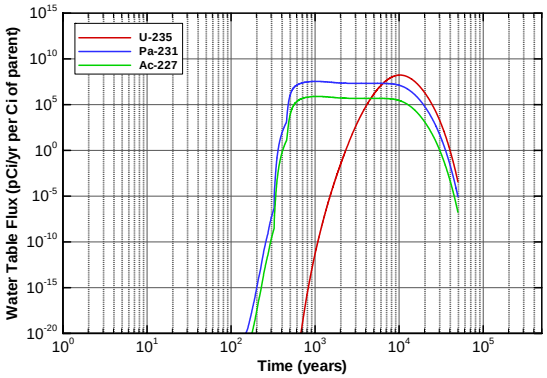

Figure A2A-24. Baseline CIG Segment 123 Inventory Water Table Flux for U-235

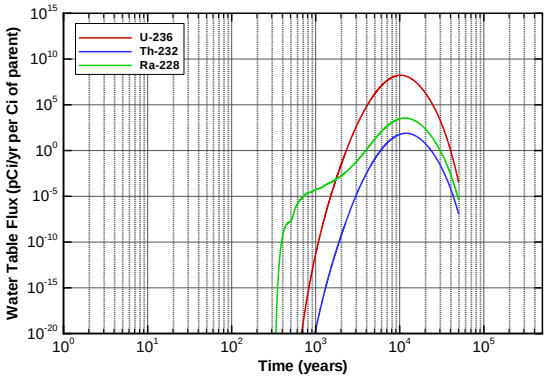

Figure A2A-25. Baseline CIG Segment 123 Inventory Water Table Flux for U-236

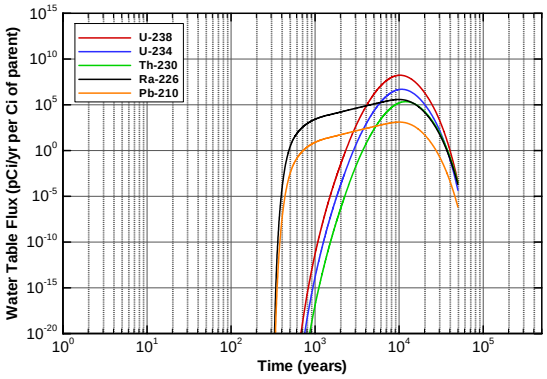

Figure A2A-26. Baseline CIG Segment 123 Inventory Water Table Flux for U-238

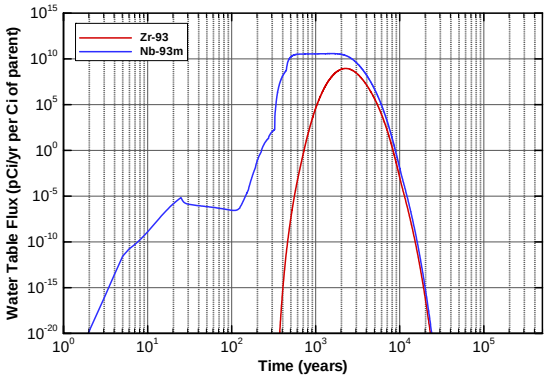

Figure A2A-27. Baseline CIG Segment 123 Inventory Water Table Flux for Zr-93

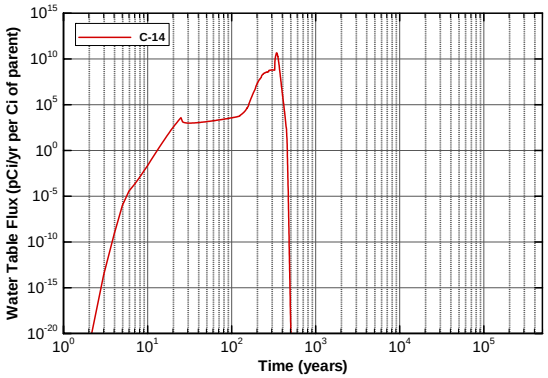

Figure A2A-28. Baseline CIG Segment 4 Inventory Water Table Flux for C-14

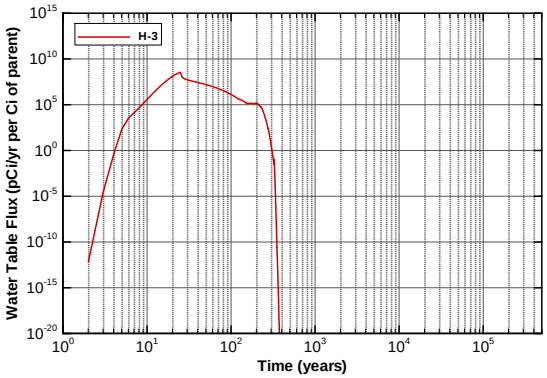

Figure A2A-29. Baseline CIG Segment 4 Inventory Water Table Flux for H-3

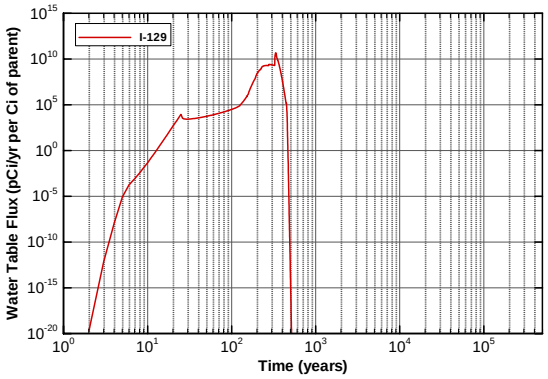

Figure A2A-30. Baseline CIG Segment 4 Inventory Water Table Flux for I-129

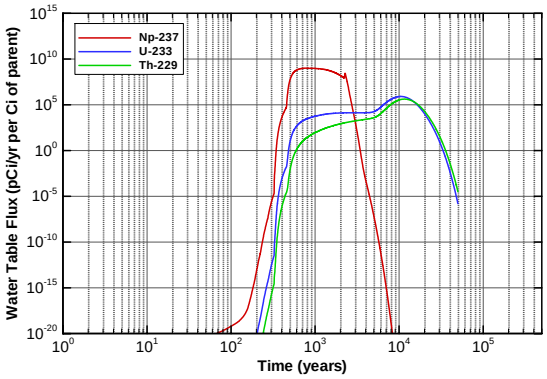

Figure A2A-31. Baseline CIG Segment 4 Inventory Water Table Flux for Np-237

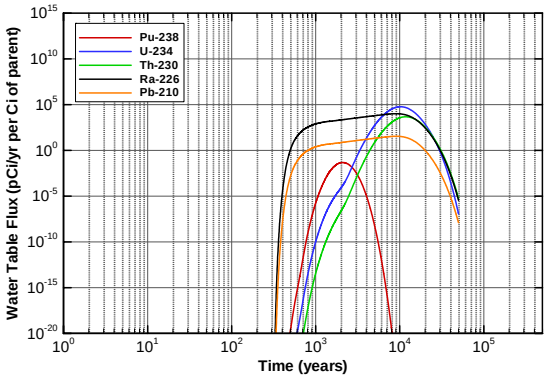

Figure A2A-32. Baseline CIG Segment 4 Inventory Water Table Flux for Pu-238

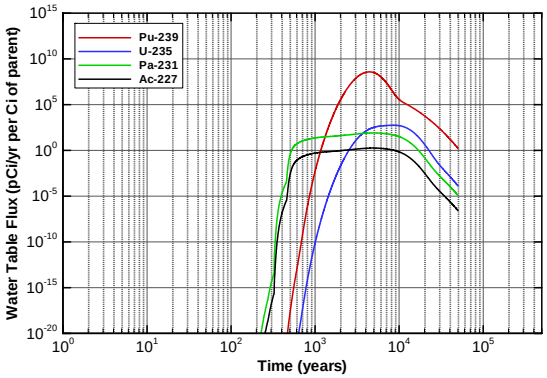

Figure A2A-33. Baseline CIG Segment 4 Inventory Water Table Flux for Pu-239

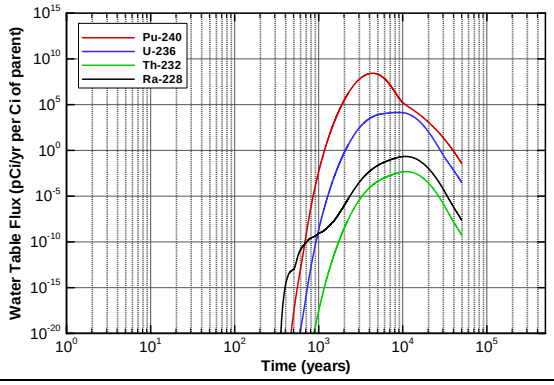

Figure A2A-34. Baseline CIG Segment 4 Inventory Water Table Flux for Pu-240

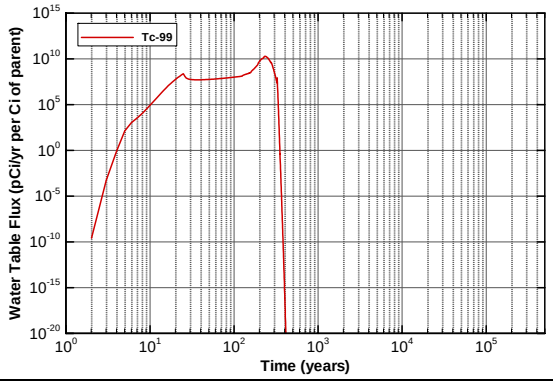

Figure A2A-35. Baseline CIG Segment 4 Inventory Water Table Flux for Tc-99

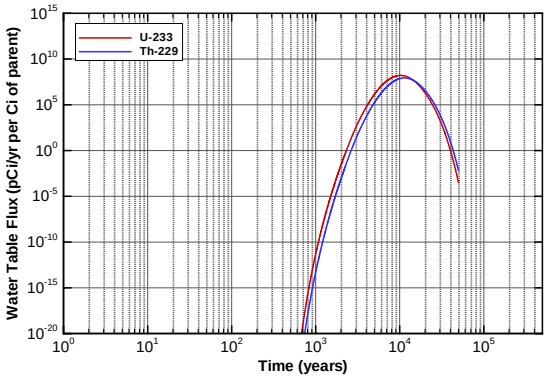

Figure A2A-36. Baseline CIG Segment 4 Inventory Water Table Flux for U-233

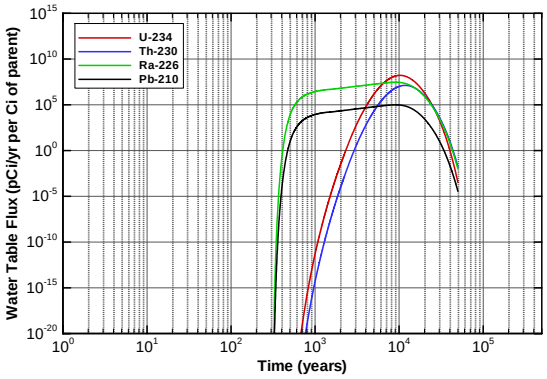

Figure A2A-37. Baseline CIG Segment 4 Inventory Water Table Flux for U-234

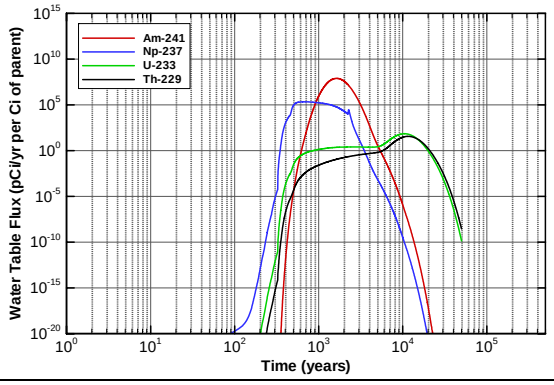

Figure A2A-38. Baseline CIG Segment 5 Inventory Water Table Flux for Am-241

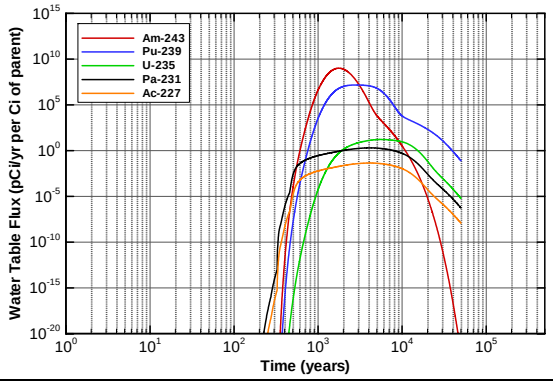

Figure A2A-39. Baseline CIG Segment 5 Inventory Water Table Flux for Am-243

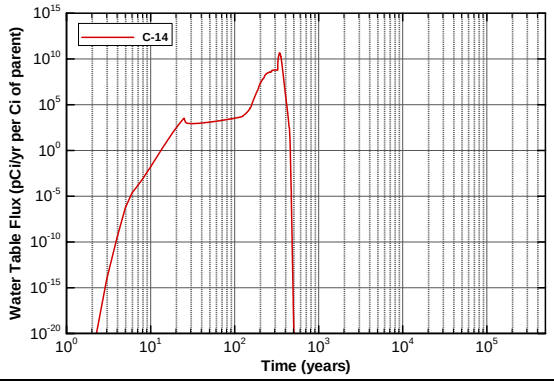

Figure A2A-40. Baseline CIG Segment 5 Inventory Water Table Flux for C-14

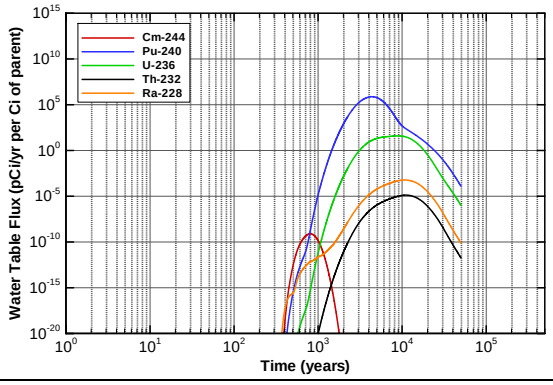

Figure A2A-41. Baseline CIG Segment 5 Inventory Water Table Flux for Cm-244

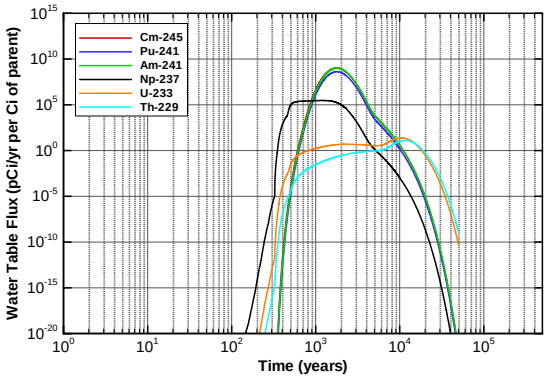

Figure A2A-42. Baseline CIG Segment 5 Inventory Water Table Flux for Cm-245

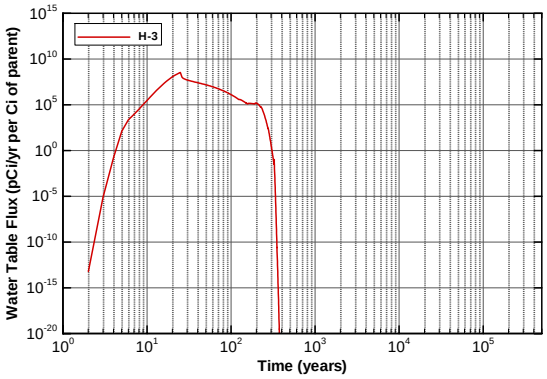

Figure A2A-43. Baseline CIG Segment 5 Inventory Water Table Flux for H-3

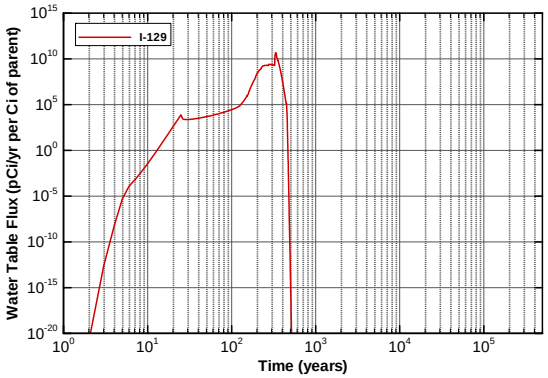

Figure A2A-44. Baseline CIG Segment 5 Inventory Water Table Flux for I-129

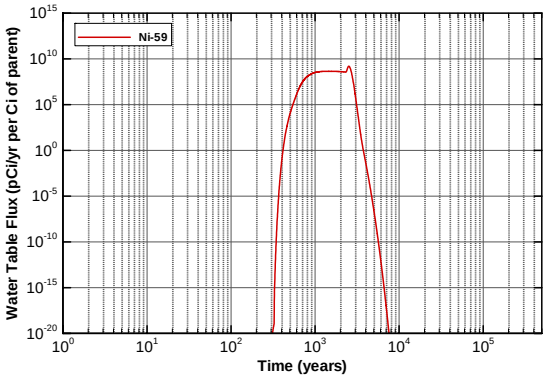

Figure A2A-45. Baseline CIG Segment 5 Inventory Water Table Flux for Ni-59

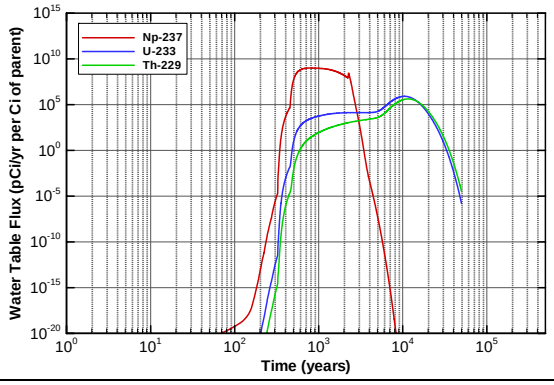

Figure A2A-46. Baseline CIG Segment 5 Inventory Water Table Flux for Np-237

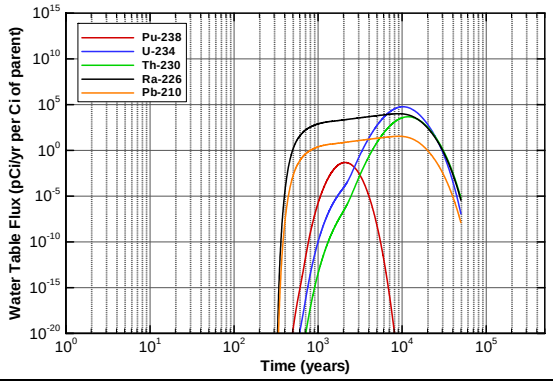

Figure A2A-47. Baseline CIG Segment 5 Inventory Water Table Flux for Pu-238

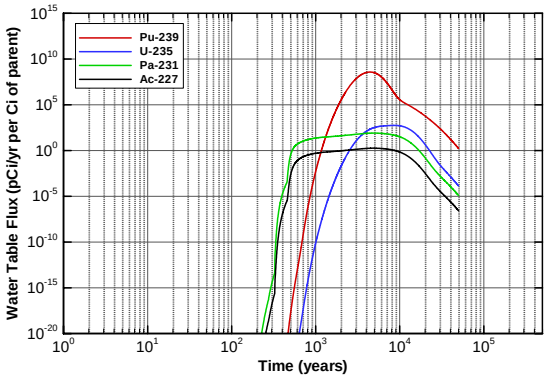

Figure A2A-48. Baseline CIG Segment 5 Inventory Water Table Flux for Pu-239

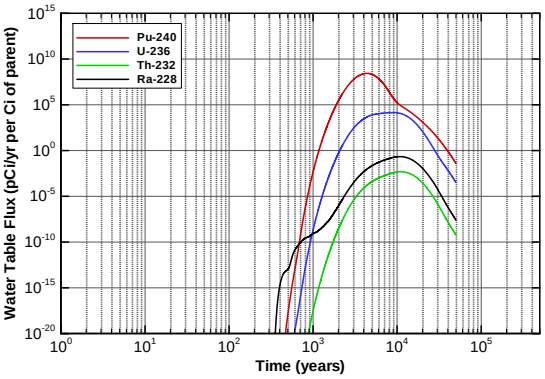

Figure A2A-49. Baseline CIG Segment 5 Inventory Water Table Flux for Pu-240

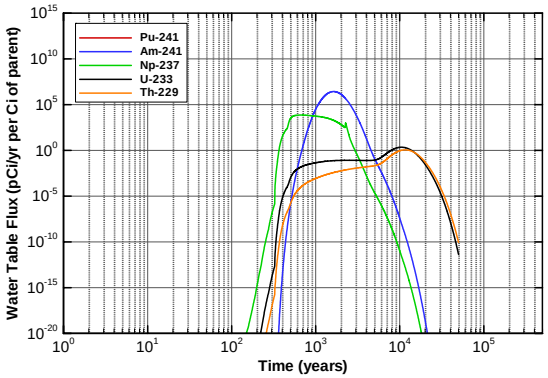

Figure A2A-50. Baseline CIG Segment 5 Inventory Water Table Flux for Pu-241

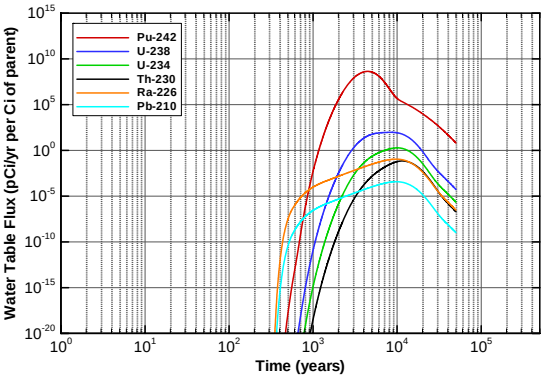

Figure A2A-51. Baseline CIG Segment 5 Inventory Water Table Flux for Pu-242

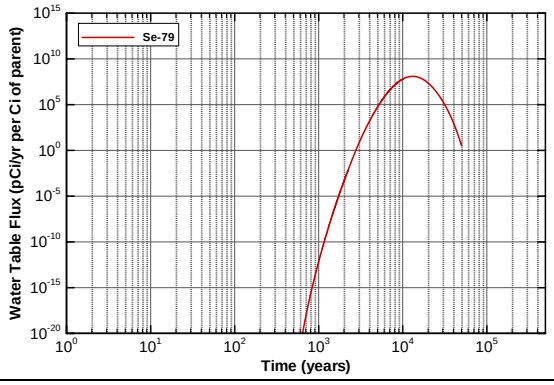

Figure A2A-52. Baseline CIG Segment 5 Inventory Water Table Flux for Se-79

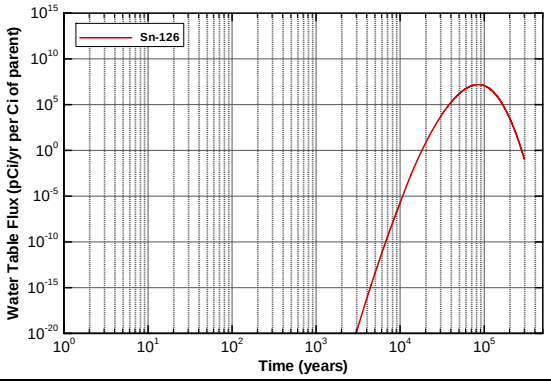

Figure A2A-53. Baseline CIG Segment 5 Inventory Water Table Flux for Sn-126

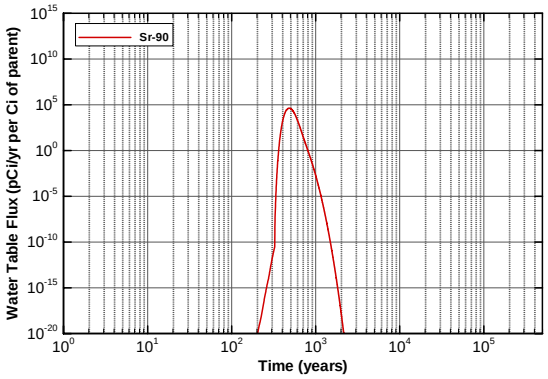

Figure A2A-54. Baseline CIG Segment 5 Inventory Water Table Flux for Sr-90

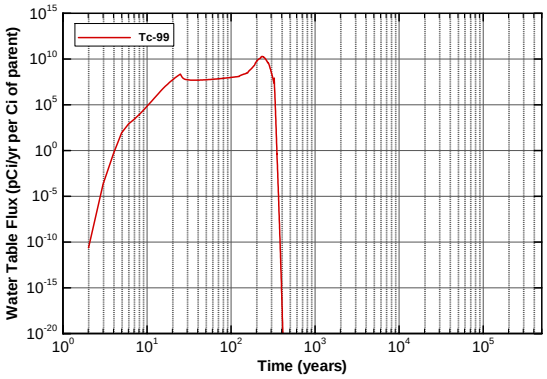

Figure A2A-55. Baseline CIG Segment 5 Inventory Water Table Flux for Tc-99

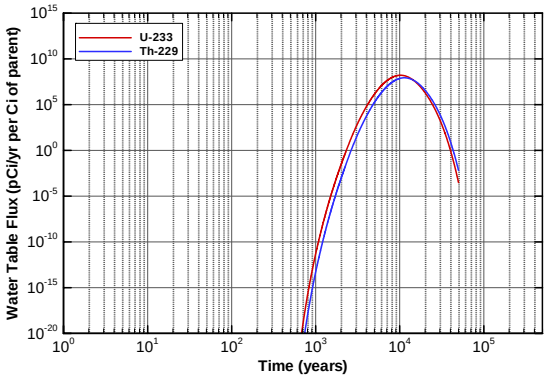

Figure A2A-56. Baseline CIG Segment 5 Inventory Water Table Flux for U-233

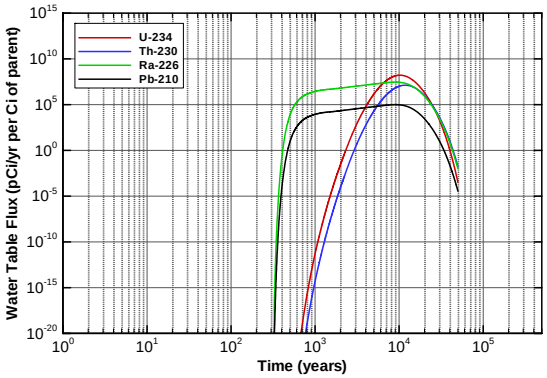

Figure A2A-57. Baseline CIG Segment 5 Inventory Water Table Flux for U-234

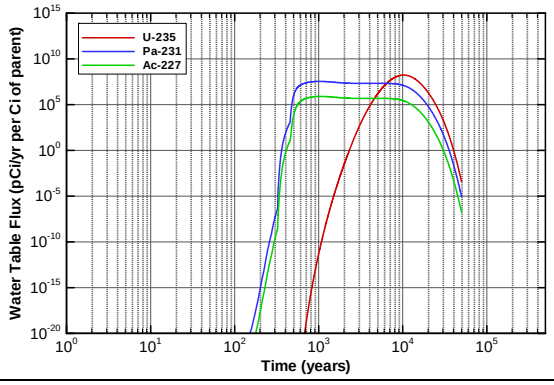

Figure A2A-58. Baseline CIG Segment 5 Inventory Water Table Flux for U-235

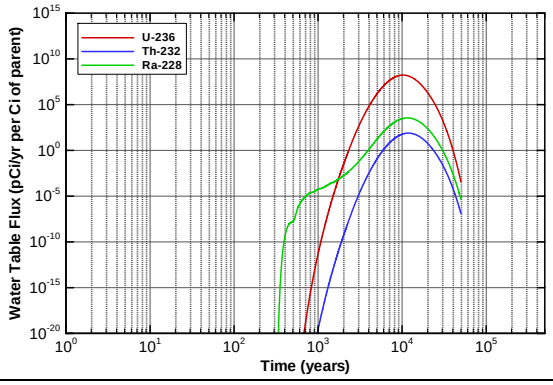

Figure A2A-59. Baseline CIG Segment 5 Inventory Water Table Flux for U-236

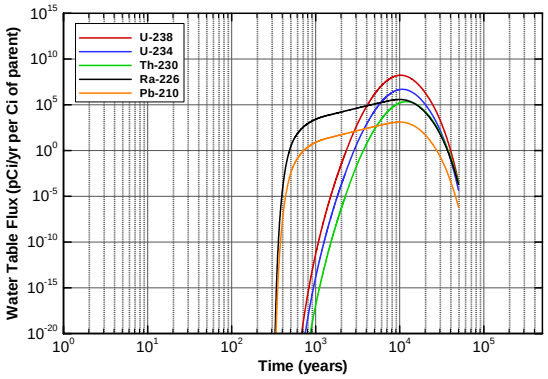

Figure A2A-60. Baseline CIG Segment 5 Inventory Water Table Flux for U-238

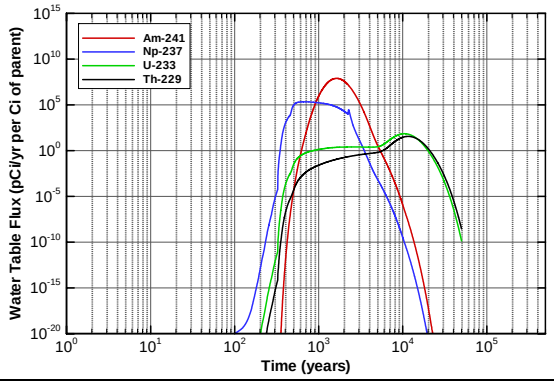

Figure A2A-61. Baseline CIG Segment 6 Inventory Water Table Flux for Am-241

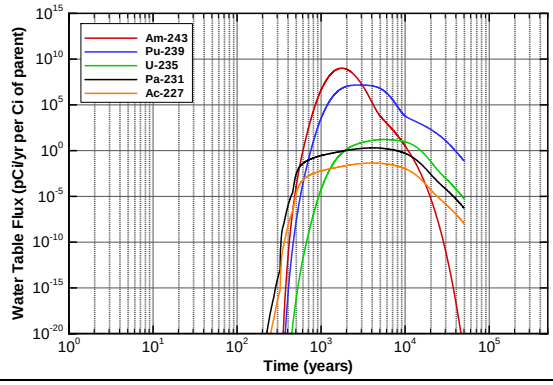

Figure A2A-62. Baseline CIG Segment 6 Inventory Water Table Flux for Am-243

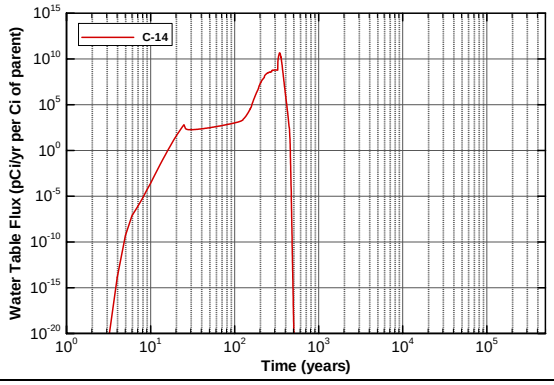

Figure A2A-63. Baseline CIG Segment 6 Inventory Water Table Flux for C-14

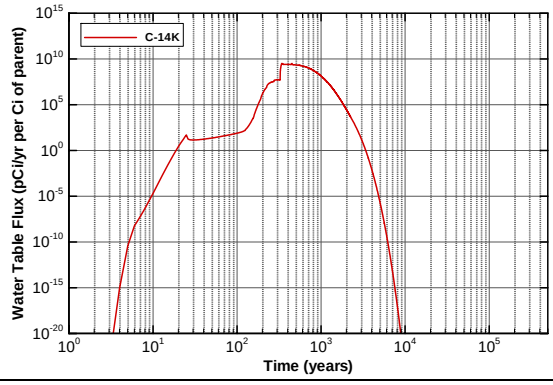

Figure A2A-64. Baseline CIG Segment 6 Inventory Water Table Flux for C-14K

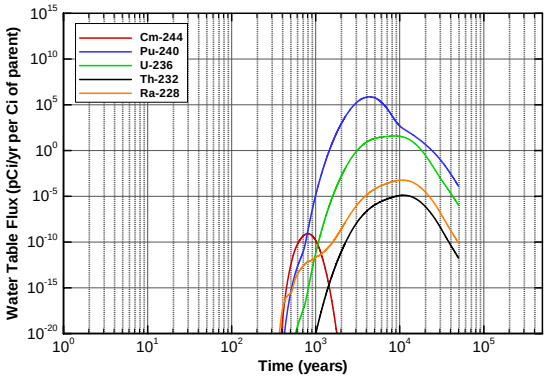

Figure A2A-65. Baseline CIG Segment 6 Inventory Water Table Flux for Cm-244

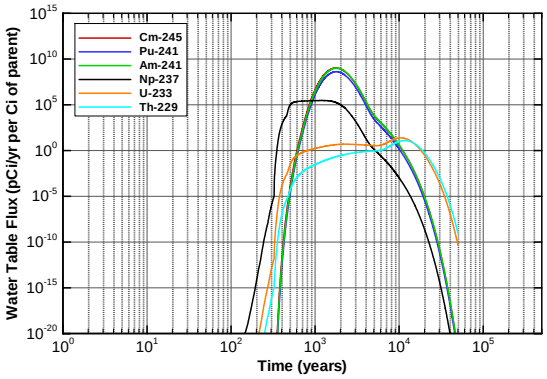

Figure A2A-66. Baseline CIG Segment 6 Inventory Water Table Flux for Cm-245

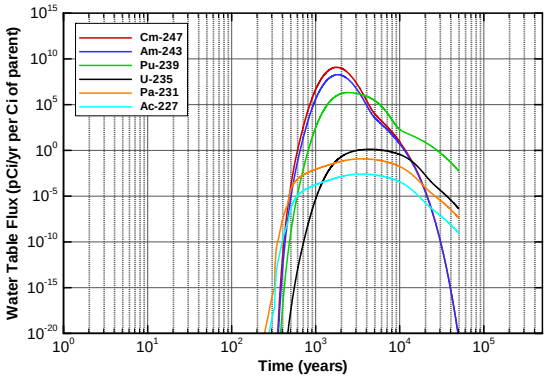

Figure A2A-67. Baseline CIG Segment 6 Inventory Water Table Flux for Cm-247

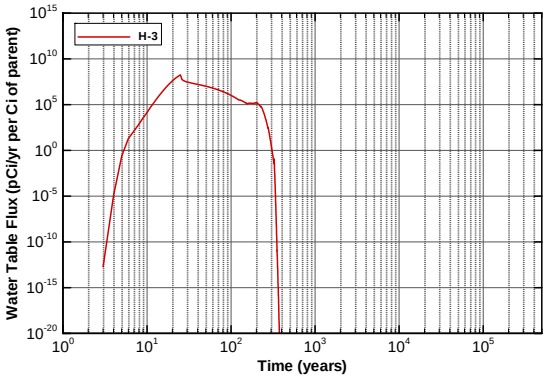

Figure A2A-68. Baseline CIG Segment 6 Inventory Water Table Flux for H-3

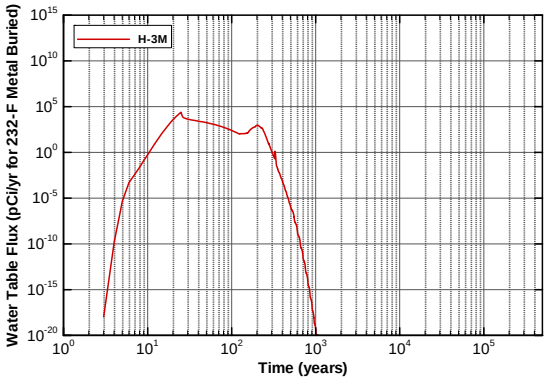

Figure A2A-69. Baseline CIG Segment 6 Inventory Water Table Flux for H-3M

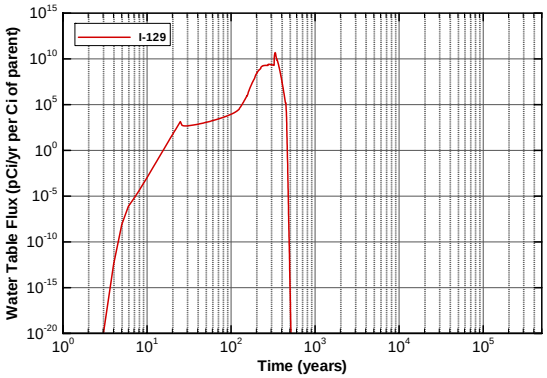

Figure A2A-70. Baseline CIG Segment 6 Inventory Water Table Flux for I-129

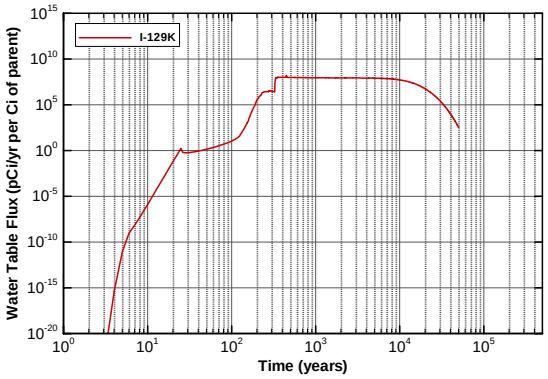

Figure A2A-71. Baseline CIG Segment 6 Inventory Water Table Flux for I-129K

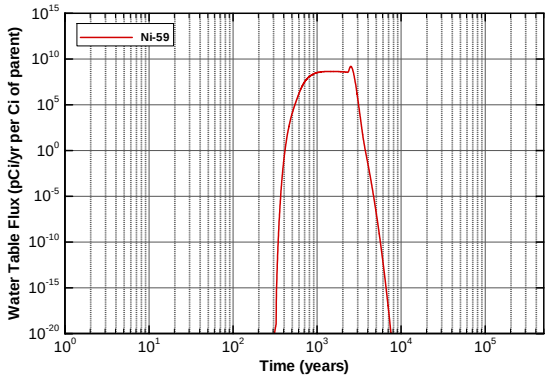

Figure A2A-72. Baseline CIG Segment 6 Inventory Water Table Flux for Ni-59

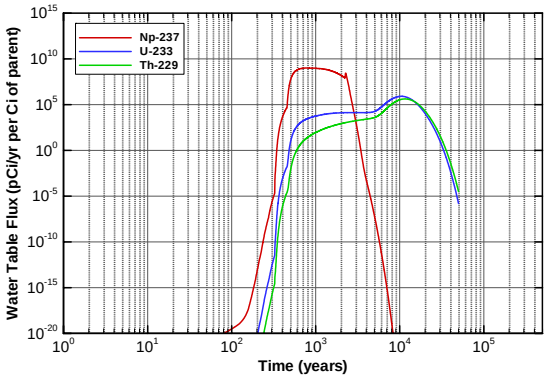

Figure A2A-73. Baseline CIG Segment 6 Inventory Water Table Flux for Np-237

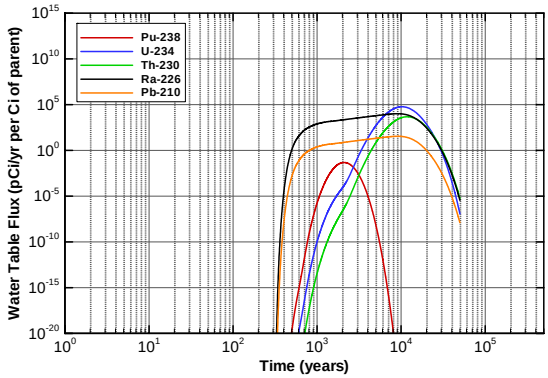

Figure A2A-74. Baseline CIG Segment 6 Inventory Water Table Flux for Pu-238

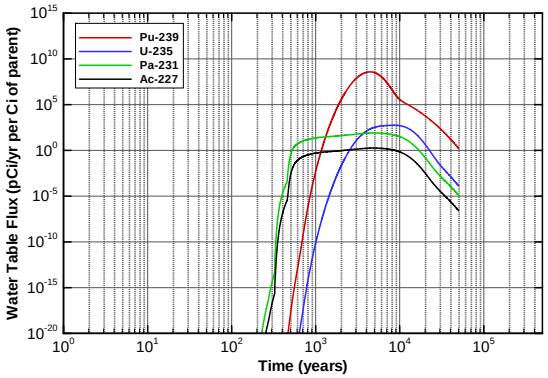

Figure A2A-75. Baseline CIG Segment 6 Inventory Water Table Flux for Pu-239

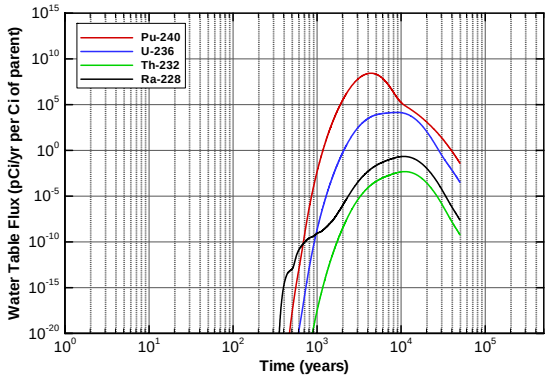

Figure A2A-76. Baseline CIG Segment 6 Inventory Water Table Flux for Pu-240

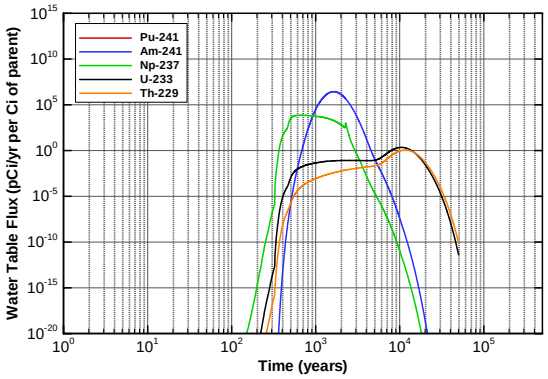

Figure A2A-77. Baseline CIG Segment 6 Inventory Water Table Flux for Pu-241

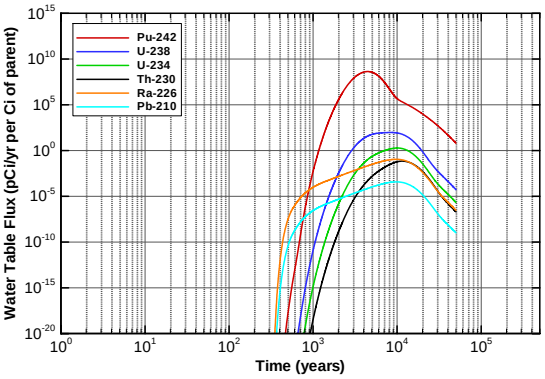

Figure A2A-78. Baseline CIG Segment 6 Inventory Water Table Flux for Pu-242

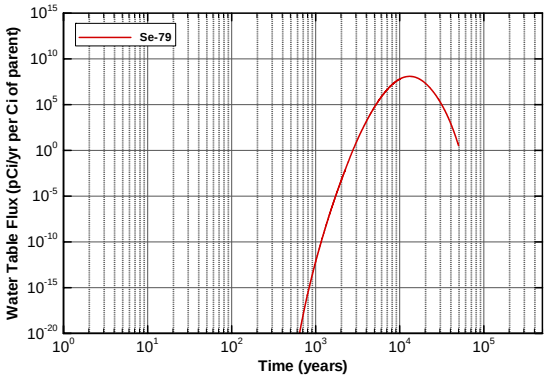

Figure A2A-79. Baseline CIG Segment 6 Inventory Water Table Flux for Se-79

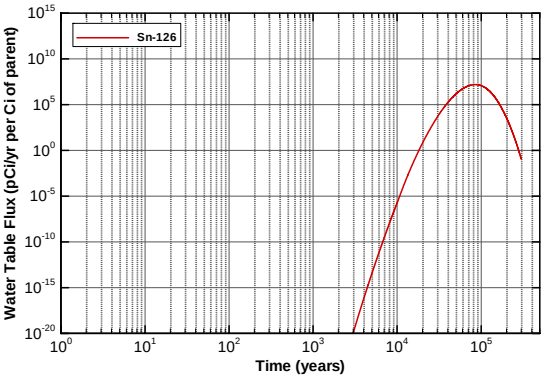

Figure A2A-80. Baseline CIG Segment 6 Inventory Water Table Flux for Sn-126

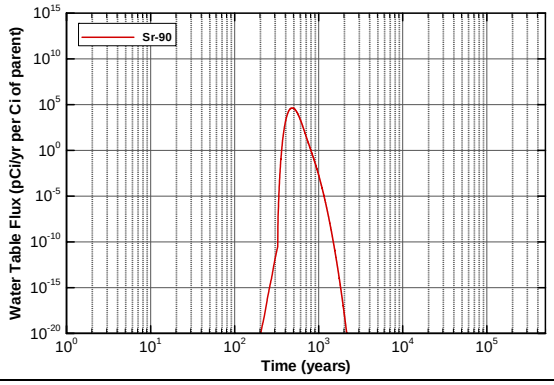

Figure A2A-81. Baseline CIG Segment 6 Inventory Water Table Flux for Sr-90

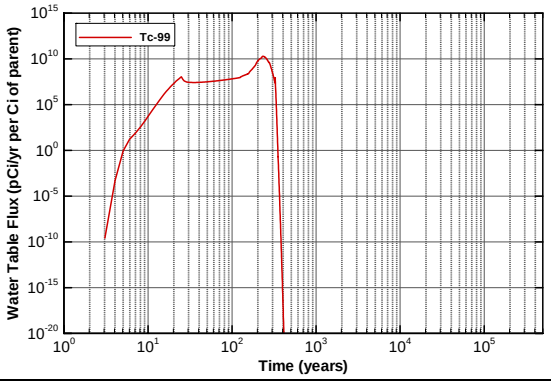

Figure A2A-82. Baseline CIG Segment 6 Inventory Water Table Flux for Tc-99

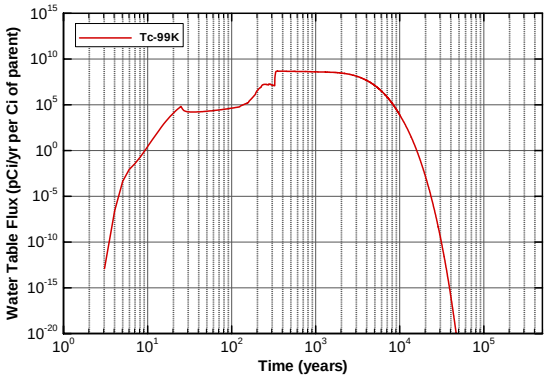

Figure A2A-83. Baseline CIG Segment 6 Inventory Water Table Flux for Tc-99K

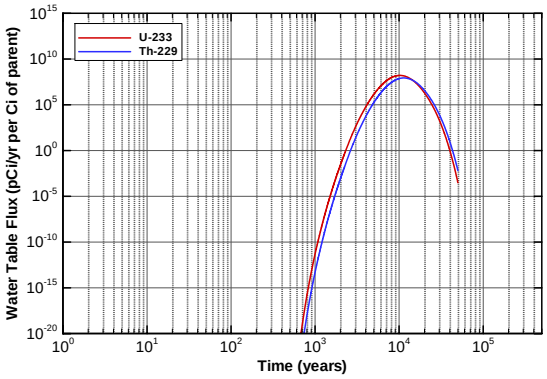

Figure A2A-84. Baseline CIG Segment 6 Inventory Water Table Flux for U-233

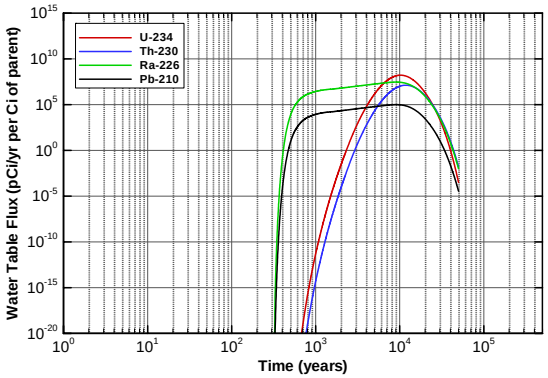

Figure A2A-85. Baseline CIG Segment 6 Inventory Water Table Flux for U-234

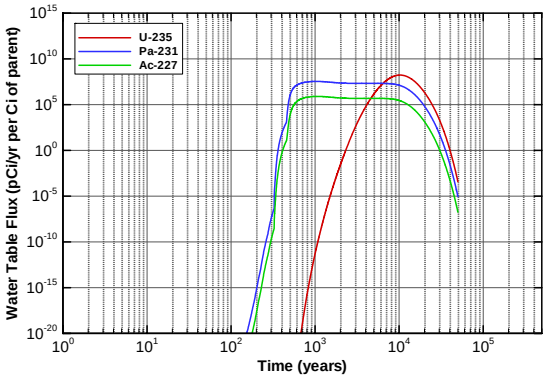

Figure A2A-86. Baseline CIG Segment 6 Inventory Water Table Flux for U-235

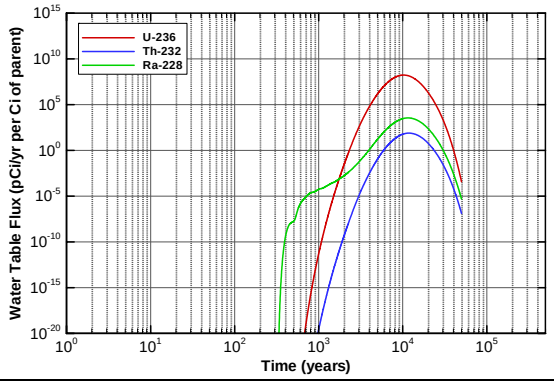

Figure A2A-87. Baseline CIG Segment 6 Inventory Water Table Flux for U-236

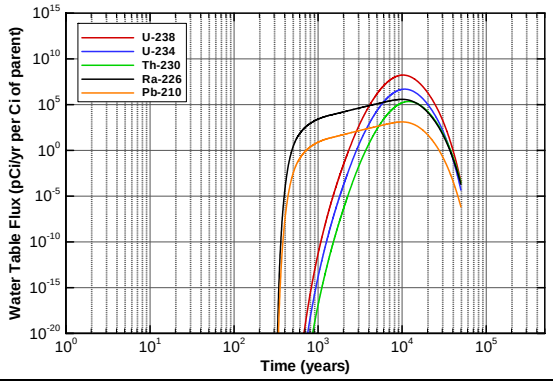

Figure A2A-88. Baseline CIG Segment 6 Inventory Water Table Flux for U-238

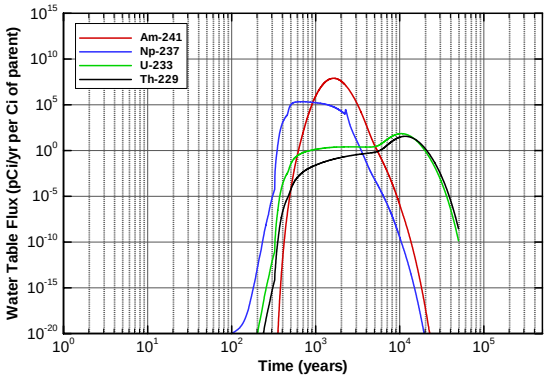

Figure A2A-89. Baseline CIG Segment 7 Inventory Water Table Flux for Am-241

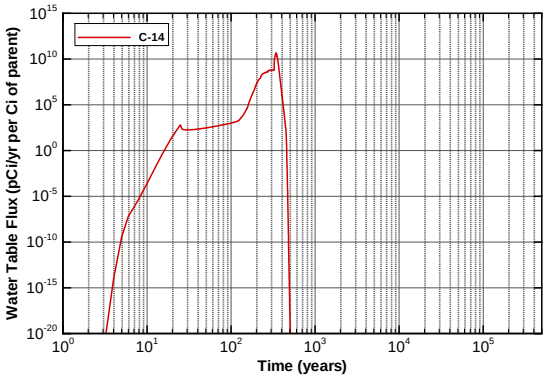

Figure A2A-90. Baseline CIG Segment 7 Inventory Water Table Flux for C-14

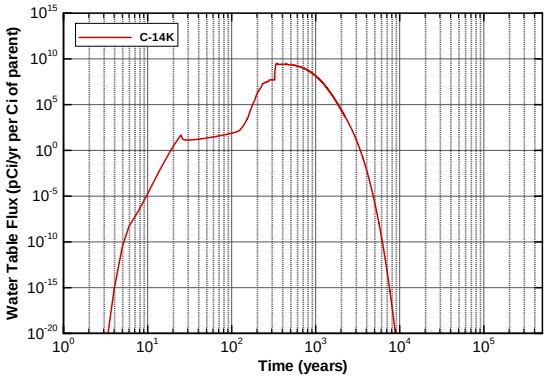

Figure A2A-91. Baseline CIG Segment 7 Inventory Water Table Flux for C-14K

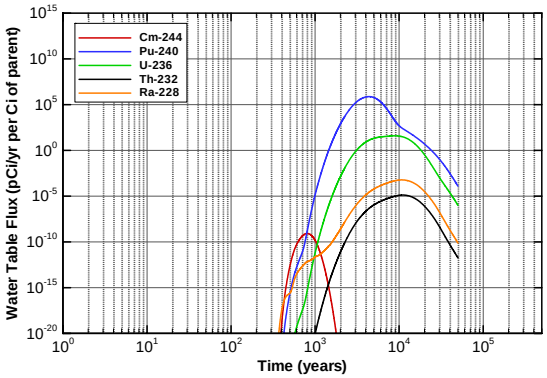

Figure A2A-92. Baseline CIG Segment 7 Inventory Water Table Flux for Cm-244

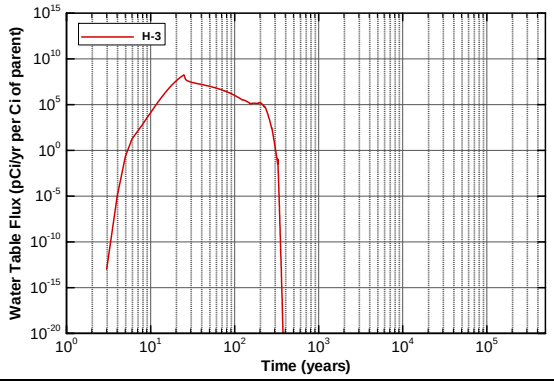

Figure A2A-93. Baseline CIG Segment 7 Inventory Water Table Flux for H-3

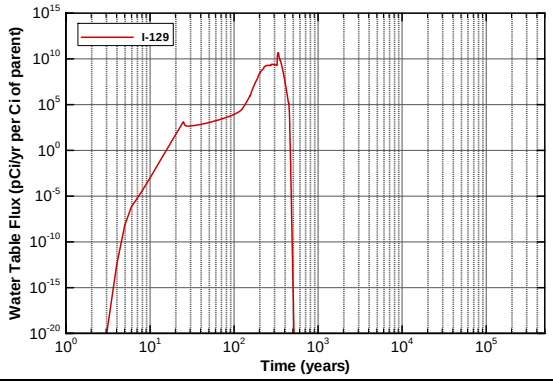

Figure A2A-94. Baseline CIG Segment 7 Inventory Water Table Flux for I-129

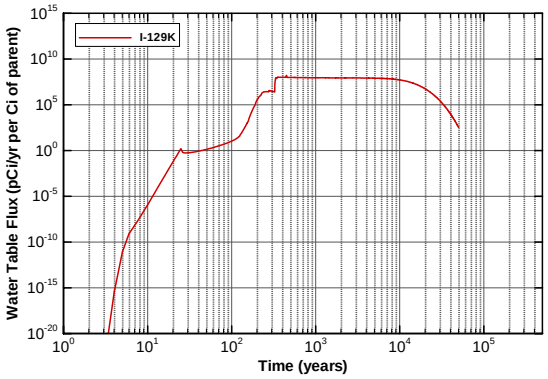

Figure A2A-95. Baseline CIG Segment 7 Inventory Water Table Flux for I-129K

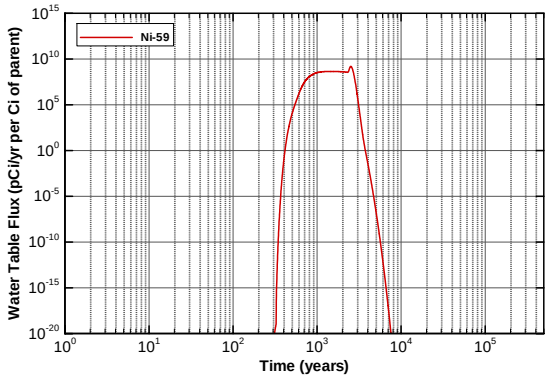

Figure A2A-96. Baseline CIG Segment 7 Inventory Water Table Flux for Ni-59

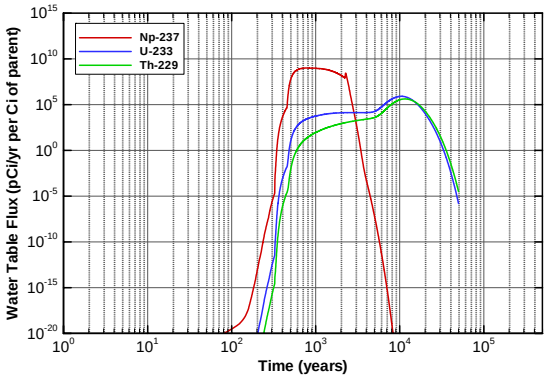

Figure A2A-97. Baseline CIG Segment 7 Inventory Water Table Flux for Np-237

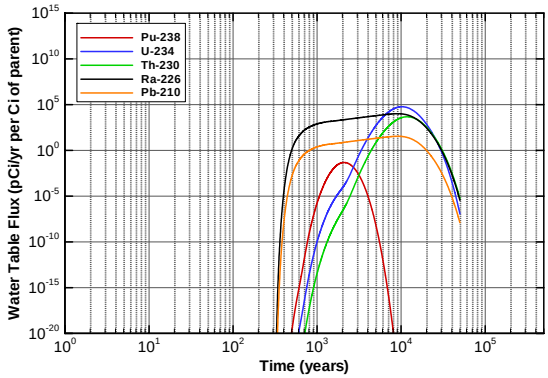

Figure A2A-98. Baseline CIG Segment 7 Inventory Water Table Flux for Pu-238

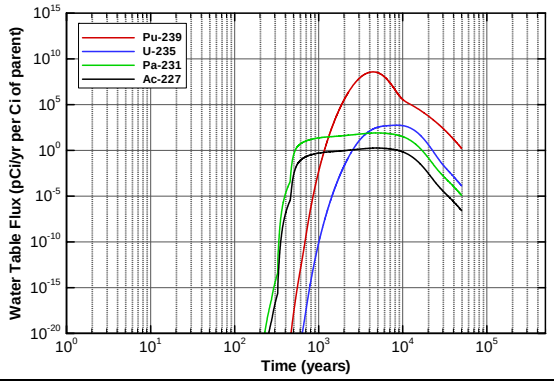

Figure A2A-99. Baseline CIG Segment 7 Inventory Water Table Flux for Pu-239

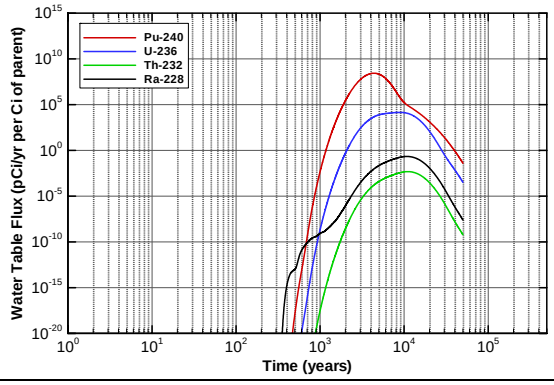

Figure A2A-100. Baseline CIG Segment 7 Inventory Water Table Flux for Pu-240

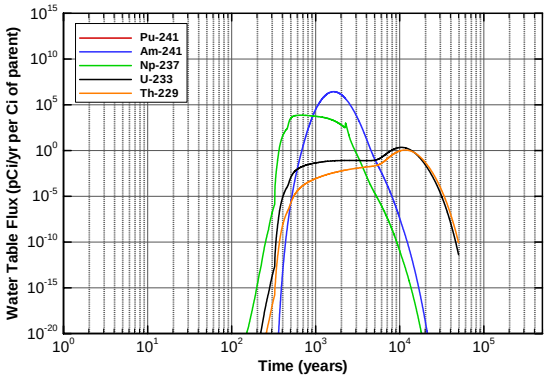

Figure A2A-101. Baseline CIG Segment 7 Inventory Water Table Flux for Pu-241

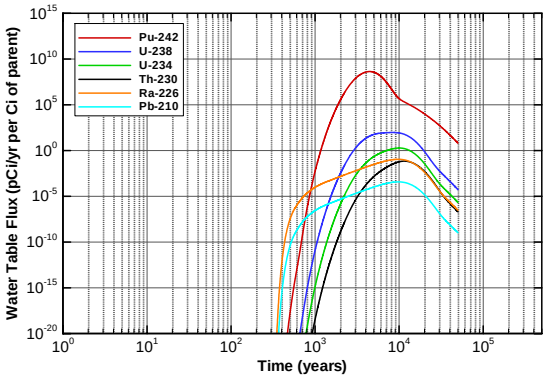

Figure A2A-102. Baseline CIG Segment 7 Inventory Water Table Flux for Pu-242

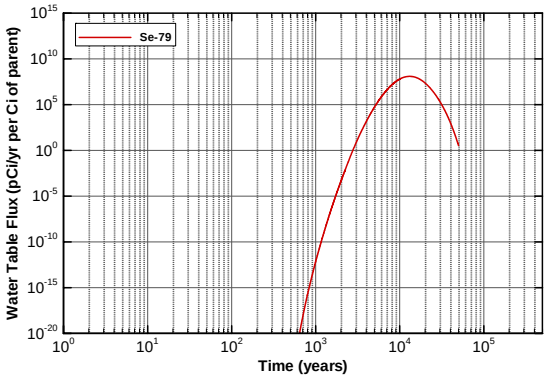

Figure A2A-103. Baseline CIG Segment 7 Inventory Water Table Flux for Se-79

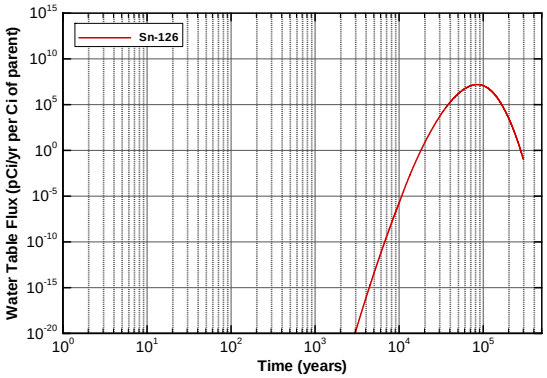

Figure A2A-104. Baseline CIG Segment 7 Inventory Water Table Flux for Sn-126

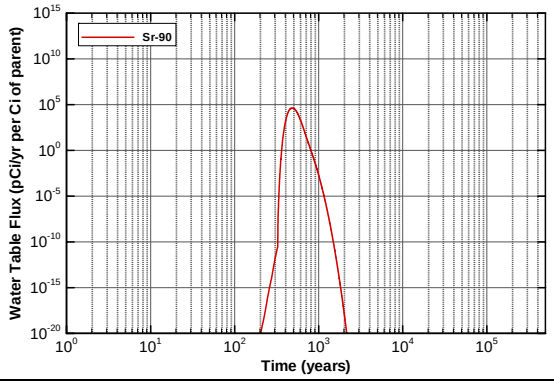

Figure A2A-105. Baseline CIG Segment 7 Inventory Water Table Flux for Sr-90

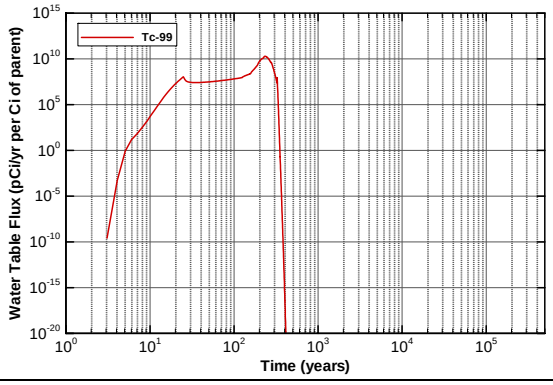

Figure A2A-106. Baseline CIG Segment 7 Inventory Water Table Flux for Tc-99

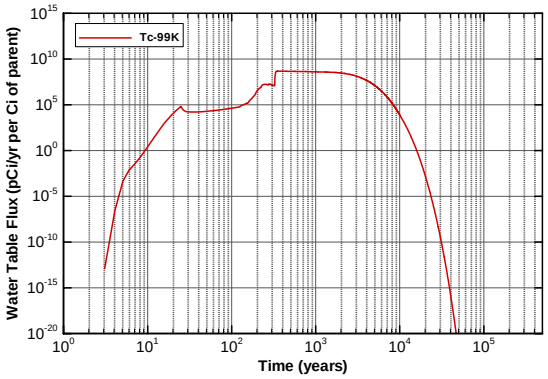

Figure A2A-107. Baseline CIG Segment 7 Inventory Water Table Flux for Tc-99K

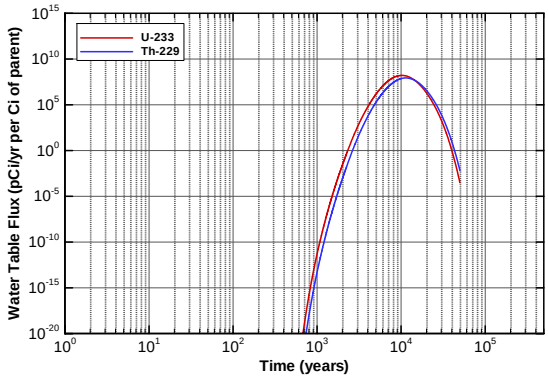

Figure A2A-108. Baseline CIG Segment 7 Inventory Water Table Flux for U-233

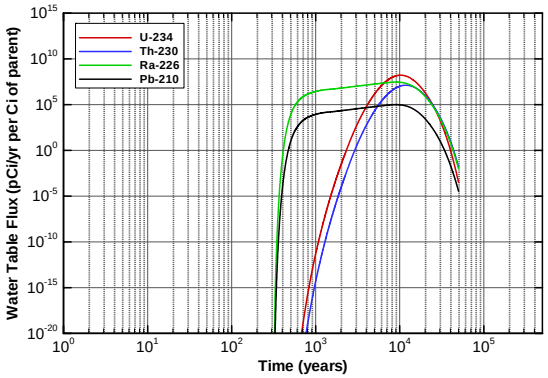

Figure A2A-109. Baseline CIG Segment 7 Inventory Water Table Flux for U-234

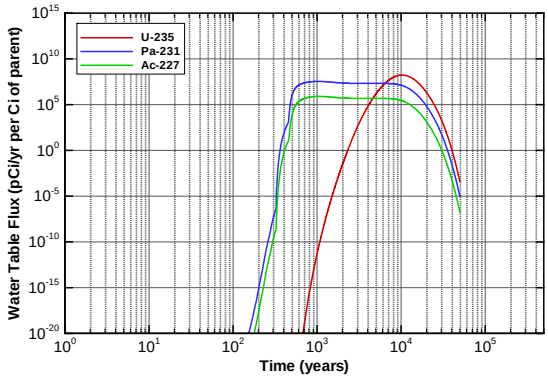

Figure A2A-110. Baseline CIG Segment 7 Inventory Water Table Flux for U-235

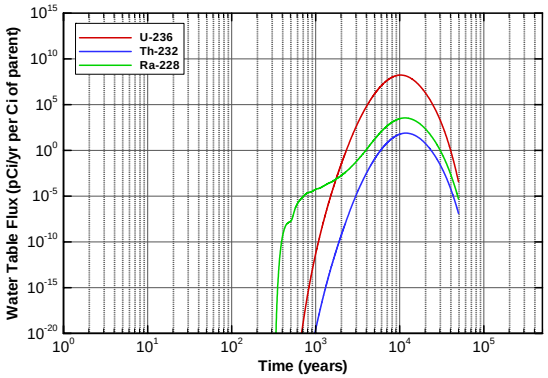

Figure A2A-111. Baseline CIG Segment 7 Inventory Water Table Flux for U-236

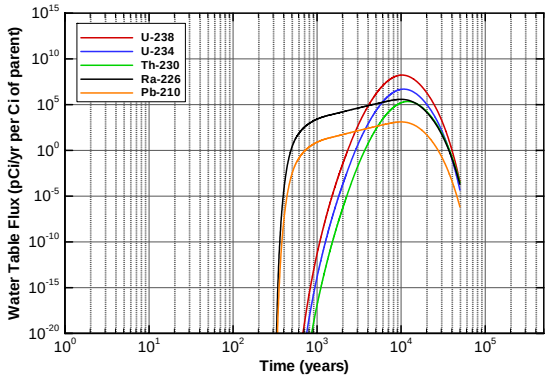

Figure A2A-112. Baseline CIG Segment 7 Inventory Water Table Flux for U-238

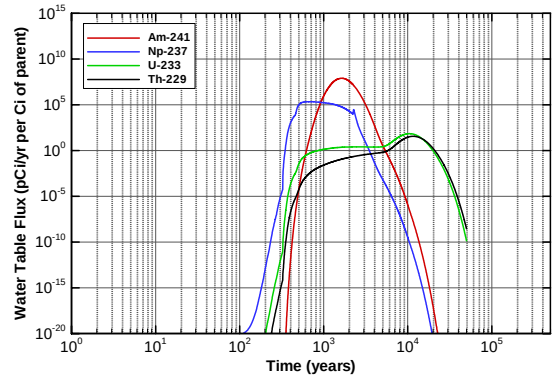

Figure A2A-113. Baseline CIG Segment 8 Inventory Water Table Flux for Am-241

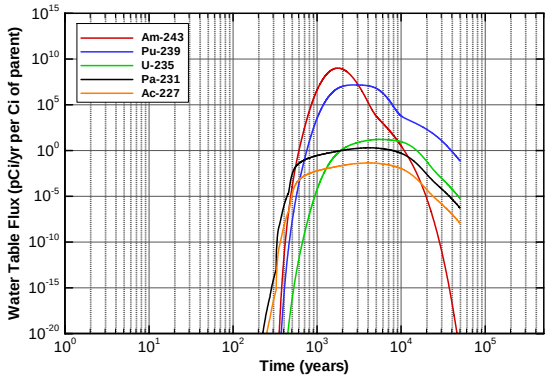

Figure A2A-114. Baseline CIG Segment 8 Inventory Water Table Flux for Am-243

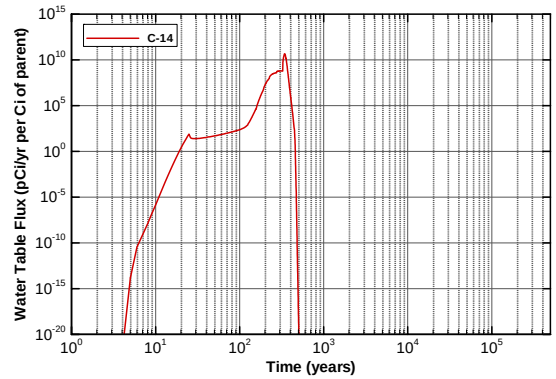

Figure A2A-115. Baseline CIG Segment 8 Inventory Water Table Flux for C-14

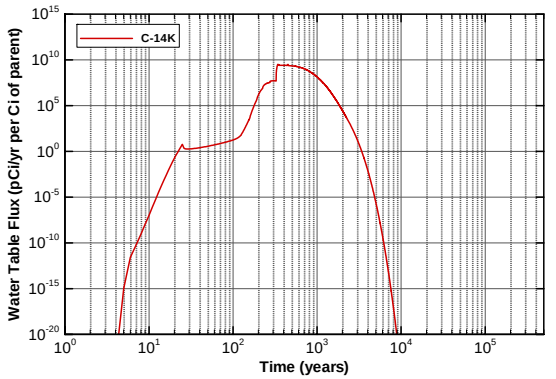

Figure A2A-116. Baseline CIG Segment 8 Inventory Water Table Flux for C-14K

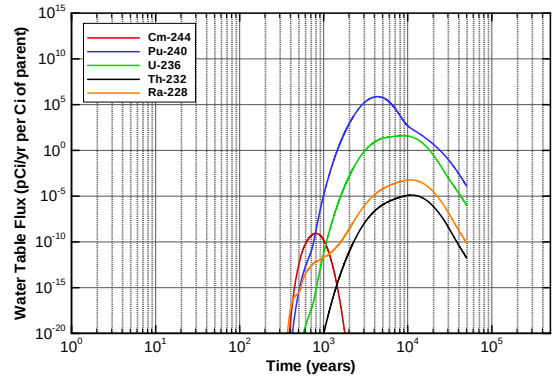

Figure A2A-117. Baseline CIG Segment 8 Inventory Water Table Flux for Cm-244

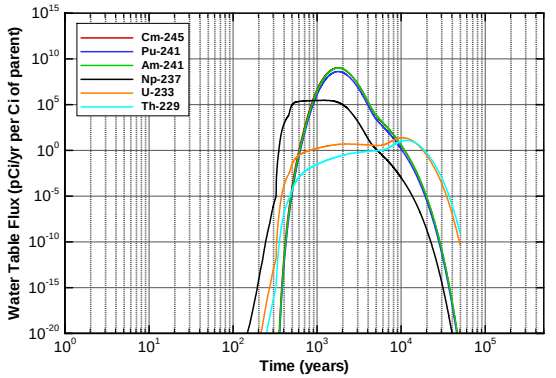

Figure A2A-118. Baseline CIG Segment 8 Inventory Water Table Flux for Cm-245

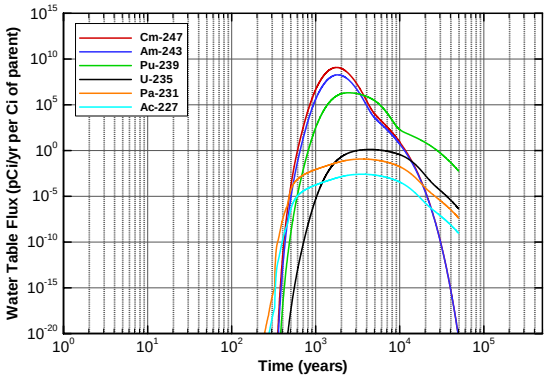

Figure A2A-119. Baseline CIG Segment 8 Inventory Water Table Flux for Cm-247

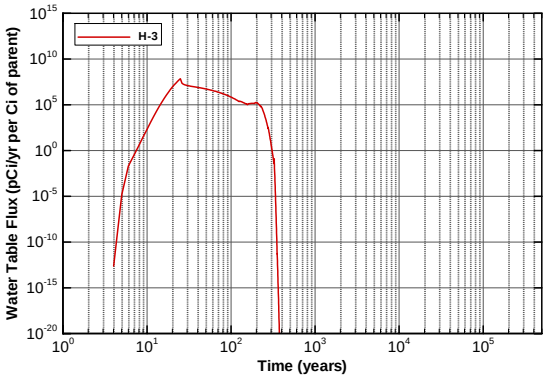

Figure A2A-120. Baseline CIG Segment 8 Inventory Water Table Flux for H-3

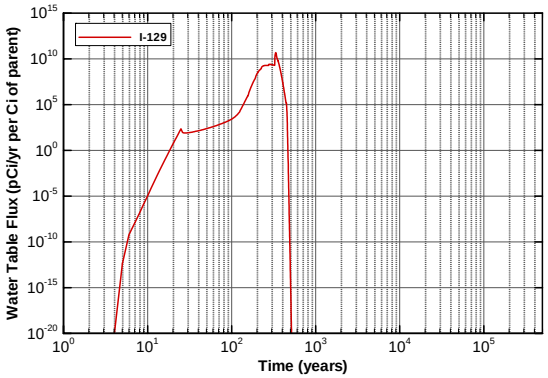

Figure A2A-121. Baseline CIG Segment 8 Inventory Water Table Flux for I-129

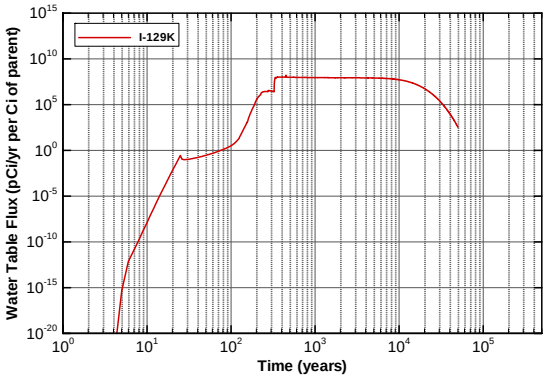

Figure A2A-122. Baseline CIG Segment 8 Inventory Water Table Flux for I-129K

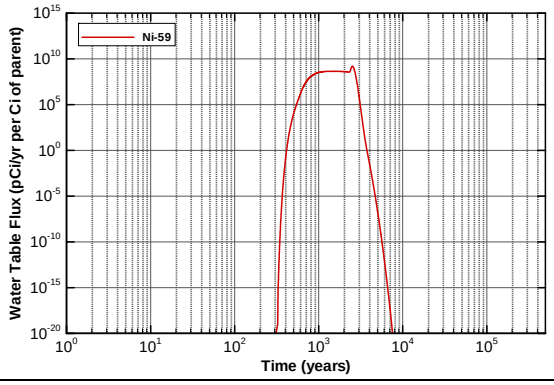

Figure A2A-123. Baseline CIG Segment 8 Inventory Water Table Flux for Ni-59

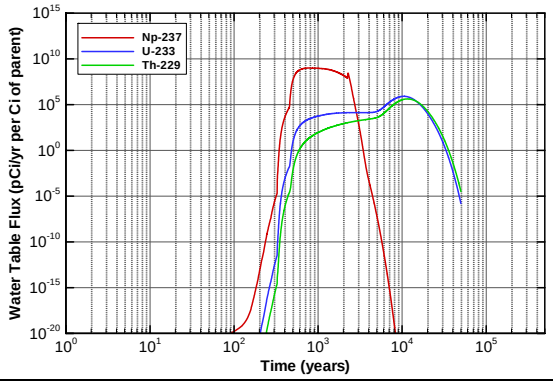

Figure A2A-124. Baseline CIG Segment 8 Inventory Water Table Flux for Np-237

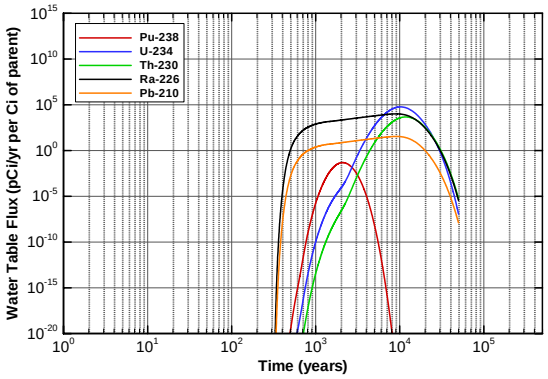

Figure A2A-125. Baseline CIG Segment 8 Inventory Water Table Flux for Pu-238

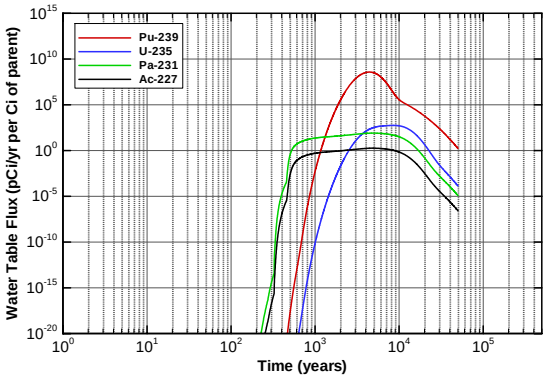

Figure A2A-126. Baseline CIG Segment 8 Inventory Water Table Flux for Pu-239

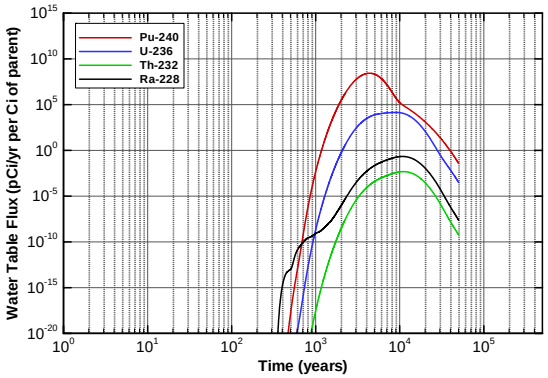

Figure A2A-127. Baseline CIG Segment 8 Inventory Water Table Flux for Pu-240

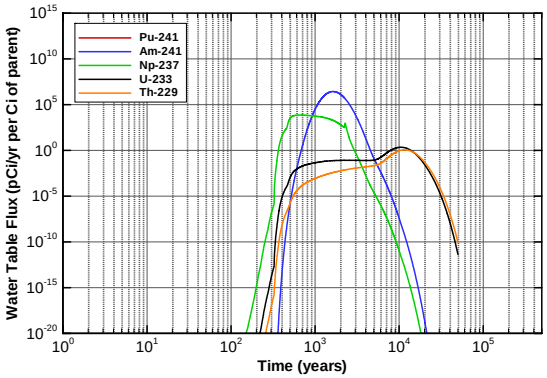

Figure A2A-128. Baseline CIG Segment 8 Inventory Water Table Flux for Pu-241

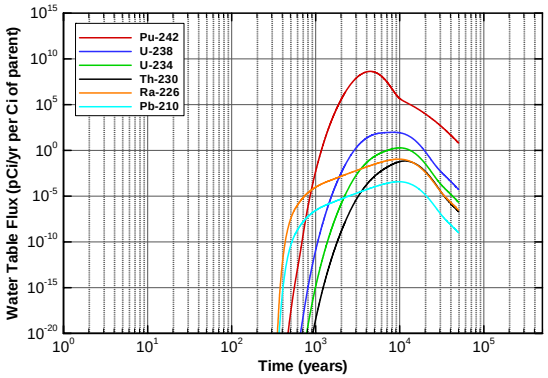

Figure A2A-129. Baseline CIG Segment 8 Inventory Water Table Flux for Pu-242

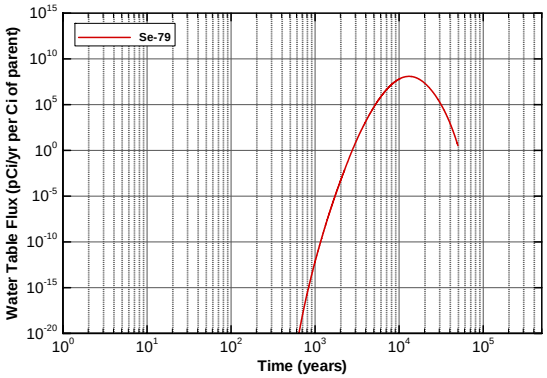

Figure A2A-130. Baseline CIG Segment 8 Inventory Water Table Flux for Se-79

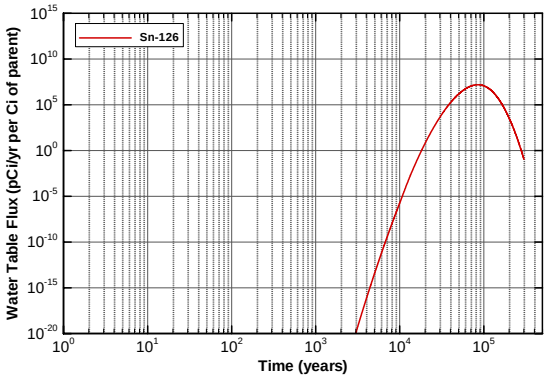

Figure A2A-131. Baseline CIG Segment 8 Inventory Water Table Flux for Sn-126

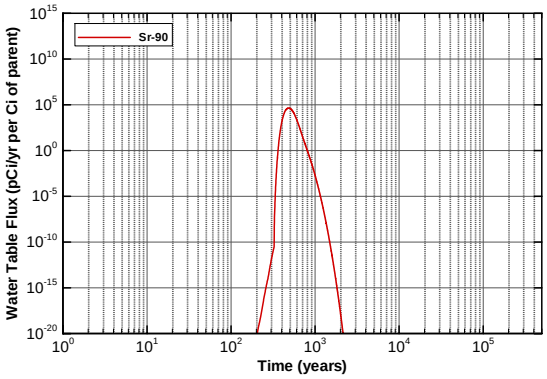

Figure A2A-132. Baseline CIG Segment 8 Inventory Water Table Flux for Sr-90

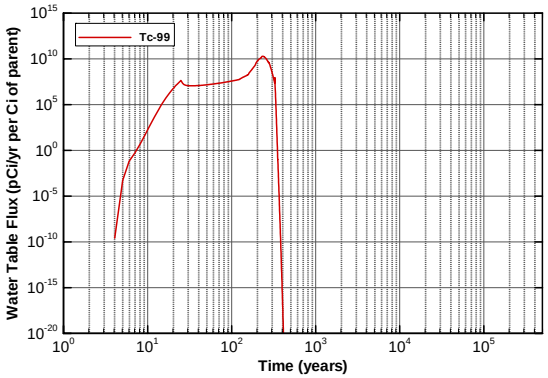

Figure A2A-133. Baseline CIG Segment 8 Inventory Water Table Flux for Tc-99

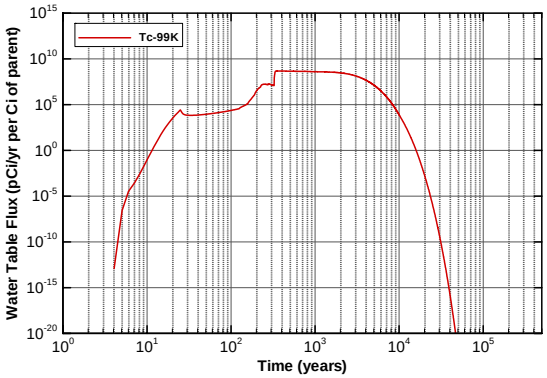

Figure A2A-134. Baseline CIG Segment 8 Inventory Water Table Flux for Tc-99K

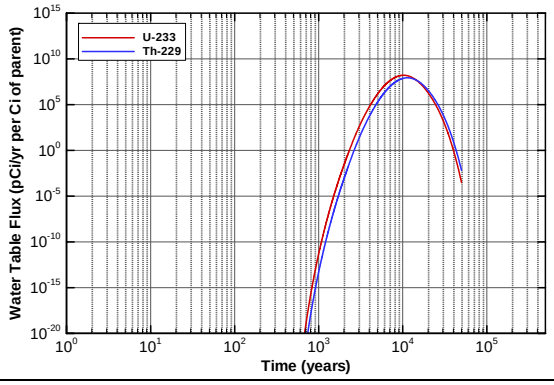

Figure A2A-135. Baseline CIG Segment 8 Inventory Water Table Flux for U-233

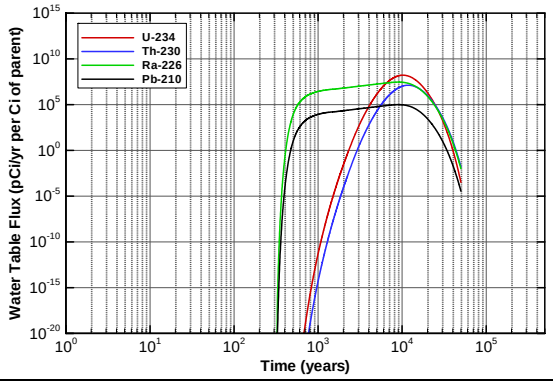

Figure A2A-136. Baseline CIG Segment 8 Inventory Water Table Flux for U-234

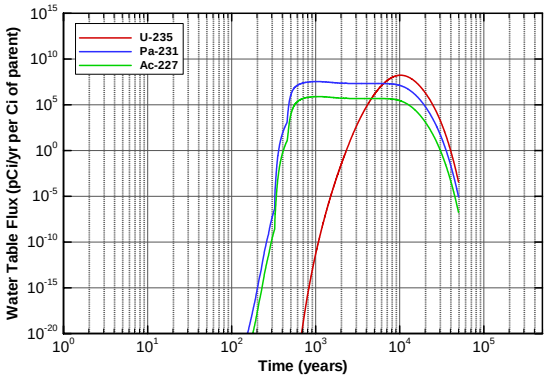

Figure A2A-137. Baseline CIG Segment 8 Inventory Water Table Flux for U-235

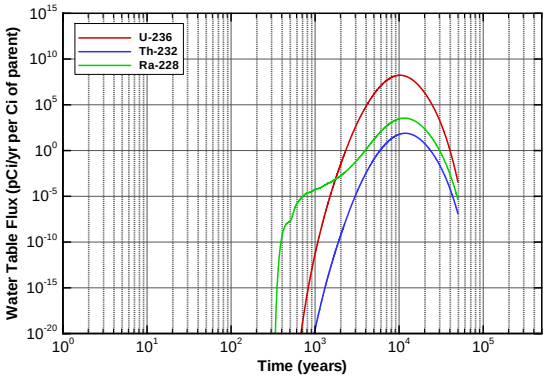

Figure A2A-138. Baseline CIG Segment 8 Inventory Water Table Flux for U-236

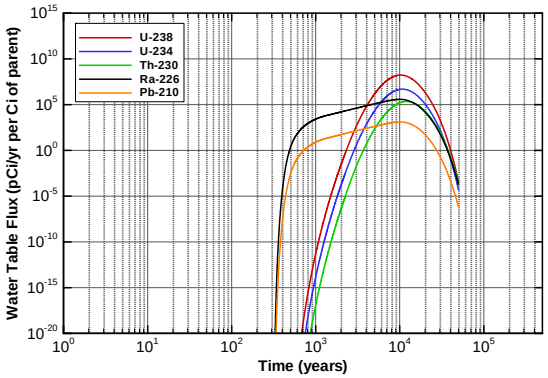

Figure A2A-139. Baseline CIG Segment 8 Inventory Water Table Flux for U-238

Flux to Water Table - Future Inventory (Flux based on unit curie inventory)

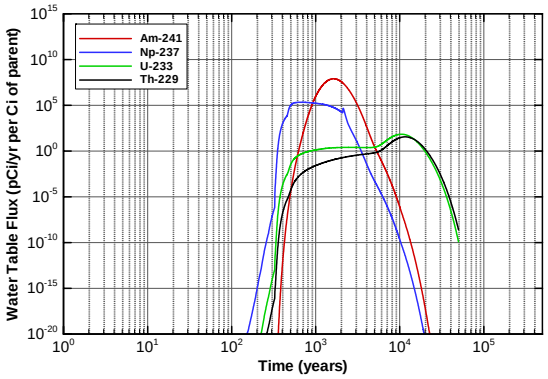

Figure A2A-140. Baseline CIG Future Inventory Water Table Flux for Am-241

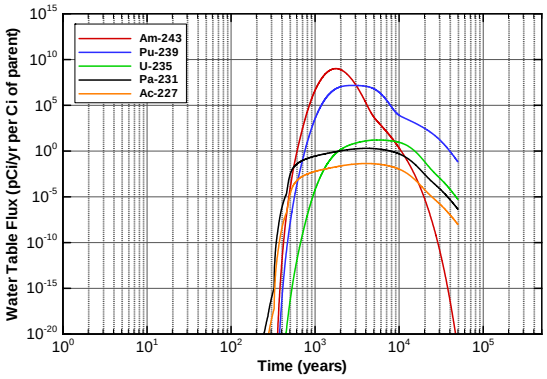

Figure A2A-141. Baseline CIG Future Inventory Water Table Flux for Am-243

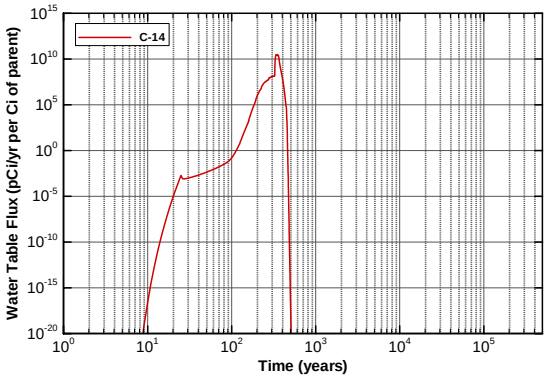

Figure A2A-142. Baseline CIG Future Inventory Water Table Flux for C-14

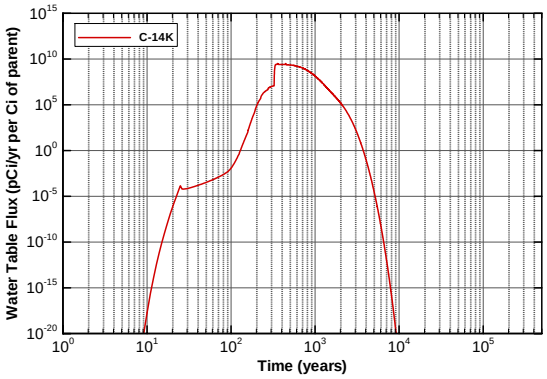

Figure A2A-143. Baseline CIG Future Inventory Water Table Flux for C-14K

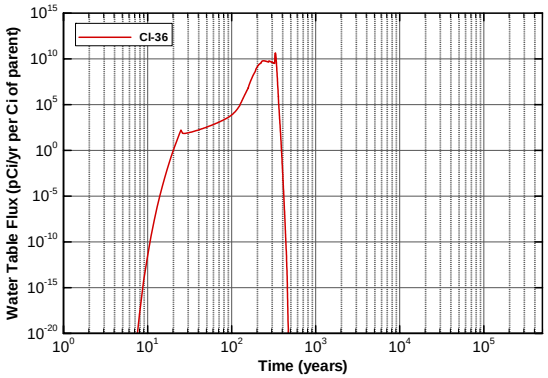

Figure A2A-144. Baseline CIG Future Inventory Water Table Flux for Cl-36

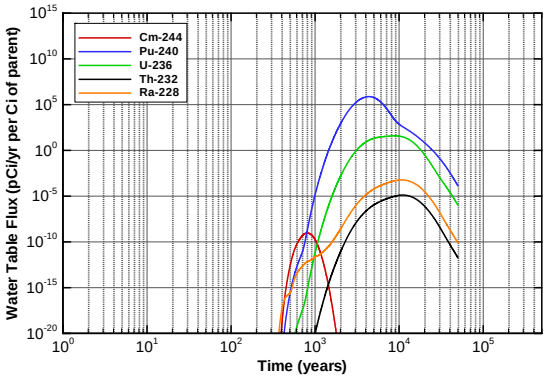

Figure A2A-145. Baseline CIG Future Inventory Water Table Flux for Cm-244

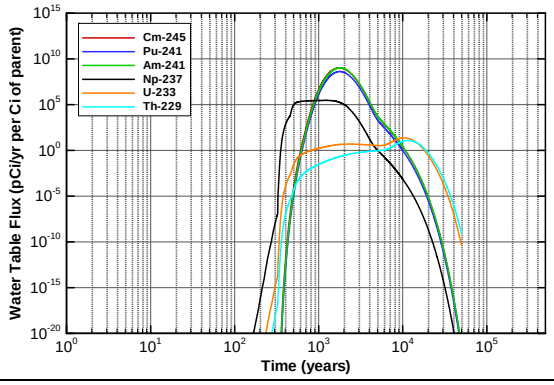

Figure A2A-146. Baseline CIG Future Inventory Water Table Flux for Cm-245

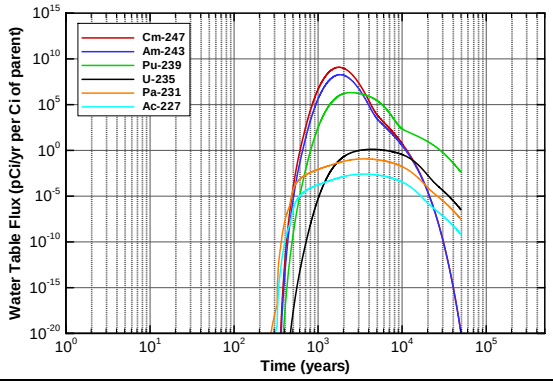

Figure A2A-147. Baseline CIG Future Inventory Water Table Flux for Cm-247

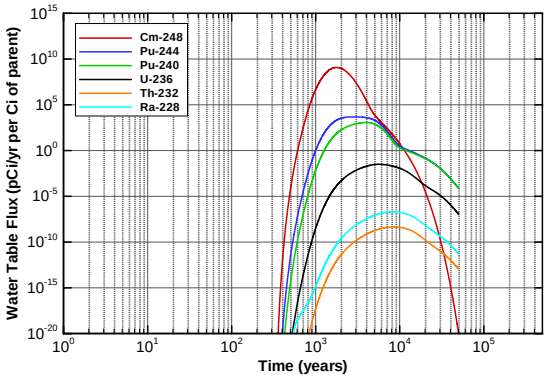

Figure A2A-148. Baseline CIG Future Inventory Water Table Flux for Cm-248

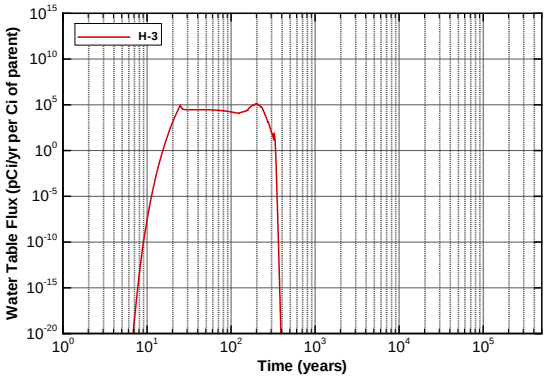

Figure A2A-149. Baseline CIG Future Inventory Water Table Flux for H-3

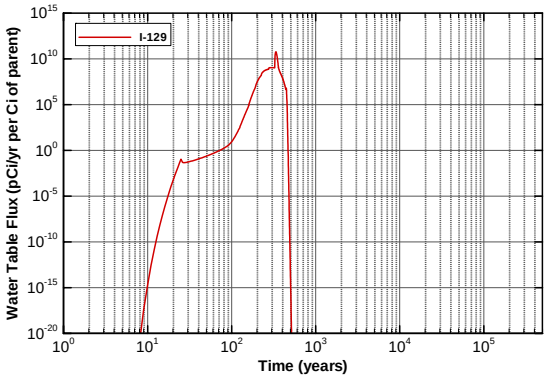

Figure A2A-150. Baseline CIG Future Inventory Water Table Flux for I-129

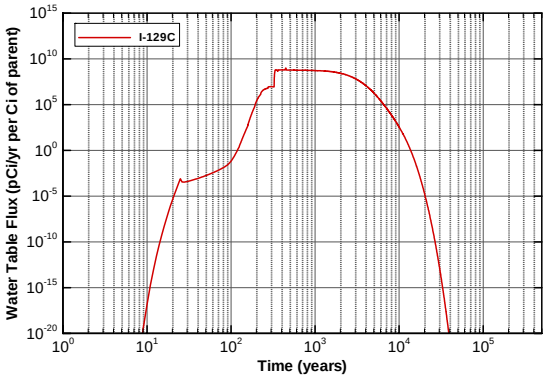

Figure A2A-151. Baseline CIG Future Inventory Water Table Flux for I-129C

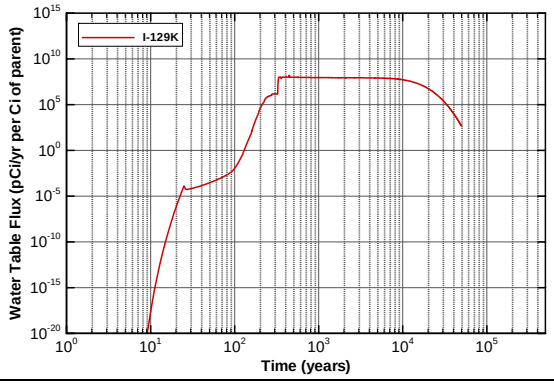

Figure A2A-152. Baseline CIG Future Inventory Water Table Flux for I-129K

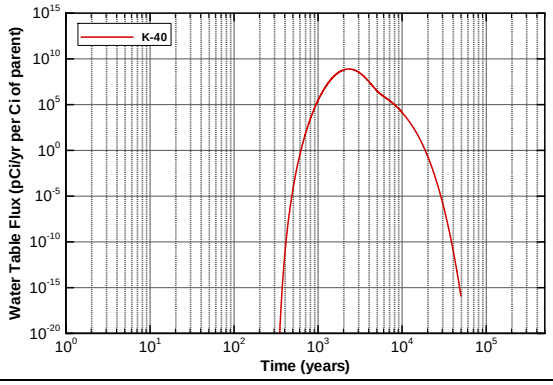

Figure A2A-153. Baseline CIG Future Inventory Water Table Flux for K-40

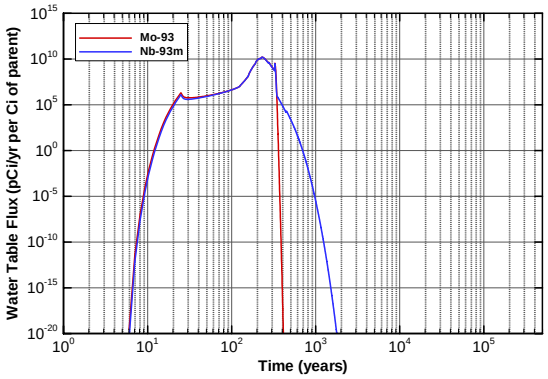

Figure A2A-154. Baseline CIG Future Inventory Water Table Flux for Mo-93

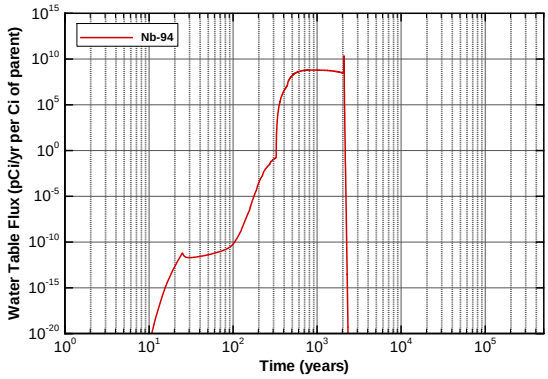

Figure A2A-155. Baseline CIG Future Inventory Water Table Flux for Nb-94

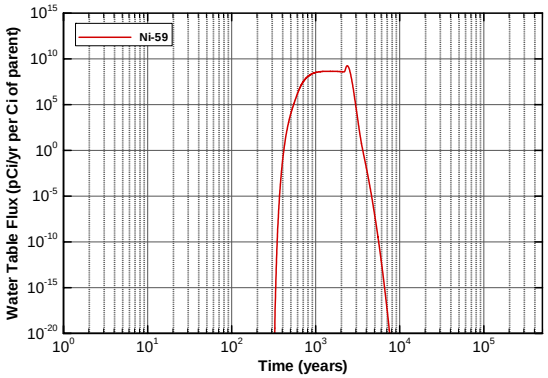

Figure A2A-156. Baseline CIG Future Inventory Water Table Flux for Ni-59

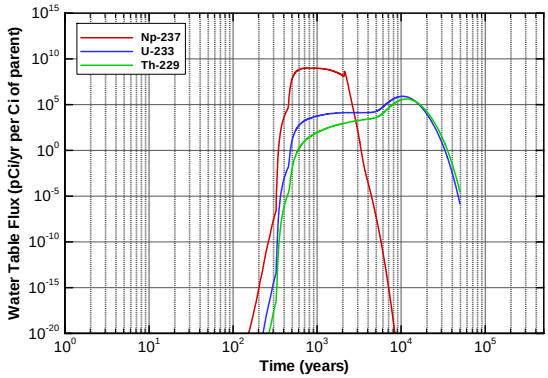

Figure A2A-157. Baseline CIG Future Inventory Water Table Flux for Np-237

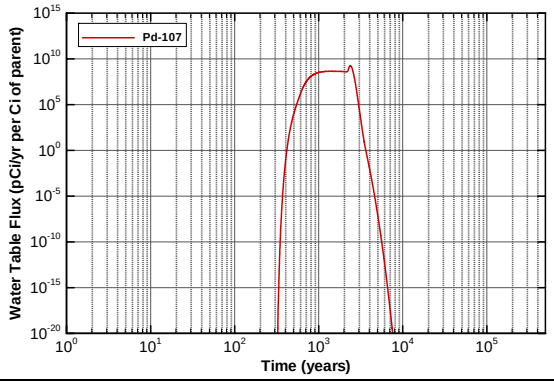

Figure A2A-158. Baseline CIG Future Inventory Water Table Flux for Pd-107

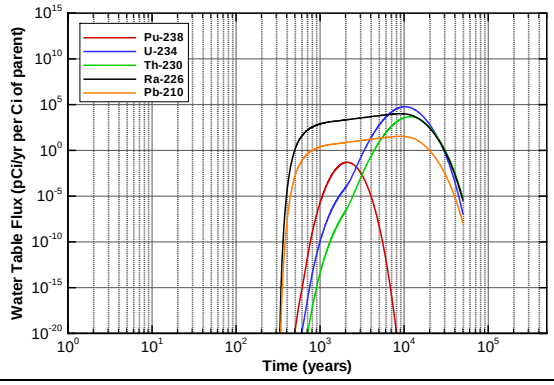

Figure A2A-159. Baseline CIG Future Inventory Water Table Flux for Pu-238

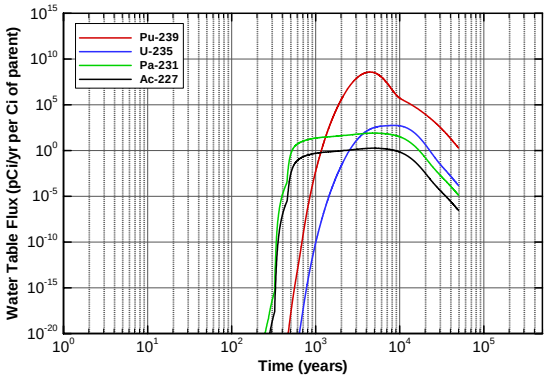

Figure A2A-160. Baseline CIG Future Inventory Water Table Flux for Pu-239

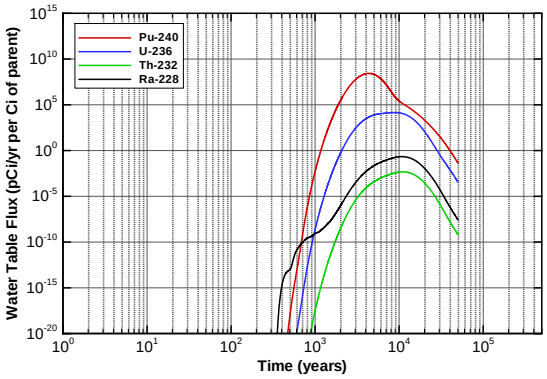

Figure A2A-161. Baseline CIG Future Inventory Water Table Flux for Pu-240

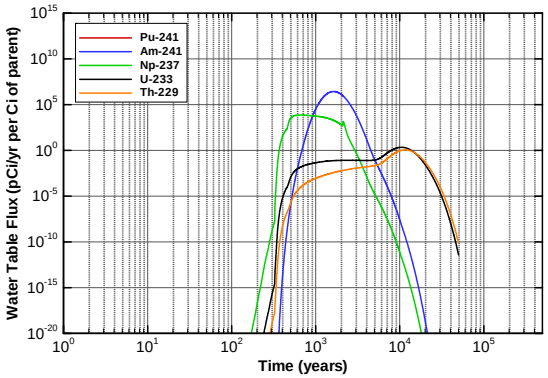

Figure A2A-162. Baseline CIG Future Inventory Water Table Flux for Pu-241

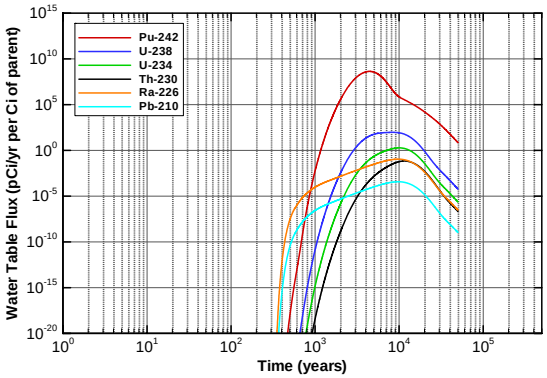

Figure A2A-163. Baseline CIG Future Inventory Water Table Flux for Pu-242

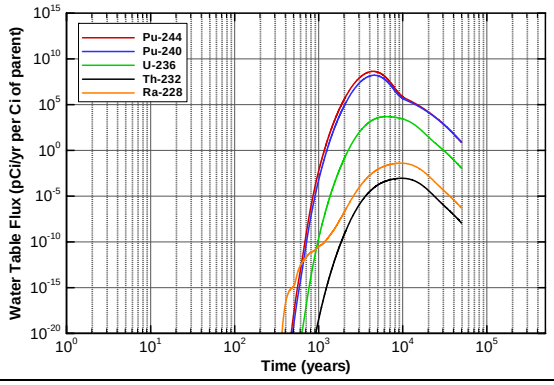

Figure A2A-164. Baseline CIG Future Inventory Water Table Flux for Pu-244

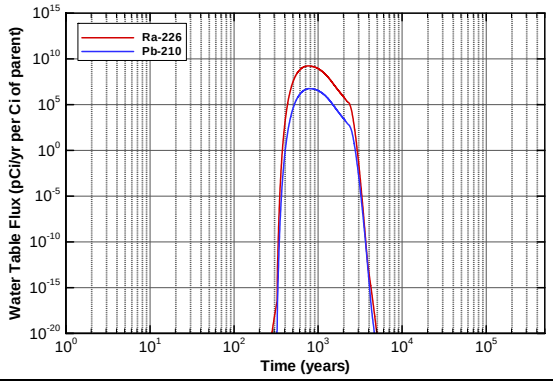

Figure A2A-165. Baseline CIG Future Inventory Water Table Flux for RA226

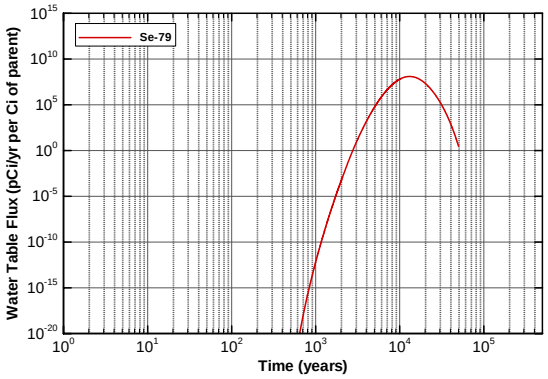

Figure A2A-166. Baseline CIG Future Inventory Water Table Flux for Se-79

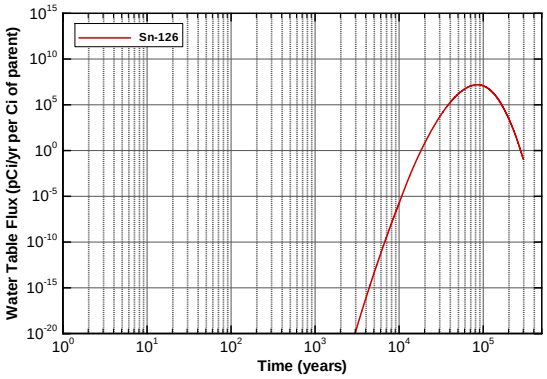

Figure A2A-167. Baseline CIG Future Inventory Water Table Flux for Sn-126

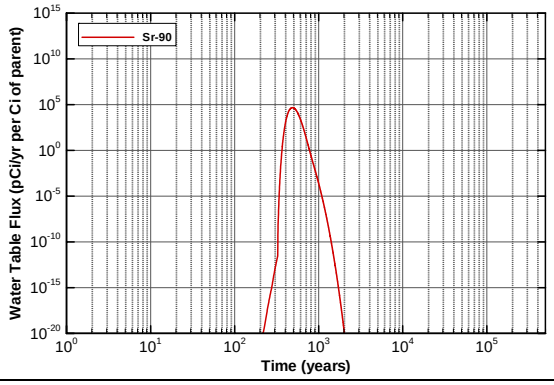

Figure A2A-168. Baseline CIG Future Inventory Water Table Flux for Sr-90

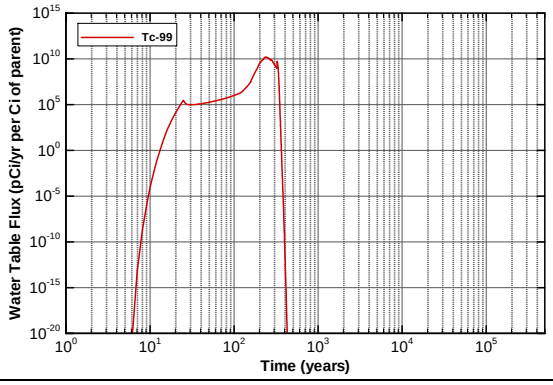

Figure A2A-169. Baseline CIG Future Inventory Water Table Flux for Tc-99

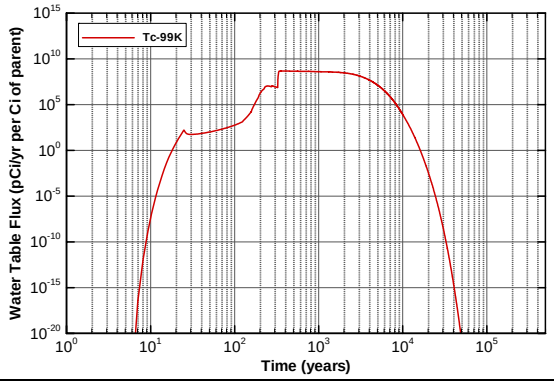

Figure A2A-170. Baseline CIG Future Inventory Water Table Flux for Tc-99K

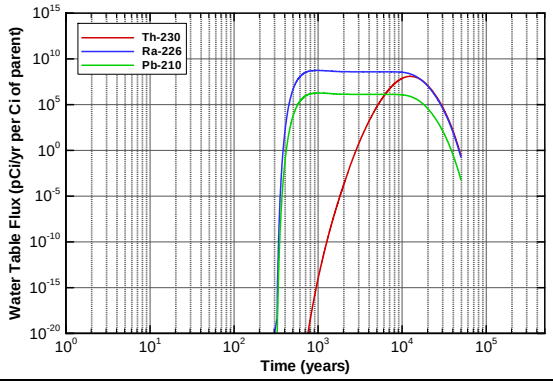

Figure A2A-171. Baseline CIG Future Inventory Water Table Flux for Th-230

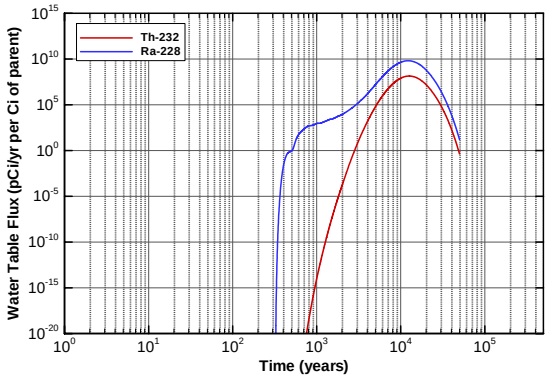

Figure A2A-172. Baseline CIG Future Inventory Water Table Flux for Th-232

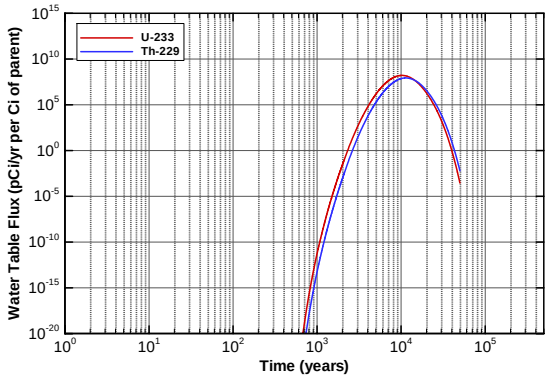

Figure A2A-173. Baseline CIG Future Inventory Water Table Flux for U-233

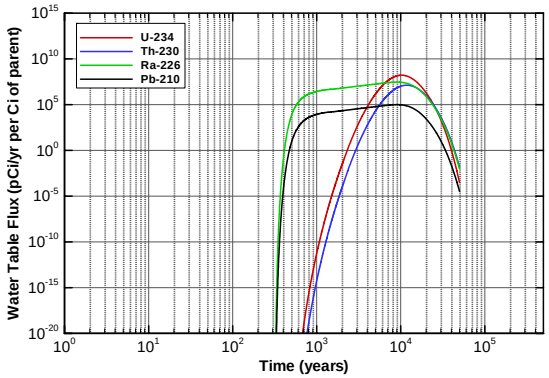

Figure A2A-174. Baseline CIG Future Inventory Water Table Flux for U-234

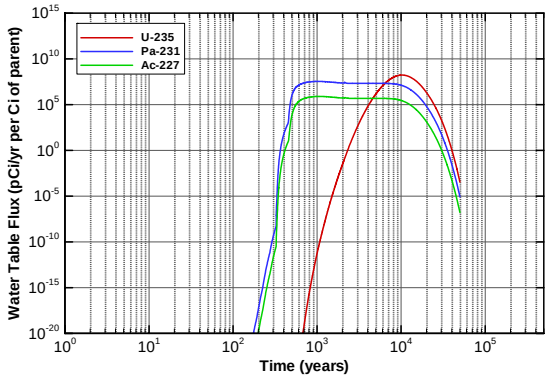

Figure A2A-175. Baseline CIG Future Inventory Water Table Flux for U-235

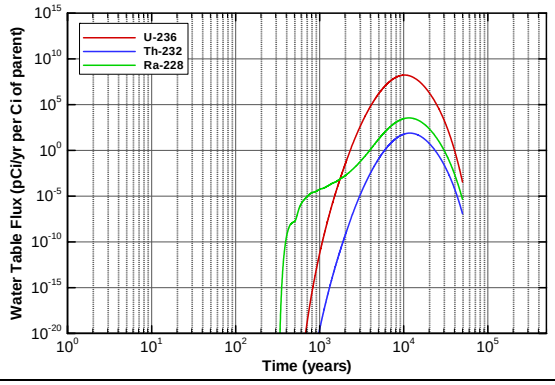

Figure A2A-176. Baseline CIG Future Inventory Water Table Flux for U-236

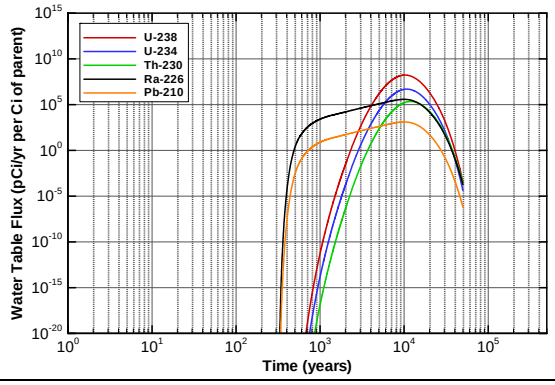

Figure A2A-177. Baseline CIG Future Inventory Water Table Flux for U-238

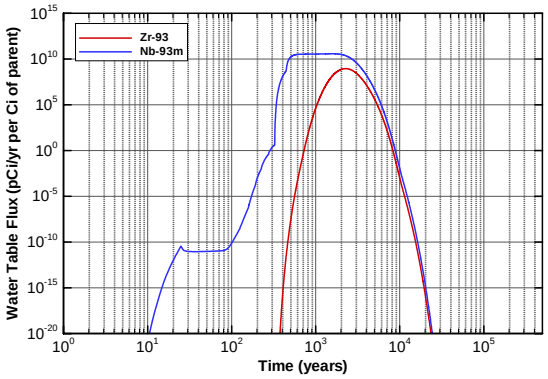

Figure A2A-178. Baseline CIG Future Inventory Water Table Flux for Zr-93

100-m Well Concentrations - Existing Inventory

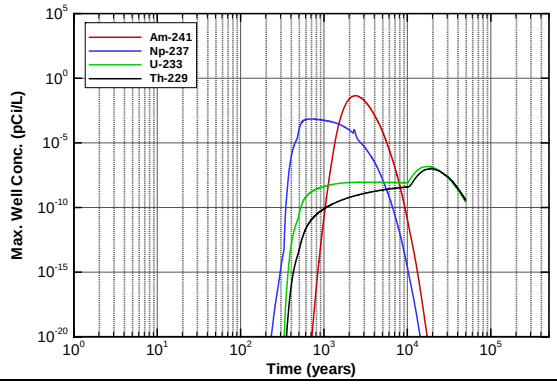

Figure A2A-179. Baseline CIG Existing Inventory Max. Well Concentration for Am-241

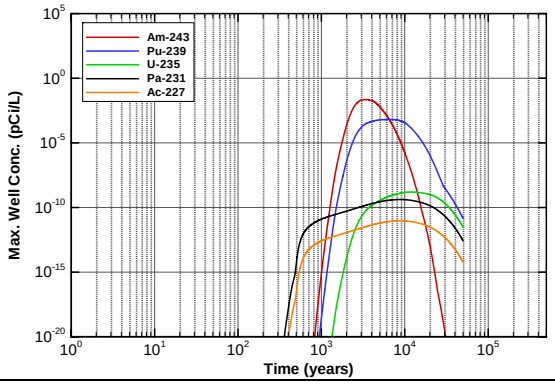

Figure A2A-180. Baseline CIG Existing Inventory Max. Well Concentration for Am-243

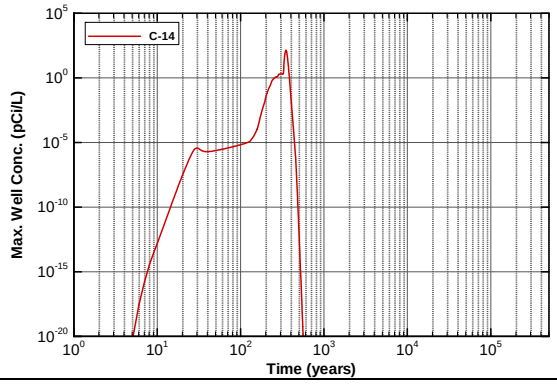

Figure A2A-181. Baseline CIG Existing Inventory Max. Well Concentration for C-14

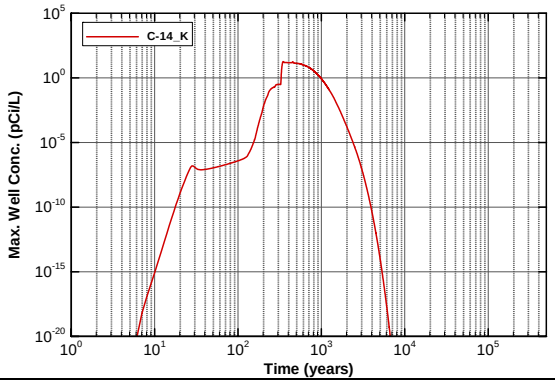

Figure A2A-182. Baseline CIG Existing Inventory Max. Well Concentration for C-14_K

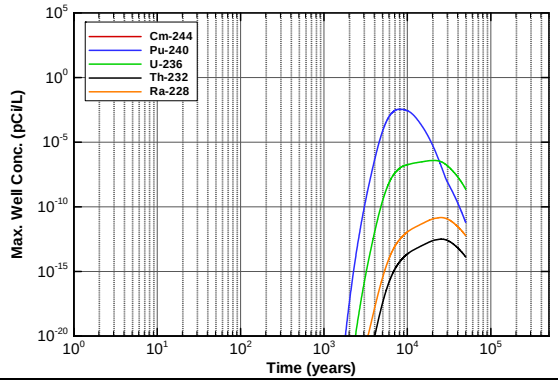

Figure A2A-183. Baseline CIG Existing Inventory Max. Well Concentration for Cm-244

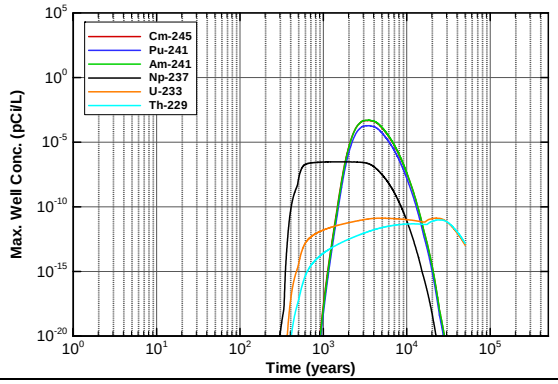

Figure A2A-184. Baseline CIG Existing Inventory Max. Well Concentration for Cm-245

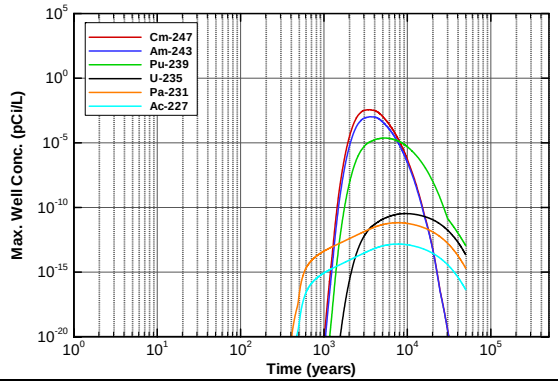

Figure A2A-185. Baseline CIG Existing Inventory Max. Well Concentration for Cm-247

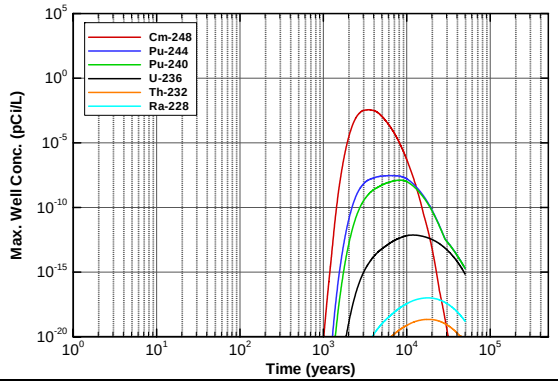

Figure A2A-186. Baseline CIG Existing Inventory Max. Well Concentration for Cm-248

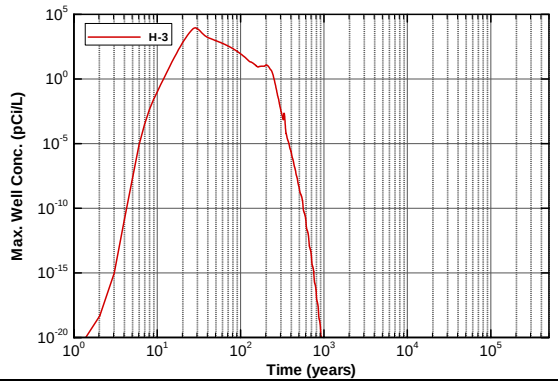

Figure A2A-187. Baseline CIG Existing Inventory Max. Well Concentration for H-3

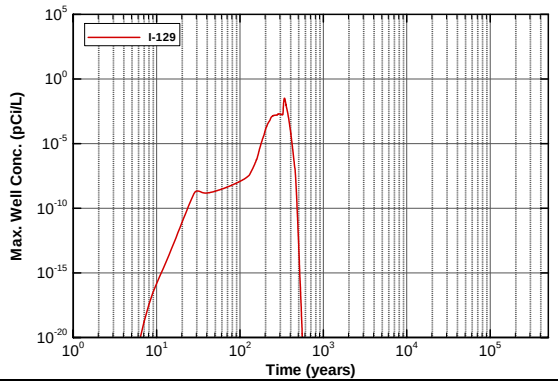

Figure A2A-188. Baseline CIG Existing Inventory Max. Well Concentration for I-129

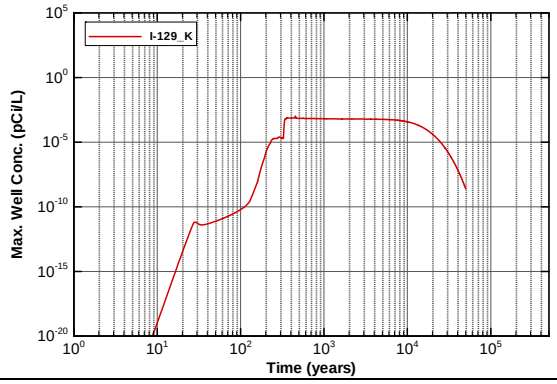

Figure A2A-189. Baseline CIG Existing Inventory Max. Well Concentration for I-129_K

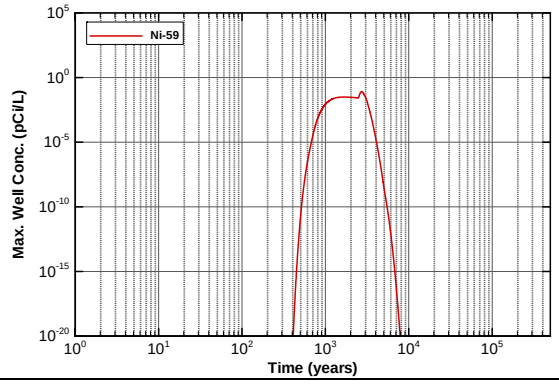

Figure A2A-190. Baseline CIG Existing Inventory Max. Well Concentration for Ni-59

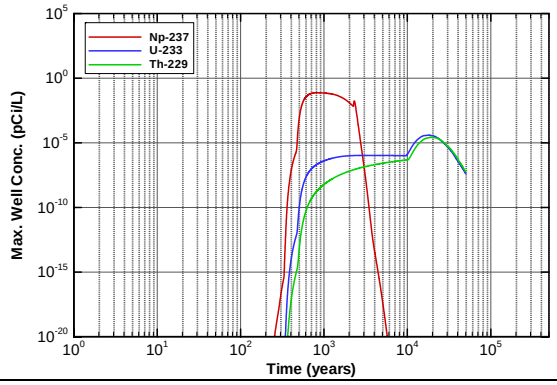

Figure A2A-191. Baseline CIG Existing Inventory Max. Well Concentration for Np-237

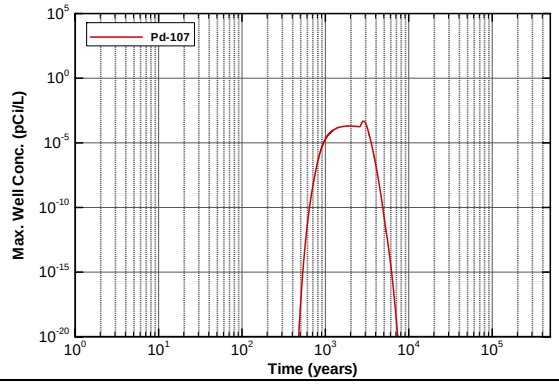

Figure A2A-192. Baseline CIG Existing Inventory Max. Well Concentration for Pd-107

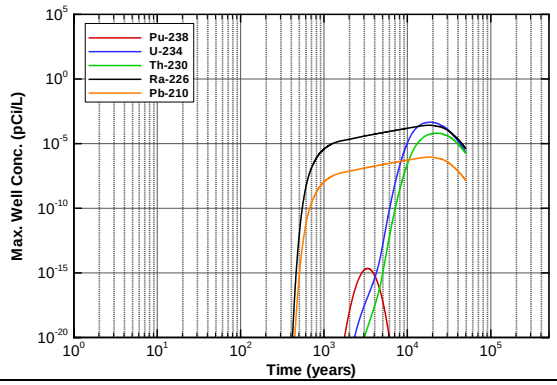

Figure A2A-193. Baseline CIG Existing Inventory Max. Well Concentration for Pu-238

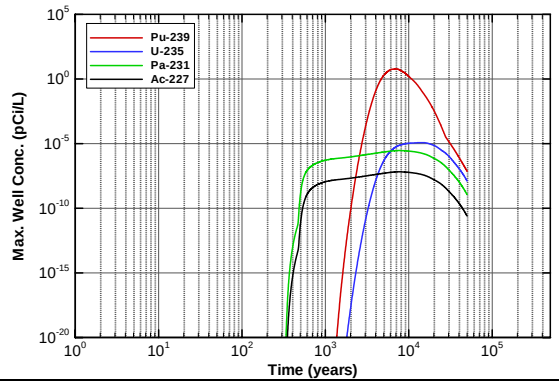

Figure A2A-194. Baseline CIG Existing Inventory Max. Well Concentration for Pu-239

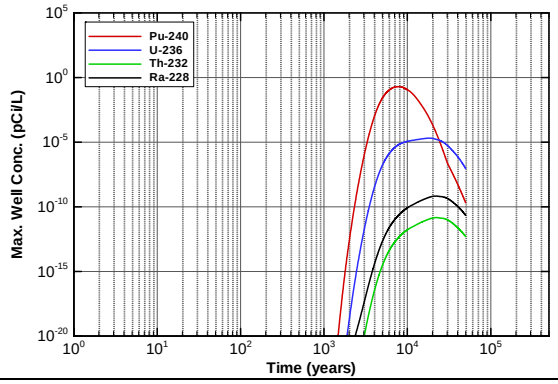

Figure A2A-195. Baseline CIG Existing Inventory Max. Well Concentration for Pu-240

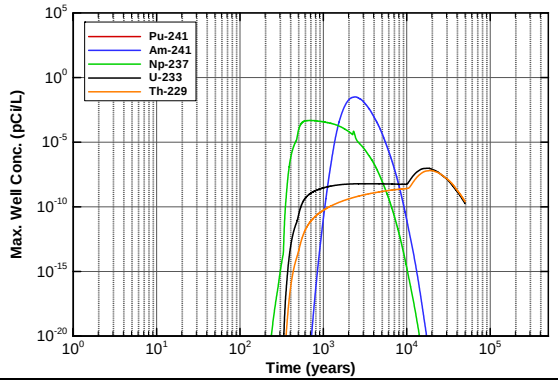

Figure A2A-196. Baseline CIG Existing Inventory Max. Well Concentration for Pu-241

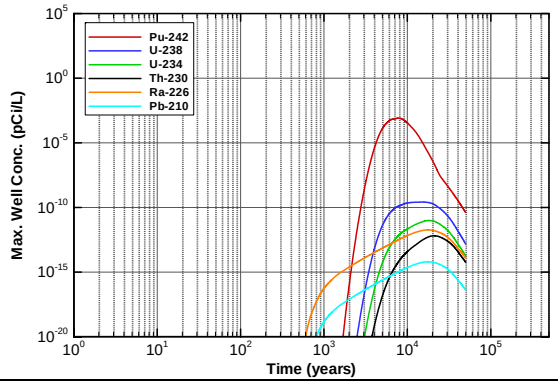

Figure A2A-197. Baseline CIG Existing Inventory Max. Well Concentration for Pu-242

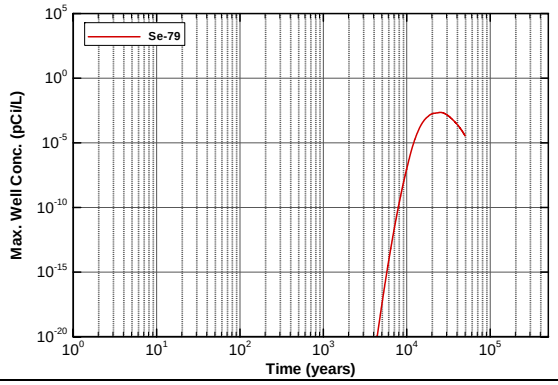

Figure A2A-198. Baseline CIG Existing Inventory Max. Well Concentration for Se-79

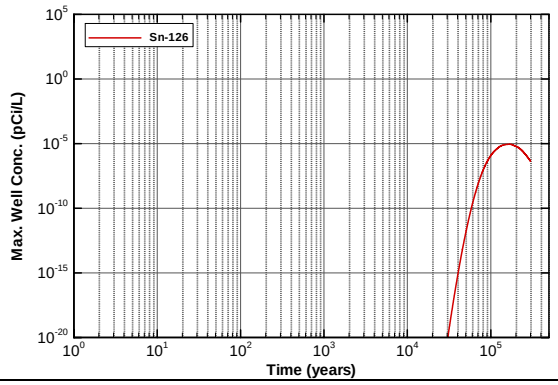

Figure A2A-199. Baseline CIG Existing Inventory Max. Well Concentration for Sn-126

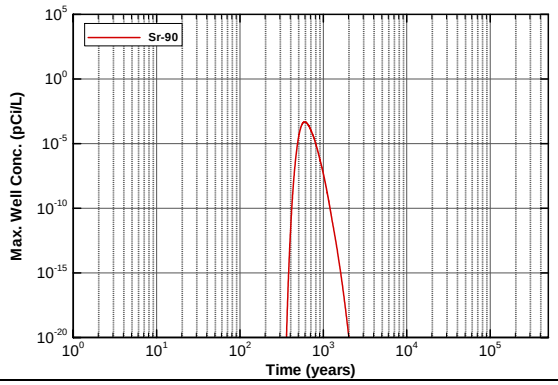

Figure A2A-200. Baseline CIG Existing Inventory Max. Well Concentration for Sr-90

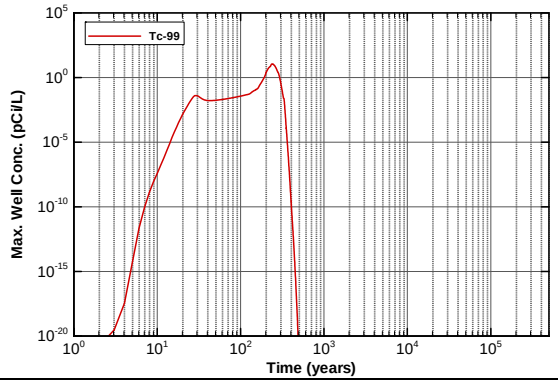

Figure A2A-201. Baseline CIG Existing Inventory Max. Well Concentration for Tc-99

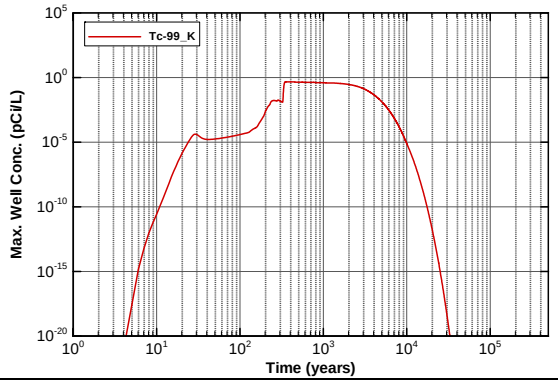

Figure A2A-202. Baseline CIG Existing Inventory Max. Well Concentration for Tc-99_K

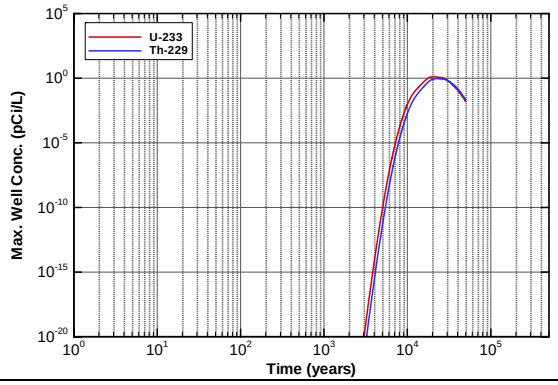

Figure A2A-203. Baseline CIG Existing Inventory Max. Well Concentration for U-233

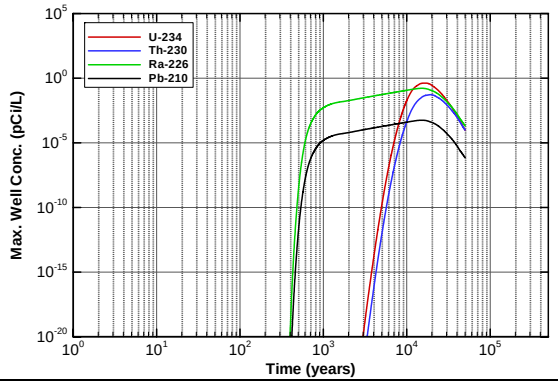

Figure A2A-204. Baseline CIG Existing Inventory Max. Well Concentration for U-234

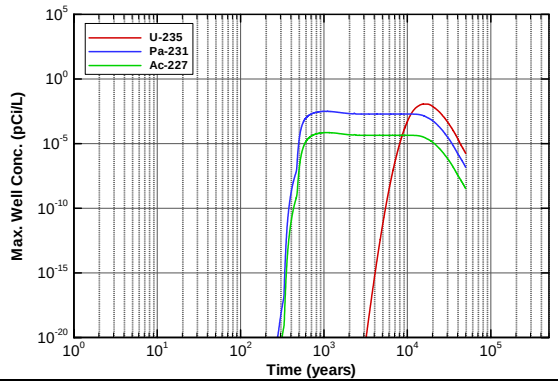

Figure A2A-205. Baseline CIG Existing Inventory Max. Well Concentration for U-235

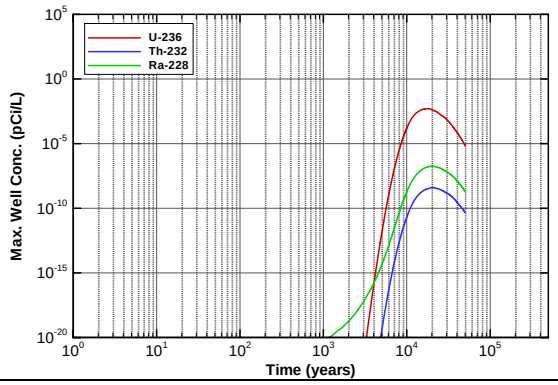

Figure A2A-206. Baseline CIG Existing Inventory Max. Well Concentration for U-236

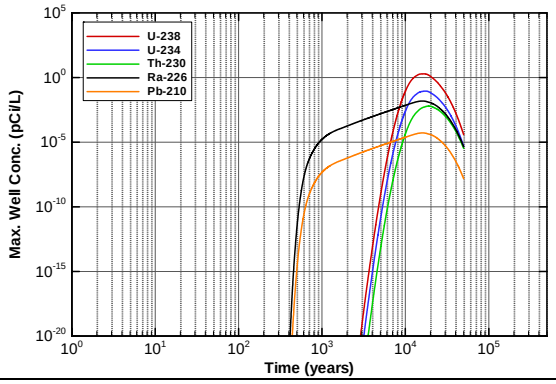

Figure A2A-207. Baseline CIG Existing Inventory Max. Well Concentration for U-238

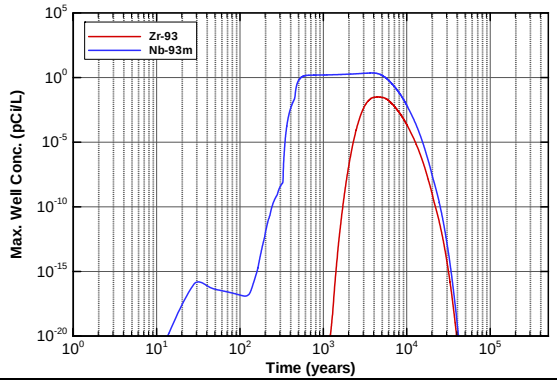

Figure A2A-208. Baseline CIG Existing Inventory Max. Well Concentration for Zr-93

100-m Well Concentrations - Future Inventory
(Concentrations based on unit curie inventory.)

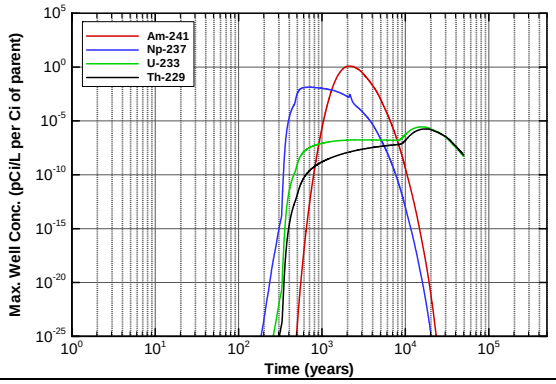

Figure A2A-209. Baseline CIG Future Inventory Max. Well Concentration for Am-241

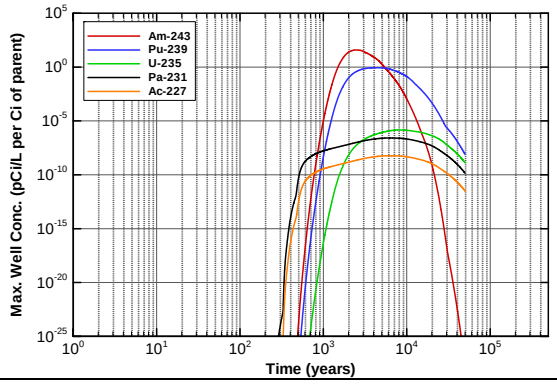

Figure A2A-210. Baseline CIG Future Inventory Max. Well Concentration for Am-243

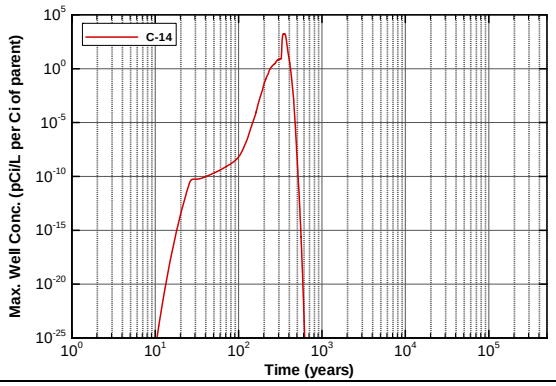

Figure A2A-211. Baseline CIG Future Inventory Max. Well Concentration for C-14

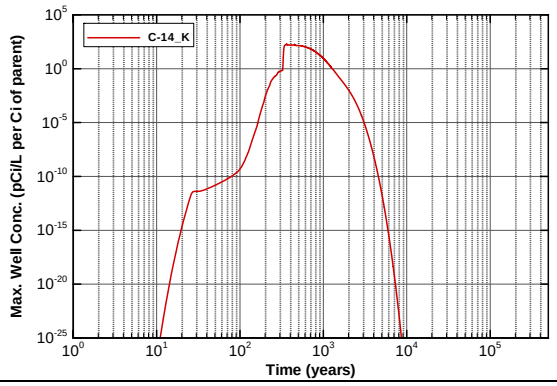

Figure A2A-212. Baseline CIG Future Inventory Max. Well Concentration for C-14_K

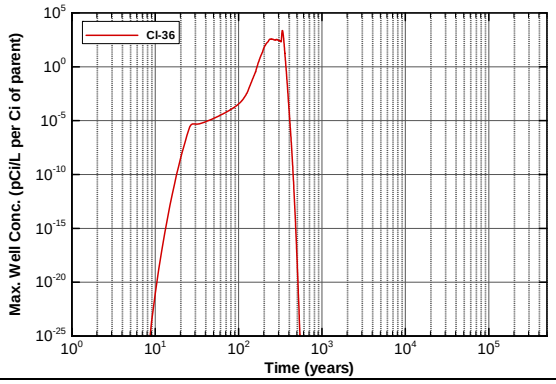

Figure A2A-213. Baseline CIG Future Inventory Max. Well Concentration for Cl-36

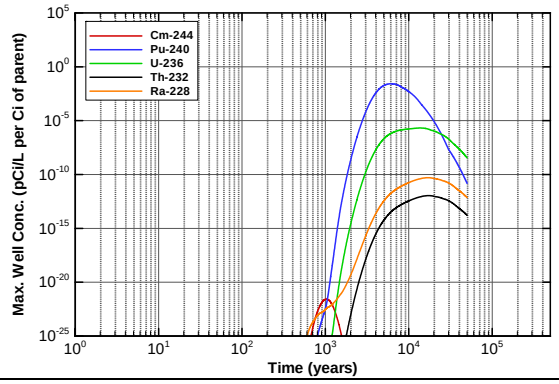

Figure A2A-214. Baseline CIG Future Inventory Max. Well Concentration for Cm-244

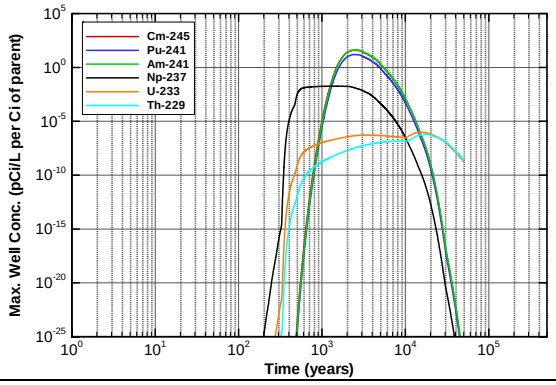

Figure A2A-215. Baseline CIG Future Inventory Max. Well Concentration for Cm-245

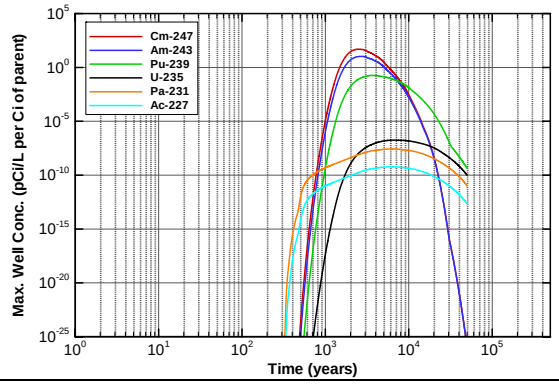

Figure A2A-216. Baseline CIG Future Inventory Max. Well Concentration for Cm-247

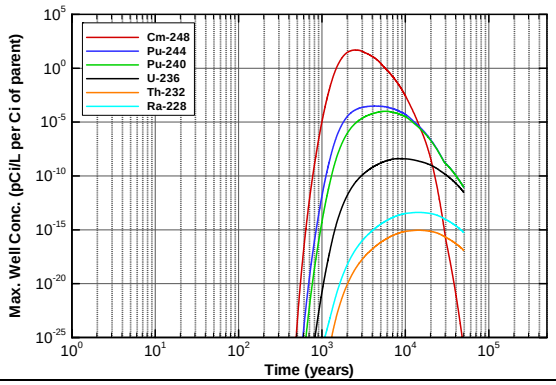

Figure A2A-217. Baseline CIG Future Inventory Max. Well Concentration for Cm-248

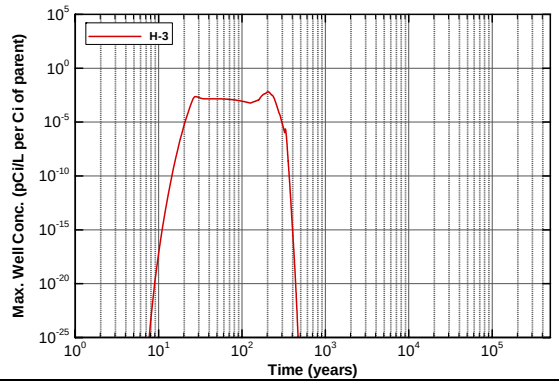

Figure A2A-218. Baseline CIG Future Inventory Max. Well Concentration for H-3

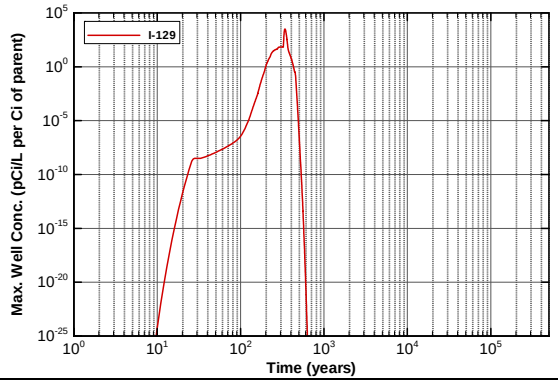

Figure A2A-219. Baseline CIG Future Inventory Max. Well Concentration for I-129

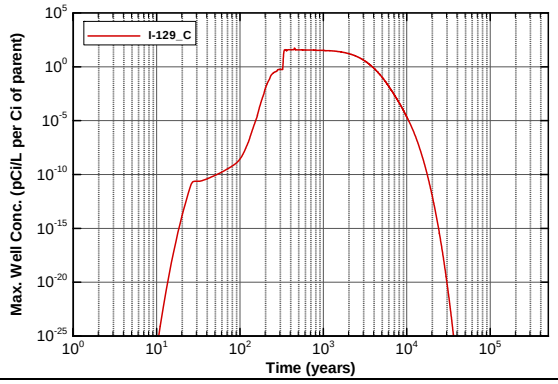

Figure A2A-220. Baseline CIG Future Inventory Max. Well Concentration for I-129_C

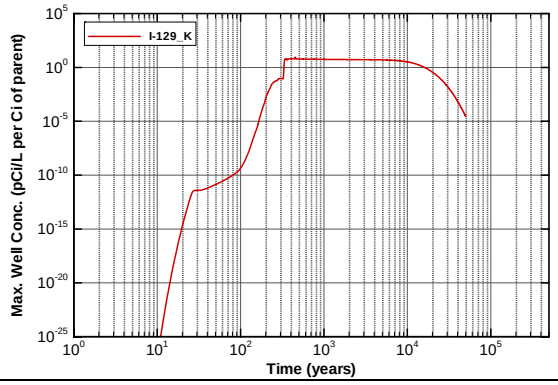

Figure A2A-221. Baseline CIG Future Inventory Max. Well Concentration for I-129_K

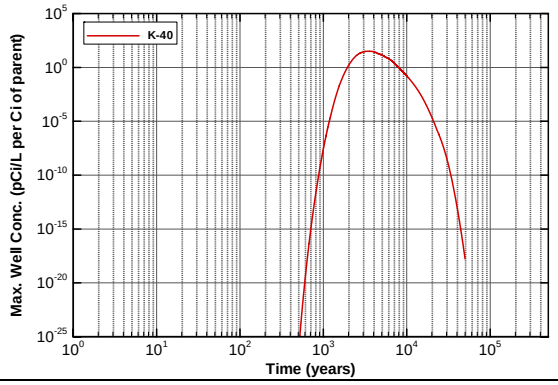

Figure A2A-222. Baseline CIG Future Inventory Max. Well Concentration for K-40

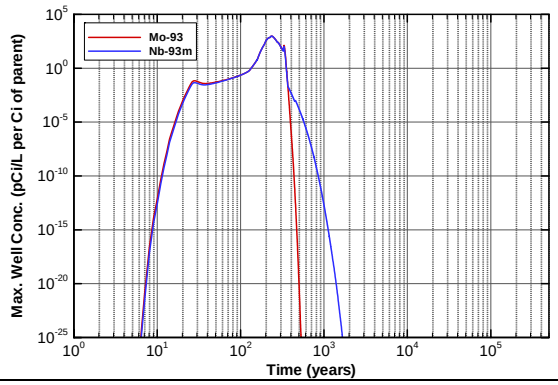

Figure A2A-223. Baseline CIG Future Inventory Max. Well Concentration for Mo-93

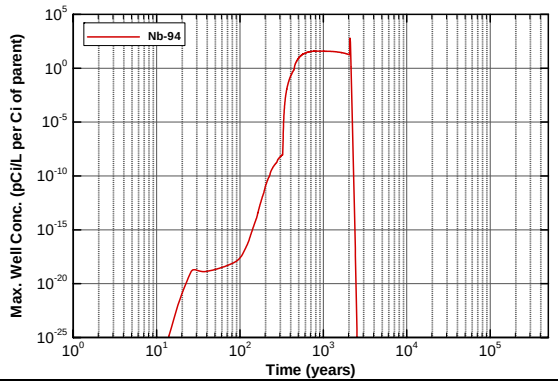

Figure A2A-224. Baseline CIG Future Inventory Max. Well Concentration for Nb-94

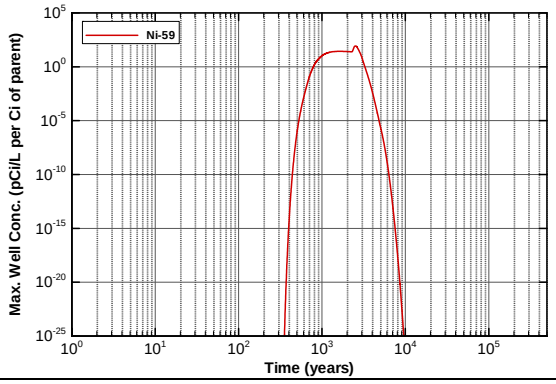

Figure A2A-225. Baseline CIG Future Inventory Max. Well Concentration for Ni-59

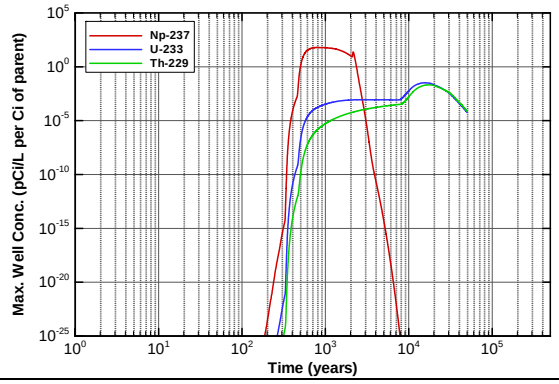

Figure A2A-226. Baseline CIG Future Inventory Max. Well Concentration for Np-237

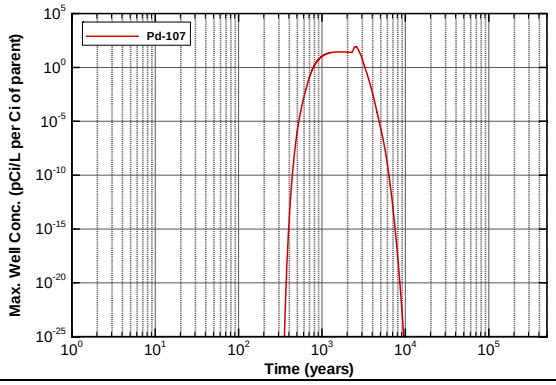

Figure A2A-227. Baseline CIG Future Inventory Max. Well Concentration for Pd-107

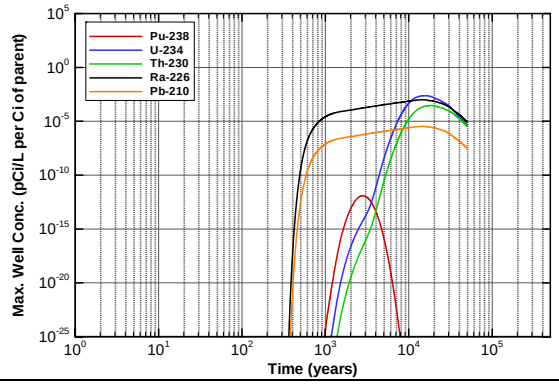

Figure A2A-228. Baseline CIG Future Inventory Max. Well Concentration for Pu-238

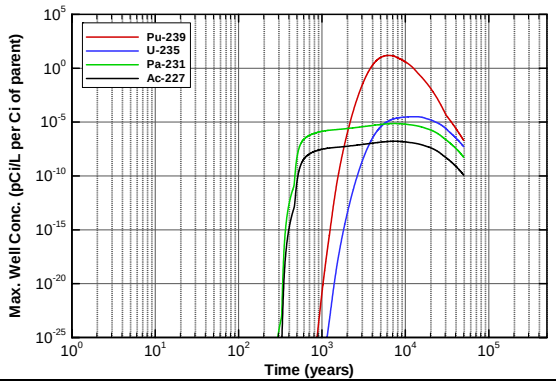

Figure A2A-229. Baseline CIG Future Inventory Max. Well Concentration for Pu-239

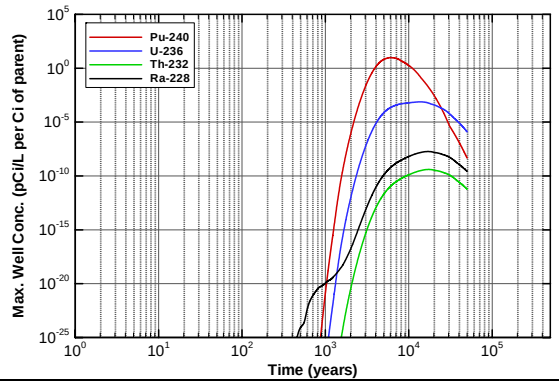

Figure A2A-230. Baseline CIG Future Inventory Max. Well Concentration for Pu-240

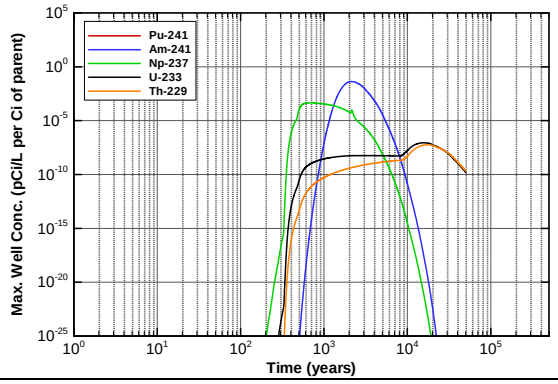

Figure A2A-231. Baseline CIG Future Inventory Max. Well Concentration for Pu-241

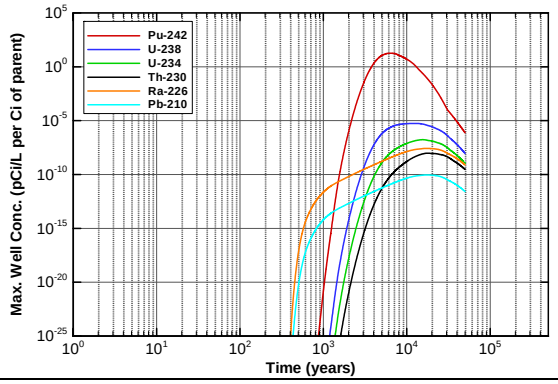

Figure A2A-232. Baseline CIG Future Inventory Max. Well Concentration for Pu-242

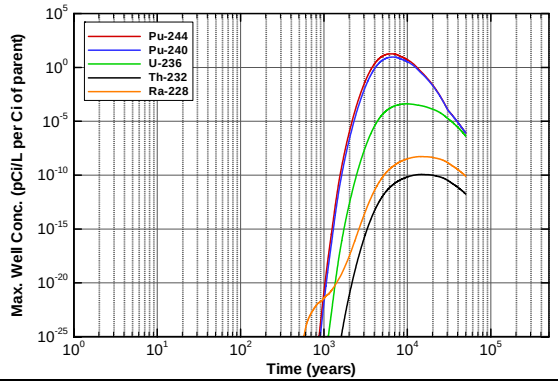

Figure A2A-233. Baseline CIG Future Inventory Max. Well Concentration for Pu-244

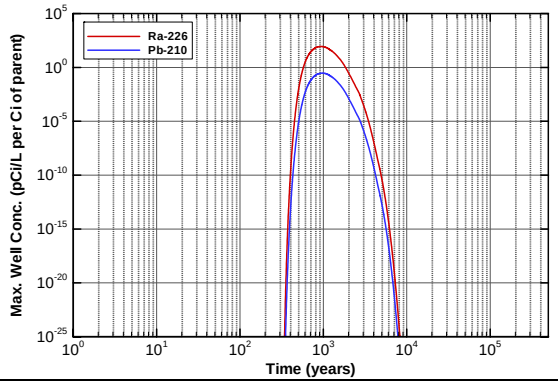

Figure A2A-234. Baseline CIG Future Inventory Max. Well Concentration for RA226

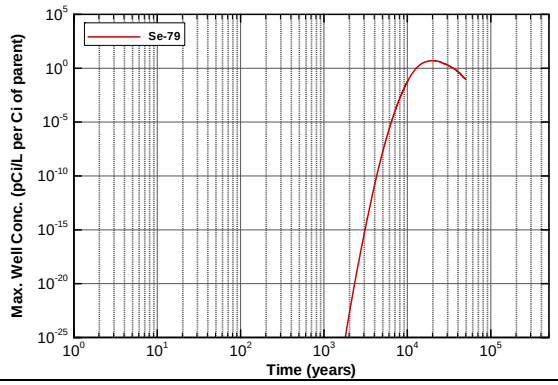

Figure A2A-235. Baseline CIG Future Inventory Max. Well Concentration for Se-79

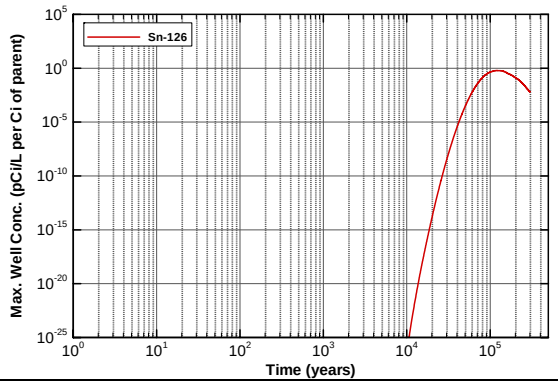

Figure A2A-236. Baseline CIG Future Inventory Max. Well Concentration for Sn-126

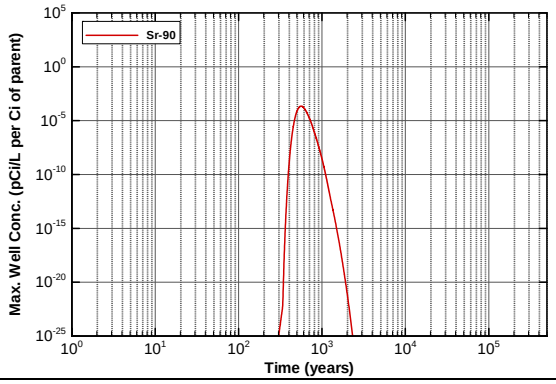

Figure A2A-237. Baseline CIG Future Inventory Max. Well Concentration for Sr-90

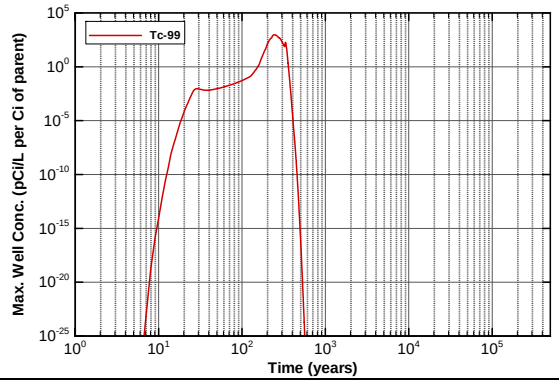

Figure A2A-238. Baseline CIG Future Inventory Max. Well Concentration for Tc-99

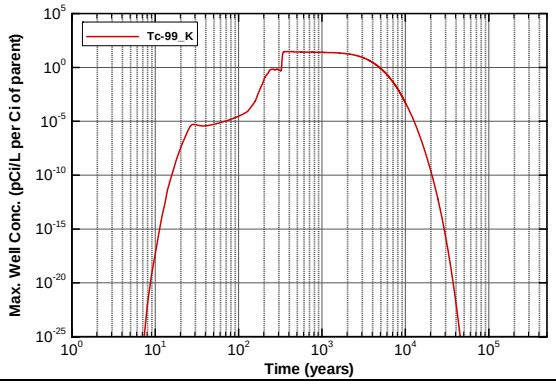

Figure A2A-239. Baseline CIG Future Inventory Max. Well Concentration for Tc-99_K

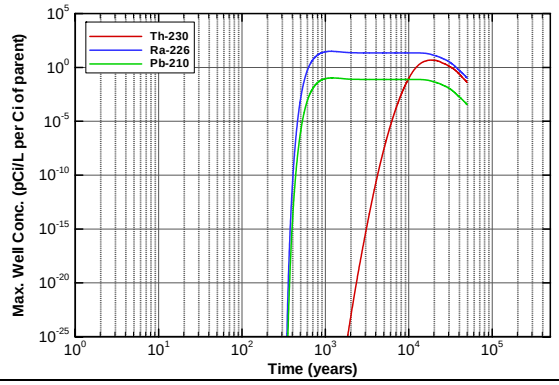

Figure A2A-240. Baseline CIG Future Inventory Max. Well Concentration for Th-230

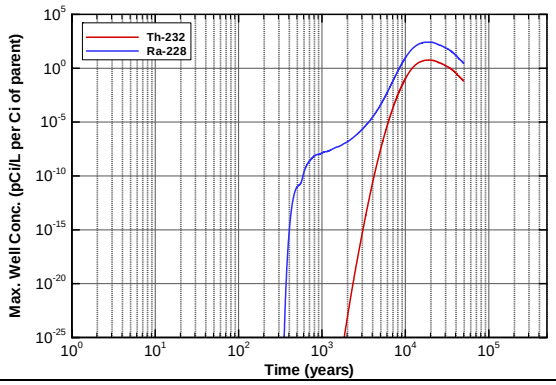

Figure A2A-241. Baseline CIG Future Inventory Max. Well Concentration for Th-232

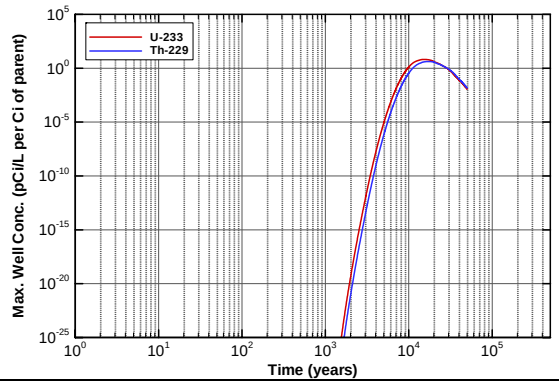

Figure A2A-242. Baseline CIG Future Inventory Max. Well Concentration for U-233

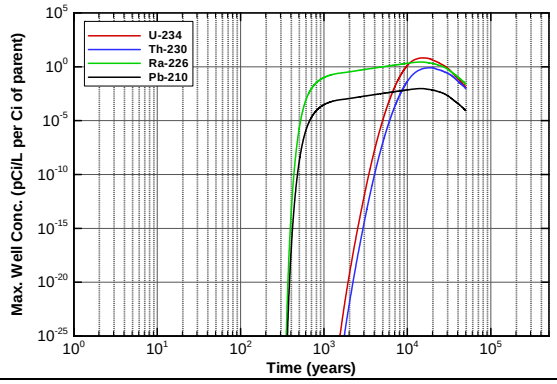

Figure A2A-243. Baseline CIG Future Inventory Max. Well Concentration for U-234

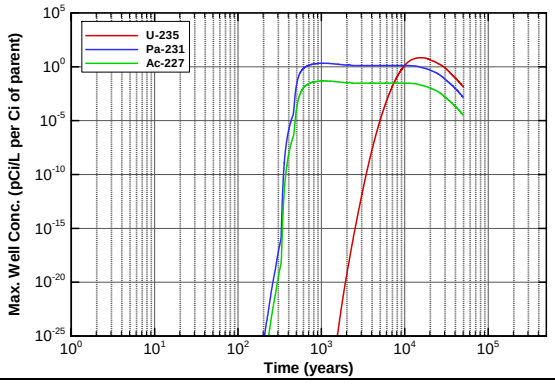

Figure A2A-244. Baseline CIG Future Inventory Max. Well Concentration for U-235

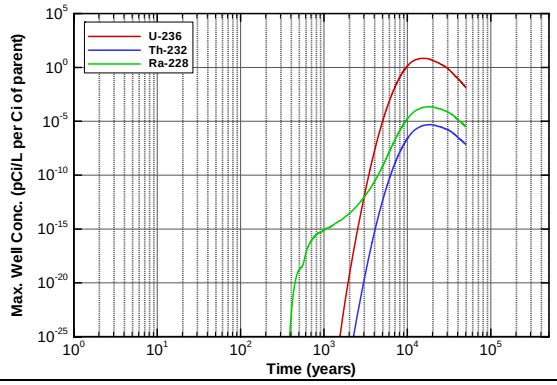

Figure A2A-245. Baseline CIG Future Inventory Max. Well Concentration for U-236

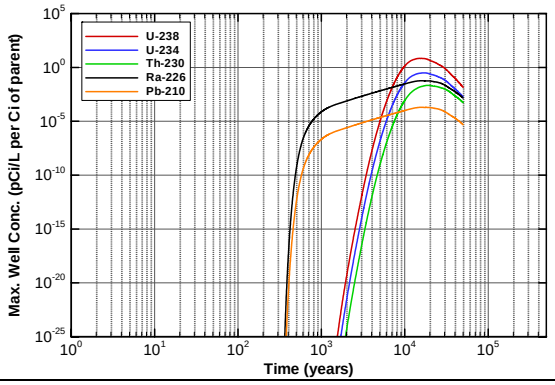

Figure A2A-246. Baseline CIG Future Inventory Max. Well Concentration for U-238

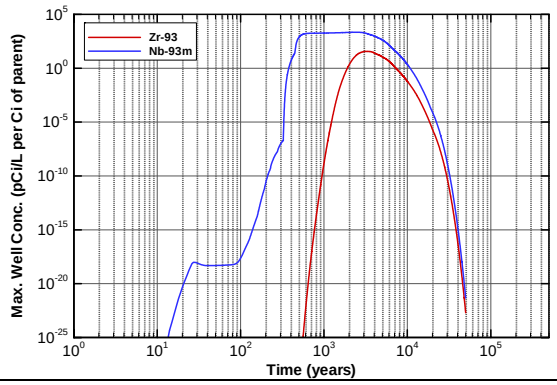

Figure A2A-247. Baseline CIG Future Inventory Max. Well Concentration for Zr-93

This page intentionally left blank.

APPENDIX A2B

Probabilistic Model

Uncertainty and Maximum Impact

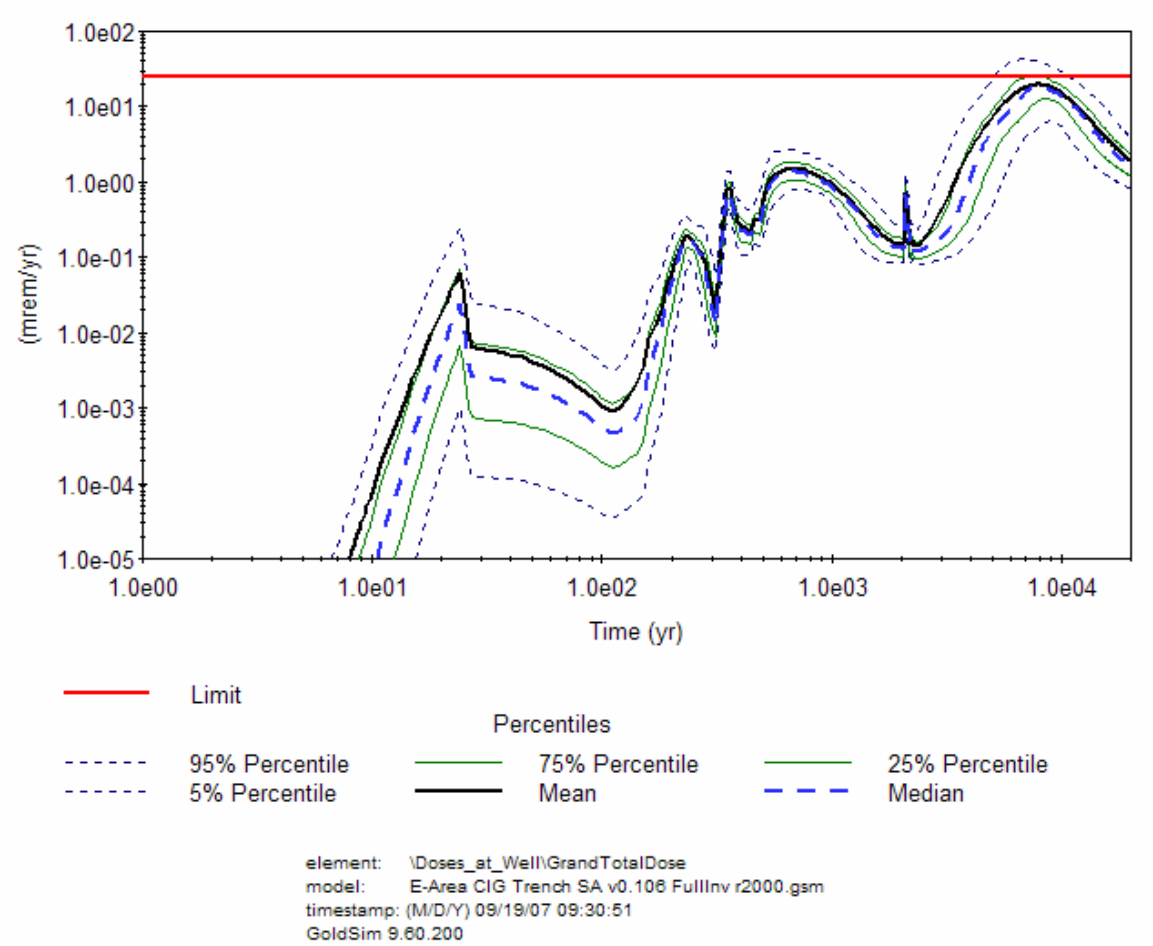

Figure A2B-1. All-Pathways Total Dose Statistics

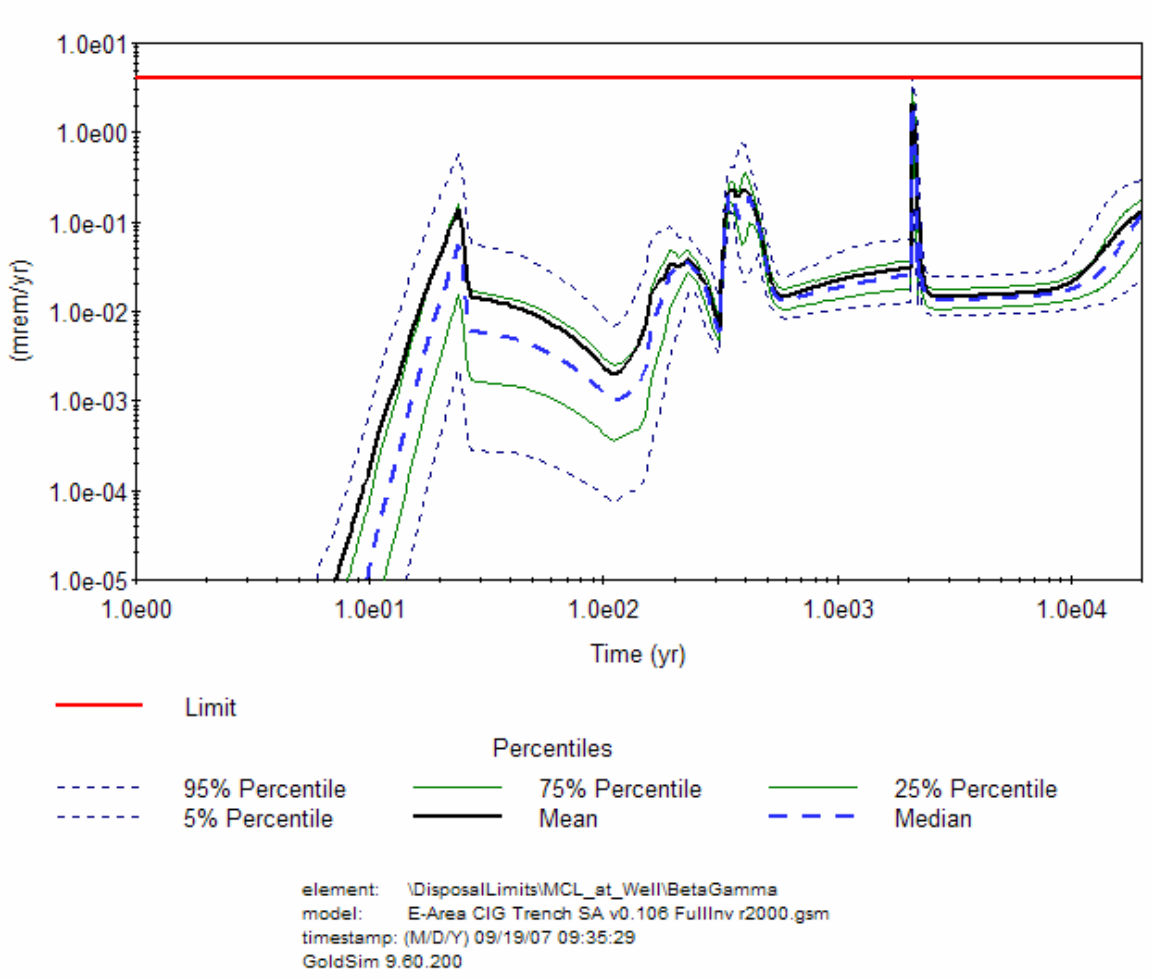

Figure A2B-2. Dose from Beta - Gamma in Well Water Statistics

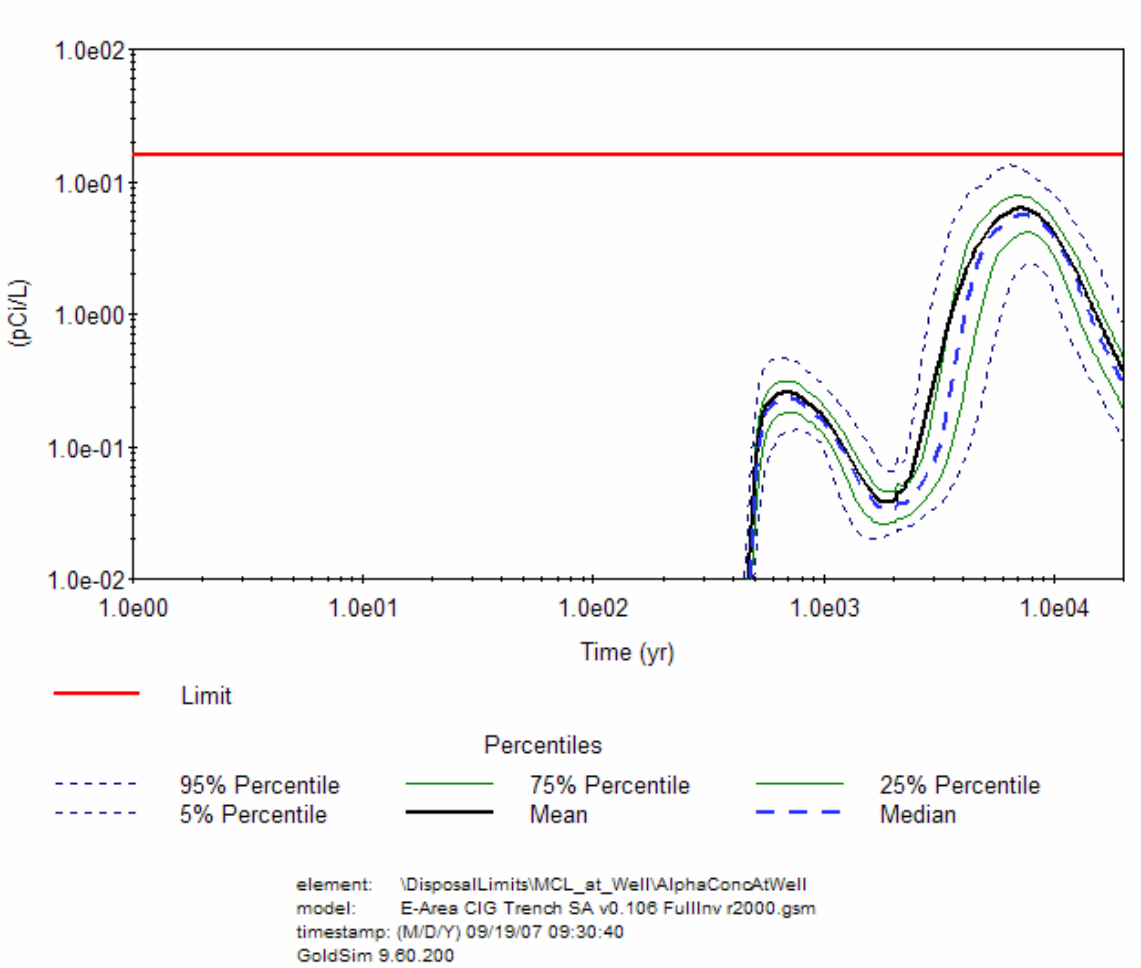

Figure A2B-3. Gross Alpha Well Water Concentration Statistics

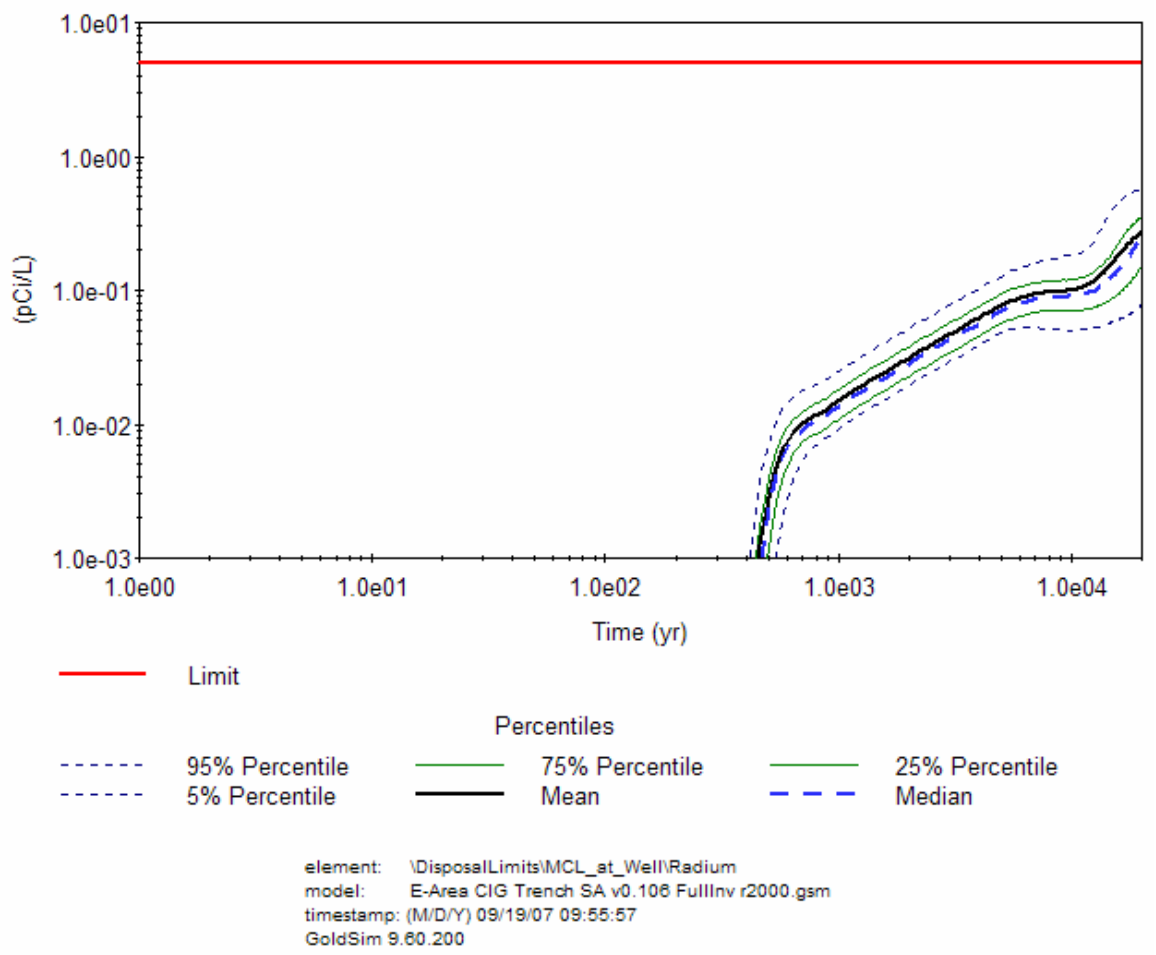

Figure A2B-4. Radium Well Water Concentration Statistics

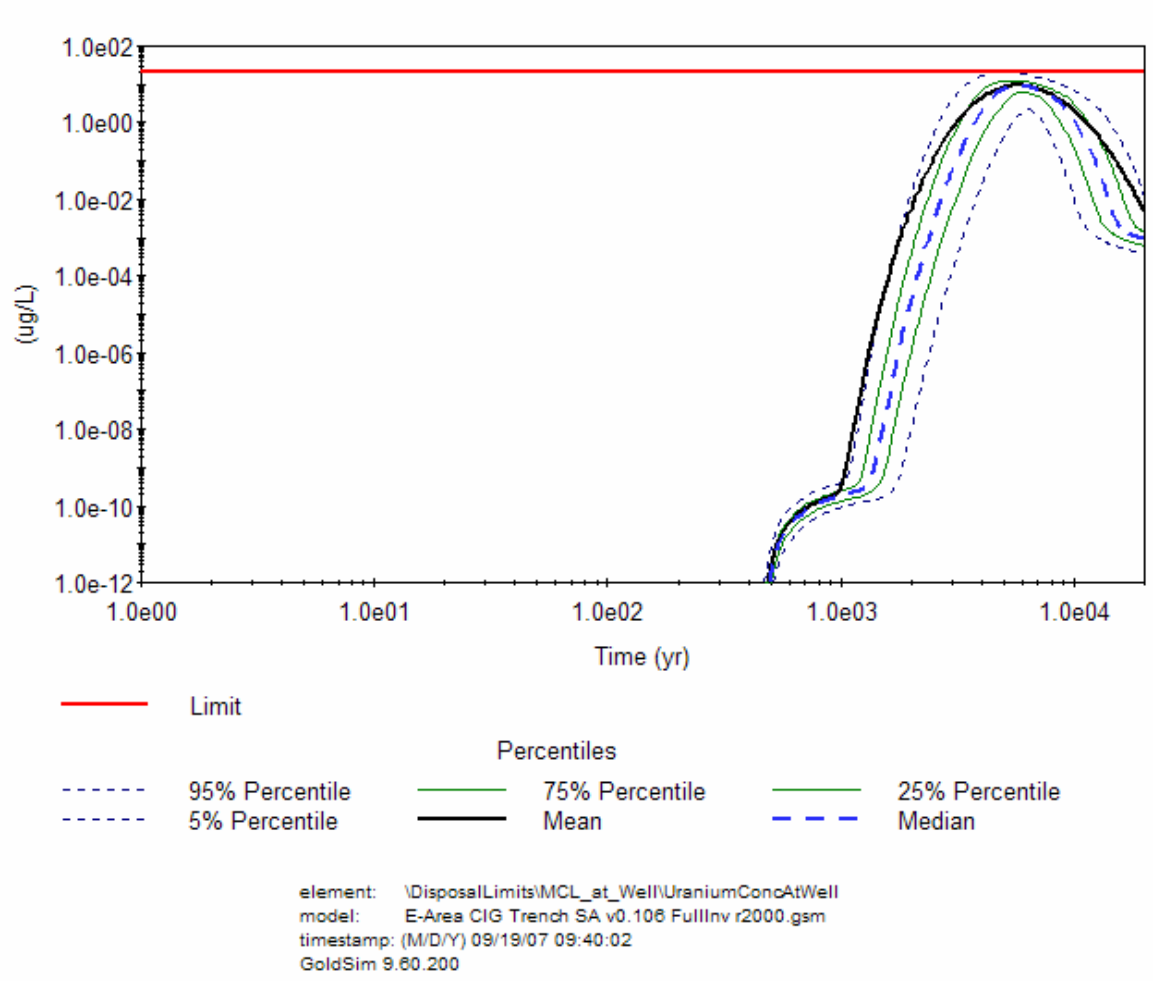

Figure A2B-5. Uranium Well Water Concentration Statistics

APPENDIX A2C

Radon Model

10,000-year Simulation of Rn-222 Flux at Land Surface

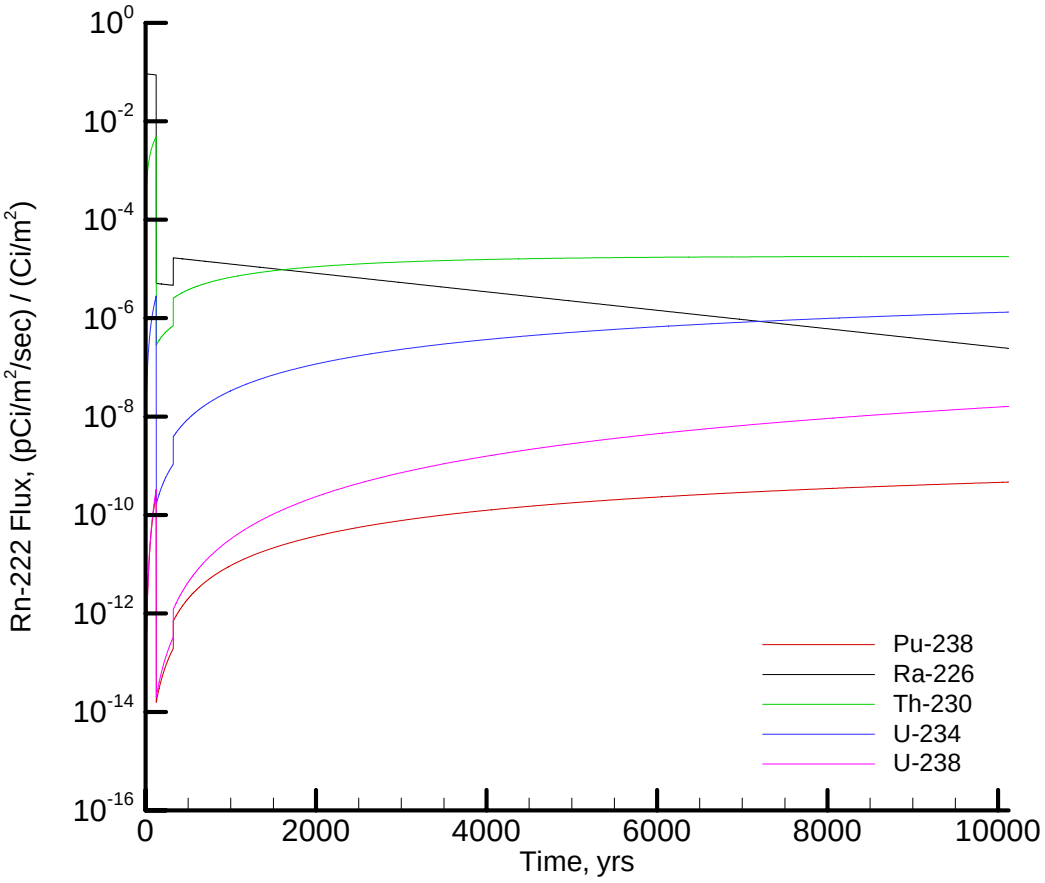

Figure A2C-1. Rn-222 Flux at Land Surface Resulting from Unit Source Term for CIG

APPENDIX A3 - LAW VAULT

GRAPHICS FOR GROUNDWATER AND RADON

This page intentionally left blank.

TABLE OF CONTENTS

APPENDIX A3A

Vadose Zone and Aquifer Models

Flux to the Water Table

100-m Well Concentrations

Flux to Water Table - Cracked Sections with CDP

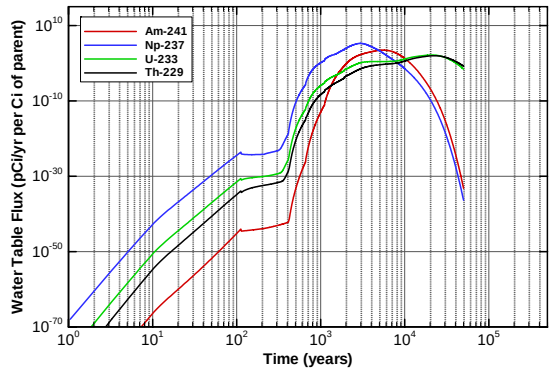

Figure A3A-1. Flux to Water Table: Cracked with CDP for Am-241

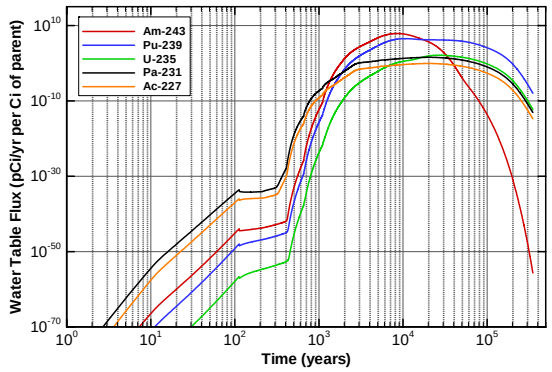

Figure A3A-2. Flux to Water Table: Cracked with CDP for Am-243

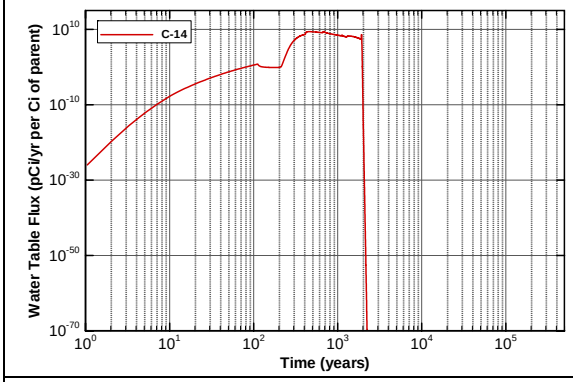

Figure A3A-3. Flux to Water Table: Cracked with CDP for C-14

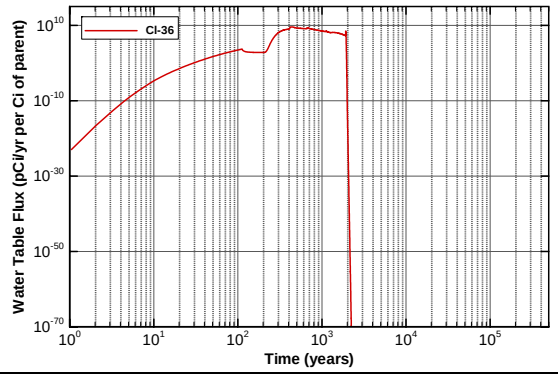

Figure A3A-4. Flux to Water Table: Cracked with CDP for Cl-36

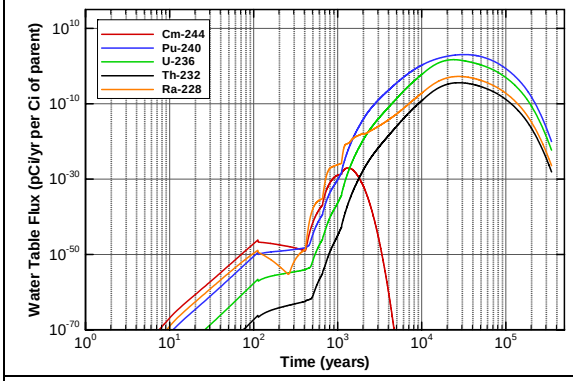

Figure A3A-5. Flux to Water Table: Cracked with CDP for Cm-244

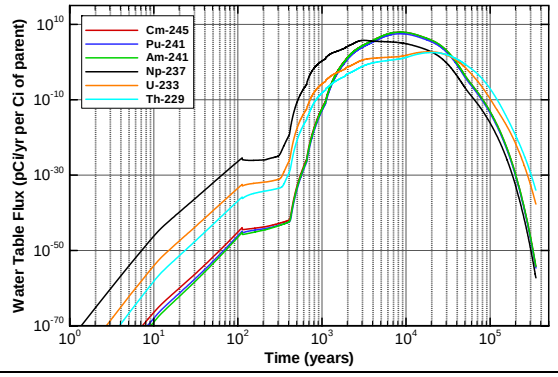

Figure A3A-6. Flux to Water Table: Cracked with CDP for Cm-245

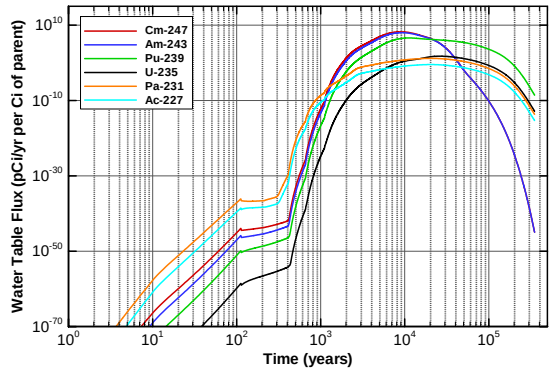

Figure A3A-7. Flux to Water Table: Cracked with CDP for Cm-247

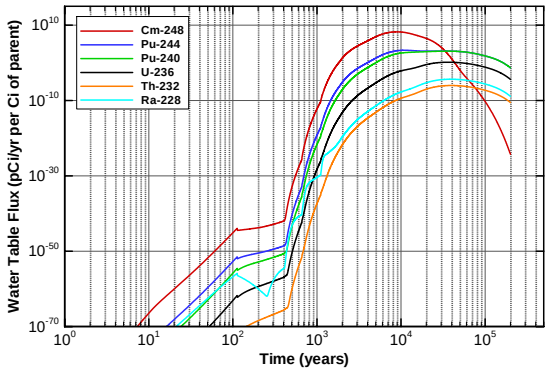

Figure A3A-8. Flux to Water Table: Cracked with CDP for Cm-248

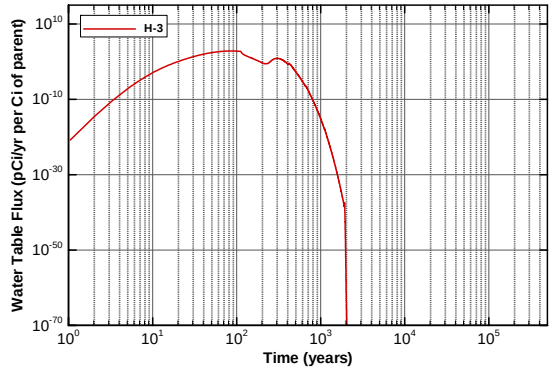

Figure A3A-9. Flux to Water Table: Cracked with CDP for H-3

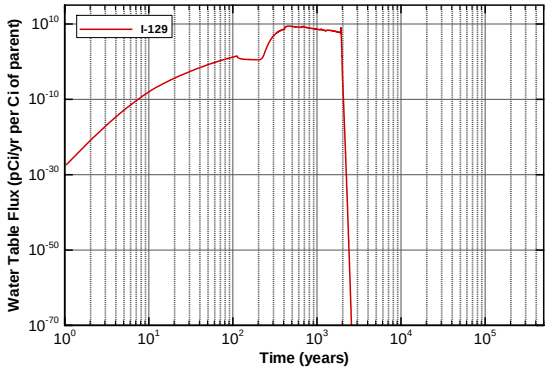

Figure A3A-10. Flux to Water Table: Cracked with CDP for I-129

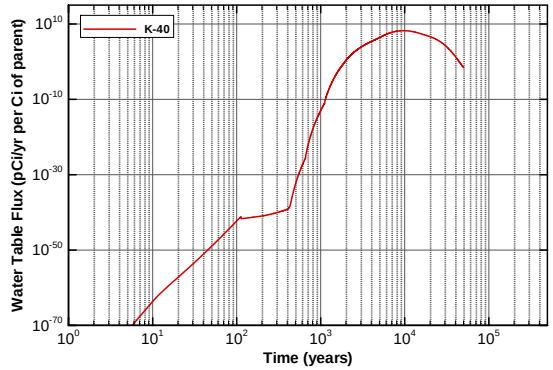

Figure A3A-11. Flux to Water Table: Cracked with CDP for K-40

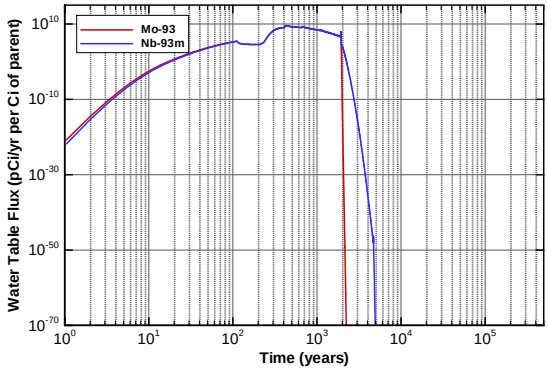

Figure A3A-12. Flux to Water Table: Cracked with CDP for Mo-93

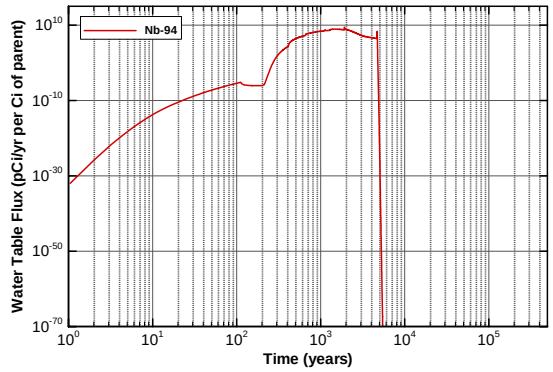

Figure A3A-13. Flux to Water Table: Cracked with CDP for Nb-94

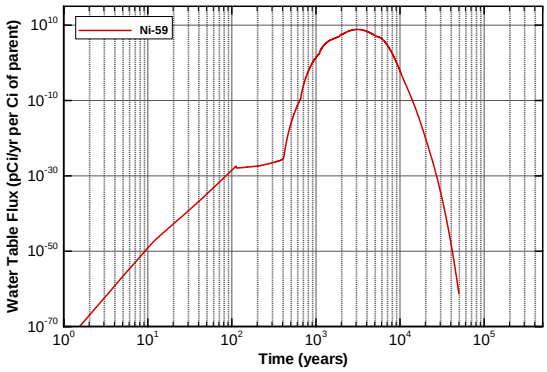

Figure A3A-14. Flux to Water Table: Cracked with CDP for Ni-59

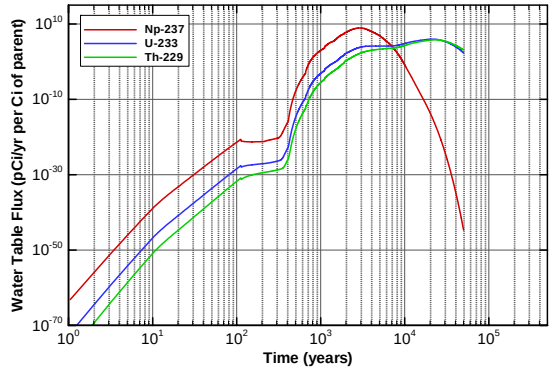

Figure A3A-15. Flux to Water Table: Cracked with CDP for Np-237

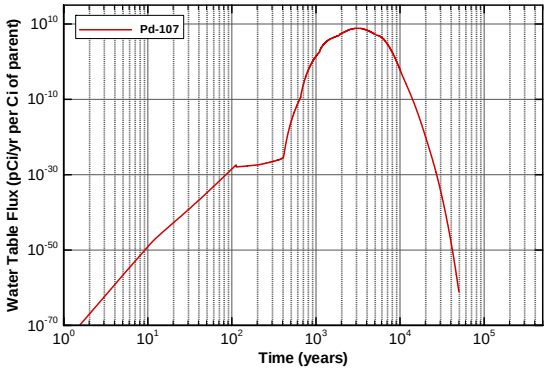

Figure A3A-16. Flux to Water Table: Cracked with CDP for Pd-107

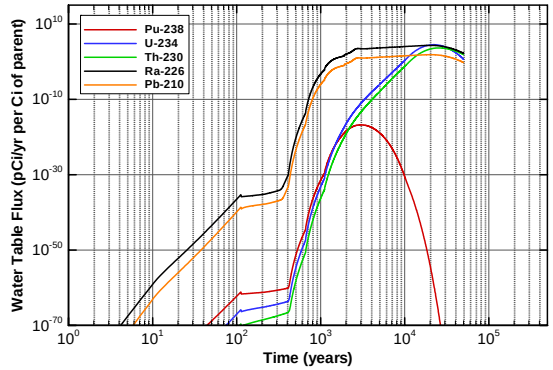

Figure A3A-17. Flux to Water Table: Cracked with CDP for Pu-238

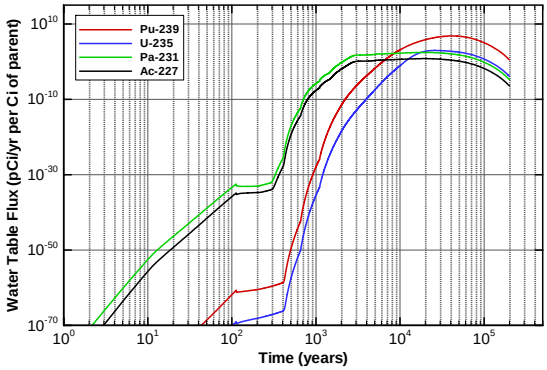

Figure A3A-18. Flux to Water Table: Cracked with CDP for Pu-239

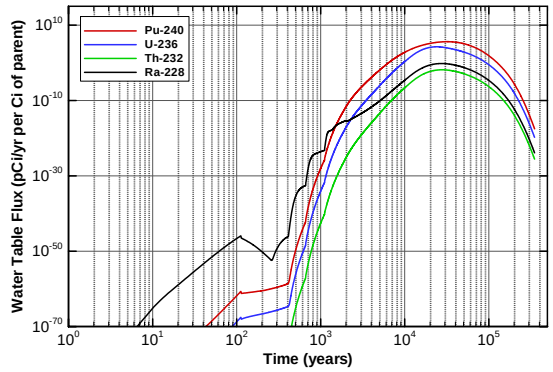

Figure A3A-19. Flux to Water Table: Cracked with CDP for Pu-240

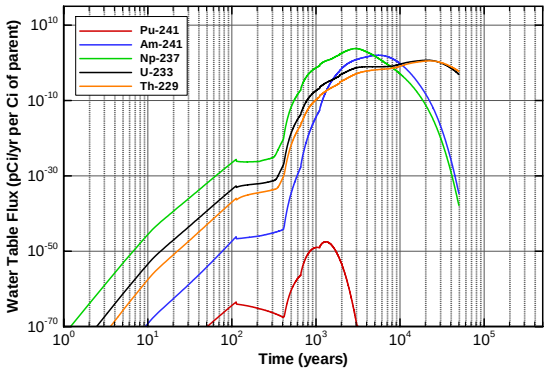

Figure A3A-20. Flux to Water Table: Cracked with CDP for Pu-241

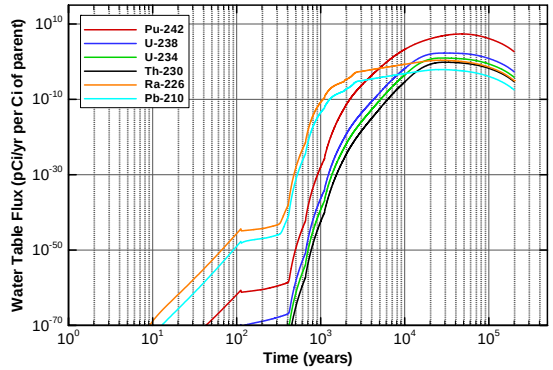

Figure A3A-21. Flux to Water Table: Cracked with CDP for Pu-242

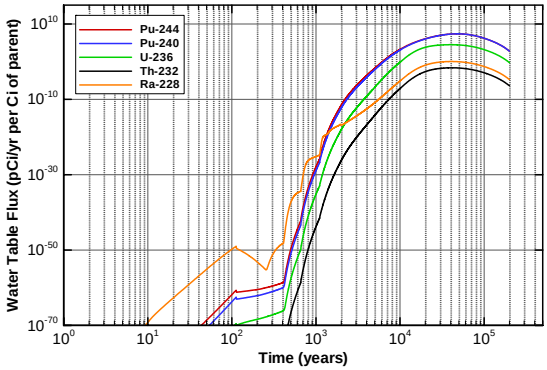

Figure A3A-22. Flux to Water Table: Cracked with CDP for Pu-244

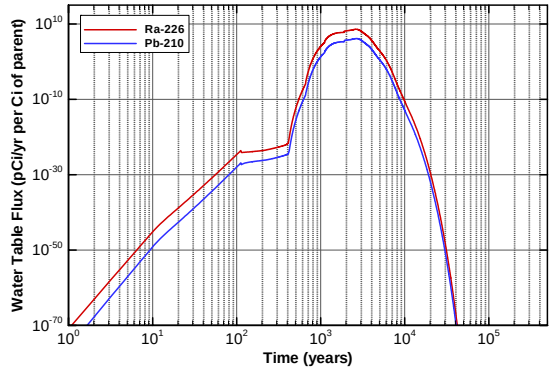

Figure A3A-23. Flux to Water Table: Cracked with CDP for Ra-226

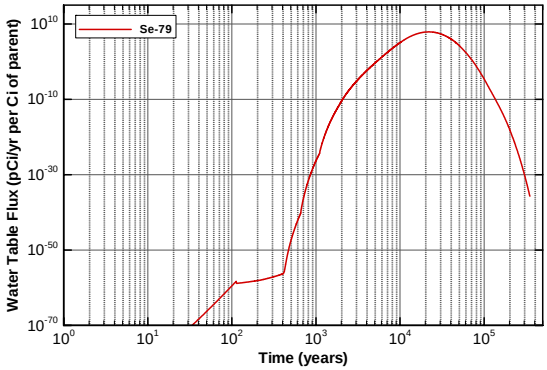

Figure A3A-24. Flux to Water Table: Cracked with CDP for Se-79

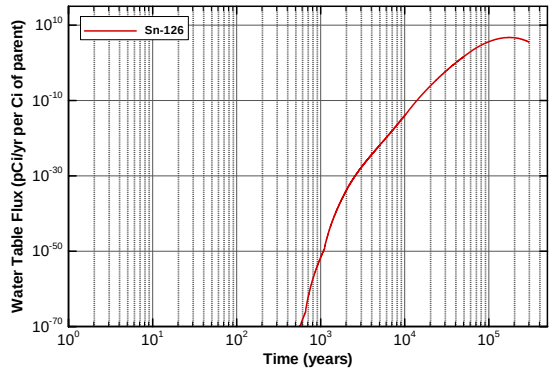

Figure A3A-25. Flux to Water Table: Cracked with CDP for Sn-126

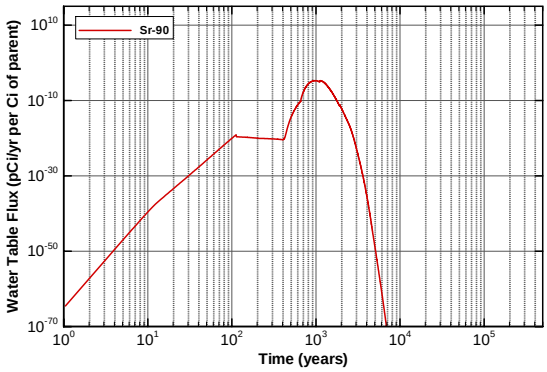

Figure A3A-26. Flux to Water Table: Cracked with CDP for Sr-90

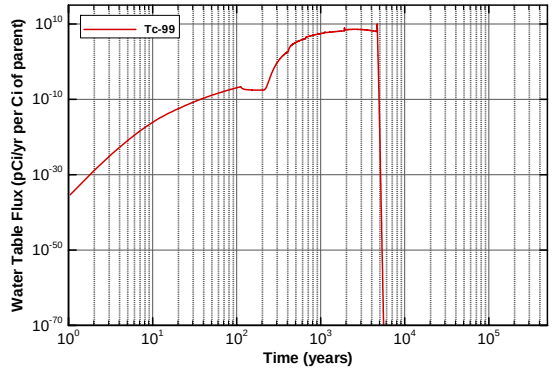

Figure A3A-27. Flux to Water Table: Cracked with CDP for Tc-99

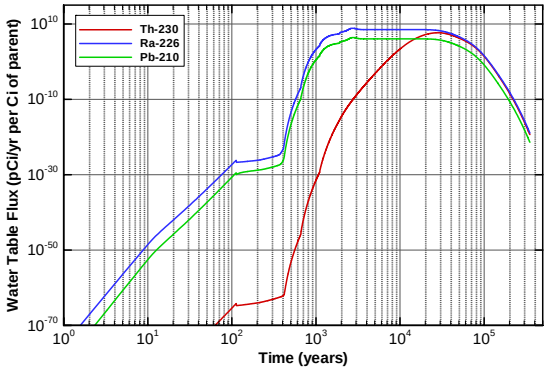

Figure A3A-28. Flux to Water Table: Cracked with CDP for Th-230

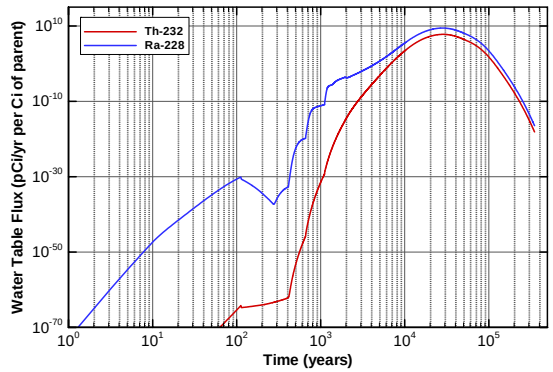

Figure A3A-29. Flux to Water Table: Cracked with CDP for Th-232

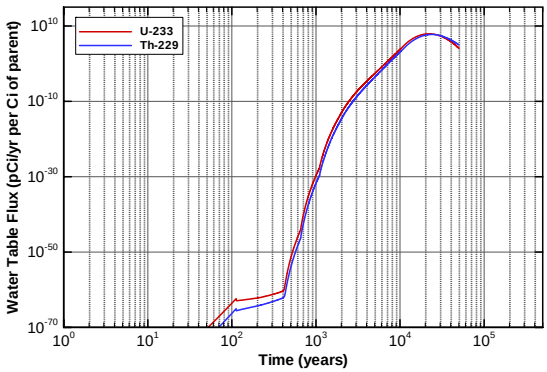

Figure A3A-30. Flux to Water Table: Cracked with CDP for U-233

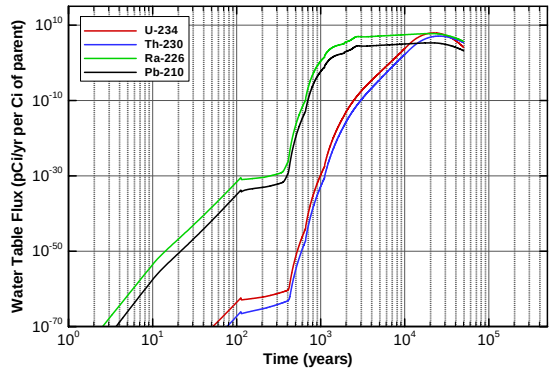

Figure A3A-31. Flux to Water Table: Cracked with CDP for U-234

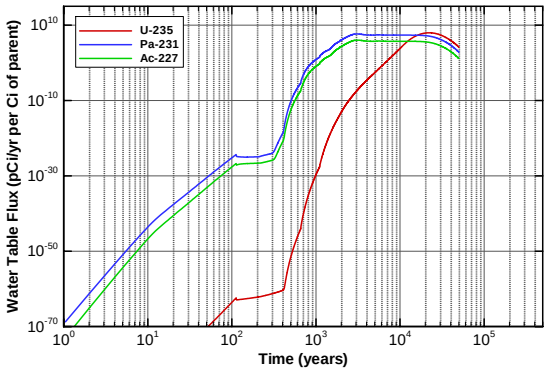

Figure A3A-32. Flux to Water Table: Cracked with CDP for U-235

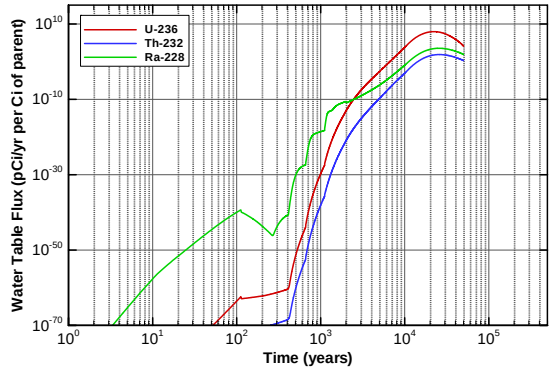

Figure A3A-33. Flux to Water Table: Cracked with CDP for U-236

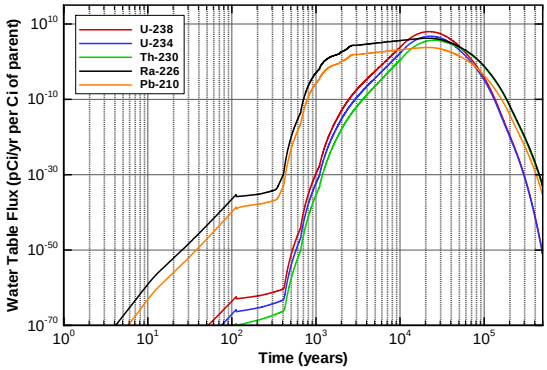

Figure A3A-34. Flux to Water Table: Cracked with CDP for U-238

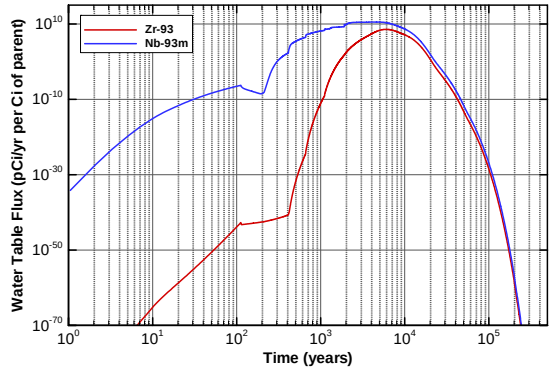

Figure A3A-35. Flux to Water Table: Cracked with CDP for Zr-93

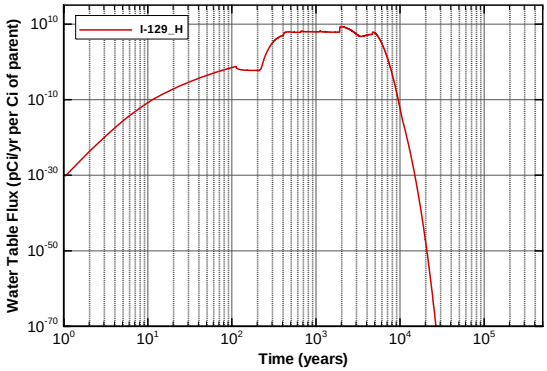

Figure A3A-36. Flux to Water Table: Cracked with CDP for I-129_H

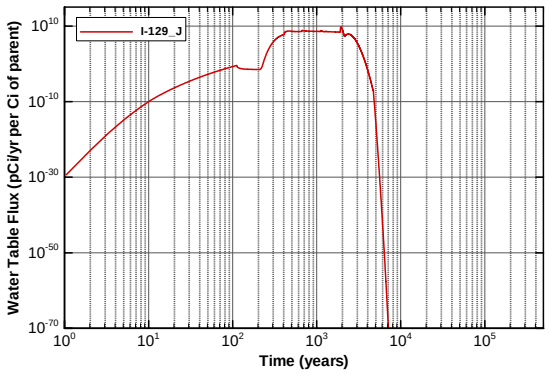

Figure A3A-37. Flux to Water Table: Cracked with CDP for I-129_J

Flux to Water Table - Uncracked Sections with CDP

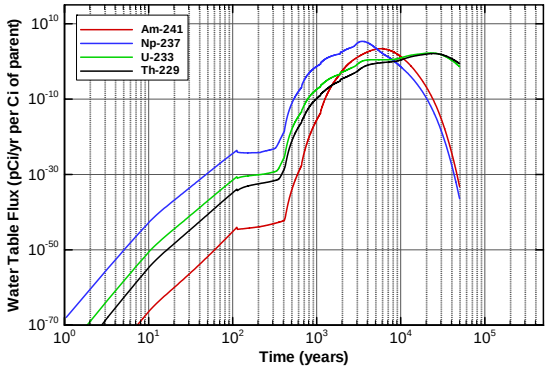

Figure A3A-38. Flux to Water Table: Uncracked with CDP for Am-241

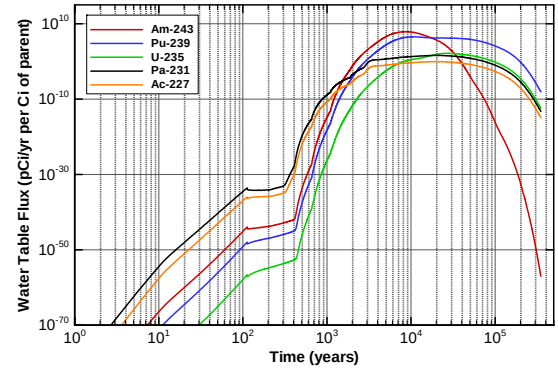

Figure A3A-39. Flux to Water Table: Uncracked with CDP for Am-243

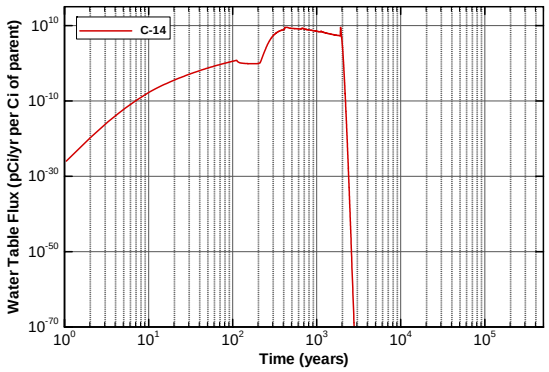

Figure A3A-40. Flux to Water Table: Uncracked with CDP for C-14

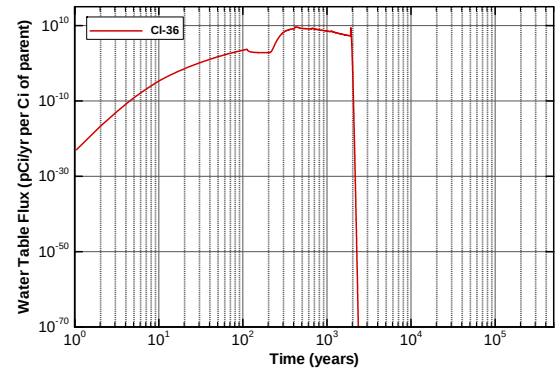

Figure A3A-41. Flux to Water Table: Uncracked with CDP for Cl-36

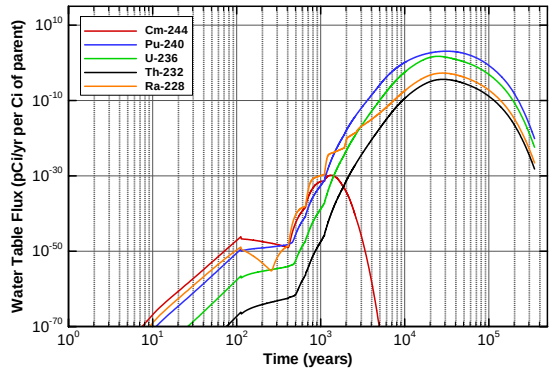

Figure A3A-42. Flux to Water Table: Uncracked with CDP for Cm-244

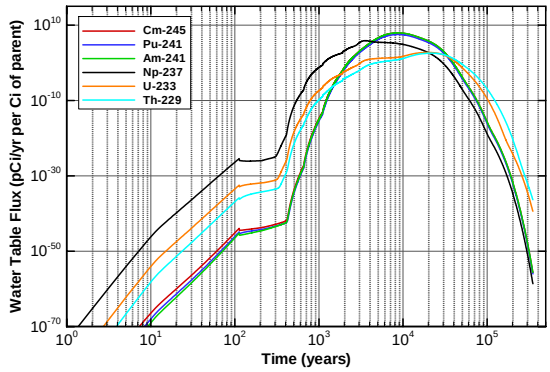

Figure A3A-43. Flux to Water Table: Uncracked with CDP for Cm-245

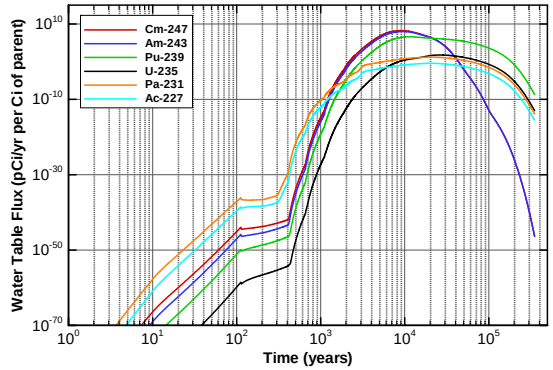

Figure A3A-44. Flux to Water Table: Uncracked with CDP for Cm-247

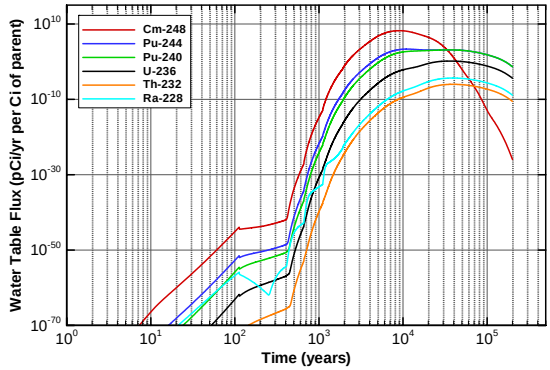

Figure A3A-45. Flux to Water Table: Uncracked with CDP for Cm-248

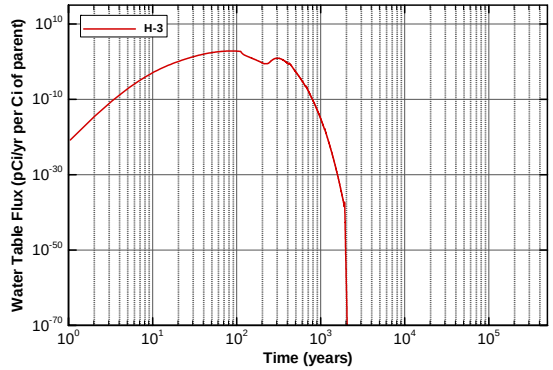

Figure A3A-46. Flux to Water Table: Uncracked with CDP for H-3

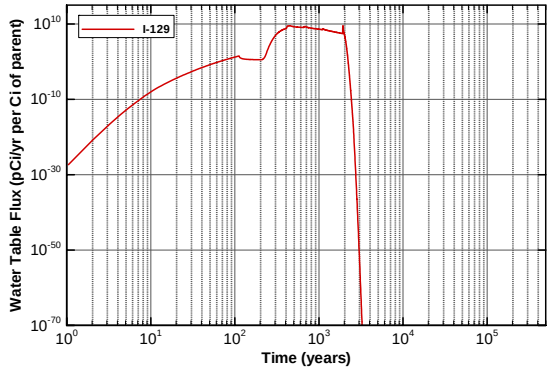

Figure A3A-47. Flux to Water Table: Uncracked with CDP for I-129

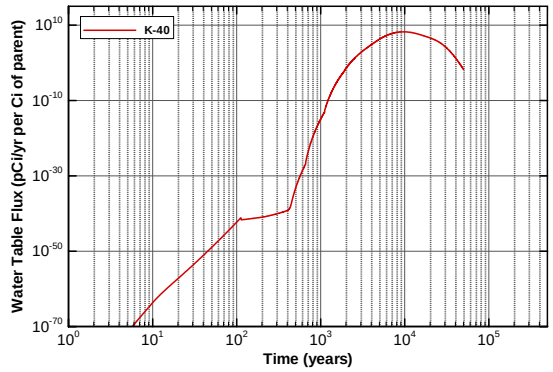

Figure A3A-48. Flux to Water Table: Uncracked with CDP for K-40

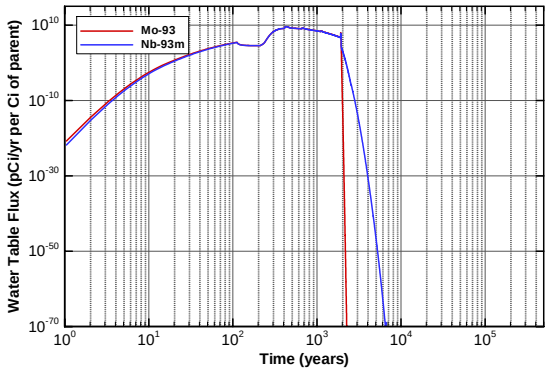

Figure A3A-49. Flux to Water Table: Uncracked with CDP for Mo-93

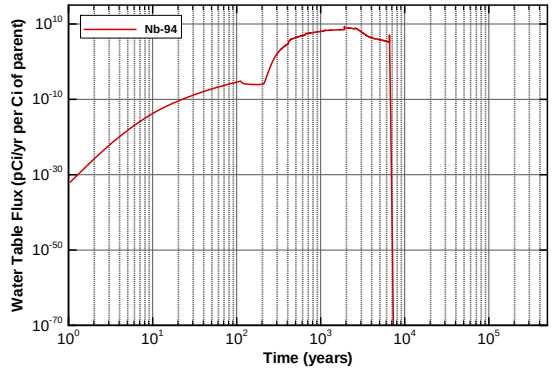

Figure A3A-50. Flux to Water Table: Uncracked with CDP for Nb-94

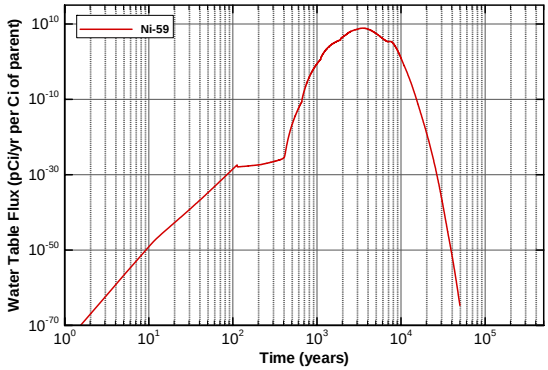

Figure A3A-51. Flux to Water Table: Uncracked with CDP for Ni-59

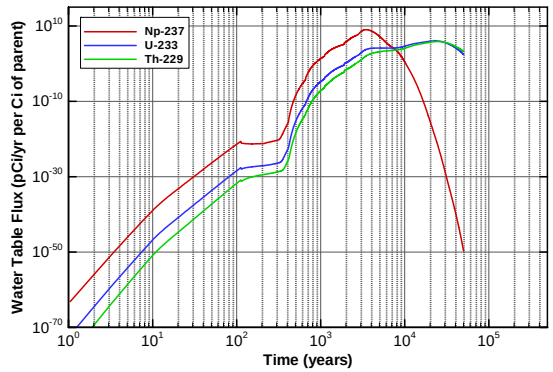

Figure A3A-52. Flux to Water Table: Uncracked with CDP for Np-237

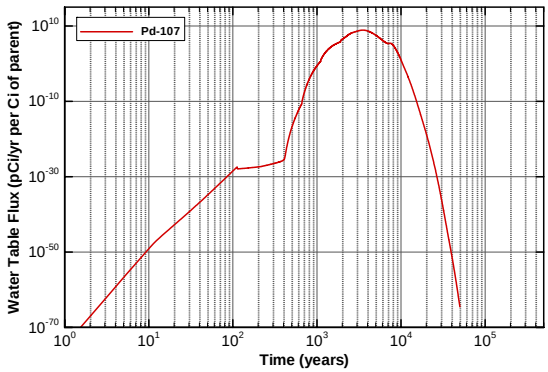

Figure A3A-53. Flux to Water Table: Uncracked with CDP for Pd-107

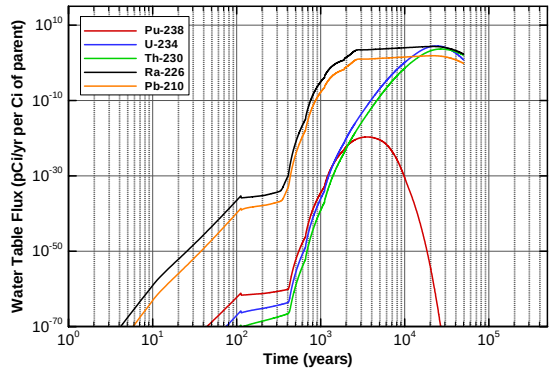

Figure A3A-54. Flux to Water Table: Uncracked with CDP for Pu-238

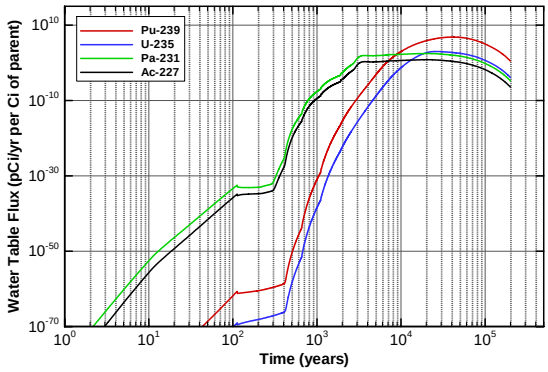

Figure A3A-55. Flux to Water Table: Uncracked with CDP for Pu-239

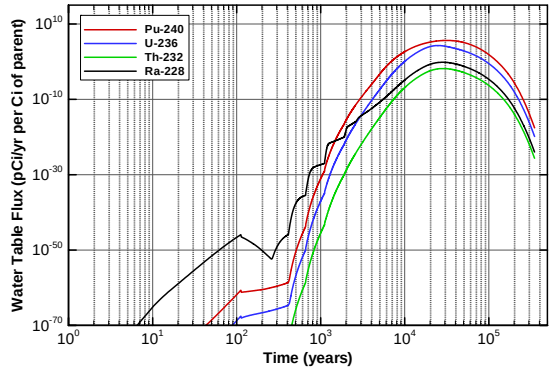

Figure A3A-56. Flux to Water Table: Uncracked with CDP for Pu-240

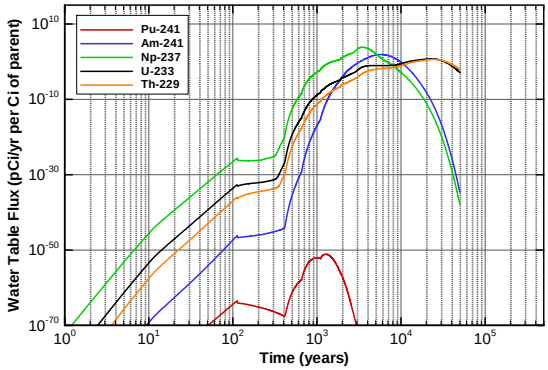

Figure A3A-57. Flux to Water Table: Uncracked with CDP for Pu-241

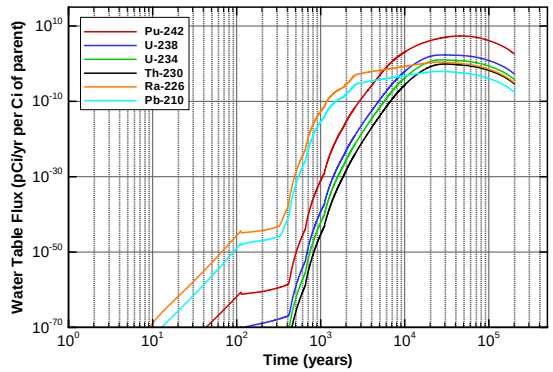

Figure A3A-58. Flux to Water Table: Uncracked with CDP for Pu-242

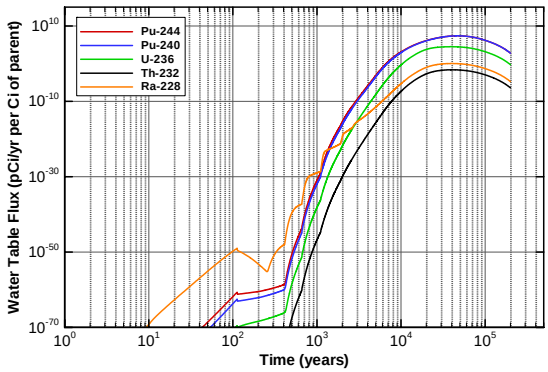

Figure A3A-59. Flux to Water Table: Uncracked with CDP for Pu-244

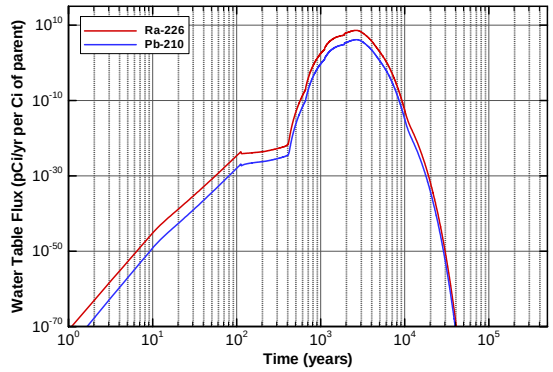

Figure A3A-60. Flux to Water Table: Uncracked with CDP for Ra-226

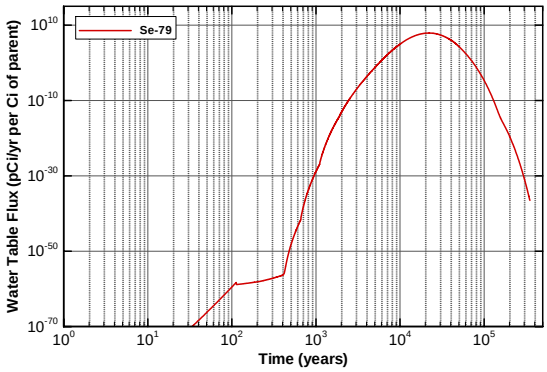

Figure A3A-61. Flux to Water Table: Uncracked with CDP for Se-79

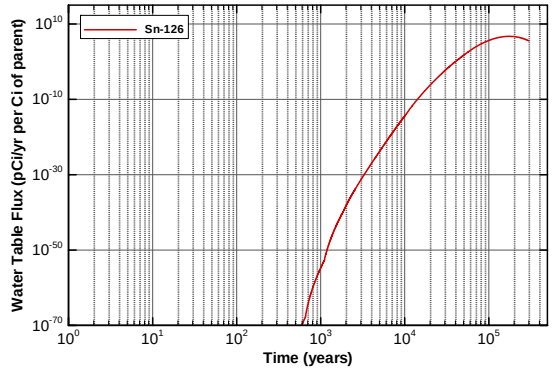

Figure A3A-62. Flux to Water Table: Uncracked with CDP for Sn-126

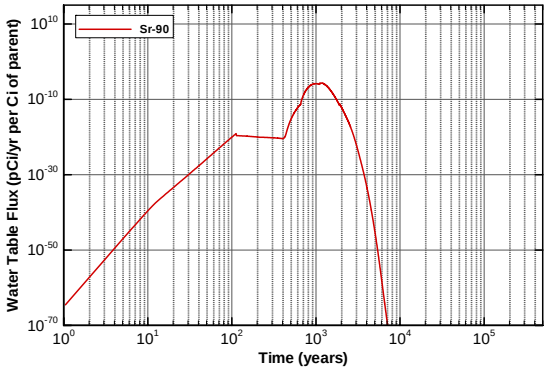

Figure A3A-63. Flux to Water Table: Uncracked with CDP for Sr-90

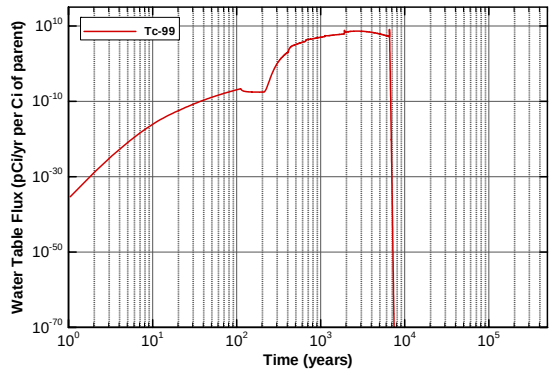

Figure A3A-64. Flux to Water Table: Uncracked with CDP for Tc-99

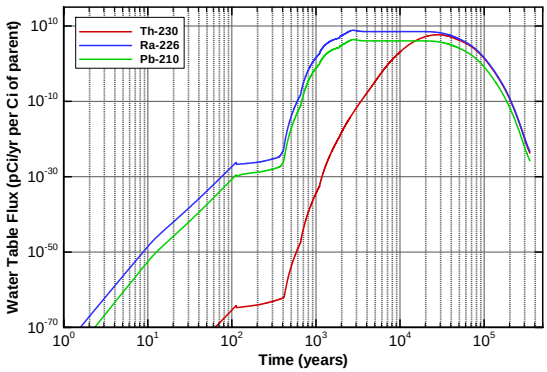

Figure A3A-65. Flux to Water Table: Uncracked with CDP for Th-230

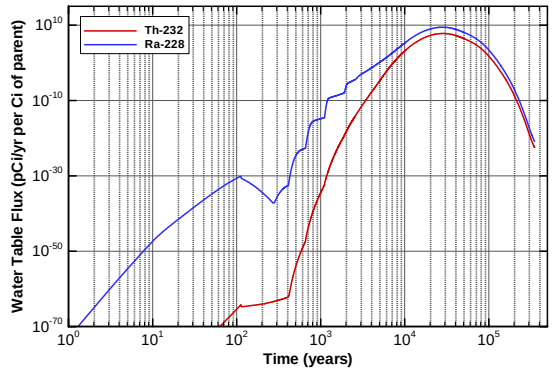

Figure A3A-66. Flux to Water Table: Uncracked with CDP for Th-232

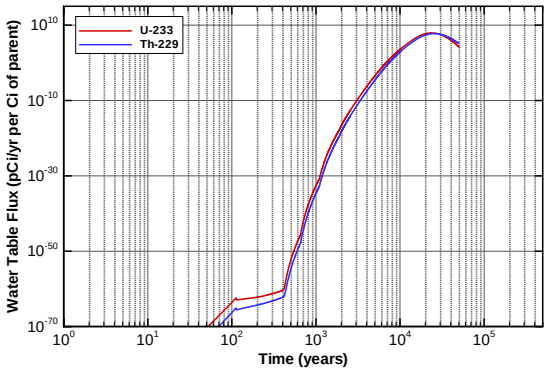

Figure A3A-67. Flux to Water Table: Uncracked with CDP for U-233

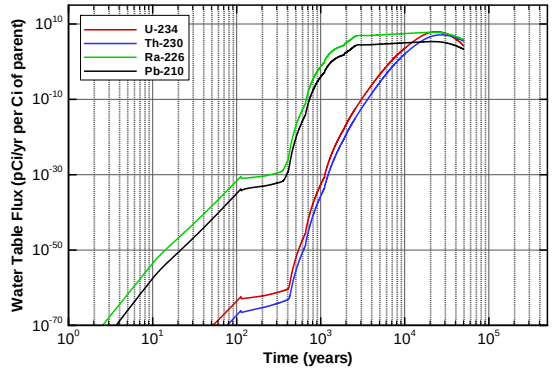

Figure A3A-68. Flux to Water Table: Uncracked with CDP for U-234

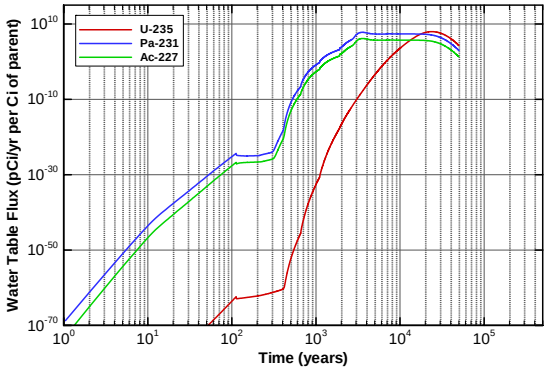

Figure A3A-69. Flux to Water Table: Uncracked with CDP for U-235

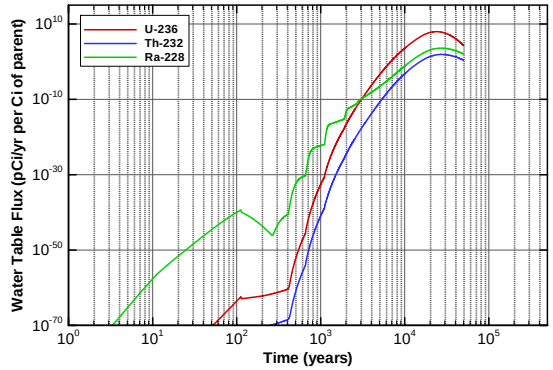

Figure A3A-70. Flux to Water Table: Uncracked with CDP for U-236

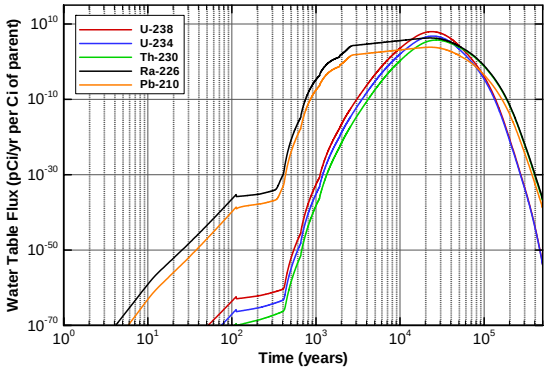

Figure A3A-71. Flux to Water Table: Uncracked with CDP for U-238

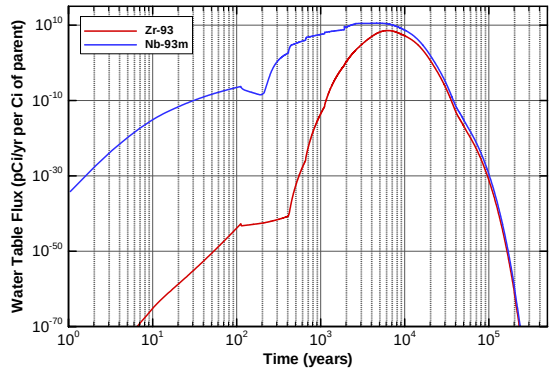

Figure A3A-72. Flux to Water Table: Uncracked with CDP for Zr-93

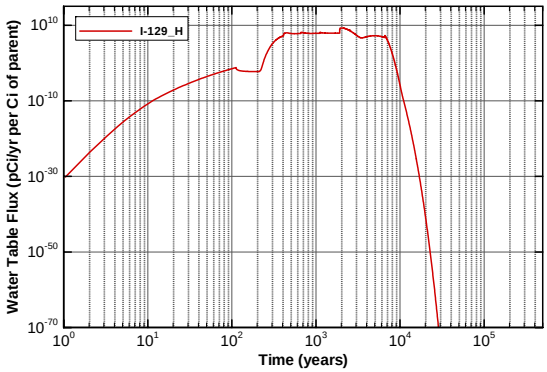

Figure A3A-73. Flux to Water Table: Uncracked with CDP for I-129_H

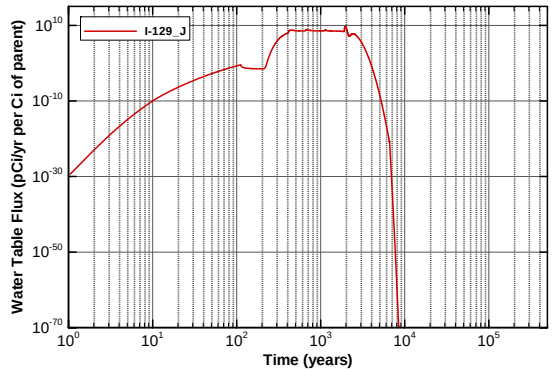

Figure A3A-74. Flux to Water Table: Uncracked with CDP for I-129_J

100-m Well Concentrations

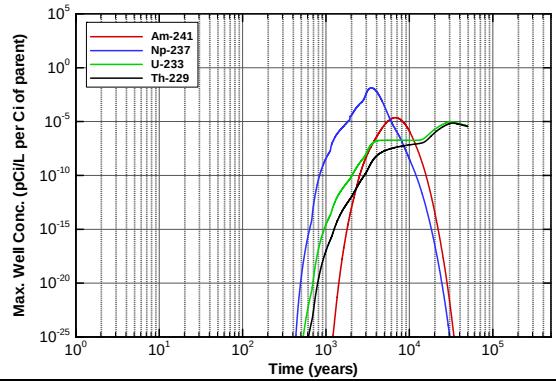

Figure A3A-75. CDP LAW Vault Well Concentration for Am-241

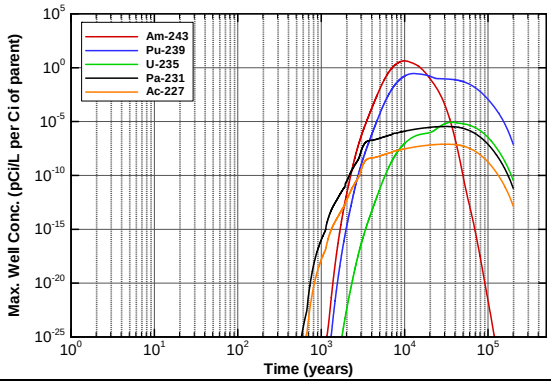

Figure A3A-76. CDP LAW Vault Well Concentration for Am-243

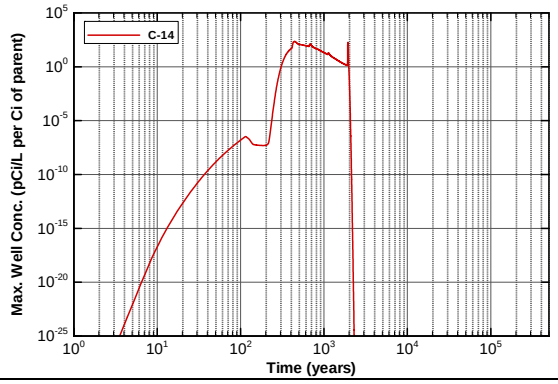

Figure A3A-77. CDP LAW Vault Well Concentration for C-14

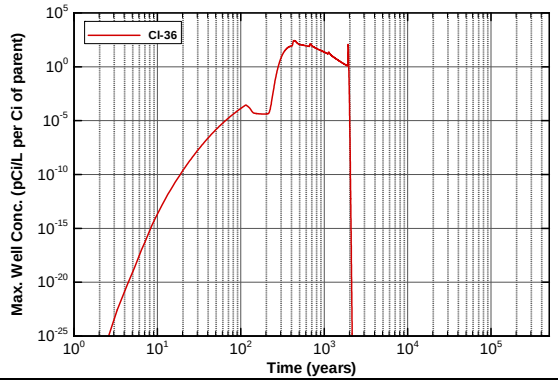

Figure A3A-78. CDP LAW Vault Well Concentration for Cl-36

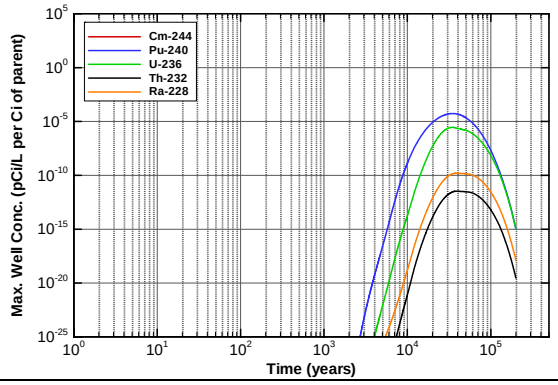

Figure A3A-79. CDP LAW Vault Well Concentration for Cm-244

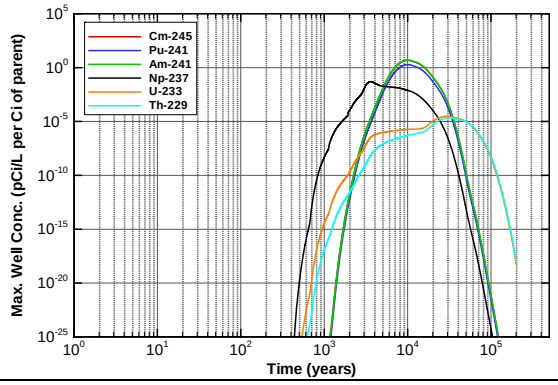

Figure A3A-80. CDP LAW Vault Well Concentration for Cm-245

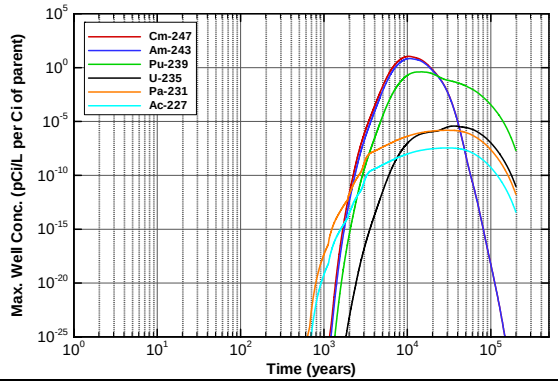

Figure A3A-81. CDP LAW Vault Well Concentration for Cm-247

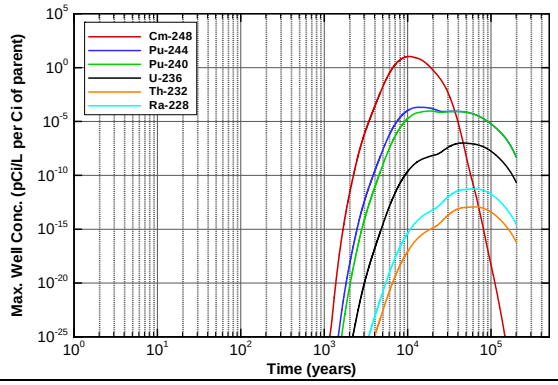

Figure A3A-82. CDP LAW Vault Well Concentration for Cm-248

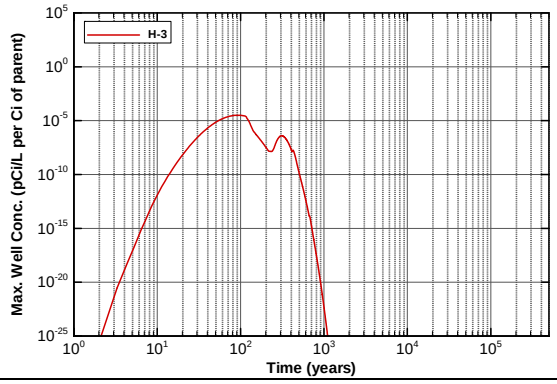

Figure A3A-83. CDP LAW Vault Well Concentration for H-3

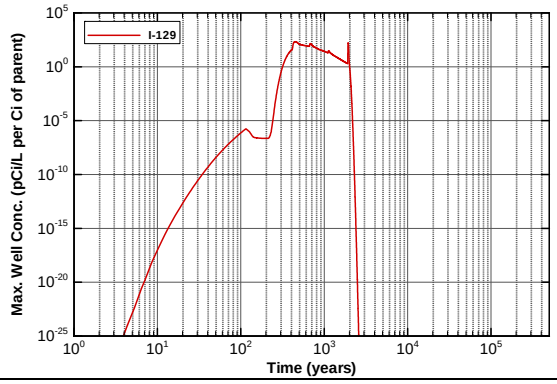

Figure A3A-84. CDP LAW Vault Well Concentration for I-129

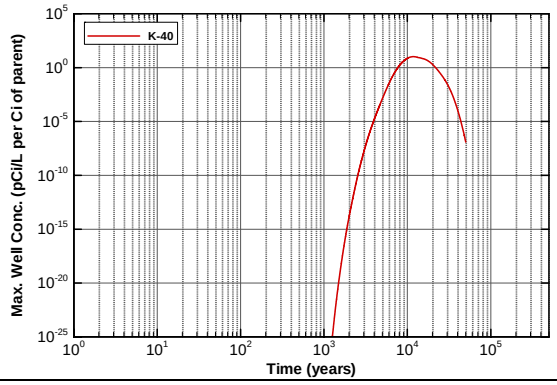

Figure A3A-85. CDP LAW Vault Well Concentration for K-40

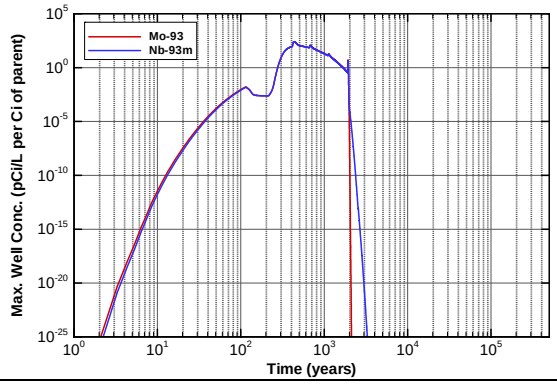

Figure A3A-86. CDP LAW Vault Well Concentration for Mo-93

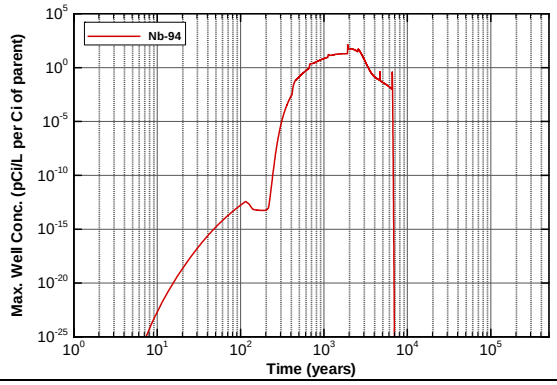

Figure A3A-87. CDP LAW Vault Well Concentration for Nb-94

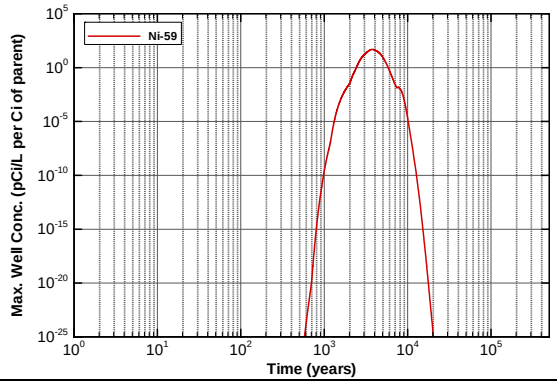

Figure A3A-88. CDP LAW Vault Well Concentration for Ni-59

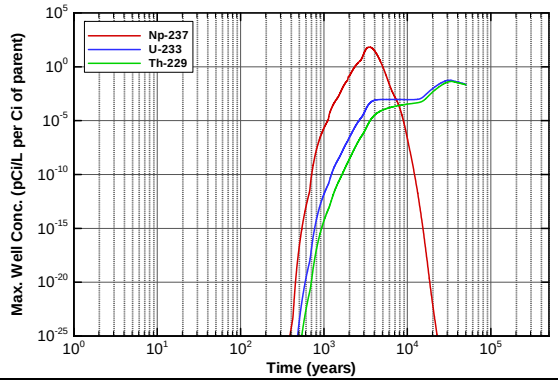

Figure A3A-89. CDP LAW Vault Well Concentration for Np-237

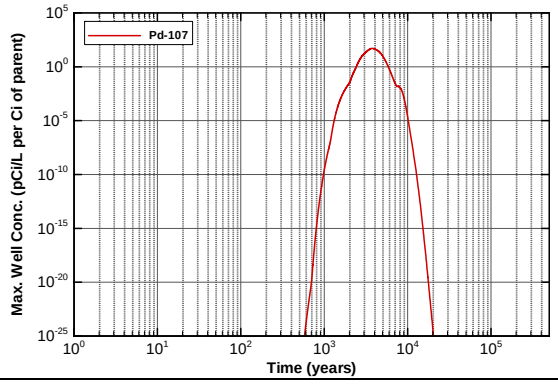

Figure A3A-90. CDP LAW Vault Well Concentration for Pd-107

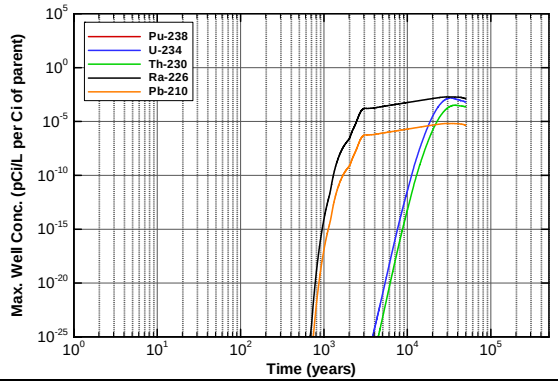

Figure A3A-91. CDP LAW Vault Well Concentration for Pu-238

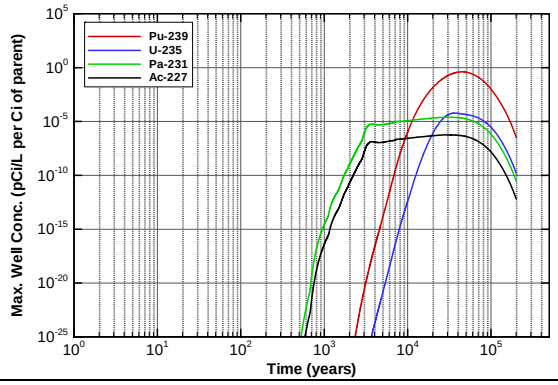

Figure A3A-92. CDP LAW Vault Well Concentration for Pu-239

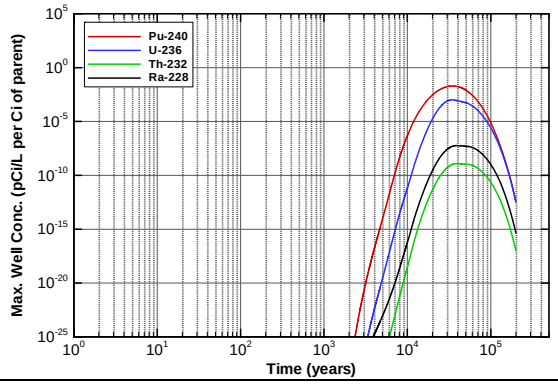

Figure A3A-93. CDP LAW Vault Well Concentration for Pu-240

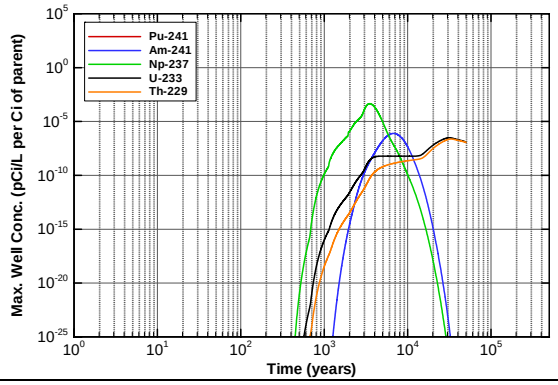

Figure A3A-94. CDP LAW Vault Well Concentration for Pu-241

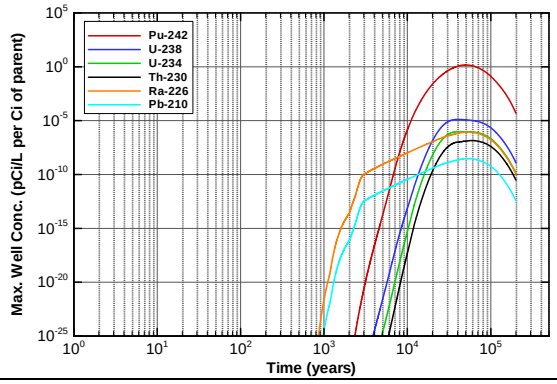

Figure A3A-95. CDP LAW Vault Well Concentration for Pu-242

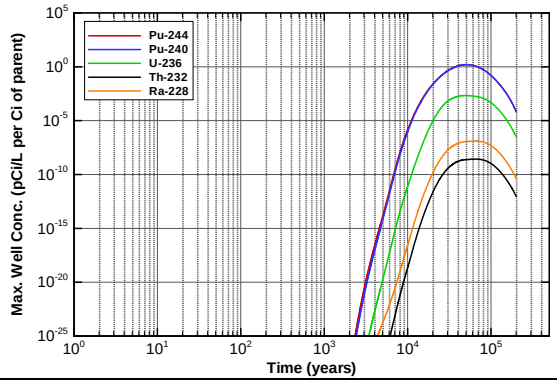

Figure A3A-96. CDP LAW Vault Well Concentration for Pu-244

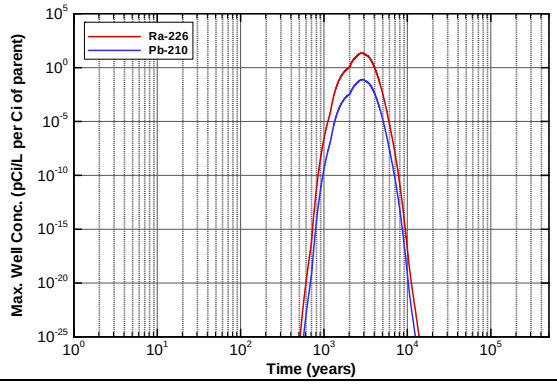

Figure A3A-97. CDP LAW Vault Well Concentration for Ra-226

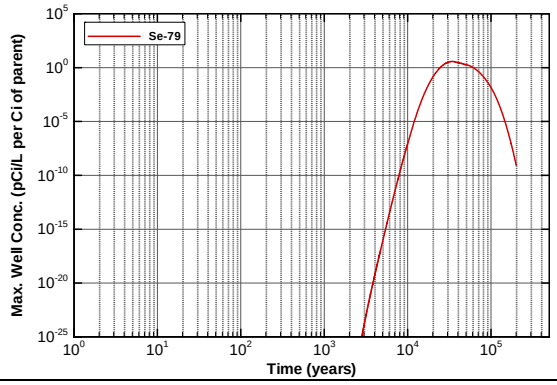

Figure A3A-98. CDP LAW Vault Well Concentration for Se-79

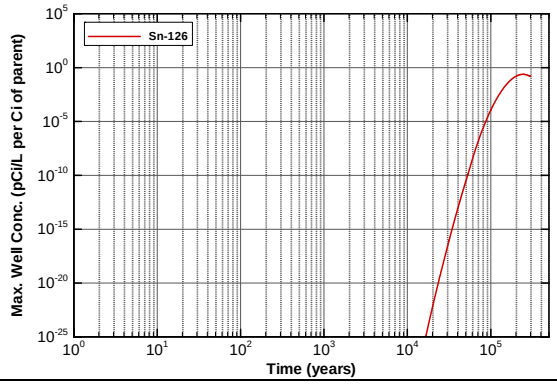

Figure A3A-99. CDP LAW Vault Well Concentration for Sn-126

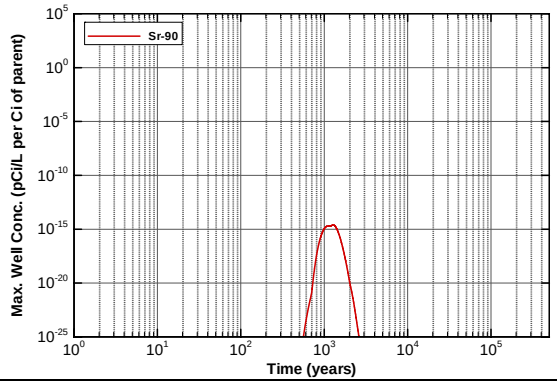

Figure A3A-100. CDP LAW Vault Well Concentration for Sr-90

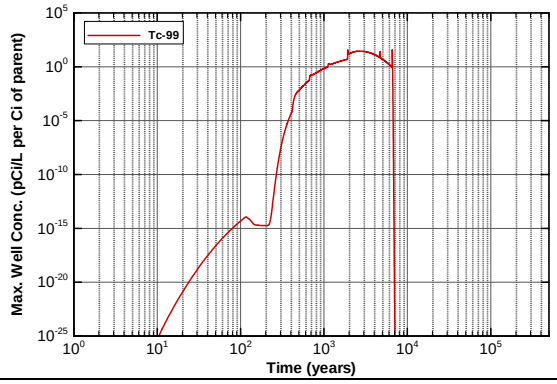

Figure A3A-101. CDP LAW Vault Well Concentration for Tc-99

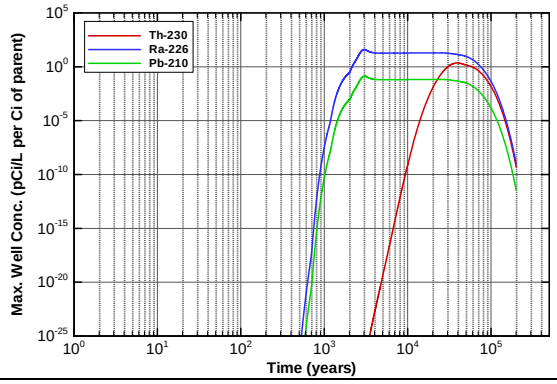

Figure A3A-102. CDP LAW Vault Well Concentration for Th-230

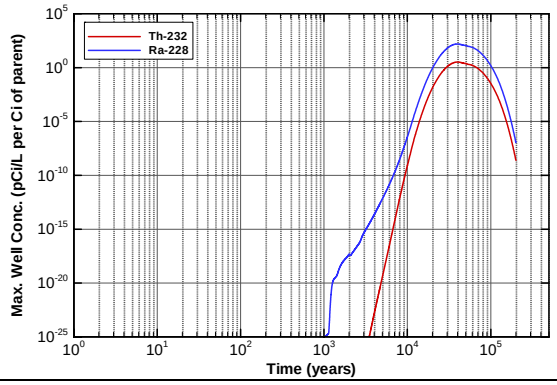

Figure A3A-103. CDP LAW Vault Well Concentration for Th-232

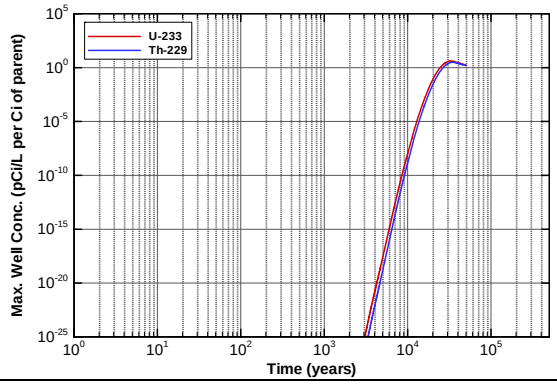

Figure A3A-104. CDP LAW Vault Well Concentration for U-233

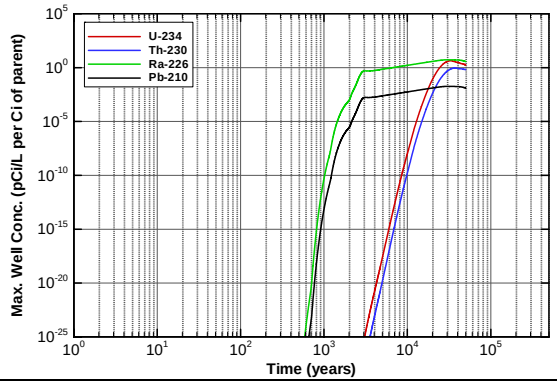

Figure A3A-105. CDP LAW Vault Well Concentration for U-234

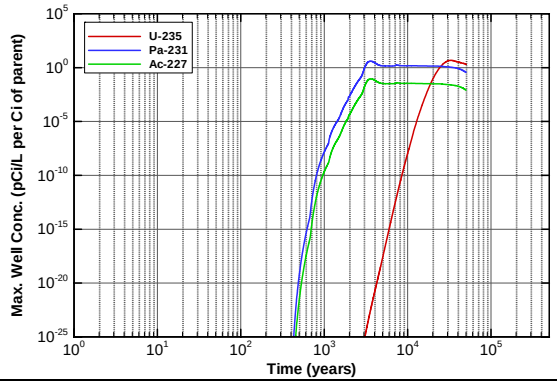

Figure A3A-106. CDP LAW Vault Well Concentration for U-235

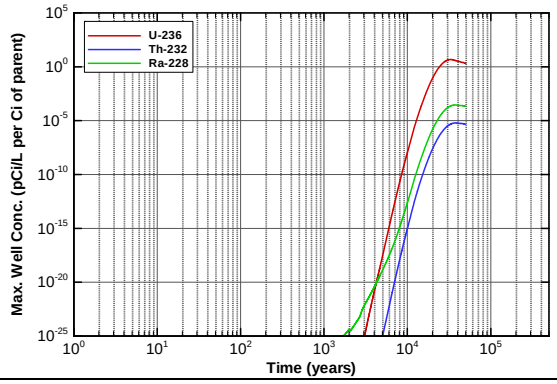

Figure A3A-107. CDP LAW Vault Well Concentration for U-236

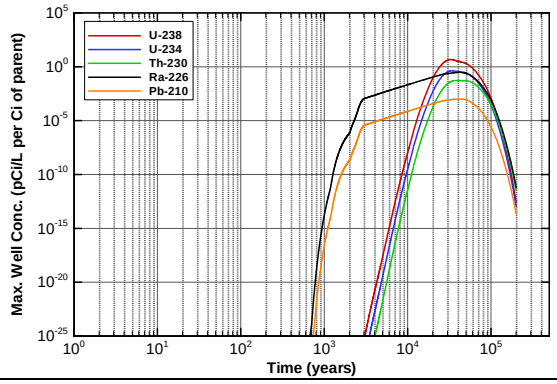

Figure A3A-108. CDP LAW Vault Well Concentration for U-238

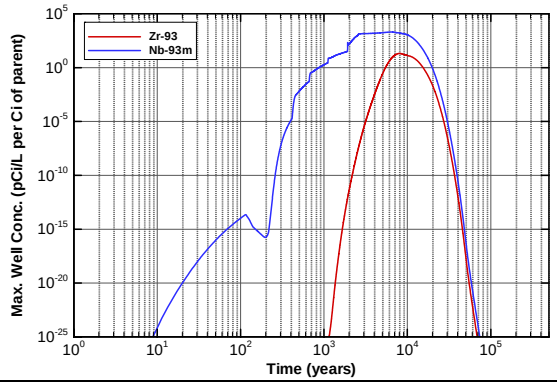

Figure A3A-109. CDP LAW Vault Well Concentration for Zr-93

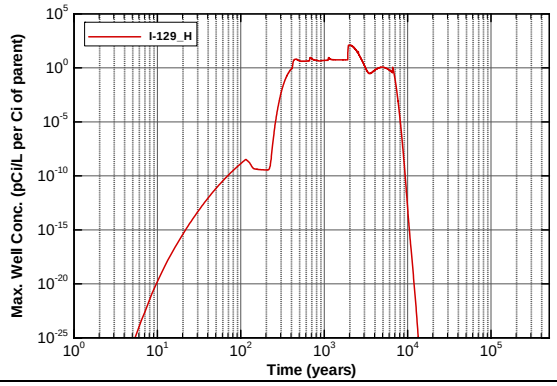

Figure A3A-110. CDP LAW Vault Well Concentration for I-129_H

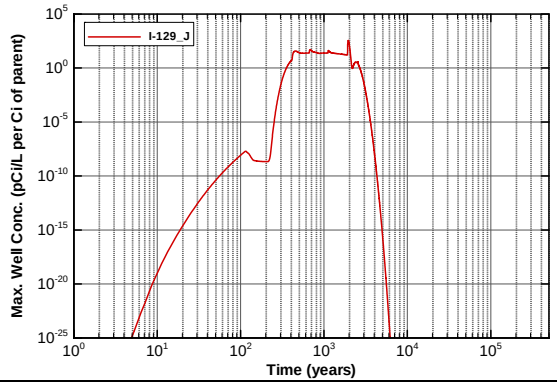

Figure A3A-111. CDP LAW Vault Well Concentration for I-129_J

APPENDIX A3B

Radon Model

10,000-year Simulation of Rn-222 Flux at Land Surface

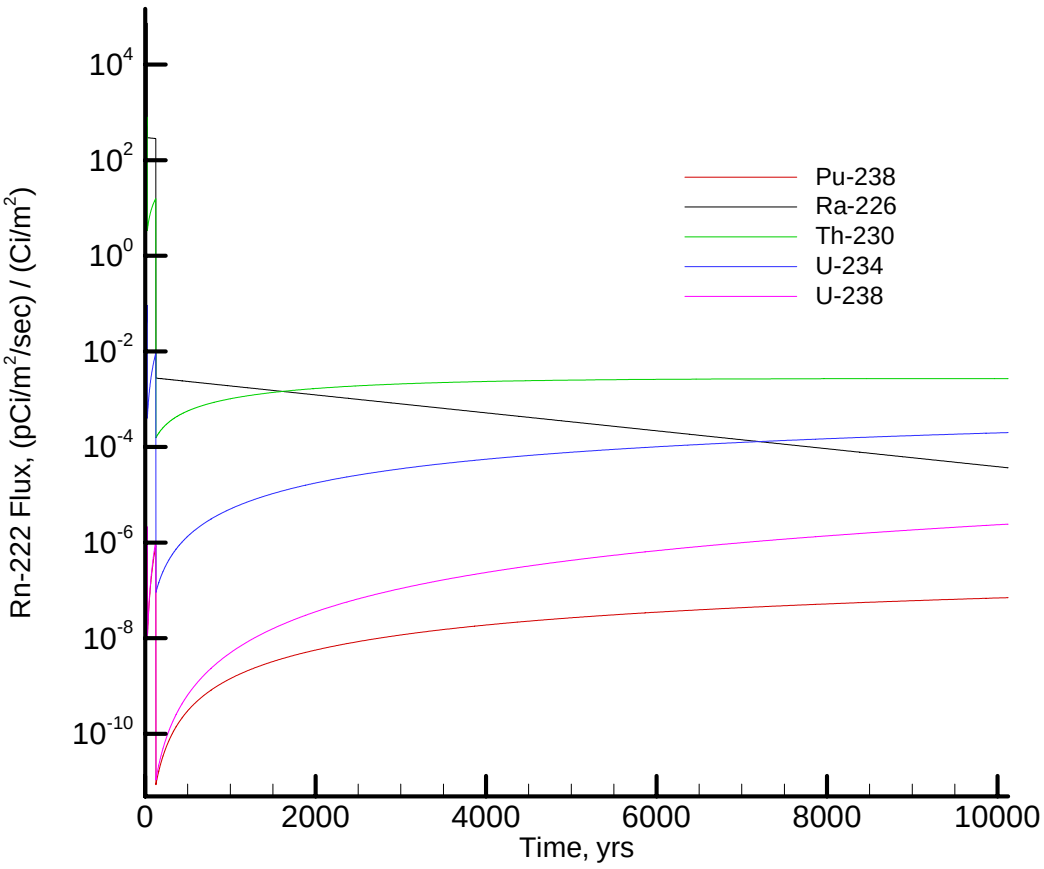

Figure A3B-1. Rn-222 Flux at Land Surface Resulting from Unit Source Term for LAW Vault

This page intentionally left blank.

APPENDIX A4 - IL VAULT

GRAPHICS FOR GROUNDWATER AND RADON

This page intentionally left blank.

TABLE OF CONTENTS

APPENDIX A4A

Vadose Zone and Aquifer Models

Typical Cell Saturation and Velocity Fields

Flux to the Water Table

100-m Well Concentrations

Typical Cell Saturation and Velocity Fields

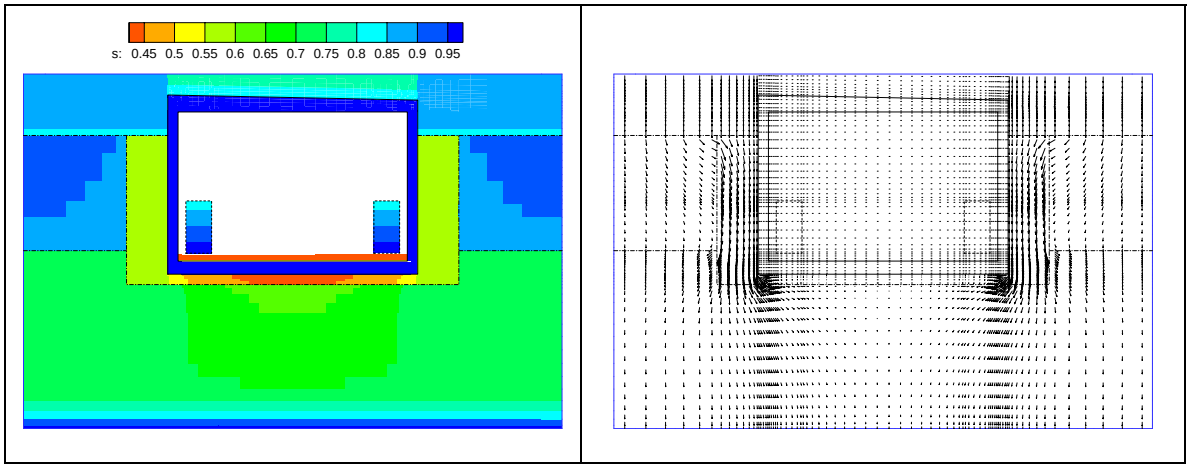

Figure A4A-1. Typical Cell saturation and velocity fields for -25 to 0 years.

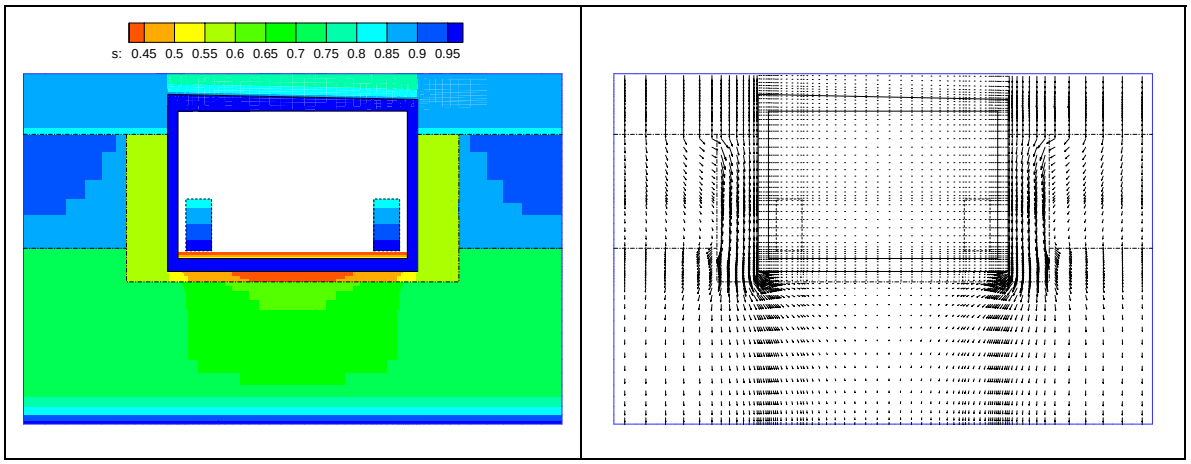

Figure A4A-2. Typical Cell saturation and velocity fields for 0 to 100 years

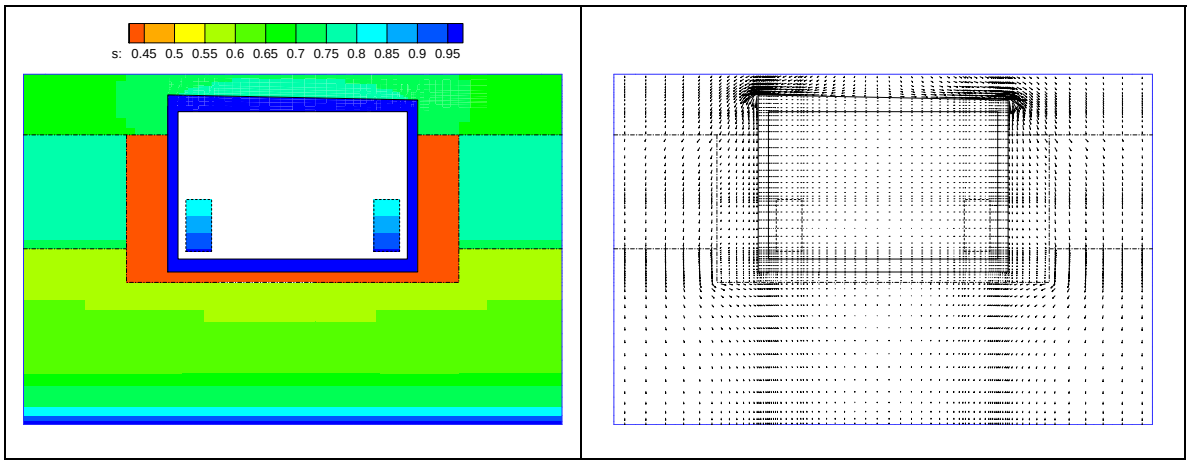

Figure A4A-3. Typical Cell saturation and velocity fields for 100 to 200 years

Note: 1. Color blanking implemented for saturations < 0.4 in waste zone.
2. Velocity vectors lengths selected independently for each steady-state period.

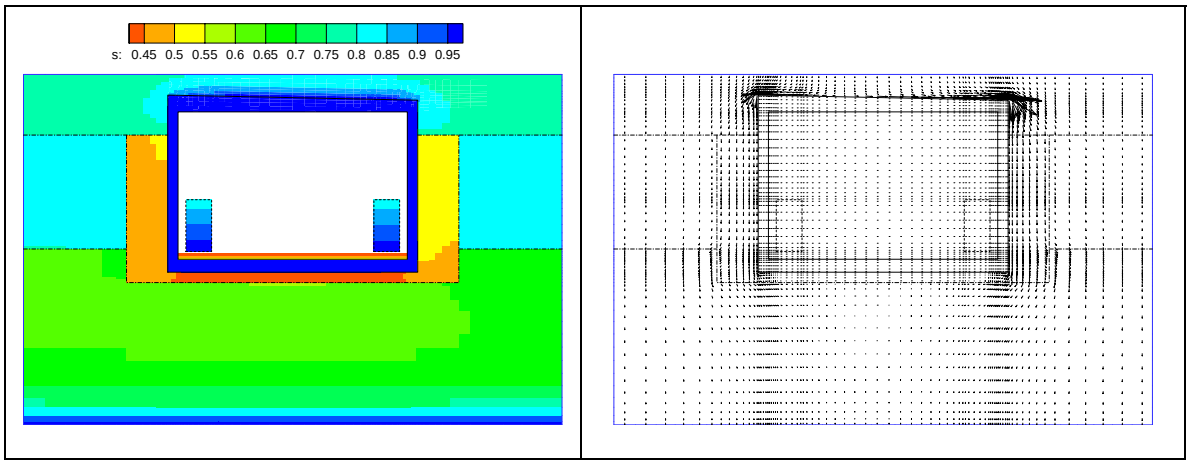

Figure A4A-4. Typical Cell saturation and velocity fields for 200 to 400 years.

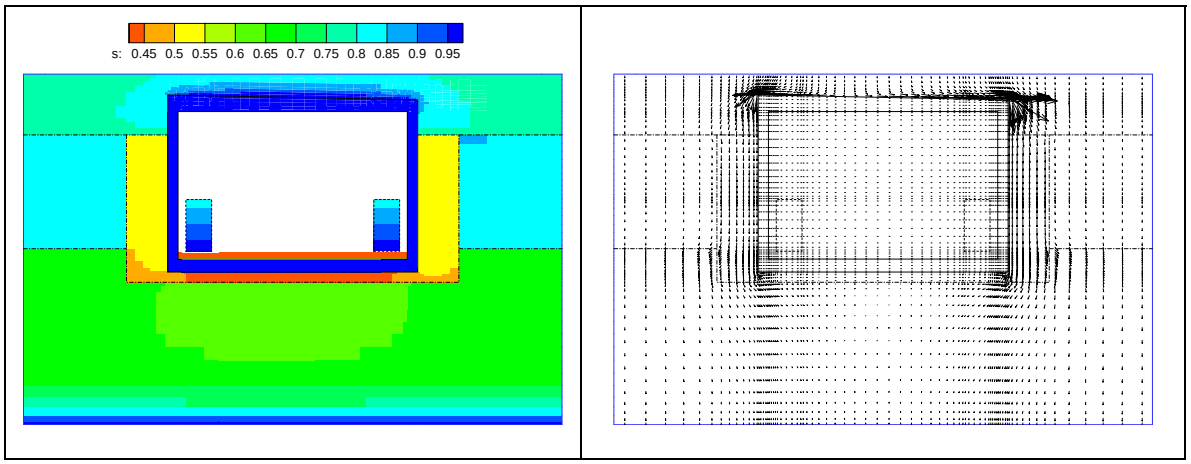

Figure A4A-5. Typical Cell saturation and velocity fields for 400 to 650 years

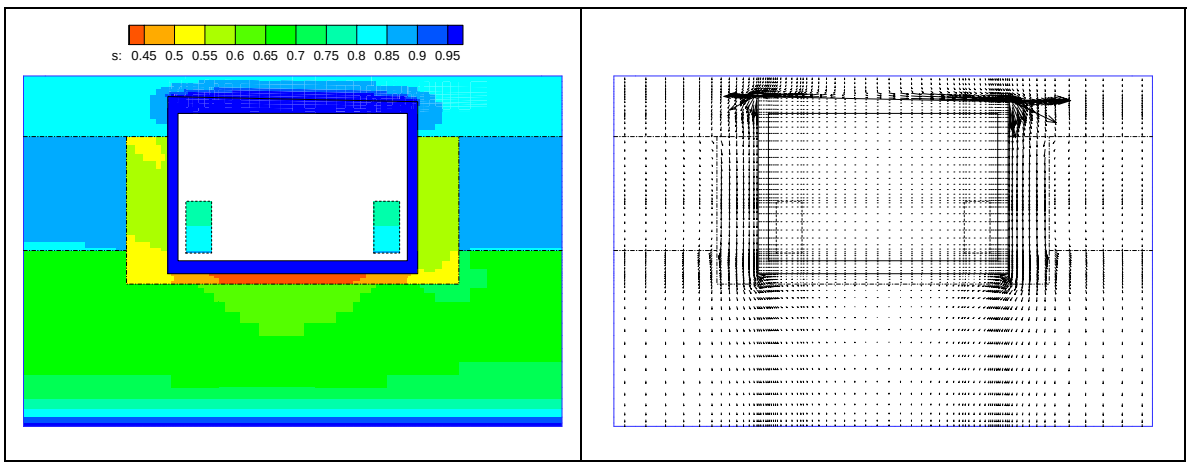

Figure A4A-6. Typical Cell saturation and velocity fields for 650 to 1100 years

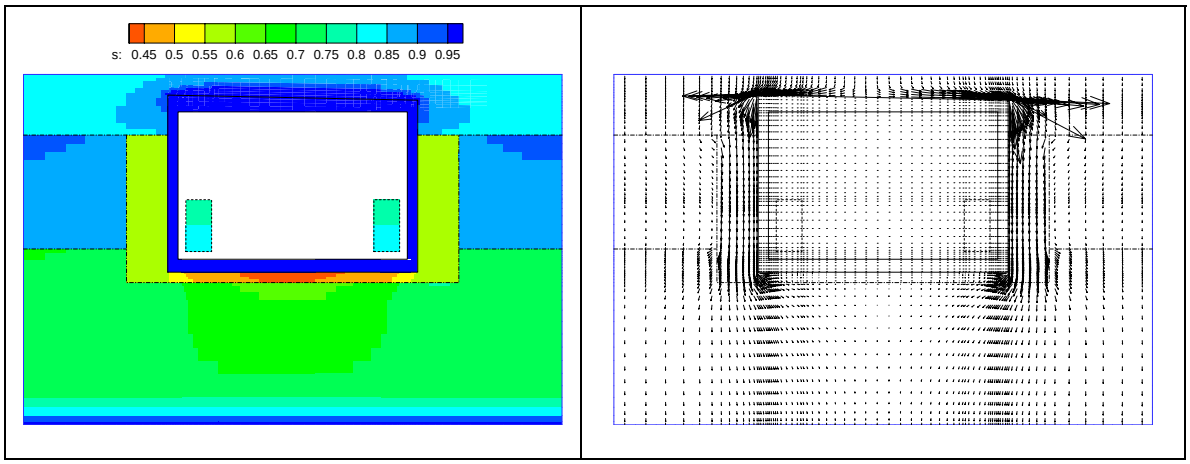

Figure A4A-7. Typical Cell saturation and velocity fields for 1100 to 1900 years.

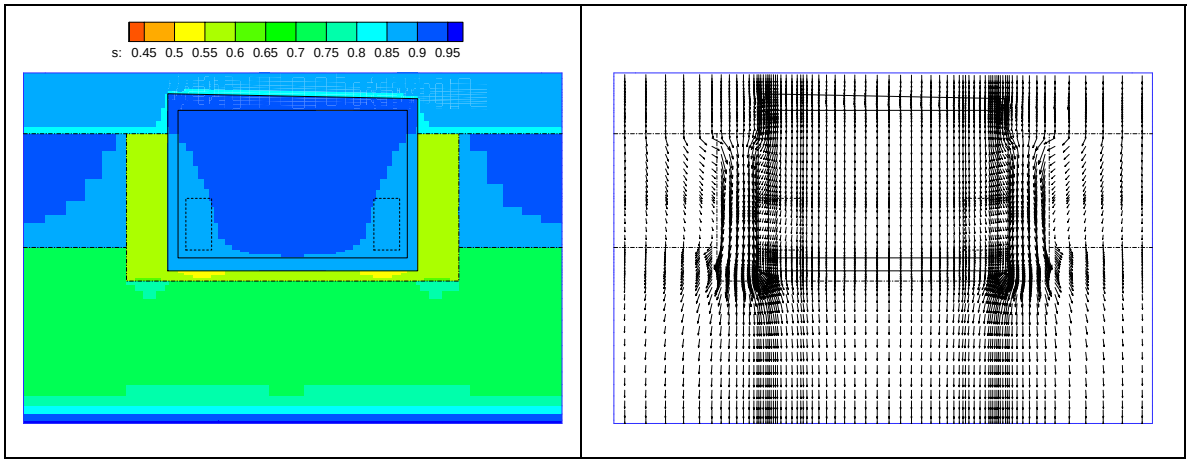

Figure A4A-8. Typical Cell saturation and velocity fields for 1900 to 10000 years

Saturation and velocity fields for Cell 4 are the same as the Typical Cell for time periods -25 to 0 years, 0 to 100 years, 100 to 200 years and 200 to 400 years and are not presented again. However, Cell 4 flow fields for the later time periods 400 to 650 years, 650 to 1100 years, 1100 to 1900 years and 1900 to 10000 years are presented.

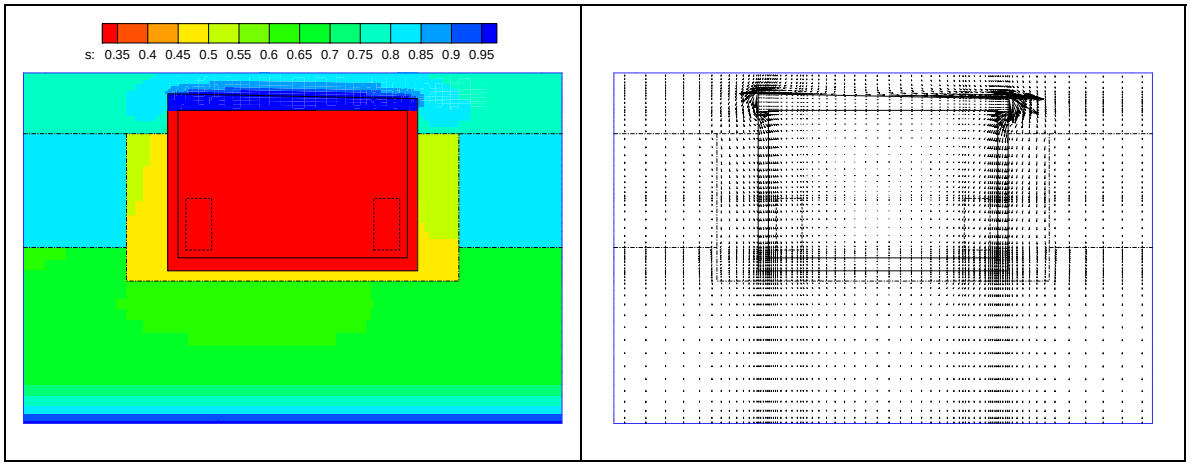

Figure A4A-9. Cell 4 saturation and velocity fields for 400 to 650 years

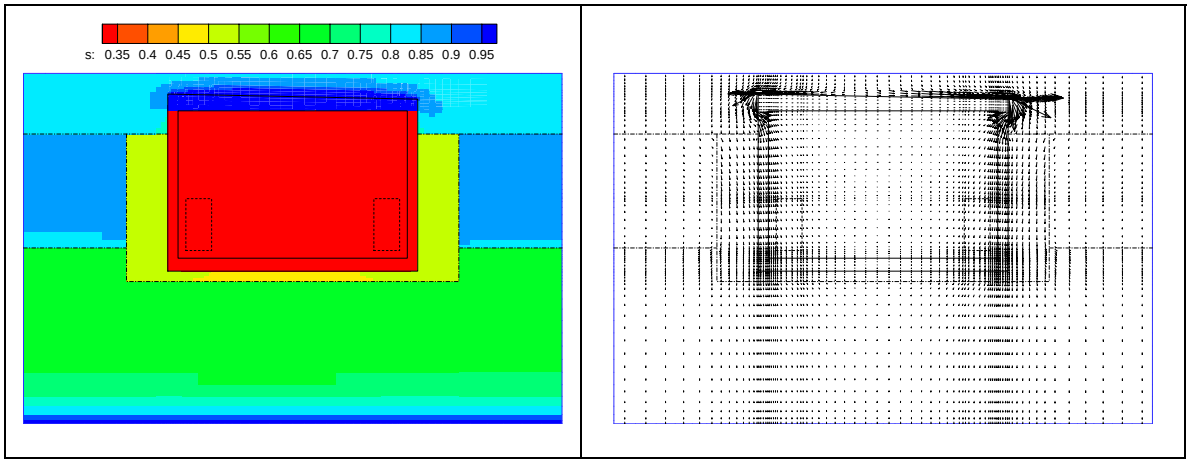

Figure A4A-10. Cell 4 saturation and velocity fields for 650 to 1100 years

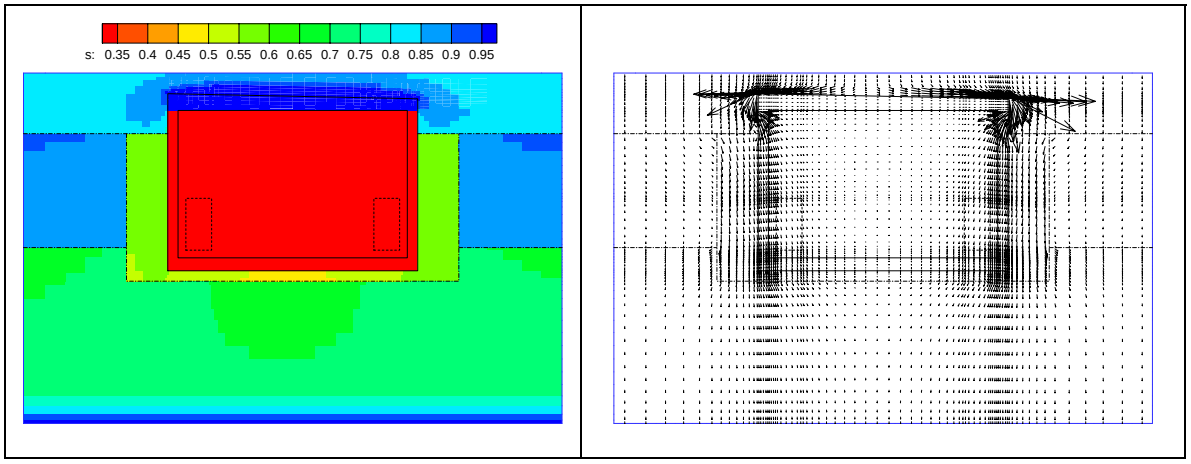

Figure A4A-11. Cell 4 saturation and velocity fields for 1100 to 1900 years

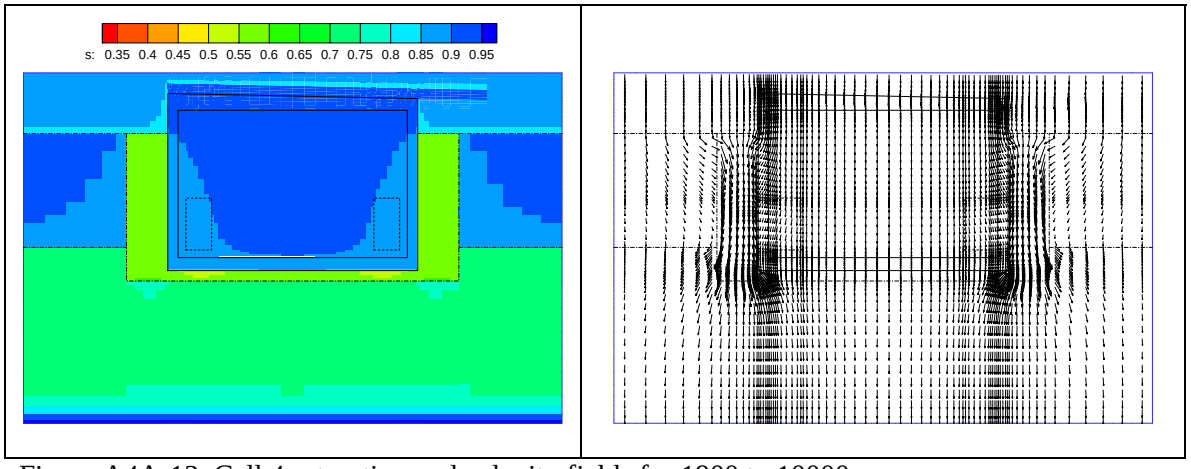

Figure A4A-12. Cell 4 saturation and velocity fields for 1900 to 10000 years

Flux to Water Table

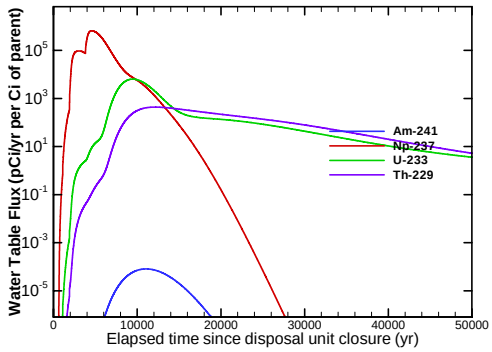

Figure A4A-13. ILV water table flux for Am-241

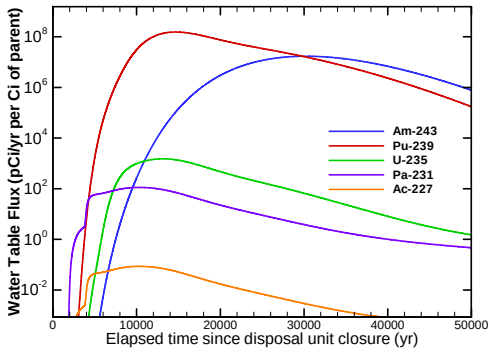

Figure A4A-14. ILV water table flux for Am-243

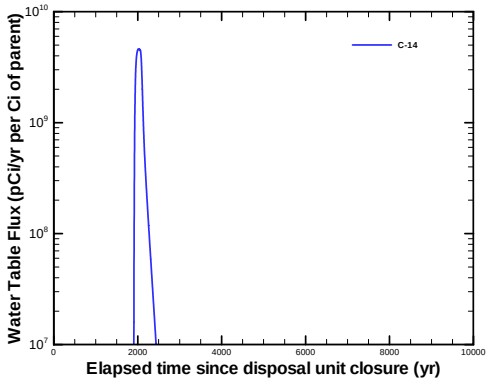

Figure A4A-15. ILV water table flux for C-14

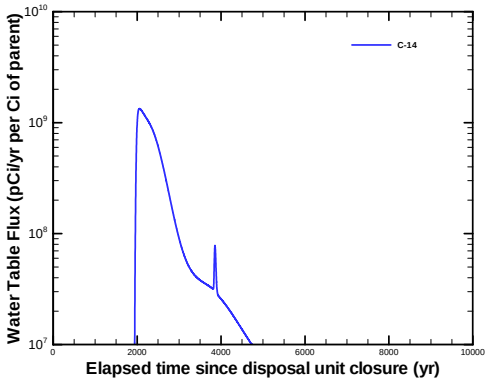

Figure A4A-16. ILV water table flux for C-14_KB

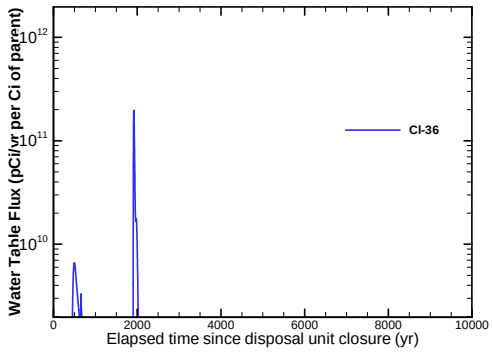

Figure A4A-17. ILV water table flux for Cl-36

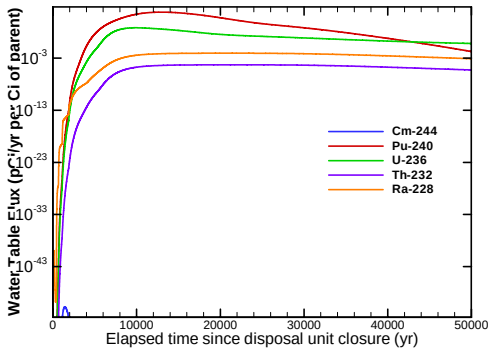

Figure A4A-18. ILV water table flux for Cm-244

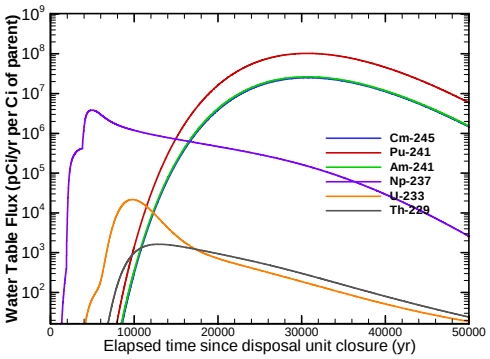

Figure A4A-19. ILV water table flux for Cm-245

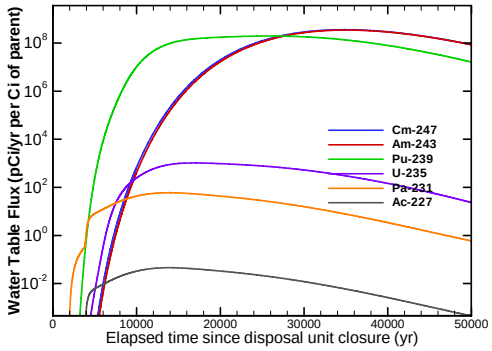

Figure A4A-20. ILV water table flux for Cm-247

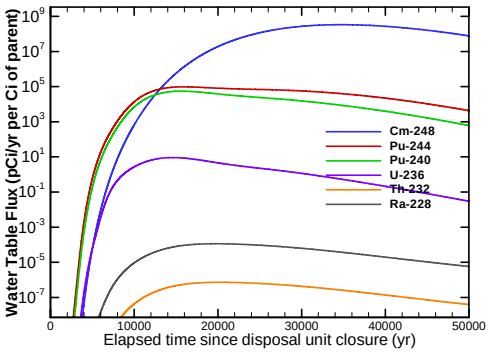

Figure A4A-21. ILV water table flux for Cm-248

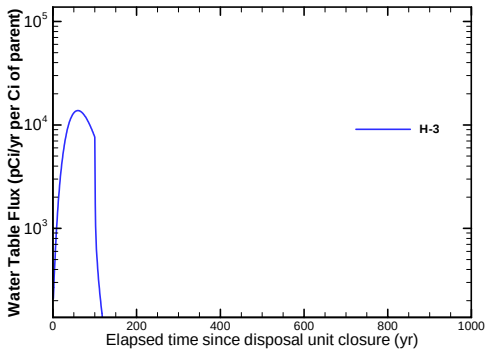

Figure A4A-22. ILV water table flux for H-3

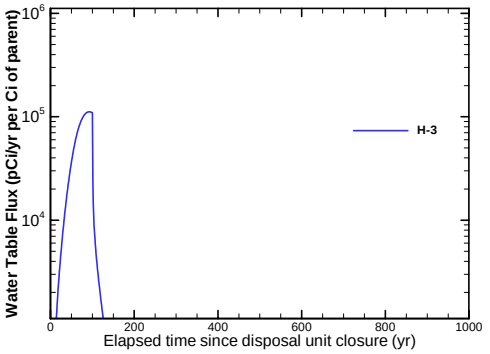

Figure A4A-23. ILV water table flux for H-3_TPBAR

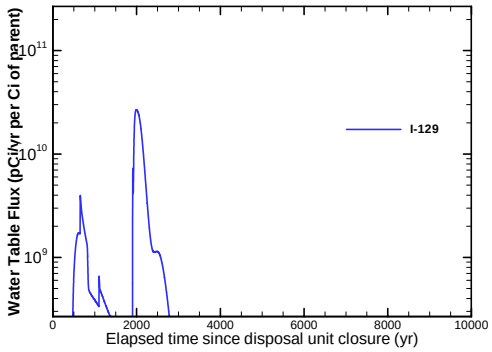

Figure A4A-24. ILV water table flux for I-129

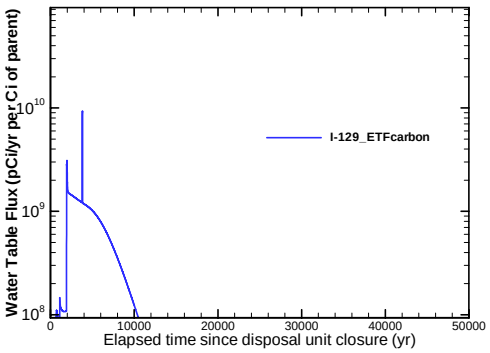

Figure A4A-25. ILV water table flux for I-129_ETFcarbon

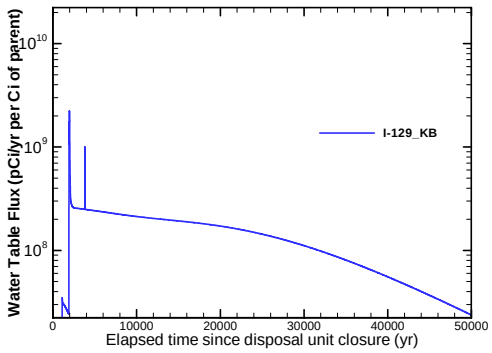

Figure A4A-26. ILV water table flux for I-129_KB

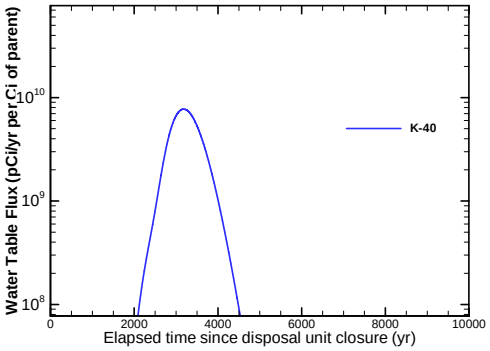

Figure A4A-27. ILV water table flux for K-40

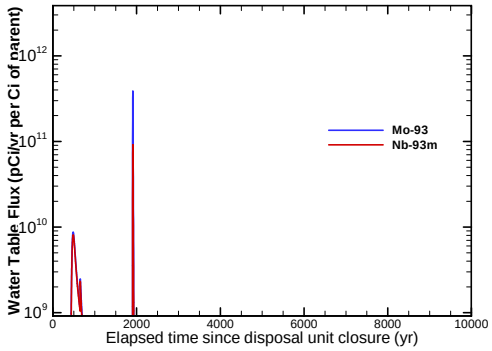

Figure A4A-28. ILV water table flux for Mo-93

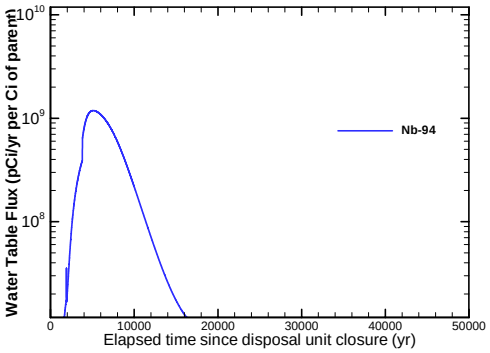

Figure A4A-29. ILV water table flux for Nb-94

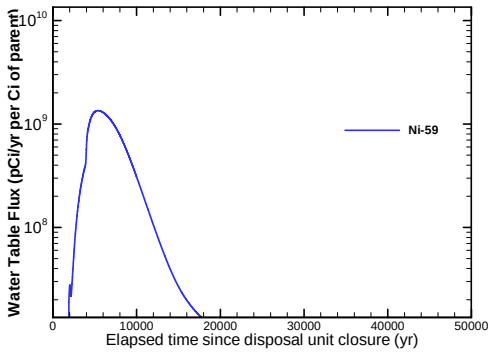

Figure A4A-30. ILV water table flux for Ni-59

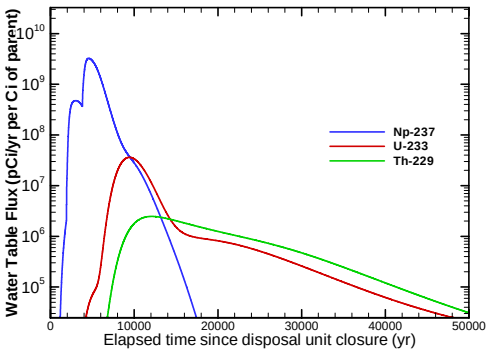

Figure A4A-31. ILV water table flux for Np-237

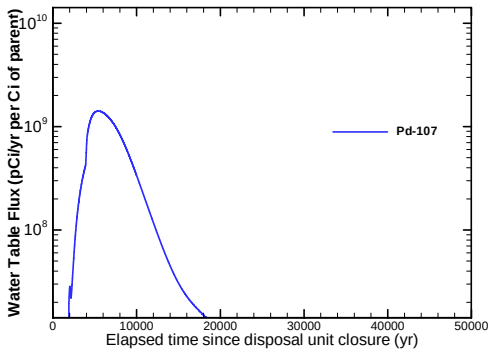

Figure A4A-32. ILV water table flux for Pd-107

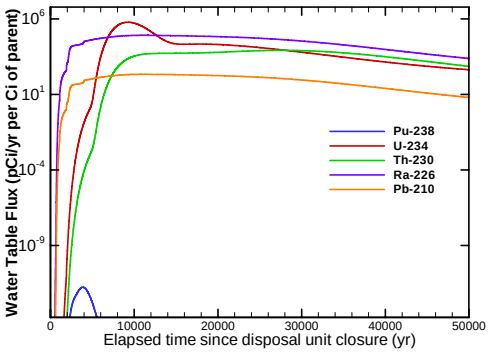

Figure A4A-33. ILV water table flux for Pu-238

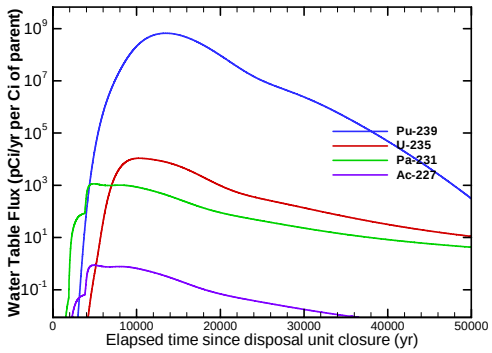

Figure A4A-34. ILV water table flux for Pu-239

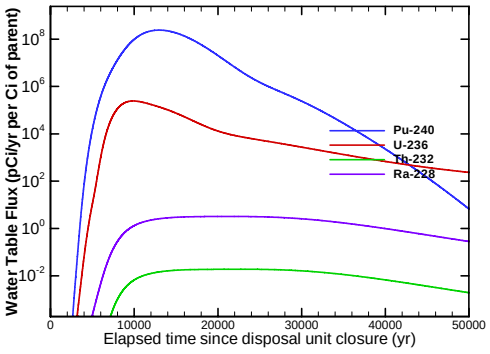

Figure A4A-35. ILV water table flux for Pu-240

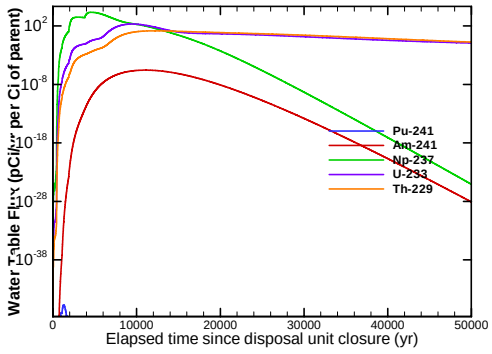

Figure A4A-36. ILV water table flux for Pu-241

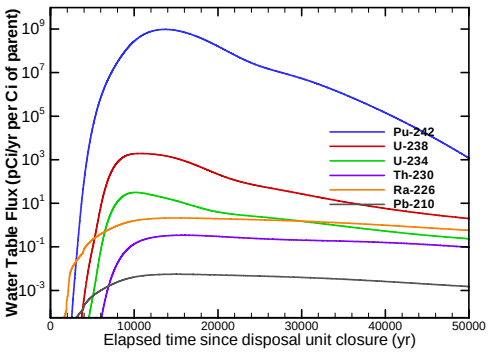

Figure A4A-37. ILV water table flux for Pu-242

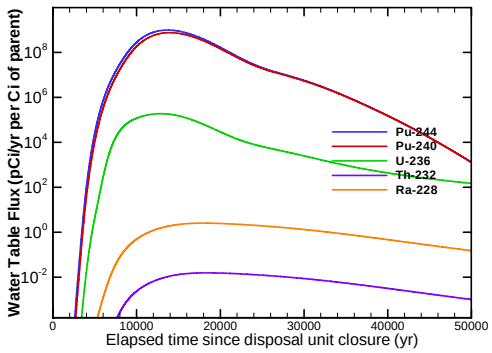

Figure A4A-38. ILV water table flux for Pu-244

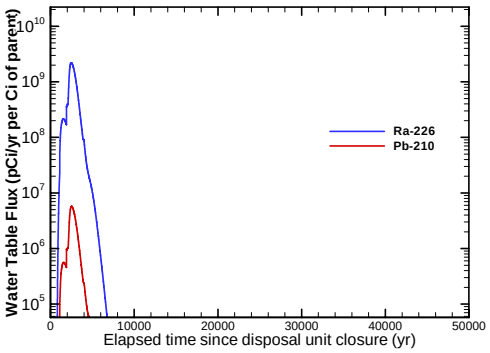

Figure A4A-39. ILV water table flux for Ra-226

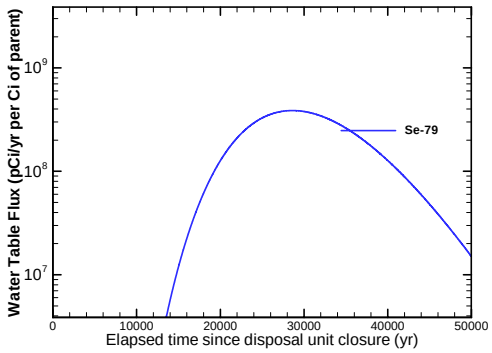

Figure A4A-40. ILV water table flux for Se-79

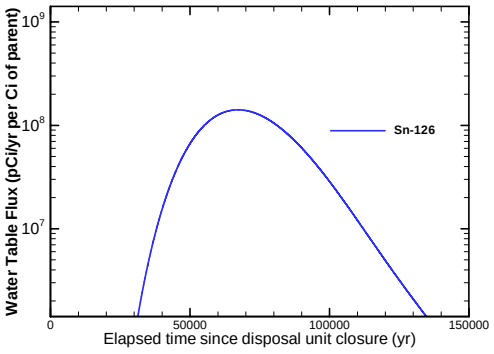

Figure A4A-41. ILV water table flux for Sn-126

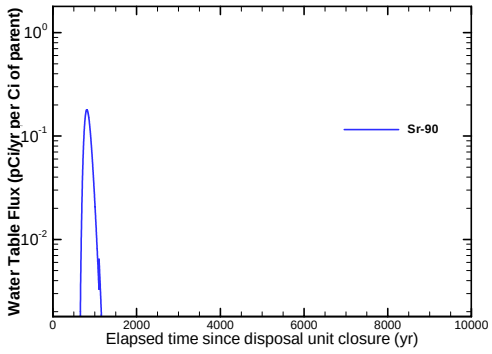

Figure A4A-42. ILV water table flux for Sr-90

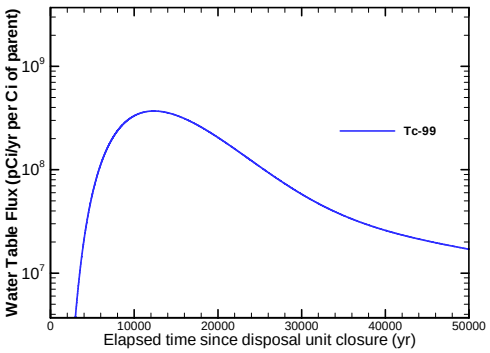

Figure A4A-43. ILV water table flux for Tc-99

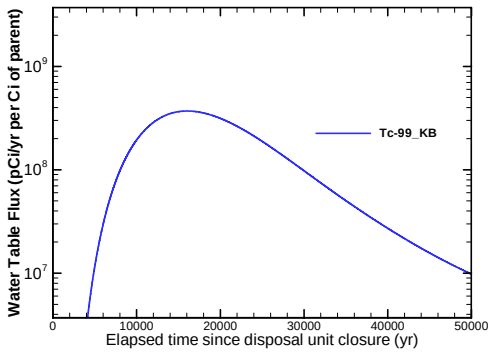

Figure A4A-44. ILV water table flux for Tc-99_KB

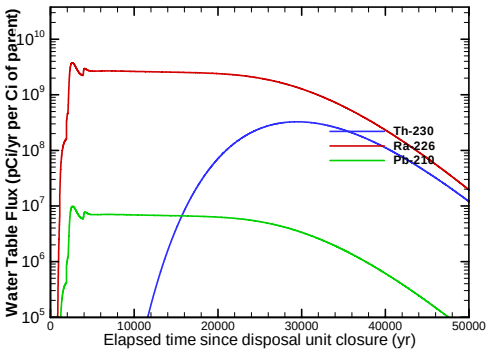

Figure A4A-45. ILV water table flux for Th-230

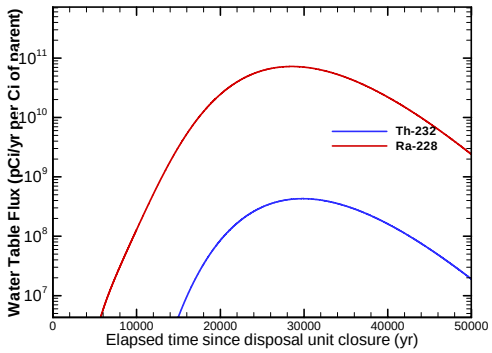

Figure A4A-46. ILV water table flux for Th-232

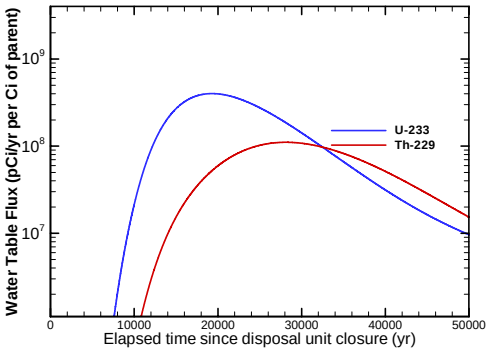

Figure A4A-47. ILV water table flux for U-233

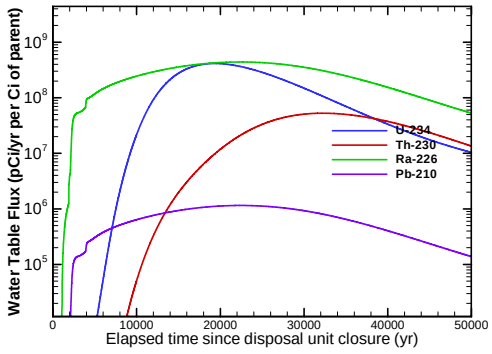

Figure A4A-48. ILV water table flux for U-234

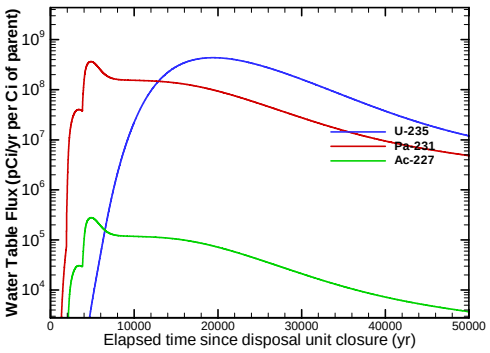

Figure A4A-49. ILV water table flux fo U-235

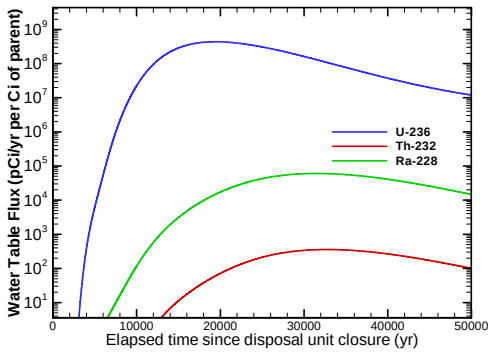

Figure A4A-50. ILV water table flux for U-236

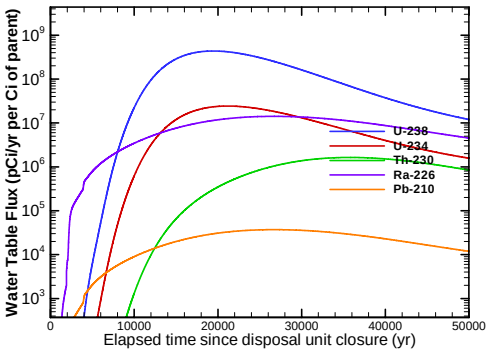

Figure A4A-51. ILV water table flux for U-238

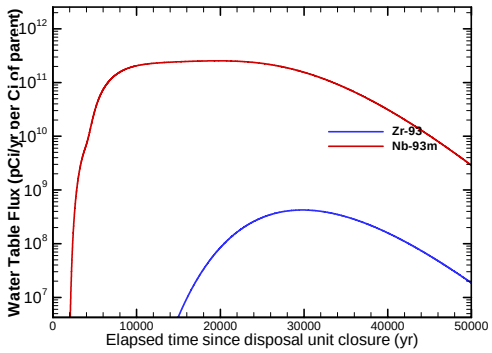

Figure A4A-52. ILV water table flux for Zr-93

100-m Well Concentrations

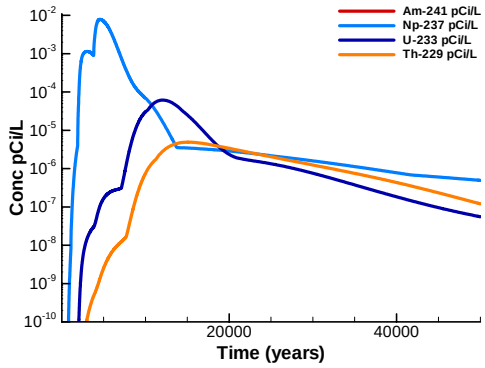

Figure A4A-53. ILV well concentration for Am-241

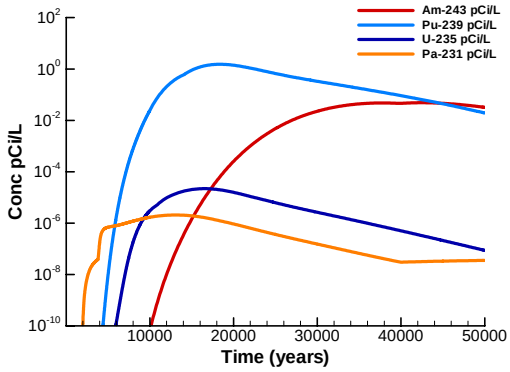

Figure A4A-54. ILV well concentration for Am-243

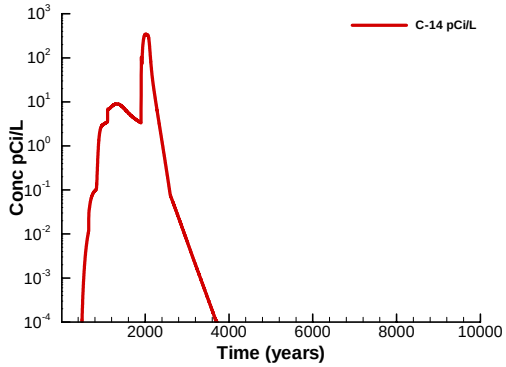

Figure A4A-55. ILV well concentration for C-14

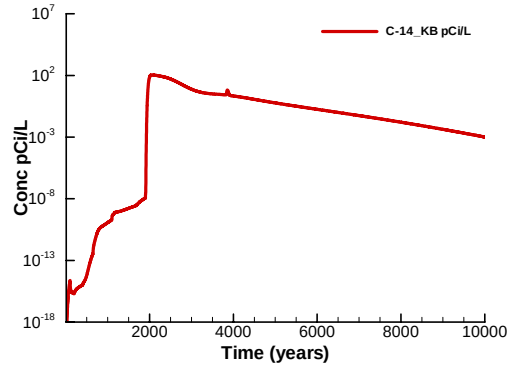

Figure A4A-56. ILV well concentration for C-14_KB

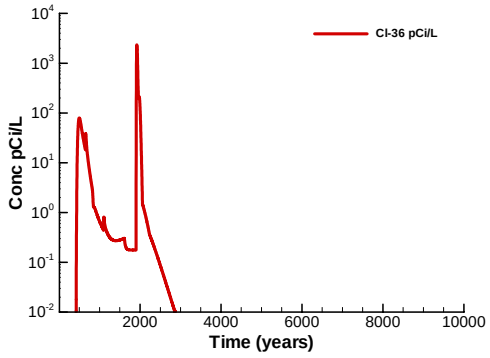

Figure A4A-57. ILV well concentration for Cl-36

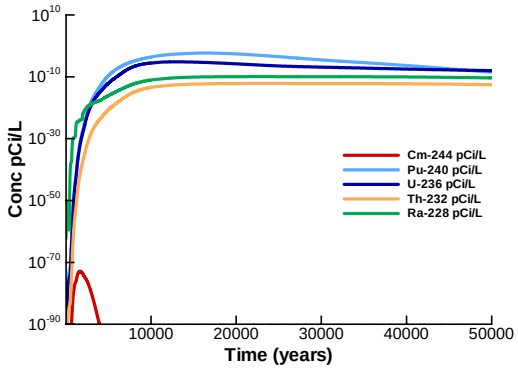

Figure A4A-58. ILV well concentration for Cm-244

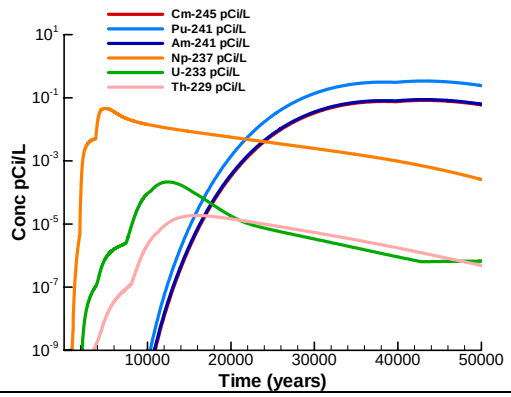

Figure A4A-59. ILV well concentration for Cm-245

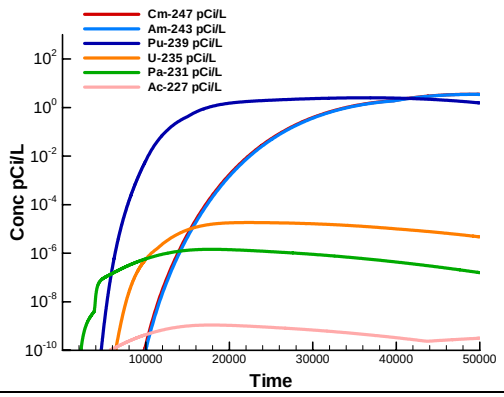

Figure A4A-60. ILV well concentration for Cm-247

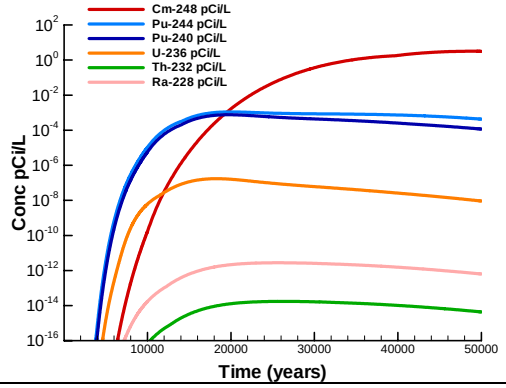

Figure A4A-61. ILV well concentration for Cm-248

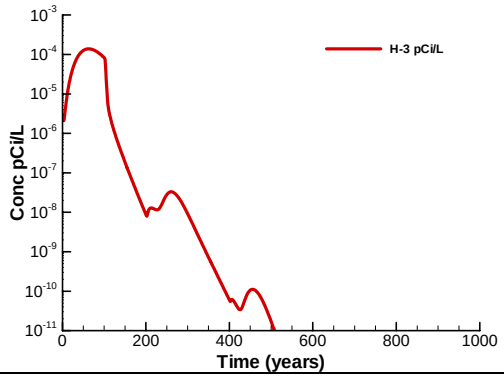

Figure A4A-62. ILV well concentration for H-3

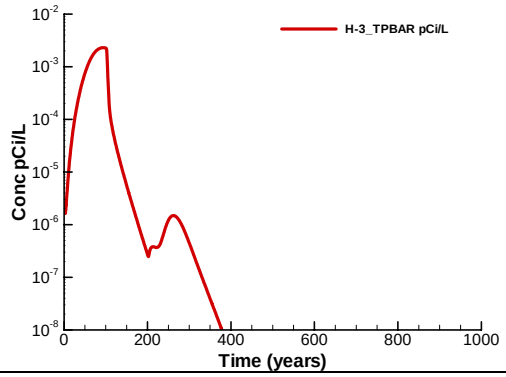

Figure A4A-63. ILV well concentration for H-3_TPBAR

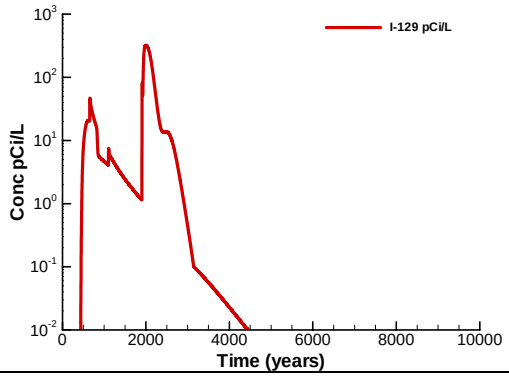

Figure A4A-64. ILV well concentration for I-129

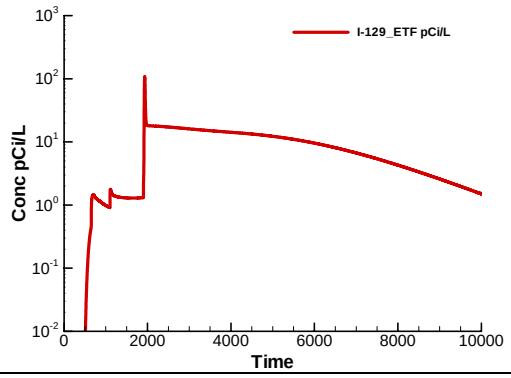

Figure A4A-65. ILV well concentration for I-129_ETFcarbon

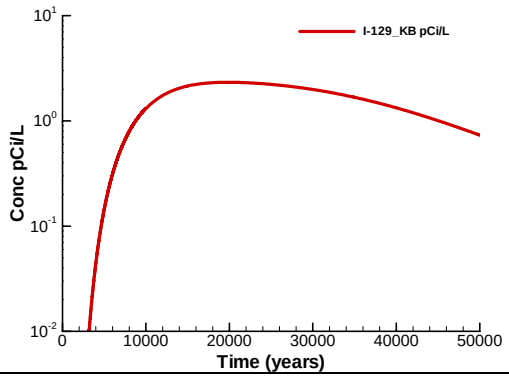

Figure A4A-66. ILV well concentration for I-129_KB

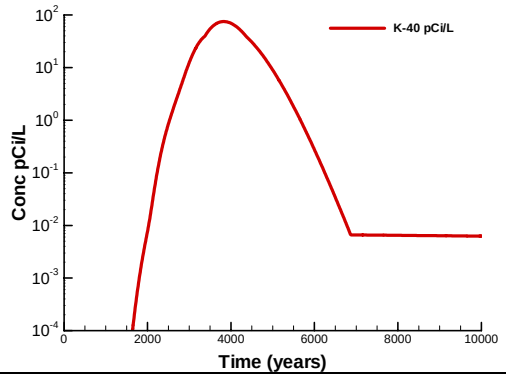

Figure A4A-67. ILV well concentration for K-40

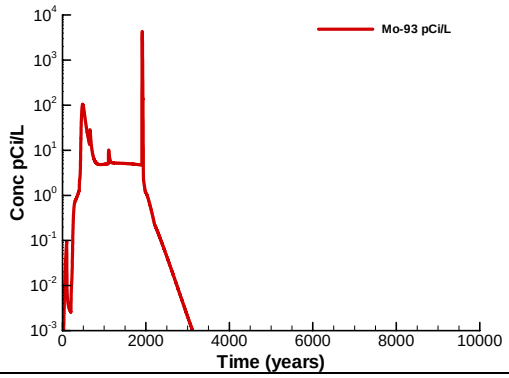

Figure A4A-68. ILV well concentration for Mo-93

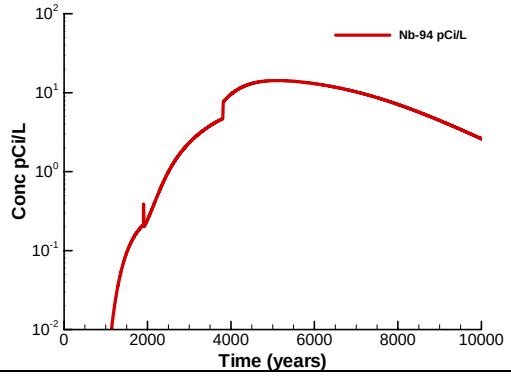

Figure A4A-69. ILV well concentration for Nb-94

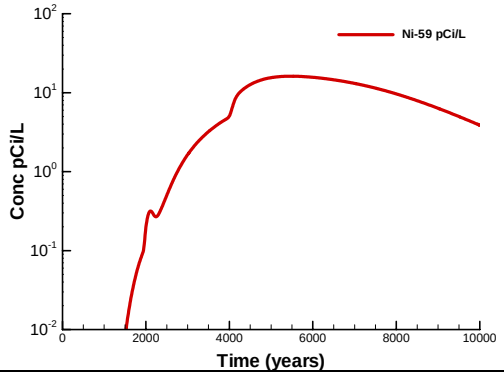

Figure A4A-70. ILV well concentration for Ni-59

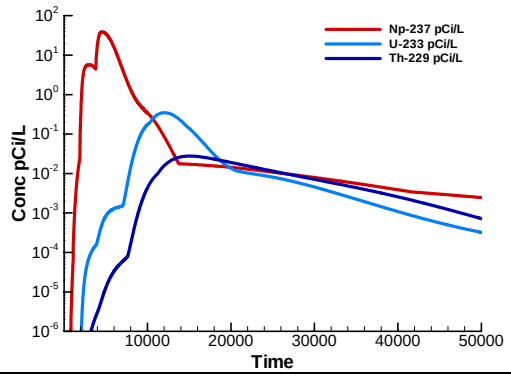

Figure A4A-71. ILV well concentration for Np-237

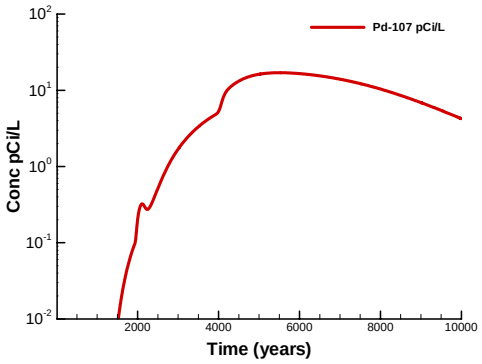

Figure A4A-72. ILV well concentration for Pd-107

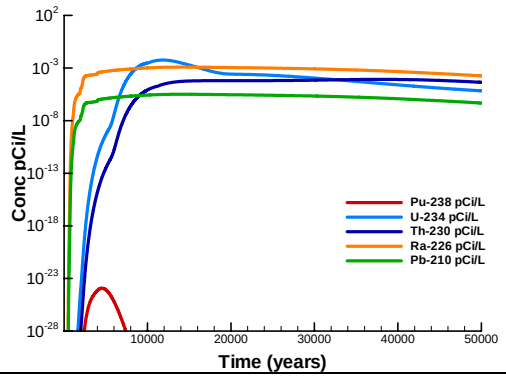

Figure A4A-73. ILV well concentration for Pu-238

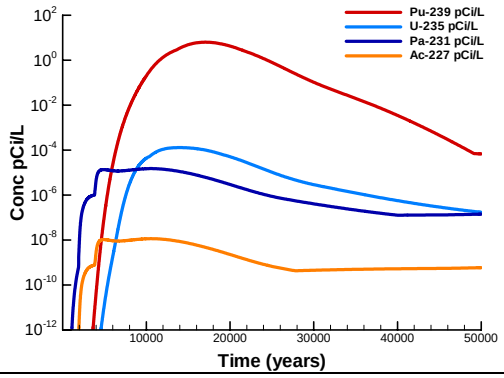

Figure A4A-74. ILV well concentration for Pu-239

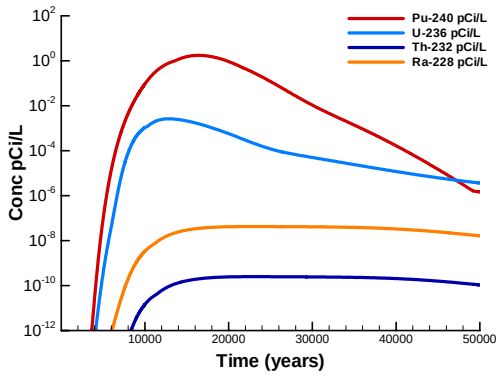

Figure A4A-75. ILV well concentration for Pu-240

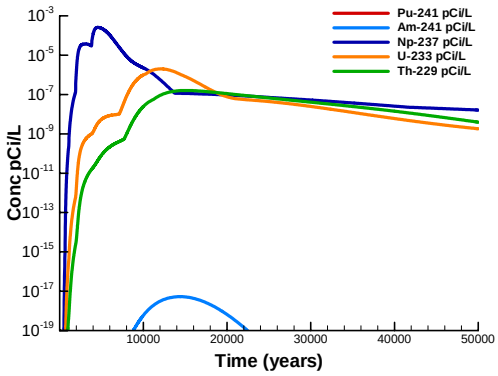

Figure A4A-76. ILV well concentration for Pu-241

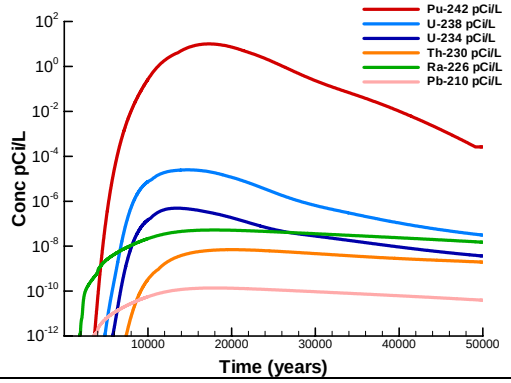

Figure A4A-77. ILV well concentration for Pu-242

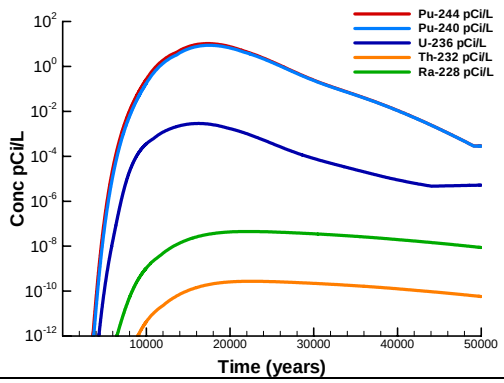

Figure A4A-78. ILV well concentration for Pu-244

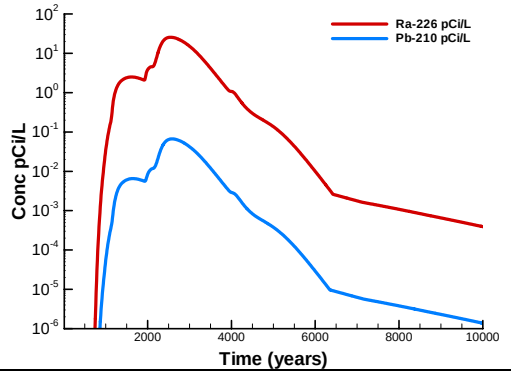

Figure A4A-79. ILV well concentration for Ra-226

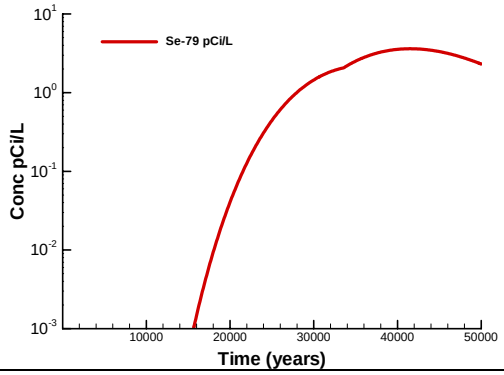

Figure A4A-80. ILV well concentration for Se-79

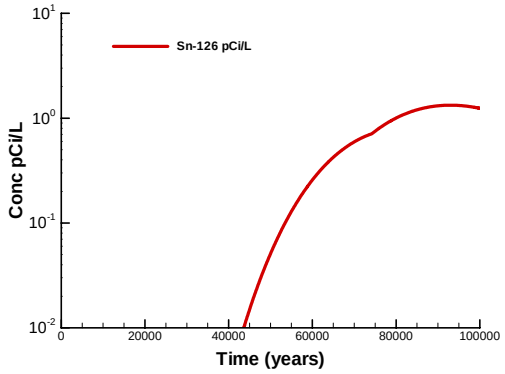

Figure A4A-81. ILV well concentration for Sn-126

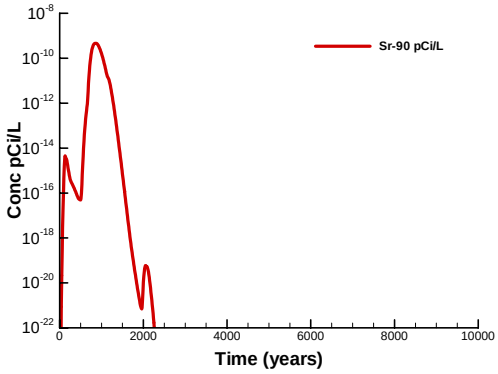

Figure A4A-82. ILV well concentration for Sr-90

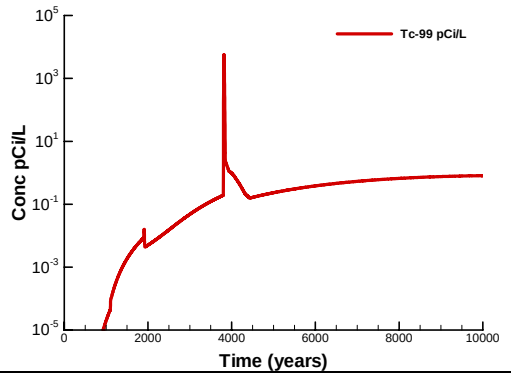

Figure A4A-83. ILV well concentration for Tc-99

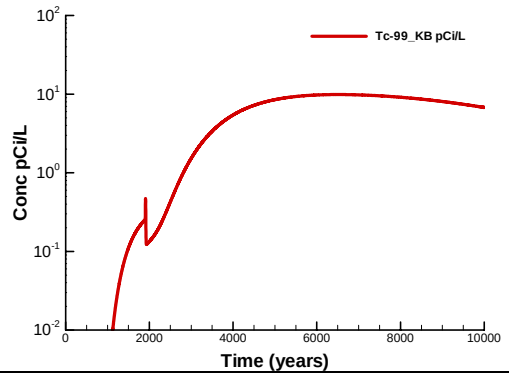

Figure A4A-84. ILV well concentration for Tc-99_KB

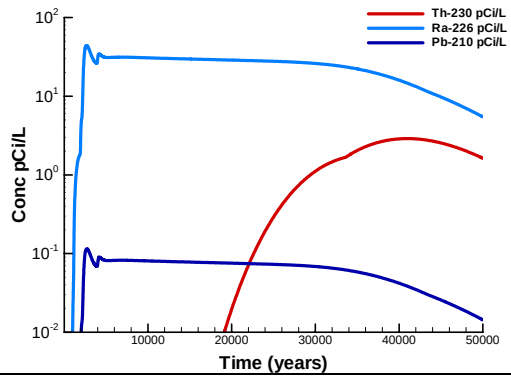

Figure A4A-85. ILV well concentration for Th-230

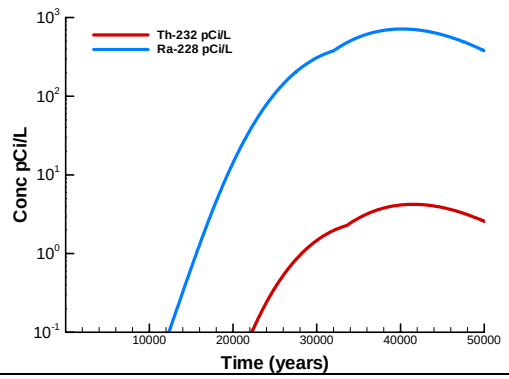

Figure A4A-86. ILV well concentration for Th-232

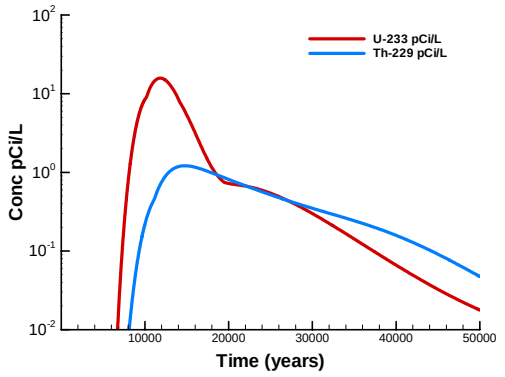

Figure A4A-87. ILV well concentration for U-233

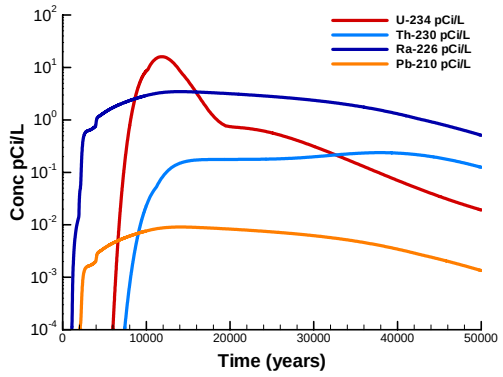

Figure A4A-88. ILV well concentration for U-234

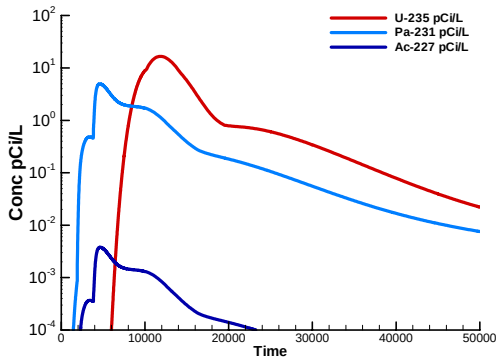

Figure A4A-89. ILV well concentration for U-235

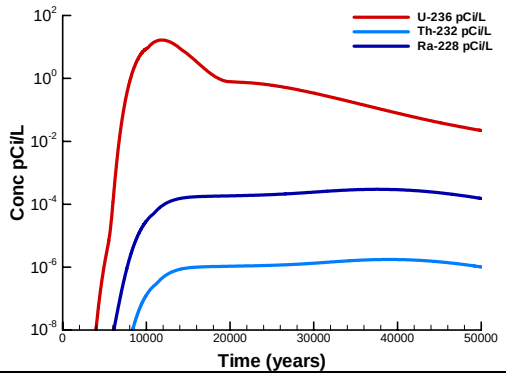

Figure A4A-90. ILV well concentration for U-236

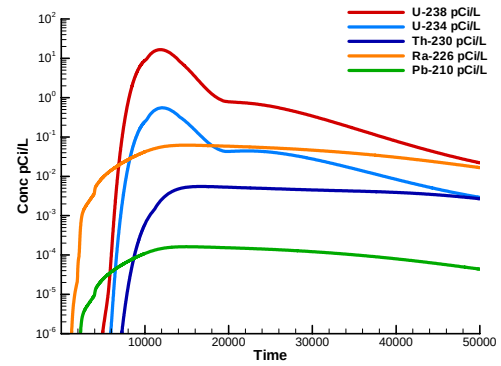

Figure A4A-91. ILV well concentration for U-238

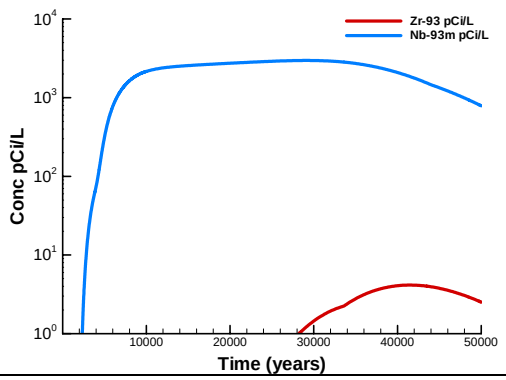

Figure A4A-92. ILV well concentration for Zr-93

APPENDIX A4B

Radon Model

10,000-year Simulation of Rn-222 Flux at Land Surface

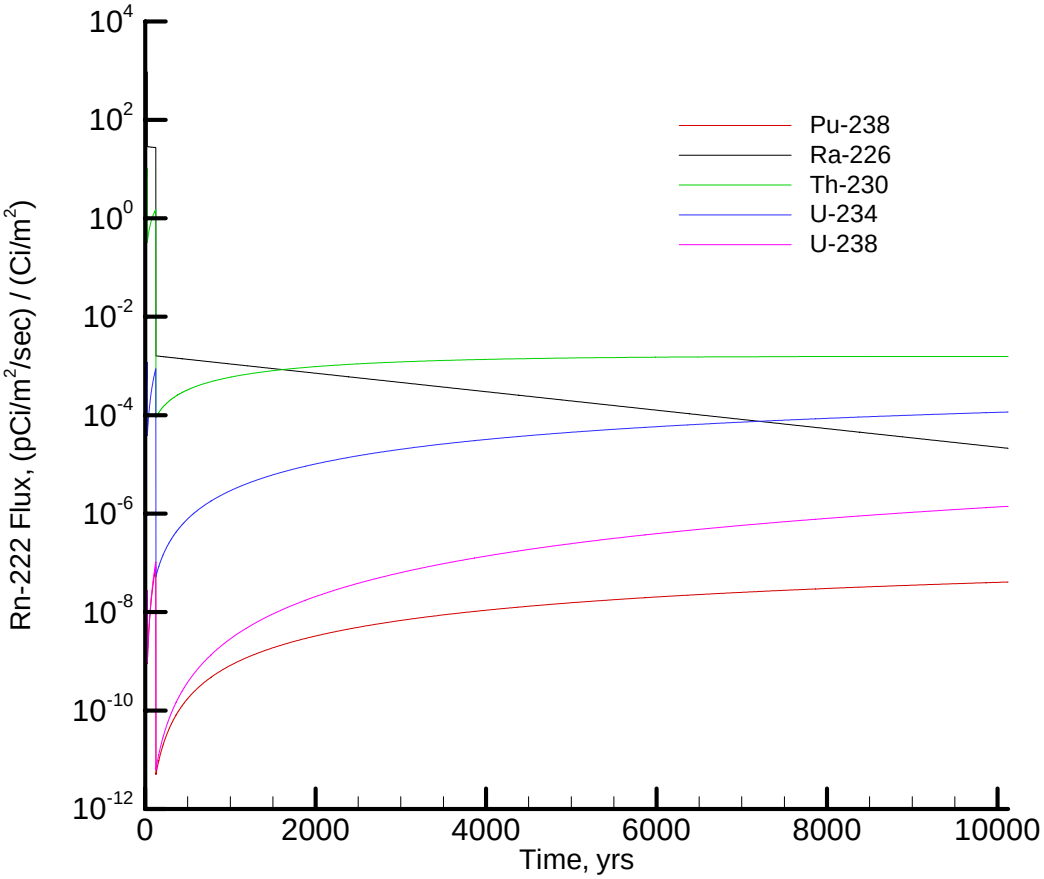

Figure A4B-1. Rn-222 Flux at Land Surface Resulting from Unit Source Term for IL Vault

APPENDIX A5

NAVAL REACTOR PADS

Radon Model

10,000-year Simulation of Rn-222 Flux at Land Surface

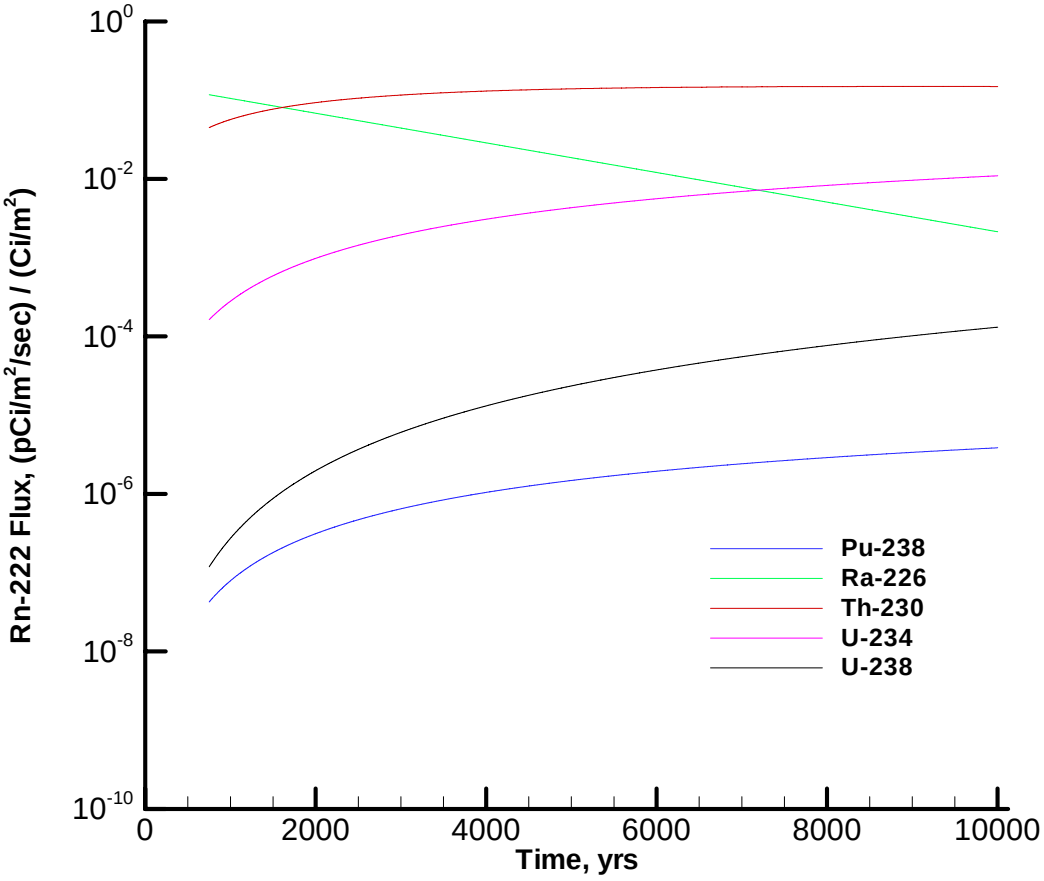

Figure A5-1. Rn-222 Flux at Land Surface Resulting from Unit Source Term for NRCDAs

APPENDIX B –

KEY INPUTS AND ASSUMPTIONS TO THE PA

Key Inputs and Assumptions to the PA

Appendix B contains a table with key inputs and assumptions made in the analysis of the various transport pathways. The table is organized by topical area or specific pathway and disposal unit. Those inputs and assumptions that may need to be protected by ELLWF Operations in order to maintain the radioactive waste management basis for the facility are identified under the Ops Parameter column. The table also contains key I&A that define disposal system or model properties that are outside of operational controls (e.g., hydraulic properties of the subsurface soil zones) but important to the analysis. If the source of the input or assumption, or a more complete description, is provided outside the PA the appropriate reference is identified in the far right column and listed at the back of the appendix. If a section, table or figure number is noted in the key I&A (far left) column, the source of that citation is the reference in far right column. If no reference is provided in the far right column, the section number cited is understood to be within the PA itself.

Table B-1. Key Inputs and Assumptions to the PA

	Key Input or Assumption	S&ET	CIG	LAWV	ILV	NRCDA	IFA	Ops Parameter	References
1.0	**General**								
1.1	The limits developed for each radionuclide (including those for special waste forms) will be applicable upon approval of this PA. Therefore, all limits currently in use (limits from previous PAs, SAs, UDQEs and/or other sources) will be superceded by this PA.	✓	✓	✓	✓	✓	✓	✓	
1.2	SOFs are calculated for each disposal unit assuming the closure inventory estimates provided in Appendix C of this PA. Changes to these estimates should never result in a SOF exceeding a value of 1 for any disposal unit.	✓	✓	✓	✓	✓	✓	✓	
1.3	The NRCDAs have no significant impact on adjacent disposal units.						✓		
1.4	Impacts from radionuclides will be no greater than that calculated for a non-depleting, non-decaying, non-sorbing tracer.						✓		
1.5	Future trench disposal units are situated according to Figures 1-1 and 2-1 in Part B Chapters 1 and 2 of this PA.	✓	✓				✓	✓	
1.6	Model assumes that each disposal unit has been filled to its radionuclide capacity in calculating plume overlap effects.						✓		

	Key Input or Assumption	S&ET	CIG	LAWV	ILV	NRCDA	IFA	Ops Parameter	References
1.7	The operations period is assumed to last for 30 years as documented in this PA in order to coincide closure with CIG for installation of final closure cap over both units because S&ET began operations 5 years prior to CIG. Assumption developed by consensus of modelers.	✓							
1.8	The operations period is assumed to last for 25 years (Section 4.5).The actual start dates and end dates for this 25-year period may vary among units.		✓	✓	✓	✓		✓	Phifer et al. 2006
1.9	The Institutional Control period is assumed to last for 100 years (Section 4.5).	✓	✓	✓	✓	✓			Phifer et al. 2006
2.0	**Construction/Closure**								
2.1	**General**								
2.1.1	The facility/unit dimensions are assumed to be those identified in Section 4.5.	✓	✓	✓	✓	✓	✓	✓	Phifer et al. 2006
2.1.2	The size of the footprint for the conceptual LAWV that is used to represent a trench disposal unit boundary is 656 ft long by 157 ft wide.	✓	✓						
2.1.3	The layout of the Slit and Engineered Trench Units is such that waste is disposed in approximately 64% and 100% respectively of the area assigned to the conceptual LAWV footprint.	✓							

	Key Input or Assumption	S&ET	CIG	LAWV	ILV	NRCDA	IFA	Ops Parameter	References
2.1.4	It is assumed that 5 individual Slit trenches make up one Trench Unit. The area of 5 nominal individual trenches make up 64% (or 0.64) of the area of the nominal trench Unit footprint. Individual trench dimensions may be adjusted as long as the total area within a Unit does not make up less than 64% of the Unit area and the individual trenches are spread out, i.e. not inordinately clustered together within the Unit footprint.	✓							
2.1.5	The layout of the CIG and any future adjacent disposal units will be such that the CIG footprint takes up approximately 57% of the area assigned to the conceptual LAWV footprint.		✓						
2.1.6	The layout of the LAW Vault and any future adjacent disposal units will be such that the actual area taken up by the LAW Vault (i.e. 145 ft by 643.33 ft) takes up 80% of the area assigned to the vault (i.e. ~116,600 ft^2).			✓					
2.1.7	The layout of the IL Vault and any future adjacent disposal units will be such that the actual area taken up by the IL Vault (i.e., 48.5 ft by 278.83 ft) takes up 80% of the area assigned to the vault (i.e., ~16,900 ft^2).				✓				

	Key Input or Assumption	S&ET	CIG	LAWV	ILV	NRCDA	IFA	Ops Parameter	References
2.2	**Operational Closure**								
2.2.1	Operational closure will be conducted in stages during the 30-year operational period of the S&E Trenches. Implement operational closure of the Engineered and Slit Trenches as described in sections 4.2.3 and 4.2.4, respectively, in Cook et al. 2004. Further elaboration is contained in sections 4.5.1 and 4.5.2 of Phifer et al. 2006.	✓						✓	Cook et al. 2004 Phifer et al. 2006
2.2.2	Operational closure will be conducted in stages during the 25-year operational period of the CIG Trenches. Implement operational closure of the CIG Trenches as described in section 4.5.3 of Phifer et al. The operational closure described in section 4.2.5 of Cook et al. 2004 is superceded by this later description.		✓					✓	Phifer et al. 2006
2.2.3	Operational closure will be conducted in stages during the 25-year operational period of the LAW and IL Vaults. Implement operational closure of the LAW and IL Vaults as described in sections 4.2.1 and 4.2.2, respectively, in Cook et al. 2004. Further elaboration is contained in sections 4.5.4 and 4.5.25 of Phifer et al. 2006.			✓	✓			✓	Cook et al. 2004 Phifer et al. 2006

	Key Input or Assumption	S&ET	CIG	LAWV	ILV	NRCDA	IFA	Ops Parameter	References
2.2.4	The operational norm shall be a 4-foot "clean backfill" without intrusions. No foreign material is allowed within the upper 2 feet of the 4-foot clean backfill. The intrusion of uncontaminated metals (such as carbon steel, stainless steel, aluminum) into the lower 2 feet of the 4-foot clean backfill can be tolerated, if it is determined that rectifying the condition is not feasible on a case-by-case basis. This does not address the intrusion of any types of materials other than metals.	✓						✓	Phifer 2003
2.2.5	Administratively close SLIT1 and SLIT2 by ensuring no further waste is emplaced. If the remaining available trench volume is to be used, perform another SA or review.	✓						✓	Flach et al. 2005
2.2.6	Maintain operational cover to ensure positive drainage away from the trenches.	✓						✓	
2.2.7	Interim runoff cover was established by 4/1/2006 covering existing CIG segments 1 through 8 containing a 10 foot wide overhang. Runoff is assumed to be diverted away from the CIG footprint area. These drainage systems are assumed to be maintained.		✓					✓	
2.2.8	Interim runoff cover is assumed to be in place for future CIG segments within 3 months of their creation.		✓					✓	

	Key Input or Assumption	S&ET	CIG	LAWV	ILV	NRCDA	IFA	Ops Parameter	References
2.2.9	All vault penetrations will be addressed during operational closure of the LAW Vault. Penetrations (e.g., in-cell sump collection systems, exterior doors and vent openings, equipment fastening bolts, through-wall electrical panels, etc.) will be restored to original/equivalent condition by removing as much of the foreign material as possible and filling in the void with an appropriate cementitious grout/patch material. Where applicable, reinforcing steel will be tied in to stub outs in cell and/or vault itself to form a unified structure to provide continuous, structurally sound walls to isolate the waste from the environment (section 4.2.1 of Cook et al. 2004 and Section 3.6.4.4 in the PA).			✓				✓	Cook et al. 2004
2.2.10	NR Waste Shipping/Disposal Casks are considered watertight requiring no operational closure measures. However, if radiation shielding is required for personnel protection during the Operational or Institutional Control period, the NRCDA or a portion of it could be operationally closed per Section 4.2.6 which allows for filling the space around, between, and over the casks with structurally suitable material. Options for achieving this objective are listed in Section 4.4.2.1.					✓		✓	Cook et al. 2004

	Key Input or Assumption	S&ET	CIG	LAWV	ILV	NRCDA	IFA	Ops Parameter	References
2.3	**Interim Closure**								
2.3.1	Implement interim closure at the end of operations. This period extends through the 100-year Institutional Control Period.	✓	✓					✓	
2.3.2	Implement interim closure of the S&E and CIG Trenches as described in section 4.3 in Cook et al. 2004. Further elaboration is contained in sections 4.5.1, 4.5.2, and 4.5.3 of Phifer et al. 2006.	✓	✓					✓	Cook et al. 2004 Phifer et al. 2006
2.3.3	The interim closure cap is assumed to be properly maintained during the Institutional Control period (100 years after placement).	✓	✓				✓	✓	
2.3.4	No interim closure actions are planned beyond that of operational closure during the 100-year institutional control period for the LAWV, ILV and NRCDAs other than monitoring and maintenance activities.			✓	✓	✓			
2.4	**Final Closure**								
2.4.1	Implement final closure at the end of the 100-year Institutional Control Period.	✓	✓	✓	✓	✓		✓	
2.4.2	Implement final closure as described in section 4.4 in Cook et al. 2004. The closure cap configuration in Figure 4-1 is superceded by similar figures for each unit in section 4.5 in Phifer et al. 2006.	✓	✓	✓	✓	✓		✓	Cook et al. 2004 Phifer et al. 2006
2.4.3	The final closure cap must be installed with the crestline running lengthwise down the center of the unit as described in sections 1.3, 2.3, and 3.3 of this PA.	✓	✓	✓				✓	

	Key Input or Assumption	S&ET	CIG	LAWV	ILV	NRCDA	IFA	Ops Parameter	References
2.4.4	The final closure cap is assumed to be installed 125 years after (2120) start of disposal operations in 1995.			✓				✓	
3.0	**Waste Form, Waste Zone, Waste Inventory/Volume and Waste Placement**								
3.1	For the purpose of this PA a non-crushable container is defined as a container with significant void space placed within a Slit or Engineered Trench which is not deemed compactable with the performance of dynamic compaction at the end of the 100-year Institutional Control period (See Section 1.6.5 of the PA).	✓						✓	
3.2	Waste forms are assumed to be primarily crushable steel containers (Section 4.5). The non-crushable content is assumed to consume no more than 10% of a Slit or Engineered Trench unit footprint and be uniformly distributed across each unit (i.e., one set of five individual slit trenches or a single Engineered Trench).	✓						✓	Phifer et al. 2006

	Key Input or Assumption	S&ET	CIG	LAWV	ILV	NRCDA	IFA	Ops Parameter	References
3.3	From modeling of the Engineered Trench unit in the PA it can be reasonably concluded that disposal of non-crushable containers can be allowed in the 10-ft buffer zones between individual slit trenches in a Slit Trench unit (i.e., set of 5 slit trenches). If contemplating use of the 10-ft buffer between trenches for waste then intruder limits from the Engineered Trenches must be applied to Slit Trench disposals. Any expansion within the current footprint must be made with the restriction that the trench excavation must be dug to the minimum 20-ft depth (i.e., at least 4 ft of operational soil cover over the waste and at least the nominal 16-ft waste depth) along with the approved closure cap. It is recognized that sloughing may reduce the depth of the trench, and this is acceptable. Finally a minimum distance of 25 ft between the bottom of the waste zone and aquifer must be maintained.	✓						✓	
3.4	Material filling the ET side slopes can include soil and waste. Waste can include crushable containers, non-containerized bulk waste, and non-crushable containers. The following four criteria apply to waste in general placed in the ET side slopes.	✓						✓	
3.4.1	No waste is to be placed >24 ft from the edge of the original waste zone footprint (i.e., bottom dimensions of the trench).	✓						✓	
3.4.2	Waste cannot extend above the waste in the original waste zone footprint.	✓						✓	

	Key Input or Assumption	S&ET	CIG	LAWV	ILV	NRCDA	IFA	Ops Parameter	References
3.4.3	At least 4 ft of operational soil cover is placed over top of all waste.	✓						✓	
3.4.4	Waste placed in the side slopes of the ET shall not exceed half the allowed concentration of levels of waste placed in the main footprint.	✓						✓	
3.5	If the above general conditions are used then the following would be an additional five specific criteria applicable to the disposal of non-crushable containers in the ET side slopes.	✓						✓	
3.5.1	The crestline of the final closure cap runs lengthwise down the center of the Engineered Trench.	✓						✓	
3.5.2	No more than 10% of the length of the side slope is used for non-crushable containers.	✓						✓	
3.5.3	To the extent practical, non-crushable containers are not clustered together but, spaced out along the length of the side slopes.	✓						✓	
3.5.4	The balance of the length of the side slope can be filled with crushable containers, non-containerized bulk waste, and/or soil.	✓						✓	
3.5.5	A shelf can be excavated into the side slopes as needed to support containers that are less than the nominal 16-ft waste zone thickness as long as the concentration of radionuclides within the waste package is consistent with item 3.4.4 above of the general ET side-slope disposal criteria.	✓						✓	

	Key Input or Assumption	S&ET	CIG	LAWV	ILV	NRCDA	IFA	Ops Parameter	References
3.6	The waste material within the side slopes of the ET are assumed to compact into a thin layer at the base of the side slope when compaction is applied to the ET at the end of Institutional Control. An assumption was made to transfer all contaminant mass from the side slopes into the Lower Waste Zone beneath the non-sloped portion of the ETs at that time since there was no way to explicitly simulate a "lower waste zone" within the sloped sides. This is thought to be conservative because it concentrates contaminant mass beneath the non-sloped part of the ET and would likely cause an incrementally higher peak because the source is then less spread out.	✓							
3.7	Waste forms are assumed to be primarily crushable steel containers (Section 4.5).				✓				Phifer et al. 2006
3.8	Co-disposal of CDPs is assumed to potentially occur with any disposal unless otherwise noted as a special wasteform restriction.	✓	✓	✓					
3.9	CDPs are not considered because very little waste containing cellulose has been disposed (communication with Solid Waste Division).				✓	✓		✓	
3.10	Waste material is assumed to collapse into the lower 2.5 ft of the Slit and Engineered Trenches at the end of institutional control when dynamic compaction and/or static surcharge is applied to compact the waste.	✓							

	Key Input or Assumption	S&ET	CIG	LAWV	ILV	NRCDA	IFA	Ops Parameter	References
3.11	Soil fill above the compacted waste is assumed to be compacted as well, prior to placement of the final closure cap for crushable waste. For non-crushable waste, backfilled soil is assumed to remain uncompacted. This assumption is made to represent the change in the hydraulic properties for this layer as a result of compaction and does not require operations to protect this assumption.	✓							
3.12	Disposal segments 1-8 in CIG-1 used a grout layer surrounding the components with a saturated hydraulic conductivity of 6E-04 cm/s.		✓						
3.13	Future segments will use a grout layer surrounding the components with a saturated hydraulic conductivity less than or equal to 1E-08 cm/s with moisture characteristic curves that are consistent with or better than those for low quality concrete.		✓						
3.14	Existing CIG inventory is handled on a segment basis with dates for each disposal consistent with the final closure of each segment.		✓						
3.15	Many low-strength containers (B-25 boxes, tankers, and SeaLands) with significant interior void space were placed within CIG-1 segments 4, 5, 6 and 7. Installation of reinforced concrete mats over these segments is planned at the end of the 100-year Institutional Control period prior to installation of the final ELLWF closure cap. These segments must be delineated and protected from significant loads (e.g., soil stockpiles and heavy equipment) in the interim.		✓					✓	

	Key Input or Assumption	S&ET	CIG	LAWV	ILV	NRCDA	IFA	Ops Parameter	References
3.16	Allow actual trench dimensions to accommodate the specific item being disposed so long as a minimum distance of 25 ft exists between the bottom of the excavation and the water table, 4 ft of clean material (i.e., soil, concrete, CLSM) is placed over the disposal and the overall set of CIG disposals is kept within the prescribed disposal unit footprint (656 ft x 157 ft).		✓						Cook 2003
3.17	Multiple components disposed and grouted in the same excavation shall be considered equivalent to disposal of a single component and subject to the same operational and engineering requirements.		✓						Wilhite 2002
3.18	The volume of disposed waste will be approximately 1,040,000 ft^3 for a Slit Trench unit (16 ft deep x 20 ft wide x 650 ft long x 5 trenches) and approximately 1,700,000 ft^3 for a single Engineered Trench (equivalent of 19,000 B25 boxes) as described in Section 1.5 of this PA.	✓							
3.19	The volume of disposed waste will be approximately 819,000 ft^3 (14 ft deep x 18 ft wide x 650 ft long x 5 trenches) as noted in Section 2.5 of this PA.		✓						
3.20	The volume of disposed waste will be approximately 1,080,000 ft^3 (equivalent of 12,000 B25 boxes) as noted in Section 3.5 of this PA.			✓					

	Key Input or Assumption	S&ET	CIG	LAWV	ILV	NRCDA	IFA	Ops Parameter	References
3.21	The volume of disposed waste will be approximately 257,000 ft^3 as noted in Section 4.5 of this PA.				✓				
3.22	The PA analysis assumed two types of NR waste components, the KAPL core barrel/thermal shields (CB/TS) and KAPL Head units, are representative of all NR components sent by the navy nuclear program to SRS for disposal. The KAPL CB/TS are predominantly activated-metal components shipped/disposed in heavily shielded casks. Figure 5-3 and section 5.4.1 provide a description of a representative heavily shielded cask. The KAPL Head units, on the other hand, are predominantly surface contaminated with activated corrosion products (crud) and contained in thinner, less robust casks. The following five requirements apply only to the heavily shielded casks for activated metal components.					✓		✓	
3.22.1	Welds are assumed to be of material and thickness such that no less than 1 cm of the material remains after 500 years. A weld that is nominally 1.6 in. thick, but no less than 1.25 in. thick, on the representative cask meets this minimum requirement.					✓		✓	
3.22.2	The minimum acceptable thickness for the top of casks is 13.8 in.					✓		✓	
3.22.3	The minimum acceptable thickness for the sides of casks is 13.8 in.					✓		✓	

	Key Input or Assumption	S&ET	CIG	LAWV	ILV	NRCDA	IFA	Ops Parameter	References
3.22.4	External dose rate at receipt is assumed to be less than 200 mR/hour.					✓		✓	
3.23	Disposal casks for surface (crud) contaminated auxiliary equipment such as pumps and closure heads are less robust and may be disposed on the NRCDA without meeting the aforementioned requirements.					✓			
3.24	In the PA analysis the radionuclide inventories for both types of NR components (surface or crud contaminated components and activated metal components) are combined and conceptually placed in the representative heavily shielded cask. In effect, this simplified approach assumes that both types of containers fail and begin contaminant release at the same time.					✓			
3.25	Limits have been developed in this PA for all previously disposed I-129 special waste forms that were evaluated in prior analyses. The limits in this PA are applicable to past and future disposal of these special waste forms. Any disposal restrictions (e.g., waste placement restrictions, waste container restrictions, etc.) apply as noted in this list of key inputs and assumptions.	✓	✓	✓	✓			✓	

	Key Input or Assumption	S&ET	CIG	LAWV	ILV	NRCDA	IFA	Ops Parameter	References
3.26	In order to protect the critical assumption of K_ds based on a natural "acidic" trench disposal environment no cementitious-type waste may be placed above these high-concentration I-129 waste forms or within a horizontal distance equal to the height of the cementitious-type wastes above the base of the trench (or minimum of 4 feet). The connection of this special waste form restriction to this PA is made in Section 1.6.3.3.	✓						✓	
3.27	The generic I-129 disposal limit will be assigned to new high-concentration I-129 waste forms disposed in the future unless groundwater modeling is performed with the waste-specific Kd measured in the lab. Thus, the equation-derived limits developed in previous SA's (WSRC-TR-2001-00021, WSRC-RP-2000-00138, WSRC-RP-99-01070) no longer apply.	✓		✓	✓			✓	
3.28	In order to protect the critical assumption of K_ds based on 1) a natural "acidic" trench disposal environment and 2) absence of CDP leachate, no concrete or cellulose-containing waste materials may be placed within 20 feet of the Paducah Demonstration Cask within the same trench. The connection of this special waste form restriction to this PA is made in Section 1.6.3.3.	✓						✓	

	Key Input or Assumption	S&ET	CIG	LAWV	ILV	NRCDA	IFA	Ops Parameter	References
3.29	In order to protect the critical assumptions of K_ds and glass dissolution rates based on 1) a natural "acidic" trench disposal environment and 2) absence of CDP leachate, no concrete or cellulose-containing waste materials may be placed in the vicinity of the M-Area Glass. The connection of this special waste form restriction to this PA is made in Section 1.6.3.3.	✓						✓	
3.30	All previously disposed M-Area Glass waste forms are bounded by this PA based on the description provided in Table 3 and the associated text. The connection of this special waste form restriction to this PA is made in Section 1.6.3.3.	✓						✓	Wilhite 2003

	Key Input or Assumption	S&ET	CIG	LAWV	ILV	NRCDA	IFA	Ops Parameter	References
3.31	In order to protect the critical assumption of a 30-year delayed release of tritium from ETF activated carbon vessels buried in Slit Trenches as follows; 1) Ensure generator seals all openings to ETF activated carbon vessels with a ¼-inch weld or equivalent closure. 2) Place ETF carbon columns vertically in an upright position in the trench to help ensure that the vessel can withstand earth pressure in a Slit Trench environment during the operational period. 3) Prohibit dynamic compaction of Slit Trench areas containing ETF carbon columns until the end of the 30-year operational period. 4) Do not place ETF vessels within a minimum of 16 feet of wastes with high chloride content or cementitious waste to protect the assumed corrosion rate and waste-specific I-129 K_d, respectively. 5) Distribute ETF carbon vessels throughout the trenches to protect the assumption of uniform spreading of radionuclide inventory throughout the trenches. The connection of this special waste form restriction to this PA is made in Section 1.6.3.3.	✓						✓	
3.32	It is assumed that the time lag between characterization and disposal is short enough that decay to potentially more problematic daughters during the time lag can be ignored.	✓	✓	✓	✓	✓		✓	
3.33	It is assumed that only contaminants/waste forms that are properly screened out and/or analyzed as described in this PA are disposed.	✓	✓	✓	✓	✓		✓	

	Key Input or Assumption	S&ET	CIG	LAWV	ILV	NRCDA	IFA	Ops Parameter	References
3.34	Waste inventories, including special waste forms, are assumed to be uniformly distributed throughout the unit.	✓		✓		✓		✓	
3.35	For all future disposals, the inventory of radionuclide parents is assumed to be distributed uniformly over the remaining waste zone footprint available within CIG Units 1 and 2. For existing disposal segments in CIG-1 radionuclide parent inventories are assumed to be distributed uniformly within each segment.		✓					✓	
3.36	Waste inventories are assumed to be uniformly distributed throughout the unit with the exceptions noted in following two I&A.				✓			✓	
3.36.1	TPBAR disposal containers are assumed to be placed in stacks of two near the outer walls of the ILV cells as described in Section 4.				✓				Hiergesell 2005
3.36.2	The groundwater analysis assumes that K and L basin resins disposed in the ILV beyond what is reported in WITS as of 3/24/08 are to be placed in any vault cell except cell 4. Inventory of C-14K disposed in ILV cell 4 prior to that date shall be managed as generic C-14, i.e., utilizing the generic C-14 limit.				✓				
3.37	Minimum spacing of 12 inches maintained between TPBAR containers and ILV cell walls to ensure CLSM maintains intimate contact with the container, as described in Section 4.				✓			✓	Hiergesell 2005
3.38	Cumulative heat load introduced by multiple TPBAR disposal containers is assumed to be managed to minimize excessive heat buildup, as described in Section 4.				✓			✓	Hiergesell 2005

	Key Input or Assumption	S&ET	CIG	LAWV	ILV	NRCDA	IFA	Ops Parameter	References
3.39	CLSM pH assumed to be sufficiently high (i.e., > 10) to delay onset of TPBAR container steel corrosion during PA period of compliance.				✓			✓	Hiergesell 2005
3.40	The waste inventory will not exceed that projected by the Navy.					✓		✓	
3.41	Large quantities of activation products are associated with the metal matrix of the waste forms within the disposal containers. Lesser amounts of radioactive contaminants are present in corrosion products.					✓			
3.42	Assumptions concerning corrosion, container failure and release of contaminants are based on the forecast and description of NR components and associated casks provided in Table 5-5 of the PA.					✓		✓	
3.43	The NR components disposed on the 643-7E NRCDA are of the same type as those on the 643-26E NRCDA. No additional disposals of NR components are planned for the 643-7E NRCDA.					✓		✓	
3.44	The amount of free liquid in a waste container does not exceed 1% of the waste container volume. This restriction is required so that the rate of release assumed in the PA for constituent release is not exceeded.	✓	✓	✓	✓	✓	✓	✓	
3.45	No materials (organic or inorganic) known to enhance radionuclide mobility or solubility (e.g. chelating agents) beyond that assumed by the Performance Assessment shall be disposed in the waste stream.	✓	✓	✓	✓	✓	✓	✓	

	Key Input or Assumption	S&ET	CIG	LAWV	ILV	NRCDA	IFA	Ops Parameter	References
3.46	The properties of the waste as specified by the generator are the same as or bounded by those analyzed in the PA.	✓	✓	✓	✓	✓	✓	✓	

	Key Input or Assumption	S&ET	CIG	LAWV	ILV	NRCDA	IFA	Ops Parameter	References
4.0	**Facility Structural Stability**								
4.1	CIG waste containers are assumed to be hydraulically intact for first 40 years of burial.		✓						
4.2	CIG segment grout chambers are assumed to remain intact for 300 years beyond the operational period. At this point in time subsidence of all CIG segments is assumed where no hydraulic credit for the grout chamber materials is employed.		✓						
4.3	Static cracking in ILV concrete is assumed to result from the weight load associated with placement of the closure cap, as described in Section 5.				✓				Peregoy 2006
4.4	Static cracking realized at time = 5000 years is conservatively assumed to occur at time = 0 per Table 3, Section 5.				✓				Peregoy 2006
4.5	Central cell of ILV (Cell 4) is assumed to be affected differently by seismic events than other ILV cells ("Typical" cells) due to the presence of two construction joints in the walls and floor rather than a single joint, as noted in Section 5.				✓				Peregoy 2006
4.6	Cell 4 through-cracks in concrete walls and floor are assumed to occur at year 400 by consensus of modelers.				✓				
4.7	The ILV is conservatively assumed to undergo collapse at 1900 years by a consensus of modelers.				✓				
4.8	NR disposal casks will be structurally stable for at least 8000 years.					✓			

	Key Input or Assumption	S&ET	CIG	LAWV	ILV	NRCDA	IFA	Ops Parameter	References
5.0	**Pathway Specific**								
5.1	**Groundwater Pathway - General**								
5.1.1	Prior to final closure it is assumed that all LAW Vault openings and penetrations are sealed with material that provides a saturated hydraulic conductivity (Ksat) that is not greater than 1E-12 cm/s and that does not exceed that level for 1800 years. Said material must have material characteristic curves similar to that of the LAW Vault concrete, especially in producing an unsaturated hydraulic conductivity curve with values equal to or lower than those for the concrete.			✓				✓	
5.1.2	Disposal casks will be watertight for 750 years.					✓			
5.1.3	Radionuclides associated with the crud (activated metal corrosion products) will be released in year 750 when the representative cask is assumed to fail as a moisture barrier.					✓			
5.1.4	Radionuclides associated with activated metal will be released at a rate determined by the corrosion rate of the alloy beginning at year 750.					✓			
5.1.5	The 643-26E NRCDA groundwater model can be used to simulate the 643-7E NRCDA. The 643-26E analysis is considered bounding because the important elements of the analysis have been shown to be the same as, or no worse than conditions at the 643-7E NRCDA. This comparison is provided in Section 5.6.5.1 of the PA.					✓			

	Key Input or Assumption	S&ET	CIG	LAWV	ILV	NRCDA	IFA	Ops Parameter	References
5.1.6	The U.S. EPA primary drinking water standards for radionuclides are the performance measures for groundwater protection.	✓	✓	✓	✓	✓	✓		EPA 2000 EPA 2001
5.2	**Groundwater Pathway – Material Flow Properties**								
5.2.1	The physical and hydraulic properties of the materials comprising the disposal system were selected based on a hierarchy of best available data (Section 3.0). Selection and assignment of material properties where data were lacking (e.g., waste zone properties) was based on professional judgment after considerable debate among modelers and analysts. Thus, these inputs are assumed to be most valid for incorporation into the vadose zone and aquifer zone models, as described in Sections 5 and 6.	✓	✓	✓	✓	✓	✓		Phifer et al. 2006
5.2.2	Cementitious materials are assumed to retain intact physical and hydraulic properties until structural damage occurs.		✓	✓	✓				
5.2.3	The parameters and distributions in Table 5-13 of this PA are assumed to account for the uncertainty in the groundwater calculations.					✓			
5.2.4	It is assumed that the material properties used for waste zone in this PA are adequate. For example, hydraulic properties for CLSM were assigned to the waste zone. If testing is performed, the material properties likely will change.			✓					

	Key Input or Assumption	S&ET	CIG	LAWV	ILV	NRCDA	IFA	Ops Parameter	References
5.2.5	It is assumed that the material properties used for all other (nonwaste) zones in this PA are adequate. For example, anisotropy has been introduced since the latest published analysis. Field testing could modify those properties.			✓					
5.2.6	Cracking has no effect on hydraulic properties other than to change Ksat in the manner assumed in Section 3.6.4.2 of this PA. The cracking pattern, extent of cracking, roughness, and crack widths and depths are uncertain. This key assumption follows the National Institute of Standards and Technology approach. No crack healing or infilling is assumed. Infilling will reduce the Ksat for the crack, which typically will produce slower water movement and slower transport of contaminants.			✓					Snyder 2003
5.2.7	Future cracking (after installation of closure cap) is assumed to be confined to "cracked" sections analyzed by the model.			✓					
5.3	**Groundwater Pathway – Material Transport Properties**								
5.3.1	Although PORFLOW allows the flexibility of specifying different values for effective, total, and diffusive porosities, it was the consensus of the modelers to select the porosity values from tables 5-18 and 6-47 and assume effective, total, and diffusive porosity each to be equal to that value.	✓	✓	✓	✓				Phifer et al. 2006
5.3.2	Particle density values obtained from Sections 5 & 6.	✓	✓	✓	✓	✓			Phifer et al. 2006

	Key Input or Assumption	S&ET	CIG	LAWV	ILV	NRCDA	IFA	Ops Parameter	References
5.3.3	Molecular diffusivity is assumed to apply to all elements.	✓	✓	✓	✓	✓			
5.3.4	Distribution coefficient (K_d) values are element-specific and are obtained from the appropriate "Best" estimate values column in Tables 10, 13 and 14. Best estimate K_d and/or solubility values (i.e., central value of multiple measurements as noted in Section 4.0) are assumed to be most appropriate by consensus of the modelers. It is assumed that using distribution coefficient values for similar elements is adequate when element-specific K_ds are not available.	✓	✓	✓	✓	✓			Kaplan 2006
5.3.5	K_d values are adjusted with a correction factor as described in Section 5.1 and Table 15 to account for the presence of CDPs. It is assumed that CDPs are present forever at the concentration level of 95 mg/L as noted in Section 5.1.	✓	✓	✓					Kaplan 2006
5.3.6	It is assumed that stochastic treatment of longitudinal and transverse dispersivity coefficients is appropriate.					✓			
5.3.7	Backfill and natural soil material are assumed to acquire K_d values assigned to Sandy sediment or Clayey sediment, as presented in Table 10. Kd assignments for these material zones are described in the applicable sections of each disposal unit chapter of the PA.	✓	✓	✓	✓	✓			Kaplan, 2006
5.3.8	Half-lives of specific radionuclides are assumed to be as presented in Appendix A.	✓	✓	✓	✓	✓			Cook 2007

	Key Input or Assumption	S&ET	CIG	LAWV	ILV	NRCDA	IFA	Ops Parameter	References
5.3.9	In-growth of radionuclide progeny is implemented in PORFLOW using the REGEN command developed for specific radionuclides based on a compilation of radionuclide data sources (see reference).	✓	✓	✓	✓	✓			Cook 2007
5.3.10	It is assumed that no plume interactions are taking place (i.e., no upstream source plume is being addressed or plume interactions with other units) in the development of preliminary groundwater limits.	✓	✓	✓	✓	✓			
5.3.11	Cementitious material aging consistent with that outlined in Kaplan 2006.		✓						Kaplan 2006
5.3.12	Cementitious materials are assumed to proceed through three geochemical stages as they age and the transition from Stage 1 to Stage 2 is assumed to occur at 50 pore volumes and from Stage 2 to Stage 3 at 500 pore volumes, as described in Section 4.2. Quantification as to when those transitions occur for Cell 4 and typical cells is depicted in Figures 4-12 and 4-13 of this PA.				✓				Kaplan 2006
5.3.13	CLSM is assumed to have characteristics of a cementitious material with respect to contaminant transport (i.e., pH range of >10).				✓				Hiergesell 2005
5.4	**Groundwater Pathway – Model Spatial**								
5.4.1	Model gridding is assumed to conform sufficiently closely with the dimensions and the configuration of backfill materials identified in the closure design (Section 4.5) to adequately simulate flow and transport.	✓	✓	✓	✓		✓		Phifer et al. 2006

	Key Input or Assumption	S&ET	CIG	LAWV	ILV	NRCDA	IFA	Ops Parameter	References
5.4.2	Lateral extent of vadose zone model is assumed to be sufficiently beyond the exterior walls of the unit to ensure vertical flow along the boundary, and therefore, justify a "no-flow" boundary condition.	✓	✓	✓	✓				
5.4.3	No explicit account is being taken for actual plume dispersion within the CIG set of analyses. Numerical dispersion is occurring to the degree consistent with the mesh and time spacings being employed.		✓						
5.4.4	For all future burials the CIG grout chamber's bottom is not placed closer than 35 ft to the time-averaged water table elevation.		✓					✓	
5.4.5	For all future burials the CIG grout chambers are 20 ft wide by 16 ft deep (i.e., vertical depth) with a minimum grout wall thickness of 1 ft.		✓					✓	
5.4.6	For modeling purposes all future CIG disposals, filling the remaining CIG waste zone footprint, are assumed to occur on 1/1/2007 and have 10 ft interim runoff covers in place within 3 months of their creation. This is considered a conservative assumption as actual CIG disposals in this area will occur over a period of years resulting in temporal spacing of contaminant release.		✓					✓	

	Key Input or Assumption	S&ET	CIG	LAWV	ILV	NRCDA	IFA	Ops Parameter	References
5.5	**Groundwater Pathway – Model Temporal Change**								
5.5.1	Model infiltration rates associated with both Case01 (all crushable containers) and Case11 (all non-crushable containers) are assumed to bound all plausible infiltration rate scenarios above the trenches during the PA period of compliance by consensus of the modelers.	✓							
5.5.2	Infiltration rates for Case01 over the Slit and Engineered Trenches are assumed to change as calculated using HELP model (see reference) and documented in Figure 1-5, Section 1.6.3.2 of the PA.	✓							Flach et al. 2005
5.5.3	Infiltration rates for Case11 over the Slit and Engineered Trenches are assumed to change as calculated in this PA and incorporated in the steady-state flow period models. (See Figure 1-5, Section 1.6.3.2 of the PA.)	✓							
5.5.4	Infiltration rates for all steady-state time periods are calculated by taking the average of the estimated infiltration rates from the start and end of each period.	✓			✓				
5.5.5	Infiltration rates over the unit and side soil are assumed to change as calculated using HELP model and documented in the reference.				✓				Jones and Phifer 2006
5.5.6	Infiltration rates are assumed to remain constant after 1900 years as discussed in Section 4.6.3.3.				✓				

	Key Input or Assumption	S&ET	CIG	LAWV	ILV	NRCDA	IFA	Ops Parameter	References
5.5.7	ILV wall and floor concrete flow properties are assumed to change to those of gravel for Cell 4 after 400 years, when through-cracking occurs, by consensus of modelers.				✓				
5.5.8	ILV concrete and waste zone material flow properties are assumed to change to those of Operational Soil Cover, Pre-compaction at the time of ILV collapse (1900 years) – by consensus of modelers.				✓				
5.5.9	ILV concrete and waste zone distribution coefficient (K_d) values are assumed to retain transport properties (K_ds) of cementitious material despite the re-assignment of flow properties to those of Operational Soil Cover, Pre-compaction at the time of ILV collapse (1900 years) – by consensus of modelers.				✓				
5.5.10	It is assumed that the depth to water table (of 40.5 ft) does not diminish from the base case value.			✓					
5.5.11	The PA analysis assumed that major climate change does not occur.	✓	✓	✓	✓	✓	✓		

	Key Input or Assumption	S&ET	CIG	LAWV	ILV	NRCDA	IFA	Ops Parameter	References
5.6	**Groundwater Pathway - Other**								
5.6.1	It is assumed that a two-dimensional cross-section representation of the LAW Vault in the vadose zone is adequate. The LAWV model does not include a HDPE layer directly over the vault. Such a HDPE layer would reduce the infiltration while it was operational. If it performs for the 1000-yr period, then it would tend to be conservative for that time period. Subsequent peaks could be higher after a sudden failure, such as roof collapse.			✓				✓	
5.6.2	It is assumed that secular equilibrium for decay chain members with half-lives of less than 5 years is adequate.	✓	✓	✓	✓	✓			
5.6.3	It is assumed that time step sizes and mesh sizes are adequate, therefore numerical dispersion is insignificant.	✓	✓	✓	✓				
5.6.4	It is assumed that one-dimensional infiltration analysis and the use of a series of steady-state flow fields, rather than transient flow analysis, is adequate.	✓	✓	✓	✓	✓			
5.6.5	It is assumed that bias in conceptual model (e.g., CDP vs. no CDP) is insignificant.	✓	✓	✓	✓	✓			

	Key Input or Assumption	S&ET	CIG	LAWV	ILV	NRCDA	IFA	Ops Parameter	References
5.7	**Intruder Pathway**								
5.7.1	It is assumed that the erosion barrier in the closure cap, as depicted in Figures 4-10 (S&ET) and 4-12 (CIG) will prevent excavation into the disposed waste and make the intrusive agriculture scenario not credible by providing at least 10 ft of soil material from the top of the erosion barrier to the top of the disposed waste.	✓	✓					✓	Phifer et al. 2006
5.7.2	It is assumed that the reinforced concrete roofs of the LAWV and ILV prevent excavation and drilling into the disposed waste for at least 1,000 years, which makes intrusive intruder scenarios – agriculture and post-drilling – not credible.			✓	✓				
5.7.3	Casks and waste forms are of material and thickness such that complete corrosion will not occur until well after the 1,000 year time of compliance (9,500 years) precluding the possibility of an intruder excavating into the waste.					✓		✓	
5.7.4	External dose at the exposed surfaces of the disposal cask after placement on the pad is less than 200 mrem/hr at 5 cm.					✓		✓	
5.7.5	Table 5-2 is representative of the inventory of Co-60 relative to that of Nb-94 in activated metal components shipped/disposed at SRS.					✓		✓	
5.7.6	It is assumed that radionuclide decay is the only mechanism by which the source is reduced; no leaching of radionuclides to the groundwater is assumed in the intruder analysis in this PA.	✓	✓	✓	✓	✓			

	Key Input or Assumption	S&ET	CIG	LAWV	ILV	NRCDA	IFA	Ops Parameter	References
5.7.7	Probability is assumed to be 1 that inadvertent intrusion will occur into each disposal unit after engineered barriers fail.	✓	✓	✓	✓	✓			
5.8	**Atmospheric (Air) Pathway**								
5.8.1	Radionuclide migration from the waste zone to the land surface is assumed to occur by diffusion in vapor-filled pores only, as described in Sections 1.7.5, 2.7.5, 3.7.5, 4.7.5, and 5.7.5 of this PA.	✓	✓	✓	✓	✓			
5.8.2	The closure cap depicted in Figure 1-3 (from Section 1.3 of this PA) is assumed to overlie the Slit and Engineered Trench disposal units for the 130- to 1,130-year time period.	✓							
5.8.3	The air analysis assumes the diffusion of the entire inventory of tritium through containers over a one-year time frame and subsequent transport to the SRS boundary during the 25-year operational period. This permits the use of an annual atmospheric tritium limit (if needed) as well as a total atmospheric tritium limit. The total atmospheric tritium limit would be 25x the annual limit over a 25-year period of operation.			✓		✓		✓	
5.8.4	This PA interpreted the air pathway performance objectives as applying during operations only after the containers are covered with CLSM.				✓				
5.8.5	During the operational period (0 to 25 years), there is a minimum 3-inch thick layer of CLSM above the top layer of ILV waste based on consensus of the modelers and WMAP Engineering.				✓			✓	

	Key Input or Assumption	S&ET	CIG	LAWV	ILV	NRCDA	IFA	Ops Parameter	References
5.8.6	During the institutional control period (25 to 125 years), there is a minimum 3-inch thick layer of CLSM and a reinforced concrete roof above the ILV waste.				✓			✓	
5.8.7	During the post-closure compliance period (125 to 1,125 years), there is a minimum 3-inch thick layer of CLSM, a reinforced concrete roof, and a closure cap as depicted in Figure 4-6 of this PA above the ILV waste.				✓			✓	
5.8.8	The ILV is assumed to remain structurally intact for the 1,125-year evaluation period.				✓				
5.8.9	The NR Waste Shipping/Disposal Casks are assumed to remain water and air-tight for a period of 750 years.					✓			
5.8.10	All NR Waste Shipping/Disposal Casks are assumed to remain structurally intact beyond the 1125 year period of analysis.					✓			
5.8.11	The closure cap as depicted in Figure 5-4 of this PA is assumed to overlie the casks prior to their being breached.					✓			
5.8.12	It is assumed that C-14 exists as part of the CO_2 molecule. Therefore the gas phase concentration of C-14 in the waste zone is controlled by carbonate chemistry.	✓	✓	✓	✓	✓			
5.8.13	It is assumed that Cl-36, H-3 and I-129 exist as diatomic gasses.	✓	✓	✓	✓	✓			
5.8.14	It is assumed that S-35, Sb-124, Sb-125, Se-75, Se-79, Sn-113, Sn-119m, Sn-121, Sn-121m, Sn-123, and Sn-126 exist as monatomic gasses.	✓	✓	✓	✓	✓			

	Key Input or Assumption	S&ET	CIG	LAWV	ILV	NRCDA	IFA	Ops Parameter	References
5.8.15	The SOF for the air pathway at the SRS boundary for all units combined shall not exceed a value of 1.						✓	✓	

	Key Input or Assumption	S&ET	CIG	LAWV	ILV	NRCDA	IFA	Ops Parameter	References
5.9	**Radon Pathway**								
5.9.1	Radon migration from the waste zone to the land surface is assumed to occur by diffusion in vapor-filled pores only, as described in Sections 1.7.5, 2.7.5, 3.7.5, 4.7.5, and 5.7.5 of this PA.	✓	✓	✓	✓	✓			
5.9.2	The closure cap up to the top of the erosion barrier as outlined in Figure 4-6 (from Section 4.3) is assumed to overlie the ILV during the entire 130 to 1,130 year time period.				✓				
5.9.3	This PA interpreted the radon emanation performance objectives as applying during operations only after the containers are covered with CLSM.				✓				
5.9.4	Representing the vault as a waste zone overlain by a minimum 27 inches of concrete during the institutional control period (25 to 125 years) is appropriate.				✓				
5.9.5	Representing the vault as a waste zone overlain by a minimum 27 inches of concrete and a minimum of 60 inches of soil materials forming the closure cap during the post-closure compliance period (125 to 1,125 years) is appropriate.				✓				
5.9.6	The closure cap up to the top of the erosion barrier as depicted in Sections 3.3 and 4.3 of this PA is assumed to overlie the ILV and LAW Vault during the entire 125- to 1,125-year time period.			✓	✓				

	Key Input or Assumption	S&ET	CIG	LAWV	ILV	NRCDA	IFA	Ops Parameter	References
5.9.7	The ILV is assumed to remain structurally intact during the entire 1,125-year evaluation period.				✓				
5.9.8	During the operational period (0 to 25 years), it is assumed that waste containers are placed in the vault and the vault is open to the atmosphere.				✓				
5.9.9	During the institutional control period (25 to 125 years), it is assumed that the exterior vault openings are sealed with reinforced concrete.				✓				
5.9.10	During the 125- to 1125-year post-closure compliance period, it is assumed that a closure cap is placed over the vault.				✓				
5.9.11	The vault is assumed to remain structurally intact for the 1125-year evaluation period.				✓				
5.9.12	The radon emanation factor is assumed to be 0.25.	✓	✓	✓	✓				
5.9.13	The air flow field is assumed to be isobaric and isothermal.	✓	✓	✓	✓	✓			
5.9.14	The impact of naturally occurring fluctuations of atmospheric pressure is assumed to have a zero net effect.	✓	✓	✓	✓				
5.9.15	PORFLOW modeling from the waste zone to the ground surface assumes that air-diffusion is the only transport mechanism simulated and advective air-transport is assumed to be negligible.	✓	✓	✓	✓				

	Key Input or Assumption	S&ET	CIG	LAWV	ILV	NRCDA	IFA	Ops Parameter	References
5.10	**All-Pathways**								
5.10.1	Because exposures via the air pathway will occur at different times and locations than exposures via groundwater, contributions from the air transport pathway are considered separately.	✓	✓	✓	✓	✓			
5.10.2	Exposure pathways to be assessed are those determined by pathway screening in Section C.4.2 of this PA.	✓	✓	✓	✓	✓			
5.10.3	The all-pathways analysis starts with the PORFLOW ideal files generated by the groundwater modeling for each disposal unit. These ideal files contain the groundwater concentrations as a function of time of each parent radionuclide and progeny radionuclides analyzed.	✓	✓	✓	✓	✓			
5.10.4	The all-pathways analysis assumes the exposure parameters shown in Table 1.	✓	✓	✓	✓	✓			Koffman 2006
5.10.5	The all-pathways analysis assumes the bio-accumulation factors shown in Table 1.	✓	✓	✓	✓	✓			Jannik and Dixon 2006

REFERENCES

Cook, J. R. 2007. *Radionuclide Data Package*, WSRC-STI-2006-00162. Westinghouse Savannah River Company, Aiken, South Carolina. March 20, 2007

Cook, J. R., Phifer, M. A., Wilhite, E. L., Young, K. E., and Jones, W. E. 2004. *Closure Plan for the E-Area Low-Level Waste Facility*, Revision 4, WSRC-RP-2000-00425. Westinghouse Savannah River Company, Aiken, South Carolina. May, 2004.

Cook, J. R. 2003. *Variations in Trench Dimensions for Components in Grout Disposal (U)*, WSRC-RP-2003-00394. Westinghouse Savannah River Company, Aiken, South Carolina. April 15, 2003.

EPA. 2000. *National Primary Drinking Water Regulations; Radionuclides; Final Rule,* 40 CFR Parts 141 and 142, U. S. Environmental Protection Agency, Washington, DC.

EPA. 2001. Implementation Guidance for Radionuclides, Appendix I, Comparison of Derived Values of Beta and Photon Emitters, EPA 816-D-00-002, U. S. Environmental Protection Agency, Washington, DC.

Flach G. P., Collard, L.B., Phifer, M. A., Crapse, K.P., Dixon, K.L., Koffman, L.D., and Wilhite, E. L. 2005. Preliminary *Closure Analysis for Slit Trenches #1 and #2*, WSRC-TR-2005-00093. Westinghouse Savannah River Company, Aiken, South Carolina. March, 2005.

Hiergesell, R.A. 2005. Special Analysis: *Production TPBAR Waste Container Disposal Within the Intermediate Level Vault. WSRC-TR-00531, Revision 0*. Westinghouse Savannah River Company, Aiken, SC 29808.

Jannik, G. T. and Dixon, K. L. 2006. *LADTAP-PA: A Spreadsheet for Estimating Dose Resulting from E-Area Groundwater Contamination at the Savannah River Site*. WSRC-STI-2006-00123, Savannah River National Laboratory, Aiken, SC.

Jones, W. E. and Phifer, M. A. 2006. E-Area Low-Level Waste Vault Subsidence Potential and Closure Cap Performance (U), WSRC-TR-2005-00405, Washington Savannah River Company, Aiken SC 29808. 2006 (draft)

Kaplan, D.I. 2006. *Geochemical Data Package for Performance Assessment Calculations Related to the Savannah River Site (U*). WSRC-TR-2006-00004, Revision 0. Washington Savannah River Company, Aiken, SC 29808.

Koffman, L.D. 2006. *SRNL All-Pathways Application*, WSRC-STI-2006-00179, Rev. 0. SRNL, Washington Savannah River Company, Aiken, SC 29808

Peregoy, W. 2006. Structural Evaluation of Intermediate Level Waste Disposal Vaults for Long-Term Behavior, T-CLC-E-00024, Rev. 0. Washington Savannah River Company, Aiken, South Carolina. June 27, 2006.

Phifer, M.A. 2003. *Unreviewed Disposal Question Evaluation: Uncontaminated Lifting Attachments and Rigging within Four-foot Slit Trench "Clean" Backfill.* WSRC-TR-2004-00139. Washington Savannah River Company, Aiken, South Carolina. March 2003.

Phifer, M.A., M. A. Millings, G. P. Flach, 2006. *Hydraulic Property Data Package for the E-Area and Z-Area Vadose Zone Soils, Cementitious Materials, and Waste Zones (U).* WSRC-STI-2006-00198. Washington Savannah River Company, Aiken, South Carolina. September 2006.

Snyder, K. A., 2003. *Condition Assessment of Concrete Nuclear Structures Considered for Entombment*, NISTIR 7026, National Institute of Standards and Technology (NIST), Version 20030108:1545. July 14, 2003.

Swingle, R. F. and Phifer, M. A. 2006. *Unreviewed Disposal Question Evaluation: Increased Disposal Volume in Slit and Engineered Trenches*, Revision 0, WSRC-TR-2006-00186. Washington Savannah River Company, Aiken, South Carolina. June 2006.

Wilhite, E. L. 2002. *Evaluation of Proposed New LLW Disposal Activity: Disposal of Multiple Components as Cement-Stabilized Encapsulated Waste*, WSRC-RP-2002-00047. Washington Savannah River Company, Aiken, South Carolina. February 2002.

Wilhite, E. L. 2003. *Unreviewed Disposal Question Evaluation: Discovery of Apparent Omission of Miscellaneous Glass Forms in M-Area Glass Special Analysis*, WSRC-TR-2002-00581. Washington Savannah River Company, Aiken, South Carolina. January 2003.

APPENDIX C

CLOSURE INVENTORY ESTIMATES

This page intentionally left blank.

CLOSURE INVENTORY ESTIMATES

LIST OF TABLES

This page intentionally left blank.

Inventory Estimation Methodology

WMAP LLW Engineering reviewed the PA limits for all ELLWF disposal units. Using this data, projected disposal inventories at closure were developed for each ELLWF unit. In the case of the closed Naval Reactor Component Disposal Area in 643-7E actual disposed inventories are given. The United States Naval Reactor program was contacted and has confirmed to continue to use the projected inventories found in WSRC-RP-2001-00948, *Special Analysis: Naval Reactor Waste Disposal Pad*, for the operational NRCDA in 643-26E.

The closure inventory estimates (Sink 2007) were developed using the radionuclide distribution received for each ELLWF disposal unit and the PA radionuclide limits developed for each disposal unit. Comparisons to waste volumes disposed to date versus radionuclide inventories disposed to date for each unit were considered for averaging purposes to project closure inventories. In addition, key LLW Waste Acceptance Criteria (WAC) radionuclides were reviewed in detail for adjusting closure inventory estimates. Also, process knowledge of past disposals was used to evaluate key radionuclides where disposal campaigns have been completed for the site (i.e., M Area Glass waste forms, etc.). These methodologies produced upper-bound curie inventory estimates. Implementation of the ELLWF WAC provides assurance that inventories in disposal units comply with PA requirements. It serves as the principal means of communicating PA assumptions, radionuclide limits, waste form and waste packaging requirements to waste generators. In capturing these necessary PA requirements, the WAC also incorporates criteria derived from DOE Order 435.1, facility safety documentation and operational constraints (e.g., compatibility with waste handling equipment). In accordance with site procedures, the WAC is revised and updated at least every two to three years through revisions or more frequently to implement new PA analyses or facility operational changes. Based on the many Special Analyses issued and approved in FY2004, the WAC revision was issued with new package limits on January 14, 2005. The WAC also allows for generator submitted deviation requests which, if approved, allow generators to deviate from specific criteria. All WAC revisions and deviation requests require documented technical reviews to ensure compliance with source documents (i.e., PA, safety, DOE Orders) (Swingle et al. 2008).

The radionuclide inventory limits calculated in the PA, implemented via a set of waste acceptance criteria, are managed through the computerized Waste Information Tracking System (WITS). Before containers are shipped for emplacement in the various vaults or trenches, the contents are entered into WITS by the waste generators. The WITS compares the package contents with the WAC container limits, calculates the cell/facility inventory (to ensure compliance with the cell criticality and safety-based limits), and calculates the total inventory for each radionuclide to ensure compliance with the limits derived from all pathways in the PA. The limits are tracked as fractions of the individual radionuclide limits. The sum of these fractions for each disposal unit is maintained less than or equal to one to ensure compliance with all of the limits (Swingle et al. 2008).

Because waste receipts, disposal unit inventories and sums of fractions are tracked on a per shipment basis using the WITS software, it is unlikely that the estimated closure inventories will be exceeded.

The waste form/type and packaging or container requirements as specified by the PA and safety-related documents are also controlled through WITS. All approved waste containers and types are listed in WITS requiring the generator to select the appropriate one. If the generator's waste type/container is not listed in WITS, a Container Approval Request is submitted. A WMAP engineer for the affected facility evaluates the request and performs a technical review that will include an Unreviewed Safety Question for review under Safety Authorization requirements and an Unreviewed Disposal Questions for review under PA requirements (Swingle et al. 2008).

Two elements of WITS that ensure that the PA limits are being protected are the software quality assurance and the self-programmed "limit-checking system." WITS software was developed under QAP 20-1 and the WSRC *E7 Manual, Conduct of Engineering and Technical Support* (E7 Manual) to ensure it met the standards of the most rigorous software configuration control. Maintenance of WITS is conducted to high quality assurance and configuration control software standards as required by the *WSRC E7 Manual* (Swingle et al. 2008)

Waste certification is the process used at SRS to ensure the waste is characterized properly and that Treatment, Storage and Disposal WAC requirements are met prior to disposal. The waste certification process includes generator waste management program development, WMAP assessment and approval of the generator program, and a continuous improvement process consisting of periodic assessment by the WSRC Facility Evaluation Board, generator self-assessments & waste certification surveillances, WMAP Point-of Contact feedback, and SWMF receipt inspection/verification. A quarterly waste certification performance metrics and integrated management evaluation provides an effective and timely means to gauge the status of both individual generator programs and the waste certification program (Swingle et al. 2008).

In the tables that follow, only those radionuclides and special waste forms that have both a limit less that 1E+20 Ci given in Section 7 and a non-zero closure inventory are shown, and only pathways which are applicable to the waste unit are shown.

References

Sink, D. F. 2007. *ELLWF Low Level Waste (LLW) Disposed Inventories at Facility Closure*, CBU-GEN-2007-00063, Rev. 1.

Swingle, R. F., II, Sink, D. F, Millings, M. R., and Crapse, K. P. 2008. *FY2007 Annual Review, E-Area Low-level Waste Facility Performance Assessment and Composite Analysis*, WSRC-RP-2008-00228, Rev. 0, Washington Savannah River Company, Aiken, SC, February 22, 2008.

SLIT AND ENGINEERED TRENCHES

Table C- 1. Fraction of Groundwater Protection Limits for East Slit Trenches

		Beta-Gamma Fraction of Limit			Gross Alpha Fraction of Limit			Radium Fraction of Limit			Uranium Fraction of Limit
Radionuclide	Closure Inventory (Ci)	0-12 yrs	12-100 yrs	100-1130 yrs	0-1000 yrs	1000-1120 yrs	1120-1130 yrs	0-1000 yrs	1000-1120 yrs	1120-1130 yrs	All Years
Am-241	5.3E-01	2.8E-11	3.1E-07	8.5E-05	1.7E-03	1.4E-03	1.5E-03	0.0E+00	0.0E+00	0.0E+00	5.8E-13
Am-243	4.3E-02	0.0E+00	1.1E-18	1.8E-05	9.8E-05	3.4E-04	3.7E-04	0.0E+00	0.0E+00	0.0E+00	5.0E-15
C-14	3.0E-02	1.2E-01	1.4E-01	6.3E-03	0.0E+00	0.0E+00	0.0E+00	0.0E+00	0.0E+00	0.0E+00	0.0E+00
C-14_NR.Pump	8.2E-02	0.0E+00	0.0E+00	5.8E-02	0.0E+00	0.0E+00	0.0E+00	0.0E+00	0.0E+00	0.0E+00	0.0E+00
Cf-249	8.3E-02	1.4E-19	2.7E-14	7.4E-07	4.3E-05	1.2E-04	1.3E-04	0.0E+00	0.0E+00	0.0E+00	1.6E-15
Cf-251	7.5E-02	0.0E+00	0.0E+00	9.3E-11	8.7E-05	2.7E-04	3.0E-04	0.0E+00	0.0E+00	0.0E+00	1.4E-20
Cl-36	1.1E-05	1.2E-04	1.4E-04	6.4E-06	0.0E+00	0.0E+00	0.0E+00	0.0E+00	0.0E+00	0.0E+00	0.0E+00
Cm-244	3.2E+00	0.0E+00	0.0E+00	5.2E-19	1.4E-12	1.2E-11	1.5E-11	2.9E-19	3.7E-19	3.8E-19	1.1E-19
Cm-245	1.1E-03	1.3E-17	1.0E-12	3.1E-07	7.0E-06	1.8E-05	1.9E-05	0.0E+00	0.0E+00	0.0E+00	1.1E-15
Cm-246	4.1E-04	0.0E+00	0.0E+00	7.5E-20	8.8E-07	3.0E-06	3.3E-06	3.8E-20	1.1E-19	1.2E-19	3.0E-18
Cm-247	1.1E-03	0.0E+00	0.0E+00	6.1E-08	2.9E-06	1.0E-05	1.1E-05	0.0E+00	0.0E+00	0.0E+00	1.2E-17
Cm-248	6.1E-05	0.0E+00	0.0E+00	3.2E-15	1.4E-07	4.8E-07	5.3E-07	0.0E+00	0.0E+00	0.0E+00	2.6E-23
H-3	1.2E+00	2.5E-01	2.6E-01	9.4E-05	0.0E+00	0.0E+00	0.0E+00	0.0E+00	0.0E+00	0.0E+00	0.0E+00
I-129	5.0E-05	3.0E-01	4.4E-01	1.5E-02	0.0E+00	0.0E+00	0.0E+00	0.0E+00	0.0E+00	0.0E+00	0.0E+00
I-129_ETF.GT.73	8.6E-05	6.8E-05	2.6E-04	6.7E-04	0.0E+00	0.0E+00	0.0E+00	0.0E+00	0.0E+00	0.0E+00	0.0E+00
K-40	1.0E-04	7.6E-04	1.2E-03	1.1E-04	0.0E+00	0.0E+00	0.0E+00	0.0E+00	0.0E+00	0.0E+00	0.0E+00
Mo-93	1.0E-03	5.4E-03	6.8E-03	5.2E-04	0.0E+00	0.0E+00	0.0E+00	0.0E+00	0.0E+00	0.0E+00	0.0E+00
Nb-94	5.0E-04	5.3E-03	6.2E-03	2.8E-04	0.0E+00	0.0E+00	0.0E+00	0.0E+00	0.0E+00	0.0E+00	0.0E+00
Ni-59	3.6E-02	0.0E+00	4.2E-12	6.4E-03	0.0E+00	0.0E+00	0.0E+00	0.0E+00	0.0E+00	0.0E+00	0.0E+00
Np-237	8.0E-03	7.0E-07	2.2E-03	8.2E-03	1.6E-01	9.9E-02	4.6E-02	0.0E+00	0.0E+00	0.0E+00	5.6E-11
Pd-107	1.1E-07	0.0E+00	1.0E-19	1.6E-10	0.0E+00	0.0E+00	0.0E+00	0.0E+00	0.0E+00	0.0E+00	0.0E+00

Table C- 1. Fraction of Groundwater Protection Limits for East Slit Trenches - continued

		Beta-Gamma Fraction of Limit			Gross Alpha Fraction of Limit			Radium Fraction of Limit			Uranium Fraction of Limit
Radionuclide	**Closure Inventory (Ci)**	**0-12 yrs**	**12-100 yrs**	**100-1130 yrs**	**0-1000 yrs**	**1000-1120 yrs**	**1120-1130 yrs**	**0-1000 yrs**	**1000-1120 yrs**	**1120-1130 yrs**	**All Years**
Pu-238	2.5E+01	0.0E+00	0.0E+00	2.4E-06	6.6E-05	2.1E-04	2.3E-04	6.6E-05	2.1E-04	2.3E-04	3.7E-18
Pu-239	1.6E+00	3.5E-19	3.3E-13	2.8E-07	3.1E-07	3.6E-07	3.6E-07	0.0E+00	0.0E+00	0.0E+00	1.6E-17
Pu-240	4.5E-01	0.0E+00	0.0E+00	2.8E-17	4.9E-11	4.8E-10	5.7E-10	1.6E-17	2.0E-17	2.1E-17	4.1E-18
Pu-241	8.4E+00	1.1E-12	3.5E-08	4.4E-05	8.7E-04	7.7E-04	7.7E-04	0.0E+00	0.0E+00	0.0E+00	3.0E-13
Pu-242	1.5E-02	0.0E+00	0.0E+00	1.5E-16	1.8E-12	1.8E-11	2.1E-11	4.4E-15	1.2E-14	1.4E-14	1.5E-19
Pu-244	5.1E-15	0.0E+00	0.0E+00	8.5E-26	6.8E-25	6.8E-24	8.1E-24	4.3E-33	5.9E-33	6.1E-33	5.5E-33
Ra-226	3.2E-03	6.2E-22	6.2E-11	1.3E-03	4.3E-02	1.0E-01	1.1E-01	4.3E-02	1.0E-01	1.1E-01	0.0E+00
Sr-90	1.2E+01	5.5E-16	1.7E-06	8.6E-02	0.0E+00	0.0E+00	0.0E+00	0.0E+00	0.0E+00	0.0E+00	0.0E+00
Tc-99	7.0E-03	2.8E-02	6.1E-02	2.8E-03	0.0E+00	0.0E+00	0.0E+00	0.0E+00	0.0E+00	0.0E+00	0.0E+00
Th-230	3.9E-04	0.0E+00	9.5E-15	4.3E-05	1.1E-03	3.7E-03	4.0E-03	1.1E-03	3.7E-03	4.0E-03	0.0E+00
Th-232	1.1E-02	7.5E-21	3.4E-13	5.9E-07	5.8E-07	2.5E-07	2.0E-07	4.3E-07	1.9E-07	1.5E-07	0.0E+00
U-233	2.0E+00	0.0E+00	0.0E+00	1.2E-13	4.5E-14	4.8E-13	5.7E-13	0.0E+00	0.0E+00	0.0E+00	3.7E-15
U-234	1.8E+00	0.0E+00	1.2E-15	7.0E-04	1.9E-02	6.0E-02	6.5E-02	1.9E-02	6.0E-02	6.5E-02	1.1E-15
U-235	3.9E-02	4.6E-12	1.8E-06	1.1E-02	1.4E-02	1.4E-02	1.2E-02	0.0E+00	0.0E+00	0.0E+00	4.5E-14
U-236	2.6E-02	0.0E+00	0.0E+00	1.6E-13	1.2E-13	1.5E-13	1.6E-13	9.1E-14	1.1E-13	1.2E-13	1.5E-15
U-238	3.3E+00	0.0E+00	0.0E+00	9.7E-07	2.8E-05	8.2E-05	9.0E-05	2.8E-05	8.2E-05	9.0E-05	3.6E-11
Zr-93	2.7E-05	1.5E-05	6.3E-05	5.4E-05	0.0E+00	0.0E+00	0.0E+00	0.0E+00	0.0E+00	0.0E+00	0.0E+00
Sum of Fractions		**7.1E-01**	**9.3E-01**	**2.0E-01**	**2.4E-01**	**2.8E-01**	**2.4E-01**	**6.3E-02**	**1.7E-01**	**1.8E-01**	**9.3E-11**

Table C- 2. Fraction of Groundwater Protection Limits for Center Slit Trenches

		Beta-Gamma Fraction of Limit			Gross Alpha Fraction of Limit			Radium Fraction of Limit			Uranium Fraction of Limit
Radionuclide	Closure Inventory (Ci)	0-12 yrs	12-100 yrs	100-1130 yrs	0-1000 yrs	1000-1120 yrs	1120-1130 yrs	0-1000 yrs	1000-1120 yrs	1120-1130 yrs	All Years
Am-241	5.3E-01	1.4E-10	3.0E-07	4.8E-05	2.4E-03	4.2E-03	4.4E-03	0.0E+00	0.0E+00	0.0E+00	3.2E-13
Am-243	4.3E-02	0.0E+00	8.1E-19	9.0E-05	6.5E-04	1.7E-03	1.8E-03	0.0E+00	0.0E+00	0.0E+00	3.5E-14
C-14	1.0E-02	4.1E-02	4.0E-02	1.2E-03	0.0E+00	0.0E+00	0.0E+00	0.0E+00	0.0E+00	0.0E+00	0.0E+00
C-14_NR.Pump	8.2E-02	0.0E+00	0.0E+00	3.3E-02	0.0E+00	0.0E+00	0.0E+00	0.0E+00	0.0E+00	0.0E+00	0.0E+00
Cf-249	8.3E-02	6.8E-19	2.6E-14	2.5E-06	2.6E-04	5.9E-04	6.3E-04	0.0E+00	0.0E+00	0.0E+00	8.9E-16
Cf-251	7.5E-02	0.0E+00	0.0E+00	4.5E-10	5.7E-04	1.4E-03	1.4E-03	0.0E+00	0.0E+00	0.0E+00	9.3E-20
Cl-36	1.1E-05	1.2E-04	1.2E-04	3.5E-06	0.0E+00	0.0E+00	0.0E+00	0.0E+00	0.0E+00	0.0E+00	0.0E+00
Cm-244	3.2E+00	0.0E+00	0.0E+00	3.6E-18	4.5E-11	3.5E-10	4.0E-10	2.0E-18	2.5E-18	2.6E-18	3.2E-18
Cm-245	1.1E-03	6.4E-17	1.0E-12	9.0E-07	3.0E-05	7.7E-05	8.3E-05	0.0E+00	0.0E+00	0.0E+00	6.1E-16
Cm-246	4.1E-04	0.0E+00	0.0E+00	5.3E-19	5.8E-06	1.5E-05	1.6E-05	3.6E-20	1.1E-19	1.2E-19	2.1E-17
Cm-247	1.1E-03	0.0E+00	0.0E+00	3.0E-07	1.9E-05	5.1E-05	5.5E-05	0.0E+00	0.0E+00	0.0E+00	7.9E-17
Cm-248	6.1E-05	0.0E+00	0.0E+00	1.9E-14	9.2E-07	2.4E-06	2.6E-06	0.0E+00	0.0E+00	0.0E+00	2.1E-22
H-3	1.0E+00	2.1E-01	2.1E-01	4.3E-05	0.0E+00	0.0E+00	0.0E+00	0.0E+00	0.0E+00	0.0E+00	0.0E+00
H-3_ETF.Carbon	2.8E-01	2.5E-02	2.5E-02	5.1E-06	0.0E+00	0.0E+00	0.0E+00	0.0E+00	0.0E+00	0.0E+00	0.0E+00
H-3_Concrete	3.9E+00	0.0E+00	0.0E+00	6.8E-05	0.0E+00	0.0E+00	0.0E+00	0.0E+00	0.0E+00	0.0E+00	0.0E+00
I-129	3.0E-05	2.1E-01	2.2E-01	4.7E-03	0.0E+00	0.0E+00	0.0E+00	0.0E+00	0.0E+00	0.0E+00	0.0E+00
I-129_ETF.Carbon	1.6E-02	0.0E+00	0.0E+00	9.5E-02	0.0E+00	0.0E+00	0.0E+00	0.0E+00	0.0E+00	0.0E+00	0.0E+00
I-129_ETF.GT.73	8.6E-05	7.4E-05	1.5E-04	3.8E-04	0.0E+00	0.0E+00	0.0E+00	0.0E+00	0.0E+00	0.0E+00	0.0E+00
I-129_F.CG.8	5.2E-05	8.7E-03	1.7E-02	1.5E-02	0.0E+00	0.0E+00	0.0E+00	0.0E+00	0.0E+00	0.0E+00	0.0E+00
I-129_F.Dowex.21K	4.4E-03	5.6E-03	1.1E-02	2.8E-02	0.0E+00	0.0E+00	0.0E+00	0.0E+00	0.0E+00	0.0E+00	0.0E+00
I-129_F.Filtercake	7.0E-05	1.0E-02	2.1E-02	1.8E-02	0.0E+00	0.0E+00	0.0E+00	0.0E+00	0.0E+00	0.0E+00	0.0E+00
I-129_H.CG.8	1.2E-04	2.7E-03	5.3E-03	8.3E-03	0.0E+00	0.0E+00	0.0E+00	0.0E+00	0.0E+00	0.0E+00	0.0E+00
I-129_H.Filtercake	2.8E-07	3.7E-06	7.3E-06	1.3E-05	0.0E+00	0.0E+00	0.0E+00	0.0E+00	0.0E+00	0.0E+00	0.0E+00
I-129_Mk50A	8.2E-06	2.3E-06	5.7E-06	2.1E-05	0.0E+00	0.0E+00	0.0E+00	0.0E+00	0.0E+00	0.0E+00	0.0E+00
K-40	1.0E-04	5.3E-04	7.1E-04	6.3E-05	0.0E+00	0.0E+00	0.0E+00	0.0E+00	0.0E+00	0.0E+00	0.0E+00
Mo-93	1.0E-03	5.3E-03	5.4E-03	2.9E-04	0.0E+00	0.0E+00	0.0E+00	0.0E+00	0.0E+00	0.0E+00	0.0E+00

Table C- 2. Fraction of Groundwater Protection Limits for Center Slit Trenches - continued

Radionuclide	Closure Inventory (Ci)	Beta-Gamma Fraction of Limit			Gross Alpha Fraction of Limit			Radium Fraction of Limit			Uranium Fraction of Limit
		0-12 yrs	12-100 yrs	100-1130 yrs	0-1000 yrs	1000-1120 yrs	1120-1130 yrs	0-1000 yrs	1000-1120 yrs	1120-1130 yrs	All Years
Nb-94	5.0E-04	5.3E-03	5.3E-03	1.5E-04	0.0E+00	0.0E+00	0.0E+00	0.0E+00	0.0E+00	0.0E+00	0.0E+00
Ni-59	3.6E-02	6.3E-22	1.1E-11	8.9E-03	0.0E+00	0.0E+00	0.0E+00	0.0E+00	0.0E+00	0.0E+00	0.0E+00
Np-237	8.0E-03	3.3E-06	2.1E-03	4.6E-03	9.3E-02	4.9E-02	2.1E-02	0.0E+00	0.0E+00	0.0E+00	3.7E-11
Pd-107	1.1E-07	0.0E+00	2.6E-19	2.2E-10	0.0E+00	0.0E+00	0.0E+00	0.0E+00	0.0E+00	0.0E+00	0.0E+00
Pu-238	2.5E+01	0.0E+00	0.0E+00	2.5E-06	6.5E-05	2.1E-04	2.2E-04	6.5E-05	2.1E-04	2.2E-04	1.6E-16
Pu-239	1.6E+00	1.7E-18	2.4E-13	1.5E-07	1.7E-07	2.4E-07	2.5E-07	0.0E+00	0.0E+00	0.0E+00	4.9E-16
Pu-240	4.5E-01	0.0E+00	0.0E+00	2.0E-16	1.7E-09	1.4E-08	1.6E-08	1.1E-16	1.4E-16	1.5E-16	1.3E-16
Pu-241	8.4E+00	5.8E-12	3.4E-08	2.5E-05	1.3E-03	2.2E-03	2.3E-03	0.0E+00	0.0E+00	0.0E+00	1.7E-13
Pu-242	1.5E-02	0.0E+00	0.0E+00	1.5E-16	6.2E-11	5.2E-10	6.0E-10	4.0E-15	1.3E-14	1.4E-14	4.7E-18
Pu-244	5.1E-15	0.0E+00	0.0E+00	2.4E-24	2.3E-23	1.9E-22	2.3E-22	3.0E-32	4.1E-32	4.3E-32	1.7E-31
Ra-226	3.2E-03	1.4E-20	1.2E-10	1.1E-03	5.0E-02	8.1E-02	8.1E-02	5.0E-02	8.1E-02	8.1E-02	0.0E+00
Ra-226_Cooling.Tower	4.0E-02	0.0E+00	3.3E-14	2.9E-03	1.7E-01	4.0E-02	4.7E-02	3.3E-03	4.0E-02	4.7E-02	0.0E+00
Se-79	8.6E-03	0.0E+00	0.0E+00	2.7E-22	0.0E+00	0.0E+00	0.0E+00	0.0E+00	0.0E+00	0.0E+00	0.0E+00
Sr-90	1.2E+01	1.2E-14	3.6E-06	1.7E-01	0.0E+00	0.0E+00	0.0E+00	0.0E+00	0.0E+00	0.0E+00	0.0E+00
Sr-90_Mk50A	7.4E+00	5.4E-18	2.3E-09	1.8E-04	0.0E+00	0.0E+00	0.0E+00	0.0E+00	0.0E+00	0.0E+00	0.0E+00
Tc-99	5.0E-02	3.0E-01	3.8E-01	1.1E-02	0.0E+00	0.0E+00	0.0E+00	0.0E+00	0.0E+00	0.0E+00	0.0E+00
Tc-99_Mk50A	1.8E-03	3.4E-07	1.4E-06	5.2E-06	0.0E+00	0.0E+00	0.0E+00	0.0E+00	0.0E+00	0.0E+00	0.0E+00
Th-230	3.9E-04	0.0E+00	1.9E-14	4.4E-05	1.3E-03	3.6E-03	3.8E-03	1.2E-03	3.6E-03	3.8E-03	0.0E+00
Th-230_Cooling.Tower	4.0E-02	0.0E+00	3.9E-17	3.7E-04	2.0E-02	2.2E-02	2.4E-02	2.0E-02	2.2E-02	2.4E-02	0.0E+00
Th-232	1.1E-02	1.8E-19	2.7E-12	4.0E-06	3.9E-06	1.7E-06	1.3E-06	2.9E-06	1.3E-06	9.9E-07	0.0E+00
U-233	2.0E+00	0.0E+00	0.0E+00	4.3E-12	1.7E-12	1.7E-11	2.0E-11	0.0E+00	0.0E+00	0.0E+00	1.3E-13
U-234	1.8E+00	0.0E+00	2.4E-15	7.1E-04	1.9E-02	5.9E-02	6.3E-02	1.9E-02	5.9E-02	6.3E-02	4.8E-14
U-234_MGlass	2.8E+00	0.0E+00	2.6E-18	2.6E-06	7.7E-05	2.2E-04	2.3E-04	7.7E-05	2.2E-04	2.3E-04	1.3E-16
U-235	3.9E-02	2.3E-11	1.3E-06	6.3E-03	8.1E-03	7.8E-03	6.6E-03	0.0E+00	0.0E+00	0.0E+00	3.0E-12
U-235_MGlass	1.9E-01	8.2E-14	1.1E-08	7.7E-05	9.0E-05	9.8E-05	9.7E-05	0.0E+00	0.0E+00	0.0E+00	2.4E-14
U-235_Paducah.Cask	3.9E-01	6.9E-15	9.6E-10	1.5E-05	1.7E-05	1.9E-05	1.9E-05	0.0E+00	0.0E+00	0.0E+00	4.6E-15

Table C- 2. Fraction of Groundwater Protection Limits for Center Slit Trenches - continued

		Beta-Gamma Fraction of Limit			Gross Alpha Fraction of Limit			Radium Fraction of Limit			Uranium Fraction of Limit
Radionuclide	**Closure Inventory (Ci)**	**0-12 yrs**	**12-100 yrs**	**100-1130 yrs**	**0-1000 yrs**	**1000-1120 yrs**	**1120-1130 yrs**	**0-1000 yrs**	**1000-1120 yrs**	**1120-1130 yrs**	**All Years**
U-236	2.6E-02	0.0E+00	1.1E-21	1.1E-12	8.3E-13	1.0E-12	1.1E-12	6.2E-13	7.8E-13	8.1E-13	6.5E-14
U-236_MGlass	1.4E-01	0.0E+00	0.0E+00	8.7E-15	6.8E-15	8.3E-15	8.6E-15	5.1E-15	6.2E-15	6.5E-15	6.2E-16
U-238	3.3E+00	0.0E+00	0.0E+00	9.8E-07	2.6E-05	8.3E-05	9.0E-05	2.6E-05	8.3E-05	9.0E-05	1.6E-09
U-238_MGlass	1.1E+01	0.0E+00	0.0E+00	8.2E-09	2.2E-07	6.9E-07	7.4E-07	2.2E-07	6.9E-07	7.4E-07	8.8E-12
Zr-93	2.7E-05	1.8E-05	4.2E-05	3.6E-05	0.0E+00	0.0E+00	0.0E+00	0.0E+00	0.0E+00	0.0E+00	0.0E+00
Sum of Fractions		**8.2E-01**	**9.3E-01**	**4.1E-01**	**1.8E-01**	**2.6E-01**	**2.4E-01**	**7.4E-02**	**1.9E-01**	**2.0E-01**	**1.6E-09**

Table C- 3. Fraction of Groundwater Protection Limits for West Slit Trenches

		Beta-Gamma Fraction of Limit			Gross Alpha Fraction of Limit			Radium Fraction of Limit			Uranium Fraction of Limit
Radionuclide	Closure Inventory (Ci)	0-12 yrs	12-100 yrs	100-1130 yrs	0-1000 yrs	1000-1120 yrs	1120-1130 yrs	0-1000 yrs	1000-1120 yrs	1120-1130 yrs	All Years
Am-241	4.8E-01	5.9E-10	3.8E-07	5.3E-05	8.7E-03	1.3E-02	1.4E-02	0.0E+00	0.0E+00	0.0E+00	0.0E+00
Am-243	2.1E-01	0.0E+00	5.1E-18	1.6E-03	1.6E-02	3.1E-02	3.2E-02	0.0E+00	0.0E+00	0.0E+00	0.0E+00
C-14	1.8E-02	9.5E-02	9.2E-02	2.2E-03	0.0E+00	0.0E+00	0.0E+00	0.0E+00	0.0E+00	0.0E+00	0.0E+00
C-14_NR.Pump	1.0E-03	0.0E+00	0.0E+00	4.5E-04	0.0E+00	0.0E+00	0.0E+00	0.0E+00	0.0E+00	0.0E+00	0.0E+00
Cf-249	4.2E-01	2.0E-17	1.9E-13	4.7E-05	6.8E-03	1.1E-02	1.2E-02	0.0E+00	0.0E+00	0.0E+00	0.0E+00
Cf-251	3.8E-01	0.0E+00	0.0E+00	8.4E-09	1.5E-02	2.6E-02	2.7E-02	0.0E+00	0.0E+00	0.0E+00	0.0E+00
Cl-36	1.0E-06	1.5E-05	1.4E-05	3.5E-07	0.0E+00	0.0E+00	0.0E+00	0.0E+00	0.0E+00	0.0E+00	0.0E+00
Cm-244	1.5E+01	0.0E+00	0.0E+00	1.1E-16	4.7E-09	3.1E-08	3.6E-08	5.7E-17	7.5E-17	7.8E-17	5.7E-17
Cm-245	7.3E-03	2.3E-15	9.7E-12	2.2E-05	9.9E-04	2.0E-03	2.0E-03	0.0E+00	0.0E+00	0.0E+00	0.0E+00
Cm-246	9.6E-06	0.0E+00	0.0E+00	7.0E-20	6.9E-07	1.3E-06	1.4E-06	1.1E-21	3.6E-21	3.9E-21	1.1E-21
Cm-247	1.6E-02	0.0E+00	0.0E+00	1.6E-05	1.5E-03	2.8E-03	3.0E-03	0.0E+00	0.0E+00	0.0E+00	0.0E+00
Cm-248	3.0E-05	0.0E+00	0.0E+00	4.5E-14	2.3E-06	4.4E-06	4.6E-06	0.0E+00	0.0E+00	0.0E+00	0.0E+00
H-3	5.5E-01	1.6E-01	1.4E-01	2.5E-05	0.0E+00	0.0E+00	0.0E+00	0.0E+00	0.0E+00	0.0E+00	0.0E+00
I-129	1.3E-04	6.4E-01	6.5E-01	1.4E-02	0.0E+00	0.0E+00	0.0E+00	0.0E+00	0.0E+00	0.0E+00	0.0E+00
K-40	1.0E-04	6.0E-04	8.0E-04	7.2E-05	0.0E+00	0.0E+00	0.0E+00	0.0E+00	0.0E+00	0.0E+00	0.0E+00
Mo-93	1.0E-03	6.6E-03	6.5E-03	3.0E-04	0.0E+00	0.0E+00	0.0E+00	0.0E+00	0.0E+00	0.0E+00	0.0E+00
Nb-94	1.0E-04	1.4E-03	1.3E-03	3.2E-05	0.0E+00	0.0E+00	0.0E+00	0.0E+00	0.0E+00	0.0E+00	0.0E+00
Ni-59	5.1E-05	1.0E-22	2.6E-14	1.8E-05	0.0E+00	0.0E+00	0.0E+00	0.0E+00	0.0E+00	0.0E+00	0.0E+00
Np-237	4.6E-04	8.5E-07	1.6E-04	3.2E-04	6.4E-03	3.4E-03	1.4E-03	0.0E+00	0.0E+00	0.0E+00	0.0E+00
Pd-107	1.0E-07	0.0E+00	4.1E-19	2.9E-10	0.0E+00	0.0E+00	0.0E+00	0.0E+00	0.0E+00	0.0E+00	0.0E+00
Pu-238	9.9E+00	0.0E+00	0.0E+00	1.3E-06	3.6E-05	1.1E-04	1.2E-04	3.6E-05	1.1E-04	1.2E-04	3.6E-05
Pu-239	3.1E+00	1.7E-17	5.8E-13	3.5E-07	6.6E-07	2.4E-06	2.8E-06	0.0E+00	0.0E+00	0.0E+00	0.0E+00
Pu-240	9.3E-01	0.0E+00	0.0E+00	2.6E-15	7.8E-08	5.5E-07	6.4E-07	1.4E-15	1.8E-15	1.9E-15	1.4E-15
Pu-241	9.4E+00	3.4E-11	5.4E-08	3.4E-05	5.8E-03	8.9E-03	9.1E-03	0.0E+00	0.0E+00	0.0E+00	0.0E+00
Pu-242	5.9E-01	0.0E+00	0.0E+00	7.9E-15	5.6E-08	4.0E-07	4.6E-07	2.1E-13	6.8E-13	7.4E-13	2.1E-13
Pu-244	1.0E-15	0.0E+00	0.0E+00	9.1E-24	1.0E-22	7.5E-22	8.7E-22	3.7E-32	5.1E-32	5.3E-32	3.7E-32

Table C- 3. Fraction of Groundwater Protection Limits for West Slit Trenches - continued

		Beta-Gamma Fraction of Limit			Gross Alpha Fraction of Limit			Radium Fraction of Limit			Uranium Fraction of Limit
Radionuclide	**Closure Inventory (Ci)**	**0-12 yrs**	**12-100 yrs**	**100-1130 yrs**	**0-1000 yrs**	**1000-1120 yrs**	**1120-1130 yrs**	**0-1000 yrs**	**1000-1120 yrs**	**1120-1130 yrs**	**All Years**
Ra-226	1.0E-04	2.8E-20	6.4E-12	4.1E-05	2.1E-03	3.1E-03	3.1E-03	2.1E-03	3.1E-03	3.1E-03	2.1E-03
Se-79	4.1E-05	0.0E+00	0.0E+00	1.2E-22	0.0E+00	0.0E+00	0.0E+00	0.0E+00	0.0E+00	0.0E+00	0.0E+00
Sr-90	4.1E+00	2.7E-13	3.5E-06	1.3E-01	0.0E+00	0.0E+00	0.0E+00	0.0E+00	0.0E+00	0.0E+00	0.0E+00
Tc-99	5.4E-03	4.6E-02	5.1E-02	1.4E-03	0.0E+00	0.0E+00	0.0E+00	0.0E+00	0.0E+00	0.0E+00	0.0E+00
Th-230	1.0E-04	1.8E-23	8.0E-15	1.5E-05	4.5E-04	1.2E-03	1.2E-03	4.5E-04	1.2E-03	1.2E-03	4.5E-04
Th-232	5.7E-08	7.1E-23	1.1E-16	1.3E-10	1.3E-10	5.4E-11	4.3E-11	9.6E-11	4.0E-11	3.2E-11	9.6E-11
U-233	8.3E-01	0.0E+00	0.0E+00	5.2E-11	2.4E-11	2.1E-10	2.5E-10	0.0E+00	0.0E+00	0.0E+00	0.0E+00
U-234	6.2E-01	0.0E+00	1.3E-15	3.2E-04	8.9E-03	2.6E-02	2.8E-02	8.9E-03	2.6E-02	2.8E-02	8.9E-03
U-235	2.5E-04	7.7E-13	1.1E-08	4.9E-05	6.3E-05	6.0E-05	5.1E-05	0.0E+00	0.0E+00	0.0E+00	0.0E+00
U-236	1.7E-06	0.0E+00	5.9E-25	4.7E-16	3.5E-16	4.4E-16	4.6E-16	2.6E-16	3.3E-16	3.4E-16	2.6E-16
U-238	2.9E-01	0.0E+00	0.0E+00	1.2E-07	3.1E-06	9.8E-06	1.1E-05	3.1E-06	9.8E-06	1.1E-05	3.1E-06
Zr-93	1.0E-06	9.2E-07	1.8E-06	1.5E-06	0.0E+00	0.0E+00	0.0E+00	0.0E+00	0.0E+00	0.0E+00	0.0E+00
Sum of Fractions		**9.5E-01**	**9.4E-01**	**1.5E-01**	**7.3E-02**	**1.3E-01**	**1.3E-01**	**1.2E-02**	**3.1E-02**	**3.2E-02**	**1.2E-02**

Table C- 4. Fraction of Groundwater Protection Limits for Engineered Trenches

		Beta-Gamma Fraction of Limit			Gross Alpha Fraction of Limit			Radium Fraction of Limit			Uranium Fraction of Limit
Radionuclide	Closure Inventory (Ci)	0-12 yrs	12-100 yrs	100-1130 yrs	0-1000 yrs	1000-1120 yrs	1120-1130 yrs	0-1000 yrs	1000-1120 yrs	1120-1130 yrs	All Years
Am-241	3.3E+00	1.6E-11	3.0E-07	1.5E-04	3.0E-03	2.8E-03	2.9E-03	0.0E+00	0.0E+00	0.0E+00	1.2E-12
Am-243	6.3E-02	0.0E+00	1.5E-19	3.4E-06	1.5E-05	6.2E-05	6.9E-05	0.0E+00	0.0E+00	0.0E+00	7.6E-16
C-14	1.3E-01	1.4E-01	2.5E-01	1.1E-02	0.0E+00	0.0E+00	0.0E+00	0.0E+00	0.0E+00	0.0E+00	0.0E+00
Cf-249	7.1E-02	9.7E-21	3.0E-15	1.2E-07	4.4E-06	1.4E-05	1.5E-05	0.0E+00	0.0E+00	0.0E+00	3.9E-16
Cf-251	6.4E-02	0.0E+00	0.0E+00	1.0E-11	7.7E-06	3.0E-05	3.2E-05	0.0E+00	0.0E+00	0.0E+00	1.3E-21
Cl-36	9.1E-05	2.9E-04	4.9E-04	2.1E-05	0.0E+00	0.0E+00	0.0E+00	0.0E+00	0.0E+00	0.0E+00	0.0E+00
Cm-244	5.3E+00	0.0E+00	0.0E+00	1.1E-19	7.6E-14	7.9E-13	9.5E-13	6.7E-20	8.2E-20	8.4E-20	0.0E+00
Cm-245	1.3E-03	1.4E-18	1.7E-13	8.0E-08	1.4E-06	3.4E-06	3.7E-06	0.0E+00	0.0E+00	0.0E+00	4.0E-16
Cm-246	5.9E-04	0.0E+00	0.0E+00	1.1E-20	1.3E-07	5.5E-07	6.0E-07	1.9E-20	4.6E-20	5.0E-20	4.4E-19
Cm-247	7.0E-04	0.0E+00	0.0E+00	5.1E-09	2.0E-07	8.4E-07	9.4E-07	0.0E+00	0.0E+00	0.0E+00	8.0E-19
Cm-248	1.0E-14	0.0E+00	0.0E+00	6.3E-26	2.5E-18	1.0E-17	1.1E-17	0.0E+00	0.0E+00	0.0E+00	4.3E-34
H-3	1.5E+00	8.3E-02	1.2E-01	4.6E-05	0.0E+00	0.0E+00	0.0E+00	0.0E+00	0.0E+00	0.0E+00	0.0E+00
I-129	7.0E-05	8.6E-02	2.2E-01	7.8E-03	0.0E+00	0.0E+00	0.0E+00	0.0E+00	0.0E+00	0.0E+00	0.0E+00
I-129_ETF.GT.73	7.4E-07	1.3E-07	4.4E-07	1.2E-06	0.0E+00	0.0E+00	0.0E+00	0.0E+00	0.0E+00	0.0E+00	0.0E+00
I-129_F.CG.8	1.6E-06	5.5E-05	1.8E-04	1.8E-04	0.0E+00	0.0E+00	0.0E+00	0.0E+00	0.0E+00	0.0E+00	0.0E+00
I-129_F.Dowex.21K	1.3E-03	3.5E-04	1.2E-03	3.0E-03	0.0E+00	0.0E+00	0.0E+00	0.0E+00	0.0E+00	0.0E+00	0.0E+00
I-129_F.Filtercake	3.6E-05	1.1E-03	3.7E-03	3.8E-03	0.0E+00	0.0E+00	0.0E+00	0.0E+00	0.0E+00	0.0E+00	0.0E+00
I-129_H.CG.8	9.6E-06	4.5E-05	1.5E-04	2.7E-04	0.0E+00	0.0E+00	0.0E+00	0.0E+00	0.0E+00	0.0E+00	0.0E+00
I-129_H.Dowex.21K	9.0E-04	1.0E-04	3.5E-04	9.0E-04	0.0E+00	0.0E+00	0.0E+00	0.0E+00	0.0E+00	0.0E+00	0.0E+00
K-40	1.7E-04	4.0E-04	6.7E-04	7.0E-05	0.0E+00	0.0E+00	0.0E+00	0.0E+00	0.0E+00	0.0E+00	0.0E+00
Mo-93	2.7E-03	3.9E-03	7.6E-03	5.4E-04	0.0E+00	0.0E+00	0.0E+00	0.0E+00	0.0E+00	0.0E+00	0.0E+00
Nb-94	2.8E-03	8.0E-03	1.4E-02	5.9E-04	0.0E+00	0.0E+00	0.0E+00	0.0E+00	0.0E+00	0.0E+00	0.0E+00
Ni-59	9.2E-02	0.0E+00	3.0E-13	5.1E-03	0.0E+00	0.0E+00	0.0E+00	0.0E+00	0.0E+00	0.0E+00	0.0E+00
Np-237	1.3E-02	1.1E-07	5.8E-04	3.4E-03	6.8E-02	5.5E-02	4.8E-02	0.0E+00	0.0E+00	0.0E+00	3.2E-11
Pd-107	1.0E-03	0.0E+00	2.6E-17	4.6E-07	0.0E+00	0.0E+00	0.0E+00	0.0E+00	0.0E+00	0.0E+00	0.0E+00

Table C- 4. Fraction of Groundwater Protection Limits for Engineered Trenches - continued

		Beta-Gamma Fraction of Limit			Gross Alpha Fraction of Limit			Radium Fraction of Limit			Uranium Fraction of Limit
Radionuclide	**Closure Inventory (Ci)**	**0-12 yrs**	**12-100 yrs**	**100-1130 yrs**	**0-1000 yrs**	**1000-1120 yrs**	**1120-1130 yrs**	**0-1000 yrs**	**1000-1120 yrs**	**1120-1130 yrs**	**All Years**
Pu-238	5.6E+00	0.0E+00	0.0E+00	1.5E-07	4.4E-06	1.2E-05	1.4E-05	4.4E-06	1.2E-05	1.4E-05	0.0E+00
Pu-239	1.7E+01	3.0E-19	3.3E-13	8.0E-07	1.0E-06	1.2E-06	1.2E-06	0.0E+00	0.0E+00	0.0E+00	5.9E-18
Pu-240	3.6E+00	0.0E+00	0.0E+00	3.0E-17	1.3E-11	1.5E-10	1.8E-10	1.8E-17	2.2E-17	2.2E-17	1.2E-18
Pu-241	9.9E+00	1.3E-13	6.1E-09	1.5E-05	2.9E-04	2.8E-04	2.8E-04	0.0E+00	0.0E+00	0.0E+00	1.2E-13
Pu-242	1.0E-01	0.0E+00	0.0E+00	2.9E-16	4.2E-13	4.7E-12	5.6E-12	1.0E-14	2.4E-14	2.6E-14	3.8E-20
Pu-244	5.2E-15	0.0E+00	0.0E+00	3.3E-27	2.3E-26	2.6E-25	3.1E-25	6.0E-34	7.8E-34	8.1E-34	2.0E-34
Ra-226	5.2E-03	0.0E+00	3.3E-12	5.9E-04	2.1E-02	5.0E-02	5.3E-02	2.1E-02	5.0E-02	5.3E-02	0.0E+00
Sr-90	7.2E+01	3.5E-17	3.2E-07	1.5E-01	0.0E+00	0.0E+00	0.0E+00	0.0E+00	0.0E+00	0.0E+00	0.0E+00
Tc-99	1.0E-01	7.6E-02	3.5E-01	1.6E-02	0.0E+00	0.0E+00	0.0E+00	0.0E+00	0.0E+00	0.0E+00	0.0E+00
Th-230	8.6E-03	0.0E+00	6.7E-15	2.4E-04	5.3E-03	2.1E-02	2.3E-02	5.3E-03	2.1E-02	2.3E-02	0.0E+00
Th-232	5.5E-03	0.0E+00	5.9E-15	4.5E-08	4.4E-08	1.8E-08	1.3E-08	3.3E-08	1.3E-08	9.9E-09	0.0E+00
U-233	2.3E+00	0.0E+00	0.0E+00	3.6E-15	1.2E-15	1.4E-14	1.7E-14	0.0E+00	0.0E+00	0.0E+00	1.2E-16
U-234	5.2E-01	0.0E+00	1.0E-17	5.2E-05	1.4E-03	4.4E-03	4.9E-03	1.4E-03	4.4E-03	4.9E-03	7.8E-18
U-235	1.7E-02	1.9E-13	8.4E-08	1.6E-03	2.1E-03	2.0E-03	2.0E-03	0.0E+00	0.0E+00	0.0E+00	7.6E-16
U-236	3.3E-02	0.0E+00	0.0E+00	2.7E-14	2.2E-14	2.6E-14	2.7E-14	1.6E-14	1.9E-14	2.0E-14	4.7E-17
U-238	4.4E-01	0.0E+00	0.0E+00	3.5E-08	1.1E-06	3.0E-06	3.2E-06	1.1E-06	3.0E-06	3.2E-06	1.2E-13
Zr-93	2.2E-05	3.3E-06	1.8E-05	1.6E-05	0.0E+00	0.0E+00	0.0E+00	0.0E+00	0.0E+00	0.0E+00	0.0E+00
Sum of Fractions		**4.0E-01**	**9.6E-01**	**2.1E-01**	**1.0E-01**	**1.4E-01**	**1.3E-01**	**2.8E-02**	**7.5E-02**	**8.1E-02**	**3.4E-11**

Table C- 5. Fraction of All-Pathways Radionuclide Disposal Limits for East Slit Trenches

Radionuclide	Closure Inventory (Ci)	Fraction of Limit		
		130 - 200 yrs	200-1000 yrs	1000-1130 yrs
Am-241	5.3E-01	1.1E-03	5.5E-03	4.4E-03
Am-243	4.3E-02	2.4E-12	2.6E-04	9.7E-04
C-14	3.0E-02	4.9E-03	4.9E-03	4.9E-03
C-14_NR.Pump	8.2E-02	3.3E-02	5.5E-02	1.9E-04
Cf-249	8.3E-02	7.3E-08	1.4E-04	4.2E-04
Cf-251	7.5E-02	2.9E-20	3.0E-04	1.0E-03
Cl-36	1.1E-05	9.8E-06	9.8E-06	9.8E-06
Cm-244	3.2E+00	0.0E+00	3.5E-12	3.7E-11
Cm-245	1.1E-03	2.3E-07	2.0E-05	5.4E-05
Cm-246	4.1E-04	0.0E+00	2.4E-06	8.8E-06
Cm-247	1.1E-03	2.6E-16	7.3E-06	2.8E-05
Cm-248	6.1E-05	0.0E+00	1.5E-06	5.7E-06
H-3	1.2E+00	5.5E-07	5.5E-07	5.5E-07
I-129	5.0E-05	2.0E-04	2.0E-04	2.0E-04
I-129_ETF.GT.73	8.6E-05	5.5E-06	1.1E-05	1.1E-05
K-40	1.0E-04	4.2E-05	3.2E-05	2.1E-06
Mo-93	1.0E-03	9.0E-05	9.0E-05	9.0E-05
Nb-94	5.0E-04	4.0E-04	4.0E-04	4.0E-04
Ni-59	3.6E-02	3.3E-09	1.7E-05	2.5E-05
Np-237	8.0E-03	3.7E-01	5.3E-01	3.2E-01
Pd-107	1.1E-07	6.5E-15	3.4E-11	5.0E-11
Pu-238	2.5E+01	1.4E-09	2.3E-05	7.7E-05
Pu-239	1.6E+00	5.2E-08	2.6E-06	2.8E-06
Pu-240	4.5E-01	3.2E-20	1.3E-10	1.5E-09
Pu-241	8.4E+00	5.0E-04	2.8E-03	2.3E-03
Pu-242	1.5E-02	5.9E-21	4.4E-12	5.2E-11
Pu-244	5.1E-15	0.0E+00	1.6E-24	1.9E-23
Ra-226	3.2E-03	9.9E-05	1.5E-02	3.7E-02
Sr-90	1.2E+01	3.2E-04	4.5E-03	4.3E-10
Tc-99	7.0E-03	1.6E-03	1.6E-03	1.6E-03
Th-230	3.9E-04	3.7E-07	3.6E-04	1.4E-03
Th-232	1.1E-02	5.7E-08	2.2E-07	9.6E-08
U-233	2.0E+00	0.0E+00	1.4E-12	1.5E-11
U-234	1.8E+00	1.0E-06	6.3E-03	2.2E-02
U-235	3.9E-02	1.6E-02	1.2E-01	1.1E-01
U-236	2.6E-02	9.3E-16	4.8E-14	9.7E-14
U-238	3.3E+00	2.4E-10	9.4E-06	3.1E-05
Zr-93	2.7E-05	3.4E-06	8.4E-06	9.1E-06
Sum of Fractions		**4.3E-01**	**7.4E-01**	**5.1E-01**

Table C- 6. Fraction of All-Pathways Radionuclide Disposal Limits for Center Slit Trenches

Radionuclide	Closure Inventory (Ci)	Fraction of Limit		
		130 - 200 yrs	200-1000 yrs	1000-1130 yrs
Am-241	5.3E-01	8.4E-04	6.7E-03	1.2E-02
Am-243	4.3E-02	1.5E-12	1.7E-03	4.7E-03
C-14	1.0E-02	8.8E-04	8.8E-04	8.8E-04
C-14_NR.Pump	8.2E-02	2.7E-02	3.2E-02	8.2E-04
Cf-249	8.3E-02	4.5E-08	8.5E-04	2.0E-03
Cf-251	7.5E-02	2.1E-20	2.0E-03	5.1E-03
Cl-36	1.1E-05	5.3E-06	5.3E-06	5.3E-06
Cm-244	3.2E+00	0.0E+00	1.2E-10	1.0E-09
Cm-245	1.1E-03	1.6E-07	8.1E-05	2.2E-04
Cm-246	4.1E-04	0.0E+00	1.6E-05	4.3E-05
Cm-247	1.1E-03	1.7E-16	4.8E-05	1.4E-04
Cm-248	6.1E-05	2.6E-24	1.0E-05	2.8E-05
H-3	1.0E+00	2.5E-07	2.5E-07	2.5E-07
H-3_ETF.Carbon	2.8E-01	2.9E-08	2.9E-08	2.9E-08
H-3_Concrete	3.9E+00	2.6E-06	3.5E-09	0.0E+00
I-129	3.0E-05	6.6E-05	6.6E-05	6.6E-05
I-129_ETF.Carbon	1.6E-02	7.8E-04	1.5E-03	1.6E-03
I-129_ETF.GT.73	8.6E-05	3.1E-06	5.9E-06	6.2E-06
I-129_F.CG.8	5.2E-05	2.4E-04	1.5E-04	4.8E-05
I-129_F.Dowex.21K	4.4E-03	2.3E-04	4.3E-04	4.6E-04
I-129_F.Filtercake	7.0E-05	3.1E-04	1.9E-04	6.8E-05
I-129_H.CG.8	1.2E-04	1.1E-04	1.3E-04	1.4E-04
I-129_H.Filtercake	2.8E-07	1.5E-07	1.9E-07	2.1E-07
I-129_Mk50A	8.2E-06	1.3E-07	3.4E-07	1.1E-07
K-40	1.0E-04	2.4E-05	1.9E-05	3.8E-06
Mo-93	1.0E-03	4.8E-05	4.8E-05	4.8E-05
Nb-94	5.0E-04	2.1E-04	2.1E-04	2.1E-04
Ni-59	3.6E-02	3.7E-08	1.7E-05	3.6E-05
Np-237	8.0E-03	2.9E-01	3.0E-01	1.6E-01
Pd-107	1.1E-07	7.3E-14	3.3E-11	7.1E-11
Pu-238	2.5E+01	1.1E-08	2.2E-05	7.7E-05
Pu-239	1.6E+00	3.8E-08	1.4E-06	1.6E-06
Pu-240	4.5E-01	3.6E-19	4.3E-09	4.1E-08
Pu-241	8.4E+00	3.8E-04	3.5E-03	6.3E-03
Pu-242	1.5E-02	4.6E-20	1.5E-10	1.5E-09
Pu-244	5.1E-15	0.0E+00	5.6E-23	5.5E-22
Ra-226	3.2E-03	6.0E-04	1.7E-02	2.8E-02
Ra-226_Cooling.Tower	4.0E-02	3.9E-06	6.0E-02	1.6E-02

Table C- 6. Fraction of All-Pathways Radionuclide Disposal Limits for Center Slit Trenches - continued

Radionuclide	Closure Inventory (Ci)	Fraction of Limit		
		130 - 200 yrs	200-1000 yrs	1000-1130 yrs
Se-79	8.6E-03	0.0E+00	0.0E+00	2.5E-22
Sr-90	1.2E+01	2.0E-03	8.9E-03	5.2E-10
Sr-90_Mk50A	7.4E+00	2.4E-06	9.5E-06	2.2E-12
Tc-99	5.0E-02	6.5E-03	6.5E-03	6.5E-03
Tc-99_Mk50A	1.8E-03	1.1E-06	3.5E-06	1.1E-06
Th-230	3.9E-04	2.7E-06	4.3E-04	1.3E-03
Th-230_Cooling.Tower	4.0E-02	8.0E-08	7.0E-03	8.1E-03
Th-232	1.1E-02	6.3E-07	1.5E-06	6.3E-07
U-233	2.0E+00	0.0E+00	5.3E-11	5.3E-10
U-234	1.8E+00	7.7E-06	6.5E-03	2.1E-02
U-234_MGlass	2.8E+00	7.1E-09	2.6E-05	7.9E-05
U-235	3.9E-02	1.2E-02	6.7E-02	6.2E-02
U-235_MGlass	1.9E-01	2.5E-05	7.1E-04	7.8E-04
U-235_Paducah.Cask	3.9E-01	3.8E-06	1.4E-04	1.5E-04
U-236	2.6E-02	1.0E-14	4.4E-13	2.1E-12
U-236_MGlass	1.4E-01	4.3E-17	3.8E-15	1.9E-14
U-238	3.3E+00	1.8E-09	8.9E-06	3.1E-05
U-238_MGlass	1.1E+01	3.5E-12	7.6E-08	2.5E-07
Zr-93	2.7E-05	3.0E-06	5.6E-06	6.1E-06
Sum of Fractions		**3.4E-01**	**5.2E-01**	**3.4E-01**

Table C- 7. Fraction of All-Pathways Radionuclide Disposal Limits for West Slit Trenches

Radionuclide	Closure Inventory (Ci)	Fraction of Limit		
		130 - 200 yrs	200-1000 yrs	1000-1130 yrs
Am-241	4.8E-01	9.6E-04	2.3E-02	3.6E-02
Am-243	2.1E-01	8.7E-12	4.2E-02	8.5E-02
C-14	1.8E-02	1.9E-03	1.9E-03	1.9E-03
C-14_NR.Pump	1.0E-03	4.1E-04	4.3E-04	9.0E-06
Cf-249	4.2E-01	2.8E-07	2.2E-02	3.7E-02
Cf-251	3.8E-01	7.9E-19	5.2E-02	9.5E-02
Cl-36	1.0E-06	6.0E-07	6.0E-07	6.0E-07
Cm-244	1.5E+01	0.0E+00	1.2E-08	9.2E-08
Cm-245	7.3E-03	1.4E-06	2.7E-03	5.5E-03
Cm-246	9.6E-06	1.5E-23	1.9E-06	3.7E-06
Cm-247	1.6E-02	3.1E-15	3.6E-03	7.4E-03
Cm-248	3.0E-05	1.8E-22	2.5E-05	5.0E-05
H-3	5.5E-01	1.6E-07	1.6E-07	1.6E-07
I-129	1.3E-04	2.0E-04	2.0E-04	2.0E-04
K-40	1.0E-04	2.9E-05	2.2E-05	4.2E-06
Mo-93	1.0E-03	5.6E-05	5.6E-05	5.6E-05
Nb-94	1.0E-04	5.1E-05	5.1E-05	5.1E-05
Ni-59	5.1E-05	4.9E-10	3.5E-08	7.3E-08
Np-237	4.6E-04	2.1E-02	2.1E-02	1.1E-02
Pd-107	1.0E-07	6.2E-13	4.4E-11	9.3E-11
Pu-238	9.9E+00	2.6E-08	1.2E-05	4.1E-05
Pu-239	3.1E+00	8.8E-08	3.7E-06	9.4E-06
Pu-240	9.3E-01	6.8E-18	2.0E-07	1.6E-06
Pu-241	9.4E+00	5.4E-04	1.6E-02	2.4E-02
Pu-242	5.9E-01	1.1E-17	1.4E-07	1.1E-06
Pu-244	1.0E-15	3.6E-35	2.5E-22	2.1E-21
Ra-226	1.0E-04	9.4E-05	7.3E-04	1.1E-03
Se-79	4.1E-05	0.0E+00	8.1E-24	1.1E-22
Sr-90	4.1E+00	3.5E-03	6.8E-03	2.4E-10
Tc-99	5.4E-03	7.4E-04	7.4E-04	7.4E-04
Th-230	1.0E-04	4.1E-06	1.5E-04	4.2E-04
Th-232	5.7E-08	3.0E-11	4.8E-11	2.0E-11
U-233	8.3E-01	0.0E+00	7.0E-10	6.1E-09
U-234	6.2E-01	1.6E-05	3.0E-03	9.5E-03
U-235	2.5E-04	9.7E-05	5.2E-04	4.8E-04
U-236	1.7E-06	6.2E-18	3.9E-16	3.3E-15
U-238	2.9E-01	1.0E-09	1.1E-06	3.6E-06
Zr-93	1.0E-06	1.4E-07	2.4E-07	2.6E-07
Sum of Fractions		**2.9E-02**	**2.0E-01**	**3.2E-01**

Table C- 8. Fraction of All-Pathways Radionuclide Disposal Limits for Engineered Trenches

Radionuclide	Closure Inventory (Ci)	Fraction of Limit 130 - 200 yrs	Fraction of Limit 200-1000 yrs	Fraction of Limit 1000-1130 yrs
Am-241	3.3E+00	2.2E-03	9.6E-03	8.8E-03
Am-243	6.3E-02	1.2E-12	4.0E-05	1.8E-04
C-14	1.3E-01	7.8E-03	7.8E-03	7.8E-03
Cf-249	7.1E-02	2.1E-08	1.4E-05	4.8E-05
Cf-251	6.4E-02	7.8E-21	2.7E-05	1.1E-04
Cl-36	9.1E-05	3.1E-05	3.1E-05	3.1E-05
Cm-244	5.3E+00	0.0E+00	2.0E-13	2.4E-12
Cm-245	1.3E-03	9.5E-08	4.2E-06	1.0E-05
Cm-246	5.9E-04	0.0E+00	3.6E-07	1.6E-06
Cm-247	7.0E-04	5.4E-17	5.0E-07	2.3E-06
Cm-248	1.0E-14	0.0E+00	2.7E-17	1.2E-16
H-3	1.5E+00	2.5E-07	2.5E-07	2.5E-07
I-129	7.0E-05	1.1E-04	1.1E-04	1.1E-04
I-129_ETF.GT.73	7.4E-07	9.1E-09	1.8E-08	1.9E-08
I-129_F.CG.8	1.6E-06	2.9E-06	2.1E-06	1.3E-06
I-129_F.Dowex.21K	1.3E-03	2.4E-05	4.6E-05	5.0E-05
I-129_F.Filtercake	3.6E-05	6.2E-05	4.8E-05	3.1E-05
I-129_H.CG.8	9.6E-06	3.0E-06	3.9E-06	4.5E-06
I-129_H.Dowex.21K	9.0E-04	7.1E-06	1.4E-05	1.5E-05
K-40	1.7E-04	2.7E-05	2.1E-05	1.3E-06
Mo-93	2.7E-03	8.7E-05	8.7E-05	8.7E-05
Nb-94	2.8E-03	8.1E-04	8.1E-04	8.1E-04
Ni-59	9.2E-02	7.2E-10	2.0E-05	1.1E-05
Np-237	1.3E-02	1.9E-01	2.2E-01	1.8E-01
Pd-107	1.0E-03	5.0E-12	1.4E-07	8.0E-08
Pu-238	5.6E+00	3.7E-11	1.5E-06	4.7E-06
Pu-239	1.7E+01	1.8E-07	8.6E-06	9.9E-06
Pu-240	3.6E+00	0.0E+00	3.3E-11	4.5E-10
Pu-241	9.9E+00	1.9E-04	9.4E-04	8.8E-04
Pu-242	1.0E-01	4.7E-21	1.0E-12	1.4E-11
Pu-244	5.2E-15	0.0E+00	5.5E-26	7.6E-25
Ra-226	5.2E-03	2.0E-05	7.1E-03	1.8E-02
Sr-90	7.2E+01	2.2E-04	8.0E-03	4.7E-10
Tc-99	1.0E-01	9.2E-03	9.2E-03	9.2E-03
Th-230	8.6E-03	9.6E-07	1.8E-03	7.9E-03
Th-232	5.5E-03	2.8E-09	1.7E-08	6.6E-09
U-233	2.3E+00	0.0E+00	3.8E-14	4.9E-13
U-234	5.2E-01	3.4E-08	4.9E-04	1.7E-03
U-235	1.7E-02	2.3E-03	1.7E-02	1.7E-02
U-236	3.3E-02	1.1E-16	8.3E-15	1.1E-14
U-238	4.4E-01	3.7E-12	3.9E-07	1.1E-06
Zr-93	2.2E-05	1.0E-06	2.4E-06	2.7E-06
Sum of Fractions		**2.1E-01**	**2.8E-01**	**2.5E-01**

Table C- 9. Fraction of Intruder-Based Radionuclide Disposal Limits for East Slit Trenches – Resident and Post-drilling Scenarios for 1000 Years

Radionuclide	Closure Inventory (Ci)	Resident Fraction of Limit	Post-drilling Fraction of Limit
Ac-227	1.0E-03	3.2E-11	2.4E-07
Ag-108m	3.2E-09	8.8E-11	1.4E-12
Al-26	1.0E-03	2.6E-04	6.3E-07
Am-241	5.3E-01	8.6E-07	3.8E-04
Am-242m	3.5E-01	2.2E-06	2.6E-04
Am-243	4.3E-02	1.1E-04	3.8E-05
Ar-39	1.0E-03	0.0E+00	2.8E-11
Ba-133	8.3E-06	1.9E-15	1.0E-12
Bi-207	1.0E-03	1.0E-08	4.3E-08
Bk-249	1.0E-03	7.0E-09	2.0E-09
C-14	3.0E-02	0.0E+00	1.5E-05
C-14_NR.Pump	8.2E-02	0.0E+00	4.1E-05
Cd-113m	2.2E-09	0.0E+00	7.5E-14
Cf-249	8.3E-02	2.3E-04	6.6E-05
Cf-250	3.6E-02	9.6E-16	1.4E-07
Cf-251	7.5E-02	5.5E-05	6.5E-05
Cf-252	5.1E-03	6.8E-15	9.5E-11
Cl-36	1.1E-05	0.0E+00	4.2E-07
Cm-242	1.7E-04	6.2E-14	2.4E-10
Cm-243	1.0E-03	2.6E-11	4.8E-08
Cm-244	3.2E+00	7.4E-12	3.2E-05
Cm-245	1.1E-03	4.6E-07	1.4E-06
Cm-246	4.1E-04	4.0E-15	2.8E-07
Cm-247	1.1E-03	1.4E-05	8.5E-07
Cm-248	6.1E-05	1.1E-11	1.5E-07
Co-60	1.3E+05	6.3E-05	1.5E-04
Cs-134	1.9E-01	1.3E-20	3.9E-19
Cs-135	7.1E-08	0.0E+00	2.9E-12
Cs-137	2.8E+01	1.3E-05	1.2E-03
Eu-152	7.1E-02	3.1E-08	1.1E-07
Eu-154	2.2E+01	5.5E-07	2.0E-06
Eu-155	9.3E-01	2.3E-19	4.0E-12
H-3	1.2E+00	0.0E+00	5.8E-07
I-129	5.0E-05	6.8E-15	1.3E-07
I-129 ETF GT73	8.6E-05	1.2E-14	2.3E-07
K-40	1.0E-04	1.5E-06	2.0E-07
Kr-85	2.8E-02	2.8E-13	2.4E-11
Mo-93	1.0E-03	0.0E+00	2.2E-09

Table C- 9. Fraction of Intruder-Based Radionuclide Disposal Limits for East Slit Trenches – Resident and Post-drilling Scenarios for 1000 Years - continued

Radionuclide	Closure Inventory (Ci)	Resident Fraction of Limit	Post-drilling Fraction of Limit
Na-22	7.9E-07	2.9E-22	1.3E-21
Nb-93m	1.6E-01	0.0E+00	1.3E-09
Nb-94	5.0E-04	5.2E-05	1.8E-07
Ni-59	3.6E-02	0.0E+00	8.7E-08
Ni-63	6.5E+00	0.0E+00	2.1E-05
Np-237	8.0E-03	4.8E-05	7.4E-05
Pa-231	1.0E-03	1.2E-05	8.2E-06
Pb-210	4.0E-02	2.8E-13	1.9E-05
Pd-107	1.1E-07	0.0E+00	1.3E-13
Pu-238	2.5E+01	1.8E-06	6.9E-03
Pu-239	1.6E+00	4.3E-07	1.1E-03
Pu-240	4.5E-01	3.8E-10	3.1E-04
Pu-241	8.4E+00	4.5E-07	2.0E-04
Pu-242	1.5E-02	2.2E-11	9.8E-06
Pu-244	5.1E-15	1.2E-16	4.0E-18
Ra-226	3.2E-03	3.5E-04	4.5E-05
Ra-228	1.1E-02	8.1E-11	4.3E-10
Rb-87	8.6E-14	0.0E+00	5.6E-18
Sb-125	7.9E-01	1.6E-17	1.1E-15
Se-79	8.6E-03	0.0E+00	3.6E-07
Sm-151	1.2E-01	0.0E+00	2.0E-08
Sn-121m	5.1E-15	0.0E+00	3.2E-21
Sn-126	1.8E-04	2.1E-05	8.8E-08
Sr-90	1.2E+01	0.0E+00	7.5E-03
Tc-99	7.0E-03	6.7E-12	2.9E-06
Th-228	1.1E-02	1.6E-21	3.1E-21
Th-229	2.2E-04	2.5E-06	4.4E-07
Th-230	3.9E-04	2.1E-05	2.1E-06
Th-232	1.1E-02	2.4E-03	7.1E-05
U-232	3.8E-02	1.2E-05	4.0E-05
U-233	2.0E+00	2.2E-03	9.2E-04
U-234	1.8E+00	4.8E-04	5.3E-04
U-235	3.9E-02	7.8E-05	1.8E-05
U-236	2.6E-02	9.3E-10	6.6E-06
U-238	3.3E+00	3.4E-03	8.2E-04
Zr-93	2.7E-05	0.0E+00	2.9E-11
Sum of Fractions		**9.7E-03**	**2.1E-02**

Table C- 10. Fraction of Intruder-Based Radionuclide Disposal Limits for Center Slit Trenches – Resident and Post-drilling Scenarios for 1000 Years

Radionuclide	Closure Inventory (Ci)	Resident Fraction of Limit	Post-drilling Fraction of Limit
Ac-227	1.0E-03	3.2E-11	2.4E-07
Ag-108m	3.2E-09	8.8E-11	1.4E-12
Al-26	1.0E-03	2.6E-04	6.3E-07
Am-241	5.3E-01	8.6E-07	3.8E-04
Am-242m	3.5E-01	2.2E-06	2.6E-04
Am-243	4.3E-02	1.1E-04	3.8E-05
Ar-39	1.0E-03	0.0E+00	2.8E-11
Ba-133	8.3E-06	1.9E-15	1.0E-12
Bi-207	1.0E-03	1.0E-08	4.3E-08
Bk-249	1.0E-03	7.0E-09	2.0E-09
C-14	1.0E-02	0.0E+00	5.1E-06
C-14_NR.Pump	8.2E-02	0.0E+00	4.1E-05
Ca-41	1.0E-03	0.0E+00	8.4E-08
Cd-113m	2.2E-09	0.0E+00	7.5E-14
Cf-249	8.3E-02	2.3E-04	6.6E-05
Cf-250	3.6E-02	9.6E-16	1.4E-07
Cf-251	7.5E-02	5.5E-05	6.5E-05
Cf-252	5.1E-03	6.8E-15	9.5E-11
Cl-36	1.1E-05	0.0E+00	4.2E-07
Cm-242	1.7E-04	6.2E-14	2.4E-10
Cm-243	1.0E-03	2.6E-11	4.8E-08
Cm-244	3.2E+00	7.4E-12	3.2E-05
Cm-245	1.1E-03	4.6E-07	1.4E-06
Cm-246	4.1E-04	4.0E-15	2.8E-07
Cm-247	1.1E-03	1.4E-05	8.5E-07
Cm-248	6.1E-05	1.1E-11	1.5E-07
Co-60	1.3E+05	6.3E-05	1.5E-04
Cs-134	1.9E-01	1.3E-20	3.9E-19
Cs-135	7.1E-08	0.0E+00	2.9E-12
Cs-137	2.8E+01	1.3E-05	1.2E-03
Eu-152	7.1E-02	3.1E-08	1.1E-07
Eu-154	2.2E+01	5.5E-07	2.0E-06
Eu-155	9.3E-01	2.3E-19	4.0E-12
H-3	1.0E+00	0.0E+00	4.8E-07
H-3 Concrete	3.9E+00	0.0E+00	1.9E-06
H-3 ETF Carbon	2.8E-01	0.0E+00	1.3E-07

Table C- 10. Fraction of Intruder-Based Radionuclide Disposal Limits for Center Slit Trenches – Resident and Post-drilling Scenarios for 1000 Years - continued

Radionuclide	Closure Inventory (Ci)	Resident Fraction of Limit	Post-drilling Fraction of Limit
I-129	3.0E-05	4.1E-15	7.9E-08
I-129 ETF Carbon	1.6E-02	2.2E-12	4.3E-05
I-129 ETF GT73	8.6E-05	1.2E-14	2.3E-07
I-129 F CG8	5.2E-05	7.0E-15	1.3E-07
I-129 F Dowex 21K	4.4E-03	6.0E-13	1.2E-05
I-129 F Filtercake	7.0E-05	9.5E-15	1.8E-07
I-129 H CG8	1.2E-04	1.6E-14	3.1E-07
I-129 H Filtercake	2.8E-07	0.0E+00	7.3E-10
I-129 Mk50A	8.2E-06	0.0E+00	2.1E-08
K-40	1.0E-04	1.5E-06	2.0E-07
Kr-85	2.8E-02	2.8E-13	2.4E-11
Mo-93	1.0E-03	0.0E+00	2.2E-09
Na-22	7.9E-07	2.9E-22	1.3E-21
Nb-93m	1.6E-01	0.0E+00	1.3E-09
Nb-94	5.0E-04	5.2E-05	1.8E-07
Ni-59	3.6E-02	0.0E+00	8.7E-08
Ni-63	6.5E+00	0.0E+00	2.1E-05
Np-237	8.0E-03	4.8E-05	7.4E-05
Pa-231	1.0E-03	1.2E-05	8.2E-06
Pb-210	4.0E-02	2.8E-13	1.9E-05
Pd-107	1.1E-07	0.0E+00	1.3E-13
Pu-238	2.5E+01	1.8E-06	6.9E-03
Pu-239	1.6E+00	4.3E-07	1.1E-03
Pu-240	4.5E-01	3.8E-10	3.1E-04
Pu-241	8.4E+00	4.5E-07	2.0E-04
Pu-242	1.5E-02	2.2E-11	9.8E-06
Pu-244	5.1E-15	1.2E-16	4.0E-18
Ra-226	3.2E-03	3.5E-04	4.5E-05
Ra-226 Cooling Tower	4.0E-02	4.3E-03	5.5E-04
Ra-228	1.1E-02	8.1E-11	4.3E-10
Rb-87	8.6E-14	0.0E+00	5.6E-18
Sb-125	7.9E-01	1.6E-17	1.1E-15
Se-79	8.6E-03	0.0E+00	3.6E-07
Sm-151	1.2E-01	0.0E+00	2.0E-08
Sn-121m	5.1E-15	0.0E+00	3.2E-21
Sn-126	1.8E-04	2.1E-05	8.8E-08
Sr-90	1.2E+01	0.0E+00	7.5E-03
Sr-90 Mk50A	7.4E+00	0.0E+00	4.5E-03

Table C- 10. Fraction of Intruder-Based Radionuclide Disposal Limits for Center Slit Trenches – Resident and Post-drilling Scenarios for 1000 Years - continued

Radionuclide	Closure Inventory (Ci)	Resident Fraction of Limit	Post-drilling Fraction of Limit
Tc-99	5.0E-02	4.8E-11	2.1E-05
Tc-99 MK50A	1.8E-03	1.7E-12	7.3E-07
Th-228	1.1E-02	1.6E-21	3.1E-21
Th-229	2.2E-04	2.5E-06	4.4E-07
Th-230	3.9E-04	2.1E-05	2.1E-06
Th-230 Cooling Tower	4.0E-02	2.1E-03	2.1E-04
Th-232	1.1E-02	2.4E-03	7.1E-05
U-232	3.8E-02	1.2E-05	4.0E-05
U-233	2.0E+00	2.2E-03	9.2E-04
U-234	1.8E+00	4.8E-04	5.3E-04
U-234 M Glass	2.8E+00	7.3E-04	8.1E-04
U-235	3.9E-02	7.8E-05	1.8E-05
U-235 M Glass	1.9E-01	3.7E-04	8.4E-05
U-235 Paducah Cask	3.9E-01	7.7E-04	1.8E-04
U-236	2.6E-02	9.3E-10	6.6E-06
U-236 M Glass	1.4E-01	5.1E-09	3.6E-05
U-238	3.3E+00	3.4E-03	8.2E-04
U-238 M Glass	1.1E+01	1.1E-02	2.6E-03
Zr-93	2.7E-05	0.0E+00	2.8E-11
Sum of Fractions		**2.9E-02**	**3.0E-02**

Table C- 11. Fraction of Intruder-Based Radionuclide Disposal Limits for West Slit Trenches – Resident and Post-drilling Scenarios for 1000 Years

Radionuclide	Closure Inventory (Ci)	Resident Fraction of Limit	Post-drilling Fraction of Limit
Ac-227	1.0E-03	3.2E-11	2.4E-07
Ag-108m	1.0E-09	2.7E-11	4.4E-13
Al-26	1.0E-03	2.6E-04	6.3E-07
Am-241	4.8E-01	7.8E-07	3.5E-04
Am-242m	1.8E+00	1.1E-05	1.3E-03
Am-243	2.1E-01	5.4E-04	1.9E-04
Ar-39	1.0E-03	0.0E+00	2.8E-11
Ba-133	1.0E-06	2.3E-16	1.2E-13
Bi-207	1.0E-03	1.0E-08	4.3E-08
C-14	1.8E-02	0.0E+00	9.3E-06
C-14_NR.Pump	1.0E-03	0.0E+00	5.0E-07
Ca-41	1.0E-03	0.0E+00	8.4E-08
Cd-113m	1.0E-13	0.0E+00	3.4E-18
Cf-249	4.2E-01	1.1E-03	3.3E-04
Cf-250	4.1E-02	1.1E-15	1.6E-07
Cf-251	3.8E-01	2.8E-04	3.3E-04
Cf-252	5.7E-03	7.6E-15	1.1E-10
Cl-36	1.0E-06	0.0E+00	4.0E-08
Cm-242	1.0E-04	3.8E-14	1.4E-10
Cm-243	7.9E-03	1.9E-10	3.6E-07
Cm-244	1.5E+01	3.5E-11	1.5E-04
Cm-245	7.3E-03	3.1E-06	9.5E-06
Cm-246	9.6E-06	9.3E-17	6.5E-09
Cm-247	1.6E-02	2.0E-04	1.3E-05
Cm-248	3.0E-05	5.4E-12	7.6E-08
Co-60	1.7E-02	8.6E-12	2.1E-11
Cs-134	1.0E-02	6.7E-22	2.1E-20
Cs-135	1.0E-14	0.0E+00	4.1E-19
Cs-137	5.5E+00	2.6E-06	2.3E-04
Eu-152	1.1E-05	5.0E-12	1.7E-11
Eu-154	1.2E+01	3.0E-07	1.1E-06
Eu-155	1.0E+00	2.6E-19	4.4E-12
H-3	5.5E-01	0.0E+00	2.7E-07
I-129	1.3E-04	1.8E-14	3.4E-07
K-40	1.0E-04	1.5E-06	2.0E-07
Kr-85	1.0E-02	1.0E-13	8.6E-12
Mo-93	1.0E-03	0.0E+00	2.1E-09

Table C- 11. Fraction of Intruder-Based Radionuclide Disposal Limits for West Slit Trenches – Resident and Post-drilling Scenarios for 1000 Years - continued

Radionuclide	Closure Inventory (Ci)	Resident Fraction of Limit	Post-drilling Fraction of Limit
Na-22	1.0E-07	3.7E-23	1.7E-22
Nb-93m	1.0E-02	0.0E+00	8.0E-11
Nb-94	1.0E-04	1.0E-05	3.7E-08
Ni-59	5.1E-05	0.0E+00	1.2E-10
Ni-63	5.1E-08	0.0E+00	1.7E-13
Np-237	4.6E-04	2.8E-06	4.2E-06
Pa-231	1.0E-03	1.2E-05	8.2E-06
Pb-210	1.0E-04	7.1E-16	4.7E-08
Pd-107	1.0E-07	0.0E+00	1.1E-13
Pu-238	9.9E+00	7.4E-07	2.8E-03
Pu-239	3.1E+00	8.2E-07	2.1E-03
Pu-240	9.3E-01	7.7E-10	6.3E-04
Pu-241	9.4E+00	5.1E-07	2.3E-04
Pu-242	5.9E-01	8.5E-10	3.8E-04
Pu-244	1.0E-15	2.3E-17	7.9E-19
Ra-226	1.0E-04	1.1E-05	1.4E-06
Ra-228	1.0E-05	7.6E-14	4.0E-13
Rb-87	1.0E-14	0.0E+00	6.5E-19
Sb-125	2.9E-03	5.9E-20	4.0E-18
Se-79	4.1E-05	0.0E+00	1.8E-09
Sm-151	2.4E-07	0.0E+00	4.0E-14
Sn-121m	1.0E-15	0.0E+00	6.2E-22
Sn-126	6.0E-08	6.9E-09	2.9E-11
Sr-90	4.1E+00	0.0E+00	2.5E-03
Tc-99	5.4E-03	5.2E-12	2.2E-06
Th-228	1.0E-03	1.5E-22	2.9E-22
Th-229	1.0E-04	1.1E-06	2.0E-07
Th-230	1.0E-04	5.3E-06	5.2E-07
Th-232	5.7E-08	1.3E-08	3.8E-10
U-232	1.0E-03	3.2E-07	1.1E-06
U-233	8.3E-01	8.9E-04	3.8E-04
U-234	6.2E-01	1.6E-04	1.8E-04
U-235	2.5E-04	5.0E-07	1.1E-07
U-236	1.7E-06	6.3E-14	4.4E-10
U-238	2.9E-01	3.0E-04	7.2E-05
Zr-93	1.0E-06	0.0E+00	1.1E-12
Sum of Fractions		**3.8E-03**	**1.2E-02**

Table C- 12. Fraction of Intruder-Based Radionuclide Disposal Limits for Engineered Trenches – Resident and Post-drilling Scenarios for 1000 Years

Radionuclide	Closure Inventory (Ci)	Resident Fraction of Limit	Post-drilling Fraction of Limit
Ac-227	1.0E-03	4.9E-11	2.3E-07
Ag-108m	2.0E-07	8.1E-09	8.2E-11
Al-26	6.5E-11	2.5E-11	3.9E-14
Am-241	3.3E+00	8.1E-06	2.3E-03
Am-242m	3.1E-01	2.9E-06	2.1E-04
Am-243	6.3E-02	2.4E-04	5.3E-05
Ar-39	1.0E-03	0.0E+00	2.7E-11
Ba-133	1.0E-04	3.7E-14	1.2E-11
Bi-207	1.0E-05	1.6E-10	4.2E-10
Bk-249	1.0E-03	1.1E-08	2.0E-09
C-14	1.3E-01	0.0E+00	6.3E-05
Ca-41	1.0E-03	0.0E+00	8.1E-08
Cd-113m	4.3E-11	0.0E+00	1.4E-15
Cf-249	7.1E-02	2.9E-04	5.4E-05
Cf-250	1.8E-04	7.3E-18	6.7E-10
Cf-251	6.4E-02	7.1E-05	5.3E-05
Cf-252	8.6E-04	1.7E-15	1.6E-11
Cl-36	9.1E-05	0.0E+00	3.5E-06
Cm-242	4.1E-05	2.3E-14	5.6E-11
Cm-243	1.0E-03	3.7E-11	4.5E-08
Cm-244	5.3E+00	1.9E-11	5.1E-05
Cm-245	1.3E-03	8.4E-07	1.7E-06
Cm-246	5.9E-04	8.6E-15	3.9E-07
Cm-247	7.0E-04	1.3E-05	5.3E-07
Cm-248	1.0E-14	2.8E-21	2.5E-17
Co-60	1.3E+01	1.0E-08	1.6E-08
Cs-134	5.8E-02	5.9E-21	1.2E-19
Cs-135	1.7E-11	0.0E+00	6.8E-16
Cs-137	4.5E+01	3.2E-05	1.8E-03
Eu-152	3.0E+01	2.0E-05	4.5E-05
Eu-154	1.2E+01	4.5E-07	1.1E-06
Eu-155	4.0E-01	1.5E-19	1.6E-12
H-3	1.5E+00	0.0E+00	7.0E-07
I-129	2.3E-03	4.8E-13	6.0E-06
K-40	1.7E-04	3.9E-06	3.2E-07
Kr-85	5.0E-02	7.7E-13	4.2E-11
Mo-93	2.7E-03	0.0E+00	5.5E-09

Table C- 12. Fraction of Intruder-Based Radionuclide Disposal Limits for Engineered Trenches – Resident and Post-drilling Scenarios for 1000 Years - continued

Radionuclide	Closure Inventory (Ci)	Resident Fraction of Limit	Post-drilling Fraction of Limit
Na-22	5.2E-06	2.9E-21	8.4E-21
Nb-93m	7.9E-02	0.0E+00	6.1E-10
Nb-94	2.8E-03	4.4E-04	9.8E-07
Ni-59	9.2E-02	0.0E+00	2.1E-07
Ni-63	8.6E+00	0.0E+00	2.7E-05
Np-237	1.3E-02	1.1E-04	1.1E-04
Pa-231	1.0E-03	1.9E-05	7.9E-06
Pb-210	4.7E-03	5.0E-14	2.1E-06
Pd-107	1.0E-03	0.0E+00	1.1E-09
Pu-238	5.6E+00	6.3E-07	1.5E-03
Pu-239	1.7E+01	6.7E-06	1.1E-02
Pu-240	3.6E+00	4.6E-09	2.4E-03
Pu-241	9.9E+00	8.1E-07	2.3E-04
Pu-242	1.0E-01	2.3E-10	6.5E-05
Pu-244	5.2E-15	1.8E-16	3.9E-18
Ra-226	5.2E-03	8.6E-04	7.0E-05
Ra-228	5.3E-03	6.1E-11	2.1E-10
Rb-87	1.0E-14	0.0E+00	6.3E-19
Sb-125	1.3E-01	3.8E-18	1.6E-16
Se-79	9.8E-03	0.0E+00	4.0E-07
Sm-151	4.3E-05	0.0E+00	6.9E-12
Sn-121m	7.9E-06	0.0E+00	4.7E-12
Sn-126	6.5E-05	1.1E-05	3.0E-08
Sr-90	7.2E+01	0.0E+00	4.2E-02
Tc-99	1.0E-01	1.4E-10	4.0E-05
Th-228	3.7E-02	8.4E-21	1.0E-20
Th-229	5.9E-03	1.0E-04	1.1E-05
Th-230	8.6E-03	6.9E-04	4.3E-05
Th-232	5.5E-03	1.9E-03	3.6E-05
U-232	3.1E-02	1.5E-05	3.2E-05
U-233	2.3E+00	3.8E-03	1.0E-03
U-234	5.2E-01	2.1E-04	1.5E-04
U-235	1.7E-02	5.2E-05	7.6E-06
U-236	3.3E-02	1.8E-09	8.0E-06
U-238	4.4E-01	6.8E-04	1.1E-04
Zr-93	2.2E-05	0.0E+00	2.2E-11
Sum of Fractions		**9.5E-03**	**6.4E-02**

Table C- 13. Fraction of East Slit Trench Air Pathway Disposal Limits

Radionuclide	Closure Inventory (Ci)	Fraction of Limit
C-14	3.0E-02	1.0E-07
C-14_NR.Pump	8.2E-02	2.8E-07
Cl-36	1.1E-05	7.0E-11
H-3	1.2E+00	1.1E-07
I-129	1.4E-04	1.4E-07
I-129 ETF GT73	8.6E-05	9.1E-08
S-35	3.0E-03	6.6E-10
Sb-125	7.9E-01	1.2E-04
Se-79	8.6E-03	1.6E-07
Sn-121m	5.1E-15	8.8E-20
Sn-126	1.8E-04	1.4E-06
Sum of Fractions		**1.2E-04**

Table C- 14. Fraction of Center Slit Trench Air Pathway Disposal Limits

Radionuclide	Closure Inventory (Ci)	Fraction of Limit
C-14	1.0E-02	3.4E-08
C-14_NR.Pump	8.2E-02	2.8E-07
Cl-36	1.1E-05	7.0E-11
H-3	3.9E+00	3.5E-07
H-3 Concrete	2.8E-01	2.5E-08
H-3 ETF Carbon	3.0E-05	3.2E-08
I-129	3.0E-05	3.2E-08
I-129 ETF Carbon	1.6E-02	1.7E-05
I-129 ETF GT73	8.6E-05	9.1E-08
I-129 F CG8	5.2E-05	5.4E-08
I-129 F Dowex 21K	4.4E-03	4.6E-06
I-129 F Filtercake	7.0E-05	7.4E-08
I-129 H CG8	1.2E-04	1.2E-07
I-129 H Filtercake	2.8E-07	2.9E-10
I-129 Mk50A	8.2E-06	8.6E-09
S-35	3.0E-03	6.6E-10
Sb-125	7.9E-01	1.2E-04
Se-79	8.6E-03	1.6E-07
Sn-121m	5.1E-15	8.8E-20
Sn-126	1.8E-04	1.4E-06
Sum of Fractions		**1.4E-04**

Table C- 15. Fraction of West Slit Trench Air Pathway Disposal Limits

Radionuclide	Closure Inventory (Ci)	Fraction of Limit
C-14	1.8E-02	6.3E-08
C-14_NR.Pump	1.0E-03	3.4E-09
Cl-36	1.0E-06	6.7E-12
H-3	5.5E-01	5.0E-08
I-129	1.3E-04	1.4E-07
S-35	1.0E-03	2.2E-10
Sb-125	2.9E-03	4.4E-07
Se-79	4.1E-05	7.5E-10
Sn-121m	1.0E-15	1.7E-20
Sn-126	6.0E-08	4.6E-10
Sum of Fractions		**7.0E-07**

Table C- 16. Fraction of Engineered Trench Air Pathway Disposal Limits

Radionuclide	Closure Inventory (Ci)	Fraction of Limit
C-14	1.3E-01	4.5E-07
Cl-36	9.1E-05	6.1E-10
H-3	1.5E+00	1.4E-07
I-129	7.0E-05	7.4E-08
I-129 ETF GT73	7.4E-07	7.8E-10
I-129 F CG8	1.6E-06	1.6E-09
I-129 F Dowex 21K	1.3E-03	1.4E-06
I-129 F Filtercake	3.6E-05	3.8E-08
I-129 H CG8	9.6E-06	1.0E-08
I-129 H Dowex 21K	9.0E-04	9.5E-07
S-35	4.7E-21	1.0E-27
Sb-125	1.3E-01	1.9E-05
Se-79	9.8E-03	1.8E-07
Sn-121m	7.9E-06	1.4E-10
Sn-126	6.5E-05	5.0E-07
Sum of Fractions		**2.3E-05**

Table C- 17. East Slit Trenches Disposal Limits for Radon Parent Radionuclides

Radionuclide	Closure Inventory (Ci)	Fraction of Limit
Pu-238	2.5E+01	3.2E-12
Ra-226	3.2E-03	1.4E-07
Th-230	3.9E-04	9.4E-10
U-234	1.8E+00	2.5E-09
U-238	3.3E+00	5.4E-13
Sum of Fractions		**1.5E-07**

Table C- 18. Center Slit Trenches Disposal Limits for Radon Parent Radionuclides

Radionuclide	Closure Inventory (Ci)	Fraction of Limit
Pu-238	2.5E+01	3.2E-12
Ra-226	3.2E-03	1.4E-07
Ra-226 Cooling Tower	4.0E-02	1.8E-06
Th-230	3.9E-04	9.4E-10
U-234	1.8E+00	2.5E-09
U-234 M Glass	2.8E+00	3.9E-09
U-238	3.3E+00	5.4E-13
U-238 M Glass	1.1E+01	1.7E-12
Sum of Fractions		**1.9E-06**

Table C- 19. West Slit Trenches Disposal Limits for Radon Parent Radionuclides

Radionuclide	Closure Inventory (Ci)	Fraction of Limit
Pu-238	9.9E+00	1.3E-12
Ra-226	1.0E-04	4.5E-09
Th-230	1.0E-04	2.4E-10
U-234	6.2E-01	8.5E-10
U-238	2.9E-01	4.7E-14
Sum of Fractions		**5.6E-09**

Table C- 20. Engineered Trench Disposal Limits for Radon Parent Radionuclides

Radionuclide	Closure Inventory (Ci)	Fraction of Limit
Pu-238	5.6E+00	4.9E-13
Ra-226	5.2E-03	1.6E-07
Th-230	8.6E-03	1.4E-08
U-234	5.2E-01	4.8E-10
U-238	4.4E-01	4.8E-14
Sum of Fractions		**1.7E-07**

COMPONENTS IN GROUT TRENCHES

Table C- 21. Components in Grout Fraction of Limits for Years 0-125

Radionuclide	Closure Inventory (Ci)	Fraction of Beta-Gamma Limit	Fraction of Gross Alpha Limit	Fraction of Radium Limit	Fraction of Uranium Limit	Fraction of All Pathways Limit	Fraction of Resident Intruder Limit	Fraction of Post-drilling Intruder Limit	Fraction of Air Limit	Fraction of Radon Limit
Am-241	2.4E-01	0.0E+00	0.0E+00	0.0E+00	0.0E+00	0.0E+00	1.1E-05	1.6E-04	0.0E+00	0.0E+00
Am-243	2.5E-03	0.0E+00	0.0E+00	0.0E+00	0.0E+00	0.0E+00	3.6E-05	2.8E-06	0.0E+00	0.0E+00
C-14	1.1E-01	3.8E-11	0.0E+00	0.0E+00	0.0E+00	0.0E+00	0.0E+00	6.8E-05	6.4E-08	0.0E+00
C-14_K	2.3E-01	6.2E-12	0.0E+00	0.0E+00	0.0E+00	0.0E+00	0.0E+00	0.0E+00	1.4E-07	0.0E+00
Cl-36	1.0E-03	1.6E-08	0.0E+00	0.0E+00	0.0E+00	0.0E+00	0.0E+00	5.0E-05	1.0E-09	0.0E+00
Cm-244	6.6E-01	0.0E+00	0.0E+00	0.0E+00	0.0E+00	0.0E+00	1.8E-10	1.5E-06	0.0E+00	0.0E+00
Cm-245	5.1E-05	0.0E+00	0.0E+00	0.0E+00	0.0E+00	0.0E+00	1.9E-07	8.6E-08	0.0E+00	0.0E+00
Cm-247	2.9E-04	0.0E+00	0.0E+00	0.0E+00	0.0E+00	0.0E+00	1.6E-05	2.9E-07	0.0E+00	0.0E+00
Cm-248	2.9E-04	0.0E+00	0.0E+00	0.0E+00	0.0E+00	0.0E+00	1.8E-10	9.4E-07	0.0E+00	0.0E+00
H-3	1.1E+04	7.6E-02	0.0E+00	0.0E+00	0.0E+00	0.0E+00	0.0E+00	8.2E-08	3.4E-04	0.0E+00
I-129	2.7E-05	1.0E-09	0.0E+00	0.0E+00	0.0E+00	0.0E+00	1.0E-09	4.1E-06	7.3E-06	0.0E+00
I-129_K	1.2E-03	5.8E-11	0.0E+00	0.0E+00	0.0E+00	0.0E+00	0.0E+00	0.0E+00	7.1E-06	0.0E+00
K-40	4.5E-09	0.0E+00	0.0E+00	0.0E+00	0.0E+00	0.0E+00	1.7E-10	1.1E-11	0.0E+00	0.0E+00
Mo-93	1.0E-03	2.2E-06	0.0E+00	0.0E+00	0.0E+00	0.0E+00	0.0E+00	0.0E+00	0.0E+00	0.0E+00
Nb-94	4.6E-04	1.3E-22	0.0E+00	0.0E+00	0.0E+00	0.0E+00	1.5E-04	2.1E-07	0.0E+00	0.0E+00
Ni-59	5.8E-03	0.0E+00	0.0E+00	0.0E+00	0.0E+00	0.0E+00	0.0E+00	1.8E-08	0.0E+00	0.0E+00
Np-237	4.2E-03	0.0E+00	0.0E+00	0.0E+00	0.0E+00	0.0E+00	1.2E-04	4.8E-05	0.0E+00	0.0E+00
Pd-107	2.3E-05	0.0E+00	0.0E+00	0.0E+00	0.0E+00	0.0E+00	0.0E+00	3.3E-11	0.0E+00	0.0E+00
Pu-238	7.6E-01	0.0E+00	0.0E+00	0.0E+00	0.0E+00	0.0E+00	1.5E-07	5.4E-05	0.0E+00	1.7E-15
Pu-239	1.0E+00	0.0E+00	0.0E+00	0.0E+00	0.0E+00	0.0E+00	2.9E-06	8.6E-04	0.0E+00	0.0E+00
Pu-240	9.8E-02	0.0E+00	0.0E+00	0.0E+00	0.0E+00	0.0E+00	9.8E-09	8.2E-05	0.0E+00	0.0E+00
Pu-241	3.1E+00	0.0E+00	0.0E+00	0.0E+00	0.0E+00	0.0E+00	4.7E-06	7.0E-05	0.0E+00	0.0E+00
Pu-242	4.5E-04	0.0E+00	0.0E+00	0.0E+00	0.0E+00	0.0E+00	5.3E-11	3.8E-07	0.0E+00	0.0E+00
Pu-244	1.0E-15	0.0E+00	0.0E+00	0.0E+00	0.0E+00	0.0E+00	6.7E-17	1.0E-18	0.0E+00	0.0E+00
Ra-226	2.6E-11	0.0E+00	0.0E+00	0.0E+00	0.0E+00	0.0E+00	7.5E-12	4.4E-13	0.0E+00	2.0E-17
Se-79	1.3E-03	0.0E+00	0.0E+00	0.0E+00	0.0E+00	0.0E+00	0.0E+00	6.8E-08	3.4E-09	0.0E+00
Sn-126	1.4E-04	0.0E+00	0.0E+00	0.0E+00	0.0E+00	0.0E+00	5.8E-05	9.0E-08	1.8E-07	0.0E+00
Sr-90	3.0E+01	0.0E+00	0.0E+00	0.0E+00	0.0E+00	0.0E+00	0.0E+00	1.9E-04	0.0E+00	0.0E+00

Table C- 21. Components in Grout Fraction of Limits for Years 0-125 – continued

Radionuclide	Closure Inventory (Ci)	Fraction of Beta-Gamma Limit	Fraction of Gross Alpha Limit	Fraction of Radium Limit	Fraction of Uranium Limit	Fraction of All Pathways Limit	Fraction of Resident Intruder Limit	Fraction of Post-drilling Intruder Limit	Fraction of Air Limit	Fraction of Radon Limit
Tc-99	1.3E-02	6.1E-06	0.0E+00	0.0E+00	0.0E+00	0.0E+00	7.7E-10	2.7E-05	0.0E+00	0.0E+00
Tc-99_K	3.8E-02	1.0E-08	0.0E+00	0.0E+00	0.0E+00	0.0E+00	0.0E+00	0.0E+00	0.0E+00	0.0E+00
Th-230	1.0E-04	0.0E+00	0.0E+00	0.0E+00	0.0E+00	0.0E+00	1.4E-05	6.7E-07	0.0E+00	4.0E-12
Th-232	1.0E-03	0.0E+00	0.0E+00	0.0E+00	0.0E+00	0.0E+00	5.6E-04	8.3E-06	0.0E+00	0.0E+00
U-233	8.4E-01	0.0E+00	0.0E+00	0.0E+00	0.0E+00	0.0E+00	3.2E-03	5.0E-04	0.0E+00	0.0E+00
U-234	1.3E-01	0.0E+00	0.0E+00	0.0E+00	0.0E+00	0.0E+00	9.3E-05	4.8E-05	0.0E+00	3.0E-12
U-235	3.2E-03	0.0E+00	0.0E+00	0.0E+00	0.0E+00	0.0E+00	4.5E-05	1.9E-06	0.0E+00	0.0E+00
U-236	3.3E-03	0.0E+00	0.0E+00	0.0E+00	0.0E+00	0.0E+00	3.0E-09	1.1E-06	0.0E+00	0.0E+00
U-238	4.7E-01	0.0E+00	0.0E+00	0.0E+00	0.0E+00	0.0E+00	1.5E-03	0.0E+00	0.0E+00	1.3E-15
Zr-93	3.4E-03	1.0E-21	0.0E+00	0.0E+00	0.0E+00	0.0E+00	0.0E+00	0.0E+00	0.0E+00	0.0E+00
Sum of Fractions		**7.6E-02**	**0.0E+00**	**0.0E+00**	**0.0E+00**	**0.0E+00**	**5.9E-03**	**2.2E-03**	**3.6E-04**	**7.0E-12**

Table C- 22. Components in Grout Fraction of Limits for Years 125-1125

Radionuclide	Closure Inventory (Ci)	Fraction of Beta-Gamma Limit	Fraction of Gross Alpha Limit	Fraction of Radium Limit	Fraction of Uranium Limit	Fraction of All Pathways Limit	Fraction of Resident Intruder Limit	Fraction of Post-Drilling Intruder Limit	Fraction of Air Limit	Fraction of Radon Limit
Am-241	2.4E-01	3.6E-05	7.3E-04	0.0E+00	2.8E-13	2.4E-03	1.1E-05	1.6E-04	0.0E+00	0.0E+00
Am-243	2.5E-03	2.0E-08	4.0E-07	0.0E+00	7.1E-19	1.1E-06	3.6E-05	2.8E-06	0.0E+00	0.0E+00
C-14	1.1E-01	3.4E-01	0.0E+00	0.0E+00	0.0E+00	3.2E-01	0.0E+00	6.8E-05	6.4E-08	0.0E+00
C-14_K	2.3E-01	7.6E-02	0.0E+00	0.0E+00	0.0E+00	7.2E-02	0.0E+00	1.4E-04	1.4E-07	0.0E+00
Cl-36	1.0E-03	1.2E-02	0.0E+00	0.0E+00	0.0E+00	2.1E-02	0.0E+00	5.0E-05	1.0E-09	0.0E+00
Cm-244	6.6E-01	0.0E+00	0.0E+00	0.0E+00	0.0E+00	0.0E+00	1.8E-10	1.5E-06	0.0E+00	0.0E+00
Cm-245	5.1E-05	1.1E-08	2.2E-07	0.0E+00	8.1E-17	7.2E-07	1.9E-07	8.6E-08	0.0E+00	0.0E+00
Cm-247	2.9E-04	3.1E-10	5.7E-08	0.0E+00	8.8E-21	1.5E-07	1.6E-05	2.9E-07	0.0E+00	0.0E+00
Cm-248	2.9E-04	1.0E-16	4.8E-08	0.0E+00	0.0E+00	5.2E-07	1.8E-10	9.4E-07	0.0E+00	0.0E+00
H-3	1.1E+04	1.1E-01	0.0E+00	0.0E+00	0.0E+00	4.4E-04	0.0E+00	8.2E-08	3.4E-04	0.0E+00
I-129	2.7E-05	2.9E-01	0.0E+00	0.0E+00	0.0E+00	5.1E-03	2.3E-11	9.0E-08	7.3E-06	0.0E+00
I-129_K	1.2E-03	3.7E-02	0.0E+00	0.0E+00	0.0E+00	6.1E-04	1.0E-09	4.0E-06	7.1E-06	0.0E+00
K-40	4.5E-09	1.1E-16	0.0E+00	0.0E+00	0.0E+00	5.3E-17	1.7E-10	1.1E-11	0.0E+00	0.0E+00
Mo-93	1.0E-03	4.1E-03	0.0E+00	0.0E+00	0.0E+00	8.5E-04	0.0E+00	2.6E-09	0.0E+00	0.0E+00
Nb-94	4.6E-04	8.0E-05	0.0E+00	0.0E+00	0.0E+00	1.4E-04	1.5E-04	2.1E-07	0.0E+00	0.0E+00
Ni-59	5.8E-03	1.1E-03	0.0E+00	0.0E+00	0.0E+00	4.6E-06	0.0E+00	1.8E-08	0.0E+00	0.0E+00
Np-237	4.2E-03	2.9E-03	5.9E-02	0.0E+00	2.2E-11	1.9E-01	1.2E-04	4.8E-05	0.0E+00	0.0E+00
Pd-107	2.3E-05	3.7E-08	0.0E+00	0.0E+00	0.0E+00	1.2E-08	0.0E+00	3.3E-11	0.0E+00	0.0E+00
Pu-238	7.6E-01	3.4E-07	2.8E-05	2.1E-05	0.0E+00	7.4E-06	1.5E-07	5.4E-05	0.0E+00	1.7E-15
Pu-239	1.0E+00	3.1E-07	4.2E-07	0.0E+00	0.0E+00	3.3E-06	2.9E-06	8.6E-04	0.0E+00	0.0E+00
Pu-240	9.8E-02	0.0E+00	5.1E-20	0.0E+00	0.0E+00	1.3E-19	9.8E-09	8.2E-05	0.0E+00	0.0E+00
Pu-241	3.1E+00	1.6E-05	3.1E-04	0.0E+00	1.2E-13	1.0E-03	4.7E-06	7.0E-05	0.0E+00	0.0E+00
Pu-242	4.5E-04	2.4E-17	2.1E-15	1.6E-15	0.0E+00	5.5E-16	5.3E-11	3.8E-07	0.0E+00	0.0E+00
Pu-244	1.0E-15	0.0E+00	6.2E-34	0.0E+00	0.0E+00	1.5E-33	6.7E-17	1.0E-18	0.0E+00	0.0E+00
Ra-226	2.6E-11	2.7E-11	2.1E-09	1.5E-09	0.0E+00	5.4E-10	7.5E-12	4.4E-13	0.0E+00	2.0E-17
Se-79	1.3E-03	0.0E+00	0.0E+00	0.0E+00	0.0E+00	0.0E+00	0.0E+00	6.8E-08	3.4E-09	0.0E+00
Sn-126	1.4E-04	0.0E+00	0.0E+00	0.0E+00	0.0E+00	0.0E+00	5.8E-05	9.0E-08	1.8E-07	0.0E+00
Sr-90	3.0E+01	3.2E-03	0.0E+00	0.0E+00	0.0E+00	1.6E-04	0.0E+00	1.9E-04	0.0E+00	0.0E+00

Table C- 22. Components in Grout Fraction of Limits for Years 125-1125 – continued

Radionuclide	Closure Inventory (Ci)	Fraction of Beta-Gamma Limit	Fraction of Gross Alpha Limit	Fraction of Radium Limit	Fraction of Uranium Limit	Fraction of All Pathways Limit	Fraction of Resident Intruder Limit	Fraction of Post-Drilling Intruder Limit	Fraction of Air Limit	Fraction of Radon Limit
Tc-99	1.3E-02	4.6E-02	0.0E+00	0.0E+00	0.0E+00	3.0E-02	2.0E-10	6.8E-06	0.0E+00	0.0E+00
Tc-99_K	3.8E-02	4.5E-03	0.0E+00	0.0E+00	0.0E+00	2.9E-03	5.7E-10	2.0E-05	0.0E+00	0.0E+00
Th-230	1.0E-04	3.7E-05	2.8E-03	2.1E-03	0.0E+00	7.3E-04	1.4E-05	6.7E-07	0.0E+00	4.0E-12
Th-232	1.0E-03	1.7E-11	1.6E-11	1.2E-11	0.0E+00	6.2E-12	5.6E-04	8.3E-06	0.0E+00	0.0E+00
U-233	8.4E-01	0.0E+00	0.0E+00	0.0E+00	0.0E+00	0.0E+00	3.2E-03	5.0E-04	0.0E+00	0.0E+00
U-234	1.3E-01	2.1E-04	1.7E-02	1.3E-02	0.0E+00	4.5E-03	9.3E-05	4.8E-05	0.0E+00	3.0E-12
U-235	3.2E-03	1.3E-03	1.7E-03	0.0E+00	0.0E+00	1.4E-02	4.5E-05	1.9E-06	0.0E+00	0.0E+00
U-236	3.3E-03	3.8E-18	3.8E-18	2.8E-18	0.0E+00	1.4E-18	3.0E-09	1.1E-06	0.0E+00	0.0E+00
U-238	4.7E-01	6.8E-07	5.8E-05	4.4E-05	0.0E+00	1.5E-05	1.5E-03	1.5E-04	0.0E+00	1.3E-15
Zr-93	3.4E-03	2.1E-02	0.0E+00	0.0E+00	0.0E+00	3.7E-03	0.0E+00	4.5E-09	0.0E+00	0.0E+00
Sum of Fractions		**9.6E-01**	**8.1E-02**	**1.5E-02**	**2.2E-11**	**6.7E-01**	**5.9E-03**	**2.5E-03**	**3.6E-04**	**7.0E-12**

This page intentionally left blank.

LOW ACTIVITY WASTE VAULT

Table C- 23. LAWV Fraction of Limits

Radionuclide	Closure Inventory (Ci)	Beta-Gamma Fraction	Gross Alpha Fraction	Radium Fraction	Uranium Fraction	All-Pathways Fraction	Resident Intruder Fraction	Air Fraction	Radon Fraction
Am-241	3.3E+00	4.6E-10	9.1E-09		5.0E-19	2.9E-08	8.2E-08		
Am-242m	2.4E-02						2.5E-07		
Am-243	8.9E-03	6.1E-19	1.1E-18			8.9E-18	4.5E-07		
Ba-133	3.3E-01						1.5E-07		
C-14	1.5E+00	3.5E-01				3.4E-01		4.4E-04	
Cf-249	7.3E-05						2.3E-08		
Cf-250	4.8E-03						2.5E-16		
Cf-251	3.0E-04						4.7E-09		
Cf-252	2.9E-02						3.1E-15		
Cl-36	4.0E-03	3.3E-03				6.2E-03		2.0E-06	
Cm-242	2.8E-04						1.3E-14		
Cm-243	2.8E-04						8.5E-10		
Cm-244	5.5E+00						2.6E-15		
Cm-245	1.1E-02	2.3E-12	4.6E-11		2.3E-21	1.5E-10	3.4E-08		
Cm-246	2.0E-02						2.3E-16		
Cm-247	4.1E-11	1.4E-28	2.5E-28			2.0E-27	1.7E-14		
Cm-248	1.3E-11						1.9E-19		
Co-60	1.7E+01						7.8E-07		
Cs-134	1.3E+01						2.3E-16		
Cs-137	3.5E+02						6.6E-02		
Eu-152	1.2E+01						5.9E-04		
Eu-154	1.0E+01						3.0E-05		
Eu-155	6.9E-02						1.2E-14		
H-3	2.1E+07	7.2E-02				8.2E-04		1.9E-01	

Table C- 23. LAWV Fraction of Limits - continued

Radionuclide	Closure Inventory (Ci)	Beta-Gamma Fraction	Gross Alpha Fraction	Radium Fraction	Uranium Fraction	All-Pathways Fraction	Resident Intruder Fraction	Air Fraction	Radon Fraction
I-129	1.1E-03	4.9E-01				8.1E-03	1.1E-22	6.4E-05	
I-129_H	1.7E-04					5.2E-05	1.8E-23	9.9E-06	
I-129_J	1.5E-04					2.6E-04	1.6E-23	8.9E-06	
K-40	2.9E-05						5.2E-08		
Kr-85	1.1E+01						8.4E-08		
Na-22	3.3E-06						1.5E-19		
Nb-94	4.5E-02	2.0E-03				3.5E-03	3.4E-04		
Ni-59	1.5E-01	2.2E-11				8.8E-14			
Np-237	2.1E-01	1.9E-08	3.7E-07		1.9E-17	1.2E-06	3.3E-05		
Pu-238	2.0E+01	4.6E-14	6.3E-12	4.7E-12		1.6E-12	1.8E-07		2.4E-10
Pu-239	8.7E+00	1.4E-14	2.5E-14			2.0E-13	9.0E-09		
Pu-240	2.4E+00						7.3E-14		
Pu-241	8.0E+01	3.8E-10	7.6E-09			2.4E-08	6.6E-08		
Pu-242	1.4E-02						1.9E-13		
Pu-244	2.2E-15						4.1E-18		
Ra-226	1.3E-06	6.9E-14	9.3E-12	6.9E-12		2.4E-12	2.2E-08		5.2E-07
Ra-228	9.1E-03						2.4E-09		
Sb-125	1.2E+00						1.5E-14	1.3E-02	
Se-79	4.6E-01							6.2E-04	
Sn-113	3.6E-06							1.5E-09	
Sn-126	1.7E-03						1.2E-05	8.5E-04	
Sr-90	1.2E+03	7.4E-13				3.8E-14			
Tc-99	5.2E-01	2.1E-03				1.4E-03	7.4E-13		

Table C- 23. LAWV Fraction of Limits - continued

Radionuclide	Closure Inventory (Ci)	Beta-Gamma Fraction	Gross Alpha Fraction	Radium Fraction	Uranium Fraction	All-Pathways Fraction	Resident Intruder Fraction	Air Fraction	Radon Fraction
Th-228	3.3E-02						1.5E-19		
Th-229	8.7E-04						7.2E-07		
Th-230	3.1E-04	2.4E-12	3.2E-10	2.4E-10		8.2E-11	2.0E-06		1.4E-06
Th-232	1.7E-03						5.6E-05		
U-232	3.9E-02						3.7E-04		
U-233	2.1E+00						1.6E-04		
U-234	1.8E+01	2.1E-10		2.2E-08		7.4E-09	5.5E-04		9.2E-06
U-235	5.9E-01	4.7E-09	8.4E-09			6.7E-08	1.5E-05		
U-236	3.0E-01						4.6E-10		
U-238	4.8E+00	2.0E-14	2.8E-12	2.1E-12		7.1E-13	4.0E-04		5.9E-11
Zr-93	2.8E-05	4.1E-07				6.9E-08			
Sum of Fractions		**9.2E-01**	**4.0E-07**	**2.2E-08**	**2.0E-17**	**3.6E-01**	**6.9E-02**	**2.0E-01**	**1.1E-05**

INTERMEDIATE LEVEL VAULT

Table C- 24. Intermediate Level Vault Fraction of Limits Years 0 - 200

Radionuclide	Closure Inventory (Ci)	Beta-Gamma Fraction of Limit	All Pathways Fraction of Limit	Resident Intruder Fraction of Limit	Air Fraction of Limit	Radon Fraction of Limit
Am-241	1.5E+00			2.8E-09		
Am-242m	2.8E-03			7.9E-09		
Am-243	4.2E-03			1.1E-08		
C-14	3.9E+00	1.4E-16	1.3E-16		1.8E-05	
C-14KB	1.0E+03	2.2E-15	2.1E-15		7.8E-05	
Cf-249	2.2E-06			6.2E-11		
Cf-251	6.8E-06			3.4E-12		
Cm-242	8.1E-05			1.5E-15		
Cm-243	2.9E-02			3.8E-09		
Cm-244	2.4E+00			7.2E-17		
Cm-245	4.2E-05			1.9E-12		
Cm-246	6.7E-05			2.0E-19		
Cm-247	9.5E-10			3.6E-14		
Cm-248	1.2E-14			4.7E-23		
Co-60	2.8E+06			4.4E-02		
Cs-134	3.7E+00			1.4E-17		
Cs-137	9.9E+02			3.3E-02		
Eu-152	1.7E-04			2.6E-09		
Eu-154	9.0E-01			8.2E-07		
Eu-155	6.1E-02			5.6E-17		
H-3*	1.5E+06	2.0E-02	7.7E-04		3.9E-01	
H-3 TPB	2.7E+06	2.2E-02	8.4E-04		2.9E-05	
I-129	4.4E-03	1.4E-13	2.4E-15		4.0E-06	
I-129 ETF	1.6E-01	7.9E-14	1.3E-15		1.4E-04	
I-129KB	6.0E-04	5.5E-08	9.2E-20		5.5E-07	
K-40	3.1E-06			2.2E-09		
Kr-85	8.1E+01			8.1E-08		
Mn-54	1.7E+00					
Nb-94	3.9E+01			6.3E-02		
Np-237	2.0E-02			2.2E-07		
Pb-210	3.1E+00			1.2E-09		
Pu-238	5.8E+00			2.2E-08		2.5E-11
Pu-239	1.5E+00			1.3E-11		
Pu-240	2.5E-01			2.9E-15		
Pu-241	6.1E+00			3.6E-10		
Pu-242	1.3E-02			4.6E-14		
Pu-244	4.6E-02			2.2E-05		

Table C- 24. Intermediate Level Vault Fraction of Limits Years 0 - 200 - continued

Radionuclide	Closure Inventory (Ci)	Beta-Gamma Fraction of Limit	All Pathways Fraction of Limit	Resident Intruder Fraction of Limit	Air Fraction of Limit	Radon Fraction of Limit
Ra-226	3.1E+00			2.2E-02		1.5E-01
Ra-228	7.2E-05			1.0E-11		
Sb-125	4.1E-01			7.2E-16	6.7E-05	
Se-79	4.0E-04				8.2E-09	
Sm-151	0.0E+00					
Sn-113	2.0E-05				1.2E-10	
Sn-126	1.9E-03			2.4E-06	1.5E-05	
Sr-90	1.1E+02	1.4E-13	7.2E-15			
Tc-99	6.7E-01			2.6E-15		
Tc-99 KB	8.2E-02			3.1E-16		
Th-228	5.1E-04			1.4E-21		
Th-229	0.0E+00			0.0E+00		
Th-230	7.3E-05			1.9E-07		4.0E-08
Th-232	2.0E-04			3.3E-06		
U-232	4.3E-04			2.4E-06		
U-233	4.9E-01			1.1E-05		
U-234	9.6E-01			1.3E-05		6.0E-08
U-235	3.4E-02			5.3E-08		
U-236	6.8E-03			5.6E-12		
U-238	2.3E+00			5.1E-05		1.3E-11
Sum of Fractions		**4.2E-02**	**1.6E-03**	**1.6E-01**	**4.0E-01**	**1.5E-01**

*The projected inventory of H-3 at closure was reduced to ensure that the sum-of-fractions of air limits at the SRS boundary across all disposal units is <1.

Table C- 25. Intermediate Level Vault Fraction of Limits Years 200 – 1100

Radionuclide	Closure Inventory (Ci)	Beta-Gamma Fraction of Limit	Gross Alpha Fraction of Limit	Radium Fraction of Limit	Uranium Fraction of Limit	All Pathways Fraction of Limit	Resident Intruder Fraction of Limit	Air Fraction of Limit	Radon Fraction of Limit
Am-241	1.5E+00	8.0E-11	1.6E-09		1.3E-19	5.2E-09	2.8E-09		
Am-243	4.2E-03	4.2E-20	2.0E-18			1.7E-17	1.1E-08		
C-14	3.9E+00	1.3E-02				1.3E-02		1.8E-05	
C-14KB	1.0E+03	1.9E-10				1.8E-10		7.8E-05	
Cf-249	2.2E-06						6.2E-11		
Cf-251	6.8E-06						3.4E-12		
Cm-242	8.1E-05						1.5E-15		
Cm-243	2.9E-02						3.8E-09		
Cm-244	2.4E+00						7.2E-17		
Cm-245	4.2E-05	1.3E-15	2.7E-14		2.1E-24	8.7E-14	1.9E-12		
Cm-246	6.7E-05						2.0E-19		
Cm-247	9.5E-10	1.7E-28	8.4E-27			7.1E-26	3.6E-14		
Cm-248	1.2E-14						4.7E-23		
Co-60	2.8E+06						4.4E-02		
Cs-134	3.7E+00						1.4E-17		
Cs-137	9.9E+02						3.3E-02		
Eu-152	1.7E-04						2.6E-09		
Eu-154	9.0E-01						8.2E-07		
Eu-155	6.1E-02						5.6E-17		
H-3*	1.5E+06	4.8E-06				1.8E-07		3.9E-01	
H-3 TPB	2.7E+06	1.6E-05				6.3E-07		2.9E-05	

Table C- 25. Intermediate Level Vault Fraction of Limits Years 200 – 1100 - continued

Radionuclide	Closure Inventory (Ci)	Beta-Gamma Fraction of Limit	Gross Alpha Fraction of Limit	Radium Fraction of Limit	Uranium Fraction of Limit	All Pathways Fraction of Limit	Resident Intruder Fraction of Limit	Air Fraction of Limit	Radon Fraction of Limit
I-129	4.4E-03	4.0E-01				6.6E-03		4.0E-06	
I-129 ETF	1.6E-01	4.1E-01				6.7E-03		1.4E-04	
I-129KB	6.0E-04	2.6E-04				4.3E-06		5.5E-07	
K-40	3.1E-06	2.6E-19				1.2E-19	2.2E-09		
Kr-85	8.1E+01						8.1E-08		
Nb-94	3.9E+01	3.5E-04				6.1E-04	6.3E-02		
Ni-59	2.8E-01	2.5E-09				1.0E-11			
Np-237	2.0E-02	7.8E-09	1.6E-07		1.3E-17	5.1E-07	2.2E-07		
Pb-210	3.1E+00						1.2E-09		
Pu-238	5.8E+00	5.9E-10	8.1E-08	6.1E-08		2.1E-08	2.2E-08		2.5E-11
Pu-239	1.5E+00	2.0E-15	9.4E-14			7.9E-13	1.3E-11		
Pu-240	2.5E-01						2.9E-15		
Pu-241	6.1E+00	1.0E-11	2.1E-10			6.7E-10	3.6E-10		
Pu-242	1.3E-02	7.7E-20	1.1E-17	8.3E-18		2.8E-18	4.6E-14		
Pu-244	4.6E-02						2.2E-05		
Ra-226	3.1E+00	1.8E-03	2.3E-01	1.7E-01		5.9E-02	2.2E-02		1.5E-01
Ra-228	7.2E-05						1.0E-11		
Sb-125	4.1E-01						7.2E-16		
Se-79	4.0E-04							8.2E-09	
Sn-126	1.9E-03						2.4E-06	1.5E-05	
Sr-90	1.1E+02	1.4E-08				7.4E-10			
Tc-99	6.7E-01	6.4E-08				4.3E-08	2.6E-15		
Tc-99KB	8.2E-02	5.6E-10				3.8E-10			

Table C- 25. Intermediate Level Vault Fraction of Limits Years 200 – 1100 - continued

Radionuclide	Closure Inventory (Ci)	Beta-Gamma Fraction of Limit	Gross Alpha Fraction of Limit	Radium Fraction of Limit	Uranium Fraction of Limit	All Pathways Fraction of Limit	Resident Intruder Fraction of Limit	Air Fraction of Limit	Radon Fraction of Limit
Th-228	5.1E-04						1.4E-21		
Th-230	7.3E-05	1.1E-08	1.5E-06	1.1E-06		3.9E-07	1.9E-07		4.0E-08
Th-232	2.0E-04	1.8E-19	1.8E-19	1.3E-19		6.6E-20	3.3E-06		
U-232	4.3E-04						2.4E-06		
U-233	4.9E-01						1.1E-05		
U-234	9.6E-01	4.1E-07	5.6E-05	4.2E-05		1.4E-05	1.3E-05		6.0E-08
U-235	3.4E-02	1.2E-10	5.5E-09			4.6E-08	5.3E-08		
U-236	6.8E-03						5.6E-12		
U-238	2.3E+00	5.6E-10	7.8E-08	5.9E-08		2.0E-08	5.1E-05		1.3E-11
Zr-93	2.6E-05	1.9E-13				3.2E-14			
Sum of Fractions		**8.2E-01**	**2.3E-01**	**1.7E-01**	**1.3E-17**	**8.6E-02**	**1.6E-01**	**4.0E-01**	**1.5E-01**

* The projected inventory of H-3 at closure was reduced to ensure that the sum-of-fractions of air limits at the SRS boundary across all disposal units is <1.

NAVAL REACTOR COMPONENTS DISPOSAL AREAS

643-26E NRCDA

Table C- 26. Closure Inventory and Fraction of Limits for 643-26E NRCDA

	Closure Inventory	Beta-Gamma Fraction	Gross Alpha Fraction	All-Pathways Fraction	Air Fraction	Radon Fraction
Radionuclide	**(Ci)**	**of Limit**	**of Limit**	**of Limit**	**of Limit**	**of Limit**
C-14	3.4E+02	2.6E-02		2.4E-02	1.3E-01	
I-129	9.4E-06	6.3E-04		1.0E-05	2.4E-06	
Nb-94	1.6E+01	1.0E-02		1.8E-02		
Ni-59	3.9E+03	4.0E-02		1.6E-04		
Pu-238	6.7E-01					6.1E-13
Pu-239	3.1E-01	4.8E-11	6.9E-09	1.3E-08		
Se-79	3.1E-03				3.1E-06	
Sn-126	1.9E-03				6.1E-04	
Tc-99	3.6E-01	5.8E-04		3.9E-04		
U-234	7.0E-04					2.1E-12
U-238	5.8E-05					1.9E-16
Sum of Fractions		**7.8E-02**	**6.9E-09**	**4.3E-02**	**1.3E-01**	**2.7E-12**

643-7E Naval Reactor Component Disposal Area

Table C- 27. Estimated Closure Inventory and fraction of Limit for 643-7E NRCDA

Radionuclide	Closure Inventory (Ci)	Beta-Gamma	Gross Alpha	All Pathways	Air-Pathway	Radon
C-14	1.4E+02	1.1E-02		9.9E-03	2.6E-01	
Cl-36	1.8E-05				4.9E-08	
I-129	1.5E-05	9.9E-04		1.6E-05	1.9E-05	
Nb-94	6.5E+00	4.1E-03		7.4E-03		
Ni-59	1.6E+03	1.6E-02		6.5E-05		
Pu-238	2.7E-01					1.1E-12
Pu-239	1.2E-01	1.9E-11	2.7E-09	5.3E-09		
Se-79	1.2E-03				6.1E-06	
Sn-126	8.6E-06				1.4E-05	
Tc-99	1.5E-01	2.4E-04		1.6E-04		
U-234	3.6E-06					5.2E-14
U-238	2.3E-05					3.6E-16
Sum of Fractions		**3.2E-02**	**2.7E-09**	**1.8E-02**	**2.6E-01**	**1.2E-12**

This page intentionally left blank.

APPENDIX D

PERFORMANCE ASSESSMENT REVIEW CRITERIA MATRIX

Table D-1 Performance Assessment Review Matrix

Criteria	Where to find[1]	Criteria met?	Response	Issues
3.1.1. Facility/Site Characteristics				
3.1.1.1 PA presents information on the site geography, land use plans, meteorology, ecology, geology, seismology, volcanology, surface water and groundwater hydrology, geochemistry, geologic resources, and water resources sufficient to support the design of the facility.	C.2 and C.3	Yes	Information relevant to all of these subjects, which was considered in design of the ELLWF is provided in Sections 2 and 3 of the Background Chapter in Part C.	
3.1.1.2 PA presents information on the facility design features the waste disposal configuration operational and protection (e.g., flood protection, inadvertent intrusion barrier) features for the facility that affect long-term stability and design/engineering features of the operational and closure covers at a level sufficient to support the analysis presented in the PA.	B.X.4	Yes	Features of each disposal unit and the covers, which affect long-term stability, operations, and protection of the ELLWF are described in Chapters 1 through 5 of Part B.	
3.1.1.3 PA identifies Federal, state, and local statutes or regulations or agreements that impact site engineering, facility design, facility operations, and the relationship and/or impact of the results of the PA on site engineering, facility design, or facility operations because of these factors.	C.2	Yes	In addition to the DOE Order, Section 2 of the Background Chapter of Part C identifies and notes the impact of other federal, state, and local regulations on the PA, including the Groundwater Protection Management Plan (which addresses federal, state and local regulations), the Composite Analysis (which addresses federal regulations), and the EIS for waste management (which addresses federal regulations).	

Criteria	Where to find[1]	Criteria met?	Response	Issues
3.1.1.4 PA identifies procedures and facility related documentation that may impact site engineering, facility design, or facility operations and the relationship and/or impact of the results of the PA on the documents and site engineering, facility design, or facility operations.	C.2	Yes	Section 2 of the Background Chapter of Part C identifies procedures and facility related documentation, including the SRS Land Use Plan, the E-Area Closure Plan, and the Disposal Authorization Statement, which influence, and may be influenced by, the PA results in terms of site engineering and facility design (e.g., closure plan), and facility operations (e.g., disposal authorization).	
3.1.1.5 PA identifies and justifies key assumptions included in the analysis that are used to model and evaluate the performance of the disposal facility. The assumptions of the PA related to the waste, site, and facility design and operations which are critical to the conclusions of the performance assessment are supported.	Appendix B	Yes	Appendix B lists key assumptions for PA analyses of all disposal unit types, and the facility as a whole. Justification for each assumption is provided in part in the Appendix B list, and in part in the relevant Chapter (i.e., ILV or CIG, etc.), the latter being noted in the list. Although all of the assumptions in the Appendix B list are considered key, those that may need to be protected by the operations in order to preserve the conclusions are also specifically identified.	
3.1.1.6 PA includes any necessary limitations on facility design or operations that are required to meet the performance objectives. The conclusions of the PA are applied to the facility design and operations. The resulting design constraints and limitations on operations can be reasonably accomplished at the disposal facility.	B.7	Yes	The conclusions of the PA are presented in Chapter 7 of Part B, and address any design constraints and limitations on operations based on comparison of results to the performance objectives. Consideration is given to plume overlap, uncertainty and parameter sensitivity in developing the conclusions in this chapter.	

Criteria	Where to find[1]	Criteria met?	Response	Issues
3.1.2 Radioactive Sources/Release Mechanism				
3.1.2.1 The PA presents an estimate of the radionuclide inventory in the waste disposed and forecasted to be disposed at the facility which is quantified and technically supported by records, data, studies and evaluations. The PA should include a thorough analysis of waste disposal records with sufficient documentation to ensure that all of the radionuclides disposed and anticipated to be present in forecast wastes are evaluated. Radionuclides screened from the PA or having no inventory limit should be clearly identified, and the bases for screening and exclusion should be fully documented and defensible (for example, NCRP screening criteria). The technical bases for estimates of the radionuclide concentrations for past and future waste disposal should be described and documented.	Appendix C C.4.1, C.4.4	Unknown Yes	Appendix C references the source of the inventory estimates provided. A brief description of the process leading to the development of these estimates is provided, as is citation of the Solid Waste Management Facility Waste Characterization Program report. Identification of radionuclides screened from the PA, and the bases for screening and exclusion, is documented in Sections 4.1 and 4.4 of the Background Chapter in Part C. Reference is made in Section 4.1 and 4.4 to the data packages which fully described the screening methodologies and the bases for the estimated of radionuclide concentrations used.	A separate analysis of waste disposal records is not included in the PA, but the process is cited.

Criteria	Where to find[1]	Criteria met?	Response	Issues
3.1.2.2 The physical and chemical characteristics of the disposed waste that affect the release should be described including presence or absence and degradation of containers, the characteristics of the waste form, waste treatments that affect contaminant release, and potential interactions of chemical or hazardous constituents. The expected effects of waste form and container degradation should be included. The assessments of the physical and chemical characteristics of the waste form should be documented, and supported by laboratory or field studies. Any assumptions concerning release mechanisms should be specified.	B.X.5.1, B.X.6, Data Packages [2] (see Phifer et al. 2006; Kaplan 2006)	Yes	Sections 5 and 6 of Chapters 1 through 5 in Part B address the physical and chemical characteristics of the disposed waste that affect release. The containment present, the waste form characteristics, and interactions of other constituents such as wood products that affect release are discussed to a limited extent in those sections, but in more detail in the supporting data packages referenced (Phifer et al. 2006 and Kaplan 2006). Both of these references and PA Sections consider physical and chemical characteristics of the waste form, and discuss assumptions pertinent to the ELLWF PA.	
3.1.3 Performance Objectives/Measures				
3.1.3.1 PA identifies the performance measures used in the PA; justifies those performance measures as site-specific applications of the performance objectives and requirements; and presents valid conclusions that the PA meets the performance objectives of DOE O 435.1 identified below:	A B.7 C.4.5	Yes	The performance measures used in the PA are identified in the Synopsis (Part A), Chapter 7 of Part B, and in Section 4.5 of the Background Chapter (Part C). The relationship of the performance measures to the performance objectives and assessment requirements of DOE Order 435.1 is provided in Chapter 7 of Part B, as are the conclusions that the performance objectives are met.	

Criteria	Where to find[1]	Criteria met?	Response	Issues
3.1.3.2 The all pathways performance objective of 25 mrem/year effective dose equivalent is met over the performance period of 1000 years after closure for all radionuclides disposed of in the disposal facility.	B.7 B.X.8	Yes	The preliminary results of the all-pathways analysis (i.e., prior to consideration of plume interaction, sensitivity/uncertainty analysis, and SOF) are presented for each disposal unit in Section 8 of Chapters 1 through 5 of Part B in terms of disposal limits. The final conclusions for all disposal units with respect to the all-pathways performance objective, taking into account the projected inventory, are provided in Chapter 7 of Part B.	
3.1.3.3 The air pathways performance objective of 10 mrem/year effective dose equivalent is met over the performance period of 1000 years after closure for post-September 1988 radionuclides disposed of in the disposal facility.	B.7 B.X.7	Yes	The preliminary results of the air pathway analysis (i.e., prior to consideration of SOF) are presented for each disposal unit in Section 7 of Chapters 1 through 5 of Part B in terms of disposal limits. The final conclusions for all disposal units with respect to the air pathways performance objective, taking into account the projected inventory, are provided in Chapter 7 of Part B.	
3.1.3.4 The radon performance objective of an average flux of 20 pCi/m^2/s at the disposal surface or 0.5 pCi/L in air at the point of compliance is met over the performance period of 1,000 years after closure for all radionuclides disposed of in the disposal facility.	B.7 B.X.10	Yes	The preliminary results of the radon analysis (i.e., prior to consideration of projected inventory) are presented for each disposal unit in Section 10 of Chapters 1 through 5 of Part B in terms of disposal limits. The final conclusions for all disposal units with respect to the radon performance objective, taking into account the projected inventory, are provided in Chapter 7 of Part B.	

Criteria	Where to find[1]	Criteria met?	Response	Issues
3.1.3.5 The groundwater resource performance measures for all radionuclides to be disposed of in the disposal facility are met over the performance period of 1,000 years after closure at the prescribed point of compliance. Impacts to the water resource protection should be assessed using the following hierarchical approach:	B.7 B.X.6	Yes	The preliminary results of the groundwater resource analysis (i.e., prior to consideration of plume interaction, sensitivity/uncertainty analysis, and SOF) are presented for each disposal unit in Section 6 of Chapters 1 through 5 of Part B in terms of disposal limits. The final conclusions for all disposal units with respect to the groundwater resource performance measures, taking into account the projected inventory, are provided in Chapter 7 of Part B.	
• First, the disposal site must comply with any applicable State or local law, regulation, or other legally applicable requirement.	B.7	Yes	The SCDHEC drinking water regulations (in the form of MCLs) are consistent with the EPA MCLs which are interpreted as the performance measure for groundwater protection.	
• Second, the disposal site should comply with any formal agreement applicable to water resource protection that is made with appropriate State or local officials.	B.7	Yes	The SCDHEC drinking water regulations (in the form of MCLs) are consistent with the EPA MCLs which are interpreted as the performance measure for groundwater protection.	
• Third, if neither of the above conditions applies, the site should select assumptions for use in the PA based on criteria established in the site groundwater protection management program and any formal land-use plans.	B.7	NA	Both of the “above conditions” apply.	
• If none of the above applies, the site may select assumptions for use in the PA for the protection of water resources that are consistent with the use of water as a drinking water source.	B.7	NA	Both of the “above conditions” apply.	

Criteria	Where to find[1]	Criteria met?	Response	Issues
In terms of protecting the groundwater as a resource, assuming some volume averaging based on projected use may be appropriate. Applying the performance measure at an assumed wellhead mixed with a reasonable volume of groundwater based on site-specific assumptions regarding groundwater use is appropriate, provided the assumption of mixing is consistent with State or local laws, regulations, or agreements. The point of compliance for groundwater protection may consider institutional controls.	NA	NA	No volume averaging in addition to that imposed by the finite size of the modeling grid elements was considered, nor were institutional controls considered.	
3.1.3.6 The inadvertent intruder performance measures of 100 mrem/year effective dose equivalent for chronic exposure and 500 mrem effective dose equivalent for acute exposure (regional social customs and well drilling, excavation, and construction practices should be considered) are met within the disposal facility over the performance period after the end of active institutional controls.	B.7 B.X.9	Yes	The preliminary results of the intruder analysis (i.e., prior to consideration of projected inventory) are presented for each disposal unit in Section 9 of Chapters 1 through 5 of Part B in terms of disposal limits. The final conclusions for all disposal units with respect to the intruder performance measures, taking into account the projected inventory, are provided in Chapter 7 of Part B.	
3.1.3.7 The PA shall include a determination that projected releases of radionuclides to the environment shall be maintained as low as reasonably achievable (ALARA). The goal of the ALARA process is attainment of the lowest practical release level after taking into account social, technical, economic, and public policy considerations.	A B.7	Yes	A qualitative discussion of how the ALARA principle is applied in the PA process is provided in Chapter 7 of Part B, and summarized in the Synopsis (Part A).	
3.1.4 Point of Assessment				

Criteria	Where to find[1]	Criteria met?	Response	Issues
3.1.4.1 PA identifies the point of assessment for each performance objective and measure, and justifies the selection of each point of assessment considering current and future land use and institutional controls.	C.4.5 B.7	Yes	The point of assessment is identified in Section 4.5 of the Background Chapter (Part C) and in the table provided in Chapter 7 of Part B. Justification for the selection of points of assessment in light of the DOE O 435.1 requirements is provided in Sections 7 and 8 of Chapters 1 through 5, as well as Chapter 7, of Part B.	
3.1.4.2 The point of assessment for all-pathways, the air pathway excluding radon, and groundwater resource protection shall correspond to the point of highest projected dose or concentration beyond a 100 meter buffer zone surrounding the disposed waste. A larger or smaller buffer zone may be used if adequate justification (e.g., land use) is provided.	C.4.5 B.X.7 B.X.8 B.7	Yes	The point of assessment for the all-pathways, the air pathway, and the groundwater resource protection corresponds to the point of highest projected dose or concentration beyond a 100 meter buffer zone surrounding the disposed waste, as noted in Section 4.5 of the Part C Background Chapter, Sections 7 and 8 of Part B Chapters 1 through 5, and Part B Chapter 7. A larger or smaller buffer zone is not used.	
3.1.4.3 The default point of assessment for the performance measure for radon exposure that is based on a limit on the average flux of radon of 20 $pCi/m^2/s$ at the ground surface is the ground surface over the disposal unit.	C.4.5 B.X.10 B.7	Yes	The point of assessment for the radon performance measure is the ground surface over each of the disposal units, and is noted in Section 4.5 of the Part C Background Chapter, Section 10 of Chapters 1 through 5 of Part B, and Chapter 7 of Part B.	
3.1.4.4 The default point of assessment for the alternative performance measure for radon exposure that is based on a limit on air concentration of radioactive material of 0.5 pCi/L is 100-m from the edge of the disposal unit.	NA	NA	The alternative performance measure for radon was not used.	

Criteria	Where to find[1]	Criteria met?	Response	Issues
3.1.5 Conceptual Model				
3.1.5.1 PA provides a clear description of the conceptual model of the hydrogeological setting of the disposal facility. The PA accounts for all relevant processes for the release of radionuclides from the waste materials for environmental transport. The processes analyzed are justified by reference to relevant studies, available data, or supporting analyses in the PA.	C.3.1 B.X.6 B.X.7 B.X.10 Phifer et al. (2006) Kaplan (2006)	Yes	The hydrogeologic setting is described in Section 3.1 of the Background Chapter in Part C. The conceptual models for release of radionuclides to the subsurface environment are described in Sections 6 (for nonvolatile radionuclides) and 7 (for volatile radionuclides) of Chapters 1 through 5 in Part B. Conceptual models relevant to radon release are described in Section 10 of Chapters 1 through 5 (Part B). These conceptual models rely largely on relevant information provided in two of the supporting data packages developed for the ELLWF PA, Phifer et al. (2006) and Kaplan (2006).	
3.1.5.2 The conceptual model incorporates alternative interpretations of the composite processes that control the transport of radionuclides at the disposal site.	B.X.6	Yes	Due to uncertainty in assigning model parameters and their importance, either uncertainty or sensitivity analyses were conducted to address the possibility of alternative interpretations of controlling processes. The configuration and results of the analyses are presented in Section 6 of Chapters 1 through 5, and the results are interpreted in Chapter 7, of Part B.	

Criteria	Where to find[1]	Criteria met?	Response	Issues
3.1.5.3 The conceptual model is a reasonable interpretation of the existing geochemical geologic, meteorologic, hydrologic, and monitoring data for the site and disposal facility. Monitoring data can be used to test the validity of the conceptual model.	B.X.4 B.X.6 B.X.7 B.X.10 C.4.3 Phifer et al. (2006) Kaplan (2006)	Yes	The conceptual models described in Sections 4, 6, 7, and 10 of Chapters 1 through 5 in Part B rely heavily on site-specific geologic, meteorologic, hydrologic, and monitoring data. Much of this data is described in detail in the supporting data packages authored by Phifer et al. (2006) and Kaplan (2006). Monitoring data has already been used to evaluate the groundwater flow simulations as described in Section 4.3 of the Background Chapter (Part C) and can be used to test the validity of the conceptual models.	
3.1.5.4 The conceptual model includes evaluation of institutional controls, design and engineered features of the facility and closure plans or reasonable assumptions for facility closure. Credits for the performance of engineered features and site closure included in the conceptual model are based on data derived from field investigations, related investigations, or documented sources of information relevant to the site and disposal facility. Credits for engineered features include a reasonable representation of the degradation of the engineered features that is justified by supporting investigations and data.	B.X.4 B.X.6 B.X.7 B.X.9 B.X.10	Yes	Evaluation of, and credit for, the institutional controls, design and engineered features of the disposal units and ELLWF cover system are accounted for in the conceptual models, as discussed in Sections 4, 6, 7, 9, and 10 of Chapters 1 through 5 in Part B.	

Criteria	Where to find[1]	Criteria met?	Response	Issues
3.1.5.5 The conceptual model includes assessment of natural processes that could affect the long-term stability of a disposal facility (e.g., flooding, mass wasting, erosion, weathering) over the time period considered in the analysis. The assessments are justified based on referenced investigations and supporting analysis.	B.X.6 B.X.7 B.X.9 B.X.10 Phifer et al. (2006)	Yes	The conceptual models for each disposal type include consideration of long-term natural degradation processes that influence stability and integrity, as well as processes that may affect shorter-term stability. Numerous references are made to data supporting the assumptions with respect to material (metal containment, grout, wasteform etc.) degradation. Discussions and references are in Sections 6, 7, 9, and 10 of Chapters 1 through 5 of Part B, and in the data package by Phifer et al. (2006).	
3.1.6 Mathematical Models				
3.1.6.1 The analytical and numerical models used for the PA are reasonable representations of the conceptual model(s). There is sufficient documentation and verification of the analytical and numerical models to provide reasonable confidence in the model results. The complexity of the mathematical models selected is commensurate with the available site data.	C.4.1 and C.4.3	Yes	The identification of analytical and numerical models used in calculating releases from the waste and transport in the environment are described in Sections 4.1 and 4.3 of the Background Chapter (Part C). Reference is made to the detailed reports that document the model structure as well as the verification work on each model. Different levels of model complexity were chosen based on support data availability, and how the results are utilized.	

Criteria	Where to find[1]	Criteria met?	Response	Issues
3.1.6.2 The input data used in the analytical and numerical models are described and are traceable to sources derived from field data from the site, laboratory data interpreted for field applications, and referenced literature sources which are applicable to the site. Assumptions which are used to formulate input data are justified and have a defensible technical basis.	B.X.6 B.X.7 B.X.10 C.4.1 C.4.3 Data Packages (Phifer et al. 2006, Kaplan 2006, Lee 2006)	Yes	The input data used in the models are derived from site-specific field data, lab data, and referenced literature sources (as documented in Phifer et al. 2006 for geohydrologic data, and in Kaplan 2006 for geochemical data). The data packages and Lee 2006 air modeling report provided relevant detailed information regarding input data, but Sections 6, 7 and 10 of Chapters 1 through 5 in Part B, and Sections 4.1 and 4.3 in the Background Chapter of Part C provide and overview of how the data were used, and justification for assumptions made.	
3.1.6.3 The computational steps in the implementation of analytical and numerical models are clearly described and traceable.	B.X.6 B.X.7 B.X.10	Yes	Descriptions of how conceptual models were represented by the computational models are provided in Sections 6, 7, and 10 of Chapters 1 through 5 in Part B.	

Criteria	Where to find[1]	Criteria met?	Response	Issues
3.1.6.4 Intermediate calculations are performed and results are presented that demonstrate, by comparison to site data or related investigations, the calculations used in the PA are representative of disposal site and facility behavior for important mechanisms represented in the mathematical models.	B.X.6 C.4.3	Yes	Intermediate calculations involving simulation of the groundwater flow field are compared to field observations of seepage faces and potentiometric surfaces, and the favorable comparisons are noted in Section 4.3 of the Background Chapter, Part C. In Section 6 of Chapters 1 through 4, where detailed descriptions of the vadose zone flow and transport modeling are provided, a number of intermediate results are presented, generally in the form of infiltration rates and saturation and pressure profiles which demonstrate that the calculations provide a reasonable representation of the site-specific behavior of vadose zone flow in the presence of the disposal units and cover systems.	
3.1.6.5 The analytical and numerical models are tested, by comparison to benchmarked analytical calculations or results of other well-established models and demonstrate that the results are consistent with the conceptual model and available site data. The models are evaluated for defensibility and are reasonable representations of the disposal site and facility performance by comparison to available site data, related technical investigations, or referenced documentation or literature.	C.7.1 SQAPs	Yes	The Software Quality Assurance Plans, referenced in Section 7 of the Part C Background Chapter, address benchmarking, verification and validation for the models. The models were selected based on defensibility and acceptance in the technical community, as well as for their utility in the ELLWF PA.	

Criteria	Where to find[1]	Criteria met?	Response	Issues
3.1.6.6 The initial conditions, the boundary conditions, and the upscaling (i.e., normalization to field scale) of parameter data are applicable to the disposal facility and the expected range of changes in the physical and hydrologic properties of the site over 1,000 years.	B.X.6 B.X.7 B.X.10 Phifer et al. (2006)	Yes	Boundary conditions are described in Sections 6, 7 and 10 of Chapters 1 through 5 in Part B. Boundary conditions such as infiltration rates are modified according to changes in waste (e.g., subsidence) and cover systems over the 1000-yr period. Phifer et al. (2006) discusses the stochastic upscaling of conductivities done in support of this PA, as well as the methods for representing degraded engineered properties of the site (e.g., cracked concrete).	
3.1.7 Exposure Pathways and Dose Analysis				
3.1.7.1 PA provides a complete description of the important exposure pathways and scenarios for the specific disposal facility that are used in the evaluation of the potential doses to the hypothetical, individual member of the public and inadvertent intruder consistent with site-specific environmental conditions and local and regional practices. The dose analysis is conducted for realistic and/or accepted scenarios for the setting of the facility and surrounding areas that represent the long-term performance of the LLW disposal facility. The exposure pathways and scenarios selected for detailed analysis are justified as representative.	C.4.2	Yes	Of the forty-seven potential pathways leading to human exposure considered, two were identified as being of possible consequence: the groundwater pathway (due to leaching of waste) and the atmospheric pathway (due to volatilization of radionuclides from buried waste). The rationale for the selection of these two pathways is provided in Section 4.2 of the Background Chapter (Part C), and considers the ELLWF setting and local practices. The resulting dose analysis is conducted for realistic and accepted scenarios consistent with the facility setting.	

Criteria	Where to find[1]	Criteria met?	Response	Issues
3.1.7.2 Exposure pathways from the transport of contamination in groundwater and surface water that may be considered include potential exposures from the ingestion of contaminated water, the use of contaminated water for drinking, for irrigation and livestock watering, and the biotic uptake and transport of contamination from groundwater and surface water. The ingestion of dairy products, livestock, fish, crops, and soil, the inhalation of resuspended particles, and external exposure should be considered. Representations of groundwater well performance (e.g., construction, diameter, yield, depth of penetration, screen length) are reasonable reflections of regional practices and are justified.	C.4.2 C.4.5	Yes	Although contamination of surface water was excluded as a pathway of consequence, groundwater contamination and the pathways associated with it, are considered in the all-pathways dose analysis, as explained in Section 4.5 of the Background Chapter (Part C).	
3.1.7.3 If radiation dose is used as a measure of groundwater resource protection, the exposure scenarios consider the ingestion of water (at 2 liters per day or an alternative rate, if a justification is included) at the point of assessment, which represents the location of maximum exposure from a well constructed and developed using current practices typical for the local area.	C.4.5	Yes	For the beta-gamma performance measure associated with groundwater resource protection, radiation dose is used as the measure of protection (see Section 4.5 of the Background Chapter, Part C). For radionuclides falling into that category, ingestion of groundwater is considered the pathway of exposure, and by adopting the MCLs as the performance measure, the assumed ingestion rate is 2 L/d.	
3.1.7.4 Exposure scenarios from the transport of contamination in air that may be considered include residential and gardening activities which include the direct inhalation of volatile and nonvolatile radionuclides, external exposure, ingestion of crops, soil, livestock, dairy products, and inhalation of re-suspended particles.	C.4.3	Yes	The CAP-88 code considers direct inhalation, external exposure, ingestion of crops, livestock and dairy products, as noted in Section 4.5 of the Background Chapter (Part C).	

Criteria	Where to find[1]	Criteria met?	Response	Issues
3.1.7.5 The inadvertent intruder analysis considers the natural and man-made processes that impact the possible exposure to an intruder and calculates the dose using acceptable methodologies and parameters. Exposure pathways from inadvertent intrusion into the waste disposal units identify the chronic (no more than one year) and acute exposure pathways for each of the exposure scenarios considered. The exposure pathways include all relevant ingestion, external exposure, and inhalation pathways for each exposure scenario. [Direct ingestion of contaminated groundwater and exposures to radon should not be considered for inadvertent intrusion, because they are considered separately.]	C.4.4	Yes	A description of the intruder scenarios considered, and the justification for selection of relevant scenarios to this PA is provided in Section 4.4 of the Background Chapter in Part C. Both chronic and acute scenarios are described, and the justification for selecting only chronic scenarios is provided.	
3.1.7.6 The inadvertent intruder analysis specifies the reductions in concentrations of radioactive material from mixing with uncontaminated material or the transport of radionuclides from the disposed waste mass, and justifies the parameters used in the analysis with site data, supporting analysis or referenced information.	C.4.4 Lee, 2004	Yes	Dilution factors relevant to mixing radionuclide-contaminated material with uncontaminated soil are provided and justified in a supporting document for the intruder analysis (Lee 2004), which is cited in Section 4.4 of the Background Chapter of Part C.	
3.1.7.7 The inadvertent intruder analysis accounts for naturally occurring processes (e.g., erosion, precipitation, flooding) and the degradation of engineered barriers in the calculation of results.	B.X.9	Yes	Details of the inadvertent intruder analysis specific to each disposal unit's degradation scenario are provided in Section 9 of Chapters 1 through 5 (Part B).	

Criteria	Where to find[1]	Criteria met?	Response	Issues
3.1.7.8 The inadvertent intruder analysis calculates the maximum dose from disposed waste during the period from the end of active institutional controls to 1,000 years after site closure using the recommendations of ICRP-30 (1979) and DOE-approved dose conversion factors from recognized published sources.	B.X.9 Lee (2004)	Yes	Dose is calculated through the 1,000-yr period after institutional control (Section 9 of Chapters 1 through 5, Part B) using dose conversion factors from the EPA Federal Guidance Reports (1988 and 1993), as cited in the supporting document by Lee (2004).	
3.1.7.9 Acute exposure scenarios for inadvertent intrusion consider direct intrusion into the disposal site and exhumation of accessible waste material. Relevant scenarios that may be considered include discovery, residential construction, and well drilling that incorporate external exposure, inhalation of resuspended particles, and ingestion of particles. The scenarios used shall be justified.	C.4.4	Yes	Construction, discovery, and well drilling acute exposure scenarios are defined and considered, but rejected as irrelevant because the three chronic scenarios will always be more restrictive (Section 4.4 of the Background Chapter in Part C).	
3.1.7.10 Chronic exposure scenarios for inadvertent intrusion consider direct intrusion into the disposal site and exhumation of accessible waste material for period of up to 1 year. Relevant scenarios that may be considered include residential use and post-construction, and post drilling agricultural use that incorporate the ingestion of foodstuffs, ingestion of soil, external exposure, and inhalation of re-suspended particles. The scenarios used shall be justified.	C.4.4	Yes	Agriculture, resident, and post-drilling chronic scenarios are defined and considered, but only the resident and post-drilling scenarios are retained as relevant (Section 4.4 of the Background Chapter in Part C). The agriculture scenario was rejected based on implausibility in light of the permanent erosion barrier placed over the ELLWF.	

Criteria	Where to find[1]	Criteria met?	Response	Issues
3.1.7.11 The dose analysis considers the exposure pathways and transfer factors between media and calculates the maximum dose using acceptable methodologies and parameters. Parameters used in the analysis are justified with supporting data or references.	B.X.7 B.X.8 B.X.9 C.4.4 C.4.5 Data packages (Lee 2004, Lee 2006, Koffman 2006, Jannik and Dixon 2006)	Yes	Overviews of the dose analyses are included in Sections 4.4 and 4.5 of the Background Chapter in Part C, and Sections 7, 8, and 9 of Chapters 1 through 5 of Part B. Dose analyses were conducted for the all-pathways, intruder, and air pathway analyses. For the all-pathways analysis, methodologies, transfer factors and other parameter values are justified in the supporting documents by Koffman (2006) and Jannik and Dixon (2006). Similarly, such justifications are provided in Lee (2004) for the intruder analyses, and in Lee (2006) for the air pathway analysis.	
3.1.7.12 The dose analysis specifies the consumption of radioactively contaminated materials for the exposure pathways evaluated, the inhalation rates of contaminated materials, and the external exposure rates and conditions to radioactive materials. These parameters are justified using references to the literature or site-specific investigations.	B.X.7 B.X.8 B.X.9 C.4.4 C.4.5 Data packages (Lee 2004, Lee 2006, Koffman 2006, Jannik and Dixon 2006)	Yes	Consumption, inhalation, and external exposure rates and conditions are provided in the supporting documents for the all-pathways analysis (Koffman 2006 and Jannik and Dixon 2006), the intruder analyses (Lee 2004), and the air pathway analysis (Lee 2006). Reference is made to these supporting reports in Sections 4.4 and 4.5 of the Background Chapter of Part C, and Sections 7, 8, and 9 of Chapters 1 through 5 in Part B.	

Criteria	Where to find[1]	Criteria met?	Response	Issues
3.1.8 Sensitivity and Uncertainty				
3.1.8.1 The PA includes sensitivity and uncertainty analysis at a sufficient level of detail to increase confidence in model results.	C.5 B.X.6 B.7	Yes	An overview of the sensitivity and uncertainty analyses conducted for the ELLWF disposal units is provided in Section 5 of the Background Chapter of Part C. Results of sensitivity and uncertainty analyses are included in Section 6 of Chapters 1 through 5 in Part B. Chapter 7 of Part B interprets the results of these analyses, which prove to add confidence that the performance measures will be met with the projected inventory.	
3.1.8.2 Acceptable methods of sensitivity analysis are used to identify and rank sensitivity parameters at a sufficient level of detail to use the results to screen future data needs or evaluate data sufficiency. Efforts are made to apply sensitivity analysis across all components of complex models to fully represent model variance. Variations analyzed in the uncertainty analysis that are important to the conclusions are justified as reasonable for the site and facility using data or related field investigations.	C.5 B.X.6 Appendix F	Yes	The scheme of selection of sensitivity parameters is described in Section 5 of the Background Section of Part C. Those parameters that have not been assigned a bounding ("worst case") value were qualitatively ranked, based on past experience and professional judgment, with respect to anticipated contribution to model uncertainty. Complete transport runs are made with the unsaturated and saturated zone models using altered values for the selected parameters, and results are compared to baseline results, to elucidate model sensitivity (Section 6 of Chapters 2 through 4 of Part B). For the uncertainty analysis, parameters selected for variation were assigned reasonable distributions based on site-relevant data or professional judgment, as described in Appendix F and Section 6 of Chapters 1 and 5 of Part B.	

Criteria	Where to find[1]	Criteria met?	Response	Issues
3.1.8.3 The results of the sensitivity and uncertainty analyses are used to assess model uncertainty and the effects of uncertainty on interpretations of model results. The analyses are based on currently accepted methodologies (probabilistic and deterministic) used in modeling studies. The results of the analysis are used to test confidence in the assumptions and conclusions of the PA.	B.X.6 B.7 Appendix F	Yes	Probabilistic uncertainty analyses were conducted for the Slit Trenches and the NRCDA's (Section 6 of Chapters 1 and 5 of Part B and Appendix F). Deterministic modeling was used in the sensitivity analyses done for the CIG Trenches, ILV and LAWV (Section 6 of Chapters 2 through 4 of Part B). A discussion is provided in Chapter 7 of Part B addressing the interpretation of uncertainty and sensitivity analysis results in terms of confidence in PA results.	
3.1.8.4 Estimates of the uncertainty in disposed and forecast waste inventory should be described with the methods used to quantify uncertainty, including decay corrections.	Appendix C	Unknown	In this PA, uncertainties in the waste inventory are addressed by applying a number of methodologies (see Appendix C) to bound forecast curie inventory estimates. These methodologies include using PA disposal limits, for which uncertainty and sensitivity analyses were carried out, the knowledge of past disposals, and LLW WAC to produce upper-bound estimates. Waste receipts, current inventories, and sums of fractions are tracked with the WITS software, allowing information from these sources to be compared to the upper-bound estimate. This process of comparison between what has been disposed and the limit on disposal diminishes the likelihood that estimated closure inventories will be exceeded.	Recognizing that inventory uncertainty is difficult to quantify, the approach has been to set conservative limits based on PA results and other constraints, to lessen the impact of uncertainty

Criteria	Where to find[1]	Criteria met?	Response	Issues
3.1.8.5 The maximum projected dose, flux, or radionuclide concentration and time of occurrence is presented in the PA to provide for understanding of the natural system being modeled and the behavior of the model.	Appendix A	Yes	The maximum projected radionuclide concentrations in groundwater are included in graphical form in Appendix A.	

Criteria	Where to find[1]	Criteria met?	Response	Issues
3.1.9 Results Integration				
3.1.9.1 The calculated results presented in the PA are consistent with the site characteristics, the waste characteristics, and the conceptual model of the facility. The demonstration of consistency is supported by available site monitoring data and supporting field investigations. The results of the analyses for transport of radionuclides and the inadvertent intrusion into the disposal facility, and the sensitivity and uncertainty of the calculated results are comprehensive representations of the existing knowledge of the site and the disposal facility design and operations.	B.1 through B.5 Data pkgs (Phifer et al. 2006, Kaplan 2006)	Yes	The conceptual models for which results are calculated for each disposal unit type are described in Chapters 1 through 5 of Part B. These models incorporate site characteristics and waste characteristics, most of which are described in detail in the supporting data packages (Phifer et al. 2006 and Kaplan 2006). These data packages review site monitoring data as well as field investigations that provide the source of the assumed characteristics. Thus, the results for transport and inadvertent intrusion, as well as for the sensitivity and uncertainty analyses, represent the existing knowledge of the site, the design, and the operations.	

Criteria	Where to find[1]	Criteria met?	Response	Issues
3.1.9.2 Any inventory limits are developed from reasonable projections of waste to be disposed and analyses that consider the physical and chemical characteristics of the wastes if those characteristics affect the release and transport of the radionuclides.	B.1 through B.5 C.4.1 Data pkgs (Craps and Cook 2006, Cook 2007, Kaplan 2006, Phifer et al. 2006)	Yes	Inventory limits are developed for all radionuclides identified in the screening procedure (Section 4.1 of the Background Chapter in Part C and the supporting data packages Crapse and Cook 2006 and Cook 2007). The Cook 2007 document reasonably took into account the total current disposed inventory of each radionuclide in identifying radionuclides of potential significance, for which detailed analyses were conducted. These detailed analyses, documented in Chapters 1 through 5 in Part B, account for physical and chemical characteristics of the waste that are projected to influence release and transport (see Kaplan 2006 and Phifer et al. 2006). For radionuclides of lesser significance, Trigger Values were calculated which serve as very conservative disposal limits, unless future inventory projections prompt a more detailed analysis.	

Criteria	Where to find[1]	Criteria met?	Response	Issues
3.1.9.3 The conclusions of the PA address and incorporate any constraints included in any Federal, state, and local statutes or regulations or agreements that impact the site design, facility design, or facility operations. The conclusions also address and incorporate any procedural or site documentation changes or constraints due to the results of the facility PA. Reasonable assurance exists that these constraints and impacts are appropriately addressed in the PA.	A.2 B.7 C.2 C.5.2	Yes	The conclusions of the PA rely directly on the projected inventory and the performance objectives and assessment requirements of the DOE Order (Chapter 2 of Part A and Chapter 7 of Part B). The projected inventory is developed in consideration of the PA disposal limits, as well as other WAC criteria such as the DSA, criticality limits and other regulatory criteria (as discussed in Section 5.2 of the Background Chapter of Part C). The PA is also influenced by other statutes, regulations and agreements, as noted in Section 2 of the Background Chapter). Some of these constraints affect the performance measures (groundwater resource protection); others affect design and operations developed for the ELLWF. The effect of the PA conclusions on the CA is discussed in Chapter 7 of Part B. Reasonable assurance does exist that these constraints and impacts are appropriately addressed, in part as a result of the extensive internal PA review process.	

Criteria	Where to find[1]	Criteria met?	Response	Issues
3.1.9.4 The PA integrates the results of the analysis, the sensitivity and uncertainty analysis, the comparisons with the performance measures, WAC, operating procedures, and applicable laws, regulations, policies and agreements to formulate conclusions.	B.7 C.5.2	Yes	In Chapter 7 of Part B, the projected inventory, which was developed with consideration given to other WAC criteria, operating procedures, laws, regulations and agreements (see Section 5.2 of the Background Chapter in Part C) as well as PA disposal limits, is compared to the PA results, which include disposal limits, plume interaction factors, and sensitivity and uncertainty analysis results. The disposal limits were derived with explicit consideration of performance measures, which also account for applicable laws, regulations and agreements. Thus, the required integration of PA results is accomplished.	
3.1.9.5 The PA conclusions incorporate the findings of the calculated results for the all pathways analysis, air pathway analysis, groundwater resource protection analysis, inadvertent intruder analysis, and sensitivity and uncertainty analysis. The results are interpreted and integrated to formulate conclusions which are supported by the results and the uncertainties in the results. The conclusions are consistent with the uncertainty of the results.	A.2 B.7	Yes	Chapter 7 addresses this criterion explicitly. The PA results are discussed for all performance objectives and assessment requirements with due consideration of uncertainty results, and conclusions are drawn based on these considerations.	

Criteria	Where to find[1]	Criteria met?	Response	Issues
3.1.9.6 The analysis, results, and conclusions of the PA provide both a reasonable representation of the disposal facility's long-term performance and a reasonable expectation that the disposal facility will remain in compliance with DOE Order 435.1.	A.2 B.7	Yes	The conceptual models forming the bases of the analyses are a reasonable representation of the facility and the long-term processes affecting its performance. The results derived from implementing this model quantitatively show a reasonable likelihood of compliance with performance objectives and assessment requirements in DOE Order 435.1, as discussed in Chapter 7 of Part B and the Synopsis (Chapter 2 of Part A).	
3.1.9.7 The maximum projected impacts during the 1000-year compliance period after facility closure at the point of compliance is used in the analysis for evaluating disposal of LLW and establishing WAC for future disposal.	B.7 C.5.2	Yes	The projected impacts during the 1000-yr period following institutional control are used to evaluate compliance with DOE Order 435.1's objectives and requirements, as described in Chapter 7 of Part B. This is done by comparing calculated disposal limits based on the projected impacts to projected inventories of LLW in the ELLWF. As described in Section 5.2 of the Background Section in Part C, these inventory limits are implemented through a set of WACs, and thus are used along with other criteria in determining future disposal.	

Criteria	Where to find[1]	Criteria met?	Response	Issues
3.1.10 Quality Assurance				
3.1.10.1 The PA discusses quality assurance measures applied to the preparation of the analysis and its documentation (e.g., software quality assurance). The PA included appendices or references to published documents and/or data that provide a basis for the discussions and analysis in the PA.	C.7 SQAPs	Yes	An overview of the QA process and references to the appropriate information is provided in Section 7 of the Background Chapter in Part C.	

[1] B.X is a reference to disposal unit chapters in Part B. 1=Slit and Engineered Trench, 2 =CIG, 3 = LAWV, 4 = ILV, 5 = NRCDA.
[2] Data packages include Phifer et al. 2006 (hydraulic property data), Kaplan 2006 (geochemical data), Lee 2004 (intruder equations), Lee 2006 (air pathway calculations), Koffman 2006 (all pathway calculations), Jannik and Dixon 2006 (all pathway calculations), Crapse and Cook 2006 (atmospheric pathway screening) and Cook 2007 (groundwater screening).

REFERENCES

Cook, J.R. 2007. *Radionuclide Data Package for Performance Assessment Calculations Related to the E-Area Low-Level Waste Facility at the Savannah River Site*, WSRC-STI-2006-00162, Rev. 0, Savannah River National Laboratory, Aiken, SC

Crapse, K. P. and Cook, J. R. 2006. *Atmospheric Pathway Screening Analysis for the E-Area Low Level Waste Facility*, WSRC-TR-2006-00159, Rev 0**,** Westinghouse Savannah River Company, Aiken, SC.

Jannik, G.T. and Dixon, K.L. 2006. *LADTAP-PA: A Spreadsheet for Estimating Dose Resulting from E-Area Groundwater Contamination at the Savannah River Site*, WSRC-STI-2006-00123, Savannah River National Laboratory, Aiken, SC.

Kaplan, D. I. 2006. *Geochemical Data Package for Performance Assessment Calculations Related to the Savannah River Site*, WSRC-TR-2006-00004, Rev. 0, Washington Savannah River Company, Aiken, SC

Koffman, L. D. 2006. *SRNL All-Pathways Application.* WSRC-STI-2006-000179, Rev. 0, Washington Savannah River Company, Aiken, SC

Lee, P. L. 2004. Inadvertent *Intruder Analysis Input for Radiological Performance Assessments*, WSRC-TR-2004-00295, Westinghouse Savannah River Company, Aiken, SC.

Lee, P. L. 2006. *Air Pathway Dose Modeling for the E-Area Low level Waste Facility*, WSRC-STI-2006-00262, Rev. 0, Washington Savannah River Company, Aiken, SC.

Phifer, M. A., Millings, M. R., and Flach, G. P. 2006. *Hydraulic Property Data Package for the E-Area and Z-Area Soils, Cementitious Materials, and Waste Zones*, WSRC-STI-2006-00198, Rev. 0, Washington Savannah River Company, Aiken, SC

This page intentionally left blank.

APPENDIX E -
LIST OF ORIGINAL RADIONUCLIDES USED IN SCREENING ANALYSES

Table E-1. Radionuclides to be Considered in the PA Process (from Cook, 2007)

Ac-223	As-70	Bi-202	Cd-117m	Co-61
Ac-224	As-71	Bi-203	Ce-134	Co-62m
Ac-225	As-72	Bi-205	Ce-135	Cr-48
Ac-226	As-73	Bi-206	Ce-137	Cr-49
Ac-227	As-74	Bi-207	Ce-137m	Cr-51
Ac-228	As-76	Bi-210	Ce-139	Cs-125
Ag-102	As-77	Bi-210m	Ce-141	Cs-126
Ag-103	As-78	Bi-211	Ce-143	Cs-127
Ag-104	At-207	Bi-212	Ce-144	Cs-128
Ag-104m	At-211	Bi-213	Cf-244	Cs-129
Ag-105	At-215	Bi-214	Cf-246	Cs-130
Ag-106	At-216	Bk-245	Cf-248	Cs-131
Ag-106m	At-217	Bk-246	Cf-249	Cs-132
Ag-108	At-218	Bk-247	Cf-250	Cs-134
Ag-108m	Au-193	Bk-249	Cf-251	Cs-134m
Ag-109m	Au-194	Bk-250	Cf-252	Cs-135
Ag-110	Au-195	Br-74	Cf-253	Cs-135m
Ag-110m	Au-195m	Br-74m	Cf-254	Cs-136
Ag-111	Au-198	Br-75	Cl-36	Cs-137
Ag-112	Au-198m	Br-76	Cl-38	Cs-138
Ag-115	Au-199	Br-77	Cl-39	Cu-60
Al-26	Au-200	Br-80	Cm-238	Cu-61
Al-28	Au-200m	Br-80m	Cm-240	Cu-62
Am-237	Au-201	Br-82	Cm-241	Cu-64
Am-238	Ba-126	Br-83	Cm-242	Cu-66
Am-239	Ba-128	Br-84	Cm-243	Cu-67
Am-240	Ba-131	C-11	Cm-244	Dy-155
Am-241	Ba-131m	C-14	Cm-245	Dy-157
Am-242	Ba-133	Ca-41	Cm-246	Dy-159
Am-242m	Ba-133m	Ca-45	Cm-247	Dy-165
Am-243	Ba-135m	Ca-47	Cm-248	Dy-166
Am-244	Ba-137m	Ca-49	Cm-249	Er-161
Am-244m	Ba-139	Cd-104	Cm-250	Er-165
Am-245	Ba-140	Cd-107	Co-55	Er-169
Am-246	Ba-141	Cd-109	Co-56	Er-171
Am-246m	Ba-142	Cd-113	Co-57	Er-172
Ar-37	Be-10	Cd-113m	Co-58	Es-250
Ar-39	Be-7	Cd-115	Co-58m	Es-251
Ar-41	Bi-200	Cd-115m	Co-60	Es-253
As-69	Bi-201	Cd-117	Co-60m	Es-254

Table E-1. Radionuclides to be Considered in the PA Process (from Cook, 2007) - continued

Es-254m	Gd-148	Ho-159	In-119m	La-137
Eu-145	Gd-149	Ho-161	Ir-182	La-138
Eu-146	Gd-151	Ho-162	Ir-184	La-140
Eu-147	Gd-152	Ho-162m	Ir-185	La-141
Eu-148	Gd-153	Ho-164	Ir-186a	La-142
Eu-149	Gd-159	Ho-164m	Ir-186b	La-143
Eu-150a	Ge-66	Ho-166	Ir-187	Lu-169
Eu-150b	Ge-67	Ho-166m	Ir-188	Lu-170
Eu-152	Ge-68	Ho-167	Ir-189	Lu-171
Eu-152m	Ge-69	I-120	Ir-190	Lu-172
Eu-154	Ge-71	I-120m	Ir-190m	Lu-173
Eu-155	Ge-75	I-121	Ir-190n	Lu-174
Eu-156	Ge-77	I-122	Ir-191m	Lu-174m
Eu-157	Ge-78	I-123	Ir-192	Lu-176
Eu-158	H-3	I-124	Ir-192m	Lu-176m
F-18	Hf-170	I-125	Ir-194	Lu-177
Fe-52	Hf-172	I-126	Ir-194m	Lu-177m
Fe-55	Hf-173	I-128	Ir-195	Lu-178
Fe-59	Hf-174	I-129	Ir-195m	Lu-178m
Fe-60	Hf-175	I-130	K-38	Lu-179
Fm-252	Hf-177m	I-131	K-40	Md-257
Fm-253	Hf-178m	I-132	K-42	Md-258
Fm-254	Hf-179m	I-132m	K-43	Mg-28
Fm-255	Hf-180m	I-133	K-44	Mn-51
Fm-257	Hf-181	I-134	K-45	Mn-52
Fr-219	Hf-182	I-135	Kr-74	Mn-52m
Fr-220	Hf-182m	In-109	Kr-76	Mn-53
Fr-221	Hf-183	In-110a	Kr-77	Mn-54
Fr-222	Hf-184	In-110b	Kr-79	Mn-56
Fr-223	Hg-193	In-111	Kr-81	Mo-101
Ga-65	Hg-193m	In-112	Kr-81m	Mo-90
Ga-66	Hg-194	In-113m	Kr-83m	Mo-93
Ga-67	Hg-195	In-114	Kr-85	Mo-93m
Ga-68	Hg-195m	In-114m	Kr-85m	Mo-99
Ga-70	Hg-197	In-115	Kr-87	N-13
Ga-72	Hg-197m	In-115m	Kr-88	Na-22
Ga-73	Hg-199m	In-116m	La-131	Na-24
Gd-145	Hg-203	In-117	La-132	Nb-88
Gd-146	Ho-155	In-117m	La-134	Nb-89a
Gd-147	Ho-157	In-119	La-135	Nb-89b

Table E-1. Radionuclides to be Considered in the PA Process (from Cook, 2007) - continued

Nb-90	Os-185	Pm-144	Pt-197m	Re-182b
Nb-93m	Os-189m	Pm-145	Pt-199	Re-184
Nb-94	Os-190m	Pm-146	Pt-200	Re-184m
Nb-95	Os-191m	Pm-147	Pu-234	Re-186
Nb-95m	Os-191	Pm-148	Pu-235	Re-186m
Nb-96	Os-193	Pm-148m	Pu-236	Re-187
Nb-97	Os-194	Pm-149	Pu-237	Re-188
Nb-97m	P-30	Pm-150	Pu-238	Re-188m
Nb-98	P-32	Pm-151	Pu-239	Re-189
Nd-136	P-33	Po-203	Pu-240	Rh-100
Nd-138	Pa-227	Po-205	Pu-241	Rh-101
Nd-139	Pa-228	Po-207	Pu-242	Rh-101m
Nd-139m	Pa-230	Po-210	Pu-243	Rh-102
Nd-141	Pa-231	Po-211	Pu-244	Rh-102m
Nd-141m	Pa-232	Po-212	Pu-245	Rh-103m
Nd-147	Pa-233	Po-213	Pu-246	Rh-105
Nd-149	Pa-234	Po-214	Ra-222	Rh-106
Nd-151	Pa-234m	Po-215	Ra-223	Rh-106m
Ne-19	Pb-195m	Po-216	Ra-224	Rh-107
Ni-56	Pb-198	Po-218	Ra-225	Rh-99
Ni-57	Pb-199	Pr-136	Ra-226	Rh-99m
Ni-59	Pb-200	Pr-137	Ra-227	Rn-218
Ni-63	Pb-201	Pr-138	Ra-228	Rn-219
Ni-65	Pb-202	Pr-138m	Rb-79	Rn-220
Ni-66	Pb-202m	Pr-139	Rb-80	Rn-222
Np-232	Pb-203	Pr-142	Rb-81	Ru-103
Np-233	Pb-205	Pr-142m	Rb-81m	Ru-105
Np-234	Pb-209	Pr-143	Rb-82	Ru-106
Np-235	Pb-210	Pr-144	Rb-82m	Ru-94
Np-236a	Pb-211	Pr-144m	Rb-83	Ru-97
Np-236b	Pb-212	Pr-145	Rb-84	S-35
Np-237	Pb-214	Pr-147	Rb-86	Sb-115
Np-238	Pd-100	Pt-186	Rb-87	Sb-116
Np-239	Pd-101	Pt-188	Rb-88	Sb-116m
Np-240	Pd-103	Pt-189	Rb-89	Sb-117
Np-240m	Pd-107	Pt-191	Re-177	Sb-118m
O-15	Pd-109	Pt-193	Re-178	Sb-119
Os-180	Pm-141	Pt-193m	Re-180	Sb-120a
Os-181	Pm-142	Pt-195m	Re-181	Sb-120b
Os-182	Pm-143	Pt-197	Re-182a	Sb-122

Table E-1. Radionuclides to be Considered in the PA Process (from Cook, 2007) - continued

Sb-124	Sn-110	Ta-186	Te-131	U-231
Sb-124m	Sn-111	Tb-147	Te-131m	U-232
Sb-124n	Sn-113	Tb-149	Te-132	U-233
Sb-125	Sn-117m	Tb-150	Te-133	U-234
Sb-126	Sn-119m	Tb-151	Te-133m	U-235
Sb-126m	Sn-121	Tb-153	Te-134	U-236
Sb-127	Sn-121m	Tb-154	Th-226	U-237
Sb-128a	Sn-123	Tb-155	Th-227	U-238
Sb-128b	Sn-123m	Tb-156m	Th-228	U-239
Sb-129	Sn-125	Tb-156n	Th-229	U-240
Sb-130	Sn-126	Tb-157	Th-230	V-47
Sb-131	Sn-127	Tb-158	Th-231	V-48
Sc-43	Sn-128	Tb-160	Th-232	V-49
Sc-44	Sr-80	Tb-161	Th-234	W-176
Sc-44m	Sr-81	Tb-156	Ti-44	W-177
Sc-46	Sr-82	Tc-101	Ti-45	W-178
Sc-47	Sr-83	Tc-104	Tl-194	W-179
Sc-48	Sr-85	Tc-93	Tl-194m	W-181
Sc-49	Sr-85m	Tc-93m	Tl-195	W-185
Se-70	Sr-87m	Tc-94	Tl-197	W-187
Se-73	Sr-89	Tc-94m	Tl-198	W-188
Se-73m	Sr-90	Tc-95	Tl-198m	Xe-120
Se-75	Sr-91	Tc-95m	Tl-199	Xe-121
Se-77m	Sr-92	Tc-96	Tl-200	Xe-122
Se-79	Ta-172	Tc-96m	Tl-201	Xe-123
Se-81	Ta-173	Tc-97	Tl-202	Xe-125
Se-81m	Ta-174	Tc-97m	Tl-204	Xe-127
Se-83	Ta-175	Tc-98	Tl-206	Xe-129m
Si-31	Ta-176	Tc-99	Tl-207	Xe-131m
Si-32	Ta-177	Tc-99m	Tl-208	Xe-133
Sm-141	Ta-178a	Te-116	Tl-209	Xe-133m
Sm-141m	Ta-178b	Te-121	Tm-162	Xe-135
Sm-142	Ta-179	Te-121m	Tm-166	Xe-135m
Sm-145	Ta-180	Te-123	Tm-167	Xe-138
Sm-146	Ta-180m	Te-123m	Tm-170	Y-86
Sm-147	Ta-182	Te-125m	Tm-171	Y-86m
Sm-151	Ta-182m	Te-127	Tm-172	Y-87
Sm-153	Ta-183	Te-127m	Tm-173	Y-88
Sm-155	Ta-184	Te-129	Tm-175	Y-90
Sm-156	Ta-185	Te-129m	U-230	Y-90m

Table E-1. Radionuclides to be Considered in the PA Process (from Cook, 2007) - continued

Y-91
Y-91m
Y-92
Y-93
Y-94
Y-95
Yb-162
Yb-166
Yb-167
Yb-169
Yb-175
Yb-177
Yb-178
Zn-62
Zn-63
Zn-65
Zn-69
Zn-69m
Zn-71m
Zn-72
Zr-86
Zr-88
Zr-89
Zr-93
Zr-95
Zr-97

APPENDIX F

SENSITIVITY AND UNCERTAINTY STUDY OF THE E-AREA TRENCHES

This page intentionally left blank.

TABLE OF CONTENTS

LIST OF FIGURES

LIST OF TABLES

1.0 SENSITIVITY AND UNCERTAINTY STUDY OF THE E-AREA TRENCHES

1.1 SLIT TRENCHES

1.1.1 Model Description

The Slit Trench uncertainty and sensitivity analysis was performed using a preliminary model build with the GoldSim™ version 9.60 SP1 (service pack 1) computational platform. This draft model consists of a transport section and a dose and disposal limits section. The transport section tracks the concentration of contaminants as they move through the waste zone, unsaturated zone, and saturated zone. The dose section takes the contaminant concentrations in the aquifer 100 m downstream of the disposal unit and uses those aqueous concentrations to determine an all pathways dose and to compare to water quality standards. Stochastic variables are used in the subsurface waterborne transport section only.

Values of parameters mentioned in the following sections are the deterministic values, which are always the mean (or geometric mean) value for this model. Distributions about those means will be discussed in a later section.

Figure F-1 shows the top-level view of the model. The GoldSim containers of interest shown in the figure will be discussed below. Those containers dealing with the mechanics of running the model will not be discussed in this document.

The conversion of the 2- and 3-dimensional flow fields from PORFLOW into an equivalent 1-D flow field in GoldSim was of prime importance. This will be discussed in the Calibration section.

1.1.1.1 Container Materials

The container Materials, Figure F-2, is where the model's material properties are defined. This includes definition of physical properties such as porosity, density, etc., and the geochemical properties such as soil/water partition coefficients (K_d). The model uses three porous media: sandy soil, clayey soil and saturated sandy soil. The saturated sandy soil is designed to mimic the material properties used in the PORFLOW aquifer model.

An additional porous medium, Waste, is included to allow flexibility in defining properties unique to wastes. The current model assumes that Waste is equivalent to ClayeySoil, so the properties of the waste are set to be identical to those of clayey soil.

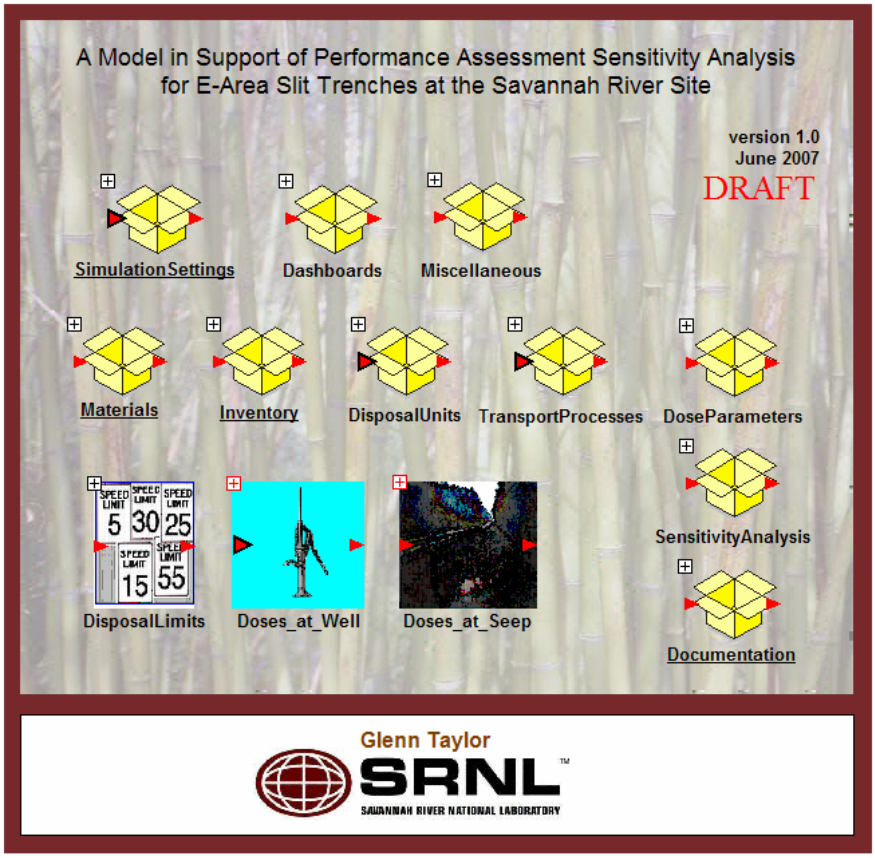

Figure F-1. Top View of the Slit Trench Sensitivity Analysis Model

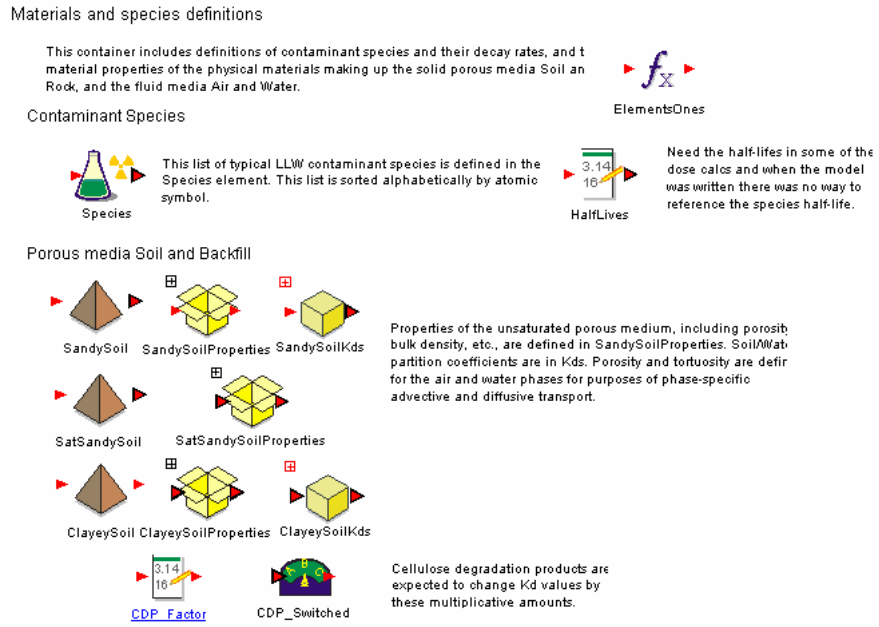

Figure F-2. Materials Container

The CDP (cellulose degradation product) switch is set by the user in a Dashboard – a control panel of sorts. The CDP factor, which adjusts the values of K_ds to be those expected in a geochemical environment dominated by CDPs, is applied to all radionuclides based on values from Kaplan (2006). This switch was not engaged for the current sensitivity analysis.

The radionuclides (defined in the GoldSim Species element) used in this model are shown in Table F-1. The model computes the mass of all radionuclides in various model compartments at all times, calculated as a solution to the many equations governing fate and transport (including radioactive decay and ingrowth). In contrast, a PORFLOW transport run is performed for a single parent and its progeny. In the GoldSim model the entire suite of radionuclides is run for each realization.

1.1.1.2 Species

This model contains 80 radioactive species. Decay chains are implemented where appropriate. This number of species was chosen to balance accuracy of the results with run-time considerations. A deterministic run with complete decay chains (approximately 120 species) for all parent species was made and compared to the results based on this species list. The difference was less than 0.2% in the all-pathways total dose with a 50+% increase in run time. It was felt that this small difference in dose did not justify the increase in run time.

Table F-1. Radionuclide Species Modeled in the Slit Trench Model

Species ID	Isotope	Atomic Weight	Half-life	Radioactive	Daughter1	Fraction1	Daughter2	Fraction2	Description
Ac227	Y	227	2.1772E+01 yr	Y					Ac-227
Al26	Y	26	7.16e5 yr	Y					
Am241	Y	241	432.2 yr	Y	Np237	1			Am-241 - Parent # 1
Am242	Y	242	16 hr	Y	Cm242	1			
Am242m	Y	242	152 yr	Y	Am242	1			
Am243	Y	243	7.3700E+03 yr	Y	Np239	1			Am-243 - Parent # 2
Am245	Y	245	2.05 hr	Y	Cm245	1			
Ba137m	Y	137	2.55 min	Y					
Bk249	Y	249	320 d	Y	Cf249	1			
C14	Y	14	5.7300E+03 yr	Y					C-14 - Parent # 3
Ce134	Y	134	72 hr	Y	La134	1			
Ce144	Y	144	284 d	Y	Pr144m	0.018	Pr144	0.982	
Cf249	Y	249	351 yr	Y	Am245	1			
Cl36	Y	36	3.0100E+05 yr	Y					Cl-36
Cm242	Y	242	163 d	Y	Np238	1			
Cm243	Y	243	28.5 yr	Y	Am243	1			
Cm244	Y	244	1.8100E+01 yr	Y	Pu240	1			Cm-244 - Parent #5
Cm245	Y	245	8.5000E+03 yr	Y	Pu241	1			Cm-245 - Parent # 6
Cm247	Y	247	1.5600E+07 yr	Y	Am243	1			Cm-247 - Parent # 7
Cm248	Y	248	3.4900E+05 yr	Y	Pu244	1			Cm-248 - Parent #8
Co60	Y	60	5.27 yr	Y					
Cs134	Y	134	2.06 yr	Y					
Cs135	Y	135	2.3e6 yr	Y					
Cs137	Y	137	30 yr	Y	Ba137m	1			
Eu152	Y	152	13.3 yr	Y					omit daughter, Gd152, has half life 1E14 yr
Eu154	Y	154	8.80 yr	Y					
Eu155	Y	155	4.96 yr	Y					
Eu156	Y	156	15.2 d	Y					

Table F-1. Radionuclide Species Modeled in the Slit Trench Model - continued

Species ID	Isotope	Atomic Weight	Half-life	Radioactive	Daughter1	Fraction1	Daughter2	Fraction2	Description
H3	Y	3	1.232e1 yr	Y					H-3 - Parent # 9
I129	Y	129	1.5700E+07 yr	Y					I-129 - Parent # 10
K40	Y	40	1.2500E+09 yr	Y					K-40 - Parent # 11
La134	Y	134	6.67 min	Y					
Mo93	Y	93	4.0000E+03 yr	Y	Nb93m	1			Mo-93 - Parent # 12
Na22	Y	22	2.6 yr	Y					
Nb93m	Y	93	1.6100E+01yr	Y					Nb-93m
Nb94	Y	94	2.0300E+04 yr	Y					Nb-94 - Parent # 13
Ni59	Y	59	7.6100E+04 yr	Y					Ni-59 - Parent # 14
Ni63	Y	63	96.0 yr	Y					
Np237	Y	237	2.1500E+06 yr	Y	U233	1			Np-237 - Parent # 15
Np238	Y	238	2.12 d	Y	Pu238	1			
Np239	Y	239	2.35 d	Y	Pu239	1			
Pa231	Y	231	3.2700E+04 yr	Y	Ac227	1			Pa-231
Pb210	Y	210	2.2200E+01yr	Y					Pb-210
Pd107	Y	107	6.5000E+06 yr	Y					Pd-107 - Parent # 16
Pm147	Y	147	2.62 yr	Y					
Pr144	Y	144	17.3 min	Y					
Pr144m	Y	144	7.2 min	Y					
Pu238	Y	238	8.7800E+01 yr	Y	U234	1			Pu-238 - Parent # 17
Pu239	Y	239	2.4100E+04 yr	Y	U235	1			Pu-239 - Parent # 18
Pu240	Y	240	6.5600E+03 yr	Y	U236	1			Pu-240 - Parent # 19
Pu241	Y	241	1.4300E+01yr	Y	Am241	1			Pu-241 - Parent # 20
Pu242	Y	242	3.7400E+05 yr	Y	U238	1			Pu-242 - Parent # 21
Pu244	Y	244	7.9900E+07 yr	Y	Pu240	1			Pu-244 - Parent # 22
Ra226	Y	226	1.6000E+03 yr	Y	Rn222	1			Ra-226 - Parent # 23
Ra228	Y	228	5.7400E+00 yr	Y	Th228	1			Ra-228
Rh106	Y	106	29.9 s	Y					

Table F-1. Radionuclide Species Modeled in the Slit Trench Model - continued

Species ID	Isotope	Atomic Weight	Half-life	Radioactive	Daughter1	Fraction1	Daughter2	Fraction2	Description
Rh106	Y	106	29.9 s	Y					
Rn222	Y	222	1.0500E-02 yr	Y	Pb210	1			Rn-222
Ru106	Y	106	368 d	Y	Rh106	1			
Sb125	Y	125	2.77 yr	Y	Te125m	1			
Sb126	Y	126	12.4 d	Y					
Sb126m	Y	126	19 min	Y	Sb126	1			
Se79	Y	79	2.9500E+05 yr	Y					Se-79 - Parent # 24
Sm151	Y	151	90 yr	Y					
Sn126	Y	126	2.3000E+05 yr	Y					Sn-126 - Parent # 25
Sr90	Y	90	2.8900E+01 yr	Y					Sr-90 - Parent # 26
Tc99	Y	99	2.1110E+05 yr	Y					Tc-99 - Parent # 27
Te125m	Y	125	58 d	Y					
Th228	Y	228	1.9100E+00 yr	Y					Th-228
Th229	Y	229	7.3600E+03 yr	Y					Th-229
Th230	Y	230	7.5500E+04yr	Y	Ra226	1			Th-230 - Parent # 28
Th231	Y	231	25.5 hr	Y	Pa231	1			
Th232	Y	232	1.4050E+10 yr	Y	Ra228	1			Th-232 - Parent # 29
U232	Y	232	72 yr	Y	Th228	1			
U233	Y	233	1.5920E+05 yr	Y	Th229	1			U-233 - Parent # 30
U234	Y	234	2.4550E+05 yr	Y	Th230	1			U-234 - Parent # 31
U235	Y	235	7.0400E+08 yr	Y	Th231	1			U-235 - Parent # 32
U236	Y	236	2.3420E+07 yr	Y	Th232	1			U-236 - Parent # 33
U238	Y	238	4.4680E+09 yr	Y	U234	1			U-238 - Parent # 34
Y90	Y	90	64 hr	Y					
Zr93	Y	93	1.5300E+06 yr	Y	Nb93m	1			Zr-93

The physical properties of the various porous media are treated the same, so Sandy Soil is chosen as a representative example. the GoldSim dialog box used to define these properties is shown in Figure F-3.

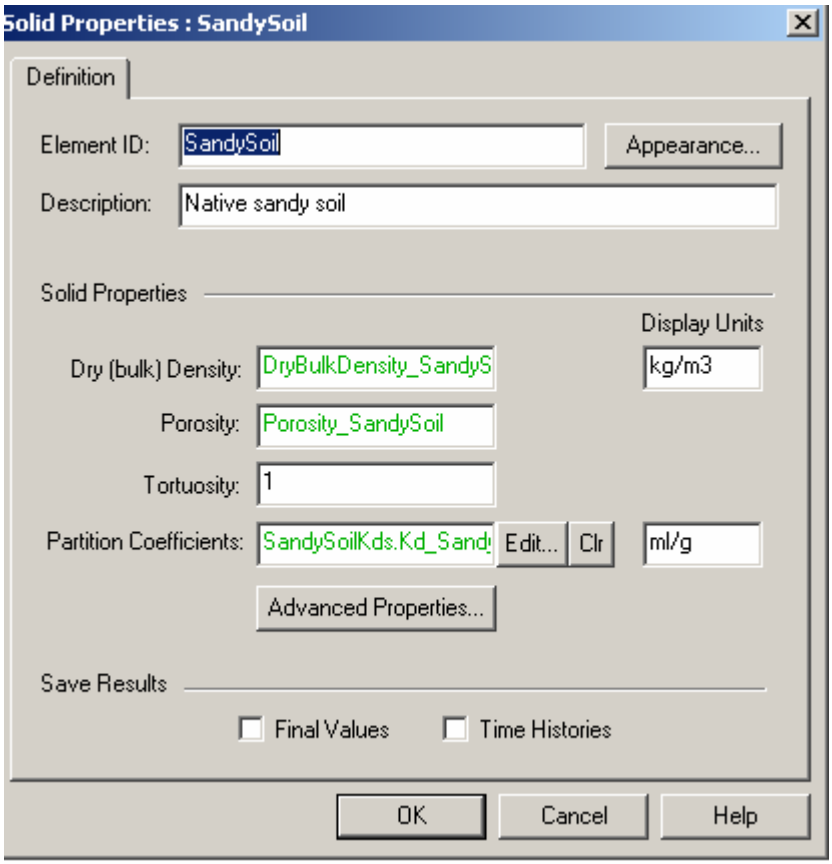

Figure F-3. Sandy Soil properties definition

The first two properties are taken from the SandySoilProperties container, Figure F-4.

The soil/water partition coefficients (K_d) determination is shown in Figure F-5. The first group, seen as data elements, includes those radionuclides which have a distribution coefficient of zero and, therefore, have no distribution applied to the K_d value. The two containers are for those K_ds with a value above 1000 mL/g and those less than 1000 mL/g. This break was chosen to correspond to the different probabilistic input distributions, per Kaplan (2006). Figure F-6 shows an example of a K_d with a log-normal distribution and a mean value less than 1000 mL/g.

Figure F-7 shows an example of a K_d with a mean value greater than 1000 mL/g. The data element Value collects the K_ds. The two K_d containers are based on chemical elements. The data element Value appropriately assigns the element K_d to each of the species[1]. Each species has a K_d explicitly assigned. GoldSim will assign a K_d based on the first isotope, but the model explicitly assigns them so there is no doubt as to what value is used for each species.

The difference between the two K_d distributions is the standard deviation. This will be discussed in the Chemical Properties Stochastics section.

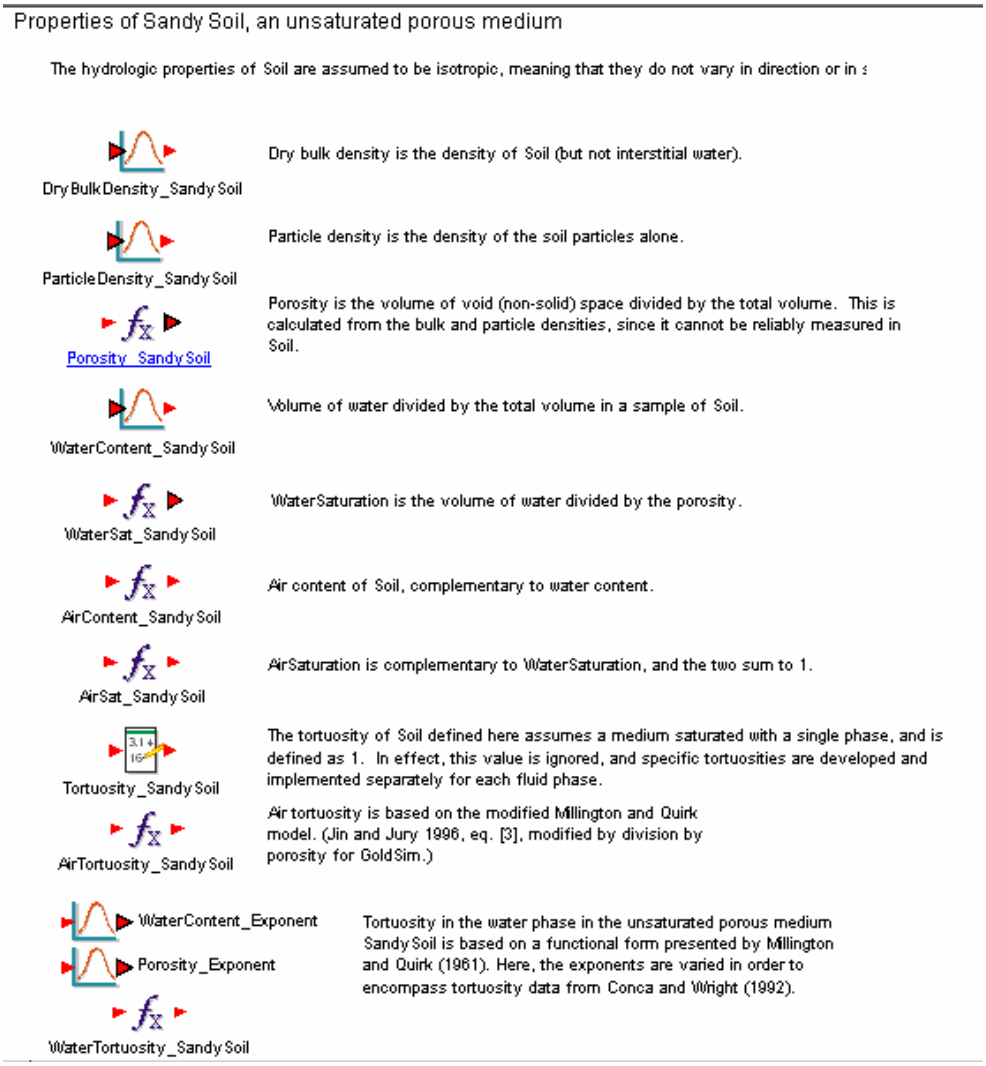

Figure F-4. SandySoilProperties Container

[1] In GoldSim nomenclature, vectors are defined by labels. This model contains an "Element" vector, which contains chemical element names (e.g., Pu, Tc, H) for labels and a "Species" vector which uses isotope names (e.g., Pu238, Pu242, U235, H3) for labels.

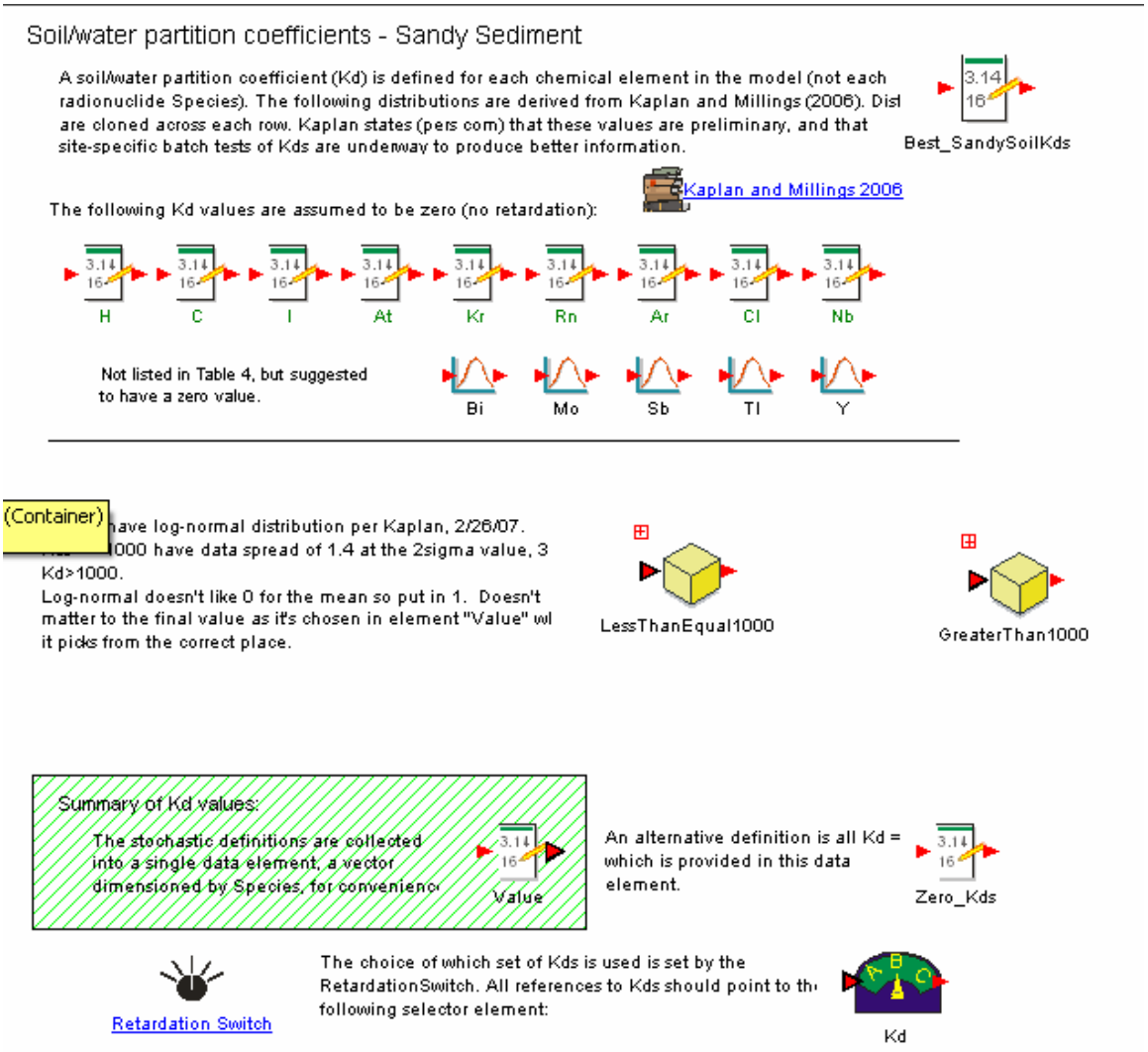

Figure F-5. Kd Container

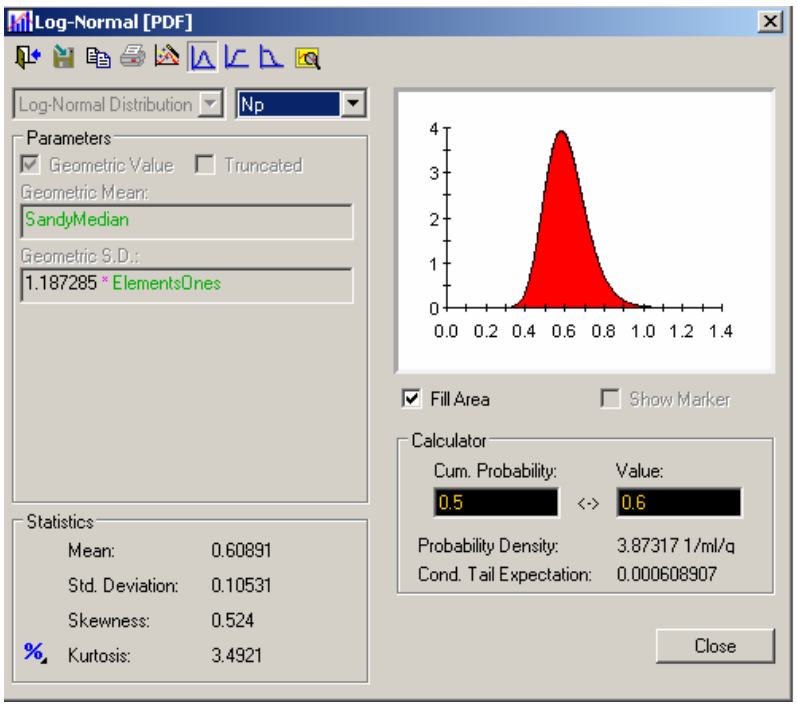

Figure F-6. Neptunium Kd

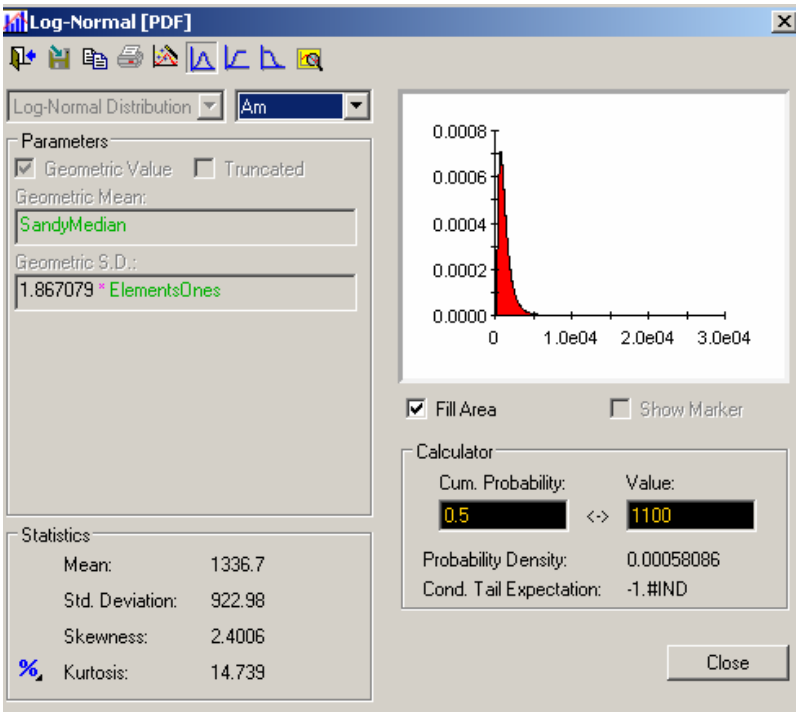

Figure F-7. Americium Kd

1.1.1.3 Container Inventory

The radionuclide inventory is supplied to the waste zone in one of two ways. The first is the option of using a unit curie for each species. By using this option a ready comparison can be made with the PORFLOW results. The other option is a user-selected inventory. The container contains a Data element, called SlitsInventories, with the projected closure inventories for each of the eight slit trenches. The expression AverageSlitsInventory generates an average of these eight. The data element InventoryUsed is defined in a dashboard and selects which column in the SlitsInventories element is used. The inventories are run in both deterministic and stochastic mode one at a time, or may be configured to sample different trenches at random in stochastic mode. The inventories are input as activities and then converted to mass for the transport model.

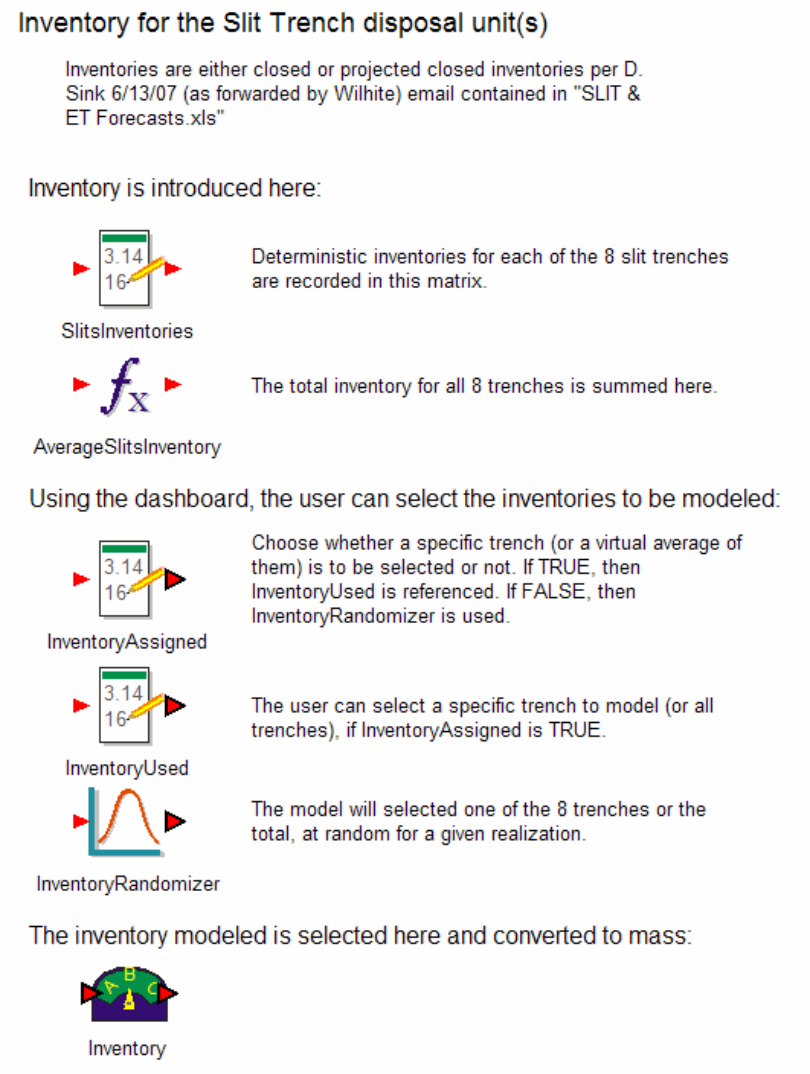

Figure F-8. Container Inventory

1.1.1.4 Container TransportProcesses

The TransportProcesses container contains the flow conditions for the GoldSim model. In addition, it contains the GoldSim Plume() function, used to adjust the mixing cell concentrations to account for transverse dispersion.

Figure F-9 shows the contents of the ClosureCap container. The WarpFactor is used to adjust the uncertain timing of the cap degradation. The flow rates are input as a time table (see Figure F-10) so the WarpFactor is applied to those times. The three containers are to simulate the three cap degradation scenarios, which determine the infiltration. The stochastic element, ScenarioSelector, picks which one of the three cap degradation scenarios to select.

The saturated zone flow is constant in time and space for a given realization. A stochastic is applied so that each realization can have a different value.

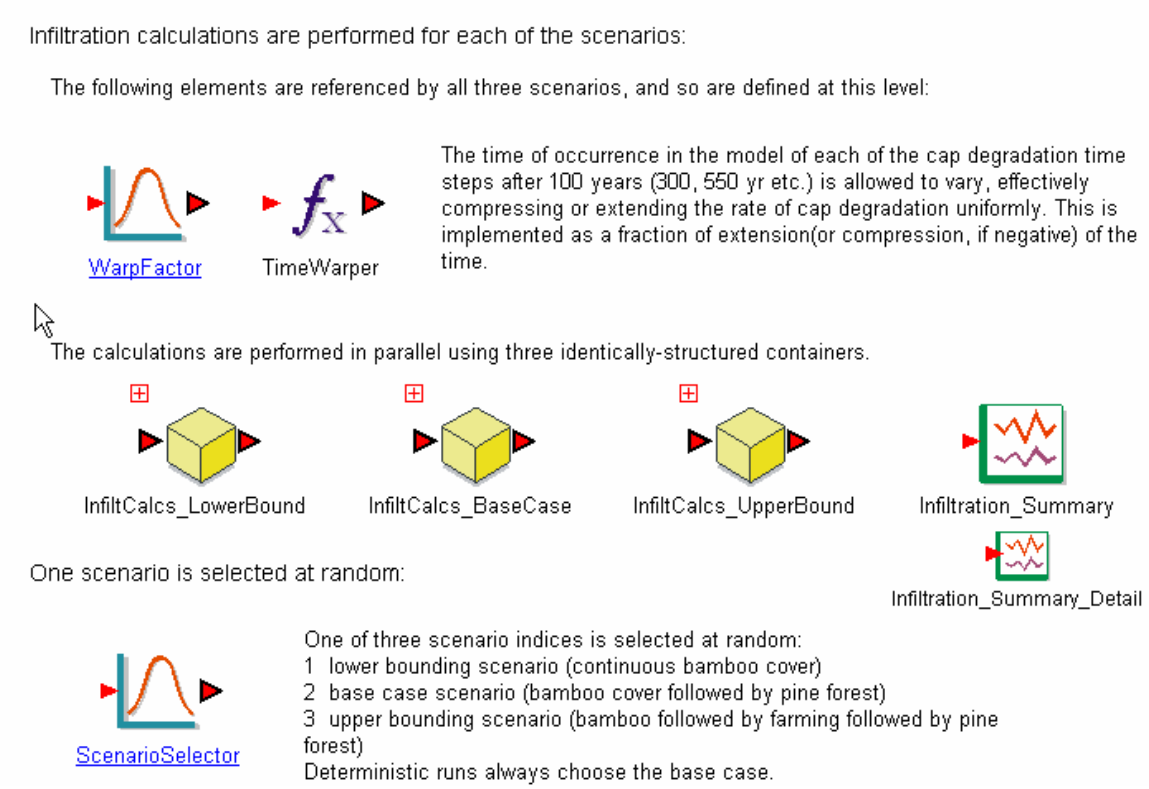

Figure F-9. ClosureCap Container

The flow conditions were taken from the PORFLOW simulations. Figure F-10 shows the unsaturated zone's flow. The flow is applied to all cells in the waste and unsaturated zones. The two cases, Case1 and Case11, are based on the PORFLOW cases of those names. The appropriately named data elements contain the PORFLOW boundary condition flow rates. The CalibrationMultiplier is used to account for the fact that the PORFLOW simulation shows an increased flow through the waste zone when compared to the inlet boundary condition. The details of the calibration will be discussed later.

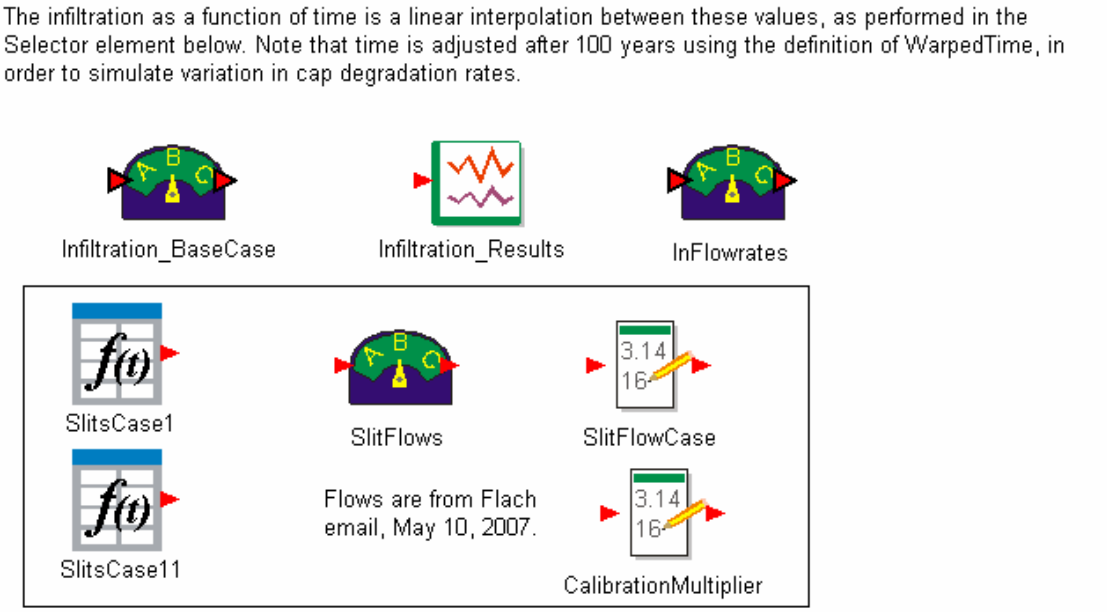

Figure F-10. Unsaturated Zone Flow

Dispersion perpendicular to the flow direction is accounted for by the use of the GoldSim Plume() function. This function requires the definition of 11 parameters. Two of those parameters, D_h and D_v, are based on values defined in container Dispersion (Figure F-11) as described in Tauxe (1994).

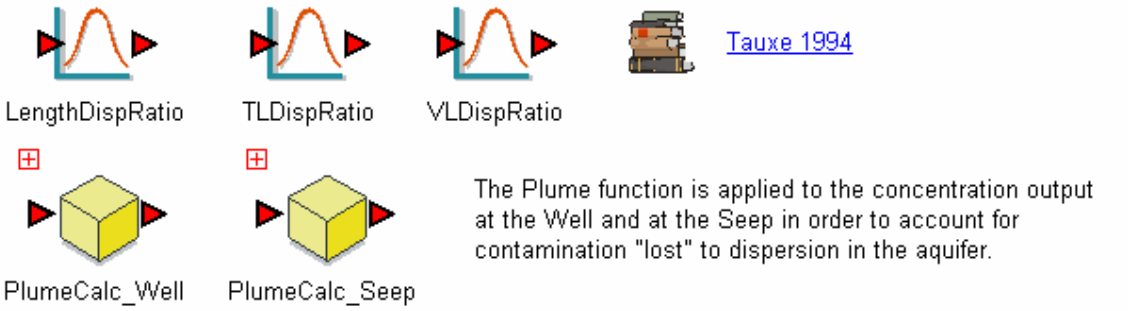

Figure F-11. Dispersion

The Plume() function is calculated in container PlumeCalc_Well, as shown in Figure F-12. The function element PlumeCorrection is the factor applied to the mixing cell concentrations to account for the transverse dispersion.

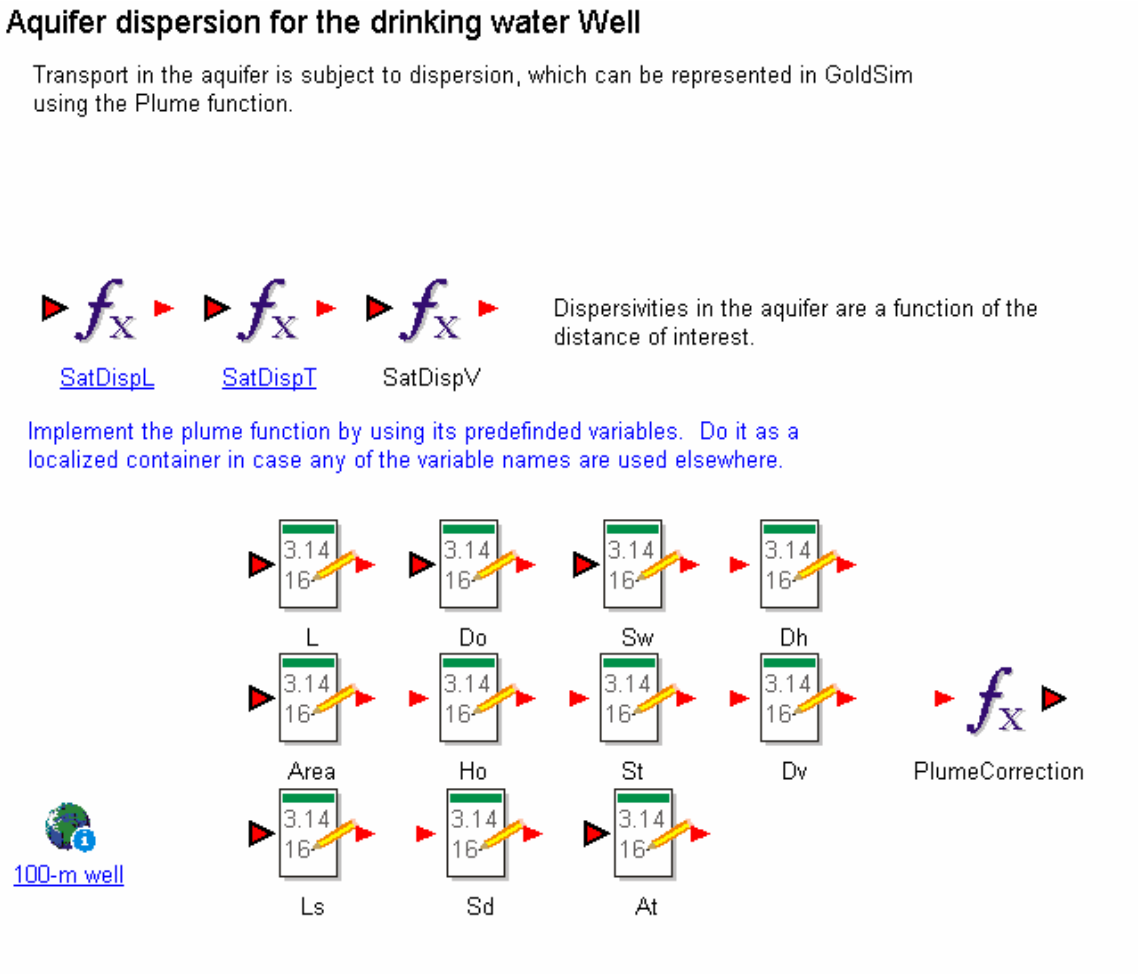

Figure F-12. Plume Function

1.1.1.5 Container DisposalUnits

The container DisposalUnits contains the E-Area Slit Trenches Model, but is configured to accommodate other disposal unit models in the future. Figure F-14 is the upper level container for the transport section of the model. Following is a discussion of the containers of interest.

All flow paths are specified as advective. There is no diffusion in this model. Figure F-13 shows an example of how all the flow paths are defined.

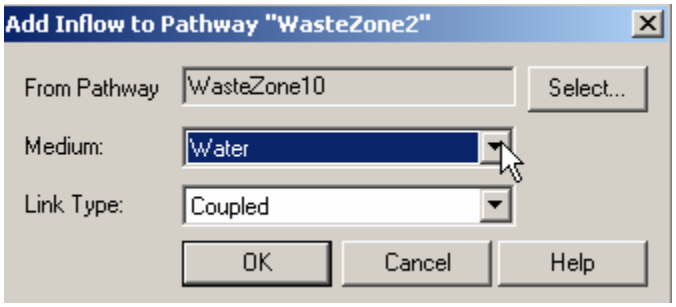

Figure F-13. Representative Flow Path

Sub-Containers SiteGeometry and Subsidence

These two sub-containers define the geometry of the unsaturated and saturated section of the model. SiteGeometry defines the geometric parameters primarily by data and stochastic elements. Subsidence determines the time of dynamic compaction and its probability of occurrence (currently set to 1), and then adjusts the waste volumes accordingly. The waste zone begins with a thickness of 4.9 m and is dynamically compacted to a mean of 1.7 m (the actual distribution is uniform, 1.2 to 2.1 m). The final, compacted thickness is a stochastic element. The final thickness of each waste element is (final thickness)/(number of waste cells). Subsidence rates and final thicknesses are also defined stochastically, with placeholder distributions for now.

In plan view, a slit trench unit has a footprint of about 200 m × 50 m (~1 ha), containing five long individual slit trenches oriented along the long axis. The long axis is also subparallel to the local groundwater flow direction.

Sub-container WasteCells

This sub-container represents the waste region of the slit trench. As shown in Figure F-15 it consists of twenty mixing cell elements and a discrete change element, AllocatedInventory. The radionuclide inventory is evenly distributed throughout the 20 mixing cells at a time determined by AllocatedInventory, which for this analysis happens to be at t = 0 yrs, i.e., the time of waste emplacement. WasteZone1 is the top layer of the waste zone and its top represents the bottom of the closure cap, and hence, the inlet boundary condition for flow in the model.

Figure F-16 shows an example of a waste zone mixing cell element. Each cell consists of two media: Water and Waste (recall that Waste shares for now the properties of ClayeySoil). The initial radionuclide inventory is entered as a discrete change at the beginning of the model.

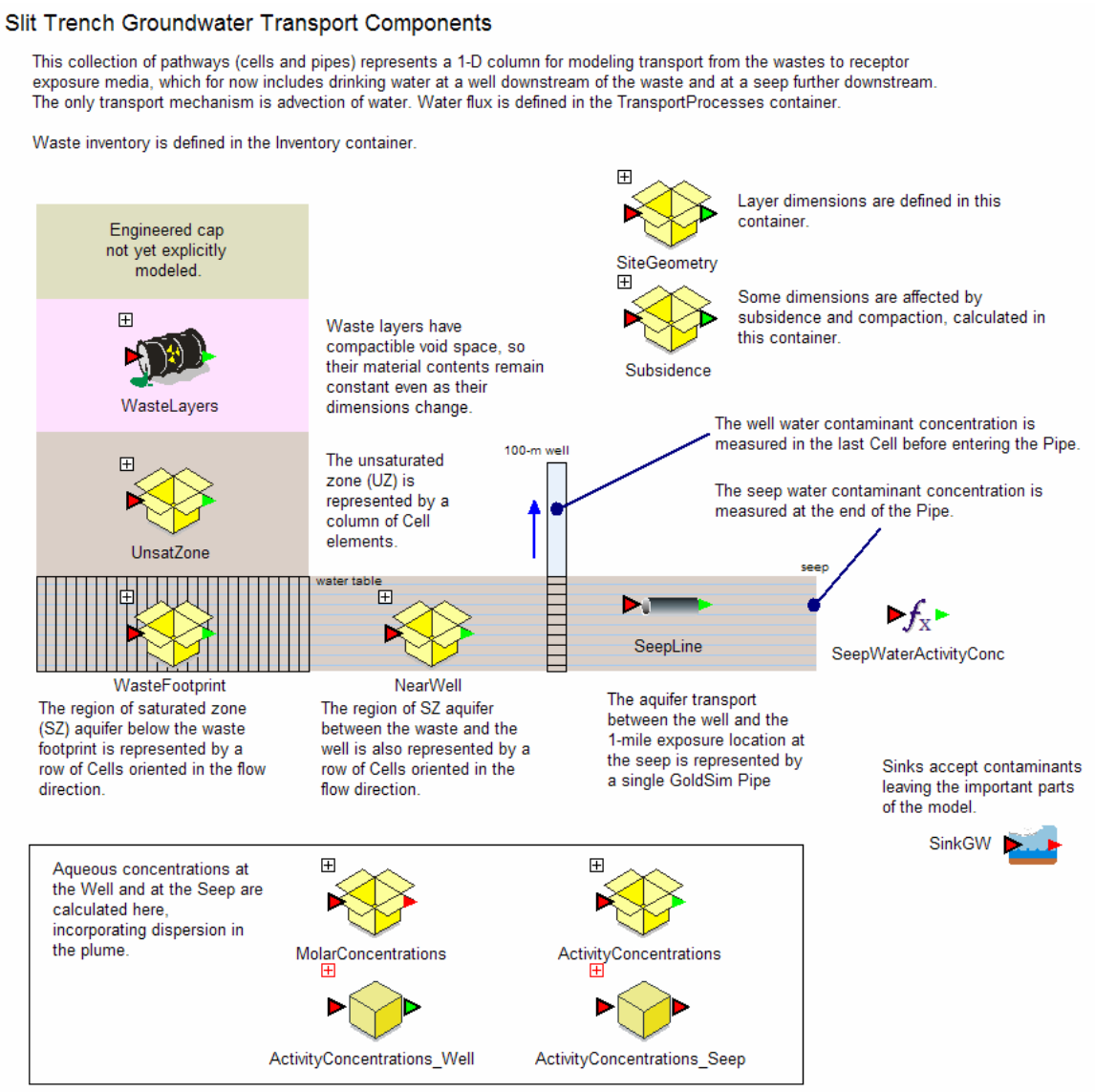

Figure F-14. SlitTrench Sub-container

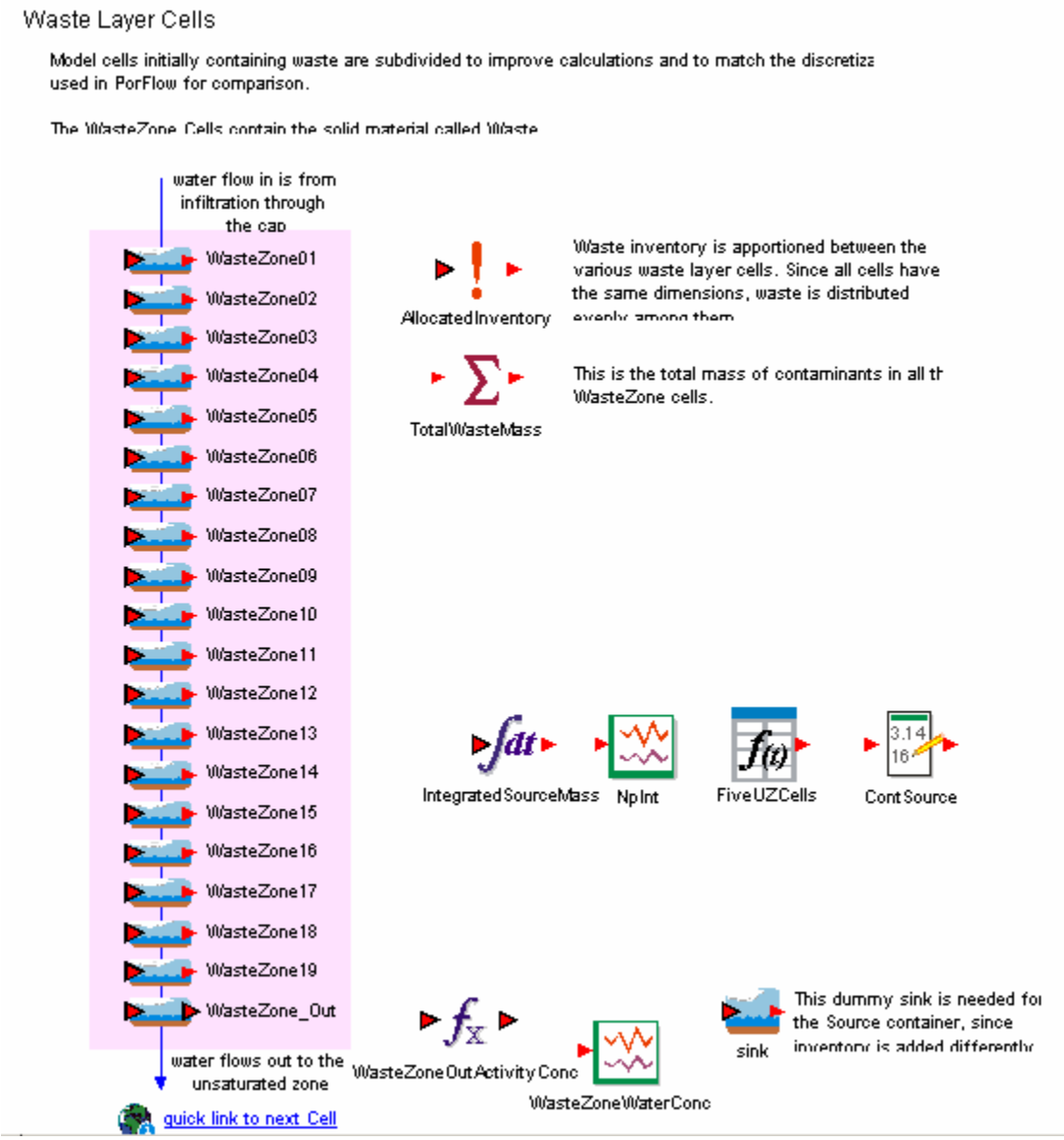

Figure F-15. WasteCells Sub-container

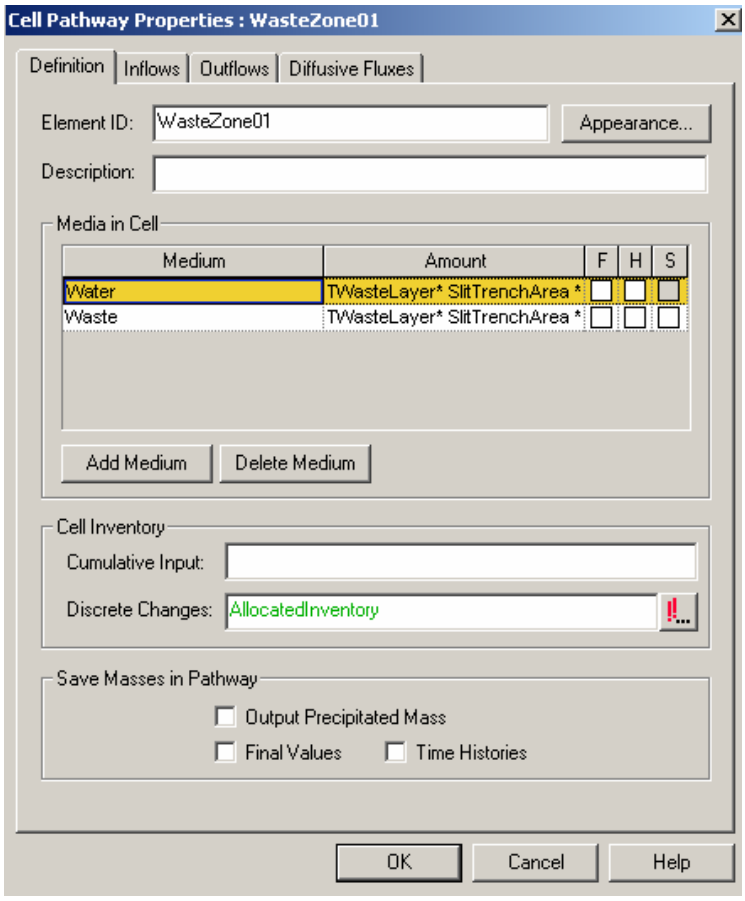

Figure F-16. WasteZone Mixing Cell

Sub-container UnsatZone

This container performs the transport in the unsaturated zone and is shown in Figure F-17. It contains 30 mixing cell elements (compartments) to represent the unsaturated zone between the bottom of the trenches and the water table. Figure F-18 shows a representative cell. Its two media are Water and SandySoil. In plan view it is the same dimensions as the waste zone cells. All unsaturated flow from the bottom waste cell enters the top unsaturated zone flow, and carries radionuclides in the water. The outflow from the unsaturated zone will be discussed in the following section.

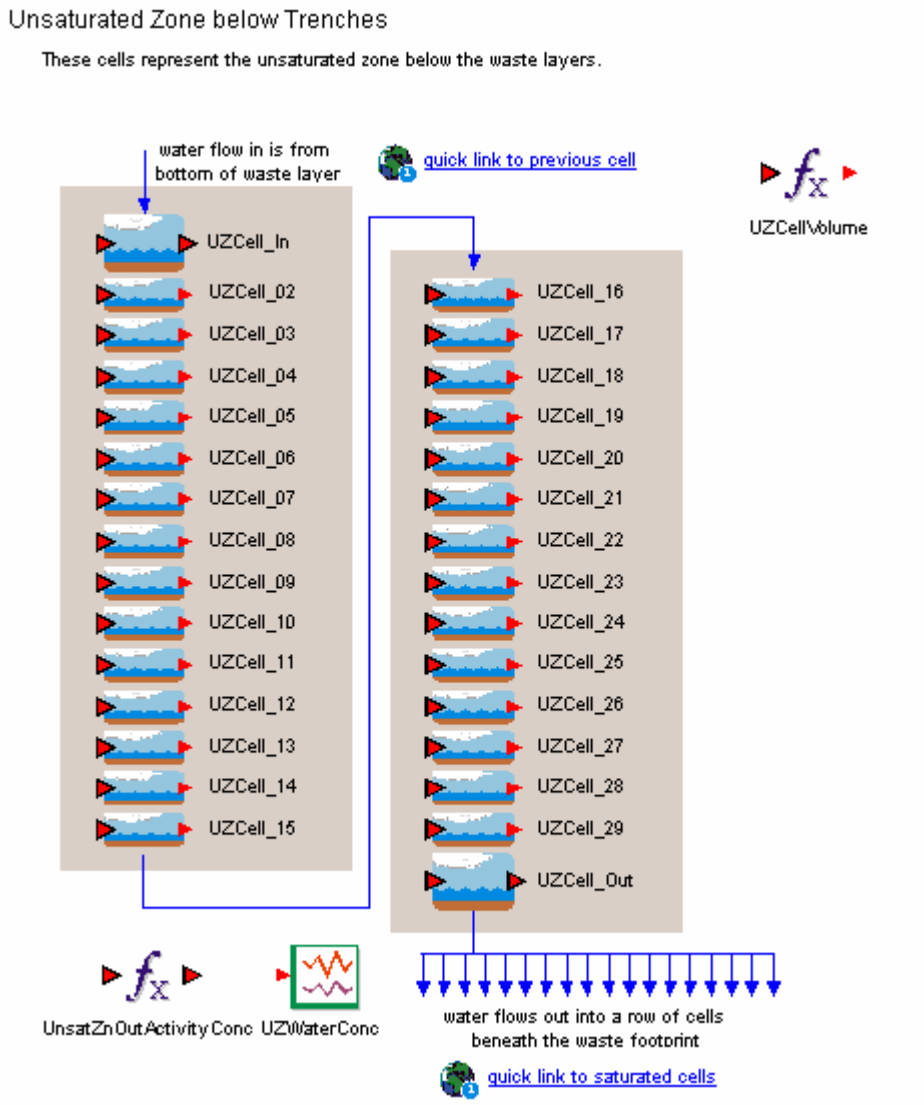

Figure F-17. UnsatZone Container

Sub-container WasteFootprint

This container represents the part of the saturated zone directly underneath the disposal unit. In plan view it is the same dimensions as the waste and unsaturated zones. Its thickness is that of the saturated zone. It is felt that modeling the entry of the waste into the saturated zone by this method is consistent with PORFLOW and more representative of what happens in the real world. It is divided horizontally into 25 mixing cells with each one receiving an equal fraction of the radionuclide flow from the bottom cell of the unsaturated region (recharge to the water table). Its media are Water and SatSandySoil (saturated sandy soil).

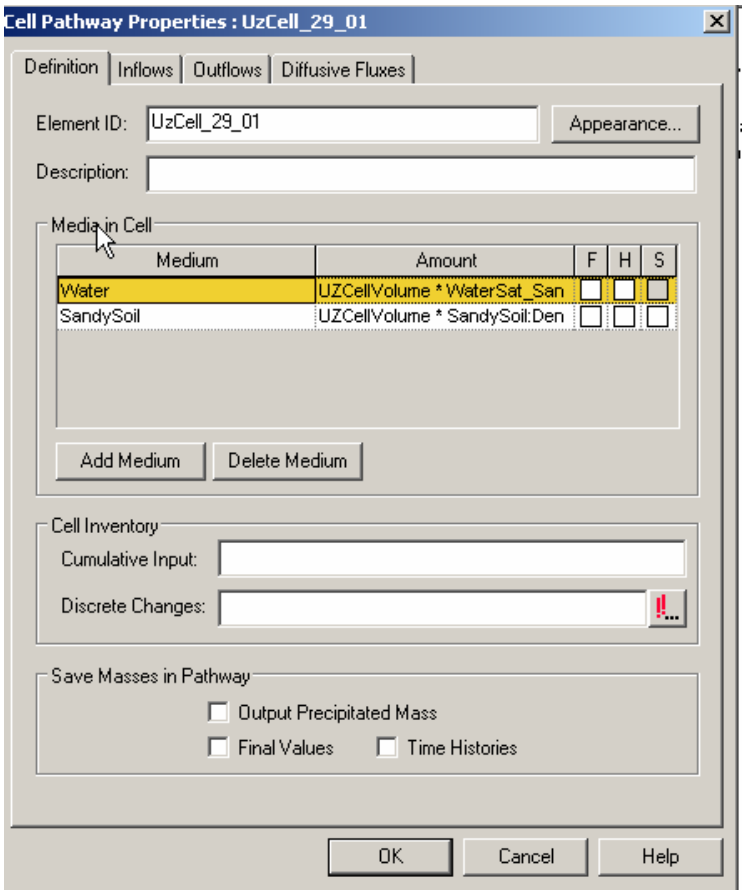

Figure F-18. Unsaturated zone mixing cell definition

This region can be thought of as a recharge entry length with the distance to the point of compliance beginning at the end of these cells and extending 100 m.

A point to be mentioned is that the GoldSim model reports a flow imbalance for these elements. As the note in Figure F-19 states, this imbalance is intended. A basic assumption of the model is that the flow in the saturated region is constant. With the sequential addition of a small flow into each mixing cell, the flow would necessarily have to increase. By setting the mixing cell outlet flows the same, i.e., the same as the saturated region flow, GoldSim essentially throws away clean water and keeps all the radionuclides. It provides a neat way to handle what could be a very messy problem.

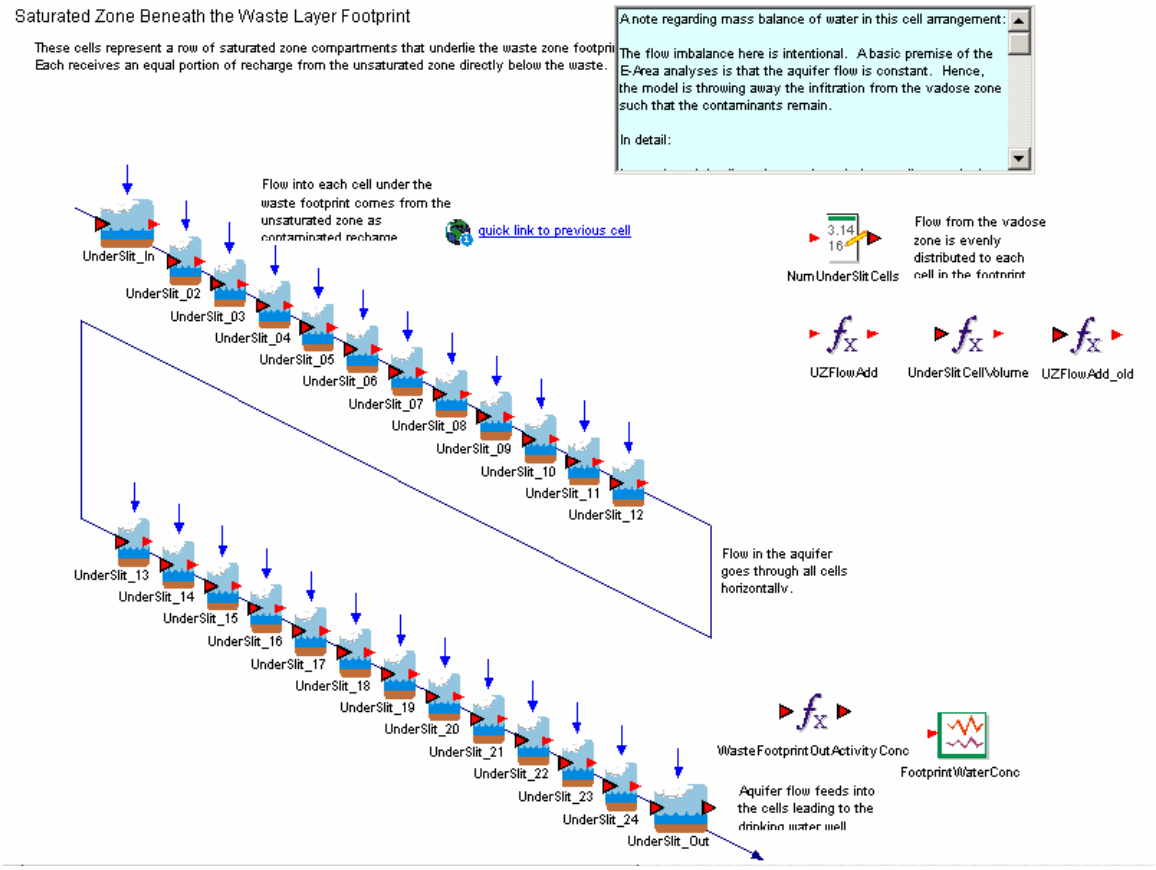

Figure F-19. Sub-container WasteFootprint

Sub-container NearWell

This container represents the saturated zone from the downstream edge of the disposal unit to the point of compliance, in this case the 100-m well. It consists of 50 equally sized mixing cell elements. The vertical faces of the elements are the same size as those in WasteFootprint. Its media are Water and SatSandySoil. The last element, NearWell_01_50, is the element upon which the limit calculations are based.

1.1.1.6 All Pathways Dose

The All-Pathways dose is calculated using the two containers shown in Figure F-20. The methodology used is described in Jannik and Dixon (2006). Two containers shown in Figure F-21, LADTAPFactors and IRRIDOSEFactors, hold the constants used in the dose calculation. The third container, ExposureMediaConc, consolidates the radionuclide concentrations in units appropriate for the dose calculation. The actual dose calculation is performed in container Dose_at_Well. Note that although some stochastic elements appear in these containers they are all set to single-value, discrete distributions. They were modeled as stochastic elements to add the flexibility if data were to become available.

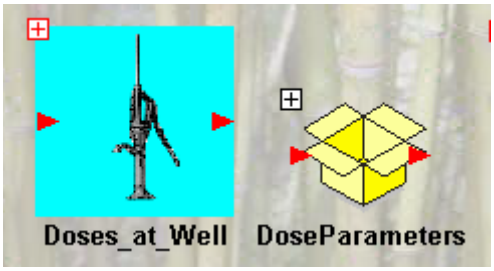

Figure F-20. All Pathways Containers

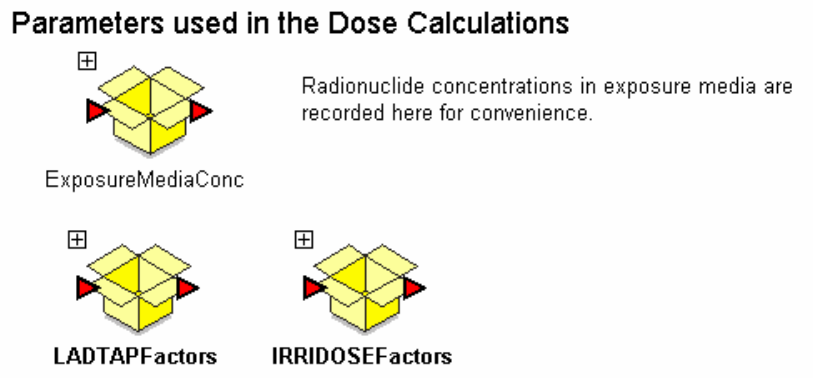

Figure F-21. DoseParameters Container

1.1.1.7 Groundwater Protection Limits

Groundwater protection limits are calculated in the container named Limits. The Radium, Uranium, and Gross Alpha concentrations, in appropriate units, are calculated by $\vec{c} \cdot \vec{M}$ (a term-by-term multiplication), where $\vec{c}$ is the concentration vector and $\vec{M}$ is the mask vector[2] with each of the three limits having its own mask.

The β/γ dose calculation is somewhat more involved and can be seen in Figure F-22

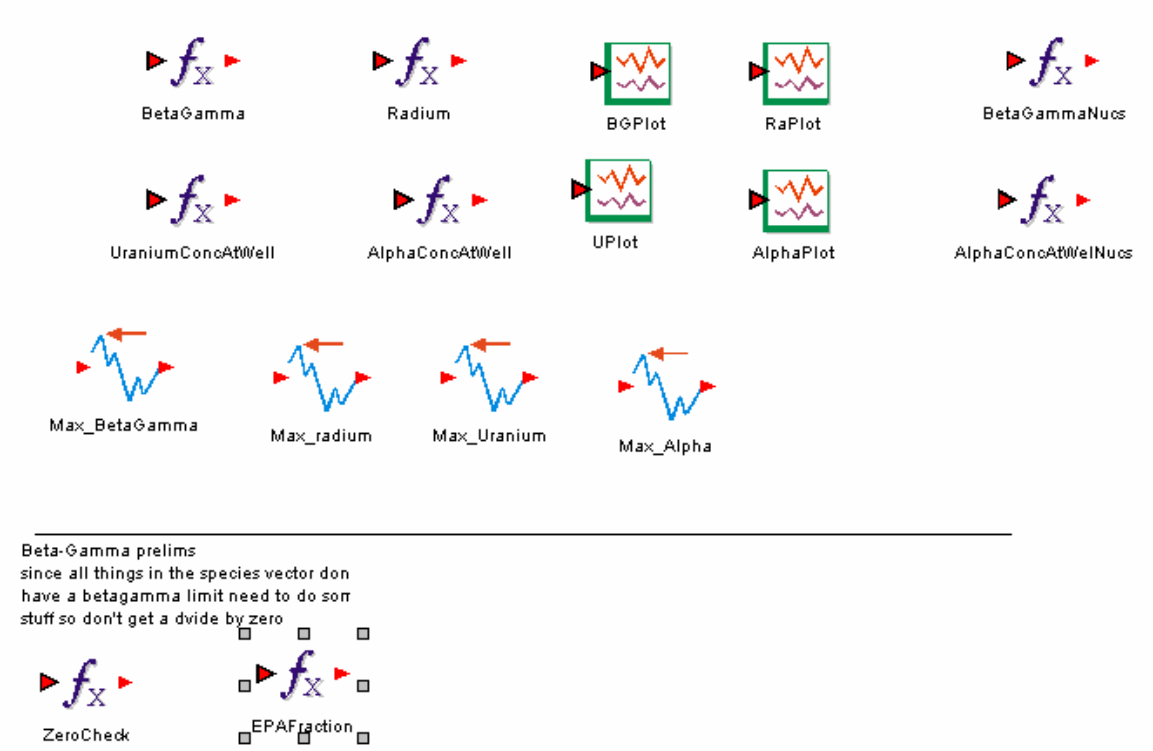

Figure F-22. β/γ Calculation

Function element EPAFraction is the GoldSim-calculated concentration divided by the EPA Maximum Concentration Level (MCL) (EPA 2001). In other words, it is the fraction of the MCL expressed as a mass (or activity) ratio. The Expression element BetaGamma calculates the total dose based on the EPA fraction.

[2] A Mask Vector is a vector consisting of zeros and ones, used as a term-by-term multiplier to screen out unwanted Species. Species not wanted in the product are given a value of zero in the Mask vector.

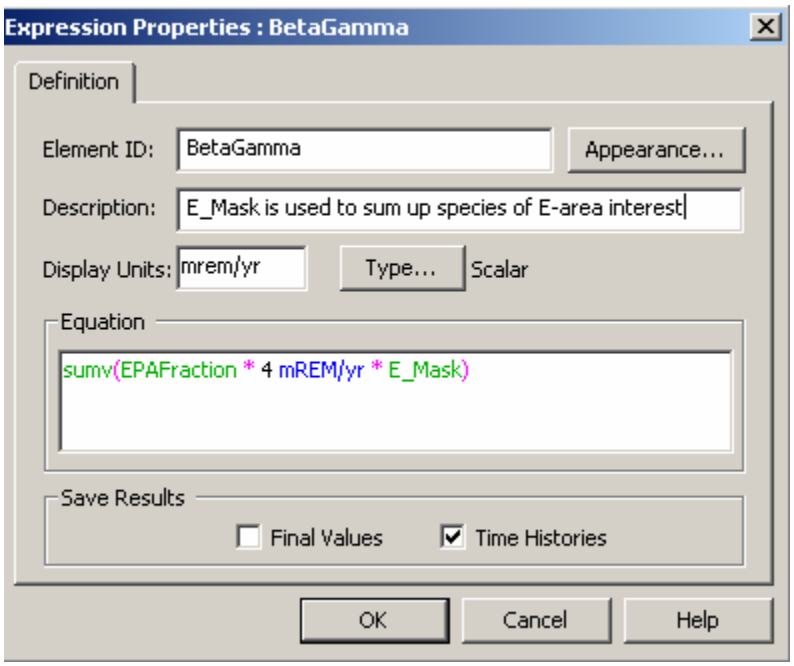

Figure F-23. β/γ Dose Calculation

1.1.1.8 Prescribed Flow Rates

There are two flow rates imposed on the GoldSim model, based on the flow calculations of PORFLOW, since GoldSim is not a flow solver. Flow rates for the unsaturated zone flow and the saturated zone flow are discussed in the following sections.

Unsaturated Zone Flow Rate

This rate is imposed on all flow paths in the waste and unsaturated zones. It is based on the closure cap infiltration as defined by HELP and PORFLOW simulations. The infiltration through the slit and engineered trenches is identical to the closure cap exfiltration as there are no engineered barriers to affect the flow. Because of the definition of the waste zone in the PORFLOW model, it has a slightly greater hydraulic conductivity than the soil surrounding it. This leads to a slight increase in flow through the waste when compared to the boundary condition. A multiplier is used to account for this and will be discussed in more detail in the Calibration section.

Three land use scenarios were evaluated for their effects on the closure cap infiltration with the HELP code. The "Base Case" was evaluated with HELP to develop uncertainties. The selection of which case to use and application of the flow uncertainties are discussed in detail in the Stochastics section.

Figure F-24 shows the base case infiltration rate. Note that it is highly time dependent, increasing as the cap degrades. This greatly affects the way in which the model can be constructed. The time-varying flow precludes the use of a pipe element. This is certainly the case for the waste and unsaturated zone where this time-varying flow rate is explicitly imposed. The saturated zone downstream of the waste footprint was modeled using cells for consistency and if in some future use a time-varying flow is desired.

The saturated zone flow rate is applied to all cells uniformly. It represents the flow calculated by PORFLOW. The upstream end of the row of cells in the saturated zone receives water at the regional aquifer flow rate, and this rate of horizontal water flow is maintained through the well location and beyond.

The columns of cells in the unsaturated zone and the rows of cells in the saturated zone also have implied no-flow boundaries on their edges. One exception to this is the cells in the WasteFootprint container, which receive recharge from the unsaturated zone above, and implicitly leak the same volume of clean water, in order to preserve mass balance of water.

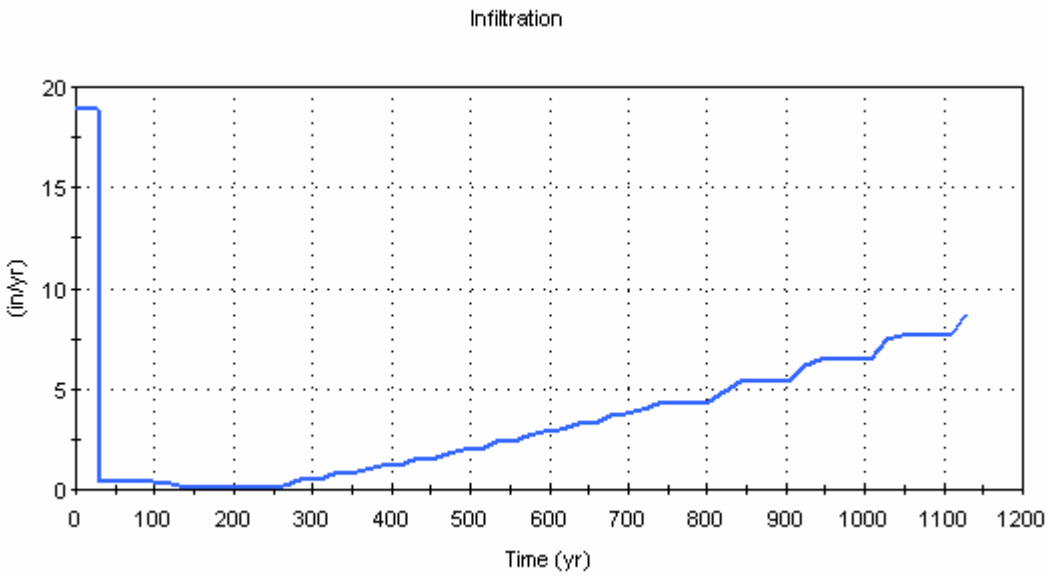

Figure F-24. Base Case Closure Cap Infiltration

1.1.1.9 Stochastics

The stochastic elements fall into two primary categories: those which act on flow parameters and those which act on physical and chemical properties.

Flow Stochastics

Scenario selector

ScenarioSelector determines which of the land use scenarios, and hence the infiltration rate, is chosen. Its distribution is currently a placeholder and can be seen in Figure F-25.

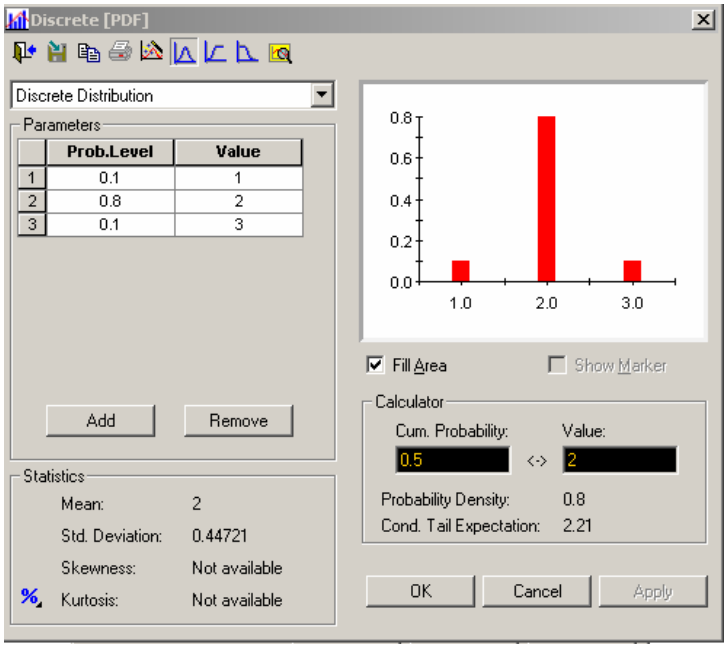

Figure F-25. Stochastic ScenarioSelector

Closure Cap Infiltration

Two flow distributions were generated for the base case land use scenario by the HELP computer program. Figure F-26 shows the form of the distribution. The mean "InFlowRates" is taken from PORFLOW and is time-dependent (see Figure F-10). The standard deviation is given as a fraction of the flow rate divided by the length of the time period of the flow. For time less than 550 years the fraction is 40%, for time greater than 550 years the fraction is 30%. (The yellow "Current Value" in Figure F-26 is for the standard deviation, defined in the text immediately below it.)

Distributions have not yet been developed for the other two cap degradation scenarios. An uncertainty is applied to them by dividing their flow by the base case nominal flow and applying that fraction to the stochastic.

Table F-2. Infiltration Flow Ratios

time (yr)	scenario1 (in/yr)	scenario3 (in/yr)
0	0.994475	0.994475
100	0.992736	1.041162
300	0.180505	0.183787
550	0.101343	0.154548
602	0.108659	0.163626
802	0.130408	1.578214
1000	0.145385	1.616682
1800	0.366952	1.549193
3400	0.460278	1.526185
5600	0.458853	1.505522
10000	0.454126	1.422692
100000	0.454126	1.422692

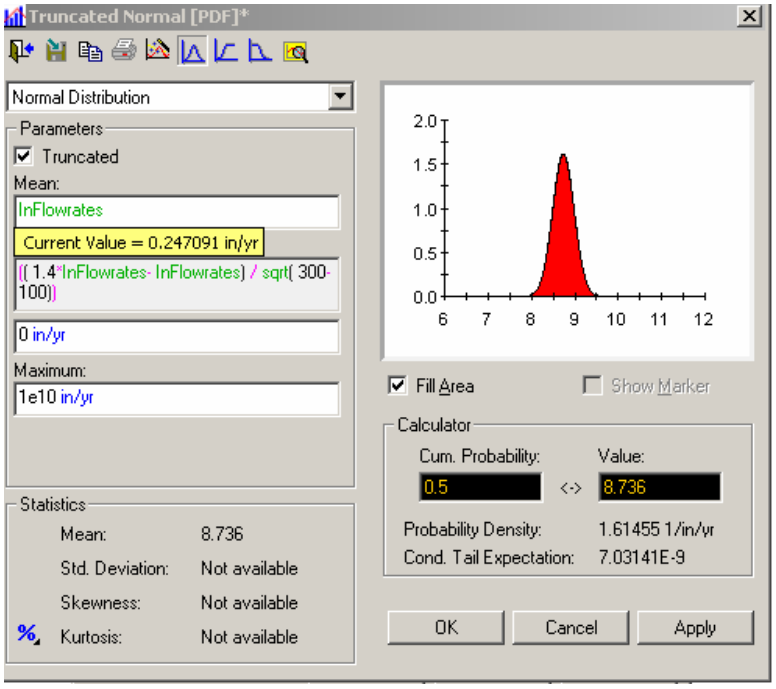

Figure F-26. Base Case Flow distribution

Cap Degradation Stochastic

The stochastic element WarpFactor is used to simulate the uncertainty in the timing of degradation of the cap. It is applied as a multiplicative factor (through the TimeWarper, which equals 1 + WarpFactor) to the simulation time when selecting the appropriate infiltration flow. It is shown in Figure F-27. The value is a placeholder, currently based on engineering judgment.

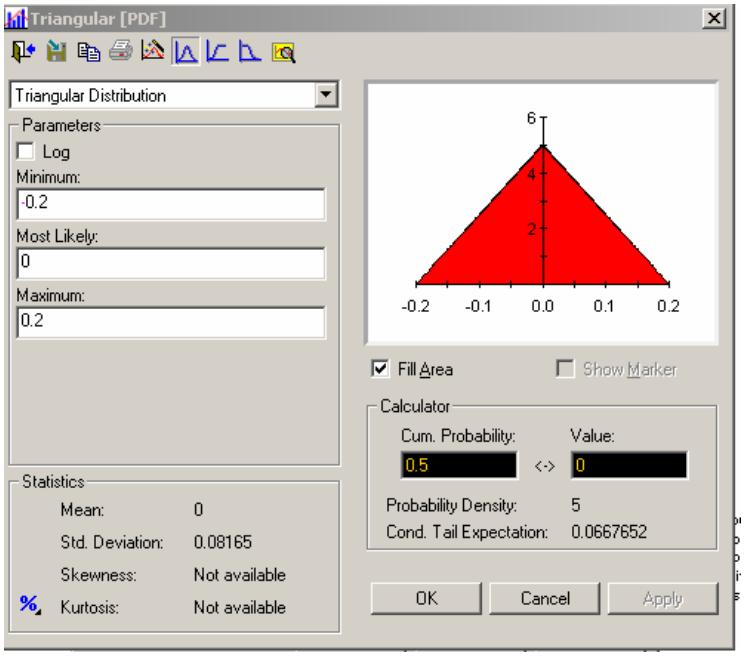

Figure F-27. WarpFactor Stochastic

Waste Zone Compaction Stochastic

This stochastic element varies the compacted thickness of the waste zone between 4 and 7 feet using a uniform distribution. As a placeholder, there are no data to support this value, but it is felt that by having it as a stochastic, during the sensitivity analysis one can determine if it is an important parameter.

Physical and Chemical Property Stochastics

The stochastic elements, and calculation method, are the same for all media. The GoldSim Solid SandySoil will be used to illustrate.

Physical Properties Stochastics

Three physical properties are treated as stochastic elements. These are dry bulk density (Figure F-28), particle density (Figure F-29), and water content (Figure F-30). The distributions are based on engineering judgment, and need to be supported by actual data in the future.

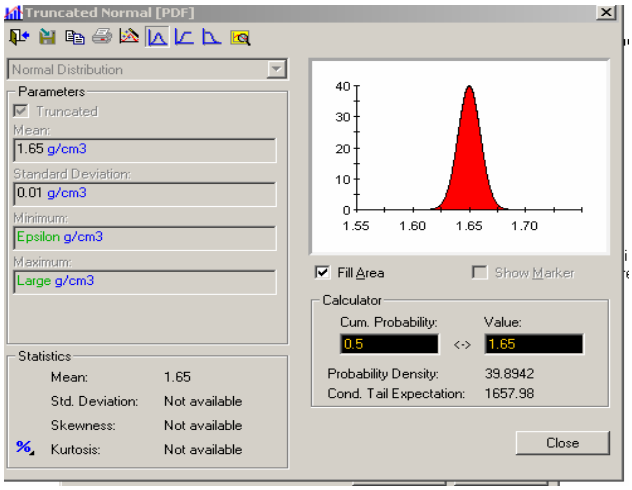

Figure F-28. Dry Bulk Density Stochastic

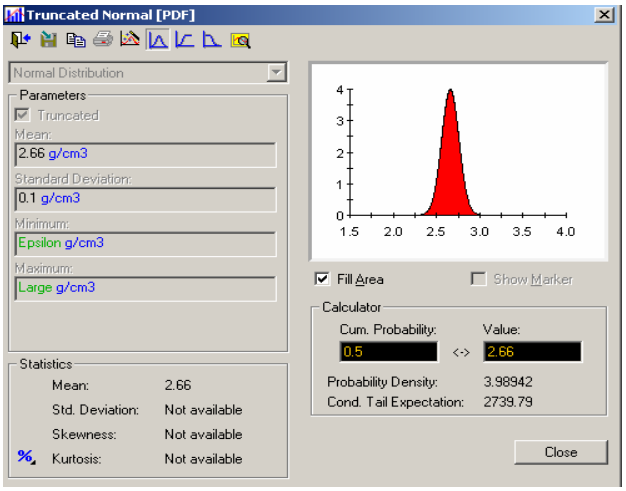

Figure F-29. Particle Density Stochastic

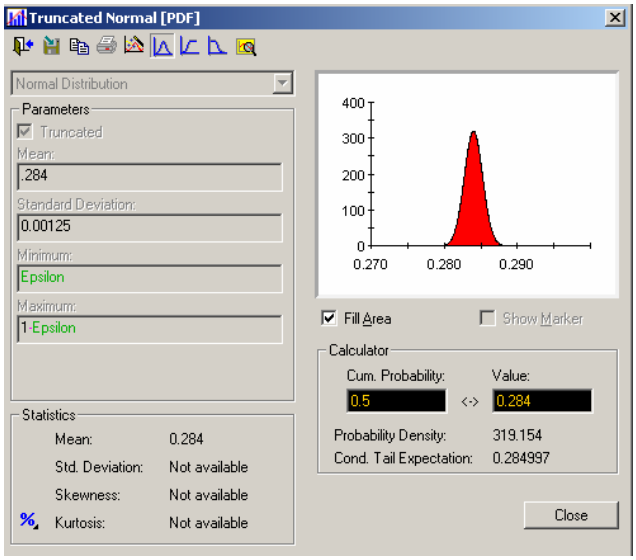

Figure F-30. Water Content Stochastic

Chemical Properties Stochastics

The chemical property of interest for this analysis is the soil/water distribution coefficient (K_d). The distribution coefficients for all media are treated similarly so only one will be discussed.

Based on the work of Kaplan (2006) and Shine (2007), the distribution coefficients are divided into two classes, those with K_d <1000 mL/g and those with $K_d \geq 1000$ mL/g. The statistical F value is 1.4 for the former and 3.4 for the latter. The log-normal distribution assigned to the K_ds, translates to approximately 1.19 and 1.87 factor on the standard deviation. For those species with $K_d = 0$ no distribution is applied.

Figure F-31 shows the stochastic element used to generate the distributions for those species with $K_d < 1000$ mL/g. The geometric mean is the expected value for Kaplan (2006). The "ElementOnes" variable in the "Geometric S.D." box is there to turn the scalar value into a vector that is applied to all the species in the species vector. Note that each element's isotopes have the same distribution coefficient.

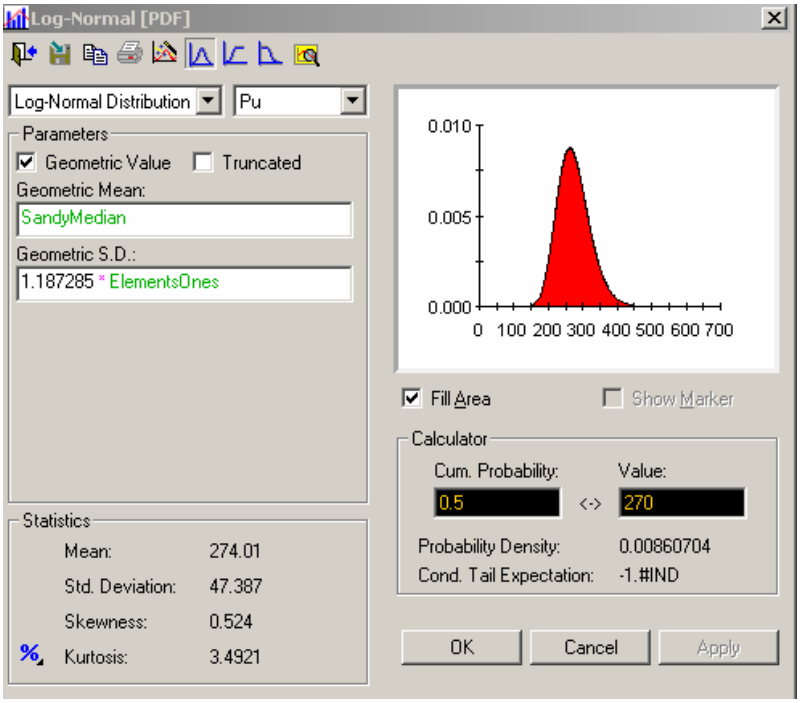

Figure F-31. Pu Soil/Water Distribution Coefficient Distribution

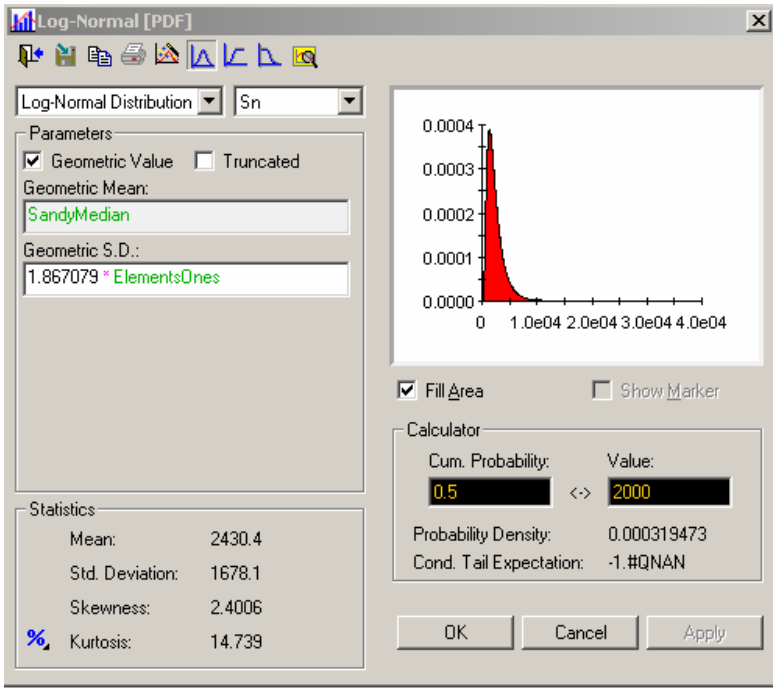

Figure F-32. Sn Soil/Water Distribution Coefficient Distribution

1.1.1.10 Calibration

The basic premise of this calibration exercise is that PORFLOW is the standard by which to set the GoldSim flow. The calibration between GoldSim and PORFLOW was performed in several steps. At the end of these steps a good match was achieved between the results of the codes.

The calibration comparisons referred to below are made by comparing species concentrations at the appropriate locations.

Calibration Step 1

The first step of the calibration was to set up a simple model with both codes in order to assess their ability to calculate transport and compare those results with an analytical solution. Two cases were run: 1) a pulse source, non-sorbing, non-decaying, and 2) a constant source, sorbing and decaying. Both codes were shown to be able to faithfully calculate the expected response for the first case. For the second case, involving sorption (retardation) PORFLOW apparently calculates retardation using the porosity instead of the water content. Once this error was accounted for both codes calculated the expected response.

Calibration Step 2

This step is seen as the first estimate of the calibration of the actual disposal unit's time-dependent scenario, and used the two codes' models of the slit trenches with a constant infiltration rate and a non-sorbing, non-decaying source. Iodine-129 was chosen as the transport species due to its lack of sorption and long half-life. The calibration continued with two phases, the first being the calibration of the unsaturated zone flow and the second being the calibration of the saturated zone flow. These two phases were deemed necessary as the PORFLOW analyses are performed as a 2-D unsaturated zone flow and a 3-D saturated zone flow.

The goal of the first phase was for the GoldSim model to match the shape, timing, and magnitude of the PORFLOW model at the exit of the unsaturated zone. The timing of the peak's arrival was primarily dependent on the velocity of the water. The shape and magnitude, and to a lesser extent, the timing, were dependent on dispersion, both hydrodynamic (physical) and numerical (added by the computational model). In this configuration, both GoldSim and PORFLOW are finite difference models, wherein numerical dispersion adds to physical dispersion. Numerical dispersion is dependent upon the dimensions of mixing cells, as well as the retardation and decay coefficient of each Species subject to transport. Short-lived and strongly-retarded radionuclides will experience relatively more severe numerical dispersion than long-lived and unretarded ones. A noding sensitivity was performed as part of this calibration and it was determined that a minimum of 30 cells was necessary to achieve the desired results.

The second phase was essentially the same as the first, but with the saturated zone. A noding sensitivity was performed so that the two codes' breakthrough curves matched. The velocity was adjusted so that the arrival times corresponded.

Calibration Step 3

The final calibration step was to compare the two actual slit trench models and adjust the GoldSim model as necessary. The calibration was performed using elements with low, or zero, soil/water distribution coefficients. Because of some sorption issues the calibration of species with higher values was not attempted. Slit 5 was chosen because it is essentially full and its final inventory is known.

The calibration was then carried one step further, to the dose calculation, as can be seen in Figure F-33. Curves of the same color represent the same species. The dashed line is the PORFLOW results and the solid line is the GoldSim results. The two non-sorbing species, I-129 (Texas burnt orange) and C-14 (purple) are in good agreement. The two sorbing species, Tc-99 (blue) and Np-237 (green) are somewhat similar and exhibit the same trends. With the PORFLOW unsaturated zone distribution coefficient issue and the fact that this is a comparison of a deterministic value for a probabilistic model, the results were deemed good enough to perform the uncertainty and sensitivity analyses. The remaining question, "Where do the PORFLOW results fit into the GoldSim results distribution?" will be addressed in the Uncertainty Analysis Preliminary Results section.

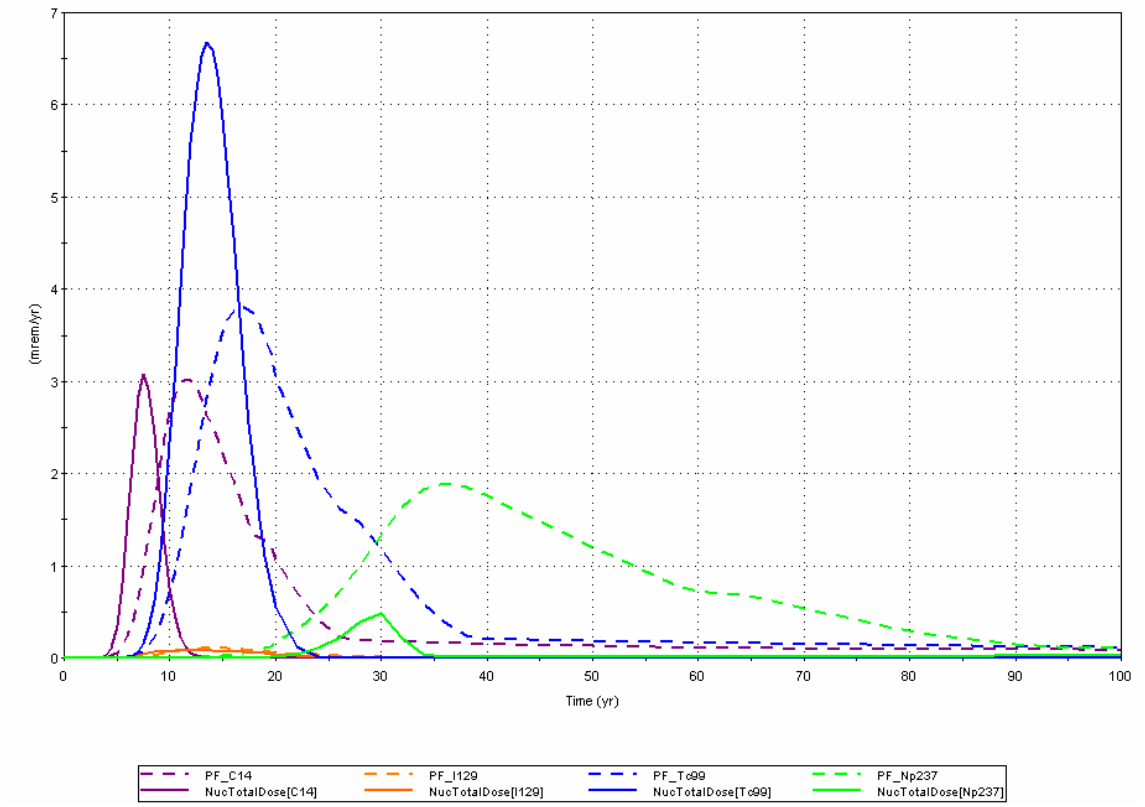

Figure F-33. PORFLOW-GoldSim Dose Comparison

1.1.2 Uncertainty Analysis

1.1.2.1 Uncertainty Analysis Preliminary Results

This section discusses the results of the preliminary uncertainty analysis. A summary of the results will first be presented followed by results for each of the slit trenches. Slit Trench 5 was run using both PORFLOW and GoldSim and its results will be discussed in more detail than the other seven trenches. All trenches behaved similarly. Any significant differences will be discussed.

The results for each trench are presented in terms of the mean value, the median value, and the 95th percentile value for each of the performance objectives. The values are based on 1000 realizations (runs) using the stochastic elements described in the Stochastics section. The plots are for the 100-m water well point of compliance.

It should be noted, however, that these results are from a preliminary GoldSim model that has many placeholder distributions in sensitive roles. The absolute values of the results, therefore, are not to be given too much credence until the model has undergone further development and review.

1.1.2.2 Summary of Uncertainty Analysis Results

Table F-3 shows that the mean and median values do not exceed any of the performance objectives for any of the trenches. The all-pathways dose, the α, uranium, and radium concentration limits were not exceeded at the 95th percentile for any trench. The β/γ limit of 4 mrem in a year was exceeded at the 95th percentile in Trench 3 with a value of 4.5 mrem in a year.

Table F-3. Summary of Preliminary Uncertainty Results

		Slit 1				Slit 2				Slit 3		
Performance measure	**limit**	**mean**	**median**	**95%**		**mean**	**median**	**95%**		**mean**	**median**	**95%**
All pathways, mrem/yr	25.0	0.7	0.6	1.5		6.7	6.5	10.8		10.9	10.6	20.8
βγ, mrem/yr	4.0	1.7	1.6	2.7		2.8	2.7	4.5		2.0	1.9	3.3
α, pCi/L	15.0	0.2	0.2	0.6		0.2	0.2	0.5		1.8	1.7	3.6
Uranium, µg/L	30	7.29E-11	6.83E-11	1.44E-10		1.35E-10	1.27E-10	2.68E-10		1.32E-09	1.24E-09	2.62E-09
Radium, pCi/L	5.00	0.20	0.16	0.52		0.02	0.01	0.08		0.09	0.04	0.33
		Slit 4				Slit 5				Slit 6		
Performance measure	limit	mean	median	95%		mean	median	95%		mean	median	95%
All pathways, mrem /yr	25.0	2.6	2.4	5.2		3.5	3.2	6.9		1.4	1.3	2.7
βγ, mrem/yr	4.0	2.1	2.0	3.4		1.9	1.8	3.0		1.9	1.8	3.0
α, pCi/L	15.0	0.3	0.3	0.8		0.5	0.5	1.1		0.2	0.2	0.5
Uranium, µg/L	30	1.7E-10	1.59E-10	3.36E-10		3.6E-10	3.37E-10	7.13E-10		1.78E-10	1.67E-10	3.52E-10
Radium, pCi/L	5.00	0.16	0.08	0.59		0.14	0.08	0.48		0.09	0.07	0.24
		Slit 7				Slit 8						
Performance measure	limit	mean	median	95%		mean	median	95%				
All pathways, mrem /yr	25.0	11.4	10.6	22.8		0.3	0.2	0.5				
βγ, mrem/yr	4.0	1.7	1.6	2.7		2.0	1.9	3.1				
α, pCi/L	15.0	1.8	1.7	3.7		0.1	0.1	0.2				
Uranium, µg/L	30	1.31E-09	1.22E-09	2.59E-09		3.85E-11	3.61E-11	7.6E-11				
Radium, pCi/L	5.00	0.17	0.08	0.64		0.04	0.02	0.16				

1.1.2.3 Slit Trench 5 Uncertainty Analysis

An explicit Slit 5 performance objective case was run with PORFLOW in order to compare results with the GoldSim analysis. When PORFLOW results are referred to, what is implied is the Automated All-Pathways analysis which used PORFLOW-generated concentrations.

All pathways dose

The all-pathways dose calculation begins at 130 years, the time of expected loss of institutional control. Before the loss of institutional control it is not credible for a well to be drilled in the disposal unit. The timing of the PORFLOW and GoldSim peaks is different due to the different manners which the codes use to calculate the effect of the distribution coefficients.

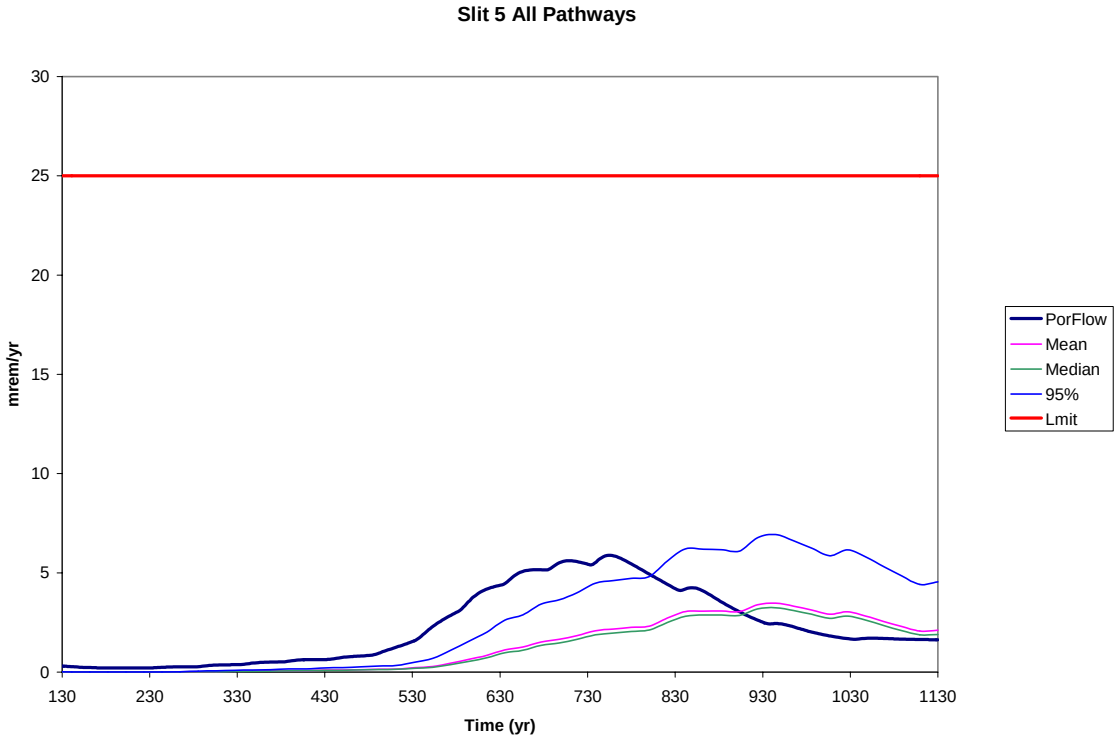

Figure F-34. Slit Trench 5 All-Pathways dose uncertainties

Figure F-35 shows the major contributors to the All-Pathways dose. Np-237 is the major contributor with Pa-231 being the second largest. Both these are long lived, mobile species. Np-237 is present in the initial inventory and also as a decay product of Am-241. Pa-231, not present in the disposed inventory, appears as an ingrowth decay product from U-235. Both are α-emitters and figure in the α concentration performance limit. Note that Figure F-35 shows only one realization.

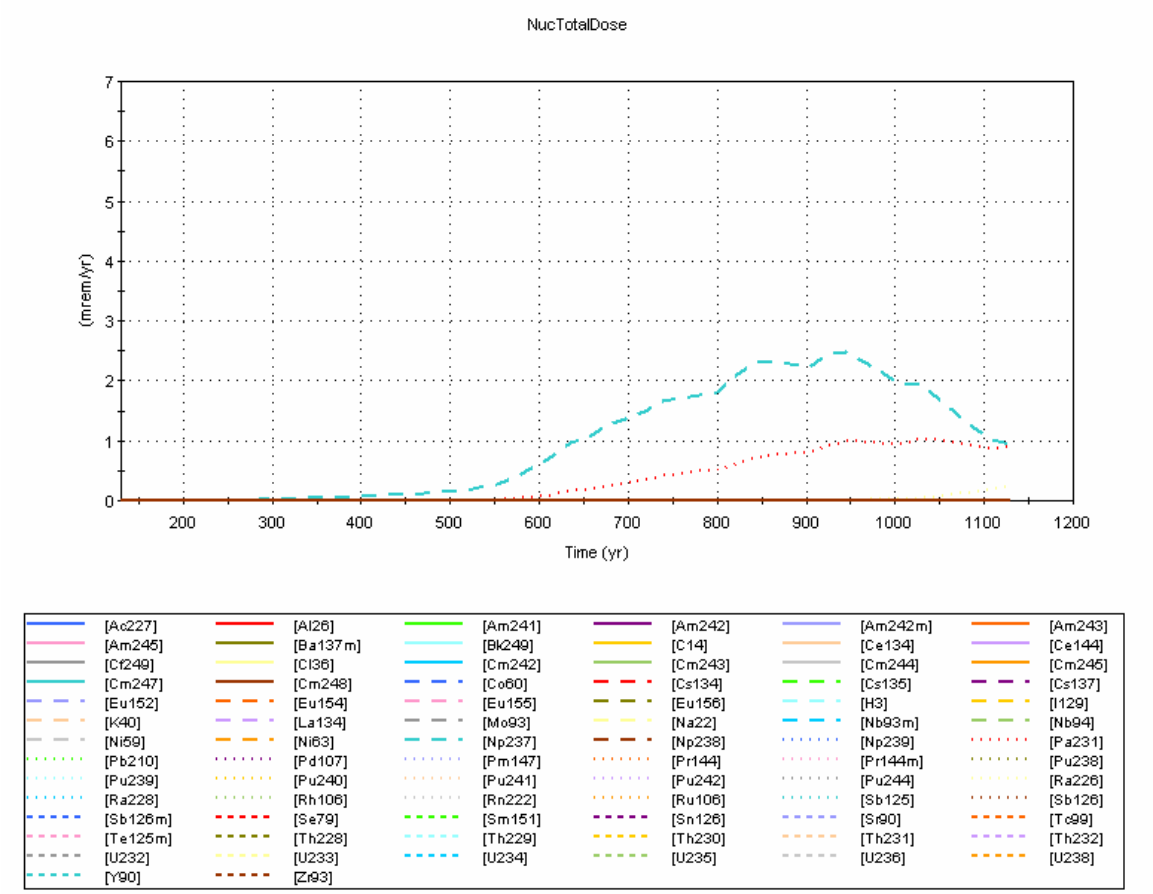

Figure F-35. Slit Trench 5 Major Contributors to All pathways Dose

Beta/Gamma-Emitter Performance Objective

As can be seen in Figure F-36, all the β/γ dose occurs within the first 50 years of the analysis. Figure F-37 shows the β/γ dose comparison for the first 50 years. This dose comes from short lived, mobile species.

The first GoldSim peak is caused by those radionuclides which have a K_d = 0 mL/g. In this case the major contributors are C-14 and Nb-94. The second peak is caused by Tc-99 which has a K_d = 0.1 mL/g.

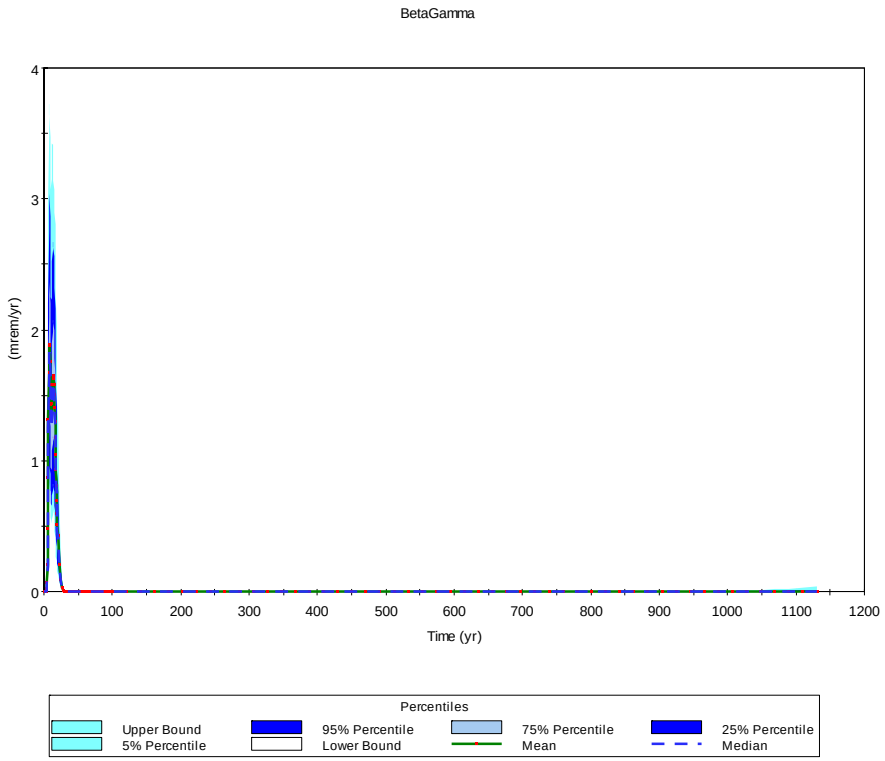

Figure F-36. GoldSim β/γ uncertainty

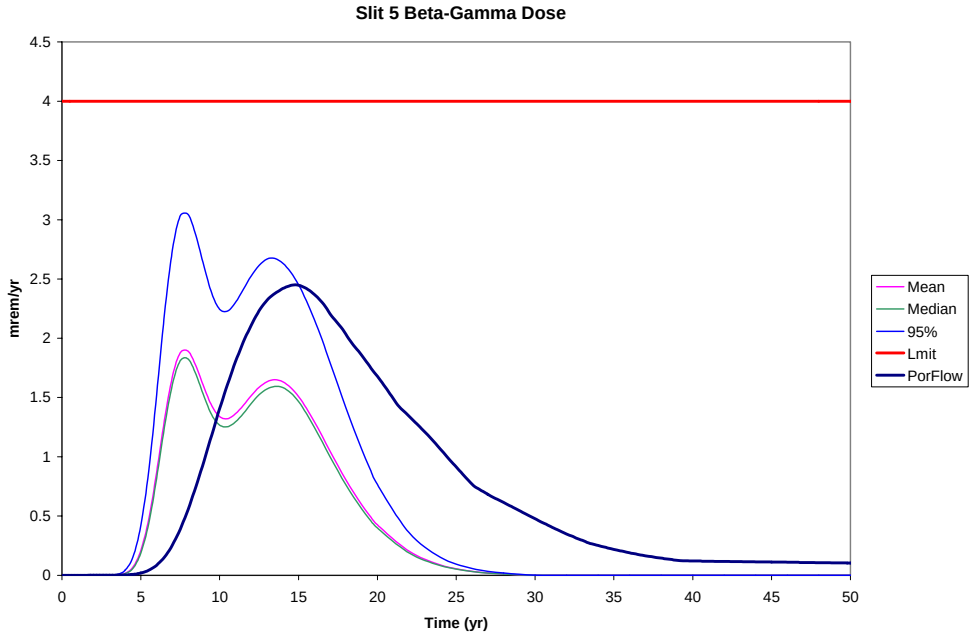

Figure F-37. Slit Trench 5 β/γ Uncertainty

Alpha-Emitter Performance Objective

The major contributors in Figure F-38 are Np-237 for both the early and late concentrations and Pa-231 for the late concentration. The late concentration was discussed in the all-pathways dose section. The early concentration is due to the high mobility of Np-237 (K_d = 0.6 mL/g) and the fact that the closure cap is not in place for 130 years, allowing rapid infiltration.

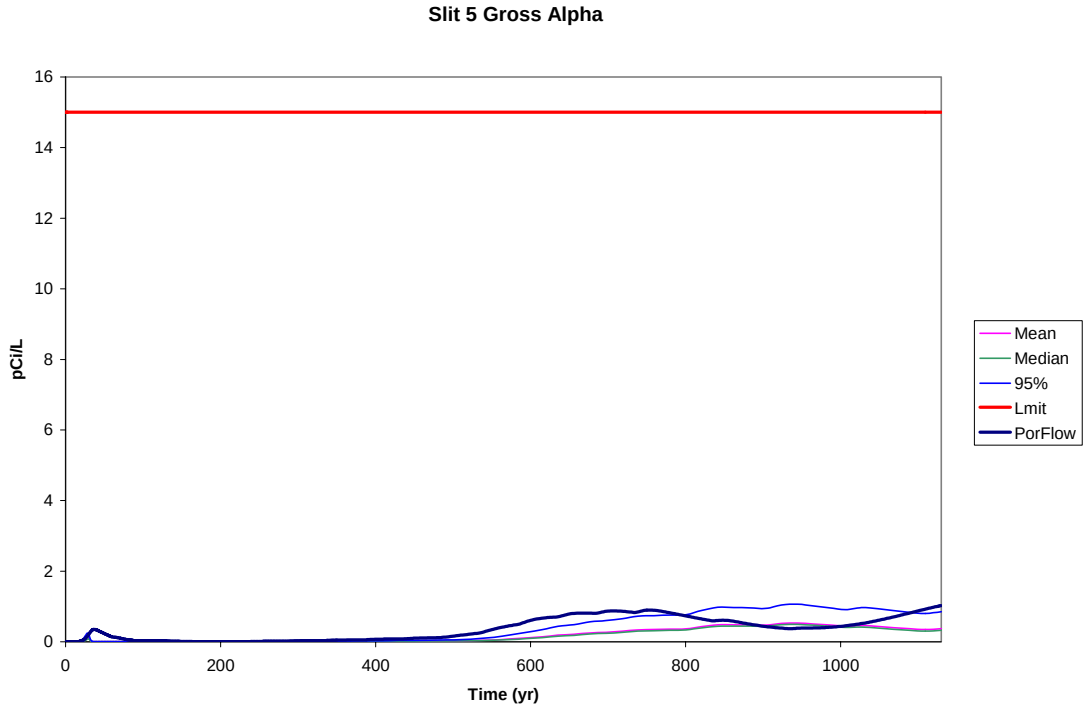

Figure F-38. Slit Trench 5 α Uncertainty

Uranium Performance Objective

The uranium concentration, as seen in Figure F-39, is about 10 orders of magnitude below the objective.

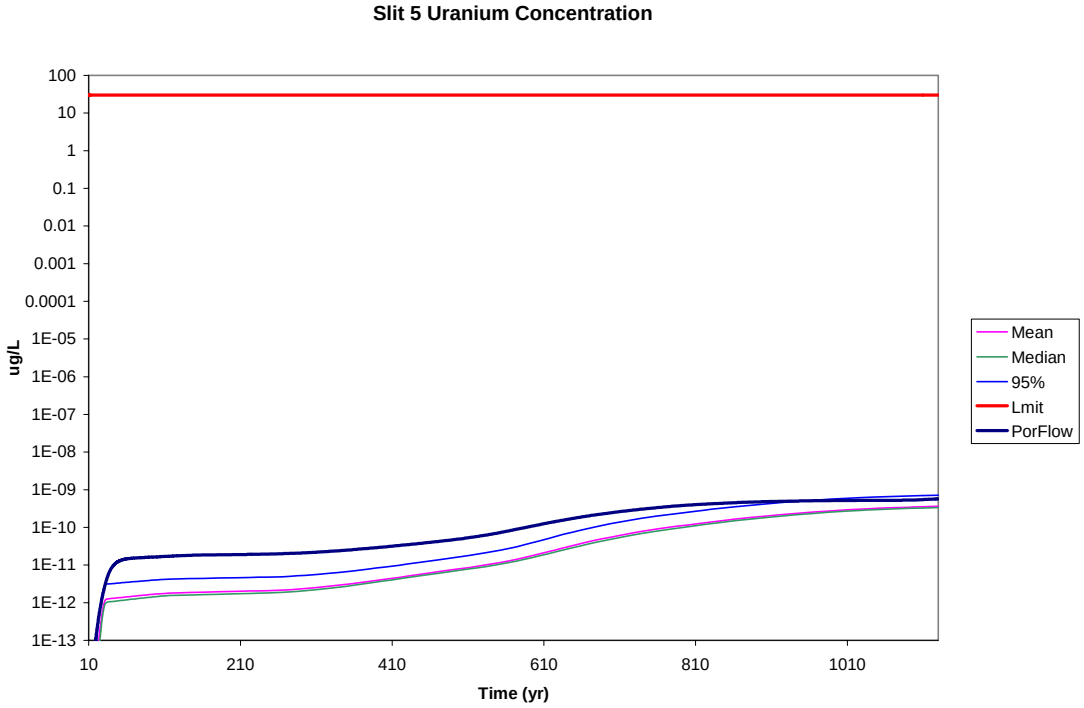

Figure F-39. Uranium Performance Objective Uncertainty

Radium Performance Objective

Radium is a daughter of relatively slow-moving radionuclides and does not appear at the compliance point until near the end of the period of concern. Its concentrations remain well below the performance objective (Figure F-40).

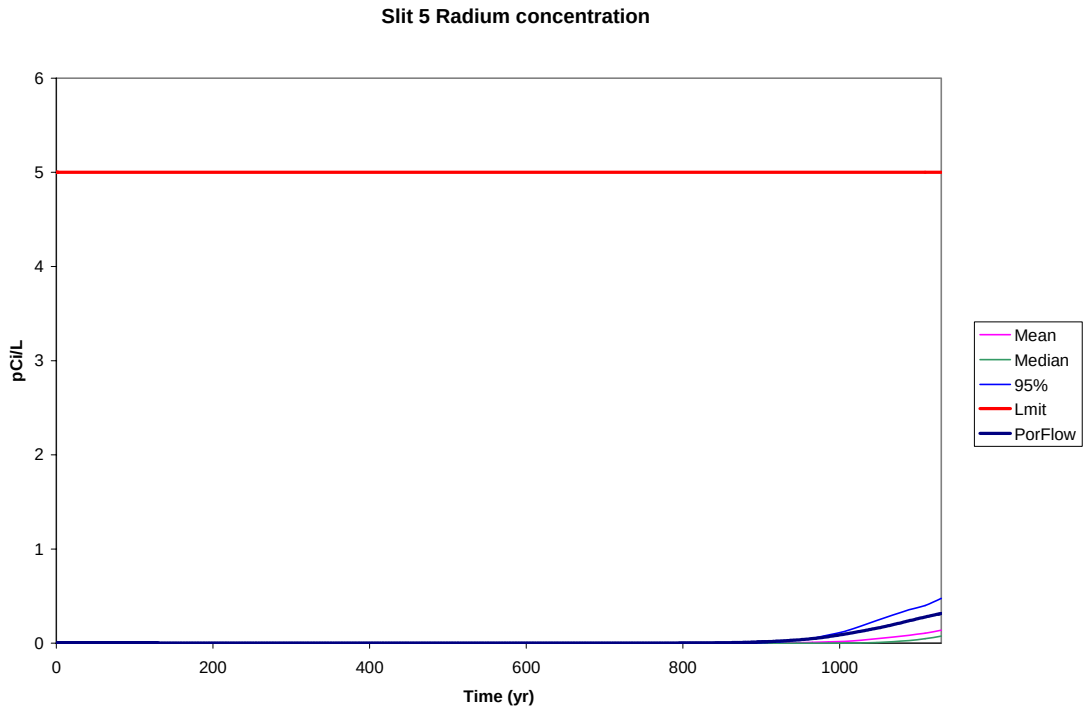

Figure F-40. Radium Performance Objective Uncertainty

1.1.2.4 Slit Trench 1 Uncertainty Analysis

Slit Trench 1 uncertainties are shown in Figure F-41. The β/γ performance objective does not exhibit the double peak as its inventory of Tc-99 is much lower than that of Slit Trench 5.

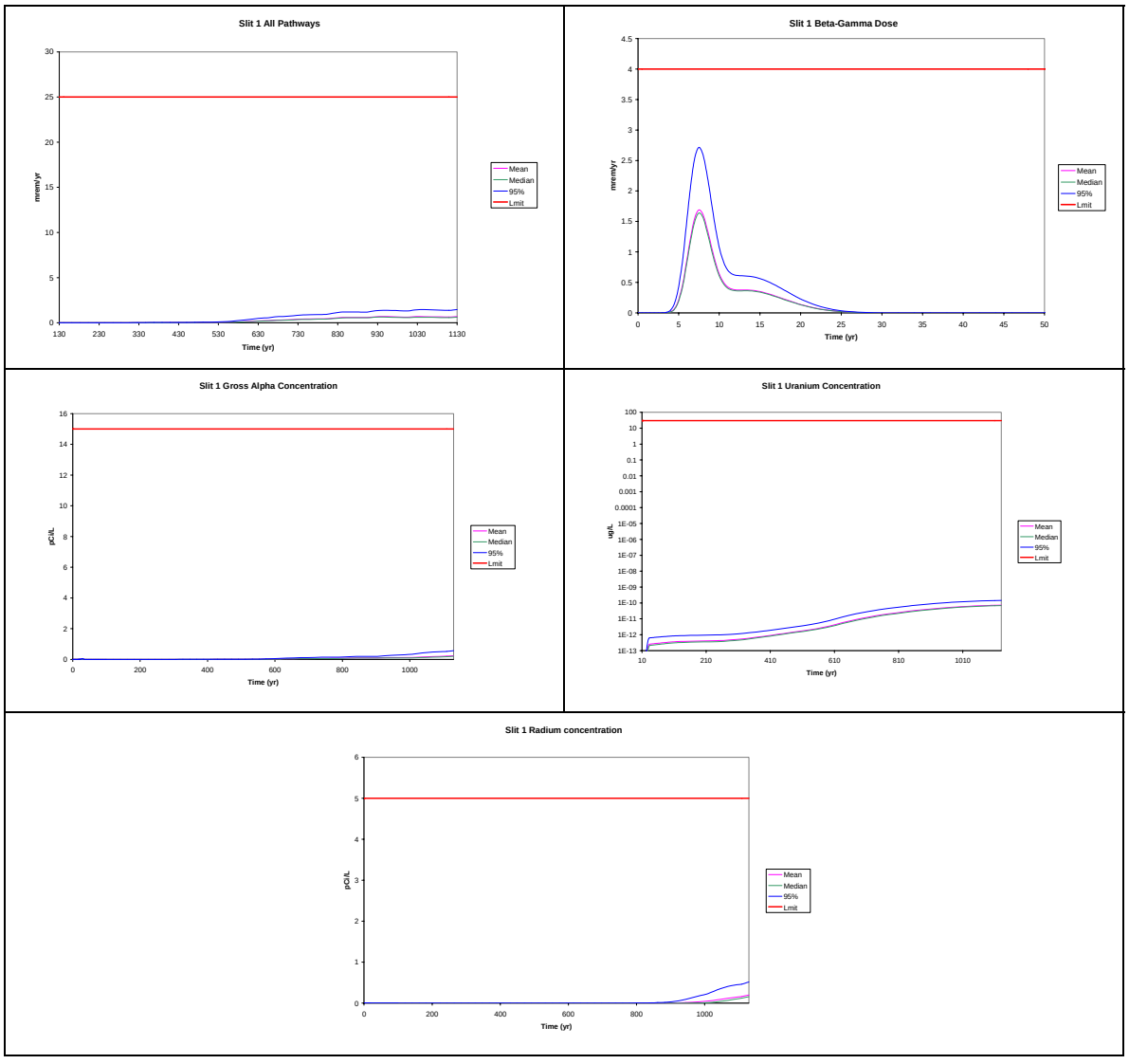

Figure F-41. Slit Trench 1 Uncertainty Analyses

1.1.2.5 Slit Trench 2 Uncertainty Analysis

The 95th percentile of the β/γ dose exceeds the performance objective. However, the mean and median doses are 2.7 and 2.8 mrem in a yr respectively. From these results it appears that the trench contains short–lived, mobile radionuclides as there is no appreciable late dose (see all-pathways dose).

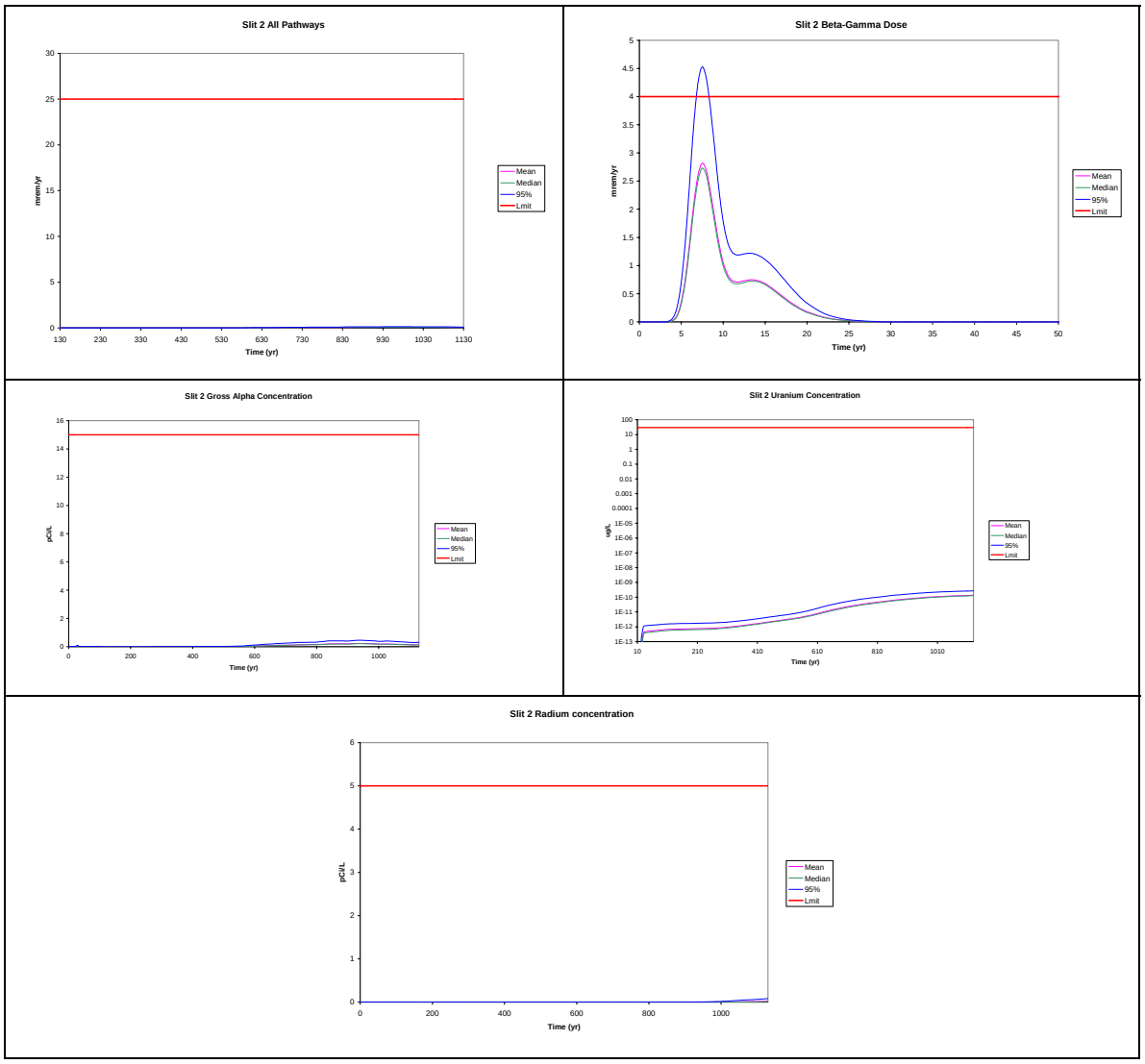

Figure F-42. Slit Trench 2 Uncertainty Analyses

1.1.2.6 Slit Trench 3 Uncertainty Analysis

Slit Trench 3 (Figure F-43) gives the second highest α concentration of the eight trenches, 3.6 pCi/L at the 95th percentile, but is still well below the performance objective.

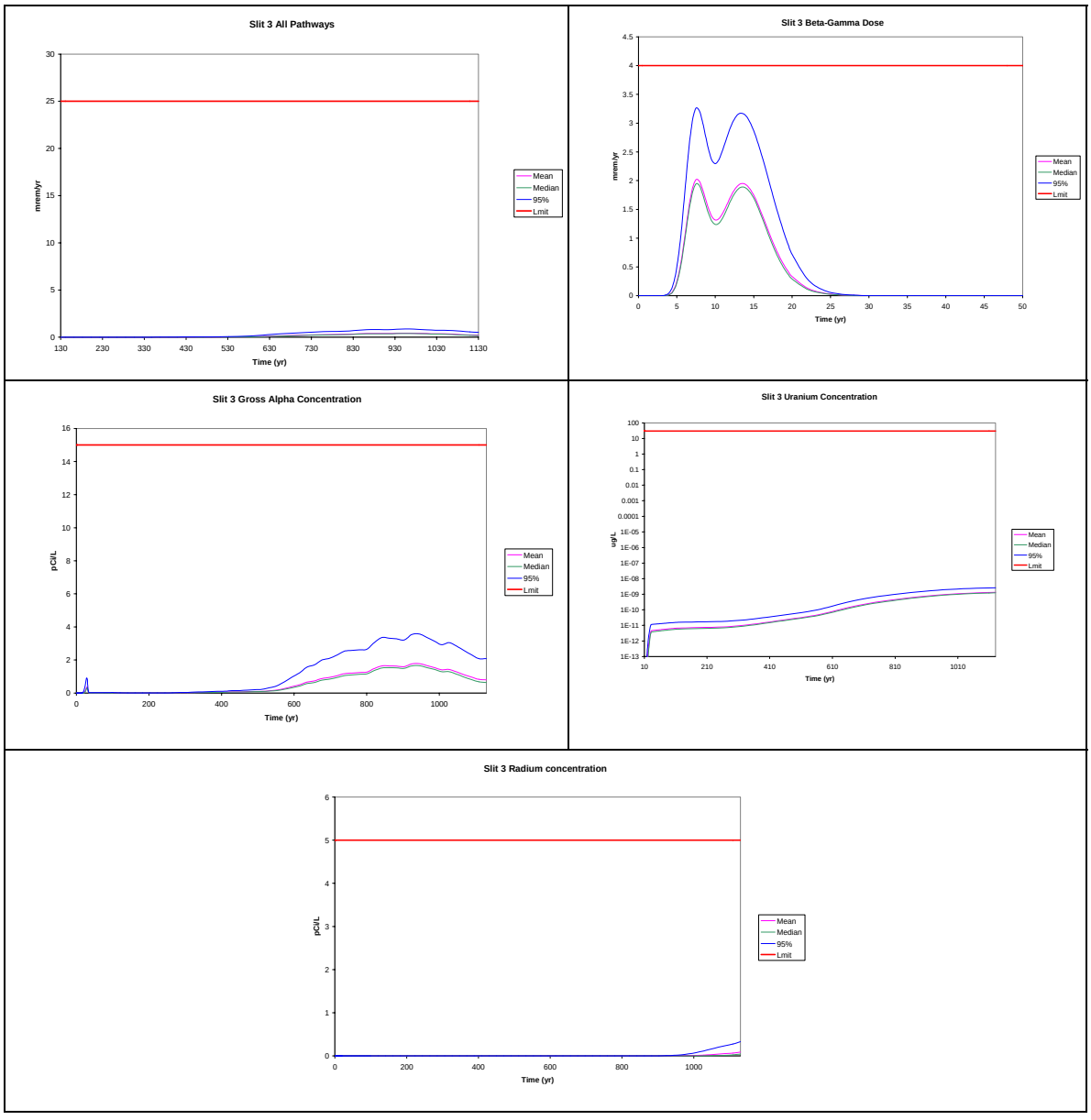

Figure F-43. Slit Trench 3 Uncertainty Analyses

1.1.2.7 Slit Trench 4 Uncertainty Analysis

Slit Trench 4 uncertainty analyses (Figure F-44) provided no challenge to any of the performance objectives.

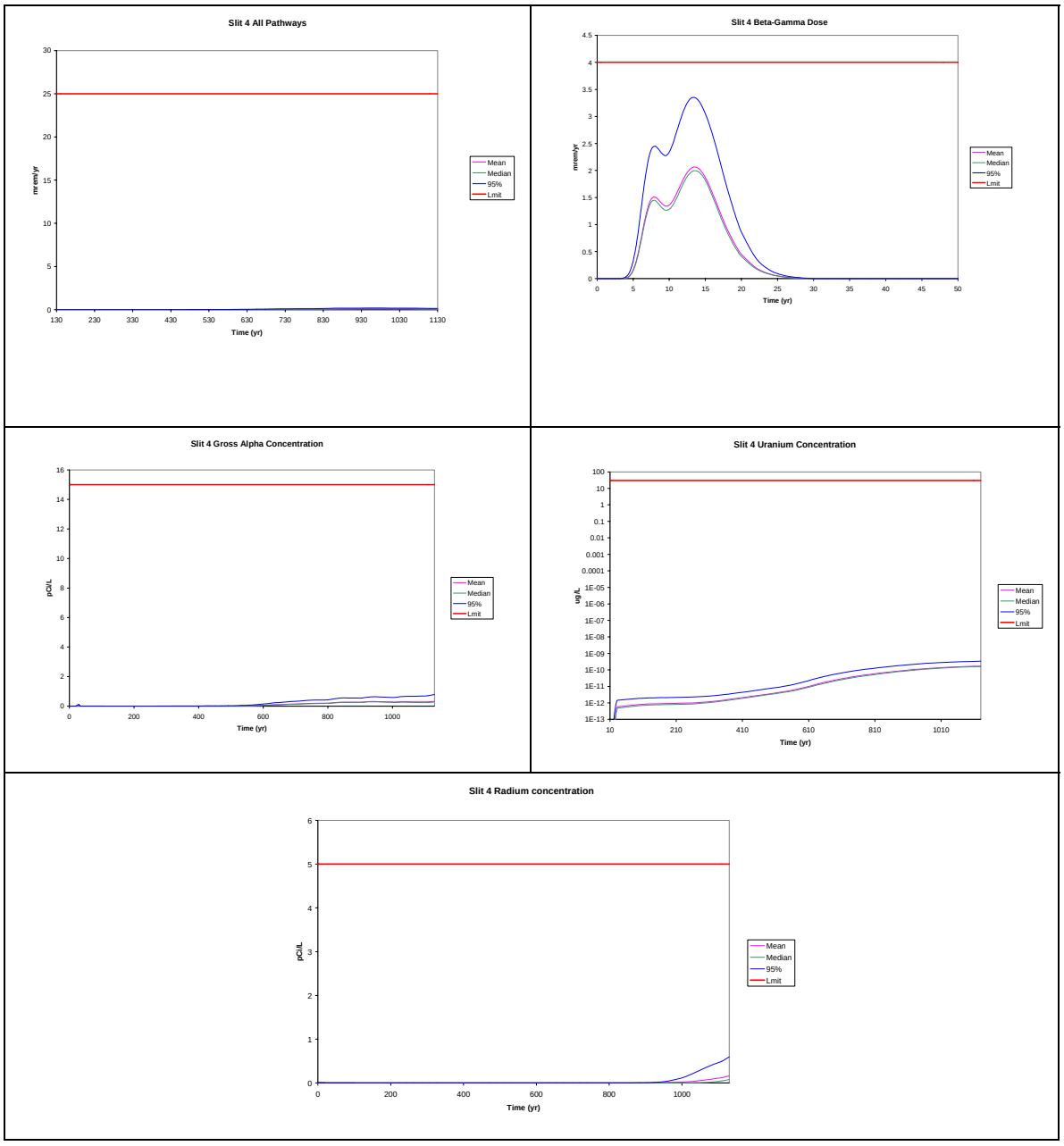

Figure F-44. Slit Trench 4 Uncertainty Analyses

1.1.2.8 Slit Trench 6 Uncertainty Analysis

Slit Trench 6 uncertainty analyses (Figure F-45) provided no challenge to any of the performance objectives.

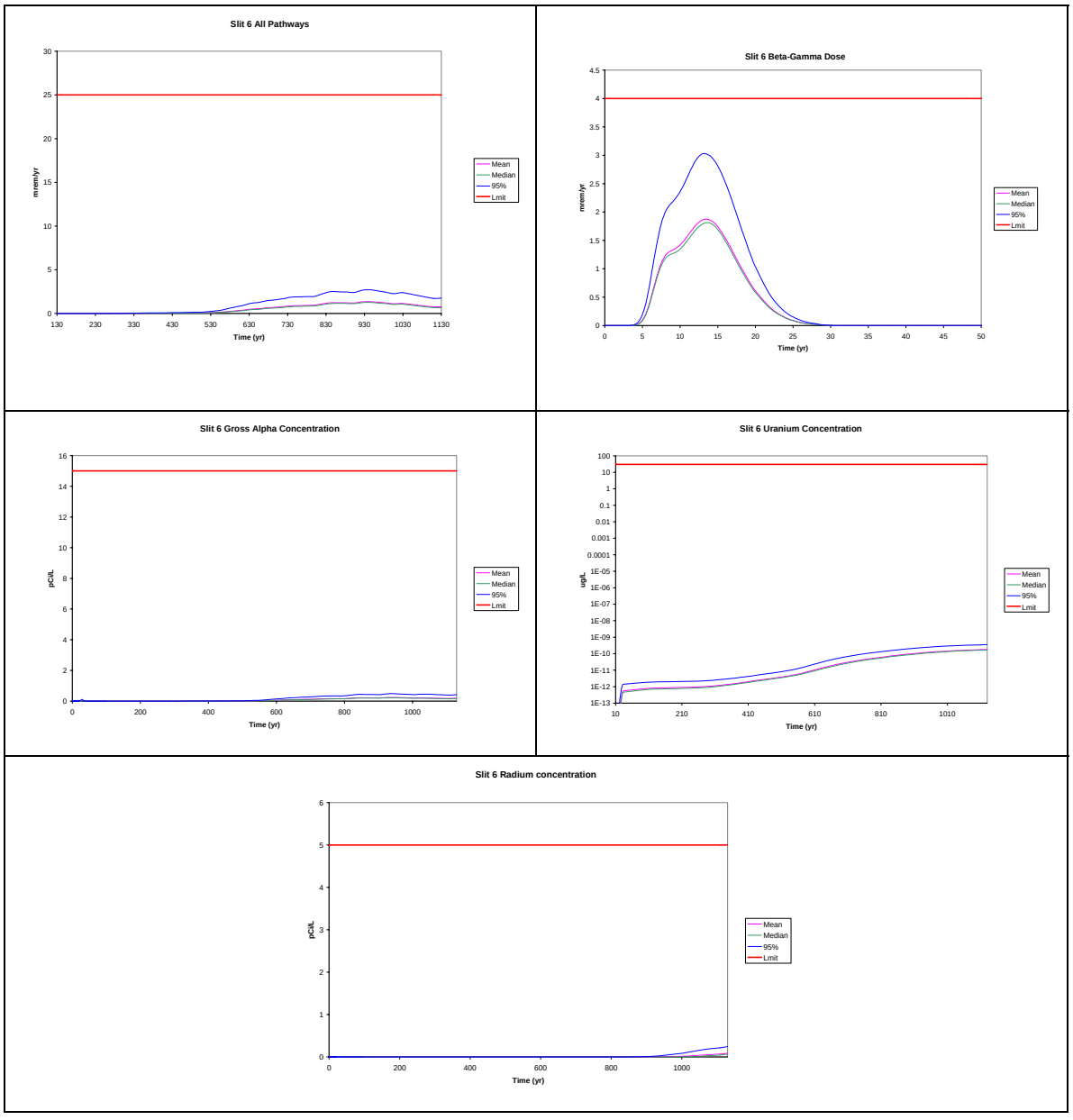

Figure F-45. Slit Trench 6 Uncertainty Analyses

1.1.2.9 Slit Trench 7 Uncertainty Analysis

Slit Trench 7 gives the highest all pathways dose and α concentration at the 95th percentile of all eight slit trenches (Figure F-46). Both of these are due to Np-237 and Pa-231, α-emitters.

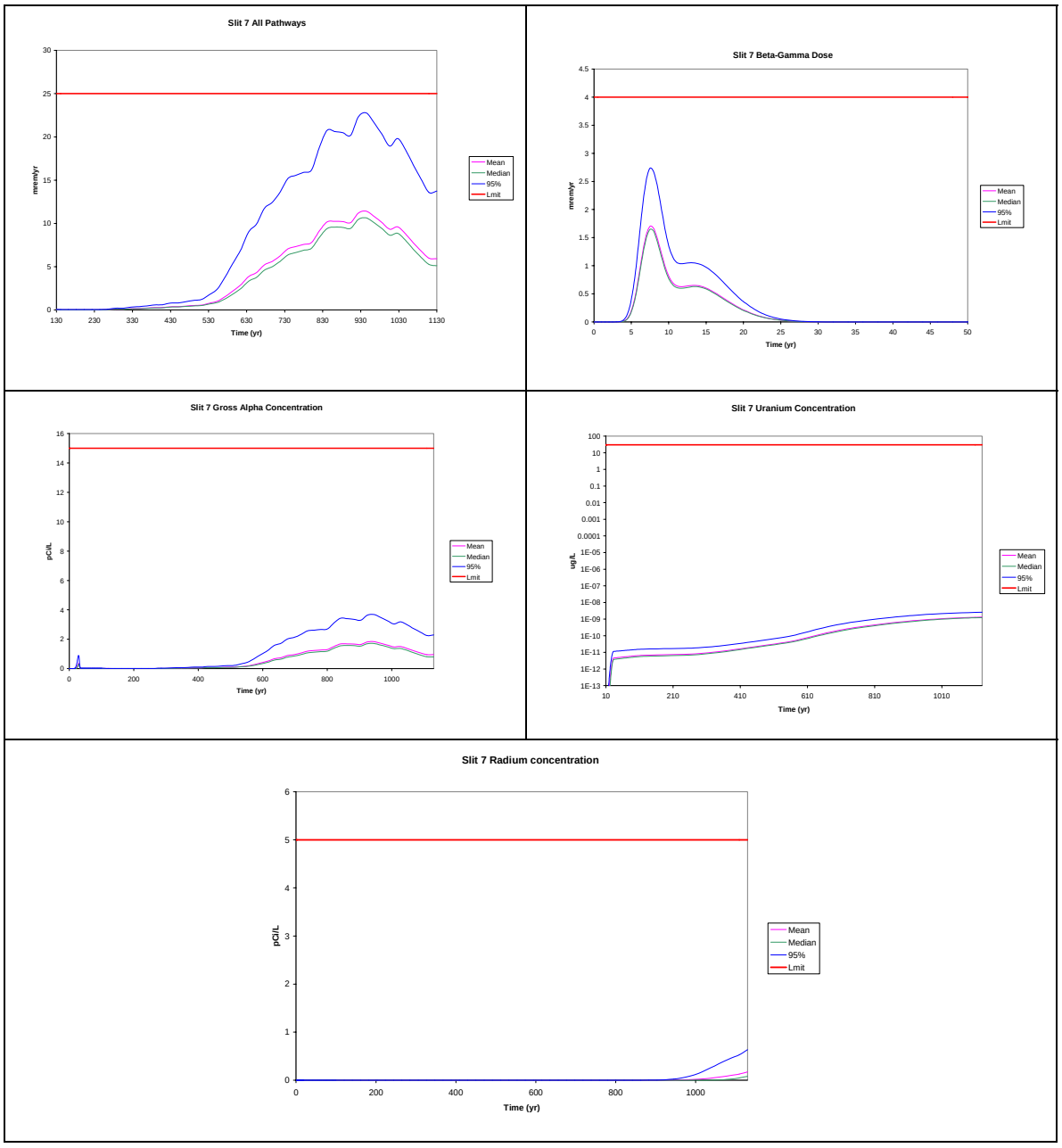

Figure F-46. Slit Trench 7 Uncertainty analyses

1.1.2.10 Slit Trench 8 Uncertainty Analysis

Slit Trench 8 uncertainty analyses (Figure F-47) provide no challenge to the performance objectives.

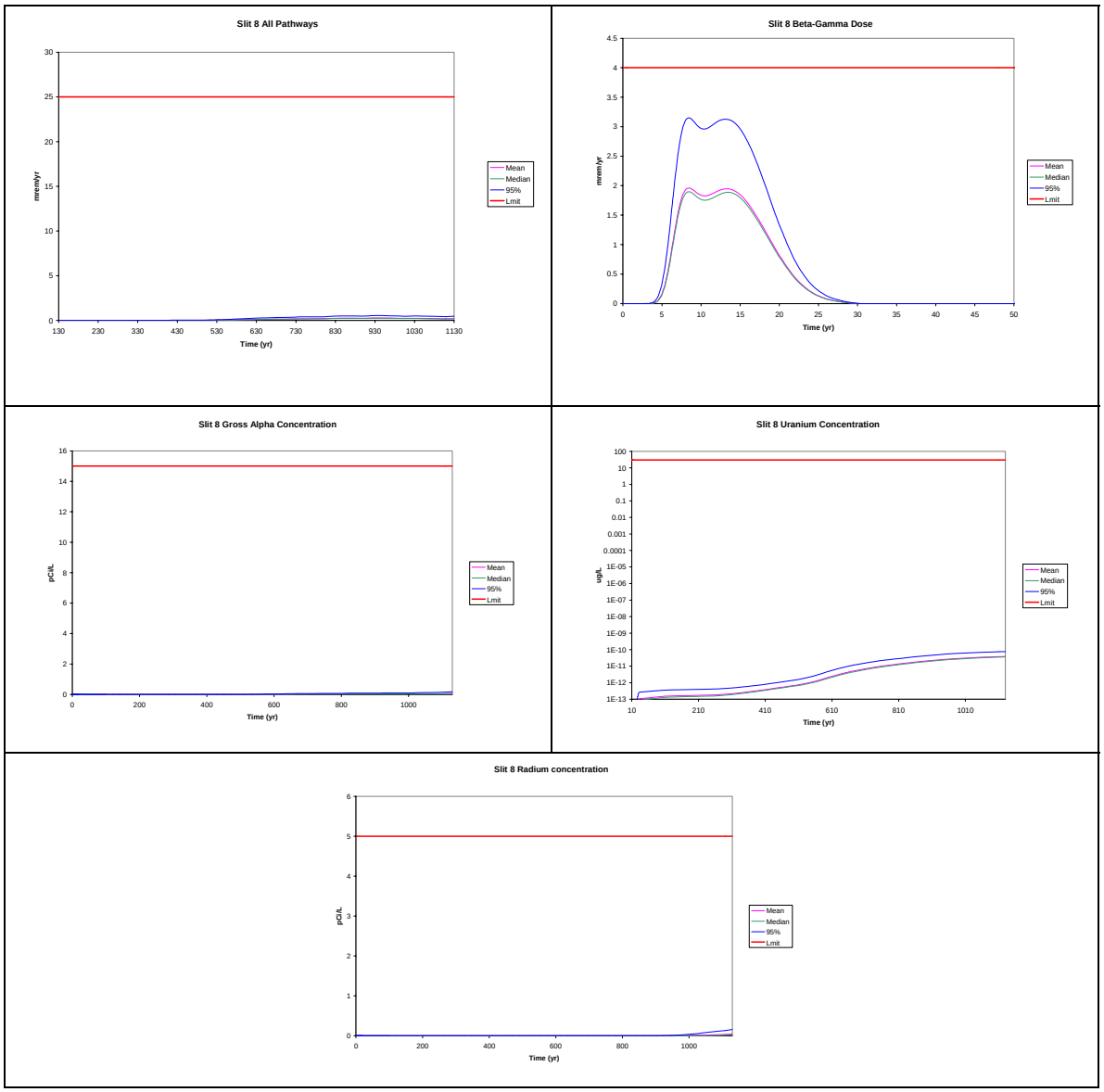

Figure F-47. Slit Trench 8 Uncertainty Analyses

1.1.3 Sensitivity Analysis

This sensitivity analysis is intended to identify relationships between stochastic inputs and selected results in a preliminary model of the Savannah River Site (SRS) E-Area Slit Trenches, in support of the E-Area Performance Assessment (PA) Maintenance Program. A special model was developed for performing the sensitivity analysis using the GoldSim systems analysis software. Results from this model were exported to a text file for sensitivity analysis in post-processing. This model is not intended to predict future potential doses—rather the goal is to characterize the context of uncertainty and sensitivity surrounding the PA calculations.

1.1.3.1 Introduction to Sensitivity Analysis

The results of the model output were analyzed using Gradient Boosting Models (GBM). The GBM modeling approach utilizes binary recursive partitioning algorithms that deconstruct a response into the relative influence from a given set of explanatory variables (stochastic model input parameters). This sensitivity analysis methodology identifies which stochastic model input parameters are most influential in determining the results, such as media concentrations or future potential doses. It should be noted that only those input parameters that are defined using a distribution of values can be analyzed for sensitivity. Many parameters in this preliminary model have not yet had distributions developed, and are defined with only a single value. Such definitions (e.g., radionuclide inventories, thickness of the vadose zone, and all the dose-related parameters) cannot be considered in the sensitivity analysis, so the influence of these deterministic parameters is not known, even though it may be significant.

Complex modeling, such as the GoldSim modeling of the E-Area Trenches, is needed to explore dynamics of systems where multiple variables interact in a nonlinear manner. The probabilistic simulation approach used in the GoldSim model propagates uncertainty regarding the explanatory variables (e.g., physical soil characteristics, inventory mass) through the model to the predicted response (e.g., dose). Quantitative assessment of the importance of inputs is necessary when the level of uncertainty in the system response exceeds the acceptable threshold specified in the decision-making framework. One of the goals of sensitivity analysis is to identify which explanatory variables have distributions that exert the greatest influence on the response.

Sensitivity analysis deals with estimating influence measures for input variables (Saltelli et al. 2000). Influence measures can be estimated in either a qualitative or quantitative context. A qualitative sensitivity analysis provides a relative ranking of the importance of input factors without incurring the computational cost of quantitatively estimating the percentage of the output variation accounted for by each input factor. For either approach the estimates can be obtained either locally or globally within the parameter space.

A local sensitivity analysis involves varying one explanatory variable while holding all other explanatory variables constant and assessing the impact on the model response. This is local in the sense that only a minimal portion of the explanatory variable space is explored (i.e., the point at which the explanatory variables are held constant). Although local sensitivity analysis is useful in some applications, the region of possible realizations for the model of interest is left largely unexplored.

Global sensitivity analysis attempts to explore the possible realizations of the model more completely. The space of possible realizations for the model can be explored through the use of search curves or evaluation of multi-dimensional integrals using Monte Carlo methods. However, these approaches to global sensitivity analysis become more computationally intensive as the dimensionality of the model (i.e., the number of observations and explanatory variables) increases.

Because of the computational cost, sensitivity analysis of high-dimensional probabilistic models requires efficient algorithms for practical application. In this work, GBMs are used to perform a global sensitivity analysis that quantifies the importance of explanatory variables using sensitivity indices, which are metrics based on the explained variance in the response (Borra and DiCiaccio 2002; Diettrich 2000; Breiman 1996). The implementation of GBM used here comes from the ***R*** statistical package named GBM and closely follows the gradient boosting method development presented by Friedman (2001, 2002).

1.1.3.2 Model Fitting and Validation

Global sensitivity is estimated here as the proportion of the variance of the response accounted for by each explanatory variable. This estimation is conducted by fitting GBM model predictions to realizations from the GoldSim model. Variance decomposition of the fitted GBM model is then used to estimate sensitivity indices. Under this decomposition approach, the goal is to identify the most influential explanatory variables that are identified within a parsimonious model. The necessary degree of model complexity is assessed using validation metrics based on comparison of model predictions with randomly selected subsets of the data. This approach uses the "deviance" of the model as a measure of goodness of fit. The concept of deviance is fundamental to classical statistical hypothesis tests (e.g., the common t-test can be derived using a deviance-based framework) and guides the model selection process applied here.

The GBM model-fitting approach is based on finding the values of each explanatory variable that result in the greatest difference in means for the corresponding subsets of the response. For example, if there were only a single explanatory variable, the GBM would identify the value of the explanatory variable that corresponds to a split of the response into two parts such that no other split would result in corresponding groups of the response variable with a greater difference in means.

When multiple explanatory variables are present, these multiple splits are referred to as "trees" and the each tree results in an estimate (e.g., prediction) of the response. As multiple potential trees are evaluated, they are compared to the observed data using a loss function. The selection of the loss function is an influential aspect of the GBM process and depends on the distribution of the response variable. For data that are sufficiently skewed (e.g., non-normal), the absolute error loss function tends to produce more reliable results.

There is a trade-off that exists when considering which loss function to use. The squared-error loss function tends to result in better-fitting models, but does so at the expense of introducing spurious variables into the model selection process when the response distribution is sufficiently skewed. The absolute error loss function tends to produce model predictions with more variability but is less likely to result in the selection of spurious variables into the model. For this application, the focus has been on using a deviance-based method to obtain parsimonious models that identify the most important explanatory variables with respect to the observed variability in the response. To this end, the squared-error function was used in these applications.

Once a GBM model is constructed, each of the explanatory variables that exist in the model can be assigned a sensitivity index. The sensitivity index is obtained through variance decomposition and can be interpreted as the percentage of variability explained in the model by a given explanatory variable. The sum of the sensitivity indices across the entire set of explanatory variables in the model will approximately equal the R^2 of the linear regression of the GoldSim output versus the GBM predictions. These "observed vs. predicted" scatterplots are presented for each of the response variables of interest.

In order to assess the relationship between an individual explanatory variable and the response of interest, partial dependence plots are used. A partial dependence plot shows the distribution of the explanatory variable and the partial dependence curve, which indentifies changes in the response as a function of the explanatory variable. The partial dependence is obtained through the integration across the joint density to obtain a marginal distribution. The integration is performed using a "weighted tree traversal" measure (Friedman 2001) that is analogous to more common integration procedures performed with Riemann or Lebesgue measures. The vertical axis of the partial dependence plot shows the change in the response variable as a function of the changes in the explanatory variable of interest. With standard linear regression techniques, it is assumed that the relationship between the response and the explanatory variable is a constant (e.g., the parameter estimates in the linear model). With the GBM approach, this relationship is not constrained by assumptions of linearity and the partial dependence plots show the data-based estimate of the relationship between the response and explanatory variable. This is especially useful for understanding the influence of changes in a single explanatory variable on the response, when integrating across all other explanatory variables.

Although not presented here, partial dependence plots can be constructed in three dimensions, useful in examining the effects of interactions between two variables on the response. Finally, these plots are especially useful for the identification of thresholds and non-linear relationships between response and explanatory variables.

1.1.3.3 Summary Statistics for Endpoints

The particular model setup used for the sensitivity analysis included an average slit trench inventory in a single set of five slit trenches. That is, rather than execute eight separate analyses for the eight different inventories, the sum of radionuclides in all eight slit trench sets was divided by 8 to arrive at a virtual inventory, modeled as being in one trench set.

The model was run using a Monte-Carlo scheme, where each stochastic input parameter is sampled in different ways, and these sampled values are combined to produce many realizations (in this case 5000 realizations.) Most of the resulting dose estimates are near some central value, and a few are extremely high or low. The probability of occurrence of any particular result is defined by where that result lives in the context of all the results.

The following modeled performance objective results, called endpoints, were selected for sensitivity analysis. That is, those stochastic input parameters that are most significant in determining the values of each result are identified.

DoseMaxEarly is the maximum potential All-Pathways (i.e., all exposure pathways from the use of contaminated groundwater) dose to an individual member of the public achieved before 200 years. Due to the timing of construction and subsequent degradation of the engineered cap, doses tend to occur either early on, before the cap is installed, or much later, once it has degraded sufficiently. It is recognized that the early doses would be precluded by effective institutional controls, but they are included here for purposes of illustration and insight into model behavior.

DoseMaxLate is the maximum potential All-Pathways dose occurring after 200 years but still within the period of performance (1130 yr). Since all engineered features of the site fail in the long term, these doses are representative of problems that would occur after the loss of institutional control, and should be used in making decisions related to dose reduction. Note that for the other models (Engineered and CIG Trenches the model duration was extended well past the period of performance, so the equivalent endpoint is called MaxDoseMidtime. For those analyses, MaxDoseLate occurs between 10,000 and 20,000 years).

MaxAlpha is the maximum concentration in well water resulting of all alpha-emitting radionuclides within the period of performance, to be compared to the MCL.

MaxBetaGamma is the maximum drinking water dose from all beta- and gamma-emitting radionuclides in the well water within the period of performance, calculated by the ratio of the EPA-derived concentration that is equivalent to a dose of 40 μSv (4 mrem) in a year.

For the Engineered Trenches and Components-in-Grout Trenches, the maximum radium and uranium groundwater concentration endpoints were also evaluated for comparison to MCLs. Although these endpoints were not subjected to sensitivity analysis, they were evaluated in the model, and so appear in the summary Table F-4 .

The results of the sensitivity analysis indicate that overwhelmingly the most significant stochastic parameter in the model for all the above endpoints is the assumed thickness of the saturated zone, or aquifer. In effect, this parameter controls the amount of water into which contaminated recharge is mixed on its way into the drinking water well, as well as the mixing hydraulics for the well capture zone, since these effects are not otherwise modeled. It is expected that this sensitivity would be important for any of the eight inventories, since the effects of inventory could not be considered in the sensitivity analysis. Other less significant sensitive parameters include soil/water partition coefficients (K_ds) for dose-significant radionuclides, aquifer dispersivity ratios (also related to mixing), and the final thickness of the waste after subsidence. As discussed in the model description section (1.1.1) all of these parameters except the K_ds are placeholder distributions based on engineering judgment.

The GoldSim model that was run for this sensitivity analysis has the file name “E-Area Slit Trench SA v1.0 InvAvg r5000.gsm”. This is a copy of v1.0 of the model, set to use an average slit trench inventory and 5000 realizations, with Latin Hypercube Sampling enabled and a seed value of 1. The exporting of results follows the simple procedure outlined in the model, in the SensitivityAnalysis container, wherein the tabulated raw data contents of the element Endpoints_SA are exported to the file “E-Area Slit Trench SA v1.0 InvAvg r5000.gsd” (note the different extension, .gsd, for “GoldSim data”) a 29 MB tab-delimited text file containing values of modeling endpoints and all stochastic input values for each of the 5000 realizations. This file is read directly by the sensitivity analysis processing program developed in ***R*** by Neptune and Company.

Figure F-48 provides some context to the subsequent discussion. This shows the dose potential from the use of well water (drinking, livestock, irrigation, etc.), summed over all radionuclides, for all 5000 realizations. The depiction of all realizations is in this case more illustrative than a plot of statistical summaries. The early doses occur within the first 30 years (ignoring institutional control) while the trenches are open to the elements. At 130 years, the engineered cap is emplaced, and infiltration rates and doses drop dramatically, remaining low until the cap begins to fail at around 270 years. At that point in time, they follow two distinct paths – the higher being associated with the base case cap degradation scenario: bamboo cover followed by pine forest.

The lower doses result from the continuous bamboo cover scenario, and the time histories that cross over from lower to higher between about 500 and 800 years are a result of the scenario of bamboo cover followed by farming and then by pine forest. By the end of the model duration, these scenarios tend to converge. This may indicate that the higher infiltration resulting from the forest tends to "wash out" the contamination, with peak concentrations at about 900 years, where the lower infiltration of the bamboo cover seems to suppress transport until later times, with a peak somewhere after 1130 years.

Summary statistics for the endpoints of interest are tabulated in Table F-4. It should be kept in mind that the absolute values for dose are not to be given a great deal of credence, in that the analysis considers a virtual average inventory in only one set of Slit Trenches, and ignores the presence of other disposals in proximity. The purpose of this model is not to predict doses, but rather to characterize the uncertainty and sensitivity context of the actual PA model. The summary statistics quantify the uncertainty surrounding the dose calculations.

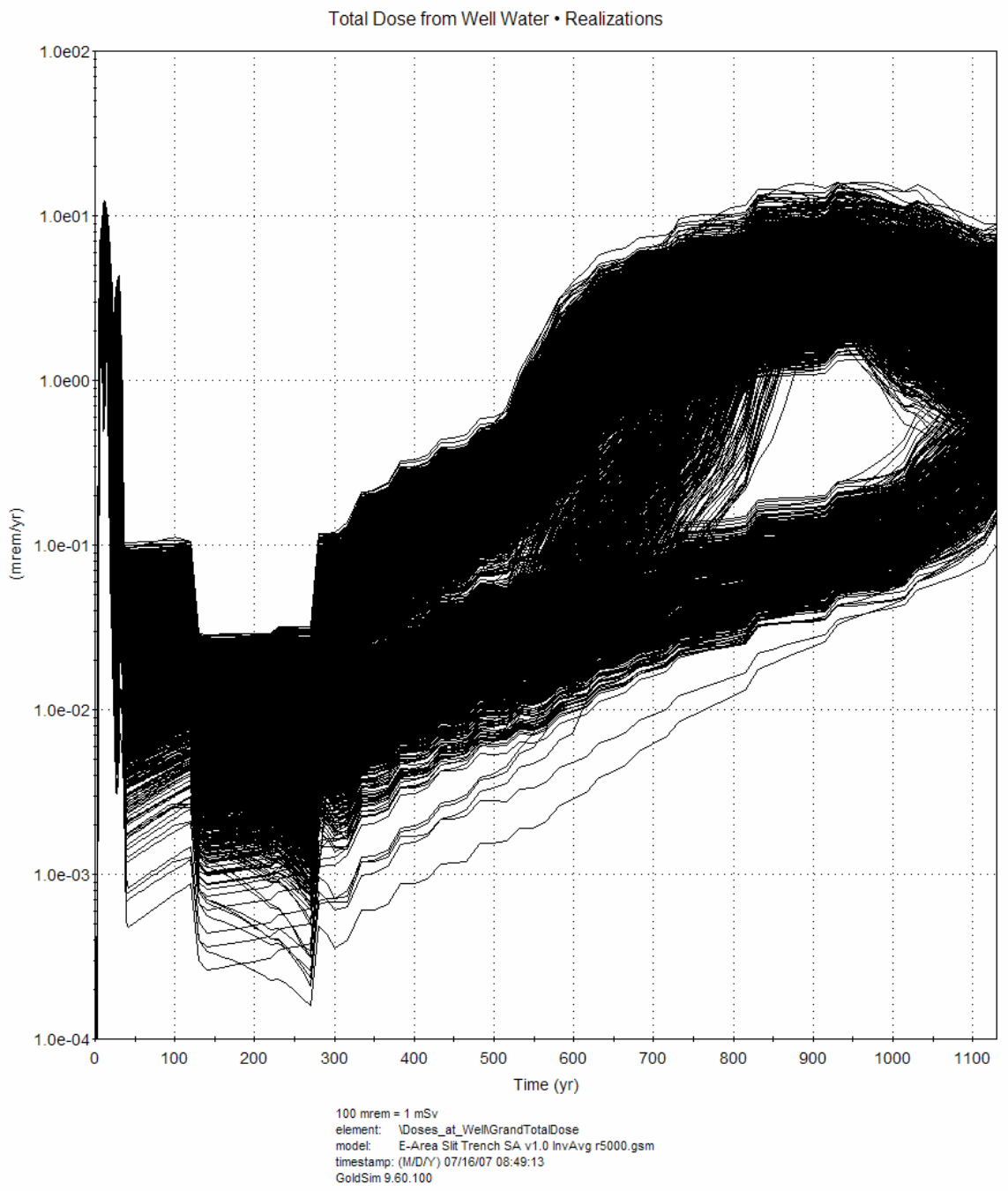

Figure F-48. Time history of Slit Trench total dose from use of well water, all 5000 realizations, averaged inventory

Table F-4. Summary statistics from 5000 realizations for the Slit Trench endpoints of interest

Endpoint	Mean	Standard Deviation	Min	1st Qu.	Median 2nd Qu.	3rd Qu.	Max
Max. Total Dose (Early)	5.7	2.0	2.1	4.1	5.2	7.0	12
Max. Total Dose (Late)	4.4	2.3	0.10	3.1	4.2	5.7	16
Max. Alpha Conc (pCi/L)	0.73	0.36	0.016	0.50	0.68	0.93	2.7
Maximum Beta-Gamma Dose	1.8	0.63	0.79	1.3	1.7	2.3	3.5
Max. Radium Conc (pCi/L)	0.11	0.13	3.5e-18	0.024	0.07	0.15	0.97
Max. Uranium Conc (μg/L)	4.5e-10	2.4e-10	6.5e-12	3.0e-10	4.2e-10	5.8e-10	1.9e-9

1 mrem = 10 μSv
All dose units are mrem in a year.

1.1.3.4 Endpoints and most influential explanatory variables

Each of the modeling endpoints discussed above and listed in the table (except for Ra dn U concentrations) was analyzed to identify those stochastic parameters having the most influence on that endpoint. In all cases, the most significant parameter was the saturated thickness of the aquifer, as shown in Table F-5. Graphs of the partial dependence are also presented.

Discussions of particular results are provided following the figures below. For each of the endpoints, a graph is provided showing the predictive power of the GBM estimate as compared to the GoldSim results. Less scatter along the line of slope = 1 reflects a better fit of the statistical model that is constructed to predict the GoldSim results. Following the scatterplot is a collection of four graphs showing the SI of the top four sensitive parameters for the endpoint. The shaded green background shows the distribution of the 5000 samples from the input distribution, and closely reflects the defined input distribution. The blue solid line (partial dependence) shows the degree of sensitivity as a function of the parameter value. The parameter is most sensitive where the partial dependence is high, and is least sensitive where it is low.

Table F-5. Identification of the four most sensitive parameters for the Slit Trench endpoints of interest

Endpoint	SI rank	input parameter	Sensitivity Index	R^2
Max. Total Dose (Early)	1	saturated thickness of aquifer	94.7	99%
	2	Tc K_d in clayey soil (and the waste)	3.69	
	3	Tc K_d in sandy soil	1.04	
	4	longitudinal dispersivity ratio	0.21	
Max. Total Dose (Late)	1	saturated thickness of aquifer	72.9	55%
	2	final subsided waste thickness	4.23	
	3	Np K_d in clayey soil (and the waste)	1.88	
	4	Fr K_d in reducing (young) concrete	0.79	
Max. Alpha Concentration	1	saturated thickness of aquifer	45.8	84%
	2	final subsided waste thickness	2.67	
	3	Np K_d in clayey soil (and the waste)	2.03	
	4	Ra K_d in sandy soil	0.58	
Maximum Beta-Gamma Dose	1	saturated thickness of aquifer	98.9	99%
	2	longitudinal dispersivity ratio	0.25	
	3	transverse/longitudinal dispersivity ratio	0.21	
	4	particle density of sandy soil	0.21	

Sensitivity indices provide a measure of the relative importance of explanatory variables with respect to the response of interest. The most important part of the sensitivity analysis is the ability for the sensitivity analysis method to predict the response given a specific set of explanatory variables. A simple way to assess the goodness-of-fit is to look at a plot of the observed output from the GoldSim model versus the predicted values from the GBM model. Quantitatively, this fit can be measured using the R-squared of a regression of the GoldSim model output on the GBM model predicted values. To the extent that the R-squared is high and the relationship between the GBM predictions and the GoldSim model output is linear, the SI values will provide a reliable measure of the relative importance of explanatory variables in the model. If the fit is poor (e.g., characterized by non-linearity, bifurcations, or excessive spread around the regression line), then the reliability of the sensitivity analysis procedure decreases.

These sensitivity analysis procedures are exploratory in nature and sort through hundreds of potential explanatory variables in order to find the most important variables in a model. If the distribution of the response is skewed such that most of the values are very small (near zero), the potential increases for the spurious identification of variables that are important in the model. When the response variable is skewed in this way, it only takes a few values that are randomly correlated with the large values in the response to produce a spuriously identified response variable. If we consider this in the context of the interpretation of parameter significance, we see that the sensitivity analysis methods presented here are less likely to produce spurious results. For example, if we take a response variable and randomly generate 100 sets of potential explanatory variables that have nothing to do with the response (i.e., they are randomly generated numbers), we would expect that on average 5 out of those 100 variables would be erroneously selected as significant at a 0.05 significance level just by chance alone. In this application we are sorting through several hundred potential explanatory variables for each endpoint within a model. Essentially we are evaluating thousands of potential explanatory variables for each model and we are observing only a few variables that have been spuriously selected. As with any modeling approach, application of process-based knowledge, along with the removal of extraneous explanatory variables from the model will result in improved performance from the application of the sensitivity analysis techniques.

Maximum All-Pathways Dose (Early)

The maximum all-pathways (water use) dose from all radionuclides in early time is that maximum achieved before 200 years. Figure F-49 shows excellent ability of the GBM to predict the GoldSim results. This means that there is high confidence in the sensitivity analysis. The R^2 for this relationship is 99%.

By far, the most significant parameter here (as well as for other Slit Trench endpoints) is the saturated thickness of the aquifer. This value defines the vertical dimension of the compartments (or Cells, as they are called in GoldSim) used to model lateral waterborne advective transport from beneath the waste zone to the exposure point, a water well located 100 meters directly downstream of the border of the modeled Slit Trench. Since these Cells assume instantaneous mixing throughout, the vertical dimension is effectively the depth over which the plume of contamination is mixed—the volume of water that dilutes the contaminated recharge as it gets extracted by the well. The saturated thickness input distribution was set to be uniform, from 5 to 15 meters, as reflected in the green background. Since the same mass of radionuclide contaminants is introduced into the aquifer regardless of its thickness, their concentration is inversely proportional to the thickness. The potential dose through water-related pathways is also a generally linear response to concentration, since none of the dose calculation parameters are defined stochastically. Hence, the strong dependence of dose on saturated thickness is not surprising.

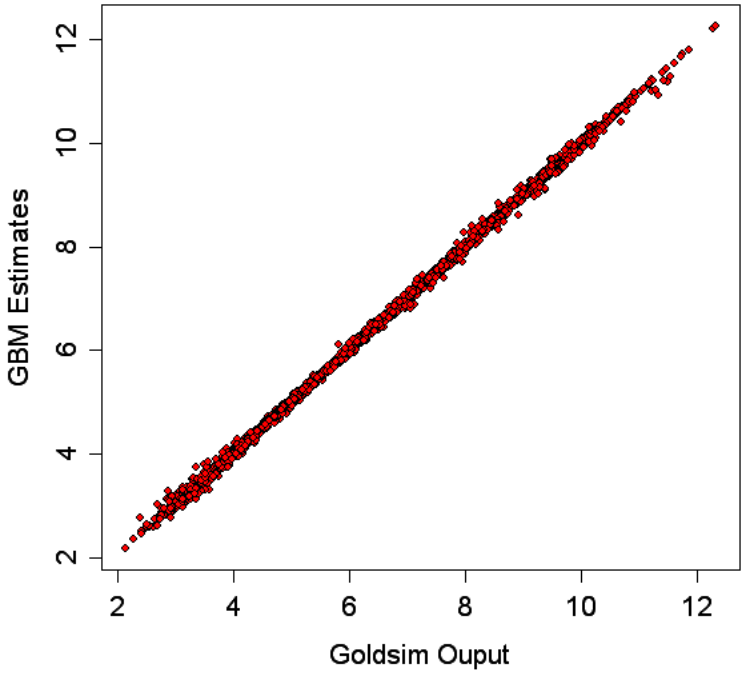

Figure F-49. Scatterplot of GBM estimate for Slit Trench maximum total dose (mrem in a year) in early time

The range of sensitivity (very sensitive in the low range of K_d, and insensitive to higher K_d values) is consistent with what we know about K_ds. Contaminants are most mobile at $K_d = 0$ or near zero. As we can see with Tc, even very small K_d values (0.1 to 0.2 mL/g) can strongly influence the ability of Tc to causes doses in early time. Vales above 0.2 or 0.3 mL/g are sufficient to remove the sensitivity of early dose to Tc K_d altogether: It is no longer sensitive because these values are capable of keeping Tc out of the picture.

The second- and third-ranking parameters are K_d for Tc in clayey and sandy soils, both of which are given a log-normal input distribution. The waste layers are assumed to have the same physicochemical properties as clayey soil, including K_d, so it is likely that this influence on the result is from retardation of Tc in the waste layer. While the influence of Tc K_d is much less than that of saturated thickness, it also is not surprising, since early doses are dominated by Tc in this average inventory setup.

The fourth-ranked parameter has a very low sensitivity index and is likely to be spurious, though as a parameter that contributes to the dispersion of the peak concentration at the well it is not implausible. The longitudinal dispersivity ratio is the ratio of the model scale (in this case the fixed distance between the waste footprint and the well) to longitudinal dispersivity, and is normally distributed around the value 27.5, a value derived from a wide variety of values reported in the dispersivity literature (Tauxe 1994).

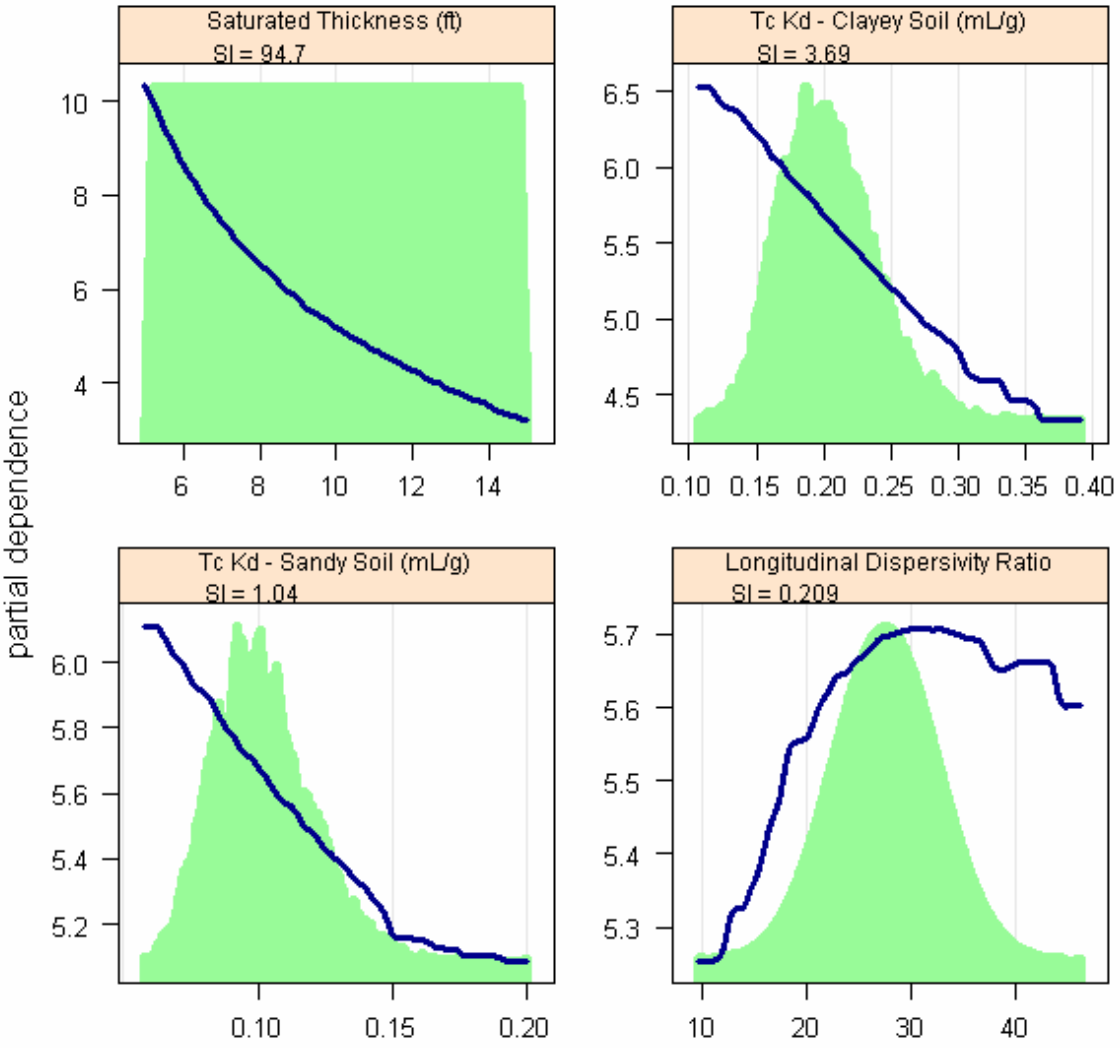

Figure F-50. Partial dependence plots for Slit Trench maximum total dose in early time

Maximum All-Pathways Dose (Late)

The maximum total dose in late time is the maximum all-pathways (water use) dose from all radionuclides achieved after 200 years, but still within the period of performance of 1130 years.

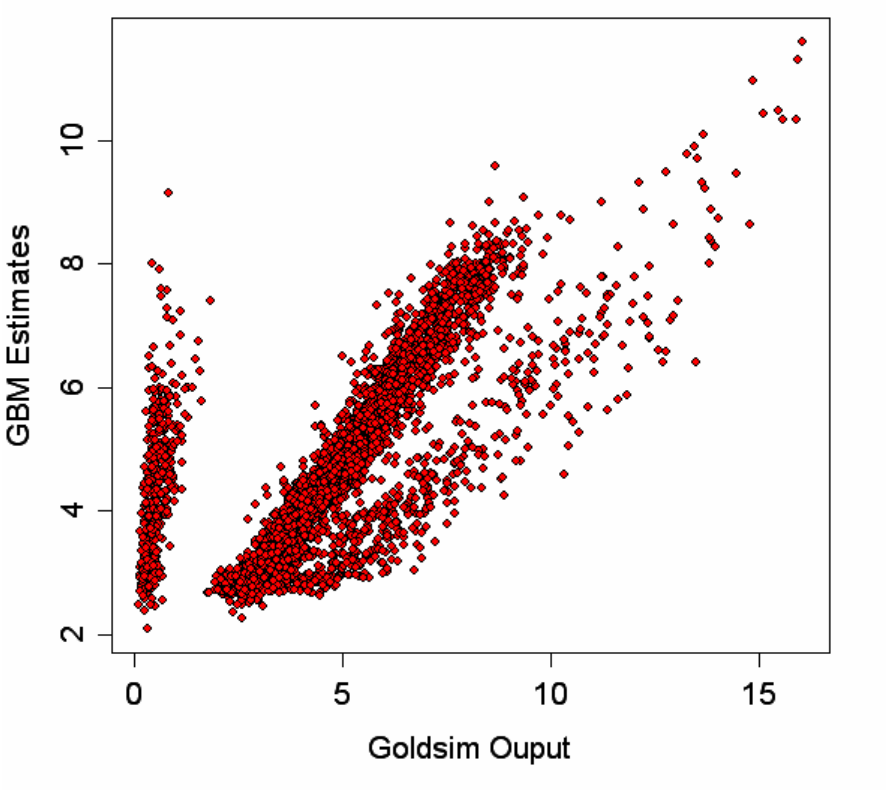

Figure F-51. Scatterplot of GBM estimate for Slit Trench maximum total dose (mrem in a year) in late time

This scatterplot shows a lower confidence in the sensitivity analysis, but the relationship is still clear. The difficulty in the GBM's ability to capture the GoldSim output may arise from the large number of late doses that are low in value compared to early maxima - a hypothesis worthy of additional investigation. The R^2 for this relationship is only 55%.

The band of points along the left-hand edge of the graph represents dose estimates ranging from 20 to over 80 μSv (2 to over 8 mrem) in a year as predicted by the GBM, where GoldSim had predicted doses between 0 and 10 μSv (1 mrem) in a year. The opposite effect (GBM underpredicting doses) is represented by the scatter of points to the right of the 1:1 line.

Again, we see the effects of the cap degradation scenario selection.

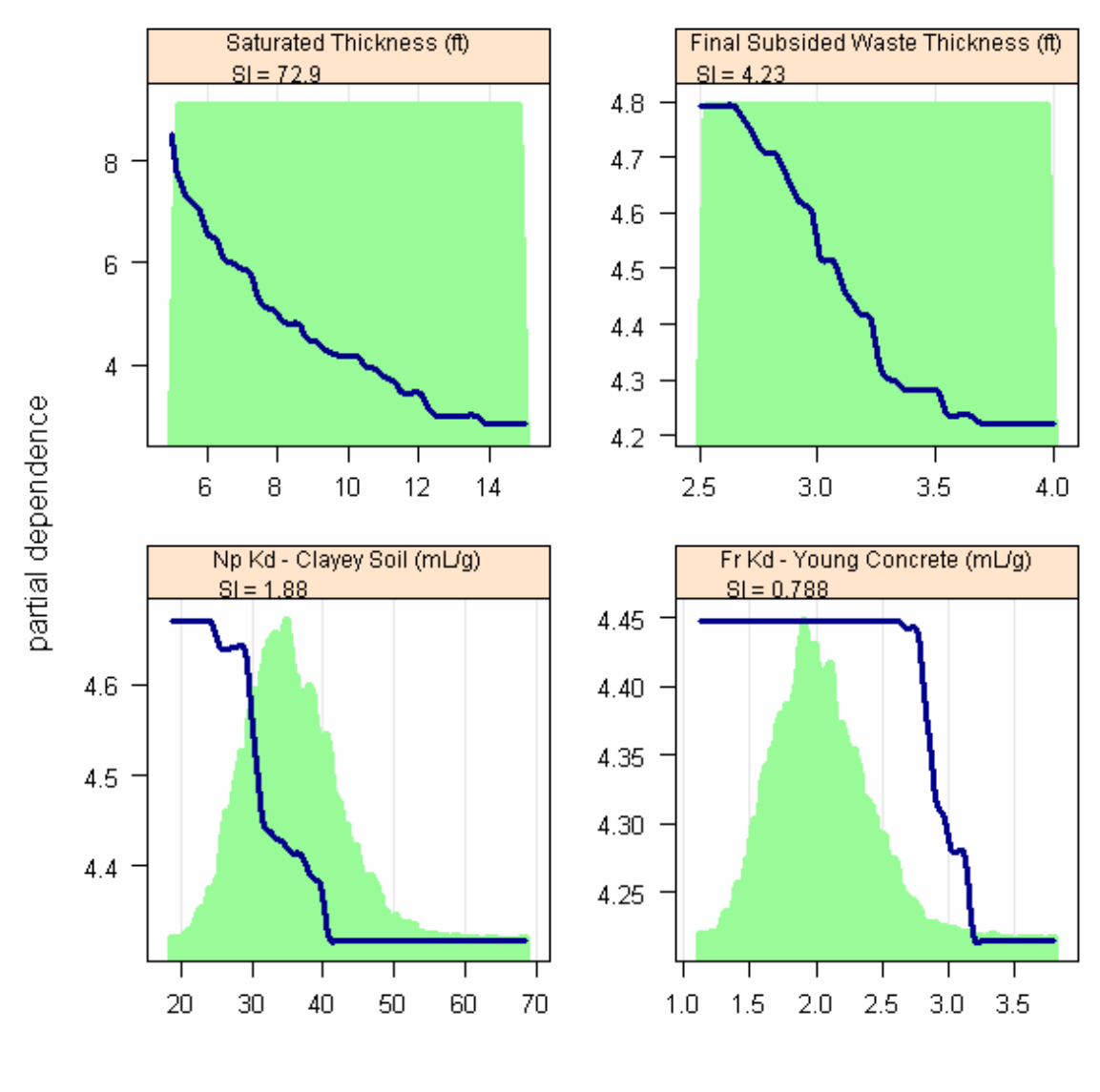

Figure F-52. Partial dependence plots for Slit Trench maximum total dose in late time

Again, the thickness of the aquifer dominates the sensitivity. Following that is the final subsided waste thickness, which has a uniform "placeholder" distribution of 2.5 to 4.0 meters. This is the estimated thickness of the waste layer after all subsidence is complete and all void space in the waste is gone, and higher doses are correlated with smaller values of final thickness. This is an example of how the later doses are influenced by parameters different from those influencing early doses: Waste subsidence does not occur until later time, and so could not possibly influence the early doses. The influence on later doses may come from the concentrating of contaminants in the waste layer from having the same mass of waste in a smaller volume. This is also an effect worthy of further investigation.

The third-ranking parameter is Np K_d, which is consistent with neptunium's domination of later doses. The K_d for francium (Fr) in concrete is necessarily a spurious result, since concrete K_ds were not implemented in the calculation. The fourth plot shows the form typical of a poor result: a sharp change in the partial dependence from one value to another.

Maximum Alpha Concentration

This is the maximum gross alpha concentration in well water for the entire duration of the model.

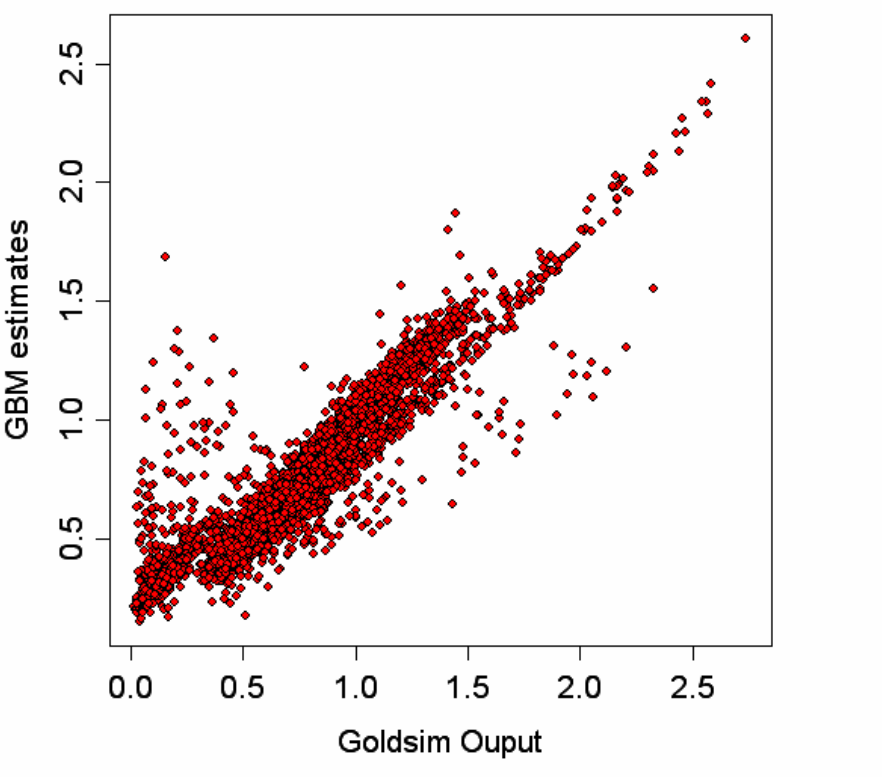

Figure F-53. Scatterplot of GBM estimate for Slit Trench maximum concentration (pCi/L) of alpha-emitters

The GBM estimates for alpha-emitter concentration is quite similar to that for late dose. Since the late dose is dominated by alpha-emitting radionuclides, this is no surprise. The R^2 for this relationship is 84.3%. Here the trifurcation of cap degradation scenarios is less pronounced. Recall from the dose time histories that this effect is less pronounced in later time, and the alpha-emitters break through at the well in those later times.

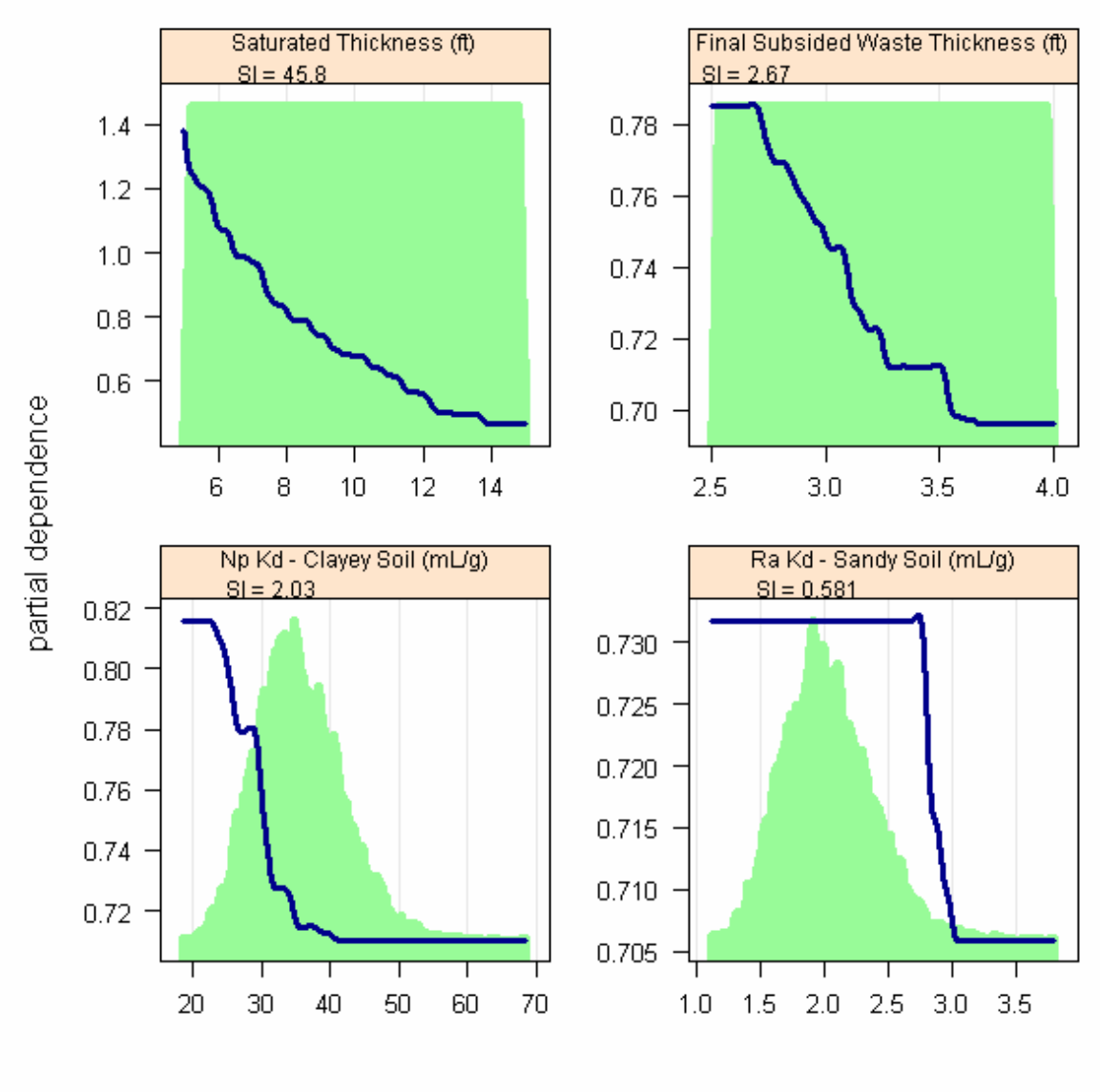

Figure F-54. Partial dependence plots for Slit Trench maximum concentration of alpha-emitters

The first three of the sensitive parameters shown below are identical to those selected for the maximum dose in late time. Since that dose is dominated by alpha-emitting radionuclides, this makes sense. The fourth, Ra K_d, is likely to be spurious given its low sensitivity index—lower even that the Fr K_d in the previous plots, which we know is noise based on what we know about connections in the model. The fourth plot here also has the appearance of a poor fit.

Maximum Beta-Gamma Water Ingestion Dose

The maximum beta-gamma dose is the maximum drinking water dose from beta- and gamma-emitting radionuclides in well water within the period of performance.

The results for beta- and gamma-emitters are similar to that of the maximum early doses, which are dominated by those same radionuclides. The R^2 for this relationship is 99%.

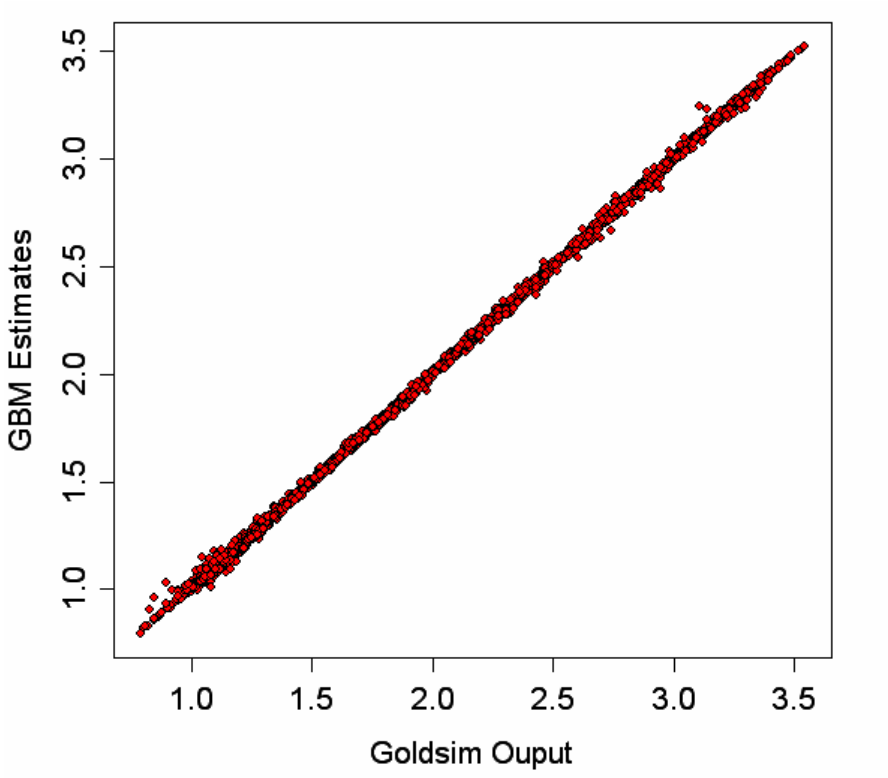

Figure F-55. Scatterplot of GBM estimate for Slit Trench maximum dose (mrem in a year) from beta- and gamma-emitters

The sensitivity index for saturated thickness completely dominates the sensitivity, and the other SI values are all very low.

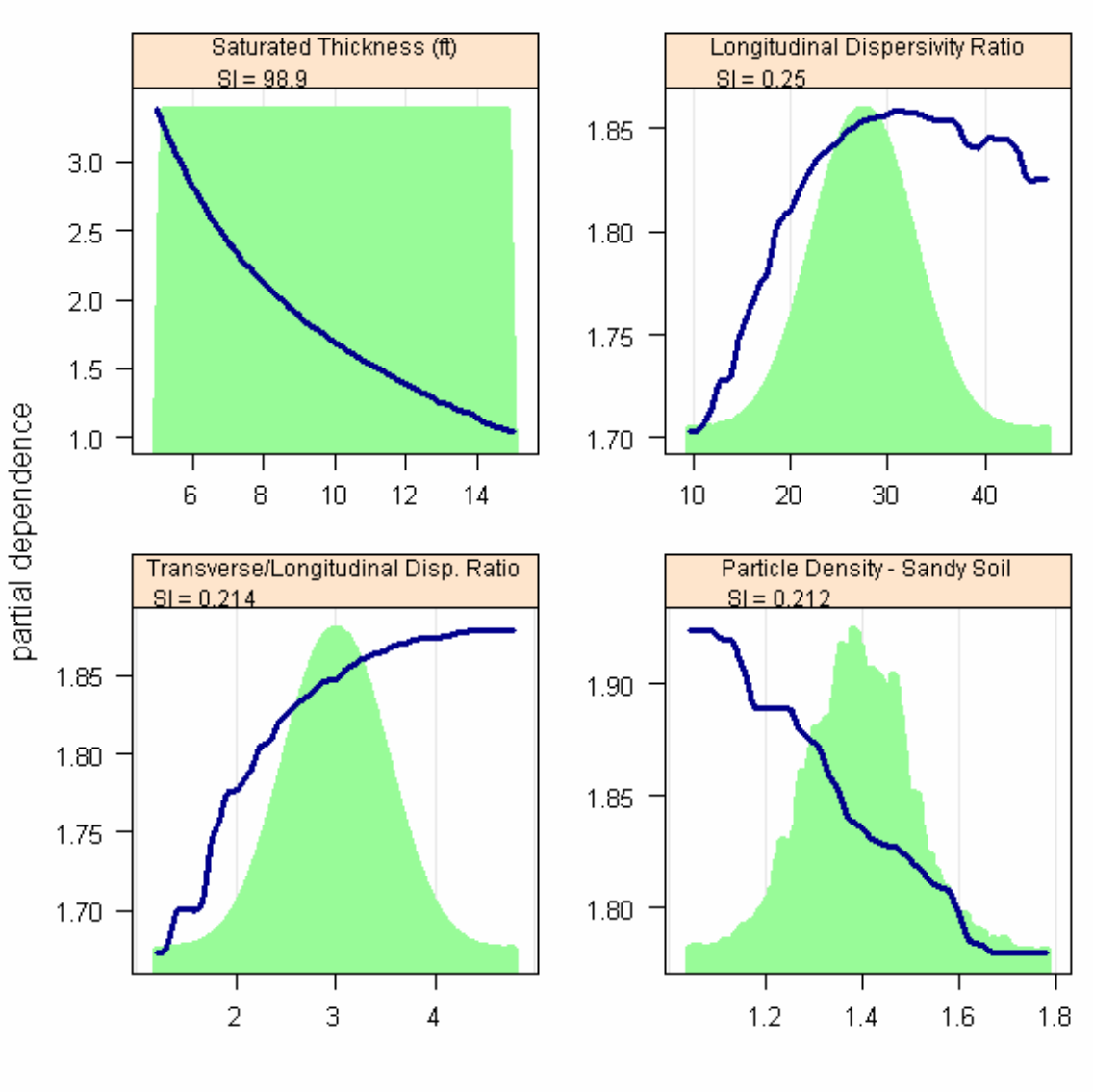

Figure F-56. Partial dependence plots for Slit Trench maximum total dose from beta- and gamma-emitters

1.2 ENGINEERED TRENCHES

The Engineered Trenches of E-Area are two 1-hectare trenches, each the dimensions of a set of five slit trenches. Engineered Trench #2 was analyzed for sensitivity using a separate GoldSim model (shown in Figure F-57.)

1.2.1 Model Description

The draft E-Area Engineered Trenches Sensitivity Analysis Model is very similar in layout, operation, and execution to the Slit Trench model described in Section 1.1.1. In fact, the Slit Trench model was given only a few modifications to produce the ET model, including

- new inventories for the two engineered trenches,
- modified trench dimensions, and
- a different value of the element CalibrationMultiplier in the ClosureCap container (0.5 rather than 1.2 for the Slit Trenches).

Doses and concentrations are calculated out to peak (to 20,000 years) instead of just to the period of performance (1130 yr) as was done for the Slit Trenches in an attempt to capture the peak dose. The Species list, materials and material properties, and the general model structure remain unchanged. The ET model was developed using GoldSim version 9.60 service pack 2.

1.2.2 Uncertainty Analysis

The Engineered Trench Sensitivity Analysis Model has several uncertain parameters, represented as probability distributions. Some of these are rather loosely defined in this early draft of the GoldSim model, with the aim being to first identify simply what some sensitive parameters might be. On the other hand, there are many other parameters that are not defined stochastically, even though they are known to be uncertain, simply because their uncertainties have yet to be evaluated. For example, radionuclide inventories, although uncertain, are defined deterministically. Such definitions will cause the model to underpredict uncertainty, and will exclude these important parameters from the sensitivity analysis. All parameter distributions will be given more defensible distributions under the PA maintenance program.

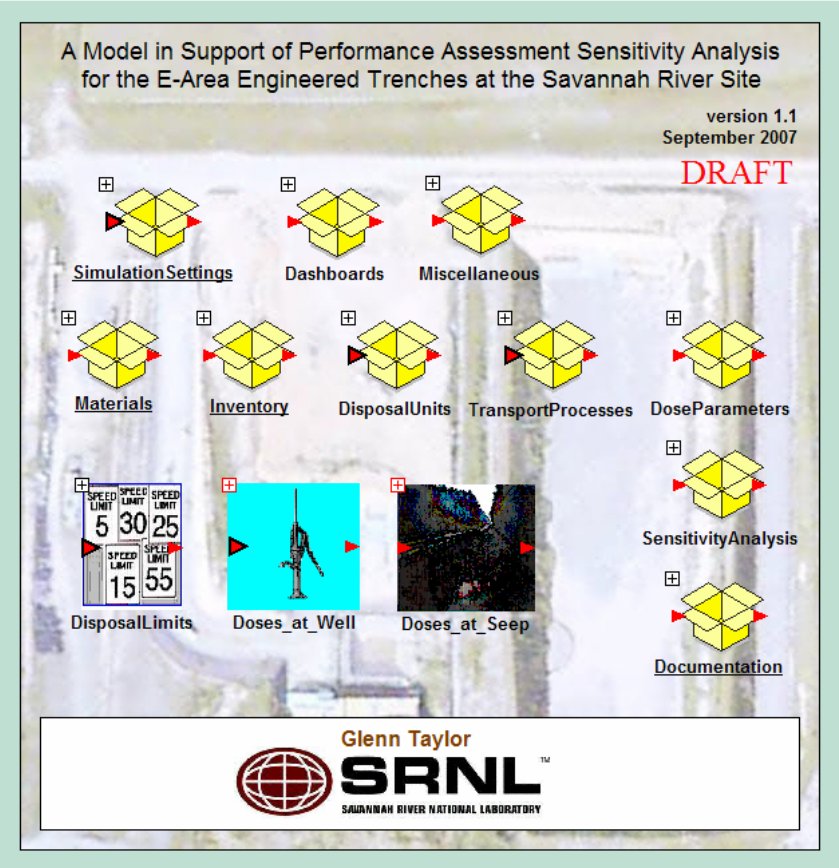

Figure F-57. Top View of the Engineered Trench Sensitivity Analysis Model

The uncertainty in the modeling results is illustrated by Figure F-58, which shows a statistical summary of the potential dose from water use from a hypothetical well located 100 meters downstream of the edge of the disposal unit, summed over all radionuclides, for all 5000 realizations. At each time step, the mean, median, 5th, 25th, 75th, and 95th percentiles are shown. Note that both axes are on a logarithmic scale. The early doses peak at about 20 years (ignoring institutional control) while the trenches are open to the elements. At 130 years, the engineered cap is emplaced, and doses drop dramatically, remaining low until the cap begins to fail at around 270 years. A second peak (the "midtime" dose, which corresponds to the "late dose" discussed for the Slit Trenches) occurs at about 1100 years, though this is not quite as high as the early peak for the ETs. In later time the third dose peak is found, past the 20,000-year model duration. (A subsequent run determine the actual peak dose to be in the neighborhood of 27,000 years.) This one is the highest and final dose, occurring after the period of performance.

As seen in the graph and summarized in Table F-6 below, the maximum potential doses in early time have a mean of about 72 μSv (7.2 mrem) in a year. Given the time relative to final closure, these doses are highly unlikely to be achieved. The second dose peak, at around 1000 years, has a mean value of about 35 μSv (3.5 mrem) in a year. Since institutional controls are not likely to have retained effectiveness that long, this dose could be considered as the dose to the member of the public required by DOE O 435.1-1. The maximum dose from all 2000 realizations at this midtime peak is just over 130 μSv (13 mrem) in a year.

The actual peak dose (for all time) occurs after 20,000 years after closure, which is the duration of the model. At 20,000 years, the all-pathways dose has a mean value of about 640 μSv (64 mrem) in a year. This is well beyond the period of performance of 1000 years after site closure, but is still useful for decision making purposes and for ALARA analysis.

In order to determine which radionuclides are causing doses at different times, the model is configured to break down the dose contributions by radionuclide. Figure F-59 is a graph of the mean dose through time, broken down by (selected) radionuclide. The early doses are dominated by C-14 and Tc-99, midtime doses by Np-237, and later doses by Pu-239.

1.2.3 Sensitivity Analysis

A sensitivity analysis for the E-Area Engineered Trenches (ETs), was also performed in support of the E-Area PA Maintenance Program. Like the Slit Trenches, a GoldSim model was developed for performing the sensitivity analysis. Again, the results of the model output were analyzed using GBM, and the discussion of the sensitivity analysis methodology provided for the Slit Trenches in Section 1.1.3 applies here.

The following ET model endpoints were selected for sensitivity analysis. A modification in endpoints was made between the running of the Slit Trench sensitivity analysis and this analysis. Specifically, the model duration was extended in an attempt to capture the peak all-pathways dose, though the concentrations of radium, uranium, and alpha emitters, as well as the dose from beta-gamma emitters, was restricted to those maxima occurring within the period of performance.

DoseMaxEarly is the maximum potential dose from well water use achieved before 200 years, a local minimum resulting from the engineered cap construction and degradation history. DoseMaxEarly is very similar to the maximum dose achieved during the period of performance (1130 years). These early maxima occur generally within the first 100 years, and will likely be precluded by effective institutional control.

DoseMaxMidtime is the maximum potential dose from well water use achieved after 200 years but before 3000 years, both local minima. This was selected for study since the dose calculations showed a strong tendency to have a dose maximum that came and went during this time. The timing of the midtime peak at about 1100 years is just within the period of performance, and beyond the time of effectiveness of institutional controls. Therefore, this midtime dose is the one to be evaluated for maximum dose to a member of the public within the period of performance.

DoseMaxLate is the maximum potential dose from well water use occurring after the 3000-year minimum. This is the peak dose for all time from the model, and would be used in making decisions related to dose reduction. The Slit Trenches are likely to have shown a similar result had the analysis been run for a sufficient length of time.

MaxAlpha is the maximum water well concentration of all alpha-emitting radionuclides. This model run restricted the maximum to that reached during the period of performance.

MaxBetaGamma is the maximum dose from all beta- and/or gamma-emitting radionuclides in the well water, within the period of performance.

MaxRadium is the maximum concentration of Ra-226 and Ra-228 in the well water, within the period of performance.

MaxUranium is the maximum concentration of from all uranium isotopes in the well water, within the period of performance.

As was found for the Slit Trenches, the results of the sensitivity analysis indicate that overwhelmingly the most significant stochastic parameter in the model for nearly all the above endpoints is the assumed thickness of the saturated zone, or aquifer. Other less significant sensitive parameters include soil/water partition coefficients for dose-significant (or concentration-significant) radionuclides, aquifer dispersivity ratios (also related to mixing), and the rate of natural compaction and final thickness of the waste after subsidence.

1.2.3.1 Summary Statistics for Endpoints

The GoldSim model that was run for this sensitivity analysis has the file name “E-Area Engd Trench SA v1.1 et2 r2000.gsm”. This is a copy of version 1.1 of the model, set to use one of the two engineered trench inventories and 2000 realizations, with Latin Hypercube Sampling enabled. The exporting of results is done the same way as for the Slit Trenches. The inventory used is the closed/projected inventory for Engineered Trench #2.

Summary statistics for the endpoints of interest are tabulated in Table F-6. It should be kept in mind that the all-pathways dose calculation considers only one of the two ET inventories, and ignores the presence of other disposals in proximity. The purpose of this preliminary model is not to predict doses, but rather to characterize the uncertainty and sensitivity context of the actual PA model. The summary statistics quantify the uncertainty surrounding the dose calculations.

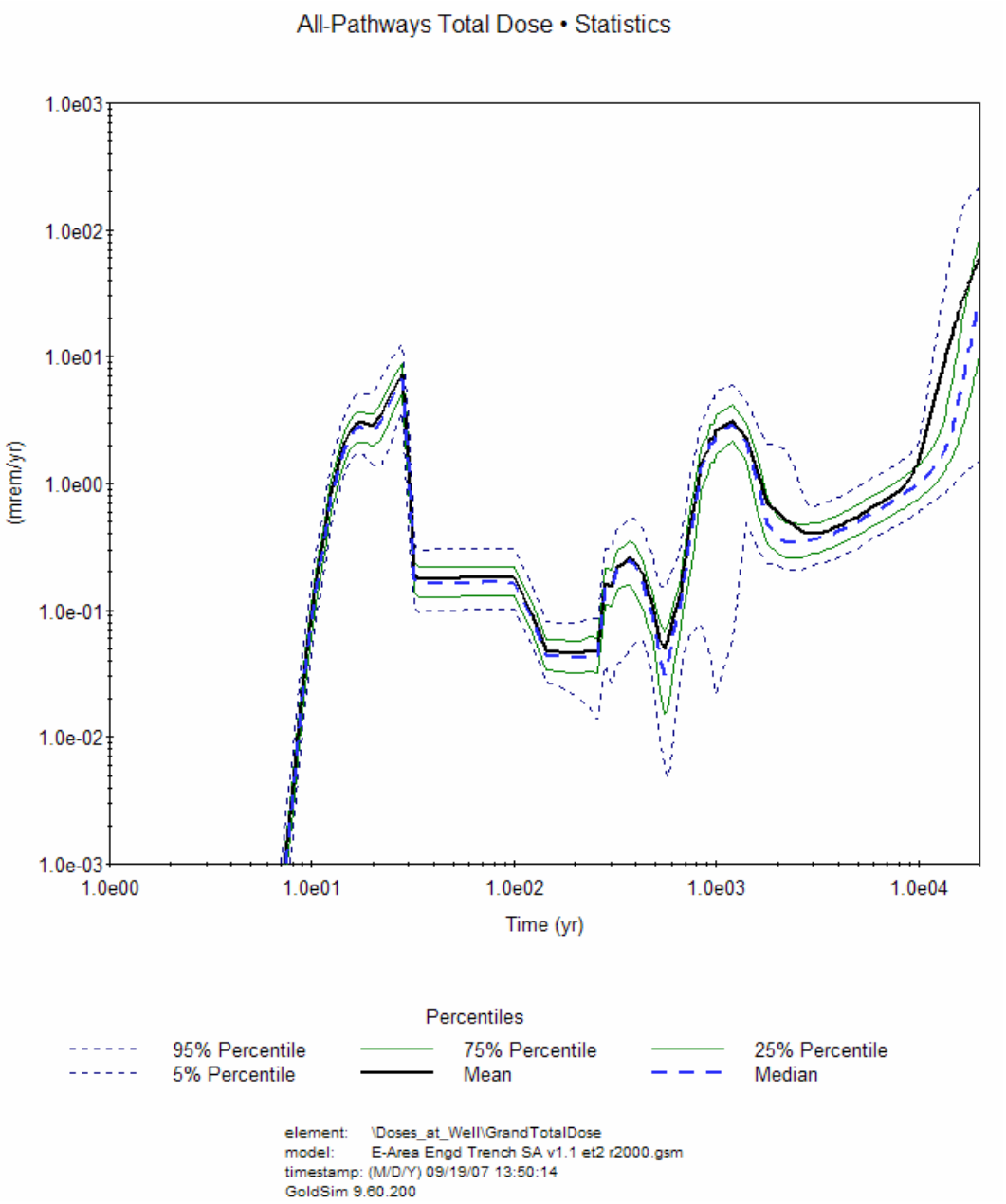

Figure F-58. Time history of total all-pathways dose from Engineered Trench 2 well water, statistical summary of 2000 realizations

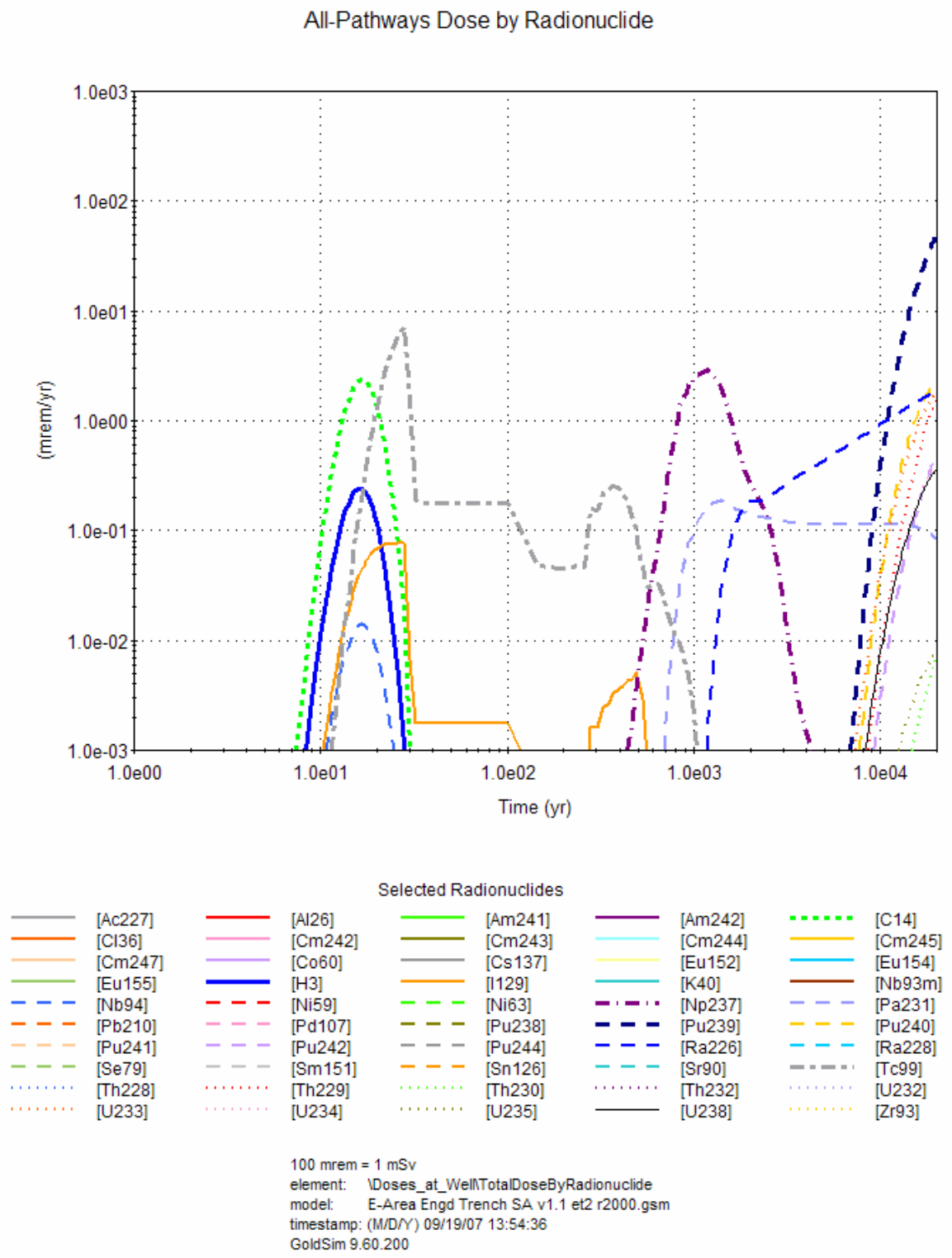

Figure F-59. Time history of mean all-pathways dose by radionuclide from Engineered Trench 2 well water, selected radionuclides shown

Table F-6. Summary statistics from 2000 realizations for the Engineered Trench #2 endpoints of interest

Endpoint	Mean	Standard Deviation	Min	1st Qu.	Median 2nd Qu.	3rd Qu.	Max
max. dose early (within period of performance) (mrem/yr)	7.2	2.8	1.8	5.1	6.6	8.9	17
max. dose – midtime (mrem/yr)	3.5	1.5	1.1	2.4	3.2	4.4	13
max. dose – late (mrem/yr)	64	83	0.75	9.8	28	85	600
max. alpha conc. at well within per. of performance (pCi/L)	0.51	0.30	1.6e-6	3.3e-1	4.7e-1	6.7e-1	2.4
max. beta - gamma dose at well within per. of performance (mrem/yr)	1.7	0.59	0.75	1.2	1.6	2.1	3.6
max. radium conc. at well within per. of perf'ce (pCi/L)	8.7e-6	1.2e-4	1.4e-29	5.5e-11	2.1e-9	4.2e-8	3.1e-3
max. uranium conc. at well within per. of performance (μg/L)	1.7e-10	1.2e-10	2.1e-16	1.1e-10	1.5e-10	2.3e-10	9.5e-10

1 mrem = 10 μSv
27 pCi = 1 Bq

1.2.3.2 Endpoints and most influential explanatory variables

Each of the modeling endpoints discussed above and listed in the table was analyzed to identify those stochastic parameters having the most influence on that endpoint. In most cases, the most significant parameter was the saturated thickness of the aquifer, as shown in Table F-7. Graphs of the goodness of fit of the statistical model and the partial dependence are also presented. The occurrence of Ra at the well is uncommon within the period of performance, and sufficient information is not available for performing a sensitivity analysis.

Discussions of particular results are provided following the figures below. For each of the endpoints, a graph is provided showing the predictive power of the GBM estimate as compared to the GoldSim results, followed by a collection of four graphs showing the SI of the top four sensitive parameters for the endpoint.

Maximum All-Pathways Dose (Early Time)

The maximum total dose from well water use within the period of performance is that encountered before 1130 years. It is usually achieved within 200 years of closure, the "early" dose time cutoff. The figure below shows excellent ability of the GBM to predict the GoldSim results for this endpoint. This means that there is high confidence in the sensitivity analysis. The R^2 for this relationship is greater than 98%.

Table F-7. Identification of the most sensitive parameters for the Engineered Trench #2 endpoints of interest

Endpoint	SI rank	input parameter	Sensitivity Index	R^2
max. dose early (within period of performance) (mrem/yr)	1	saturated thickness of aquifer	75.9	98%
	2	Tc K_d in sandy soil	16.6	
	3	Tc K_d in clayey soil (and the waste)	7.4	
	4	transverse/longitudinal disp'y ratio	0.043	
max. dose – midtime (mrem/yr)	1	saturated thickness of aquifer	75.5	82%
	2	final subsided waste thickness	7.61	
	3	Np K_d in clayey soil (and the waste)	7.36	
	4	post-compaction subsidence rate	1.17	
max. dose – late time (mrem/yr)	1	Pu K_d in sandy soil	44.3	76%
	2	saturated thickness of aquifer	12.0	
	3	Pu K_d in clayey soil (and the waste)	1.61	
	4	Ni K_d in sandy soil	0.919	
max. alpha conc. at well (pCi/L)	1	saturated thickness of aquifer	29.5	84%
	2	Np K_d in clayey soil (and the waste)	7.82	
	3	final subsided waste thickness	5.67	
	4	post-compaction subsidence rate	5.14	
max. beta - gamma dose at well (mrem/yr)	1	saturated thickness of aquifer	92.2	99%
	2	Tc K_d in sandy soil	4.34	
	3	Tc K_d in clayey soil (and the waste)	2.58	
	4	longitudinal dispersivity ratio	0.243	
max. radium conc. at well		insufficient information		49%
max. uranium conc. at well (μg/L)	1	saturated thickness of aquifer	24.9	88%
	2	infiltration rate timing warp factor	13.1	
	3	U K_d in sandy soil	8.24	
	4	Np K_d in clayey soil (and the waste)	5.98	

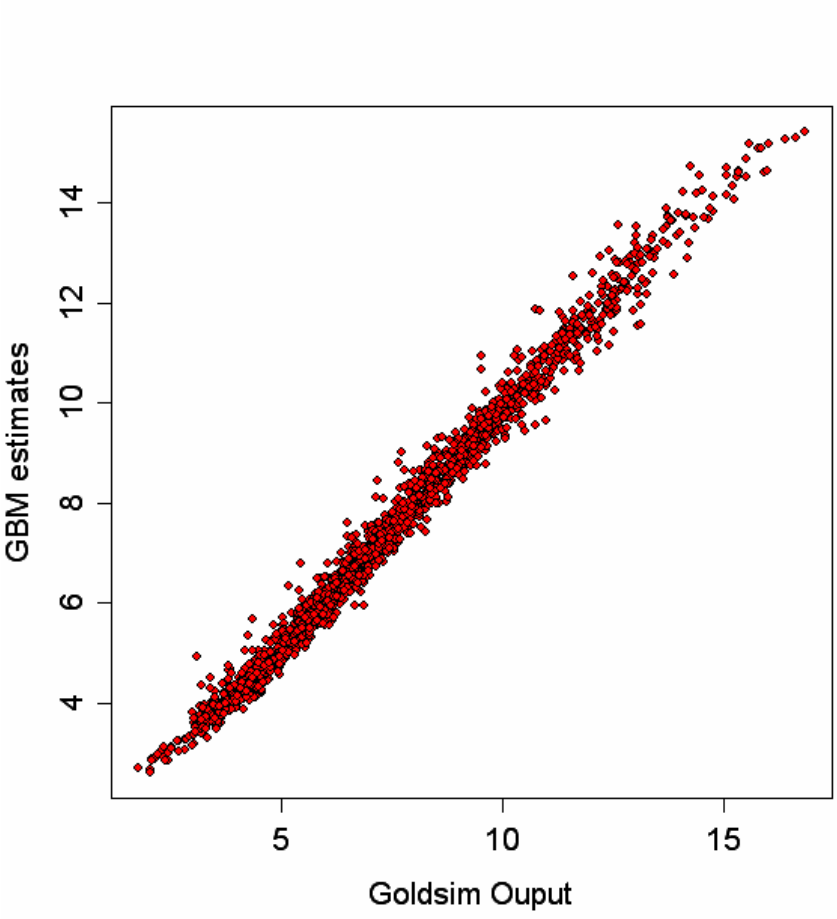

Figure F-60. Scatterplot of GBM estimate for Engineered Trench 2 maximum all-pathways dose in early time (mrem in a year)

Similar to the Slit trenches, the most significant parameter here is the saturated thickness of the aquifer. This parameter has the same value in both models, and its influence is described above. Also mimicking the Slit Trench model, the second- and third-ranking parameters are K_d for Tc in sandy and clayey soils. The waste layers are assumed to have the same physicochemical properties as clayey soil, including K_d, so it is likely that this influence on the result is from retardation of Tc in the waste layer. While the influence of Tc K_d is much less than that of saturated thickness, it also is not surprising, since early doses are dominated by Tc in this average inventory setup.

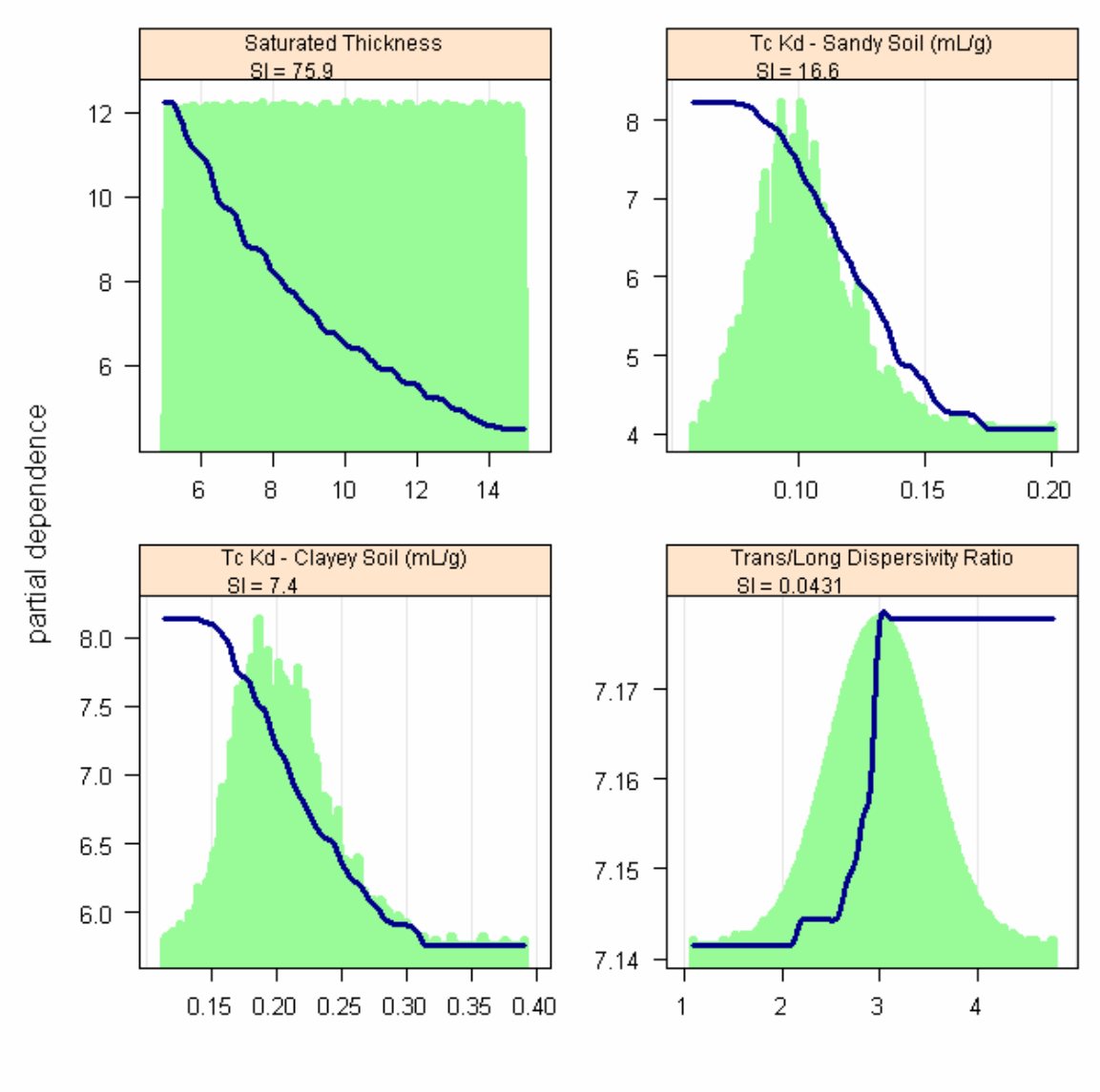

Figure F-61. Partial dependence plots for Engineered Trench 2 maximum all-pathways dose within the period of performance

The fourth-ranked parameter has a very low sensitivity index and is likely to be spurious, though as a parameter that contributes to the dispersion of the peak concentration at the well it is not implausible. The transverse/longitudinal dispersivity ratio is the ratio of the longitudinal dispersivity to the transverse (horizontal) component, and is normally distributed around the value 3.0, a value derived from a wide variety of values reported in the dispersivity literature (Tauxe, 1994).

Maximum All-Pathways Dose (Midtime)

The maximum total dose in late time is the maximum all-pathways dose achieved after 200 years and before 3000 years, both local minima. As seen in Figure F-58, most of these midtime doses occur before the end of the period of performance. Even if institutional controls prevent the early potential doses from actually occurring, these controls will not likely have any remaining effectiveness after nearly 1000 years. Therefore, these midtime doses might be considered the most likely to occur within the period of performance.

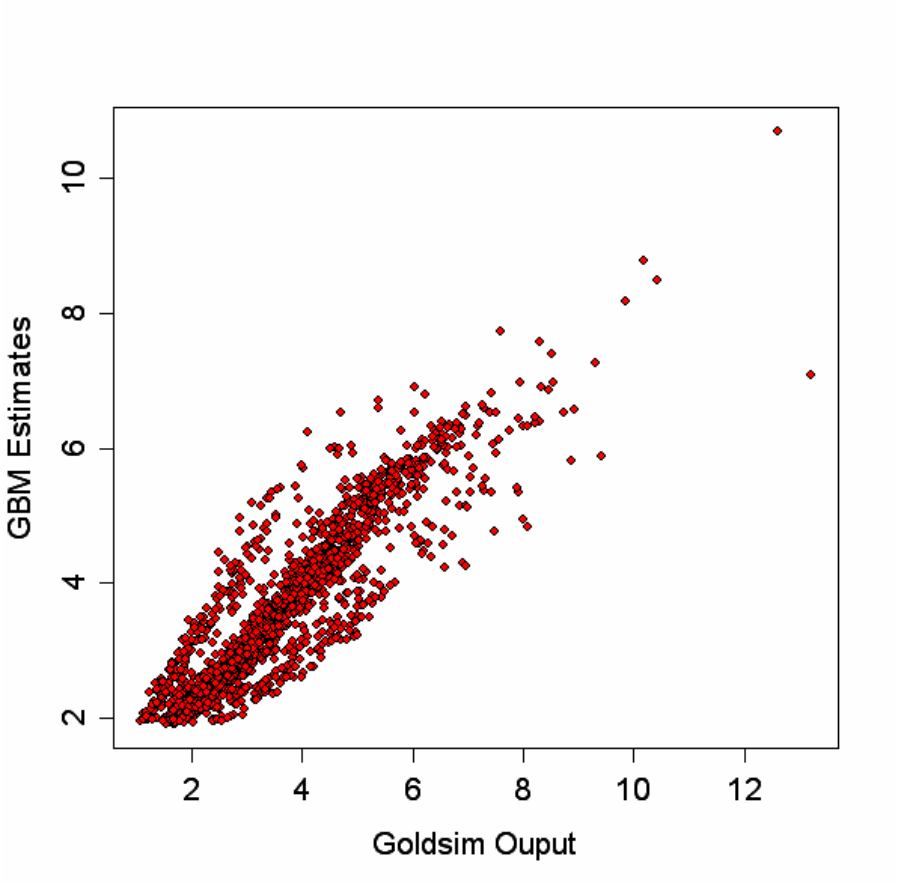

Figure F-62. Scatterplot of GBM estimate for Engineered Trench 2 maximum all-pathways dose (mrem in a year) in midtime

This scatterplot shows a lower confidence in the sensitivity analysis, but the relationship is still clear. The difficulty in the GBM's ability to mimic the GoldSim model is likely to arise from the trifurcation of results. These three "bands" of results come from the random selection between the three cap degradation scenarios. The data could be further subdivided based on scenario and re-examined. The R^2 for this relationship is 82%.

Again, the thickness of the aquifer dominates the sensitivity. Following that is the final subsided waste thickness, which has a uniform "placeholder" distribution of 2.5 to 4.0 meters. Third is Np K_d in clayey soils and the waste, which is consistent with neptunium's domination of midtime doses, and therefore its key role in determining the performance of the facility with respect to doses to members of the public. These first three are also the top three for the Slit Trenches' late dose (which is of the same time period). The fourth-ranking has a low SI, but would be a credible player for the same reason that the final subsided waste thickness is important.

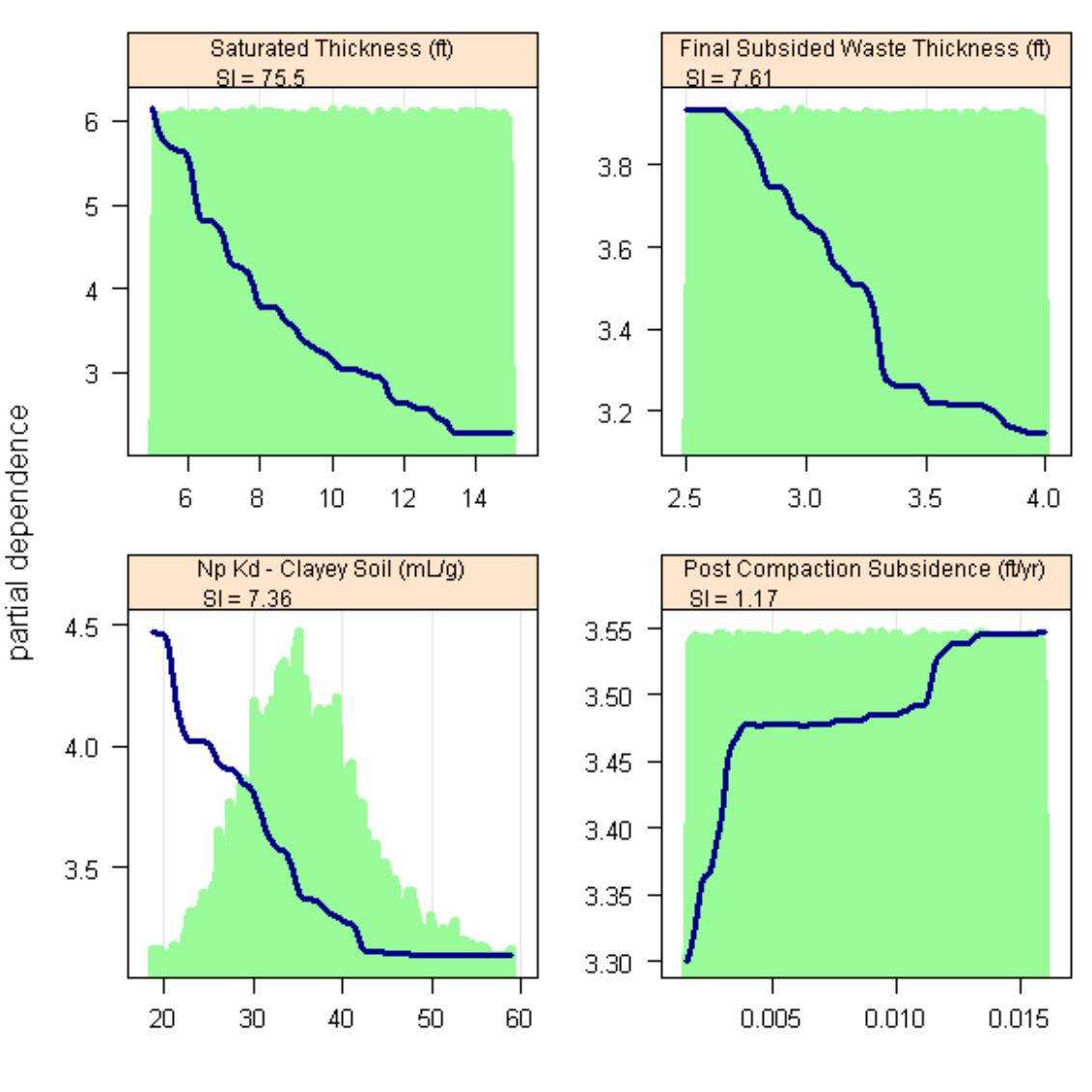

Figure F-63. Partial dependence plots for Engineered Trench 2 maximum all-pathways dose in midtime

Maximum All-Pathways Dose (Late)

The maximum total dose in late time is the maximum all-pathways dose achieved after 3000 years. This is the peak dose for all time, although it occurs well after the period of performance as defined in DOE O 435.1-1.

In this graph we can again see the splitting of results with the cap degradation scenario, and the result is still a challenge for the GBM to model. The R^2 for this relationship is 76%.

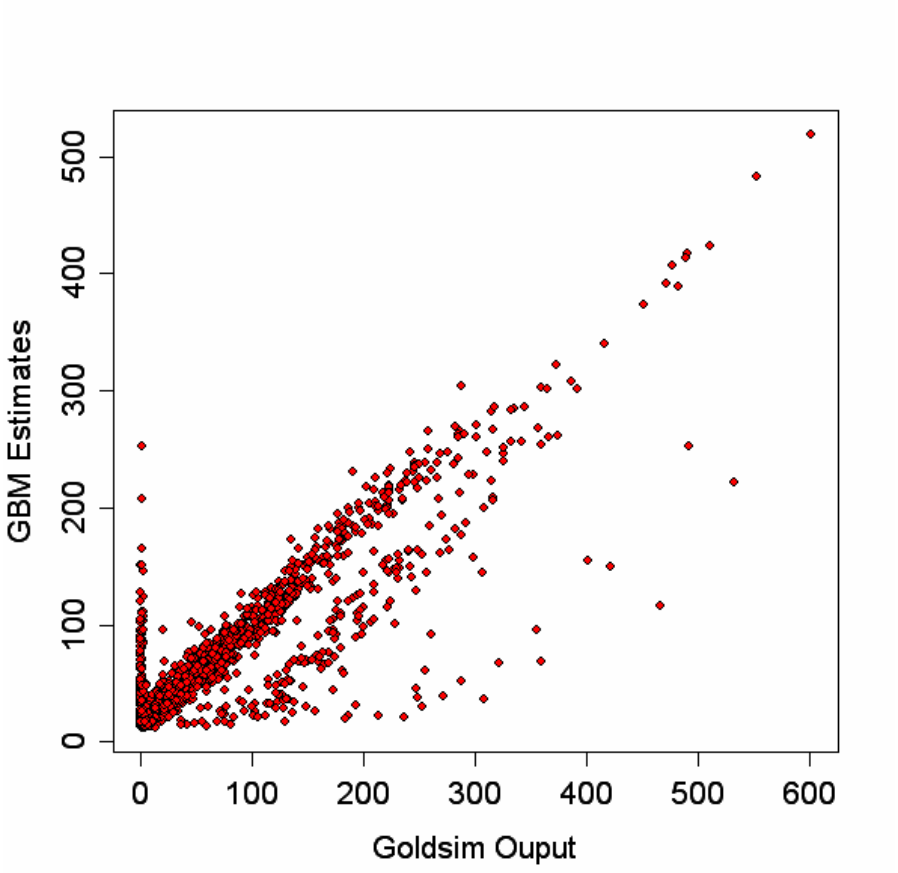

Figure F-64. Scatterplot of GBM estimate for Engineered Trench 2 maximum all-pathways dose (mrem in a year) in late time

For the late time dose, the Pu K_d in sandy soil is the most significant parameter, consistent with Pu-239's domination of doses in later time. Again, we see the inverse relationship of K_d with dose. This is followed by the thickness of the aquifer.

The third and fourth ranking parameters have a low SI and are likely to be spurious. The response of the endpoint to the range of the parameter (the blue line) is difficult to interpret.

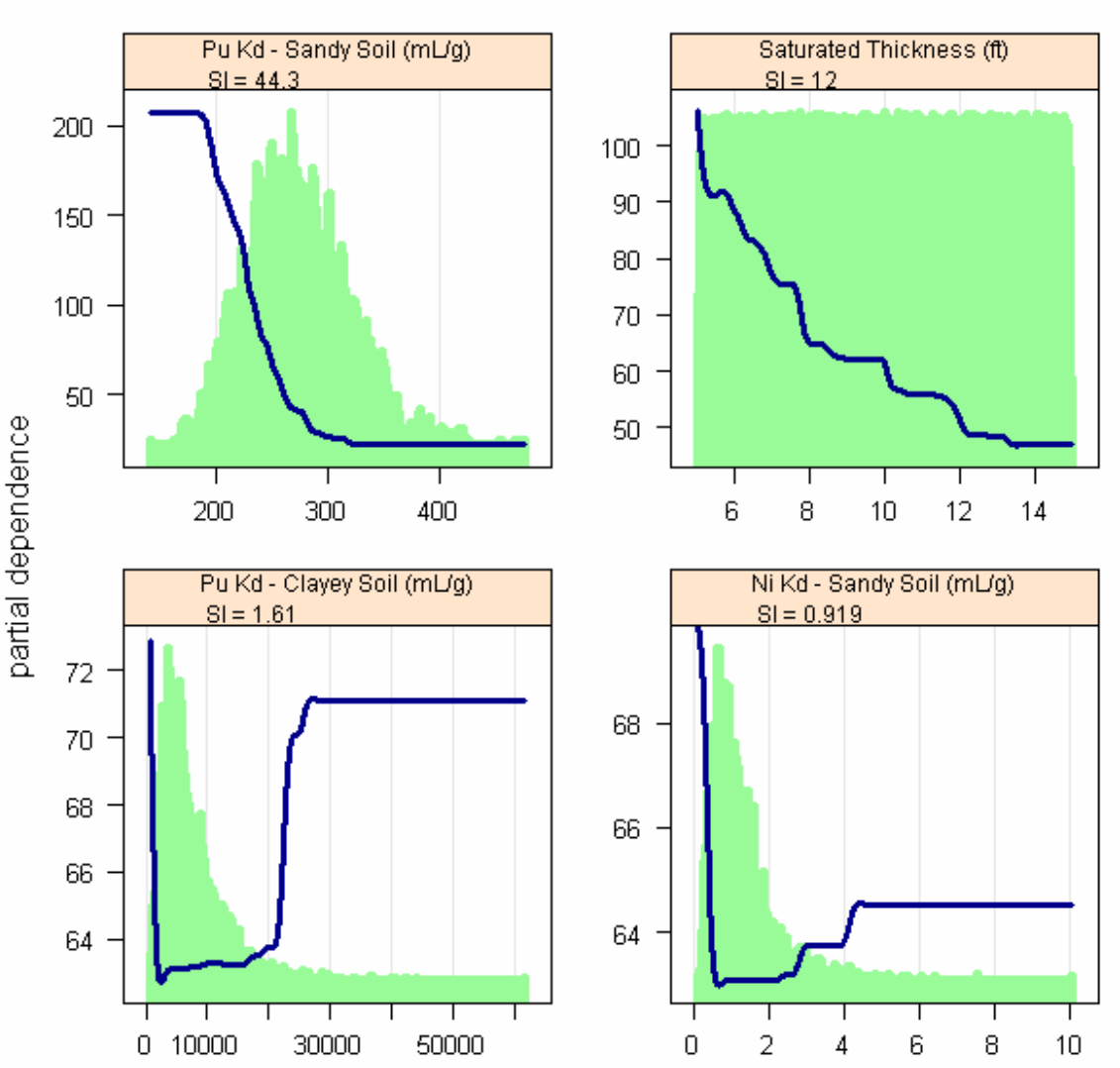

Figure F-65. Partial dependence plots for Engineered Trench 2 maximum all-pathways dose in late time

Maximum Alpha Concentration

This is the maximum gross alpha concentration in well water within the period of performance.

The GBM estimate for alpha concentration is similar to that for late dose, consistent with the domination of later doses by alpha-emitting radionuclides. The R^2 for this relationship is 84%.

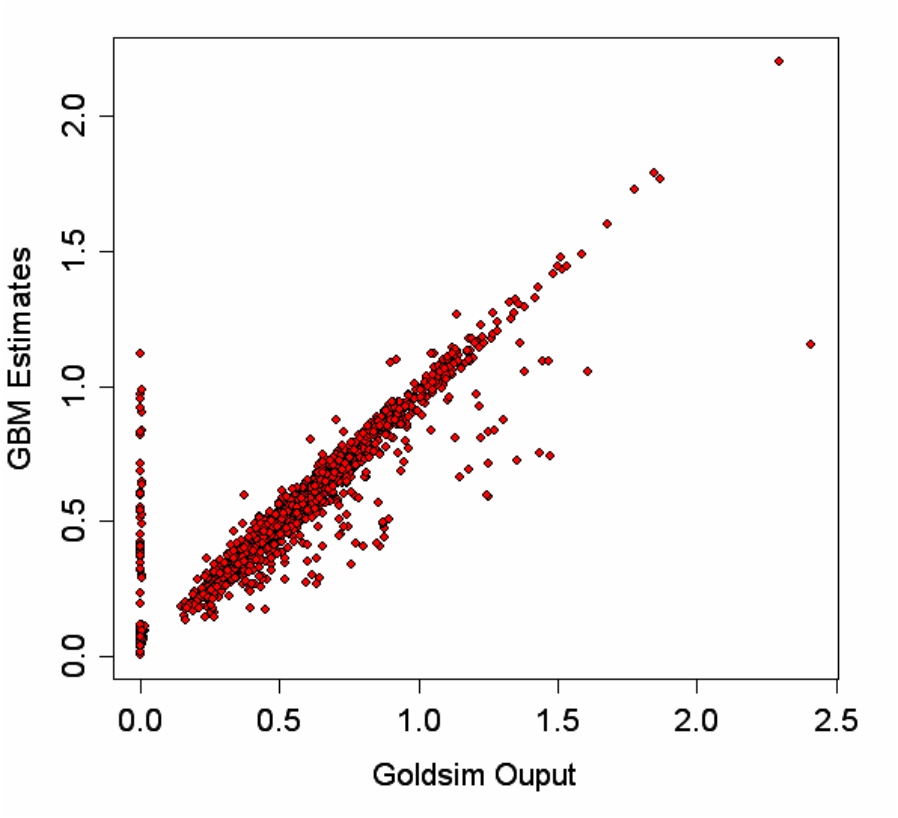

Figure F-66. Scatterplot of GBM estimate for Engineered Trench 2 maximum concentration of alpha-emitters (pCi/L)

All of these parameters were also selected as sensitive for the maximum dose in midtime, which is dominated by neptunium. The timing of the maximum alpha concentration is here constrained to be that maximum achieved within the period of performance, so alpha-emitters occurring later (e.g., plutonium) are not seen.

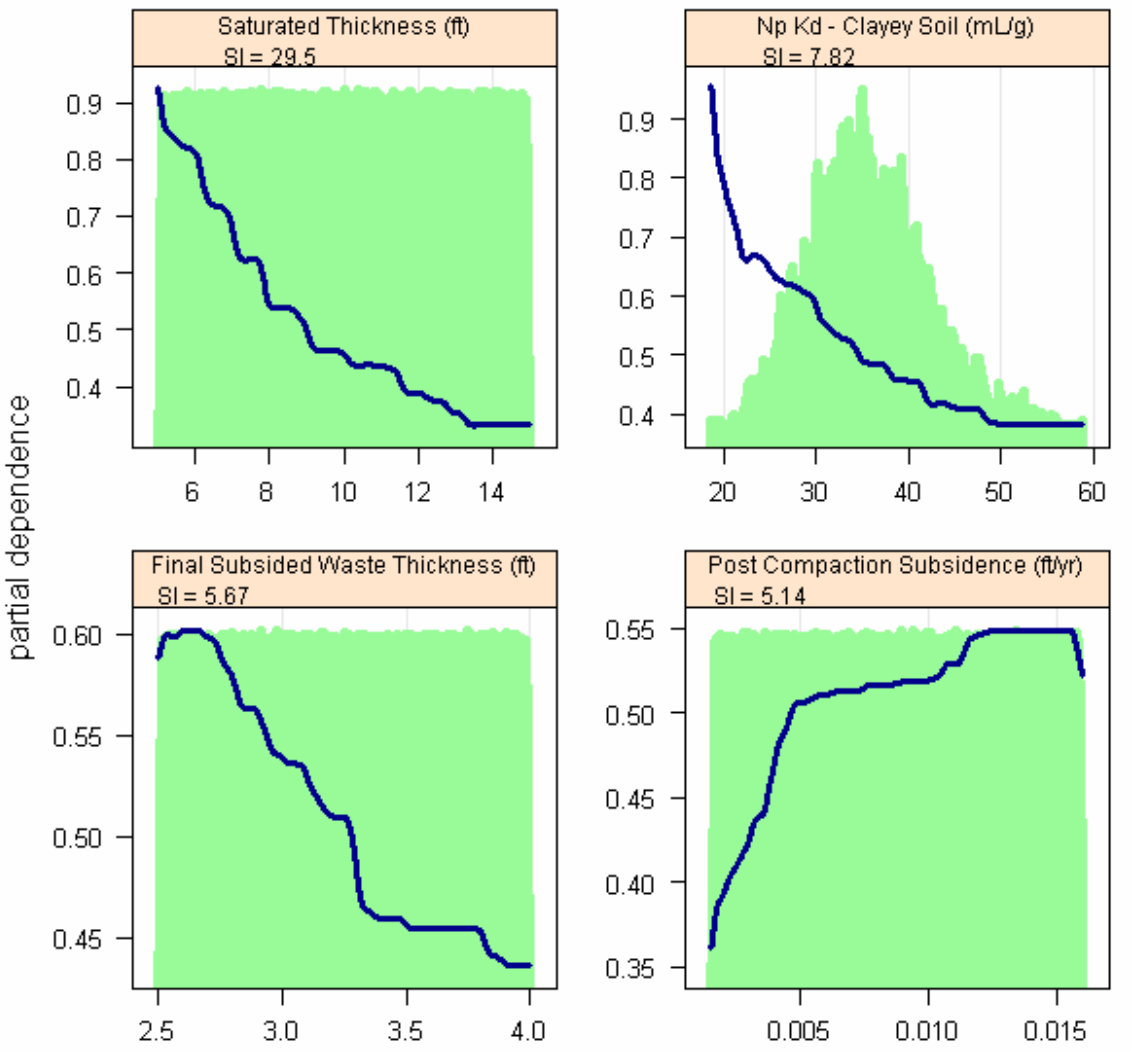

Figure F-67. Partial dependence plots for Engineered Trench 2 maximum concentration of alpha-emitters

Maximum Beta-Gamma Water Ingestion Dose

The maximum beta/gamma dose is the maximum beta-gamma drinking water dose received from groundwater at the 100-m well within the period of performance.

The results for beta- and gamma-emitters are similar to that of the maximum early doses, which are dominated by Tc-99. The R^2 for this relationship is over 99%.

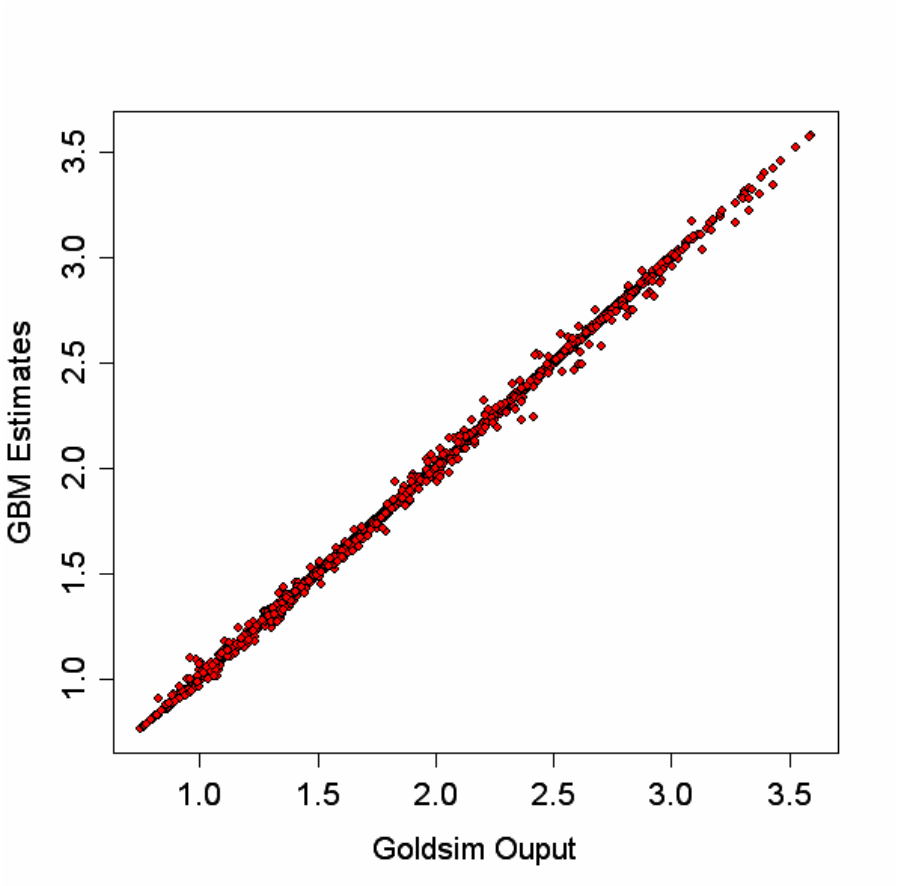

Figure F-68. Scatterplot of GBM estimate for Engineered Trench 2 maximum dose from beta-gamma-emitters

The saturated thickness is clearly dominant for this endpoint, followed by the K_d of Tc. While the ratio of longitudinal dispersivity to the transport distance is credible, its SI is too low to consider it seriously.

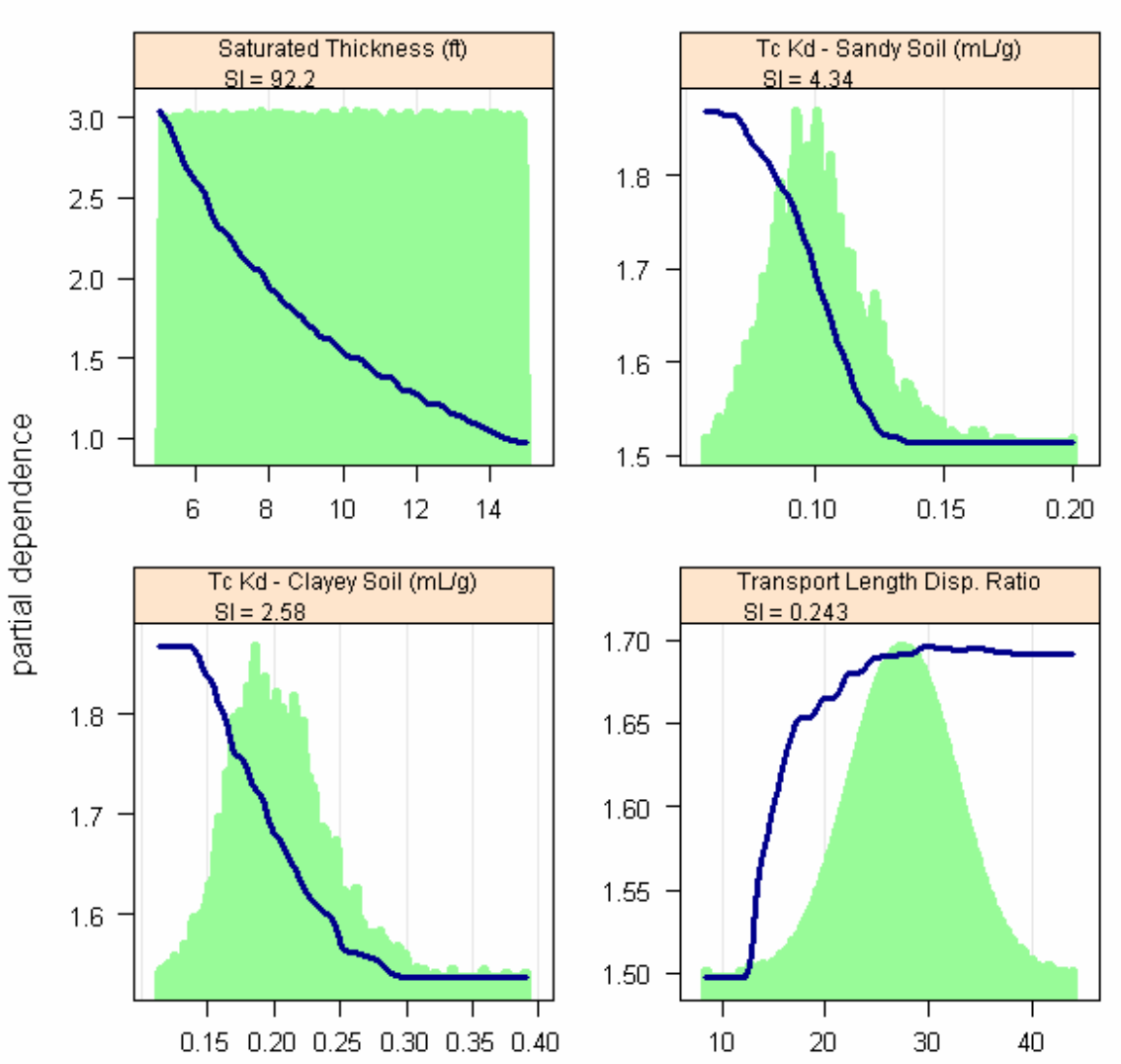

Figure F-69. Partial dependence plots for Engineered Trench 2 maximum total dose from beta- and gamma-emitters

Maximum Radium Concentration

This is the maximum radium concentration in well water within the period of performance.

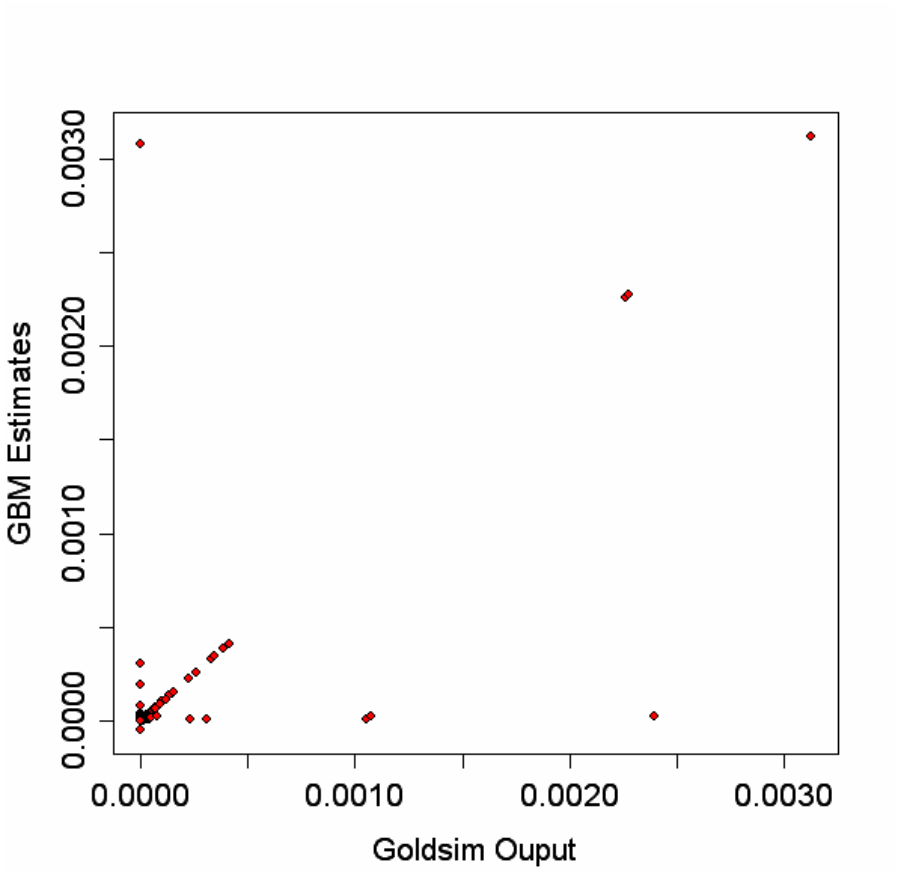

Figure F-70. Scatterplot of GBM estimate for Engineered Trench 2 maximum concentration of radium isotopes (pCi/L)

The GBM estimate for radium concentration is scattered and sparse, showing the difficulty in getting the GBM to mimic the GoldSim results. The R^2 for this relationship is only 49%. The number of points and their low value precluded being able to do an effective sensitivity analysis for this endpoint.

Maximum Uranium Concentration

This is the maximum concentration of uranium (all isotopes) in well water within the period of performance.

The GBM estimate for uranium concentration is better constrained than that for radium. The R^2 for this relationship is 88%.

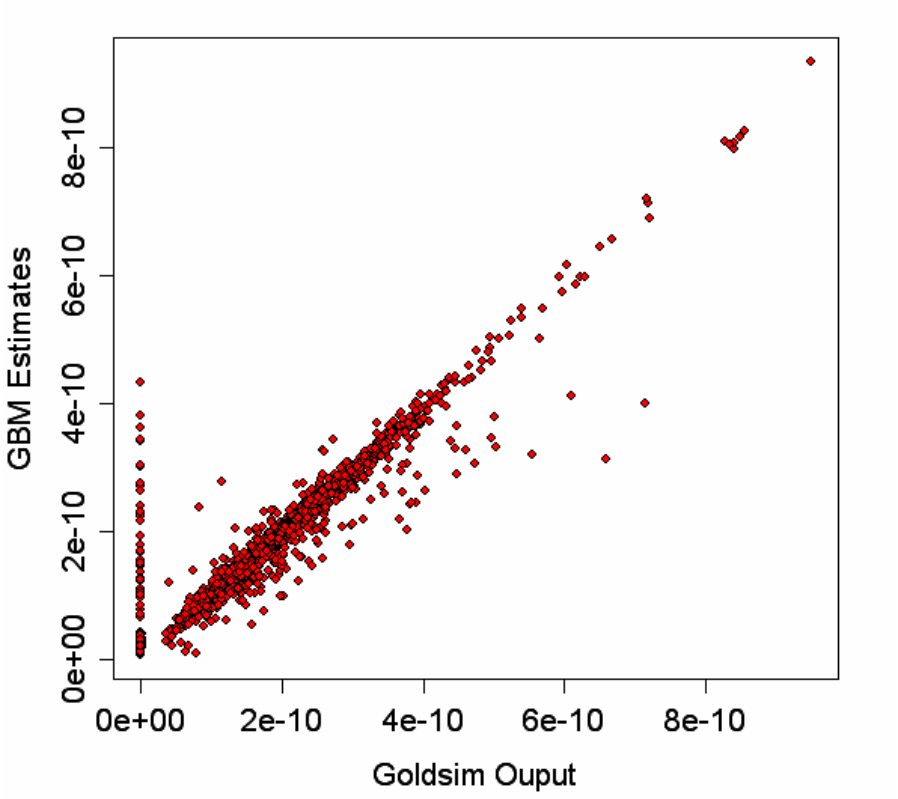

Figure F-71. Scatterplot of GBM estimate for Engineered Trench 2 maximum concentration of uranium (µg/L)

In addition to the dominant role of aquifer thickness, this endpoint identifies a new parameter for sensitivity: the closure cap infiltration timing warp factor. The WarpFactor modifies the timing of the infiltration rate through the cap, which is defined as time series. One could speculate that there is some edge-effect interplay between the timing of the change in infiltration rate at about 1000 years and the period of performance of 1130 years, but this does not explain why negative values of WarpFactor seem to have little effect. This is a case that could warrant further investigation, if there is sufficient value in doing so. The value can be evaluated using a value-of-information analysis (VOI), where the benefit of, for example, reducing model uncertainty, is weighed against the cost of developing a more robust input distribution for the parameter.

The sensitivity of uranium concentrations to the K_ds of U and Np is not surprising, since U is present in the inventory, and Np-237 is a parent of the U-233 isotope.

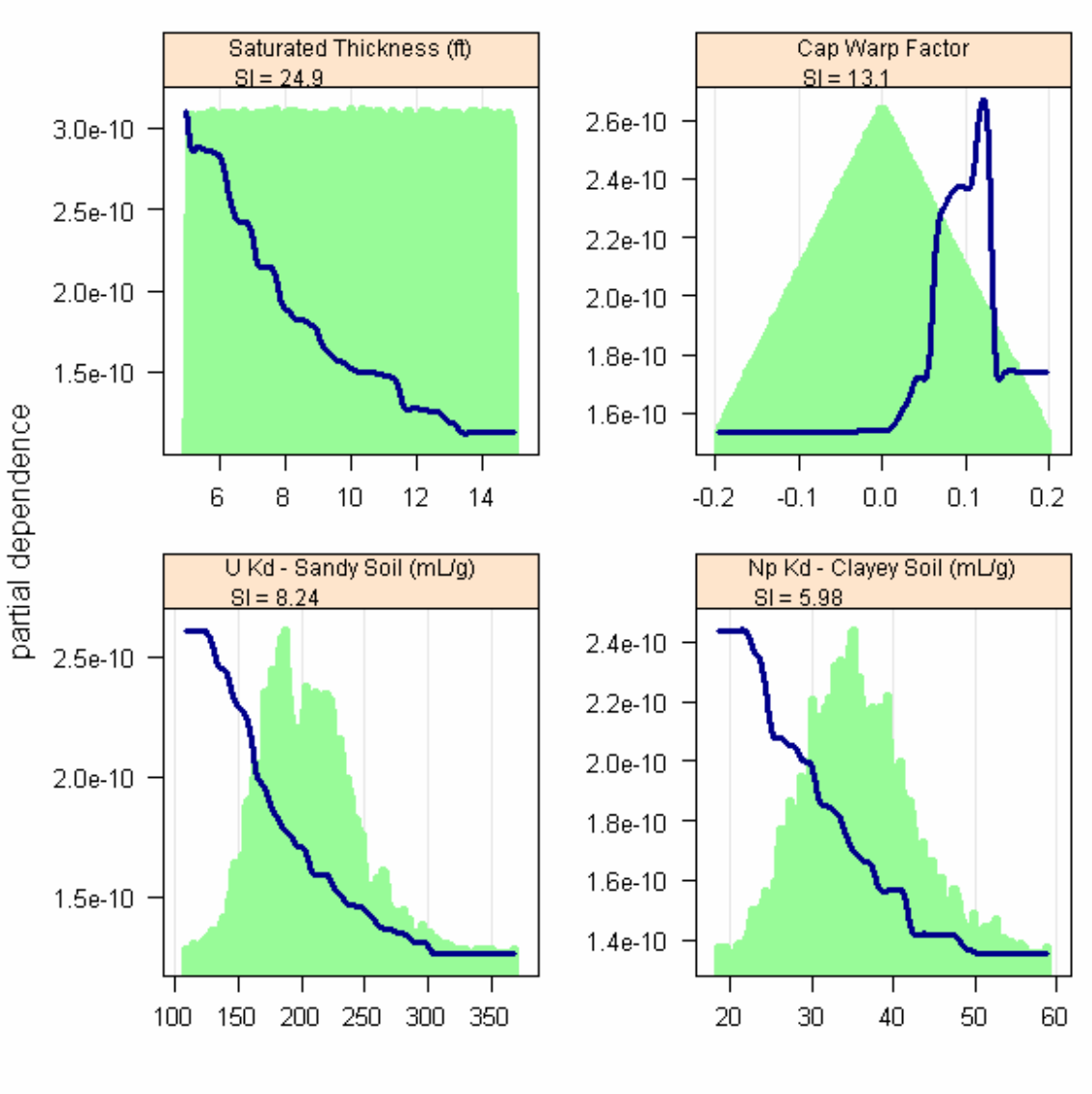

Figure F-72. Partial dependence plots for Engineered Trench 2 maximum concentration of uranium

1.3 COMPONENTS-IN-GROUT TRENCHES

The E-Area Burial Grounds include two specialized trenches that are similar in layout to the Slit Trenches. The two Components-in-Grout (CIG) Trenches each have five narrow trenches within them, similar in dimension to the individual slit trenches: nominally 6 m wide by 200 m long. Each set of five sits within the larger footprint of CIG#1 and CIG#2, about 50 m × 200 m, which is the same overall dimension of the engineered trench and slit trench unit.

Within each CIG "slit" are disposed components surrounded by grout on all sides. Each collection of components disposed at once comprises a Segment. The GoldSim model devised to assess sensitivity analysis of the CIG Trenches assumes that eight such segments are disposed. A screen shot of the model's top level is shown in Figure F-73.

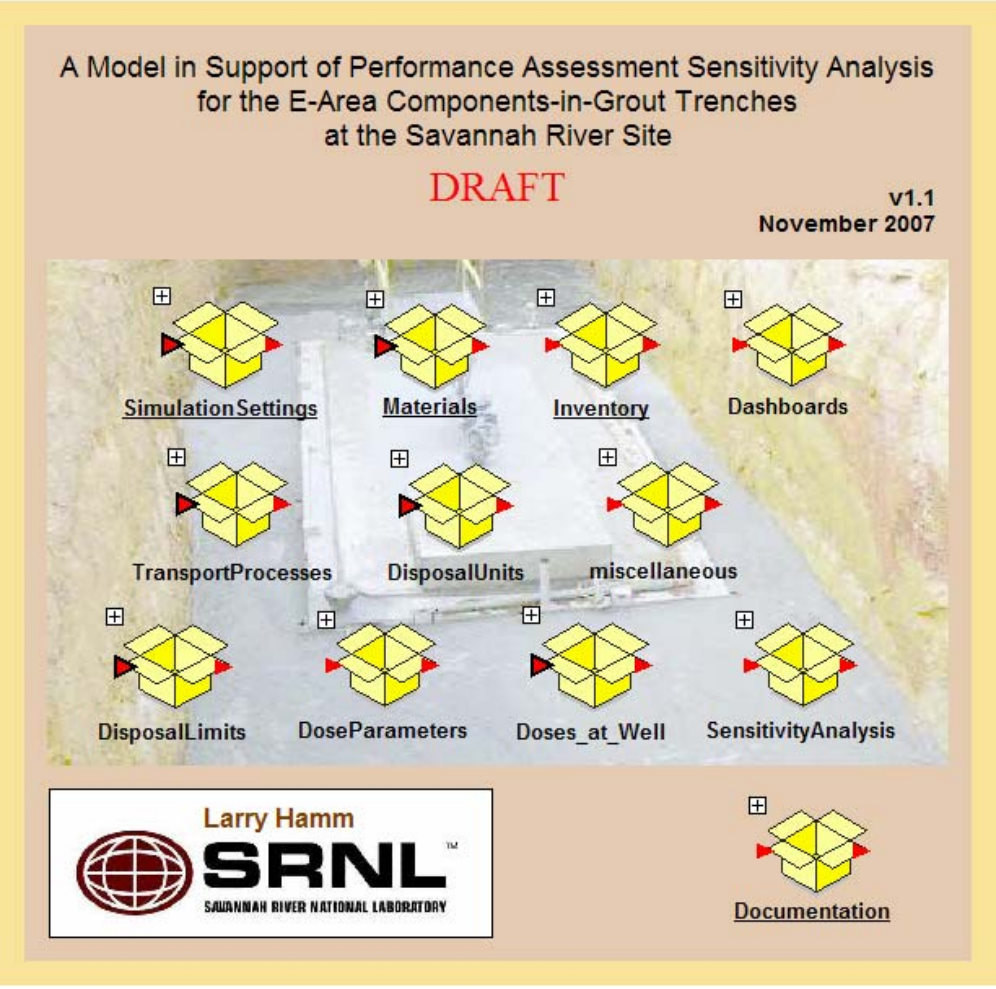

Figure F-73. Top View of the Components-in-Grout Trenches Sensitivity Analysis Model

1.3.1 Model Description

The draft E-Area CIG Trenches Sensitivity Analysis Model is similar in general layout, operation, and execution to the Slit and Engineered Trench models, though it differs a great deal in the treatment of the contaminant transport in the near field—that is, in the region near the trenches themselves. The principal differences are necessary in order to model the contaminant transport within the concrete that immediately surrounds the radioactive materials.

The many modifications to the model include

- new materials and properties for both the older and newer formulations of grout in both oxidized and reduced conditions, and current and future waste forms
- the division of the trenches into Segments, in order to model segments individually or in groups
- low-resolution two-dimensional finite difference modeling, with a transient flow field imported from PORFLOW calculations, taking advantage of geometrical symmetry
- a reduced Species list, screened for radionuclides with half-lives over five years, plus Rn-222 and four special waste forms for C-14, Tc-99, and I-129

A flowable, low-strength grout was used in the emplacement of Segments 1 through 8, and its relatively rapid degradation to a highly transmissive porous medium is accounted for in both the PORFLOW and GoldSim modeling. Later CIG segments are assumed to use a higher-strength grout, which will retain its physical (mechanical, hydraulic) and chemical properties for a longer period of time.

The aqueous contaminant transport calculations in the GoldSim model were benchmarked to the PORFLOW model by comparing the breakthrough of various radionuclides at the point of recharge to the aquifer and at the well in Segment 6. In addition to the flow field, PORFLOW concentration results were imported into the GoldSim model so that they could be compared directly (within the same Result element) in the GoldSim CIG Model version 0.102. Good agreement was obtained for nearly all conditions, though calibration exercises are ongoing as an optimal GoldSim mesh is obtained and PORFLOW gets updated to perform correct unsaturated zone retardation calculations. The PORFLOW results were removed from the release versions v1.0 and v1.1 in order to reduce the size of GoldSim model results, though they could be reintroduced at any time in order to revisit the benchmarking.

All-pathways doses are again calculated using all exposure pathways from the use of contaminated ground water. The CIG model v1.1 was developed using GoldSim version 9.60 service pack 2.

A specific point must be made about a unique feature of the CIG model: geometrical symmetry. In order to reduce redundant calculations, the vadose zone model domain covers only half of the CIG trench, sliced vertically transverse to the long axis of the segments and trenches. In order to preserve the proper concentrations within the model (necessary to capture the correct nonlinear interactions of diffusion and advection under the influence of retardation and solubility in the unsaturated zone), one half of the specified inventory is put into the model. This modification is corrected for, so that the flux to the water table from the half-model unsaturated zone is doubled, and all concentrations in the aquifer (the saturated zone) are consistent with the full inventory.

1.3.1.1 Disposal Segment Selection

A dashboard was constructed in order to facilitate the selection of inventories to use and trench segments to be modeled, as shown in Figure F-74. Here the user can select any combination of existing segments (1 through 8) or the future inventory, identified as SegX.

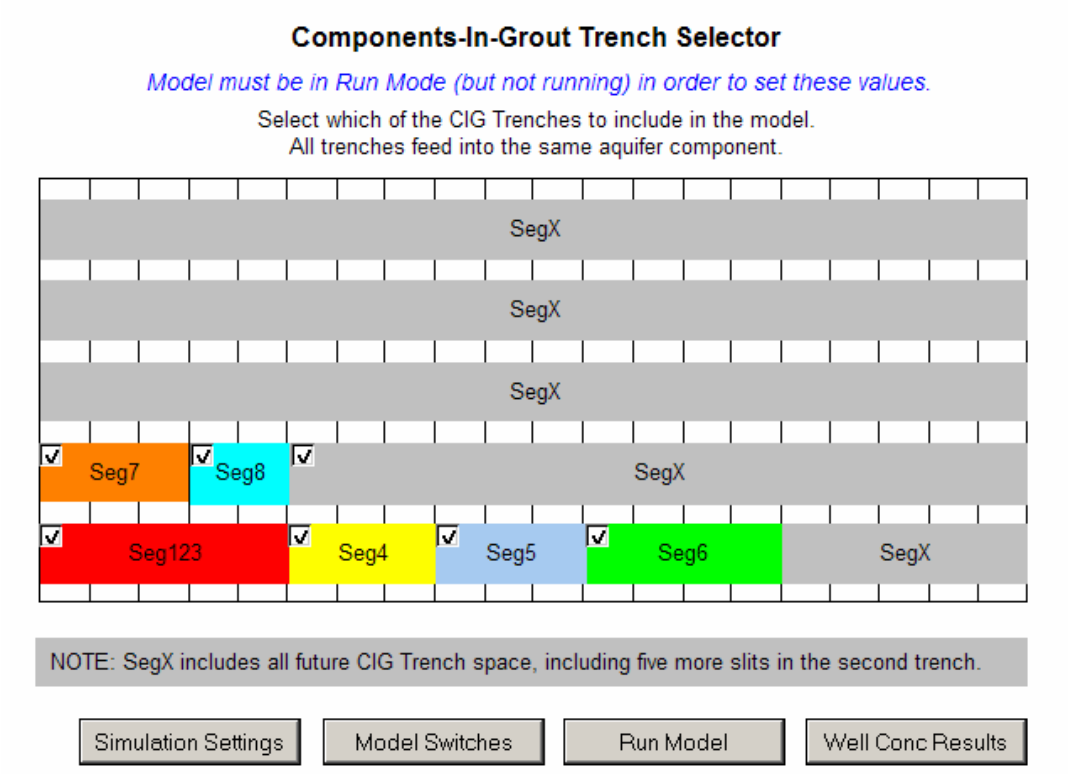

Figure F-74. Dashboard for selecting segments to run in the CIG Model

Segment 9, which was recently emplaced, is considered part of the future inventory for the purposes of this PA. SegX fills the space in CIG Trench #1 that is not occupied by Segments 1 through 8, as well as all of CIG#2, which is not shown, but has the same overall dimensions and layout as CIG#1, with five long individual trenches in the larger CIG Trench. If the SegX inventory is selected, the inventory from CIG#2 is added to that shown in the Figure, as if it were simply placed on top of it. Groundwater flow is to the right, subparallel to the long dimension of the trenches, in this figure.

1.3.1.2 Modeling the Near Field

The CIG contaminant transport calculations are performed for the waste layer and vadose zone for each Segment individually (including SegX), assuming columnar flow in the vadose zone below the footprint of the segment. The recharge to the aquifer is combined, as discussed below. The waste layer is separated from the underlying vadose zone simply to aid in model organization and presentation, and consists of the Cells and associated GoldSim elements shown in Figure F-75. The cells in the olive rectangle (upper left) handle the introduction of inventory into the Cells Waste1 through Waste8, given a burial time and inventory specific to each Segment. This WasteLayers GoldSim container is duplicated for each of the Segments, with only the BurialTime and FreeInventory elements having Segment-specific definitions.

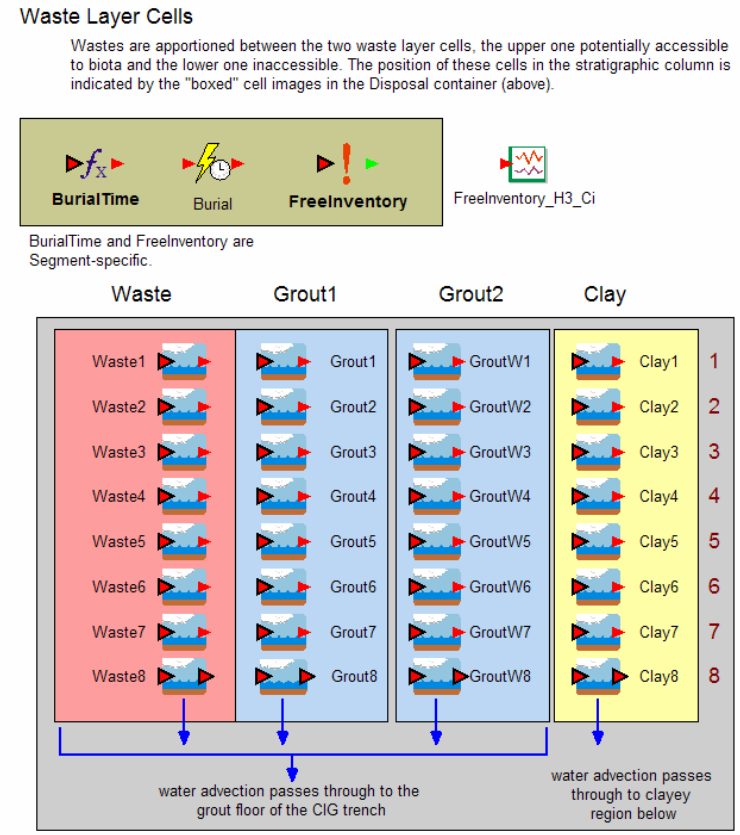

Figure F-75. An Example WasteLayers Container in the CIG Model

The column of Cells in the salmon colored rectangle (left) are labeled Waste1 through Waste8, representing eight separate vertically-stacked Cells that initially contain a homogeneous average of the radioactive waste. These are connected, through advective and diffusive water connections, to each other and to the neighboring cells Grout1 through Grout8 in the blue rectangle (center left). These, in turn, are connected to each other and to the GroutW Cells (center right), which are likewise connected to the Clay cells (in the yellow rectangle on the right).

All Cell elements in the container are connected to each neighboring Cell, creating a coarsely-discretized waterborne contaminant transport finite-difference model in GoldSim. The Grout cells represent the wall of grout that surrounds the waste (subdivided into two columns), and the Clay cells represent the surrounding native clayey soils. The physical properties of grout (both old and new formulations) and the flow field within it change in time by referencing flow field information generated by PORFLOW.

The finite-difference model thus constructed in GoldSim is a coarse version of the same model constructed in PORFLOW. The finer PORFLOW mesh is coarsened, but the material properties and dimensions of the materials are maintained. Transient water saturations and flow rates are calculated in PORFLOW (which unlike GoldSim has a flow solver) and are exported from PORFLOW, resampled to the coarser GoldSim "mesh" of Cells, and are assigned values in the GoldSim Cells, which refer to lookup tables of water saturations and flow rates for each Cell and each advective connection. The PORFLOW CIG modeling is described fully in Chapter 2, with Figure 2-23 showing the PORFLOW mesh.

In its flow calculations, the PORFLOW model assumes that a concrete cap or "roof" has been constructed above each CIG segment. Given this substrate of material properties and water saturations within Cells, and water fluxes between Cells, GoldSim performs the fully-coupled contaminant transport calculations natively.

The bottom layer of Cells in the WasteLayer container are in turn connected to the top layer of Cells in the vadose zone, discussed in the following section. These vadose zone Cells are in the next container up in the hierarchy of the model.

1.3.1.3 Integration of Contaminant Flux to the Aquifer

Within each Segment submodel, the WasteLayer container, described above, feeds into the parent container, which is named Seg123, Seg4, Seg5, ..., Seg8, or SegX, an example of which is shown in Figure F-76. Imagine the Cells in Figure F-75 nested in the upper left WasteLayers Source container in Figure F-76. Each of the columns in the WasteLayers container feeds into a similar column in the Segment container, which contains GoldSim contaminant transport Cells representing the vadose zone below the waste trenches. The Grout wall and floor (emplaced below the waste) are in the blue background, and the surrounding native clayey soil in green. All of these overlie the native sandy soils, shown in brown.

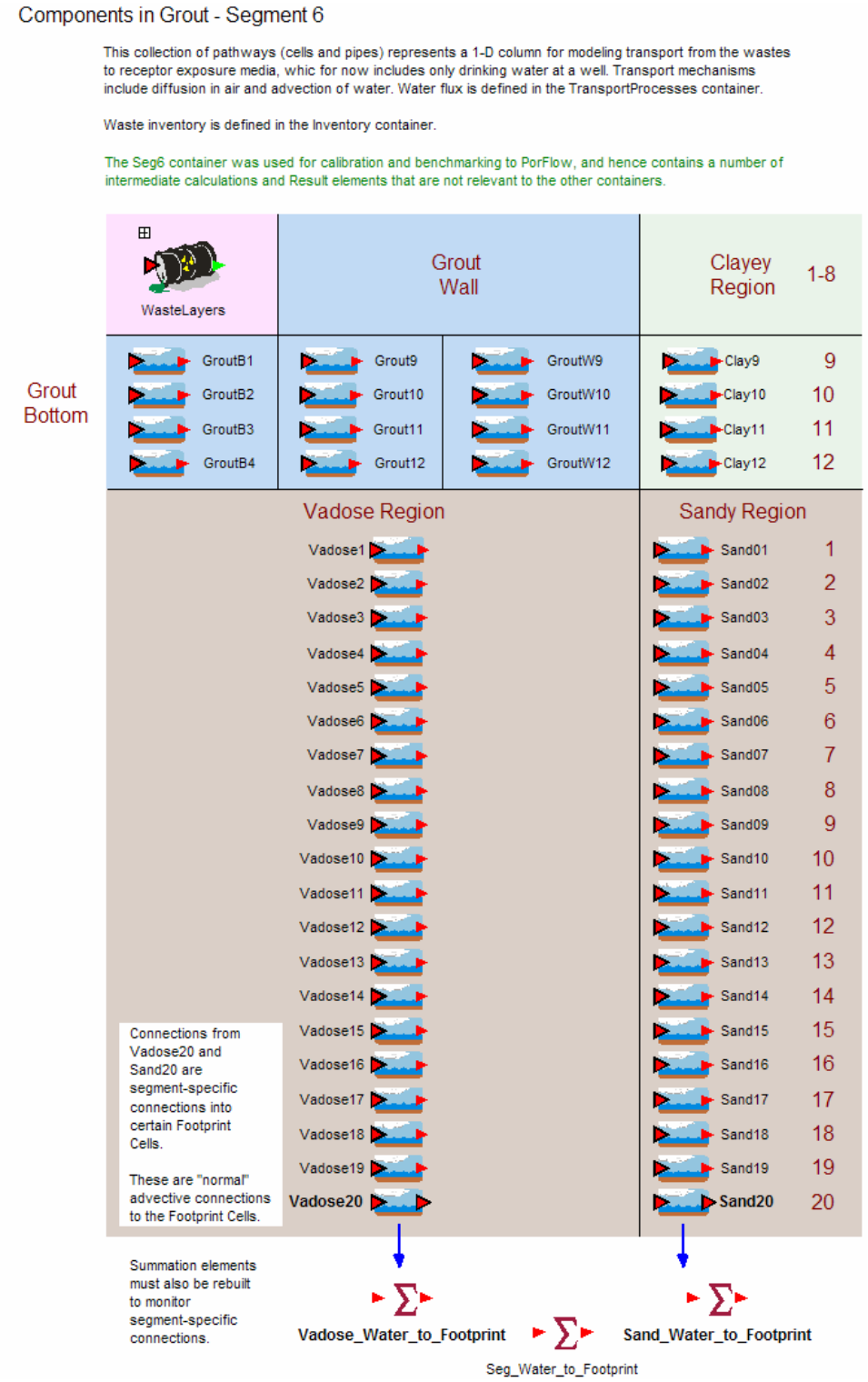

Figure F-76. An Example Segment Container in the CIG Model

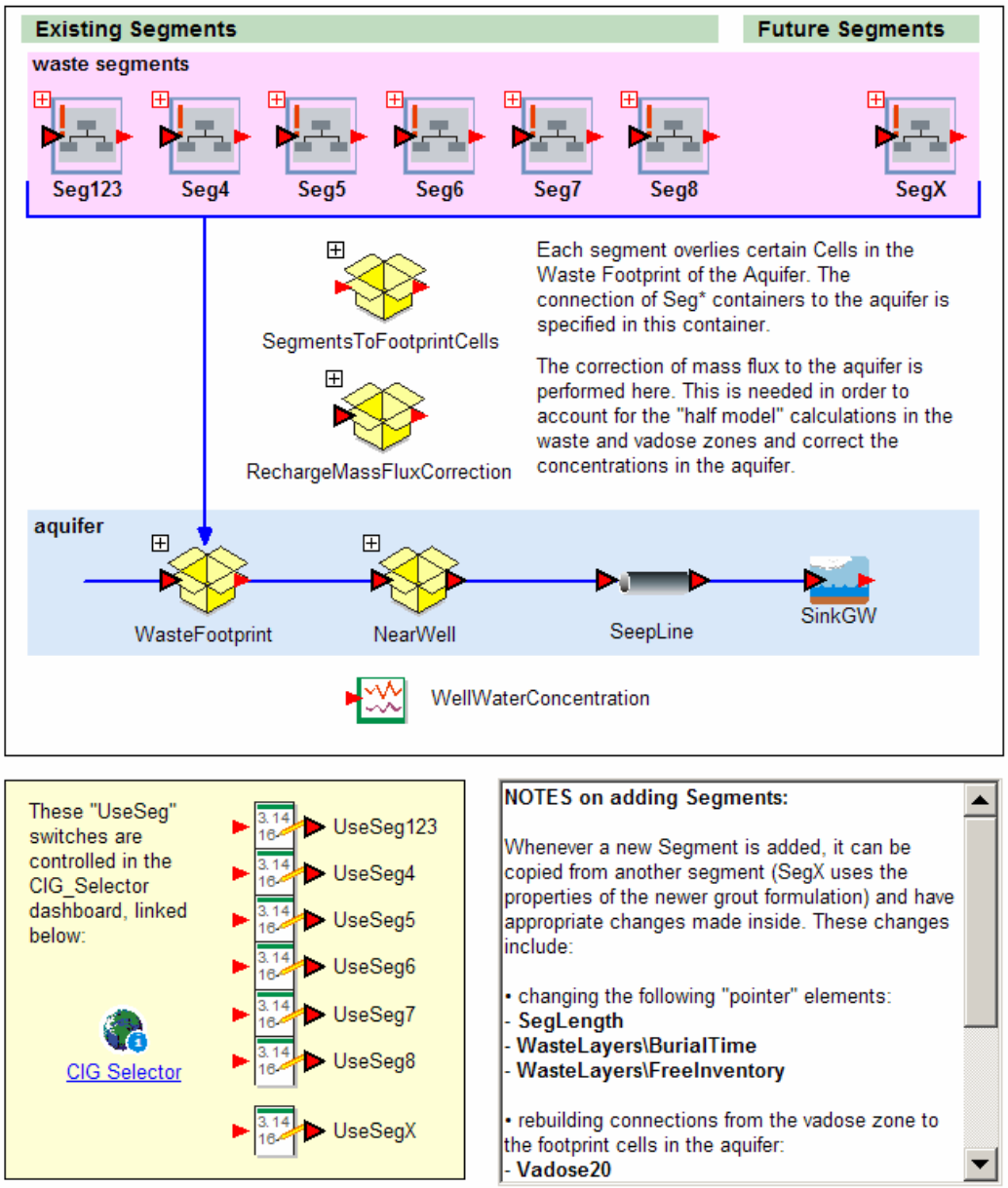

Figure F-77. Segment Integration Into the Aquifer in the CIG Model

This part of the model is represented by two columns, one below the trench (which includes the grout walls and floor) and one below the clayey soil. Like the WasteLayers described above, all these Cells have water advective and diffusive connections to their neighbors. This completes the GoldSim finite difference model representing each of the Segments' waste zones and vadose zones.

Each of these vadose zone columns is connected to the aquifer below. For simplicity, all of them feed into the aquifer in line with each other, since the aquifer is assumed to have the same width as a full CIG Trench. This connection and subsequent transport is discussed in the following section.

1.3.1.4 Combining Segments

The previous sections have discussed the particular arrangements and connections of Cells and associated GoldSim elements within each Segment's container. Moving up one more level, as shown in Figure F-77, the model has each Segment container in the pink rectangle (labeled "waste segments"). These have a different icon because they are Conditional Containers (GoldSim submodels). That is, they are used in the model only on the condition that each of them is selected in the dashboard shown in Figure F-74, through which the user manipulates the true/false conditional values of the Data elements UseSeg123, UseSeg4, ..., UseSegX. Making the Containers conditional saves a great deal of computer time if segments are turned off, since the calculations are not performed for deselected segments.

The first three CIG segments are combined into Seg123, accompanied by Seg4 through Seg8 as disposed wastes. Segments 1 through 8 all share the materials representing an older grout formulation, and use the water saturations and flow fields from PORFLOW runs for that formulation. Future wastes, including Segment 9, all assumed to be in SegX, use a newer, stronger grout formulation, with water saturations and flow fields from PORFLOW runs assuming that formulation.

All segments feed water into the aquifer as recharge, in the WasteFootprint container. This container is analogous to that shown in Figure F-19 for the Slit and Engineered Trenches, except that each Segment's vadose zone Cells feeds into different Footprint Cells, depending on its location. The Footprint Cells that are fed by each Segment are shown in the diagram on the dashboard shown in Figure F-74. For example, Seg4 feeds into Footprint Cells 6, 7, and 8. Seg8 feeds into 4 and 5, overlapping with contributions from Seg123. In v1.1 of the Model, the underlying aquifer Cells span the entire width of the CIG Trench, introducing instantaneous and complete mixing (numerical dispersion) in later and vertical directions, perpendicular to flow. At this point, the rest of the contaminant transport pathway and dose assessment for the CIG Trenches follows the same pattern as that for the Slit and Engineered Trenches.

1.3.2 Uncertainty Analysis

The CIG Trench Sensitivity Analysis Model has several uncertain parameters, represented as probability distributions. Like the Slit and Engineered Trench Models, some of these are rather loosely defined in this early draft of the GoldSim model, and some are not defined stochastically at all. Again, the lack of stochastic parameters will cause the model to underpredict uncertainty, and will exclude some potentially important parameters from the sensitivity analysis. All parameter distributions will be given more defensible distributions under the PA maintenance program.

1.3.2.1 CIG with Full Closure Inventory

The CIG Model was run with two different inventory scenarios: 1) with the inventory that is expected to occupy CIG#1 and CIG#2 at closure, and 2) with just the inventory of Segments 1 through 8. Each of these inventory options is considered separately in the following discussion. Figure F-78 and Figure F-79 show the uncertainty in the modeling of future all-pathways dose (i.e. potential dose from the use of water from a hypothetical well located 100 m downstream of the edge of the disposal unit). The former shows the statistical summary as a time history of total dose, summed across all radionuclides. The latter shows a time history of the dose attributable to each radionuclide, so that one can see which are the most significant contributors to the dose. Note how the two forms of Tc-99 (Tc99 and Tc99K) come out simultaneously, and should be added to arrive at the total dose from Tc-99. Similarly behaved are the two forms of C-14. The three source forms of I-129 are not significant dose contributors in this graph.

1.3.2.2 CIG with Segments 1 through 8 Inventory

The same calculation was performed for just the currently-disposed inventory, which for the purposes of this PA is assumed to include only Segments 1 through 8. The total projected dose time history statistics are shown in Figure F-80, followed by mean value time histories of dose from each radionuclide, in Figure F-81. The various source forms of Tc-99 and C-14 behave as they do for the full inventory.

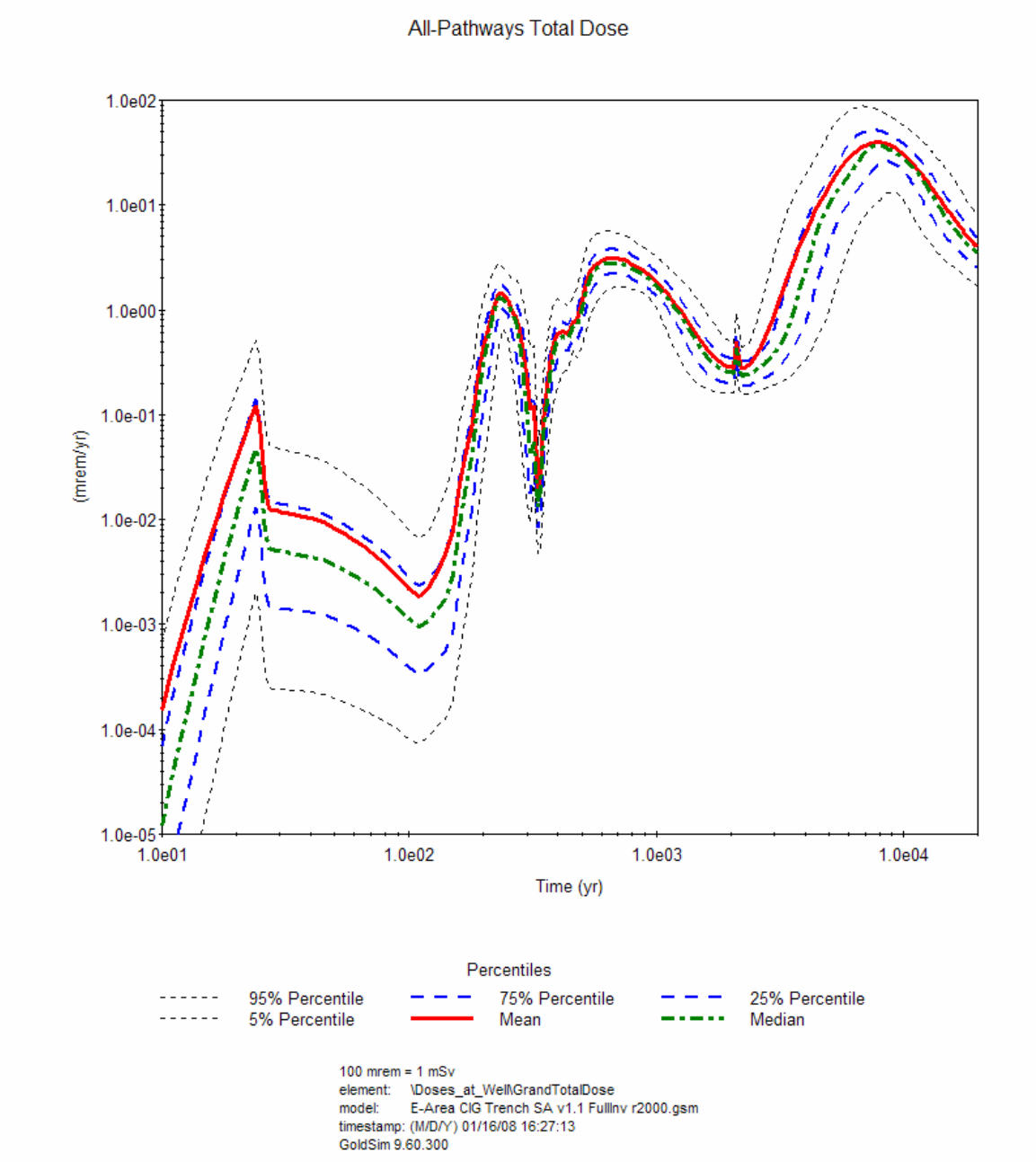

Figure F-78. Time history of total all-pathways dose from CIG Trench well water statistical summary of 2000 realizations (full projected inventory)

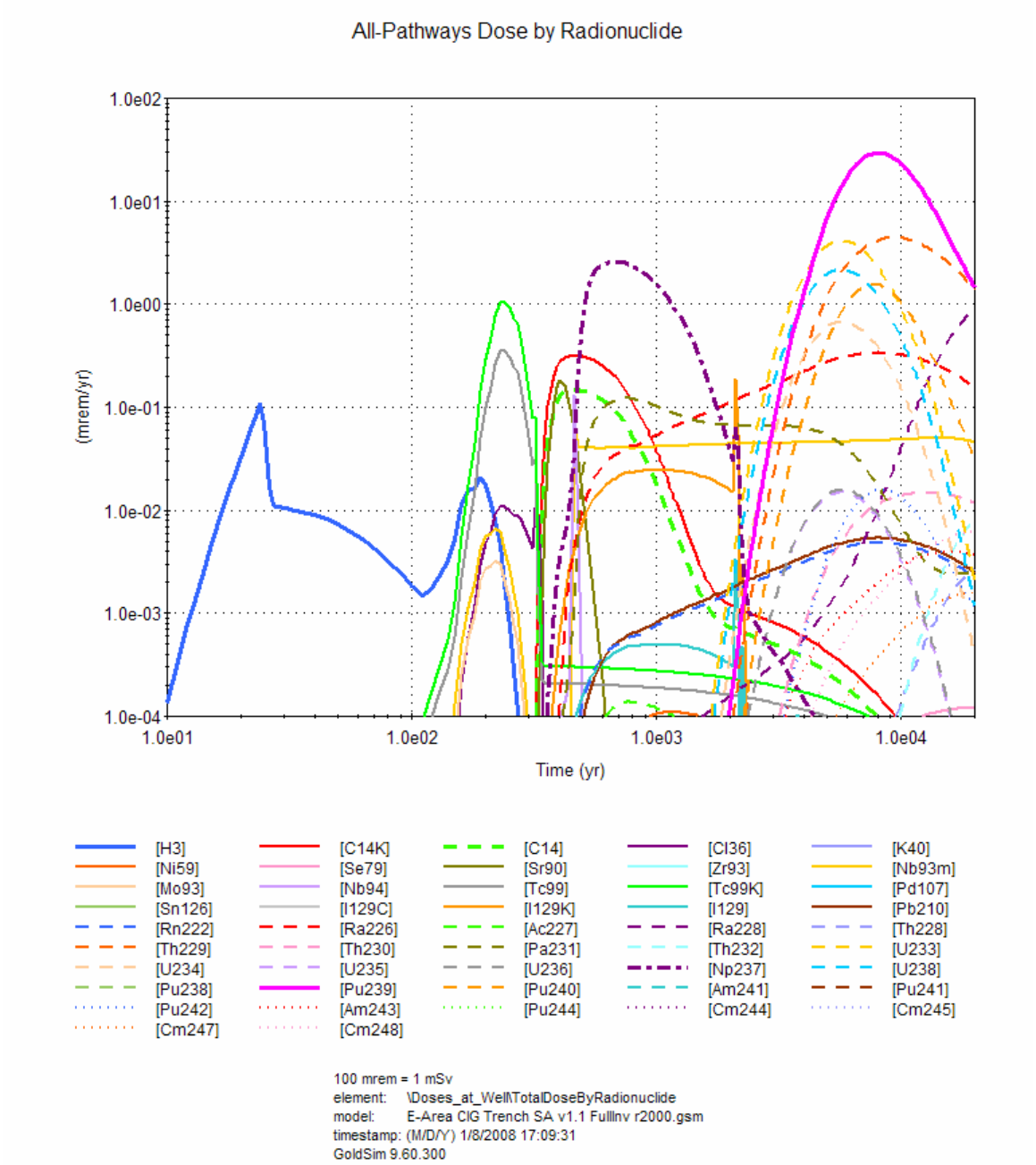

Figure F-79. Time history of mean all-pathways dose by radionuclide from CIG Trench well water (full projected inventory); selected radionuclides shown

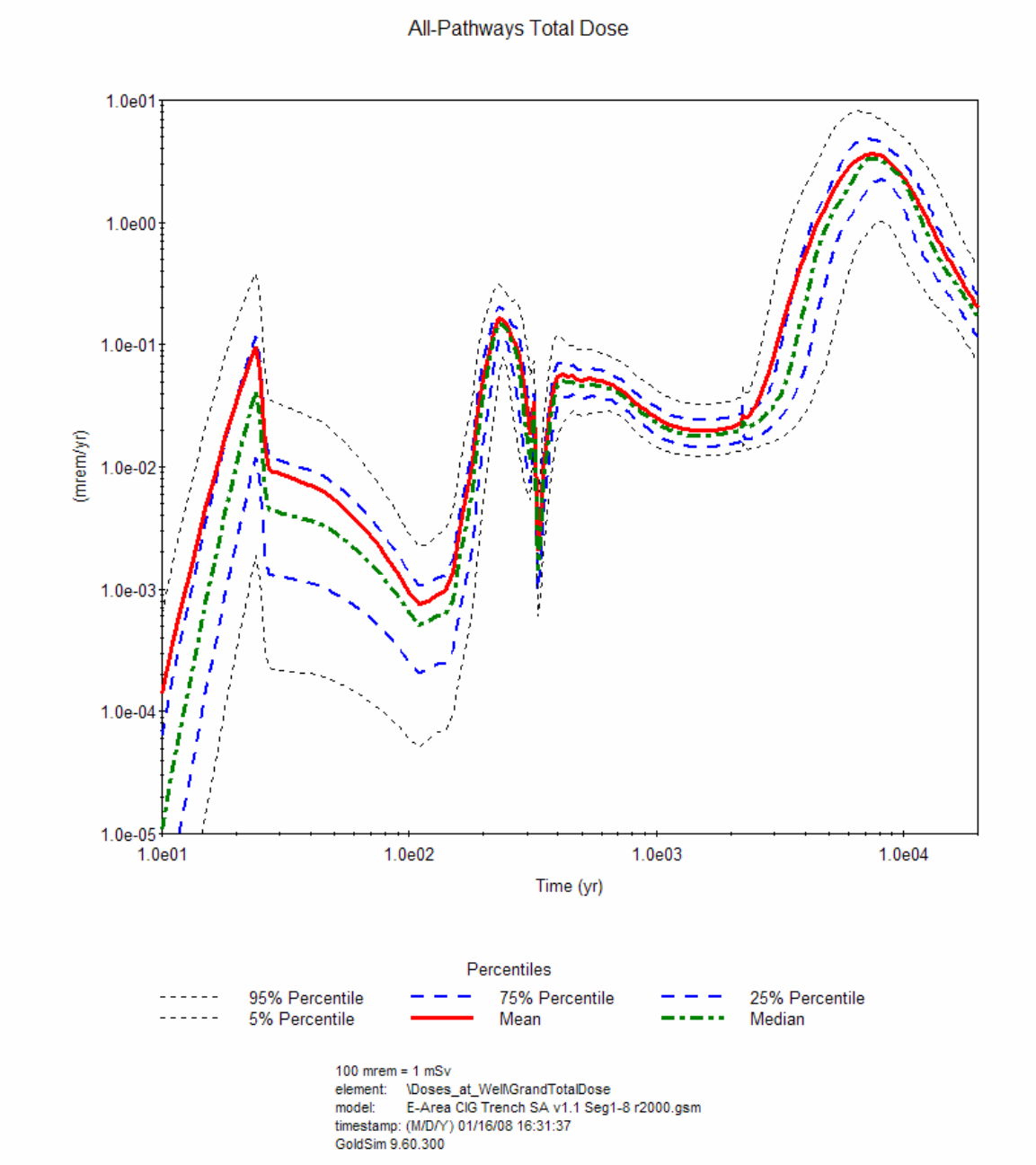

Figure F-80. Time history of total all-pathways dose from CIG Trench well water statistical summary of 2000 realizations (segments 1-8 inventory)

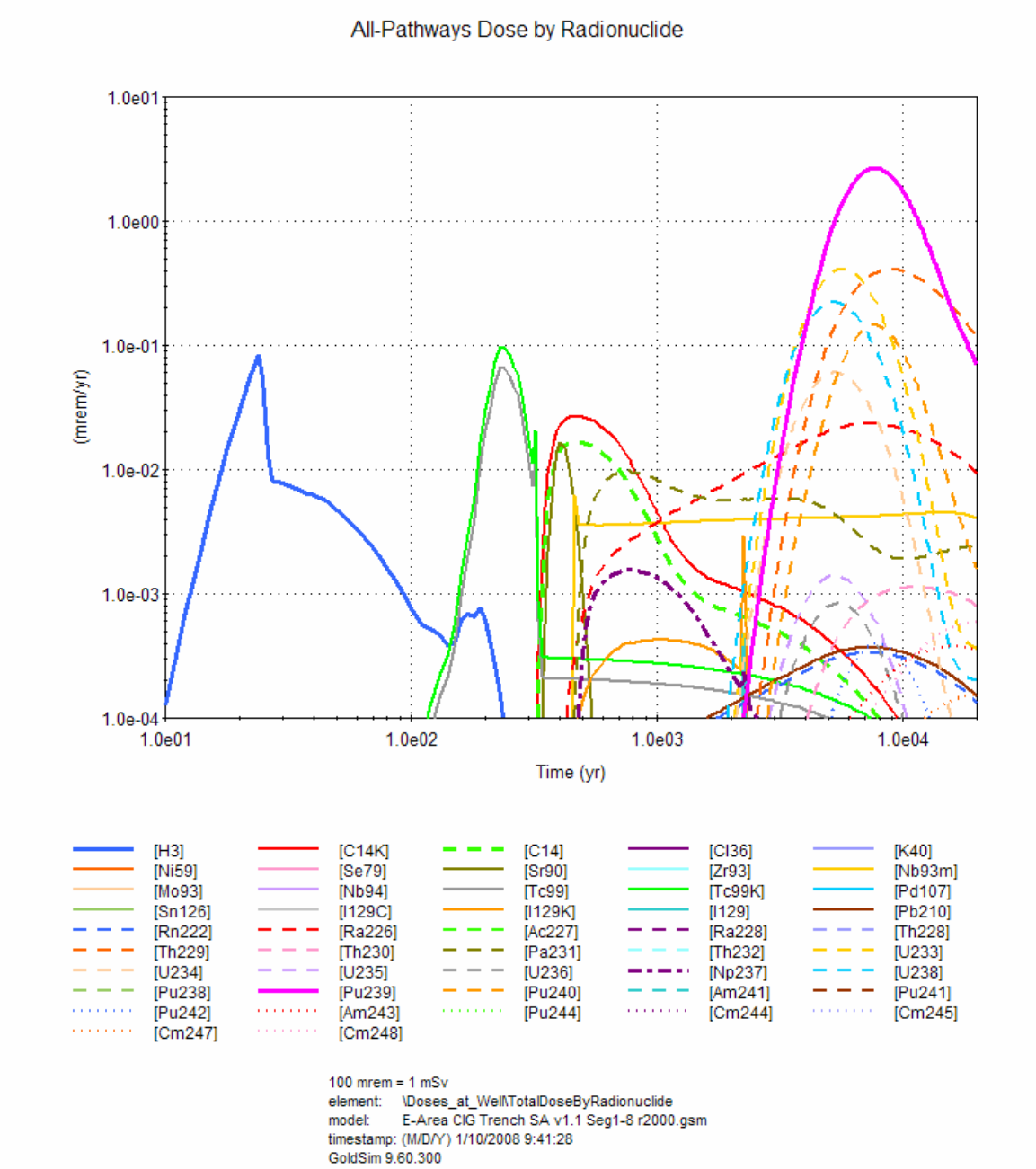

Figure F-81. Time history of mean all-pathways dose by radionuclide from CIG Trench well water (segments 1-8 inventory); selected radionuclides shown

1.3.3 Sensitivity Analysis

A sensitivity analysis for the E-Area CIG Trenches was also performed in support of the E-Area PA Maintenance Program. Like the Slit and Engineered Trenches, a GoldSim model was developed for performing the sensitivity analysis. Again, the results of the model output were analyzed using GBM, and the discussion of the sensitivity analysis methodology provided for the Slit Trenches in Section 1.1.3 applies here. The same model endpoints were selected for sensitivity analysis as were discussed for the Engineered Trenches in Section 1.2.3.

As was found for the Slit and Engineered Trenches, the results of the sensitivity analysis indicate that the most significant stochastic parameters in the model are related to water flow: the assumed thickness of the saturated zone, or aquifer, and the infiltration rate multiplier, an *ad hoc* factor introduced to add some uncertainty to the rate of infiltration through the concrete slabs overlying each of the CIG trenches. Recall that the CIG Trenches do not share the infiltration model arising from the HELP closure cap modeling that is used for the Slit and Engineered Trenches—rather the CIG model uses the infiltration calculated by PORFLOW, assuming the presence of a concrete slab over the CIG segments. The infiltration multiplier is an *ad hoc* distribution (uniform 0.75 to 1.25) designed to artificially add uncertainty as a multiplier to the value of infiltration, in order to determine whether it is sensitive in the model. Indeed it is.

Other less significant sensitive parameters include soil/water partition coefficients for dose-significant radionuclides, the porosity of sandy soil, and the molecular diffusivity in water.

These results suggest that uncertainty most effectively be reduced by determining reasonable values for the input distributions for the aquifer thickness and the infiltration through the concrete slab.

1.3.3.1 Summary Statistics for Endpoints

Two inventory scenarios were run for this sensitivity analysis. The first assumed the full closed/projected inventory for both CIG#1 and CIG#2, including all currently disposed Segments, and has the file name “E-Area CIG Trench SA v1.1 FullInv r2000.gsm”. The second model, which was configured to include only the inventory from disposed Segments 1 through 8, has the file name “E-Area CIG Trench SA v1.1 Seg1-8 r2000.gsm”. Both models executed 2000 realizations, with Latin Hypercube Sampling enabled and a seed value of 1. The exporting of results is done the same way as for the Slit and Engineered Trenches.

Summary statistics for the endpoints of interest are tabulated in Table F-8 for the full inventory and Table F-9 for Segments 1 through 8. It should be kept in mind that the all-pathways (water use) dose calculation considers the CIG inventories as if they were directly in line, and ignores the presence of other disposals in proximity. The purpose of this preliminary model is not to predict doses, but rather to characterize the uncertainty and sensitivity context of the actual PA model. The summary statistics quantify the uncertainty surrounding the dose calculations.

1.3.3.2 Endpoints and most influential explanatory variables (full CIG inventory)

The endpoints selected for sensitivity analysis include doses and maximum contaminant levels (MCLs). The maximum dose to a hypothetical member of the public is examined both within the period of performance (1130 y) and for all time. Note that for the model v1.1, the all-time doses were recorded as the maximum dose achieved after 2000 y, but this is seen (by examination of Figure F-78 through Figure F-81) to always bracket the largest does. The MCLs for gross alpha concentration, dose from beta and gamma emitters, and concentrations of total radium and total uranium are also subjected to analysis.

Each of the modeling endpoints listed in the tables was analyzed to identify those stochastic parameters having the most influence on that endpoint. In most cases, the most significant parameter was the saturated thickness of the aquifer, as shown in Table F-10. Graphs of the goodness of fit of the statistical model and the partial dependence are also presented.

Discussions of particular results are provided following the figures below. For each of the endpoints, a graph is provided showing the predictive power of the GBM estimate as compared to the GoldSim results. Less scatter along the line of slope = 1 reflects a better fit of the statistical model that is constructed to predict the GoldSim results. Following the scatterplot is a collection of four graphs showing the SI of the top four sensitive parameters for the endpoint. The shaded green background shows the distribution of the 2000 samples from the input distribution, and closely reflects the defined input distribution. The blue solid line (partial dependence) shows the degree of sensitivity as a function of the parameter value. The parameter is most sensitive where the partial dependence is high, and is least sensitive where it is low.

The following sections are grouped first for all the CIG full inventory runs, followed by another section for the CIG Segments 1 through 8 runs.

Table F-8. Summary statistics from 2000 realizations for the CIG Trenches endpoints of interest (full projected inventory)

Endpoint	Mean	Standard Deviation	Min	1st Qu.	Median (2nd Qu.)	3rd Qu.	Max
max. dose in period of performance (mrem/yr)	3.2	1.3	1.1	2.2	2.9	3.6	12
max. dose – all time (mrem/yr)	50	24	11	33	44	61	210
max. alpha concentration at well within period of performance (pCi/L)	0.52	0.21	0.18	0.36	0.47	0.63	2.0
max. beta - gamma dose at well within period of performance (mrem/yr)	0.69	0.60	0.14	0.30	0.50	0.87	5.7
max. radium concentration at well within period of performance (pCi/L)	0.034	0.011	0.017	0.025	0.031	0.041	0.067
max. uranium concentration at well within period of performance (μg/L)	1.6e-8	3.6e-7	1.1e-10	3.2e-10	4.4e-10	6.3e-10	1.5e-5

1 mrem = 10 μSv
27 pCi = 1 Bq

Table F-9. Summary statistics from 2000 realizations for the CIG Trenches endpoints of interest (segments 1 through 8 inventory)

Endpoint	Mean	Standard Deviation	Min	1st Qu.	Median 2nd Qu.	3rd Qu.	Max
max. dose in period of performance (mrem/yr)	0.22	0.12	0.098	0.14	0.19	0.22	1.4
max. dose – all time (mrem/yr)	4.8	2.2	1.1	3.2	4.3	5.9	19
max. alpha concentration at well within period of performance (pCi/L)	3.1e-3	1.0e-3	1.7e-3	2.3e-3	2.9e-3	3.8e-3	5.9e-3
max. beta - gamma dose at well within period of performance (mrem/yr)	0.23	0.33	0.016	0.045	0.11	0.28	3.2
max. radium concentration at well within period of performance (pCi/L)	2.4e-3	8.0e-4	1.3e-3	1.8e-3	2.2e-3	3.0e-3	4.7e-3
max. uranium concentration at well within period of performance (μg/L)	7.5e-10	2.0e-8	7.0e-14	2.1e-13	3.1e-13	5.7e-13	8.4e-7

1 mrem = 10 μSv
27 pCi = 1 Bq

Table F-10. Identification of the most sensitive parameters for the CIG Trenches endpoints of interest (full projected inventory)

Endpoint	SI rank	input parameter	Sensitivity Index	R^2
max. dose within period of performance (mrem/yr)	1	saturated thickness of aquifer	65	99%
	2	Np K_d in oxidized old concrete	17	
	3	infiltration multiplier	13	
	4	porosity of future waste	4.1	
max. dose – late time (mrem/yr)	1	saturated thickness of aquifer	50	98%
	2	infiltration multiplier	22	
	3	Pu K_d in sandy soil	20	
	4	Pu K_d in oxidized old concrete	3.1	
max. alpha conc. at well (pCi/L)	1	saturated thickness of aquifer	63	99%
	2	Np K_d in oxidized old concrete	18	
	3	infiltration multiplier	13	
	4	porosity of future waste	4.8	
max. beta - gamma dose at well (mrem/yr)	1	infiltration multiplier	33	96%
	2	Sr K_d in sandy soil	26	
	3	saturated thickness of aquifer	18	
	4	porosity of sandy soil	15	
max. radium conc. at well (pCi/L)	1	saturated thickness of aquifer	97	99%
	2	infiltration multiplier	1.1	
	3	Ra K_d in sandy soil	1.1	
	4	porosity of sandy soil	0.22	
maximum uranium concentration at well		insufficient information		

Maximum All-Pathways Dose within the Period of Performance

The maximum total dose within the period of performance occurs at about 700 years, clearly dominated by Np-237 (as seen in Figure F-79).

This scatterplot again shows a good fit between the GBM and the GoldSim model results. The R^2 for this relationship is over 99%.

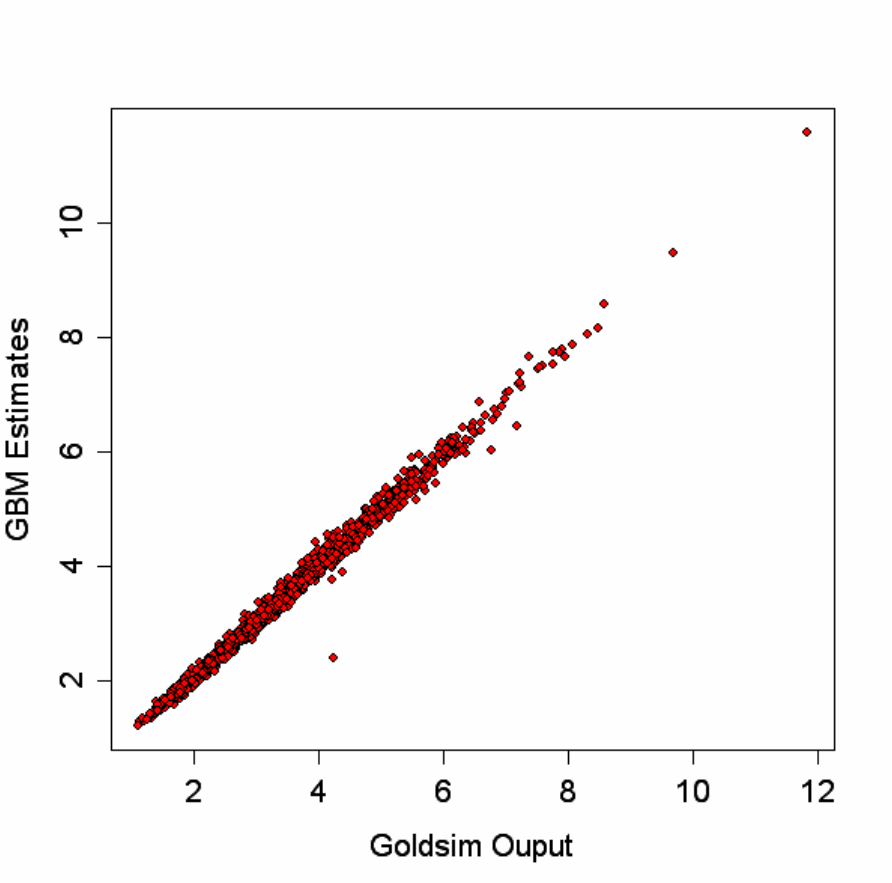

Figure F-82. Scatterplot of GBM estimate for CIG Trenches (full projected inventory) maximum all-pathways dose (mrem in a year) within the period of performance

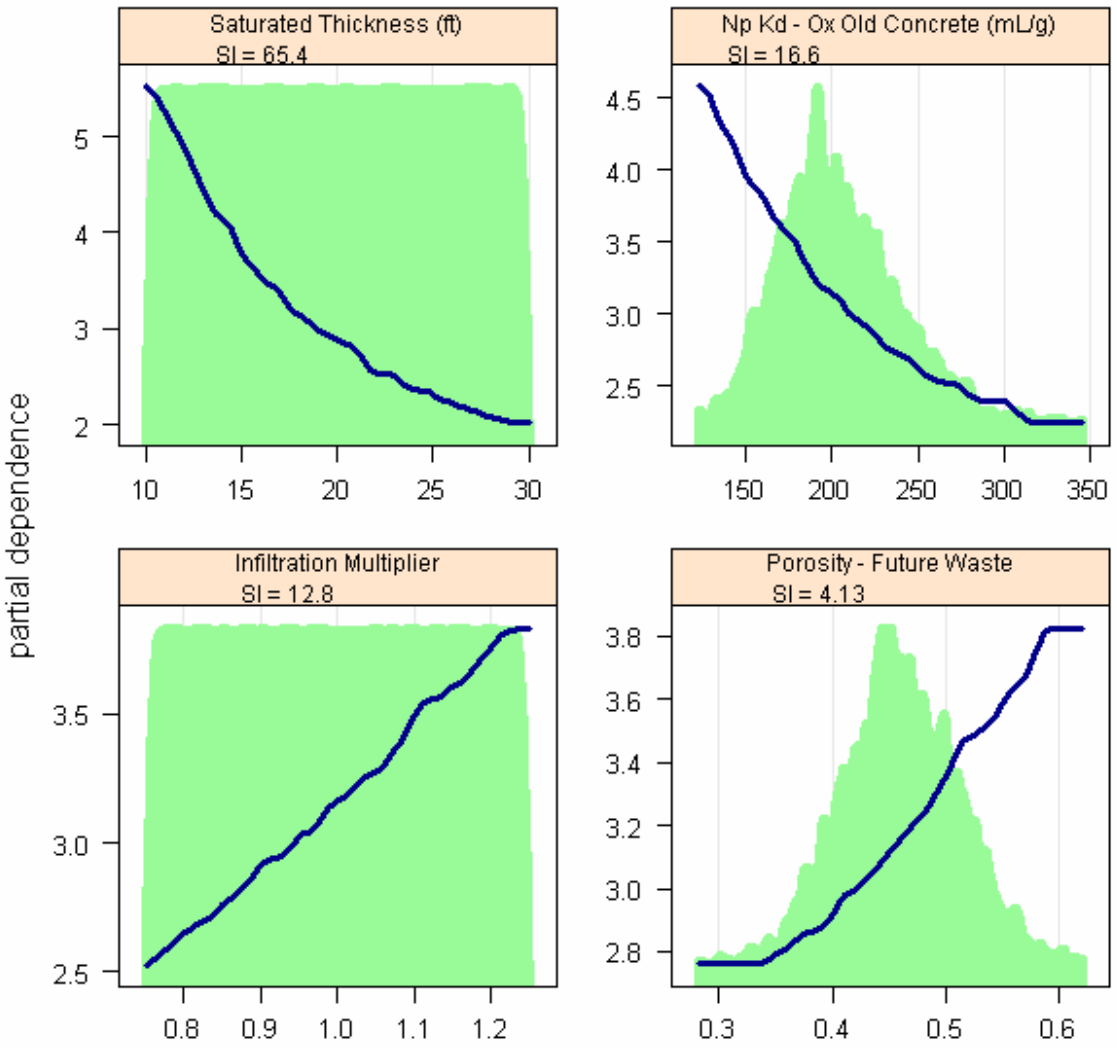

Figure F-83. Partial dependence plots for CIG Trench (full projected inventory) maximum all-pathways dose within the period of performance

As was found for the Slit and Engineered Trenches, the thickness of the aquifer is the most significant contributor to parameter uncertainty. Second is the K_d of Np in oxidized old concrete, which is consistent with neptunium's domination of doses. This is followed by the infiltration multiplier. The fourth-ranked parameter is the assumed porosity of future waste, a waste form found only in SegX.

Maximum All-Pathways Dose in All Time

The maximum total dose in late time is the maximum all-pathways dose achieved after 2000 years. This is the peak dose for all time, driven by Pu-239, although it occurs well after the period of performance as defined in DOE O 435.1-1.

A good fit is seen between the statistical model and the GoldSim results. The R^2 for this relationship is over 98%.

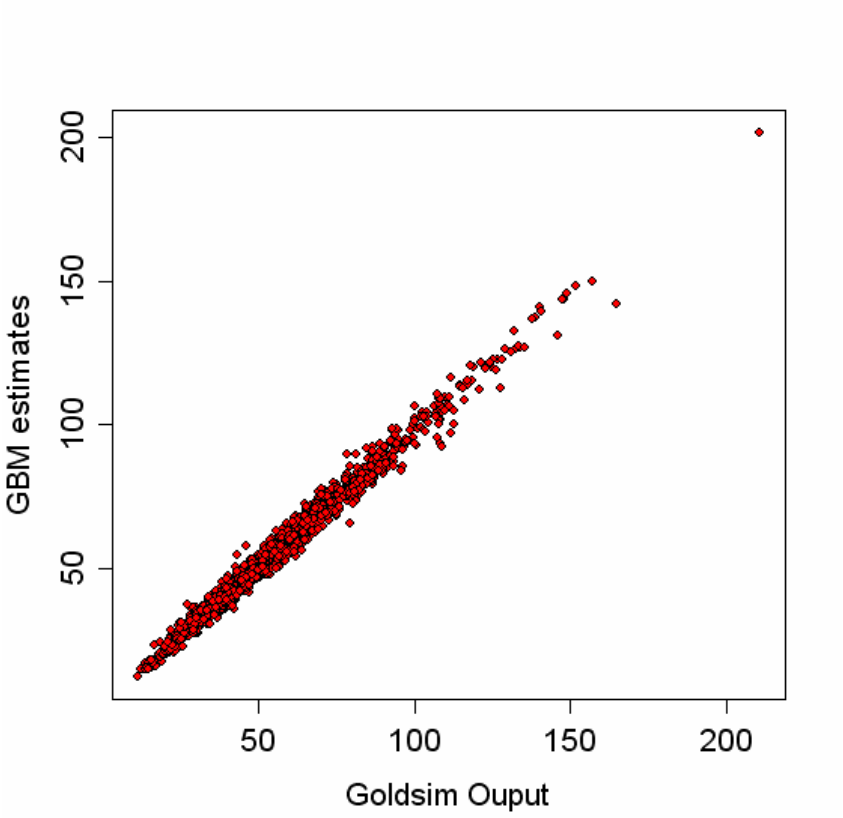

Figure F-84. Scatterplot of GBM estimate for CIG Trenches (full projected inventory) maximum all-pathways dose (mrem in a year) in all time

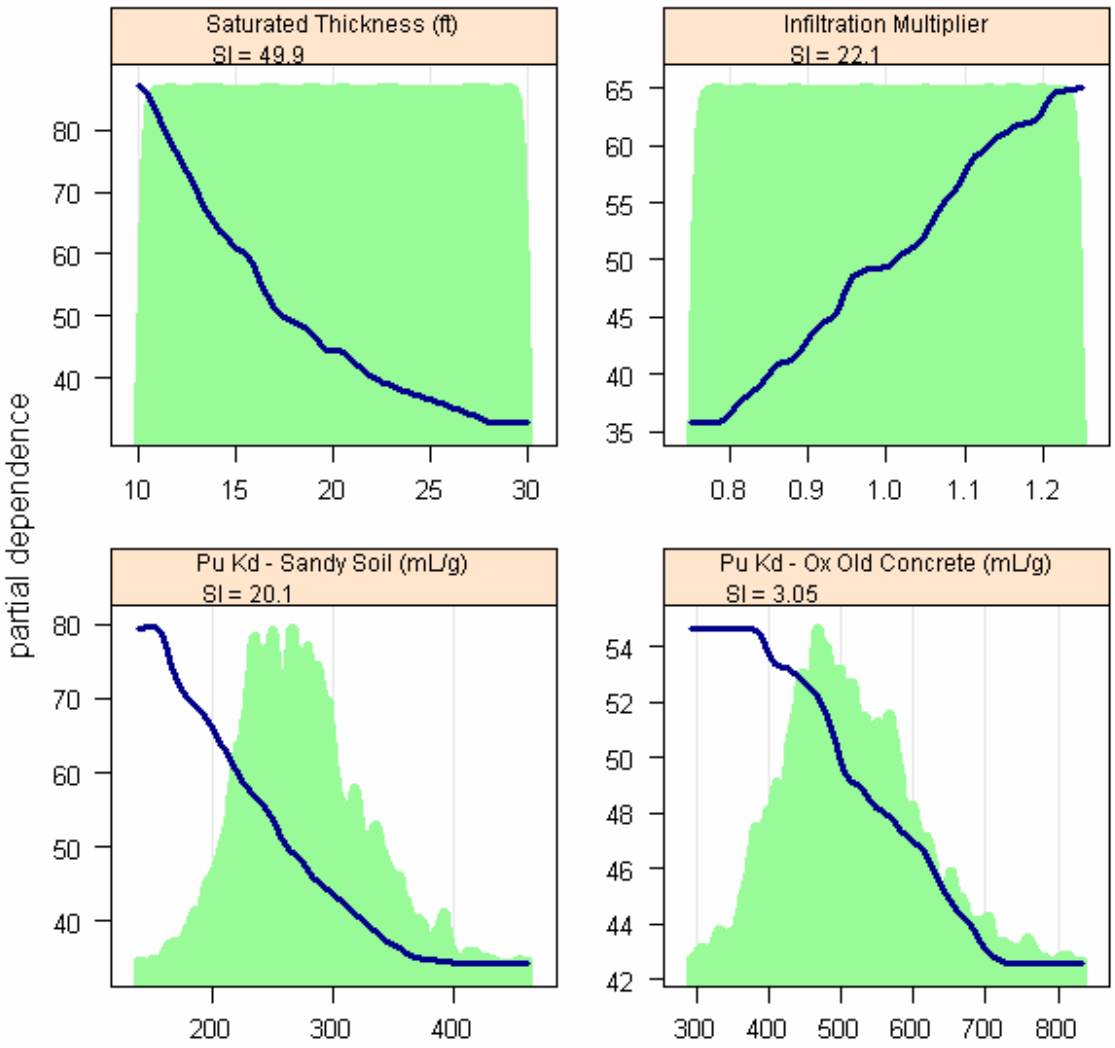

Figure F-85. Partial dependence plots for CIG Trenches (full projected inventory) maximum all-pathways dose in late time

For the maximum dose in all time, the thickness of the aquifer and the infiltration multiplier dominate the sensitivity. These are followed by Pu K_d, in both sandy soil and in oxidized old concrete, consistent with Pu-239's domination of doses in later time. Again, we see the typical inverse relationship of K_d with dose.

Maximum Alpha Concentration

This is the maximum alpha concentration in well water within the period of performance.

The GBM estimate for alpha concentration within the period of performance is again quite good, with an R^2 of over 99%. Note that although U and Pu are the major alpha contributors in later time, they play a minor role here, with Np being the largest contributor during the limited period of performance.

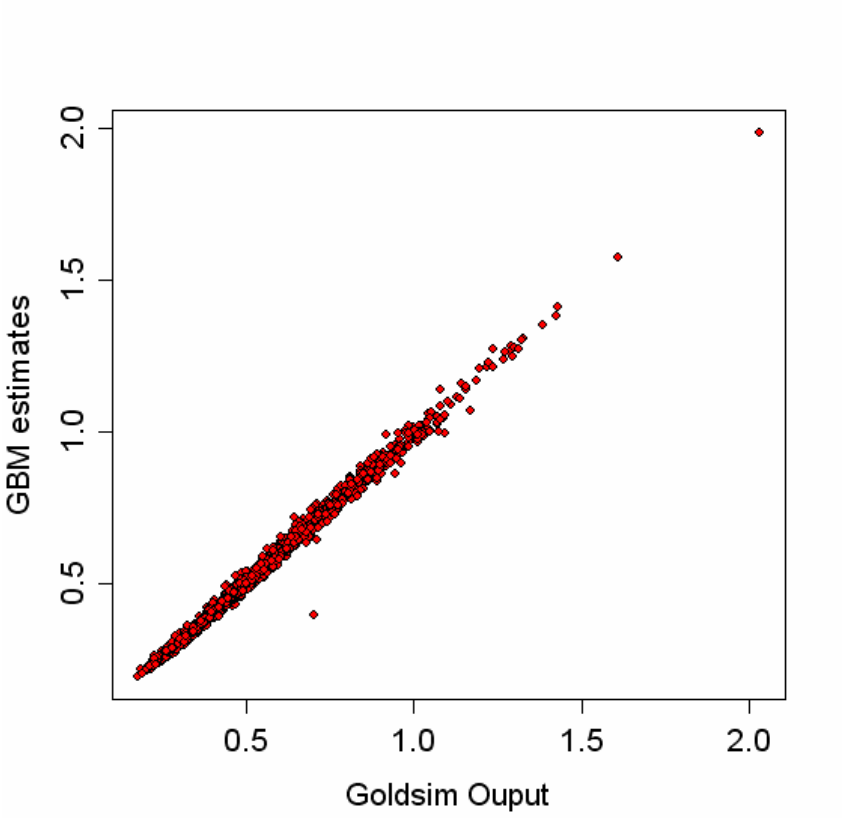

Figure F-86. Scatterplot of GBM estimate for CIG Trench (full projected inventory) maximum concentration of alpha-emitters (pCi/L)

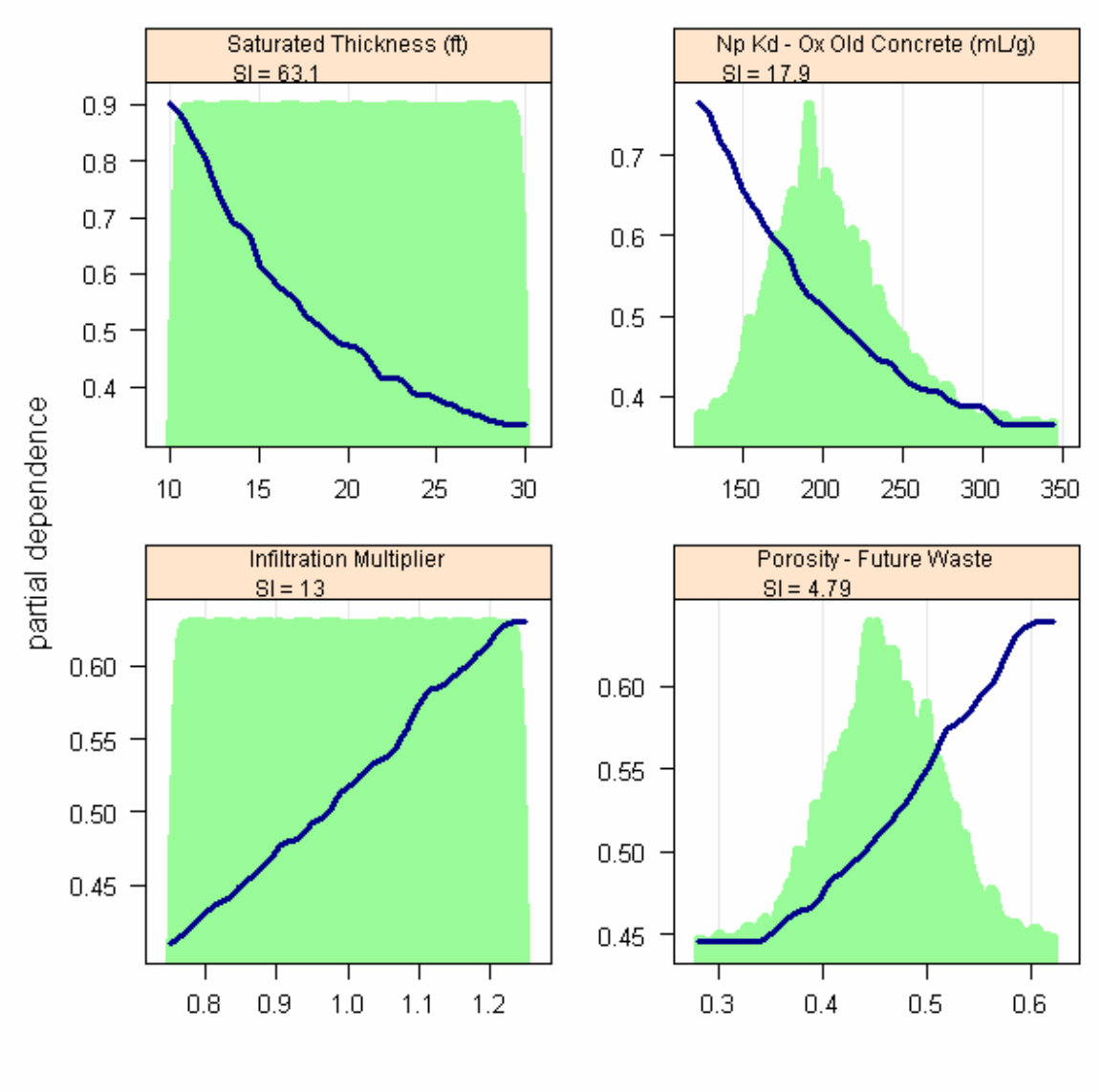

Figure F-87. Partial dependence plots for CIG Trench (full projected inventory) maximum concentration of alpha-emitters

All of these parameters are identical to those selected for the maximum dose within the period of performance, which is dominated by ^{237}Np. Even the partial dependence and SI values are essentially the same. The timing of the maximum alpha concentration is here constrained to be that maximum achieved within the period of performance, so alpha-emitters occurring later (e.g., plutonium) are not considered. If we were to examine the maximum alpha concentration in all time, it would be expected to mimic the sensitivities for the dose in all time.

Maximum Beta-Gamma Water Ingestion Dose

The maximum beta-gamma dose is the maximum dose from beta- and gamma-emitting radionuclides within the period of performance, using the EPA scenario for exposure to groundwater as a drinking water source.

The results for beta- and gamma-emitters show a bit more scatter, but the R^2 for this relationship is still over 96%.

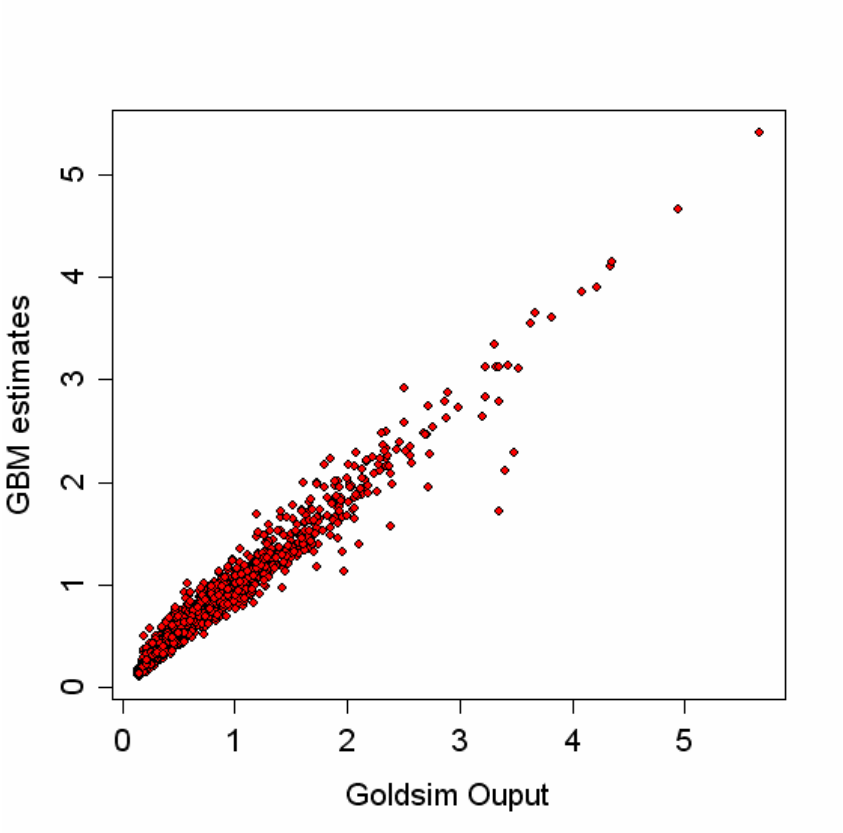

Figure F-88. Scatterplot of GBM estimate for CIG Trenches (full projected inventory) maximum dose from beta- and gamma-emitters

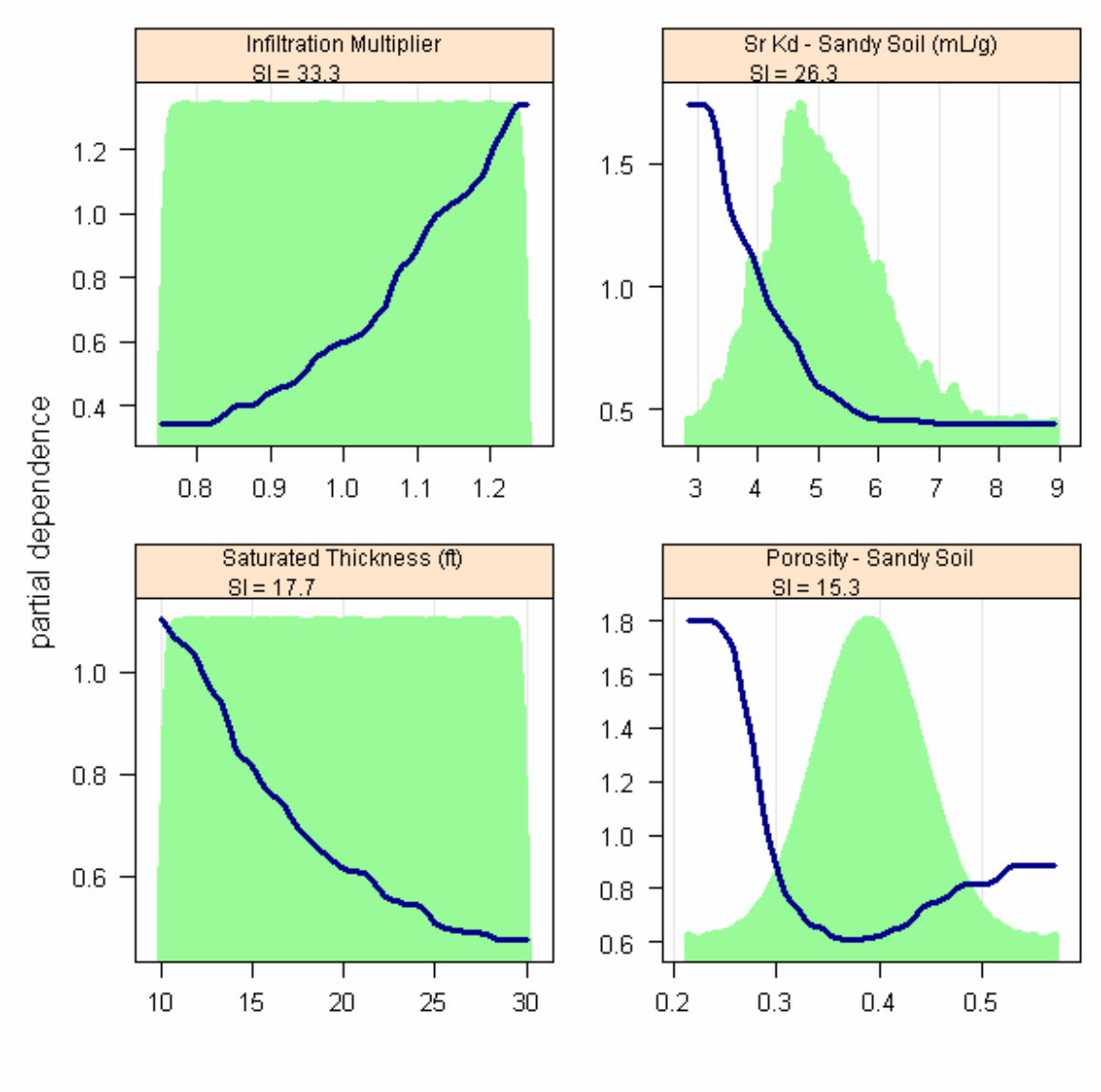

Figure F-89. Partial dependence plots for CIG Trenches (full projected inventory) maximum dose from beta- and gamma-emitters

In addition to the now-familiar infiltration multiplier and saturated aquifer thickness, we see a new parameter for sensitivity of dose from beta-gamma emitters: The K_d of strontium in sandy soil exhibits the typical behavior for K_d, being most sensitive at low values. Strontium-90 is a strong beta emitter, so its appearance here is not surprising. The dependence on the lowest-ranked parameter, sandy soil porosity, does not appear to make much sense, however, showing some sensitivity at the higher values as well as strong sensitivities at low values.

Maximum Radium Concentration

This is the maximum radium concentration in well water within the period of performance.

The GBM estimate for radium concentration is excellent, with an R^2 of over 99%.

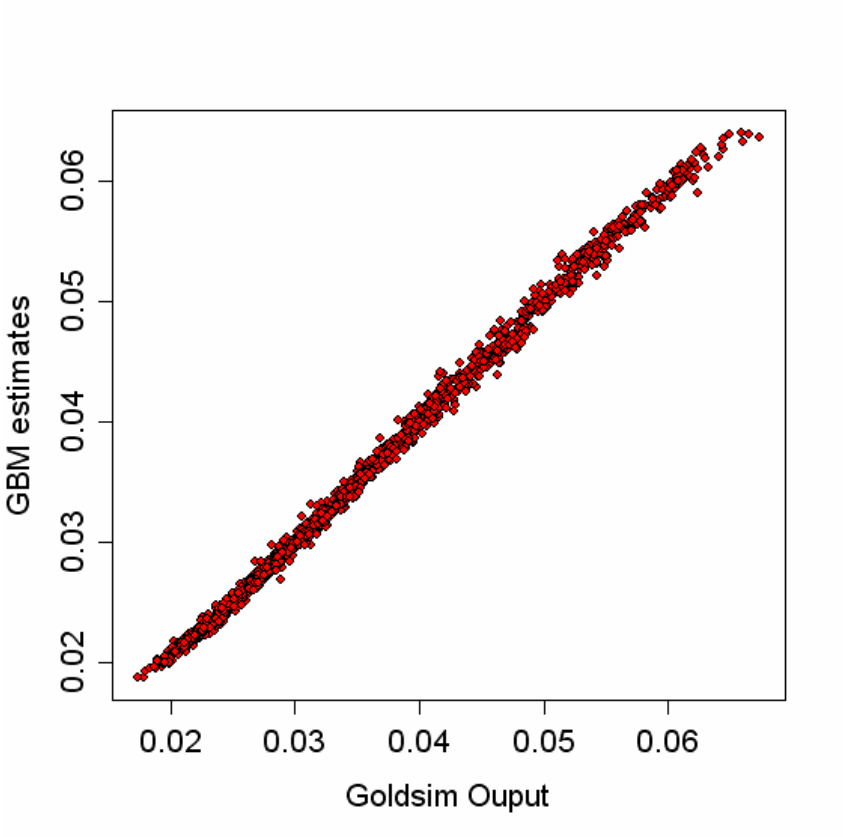

Figure F-90. Scatterplot of GBM estimate for CIG Trenches (full projected inventory) maximum concentration of radium isotopes (pCi/L)

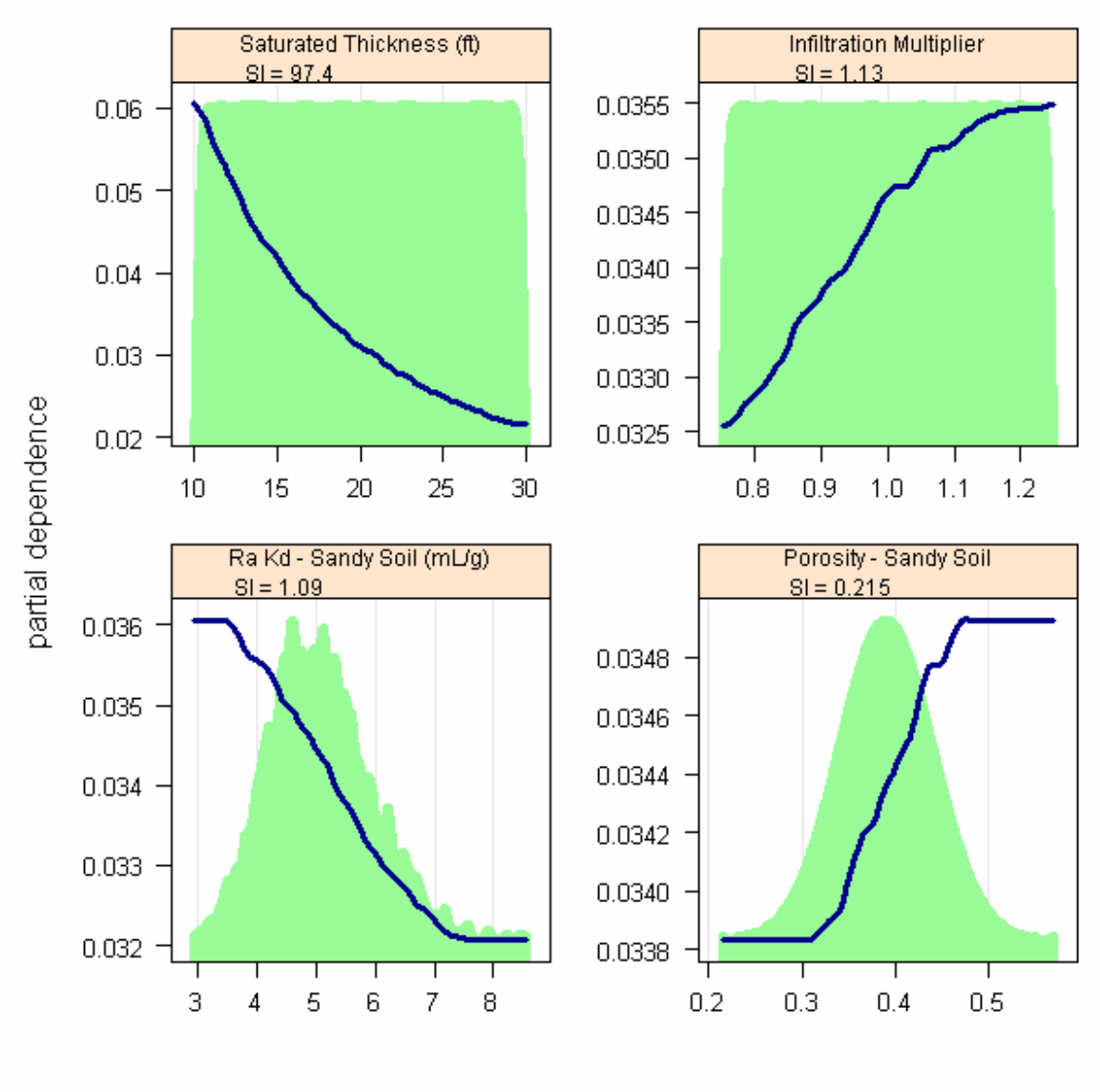

Figure F-91. Partial dependence plots for CIG Trenches (full projected inventory) maximum concentration of radium

The concentration of radium in well water is here heavily dominated by the saturated thickness of the aquifer. Secondary to that, is the infiltration multiplier, the K_d of Ra in sandy soil, and the porosity of the sandy soil, all of which are plausible contributors, but with very low SI values.

Maximum Uranium Concentration

This is the maximum concentration of uranium (all isotopes) in well water within the period of performance.

The GBM estimate for uranium concentration is similar to that of radium in the Engineered Trenches, in that very few non-zero data points were available for analysis. The R^2 of 97% is deceptive, since it is based on the three points (out of the 2000 points that are actually in this plot) that are furthest from the origin, and these are in line. This problematic fit results from the fact that within the period of performance, very little U escapes to the well. The sensitivity analysis, therefore, is poorly constrained. This is perhaps acceptable, since apparently the water concentration of U from the CIG Trenches is not a cause for alarm.

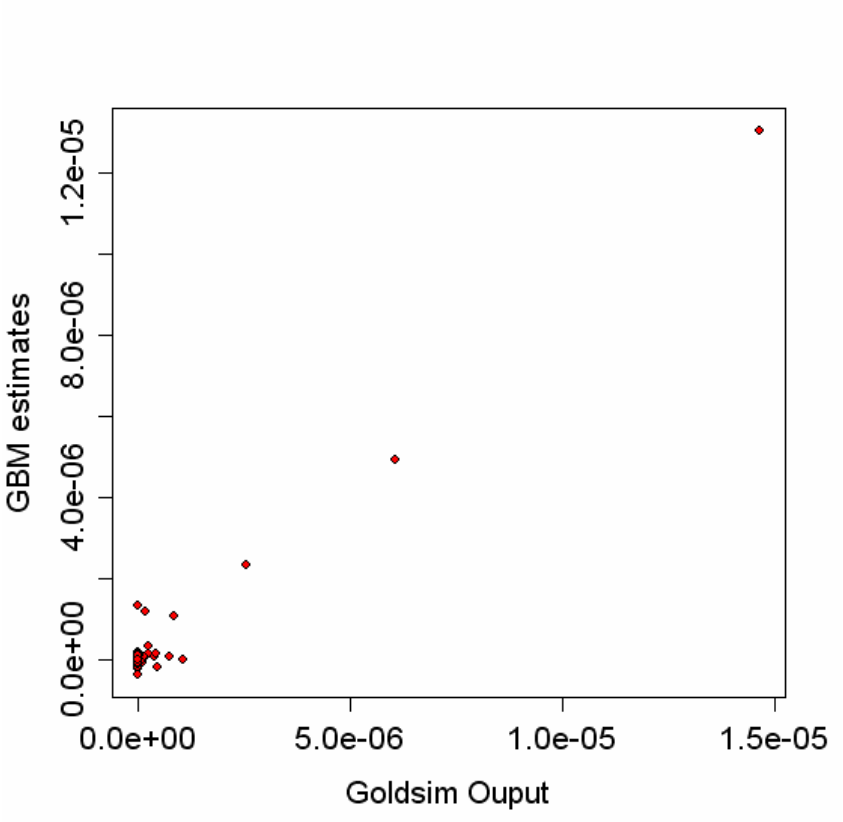

Figure F-92. Scatterplot of GBM estimate for CIG Trenches (full projected inventory) maximum concentration of uranium (µg/L)

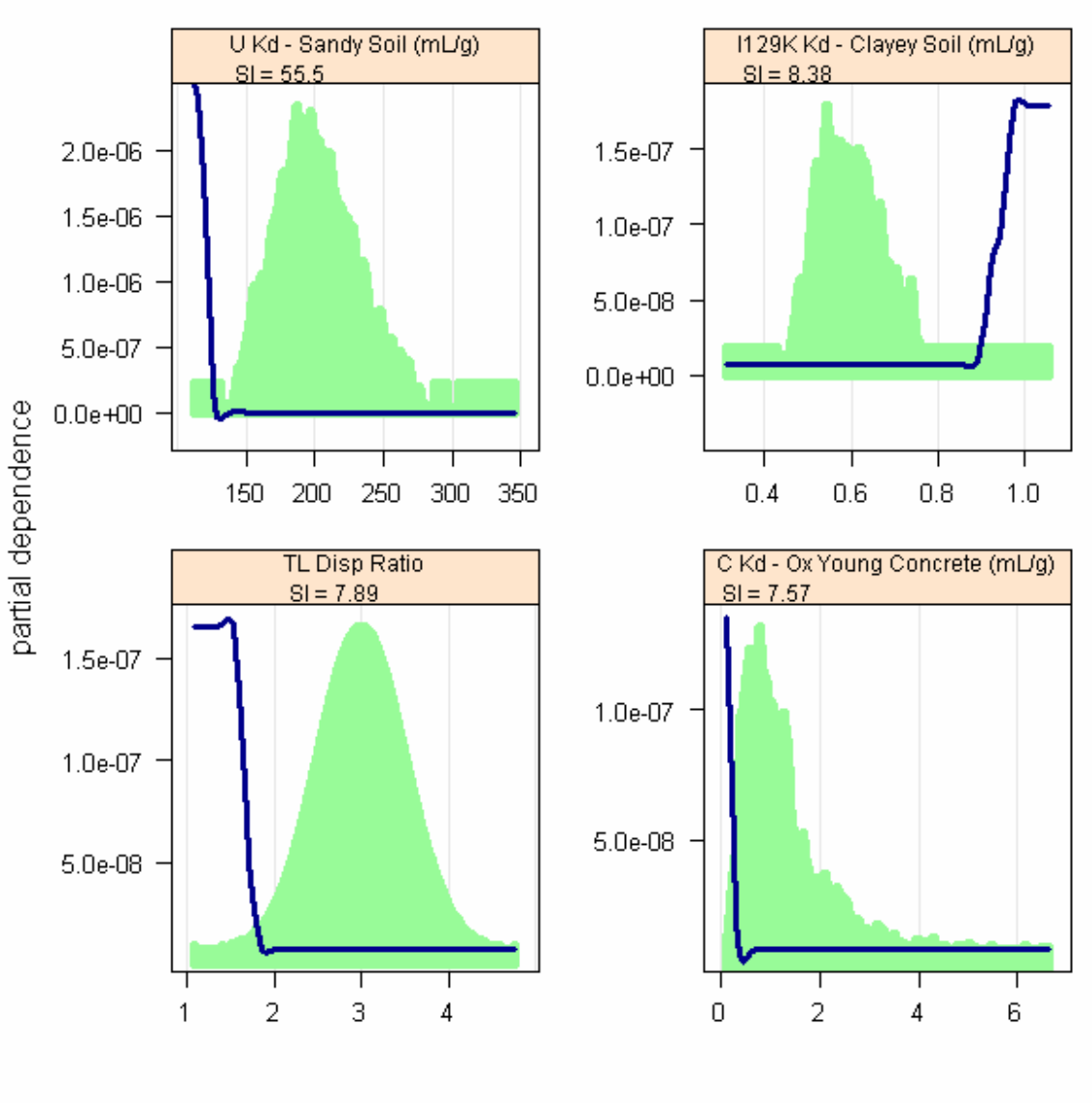

Figure F-93. Partial dependence plots for CIG Trenches (full projected inventory) maximum concentration of uranium

As can be seen in the partial dependence plots, the information available for sensitivity analysis of uranium concentration is inadequate. These plots are typical of a poor result, showing some sensitivity over only isolated ranges, and with unreasonable choices for sensitivities. For example, I-129 and C-14 could not possibly have any influence on uranium concentrations, and yet they appear. For this reason, the sensitivity analysis for uranium MCL is considered inadequate, and these results cannot inform decision making.

1.3.3.3 Endpoints and most influential explanatory variables (CIG Segments 1 through 8 inventory)

A similar analysis was developed for the CIG Trenches with the disposed inventory in Segments 1 through 8. The results are summarized in Table F-11, and the detailed discussions of the results follow.

Table F-11. Identification of the most sensitive parameters for the CIG Trenches endpoints of interest (segments 1 through 8 inventory)

Endpoint	SI rank	input parameter	Sensitivity Index	R^2
max. dose within period of performance (mrem/yr)	1	porosity of sandy soil	35	97%
	2	saturated thickness of aquifer	35	
	3	infiltration multiplier	19	
	4	molecular diffusivity in water	3.0	
max. dose – all time (mrem/yr)	1	saturated thickness of aquifer	51	98%
	2	infiltration multiplier	21	
	3	Pu K_d in sandy soil	21	
	4	Pu K_d in oxidized old concrete	2.7	
max. alpha concentration at well (pCi/L)	1	saturated thickness of aquifer	99	99%
	2	Ra K_d in sandy soil	0.59	
	3	porosity of sandy soil	0.18	
	4	infiltration multiplier	0.15	
max. beta - gamma dose at well (mrem/yr)	1	porosity of sandy soil	46	98%
	2	infiltration multiplier	37	
	3	saturated thickness of aquifer	9.1	
	4	molecular diffusivity in water	3.5	
max. radium concentration at well (pCi/L)	1	saturated thickness of aquifer	98	99%
	2	infiltration multiplier	0.92	
	3	Ra K_d in sandy soil	0.90	
	4	porosity of sandy soil	0.20	
maximum uranium concentration at well		insufficient information		

Maximum All-Pathways Dose within the Period of Performance

This is the maximum all-pathways (water use) dose in early time is that achieved within the period of performance.

Figure F-94 shows excellent ability of the GBM to predict the GoldSim results for this endpoint. This means that there is high confidence in the sensitivity analysis, as was the case for most the CIG sensitivity analysis work. The R^2 for this relationship is greater than 97%. Doses in early time are driven by a very early peak of H-3 at 24 yr or so, followed by Tc-99 (Tc99 plus Tc99K), which actually peaks at 240 years.

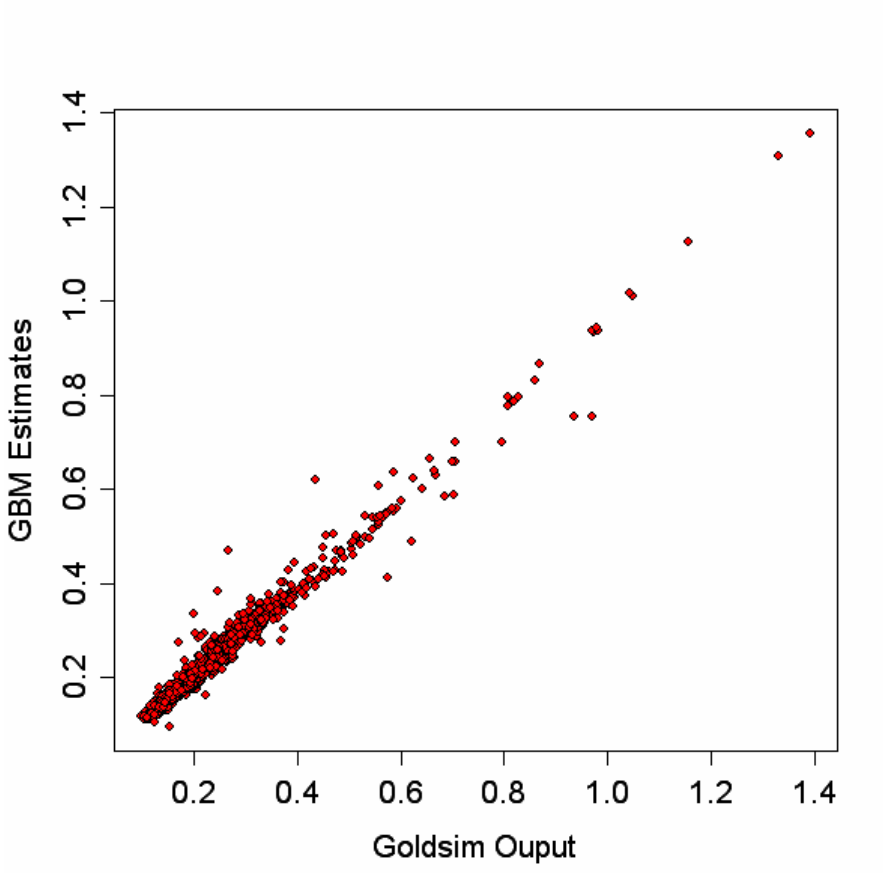

Figure F-94. Scatterplot of GBM estimate for CIG Trenches (segments 1-8 inventory) maximum all-pathways dose (mrem in a year) within the period of performance

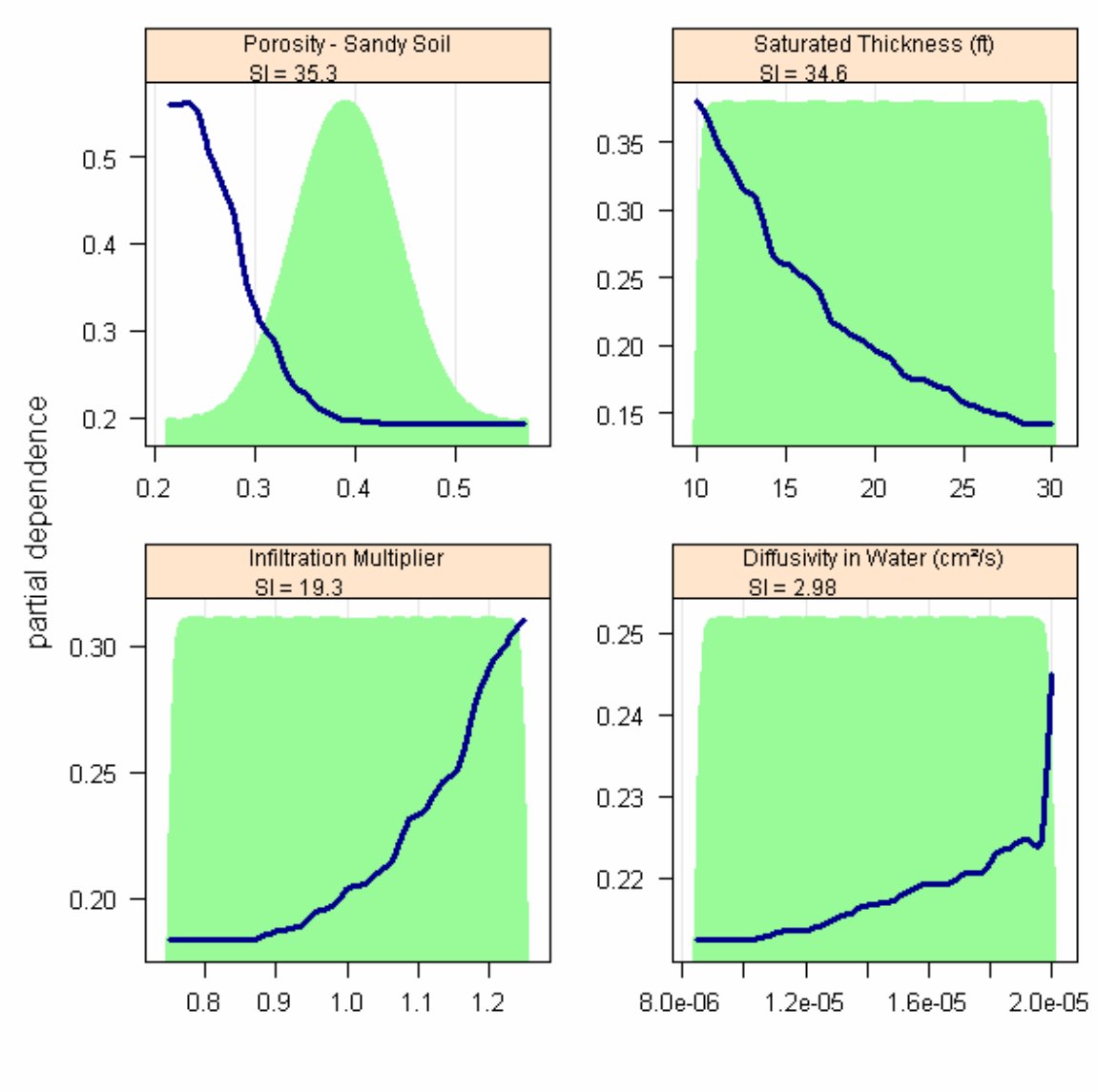

Figure F-95. Partial dependence plots for CIG Trenches (segments 1-8 inventory) maximum all-pathways dose within the period of performance

The most sensitive parameter for the CIG maximum dose endpoint is the porosity of sandy soil, but this is closely followed by the saturated thickness. The last two parameters are also water-related: the infiltration multiplier and the molecular diffusivity in water.

Maximum All-Pathways Dose in All Time

This is the peak dose for all time, although it occurs well after the period of performance as defined in DOE O 435.1-1.

Again a good fit is seen between the statistical model and the GoldSim results. The R^2 for this relationship is over 98%.

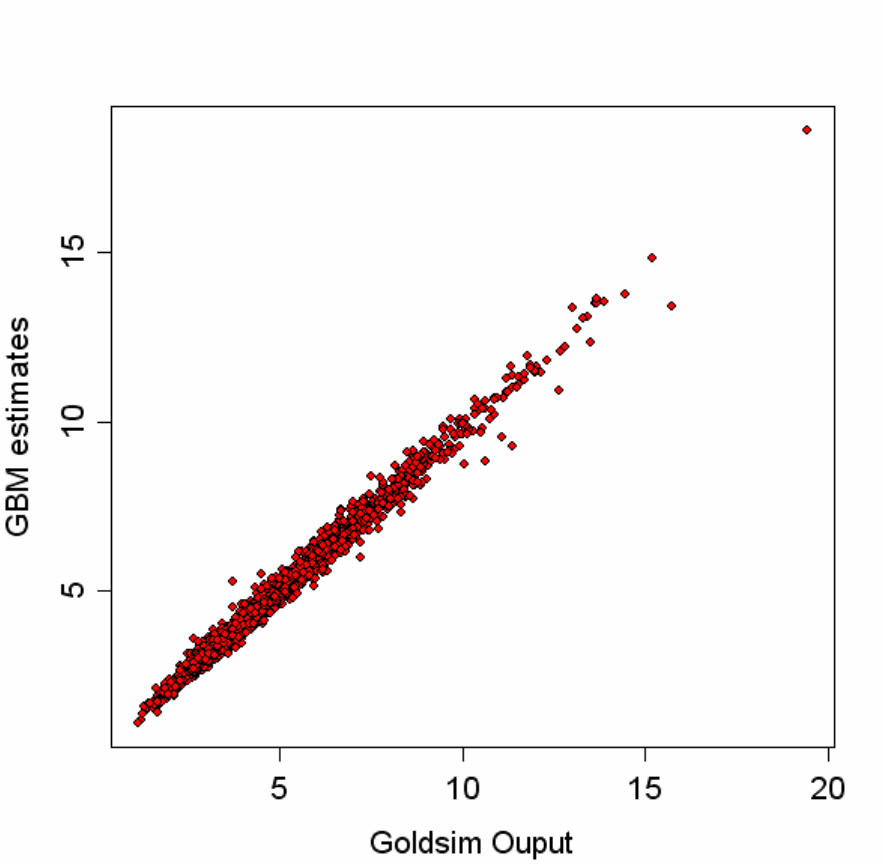

Figure F-96. Scatterplot of GBM estimate for CIG Trenches (segments 1-8 inventory) maximum all-pathways dose (mrem in a year) in late time

This graph illustrates an example of how the analysis can be heavily influenced by a single extreme value. In this case, a dose of nearly 20 mrem in a year, a seeming outlier, drives up the mean value of doses. This probably warrants further investigation as to its cause.

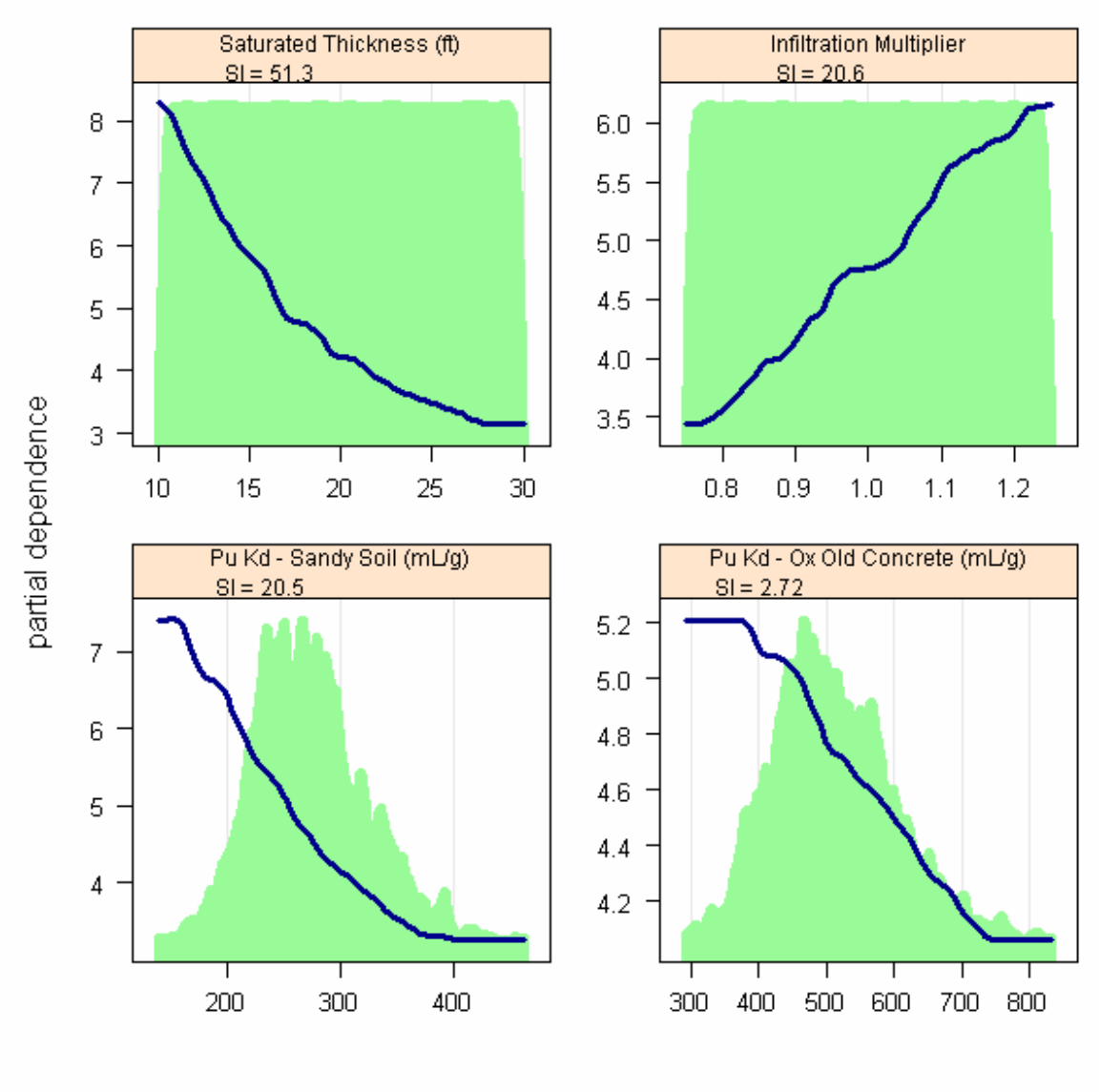

Figure F-97. Partial dependence plots for CIG Trenches (segments 1-8 inventory) maximum all-pathways dose in all time

Again, the thickness of the aquifer and the infiltration multiplier dominate the sensitivity. These are followed by Pu K_d, in both sandy soil and in oxidized old concrete, consistent with Pu-239's domination of doses in later time. The typical inverse relationship of K_d with dose is observed.

Maximum Alpha Concentration

This is the maximum gross alpha concentration in well water within the period of performance.

The GBM estimate for alpha concentration within the period of performance is again quite good, with an R^2 of over 99%. Note that although U and Pu are the major alpha contributors in later time, they play a minor role here, with Pa-231, Ra-226, and Np-237 being the largest contributors to gross alpha during the limited period of performance of 1130 yr (see Figure F-81).

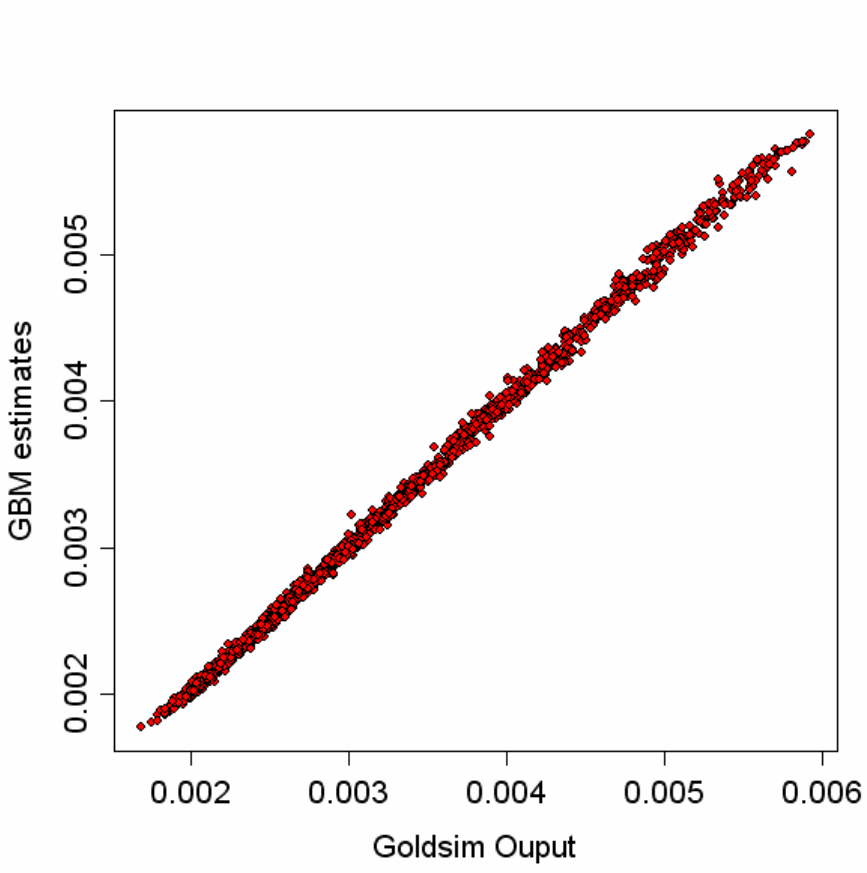

Figure F-98. Scatterplot of GBM estimate for CIG Trench (segments 1-8 inventory) maximum concentration of alpha-emitters (pCi/L)

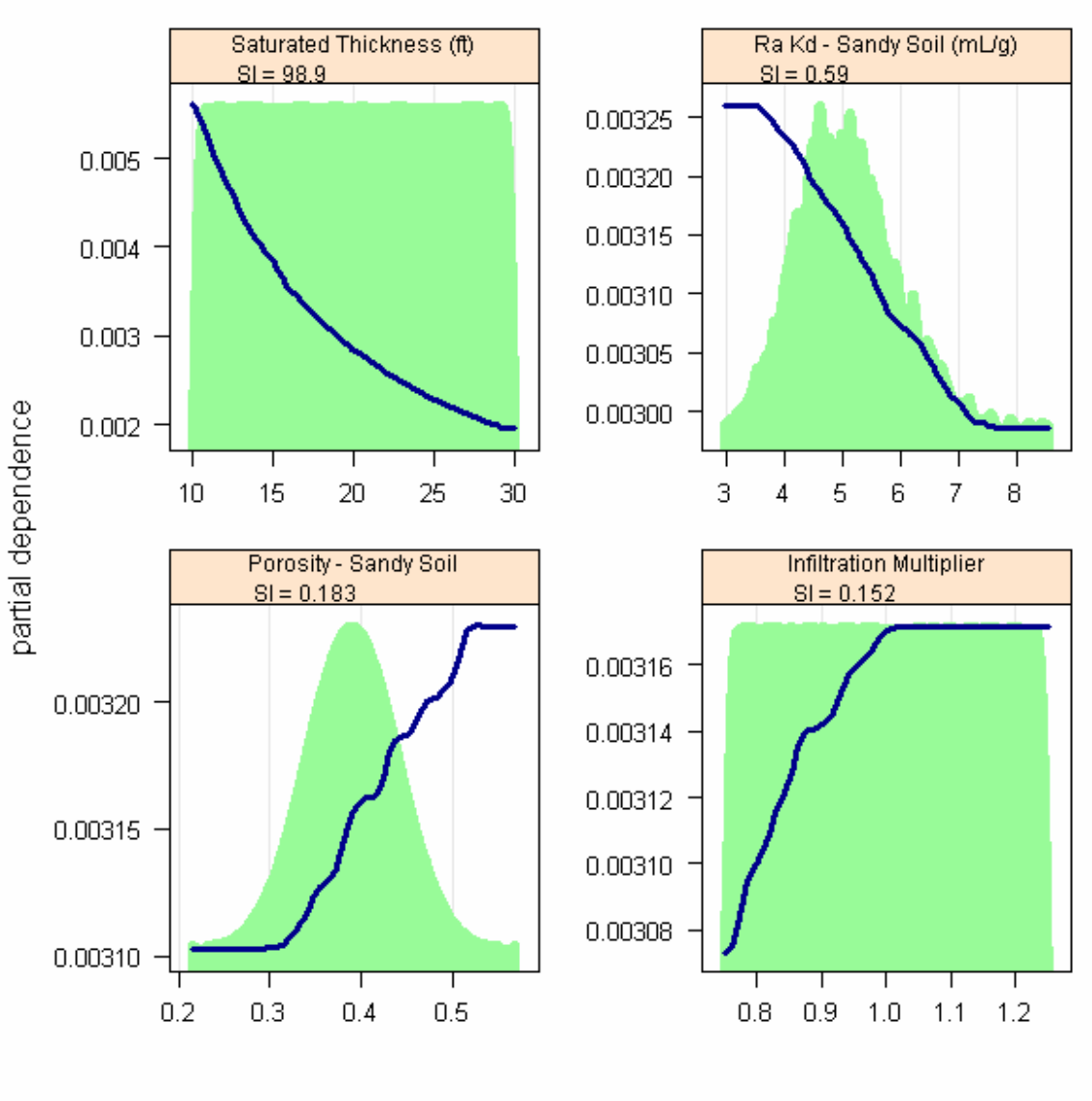

Figure F-99. Partial dependence plots for CIG Trench (segments 1-8 inventory) maximum concentration of alpha-emitters

The timing of the maximum alpha concentration is here constrained to be that maximum achieved within the period of performance, so alpha-emitters occurring later (e.g., plutonium) are not seen. Instead, we see the K_d for Ra playing a sensitive role, and indeed Ra-226 is a dominant alpha-emitting radionuclide within the period of performance. If we were to examine the maximum alpha concentration in late time, it would be expected to mimic the sensitivities for the dose in late time.

The infiltration multiplier graph illustrates the limit of range on the influence of a parameter: above the value of 1, the value does not matter in its effect on doses.

Maximum Beta-Gamma Water Ingestion Dose

The maximum beta-gamma dose is the maximum dose from beta- and gamma-emitting radionuclides within the period of performance.

The results for beta- and gamma-emitters show a bit more scatter, but the R^2 for this relationship is still over 98%.

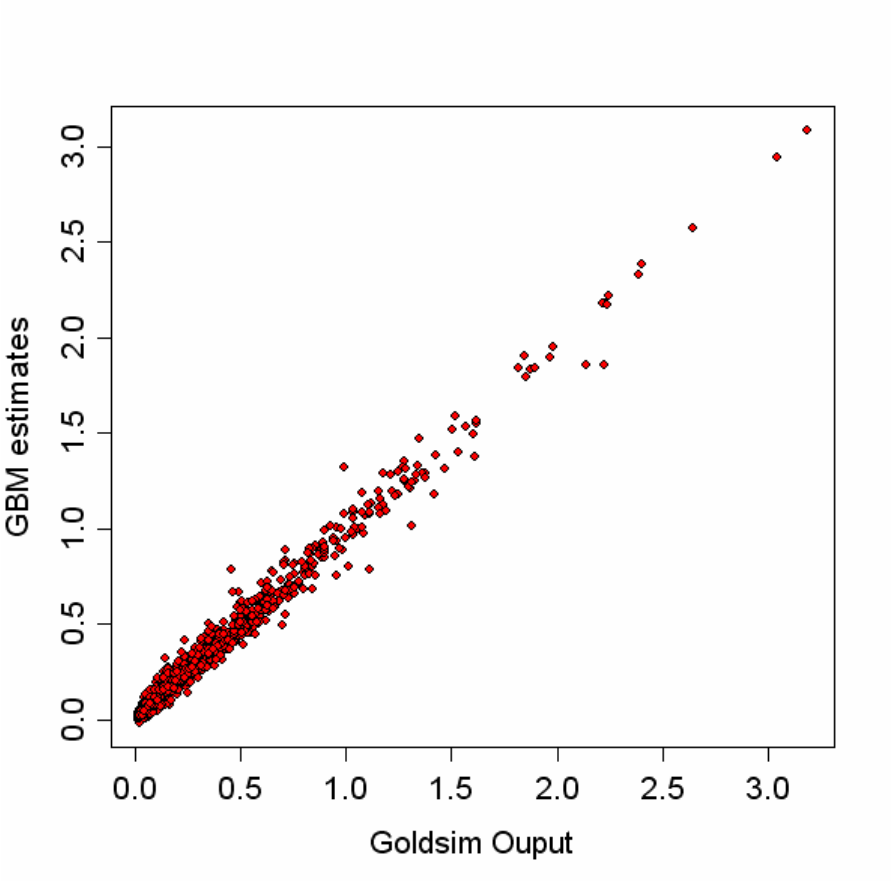

Figure F-100. Scatterplot of GBM estimate for CIG Trenches (segments 1-8 inventory) maximum dose from beta- and gamma-emitters

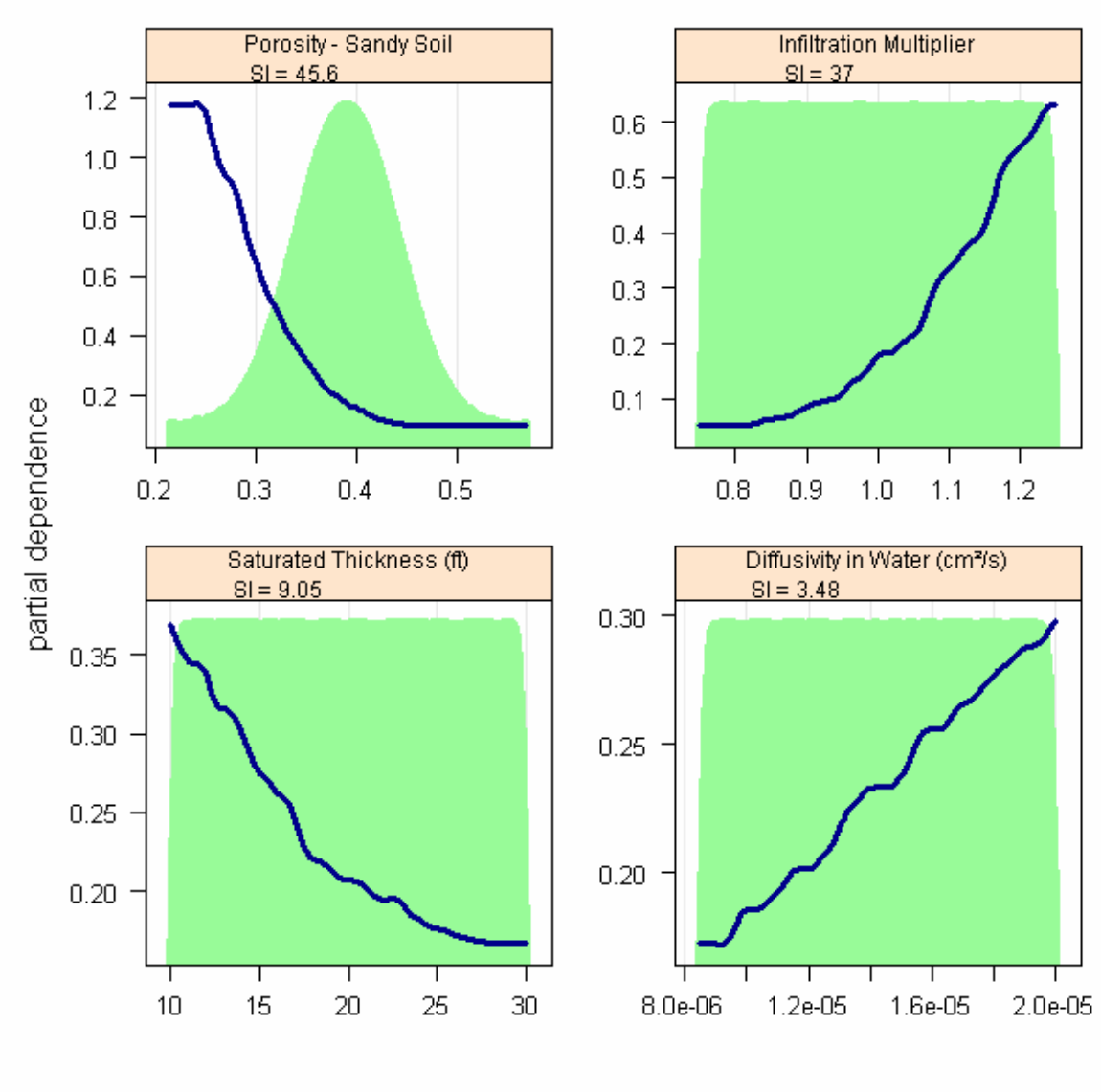

Figure F-101. Partial dependence plots for CIG Trenches (segments 1-8 inventory) maximum dose from beta- and gamma-emitters

The sensitivity of dose from beta-gamma emitters for Segments 1 through 8 is explained entirely by water-related variables: porosity of sandy soil, the infiltration multiplier, the saturated thickness, and the molecular diffusivity in water. No partition coefficients played a significant role.

Note how porosity values above 0.45 no longer have a differential influence on beta-gamma dose.

Maximum Radium Concentration

This is the maximum radium concentration in well water within the period of performance.

The GBM estimate for radium concentration is excellent, with an R^2 of over 99%.

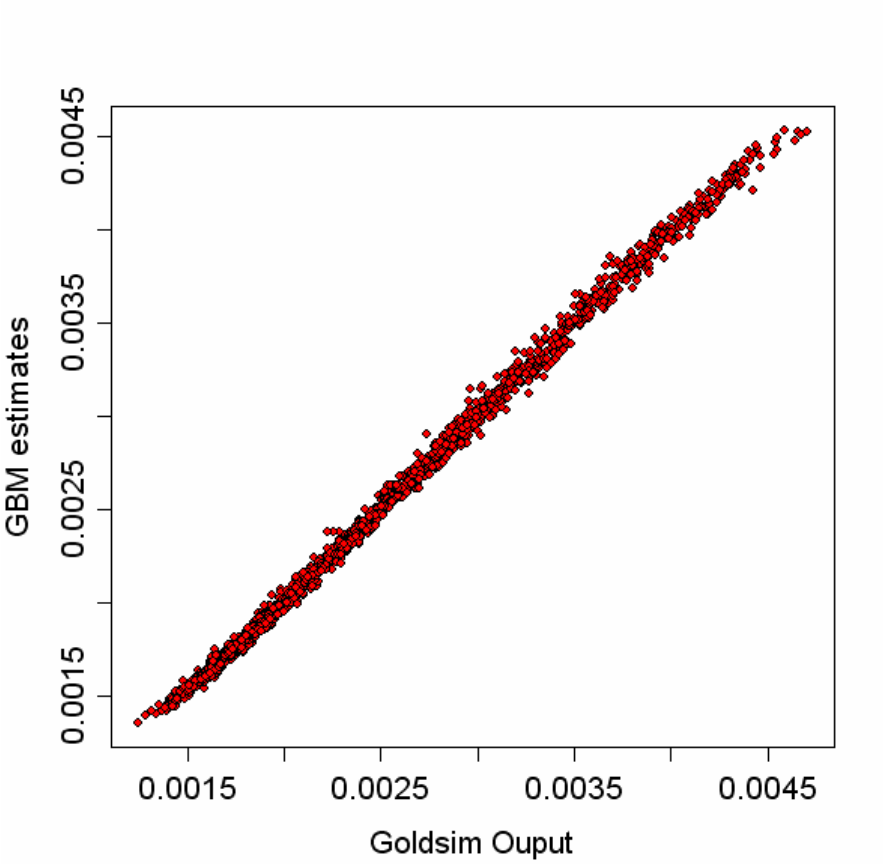

Figure F-102. Scatterplot of GBM estimate for CIG Trenches (segments 1-8 inventory) maximum concentration of radium isotopes (pCi/L)

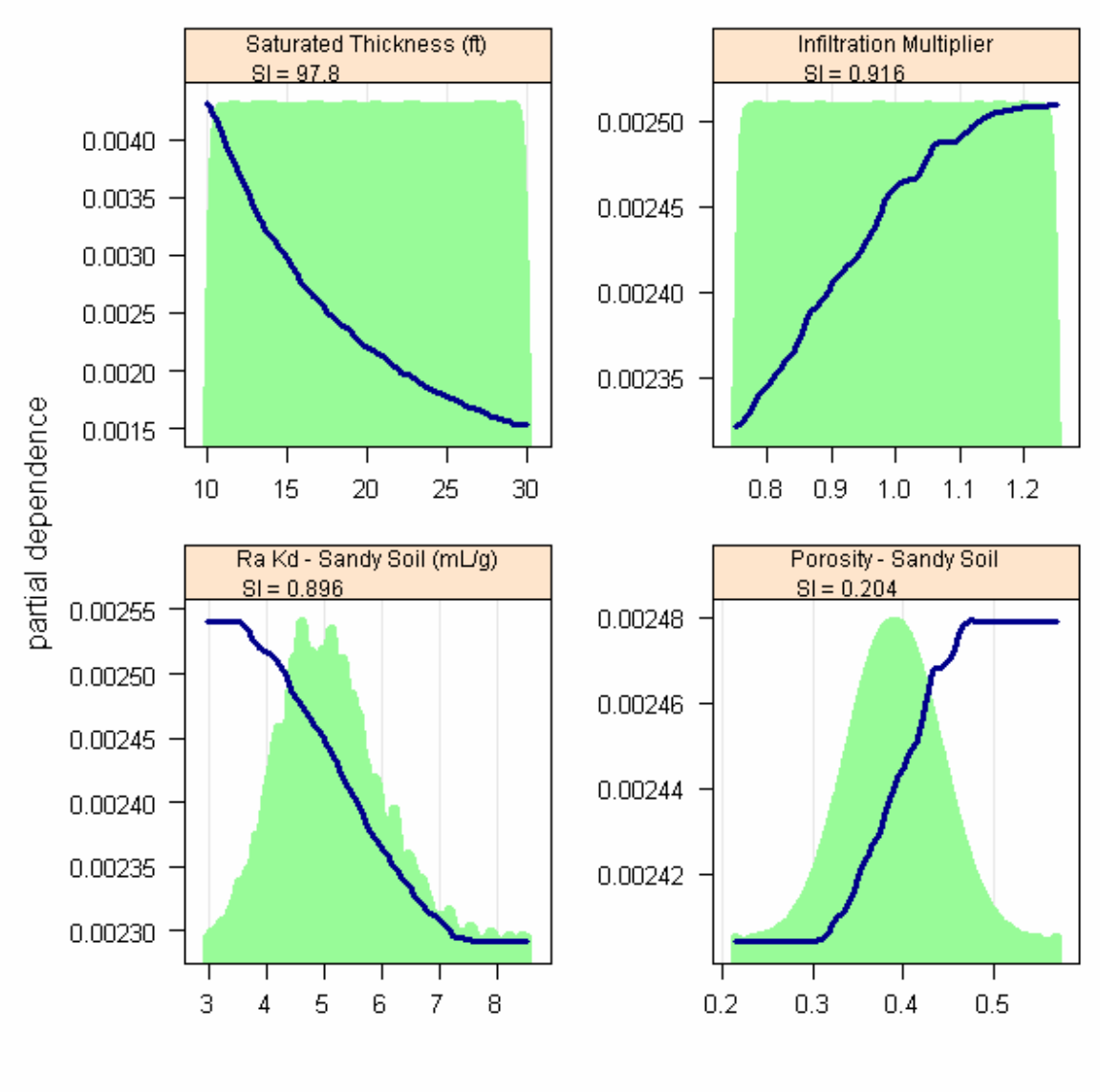

Figure F-103. Partial dependence plots for CIG Trenches (segments 1-8 inventory) maximum concentration of radium

The maximum concentration of Ra in well water during the period of performance is, like the alpha concentration, dominated by the saturated thickness of the aquifer to the exclusion of any other significant explanatory variables.

Maximum Uranium Concentration

This is the maximum concentration of uranium (all isotopes) in well water within the period of performance.

As with the uranium analysis for the full inventory, there are very few non-zero data points were available for Segments 1 through 8. The sensitivity analysis is too poorly constrained to be reliable.

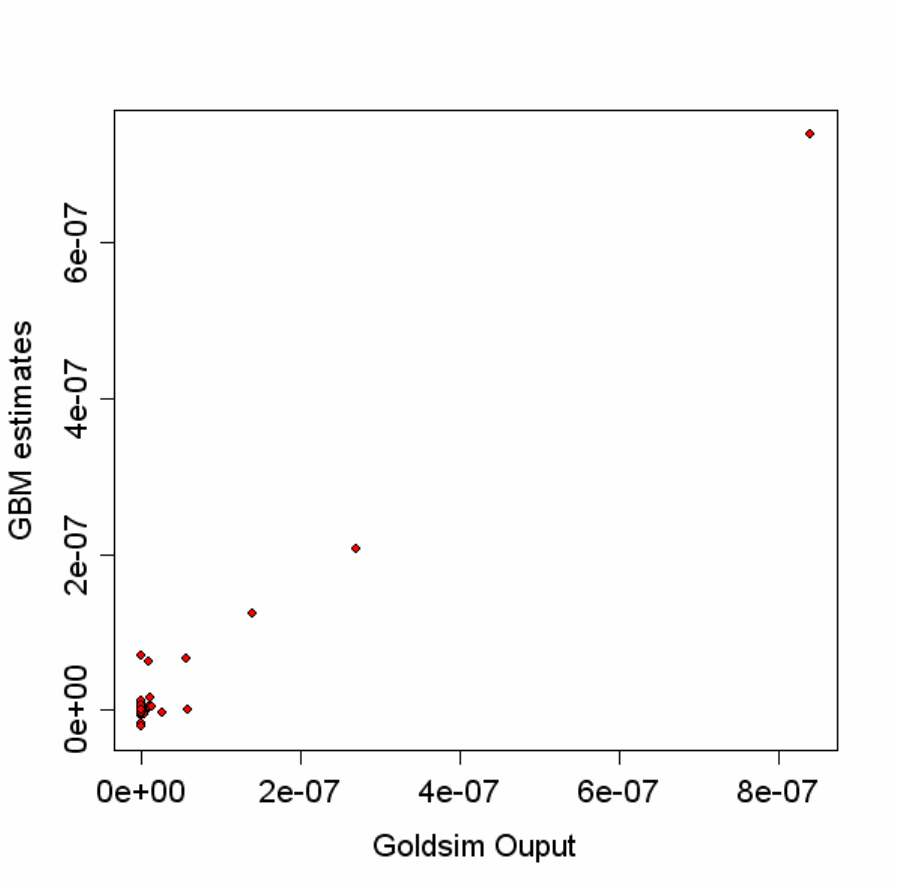

Figure F-104. Scatterplot of GBM estimate for CIG Trenches (segments 1-8 inventory) maximum concentration of uranium (µg/L)

The results for maximum uranium MCLs within the period of performance are equally poor for Segments 1-8 as they are for the full inventory. For this reason, the partial dependence plots are not presented.

1.4 FUTURE WORK

This sensitivity analysis indicates that additional investigations are warranted to better define the value and role of the several parameters in determining dose estimates. Primary among these seems to be the saturated thickness, or, more generally, the well hydraulics for the drinking water well, including capture zone as well as the hydrodynamics of the aquifer. This would include a study of dispersivities in the aquifer and how they will need to be modeled and calibrated in the GoldSim model. Nearly as significant is the distribution for the infiltration multiplier. Both of these distributions were selected as *ad hoc* ranges simply to see if they were significant. As it turns out, they are indeed significant, and defensible distributions need to be developed for these parameters.

Porosities of various materials are also sensitive parameters related to water flow. Some of these are based on measurements (e.g. native sandy soil) and others are assumed (e.g., future waste in the CIG trenches). Both need to be modified to capture spatial averaging so that the model is working with distributions of the mean values. This improvement will reduce their uncertainty and their influence on the results of interest.

Other parameters identified in the sensitivity analysis as worthy of consideration are the K_ds for those radionuclides that contribute significantly to dose (Pu, I, C, U, Ra, Np and Tc at a minimum). While a good bit of work has been put into better quantifying K_ds, this work is worth revisiting to see if better distributions can be developed from the information available.

In addition to these parameters identified by the sensitivity analysis are all other parameters in the model that do not yet have distributions defined since they are simply not addressed by the sensitivity analysis, though they may still be significant in determining doses (e.g., inventory, flow field definitions, and dose assessment parameters), and those that were defined with poorly supported *ad hoc* distributions (e.g. saturated thickness, infiltration calibration multiplier). Once these concerns have been addressed, another sensitivity analysis would be in order to evaluate the behavior of the better-defined model.

Several other parts of the sensitivity analysis models need to be developed more rigorously in order to better simulate the entire risk assessment, from source release to dose. A natural place in the model development process for this to take place would be at the combining of these Slit, Engineered, and CIG Trench models into one E-Area Model. This would be done in consideration of other sources as well, such as the ILW and LAW vaults and the NRCDA. Such a model could take advantage of the conditional submodel approach used in the CIG Trench Sensitivity Analysis Model. A more complete implementation of dashboards could also help tremendously in efficiency of model operation and comprehension.

Once sufficiently developed, an E-Area GoldSim model might supplant the primary role of PORFLOW as the definitive PA support computer program, relegating PORFLOW (or other process-level groundwater flow solver) to a supporting role in defining flow fields with which to inform GoldSim, and a check on fate and transport calculations. Process model information will be critical to informing a probabilistic implementation of flow fields in GoldSim.

The draft sensitivity analysis models presented here form a good foundation for future modeling, as the basic model structure has been well-tested. What remains is to populate the models with robust input distributions in order to generate defensible probabilistic results.

1.5 REFERENCES

Borra, S., and DiCiaccio, A., (2002) Improving nonparametric regression methods by bagging and boosting. *Computational Statistics and Data Analysis*, 38(4), p 407-420.

Breiman, L. (1996). Bagging predictors. *Machine Learning* 26, 123–140.

Dietterich, T. G. (2000). An experimental comparison of three methods for constructing ensembles of decision trees: Bagging, boosting, and randomization. *Machine Learning*, 40(2), 139–158.

Friedman, J. (2001). Greedy function approximation: A gradient boosting machine. *The Annals of Statistics* 29(5) p.1189-1232.

Friedman, J. (2002). Stochastic gradient boosting. *Computational Statistics and Data Analysis* 38(4) p.367-378.

Kaplan, D. and M. Millings, 2006, *Early Guidance for Assigning Distribution Parameters to Geochemical Input Terms to Stochastic Transport Models*, WSRC-STI-2006-00019, Washington Savannah River Company, June 2006

Saltelli, A., Chan, K., and Scott, E.M. (2000) *Sensitivity Analysis* Wiley, New York. *pp*. 475.

Tauxe, J.D. (1994). Porous Medium Advection-Dispersion Modeling in a Geographic Information System, *Center for Research in Water Resources Technical Report No. 253*, Bureau of Engineering Research, The University of Texas at Austin, Austin, Texas, May 1994

This page intentionally left blank.

APPENDIX G

DATA SUPPORTING THE HYDROGEOLOGIC CONCEPTUAL MODEL

This page intentionally left blank.

TABLE OF CONTENTS

LIST OF FIGURES

LIST OF TABLES

1.0 OVERVIEW OF E-AREA HYDROGEOLOGIC ENVIRONMENT

Development of the conceptual hydrogeologic model for the E-Area PA was based on consideration of all of the aquifers and confining units that might affect the subsurface distribution of contaminants potentially released from the E-Area LLWF. A brief overview of that information is provided here.

The hydrostratigraphic classification system used in developing the model is consistent with the system established by Aadland et al. (1995) and in Smits et al. (1997) and Denham (1999). This classification is now widely used as the standard (Mamatey 2006). Figure G-1 shows the regional lithologic units and their corresponding hydrostratigraphic units at the SRS. A detailed description of the lithologic units is provided in Section 3.1.4.1 of the Background Chapter (Part C).

The hydrogeologic conceptual model for the E-Area PA included only hydrostratigraphic units above the Meyers Branch confining system because units below that system are considered protected from contamination. The justification for this assumption is as follows. The Meyers Branch confining system overlies the Dublin-Midville aquifer system (Figure G- 1). At the SRS, the Meyers Branch system consists of a single hydrostratigraphic unit, known as the Crouch Branch confining unit, which includes several thick and relatively continuous (over several miles) clay beds. The Crouch Branch confining unit ranges in thickness from 17 m to 56 m. East of E-Area, the Meyers Branch confining system is 41 m thick, 21 m of which are clay beds.

Areas of the SRS which are adjacent to the Savannah River flood plain and the Upper Three Runs drainage systems, including E-Area, exhibit an “upward” hydraulic gradient across the Crouch Branch confining unit. Hydraulic heads in the underlying Crouch Branch aquifer are higher than those in the overlying Gordon aquifer in these areas, due to the incisement of the overlying aquifer by these two river systems. The magnitude of this upward gradient is shown in Figure G- 2, where the head differential contours are plotted. Positive values in the contours indicate upward flow from the Crouch Branch into the overlying aquifer. As shown in Figure G- 2, this area of upward gradient encompasses all of E-Area. The magnitude of the upward gradient varies from 2 to 5 m in the vicinity of E-Area, but the low transmissivity of the Meyers Branch confining system results in a low water flux into the Gordon aquifer. Thus, in E-Area, the confining nature of the Crouch Branch confining unit along with the head-reversal phenomenon provides a natural protection of aquifers beneath the Floridan aquifer system from contamination.

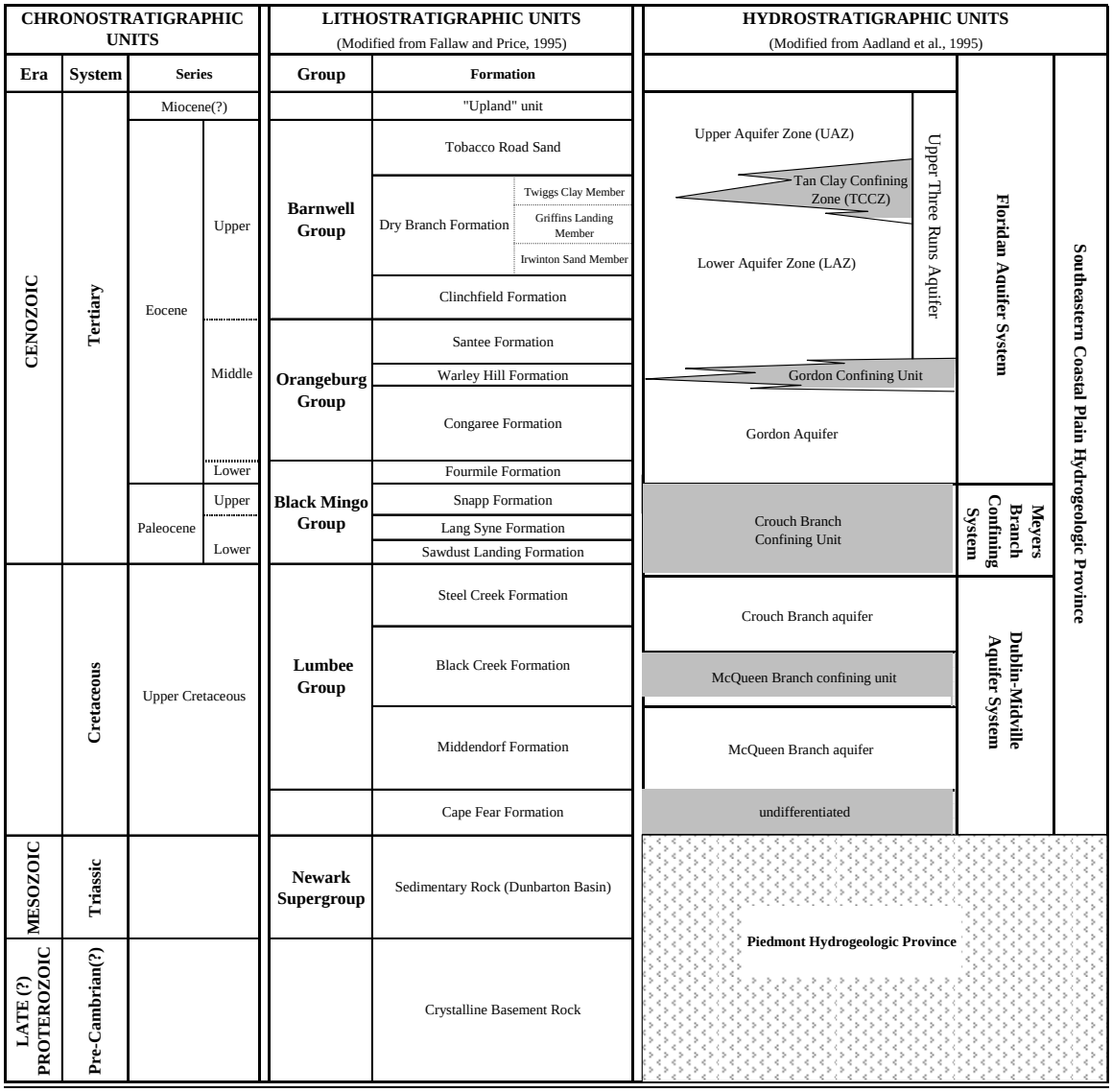

Figure G- 1. Comparison of Lithostratigraphic and Hydrostratigraphic Units at SRS

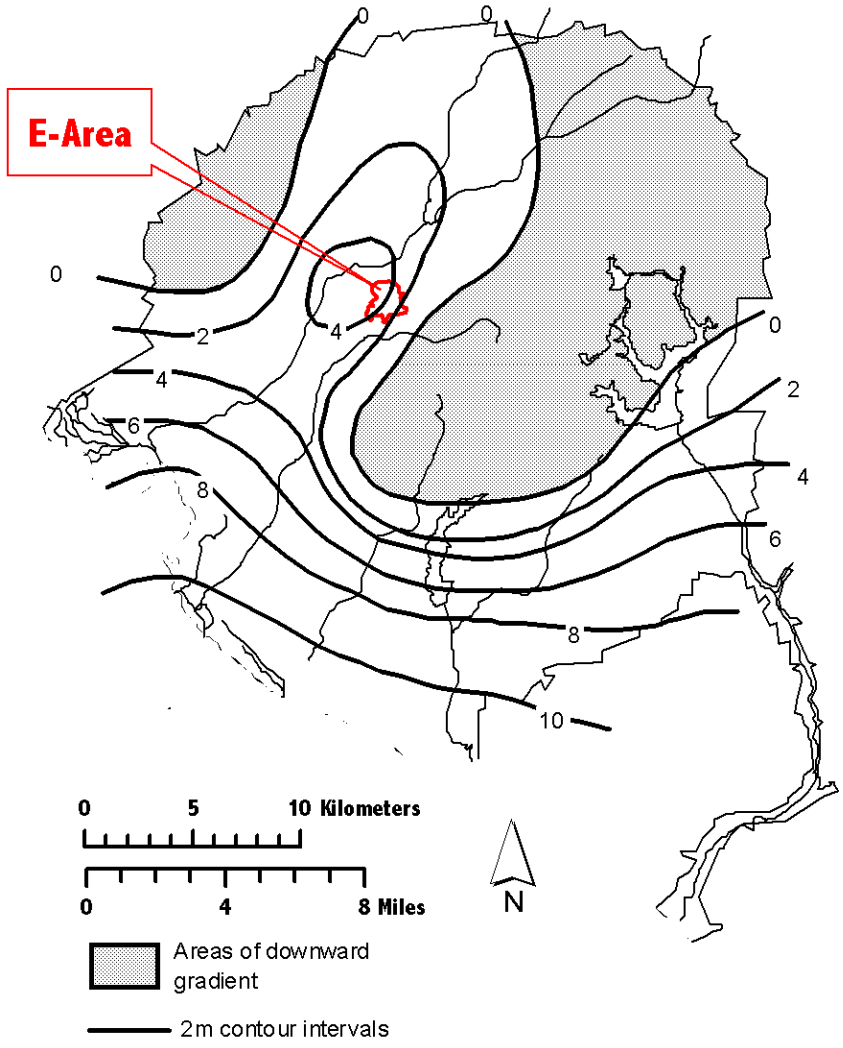

Figure G- 2. Hydraulic head difference between the Crouch Branch Aquifer and the overlying confined aquifer (difference in m; positive values indicate areas of upward flow from the Crouch Branch into the overlying aquifers – from Denham 1999)

Because of relative hydrologic isolation due to the Meyers Branch confining system (i.e. Crouch Branch confining unit), only the Floridan aquifer system (see Figure G- 1) is of interest in the performance assessment of potential groundwater contamination from operations at E-Area. The Floridan aquifer system is comprised of the Gordon aquifer unit, the Gordon confining unit, and the uppermost Upper Three Runs aquifer unit. The Upper Three Runs aquifer unit, in which the water table occurs, is divided into the "lower" aquifer zone, the "tan clay" confining zone, and the "upper" aquifer zone.

1.1 GORDON AQUIFER

The Gordon aquifer unit overlies the Meyers Branch confining system and is approximately 23 m thick at E Area. The hydraulic gradient in the Gordon aquifer across the SRS is generally from northeast to southwest, averaging 0.9 m/km, towards the Savannah River. However, the potentiometric surface indicates considerable deflection of the contours due to incisement of aquifer sediments by Upper Three Runs such that flow from E-Area is westerly. Horizontal hydraulic conductivity for the Gordon aquifer reported from aquifer tests and modeling studies of the GSA ranges from 8.5×10^{-5} to 1.4×10^{-4} m/s (Aadland et al. 1995; Denham 1999; Flach and Harris 1999; Flach 2004). According to Aadland et al. (1995) and Denham (1999), a representative horizontal hydraulic conductivity for the Gordon aquifer in the GSA is 1.2×10^{-4} m/s based on pumping test data. The horizontal hydraulic conductivity value used in the aquifer transport simulations for the E-Area PA was consistent with these previously reported values (Table G- 1).

1.1.1 Gordon Confining Unit

The Gordon confining unit separates the underlying Gordon aquifer unit from the Upper Three Runs aquifer unit. This confining unit is informally known as the "green clay." Thickness of the Gordon confining unit in the vicinity of the SRS varies from 1.5 to 25 m. In the vicinity of E-Area, it is from 0.6 to 9 m thick. Recent studies indicate the unit is composed of several lenses of green and gray clays and silty sands that thicken, thin, and pinch out abruptly. Extensive carbonate sediments associated with areas of thin or truncated clay beds are present in E-Area.

Laboratory and model-derived vertical hydraulic conductivities ranging from 4.0×10^{-12} to 9.5×10^{-9} m/s have been reported for the Gordon confining unit for the GSA (Aadland et al. 1995; Flach and Harris 1999; Flach 2004), suggesting that the Gordon confining unit is an effective aquitard in this region. The vertical hydraulic conductivity value used in the aquifer transport simulations for the E-Area PA falls within the range of these previously reported values (Table G- 1).

1.1.2 Upper Three Runs Aquifer

The Upper Three Runs aquifer unit overlies the Gordon confining unit and is the water table unit. This unit includes the sandy sediments of the Tinker/Santee Formation and all of the heterogeneous sediments in the Late Eocene Barnwell Group. In the center of the SRS, the aquifer unit is 40 m thick. In E-Area, the aquifer unit is divided into three hydrostratigraphic zones with respect to hydraulic properties (Aadland et al. 1995): a "lower" aquifer zone, a "tan clay" confining zone, and an "upper" aquifer zone (Figure G- 1). Within the bounds of E-Area proper, the water table occurs within the "upper" aquifer zone; but as Upper Three Runs is approached and these three zones are incised, the water table is found within the "lower" aquifer zone.

In E-Area, the "lower" aquifer zone occurs between the overlying "tan clay" confining zone and the Gordon confining unit. Groundwater that leaks across the "tan clay" confining zone recharges this zone. Most of the recharge water moves laterally toward the bounding streams that incise this zone; the remainder of the groundwater flows vertically downward across the Gordon confining unit. Hydraulic conductivity of the "lower" zone has been estimated for the E-Area vicinity by several methods including slug tests, pumping tests, and minipermeameter tests. Average values for the various methods range from 3×10^{-6} m/s to 1×10^{-4} m/s (Aadland et al. 1995). As reported by Aadland et al. (1995) and Denham (1999), the hydraulic conductivity of the "lower" aquifer zone near E-Area is on the order of 3.5×10^{-5} m/s based on pumping test data. The horizontal hydraulic conductivity value used in the aquifer transport simulations for the E-Area PA for the "lower" aquifer zone is consistent with the lower reported, field-based values (Table G- 1).

The "tan clay" confining zone is a leaky confining zone, ranging in thickness from 0 to approximately 10 m throughout the E-Area vicinity. The average thickness is about 3 m. The clay beds of this confining zone, when present, generally support a head difference (up to 5 m) in E-Area between the "upper" and "lower" aquifer zones of the Upper Three Runs aquifer unit and thus retard the movement of water downward across this zone. Laboratory analyses of undisturbed samples of the "tan clay" confining zone yielded a range of vertical hydraulic conductivities from 1.2×10^{-11} to 4.2×10^{-7} m/s (Aadland et al. 1995). The vertical hydraulic conductivity for the "tan clay" used in the aquifer transport simulations for the E-Area PA falls within this range of reported values (Table G- 1).

Within the bounds of E-Area proper, the water table occurs in the "upper" aquifer zone. This zone overlies the "tan clay" confining zone, when present, or the "lower" aquifer zone when the confining zone is absent. Units below the "upper" aquifer zone are always saturated and therefore the "upper" aquifer is not considered a perched system. According to Aadland et al. (1995) and Denham (1999), the hydraulic conductivity of the "upper" aquifer zone near E-Area is on the order of 4.5×10^{-5} m/s based on reliable pumping test data. The horizontal hydraulic conductivity value used in the aquifer transport simulations for the E-Area PA is consistent with this reported value (Table G- 1).

Table G- 1. Hydraulic Conductivity Values Used in Aquifer Transport Simulations

UNIT	Approximate Hydraulic Conductivity in Transport Simulations m/s	Cited Representative Hydraulic Conductivity Values m/s
Upper Aquifer Zone[1]	$3.5x10^{-5}$ m/s	4.5×10^{-5} m/s[3]
Tan Clay Confining Unit[2]	$2.1x10^{-8}$ m/s	$1.2x10^{-11}$ to $4.2x10^{-7}$ m/s[4]
Lower Aquifer Zone[1]	$4.6x10^{-5}$ m/s	3.5×10^{-5} m/s[3]
Gordon Confining Unit[2]	$3.5x10^{-11}$ m/s	$4.0x10^{-12}$ to $9.5x10^{-9}$ m/s[5]
Gordon Aquifer[1]	$1.3x10^{-4}$ m/s	1.2×10^{-4} m/s[3]

[1]values reflect horizontal hydraulic conductivity for the aquifers
[2]values reflect vertical hydraulic conductivity for the confining zones
[3]representative value based on pumping test data from GSA as summarized in Aadland et al., 1995 and Denham, 1999
[4]range based on laboratory tests of core from the GSA as summarized in Aadland et al., 1995
[5]range based on laboratory and model-derived vertical hydraulic conductivities for the GSA as reported by Aadland et al., 1995; Flach and Harris, 1999; and Flach, 2004

1.1.3 Vadose Zone

The vadose zone, which extends from the ground surface downward to the water table, primarily consists of sediments from the Upland unit (where it is present) and the Tobacco Road formation (Figure G- 1). Phifer et al. (2006) compiled and analyzed existing characterization data for the vadose zone in E-Area. Data included grain size (sieve) analyses, hydraulic property data (laboratory measurements of vertical hydraulic conductivity and water retention), bulk property laboratory measurements, CPT data, continuous core descriptions and geophysical logs.

Using the laboratory and field data, Phifer et al. (2006) recognized two zones (an “upper” and “lower” zone) within the vadose zone. The “upper” zone is characterized as having a higher clay content and lower saturated hydraulic conductivity than the “lower” zone.

Table G- 2 provides representative saturated hydraulic conductivity values based on laboratory falling head analyses for the "upper" and "lower" zones. In addition to these values, Phifer et al. (2006) also reported nominal or "best estimate" values for porosity (η), dry bulk density (ρ_b), particle density (ρ_p), saturated hydraulic conductivity (K_{sat}), characteristic curves (suction head, saturation, and relative permeability), and effective diffusion coefficient (D_e) for use in the deterministic and sensitivity modeling of the E- Area PA. Moreover, they provided uncertainty estimates for the properties based on exiting laboratory data.

Both the "upper" and "lower" zones were identifiable on CPT and geophysical logs. Using these logs, the two zones were defined for the E-Area disposal units where soil property data was not available. In E-Area, the "upper zone" extends from the land surface down to approximately 111 m above msl and the "lower" zone continues from 111 m above msl to the water table, which varies from 64 to 73 m above msl near the disposal units (Phifer et al. 2006).

Table G- 2. Saturated Hydraulic Conductivity Values for the Vadose Zone

Zone	Horizontal Hydraulic Conductivity m/s	Vertical Hydraulic Conductivity m/s
Upper Vadose Zone	6.2×10^{-7} m/s	8.7×10^{-8} m/s
Lower Vadose Zone	3.3×10^{-6} m/s	9.1×10^{-7} m/s

from Phifer et al (2006)

1.1.4 Water Balance and Infiltration

Numerous water balance and infiltration studies have been conducted in and around the Savannah River Site (SRS) by various organizations (Phifer et al. 2007). Nominal water balance and infiltration estimates from eight water balance and infiltration studies are summarized in Table G- 3. As seen in Table G- 3, precipitation is distributed, in decreasing order, into evapotranspiration, infiltration, and runoff. Average precipitation is seen to range very little between the eight studies, with a median of 47.79 inches/year. Evapotranspiration is seen to range from 30 to 33.5 inches/year with a median of the eight studies nominal values of 31.2 inches/year. Infiltration is seen to range from 9.1 to 16 inches/year with a median of the eight studies nominal values of 14.85 inches/year, or approximately 1/3 of the yearly rainfall. Runoff constitutes very little of the water balance; it is seen to range from 0 to 2 inches/year.

Table G- 3. Nominal Water Balance and Infiltration Estimate Produced from each of Eight Studies [1]

Source	Nominal Annual Precipitation (inches/year)	Nominal Annual Runoff (inches/year)	Nominal Annual Evapotranspiration (inches/year)	Nominal Annual Infiltration (inches/year)
Cahill (1982)	46.62	0	31.62	15
Hubbard and Emslie (1984)	47	2	30	15
Hubbard (1986)	48	2	30	16
Parizek and Root (1986)	47.78	2	30.78	15
Hubbard and Englehardt (1987)	48.51	1.21	32.60	14.70
Dennehy and McMahon (1989)	47.8	0	33.5	14.3
Young and Pohlmann (2001)	10-year Augusta, GA data from 1977 to 1987	Assumed to be 0	Determined but not reported within the document [2]	9.1
Young and Pohlmann (2003)	10-year Augusta, GA data from 1977 to 1987	Assumed to be 0	Determined but not reported within the document [2]	11.7
Median of the eight Studies Nominal Values [3]	47.79	1.6	31.2	14.85

[1] All of these studies assumed that the change in water storage was a minor water budget component

[2] Based upon the infiltration estimates, the associated evapotranspiration estimates would have had to be relatively high (at least in the 30s of inches/year range).

[3] The median of the eight studies nominal values does not include precipitation, runoff, and evapotranspiration from Young and Pohlmann (2001 and 2003)

1.1.5 Surface Water Influences on Groundwater Flow

In the GSA, the surrounding streams influence groundwater flow. Figure G- 3 provides a generalized cross section illustrating the GSA hydrogeology, although the incisement of the "upper" aquifer zone, "tan clay" confining zone, and "lower" aquifer zone by the local streams is not shown in this figure. Three streams (Upper Three Runs to the north; McQueen Branch, a tributary of Upper Three Runs to the northeast; and Fourmile Branch to the south) are natural boundaries to groundwater flow in the Upper Three Runs aquifer unit. All creeks cut into this unit, and thus groundwater is either intercepted by the creeks or recharges the underlying Gordon aquifer unit. Also important to note is a groundwater divide, which occurs in this water table unit due to the influence of these streams. Figure G- 4 shows the influence of the creeks on groundwater flow directions local to E-Area.

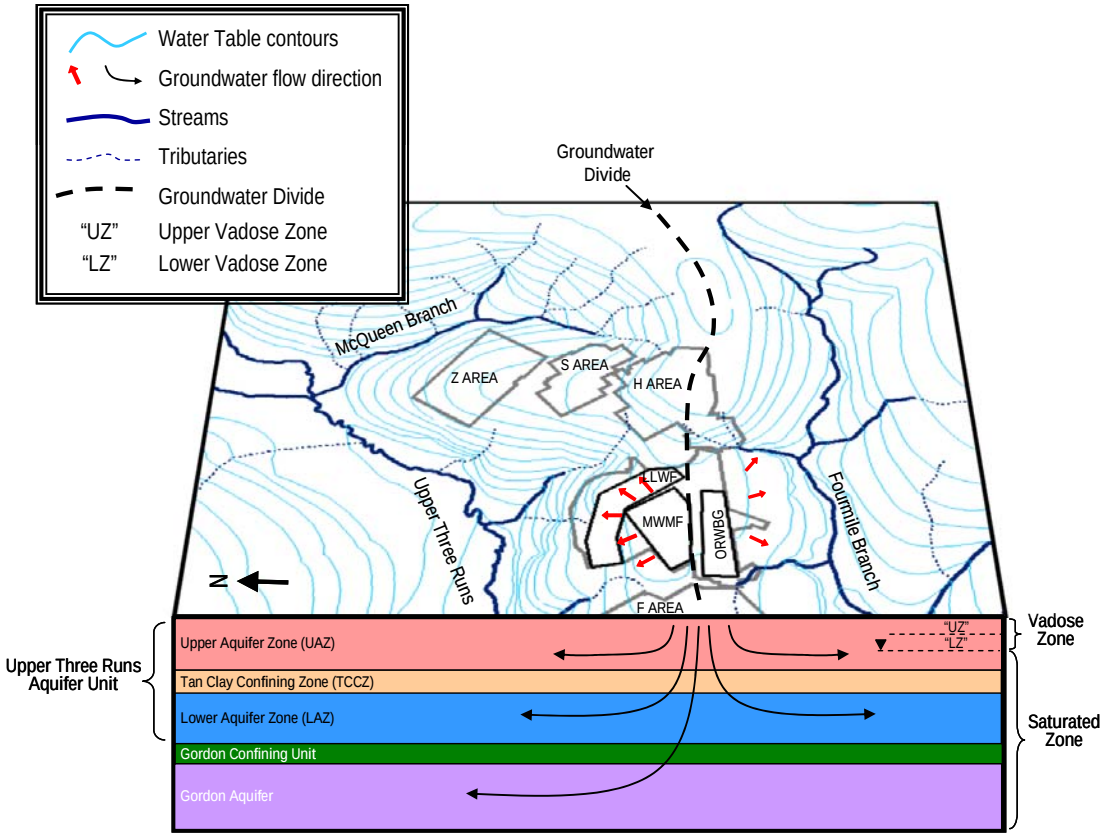

Figure G- 3. Generalized Hydrogeology at the General Separations Area (incisement of UTR aquifer unit by local streams not depicted)

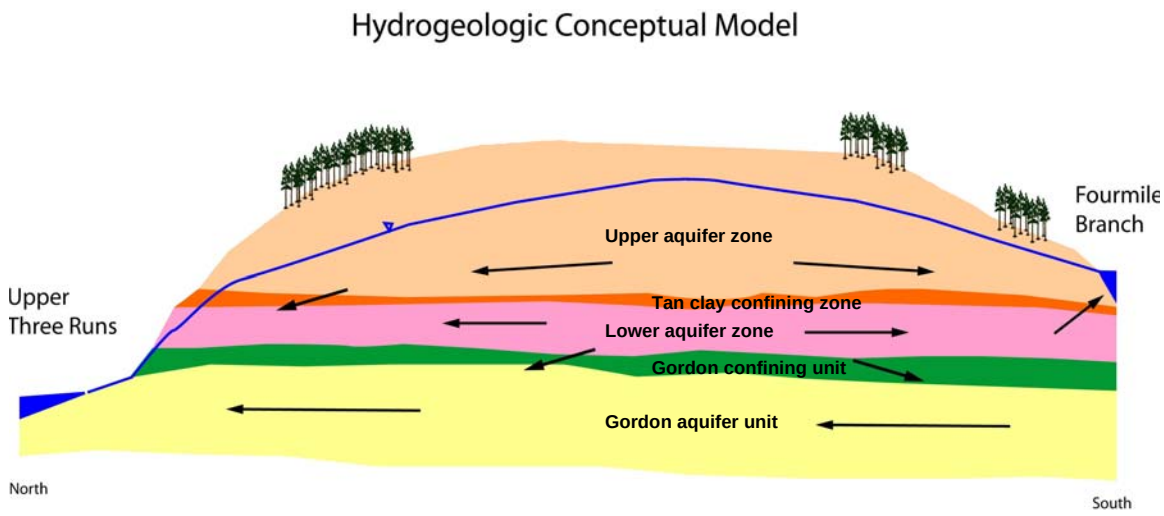

Figure G- 4. Generalized hydrogeologic cross-section near E-Area, showing Influence of Streams on Groundwater Flow

1.2 HYDROGEOLOGIC CHARACTERIZATION AND MONITORING DATA

Typical hydrologic characterization and monitoring data collected and used in hydrogeologic conceptual model development include the results of:

- Visual core descriptions
- Geophysical logs (caliper, gamma, resistivity)
- Cone Penetration Testing (sleeve friction, tip pressure, pore pressure)
- Water levels
- Water quality
- Pump tests
- Slug tests
- Laboratory measurements (permeability, moisture retention, grain size, porosity, bulk density)
- Stream flow measurements
- Lysimeter infiltration measurements
- Watershed water budgets
- Water content and matrix potential (suction head)
- Weather data (rainfall, temperature, etc.)

These data were used to: 1) define the various hydrostratigraphic units in the GSA (visual core descriptions, geophysical logs, and CPT); 2) support assignment of appropriate hydraulic conductivity fields in the model (pump tests, slug tests); 3) provide water level data for model calibration and validation (water levels and stream flow measurements); 4) characterize vadose zone flow (laboratory measurements); 5) provide data for estimating infiltration at the surface (lysimeter infiltration measurements, watershed water budgets, water content and matrix potential, and weather data); and 6) characterize contaminant sorption potential and monitor contaminant plumes (water quality).

Hydrogeologic, geotechnical, and contaminant monitoring data have been collected from the locations denoted in Figure G- 5. Hydrostratigraphic data have been collected from over 100 locations within a 500-meter area surrounding E-Area with over 900 wells providing water level data.

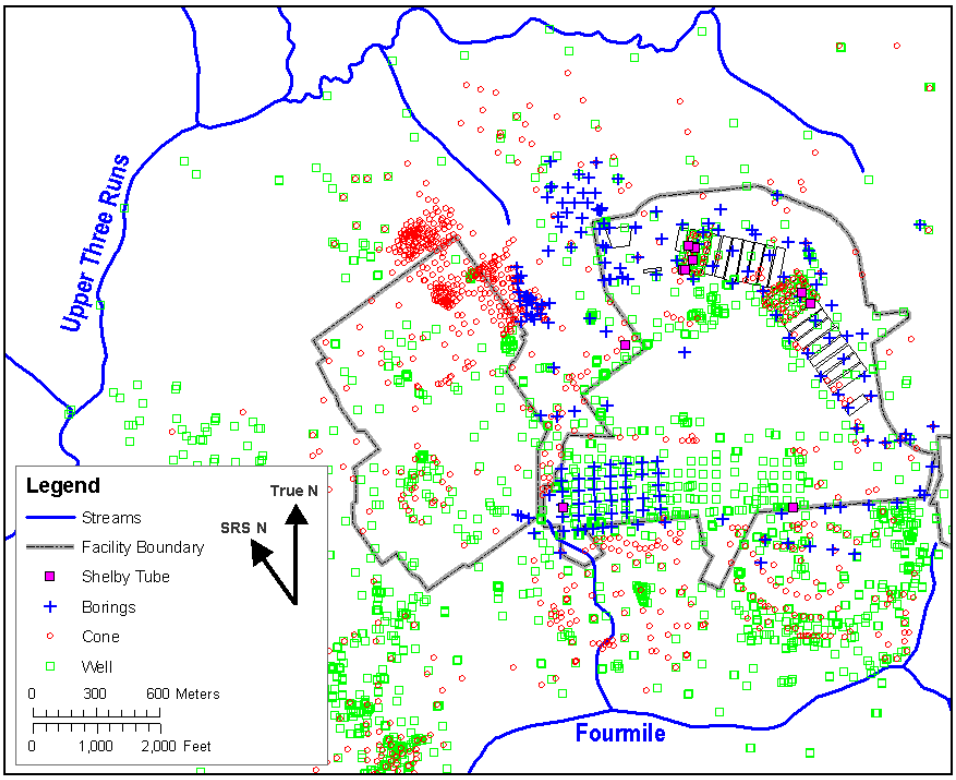

Figure G- 5. Characterization and Monitoring Locations in the GSA Region of the SRS (from the SRS Landmark database)

In general, because of the extensive amount of data, the hydrogeology at the SRS, and at the GSA in particular, is fairly well understood, when compared with many other DOE sites. Although it is quite heterogeneous, the hydrogeology is simpler than some other systems (e.g., fractured rock); and is well-characterized due to the diverse needs driving characterization and monitoring at the SRS and the relatively inexpensive methods (e.g., CPT) employed.

1.2.1 Use of Characterization Data

From characterization data collected, geologic cross-sections were constructed to provide a two-dimensional vertical view of the subsurface. With numerous such cross-sections, a three-dimensional view begins to emerge. The locations of three such cross-sections constructed for the GSA are identified in Figure G- 6 (Smits et al. 1997).

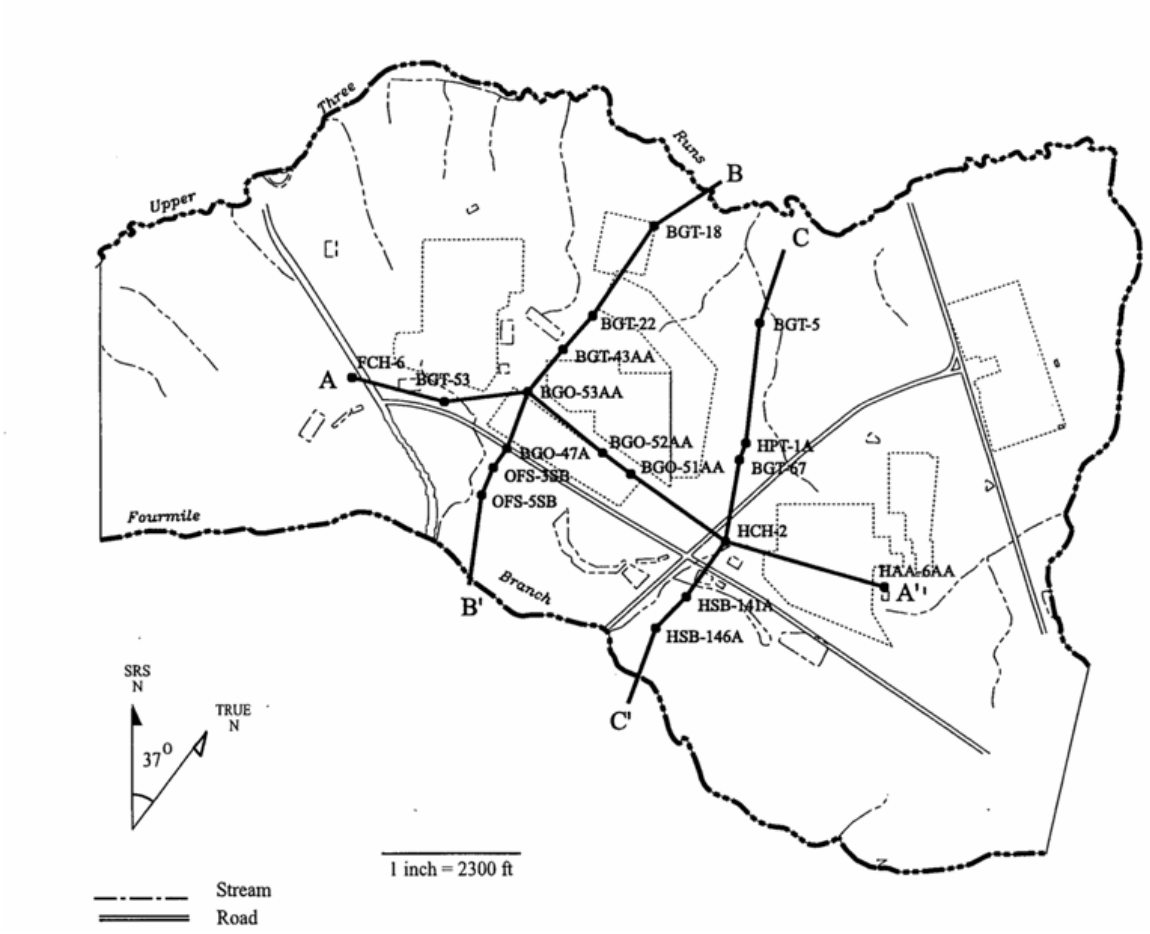

Figure G- 6. Hydrogeologic Cross Sections Constructed for the GSA (from Smits et al. 1997)

Figure G- 7 shows an example of the two-dimensional view of the subsurface that can be constructed, for the north-south cross-section B-B' (Smits et al. 1997).

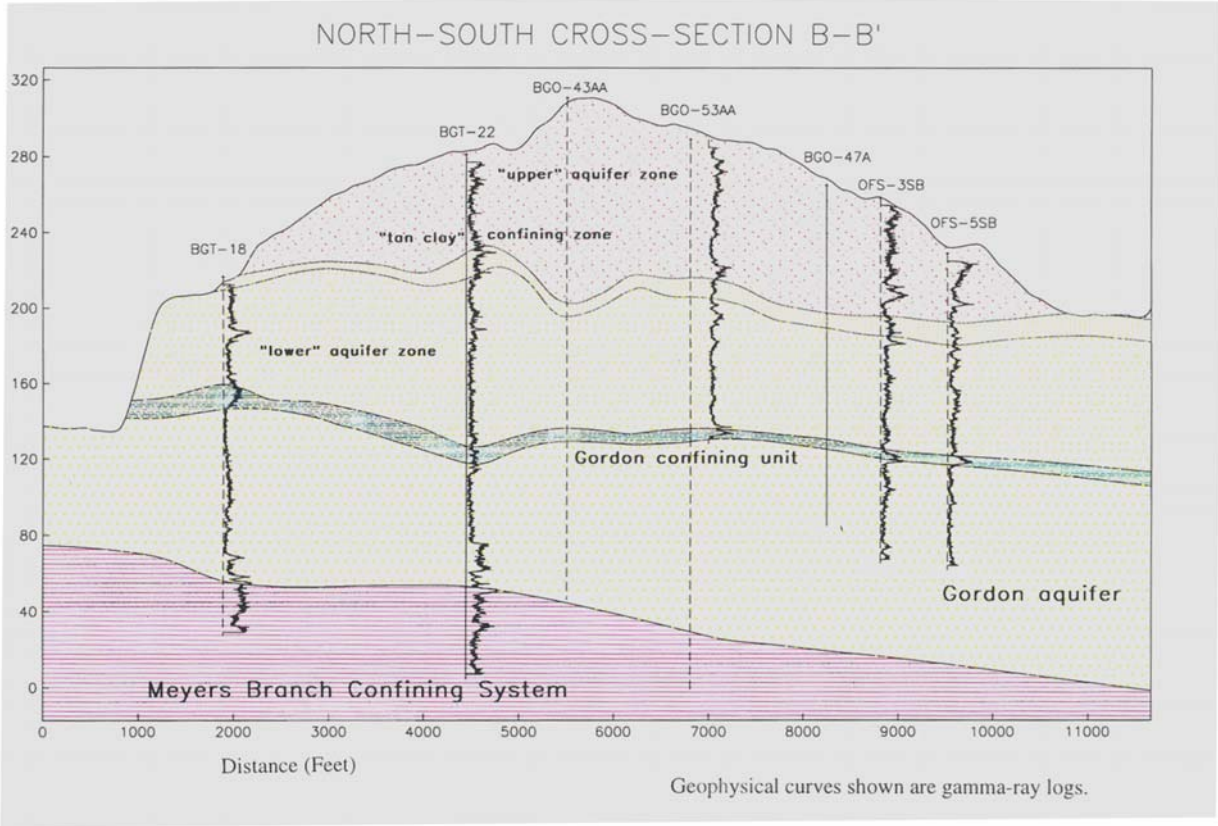

Figure G- 7. Hydrogeologic Cross Section B-B' (refer to Figure G- 6 for location; geophysical curves shown are gamma-ray logs) (from Smits et al. 1997)

Another way to interpret characterization data collected is through mapping of hydraulic head contours of water levels measured in wells completed in the aquifers of interest. Figure G- 8 shows the results of this technique for the water table aquifer. The contours shown in Figure G- 8 represent long-term head data, from which the median values were mapped. The location of the groundwater divide associated with this long-term data is noted.

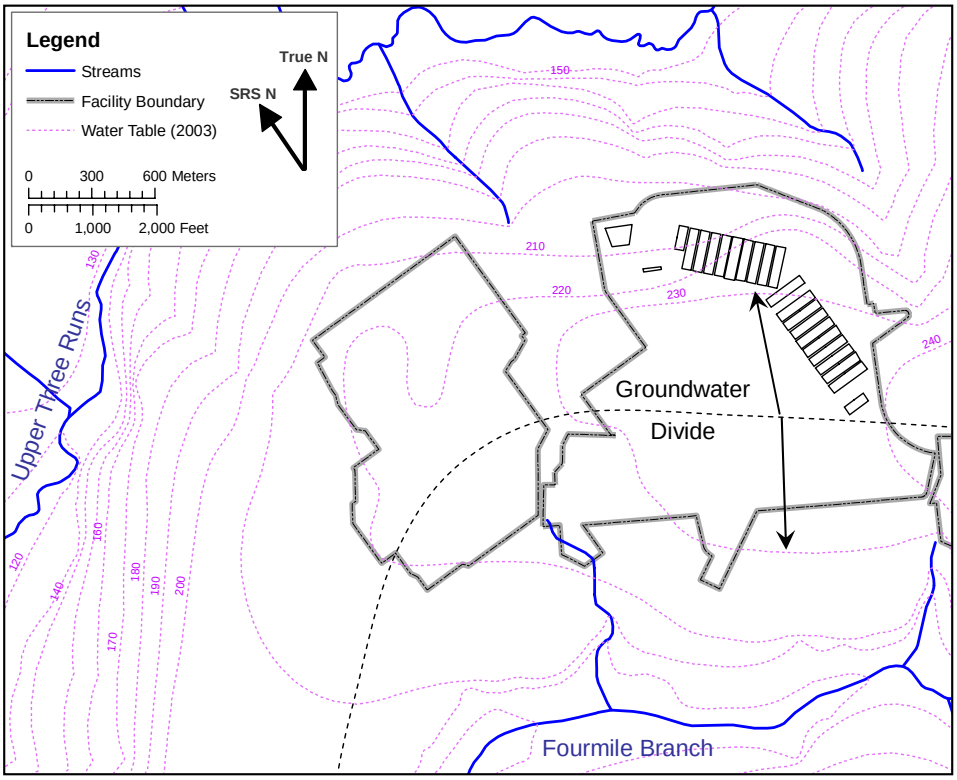

Figure G- 8. Hydraulic Head Contours for the Water Table Aquifer in the GSA, reflecting medians of long-term data

Figure G- 9 shows hydraulic head contours for the confined Gordon aquifer. The locations of measured data, from which the contours were mapped, are show as solid dots.

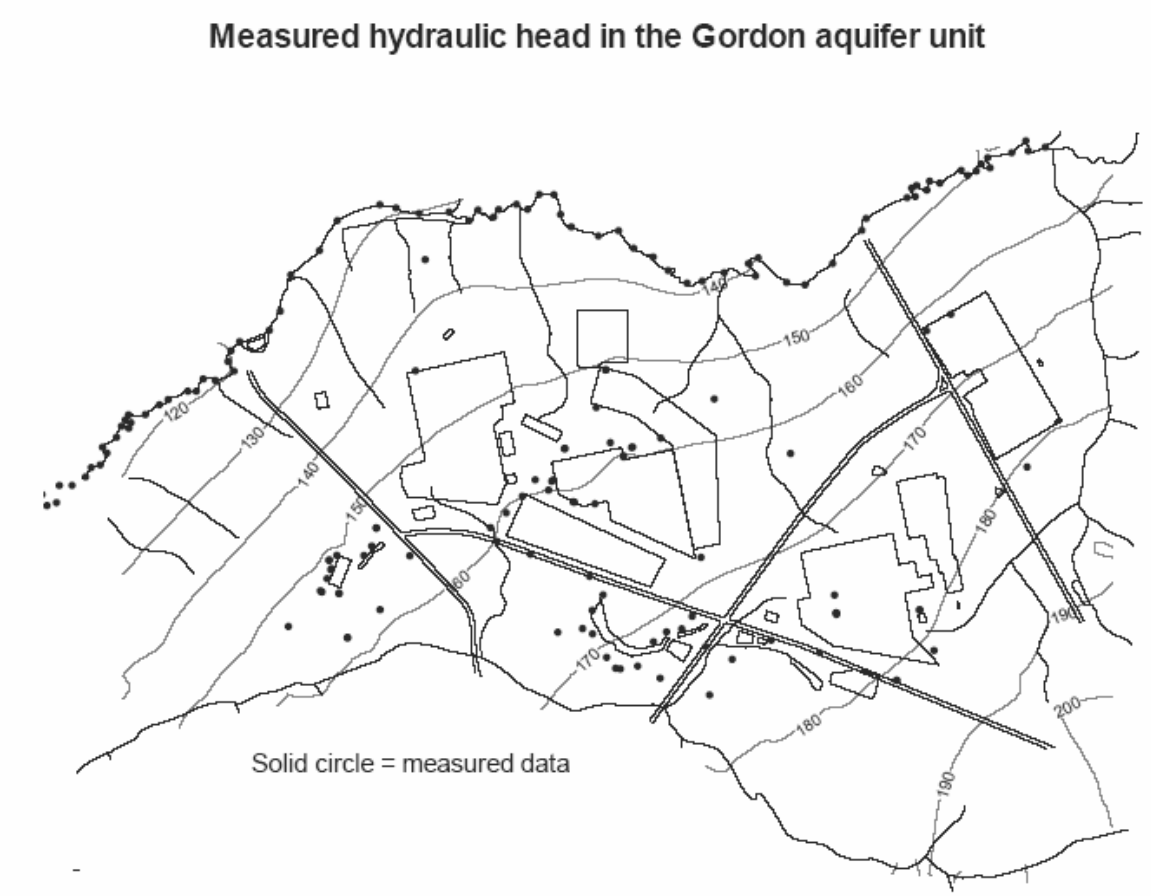

Figure G- 9. Hydraulic Head Contours for the Gordon Aquifer Unit in the GSA

1.2.2 Use of Monitoring Data

The E-Area Monitoring Program has been in operation since 1999 and is designed to evaluate waste disposal operations versus criteria established by the facility Performance Assessment and the Composite Analysis (Swingle et al. 2008). The EMOP is in accordance with DOE Order 435.1. The objective of the EMOP is twofold: (1) to monitor trends in performance and (2) to evaluate the need for corrective action prior to exceeding PA performance objectives.

According to the current PA analyses, groundwater is the most significant pathway for release from the ELLWF. Therefore, the EMOP includes the monitoring of various areas that have the potential of contributing constituents of concern to the groundwater. Sections 2.2.1 and 2.2.2 briefly describe the monitoring programs for the vadose zone and groundwater. Table G- 4 shows a summary of the monitoring plan for each program (Cook 2002; Cook and Crapse 2005).

1.2.2.1 Vadose Zone Monitoring

In 1999 a vadose zone monitoring system (VZMS) was initiated to collect soil property data and soil moisture samples. As part of this program, a network of suction lysimeters were installed within the vadose zone that allow repeated sampling of soil moisture from the soil beneath and adjacent to the trench disposal units. Since 1999, new lysimeters have been installed and sampled as new disposal units were built in the ELLWF. Lysimeter clusters are spaced around the trench perimeters based on as-built data obtained from the construction layout department. Locations are kept as close as possible to the side of the trench wall without interfering with daily construction operations. Figure G- 10 shows the current VZMS for the Slit Trenches, Engineered Trenches, and CIG Trenches.

In the monitoring plan for the VZMS, tritium was selected for monitoring because its mobility makes it a good early indicator for contaminant movement. According to PA modeling predictions, elevated tritium concentrations are expected in the vadose zone beneath the ELLWF. A tritium action level of 100 pCi/ml (Table G- 4) was established based on consideration of the established drinking water standard and previous PA modeling (Swingle et al. 2008). Tritium activity concentrations in the lower lysimeters that exceed this action level (100 pCi/ml) will be evaluated in terms of temporal, depth, and geographic occurrence to determine whether further action is needed.

Results of the VZMS since 1999 indicate that the tritium concentrations in the lower vadose zone for lysimeters not affected by the tritium plume emanating from the MWMF are below the Action Level of 100 pCi/mL, and most such lysimeters had tritium concentration near or below the 10 pCi/ml baseline (‘background”) tritium concentration associated with infiltrating rainfall (Swingle et al. 2008). Three lysimeters at the ET1 location (Figure G- 10) are located in or near the water table in an area known to have elevated tritium concentrations (100 to 1000 pCi/ml in that region) attributed to the MWMF plume (see Section G.4.3).

1.2.2.2 Groundwater Monitoring

Groundwater is currently monitored at the ELLWF by sampling from the BGX well series at the ELLWF fence line (i.e., the perimeter wells). The perimeter well samples are analyzed for gross alpha, nonvolatile beta, and tritium on an annual basis. Figure G- 11 shows the location of the BGX water table wells near the ELLWF.

The ELLWF is sited downgradient of an older disposal facility, the Mixed Waste Management Facility (MWMF), which is the source of a tritium plume extending beneath portions of the ELLWF. Groundwater monitoring data from the ELLWF perimeter wells, evaluated with respect to the Action Levels shown in Table G- 4, take this into consideration.

The MWMF and ELLWF are located near a groundwater divide. Figure G- 4 depicts the downward and lateral flow to either side of the groundwater divide that results from the topographic ridge along which the ELLWF and MWMF are located. Shallow groundwater beneath the Old Radioactive Waste Burial Ground (ORWBG) flows southerly, toward Fourmile Branch. Shallow groundwater beneath the ELLWF and MWMF flows northerly, toward Upper Three Runs. Figure G-12 depicts tritium plumes in the Upper Aquifer Zone (UAZ) showing the movement of the plumes to the north and south of the groundwater divide.

Figure G- 13 shows a closeup of the tritium plumes in the UAZ from beneath the closed and capped MWMF moving to the north beneath the ELLWF. Colors designate approximate plume concentrations with orange representing groundwater concentrations greater than 10,000 pCi/ml, green representing concentrations 1,000-10,000 pCi/ml, blue representing concentrations 100-1,000 pCi/ml and yellow representing concentrations 20-100 pCi/ml. These plume maps are based on 1st quarter 2006 groundwater data from the General Separations Area (GSA) and are documented in the GSA Corrective Action Report (WSRC 2006). It is important to note that the tritium plume emanating from the MWMF flows under parts of the Engineered Trenches, Slit Trenches, and Components-in-Grout Trenches. Tritium concentrations in the groundwater (UAZ) can potentially affect tritium levels observed in the lower lysimeters if the lysimeters are located near or in the water table. Figure G- 14 shows tritium in the lower aquifer zone (LAZ), again depicting plumes emanating from the MWMF.

Table G- 4. E-Area PA Vadose Zone and Groundwater Monitoring Plan Summary

Area	Monitoring Location	Sampling Frequency	Radionuclide/ Other Substance	Action Levels
Vadose Zone	Beneath and adjacent to the trenches	Twice per year	Tritium	1.0E+5 pCi/L (or 100 pCi/ml)
Groundwater	BGX Well Series bordering the ELLWF	Once per year	Gross Alpha	7.56E+2 pCi/L
			Nonvolatile Beta	1.63E+3 pCi/L
			Tritium	7.53E+7 pCi/L

Source: Swingle et al. 2008 (*FY2007 Annual Review, E-Area Low-Level Waste Facility Performance Assessment and Composite Analysis*)

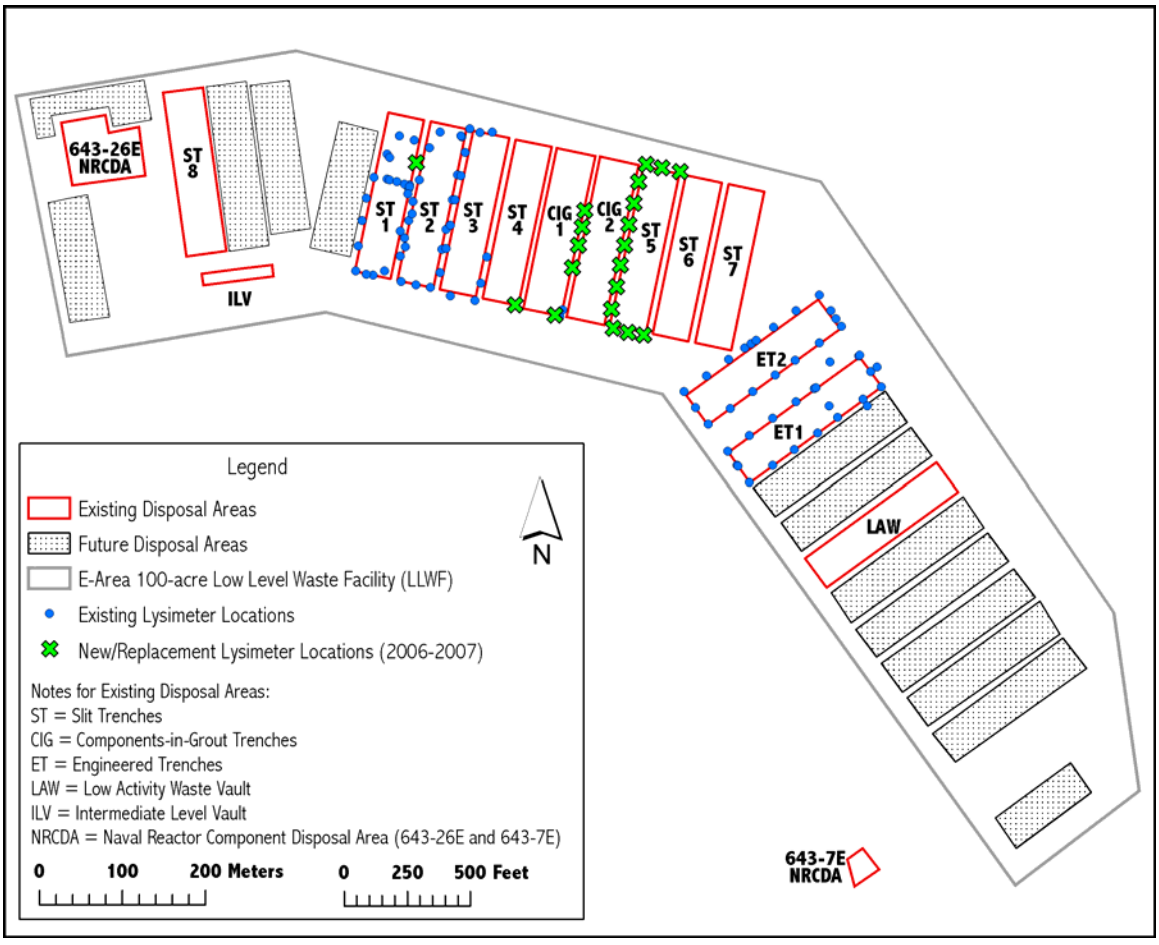

Figure G- 10. Location of lysimeters in the VZMS (from Swingle et al. 2008)

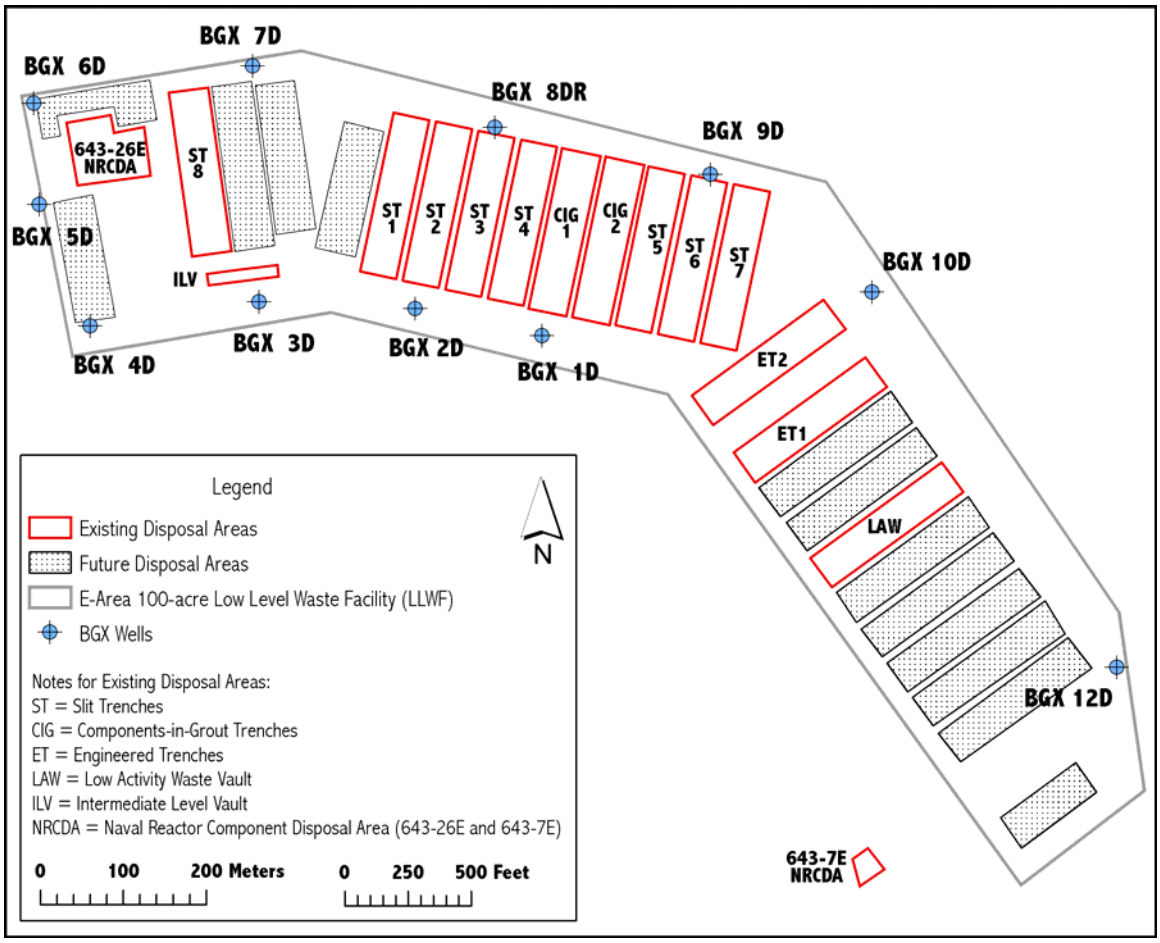

Figure G- 11. Location of BGX Perimeter Wells for Groundwater Monitoring in E-Area (from Swingle et al. 2008)

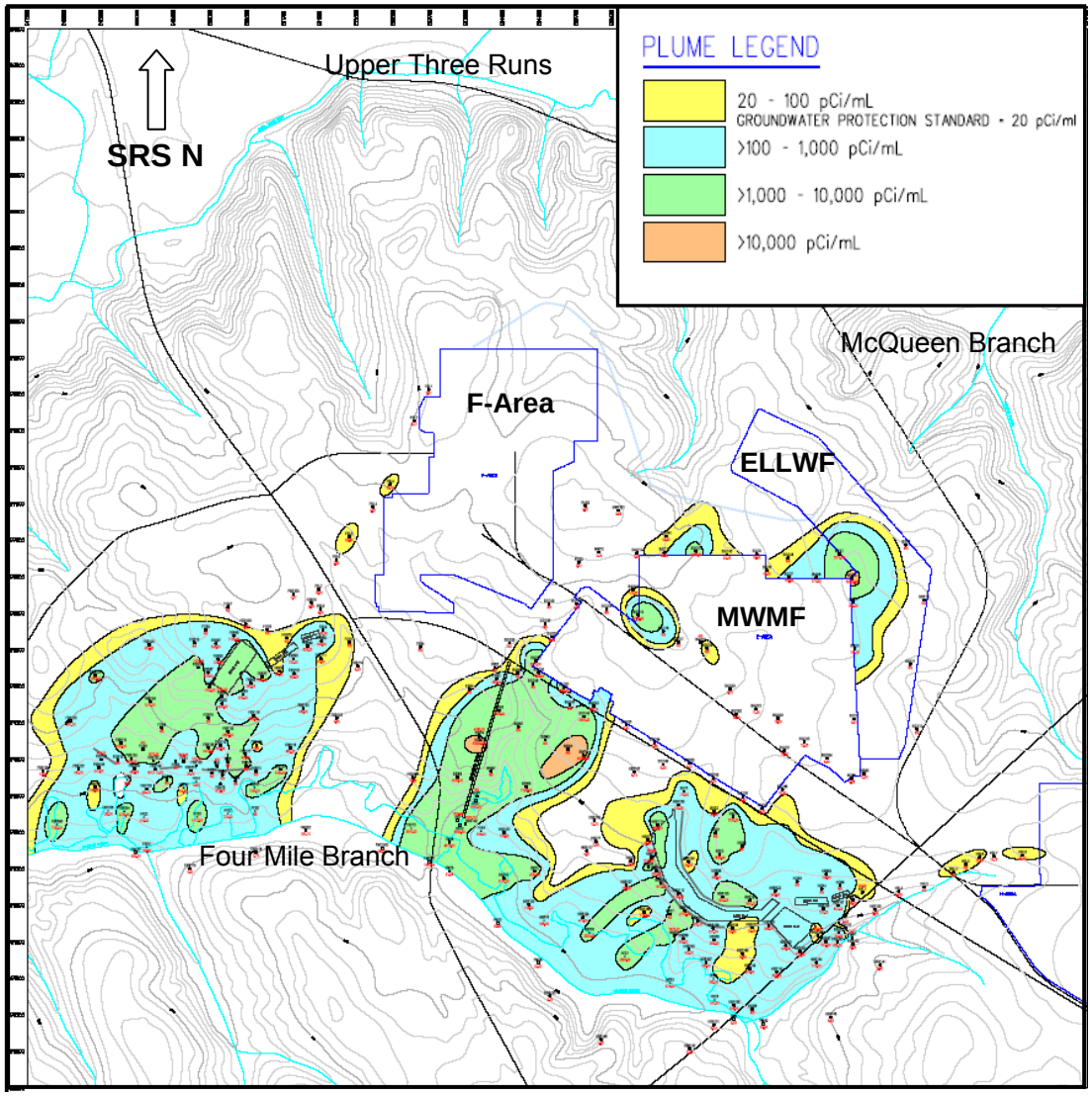

Figure G- 12. E-Area Vicinity Tritium Plumes Moving to North and South Sides of Groundwater Divide in the Upper Aquifer Zone (UAZ) of the UTRA

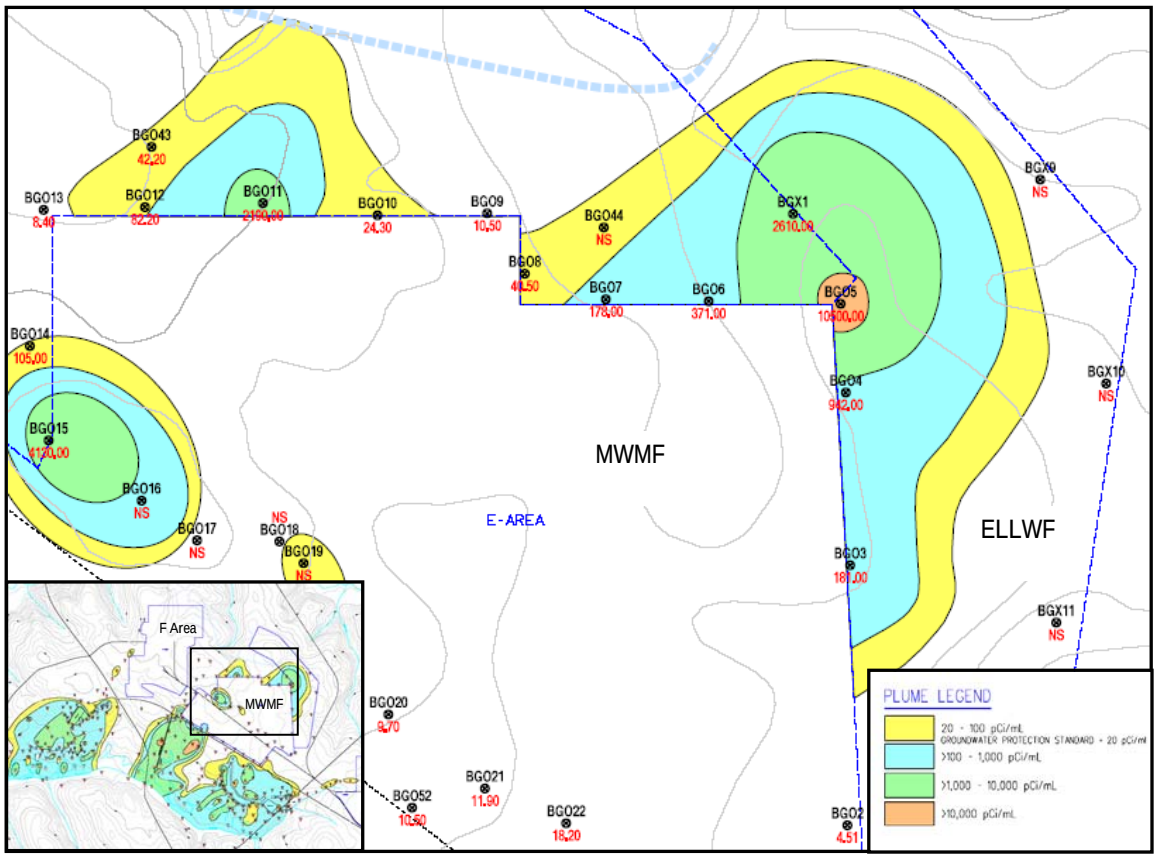

Figure G- 13. Closeup of Tritium Plumes Moving from MWMF to ELLWF in the Upper Aquifer Zone (UAZ) of the UTRA

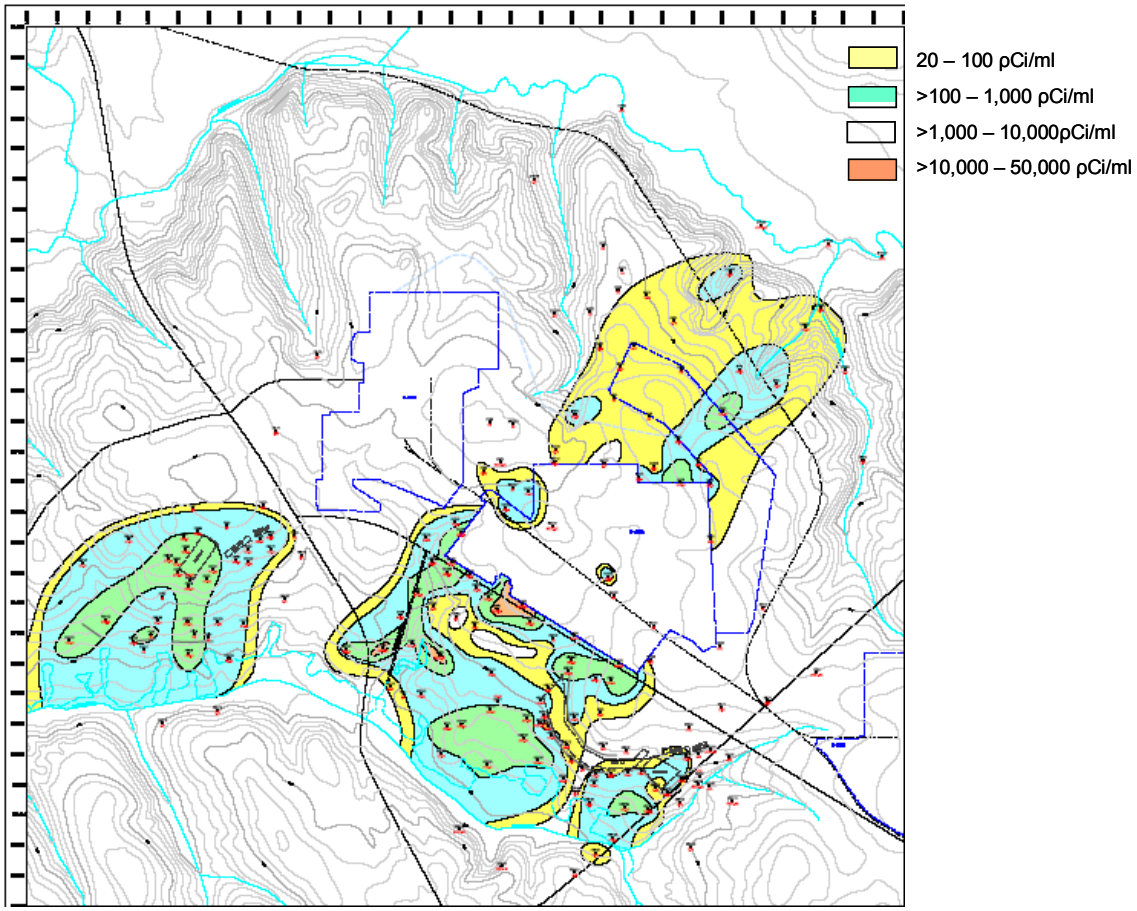

Figure G- 14. E-Area Vicinity Tritium Plumes Moving to North and South Sides of Groundwater Divide in the Lower Aquifer Zone (LAZ) of the UTRA

1.3 CONCEPTUAL MODEL SUPPORT

Summarizing the implications of the foregoing information in this appendix, the following general points form the basis of the hydrologic conceptual model for E-Area:

- Shallow groundwater flow is controlled by local recharge and topographic features (e.g., stream elevations)
- Shallow groundwater flow is driven primarily by local recharge (~ 1/3 of rainfall), and to a lesser extent by leakage through the Gordon confining unit
- Contamination in the GSA migrates primarily through the UTR aquifer and discharges to the local surface water (Upper Three Runs and/or Fourmile Branch)
- Nearly all contamination from E-Area disposal units migrates to Upper Three Runs above the Gordon confining unit, with only trace amounts entering the Gordon aquifer

The UAZ and LAZ tritium plume maps (Figure G- 12 and Figure G- 14) support these points, by illustrating the interception of the plumes by UTR and Four Mile Branch. A comparison of the UAZ tritium plume from the MWMF with the LAZ tritium plume from the MWMF clearly demonstrates a downward gradient from the UAZ to the LAZ, and indicates that the UAZ does not extend to Upper Three Runs or Crouch Branch (a tributary to UTR).

Precipitation at the SRS tends to be less variable when compared to other sites. Although seasonal variations may affect hydraulic head gradients, significant changes in flow direction have not been observed. Since transport is advection dominated in this environment, the flow directions are not significantly different throughout the year, and precipitation is fairly constant from year to year, it was determined that a steady state solution of the computational implementation of the model would be suitable. While the location of the groundwater divide may move slightly from year to year, the fact that the vertical flux in the vicinity of the divide is much more significant than the lateral flux (see Figure G- 3) does not argue against the use of the steady-state flow assumption. The groundwater divide is clearly shown as existing between the MWMF and the OBG in Figure G- 12 and Figure G- 14, and there is no indication from the plume maps that the groundwater divide shifts significantly in one direction or another with changes in the water table elevation.

The PORFLOW code (ACRI 2004) was selected for implementing the conceptual model for several reasons. PORFLOW has the ability to simulate first-order decay and progeny ingrowth associated with radionuclide chains. PORFLOW implements a variably-saturated equation set, so is useful for simulating flow and transport in both the vadose zone and saturated zone. This code also employs an extensive set of powerful “keyword” commands that minimize data pre- and post-processing.

Finally, the SRS has a considerable base of personnel with experience using the PORFLOW code, and code verification and limited site-specific model validation work has been carried out at the SRS with satisfactory results for the E-Area application. The model verification work is documented in Aleman (2007), and includes ten problems specified to determine the accuracy of solutions addressing saturated and variably saturated groundwater flow in one and two dimensions (under steady-state and transient conditions), five problems addressing contaminant transport in one, two and three dimensions (transient), one problem designed to evaluate numerical dispersion, and problems posed to evaluate the accuracy of implementation of some of the Keyword Commands. Validation work is described in the following section.

1.4 PRELIMINARY PORFLOW MODEL VALIDATION

Validation of the PORFLOW-based model for use in the ELLWF PA has addressed both vadose zone and groundwater modeling applications. Results, to date, of validation studies relevant to the ELLWF PA are summarized below.

1.4.1 Vadose Zone Flow Model Validation Studies

For the vadose zone, comparison of VZMS data with PORFLOW-derived values of suction head and saturation were made. A suction head of 83 cm and saturation of 91% were predicted by the numerical simulations for the upper vadose zone, as were a suction head of 170 cm and 72% saturation for the lower vadose zone (Phifer et al. 2006). These results show reasonable agreement with field measurements of the same parameters from the VZMS, which indicate an approximate range of soil suction from 50 to 200 cm, and a water content of 15 to 30% (which suggests saturation levels between 35 to 75%) (Phifer et al. 2006).

Using the PORFLOW-derived saturation values, the recommended value of porosity based on measurements (0.39 from Phifer et al. 2006), and the estimated infiltration over the local area (12 in/yr from Phifer et al. 2006), pore water velocity can be estimated from:

$$Pore\ water\ velocity = \frac{Infiltration}{(Porosity) * (Saturation)},$$

where infiltration is the flux of water into the vadose zone, and the denominator [(porosity) * (saturation)] represents the amount of water-filled space through which movement of soil moisture in the subsurface can occur (Millings and Flach 2007). Calculations for the upper and lower vadose zones yield the following estimates of pore water velocity:

- Upper vadose zone pore water velocity = (12 in/yr) / [(0./39)*(0.91)] = ~ 34 in/yr
- Lower vadose zone pore water velocity = (12 in/yr) / [(0.39)*0.72)] = ~ 43 in/yr

These estimates are consistent with field measurements using a deuterium tracer made by Haskell and Hawkins (1964) and Hawkins and Horton (1967) for a sandy loam to sandy clay sediment near the SRS Burial Grounds. These researchers reported downward movements of water of 0.94 and 0.96 in per in of rainfall, respectively. For an average rainfall of 48 in/yr, this yields a pore velocity of approximately 46 in/yr, which is similar to the estimates for the upper and lower vadose zones.

1.4.2 Vadose Zone Transport Model Validation Studies

As the disposal in Slit Trenches #1 and #2 neared volume capacity, a preliminary closure analysis focusing on the groundwater pathway was conducted (Flach et al. 2005). Part of this analysis involved comparison of VZMS measurements made to monitor the downward flux of water and contaminants in the vadose zone near Slit Trenches #1. A graphical layout of the VZMS for Slit Trenches #1 is depicted in Figure G- 15. Vertical and angled lysimeters, installed as part of the VZMS, are routinely sampled and analyzed for tritium. In order to compare the tritium monitoring data to model predictions of tritium migration from the slit trenches, it was necessary to adjust the raw tritium data collected to account for background contributions of tritium from rainwater. Further, the concentration data collected had to be transformed to correspond to the 1-cm (implied by using a 2-dimensional representation) vertical slice through trench segments represented by the flow and transport model implemented with PORFLOW, as well as to the elapsed time scale of the model (Flach et al. 2005).

From the standpoint of model manipulations done to accomplish the comparison, concentration histories at four nodes corresponding to lysimeter locations were recorded during simulations. Data from lysimeters located on the edge of the trench segment were assigned the position category “edge”; data from angled lysimeter were assigned the category “center”. With respect to depth, data from lysimeters located below a depth of 30 ft bgs were assigned an elevation category of “low”; those above 30 ft bgs were assigned an elevation category of “high”. These groupings are depicted in Figure G- 16.

In Figure G- 17, the VZMS adjusted data for tritium are plotted against the predicted values at the corresponding center and edge high and low locations using PORFLOW. In this figure, “Generic” refers to segments of the slit trenches in which the maximum radioactivity is associated with generic waste (i.e., not concrete rubble). For segments in which the maximum activity is associated with concrete rubble, the data were assigned the designation “Concrete”.

Differences between the VZMS data and the model predictions can possibly be attributed to the heterogeneity of the sediments beneath Slit Trench #1. Heterogeneous sediments beneath the trench segments would cause lateral spreading of the tritium plume to the edge of the trench where it would be subsequently measured in the VZMS lysimeters. Since the model does not account for this heterogeneity, it would tend to under predict concentrations at the edge of the trench at shallow depths.

Therefore, it is reasonable to expect the model output from the center and edge position to bracket the VZMS results. Figure G- 17 shows that the predicted concentrations for the center and edge positions bracket the VZMS results well for the concrete waste type. However, for the generic waste type, the data is more scattered but generally less than the predicted concentrations.

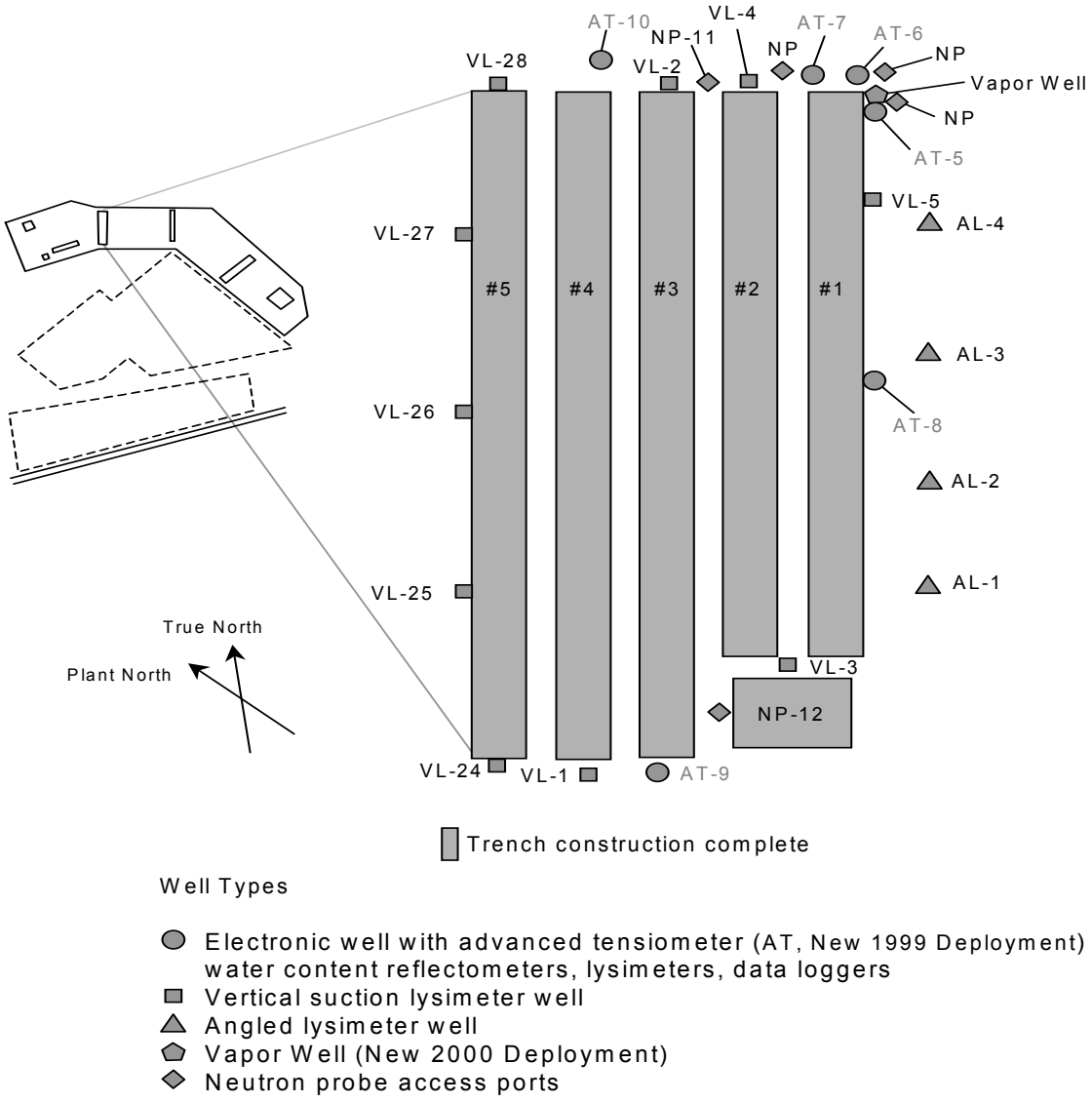

Figure G- 15. Layout of VZMS for Slit Trenches #1, showing lysimeter locations

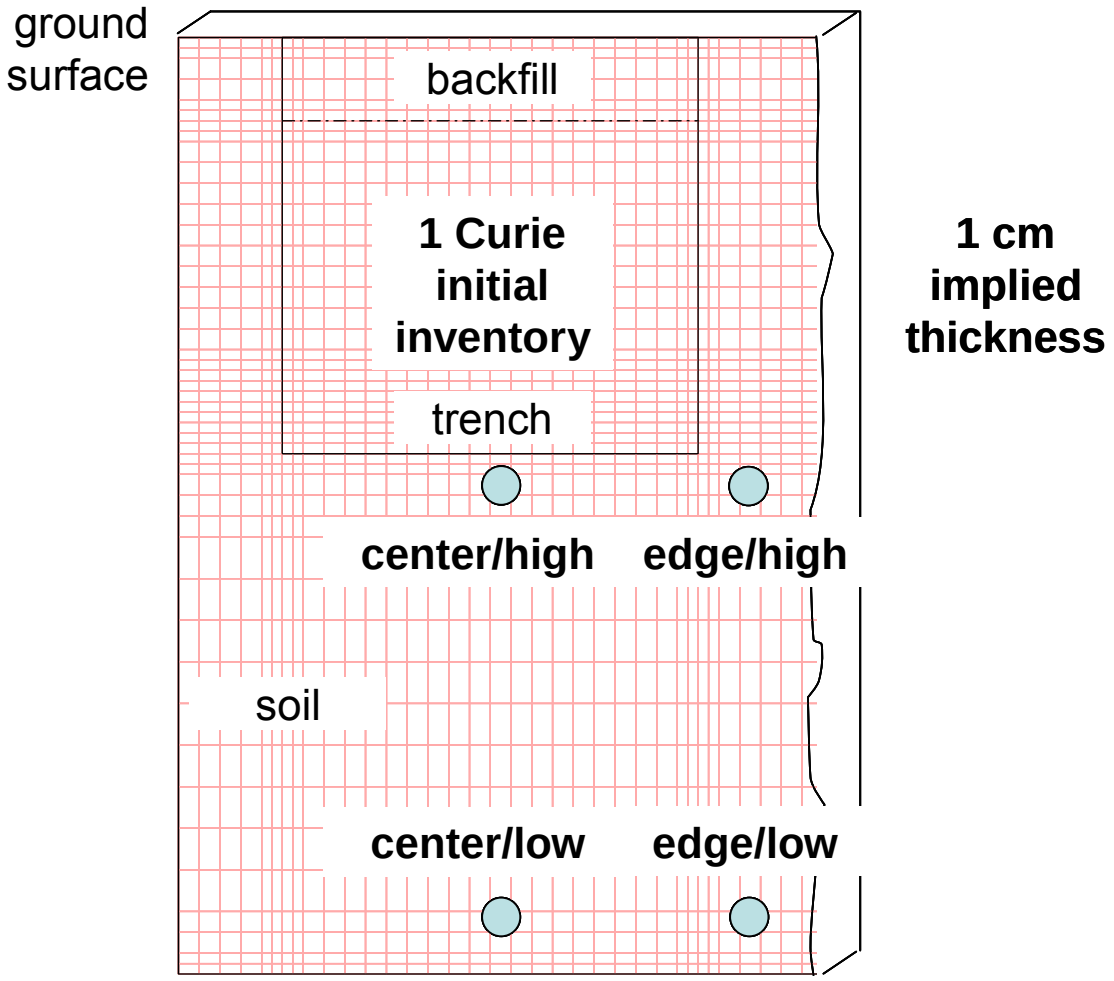

Figure G- 16. Basis for Comparison of PORFLOW Results and VZMS Data

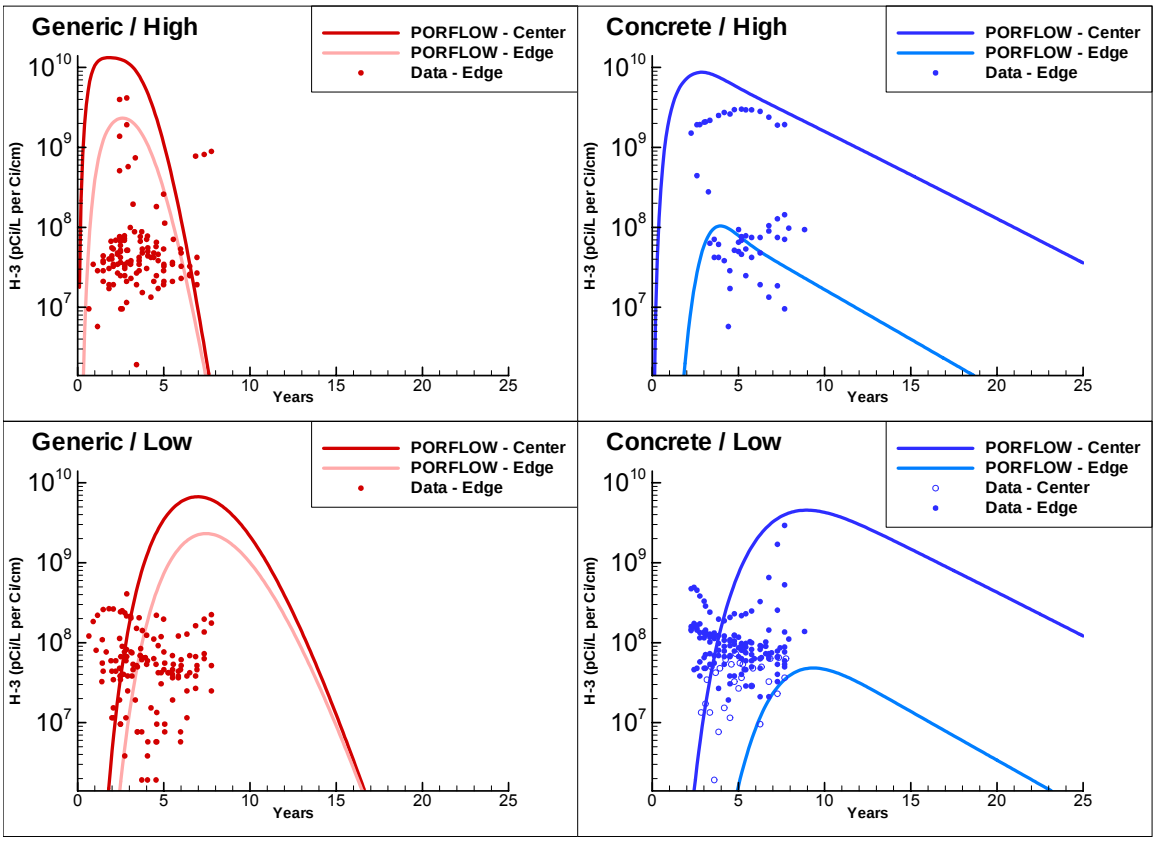

Figure G- 17. VZMS Data versus PORFLOW Vadose Zone Predictions

In general, model predictions from the center and edge of the trench can be expected to bracket the VZMS field data. More scatter is observed in the field data for the generic waste type than the concrete waste type. This is because the generic waste type has a higher conductivity than the native sediments which results in a flow field conducive to spreading of the contaminant plume beneath the trench. Because the concrete waste type has a low conductivity, water tends to flow around the trench and bend sharply in towards the centerline once below the trench. This limits plume spreading and scatter in the field data.

1.4.3 Saturated Zone Flow and Transport Model Validation Studies

Model validation work on the saturated zone has involved comparison of predicted versus measured seepage faces near E-Area (Figure G- 18), and comparison of predicted flow pathlines with measured tritium plumes emanating from the MWMF (Figure G- 19). Figure G- 18 defines seepage faces simulated by the GSA/PORFLOW model (Flach 2004). The seepline predicted by the model is the border between recharge (red) and discharge (blue) areas. A survey of the seepline in the early 1990s is shown in the figure for comparison. The surveyed seepline and simulated seepline show good agreement.

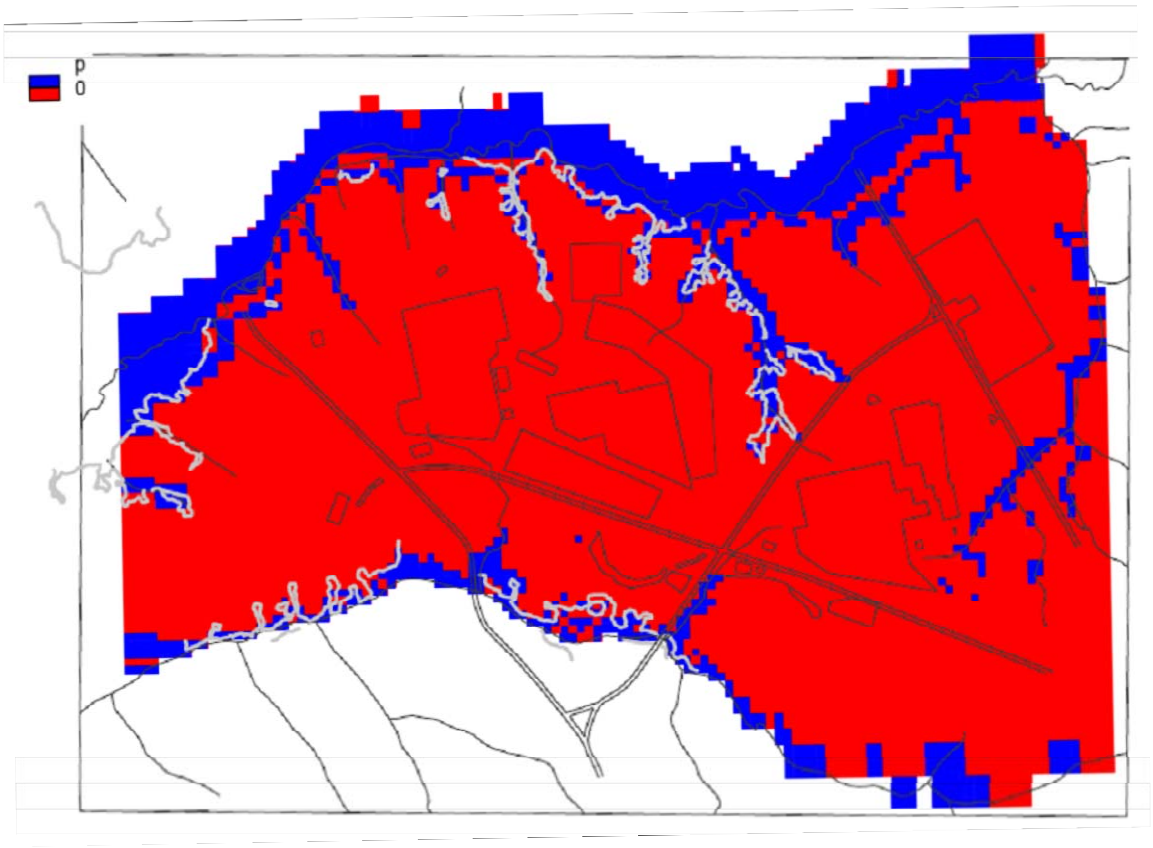

Figure G- 18. Surveyed Seepline (gray line) and Predicted Seepline (border between red and blue areas)

The results of particle tracking simulations based on the velocity fields from the GSA/PORFLOW model are shown in Figure G- 19. The dots on the particle trajectory lines represent 5-year travel times. This figure shows, by comparing the predicted particle trajectories with the measured tritium plume shape, that the PORFLOW model is reasonably predicting the direction of mass (i.e., particle) transport.

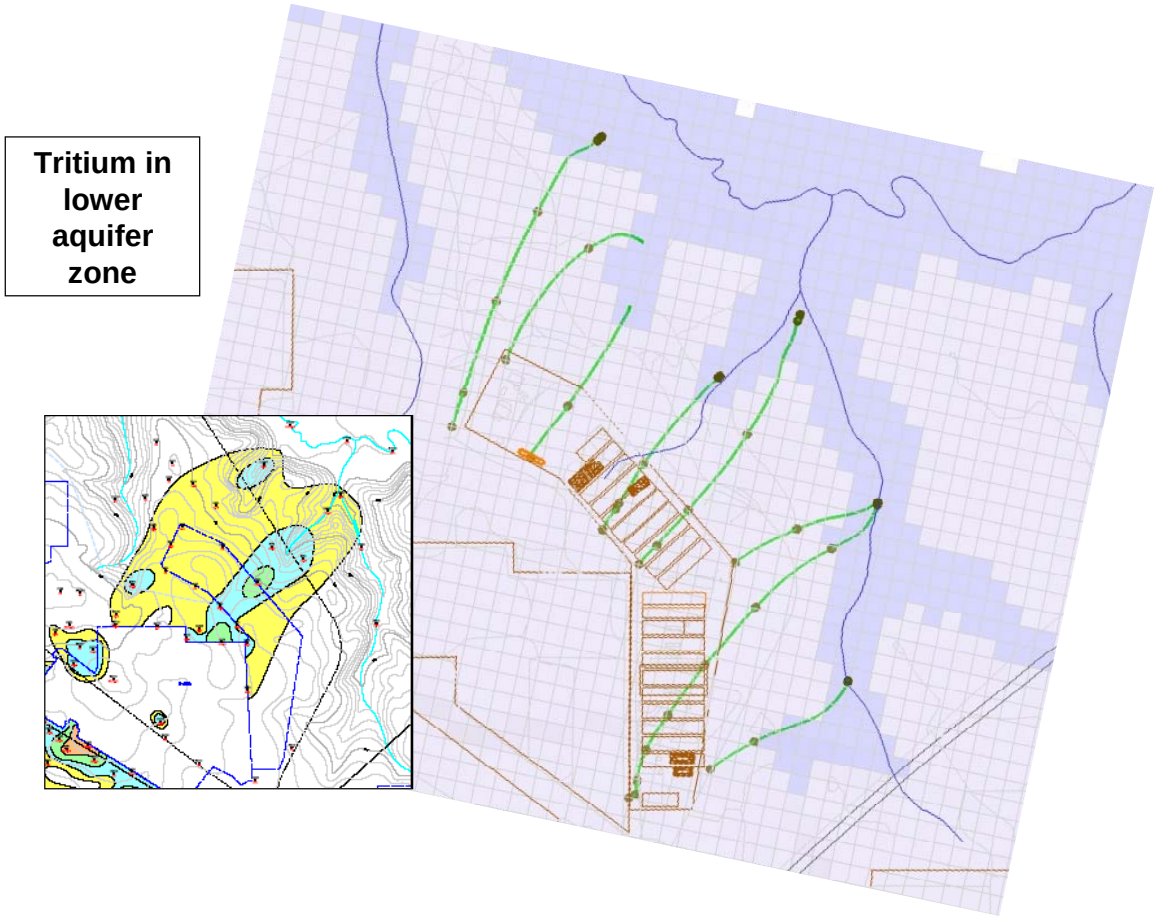

Figure G- 19. Tritium Plume versus Model-predicted Groundwater Pathlines (5-year time markers shown)

1.5 REFERENCES

Aadland, R. K., Harris, M. K., Lewis, C. M., Gaughan, T. F. and Westbrook, T. M. 1991. *Hydrostratigraphy of the General Separations Area, Savannah River Site (SRS), South Carolina*, WSRC-RP-91-13, Westinghouse Savannah River Company, Aiken, SC.

ACRI (Analytic & Computational Research, Inc.). 2004. *PORFLOW User's Manual*, Version 5.0, Rev: 5. Available at http://www.acricfd.com/download/papers/PORFLOW.pdf

Aleman, S. E. 2007. *PORFLOW Testing and Verification Document*, WSRC-STI-2007-00159, Rev. 0, Washington Savannah River Company, Aiken, SC, June 2007.

Cahill, J. M. 1982. *Hydrology of the Low-Level Radioactive-Solid-Waste Burial Site and Vicinity near Barnwell, South Carolina*, open-File Report 82-863" Columbia, South Carolina, U. S. Geological survey, 101 p.

Cook, J. R. 2002. *Performance Assessment Monitoring Plan for the E-Area Low-Level Waste Facility*, SW&I-SWE-98-0153, Rev. 4, December 2002.

J. R. Cook and K. P. Crapse. 2005. *Composite Analysis Monitoring Plan.* WSRC-RP-2000-00326, Westinghouse Savannah River Company, Revision 2, February, 2005.

Denham, M. E. 1999. *SRS Geology/Hydrogeology Environmental Information Document*, WSRC-TR-95-0046, Westinghouse Savannah River Company, Aiken, SC.

Dennehy, K. F. and McMahon, P. B. 1989. *Water Movement in the Unsaturated Zone at a Low-Level Radioactive-Waste Burial Site near Barnwell, South Carolina*, United States Geological Survey Water-Supply Paper 2345: Denver, Colorado, U. S. Geological Survey, United States Government Printing Office, 40 p.

Flach, G. P. and Harris, M. K. 1999. *Integrated Hydrogeological Model of the General Separations Area (U), Volume 2: Groundwater Flow Model (U)*, WSRC-TR-96-0399, Rev. 1, Westinghouse Savannah River Company, Aiken, SC.

Flach, G. P. 2004. *Groundwater Flow Model of the General Separations Area Using PORFLOW (U)*, WSRC-TR-2004-00106, Westinghouse Savannah River Company LLC, Aiken, SC, July 15, 2004.

Flach, G. P., Collard, L. B., Phifer, M. A., Crapse, K. P., Dixon, K. L., Koffman, L. D. and Wilhite, E. L. 2005. *Preliminary Closure Analysis for Slit Trenches #1 and #2*, WSRC-TR-2005-00093, Westinghouse Savannah River Company, Aiken, SC, March 9, 2005.

Haskell, C. C. and Hawkins, R. H., 1964. *D_2O-Na^{24} Method for Tracing Soil Moisture Movement in the Field*, Soil Science Society of America Proceedings, vol 28, p 725-728.

Hawkins, R. H. and Horton, H. H., 1967. *Bentonite as a Protective Cover for Buried Radioactive Waste,* Health Physics, vol 13, p 287-292.

Hubbard, J. E. and Emslie, R. H. 1984. *Water Budget for SRP Burial Ground Area*, DPST-83-742, E. I. du Pont de Nemours and Company, Savannah River Plant, Aiken, South Carolina, March 19, 1984.

Hubbard, J. E. 1986. *An Update on the SRP Burial Ground Area Water Balance and Hydrology*, DPST-95-958. E. I. du Pont de Nemours and Company, Savannah River Plant, Aiken, South Carolina, January 9, 1986.

Hubbard, J. E. and Englehardt M. 1987. *Calculation of Groundwater Recharge at the old SRP Burial Ground Using the CREAMS Model (1961-1986),* State University of New York, Brockport, New York, Summer 1987 (report prepared for E. I. du Pont de Nemours and Company, Savannah River Plant, Aiken, South Carolina and given DuPont document number DP-MS-87-126)

Mamatey, A. R. 2006. *Savannah River Site Environmental Report for 2005*, WSRC-TR-2006-00007, Washington Savannah River Company, Savannah River Site, Aiken, SC.

McDowell-Boyer, L. A. D. Yu, J. R. Cook, D. C. Kocher, E. L. Wilhite, H. Holmes-Burns, and K. E. Young. 2000. *Radiological Performance Assessment for the E-Area Low-Level Waste Facility*, WSRC-RP-94-218, Rev. 1. Westinghouse Savannah River Company, Aiken, SC.

Millings, M. R. and Flach, G. P. 2007. *Hydrogeologic Data Summary in Support of the F-Area Tank Farm (FTF) Performance Assessment (PA),* WSRC-TR-2007-00283, Revision 0, Washington Savannah River Company, Aiken, SC, July 2007.

Parizek, R. R. and Root, R. W. 1986. *Development of a Ground-Water Velocity Model for the Radioactive Waste Management Facility Savannah River Plant,* South Carolina, The Pennsylvania State University, University Park, Pennsylvania, June 1986 (report prepared for E. I. du Pont de Nemours and Company, Savannah River Plant, Aiken, South Carolina and given DuPont document number DPST-86-658)

Phifer, M. A., Millings, M. R., and Flach, G. P. 2006. *Hydraulic Property Data Package for the E-Area and Z-Area Vadose Zone Soils, Cementitious Materials, and Waste Zones,* WSRC-STI-2006-00198, Rev. 0, Washington Savannah River Company, Aiken, SC.

Phifer, M. A., Jones, W. E., Nelson, E. A., Denham, M. E., Lewis, M. R., Shine, E. P. 2007. *FTF Closure Cap Concept and Infiltration Estimates*, WSRC-STI-2007-00184, Revision 2, Washington Savannah River Company, Aiken, SC, October 2007.

Smits, A. D., Harris, M. K., Hawkins, K. L., and Flach, G. P. 1997. *Integrated Hydrogeological Model of the General Separations Area, Volume 1: Hydrogeologic Framework*, WSRC-TR-96-0399, Rev. 0, Westinghouse Savannah River Company, Aiken, SC.

Swingle, R. F., II, Sink, D. F, Milllings, M. R., and Crapse, K. P. 2008. *FY2007 Annual Review, E-Area Low-level Waste Facility Performance Assessment and Composite Analysis*, WSRC-RP-2008-00228, Rev. 0, Washington Savannah River Company, Aiken, SC, February 22, 2008.

WSRC (Westinghouse Savannah River Company). 1997. *Composite Analysis, E-Area Vaults and Saltstone Disposal Facilities*, WSRC-RP-97-311, Rev. 0, Westinghouse Savannah River Company, Aiken, SC.

WSRC (Washington Savannah River Company). 2006. *Semi-Annual Corrective Action Report for the F-Area Hazardous Waste Management Facility, the H-Area Hazardous Waste Management Facility, and the Mixed Waste Management Facility (U)*, WSRC-RP-2006-04043, Revision 0, Washington Savannah River Company, Aiken, SC, October, 2006.

Young, M. H. and Pohlmann, K. F. 2001. *Analysis of Vadose Zone Monitoring System: Computer Simulation of Water Flux: E-Area Disposal Trenches*, Task Order GA0074 (KG43360-0). Division of Hydrologic Sciences, Desert Research Institute, Las Vegas, NV. August 2001.

Young, M. H. and Pohlmann, K. F. 2003. *Analysis of Vadose Zone Monitoring System: Computer Simulation of Water Flux under Conditions of Variable Vegetative Cover: E-Area Disposal Trenches*, Publication No. 41188. Division of Hydrologic Sciences, Desert Research Institute, Las Vegas, NV. August 2001.

This page intentionally left blank.